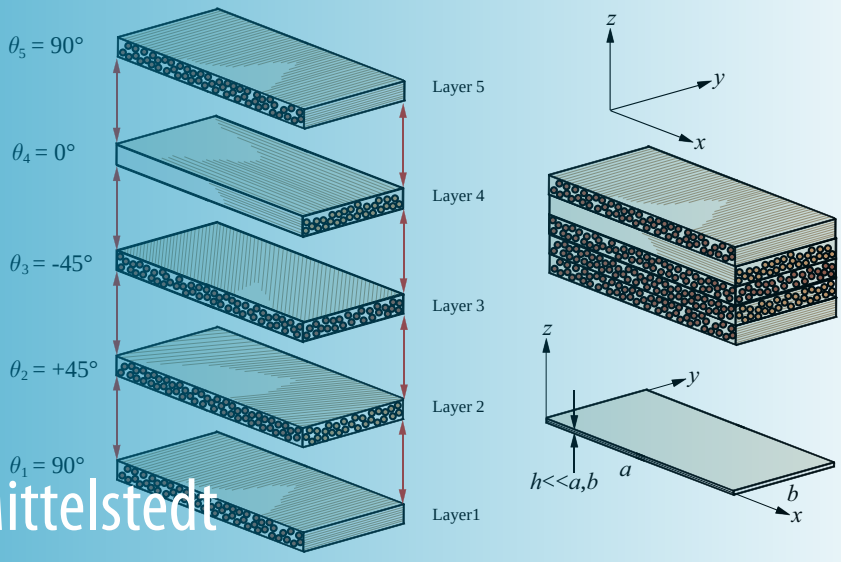


Christian Mittelstedt

Mechanics of Composite Structures

Springer

Mechanics of Composite Structures

Christian Mittelstedt

Mechanics of Composite Structures

Springer

Christian Mittelstedt
Fachbereich Maschinenbau
Technical University of Darmstadt
Darmstadt, Hessen, Germany

ISBN 978-3-662-70787-6 ISBN 978-3-662-70788-3 (eBook)
https://doi.org/10.1007/978-3-662-70788-3

Translation from the German language edition: “Mechanik geschichteter Strukturen” by Christian Mittelstedt, © Der/die Herausgeber bzw. der/die Autor(en), exklusiv lizenziert an Springer-Verlag GmbH, DE, ein Teil von Springer Nature 2025. Published by Springer Berlin Heidelberg. All Rights Reserved.

© The Editor(s) (if applicable) and The Author(s), under exclusive license to Springer-Verlag GmbH, DE, part of Springer Nature 2025

This work is subject to copyright. All rights are solely and exclusively licensed by the Publisher, whether the whole or part of the material is concerned, specifically the rights of translation, reprinting, reuse of illustrations, recitation, broadcasting, reproduction on microfilms or in any other physical way, and transmission or information storage and retrieval, electronic adaptation, computer software, or by similar or dissimilar methodology now known or hereafter developed.
The use of general descriptive names, registered names, trademarks, service marks, etc. in this publication does not imply, even in the absence of a specific statement, that such names are exempt from the relevant protective laws and regulations and therefore free for general use.
The publisher, the authors and the editors are safe to assume that the advice and information in this book are believed to be true and accurate at the date of publication. Neither the publisher nor the authors or the editors give a warranty, expressed or implied, with respect to the material contained herein or for any errors or omissions that may have been made. The publisher remains neutral with regard to jurisdictional claims in published maps and institutional affiliations.

This Springer imprint is published by the registered company Springer-Verlag GmbH, DE, part of Springer Nature
The registered company address is: Heidelberger Platz 3, 14197 Berlin, Germany

If disposing of this product, please recycle the paper.

Preface

This book is a significantly expanded version of the book ‘Structural Mechanics of Plane Composite Laminates’ (in German ‘Strukturmechanik ebener Laminate’), which was published in 2016 by the Mechanics Department of the Technical University of Darmstadt, Germany, in collaboration with my esteemed colleague Wilfried Becker. However, the further development of my teaching in the field of composites structures since the first edition was published has made a new edition necessary. In addition, the publishing house of the Mechanics Department of the Technical University of Darmstadt has ceased its work, so that alternative ways of distribution had to be found. In the course of revising this book, some significant new content was added, so that the title was adapted to ‘Mechanics of Composite Structures’. This significantly expanded version of the original book is a further contribution to a series of books on structural mechanics in lightweight engineering, which began with the book ‘Structural Mechanics in Lightweight Engineering’ and was continued with the two books ‘Theory of Plates and Shells’ and ‘Buckling of Beams, Plates and Shells’.

I would like to take this opportunity to thank my colleague Wilfried Becker for his understanding of my wish to develop this book further on my own initiative. I would also like to thank the research assistants and students whose work forms the basis of some of the content of this book.

Darmstadt, Germany
Winter 2024

Christian Mittelstedt

Competing Interests The author has no competing interests to declare that are relevant to the content of this manuscript.

Contents

1 Introduction 1
- 1.1 Basic Concepts 1
- 1.2 Motivation and Structure of This Book 4
- 1.3 Further Literature References 9
- 1.4 Nomenclature 10
- References 11

Part I Theory of Elasticity

2 Some Basic Concepts of the Theory of Elasticity 15
- 2.1 Introduction 15
- 2.2 State of Stress 18
  - 2.2.1 Stress Vector and Stress Tensor 18
  - 2.2.2 Transformation Rules 22
  - 2.2.3 Principal Stresses, Invariants, Mohr's Circles 24
  - 2.2.4 Hydrostatic Stress State, Deviator 26
  - 2.2.5 Equilibrium Conditions 27
- 2.3 Deformation and Strains 29
  - 2.3.1 Introduction 29
  - 2.3.2 Green-Lagrange Strain Tensor 32
  - 2.3.3 Von-Kármán Strains 34
  - 2.3.4 Infinitesimal Strain Tensor 34
  - 2.3.5 Compatibility Conditions 37
- 2.4 Constitutive Law 38
  - 2.4.1 Introduction 38
  - 2.4.2 The Generalized Hooke's Law 39
  - 2.4.3 Strain Energy 42
- 2.5 Boundary Value Problems 45
- 2.6 Thermal Strains 47
- References 49

3 Plane Problems and Surface Structures 51
3.1 Surface Structures 52
3.2 Plane State of Strain 56
3.3 Plane State of Stress 58
3.4 Analysis of Isotropic Disks 59
3.4.1 Airy's Stress Function, Bipotential Equation 59
3.4.2 Selected Examples for Solving Disk Problems 62
3.5 Analysis of Shear-Rigid Isotropic Plates 67
3.5.1 Kinematics in the Context of Kirchhoff's Plate Theory 67
3.5.2 Internal Forces, Equilibrium, Plate Equation 70
3.5.3 Equivalent Transverse Shear Forces and Boundary Conditions 73
3.5.4 Navier Solution 76
3.5.5 Lévy Solution 79
References 82

4 Variational Principles and Approximation Methods in Structural Mechanics 85
4.1 General Theorem of Work 86
4.2 Principle of Virtual Displacements 88
4.3 Principle of Virtual Forces 89
4.4 Extremal Principles 91
4.4.1 The Principle of the Stationary Value of the Total Potential 91
4.4.2 The Principle of the Stationary Value of the Total Complementary Potential 92
4.5 Analysis Rules for the δ-Operator 93
4.6 Application to Simple Mechanical Systems 94
4.6.1 Beam Under Line Load $n(x)$ and Single Force F 94
4.6.2 Beam Under Line Load $q(x)$ and Single Force F 100
4.7 Approximation Methods 104
4.7.1 The Ritz Method 105
4.7.2 The Galerkin Method 114
4.7.3 The Finite Element Method 115
References 121

5 Strength Hypotheses for Isotropic Materials 123
5.1 Introduction 123
5.2 Principal Stress Hypothesis 126
5.3 Principal Strain Hypothesis 127
5.4 Beltrami Strain Energy Hypothesis 128
5.5 von Mises Strain Energy Hypothesis 129
5.6 Tresca Yield Criterion 131
5.7 Coulomb-Mohr Hypothesis 131
5.8 Drucker-Prager Hypothesis 134
5.9 Cuntze's Failure Mode Concept (FMC) 135
References 138

Part II Analysis of Plane Composite Laminates

6 Mechanics of a Laminate Layer 141
6.1 Introduction 141
6.2 Material Law of a Single Laminate Layer 142
6.2.1 Full Anisotropy 142
6.2.2 Monoclinic Material 143
6.2.3 Orthogonal Anisotropy/Orthotropy 145
6.2.4 Transversal Isotropy 146
6.2.5 Isotropy 147
6.2.6 Representation Using Engineering Constants 148
6.2.7 Transformation Rules 150
6.3 Formulation for the Plane Case 154
6.4 Effective Stiffnesses of a Unidirectional Single Layer, Rules of Mixture 157
6.4.1 Introduction 157
6.4.2 Modulus of Elasticity in Fiber Direction 159
6.4.3 Modulus of Elasticity Perpendicular to the Fiber Direction 160
6.4.4 Poisson's Ratio 162
6.4.5 Shear Modulus 162
6.4.6 Improved Rules of Mixture, Limit Values 163
References 164

7 Classical Laminated Plate Theory 165
7.1 Introduction 165
7.2 Assumptions and Kinematics 167
7.3 Strains and Stresses 170
7.4 Constitutive Law 173

7.5 Coupling Effects 176
7.5.1 Shear Coupling 177
7.5.2 Bending-Twisting Coupling 178
7.5.3 Bending-Extension Coupling 178
7.5.4 Remarks on Coupling Effects 179
7.6 Special Laminates 180
7.6.1 Isotropic Single Layer 180
7.6.2 Orthotropic Single Layer 181
7.6.3 Anisotropic Single Layer/Off-Axis Single Layer 181
7.6.4 Symmetric Laminates 181
7.6.5 Cross-Ply Laminates 182
7.6.6 Angle-Ply Laminates 182
7.6.7 Quasi-isotropic Laminate 183
7.7 Change of the Reference Plane 184
7.8 Effective Properties of Laminates 185
7.8.1 Inplane Modulus of Elasticity E_{xx} 186
7.8.2 Inplane Modulus of Elasticity E_{yy} 186
7.8.3 Inplane Shear Modulus G_{xy} 187
7.8.4 Inplane Poisson's Ratio ν_{xy} 187
7.8.5 Modulus of Elasticity $E_{xx,B}$ Under Bending 188
7.8.6 Modulus of Elasticity $E_{yy,B}$ Under Bending 189
7.8.7 Approximate Calculation of Effective Properties 190
7.9 Strain Energy of a Laminate 190
7.10 Consideration of the Bending-Extension Coupling for Unsymmetric Laminates 193
References 194

8 Static and Dynamic Laminate Problems 197
8.1 Static Equilibrium and Displacement Differential Equations of a Laminate 197
8.2 Laminate Boundary Conditions 201
8.3 Energetic Derivation of the Governing Equations 203
8.4 Dimensionless Notation 209
8.5 Examples for Exact Solutions 213
8.5.1 Navier Solutions 213
8.5.2 Lévy Solutions 224
8.6 The Ritz Method 229
8.6.1 Energetic Considerations and Ritz Equations 229
8.6.2 Shape Functions for Symmetric Orthotropic Laminates 233
8.6.3 Selected Closed-Form Analytical Approximate Solutions 237

8.6.4 Bending of a Laminate with Arbitrary Symmetric Layup Using the Ritz Method 243
8.7 Nonlinear Equations of Motion 252
8.8 Vibrations 263
8.8.1 Navier Solution for Symmetric Orthotropic Laminates 263
8.8.2 Navier Solution for Unsymmetric Cross-Ply Laminates 263
8.8.3 Navier Solution for Unsymmetric Angle-Ply Laminates 266
8.9 The Finite Element Method 269
References 271

9 Strength Hypotheses for Unidirectionally Fiber-Reinforced Laminate Layers 273
9.1 Introduction 273
9.2 Maximum Stress Criterion 274
9.3 Maximum Strain Criterion 274
9.4 Tsai-Hill Criterion 275
9.5 Tsai-Wu Criterion 275
9.6 Puck Criterion 277
9.7 Hashin Criterion 278
9.8 Puck's Action Plane Fracture Criterion 279
9.9 Cuntze's Failure Mode Concept (FMC) 283
References 288

10 Hygrothermal Problems 289
10.1 Introduction 289
10.2 Thermomechanical Problems 290
10.3 Hygromechanical Problems 293
References 298

11 Higher-Order Laminate Theories 299
11.1 Introduction 299
11.2 Three-Dimensional Local Equilibrium 301
11.3 First-Order Shear Deformation Theory 302
11.3.1 Kinematics and Constitutive Equations 302
11.3.2 Equilibrium and Boundary Conditions 307
11.3.3 Strain Energy 309
11.3.4 Determination of the Shear Correction Factor K 310
11.3.5 Selected Solutions for Boundary Value Problems of Static Laminate Problems 312

11.3.6 The Ritz Method 321
11.3.7 Nonlinear Equations of Motion 328
11.4 Third-Order Shear Deformation Theory According to Reddy 333
11.4.1 Introduction 333
11.4.2 Kinematics 334
11.4.3 Strains and Constitutive Equations 336
11.4.4 Equilibrium Conditions 340
11.4.5 Special Laminates 342
11.4.6 Navier Solutions 343
11.4.7 The Ritz Method 351
11.4.8 Equations of Motion 356
11.5 Layerwise Approaches 357
11.5.1 Introduction 357
11.5.2 Displacement Field 359
11.5.3 Kinematics and Stresses 361
11.5.4 Cylindrical Bending of a Cross-Ply Laminate: Exact Solution According to Pagano (1969) 362
References 365

Part III Buckling of Laminates

12 Navier-Type Solutions for Laminate Buckling Problems 369
12.1 Basic Equations in the Context of Classical Laminated Plate Theory 369
12.2 Navier Solutions in the Context of Classical Laminated Plate Theory 374
12.2.1 Navier Solution for a Simply-Supported Symmetric Cross-Ply Laminate Under Uniaxial Compressive Load 374
12.2.2 Navier Solution for a Simply-Supported Symmetric Cross-Ply Laminate Under Biaxial Load 380
12.2.3 Navier Solution for a Simply-Supported Unsymmetric Cross-Ply Laminate Under Uniaxial Compressive Load 383
12.2.4 Navier Solution for a Simply-Supported Unsymmetric Angle-Ply Laminate Under Uniaxial Compressive Load 386
12.3 Governing Equations for First-Order Shear Deformation Theory 390
12.4 Navier Solutions for First-Order Shear Deformation Theory 393

12.4.1 Navier Solution for a Simply Supported Symmetric Cross-Ply Laminate Under Uniaxial Compressive Load 393
12.4.2 Navier Solution for a Simply Supported Unsymmetric Cross-Ply Laminate Under Uniaxial Compressive Load 397
12.4.3 Navier Solution for a Simply Supported Unsymmetric Angle-Ply Laminate Under Uniaxial Compressive Load 399
References 402

13 Lévy-Type Solutions for Laminate Buckling Problems 403
13.1 Introduction 403
13.2 Case Distinctions and Alternative Solution Representations 405
13.3 Selected Lévy Solutions 408
13.3.1 Laminate with Three Simply Supported Edges and One Free Edge 408
13.3.2 Laminate with One Clamped and One Free Unloaded Edge 411
13.3.3 Laminate with One Elastically Restrained and One Free Unloaded Edge 413
13.3.4 Laminate with Two Elastically Restrained Unloaded Edges 416
13.3.5 Laminate with Two Clamped Unloaded Edges 417
13.3.6 Laminate with One Clamped and One Simply Supported Unloaded Edge 419
13.3.7 Laminate with One Elastically Restrained and One Simply Supported Unloaded Edge 420
13.3.8 Laminate with One Elastically Restrained and One Clamped Unloaded Edge 420
13.4 Lévy Solutions for Shear-Deformable Laminates 421
References 430

14 Energy Methods for Laminate Buckling Problems 431
14.1 Energetic Derivation of the Governing Equations 431
14.2 The Rayleigh Quotient for Laminates Without Bending-Twisting Coupling 437
14.2.1 Methodology 437
14.2.2 Simply Supported Laminate 440
14.2.3 Laminate with Clamped Unloaded Edges 442
14.2.4 Laminate with Elastically Restrained Unloaded Edges 445

14.2.5 Laminate with Three Simply Supported Edges and One Free Unloaded Edge 450
14.2.6 Laminate with One Clamped and One Free Unloaded Edge 452
14.2.7 Laminate with One Elastically Restrained and One Free Unloaded Edge 454
14.2.8 Laminate with One Simply Supported and One Clamped Unloaded Edge 457
14.2.9 Laminate with an Elastically Restrained and a Simply Supported Unloaded Edge 458
14.2.10 Laminate with One Elastically Restrained and One Clamped Unloaded Edge 459
14.3 The Rayleigh Quotient in the Framework of First-Order Shear Deformation Theory 461
14.4 The Rayleigh Quotient in the Framework of Third-Order Shear Deformation Theory 463
14.5 The Ritz Method for Arbitrary Symmetric Laminates 477
14.6 Laminates Under Inplane Shear Load 490
14.7 Laminates Under Inplane Bending 493
14.8 Load Case Interactions 494
14.9 Influence of Bending-Twisting Coupling on Buckling of Laminates 497
14.9.1 Influence of Bending-Twisting Coupling on Laminates Under Compression 497
14.9.2 Sign Dependence of the Buckling Load Under Inplane Shear Load 500
14.10 The Finite Element Method for Linear Buckling Problems 507
References 508

15 The Ritz Method for Buckling Analysis of Shear-Deformable Laminates 511
15.1 The Ritz Method in the Framework of FSDT 511
15.1.1 Structural Situation and Basic Equations 511
15.1.2 Shape Functions and Energy Formulations 514
15.1.3 Eigenvalue Problem 519
15.2 Considered Boundary Conditions 521
15.2.1 Shape Functions for Case 1 521
15.2.2 Shape Functions for Case 2 522
15.2.3 Shape Functions for Case 3 523
15.2.4 Shape Functions for Case 4 523
15.2.5 Resultants of the Shape Functions 524
15.3 The Ritz Method in the Framework of TSDT 536

15.3.1 Resultants of the Shape Functions 542
Reference 563

16 Buckling of Unsymmetric Laminates 565
16.1 Closed-Form Analysis Approach 565
16.1.1 Analysis Approach 565
16.1.2 Shape Functions 573
16.1.3 Reduced Bending Stiffness Method 577
16.1.4 Results and Discussion 578
16.2 Lévy Solutions 584
16.2.1 Fundamental Equations 584
16.2.2 Lévy Solution 591
References 603

17 Buckling of Stiffened Laminates 605
17.1 Introduction 605
17.2 The Ritz Method for Longitudinally and Transversely Stiffened Laminates 607
17.3 Lévy Solution for Uniaxially Compressed Longitudinally Stiffened Laminates 612
17.3.1 Basic Equations 612
17.3.2 Continuity Conditions at Stiffener *i* 615
17.3.3 Boundary Conditions 618
17.3.4 Evaluation of the Boundary and Continuity Conditions 618
17.3.5 Buckling Conditions 620
17.4 Closed-Form Analytical Solutions for Longitudinally Stiffened Laminates Under Uniaxial Compressive Load 624
17.4.1 Determination of the Buckling Load 624
17.4.2 Determination of the Minimum Stiffness 627
17.4.3 Verification and Discussion 628
17.4.4 Dimensionless Representation 634
17.5 Buckling Curves for Longitudinally Stiffened Laminates Under Compression 635
17.6 Laminates with Transverse Stiffeners 636
17.6.1 Introduction 636
17.6.2 Boundary and Continuity Conditions 641

17.6.3 Buckling Condition 642
17.6.4 Selected Configurations 643
17.7 Laminate Simply Supported at Three Edges with a Reinforced Free Edge 649
17.8 Laminate with Simply Supported Loaded Edges, One Elastically Restrained 658
17.9 Local Buckling Analysis Taking Into Account Plate-Stiffener Interaction 662
17.9.1 Structural Situation 662
17.9.2 Boundary and Continuity Conditions 664
17.9.3 Shape Functions 666
17.9.4 Inner and External Potential 672
17.9.5 Closed-Form Analytical Solution 677
17.9.6 Lévy Solution 678
17.9.7 Verification 684
17.10 Buckling of Stiffened Laminates Under Shear Load 687
17.11 Global Buckling of Stiffened Plates 692
References 695

18 Postbuckling of Laminates 697
18.1 Introduction 697
18.2 Postbuckling Behaviour of Laminates Under Uniaxial Compression 698
18.2.1 Material Law and Boundary Conditions 698
18.2.2 Fundamental Equations: Strains, Equilibrium and Compatibility 700
18.2.3 Postbuckling Behaviour of the Simply Supported Plate 704
18.2.4 Postbuckling Behaviour of the Clamped Plate 710
18.2.5 Verification of the Closed-Form Analysis Methods 713
18.3 Postbuckling Behaviour of Laminates Under Shear 717
18.3.1 Given Situation and Boundary Conditions 718
18.3.2 Basic Equations 719
18.3.3 Laminates with Simply Supported Longitudinal Edges (SSSS Plates) 720
18.3.4 Laminates with Clamped Longitudinal Edges (CCCC Plates) 724
18.3.5 Results and Discussion 727
18.4 Semi-analytical Method 730
18.5 Postbuckling Analysis of Shear-Deformable Laminates 733
References 743

Part IV Advanced Topics

19 Sandwich Structures 749
19.1 Load-Bearing Behaviour of Sandwich Structures 749
19.2 Idealization for an Orthotropic Sandwich Panel 754
19.3 General Formulation 762
References 764

20 The Free-Edge Effect 767
20.1 Introduction 767
20.2 The Nature of the Free-Edge Effect 768
20.2.1 The Free-Edge Effect in a Cross-Ply Laminate 769
20.2.2 The Free-Edge Effect in an Angle-Ply Laminate 772
20.2.3 The Free-Edge Effect in an Arbitrary Symmetric Laminate 774
20.3 Methods for Analyzing the Free-Edge Effect 778
20.3.1 Delamination Forces and Moments 778
20.3.2 Finite Element Analyses 779
20.3.3 Closed-Form Analysis According to Kassapoglou and Lagace (1986) 782
20.3.4 Semi-Analytical Free-Edge Effect Analysis According to Mittelstedt and Becker (2006a, 2007a) 784
20.4 Benefits of the Free-Edge Effect Analyses 787
20.5 Results and Discussion 788
20.6 Recommendations for Practical Applications 791
20.7 Related Problems 792
20.8 Free-Edge Effects in Piezoelectric Laminates 793
20.9 The Scaled Boundary Finite Element Method 795
References 797

21 Laminated Shells 801
21.1 Introduction 801
21.2 Membrane Theory of Shells of Revolution 811
21.3 Bending Theory of Shells of Revolution 826
21.4 Bending Theory of a Cross-Ply Circular Cylindrical Shell Within the Framework of Classical Laminated Plate Theory 832
21.5 Bending Theory of a Cross-Ply Circular Cylindrical Shell in the Context of First-Order Shear Deformation Theory 836
21.6 Sandwich Shells 841
21.7 Vibrations of Circular Cylindrical Shells 844
21.8 Buckling of Circular Cylindrical Shells 846

21.9 Postbuckling Behaviour of Imperfect Circular Cylindrical Shells ... 847
21.9.1 Introduction ... 847
21.9.2 Basic Equations ... 848
21.9.3 Dimensionless Notation ... 851
21.9.4 Inplane Displacements ... 853
21.9.5 Closed-Form Analytical Solution ... 854
21.9.6 Results and Discussion ... 858
References ... 863

22 Interlaminar Stresses in Curved Laminates ... 867
22.1 Interlaminar Stresses in Curved Laminates ... 867
22.2 Isotropic Cylindrically Curved Shells ... 869
22.3 Orthotropic Cylindrically Curved Shells ... 872
22.4 Layered Cylindrically Curved Shells ... 874
22.5 Three-Dimensional Stress Analysis ... 877
22.6 Coefficient Matrices and Perturbation Terms ... 888
References ... 892

Part V Laminated Beams

23 Laminate and Sandwich Beams ... 895
23.1 Classical Laminated Plate Theory ... 895
23.2 First-Order Shear Deformation Theory ... 905
23.3 Sandwich Beams ... 911
23.4 Finite Rod and Beam Elements ... 916
23.4.1 The Two-Noded Rod Element ... 917
23.4.2 The Three-Noded Rod Element ... 919
23.4.3 The Two-Noded Beam Element in the Framework of Classical Laminated Plate Theory ... 921
23.4.4 The Three-Noded Beam Element in the Framework of Classical Laminated Plate Theory ... 926
23.4.5 Finite Beam Element in the Framework of First-Order Shear Deformation Theory ... 929
References ... 933

24 Thin-Walled Laminated Beams ... 935
24.1 Introduction ... 935
24.2 Beams Under Normal Force and Bending ... 938
24.2.1 Basic Equations for an Arbitrary Reference System ... 938
24.2.2 First Cross-Sectional Normalization ... 945
24.2.3 Selected Cross-Sections ... 949
24.2.4 Second Cross-Sectional Normalization ... 955

24.2.5 Stresses and Strains 956
24.2.6 Arbitrary Cross-Sections 958
24.3 Transverse Shear 959
24.3.1 Shear Flow in Open Cross-Sections 959
24.3.2 Shear Force Flow in Single-Cell Closed Cross-Sections 961
24.3.3 Shear Flow in Multicellular Closed Cross-Sections 964
24.3.4 Shear Center 968
24.4 Torsion 968
24.4.1 Introduction 968
24.4.2 Closed Single-Cell Profiles 971
24.4.3 Closed Multi-cell Profiles 975
24.4.4 Open Thin-Walled Cross-Sections 978
24.4.5 Thin-Walled Cross-Sections 979
24.4.6 Warping Torsion 980
24.4.7 Selected Cross-Sections 985
References 988

25 Buckling of Laminated Beams 989
25.1 Introduction 989
25.2 Global Buckling of Thin-Walled Beams 994
25.2.1 Basic Equations 994
25.2.2 Flexural-Torsional Buckling 998
25.2.3 Flexural Buckling and Torsional Buckling 998
25.2.4 Exact Solutions 999
25.2.5 Approximate Methods 1000
25.3 Local Buckling of Thin-Walled Beam Structures 1004
References 1010

26 Generalized Beam Theory 1013
26.1 Introduction 1013
26.2 Conventional GBT According to Schardt 1014
26.2.1 The Elementary Cases for the Straight Prismatic Beam 1014
26.2.2 Introduction of Higher-Order Deformation Terms 1020
26.2.3 Cross-Sectional Analysis 1021
26.2.4 Differential Equations and Boundary Conditions 1024
26.2.5 Further Work from Schardt's Working Group 1027
26.3 Application of the Generalized Beam Theory to Layered Thin-Walled Beams 1031
References 1033

Index 1037



Introduction

1

1.1 Basic Concepts

A composite material is a compound material of at least two components (constituents) or materials that are joined together using a specific manufacturing process to form a new material. The mechanical behaviour of the resulting new material is naturally determined by the properties of the constituents and, in contrast to the individual constituents, generally has improved or optimized properties. Such composite materials can be found in a whole range of engineering applications. For example, reinforced concrete components in civil engineering are structures in which the concrete is reinforced by steel reinforcements. The strength and stiffness properties of structural steel are many times higher than those of unreinforced concrete. Composite materials in the form of fiber-reinforced plastics are widely used in lightweight engineering and construction, particularly in the aerospace industry. In this case, fibers are embedded in a matrix material. What all composite materials have in common is that the reinforcement or fibers essentially have high strength and high stiffness properties and give the composite material its advantageous properties, while the generally 'weaker' matrix material (or, to put it more briefly, the matrix) has the task of holding the reinforcement or fibers in their intended position, ensuring force transmission between the fibers and protecting the fibers from external influences. In the following, we will only talk about fiber-reinforced plastics, which are often summarized under the generic terms 'composite materials' or 'composites'. Composite materials are fundamentally characterised by the properties, the arrangement and the respective quantity of their components. In the case of a fiber composite materials, the type of fiber reinforcements is also important. In addition to unidirectional continuous fibers, there are also plastics that are reinforced by fibers in two or more directions. In addition, there are also so-called fiber fabrics, particle-reinforced plastics and also reinforcements by short random fibers.

A 'layer' or 'single layer' of a fiber composite material is the 'basic unit' from which fiber composite components are assembled. If several layers of a fiber-reinforced plastic are

© The Author(s), under exclusive license to Springer-Verlag GmbH, DE, part of Springer Nature 2025

C. Mittelstedt, *Mechanics of Composite Structures*,
https://doi.org/10.1007/978-3-662-70788-3_1

joined together to form a layered component in order to achieve the desired thickness and mechanical properties, this is known as a 'laminate' (Fig. 1.1). The layers can be arranged at different fiber orientation angles. The layers can also have any arbitrary thickness and be made of different materials. It can be seen that the use of laminate structures gives designing and planning engineers a great deal of freedom and flexibility to design a laminate in such a way that the desired mechanical properties can be achieved by skilful selection of the material, the type of reinforcement, the arrangement and orientation of the individual layers in the laminate, etc. Due to the large number of possible combinations of the above-mentioned design parameters, laminate structures therefore offer great potential for optimization, which is an important point, especially in lightweight engineering and construction with its extreme demands on the weight of a structure.

Early examples of the use of laminates can be found in wood engineering, for example. Plywood consists of many so-called veneers (i.e. very thin layers of wood), which are glued together to form a plywood panel. Such plywood generally has significantly better mechanical properties than the original solid wood. Another example is glulam, in which a number of boards are glued together to form a layered wooden beam (sometimes with cross-sectional heights of up to 2 m). Here, too, it can be seen that the resulting glulam generally has significantly more favourable properties than the properties of the individual boards.

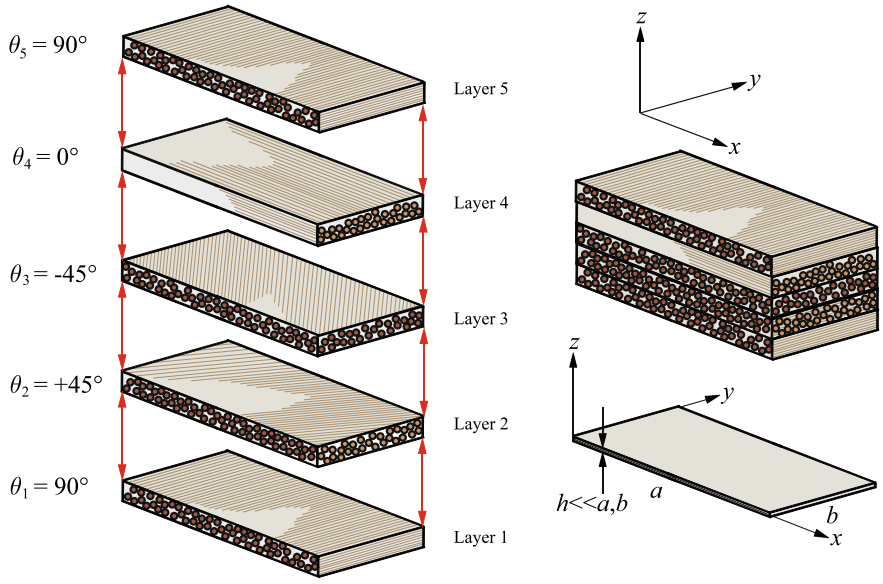


Fig. 1.1 Assembly of a number of layers to form a laminate (note that the thickness dimensions of the layers and the laminate are greatly exaggerated, as laminates are generally classified as very thin)

As far as the aviation industry is concerned, fiber-reinforced plastics have enjoyed steadily growing popularity for decades. The main reason for this is the advantageous mechanical behaviour with high stiffness and strength at a very low density of the material, which makes such fiber-reinforced plastics very attractive, especially for lightweight engineering. Some examples are shown in the following illustrations. The AIRBUS A380 is currently the world's largest passenger aircraft and has some components of its primary structure in composite laminate construction. Examples are the upper fuselage shells, which consist of so-called GLARE laminates. These are hybrid laminates that contain layers of both aluminium and glass fiber-reinforced plastics. Another example is the rear fuselage section (so-called 'section 19'), which consists almost entirely of laminated composites. The vertical tail planes of the AIRBUS fleet have also been manufactured using fiber-reinforced plastics for decades (Figs. 1.2 and 1.3).

Another example of the use of composite laminates in aircraft construction is the AIRBUS A350 XWB, which is the first AIRBUS aircraft whose fuselage and wing structures are made of fiber-reinforced plastics. However, the US aircraft manufacturer BOEING has also shown itself to be open to this trend and, with the BOEING 787 ('Dreamliner'), has also launched a major project in which the entire aircraft fuselage is made of fiber-reinforced plastics (Fig. 1.4).

However, fiber-reinforced plastics do not only have advantages. Effects 'on a small scale', such as the quality of the fiber-matrix bonding, deviations of the fibers from the ideal straight shape (so-called fiber waviness), delaminations, microdamage such as pores, inclusions or cracks and many others also have a decisive influence on the mechanical behaviour of a fiber



Fig. 1.2 Sketch of the AIRBUS A380 (*Source* www.flightglobal.com)



Fig. 1.3 The AIRBUS A350 XWB (*Source* www.airbus.com)



Fig. 1.4 BOEING 787 ('Dreamliner') (*Source* www.boeing.com)

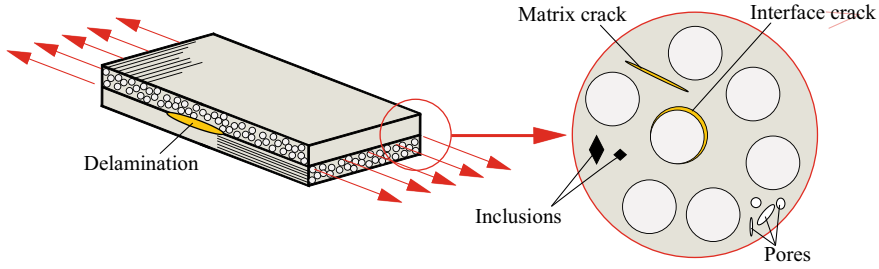


Fig. 1.5 Microdamage in a fiber composite laminate

composite material (see also Fig. 1.5). This also explains the concept of the so-called plane of reference, which is used in many different ways. While the composite laminate is viewed 'as a whole' on the macroscopic plane and thus it is assumed that the individual layers have been 'smeared' to form a homogeneous body with effective properties, the mesoscopic plane turns to the individual layer, which in turn is assumed to be a structure with smeared effective characteristic values. Finally, the microscopic level of observation turns to the real microstructure of a fiber composite material, taking into account the heterogeneity that always exists in reality. While the mesoscopic level of observation assumes effective smeared properties of a single laminate layer, the microscopic level of observation considers fibers, matrix and interfaces as well as microscopic effects as separate from each other (see Fig. 1.6).

1.2 Motivation and Structure of This Book

This book is dedicated to the fundamentals of mechanics and, based on this, the analysis of fiber-reinforced composite laminates, primarily with regard to the determination of the mechanical properties as well as the static and dynamic behaviour of laminates. Another

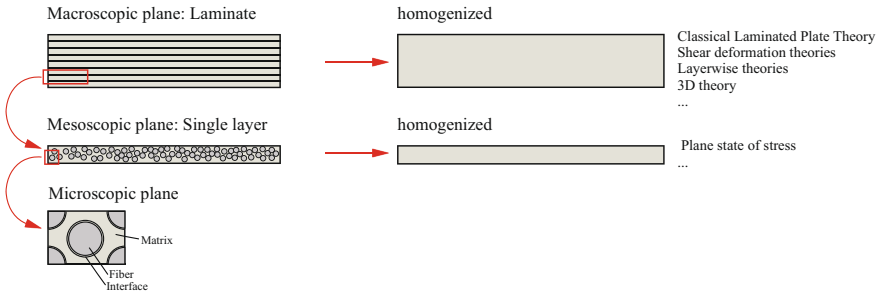


Fig. 1.6 Macroscopic, mesoscopic and microscopic planes of reference for a composite laminate

aspect that is dealt with in detail in this book and is of fundamental interest, especially for very thin laminate structures in lightweight engineering, is the stability behaviour of layered structures. Therefore, the statics and the stability of laminated composite structures are dealt with, with a focus on macroscopic and mesoscopic approaches. The author is well aware that the microscopic approach is also of paramount importance with regard to the practical application of composite laminates. However, the treatment of this subfield of mechanics, i.e. micromechanics (which has developed into a very unique and extremely active branch of research in recent decades), would go beyond the scope of this book, so that interested readers are referred to the widely available specialized literature (see e.g. Gross and Seelig (2011), Nemat-Nasser and Hori (1999), Mura (2008), Buryachenko (2007)).

In line with the above, this book is divided into five parts. *Part I—Theory of Elasticity* contains Chaps. 2–5 and is devoted to the theoretical foundations that provide the tools for understanding the analysis principles of laminate structures. Chapter 2: *Some Basic Concepts of the Theory of Elasticity* introduces some important basic concepts such as stress, strain and displacement states as well as the constitutive behaviour of elastic bodies. In Chap. 3: *Plane Problems and Surface Structures*, the considerations are specialized to thin plane structures, namely disks and plates, and the corresponding mechanical principles, which are also important for the consideration of composite laminates, are explained. Chapter 4: *Variational Principles and Approximation Methods in Structural Mechanics* is then devoted to fundamental work and energy considerations in the context of general structural mechanics, and the classical approximation methods based on this, such as the Ritz and Galerkin methods and the Finite Element Method, all of which also play an important role in the mechanics of composite structures, are explained. Chapter 5: *Strength Hypotheses for Isotropic Materials* concludes the first main part of this book and deals with very basic classical strength criteria, as they are employed when considering isotropic materials.

After Part I of this book has explained the basic theoretical relationships, *Part II—Analysis of Plane Composite Laminates* tackles one of the actual concerns of this book, namely the communication of all those theoretical backgrounds and the corresponding analysis methods that form the 'basic framework' of the calculation of plane laminated structures. Chapter 6:

Mechanics of a Laminate Layer starts with some considerations of generalized Hooke's law and practically relevant cases of material symmetries, before specializing the considerations to two-dimensional cases as they are usually considered in the treatment of plane composite laminates. This chapter concludes with some basic rules of mixture that can be used to calculate the effective properties of a single layer of a laminate from the properties of the constituents (i.e. fibers and matrix) and their volume fractions. This is followed by Chap. 7: *Classical Laminated Plate Theory*, in which the basic assumptions within the framework of this widely used laminate theory are explained and the corresponding constitutive behaviour of a laminate is derived step by step. The associated coupling effects are discussed in detail and the constitutive behaviour of specific laminate types is explained in detail. Other topics in this chapter include energy considerations, effective stiffnesses of laminates, analysis rules for changing reference planes, and the simplified consideration of coupling effects. Chapter 8: *Static and Dynamic Laminate Problems* then goes into detail on various exact-analytical and approximate solutions for static and dynamic laminate problems. First, the governing differential equations are derived both from equilibrium and from energy considerations. The dimensionless representation of all formulaic relationships, which is very helpful in many cases, is then explained. This is followed by a discussion of some selected exact analytical solutions for laminate bending problems, namely Navier-type solutions on the one hand and Lévy-type solutions on the other hand. This is followed by a detailed explanation of the Ritz method for static laminate problems. After a detailed consideration of the energy fundamentals, shape functions for this approximation method are explained for many types of boundary conditions and, based on this, some closed-form analytical approximation solutions for laminate bending problems are also discussed. This is followed by a derivation of the nonlinear equations of motion in the context of Classical Laminated Plate Theory, before a very basic consideration of vibration problems and a brief insight into the finite element method conclude this chapter. In Chap. 9: *Strength Hypotheses for Unidirectionally Fiber-Reinforced Laminate Layers*, corresponding strength hypotheses are then provided, with the help of which an assessment of the stress state in a laminate is made possible. In addition to purely static load cases, the influences of temperature and moisture on the state of stress and the strength behaviour are also of interest in practice, so that the corresponding analysis principles are explained in Chap. 10: *Hygrothermal Problems*. In cases where Classical Laminated Plate Theory provides unsatisfactory results, e.g. for very thick laminates or sandwich structures, advanced laminate theories must be used in order to take into account the transverse shear strains as they are typical for composite laminates in particular. This topic is then addressed in Chap. 11: *Higher-Order Laminate Theories*, and in addition to the so-called First-Order Shear Deformation Theory and the Third-Order Shear Deformation Theory according to Reddy, layerwise approaches are also discussed and hints for practical application are given.

The third part of this book, namely *Part III—Buckling of Laminates*, is then dedicated to the analysis of the stability behaviour, here essentially the buckling behaviour of plane composite laminates. The presentation of the stability analysis of plane laminates begins

with Chap. 12: *Navier-Type Solutions for Laminate Buckling Problems*. The governing differential equations are first derived from the equilibrium of a deformed laminate element, which can be solved exactly for a few elementary cases. The typical buckling behaviour of plane laminates is discussed in detail using these exact solutions, whereby solutions according to both Classical Laminated Plate Theory and First-Order Shear Deformation Theory are examined here. Another class of solutions for laminate buckling problems, namely the so-called Lévy solutions, are discussed in Chap. 13: *Lévy-Type Solutions for Laminate Buckling Problems* within the framework of Classical Laminated Plate Theory and also with regard to higher-order shear deformation theories. Although such solutions generally lead to implicit solutions for the buckling loads of laminates, they are important for the verification of approximate solutions on the one hand, and Lévy solutions play an important role in the consideration of so-called minimum stiffness problems for stiffened laminates on the other hand. Energy methods which are also important for the stability analysis of laminates are explained in detail in Chap. 14: *Energy Methods for Laminate Buckling Problems*. Firstly, the governing equations and the boundary conditions for laminate buckling problems are derived from the consideration of the energy balance of a buckled laminate. This is followed by a discussion of important approximation methods such as the Rayleigh quotient and the Ritz method, and the methods considered are applied to a variety of special situations. In addition, the Ritz method in particular enables the buckling analysis of laminates under complex load cases, especially in the presence of laminate-specific coupling effects, for which no exact analytical solutions are generally available. Chapter 15: *The Ritz Method for Buckling Analysis of Shear-Deformable Laminates* provides a complete description of the Ritz method for shear-deformable laminates in the context of First-Order Shear Deformation Theory and Third-Order Shear Deformation Theory for different types of boundary conditions, which is a very important point especially for practical applications. In Chap. 16: *Buckling of Unsymmetric Laminates*, the buckling behaviour of unsymmetric cross-ply and angle-ply laminates is investigated, whereby the associated Lévy solutions are considered in addition to closed-form analysis approaches. Finally, Chap. 17: *Buckling of Stiffened Laminates* deals with the practically extremely important topic of the stability of thin plate structures reinforced by stiffeners. In addition to Lévy-type solutions for some selected cases, approximation methods for buckling analysis are also presented. In addition, for some structural situations, the calculation of the minimum stiffness of the stiffening elements is also discussed—i.e. the stiffness required for the stiffening elements to prevent a global and thus potentially catastrophic buckling pattern and rather to enforce local buckling patterns. The last chapter of this part of the book—Chap. 18: *Postbuckling of Laminates* firstly provides all the theoretical foundations for a geometrically nonlinear analysis of laminates, based on v. Kármán's plate theory. For some basic structural situations, closed-form analytical approximation methods are derived, which can be used conveniently in everyday engineering practice. The chapter then concludes with a presentation of a semi-analytical method that can also be used to tackle more complicated tasks, and the postbuckling analysis of shear-deformable laminates is treated in a closed-form analytical manner.

The fourth part of this book *Part IV—Advanced Topics* is dedicated to the consideration of sandwich construction in Chap. 19: *Sandwich Structures*. It deals fundamentally with the load-bearing effect and the division of tasks of the individual components of a sandwich before an orthotropic sandwich panel is considered. The chapter concludes with a very general treatment of sandwich mechanics. Chapter 20: *The Free-Edge Effect* deals in detail with this stress problem typical of layered structures. Some analytical methods are explained and a brief outlook on related and further topics is given. Chapter 21: *Laminated Shells* deals with the mechanics of curved surface structures, the so-called shells. This chapter provides a fundamental introduction to the load-bearing behaviour of such structures and follows the 'classical' division into membrane and bending theory. The chapter then specializes the considerations to the treatment of unsymmetric cross-ply composite shells and provides all the necessary equations according to both Classical Laminated Plate Theory and First-Order Shear Deformation Theory. Finally, vibrations, buckling and postbuckling of such shells are analysed. The last chapter of this part of the book—Chap. 22: *Interlaminar Stresses in Curved Laminates* finally deals with the analysis of interlaminar stresses in curved laminates, a problem that is particularly important in lightweight engineering practice.

The last part of this book *Part V—Laminated Beams* introduces the mechanics of laminated beams, and Chap. 23: *Laminate and Sandwich Beams* presents the fundamentals of the mechanics of rods and beams in the form of laminated structures and sandwiches. In addition to all the necessary governing equations, formulations for finite elements are also provided. Chapter 24: *Thin-Walled Laminated Beams* is dedicated to the load-bearing behaviour of thin-walled beams with arbitrary cross-sectional shapes whose walls consist of laminates. Both beams under normal force and bending as well as the topics of transverse shear and torsion are considered. In Chap. 25: *Buckling of Laminated Beams*, the global and local buckling behaviour of such laminated beams is discussed. Finally, Chap. 26: *Generalized Beam Theory* concludes this part of the book and presents the so-called Generalized Beam Theory for the analysis of thin-walled beam structures.

In addition to the mechanics and analysis principles of composite laminated structures, users are also interested in aspects such as production, general design principles and specific design regulations. A completely separate field of knowledge deals with the fundamentals of materials science and the associated investigations. Other extremely important topics include operational stability, joining technology, semi-finished products, fire protection, quality management, recycling, and many more. However, these are all aspects that cannot be covered in this book and for which there is a wealth of excellent standard works. Interested readers are referred, for example, to the works of Ashby and Jones (1986), Michaeli and Wegener (1990), Ehrenstein (1992), Bergmann (1992), Moser (1990), Michaeli et al. (1994) or Schürmann (2007) (without any claim to completeness).

1.3 Further Literature References

Finally, reference should be made to journals that are regularly published worldwide which are dedicated to composites science and technology and specifically to the analysis of composite laminates and which should be studied regularly in order to obtain an overview of current research. This is also and especially important for users in lightweight engineering practice. Without claiming to be exhaustive, the reader is referred to the following journals:

- *Composites Part A: Applied Science and Manufacturing*,
- *Composites Part B: Engineering*,
- *Composites Part C: Open Access*,
- *Composites Science and Technology*,
- *Composite Structures*,
- *Journal of Composite Materials*.

Furthermore, mechanics journals and journals of applied engineering sciences should also be mentioned, which also deal with the mechanics of composite structures to a considerable extent. The following journals provide a selection:

- *Archive of Applied Mechanics*,
- *Applied Mechanics Reviews*,
- *European Journal of Mechanics A—Solids*,
- *Engineering Structures*,
- *International Journal of Engineering Science*,
- *International Journal of Mechanical Sciences*,
- *International Journal of Non-Linear Mechanics*,
- *International Journal of Solids and Structures*,
- *International Journal of Structural Stability and Dynamics*,
- *Journal of Applied Mechanics*,
- *Journal of Engineering Mechanics*,
- *Journal of Mechanics of Materials and Structures*,
- *Journal of the Mechanics and Physics of Solids*,
- *Journal of Structural Engineering*,
- *Mechanics of Advanced Materials and Structures*,
- *Zeitschrift für Angewandte Mathematik und Mechanik (ZAMM)*.

In addition, journals that focus on the mechanics and analysis of thin-walled structures are of particular interest to users in lightweight engineering practice. The following journals provide a selection:

- *Aerospace Science and Technology*,
- *AIAA Journal*,

– *Journal of Aircraft*,
– *Marine Structures*,
– *Thin-Walled Structures*.

Finally, publications that focus on the rapidly growing field of numerical analysis of structures, including composite laminates, should be mentioned:

– *Computational Materials Science*,
– *Computational Mechanics*,
– *Computer Methods in Applied Mechanics and Engineering*,
– *Computers and Structures*,
– *International Journal for Numerical Methods in Engineering*.

1.4 Nomenclature

Naturally, mathematical quantities in the form of tensors, vectors and matrices are frequently used in this book. The following notation is agreed for this. First-level vectors/tensors are shown with an underline. The vector $\underline{a}$ with the components a_x, a_y, a_z is then written as

$$\underline{a} = \begin{pmatrix} a_x \\ a_y \\ a_z \end{pmatrix}. \tag{1.1}$$

Second-level matrices/tensors are labelled with two underlines:

$$\underline{\underline{A}} = \begin{bmatrix} A_{11} & A_{12} & A_{13} \\ A_{21} & A_{22} & A_{23} \\ A_{31} & A_{32} & A_{33} \end{bmatrix}. \tag{1.2}$$

In some instances, it will prove helpful to refer to a compact representation of the formulaic relationships. Here, the so-called Einstein[1] summation convention has proven to be useful. This consists of simply omitting the summation signs from sums to be formed and summing over identical indices. An example:

$$a_{11} + a_{22} + a_{33} = \sum_{i=1}^{i=3} a_{ii}. \tag{1.3}$$

Using Einstein's summation convention, this relationship simplifies to:

$$a_{11} + a_{22} + a_{33} \equiv a_{ii}, \tag{1.4}$$

[1] Albert Einstein, 1879–1955, German physicist.

and it is summed from 1 to 3 using the index i that appears twice. Another example:

$$a_1 b_1 + a_2 b_2 + a_3 b_3 = \sum_{i=1}^{i=3} a_i b_i \equiv a_i b_i . \tag{1.5}$$

The notation $a_i b_i$ is also referred to as the so-called index notation, which always assumes that sums are performed over identical indices.

If a summation is only to be carried out from 1 to 2, Greek letters are often used instead of Latin letters for the indices:

$$a_{11} + a_{22} = \sum_{\alpha=1}^{\alpha=2} a_{\alpha\alpha} \equiv a_{\alpha\alpha}. \tag{1.6}$$

Another example: The expression

$$\frac{\partial \sigma_{11}}{\partial x_1} + \frac{\partial \sigma_{12}}{\partial x_2} + f_1 = 0 \tag{1.7}$$

reads in index notation:

$$\frac{\partial \sigma_{1\alpha}}{\partial x_\alpha} + f_1 = 0. \tag{1.8}$$

References

Ashby MF, Jones DRH (1986): *Ingenieurwerkstoffe*, Springer, Berlin et al., Germany.

Bergmann HW (1992): *Konstruktionsgrundlagen für Faserverbundbauteile*, Springer, Berlin et al., Germany.

Buryachenko V (2007): *Micromechanics of Heterogeneous Materials*, Springer, Berlin et al., Germany.

Ehrenstein GW (1992): *Faserverbund-Kunststoffe*, Hanser, Munich et al., Germany.

Gross D, Seelig T (2011): *Bruchmechanik - Mit einer Einführung in die Mikromechanik*, 5th edition, Springer, Berlin et al., Germany.

Michaeli W, Wegener M (Hrsg.) (1990): *Technologie der Faserverbundwerkstoffe*, Hanser, Munich et al., Germany.

Michaeli W, Huybrechts D, Wegener M (1994): *Dimensionieren mit Faserverbundkunststoffen*, Hanser, Munich et al., Germany.

Moser K (1990): *Faser-Kunststoff-Verbund*, VDI-Verlag, Düsseldorf, Germany.

Mura T (2008): *Micromechanics of Defects in Solids*, 2nd Edition, Springer, Berlin et al., Germany.

Nemat-Nasser S, Hori M (1999): *Micromechanics: Overall Properties of Heterogeneous Materials*, North-Holland Series in Applied Mathematics and Mechanics, 2nd Edition, Elsevier Ltd., Amsterdam et al., The Netherlands.

Schürmann H (2007): *Konstruieren mit Faser-Kunststoff-Verbunden*, 2nd edition, Springer, Berlin, Heidelberg, Germany.

Part I
Theory of Elasticity

Check for updates

Some Basic Concepts of the Theory of Elasticity

2

Theory of elasticity forms the basis of many engineering disciplines, including composites science and technology, especially from the perspective of engineers who plan, analyze and design lightweight structures. This chapter provides the basics for analyzing the stresses and deformations of elastic structures, which are also the basics for analyzing composite laminated structures. A selection of relevant references in this field can be found in the bibliography of this chapter.

2.1 Introduction

A component that is under load develops an internal state of stress. This causes deformations (i.e. displacements of the component) or strains. The stresses and strains of the elastic body are coupled with each other via the so-called constitutive law. In the case of linear elasticity, this is the well-known Hooke's law.[1] In the following, these terms will be defined and described in more detail for the general case of a three-dimensional elastic body.

In order to determine the state of an elastic body under given loads, the following equations are required, in addition to the given specific boundary conditions:

(1) kinematic equations,
(2) constitutive equations,
(3) equilibrium conditions.

[1] Robert Hooke, 1635–1703, English physicist.

© The Author(s), under exclusive license to Springer-Verlag GmbH, DE, part of Springer Nature 2025

C. Mittelstedt, *Mechanics of Composite Structures*,
https://doi.org/10.1007/978-3-662-70788-3_2

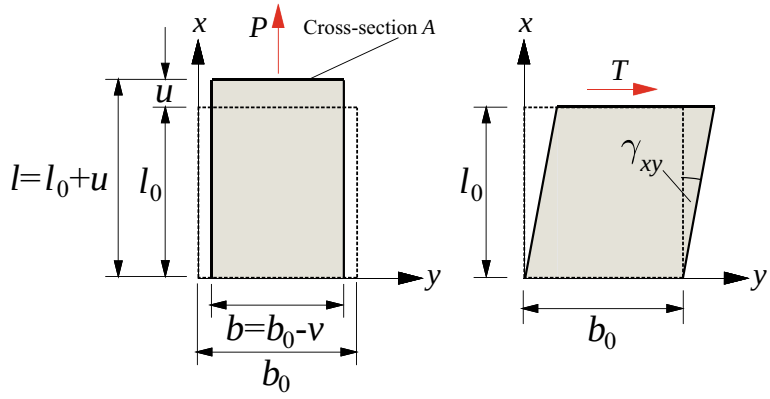


Fig. 2.1 Plate under tensile load (left), plate under shear load (right)

The kinematic equations establish a correlation between the displacements that occur on the one hand, and the resulting strains on the other hand. The constitutive equations then connect the strains with the stresses in the body. To clarify these basic concepts, two elementary examples are considered in the following.

First, a plate under a tensile force P is considered (Fig. 2.1, left). The plate has the length l_0 and the width b_0 in the unloaded state and consists of a homogeneous isotropic material (e.g. steel or aluminium). It is assumed that the plate material behaves in a linear elastic manner, so that Hooke's law is valid. It is assumed that the load P represented as a point force is distributed uniformly as the so-called normal stress σ_{xx} over the cross-sectional area A of the plate:

$$\sigma_{xx} = \frac{P}{A}, \tag{2.1}$$

whereby here and also in the further course of this book, stresses are always written with double indices. The indexing of the stress is explained as follows. The first index indicates the area on which the considered stress acts. In this case, it is the area of the plate that is penetrated by the x axis, which explains the first index x. The second index, on the other hand, indicates the direction in which the stress acts. This explains the second index x here. This definition of a stress and its designation is sufficient at this point, but it will be made more precise later.

Due to the applied load P or the stress σ_{xx}, the plate will experience a positive displacement u in the x direction and thus stretch. The resulting normal strain ε_{xx} is the ratio between the change in length $u = l - l_0$ and the original length l_0. The indexing of the strain ε_{xx} is explained analogously to the indices of the acting stress σ_{xx}. Thus, we obtain:

$$\varepsilon_{xx} = \frac{l - l_0}{l_0} = \frac{u}{l_0}. \tag{2.2}$$

At this point, the following definition is given: Normal strain means that the body changes its dimensions/volume but not its shape. At present, this means that the plate has a rectangular

shape both in the undeformed state and in the deformed state, although the dimensions l_0 and b_0 in the undeformed state have changed to the values l and b in the deformed state. Since the Eq. (2.2) establishes a relationship between the normal strain ε_{xx} and the displacement u, it is a representative of a kinematic equation.

The normal strain ε_{xx} can be related to the acting normal stress σ_{xx} using the constitutive law in the form of Hooke's law. The following applies:

$$\sigma_{xx} = E\varepsilon_{xx}. \tag{2.3}$$

In this equation, E is the modulus of elasticity or the so-called Young's[2] modulus. The relationship (2.3) is thus a constitutive equation.

In addition to the change in length in the x-direction, the plate will also experience a contraction v in the y-direction. The accompanying transverse normal strain ε_{yy} can be calculated as follows from the occurring longitudinal normal strain ε_{xx}:

$$\varepsilon_{yy} = -\nu\varepsilon_{xx}. \tag{2.4}$$

Here, ν is the so-called Poisson's[3] ratio. Here, it establishes a correlation between the longitudinal normal strain and the lateral normal strain and is therefore defined as follows:

$$\nu = -\frac{\varepsilon_{yy}}{\varepsilon_{xx}}. \tag{2.5}$$

It turns out that for the rather simple example presented here, two material constants (E and ν) are sufficient to fully describe the behaviour of the isotropic plate. For the general three-dimensional case, taking into account anisotropy, which is extremely important for fiber-reinforced composite structures, there are considerably more material parameters to be considered and, consequently, more detailed governing equations. This will be discussed in detail in the further course of this chapter.

The second introductory example is a plate under a shear force T (see Fig. 2.1, right). The resulting shear stress τ_{xy} can be calculated as follows:

$$\tau_{xy} = \frac{T}{A}. \tag{2.6}$$

The indexing of the shear stress τ_{xy} in (2.6) can be explained in a similar way to the normal stress σ_{xx}. Although the shear stress τ_{xy} acts on the surface of the plate that is penetrated by the x axis, τ_{xy} acts in the y direction, which explains the indexing with xy.

The plate experiences a horizontal displacement v due to the shear stress τ_{xy}, which gradually increases starting from the support at the lower edge. This is accompanied by a shear strain γ_{xy}, which here corresponds to the angle between the unloaded vertical plate edge and the obliquely positioned deformed edge:

[2] Thomas Young, 1773–1829, British polymath.

[3] Siméon Denis Poisson, 1781–1840, French mathematician and physicist.

$$\tan \gamma_{xy} = \frac{v}{l_0}. \tag{2.7}$$

The relation (2.7) is the necessary kinematic equation for this case. If we further assume, for the sake of simplicity, that the shear stress is sufficiently small, so that the angle/the shear strain γ_{xy} also remains small, it is usually assumed that the sine of a small angle approximately corresponds to the angle itself, while the cosine of the angle tends towards the value 1. Furthermore, the tangent of a small angle also approaches the angle itself. Here, then:

$$\sin \gamma_{xy} \simeq \gamma_{xy}, \quad \cos \gamma_{xy} \simeq 1, \quad \tan \gamma_{xy} = \frac{\sin \gamma_{xy}}{\cos \gamma_{xy}} \simeq \gamma_{xy}. \tag{2.8}$$

Ultimately, the following can then be written for the shear strain γ_{xy}:

$$\gamma_{xy} = \frac{v}{l_0}. \tag{2.9}$$

A shear strain means that the body changes its shape but not its volume.

The relationship between the shear stress τ_{xy}, on the one hand, and the shear strain γ_{xy}, on the other hand, is established here by Hooke's law as follows:

$$\tau_{xy} = G\gamma_{xy}. \tag{2.10}$$

Herein, G is the so-called shear modulus.

This introductory example has now explained the basic concepts for analysing a linear-elastic solid in an elementary way. In the further course of this chapter, the definitions will be specified and presented for the general case of a three-dimensional anisotropic solid. From this, all the necessary basics for the analysis of laminated composite structures can be clearly derived.

2.2 State of Stress

2.2.1 Stress Vector and Stress Tensor

To motivate the concept of the state of stress, an arbitrary three-dimensional body under a given load is considered (Fig. 2.2, left). The Cartesian reference system has the spatial directions x, y, z. Different types of load can now occur in a practical application. First of all, the so-called volume forces are to be mentioned here. These include all types of loads that can be imagined as distributed throughout the body. One example is the gravitational force. Volume forces can, of course, occur in all three spatial directions; the corresponding components are denoted f_x, f_y, f_z. These components are then summarised in the vector $\underline{f}$:

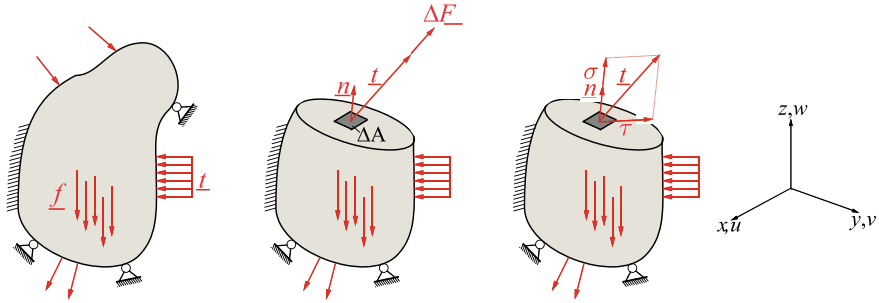


Fig. 2.2 Three-dimensional solid under load (left), section through an arbitrary solid point (middle), decomposition of the stress vector into normal and shear stress (right)

$$\underline{f} = \begin{pmatrix} f_x \\ f_y \\ f_z \end{pmatrix}. \tag{2.11}$$

Furthermore, loads can occur in the form of distributed surface loads that act on the entire surface of the component or only on a part of the surface. If the components of a surface load are named t_x, t_y, t_z, such a surface load can be written in vector form as follows:

$$\underline{t} = \begin{pmatrix} t_x \\ t_y \\ t_z \end{pmatrix}. \tag{2.12}$$

In addition, (at least in an idealised form) loads can occur in the form of line loads, which act along a line, and in the form of point loads, which act in a concentrated manner at a point in the body or on its surface.

The loading of a body, in turn, causes internal forces. If these internal forces are applied to an imaginary section, one also speaks of the so-called stresses, which act inside the body. For this purpose, an arbitrary section is made at any point in the body and an infinitesimal section area ΔA is considered (Fig. 2.2, middle). The orientation of the area ΔA is described by the unit normal vector $\underline{n}$:

$$\underline{n} = \begin{pmatrix} n_x \\ n_y \\ n_z \end{pmatrix}. \tag{2.13}$$

Cutting free exposes a force $\Delta\underline{F}$. The stress vector $\underline{t}$ is then defined as:

$$\underline{t} = \lim_{\Delta A \to 0} \frac{\Delta \underline{F}}{\Delta A}. \tag{2.14}$$

Depending on how the cut is made through the point on the body and which cutting surface is observed, a different stress vector will result. The stress vector $\underline{t}$ is therefore

dependent on the orientation of the normal vector $\underline{n}$, i.e. $\underline{t} = \underline{t}\,(\underline{n})$. This will be discussed in more detail later.

It is common practice to decompose the stress vector into a component parallel to the normal vector—the so-called normal stress σ—and a component tangential to the section plane, namely the so-called shear stress τ (see Fig. 2.2, right). The normal stress and the shear stress can be calculated as follows:

$$\sigma = \underline{t} \cdot \underline{n}, \quad \tau = \sqrt{\underline{t} \cdot \underline{t} - \sigma^2}. \tag{2.15}$$

The state of stress at any point in the body under consideration is fully defined if the stresses or the stress vector in three independent sections are known, where the three normal vectors involved, which characterise the sectional areas, must be linearly independent of each other. From the known stress vectors, the stress vector for any other section at the point under consideration can be calculated. It is useful to choose the sections so that they are perpendicular to the coordinate axes x, y, z. Figure 2.3, left, shows an infinitesimal cube that has been cut out of the body under consideration in this way. The stress vectors $\underline{t}_x$, $\underline{t}_y$, $\underline{t}_z$ can then be specified as follows:

$$\underline{t}_x = \begin{pmatrix} \sigma_{xx} \\ \tau_{xy} \\ \tau_{xz} \end{pmatrix}, \quad \underline{t}_y = \begin{pmatrix} \tau_{yx} \\ \sigma_{yy} \\ \tau_{yz} \end{pmatrix}, \quad \underline{t}_z = \begin{pmatrix} \tau_{zx} \\ \tau_{zy} \\ \sigma_{zz} \end{pmatrix}. \tag{2.16}$$

The indexing of the stresses corresponds to that already explained in the introductory example. While the first index indicates the direction of the surface normal of the considered section, the second index indicates the direction of action of the stress component. Accordingly, stresses with identical indices are normal stresses that are perpendicular to the considered section. In contrast, stresses with two different indices are shear stresses that run tangentially to the section surface under consideration. It can be seen that, for a complete description of the three-dimensional state of stress, knowledge of nine different stress components is necessary.

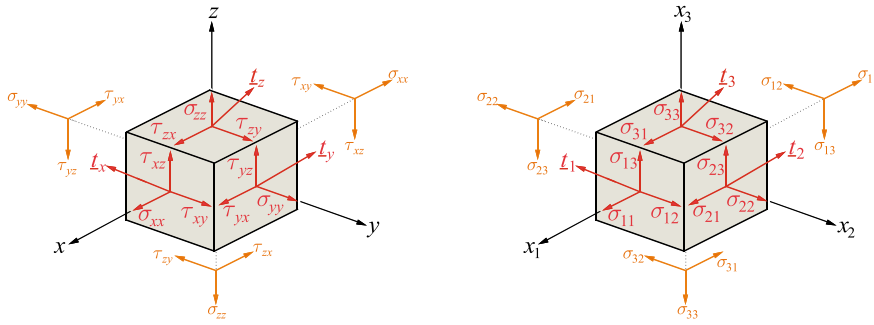


Fig. 2.3 Infinitesimal cube and associated stress components (left), alternative notations (right)

A fairly common alternative notation is to denote the coordinate axes as x_1, x_2, x_3 and to name the stress components accordingly (Fig. 2.3, right). Often, all stress components, i.e. both the normal stresses and the shear stresses, are denoted by σ. The stress vectors are then called $\underline{t}_1, \underline{t}_2, \underline{t}_3$ and are assigned as follows:

$$\underline{t}_1 = \begin{pmatrix} \sigma_{11} \\ \sigma_{12} \\ \sigma_{13} \end{pmatrix}, \quad \underline{t}_2 = \begin{pmatrix} \sigma_{21} \\ \sigma_{22} \\ \sigma_{23} \end{pmatrix}, \quad \underline{t}_3 = \begin{pmatrix} \sigma_{31} \\ \sigma_{32} \\ \sigma_{33} \end{pmatrix}. \tag{2.17}$$

The following sign convention is common when dealing with stresses. A stress is considered positive if it points in the positive coordinate direction on the positive cutting surface. A cutting surface is positive if the outward-pointing normal vector points in positive coordinate direction.

If one considers the sectional element of Fig. 2.3 and forms the equilibrium of moments around all three spatial axes with respect to the center of gravity of the sectional element, it is easy to see that to maintain the equilibrium of moments, shear stresses with the same but swapped indices must be identical. Therefore, the following applies:

$$\tau_{xy} = \tau_{yx}, \quad \tau_{xz} = \tau_{zx}, \quad \tau_{yz} = \tau_{zy}, \tag{2.18}$$

or

$$\sigma_{12} = \sigma_{21}, \quad \sigma_{13} = \sigma_{31}, \quad \sigma_{23} = \sigma_{32}. \tag{2.19}$$

This property of the state of stress will be used in all further explanations in this book. The number of independent stress components is thus reduced to six.

To characterize the state of stress in any body point, the stress components are usually summarized in a symmetric matrix as follows:

$$\underline{\underline{\sigma}} = \begin{bmatrix} \sigma_{xx} & \tau_{xy} & \tau_{xz} \\ \tau_{xy} & \sigma_{yy} & \tau_{yz} \\ \tau_{xz} & \tau_{yz} & \sigma_{zz} \end{bmatrix} = \begin{bmatrix} \sigma_{11} & \sigma_{12} & \sigma_{13} \\ \sigma_{12} & \sigma_{22} & \sigma_{23} \\ \sigma_{13} & \sigma_{23} & \sigma_{33} \end{bmatrix}. \tag{2.20}$$

The matrix $\underline{\underline{\sigma}}$ is the Cauchy[4] stress tensor, in which the stress vectors involved $\underline{t}_x$, $\underline{t}_y$, $\underline{t}_z$ or $\underline{t}_1$, $\underline{t}_2$, $\underline{t}_3$ are arranged column by column. From a mathematical point of view, $\underline{\underline{\sigma}}$ is a symmetric second-order tensor.

Instead of the infinitesimal cube, a tetrahedron cut out of the continuum (see Fig. 2.4) is considered, which is marked by the three cube intersection surfaces $\mathrm{d}A_x, \mathrm{d}A_y, \mathrm{d}A_z$ and the arbitrarily oriented tetrahedral surface $\mathrm{d}A$. The angles $\varphi_x, \varphi_y, \varphi_z$ characterize the direction of the normal vector $\underline{n}$ of the tetrahedron surface to the reference system x, y, z. The vector $\underline{t} = \left(t_x, t_y, t_z\right)^T$ is the vector of stresses related to the tetrahedron surface $\mathrm{d}A$. The normal vector $\underline{n}$ is defined as $\underline{n} = \left(n_x, n_y, n_z\right)^T = \left(\cos\varphi_x, \cos\varphi_y, \cos\varphi_z\right)^T$. Equilibrium in x-, y- and in z-direction results in:

[4] Augustin-Louis Cauchy, 1789–1857, French mathematician.

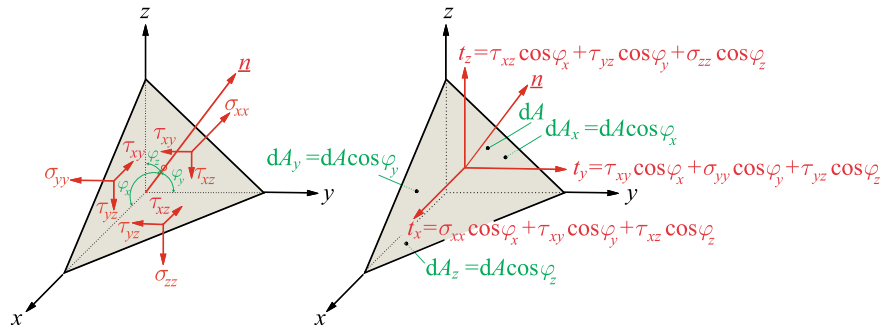


Fig. 2.4 Forces on an infinitesimal tetrahedral element

$$
\begin{aligned}
t_x \mathrm{d}A &= \sigma_{xx}\mathrm{d}A_x + \tau_{xy}\mathrm{d}A_y + \tau_{xz}\mathrm{d}A_z,\\
t_y \mathrm{d}A &= \tau_{xy}\mathrm{d}A_x + \sigma_{yy}\mathrm{d}A_y + \tau_{yz}\mathrm{d}A_z,\\
t_z \mathrm{d}A &= \tau_{xz}\mathrm{d}A_x + \tau_{yz}\mathrm{d}A_y + \sigma_{zz}\mathrm{d}A_z,
\end{aligned}
\tag{2.21}
$$

where $\tau_{ij} = \tau_{ji}$ has already been taken into account. Taking into account $\mathrm{d}A_x = \mathrm{d}An_x$, $\mathrm{d}A_y = \mathrm{d}An_y$, $\mathrm{d}A_z = \mathrm{d}An_z$ we obtain:

$$
\begin{aligned}
t_x &= \sigma_{xx}n_x + \tau_{xy}n_y + \tau_{xz}n_z,\\
t_y &= \tau_{xy}n_x + \sigma_{yy}n_y + \tau_{yz}n_z,\\
t_z &= \tau_{xz}n_x + \tau_{yz}n_y + \sigma_{zz}n_z,
\end{aligned}
\tag{2.22}
$$

or in vector-matrix notation:

$$
\underline{t} = \underline{\underline{\sigma}}\,\underline{n}. \tag{2.23}
$$

Using the reference system x_1, x_2, x_3 and denoting all stress components as σ, we can also write in index notation:

$$
t_i = \sigma_{ij}n_j. \tag{2.24}
$$

This relationship is also known as Cauchy's formula or Cauchy's theorem. It can be seen that if the stress tensor $\underline{\underline{\sigma}}$ is known, the stress vector can be calculated for any section through the body point under consideration.

2.2.2 Transformation Rules

The considerations in the previous section on the stress transformation assumes that the stresses related to the axes x, y, z or their base vectors $\underline{e}_x$, $\underline{e}_y$, $\underline{e}_z$ are known. Now, consider

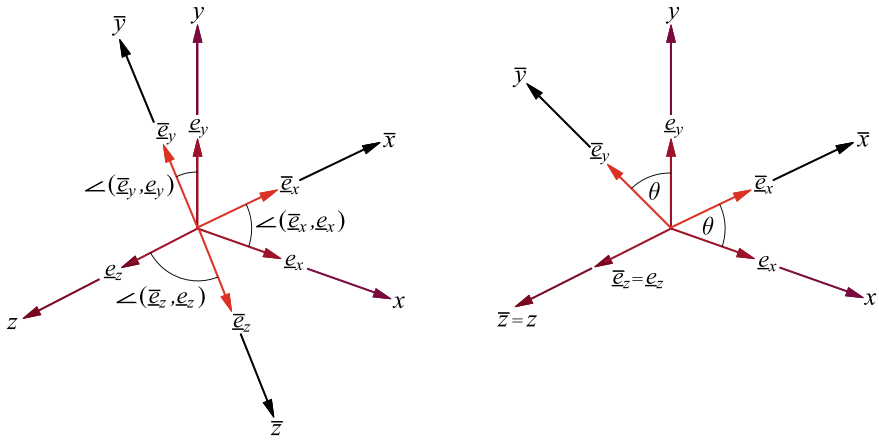


Fig. 2.5 Rotation of an orthonormal basis $\underline{e}_x, \underline{e}_y, \underline{e}_z$ into an arbitrary basis $\underline{\bar{e}}_x, \underline{\bar{e}}_y, \underline{\bar{e}}_z$ (left), and rotation of an orthonormal basis $\underline{e}_x, \underline{e}_y, \underline{e}_z$ into an orthonormal basis $\underline{\bar{e}}_x, \underline{\bar{e}}_y, \underline{\bar{e}}_z$ with the z-axis fixed

an orthonormal basis consisting of $\underline{e}_x, \underline{e}_y, \underline{e}_z$, which is transformed by a pure vector rotation into an arbitrary basis $\underline{\bar{e}}_x, \underline{\bar{e}}_y, \underline{\bar{e}}_z$ or the reference system $\bar{x}, \bar{y}, \bar{z}$ (see Fig. 2.5, left). The origin of the orthonormal basis $\underline{e}_x, \underline{e}_y, \underline{e}_z$ and the basis $\underline{\bar{e}}_x, \underline{\bar{e}}_y, \underline{\bar{e}}_z$ is thus assumed to be identical. In this case, for example, the basis vectors $\underline{e}_x$ and $\underline{\bar{e}}_y$ enclose the directional angle $\angle\left(\underline{\bar{e}}_y, \underline{e}_x\right)$. The cosine of this angle is called the direction cosine R_{yx} (analogously for all other R_{ij}). The first index denotes the base vector considered from the transformed coordinate system $\bar{x}, \bar{y}, \bar{z}$, the second index denotes that from the original coordinate system x, y, z ($i, j = x, y, z$):

$$R_{ij} = \cos\left(\angle\underline{\bar{e}}_i, \underline{e}_j\right). \tag{2.25}$$

The direction cosine R_{ij} follows from the scalar product of the two basis vectors involved:

$$R_{ij} = \frac{\underline{\bar{e}}_i \cdot \underline{e}_j}{\left|\underline{\bar{e}}_i\right| \left|\underline{e}_j\right|}. \tag{2.26}$$

If the stresses are arranged in a column vector $\underline{\sigma} = \left(\sigma_{xx}, \sigma_{yy}, \sigma_{zz}, \tau_{yz}, \tau_{xz}, \tau_{xy}\right)^T$, then the transformation of the stresses from $\underline{e}_x, \underline{e}_y, \underline{e}_z$ to $\underline{\bar{e}}_x, \underline{\bar{e}}_y, \underline{\bar{e}}_z$ follows from the equilibrium at the tetrahedron:

$$\underline{\bar{\sigma}} = \underline{\underline{T}}_\sigma \underline{\sigma}, \tag{2.27}$$

wherein the transformation matrix $\underline{\underline{T}}_\sigma$ can be written as:

$$\underline{\underline{T}}_{\sigma} = \begin{bmatrix} R_{11}^2 & R_{12}^2 & R_{13}^2 & 2R_{12}R_{13} & 2R_{11}R_{13} & 2R_{11}R_{12} \\ R_{21}^2 & R_{22}^2 & R_{23}^2 & 2R_{22}R_{23} & 2R_{21}R_{23} & 2R_{21}R_{22} \\ R_{31}^2 & R_{32}^2 & R_{33}^2 & 2R_{32}R_{33} & 2R_{31}R_{33} & 2R_{31}R_{32} \\ R_{21}R_{31} & R_{22}R_{32} & R_{23}R_{33} & R_{22}R_{33}+R_{23}R_{32} & R_{21}R_{33}+R_{23}R_{31} & R_{21}R_{32}+R_{22}R_{31} \\ R_{11}R_{31} & R_{12}R_{32} & R_{13}R_{33} & R_{12}R_{33}+R_{13}R_{32} & R_{11}R_{33}+R_{13}R_{31} & R_{11}R_{32}+R_{12}R_{31} \\ R_{11}R_{21} & R_{12}R_{22} & R_{13}R_{23} & R_{12}R_{23}+R_{13}R_{22} & R_{11}R_{23}+R_{13}R_{21} & R_{11}R_{22}+R_{12}R_{21} \end{bmatrix}. \tag{2.28}$$

In the event that $\underline{\bar{e}}_x, \underline{\bar{e}}_y, \underline{\bar{e}}_z$ form an orthonormal basis and the rotation of $\underline{e}_x, \underline{e}_y, \underline{e}_z$ takes place around the fixed z-axis by the angle θ (see Fig. 2.5, right), then some simplifications apply:

$$\begin{pmatrix} \bar{\sigma}_{xx} \\ \bar{\sigma}_{yy} \\ \bar{\sigma}_{zz} \\ \bar{\tau}_{yz} \\ \bar{\tau}_{xz} \\ \bar{\tau}_{xy} \end{pmatrix} = \begin{bmatrix} \cos^2\theta & \sin^2\theta & 0 & 0 & 0 & 2\cos\theta\sin\theta \\ \sin^2\theta & \cos^2\theta & 0 & 0 & 0 & -2\cos\theta\sin\theta \\ 0 & 0 & 1 & 0 & 0 & 0 \\ 0 & 0 & 0 & \cos\theta & -\sin\theta & 0 \\ 0 & 0 & 0 & \sin\theta & \cos\theta & 0 \\ -\cos\theta\sin\theta & \cos\theta\sin\theta & 0 & 0 & 0 & \cos^2\theta-\sin^2\theta \end{bmatrix} \begin{pmatrix} \sigma_{xx} \\ \sigma_{yy} \\ \sigma_{zz} \\ \tau_{yz} \\ \tau_{xz} \\ \tau_{xy} \end{pmatrix}. \tag{2.29}$$

This transformation rule will be used several times in the remainder of this book.

2.2.3 Principal Stresses, Invariants, Mohr's Circles

The stress tensor $\underline{\underline{\sigma}}$ can be written in any arbitrary system of coordinates. A special reference system is the principal axis system x_h, y_h, z_h, in whose sections the stress vectors are parallel to the unit vectors $\underline{e}_{x,h}, \underline{e}_{y,h}, \underline{e}_{z,h}$ or to the normal vectors of the cut surfaces. This is only possible if the shear stress components vanish: $\tau_{yz} = \tau_{xz} = \tau_{xy} = 0$. The remaining normal stress components $\sigma_{xx}, \sigma_{yy}, \sigma_{zz}$ are called principal stresses and are denoted as $\sigma_1, \sigma_2, \sigma_3$. The requirement that the principal stresses $\sigma_1, \sigma_2, \sigma_3$ simultaneously form the corresponding stress vectors of their section and are therefore perpendicular to the section, means that the components of $\underline{t}$ are each a multiple of the corresponding normal vector, multiplied by the corresponding principal stress σ:

$$\underline{t} = \sigma \underline{n}, \tag{2.30}$$

or in compliance with (2.23):

$$\underline{\underline{\sigma}}\,\underline{n} = \sigma \underline{n}. \tag{2.31}$$

Rearranging yields:

$$\left[\underline{\underline{\sigma}} - \sigma \underline{\underline{I}}\right] \underline{n} = 0. \tag{2.32}$$

This represents an eigenvalue problem in which σ represents the eigenvalues to be determined and $\underline{n}$ the associated eigenvectors. The matrix $\underline{\underline{I}}$ is the unit matrix, which is populated with the value 1 on its main diagonal, while all other entries in $\underline{\underline{I}}$ are zero. To obtain a non-trivial solution, it is required that the coefficient determinant in (2.32) vanishes:

$$\det\left[\underline{\underline{\sigma}} - \sigma\underline{\underline{I}}\right] = 0, \tag{2.33}$$

or in expanded form:

$$\det\begin{bmatrix} \sigma_{xx}-\sigma & \tau_{xy} & \tau_{xz} \\ \tau_{xy} & \sigma_{yy}-\sigma & \tau_{yz} \\ \tau_{xz} & \tau_{yz} & \sigma_{zz}-\sigma \end{bmatrix} = 0. \tag{2.34}$$

This leads to the following cubic polynomial, whose zeros represent the principal stresses $\sigma_1, \sigma_2, \sigma_3$:

$$\sigma^3 - I_1\sigma^2 - I_2\sigma - I_3 = 0, \tag{2.35}$$

wherein:

$$\begin{aligned} I_1 &= \sigma_{xx} + \sigma_{yy} + \sigma_{zz} = \text{spur}\left[\underline{\underline{\sigma}}\right], \\ I_2 &= \tau_{xy}^2 + \tau_{yz}^2 + \tau_{xz}^2 - \left(\sigma_{xx}\sigma_{yy} + \sigma_{yy}\sigma_{zz} + \sigma_{xx}\sigma_{zz}\right), \\ I_3 &= \det\underline{\underline{\sigma}}. \end{aligned} \tag{2.36}$$

The Eq. (2.35) always provides real values for the principal stresses $\sigma_1, \sigma_2, \sigma_3$ and is not dependent on the reference system. This must therefore also apply to the variables I_1, I_2, I_3, which is why these variables are also called invariants of the stress state. The result from (2.35) can be interpreted as follows for $\sigma_1, \sigma_2, \sigma_3$. One of these stresses is the maximum normal stress σ_1 occurring at the body point under consideration. Another stress σ_3 describes the minimum occurring value, the remaining value σ_2 is a value between σ_1 and σ_3. The unit vectors of the principal axis system result from the eigenvectors of $\underline{\underline{\sigma}}$ to the corresponding eigenvalues, which always form an orthogonal basis. The calculation of the principal stresses and the principal axis system is called principal axis transformation. The stress tensor takes the following form in this axis system:

$$\underline{\underline{\sigma}} = \begin{bmatrix} \sigma_1 & 0 & 0 \\ 0 & \sigma_2 & 0 \\ 0 & 0 & \sigma_3 \end{bmatrix}. \tag{2.37}$$

The invariants I_1, I_2, I_3 of the stress tensor can then also be written in the following form:

$$\begin{aligned} I_1 &= \sigma_1 + \sigma_2 + \sigma_3, \\ I_2 &= \sigma_1\sigma_2 + \sigma_2\sigma_3 + \sigma_1\sigma_3, \\ I_3 &= \sigma_1\sigma_2\sigma_3. \end{aligned} \tag{2.38}$$

Similarly, the maximum shear stresses (principal shear stresses) τ_1, τ_2, τ_3 can be calculated, which result in sections whose normal lines are each perpendicular to a principal axis and form an angle of 45° with the remaining ones. In general, the normal stresses in these sections are not equal to zero. The following applies to the principal shear stresses:

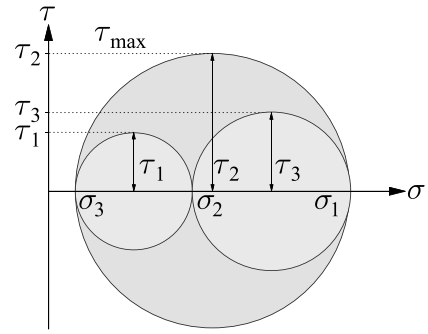


Fig. 2.6 Mohr's circles for the three-dimensional stress state

$$\tau_1 = \frac{1}{2}(\sigma_2 - \sigma_3)\,, \quad \tau_2 = \frac{1}{2}(\sigma_1 - \sigma_3)\,, \quad \tau_3 = \frac{1}{2}(\sigma_1 - \sigma_2)\,. \tag{2.39}$$

As can be easily verified, τ_2 is the maximum shear stress. A graphical interpretation of the spatial stress state is possible with the help of Mohr's[5] circles. The three circles shown in Fig. 2.6 represent the state of stress in one of the three sections characterised by the unit vectors $\underline{e}_{x,h}$, $\underline{e}_{y,h}$, $\underline{e}_{z,h}$ of the principal axis system. The tangent points of the circles are determined by the three principal normal stresses. All other stress states whose reference axis systems deviate from $\underline{e}_{x,h}$, $\underline{e}_{y,h}$, $\underline{e}_{z,h}$ can only be found in the shaded area. The Mohr circle marked by σ_1 and σ_3 with the centre $\frac{1}{2}(\sigma_1 - \sigma_3)$ limits the stress state on both diagram axes.

2.2.4 Hydrostatic Stress State, Deviator

If the stress tensor $\underline{\underline{\sigma}}$ on its principal diagonal only contains identical stresses $\sigma_{xx} = \sigma_{yy} = \sigma_{zz} = \sigma_0$ and all the shear stresses are all equal to zero, this is also referred to as the so-called hydrostatic stress state. The stress tensor $\underline{\underline{\sigma}}$ can then also be written as follows:

$$\underline{\underline{\sigma}} = \begin{bmatrix} \sigma_0 & 0 & 0 \\ 0 & \sigma_0 & 0 \\ 0 & 0 & \sigma_0 \end{bmatrix}. \tag{2.40}$$

In this state, σ_0 is also the principal stress. Since this applies to all normal stresses that occur, Mohr's circle in the hydrostatic stress state degenerates into a point on the σ axis. Accordingly, all normal stresses in every section are identical to σ_0, while the shear stresses in any reference system vanish. Thus, any axis system is a principal axis system.

It is useful to break down the stress tensor $\underline{\underline{\sigma}}$ into two components. These are the hydrostatic component $\underline{\underline{\sigma}}_0$ and the deviatoric part ('stress deviator') $\underline{\underline{\sigma}}_1$. To do this, an average

[5] Christian Otto Mohr, 1835–1918, German engineer.

stress σ_m is introduced as follows:

$$\sigma_m = \frac{1}{3}\left(\sigma_{xx} + \sigma_{yy} + \sigma_{zz}\right) = \frac{1}{3} I_1. \tag{2.41}$$

The stress tensor $\underline{\underline{\sigma}}$ can then be formulated as follows:

$$\underline{\underline{\sigma}} = \underline{\underline{\sigma}}_0 + \underline{\underline{\sigma}}_1, \tag{2.42}$$

or

$$\begin{bmatrix} \sigma_{xx} & \tau_{xy} & \tau_{xz} \\ \tau_{xy} & \sigma_{yy} & \tau_{yz} \\ \tau_{xz} & \tau_{yz} & \sigma_{zz} \end{bmatrix} = \begin{bmatrix} \sigma_m & 0 & 0 \\ 0 & \sigma_m & 0 \\ 0 & 0 & \sigma_m \end{bmatrix} + \begin{bmatrix} (\sigma_{xx} - \sigma_m) & \tau_{xy} & \tau_{xz} \\ \tau_{xy} & (\sigma_{yy} - \sigma_m) & \tau_{yz} \\ \tau_{xz} & \tau_{yz} & (\sigma_{zz} - \sigma_m) \end{bmatrix}. \tag{2.43}$$

While the so-called spherical tensor $\underline{\underline{\sigma}}_0$ leads to a volume strain in isotropic materials, the so-called stress deviator $\underline{\underline{\sigma}}_1$ is the cause of pure shape change. The spherical tensor $\underline{\underline{\sigma}}_0$ describes a hydrostatic stress state due to σ_m, while the stress deviator $\underline{\underline{\sigma}}_1$ can be interpreted as the deviation. In the hydrostatic state of stress $\underline{\underline{\sigma}}_0$, the structure undergoes a pure volume change, but no change in shape. In contrast, the state of stress described by $\underline{\underline{\sigma}}_1$ stress state can be interpreted as the partial stress state that causes a pure change in shape at a constant volume.

Since the stress deviator $\underline{\underline{\sigma}}_1$ represents a symmetrical second-order tensor analogous to $\underline{\underline{\sigma}}$, some properties of $\underline{\underline{\sigma}}$ can be transferred to $\underline{\underline{\sigma}}_1$. Thus $\underline{\underline{\sigma}}_1$ also has three invariant quantities, which are denoted below as J_1, J_2, J_3. They result in:

$$\begin{aligned} J_1 &= (\sigma_{xx} - \sigma_m) + \left(\sigma_{yy} - \sigma_m\right) + (\sigma_{zz} - \sigma_m) = \text{spur}\left[\underline{\underline{\sigma}}_1\right] = 0, \\ J_2 &= \frac{1}{6}\left[\left(\sigma_{xx} - \sigma_{yy}\right)^2 + \left(\sigma_{yy} - \sigma_{zz}\right)^2 + (\sigma_{zz} - \sigma_{xx})^2 + \tau_{xy}^2 + \tau_{yz}^2 + \tau_{xz}^2\right] \\ &= \frac{1}{6}\left[(\sigma_1 - \sigma_2)^2 + (\sigma_2 - \sigma_3)^2 + (\sigma_3 - \sigma_1)^2\right], \\ J_3 &= \det \underline{\underline{\sigma}}_1. \end{aligned} \tag{2.44}$$

2.2.5 Equilibrium Conditions

So far, the state of stress at any point in a body has been dealt with. If we now consider two neighbouring points in a body, infinitesimally distant from each other, the stresses at these two points must be in equilibrium with each other and fulfil the local equilibrium conditions. If one cuts out an infinitesimally small cube from an elastic body, the stresses released in the process must be in equilibrium with each other. For this purpose, the infinitesimal volume element of Fig. 2.7 with the edge dimensions $\mathrm{d}x$, $\mathrm{d}y$, $\mathrm{d}z$ is considered. The volume forces f_x, f_y, f_z are not shown here. The stress components at the positive and negative cutting

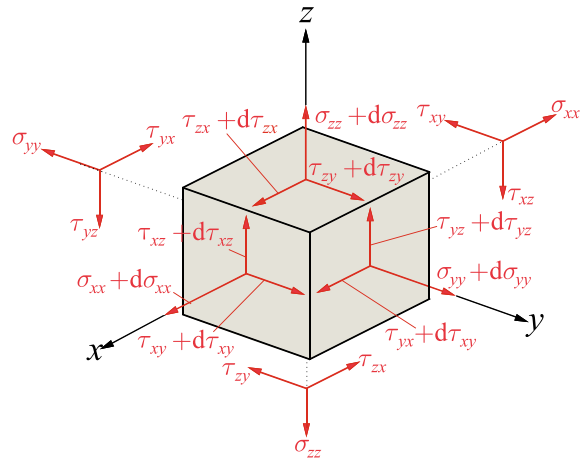


Fig. 2.7 Stresses on the infinitesimal volume element

surfaces differ by an infinitesimal increment $d\sigma_{xx}$, $d\sigma_{yy}$, $d\sigma_{zz}$ and $d\tau_{xy}$, $d\tau_{xz}$, $d\tau_{yz}$. For example, at the negative cutting surface in the x-direction, the normal stress $\sigma_{xx}(x)$ acts, while at the opposite positive cutting surface, the stress $\sigma_{xx}(x + dx) = \sigma_{xx} + d\sigma_{xx}$ occurs. The infinitesimal increment can be developed in the form of a Taylor series which is truncated after the first term. We then obtain:

$$\begin{aligned}
d\sigma_{xx} &= \frac{\partial \sigma_{xx}}{\partial x} dx, \quad d\sigma_{yy} = \frac{\partial \sigma_{yy}}{\partial y} dy, \quad d\sigma_{zz} = \frac{\partial \sigma_{zz}}{\partial z} dz, \\
d\tau_{xy} &= \frac{\partial \tau_{xy}}{\partial x} dx, \quad d\tau_{yx} = \frac{\partial \tau_{yx}}{\partial y} dy, \quad d\tau_{xz} = \frac{\partial \tau_{xz}}{\partial x} dx, \\
d\tau_{zx} &= \frac{\partial \tau_{zx}}{\partial z} dz, \quad d\tau_{yz} = \frac{\partial \tau_{yz}}{\partial y} dy, \quad d\tau_{zy} = \frac{\partial \tau_{zy}}{\partial z} dz.
\end{aligned} \tag{2.45}$$

If we now formulate the equilibrium of forces in the x-direction, we obtain the following after adding up all resulting stresses:

$$\begin{aligned}
&\left(\sigma_{xx} + \frac{\partial \sigma_{xx}}{\partial x} dx\right) dy dz - \sigma_{xx} dy dz + \left(\tau_{yx} + \frac{\partial \tau_{yx}}{\partial y} dy\right) dx dz - \tau_{yx} dx dz \\
&+ \left(\tau_{zx} + \frac{\partial \tau_{zx}}{\partial z} dz\right) dx dy - \tau_{zx} dx dy + f_x dx dy dz = 0.
\end{aligned} \tag{2.46}$$

Observing $\tau_{ij} = \tau_{ji}$ yields:

$$\frac{\partial \sigma_{xx}}{\partial x} + \frac{\partial \tau_{xy}}{\partial y} + \frac{\partial \tau_{xz}}{\partial z} + f_x = 0. \tag{2.47}$$

We proceed in the same way when forming the force balances in the y- and z-directions. In total, the following three local equilibrium conditions are obtained:

$$\begin{aligned}\frac{\partial \sigma_{xx}}{\partial x}+\frac{\partial \tau_{xy}}{\partial y}+\frac{\partial \tau_{xz}}{\partial z}+f_x&=0,\\ \frac{\partial \tau_{xy}}{\partial x}+\frac{\partial \sigma_{yy}}{\partial y}+\frac{\partial \tau_{yz}}{\partial z}+f_y&=0,\\ \frac{\partial \tau_{xz}}{\partial x}+\frac{\partial \tau_{yz}}{\partial y}+\frac{\partial \sigma_{zz}}{\partial z}+f_z&=0,\end{aligned} \tag{2.48}$$

or in compact index notation when using the reference system x_1, x_2, x_3 and the notation $\tau_{ij}=\sigma_{ij}$:

$$\frac{\partial \sigma_{ij}}{\partial x_j}+f_i=0. \tag{2.49}$$

These are three coupled partial differential equations for six unknown stress components. It can therefore be concluded that the problem under consideration is statically indeterminate—there are only three equilibrium equations for six unknown stress components. Therefore, the local equilibrium conditions alone are generally not sufficient to determine the stress state.

2.3 Deformation and Strains

2.3.1 Introduction

The deformation state of an elastic body is described by the displacements u, v, w of the body points and the resulting local strains. For this purpose, it is necessary to refer to a specific configuration or a specific deformation state for further considerations. It is common to distinguish between the undeformed initial state C_0 (also: reference configuration) and the current state C_1 (also: momentary configuration), which occurs after the deformation (Fig. 2.8). A fixed Cartesian coordinate system X, Y, Z is defined, with the help of which the position of each body point P in the initial configuration C_0 can be described by the position vector $\underline{X}$ with the components X, Y, Z. The components X, Y, Z are also called material coordinates or Lagrangian[6] coordinates. The set of all body points P or the set of all position vectors $\underline{X}$ in the initial state C_0 forms the undeformed body. The volume of the undeformed body is labelled V_0, its surface is called ∂V_0.

[6] Joseph-Louis de Lagrange, 1736–1813, Italian mathematician.

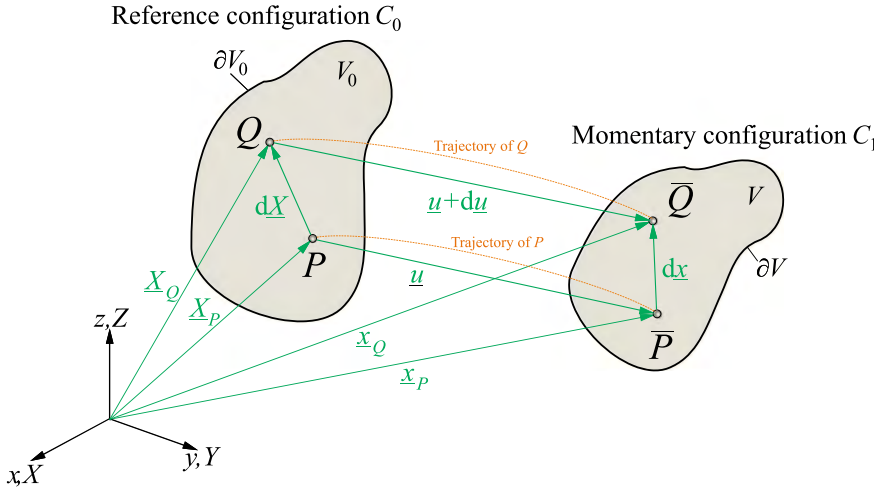


Fig. 2.8 Deformation of an elastic body

If the body is now deformed, each point P generally shifts by a certain amount $\underline{u}$ and then assumes a new position in the momentary configuration C_1, described by the position vector $\underline{x}$ or its components x, y, z. The following therefore applies:

$$\underline{x} = \begin{pmatrix} x \\ y \\ z \end{pmatrix} = \begin{pmatrix} X \\ Y \\ Z \end{pmatrix} + \begin{pmatrix} u \\ v \\ w \end{pmatrix} = \underline{X} + \underline{u}. \tag{2.50}$$

The deformation of a body is thus clearly defined by the displacement vector $\underline{u}$ at every point:

$$\underline{u} = \underline{x} - \underline{X}. \tag{2.51}$$

The coordinates x, y, z are also called Eulerian[7] coordinates. The set of all body points $\bar{P}$ in the momentary configuration C_1 forms the deformed body and is referred to as V. Let the surface of V be ∂V.

Two different approaches are commonly used to describe the deformation process of a solid. One is the so-called Lagrangian approach, in which all state variables such as the displacements u, v, w are understood as functions of the coordinates X, Y, Z, in other words:

$$u = u(X, Y, Z), \quad v = v(X, Y, Z), \quad w = w(X, Y, Z), \tag{2.52}$$

or

$$\underline{u} = \underline{u}(X, Y, Z). \tag{2.53}$$

[7] Leonhard Euler, 1707–1783, Swiss polymath.

This means that the coordinate system X, Y, Z remains in the same position during the entire deformation process and the deformation process is always related to the original coordinates.

On the other hand, there is the so-called Eulerian approach, in which all state variables such as the displacements u, v, w are described as functions of the spatial coordinates x, y, z:

$$u = u(x, y, z), \quad v = v(x, y, z), \quad w = w(x, y, z), \tag{2.54}$$

or

$$\underline{u} = \underline{u}(x, y, z). \tag{2.55}$$

This approach is particularly widespread in the dynamics of fluids and gases, while the Lagrangian approach is generally favoured in the theory of elasticity, so that both the location $\underline{x}$ of a body point and its displacements $\underline{u}$ are understood as functions of the material coordinates X, Y, Z. Therefore, $\underline{u} = \underline{u}(X, Y, Z)$ and $\underline{x} = \underline{x}(X, Y, Z)$ apply.

Let us take another look at the situation in Fig. 2.8. Let P and Q be two infinitesimally neighbouring points in the initial state C_0 with the position vectors $\underline{X}_P = (X, Y, Z)^T$ and $\underline{X}_Q = (X + \mathrm{d}X, Y + \mathrm{d}Y, Z + \mathrm{d}Z)^T$. The difference vector $\mathrm{d}\underline{X}$ is then as follows:

$$\mathrm{d}\underline{X} = \begin{pmatrix} \mathrm{d}X \\ \mathrm{d}Y \\ \mathrm{d}Z \end{pmatrix} = \underline{X}_Q - \underline{X}_P, \tag{2.56}$$

whereby its magnitude can be determined as follows:

$$|\mathrm{d}\underline{X}| = \mathrm{d}S = \sqrt{\mathrm{d}X^2 + \mathrm{d}Y^2 + \mathrm{d}Z^2}. \tag{2.57}$$

In the momentary configuration C_1, the two points P and Q transform into the points $\bar{P}$ and $\bar{Q}$. The position vectors in the momentary configuration are then $\underline{x}_P = (x, y, z)^T$ and $\underline{x}_Q = (x + \mathrm{d}x, y + \mathrm{d}y, z + \mathrm{d}z)^T$. The difference vector $\mathrm{d}\underline{x}$ can be written as:

$$\mathrm{d}\underline{x} = \begin{pmatrix} \mathrm{d}x \\ \mathrm{d}y \\ \mathrm{d}z \end{pmatrix} = \underline{x}_Q - \underline{x}_P, \tag{2.58}$$

with the magnitude:

$$|\mathrm{d}\underline{x}| = \mathrm{d}s = \sqrt{\mathrm{d}x^2 + \mathrm{d}y^2 + \mathrm{d}z^2}. \tag{2.59}$$

The deformation process at the transition of the points P and Q in the initial configuration C_0 to the points $\bar{P}$ and $\bar{Q}$ in the momentary configuration C_1 can be determined from Fig. 2.8:

$$\mathrm{d}\underline{X} + \underline{u} + \mathrm{d}\underline{u} = \underline{u} + \mathrm{d}\underline{x}, \tag{2.60}$$

or

$$\mathrm{d}\underline{u} = \mathrm{d}\underline{x} - \mathrm{d}\underline{X}, \tag{2.61}$$

or expanded:

$$\begin{pmatrix} \mathrm{d}u \\ \mathrm{d}v \\ \mathrm{d}w \end{pmatrix} = \begin{pmatrix} \mathrm{d}x \\ \mathrm{d}y \\ \mathrm{d}z \end{pmatrix} - \begin{pmatrix} \mathrm{d}X \\ \mathrm{d}Y \\ \mathrm{d}Z \end{pmatrix}. \tag{2.62}$$

The components $\mathrm{d}u, \mathrm{d}v, \mathrm{d}w$ of $\mathrm{d}\underline{u}$ can be written as total differentials of the displacement components u, v, w:

$$\begin{aligned} \mathrm{d}u &= \frac{\partial u}{\partial X}\mathrm{d}X + \frac{\partial u}{\partial Y}\mathrm{d}Y + \frac{\partial u}{\partial Z}\mathrm{d}Z, \\ \mathrm{d}v &= \frac{\partial v}{\partial X}\mathrm{d}X + \frac{\partial v}{\partial Y}\mathrm{d}Y + \frac{\partial v}{\partial Z}\mathrm{d}Z, \\ \mathrm{d}w &= \frac{\partial w}{\partial X}\mathrm{d}X + \frac{\partial w}{\partial Y}\mathrm{d}Y + \frac{\partial w}{\partial Z}\mathrm{d}Z. \end{aligned} \tag{2.63}$$

It is common to summarise the partial derivatives of the displacements u, v, w according to the material coordinates X, Y, Z in a second-order tensor $\underline{\underline{H}}$, the so-called displacement gradient:

$$\underline{\underline{H}} = \begin{bmatrix} H_{xx} & H_{xy} & H_{xz} \\ H_{yx} & H_{yy} & H_{yz} \\ H_{zx} & H_{zy} & H_{zz} \end{bmatrix} = \begin{bmatrix} \frac{\partial u}{\partial X} & \frac{\partial u}{\partial Y} & \frac{\partial u}{\partial Z} \\ \frac{\partial v}{\partial X} & \frac{\partial v}{\partial Y} & \frac{\partial v}{\partial Z} \\ \frac{\partial w}{\partial X} & \frac{\partial w}{\partial Y} & \frac{\partial w}{\partial Z} \end{bmatrix}. \tag{2.64}$$

2.3.2 Green-Lagrange Strain Tensor

The so-called Green[8]-Lagrangian strain tensor is obtained by considering the difference of the squares of the lengths $\mathrm{d}s^2$ and $\mathrm{d}S^2$:

$$\begin{aligned} \mathrm{d}s^2 - \mathrm{d}S^2 &= \mathrm{d}x^2 + \mathrm{d}y^2 + \mathrm{d}z^2 - \left(\mathrm{d}X^2 + \mathrm{d}Y^2 + \mathrm{d}Z^2\right) \\ &= (\mathrm{d}u + \mathrm{d}X)^2 + (\mathrm{d}v + \mathrm{d}Y)^2 + (\mathrm{d}w + \mathrm{d}Z)^2 - \left(\mathrm{d}X^2 + \mathrm{d}Y^2 + \mathrm{d}Z^2\right) \\ &= \left(\frac{\partial u}{\partial X}\mathrm{d}X + \frac{\partial u}{\partial Y}\mathrm{d}Y + \frac{\partial u}{\partial Z}\mathrm{d}Z + \mathrm{d}X\right)^2 \\ &\quad + \left(\frac{\partial v}{\partial X}\mathrm{d}X + \frac{\partial v}{\partial Y}\mathrm{d}Y + \frac{\partial v}{\partial Z}\mathrm{d}Z + \mathrm{d}Y\right)^2 \\ &\quad + \left(\frac{\partial w}{\partial X}\mathrm{d}X + \frac{\partial w}{\partial Y}\mathrm{d}Y + \frac{\partial w}{\partial Z}\mathrm{d}Z + \mathrm{d}Z\right)^2 - \left(\mathrm{d}X^2 + \mathrm{d}Y^2 + \mathrm{d}Z^2\right). \end{aligned} \tag{2.65}$$

After a few elementary transformations, the following representation is obtained for the difference between the squares of length:

[8] George Green, 1793–1841, British mathematician and physicist.

$$\begin{aligned} \mathrm{d}s^2 - \mathrm{d}S^2 &= 2E_{xx}\mathrm{d}X^2 + 2E_{yy}\mathrm{d}Y^2 + 2E_{zz}\mathrm{d}Z^2 \\ &\quad + 4E_{xy}\mathrm{d}X\mathrm{d}Y + 4E_{xz}\mathrm{d}X\mathrm{d}Z + 4E_{yz}\mathrm{d}Y\mathrm{d}Z, \end{aligned} \tag{2.66}$$

or in index notation

$$\mathrm{d}s^2 - \mathrm{d}S^2 = 2E_{ij}\mathrm{d}X_i\mathrm{d}X_j, \tag{2.67}$$

wherein:

$$\begin{aligned} E_{xx} &= \frac{\partial u}{\partial X} + \frac{1}{2}\left(\frac{\partial u}{\partial X}\right)^2 + \frac{1}{2}\left(\frac{\partial v}{\partial X}\right)^2 + \frac{1}{2}\left(\frac{\partial w}{\partial X}\right)^2, \\ E_{yy} &= \frac{\partial v}{\partial Y} + \frac{1}{2}\left(\frac{\partial u}{\partial Y}\right)^2 + \frac{1}{2}\left(\frac{\partial v}{\partial Y}\right)^2 + \frac{1}{2}\left(\frac{\partial w}{\partial Y}\right)^2, \\ E_{zz} &= \frac{\partial w}{\partial Z} + \frac{1}{2}\left(\frac{\partial u}{\partial Z}\right)^2 + \frac{1}{2}\left(\frac{\partial v}{\partial Z}\right)^2 + \frac{1}{2}\left(\frac{\partial w}{\partial Z}\right)^2, \\ E_{xy} &= \frac{1}{2}\left(\frac{\partial u}{\partial Y} + \frac{\partial v}{\partial X} + \frac{\partial u}{\partial X}\frac{\partial u}{\partial Y} + \frac{\partial v}{\partial X}\frac{\partial v}{\partial Y} + \frac{\partial w}{\partial X}\frac{\partial w}{\partial Y}\right), \\ E_{xz} &= \frac{1}{2}\left(\frac{\partial u}{\partial Z} + \frac{\partial w}{\partial X} + \frac{\partial u}{\partial X}\frac{\partial u}{\partial Z} + \frac{\partial v}{\partial X}\frac{\partial v}{\partial Z} + \frac{\partial w}{\partial X}\frac{\partial w}{\partial Z}\right), \\ E_{yz} &= \frac{1}{2}\left(\frac{\partial v}{\partial Z} + \frac{\partial w}{\partial Y} + \frac{\partial u}{\partial Y}\frac{\partial u}{\partial Z} + \frac{\partial v}{\partial Y}\frac{\partial v}{\partial Z} + \frac{\partial w}{\partial Y}\frac{\partial w}{\partial Z}\right). \end{aligned} \tag{2.68}$$

The variables E_{xx}, E_{yy}, E_{zz}, E_{xy}, E_{xz}, E_{yz} are the components of the (symmetrical) Green-Lagrangian strain tensor $\underline{\underline{E}}$, which describes large ('finite') deformations:

$$\underline{\underline{E}} = \begin{bmatrix} E_{xx} & E_{xy} & E_{xz} \\ E_{xy} & E_{yy} & E_{yz} \\ E_{xz} & E_{yz} & E_{zz} \end{bmatrix}. \tag{2.69}$$

We can formulate (2.68) in index notation as follows:

$$E_{ij} = \frac{1}{2}\left(\frac{\partial u_i}{\partial X_j} + \frac{\partial u_j}{\partial X_i} + \frac{\partial u_k}{\partial X_i}\frac{\partial u_k}{\partial X_j}\right). \tag{2.70}$$

Caution is required with regard to the later explanations in this book—here E_{xx}, E_{yy}, E_{zz} also denote the moduli of elasticity of an orthotropic material. However, the material discussed later in the relevant sections should not harbour any risk of confusion.

2.3.3 Von-Kármán Strains

When considering thin-walled composite laminated structures, the so-called von-Kármán[9] theory is of considerable importance. The von-Kármán strains are obtained by assuming that all three displacement components u, v, w occur in a thin plate structure, but that the inplane displacements u and v are small compared to the deflection w of the plate structure. This justifies the assumption that all quadratic terms containing u and v can be neglected in the Green-Lagrangian strain tensor, and one obtains:

$$
\begin{aligned}
E_{xx} &= \frac{\partial u}{\partial x} + \frac{1}{2}\left(\frac{\partial w}{\partial x}\right)^2, \\
E_{yy} &= \frac{\partial v}{\partial y} + \frac{1}{2}\left(\frac{\partial w}{\partial y}\right)^2, \\
E_{zz} &= \frac{\partial w}{\partial z} + \frac{1}{2}\left(\frac{\partial w}{\partial z}\right)^2, \\
E_{xy} &= \frac{1}{2}\left(\frac{\partial u}{\partial y} + \frac{\partial v}{\partial x} + \frac{\partial w}{\partial x}\frac{\partial w}{\partial y}\right), \\
E_{xz} &= \frac{1}{2}\left(\frac{\partial u}{\partial z} + \frac{\partial w}{\partial x} + \frac{\partial w}{\partial x}\frac{\partial w}{\partial z}\right), \\
E_{yz} &= \frac{1}{2}\left(\frac{\partial v}{\partial z} + \frac{\partial w}{\partial y} + \frac{\partial w}{\partial y}\frac{\partial w}{\partial z}\right).
\end{aligned}
\tag{2.71}
$$

This strain measure is usually used, for example, when considering buckling and post-buckling problems of thin-walled structures, whereby the practical value of such analyses is primarily to examine the condition of the structure at load levels that do not exceed the critical load too far. Therefore, the distinction between material and Euler coordinates is generally no longer made here, and the coordinates X, Y, Z are exchanged for x, y, z. Depending on the type of laminate theory used, further terms can be omitted, which will be discussed in more detail later.

2.3.4 Infinitesimal Strain Tensor

The infinitesimal or linearized strain tensor is obtained assuming that the components of the displacement gradient are very small ($H_{ij} \ll 1$). This means that all products and all quadratic terms can be neglected in the Green-Lagrangian strain tensor. In addition, the distinction between derivatives according to the material coordinates X, Y, Z and spatial coordinates x, y, z can be omitted, i.e. the Lagrangian and Eulerian approaches coincide ($x_i \rightarrow X_i$). Accordingly, the displacements u, v, w can be understood as functions of the

[9] Theodore von Kármán, 1881–1963, Austro-Hungarian engineer and physicist.

spatial coordinates x, y, z, which then describe the initial configuration: $u = u(x, y, z)$, $v = v(x, y, z)$, $w = w(x, y, z)$. The components of the infinitesimal strain tensor $\underline{\underline{\varepsilon}}$ are then obtained as follows:

$$\begin{aligned}
\varepsilon_{xx} &= \frac{\partial u}{\partial x}, \quad \varepsilon_{yy} = \frac{\partial v}{\partial y}, \quad \varepsilon_{zz} = \frac{\partial w}{\partial z}, \\
\gamma_{xy} &= 2\varepsilon_{xy} = \frac{\partial u}{\partial y} + \frac{\partial v}{\partial x}, \\
\gamma_{xz} &= 2\varepsilon_{xz} = \frac{\partial u}{\partial z} + \frac{\partial w}{\partial x}, \\
\gamma_{yz} &= 2\varepsilon_{yz} = \frac{\partial v}{\partial z} + \frac{\partial w}{\partial y},
\end{aligned} \tag{2.72}$$

where the variables $\gamma_{xy}, \gamma_{xz}, \gamma_{yz}$ represent the so-called technical shear strains. The following representation is common for the (symmetric) infinitesimal strain tensor $\underline{\underline{\varepsilon}}$:

$$\underline{\underline{\varepsilon}} = \begin{bmatrix} \varepsilon_{11} & \varepsilon_{12} & \varepsilon_{13} \\ \varepsilon_{12} & \varepsilon_{22} & \varepsilon_{23} \\ \varepsilon_{13} & \varepsilon_{23} & \varepsilon_{33} \end{bmatrix} = \begin{bmatrix} \varepsilon_{xx} & \frac{1}{2}\gamma_{xy} & \frac{1}{2}\gamma_{xz} \\ \frac{1}{2}\gamma_{xy} & \varepsilon_{yy} & \frac{1}{2}\gamma_{yz} \\ \frac{1}{2}\gamma_{xz} & \frac{1}{2}\gamma_{yz} & \varepsilon_{zz} \end{bmatrix}. \tag{2.73}$$

Its diagonal elements $\varepsilon_{xx}, \varepsilon_{yy}, \varepsilon_{zz}$ are called normal strains. The other elements $\gamma_{xy} = 2\varepsilon_{xy}, \gamma_{xz} = 2\varepsilon_{xz}, \gamma_{yz} = 2\varepsilon_{yz}$ are referred to as shear strains. All tensor components together fall under the term strains. The relationships (2.72) can be written in compact index notation as follows:

$$\varepsilon_{ij} = \frac{1}{2}\left(\frac{\partial u_i}{\partial x_j} + \frac{\partial u_j}{\partial x_i}\right). \tag{2.74}$$

The components of the infinitesimal strain tensor are accessible to a particularly clear geometric interpretation. Firstly, the strains in the xy-plane of an infinitesimal cube are considered (Fig. 2.9). The normal strain in the x-direction is calculated as follows:

$$\varepsilon_{xx} = \frac{\Delta l}{l} = \frac{\left[u(x) + \frac{\partial u}{\partial x}\mathrm{d}x\right] - u(x)}{\mathrm{d}x} = \frac{\partial u}{\partial x}. \tag{2.75}$$

This corresponds to the relationship already derived above. We can proceed in the same way for the normal strains ε_{yy} and ε_{zz}.

Furthermore, the shear strain in the xy-plane of an infinitesimal cube is analyzed (see Fig. 2.10). We obtain:

$$\tan\alpha \simeq \alpha = \frac{\frac{\partial v}{\partial x}\mathrm{d}x}{\mathrm{d}x} = \frac{\partial v}{\partial x}, \quad \tan\beta \simeq \beta = \frac{\frac{\partial u}{\partial y}\mathrm{d}y}{\mathrm{d}y} = \frac{\partial u}{\partial y}. \tag{2.76}$$

Therefore, for the shear strain γ_{xy} it follows:

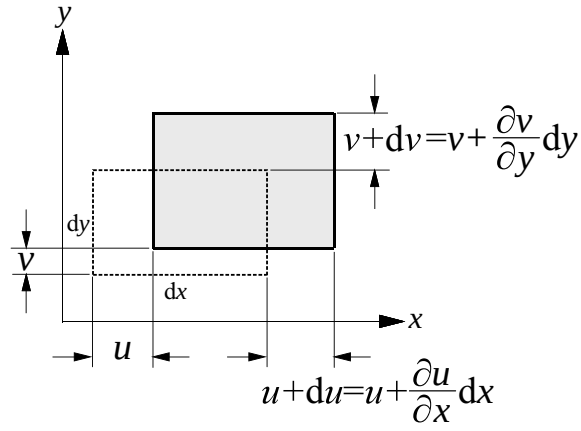


Fig. 2.9 Definition of the infinitesimal normal strains

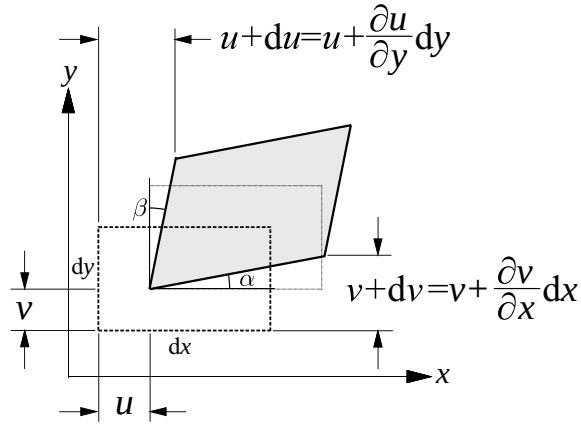


Fig. 2.10 Definition of the infinitesimal shear strains

$$\gamma_{xy} = \frac{\partial u}{\partial y} + \frac{\partial v}{\partial x}. \tag{2.77}$$

An analogue procedure then leads to the corresponding relationships for the shear strains γ_{xz} and γ_{yz}.

The relationships (2.72) establish a connection between the displacements u, v, w on the one hand and the strains ε_{xx}, ε_{yy}, ε_{zz}, γ_{xy}, γ_{xz}, γ_{yz} on the other hand, which is why they are often referred to as the so-called kinematic equations.

Finally, reference should be made to the transformation relationships, which can be derived analogously to the transformation of the stress components, whereby slight changes to (2.28) result when using the technical shear strains. The transformation matrix $\underline{\underline{T}}_{\varepsilon}$ to perform the transformation $\bar{\underline{\varepsilon}} = \underline{\underline{T}}_{\varepsilon}\,\underline{\varepsilon}$ with an arrangement of the strains in the vector $\underline{\varepsilon} = \left(\varepsilon_{xx}, \varepsilon_{yy}, \varepsilon_{zz}, \gamma_{yz}, \gamma_{xz}, \gamma_{xy}\right)^T$ reads:

$$\underline{\underline{T}}_{\varepsilon} = \begin{bmatrix} R_{11}^2 & R_{12}^2 & R_{13}^2 & R_{12}R_{13} & R_{11}R_{13} & R_{11}R_{12} \\ R_{21}^2 & R_{22}^2 & R_{23}^2 & R_{22}R_{23} & R_{21}R_{23} & R_{21}R_{22} \\ R_{31}^2 & R_{32}^2 & R_{33}^2 & R_{32}R_{33} & R_{31}R_{33} & R_{31}R_{32} \\ 2R_{21}R_{31} & 2R_{22}R_{32} & 2R_{23}R_{33} & R_{22}R_{33}+R_{23}R_{32} & R_{21}R_{33}+R_{23}R_{31} & R_{21}R_{32}+R_{22}R_{31} \\ 2R_{11}R_{31} & 2R_{12}R_{32} & 2R_{13}R_{33} & R_{12}R_{33}+R_{13}R_{32} & R_{11}R_{33}+R_{13}R_{31} & R_{11}R_{32}+R_{12}R_{31} \\ 2R_{11}R_{21} & 2R_{12}R_{22} & 2R_{13}R_{23} & R_{12}R_{23}+R_{13}R_{22} & R_{11}R_{23}+R_{13}R_{21} & R_{11}R_{22}+R_{12}R_{21} \end{bmatrix}. \tag{2.78}$$

In the case of a pure coordinate rotation around the angle θ with a fixed z-axis, the result is

$$\begin{pmatrix} \bar{\varepsilon}_{xx} \\ \bar{\varepsilon}_{yy} \\ \bar{\varepsilon}_{zz} \\ \bar{\gamma}_{yz} \\ \bar{\gamma}_{xz} \\ \bar{\gamma}_{xy} \end{pmatrix} = \begin{bmatrix} \cos^2\theta & \sin^2\theta & 0 & 0 & 0 & \cos\theta\sin\theta \\ \sin^2\theta & \cos^2\theta & 0 & 0 & 0 & -\cos\theta\sin\theta \\ 0 & 0 & 1 & 0 & 0 & 0 \\ 0 & 0 & 0 & \cos\theta & -\sin\theta & 0 \\ 0 & 0 & 0 & \sin\theta & \cos\theta & 0 \\ -2\cos\theta\sin\theta & 2\cos\theta\sin\theta & 0 & 0 & 0 & \cos^2\theta-\sin^2\theta \end{bmatrix} \begin{pmatrix} \varepsilon_{xx} \\ \varepsilon_{yy} \\ \varepsilon_{zz} \\ \gamma_{yz} \\ \gamma_{xz} \\ \gamma_{xy} \end{pmatrix}. \tag{2.79}$$

It is found that the following relationships exist between the transformation matrices $\underline{\underline{T}}_{\sigma}$ and $\underline{\underline{T}}_{\varepsilon}$:

$$\underline{\underline{T}}_{\sigma}^{-1} = \underline{\underline{T}}_{\varepsilon}^{T}, \quad \underline{\underline{T}}_{\varepsilon}^{-1} = \underline{\underline{T}}_{\sigma}^{T}. \tag{2.80}$$

Analogous invariants can be determined for the infinitesimal strain tensor as in the case of the stress tensor. Principal strains and the corresponding principal strain directions can also be determined analogously. In the corresponding equations, only the stress components must then be exchanged for the associated strain components. In the same way, the infinitesimal strain tensor can be split into a spherical tensor and a deviator. However, this will not be discussed in detail in this book.

2.3.5 Compatibility Conditions

If the three displacement components u, v, w are known, the six strain components $\varepsilon_{xx}, \varepsilon_{yy}, \varepsilon_{zz}, \gamma_{yz}, \gamma_{xz}, \gamma_{xy}$ of the infinitesimal strain tensor $\underline{\underline{\varepsilon}}$ can be determined from the kinematic equations (2.72). However, if the six strain components are known first, six kinematic equations are available to determine the displacements u, v, w. This system of equations is therefore kinematically overdetermined, so that the components of $\underline{\underline{\varepsilon}}$ cannot be independent of each other. Rather, the six strain components $\varepsilon_{xx}, \varepsilon_{yy}, \varepsilon_{zz}, \gamma_{yz}, \gamma_{xz}, \gamma_{xy}$ must satisfy the so-called compatibility conditions, which are necessary and sufficient conditions for a unique displacement field. These are obtained by eliminating the displacements in the kinematic equations. Ultimately, the following compatibility conditions must apply:

$$\frac{\partial^2\varepsilon_{ij}}{\partial x_k \partial x_l} + \frac{\partial^2\varepsilon_{kl}}{\partial x_i \partial x_j} - \frac{\partial^2\varepsilon_{ik}}{\partial x_j \partial x_l} - \frac{\partial^2\varepsilon_{jl}}{\partial x_i \partial x_k} = 0, \tag{2.81}$$

where the notation $\varepsilon_{ij} = \frac{1}{2}\gamma_{ij}$ for the shear strains and the reference system x_1, x_2, x_3 were used. For the index pairings $(i, j), (k, l) = (1, 1), (2, 2), (3, 3), (1, 2), (1, 3), (2, 3)$, a total of six different compatibility conditions are obtained, three of which are independent of each other.

In the case of a plane problem in which the strain components $\gamma_{xz}, \gamma_{yz}, \varepsilon_{zz}$ disappear and all partial derivatives to x_3 or z disappear, five of the six compatibility conditions are automatically satisfied, and the only remaining requirement is:

$$\frac{\partial^2 \varepsilon_{xx}}{\partial y^2} + \frac{\partial^2 \varepsilon_{yy}}{\partial x^2} - \frac{\partial^2 \gamma_{xy}}{\partial x \partial y} = 0. \tag{2.82}$$

Finally, it should be noted that a number of other strain tensors exist within the framework of continuum mechanics. However, these do not play a role in the context of this book and are therefore not discussed further.

2.4 Constitutive Law

2.4.1 Introduction

The relationships derived so far in the form of kinematic equations and equilibrium conditions are material-independent and apply to any material. Accordingly, these equations alone are not sufficient to describe the mechanical behaviour of an elastic body. Rather, material-specific equations must be considered as well that take the material properties into account and establish a relationship between the stresses on the one hand and the strains or displacements on the other hand. Such equations are also referred to as the so-called constitutive equations, but also as constitutive law or material law.

In the context of this book, ideally elastic material behavior is considered. In particular, the state of stress is then independent of time and also independent of the load history and is uniquely determined by the momentary state of deformation. Elasticity also means that after a complete relief of the considered structure, no permanent deformations remain. If we initially limit ourselves to the case of small deformations and work within the framework of a geometrically linear theory, whereby the distinction between the initial and momentary configuration is unnecessary, the strain state can be expressed by the infinitesimal strain tensor $\underline{\underline{\varepsilon}}$. The elasticity law is then assumed in the following general form:

$$\underline{\underline{\sigma}} = \underline{\underline{\sigma}}\left(\underline{\underline{\varepsilon}}\right), \tag{2.83}$$

where the specific form of (2.83) for the case of linear-elastic material behaviour is considered in more detail in the following section.

2.4.2 The Generalized Hooke's Law

Assuming Hooke's law to be valid, we are not only assuming elastic material behaviour, but we are also assuming that the state of stress will be proportional to the strains. There is then a linear relationship between the stresses and the strains, as already shown in the first section of this chapter using the introductory example. However, this representation is not sufficient for the general three-dimensional case and anisotropic (i.e. direction-dependent) material behaviour, so that the representation (2.83) is replaced by the following formulation:

$$\sigma_{ij} = C_{ijkl}\varepsilon_{kl}. \tag{2.84}$$

Herein, Einstein's summation convention has been employed, the indices i, j, k, l run from 1 to 3. The quantity C_{ijkl} is the so-called elasticity tensor of fourth order with a total of $3^4 = 81$ components. Note that the reference system x_1, x_2, x_3 and the designations σ_{ij} for shear stresses and $2\varepsilon_{ij} = \gamma_{ij}$ for shear strains are used here. If (2.84) is written out completely with regard to the indices k, l, the following is obtained for the stress component σ_{ij}:

$$\begin{aligned}\sigma_{ij} = {} & C_{ij11}\varepsilon_{11} + C_{ij12}\varepsilon_{12} + C_{ij13}\varepsilon_{13} \\ & + C_{ij21}\varepsilon_{21} + C_{ij22}\varepsilon_{22} + C_{ij23}\varepsilon_{23} \\ & + C_{ij31}\varepsilon_{31} + C_{ij32}\varepsilon_{32} + C_{ij33}\varepsilon_{33}.\end{aligned} \tag{2.85}$$

Further expanded we obtain:

$$\begin{aligned}
\sigma_{11} &= C_{1111}\varepsilon_{11} + C_{1112}\varepsilon_{12} + C_{1113}\varepsilon_{13} + C_{1121}\varepsilon_{21} + C_{1122}\varepsilon_{22} + C_{1123}\varepsilon_{23} \\
&\quad + C_{1131}\varepsilon_{31} + C_{1132}\varepsilon_{32} + C_{1133}\varepsilon_{33}, \\
\sigma_{22} &= C_{2211}\varepsilon_{11} + C_{2212}\varepsilon_{12} + C_{2213}\varepsilon_{13} + C_{2221}\varepsilon_{21} + C_{2222}\varepsilon_{22} + C_{2223}\varepsilon_{23} \\
&\quad + C_{2231}\varepsilon_{31} + C_{2232}\varepsilon_{32} + C_{2233}\varepsilon_{33}, \\
\sigma_{33} &= C_{3311}\varepsilon_{11} + C_{3312}\varepsilon_{12} + C_{3313}\varepsilon_{13} + C_{3321}\varepsilon_{21} + C_{3322}\varepsilon_{22} + C_{3323}\varepsilon_{23} \\
&\quad + C_{3331}\varepsilon_{31} + C_{3332}\varepsilon_{32} + C_{3333}\varepsilon_{33}, \\
\sigma_{12} &= C_{1211}\varepsilon_{11} + C_{1212}\varepsilon_{12} + C_{1213}\varepsilon_{13} + C_{1221}\varepsilon_{21} + C_{1222}\varepsilon_{22} + C_{1223}\varepsilon_{23} \\
&\quad + C_{1231}\varepsilon_{31} + C_{1232}\varepsilon_{32} + C_{1233}\varepsilon_{33}, \\
\sigma_{13} &= C_{1311}\varepsilon_{11} + C_{1312}\varepsilon_{12} + C_{1313}\varepsilon_{13} + C_{1321}\varepsilon_{21} + C_{1322}\varepsilon_{22} + C_{1323}\varepsilon_{23} \\
&\quad + C_{1331}\varepsilon_{31} + C_{1332}\varepsilon_{32} + C_{1333}\varepsilon_{33}, \\
\sigma_{21} &= C_{2111}\varepsilon_{11} + C_{2112}\varepsilon_{12} + C_{2113}\varepsilon_{13} + C_{2121}\varepsilon_{21} + C_{2122}\varepsilon_{22} + C_{2123}\varepsilon_{23} \\
&\quad + C_{2131}\varepsilon_{31} + C_{2132}\varepsilon_{32} + C_{2133}\varepsilon_{33}, \\
\sigma_{23} &= C_{2311}\varepsilon_{11} + C_{2312}\varepsilon_{12} + C_{2313}\varepsilon_{13} + C_{2321}\varepsilon_{21} + C_{2322}\varepsilon_{22} + C_{2323}\varepsilon_{23} \\
&\quad + C_{2331}\varepsilon_{31} + C_{2332}\varepsilon_{32} + C_{2333}\varepsilon_{33}, \\
\sigma_{31} &= C_{3111}\varepsilon_{11} + C_{3112}\varepsilon_{12} + C_{3113}\varepsilon_{13} + C_{3121}\varepsilon_{21} + C_{3122}\varepsilon_{22} + C_{3123}\varepsilon_{23}
\end{aligned}$$

$$
\begin{aligned}
&+ C_{3131}\varepsilon_{31} + C_{3132}\varepsilon_{32} + C_{3133}\varepsilon_{33},\\
\sigma_{32} &= C_{3211}\varepsilon_{11} + C_{3212}\varepsilon_{12} + C_{3213}\varepsilon_{13} + C_{3221}\varepsilon_{21} + C_{3222}\varepsilon_{22} + C_{3223}\varepsilon_{23}\\
&+ C_{3231}\varepsilon_{31} + C_{3232}\varepsilon_{32} + C_{3233}\varepsilon_{33}.
\end{aligned} \tag{2.86}
$$

It is found that not all 81 components of the elasticity tensor C_{ijkl} are independent of each other, but that certain symmetry properties can be demonstrated. If, for example, we take a closer look at the stress components σ_{12} and σ_{21} in (2.86) (which must be identical due to the symmetry of the stress tensor, since $\sigma_{ij} = \sigma_{ij}$), we can see directly from this that $C_{12kl} = C_{21kl}$ must apply. In general, it follows that:

$$C_{ijkl} = C_{jikl}. \tag{2.87}$$

If we also consider that the infinitesimal strain tensor is symmetric (because $\varepsilon_{ij} = \varepsilon_{ji}$ applies), then, for example, when considering the stress component σ_{12}, it is easy to see that $C_{12kl} = C_{12lk}$ must apply. In general, this means:

$$C_{ijkl} = C_{ijlk}. \tag{2.88}$$

Of the 81 components of the elasticity tensor C_{ijkl}, only 36 independent components remain. It is useful and common in engineering practice not to use the notation (2.84) for the generalised Hooke's law, but to use a compact notation as follows (so-called Voigt[10] notation):

$$
\begin{pmatrix} \sigma_{11} \\ \sigma_{22} \\ \sigma_{33} \\ \sigma_{23} \\ \sigma_{13} \\ \sigma_{12} \end{pmatrix}
=
\begin{bmatrix}
C_{11} & C_{12} & C_{13} & C_{14} & C_{15} & C_{16} \\
C_{21} & C_{22} & C_{23} & C_{24} & C_{25} & C_{26} \\
C_{31} & C_{32} & C_{33} & C_{34} & C_{35} & C_{36} \\
C_{41} & C_{42} & C_{43} & C_{44} & C_{45} & C_{46} \\
C_{51} & C_{52} & C_{53} & C_{54} & C_{55} & C_{56} \\
C_{61} & C_{62} & C_{63} & C_{64} & C_{65} & C_{66}
\end{bmatrix}
\begin{pmatrix} \varepsilon_{11} \\ \varepsilon_{22} \\ \varepsilon_{33} \\ 2\varepsilon_{23} \\ 2\varepsilon_{13} \\ 2\varepsilon_{12} \end{pmatrix}. \tag{2.89}
$$

The relationship between the quantities C_{ij} and the components C_{ijkl} of the elasticity tensor can be easily determined by comparison. If, for example, we investigate the stress component σ_{11} according to both (2.84) and (2.86) and (2.89), then we find that the identities $C_{11} = C_{1111}$, $C_{12} = C_{1122}$, $C_{16} = \frac{1}{2}(C_{1112} + C_{1121}) = C_{1112}$ hold.

In symbolic notation, we can also write (2.89) as:

$$\underline{\sigma} = \underline{\underline{C}}\,\underline{\varepsilon}. \tag{2.90}$$

In this, $\underline{\underline{C}}$ is the so-called stiffness matrix. The components C_{ij} $(i, j = 1, 2, 3, 4, 5, 6)$ are called stiffnesses. In anticipation of the following explanations, it can be stated that both the elasticity tensor C_{ijkl} and the stiffness matrix $\underline{\underline{C}}$ are always symmetric, so that the following always applies:

[10] Woldemar Voigt, 1850–1919, German physicist.

$$C_{ijkl} = C_{klij} \quad \text{and} \quad C_{ij} = C_{ji}. \tag{2.91}$$

Accordingly, general anisotropic and linear-elastic material behaviour is always described by 21 independent material constants.

The coupling effects, which can be easily deduced from the representation (2.89), are also important in the presence of anisotropy. Accordingly, any strain component ε_{ij} causes all stress components σ_{ij}, which makes the analysis of a structure made of an anisotropic material considerably more difficult than in the case of isotropic material. This also has significant effects on the calculation of composite laminated structures, which will be discussed in detail in the further course of this book.

The generalized Hooke's law can also be stated in an inverted form as follows:

$$\varepsilon_{ij} = S_{ijkl}\sigma_{kl}. \tag{2.92}$$

Therein, S_{ijkl} is the so-called compliance tensor, which has the same symmetry properties as the elasticity tensor C_{ijkl} and thus also has a maximum of 21 components that are independent of one another:

$$S_{ijkl} = S_{jikl} = S_{ijlk} = S_{klij}. \tag{2.93}$$

In condensed vector-matrix-notation, we obtain:

$$\begin{pmatrix} \varepsilon_{11} \\ \varepsilon_{22} \\ \varepsilon_{33} \\ 2\varepsilon_{23} \\ 2\varepsilon_{13} \\ 2\varepsilon_{12} \end{pmatrix} = \begin{bmatrix} S_{11} & S_{12} & S_{13} & S_{14} & S_{15} & S_{16} \\ S_{21} & S_{22} & S_{23} & S_{24} & S_{25} & S_{26} \\ S_{31} & S_{32} & S_{33} & S_{34} & S_{35} & S_{36} \\ S_{41} & S_{42} & S_{43} & S_{44} & S_{45} & S_{46} \\ S_{51} & S_{52} & S_{53} & S_{54} & S_{55} & S_{56} \\ S_{61} & S_{62} & S_{63} & S_{64} & S_{65} & S_{66} \end{bmatrix} \begin{pmatrix} \sigma_{11} \\ \sigma_{22} \\ \sigma_{33} \\ \sigma_{23} \\ \sigma_{13} \\ \sigma_{12} \end{pmatrix}, \tag{2.94}$$

or in symbolic form:

$$\underline{\varepsilon} = \underline{\underline{S}}\,\underline{\sigma}, \tag{2.95}$$

where $\underline{\underline{S}}$ is the so-called compliance matrix, which, like the stiffness matrix $\underline{\underline{C}}$, is symmetric, i.e. $S_{ij} = S_{ji}$.

It should also be noted that the case of a fully populated stiffness matrix $\underline{\underline{C}}$ is rather rare in technical applications. This also applies to applications in composites science and technology. In many technically relevant examples, so-called material symmetries can be found, which lead to some components of the stiffness matrix $\underline{\underline{C}}$ and thus also of the compliance matrix $\underline{\underline{S}}$ becoming zero. This will be discussed in detail in the following chapters of this book.

An important special case is the so-called isotropy. A material is isotropic if, in contrast to anisotropy, its behaviour is not direction-dependent, but rather its behaviour is the same in all directions. The generalised Hooke's law for isotropy is given here in anticipation of the explanations on material symmetries that will follow later:

$$\begin{pmatrix}\sigma_{11}\\ \sigma_{22}\\ \sigma_{33}\\ \sigma_{23}\\ \sigma_{13}\\ \sigma_{12}\end{pmatrix} = \frac{E}{(1+\nu)(1-2\nu)} \begin{bmatrix} 1-\nu & \nu & \nu & 0 & 0 & 0\\ \nu & 1-\nu & \nu & 0 & 0 & 0\\ \nu & \nu & 1-\nu & 0 & 0 & 0\\ 0 & 0 & 0 & G & 0 & 0\\ 0 & 0 & 0 & 0 & G & 0\\ 0 & 0 & 0 & 0 & 0 & G \end{bmatrix} \begin{pmatrix}\varepsilon_{11}\\ \varepsilon_{22}\\ \varepsilon_{33}\\ 2\varepsilon_{23}\\ 2\varepsilon_{13}\\ 2\varepsilon_{12}\end{pmatrix}, \tag{2.96}$$

where E, ν, G are the engineering constants already mentioned in the introductory section. Note that the following relationship exists between the modulus of elasticity E, the Poisson's ratio ν and the shear modulus G:

$$G = \frac{E}{2(1+\nu)}. \tag{2.97}$$

The inverse of (2.96) can be written as follows:

$$\begin{pmatrix}\varepsilon_{11}\\ \varepsilon_{22}\\ \varepsilon_{33}\\ 2\varepsilon_{23}\\ 2\varepsilon_{13}\\ 2\varepsilon_{12}\end{pmatrix} = \begin{bmatrix} \frac{1}{E} & -\frac{\nu}{E} & -\frac{\nu}{E} & 0 & 0 & 0\\ -\frac{\nu}{E} & \frac{1}{E} & -\frac{\nu}{E} & 0 & 0 & 0\\ -\frac{\nu}{E} & -\frac{\nu}{E} & \frac{1}{E} & 0 & 0 & 0\\ 0 & 0 & 0 & \frac{1}{G} & 0 & 0\\ 0 & 0 & 0 & 0 & \frac{1}{G} & 0\\ 0 & 0 & 0 & 0 & 0 & \frac{1}{G} \end{bmatrix} \begin{pmatrix}\sigma_{11}\\ \sigma_{22}\\ \sigma_{33}\\ \sigma_{23}\\ \sigma_{13}\\ \sigma_{12}\end{pmatrix}. \tag{2.98}$$

The example of isotropy clearly shows that certain properties of the elastic material under consideration sometimes result in considerable simplifications in the material law (2.89) or (2.94).

A widely used notation is to summarise pairs of indices so that the stresses and strains arranged in column vectors can be written as follows:

$$\begin{pmatrix}\sigma_{xx}\\ \sigma_{yy}\\ \sigma_{zz}\\ \tau_{yz}\\ \tau_{xz}\\ \tau_{xy}\end{pmatrix} = \begin{pmatrix}\sigma_{11}\\ \sigma_{22}\\ \sigma_{33}\\ \sigma_{23}\\ \sigma_{13}\\ \sigma_{12}\end{pmatrix} = \begin{pmatrix}\sigma_{1}\\ \sigma_{2}\\ \sigma_{3}\\ \sigma_{4}\\ \sigma_{5}\\ \sigma_{6}\end{pmatrix}, \quad \begin{pmatrix}\varepsilon_{xx}\\ \varepsilon_{yy}\\ \varepsilon_{zz}\\ \gamma_{yz}\\ \gamma_{xz}\\ \gamma_{xy}\end{pmatrix} = \begin{pmatrix}\varepsilon_{11}\\ \varepsilon_{22}\\ \varepsilon_{33}\\ 2\varepsilon_{23}\\ 2\varepsilon_{13}\\ 2\varepsilon_{12}\end{pmatrix} = \begin{pmatrix}\varepsilon_{1}\\ \varepsilon_{2}\\ \varepsilon_{3}\\ \varepsilon_{4}\\ \varepsilon_{5}\\ \varepsilon_{6}\end{pmatrix}. \tag{2.99}$$

This notation is used frequently in the literature, but is not used in this book.

2.4.3 Strain Energy

If an elastic body is deformed, the internal stresses perform work. In general, it should be noted that work concepts and the energy principles based on them play an extremely important role not only in general mechanics, but also form the basis of many calculation methods used in everyday engineering practice. For example, the widely used Finite Element

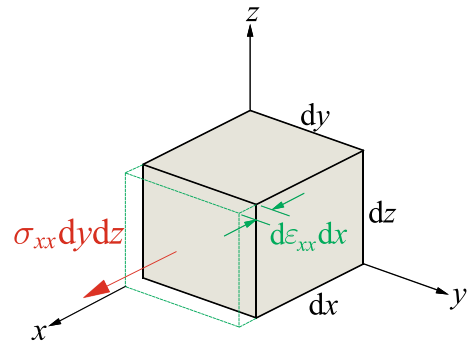


Fig. 2.11 Infinitesimal volume element under normal stress σ_{xx} and the resulting infinitesimal strain $d\varepsilon_{xx}$

Method, which is used today at all levels to model and calculate composite structures, is based on certain work and energy principles. It is therefore important to introduce and explain some of the basic concepts in this regard (which will be referred to repeatedly in this book) at the very beginning.

Consider an infinitesimal volume element with edge lengths $\mathrm{d}x$, $\mathrm{d}y$, $\mathrm{d}z$ cut out of an elastic body (see Fig. 2.11). The volume element is subjected to a normal stress σ_{xx} and experiences an infinitesimal strain $\mathrm{d}\varepsilon_{xx}$ as a result. The associated change in length is given by $\mathrm{d}\varepsilon_{xx}\mathrm{d}x$. The force resulting from σ_{xx} can be calculated as $\sigma_{xx}\mathrm{d}y\mathrm{d}z$ (stress times area) and performs the work increment (force times displacement) $\mathrm{d}\varepsilon_{xx}\mathrm{d}x$ along the length change $\sigma_{xx}\mathrm{d}\varepsilon_{xx}\mathrm{d}x\mathrm{d}y\mathrm{d}z$. The work can also be related to the volume $\mathrm{d}V = \mathrm{d}x\mathrm{d}y\mathrm{d}z$, so that the work increment per volume is obtained:

$$\mathrm{d}W_{xx} = \sigma_{xx}\mathrm{d}\varepsilon_{xx}. \tag{2.100}$$

If not only the stress σ_{xx} occurs, but all other components of the stress tensor are also present, then these also perform work corresponding to the strain components assigned to them. The total work increment per unit volume can then be written as:

$$\mathrm{d}W = \sigma_{xx}\mathrm{d}\varepsilon_{xx} + \sigma_{yy}\mathrm{d}\varepsilon_{yy} + \sigma_{zz}\mathrm{d}\varepsilon_{zz} + \tau_{yz}\mathrm{d}\gamma_{yz} + \tau_{xz}\mathrm{d}\gamma_{xz} + \tau_{xy}\mathrm{d}\gamma_{xy}, \tag{2.101}$$

or in index notation:

$$\mathrm{d}W = \sigma_{ij}\mathrm{d}\varepsilon_{ij}. \tag{2.102}$$

If we want to determine the work W done in the elastic body from the undeformed state to the current deformed state with the strains $\varepsilon_{xx}, \varepsilon_{yy}, \varepsilon_{zz}, \gamma_{yz}, \gamma_{xz}, \gamma_{xy}$, the integral is formed over the total work increment $\mathrm{d}W$, from the undeformed initial state to the deformed state with the current strains:

$$W = \int_0^{\varepsilon_{xx}} \sigma_{xx} \mathrm{d}\varepsilon_{xx} + \int_0^{\varepsilon_{yy}} \sigma_{yy} \mathrm{d}\varepsilon_{yy} + \int_0^{\varepsilon_{zz}} \sigma_{zz} \mathrm{d}\varepsilon_{zz} + \int_0^{\gamma_{yz}} \tau_{yz} \mathrm{d}\gamma_{yz} + \int_0^{\gamma_{xz}} \tau_{xz} \mathrm{d}\gamma_{xz} + \int_0^{\gamma_{xy}} \tau_{xy} \mathrm{d}\gamma_{xy}. \tag{2.103}$$

This is also referred to as the strain energy density W, whereby the term 'density' indicates that the work is related to the volume. In the case of elastic material, the energy density W does not depend on the deformation history, but only on the current strains ε_{xx}, ε_{yy}, ε_{zz}, γ_{yz}, γ_{xz}, γ_{xy}. In this case, the work increment $\mathrm{d}W$ is the complete differential $\mathrm{d}U$ of the so-called strain energy density U:

$$\begin{aligned} &\sigma_{xx}\mathrm{d}\varepsilon_{xx} + \sigma_{yy}\mathrm{d}\varepsilon_{yy} + \sigma_{zz}\mathrm{d}\varepsilon_{zz} + \tau_{yz}\mathrm{d}\gamma_{yz} + \tau_{xz}\mathrm{d}\gamma_{xz} + \tau_{xy}\mathrm{d}\gamma_{xy} \\ &= \frac{\partial U}{\partial \varepsilon_{xx}}\mathrm{d}\varepsilon_{xx} + \frac{\partial U}{\partial \varepsilon_{yy}}\mathrm{d}\varepsilon_{yy} + \frac{\partial U}{\partial \varepsilon_{zz}}\mathrm{d}\varepsilon_{zz} + \frac{\partial U}{\partial \gamma_{yz}}\mathrm{d}\gamma_{yz} + \frac{\partial U}{\partial \gamma_{xz}}\mathrm{d}\gamma_{xz} + \frac{\partial U}{\partial \gamma_{xy}}\mathrm{d}\gamma_{xy}, \end{aligned} \tag{2.104}$$

or

$$\sigma_{ij}\mathrm{d}\varepsilon_{ij} = \frac{\partial U}{\partial \varepsilon_{ij}}\mathrm{d}\varepsilon_{ij}, \tag{2.105}$$

if the index notation is used. By comparison, it can then be determined that the stresses can be calculated as partial derivatives of the potential U with respect to the respective strains, i.e.:

$$\begin{aligned} \sigma_{xx} &= \frac{\partial U}{\partial \varepsilon_{xx}}, \quad \sigma_{yy} = \frac{\partial U}{\partial \varepsilon_{yy}}, \quad \sigma_{zz} = \frac{\partial U}{\partial \varepsilon_{zz}}, \\ \tau_{yz} &= \frac{\partial U}{\partial \gamma_{yz}}, \quad \tau_{xz} = \frac{\partial U}{\partial \gamma_{xz}}, \quad \tau_{xy} = \frac{\partial U}{\partial \gamma_{xy}}, \end{aligned} \tag{2.106}$$

or

$$\sigma_{ij} = \frac{\partial U}{\partial \varepsilon_{ij}}. \tag{2.107}$$

If the material under consideration is linearly elastic, then the stiffnesses C_{ijkl} are obtained as partial derivatives of the stresses σ_{ij} with respect to the strains ε_{kl}:

$$C_{ijkl} = \frac{\partial \sigma_{ij}}{\partial \varepsilon_{kl}}. \tag{2.108}$$

Because the stresses σ_{ij} are obtained with (2.107) as the first partial derivatives of the potential U, the stiffnesses C_{ijkl} are obtained as the second partial derivatives of the potential U:

$$C_{ijkl} = \frac{\partial^2 U}{\partial \varepsilon_{ij} \partial \varepsilon_{kl}}. \tag{2.109}$$

Since the sequence of the differentiations is arbitrary, we can also write:

$$C_{ijkl} = \frac{\partial \sigma_{ij}}{\partial \varepsilon_{kl}} = \frac{\partial^2 U}{\partial \varepsilon_{ij} \partial \varepsilon_{kl}} = \frac{\partial^2 U}{\partial \varepsilon_{kl} \partial \varepsilon_{ij}} = \frac{\partial \sigma_{kl}}{\partial \varepsilon_{ij}} = C_{klij}, \tag{2.110}$$

which proves the symmetry property $C_{ijkl} = C_{klij}$ of the elasticity tensor described above and thus also the symmetry of the stiffness matrix $\underline{\underline{C}}$.

Finally, it should be mentioned that the strain energy density U results as a quadratic form in the strains in the case of linear elasticity. In index notation one obtains

$$U = \int_0^{\varepsilon} \sigma_{ij} \mathrm{d}\varepsilon_{ij} = C_{ijkl} \int_0^{\varepsilon} \varepsilon_{kl} \mathrm{d}\varepsilon_{ij} = \frac{1}{2} C_{ijkl} \varepsilon_{ij} \varepsilon_{kl} = \frac{1}{2} \sigma_{ij} \varepsilon_{ij}, \tag{2.111}$$

or in detailed notation:

$$U = \frac{1}{2} \left(\sigma_{xx} \varepsilon_{xx} + \sigma_{yy} \varepsilon_{yy} + \sigma_{zz} \varepsilon_{zz} + \tau_{yz} \gamma_{yz} + \tau_{xz} \gamma_{xz} + \tau_{xy} \gamma_{xy} \right). \tag{2.112}$$

This fact will be of more use later in this book.

2.5 Boundary Value Problems

A problem of elasticity theory is covered by the basic equations given in the previous sections. If we restrict ourselves to linear elasticity ('material linearity') and small deformations ('geometric linearity'), the basic equations can be summarised as follows. Firstly, the local equilibrium conditions must be fulfilled:

$$\begin{aligned} \frac{\partial \sigma_{xx}}{\partial x} + \frac{\partial \tau_{xy}}{\partial y} + \frac{\partial \tau_{xz}}{\partial z} + f_x &= 0, \\ \frac{\partial \tau_{xy}}{\partial x} + \frac{\partial \sigma_{yy}}{\partial y} + \frac{\partial \tau_{yz}}{\partial z} + f_y &= 0, \\ \frac{\partial \tau_{xz}}{\partial x} + \frac{\partial \tau_{yz}}{\partial y} + \frac{\partial \sigma_{zz}}{\partial z} + f_z &= 0, \end{aligned} \tag{2.113}$$

or in index notation:

$$\frac{\partial \sigma_{ij}}{\partial x_j} + f_i = 0. \tag{2.114}$$

The kinematic equations must also be observed:

$$\begin{aligned} &\varepsilon_{xx} = \frac{\partial u}{\partial x}, \quad \varepsilon_{yy} = \frac{\partial v}{\partial y}, \quad \varepsilon_{zz} = \frac{\partial w}{\partial z}, \\ &\gamma_{xy} = 2\varepsilon_{xy} = \frac{\partial u}{\partial y} + \frac{\partial v}{\partial x}, \quad \gamma_{xz} = 2\varepsilon_{xz} = \frac{\partial u}{\partial z} + \frac{\partial w}{\partial x}, \quad \gamma_{yz} = 2\varepsilon_{yz} = \frac{\partial v}{\partial z} + \frac{\partial w}{\partial y}, \end{aligned} \tag{2.115}$$

or in compact index notation:

$$\varepsilon_{ij} = \frac{1}{2}\left(\frac{\partial u_i}{\partial x_j} + \frac{\partial u_j}{\partial x_i}\right). \tag{2.116}$$

Finally, Hooke's law must be observed, which can be expressed in vector-matrix notation as follows:

$$\begin{pmatrix} \sigma_{11} \\ \sigma_{22} \\ \sigma_{33} \\ \sigma_{23} \\ \sigma_{13} \\ \sigma_{12} \end{pmatrix} = \begin{bmatrix} C_{11} & C_{12} & C_{13} & C_{14} & C_{15} & C_{16} \\ C_{21} & C_{22} & C_{23} & C_{24} & C_{25} & C_{26} \\ C_{31} & C_{32} & C_{33} & C_{34} & C_{35} & C_{36} \\ C_{41} & C_{42} & C_{43} & C_{44} & C_{45} & C_{46} \\ C_{51} & C_{52} & C_{53} & C_{54} & C_{55} & C_{56} \\ C_{61} & C_{62} & C_{63} & C_{64} & C_{65} & C_{66} \end{bmatrix} \begin{pmatrix} \varepsilon_{11} \\ \varepsilon_{22} \\ \varepsilon_{33} \\ 2\varepsilon_{23} \\ 2\varepsilon_{13} \\ 2\varepsilon_{12} \end{pmatrix}, \tag{2.117}$$

or in index notation:

$$\sigma_{ij} = C_{ijkl}\varepsilon_{kl}. \tag{2.118}$$

The set of Eqs. (2.113)–(2.118) are the governing equations since they determine the state variables u_i, ε_{ij} and σ_{ij} inside the structure. The governing equations represent a set of 15 equations for the total of 15 unknown state variables u_i, ε_{ij} and σ_{ij}.

However, in addition to the governing equations boundary values for the state variables need to be specified for static problems. If ∂V is the entire body surface, boundary conditions usually consist of the fact that on a part ∂V_t of the body surface ∂V loads are given in the form of the stress vector, i.e. $\underline{t} = \underline{t}_0$ applies. Values for the displacements are then prescribed for the remaining part ∂V_u, i.e. $u_i = u_{i0}$. Herein, we have $\partial V_t \cup \partial V_u = \partial V$. A boundary value problem can be formulated in detail as follows. On the partial surface ∂V_t applies

$$\begin{aligned} \sigma_{xx}n_x + \tau_{xy}n_y + \tau_{xz}n_z &= t_{x0}, \\ \tau_{xy}n_x + \sigma_{yy}n_y + \tau_{yz}n_z &= t_{y0}, \\ \tau_{xz}n_x + \tau_{yz}n_y + \sigma_{zz}n_z &= t_{z0}, \end{aligned} \tag{2.119}$$

or in index notation:

$$\sigma_{ij}n_j = t_{i0}. \tag{2.120}$$

On the partial surface ∂V_u then applies:

$$u_1 = u_{10}, \quad u_2 = u_{20}, \quad u_3 = u_{30}. \tag{2.121}$$

In addition to the governing equations already mentioned, the compatibility conditions (2.81) can also be used as an alternative or in addition to the kinematic relationships.

2.6 Thermal Strains

In addition to purely mechanical stresses in an elastic body, thermal influences can also play a decisive role in the analysis and design. This also applies in particular to components made of fiber-reinforced plastics. If we consider a body that experiences a change ΔT in its initial temperature T_0 and assumes the current temperature T, thermal strains ε_{ij}^T will result. For many technically relevant purposes, it is sufficient to assume a linear correlation between the temperature change ΔT and the resulting thermal strains. The thermal strains ε_{ij}^T are then assumed to be proportional to the temperature change $\Delta T = T - T_0$. The associated material constant is the so-called coefficient of thermal expansion, α_{ij}^T, and the corresponding relationship can be written as follows:

$$\varepsilon_{ij}^T = \alpha_{ij}^T \Delta T. \tag{2.122}$$

It should be noted that the thermal behaviour, like the elastic behaviour already discussed, can be anisotropic within the framework of the generalised Hooke's law. Therefore, the thermal expansion coefficients α_{ij}^T can be different in each case. Consequently, in an anisotropic body, a temperature change ΔT can also cause shear strains, which is not the case for an isotropic structure.

If not only thermal strains ε_{ij}^T are present, but mechanical strains also occur, the total strains ε_{ij} result from the addition of the two components. The following then applies:

$$\varepsilon_{ij} = S_{ijkl}\sigma_{kl} + \alpha_{ij}^T \Delta T. \tag{2.123}$$

In condensed vector-matrix notation, the following is obtained:

$$\begin{pmatrix} \varepsilon_{11} \\ \varepsilon_{22} \\ \varepsilon_{33} \\ \gamma_{23} \\ \gamma_{13} \\ \gamma_{12} \end{pmatrix} = \begin{bmatrix} S_{11} & S_{12} & S_{13} & S_{14} & S_{15} & S_{16} \\ S_{21} & S_{22} & S_{23} & S_{24} & S_{25} & S_{26} \\ S_{31} & S_{32} & S_{33} & S_{34} & S_{35} & S_{36} \\ S_{41} & S_{42} & S_{43} & S_{44} & S_{45} & S_{46} \\ S_{51} & S_{52} & S_{53} & S_{54} & S_{55} & S_{56} \\ S_{61} & S_{62} & S_{63} & S_{64} & S_{65} & S_{66} \end{bmatrix} \begin{pmatrix} \sigma_{11} \\ \sigma_{22} \\ \sigma_{33} \\ \sigma_{23} \\ \sigma_{13} \\ \sigma_{12} \end{pmatrix} + \Delta T \begin{pmatrix} \alpha_{11}^T \\ \alpha_{22}^T \\ \alpha_{33}^T \\ \alpha_{23}^T \\ \alpha_{13}^T \\ \alpha_{12}^T \end{pmatrix}. \tag{2.124}$$

The inverse relationship is as follows:

$$\begin{pmatrix} \sigma_{11} \\ \sigma_{22} \\ \sigma_{33} \\ \sigma_{23} \\ \sigma_{13} \\ \sigma_{12} \end{pmatrix} = \begin{bmatrix} C_{11} & C_{12} & C_{13} & C_{14} & C_{15} & C_{16} \\ C_{21} & C_{22} & C_{23} & C_{24} & C_{25} & C_{26} \\ C_{31} & C_{32} & C_{33} & C_{34} & C_{35} & C_{36} \\ C_{41} & C_{42} & C_{43} & C_{44} & C_{45} & C_{46} \\ C_{51} & C_{52} & C_{53} & C_{54} & C_{55} & C_{56} \\ C_{61} & C_{62} & C_{63} & C_{64} & C_{65} & C_{66} \end{bmatrix} \begin{pmatrix} \varepsilon_{11} - \alpha_{11}^T \Delta T \\ \varepsilon_{22} - \alpha_{22}^T \Delta T \\ \varepsilon_{33} - \alpha_{33}^T \Delta T \\ \gamma_{23} - \alpha_{23}^T \Delta T \\ \gamma_{13} - \alpha_{13}^T \Delta T \\ \gamma_{12} - \alpha_{12}^T \Delta T \end{pmatrix}. \tag{2.125}$$

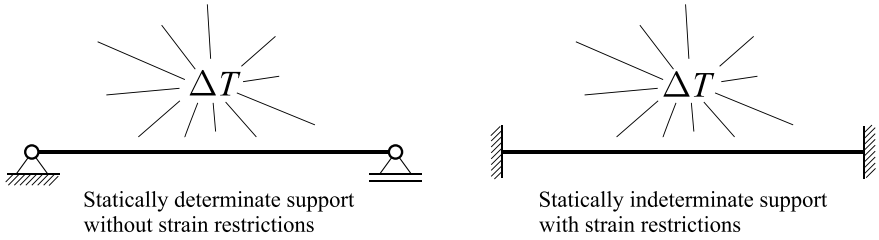


Fig. 2.12 Statically determinate beam (left) and statically indeterminate beam (right) under thermal load

This shows that only the difference between the total strains and the thermal strains, i.e. the mechanical strains, cause stresses. This can be explained using the simple one-dimensional example of a beam under a constant temperature change ΔT (Fig. 2.12). The thermal expansion ε^T then results in the beam as:

$$\varepsilon^T = \alpha^T \Delta T. \tag{2.126}$$

If mechanical strains ε^M occur at the same time, the total strains result from the superposition of both strain components:

$$\varepsilon = \varepsilon^M + \varepsilon^T = \frac{\sigma}{E} + \alpha^T \Delta T. \tag{2.127}$$

If the elongation of the bar is unrestricted (Fig. 2.12, left), the expansion or shortening of the bar as a result of the temperature change will not cause any stresses. The following then applies:

$$\sigma = E\left(\varepsilon - \alpha^T \Delta T\right) = 0. \tag{2.128}$$

The total strains occurring as a result of the temperature stress can be determined as:

$$\varepsilon = \alpha^T \Delta T. \tag{2.129}$$

If, on the other hand, the elongation of the bar is completely restricted (Fig. 2.12, right), the following applies

$$\varepsilon = \frac{\sigma}{E} + \alpha^T \Delta T = 0. \tag{2.130}$$

Stresses will occur in the bar which can be calculated as:

$$\sigma = -E\alpha^T \Delta T. \tag{2.131}$$

It should be noted again that in the case of full anisotropy of a material, in general, all temperature coefficients of expansion α_{ij}^T can be unequal to zero. However, the complexity

of the thermomechanical behaviour is significantly reduced when considering an isotropic material. Then it turns out that all α_{ij}^T for $i \neq j$ are zero. Furthermore, the remaining thermal expansion coefficients are identical, and the following applies: $\alpha_{11}^T = \alpha_{22}^T = \alpha_{33}^T = \alpha^T$. The following is then obtained for the total strains:

$$\begin{pmatrix} \varepsilon_{11} \\ \varepsilon_{22} \\ \varepsilon_{33} \\ \gamma_{23} \\ \gamma_{13} \\ \gamma_{12} \end{pmatrix} = \begin{bmatrix} \frac{1}{E} & -\frac{\nu}{E} & -\frac{\nu}{E} & 0 & 0 & 0 \\ -\frac{\nu}{E} & \frac{1}{E} & -\frac{\nu}{E} & 0 & 0 & 0 \\ -\frac{\nu}{E} & -\frac{\nu}{E} & \frac{1}{E} & 0 & 0 & 0 \\ 0 & 0 & 0 & \frac{1}{G} & 0 & 0 \\ 0 & 0 & 0 & 0 & \frac{1}{G} & 0 \\ 0 & 0 & 0 & 0 & 0 & \frac{1}{G} \end{bmatrix} \begin{pmatrix} \sigma_{11} \\ \sigma_{22} \\ \sigma_{33} \\ \sigma_{23} \\ \sigma_{13} \\ \sigma_{12} \end{pmatrix} + \Delta T \begin{pmatrix} \alpha^T \\ \alpha^T \\ \alpha^T \\ 0 \\ 0 \\ 0 \end{pmatrix}. \tag{2.132}$$

Apparently, in an isotropic structure the temperature strains that occur mean a pure normal strain state, whereby the strains are the same in all directions and no change in shape is associated with a change in temperature.

References

Altenbach H, Altenbach J, Rikards R (1996): *Einführung in die Mechanik der Laminat- und Sandwichtragwerke*, Deutscher Verlag der Grundstoffindustrie, Stuttgart, Germany.

Altenbach H, Altenbach J, Naumenko K (1998): *Ebene Flächentragwerke*, Springer Verlag, Berlin et al., Germany

Ambartsumyan SA (1970): *Theory of anisotropic plates*, Technomic Publishing Co., Inc., Stamford, USA.

Ashton JE, Whitney JM (1970): *Theory of laminated plates*, Technomic Publishing Co., Inc., Stamford, USA.

Becker W, Gross D (2002): *Mechanik elastischer Körper und Strukturen*, Springer Verlag, Berlin et al., Germany.

Eschenauer H, Schnell W (1986): *Elastizitätstheorie I*, 2. Auflage, Bibliographisches Institut, Mannheim et al., Germany.

Göldner H, Altenbach J, Eschke K, Garz KF, Sähn S (1979): *Lehrbuch Höhere Festigkeitslehre Band 1*, Physik Verlag, Weinheim, Germany.

Göldner H, Altenbach J, Eschke K, Garz KF, Sähn S (1985): *Lehrbuch Höhere Festigkeitslehre Band 2*, Physik Verlag, Weinheim, Germany.

Gross D, Hauger W, Schnell W, Wriggers P (1995): *Technische Mechanik 4: Hydromechanik, Elemente der Höheren Mechanik, Numerische Methoden*, 2nd edition, Springer Verlag, Berlin et al., Germany.

Hahn HG (1985): *Elastizitätstheorie*, BG Teubner Verlag, Stuttgart, Germany.

Herakovich CT (1998): *Mechanics of fibrous composites*, John Wiley and Sons, Inc., New York et al., USA.

Jones RM (1975): *Mechanics of composite materials*, Scripta Book Co., Washington, USA.

Lekhnitskii SG (1968): *Anisotropic plates*, Gordon and Breach, New York et al., USA.

Mittelstedt C (2021): *Structural mechanics in lightweight engineering*, Springer Nature, Cham, Switzerland.

Reddy JN (2004): *Mechanics of laminated composite plates and shells (2nd edition)*, CRC Press Boca Raton et al., USA.

Tsai SW, Hahn HT (1980): *Introduction to composite materials*, Technomic Publishing Co., Inc., Lancaster et al., UK.



Plane Problems and Surface Structures

3

Finding a closed-form solution in the context of a three-dimensional stress and strain analysis for elastic and anisotropic material behaviour is only possible in a few special cases. In many technically relevant cases, simplifying assumptions help to ensure a successful calculation. Under certain conditions, this includes considering a two-dimensional problem instead of the actual three-dimensional case. This enables a considerable reduction of the unknown state variables to be determined (displacements, strains, stresses) and leads to a considerable simplification of the governing equations. The result is then, in all cases, a significant saving in computing time compared to a fully three-dimensional approach. In this context, the concept of so-called 'surface structures' is important, which will be defined in more detail below.

The following chapters of this book will show that the approximate two-dimensional treatment also has its justification in the case of thin-walled composite structures. Within the framework of the usual and practically relevant analysis approaches, both individual laminate layers and entire laminates are regarded as essentially two-dimensional structures, which ensures some quite considerable simplifications in the calculation. Practical experience shows that such simplifying assumptions are justified in the vast majority of cases and that calculation approaches based on them have proven to be very effective.

A distinction is made in two-dimensional analysis approaches between the so-called 'plane strain state' and the so-called 'plane stress state', which will also be outlined below.

© The Author(s), under exclusive license to Springer-Verlag GmbH, DE, part of Springer Nature 2025

C. Mittelstedt, *Mechanics of Composite Structures*,
https://doi.org/10.1007/978-3-662-70788-3_3

3.1 Surface Structures

If it is assumed that the structure under consideration can essentially be described in two dimensions, it is also referred to as a surface structure. A distinction is made here between the so-called 'disks', 'plates' and 'shells'.

A disk (see Fig. 3.1, top) is a flat and planar structure whose thickness h is significantly smaller than its other characteristic dimensions in the directions perpendicular to the thickness and which is only loaded by forces in its plane that are constant over the thickness h and, if applicable, by volume forces f_x, f_y. Individual forces acting in the plane of the disk are also possible. In contrast, a plate (see Fig. 3.1, bottom) is a flat and thin load-bearing structure that is loaded by a load p perpendicular to its plane. In the case of a plate, individual forces perpendicular to the plate plane and moments about the inplane axes are also possible. The plane that bisects the disk/plate at each point is also called the middle plane. It can therefore be seen that a disk and a plate differ only in the way they are loaded, but not in their geometry. If we work within the framework of a geometrically linear theory (small deformations), then the disk behaviour (deformations in the plane) is decoupled from the plate behaviour (deformations out of the plane), and consequently the 'disk effect' and the 'plate effect' can be investigated separately, even if loads occur simultaneously in the plane and transversely to the plane.

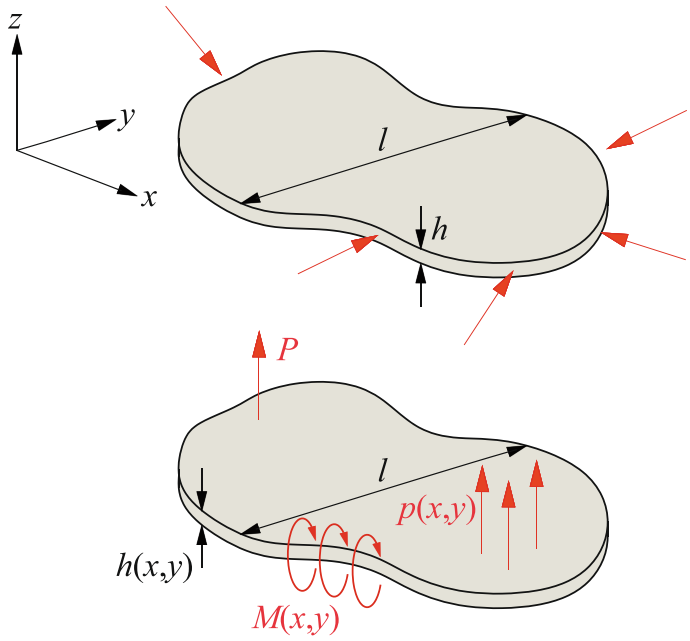


Fig. 3.1 Disk (top), plate (bottom)

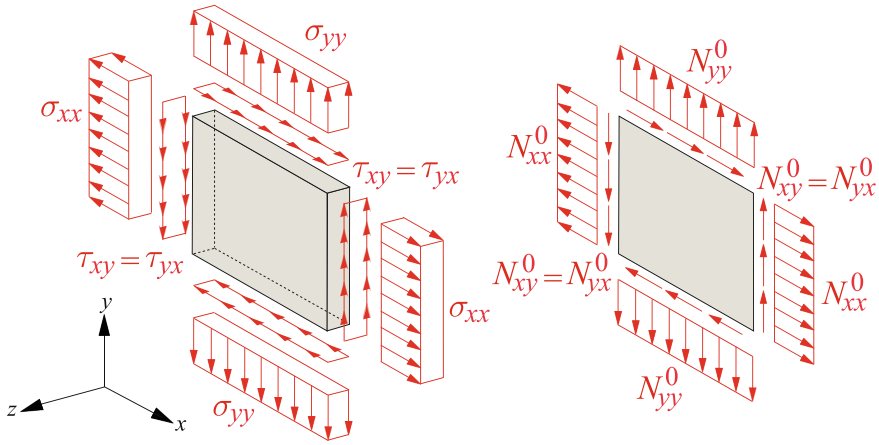


Fig. 3.2 Stresses and internal forces in a disk

In a disk, only the plane stress components σ_{xx}, σ_{yy} and τ_{xy} occur (Fig. 3.2). Whether a normal stress σ_{zz} also occurs in addition to these stresses depends on whether the disk is in the plane strain state or in the plane stress state. These terms will be defined in more detail later. The stresses σ_{xx}, σ_{yy} and τ_{xy} are constant for a disk over the thickness h, i.e. $\sigma_{xx} = \sigma_{xx}(x, y)$, $\sigma_{yy} = \sigma_{yy}(x, y)$ and $\tau_{xy} = \tau_{xy}(x, y)$. The disk stresses σ_{xx}, σ_{yy} and τ_{xy} are often integrated through the disk thickness to form the resultant internal forces N_{xx}, N_{yy}, N_{xy}, which can be obtained by integrating the stresses σ_{xx}, σ_{yy} and τ_{xy} in the thickness direction:

$$N_{xx} = \int_{-\frac{h}{2}}^{+\frac{h}{2}} \sigma_{xx} \mathrm{d}z, \quad N_{yy} = \int_{-\frac{h}{2}}^{+\frac{h}{2}} \sigma_{yy} \mathrm{d}z, \quad N_{xy} = \int_{-\frac{h}{2}}^{+\frac{h}{2}} \tau_{xy} \mathrm{d}z. \tag{3.1}$$

The internal forces N_{xx}, N_{yy}, N_{xy} are therefore distributed forces ('force per unit length') with a corresponding unit, e.g. N/mm. To make it clear that these internal forces are related to the middle plane of the disk, they are often given the superscript '0', i.e. N^0_{xx}, N^0_{yy}, N^0_{xy}.

In a plate, in addition to the stresses σ_{xx}, σ_{yy} and τ_{xy}, shear stresses τ_{yz} and τ_{xz} must also act in the thickness direction z for reasons of equilibrium. Due to the load being perpendicular to the middle plane, the plane stress components σ_{xx}, σ_{yy} and τ_{xy} will show linearly variable distributions across the thickness, while the shear stresses τ_{yz} and τ_{xz} will show a parabolic distribution. The internal forces occurring in the plate are the two bending moments M_{xx} and M_{yy}, the twisting moment M_{xy} and the two transverse shear forces Q_x and Q_y (Fig. 3.3). They can be calculated as follows by thickness integration from the occurring stresses:

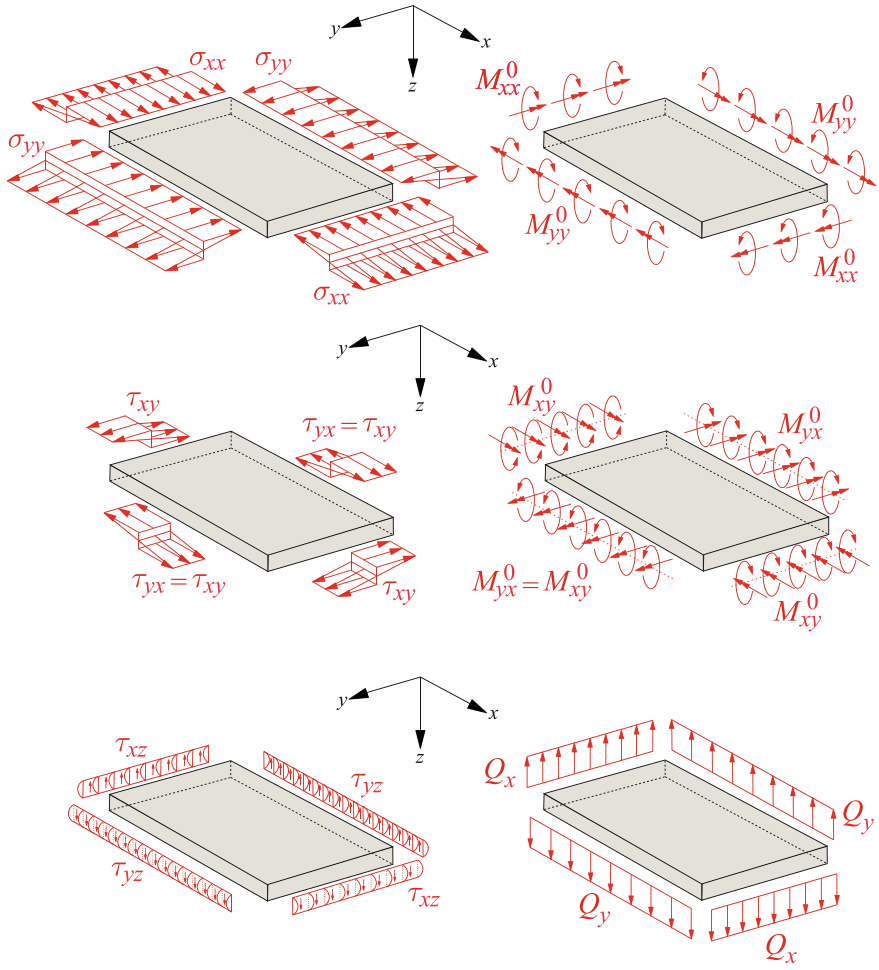


Fig. 3.3 Stresses and internal forces in a plate

$$M_{xx} = \int_{-\frac{h}{2}}^{+\frac{h}{2}} \sigma_{xx} z \mathrm{d}z, \quad M_{yy} = \int_{-\frac{h}{2}}^{+\frac{h}{2}} \sigma_{yy} z \mathrm{d}z, \quad M_{xy} = \int_{-\frac{h}{2}}^{+\frac{h}{2}} \tau_{xy} z \mathrm{d}z,$$

$$Q_x = \int_{-\frac{h}{2}}^{+\frac{h}{2}} \tau_{xz} \mathrm{d}z, \quad Q_y = \int_{-\frac{h}{2}}^{+\frac{h}{2}} \tau_{yz} \mathrm{d}z. \tag{3.2}$$

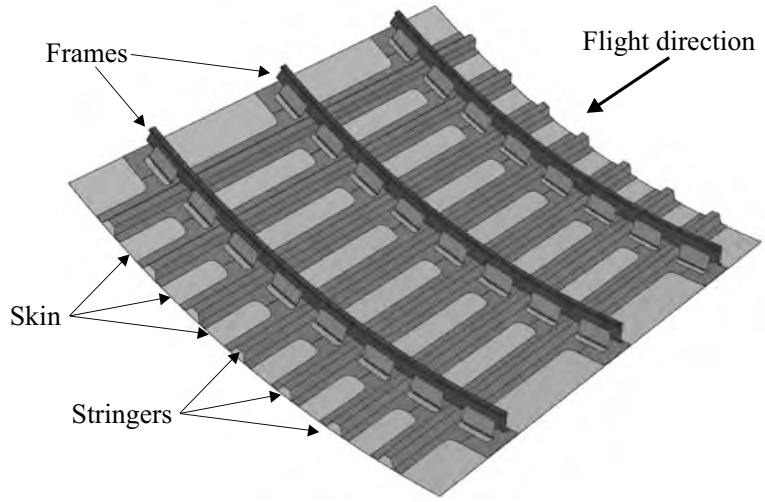


Fig. 3.4 Typical fuselage segment of a modern passenger aircraft

While the shear forces, like the plane internal forces, have the unit of a line load, the internal moments, due to their line-like distribution ('moment per unit length'), result in the unit of a force, e.g. Nmm/mm = N. Here, too, the superscript '0' is often found.

Finally, the term shell must be defined. A shell is a load-bearing structure that, in contrast to a disk or plate, is not flat but has an arbitrarily curved geometry. Examples of shell-like load-bearing structures can already be found very frequently in nature, for example in the form of eggshells, snail shells or mussel shells. However, it has also been shown in technical applications that shell structures have extremely advantageous properties and are therefore very common, be it in container construction, in aircraft and rocket construction, e.g. as fuselage structures (Fig. 3.4 shows a typical fuselage segment of a modern passenger aircraft), or in civil engineering in the form of curved roof structures. An important difference between a flat surface structure (disk/plate) and a shell structure is that the disk behaviour and the plate behaviour cannot be treated separately from each other, but the membrane and plate load-bearing effect generally occur simultaneously as a result of the curved structure, regardless of the type of load. The load-bearing behaviour of a shell is therefore much more complex compared to the calculation of disks and plates, so that shell structures are only dealt with at a later point of this book. Interested readers are referred to the wide range of specialized literature available, a selection of which is cited in the bibliography of this chapter.

Finally, it should be noted that in engineering practice one often refers to 'flat plates' or 'curved shells'. The definitions now introduced show that this use of language is not appropriate. A plate is always flat by definition, just as a shell is always curved by definition.

3.2 Plane State of Strain

Consider a linear-elastic and isotropic structure in which the two displacements u and v are non-zero, while the third displacement component w vanishes. Furthermore, the two displacements u and v are independent of the coordinate z, so that

$$u = u(x, y), \quad v = v(x, y), \quad w = 0. \tag{3.3}$$

In this case, all strains containing the index z disappear:

$$\gamma_{xz} = \gamma_{yz} = \varepsilon_{zz} = 0. \tag{3.4}$$

If the conditions (3.3) and (3.4) are given, this is referred to as the 'plane strain state'. The only remaining strains are the components $\varepsilon_{xx}, \varepsilon_{yy}$ and γ_{xy}, which are exclusively functions of x and y:

$$\varepsilon_{xx}(x, y) = \frac{\partial u}{\partial x}, \quad \varepsilon_{yy}(x, y) = \frac{\partial v}{\partial y}, \quad \gamma_{xy}(x, y) = \frac{\partial u}{\partial y} + \frac{\partial v}{\partial x}. \tag{3.5}$$

A plane strain state occurs in components in which both the shape and the load in the z direction do not change and in which the displacement w is prevented. An example of a structure in the plane strain state is shown in Fig. 3.5, which is supported between two rigid restraints and loaded, for example, by stresses σ_{xx} and σ_{yy}.

If Hooke's law (2.96) is considered for a linear-elastic and isotropic body, the two shear stresses τ_{yz} and τ_{xz} are zero in the plane strain state. However, the normal stress σ_{zz} is generally not equal to zero. Consider the third line in (2.98):

$$\varepsilon_{zz} = -\frac{\nu}{E}\sigma_{xx} - \frac{\nu}{E}\sigma_{yy} + \frac{1}{E}\sigma_{zz} = 0. \tag{3.6}$$

From this, the normal stress σ_{zz} can be calculated as a further stress component that does not vanish in the plane strain state as:

$$\sigma_{zz} = \nu\left(\sigma_{xx} + \sigma_{yy}\right). \tag{3.7}$$

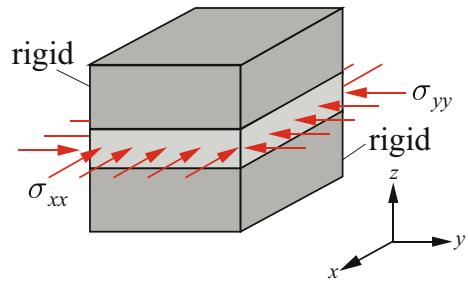


Fig. 3.5 Elastic block between two rigid fixtures

This allows the normal stress σ_{zz} in the elasticity law to be eliminated, and the following form of the material law (2.98) is obtained in the plane strain state:

$$\begin{aligned}
\varepsilon_{xx} &= \frac{1-\nu^2}{E}\left(\sigma_{xx} - \frac{\nu}{1-\nu}\sigma_{yy}\right), \\
\varepsilon_{yy} &= \frac{1-\nu^2}{E}\left(\sigma_{yy} - \frac{\nu}{1-\nu}\sigma_{xx}\right), \\
\gamma_{xy} &= \frac{2\,(1+\nu)}{E}\tau_{xy}.
\end{aligned} \tag{3.8}$$

In (3.8) we can introduce an 'equivalent modulus of elasticity' $\overline{E}$ and an 'equivalent Poisson's ratio' $\overline{\nu}$ as follows:

$$\overline{E} = \frac{E}{1-\nu^2}, \quad \overline{\nu} = \frac{\nu}{1-\nu}, \tag{3.9}$$

and from (3.8) we obtain:

$$\begin{aligned}
\varepsilon_{xx} &= \frac{1}{\overline{E}}\left(\sigma_{xx} - \overline{\nu}\sigma_{yy}\right), \\
\varepsilon_{yy} &= \frac{1}{\overline{E}}\left(\sigma_{yy} - \overline{\nu}\sigma_{xx}\right), \\
\gamma_{xy} &= \frac{2\,(1+\overline{\nu})}{\overline{E}}\tau_{xy}.
\end{aligned} \tag{3.10}$$

Finally, in the plane strain state, the stresses also result as variables independent of z due to the strains being independent of z. If we also assume that no volume forces act in the z-direction, we can show that the equilibrium condition (2.48) in the z-direction is automatically fulfilled. The two remaining equilibrium conditions are simplified to:

$$\begin{aligned}
\frac{\partial \sigma_{xx}}{\partial x} + \frac{\partial \tau_{xy}}{\partial y} + f_x &= 0, \\
\frac{\partial \tau_{xy}}{\partial x} + \frac{\partial \sigma_{yy}}{\partial y} + f_y &= 0.
\end{aligned} \tag{3.11}$$

Of the compatibility conditions, only the condition (2.82) remains:

$$\frac{\partial^2 \varepsilon_{xx}}{\partial y^2} + \frac{\partial^2 \varepsilon_{yy}}{\partial x^2} - \frac{\partial^2 \gamma_{xy}}{\partial x \partial y} = 0. \tag{3.12}$$

A problem of the plane strain state is thus completely described by the set of Eqs. (3.5), (3.8), (3.11), (3.12). In addition, there are always corresponding boundary conditions. It should be noted at this point that no approximations or simplifications were made in the considerations of the plane strain state. All Eqs. (3.5), (3.8), (3.11), (3.12) are therefore exact within the framework of linear elasticity theory assumed here.

3.3 Plane State of Stress

Of great technical relevance, particularly in the context of composite structures, is the so-called plane stress state. The resulting equations are not exact in the sense of the theory of elasticity assumed here, but experience in practical applications shows that very useful results can often be achieved by assuming a plane stress state. The plane state of stress occurs in a good approximation in disk structures. In a disk, that is, in a thin surface structure that is only stressed by forces in its plane, the stress components σ_{zz}, τ_{xz} and τ_{yz} must vanish at the free surfaces at $z = \pm\frac{h}{2}$. Since it is assumed that the disk is thin, i.e. its thickness h is considerably smaller than its two dimensions in the plane, it can be assumed to a good approximation that the stresses σ_{zz}, τ_{xz} and τ_{yz} not only disappear at the surfaces, but are zero throughout the disk. Thus, we obtain:

$$\sigma_{zz} = \tau_{xz} = \tau_{yz} = 0. \tag{3.13}$$

This means that only the three inplane stress components σ_{xx}, σ_{yy} and τ_{xy} remain in a disk in the plane stress state. These are also independent of the thickness coordinate z:

$$\sigma_{xx} = \sigma_{xx}(x, y), \quad \sigma_{yy} = \sigma_{yy}(x, y), \quad \tau_{xy} = \tau_{xy}(x, y). \tag{3.14}$$

Hooke's law (2.98) is simplified as follows in the presence of a plane stress state:

$$\begin{aligned}
\varepsilon_{xx} &= \frac{1}{E}\left(\sigma_{xx} - \nu\sigma_{yy}\right), \\
\varepsilon_{yy} &= \frac{1}{E}\left(\sigma_{yy} - \nu\sigma_{xx}\right), \\
\varepsilon_{zz} &= -\frac{\nu}{E}\left(\sigma_{xx} + \sigma_{yy}\right), \\
\gamma_{xy} &= \frac{2(1+\nu)}{E}\tau_{xy}, \\
\gamma_{xz} &= \gamma_{yz} = 0,
\end{aligned} \tag{3.15}$$

where the relationship $G = \frac{E}{2(1+\nu)}$ was used for the shear modulus G. If we compare this set of equations with the relationships (3.10) for the plane strain state, we see that the relationships for ε_{xx}, ε_{yy} and γ_{xy} are completely analogous if we use the 'equivalent parameters' $\overline{E}$ and $\overline{\nu}$ in (3.15). The relationship for ε_{zz} in (3.15) indicates that a disk in a plane stress state can also stretch or contract in the thickness direction.

The relationships (3.15) can be solved for the stresses and we obtain:

$$\begin{aligned}
\sigma_{xx} &= \frac{E}{1-\nu^2}\left(\varepsilon_{xx} + \nu\varepsilon_{yy}\right), \\
\sigma_{yy} &= \frac{E}{1-\nu^2}\left(\varepsilon_{yy} + \nu\varepsilon_{xx}\right), \\
\tau_{xy} &= G\gamma_{xy}.
\end{aligned} \tag{3.16}$$

The only kinematic equations that remain in the plane stress state are the following:

$$\varepsilon_{xx} = \frac{\partial u}{\partial x}, \quad \varepsilon_{yy} = \frac{\partial v}{\partial y}, \quad \gamma_{xy} = \frac{\partial u}{\partial y} + \frac{\partial v}{\partial x}. \tag{3.17}$$

The equilibrium conditions are reduced as follows:

$$\begin{aligned} \frac{\partial \sigma_{xx}}{\partial x} + \frac{\partial \tau_{xy}}{\partial y} + f_x &= 0, \\ \frac{\partial \tau_{xy}}{\partial x} + \frac{\partial \sigma_{yy}}{\partial y} + f_y &= 0. \end{aligned} \tag{3.18}$$

The following compatibility condition remains:

$$\frac{\partial^2 \varepsilon_{xx}}{\partial y^2} + \frac{\partial^2 \varepsilon_{yy}}{\partial x^2} - \frac{\partial^2 \gamma_{xy}}{\partial x \partial y} = 0. \tag{3.19}$$

The plane stress state is fully described with the introduced equation set. Of course, the respective boundary conditions must then be taken into account as well.

If we compare the equations for the plane stress state with those for the plane strain state, we find that the equations are completely identical except for the respective elasticity constants. Hence, if we have found a solution to a problem for the plane strain state, we can determine the corresponding solution for the plane stress state by exchanging the elasticity constants $\overline{E}$ and $\overline{\nu}$ for E and ν.

3.4 Analysis of Isotropic Disks

3.4.1 Airy's Stress Function, Bipotential Equation

If a plane load-bearing structure is only loaded in its plane, it is referred to as a disk. In the following, the case of a disk in the plane stress state will be considered in detail. The equilibrium conditions for a disk represent two partial differential equations in the stresses $\sigma_{xx}, \sigma_{yy}, \tau_{xy}$ and are as follows:

$$\frac{\partial \sigma_{xx}}{\partial x} + \frac{\partial \tau_{xy}}{\partial y} + f_x = 0, \quad \frac{\partial \tau_{xy}}{\partial x} + \frac{\partial \sigma_{yy}}{\partial y} + f_y = 0. \tag{3.20}$$

Another differential equation is obtained by applying the law of elasticity

$$\begin{aligned} \varepsilon_{xx} &= \frac{1}{E}\left(\sigma_{xx} - \nu \sigma_{yy}\right), \quad \varepsilon_{yy} = \frac{1}{E}\left(\sigma_{yy} - \nu \sigma_{xx}\right), \\ \varepsilon_{zz} &= -\frac{\nu}{E}\left(\sigma_{xx} + \sigma_{yy}\right), \quad \gamma_{xy} = \frac{2\,(1+\nu)}{E}\tau_{xy} \end{aligned} \tag{3.21}$$

in the compatibility condition

$$\frac{\partial^2 \varepsilon_{xx}}{\partial y^2} + \frac{\partial^2 \varepsilon_{yy}}{\partial x^2} - \frac{\partial^2 \gamma_{xy}}{\partial x \partial y} = 0, \tag{3.22}$$

which leads to the following equation:

$$\frac{\partial^2 \sigma_{xx}}{\partial y^2} - \nu \frac{\partial^2 \sigma_{yy}}{\partial y^2} + \frac{\partial^2 \sigma_{yy}}{\partial x^2} - \nu \frac{\partial^2 \sigma_{xx}}{\partial x^2} - 2\,(1+\nu)\,\frac{\partial^2 \tau_{xy}}{\partial x \partial y} = 0. \tag{3.23}$$

This equation can be simplified further by using the two equilibrium conditions (3.20). If we differentiate the first equilibrium condition with respect to x and the second with respect to y and add up the two resulting expressions, we obtain

$$2\frac{\partial^2 \tau_{xy}}{\partial x \partial y} = -\frac{\partial^2 \sigma_{xx}}{\partial x^2} - \frac{\partial^2 \sigma_{yy}}{\partial y^2} - \frac{\partial f_x}{\partial x} - \frac{\partial f_y}{\partial y}. \tag{3.24}$$

Inserting (3.24) into the compatibility condition (3.22) then results in:

$$\frac{\partial^2}{\partial x^2}\left(\sigma_{xx} + \sigma_{yy}\right) + \frac{\partial^2}{\partial y^2}\left(\sigma_{xx} + \sigma_{yy}\right) = -\,(1+\nu)\left(\frac{\partial f_x}{\partial x} + \frac{\partial f_y}{\partial y}\right). \tag{3.25}$$

A common notation is to use the so-called Laplace operator Δ as follows:

$$\Delta = \frac{\partial^2}{\partial x^2} + \frac{\partial^2}{\partial y^2}, \tag{3.26}$$

with which (3.25) can also be written as follows:

$$\Delta\left(\sigma_{xx} + \sigma_{yy}\right) = -\,(1+\nu)\left(\frac{\partial f_x}{\partial x} + \frac{\partial f_y}{\partial y}\right). \tag{3.27}$$

With vanishing volume forces f_x and f_y we get

$$\Delta\left(\sigma_{xx} + \sigma_{yy}\right) = 0, \tag{3.28}$$

which is also known as the potential equation or the disk equation. With the equilibrium conditions (3.20) and the relationship (3.25) or (3.27) or (3.28), there are a total of three differential equations for the three unknown stress components σ_{xx}, σ_{yy} and τ_{xy}.

If the volume forces f_x and f_y are not equal to zero, then the differential equation system composed by (3.20) and (3.25) and (3.27) is inhomogeneous, and the stress solutions are composed of a homogeneous and a particular solution. The latter is a result of the volume forces. For all further explanations, the particular solution is assumed to be known (it will in fact be quite easy to determine for many technically relevant cases), and the focus is on the solution of the homogeneous system of differential equations

$$\Delta\left(\sigma_{xx} + \sigma_{yy}\right) = 0, \quad \frac{\partial \sigma_{xx}}{\partial x} + \frac{\partial \tau_{xy}}{\partial y} = 0, \quad \frac{\partial \tau_{xy}}{\partial x} + \frac{\partial \sigma_{yy}}{\partial y} = 0. \tag{3.29}$$

The system of differential equations (3.29) can be significantly reduced by using a function F, the so-called Airy's[1] stress function, which is related to the stresses σ_{xx}, σ_{yy} and τ_{xy} in the following manner:

$$\sigma_{xx} = \frac{\partial^2 F}{\partial y^2}, \quad \sigma_{yy} = \frac{\partial^2 F}{\partial x^2}, \quad \tau_{xy} = -\frac{\partial^2 F}{\partial x \partial y}, \tag{3.30}$$

where F is a function of the two plane coordinates x, y: $F = F(x, y)$. It is easy to see that by introducing Airy's stress function, the two equilibrium conditions are fulfilled identically for any choice of F:

$$\begin{aligned} \frac{\partial \sigma_{xx}}{\partial x} + \frac{\partial \tau_{xy}}{\partial y} &= \frac{\partial^3 F}{\partial x \partial y^2} - \frac{\partial^3 F}{\partial x \partial y^2} = 0, \\ \frac{\partial \tau_{xy}}{\partial x} + \frac{\partial \sigma_{yy}}{\partial y} &= -\frac{\partial^3 F}{\partial x^2 \partial y} + \frac{\partial^3 F}{\partial x^2 \partial y} = 0, \end{aligned} \tag{3.31}$$

and the only remaining equation to be fulfilled is the compatibility condition, which can be written using the relationship $\Delta F = \sigma_{xx} + \sigma_{yy}$ as:

$$\Delta \Delta F = 0, \tag{3.32}$$

or

$$\frac{\partial^4 F}{\partial x^4} + 2\frac{\partial^4 F}{\partial x^2 \partial y^2} + \frac{\partial^4 F}{\partial y^4} = 0. \tag{3.33}$$

The Eq. (3.32) or (3.33) is also called the bipotential equation or simply disk equation, which is valid regardless of the type of coordinate system. Thus, (3.32) or (3.33) can also be used for a polar coordinate system r, φ (see Fig. 3.6). The Laplace operator is then:

$$\Delta = \frac{\partial^2}{\partial r^2} + \frac{1}{r^2}\frac{\partial^2}{\partial \varphi^2} + \frac{1}{r}\frac{\partial}{\partial r}, \tag{3.34}$$

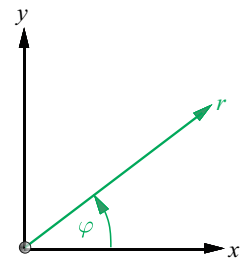


Fig. 3.6 Polar coordinate system r, φ

[1] George Biddell Airy, 1801–1892, English mathematician and astronomer.

and the disk equation $\Delta\Delta F = 0$ then changes to the following form:

$$\frac{\partial^4 F}{\partial r^4} + \frac{2}{r}\frac{\partial^3 F}{\partial r^3} - \frac{1}{r^2}\left(\frac{\partial^2 F}{\partial r^2} - 2\frac{\partial^4 F}{\partial r^2 \partial \varphi^2}\right) + \frac{1}{r^3}\left(\frac{\partial F}{\partial r} - 2\frac{\partial^3 F}{\partial r \partial \varphi^2}\right) + \frac{1}{r^4}\left(4\frac{\partial^2 F}{\partial \varphi^2} + \frac{\partial^4 F}{\partial \varphi^4}\right) = 0. \tag{3.35}$$

The stress components σ_{rr}, $\sigma_{\varphi\varphi}$ and $\tau_{r\varphi}$ can then be expressed by Airy's stress function as follows:

$$\sigma_{rr} = \frac{1}{r^2}\frac{\partial^2 F}{\partial \varphi^2} + \frac{1}{r}\frac{\partial F}{\partial r}, \quad \sigma_{\varphi\varphi} = \frac{\partial^2 F}{\partial r^2}, \quad \sigma_{r\varphi} = -\frac{\partial}{\partial r}\left(\frac{1}{r}\frac{\partial F}{\partial \varphi}\right). \tag{3.36}$$

The elasticity law can be written in the polar coordinate system in a similar manner as in Cartesian coordinates:

$$\varepsilon_{rr} = \frac{1}{E}\left(\sigma_{rr} - \nu\sigma_{\varphi\varphi}\right), \quad \varepsilon_{\varphi\varphi} = \frac{1}{E}\left(\sigma_{\varphi\varphi} - \nu\sigma_{rr}\right), \quad \gamma_{r\varphi} = \frac{1}{G}\tau_{r\varphi}. \tag{3.37}$$

The infinitesimal strains, expressed by the displacements u_r and u_φ, are as follows in polar coordinates:

$$\varepsilon_{rr} = \frac{\partial u_r}{\partial r}, \quad \varepsilon_{\varphi\varphi} = \frac{1}{r}\frac{\partial u_\varphi}{\partial \varphi} + \frac{u_r}{r}, \quad \gamma_{r\varphi} = \frac{1}{r}\frac{\partial u_r}{\partial \varphi} + \frac{\partial u_\varphi}{\partial r} - \frac{u_\varphi}{r}. \tag{3.38}$$

To solve the bipotential equation (3.33) or (3.35), a whole series of special solutions can be used, which will not be discussed in detail here. However, to illustrate the general procedure for solving disk problems, a few selected examples are briefly discussed below.

3.4.2 Selected Examples for Solving Disk Problems

3.4.2.1 Isotropic Disk Under Uniaxial Tension and Under Plane Bending

Consider an isotropic disk under uniaxial tension as shown in Fig. 3.7, left. Furthermore, the same disk is considered under a plane bending load (Fig. 3.7, right).

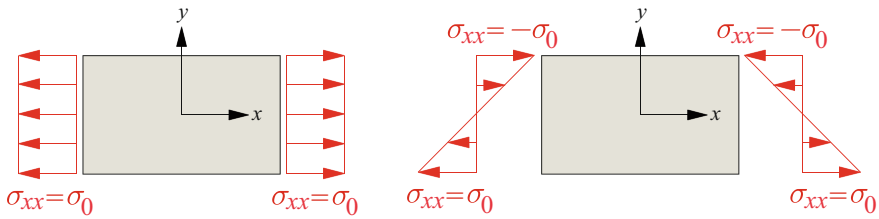


Fig. 3.7 Disk under uniaxial tension (left) and under plane bending (right)

If we first consider the disk under uniaxial tensile load σ_0, we can show that a quadratic approach for the Airy stress function of the form

$$F = \frac{1}{2}\sigma_0 y^2 \tag{3.39}$$

leads to the following stress components in the disk:

$$\sigma_{xx} = \frac{\partial^2 F}{\partial y^2} = \sigma_0, \quad \sigma_{yy} = \frac{\partial^2 F}{\partial x^2} = 0, \quad \tau_{xy} = -\frac{\partial^2 F}{\partial x \partial y} = 0, \tag{3.40}$$

which corresponds to the exact solution for the disk problem under consideration.

In the case of the plane bending load, an approach of the form

$$F = \frac{1}{6}Cy^3 \tag{3.41}$$

leads to the following stresses in the disk under consideration:

$$\sigma_{xx} = \frac{\partial^2 F}{\partial y^2} = Cy, \quad \sigma_{yy} = \frac{\partial^2 F}{\partial x^2} = 0, \quad \tau_{xy} = -\frac{\partial^2 F}{\partial x \partial y} = 0, \tag{3.42}$$

which corresponds exactly to the expected solution (i.e. normal stresses σ_{xx} distributed linearly over the disk height and vanishing stresses $\sigma_{yy} = \tau_{xy} = 0$).

3.4.2.2 Cantilever Isotropic Disk Under Constant Line Load

Let an isotropic disk be given, which is free at its end $x = 0$ and clamped at its end $x = a$ (Fig. 3.8). The disk (thickness h) is subjected to a constant surface load p_0, which acts on the upper edge at $y = b$. The lower edge at $y = -b$ is unloaded.

An approach in the form of a biharmonic polynomial is made for the Airy stress function F:

$$F = C_1 x^2 + C_2 x^2 y + C_3 y^3 + C_4 \left(y^5 - 5x^2 y^3\right). \tag{3.43}$$

From this, the stress components in the disk can be calculated as:

$$\begin{aligned}
\sigma_{xx} &= \frac{\partial^2 F}{\partial y^2} = 6C_3 y + C_4 \left(20y^3 - 30x^2 y\right), \\
\sigma_{yy} &= \frac{\partial^2 F}{\partial x^2} = 2C_1 + 2C_2 y - 10C_4 y^3, \\
\tau_{xy} &= -\frac{\partial^2 F}{\partial x \partial y} = -2C_2 x + 30C_4 x y^2.
\end{aligned} \tag{3.44}$$

The constants C_1, C_2, C_3, C_4 are adjusted to the given boundary conditions. These are as follows with regard to the stresses:

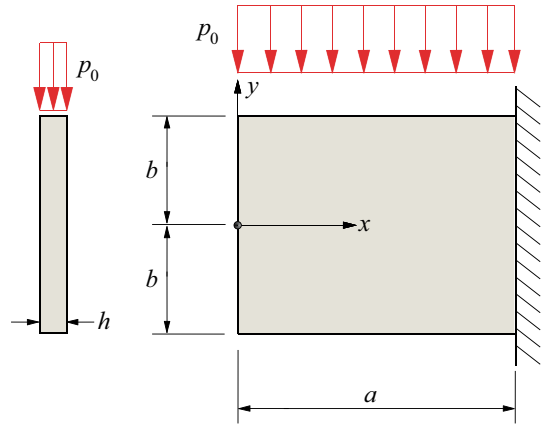


Fig. 3.8 Cantilever disk

$$\begin{aligned}
&\sigma_{yy}\,(y=b)=-p_0, \quad \tau_{xy}\,(y=b)=0,\\
&\sigma_{yy}\,(y=-b)=0, \quad \tau_{xy}\,(y=-b)=0,\\
&\sigma_{xx}\,(x=0)=0, \quad \tau_{xy}\,(x=0)=0.
\end{aligned} \tag{3.45}$$

First, the stress boundary conditions at the upper edge of the disk at $y = b$ are considered. Inserting the stresses according to (3.44) into the first two boundary conditions in (3.45) results in the following two equations:

$$\begin{aligned}
2C_1 + 2C_2 b - 10C_4 b^3 &= -p_0,\\
-2C_2 x + 30C_4 x b^2 &= 0.
\end{aligned} \tag{3.46}$$

Furthermore, the fulfilment of the boundary conditions at the lower edge of the disk at $y = -b$ is required. It can be seen that the approach (3.43) leads to a shear stress distribution τ_{xy} that automatically fulfils the requirement $\tau_{xy}\,(y=-b)=0$. Evaluating the boundary condition $\sigma_{yy}\,(y=-b)=0$ leads to the following equation:

$$2C_1 - 2C_2 b + 10C_4 b^3 = 0. \tag{3.47}$$

Finally, the requirements $\sigma_{xx} = 0$ and $\tau_{xy} = 0$ must be fulfilled at the free disk end at $x = 0$. This is not exactly possible with the chosen approach, but can at least be fulfilled in the integral sense by demanding that the resulting internal forces N, M and Q disappear instead of the stresses σ_{xx} and τ_{xy}. Thus:

$$N = \int_{-b}^{b} \sigma_{xx} \mathrm{d}y = 0, \quad M = \int_{-b}^{b} \sigma_{xx} y \mathrm{d}y = 0, \quad Q = \int_{-b}^{b} \tau_{xy} \mathrm{d}y = 0. \tag{3.48}$$

It can be seen that the resulting normal force N and the resulting shear force Q automatically disappear at $x = 0$ due to the choice of approach (3.43). However, the requirement for the disappearance of the resulting moment M leads to the following equation:

$$4C_3 b^3 + 8C_4 b^5 = 0. \tag{3.49}$$

With the Eqs. (3.46), (3.47) and (3.49), four equations for the four constants C_1, C_2, C_3, C_4 are found. The resulting system of equations is easy to solve and results in

$$C_1 = -\frac{p_0}{4}, \quad C_2 = -\frac{3p_0}{8b}, \quad C_3 = \frac{p_0}{20b}, \quad C_4 = -\frac{p_0}{40b^3}. \tag{3.50}$$

This allows the stresses (3.44) in the disk to be written as:

$$\begin{aligned} \sigma_{xx} &= p_0 \frac{y}{b} \left(\frac{3}{10} + \frac{3x^2}{4b^2} - \frac{y^2}{2b^2} \right), \\ \sigma_{yy} &= p_0 \left(-\frac{1}{2} - \frac{3y}{4b} + \frac{y^3}{4b^3} \right), \\ \tau_{xy} &= p_0 \frac{x}{b} \left(\frac{3}{4} - \frac{3y^2}{4b^2} \right). \end{aligned} \tag{3.51}$$

This solves the considered disk problem at least to a good approximation (note the approximate nature of the conditions (3.48)).

3.4.2.3 Infinitely Extended Perforated Isotropic Disk Under Uniaxial Tension

In many technical applications, it is necessary to provide circular holes in a disk structure. An isotropic disk is now considered, which is assumed to be infinitely extended in both directions x and y and is loaded by a tensile stress $\sigma_{xx} = \sigma_0$ acting at infinity. The disk is weakened by a circular hole of radius a (Fig. 3.9). The following approach is used for Airy's stress function:

$$F = C_1 r^2 + C_2 \ln\left(\frac{r}{a}\right) + C_3 r^2 \ln\left(\frac{r}{a}\right) + f(r) \cos(2\varphi). \tag{3.52}$$

It can be seen that the first three terms in (3.52) describe a purely axially symmetric state, since these terms depend only on r. In contrast, the fourth term in (3.52) represents a non-axially symmetric partial solution, which contains an as of yet unknown function $f(r)$ that is to be determined. If the approach (3.52) is inserted into the disk equation (3.35), a homogeneous Euler differential equation is obtained for the unknown function $f(r)$:

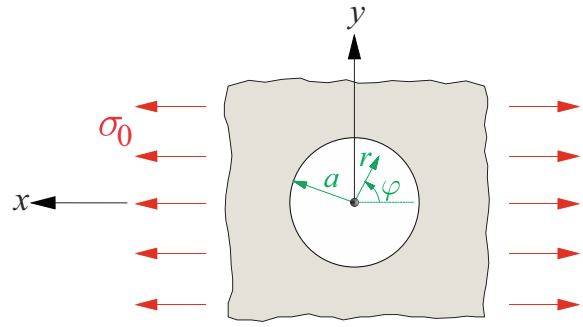


Fig. 3.9 Infinitely extended perforated disk under uniaxial tensile load

$$\frac{\mathrm{d}^4 f}{\mathrm{d}r^4} + \frac{2}{r}\frac{\mathrm{d}^3 f}{\mathrm{d}r^3} - \frac{9}{r^2}\frac{\mathrm{d}^2 f}{\mathrm{d}r^2} + \frac{9}{r^3}\frac{\mathrm{d}f}{\mathrm{d}r} = 0. \tag{3.53}$$

The differential equation (3.53) has the following general solution:

$$f(r) = D_1 r^2 + D_2 r^4 + D_3 \frac{1}{r^2} + D_4, \tag{3.54}$$

in which the variables D_1, D_2, D_3, D_4 are free constants that must be adapted to the given boundary conditions with the constants C_1, C_2, C_3. In the present example, the radial stresses σ_{rr} as well as the shear stresses $\tau_{r\varphi}$ must disappear at the hole edge. It must also be ensured that the constant stress state $\sigma_{xx} = \sigma_0$ and $\sigma_{yy} = \tau_{xy} = 0$ occurs at a sufficient distance from the hole edge. The following result is obtained:

$$\begin{aligned} C_1 &= \frac{\sigma_0}{4}, \quad C_2 = -a^2\frac{\sigma_0}{2}, \quad C_3 = 0, \\ D_1 &= -\frac{\sigma_0}{4}, \quad D_2 = 0, \quad D_3 = -a^4\frac{\sigma_0}{4}, \quad D_4 = a^2\frac{\sigma_0}{2}. \end{aligned} \tag{3.55}$$

The Airy stress function (3.52) is then as follows:

$$F = \frac{\sigma_0}{4}\left[r^2 - 2a^2 \ln\left(\frac{r}{a}\right) - \frac{\left(r^2 - a^2\right)^2}{r^2}\cos(2\varphi)\right], \tag{3.56}$$

and the stress components in the perforated disk can be written as:

$$\begin{aligned} \sigma_{rr} &= \frac{\sigma_0}{2}\left[1 - \frac{a^2}{r^2} + \left(1 - 4\frac{a^2}{r^2} + 3\frac{a^4}{r^4}\right)\cos(2\varphi)\right], \\ \sigma_{\varphi\varphi} &= \frac{\sigma_0}{2}\left[1 + \frac{a^2}{r^2} - \left(1 + 3\frac{a^4}{r^4}\right)\cos(2\varphi)\right], \\ \tau_{r\varphi} &= \frac{\sigma_0}{2}\left(-1 - 2\frac{a^2}{r^2} + 3\frac{a^4}{r^4}\right)\sin(2\varphi). \end{aligned} \tag{3.57}$$

Of particular importance is the circumferential stress $\sigma_{\varphi\varphi}$ directly at the edge of the hole at $r = a$, which is calculated as follows:

$$\sigma_{\varphi\varphi}(r = a) = \sigma_0 [1 - 2\cos(2\varphi)] . \tag{3.58}$$

If this stress component is discussed, it is easy to see that the maximum of $\sigma_{\varphi\varphi} = 3\sigma_0$ occurs at the edge of the hole at the point $\varphi = \pm\frac{\pi}{2}$, i.e. in a section along the y-axis. The minimum of $\sigma_{\varphi\varphi} = -\sigma_0$, on the other hand, occurs at the points $\varphi = 0$ and $\varphi = \pi$, i.e. in sections along the x-axis. The result shows that the resulting stress increase by a factor of 3 compared to the applied load σ_0 near the hole is of central importance with regard to the strength of a perforated disk. It should be noted that in the case of composite laminates, even considerably higher stress concentrations can sometimes occur at the edges of holes.

3.5 Analysis of Shear-Rigid Isotropic Plates

3.5.1 Kinematics in the Context of Kirchhoff's Plate Theory

For many technical applications, the so-called Kirchhoff[2] plate theory has proven itself in many applications. To derive this specific plate theory, we consider a thin plate (thickness h) whose middle plane is spanned at $z = 0$ by the x-axis and the y-axis (Fig. 3.1).

Kirchhoff's plate theory is essentially based on the following assumptions

(1) The displacement w of any point on the plate is always independent of the thickness coordinate z. This means that the deflection w is only a function of the two inplane coordinates x and y, but not of the thickness coordinate z. The following therefore applies: $w = w(x, y)$. This means that the thickness h of the plate does not change during the deformation process.
(2) The hypothesis that the cross-sections remain plane and the normal hypothesis are assumed to be valid. A straight line that is normal to the middle plane of the plate before the deformation remains a straight line after the deformation and also normal to the middle plane of the plate.
(3) A plane stress state in the plate is considered. In particular, the normal stress σ_{zz} in the thickness direction z is assumed to be negligibly small and is therefore neglected in Kirchhoff's plate theory.

A graphical interpretation of assumptions (1) and (2) can be found in Fig. 3.10, in which a plate element is shown in the undeflected and deflected state according to Kirchhoff's plate theory. A point on the middle plane of the plate has moved by the deflection w. The inclination of the deflected plate element is then $\frac{\partial w}{\partial x}$ to the middle plane.

[2] Gustav Robert Kirchhoff, 1824–1887, German physicist.

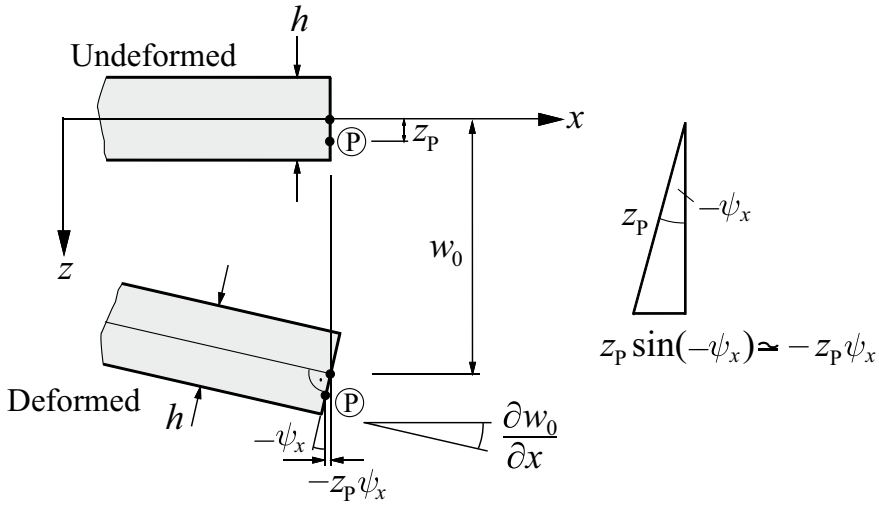


Fig. 3.10 Kinematics of the Kirchhoff plate

Now let $w_0\,(x, y)$ be the deflection of the middle plane of the plate. Furthermore, let $u\,(x, y, z)$, $v\,(x, y, z)$, $w\,(x, y, z)$ be the displacements at any point, all of which can be functions of all three plate coordinates x, y, z. Due to the deformation of the plate, a bending angle ψ_x occurs, which represents the rotation of the cross-section around the y-axis. Since it is required that the cross-sections of the plate remain plane, ψ_x will only result as a function of the coordinates x, y, so that $\psi_x = \psi_x\,(x, y)$ applies. Similarly, another bending angle $\psi_y\,(x, y)$ occurs, which is used to describe the rotation of the cross-section around the x-axis.

The displacement of the point P in Fig. 3.10 is now examined in more detail. The displacement u of point P can be determined directly from Fig. 3.10 as:

$$u_P = -z_P \sin(-\psi_x)\,. \tag{3.59}$$

Small bending angles of the cross-sections are assumed, so that one can approximately assume $\sin(-\psi_x) \simeq -\psi_x$ (Fig. 3.10, right). Then we obtain u_P as:

$$u_P = z_P \psi_x. \tag{3.60}$$

This relationship applies to any other point in the plate, so that it can be written in general terms:

$$u = z\psi_x. \tag{3.61}$$

The same applies to the displacement v:

$$v = z\psi_y. \tag{3.62}$$

Finally, the normal hypothesis must be taken into account, according to which a straight line that is a normal to the middle plane in the undeformed state also remains a straight line in the deformed state and also a normal to the middle plane. From Fig. 3.10 we obtain:

$$-\psi_x = \frac{\partial w_0}{\partial x}. \tag{3.63}$$

Also:

$$-\psi_y = \frac{\partial w_0}{\partial y}. \tag{3.64}$$

The displacement field according to Kirchhoff's plate theory is therefore as follows:

$$\begin{aligned} u(x, y, z) &= z\psi_x(x, y) = -z\frac{\partial w_0}{\partial x}, \\ v(x, y, z) &= z\psi_y(x, y) = -z\frac{\partial w_0}{\partial y}, \\ w(x, y, z) &= w_0(x, y). \end{aligned} \tag{3.65}$$

With the displacement field (3.65) we can calculate the corresponding strains in the plate:

$$\begin{aligned} &\varepsilon_{xx} = \frac{\partial u}{\partial x} = -z\frac{\partial^2 w_0}{\partial x^2}, \quad \varepsilon_{yy} = \frac{\partial v}{\partial y} = -z\frac{\partial^2 w_0}{\partial y^2}, \quad \varepsilon_{zz} = \frac{\partial w}{\partial z} = 0, \\ &\gamma_{xy} = \frac{\partial u}{\partial y} + \frac{\partial v}{\partial x} = -2z\frac{\partial^2 w_0}{\partial x \partial y}, \quad \gamma_{xz} = \frac{\partial u}{\partial z} + \frac{\partial w}{\partial x} = 0, \quad \gamma_{yz} = \frac{\partial v}{\partial z} + \frac{\partial w}{\partial y} = 0. \end{aligned} \tag{3.66}$$

It can be seen that the two transverse shear strains γ_{xz} and γ_{yz} disappear due to the requirement for the cross-sections to remain plane in conjunction with the normal hypothesis. In addition, the assumption that the thickness h of the plate remains constant also results in vanishing strains ε_{zz} in the thickness direction.

The stress field in the plate according to Kirchhoff's plate theory can be written with $\sigma_{zz} = 0$ analogous to the plane stress state:

$$\sigma_{xx} = \frac{E}{1-\nu^2}\left(\varepsilon_{xx} + \nu\varepsilon_{yy}\right), \quad \sigma_{yy} = \frac{E}{1-\nu^2}\left(\varepsilon_{yy} + \nu\varepsilon_{xx}\right), \quad \tau_{xy} = G\gamma_{xy}. \tag{3.67}$$

It should be noted at this point that Kirchhoff's plate theory simultaneously requires that both the normal stress σ_{zz} and the strain ε_{zz} disappear in the thickness direction z. However, since the strain ε_{zz} can now be calculated according to $\varepsilon_{zz} = -\nu\left(\sigma_{xx} + \sigma_{yy}\right)$ and this will generally result in a non-zero value, Kirchhoff's plate theory contains a certain contradiction. However, practical experience shows that this error is very small for thin plates and not too large deformations, so that this contradiction can be accepted in many technical applications. In fact, the everyday reality of engineering practice shows that Kirchhoff's plate theory has

proven itself for a large number of technical applications and is an important basis for many calculations.

Another contradiction in Kirchhoff's plate theory is that, although no transverse shear strains γ_{xz} and γ_{yz} occur in the plate due to the assumption of the normal hypothesis and the requirement that the cross-sections remain plane (which is why a plate calculation according to Kirchhoff's plate theory is also referred to as a shear-rigid plate), but for reasons of equilibrium alone, shear stresses τ_{xz} and τ_{yz} must occur. For τ_{xz} and τ_{yz}, however, it is not possible to calculate them from the material law due to the disappearance of γ_{xz} and γ_{yz}.

3.5.2 Internal Forces, Equilibrium, Plate Equation

The stresses in a plate according to Kirchhoff's plate theory can be calculated by inserting the kinematic relationships (3.66) into the material law (3.67). One then obtains

$$\begin{aligned}
\sigma_{xx} &= -\frac{Ez}{1-\nu^2}\left(\frac{\partial^2 w_0}{\partial x^2} + \nu\frac{\partial^2 w_0}{\partial y^2}\right),\\
\sigma_{yy} &= -\frac{Ez}{1-\nu^2}\left(\frac{\partial^2 w_0}{\partial y^2} + \nu\frac{\partial^2 w_0}{\partial x^2}\right),\\
\tau_{xy} &= -\frac{Ez}{1+\nu}\frac{\partial^2 w_0}{\partial x \partial y}.
\end{aligned} \tag{3.68}$$

Obviously, there is a linear relationship between the stresses and the thickness coordinate z, which is a plausible result when a plate is subjected to a bending load.

The internal force flows Q_x and Q_y as well as bending moment flows M^0_{xx} and M^0_{yy} and a twisting moment flow M^0_{xy} occur in a plate as internal force quantities (Fig. 3.3). The internal forces can be calculated as resultants of the stresses as follows. On the one hand, the bending moments M^0_{xx}, M^0_{yy} and the twisting moment M^0_{xy} can be obtained from the integration of the stresses σ_{xx}, σ_{yy} and τ_{xy} multiplied by the 'lever arm' z:

$$M^0_{xx} = \int_{-\frac{h}{2}}^{\frac{h}{2}} \sigma_{xx} z \mathrm{d}z, \quad M^0_{yy} = \int_{-\frac{h}{2}}^{\frac{h}{2}} \sigma_{yy} z \mathrm{d}z, \quad M^0_{xy} = M^0_{yx} = \int_{-\frac{h}{2}}^{\frac{h}{2}} \tau_{xy} z \mathrm{d}z. \tag{3.69}$$

The sectional moments obtained in this way have the unit of a moment per unit length, i.e. the unit of a force. If the material law (3.68) is inserted into the moment equations (3.69), the constitutive equations for the bending moments and the twisting moment are obtained:

$$M_{xx}^0 = -D\left(\frac{\partial^2 w_0}{\partial x^2} + \nu\frac{\partial^2 w_0}{\partial y^2}\right),$$
$$M_{yy}^0 = -D\left(\frac{\partial^2 w_0}{\partial y^2} + \nu\frac{\partial^2 w_0}{\partial x^2}\right),$$
$$M_{xy}^0 = -(1-\nu)D\frac{\partial^2 w_0}{\partial x \partial y}. \tag{3.70}$$

Therein

$$D = \frac{Eh^3}{12(1-\nu^2)} \tag{3.71}$$

is the so-called plate stiffness.

On the other hand, the plate shear forces Q_x and Q_y can be calculated as the resultants of the transverse shear stresses τ_{xz} and τ_{yz}:

$$Q_x = \int_{-\frac{h}{2}}^{\frac{h}{2}} \tau_{xz}\mathrm{d}z, \quad Q_y = \int_{-\frac{h}{2}}^{\frac{h}{2}} \tau_{yz}\mathrm{d}z. \tag{3.72}$$

The transverse forces have the unit force per unit length, i.e. a line load. However, since no material law is available for calculating the transverse shear stresses τ_{xz} and τ_{yz} from the shear strains within the framework of Kirchhoff's plate theory (because it was explicitly required for the assigned shear strains γ_{xz} and γ_{yz} that they disappear), a calculation of the transverse forces according to (3.72) does not lead to any result. However, the transverse forces Q_x and Q_y can be determined from the equilibrium conditions in a post-calculation. For this purpose, the infinitesimal section element with the edge lengths $\mathrm{d}x$ and $\mathrm{d}y$ according to Fig. 3.11 under a surface load $p(x, y)$ is considered. The internal force and moment flows $M_{xx}^0, M_{yy}^0, M_{xy}^0, Q_x, Q_y$ are plotted on the negative cutting edges, whereas the internal forces and moments with the respective infinitesimal increments are plotted on the positive cutting edges, i.e. $M_{xx}^0 + \frac{\partial M_{xx}^0}{\partial x}\mathrm{d}x$, $M_{yy}^0 + \frac{\partial M_{yy}^0}{\partial y}\mathrm{d}y$, $M_{xy}^0 + \frac{\partial M_{xy}^0}{\partial x}\mathrm{d}x$, $M_{xy}^0 + \frac{\partial M_{xy}^0}{\partial y}\mathrm{d}y$, $Q_x + \frac{\partial Q_x}{\partial x}\mathrm{d}x$ and $Q_y + \frac{\partial Q_y}{\partial y}\mathrm{d}y$. If we calculate the sum of all forces in the z-direction, we obtain

$$\left(Q_x + \frac{\partial Q_x}{\partial x}\mathrm{d}x\right)\mathrm{d}y + \left(Q_y + \frac{\partial Q_y}{\partial y}\mathrm{d}y\right)\mathrm{d}x - Q_x\mathrm{d}y - Q_y\mathrm{d}x + p\mathrm{d}x\mathrm{d}y = 0, \tag{3.73}$$

or after shortening and dividing by $\mathrm{d}A = \mathrm{d}x\mathrm{d}y$:

$$\frac{\partial Q_x}{\partial x} + \frac{\partial Q_y}{\partial y} + p = 0. \tag{3.74}$$

In addition, the moment equilibrium about the y-axis with reference point in the center of gravity of the infinitesimal sectional element is considered:

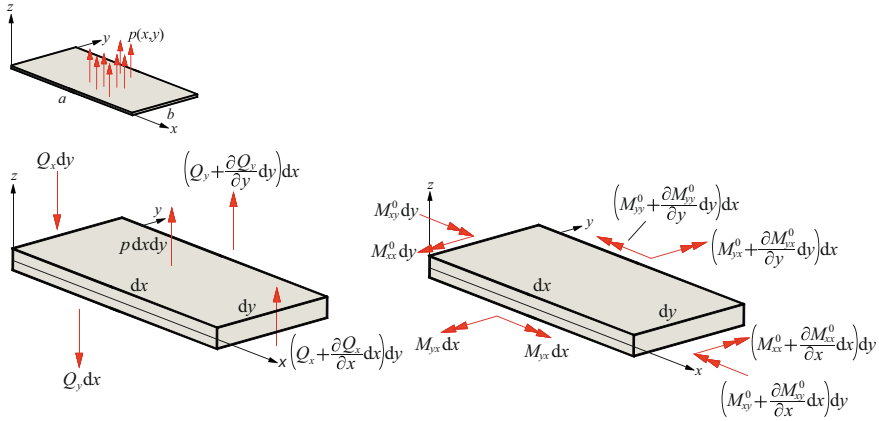


Fig. 3.11 Infinitesimal sectional element

$$\left(M^0_{xx}+\frac{\partial M^0_{xx}}{\partial x}\mathrm{d}x\right)\mathrm{d}y+\left(M^0_{xy}+\frac{\partial M^0_{yx}}{\partial y}\mathrm{d}y\right)\mathrm{d}x-M^0_{xx}\mathrm{d}y-M^0_{yx}\mathrm{d}x$$
$$-\left(Q_x+\frac{\partial Q_x}{\partial x}\mathrm{d}x\right)\mathrm{d}y\frac{\mathrm{d}x}{2}-Q_x\mathrm{d}y\frac{\mathrm{d}x}{2}=0, \tag{3.75}$$

or after shortening:

$$\frac{\partial M^0_{xx}}{\partial x}\mathrm{d}x\mathrm{d}y+\frac{\partial M^0_{xy}}{\partial y}\mathrm{d}x\mathrm{d}y-Q_x\mathrm{d}x\mathrm{d}y-\frac{\partial Q_x}{\partial x}\frac{\mathrm{d}x^2\mathrm{d}y}{2}=0. \tag{3.76}$$

Here, the last term can be assumed to be of higher order than the other terms, so that the final result is obtained:

$$\frac{\partial M^0_{xx}}{\partial x}+\frac{\partial M^0_{xy}}{\partial y}=Q_x. \tag{3.77}$$

The moment equilibrium around the x-axis can be formed in the same way:

$$\frac{\partial M^0_{xy}}{\partial x}+\frac{\partial M^0_{yy}}{\partial y}=Q_y. \tag{3.78}$$

From the two moment equilibrium relationships (3.77), (3.78), the shear forces Q_x and Q_y of the plate can then also be calculated if the moments are known.

The equilibrium requirements (3.74), (3.77), (3.78) can be represented in a more compact manner. If we differentiate the first moment equilibrium (3.77) partially with respect to x and the second moment equilibrium (3.78) partially with respect to y and insert this into the transverse force sum (3.74), we obtain the so-called 'condensed plate equilibrium':

$$\frac{\partial^2 M_{xx}^0}{\partial x^2} + 2\frac{\partial^2 M_{xy}^0}{\partial x \partial y} + \frac{\partial^2 M_{yy}^0}{\partial y^2} + p = 0. \tag{3.79}$$

If the constitutive equations (3.70) are finally inserted into the condensed plate equilibrium (3.79), the so-called Kirchhoff plate equation or plate differential equation is obtained after a few transformations:

$$\frac{\partial^4 w_0}{\partial x^4} + 2\frac{\partial^4 w_0}{\partial x^2 \partial y^2} + \frac{\partial^4 w_0}{\partial y^4} = \frac{p}{D}. \tag{3.80}$$

This is a fourth-order inhomogeneous linear partial differential equation/a bipotential equation for the plate deflection or the deflection of the plate middle plane $w_0(x, y)$. It can also be represented compactly using the Laplace operator Δ as:

$$\Delta\Delta w_0 = \frac{p}{D}. \tag{3.81}$$

3.5.3 Equivalent Transverse Shear Forces and Boundary Conditions

In order to fully describe a boundary value problem within the framework of Kirchhoff's plate theory, the respective boundary conditions are required in addition to the basic equations provided. A distinction is made here between the so-called geometric boundary conditions and the so-called dynamic boundary conditions. While the former place demands on kinematic boundary variables (i.e. generally displacements and rotations), the latter require the fulfilment of boundary conditions for force quantities (i.e. transverse forces and moments). Since the plate equation (3.80) or (3.81) is a fourth-order differential equation, two boundary conditions must be fulfilled at each boundary.

If we consider a plate boundary at the point $x = \text{const.}$, then both a given boundary displacement $\widehat{w}_0$ or a given boundary rotation $\widehat{\frac{\partial w_0}{\partial x}}$ (where the symbol $\widehat{...}$ denotes a given quantity) can be specified. Similarly, we can specify a plate deflection $\widehat{w}_0$ or an edge rotation $\widehat{\frac{\partial w_0}{\partial y}}$ at an edge with $y = \text{const.}$

As far as the dynamic boundary conditions are concerned, statements about the boundary quantities Q_x, M_{xx}^0, M_{xy}^0 can be specified at a boundary $x = \text{const.}$ At a boundary $y = \text{const.}$, statements about the boundary force and moment flows Q_y, M_{yy}^0, M_{xy}^0 would then be possible in the same way. However, it turns out that within the framework of Kirchhoff's plate theory, only two boundary force quantities can be used in each case. It has therefore become established practice to summarise the transverse forces Q_x, Q_y and the twisting moments M_{xy}^0 to form the so-called Kirchhoff equivalent transverse shear forces. The procedure is shown in Fig. 3.12 using the example of the twisting moment M_{xy}^0 for a boundary at the point x=const. Consider the twisting moment M_{xy}^0 occurring at this edge at a point $y = y_1$. If we now also consider an infinitesimally neighbouring point on the y-axis at the point $y = y_2$, then the twisting moment plus an additional infinitesimal term occurs here,

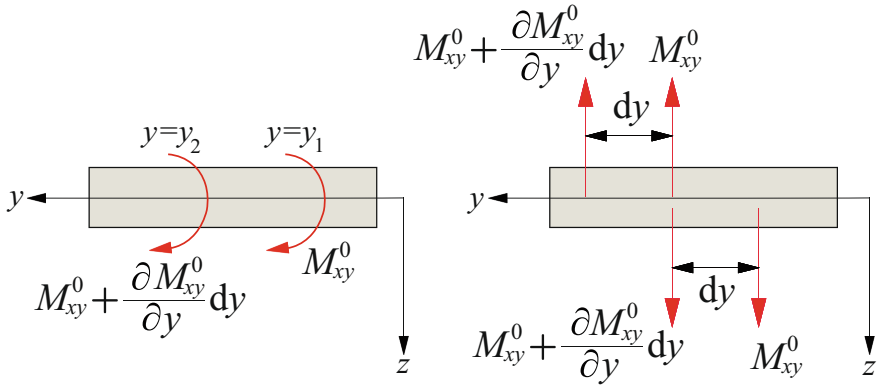


Fig. 3.12 Kirchhoff equivalent transverse shear force

i.e. $M^0_{xy}+\frac{\partial M^0_{xy}}{\partial y}\mathrm{d}y$. The twisting moment can be interpreted as a pair of forces with the lever arm $\mathrm{d}y$. A pair of forces M^0_{xy} then occurs at the point $y=y_1$ and a pair of forces $M^0_{xy}+\frac{\partial M^0_{xy}}{\partial y}\mathrm{d}y$ at the point $y=y_2$. It can then be seen that the forces partially cancel each other out in their effect and that the only remaining force component in the z-direction is precisely the component due to the infinitesimal term $\frac{\partial M^0_{xy}}{\partial y}\mathrm{d}y$. If this force component is related to the length $\mathrm{d}y$ and added to the shear force Q_x, the so-called Kirchhoff equivalent shear force $\bar{Q}_x$ is obtained:

$$\bar{Q}_x = Q_x + \frac{\partial M^0_{xy}}{\partial y}. \tag{3.82}$$

We proceed in the same way for the second shear force:

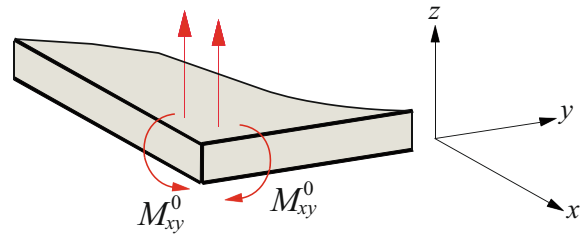
$$\bar{Q}_y = Q_y + \frac{\partial M^0_{xy}}{\partial x}. \tag{3.83}$$

With the Eqs. (3.77) and (3.78) we obtain:

$$\begin{aligned}\bar{Q}_x &= \frac{\partial M^0_{xx}}{\partial x} + 2\frac{\partial M^0_{xy}}{\partial y},\\ \bar{Q}_y &= 2\frac{\partial M^0_{xy}}{\partial x} + \frac{\partial M^0_{yy}}{\partial y}.\end{aligned} \tag{3.84}$$

If the constitutive equations (3.70) for the plate moments are also used here, the following expressions for Kirchhoff's equivalent transverse shear forces are obtained from (3.84):

Fig. 3.13 Corner forces



$$\bar{Q}_x = -D\left(\frac{\partial^3 w_0}{\partial x^3} + (2-\nu)\frac{\partial^3 w_0}{\partial x \partial y^2}\right),$$
$$\bar{Q}_y = -D\left(\frac{\partial^3 w_0}{\partial y^3} + (2-\nu)\frac{\partial^3 w_0}{\partial x^2 \partial y}\right). \tag{3.85}$$

Finally, a special feature should be pointed out that arises when looking at the corners of a plate (Fig. 3.13). If the twisting moments are replaced by equivalent transverse shear forces as explained, individual forces remain at the plate corners in the z-direction, which do not cancel each other out in their effect. The resulting force is also called corner force and is calculated for a right-angled corner as:

$$F = -2M^0_{xy} = 2D(1-\nu)\frac{\partial^2 w_0}{\partial x \partial y}. \tag{3.86}$$

Finally, a few examples of plate boundary conditions are given.

(1) If an edge is free at the point $x = \text{const.}$, then both the Kirchhoff equivalent transverse shear force $\bar{Q}_x$ and the bending moment M^0_{xx} must disappear there:

$$\bar{Q}_x = 0, \quad M^0_{xx} = 0, \tag{3.87}$$

which can also be written as follows when using the constitutive law:

$$\frac{\partial^3 w_0}{\partial x^3} + (2-\nu)\frac{\partial^3 w_0}{\partial x \partial y^2} = 0, \quad \frac{\partial^2 w_0}{\partial x^2} + \nu\frac{\partial^2 w_0}{\partial y^2} = 0. \tag{3.88}$$

(2) If a plate edge is simply supported and thus free to rotate at the point $x = \text{const.}$, then both the deflection w_0 and the bending moment M^0_{xx} must disappear there:

$$w_0 = 0, \quad M^0_{xx} = 0. \tag{3.89}$$

When using the constitutive law, the second condition can also be written as:

$$\frac{\partial^2 w_0}{\partial x^2} + \nu\frac{\partial^2 w_0}{\partial y^2} = 0. \tag{3.90}$$

It should be noted that a simple support at an edge at the point $x = \text{const.}$ means that both the slope $\frac{\partial w_0}{\partial y}$ and the curvature $\frac{\partial^2 w_0}{\partial y^2}$ disappear there. For the condition (3.90) then remains:

$$\frac{\partial^2 w_0}{\partial x^2} = 0. \tag{3.91}$$

(3) If an edge is clamped at the point $x = \text{const.}$, then the plate deflection w_0 and the edge rotation $\frac{\partial w_0}{\partial x}$ must disappear there:

$$w_0 = 0, \quad \frac{\partial w_0}{\partial x} = 0. \tag{3.92}$$

Furthermore, no twisting moments M^0_{xy} occur at clamped plate edges.

In the following, the solution of the plate equation (3.80) or (3.81) for some selected plate situations will be discussed. The plate equation (3.80) or (3.81) is an inhomogeneous partial differential equation whose solution w_0 is composed of a homogeneous part w_h and a particular part w_p:

$$w_0 = w_h + w_p. \tag{3.93}$$

There are a large number of potential solution functions that fulfil (3.80) or (3.81), but of course the underlying boundary conditions must always be fulfilled, which makes it difficult to specify a generally valid solution. Two specific cases, which will also be referred to frequently in this book, will be discussed below. One is the so-called Navier solution for plate problems and the other is the so-called Lévy solution. It can be seen that these approaches can be used to tackle a large number of technically relevant plate problems, also in relation to composite structures.

3.5.4 Navier Solution

Consider a rectangular plate (length a, width b) that is simply supported at all edges (Fig. 3.14). Such a plate is often referred to as a Navier[3] plate. The following boundary conditions apply to such a plate. Firstly, the deflections of the plate's middle plane must disappear at all edges:

$$w_0(x = 0) = 0, \quad w_0(x = a) = 0, \quad w_0(y = 0) = 0, \quad w_0(y = b) = 0. \tag{3.94}$$

Furthermore, the bending moments M^0_{xx} must disappear at the edges $x = 0$ and $x = a$:

$$M^0_{xx}(x = 0) = 0, \quad M^0_{xx}(x = a) = 0, \tag{3.95}$$

[3] Claude Louis Marie Henri Navier, 1785–1836, French mathematician, engineer and physicist.

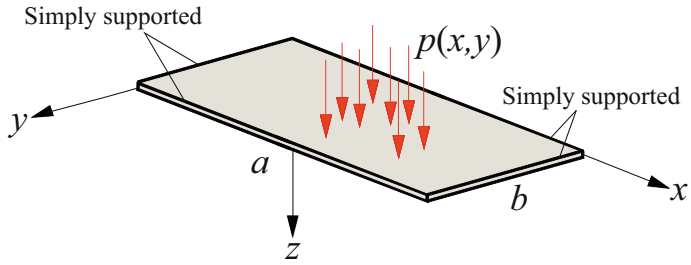


Fig. 3.14 Simply supported plate under arbitrary distributed load $p(x, y)$

which, after the application of the constitutive law and in compliance with

$$\left.\frac{\partial^2 w_0}{\partial y^2}\right|_{x=0} = 0, \quad \left.\frac{\partial^2 w_0}{\partial y^2}\right|_{x=a} = 0 \tag{3.96}$$

leads to the following boundary conditions:

$$\left.\frac{\partial^2 w_0}{\partial x^2}\right|_{x=0} = 0, \quad \left.\frac{\partial^2 w_0}{\partial x^2}\right|_{x=a} = 0. \tag{3.97}$$

The same applies to the edges $y = 0$ and $y = b$:

$$\left.\frac{\partial^2 w_0}{\partial y^2}\right|_{y=0} = 0, \quad \left.\frac{\partial^2 w_0}{\partial y^2}\right|_{y=b} = 0. \tag{3.98}$$

The plate is under a load $p(x, y)$, which is represented as a Fourier series[4]:

$$p = \sum_{m=1}^{m=\infty} \sum_{n=1}^{n=\infty} P_{mn} \sin\left(\frac{m\pi x}{a}\right) \sin\left(\frac{n\pi y}{b}\right), \tag{3.99}$$

where the coefficients P_{mn} can be calculated as:

$$P_{mn} = \frac{4}{ab} \int_0^b \int_0^a p\,(x, y) \sin\left(\frac{m\pi x}{a}\right) \sin\left(\frac{n\pi y}{b}\right) \mathrm{d}x\mathrm{d}y. \tag{3.100}$$

Some selected technically important load types are shown in Fig. 3.15.

In the case of a uniformly distributed surface load $p(x, y) = p_0$, the Fourier coefficients P_{mn} can be determined as follows:

$$P_{mn} = \frac{16 p_0}{mn\pi^2} \quad (m, n = 1, 3, 5, \ldots). \tag{3.101}$$

[4] Jean Baptiste Joseph Fourier, 1768–1830, French mathematician and physicist.

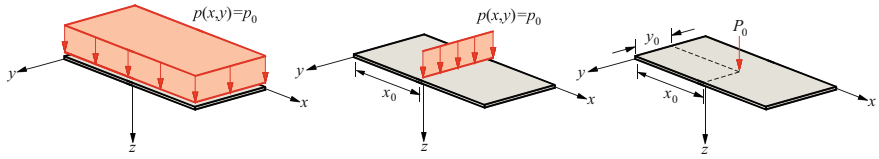


Fig. 3.15 Some elementary load cases

If the load on the plate consists of a linearly distributed load $p(x, y) = p_0$, which is uniformly distributed at the point $x = x_0$, then the following is obtained:

$$P_{mn} = \frac{8p_0}{an\pi} \sin\left(\frac{m\pi x_0}{a}\right) \quad (m = 1, 3, 5, \ldots; n = 1, 2, 3, \ldots). \tag{3.102}$$

If the load is given in the form of a single force $p(x, y) = P_0$, which acts at the point $x = x_0$ and $y = y_0$, then the Fourier coefficients can be written as follows:

$$P_{mn} = \frac{4P_0}{ab} \sin\left(\frac{m\pi x_0}{a}\right) \sin\left(\frac{n\pi y_0}{b}\right) \quad (m, n = 1, 2, 3, \ldots). \tag{3.103}$$

With the help of a Fourier series expansion, any type of load can be approximated as accurately as desired if the degree of series expansion is chosen high enough.

The deflection w_0 of the plate is also approximated in the form of a Fourier series:

$$w_0 = \sum_{m=1}^{m=\infty} \sum_{n=1}^{n=\infty} W_{mn} \sin\left(\frac{m\pi x}{a}\right) \sin\left(\frac{n\pi y}{b}\right). \tag{3.104}$$

If the series expansions for $w_0(x, y)$ and $p(x, y)$ are inserted into the plate equation (3.80), the following representation is obtained:

$$\sum_{m=1}^{m=\infty} \sum_{n=1}^{n=\infty} \left[W_{mn} \left(\frac{m^4\pi^4}{a^4} + 2\frac{m^2n^2\pi^4}{a^2b^2} + \frac{n^4\pi^4}{b^4} \right) - \frac{P_{mn}}{D} \right] \times \sin\left(\frac{m\pi x}{a}\right) \sin\left(\frac{n\pi y}{b}\right) = 0. \tag{3.105}$$

For any x and y, this equation can only be fulfilled if the expression in the square bracket becomes zero. We can solve the expression in brackets directly for the unknown coefficients W_{mn} of the plate deflection and obtain

$$W_{mn} = \frac{P_{mn}}{D} \frac{a^4b^4}{\pi^4 \left(m^2b^2 + n^2a^2\right)^2}. \tag{3.106}$$

The following solution can then be written for the plate deflection $w_0(x, y)$:

$$w_0 = \sum_{m=1}^{m=\infty} \sum_{n=1}^{n=\infty} \frac{P_{mn}}{D} \frac{a^4 b^4}{\pi^4 \left(m^2 b^2 + n^2 a^2\right)^2} \sin\left(\frac{m\pi x}{a}\right) \sin\left(\frac{n\pi y}{b}\right). \tag{3.107}$$

This solution for a plate problem is called Navier solution. The series expansion for $w(x, y)$ generally converges quite quickly, as the coefficients W_{mn} only take on small values quite quickly with increasing degrees of approach due to the terms m^4 and n^4 appearing in the denominator. However, a certain amount of caution is required with regard to the convergence behaviour when considering the internal force and moment flows. Moments and transverse shear forces are quantities that arise from partial derivatives of the second or third order of the plate deflection w_0. Therefore, the convergence behaviour of the moments and shear forces is characterised by $\frac{1}{m^2}$, $\frac{1}{n^2}$ and $\frac{1}{m}$, $\frac{1}{m}$, respectively.

3.5.5 Lévy Solution

The Navier solution is only valid for rectangular plates that are simply supported at all edges. In technical applications, however, many other boundary conditions and their combinations are of considerable importance. One way to analyze some of these plate situations is to use so-called Lévy[5] solutions. Lévy solutions can be derived for plates in which two opposite edges (e.g. the two plate edges $x = 0$ and $x = a$) are simply supported, and the two remaining edges at $y = 0$ and $y = b$ can have any type of support (hinged, clamped, free, elastically supported, reinforced by stiffeners, …). The plate load $p(x, y)$ is again represented in the form of a Fourier series:

$$p = \sum_{m=1}^{m=\infty} \sin\left(\frac{m\pi x}{a}\right) P_m(y), \tag{3.108}$$

where the coefficient functions P_m can be calculated as follows:

$$P_m(y) = \frac{2}{a} \int_0^a p(x, y) \sin\left(\frac{m\pi x}{a}\right) \mathrm{d}x. \tag{3.109}$$

For a uniformly distributed surface load $p(x, y) = p_0$, the following is obtained for P_m, for example

$$P_m = \frac{4p_0}{m\pi} \quad (m = 1, 3, 5, \ldots). \tag{3.110}$$

Further load cases will not be considered in detail at this point. A Fourier series approach is also used for the plate deflection:

$$w_0 = \sum_{m=1}^{m=\infty} \sin\left(\frac{m\pi x}{a}\right) W_m(y). \tag{3.111}$$

[5] Maurice Lévy, 1838–1910, French mathematician, physicist and engineer.

If the approaches for the load p and the plate deflection w_0 are inserted into the plate equation (3.80), the following equation is obtained:

$$\sum_{m=1}^{m=\infty} \left(\frac{\mathrm{d}^4 W_m(y)}{\mathrm{d}y^4} - 2\frac{m^2\pi^2}{a^2}\frac{\mathrm{d}^2 W_m(y)}{\mathrm{d}y^2} + \frac{m^4\pi^4}{a^4} W_m(y) - \frac{1}{D} P_m(y) \right) \times \sin\left(\frac{m\pi x}{a}\right) = 0. \tag{3.112}$$

Since this equation must be valid for any value of x, the bracket term must disappear:

$$\frac{\mathrm{d}^4 W_m(y)}{\mathrm{d}y^4} - 2\frac{m^2\pi^2}{a^2}\frac{\mathrm{d}^2 W_m(y)}{\mathrm{d}y^2} + \frac{m^4\pi^4}{a^4} W_m(y) = \frac{1}{D} P_m(y). \tag{3.113}$$

This is an ordinary linear inhomogeneous differential equation of fourth order for the function $W_m(y)$ yet to be determined. Several methods are generally available for its determination. At this point, we will only discuss the direct analytical solution.

The solution of (3.113) requires knowledge of two solutions, namely the homogeneous solution on the one hand and the particular solution on the other. For the homogeneous solution, an approach of the form

$$W_{m,h} = Ce^{\lambda y} \tag{3.114}$$

is used which leads to the following characteristic equation for the exponent λ after insertion into (3.113) and truncation of the constants C and the exponential functions:

$$\lambda^4 - 2\frac{m^2\pi^2}{a^2}\lambda^2 + \frac{m^4\pi^4}{a^4} = 0. \tag{3.115}$$

This equation has four solutions, two of which are identical. They are as follows:

$$\lambda_1 = \lambda_2 = -\lambda_3 = -\lambda_4 = \frac{m\pi}{a}. \tag{3.116}$$

This allows us to write the homogeneous solution of the differential equation (3.113) as:

$$W_{m,h} = \left(C_{1,m} + C_{2,m}y\right)\cosh\left(\frac{m\pi y}{a}\right) + \left(C_{3,m} + C_{4,m}y\right)\sinh\left(\frac{m\pi y}{a}\right). \tag{3.117}$$

The type of particular solution $W_{m,p}$ depends on the specific load case and cannot be generally described a priori. In many cases, standard mathematical methods will be used, e.g. a right-hand side approach. The total solution for W_m is then obtained by adding the homogeneous and the particular solution: $W_m = W_{m,h} + W_{m,p}$. The total solution for the plate deflection $w_0(x, y)$ is therefore obtained as:

$$w_0 = \sum_{m=1}^{m=\infty} \sin\left(\frac{m\pi x}{a}\right)\left[\left(C_{1,m} + C_{2,m}y\right)\cosh\left(\frac{m\pi y}{a}\right) + \left(C_{3,m} + C_{4,m}y\right)\sinh\left(\frac{m\pi y}{a}\right) + W_{m,p}\right]. \tag{3.118}$$

The constants $C_{1,m}$, $C_{2,m}$, $C_{3,m}$, $C_{4,m}$ can be determined from the boundary conditions at the edges $y = 0$ and $y = b$.

For the case of a plate under a uniform load $p(x, y) = p_0$, a Lévy-type solution is to be derived below. The differential equation (3.113) then changes into the form

$$\frac{\mathrm{d}^4 W_m(y)}{\mathrm{d}y^4} - 2\frac{m^2\pi^2}{a^2}\frac{\mathrm{d}^2 W_m(y)}{\mathrm{d}y^2} + \frac{m^4\pi^4}{a^4}W_m(y) = \frac{1}{D}\frac{4p_0}{m\pi}. \tag{3.119}$$

The plate is assumed to be simply supported at the edges $x = 0$ and $x = a$. The plate is clamped at the edges $y = 0$ and $y = b$, so the following applies there:

$$w_0(y = 0) = 0, \quad w_0(y = b) = 0, \quad \left.\frac{\partial w_0}{\partial y}\right|_{y=0} = 0, \quad \left.\frac{\partial w_0}{\partial y}\right|_{y=b} = 0. \tag{3.120}$$

First, a particular solution is sought for the inhomogeneous differential equation (3.119), which can be easily applied here as a constant $W_{m,p} = k$. Inserting it into (3.119) results in:

$$W_{m,p} = \frac{4p_0a^4}{Dm^5\pi^5}, \tag{3.121}$$

so that the solution for the plate deflection takes the following form:

$$w_0 = \sum_{m=1}^{m=\infty} \sin\left(\frac{m\pi x}{a}\right)\left[\left(C_{1,m} + C_{2,m}y\right)\cosh\left(\frac{m\pi y}{a}\right) + \left(C_{3,m} + C_{4,m}y\right)\sinh\left(\frac{m\pi y}{a}\right) + \frac{4p_0a^4}{Dm^5\pi^5}\right]. \tag{3.122}$$

The constants $C_{1,m}$, $C_{2,m}$, $C_{3,m}$, $C_{4,m}$ are determined from the boundary conditions at the edges $y = 0$ and $y = b$. The requirement $w_0(y = 0) = 0$ immediately leads to

$$C_{1,m} = -\frac{4p_0a^4}{Dm^5\pi^5}. \tag{3.123}$$

If we insert the remaining boundary conditions at the edges $y = 0$ and $y = b$ into the solution (3.122), we obtain the following three equations for the three remaining constants $C_{2,m}$, $C_{3,m}$, $C_{4,m}$:

$$
\begin{aligned}
C_{2,m} b \cosh\left(\frac{m\pi b}{a}\right) + C_{3,m} \sinh\left(\frac{m\pi b}{a}\right) + C_{4,m} b \sinh\left(\frac{m\pi b}{a}\right) &= \frac{4p_0 a^4}{Dm^5\pi^5}\left[\cosh\left(\frac{m\pi b}{a}\right) - 1\right], \\
C_{2,m} + C_{3,m}\frac{m\pi}{a} &= 0, \\
C_{2,m}\left[\cosh\left(\frac{m\pi b}{a}\right) + \frac{m\pi b}{a}\sinh\left(\frac{m\pi b}{a}\right)\right] + C_{3,m}\frac{m\pi}{a}\cosh\left(\frac{m\pi b}{a}\right) & \\
+C_{4,m}\left[\sinh\left(\frac{m\pi b}{a}\right) + \frac{m\pi b}{a}\cosh\left(\frac{m\pi b}{a}\right)\right] &= \frac{4p_0 a^3}{Dm^4\pi^4}\sinh\left(\frac{m\pi b}{a}\right). \qquad (3.124)
\end{aligned}
$$

The system of Eq. (3.124) can then be solved quite easily:

$$
\begin{aligned}
C_{2,m} &= \frac{4p_0 a^2}{Dm^4\pi^4\Delta}\left[a\sinh\left(\frac{m\pi b}{a}\right) - m\pi b\right]\left[\cosh\left(\frac{m\pi b}{a}\right) - 1\right], \\
C_{3,m} &= -\frac{4p_0 a^3}{Dm^5\pi^5\Delta}\left[a\sinh\left(\frac{m\pi b}{a}\right) - m\pi b\right]\left[\cosh\left(\frac{m\pi b}{a}\right) - 1\right], \\
C_{4,m} &= \frac{4a^2 p_0}{Dm^4\pi^4\Delta}\left[a + m\pi b\sinh\left(\frac{m\pi b}{a}\right) - a\cosh^2\left(\frac{m\pi b}{a}\right)\right], \qquad (3.125)
\end{aligned}
$$

where Δ is the determinant of the coefficient matrix of the system of Eq. (3.124):

$$
\Delta = \frac{m^2\pi^2 b^2}{a^2} + 1 - \cosh^2\left(\frac{m\pi b}{a}\right). \qquad (3.126)
$$

Other Lévy-type solutions can be constructed in the same way. This will be discussed in more detail in connection with composite structures in the further course of this book.

References

Altenbach H, Altenbach J, Naumenko K (1998): *Ebene Flächentragwerke*, Springer Verlag, Berlin et al., Germany.

Becker W, Gross D (2002): *Mechanik elastischer Körper und Strukturen*, Springer Verlag, Berlin et al., Germany.

Eschenauer H, Schnell W (1986): *Elastizitätstheorie I*, 2nd edition, Bibliographisches Institut, Mannheim et al., Germany.

Eschenauer H, Olhoff N, Schnell W (1997): *Applied Structural Mechanics*, Springer Verlag, Berlin et al., Germany.

Flügge W (1981): *Statik und Dynamik der Schalen*, 3rd edition, Springer Verlag, Berlin et al., Germany.

Girkmann K (1974): *Flächentragwerke*, 6th edition, Springer Verlag, Wien et al., Austria.

Göldner H, Altenbach J, Eschke K, Garz KF, Sähn S (1979): *Lehrbuch Höhere Festigkeitslehre Band 1*, Physik Verlag, Weinheim, Germany.

Göldner H, Altenbach J, Eschke K, Garz KF, Sähn S (1985): *Lehrbuch Höhere Festigkeitslehre Band 2*, Physik Verlag, Weinheim, Germany.

Gross D, Hauger W, Schnell W, Wriggers P (1995): *Technische Mechanik 4: Hydromechanik, Elemente der Höheren Mechanik, Numerische Methoden*, 2nd edition, Springer Verlag, Berlin et al., Germany.

Mazurkiewicz EM, Nagorski RT (1991): *Shells of revolution*, Elsevier Science Publ., Amsterdam, The Netherlands.

Pflüger A (1967): *Elementare Schalenstatik*, 4th edition, Springer Verlag, Berlin et al., Germany.

Reddy JN (2006): *Theory and Analysis of Elastic Plates and Shells*, CRC Press Boca Raton et al., USA.

Wlassow WS (1958): *Allgemeine Schalentheorie und ihre Anwendung in der Technik*, Akademie-Verlag, Berlin, Germany.



Variational Principles and Approximation Methods in Structural Mechanics

4

The behaviour of a solid is described by differential equations that depend on location and time. As an example, the linear elastic and anisotropic structural behaviour in the three-dimensional case is defined with the equation systems shown in Chap. 2. The problem is fully described when all boundary conditions (support conditions, geometry, load) are taken into account. Nevertheless, only in the rarest of cases is it possible to determine a mathematically rigorous solution for a given engineering problem. By rigorous, we mean that a problem can be solved in such a way that all governing equations as well as all underlying boundary conditions are exactly fulfilled. For this reason, a whole range of solution methods have been developed that can be used to find at least approximate solutions for a large number of engineering problems. In addition to the classic methods such as the Ritz method or the Galerkin method, the Finite Element Method (FEM) should be mentioned in particular, which has become an indispensable part of everyday engineering work and is a valuable tool for a large number of problems. What all of these approximation methods have in common is that they are based on certain variational and energy principles that are of fundamental importance both from a purely mechanical point of view and for practical applications. Some selected principles will be considered below, and the connection to the fundamentals of the approximation methods mentioned will be established, whereby the Ritz method, the Galerkin method and the Finite Element Method will be considered in more detail. The considerations are limited to geometric and material linearity.

© The Author(s), under exclusive license to Springer-Verlag GmbH, DE, part of Springer Nature 2025

C. Mittelstedt, *Mechanics of Composite Structures*,
https://doi.org/10.1007/978-3-662-70788-3_4

4.1 General Theorem of Work

A general theorem of work is derived from the equilibrium conditions (2.48) and the kinematic equations (2.72), which establishes a relationship between any equilibrium group of stresses and forces on the one hand, and any kinematically permissible field of strains and displacements on the other.

Consider an equilibrium group consisting of the stresses $\sigma_{xx}^{(1)}$, $\sigma_{yy}^{(1)}$, $\sigma_{zz}^{(1)}$, $\tau_{xy}^{(1)}$, $\tau_{xz}^{(1)}$, $\tau_{yz}^{(1)}$, the volume forces $f_x^{(1)}$, $f_y^{(1)}$, $f_z^{(1)}$, and the stress vectors $t_x^{(1)}$, $t_y^{(1)}$, $t_z^{(1)}$. The stresses are required to fulfil the equilibrium conditions (2.48) and the corresponding boundary conditions $t_x = t_{x0}$, $t_y = t_{y0}$, $t_z = t_{z0}$. In addition, a kinematic field is given that consists of the displacements $u^{(2)}$, $v^{(2)}$, $w^{(2)}$ and the resulting strains $\varepsilon_{xx}^{(2)}$, $\varepsilon_{yy}^{(2)}$, $\varepsilon_{zz}^{(2)}$, $\gamma_{yz}^{(2)}$, $\gamma_{xz}^{(2)}$, $\gamma_{xy}^{(2)}$ that can be calculated using the kinematic relationships (2.72) and which fulfils any existing displacement boundary conditions $u = u_0$, $v = v_0$, $w = w_0$. To derive the general theorem of work, the local equilibrium conditions are used (2.48)

$$\begin{aligned}
\frac{\partial \sigma_{xx}^{(1)}}{\partial x} + \frac{\partial \tau_{xy}^{(1)}}{\partial y} + \frac{\partial \tau_{xz}^{(1)}}{\partial z} + f_x^{(1)} &= 0, \\
\frac{\partial \tau_{xy}^{(1)}}{\partial x} + \frac{\partial \sigma_{yy}^{(1)}}{\partial y} + \frac{\partial \tau_{yz}^{(1)}}{\partial z} + f_y^{(1)} &= 0, \\
\frac{\partial \tau_{xz}^{(1)}}{\partial x} + \frac{\partial \tau_{yz}^{(1)}}{\partial y} + \frac{\partial \sigma_{zz}^{(1)}}{\partial z} + f_z^{(1)} &= 0.
\end{aligned} \tag{4.1}$$

For further considerations, it is advantageous to make use of the index notation and Einstein's summation convention. We can then write (4.1) using the reference coordinates x_1, x_2, x_3 as follows ($i, j = 1, 2, 3$):

$$\frac{\partial \sigma_{ij}^{(1)}}{\partial x_j} + f_i^{(1)} = 0. \tag{4.2}$$

If we multiply (4.2) by the displacements $u_i^{(2)}$ and integrate over the volume V of the body, we obtain

$$\int_V \frac{\partial \sigma_{ij}^{(1)}}{\partial x_j} u_i^{(2)} \mathrm{d}V + \int_V f_i^{(1)} u_i^{(2)} \mathrm{d}V = 0. \tag{4.3}$$

The integrand in the first integral can be transformed as follows using the product rule of differential calculus:

$$\frac{\partial \sigma_{ij}^{(1)}}{\partial x_j} u_i^{(2)} = \frac{\partial}{\partial x_j} \left(\sigma_{ij}^{(1)} u_i^{(2)} \right) - \sigma_{ij}^{(1)} \frac{\partial u_i^{(2)}}{\partial x_j}, \tag{4.4}$$

which leads to the following equation:

$$\int_V \frac{\partial}{\partial x_j}\left(\sigma_{ij}^{(1)} u_i^{(2)}\right) \mathrm{d}V - \int_V \sigma_{ij}^{(1)} \frac{\partial u_i^{(2)}}{\partial x_j} \mathrm{d}V + \int_V f_i^{(1)} u_i^{(2)} \mathrm{d}V = 0. \tag{4.5}$$

At this point, the first integral is transformed from a volume integral over V into an integral on the boundary ∂V using the Gaussian[1] integral theorem as follows:

$$\int_V \frac{\partial}{\partial x_j}\left(\sigma_{ij}^{(1)} u_i^{(2)}\right) \mathrm{d}V = \int_{\partial V} \sigma_{ij}^{(1)} u_i^{(2)} n_j \mathrm{d}A, \tag{4.6}$$

where n_j is the component of the normal vector $\underline{n}$ in coordinate direction x_j. Thus:

$$\int_{\partial V} \sigma_{ij}^{(1)} u_i^{(2)} n_j \mathrm{d}A - \int_V \sigma_{ij}^{(1)} \frac{\partial u_i^{(2)}}{\partial x_j} \mathrm{d}V + \int_V f_i^{(1)} u_i^{(2)} \mathrm{d}V = 0. \tag{4.7}$$

At this point, we can make use of the relationship $\sigma_{ij}^{(1)} n_j = t_i^{(1)}$, where t_i is the i-th component of the stress vector $\underline{t}$. Furthermore, the relation $\sigma_{ij}^{(1)} \frac{\partial u_i^{(2)}}{\partial x_j} = \sigma_{ij}^{(1)} \varepsilon_{ij}^{(2)}$, and finally the following relationship is obtained, which is also referred to as the 'general theorem of work':

$$\int_{\partial V} t_i^{(1)} u_i^{(2)} \mathrm{d}A - \int_V \sigma_{ij}^{(1)} \varepsilon_{ij}^{(2)} \mathrm{d}V + \int_V f_i^{(1)} u_i^{(2)} \mathrm{d}V = 0, \tag{4.8}$$

or

$$\int_V \sigma_{ij}^{(1)} \varepsilon_{ij}^{(2)} \mathrm{d}V = \int_V f_i^{(1)} u_i^{(2)} \mathrm{d}V + \int_{\partial V} t_i^{(1)} u_i^{(2)} \mathrm{d}A. \tag{4.9}$$

If the boundary of the solid ∂V is divided into a section ∂V_t and a section ∂V_u, on which boundary loads t_{i0} or displacements u_{i0} are specified, then the general work theorem can also be written as follows:

$$\int_V \sigma_{ij}^{(1)} \varepsilon_{ij}^{(2)} \mathrm{d}V = \int_V f_i^{(1)} u_i^{(2)} \mathrm{d}V + \int_{\partial V_t} t_{i0}^{(1)} u_i^{(2)} \mathrm{d}A + \int_{\partial V_u} t_i^{(1)} u_{i0}^{(2)} \mathrm{d}A. \tag{4.10}$$

Using the reference coordinates x, y, z we have:

$$\begin{aligned} &\int_V \left(\sigma_{xx}^{(1)} \varepsilon_{xx}^{(2)} + \sigma_{yy}^{(1)} \varepsilon_{yy}^{(2)} + \sigma_{zz}^{(1)} \varepsilon_{zz}^{(2)} + \tau_{yz}^{(1)} \gamma_{yz}^{(2)} + \tau_{xz}^{(1)} \gamma_{xz}^{(2)} + \tau_{xy}^{(1)} \gamma_{xy}^{(2)}\right) \mathrm{d}V \\ &= \int_V \left(f_x^{(1)} u^{(2)} + f_y^{(1)} v^{(2)} + f_z^{(1)} w^{(2)}\right) \mathrm{d}V \end{aligned}$$

[1] Johann Carl Friedrich Gauss, 1777–1855, German polymath.

$$+\int_{\partial V_t}\left(t_{x0}^{(1)}u^{(2)}+t_{y0}^{(1)}v^{(2)}+t_{z0}^{(1)}w^{(2)}\right)\mathrm{d}A$$
$$+\int_{\partial V_u}\left(t_{x}^{(1)}u_0^{(2)}+t_{y}^{(1)}v_0^{(2)}+t_{z}^{(1)}w_0^{(2)}\right)\mathrm{d}A. \tag{4.11}$$

Here, the integral on the left side of (4.11) represents the work of the internal forces or stresses that is performed on the strains assigned to them. The first integral on the right-hand side of (4.11) is the work of the volume forces. The remaining two integrals are then the work done by the surface loads. It should also be noted that the general work theorem is valid regardless of the material behaviour. It is the basis for the derivation of a whole series of other theorems that are also very important for the analysis of composite structures, which are explained below.

4.2 Principle of Virtual Displacements

A specific boundary value problem will now be considered in the context of elastostatics. A stress field σ_{ij} is caused by a given surface load t_i and given volume loads f_i in the body under consideration, which is in equilibrium. It is now assumed that the body is deflected infinitesimally from its equilibrium position and thus subjected to virtual displacements δu_i and virtual strains $\delta\varepsilon_{ij}$. The following requirements are placed on the virtual displacements and strains:

(1) The virtual displacements δu_i and the virtual strains $\delta\varepsilon_{ij}$ do not occur in reality, they are imaginary, i.e. virtual. This is illustrated by the δ-symbol.
(2) The virtual displacements δu_i and the virtual strains $\delta\varepsilon_{ij}$ are infinitesimally small.
(3) The virtual displacements δu_i and the virtual strains $\delta\varepsilon_{ij}$ cannot be chosen arbitrarily, but must be potentially possible, i.e. satisfy the geometric boundary conditions of the respective system.

The principle of virtual displacements can now be derived by replacing the force quantities $\sigma_{ij}^{(1)}, f_i^{(1)}, t_i^{(1)}$ with the real force quantities σ_{ij} in the general work theorem (4.10), f_i, t_i and the kinematic variables $u_i^{(2)}, \varepsilon_{ij}^{(2)}$ are substituted by the virtual kinematic variables $\delta u_i, \delta\varepsilon_{ij}$. The restriction here is that no virtual displacements δu_i may occur on edges ∂V_u on which displacements are already specified. The principle of virtual displacements can therefore be written as follows:

$$\int_V \sigma_{ij}\delta\varepsilon_{ij}\mathrm{d}V=\int_V f_i\delta u_i\mathrm{d}V+\int_{\partial V_t} t_{i0}\delta u_i\mathrm{d}A. \tag{4.12}$$

In the reference system x, y, z we have:

$$\int_V \left(\sigma_{xx}\delta\varepsilon_{xx} + \sigma_{yy}\delta\varepsilon_{yy} + \sigma_{zz}\delta\varepsilon_{zz} + \tau_{yz}\delta\gamma_{yz} + \tau_{xz}\delta\gamma_{xz} + \tau_{xy}\delta\gamma_{xy}\right) \mathrm{d}V$$
$$= \int_V \left(f_x\delta u + f_y\delta v + f_z\delta w\right) \mathrm{d}V + \int_{\partial V_t} \left(t_{x0}\delta u + t_{y0}\delta v + t_{z0}\delta w\right) \mathrm{d}A. \tag{4.13}$$

At this point, it is customary to describe the work performed by the internal forces or the stresses along the virtual strains as 'internal virtual work' δW_i. Similarly, the work performed by the surface forces and the volume forces along the virtual displacements is referred to as 'external virtual work' δW_a:

$$\delta W_i = \int_V \sigma_{ij}\delta\varepsilon_{ij}\mathrm{d}V,$$
$$\delta W_a = \int_V f_i\delta u_i\mathrm{d}V + \int_{\partial V_t} t_{i0}\delta u_i\mathrm{d}A. \tag{4.14}$$

This means that the principle of virtual displacements can also be formulated as follows:

$$\delta W_i = \delta W_a. \tag{4.15}$$

Note that the principle of virtual displacements applies to any permissible virtual displacements. As the derivation of both the general theorem of work and the principle of virtual displacements has shown, it is not only a consequence of the equilibrium conditions, but is completely equivalent to them. The principle of virtual displacements can thus be described verbally as follows:

A deformable body is in equilibrium precisely when the virtual internal work is equal to the virtual external work for any permissible virtual displacement from the equilibrium position.

The principle of virtual displacements is therefore an equilibrium statement formulated via corresponding virtual work and applies to any material law. It is of fundamental importance for a large number of applications in the context of applied structural mechanics and will be used frequently in the remainder of this book.

4.3 Principle of Virtual Forces

The so-called principle of virtual forces is obtained in a completely analogous way. For this purpose, it is assumed in the general work theorem that the forces or stresses are now varied and that the kinematic field consists of the real displacements and strains. The force variables are assumed to be virtual variables, i.e. the virtual changes $\delta\sigma_{ij}$, δf_i and δt_i are assumed. On the edges ∂V_t of the body, on which stresses are specified, the virtual surface forces δt_i must disappear.

The virtual forces have the following properties analogous to the virtual displacements:

(1) The virtual forces are only imaginary and do not really exist, they are virtual quantities.
(2) The virtual forces are infinitesimally small.
(3) The virtual forces must fulfil the equilibrium conditions and the specified stress boundary conditions.

If we now insert the actual/real displacements and strains u_i and ε_{ij} as well as the virtual force variables $\delta\sigma_{ij}$, δf_i and δt_i into the general work theorem, we obtain the principle of virtual forces in the following form:

$$\int_V \varepsilon_{ij}\delta\sigma_{ij}\mathrm{d}V = \int_V u_i\delta f_i\mathrm{d}V + \int_{\partial V_u} u_{i0}\delta t_i\mathrm{d}A. \tag{4.16}$$

If the abbreviations $\delta\widetilde{W}_i$ and $\delta\widetilde{W}_a$ are used for the so-called inner complementary work and the so-called external complementary work according to

$$\begin{aligned}\delta\widetilde{W}_i &= \int_V \varepsilon_{ij}\delta\sigma_{ij}\mathrm{d}V,\\ \delta\widetilde{W}_a &= \int_V u_i\delta f_i\mathrm{d}V + \int_{\partial V_u} u_{i0}\delta t_i\mathrm{d}A,\end{aligned} \tag{4.17}$$

then the principle of virtual forces can also be written as follows:

$$\delta\widetilde{W}_i = \delta\widetilde{W}_a. \tag{4.18}$$

The variables $\delta\widetilde{W}_i$ and $\delta\widetilde{W}_a$ are often also referred to as virtual complementary work, so that the principle of virtual forces is also known as the principle of virtual complementary work.

The principle of virtual forces applies to any virtual force quantities that are consistent with the given stress boundary conditions. It is therefore not only a consequence of the kinematic compatibility of the displacements and strains, but is completely equivalent to them. The principle of virtual forces can be verbalised as follows:

A deformable body is in a kinematically compatible state of displacement and strain if, for any equilibrium system of virtual forces, the inner complementary work corresponds to the external complementary work.

The principle of virtual forces applies to any material law of the body under consideration.

4.4 Extremal Principles

The principles already discussed can be used to derive some other important theorems that are of fundamental importance in mechanics in general, but also for composite structures in particular. For a broader overview and further special energy principles and theorems, the interested reader is referred to the relevant specialist literature (see e.g. Becker and Gross (2002), Göldner et al. (1985), Reddy (2002), Oden and Reddy (1982), Washizu (1982), Tauchert (1974), Langhaar (1962), Bauchau and Craig (2009), Lanczos (1986), Mittelstedt (2021)).

4.4.1 The Principle of the Stationary Value of the Total Potential

The principle of the stationary value of the total potential plays a very important role in the derivation of various approximation methods in mechanics and therefore also for composite structures. The prerequisite is elastic behaviour of the body under consideration, although linear elasticity is not necessarily a prerequisite. If the structure under consideration behaves elastically, the virtual internal work δW_i corresponds exactly to the virtual change $\delta \Pi_i$ of the total strain energy or inner potential stored in the body:

$$\delta W_i = \int_V \sigma_{ij} \delta \varepsilon_{ij} \mathrm{d}V = \int_V \delta U \mathrm{d}V = \delta \Pi_i. \tag{4.19}$$

If the acting external forces also have a potential Π_a, then its virtual change $\delta \Pi_a$ corresponds exactly to the external virtual work δW_a, but with the opposite sign:

$$\delta W_a = \int_V f_i \delta u_i \mathrm{d}V + \int_{\partial V_t} t_{i0} \delta u_i \mathrm{d}A = -\delta \Pi_a. \tag{4.20}$$

The total potential Π of the elastic system under consideration is made up of the inner potential Π_i and the external potential Π_a:

$$\Pi = \Pi_i + \Pi_a. \tag{4.21}$$

The principle of the virtual total potential thus follows from the principle of virtual displacements:

$$\delta \Pi = \delta \left(\Pi_i + \Pi_a \right) = 0. \tag{4.22}$$

This means that an elastic body is in equilibrium when the change in the overall potential is zero for all kinematically permissible variations in displacements and strains. In this context, it is also said that the first variation of the total potential must disappear in order to ensure equilibrium of the system. The disappearance of the change $\delta \Pi$ of the potential

for any permissible virtual displacements and strains is equivalent to the fact that the total potential Π must assume an extremal value in the state of equilibrium:

$$\Pi = \Pi_i + \Pi_a = \text{Extremum}. \tag{4.23}$$

This relationship is known as the principle of the stationary value of the total potential.

If not only elastic material behaviour is present, but also linear elasticity as a special case (so that Hooke's law is valid), then the inner potential Π_i depends quadratically on the strains. The extremal value required by (4.23) then becomes a minimum, and the result is for linear elasticity:

$$\Pi = \Pi_i + \Pi_a = \text{Minimum}. \tag{4.24}$$

This relationship is also known as the principle of the minimum of the total potential or as the Green-Dirichlet[2] minimum principle.

4.4.2 The Principle of the Stationary Value of the Total Complementary Potential

The derivation of the principle of the stationary value of the total complementary potential is analogous to the previous section. If the structure under consideration is elastic, then the virtual inner complementary work $\delta\widetilde{W}_i$ is identical to the virtual change $\delta\widetilde{\Pi}_i$ of the inner complementary potential $\widetilde{\Pi}_i$:

$$\delta\widetilde{W}_i = \int_V \varepsilon_{ij}\delta\sigma_{ij}\mathrm{d}V = \delta\widetilde{\Pi}_i. \tag{4.25}$$

If the resulting displacements have a complementary potential, this corresponds to the virtual external complementary work except for the sign and is referred to as the external complementary potential $\widetilde{\Pi}_a$:

$$\delta\widetilde{W}_a = \int_V u_i\delta f_i\mathrm{d}V + \int_{\partial V_u} u_{i0}\delta t_i\mathrm{d}A = -\widetilde{\Pi}_a. \tag{4.26}$$

The total complementary potential $\widetilde{\Pi}$ is then composed of the inner and external complementary potential (i.e. $\widetilde{\Pi} = \widetilde{\Pi}_i + \widetilde{\Pi}_a$), and the principle of virtual forces leads to the principle of the virtual total complementary potential:

$$\delta\widetilde{\Pi} = \delta\left(\widetilde{\Pi}_i + \widetilde{\Pi}_a\right) = 0. \tag{4.27}$$

The disappearance of the variation $\delta\widetilde{\Pi}$ for any virtual forces is equivalent to the fact that the total complementary potential assumes an extremum in the real state of deformation:

[2] Johann Peter Gustav Lejeune Dirichlet, 1805–1859, German mathematician.

$$\widetilde{\Pi} = \widetilde{\Pi}_i + \widetilde{\Pi}_a = \text{Extremum}. \tag{4.28}$$

This theorem is also known as the principle of the stationary value of the total complementary potential.

Furthermore, if the material behaviour is not only elastic, but if there is even linear elasticity, then the inner complementary potential proves to be a quadratic form of the stresses, and the extremal value required with (4.28) is always a minimum. The principle of the stationary value of the total complementary potential then becomes the principle of the minimum of the total complementary potential (also known as the principle of Castigliano[3] and Menabrea[4]):

$$\widetilde{\Pi} = \widetilde{\Pi}_i + \widetilde{\Pi}_a = \text{Minimum}. \tag{4.29}$$

4.5 Analysis Rules for the δ-Operator

The variation operator δ (often simply called δ-operator) characterizes a very small 'change' or the variation of a certain dependent variable, e.g. a displacement u, which can depend on one or more variables. This is also referred to as the 'first variation' δu if, for example, a virtual displacement is applied to a static system. Similarly, in the context of differential calculus, we speak of a change $\mathrm{d}x$ with respect to x if we want to describe an infinitesimally small increase in x. For the variation operator δ, which describes the change of a dependent quantity (e.g. u) and thus represents a differential operator, some analogies to the calculation rules of differential calculus can therefore be found, which are presented below. For further details, the interested reader is referred to the widely available specialized literature. The functions f_1, f_2, f_3, …, f_n are dependent quantities, e.g. on the displacement u.

(1) The order of variation and differentiation is interchangeable, i.e.:

$$\delta\left(\nabla u\right) = \nabla\left(\delta u\right), \tag{4.30}$$

where ∇ is the so-called nabla operator or gradient: $\nabla = \left(\frac{\partial}{\partial x}, \frac{\partial}{\partial y}, \frac{\partial}{\partial z}\right)^T$.

(2) The order of integration and variation is interchangeable:

$$\delta\left[\int_V u\mathrm{d}V\right] = \int_V \delta u\mathrm{d}V. \tag{4.31}$$

(3) The first variation of the sum of several functions f_1, f_2, f_3, …, f_n can be formed according to the sum rule of differential calculus:

[3] Carlo Alberto Castigliano, 1847–1884, Italian civil engineer.

[4] Federico Luigi Conte di Menabrea, 1809–1896, Italian scientist.

$$\delta [f_1 \pm f_2 \pm f_3 \pm \cdots \pm f_n] = \delta f_1 \pm \delta f_2 \pm \delta f_3 \pm \cdots \pm \delta f_n. \tag{4.32}$$

(4) The first variation of a product of two functions f_1, f_2 can be formed analogously to the product rule of differential calculus:

$$\delta [f_1 f_2] = f_2 \delta f_1 + f_1 \delta f_2. \tag{4.33}$$

(5) The first variation of a quotient of two functions f_1, f_2 can be formed according to the quotient rule of differential calculus:

$$\delta \left[\frac{f_1}{f_2} \right] = \frac{\delta f_1}{f_2} - \frac{f_1 \delta f_2}{f_2^2}. \tag{4.34}$$

(6) The first variation of a function f_1 with a power law can be formed according to the chain rule of differential calculus:

$$\delta \left[f_1^n \right] = n f_1^{n-1} \delta f_1. \tag{4.35}$$

(7) If the function f is a function of several dependent variables (for example the displacements u, v, w), then the total variation δf can be composed of the sum of the partial variations:

$$\delta f\,(u, v, w) = \delta_u f + \delta_v f + \delta_w f, \tag{4.36}$$

where the operators δ_u, δ_v, δ_w symbolize the partial variations according to u, v, w.

4.6 Application to Simple Mechanical Systems

In this section, the previous explanations will be illustrated using concrete, simple mechanical systems.

4.6.1 Beam Under Line Load $n(x)$ and Single Force F

Consider a beam of length l and constant extensional stiffness EA (Fig. 4.1). The beam is loaded by a constant line load $n(x)$ and a single force F at the free end. The governing equations are to be derived using both the principle of virtual displacements and the principle of the minimum of the total elastic potential.

If an infinitesimal section element of length $\mathrm{d}x$ is first cut out of the beam (Fig. 4.2), equilibrium of forces in the horizontal direction yields:

$$N + \frac{\mathrm{d}N}{\mathrm{d}x}\mathrm{d}x - N + n\mathrm{d}x = 0, \tag{4.37}$$

or

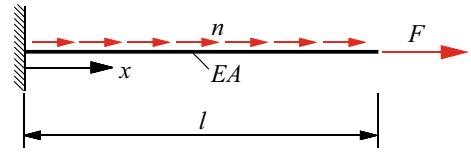


Fig. 4.1 Beam under line load $n\,(x)$ and single force F

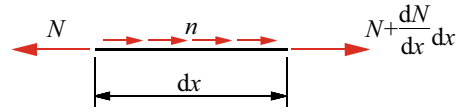


Fig. 4.2 Infinitesimal element of the beam under consideration

$$\frac{\mathrm{d}N}{\mathrm{d}x} = -n. \tag{4.38}$$

The first derivative of the normal force N acting in the beam therefore corresponds to the negative external line load n. The boundary conditions can be deduced immediately from the given situation. Firstly, the displacement u must disappear at the clamping point, and secondly, the normal force N at the free end of the beam corresponds to the tensile force F:

$$u(x = 0) = 0, \quad N(x = l) = F. \tag{4.39}$$

Firstly, the principle of the minimum of the total potential is used: $\Pi = \Pi_i + \Pi_a =$ Minimum. The following currently applies to the external potential Π_a:

$$\Pi_a = -\int_0^l n(x)u(x)\mathrm{d}x - Fu(x = l). \tag{4.40}$$

In the formulation for the inner potential Π_i, only the portion of the normal stress σ_{xx} multiplied by the strain ε_{xx} currently remains:

$$\Pi_i = \frac{1}{2}\int_V \sigma_{xx}\varepsilon_{xx}\mathrm{d}V = \frac{1}{2}\int_V \sigma\varepsilon\mathrm{d}V, \tag{4.41}$$

whereby the indexing is omitted in the rest of the example for the sake of a better readability. The volume integral can be split into an integral over the cross-sectional area A and an integral over the beam length l:

$$\Pi_i = \frac{1}{2}\int_A \int_0^l \sigma\varepsilon\mathrm{d}x\mathrm{d}A. \tag{4.42}$$

Since stresses and strains in the given situation are not dependent on the coordinates y, z, the area integral can be calculated according to

$$\int_A \mathrm{d}A = A, \tag{4.43}$$

and we obtain:

$$\Pi_i = \frac{1}{2}\int_0^l \sigma\varepsilon A \mathrm{d}x. \tag{4.44}$$

Using Hooke's law $\sigma = E\varepsilon$ for the beam then results in the following with $EA = \text{const.}$:

$$\Pi_i = \frac{EA}{2}\int_0^l \varepsilon^2 \mathrm{d}x. \tag{4.45}$$

After inserting the kinematic equation $\varepsilon = \frac{\partial u}{\partial x} = u'$ we obtain

$$\Pi_i = \frac{EA}{2}\int_0^l u'^2 \mathrm{d}x, \tag{4.46}$$

where the notation $(\ldots)'$ was used here for a derivation with respect to the coordinate x for the sake of simplicity. This allows the total elastic potential to be written as (note that the line load n was assumed to be constant in this example and could therefore also be drawn in front of the integral):

$$\Pi = \frac{EA}{2}\int_0^l u'^2 \mathrm{d}x - \int_0^l n(x)u(x)\mathrm{d}x - Fu(x=l). \tag{4.47}$$

The first variation $\delta\Pi$ of the total elastic potential Π then results as follows:

$$\delta\Pi = \delta\left[\frac{EA}{2}\int_0^l u'^2 \mathrm{d}x - \int_0^l n(x)u(x)\mathrm{d}x - Fu(x=l)\right]. \tag{4.48}$$

Since the order of variation and integration is interchangeable, we can also write:

$$\delta\Pi = \frac{EA}{2}\int_0^l \delta\left(u'^2\right)\mathrm{d}x - \int_0^l n\delta u \mathrm{d}x - F\delta u(x=l) = 0, \tag{4.49}$$

where it is required that the first variation disappears. Note that the first integrand can be written as

$$\delta\left(u'^2\right) = 2u'\delta u', \tag{4.50}$$

so that we obtain:

$$\delta\Pi = EA \int_0^l u'\delta u' \mathrm{d}x - \int_0^l n\delta u \mathrm{d}x - F\delta u(x = l) = 0. \tag{4.51}$$

The first term in Eq. (4.51) is now partially integrated in order to reduce the order of the derivative appearing there by one. For this purpose, the elementary calculation rule of integral calculus

$$\int_0^l vw' \mathrm{d}x = vw|_0^l - \int_0^l v'w \mathrm{d}x \tag{4.52}$$

is employed, where v and w are any two functions of x. In the example, the first integral term in (4.51) follows as:

$$EA \int_0^l u'\delta u' \mathrm{d}x = EAu'\delta u|_0^l - EA \int_0^l u''\delta u \mathrm{d}x. \tag{4.53}$$

If we note that Hooke's law $\sigma = E\varepsilon$ can also be used to write $N = EAu'$ and $N' = EAu''$, the first variation $\delta\Pi$ of the total elastic potential follows as:

$$\delta\Pi = N\delta u|_0^l - \int_0^l N'\delta u \mathrm{d}x - \int_0^l n\delta u \mathrm{d}x - F\delta u(x = l) = 0, \tag{4.54}$$

or:

$$\delta\Pi = N\delta u|_0^l - \int_0^l \left(N' + n\right) \delta u \mathrm{d}x - F\delta u(x = l) = 0. \tag{4.55}$$

The first term $N\delta u|_0^l$ can also be written as:

$$N\delta u|_0^l = N\delta u(x = l) - N\delta u(x = 0), \tag{4.56}$$

so that the following form of the first variation $\delta\Pi$ is ultimately obtained:

$$\delta\Pi = -\int_0^l \left(N' + n\right) \delta u \mathrm{d}x - N\delta u(x = 0) + (N - F)\, \delta u(x = l) = 0. \tag{4.57}$$

For any permissible variation δu of the displacement u, this can only be fulfilled if the individual terms in (4.57) each disappear on their own. If we first consider the integral term in (4.57), we obtain

$$\int_0^l \left(N' + n\right) \delta u \mathrm{d}x = 0. \tag{4.58}$$

If the possible trivial solution $\delta u = 0$ is ignored, this condition can only be fulfilled if the bracket term in the integral in (4.58) disappears:

$$N' + n = 0. \tag{4.59}$$

We find that this corresponds to the differential equation of the beam derived above from simple equilibrium requirements.

Furthermore, the second term in (4.57) provides the statement that at the point $x = 0$ either the normal force N disappears (which would correspond to a free end), or that the variation δu disappears, meaning that the displacement u is given with a fixed value:

$$\text{either} \quad \delta u(x = 0) = 0 \quad \text{or} \quad N(x = 0) = 0. \tag{4.60}$$

The case that the variation δu of the displacement u disappears corresponds to the requirement that the displacement u itself must assume a fixed specified value $u\,(x = 0) = u_0$ at the point, e.g. the value $u_0 = 0$. As only the first option is possible for the given example, the first boundary condition is obtained:

$$u(x = 0) = u_0, \tag{4.61}$$

where $u_0 = 0$ applies for the clamping given here, and then $N(x = 0) \neq 0$ will generally apply (in fact, a reaction force will result at this point due to the given load). This corresponds to the first boundary condition already derived elementarily.

Finally, the third term in (4.57) provides the following statement based on the same considerations:

$$\text{either} \quad \delta u(x = l) = 0 \quad \text{or} \quad N(x = l) - F = 0. \tag{4.62}$$

At present, only the second condition can be considered, as no displacement is specified at the free beam end, so that the following result is obtained:

$$N(x = l) = F. \tag{4.63}$$

This is identical to the second elementarily derived boundary condition of the current beam situation.

It can therefore be seen that the principle of the minimum of the total elastic potential can be used not only to obtain the equilibrium conditions of the system under consideration, but also to determine all possible boundary conditions in a natural and unambiguous way.

Finally, it will be shown that the same solution can also be obtained using the principle of virtual displacements. The virtual internal work δW_i is in this case:

$$\delta W_i = \int_V \sigma \delta \varepsilon \mathrm{d}V. \tag{4.64}$$

Since the variation of the longitudinal displacement δu is performed from the (as yet unknown) equilibrium position with the stresses kept constant, the stresses σ are not part of the variation to be performed. Splitting the integral into a surface integral and an integral with respect to the longitudinal axis x results in

$$\delta W_i = \int_0^l \sigma A \delta u' \mathrm{d}x = \int_0^l N \delta u' \mathrm{d}x. \tag{4.65}$$

Since $N = EAu'$ applies, we obtain:

$$\delta W_i = EA \int_0^l u' \delta u' \mathrm{d}x, \tag{4.66}$$

or after partial integration:

$$\delta W_i = EAu' \delta u|_0^l - EA \int_0^l u'' \delta u \mathrm{d}x. \tag{4.67}$$

If the relationships $N = EAu'$ and $N' = EAu''$ are also taken into account, the result is

$$\delta W_i = N \delta u|_0^l - \int_0^l N' \delta u \mathrm{d}x. \tag{4.68}$$

The virtual external work can be written as:

$$\delta W_a = \int_0^l n \delta u \mathrm{d}x + F \delta u(x = l). \tag{4.69}$$

The requirement for equality of the internal and external virtual work, i.e. $\delta W_i = \delta W_a$, then provides the following expression:

$$N \delta u|_0^l - \int_0^l N' \delta u \mathrm{d}x - \int_0^l n \delta u \mathrm{d}x - F \delta u(x = l) = 0, \tag{4.70}$$

or:

$$-\int_0^l (N' + n) \delta u \mathrm{d}x - N \delta u(x = 0) + (N - F)\, \delta u(x = l) = 0. \tag{4.71}$$

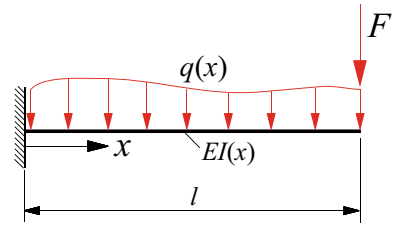


Fig. 4.3 Beam under line load $q\,(x)$ and single force F

Obviously, this expression corresponds to the requirement already determined using the principle of the minimum of the total potential. As expected, both methods therefore deliver identical results.

4.6.2 Beam Under Line Load $q\,(x)$ and Single Force F

As a further example, consider the beam shown in Fig. 4.3 under a line load $q(x)$ and a single force F. The beam has the length l and the bending stiffness $EI = EI(x)$, which is an arbitrary function of the beam length coordinate x. It is also assumed that we are dealing with a shear-rigid beam according to the Euler-Bernoulli theory,[5] so that shear deformations in the thickness direction z can be neglected.

The beam differential equation can be written as (no derivation is given here, the reader is referred to the widely available literature on engineering mechanics):

$$\left(EIw''\right)'' - q = 0. \tag{4.72}$$

The boundary conditions can be read directly from the given situation and are as follows:

$$w(x=0) = 0, \quad w'(x=0) = 0, \quad M(x=l) = 0, \quad Q(x=l) = F. \tag{4.73}$$

The beam differential equation and the associated boundary conditions are now to be derived using the principle of the minimum of the total elastic potential.

The inner potential Π_i is reduced to the following term due to the assumed shear rigidity of the beam:

$$\Pi_i = \frac{1}{2}\int_V \sigma_{xx}\varepsilon_{xx}\mathrm{d}V = \frac{1}{2}\int_V \sigma\varepsilon\mathrm{d}V, \tag{4.74}$$

whereby the stresses and strains involved are again not indexed in order to improve readability. Firstly, Hooke's law $\sigma = E\varepsilon$ and the splitting of the volume integral already used for the beam are used. The result is

[5] Jakob Bernoulli, 1654–1705, Swiss polymath.

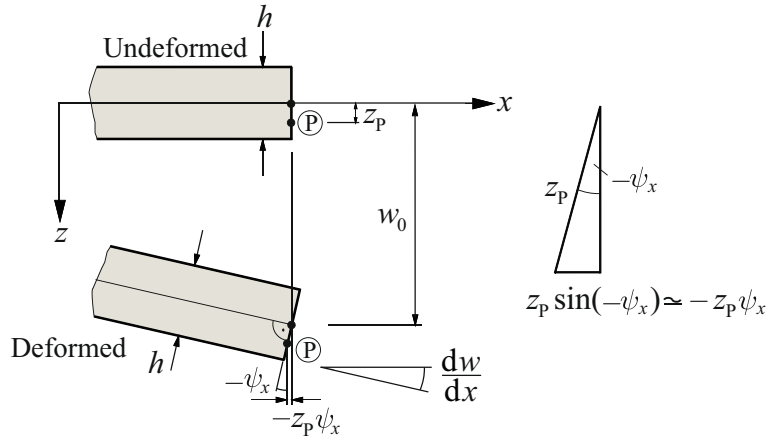


Fig. 4.4 Kinematics of the Euler-Bernoulli beam

$$\Pi_i = \frac{1}{2}\int_0^l \int_A E\varepsilon^2 \mathrm{d}A\mathrm{d}x. \tag{4.75}$$

At this point, it is worth taking a brief look at the kinematics of the Euler-Bernoulli beam (see Fig. 4.4).

(1) In the case of a shear-rigid beam, the beam cross-section remains plane and perpendicular to the longitudinal axis of the beam even when deformed (i.e. the so-called hypothesis that the cross-sections remain plane and the so-called normal hypothesis (i.e. $\psi_x = -w'$) are assumed to be valid).
(2) The thickness h of the beam does not change during the deformation process.

This means that the displacement u of any point P on the cross-section can be determined as $u = -z_P \frac{\mathrm{d}w}{\mathrm{d}x} = -z_P w'$, or in general $u = -zw'$. The following then applies for the elongation ε:

$$\varepsilon = u' = -zw''. \tag{4.76}$$

If this expression is inserted into the inner potential according to (4.75), the result is

$$\Pi_i = \frac{1}{2}\int_0^l \int_A E\left(-zw''\right)^2 \mathrm{d}A\mathrm{d}x = \frac{1}{2}\int_0^l \int_A Ez^2 w''^2 \mathrm{d}A\mathrm{d}x. \tag{4.77}$$

Since neither the modulus of elasticity E nor w'' are functions of the cross-section coordinates y, z, we can also write

$$\Pi_i = \frac{1}{2} \int_0^l E w''^2 \mathrm{d}x \int_A z^2 \mathrm{d}A. \tag{4.78}$$

Here, $\int_A z^2 \mathrm{d}A$ is the moment of inertia I of the cross-section with regard to bending about the y-axis, so that we finally obtain

$$\Pi_i = \frac{1}{2} \int_0^l E I w''^2 \mathrm{d}x. \tag{4.79}$$

The external potential for the current example can be written as follows:

$$\Pi_a = -\int_0^l q w \mathrm{d}x - F w(x = l). \tag{4.80}$$

The requirement for a minimum of the total elastic potential Π requires the disappearance of the first variation $\delta\Pi$, i.e. $\delta\Pi = \delta\Pi_i + \delta\Pi_a = 0$. At present we have:

$$\delta\Pi = \frac{1}{2} \int_0^l E I \delta(w'')^2 \mathrm{d}x - \int_0^l q \delta w \mathrm{d}x - F \delta w(x = l) = 0, \tag{4.81}$$

or after applying the chain rule for the first term:

$$\int_0^l E I w'' \delta w'' \mathrm{d}x - \int_0^l q \delta w \mathrm{d}x - F \delta w(x = l) = 0. \tag{4.82}$$

Partial integration of the first term in (4.82) results in:

$$E I w'' \delta w'|_0^l - \int_0^l (E I w'')' \delta w' \mathrm{d}x - \int_0^l q \delta w \mathrm{d}x - F \delta w(x = l) = 0. \tag{4.83}$$

Renewed partial integration leads to:

$$E I w'' \delta w'|_0^l - (E I w'')' \delta w|_0^l + \int_0^l (E I w'')'' \delta w \mathrm{d}x - \int_0^l q \delta w \mathrm{d}x - F \delta w(x = l) = 0, \tag{4.84}$$

or:

$$\int_0^l \left[(EIw'')'' - q\right]\delta w \mathrm{d}x + (EIw'')'\delta w(x=0) - EIw''\delta w'(x=0) + EIw''\delta w'(x=l) - \left[(EIw'')' + F\right]\delta w(x=l) = 0. \tag{4.85}$$

If the relationships $EIw'' = -M$ and $(EIw'')' = -Q$ are used here, the result is

$$\int_0^l \left[(EIw'')'' - q\right]\delta w \mathrm{d}x - Q\delta w(x=0) + M\delta w'(x=0) - M\delta w'(x=l) - (-Q+F)\,\delta w(x=l) = 0. \tag{4.86}$$

Again, this condition can only be fulfilled for any permissible variation δw of the beam deflection and its derivative $\delta w'$ if the individual terms in (4.86) each disappear on their own. The integral term in (4.86) then results in

$$\int_0^l \left[(EIw'')'' - q\right]\delta w \mathrm{d}x = 0. \tag{4.87}$$

This is fulfilled either if $\delta w = 0$ (which is the trivial solution) or if the bracket term disappears:

$$(EIw'')'' - q = 0. \tag{4.88}$$

It is easy to see that (4.88) is the well-known beam differential equation.

Similarly, the remaining terms in (4.86) lead to the boundary conditions of the beam problem under consideration:

$$\begin{aligned} Q\delta w(x=0) &= 0, \\ M\delta w'(x=0) &= 0, \\ M\delta w'(x=l) &= 0, \\ (-Q+F)\,\delta w(x=l) &= 0. \end{aligned} \tag{4.89}$$

The boundary conditions of the system can be deduced from this. At the point $x = 0$ therefore applies:

$$\begin{aligned} &\text{either} \quad \delta w(x=0) = 0 \quad \text{or} \quad Q(x=0) = 0, \\ &\text{either} \quad \delta w'(x=0) = 0 \quad \text{or} \quad M(x=0) = 0. \end{aligned} \tag{4.90}$$

At $x = l$ we have:

$$\begin{aligned} &\text{either} \quad \delta w(x=l)=0 \quad \text{or} \quad Q(x=l)=F, \\ &\text{either} \quad \delta w'(x=l)=0 \quad \text{or} \quad M(x=l)=0. \end{aligned} \tag{4.91}$$

It is easy to see that from the set of potential boundary conditions shown above, only the following conditions can currently be considered:

$$w(x=0)=0, \quad w'(x=0)=0, \quad M(x=l)=0, \quad Q(x=l)=F, \tag{4.92}$$

which corresponds to the boundary conditions already described.

4.7 Approximation Methods

In the vast majority of practical engineering applications, a given boundary value problem cannot be solved in a closed-form analytical way. Specifically, this means that it is only possible in a few exceptional cases to find a solution to a boundary value problem that exactly satisfies all the underlying equations—equilibrium, kinematics, constitutive equations—as well as all given boundary conditions. This also and especially applies to the common and very complex lightweight structures used, for example, in aircraft construction. For this reason, approximation methods are very often used, which have become increasingly prevalent in recent decades with ever-increasing computer power and for which enormous research and development efforts have been made worldwide. In addition to the more 'classical' methods such as the Galerkin method or the Ritz method, the so-called discretizing methods should be mentioned here of which the Finite Element Method (FEM) is the most common, but also more specialised methods such as the Boundary Element Method, or, as a fairly new method, the so-called Scaled Boundary Finite Element Method. All the methods mentioned have in common the fact that they assume certain approximations for one or more variables and use an energy principle to solve the problem under consideration. A fundamental way of differentiating approximation methods is based on the type of approach. In the case of the so-called continuous methods, an attempt is made to find an approximation approach that is valid for the entire structure. One such continuous method is the Ritz method, which will be discussed in more detail below. In the case of discretizing methods, on the other hand, the structure is not considered as a whole, but rather it is divided into subareas (the so-called elements) and approximation approaches are formulated in these elements. The elements are then assembled using continuity conditions to represent the complete structure. Probably the most important representative of discretizing methods is the Finite Element Method, which will also be discussed later. In general, when using discretizing methods, one quickly encounters relatively large equation systems, which, in particular when considering nonlinear problems, can result in a considerable computational effort. For this reason, despite the large computing resources available today, the continuous methods are still indispensable in the practical work of engineers in many areas.

4.7.1 The Ritz Method

The Ritz method[6] (see the original work by Ritz (1908)) is based on the principle of the stationary value of the total elastic potential and assumes that the total potential is known as a function of the displacements of the system under consideration. The procedure is then to use an approach for the displacements u, v, w of the elastic structure of the following form:

$$\begin{aligned} u(x,y,z) \simeq U(x,y,z) &= \sum_{i=1}^{i=n_u} A_i U_i(x,y,z), \\ v(x,y,z) \simeq V(x,y,z) &= \sum_{i=1}^{i=n_v} B_i V_i(x,y,z), \\ w(x,y,z) \simeq W(x,y,z) &= \sum_{i=1}^{i=n_w} C_i W_i(x,y,z). \end{aligned} \tag{4.93}$$

Herein, $U(x,y,z)$, $V(x,y,z)$, $W(x,y,z)$ represent the approximation functions to be selected by the user, which must at least fulfil the given kinematic boundary conditions. This also applies to the shape functions $U_i(x,y,z)$, $V_i(x,y,z)$, $W_i(x,y,z)$. The variables n_u, n_v, n_w are the numbers of the shape functions, which are also to be defined by the user, the variables A_i, B_i, C_i are free constants and the actual target of the calculation. In addition, the shape functions should be as plausible as possible. This means that users should try to find functions that describe the given problem as closely as possible according to engineering intuition. While this may be reasonably feasible for simple problems, it may be difficult to fulfil this requirement for difficult multidimensional problems. Here, test calculations must show to what extent certain classes of shape functions prove themselves in application.

If the approach (4.93) is used in the elastic total potential Π, the only degrees of freedom that are still accessible to variation are the constants A_i, B_i, C_i: $\Pi = \Pi(A_i, B_i, C_i)$. The first variation $\delta\Pi$ of the total elastic potential then changes to the following form:

$$\begin{aligned} \delta\Pi = &\frac{\partial\Pi}{\partial A_1}\delta A_1 + \frac{\partial\Pi}{\partial A_2}\delta A_2 + \frac{\partial\Pi}{\partial A_3}\delta A_3 + \cdots + \frac{\partial\Pi}{\partial A_{n_u}}\delta A_{n_u} \\ &+ \frac{\partial\Pi}{\partial B_1}\delta B_1 + \frac{\partial\Pi}{\partial B_2}\delta B_2 + \frac{\partial\Pi}{\partial B_3}\delta B_3 + \cdots + \frac{\partial\Pi}{\partial B_{n_v}}\delta B_{n_v} \\ &+ \frac{\partial\Pi}{\partial C_1}\delta C_1 + \frac{\partial\Pi}{\partial C_2}\delta C_2 + \frac{\partial\Pi}{\partial C_3}\delta C_3 + \cdots + \frac{\partial\Pi}{\partial C_{n_w}}\delta C_{n_w} = 0. \end{aligned} \tag{4.94}$$

This can only be fulfilled for any permissible variations of the otherwise independent constants A_i, B_i, C_i if

[6] Walter Ritz, 1878–1909, Swiss mathematician and physicist.

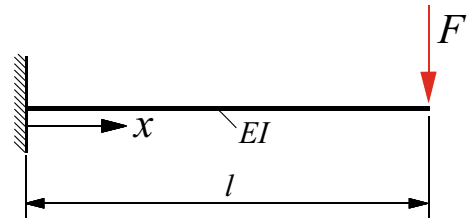


Fig. 4.5 Beam under point force F

$$\begin{aligned}
&\frac{\partial \Pi}{\partial A_1} = 0, \quad \frac{\partial \Pi}{\partial A_2} = 0, \quad \frac{\partial \Pi}{\partial A_3} = 0, \quad \ldots \quad \frac{\partial \Pi}{\partial A_{n_u}} = 0, \\
&\frac{\partial \Pi}{\partial B_1} = 0, \quad \frac{\partial \Pi}{\partial B_2} = 0, \quad \frac{\partial \Pi}{\partial B_3} = 0, \quad \ldots \quad \frac{\partial \Pi}{\partial B_{n_v}} = 0, \\
&\frac{\partial \Pi}{\partial C_1} = 0, \quad \frac{\partial \Pi}{\partial C_2} = 0, \quad \frac{\partial \Pi}{\partial C_3} = 0, \quad \ldots \quad \frac{\partial \Pi}{\partial C_{n_w}} = 0.
\end{aligned} \tag{4.95}$$

These are the so-called Ritz equations. In the case of a problem within the framework of a geometrically linear theory, the Ritz equations lead to a linear system of equations with $n_u + n_v + n_w$ equations for the total of $n_u + n_v + n_w$ unknown constants A_i, B_i, C_i. In the case of a geometrically nonlinear problem, the Ritz equations are nonlinear and can generally only be solved numerically. Approximate strains and approximate stresses can be determined for the structure under consideration using the kinematic equations and Hooke's law.

The Ritz method is illustrated using a simple example. Let an Euler-Bernoulli beam of length l and constant bending stiffness EI be clamped at one end and subjected to a single force F at the free end (Fig. 4.5). The elastic line $w(x)$ is to be determined. Firstly, the exact solution according to elementary beam theory will be determined for comparison purposes. The elastic line can be determined by integrating the beam differential equation $EIw'''' = q$ four times:

$$\begin{aligned}
EIw(x)'''' &= q(x) = 0, \\
EIw(x)''' &= -Q(x) = D_1, \\
EIw(x)'' &= -M(x) = D_1 x + D_2, \\
EIw(x)' &= \frac{1}{2} D_1 x^2 + D_2 x + D_3, \\
EIw(x) &= \frac{1}{6} D_1 x^3 + \frac{1}{2} D_2 x^2 + D_3 x + D_4.
\end{aligned} \tag{4.96}$$

The unknown constants $D_1, \ldots, D_4$ can be determined from the boundary conditions of the given beam bending problem:

$$w(x = 0) = 0, \quad w'(x = 0) = 0, \quad Q(x = l) = F, \quad M(x = l) = 0. \tag{4.97}$$

Evaluation yields:

$$D_1 = -F, \quad D_2 = Fl, \quad D_3 = 0, \quad D_4 = 0. \tag{4.98}$$

This provides the exact elastic line $w(x)$ as follows:

$$w(x) = \frac{1}{EI}\left(-\frac{F}{6}x^3 + \frac{F}{2}lx^2\right). \tag{4.99}$$

The maximum deflection $w_{\max}$ results at the end of the beam at the point $x = l$ as:

$$w_{\max} = \frac{1}{EI}\left(-\frac{F}{6}l^3 + \frac{F}{2}l^3\right) = \frac{Fl^3}{3EI}. \tag{4.100}$$

This example is now also solved using the Ritz method. The total elastic potential can currently be written as:

$$\Pi = \frac{1}{2}EI\int_0^l w''^2 \mathrm{d}x - Fw(x = l). \tag{4.101}$$

As a first approximation we use the following approach:

$$w(x) \simeq W(x) = C_1 W_1(x) + C_2 W_2(x). \tag{4.102}$$

wherein the shape functions $W_1(x)$ and $W_2(x)$ are chosen as

$$W_1(x) = x^2, \quad W_2(x) = x^3, \tag{4.103}$$

so that

$$w(x) \simeq W(x) = C_1 x^2 + C_2 x^3. \tag{4.104}$$

The constants C_1 and C_2 are now to be determined by evaluating the Ritz equations, which can be determined by inserting (4.104) into (4.101):

$$\begin{aligned}
\Pi &= \frac{1}{2}EI\int_0^l w''^2 \mathrm{d}x - Fw(x = l) \\
&= \frac{1}{2}EI\int_0^l (2C_1 + 6C_2 x)^2 \,\mathrm{d}x - F\left(C_1 l^2 + C_2 l^3\right) \\
&= 2EIl\left(C_1^2 + 3C_1 C_2 l + 3C_2^2 l^2\right) - F\left(C_1 l^2 + C_2 l^3\right) = \Pi\left(C_1, C_2\right).
\end{aligned} \tag{4.105}$$

The two Ritz equations to be employed here are then as follows:

$$\frac{\partial \Pi}{\partial C_1} = 2EIl\,(2C_1 + 3C_2 l) - Fl^2 = 0,$$
$$\frac{\partial \Pi}{\partial C_2} = 2EIl\left(3C_1 l + 6C_2 l^2\right) - Fl^3 = 0. \tag{4.106}$$

The following linear system of equations is then obtained for the two constants C_1 and C_2:

$$2C_1 + 3C_2 l = \frac{Fl}{2EI},$$
$$3C_1 + 6C_2 l = \frac{Fl}{2EI}. \tag{4.107}$$

This yields:

$$C_1 = \frac{Fl}{2EI}, \quad C_2 = -\frac{F}{6EI}, \tag{4.108}$$

and thus the following solution for the elastic line $w(x)$:

$$w(x) = \frac{1}{EI}\left(-\frac{F}{6}x^3 + \frac{F}{2}lx^2\right). \tag{4.109}$$

This solution using the Ritz method corresponds exactly to the exact solution. The reason for this is that the selected shape functions contain the exact solution, so that the requirement $\Pi = \text{Extremum}$ leads to the exact result (at this point, we note again that the principle of the minimum of the total elastic potential is not only a consequence of the local equilibrium conditions, but is also completely equivalent to them).

Next we want to determine which result is obtained if an alternative admissible approach is used which does not contain the exact solution. We employ an approach of the form

$$w(x) \simeq W(x) = C_1 W_1(x) = C_1\left[1 - \cos\left(\frac{\pi x}{2l}\right)\right]. \tag{4.110}$$

Insertion into the total potential of the beam results in:

$$\Pi = \frac{1}{2}EI\int_0^l C_1^2\frac{\pi^4}{16l^4}\cos^2\left(\frac{\pi x}{2l}\right)\mathrm{d}x - FC_1 = C_1^2\frac{EI\pi^4}{64l^3} - FC_1 = \Pi\,(C_1)\,. \tag{4.111}$$

The corresponding Ritz equation then reads:

$$\frac{\mathrm{d}\Pi}{\mathrm{d}C_1} = \frac{EI\pi^4}{32l^3}C_1 - F = 0, \tag{4.112}$$

which can be immediately solved for C_1:

$$C_1 = \frac{32Fl^3}{EI\pi^4}. \tag{4.113}$$

This provides an approximate solution for the elastic line $w(x)$ as follows:

$$w(x) = \frac{32Fl^3}{EI\pi^4}\left[1 - \cos\left(\frac{\pi x}{2l}\right)\right]. \tag{4.114}$$

The maximum deflection can then be approximated as:

$$w_{\max} = \frac{32Fl^3}{EI\pi^4} = 0.3285\frac{Fl^3}{EI}. \tag{4.115}$$

Comparison with the exact value for the maximum deflection

$$w_{\max} = \frac{Fl^3}{3EI} \tag{4.116}$$

results in a fairly good match, although only a single shape function was used in the Ritz approximation.

The Ritz method will now be generalized for the case of bending of an Euler-Bernoulli beam. Consider a beam of length l simply supported on both sides and with a (variable) bending stiffness $EI = EI(x)$ (Fig. 4.6). The beam is subjected to an arbitrary line load $q = q(x)$. We want to determine the elastic line $w(x)$. The total potential of the beam can be represented as:

$$\Pi = \Pi_i + \Pi_a = \frac{1}{2}\int_0^l EI(x)w(x)''^2 \mathrm{d}x - \int_0^l q(x)w(x)\mathrm{d}x. \tag{4.117}$$

An approximation for the bending line $w(x)$ in the form

$$w(x) \simeq W(x) = \sum_{i=1}^{i=n} C_i W_i(x) = C_1 W_1(x) + C_2 W_2(x) + \cdots + C_n W_n(x) \tag{4.118}$$

is employed. Once again, the requirement is placed on the shape functions $W_i(x)$ that they have to fulfil the given geometric boundary conditions, currently $w(x = 0) = w(x = l) = 0$. If the approach (4.118) is inserted into the total potential (4.117) of the beam, the result is

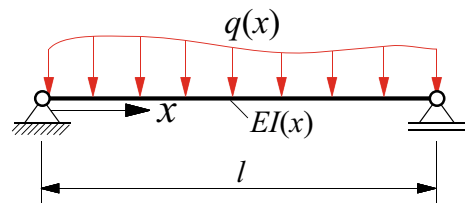


Fig. 4.6 Beam under line load $q(x)$

$$\Pi = \frac{1}{2}\int_0^l EI(x)\left(\sum_{i=1}^{i=n} C_i W_i''(x)\right)^2 \mathrm{d}x - \int_0^l q(x)\sum_{i=1}^{i=n} C_i W_i(x)\mathrm{d}x, \tag{4.119}$$

or if we reformulate the first integral:

$$\Pi = \frac{1}{2}\sum_{i=1}^{i=n}\sum_{j=1}^{j=n}\int_0^l EI(x)C_iC_j W_i''(x)W_j''(x)\mathrm{d}x - \int_0^l q(x)\sum_{i=1}^{i=n} C_i W_i(x)\mathrm{d}x. \tag{4.120}$$

Written out in full for illustrative purposes, e.g. for $n = 3$, the result is

$$\begin{aligned}\Pi = {} & \frac{1}{2}\int_0^l EI(x)C_1C_1W_1''(x)W_1''(x)\mathrm{d}x + \int_0^l EI(x)C_1C_2W_1''(x)W_2''(x)\mathrm{d}x \\ & + \int_0^l EI(x)C_1C_3W_1''(x)W_3''(x)\mathrm{d}x + \frac{1}{2}\int_0^l EI(x)C_2C_2W_2''(x)W_2''(x)\mathrm{d}x \\ & + \int_0^l EI(x)C_2C_3W_2''(x)W_3''(x)\mathrm{d}x + \frac{1}{2}\int_0^l EI(x)C_3C_3W_3''(x)W_3''(x)\mathrm{d}x \\ & - \int_0^l q(x)C_1W_1(x)\mathrm{d}x - \int_0^l q(x)C_2W_2(x)\mathrm{d}x - \int_0^l q(x)C_3W_3(x)\mathrm{d}x.\end{aligned} \tag{4.121}$$

It is useful to introduce abbreviations for the integrals appearing in (4.120) or (4.121) as follows:

$$\begin{aligned}K_{ij} &= \int_0^l EI(x)W_i''(x)W_j''(x)\mathrm{d}x, \\ F_i &= \int_0^l q(x)W_i(x)\mathrm{d}x.\end{aligned} \tag{4.122}$$

Since the shape functions $W_i(x)$ are all given and one will usually limit oneself to simple classes of shape functions for the simple applicability of the Ritz method, the integrals in (4.122) can often be solved in an exact analytical manner. The Eq. (4.121) can then be written as:

$$\begin{aligned}\Pi = {} & \frac{1}{2}C_1C_1K_{11} + C_1C_2K_{12} + C_1C_3K_{13} + \frac{1}{2}C_2C_2K_{22} + C_2C_3K_{23} + \frac{1}{2}C_3C_3K_{33} \\ & - C_1F_1 - C_2F_2 - C_3F_3.\end{aligned} \tag{4.123}$$

The Ritz equations read:

$$\begin{aligned}\frac{\partial \Pi}{\partial C_1} &= C_1 K_{11} + C_2 K_{12} + C_3 K_{13} - F_1 = 0,\\ \frac{\partial \Pi}{\partial C_2} &= C_1 K_{12} + C_2 K_{22} + C_3 K_{23} - F_2 = 0,\\ \frac{\partial \Pi}{\partial C_3} &= C_1 K_{13} + C_2 K_{23} + C_3 K_{33} - F_3 = 0.\end{aligned} \tag{4.124}$$

It can be seen that (4.124) is a linear system of equations consisting of three equations for the three unknown constants C_1, C_2, C_3. The Eq. (4.124) are summarized in a vector-matrix notation as follows:

$$\begin{bmatrix} K_{11} & K_{12} & K_{13} \\ K_{12} & K_{22} & K_{23} \\ K_{13} & K_{23} & K_{33} \end{bmatrix} \begin{pmatrix} C_1 \\ C_2 \\ C_3 \end{pmatrix} = \begin{pmatrix} F_1 \\ F_2 \\ F_3 \end{pmatrix}. \tag{4.125}$$

For an arbitrary number n of shape functions, (4.125) can also be written as:

$$\begin{bmatrix} K_{11} & K_{12} & K_{13} & \dots & K_{1n} \\ K_{12} & K_{22} & K_{23} & \dots & K_{2n} \\ K_{13} & K_{23} & K_{33} & \dots & K_{3n} \\ \vdots & \vdots & \vdots & \ddots & \vdots \\ K_{n1} & K_{n2} & K_{n3} & \dots & K_{nn} \end{bmatrix} \begin{pmatrix} C_1 \\ C_2 \\ C_3 \\ \vdots \\ C_n \end{pmatrix} = \begin{pmatrix} F_1 \\ F_2 \\ F_3 \\ \vdots \\ F_n \end{pmatrix}, \tag{4.126}$$

or in symbolic notation:

$$\underline{\underline{K}}\,\underline{C} = \underline{F}. \tag{4.127}$$

Therein, $\underline{\underline{K}}$ is the so-called stiffness matrix which is a symmetric matrix with $n \times n$ rows and columns for n shape functions. The vector $\underline{C}$ contains the constants C_i, the vector of the right-hand side $\underline{F}$ can be interpreted as a resultant force vector. Finally, the linear system of Eq. (4.127) can be solved using any solution algorithm for solving linear equation systems. The constants C_i are then determined and the approximation (4.118) of the elastic line of the beam can be analyzed.

A disadvantage of the Ritz method is that the stiffness matrix $\underline{\underline{K}}$ is generally fully populated, which may make the numerical solution of the system of equations resulting from the Ritz equations complex, especially in the case of high-degree approaches.

We conclude with the example shown in Fig. 4.7, i.e. a beam with constant bending stiffness EI which is loaded by a linear line load $q(x) = q_0 \frac{x}{l}$. An approach consisting of three shape functions is used as follows:

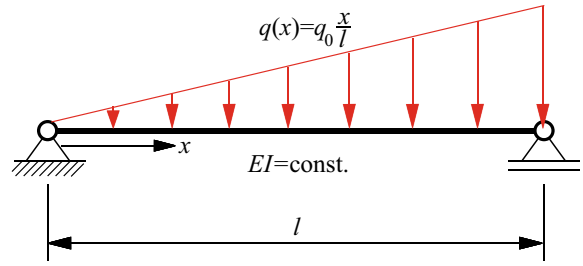


Fig. 4.7 Beam under linear line load q

$$w(x) \simeq W(x) = \sum_{i=1}^{i=3} C_i W_i(x) = C_1 W_1(x) + C_2 W_2(x) + C_3 W_3(x)$$
$$= C_1 \sin\left(\frac{\pi x}{l}\right) + C_2 \sin\left(\frac{2\pi x}{l}\right) + C_3 \sin\left(\frac{3\pi x}{l}\right), \qquad (4.128)$$

where the sine functions fulfil the underlying geometric boundary conditions $w(x = 0) = w(x = l) = 0$ identically. The entries of the stiffness matrix $\underline{\underline{K}}$ can be calculated as follows:

$$K_{11} = EI \int_0^l W_1''(x) W_1''(x) \mathrm{d}x = EI \frac{\pi^4}{l^4} \int_0^l \sin\left(\frac{\pi x}{l}\right) \sin\left(\frac{\pi x}{l}\right) \mathrm{d}x = \frac{EI\pi^4}{2l^3},$$
$$K_{12} = EI \int_0^l W_1''(x) W_2''(x) \mathrm{d}x = 2EI \frac{\pi^4}{l^4} \int_0^l \sin\left(\frac{\pi x}{l}\right) \sin\left(\frac{2\pi x}{l}\right) \mathrm{d}x = 0,$$
$$K_{13} = EI \int_0^l W_1''(x) W_3''(x) \mathrm{d}x = 3EI \frac{\pi^4}{l^4} \int_0^l \sin\left(\frac{\pi x}{l}\right) \sin\left(\frac{3\pi x}{l}\right) \mathrm{d}x = 0,$$
$$K_{22} = EI \int_0^l W_2''(x) W_2''(x) \mathrm{d}x = 16EI \frac{\pi^4}{l^4} \int_0^l \sin\left(\frac{2\pi x}{l}\right) \sin\left(\frac{2\pi x}{l}\right) \mathrm{d}x = \frac{8EI\pi^4}{l^3},$$
$$K_{23} = EI \int_0^l W_2''(x) W_3''(x) \mathrm{d}x = 6EI \frac{\pi^4}{l^4} \int_0^l \sin\left(\frac{2\pi x}{l}\right) \sin\left(\frac{3\pi x}{l}\right) \mathrm{d}x = 0,$$
$$K_{33} = EI \int_0^l W_3''(x) W_3''(x) \mathrm{d}x = 81EI \frac{\pi^4}{l^4} \int_0^l \sin\left(\frac{3\pi x}{l}\right) \sin\left(\frac{3\pi x}{l}\right) \mathrm{d}x = \frac{81EI\pi^4}{2l^3}. \qquad (4.129)$$

The entries of the vector $\underline{F}$ of the right-hand side then result as:

$$F_1 = \int_0^l q(x)W_1(x)\mathrm{d}x = \int_0^l \frac{q_0 x}{l}\sin\left(\frac{\pi x}{l}\right)\mathrm{d}x = \frac{q_0 l}{\pi},$$
$$F_2 = \int_0^l q(x)W_2(x)\mathrm{d}x = \int_0^l \frac{q_0 x}{l}\sin\left(\frac{2\pi x}{l}\right)\mathrm{d}x = -\frac{q_0 l}{2\pi},$$
$$F_3 = \int_0^l q(x)W_3(x)\mathrm{d}x = \int_0^l \frac{q_0 x}{l}\sin\left(\frac{3\pi x}{l}\right)\mathrm{d}x = \frac{q_0 l}{3\pi}. \tag{4.130}$$

The linear system of Eq. (4.126) or (4.127) can thus be written as:

$$\begin{bmatrix} \frac{EI\pi^4}{2l^3} & 0 & 0 \\ 0 & \frac{8EI\pi^4}{l^3} & 0 \\ 0 & 0 & \frac{81EI\pi^4}{2l^3} \end{bmatrix} \begin{pmatrix} C_1 \\ C_2 \\ C_3 \end{pmatrix} = \begin{pmatrix} \frac{q_0 l}{\pi} \\ -\frac{q_0 l}{2\pi} \\ \frac{q_0 l}{3\pi} \end{pmatrix}. \tag{4.131}$$

Solving for the constants C_1, C_2, C_3 yields:

$$C_1 = \frac{2q_0 l^4}{EI\pi^5}, \quad C_2 = -\frac{q_0 l^4}{16EI\pi^5}, \quad C_3 = \frac{2q_0 l^4}{243EI\pi^5}. \tag{4.132}$$

The approximated elastic line $w(x)$ of the beam is thus:

$$w(x) = \frac{2q_0 l^4}{EI\pi^5}\sin\left(\frac{\pi x}{l}\right) - \frac{q_0 l^4}{16EI\pi^5}\sin\left(\frac{2\pi x}{l}\right) + \frac{2q_0 l^4}{243EI\pi^5}\sin\left(\frac{3\pi x}{l}\right). \tag{4.133}$$

In general, the better the shape functions are able to map the actual structural behaviour, the better the results of an approximate solution using the Ritz method will be. If the selected approach is also able to fulfil not only the kinematic but also some or even all of the dynamic boundary conditions, the quality of the approximate solution will generally also increase. It has also been shown that in practical applications, even single-term approaches often lead to very good approximate solutions, which can be used well at least for the purposes of pre-design or optimization routines. In general, the Ritz method can be regarded as a very efficient and, assuming plausible and suitable shape functions, accurate method that is still very popular in practical applications. The Ritz method will also be used frequently in the remainder of this book.

4.7.2 The Galerkin Method

The Galerkin[7] method is also briefly explained using a beam structure, whereby for the sake of simplicity it is assumed here that the bending stiffness EI is constant over the beam length. The starting point of the considerations is the variational statement (4.86):

$$\int_0^l \left[EIw'''' - q\right]\delta w \mathrm{d}x - Q\delta w(x=0) + M\delta w'(x=0) \\ -M\delta w'(x=l) - (-Q+F)\,\delta w(x=l) = 0. \tag{4.134}$$

If we use an approach of the form

$$w(x) \simeq W(x) = \sum_{i=1}^{i=n} C_i W_i(x) = C_1 W_1(x) + C_2 W_2(x) + \cdots + C_n W_n(x) \tag{4.135}$$

for the elastic line, which, in contrast to a Ritz approach, is able to fulfil not only the kinematic boundary conditions, but all underlying boundary conditions, then all boundary terms disappear after insertion into (4.134), and the only requirement to be fulfilled is as follows:

$$\int_0^l \left[EIW'''' - q\right]\delta W \mathrm{d}x = 0. \tag{4.136}$$

Inserting (4.135) gives the result:

$$\int_0^l \{\left[EIC_1W_1'''' + EIC_2W_2'''' + \cdots + EIC_nW_n'''' - q\right] \\ (\delta C_1 W_1 + \delta C_2 W_2 + \cdots + \delta C_n W_n)\}\,\mathrm{d}x = 0, \tag{4.137}$$

whereby it has already been taken into account that the only variables in this approach that are accessible to variation are the constants C_1, C_2, …, C_n. Since the variations of the constants prescribed in (4.137) are independent of each other, the requirement (4.137) can only be fulfilled if the following applies:

[7] Boris Grigoryevich Galerkin, 1871–1945, Soviet engineer and mathematician.

$$\int_0^l \left[EIC_1 W_1'''' + EIC_2 W_2'''' + \cdots + EIC_n W_n'''' - q\right] W_1 \mathrm{d}x = 0,$$

$$\int_0^l \left[EIC_1 W_1'''' + EIC_2 W_2'''' + \cdots + EIC_n W_n'''' - q\right] W_2 \mathrm{d}x = 0,$$

$$\vdots$$

$$\int_0^l \left[EIC_1 W_1'''' + EIC_2 W_2'''' + \cdots + EIC_n W_n'''' - q\right] W_n \mathrm{d}x = 0. \qquad (4.138)$$

At this point, one also speaks of the so-called Galerkin equations, which represent a linear system of equations for the unknown constants C_1, C_2, …, C_n after performing the integrations. The constants can be determined by solving the above linear equation system, and the approximation approach $w(x) \simeq W(x)$ is thus completely available. A disadvantage of the Galerkin method, however, is the fact that the shape functions used must fulfil all underlying boundary conditions, which can lead to considerable difficulties in the definition of appropriate approaches in practical application, in contrast to the Ritz method, which only requires the weaker requirement of fulfilling the kinematic boundary conditions. For this reason, the Galerkin method will only be referred to very occasionally in the remainder of this book.

4.7.3 The Finite Element Method

The aim of the Finite Element Method (FEM) is to describe the physical behaviour of a structure under consideration using individual discrete numerical values. For this purpose, the structure is divided into so-called elements ('discretized', also: 'meshed', see Fig. 4.8), within which approaches are made for the physical variables to be calculated. In the context of elasticity theory, these are generally the state variables of the structure under consideration, usually the deformation state in the form of nodal displacements. At this point, one also speaks of the so-called displacement method, on which the majority of available commercial FEM programmes are based. The elements are coupled to each other at discrete points, so-called 'nodes' (see Fig. 4.8). The numerical result of an analysis using the FEM are discrete values of the required state variables in the nodes. All state variables inside each element can then be calculated from the nodal values using the selected shape functions.

The approaches for the required state variables must be such that compatibility requirements between neighbouring elements are not violated. This is associated with the requirement for a continuous distribution of the state variables in the interior of an element and on its edge. It must at least be possible to represent a constant stress or strain state, which results in requirements for the continuous differentiability of the shape functions that apply both

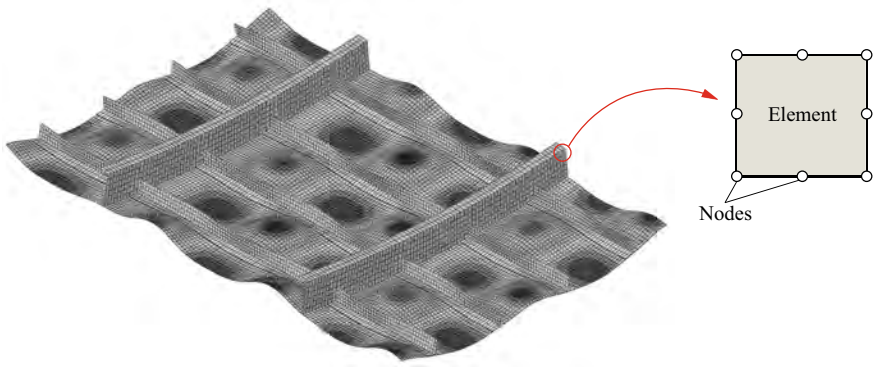


Fig. 4.8 Finite element model of a stiffened composite fuselage shell of an aircraft, the first buckling mode under longitudinal compressive load is shown

inside the element and on the element edge. Rigid body displacements must not cause any deformations in the elements. Since the approximation approaches in the FEM only extend to partial areas, mathematically very simple shape functions N are usually sufficient, which are also identical everywhere in the preferred use of similar elements on the entire structure.

This section is primarily intended to show the direct relationship between the Finite Element Method and the 'classical' energy methods; for more in-depth details and detailed introductions, interested readers are referred to the wide range of specialist literature available. Gross et al. (1995), Altenbach and Sacharov (1982), Betten (1997, 1998), Ochoa and Reddy (1992), Zienkiewicz and Taylor (2000a, b), Reddy (2004, 2005), Oden and Reddy (2011), Wriggers (2008), Crisfield (1991) and (1997), and Bathe (1996) are just a few examples.

The actual physical behaviour of the structure under consideration is approximated using element-by-element shape functions N, which interpolate between the determined values of the desired state variables in the nodes in the element. Standard element types that can be used for a variety of discretization purposes have been developed in accordance with the variety of possible shape functions and the number of nodes of an element. The number of elements and nodes, the class of the shape functions used and, consequently, the type of element are determined by the respective requirements. There are a large number of standardized element types that are used depending on the type of problem under consideration. These are differentiated according to their geometric shape (beam-shaped elements, disk elements, solid elements, etc.), the type and degree of the shape functions, special applications (elements for contact problems, composite elements, etc.) and other criteria.

The starting point for the FEM was the classic Ritz method. The Ritz method is based on an approach for the desired physical quantity on the entire structure (global approximation), whereby this approach must at least fulfil all geometric boundary conditions exactly. As this method is unsuitable for complex structures, in the middle of the last century there was

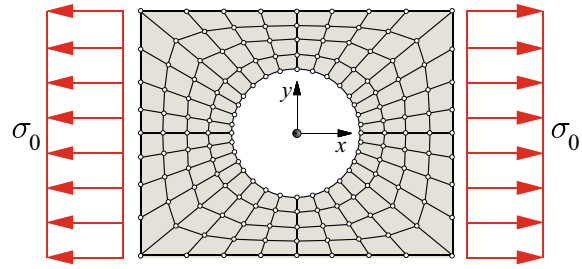


Fig. 4.9 Perforated disk, discretized by disk elements with four nodes

a demand for a Ritz approach that should only cover partial areas (local approximation). The FEM in its 'classical form' thus represents a modification or generalization of the Ritz method. This approach generally leads to very large systems of equations, which is why this idea was initially rejected decades ago and only became practicable for larger and more complex problems with the advent of powerful computer systems in about the last 50 years. In the meantime, the FEM has become established in many technical fields. For engineers working in the field of composites science and technology, relevant problems that can be solved approximately with the FEM are, for example, tasks from continuum mechanics, the mechanics of fluids and gases, the stability of structures, dynamics and much more.

A structural analysis with the aid of the FEM generally includes the following essential steps:

(1) Creating a structural model (loads, material behaviour, geometry) and adapting a suitable discretization (meshing),
(2) Deriving a suitable element formulation and setting up element equations.
(3) Summarizing the element equations into a single system of equations for the entire structure and taking into account all boundary conditions.
(4) Solving the system of equations and calculating the required state variables of the structure at all relevant points.

In the following, linear problems and conservative forces are assumed for the derivation of the basic equations of the FEM. This introductory section will be limited to a disk problem in the plane stress state (see Fig. 4.9), which can be used to demonstrate all the essential principles of the FEM. The disk structure is discretized by planar finite elements with four nodes which are located in the element corners. Depending on requirements, however, we can also use elements that have additional nodes on the element edges or inside the element.

The volume V of the disk is 'meshed' with n volume elements of volume V_e. The disk is thus geometrically approximated by the union of all elements, i.e.:

$$V \simeq \bigcup_{e=1}^{e=n} V_e. \tag{4.139}$$

The degrees of freedom of a node i are denoted as u_i (displacement of the node i in x-direction) and as v_i (displacement of the node i in y-direction) and are summarised in the vector $\underline{v}_i = \begin{pmatrix} u_i & v_i \end{pmatrix}^T$. An approximate displacement field $\underline{\tilde{u}}(x, y)$ in the element is interpolated from the (as yet unknown) displacements of the nodes using the shape functions $N_i(x, y)$ (where n_e is the number of nodes of the element under consideration):

$$\underline{\tilde{u}}(x, y) = \sum_{i=1}^{i=n_e} N_i(x, y)\underline{v}_i, \tag{4.140}$$

e.g. for the four-noded disk element:

$$\underline{\tilde{u}} = \begin{pmatrix} \tilde{u} \\ \tilde{v} \end{pmatrix} = N_1 \begin{pmatrix} u_1 \\ v_1 \end{pmatrix} + N_2 \begin{pmatrix} u_2 \\ v_2 \end{pmatrix} + N_3 \begin{pmatrix} u_3 \\ v_3 \end{pmatrix} + N_4 \begin{pmatrix} u_4 \\ v_4 \end{pmatrix}. \tag{4.141}$$

The shape functions N_i are selected in such a way that they assume the value 1 in node i, while they become zero in all other nodes. In many cases, the shape functions are selected in the form of simple polynomials.

With the displacement approach formulated with (4.140), the following approximated strain field can be written in the finite element with the help of the kinematic relations (3.17):

$$\underline{\tilde{\varepsilon}} = \begin{pmatrix} \tilde{\varepsilon}_{xx} \\ \tilde{\varepsilon}_{yy} \\ \tilde{\gamma}_{xy} \end{pmatrix} = \sum_{i=1}^{i=n_e} \begin{bmatrix} \frac{\partial N_i}{\partial x} & 0 \\ 0 & \frac{\partial N_i}{\partial y} \\ \frac{\partial N_i}{\partial y} & \frac{\partial N_i}{\partial x} \end{bmatrix} \begin{pmatrix} u_i \\ v_i \end{pmatrix} = \sum_{i=1}^{i=n_e} \underline{\underline{B}}_i \underline{v}_i. \tag{4.142}$$

We introduce the following matrices:

$$\underline{\underline{N}}_i = \begin{bmatrix} N_i & 0 \\ 0 & N_i \end{bmatrix}, \quad \underline{\underline{N}} = \begin{bmatrix} \underline{\underline{N}}_1 & \underline{\underline{N}}_2 & \underline{\underline{N}}_3 & \underline{\underline{N}}_4 \end{bmatrix},$$
$$\underline{\underline{B}} = \begin{bmatrix} \underline{\underline{B}}_1 & \underline{\underline{B}}_2 & \underline{\underline{B}}_3 & \underline{\underline{B}}_4 \end{bmatrix}. \tag{4.143}$$

In addition, the nodal displacements $u_1, v_1, \ldots, u_4, v_4$ are summarized in the vector $\underline{v}$:

$$\underline{v} = \begin{pmatrix} u_1 & v_1 & u_2 & v_2 & u_3 & v_3 & u_4 & v_4 \end{pmatrix}^T. \tag{4.144}$$

This allows us to write the displacements and strains of the element as:

$$\underline{\tilde{u}} = \underline{\underline{N}}\underline{v}, \quad \underline{\tilde{\varepsilon}} = \underline{\underline{B}}\underline{v}. \tag{4.145}$$

To derive the element equations, the principle of the minimum of the total potential (4.24) is applied:

$$\delta\Pi = \int_V \sigma_{ij}\delta\varepsilon_{ij}\mathrm{d}V - \int_V f_i\delta u_i\mathrm{d}V - \int_{\partial V_t} t_{i0}\delta u_i\mathrm{d}A = 0, \tag{4.146}$$

which can also be written as follows after inserting the approximated displacements and strains of the element:

$$\delta\Pi = \int_V \underline{\sigma}\delta\underline{\tilde{\varepsilon}}\mathrm{d}V - \int_V \underline{f}\delta\underline{\tilde{u}}\mathrm{d}V - \int_{\partial V_t} \underline{t}_0\delta\underline{\tilde{u}}\mathrm{d}A = 0, \tag{4.147}$$

where the volume forces f_x and f_y are summarised in the vector $\underline{f}$ and the specified boundary loads t_{x0} and t_{y0} are summarised in the vector $\underline{t}_0$.

The stress components, which are shown here in a vector representation $\underline{\sigma} = \left(\sigma_{xx}\ \sigma_{yy}\ \tau_{xy}\right)^T$, can be obtained from the strains $\underline{\tilde{\varepsilon}}$ with the help of Hooke's law:

$$\underline{\sigma} = \begin{pmatrix} \sigma_{xx} \\ \sigma_{yy} \\ \tau_{xy} \end{pmatrix} = \begin{bmatrix} \frac{E}{1-\nu^2} & \frac{\nu E}{1-\nu^2} & 0 \\ \frac{\nu E}{1-\nu^2} & \frac{E}{1-\nu^2} & 0 \\ 0 & 0 & G \end{bmatrix} \begin{pmatrix} \tilde{\varepsilon}_{xx} \\ \tilde{\varepsilon}_{yy} \\ \tilde{\gamma}_{xy} \end{pmatrix} = \underline{\underline{Q}}\underline{\tilde{\varepsilon}}. \tag{4.148}$$

If we insert the relationships (4.145) and (4.148) into (4.147) and take into account that the integrals in (4.147) can be split into a corresponding sum of partial integrals over the element volumes and element boundaries, then we obtain the following:

$$\sum_{e=1}^{n} \left\{ \int_{V_e} \left[\underline{\underline{Q}}\underline{\underline{B}}\underline{v}_e\right]^T \underline{\underline{B}}\mathrm{d}V - \int_{V_e} \underline{\underline{N}}^T \underline{f}\mathrm{d}V - \int_{\partial V_e} \underline{\underline{N}}^T \underline{t}_0\mathrm{d}A \right\} \delta\underline{v}_e = 0. \tag{4.149}$$

Since the variation $\delta\underline{v}_e$ of the nodal displacements is arbitrary, only the disappearance of the bracket term can be considered as a solution for (4.149):

$$\int_{V_e} \left[\underline{\underline{Q}}\underline{\underline{B}}\underline{v}_e\right]^T \underline{\underline{B}}\mathrm{d}V - \int_{V_e} \underline{\underline{N}}^T \underline{f}\mathrm{d}V - \int_{\partial V_e} \underline{\underline{N}}^T \underline{t}_0\mathrm{d}A = 0. \tag{4.150}$$

By introducing the quantities

$$\underline{\underline{K}}_e = \int_{V_e} \underline{\underline{B}}^T \underline{\underline{Q}}\underline{\underline{B}}\mathrm{d}V, \quad \underline{F}_e = \int_{V_e} \underline{\underline{N}}^T \underline{f}\mathrm{d}V + \int_{\partial V_e} \underline{\underline{N}}^T \underline{t}_0\mathrm{d}A \tag{4.151}$$

Equation (4.150) can be expressed in the following compact form:

$$\underline{\underline{K}}_e \underline{v}_e = \underline{F}_e. \tag{4.152}$$

Therein, $\underline{\underline{K}}_e$ is also referred to as element stiffness matrix and $\underline{F}_e$ as element load vector. Note that the form of the Eq. (4.152) is identical to the form of the Ritz equations (4.127). The Eq. (4.152) thus represents a constitutive equation for a finite element and describes a linear system of equations in the nodal values $\underline{v}_e$ of the element displacements. The number of rows and columns of the stiffness matrix $\underline{\underline{K}}_e$ then corresponds exactly to the number of degrees

of freedom of the element. The four-noded disk element currently under consideration has two displacements as degrees of freedom in each node, which is why $\underline{\underline{K}}_e$ would then be an 8×8-matrix. Similarly, the element load vector $\underline{\underline{F}}_e$ would then have eight components. It should be noted that the integrations to be carried out in (4.151) can generally only be carried out in a closed-form manner for simple rectangular geometries. Therefore, numerical methods are usually used for integration where Gauss integration is widely used.

Since the minimum requirement (4.149) is related to the nodal degrees of freedom, the displacement approach (4.140) is adapted to the best possible fit due to the underlying variational formulation. With the linear system of Eq. (4.152), the variation problem (4.149) for the minimization of the total potential of a finite element is then considered to be approximately solved, since an expression for $\underline{\underline{K}}_e$ has been found and $\underline{\underline{F}}_e$ can be considered to be known. In contrast to the Ritz method, the values $\underline{v}_e$ represent physically interpretable quantities, namely exactly the approximated nodal displacements themselves. After selecting the discretization, the elements and suitable shape functions, the FEM consists of simple matrix operations.

If all element matrices of the discretized structure under consideration are assembled to form total matrices (so-called assembling), a system of equations of the type

$$\underline{\underline{K}}\,\underline{v} = \underline{\underline{F}} \tag{4.153}$$

results. Here, $\underline{\underline{K}}$ can be understood as the stiffness matrix of the entire discretized system, which results from the combination of all element stiffness matrices. The degree of the system matrix $\underline{\underline{K}}$ corresponds to the number of all nodal degrees of freedom of the system discretized by finite elements. This applies analogously to the force vector $\underline{\underline{F}}$. This procedure formally corresponds to the summation of all element-wise contributions to the potential of the entire structure. The system equilibrium is guaranteed by the addition of all element-wise potential contributions, although the entries in the system stiffness matrix must be correctly assigned to those of the system force vector. The stiffness matrix of the finite element as well as that of the overall structure is diagonally symmetrical and generally band-shaped, which means a simplification of the calculation steps when solving (4.153) and a reduction of the necessary computation time. It is also singular if no boundary conditions are taken into account. By considering the kinematic conditions, the resulting system of equations becomes unique and solvable. The inverse of the remaining system stiffness matrix can be calculated, which is a necessary criterion for an unambiguous solution of (4.153). Equation (4.153) therefore solves the variation problem of a structure discretized by an arbitrary number of finite elements. Thus, even complicated structures can be approximated by a discretization adapted to the problem.

References

Altenbach J, Sacharov AS (1982): *Die Methode der finiten Elemente in der Festkörpermechanik*, Hanser Verlag, München et al., Germany.

Bathe KJ (1996): *Finite element procedures*, Prentice Hall, New Jersey, USA.

Bauchau OA, Craig JI (2009): *Structural analysis: with applications to aerospace structures*, Springer-Verlag, Dordrecht et al., The Netherlands.

Becker W, Gross D (2002): *Mechanik elastischer Körper und Strukturen*, Springer Verlag, Berlin et al., Germany.

Betten J (1997): *Finite Elemente für Ingenieure Teil 1: Grundlagen, Matrixmethoden, Elastisches Kontinuum*, Springer Verlag, Berlin et al., Germany.

Betten J (1998): *Finite Elemente für Ingenieure Teil 2: Variationsrechnung, Energie-methoden, Näherungsverfahren, Nichtlinearitäten*, Springer Verlag, Berlin et al., Germany.

Crisfield MA (1991): *Non-linear finite element analysis of solids and structures, volume 1: essentials*, John Wiley and sons, Chichester et al., UK.

Crisfield MA (1997): *Non-linear finite element analysis of solids and structures, volume 2: advanced topics*, John Wiley and sons, Chichester et al., UK.

Göldner H, Altenbach J, Eschke K, Garz KF, Sähn S (1985): *Lehrbuch Höhere Festigkeitslehre Band 2*, Physik Verlag, Weinheim, Germany.

Gross D, Hauger W, Schnell W, Wriggers P (1995): *Technische Mechanik 4: Hydromechanik, Elemente der Höheren Mechanik, Numerische Methoden*, 2nd edition, Springer Verlag, Berlin et al., Germany.

Lanczos C (1986): *The variational principles of mechanics*, 4th edition, Dover Pubn Inc., UK.

Langhaar HL (1962): *Energy methods in applied mechanics*, John Wiley and Sons Inc., New York, USA.

Mittelstedt C (2021): *Structural mechanics in lightweight engineering*, Springer Nature, Cham, Switzerland.

Ochoa OO, Reddy JN (1992): *Finite element analysis of composite laminates*, Kluwer Academic Publishers, Dordrecht et al., The Netherlands.

Oden JT, Reddy JN (1982): *Variational methods in theoretical mechanics*, 2nd edition, Springer Verlag, Berlin, Germany.

Oden JT, Reddy JN (2011): *An introduction to the mathematical theory of finite elements*, Dover Inc., UK.

Reddy JN (2002): *Energy principles and variational methods in applied mechanics*, 2nd edition, John Wiley and Sons, New York, USA.

Reddy JN (2004): *An introduction to nonlinear finite element analysis*, Oxford University Press, New York et al., USA.

Reddy JN (2005): *An introduction to the finite element method*, 3rd edition, McGraw Hill Book Co., USA.

Ritz W (1908): *Über eine neue Methode zur Lösung gewisser Variationsprobleme der mathematischen Physik*, Journal für reine und angewandte Mathematik 135:1–61.

Tauchert TR (1974): *Energy principles in structural mechanics*, McGraw-Hill Inc., USA.

Washizu K (1982): *Variational methods in elasticity and plasticity*, 3rd edition, Pergamon Press, New York, USA.

Wriggers P (2008): *Nichtlineare Finite-Element-Methoden*, Springer-Verlag, Berlin et al., Germany.

Zienkiewicz OC, Taylor RL (2000a): *The finite element method, Vol. 1: the basis*, 5th edition, Butterworth Heinemann, Oxford, USA.

Zienkiewicz OC, Taylor RL (2000b): *The finite element method, Vol. 2: solid mechanics*, 5th edition, Butterworth Heinemann, Oxford, USA.



Strength Hypotheses for Isotropic Materials

5

This chapter is dedicated to an overview of strength hypotheses for isotropic materials. After a basic overview, classical hypotheses and more advanced hypotheses are discussed.

5.1 Introduction

It is a very fundamental task of engineers to predict the load-bearing capacity of a structure under load. Thus, the elasticity-theoretical analysis of a structure with the determination of all resulting stresses is very often carried out with regard to a subsequent strength analysis of a structure or a prediction of when which type of failure is to be expected. Failure criteria based on the corresponding stress results of a structural analysis are used to predict failure.

Failure criteria for isotropic materials are mostly of an older date. They were developed over many decades in the course of the development of solid mechanics. These failure criteria are often comparatively simple, but of considerable practical importance, whereby the following will be limited to the case of static strength verifications.

As an introduction to the strength assessment, the topic of so-called 'theoretical strength' should first be examined. To estimate the theoretical strength of a solid structure, we will hypothetically assume an absolutely intact, defect-free material, i.e. a material in which the basic building blocks of the material (such as atoms, ions or molecules) are arranged periodically in a completely regular manner. Failure or fracture then manifests itself in a loosening of the bonds between the building blocks of the material, i.e. the loosening of bonds between atoms, ions or molecules.

The binding force between two neighbouring basic elements of the material can be described approximately by (Fig. 5.1)

© The Author(s), under exclusive license to Springer-Verlag GmbH, DE, part of Springer Nature 2025

C. Mittelstedt, *Mechanics of Composite Structures*,
https://doi.org/10.1007/978-3-662-70788-3_5

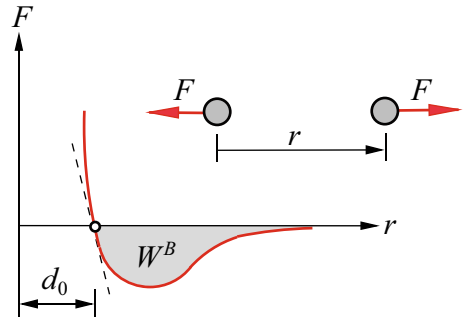


Fig. 5.1 Force-distance behaviour

$$F = -\frac{a}{r^m} + \frac{b}{r^n}, \qquad m < n, \tag{5.1}$$

with suitable constants a, b, m, n.

For small deflections from the equilibrium position, which is characterised by the mutual distance $r = d_0$ between neighbouring basic material components, a linear approximation of the mutual repelling force $F(r)$ can be applied, which corresponds macroscopically to a corresponding Hooke's law. In the ideal case of a completely regular lattice structure, the mechanical stress σ in the tensile range $x = r - d_0 > 0$ can be approximated in the first approximation by

$$\sigma \approx \sigma_c \sin\left(\frac{\pi x}{a}\right), \tag{5.2}$$

where σ_c denotes the so-called 'cohesion strength' or 'theoretical strength' (Fig. 5.2).

For small strains $\varepsilon = \frac{x}{d_0}$ it follows under the additional assumption $d_0 \approx a$:

$$\begin{aligned} \sigma &\approx \sigma_c \frac{\pi x}{a} = \sigma_c \, \pi \varepsilon, \\ \rightarrow \ \sigma_c \, \pi &= E \qquad \rightarrow \ \sigma_c \approx \frac{E}{\pi}. \end{aligned} \tag{5.3}$$

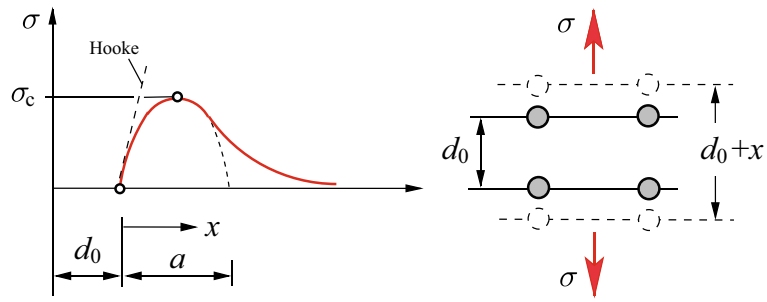


Fig. 5.2 Idealized derivation of 'theoretical strength'

The strength of a material and its elastic stiffness are closely related: The theoretical strength is of the order of one third of the modulus of elasticity. For steel with a modulus of elasticity of $E = 210{,}000$ MPa, a theoretical strength of about $\sigma_c \approx 70{,}000$ MPa can be expected. This result is far above typical strength values for real polycrystalline steels.

The reason for the enormous deviation of the real strength from the theoretical strength ultimately lies in the existing inhomogeneous microstructure of the material and in the presence of (micro) defects. Such (micro) defects include microcracks, microholes, pores, crystalline graininess, or defects in the crystal lattice. A distinction is made between point imperfections (such as voids, interstitial atoms or foreign atoms), line imperfections (such as dislocations) and surface imperfections (such as grain boundaries) in the crystal lattice. In the case of dislocations, a distinction is made between step dislocations and screw dislocations, each of which can be characterised by a corresponding Burgers[1] vector. Dislocations are also of considerable importance in another context: Macroscopic plastic behaviour is due to the movement of dislocations in the polycrystalline structure.

As far as the stress-strain behaviour and fracture behaviour of different materials are concerned, this can vary greatly from material to material. In principle, a distinction is made between a more 'ductile' behaviour and a more 'brittle' behaviour.

In the case of ductile behaviour (Fig. 5.3, left), it is typically the case that significant plastic deformations occur in a uniaxial tensile test after the so-called 'proportional stress' $R_{\text{prop.}}$ is exceeded. The ultimate fracture only occurs with comparatively large inelastic deformations. From a micromechanical point of view, plastic flow is often accompanied by pore or cavity formation and unification. The technical yield point is defined as $R_{p\,0.2}$, i.e. the stress at which a plastic strain of 0.2 per cent remains after unloading. The fracture that ultimately occurs is referred to as a 'ductile fracture'.

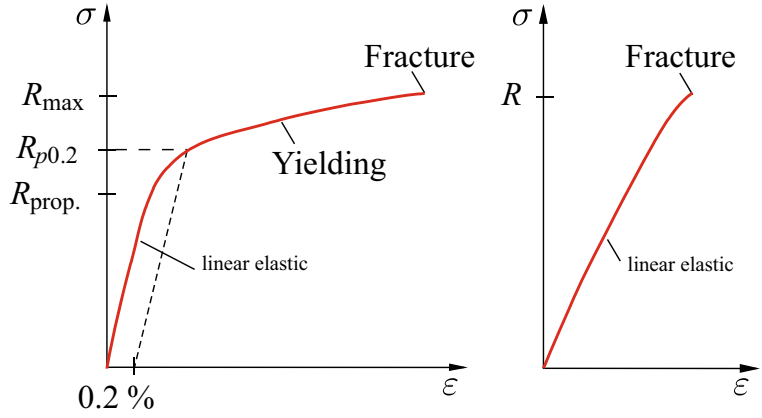


Fig. 5.3 Ductile and brittle material behaviour

[1] Johannes Martinus Burgers, 1895–1981, Dutch physicist.

In the case of a brittle behaviour (Fig. 5.3, right), it is typically the case that the material can be loaded in a uniaxial tensile test until fracture without noticeable inelastic deformation and then fails quite instantaneously. This results in what is known as 'brittle fracture' without any notable inelastic deformation.

In this context, the following properties can usually also be observed:

- Ductile or brittle behaviour or the failure type is also dependent on the stress state.
- With a largely hydrostatic tensile stress state, a comparatively brittle behaviour is often observed even with ductile materials.
- Conversely, a hydrostatic compressive stress state often exhibits a comparatively ductile behaviour, even in brittle materials.

When postulating and formulating strength or failure criteria, it is usually assumed that the failure limit at each point of the relevant solid continuum can be characterised solely by the stress state or strain state present there, namely by a failure condition of the type

$$F(\sigma_{ij}) = 1, \tag{5.4}$$

or

$$f(\varepsilon_{ij}) = 1. \tag{5.5}$$

Here, F is the so-called failure function. This description leads to a corresponding failure (hyper)surface in the 6-dimensional space of stresses or in the 3-dimensional space of principal stresses. Under certain circumstances, it may be more favourable to write $G = F - 1 = 0$.

In the following, some concrete examples of such failure criteria will be presented.

5.2 Principal Stress Hypothesis

Starting from a characterisation of the given material behaviour by its tensile strength R^t (t = tension) and compressive strength R^c (c = compression), the principal stress hypothesis according to Rankine,[2] Lamé[3] and Navier[4] postulates that failure occurs when the maximum positive principal stress reaches the value R^t or when the mathematically smallest principal stress reaches the value $-|R^c|$. This results in an associated failure surface in the space of principal stresses as shown in Fig. 5.4. In the case of a plane stress state, the cube surface is reduced to a square in the $\sigma_1 - \sigma_2$ plane.

[2] William John Macquorn Rankine, 1820–1872, Scottish physicist.

[3] Gabriel Lamé, 1795–1870, French physicist.

[4] Claude Louis Marie Henri Navier, 1785–1836, French mathematician and physicist.

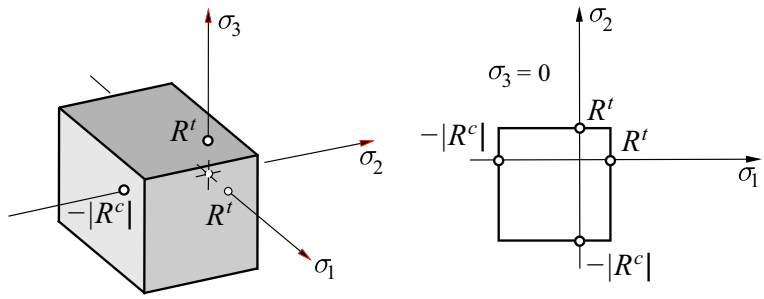


Fig. 5.4 Principal stress hypothesis

This failure criterion is best suited to brittle failure. However, it neglects any 'interaction' between the principal stresses, i.e. the magnitude of the stress σ_2, for example, does not influence the magnitude of the endurable stress σ_1. However, this does not correspond with the existing experimental findings for very many materials, and therefore the principal stress hypothesis is only applicable to a very limited extent.

5.3 Principal Strain Hypothesis

The principal strain hypothesis according to Saint-Venant[5] and Bach[6] provides for a certain interaction between the principal stresses via the existing contraction, and failure is postulated in the principal strain hypothesis if the maximum principal strain assumes a limit strain value e^t. With the corresponding tensile strength $R^t = E\,e^t$, the following failure criteria then follow

$$\begin{aligned} \sigma_1 - \nu(\sigma_2 + \sigma_3) &= R^t, \\ \sigma_2 - \nu(\sigma_3 + \sigma_1) &= R^t, \\ \sigma_3 - \nu(\sigma_1 + \sigma_2) &= R^t. \end{aligned} \tag{5.6}$$

The resulting failure surface (Fig. 5.5) is a three-sided pyramid around the hydrostatic axis ($\sigma_1 = \sigma_2 = \sigma_3$) with the apex

$$\sigma_1 = \sigma_2 = \sigma_3 = \frac{R^t}{1 - 2\nu}. \tag{5.7}$$

[5] Adhémar Jean Claude Barré de Saint-Venant, 1797–1886, French scientist.
[6] Carl Julius von Bach, 1847–1931, German engineer.

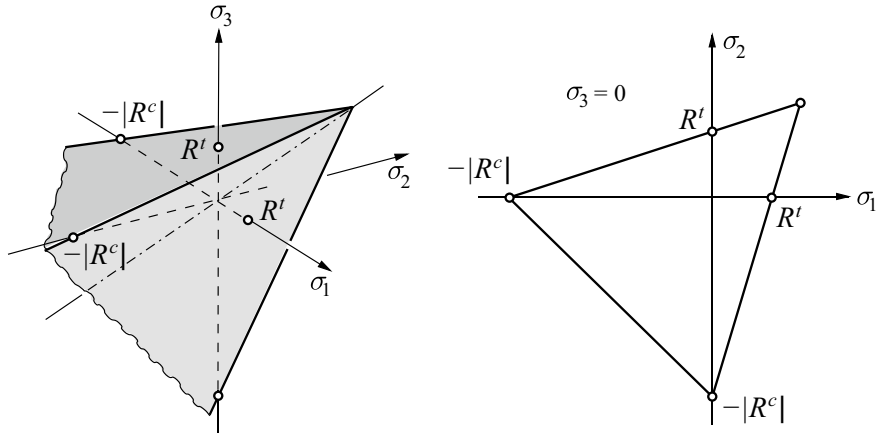


Fig. 5.5 Principal strain hypothesis

With purely uniaxial compression, failure occurs at $R^c = \frac{R^t}{\nu}$. However, this result contradicts the observable experimental experience for most materials, and therefore the principal strain hypothesis can only be recommended to a limited extent.

5.4 Beltrami Strain Energy Hypothesis

The strain energy hypothesis according to Beltrami[7] is a suitable hypothesis for the onset of flow of metallic materials. Failure (as the onset of flow) is postulated when the linear-elastic strain energy density U just reaches a critical value U_c:

$$U = U_c. \tag{5.8}$$

The relationship with the uniaxial equivalent stress R_p is then given by $U_c = \frac{R_p^2}{2E}$. If we express the strain energy density

$$U = \frac{1}{2}\frac{E}{3(1-2\nu)}\varepsilon_{kk}^2 + \frac{E}{2(1+\nu)}\varepsilon'_{ij}\varepsilon'_{ij} = U_V + U_G \tag{5.9}$$

as the sum of the volume change energy density U_V and the deformation energy density U_G over the principal strains in principal stresses, the following representation is obtained:

[7] Eugenio Beltrami, 1835–1900, Italian mathematician.

$$
\begin{aligned}
U &= \frac{1}{2}\frac{E}{3(1-2\nu)}(\varepsilon_1+\varepsilon_2+\varepsilon_3)^2 + \frac{E}{2(1+\nu)}\left[\left(\frac{2\varepsilon_1-\varepsilon_2-\varepsilon_3}{3}\right)^2\right. \\
&\quad \left. + \left(\frac{2\varepsilon_2-\varepsilon_1-\varepsilon_3}{3}\right)^2 + \left(\frac{2\varepsilon_3-\varepsilon_1-\varepsilon_2}{3}\right)^2\right] \\
&= \frac{1}{18K}\sigma_{kk}^2 + \frac{1}{4\mu}\sigma'_{ij}\sigma'_{ij} \\
&= \frac{3(1-2\nu)}{18E}(\sigma_1+\sigma_2+\sigma_3)^2 + \frac{2(1+\nu)}{4E}\left[\left(\frac{2\sigma_1-\sigma_2-\sigma_3}{3}\right)^2\right. \\
&\quad \left. + \left(\frac{2\sigma_2-\sigma_1-\sigma_3}{3}\right)^2 + \left(\frac{2\sigma_3-\sigma_1-\sigma_2}{3}\right)^2\right] \\
&= \frac{1-2\nu}{6E}(\sigma_1+\sigma_2+\sigma_3)^2 + \frac{1+\nu}{18E}\left[6\sigma_1^2+6\sigma_2^2+6\sigma_3^2\right. \\
&\quad \left. -6\sigma_1\sigma_2-6\sigma_2\sigma_3-6\sigma_1\sigma_3\right] \\
&= \frac{1-2\nu}{6E}(\sigma_1+\sigma_2+\sigma_3)^2 + \frac{1+\nu}{6E}\left[(\sigma_1-\sigma_2)^2+(\sigma_2-\sigma_3)^2+(\sigma_3-\sigma_1)^2\right] \\
&= \frac{1}{2E}\left[\frac{1-2\nu}{3}\,I_1^2 + 2\,(1+\nu)\,J_2\right]. \qquad (5.10)
\end{aligned}
$$

This results in the following failure criterion

$$
(1+\nu)\left[(\sigma_1-\sigma_2)^2+(\sigma_2-\sigma_3)^2+(\sigma_3-\sigma_1)^2\right] + (1-2\nu)(\sigma_1+\sigma_2+\sigma_3)^2 = 3R_p^2. \qquad (5.11)
$$

Geometrically, this describes an ellipsoid of rotation around the hydrostatic axis as the failure surface, with the vertices at the points

$$
\sigma_1 = \sigma_2 = \sigma_3 = \pm\frac{R_p}{\sqrt{3(1-2\nu)}}. \qquad (5.12)
$$

One consequence of this failure criterion is failure at the same hydrostatic tension and hydrostatic pressure, which, however, often contradicts experimental findings.

5.5 von Mises Strain Energy Hypothesis

The strain energy hypothesis according to von Mises[8] is obtained by omitting the volume change energy density component U_V. This means that the occurrence of plastic flow with elastic-plastic material behaviour is postulated for the case when the deformation energy density U_G reaches the critical value U_C. Using a uniaxial stress state, the uniaxial equivalent

[8] Richard Edler von Mises, 1883–1953, Austrian mathematician.

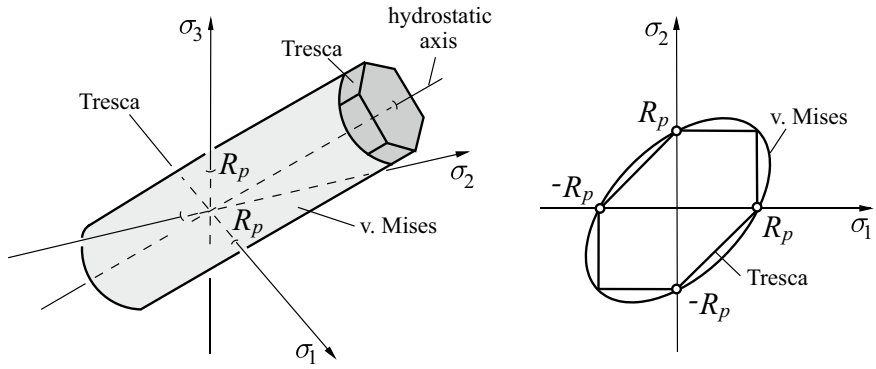


Fig. 5.6 von Mises strain energy hypothesis

stress R_p ('von Mises equivalent stress') can be introduced as follows:

$$U_C = \frac{1+\nu}{3E} R_p^2 = \frac{1+\nu}{E} J_2. \tag{5.13}$$

If the second invariant of the stress deviator is expressed using the principal stresses of the given stress state, the following form of the failure criterion is obtained:

$$(\sigma_1 - \sigma_2)^2 + (\sigma_2 - \sigma_3)^2 + (\sigma_3 - \sigma_1)^2 = 2R_p^2, \tag{5.14}$$

$$\text{or} \quad R_p^2 = \sqrt{\frac{3}{2}\sigma'_{ij}\sigma'_{ij}} = \sqrt{3J_2}.$$

Geometrically (Fig. 5.6), this describes a circular cylinder surface in the space of principal stresses, the center axis of which coincides with the hydrostatic straight line $\sigma_1 = \sigma_2 = \sigma_3$.

In the special case of a plane stress state ($\sigma_3 = 0$), this hypothesis is simplified to

$$\sigma_1^2 + \sigma_2^2 - \sigma_1\sigma_2 = R_p^2, \tag{5.15}$$

and the failure surface becomes an ellipse as a 'yield curve'.

The strain energy hypothesis is generally in good agreement with experimental findings for metals and has proven itself very well for technical applications. This criterion is probably the most widely used failure criterion in the world and is fairly well established in many standards and commercial analysis programmes. This also often leads to the use of the failure criterion where it is no longer appropriate.

5.6 Tresca Yield Criterion

The Tresca[9] yield criterion is very similar to the strain energy hypothesis. It postulates plastic flow when the maximum shear stress of a given stress state assumes a critical value. Including the uniaxial equivalent stress R_p leads to:

$$\frac{\sigma_1 - \sigma_3}{2} = \pm\frac{R_p}{2}, \qquad \frac{\sigma_2 - \sigma_1}{2} = \pm\frac{R_p}{2}, \qquad \frac{\sigma_3 - \sigma_2}{2} = \pm\frac{R_p}{2}. \tag{5.16}$$

Geometrically speaking, the associated yield surface in the space of principal stresses is a hexagonal cylinder composed of partial planes with the hydrostatic straight line as the center axis. This hexagonal cylinder is inscribed in the von Mises cylinder so that the straight edges lie on the cylinder surface. The less 'smooth' surface of the Tresca cylinder can be seen as a disadvantage compared to the von Mises cylinder. Quantitatively, there are no major differences to the strain energy hypothesis. Especially in the field of sheet metal forming, Tresca's yield condition is comparatively popular.

5.7 Coulomb-Mohr Hypothesis

The Coulomb-Mohr[10] hypothesis (Fig. 5.7) is particularly suitable for geological and granular materials (such as sand, rock or soil). Its physical motivation is to consider failure in the form of internal slip processes at suitable internal interfaces in the material. The decisive roles are played by the existing normal stress σ (especially if it is a compressive stress) and the shear stress τ that is also present in relation to the same cut surface. Based on Coulomb's law of friction, sliding along the corresponding cut surface is postulated if

$$|\tau| = \; -\sigma \tan\rho, \tag{5.17}$$

where $\rho =$ 'friction angle'. So that sliding at $\sigma = 0$ is not predicted for arbitrarily small shear stresses, but only for a finite shear stress value, and also so that cutting planes can withstand a certain tensile stress, the following modification of the sliding condition is appropriate:

$$|\tau| = \; -\sigma \tan\rho + c, \tag{5.18}$$

where c represents the 'cohesion'. This sliding condition is also called the Coulomb-Mohr hypothesis, it corresponds geometrically in the $\sigma - \tau$ diagram to two straight lines as the envelope of the admissible Mohr circles and leads to the condition

[9] Henri Édouard Tresca, 1814–1885, French engineer.

[10] Charles Augustin de Coulomb, 1736–1806, French physicist, and Christian Otto Mohr, 1835–1918, German engineer.

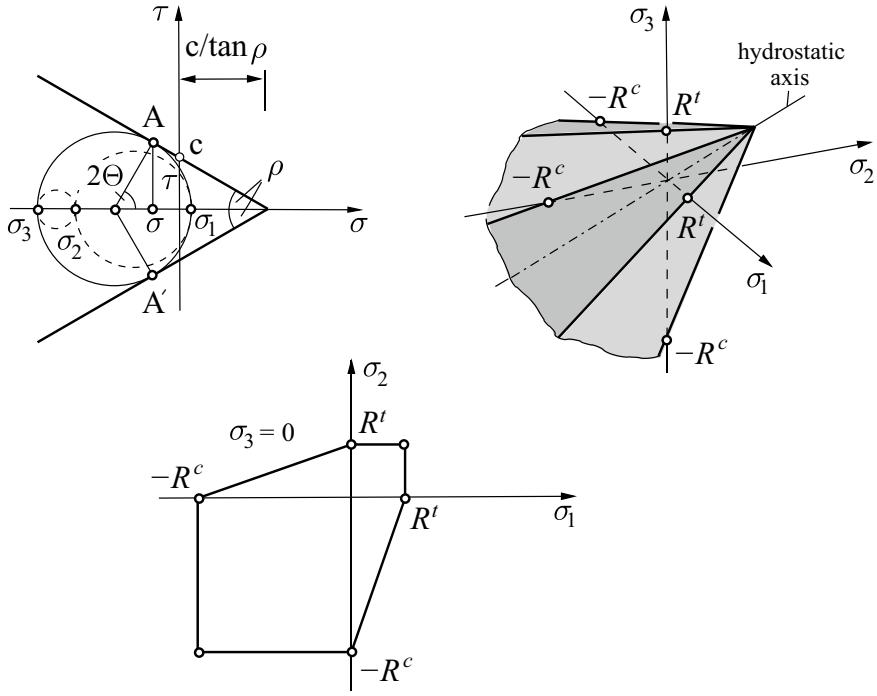


Fig. 5.7 Coulomb-Mohr-hypothesis

$$\frac{|\sigma_1 - \sigma_3|}{2} = \left[\frac{c}{\tan\rho} - \frac{\sigma_1 + \sigma_3}{2}\right] \sin\rho. \tag{5.19}$$

The relationship with the uniaxial tensile strength R^t is obtained by considering the uniaxial tensile stress state $\sigma_1 = R^t$, $\sigma_3 = 0$:

$$R^t = \frac{2c\cos\rho}{1 + \sin\rho}. \tag{5.20}$$

The relationship with the uniaxial compressive strength R^c is obtained by considering the uniaxial compressive stress state $\sigma_1 = 0$, $\sigma_3 = -R^c$:

$$R^c = \frac{2c\cos\rho}{1 - \sin\rho}. \tag{5.21}$$

From the latter two relationships, the material constants c and ρ can be identified for known tensile and compressive strength.

Geometrically, the Mohr-Coulomb failure surface in the three-dimensional space of principal stresses is a six-sided pyramid around the hydrostatic axis, whereby the prin-

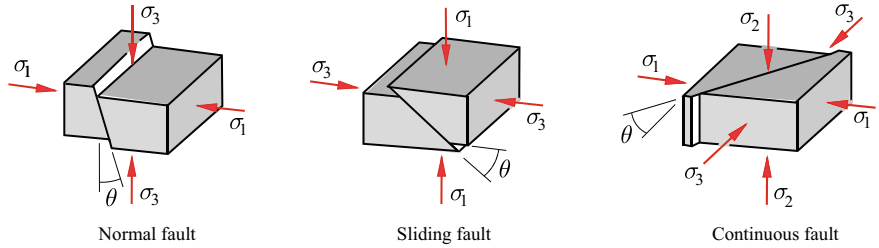


Fig. 5.8 Different types of faults in geology

cipal stresses are not to be arranged in order of size. The apex of the pyramid is then at $\sigma_1 = \sigma_2 = \sigma_3 = \frac{c}{\tan \rho}$.

On the other hand, if σ_1 is the largest principal stress and σ_3 is the smallest principal stress, then the direction of the normal to the failure plane in the $\sigma_1 - \sigma_3$ plane is in the direction $\theta_{1,2} = \pm (45° - \rho/2)$.

The Coulomb-Mohr hypothesis can be used to explain different types of faults in geology (Fig. 5.8), whereby it is assumed that the principal stresses are compressive stresses with $|\sigma_3| \geq |\sigma_2| \geq |\sigma_1|$.

It turns out that the Coulomb-Mohr hypothesis is only appropriate for many materials in the compression range. In the tensile range, a different failure mechanism is usually relevant, not sliding but, for example, separation fracture or normal decohesion. This can be taken into account by modifying the failure surface with normal stress sections (so-called 'tension cutoffs', Fig. 5.9) in the failure criterion.

One arrives at the general Mohr failure hypothesis (Fig. 5.10) if, instead of Coulomb's law of friction, a more general approach of the type

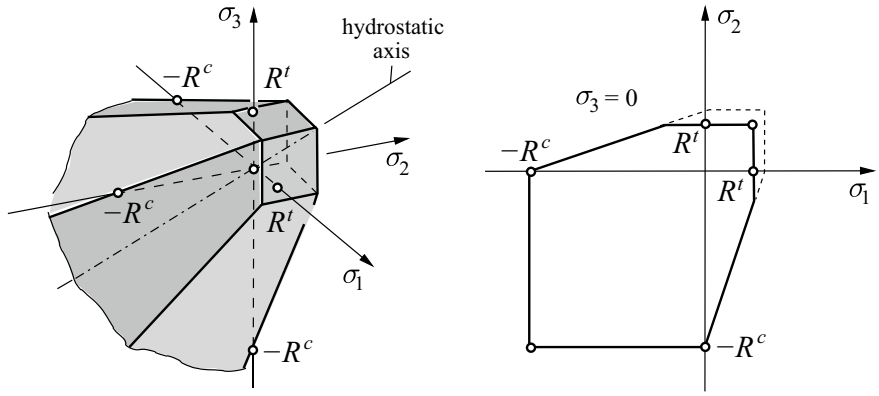


Fig. 5.9 Tension cutoffs

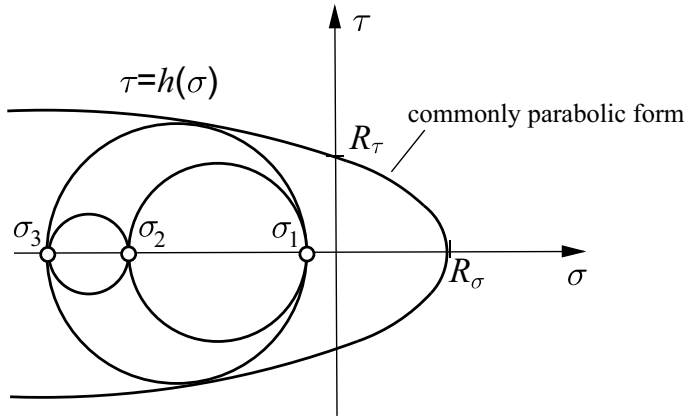


Fig. 5.10 General Mohr's failure hypothesis

$$|\tau| = h(\sigma) \tag{5.22}$$

is employed, where the function $h(\sigma)$ is to be determined experimentally. Geometrically, this function represents the envelope of the admissible Mohr circles in the $\sigma - \tau$ plane.

5.8 Drucker-Prager Hypothesis

The Drucker-Prager[11] hypothesis can be understood as a modification of the Coulomb-Mohr hypothesis. The normal stress associated with a specific direction is replaced by the 1st invariant of the stress tensor and the shear stress is replaced by the von Mises equivalent stress in the form of the square root of the 2nd invariant of the stress deviator:

$$\alpha I_1 + \sqrt{J_2} - k = 0, \tag{5.23}$$

wherein I_1 : 1st invariant of the stress tensor,

J_2 : 2nd invariant of the stress deviator,

α, k : Material parameter.

This failure condition describes a circular cone around the hydrostatic axis with the vertex $\sigma_1 = \sigma_2 = \sigma_3 = \frac{k}{3\alpha}$ (Fig. 5.11) as the failure surface in the space of principal stresses. In the special case of the plane stress state ($\sigma_3 = 0$), the failure surface is reduced to an ellipse in the $\sigma_1 - \sigma_2$ plane.

[11] Daniel Charles Drucker, 1918–2001, US-American engineer, and William Prager (born Willy Prager), 1903–1980, German-US-American mathematician.

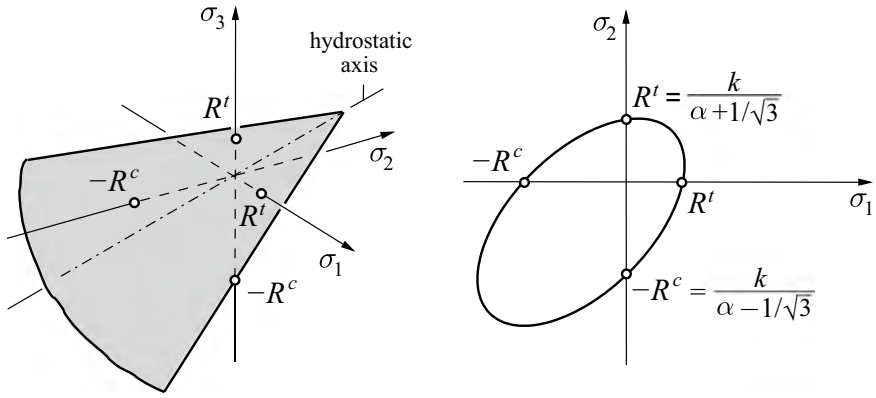


Fig. 5.11 Drucker-Prager hypothesis

The Drucker-Prager hypothesis is mainly used in the analysis of granular and geological materials. For the case $\alpha = 0$, it is converted into the von Mises yield criterion.

The failure criteria described so far reflect the fact that material behaviour, material failure and the underlying failure mechanism can be quite diverse. This depends, among other things, on whether a material is dense and compact or porous, and whether the material behaviour is rather brittle or ductile. Material behaviour is usually even more complex and varied in the case of anisotropic materials, such as fiber-reinforced composite materials in particular.

5.9 Cuntze's Failure Mode Concept (FMC)

Failure criteria should be easy to formulate, as numerically robust as possible, based on a physical foundation and, if possible, only require the standard strength parameters. Most failure criteria ($F >=< 1$) are based on so-called global failure conditions ($F = 1$). These mathematically combine several failure modes. As a result, if there is a change in one failure mode area, the failure in another mode is also affected. Physically, this makes no sense. For this reason, Cuntze[12] pursues a strict, failure mode-related formulation. Each failure mode is described separately (incidentally, the von Mises yield criterion also only describes one failure mode), so that as many conditions as there are failure modes can be set up.

$$\begin{aligned} \text{1 global failure criterion:} \quad & F\left(\underline{\sigma}, \underline{R}\right) = 1, \\ \text{Set of mode-related failure criteria:} \quad & F\left(\underline{\sigma}, R^{\text{mode}}\right) = 1 \qquad \text{(FMC)}. \end{aligned}$$

In the above equations, $\underline{\sigma}$ means the set of all stress tensor components and $\underline{R}$ means the strengths of the material under consideration summarized in a vector. In the FMC, only the

[12] Ralf Cuntze, born 1939, German engineer.

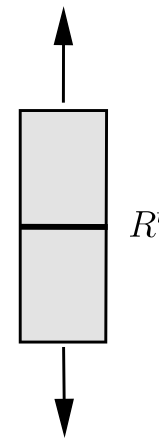


Fig. 5.12 Normal fracture under tension

associated strength must be used for each mode. The number of strengths depends on the material symmetry, i.e. whether a material is isotropic, transversely isotropic or orthotropic. For materials with brittle behaviour, failure is fracture. According to material symmetry, the number of independent elasticity constants is equal to the number of independent strength values. The failure mode concept according to Cuntze (also known as the Failure Mode Concept, FMC) is based on the following:

- Number of independent failure modes = Number of independent strength values.
- When formulating the mode failure criteria, it is often useful to use invariants related to material symmetry.

The selection of the invariant(s) to be used for the failure mode under consideration depends on the physical mechanism. This is discussed in more detail using the example of isotropic, dense, brittle materials. Characteristic for these materials is that fracture occurs with little deformation and a relatively smooth fracture surface (Fig. 5.12) under uniaxial tension.

It is also characteristic of these materials that a shear fracture occurs under sufficiently strong uniaxial pressure (Fig. 5.13).

All in all, therefore, there are:

- 2 failure modes,
- 2 Independent strength parameters,
- 2 Independent stiffness parameters, (E, ν) or (E, G).

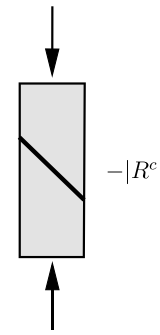


Fig. 5.13 Shear fracture under pressure

Furthermore, isotropic, porous, brittle materials such as foams or fiber-reinforced ceramics are to be considered. These materials are characterised by the fact that they lead to fracture under uniaxial tension, with little deformation and a rough fracture surface (Fig. 5.14).

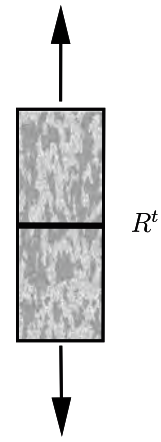


Fig. 5.14 Normal fracture under tension

On the other hand, under uniaxial pressure failure occurs in the form of crushing. Thus:

- 2 failure modes,
- 2 Independent strength parameters,
- 2 Independent stiffness parameters.

For concretization, a brittle isotropic material with 2 failure mode conditions is considered.

$$\text{Normal fracture:} \quad \frac{\frac{1}{3}I_1 + \sqrt{\frac{4}{3}J_2}}{2R^t} = 1, \tag{5.24}$$

$$\text{Shear fracture:} \quad a_\tau^d \frac{3J_2}{R^{c2}} + \left(a_\tau^d - 1\right)\frac{I_1}{3R^c} = 1. \tag{5.25}$$

The strength parameter a_τ^d must be determined either from multiaxial compression tests or from uniaxial compression tests with measurement of the fracture angle.

The individual terms in the conditions represent the efforts (stress *Eff* orts) of the material in the individual modes and, for the example above, are e.g. for the normal fracture:

$$Eff^{\text{mode}} = Eff^{NF} = \frac{\frac{1}{3}I_1 + \sqrt{\frac{4}{3}J_2}}{2R^t}. \tag{5.26}$$

To achieve a closed, multi-dimensional failure surface, the mode failure conditions must still be superimposed by means of an interaction equation, so that a closed formulation is obtained again, but without the disadvantage of the global formulation. This is carried out in an engineering manner by means of a series failure model, which summarises the efforts of all mode efforts activated by the current stress state as a failure equation:

$$Eff^m = \left(Eff^{\text{mode 1}}\right)^m + \left(Eff^{\text{mode 2}}\right)^m + \cdots = 1 = 100\%. \tag{5.27}$$

The interaction coefficient m can be set at 2.5–3. Ultimately, failure surfaces are obtained in this way that are rotationally symmetric about the hydrostatic axis.

Cuntze's failure mode concept is not very commonly used for isotropic materials. In contrast, it plays a much more important role for the assessment of fiber-reinforced composites.

References

Gross D, Seelig Th (2007): *Bruchmechanik – mit einer Einführung in die Mikromechanik, 4th edition*, Springer-Verlag, Berlin, Heidelberg, Germany.

Anderson TL (1995): *Fracture Mechanics – Fundamentals and Applications, 2nd edition*, CRC Press, Boca Raton, USA.

Lemaitre J (1992): *A Course on Damage Mechanics*. Springer-Verlag, Berlin, Heidelberg, Germany.

Kanninen MF, Popelar CH(1985): *Advanced Fracture Mechanics*, Oxford University Press, USA.

Part II
Analysis of Plane Composite Laminates



Mechanics of a Laminate Layer

6

This chapter deals with the mechanical behaviour of a single laminate layer and presents Hooke's generalised law for a variety of different material symmetries. It is presented in terms of stiffnesses and compliances as well as in terms of the so-called engineering constants. The elementary transformation rules for stiffnesses and compliances, which are essential for the treatment of layered anisotropic structures, are discussed as well as the transition to the plane case, which is relevant for many engineering applications. The chapter concludes with a brief overview of the determination of effective properties of anisotropic single layers using so-called rules of mixture.

6.1 Introduction

Having laid the general foundations in the previous chapters of this book, the following chapters now aim to substantiate the previous explanations and focus on their application in the modeling and analysis of composite structures. In doing so, it makes sense to first go into the properties of a single laminate layer in detail before the actual analysis of composite laminates. It will be shown later that many of the basic principles of this chapter also apply very similarly to the modeling and analysis of entire laminates.

In the following, the term of a laminate single layer refers to a composite of a matrix material (e.g. a polymer resin) and unidirectional fibers or a fiber fabric (e.g. made of carbon fibres). Unless otherwise agreed, x_1, x_2, x_3 are always the material principal axes (so-called on-axis system), whereby x_1 is always assumed to be parallel to the fibers. The axis x_3 is always the thickness direction (Fig. 6.1).

© The Author(s), under exclusive license to Springer-Verlag GmbH, DE, part of Springer Nature 2025

C. Mittelstedt, *Mechanics of Composite Structures*,
https://doi.org/10.1007/978-3-662-70788-3_6

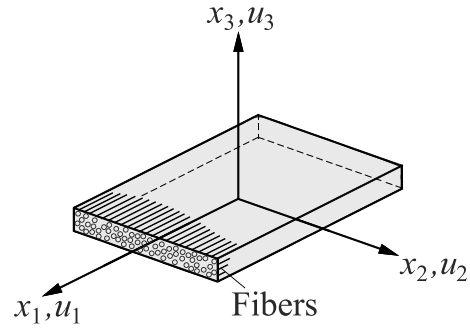


Fig. 6.1 Laminate single layer

6.2 Material Law of a Single Laminate Layer

In all further explanations, the individual layers of a laminate behave in a linear elastic manner, so that the generalized Hooke's law in the form (2.89) or (2.94) is valid.

6.2.1 Full Anisotropy

First, the most general case of Hooke's law will be considered, namely the case of full anisotropy. Accordingly, all stiffnesses C_{ij} and all compliances S_{ij} in (2.89) and (2.94) are not equal to zero. The material behaviour is then described by 21 independent material constants. The following applies:

$$\begin{pmatrix} \sigma_{11} \\ \sigma_{22} \\ \sigma_{33} \\ \tau_{23} \\ \tau_{13} \\ \tau_{12} \end{pmatrix} = \begin{bmatrix} C_{11} & C_{12} & C_{13} & C_{14} & C_{15} & C_{16} \\ C_{12} & C_{22} & C_{23} & C_{24} & C_{25} & C_{26} \\ C_{13} & C_{23} & C_{33} & C_{34} & C_{35} & C_{36} \\ C_{14} & C_{24} & C_{34} & C_{44} & C_{45} & C_{46} \\ C_{15} & C_{25} & C_{35} & C_{45} & C_{55} & C_{56} \\ C_{16} & C_{26} & C_{36} & C_{46} & C_{56} & C_{66} \end{bmatrix} \begin{pmatrix} \varepsilon_{11} \\ \varepsilon_{22} \\ \varepsilon_{33} \\ \gamma_{23} \\ \gamma_{13} \\ \gamma_{12} \end{pmatrix}, \tag{6.1}$$

or

$$\begin{pmatrix} \varepsilon_{11} \\ \varepsilon_{22} \\ \varepsilon_{33} \\ \gamma_{23} \\ \gamma_{13} \\ \gamma_{12} \end{pmatrix} = \begin{bmatrix} S_{11} & S_{12} & S_{13} & S_{14} & S_{15} & S_{16} \\ S_{12} & S_{22} & S_{23} & S_{24} & S_{25} & S_{26} \\ S_{13} & S_{23} & S_{33} & S_{34} & S_{35} & S_{36} \\ S_{14} & S_{24} & S_{34} & S_{44} & S_{45} & S_{46} \\ S_{15} & S_{25} & S_{35} & S_{45} & S_{55} & S_{56} \\ S_{16} & S_{26} & S_{36} & S_{46} & S_{56} & S_{66} \end{bmatrix} \begin{pmatrix} \sigma_{11} \\ \sigma_{22} \\ \sigma_{33} \\ \tau_{23} \\ \tau_{13} \\ \tau_{12} \end{pmatrix}. \tag{6.2}$$

The term τ_{ij} was used here for the shear stresses. It can be seen that such a form of material behaviour results in a rather complex stress-strain relation in the form of various so-

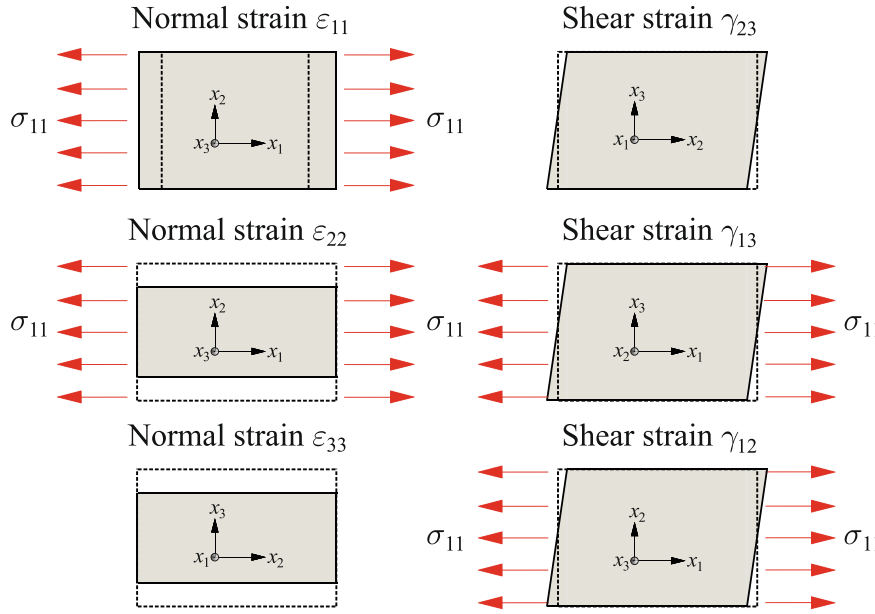


Fig. 6.2 Coupling effects in an anisotropic material

called 'coupling effects'. If one considers a cube made of a completely anisotropic material according to Fig. 6.2 and assumes a normal stress σ_{11}, it can be seen from (6.2) that the stress σ_{11} causes all strain components ε_{11}, ε_{22}, ε_{33}, γ_{23}, γ_{13} and γ_{12} (Fig. 6.2). Even if this material behaviour probably contradicts intuitive perception, there is a whole range of materials to which exactly this behaviour according to (6.1) and (6.2) applies.

However, in lightweight construction applications complete anisotropy does not occur in the materials commonly used there. Rather, due to so-called 'material symmetries' (i.e. symmetry properties with regard to rotations of the reference system), several stiffnesses C_{ij} or compliances S_{ij} become zero, which will be discussed in detail in the following subsections.

6.2.2 Monoclinic Material

A monoclinic or monotropic material is a material in which a single plane of symmetry exists. Let the x_1x_2-plane be the plane of symmetry of the material, i.e. the material properties are mirror-symmetric with respect to the plane $x_3 = 0$ (Fig. 6.3). Here, the coordinates x_1, x_2 and x_3 are not the principal axes of the material, but global reference axes that do not necessarily coincide with the principal material axes, so that in the case of a fiber-reinforced plastic, for example, the fibers form an arbitrary angle with the x_1-axis. If there is a symmetry plane,

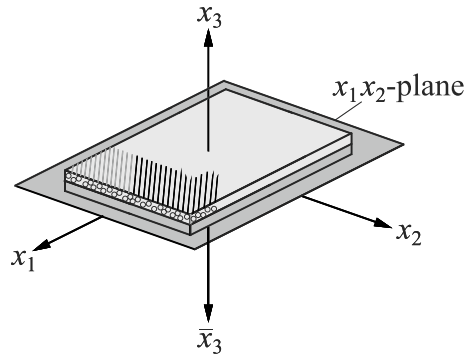


Fig. 6.3 Monoclinic material

this means that the material properties are invariant compared to a reflection of the x_3-axis on the x_1x_2-plane (i.e. a reflection of the type $x_1 = \bar{x}_1, x_2 = \bar{x}_2, x_3 = -\bar{x}_3$). Then, the signs of the shear strains γ_{23} and γ_{13} as well as the shear stresses σ_{23} and σ_{13} are reversed, i.e. $\bar{\gamma}_{23} = -\gamma_{23}$, $\bar{\gamma}_{13} = -\gamma_{13}$ and $\bar{\sigma}_{23} = -\sigma_{23}$, $\bar{\sigma}_{13} = -\sigma_{13}$, while all other stress and strain components remain unchanged. We can then write e.g. for the fourth and fifth line in (6.1):

$$\begin{aligned}\tau_{23} &= C_{14}\varepsilon_{11} + C_{24}\varepsilon_{22} + C_{34}\varepsilon_{33} + C_{44}\gamma_{23} + C_{45}\gamma_{13} + C_{46}\gamma_{12},\\ \tau_{13} &= C_{15}\varepsilon_{11} + C_{25}\varepsilon_{22} + C_{35}\varepsilon_{33} + C_{45}\gamma_{23} + C_{55}\gamma_{13} + C_{56}\gamma_{12}.\end{aligned} \tag{6.3}$$

In the mirrored reference system $\bar{x}_1, \bar{x}_2, \bar{x}_3$, on the other hand, we have

$$\begin{aligned}\bar{\tau}_{23} &= -C_{14}\varepsilon_{11} - C_{24}\varepsilon_{22} - C_{34}\varepsilon_{33} + C_{44}\gamma_{23} + C_{45}\gamma_{13} - C_{46}\gamma_{12},\\ \bar{\tau}_{13} &= -C_{15}\varepsilon_{11} - C_{25}\varepsilon_{22} - C_{35}\varepsilon_{33} + C_{45}\gamma_{23} + C_{55}\gamma_{13} - C_{56}\gamma_{12}.\end{aligned} \tag{6.4}$$

Since a constitutive law must always be invariant to a coordinate transformation or a change of the reference system, the obvious contradiction between (6.3) and (6.4) can only be eliminated if certain stiffnesses disappear, namely if the following applies:

$$C_{14} = C_{24} = C_{34} = C_{46} = C_{15} = C_{25} = C_{35} = C_{56} = 0. \tag{6.5}$$

Then Hooke's generalized law for a monoclinic material changes into the following form:

$$\begin{pmatrix}\sigma_{11}\\ \sigma_{22}\\ \sigma_{33}\\ \tau_{23}\\ \tau_{13}\\ \tau_{12}\end{pmatrix} = \begin{bmatrix}C_{11} & C_{12} & C_{13} & 0 & 0 & C_{16}\\ C_{12} & C_{22} & C_{23} & 0 & 0 & C_{26}\\ C_{13} & C_{23} & C_{33} & 0 & 0 & C_{36}\\ 0 & 0 & 0 & C_{44} & C_{45} & 0\\ 0 & 0 & 0 & C_{45} & C_{55} & 0\\ C_{16} & C_{26} & C_{36} & 0 & 0 & C_{66}\end{bmatrix} \begin{pmatrix}\varepsilon_{11}\\ \varepsilon_{22}\\ \varepsilon_{33}\\ \gamma_{23}\\ \gamma_{13}\\ \gamma_{12}\end{pmatrix}, \tag{6.6}$$

or in the inverted form:

$$\begin{pmatrix} \varepsilon_{11} \\ \varepsilon_{22} \\ \varepsilon_{33} \\ \gamma_{23} \\ \gamma_{13} \\ \gamma_{12} \end{pmatrix} = \begin{bmatrix} S_{11} & S_{12} & S_{13} & 0 & 0 & S_{16} \\ S_{12} & S_{22} & S_{23} & 0 & 0 & S_{26} \\ S_{13} & S_{23} & S_{33} & 0 & 0 & S_{36} \\ 0 & 0 & 0 & S_{44} & S_{45} & 0 \\ 0 & 0 & 0 & S_{45} & S_{55} & 0 \\ S_{16} & S_{26} & S_{36} & 0 & 0 & S_{66} \end{bmatrix} \begin{pmatrix} \sigma_{11} \\ \sigma_{22} \\ \sigma_{33} \\ \tau_{23} \\ \tau_{13} \\ \tau_{12} \end{pmatrix}. \tag{6.7}$$

An important example of monoclinic material behaviour is a laminate single layer in which the fibers and the x_1-axis are not parallel to each other. Monoclinic material behaviour is therefore described by 13 constants.

6.2.3 Orthogonal Anisotropy/Orthotropy

Of great technical importance, especially in fiber composite technology, is the case of so-called orthogonal anisotropic or orthotropic material behaviour. Orthotropy means that mirror symmetry exists with respect to the planes $x_1 = 0$, $x_2 = 0$, $x_3 = 0$ (Fig. 6.4). From here on, the axes x_1, x_2, x_3 are the principal material axes. It is easy to show that in this case further stiffnesses must become zero in order to maintain the invariance of the material law. The following then applies:

$$C_{14} = C_{24} = C_{34} = C_{46} = C_{15} = C_{25} = C_{35} = C_{56} = C_{16} = C_{26} = C_{36} = C_{45} = 0. \tag{6.8}$$

The generalized Hooke's law then changes into the following form:

$$\begin{pmatrix} \sigma_{11} \\ \sigma_{22} \\ \sigma_{33} \\ \tau_{23} \\ \tau_{13} \\ \tau_{12} \end{pmatrix} = \begin{bmatrix} C_{11} & C_{12} & C_{13} & 0 & 0 & 0 \\ C_{12} & C_{22} & C_{23} & 0 & 0 & 0 \\ C_{13} & C_{23} & C_{33} & 0 & 0 & 0 \\ 0 & 0 & 0 & C_{44} & 0 & 0 \\ 0 & 0 & 0 & 0 & C_{55} & 0 \\ 0 & 0 & 0 & 0 & 0 & C_{66} \end{bmatrix} \begin{pmatrix} \varepsilon_{11} \\ \varepsilon_{22} \\ \varepsilon_{33} \\ \gamma_{23} \\ \gamma_{13} \\ \gamma_{12} \end{pmatrix}, \tag{6.9}$$

or in inverted form:

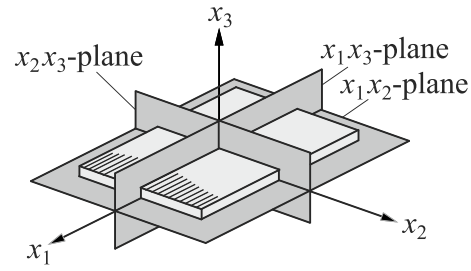


Fig. 6.4 Orthotropic material

$$\begin{pmatrix} \varepsilon_{11} \\ \varepsilon_{22} \\ \varepsilon_{33} \\ \gamma_{23} \\ \gamma_{13} \\ \gamma_{12} \end{pmatrix} = \begin{bmatrix} S_{11} & S_{12} & S_{13} & 0 & 0 & 0 \\ S_{12} & S_{22} & S_{23} & 0 & 0 & 0 \\ S_{13} & S_{23} & S_{33} & 0 & 0 & 0 \\ 0 & 0 & 0 & S_{44} & 0 & 0 \\ 0 & 0 & 0 & 0 & S_{55} & 0 \\ 0 & 0 & 0 & 0 & 0 & S_{66} \end{bmatrix} \begin{pmatrix} \sigma_{11} \\ \sigma_{22} \\ \sigma_{33} \\ \tau_{23} \\ \tau_{13} \\ \tau_{12} \end{pmatrix}. \tag{6.10}$$

Orthotropic material behaviour is therefore described by nine independent constants. Technically relevant examples are laminate single layers that are reinforced by orthogonal fiber fabrics or unidirectional fibers. However, the natural material wood or reinforced concrete also exhibit pronounced orthotropic properties.

By inverting (6.10), the following relationships are obtained between the compliances S_{ij} and the stiffnesses C_{ij} in the case of orthotropic material behaviour:

$$\begin{aligned}
C_{11} &= \frac{S_{23}^2 - S_{22}S_{33}}{S_{11}S_{23}^2 - S_{11}S_{22}S_{33} - 2S_{12}S_{13}S_{23} + S_{22}S_{13}^2 + S_{33}S_{12}^2}, \\
C_{22} &= \frac{S_{13}^2 - S_{11}S_{33}}{S_{11}S_{23}^2 - S_{11}S_{22}S_{33} - 2S_{12}S_{13}S_{23} + S_{22}S_{13}^2 + S_{33}S_{12}^2}, \\
C_{33} &= \frac{S_{12}^2 - S_{11}S_{22}}{S_{11}S_{23}^2 - S_{11}S_{22}S_{33} - 2S_{12}S_{13}S_{23} + S_{22}S_{13}^2 + S_{33}S_{12}^2}, \\
C_{12} &= \frac{S_{12}S_{33} - S_{13}S_{23}}{S_{11}S_{23}^2 - S_{11}S_{22}S_{33} - 2S_{12}S_{13}S_{23} + S_{22}S_{13}^2 + S_{33}S_{12}^2}, \\
C_{13} &= \frac{S_{13}S_{22} - S_{12}S_{23}}{S_{11}S_{23}^2 - S_{11}S_{22}S_{33} - 2S_{12}S_{13}S_{23} + S_{22}S_{13}^2 + S_{33}S_{12}^2}, \\
C_{23} &= \frac{S_{11}S_{23} - S_{12}S_{13}}{S_{11}S_{23}^2 - S_{11}S_{22}S_{33} - 2S_{12}S_{13}S_{23} + S_{22}S_{13}^2 + S_{33}S_{12}^2}, \\
C_{44} &= \frac{1}{S_{44}}, \quad C_{55} = \frac{1}{S_{55}}, \quad C_{66} = \frac{1}{S_{66}}.
\end{aligned} \tag{6.11}$$

6.2.4 Transversal Isotropy

Transversal isotropy exists when isotropy prevails with respect to a plane, e.g. the x_2x_3-plane (Fig. 6.5). This means that the material behaviour is invariant to a rotation of the reference system around the x_1-axis. The structural response is then identical in every direction perpendicular to the x_1-axis. A technically very important example is a unidirectional fiber-matrix composite (see Fig. 6.5), where the fibers run parallel to the x_1-axis. The following identities for the stiffnesses C_{ij} can be derived for transversal isotropy (the stiffnesses already omitted for orthotropy are of course also identical to zero in the case of transversal isotropy):

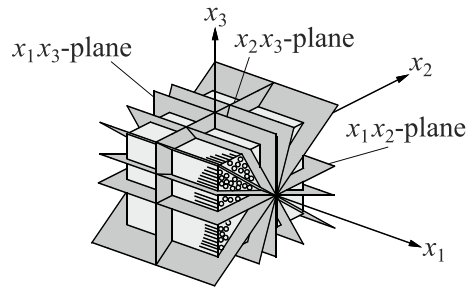


Fig. 6.5 Transversal isotropy

$$C_{13} = C_{12}, \quad C_{33} = C_{22}, \quad C_{66} = C_{55}, \quad C_{44} = \frac{1}{2}\left(C_{22} - C_{23}\right), \tag{6.12}$$

which leads to the generalized Hooke's law the following form:

$$\begin{pmatrix} \sigma_{11} \\ \sigma_{22} \\ \sigma_{33} \\ \tau_{23} \\ \tau_{13} \\ \tau_{12} \end{pmatrix} = \begin{bmatrix} C_{11} & C_{12} & C_{12} & 0 & 0 & 0 \\ C_{12} & C_{22} & C_{23} & 0 & 0 & 0 \\ C_{12} & C_{23} & C_{22} & 0 & 0 & 0 \\ 0 & 0 & 0 & \frac{1}{2}\left(C_{22} - C_{23}\right) & 0 & 0 \\ 0 & 0 & 0 & 0 & C_{55} & 0 \\ 0 & 0 & 0 & 0 & 0 & C_{55} \end{bmatrix} \begin{pmatrix} \varepsilon_{11} \\ \varepsilon_{22} \\ \varepsilon_{33} \\ \gamma_{23} \\ \gamma_{13} \\ \gamma_{12} \end{pmatrix}, \tag{6.13}$$

or in inverted form:

$$\begin{pmatrix} \varepsilon_{11} \\ \varepsilon_{22} \\ \varepsilon_{33} \\ \gamma_{23} \\ \gamma_{13} \\ \gamma_{12} \end{pmatrix} = \begin{bmatrix} S_{11} & S_{12} & S_{12} & 0 & 0 & 0 \\ S_{12} & S_{22} & S_{23} & 0 & 0 & 0 \\ S_{12} & S_{23} & S_{22} & 0 & 0 & 0 \\ 0 & 0 & 0 & 2\left(S_{22} - S_{23}\right) & 0 & 0 \\ 0 & 0 & 0 & 0 & S_{55} & 0 \\ 0 & 0 & 0 & 0 & 0 & S_{55} \end{bmatrix} \begin{pmatrix} \sigma_{11} \\ \sigma_{22} \\ \sigma_{33} \\ \tau_{23} \\ \tau_{13} \\ \tau_{12} \end{pmatrix}. \tag{6.14}$$

In the case of transversely isotropic material behaviour, only five independent material constants remain.

6.2.5 Isotropy

Finally, the case of so-called isotropy must also be considered. A material is isotropic if it behaves the same in all directions. In this case, any plane is a symmetry plane of the material. It can be shown that the generalized Hooke's law then takes the following form:

$$\begin{pmatrix}\sigma_{11}\\ \sigma_{22}\\ \sigma_{33}\\ \tau_{23}\\ \tau_{13}\\ \tau_{12}\end{pmatrix} = \begin{bmatrix} C_{11} & C_{12} & C_{12} & 0 & 0 & 0 \\ C_{12} & C_{11} & C_{12} & 0 & 0 & 0 \\ C_{12} & C_{12} & C_{11} & 0 & 0 & 0 \\ 0 & 0 & 0 & \frac{1}{2}(C_{11}-C_{12}) & 0 & 0 \\ 0 & 0 & 0 & 0 & \frac{1}{2}(C_{11}-C_{12}) & 0 \\ 0 & 0 & 0 & 0 & 0 & \frac{1}{2}(C_{11}-C_{12}) \end{bmatrix} \begin{pmatrix}\varepsilon_{11}\\ \varepsilon_{22}\\ \varepsilon_{33}\\ \gamma_{23}\\ \gamma_{13}\\ \gamma_{12}\end{pmatrix}, \tag{6.15}$$

or in inverted form:

$$\begin{pmatrix}\varepsilon_{11}\\ \varepsilon_{22}\\ \varepsilon_{33}\\ \gamma_{23}\\ \gamma_{13}\\ \gamma_{12}\end{pmatrix} = \begin{bmatrix} S_{11} & S_{12} & S_{12} & 0 & 0 & 0 \\ S_{12} & S_{11} & S_{12} & 0 & 0 & 0 \\ S_{12} & S_{12} & S_{11} & 0 & 0 & 0 \\ 0 & 0 & 0 & 2(S_{11}-S_{12}) & 0 & 0 \\ 0 & 0 & 0 & 0 & 2(S_{11}-S_{12}) & 0 \\ 0 & 0 & 0 & 0 & 0 & 2(S_{11}-S_{12}) \end{bmatrix} \begin{pmatrix}\sigma_{11}\\ \sigma_{22}\\ \sigma_{33}\\ \tau_{23}\\ \tau_{13}\\ \tau_{12}\end{pmatrix}. \tag{6.16}$$

Obviously, only two independent material constants remain for isotropic material behaviour. Technically relevant materials that can often be treated as isotropic are aluminium, steel and many other metallic materials. Matrix materials in fiber composite technology are also generally isotropic, as the anisotropy typical of fiber composites is caused by the arrangement of the fibers. Other examples of isotropic materials are glass, ceramic materials, but also (at least from a macroscopic point of view) unreinforced concrete.

6.2.6 Representation Using Engineering Constants

In order to describe the elastic stiffness properties of an orthotropic material, it is very common to use the so-called engineering constants in addition to the stiffnesses C_{ij} and the compliances S_{ij}. There are a total of twelve engineering constants:

(i) Three generalized moduli of elasticity E_{11}, E_{22}, E_{33},
(ii) six Poisson's ratios ν_{12}, ν_{13}, ν_{23}, ν_{21}, ν_{31}, ν_{32},
(iii) three shear moduli G_{23}, G_{13}, G_{12}.

The generalized Hooke's law (6.10) can be represented as follows using the engineering constants:

$$\begin{pmatrix} \varepsilon_{11} \\ \varepsilon_{22} \\ \varepsilon_{33} \\ \gamma_{23} \\ \gamma_{13} \\ \gamma_{12} \end{pmatrix} = \begin{bmatrix} \frac{1}{E_{11}} & -\frac{\nu_{21}}{E_{22}} & -\frac{\nu_{31}}{E_{33}} & 0 & 0 & 0 \\ -\frac{\nu_{12}}{E_{11}} & \frac{1}{E_{22}} & -\frac{\nu_{32}}{E_{33}} & 0 & 0 & 0 \\ -\frac{\nu_{13}}{E_{11}} & -\frac{\nu_{23}}{E_{22}} & \frac{1}{E_{33}} & 0 & 0 & 0 \\ 0 & 0 & 0 & \frac{1}{G_{23}} & 0 & 0 \\ 0 & 0 & 0 & 0 & \frac{1}{G_{13}} & 0 \\ 0 & 0 & 0 & 0 & 0 & \frac{1}{G_{12}} \end{bmatrix} \begin{pmatrix} \sigma_{11} \\ \sigma_{22} \\ \sigma_{33} \\ \tau_{23} \\ \tau_{13} \\ \tau_{12} \end{pmatrix}. \tag{6.17}$$

By comparing (6.10) and (6.17), the following relationships between the engineering constants and the compliances can be determined:

$$\begin{aligned} &S_{11} = \frac{1}{E_{11}}, \quad S_{22} = \frac{1}{E_{22}}, \quad S_{33} = \frac{1}{E_{33}}, \\ &S_{44} = \frac{1}{G_{23}}, \quad S_{55} = \frac{1}{G_{13}}, \quad S_{66} = \frac{1}{G_{12}}, \\ &S_{12} = -\frac{\nu_{12}}{E_{11}} = -\frac{\nu_{21}}{E_{22}}, \quad S_{23} = -\frac{\nu_{23}}{E_{22}} = -\frac{\nu_{32}}{E_{33}}, \quad S_{13} = -\frac{\nu_{31}}{E_{33}} = -\frac{\nu_{13}}{E_{11}}. \end{aligned} \tag{6.18}$$

The symmetry properties of the compliance matrix $\underline{\underline{S}}$ must also apply to the representation (6.17), so that the following relations can be determined:

$$\frac{\nu_{12}}{E_{11}} = \frac{\nu_{21}}{E_{22}}, \quad \frac{\nu_{23}}{E_{22}} = \frac{\nu_{32}}{E_{33}}, \quad \frac{\nu_{31}}{E_{33}} = \frac{\nu_{13}}{E_{11}}. \tag{6.19}$$

This means that only nine of the twelve engineering constants are independent of each other.

The stiffnesses C_{ij} can be expressed by the engineering constants as follows:

$$\begin{aligned} C_{11} &= \frac{(1-\nu_{23}\nu_{32})E_{11}}{1-\nu_{12}\nu_{21}-\nu_{23}\nu_{32}-\nu_{31}\nu_{13}-2\nu_{21}\nu_{13}\nu_{32}}, \\ C_{22} &= \frac{(1-\nu_{31}\nu_{13})E_{11}}{1-\nu_{12}\nu_{21}-\nu_{23}\nu_{32}-\nu_{31}\nu_{13}-2\nu_{21}\nu_{13}\nu_{32}}, \\ C_{33} &= \frac{(1-\nu_{21}\nu_{12})E_{33}}{1-\nu_{12}\nu_{21}-\nu_{23}\nu_{32}-\nu_{31}\nu_{13}-2\nu_{21}\nu_{13}\nu_{32}}, \\ C_{44} &= G_{23}, \quad C_{55} = G_{13}, \quad C_{66} = G_{12}, \\ C_{12} &= \frac{(\nu_{12}+\nu_{32}\nu_{13})E_{22}}{1-\nu_{12}\nu_{21}-\nu_{23}\nu_{32}-\nu_{31}\nu_{13}-2\nu_{21}\nu_{13}\nu_{32}} \\ &= \frac{(\nu_{21}+\nu_{31}\nu_{23})E_{11}}{1-\nu_{12}\nu_{21}-\nu_{23}\nu_{32}-\nu_{31}\nu_{13}-2\nu_{21}\nu_{13}\nu_{32}}, \end{aligned}$$

$$
\begin{aligned}
C_{13} &= \frac{(\nu_{13} + \nu_{12}\nu_{23})E_{33}}{1 - \nu_{12}\nu_{21} - \nu_{23}\nu_{32} - \nu_{31}\nu_{13} - 2\nu_{21}\nu_{13}\nu_{32}} \\
&= \frac{(\nu_{31} + \nu_{21}\nu_{32})E_{11}}{1 - \nu_{12}\nu_{21} - \nu_{23}\nu_{32} - \nu_{31}\nu_{13} - 2\nu_{21}\nu_{13}\nu_{32}}, \\
C_{23} &= \frac{(\nu_{23} + \nu_{21}\nu_{13})E_{33}}{1 - \nu_{12}\nu_{21} - \nu_{23}\nu_{32} - \nu_{31}\nu_{13} - 2\nu_{21}\nu_{13}\nu_{32}} \\
&= \frac{(\nu_{32} + \nu_{12}\nu_{31})E_{11}}{1 - \nu_{12}\nu_{21} - \nu_{23}\nu_{32} - \nu_{31}\nu_{13} - 2\nu_{21}\nu_{13}\nu_{32}},
\end{aligned} \tag{6.20}
$$

as can be determined by inverting (6.17).

In the case of isotropic material behaviour, only three engineering constants remain, namely the modulus of elasticity E, the shear modulus G and the Poisson's ratio ν, of which only two can be specified independently. The elastic compliances S_{ij} can then be specified as follows:

$$
\begin{aligned}
S_{11} = S_{22} = S_{33} &= \frac{1}{E}, \\
S_{12} = S_{13} = S_{23} &= -\frac{\nu}{E}, \\
S_{44} = S_{55} = S_{66} &= \frac{1}{G}.
\end{aligned} \tag{6.21}
$$

The elastic stiffnesses C_{ij} are obtained as:

$$
\begin{aligned}
C_{11} = C_{22} = C_{33} &= \frac{(1-\nu)\,E}{(1+\nu)\,(1-2\nu)}, \\
C_{12} = C_{13} = C_{23} &= \frac{\nu E}{(1+\nu)\,(1-2\nu)}, \\
C_{44} = C_{55} = C_{66} &= G.
\end{aligned} \tag{6.22}
$$

The following relationship exists between the engineering constants:

$$
G = \frac{E}{2(1+\nu)}, \tag{6.23}
$$

so that only two independent material constants remain in this representation of isotropic material behaviour.

6.2.7 Transformation Rules

All previous considerations have assumed the case that stresses, strains and displacements as well as the material constants S_{ij} and C_{ij} always refer to the material principal axis system x_1, x_2, x_3. The question is now to be investigated as to how the variables mentioned change as soon as the coordinate system x_1, x_2, x_3 is transferred to another orthogonal

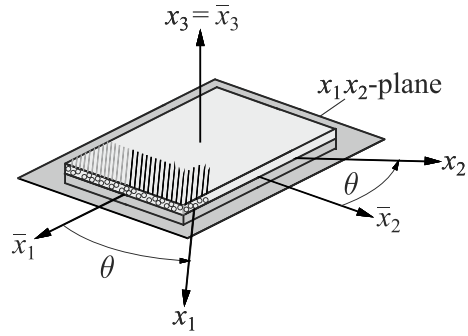


Fig. 6.6 Rotation of the reference system

coordinate system $\bar{x}_1, \bar{x}_2, \bar{x}_3$ (so-called off-axis system) by a pure rotation. The origin of both coordinate systems is identical. The rotation is performed around the axis x_3 so that x_3 and $\bar{x}_3$ are identical. In addition, the right angle between the axes x_1 and x_2 is retained so that the transformed axes $\bar{x}_1$ and $\bar{x}_2$ also include a right angle. The rotation creates an angle θ between the axes x_1 and $\bar{x}_1$ and between x_2 and $\bar{x}_2$ (see Fig. 6.6). The stiffnesses and compliances of a single laminate layer are now sought in relation to the off-axis reference system $\bar{x}_1, \bar{x}_2, \bar{x}_3$. In anticipation of the so-called Classical Laminated Plate Theory, it should be mentioned at this point that the use of the designations x, y, z is common when analyzing laminate structures for the off-axis system, but is not (yet) used in this section.

The transformation of the stresses from the coordinate system x_1, x_2, x_3 into the new coordinate system $\bar{x}_1, \bar{x}_2, \bar{x}_3$ is carried out as follows:

$$\underline{\bar{\sigma}} = \underline{\underline{T}}_{\sigma} \underline{\sigma}. \tag{6.24}$$

The transformation of the strains is written in an analogous manner:

$$\underline{\bar{\varepsilon}} = \underline{\underline{T}}_{\varepsilon} \underline{\varepsilon}. \tag{6.25}$$

Here, the transformation matrices $\underline{\underline{T}}_{\sigma}$ and $\underline{\underline{T}}_{\varepsilon}$ have the following relationships:

$$\underline{\underline{T}}_{\sigma}^{-1} = \underline{\underline{T}}_{\varepsilon}^{T}, \quad \underline{\underline{T}}_{\varepsilon}^{-1} = \underline{\underline{T}}_{\sigma}^{T}. \tag{6.26}$$

Inserting Hooke's law $\underline{\sigma} = \underline{\underline{C}}\,\underline{\varepsilon}$ into (6.24) leads to:

$$\underline{\bar{\sigma}} = \underline{\underline{T}}_{\sigma} \underline{\underline{C}}\,\underline{\varepsilon}. \tag{6.27}$$

If we introduce $\underline{\varepsilon} = \underline{\underline{T}}_{\varepsilon}^{-1} \underline{\bar{\varepsilon}}$ according to the inversion of (6.25), we obtain:

$$\underline{\bar{\sigma}} = \underline{\underline{T}}_{\sigma} \underline{\underline{C}} \underline{\underline{T}}_{\varepsilon}^{-1} \underline{\bar{\varepsilon}}. \tag{6.28}$$

Taking (6.26) into account, the result is:

$$\bar{\underline{\sigma}} = \underline{\underline{T}}_\sigma \underline{\underline{C}} \underline{\underline{T}}_\sigma^T \bar{\underline{\varepsilon}}. \tag{6.29}$$

With (6.29), a connection between the stresses and strains in the off-axis system is established. Similarly, we can proceed from (6.25) and finally obtain the inverse expression to (6.29):

$$\bar{\underline{\varepsilon}} = \underline{\underline{T}}_\varepsilon \underline{\underline{S}} \underline{\underline{T}}_\varepsilon^T \bar{\underline{\sigma}}. \tag{6.30}$$

In (6.29) and (6.30) the expressions $\underline{\underline{T}}_\sigma \underline{\underline{C}} \underline{\underline{T}}_\sigma^T$ and $\underline{\underline{T}}_\varepsilon \underline{\underline{S}} \underline{\underline{T}}_\varepsilon^T$ are the transformed stiffness matrix $\bar{\underline{\underline{C}}}$ and the transformed compliance matrix $\bar{\underline{\underline{S}}}$. The transformation of the stiffness matrix $\underline{\underline{C}}$ and the compliance matrix $\underline{\underline{S}}$ can therefore be carried out as:

$$\begin{aligned} \bar{\underline{\underline{S}}} &= \underline{\underline{T}}_\varepsilon \underline{\underline{S}} \underline{\underline{T}}_\varepsilon^T, \\ \bar{\underline{\underline{C}}} &= \underline{\underline{T}}_\sigma \underline{\underline{C}} \underline{\underline{T}}_\sigma^T. \end{aligned} \tag{6.31}$$

The transformation matrices $\underline{\underline{T}}_\sigma$ and $\underline{\underline{T}}_\varepsilon$ were already derived in Chap. 2 and are given again for the sake of clarity:

$$\underline{\underline{T}}_\sigma = \begin{bmatrix} \cos^2\theta & \sin^2\theta & 0 & 0 & 0 & 2\cos\theta\sin\theta \\ \sin^2\theta & \cos^2\theta & 0 & 0 & 0 & -2\cos\theta\sin\theta \\ 0 & 0 & 1 & 0 & 0 & 0 \\ 0 & 0 & 0 & \cos\theta & -\sin\theta & 0 \\ 0 & 0 & 0 & \sin\theta & \cos\theta & 0 \\ -\cos\theta\sin\theta & \cos\theta\sin\theta & 0 & 0 & 0 & \cos^2\theta - \sin^2\theta \end{bmatrix},$$

$$\underline{\underline{T}}_\varepsilon = \begin{bmatrix} \cos^2\theta & \sin^2\theta & 0 & 0 & 0 & \cos\theta\sin\theta \\ \sin^2\theta & \cos^2\theta & 0 & 0 & 0 & -\cos\theta\sin\theta \\ 0 & 0 & 1 & 0 & 0 & 0 \\ 0 & 0 & 0 & \cos\theta & -\sin\theta & 0 \\ 0 & 0 & 0 & \sin\theta & \cos\theta & 0 \\ -2\cos\theta\sin\theta & 2\cos\theta\sin\theta & 0 & 0 & 0 & \cos^2\theta - \sin^2\theta \end{bmatrix}. \tag{6.32}$$

In the following, the transformation rules for the stiffnesses C_{ij} and the compliancees S_{ij} for the case of an orthotropic material are given explicitly. After applying elementary matrix operations, the transformation rules for the elastic compliances S_{ij}, which are transformed into the transformed components $\bar{S}_{ij}$ in $\bar{\underline{\underline{S}}}$, can be explicitly specified with the help of (6.31) as

$$\begin{aligned} \bar{S}_{11} &= S_{11}\cos^4\theta + S_{22}\sin^4\theta + 2S_{12}\cos^2\theta\sin^2\theta + S_{66}\cos^2\theta\sin^2\theta, \\ \bar{S}_{22} &= S_{11}\sin^4\theta + 2S_{12}\cos^2\theta\sin^2\theta + S_{22}\cos^4\theta + S_{66}\cos^2\theta\sin^2\theta, \\ \bar{S}_{12} &= (S_{11} + S_{22})\cos^2\theta\sin^2\theta + S_{12}\left(\cos^4\theta + \sin^4\theta\right) - S_{66}\cos^2\theta\sin^2\theta, \\ \bar{S}_{66} &= 4\,(S_{11} + S_{22})\cos^2\theta\sin^2\theta - 8S_{12}\cos^2\theta\sin^2\theta + S_{66}\left(\cos^2\theta - \sin^2\theta\right)^2, \\ \bar{S}_{16} &= 2S_{11}\cos^3\theta\sin\theta + 2S_{12}\left(\cos\theta\sin^3\theta - \cos^3\theta\sin\theta\right) \end{aligned}$$

$$
\begin{aligned}
&\quad - 2S_{22}\cos\theta\sin^3\theta + S_{66}\left(\cos\theta\sin^3\theta - \cos^3\theta\sin\theta\right),\\
\bar{S}_{26} &= 2S_{11}\cos\theta\sin^3\theta + 2S_{12}\left(\cos^3\theta\sin\theta - \cos\theta\sin^3\theta\right)\\
&\quad - 2S_{22}\cos^3\theta\sin\theta + S_{66}\left(\cos^3\theta\sin\theta - \cos\theta\sin^3\theta\right),\\
\bar{S}_{13} &= S_{13}\cos^2\theta + S_{23}\sin^2\theta,\\
\bar{S}_{23} &= S_{13}\sin^2\theta + S_{23}\cos^2\theta,\\
\bar{S}_{33} &= S_{33},\\
\bar{S}_{36} &= 2S_{13}\cos\theta\sin\theta - 2S_{23}\cos\theta\sin\theta,\\
\bar{S}_{44} &= S_{44}\cos^2\theta + S_{55}\sin^2\theta,\\
\bar{S}_{45} &= S_{55}\cos\theta\sin\theta - S_{44}\cos\theta\sin\theta,\\
\bar{S}_{55} &= S_{44}\sin^2\theta + S_{55}\cos^2\theta.
\end{aligned}
\tag{6.33}
$$

All other compliance terms $\bar{S}_{ij}$ disappear in this case of coordinate transformation for orthotropic material. Hooke's law $\underline{\bar{\varepsilon}} = \underline{\underline{\bar{S}}}\,\underline{\bar{\sigma}}$ in the off-axis system can then be written as:

$$
\begin{pmatrix} \bar{\varepsilon}_{11}\\ \bar{\varepsilon}_{22}\\ \bar{\varepsilon}_{33}\\ \bar{\gamma}_{23}\\ \bar{\gamma}_{13}\\ \bar{\gamma}_{12} \end{pmatrix} = \begin{bmatrix} \bar{S}_{11} & \bar{S}_{12} & \bar{S}_{13} & 0 & 0 & \bar{S}_{16}\\ \bar{S}_{12} & \bar{S}_{22} & \bar{S}_{23} & 0 & 0 & \bar{S}_{26}\\ \bar{S}_{13} & \bar{S}_{23} & \bar{S}_{33} & 0 & 0 & \bar{S}_{36}\\ 0 & 0 & 0 & \bar{S}_{44} & \bar{S}_{45} & 0\\ 0 & 0 & 0 & \bar{S}_{45} & \bar{S}_{55} & 0\\ \bar{S}_{16} & \bar{S}_{26} & \bar{S}_{36} & 0 & 0 & \bar{S}_{66} \end{bmatrix} \begin{pmatrix} \bar{\sigma}_{11}\\ \bar{\sigma}_{22}\\ \bar{\sigma}_{33}\\ \bar{\sigma}_{23}\\ \bar{\sigma}_{13}\\ \bar{\sigma}_{12} \end{pmatrix}. \tag{6.34}
$$

Obviously, this form of the material law corresponds to the representation in the case of a monoclinic material with only one symmetry plane at $x_3 = 0$. It can be seen that the description of the material behaviour is considerably more complicated in the off-axis system.

The transformation rules for the stiffness components C_{ij}, from which the transformed stiffnesses $\bar{C}_{ij}$ of the stiffness matrix $\underline{\underline{\bar{C}}}$ emerge, can be written in the same way:

$$
\begin{aligned}
\bar{C}_{11} &= C_{11}\cos^4\theta + C_{22}\sin^4\theta + 2C_{12}\cos^2\theta\sin^2\theta + 4C_{66}\cos^2\theta\sin^2\theta,\\
\bar{C}_{22} &= C_{11}\sin^4\theta + C_{22}\cos^4\theta + 2C_{12}\cos^2\theta\sin^2\theta + 4C_{66}\cos^2\theta\sin^2\theta,\\
\bar{C}_{12} &= (C_{11} + C_{22})\cos^2\theta\sin^2\theta + C_{12}\left(\cos^4\theta + \sin^4\theta\right) - 4C_{66}\cos^2\theta\sin^2\theta,\\
\bar{C}_{66} &= (C_{11} + C_{22})\cos^2\theta\sin^2\theta - 2C_{12}\cos^2\theta\sin^2\theta + C_{66}\left(\cos^2\theta - \sin^2\theta\right)^2,\\
\bar{C}_{16} &= C_{11}\cos^3\theta\sin\theta + C_{12}\left(\cos\theta\sin^3\theta - \cos^3\theta\sin\theta\right)\\
&\quad - C_{22}\cos\theta\sin^3\theta + 2C_{66}\left(\cos\theta\sin^3\theta - \cos^3\theta\sin\theta\right),\\
\bar{C}_{26} &= C_{11}\cos\theta\sin^3\theta + C_{12}\left(\cos^3\theta\sin\theta - \cos\theta\sin^3\theta\right)\\
&\quad - C_{22}\cos^3\theta\sin\theta + 2C_{66}\left(\cos^3\theta\sin\theta - \cos\theta\sin^3\theta\right),\\
\bar{C}_{13} &= C_{13}\cos^2\theta + C_{23}\sin^2\theta,
\end{aligned}
$$

$$
\begin{aligned}
\bar{C}_{23} &= C_{13}\sin^2\theta + C_{23}\cos^2\theta,\\
\bar{C}_{33} &= C_{33},\\
\bar{C}_{36} &= C_{13}\cos\theta\sin\theta - C_{23}\cos\theta\sin\theta,\\
\bar{C}_{44} &= C_{44}\cos^2\theta + C_{55}\sin^2\theta,\\
\bar{C}_{45} &= C_{55}\cos\theta\sin\theta - C_{44}\cos\theta\sin\theta,\\
\bar{C}_{55} &= C_{44}\sin^2\theta + C_{55}\cos^2\theta.
\end{aligned}
\tag{6.35}
$$

All other transformed stiffnesses $\bar{C}_{ij}$ disappear. The transformed material law $\underline{\bar{\sigma}} = \underline{\underline{\bar{C}}}\,\underline{\bar{\varepsilon}}$ in the off-axis system can then be written as:

$$
\begin{pmatrix} \bar{\sigma}_{11}\\ \bar{\sigma}_{22}\\ \bar{\sigma}_{33}\\ \bar{\tau}_{23}\\ \bar{\tau}_{13}\\ \bar{\tau}_{12} \end{pmatrix} =
\begin{bmatrix}
\bar{C}_{11} & \bar{C}_{12} & \bar{C}_{13} & 0 & 0 & \bar{C}_{16}\\
\bar{C}_{12} & \bar{C}_{22} & \bar{C}_{23} & 0 & 0 & \bar{C}_{26}\\
\bar{C}_{13} & \bar{C}_{23} & \bar{C}_{33} & 0 & 0 & \bar{C}_{36}\\
0 & 0 & 0 & \bar{C}_{44} & \bar{C}_{45} & 0\\
0 & 0 & 0 & \bar{C}_{45} & \bar{C}_{55} & 0\\
\bar{C}_{16} & \bar{C}_{26} & \bar{C}_{36} & 0 & 0 & \bar{C}_{66}
\end{bmatrix}
\begin{pmatrix} \bar{\varepsilon}_{11}\\ \bar{\varepsilon}_{22}\\ \bar{\varepsilon}_{33}\\ \bar{\gamma}_{23}\\ \bar{\gamma}_{13}\\ \bar{\gamma}_{12} \end{pmatrix}.
\tag{6.36}
$$

However, it is important to note that the 13 transformed stiffnesses $\bar{C}_{ij}$ and compliances $\bar{S}_{ij}$ in the off-axis system depend on the original variables C_{ij} and S_{ij} in the on-axis system and therefore only nine independent variables are to be provided in the off-axis system.

6.3 Formulation for the Plane Case

Most technically relevant formulations of analysis approaches for laminate structures are based on more or less simplifying assumptions regarding the structural behaviour. If one is interested in methods that are easy to use in practice and lead to good results with reasonable effort, the underlying assumptions almost always include the assumption of a plane stress state (see also Chap. 3). This assumption is also particularly justified when considering a single laminate layer, because typical laminates, e.g. in aircraft construction, are always 'thin' plane components whose thickness is generally much smaller than their inplane dimensions. If one assumes a plane stress state with regard to the x_1x_2-plane, the so-called 'interlaminar' stresses τ_{23}, τ_{13} and σ_{33} disappear, and only the so-called 'intralaminar' stresses remain, i.e. the plane stresses σ_{11}, σ_{22}, τ_{12}. Hooke's law is considerably simplified in this case, and the following representation remains when considering an orthotropic laminate single layer in the on-axis system:

$$
\begin{pmatrix} \varepsilon_{11}\\ \varepsilon_{22}\\ \gamma_{12} \end{pmatrix} =
\begin{bmatrix}
S_{11} & S_{12} & 0\\
S_{12} & S_{22} & 0\\
0 & 0 & S_{66}
\end{bmatrix}
\begin{pmatrix} \sigma_{11}\\ \sigma_{22}\\ \tau_{12} \end{pmatrix},
\tag{6.37}
$$

or when using the relevant engineering constants:

$$\begin{pmatrix} \varepsilon_{11} \\ \varepsilon_{22} \\ \gamma_{12} \end{pmatrix} = \begin{bmatrix} \frac{1}{E_{11}} & -\frac{\nu_{21}}{E_{22}} & 0 \\ -\frac{\nu_{12}}{E_{11}} & \frac{1}{E_{22}} & 0 \\ 0 & 0 & \frac{1}{G_{12}} \end{bmatrix} \begin{pmatrix} \sigma_{11} \\ \sigma_{22} \\ \tau_{12} \end{pmatrix}. \tag{6.38}$$

In addition, an elongation in the thickness direction x_3 can occur, which can be calculated as follows, taking $\sigma_{33} = 0$ into account:

$$\varepsilon_{33} = S_{13}\sigma_{11} + S_{23}\sigma_{22}. \tag{6.39}$$

The inverse relationship can be written as:

$$\begin{pmatrix} \sigma_{11} \\ \sigma_{22} \\ \tau_{12} \end{pmatrix} = \begin{bmatrix} C_{11} & C_{12} & C_{13} & 0 \\ C_{12} & C_{22} & C_{23} & 0 \\ 0 & 0 & 0 & C_{66} \end{bmatrix} \begin{pmatrix} \varepsilon_{11} \\ \varepsilon_{22} \\ \varepsilon_{33} \\ \gamma_{12} \end{pmatrix}. \tag{6.40}$$

The normal stress σ_{33} must disappear in the plane stress state. This can be used to eliminate the strain ε_{33} from (6.40). From the generalized Hooke's law follows:

$$0 = C_{13}\varepsilon_{11} + C_{23}\varepsilon_{22} + C_{33}\varepsilon_{33}. \tag{6.41}$$

Solving for the strain ε_{33} results in:

$$\varepsilon_{33} = -\frac{C_{13}}{C_{33}}\varepsilon_{11} - \frac{C_{23}}{C_{33}}\varepsilon_{22}. \tag{6.42}$$

If this is inserted into the first two equations in (6.40), the result is

$$\begin{aligned} \sigma_{11} &= \left(C_{11} - \frac{C_{13}^2}{C_{33}}\right)\varepsilon_{11} + \left(C_{12} - \frac{C_{13}C_{23}}{C_{33}}\right)\varepsilon_{22}, \\ \sigma_{22} &= \left(C_{12} - \frac{C_{13}C_{23}}{C_{33}}\right)\varepsilon_{11} + \left(C_{22} - \frac{C_{23}^2}{C_{33}}\right)\varepsilon_{22}. \end{aligned} \tag{6.43}$$

The third equation in (6.40) remains unchanged. At this point, it is customary to introduce the so-called 'reduced stiffnesses' $Q_{11}, Q_{22}, Q_{12}, Q_{66}$, so that the following representation is finally obtained for (6.40):

$$\begin{pmatrix} \sigma_{11} \\ \sigma_{22} \\ \tau_{12} \end{pmatrix} = \begin{bmatrix} Q_{11} & Q_{12} & 0 \\ Q_{12} & Q_{22} & 0 \\ 0 & 0 & Q_{66} \end{bmatrix} \begin{pmatrix} \varepsilon_{11} \\ \varepsilon_{22} \\ \gamma_{12} \end{pmatrix}, \tag{6.44}$$

or symbolically as:

$$\underline{\sigma} = \underline{\underline{Q}}\,\underline{\varepsilon}. \tag{6.45}$$

The reduced stiffnesses Q_{11}, Q_{22}, Q_{12}, Q_{66} are defined as follows:

$$Q_{11} = C_{11} - \frac{C_{13}^2}{C_{33}}, \quad Q_{12} = C_{12} - \frac{C_{13}C_{23}}{C_{33}}, \quad Q_{22} = C_{22} - \frac{C_{23}^2}{C_{33}}, \quad Q_{66} = C_{66}. \tag{6.46}$$

The reduced stiffnesses can also be calculated from the engineering constants as follows:

$$Q_{11} = \frac{E_{11}}{1 - \nu_{12}\nu_{21}}, \quad Q_{22} = \frac{E_{22}}{1 - \nu_{12}\nu_{21}}, \quad Q_{12} = \frac{\nu_{12}E_{22}}{1 - \nu_{12}\nu_{21}}, \quad Q_{66} = G_{12}. \tag{6.47}$$

The relationship (6.44) refers to an on-axis layer in which the principal directions of the material coincide with the reference axes. Naturally, the principal directions of the individual layers of a laminate can have any orientation with respect to the reference system, so it is of great importance to consider the behaviour of an off-axis layer in the plane stress state. Again, the case of a plane coordinate rotation according to Fig. 6.6 is considered. The transformation rules regarding the stresses and strains are currently reduced to

$$\begin{pmatrix} \bar{\sigma}_{11} \\ \bar{\sigma}_{22} \\ \bar{\tau}_{12} \end{pmatrix} = \begin{bmatrix} \cos^2\theta & \sin^2\theta & -2\cos\theta\sin\theta \\ \sin^2\theta & \cos^2\theta & 2\cos\theta\sin\theta \\ \cos\theta\sin\theta & -\cos\theta\sin\theta & \cos^2\theta - \sin^2\theta \end{bmatrix} \begin{pmatrix} \sigma_{11} \\ \sigma_{22} \\ \tau_{12} \end{pmatrix}$$
$$= \underline{\underline{T}} \begin{pmatrix} \sigma_{11} \\ \sigma_{22} \\ \tau_{12} \end{pmatrix}, \tag{6.48}$$

and

$$\begin{pmatrix} \varepsilon_{11} \\ \varepsilon_{22} \\ \gamma_{12} \end{pmatrix} = \begin{bmatrix} \cos^2\theta & \sin^2\theta & \cos\theta\sin\theta \\ \sin^2\theta & \cos^2\theta & -\cos\theta\sin\theta \\ -2\cos\theta\sin\theta & 2\cos\theta\sin\theta & \cos^2\theta - \sin^2\theta \end{bmatrix} \begin{pmatrix} \bar{\varepsilon}_{11} \\ \bar{\varepsilon}_{22} \\ \bar{\gamma}_{12} \end{pmatrix}$$
$$= \underline{\underline{T}}^T \begin{pmatrix} \bar{\varepsilon}_{11} \\ \bar{\varepsilon}_{22} \\ \bar{\gamma}_{12} \end{pmatrix}. \tag{6.49}$$

The following relationship between the stresses and the strains in the off-axis system is obtained in the same way as previously described for the three-dimensional case:

$$\begin{pmatrix} \bar{\sigma}_{11} \\ \bar{\sigma}_{22} \\ \bar{\tau}_{12} \end{pmatrix} = \underline{\underline{T}}\,\underline{\underline{Q}}\,\underline{\underline{T}}^T \begin{pmatrix} \bar{\varepsilon}_{11} \\ \bar{\varepsilon}_{22} \\ \bar{\gamma}_{12} \end{pmatrix} = \underline{\underline{\bar{Q}}} \begin{pmatrix} \bar{\varepsilon}_{11} \\ \bar{\varepsilon}_{22} \\ \bar{\gamma}_{12} \end{pmatrix}, \tag{6.50}$$

where $\underline{\underline{\bar{Q}}} = \underline{\underline{T}}\,\underline{\underline{Q}}\,\underline{\underline{T}}^T$ is the matrix of the transformed reduced stiffnesses. It is generally fully occupied, so that one obtains

$$\begin{pmatrix} \bar{\sigma}_{11} \\ \bar{\sigma}_{22} \\ \bar{\tau}_{12} \end{pmatrix} = \begin{bmatrix} \bar{Q}_{11} & \bar{Q}_{12} & \bar{Q}_{16} \\ \bar{Q}_{12} & \bar{Q}_{22} & \bar{Q}_{26} \\ \bar{Q}_{16} & \bar{Q}_{26} & \bar{Q}_{66} \end{bmatrix} \begin{pmatrix} \bar{\varepsilon}_{11} \\ \bar{\varepsilon}_{22} \\ \bar{\gamma}_{12} \end{pmatrix}, \tag{6.51}$$

where $\bar{Q}_{11}$, $\bar{Q}_{22}$, $\bar{Q}_{12}$, $\bar{Q}_{66}$, $\bar{Q}_{16}$, $\bar{Q}_{26}$ are the transformed reduced stiffnesses. Evaluating the matrix product $\underline{\underline{T}}\,\underline{\underline{Q}}\,\underline{\underline{T}}^T$ then leads to the following transformation rules for the reduced stiffnesses:

$$\begin{aligned}
\bar{Q}_{11} &= Q_{11}\cos^4\theta + 2\,(Q_{12} + 2Q_{66})\cos^2\theta\sin^2\theta + Q_{22}\sin^4\theta, \\
\bar{Q}_{22} &= Q_{11}\sin^4\theta + 2\,(Q_{12} + 2Q_{66})\cos^2\theta\sin^2\theta + Q_{22}\cos^4\theta, \\
\bar{Q}_{12} &= (Q_{11} + Q_{22} - 4Q_{66})\cos^2\theta\sin^2\theta + Q_{12}\left(\cos^4\theta + \sin^4\theta\right), \\
\bar{Q}_{66} &= (Q_{11} + Q_{22} - 2Q_{12} - 2Q_{66})\cos^2\theta\sin^2\theta + Q_{66}\left(\cos^4\theta + \sin^4\theta\right), \\
\bar{Q}_{16} &= (Q_{11} - Q_{12} - 2Q_{66})\cos^3\theta\sin\theta + (Q_{12} - Q_{22} + 2Q_{66})\cos\theta\sin^3\theta, \\
\bar{Q}_{26} &= (Q_{11} - Q_{12} - 2Q_{66})\cos\theta\sin^3\theta + (Q_{12} - Q_{22} + 2Q_{66})\cos^3\theta\sin\theta.
\end{aligned} \tag{6.52}$$

6.4 Effective Stiffnesses of a Unidirectional Single Layer, Rules of Mixture

6.4.1 Introduction

Until now a laminate single layer was treated as a homogenized continuum with corresponding effective properties, namely e.g. the engineering constants E_{11}, E_{22}, G_{12}, ν_{12} and ν_{21}. The plane reduced stiffnesses Q_{ij} and the compliances S_{ij} can then be calculated from this. However, a fiber composite material and therefore also a laminate single layer is extremely heterogeneous and is characterized by the properties of both the matrix and the fibers. The question must therefore be answered as to how the effective engineering constants E_{11}, E_{22}, G_{12}, ν_{12} and ν_{21} of a single laminate layer can be determined as a function of the properties of the fibers and the matrix material. For this purpose, as is common in engineering practice, the actual heterogeneous structure of a laminate single layer is replaced by a homogenized single layer, generally with orthotropic properties, and an attempt is made to determine effective values for the engineering constants from the volume fractions of the constituents using simple calculation rules. The mechanical properties of the individual layers of a fiber composite are largely controlled by the volume fractions v_f and v_m of the fibres or the matrix:

$$\begin{aligned}
v_f &= \frac{V_f}{V} = \frac{\text{Volume of the fibers}}{\text{Composite volume}}, \\
v_m &= \frac{V_m}{V} = \frac{\text{Volume of the matrix}}{\text{Composite volume}},
\end{aligned} \tag{6.53}$$

where:

$$v_f + v_m = 1, \quad V_f + V_m = V. \tag{6.54}$$

The following material properties are introduced at this point:

E_{f0} Modulus of elasticity of the fibers in the longitudinal direction of the fibres,
E_{f90} Modulus of elasticity of the fibers in the transverse direction,
ν_f Poisson's ratio of the fibers,
v_f Fiber volume fraction,
E_m Modulus of elasticity of the matrix,
ν_m Poisson's ratio of the matrix,
v_m Matrix volume fraction.

In the following, simple analysis rules will be shown to deduce effective homogenized properties of the individual layers of a laminate from the properties of fibers and matrix, i.e. expressions of the type

$$\text{eff.}C_{ij} = \text{eff.}C_{ij}\left(E_f, \nu_f, v_f, E_m, \nu_m, v_m\right). \tag{6.55}$$

Such relationships are also referred to as the so-called rules of mixture, or ROM. For this purpose, a so-called representative unit cell is usually employed (see Fig. 6.7). A representative unit cell is the smallest possible unit of a laminate single layer for determining the macroscopic homogenized stresses and strains. Naturally, inhomogeneous stresses and strains occur within the unit cell, hence some simplifying assumptions are made, which are discussed in detail later.

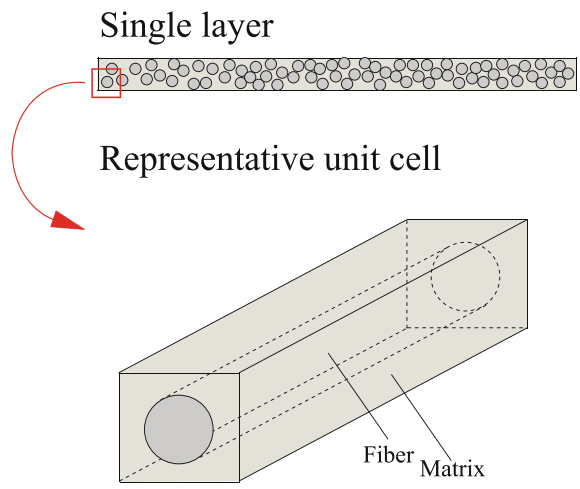


Fig. 6.7 Representative unit cell for determining the effective elastic properties of a single laminate layer

6.4.2 Modulus of Elasticity in Fiber Direction

First, the determination of the modulus of elasticity E_{11} in the fiber direction is discussed. The unit cell is stressed by a fiber-parallel stress σ_{11} and is shown in Fig. 6.8. To calculate E_{11}, it is assumed that the strains ε_f and ε_m of the fiber and the matrix under the stress σ_{11} are equal and assume the value ε_{11}:

$$\varepsilon_m = \varepsilon_f = \varepsilon_{11}. \tag{6.56}$$

If it is also assumed that homogeneous transverse strains will occur in the unit cell, the following expressions are obtained for the stresses σ_f and σ_m in the fiber and the matrix:

$$\sigma_f = E_{f0}\varepsilon_f = E_{f0}\varepsilon_{11}, \quad \sigma_m = E_m\varepsilon_m = E_m\varepsilon_{11}. \tag{6.57}$$

The resulting force P acting on the unit cell is calculated as:

$$P = \sigma_{11}A = \sigma_f A_f + \sigma_m A_m. \tag{6.58}$$

This yields:

$$\sigma_{11} = \sigma_f \frac{A_f}{A} + \sigma_m \frac{A_m}{A}. \tag{6.59}$$

The mean or effective modulus of elasticity E_{11} of the unit cell can then be calculated immediately as follows using Hooke's law:

$$E_{11} = \frac{\sigma_{11}}{\varepsilon_{11}} = \frac{\sigma_f A_f}{\varepsilon_{11} A} + \frac{\sigma_m A_m}{\varepsilon_{11} A}. \tag{6.60}$$

If the relationships $\frac{\sigma_f}{\varepsilon_{11}} = E_{f0}$ and $\frac{\sigma_m}{\varepsilon_{11}} = E_m$ are used and it is assumed, that the cross-sectional quotients $\frac{A_f}{A}$ and $\frac{A_m}{A}$ are the same as the corresponding volume quotients $\frac{V_f}{V} = v_f$ and $\frac{V_m}{V} = v_m$, the following equation for determining the effective modulus of elasticity E_{11} of the unit cell is obtained:

$$E_{11} = E_{f0}v_f + E_m v_m. \tag{6.61}$$

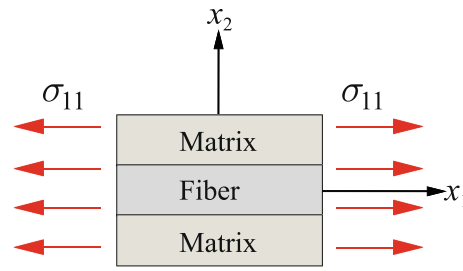


Fig. 6.8 Representative unit cell for determining the fiber-parallel modulus of elasticity E_{11} of a single laminate layer

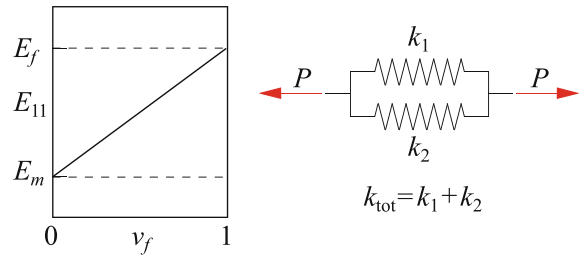


Fig. 6.9 Effective modulus of elasticity E_{11} of a laminate single layer with variable fiber volume fraction (left), analogy of the model of two elastic springs connected in parallel (right)

One recognizes the analogy of this elementary rule of mixture with the simple physical model of two springs connected in parallel (Fig. 6.9). Obviously, $E_{11}\left(v_f, v_m\right)$ is linearly dependent on the volume fractions v_f and v_m involved (Fig. 6.9, left).

6.4.3 Modulus of Elasticity Perpendicular to the Fiber Direction

The representative unit cell for determining the modulus of elasticity E_{22} perpendicular to the fiber direction is shown in Fig. 6.10. To determine the modulus of elasticity E_{22}, it is assumed for simplicity that fibers and matrix are connected in series weighted according to their volume fractions (Fig. 6.11). It is also assumed that the applied stress σ_{22} is homogeneously distributed over the entire unit cell and that the transverse contraction of both the fiber and the matrix is identical. The strains of the fiber and the matrix in the x_2-direction can then be calculated as:

$$\varepsilon_f = \frac{\sigma_{22}}{E_{f90}}, \quad \varepsilon_m = \frac{\sigma_{22}}{E_m}. \tag{6.62}$$

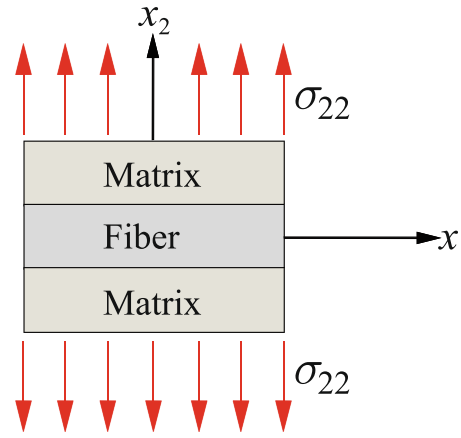


Fig. 6.10 Representative unit cell for determining the effective modulus of elasticity E_{22} of a single laminate layer

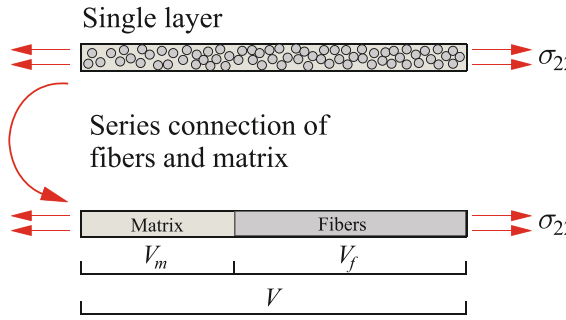


Fig. 6.11 Series connection of fibers and matrix

The total strain ε_{22} can then be calculated by adding the strains ε_f and ε_m, weighted with their specific volume fractions:

$$\varepsilon_{22} = \varepsilon_f v_f + \varepsilon_m v_m = \frac{\sigma_{22}}{E_{f90}} v_f + \frac{\sigma_{22}}{E_m} v_m. \tag{6.63}$$

If Hooke's law is assumed for the composite, then we may write:

$$\varepsilon_{22} = \frac{\sigma_{22}}{E_{22}}. \tag{6.64}$$

Comparing the two equations for ε_{22} provides:

$$E_{22} = \frac{1}{\frac{v_f}{E_{f90}} + \frac{v_m}{E_m}} = \frac{E_{f90} E_m}{v_f E_m + v_m E_{f90}}. \tag{6.65}$$

At this point, the analogy with the physical model of two springs connected in series becomes obvious (see Fig. 6.12). A non-linear distribution of $E_{22}\left(v_f, v_m\right)$ is observed here, with larger values for v_f leading to a disproportionate increase in $E_{22}\left(v_f, v_m\right)$.

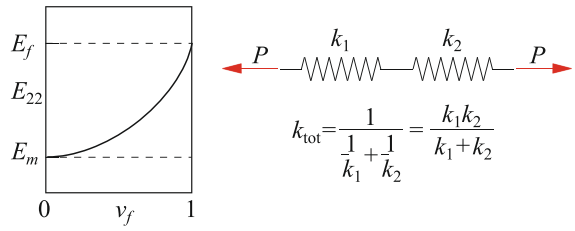


Fig. 6.12 Effective modulus of elasticity E_{22} of a laminate single layer with variable fiber volume fraction (left), analogy of the model of a series connection of two elastic springs (right)

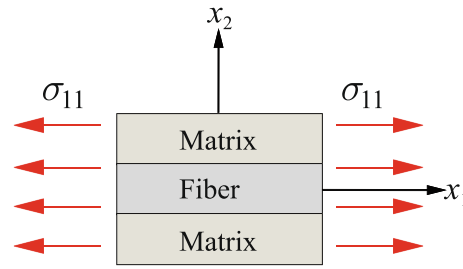


Fig. 6.13 Representative unit cell for determining the inplane Poisson's ratio ν_{12} of a single laminate layer

6.4.4 Poisson's Ratio

Figure 6.13 shows the representative unit cell for determining the inplane Poisson's ratio ν_{12}. If we assume that the fiber and matrix suffer the same longitudinal strain ε_{11} under the given load case and that the longitudinal strain ε_{11} is distributed homogeneously over the cross-section of the unit cell, then the transverse strains of the fiber and matrix can be calculated as follows:

$$\varepsilon_{22f} = -\nu_{12f}\varepsilon_{11}, \quad \varepsilon_{22m} = -\nu_{12m}\varepsilon_{11}. \tag{6.66}$$

If we note that the total transverse strain ε_{22} can be added together from the transverse strains of the fiber and the matrix according to their volume fractions, we obtain the following expression:

$$\varepsilon_{22} = \varepsilon_{22f}v_f + \varepsilon_{22m}v_m = -\left(\nu_{12f}v_f + \nu_{12m}v_m\right)\varepsilon_{11}. \tag{6.67}$$

The term in brackets can be interpreted as the effective Poisson's ratio:

$$\nu_{12} = \nu_{12f}v_f + \nu_{12m}v_m. \tag{6.68}$$

The procedure here is therefore completely analogous to the determination of the effective modulus of elasticity E_{11}.

6.4.5 Shear Modulus

Figure 6.14 shows the representative unit cell for determining the effective inplane shear modulus G_{12}. It is assumed that the applied shear stress τ_{12} is homogeneously distributed over the unit cell. Then the shear strains γ_{12f} and γ_{12m} of the fiber and the matrix can be determined as:

$$\gamma_{12f} = \frac{\tau_{12}}{G_{12f}}, \quad \gamma_{12m} = \frac{\tau_{12}}{G_{12m}}. \tag{6.69}$$

Here, G_{12f} and G_{12m} are the shear moduli of the fiber and the matrix material. The total shear strain is again determined under the assumption that the shear strains γ_{12f} and γ_{12m}

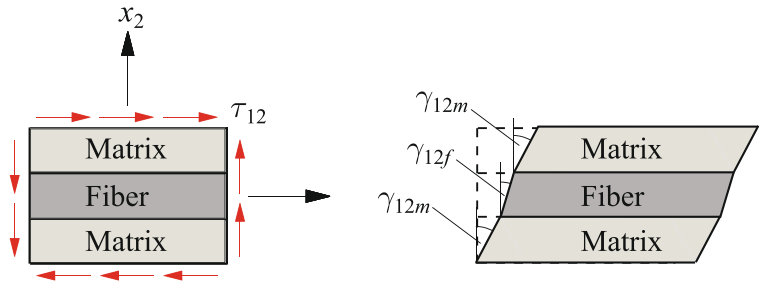


Fig. 6.14 Representative unit cell for determining the inplane shear modulus G_{12} of a laminate single layer (left), shear strains of the fiber and the matrix (right)

can be added together weighted with their volume fractions. The total shear strain is then obtained:

$$\gamma_{12} = \gamma_{12f} v_f + \gamma_{12m} v_m \quad = \left(\frac{v_f}{G_{12f}} + \frac{v_m}{G_{12m}} \right) \tau_{12}. \tag{6.70}$$

According to Hooke's law, the term in brackets represents the reciprocal of the required shear modulus G_{12}:

$$G_{12} = \frac{G_{12f} G_{12m}}{G_{12f} v_m + G_{12m} v_f}. \tag{6.71}$$

The procedure and the result obtained are therefore analogous to what was already found when determining the effective modulus of elasticity E_{22}.

6.4.6 Improved Rules of Mixture, Limit Values

The rather simple models presented above for determining the effective elastic constants of a single laminate layer provide sufficiently accurate predictions for a variety of practical applications. Improved models can generally be developed using all methods of linear elasticity theory that allow a more accurate determination of the stress and strain distribution in the fiber-matrix composite. For example, comprehensive finite element models for more accurate determination of the effective behaviour of a fiber composite material are very popular. However, when considering improved models, one must always ask about the gain in knowledge, which often comes at the price of considerably increased computational effort.

In addition to the development of improved models for estimating the effective elastic properties of a fiber composite material, the provision of limit values, i.e. maximum and minimum possible values for the effective properties, is also of interest. Such limit values can be derived from the energy principles of mechanics, namely:

(i) the principle of minimum strain energy, and
(ii) the principle of minimum complementary energy.

However, this special chapter on composite materials will not be discussed further here. Interested readers will find a large number of valuable references to more precise calculations in this independent and very active field of research in further literature on the micromechanics of inhomogeneous bodies and structures (see, for example, the books by Buryachenko (2007), Mura (2008) or Nemat-Nasser and Hori (1999)).

References

Altenbach H, Altenbach J, Rikards R (1996): *Einführung in die Mechanik der Laminat- und Sandwichtragwerke*, Deutscher Verlag der Grundstoffindustrie, Stuttgart, Germany.

Ambartsumyan SA (1970): *Theory of anisotropic plates*, Technomic Publishing Co., Inc., Stamford, USA.

Ashton JE, Whitney JM (1970): *Theory of laminated plates*, Technomic Publishing Co., Inc., Stamford, USA.

Bert CW (1975): *Analysis of plates*, in: Composite materials, volume 7, Structural design and analysis, part I, Academic Press, New York et al., USA.

Buryachenko V (2007): *Micromechanics of Heterogeneous Materials*, Springer Verlag Berlin et al., Germany.

Frick A, Klamser H (1990): *Untersuchung der Verschiebungs- und Spannungsverteilungen an unbelasteten Rändern multidirektionaler Laminate*, VDI Verlag, Düsseldorf, Germany.

Jones RM (1975): *Mechanics of composite materials*, Scripta Book Co., Washington, USA.

Lekhnitskii SG (1968): *Anisotropic plates*, Gordon and Breach, New York et al., USA.

Mura T (2008): *Micromechanics of Defects in Solids*, Second Edition, Springer Verlag Berlin et al., Germany.

Nemat-Nasser S, Hori M (1999): *Micromechanics: Overall Properties of Heterogeneous Materials*, North-Holland Series in Applied Mathematics and Mechanics, Second Edition, Elsevier Ltd. Amsterdam et al., The Netherlands.

Reddy JN (2004): *Mechanics of laminated composite plates and shells (2nd edition)*, CRC Press Boca Raton et al., USA.

Schürmann H (2007): *Konstruieren mit Faser-Kunststoff-Verbunden (2nd edition)*, Springer Verlag Berlin Heidelberg, Germany.

Tsai SW, Hahn HT (1980): *Introduction to composite materials*, Technomic Publishing Co., Inc., Lancaster et al., UK.



Classical Laminated Plate Theory

7

In this chapter, we introduce the so-called Classical Laminated Plate Theory (CLPT), which represents a very basic theoretical framework and tool for the mechanical analysis of composite laminates. After presenting the basic assumptions of this laminate theory and clarifying the kinematics and the stress state, we derive the constitutive law of a laminate within the framework of CLPT and familiarise ourselves with the so-called coupling effects that are typical for laminates. This is followed by a discussion of the constitutive law for selected classes of laminates, and the effective properties of laminates are also dealt with. The chapter ends with a presentation of the strain energy of a laminate and the treatment of unsymmetric laminates.

7.1 Introduction

Now that the previous chapters have provided all the necessary basics for dealing with the mechanical behaviour of a composite material, the basics of the analysis of thin layered structures, so-called laminates, will now be addressed. A compilation of literature that interested readers can refer to for further details can be found at the end of this chapter.

A laminate is a multi-layer composite consisting of an arbitrary number of individual layers. The properties of the individual layers (material, orientation of the principal material axes, thickness of the layers) are arbitrary. A schematic representation is shown in Fig. 7.1. In the following, only single layers reinforced with unidirectional fibers will be considered. However, the analysis rules presented below also apply, for example, to single layers that are reinforced with a fiber fabric. The direction of the unidirectional fibers in layer k is determined by specifying the fiber angle θ_k.

© The Author(s), under exclusive license to Springer-Verlag GmbH, DE, part of Springer Nature 2025

C. Mittelstedt, *Mechanics of Composite Structures*,
https://doi.org/10.1007/978-3-662-70788-3_7

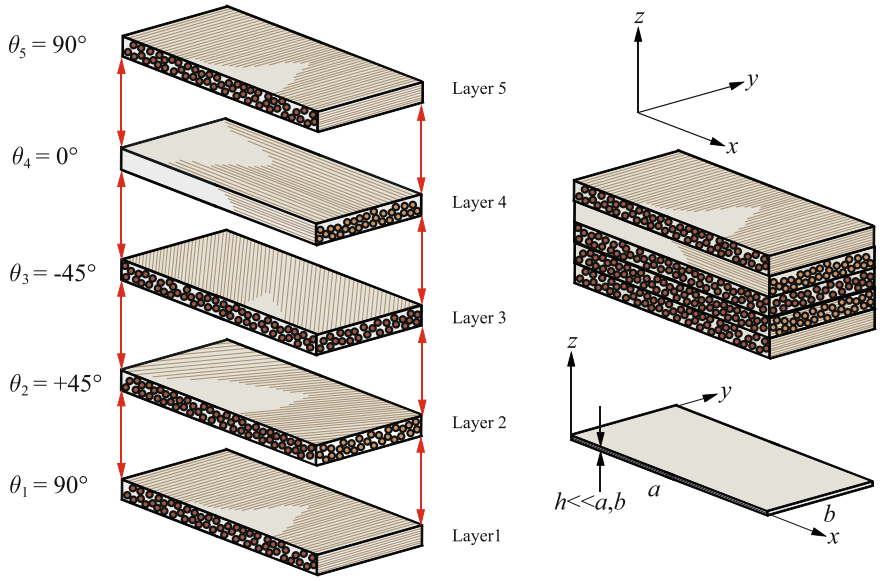


Fig. 7.1 Laminate layers (left), composite laminate (right); the illustration is greatly exaggerated in the thickness direction, real laminates are generally to be regarded as thin in comparison with the length and width, i.e. generally $h \ll a, b$

The so-called laminate code is an adequate way of clearly indicating the stacking sequence of a laminate. Here, the individual layers are labelled according to their fiber orientation, with counting starting from the bottom layer in the positive z-direction. The example in Fig. 7.1 is then labelled according to the laminate code as follows:

$$\left[90°/+45°/-45°/0°/90°\right]. \tag{7.1}$$

It is implicitly assumed that all layers have the same material properties and the same thickness. If this is not the case, this must be indicated separately. The '+' symbol is often omitted for individual layers that have a positive fiber angle. For the example above we thus have:

$$\left[90°/45°/-45°/0°/90°\right]. \tag{7.2}$$

A number of abbreviations are common within the laminate code. For example, for symmetric laminates (i.e. laminates in which the upper half of the laminate can be created by mirroring the lower half at the laminate middle plane, e.g. the bottom layer is identical to the top layer, while the second layer of the laminate is identical to the penultimate layer, and so on), it is sufficient to specify only one half of the layers and to close the square brackets with the index S. Example:

$$\left[0°/90°/90°/0°\right] = \left[0°/90°\right]_S. \tag{7.3}$$

Directly consecutive layers with the opposite fiber angles of identical magnitude are combined with the '±'-symbol. An example:

$$\left[+45^\circ/-45^\circ\right] = [\pm 45]\,. \tag{7.4}$$

Combinations of the two previous abbreviations are very common:

$$\left[+45^\circ/-45^\circ/-45^\circ/+45^\circ\right] = [\pm 45]_S\,. \tag{7.5}$$

Individual layers that occur several times in direct succession are abbreviated by an index that specifies the number of layers that occur several times:

$$\left[0^\circ/90^\circ/90^\circ/90^\circ/0^\circ\right] = \left[0^\circ/90^\circ_3/0^\circ\right]_S\,. \tag{7.6}$$

The nomenclature used in the following is shown in Fig. 7.2. The laminate has the thickness of h and consists of N arbitrary layers. The laminate is divided into two halves of equal thickness by the so-called laminate middle plane. The origin of the coordinates x, y, z can be found in this middle plane, whereby the two coordinates x and y span the laminate middle plane and z is the thickness direction. The difference between the laminate middle plane and the symmetry plane of a laminate should be emphasised here. The laminate middle plane divides the laminate into two halves of equal thickness (partial thickness $\frac{h}{2}$) and is therefore a purely geometric quantity that has nothing whatsoever to do with the stacking sequence of the laminate. On the other hand, a so-called symmetry plane only exists if we are actually dealing with a symmetric laminate. If a symmetry plane exists, it is identical to the laminate middle plane.

The contact surface between two individual layers of a laminate is also called the interface. Each individual layer k is characterised by two thickness coordinates. One is the coordinate z_{k-1}, which describes the lower interface of the individual layer k, and the other is the coordinate z_k, which characterises the upper interface of the layer k. For example, the interface between layer 1 and layer 2 is located at $z = z_1$.

7.2 Assumptions and Kinematics

The Classical Laminated Plate Theory represents a very simple form of laminate theory and is a theory that is valid for thin laminates, whereby the term 'thin' will have to be specified in more detail in quantitative terms. However, it should be noted here that a 'thin' laminate can be assumed if the thickness h is significantly smaller than the inplane dimensions a and b of the laminate, i.e. if $h \ll a, b$ applies (see also Fig. 7.1, bottom right).

The aim of the following explanations is to deduce the properties of a laminate from the knowledge of the properties of the individual layers. To derive Classical Laminated Plate Theory, some assumptions are made with regard to the kinematics. These correspond to

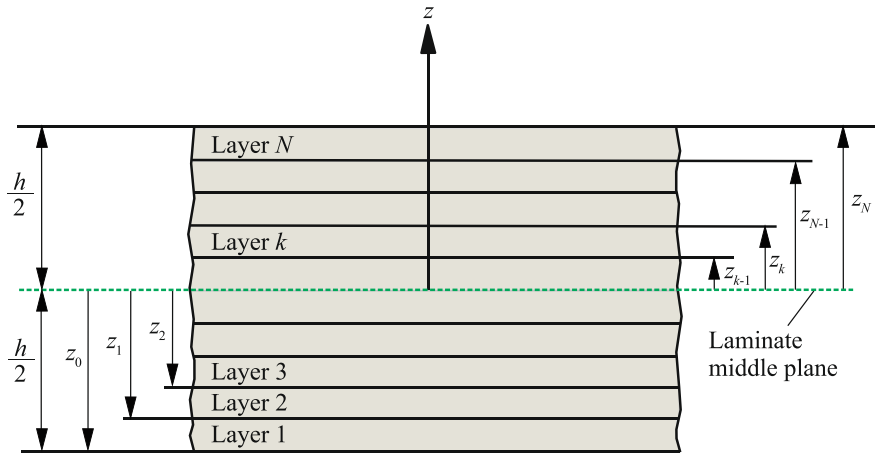


Fig. 7.2 Section through a laminate, nomenclature

the application of Kirchhoff's classical plate theory to laminates. The assumptions are as follows:

(i) A perfect laminate is required. At this point, perfect means that there is a perfect bond/perfect adhesion between the individual layers. The laminate is undamaged and there is no damage or imperfections such as delamination, porosity, fiber waviness, etc.
(ii) A plane state of stress is assumed not only in the individual laminate layers, but also in the entire laminate.
(iii) The kinematics of a Kirchhoff plate are assumed. This means that the hypothesis that the cross-sections remain plane and the normal hypothesis are assumed to be valid. A straight line that is normal to the laminate middle plane before deformation also remains a straight line after deformation and also normal to the deformed laminate middle plane.
(iv) The thickness h of the laminate does not change during the entire deformation process.

The kinematic assumptions (iii) and (iv) are illustrated in Fig. 7.3, in which a plate element is shown in the deflected state according to Classical Laminated Plate Theory. A point on the laminate middle plane is assumed to have moved by the longitudinal displacement u_0 and the transverse displacement/deflection w_0. The deflected plate element then has the inclination $\frac{\partial w_0}{\partial x}$ to the laminate middle plane. The displacements $u_0\,(x, y)$, $v_0\,(x, y)$, $w_0\,(x, y)$ of the laminate middle plane are introduced as displacement quantities, where u_0, v_0, w_0 depend exclusively on the plane coordinates x, y. Furthermore, let $u\,(x, y, z)$, $v\,(x, y, z)$, $w\,(x, y, z)$ be the displacements at any point in the laminate and therefore dependent on all three coordinates x, y, z. Furthermore, a bending angle ψ_x results, which describes the rotation of the cross-section around the y-axis. As the cross-sections are assumed to remain plane,

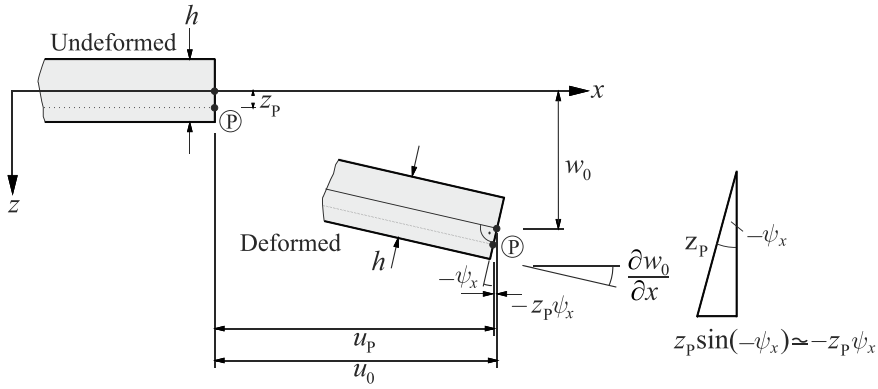


Fig. 7.3 Kinematics of a laminate according to classical laminated plate theory

ψ_x is only a function of the inplane coordinates x, y: $\psi_x = \psi_x\,(x, y)$. Similarly, a second bending angle $\psi_y\,(x, y)$ results, which describes the rotation of the cross-section around the x-axis. Due to the perspective used in Fig. 7.3, the bending angle ψ_y is not visible there.

Firstly, a relationship is sought between the longitudinal displacement u_0 of the middle plane and the longitudinal displacement u_P of the point P. From Fig. 7.3 we obtain:

$$u_P = u_0 - z_P \sin(-\psi_x) = u_0 + z_P \sin\psi_x. \tag{7.7}$$

Since small angles are assumed, $\sin\psi_x \simeq \psi_x$ can be assumed (Fig. 7.3, right), so that:

$$u_P = u_0 + z_P\psi_x. \tag{7.8}$$

This relationship applies to any point on the cross-section at any point z, so that this relationship can be generalized. The following therefore applies to the longitudinal displacement u of any point at location z:

$$u = u_0 + z\psi_x. \tag{7.9}$$

An analogous relationship can also be written for the second inplane displacement v:

$$v = v_0 + z\psi_y. \tag{7.10}$$

Since the Classical Laminated Plate Theory is based on the assumption that the thickness of the laminate h does not change, the deflection w is always identical to the deflection w_0 of the laminate middle plane:

$$w = w_0. \tag{7.11}$$

Finally, the normal hypothesis comes into play, according to which a straight line that is a normal to the laminate middle plane in the undeformed state also remains a straight line in the deformed state and also a normal to the laminate middle plane. This means that the right

angle between the cross-section and the laminate middle plane is maintained, and Fig. 7.3 yields:

$$-\psi_x = \frac{\partial w_0}{\partial x}. \tag{7.12}$$

The same applies to ψ_y:

$$-\psi_y = \frac{\partial w_0}{\partial y}. \tag{7.13}$$

With the kinematics introduced, the displacement field according to Classical Laminated Plate Theory is as follows:

$$\begin{aligned} u(x, y, z) &= u_0(x, y) + z\psi_x(x, y) = u_0 - z\frac{\partial w_0}{\partial x}, \\ v(x, y, z) &= v_0(x, y) + z\psi_y(x, y) = v_0 - z\frac{\partial w_0}{\partial y}, \\ w(x, y, z) &= w_0(x, y). \end{aligned} \tag{7.14}$$

7.3 Strains and Stresses

The associated strain field can be calculated from the displacement field according to Classical Laminated Plate Theory:

$$\begin{aligned} \varepsilon_{xx} &= \frac{\partial u}{\partial x} = \frac{\partial u_0}{\partial x} - z\frac{\partial^2 w_0}{\partial x^2}, \\ \varepsilon_{yy} &= \frac{\partial v}{\partial y} = \frac{\partial v_0}{\partial y} - z\frac{\partial^2 w_0}{\partial y^2}, \\ \varepsilon_{zz} &= \frac{\partial w}{\partial z} = 0, \\ \gamma_{xy} &= \frac{\partial u}{\partial y} + \frac{\partial v}{\partial x} = \frac{\partial u_0}{\partial y} + \frac{\partial v_0}{\partial x} - 2z\frac{\partial^2 w_0}{\partial x \partial y}, \\ \gamma_{xz} &= \frac{\partial u}{\partial z} + \frac{\partial w}{\partial x} = 0, \\ \gamma_{yz} &= \frac{\partial v}{\partial z} + \frac{\partial w}{\partial y} = 0. \end{aligned} \tag{7.15}$$

This leaves only the three inplane strains ε_{xx}, ε_{yy} and γ_{xy}. It is common practice to summarize the remaining equations above in a vector notation:

$$\begin{pmatrix} \varepsilon_{xx}(x, y, z) \\ \varepsilon_{yy}(x, y, z) \\ \gamma_{xy}(x, y, z) \end{pmatrix} = \begin{pmatrix} \varepsilon^0_{xx}(x, y) \\ \varepsilon^0_{yy}(x, y) \\ \gamma^0_{xy}(x, y) \end{pmatrix} + z \begin{pmatrix} \kappa^0_{xx}(x, y) \\ \kappa^0_{yy}(x, y) \\ \kappa^0_{xy}(x, y) \end{pmatrix}. \tag{7.16}$$

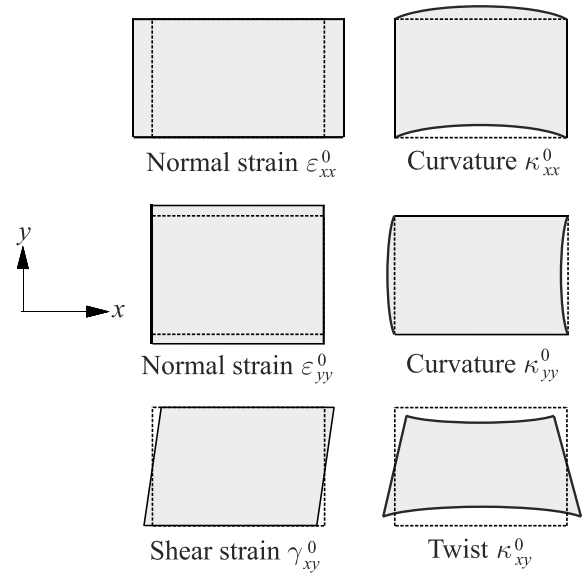


Fig. 7.4 Elementary deformation states of a laminate: strains of the laminate middle plane (left), curvatures and twist of the laminate middle plane (right)

Here $\varepsilon_{xx}(x, y, z)$, $\varepsilon_{yy}(x, y, z)$ and $\gamma_{xy}(x, y, z)$ are the normal strains and shear strains at any point in the laminate, which result from the strains $\varepsilon^0_{xx}(x, y)$, $\varepsilon^0_{yy}(x, y)$ and the shear strain $\gamma^0_{xy}(x, y)$ of the laminate middle plane, as well as the curvatures $\kappa^0_{xx}(x, y)$, $\kappa^0_{yy}(x, y)$ and the twist $\kappa^0_{xy}(x, y)$ of the laminate middle plane (see Fig. 7.4). The superscript '0' indicates that these are variables that are related to the laminate middle plane. The strains, curvatures and the twist of the laminate middle plane are defined as follows:

$$\underline{\varepsilon}^0 = \begin{pmatrix} \varepsilon^0_{xx} \\ \varepsilon^0_{yy} \\ \gamma^0_{xy} \end{pmatrix} = \begin{pmatrix} \dfrac{\partial u_0}{\partial x} \\ \dfrac{\partial v_0}{\partial y} \\ \dfrac{\partial u_0}{\partial y} + \dfrac{\partial v_0}{\partial x} \end{pmatrix}, \quad \underline{\kappa}^0 = \begin{pmatrix} \kappa^0_{xx} \\ \kappa^0_{yy} \\ \kappa^0_{xy} \end{pmatrix} = - \begin{pmatrix} \dfrac{\partial^2 w_0}{\partial x^2} \\ \dfrac{\partial^2 w_0}{\partial y^2} \\ 2\dfrac{\partial^2 w_0}{\partial x \partial y} \end{pmatrix}. \tag{7.17}$$

Once the strains, curvatures and twist of the laminate middle plane are known, the layerwise stresses can be calculated from Hooke's law. For the k-th layer of a laminate this results in

$$\begin{aligned} \begin{pmatrix} \sigma_{xx} \\ \sigma_{yy} \\ \tau_{xy} \end{pmatrix}_k &= \begin{bmatrix} \bar{Q}_{11} & \bar{Q}_{12} & \bar{Q}_{16} \\ \bar{Q}_{12} & \bar{Q}_{22} & \bar{Q}_{26} \\ \bar{Q}_{16} & \bar{Q}_{26} & \bar{Q}_{66} \end{bmatrix}_k \begin{pmatrix} \varepsilon_{xx} \\ \varepsilon_{yy} \\ \gamma_{xy} \end{pmatrix} \\ &= \begin{bmatrix} \bar{Q}_{11} & \bar{Q}_{12} & \bar{Q}_{16} \\ \bar{Q}_{12} & \bar{Q}_{22} & \bar{Q}_{26} \\ \bar{Q}_{16} & \bar{Q}_{26} & \bar{Q}_{66} \end{bmatrix}_k \left[\begin{pmatrix} \varepsilon^0_{xx} \\ \varepsilon^0_{yy} \\ \gamma^0_{xy} \end{pmatrix} + z \begin{pmatrix} \kappa^0_{xx} \\ \kappa^0_{yy} \\ \kappa^0_{xy} \end{pmatrix} \right], \end{aligned} \tag{7.18}$$

wherein $z_{k-1} \leq z \leq z_k$. Since the elastic properties of the individual layers can differ due to different materials or fiber orientations, in the case of a laminate there are generally discontinuities in the stress distributions in the interfaces of adjacent layers, as shown in Fig. 7.5, top, at the example of the normal stress σ_{xx}. In Fig. 7.5, the stresses shown were divided into membrane stresses (stress image on the left) and bending stresses (stress image on the right). While the former are the result of the normal strains ε^0_{xx}, ε^0_{yy} and the shear strain γ^0_{xy} of the laminate middle plane, the latter are the result of the curvatures κ^0_{xx}, κ^0_{yy} and the twist κ^0_{xy}. It should also be noted that a laminate behaves very similarly to a statically indeterminate beam system with regard to the distribution of stresses across the cross-section. 'Stiff' layers therefore attract large stresses, while 'compliant' layers are less stressed. For comparison, Fig. 7.5, bottom, also shows qualitative stress distributions on an isotropic structure under normal force and bending. Of course, the typical discontinuities in the stress distributions for a laminate do not occur here.

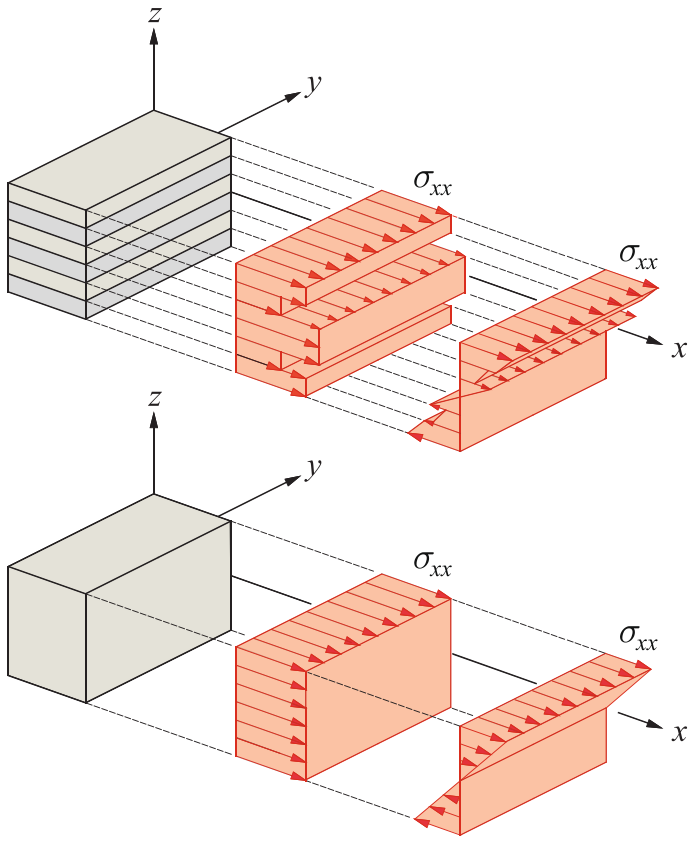


Fig. 7.5 Exemplary stress distributions in a laminate (top) and in an isotropic plate (bottom)

7.4 Constitutive Law

The aim of the constitutive equations is to establish a relationship between the internal force and moment flows in the laminate on the one hand, and the resulting strains, curvatures and twist on the other hand by means of a material law. This material law is derived step by step in this section.

The internal forces in the laminate are introduced as the laminate forces N^0_{xx}, N^0_{yy}, N^0_{xy} per unit width and the laminate moments M^0_{xx}, M^0_{yy}, M^0_{xy} per unit width (Fig. 7.6). The internal forces N^0_{xx}, N^0_{yy} are therefore normal force flows, whereas N^0_{xy} is a shear force flow. The moment flows M^0_{xx}, M^0_{yy} are bending moment flows, whereas the moment M^0_{xy} is a twisting moment flow. The internal forces always have the unit [force/unit length] (e.g. [N/mm]), while the internal moments have the unit [force · unit length/unit length] (e.g. [N]). This means that the laminate forces are forces distributed over a length unit and the laminate moments are moments distributed over a length unit. It is therefore appropriate to speak of force flows and moment flows at this point, even if the terms forces and moments are often used in the following for reasons of simplicity.

A few comments are necessary with regard to the designations of the laminate moments. In contrast to classical beam theory, the indices of the laminate bending moments denote the stress component that causes this moment. Accordingly, M^0_{xx} is a consequence of the normal stress σ_{xx} and a moment about the y-axis. In contrast, the index of the bending moments

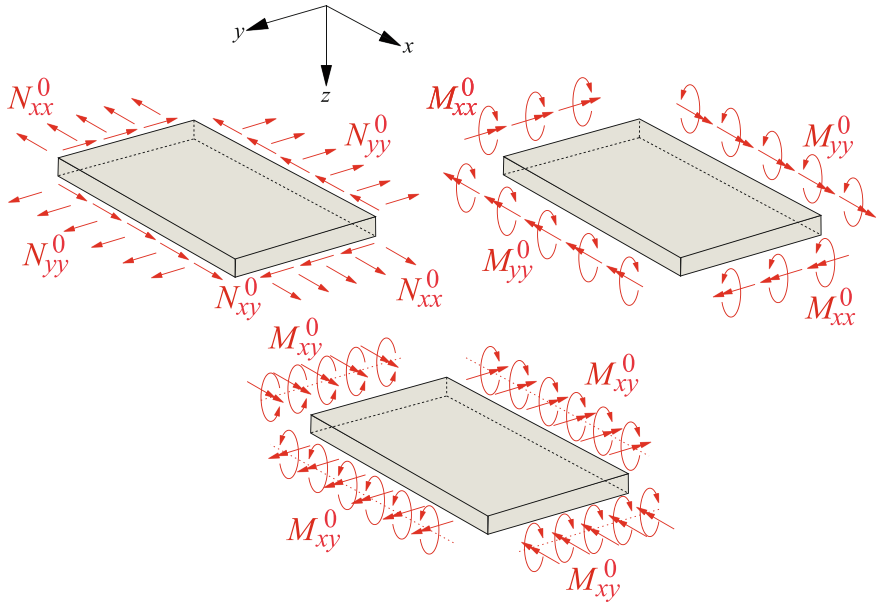


Fig. 7.6 Internal forces in laminate

of a beam is usually defined the other way round. In this case, the normal stress σ_{xx} in the beam causes a bending moment M_y that rotates the cross-section about the y-axis.

The laminate forces $N^0_{xx}, N^0_{yy}, N^0_{xy}$ can be calculated from the integration of the associated stresses over the thickness of the laminate:

$$\begin{pmatrix} N^0_{xx} \\ N^0_{yy} \\ N^0_{xy} \end{pmatrix} = \int_{-\frac{h}{2}}^{\frac{h}{2}} \begin{pmatrix} \sigma_{xx} \\ \sigma_{yy} \\ \tau_{xy} \end{pmatrix} \mathrm{d}z. \tag{7.19}$$

The integration required here through the thickness h of the laminate cannot generally be carried out continuously for a laminate, as the elastic properties can vary from layer to layer. Therefore, the integral over the thickness h is decomposed into N partial integrals:

$$\begin{pmatrix} N^0_{xx} \\ N^0_{yy} \\ N^0_{xy} \end{pmatrix} = \sum_{k=1}^{N} \int_{z_{k-1}}^{z_k} \begin{pmatrix} \sigma_{xx} \\ \sigma_{yy} \\ \tau_{xy} \end{pmatrix}_k \mathrm{d}z. \tag{7.20}$$

Similarly, the laminate section moments can be determined as the resultant of the respective stress components multiplied by the lever arm z:

$$\begin{pmatrix} M^0_{xx} \\ M^0_{yy} \\ M^0_{xy} \end{pmatrix} = \int_{-\frac{h}{2}}^{\frac{h}{2}} \begin{pmatrix} \sigma_{xx} \\ \sigma_{yy} \\ \tau_{xy} \end{pmatrix} z\mathrm{d}z = \sum_{k=1}^{N} \int_{z_{k-1}}^{z_k} \begin{pmatrix} \sigma_{xx} \\ \sigma_{yy} \\ \tau_{xy} \end{pmatrix}_k z\mathrm{d}z. \tag{7.21}$$

If the stresses are replaced by the strains with the help of Hooke's law, the result is

$$\begin{aligned} \begin{pmatrix} N^0_{xx} \\ N^0_{yy} \\ N^0_{xy} \end{pmatrix} &= \sum_{k=1}^{N} \int_{z_{k-1}}^{z_k} \begin{bmatrix} \bar{Q}_{11} & \bar{Q}_{12} & \bar{Q}_{16} \\ \bar{Q}_{12} & \bar{Q}_{22} & \bar{Q}_{26} \\ \bar{Q}_{16} & \bar{Q}_{26} & \bar{Q}_{66} \end{bmatrix}_k \left[\begin{pmatrix} \varepsilon^0_{xx} \\ \varepsilon^0_{yy} \\ \gamma^0_{xy} \end{pmatrix} + z \begin{pmatrix} \kappa^0_{xx} \\ \kappa^0_{yy} \\ \kappa^0_{xy} \end{pmatrix} \right] \mathrm{d}z, \\ \begin{pmatrix} M^0_{xx} \\ M^0_{yy} \\ M^0_{xy} \end{pmatrix} &= \sum_{k=1}^{N} \int_{z_{k-1}}^{z_k} \begin{bmatrix} \bar{Q}_{11} & \bar{Q}_{12} & \bar{Q}_{16} \\ \bar{Q}_{12} & \bar{Q}_{22} & \bar{Q}_{26} \\ \bar{Q}_{16} & \bar{Q}_{26} & \bar{Q}_{66} \end{bmatrix}_k \left[\begin{pmatrix} \varepsilon^0_{xx} \\ \varepsilon^0_{yy} \\ \gamma^0_{xy} \end{pmatrix} + z \begin{pmatrix} \kappa^0_{xx} \\ \kappa^0_{yy} \\ \kappa^0_{xy} \end{pmatrix} \right] z\mathrm{d}z. \end{aligned} \tag{7.22}$$

If the integrations prescribed herein are carried out, the result is

$$\begin{aligned} \begin{pmatrix} N^0_{xx} \\ N^0_{yy} \\ N^0_{xy} \end{pmatrix} &= \begin{bmatrix} A_{11} & A_{12} & A_{16} \\ A_{12} & A_{22} & A_{26} \\ A_{16} & A_{26} & A_{66} \end{bmatrix} \begin{pmatrix} \varepsilon^0_{xx} \\ \varepsilon^0_{yy} \\ \gamma^0_{xy} \end{pmatrix} + \begin{bmatrix} B_{11} & B_{12} & B_{16} \\ B_{12} & B_{22} & B_{26} \\ B_{16} & B_{26} & B_{66} \end{bmatrix} \begin{pmatrix} \kappa^0_{xx} \\ \kappa^0_{yy} \\ \kappa^0_{xy} \end{pmatrix}, \\ \begin{pmatrix} M^0_{xx} \\ M^0_{yy} \\ M^0_{xy} \end{pmatrix} &= \begin{bmatrix} B_{11} & B_{12} & B_{16} \\ B_{12} & B_{22} & B_{26} \\ B_{16} & B_{26} & B_{66} \end{bmatrix} \begin{pmatrix} \varepsilon^0_{xx} \\ \varepsilon^0_{yy} \\ \gamma^0_{xy} \end{pmatrix} + \begin{bmatrix} D_{11} & D_{12} & D_{16} \\ D_{12} & D_{22} & D_{26} \\ D_{16} & D_{26} & D_{66} \end{bmatrix} \begin{pmatrix} \kappa^0_{xx} \\ \kappa^0_{yy} \\ \kappa^0_{xy} \end{pmatrix}. \end{aligned} \tag{7.23}$$

The following abbreviations were introduced ($i, j = 1, 2, 6$):

$$A_{ij} = \int_{-\frac{h}{2}}^{\frac{h}{2}} \bar{Q}_{ij} \mathrm{d}z,$$
$$B_{ij} = \int_{-\frac{h}{2}}^{\frac{h}{2}} \bar{Q}_{ij} z \mathrm{d}z,$$
$$D_{ij} = \int_{-\frac{h}{2}}^{\frac{h}{2}} \bar{Q}_{ij} z^2 \mathrm{d}z. \tag{7.24}$$

The variables A_{ij} are called membrane stiffnesses. They establish a relationship between the laminate forces N^0_{xx}, N^0_{yy}, N^0_{xy} on the one hand, and the strains ε^0_{xx}, ε^0_{yy}, γ^0_{xy} of the laminate middle plane on the other. The variables D_{ij} are defined as plate stiffnesses or bending stiffnesses and connect the laminate moments M^0_{xx}, M^0_{yy}, M^0_{xy} with the curvatures κ^0_{xx}, κ^0_{yy} and the twist κ^0_{xy} of the laminate middle plane.

The terms B_{ij} on the other hand—usually referred to as coupling stiffnesses—represent a special feature of layered structures. They couple the laminate forces N^0_{xx}, N^0_{yy}, N^0_{xy} with the curvatures κ^0_{xx}, κ^0_{yy} and the twist κ^0_{xy} of the laminate middle plane. In addition, the coupling stiffnesses establish a relationship between the laminate moments M^0_{xx}, M^0_{yy}, M^0_{xy} and the strains ε^0_{xx}, ε^0_{yyy}, γ^0_{xy} of the laminate middle plane. Of course, such coupling terms do not occur in homogeneous surface structures such as an isotropic plate.

If the properties of the individual laminate layers in the respective interval $z_{k-1} \leq z \leq z_k$ are constant, the integrals in (7.24) can be easily solved and decomposed into sums:

$$A_{ij} = \sum_{k=1}^{N} \bar{Q}_{ij,k} \left(z_k - z_{k-1}\right),$$
$$B_{ij} = \frac{1}{2} \sum_{k=1}^{N} \bar{Q}_{ij,k} \left(z_k^2 - z_{k-1}^2\right),$$
$$D_{ij} = \frac{1}{3} \sum_{k=1}^{N} \bar{Q}_{ij,k} \left(z_k^3 - z_{k-1}^3\right). \tag{7.25}$$

Usually (7.23) is written in a summarized form as follows:

$$\begin{pmatrix} N^0_{xx} \\ N^0_{yy} \\ N^0_{xy} \\ M^0_{xx} \\ M^0_{yy} \\ M^0_{xy} \end{pmatrix} = \begin{bmatrix} A_{11} & A_{12} & A_{16} & B_{11} & B_{12} & B_{16} \\ A_{12} & A_{22} & A_{26} & B_{12} & B_{22} & B_{26} \\ A_{16} & A_{26} & A_{66} & B_{16} & B_{26} & B_{66} \\ B_{11} & B_{12} & B_{16} & D_{11} & D_{12} & D_{16} \\ B_{12} & B_{22} & B_{26} & D_{12} & D_{22} & D_{26} \\ B_{16} & B_{26} & B_{66} & D_{16} & D_{26} & D_{66} \end{bmatrix} \begin{pmatrix} \varepsilon^0_{xx} \\ \varepsilon^0_{yy} \\ \gamma^0_{xy} \\ \kappa^0_{xx} \\ \kappa^0_{yy} \\ \kappa^0_{xy} \end{pmatrix}. \tag{7.26}$$

The resulting 'material matrix' of the laminate is referred to as the 'laminate stiffness matrix', also known colloquially as the 'ABD matrix'. The constitutive law can also be written in symbolic form:

$$\begin{pmatrix} \underline{N}^0 \\ \underline{M}^0 \end{pmatrix} = \begin{bmatrix} \underline{\underline{A}} & \underline{\underline{B}} \\ \underline{\underline{B}} & \underline{\underline{D}} \end{bmatrix} \begin{pmatrix} \underline{\varepsilon}^0 \\ \underline{\kappa}^0 \end{pmatrix}, \tag{7.27}$$

wherein:

$$\begin{bmatrix} \underline{\underline{A}} & \underline{\underline{B}} \\ \underline{\underline{B}} & \underline{\underline{D}} \end{bmatrix} = \begin{bmatrix} \text{Membrane quadrant} & \text{Coupling quadrant} \\ \text{Coupling quadrant} & \text{Plate quadrant} \end{bmatrix}. \tag{7.28}$$

The above constitutive relationship takes into account the layered structure of the laminate as well as the elastic properties of all individual layers with (7.24). Because the stiffnesses A_{ij}, B_{ij} and D_{ij} in (7.24) are obtained by integrations over the thickness h of the laminate, they can be understood as global or effective laminate properties. Classical Laminated Plate Theory thus uses 'smeared' parameters A_{ij}, B_{ij} and D_{ij} for the laminate, which can be understood as variables averaged over the thickness. This is also referred to as a 'single-layer theory', because the laminate is mathematically reduced to its middle plane with corresponding 'effective properties' A_{ij}, B_{ij} and D_{ij}.

7.5 Coupling Effects

The constitutive law of a laminate in the framework of CLPT implies that with a fully populated laminate stiffness matrix, any internal force quantity calls forth all strains ε^0_{xx}, ε^0_{yy}, γ^0_{xy} as well as both curvatures κ^0_{xx}, κ^0_{yy} and also the twist κ^0_{xy} of the laminate middle plane. Figure 7.7 shows this for the example of the laminate force N^0_{xx}. Obviously, both the disk and the plate behaviour are generally coupled with each other for arbitrary laminate layups. At this point it becomes clear that the common distinction between 'disks' and 'plates' does not make sense for laminates, since internal forces can develop a plate effect, while internal moments can result in a membrane effect.

A closer look shows that the stiffness components that make the difference to isotropic disk and plate structures are the terms A_{16}, A_{26} in the membrane quadrant, the terms D_{16}, D_{26} in the plate quadrant, and all coupling stiffnesses B_{ij}. The coupling effects associated with them are named as follows:

A_{16}, A_{26}: Shear coupling,
D_{16}, D_{26}: Bending-twisting coupling,
B_{ij}: Bending-extension coupling.

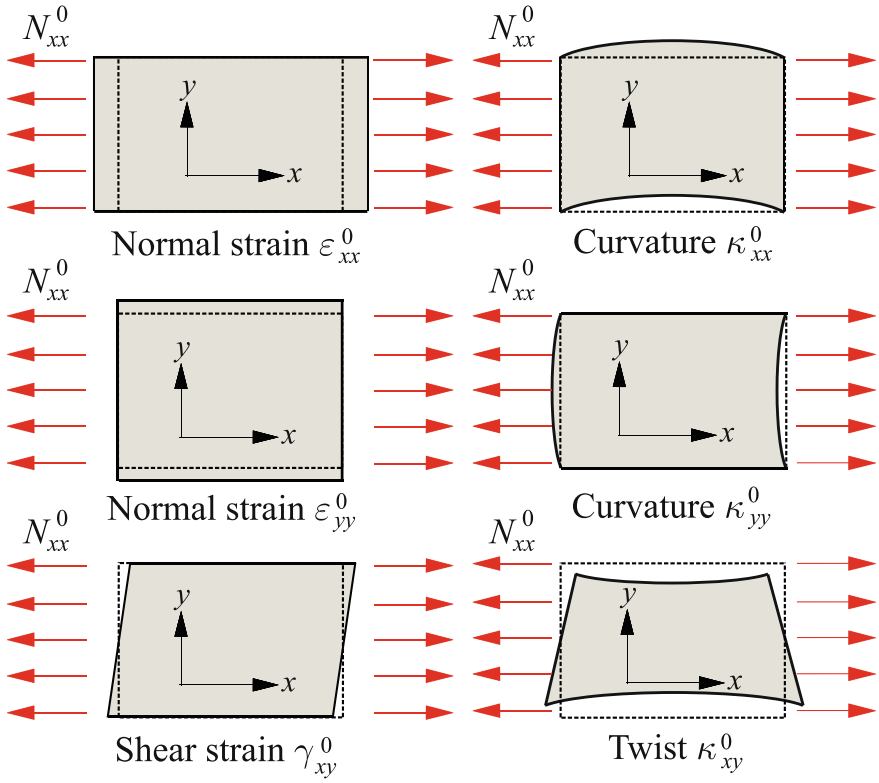


Fig. 7.7 Coupling effects in a laminate with fully populated laminate stiffness matrix: Strains of the laminate middle plane as well as curvatures and twist of the laminate middle plane caused by the laminate force N_{xx}^0

7.5.1 Shear Coupling

Shear coupling occurs in laminates in which the terms A_{16}, A_{26} do not disappear. In such laminates, normal strains ε_{xx}^0, ε_{yy}^0 cause the laminate force N_{xy}^0 to occur. A shear strain γ_{xy}^0, on the other hand, causes the two laminate forces N_{xx}^0 and N_{yy}^0. An example of the occurrence of shear coupling is a laminate single layer that is rotated by an angle θ relative to the x-axis ('off-axis layer', Fig. 7.8). A laminate whose shear coupling terms A_{16}, A_{26} disappear is called 'balanced'.

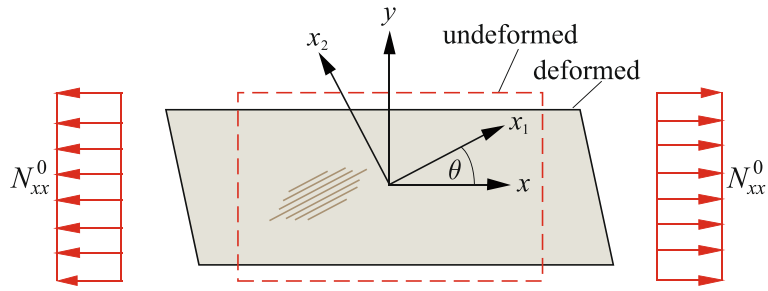


Fig. 7.8 Shear coupling at the example of an off-axis single layer

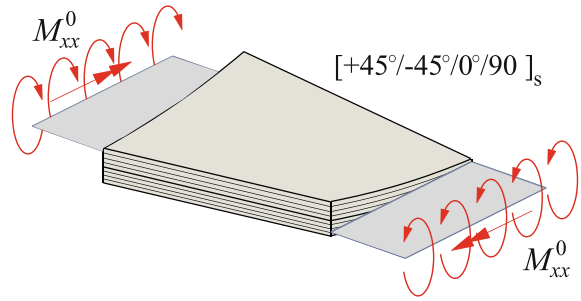


Fig. 7.9 Bending-twisting coupling at the example of a typical aircraft laminate

7.5.2 Bending-Twisting Coupling

Laminates exhibit bending-twisting coupling (Fig. 7.9) if the stiffnesses D_{16} and D_{26} are not equal to zero. The curvatures κ^0_{xx}, κ^0_{yy} of the laminate middle plane are then involved in generating the twisting moment M^0_{xy}. The twist κ^0_{xy} of the laminate middle plane, on the other hand, is then the cause of the two bending moments M^0_{xx} and M^0_{yy}.

7.5.3 Bending-Extension Coupling

A bending-extension coupling always occurs when one or more coupling stiffnesses B_{ij} are not equal to zero. The strains ε^0_{xx}, ε^0_{yy}, γ^0_{xy} of the laminate middle plane then cause the laminate moments M^0_{xx}, M^0_{yy}, M^0_{xy}. At the same time, the curvatures κ^0_{xx}, κ^0_{yy} and the twist κ^0_{xy} of the laminate middle plane cause the laminate forces N^0_{xx}, N^0_{yy}, N^0_{xy} to occur. Examples are given in Figs. 7.10 and 7.11. While the coupling stiffnesses B_{11} and B_{22} occur in the unsymmetric cross-ply laminate [0°/90°], the terms B_{16} and B_{26} are not equal to zero for the unsymmetric angle-ply laminate [±45°]. Bending-extension coupling can only occur for unsymmetric laminates. Conversely, this means that a symmetric laminate is always free of bending-extension coupling: $B_{ij} = 0$.

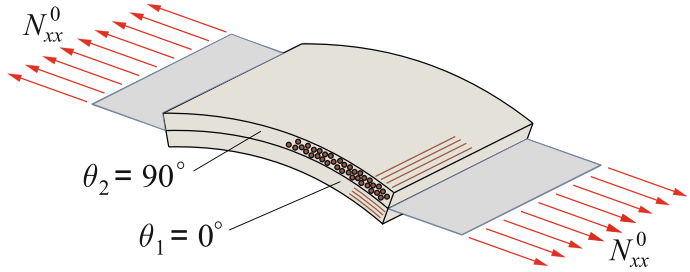


Fig. 7.10 Bending-extension coupling at the example of an unsymmetric cross-ply laminate

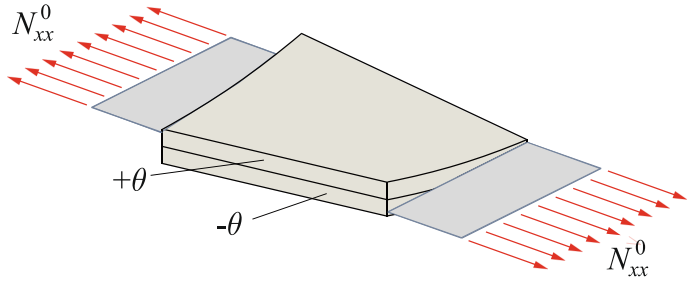


Fig. 7.11 Bending-extension coupling at the example of an unsymmetric angle-ply laminate

7.5.4 Remarks on Coupling Effects

Coupling effects are generally undesirable side effects that are a speciality when dealing with laminated structures and do not occur, for example, in homogeneous isotropic structures such as an aluminium plate. On the one hand, coupling effects sometimes make it considerably more difficult to analyze a laminate structure, especially if one is interested in simple analytical calculation methods, which are essential in practical engineering work. On the other hand, coupling effects can sometimes have serious weakening effects on the mechanical behaviour of a laminate.

As an example, consider a laminate that is under a compressive load N_{xx}^0. If the laminate is symmetric, a pure normal strain state ε_{xx}^0, ε_{yy}^0 will occur under the compressive load (whereby it is assumed here that the laminate is balanced so that no shear strain γ_{xy}^0 occurs). The curvatures κ_{xx}^0, κ_{yy}^0 and the twist κ_{xy}^0 will only occur from the load level at which the buckling load of the laminate is exceeded. If, on the other hand, the laminate is unsymmetric, no matter how small the load, it will cause curvatures κ_{xx}^0, κ_{yy}^0 and/or a twist κ_{xy}^0. For this specific case, it can therefore be stated that an unsymmetric laminate potentially behaves more compliant than a similar symmetric laminate will.

However, there are also examples where coupling effects can have a favourable effect. If we look again at the buckling behaviour of a laminate, but this time under an inplane shear load, the bending-twisting coupling can have both an advantageous and a disadvantageous

effect on the level of the achievable buckling load, which basically depends on the individual layup of the laminate. This is explained in more detail in the relevant sections of this book on the buckling of laminates.

It is therefore always at the discretion of the user to decide whether coupling effects can be tolerated, whether they must be completely avoided, or whether they may even be desirable.

7.6 Special Laminates

The case of a fully populated laminate stiffness matrix in the constitutive law is rather rare in practical application. In many cases, the constitutive law is considerably simplified.

7.6.1 Isotropic Single Layer

In the case of an isotropic single layer (which corresponds to an isotropic plate or disk), the stiffness matrix is considerably simplified:

$$\begin{bmatrix} \underline{\underline{A}} & \underline{\underline{B}} \\ \underline{\underline{B}} & \underline{\underline{D}} \end{bmatrix} = \begin{bmatrix} A_{11} & A_{12} & 0 & 0 & 0 & 0 \\ A_{12} & A_{22} & 0 & 0 & 0 & 0 \\ 0 & 0 & A_{66} & 0 & 0 & 0 \\ 0 & 0 & 0 & D_{11} & D_{12} & 0 \\ 0 & 0 & 0 & D_{12} & D_{22} & 0 \\ 0 & 0 & 0 & 0 & 0 & D_{66} \end{bmatrix}. \tag{7.29}$$

Such a surface structure is therefore free of all laminate-specific coupling effects, so there is no shear coupling, no bending-extension coupling and no bending-twisting coupling.

The individual entries of the stiffness matrix in (7.29) can be further specified using the engineering constants E, G and ν:

$$\begin{aligned} A_{11} &= Q_{11}h = \frac{Eh}{1-\nu^2}, \quad A_{22} = Q_{22}h = \frac{Eh}{1-\nu^2}, \\ A_{12} &= Q_{12}h = \frac{\nu Eh}{1-\nu^2}, \quad A_{66} = Q_{66}h = Gh, \\ D_{11} &= Q_{11}\frac{h^3}{12} = \frac{Eh^3}{12\left(1-\nu^2\right)}, \quad D_{22} = Q_{22}\frac{h^3}{12} = \frac{Eh^3}{12\left(1-\nu^2\right)}, \\ D_{12} &= Q_{12}\frac{h^3}{12} = \frac{\nu Eh^3}{12\left(1-\nu^2\right)}, \quad D_{66} = Q_{66}\frac{h^3}{12} = \frac{Gh^3}{12}. \end{aligned} \tag{7.30}$$

7.6.2 Orthotropic Single Layer

An orthotropic single layer shows the same assignment of the stiffness matrix as in (7.29), but the engineering constants E_{11}, E_{22}, ν_{12}, ν_{21} and G_{12} must now be taken into account in the individual components in $\underline{\underline{A}}$ and $\underline{\underline{D}}$:

$$\begin{aligned}
A_{11} &= Q_{11}h = \frac{E_{11}h}{1-\nu_{12}\nu_{21}}, \quad A_{22} = Q_{22}h = \frac{E_{22}h}{1-\nu_{12}\nu_{21}}, \\
A_{12} &= Q_{12}h = \frac{\nu_{12}E_{22}h}{1-\nu_{12}\nu_{21}}, \quad A_{66} = Q_{66}h = G_{12}h, \\
D_{11} &= Q_{11}\frac{h^3}{12} = \frac{E_{11}h^3}{12\,(1-\nu_{12}\nu_{21})}, \quad D_{22} = Q_{22}\frac{h^3}{12} = \frac{E_{22}h^3}{12\,(1-\nu_{12}\nu_{21})}, \\
D_{12} &= Q_{12}\frac{h^3}{12} = \frac{\nu_{12}E_{22}h^3}{12\,(1-\nu_{12}\nu_{21})}, \quad D_{66} = Q_{66}\frac{h^3}{12} = \frac{G_{12}h^3}{12}.
\end{aligned} \tag{7.31}$$

7.6.3 Anisotropic Single Layer/Off-Axis Single Layer

The following population of the stiffness matrix results for an anisotropic single layer:

$$\begin{bmatrix} \underline{\underline{A}} & \underline{\underline{B}} \\ \underline{\underline{B}} & \underline{\underline{D}} \end{bmatrix} = \begin{bmatrix} A_{11} & A_{12} & A_{16} & 0 & 0 & 0 \\ A_{12} & A_{22} & A_{26} & 0 & 0 & 0 \\ A_{16} & A_{26} & A_{66} & 0 & 0 & 0 \\ 0 & 0 & 0 & D_{11} & D_{12} & D_{16} \\ 0 & 0 & 0 & D_{12} & D_{22} & D_{26} \\ 0 & 0 & 0 & D_{16} & D_{26} & D_{66} \end{bmatrix}. \tag{7.32}$$

Although an anisotropic single layer does not exhibit bending-extension coupling, both shear coupling and bending-twisting coupling generally occur. The individual terms in (7.32) can be written as follows:

$$A_{ij} = \bar{Q}_{ij}h, \quad D_{ij} = \bar{Q}_{ij}\frac{h^3}{12}. \tag{7.33}$$

7.6.4 Symmetric Laminates

A symmetric laminate is always free of bending-extension coupling. However, both shear coupling and bending-twisting coupling cannot be ruled out from the outset for an arbitrary laminate:

$$\begin{bmatrix} \underline{\underline{A}} & \underline{\underline{B}} \\ \underline{\underline{B}} & \underline{\underline{D}} \end{bmatrix} = \begin{bmatrix} A_{11} & A_{12} & A_{16} & 0 & 0 & 0 \\ A_{12} & A_{22} & A_{26} & 0 & 0 & 0 \\ A_{16} & A_{26} & A_{66} & 0 & 0 & 0 \\ 0 & 0 & 0 & D_{11} & D_{12} & D_{16} \\ 0 & 0 & 0 & D_{12} & D_{22} & D_{26} \\ 0 & 0 & 0 & D_{16} & D_{26} & D_{66} \end{bmatrix}. \tag{7.34}$$

7.6.5 Cross-Ply Laminates

A cross-ply laminate consists of layers with the orientation angles $\theta_k = 0°$ or $\theta_k = 90°$. Such laminates are always balanced (shear coupling terms $A_{16} = A_{26} = 0$) and free of bending-twisting coupling, i.e. $D_{16} = D_{26} = 0$. Whether a cross-ply laminate exhibits bending-extension coupling depends on whether it has symmetry properties or not.

An example of an unsymmetric cross-ply laminate is the $[0°/90°]$ laminate. In this case, the laminate stiffness matrix is populated as follows:

$$\begin{bmatrix} \underline{\underline{A}} & \underline{\underline{B}} \\ \underline{\underline{B}} & \underline{\underline{D}} \end{bmatrix} = \begin{bmatrix} A_{11} & A_{12} & 0 & B_{11} & 0 & 0 \\ A_{12} & A_{22} & 0 & 0 & -B_{11} & 0 \\ 0 & 0 & A_{66} & 0 & 0 & 0 \\ B_{11} & 0 & 0 & D_{11} & D_{12} & 0 \\ 0 & -B_{11} & 0 & D_{12} & D_{22} & 0 \\ 0 & 0 & 0 & 0 & 0 & D_{66} \end{bmatrix}. \tag{7.35}$$

A symmetric cross-ply laminate of the type $[0°/90°]_S$, on the other hand, is free of any bending-extension coupling, and the following remains:

$$\begin{bmatrix} \underline{\underline{A}} & \underline{\underline{B}} \\ \underline{\underline{B}} & \underline{\underline{D}} \end{bmatrix} = \begin{bmatrix} A_{11} & A_{12} & 0 & 0 & 0 & 0 \\ A_{12} & A_{22} & 0 & 0 & 0 & 0 \\ 0 & 0 & A_{66} & 0 & 0 & 0 \\ 0 & 0 & 0 & D_{11} & D_{12} & 0 \\ 0 & 0 & 0 & D_{12} & D_{22} & 0 \\ 0 & 0 & 0 & 0 & 0 & D_{66} \end{bmatrix}. \tag{7.36}$$

7.6.6 Angle-Ply Laminates

An angle-ply laminate is a laminate in which for every layer with the angle θ there is a layer with the opposite angle $-\theta$. Such laminates are always balanced ($A_{16} = A_{26} = 0$). Whether

bending-twisting coupling and/or bending-extension coupling occur depends on the specific laminate layup.

An example of an unsymmetric angle-ply laminate is a laminate of the type $[\pm\theta]$. The laminate stiffness matrix has the following assignment here:

$$\begin{bmatrix} \underline{\underline{A}} & \underline{\underline{B}} \\ \underline{\underline{B}} & \underline{\underline{D}} \end{bmatrix} = \begin{bmatrix} A_{11} & A_{12} & 0 & 0 & 0 & B_{16} \\ A_{12} & A_{22} & 0 & 0 & 0 & B_{26} \\ 0 & 0 & A_{66} & B_{16} & B_{26} & 0 \\ 0 & 0 & B_{16} & D_{11} & D_{12} & 0 \\ 0 & 0 & B_{26} & D_{12} & D_{22} & 0 \\ B_{16} & B_{26} & 0 & 0 & 0 & D_{66} \end{bmatrix}. \tag{7.37}$$

Interestingly, such a laminate is free of bending-twisting coupling ($D_{16} = D_{26} = 0$), but exhibits the bending-extension coupling terms B_{16} and B_{26}.

A symmetric angle-ply laminate of the type $[\pm\theta]_S$ is naturally free of any bending-extension coupling, but bending-twisting coupling does occur:

$$\begin{bmatrix} \underline{\underline{A}} & \underline{\underline{B}} \\ \underline{\underline{B}} & \underline{\underline{D}} \end{bmatrix} = \begin{bmatrix} A_{11} & A_{12} & 0 & 0 & 0 & 0 \\ A_{12} & A_{22} & 0 & 0 & 0 & 0 \\ 0 & 0 & A_{66} & 0 & 0 & 0 \\ 0 & 0 & 0 & D_{11} & D_{12} & D_{16} \\ 0 & 0 & 0 & D_{12} & D_{22} & D_{26} \\ 0 & 0 & 0 & D_{16} & D_{26} & D_{66} \end{bmatrix}. \tag{7.38}$$

7.6.7 Quasi-isotropic Laminate

Quasi-isotropic laminates are widely used in aircraft construction, for example, and are laminates whose membrane quadrant has isotropic properties. The following then applies: $A_{11} = A_{22}$ and $A_{66} = \frac{1}{2}(A_{11} - A_{12})$. If the laminate is symmetric, the following population of the laminate stiffness matrix results:

$$\begin{bmatrix} \underline{\underline{A}} & \underline{\underline{B}} \\ \underline{\underline{B}} & \underline{\underline{D}} \end{bmatrix} = \begin{bmatrix} A_{11} & A_{12} & 0 & 0 & 0 & 0 \\ A_{12} & A_{11} & 0 & 0 & 0 & 0 \\ 0 & 0 & \frac{1}{2}(A_{11} - A_{12}) & 0 & 0 & 0 \\ 0 & 0 & 0 & D_{11} & D_{12} & D_{16} \\ 0 & 0 & 0 & D_{12} & D_{22} & D_{26} \\ 0 & 0 & 0 & D_{16} & D_{26} & D_{66} \end{bmatrix}. \tag{7.39}$$

Quasi-isotropic laminates are also always balanced and therefore free of shear coupling. However, it is very important to note that the term ‘quasi-isotropy’ only refers to the membrane quadrant and no conclusions can be drawn from this about the properties of

the plate quadrant which generally remains anisotropic in its properties, i.e. $D_{11} \neq D_{22}$. In addition, bending-twisting coupling cannot generally be ruled out, which generally means $D_{16}, D_{26} \neq 0$. Whether a quasi-isotropic laminate shows bending-extension coupling depends on its symmetry properties.

Examples for quasi-isotropic laminates are $[-60°/0°/60°]$, $[-60°/0°/60°]_S$, $[0°/\pm 45°/90°]$, $[0°/\pm 45°/90°]_S$, $[0°/-36°/-72°/36°/72°]$, and many more.

7.7 Change of the Reference Plane

Many technical applications involve joining two laminated components together. The question then arises as to how the different middle planes of the laminate structures involved can be mathematically connected. This can be done by shifting the reference plane of one of the two components or of both components (see Fig. 7.12). We will now consider the case where the location $z = 0$ is not the location of the laminate middle plane, but rather the laminate middle plane is shifted by the amount d, and we will clarify how the laminate stiffness matrix can be calculated in this case. The relationship $\bar{z} = z + d$ applies between the shifted axis $\bar{z}$ and the original axis z.

Firstly, the resulting laminate forces are considered:

$$\begin{aligned}\begin{pmatrix} N_{xx}^0 \\ N_{yy}^0 \\ N_{xy}^0 \end{pmatrix} &= \int_{d-\frac{h}{2}}^{d+\frac{h}{2}} \begin{bmatrix} \bar{Q}_{11} & \bar{Q}_{12} & \bar{Q}_{16} \\ \bar{Q}_{12} & \bar{Q}_{22} & \bar{Q}_{26} \\ \bar{Q}_{16} & \bar{Q}_{26} & \bar{Q}_{66} \end{bmatrix} \left[\begin{pmatrix} \varepsilon_{xx}^0 \\ \varepsilon_{yy}^0 \\ \gamma_{xy}^0 \end{pmatrix} + \bar{z} \begin{pmatrix} \kappa_{xx}^0 \\ \kappa_{yy}^0 \\ \kappa_{xy}^0 \end{pmatrix} \right] \mathrm{d}\bar{z} \\ &= \int_{d-\frac{h}{2}}^{d+\frac{h}{2}} \underline{\underline{\bar{Q}}} \left(\underline{\varepsilon}^0 + \bar{z}\underline{\kappa}^0 \right) \mathrm{d}\bar{z} = \int_{-\frac{h}{2}}^{+\frac{h}{2}} \underline{\underline{\bar{Q}}} \underline{\varepsilon}^0 \mathrm{d}z + \int_{-\frac{h}{2}}^{+\frac{h}{2}} \underline{\underline{\bar{Q}}} \, (z+d) \, \underline{\kappa}^0 \mathrm{d}z. \end{aligned} \tag{7.40}$$

In the last two integral expressions, both the membrane stiffness matrix $\underline{\underline{A}}$ and the coupling stiffness matrix $\underline{\underline{B}}$ appear, so that the following result is obtained:

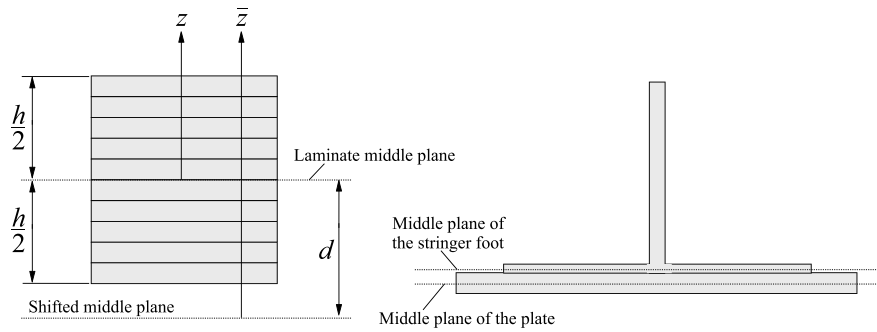


Fig. 7.12 Shift of the reference plane of a laminate (left), application: panel with stringer (right)

$$\underline{N} = \begin{pmatrix} N_{xx}^0 \\ N_{yy}^0 \\ N_{xy}^0 \end{pmatrix} = \begin{bmatrix} A_{11} & A_{12} & A_{16} \\ A_{12} & A_{22} & A_{26} \\ A_{16} & A_{26} & A_{66} \end{bmatrix} \begin{pmatrix} \varepsilon_{xx}^0 \\ \varepsilon_{yy}^0 \\ \gamma_{xy}^0 \end{pmatrix} + \left[\begin{bmatrix} B_{11} & B_{12} & B_{16} \\ B_{12} & B_{22} & B_{26} \\ B_{16} & B_{26} & B_{66} \end{bmatrix} + d \begin{bmatrix} A_{11} & A_{12} & A_{16} \\ A_{12} & A_{22} & A_{26} \\ A_{16} & A_{26} & A_{66} \end{bmatrix} \right] \begin{pmatrix} \kappa_{xx}^0 \\ \kappa_{yy}^0 \\ \kappa_{xy}^0 \end{pmatrix} = \underline{\underline{A}}\,\underline{\varepsilon}^0 + \left(\underline{\underline{B}} + d\,\underline{\underline{A}} \right) \underline{\kappa}^0. \tag{7.41}$$

The same procedure can be used to determine the laminate moments:

$$\begin{aligned} \underline{M} = \begin{pmatrix} M_{xx}^0 \\ M_{yy}^0 \\ M_{xy}^0 \end{pmatrix} &= \int_{d-\frac{h}{2}}^{d+\frac{h}{2}} \begin{bmatrix} \bar{Q}_{11} & \bar{Q}_{12} & \bar{Q}_{16} \\ \bar{Q}_{12} & \bar{Q}_{22} & \bar{Q}_{26} \\ \bar{Q}_{16} & \bar{Q}_{26} & \bar{Q}_{66} \end{bmatrix} \left[\begin{pmatrix} \varepsilon_{xx}^0 \\ \varepsilon_{yy}^0 \\ \gamma_{xy}^0 \end{pmatrix} + \bar{z} \begin{pmatrix} \kappa_{xx}^0 \\ \kappa_{yy}^0 \\ \kappa_{xy}^0 \end{pmatrix} \right] \bar{z}\,\mathrm{d}\bar{z} \\ &= \int_{d-\frac{h}{2}}^{d+\frac{h}{2}} \underline{\underline{\bar{Q}}} \left(\underline{\varepsilon}^0 + \bar{z}\underline{\kappa}^0 \right) \bar{z}\,\mathrm{d}\bar{z} \\ &= \int_{-\frac{h}{2}}^{+\frac{h}{2}} \underline{\underline{\bar{Q}}}\underline{\varepsilon}^0 \,(z+d)\,\mathrm{d}z + \int_{-\frac{h}{2}}^{+\frac{h}{2}} \underline{\underline{\bar{Q}}}\underline{\kappa}^0 \,(z+d)^2\,\mathrm{d}z. \end{aligned} \tag{7.42}$$

The following representation is obtained for the laminate moments:

$$\underline{M} = \left(\underline{\underline{B}} + d\,\underline{\underline{A}} \right) \underline{\varepsilon}^0 + \left(\underline{\underline{D}} + 2d\,\underline{\underline{B}} + \mathrm{d}^2\,\underline{\underline{A}} \right) \underline{\kappa}^0. \tag{7.43}$$

Thus, for the case of the laminate middle plane shifted by the amount d, the constitutive law for the laminate can be written as:

$$\begin{pmatrix} \underline{N} \\ \underline{M} \end{pmatrix} = \begin{bmatrix} \underline{\underline{A}} & \left(\underline{\underline{B}} + d\,\underline{\underline{A}} \right) \\ \left(\underline{\underline{B}} + d\,\underline{\underline{A}} \right) & \left(\underline{\underline{D}} + 2d\,\underline{\underline{B}} + \mathrm{d}^2\,\underline{\underline{A}} \right) \end{bmatrix} \begin{pmatrix} \underline{\varepsilon}^0 \\ \underline{\kappa}^0 \end{pmatrix}. \tag{7.44}$$

7.8 Effective Properties of Laminates

For practical application, it is often necessary to make statements about the engineering constants E_{xx}, E_{yy}, G_{xy} and ν_{xy} of a laminate. The following shows how these so-called effective properties can be calculated from the entries of the laminate stiffness matrix.

For the sake of simplicity, only symmetric laminates that have no shear coupling and no bending-twisting coupling will be considered in this section. The laminate stiffness matrix is then described by (7.36). However, the extension to laminate structures that exhibit coupling effects is easily possible in the same way.

7.8.1 Inplane Modulus of Elasticity E_{xx}

A laminate is considered under a uniaxial load N^0_{xx}. The laminate internal forces N^0_{yy} and N^0_{xy} are zero:

$$\begin{pmatrix} N^0_{xx} \\ 0 \\ 0 \end{pmatrix} = \begin{bmatrix} A_{11} & A_{12} & 0 \\ A_{12} & A_{22} & 0 \\ 0 & 0 & A_{66} \end{bmatrix} \begin{pmatrix} \varepsilon^0_{xx} \\ \varepsilon^0_{yy} \\ \gamma^0_{xy} \end{pmatrix}. \tag{7.45}$$

From the second equation we obtain:

$$\varepsilon^0_{yy} = -\frac{A_{12}}{A_{22}} \varepsilon^0_{xx}. \tag{7.46}$$

Inserting this into the first equation yields

$$N^0_{xx} = A_{11}\varepsilon^0_{xx} - \frac{A^2_{12}}{A_{22}} \varepsilon^0_{xx} = \left(A_{11} - \frac{A^2_{12}}{A_{22}} \right) \varepsilon^0_{xx}. \tag{7.47}$$

If this expression is divided by the laminate thickness h, the corresponding stress σ_{xx} is obtained:

$$\sigma_{xx} = \frac{N^0_{xx}}{h} = \frac{1}{h} \left(A_{11} - \frac{A^2_{12}}{A_{22}} \right) \varepsilon^0_{xx}. \tag{7.48}$$

If we compare this expression for the stress σ_{xx} with Hooke's law $\sigma_{xx} = E_{xx}\varepsilon_{xx}$, we can determine the effective plane modulus of elasticity for the laminate:

$$E_{xx} = \frac{1}{h} \left(A_{11} - \frac{A^2_{12}}{A_{22}} \right). \tag{7.49}$$

7.8.2 Inplane Modulus of Elasticity E_{yy}

The procedure for determining the effective modulus of elasticity E_{yy} is analogous to the calculation of E_{xx}. Starting from

$$\begin{pmatrix} 0 \\ N^0_{yy} \\ 0 \end{pmatrix} = \begin{bmatrix} A_{11} & A_{12} & 0 \\ A_{12} & A_{22} & 0 \\ 0 & 0 & A_{66} \end{bmatrix} \begin{pmatrix} \varepsilon^0_{xx} \\ \varepsilon^0_{yy} \\ \gamma^0_{xy} \end{pmatrix}, \tag{7.50}$$

we obtain from the first equation:

$$\varepsilon^0_{xx} = -\frac{A_{12}}{A_{11}} \varepsilon^0_{yy}. \tag{7.51}$$

Inserting into the second equation yields:

$$N_{yy}^0 = -\frac{A_{12}^2}{A_{11}}\varepsilon_{yy}^0 + A_{22}\varepsilon_{yy}^0 = \left(A_{22} - \frac{A_{12}^2}{A_{11}}\right)\varepsilon_{yy}^0. \tag{7.52}$$

Division by the laminate thickness h and comparison with Hooke's law yields the following expression for the effective inplane modulus of elasticity E_{yy} of the laminate:

$$E_{yy} = \frac{1}{h}\left(A_{22} - \frac{A_{12}^2}{A_{11}}\right). \tag{7.53}$$

7.8.3 Inplane Shear Modulus G_{xy}

If we now consider the laminate under a plane shear force N_{xy}^0 and assume

$$\begin{pmatrix} 0 \\ 0 \\ N_{xy}^0 \end{pmatrix} = \begin{bmatrix} A_{11} & A_{12} & 0 \\ A_{12} & A_{22} & 0 \\ 0 & 0 & A_{66} \end{bmatrix} \begin{pmatrix} \varepsilon_{xx}^0 \\ \varepsilon_{yy}^0 \\ \gamma_{xy}^0 \end{pmatrix}, \tag{7.54}$$

then the third equation gives:

$$N_{xy}^0 = A_{66}\gamma_{xy}^0. \tag{7.55}$$

If this expression is divided by the laminate thickness h, the associated shear stress τ_{xy} is obtained:

$$\tau_{xy} = \frac{A_{66}}{h}\gamma_{xy}^0. \tag{7.56}$$

The comparison with Hooke's law $\tau_{xy} = G_{xy}\gamma_{xy}$ then leads to the following effective shear modulus of the laminate:

$$G_{xy} = \frac{A_{66}}{h}. \tag{7.57}$$

7.8.4 Inplane Poisson's Ratio ν_{xy}

A laminate under uniaxial stress N_{xx}^0 is now considered again:

$$\begin{pmatrix} N_{xx}^0 \\ 0 \\ 0 \end{pmatrix} = \begin{bmatrix} A_{11} & A_{12} & 0 \\ A_{12} & A_{22} & 0 \\ 0 & 0 & A_{66} \end{bmatrix} \begin{pmatrix} \varepsilon_{xx}^0 \\ \varepsilon_{yy}^0 \\ \gamma_{xy}^0 \end{pmatrix}. \tag{7.58}$$

By definition, the following applies to the Poisson's ratio ν_{xy}:

$$\nu_{xy} = -\frac{\varepsilon_{yy}^0}{\varepsilon_{xx}^0}. \tag{7.59}$$

The following expressions for the strains ε^0_{xx} and ε^0_{yy} of the laminate middle plane are obtained from the above constitutive law:

$$\varepsilon^0_{xx} = N^0_{xx}\frac{A_{22}}{A_{11}A_{22} - A_{12}^2}, \quad \varepsilon^0_{yy} = -N^0_{xx}\frac{A_{12}}{A_{11}A_{22} - A_{12}^2}. \tag{7.60}$$

This results in the inplane Poisson's ratio ν_{xy} of the laminate:

$$\nu_{xy} = -\frac{\varepsilon^0_{yy}}{\varepsilon^0_{xx}} = \frac{A_{12}}{A_{22}}. \tag{7.61}$$

7.8.5 Modulus of Elasticity $E_{xx,B}$ Under Bending

It is important to distinguish between membrane stress and bending stress when determining an effective modulus of elasticity. If a symmetric laminate without bending-twisting coupling is considered under the bending moment M^0_{xx}, then the constitutive law reads:

$$\begin{pmatrix} M^0_{xx} \\ 0 \\ 0 \end{pmatrix} = \begin{bmatrix} D_{11} & D_{12} & 0 \\ D_{12} & D_{22} & 0 \\ 0 & 0 & D_{66} \end{bmatrix} \begin{pmatrix} \kappa^0_{xx} \\ \kappa^0_{yy} \\ \kappa^0_{xy} \end{pmatrix}. \tag{7.62}$$

From the second equation follows:

$$D_{12}\kappa^0_{xx} + D_{22}\kappa^0_{yy} = 0. \tag{7.63}$$

Solving for κ^0_{yy} and inserting into the first equation gives:

$$M^0_{xx} = D_{11}\kappa^0_{xx} - \frac{D_{12}^2}{D_{22}}\kappa^0_{xx} = \left(D_{11} - \frac{D_{12}^2}{D_{22}}\right)\kappa^0_{xx} = -\left(D_{11} - \frac{D_{12}^2}{D_{22}}\right)\frac{\partial^2 w_0}{\partial x^2}. \tag{7.64}$$

If we compare this expression with the differential equation of the elastic line of the Euler-Bernoulli beam $-EI\frac{\mathrm{d}^2 w}{\mathrm{d}x^2} = M$, we obtain the following result:

$$E_{xx,B}I = D_{11} - \frac{D_{12}^2}{D_{22}}, \tag{7.65}$$

where $I = \frac{h^3}{12}$ is the moment of inertia of the laminate cross-section per unit length. The effective modulus of elasticity $E_{xx,B}$ of the laminate under bending is then

$$E_{xx,B} = \frac{1}{I}\left(D_{11} - \frac{D_{12}^2}{D_{22}}\right) = \frac{12}{h^3}\left(D_{11} - \frac{D_{12}^2}{D_{22}}\right). \tag{7.66}$$

7.8.6 Modulus of Elasticity $E_{yy,B}$ Under Bending

The derivation of an expression for $E_{yy,B}$ is analogous to that for $E_{xx,B}$. It follows:

$$E_{yy,B} = \frac{12}{h^3}\left(D_{22} - \frac{D_{12}^2}{D_{11}}\right). \tag{7.67}$$

With regard to the effective properties E_{xx}, E_{yy}, $E_{xx,B}$ and $E_{yy,B}$, a few comments are necessary. In general, the anisotropy of a laminate will not only cause the effective properties E_{xx} and E_{yy} to differ from each other, but there will also be differences between the effective properties under pure membrane stress and pure bending. This is of course different for a purely isotropic structure, where the plane modulus of elasticity E and the modulus of elasticity under bending E_B are always the same and, of course, not direction-dependent.

To illustrate this, we consider two simple cross-ply laminates with the layups $[0°/90°]_S$ and $[90°/0°]_S$ (Fig. 7.13). If the two cross-ply laminates are subjected to a uniaxial force N_{xx}^0, it will be shown that the effective modulus of elasticity E_{xx} will be identical in both cases. In this case, the tensile stiffness is not influenced by the order of the layers. However, the behaviour will be different if the two laminates are considered under a bending moment M_{xx}^0. Here, not only will different values for the effective properties $E_{xx,B}$ result compared to the plane stiffnesses E_{xx}, but these will even be different for the two laminates under consideration. Specifically, it will turn out that $E_{xx,B}^{[0/90]_S} > E_{xx,B}^{[90/0]_S}$ applies. The reason for this is that the 0°-layers have a high stiffness, whereas the 90°-layers have a much lower stiffness in the x-direction in comparison. As the 0° layers in the $[0°/90°]_S$-laminate are on the outside, they have a correspondingly high lever arm to the laminate middle, which ensures a high bending stiffness of the laminate. In contrast, the 0°-layers in the $[90°/0°]_S$ cross-ply laminate are close to the laminate middle plane, so that their contribution to the bending stiffness is lower here. It can therefore be concluded that when determining the effective properties of a laminate, it may not only be necessary to differentiate according to the direction of the stress, but also carefully according to the type of stress.

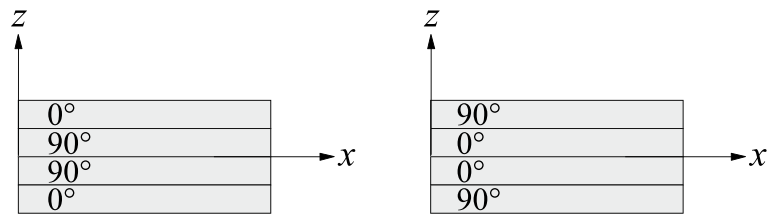


Fig. 7.13 Cross-ply laminates $[0°/90°]_S$ and $[90°/0°]_S$

7.8.7 Approximate Calculation of Effective Properties

The following approximate formulae are often used for pure inplane loading of symmetric cross-ply laminates:

$$E_{xx} = \frac{N_0}{N} E_{11} + \frac{N_{90}}{N} E_{22},$$
$$E_{yy} = \frac{N_{90}}{N} E_{11} + \frac{N_0}{N} E_{22}. \tag{7.68}$$

Here N, N_0, N_{90} are the total number of layers in the cross-ply laminate, as well as the number of 0°-layers and 90°-layers.

The following formulae are widely used for symmetric laminates of arbitrary layup:

$$E_{xx} = \frac{1}{N} \sum_{i=1}^{i=N} E_{xx,i},$$
$$E_{yy} = \frac{1}{N} \sum_{i=1}^{i=N} E_{yy,i}. \tag{7.69}$$

7.9 Strain Energy of a Laminate

For the application of energy-based methods for analyzing laminate problems, the strain energy or the internal potential Π_i is required. The strain energy Π_i is obtained from

$$\Pi_i = \frac{1}{2} \int \int \int_V \left(\sigma_{xx}\varepsilon_{xx} + \sigma_{yy}\varepsilon_{yy} + \sigma_{zz}\varepsilon_{zz} + \tau_{yz}\gamma_{yz} + \tau_{xz}\gamma_{xz} + \tau_{xy}\gamma_{xy} \right) \mathrm{d}V, \tag{7.70}$$

whereby in the context of Classical Laminated Plate Theory, only the following expression remains due to the assumed shear rigidity with respect to the thickness direction and the assumption of a plane stress state in the entire laminate:

$$\Pi_i = \frac{1}{2} \int \int \int_V \left(\sigma_{xx}\varepsilon_{xx} + \sigma_{yy}\varepsilon_{yy} + \tau_{xy}\gamma_{xy} \right) \mathrm{d}V. \tag{7.71}$$

If the strains are expressed according to the Classical Laminated Plate Theory

$$\varepsilon_{xx} = \frac{\partial u_0}{\partial x} - z\frac{\partial^2 w_0}{\partial x^2}, \quad \varepsilon_{yy} = \frac{\partial v_0}{\partial y} - z\frac{\partial^2 w_0}{\partial y^2}, \quad \gamma_{xy} = \frac{\partial u_0}{\partial y} + \frac{\partial v_0}{\partial x} - 2z\frac{\partial^2 w_0}{\partial x \partial y}, \tag{7.72}$$

then (7.71) transforms into:

$$\Pi_i = \frac{1}{2}\int\int\int_V \left[\sigma_{xx}\left(\frac{\partial u_0}{\partial x} - z\frac{\partial^2 w_0}{\partial x^2}\right) + \sigma_{yy}\left(\frac{\partial v_0}{\partial y} - z\frac{\partial^2 w_0}{\partial y^2}\right) + \tau_{xy}\left(\frac{\partial u_0}{\partial y} + \frac{\partial v_0}{\partial x} - 2z\frac{\partial^2 w_0}{\partial x \partial y}\right)\right] \mathrm{d}V. \tag{7.73}$$

If we split the volume integral in (7.73) into integrals with respect to x, y, z, we obtain:

$$\Pi_i = \frac{1}{2}\int_0^a \int_0^b \int_{-\frac{h}{2}}^{+\frac{h}{2}} \left[\sigma_{xx}\frac{\partial u_0}{\partial x} - \sigma_{xx} z\frac{\partial^2 w_0}{\partial x^2} + \sigma_{yy}\frac{\partial v_0}{\partial y} - \sigma_{yy} z\frac{\partial^2 w_0}{\partial y^2} + \tau_{xy}\left(\frac{\partial u_0}{\partial y} + \frac{\partial v_0}{\partial x}\right) - 2\tau_{xy} z\frac{\partial^2 w_0}{\partial x \partial y}\right] \mathrm{d}z\mathrm{d}y\mathrm{d}x. \tag{7.74}$$

Taking into account the definitions of the laminate internal forces and moments

$$\begin{pmatrix} N_{xx}^0 \\ N_{yy}^0 \\ N_{xy}^0 \end{pmatrix} = \int_{-\frac{h}{2}}^{+\frac{h}{2}} \begin{pmatrix} \sigma_{xx} \\ \sigma_{yy} \\ \tau_{xy} \end{pmatrix} \mathrm{d}z, \quad \begin{pmatrix} M_{xx}^0 \\ M_{yy}^0 \\ M_{xy}^0 \end{pmatrix} = \int_{-\frac{h}{2}}^{+\frac{h}{2}} \begin{pmatrix} \sigma_{xx} \\ \sigma_{yy} \\ \tau_{xy} \end{pmatrix} z\mathrm{d}z, \tag{7.75}$$

the integration prescribed in (7.74) can be carried out with respect to z, and we obtain in vector notation:

$$\Pi_i = \frac{1}{2}\int_0^b \int_0^a \begin{pmatrix} N_{xx}^0 \\ N_{yy}^0 \\ N_{xy}^0 \\ M_{xx}^0 \\ M_{yy}^0 \\ M_{xy}^0 \end{pmatrix}^T \begin{pmatrix} \frac{\partial u_0}{\partial x} \\ \frac{\partial v_0}{\partial y} \\ \frac{\partial u_0}{\partial y} + \frac{\partial v_0}{\partial x} \\ -\frac{\partial^2 w_0}{\partial x^2} \\ -\frac{\partial^2 w_0}{\partial y^2} \\ -2\frac{\partial^2 w_0}{\partial x \partial y} \end{pmatrix} \mathrm{d}x\mathrm{d}y. \tag{7.76}$$

Implementation of the constitutive law

$$\begin{pmatrix} N_{xx}^0 \\ N_{yy}^0 \\ N_{xy}^0 \\ M_{xx}^0 \\ M_{yy}^0 \\ M_{xy}^0 \end{pmatrix} = \begin{bmatrix} A_{11} & A_{12} & A_{16} & B_{11} & B_{12} & B_{16} \\ A_{12} & A_{22} & A_{26} & B_{12} & B_{22} & B_{26} \\ A_{16} & A_{26} & A_{66} & B_{16} & B_{26} & B_{66} \\ B_{11} & B_{12} & B_{16} & D_{11} & D_{12} & D_{16} \\ B_{12} & B_{22} & B_{26} & D_{12} & D_{22} & D_{26} \\ B_{16} & B_{26} & B_{66} & D_{16} & D_{26} & D_{66} \end{bmatrix} \begin{pmatrix} \frac{\partial u_0}{\partial x} \\ \frac{\partial v_0}{\partial y} \\ \frac{\partial u_0}{\partial y} + \frac{\partial v_0}{\partial x} \\ -\frac{\partial^2 w_0}{\partial x^2} \\ -\frac{\partial^2 w_0}{\partial y^2} \\ -2\frac{\partial^2 w_0}{\partial x \partial y} \end{pmatrix} \tag{7.77}$$

yields:

$$\Pi_i = \frac{1}{2}\int_0^b \int_0^a \begin{pmatrix} \frac{\partial u_0}{\partial x} \\ \frac{\partial v_0}{\partial y} \\ \frac{\partial u_0}{\partial y} + \frac{\partial v_0}{\partial x} \\ -\frac{\partial^2 w_0}{\partial x^2} \\ -\frac{\partial^2 w_0}{\partial y^2} \\ -2\frac{\partial^2 w_0}{\partial x \partial y} \end{pmatrix}^T \begin{bmatrix} A_{11} & A_{12} & A_{16} & B_{11} & B_{12} & B_{16} \\ A_{12} & A_{22} & A_{26} & B_{12} & B_{22} & B_{26} \\ A_{16} & A_{26} & A_{66} & B_{16} & B_{26} & B_{66} \\ B_{11} & B_{12} & B_{16} & D_{11} & D_{12} & D_{16} \\ B_{12} & B_{22} & B_{26} & D_{12} & D_{22} & D_{26} \\ B_{16} & B_{26} & B_{66} & D_{16} & D_{26} & D_{66} \end{bmatrix} \begin{pmatrix} \frac{\partial u_0}{\partial x} \\ \frac{\partial v_0}{\partial y} \\ \frac{\partial u_0}{\partial y} + \frac{\partial v_0}{\partial x} \\ -\frac{\partial^2 w_0}{\partial x^2} \\ -\frac{\partial^2 w_0}{\partial y^2} \\ -2\frac{\partial^2 w_0}{\partial x \partial y} \end{pmatrix} \mathrm{d}x\mathrm{d}y$$

$$= \frac{1}{2}\int_0^b \int_0^a \left[A_{11}\left(\frac{\partial u_0}{\partial x}\right)^2 + 2A_{12}\frac{\partial u_0}{\partial x}\frac{\partial v_0}{\partial y} + \cdots \right] \mathrm{d}x\mathrm{d}y, \tag{7.78}$$

or expanded:

$$\begin{aligned} \Pi_i = \frac{1}{2}\int_0^b \int_0^a \Bigg[& A_{11}\left(\frac{\partial u_0}{\partial x}\right)^2 + A_{22}\left(\frac{\partial v_0}{\partial y}\right)^2 + 2A_{12}\frac{\partial u_0}{\partial x}\frac{\partial v_0}{\partial y} \\ & + 2A_{16}\left(\frac{\partial u_0}{\partial y} + \frac{\partial v_0}{\partial x}\right)\frac{\partial u_0}{\partial x} + 2A_{26}\left(\frac{\partial u_0}{\partial y} + \frac{\partial v_0}{\partial x}\right)\frac{\partial v_0}{\partial y} \\ & + A_{66}\left[\left(\frac{\partial u_0}{\partial y}\right)^2 + 2\frac{\partial u_0}{\partial y}\frac{\partial v_0}{\partial x} + \left(\frac{\partial v_0}{\partial x}\right)^2\right] \\ & - 2B_{11}\frac{\partial u_0}{\partial x}\frac{\partial^2 w_0}{\partial x^2} - 2B_{22}\frac{\partial v_0}{\partial y}\frac{\partial^2 w_0}{\partial y^2} \\ & - 2B_{12}\left(\frac{\partial u_0}{\partial x}\frac{\partial^2 w_0}{\partial y^2} + \frac{\partial v_0}{\partial y}\frac{\partial^2 w_0}{\partial x^2}\right) \\ & - 2B_{16}\left[\left(\frac{\partial u_0}{\partial y} + \frac{\partial v_0}{\partial x}\right)\frac{\partial^2 w_0}{\partial x^2} + 2\frac{\partial u_0}{\partial x}\frac{\partial^2 w_0}{\partial x \partial y}\right] \\ & - 2B_{26}\left[\left(\frac{\partial u_0}{\partial y} + \frac{\partial v_0}{\partial x}\right)\frac{\partial^2 w_0}{\partial y^2} + 2\frac{\partial v_0}{\partial y}\frac{\partial^2 w_0}{\partial x \partial y}\right] \\ & - 4B_{66}\left(\frac{\partial u_0}{\partial y} + \frac{\partial v_0}{\partial x}\right)\frac{\partial^2 w_0}{\partial x \partial y} \\ & + D_{11}\left(\frac{\partial^2 w_0}{\partial x^2}\right)^2 + D_{22}\left(\frac{\partial^2 w_0}{\partial y^2}\right)^2 + 2D_{12}\frac{\partial^2 w_0}{\partial x^2}\frac{\partial^2 w_0}{\partial y^2} \\ & + \left(D_{16}\frac{\partial^2 w_0}{\partial x^2} + D_{26}\frac{\partial^2 w_0}{\partial y^2} + D_{66}\frac{\partial^2 w_0}{\partial x \partial y}\right)\frac{\partial^2 w_0}{\partial x \partial y} \Bigg] \mathrm{d}x\mathrm{d}y. \end{aligned} \tag{7.79}$$

The expressions (7.78) and (7.79) will be used for many applications in the remainder of this book.

7.10 Consideration of the Bending-Extension Coupling for Unsymmetric Laminates

The influence of the bending-extension coupling can be significant when analyzing an unsymmetric laminate. For example, a laminate problem with bending-extension coupling present will generally show larger deformations and thus lower stiffness compared to a similar but symmetric laminate. In addition, bending-extension coupling may be the reason why an unsymmetric laminate exhibits lower buckling loads and lower natural frequencies than a comparable laminate without bending-extension coupling. Naturally, the bending-extension coupling must therefore be suitably taken into account in the analysis. However—and this will be shown in the following chapters of this book—this sometimes causes considerable difficulties in the analysis, especially if one is interested in simple closed-form analytical methods that do not require a great deal of numerical effort. A good compromise for a whole series of practically relevant engineering problems has therefore proved to be the approximate consideration of the bending-extension coupling, which is based on the application of so-called 'reduced plate stiffnesses' and the analysis of a 'similar' symmetric laminate. This will be explained below. The starting point for the considerations is the constitutive law for the laminate according to

$$\begin{pmatrix} \underline{N}^0 \\ \underline{M}^0 \end{pmatrix} = \begin{bmatrix} \underline{\underline{A}} & \underline{\underline{B}} \\ \underline{\underline{B}} & \underline{\underline{D}} \end{bmatrix} \begin{pmatrix} \underline{\varepsilon}^0 \\ \underline{\kappa}^0 \end{pmatrix}. \tag{7.80}$$

The following applies to the laminate forces:

$$\underline{N}^0 = \underline{\underline{A}}\,\underline{\varepsilon}^0 + \underline{\underline{B}}\,\underline{\kappa}^0. \tag{7.81}$$

If this expression is solved for the strains of the laminate middle plane, the result is

$$\underline{\varepsilon}^0 = \underline{\underline{A}}^{-1}\underline{N}^0 - \underline{\underline{A}}^{-1}\underline{\underline{B}}\,\underline{\kappa}^0. \tag{7.82}$$

If this is used in the laminate moments, the result is

$$\begin{aligned} \underline{M}^0 &= \underline{\underline{B}}\,\underline{\varepsilon}^0 + \underline{\underline{D}}\,\underline{\kappa}^0 \\ &= \underline{\underline{B}}\left(\underline{\underline{A}}^{-1}\underline{N}^0 - \underline{\underline{A}}^{-1}\underline{\underline{B}}\,\underline{\kappa}^0\right) + \underline{\underline{D}}\,\underline{\kappa}^0 \\ &= \underline{\underline{B}}\,\underline{\underline{A}}^{-1}\underline{N}^0 + \left(\underline{\underline{D}} - \underline{\underline{B}}\,\underline{\underline{A}}^{-1}\underline{\underline{B}}\right)\underline{\kappa}^0. \end{aligned} \tag{7.83}$$

This allows the constitutive law (7.80) to be written in partially inverted form as:

$$\begin{pmatrix} \underline{\varepsilon}^0 \\ \underline{M}^0 \end{pmatrix} = \begin{bmatrix} \underline{\underline{\widehat{A}}} & \underline{\underline{\widehat{B}}} \\ \underline{\underline{\widehat{B}}} & \underline{\underline{\widehat{D}}} \end{bmatrix} \begin{pmatrix} \underline{N}^0 \\ \underline{\kappa}^0 \end{pmatrix}, \tag{7.84}$$

wherein:

$$\underline{\underline{\widehat{A}}} = \underline{\underline{A}}^{-1}, \quad \underline{\underline{\widehat{B}}} = -\underline{\underline{A}}^{-1}\underline{\underline{B}}, \quad \underline{\underline{\widehat{D}}} = \underline{\underline{D}} - \underline{\underline{B}}\,\underline{\underline{A}}^{-1}\underline{\underline{B}}. \tag{7.85}$$

The strain energy Π_i can be represented as:

$$\Pi_i = \frac{1}{2}\int_0^b \int_0^a \left(N_{xx}^0 \varepsilon_{xx}^0 + N_{yy}^0 \varepsilon_{yy}^0 + N_{xy}^0 \gamma_{xy}^0 + M_{xx}^0 \kappa_{xx}^0 + M_{yy}^0 \kappa_{yy}^0 + M_{xy}^0 \kappa_{xy}^0 \right) \mathrm{d}x\mathrm{d}y. \tag{7.86}$$

If the strains of the laminate middle plane and the laminate moments according to (7.84) are used, it results that all terms associated with the partially inverted coupling stiffnesses are removed from the strain energy and the following expression remains:

$$\begin{aligned}\Pi_i = \frac{1}{2}\int_0^b \int_0^a \Big(& \widehat{A}_{11} {N_{xx}^0}^2 + \widehat{A}_{22} {N_{yy}^0}^2 + \widehat{A}_{66} {N_{xy}^0}^2 + 2\widehat{A}_{12} N_{xx}^0 N_{yy}^0 + 2\widehat{A}_{16} N_{xx}^0 N_{xy}^0 \\ & + 2\widehat{A}_{26} N_{yy}^0 N_{xy}^0 + \widehat{D}_{11} {\kappa_{xx}^0}^2 + \widehat{D}_{22} {\kappa_{yy}^0}^2 + \widehat{D}_{66} {\kappa_{xy}^0}^2 + 2\widehat{D}_{12} \kappa_{xx}^0 \kappa_{yy}^0 \\ & + 2\widehat{D}_{16} \kappa_{xx}^0 \kappa_{xy}^0 + 2\widehat{D}_{26} \kappa_{yy}^0 \kappa_{xy}^0 \Big) \mathrm{d}x\mathrm{d}y. \end{aligned} \tag{7.87}$$

It can therefore be seen that it has no influence on the energy balance of the laminate whether the partially inverted coupling stiffnesses $\underline{\underline{\widehat{B}}}$ are taken into account or not, so that an unsymmetric laminate can be regarded as a symmetric laminate to a good approximation when the plate stiffnesses $\underline{\underline{D}}$ are replaced by the 'reduced plate stiffnesses'

$$\underline{\underline{\widehat{D}}} = \underline{\underline{D}} - \underline{\underline{B}}\,\underline{\underline{A}}^{-1}\,\underline{\underline{B}}. \tag{7.88}$$

In fact, many examples from engineering practice show that good results are often achieved with this concept.

References

Altenbach H, Altenbach J, Rikards R (1996): *Einführung in die Mechanik der Laminat- und Sandwichtragwerke*, Deutscher Verlag der Grundstoffindustrie, Stuttgart, Germany.

Altenbach H, Altenbach J, Naumenko K (1998): *Ebene Flächentragwerke*, Springer Verlag, Berlin et al., Germany.

Ambartsumyan SA (1970): *Theory of anisotropic plates*, Technomic Publishing Co., Inc., Stamford, USA.

Ashton JE, Whitney JM (1970): *Theory of laminated plates*, Technomic Publishing Co., Inc., Stamford, USA.

Bert CW (1975): *Analysis of plates*, in: Composite materials, volume 7, Structural design and analysis, part I, Academic Press, New York et al., USA.

Frick A, Klamser H (1990): *Untersuchung der Verschiebungs- und Spannungsverteilungen an unbelasteten Rändern multidirektionaler Laminate*, VDI Verlag, Düsseldorf, Germany.

Herakovich CT (1998): *Mechanics of fibrous composites*, John Wiley and Sons, Inc., New York et al., USA.

Jones RM (1975): *Mechanics of composite materials*, Scripta Book Co., Washington, USA.

Lekhnitskii SG (1968): *Anisotropic plates*, Gordon and Breach, New York et al., USA.

Niederstadt G, Block J, Geier B, Rohwer K, Weiß R (1985): *Leichtbau mit kohlenstofffaserverstärkten Kunststoffen*, Expert Verlag, Sindelfingen, Germany.

Ochoa OO, Reddy JN (1992): *Mechanics of composite materials*, Kluwer Academic Publishers, Dordrecht et al., The Netherlands.

Reddy JN (2004): *Mechanics of laminated composite plates and shells (2nd edition)*, CRC Press Boca Raton et al., USA.

Reissner E, Stavsky Y (1961): *Bending and stretching of certain types of heterogeneous aelotropic elastic plates*, Journal of Applied Mechanics 28:402–408.

Tsai SW, Hahn HT (1980): *Introduction to composite materials*, Technomic Publishing Co., Inc., Lancaster et al., UK.

Wiedemann J (1962a): *Beitrag zum Problem orthotroper Platten ohne allgemeine Neutralebene - I: Elastische Symmetrieeigenschaften anisotroper Platten und ihr Einfluß auf die Besetzung der Elastizitätsmatrix der Platte*, Luftfahrttechnik 8:283–289.

Wiedemann J (1962b): *Beitrag zum Problem orthotroper Platten ohne allgemeine Neutralebene - III: Zum Beulproblem antimetrischer und exzentrischer orthotroper Rechteckplatten*, Luftfahrttechnik 9:118–130.

Wiedemann J (1963): *Beitrag zum Problem orthotroper Platten ohne allgemeine Neutralebene - II: Zur Bestimmung der Elastizitätskonstanten anisotroper Platten*, Luftfahrttechnik 9:73–82.

Wiedemann J (1996): *Leichtbau 1 -Elemente*, 2.Auflage, Springer Verlag, Berlin et al., Germany.



Static and Dynamic Laminate Problems

8

This chapter deals with the solution of static and dynamic boundary value problems of plane laminates within the framework of Classical Laminated Plate Theory. From the equilibrium conditions, in conjunction with the constitutive law, the displacement differential equations describing static problems can be obtained. In addition, laminate boundary conditions are discussed and an energetic derivation of the basic equations is carried out, followed by a dimensionless presentation of the relationships. Closed-form analytical solutions for static boundary value problems are presented in the form of Navier-type solutions and Lévy-type solutions, and the Ritz method for static problems is discussed in detail. The chapter concludes with the provision of the nonlinear equations of motion according to Classical Laminated Plate Theory as well as an overview of elementary vibration problems and a brief presentation of the Finite Element Method.

8.1 Static Equilibrium and Displacement Differential Equations of a Laminate

Composite structures, and laminate structures in particular, are generally thin compared to their other characteristic dimensions (i.e. $h \ll a, b$ applies to a rectangular structure). Accordingly, these are thin surface structures, and more specifically, in the case of symmetric laminates, disks or plates depending on the type of load, provided there is no curvature of the laminate. The differentiation of a plane laminate structure naturally no longer makes sense with unsymmetric laminates due to the bending-extension coupling that then occurs and the resulting coupling of the disk and plate behaviour. Nevertheless, the terms ‘disk’ and ‘plate’ are still used in accordance with the classical theory of plane isotropic surface structures in order to demonstrate analogies.

© The Author(s), under exclusive license to Springer-Verlag GmbH, DE, part of Springer Nature 2025

C. Mittelstedt, *Mechanics of Composite Structures*,
https://doi.org/10.1007/978-3-662-70788-3_8

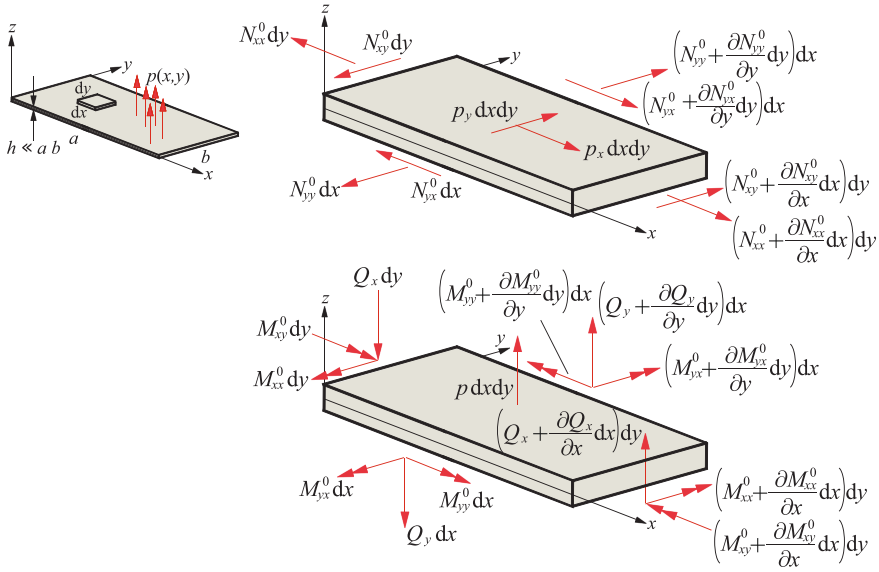


Fig. 8.1 Infinitesimal element of a laminate

In order to derive the local equilibrium conditions of a plane laminate, an infinitesimal element is cut out of a laminate as in the case of the three-dimensional equilibrium conditions (Fig. 8.1). The resulting forces and moments are shown in Fig. 8.1. In addition to the tangential forces p_x and p_y, there is also a surface force p in the z direction perpendicular to the laminate plane.

If the equilibrium of forces is formulated in the x-direction, the result is

$$\left(N^0_{xx}+\frac{\partial N^0_{xx}}{\partial x}\mathrm{d}x\right)\mathrm{d}y+\left(N^0_{yx}+\frac{\partial N^0_{yx}}{\partial y}\mathrm{d}y\right)\mathrm{d}x-N^0_{xx}\mathrm{d}y-N^0_{yx}\mathrm{d}x+p_x\mathrm{d}x\mathrm{d}y=0, \tag{8.1}$$

or:

$$\frac{\partial N^0_{xx}}{\partial x}\mathrm{d}x\mathrm{d}y+\frac{\partial N^0_{yx}}{\partial y}\mathrm{d}x\mathrm{d}y+p_x\mathrm{d}x\mathrm{d}y=0, \tag{8.2}$$

and considering $N^0_{yx}=N^0_{xy}$:

$$\frac{\partial N^0_{xx}}{\partial x}+\frac{\partial N^0_{xy}}{\partial y}=-p_x. \tag{8.3}$$

Similarly, the following equation is obtained from the equilibrium of forces in the y-direction:

$$\left(N_{yy}^0 + \frac{\partial N_{yy}^0}{\partial y}\mathrm{d}y\right)\mathrm{d}x + \left(N_{xy}^0 + \frac{\partial N_{xy}^0}{\partial x}\mathrm{d}x\right)\mathrm{d}y - N_{yy}^0\mathrm{d}x - N_{xy}^0\mathrm{d}y + p_y\mathrm{d}x\mathrm{d}y = 0, \tag{8.4}$$

or:

$$\frac{\partial N_{xy}^0}{\partial x} + \frac{\partial N_{yy}^0}{\partial y} = -p_y. \tag{8.5}$$

The two Eqs. (8.3) and (8.5) form the so-called 'disk equilibrium'.

Furthermore, the force equilibrium in the z-direction is considered:

$$\left(Q_x + \frac{\partial Q_x}{\partial x}\mathrm{d}x\right)\mathrm{d}y + \left(Q_y + \frac{\partial Q_y}{\partial y}\mathrm{d}y\right)\mathrm{d}x - Q_x\mathrm{d}y - Q_y\mathrm{d}x + p\mathrm{d}x\mathrm{d}y = 0. \tag{8.6}$$

This yields:

$$\frac{\partial Q_x}{\partial x}\mathrm{d}x\mathrm{d}y + \frac{\partial Q_y}{\partial y}\mathrm{d}x\mathrm{d}y + p\mathrm{d}x\mathrm{d}y = 0, \tag{8.7}$$

or

$$\frac{\partial Q_x}{\partial x} + \frac{\partial Q_y}{\partial y} = -p. \tag{8.8}$$

In addition, the moment equilibrium is formed around the y-axis with the reference point in the center of gravity of the infinitesimal element:

$$\left(M_{xx}^0 + \frac{\partial M_{xx}^0}{\partial x}\mathrm{d}x\right)\mathrm{d}y + \left(M_{yx}^0 + \frac{\partial M_{yx}^0}{\partial y}\mathrm{d}y\right)\mathrm{d}x - M_{xx}^0\mathrm{d}y - M_{yx}^0\mathrm{d}x$$
$$- \left(Q_x + \frac{\partial Q_x}{\partial x}\mathrm{d}x\right)\mathrm{d}y\frac{\mathrm{d}x}{2} - Q_x\mathrm{d}y\frac{\mathrm{d}x}{2} = 0. \tag{8.9}$$

If we shorten this equilibrium requirement appropriately and note that $M_{yx}^0 = M_{xy}^0$, we obtain the following:

$$\frac{\partial M_{xx}^0}{\partial x}\mathrm{d}x\mathrm{d}y + \frac{\partial M_{xy}^0}{\partial y}\mathrm{d}x\mathrm{d}y - Q_x\mathrm{d}x\mathrm{d}y - \frac{\partial Q_x}{\partial x}\frac{\mathrm{d}x^2\mathrm{d}y}{2} = 0. \tag{8.10}$$

If we now assume that the last term in (8.10) is small compared to the other terms, then (8.10) becomes:

$$\frac{\partial M_{xx}^0}{\partial x} + \frac{\partial M_{xy}^0}{\partial y} = Q_x. \tag{8.11}$$

Similarly, the sum of moments about the x-axis yields:

$$\frac{\partial M_{xy}^0}{\partial x} + \frac{\partial M_{yy}^0}{\partial y} = Q_y. \tag{8.12}$$

The two Eqs. (8.11) and (8.12), in conjunction with the force equilibrium condition (8.8), form the so-called 'plate equilibrium'.

The plate equilibrium can be summarized even further. Partial differentiation of the first moment equilibrium (8.11) with respect to x results in:

$$\frac{\partial^2 M^0_{xx}}{\partial x^2} + \frac{\partial^2 M^0_{xy}}{\partial x \partial y} = \frac{\partial Q_x}{\partial x}. \tag{8.13}$$

If the second sum of moments (8.12) is derived partially with respect to y, the result is

$$\frac{\partial^2 M^0_{xy}}{\partial x \partial y} + \frac{\partial^2 M^0_{yy}}{\partial y^2} = \frac{\partial Q_y}{\partial y}. \tag{8.14}$$

Inserting the two Eqs. (8.13) and (8.14) into the force equilibrium (8.8) leads to the so-called 'condensed plate equilibrium':

$$\frac{\partial^2 M^0_{xx}}{\partial x^2} + \frac{\partial^2 M^0_{yy}}{\partial y^2} + 2\frac{\partial^2 M^0_{xy}}{\partial x \partial y} = -p. \tag{8.15}$$

If we use the constitutive law in the 'disk equilibrium' (8.3) and (8.5) as well as in the 'condensed plate equilibrium' (8.15)

$$\begin{pmatrix} N^0_{xx} \\ N^0_{yy} \\ N^0_{xy} \\ M^0_{xx} \\ M^0_{yy} \\ M^0_{xy} \end{pmatrix} = \begin{bmatrix} A_{11} & A_{12} & A_{16} & B_{11} & B_{12} & B_{16} \\ A_{12} & A_{22} & A_{26} & B_{12} & B_{22} & B_{26} \\ A_{16} & A_{26} & A_{66} & B_{16} & B_{26} & B_{66} \\ B_{11} & B_{12} & B_{16} & D_{11} & D_{12} & D_{16} \\ B_{12} & B_{22} & B_{26} & D_{12} & D_{22} & D_{26} \\ B_{16} & B_{26} & B_{66} & D_{16} & D_{26} & D_{66} \end{bmatrix} \begin{pmatrix} \frac{\partial u_0}{\partial x} \\ \frac{\partial v_0}{\partial y} \\ \frac{\partial u_0}{\partial y} + \frac{\partial v_0}{\partial x} \\ -\frac{\partial^2 w_0}{\partial x^2} \\ -\frac{\partial^2 w_0}{\partial y^2} \\ -2\frac{\partial^2 w_0}{\partial x \partial y} \end{pmatrix}, \tag{8.16}$$

then from (8.3), (8.5) and (8.15) the displacement differential equations are obtained, which describe the static laminate problem in the form of the displacements u_0, v_0, w_0 of the laminate middle plane:

$$\begin{aligned} &A_{11}\frac{\partial^2 u_0}{\partial x^2} + 2A_{16}\frac{\partial^2 u_0}{\partial x \partial y} + A_{66}\frac{\partial^2 u_0}{\partial y^2} + A_{16}\frac{\partial^2 v_0}{\partial x^2} + (A_{12} + A_{66})\frac{\partial^2 v_0}{\partial x \partial y} + A_{26}\frac{\partial^2 v_0}{\partial y^2} \\ &\qquad - B_{11}\frac{\partial^3 w_0}{\partial x^3} - 3B_{16}\frac{\partial^3 w_0}{\partial x^2 \partial y} - (B_{12} + 2B_{66})\frac{\partial^3 w_0}{\partial x \partial y^2} - B_{26}\frac{\partial^3 w_0}{\partial y^3} + p_x = 0, \\ &A_{16}\frac{\partial^2 u_0}{\partial x^2} + (A_{12} + A_{66})\frac{\partial^2 u_0}{\partial x \partial y} + A_{26}\frac{\partial^2 u_0}{\partial y^2} + A_{66}\frac{\partial^2 v_0}{\partial x^2} + 2A_{26}\frac{\partial^2 v_0}{\partial x \partial y} + A_{22}\frac{\partial^2 v_0}{\partial y^2} \\ &\qquad - B_{16}\frac{\partial^3 w_0}{\partial x^3} - (B_{12} + 2B_{66})\frac{\partial^3 w_0}{\partial x^2 \partial y} - 3B_{26}\frac{\partial^3 w_0}{\partial x \partial y^2} - B_{22}\frac{\partial^3 w_0}{\partial y^3} + p_y = 0, \end{aligned}$$

$$D_{11}\frac{\partial^4 w_0}{\partial x^4} + 4D_{16}\frac{\partial^4 w_0}{\partial x^3 \partial y} + 2\left(D_{12} + 2D_{66}\right)\frac{\partial^4 w_0}{\partial x^2 \partial y^2} + 4D_{26}\frac{\partial^4 w_0}{\partial x \partial y^3} + D_{22}\frac{\partial^4 w_0}{\partial y^4}$$
$$- B_{11}\frac{\partial^3 u_0}{\partial x^3} - 3B_{16}\frac{\partial^3 u_0}{\partial x^2 \partial y} - \left(B_{12} + 2B_{66}\right)\frac{\partial^3 u_0}{\partial x \partial y^2} - B_{26}\frac{\partial^3 u_0}{\partial y^3}$$
$$- B_{16}\frac{\partial^3 v_0}{\partial x^3} - \left(B_{12} + 2B_{66}\right)\frac{\partial^3 v_0}{\partial x^2 \partial y} - 3B_{26}\frac{\partial^3 v_0}{\partial x \partial y^2} - B_{22}\frac{\partial^3 v_0}{\partial y^3} - p = 0. \tag{8.17}$$

It is clear from (8.17) that the three displacement differential equations are coupled with each other. Each of the displacement components u_0, v_0, w_0 appears in each differential equation. The disk and plate behaviour are therefore coupled with each other for arbitrary laminates, and here in particular for unsymmetric laminates. However, the differential equation system (8.17) is considerably simplified if symmetric laminates and thus vanishing bending-extension coupling stiffnesses B_{11}, B_{22}, B_{12}, B_{16}, B_{26} and B_{66} are assumed:

$$\begin{aligned}
A_{11}\frac{\partial^2 u_0}{\partial x^2} + 2A_{16}\frac{\partial^2 u_0}{\partial x \partial y} + A_{66}\frac{\partial^2 u_0}{\partial y^2} + A_{16}\frac{\partial^2 v_0}{\partial x^2} + \left(A_{12} + A_{66}\right)\frac{\partial^2 v_0}{\partial x \partial y} \\
+ A_{26}\frac{\partial^2 v_0}{\partial y^2} + p_x = 0, \\
A_{16}\frac{\partial^2 u_0}{\partial x^2} + \left(A_{12} + A_{66}\right)\frac{\partial^2 u_0}{\partial x \partial y} + A_{26}\frac{\partial^2 u_0}{\partial y^2} + A_{66}\frac{\partial^2 v_0}{\partial x^2} + 2A_{26}\frac{\partial^2 v_0}{\partial x \partial y} \\
+ A_{22}\frac{\partial^2 v_0}{\partial y^2} + p_y = 0, \\
D_{11}\frac{\partial^4 w_0}{\partial x^4} + 4D_{16}\frac{\partial^4 w_0}{\partial x^3 \partial y} + 2\left(D_{12} + 2D_{66}\right)\frac{\partial^4 w_0}{\partial x^2 \partial y^2} + 4D_{26}\frac{\partial^4 w_0}{\partial x \partial y^3} \\
+ D_{22}\frac{\partial^4 w_0}{\partial y^4} - p = 0.
\end{aligned} \tag{8.18}$$

It can be seen that in this case the first two equations in (8.18) describe a pure membrane behaviour of the laminate—here only the two inplane displacements u_0, v_0 of the laminate middle plane appear. In contrast, the third equation in (8.18) describes a pure plate behaviour, because here only the deflection w_0 of the laminate middle plane is included.

8.2 Laminate Boundary Conditions

To define a laminate problem, the given boundary conditions must be considered. On the one hand, the so-called geometric or kinematic boundary conditions must be considered, which place demands on kinematic variables. On the other hand, so-called physical or dynamic

boundary conditions can be established, which place demands on forces and moments at the boundary.

On a boundary with $x = \text{const.}$ the following boundary conditions are possible:

$$\begin{aligned} u_0 &= \widehat{u}_0 \quad \text{or } N^0_{xx} = \widehat{N}^0_{xx}, \\ v_0 &= \widehat{v}_0 \quad \text{or } N^0_{xy} = \widehat{N}^0_{xy}, \\ \frac{\partial w_0}{\partial x} &= \widehat{\frac{\partial w_0}{\partial x}} \quad \text{or } M^0_{xx} = \widehat{M}^0_{xx}, \\ w_0 &= \widehat{w}_0 \quad \text{or } \bar{Q}_x = \widehat{\bar{Q}}_x. \end{aligned} \tag{8.19}$$

Similarly, the following boundary conditions can occur on a boundary with $y = \text{const.}$:

$$\begin{aligned} u_0 &= \widehat{u}_0 \quad \text{or } N^0_{xy} = \widehat{N}^0_{xy}, \\ v_0 &= \widehat{v}_0 \quad \text{or } N^0_{yy} = \widehat{N}^0_{yy}, \\ \frac{\partial w_0}{\partial y} &= \widehat{\frac{\partial w_0}{\partial y}} \quad \text{or } M^0_{yy} = \widehat{M}^0_{yy}, \\ w_0 &= \widehat{w}_0 \quad \text{or } \bar{Q}_y = \widehat{\bar{Q}}_y. \end{aligned} \tag{8.20}$$

Here, $\bar{Q}_x$ and $\bar{Q}_y$ are Kirchhoff's equivalent transverse forces, and the notation $\widehat{(\ldots)}$ indicates a given quantity. Note that, in contrast to isotropic plates, boundary conditions for laminates require a more detailed consideration. This will be explained in more detail using the example of a simply supported rectangular isotropic plate (length a, width b). A simply supported isotropic plate naturally has no bending-extension coupling, so that a hinged support at all four edges means that both the deflections w_0 and the bending moments M^0_{xx} or M^0_{yy} must disappear there:

$$\begin{aligned} &w_0(x=0) = 0, \quad w_0(x=a) = 0, \quad w_0(y=0) = 0, \quad w_0(y=b) = 0, \\ &M^0_{xx}(x=0) = 0, \quad M^0_{xx}(x=a) = 0, \quad M^0_{yy}(y=0) = 0, \quad M^0_{yy}(y=b) = 0. \end{aligned} \tag{8.21}$$

On the other hand, for an arbitrary laminate, due to the bending-extension coupling that is always possible there (and thus the coupling of the disk and plate behaviour), conditions must also be specified with regard to the inplane displacements u_0, v_0 and the associated laminate forces. Thus, when considering laminates, a hinged support e.g. at the edge $x = 0$ can mean the following:

$$\begin{aligned} \text{either} \quad & w_0(x=0) = 0, \quad M^0_{xx}(x=0) = 0, \quad u_0 = \widehat{u}_0, \quad v_0 = \widehat{v}_0, \\ \text{or} \quad & w_0(x=0) = 0, \quad M^0_{xx}(x=0) = 0, \quad N^0_{xx} = \widehat{N}^0_{xx}, \quad v_0 = \widehat{v}_0, \\ \text{or} \quad & w_0(x=0) = 0, \quad M^0_{xx}(x=0) = 0, \quad u_0 = \widehat{u}_0, \quad N^0_{xy} = \widehat{N}^0_{xy}, \\ \text{or} \quad & w_0(x=0) = 0, \quad M^0_{xx}(x=0) = 0, \quad N^0_{xx} = \widehat{N}^0_{xx}, \quad N^0_{xy} = \widehat{N}^0_{xy}. \end{aligned} \tag{8.22}$$

8.3 Energetic Derivation of the Governing Equations

The equilibrium conditions (8.3), (8.5) and (8.15) as well as the boundary conditions (8.22) can also be obtained in an energetic manner. For this purpose, the principle of the minimum of the elastic potential is used. Specifically, a rectangular laminate with the dimensions a, b in x- and in y-direction and the thickness h is considered here. The laminate is stressed by arbitrarily distributed tangential forces p_x and p_y as well as the surface load p.

The total potential Π is calculated by adding the strain energy Π_i and the potential Π_a of the applied loads:

$$\Pi = \Pi_i + \Pi_a. \tag{8.23}$$

The strain energy Π_i is obtained from

$$\Pi_i = \frac{1}{2}\int\int\int_V \left(\sigma_{xx}\varepsilon_{xx} + \sigma_{yy}\varepsilon_{yy} + \sigma_{zz}\varepsilon_{zz} + \tau_{yz}\gamma_{yz} + \tau_{xz}\gamma_{xz} + \tau_{xy}\gamma_{xy}\right) \mathrm{d}V, \tag{8.24}$$

whereby in the context of Classical Laminated Plate Theory, only the following expression remains due to the assumed shear rigidity with respect to the thickness direction and the assumption of a plane stress state in the entire laminate:

$$\Pi_i = \frac{1}{2}\int\int\int_V \left(\sigma_{xx}\varepsilon_{xx} + \sigma_{yy}\varepsilon_{yy} + \tau_{xy}\gamma_{xy}\right) \mathrm{d}V. \tag{8.25}$$

If the strains are expressed according to Classical Laminated Plate Theory

$$\varepsilon_{xx} = \frac{\partial u_0}{\partial x} - z\frac{\partial^2 w_0}{\partial x^2}, \quad \varepsilon_{yy} = \frac{\partial v_0}{\partial y} - z\frac{\partial^2 w_0}{\partial y^2}, \quad \gamma_{xy} = \frac{\partial u_0}{\partial y} + \frac{\partial v_0}{\partial x} - 2z\frac{\partial^2 w_0}{\partial x \partial y}, \tag{8.26}$$

Equation (8.25) takes on the following form:

$$\begin{aligned}\Pi_i = \frac{1}{2}\int\int\int_V \Bigg[&\sigma_{xx}\left(\frac{\partial u_0}{\partial x} - z\frac{\partial^2 w_0}{\partial x^2}\right) + \sigma_{yy}\left(\frac{\partial v_0}{\partial y} - z\frac{\partial^2 w_0}{\partial y^2}\right) \\ &+ \tau_{xy}\left(\frac{\partial u_0}{\partial y} + \frac{\partial v_0}{\partial x} - 2z\frac{\partial^2 w_0}{\partial x \partial y}\right)\Bigg] \mathrm{d}V.\end{aligned} \tag{8.27}$$

If we split the volume integral in (8.27) into integrals with respect to x, y, z we obtain

$$\begin{aligned}\Pi_i = \frac{1}{2}\int_0^a \int_0^b \int_{-\frac{h}{2}}^{+\frac{h}{2}} \Bigg[&\sigma_{xx}\frac{\partial u_0}{\partial x} - \sigma_{xx}z\frac{\partial^2 w_0}{\partial x^2} + \sigma_{yy}\frac{\partial v_0}{\partial y} - \sigma_{yy}z\frac{\partial^2 w_0}{\partial y^2} \\ &+ \tau_{xy}\left(\frac{\partial u_0}{\partial y} + \frac{\partial v_0}{\partial x}\right) - 2\tau_{xy}z\frac{\partial^2 w_0}{\partial x \partial y}\Bigg] \mathrm{d}z\mathrm{d}y\mathrm{d}x.\end{aligned} \tag{8.28}$$

Taking into account the definitions of the laminate forces and moments

$$\begin{pmatrix} N_{xx}^0 \\ N_{yy}^0 \\ N_{xy}^0 \end{pmatrix} = \int_{-\frac{h}{2}}^{+\frac{h}{2}} \begin{pmatrix} \sigma_{xx} \\ \sigma_{yy} \\ \tau_{xy} \end{pmatrix} \mathrm{d}z, \quad \begin{pmatrix} M_{xx}^0 \\ M_{yy}^0 \\ M_{xy}^0 \end{pmatrix} = \int_{-\frac{h}{2}}^{+\frac{h}{2}} \begin{pmatrix} \sigma_{xx} \\ \sigma_{yy} \\ \tau_{xy} \end{pmatrix} z \mathrm{d}z \tag{8.29}$$

the integration required in (8.28) can be carried out with respect to z:

$$\Pi_i = \frac{1}{2} \int_0^b \int_0^a \begin{pmatrix} N_{xx}^0 \\ N_{yy}^0 \\ N_{xy}^0 \\ M_{xx}^0 \\ M_{yy}^0 \\ M_{xy}^0 \end{pmatrix}^T \begin{pmatrix} \frac{\partial u_0}{\partial x} \\ \frac{\partial v_0}{\partial y} \\ \frac{\partial u_0}{\partial y} + \frac{\partial v_0}{\partial x} \\ -\frac{\partial^2 w_0}{\partial x^2} \\ -\frac{\partial^2 w_0}{\partial y^2} \\ -2\frac{\partial^2 w_0}{\partial x \partial y} \end{pmatrix} \mathrm{d}x\mathrm{d}y. \tag{8.30}$$

Insertion of the constitutive law (8.16) yields:

$$\begin{aligned} \Pi_i &= \frac{1}{2} \int_0^b \int_0^a \begin{pmatrix} \frac{\partial u_0}{\partial x} \\ \frac{\partial v_0}{\partial y} \\ \frac{\partial u_0}{\partial y} + \frac{\partial v_0}{\partial x} \\ -\frac{\partial^2 w_0}{\partial x^2} \\ -\frac{\partial^2 w_0}{\partial y^2} \\ -2\frac{\partial^2 w_0}{\partial x \partial y} \end{pmatrix}^T \begin{bmatrix} \underline{\underline{A}} & \underline{\underline{B}} \\ \underline{\underline{B}} & \underline{\underline{D}} \end{bmatrix} \begin{pmatrix} \frac{\partial u_0}{\partial x} \\ \frac{\partial v_0}{\partial y} \\ \frac{\partial u_0}{\partial y} + \frac{\partial v_0}{\partial x} \\ -\frac{\partial^2 w_0}{\partial x^2} \\ -\frac{\partial^2 w_0}{\partial y^2} \\ -2\frac{\partial^2 w_0}{\partial x \partial y} \end{pmatrix} \mathrm{d}x\mathrm{d}y \\ &= \frac{1}{2} \int_0^b \int_0^a \left[A_{11} \left(\frac{\partial u_0}{\partial x} \right)^2 + 2A_{12} \frac{\partial u_0}{\partial x} \frac{\partial v_0}{\partial y} + \cdots \right] \mathrm{d}x\mathrm{d}y. \end{aligned} \tag{8.31}$$

The potential of the external loads of the laminate Π_a is made up of the contribution of the transverse load p and the contributions of the tangential loads p_x and p_y as follows:

$$\Pi_a = -\int_0^b \int_0^a \left(p w_0 + p_x u_0 + p_y v_0 \right) \mathrm{d}x\mathrm{d}y. \tag{8.32}$$

The principle of the minimum of the total elastic potential of the considered laminate requires a disappearance of the first variation $\delta\Pi$ of Π:

$$\delta\Pi = \delta\Pi_i + \delta\Pi_a = 0. \tag{8.33}$$

The first variation of the strain energy Π_i is calculated using the rules of the calculus of variations as follows:

$$\begin{aligned}
\delta\Pi_i &= \frac{1}{2}\delta \int_0^b \int_0^a \left[A_{11}\left(\frac{\partial u_0}{\partial x}\right)^2 + 2A_{12}\left(\frac{\partial u_0}{\partial x}\frac{\partial v_0}{\partial y}\right) + \cdots \right] \mathrm{d}x\mathrm{d}y \\
&= \frac{1}{2}\int_0^b \int_0^a \left[A_{11}\delta\left(\frac{\partial u_0}{\partial x}\right)^2 + 2A_{12}\delta\left(\frac{\partial u_0}{\partial x}\frac{\partial v_0}{\partial y}\right) + \cdots \right] \mathrm{d}x\mathrm{d}y \\
&= \frac{1}{2}\int_0^b \int_0^a \left[2A_{11}\frac{\partial u_0}{\partial x}\delta\left(\frac{\partial u_0}{\partial x}\right) + 2A_{12}\frac{\partial v_0}{\partial y}\delta\left(\frac{\partial u_0}{\partial x}\right) \right. \\
&\quad \left. + \; 2A_{12}\frac{\partial u_0}{\partial x}\delta\left(\frac{\partial v_0}{\partial y}\right) + \cdots \right] \mathrm{d}x\mathrm{d}y \\
&= \int_0^b \int_0^a \begin{pmatrix} \frac{\partial u_0}{\partial x} \\ \frac{\partial v_0}{\partial y} \\ \frac{\partial u_0}{\partial y} + \frac{\partial v_0}{\partial x} \\ -\frac{\partial^2 w_0}{\partial x^2} \\ -\frac{\partial^2 w_0}{\partial y^2} \\ -2\frac{\partial^2 w_0}{\partial x \partial y} \end{pmatrix}^T \begin{bmatrix} \underline{\underline{A}} & \underline{\underline{B}} \\ \underline{\underline{B}} & \underline{\underline{D}} \end{bmatrix} \begin{pmatrix} \delta\frac{\partial u_0}{\partial x} \\ \delta\frac{\partial v_0}{\partial y} \\ \delta\frac{\partial u_0}{\partial y} + \delta\frac{\partial v_0}{\partial x} \\ -\delta\frac{\partial^2 w_0}{\partial x^2} \\ -\delta\frac{\partial^2 w_0}{\partial y^2} \\ -2\delta\frac{\partial^2 w_0}{\partial x \partial y} \end{pmatrix} \mathrm{d}x\mathrm{d}y \\
&= \int_0^b \int_0^a \begin{pmatrix} N_{xx}^0 \\ N_{yy}^0 \\ N_{xy}^0 \\ M_{xx}^0 \\ M_{yy}^0 \\ M_{xy}^0 \end{pmatrix}^T \begin{pmatrix} \delta\frac{\partial u_0}{\partial x} \\ \delta\frac{\partial v_0}{\partial y} \\ \delta\frac{\partial u_0}{\partial y} + \delta\frac{\partial v_0}{\partial x} \\ -\delta\frac{\partial^2 w_0}{\partial x^2} \\ -\delta\frac{\partial^2 w_0}{\partial y^2} \\ -2\delta\frac{\partial^2 w_0}{\partial x \partial y} \end{pmatrix} \mathrm{d}x\mathrm{d}y \\
&= \int_0^b \int_0^a \left(N_{xx}\delta u_{,x} + N_{yy}\delta v_{,y} + N_{xy}\delta u_{,y} + N_{xy}\delta v_{,x} \right. \\
&\quad \left. - \; M_{xx}\delta w_{,xx} - M_{yy}\delta w_{,yy} - 2M_{xy}\delta w_{,xy} \right) \mathrm{d}x\mathrm{d}y,
\end{aligned} \tag{8.34}$$

whereby here, for the sake of better readability, the notation e.g. $u_{,x} = \frac{\partial u}{\partial x}$ was used for a partial derivative and, in addition, the indices '0' were omitted for the following calculation steps.

The first variation of the external potential Π_a results as:

$$\delta\Pi_a = -\int_0^b \int_0^a \left(p\delta w + f_x \delta u + f_y \delta v\right) \mathrm{d}x\mathrm{d}y. \tag{8.35}$$

The individual terms in the first variation of the strain energy are partially integrated step by step. The result is

$$\begin{aligned}
\int_0^b \int_0^a N_{xx}\delta u_{,x}\mathrm{d}x\mathrm{d}y &= \int_0^b N_{xx}\delta u|_0^a \mathrm{d}y - \int_0^b \int_0^a N_{xx,x}\delta u\mathrm{d}x\mathrm{d}y,\\
\int_0^b \int_0^a N_{yy}\delta v_{,y}\mathrm{d}x\mathrm{d}y &= \int_0^a N_{yy}\delta v|_0^b \mathrm{d}x - \int_0^b \int_0^a N_{yy,y}\delta v\mathrm{d}x\mathrm{d}y,\\
\int_0^b \int_0^a N_{xy}\delta u_{,y}\mathrm{d}x\mathrm{d}y &= \int_0^a N_{xy}\delta u|_0^b \mathrm{d}x - \int_0^b \int_0^a N_{xy,y}\delta u\mathrm{d}x\mathrm{d}y,\\
\int_0^b \int_0^a N_{xy}\delta v_{,x}\mathrm{d}x\mathrm{d}y &= \int_0^b N_{xy}\delta v|_0^a \mathrm{d}y - \int_0^b \int_0^a N_{xy,x}\delta v\mathrm{d}x\mathrm{d}y,\\
-\int_0^b \int_0^a M_{xx}\delta w_{,xx}\mathrm{d}x\mathrm{d}y &= -\left(\int_0^b M_{xx}\delta w_{,x}|_0^a \mathrm{d}y - \int_0^b \int_0^a M_{xx,x}\delta w_{,x}\mathrm{d}x\mathrm{d}y\right)\\
&= -\int_0^b M_{xx}\delta w_{,x}|_0^a \mathrm{d}y + \int_0^b M_{xx,x}\delta w|_0^a \mathrm{d}y\\
&\quad - \int_0^b \int_0^a M_{xx,xx}\delta w\mathrm{d}x\mathrm{d}y,
\end{aligned}$$

$$
\begin{aligned}
-\int_0^b\int_0^a M_{yy}\delta w_{,yy}\mathrm{d}x\mathrm{d}y &= -\left(\int_0^a M_{yy}\delta w_{,y}|_0^b\mathrm{d}x - \int_0^b\int_0^a M_{yy,y}\delta w_{,y}\mathrm{d}x\mathrm{d}y\right)\\
&= -\int_0^a M_{yy}\delta w_{,y}|_0^b\mathrm{d}x + \int_0^a M_{yy,y}\delta w|_0^b\mathrm{d}x\\
&\quad -\int_0^b\int_0^a M_{yy,yy}\delta w\mathrm{d}x\mathrm{d}y,\\
-2\int_0^b\int_0^a M_{xy}\delta w_{,xy}\mathrm{d}x\mathrm{d}y &= -2\left(\int_0^b M_{xy}\delta w_{,y}|_0^a\mathrm{d}y - \int_0^b\int_0^a M_{xy,x}\delta w_{,y}\mathrm{d}x\mathrm{d}y\right)\\
&= -2M_{xy}\delta w|_0^a|_0^b + 2\int_0^b M_{xy,y}\delta w|_0^a\mathrm{d}y\\
&\quad + 2\int_0^a M_{xy,x}\delta w|_0^b\mathrm{d}x - 2\int_0^b\int_0^a M_{xy,xy}\delta w\mathrm{d}x\mathrm{d}y. \qquad (8.36)
\end{aligned}
$$

Partial integration of the terms in the external potential Π_a is not necessary, as no derivatives of the displacements u, v, w appear here. After sorting according to the variations δu_0, δv_0, δw_0 we eventually obtain:

$$
\begin{aligned}
&-\int_0^a\int_0^b\left[\left(\frac{\partial N_{xx}^0}{\partial x}+\frac{\partial N_{xy}^0}{\partial y}+p_x\right)\delta u_0+\left(\frac{\partial N_{xy}^0}{\partial x}+\frac{\partial N_{yy}^0}{\partial y}+p_y\right)\delta v_0\right.\\
&\left.+\left(\frac{\partial^2 M_{xx}^0}{\partial x^2}+2\frac{\partial^2 M_{xy}^0}{\partial x\partial y}+\frac{\partial^2 M_{yy}^0}{\partial y^2}+p\right)\delta w_0\right]\mathrm{d}y\mathrm{d}x\\
&+\int_0^a\left\{\left[N_{xy}^0\delta u_0+N_{yy}^0\delta v_0-M_{yy}^0\delta\left(\frac{\partial w_0}{\partial y}\right)+\left(\frac{\partial M_{yy}^0}{\partial y}+2\frac{\partial M_{xy}^0}{\partial x}\right)\delta w_0\right]\Big|_0^b\right\}\mathrm{d}x\\
&+\int_0^b\left\{\left[N_{xx}^0\delta u_0+N_{xy}^0\delta v_0-M_{xx}^0\delta\left(\frac{\partial w_0}{\partial x}\right)+\left(\frac{\partial M_{xx}^0}{\partial x}+2\frac{\partial M_{xy}^0}{\partial y}\right)\delta w_0\right]\Big|_0^a\right\}\mathrm{d}y\\
&-\left(2M_{xy}^0\delta w_0\right)\Big|_0^a\Big|_0^b=0. \qquad (8.37)
\end{aligned}
$$

Since all variations δ of the displacements u_0, v_0, w_0 and their derivatives are completely arbitrary (taking into account the given geometric boundary conditions of the laminate) and also independent of each other, the condition (8.37) can only be fulfilled if the variations

$\delta u_0 = 0, \delta v_0 = 0, \delta w_0 = 0, \delta \frac{\partial w_0}{\partial x} = 0, \delta \frac{\partial w_0}{\partial y} = 0$, or if the associated terms disappear. While the former is a trivial solution, the latter results in both the equilibrium conditions of the laminate and all associated boundary conditions.

The integral expressions in the first two lines of the Eq. (8.37) are considered first. The equilibrium conditions of the laminate under consideration can be read from this:

$$\begin{aligned} \frac{\partial N^0_{xx}}{\partial x} + \frac{\partial N^0_{xy}}{\partial y} + p_x &= 0, \\ \frac{\partial N^0_{xy}}{\partial x} + \frac{\partial N^0_{yy}}{\partial y} + p_y &= 0, \\ \frac{\partial^2 M^0_{xx}}{\partial x^2} + 2\frac{\partial^2 M^0_{xy}}{\partial x \partial y} + \frac{\partial^2 M^0_{yy}}{\partial y^2} + p &= 0. \end{aligned} \tag{8.38}$$

It can be seen that these differential equations correspond exactly to the equilibrium conditions of the laminate, as already given with (8.3), (8.5) and (8.15). If the laminate constitutive law (8.16) is also used here, we obtain the displacement differential equations (8.17), or in the case of symmetric laminates (8.18).

The remaining boundary terms in (8.37) describe the boundary conditions of the laminate under consideration as follows:

For $x = 0$ and $x = a$ for $0 \leq y \leq b$:

$$\begin{aligned} N^0_{xx} &= 0 \text{ or } u_0 = \widehat{u}_0, \\ N^0_{xy} &= 0 \text{ or } v_0 = \widehat{v}_0, \\ M^0_{xx} &= 0 \text{ or } \frac{\partial w_0}{\partial x} = \widehat{\frac{\partial w_0}{\partial x}}, \\ \frac{\partial M^0_{xx}}{\partial x} + 2\frac{\partial M^0_{xy}}{\partial y} &= 0 \text{ or } w_0 = \widehat{w}_0. \end{aligned}$$

For $y = 0$ and $y = b$ for $0 \leq x \leq a$:

$$\begin{aligned} N^0_{xy} &= 0 \text{ or } u_0 = \widehat{u}_0, \\ N^0_{yy} &= 0 \text{ or } v_0 = \widehat{v}_0, \\ M^0_{yy} &= 0 \text{ or } \frac{\partial w_0}{\partial y} = \widehat{\frac{\partial w_0}{\partial y}}, \\ \frac{\partial M^0_{yy}}{\partial y} + 2\frac{\partial M^0_{xy}}{\partial x} &= 0 \text{ or } w_0 = \widehat{w}_0. \end{aligned}$$

For $x = 0$, $y = 0$, at $x = a$, $y = 0$, at $x = 0$, $y = b$ and at $x = a$, $y = b$:

$$M^0_{xy} = 0 \quad \text{or} \quad \widehat{w}_0 = 0. \tag{8.39}$$

Obviously, the boundary conditions that were previously specified 'intuitively' can also be obtained by energetic means.

8.4 Dimensionless Notation

It has proven useful in many applications to use a dimensionless notation instead of the previous representation. The advantage of this type of notation is that it often allows formulaic relationships to be represented much more compactly. In addition, results generated in a dimensionless formulation are generic in nature and therefore allow for easier comparability.

The procedure is demonstrated using a rectangular laminate of length a and width b. The starting point is a coordinate transformation such that the coordinates x and y are transformed to the natural coordinates ξ_1 and ξ_2:

$$\xi_1 = \frac{x}{a}, \quad \xi_2 = \frac{y}{b}. \tag{8.40}$$

While $0 \leq x \leq a$ and $0 \leq y \leq b$ apply, for the natural coordinates ξ_1 and ξ_2 the relationships $0 \leq \xi_1 \leq 1$ and $0 \leq \xi_2 \leq 1$ exist.

The explanations here are limited to symmetric laminates with $B_{ij} = 0$. The differential equation (8.18) is considered first:

$$D_{11}\frac{\partial^4 w_0}{\partial x^4} + 4D_{16}\frac{\partial^4 w_0}{\partial x^3 \partial y} + 2\left(D_{12} + 2D_{66}\right)\frac{\partial^4 w_0}{\partial x^2 \partial y^2} + 4D_{26}\frac{\partial^4 w_0}{\partial x \partial y^3} + D_{22}\frac{\partial^4 w_0}{\partial y^4} - p = 0. \tag{8.41}$$

Using the coordinate transformation (8.40), the partial differentiations in (8.41) can be written as follows:

$$\frac{\partial^{i+j} w_0}{\partial x^i \partial y^j} = \frac{\partial^{i+j} w_0}{a^i b^j \partial \xi_1^i \partial \xi_2^j}. \tag{8.42}$$

It will also prove useful to choose a dimensionless representation for the deflection w_0 as follows:

$$\overline{w}_0 = \frac{w_0}{\sqrt{ab}}. \tag{8.43}$$

Inserting (8.42) and (8.43) into (8.41) and multiplying (8.41) by the factor $\frac{a^2 b^2}{\sqrt{D_{11} D_{22}}}$, we obtain the following representation for the differential equation (8.41):

$$\frac{1}{\alpha^2}\frac{\partial^4 \overline{w}_0}{\partial \xi_1^4} + 2\beta\frac{\partial^4 \overline{w}_0}{\partial \xi_1^2 \partial \xi_2^2} + \alpha^2\frac{\partial^4 \overline{w}_0}{\partial \xi_2^4} + 4\frac{\gamma}{\alpha}\frac{\partial^4 \overline{w}_0}{\partial \xi_1^3 \partial \xi_2} + 4\alpha\delta\frac{\partial^4 \overline{w}_0}{\partial \xi_1 \partial \xi_2^3} - \overline{p} = 0. \tag{8.44}$$

The new dimensionless variables are defined as follows:

$$\alpha = \frac{a}{b}\sqrt[4]{\frac{D_{22}}{D_{11}}}, \quad \beta = \frac{D_{12}+2D_{66}}{\sqrt{D_{11}D_{22}}},$$
$$\gamma = \frac{D_{16}}{\sqrt[4]{D_{11}^3 D_{22}}}, \quad \delta = \frac{D_{26}}{\sqrt[4]{D_{11}D_{22}^3}},$$
$$\overline{p} = \frac{pa^2b^2}{\sqrt{D_{11}D_{22}}ab}. \tag{8.45}$$

These quantities are also referred to as the aspect ratio α, the so-called Seydel's orthotropy parameter β, the two bending-twisting coupling ratios γ and δ, as well as the dimensionless surface load $\overline{p}$. It is easy to see that these variables are all dimensionless. In the special case of an isotropic plate, these quantities take the following form:

$$\alpha = \frac{a}{b}, \quad \beta = 1, \quad \gamma = 0, \quad \delta = 0, \quad \overline{p} = \frac{pa^2b^2}{D\sqrt{ab}}. \tag{8.46}$$

In particular, the two bending-twisting coupling ratios γ and δ disappear. In addition, the orthotropy parameter β always assumes the value $\beta = 1$ for isotropic plates. The aspect ratio α also loses its dependence on the two bending stiffnesses of the laminate and changes to the aspect ratio $\alpha = \frac{a}{b}$ familiar from isotropic plate structures.

Furthermore, the total elastic potential Π of the laminate is considered. The inner potential Π_i is currently:

$$\Pi_i = \frac{1}{2}\int_0^a\int_0^b \left[D_{11}\left(\frac{\partial^2 w_0}{\partial x^2}\right)^2 + D_{22}\left(\frac{\partial^2 w_0}{\partial y^2}\right)^2 + 2D_{12}\frac{\partial^2 w_0}{\partial x^2}\frac{\partial^2 w_0}{\partial y^2} \right.$$
$$\left. + \; 4D_{16}\frac{\partial^2 w_0}{\partial x^2}\frac{\partial^2 w_0}{\partial x \partial y} + 4D_{26}\frac{\partial^2 w_0}{\partial y^2}\frac{\partial^2 w_0}{\partial x \partial y} + 4D_{66}\left(\frac{\partial^2 w_0}{\partial x \partial y}\right)^2 \right] \mathrm{d}y\mathrm{d}x. \tag{8.47}$$

If the dimensionless representation $\overline{w}_0 = \frac{w_0}{\sqrt{ab}}$ is used for the deflection and the dimensionless notation $\overline{\Pi}_i = \frac{\Pi_i}{\sqrt{D_{11}D_{22}}}$ for the inner potential, if the substitution rule (8.42) and $\mathrm{d}x = a\mathrm{d}\xi_1$ and $\mathrm{d}y = b\mathrm{d}\xi_2$ due to the coordinate transformation are also observed, and if the integral limits in (8.47) are substituted accordingly, then the following dimensionless representation for the inner potential is finally obtained:

$$\overline{\Pi}_i = \frac{1}{2}\int_0^1\int_0^1 \left[\frac{1}{\alpha^2}\left(\frac{\partial^2 \overline{w}_0}{\partial \xi_1^2}\right)^2 + \alpha^2\left(\frac{\partial^2 \overline{w}_0}{\partial \xi_2^2}\right)^2 + 2\beta\zeta\frac{\partial^2 \overline{w}_0}{\partial \xi_1^2}\frac{\partial^2 \overline{w}_0}{\partial \xi_2^2} \right.$$
$$\left. + \; 4\frac{\gamma}{\alpha}\frac{\partial^2 \overline{w}_0}{\partial \xi_1^2}\frac{\partial^2 \overline{w}_0}{\partial \xi_1 \partial \xi_2} + 4\alpha\delta\frac{\partial^2 \overline{w}_0}{\partial \xi_2^2}\frac{\partial^2 \overline{w}_0}{\partial \xi_1 \partial \xi_2} + 2\left(1-\zeta\right)\beta\left(\frac{\partial^2 \overline{w}_0}{\partial \xi_1 \partial \xi_2}\right)^2 \right] \mathrm{d}\xi_2\mathrm{d}\xi_1. \tag{8.48}$$

This representation contains another dimensionless variable, namely the so-called generalized Poisson's ratio ζ, which is defined as follows:

$$\zeta = \frac{D_{12}}{D_{12} + 2D_{66}}. \tag{8.49}$$

It should be mentioned at this point that this variable only has an influence on the static analysis of a laminate if a laminate situation is considered in which dynamic boundary conditions (i.e. conditions for force variables) must be taken into account, such as those that occur at free edges. In the case of an isotropic plate, ζ becomes the Poisson's ratio ν of the isotropic material.

The external potential Π_a in the presence of a surface load p is:

$$\Pi_a = -\int_0^a \int_0^b p w_0 \mathrm{d}y \mathrm{d}x. \tag{8.50}$$

Performing the corresponding substitutions provides the following dimensionless representation:

$$\overline{\Pi}_a = -\int_0^1 \int_0^1 \overline{pw}_0 \mathrm{d}\xi_2 \mathrm{d}\xi_1. \tag{8.51}$$

A few comments need to be made regarding permissible and technically relevant parameter spaces. For further details, interested readers are referred to e.g. Weaver and Nemeth (2007). It is always required that the strain energy of a laminate or the inner potential is positive—it is always the case that an elastic laminate can store energy, which in turn can be converted into work. The inner potential in its dimensionless representation (8.48) can also be represented as follows:

$$\overline{\Pi}_i = \frac{1}{2}\int_0^1 \int_0^1 \begin{pmatrix} \frac{\partial^2 \overline{w}_0}{\partial \xi_1^2} \\ \frac{\partial^2 \overline{w}_0}{\partial \xi_2^2} \\ 2\frac{\partial^2 \overline{w}_0}{\partial \xi_1 \partial \xi_2} \end{pmatrix}^T \begin{bmatrix} \frac{1}{\alpha^2} & \beta\zeta & \frac{\gamma}{\alpha} \\ \beta\zeta & \alpha^2 & \alpha\delta \\ \frac{\gamma}{\alpha} & \alpha\delta & \frac{1}{2}(1-\zeta)\beta \end{bmatrix} \begin{pmatrix} \frac{\partial^2 \overline{w}_0}{\partial \xi_1^2} \\ \frac{\partial^2 \overline{w}_0}{\partial \xi_2^2} \\ 2\frac{\partial^2 \overline{w}_0}{\partial \xi_1 \partial \xi_2} \end{pmatrix} \mathrm{d}\xi_2 \mathrm{d}\xi_1. \tag{8.52}$$

In order to fulfil the requirement for a positive strain energy, it must be required that the matrix occurring in (8.52) is positive definite. From this, some conclusions can be drawn regarding admissible parameter spaces for the characteristic dimensionless quantities introduced. Without going into further details at this point (the interested reader is referred to the work of Weaver and Nemeth (2007)), some parameter spaces are discussed here.

On the one hand, the aspect ratio α must always be greater than zero (neither the dimensions a, b, nor the stiffnesses D_{11}, D_{22} can assume negative values), but is theoretically not limited upwards:

$$0 < \alpha < \infty. \tag{8.53}$$

However, an upper limit for α will always be specified by the specific technical task.

Furthermore, the following interval can be specified for Seydel's orthotropy factor β:

$$-1 < \beta < 3.0. \tag{8.54}$$

While the lower limit results from energy considerations, the upper limit can be derived from purely technical considerations (see e.g. Wiedemann (1996)). However, real laminates will always have $\beta > 0$, so that the following interval is relevant from a technical point of view:

$$0 < \beta < 3.0. \tag{8.55}$$

The two bending-twisting coupling ratios γ and δ can be delimited as follows:

$$-1.0 < \gamma < 1.0, \quad -1.0 < \delta < 1.0. \tag{8.56}$$

It is interesting to note that β, γ and δ cannot be varied independently of each other in the above-mentioned intervals. Rather, there is a mutually limiting relationship between β, γ and δ, which will not be discussed in more detail here. In Chap. 14 some hints on this topic are given. Interested readers are again referred to Weaver and Nemeth (2007). Only in the rarest of cases do technically relevant laminates have bending-twisting coupling coefficients γ and δ that are close to the value 1.

For the generalised Poisson's ratio ζ, a mechanically strictly justified limit cannot be specified. From a purely technical point of view, however, ζ will mostly be found in the following typical interval in the vast majority of cases:

$$0.1 < \zeta < 0.4. \tag{8.57}$$

The extent to which an energetically permissible parameter space exists for ζ and whether restrictive interactions with β, γ and δ exist has not yet been exhaustively investigated.

Finally, the benefits of such a dimensionless representation should be emphasized once again. In technical applications, there are almost unlimited possibilities for assembling a laminate from its individual layers. In addition, each layer can have any fiber orientation, any material properties and any thickness. Thus, assuming symmetry, each laminate is characterized by its dimensions and plate stiffnesses D_{ij} when subjected to bending. If, for example, technical requirements result in changes, e.g. to the layup, all calculations must be carried out again and all results must be worked out and presented again. This shows the benefit of dimensionless representation, because once results have been generated for specific values for $\alpha, \beta, \zeta, \gamma, \delta$, then these results apply to every laminate that has exactly these values for $\alpha, \beta, \zeta, \gamma, \delta$. Results obtained once in a dimensionless representation are therefore

generic and can always be used again. If we determine a set of results for a specific technical task, taking into account the relevant parameter spaces for the characteristic dimensionless variables α, β, ζ, γ, δ, we can present these results in the form of design diagrams or a design manual and can dispense with a new calculation if a change is made to the laminate in question. Such results are therefore universally valid, which is also the reason why textbooks and technical design documents very often refer to such a dimensionless representation (note the consistent dimensionless representation of all results, e.g. in Wiedemann (1996)).

8.5 Examples for Exact Solutions

For some laminate problems, it is possible to find exact solutions for boundary value problems of static laminate problems given specific boundary conditions. Exact means here that both the governing differential equations and the specified boundary conditions are exactly fulfilled. A selection of such solutions is presented below. The value of these exact solutions lies not only in their often high technical significance, but also in the fact that they can be used as reference solutions for verifying approximate methods.

8.5.1 Navier Solutions

All following examples assume that the considered rectangular laminate (length a, width b, thickness h) is simply supported at all edges. The ambiguity that this condition may entail has already been discussed at the beginning of this chapter, so that special attention must be paid to the boundary conditions in each case. The laminates under consideration are subject to an arbitrary surface load $p(x, y)$, which can usually be represented in the form of a Fourier series:

$$p(x, y) = \sum_{m=1}^{m=\infty} \sum_{n=1}^{n=\infty} P_{mn} \sin\left(\frac{m\pi x}{a}\right) \sin\left(\frac{n\pi y}{b}\right). \tag{8.58}$$

The coefficients P_{mn} can be determined as:

$$P_{mn} = \frac{4}{ab} \int_0^b \int_0^a p(x, y) \sin\left(\frac{m\pi x}{a}\right) \sin\left(\frac{n\pi y}{b}\right) \mathrm{d}x\mathrm{d}y. \tag{8.59}$$

In the following it is shown how exact solutions for the given laminate bending problem can be derived.

8.5.1.1 Bending of a Symmetric Cross Composite

A symmetric cross-ply laminate is a laminate in which the individual layers only have orientation angles $\theta_k = 0°$ or $\theta_k = 90°$. Symmetric cross-ply laminates are thus always balanced (i.e. shear coupling terms $A_{16} = A_{26} = 0$) and also free of any bending-twisting coupling ($D_{16} = D_{26} = 0$). As a special case, this contains a single orthotropic layer or an orthotropic plate whose material principal axes coincide with the coordinate directions x, y. The laminate stiffness matrix then takes the following form:

$$\begin{bmatrix} \underline{\underline{A}} & \underline{\underline{B}} \\ \underline{\underline{B}} & \underline{\underline{D}} \end{bmatrix} = \begin{bmatrix} A_{11} & A_{12} & 0 & 0 & 0 & 0 \\ A_{12} & A_{22} & 0 & 0 & 0 & 0 \\ 0 & 0 & A_{66} & 0 & 0 & 0 \\ 0 & 0 & 0 & D_{11} & D_{12} & 0 \\ 0 & 0 & 0 & D_{12} & D_{22} & 0 \\ 0 & 0 & 0 & 0 & 0 & D_{66} \end{bmatrix}. \tag{8.60}$$

For the present problem, the displacement differential equations are considerably simplified, because the disk and plate behaviour are decoupled from each other, so that it is sufficient to consider only the third equation in (8.17) or (8.18), which then reads as follows:

$$D_{11}\frac{\partial^4 w_0}{\partial x^4} + 2\left(D_{12} + 2D_{66}\right)\frac{\partial^4 w_0}{\partial x^2 \partial y^2} + D_{22}\frac{\partial^4 w_0}{\partial y^4} - p = 0. \tag{8.61}$$

For this elementary example, simply supported boundary conditions mean that for $x = 0$ and $x = a$ for $0 \leq y \leq b$

$$w_0 = 0, \quad M_{xx}^0 = -D_{11}\frac{\partial^2 w_0}{\partial x^2} - D_{12}\frac{\partial^2 w_0}{\partial y^2} = 0, \tag{8.62}$$

whereas at the edges $y = 0$ and $y = b$ for $0 \leq x \leq a$ it is required that

$$w_0 = 0, \quad M_{yy}^0 = -D_{12}\frac{\partial^2 w_0}{\partial x^2} - D_{22}\frac{\partial^2 w_0}{\partial y^2} = 0 \tag{8.63}$$

holds. Since the disk and plate effects are decoupled for the current problem, it is not necessary to specify boundary conditions for the inplane displacements u_0, v_0.

A displacement approach of the form

$$w_0 = \sum_{m=1}^{m=\infty}\sum_{n=1}^{n=\infty} W_{mn} \sin\left(\frac{m\pi x}{a}\right)\sin\left(\frac{n\pi y}{b}\right) \tag{8.64}$$

fulfils all given boundary conditions (8.62) and (8.63) identically. If this approach is inserted into the differential equation (8.61), the following expression is obtained:

$$\sum_{m=1}^{m=\infty}\sum_{n=1}^{n=\infty}\left\{-W_{mn}\left[D_{11}\left(\frac{m\pi}{a}\right)^4+2\left(D_{12}+2D_{66}\right)\left(\frac{m\pi}{a}\right)^2\left(\frac{n\pi}{b}\right)^2 +D_{22}\left(\frac{n\pi}{b}\right)^4\right]+P_{mn}\right\}\sin\left(\frac{m\pi x}{a}\right)\sin\left(\frac{n\pi y}{b}\right)=0. \tag{8.65}$$

This requirement is fulfilled if the expression in the curly brackets disappears. This can be solved directly for the coefficients W_{mn}, and the result is:

$$W_{mn}=\frac{P_{mn}}{\pi^4\left[D_{11}\frac{m^4}{a^4}+2\left(D_{12}+2D_{66}\right)\frac{m^2n^2}{a^2b^2}+D_{22}\frac{n^4}{b^4}\right]}. \tag{8.66}$$

Thus, the series expansion (8.64) can generally be represented as:

$$w_0=\sum_{m=1}^{m=\infty}\sum_{n=1}^{n=\infty}\frac{P_{mn}\sin\left(\frac{m\pi x}{a}\right)\sin\left(\frac{n\pi y}{b}\right)}{\pi^4\left[D_{11}\frac{m^4}{a^4}+2\left(D_{12}+2D_{66}\right)\frac{m^2n^2}{a^2b^2}+D_{22}\frac{n^4}{b^4}\right]}. \tag{8.67}$$

It should be noted that the form of the solution (8.67) could suggest at first glance that this is an approximate solution, because after all, a series expansion is evaluated here, as is often the case in the context of approximating methods. However, it should be noted that the solution (8.67) is not only the result of the evaluation of the differential equation (8.61), but also fulfils all underlying boundary conditions (8.62) and (8.63) identically. Thus, the solution (8.67) is exact in the framework of Classical Laminated Plate Theory. During the evaluation, it is only necessary to ensure that the series expansion is sufficiently expanded. Of course, the upper limits $m=\infty, n=\infty$ are practically unrealizable. However, the quality of the solution naturally always increases as the degree of series expansion increases. However, this must always be verified by convergence studies.

For the special case of a constant load p it can be shown that the deflection of the laminate can be described by the following series expansion:

$$w_0=\frac{16p}{\pi^6}\sum_{m=1,3,5,\ldots}^{m=\infty}\sum_{n=1,3,5,\ldots}^{n=\infty}\frac{\frac{1}{mn}\sin\left(\frac{m\pi x}{a}\right)\sin\left(\frac{n\pi y}{b}\right)}{D_{11}\frac{m^4}{a^4}+2\left(D_{12}+2D_{66}\right)\frac{m^2n^2}{a^2b^2}+D_{22}\frac{n^4}{b^4}}. \tag{8.68}$$

An interesting special case is when the load p is in the form of a sinusoidal distribution of the type

$$p\left(x,y\right)=P_0\sin\left(\frac{\pi x}{a}\right)\sin\left(\frac{\pi y}{b}\right). \tag{8.69}$$

Then it turns out that a series expansion is not necessary, but that for $m = 1$ and $n = 1$ we are dealing with a closed-form analytical solution. The other load coefficients P_{mn} are identical to zero, the only remaining coefficient is $P_{11} = P_0$. Then the only remaining coefficient W_{11} of the deflection of the laminate is

$$W_{11} = \frac{P_0}{\pi^4 \left[\frac{D_{11}}{a^4} + \frac{2}{a^2 b^2} (D_{12} + 2D_{66}) + \frac{D_{22}}{b^4} \right]}, \tag{8.70}$$

and the exact solution of the deflection w_0 can be written as:

$$w_0 = \frac{P_0 \sin\left(\frac{\pi x}{a}\right) \sin\left(\frac{\pi y}{b}\right)}{\pi^4 \left[\frac{D_{11}}{a^4} + \frac{2}{a^2 b^2} (D_{12} + 2D_{66}) + \frac{D_{22}}{b^4} \right]}. \tag{8.71}$$

Once the exact solution for the deflection w_0 has been determined, the laminate moments M^0_{xx}, M^0_{yy} and M^0_{xy} can be calculated as follows:

$$\begin{aligned}
M^0_{xx} &= -D_{11} \frac{\partial^2 w_0}{\partial x^2} - D_{12} \frac{\partial^2 w_0}{\partial y^2} \\
&= \sum_{m=1}^{m=\infty} \sum_{n=1}^{n=\infty} \left(D_{11} \frac{m^2 \pi^2}{a^2} + D_{12} \frac{n^2 \pi^2}{b^2} \right) W_{mn} \sin\left(\frac{m\pi x}{a}\right) \sin\left(\frac{n\pi y}{b}\right), \\
M^0_{yy} &= -D_{12} \frac{\partial^2 w_0}{\partial x^2} - D_{22} \frac{\partial^2 w_0}{\partial y^2} \\
&= \sum_{m=1}^{m=\infty} \sum_{n=1}^{n=\infty} \left(D_{12} \frac{m^2 \pi^2}{a^2} + D_{22} \frac{n^2 \pi^2}{b^2} \right) W_{mn} \sin\left(\frac{m\pi x}{a}\right) \sin\left(\frac{n\pi y}{b}\right), \\
M^0_{xy} &= -2 D_{66} \frac{\partial^2 w_0}{\partial x \partial y} \\
&= -2 \sum_{m=1}^{m=\infty} \sum_{n=1}^{n=\infty} \frac{m\pi}{a} \frac{n\pi}{b} D_{66} W_{mn} \cos\left(\frac{m\pi x}{a}\right) \cos\left(\frac{n\pi y}{b}\right).
\end{aligned} \tag{8.72}$$

The layerwise intralaminar stresses can then be calculated as:

$$
\begin{aligned}
\begin{pmatrix}\sigma_{xx}\\ \sigma_{yy}\\ \tau_{xy}\end{pmatrix}_k &= -z\begin{bmatrix}Q_{11} & Q_{12} & 0\\ Q_{12} & Q_{22} & 0\\ 0 & 0 & Q_{66}\end{bmatrix}_k \begin{pmatrix}\dfrac{\partial^2 w_0}{\partial x^2}\\ \dfrac{\partial^2 w_0}{\partial y^2}\\ 2\dfrac{\partial^2 w_0}{\partial x \partial y}\end{pmatrix}\\
&= z\sum_{m=1}^{m=\infty}\sum_{n=1}^{n=\infty} W_{mn}\begin{bmatrix}Q_{11} & Q_{12} & 0\\ Q_{12} & Q_{22} & 0\\ 0 & 0 & Q_{66}\end{bmatrix}_k \begin{pmatrix}\dfrac{m^2\pi^2}{a^2}\sin\left(\dfrac{m\pi x}{a}\right)\sin\left(\dfrac{n\pi y}{b}\right)\\ \dfrac{n^2\pi^2}{b^2}\sin\left(\dfrac{m\pi x}{a}\right)\sin\left(\dfrac{n\pi y}{b}\right)\\ -2\dfrac{m\pi}{a}\dfrac{n\pi}{b}\cos\left(\dfrac{m\pi x}{a}\right)\cos\left(\dfrac{n\pi y}{b}\right)\end{pmatrix}\\
&= z\sum_{m=1}^{m=\infty}\sum_{n=1}^{n=\infty} W_{mn}\begin{pmatrix}\left(Q_{11,k}\dfrac{m^2\pi^2}{a^2}+Q_{12,k}\dfrac{n^2\pi^2}{b^2}\right)\sin\left(\dfrac{m\pi x}{a}\right)\sin\left(\dfrac{n\pi y}{b}\right)\\ \left(Q_{12,k}\dfrac{m^2\pi^2}{a^2}+Q_{22,k}\dfrac{n^2\pi^2}{b^2}\right)\sin\left(\dfrac{m\pi x}{a}\right)\sin\left(\dfrac{n\pi y}{b}\right)\\ -2Q_{66,k}\dfrac{m\pi}{a}\dfrac{n\pi}{b}\cos\left(\dfrac{m\pi x}{a}\right)\cos\left(\dfrac{n\pi y}{b}\right)\end{pmatrix}.
\end{aligned}
\tag{8.73}
$$

If (8.73) is discussed in more detail, it can be seen that, for example, in the case of a uniformly distributed load p, the largest normal stresses in terms of magnitude occur in the center of the plate and usually (but not necessarily in every case) at the laminate surfaces. The maximum shear stresses, on the other hand, occur at the four laminate corners. In addition, the stresses in each individual layer are piecewise linear over the thickness direction z.

There is no constitutive law for the interlaminar stresses τ_{xz}, τ_{yz} and σ_{zz} within the framework of Classical Laminated Plate Theory. However, the interlaminar stresses can be obtained in a post-processing analysis (some more detailed comments on this follow later in this book) by integrating the three-dimensional local equilibrium conditions

$$
\begin{aligned}
\frac{\partial \sigma_{xx}}{\partial x}+\frac{\partial \tau_{xy}}{\partial y}+\frac{\partial \tau_{xz}}{\partial z} &= 0,\\
\frac{\partial \tau_{xy}}{\partial x}+\frac{\partial \sigma_{yy}}{\partial y}+\frac{\partial \tau_{yz}}{\partial z} &= 0,\\
\frac{\partial \tau_{xz}}{\partial x}+\frac{\partial \tau_{yz}}{\partial y}+\frac{\partial \sigma_{zz}}{\partial z} &= 0
\end{aligned}
\tag{8.74}
$$

through the thickness (whereby it is assumed here that no volume forces are present):

$$\tau_{xz,k} = -\int_{z_{k-1}}^{z} \left(\frac{\partial \sigma_{xx,k}}{\partial x} + \frac{\partial \tau_{xy,k}}{\partial y} \right) \mathrm{d}z + F_{1,k}(x, y),$$

$$\tau_{yz,k} = -\int_{z_{k-1}}^{z} \left(\frac{\partial \tau_{xy,k}}{\partial x} + \frac{\partial \sigma_{yy,k}}{\partial y} \right) \mathrm{d}z + F_{2,k}(x, y),$$

$$\sigma_{zz,k} = -\int_{z_{k-1}}^{z} \left(\frac{\partial \tau_{xz,k}}{\partial x} + \frac{\partial \tau_{yz,k}}{\partial y} \right) \mathrm{d}z + F_{3,k}(x, y). \tag{8.75}$$

Since the intralaminar stresses $\sigma_{xx,k}$, $\sigma_{yy,k}$ and $\tau_{xy,k}$ are given in each layer with (8.73), the integrals in (8.75) can be evaluated relatively easily. The functions $F_{1,k}$, $F_{2,k}$, $F_{3,k}$ result from the integration in the z-direction and must be adapted to the given requirements for stress-free surfaces and continuous interlaminar stresses across the layer interfaces. Finally, the following compact expressions are obtained for the interlaminar stresses τ_{xz}, τ_{yz} and σ_{zz} in the layer k ($z_{k-1} \leq z \leq z_k$):

$$\tau_{xz,k} = -X(z) \sum_{m=1}^{m=\infty} \sum_{n=1}^{n=\infty} \left[T_{x,k} W_{mn} \cos\left(\frac{m\pi x}{a}\right) \sin\left(\frac{n\pi y}{b}\right) \right] + \tau_{xz,k-1}(z = z_{k-1}),$$

$$\tau_{yz,k} = -Y(z) \sum_{m=1}^{m=\infty} \sum_{n=1}^{n=\infty} \left[T_{y,k} W_{mn} \sin\left(\frac{m\pi x}{a}\right) \cos\left(\frac{n\pi y}{b}\right) \right] + \tau_{yz,k-1}(z = z_{k-1}),$$

$$\sigma_{zz,k} = -Z(z) \sum_{m=1}^{m=\infty} \sum_{n=1}^{n=\infty} \left[T_{z,k} W_{mn} \sin\left(\frac{m\pi x}{a}\right) \sin\left(\frac{n\pi y}{b}\right) \right] + \sigma_{zz,k-1}(z = z_{k-1})$$
$$+ (z - z_{k-1}) \left(\frac{\partial \tau_{xz,k}}{\partial x} + \frac{\partial \tau_{yz,k}}{\partial y} \right) \Bigg|_{z=z_{k-1}}, \tag{8.76}$$

wherein

$$X(z) = Y(z) = \frac{z^2 - z_{k-1}^2}{2}, \quad Z(z) = \frac{z_{k-1}^3}{3} + \frac{z}{6}\left(z^2 - 3z_{k-1}^2\right), \tag{8.77}$$

and

$$T_{x,k} = \frac{m^3\pi^3}{a^3} Q_{11,k} + \frac{m\pi}{a} \frac{n^2\pi^2}{b^2} \left(2Q_{66,k} + Q_{12,k}\right),$$

$$T_{y,k} = \frac{n^3\pi^3}{b^3} Q_{22,k} + \frac{m^2\pi^2}{a^2} \frac{n\pi}{b} \left(2Q_{66,k} + Q_{12,k}\right),$$

$$T_{z,k} = \frac{m^4\pi^4}{a^4} Q_{11,k} + 2\frac{m^2\pi^2}{a^2} \frac{n^2\pi^2}{b^2} \left(2Q_{66,k} + Q_{12,k}\right) + \frac{n^4\pi^4}{b^4} Q_{22,k}. \tag{8.78}$$

8.5.1.2 Bending of an Unsymmetric Cross-Ply Laminate $\left[(0°/90°)_N\right]$

As a further example of an exact solution, the bending of an unsymmetric cross-ply laminate $\left[(0°/90°)_N\right]$ will be considered. For such a laminate, the laminate stiffness matrix is populated as follows:

$$\begin{bmatrix} \underline{\underline{A}} & \underline{\underline{B}} \\ \underline{\underline{B}} & \underline{\underline{D}} \end{bmatrix} = \begin{bmatrix} A_{11} & A_{12} & 0 & B_{11} & 0 & 0 \\ A_{12} & A_{11} & 0 & 0 & -B_{11} & 0 \\ 0 & 0 & A_{66} & 0 & 0 & 0 \\ B_{11} & 0 & 0 & D_{11} & D_{12} & 0 \\ 0 & -B_{11} & 0 & D_{12} & D_{11} & 0 \\ 0 & 0 & 0 & 0 & 0 & D_{66} \end{bmatrix}. \tag{8.79}$$

In this case, the displacement differential equations can be specified as (the tangential forces p_x and p_y are zero here):

$$\begin{aligned} A_{11}\frac{\partial^2 u_0}{\partial x^2} + A_{66}\frac{\partial^2 u_0}{\partial y^2} + (A_{12}+A_{66})\frac{\partial^2 v_0}{\partial x \partial y} - B_{11}\frac{\partial^3 w_0}{\partial x^3} &= 0, \\ (A_{12}+A_{66})\frac{\partial^2 u_0}{\partial x \partial y} + A_{66}\frac{\partial^2 v_0}{\partial x^2} + A_{11}\frac{\partial^2 v_0}{\partial y^2} + B_{11}\frac{\partial^3 w_0}{\partial y^3} &= 0, \\ D_{11}\left(\frac{\partial^4 w_0}{\partial x^4} + \frac{\partial^4 w_0}{\partial y^4}\right) + 2\,(D_{12}+2D_{66})\frac{\partial^4 w_0}{\partial x^2 \partial y^2} - B_{11}\left(\frac{\partial^3 u_0}{\partial x^3} - \frac{\partial^3 v_0}{\partial y^3}\right) &= p. \end{aligned} \tag{8.80}$$

For the given laminate bending problem, plate and disk behaviour remain coupled with each other.

The following requirements are specified as boundary conditions (this type of boundary condition is also known as SS1 boundary conditions, where 'SS' is derived from 'simply supported'). For $x = 0$ and $x = a$ for $0 \le y \le b$ it is required that

$$\begin{aligned} w_0 &= 0, \\ v_0 &= 0, \\ M^0_{xx} &= B_{11}\frac{\partial u_0}{\partial x} - D_{11}\frac{\partial^2 w_0}{\partial x^2} - D_{12}\frac{\partial^2 w_0}{\partial y^2} = 0, \\ N^0_{xx} &= A_{11}\frac{\partial u_0}{\partial x} + A_{12}\frac{\partial v_0}{\partial y} - B_{11}\frac{\partial^2 w_0}{\partial x^2} = 0, \end{aligned} \tag{8.81}$$

whereas for $y = 0$ and $y = b$ for $0 \le x \le a$ it is required that

$$
\begin{aligned}
w_0 &= 0, \\
u_0 &= 0, \\
M^0_{yy} &= -B_{11}\frac{\partial v_0}{\partial y} - D_{12}\frac{\partial^2 w_0}{\partial x^2} - D_{11}\frac{\partial^2 w_0}{\partial y^2} = 0, \\
N^0_{yy} &= A_{12}\frac{\partial u_0}{\partial x} + A_{11}\frac{\partial v_0}{\partial y} + B_{11}\frac{\partial^2 w_0}{\partial y^2} = 0.
\end{aligned} \tag{8.82}
$$

These could be typical boundary conditions for a skin panel of a stiffened aircraft panel.

The procedure is that a series approach of the following form is made for the displacements u_0, v_0, w_0:

$$
\begin{aligned}
u_0 &= \sum_{m=1}^{m=\infty}\sum_{n=1}^{n=\infty} U_{mn}\cos\left(\frac{m\pi x}{a}\right)\sin\left(\frac{n\pi y}{b}\right), \\
v_0 &= \sum_{m=1}^{m=\infty}\sum_{n=1}^{n=\infty} V_{mn}\sin\left(\frac{m\pi x}{a}\right)\cos\left(\frac{n\pi y}{b}\right), \\
w_0 &= \sum_{m=1}^{m=\infty}\sum_{n=1}^{n=\infty} W_{mn}\sin\left(\frac{m\pi x}{a}\right)\sin\left(\frac{n\pi y}{b}\right).
\end{aligned} \tag{8.83}
$$

Here, too, it makes sense to develop the applied surface load p in the form of a Fourier series according to (8.58) with (8.59). If this is inserted into the displacement differential equations (8.80) using the approach (8.83), the following relationships are obtained:

$$
\begin{aligned}
&\sum_{m=1}^{m=\infty}\sum_{n=1}^{n=\infty}\left[-\left(A_{11}\frac{m^2\pi^2}{a^2} + A_{66}\frac{n^2\pi^2}{b^2}\right)U_{mn} - (A_{12}+A_{66})\frac{m\pi}{a}\frac{n\pi}{b}V_{mn}\right. \\
&\left. + B_{11}\frac{m^3\pi^3}{a^3}W_{mn}\right]\cos\left(\frac{m\pi x}{a}\right)\sin\left(\frac{n\pi y}{b}\right) = 0, \\
&\sum_{m=1}^{m=\infty}\sum_{n=1}^{n=\infty}\left[-(A_{12}+A_{66})\frac{m\pi}{a}\frac{n\pi}{b}U_{mn} - \left(A_{66}\frac{m^2\pi^2}{a^2} + A_{11}\frac{n^2\pi^2}{b^2}\right)V_{mn}\right. \\
&\left. - B_{11}\frac{n^3\pi^3}{b^3}W_{mn}\right]\sin\left(\frac{m\pi x}{a}\right)\cos\left(\frac{n\pi y}{b}\right) = 0, \\
&\sum_{m=1}^{m=\infty}\sum_{n=1}^{n=\infty}\left\{B_{11}\frac{m^3\pi^3}{a^3}U_{mn} - B_{11}\frac{n^3\pi^3}{b^3}V_{mn}\right. \\
&\left. - \left[D_{11}\frac{m^4\pi^4}{a^4} + 2\,(D_{12}+2D_{66})\frac{m^2\pi^2}{a^2}\frac{n^2\pi^2}{b^2} + D_{11}\frac{n^4\pi^4}{b^4}\right]W_{mn}\right\} \\
&\times\sin\left(\frac{m\pi x}{a}\right)\sin\left(\frac{n\pi y}{b}\right) = -p.
\end{aligned} \tag{8.84}
$$

As with the bending problem of the symmetric orthotropic laminate, the terms contained in brackets must also disappear at this point in order to fulfil (8.84). This ultimately leads

to a system of three linear equations for the three unknown coefficients U_{mn}, V_{mn}, W_{mn}:

$$
\begin{aligned}
&-\left(A_{11}\frac{m^2\pi^2}{a^2}+A_{66}\frac{n^2\pi^2}{b^2}\right)U_{mn}-(A_{12}+A_{66})\,\frac{m\pi}{a}\frac{n\pi}{b}V_{mn}+B_{11}\frac{m^3\pi^3}{a^3}W_{mn}=0,\\
&-(A_{12}+A_{66})\,\frac{m\pi}{a}\frac{n\pi}{b}U_{mn}-\left(A_{66}\frac{m^2\pi^2}{a^2}+A_{11}\frac{n^2\pi^2}{b^2}\right)V_{mn}-B_{11}\frac{n^3\pi^3}{b^3}W_{mn}=0,\\
&B_{11}\frac{m^3\pi^3}{a^3}U_{mn}-B_{11}\frac{n^3\pi^3}{b^3}V_{mn}\\
&-\left[D_{11}\frac{m^4\pi^4}{a^4}+2\,(D_{12}+2D_{66})\,\frac{m^2\pi^2}{a^2}\frac{n^2\pi^2}{b^2}+D_{11}\frac{n^4\pi^4}{b^4}\right]W_{mn}=-P_{mn}.
\end{aligned}
\tag{8.85}
$$

If the linear system of equations (8.85) is solved for a given pair of values m, n, then the corresponding coefficients U_{mn}, V_{mn}, W_{mn} are found. Equations (8.85) can also be represented in a vector-matrix form as follows:

$$
\begin{bmatrix}\lambda_{11} & \lambda_{12} & \lambda_{13}\\ \lambda_{12} & \lambda_{22} & \lambda_{23}\\ \lambda_{13} & \lambda_{23} & \lambda_{33}\end{bmatrix}\begin{pmatrix}U_{mn}\\ V_{mn}\\ W_{mn}\end{pmatrix}=\begin{pmatrix}0\\ 0\\ -P_{mn}\end{pmatrix},
\tag{8.86}
$$

where the following abbreviations were used for the matrix entries:

$$
\begin{aligned}
&\lambda_{11}=-A_{11}\frac{m^2\pi^2}{a^2}-A_{66}\frac{n^2\pi^2}{b^2},\quad \lambda_{12}=-(A_{12}+A_{66})\,\frac{mn\pi^2}{ab},\\
&\lambda_{13}=B_{11}\frac{m^3\pi^3}{a^3},\quad \lambda_{22}=-A_{66}\frac{m^2\pi^2}{a^2}-A_{11}\frac{n^2\pi^2}{b^2},\quad \lambda_{23}=-B_{11}\frac{n^3\pi^3}{b^3},\\
&\lambda_{33}=-\left[D_{11}\left(\frac{m^4\pi^4}{a^4}+\frac{n^4\pi^4}{b^4}\right)+2\,(D_{12}+2D_{66})\,\frac{m^2n^2\pi^4}{a^2b^2}\right].
\end{aligned}
\tag{8.87}
$$

The Navier solution for the bending of an unsymmetric cross-ply laminate is now complete and all displacements, internal forces and stresses in the laminate can be calculated. This will not be formulated further here. A convergence analysis must show at which degree of series development for load and displacements the results achieve a satisfactory quality.

For the special case of a sinusoidal load p of the form

$$
p\,(x,\,y)=P_0\sin\left(\frac{\pi x}{a}\right)\sin\left(\frac{\pi y}{b}\right)
\tag{8.88}
$$

a displacement approach of the following type is sufficient:

$$
\begin{aligned}
u_0&=U_{11}\cos\left(\frac{\pi x}{a}\right)\sin\left(\frac{\pi y}{b}\right),\\
v_0&=V_{11}\sin\left(\frac{\pi x}{a}\right)\cos\left(\frac{\pi y}{b}\right),\\
w_0&=W_{11}\sin\left(\frac{\pi x}{a}\right)\sin\left(\frac{\pi y}{b}\right).
\end{aligned}
\tag{8.89}
$$

If this is inserted into the displacement differential equations (8.80), the following linear system of equations is obtained to determine the coefficients U_{11}, V_{11}, W_{11} (all other coefficients U_{mn}, V_{mn}, W_{mn} would result in zero in this case):

$$\begin{bmatrix} -A_{11}\frac{\pi^2}{a^2} - A_{66}\frac{\pi^2}{b^2} & -(A_{12}+A_{66})\frac{\pi^2}{ab} & B_{11}\frac{\pi^3}{a^3} \\ -(A_{12}+A_{66})\frac{\pi^2}{ab} & -A_{66}\frac{\pi^2}{a^2} - A_{11}\frac{\pi^2}{b^2} & -B_{11}\frac{\pi^3}{b^3} \\ -B_{11}\frac{\pi^3}{a^3} & B_{11}\frac{\pi^3}{b^3} & D_{11}\left(\frac{\pi^4}{a^4}+\frac{\pi^4}{b^4}\right) + 2\,(D_{12}+2D_{66})\,\frac{\pi^4}{a^2b^2} \end{bmatrix} \times \begin{pmatrix} U_{11} \\ V_{11} \\ W_{11} \end{pmatrix} = \begin{pmatrix} 0 \\ 0 \\ P_0 \end{pmatrix}. \tag{8.90}$$

If this is solved for the coefficients U_{11}, V_{11}, W_{11}, the displacements of each laminate point are determined, and the strains and stresses of the laminate can be calculated.

8.5.1.3 Bending of an Unsymmetric Angle-Ply Laminate $\left[(\pm\theta)_N\right]$

For an angle-ply laminate of the kind $\left[(\pm\theta)_N\right]$, the laminate stiffness matrix reads:

$$\begin{bmatrix} \underline{\underline{A}} & \underline{\underline{B}} \\ \underline{\underline{B}} & \underline{\underline{D}} \end{bmatrix} = \begin{bmatrix} A_{11} & A_{12} & 0 & 0 & 0 & B_{16} \\ A_{12} & A_{22} & 0 & 0 & 0 & B_{26} \\ 0 & 0 & A_{66} & B_{16} & B_{26} & 0 \\ 0 & 0 & B_{16} & D_{11} & D_{12} & 0 \\ 0 & 0 & B_{26} & D_{12} & D_{22} & 0 \\ B_{16} & B_{26} & 0 & 0 & 0 & D_{66} \end{bmatrix}. \tag{8.91}$$

The displacement differential equations (8.17) are as follows for this case:

$$\begin{aligned} A_{11}\frac{\partial^2 u_0}{\partial x^2} + A_{66}\frac{\partial^2 u_0}{\partial y^2} + (A_{12}+A_{66})\frac{\partial^2 v_0}{\partial x \partial y} - 3B_{16}\frac{\partial^3 w_0}{\partial x^2 \partial y} - B_{26}\frac{\partial^3 w_0}{\partial y^3} &= 0, \\ (A_{12}+A_{66})\frac{\partial^2 u_0}{\partial x \partial y} + A_{66}\frac{\partial^2 v_0}{\partial x^2} + A_{22}\frac{\partial^2 v_0}{\partial y^2} - B_{16}\frac{\partial^3 w_0}{\partial x^3} - 3B_{26}\frac{\partial^3 w_0}{\partial x \partial y^2} &= 0, \\ D_{11}\frac{\partial^4 w_0}{\partial x^4} + 2\,(D_{12}+2D_{66})\frac{\partial^4 w_0}{\partial x^2 \partial y^2} + D_{22}\frac{\partial^4 w_0}{\partial y^4} & \\ -B_{16}\left(3\frac{\partial^3 u_0}{\partial x^2 \partial y} + \frac{\partial^3 v_0}{\partial x^3}\right) - B_{26}\left(3\frac{\partial^3 v_0}{\partial x \partial y^2} + \frac{\partial^3 u_0}{\partial y^3}\right) - p &= 0. \end{aligned} \tag{8.92}$$

With regard to the boundary conditions (here these are the so-called SS2 boundary conditions), for $x = 0$ and $x = a$ for $0 \le y \le b$ it is required that

$$
\begin{aligned}
w_0 &= 0, \\
u_0 &= 0, \\
M_{xx}^0 &= B_{16}\left(\frac{\partial u_0}{\partial y} + \frac{\partial v_0}{\partial x}\right) - D_{11}\frac{\partial^2 w_0}{\partial x^2} - D_{12}\frac{\partial^2 w_0}{\partial y^2} = 0, \\
N_{xy}^0 &= A_{66}\left(\frac{\partial u_0}{\partial y} + \frac{\partial v_0}{\partial x}\right) - B_{16}\frac{\partial^2 w_0}{\partial x^2} - B_{26}\frac{\partial^2 w_0}{\partial y^2} = 0,
\end{aligned} \tag{8.93}
$$

while for $y = 0$ and $y = b$ the following is required for $0 \le x \le a$:

$$
\begin{aligned}
w_0 &= 0, \\
v_0 &= 0, \\
M_{yy}^0 &= B_{26}\left(\frac{\partial u_0}{\partial y} + \frac{\partial v_0}{\partial x}\right) - D_{12}\frac{\partial^2 w_0}{\partial x^2} - D_{22}\frac{\partial^2 w_0}{\partial y^2} = 0, \\
N_{xy}^0 &= A_{66}\left(\frac{\partial u_0}{\partial y} + \frac{\partial v_0}{\partial x}\right) - B_{16}\frac{\partial^2 w_0}{\partial x^2} - B_{26}\frac{\partial^2 w_0}{\partial y^2} = 0.
\end{aligned} \tag{8.94}
$$

As with the bending problem of the unsymmetric cross-ply laminate, it is easy to show that a displacement approach of the form

$$
\begin{aligned}
u_0 &= \sum_{m=1}^{m=\infty}\sum_{n=1}^{n=\infty} U_{mn} \sin\left(\frac{m\pi x}{a}\right)\cos\left(\frac{n\pi y}{b}\right), \\
v_0 &= \sum_{m=1}^{m=\infty}\sum_{n=1}^{n=\infty} V_{mn} \cos\left(\frac{m\pi x}{a}\right)\sin\left(\frac{n\pi y}{b}\right), \\
w_0 &= \sum_{m=1}^{m=\infty}\sum_{n=1}^{n=\infty} W_{mn} \sin\left(\frac{m\pi x}{a}\right)\sin\left(\frac{n\pi y}{b}\right)
\end{aligned} \tag{8.95}
$$

fulfills both the displacement differential equations (8.92) and the boundary conditions (8.93) and (8.94) identically. The system of equations for determining the coefficients U_{mn}, V_{mn}, W_{mn} can then be specified as follows:

$$
\begin{bmatrix}
\lambda_{11} & \lambda_{12} & \lambda_{13} \\
\lambda_{12} & \lambda_{22} & \lambda_{23} \\
\lambda_{13} & \lambda_{23} & \lambda_{33}
\end{bmatrix}
\begin{pmatrix}
U_{mn} \\ V_{mn} \\ W_{mn}
\end{pmatrix}
=
\begin{pmatrix}
0 \\ 0 \\ P_{mn}
\end{pmatrix}, \tag{8.96}
$$

wherein:

$$\lambda_{11} = A_{11}\frac{m^2\pi^2}{a^2} + A_{66}\frac{n^2\pi^2}{b^2}, \quad \lambda_{12} = (A_{12} + A_{66})\frac{m\pi}{a}\frac{n\pi}{b},$$
$$\lambda_{13} = -\left(3B_{16}\frac{m^2\pi^2}{a^2} + B_{26}\frac{n^2\pi^2}{b^2}\right)\frac{n\pi}{b}, \quad \lambda_{22} = A_{66}\frac{m^2\pi^2}{a^2} + A_{22}\frac{n^2\pi^2}{b^2},$$
$$\lambda_{23} = -\left(B_{16}\frac{m^2\pi^2}{a^2} + 3B_{26}\frac{n^2\pi^2}{b^2}\right)\frac{m\pi}{a},$$
$$\lambda_{33} = D_{11}\frac{m^4\pi^4}{a^4} + 2\left(D_{12} + 2D_{66}\right)\frac{m^2\pi^2}{a^2}\frac{n^2\pi^2}{b^2} + D_{22}\frac{n^4\pi^4}{b^4}. \tag{8.97}$$

If we again consider the special case of a sinusoidally distributed load p according to

$$p(x, y) = P_0 \sin\left(\frac{\pi x}{a}\right)\sin\left(\frac{\pi y}{b}\right) \tag{8.98}$$

and assume that a single-term approach of the type

$$u_0 = U_{11}\sin\left(\frac{\pi x}{a}\right)\cos\left(\frac{\pi y}{b}\right),$$
$$v_0 = V_{11}\cos\left(\frac{\pi x}{a}\right)\sin\left(\frac{\pi y}{b}\right),$$
$$w_0 = W_{11}\sin\left(\frac{\pi x}{a}\right)\sin\left(\frac{\pi y}{b}\right) \tag{8.99}$$

is sufficient for each displacement component, then after inserting (8.99) into the displacement differential equations (8.92), the following linear system of equations is obtained for the coefficients U_{11}, V_{11}, W_{11}:

$$\begin{bmatrix} -A_{11}\frac{\pi^2}{a^2} - A_{66}\frac{\pi^2}{b^2} & -(A_{12} + A_{66})\frac{\pi^2}{ab} & 3B_{16}\frac{\pi^3}{a^2b} + B_{26}\frac{\pi^3}{b^3} \\ -(A_{12} + A_{66})\frac{\pi^2}{ab} & -A_{66}\frac{\pi^2}{a^2} - A_{22}\frac{\pi^2}{b^2} & 3B_{26}\frac{\pi^3}{ab^2} + B_{16}\frac{\pi^3}{a^3} \\ -3B_{16}\frac{\pi^3}{a^2b} - B_{26}\frac{\pi^3}{b^3} & -3B_{26}\frac{\pi^3}{ab^2} - B_{16}\frac{\pi^3}{a^3} & D_{11}\frac{\pi^4}{a^4} + 2\left(D_{12} + 2D_{66}\right)\frac{\pi^4}{a^2b^2} + D_{22}\frac{\pi^4}{b^4} \end{bmatrix}$$
$$\times \begin{pmatrix} U_{11} \\ V_{11} \\ W_{11} \end{pmatrix} = \begin{pmatrix} 0 \\ 0 \\ P_0 \end{pmatrix}. \tag{8.100}$$

8.5.2 Lévy Solutions

Lévy-type solutions can be specified for the problem of laminate bending in the same way as for isotropic structures. Rectangular laminates are considered whose edges are simply supported at $x = 0$ and $x = a$. The two remaining edges $y = 0$ and $y = b$ can have any support conditions, e.g. free, hinged, clamped, elastically supported, reinforced by stiffeners, etc. Navier-type solutions cannot be derived for such situations, and an alternative form of

solution must be found. One possibility is to utilise the fact that the opposite edges at $x = 0$ and $x = a$ are simply supported. As with the Navier solution, we can then use a very similar solution approach in the x-direction and thus reduce the governing partial differential equations to ordinary differential equations. The remaining ordinary differential equations can then be solved exactly for elementary cases, as will be shown below. For reasons of clarity, we will restrict ourselves to the case of a symmetric laminate with orthotropic plate behaviour.

Bending of a symmetric and orthotropic laminate under a surface load p in z-direction is described by the following linear partial differential equation of fourth order:

$$D_{11}\frac{\partial^4 w_0}{\partial x^4} + D_{22}\frac{\partial^4 w_0}{\partial y^4} + 2\left(D_{12} + 2D_{66}\right)\frac{\partial^4 w_0}{\partial x^2 \partial y^2} - p = 0. \tag{8.101}$$

The following approach is used for the deflection w_0 of the laminate:

$$w_0 = \sum_{m=1}^{m=\infty} \sin\left(\frac{m\pi x}{a}\right) W_m\left(y\right). \tag{8.102}$$

The surface load p is expressed in the same way:

$$p = \sum_{m=1}^{m=\infty} \sin\left(\frac{m\pi x}{a}\right) P_m\left(y\right), \tag{8.103}$$

wherein:

$$P_m\left(y\right) = \frac{2}{a}\int_0^a p\left(x, y\right) \sin\left(\frac{m\pi x}{a}\right) \mathrm{d}x. \tag{8.104}$$

If the approach (8.102) is inserted into the differential equation (8.101), the following expression is obtained:

$$\sum_{m=1}^{m=\infty} \left\{ \left[D_{22}\frac{\partial^4 W_m}{\partial y^4} - 2\left(D_{12} + 2D_{66}\right)\left(\frac{m\pi}{a}\right)^2 \frac{\partial^2 W_m}{\partial y^2} + D_{11}\left(\frac{m\pi}{a}\right)^4 W_m - P_m \right] \sin\left(\frac{m\pi x}{a}\right) \right\} = 0. \tag{8.105}$$

The condition (8.105) must be fulfilled regardless of the value x, so that the term in the square brackets is required to disappear:

$$D_{22}\frac{\mathrm{d}^4 W_m}{\mathrm{d}y^4} - 2\left(D_{12} + 2D_{66}\right)\left(\frac{m\pi}{a}\right)^2 \frac{\mathrm{d}^2 W_m}{\mathrm{d}y^2} + D_{11}\left(\frac{m\pi}{a}\right)^4 W_m = P_m. \tag{8.106}$$

This is an ordinary differential equation of the fourth order, from which the displacement function W_m can be determined.

Firstly, the homogeneous solution $W_{m,h}$ is to be determined. To do this, we use an approach of the form

$$W_{m,h} = C_m e^{\lambda y}, \tag{8.107}$$

which, after insertion into (8.106), leads to the following fourth-order polynomial for the exponent λ:

$$D_{22}\lambda^4 - 2\left(D_{12} + 2D_{66}\right)\left(\frac{m\pi}{a}\right)^2 \lambda^2 + D_{11}\left(\frac{m\pi}{a}\right)^4 = 0. \tag{8.108}$$

The four solutions of (8.108) are:

$$\lambda_{1,2,3,4} = \pm\frac{m\pi}{a\sqrt{D_{22}}}\sqrt{D_{12} + 2D_{66} \pm \sqrt{\left(D_{12} + 2D_{66}\right)^2 - D_{11}D_{22}}}. \tag{8.109}$$

In order to determine the type of displacement solution $W_{m,h}$ in more detail, a case differentiation is carried out. The decisive factor here is the term under the second root in (8.109), and the following three cases must be distinguished.

1. if $\left(D_{12} + 2D_{66}\right)^2 > D_{11}D_{22}$ holds, then all solutions for λ are both real-valued and different from each other, and $\lambda_1 = -\lambda_2$ and $\lambda_3 = -\lambda_4$ hold. The displacement function $W_{m,h}$ can then be written as:

$$W_{m,h} = C_{m,1}e^{\lambda_1 y} + C_{m,2}e^{\lambda_2 y} + C_{m,3}e^{\lambda_3 y} + C_{m,4}e^{\lambda_4 y}. \tag{8.110}$$

A representation in the form

$$W_{m,h} = C_{m,1}\cosh\left(\lambda_1 y\right) + C_{m,2}\sinh\left(\lambda_1 y\right) + C_{m,3}\cosh\left(\lambda_3 y\right) + C_{m,4}\sinh\left(\lambda_3 y\right) \tag{8.111}$$

is just as common and equivalent.

2. if $\left(D_{12} + 2D_{66}\right)^2 = D_{11}D_{22}$ applies, then all exponents λ are real-valued and result as

$$\lambda = \pm\frac{m\pi}{a\sqrt{D_{22}}}\sqrt{D_{12} + 2D_{66}}, \tag{8.112}$$

where two pairs are identical, i.e. $\lambda_1 = \lambda_2 = -\lambda_3 = -\lambda_4 = \lambda$. In this case, the displacement function $W_{m,h}$ can be represented as:

$$W_{m,h} = \left(C_{m,1} + C_{m,2}y\right)\cosh\left(\lambda y\right) + \left(C_{m,3} + C_{m,4}y\right)\sinh\left(\lambda y\right). \tag{8.113}$$

3. if $\left(D_{12} + 2D_{66}\right)^2 < D_{11}D_{22}$ applies, then the exponents λ are complex-valued and appear in complex conjugate pairs: $\pm\lambda_1 \pm i\lambda_2$. The function $W_{m,h}$ then takes the following form:

$$\begin{aligned} W_{m,h} = &\left[C_{m,1}\cos\left(\lambda_2 y\right) + C_{m,2}\sin\left(\lambda_2 y\right)\right]\cosh\left(\lambda_1 y\right) \\ &+ \left[C_{m,3}\cos\left(\lambda_2 y\right) + C_{m,4}\sin\left(\lambda_2 y\right)\right]\sinh\left(\lambda_1 y\right). \end{aligned} \tag{8.114}$$

In all three cases, the constants C_m are determined from the boundary conditions at the edges at $y = 0$ and $y = b$.

The particular solution $W_{m,p}$ of (8.106) cannot be given universally, but rather depends on the specific mathematical form of the term P_m. In many cases, a solution can be determined with a right-hand side approach and a final comparison of coefficients. The special case of a constant P_m can be solved quite easily in a generalised way. The approach for $W_{m,p}$ is chosen in the form of a constant k. Insertion into (8.106) and coefficient comparison leads to:

$$W_{m,p} = \frac{P_m}{D_{11}} \left(\frac{a}{m\pi} \right)^4 . \tag{8.115}$$

This special case will be considered exclusively in the following. However, all other (also technically) relevant cases can be solved in a similar way. The homogeneous solutions determined remain valid in all cases.

To illustrate the procedure when using a Lévy solution approach, the deflection of a symmetric and orthotropic laminate under a constant surface load p is considered, assuming that $(D_{12} + 2D_{66})^2 > D_{11}D_{22}$ applies. The overall solution w_0 for the deflection of the laminate is then

$$\begin{aligned} w_0 = \sum_{m=1}^{m=\infty} \Bigg\{ \sin\left(\frac{m\pi x}{a} \right) \Bigg[& C_{m,1} e^{\lambda_1 y} + C_{m,2} e^{\lambda_2 y} + C_{m,3} e^{\lambda_3 y} \\ & + C_{m,4} e^{\lambda_4 y} + \frac{P_m}{D_{11}} \left(\frac{a}{m\pi} \right)^4 \Bigg] \Bigg\} . \end{aligned} \tag{8.116}$$

The laminate is assumed to be simply supported at the edges $x = 0$ and $x = a$. Clamped edges are considered at $y = 0$ and $y = b$. The corresponding boundary conditions are at the edges $y = 0$ and $y = b$:

$$w_0\,(y = 0) = 0, \quad w_0\,(y = b) = 0, \quad \left. \frac{\partial w_0}{\partial y} \right|_{y=0} = 0, \quad \left. \frac{\partial w_0}{\partial y} \right|_{y=b} = 0. \tag{8.117}$$

If the solution (8.116) is inserted into the boundary conditions (8.117), the following system of four linear equations for the constants C_m is obtained:

$$\begin{aligned} C_{m,1} + C_{m,2} + C_{m,3} + C_{m,4} &= -\frac{P_m}{D_{11}} \left(\frac{a}{m\pi} \right)^4 , \\ C_{m,1} e^{\lambda_1 b} + C_{m,2} e^{\lambda_2 b} + C_{m,3} e^{\lambda_3 b} + C_{m,4} e^{\lambda_4 b} &= -\frac{P_m}{D_{11}} \left(\frac{a}{m\pi} \right)^4 , \\ \lambda_1 C_{m,1} + \lambda_2 C_{m,2} + \lambda_3 C_{m,3} + \lambda_4 C_{m,4} &= 0, \\ \lambda_1 C_{m,1} e^{\lambda_1 b} + \lambda_2 C_{m,2} e^{\lambda_2 b} + \lambda_3 C_{m,3} e^{\lambda_3 b} + \lambda_4 C_{m,4} e^{\lambda_4 b} &= 0. \end{aligned} \tag{8.118}$$

This can then be solved for the constants C_m. The total solution for the deflection w_0 then follows according to (8.116) by summing up all individual solutions for $m = 1$ up to

a certain degree of approximation $m = M$, which is to be determined by a convergence analysis.

Overall, it turns out that solving the system of equations (8.118) in closed-form analytical form is possible, but leads to rather long expressions that are difficult to handle. However, if we use the form (8.111) instead of the representation (8.110), we can show that the resulting system of equations is easier to solve in closed form. The total solution w_0 for the deflection of the laminate is obtained with (8.111) in the following form:

$$w_0 = \sum_{m=1}^{m=\infty} \left\{ \sin\left(\frac{m\pi x}{a}\right) \left[C_{m,1} \cosh(\lambda_1 y) + C_{m,2} \sinh(\lambda_1 y) \right.\right. \\ \left.\left. + \; C_{m,3} \cosh(\lambda_3 y) + C_{m,4} \sinh(\lambda_3 y) + \frac{P_m}{D_{11}} \left(\frac{a}{m\pi}\right)^4 \right] \right\}. \tag{8.119}$$

Evaluating the boundary conditions (8.117) then results in the following set of equations:

$$\begin{aligned} C_{m,1} + C_{m,3} &= -\frac{P_m}{D_{11}} \left(\frac{a}{m\pi}\right)^4, \\ C_{m,1} \cosh(\lambda_1 b) + C_{m,2} \sinh(\lambda_1 b) & \\ + C_{m,3} \cosh(\lambda_3 b) + C_{m,4} \sinh(\lambda_3 b) &= -\frac{P_m}{D_{11}} \left(\frac{a}{m\pi}\right)^4, \\ \lambda_1 C_{m,2} + \lambda_3 C_{m,4} &= 0, \\ \lambda_1 C_{m,1} \sinh(\lambda_1 b) + \lambda_1 C_{m,2} \cosh(\lambda_1 b) & \\ + \lambda_3 C_{m,3} \sinh(\lambda_3 b) + \lambda_3 C_{m,4} \cosh(\lambda_3 b) &= 0. \end{aligned} \tag{8.120}$$

This can be solved immediately for the coefficients, and the result is

$$\begin{aligned} C_{m,1} &= -\frac{a^4 P_m \lambda_3}{D_{11} m^4 \pi^4 \Delta} \left[-\lambda_1 \cosh(\lambda_1 b) + \lambda_1 \cosh(\lambda_3 b) \right. \\ &\quad \left. + \; \lambda_1 \cosh(\lambda_1 b) \cosh(\lambda_3 b) - \lambda_3 \sinh(\lambda_1 b) \sinh(\lambda_3 b) - \lambda_1 \right], \\ C_{m,2} &= \frac{\lambda_3 P_m a^4}{D_{11} m^4 \pi^4 \Delta} \left[-\lambda_1 \sinh(\lambda_1 b) + \lambda_3 \sinh(\lambda_3 b) \right. \\ &\quad \left. - \; \lambda_3 \cosh(\lambda_1 b) \sinh(\lambda_3 b) + \lambda_1 \cosh(\lambda_3 b) \sinh(\lambda_1 b) \right], \\ C_{m,3} &= \frac{P_m a^4 \lambda_1}{D_{11} m^4 \pi^4 \Delta} \left[-\lambda_3 \cosh(\lambda_1 b) + \lambda_3 \cosh(\lambda_3 b) \right. \\ &\quad \left. - \; \lambda_3 \cosh(\lambda_1 b) \cosh(\lambda_3 b) + \lambda_1 \sinh(\lambda_1 b) \sinh(\lambda_3 b) + \lambda_3 \right], \\ C_{m,4} &= -\frac{\lambda_1 P_m a^4}{D_{11} m^4 \pi^4 \Delta} \left[-\lambda_1 \sinh(\lambda_1 b) + \lambda_3 \sinh(\lambda_3 b) \right. \\ &\quad \left. - \; \lambda_3 \cosh(\lambda_1 b) \sinh(\lambda_3 b) + \lambda_1 \cosh(\lambda_3 b) \sinh(\lambda_1 b) \right], \end{aligned} \tag{8.121}$$

where Δ is the determinant of the coefficient matrix:

$$\Delta = -\left(\lambda_1^2 + \lambda_3^2\right) \sinh(\lambda_1 b) \sinh(\lambda_3 b) + 2\lambda_1 \lambda_3 \cosh(\lambda_1 b) \cosh(\lambda_3 b) - 1. \tag{8.122}$$

8.6 The Ritz Method

The Ritz method (see also Chap. 4 of this book) is a traditional method that is still very popular in practical industrial applications despite the immense computing power available today—it often delivers very convincing results with a fraction of the computational effort that would be necessary for a finite element analysis, provided that suitable approaches are used. The Ritz method is extended below to the case of laminate structures.

8.6.1 Energetic Considerations and Ritz Equations

The starting point for the analysis using the Ritz method is the principle of the minimum of the total elastic potential Π:

$$\Pi = \Pi_i + \Pi_a = \text{Min.} \tag{8.123}$$

For the sake of simplicity, the prerequisite here is that only symmetric laminates with an otherwise arbitrary layup are considered. The strain energy or the internal potential can then be determined for a pure bending load as:

$$\begin{aligned}\Pi_i = \frac{1}{2} \int_0^b \int_0^a \Bigg[& D_{11} \left(\frac{\partial^2 w_0}{\partial x^2}\right)^2 + D_{22} \left(\frac{\partial^2 w_0}{\partial y^2}\right)^2 + 2D_{12} \frac{\partial^2 w_0}{\partial x^2} \frac{\partial^2 w_0}{\partial y^2} \\ & + 4D_{66} \left(\frac{\partial^2 w_0}{\partial x \partial y}\right)^2 + 4D_{16} \frac{\partial^2 w_0}{\partial x^2} \frac{\partial^2 w_0}{\partial x \partial y} + 4D_{26} \frac{\partial^2 w_0}{\partial y^2} \frac{\partial^2 w_0}{\partial x \partial y} \Bigg] \mathrm{d}x \mathrm{d}y. \end{aligned} \tag{8.124}$$

The laminate is stressed by a surface load $p(x, y)$. Then the potential of the surface load p or the external potential can be determined as:

$$\Pi_a = -\int_0^b \int_0^a p w_0 \mathrm{d}x \mathrm{d}y. \tag{8.125}$$

Specific boundary conditions are not specified at this point, but the Ritz formulation will first be described in general terms.

A displacement approach of the form

$$w_0(x, y) = \sum_{m=1}^{\infty} \sum_{n=1}^{\infty} W_{mn} w_{1m}(x) w_{2n}(y) \tag{8.126}$$

contains the shape functions $w_{1m}(x)$ and $w_{2n}(y)$, which are required to fulfil the underlying kinematic boundary conditions. The dynamic boundary conditions do not have to be fulfilled explicitly, but are fulfilled better and better in the average sense with increasing degrees of series expansion by using the underlying energy principle. In practical application, one will always endeavour to keep the computational effort as low as possible, so that the series expansion in (8.126) will be terminated at a certain degree $m = M$ and $n = N$, so that:

$$w_0(x, y) = \sum_{m=1}^{M} \sum_{n=1}^{N} W_{mn} w_{1m}(x) w_{2n}(y) . \tag{8.127}$$

If the approach (8.127) is inserted into the inner potential (8.124), the following representation of Π_i is obtained:

$$\begin{aligned}
\Pi_i = & \sum_{m=1}^{M} \sum_{n=1}^{N} \sum_{p=1}^{M} \sum_{q=1}^{N} W_{mn} W_{pq} \\
& \times \left[\frac{1}{2} D_{11} \int_0^a \frac{\mathrm{d}^2 w_{1m}}{\mathrm{d}x^2} \frac{\mathrm{d}^2 w_{1p}}{\mathrm{d}x^2} \mathrm{d}x \int_0^b w_{2n} w_{2q} \mathrm{d}y \right. \\
& + \frac{1}{2} D_{22} \int_0^a w_{1m} w_{1p} \mathrm{d}x \int_0^b \frac{\mathrm{d}^2 w_{2n}}{\mathrm{d}y^2} \frac{\mathrm{d}^2 w_{2q}}{\mathrm{d}y^2} \mathrm{d}y \\
& + D_{12} \int_0^a \frac{\mathrm{d}^2 w_{1m}}{\mathrm{d}x^2} w_{1p} \mathrm{d}x \int_0^b w_{2n} \frac{\mathrm{d}^2 w_{2q}}{\mathrm{d}y^2} \mathrm{d}y \\
& + 2 D_{66} \int_0^a \frac{\mathrm{d}w_{1m}}{\mathrm{d}x} \frac{\mathrm{d}w_{1p}}{\mathrm{d}x} \mathrm{d}x \int_0^b \frac{\mathrm{d}w_{2n}}{\mathrm{d}y} \frac{\mathrm{d}w_{2q}}{\mathrm{d}y} \mathrm{d}y \\
& + 2 D_{16} \int_0^a \frac{\mathrm{d}^2 w_{1m}}{\mathrm{d}x^2} \frac{\mathrm{d}w_{1p}}{\mathrm{d}x} \mathrm{d}x \int_0^b w_{2n} \frac{\mathrm{d}w_{2q}}{\mathrm{d}y} \mathrm{d}y \\
& \left. + 2 D_{26} \int_0^a w_{1m} \frac{\mathrm{d}w_{1p}}{\mathrm{d}x} \mathrm{d}x \int_0^b \frac{\mathrm{d}^2 w_{2n}}{\mathrm{d}y^2} \frac{\mathrm{d}w_{2q}}{\mathrm{d}y} \mathrm{d}y \right] .
\end{aligned} \tag{8.128}$$

With the abbreviations

$$\lambda_{x,ij}^{mp} = \int_0^a \frac{\mathrm{d}^i w_{1m}}{\mathrm{d}x^i} \frac{\mathrm{d}^j w_{1p}}{\mathrm{d}x^j} \mathrm{d}x, \quad \lambda_{y,ij}^{nq} = \int_0^b \frac{\mathrm{d}^i w_{2n}}{\mathrm{d}y^i} \frac{\mathrm{d}^j w_{2q}}{\mathrm{d}y^j} \mathrm{d}y \tag{8.129}$$

(8.128) can also be represented as:

$$\Pi_i = \sum_{m=1}^{M}\sum_{n=1}^{N}\sum_{p=1}^{M}\sum_{q=1}^{N} W_{mn}W_{pq}\left[\frac{1}{2}D_{11}\lambda_{x,22}^{mp}\lambda_{y,00}^{nq} + \frac{1}{2}D_{22}\lambda_{x,00}^{mp}\lambda_{y,22}^{nq}\right.$$
$$\left. + \; D_{12}\lambda_{x,20}^{mp}\lambda_{y,02}^{nq} + 2D_{16}\lambda_{x,21}^{mp}\lambda_{y,01}^{nq} + 2D_{26}\lambda_{x,01}^{mp}\lambda_{y,21}^{nq} + 2D_{66}\lambda_{x,11}^{mp}\lambda_{y,11}^{nq}\right]. \tag{8.130}$$

If the displacement approach (8.127) is inserted into the potential Π_a of the surface load p according to (8.125), the following result is obtained:

$$\Pi_a = -\int_0^b\int_0^a p\sum_{m=1}^{M}\sum_{n=1}^{N} W_{mn}w_{1m}w_{2n}\mathrm{d}x\mathrm{d}y. \tag{8.131}$$

Introducing the abbreviation

$$\Omega_{mn} = \int_0^b\int_0^a p w_{1m}w_{2n}\mathrm{d}x\mathrm{d}y \tag{8.132}$$

yields:

$$\Pi_a = -\sum_{m=1}^{M}\sum_{n=1}^{N} W_{mn}\Omega_{mn}. \tag{8.133}$$

For the special case of a constant load $p = \text{const.} = p_0$ we obtain:

$$\Pi_a = -p_0\sum_{m=1}^{M}\sum_{n=1}^{N} W_{mn}\int_0^a w_{1m}\mathrm{d}x\int_0^b w_{2n}\mathrm{d}y. \tag{8.134}$$

With the abbreviations

$$\omega_x^m = \int_0^a w_{1m}\mathrm{d}x, \quad \omega_y^n = \int_0^b w_{2n}\mathrm{d}y \tag{8.135}$$

this leads to:

$$\Pi_a = -p_0\sum_{m=1}^{M}\sum_{n=1}^{N} W_{mn}\omega_x^m\omega_y^n. \tag{8.136}$$

The necessary condition for a stationary value (here specifically a minimum) of the total elastic potential is the vanishing of the first variation of the potential Π:

$$\delta\Pi = 0. \tag{8.137}$$

Since the functional form of the deflection w_0 is already completely determined by the approach (8.127), the only quantities of the potential that are still accessible to variation are the coefficients W_{mn}, i.e. $\Pi = \Pi(W_{mn})$. The requirement (8.137) thus transforms into the Ritz equations, which then read as follows:

$$\frac{\partial \Pi}{\partial W_{11}} = 0, \quad \frac{\partial \Pi}{\partial W_{12}} = 0, \quad \frac{\partial \Pi}{\partial W_{13}} = 0, \ldots \tag{8.138}$$

or more compact:

$$\frac{\partial \Pi}{\partial W_{mn}} = 0. \tag{8.139}$$

The requirement (8.139) evaluated for all coefficients W_{mn} leads to a linear system of equations of the form

$$\underline{\underline{K}}\,\underline{W} = \underline{P} \tag{8.140}$$

with the dimension $M \times N$, from which the values W_{mn} can be determined. The stiffness matrix $\underline{\underline{K}}$ has the form

$$\underline{\underline{K}} = \begin{bmatrix} \underline{\underline{K}}^{11} & \underline{\underline{K}}^{12} & \underline{\underline{K}}^{13} & \cdots & \underline{\underline{K}}^{1M} \\ \underline{\underline{K}}^{21} & \underline{\underline{K}}^{22} & \underline{\underline{K}}^{23} & \cdots & \underline{\underline{K}}^{2M} \\ \underline{\underline{K}}^{31} & \underline{\underline{K}}^{32} & \underline{\underline{K}}^{33} & \cdots & \underline{\underline{K}}^{3M} \\ \vdots & \vdots & \vdots & \ddots & \vdots \\ \underline{\underline{K}}^{M1} & \underline{\underline{K}}^{M2} & \underline{\underline{K}}^{M3} & \cdots & \underline{\underline{K}}^{MM} \end{bmatrix}, \tag{8.141}$$

where the components K_{nq}^{mp} ($m, p = 1, 2, 3, \ldots, M$ and $n, q = 1, 2, 3, \ldots, N$) of the submatrices $\underline{\underline{K}}^{mp}$ with dimension $N \times N$ are composed as follows:

$$\begin{aligned} K_{nq}^{mp} = {} & \frac{1}{2} D_{11} \left(\lambda_{x,22}^{mp} \lambda_{y,00}^{nq} + \lambda_{x,22}^{pm} \lambda_{y,00}^{qn} \right) + \frac{1}{2} D_{22} \left(\lambda_{x,00}^{mp} \lambda_{y,22}^{nq} + \lambda_{x,00}^{pm} \lambda_{y,22}^{qn} \right) \\ & + D_{12} \left(\lambda_{x,20}^{mp} \lambda_{y,02}^{nq} + \lambda_{x,20}^{pm} \lambda_{y,02}^{qn} \right) + 2 D_{16} \left(\lambda_{x,21}^{mp} \lambda_{y,01}^{nq} + \lambda_{x,21}^{pm} \lambda_{y,01}^{qn} \right) \\ & + 2 D_{26} \left(\lambda_{x,01}^{mp} \lambda_{y,21}^{nq} + \lambda_{x,01}^{pm} \lambda_{y,21}^{qn} \right) + 2 D_{66} \left(\lambda_{x,11}^{mp} \lambda_{y,11}^{nq} + \lambda_{x,11}^{pm} \lambda_{y,11}^{qn} \right). \end{aligned} \tag{8.142}$$

The vector $\underline{W} = (W_{11}, W_{12}, W_{13}, \ldots, W_{MN})^T$ contains all coefficients. The vector $\underline{P} = \left(\underline{P}^1, \underline{P}^2, \underline{P}^3, \ldots, \underline{P}^M\right)^T$ is divided into the subvectors $\underline{P}^m$, whose components P_n^m are as follows:

$$P_n^m = -\Omega_{mn}, \tag{8.143}$$

or for a constantly distributed surface load $p = p_0$:

$$P_n^m = -p_0 \omega_x^m \omega_y^n. \tag{8.144}$$

If the laminate under consideration is unsymmetric, the displacement approach (8.127) must be extended accordingly by approaches for the inplane displacements u_0, v_0:

$$\begin{aligned} u_0(x, y) &= \sum_{m=1}^{M_u} \sum_{n=1}^{N_u} U_{mn} u_{1m}(x)\, u_{2n}(y), \\ v_0(x, y) &= \sum_{m=1}^{M_v} \sum_{n=1}^{N_v} V_{mn} v_{1m}(x)\, v_{2n}(y), \\ w_0(x, y) &= \sum_{m=1}^{M_w} \sum_{n=1}^{N_w} W_{mn} w_{1m}(x)\, w_{2n}(y). \end{aligned} \tag{8.145}$$

The Ritz equations are then as follows:

$$\frac{\partial \Pi}{\partial U_{mn}} = 0, \quad \frac{\partial \Pi}{\partial V_{mn}} = 0, \quad \frac{\partial \Pi}{\partial W_{mn}} = 0. \tag{8.146}$$

8.6.2 Shape Functions for Symmetric Orthotropic Laminates

The Ritz method can be used quite universally for a variety of laminate problems. If the bending problem under consideration is a rectangular symmetric and orthotropic laminate with the dimensions a and b, the following shape functions can be used in the approach for various combinations of boundary conditions (see e.g. Reddy (2004)):

$$w_0(x, y) = \sum_{m=1}^{M} \sum_{n=1}^{N} W_{mn} w_{1m}(x)\, w_{2n}(y). \tag{8.147}$$

(1) Simple supports at all four edges:

$$w_{1m}(x) = \sin\left(\frac{m\pi x}{a}\right), \quad w_{2n}(y) = \sin\left(\frac{n\pi y}{b}\right). \tag{8.148}$$

(2) Clamping at all four edges:
In this case, several potential shape functions can be specified:

$$\begin{aligned} w_{1m}(x) &= \left(\frac{x}{a}\right)^{m+1} \left(1 - \frac{x}{a}\right)^2, \\ w_{2n}(y) &= \left(\frac{y}{b}\right)^{n+1} \left(1 - \frac{y}{b}\right)^2, \end{aligned} \tag{8.149}$$

or

$$w_{1m}(x) = \sin(\lambda_m x) - \sinh(\lambda_m x) + \alpha_m\Big[\cosh(\lambda_m x) - \cos(\lambda_m x)\Big],$$
$$w_{2n}(y) = \sin(\lambda_n y) - \sinh(\lambda_n y) + \alpha_n\Big[\cosh(\lambda_n y) - \cos(\lambda_n y)\Big], \tag{8.150}$$

where the variables λ_m and λ_n are the roots of the characteristic equations

$$\cos(\lambda_m a)\cosh(\lambda_m a) - 1 = 0,$$
$$\cos(\lambda_n b)\cosh(\lambda_n b) - 1 = 0, \tag{8.151}$$

and the variables α_m and α_n are defined as follows:

$$\alpha_m = \frac{\sinh(\lambda_m a) - \sin(\lambda_m a)}{\cosh(\lambda_m a) - \cos(\lambda_m a)} = \frac{\cosh(\lambda_m a) - \cos(\lambda_m a)}{\sinh(\lambda_m a) + \sin(\lambda_m a)},$$
$$\alpha_n = \frac{\sinh(\lambda_n b) - \sin(\lambda_n b)}{\cosh(\lambda_n b) - \cos(\lambda_n b)} = \frac{\cosh(\lambda_n b) - \cos(\lambda_n b)}{\sinh(\lambda_n b) + \sin(\lambda_n b)}. \tag{8.152}$$

Other potential shape functions are

$$w_{1m}(x) = \cos\left(\frac{(m-2)\pi x}{a}\right) - \cos\left(\frac{m\pi x}{a}\right),$$
$$w_{2n}(y) = \cos\left(\frac{(n-2)\pi y}{b}\right) - \cos\left(\frac{n\pi y}{b}\right), \tag{8.153}$$

whereby the summation is then to be carried out as follows:

$$w_0(x, y) = \sum_{m=2}^{M+1}\sum_{n=2}^{N+1} W_{mn} w_{1m}(x) w_{2n}(y). \tag{8.154}$$

(3) Clamping at $x = 0$ and $x = a$, simple supports at $y = 0$ and $y = b$:

$$w_{1m}(x) = \sin(\lambda_m x) - \sinh(\lambda_m x) + \alpha_m\Big[\cosh(\lambda_m x) - \cos(\lambda_m x)\Big],$$
$$w_{2n}(y) = \sin\left(\frac{n\pi y}{b}\right). \tag{8.155}$$

Here, the variables λ_m are the roots of the characteristic equation

$$\cos(\lambda_m a)\cosh(\lambda_m a) - 1 = 0, \tag{8.156}$$

and the variables α_m are defined as follows:

$$\alpha_m = \frac{\sinh(\lambda_m a) - \sin(\lambda_m a)}{\cosh(\lambda_m a) - \cos(\lambda_m a)}. \tag{8.157}$$

(4) Clamping at $x = 0$, free edge at $x = a$, simple supports at $y = 0$ and $y = b$:

$$w_{1m}(x) = \sin(\lambda_m x) - \sinh(\lambda_m x) + \alpha_m \Big[\cosh(\lambda_m x) - \cos(\lambda_m x)\Big],$$
$$w_{2n}(y) = \sin\left(\frac{n\pi y}{b}\right). \tag{8.158}$$

The variables λ_m are the roots of the characteristic equation

$$\cos(\lambda_m a)\cosh(\lambda_m a) + 1 = 0, \tag{8.159}$$

the values α_m are calculated as follows:

$$\alpha_m = \frac{\sinh(\lambda_m a) + \sin(\lambda_m a)}{\cosh(\lambda_m a) + \cos(\lambda_m a)}. \tag{8.160}$$

(5) Free edges at $x = 0$ and $x = a$, simple supports at $y = 0$ and $y = b$:

$$w_{1m}(x) = \sin(\lambda_m x) + \sinh(\lambda_m x) - \alpha_m \Big[\cosh(\lambda_m x) + \cos(\lambda_m x)\Big],$$
$$w_{2n}(y) = \sin\left(\frac{n\pi y}{b}\right). \tag{8.161}$$

The variables λ_m result as roots of the characteristic equation

$$\cos(\lambda_m a)\cosh(\lambda_m a) - 1 = 0, \tag{8.162}$$

the values α_m are calculated as follows:

$$\alpha_m = \frac{\sinh(\lambda_m a) - \sin(\lambda_m a)}{\cosh(\lambda_m a) - \cos(\lambda_m a)}. \tag{8.163}$$

(6) Simple supports at $x = 0$, $y = 0$ and $y = b$, clamping at $x = a$:

$$w_{1m}(x) = \sinh(\lambda_m a)\sin(\lambda_m x) + \sin(\lambda_m a)\sinh(\lambda_m x),$$
$$w_{2n}(y) = \sin\left(\frac{n\pi y}{b}\right). \tag{8.164}$$

The variables λ_m result from the characteristic equation

$$\tan(\lambda_m a) - \tanh(\lambda_m a) = 0. \tag{8.165}$$

(7) Simple supports at $x = 0$, $y = 0$ and $y = b$, free edge at $x = a$:

$$w_{1m}(x) = \sinh(\lambda_m a)\sin(\lambda_m x) - \sin(\lambda_m a)\sinh(\lambda_m x),$$
$$w_{2n}(y) = \sin\left(\frac{n\pi y}{b}\right). \tag{8.166}$$

The variables λ_m can be derived from the characteristic equation

$$\tan(\lambda_m a) - \tanh(\lambda_m a) = 0. \tag{8.167}$$

(8) Clamping at $x = 0$, free edges at $x = a$, $y = 0$ and $y = b$:

$$\begin{aligned} w_{1m}(x) &= \sin(\lambda_m x) - \sinh(\lambda_m x) + \alpha_m\Big[\cosh(\lambda_m x) - \cos(\lambda_m x)\Big], \\ w_{2n}(y) &= \sin(\lambda_n y) + \sinh(\lambda_n y) - \alpha_n\Big[\cosh(\lambda_n y) + \cos(\lambda_n y)\Big], \end{aligned} \tag{8.168}$$

where the variables λ_m and λ_n are the roots of the characteristic equations

$$\begin{aligned} \cos(\lambda_m a)\cosh(\lambda_m a) + 1 &= 0, \\ \cos(\lambda_n b)\cosh(\lambda_n b) - 1 &= 0. \end{aligned} \tag{8.169}$$

The values α_m and α_n are calculated as follows:

$$\begin{aligned} \alpha_m &= \frac{\sinh(\lambda_m a) + \sin(\lambda_m a)}{\cosh(\lambda_m a) + \cos(\lambda_m a)}, \\ \alpha_n &= \frac{\sinh(\lambda_n b) - \sin(\lambda_n b)}{\cosh(\lambda_n b) - \cos(\lambda_n b)}. \end{aligned} \tag{8.170}$$

(9) Clamping at $x = 0$, simple support at $y = 0$, free edges at $x = a$ and $y = b$:

$$\begin{aligned} w_{1m}(x) &= \sin(\lambda_m x) - \sinh(\lambda_m x) + \alpha_m\Big[\cosh(\lambda_m x) - \cos(\lambda_m x)\Big], \\ w_{2n}(y) &= \sinh(\lambda_n b)\sin(\lambda_n y) - \sin(\lambda_n b)\sinh(\lambda_n y)\,. \end{aligned} \tag{8.171}$$

The variables λ_m and λ_n are the zeros of the following characteristic equations:

$$\begin{aligned} \cos(\lambda_m a)\cosh(\lambda_m a) + 1 &= 0, \\ \tan(\lambda_n b) - \tanh(\lambda_n b) &= 0. \end{aligned} \tag{8.172}$$

The quantity α_m is defined as

$$\alpha_m = \frac{\sinh(\lambda_m a) + \sin(\lambda_m a)}{\cosh(\lambda_m a) + \cos(\lambda_m a)}. \tag{8.173}$$

In an analogous way, further combinations of shape functions can be found for any other combination of boundary conditions. The real difficulty will lie in solving the integrals involved in the shape functions and their derivatives. Tables or mathematical programme packages should be consulted for this purpose or, in extreme cases, numerical integration methods should be used.

8.6.3 Selected Closed-Form Analytical Approximate Solutions

The Ritz method often proves its worth in industrial practice when problems are considered that can be tackled with the simplest possible approach functions. At best, it is even possible to dispense with series developments for the displacements so that, depending on the problem, it may be possible to derive quite simple closed-form analytical approximate solutions. This will be illustrated below using a few examples, whereby we will restrict ourselves here to symmetric and orthotropic laminates. Essentially, two requirements are placed on the shape functions used. On the one hand, there is the mechanically based requirement to fulfil all kinematic boundary conditions. On the other hand, the 'engineering' requirement must be met that the shape functions should be as plausible as possible, which means that the approaches should represent the structural behaviour expected from engineering intuition as well as possible. Accordingly, approaches should be chosen that come as close as possible to the assumed reality.

The reason for the restriction to purely orthotropic laminates is that similar closed-form solutions for other laminate classes are often much more difficult to determine or may even be impossible to identify for purely mathematical reasons. For example, the bending-twisting coupling (characterised by the terms D_{16} and D_{26}) prevents the derivation of simple closed-form analytical solutions for laminate bending problems in very many cases, so that in practical implementation one is often forced to ignore these terms in the sense of an easy-to-handle and efficient procedure (i.e. assuming an orthotropy of the plate behaviour that does not exist in reality), although the bending-twisting coupling can certainly play an important role in the structural response. In all cases, however, closed-form approximate solutions must always be verified by means of more complex numerical analyses or, at best, validated by experiments.

What all the following solutions have in common is that they are based on a one-term displacement approach of the form

$$w_0(x, y) = W w_1(x) w_2(y). \tag{8.174}$$

The inner potential Π_i of the laminate (8.124) can then be written as:

$$\Pi_i = \frac{1}{2} \int_0^b \int_0^a \left[D_{11} \left(\frac{\partial^2 w_0}{\partial x^2} \right)^2 + D_{22} \left(\frac{\partial^2 w_0}{\partial y^2} \right)^2 + 2 D_{12} \frac{\partial^2 w_0}{\partial x^2} \frac{\partial^2 w_0}{\partial y^2} + 4 D_{66} \left(\frac{\partial^2 w_0}{\partial x \partial y} \right)^2 \right] \mathrm{d}x \mathrm{d}y. \tag{8.175}$$

Inserting (8.174) into the inner potential gives the following expression:

$$\begin{aligned}\Pi = &\frac{1}{2}D_{11}W^2\int_0^a\left(\frac{\mathrm{d}^2w_1}{\mathrm{d}x^2}\right)^2\mathrm{d}x\int_0^b w_2^2\mathrm{d}y\\ &+\frac{1}{2}D_{22}W^2\int_0^a w_1^2\mathrm{d}x\int_0^b\left(\frac{\mathrm{d}^2w_2}{\mathrm{d}y^2}\right)^2\mathrm{d}y\\ &+D_{12}W^2\int_0^a w_1\frac{\mathrm{d}^2w_1}{\mathrm{d}x^2}\mathrm{d}x\int_0^b w_2\frac{\mathrm{d}^2w_2}{\mathrm{d}y^2}\mathrm{d}y\\ &+2D_{66}W^2\int_0^a\left(\frac{\mathrm{d}w_1}{\mathrm{d}x}\right)^2\mathrm{d}x\int_0^b\left(\frac{\mathrm{d}w_2}{\mathrm{d}y}\right)^2\mathrm{d}y.\end{aligned}\tag{8.176}$$

The external potential Π_a is given here for two special cases. Firstly, the case where the laminate is loaded by a constant surface load $p = p_0$ is considered. Then we can write for Π_a:

$$\Pi_a = -p_0\int_0^b\int_0^a w_0\mathrm{d}x\mathrm{d}y,\tag{8.177}$$

which, after inserting the displacement approach (8.174), changes into:

$$\Pi_a = -p_0W\int_0^a w_1\mathrm{d}x\int_0^b w_2\mathrm{d}y.\tag{8.178}$$

In the case of a single load F_0 at the point $x = x_0$, $y = y_0$, the external potential results as:

$$\Pi_a = -F_0w_0\left(x_0, y_0\right).\tag{8.179}$$

After inserting the formula (8.174) we obtain

$$\Pi_a = -F_0Ww_1\left(x_0\right)w_2\left(y_0\right).\tag{8.180}$$

The solution for the constant W can then be obtained quite simply from Ritz's equation

$$\frac{\partial\Pi}{\partial W} = 0.\tag{8.181}$$

8.6.3.1 Bending of a Symmetric Orthotropic Laminate Clamped at All Edges Under Constant Surface Load $p = p_0$

A symmetric orthotropic laminate is considered, which is rigidly clamped at all four edges. The boundary conditions are then as follows:

$$w_0(x=0)=0, \quad w_0(x=a)=0, \quad w_0(y=0)=0, \quad w_0(y=b)=0,$$
$$\left.\frac{\partial w_0}{\partial x}\right|_{x=0}=0, \quad \left.\frac{\partial w_0}{\partial x}\right|_{x=a}=0, \quad \left.\frac{\partial w_0}{\partial y}\right|_{y=0}=0, \quad \left.\frac{\partial w_0}{\partial y}\right|_{y=b}=0. \tag{8.182}$$

The following approaches w_1, w_2 can be proposed for such a situation with regard to the shape functions (8.149):

$$w_1=\left(\frac{x}{a}\right)^2\left(1-\frac{x}{a}\right)^2, \quad w_2=\left(\frac{y}{b}\right)^2\left(1-\frac{y}{b}\right)^2. \tag{8.183}$$

In order to solve the problem, the integrals of the shape functions in the inner potential are first analyzed:

$$\begin{aligned}
&\int_0^a\left(\frac{\mathrm{d}^2w_1}{\mathrm{d}x^2}\right)^2\mathrm{d}x=\frac{4}{5a^3}, \quad \int_0^a w_1^2\mathrm{d}x=\frac{a}{630},\\
&\int_0^a w_1\frac{\mathrm{d}^2w_1}{\mathrm{d}x^2}\mathrm{d}x=-\frac{2}{105a}, \quad \int_0^a\left(\frac{\mathrm{d}w_1}{\mathrm{d}x}\right)^2\mathrm{d}x=\frac{2}{105a},\\
&\int_0^b w_2^2\mathrm{d}y=\frac{b}{630}, \quad \int_0^b\left(\frac{\mathrm{d}^2w_2}{\mathrm{d}y^2}\right)^2\mathrm{d}y=\frac{4}{5b^3},\\
&\int_0^b w_2\frac{\mathrm{d}^2w_2}{\mathrm{d}y^2}\mathrm{d}y=-\frac{2}{105b}, \quad \int_0^b\left(\frac{\mathrm{d}w_2}{\mathrm{d}y}\right)^2\mathrm{d}y=\frac{2}{105b}.
\end{aligned} \tag{8.184}$$

The inner potential Π_i (8.176) can thus be summarized as:

$$\Pi_i=\left(\frac{D_{11}b}{1575a^3}+\frac{D_{22}a}{1575b^3}+\frac{4D_{12}}{11025ab}+\frac{8D_{66}}{11025ab}\right)W^2. \tag{8.185}$$

The external potential Π_a can be determined according to (8.178) as follows:

$$\Pi_a=-p_0W\int_0^a\left(\frac{x}{a}\right)^2\left(1-\frac{x}{a}\right)^2\mathrm{d}x\int_0^b\left(\frac{y}{b}\right)^2\left(1-\frac{y}{b}\right)^2\mathrm{d}y=-\frac{p_0ab}{900}W. \tag{8.186}$$

The total potential of the laminate is then obtained as:

$$\Pi = \Pi_i + \Pi_a = \left(\frac{D_{11} b}{1575 a^3} + \frac{D_{22} a}{1575 b^3} + \frac{4 D_{12}}{11025 ab} + \frac{8 D_{66}}{11025 ab} \right) W^2 - \frac{p_0 ab}{900} W. \tag{8.187}$$

Evaluating the Ritz equation (8.181) then leads to the following solution for the constant W:

$$W = \frac{49}{8} \frac{p_0 a^4 b^4}{7 D_{11} b^4 + 7 D_{22} a^4 + 4 a^2 b^2 \left(D_{12} + 2 D_{66} \right)}, \tag{8.188}$$

and the approximate solution for the deflection w_0 of the symmetric and orthotropic laminate clamped at all edges can be specified as follows:

$$w_0 \left(x, y \right) = \frac{49}{8} \frac{p_0 a^4 b^4 \left(\frac{x}{a} \right)^2 \left(1 - \frac{x}{a} \right)^2 \left(\frac{y}{b} \right)^2 \left(1 - \frac{y}{b} \right)^2}{7 D_{11} b^4 + 7 D_{22} a^4 + 4 a^2 b^2 \left(D_{12} + 2 D_{66} \right)}. \tag{8.189}$$

The maximum deflection will occur in the center of the laminate at $x = \frac{a}{2}$, $y = \frac{b}{2}$:

$$w_{0,\max} = \frac{49}{2048} \frac{p_0 a^4 b^4}{\left[7 D_{11} b^4 + 7 D_{22} a^4 + 4 a^2 b^2 \left(D_{12} + 2 D_{66} \right) \right]}. \tag{8.190}$$

Alternatively, an approach of the form

$$w_1 = 1 - \cos \left(\frac{2 \pi x}{a} \right), \quad w_2 = 1 - \cos \left(\frac{2 \pi y}{b} \right) \tag{8.191}$$

can be used. The integrals in the inner potential can then be determined as:

$$\begin{aligned}
\int_0^a \left(\frac{\mathrm{d}^2 w_1}{\mathrm{d}x^2} \right)^2 \mathrm{d}x &= \frac{8 \pi^4}{a^3}, \quad \int_0^a w_1^2 \mathrm{d}x = \frac{3a}{2}, \\
\int_0^a w_1 \frac{\mathrm{d}^2 w_1}{\mathrm{d}x^2} \mathrm{d}x &= -\frac{2 \pi^2}{a}, \quad \int_0^a \left(\frac{\mathrm{d}w_1}{\mathrm{d}x} \right)^2 \mathrm{d}x = \frac{2 \pi^2}{a}, \\
\int_0^b w_2^2 \mathrm{d}y &= \frac{3b}{2}, \quad \int_0^b \left(\frac{\mathrm{d}^2 w_2}{\mathrm{d}y^2} \right)^2 \mathrm{d}y = \frac{8 \pi^4}{b^3}, \\
\int_0^b w_2 \frac{\mathrm{d}^2 w_2}{\mathrm{d}y^2} \mathrm{d}y &= -\frac{2 \pi^2}{b}, \quad \int_0^b \left(\frac{\mathrm{d}w_2}{\mathrm{d}y} \right)^2 \mathrm{d}y = \frac{2 \pi^2}{b},
\end{aligned} \tag{8.192}$$

so that the inner potential Π_i can be represented as:

$$\Pi_i = \pi^4 \left[6D_{11}\frac{b}{a^3} + 6D_{22}\frac{a}{b^3} + \frac{4}{ab}\left(D_{12} + 2D_{66}\right) \right] W^2. \tag{8.193}$$

For the external potential we obtain:

$$\Pi_a = -p_0 W \int_0^a \left[1 - \cos\left(\frac{2\pi x}{a}\right) \right] \mathrm{d}x \int_0^b \left[1 - \cos\left(\frac{2\pi y}{b}\right) \right] \mathrm{d}y = -p_0 W ab. \tag{8.194}$$

Evaluating the Ritz equation then finally results in the following expression for the constant W:

$$W = \frac{p_0 a^4 b^4}{4\pi^4 \left(3D_{11}b^4 + 3D_{22}a^4 + 2D_{12}a^2b^2 + 4D_{66}a^2b^2\right)}, \tag{8.195}$$

with which the closed-form approximate solution for the deflection w_0 of the laminate is determined:

$$w_0 = \frac{p_0 a^4 b^4 \left[1 - \cos\left(\frac{2\pi x}{a}\right) \right] \left[1 - \cos\left(\frac{2\pi y}{b}\right) \right]}{4\pi^4 \left(3D_{11}b^4 + 3D_{22}a^4 + 2D_{12}a^2b^2 + 4D_{66}a^2b^2\right)}. \tag{8.196}$$

The maximum deflection in the center of the laminate is then calculated as:

$$w_{0,\max} = \frac{p_0 a^4 b^4}{\pi^4 \left(3D_{11}b^4 + 3D_{22}a^4 + 2D_{12}a^2b^2 + 4D_{66}a^2b^2\right)}. \tag{8.197}$$

8.6.3.2 Bending of a Clamped Symmetric Orthotropic Laminate Under Point Load $F = F_0$ at the Free Corner

The laminate situation as shown in Fig. 8.2 is considered. The boundary conditions occurring here at the clamped edges at $x = 0$ and $y = 0$ are as follows:

$$w_0\,(x = 0) = 0, \quad w_0\,(y = 0) = 0, \quad \left.\frac{\partial w_0}{\partial x}\right|_{x=0} = 0, \quad \left.\frac{\partial w_0}{\partial y}\right|_{y=0} = 0. \tag{8.198}$$

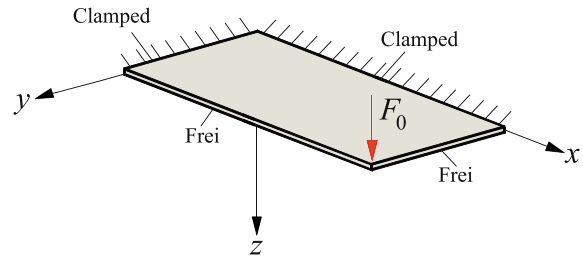


Fig. 8.2 Laminate clamped at two edges with two free edges loaded by a single force F_0

At the free edges at $x = a$ and $y = b$, the respective bending moments and Kirchhoff's equivalent shear forces must disappear:

$$M^0_{xx}\,(x = a) = 0, \quad M^0_{yy}\,(y = b) = 0, \quad \bar{Q}_x\,(x = a) = 0, \quad \bar{Q}_y\,(y = b) = 0. \tag{8.199}$$

The approach to be selected for w_0 must fulfil the boundary conditions (8.198). The dynamic boundary conditions (8.199) are approximately fulfilled by the energy principle to be applied, depending on the quality of the selected shape functions. The following approach is currently used:

$$w_1 = 1 - \cos\left(\frac{\pi x}{2a}\right), \quad w_2 = 1 - \cos\left(\frac{\pi y}{2b}\right). \tag{8.200}$$

The integrals occurring in the inner potential Π_i are then as follows:

$$\begin{aligned}
&\int_0^a \left(\frac{\mathrm{d}^2 w_1}{\mathrm{d}x^2}\right)^2 \mathrm{d}x = \frac{\pi^4}{32a^3}, \quad \int_0^a w_1^2 \mathrm{d}x = \frac{a\,(3\pi - 8)}{2\pi}, \\
&\int_0^a w_1 \frac{\mathrm{d}^2 w_1}{\mathrm{d}x^2} \mathrm{d}x = -\frac{(\pi - 4)\,\pi}{8a}, \quad \int_0^a \left(\frac{\mathrm{d}w_1}{\mathrm{d}x}\right)^2 \mathrm{d}x = \frac{\pi^2}{8a}, \\
&\int_0^b w_2^2 \mathrm{d}y = \frac{b\,(3\pi - 8)}{2\pi}, \quad \int_0^b \left(\frac{\mathrm{d}^2 w_2}{\mathrm{d}y^2}\right)^2 \mathrm{d}y = \frac{\pi^4}{32b^3}, \\
&\int_0^b w_2 \frac{\mathrm{d}^2 w_2}{\mathrm{d}y^2} \mathrm{d}y = -\frac{(\pi - 4)\,\pi}{8b}, \quad \int_0^b \left(\frac{\mathrm{d}w_2}{\mathrm{d}y}\right)^2 \mathrm{d}y = \frac{\pi^2}{8b}.
\end{aligned} \tag{8.201}$$

Then the inner potential Π_i can be represented as:

$$\begin{aligned}
\Pi_i = \frac{\pi^2}{128a^3b^3} &\left[\left(D_{11}b^4 + D_{22}a^4\right)\pi\,(3\pi - 8) + 2D_{12}a^2b^2\,(\pi - 4)^2\right. \\
&\left. +\ 4D_{66}\pi^2 a^2 b^2\right] W^2.
\end{aligned} \tag{8.202}$$

For the external potential we then obtain:

$$\Pi_a = -F_0 W w_1\,(x = a)\, w_2\,(y = b) = -F_0 W, \tag{8.203}$$

and evaluating the Ritz equation (8.181) finally results in the following expression for the constant W:

$$W = \frac{64 F_0 a^3 b^3}{\pi^2\left[\left(D_{11}b^4 + D_{22}a^4\right)\pi\,(3\pi - 8) + 2D_{12}a^2b^2\,(\pi - 4)^2 + 4D_{66}a^2b^2\pi^2\right]}. \tag{8.204}$$

The approximate solution for the deflection w_0 of the current laminate situation can be specified as:

$$w_0 = \frac{64F_0a^3b^3\left[1-\cos\left(\frac{\pi x}{2a}\right)\right]\left[1-\cos\left(\frac{\pi y}{2b}\right)\right]}{\pi^2\left[\left(D_{11}b^4+D_{22}a^4\right)\pi\left(3\pi-8\right)+2D_{12}a^2b^2\left(\pi-4\right)^2+4D_{66}a^2b^2\pi^2\right]}. \quad (8.205)$$

The maximum deflection is obtained at the corner at $x = a$, $y = b$ and is as follows:

$$w_{0,\max} = \frac{64F_0a^3b^3}{\pi^2\left[\left(D_{11}b^4+D_{22}a^4\right)\pi\left(3\pi-8\right)+2D_{12}a^2b^2\left(\pi-4\right)^2+4D_{66}a^2b^2\pi^2\right]}. \quad (8.206)$$

8.6.4 Bending of a Laminate with Arbitrary Symmetric Layup Using the Ritz Method

We illustrate the application of the Ritz method using an elementary example. Consider a rectangular (length a, width b), symmetric, but otherwise arbitrarily constructed laminate, which is simply supported at all four edges. The laminate is subject to a constant surface load $p = p_0$. The deflection w_0 is sought, whereby the Ritz method is to be applied. We use a four-term approach of the form

$$w_0(x, y) = \sum_{m=1}^{2}\sum_{n=1}^{2} W_{mn}w_{1m}(x)\,w_{2n}(y). \quad (8.207)$$

First, the inner potential Π_i of the laminate according to (8.130) is considered, which can currently be written as follows:

$$\begin{aligned}\Pi_i = \sum_{m=1}^{2}\sum_{n=1}^{2}\sum_{p=1}^{2}\sum_{q=1}^{2} W_{mn}W_{pq}\Bigg[&\frac{1}{2}D_{11}\lambda_{x,22}^{mp}\lambda_{y,00}^{nq}+\frac{1}{2}D_{22}\lambda_{x,00}^{mp}\lambda_{y,22}^{nq}\\ &+ D_{12}\lambda_{x,20}^{mp}\lambda_{y,02}^{nq}+2D_{16}\lambda_{x,21}^{mp}\lambda_{y,01}^{nq}+2D_{26}\lambda_{x,01}^{mp}\lambda_{y,21}^{nq}+2D_{66}\lambda_{x,11}^{mp}\lambda_{y,11}^{nq}\Bigg].\end{aligned} \quad (8.208)$$

After performing the summations and sorting the resulting expression, the following representation is obtained:

$$\begin{aligned}\Pi_i = W_{11}^2\Bigg(&\frac{1}{2}D_{11}\lambda_{x,22}^{11}\lambda_{y,00}^{11}+\frac{1}{2}D_{22}\lambda_{x,00}^{11}\lambda_{y,22}^{11}+D_{12}\lambda_{x,20}^{11}\lambda_{y,02}^{11}\\ &+ 2D_{16}\lambda_{x,21}^{11}\lambda_{y,01}^{11}+2D_{26}\lambda_{x,01}^{11}\lambda_{y,21}^{11}+2D_{66}\lambda_{x,11}^{11}\lambda_{y,11}^{11}\Bigg)\\ &+ W_{11}W_{12}\Bigg(\frac{1}{2}D_{11}\lambda_{x,22}^{11}\left(\lambda_{y,00}^{12}+\lambda_{y,00}^{21}\right)+\frac{1}{2}D_{22}\lambda_{x,00}^{11}\left(\lambda_{y,22}^{12}+\lambda_{y,22}^{21}\right)\end{aligned}$$

$$
\begin{aligned}
&+\ D_{12}\lambda^{11}_{x,20}\left(\lambda^{12}_{y,02}+\lambda^{21}_{y,02}\right)+2D_{16}\lambda^{11}_{x,21}\left(\lambda^{12}_{y,01}+\lambda^{21}_{y,01}\right)\\
&+\ 2D_{26}\lambda^{11}_{x,01}\left(\lambda^{12}_{y,21}+\lambda^{21}_{y,21}\right)+2D_{66}\lambda^{11}_{x,11}\left(\lambda^{12}_{y,11}+\lambda^{21}_{y,11}\right)\Big)\\
&+\ W_{11}W_{21}\Big(\frac{1}{2}D_{11}\left(\lambda^{12}_{x,22}+\lambda^{21}_{x,22}\right)\lambda^{11}_{y,00}+\frac{1}{2}D_{22}\left(\lambda^{12}_{x,00}+\lambda^{21}_{x,00}\right)\lambda^{11}_{y,22}\\
&+\ D_{12}\left(\lambda^{12}_{x,20}+\lambda^{21}_{x,20}\right)\lambda^{11}_{y,02}+2D_{16}\left(\lambda^{12}_{x,21}+\lambda^{21}_{x,21}\right)\lambda^{11}_{y,01}\\
&+\ 2D_{26}\left(\lambda^{12}_{x,01}+\lambda^{21}_{x,01}\right)\lambda^{11}_{y,21}+2D_{66}\left(\lambda^{12}_{x,11}+\lambda^{21}_{x,11}\right)\lambda^{11}_{y,11}\Big)\\
&+\ W_{11}W_{22}\Big(\frac{1}{2}D_{11}\left(\lambda^{12}_{x,22}\lambda^{12}_{y,00}+\lambda^{21}_{x,22}\lambda^{21}_{y,00}\right)+\frac{1}{2}D_{22}\left(\lambda^{12}_{x,00}\lambda^{12}_{y,22}+\lambda^{21}_{x,00}\lambda^{21}_{y,22}\right)\\
&+\ D_{12}\left(\lambda^{12}_{x,20}\lambda^{12}_{y,02}+\lambda^{21}_{x,20}\lambda^{21}_{y,02}\right)+2D_{16}\left(\lambda^{12}_{x,21}\lambda^{12}_{y,01}+\lambda^{21}_{x,21}\lambda^{21}_{y,01}\right)\\
&+\ 2D_{26}\left(\lambda^{12}_{x,01}\lambda^{12}_{y,21}+\lambda^{21}_{x,01}\lambda^{21}_{y,21}\right)+2D_{66}\left(\lambda^{12}_{x,11}\lambda^{12}_{y,11}+\lambda^{21}_{x,11}\lambda^{21}_{y,11}\right)\Big)\\
&+\ W^2_{12}\Big(\frac{1}{2}D_{11}\lambda^{11}_{x,22}\lambda^{22}_{y,00}+\frac{1}{2}D_{22}\lambda^{11}_{x,00}\lambda^{22}_{y,22}+D_{12}\lambda^{11}_{x,20}\lambda^{22}_{y,02}\\
&+\ 2D_{16}\lambda^{11}_{x,21}\lambda^{22}_{y,01}+2D_{26}\lambda^{11}_{x,01}\lambda^{22}_{y,21}+2D_{66}\lambda^{11}_{x,11}\lambda^{22}_{y,11}\Big)\\
&+\ W_{12}W_{21}\Big(\frac{1}{2}D_{11}\left(\lambda^{12}_{x,22}\lambda^{21}_{y,00}+\lambda^{21}_{x,22}\lambda^{12}_{y,00}\right)+\frac{1}{2}D_{22}\left(\lambda^{12}_{x,00}\lambda^{21}_{y,22}+\lambda^{21}_{x,00}\lambda^{12}_{y,22}\right)\\
&+\ D_{12}\left(\lambda^{12}_{x,20}\lambda^{21}_{y,02}+\lambda^{21}_{x,20}\lambda^{12}_{y,02}\right)+2D_{16}\left(\lambda^{12}_{x,21}\lambda^{21}_{y,01}+\lambda^{21}_{x,21}\lambda^{12}_{y,01}\right)\\
&+\ 2D_{26}\left(\lambda^{12}_{x,01}\lambda^{21}_{y,21}+\lambda^{21}_{x,01}\lambda^{12}_{y,21}\right)+2D_{66}\left(\lambda^{12}_{x,11}\lambda^{21}_{y,11}+\lambda^{21}_{x,11}\lambda^{12}_{y,11}\right)\Big)\\
&+\ W_{12}W_{22}\Big(\frac{1}{2}D_{11}\left(\lambda^{12}_{x,22}+\lambda^{21}_{x,22}\right)\lambda^{22}_{y,00}+\frac{1}{2}D_{22}\left(\lambda^{12}_{x,00}+\lambda^{21}_{x,00}\right)\lambda^{22}_{y,22}\\
&+\ D_{12}\left(\lambda^{12}_{x,20}+\lambda^{21}_{x,20}\right)\lambda^{22}_{y,02}+2D_{16}\left(\lambda^{12}_{x,21}+\lambda^{21}_{x,21}\right)\lambda^{22}_{y,01}\\
&+\ 2D_{26}\left(\lambda^{12}_{x,01}+\lambda^{21}_{x,01}\right)\lambda^{22}_{y,21}+2D_{66}\left(\lambda^{12}_{x,11}+\lambda^{21}_{x,11}\right)\lambda^{22}_{y,11}\Big)\\
&+\ W^2_{21}\Big(\frac{1}{2}D_{11}\lambda^{22}_{x,22}\lambda^{11}_{y,00}+\frac{1}{2}D_{22}\lambda^{22}_{x,00}\lambda^{11}_{y,22}+D_{12}\lambda^{22}_{x,20}\lambda^{11}_{y,02}\\
&+\ 2D_{16}\lambda^{22}_{x,21}\lambda^{11}_{y,01}+2D_{26}\lambda^{22}_{x,01}\lambda^{11}_{y,21}+2D_{66}\lambda^{22}_{x,11}\lambda^{11}_{y,11}\Big)\\
&+\ W_{21}W_{22}\Big(\frac{1}{2}D_{11}\lambda^{22}_{x,22}\left(\lambda^{12}_{y,00}+\lambda^{21}_{y,00}\right)+\frac{1}{2}D_{22}\lambda^{22}_{x,00}\left(\lambda^{12}_{y,22}+\lambda^{21}_{y,22}\right)\\
&+\ D_{12}\lambda^{22}_{x,20}\left(\lambda^{12}_{y,02}+\lambda^{21}_{y,02}\right)+2D_{16}\lambda^{22}_{x,21}\left(\lambda^{12}_{y,01}+\lambda^{21}_{y,01}\right)\\
&+\ 2D_{26}\lambda^{22}_{x,01}\left(\lambda^{12}_{y,21}+\lambda^{21}_{y,21}\right)+2D_{66}\lambda^{22}_{x,11}\left(\lambda^{12}_{y,11}+\lambda^{21}_{y,11}\right)\Big)\\
&+\ W^2_{22}\Big(\frac{1}{2}D_{11}\lambda^{22}_{x,22}\lambda^{22}_{y,00}+\frac{1}{2}D_{22}\lambda^{22}_{x,00}\lambda^{22}_{y,22}+D_{12}\lambda^{22}_{x,20}\lambda^{22}_{y,02}\\
&+\ 2D_{16}\lambda^{22}_{x,21}\lambda^{22}_{y,01}+2D_{26}\lambda^{22}_{x,01}\lambda^{22}_{y,21}+2D_{66}\lambda^{22}_{x,11}\lambda^{22}_{y,11}\Big).
\end{aligned}
\tag{8.209}
$$

The external potential Π_a (8.136) can be written as:

$$\Pi_a = -p_0 \sum_{m=1}^{2} \sum_{n=1}^{2} W_{mn} \omega_x^m \omega_y^n, \tag{8.210}$$

which results in the following after performing the summation:

$$\Pi_a = -p_0 \left(W_{11} \omega_x^1 \omega_y^1 + W_{12} \omega_x^1 \omega_y^2 + W_{21} \omega_x^2 \omega_y^1 + W_{22} \omega_x^2 \omega_y^2 \right). \tag{8.211}$$

At this point, the Ritz equations can be analysed, which are currently as follows:

$$\frac{\partial \Pi}{\partial W_{11}} = 0, \quad \frac{\partial \Pi}{\partial W_{12}} = 0, \quad \frac{\partial \Pi}{\partial W_{21}} = 0, \quad \frac{\partial \Pi}{\partial W_{22}} = 0. \tag{8.212}$$

This leads to a linear system of equations consisting of four equations for the four unknown coefficients W_{11}, W_{12}, W_{21}, W_{22}:

$$\begin{aligned}
\frac{\partial \Pi}{\partial W_{11}} = 2W_{11} \Bigg(& \frac{1}{2} D_{11} \lambda_{x,22}^{11} \lambda_{y,00}^{11} + \frac{1}{2} D_{22} \lambda_{x,00}^{11} \lambda_{y,22}^{11} + D_{12} \lambda_{x,20}^{11} \lambda_{y,02}^{11} \\
& + 2D_{16} \lambda_{x,21}^{11} \lambda_{y,01}^{11} + 2D_{26} \lambda_{x,01}^{11} \lambda_{y,21}^{11} + 2D_{66} \lambda_{x,11}^{11} \lambda_{y,11}^{11} \Bigg) \\
& + W_{12} \Bigg(\frac{1}{2} D_{11} \lambda_{x,22}^{11} \left(\lambda_{y,00}^{12} + \lambda_{y,00}^{21} \right) + \frac{1}{2} D_{22} \lambda_{x,00}^{11} \left(\lambda_{y,22}^{12} + \lambda_{y,22}^{21} \right) \\
& + D_{12} \lambda_{x,20}^{11} \left(\lambda_{y,02}^{12} + \lambda_{y,02}^{21} \right) + 2D_{16} \lambda_{x,21}^{11} \left(\lambda_{y,01}^{12} + \lambda_{y,01}^{21} \right) \\
& + 2D_{26} \lambda_{x,01}^{11} \left(\lambda_{y,21}^{12} + \lambda_{y,21}^{21} \right) + 2D_{66} \lambda_{x,11}^{11} \left(\lambda_{y,11}^{12} + \lambda_{y,11}^{21} \right) \Bigg) \\
& + W_{21} \Bigg(\frac{1}{2} D_{11} \left(\lambda_{x,22}^{12} + \lambda_{x,22}^{21} \right) \lambda_{y,00}^{11} + \frac{1}{2} D_{22} \left(\lambda_{x,00}^{12} + \lambda_{x,00}^{21} \right) \lambda_{y,22}^{11} \\
& + D_{12} \left(\lambda_{x,20}^{12} + \lambda_{x,20}^{21} \right) \lambda_{y,02}^{11} + 2D_{16} \left(\lambda_{x,21}^{12} + \lambda_{x,21}^{21} \right) \lambda_{y,01}^{11} \\
& + 2D_{26} \left(\lambda_{x,01}^{12} + \lambda_{x,01}^{21} \right) \lambda_{y,21}^{11} + 2D_{66} \left(\lambda_{x,11}^{12} + \lambda_{x,11}^{21} \right) \lambda_{y,11}^{11} \Bigg) \\
& + W_{22} \Bigg(\frac{1}{2} D_{11} \left(\lambda_{x,22}^{12} \lambda_{y,00}^{12} + \lambda_{x,22}^{21} \lambda_{y,00}^{21} \right) + \frac{1}{2} D_{22} \left(\lambda_{x,00}^{12} \lambda_{y,22}^{12} + \lambda_{x,00}^{21} \lambda_{y,22}^{21} \right) \\
& + D_{12} \left(\lambda_{x,20}^{12} \lambda_{y,02}^{12} + \lambda_{x,20}^{21} \lambda_{y,02}^{21} \right) + 2D_{16} \left(\lambda_{x,21}^{12} \lambda_{y,01}^{12} + \lambda_{x,21}^{21} \lambda_{y,01}^{21} \right) \\
& + 2D_{26} \left(\lambda_{x,01}^{12} \lambda_{y,21}^{12} + \lambda_{x,01}^{21} \lambda_{y,21}^{21} \right) + 2D_{66} \left(\lambda_{x,11}^{12} \lambda_{y,11}^{12} + \lambda_{x,11}^{21} \lambda_{y,11}^{21} \right) \Bigg) \\
& - p_0 \omega_x^1 \omega_y^1 = 0, \\
\frac{\partial \Pi}{\partial W_{12}} = W_{11} \Bigg(& \frac{1}{2} D_{11} \lambda_{x,22}^{11} \left(\lambda_{y,00}^{12} + \lambda_{y,00}^{21} \right) + \frac{1}{2} D_{22} \lambda_{x,00}^{11} \left(\lambda_{y,22}^{12} + \lambda_{y,22}^{21} \right) \\
& + D_{12} \lambda_{x,20}^{11} \left(\lambda_{y,02}^{12} + \lambda_{y,02}^{21} \right) + 2D_{16} \lambda_{x,21}^{11} \left(\lambda_{y,01}^{12} + \lambda_{y,01}^{21} \right)
\end{aligned}$$

$$
\begin{aligned}
&+2D_{26}\lambda^{11}_{x,01}\left(\lambda^{12}_{y,21}+\lambda^{21}_{y,21}\right)+2D_{66}\lambda^{11}_{x,11}\left(\lambda^{12}_{y,11}+\lambda^{21}_{y,11}\right)\Big)\\
&+2W_{12}\Big(\frac{1}{2}D_{11}\lambda^{11}_{x,22}\lambda^{22}_{y,00}+\frac{1}{2}D_{22}\lambda^{11}_{x,00}\lambda^{22}_{y,22}+D_{12}\lambda^{11}_{x,20}\lambda^{22}_{y,02}\\
&+2D_{16}\lambda^{11}_{x,21}\lambda^{22}_{y,01}+2D_{26}\lambda^{11}_{x,01}\lambda^{22}_{y,21}+2D_{66}\lambda^{11}_{x,11}\lambda^{22}_{y,11}\Big)\\
&+W_{21}\Big(\frac{1}{2}D_{11}\left(\lambda^{12}_{x,22}\lambda^{21}_{y,00}+\lambda^{21}_{x,22}\lambda^{12}_{y,00}\right)+\frac{1}{2}D_{22}\left(\lambda^{12}_{x,00}\lambda^{21}_{y,22}+\lambda^{21}_{x,00}\lambda^{12}_{y,22}\right)\\
&+D_{12}\left(\lambda^{12}_{x,20}\lambda^{21}_{y,02}+\lambda^{21}_{x,20}\lambda^{12}_{y,02}\right)+2D_{16}\left(\lambda^{12}_{x,21}\lambda^{21}_{y,01}+\lambda^{21}_{x,21}\lambda^{12}_{y,01}\right)\\
&+2D_{26}\left(\lambda^{12}_{x,01}\lambda^{21}_{y,21}+\lambda^{21}_{x,01}\lambda^{12}_{y,21}\right)+2D_{66}\left(\lambda^{12}_{x,11}\lambda^{21}_{y,11}+\lambda^{21}_{x,11}\lambda^{12}_{y,11}\right)\Big)\\
&+W_{22}\Big(\frac{1}{2}D_{11}\left(\lambda^{12}_{x,22}+\lambda^{21}_{x,22}\right)\lambda^{22}_{y,00}+\frac{1}{2}D_{22}\left(\lambda^{12}_{x,00}+\lambda^{21}_{x,00}\right)\lambda^{22}_{y,22}\\
&+D_{12}\left(\lambda^{12}_{x,20}+\lambda^{21}_{x,20}\right)\lambda^{22}_{y,02}+2D_{16}\left(\lambda^{12}_{x,21}+\lambda^{21}_{x,21}\right)\lambda^{22}_{y,01}\\
&+2D_{26}\left(\lambda^{12}_{x,01}+\lambda^{21}_{x,01}\right)\lambda^{22}_{y,21}+2D_{66}\left(\lambda^{12}_{x,11}+\lambda^{21}_{x,11}\right)\lambda^{22}_{y,11}\Big)\\
&-p_0\omega^1_x\omega^2_y=0,
\end{aligned}
$$

$$
\begin{aligned}
\frac{\partial\Pi}{\partial W_{21}}=\;&W_{11}\Big(\frac{1}{2}D_{11}\left(\lambda^{12}_{x,22}+\lambda^{21}_{x,22}\right)\lambda^{11}_{y,00}+\frac{1}{2}D_{22}\left(\lambda^{12}_{x,00}+\lambda^{21}_{x,00}\right)\lambda^{11}_{y,22}\\
&+D_{12}\left(\lambda^{12}_{x,20}+\lambda^{21}_{x,20}\right)\lambda^{11}_{y,02}+2D_{16}\left(\lambda^{12}_{x,21}+\lambda^{21}_{x,21}\right)\lambda^{11}_{y,01}\\
&+2D_{26}\left(\lambda^{12}_{x,01}+\lambda^{21}_{x,01}\right)\lambda^{11}_{y,21}+2D_{66}\left(\lambda^{12}_{x,11}+\lambda^{21}_{x,11}\right)\lambda^{11}_{y,11}\Big)\\
&+W_{12}\Big(\frac{1}{2}D_{11}\left(\lambda^{12}_{x,22}\lambda^{21}_{y,00}+\lambda^{21}_{x,22}\lambda^{12}_{y,00}\right)+\frac{1}{2}D_{22}\left(\lambda^{12}_{x,00}\lambda^{21}_{y,22}+\lambda^{21}_{x,00}\lambda^{12}_{y,22}\right)\\
&+D_{12}\left(\lambda^{12}_{x,20}\lambda^{21}_{y,02}+\lambda^{21}_{x,20}\lambda^{12}_{y,02}\right)+2D_{16}\left(\lambda^{12}_{x,21}\lambda^{21}_{y,01}+\lambda^{21}_{x,21}\lambda^{12}_{y,01}\right)\\
&+2D_{26}\left(\lambda^{12}_{x,01}\lambda^{21}_{y,21}+\lambda^{21}_{x,01}\lambda^{12}_{y,21}\right)+2D_{66}\left(\lambda^{12}_{x,11}\lambda^{21}_{y,11}+\lambda^{21}_{x,11}\lambda^{12}_{y,11}\right)\Big)\\
&+2W_{21}\Big(\frac{1}{2}D_{11}\lambda^{22}_{x,22}\lambda^{11}_{y,00}+\frac{1}{2}D_{22}\lambda^{22}_{x,00}\lambda^{11}_{y,22}+D_{12}\lambda^{22}_{x,20}\lambda^{11}_{y,02}\\
&+2D_{16}\lambda^{22}_{x,21}\lambda^{11}_{y,01}+2D_{26}\lambda^{22}_{x,01}\lambda^{11}_{y,21}+2D_{66}\lambda^{22}_{x,11}\lambda^{11}_{y,11}\Big)\\
&+W_{22}\Big(\frac{1}{2}D_{11}\lambda^{22}_{x,22}\left(\lambda^{12}_{y,00}+\lambda^{21}_{y,00}\right)+\frac{1}{2}D_{22}\lambda^{22}_{x,00}\left(\lambda^{12}_{y,22}+\lambda^{21}_{y,22}\right)\\
&+D_{12}\lambda^{22}_{x,20}\left(\lambda^{12}_{y,02}+\lambda^{21}_{y,02}\right)+2D_{16}\lambda^{22}_{x,21}\left(\lambda^{12}_{y,01}+\lambda^{21}_{y,01}\right)\\
&+2D_{26}\lambda^{22}_{x,01}\left(\lambda^{12}_{y,21}+\lambda^{21}_{y,21}\right)+2D_{66}\lambda^{22}_{x,11}\left(\lambda^{12}_{y,11}+\lambda^{21}_{y,11}\right)\Big)\\
&-p_0\omega^2_x\omega^1_y=0,
\end{aligned}
$$

$$
\frac{\partial\Pi}{\partial W_{22}}=W_{11}\Big(\frac{1}{2}D_{11}\left(\lambda^{12}_{x,22}\lambda^{12}_{y,00}+\lambda^{21}_{x,22}\lambda^{21}_{y,00}\right)+\frac{1}{2}D_{22}\left(\lambda^{12}_{x,00}\lambda^{12}_{y,22}+\lambda^{21}_{x,00}\lambda^{21}_{y,22}\right)
$$

$$
\begin{aligned}
&+D_{12}\left(\lambda^{12}_{x,20}\lambda^{12}_{y,02}+\lambda^{21}_{x,20}\lambda^{21}_{y,02}\right)+2D_{16}\left(\lambda^{12}_{x,21}\lambda^{12}_{y,01}+\lambda^{21}_{x,21}\lambda^{21}_{y,01}\right)\\
&+2D_{26}\left(\lambda^{12}_{x,01}\lambda^{12}_{y,21}+\lambda^{21}_{x,01}\lambda^{21}_{y,21}\right)+2D_{66}\left(\lambda^{12}_{x,11}\lambda^{12}_{y,11}+\lambda^{21}_{x,11}\lambda^{21}_{y,11}\right)\Big)\\
&+W_{12}\Big(\frac{1}{2}D_{11}\left(\lambda^{12}_{x,22}+\lambda^{21}_{x,22}\right)\lambda^{22}_{y,00}+\frac{1}{2}D_{22}\left(\lambda^{12}_{x,00}+\lambda^{21}_{x,00}\right)\lambda^{22}_{y,22}\\
&+D_{12}\left(\lambda^{12}_{x,20}+\lambda^{21}_{x,20}\right)\lambda^{22}_{y,02}+2D_{16}\left(\lambda^{12}_{x,21}+\lambda^{21}_{x,21}\right)\lambda^{22}_{y,01}\\
&+2D_{26}\left(\lambda^{12}_{x,01}+\lambda^{21}_{x,01}\right)\lambda^{22}_{y,21}+2D_{66}\left(\lambda^{12}_{x,11}+\lambda^{21}_{x,11}\right)\lambda^{22}_{y,11}\Big)\\
&+W_{21}\Big(\frac{1}{2}D_{11}\lambda^{22}_{x,22}\left(\lambda^{12}_{y,00}+\lambda^{21}_{y,00}\right)+\frac{1}{2}D_{22}\lambda^{22}_{x,00}\left(\lambda^{12}_{y,22}+\lambda^{21}_{y,22}\right)\\
&+D_{12}\lambda^{22}_{x,20}\left(\lambda^{12}_{y,02}+\lambda^{21}_{y,02}\right)+2D_{16}\lambda^{22}_{x,21}\left(\lambda^{12}_{y,01}+\lambda^{21}_{y,01}\right)\\
&+2D_{26}\lambda^{22}_{x,01}\left(\lambda^{12}_{y,21}+\lambda^{21}_{y,21}\right)+2D_{66}\lambda^{22}_{x,11}\left(\lambda^{12}_{y,11}+\lambda^{21}_{y,11}\right)\Big)\\
&+2W_{22}\Big(\frac{1}{2}D_{11}\lambda^{22}_{x,22}\lambda^{22}_{y,00}+\frac{1}{2}D_{22}\lambda^{22}_{x,00}\lambda^{22}_{y,22}+D_{12}\lambda^{22}_{x,20}\lambda^{22}_{y,02}\\
&+2D_{16}\lambda^{22}_{x,21}\lambda^{22}_{y,01}+2D_{26}\lambda^{22}_{x,01}\lambda^{22}_{y,21}+2D_{66}\lambda^{22}_{x,11}\lambda^{22}_{y,11}\Big)\\
&-p_0\omega_x^2\omega_y^2=0.
\end{aligned}
\tag{8.213}
$$

This can be expressed in a more compact vector-matrix notation as:

$$
\begin{bmatrix}\underline{\underline{K}}^{11} & \underline{\underline{K}}^{12}\\ \underline{\underline{K}}^{21} & \underline{\underline{K}}^{22}\end{bmatrix}\begin{pmatrix}\underline{W}^1\\ \underline{W}^2\end{pmatrix}=\begin{pmatrix}\underline{P}^1\\ \underline{P}^2\end{pmatrix},
\tag{8.214}
$$

where the submatrices and subvectors according to (8.142) and (8.144) are assigned as follows:

$$
\begin{aligned}
\underline{\underline{K}}^{11}&=\begin{bmatrix}K^{11}_{11} & K^{11}_{12}\\ K^{11}_{21} & K^{11}_{22}\end{bmatrix},\quad \underline{\underline{K}}^{12}=\begin{bmatrix}K^{12}_{11} & K^{12}_{12}\\ K^{12}_{21} & K^{12}_{22}\end{bmatrix},\\
\underline{\underline{K}}^{21}&=\begin{bmatrix}K^{21}_{11} & K^{21}_{12}\\ K^{21}_{21} & K^{21}_{22}\end{bmatrix},\quad \underline{\underline{K}}^{22}=\begin{bmatrix}K^{22}_{11} & K^{22}_{12}\\ K^{22}_{21} & K^{22}_{22}\end{bmatrix},\\
\underline{W}^1&=\begin{pmatrix}W_{11}\\ W_{12}\end{pmatrix},\quad \underline{W}^2=\begin{pmatrix}W_{21}\\ W_{22}\end{pmatrix},\quad \underline{P}^1=\begin{pmatrix}P^1_1\\ P^1_2\end{pmatrix},\quad \underline{P}^2=\begin{pmatrix}P^2_1\\ P^2_2\end{pmatrix}.
\end{aligned}
\tag{8.215}
$$

The respective entries are as follows:

$$
\begin{aligned}
K_{11}^{11} &= D_{11}\lambda_{x,22}^{11}\lambda_{y,00}^{11} + D_{22}\lambda_{x,00}^{11}\lambda_{y,22}^{11} + 2D_{12}\lambda_{x,20}^{11}\lambda_{y,02}^{11} \\
&\quad + 4D_{16}\lambda_{x,21}^{11}\lambda_{y,01}^{11} + 4D_{26}\lambda_{x,01}^{11}\lambda_{y,21}^{11} + 4D_{66}\lambda_{x,11}^{11}\lambda_{y,11}^{11}, \\
K_{12}^{11} &= \frac{1}{2}D_{11}\lambda_{x,22}^{11}\left(\lambda_{y,00}^{12} + \lambda_{y,00}^{21}\right) + \frac{1}{2}D_{22}\lambda_{x,00}^{11}\left(\lambda_{y,22}^{12} + \lambda_{y,22}^{21}\right) \\
&\quad + D_{12}\lambda_{x,20}^{11}\left(\lambda_{y,02}^{12} + \lambda_{y,02}^{21}\right) + 2D_{16}\lambda_{x,21}^{11}\left(\lambda_{y,01}^{12} + \lambda_{y,01}^{21}\right) \\
&\quad + 2D_{26}\lambda_{x,01}^{11}\left(\lambda_{y,21}^{12} + \lambda_{y,21}^{21}\right) + 2D_{66}\lambda_{x,11}^{11}\left(\lambda_{y,11}^{12} + \lambda_{y,11}^{21}\right), \\
K_{21}^{11} &= \frac{1}{2}D_{11}\lambda_{x,22}^{11}\left(\lambda_{y,00}^{12} + \lambda_{y,00}^{21}\right) + \frac{1}{2}D_{22}\lambda_{x,00}^{11}\left(\lambda_{y,22}^{12} + \lambda_{y,22}^{21}\right) \\
&\quad + D_{12}\lambda_{x,20}^{11}\left(\lambda_{y,02}^{12} + \lambda_{y,02}^{21}\right) + 2D_{16}\lambda_{x,21}^{11}\left(\lambda_{y,01}^{12} + \lambda_{y,01}^{21}\right) \\
&\quad + 2D_{26}\lambda_{x,01}^{11}\left(\lambda_{y,21}^{12} + \lambda_{y,21}^{21}\right) + 2D_{66}\lambda_{x,11}^{11}\left(\lambda_{y,11}^{12} + \lambda_{y,11}^{21}\right), \\
K_{22}^{11} &= D_{11}\lambda_{x,22}^{11}\lambda_{y,00}^{22} + D_{22}\lambda_{x,00}^{11}\lambda_{y,22}^{22} + 2D_{12}\lambda_{x,20}^{11}\lambda_{y,02}^{22} \\
&\quad + 4D_{16}\lambda_{x,21}^{11}\lambda_{y,01}^{22} + 4D_{26}\lambda_{x,01}^{11}\lambda_{y,21}^{22} + 4D_{66}\lambda_{x,11}^{11}\lambda_{y,11}^{22}, \\
K_{11}^{12} &= \frac{1}{2}D_{11}\left(\lambda_{x,22}^{12} + \lambda_{x,22}^{21}\right)\lambda_{y,00}^{11} + \frac{1}{2}D_{22}\left(\lambda_{x,00}^{12} + \lambda_{x,00}^{21}\right)\lambda_{y,22}^{11} \\
&\quad + D_{12}\left(\lambda_{x,20}^{12} + \lambda_{x,20}^{21}\right)\lambda_{y,02}^{11} + 2D_{16}\left(\lambda_{x,21}^{12} + \lambda_{x,21}^{21}\right)\lambda_{y,01}^{11} \\
&\quad + 2D_{26}\left(\lambda_{x,01}^{12} + \lambda_{x,01}^{21}\right)\lambda_{y,21}^{11} + 2D_{66}\left(\lambda_{x,11}^{12} + \lambda_{x,11}^{21}\right)\lambda_{y,11}^{11}, \\
K_{12}^{12} &= \frac{1}{2}D_{11}\left(\lambda_{x,22}^{12}\lambda_{y,00}^{12} + \lambda_{x,22}^{21}\lambda_{y,00}^{21}\right) + \frac{1}{2}D_{22}\left(\lambda_{x,00}^{12}\lambda_{y,22}^{12} + \lambda_{x,00}^{21}\lambda_{y,22}^{21}\right) \\
&\quad + D_{12}\left(\lambda_{x,20}^{12}\lambda_{y,02}^{12} + \lambda_{x,20}^{21}\lambda_{y,02}^{21}\right) + 2D_{16}\left(\lambda_{x,21}^{12}\lambda_{y,01}^{12} + \lambda_{x,21}^{21}\lambda_{y,01}^{21}\right) \\
&\quad + 2D_{26}\left(\lambda_{x,01}^{12}\lambda_{y,21}^{12} + \lambda_{x,01}^{21}\lambda_{y,21}^{21}\right) + 2D_{66}\left(\lambda_{x,11}^{12}\lambda_{y,11}^{12} + \lambda_{x,11}^{21}\lambda_{y,11}^{21}\right), \\
K_{21}^{12} &= \frac{1}{2}D_{11}\left(\lambda_{x,22}^{12}\lambda_{y,00}^{21} + \lambda_{x,22}^{21}\lambda_{y,00}^{12}\right) + \frac{1}{2}D_{22}\left(\lambda_{x,00}^{12}\lambda_{y,22}^{21} + \lambda_{x,00}^{21}\lambda_{y,22}^{12}\right) \\
&\quad + D_{12}\left(\lambda_{x,20}^{12}\lambda_{y,02}^{21} + \lambda_{x,20}^{21}\lambda_{y,02}^{12}\right) + 2D_{16}\left(\lambda_{x,21}^{12}\lambda_{y,01}^{21} + \lambda_{x,21}^{21}\lambda_{y,01}^{12}\right) \\
&\quad + 2D_{26}\left(\lambda_{x,01}^{12}\lambda_{y,21}^{21} + \lambda_{x,01}^{21}\lambda_{y,21}^{12}\right) + 2D_{66}\left(\lambda_{x,11}^{12}\lambda_{y,11}^{21} + \lambda_{x,11}^{21}\lambda_{y,11}^{12}\right), \\
K_{22}^{12} &= \frac{1}{2}D_{11}\left(\lambda_{x,22}^{12} + \lambda_{x,22}^{21}\right)\lambda_{y,00}^{22} + \frac{1}{2}D_{22}\left(\lambda_{x,00}^{12} + \lambda_{x,00}^{21}\right)\lambda_{y,22}^{22} \\
&\quad + D_{12}\left(\lambda_{x,20}^{12} + \lambda_{x,20}^{21}\right)\lambda_{y,02}^{22} + 2D_{16}\left(\lambda_{x,21}^{12} + \lambda_{x,21}^{21}\right)\lambda_{y,01}^{22} \\
&\quad + 2D_{26}\left(\lambda_{x,01}^{12} + \lambda_{x,01}^{21}\right)\lambda_{y,21}^{22} + 2D_{66}\left(\lambda_{x,11}^{12} + \lambda_{x,11}^{21}\right)\lambda_{y,11}^{22}, \\
K_{11}^{21} &= \frac{1}{2}D_{11}\left(\lambda_{x,22}^{12} + \lambda_{x,22}^{21}\right)\lambda_{y,00}^{11} + \frac{1}{2}D_{22}\left(\lambda_{x,00}^{12} + \lambda_{x,00}^{21}\right)\lambda_{y,22}^{11} \\
&\quad + D_{12}\left(\lambda_{x,20}^{12} + \lambda_{x,20}^{21}\right)\lambda_{y,02}^{11} + 2D_{16}\left(\lambda_{x,21}^{12} + \lambda_{x,21}^{21}\right)\lambda_{y,01}^{11} \\
&\quad + 2D_{26}\left(\lambda_{x,01}^{12} + \lambda_{x,01}^{21}\right)\lambda_{y,21}^{11} + 2D_{66}\left(\lambda_{x,11}^{12} + \lambda_{x,11}^{21}\right)\lambda_{y,11}^{11},
\end{aligned}
$$

$$
\begin{aligned}
K_{12}^{21} &= \frac{1}{2}D_{11}\left(\lambda_{x,22}^{12}\lambda_{y,00}^{21}+\lambda_{x,22}^{21}\lambda_{y,00}^{12}\right)+\frac{1}{2}D_{22}\left(\lambda_{x,00}^{12}\lambda_{y,22}^{21}+\lambda_{x,00}^{21}\lambda_{y,22}^{12}\right)\\
&+ D_{12}\left(\lambda_{x,20}^{12}\lambda_{y,02}^{21}+\lambda_{x,20}^{21}\lambda_{y,02}^{12}\right)+2D_{16}\left(\lambda_{x,21}^{12}\lambda_{y,01}^{21}+\lambda_{x,21}^{21}\lambda_{y,01}^{12}\right)\\
&+ 2D_{26}\left(\lambda_{x,01}^{12}\lambda_{y,21}^{21}+\lambda_{x,01}^{21}\lambda_{y,21}^{12}\right)+2D_{66}\left(\lambda_{x,11}^{12}\lambda_{y,11}^{21}+\lambda_{x,11}^{21}\lambda_{y,11}^{12}\right),\\
K_{21}^{21} &= \frac{1}{2}D_{11}\left(\lambda_{x,22}^{12}\lambda_{y,00}^{12}+\lambda_{x,22}^{21}\lambda_{y,00}^{21}\right)+\frac{1}{2}D_{22}\left(\lambda_{x,00}^{12}\lambda_{y,22}^{12}+\lambda_{x,00}^{21}\lambda_{y,22}^{21}\right)\\
&+ D_{12}\left(\lambda_{x,20}^{12}\lambda_{y,02}^{12}+\lambda_{x,20}^{21}\lambda_{y,02}^{21}\right)+2D_{16}\left(\lambda_{x,21}^{12}\lambda_{y,01}^{12}+\lambda_{x,21}^{21}\lambda_{y,01}^{21}\right)\\
&+ 2D_{26}\left(\lambda_{x,01}^{12}\lambda_{y,21}^{12}+\lambda_{x,01}^{21}\lambda_{y,21}^{21}\right)+2D_{66}\left(\lambda_{x,11}^{12}\lambda_{y,11}^{12}+\lambda_{x,11}^{21}\lambda_{y,11}^{21}\right),\\
K_{22}^{21} &= \frac{1}{2}D_{11}\left(\lambda_{x,22}^{12}+\lambda_{x,22}^{21}\right)\lambda_{y,00}^{22}+\frac{1}{2}D_{22}\left(\lambda_{x,00}^{12}+\lambda_{x,00}^{21}\right)\lambda_{y,22}^{22}\\
&+ D_{12}\left(\lambda_{x,20}^{12}+\lambda_{x,20}^{21}\right)\lambda_{y,02}^{22}+2D_{16}\left(\lambda_{x,21}^{12}+\lambda_{x,21}^{21}\right)\lambda_{y,01}^{22}\\
&+ 2D_{26}\left(\lambda_{x,01}^{12}+\lambda_{x,01}^{21}\right)\lambda_{y,21}^{22}+2D_{66}\left(\lambda_{x,11}^{12}+\lambda_{x,11}^{21}\right)\lambda_{y,11}^{22},\\
K_{11}^{22} &= D_{11}\lambda_{x,22}^{22}\lambda_{y,00}^{11}+D_{22}\lambda_{x,00}^{22}\lambda_{y,22}^{11}+2D_{12}\lambda_{x,20}^{22}\lambda_{y,02}^{11}\\
&+ 4D_{16}\lambda_{x,21}^{22}\lambda_{y,01}^{11}+4D_{26}\lambda_{x,01}^{22}\lambda_{y,21}^{11}+4D_{66}\lambda_{x,11}^{22}\lambda_{y,11}^{11},\\
K_{12}^{22} &= \frac{1}{2}D_{11}\lambda_{x,22}^{22}\left(\lambda_{y,00}^{12}+\lambda_{y,00}^{21}\right)+\frac{1}{2}D_{22}\lambda_{x,00}^{22}\left(\lambda_{y,22}^{12}+\lambda_{y,22}^{21}\right)\\
&+ D_{12}\lambda_{x,20}^{22}\left(\lambda_{y,02}^{12}+\lambda_{y,02}^{21}\right)+2D_{16}\lambda_{x,21}^{22}\left(\lambda_{y,01}^{12}+\lambda_{y,01}^{21}\right)\\
&+ 2D_{26}\lambda_{x,01}^{22}\left(\lambda_{y,21}^{12}+\lambda_{y,21}^{21}\right)+2D_{66}\lambda_{x,11}^{22}\left(\lambda_{y,11}^{12}+\lambda_{y,11}^{21}\right),\\
K_{21}^{22} &= \frac{1}{2}D_{11}\lambda_{x,22}^{22}\left(\lambda_{y,00}^{12}+\lambda_{y,00}^{21}\right)+\frac{1}{2}D_{22}\lambda_{x,00}^{22}\left(\lambda_{y,22}^{12}+\lambda_{y,22}^{21}\right)\\
&+ D_{12}\lambda_{x,20}^{22}\left(\lambda_{y,02}^{12}+\lambda_{y,02}^{21}\right)+2D_{16}\lambda_{x,21}^{22}\left(\lambda_{y,01}^{12}+\lambda_{y,01}^{21}\right)\\
&+ 2D_{26}\lambda_{x,01}^{22}\left(\lambda_{y,21}^{12}+\lambda_{y,21}^{21}\right)+2D_{66}\lambda_{x,11}^{22}\left(\lambda_{y,11}^{12}+\lambda_{y,11}^{21}\right),\\
K_{22}^{22} &= D_{11}\lambda_{x,22}^{22}\lambda_{y,00}^{22}+D_{22}\lambda_{x,00}^{22}\lambda_{y,22}^{22}+2D_{12}\lambda_{x,20}^{22}\lambda_{y,02}^{22}\\
&+ 4D_{16}\lambda_{x,21}^{22}\lambda_{y,01}^{22}+4D_{26}\lambda_{x,01}^{22}\lambda_{y,21}^{22}+4D_{66}\lambda_{x,11}^{22}\lambda_{y,11}^{22},\\
P_1^1 &= p_0\omega_x^1\omega_y^1,\quad P_2^1 = p_0\omega_x^1\omega_y^2 m,\quad P_1^2 = p_0\omega_x^2\omega_y^1,\quad P_2^2 = p_0\omega_x^2\omega_y^2.
\end{aligned}
\tag{8.216}
$$

The system of equations (8.214) can then be easily solved using any method for solving linear systems of equations. The coefficients W_{11}, W_{12}, W_{21}, W_{22} and the approximate solution for the deflection w_0 of the laminate are then known. This can then be used to calculate approximate internal forces and stresses in the laminate.

As an approach for the deflection w_0, a series development of the following form is now used:

$$w_0(x, y) = \sum_{m=1}^{2} \sum_{n=1}^{2} W_{mn} \sin\left(\frac{m\pi x}{a}\right) \sin\left(\frac{n\pi y}{b}\right). \tag{8.217}$$

To evaluate the integrals $\lambda_{x,ij}^{mp}$ and $\lambda_{y,ij}^{nq}$, the following regularities can then be determined:

$$\lambda_{x,00}^{mp} = \int_0^a w_{1m} w_{1p} \mathrm{d}x = \int_0^a \sin\left(\frac{m\pi x}{a}\right) \sin\left(\frac{p\pi x}{a}\right) \mathrm{d}x,$$

$$\lambda_{x,01}^{mp} = \int_0^a w_{1m} \frac{\partial w_{1p}}{\partial x} \mathrm{d}x = \frac{p\pi}{a} \int_0^a \sin\left(\frac{m\pi x}{a}\right) \cos\left(\frac{p\pi x}{a}\right) \mathrm{d}x,$$

$$\lambda_{x,02}^{mp} = \int_0^a w_{1m} \frac{\partial^2 w_{1p}}{\partial x^2} \mathrm{d}x = -\frac{p^2\pi^2}{a^2} \int_0^a \sin\left(\frac{m\pi x}{a}\right) \sin\left(\frac{p\pi x}{a}\right) \mathrm{d}x,$$

$$\lambda_{x,10}^{mp} = \int_0^a \frac{\partial w_{1m}}{\partial x} w_{1p} \mathrm{d}x = \frac{m\pi}{a} \int_0^a \cos\left(\frac{m\pi x}{a}\right) \sin\left(\frac{p\pi x}{a}\right) \mathrm{d}x,$$

$$\lambda_{x,11}^{mp} = \int_0^a \frac{\partial w_{1m}}{\partial x} \frac{\partial w_{1p}}{\partial x} \mathrm{d}x = \frac{m\pi}{a} \frac{p\pi}{a} \int_0^a \cos\left(\frac{m\pi x}{a}\right) \cos\left(\frac{p\pi x}{a}\right) \mathrm{d}x,$$

$$\lambda_{x,12}^{mp} = \int_0^a \frac{\partial w_{1m}}{\partial x} \frac{\partial^2 w_{1p}}{\partial x^2} \mathrm{d}x = -\frac{m\pi}{a} \frac{p^2\pi^2}{a^2} \int_0^a \cos\left(\frac{m\pi x}{a}\right) \sin\left(\frac{p\pi x}{a}\right) \mathrm{d}x,$$

$$\lambda_{x,20}^{mp} = \int_0^a \frac{\partial^2 w_{1m}}{\partial x^2} w_{1p} \mathrm{d}x = -\frac{m^2\pi^2}{a^2} \int_0^a \sin\left(\frac{m\pi x}{a}\right) \sin\left(\frac{p\pi x}{a}\right) \mathrm{d}x,$$

$$\lambda_{x,21}^{mp} = \int_0^a \frac{\partial^2 w_{1m}}{\partial x^2} \frac{\partial w_{1p}}{\partial x} \mathrm{d}x = -\frac{m^2\pi^2}{a^2} \frac{p\pi}{a} \int_0^a \sin\left(\frac{m\pi x}{a}\right) \cos\left(\frac{p\pi x}{a}\right) \mathrm{d}x,$$

$$\lambda_{x,22}^{mp} = \int_0^a \frac{\partial^2 w_{1m}}{\partial x^2} \frac{\partial^2 w_{1p}}{\partial x^2} \mathrm{d}x = \frac{m^2\pi^2}{a^2} \frac{p^2\pi^2}{a^2} \int_0^a \sin\left(\frac{m\pi x}{a}\right) \sin\left(\frac{p\pi x}{a}\right) \mathrm{d}x,$$

$$\lambda_{y,00}^{nq} = \int_0^b w_{2n} w_{2q} \mathrm{d}y = \int_0^b \sin\left(\frac{n\pi y}{b}\right) \sin\left(\frac{q\pi y}{b}\right) \mathrm{d}y,$$

$$\lambda_{y,01}^{nq} = \int_0^b w_{2n} \frac{\partial w_{2q}}{\partial y} \mathrm{d}y = \frac{q\pi}{b} \int_0^b \sin\left(\frac{n\pi y}{b}\right) \cos\left(\frac{q\pi y}{b}\right) \mathrm{d}y,$$

$$\lambda_{y,02}^{nq} = \int_0^b w_{2n} \frac{\partial^2 w_{2q}}{\partial y^2} \mathrm{d}y = -\frac{q^2\pi^2}{b^2} \int_0^b \sin\left(\frac{n\pi y}{b}\right) \sin\left(\frac{q\pi y}{b}\right) \mathrm{d}y,$$

$$\lambda_{y,10}^{nq} = \int_0^b \frac{\partial w_{2n}}{\partial y} w_{2q} \mathrm{d}y = \frac{n\pi}{b} \int_0^b \cos\left(\frac{n\pi y}{b}\right) \sin\left(\frac{q\pi y}{b}\right) \mathrm{d}y,$$

$$\lambda_{y,11}^{nq} = \int_0^b \frac{\partial w_{2n}}{\partial y} \frac{\partial w_{2q}}{\partial y} \mathrm{d}y = \frac{n\pi}{b} \frac{q\pi}{b} \int_0^b \cos\left(\frac{n\pi y}{b}\right) \cos\left(\frac{q\pi y}{b}\right) \mathrm{d}y,$$

$$\lambda_{y,12}^{nq} = \int_0^b \frac{\partial w_{2n}}{\partial y} \frac{\partial^2 w_{2q}}{\partial y^2} \mathrm{d}y = -\frac{n\pi}{b} \frac{q^2\pi^2}{b^2} \int_0^b \cos\left(\frac{n\pi y}{b}\right) \sin\left(\frac{q\pi y}{b}\right) \mathrm{d}y,$$

$$\lambda_{y,20}^{nq} = \int_0^b \frac{\partial^2 w_{2n}}{\partial y^2} w_{2q} \mathrm{d}y = -\frac{n^2\pi^2}{b^2} \int_0^b \sin\left(\frac{n\pi y}{b}\right) \sin\left(\frac{q\pi y}{b}\right) \mathrm{d}y,$$

$$\lambda_{y,21}^{nq} = \int_0^b \frac{\partial^2 w_{2n}}{\partial y^2} \frac{\partial w_{2q}}{\partial y} \mathrm{d}y = -\frac{n^2\pi^2}{b^2} \frac{q\pi}{b} \int_0^b \sin\left(\frac{n\pi y}{b}\right) \cos\left(\frac{q\pi y}{b}\right) \mathrm{d}y,$$

$$\lambda_{y,22}^{nq} = \int_0^b \frac{\partial^2 w_{2n}}{\partial y^2} \frac{\partial^2 w_{2q}}{\partial y^2} \mathrm{d}x_2 = \frac{n^2\pi^2}{b^2} \frac{q^2\pi^2}{b^2} \int_0^b \sin\left(\frac{n\pi y}{b}\right) \sin\left(\frac{q\pi y}{b}\right) \mathrm{d}y. \quad (8.218)$$

The integrals can be solved exactly, and the result is

$$\lambda_{x,00}^{mp} = \begin{cases} 0 \text{ if } m \neq p \\ \frac{a}{2} \text{ if } m = p \end{cases},$$

$$\lambda_{x,01}^{mp} = \begin{cases} 0 \text{ if } m+p \text{ even} \\ \frac{2mp}{m^2-p^2} \text{ if } m+p \text{ odd} \end{cases},$$

$$\lambda_{x,02}^{mp} = \begin{cases} 0 \text{ if } m \neq p \\ -\frac{p^2\pi^2}{2a} \text{ if } m = p \end{cases},$$

$$\lambda_{x,10}^{mp} = \begin{cases} 0 \text{ if } m+p \text{ even} \\ \frac{2mp}{p^2-m^2} \text{ if } m+p \text{ odd} \end{cases},$$

$$\lambda_{x,11}^{mp} = \begin{cases} 0 \text{ if } m \neq p \\ \frac{mp\pi^2}{2a} \text{ if } m = p \end{cases},$$

$$\lambda_{x,12}^{mp} = \begin{cases} 0 \text{ if } m+p \text{ even} \\ -\frac{2mp^3\pi^2}{a^2(p^2-m^2)} \text{ if } m+p \text{ odd} \end{cases},$$

$$\lambda_{x,20}^{mp} = \begin{cases} 0 \text{ if } m \neq p \\ -\frac{m^2\pi^2}{2a} \text{ if } m = p \end{cases},$$
$$\lambda_{x,21}^{mp} = \begin{cases} 0 \text{ if} m+p \text{ even} \\ -\frac{2m^3 p\pi^2}{a^2(m^2-p^2)} \text{ if} m+p \text{ odd} \end{cases},$$
$$\lambda_{x,22}^{mp} = \begin{cases} 0 \text{ if } m \neq p \\ \frac{m^2p^2\pi^4}{2a^3} \text{ if} m = p \end{cases}. \tag{8.219}$$

The integrals λ_{00}^{nq}, λ_{01}^{nq}, λ_{02}^{nq}, λ_{10}^{nq}, λ_{11}^{nq}, λ_{12}^{nq}, λ_{20}^{nq}, λ_{21}^{nq} and λ_{22}^{nq} can be determined directly from this by replacing the geometric quantity a with b. Furthermore, the indices m and p must be replaced by n and q. This is not shown here.

The integrals ω_x^m and ω_y^n currently result in:

$$\omega_x^m = \int_0^a \sin\left(\frac{m\pi x}{a}\right) \mathrm{d}x = \begin{cases} 0 \text{ if } m \text{ even} \\ \frac{2a}{m\pi} \text{ if} m \text{ odd} \end{cases},$$
$$\omega_y^n = \int_0^b \sin\left(\frac{n\pi y}{b}\right) \mathrm{d}y \begin{cases} 0 \text{ if} n \text{ even} \\ \frac{2b}{n\pi} \text{ if } n \text{ odd} \end{cases}. \tag{8.220}$$

8.7 Nonlinear Equations of Motion

In this section, we derive the equations of motion for a geometrically nonlinear approach to dynamic problems within the framework of Classical Laminated Plate Theory and essentially follow the procedure as found in Reddy (2004). For this purpose, we use Hamilton's principle[1], which can be interpreted as a dynamic variant of the principle of virtual displacements. It reads:

$$\int_0^T (\delta\Pi_i + \delta\Pi_a - \delta K)\,\mathrm{d}t = 0. \tag{8.221}$$

Here $\delta\Pi_i$ is the virtual strain energy, whereas $\delta\Pi_a$ is the virtual potential of the external loads/the virtual external potential. The expression δK is the virtual kinetic energy.

We now consider the displacement field according to Classical Laminated Plate Theory (7.14), which is given again here for the sake of better readability:

[1] Sir William Rowan Hamilton, 1805–1865, Irish mathematician and physicist.

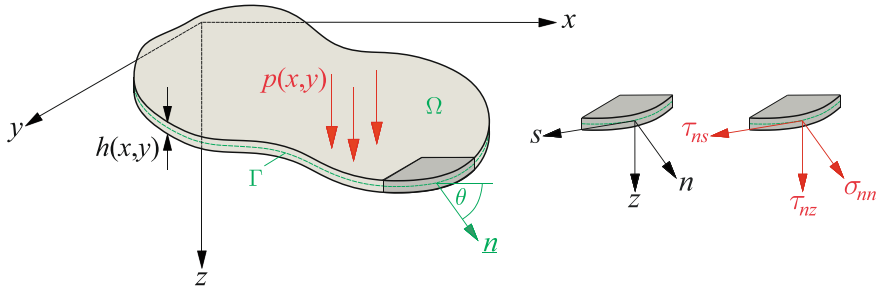


Fig. 8.3 Considered laminate

$$
\begin{aligned}
u\,(x,\,y,\,z,\,t) &= u_0\,(x,\,y,\,t) + z\psi_x\,(x,\,y,\,t) = u_0 - z\frac{\partial w_0}{\partial x},\\
v\,(x,\,y,\,z,\,t) &= v_0\,(x,\,y,\,t) + z\psi_y\,(x,\,y,\,t) = v_0 - z\frac{\partial w_0}{\partial y},\\
w\,(x,\,y,\,z,\,t) &= w_0\,(x,\,y,\,t)\,.
\end{aligned}
\tag{8.222}
$$

All kinematic variables are now assumed to be functions of time t.
We also use the v. Kármán strains (2.71), which we also give again at this point:

$$
\begin{aligned}
E_{xx} &= \frac{\partial u}{\partial x} + \frac{1}{2}\left(\frac{\partial w}{\partial x}\right)^2,\\
E_{yy} &= \frac{\partial v}{\partial y} + \frac{1}{2}\left(\frac{\partial w}{\partial y}\right)^2,\\
E_{zz} &= \frac{\partial w}{\partial z} + \frac{1}{2}\left(\frac{\partial w}{\partial z}\right)^2,\\
E_{xy} &= \frac{1}{2}\left(\frac{\partial u}{\partial y} + \frac{\partial v}{\partial x} + \frac{\partial w}{\partial x}\frac{\partial w}{\partial y}\right),\\
E_{xz} &= \frac{1}{2}\left(\frac{\partial u}{\partial z} + \frac{\partial w}{\partial x} + \frac{\partial w}{\partial x}\frac{\partial w}{\partial z}\right),\\
E_{yz} &= \frac{1}{2}\left(\frac{\partial v}{\partial z} + \frac{\partial w}{\partial y} + \frac{\partial w}{\partial y}\frac{\partial w}{\partial z}\right).
\end{aligned}
\tag{8.223}
$$

If we assume here that, according to the assumptions of Classical Laminated Plate Theory, both the strain in the z-direction and the two transverse shear strains become zero, then we obtain the non-vanishing strain components as:

$$\begin{aligned}
\varepsilon_{xx} &= \frac{\partial u_0}{\partial x} + \frac{1}{2}\left(\frac{\partial w_0}{\partial x}\right)^2 - z\frac{\partial^2 w_0}{\partial x^2},\\
\varepsilon_{yy} &= \frac{\partial v_0}{\partial y} + \frac{1}{2}\left(\frac{\partial w_0}{\partial y}\right)^2 - z\frac{\partial^2 w_0}{\partial y^2},\\
\gamma_{xy} &= \frac{\partial u_0}{\partial y} + \frac{\partial v_0}{\partial x} + \frac{\partial w_0}{\partial x}\frac{\partial w_0}{\partial y} - 2z\frac{\partial^2 w_0}{\partial x \partial y}.
\end{aligned} \tag{8.224}$$

We can write in vector-matrix notation:

$$\begin{pmatrix} \varepsilon_{xx} \\ \varepsilon_{yy} \\ \gamma_{xy} \end{pmatrix} = \begin{pmatrix} \varepsilon^0_{xx} \\ \varepsilon^0_{yy} \\ \gamma^0_{xy} \end{pmatrix} + z \begin{pmatrix} \kappa^0_{xx} \\ \kappa^0_{yy} \\ \kappa^0_{xy} \end{pmatrix}. \tag{8.225}$$

Here, ε^0_{xx}, ε^0_{yy}, γ^0_{xy} are the strains of the laminate middle plane, whereas κ^0_{xx}, κ^0_{yy}, κ^0_{xy} represent the curvatures and the twist of the laminate middle plane. The symbolic notation for (8.225) is:

$$\underline{\varepsilon} = \underline{\varepsilon}_0 + z\underline{\kappa}, \tag{8.226}$$

with

$$\underline{\varepsilon}^0 = \begin{pmatrix} \varepsilon^0_{xx} \\ \varepsilon^0_{yy} \\ \gamma^0_{xy} \end{pmatrix} = \begin{pmatrix} \dfrac{\partial u_0}{\partial x} + \dfrac{1}{2}\left(\dfrac{\partial w_0}{\partial x}\right)^2 \\ \dfrac{\partial v_0}{\partial y} + \dfrac{1}{2}\left(\dfrac{\partial w_0}{\partial y}\right)^2 \\ \dfrac{\partial u_0}{\partial y} + \dfrac{\partial v_0}{\partial x} + \dfrac{\partial w_0}{\partial x}\dfrac{\partial w_0}{\partial y} \end{pmatrix}, \quad \underline{\kappa}^0 = \begin{pmatrix} \kappa^0_{xx} \\ \kappa^0_{yy} \\ \kappa^0_{xy} \end{pmatrix} = - \begin{pmatrix} \dfrac{\partial^2 w_0}{\partial x^2} \\ \dfrac{\partial^2 w_0}{\partial y^2} \\ 2\dfrac{\partial^2 w_0}{\partial x \partial y} \end{pmatrix}. \tag{8.227}$$

The equations of motion for a laminate in the context of Classical Laminated Plate Theory are obtained from Hamilton's principle (8.221). The virtual strain energy is:

$$\begin{aligned}
\delta\Pi_i &= \int_{\Omega_0} \int_{-\frac{h}{2}}^{\frac{h}{2}} \left(\sigma_{xx}\delta\varepsilon_{xx} + \sigma_{yy}\delta\varepsilon_{yy} + \tau_{xy}\delta\gamma_{xy}\right) \mathrm{d}z\mathrm{d}x\mathrm{d}y \\
&= \int_{\Omega_0} \int_{-\frac{h}{2}}^{\frac{h}{2}} \left(\sigma_{xx}\left(\delta\varepsilon^0_{xx} + z\delta\kappa^0_{xx}\right) + \sigma_{yy}\left(\delta\varepsilon^0_{yy} + z\delta\kappa^0_{yy}\right) + \tau_{xy}\left(\delta\gamma^0_{xy} + z\delta\kappa^0_{xy}\right)\right) \mathrm{d}z\mathrm{d}x\mathrm{d}y.
\end{aligned} \tag{8.228}$$

The following applies to the virtual external potential:

$$\begin{aligned}\delta\Pi_a &= -\int_{\Omega_0} p\delta w_0 \mathrm{d}x\mathrm{d}y \\ &\quad -\int_{\Gamma_\sigma}\int_{-\frac{h}{2}}^{\frac{h}{2}} \left(\hat{\sigma}_{nn}\delta u_n + \hat{\tau}_{ns}\delta u_s + \hat{\tau}_{nz}\delta w_0\right)\mathrm{d}z\mathrm{d}s \\ &= -\int_{\Omega_0} q\delta w_0 \mathrm{d}x\mathrm{d}y - \int_{\Gamma_\sigma}\int_{-\frac{h}{2}}^{\frac{h}{2}} \left[\hat{\sigma}_{nn}\left(\delta u_{0n} - z\frac{\partial\delta w_0}{\partial n}\right)\right. \\ &\quad \left. + \hat{\tau}_{ns}\left(\delta u_{0s} - z\frac{\partial\delta w_0}{\partial s}\right) + \hat{\tau}_{nz}\delta w_0\right]\mathrm{d}z\mathrm{d}s. \end{aligned} \tag{8.229}$$

Here p is the surface load acting on the laminate in z-direction, σ_{nn}, τ_{ns}, τ_{nz} are edge stresses prescribed on the edge Γ_σ, and u_{0n}, u_{0s} are the edge displacements normal and tangential to the edge of the laminate. The following applies to the virtual kinetic energy:

$$\begin{aligned}\delta K = \int_{\Omega_0}\int_{-\frac{h}{2}}^{\frac{h}{2}} \rho_0 &\left[\left(\dot{u}_0 - z\frac{\partial\dot{w}_0}{\partial x}\right)\left(\delta\dot{u}_0 - z\frac{\partial\delta\dot{w}_0}{\partial x}\right)\right. \\ &\left. + \left(\dot{v}_0 - z\frac{\partial\dot{w}_0}{\partial y}\right)\left(\delta\dot{v}_0 - z\frac{\partial\delta\dot{w}_0}{\partial y}\right)\right]\mathrm{d}z\mathrm{d}x\mathrm{d}y. \end{aligned} \tag{8.230}$$

Here ρ_0 is the density of the material under consideration. A superscript indicates a time derivative, e.g. $\dot{u}_0 = \frac{\partial u_0}{\partial t}$.

It should be noted that the virtual displacements are zero on those regions Γ_u of the edge on which displacements are prescribed. If (8.228), (8.229) and (8.230) are inserted into (8.221), the following result is obtained after performing the integration with respect to the thickness direction z:

$$\begin{aligned}\int_0^T \Bigg\{ \int_{\Omega_0} \Big[& N^0_{xx}\delta\varepsilon^0_{xx} + M^0_{xx}\delta\kappa^0_{xx} + N^0_{yy}\delta\varepsilon^0_{yy} + M^0_{yy}\delta\kappa^0_{yy} + N^0_{xy}\delta\gamma^0_{xy} \\ & + M^0_{xy}\delta\kappa^0_{xy} - q\delta w_0 - I_0\left(\dot{u}_0\delta\dot{u}_0 + \dot{v}_0\delta\dot{v}_0 + \dot{w}_0\delta\dot{w}_0\right) \\ & + I_1\left(\frac{\partial\delta\dot{w}_0}{\partial x}\dot{u}_0 + \frac{\partial\dot{w}_0}{\partial x}\delta\dot{u}_0 + \frac{\partial\delta\dot{w}_0}{\partial y}\dot{v}_0 + \frac{\partial\dot{w}_0}{\partial y}\delta\dot{v}_0\right) \\ & - I_2\left(\frac{\partial\dot{w}_0}{\partial x}\frac{\partial\delta\dot{w}_0}{\partial x} + \frac{\partial\dot{w}_0}{\partial y}\frac{\partial\delta\dot{w}_0}{\partial y}\right)\Big]\mathrm{d}x\mathrm{d}y \\ - \int_{\Gamma_\sigma} \Big(& \hat{N}^0_{nn}\delta u_{0n} + \hat{N}^0_{ns}\delta u_{0s} - \hat{M}_{nn}\frac{\partial\delta w_0}{\partial n} - \hat{M}_{ns}\frac{\partial\delta w_0}{\partial s} + \hat{Q}_n\delta w_0\Big)\mathrm{d}s \Bigg\}\,\mathrm{d}t = 0. \end{aligned} \tag{8.231}$$

Here, the variables I_0, I_1, I_2 are the mass moments of inertia, defined as:

$$I_0 = \int_{-\frac{h}{2}}^{\frac{h}{2}} \rho_0 \mathrm{d}z, \quad I_1 = \int_{-\frac{h}{2}}^{\frac{h}{2}} \rho_0 z \mathrm{d}z, \quad I_2 = \int_{-\frac{h}{2}}^{\frac{h}{2}} \rho_0 z^2 \mathrm{d}z. \tag{8.232}$$

The virtual strains are as follows:

$$\begin{aligned}
\delta\varepsilon^0_{xx} &= \frac{\partial \delta u_0}{\partial x} + \frac{\partial w_0}{\partial x}\frac{\partial \delta w_0}{\partial x}, \\
\delta\varepsilon^0_{yy} &= \frac{\partial \delta v_0}{\partial y} + \frac{\partial w_0}{\partial y}\frac{\partial \delta w_0}{\partial y}, \\
\delta\gamma^0_{xy} &= \frac{\partial \delta u_0}{\partial y} + \frac{\partial \delta v_0}{\partial x} + \frac{\partial \delta w_0}{\partial x}\frac{\partial w_0}{\partial y} + \frac{\partial w_0}{\partial x}\frac{\partial \delta w_0}{\partial y}, \\
\delta\kappa^0_{xx} &= -\frac{\partial^2 \delta w_0}{\partial x^2}, \\
\delta\kappa^0_{yy} &= -\frac{\partial^2 \delta w_0}{\partial y^2}, \\
\delta\kappa^0_{xy} &= -2\frac{\partial^2 \delta w_0}{\partial x \partial y}.
\end{aligned} \tag{8.233}$$

Inserting (8.233) into (8.231) and performing partial integration yields the following expression after a few transformations:

$$\int_0^T \left\{ \int_{\Omega_0} \left[-\frac{\partial N_{xx}^0}{\partial x}\delta u_0 - \frac{\partial}{\partial x}\left(N_{xx}^0 \frac{\partial w_0}{\partial x}\right)\delta w_0 - \frac{\partial^2 M_{xx}^0}{\partial x^2}\delta w_0 \right.\right.$$
$$-\frac{\partial N_{yy}^0}{\partial y}\delta v_0 - \frac{\partial}{\partial y}\left(N_{yy}^0 \frac{\partial w_0}{\partial y}\right)\delta w_0 - \frac{\partial^2 M_{yy}^0}{\partial y^2}\delta w_0$$
$$-\frac{\partial N_{xy}^0}{\partial y}\delta u_0 - \frac{\partial N_{xy}^0}{\partial x}\delta v_0 - \frac{\partial}{\partial x}\left(N_{xy}^0 \frac{\partial w_0}{\partial y}\right)\delta w_0$$
$$-\frac{\partial}{\partial y}\left(N_{xy}^0 \frac{\partial w_0}{\partial x}\right)\delta w_0 - 2\frac{\partial M_{xy}^0}{\partial x \partial y}\delta w_0 - p\delta w_0$$
$$+I_0\left(\ddot{u}_0\delta u_0 + \ddot{v}_0\delta v_0 + \ddot{w}_0\delta w_0\right) - I_2\left(\frac{\partial^2 \ddot{w}_0}{\partial x^2} + \frac{\partial^2 \ddot{w}_0}{\partial y^2}\right)\delta w_0$$
$$\left. +I_1\left(\frac{\partial \ddot{u}_0}{\partial x}\delta w_0 - \frac{\partial \ddot{w}_0}{\partial x}\delta u_0 + \frac{\partial \ddot{v}_0}{\partial y}\delta w_0 - \frac{\partial \ddot{w}_0}{\partial y}\delta v_0\right)\right] \mathrm{d}x\mathrm{d}y$$
$$+\oint_\Gamma \left[N_{xx}^0 n_x \delta u_0 + \left(N_{xx}^0 \frac{\partial w_0}{\partial x}\right) n_x \delta w_0 - M_{xx}^0 n_x \frac{\partial \delta w_0}{\partial x} + \frac{\partial M_{xx}^0}{\partial x} n_x \delta w_0 \right.$$
$$+N_{yy}^0 n_y \delta v_0 + \left(N_{yy}^0 \frac{\partial w_0}{\partial y}\right) n_y \delta w_0 - M_{yy}^0 n_y \frac{\partial \delta w_0}{\partial y} + \frac{\partial M_{yy}^0}{\partial y} n_y \delta w_0$$
$$-M_{xy}^0 n_x \frac{\partial \delta w_0}{\partial y} + \frac{\partial M_{xy}^0}{\partial x} n_y \delta w_0 - M_{xy}^0 n_y \frac{\partial \delta w_0}{\partial x} + \frac{\partial M_{xy}^0}{\partial y} n_x \delta w_0$$
$$\left. + N_{xy}^0 n_y \delta u_0 + N_{xy}^0 n_x \delta v_0 - N_{xy}^0 \frac{\partial w_0}{\partial y} n_x \delta w_0 + N_{xy}^0 \frac{\partial w_0}{\partial x} n_y \delta w_0 \right] \mathrm{d}s$$
$$-\oint_{\Gamma_\sigma} \left(\hat{N}_{nn}^0 \delta u_{0n} + \hat{N}_{ns}\delta u_{0s} - \hat{M}_{nn}\frac{\partial \delta w_0}{\partial n} - \hat{M}_{ns}\frac{\partial \delta w_0}{\partial s} + \hat{Q}_n \delta w_0 \right) \mathrm{d}s$$
$$\left. + \oint_\Gamma \left[-I_1\left(\ddot{u}_0 n_x + \ddot{v}_0 n_y\right) + I_2\left(\frac{\partial \ddot{w}_0}{\partial x} n_x + \frac{\partial \ddot{w}_0}{\partial y} n_y\right)\right] \delta w_0 \mathrm{d}s \right\} \mathrm{d}t = 0. \quad (8.234)$$

Boundary terms at the times $t = 0$ and $t = T$ disappear. Sorting terms with identical virtual displacements and noting that the virtual displacements become zero on Γ_u, leads to an expression as follows:

$$\int_0^T \left\{ \int_{\Omega_0} \left[-\left(\frac{\partial N_{xx}^0}{\partial x} + \frac{\partial N_{xy}^0}{\partial y} - I_0 \ddot{u}_0 + I_1 \frac{\partial \ddot{w}_0}{\partial x}\right)\delta u_0 \right.\right.$$
$$-\left(\frac{\partial N_{xy}^0}{\partial x} + \frac{\partial N_{yy}^0}{\partial y} - I_0 \ddot{v}_0 + I_1 \frac{\partial \ddot{w}_0}{\partial y}\right)\delta v_0$$
$$-\left(\frac{\partial^2 M_{xx}^0}{\partial x^2} + 2\frac{\partial^2 M_{xy}^0}{\partial x \partial y} + \frac{\partial M_{yy}^0}{\partial y^2} + p\right.$$

$$
\begin{aligned}
&+\frac{\partial}{\partial x}\left(N^0_{xx}\frac{\partial w_0}{\partial x}+N^0_{xy}\frac{\partial w_0}{\partial y}\right)+\frac{\partial}{\partial y}\left(N^0_{xy}\frac{\partial w_0}{\partial x}+N^0_{yy}\frac{\partial w_0}{\partial y}\right)\\
&-I_0\ddot{w}_0-I_1\frac{\partial \ddot{u}_0}{\partial x}-I_1\frac{\partial \ddot{v}_0}{\partial y}+I_2\frac{\partial^2\ddot{w}_0}{\partial x^2}+I_2\frac{\partial^2\ddot{w}_0}{\partial y^2}\Big)\,\delta w_0\Big]\,\mathrm{d}x\mathrm{d}y\\
&+\int_{\Gamma_\sigma}\Big[\Big(N^0_{xx}n_x+N^0_{xy}n_y\Big)\,\delta u_0+\Big(N^0_{xy}n_x+N^0_{yy}n_y\Big)\,\delta v_0\\
&+\Big(\frac{\partial M^0_{xx}}{\partial x}n_x+\frac{\partial M^0_{xy}}{\partial y}n_x+\frac{\partial M^0_{yy}}{\partial y}n_y+\frac{\partial M^0_{xy}}{\partial x}n_y\\
&+\Big(N^0_{xx}\frac{\partial w_0}{\partial x}+N^0_{xy}\frac{\partial w_0}{\partial y}\Big)n_x+\Big(N^0_{xy}\frac{\partial w_0}{\partial x}+N^0_{yy}\frac{\partial w_0}{\partial y}\Big)n_y\quad v\\
&-I_1\ddot{u}_0n_x-I_1\ddot{v}_0n_y+I_2\frac{\partial\ddot{w}_0}{\partial x}n_x+I_2\frac{\partial\ddot{w}_0}{\partial y}n_y\Big)\,\delta w_0\\
&-\Big(M^0_{xx}n_x+M^0_{xy}n_y\Big)\frac{\partial\delta w_0}{\partial x}-\Big(M^0_{xy}n_x+M^0_{yy}n_y\Big)\frac{\partial\delta w_0}{\partial y}\Big]\,\mathrm{d}s\\
&-\int_{\Gamma_\sigma}\Big(\hat{N}^0_{nn}\delta u_{0n}+\hat{N}_{ns}\delta u_{0s}-\hat{M}_{nn}\frac{\partial\delta w_0}{\partial n}-\hat{M}_{ns}\frac{\partial\delta w_0}{\partial s}+\hat{Q}_n\delta w_0\Big)\,\mathrm{d}s\Bigg\}\,\mathrm{d}t. \qquad (8.235)
\end{aligned}
$$

The Euler-Lagrange equations can be read from the integral terms with respect to the laminate middle plane:

$$
\begin{aligned}
\delta u_0:\ &\frac{\partial N^0_{xx}}{\partial x}+\frac{\partial N^0_{xy}}{\partial y}=I_0\ddot{u}_0-I_1\frac{\partial\ddot{w}_0}{\partial x},\\
\delta v_0:\ &\frac{\partial N^0_{xy}}{\partial x}+\frac{\partial N^0_{yy}}{\partial y}=I_0\ddot{v}_0-I_1\frac{\partial\ddot{w}_0}{\partial y},\\
\delta w_0:\ &\frac{\partial^2 M^0_{xx}}{\partial x^2}+2\frac{\partial^2 M^0_{xy}}{\partial x\partial y}+\frac{\partial M^0_{yy}}{\partial y^2}+p\\
&+\frac{\partial}{\partial x}\left(N^0_{xx}\frac{\partial w_0}{\partial x}+N^0_{xy}\frac{\partial w_0}{\partial y}\right)+\frac{\partial}{\partial y}\left(N^0_{xy}\frac{\partial w_0}{\partial x}+N^0_{yy}\frac{\partial w_0}{\partial y}\right)\\
&=I_0\ddot{w}_0+I_1\frac{\partial\ddot{u}_0}{\partial x}+I_1\frac{\partial\ddot{v}_0}{\partial y}-I_2\frac{\partial^2\ddot{w}_0}{\partial x^2}-I_2\frac{\partial^2\ddot{w}_0}{\partial y^2}. \qquad (8.236)
\end{aligned}
$$

To discuss the boundary terms in (8.235), we use the relationship $u_0 = n_x u_{0n} - n_y u_{0s}$ and $v_0 = n_y u_{0n} + n_x u_{0s}$ and express derivatives of the deflection w_0 by derivatives with respect to the boundary coordinates as follows:

$$
\frac{\partial w_0}{\partial x}=n_x\frac{\partial w_0}{\partial n}-n_y\frac{\partial w_0}{\partial s},\quad \frac{\partial w_0}{\partial y}=n_y\frac{\partial w_0}{\partial n}+n_x\frac{\partial w_0}{\partial s}. \qquad (8.237)
$$

The boundary terms in (8.235) can then be written as:

$$\begin{aligned}&\left(N_{xx}^0 n_x + N_{xy}^0 n_y\right)\delta u_0 + \left(N_{xy}^0 n_x + N_{yy}^0 n_y\right)\delta v_0\\ &= \left(N_{xx}^0 n_x^2 + 2N_{xy}^0 n_x n_y + N_{yy}^0 n_y^2\right)\delta u_{0n} + \left[\left(N_{yy}^0 - N_{xx}^0\right)n_x n_y + N_{xy}^0\left(n_x^2 - n_y^2\right)\right]\delta u_{0s}.\end{aligned} \tag{8.238}$$

Here, the bracket terms in front of the virtual displacements δu_{0n} and δ_{0s} are exactly the boundary force flows N_{nn}^0 and N_{ns}^0, as can be seen from the transformation equations

$$\begin{aligned}N_{nn}^0 &= n_x^2 N_{xx}^0 + n_y^2 N_{yy}^0 + 2n_x n_y N_{xy}^0,\\ N_{ns}^0 &= -n_x n_y N_{xx}^0 + n_x n_y N_{yy}^0 + \left(n_x^2 - n_y^2\right)N_{xy}^0.\end{aligned} \tag{8.239}$$

The same applies to the moment flows:

$$\begin{aligned}M_{nn}^0 &= n_x^2 M_{xx}^0 + n_y^2 M_{yy}^0 + 2n_x n_y M_{xy}^0,\\ M_{ns}^0 &= -n_x n_y M_{xx}^0 + n_x n_y M_{yy}^0 + \left(n_x^2 - n_y^2\right)M_{xy}^0.\end{aligned} \tag{8.240}$$

The boundary integrals in (8.235) can be written as:

$$\begin{aligned}&\int_0^T \int_{\Gamma_\sigma} \Bigg[\left(N_{nn}^0 - \hat{N}_{nn}^0\right)\delta u_{0n} + \left(N_{ns}^0 - \hat{N}_{ns}^0\right)\delta u_{0s}\\ &+ \left(\frac{\partial M_{xx}^0}{\partial x}n_x + \frac{\partial M_{xy}^0}{\partial y}n_x + \frac{\partial M_{yy}^0}{\partial y}n_y + \frac{\partial M_{xy}}{\partial x}n_y\right.\\ &+ \left(N_{xx}^0\frac{\partial w_0}{\partial x} + N_{xy}^0\frac{\partial w_0}{\partial y}\right)n_x + \left(N_{xy}^0\frac{\partial w_0}{\partial x} + N_{yy}^0\frac{\partial w_0}{\partial y}\right)n_y\\ &\left.- I_1\ddot{u}_0 n_x - I_1\ddot{v}_0 n_y + I_2\frac{\partial\ddot{w}_0}{\partial x}n_x + I_2\frac{\partial\ddot{w}_0}{\partial y}n_y - \hat{Q}_n\right)\delta w_0\\ &- \left(M_{nn}^0 - \hat{M}_{nn}^0\right)\frac{\partial\delta w_0}{\partial n} - \left(M_{ns}^0 - \hat{M}_{ns}^0\right)\frac{\partial\delta w_0}{\partial s}\Bigg]\mathrm{d}s\mathrm{d}t.\end{aligned} \tag{8.241}$$

The boundary conditions of the given problem can be determined from this:

$$\begin{aligned}\delta u_{0n}:&\quad N_{nn}^0 = \hat{N}_{nn}^0,\\ \delta u_{0s}:&\quad N_{ns}^0 = \hat{N}_{ns}^0,\\ \delta w_0:&\quad Q_n = \hat{Q}_n,\\ \frac{\partial\delta w_0}{\partial n}:&\quad M_{nn}^0 = \hat{M}_{nn}^0,\\ \frac{\partial\delta w_0}{\partial s}:&\quad M_{ns}^0 = \hat{M}_{ns}^0,\end{aligned} \tag{8.242}$$

with

$$
\begin{aligned}
Q_n = & \left(\frac{\partial M_{xx}^0}{\partial x} + \frac{\partial M_{xy}^0}{\partial y} - I_1 \ddot{u}_0 + I_2 \frac{\partial \ddot{w}_0}{\partial x} \right) n_x \\
& + \left(\frac{\partial M_{yy}^0}{\partial y} + \frac{\partial M_{xy}^0}{\partial x} - I_1 \ddot{v}_0 + I_2 \frac{\partial \ddot{w}_0}{\partial y} \right) n_y \\
& + \left(N_{xx}^0 \frac{\partial w_0}{\partial x} + N_{xy}^0 \frac{\partial w_0}{\partial y} \right) n_x + \left(N_{xy}^0 \frac{\partial w_0}{\partial x} + N_{yy}^0 \frac{\partial w_0}{\partial y} \right) n_y .
\end{aligned} \tag{8.243}
$$

The boundary term $-\oint_\Gamma M_{ns}^0 \frac{\partial \delta w_0}{\partial s} \mathrm{d}s$ is partially integrated as follows:

$$
-\oint_\Gamma M_{ns}^0 \frac{\partial \delta w_0}{\partial s} \mathrm{d}s = \oint_\Gamma \frac{\partial M_{ns}^0}{\partial s} \delta w_0 \mathrm{d}s - M_{ns}^0 \delta w_0 \big|_\Gamma . \tag{8.244}
$$

The last term appearing here is identical to zero due to the closed boundary curve. The remaining term on the right-hand side is now added to Q_n and we obtain the Kirchhoff equivalent shear force as follows:

$$
\bar{Q}_n = Q_n + \frac{\partial M_{ns}^0}{\partial s} . \tag{8.245}
$$

We now use the constitutive law of Classical Laminated Plate Theory and obtain with (8.227):

$$
\begin{aligned}
\begin{pmatrix} N_{xx}^0 \\ N_{yy}^0 \\ N_{xy}^0 \end{pmatrix} = & \begin{bmatrix} A_{11} & A_{12} & A_{16} \\ A_{12} & A_{22} & A_{26} \\ A_{16} & A_{26} & A_{66} \end{bmatrix} \begin{pmatrix} \dfrac{\partial u_0}{\partial x} + \dfrac{1}{2} \left(\dfrac{\partial w_0}{\partial x} \right)^2 \\ \dfrac{\partial v_0}{\partial y} + \dfrac{1}{2} \left(\dfrac{\partial w_0}{\partial y} \right)^2 \\ \dfrac{\partial u_0}{\partial y} + \dfrac{\partial v_0}{\partial x} + \dfrac{\partial w_0}{\partial x} \dfrac{\partial w_0}{\partial y} \end{pmatrix} \\
& + \begin{bmatrix} B_{11} & B_{12} & B_{16} \\ B_{12} & B_{22} & B_{26} \\ B_{16} & B_{26} & B_{66} \end{bmatrix} \begin{pmatrix} \dfrac{\partial^2 w_0}{\partial x^2} \\ \dfrac{\partial^2 w_0}{\partial y^2} \\ 2 \dfrac{\partial^2 w_0}{\partial x \partial y} \end{pmatrix} ,
\end{aligned}
$$

$$\begin{pmatrix} M^0_{xx} \\ M^0_{yy} \\ M^0_{xy} \end{pmatrix} = \begin{bmatrix} B_{11} & B_{12} & B_{16} \\ B_{12} & B_{22} & B_{26} \\ B_{16} & B_{26} & B_{66} \end{bmatrix} \begin{pmatrix} \dfrac{\partial u_0}{\partial x} + \dfrac{1}{2}\left(\dfrac{\partial w_0}{\partial x}\right)^2 \\ \dfrac{\partial v_0}{\partial y} + \dfrac{1}{2}\left(\dfrac{\partial w_0}{\partial y}\right)^2 \\ \dfrac{\partial u_0}{\partial y} + \dfrac{\partial v_0}{\partial x} + \dfrac{\partial w_0}{\partial x}\dfrac{\partial w_0}{\partial y} \end{pmatrix} + \begin{bmatrix} D_{11} & D_{12} & D_{16} \\ D_{12} & D_{22} & D_{26} \\ D_{16} & D_{26} & D_{66} \end{bmatrix} \begin{pmatrix} \dfrac{\partial^2 w_0}{\partial x^2} \\ \dfrac{\partial^2 w_0}{\partial y^2} \\ 2\dfrac{\partial^2 w_0}{\partial x \partial y} \end{pmatrix}. \tag{8.246}$$

By inserting into (8.236), we obtain the equations of motion for the laminate within the framework of Classical Laminated Plate Theory as follows:

$$\begin{aligned}
&A_{11}\left(\frac{\partial^2 u_0}{\partial x^2} + \frac{\partial w_0}{\partial x}\frac{\partial^2 w_0}{\partial x^2}\right) + A_{12}\left(\frac{\partial^2 v_0}{\partial x \partial y} + \frac{\partial w_0}{\partial y}\frac{\partial^2 w_0}{\partial x \partial y}\right) \\
&+ A_{16}\left(\frac{\partial^2 u_0}{\partial x \partial y} + \frac{\partial^2 v_0}{\partial x^2} + \frac{\partial^2 w_0}{\partial x^2}\frac{\partial w_0}{\partial y} + \frac{\partial w_0}{\partial x}\frac{\partial^2 w_0}{\partial x \partial y}\right) \\
&- B_{11}\frac{\partial^3 w_0}{\partial x^3} - B_{12}\frac{\partial^3 w_0}{\partial x \partial y^2} - 2B_{16}\frac{\partial^3 w_0}{\partial x^2 \partial y} \\
&+ A_{16}\left(\frac{\partial^2 u_0}{\partial x \partial y} + \frac{\partial w_0}{\partial x}\frac{\partial^2 w_0}{\partial x \partial y}\right) + A_{26}\left(\frac{\partial^2 v_0}{\partial y^2} + \frac{\partial w_0}{\partial y}\frac{\partial^2 w_0}{\partial y^2}\right) \\
&+ A_{66}\left(\frac{\partial^2 u_0}{\partial y^2} + \frac{\partial^2 v_0}{\partial x \partial y} + \frac{\partial^2 w_0}{\partial x \partial y}\frac{\partial w_0}{\partial y} + \frac{\partial w_0}{\partial x}\frac{\partial^2 w_0}{\partial y^2}\right) \\
&- B_{16}\frac{\partial^3 w_0}{\partial x^2 \partial y} - B_{26}\frac{\partial^3 w_0}{\partial y^3} - 2B_{66}\frac{\partial^3 w_0}{\partial x \partial y^2} = I_0\frac{\partial^2 u_0}{\partial t^2} - I_1\frac{\partial^3 w_0}{\partial x \partial t^2}, \\
&A_{16}\left(\frac{\partial^2 u_0}{\partial x^2} + \frac{\partial w_0}{\partial x}\frac{\partial^2 w_0}{\partial x^2}\right) + A_{26}\left(\frac{\partial^2 v_0}{\partial x \partial y} + \frac{\partial w_0}{\partial y}\frac{\partial^2 w_0}{\partial x \partial y}\right) \\
&+ A_{66}\left(\frac{\partial^2 u_0}{\partial x \partial y} + \frac{\partial^2 v_0}{\partial x^2} + \frac{\partial^2 w_0}{\partial x^2}\frac{\partial w_0}{\partial y} + \frac{\partial w_0}{\partial x}\frac{\partial^2 w_0}{\partial x \partial y}\right) \\
&- B_{16}\frac{\partial^3 w_0}{\partial x^3} - B_{26}\frac{\partial^3 w_0}{\partial x \partial y^2} - 2B_{6}6\frac{\partial^3 w_0}{\partial x^2 \partial y} \\
&+ A_{12}\left(\frac{\partial^2 u_0}{\partial x \partial y} + \frac{\partial w_0}{\partial x}\frac{\partial^2 w_0}{\partial x \partial y}\right) + A_{22}\left(\frac{\partial^2 v_0}{\partial y^2} + \frac{\partial w_0}{\partial y}\frac{\partial^2 w_0}{\partial y^2}\right) \\
&+ A_{26}\left(\frac{\partial^2 u_0}{\partial y^2} + \frac{\partial^2 v_0}{\partial x \partial y} + \frac{\partial^2 w_0}{\partial x \partial y}\frac{\partial w_0}{\partial y} + \frac{\partial w_0}{\partial x}\frac{\partial^2 w_0}{\partial y^2}\right)
\end{aligned}$$

$$
\begin{aligned}
&- B_{12}\frac{\partial^3 w_0}{\partial x^2\partial y} - B_{22}\frac{\partial^3 w_0}{\partial y^3} - 2B_{26}\frac{\partial^3 w_0}{\partial x\partial y^2}\\
&= I_0\frac{\partial^2 v_0}{\partial t^2} - I_1\frac{\partial^3 w_0}{\partial y\partial t^2},
\end{aligned}
$$

$$
\begin{aligned}
&B_{11}\left(\frac{\partial^3 u_0}{\partial x^3} + \frac{\partial^2 w_0}{\partial x^2}\frac{\partial^2 w_0}{\partial x^2} + \frac{\partial w_0}{\partial x}\frac{\partial^3 w_0}{\partial x^3}\right)\\
&+ B_{12}\left(\frac{\partial^3 v_0}{\partial x^2\partial y} + \frac{\partial^2 w_0}{\partial x\partial y}\frac{\partial^2 w_0}{\partial x\partial y} + \frac{\partial w_0}{\partial y}\frac{\partial^3 w_0}{\partial x^2\partial y}\right)\\
&+ B_{16}\left(\frac{\partial^3 u_0}{\partial x^2\partial y} + \frac{\partial^3 v_0}{\partial x^3} + \frac{\partial^3 w_0}{\partial x^3}\frac{\partial w_0}{\partial y} + 2\frac{\partial^2 w_0}{\partial x^2}\frac{\partial^2 w_0}{\partial x\partial y} + \frac{\partial w_0}{\partial x}\frac{\partial^3 w_0}{\partial x^2\partial y}\right)\\
&- D_{11}\frac{\partial^4 w_0}{\partial x^4} - D_{12}\frac{\partial^4 w_0}{\partial x^2\partial y^2} - 2D_{16}\frac{\partial^4 w_0}{\partial x^3\partial y}\\
&+ 2B_{16}\left(\frac{\partial^3 u_0}{\partial x^2\partial y} + \frac{\partial^2 w_0}{\partial x^2}\frac{\partial^2 w_0}{\partial x\partial y} + \frac{\partial w_0}{\partial x}\frac{\partial^3 w_0}{\partial x^2\partial y}\right)\\
&+ 2B_{26}\left(\frac{\partial^3 v_0}{\partial x\partial y^2} + \frac{\partial^2 w_0}{\partial x\partial y}\frac{\partial^2 w_0}{\partial y^2} + \frac{\partial w_0}{\partial y}\frac{\partial^3 w_0}{\partial x\partial y^2}\right)\\
&+ 2B_{66}\left(\frac{\partial^3 u_0}{\partial x\partial y^2} + \frac{\partial^3 v_0}{\partial x^2\partial y} + \frac{\partial^3 w_0}{\partial x^2\partial y}\frac{\partial w_0}{\partial y} + \frac{\partial^2 w_0}{\partial x\partial y}\frac{\partial^2 w_0}{\partial x\partial y} + \frac{\partial^2 w_0}{\partial x^2}\frac{\partial^2 w_0}{\partial y^2} + \frac{\partial w_0}{\partial x}\frac{\partial^3 w_0}{\partial x\partial y^2}\right)\\
&- 2D_{16}\frac{\partial^4 w_0}{\partial x^3\partial y} - 2D_{26}\frac{\partial^4 w_0}{\partial x\partial y^3} - 4D_{66}\frac{\partial^4 w_0}{\partial x^2\partial y^2}\\
&+ B_{12}\left(\frac{\partial^3 u_0}{\partial x\partial y^2} + \frac{\partial^2 w_0}{\partial x\partial y}\frac{\partial^2 w_0}{\partial x\partial y} + \frac{\partial w_0}{\partial x}\frac{\partial^3 w_0}{\partial x\partial y^2}\right)\\
&+ B_{22}\left(\frac{\partial^3 v_0}{\partial y^3} + \frac{\partial^2 w_0}{\partial y^2}\frac{\partial^2 w_0}{\partial y^2} + \frac{\partial w_0}{\partial y}\frac{\partial^3 w_0}{\partial y^3}\right)\\
&+ B_{26}\left(\frac{\partial^3 u_0}{\partial y^3} + \frac{\partial^3 v_0}{\partial x\partial y^2} + \frac{\partial^3 w_0}{\partial x\partial y^2}\frac{\partial w_0}{\partial y} + 2\frac{\partial^2 w_0}{\partial x\partial y}\frac{\partial^2 w_0}{\partial y^2} + \frac{\partial w_0}{\partial x}\frac{\partial^3 w_0}{\partial y^3}\right)\\
&- D_{12}\frac{\partial^4 w_0}{\partial x^2\partial y^2} - D_{22}\frac{\partial^4 w_0}{\partial y^4} - 2D_{26}\frac{\partial^4 w_0}{\partial x\partial y^3} + p\\
&+ \frac{\partial}{\partial x}\left(N^0_{xx}\frac{\partial w_0}{\partial x} + N^0_{xy}\frac{\partial w_0}{\partial y}\right) + \frac{\partial}{\partial y}\left(N^0_{xy}\frac{\partial w_0}{\partial x} + N^0_{yy}\frac{\partial w_0}{\partial y}\right)\\
&= I_0\frac{\partial^2 w_0}{\partial t^2} - I_2\frac{\partial^2}{\partial t^2}\left(\frac{\partial^2 w_0}{\partial x^2} + \frac{\partial^2 w_0}{\partial y^2}\right) + I_1\frac{\partial^2}{\partial t^2}\left(\frac{\partial u_0}{\partial x} + \frac{\partial v_0}{\partial y}\right).
\end{aligned}
\tag{8.247}
$$

8.8 Vibrations

8.8.1 Navier Solution for Symmetric Orthotropic Laminates

The following equation of motion can be derived from the nonlinear equations of motion (8.247) by neglecting higher-order terms and setting the external load to zero:

$$D_{11}\frac{\partial^4 w_0}{\partial x^4} + 2\left(D_{12}+2D_{66}\right)\frac{\partial^4 w_0}{\partial x^2 \partial y^2} + D_{22}\frac{\partial^4 w_0}{\partial y^4} + I_0\ddot{w}_0 - I_2\left(\frac{\partial^2 \ddot{w}_0}{\partial x^2} + \frac{\partial^2 \ddot{w}_0}{\partial y^2}\right) = 0, \tag{8.248}$$

with $I_0 = \sum_{k=1}^{n} \rho_0^{(k)}\left(z_k - z_{k-1}\right)$ and $I_2 = \frac{1}{3}\sum_{k=1}^{n} \rho_0^{(k)}\left(z_k^3 - z_{k-1}^3\right)$. With an approach of the type $W_{mn}(t) = W_{mn}^0 e^{i\omega t}$ (ω is the natural frequency of the laminate under consideration, $i = \sqrt{-1}$) we obtain from (8.248):

$$\left\{D_{11}\left(\frac{m\pi}{a}\right)^4 + 2\left(D_{12}+2D_{66}\right)\left(\frac{m\pi}{a}\right)^2\left(\frac{n\pi}{b}\right)^2 + D_{22}\left(\frac{n\pi}{b}\right)^4 - \omega^2\left[I_0 + I_2\left(\left(\frac{m\pi}{a}\right)^2 + \left(\frac{n\pi}{b}\right)^2\right)\right]\right\} W_{mn}\sin\left(\frac{m\pi x}{a}\right)\sin\left(\frac{n\pi y}{b}\right) = 0. \tag{8.249}$$

We set the bracket term to zero and solve for the natural frequency ω:

$$\omega_{mn}^2 = \frac{\pi^4}{b^4}\frac{D_{11}\left(\frac{mb}{a}\right)^4 + 2\left(D_{12}+2D_{66}\left(\frac{mnb}{a}\right)^2 + D_{22}n^4\right)}{I_0 + I_2\left[\left(\frac{m\pi}{a}\right)^2 + \left(\frac{n\pi}{b}\right)^2\right]}. \tag{8.250}$$

The eigenmode associated with the natural frequency ω_{mn} is as follows:

$$w_0(x,y) = W_{mn}^0 \sin\left(\frac{m\pi x}{a}\right)\sin\left(\frac{n\pi y}{b}\right). \tag{8.251}$$

8.8.2 Navier Solution for Unsymmetric Cross-Ply Laminates

We consider an unsymmetric cross-ply laminate with $A_{16} = A_{26} = B_{16} = B_{26} = D_{16} = D_{26} = 0$. The constitutive law for the laminate is then:

$$\begin{pmatrix} N_{xx}^0 \\ N_{yy}^0 \\ N_{xy}^0 \\ M_{xx}^0 \\ M_{yy}^0 \\ M_{xy}^0 \end{pmatrix} = \begin{bmatrix} A_{11} & A_{12} & 0 & B_{11} & B_{12} & 0 \\ A_{12} & A_{22} & 0 & B_{12} & B_{22} & 0 \\ 0 & 0 & A_{66} & 0 & 0 & B_{66} \\ B_{11} & B_{12} & 0 & D_{11} & D_{12} & 0 \\ B_{12} & B_{22} & 0 & D_{12} & D_{22} & 0 \\ 0 & 0 & B_{66} & 0 & 0 & D_{66} \end{bmatrix} \begin{pmatrix} \varepsilon_{xx}^0 \\ \varepsilon_{yy}^0 \\ \gamma_{xy}^0 \\ \kappa_{xx}^0 \\ \kappa_{yy}^0 \\ \kappa_{xy}^0 \end{pmatrix}. \tag{8.252}$$

The corresponding equations of motion are as follows:

$$\begin{aligned}
&A_{11}\frac{\partial^2 u_0}{\partial x^2} + A_{66}\frac{\partial^2 u_0}{\partial y^2} + (A_{12}+A_{66})\frac{\partial^2 v_0}{\partial x \partial y} \\
&- B_1\frac{\partial^3 w_0}{\partial x^3} - (B_{12}+2B_{66})\frac{\partial^3 w_0}{\partial x \partial y^2} = I_0\ddot{u}_0 - I_1\frac{\partial \ddot{w}_0}{\partial x}, \\
&(A_{12}+A_{66})\frac{\partial^2 u_0}{\partial x \partial y} + A_{66}\frac{\partial^2 v_0}{\partial x^2} + A_{22}\frac{\partial^2 v_0}{\partial y^2} \\
&- (B_{12}+2B_{66})\frac{\partial^3 w_0}{\partial x^2 \partial y} - B_{22}\frac{\partial^3 w_0}{\partial y^3} = I_0\ddot{v}_0 - I_1\frac{\partial \ddot{w}_0}{\partial y}, \\
&B_{11}\frac{\partial^3 u_0}{\partial x^3} + (B_{12}+2B_{66})\left(\frac{\partial^3 u_0}{\partial x \partial y^2} + \frac{\partial^3 v_0}{\partial x^2 \partial y}\right) + B_{22}\frac{\partial^3 v_0}{\partial y^3} \\
&- D_{11}\frac{\partial^4 w_0}{\partial x^4} - 2(D_{12}+2D_{66})\frac{\partial^4 w_0}{\partial x^2 \partial y^2} - D_{22}\frac{\partial^4 w_0}{\partial y^4} \\
&= I_0\ddot{w}_0 + I_1\left(\frac{\partial \ddot{u}_0}{\partial x} + \frac{\partial \ddot{v}_0}{\partial y}\right) - I_2\left(\frac{\partial^2 \ddot{w}_0}{\partial x^2} + \frac{\partial^2 \ddot{w}_0}{\partial y^2}\right).
\end{aligned} \tag{8.253}$$

Here we consider the so-called SS1 boundary conditions:

$$\begin{aligned}
&u_0(x,0,t) = 0, \quad u_0(x,b,t) = 0, \quad v_0(0,y,t) = 0, \quad v_0(a,y,t) = 0, \\
&w_0(x,0,t) = 0, \quad w_0(x,b,t) = 0, \quad w_0(0,y,t) = 0, \quad w_0(a,y,t) = 0, \\
&\left.\frac{\partial w_0}{\partial x}\right|_{(x,0,t)} = 0, \quad \left.\frac{\partial w_0}{\partial x}\right|_{(x,b,t)} = 0, \quad \left.\frac{\partial w_0}{\partial y}\right|_{(0,y,t)} = 0, \quad \left.\frac{\partial w_0}{\partial y}\right|_{(a,y,t)} = 0, \\
&N^0_{xx}(0,y,t) = 0, \quad N^0_{xx}(a,y,t) = 0, \quad N^0_{yy}(x,0,t) = 0, \quad N^0_{yy}(x,b,t) = 0, \\
&M^0_{xx}(0,y,t) = 0, \quad M^0_{xx}(a,y,t) = 0, \quad M^0_{yy}(x,0,t) = 0, \quad M^0_{yy}(x,b,t) = 0.
\end{aligned} \tag{8.254}$$

We choose the following approach for the displacements u_0, v_0 and w_0:

$$\begin{aligned}
u_0(x,y,t) &= \sum_{n=1}^{\infty}\sum_{m=1}^{\infty} U_{mn}(t)\cos\left(\frac{m\pi x}{a}\right)\sin\left(\frac{n\pi y}{b}\right), \\
v_0(x,y,t) &= \sum_{n=1}^{\infty}\sum_{m=1}^{\infty} V_{mn}(t)\sin\left(\frac{m\pi x}{a}\right)\cos\left(\frac{n\pi y}{b}\right), \\
w_0(x,y,t) &= \sum_{n=1}^{\infty}\sum_{m=1}^{\infty} W_{mn}(t)\sin\left(\frac{m\pi x}{a}\right)\sin\left(\frac{n\pi y}{b}\right).
\end{aligned} \tag{8.255}$$

This approach fulfils all boundary conditions in (8.254) exactly. Inserting the approach (8.255) into the equations of motion (8.253) results in the following expressions with $\alpha = \frac{m\pi}{a}$ and $\beta = \frac{n\pi}{b}$:

$$\sum_{n=1}^{\infty}\sum_{m=1}^{\infty}\left[-\left(A_{11}\alpha^2+A_{66}\beta^2\right)U_{mn}-\left(A_{12}+A_{66}\right)\alpha\beta V_{mn}\right.$$
$$\left.+\left(B_{11}\alpha^3+\left(B_{12}+2B_{66}\right)\alpha\beta^2\right)W_{mn}-I_0\ddot{U}_{mn}I_1\beta\ddot{W}_{mn}\right]\cos\alpha x\sin\beta y=0,$$
$$\sum_{n=1}^{\infty}\sum_{m=1}^{\infty}\left[-\left(A_{12}+A_{66}\right)\alpha\beta U_{mn}-\left(A_{66}\alpha^2+A_{22}\beta^2\right)V_{mn}\right.$$
$$\left.+\left(\left(B_{12}+2B_{66}\right)\alpha^2\beta+B_{22}\beta^3\right)W_{mn}-I_0\ddot{V}_{mn}+I_1\beta\ddot{W}_{mn}\right]\sin\alpha x\cos\beta y=0,$$
$$\sum_{n=1}^{\infty}\sum_{m=1}^{\infty}\left[\left(B_{11}\alpha^3+\left(B_{12}+2B_{66}\right)\alpha\beta^2\right)U_{mn}+\left(\left(B_{12}+2B_{66}\right)\alpha^2\beta+B_{22}\beta^3\right)V_{mn}\right.$$
$$-\left(D_{11}\alpha^4+2\left(D_{12}+2D_{66}\right)\alpha^2\beta^2+D_{22}\beta^4\right)W_{mn}$$
$$\left.+I_1\left(\alpha\ddot{U}_{mn}+\beta\ddot{V}_{mn}\right)-\left(I_0+I_2\left(\alpha^2+\beta^2\right)\right)\ddot{W}_{mn}\right]\sin\alpha x\sin\beta y=0. \tag{8.256}$$

These equations can be expressed in a vector-matrix notation as:

$$\begin{bmatrix}\hat{c}_{11}&\hat{c}_{12}&\hat{c}_{13}\\ \hat{c}_{12}&\hat{c}_{22}&\hat{c}_{23}\\ \hat{c}_{13}&\hat{c}_{23}&\hat{c}_{33}\end{bmatrix}\begin{pmatrix}U_{mn}\\V_{mn}\\W_{mn}\end{pmatrix}+\begin{bmatrix}\hat{m}_{11}&0&0\\0&\hat{m}_{22}&0\\0&0&\hat{m}_{33}\end{bmatrix}\begin{pmatrix}\ddot{U}_{mn}\\\ddot{V}_{mn}\\\ddot{W}_{mn}\end{pmatrix}=\begin{pmatrix}0\\0\\0\end{pmatrix}, \tag{8.257}$$

if we neglect the inertia term I_1 at this point. The individual matrix entries are as follows:

$$\begin{aligned}\hat{c}_{11}&=A_{11}\alpha^2+A_{66}\beta^2,\\ \hat{c}_{12}&=\left(A_{12}+A_{66}\right)\alpha\beta,\\ \hat{c}_{13}&=-B_{11}\alpha^3-\left(B_{12}+2B_{66}\right)\alpha\beta^2,\\ \hat{c}_{22}&=A_{66}\alpha^2+A_{22}\beta^2,\\ \hat{c}_{23}&=-\left(B_{12}+2B_{66}\right)\alpha^2\beta-B_{22}\beta^3,\\ \hat{c}_{33}&=D_{11}\alpha^4+2\left(D_{12}+2D_{66}\right)\alpha^2\beta^2+D_{22}\beta^4,\\ \hat{m}_{11}&=I_0,\\ \hat{m}_{22}&=I_0,\\ \hat{m}_{33}&=I_0+I_2\left(\alpha^2+\beta^2\right).\end{aligned} \tag{8.258}$$

At this point, we take an approach of the form

$$U_{mn}(t)=U_{mn}^0e^{i\omega t},\quad V_{mn}(t)=V_{mn}^0e^{i\omega t},\quad W_{mn}(t)=W_{mn}^0e^{i\omega t}. \tag{8.259}$$

Inserting into (8.257) leads to the following eigenvalue problem:

$$\left(\begin{bmatrix}\hat{c}_{11}&\hat{c}_{12}&\hat{c}_{13}\\ \hat{c}_{12}&\hat{c}_{22}&\hat{c}_{23}\\ \hat{c}_{13}&\hat{c}_{23}&\hat{c}_{33}\end{bmatrix}-\omega^2\begin{bmatrix}\hat{m}_{11}&0&0\\0&\hat{m}_{22}&0\\0&0&\hat{m}_{33}\end{bmatrix}\right)\begin{pmatrix}U_{mn}^0\\V_{mn}^0\\W_{mn}^0\end{pmatrix}=\begin{pmatrix}0\\0\\0\end{pmatrix}. \tag{8.260}$$

Developing and zeroing the coefficient determinant leads to the following characteristic polynomial for determining the natural frequency ω (with $\lambda = \omega^2$):

$$-C_1\lambda^3 + C_2\lambda^2 - C_3\lambda + C_4 = 0, \tag{8.261}$$

with:

$$\begin{aligned}
C_1 &= \begin{vmatrix} \hat{m}_{11} & 0 & 0 \\ 0 & \hat{m}_{22} & 0 \\ 0 & 0 & \hat{m}_{33} \end{vmatrix}, \\
C_2 &= \begin{vmatrix} \hat{c}_{11} & 0 & 0 \\ \hat{c}_{12} & \hat{m}_{22} & 0 \\ \hat{c}_{13} & 0 & \hat{m}_{33} \end{vmatrix} + \begin{vmatrix} \hat{m}_{11} & \hat{c}_{12} & 0 \\ 0 & \hat{c}_{22} & 0 \\ 0 & \hat{c}_{23} & \hat{m}_{33} \end{vmatrix} + \begin{vmatrix} \hat{m}_{11} & 0 & \hat{c}_{13} \\ 0 & \hat{m}_{22} & \hat{c}_{23} \\ 0 & 0 & \hat{c}_{33} \end{vmatrix}, \\
C_3 &= \begin{vmatrix} \hat{c}_{11} & \hat{c}_{12} & 0 \\ \hat{c}_{12} & \hat{c}_{22} & 0 \\ \hat{c}_{13} & \hat{c}_{23} & \hat{m}_{33} \end{vmatrix} + \begin{vmatrix} \hat{c}_{11} & 0 & \hat{c}_{13} \\ \hat{c}_{12} & \hat{m}_{22} & \hat{c}_{23} \\ \hat{c}_{13} & 0 & \hat{c}_{33} \end{vmatrix} + \begin{vmatrix} \hat{m}_{11} & \hat{c}_{12} & \hat{c}_{13} \\ 0 & \hat{c}_{22} & \hat{c}_{23} \\ 0 & \hat{c}_{23} & \hat{c}_{33} \end{vmatrix}, \\
C_4 &= \begin{vmatrix} \hat{c}_{11} & \hat{c}_{12} & \hat{c}_{13} \\ \hat{c}_{12} & \hat{c}_{22} & \hat{c}_{23} \\ \hat{c}_{13} & \hat{c}_{23} & \hat{c}_{33} \end{vmatrix}.
\end{aligned} \tag{8.262}$$

8.8.3 Navier Solution for Unsymmetric Angle-Ply Laminates

We also consider an unsymmetric angle-ply laminate with $A_{16} = A_{26} = B_{11} = B_{12} = B_{22} = B_{66} = D_{16} = D_{26} = 0$. The constitutive law for such a laminate is then:

$$\begin{pmatrix} N^0_{xx} \\ N^0_{yy} \\ N^0_{xy} \\ M^0_{xx} \\ M^0_{yy} \\ M^0_{xy} \end{pmatrix} = \begin{bmatrix} A_{11} & A_{12} & 0 & 0 & 0 & B_{16} \\ A_{12} & A_{22} & 0 & 0 & 0 & B_{26} \\ 0 & 0 & A_{66} & B_{16} & B_{26} & 0 \\ 0 & 0 & B_{16} & D_{11} & D_{12} & 0 \\ 0 & 0 & B_{26} & D_{12} & D_{22} & 0 \\ B_{16} & B_{26} & 0 & 0 & 0 & D_{66} \end{bmatrix} \begin{pmatrix} \varepsilon^0_{xx} \\ \varepsilon^0_{yy} \\ \gamma^0_{xy} \\ \kappa^0_{xx} \\ \kappa^0_{yy} \\ \kappa^0_{xy} \end{pmatrix}. \tag{8.263}$$

The equations of motion are given with $I_1 = 0$:

$$
\begin{aligned}
&A_{11}\frac{\partial^2 u_0}{\partial x^2} + A_{66}\frac{\partial^2 u_0}{\partial y^2} + (A_{12}+A_{66})\frac{\partial^2 v_0}{\partial x \partial y} \\
&- 3B_{16}\frac{\partial^3 w_0}{\partial x^2 \partial y} - B_{26}\frac{\partial^3 w_0}{\partial y^3} = I_0 \ddot{u}_0, \\
&+ (A_{12}+A_{66})\frac{\partial^2 u_0}{\partial x \partial y} + A_{66}\frac{\partial^2 v_0}{\partial x^2} + A_{22}\frac{\partial^2 v_0}{\partial y^2} \\
&- B_{16}\frac{\partial^3 w_0}{\partial x^3} - 3B_{26}\frac{\partial^3 w_0}{\partial x \partial y^2} = I_0 \ddot{v}_0, \\
&+ B_{16}\left(3\frac{\partial^3 u_0}{\partial x^2 \partial y} + \frac{\partial^3 v_0}{\partial x^3}\right) + B_{26}\left(\frac{\partial^3 u_0}{\partial y^3} + 3\frac{\partial^3 v_0}{\partial x \partial y^2}\right) \\
&- D_{11}\frac{\partial^4 w_0}{\partial x^4} - 2(D_{12}+2D_{66})\frac{\partial^4 w_0}{\partial x^2 \partial y^2} - D_{22}\frac{\partial^4 w_0}{\partial y^4} \\
&= I_0 \ddot{w}_0 - I_2\left(\frac{\partial^2 \ddot{w}_0}{\partial x^2} + \frac{\partial^2 \ddot{w}_0}{\partial y^2}\right).
\end{aligned}
\tag{8.264}
$$

The so-called SS2 boundary conditions are assumed here:

$$
\begin{aligned}
&u_0(0,y,t) = 0, \quad u_0(a,y,t) = 0, \quad v_0(x,0,t) = 0, \quad v_0(x,b,t) = 0, \\
&w_0(x,0,t) = 0, \quad w_0(x,b,t) = 0, \quad w_0(0,y,t) = 0, \quad w_0(a,y,t) = 0, \\
&\left.\frac{\partial w_0}{\partial x}\right|_{(x,0,t)} = 0, \quad \left.\frac{\partial w_0}{\partial x}\right|_{(x,b,t)} = 0, \quad \left.\frac{\partial w_0}{\partial y}\right|_{(0,y,t)} = 0, \quad \left.\frac{\partial w_0}{\partial y}\right|_{(a,y,t)} = 0, \\
&N^0_{xy}(0,y,t) = 0, \quad N^0_{xy}(a,y,t) = 0, \quad N^0_{xy}(x,0,t) = 0, \quad N^0_{xy}(x,b,t) = 0, \\
&M^0_{xx}(0,y,t) = 0, \quad M^0_{xx}(a,y,t) = 0, \quad M^0_{yy}(x,0,t) = 0, \quad M^0_{yy}(x,b,t) = 0.
\end{aligned}
\tag{8.265}
$$

The following approach fulfils these boundary conditions identically:

$$
\begin{aligned}
u_0(x,y,t) &= \sum_{n=1}^{\infty}\sum_{m=1}^{\infty} U_{mn}(t)\sin\left(\frac{m\pi x}{a}\right)\cos\left(\frac{n\pi y}{b}\right), \\
v_0(x,y,t) &= \sum_{n=1}^{\infty}\sum_{m=1}^{\infty} V_{mn}(t)\cos\left(\frac{m\pi x}{a}\right)\sin\left(\frac{n\pi y}{b}\right), \\
w_0(x,y,t) &= \sum_{n=1}^{\infty}\sum_{m=1}^{\infty} W_{mn}(t)\sin\left(\frac{m\pi x}{a}\right)\sin\left(\frac{n\pi y}{b}\right).
\end{aligned}
\tag{8.266}
$$

Insertion into the equations of motion (8.264) results in:

$$\sum_{n=1}^{\infty}\sum_{m=1}^{\infty}\left[-\left(A_{11}\alpha^2+A_{66}\beta^2\right)U_{mn}-\left(A_{12}+A_{66}\right)\alpha\beta V_{mn}\right.$$
$$\left.+\left(3B_{16}\alpha^2\beta+B_{26}\beta^3\right)W_{mn}-I_0\ddot{U}_{mn}\right]\sin\alpha x\cos\beta y=0,$$
$$\sum_{n=1}^{\infty}\sum_{m=1}^{\infty}\left[-\left(A_{12}+A_{66}\right)\alpha\beta U_{mn}-\left(A_{66}\alpha^2+A_{22}\beta^2\right)V_{mn}\right.$$
$$\left.+\left(B_{16}\alpha^3+3B_{26}\alpha\beta^2\right)W_{mn}-I_0\ddot{V}_{mn}\right]\cos\alpha x\sin\beta y=0,$$
$$\sum_{n=1}^{\infty}\sum_{m=1}^{\infty}\left[\left(3B_{16}\alpha^2\beta+B_{26}\beta^3\right)U_{mn}+\left(B_{16}\alpha^3+3B_{26}\alpha\beta^2\right)V_{mn}\right.$$
$$-\left(D_{11}\alpha^4+2\left(D_{12}+2D_{66}\right)\alpha^2\beta^2+D_{22}\beta^4\right)W_{mn}$$
$$\left.-\left(I_0+I_2\left(\alpha^2+\beta^2\right)\right)\ddot{W}_{mn}\right]\sin\alpha x\sin\beta y=0. \tag{8.267}$$

This system of equations can be written in a vector-matrix notation as:

$$\begin{bmatrix}\hat{c}_{11}&\hat{c}_{12}&\hat{c}_{13}\\ \hat{c}_{12}&\hat{c}_{22}&\hat{c}_{23}\\ \hat{c}_{13}&\hat{c}_{23}&\hat{c}_{33}\end{bmatrix}\begin{pmatrix}U_{mn}\\V_{mn}\\W_{mn}\end{pmatrix}+\begin{bmatrix}\hat{m}_{11}&0&0\\0&\hat{m}_{22}&0\\0&0&\hat{m}_{33}\end{bmatrix}\begin{pmatrix}\ddot{U}_{mn}\\\ddot{V}_{mn}\\\ddot{W}_{mn}\end{pmatrix}=\begin{pmatrix}0\\0\\0\end{pmatrix}, \tag{8.268}$$

if we neglect the inertia term I_1 at this point. The individual matrix entries are as follows:

$$\begin{aligned}\hat{c}_{11}&=A_{11}\alpha^2+A_{66}\beta^2,\\ \hat{c}_{12}&=\left(A_{12}+A_{66}\right)\alpha\beta,\\ \hat{c}_{13}&=-\left(3B_{16}\alpha^2+B_{26}\beta^2\right)\beta,\\ \hat{c}_{22}&=A_{66}\alpha^2+A_{22}\beta^2,\\ \hat{c}_{23}&=-\left(B_{16}\alpha^2+3B_{26}\beta^2\right)\alpha,\\ \hat{c}_{33}&=D_{11}\alpha^4+2\left(D_{12}+2D_{66}\right)\alpha^2\beta^2+D_{22}\beta^4,\\ \hat{m}_{11}&=I_0,\\ \hat{m}_{22}&=I_0,\\ \hat{m}_{33}&=I_0+I_2\left(\alpha^2+\beta^2\right).\end{aligned} \tag{8.269}$$

This again leads to an eigenvalue problem of the form:

$$\left(\begin{bmatrix}\hat{c}_{11}&\hat{c}_{12}&\hat{c}_{13}\\ \hat{c}_{12}&\hat{c}_{22}&\hat{c}_{23}\\ \hat{c}_{13}&\hat{c}_{23}&\hat{c}_{33}\end{bmatrix}-\omega^2\begin{bmatrix}\hat{m}_{11}&0&0\\0&\hat{m}_{22}&0\\0&0&\hat{m}_{33}\end{bmatrix}\right)\begin{pmatrix}U^0_{mn}\\V^0_{mn}\\W^0_{mn}\end{pmatrix}=\begin{pmatrix}0\\0\\0\end{pmatrix}. \tag{8.270}$$

Developing and setting the coefficient determinant to zero results in the following characteristic polynomial for the natural frequency ω (with $\lambda=\omega^2$):

$$-C_1\lambda^3+C_2\lambda^2-C_3\lambda+C_4=0, \tag{8.271}$$

wherein:

$$
\begin{aligned}
C_1 &= \begin{vmatrix} \hat{m}_{11} & 0 & 0 \\ 0 & \hat{m}_{22} & 0 \\ 0 & 0 & \hat{m}_{33} \end{vmatrix}, \\
C_2 &= \begin{vmatrix} \hat{c}_{11} & 0 & 0 \\ \hat{c}_{12} & \hat{m}_{22} & 0 \\ \hat{c}_{13} & 0 & \hat{m}_{33} \end{vmatrix} + \begin{vmatrix} \hat{m}_{11} & \hat{c}_{12} & 0 \\ 0 & \hat{c}_{22} & 0 \\ 0 & \hat{c}_{23} & \hat{m}_{33} \end{vmatrix} + \begin{vmatrix} \hat{m}_{11} & 0 & \hat{c}_{13} \\ 0 & \hat{m}_{22} & \hat{c}_{23} \\ 0 & 0 & \hat{c}_{33} \end{vmatrix}, \\
C_3 &= \begin{vmatrix} \hat{c}_{11} & \hat{c}_{12} & 0 \\ \hat{c}_{12} & \hat{c}_{22} & 0 \\ \hat{c}_{13} & \hat{c}_{23} & \hat{m}_{33} \end{vmatrix} + \begin{vmatrix} \hat{c}_{11} & 0 & \hat{c}_{13} \\ \hat{c}_{12} & \hat{m}_{22} & \hat{c}_{23} \\ \hat{c}_{13} & 0 & \hat{c}_{33} \end{vmatrix} + \begin{vmatrix} \hat{m}_{11} & \hat{c}_{12} & \hat{c}_{13} \\ 0 & \hat{c}_{22} & \hat{c}_{23} \\ 0 & \hat{c}_{23} & \hat{c}_{33} \end{vmatrix}, \\
C_4 &= \begin{vmatrix} \hat{c}_{11} & \hat{c}_{12} & \hat{c}_{13} \\ \hat{c}_{12} & \hat{c}_{22} & \hat{c}_{23} \\ \hat{c}_{13} & \hat{c}_{23} & \hat{c}_{33} \end{vmatrix}.
\end{aligned} \tag{8.272}
$$

8.9 The Finite Element Method

The solution methods presented so far for boundary value problems of plane laminates reach their limits when complex laminate geometries, load cases and boundary conditions are to be treated. In such cases, a calculation is generally carried out using the Finite Element Method. In this section, the necessary equations for a finite element formulation in the framework of Classical Laminated Plate Theory are presented as given by Reddy (2004). We revisit the equations of motion (8.236), multiply them by the virtual displacements δu_0, δv_0, δw_0 and integrate over the element e as follows:

$$
\begin{aligned}
&\int_{\Omega_e} \delta u_0 \left(-\frac{\partial N^0_{xx}}{\partial x} - \frac{\partial N^0_{xy}}{\partial y} + I_0 \ddot{u}_0 - I_1 \frac{\partial \ddot{w}_0}{\partial x} \right) \mathrm{d}x\mathrm{d}y = 0, \\
&\int_{\Omega_e} \delta u_0 \left(-\frac{\partial N^0_{xy}}{\partial x} - \frac{\partial N^0_{yy}}{\partial y} + I_0 \ddot{v}_0 - I_1 \frac{\partial \ddot{w}_0}{\partial y} \right) \mathrm{d}x\mathrm{d}y = 0, \\
&\int_{\Omega_e} \delta w_0 \left(-\frac{\partial^2 M^0_{xx}}{\partial x^2} - 2\frac{\partial^2 M^0_{xy}}{\partial x \partial y} - \frac{\partial M^0_{yy}}{\partial y^2} - p \right. \\
&\left. + I_0 \ddot{w}_0 + I_1 \frac{\partial \ddot{u}_0}{\partial x} + I_1 \frac{\partial \ddot{v}_0}{\partial y} - I_2 \frac{\partial^2 \ddot{w}_0}{\partial x^2} - I_2 \frac{\partial^2 \ddot{w}_0}{\partial y^2} \right) \mathrm{d}x\mathrm{d}y = 0.
\end{aligned} \tag{8.273}
$$

These equations represent the weak form of the equations of motion.

For the element e, the following approach is now provided for the displacements:

$$\begin{aligned} u_0(x,y,t) &= \sum_{j=1}^{m} u_j^e(t)\psi_j^e(x,y), \\ v_0(x,y,t) &= \sum_{j=1}^{m} v_j^e(t)\psi_j^e(x,y), \\ w_0(x,y,t) &= \sum_{k=1}^{n} \Delta_k^e(t)\varphi_k^e(x,y), \end{aligned} \tag{8.274}$$

where u_j^e, v_j^e are the nodal values of node j of the element. Similarly, Δ_k^e is the nodal value of w_0 in node k. The functions ψ_j^e, ψ_j^e are Lagrangian shape functions, whereas φ_k^e are Hermitian[2] shape functions. If this approach is used in the weak form (8.273), the following equations of motion are obtained for the element e:

$$\begin{bmatrix} \underline{\underline{K}}_{11} & \underline{\underline{K}}_{12} & \underline{\underline{K}}_{13} \\ \underline{\underline{K}}_{12}^T & \underline{\underline{K}}_{22} & \underline{\underline{K}}_{23} \\ \underline{\underline{K}}_{13}^T & \underline{\underline{K}}_{23}^T & \underline{\underline{K}}_{33} \end{bmatrix} \begin{pmatrix} \underline{u}_e \\ \underline{v}_e \\ \underline{\Delta}_e \end{pmatrix} + \begin{bmatrix} \underline{\underline{M}}_{11} & \underline{\underline{0}} & \underline{\underline{M}}_{13} \\ \underline{\underline{0}} & \underline{\underline{M}}_{22} & \underline{\underline{M}}_{23} \\ \underline{\underline{M}}_{13}^T & \underline{\underline{M}}_{23}^T & \underline{\underline{M}}_{33} \end{bmatrix} \begin{pmatrix} \ddot{\underline{u}}_e \\ \ddot{\underline{v}}_e \\ \ddot{\underline{\Delta}}_e \end{pmatrix} = \begin{pmatrix} \underline{F}_1 \\ \underline{F}_2 \\ \underline{F}_3 \end{pmatrix}. \tag{8.275}$$

The specific assignment of the individual matrices occurring here is not described at this point, they can be found in Reddy (2004).

If the given problem is a purely static task in which no boundary loads $\hat{N}_{xx}^0$, $\hat{N}_{yy}^0$, $\hat{N}_{xy}^0$ occur, then we obtain from (8.275) with vanishing time derivatives:

$$\begin{bmatrix} \underline{\underline{K}}_{11} & \underline{\underline{K}}_{12} & \underline{\underline{K}}_{13} \\ \underline{\underline{K}}_{12}^T & \underline{\underline{K}}_{22} & \underline{\underline{K}}_{23} \\ \underline{\underline{K}}_{13}^T & \underline{\underline{K}}_{23}^T & \underline{\underline{K}}_{33} \end{bmatrix} \begin{pmatrix} \underline{u}_e \\ \underline{v}_e \\ \underline{\Delta}_e \end{pmatrix} = \begin{pmatrix} \underline{F}_1 \\ \underline{F}_2 \\ \underline{F}_3 \end{pmatrix}. \tag{8.276}$$

If, on the other hand, we want to analyse free vibrations, the following eigenvalue problem arises:

$$\left(\begin{bmatrix} \underline{\underline{K}}_{11} & \underline{\underline{K}}_{12} & \underline{\underline{K}}_{13} \\ \underline{\underline{K}}_{12}^T & \underline{\underline{K}}_{22} & \underline{\underline{K}}_{23} \\ \underline{\underline{K}}_{13}^T & \underline{\underline{K}}_{23}^T & \underline{\underline{K}}_{33} \end{bmatrix} - \omega^2 \begin{bmatrix} \underline{\underline{M}}_{11} & \underline{\underline{0}} & \underline{\underline{M}}_{13} \\ \underline{\underline{0}} & \underline{\underline{M}}_{22} & \underline{\underline{M}}_{23} \\ \underline{\underline{M}}_{13}^T & \underline{\underline{M}}_{23}^T & \underline{\underline{M}}_{33} \end{bmatrix} \right) \begin{pmatrix} \underline{u}_e \\ \underline{v}_e \\ \underline{\Delta}_e \end{pmatrix} = \begin{pmatrix} \underline{0} \\ \underline{0} \\ \underline{0} \end{pmatrix}. \tag{8.277}$$

We will refrain from an in-depth discussion of the Finite Element Method at this point; interested readers will find a wealth of further information in the sources cited in Chapter 4.

[2] Charles Hermite, 1822–1901, French mathematician.

References

Altenbach H, Altenbach J, Rikards R (1996): *Einführung in die Mechanik der Laminat- und Sandwichtragwerke*, Deutscher Verlag der Grundstoffindustrie, Stuttgart, Germany.

Altenbach H, Altenbach J, Naumenko K (1998): *Ebene Flächentragwerke*, Springer Verlag, Berlin et al., Germany.

Jones RM (1975): *Mechanics of composite materials*, Scripta Book Co., Washington, USA.

Mittelstedt C (2023): *Theory of plates and shells*, Springer Vieweg, Berlin et al., Germany.

Reddy JN (2004): *Mechanics of laminated composite plates and shells (2nd edition)*, CRC Press Boca Raton et al., USA.

Weaver PM, Nemeth MP (2007): *Bounds on flexural properties and buckling response for symmetrically laminated composite plates*. Journal of Engineering Mechanics 133:1178–1191.

Wiedemann J (1996): *Leichtbau 1 - Elemente*, 2. Auflage, Springer Verlag, Berlin et al., Germany.



9 Strength Hypotheses for Unidirectionally Fiber-Reinforced Laminate Layers

The unidirectional (UD) fiber-reinforced layers frequently used in modern fiber composite laminates are special representatives of UD materials that typically consist of an isotropic matrix and a unidirectional fiber reinforcement. Due to the microstructurally inhomogeneous structure of these UD materials and the given anisotropy with regard to both the elastic properties and the strength properties, the strength analysis of a laminate with fiber-reinforced layers generally proves to be significantly more complex than with homogeneous isotropic materials. One of the reasons for this is that there are different types of failure, such as fiber fracture, matrix fracture, fiber-matrix delamination and delamination of the layers from each other. As a consequence of this, it is not necessarily the stress components with the highest magnitudes that are particularly critical to failure within a laminate; it can also be comparatively small stress components if these are associated with a relatively small anisotropic strength. This chapter provides an overview of common failure criteria for composite laminates made of layers of fiber-reinforced plastics.

9.1 Introduction

The failure criteria presented in this chapter are mostly limited to the pure inplane strength assessment of the individual layers. Failure due to interlaminar stresses σ_{33}, τ_{13}, τ_{23} must then be analysed separately.

For UD materials, it has proven to be useful to characterize the effective strength by the following basic strength parameters with respect to the principal material axes (where the 1-direction is the fiber direction, the 2-direction is the direction perpendicular to it in the plane and the 3-direction is the laminate thickness direction):

© The Author(s), under exclusive license to Springer-Verlag GmbH, DE, part of Springer Nature 2025

C. Mittelstedt, *Mechanics of Composite Structures*,
https://doi.org/10.1007/978-3-662-70788-3_9

$R_{\parallel}^{t}$ (or X_t): Axial or longitudinal tensile strength, in fiber direction,
$R_{\parallel}^{c}$ (or X_c): Axial or longitudinal compressive strength, in fiber direction,
$R_{\perp}^{t}$ (or Y_t): Transverse tensile strength,
$R_{\perp}^{c}$ (or Y_c): Transverse compressive strength,
$R_{\perp\parallel}$ (or S): Shear strength.

For the CFRP single-layer standard material T300/ epoxy (unidirectional carbon fibers of type T300 in an epoxy matrix, with a fiber volume fraction of $V_f = 60\%$), for example, the following strength properties apply:

$$R_{\parallel}^{t} = 1450\,\text{MPa},\ R_{\perp}^{t} = 55\,\text{MPa},$$
$$R_{\parallel}^{c} = 1400\,\text{MPa},\ R_{\perp}^{c} = 170\,\text{MPa},\ R_{\perp\parallel} = 90\,\text{MPa}.$$

It can be seen that in this case the transverse tensile strength $R_{\perp}^{t}$ is almost 30 times lower than the longitudinal tensile strength $R_{\parallel}^{t}$.

9.2 Maximum Stress Criterion

With the maximum stress criterion, failure is postulated in the event that at least one of the following three conditions is violated:

$$\begin{aligned} -X_c &< \sigma_{11} < X_t, \\ -Y_c &< \sigma_{22} < Y_t, \\ |\tau_{12}| &< S. \end{aligned} \tag{9.1}$$

The criterion corresponds to an obvious intuitive view and is very easy to apply. However, it is not particularly reliable for mixed stress states and shows clear discrepancies with experimental findings. This is due in particular to the fact that the criterion does not provide for any interaction between the stresses, i.e., for example, no influence of a normal stress in one direction on the remaining load-bearing capacity with respect to a normal stress in another direction.

9.3 Maximum Strain Criterion

A certain interaction between the stresses can be taken into account if the failure is not determined by maximum stresses, but by maximum strains. Then the stresses interact via the corresponding transverse contraction properties of the material. Thus, the maximum strain criterion postulates failure of the UD material if at least one of the following three conditions is violated:

$$
\begin{aligned}
-\frac{X_c}{E_{11}} < \varepsilon_{11} < \frac{X_t}{E_{11}},\\
-\frac{Y_c}{E_{22}} < \varepsilon_{22} < \frac{Y_t}{E_{22}},\\
|\gamma_{12}| < \frac{S}{G_{12}}.
\end{aligned}
\tag{9.2}
$$

Except for the influence of transverse contraction, this criterion is largely analogous to the maximum stress criterion. As far as the agreement with experimental findings is concerned, the criterion is again not particularly reliable.

9.4 Tsai-Hill Criterion

For the case of the plane stress state, the Tsai-Hill criterion[1] is given by the following failure surface in formal analogy to the von Mises yield criterion of plasticity theory:

$$
\frac{\sigma_{11}^2}{X^2} - \frac{\sigma_{11}\sigma_{22}}{X^2} + \frac{\sigma_{22}^2}{Y^2} + \frac{\tau_{12}^2}{S^2} = 1. \tag{9.3}
$$

A superposition of quadratic stresses (i.e. stresses related to strength values) is considered here. The advantage of this criterion is that it consists of only one criterion; this leads to a correspondingly smooth failure surface. Due to the superposition as well as the product term with $\sigma_{11}\sigma_{22}$, there is a very significant interaction between the occurring stresses. It is advantageous that this failure criterion also shows a significantly better agreement with experiments than the criteria according to Sects. 9.2 and 9.3. A disadvantage of the Tsai-Hill criterion is that no clear distinction is made between tensile and compressive strengths. There is also no differentiation between different types of failure, as they do exist in reality.

9.5 Tsai-Wu Criterion

A clearer distinction between tensile and compressive behaviour than in the Tsai-Hill criterion is provided in the Tsai-Wu criterion.[2] Here, the failure surface is described using a 2nd degree tensor polynomial, whereby linear terms also occur. The approach is of the following type:

$$
F_{ij}\sigma_i\sigma_j + F_i\sigma_i = 1, \quad i, j = 1, 2, 6, \tag{9.4}
$$

[1] Rodney Hill, 1921–2011, British mathematician, and Stephen Wei-Lun Tsai, born 1929, US-American engineer.

[2] Edward Ming-Chi Wu, 1938–2009, US-American engineer.

(in the original three-dimensional formulation $i, j = 1, \ldots, 6$). If, according to the internal symmetry of the material, the invariance of the failure criterion is required with a sign reversal of $\sigma_6 = \tau_{12}$, the coefficients F_{16}, F_{26} and F_6 in the tensor polynomial disappear. This leaves the following failure representation:

$$F_{11}\sigma_{11}^2 + 2F_{12}\sigma_{11}\sigma_{22} + F_{22}\sigma_{22}^2 + F_{66}\tau_{12}^2 + F_1\sigma_{11} + F_2\sigma_{22} = 1. \tag{9.5}$$

This contains a total of six free coefficients that need to be considered. For this purpose, the knowledge of the five strength values X_t, X_c, Y_t, Y_c and S is required. The following results from the consideration of a pure axial tensile stress and compressive stress state:

$$\text{tensile stress} \quad \sigma_{11} = X_t : \qquad F_{11}X_t^2 + F_1X_t = 1,$$
$$\text{compressive stress} \quad \sigma_{11} = -X_c : \qquad F_{11}X_c^2 - F_1X_c = 1.$$

From the resulting equations, the coefficients F_{11} and F_1 can be identified as:

$$F_{11} = \frac{1}{X_tX_c}, \quad F_1 = \frac{1}{X_t} - \frac{1}{X_c}. \tag{9.6}$$

Analogous results are obtained from the consideration of a pure transversal tensile and compressive stress state:

$$\text{tensile stress} \quad \sigma_{22} = Y_t : \qquad F_{22}Y_t^2 + F_2Y_t = 1,$$
$$\text{compressive stress} \quad \sigma_{22} = -Y_c : \qquad F_{22}Y_c^2 - F_2Y_c = 1.$$

From this, the coefficients F_{22} and F_2 can be identified as

$$F_{22} = \frac{1}{Y_tY_c}, \quad F_2 = \frac{1}{Y_t} - \frac{1}{Y_c}. \tag{9.7}$$

Finally, the consideration of a pure shear stress state $\tau_{12} = S$ results in the following:

$$F_{66}S^2 = 1, \tag{9.8}$$

and thus:

$$F_{66} = \frac{1}{S^2}. \tag{9.9}$$

This leaves the only undetermined coefficient to be F_{12}. To identify it, additional strength information is actually required, e.g. the strength in a biaxial tensile or compression test. In most cases, this information is not available, and an experimental campaign is mostly not desirable because it would be costly and time-consuming. The following expression is often used:

$$F_{12} = -\frac{1}{2}\frac{1}{\sqrt{X_t X_c Y_t Y_c}}. \tag{9.10}$$

Thus, the complete tensor polynomial has been determined, and the Tsai-Wu criterion reads:

$$\frac{\sigma_{11}^2}{X_t X_c} - \frac{\sigma_{11}\sigma_{22}}{\sqrt{X_t X_c Y_t Y_c}} + \frac{\sigma_{22}^2}{Y_t Y_c} + \frac{\tau_{12}^2}{S^2} + \sigma_{11}\left(\frac{1}{X_t} - \frac{1}{X_c}\right) + \sigma_{22}\left(\frac{1}{Y_t} - \frac{1}{Y_c}\right) = 1. \tag{9.11}$$

The advantage of the Tsai-Wu criterion is that it consists of only one criterion and is represented by a smooth failure surface. Different tensile and compressive strengths as well as the interaction between stresses are taken into account. A disadvantage is that no distinction is made between different types of failure.

9.6 Puck Criterion

A certain distinction of failure types is made in the criterion of Puck,[3] which has undergone various further developments, but is presented here in its original form. Puck distinguishes between two different types of failure, namely inter fiber fracture and fiber fracture, and describes these using two different sub-criteria.

Inter fiber fracture (IFF) encompasses all matrix and interface fractures and is described by a modified Tsai-Wu criterion, in which the axial strengths X_t and X_c are replaced by the fictitious strengths $E_{11}\,\varepsilon_{1t}$ and $E_{11}\,\varepsilon_{1c}$, where ε_{1t} and ε_{1c} represent the tensile and compressive fracture strains of the matrix material. In this case, the fiber failure that occurs before the inter fiber fracture is thus excluded. This leads to the following partial failure condition:

$$\begin{aligned}\frac{\sigma_{11}^2}{E_{11}\varepsilon_{1t}E_{11}\varepsilon_{1c}} - \frac{\sigma_{11}\sigma_{22}}{\sqrt{E_{11}\varepsilon_{1t}E_{11}\varepsilon_{1c}Y_t Y_c}} + \frac{\sigma_{22}^2}{Y_t Y_c} + \frac{\tau_{12}^2}{S^2} \\ + \sigma_{11}\left(\frac{1}{E_{11}\varepsilon_{1t}} - \frac{1}{E_{11}\varepsilon_{1c}}\right) + \sigma_{22}\left(\frac{1}{Y_t} - \frac{1}{Y_c}\right) = 1.\end{aligned} \tag{9.12}$$

The fiber fracture (FF), on the other hand, comprises the fracture of the fibers in tension and their buckling due to insufficient support in compression and is described quite simply by

$$\frac{\sigma_{11}^2}{X_t^2} = 1 \quad \text{for} \quad \sigma_{11} > 0, \qquad \frac{\sigma_{11}^2}{X_c^2} = 1 \quad \text{for} \quad \sigma_{11} < 0. \tag{9.13}$$

[3] Alfred Puck, 1927–2021, German engineer.

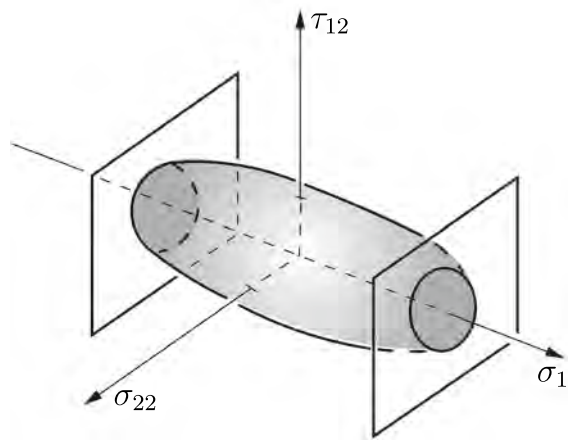


Fig. 9.1 Failure surface according to the Puck criterion

Geometrically, the failure surface associated with the inter fiber fracture is an ellipsoid in $\sigma_{11}, \sigma_{22}, \tau_{12}$ space. In contrast, the failure surface associated with the fiber fracture consists of two planes perpendicular to the σ_{11} axis. These planes intersect the IFF ellipsoid at the front and rear ends. This leads to a resulting total failure surface, which is often referred to as a 'puck cigar' (Fig. 9.1).

The advantage of Puck's criterion is certainly the distinction between different types of failure and the decision about the type of fracture that occurs, at least in the distinction between fiber fracture and inter fiber fracture. Otherwise, Puck's criterion is just as applicable as the Tsai-Wu criterion.

9.7 Hashin Criterion

A further differentiation between different types of failure is made in the criterion of Hashin.[4] Hashin's criterion provides for four types of failure, namely fiber tensile failure, fiber compressive failure, matrix tension failure and matrix compressive failure. The corresponding sub-criteria are as follows:

Tensile fiber fracture $\sigma_{11} > 0$:

$$\left(\frac{\sigma_{11}}{X_t}\right)^2 + \left(\frac{\tau_{12}}{S}\right)^2 = 1. \tag{9.14}$$

Compressive fiber failure $\sigma_{11} < 0$:

$$\sigma_{11} = -X_c. \tag{9.15}$$

[4] Zvi Hashin, 1929–2017, Israeli scientist.

Matrix tensile fracture $\sigma_{22} > 0$:

$$\left(\frac{\sigma_{22}}{Y_t}\right)^2 + \left(\frac{\tau_{12}}{S}\right)^2 = 1. \tag{9.16}$$

Matrix compressive fracture $\sigma_{22} < 0$:

$$\left(\frac{\sigma_{22}}{2S}\right)^2 + \left(\frac{\tau_{12}}{S}\right)^2 + \frac{\sigma_{22}}{Y_c}\left[\left(\frac{Y_c}{2S}\right)^2 - 1\right] = 1. \tag{9.17}$$

By intersecting the associated partial failure surfaces, a correspondingly total failure surface is created. The further differentiation of the failure types can of course be seen as an advantage of Hashin's criterion.

9.8 Puck's Action Plane Fracture Criterion

The different variants of the failure criteria further developed by Puck have been incorporated into the so-called "action plane fracture criterion" since 1996. This has the advantage that it is physically based and distinguishes between different failure mechanisms. In addition, it also provides information on the resulting fracture angle, not only for the case of the plane stress state, but also for a three-dimensional stress state.

The key idea of Puck's action plane fracture criterion is the application of Mohr's approach to the UD layer. Hypothetically, all inter fiber fractures are considered on all conceivable fiber-parallel planes. This means that all potential fracture planes resulting from the rotation of the cutting planes around the fiber-parallel 1-axis are considered. The following stresses are considered on each action plane:

- normal stress σ_{nn}
- shear stress τ_{nt}
- shear stress τ_{n1}.

These components result in the total shear stress

$$\tau_{n\psi} = \sqrt{\tau_{n1}^2 + \tau_{nt}^2} \quad \text{in direction } \psi, \qquad \text{with } \psi = \arctan\frac{\tau_{n1}}{\tau_{nt}}. \tag{9.18}$$

Both the normal stress σ_{nn} and the total shear stress $\tau_{n\psi}$ are decisive for the fracture process. A positive normal stress $\sigma_{nn} > 0$ (tensile stress) facilitates the fracture process (interaction with $\tau_{n\psi}$) or even causes the fracture on its own. A negative normal stress $\sigma_{nn} < 0$ (compressive stress), on the other hand, makes a shear fracture caused by $\tau_{n\psi}$ more

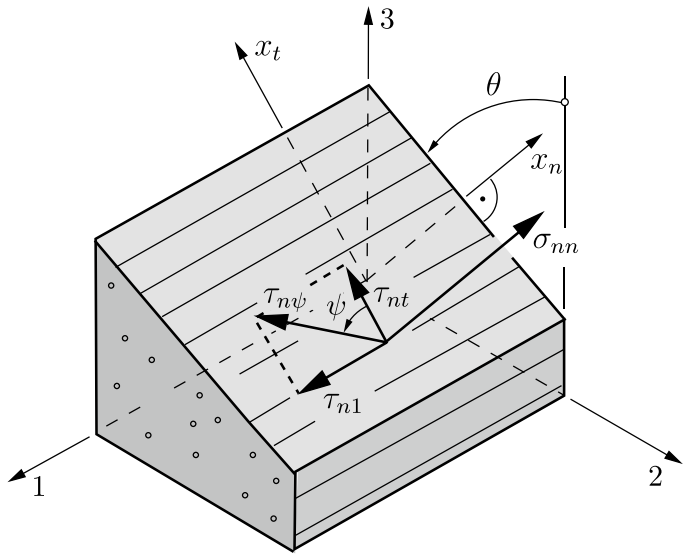


Fig. 9.2 Action plane and associated stress components

difficult. The action plane in which a fracture ultimately forms depends on the plane in which the fracture limit is reached first (Fig. 9.2).

The position of the fracture plane is determined as follows. The stresses σ_{nn}, τ_{nt} and τ_{n1} associated with the potential plane of action result from the single layer stress components σ_{22}, σ_{33}, τ_{32}, τ_{31} and τ_{21} by the corresponding tensor transformation, which can be represented as follows:

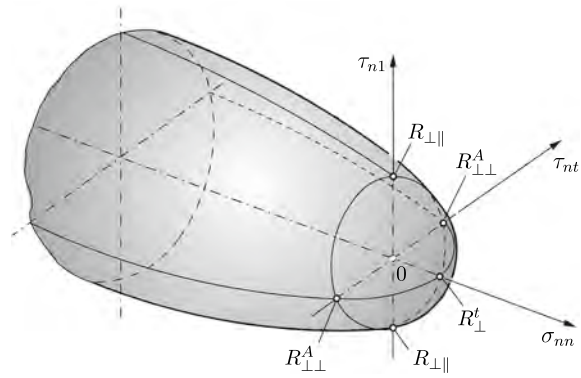
$$\begin{bmatrix} \sigma_{nn} \\ \tau_{nt} \\ \tau_{n1} \end{bmatrix} = \begin{bmatrix} c^2 & s^2 & 2cs & 0 & 0 \\ -cs & cs & (c^2 - s^2) & 0 & 0 \\ 0 & 0 & 0 & s & c \end{bmatrix} \begin{bmatrix} \sigma_{22} \\ \sigma_{33} \\ \tau_{23} \\ \tau_{31} \\ \tau_{21} \end{bmatrix}, \tag{9.19}$$

$$\text{with} \quad c = \cos\theta, \quad s = \sin\theta.$$

The angle θ at which the vector $(\sigma_{nn}, \tau_{nt}, \tau_{n1})$ comes closest to passing through the surface of the so-called master fractional body is the angle of the fracture surface θ_{fp}. In most cases, this angle θ_{fp} can be determined numerically. The fracture surface or the corresponding fracture plane that ultimately describes failure is usually open in the direction of the negative σ_{nn} axis (Fig. 9.3).

The fracture conditions for inter fiber fracture are determined as follows. For the tensile range $\sigma_{nn} \geq 0$, it has proven to be expedient to provide the interaction of the stresses σ_{nn}, τ_{n1} and τ_{nt} as follows:

Fig. 9.3 Fracture surface



$$\sqrt{\left(\frac{1}{R^t_\perp}-\frac{p^+_{\perp\psi}}{R^A_{\perp\psi}}\right)^2\sigma^2_{nn}+\left(\frac{\tau_{nt}}{R^A_{\perp\perp}}\right)^2+\left(\frac{\tau_{n1}}{R_{\perp\parallel}}\right)^2}+\frac{p^+_{\perp\psi}}{R^A_{\perp\parallel}}\sigma_{nn}=1. \tag{9.20}$$

For compressive stresses $\sigma_{nn} < 0$, it has proven expedient to employ the following interaction of stresses:

$$\sqrt{\left(\frac{\tau_{nt}}{R^A_{\perp\perp}}\right)^2+\left(\frac{\tau_{n1}}{R_{\perp\parallel}}\right)^2+\left(\frac{p^-_{\perp\psi}}{R^A_{\perp\psi}}\sigma_{nn}\right)^2}+\frac{p^-_{\perp\psi}}{R^A_{\perp\psi}}\sigma_{nn}=1. \tag{9.21}$$

Therein:

$p^+_{\perp\psi}$, $p^-_{\perp\psi}$: 'Inclination parameter', depending on Ψ,

$R^A_{\perp\psi}$: Effective action plane shear strength in the direction of Ψ,

$R^A_{\perp\perp}$: Effective action plane shear strength in the direction of $\Psi = 0$,
(Index A stands for 'action plane').

For the quotients $p^\pm_{\perp\psi}/R^A_{\perp\psi}$ occurring in the master fracture criteria, it is recommended to use the following relationships:

$$\frac{p^\pm_{\perp\psi}}{R^A_{\perp\psi}}=\frac{1}{\tau^2_{nt}+\tau^2_{n1}}\left(\frac{p^\pm_{\perp\perp}}{R^A_{\perp\perp}}\tau^2_{nt}+\frac{p^\pm_{\perp\parallel}}{R_{\perp\parallel}}\tau^2_{n1}\right) \quad \text{for} \quad \tau^2_{nt}+\tau^2_{n1}>0, \tag{9.22}$$

$$\text{or} \qquad 0 \qquad \text{for} \quad \tau^2_{nt}+\tau^2_{n1}=0. \tag{9.23}$$

The following should be noted when obtaining the required strength values: The strength parameter $R^t_\perp$ can be determined using a standard tensile test. The strength parameter $R_{\perp\parallel}$ can be identified from a standard shear test. In contrast, determining the strength parameter $R^A_{\perp\perp}$ is problematic. This characteristic value cannot be determined using a pure shear load

τ_{nt}, as pure shear leads prematurely to a normal stress crack in the 45° direction. Puck therefore made the pragmatic suggestion of using the following relationship to determine this characteristic value:

$$R^A_{\perp\perp} = \frac{R^c_\perp}{2\left(1 + p^-_{\perp\perp}\right)}. \tag{9.24}$$

In the special case of a plane stress state, the situation is simplified insofar as the orientation of the fracture surface is known ($\theta = 0$ applies for compressive stresses $\sigma_{22} < 0$ that are not too large) or can be determined by closed-form analysis. This means that the fracture surface can ultimately be represented as follows:

$$\sqrt{\left(\frac{\tau_{21}}{R_{\perp\parallel}}\right)^2 + \left(1 - p^+_{\perp\parallel}\frac{R^t_\perp}{R_{\perp\parallel}}\right)^2\left(\frac{\sigma_{22}}{R^t_\perp}\right)^2} + p^+_{\perp\parallel}\frac{\sigma_{22}}{R_{\perp\parallel}} = 1 \quad \text{for } \sigma_{22} \geq 0$$

(Mode A),

$$\frac{1}{R_{\perp\parallel}}\left(\sqrt{\tau_{21}^2 + \left(p^-_{\perp\parallel}\sigma_{22}\right)^2} + p^-_{\perp\parallel}\sigma_{22}\right) = 1 \quad \text{for } \sigma_{22} < 0$$

$$\text{with } \left|\frac{\sigma_{22}}{\tau_{12}}\right| \leq \frac{R^A_{\perp\perp}}{R_{\perp\parallel}\sqrt{1 + 2p^-_{\perp\perp}}}$$

(Mode B),

$$\left[\left(\frac{\tau_{21}}{2(1 + p^-_{\perp\perp})R_{\perp\parallel}}\right)^2 + \left(\frac{\sigma_{22}}{R^-_\perp}\right)^2\right]\frac{R^c_\perp}{-\sigma_{22}} = 1 \quad \text{for } \sigma_{22} < 0$$

$$\text{with } \left|\frac{\sigma_{22}}{\tau_{12}}\right| > \frac{R^A_{\perp\perp}}{R_{\perp\parallel}\sqrt{1 + 2p^-_{\perp\perp}}}$$

(Mode C).

Therein

$$R^A_{\perp\perp} = \frac{R_{\perp\parallel}}{2p_{\perp\parallel^-}}\left(\sqrt{1 + 2p^-_{\perp\parallel}\frac{R^c_\perp}{R_{\perp\parallel}}} - 1\right)$$

and

$$\frac{p^-_{\perp\perp}}{R^A_{\perp\perp}} = \frac{p^-_{\perp\parallel}}{R_{\perp\parallel}}$$

has been employed.

The three partial failure criteria described above correspond to three different failure modes (mode A, mode B, mode C), as shown in Fig. 9.4.

If the overall description of failure by inter fiber fracture is again combined with a fiber fracture criterion of the type $\sigma_{11} = R^t_\parallel$ for $\sigma_{11} > 0$ and $\sigma_{11} = R^c_\parallel$ for $\sigma_{11} < 0$, this results in a composite fracture surface as shown in Fig. 9.5.

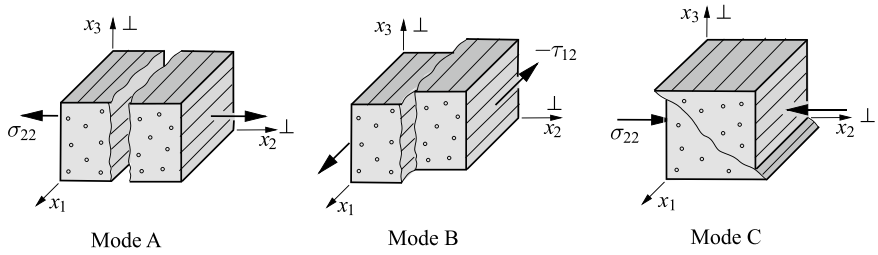


Fig. 9.4 Failure modes

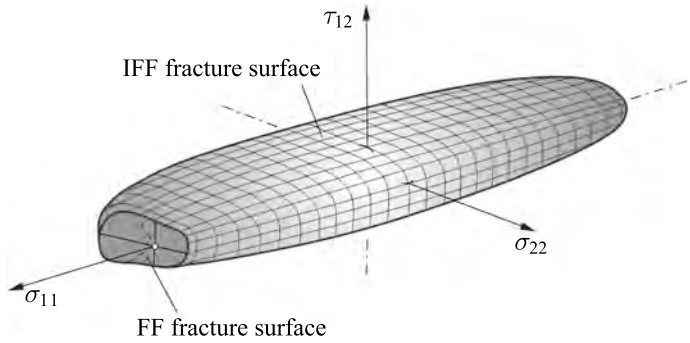


Fig. 9.5 Fracture surface

The advantage of the action plane fracture criterion is that it is physically based and that the fracture angle is included as information. In addition, the predictions that can be made with it fit experimental findings very well. The disadvantage is that the identification of the strength parameters $R^A_{\perp\perp}$ and the inclination parameters is somewhat complex. The fact that the use of the effective plane criterion requires a certain amount of familiarization can also be seen as a certain complication.

9.9 Cuntze's Failure Mode Concept (FMC)

UD materials such as unidirectional fiber-reinforced plastics are generally transversely isotropic due to their internal symmetry. This means that their linear-elastic material behaviour can be described by five independent constants. According to Cuntze's failure mode concept (FMC), the UD material is then characterised by the same number of independent strength constants and its failure is possible in the form of the same number of different failure modes. In fact, fractographic fracture patterns show that there are five different fracture failure modes, each dominated by an associated strength value. These are:

– 2 fiber failure modes, FF (Fiber Failure),
– 3 inter fiber failure modes, IFF (Inter Fiber Failure).

These failure modes are shown in Fig. 9.6.

Of the five failure modes, the fiber failure modes result in the immediate fracture of a laminate made up of UD layers. The intermediate fiber failure mode IFF2 should also be avoided as far as possible, because the entire laminate is sometimes 'blown open' by the corresponding wedge effect. It is also obvious that each failure mode is dominated by an associated strength value.

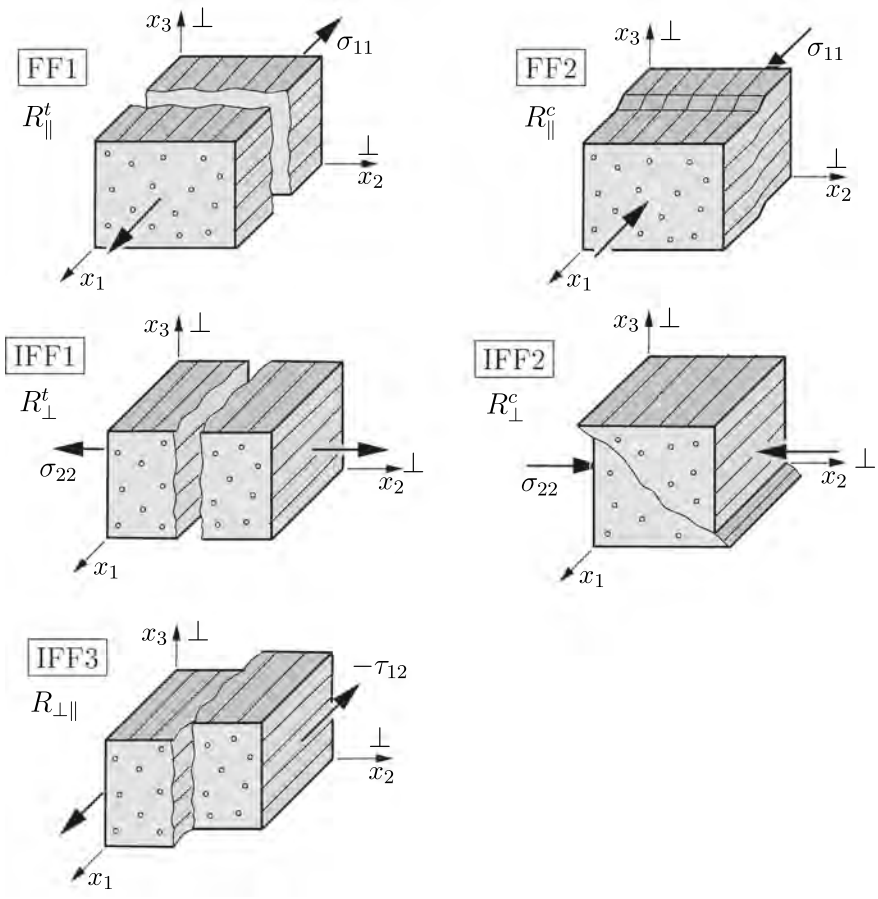


Fig. 9.6 Failure modes

There are several different options for formulating the corresponding partial failure criteria. The formulation can take place using

- layer stresses,
- Mohr's stresses,
- principal stresses,
- stress invariants.

The stress invariants must be introduced somewhat differently than in the case of isotropic material behaviour. In the case of transversely isotropic materials, only the invariance with respect to a rotation around the x_1 or fiber axis is required. This means that there are then five different, independent invariants I_1, …, I_5. These are given in the different possible stress systems as follows. With $\underline{\sigma} = (\,\sigma_{11},\ \sigma_{22},\ \sigma_{33},\ \tau_{23},\ \tau_{31},\ \tau_{12}\,)^T$ we obtain in layer coordinates (Figs. 9.7 and 9.8):

$$
\begin{aligned}
I_1 &= \sigma_{11},\\
I_2 &= \sigma_{22} + \sigma_{33},\\
I_3 &= \tau_{31}^2 + \tau_{21}^2,\\
I_4 &= (\sigma_{22} - \sigma_{33})^2 + 4\,\tau_{23}^2,\\
I_5 &= (\sigma_{22} - \sigma_{33})(\tau_{31}^2 - \tau_{21}^2) - 4\,\tau_{23}\,\tau_{31}\,\tau_{21}.
\end{aligned}
$$

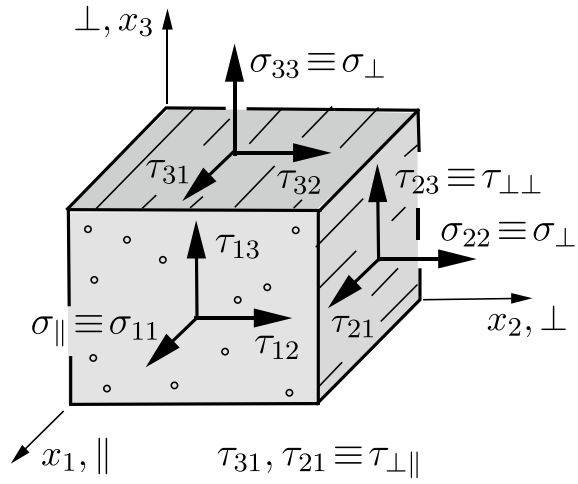
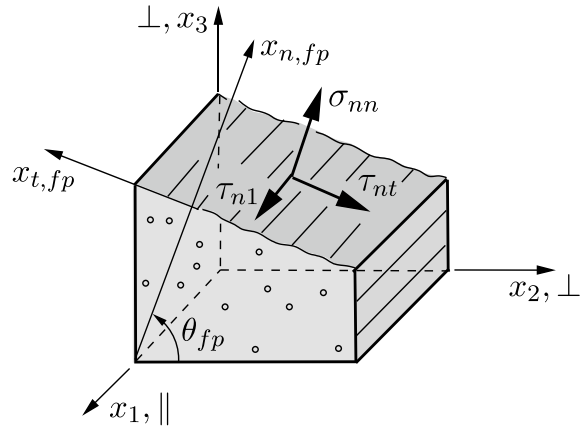


Fig. 9.7 Layer stresses

Fig. 9.8 Mohr's stresses



With respect to an arbitrary action plane with regard to Mohr's failure hypothesis, $\underline{\sigma}_{\text{Mohr}} = (\,\sigma_{ll},\ \sigma_{nn},\ \sigma_{tt},\ \tau_{nt},\ \tau_{tl},\ \tau_{ln}\,)^T$:

$$
\begin{aligned}
I_1 &= \sigma_{ll},\\
I_2 &= \sigma_{nn} + \sigma_{tt},\\
I_3 &= \tau_{tl}^2 + \tau_{nl}^2,\\
I_4 &= (\sigma_{nn} - \sigma_{tt})^2 + 4\,\tau_{nt}^2,\\
I_5 &= (\sigma_{nn} - \sigma_{tt})(\tau_{tl}^2 - \tau_{nl}^2) - 4\,\tau_{nt}\,\tau_{tl}\,\tau_{nl}.
\end{aligned}
$$

With regard to a 'principal axis transformation', in which the normal stresses σ_{22} and σ_{33} are extremalized by rotation around the x_1 axis, the following applies with $\underline{\sigma}_{\text{principal}} = (\,\sigma_{11},\ \sigma_2^p,\ \sigma_3^p, 0,\ \tau_{31}^p,\ \tau_{21}^p\,)^T$:

$$
\begin{aligned}
I_1 &= \sigma_{11},\\
I_2 &= \sigma_2^p + \sigma_3^p,\\
I_3 &= \tau_{31}^{p2} + \tau_{21}^{p2},\\
I_4 &= (\sigma_2^p - \sigma_3^p)^2 + 0,\\
I_5 &= (\sigma_2^p - \sigma_3^p)(\tau_{31}^{p2} - \tau_{21}^{p2}) + 0.
\end{aligned}
$$

The use of stress invariants is particularly advantageous for three-dimensional loads. For a plane two-dimensional load, it is easier to use the plane stress components $\sigma_{11}, \sigma_{22}, \tau_{12}$.

The following concrete FMC partial failure conditions for the case of a plane load are employed according to Cuntze:

$$\underline{\text{FF1:}} \qquad \frac{\sigma_{11}}{R_{\parallel}^{t}} = 1 \quad \text{for} \quad \sigma_{11} > 0,$$

$$\underline{\text{FF2:}} \qquad \frac{-\sigma_{11}}{R_{\parallel}^{c}} = 1 \quad \text{for} \quad \sigma_{11} < 0,$$

$$\underline{\text{IFF1:}} \qquad \frac{\sigma_{22}}{R_{\perp}^{t}} = 1 \quad \text{for} \quad \sigma_{22} > 0,$$

$$\underline{\text{IFF2:}} \qquad \frac{-\sigma_{22}}{R_{\perp}^{c}} = 1 \quad \text{for} \quad \sigma_{22} < 0,$$

$$\underline{\text{IFF3:}} \quad \frac{\tau_{21}}{R_{\perp\parallel} - \mu_{\perp\parallel}\sigma_{22}} = 1 \quad \text{with} \quad \mu_{\perp\parallel} = 0.1 \ldots 0.3$$

for CFRP and GFRP
(inner friction coefficient).

This can be generalized as follows for the case of a three-dimensional load:

$$\underline{\text{FF1:}} \qquad \frac{I_1}{R_{\parallel}^{t}} = \frac{\sigma_{11}}{R_{\parallel}^{t}} = 1 \quad \text{for} \quad \sigma_{11} > 0,$$

$$\underline{\text{FF2:}} \qquad \frac{-I_1}{R_{\parallel}^{c}} = \frac{-\sigma_{11}}{R_{\parallel}^{c}} = 1 \quad \text{for} \quad \sigma_{11} < 0,$$

$$\underline{\text{IFF1:}} \qquad \frac{I_2 + \sqrt{I_4}}{2R_{\perp}^{t}} = 1 \quad \text{for} \quad \frac{I_2 + \sqrt{I_4}}{2} > 0$$

$\hat{=}$ maximum tensile stress perpendicular to the x_1-direction,

$$\underline{\text{IFF2:}} \qquad \underbrace{\frac{\sqrt{I_4}}{R_{\perp}^{c}} = 1}_{\text{(sometimes modified)}}$$

$\hat{=}$ Ratio of the maximum shear stress to half the compressive strength (= shear strength),

$$\underline{\text{IFF3:}} \qquad \frac{\sqrt{I_3}}{R_{\perp\parallel} - \mu_{\perp\parallel} I_2} = 1 \quad \text{where} \quad I_3 \hat{=} \text{maximum shear stress}$$

in the x_1-direction.

In the practical application of the partial failure criteria, these can of course simply be checked individually and independently of each other. However, certain discrepancies with experimental findings then arise in the vicinity of the intersection curves where two partial failure criteria meet. This is where a certain interaction of the relevant partial failure modes occurs. In order to capture this, it has proven to be useful to combine the partial failure surfaces by superimposing the "partial efforts":

$$\left(\frac{\sigma_{11} + |\sigma_{11}|}{2R_{\parallel}^{t}}\right)^{m} + \left(\frac{-\sigma_{11} + |\sigma_{11}|}{2R_{\parallel}^{c}}\right)^{m} + \left(\frac{\sigma_{22} + |\sigma_{22}|}{2R_{\perp}^{t}}\right)^{m}$$

$$+ \left(\frac{-\sigma_{22} + |\sigma_{22}|}{2R_{\perp}^{c}}\right)^{m} + \left(\frac{|\tau_{21}|}{R_{\perp\parallel} - \mu_{\perp\parallel}\sigma_{22}}\right)^{m} = 1 \qquad (9.25)$$

for the case of two-dimensional loading, where $m =$ 'interaction coefficient' $= 2.5 \ldots 3$, or for the case of three-dimensional load:

$$\left(\frac{\sigma_{11}+|\sigma_{11}|}{2R_{\parallel}^{t}}\right)^{m}+\left(\frac{-\sigma_{11}+|\sigma_{11}|}{2R_{\parallel}^{c}}\right)^{m}+\left(\frac{I_2+\sqrt{I_4}+|I_2+\sqrt{I_4}|}{4R_{\perp}^{t}}\right)^{m}$$
$$+\left(\frac{\sqrt{I_4}}{R_{\perp}^{c}}\right)^{m}+\left(\frac{\sqrt{I_3}}{R_{\perp\parallel}-\mu_{\perp\parallel}I_2}\right)^{m}=1. \quad (9.26)$$

To summarize Cuntze's failure mode concept, it can be said that the failure predictions based on it fit quite well with experimental findings. The failure criterion is comparatively simple and pragmatic. Overall, Cuntze's failure mode concept can be highly recommended for use in practice.

References

Schürmann H (2005): *Konstruieren mit Faser-Kunststoff-Verbunden*, Springer-Verlag, Berlin, Heidelberg, Germany.

Becker W, Gross D (2002): *Mechanik elastischer Körper und Strukturen*, Springer-Verlag, Berlin, Heidelberg, Germany.

Cuntze RG (2006): *Efficient 3D and 2D failure conditions for UD laminae and their application within the verification of the laminate design*, Composites Science and Technology 66:1081–1096.

Hinton MJ, Kaddour AS, Soden PD (2002): *A comparison of the predictive capabilities of current failure theories for composite laminates, judged against experimental evidence*, Composites Science and Technology 62:1725–1797.



Hygrothermal Problems

10

This chapter is dedicated to the treatment of hygrothermal problems, i.e. the consideration of laminates under thermal load and moisture exposure. For both cases, the constitutive law according to Classical Laminated Plate Theory is extended, and the importance of considering such effects is emphasized.

10.1 Introduction

In fiber composite science and technology, in addition to the analysis of mechanically induced stresses and deformations, the treatment of thermomechanical behaviour and hygroscopic influences is also of great interest Schürmann (2007), Rohwer (1996). For example, in a layered structure such as a composite laminate which is made up of various individual layers made of fiber-reinforced plastics, considerable stresses can arise solely due to temperature influences or a temperature change compared to the stress-free manufacturing temperature, even without external mechanical influences, which must be taken into account appropriately in the design. This becomes particularly clear when we consider that the individual layers of a laminate generally not only have clearly anisotropic properties, but can also be arranged at any orientation angle. It is clear that the individual layers can 'tense' against each other when the temperature changes, which must not be disregarded when designing a lightweight composite structure. The same also applies to hygromechanical problems, i.e. moisture-induced stresses and deformations, because typical polymer matrices used in fiber composite technology behave hygroscopically and are therefore able to absorb or release moisture to a certain extent. Similar to thermally induced deformations, the deformations caused by moisture absorption or a change in moisture content compared to the stress-free original moisture content can lead to considerable layer stresses. Such problems fall under

© The Author(s), under exclusive license to Springer-Verlag GmbH, DE, part of Springer Nature 2025

C. Mittelstedt, *Mechanics of Composite Structures*,
https://doi.org/10.1007/978-3-662-70788-3_10

the generic term of hygrothermal problems. However, hygrothermal influences are not only interesting from the point of view of the strength of a composite laminate, but also with regard to the dimensional stability of a laminate structure.

10.2 Thermomechanical Problems

A unidirectionally reinforced single layer, which consists of an isotropic polymer matrix and embedded anisotropic fibers (e.g. carbon fibers or glass fibers), generally exhibits strongly anisotropic coefficients of thermal expansion. The reason for this is that a polymer matrix has a fairly large coefficient of thermal expansion (e.g. in the order of $\alpha^T_{\text{Matrix}} = 50 \cdot 10^{-6}\,\text{K}^{-1}$), while the corresponding material coefficient of a carbon fiber is much lower or can even be slightly negative (e.g. in the order of magnitude $\alpha^T_{\text{fiber}} = -1.2 \cdot 10^{-6}\,\text{K}^{-1}$). Overall, this can lead to the coefficients of thermal expansion of a unidirectionally reinforced single layer differing significantly in the two principal directions x_1 and x_2. As an example, consider a layer made of T300/epoxy whose coefficients of thermal expansion α^T_{11} and α^T_{22} in the x_1- and x_2-directions with a fiber volume content $v_f = 0.6$ are in the order of magnitude of about $\alpha^T_{11} = -0.6 \cdot 10^{-6}\,\text{K}^{-1}$ and $\alpha^T_{22} = 30 \cdot 10^{-6}\,\text{K}^{-1}$. It is obvious that in a laminate, in which the layers can be arranged completely arbitrarily, the layer-by-layer deformations resulting from a temperature change cannot occur freely. Instead, the individual layers of the laminate will strain against each other, so that a change in temperature compared to the manufacturing temperature can result in considerable layer stresses, even though there are no external mechanical influences. In principle, thermally induced stresses always arise as soon as the application temperature of a composite laminate deviates from the (at least theoretically) stress-free manufacturing temperature.

The total strains of an anisotropic structure consist of the mechanical strains and the thermal strains:

$$\begin{pmatrix} \varepsilon_{11} \\ \varepsilon_{22} \\ \varepsilon_{33} \\ \gamma_{23} \\ \gamma_{13} \\ \gamma_{12} \end{pmatrix} = \begin{bmatrix} S_{11} & S_{12} & S_{13} & S_{14} & S_{15} & S_{16} \\ S_{12} & S_{22} & S_{23} & S_{24} & S_{25} & S_{26} \\ S_{13} & S_{23} & S_{33} & S_{34} & S_{35} & S_{36} \\ S_{14} & S_{24} & S_{34} & S_{44} & S_{45} & S_{46} \\ S_{15} & S_{25} & S_{35} & S_{45} & S_{55} & S_{56} \\ S_{16} & S_{26} & S_{36} & S_{46} & S_{56} & S_{66} \end{bmatrix} \begin{pmatrix} \sigma_{11} \\ \sigma_{22} \\ \sigma_{33} \\ \sigma_{23} \\ \sigma_{13} \\ \sigma_{12} \end{pmatrix} + \Delta T \begin{pmatrix} \alpha^T_{11} \\ \alpha^T_{22} \\ \alpha^T_{33} \\ \alpha^T_{23} \\ \alpha^T_{13} \\ \alpha^T_{12} \end{pmatrix}. \tag{10.1}$$

This relationship is simplified considerably if an orthotropic material is considered as a special case of anisotropy. If the reference axes were chosen to be aligned with the principal material axes, the coefficients α^T_{23}, α^T_{13} and α^T_{12} are all zero, so that the following representation of (10.1) remains:

$$\begin{pmatrix} \varepsilon_{11} \\ \varepsilon_{22} \\ \varepsilon_{33} \\ \gamma_{23} \\ \gamma_{13} \\ \gamma_{12} \end{pmatrix} = \begin{bmatrix} S_{11} & S_{12} & S_{13} & 0 & 0 & 0 \\ S_{12} & S_{22} & S_{23} & 0 & 0 & 0 \\ S_{13} & S_{23} & S_{33} & 0 & 0 & 0 \\ 0 & 0 & 0 & S_{44} & 0 & 0 \\ 0 & 0 & 0 & 0 & S_{55} & 0 \\ 0 & 0 & 0 & 0 & 0 & S_{66} \end{bmatrix} \begin{pmatrix} \sigma_{11} \\ \sigma_{22} \\ \sigma_{33} \\ \sigma_{23} \\ \sigma_{13} \\ \sigma_{12} \end{pmatrix} + \Delta T \begin{pmatrix} \alpha_{11}^T \\ \alpha_{22}^T \\ \alpha_{33}^T \\ 0 \\ 0 \\ 0 \end{pmatrix}. \tag{10.2}$$

Accordingly, a temperature change ΔT in an orthotropic material does not result in any shear strains, but a pure normal strain state occurs, which can be different in all three spatial directions due to the orthotropy.

For a laminate according to Classical Laminated Plate Theory, a plane stress state is assumed with regard to the thickness direction z. Only the mechanical strains resulting from the difference between the total strains and the thermally induced strains are included in the material law for the on-axis layer:

$$\begin{pmatrix} \sigma_{11} \\ \sigma_{22} \\ \tau_{12} \end{pmatrix}_k = \begin{bmatrix} Q_{11} & Q_{12} & 0 \\ Q_{12} & Q_{22} & 0 \\ 0 & 0 & Q_{66} \end{bmatrix}_k \begin{pmatrix} \varepsilon_{11} - \alpha_{11}^T \Delta T \\ \varepsilon_{22} - \alpha_{22}^T \Delta T \\ \gamma_{12} \end{pmatrix}_k. \tag{10.3}$$

In global coordinates x, y, z we have:

$$\begin{pmatrix} \sigma_{xx} \\ \sigma_{yy} \\ \tau_{xy} \end{pmatrix}_k = \begin{bmatrix} \bar{Q}_{11} & \bar{Q}_{12} & \bar{Q}_{16} \\ \bar{Q}_{12} & \bar{Q}_{22} & \bar{Q}_{26} \\ \bar{Q}_{16} & \bar{Q}_{26} & \bar{Q}_{66} \end{bmatrix}_k \begin{pmatrix} \varepsilon_{xx} - \alpha_{xx}^T \Delta T \\ \varepsilon_{yy} - \alpha_{yy}^T \Delta T \\ \gamma_{xy} - \alpha_{xy}^T \Delta T \end{pmatrix}_k. \tag{10.4}$$

The transformation of the coefficients of thermal expansion α_{11}^T and α_{22}^T from the principal layer directions x_1 and x_2 into the coefficients of thermal expansion α_{xx}^T, α_{yy}^T, α_{xy}^T in the global laminate coordinate system x, y, z is possible by applying elementary tensor transformations, and one obtains

$$\begin{aligned} \alpha_{xx}^T &= \alpha_{11}^T \cos^2\theta + \alpha_{22}^T \sin^2\theta, \\ \alpha_{yy}^T &= \alpha_{11}^T \sin^2\theta + \alpha_{22}^T \cos^2\theta, \\ \alpha_{xy}^T &= 2\cos\theta \sin\theta \left(\alpha_{11}^T - \alpha_{22}^T\right). \end{aligned} \tag{10.5}$$

The comparison of (10.3) and (10.4) shows that the coefficient of thermal expansion α_{xy}^T or α_{12}^T for typical fiber composite materials always disappears in the on-axis system, while it will generally be unequal to zero in the off-axis system. The strain determined in this way is illustrated in Fig. 10.1.

While only strains ε_{xx} and ε_{yy} but no shear strains γ_{xy} will always occur in an on-axis layer under thermal load, all three strain components $\varepsilon_{xx}, \varepsilon_{yy}\ \gamma_{xy}$ will generally occur in an off-axis layer.

The laminate forces N_{xx}^0, N_{yy}^0, N_{xy}^0 can be calculated using the material law (10.4):

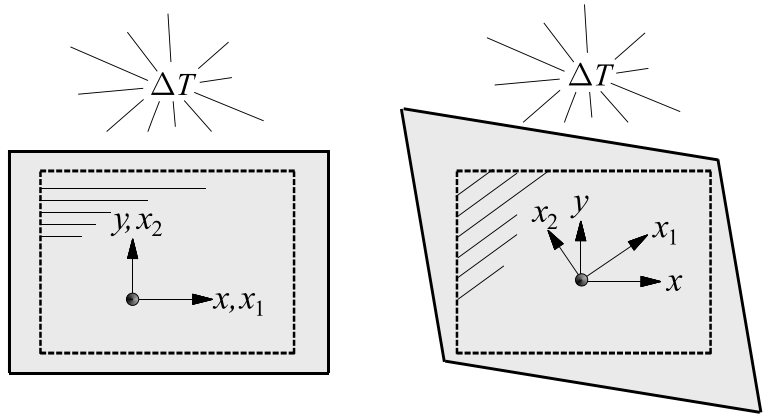


Fig. 10.1 On-axis layer (left) and off-axis layer (right) under thermal load

$$
\begin{aligned}
\begin{pmatrix} N^0_{xx} \\ N^0_{yy} \\ N^0_{xy} \end{pmatrix} &= \sum_{k=1}^{k=N} \int_{z_{k-1}}^{z_k} \begin{pmatrix} \sigma_{xx} \\ \sigma_{yy} \\ \tau_{xy} \end{pmatrix}_k \mathrm{d}z \\
&= \sum_{k=1}^{k=N} \int_{z_{k-1}}^{z_k} \begin{bmatrix} \bar{Q}_{11} & \bar{Q}_{12} & \bar{Q}_{16} \\ \bar{Q}_{12} & \bar{Q}_{22} & \bar{Q}_{26} \\ \bar{Q}_{16} & \bar{Q}_{26} & \bar{Q}_{66} \end{bmatrix}_k \begin{pmatrix} \varepsilon^0_{xx} + z\kappa^0_{xx} - \alpha^T_{xx}\Delta T \\ \varepsilon^0_{yy} + z\kappa^0_{yy} - \alpha^T_{yy}\Delta T \\ \gamma^0_{xy} + z\kappa^0_{xy} - \alpha^T_{xy}\Delta T \end{pmatrix}_k \mathrm{d}z \\
&= \begin{bmatrix} A_{11} & A_{12} & A_{16} \\ A_{12} & A_{22} & A_{26} \\ A_{16} & A_{26} & A_{66} \end{bmatrix} \begin{pmatrix} \varepsilon^0_{xx} \\ \varepsilon^0_{yy} \\ \gamma^0_{xy} \end{pmatrix} + \begin{bmatrix} B_{11} & B_{12} & B_{16} \\ B_{12} & B_{22} & B_{26} \\ B_{16} & B_{26} & B_{66} \end{bmatrix} \begin{pmatrix} \kappa^0_{xx} \\ \kappa^0_{yy} \\ \kappa^0_{xy} \end{pmatrix} \\
&\quad - \sum_{k=1}^{k=N} \int_{z_{k-1}}^{z_k} \begin{bmatrix} \bar{Q}_{11} & \bar{Q}_{12} & \bar{Q}_{16} \\ \bar{Q}_{12} & \bar{Q}_{22} & \bar{Q}_{26} \\ \bar{Q}_{16} & \bar{Q}_{26} & \bar{Q}_{66} \end{bmatrix}_k \begin{pmatrix} \alpha^T_{xx}\Delta T \\ \alpha^T_{yy}\Delta T \\ \alpha^T_{xy}\Delta T \end{pmatrix}_k \mathrm{d}z. \qquad (10.6)
\end{aligned}
$$

The last term appearing in (10.6) represents the thermal forces:

$$
\begin{pmatrix} N^T_{xx} \\ N^T_{yy} \\ N^T_{xy} \end{pmatrix} = \sum_{k=1}^{k=N} \int_{z_{k-1}}^{z_k} \begin{bmatrix} \bar{Q}_{11} & \bar{Q}_{12} & \bar{Q}_{16} \\ \bar{Q}_{12} & \bar{Q}_{22} & \bar{Q}_{26} \\ \bar{Q}_{16} & \bar{Q}_{26} & \bar{Q}_{66} \end{bmatrix}_k \begin{pmatrix} \alpha^T_{xx}\Delta T \\ \alpha^T_{yy}\Delta T \\ \alpha^T_{xy}\Delta T \end{pmatrix}_k \mathrm{d}z, \qquad (10.7)
$$

and one obtains for (10.6):

$$
\begin{pmatrix} N^0_{xx} \\ N^0_{yy} \\ N^0_{xy} \end{pmatrix} + \begin{pmatrix} N^T_{xx} \\ N^T_{yy} \\ N^T_{xy} \end{pmatrix} = \begin{bmatrix} A_{11} & A_{12} & A_{16} \\ A_{12} & A_{22} & A_{26} \\ A_{16} & A_{26} & A_{66} \end{bmatrix} \begin{pmatrix} \varepsilon^0_{xx} \\ \varepsilon^0_{yy} \\ \gamma^0_{xy} \end{pmatrix}
$$

$$+\begin{bmatrix} B_{11} & B_{12} & B_{16} \\ B_{12} & B_{22} & B_{26} \\ B_{16} & B_{26} & B_{66} \end{bmatrix} \begin{pmatrix} \kappa_{xx}^0 \\ \kappa_{yy}^0 \\ \kappa_{xy}^0 \end{pmatrix}. \tag{10.8}$$

We can proceed in the same way for the laminate moments M_{xx}^0, M_{yy}^0, M_{xy}^0:

$$\begin{pmatrix} M_{xx}^0 \\ M_{yy}^0 \\ M_{xy}^0 \end{pmatrix} + \begin{pmatrix} M_{xx}^T \\ M_{yy}^T \\ M_{xy}^T \end{pmatrix} = \begin{bmatrix} B_{11} & B_{12} & B_{16} \\ B_{12} & B_{22} & B_{26} \\ B_{16} & B_{26} & B_{66} \end{bmatrix} \begin{pmatrix} \varepsilon_{xx}^0 \\ \varepsilon_{yy}^0 \\ \gamma_{xy}^0 \end{pmatrix}$$

$$+\begin{bmatrix} D_{11} & D_{12} & D_{16} \\ D_{12} & D_{22} & D_{26} \\ D_{16} & D_{26} & D_{66} \end{bmatrix} \begin{pmatrix} \kappa_{xx}^0 \\ \kappa_{yy}^0 \\ \kappa_{xy}^0 \end{pmatrix}, \tag{10.9}$$

where the thermal moments are defined as:

$$\begin{pmatrix} M_{xx}^T \\ M_{yy}^T \\ M_{xy}^T \end{pmatrix} = \sum_{k=1}^{k=N} \int_{z_{k-1}}^{z_k} \begin{bmatrix} \bar{Q}_{11} & \bar{Q}_{12} & \bar{Q}_{16} \\ \bar{Q}_{12} & \bar{Q}_{22} & \bar{Q}_{26} \\ \bar{Q}_{16} & \bar{Q}_{26} & \bar{Q}_{66} \end{bmatrix}_k \begin{pmatrix} \alpha_{xx}^T \Delta T \\ \alpha_{yy}^T \Delta T \\ \alpha_{xy}^T \Delta T \end{pmatrix}_k z \mathrm{d}z. \tag{10.10}$$

The thermal forces and moments can be interpreted in such a way that they represent exactly those forces and moments that would have to be applied to the laminate in order to produce the same deformations by purely mechanical means that are obtained from the thermal stress state. Overall, the constitutive law for the laminate in the presence of temperature effects is as follows:

$$\begin{pmatrix} N_{xx}^0 + N_{xx}^T \\ N_{yy}^0 + N_{yy}^T \\ N_{xy}^0 + N_{xy}^T \\ M_{xx}^0 + M_{xx}^T \\ M_{yy}^0 + M_{yy}^T \\ M_{xy}^0 + M_{xy}^T \end{pmatrix} = \begin{bmatrix} A_{11} & A_{12} & A_{16} & B_{11} & B_{12} & B_{16} \\ A_{12} & A_{22} & A_{26} & B_{12} & B_{22} & B_{26} \\ A_{16} & A_{26} & A_{66} & B_{16} & B_{26} & B_{66} \\ B_{11} & B_{12} & B_{16} & D_{11} & D_{12} & D_{16} \\ B_{12} & B_{22} & B_{26} & D_{12} & D_{22} & D_{26} \\ B_{16} & B_{26} & B_{66} & D_{16} & D_{26} & D_{66} \end{bmatrix} \begin{pmatrix} \varepsilon_{xx}^0 \\ \varepsilon_{yy}^0 \\ \gamma_{xy}^0 \\ \kappa_{xx}^0 \\ \kappa_{yy}^0 \\ \kappa_{xy}^0 \end{pmatrix}. \tag{10.11}$$

10.3 Hygromechanical Problems

Hygroscopic stresses in composite laminates pose a very similar problem to thermal stresses. Many typical matrix materials of modern fiber composite materials are capable of absorbing moisture from the ambient air or releasing moisture into it. If the ambient moisture content is not equal to the (at least theoretically) stress-free curing state of the laminate, so-called moisture strains ε_{ij}^H (where the 'H' stands for hygroscopy) occur, analogous to the thermal

strains, and assuming a linear relationship we have:

$$\varepsilon_{ij}^{H} = \beta_{ij}\,\Delta c, \tag{10.12}$$

where β_{ij} are the so-called moisture expansion coefficients/swelling coefficients, which are measured in $\frac{1}{\%}$. The quantity Δc is the moisture concentration, which is defined as follows

$$\Delta c = \frac{\text{Mass of the absorbed liquid}}{\text{Mass of the dry composite volume}}. \tag{10.13}$$

Here, Δc is specified in [%]. Typical values for the relative moisture mass concentration c for composite laminates are around $c = 0.1\%$ up to $c = 0.4\%$ after the curing process and around $c = 0.6\%$ up to $c = 1.0\%$ when the laminate is used at a relative humidity of 50–60%.

Very similar to the thermal behaviour, composite materials have strongly anisotropic hygroscopic properties. As the moisture absorption capacity of typical fiber materials is usually negligible, a fairly small value for β_{11} is obtained for a single layer in the longitudinal direction of the fiber (approximately $\beta_{11} = 30 \cdot 10^{-6}\frac{1}{\%}$), while much larger values can occur transverse to the fiber direction (e.g. $\beta_{11} = 4000 \cdot 10^{-6}\frac{1}{\%}$).

The layerwise stresses in a composite laminate can be calculated in a similar way to those under thermal load. For the on-axis layer one obtains

$$\begin{pmatrix} \sigma_{11} \\ \sigma_{22} \\ \tau_{12} \end{pmatrix}_k = \begin{bmatrix} Q_{11} & Q_{12} & 0 \\ Q_{12} & Q_{22} & 0 \\ 0 & 0 & Q_{66} \end{bmatrix}_k \begin{pmatrix} \varepsilon_{11} - \beta_{11}\Delta c \\ \varepsilon_{22} - \beta_{22}\Delta c \\ \gamma_{12} \end{pmatrix}_k . \tag{10.14}$$

In global coordinates x, y, z the result is

$$\begin{pmatrix} \sigma_{xx} \\ \sigma_{yy} \\ \tau_{xy} \end{pmatrix}_k = \begin{bmatrix} \bar{Q}_{11} & \bar{Q}_{12} & \bar{Q}_{16} \\ \bar{Q}_{12} & \bar{Q}_{22} & \bar{Q}_{26} \\ \bar{Q}_{16} & \bar{Q}_{26} & \bar{Q}_{66} \end{bmatrix}_k \begin{pmatrix} \varepsilon_{xx} - \beta_{xx}\Delta c \\ \varepsilon_{yy} - \beta_{yy}\Delta c \\ \gamma_{xy} - \beta_{xy}\Delta c \end{pmatrix}_k . \tag{10.15}$$

The transformation rules for the moisture expansion coefficients from the on-axis system to the global coordinate system correspond exactly to those for the thermal expansion coefficients. Similarly, it is possible to define moisture forces and moments for the laminate, which result from the change in moisture Δc:

$$\begin{pmatrix} N_{xx}^H \\ N_{yy}^H \\ N_{xy}^H \end{pmatrix} = \sum_{k=1}^{k=N} \int_{z_{k-1}}^{z_k} \begin{bmatrix} \bar{Q}_{11} & \bar{Q}_{12} & \bar{Q}_{16} \\ \bar{Q}_{12} & \bar{Q}_{22} & \bar{Q}_{26} \\ \bar{Q}_{16} & \bar{Q}_{26} & \bar{Q}_{66} \end{bmatrix}_k \begin{pmatrix} \beta_{xx}\Delta c \\ \beta_{yy}\Delta c \\ \beta_{xy}\Delta c \end{pmatrix}_k \mathrm{d}z,$$

$$\begin{pmatrix} M_{xx}^H \\ M_{yy}^H \\ M_{xy}^H \end{pmatrix} = \sum_{k=1}^{k=N} \int_{z_{k-1}}^{z_k} \begin{bmatrix} \bar{Q}_{11} & \bar{Q}_{12} & \bar{Q}_{16} \\ \bar{Q}_{12} & \bar{Q}_{22} & \bar{Q}_{26} \\ \bar{Q}_{16} & \bar{Q}_{26} & \bar{Q}_{66} \end{bmatrix}_k \begin{pmatrix} \beta_{xx}\Delta c \\ \beta_{yy}\Delta c \\ \beta_{xy}\Delta c \end{pmatrix}_k z\mathrm{d}z. \tag{10.16}$$

The constitutive law for the laminate in the presence of both thermal and moisture strains can then be stated as:

$$\begin{pmatrix} N_{xx}^0 + N_{xx}^T + N_{xx}^H \\ N_{yy}^0 + N_{yy}^T + N_{yy}^H \\ N_{xy}^0 + N_{xy}^T + N_{xy}^H \\ M_{xx}^0 + M_{xx}^T + M_{xx}^H \\ M_{yy}^0 + M_{yy}^T + M_{yy}^H \\ M_{xy}^0 + M_{xy}^T + M_{xy}^H \end{pmatrix} = \begin{bmatrix} A_{11} & A_{12} & A_{16} & B_{11} & B_{12} & B_{16} \\ A_{12} & A_{22} & A_{26} & B_{12} & B_{22} & B_{26} \\ A_{16} & A_{26} & A_{66} & B_{16} & B_{26} & B_{66} \\ B_{11} & B_{12} & B_{16} & D_{11} & D_{12} & D_{16} \\ B_{12} & B_{22} & B_{26} & D_{12} & D_{22} & D_{26} \\ B_{16} & B_{26} & B_{66} & D_{16} & D_{26} & D_{66} \end{bmatrix} \begin{pmatrix} \varepsilon_{xx}^0 \\ \varepsilon_{yy}^0 \\ \gamma_{xy}^0 \\ \kappa_{xx}^0 \\ \kappa_{yy}^0 \\ \kappa_{xy}^0 \end{pmatrix}. \tag{10.17}$$

A numerical example is provided to illustrate the potentially serious influence of temperature on the effective strength of laminates. Consider a $[0°/90°]_S$ cross-ply laminate made of T300/epoxy with a total thickness of $h = 1.0\,\mathrm{mm}$. The laminate is subjected to a temperature change of $\Delta T = -150\,\mathrm{K}$ and a tensile stress N_{xx}^0. The elastic constants of the single-layer material are $E_{11} = 135{,}000\,\mathrm{MPa}$, $E_{22} = 10{,}000\,\mathrm{MPa}$, $G_{12} = 5000\,\mathrm{MPa}$, $\nu_{12} = 0.27$. The strength values of the individual layers are given as $X_t = 1450\,\mathrm{MPa}$, $X_c = 1400\,\mathrm{MPa}$, $Y_t = 55\,\mathrm{MPa}$, $Y_c = 170\,\mathrm{MPa}$, $S = 90\,\mathrm{MPa}$. The thermal expansion coefficients α_1^T and α_2^T are $\alpha_1^T = -0.6 \cdot 10^{-6}\,\mathrm{K}^{-1}$ and $\alpha_2^T = 30 \cdot 10^{-6}\,\mathrm{K}^{-1}$. We want to perform a strength analysis using the Tsai-Wu criterion.

The reduced on-axis stiffnesses Q_{ij} of the individual layers and thus the reduced stiffnesses of the 0°-layers are as follows:

$$\underline{\underline{Q}}_1 = \underline{\underline{Q}}_4 = \begin{bmatrix} 135733 & 2715 & 0 \\ 2715 & 10054 & 0 \\ 0 & 0 & 5000 \end{bmatrix} \quad [\mathrm{MPa}]\,. \tag{10.18}$$

For the 90°-layers we obtain:

$$\underline{\underline{Q}}_2 = \underline{\underline{Q}}_3 = \begin{bmatrix} 10054 & 2715 & 0 \\ 2715 & 135733 & 0 \\ 0 & 0 & 5000 \end{bmatrix} \quad [\mathrm{MPa}]\,. \tag{10.19}$$

The thermal expansion coefficients in the 0°-layers can be taken directly from the given values:

$$\begin{aligned}
\alpha^T_{1,1} &= \alpha^T_{1,4} = -0.6 \cdot 10^{-6}\,\mathrm{K}^{-1},\\
\alpha^T_{1,2} &= \alpha^T_{1,3} = 30 \cdot 10^{-6}\,\mathrm{K}^{-1},\\
\alpha^T_{2,1} &= \alpha^T_{2,4} = 30 \cdot 10^{-6}\,\mathrm{K}^{-1},\\
\alpha^T_{2,2} &= \alpha^T_{2,3} = -0.6 \cdot 10^{-6}\,\mathrm{K}^{-1}.
\end{aligned} \tag{10.20}$$

Next, the laminate stiffnesses are calculated. Since the laminate is symmetric and both load cases ΔT and N^0_{xx} ensure a pure disk effect, only the membrane quadrant $\underline{\underline{A}}$ is of interest here. One obtains:

$$\underline{\underline{A}} = \begin{bmatrix} 72894 & 2715 & 0 \\ 2715 & 72894 & 0 \\ 0 & 0 & 5000 \end{bmatrix} \quad \left[\frac{\mathrm{N}}{\mathrm{mm}}\right]. \tag{10.21}$$

The thermal forces can be calculated as:

$$\begin{aligned}
\begin{pmatrix} N^{0T}_{xx} \\ N^{0T}_{yy} \\ N^{0T}_{xy} \end{pmatrix} &= \int_{-\frac{h}{2}}^{\frac{h}{2}} \begin{bmatrix} \bar{Q}_{11} & \bar{Q}_{12} & \bar{Q}_{16} \\ \bar{Q}_{12} & \bar{Q}_{22} & \bar{Q}_{26} \\ \bar{Q}_{16} & \bar{Q}_{26} & \bar{Q}_{66} \end{bmatrix} \begin{pmatrix} \alpha^T_{xx} \\ \alpha^T_{yy} \\ \alpha^T_{xy} \end{pmatrix} \Delta T \,\mathrm{d}z \\
&= 2 \int_{-\frac{h}{2}}^{-\frac{h}{4}} \begin{bmatrix} \bar{Q}_{11} & \bar{Q}_{12} & \bar{Q}_{16} \\ \bar{Q}_{12} & \bar{Q}_{22} & \bar{Q}_{26} \\ \bar{Q}_{16} & \bar{Q}_{26} & \bar{Q}_{66} \end{bmatrix}_1 \begin{pmatrix} \alpha^T_{xx} \\ \alpha^T_{yy} \\ \alpha^T_{xy} \end{pmatrix}_1 \Delta T \,\mathrm{d}z \\
&\quad + 2 \int_{-\frac{h}{4}}^{0} \begin{bmatrix} \bar{Q}_{11} & \bar{Q}_{12} & \bar{Q}_{16} \\ \bar{Q}_{12} & \bar{Q}_{22} & \bar{Q}_{26} \\ \bar{Q}_{16} & \bar{Q}_{26} & \bar{Q}_{66} \end{bmatrix}_2 \begin{pmatrix} \alpha^T_{xx} \\ \alpha^T_{yy} \\ \alpha^T_{xy} \end{pmatrix}_2 \Delta T \,\mathrm{d}z,
\end{aligned} \tag{10.22}$$

whereby the symmetry of the laminate and the given load have already been explicitly utilized here. After elementary matrix operations and carrying out the integrations, the result is (note that all $\bar{Q}_{16,k}$ and $\bar{Q}_{26,k}$ are identical to zero):

$$\begin{pmatrix} N^{0T}_{xx} \\ N^{0T}_{yy} \\ N^{0T}_{xy} \end{pmatrix} = \frac{h}{2} \Delta T \begin{pmatrix} \bar{Q}_{11,1}\alpha^T_{xx,1} + \bar{Q}_{12,1}\alpha^T_{yy,1} + \bar{Q}_{11,2}\alpha^T_{xx,2} + \bar{Q}_{12,2}\alpha^T_{yy,2} \\ \bar{Q}_{12,1}\alpha^T_{xx,1} + \bar{Q}_{22,1}\alpha^T_{yy,1} + \bar{Q}_{12,2}\alpha^T_{xx,2} + \bar{Q}_{22,2}\alpha^T_{yy,2} \\ \bar{Q}_{66,1}\alpha^T_{xy,1} + \bar{Q}_{66,2}\alpha^T_{xy,2} \end{pmatrix}. \tag{10.23}$$

Evaluating provides ($\alpha^T_{xy,1} = \alpha^T_{xy,2} = 0$):

$$\begin{pmatrix} N^{0T}_{xx} \\ N^{0T}_{yy} \\ N^{0T}_{xy} \end{pmatrix} = - \begin{pmatrix} 22.5 \\ 22.5 \\ 0 \end{pmatrix} \quad \frac{\mathrm{N}}{\mathrm{mm}}. \tag{10.24}$$

The corresponding strains of the laminate middle plane $\varepsilon_{xx}^0, \varepsilon_{yy}^0, \gamma_{xy}^0$ then result from the constitutive law of the laminate:

$$\begin{pmatrix} N_{xx}^{0T} \\ N_{yy}^{0T} \\ N_{xy}^{0T} \end{pmatrix} = \begin{bmatrix} A_{11} & A_{12} & A_{16} \\ A_{12} & A_{22} & A_{26} \\ A_{16} & A_{26} & A_{66} \end{bmatrix} \begin{pmatrix} \varepsilon_{xx}^0 \\ \varepsilon_{yy}^0 \\ \gamma_{xy}^0 \end{pmatrix}. \tag{10.25}$$

Since the laminate is balanced and therefore free of shear coupling, the terms A_{16} and A_{26} (see above) vanish and the following result is obtained for the strains $\varepsilon_{xx}^0, \varepsilon_{yy}^0, \gamma_{xy}^0$:

$$\begin{pmatrix} \varepsilon_{xx}^0 \\ \varepsilon_{yy}^0 \\ \gamma_{xy}^0 \end{pmatrix} = - \begin{pmatrix} 297.6 \\ 297.6 \\ 0 \end{pmatrix} \cdot 10^{-6}. \tag{10.26}$$

The individual layer stresses then follow from

$$\begin{pmatrix} \sigma_{xx} \\ \sigma_{yy} \\ \tau_{xy} \end{pmatrix}_k = \begin{bmatrix} \bar{Q}_{11} & \bar{Q}_{12} & \bar{Q}_{16} \\ \bar{Q}_{12} & \bar{Q}_{22} & \bar{Q}_{26} \\ \bar{Q}_{16} & \bar{Q}_{26} & \bar{Q}_{66} \end{bmatrix}_k \begin{pmatrix} \varepsilon_{xx}^0 - \alpha_{xx}^T \Delta T \\ \varepsilon_{yy}^0 - \alpha_{yy}^T \Delta T \\ \gamma_{xy}^0 - \alpha_{xy}^T \Delta T \end{pmatrix}_k, \tag{10.27}$$

which leads to the following numerical result:

$$\begin{aligned} \begin{pmatrix} \sigma_{xx} \\ \sigma_{yy} \\ \tau_{xy} \end{pmatrix}_1 &= \begin{pmatrix} \sigma_{xx} \\ \sigma_{yy} \\ \tau_{xy} \end{pmatrix}_4 = \begin{pmatrix} -41.20 \\ 41.20 \\ 0 \end{pmatrix} \quad \text{MPa}, \\ \begin{pmatrix} \sigma_{xx} \\ \sigma_{yy} \\ \tau_{xy} \end{pmatrix}_2 &= \begin{pmatrix} \sigma_{xx} \\ \sigma_{yy} \\ \tau_{xy} \end{pmatrix}_3 = \begin{pmatrix} 41.20 \\ -41.20 \\ 0 \end{pmatrix} \quad \text{MPa}. \end{aligned} \tag{10.28}$$

In addition, the layer stresses due to a unit tensile stress $N_{xx}^0 = 1 \frac{\text{N}}{\text{mm}}$ must be calculated, whereby the unit load is provided with the load factor λ. The strains of the laminate middle plane $\varepsilon_{xx}^0, \varepsilon_{yy}^0, \gamma_{xy}^0$ due to the mechanical load result from

$$\begin{pmatrix} N_{xx}^0 \\ 0 \\ 0 \end{pmatrix} = \begin{bmatrix} A_{11} & A_{12} & A_{16} \\ A_{12} & A_{22} & A_{26} \\ A_{16} & A_{26} & A_{66} \end{bmatrix} \begin{pmatrix} \varepsilon_{xx}^0 \\ \varepsilon_{yy}^0 \\ \gamma_{xy}^0 \end{pmatrix}, \tag{10.29}$$

or solved for the strains:

$$\begin{pmatrix} \varepsilon_{xx}^0 \\ \varepsilon_{yy}^0 \\ \gamma_{xy}^0 \end{pmatrix} = \begin{pmatrix} 13.74 \\ -0.51 \\ 0 \end{pmatrix} \lambda \cdot 10^{-6}. \tag{10.30}$$

The layer stresses can then be calculated as:

$$\begin{pmatrix}\sigma_{xx}\\ \sigma_{yy}\\ \tau_{xy}\end{pmatrix}_1 = \begin{pmatrix}\sigma_{xx}\\ \sigma_{yy}\\ \tau_{xy}\end{pmatrix}_4 = \begin{pmatrix}1.864\\ 0.032\\ 0\end{pmatrix}\lambda \quad \text{MPa},$$
$$\begin{pmatrix}\sigma_{xx}\\ \sigma_{yy}\\ \tau_{xy}\end{pmatrix}_2 = \begin{pmatrix}\sigma_{xx}\\ \sigma_{yy}\\ \tau_{xy}\end{pmatrix}_3 = \begin{pmatrix}0.136\\ -0.032\\ 0\end{pmatrix}\lambda \quad \text{MPa}. \tag{10.31}$$

The strength assessment is now carried out using the Tsai-Wu criterion:

$$\frac{\sigma_{11}^2}{X_t X_c} - \frac{\sigma_{11}\sigma_{22}}{\sqrt{X_t X_c Y_t Y_c}} + \frac{\sigma_{22}^2}{Y_t Y_c} + \frac{\tau_{12}^2}{S_{12}^2} + \left(\frac{1}{X_t} - \frac{1}{X_c}\right)\sigma_{11} + \left(\frac{1}{Y_t} - \frac{1}{Y_c}\right)\sigma_{22} = 1. \tag{10.32}$$

Firstly, the maximum mechanical load $N^0_{xx,\max}$ is determined without the thermal load ΔT. If the Tsai-Wu criterion is analyzed numerically, the final result is $N^0_{xx,\max} = 402\ \frac{\mathrm{N}}{\mathrm{mm}}$ as the load that can be absorbed if $\Delta T = 0$.

If, on the other hand, the mechanical stress N^0_{xx} and the thermal stress ΔT act simultaneously, the strength evaluation with the Tsai-Wu criterion, evaluated in the 90°-layer, results in the following equation:

$$\frac{(-41.2 - 0.032\lambda)^2}{1450 \cdot 1400} - \frac{(-41.2 - 0.032\lambda)\,(41.2 + 0.136\lambda)}{\sqrt{1450 \cdot 1400 \cdot 55 \cdot 170}} + \frac{(41.2 + 0.136\lambda)^2}{55 \cdot 170}$$
$$+ \left(\frac{1}{1450} - \frac{1}{1400}\right)(-41.2 - 0.032\lambda) + \left(\frac{1}{55} - \frac{1}{170}\right)(41.2 + 0.136\lambda) - 1 = 0. \tag{10.33}$$

Solving results in a limit load of the laminate under combined thermomechanical stress of $N^0_{xx,\max} = 95.5\ \frac{\mathrm{N}}{\mathrm{mm}}$. It can be seen that this is only about 25% of the limit load that results from the effect of mechanical stress alone. It can therefore be stated that thermal stresses can have a considerable influence on the strength behaviour of composite laminated structures and must be taken into account appropriately when designing such structures.

References

Rohwer K (1996): *Modelle und Methoden zur Berechnung von Laminaten aus unidirektionalen Faserverbunden*. VDI Verlag, Düsseldorf, Germany.

Schürmann H (2007): *Konstruieren mit Faser-Kunststoff-Verbunden (2. Auflage)*, Springer Verlag, Berlin Heidelberg, Germany.



Higher-Order Laminate Theories

11

In this chapter, higher-order laminate theories are presented, namely the so-called First-Order Shear Deformation Theory as well as the so-called Third-Order Shear Deformation Theory according to Reddy. Both theories are so-called single-layer theories that take transverse shear strains into account and in which the laminate is reduced to its middle plane. The basic equations are derived for both theories and some exact analytical solutions for boundary value problems are discussed. The Ritz method is also introduced as an approximation method. The chapter concludes with the treatment of so-called layerwise theories for laminates.

11.1 Introduction

Classical Laminated Plate Theory (CLPT) has proven itself in many practical applications, e.g. in lightweight construction and here in particular in aerospace engineering, as a universal theoretical framework for the static and dynamic analysis of composite laminated structures. CLPT is based on the kinematic assumptions of Kirchhoff's classical plate theory—i.e. the assumption that the cross-sections remain plane and the normal hypothesis—in conjunction with the assumption of a plane stress state with regard to the thickness direction in the entire laminate. While these assumptions are justified for quite thin laminates, it turns out that for thicker laminates, especially with 'weak' transverse shear stiffnesses and especially for sandwich structures, sometimes massive errors can occur in the analysis if one also assumes that CLPT is applicable in such cases. In most cases, the resulting errors will not be conservative, so that in the case of thick laminates or sandwiches, for example, too small deflections or too high buckling loads can result according to CLPT, which is of course not acceptable in lightweight construction applications.

© The Author(s), under exclusive license to Springer-Verlag GmbH, DE, part of Springer Nature 2025

C. Mittelstedt, *Mechanics of Composite Structures*,
https://doi.org/10.1007/978-3-662-70788-3_11

When using CLPT, in addition to the points mentioned, it should also be noted that there are no constitutive relationships for the transverse shear forces in the laminate—a deficiency that arises according to CLPT, because even if transverse shear stresses and thus transverse forces do not occur in the constitutive law of CLPT, transverse shear forces are always required to maintain the equilibrium of a laminate.

The above-mentioned discrepancies between the assumptions according to CLPT and the actual conditions in thick laminates and sandwich structures have led to considerable research efforts being made worldwide in recent decades to develop improved laminate theories, often referred to in this context as higher-order laminate theories. Detailed overviews can be found, for example, in the publications of Altenbach (1998), Altenbach and Becker (2003), Kant and Swaminathan (2000), Noor and Burton (1989, 1990), Reddy (1987, 1990a, b, 2004), Reddy and Robbins (1994), or Rohwer (1996). This chapter is devoted to the documentation and discussion of several such higher-order laminate theories. First, the so-called First-Order Shear Deformation Theory is presented, which corresponds to an application of the classical Reissner-Mindlin theory[1] to laminate structures and is essentially an extension of CLPT, although the normal hypothesis is dropped here. Furthermore, the so-called Third-Order Shear Deformation Theory according to Reddy is introduced, which is based on improved displacement approaches, with the help of which the cross-sectional warping due to transverse shear stresses can be approximately modelled. Finally, for special applications, so-called layerwise theories are discussed, which use a layer-by-layer displacement approach. Where available, analytical solution methods for static bending problems are presented, which can be used to carry out a laminate analysis according to the above-mentioned higher-order theories without great effort and which can prove to be very helpful in practical applications.

Practical application shows that CLPT leads to good results in the calculation of 'thin' and/or sufficiently shear-stiff laminates (whereby the terms 'thin' and 'shear-stiff' require a more detailed definition in each application). However, the assumptions of CLPT are no longer sufficient when dealing with laminates that exceed a certain ratio between thickness and planar dimensions and/or do not have sufficient shear stiffness in the thickness direction. As an example, Fig. 11.1 shows a sandwich beam subjected to a single force P. In such a construction, the resulting bending moments are essentially absorbed by the facesheets by forming a corresponding membrane stress state. The sandwich core then has the task of absorbing the shear forces. As the shear stiffnesses of typical core materials are generally relatively weak compared to, for example, the longitudinal stiffnesses of the facesheets, such a sandwich beam will not only exhibit the typical bending deformations (Fig. 11.1, top right), but shear deformations will also occur, as shown in Fig. 11.1, bottom right. In general, it can be stated that the shear deformations (expressed by the shear strains γ_{xz} and γ_{yz}) will increase as the ratio of length l to thickness h decreases. In addition, smaller transverse shear stiffnesses also indicate larger shear deformations. This relatively simple

[1] Raymond David Mindlin, 1906–1987, US-American engineer, and Max Erich Reissner, 1913–1996, German-US-American engineer.

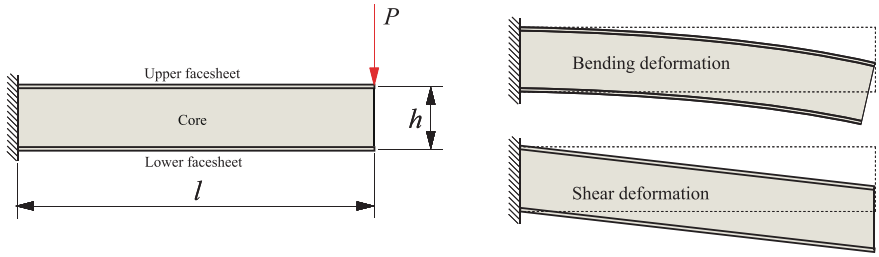


Fig. 11.1 Sandwich beam under bending

example shows the importance of considering the transverse shear strains γ_{xz} and γ_{yz} and the associated transverse shear stresses τ_{xz} and τ_{yz} in thick and compliant laminate and sandwich structures, which are neglected in CLPT. In addition, the calculation of the normal stress σ_{zz} can also be important for failure analyses.

11.2 Three-Dimensional Local Equilibrium

A stress analysis according to CLPT leads to the stresses σ_{xx}, σ_{yy} and τ_{xy} of each individual laminate layer. A first simple way to obtain a statement about the interlaminar stress components τ_{xz}, τ_{yz} and σ_{zz} neglected according to CLPT is to integrate the three-dimensional local equilibrium conditions and drawing a conclusion from the known inplane stress components σ_{xx}, σ_{yy} and τ_{xy} about the stresses in the thickness direction. From the equilibrium conditions

$$\begin{aligned} \frac{\partial \sigma_{xx}}{\partial x} + \frac{\partial \tau_{xy}}{\partial y} + \frac{\partial \tau_{xz}}{\partial z} &= 0, \\ \frac{\partial \tau_{xy}}{\partial x} + \frac{\partial \sigma_{yy}}{\partial y} + \frac{\partial \tau_{yz}}{\partial z} &= 0 \end{aligned} \tag{11.1}$$

the transverse shear stresses can be obtained by integration:

$$\begin{aligned} \tau_{xz} &= -\int_{-h/2}^{z} \left(\frac{\partial \sigma_{xx}}{\partial x} + \frac{\partial \tau_{xy}}{\partial y} \right) \mathrm{d}z, \\ \tau_{yz} &= -\int_{-h/2}^{z} \left(\frac{\partial \tau_{xy}}{\partial x} + \frac{\partial \sigma_{yy}}{\partial y} \right) \mathrm{d}z. \end{aligned} \tag{11.2}$$

Since the stresses σ_{xx}, σ_{yy} and τ_{xy} are linear with respect to z if, for example, a laminate is considered under bending, parabolic distributions for τ_{xz} and τ_{yz} will result according to (11.2). The third remaining equilibrium condition

$$\frac{\partial \tau_{xz}}{\partial x} + \frac{\partial \tau_{yz}}{\partial y} + \frac{\partial \sigma_{zz}}{\partial z} = 0 \tag{11.3}$$

can then be used to determine the behaviour of the normal stress σ_{zz} from the already calculated transverse shear stresses τ_{xz} and τ_{yz}:

$$\sigma_{zz} = -\int_{-h/2}^{z} \left(\frac{\partial \tau_{xz}}{\partial x} + \frac{\partial \tau_{yz}}{\partial y} \right) \mathrm{d}z. \tag{11.4}$$

This will generally lead to a cubic distribution of σ_{zz} with respect to z.

The evaluation of the relationships (11.2) and (11.4) is relatively easy to perform. However, it turns out that the results from the integration of the three-dimensional equilibrium conditions can become unreliable when dealing with thick and shear-compliant laminate structures. It is therefore necessary to look for alternatives that can be used in practice with a tolerable amount of effort on the one hand, but also lead to acceptable results on the other. One such improved approach is based on First-Order Shear Deformation Theory, which is presented in the next section.

11.3 First-Order Shear Deformation Theory

11.3.1 Kinematics and Constitutive Equations

A laminate theory that relaxes the assumptions of CLPT to a certain degree is the so-called First-Order Shear Deformation Theory (FSDT). As an extension of the classic Reissner-Mindlin theory (Reissner 1945; Hencky 1947; Mindlin 1951), it is based on the work of Whitney and Pagano (1970), Chow (1971) and Whitney (1973), among others, and is based on the following assumptions:

(1) A plane stress state is still assumed with regard to the thickness direction in the entire laminate, in this case with regard to the normal stress σ_{zz}.
(2) The hypothesis that the cross-sections remain plane is still valid, but the normal hypothesis is dropped. A straight line that is normal to the laminate middle plane before deformation remains a straight line in the deformed state, but is no longer necessarily normal to the laminate middle plane.
(3) The thickness h of the laminate does not change during the entire deformation process.

The main difference between FSDT and CLPT is therefore the dropping of the normal hypothesis. The deformation process according to the FSDT is shown schematically in Fig. 11.2. Figure 11.2 shows that the resulting bending angles ψ_x and ψ_y are no longer related to the inclinations $\frac{\partial w_0}{\partial x}$ or $\frac{\partial w_0}{\partial y}$. Rather, ψ_x and ψ_y must be included in the analysis as additional degrees of freedom, which increases the number of degrees of freedom to a

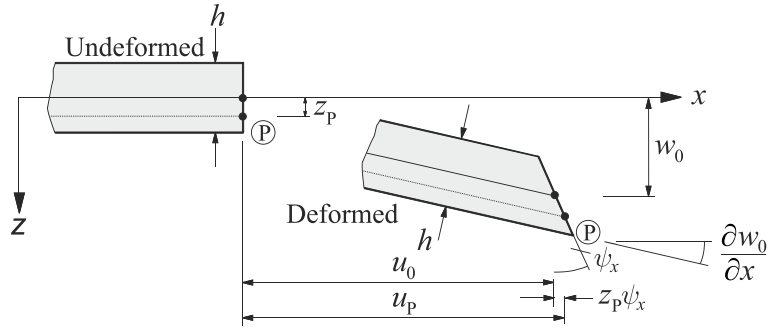


Fig. 11.2 Undeformed and deformed laminate segment according to FSDT

total of five, namely the displacements u_0, v_0, w_0 of the laminate middle plane on the one hand, and the bending angles ψ_x and ψ_y on the other. Of course, this generally requires a higher computational effort compared to an analysis using CLPT.

The displacement field according to FSDT can be deduced from Fig. 11.2:

$$\begin{aligned} u(x, y, z) &= u_0(x, y) + z\psi_x(x, y), \\ v(x, y, z) &= v_0(x, y) + z\psi_y(x, y), \\ w(x, y) &= w_0(x, y). \end{aligned} \tag{11.5}$$

This displacement field can be converted into the one according to CLPT if $\psi_x = -\frac{\partial w_0}{\partial x}$ and $\psi_y = -\frac{\partial w_0}{\partial y}$. The strain field in the framework of FSDT results as:

$$\begin{aligned} \varepsilon_{xx} &= \frac{\partial u}{\partial x} = \frac{\partial u_0}{\partial x} + z\frac{\partial \psi_x}{\partial x}, \\ \varepsilon_{yy} &= \frac{\partial v}{\partial y} = \frac{\partial v_0}{\partial y} + z\frac{\partial \psi_y}{\partial y}, \\ \varepsilon_{zz} &= \frac{\partial w}{\partial z} = 0, \\ \gamma_{xy} &= \frac{\partial u}{\partial y} + \frac{\partial v}{\partial x} = \frac{\partial u_0}{\partial y} + \frac{\partial v_0}{\partial x} + z\left(\frac{\partial \psi_x}{\partial y} + \frac{\partial \psi_y}{\partial x}\right), \\ \gamma_{xz} &= \frac{\partial u}{\partial z} + \frac{\partial w}{\partial x} = \frac{\partial w_0}{\partial x} + \psi_x, \\ \gamma_{yz} &= \frac{\partial v}{\partial z} + \frac{\partial w}{\partial y} = \frac{\partial w_0}{\partial y} + \psi_y. \end{aligned} \tag{11.6}$$

Obviously, the assumptions of FSDT lead to non-vanishing transverse shear strains γ_{xz} and γ_{yz}, but to a vanishing strain ε_{zz}. It is also easy to see that the shear strains γ_{xz} and γ_{yz} are not functions of the thickness direction z and are therefore constant over the laminate thickness h, which is a plausible result due to the assumption that the cross-sections remain

plane. However, this is associated with some special features in the stress analysis, which will be discussed in detail later.

The layerwise inplane stresses σ_{xx}, σ_{yy} and τ_{xy} can be calculated within the framework of FSDT using the relationships familiar from CLPT:

$$\begin{pmatrix} \sigma_{xx} \\ \sigma_{yy} \\ \tau_{xy} \end{pmatrix}_k = \begin{bmatrix} \bar{Q}_{11} & \bar{Q}_{12} & \bar{Q}_{16} \\ \bar{Q}_{12} & \bar{Q}_{22} & \bar{Q}_{26} \\ \bar{Q}_{16} & \bar{Q}_{26} & \bar{Q}_{66} \end{bmatrix}_k \begin{pmatrix} \varepsilon_{xx} \\ \varepsilon_{yy} \\ \gamma_{xy} \end{pmatrix}. \tag{11.7}$$

Within the framework of CLPT, the transverse shear strains γ_{xz} and γ_{yz} are zero. On the other hand, the relationships (11.6) now make it possible to calculate transverse shear stresses τ_{xz} and τ_{yz} from the given expressions for γ_{xz} and γ_{yz} using Hooke's generalised law in addition to the inplane stresses σ_{xx}, σ_{yy} and τ_{xy} as follows:

$$\begin{pmatrix} \tau_{yz} \\ \tau_{xz} \end{pmatrix}_k = \begin{bmatrix} \bar{C}_{44} & \bar{C}_{45} \\ \bar{C}_{45} & \bar{C}_{55} \end{bmatrix}_k \begin{pmatrix} \gamma_{yz} \\ \gamma_{xz} \end{pmatrix}, \tag{11.8}$$

where $\bar{C}_{44}$ and $\bar{C}_{55}$ are the transverse (off-axis) shear stiffnesses, and $\bar{C}_{45}$ is a shear coupling stiffness. The index k characterises the shear stresses and the elastic properties in the layer k. The off-axis stiffnesses can be calculated from the on-axis shear stiffnesses C_{44} and C_{55} using elementary rules of tensor transformation as:

$$\begin{aligned} \bar{C}_{44} &= C_{44} \cos^2\theta + C_{55} \sin^2\theta, \\ \bar{C}_{45} &= (C_{55} - C_{44}) \cos\theta \sin\theta, \\ \bar{C}_{55} &= C_{44} \sin^2\theta + C_{55} \cos^2\theta. \end{aligned} \tag{11.9}$$

The transverse shear stresses obtained by (11.8) are constant in each laminate layer and show discontinuities in the interfaces due to the generally different stiffnesses of the individual layers. The resulting transverse shear forces Q_x and Q_y can be calculated by integrating over the laminate cross-section:

$$\begin{pmatrix} Q_y \\ Q_x \end{pmatrix} = \int_{-\frac{h}{2}}^{+\frac{h}{2}} \begin{pmatrix} \tau_{yz} \\ \tau_{xz} \end{pmatrix} \mathrm{d}z = \int_{-\frac{h}{2}}^{+\frac{h}{2}} \begin{bmatrix} \bar{C}_{44} & \bar{C}_{45} \\ \bar{C}_{45} & \bar{C}_{55} \end{bmatrix} \begin{pmatrix} \gamma_{yz} \\ \gamma_{xz} \end{pmatrix} \mathrm{d}z. \tag{11.10}$$

Since the elastic properties are generally different for each layer, the integral is broken down into partial integrals:

$$\begin{pmatrix} Q_y \\ Q_x \end{pmatrix} = \sum_{k=1}^{k=N} \int_{z_{k-1}}^{z_k} \begin{bmatrix} \bar{C}_{44} & \bar{C}_{45} \\ \bar{C}_{45} & \bar{C}_{55} \end{bmatrix}_k \begin{pmatrix} \gamma_{yz} \\ \gamma_{xz} \end{pmatrix} \mathrm{d}z. \tag{11.11}$$

Performing the integrations and summing up finally results in:

$$\begin{pmatrix} Q_y \\ Q_x \end{pmatrix} = \begin{bmatrix} A_{44} & A_{45} \\ A_{45} & A_{55} \end{bmatrix} \begin{pmatrix} \gamma_{yz} \\ \gamma_{xz} \end{pmatrix}, \tag{11.12}$$

where the variables A_{44}, A_{55} and A_{45} are the transverse shear stiffnesses of the laminate:

$$\begin{aligned} A_{44} &= \int_{-\frac{h}{2}}^{+\frac{h}{2}} \bar{C}_{44} \mathrm{d}z = \sum_{k=1}^{k=N} \int_{z_{k-1}}^{z_k} \bar{C}_{44,k} \mathrm{d}z, \\ A_{55} &= \int_{-\frac{h}{2}}^{+\frac{h}{2}} \bar{C}_{55} \mathrm{d}z = \sum_{k=1}^{k=N} \int_{z_{k-1}}^{z_k} \bar{C}_{55,k} \mathrm{d}z, \\ A_{45} &= \int_{-\frac{h}{2}}^{+\frac{h}{2}} \bar{C}_{45} \mathrm{d}z = \sum_{k=1}^{k=N} \int_{z_{k-1}}^{z_k} \bar{C}_{45,k} \mathrm{d}z. \end{aligned} \tag{11.13}$$

If the elastic properties of the individual layers are constant over the layer thickness h_k, then the integrals in (11.13) can be solved easily, and one obtains

$$\begin{aligned} A_{44} &= \sum_{k=1}^{k=N} \bar{C}_{44,k} \left(z_k - z_{k-1}\right) = \sum_{k=1}^{k=N} \bar{C}_{44,k} h_k, \\ A_{55} &= \sum_{k=1}^{k=N} \bar{C}_{55,k} h_k, \\ A_{45} &= \sum_{k=1}^{k=N} \bar{C}_{45,k} h_k. \end{aligned} \tag{11.14}$$

The shear stresses τ_{xz} and τ_{yz} that can be calculated using (11.8) are constant in each individual laminate layer. This contradicts the elementary bending theory, according to which the transverse shear stresses have a parabolic distribution in the thickness direction and must also disappear at the free surfaces. A consequence of this inadequacy is the observation that for most laminates the transverse shear stiffnesses A_{44}, A_{55}, A_{45} are somewhat higher than the real observations in corresponding experiments. Therefore, the transverse stiffnesses are often modified by introducing a so-called shear correction factor K. The relationship (11.8) is then:

$$\begin{pmatrix} \tau_{yz} \\ \tau_{xz} \end{pmatrix}_k = K \begin{bmatrix} \bar{C}_{44} & \bar{C}_{45} \\ \bar{C}_{45} & \bar{C}_{55} \end{bmatrix}_k \begin{pmatrix} \gamma_{yz} \\ \gamma_{xz} \end{pmatrix}, \tag{11.15}$$

and the constitutive equation (11.12) changes to:

$$\begin{pmatrix} Q_y \\ Q_x \end{pmatrix} = K \begin{bmatrix} A_{44} & A_{45} \\ A_{45} & A_{55} \end{bmatrix} \begin{pmatrix} \gamma_{yz} \\ \gamma_{xz} \end{pmatrix}. \tag{11.16}$$

The introduction of the shear correction factor K does not solve the problem of constant transverse shear stresses, but this measure attempts to at least minimize the effects of this shortcoming of FSDT. The introduction of K is equivalent to a reduction of the laminate shear stiffnesses A_{44}, A_{55}, A_{45}.

The constitutive equation for the entire laminate according to the FSDT then ultimately reads:

$$\begin{pmatrix} N^0_{xx} \\ N^0_{yy} \\ N^0_{xy} \\ M^0_{xx} \\ M^0_{yy} \\ M^0_{xy} \\ Q_y \\ Q_x \end{pmatrix} = \begin{bmatrix} A_{11} & A_{12} & A_{16} & B_{11} & B_{12} & B_{16} & 0 & 0 \\ A_{12} & A_{22} & A_{26} & B_{12} & B_{22} & B_{26} & 0 & 0 \\ A_{16} & A_{26} & A_{66} & B_{16} & B_{26} & B_{66} & 0 & 0 \\ B_{11} & B_{12} & B_{16} & D_{11} & D_{12} & D_{16} & 0 & 0 \\ B_{12} & B_{22} & B_{26} & D_{12} & D_{22} & D_{26} & 0 & 0 \\ B_{16} & B_{26} & B_{66} & D_{16} & D_{26} & D_{66} & 0 & 0 \\ 0 & 0 & 0 & 0 & 0 & 0 & KA_{44} & KA_{45} \\ 0 & 0 & 0 & 0 & 0 & 0 & KA_{45} & KA_{55} \end{bmatrix} \begin{pmatrix} \frac{\partial u_0}{\partial x} \\ \frac{\partial v_0}{\partial y} \\ \frac{\partial u_0}{\partial y} + \frac{\partial v_0}{\partial x} \\ \frac{\partial \psi_x}{\partial x} \\ \frac{\partial \psi_y}{\partial y} \\ \frac{\partial \psi_x}{\partial y} + \frac{\partial \psi_y}{\partial x} \\ \frac{\partial w_0}{\partial y} + \psi_y \\ \frac{\partial w_0}{\partial x} + \psi_x \end{pmatrix}. \tag{11.17}$$

It can be seen that this form of the constitutive law for the laminate does not differ from the relationships according to CLPT with regard to the laminate forces N^0_{xx}, N^0_{yy}, N^0_{xy} and moments M^0_{xx}, M^0_{yy}, M^0_{xy}. The only new additions are the constitutive relationships for the transverse shear forces. In symbolic form, (11.17) can also be written as follows:

$$\begin{pmatrix} \underline{N}^0 \\ \underline{M}^0 \\ \underline{Q} \end{pmatrix} = \begin{bmatrix} \underline{\underline{A}} & \underline{\underline{B}} & \underline{0} \\ \underline{\underline{B}} & \underline{\underline{D}} & \underline{0} \\ \underline{0} & \underline{0} & \underline{\underline{A}}_S \end{bmatrix} \begin{pmatrix} \underline{\varepsilon}^0 \\ \underline{\kappa}^0 \\ \underline{\gamma}_S \end{pmatrix}. \tag{11.18}$$

It should be pointed out again at this point that a calculation of the transverse shear stresses τ_{yz} and τ_{xz} from the constitutive law (11.15) will lead to layerwise constant stresses in terms of z. A simple way to achieve better results here is to use the local equilibrium conditions again and to determine the transverse shear stresses τ_{yz} and τ_{xz} by integrating the intralaminar stresses σ_{xx}, σ_{yy}, τ_{xy} calculated from (11.7):

$$\tau_{xz} = -\int_{-h/2}^{z} \left(\frac{\partial \sigma_{xx}}{\partial x} + \frac{\partial \tau_{xy}}{\partial y} \right) \mathrm{d}z,$$
$$\tau_{yz} = -\int_{-h/2}^{z} \left(\frac{\partial \tau_{xy}}{\partial x} + \frac{\partial \sigma_{yy}}{\partial y} \right) \mathrm{d}z. \tag{11.19}$$

Experience shows that by applying (11.19) one can obtain quite useful results for τ_{yz} and τ_{xz} in many cases.

11.3.2 Equilibrium and Boundary Conditions

The equilibrium conditions for a laminate according to FSDT can be taken directly from CLPT. In the case of disk equilibrium conditions, these are

$$\frac{\partial N_{xx}^0}{\partial x} + \frac{\partial N_{xy}^0}{\partial y} + f_x = 0,$$
$$\frac{\partial N_{xy}^0}{\partial x} + \frac{\partial N_{yy}^0}{\partial y} + f_y = 0, \tag{11.20}$$

and for the plate equilibrium we have:

$$\frac{\partial M_{xx}^0}{\partial x} + \frac{\partial M_{xy}^0}{\partial y} = Q_x,$$
$$\frac{\partial M_{xy}^0}{\partial x} + \frac{\partial M_{yy}^0}{\partial y} = Q_y,$$
$$\frac{\partial Q_x}{\partial x} + \frac{\partial Q_y}{\partial y} + p = 0, \tag{11.21}$$

where p is a load on the laminate in the z-direction, e.g. in the form of a surface load. If the constitutive relations (11.17) are inserted into (11.20) and (11.21), the displacement differential equations are obtained, which describe the behaviour of a laminate according to FSDT:

$$A_{11}\frac{\partial^2 u_0}{\partial x^2} + 2A_{16}\frac{\partial^2 u_0}{\partial x \partial y} + A_{66}\frac{\partial^2 u_0}{\partial y^2} + A_{16}\frac{\partial^2 v_0}{\partial x^2} + (A_{12} + A_{66})\frac{\partial^2 v_0}{\partial x \partial y}$$
$$+ A_{26}\frac{\partial^2 v_0}{\partial y^2} + B_{11}\frac{\partial^2 \psi_x}{\partial x^2} + 2B_{16}\frac{\partial^2 \psi_x}{\partial x \partial y} + B_{66}\frac{\partial^2 \psi_x}{\partial y^2} + B_{16}\frac{\partial^2 \psi_y}{\partial x^2}$$
$$+ (B_{12} + B_{66})\frac{\partial^2 \psi_y}{\partial x \partial y} + B_{26}\frac{\partial^2 \psi_y}{\partial y^2} + f_x = 0,$$

$$
\begin{aligned}
&A_{16}\frac{\partial^2 u_0}{\partial x^2} + (A_{12}+A_{66})\frac{\partial^2 u_0}{\partial x\partial y} + A_{26}\frac{\partial^2 u_0}{\partial y^2} + A_{66}\frac{\partial^2 v_0}{\partial x^2} + 2A_{26}\frac{\partial^2 v_0}{\partial x\partial y}\\
&+ A_{22}\frac{\partial^2 v_0}{\partial y^2} + B_{16}\frac{\partial^2 \psi_x}{\partial x^2} + (B_{12}+B_{66})\frac{\partial^2 \psi_x}{\partial x\partial y} + B_{26}\frac{\partial^2 \psi_x}{\partial y^2}\\
&+ B_{66}\frac{\partial^2 \psi_y}{\partial x^2} + 2B_{26}\frac{\partial^2 \psi_y}{\partial x\partial y} + B_{22}\frac{\partial^2 \psi_y}{\partial y^2} + f_y = 0,\\
&B_{11}\frac{\partial^2 u_0}{\partial x^2} + 2B_{16}\frac{\partial^2 u_0}{\partial x\partial y} + B_{66}\frac{\partial^2 u_0}{\partial y^2} + B_{16}\frac{\partial^2 v_0}{\partial x^2} + (B_{12}+B_{66})\frac{\partial^2 v_0}{\partial x\partial y}\\
&+ B_{26}\frac{\partial^2 v_0}{\partial y^2} + D_{11}\frac{\partial^2 \psi_x}{\partial x^2} + 2D_{16}\frac{\partial^2 \psi_x}{\partial x\partial y} + D_{66}\frac{\partial^2 \psi_x}{\partial y^2} + D_{16}\frac{\partial^2 \psi_y}{\partial x^2} + D_{26}\frac{\partial^2 \psi_y}{\partial y^2}\\
&+ (D_{12}+D_{66})\frac{\partial^2 \psi_y}{\partial x\partial y} = K\left[A_{55}\left(\psi_x + \frac{\partial w_0}{\partial x}\right) + A_{45}\left(\psi_y + \frac{\partial w_0}{\partial y}\right)\right],\\
&B_{16}\frac{\partial^2 u_0}{\partial x^2} + (B_{12}+B_{66})\frac{\partial^2 u_0}{\partial x\partial y} + B_{26}\frac{\partial^2 u_0}{\partial y^2} + B_{66}\frac{\partial^2 v_0}{\partial x^2} + 2B_{26}\frac{\partial^2 v_0}{\partial x\partial y}\\
&+ B_{22}\frac{\partial^2 v_0}{\partial y^2} + D_{16}\frac{\partial^2 \psi_x}{\partial x^2} + (D_{12}+D_{66})\frac{\partial^2 \psi_x}{\partial x\partial y} + D_{26}\frac{\partial^2 \psi_x}{\partial y^2} + D_{66}\frac{\partial^2 \psi_y}{\partial x^2}\\
&+ 2D_{26}\frac{\partial^2 \psi_y}{\partial x\partial y} + D_{22}\frac{\partial^2 \psi_y}{\partial y^2} + f_y = K\left[A_{45}\left(\psi_x + \frac{\partial w_0}{\partial x}\right) + A_{44}\left(\psi_y + \frac{\partial w_0}{\partial y}\right)\right],\\
&K\left[A_{55}\left(\frac{\partial \psi_x}{\partial x} + \frac{\partial^2 w_0}{\partial x^2}\right) + A_{45}\left(\frac{\partial \psi_x}{\partial y} + \frac{\partial \psi_y}{\partial x} + 2\frac{\partial^2 w_0}{\partial x\partial y}\right)\right.\\
&\left.+ A_{44}\left(\frac{\partial \psi_y}{\partial y} + \frac{\partial^2 w_0}{\partial y^2}\right)\right] + p = 0.
\end{aligned}
\tag{11.22}
$$

These are five coupled partial differential equations in the five degrees of freedom according to FSDT, namely the displacements u_0, v_0, w_0 of the laminate middle plane and the bending angles ψ_x and ψ_y.

As far as the boundary conditions are concerned, one of the following variables is available at each boundary of a laminate according to FSDT (where the indices n and t indicate the directions normal and tangential to the boundary under consideration):

$$
\begin{aligned}
u_{0n} \quad &\text{or} \quad N^0_{nn},\\
u_{0t} \quad &\text{or} \quad N^0_{nt},\\
w_0 \quad &\text{or} \quad Q_n,\\
\psi_n \quad &\text{or} \quad M^0_{nn},\\
\psi_t \quad &\text{or} \quad M^0_{nt}.
\end{aligned}
\tag{11.23}
$$

If a laminate edge is simply supported (whereby the possible ambiguity of this term for laminates has already been pointed out earlier), the laminate forces N_{nn}^0 and N_{nt}^0 as well as the laminate moments M_{nn}^0 and M_{nt}^0, for example, disappear here as a possibility in addition to the deflection w_0:

$$N_{nn}^0 = N_{nt}^0 = M_{nn}^0 = M_{nt}^0 = w_0 = 0. \tag{11.24}$$

A clamped laminate edge requires the disappearance of all kinematic variables:

$$u_{0n} = u_{0t} = \psi_n = \psi_t = w_0 = 0. \tag{11.25}$$

At a free laminate edge, however, all laminate forces and moments must disappear:

$$N_{nn}^0 = N_{nt}^0 = M_{nn}^0 = M_{nt}^0 = Q_n = 0. \tag{11.26}$$

11.3.3 Strain Energy

For energy-based approximation methods, it is important to be able to determine the strain energy or the internal potential of a laminate according to FSDT. At present, one obtains

$$\Pi_i = \frac{1}{2} \int\int\int_V \left(\sigma_{xx}\varepsilon_{xx} + \sigma_{yy}\varepsilon_{yy} + \tau_{xy}\gamma_{xy} + \tau_{xz}\gamma_{xz} + \tau_{yz}\gamma_{yz}\right) \mathrm{d}V. \tag{11.27}$$

Performing the integration with regard to the thickness direction yields:

$$\begin{aligned}\Pi_i = \frac{1}{2} \int_0^b \int_0^a \Bigg[& N_{xx}^0 \frac{\partial u_0}{\partial x} + N_{yy}^0 \frac{\partial v_0}{\partial y} + N_{xy}^0 \left(\frac{\partial u_0}{\partial y} + \frac{\partial v_0}{\partial x}\right) + M_{xx}^0 \frac{\partial \psi_x}{\partial x} + M_{yy}^0 \frac{\partial \psi_y}{\partial y} \\ & + M_{xy}^0 \left(\frac{\partial \psi_x}{\partial y} + \frac{\partial \psi_y}{\partial x}\right) + Q_y \left(\frac{\partial w_0}{\partial y} + \psi_y\right) + Q_x \left(\frac{\partial w_0}{\partial x} + \psi_x\right) \Bigg] \mathrm{d}x\mathrm{d}y. \end{aligned} \tag{11.28}$$

Inserting the constitutive law according to (11.17) leads to:

$$\begin{aligned}\Pi_i = \frac{1}{2} \int_0^b \int_0^a \Bigg\{ & A_{11} \left(\frac{\partial u_0}{\partial x}\right)^2 + 2A_{12} \frac{\partial u_0}{\partial x} \frac{\partial v_0}{\partial y} + A_{22} \left(\frac{\partial v_0}{\partial y}\right)^2 \\ & + A_{66} \left(\frac{\partial u_0}{\partial y} + \frac{\partial v_0}{\partial x}\right)^2 + 2 \left(A_{16} \frac{\partial u_0}{\partial x} + A_{26} \frac{\partial v_0}{\partial y}\right) \left(\frac{\partial u_0}{\partial y} + \frac{\partial v_0}{\partial x}\right) \\ & + 2B_{11} \frac{\partial u_0}{\partial x} \frac{\partial \psi_x}{\partial x} + 2B_{12} \left(\frac{\partial u_0}{\partial x} \frac{\partial \psi_y}{\partial y} + \frac{\partial v_0}{\partial y} \frac{\partial \psi_x}{\partial x}\right) + 2B_{22} \frac{\partial v_0}{\partial y} \frac{\partial \psi_y}{\partial y} \\ & + 2B_{16} \left[\frac{\partial u_0}{\partial x} \left(\frac{\partial \psi_x}{\partial y} + \frac{\partial \psi_y}{\partial x}\right) + \left(\frac{\partial u_0}{\partial y} + \frac{\partial v_0}{\partial x}\right) \frac{\partial \psi_x}{\partial x}\right] \end{aligned}$$

$$
\begin{aligned}
&+ 2B_{26}\left[\frac{\partial v_0}{\partial y}\left(\frac{\partial \psi_x}{\partial y}+\frac{\partial \psi_y}{\partial x}\right)+\left(\frac{\partial u_0}{\partial y}+\frac{\partial v_0}{\partial x}\right)\frac{\partial \psi_y}{\partial y}\right]\\
&+ 2B_{66}\left(\frac{\partial u_0}{\partial y}+\frac{\partial v_0}{\partial x}\right)\left(\frac{\partial \psi_x}{\partial y}+\frac{\partial \psi_y}{\partial x}\right)\\
&+ D_{11}\left(\frac{\partial \psi_x}{\partial x}\right)^2+2D_{12}\frac{\partial \psi_x}{\partial x}\frac{\partial \psi_y}{\partial y}+D_{22}\left(\frac{\partial \psi_y}{\partial y}\right)^2+D_{66}\left(\frac{\partial \psi_x}{\partial y}+\frac{\partial \psi_y}{\partial x}\right)^2\\
&+ 2D_{16}\frac{\partial \psi_x}{\partial x}\left(\frac{\partial \psi_x}{\partial y}+\frac{\partial \psi_y}{\partial x}\right)+2D_{26}\frac{\partial \psi_y}{\partial y}\left(\frac{\partial \psi_x}{\partial y}+\frac{\partial \psi_y}{\partial x}\right)+KA_{44}\left(\frac{\partial w_0}{\partial y}+\psi_y\right)^2\\
&+ 2KA_{45}\left(\frac{\partial w_0}{\partial x}+\psi_x\right)\left(\frac{\partial w_0}{\partial y}+\psi_y\right)+KA_{55}\left(\frac{\partial w_0}{\partial x}+\psi_x\right)^2\Bigg\}\,\mathrm{d}x\mathrm{d}y. \qquad (11.29)
\end{aligned}
$$

11.3.4 Determination of the Shear Correction Factor K

Various methods have been proposed over the years for determining the shear correction factor, each leading to different results. A simple method is presented here using the example of a homogeneous orthotropic plate, which is based on Reissner's classical plate theory. The shear correction factor K is determined by equating the shear strain energy, as it results from the quadratic shear stress distribution, and the current shear deformation theory. The shear strain energy is generally

$$\Pi_i = \frac{1}{2}\int\int\int_V \left(\tau_{xz}\gamma_{xz}+\tau_{yz}\gamma_{yz}\right)\mathrm{d}V. \qquad (11.30)$$

Firstly, the shear strain energy is to be considered according to the quadratic shear stress distribution. The distribution of the transverse shear stresses τ_{xz} and τ_{yz} in a homogeneous plate under bending due to the transverse shear forces Q_x and Q_y is parabolic over the cross-section and can be calculated as:

$$\tau_{xz} = \frac{3Q_x}{2h}\left(1-\frac{4z^2}{h^2}\right), \quad \tau_{yz} = \frac{3Q_y}{2h}\left(1-\frac{4z^2}{h^2}\right). \qquad (11.31)$$

If the generalised Hooke's law is used for the shear stresses τ_{xz} and τ_{yz} according to $\tau_{yz} = C_{44}\gamma_{yz}$ and $\tau_{xz} = C_{55}\gamma_{xz}$ and if the volume integral is split into an integral over the cross-section A and an integral in the thickness direction, the result for (11.30) is:

$$\Pi_i = \frac{1}{2}\int\int_A\int_{-\frac{h}{2}}^{+\frac{h}{2}}\left(\frac{\tau_{xz}^2}{C_{55}}+\frac{\tau_{yz}^2}{C_{44}}\right)\mathrm{d}z\mathrm{d}A. \qquad (11.32)$$

Inserting the expressions (11.31) then results in:

$$\Pi_i = \frac{9}{8h^2} \int\int_A \left(\frac{Q_x^2}{C_{55}} + \frac{Q_y^2}{C_{44}} \right) \mathrm{d}A \int_{-\frac{h}{2}}^{+\frac{h}{2}} \left(1 - \frac{4z^2}{h^2} \right)^2 \mathrm{d}z$$

$$= \frac{9}{15h} \int\int_A \left(\frac{Q_x^2}{C_{55}} + \frac{Q_y^2}{C_{44}} \right) \mathrm{d}A. \tag{11.33}$$

Furthermore, the shear strain energy is considered according to the current shear deformation theory. For a homogeneous orthotropic plate, the constitutive law (11.17) gives the expressions $Q_x = K A_{55} \gamma_{xz}$ and $Q_y = K A_{44} \gamma_{yz}$ for the transverse shear forces. Insertion into the shear strain energy (11.30) provides:

$$\Pi_i = \frac{1}{2K} \int\int_A \int_{-\frac{h}{2}}^{+\frac{h}{2}} \left(\tau_{xz} \frac{Q_x}{A_{55}} + \tau_{yz} \frac{Q_y}{A_{44}} \right) \mathrm{d}z \mathrm{d}A. \tag{11.34}$$

Performing the integration with respect to z results in:

$$\Pi_i = \frac{1}{2K} \int\int_A \left(\frac{Q_x^2}{A_{55}} + \frac{Q_y^2}{A_{44}} \right) \mathrm{d}A. \tag{11.35}$$

Since $A_{44} = C_{44} h$ and $A_{55} = C_{55} h$ also apply to a homogeneous orthotropic plate, this results in

$$\Pi_i = \frac{1}{2hK} \int\int_A \left(\frac{Q_x^2}{C_{55}} + \frac{Q_y^2}{C_{44}} \right) \mathrm{d}A. \tag{11.36}$$

Equating the expressions (11.33) and (11.36) results in:

$$\frac{9}{15h} \int\int_A \left(\frac{Q_x^2}{C_{55}} + \frac{Q_y^2}{C_{44}} \right) \mathrm{d}A = \frac{1}{2hK} \int\int_A \left(\frac{Q_x^2}{C_{55}} + \frac{Q_y^2}{C_{44}} \right) \mathrm{d}A. \tag{11.37}$$

This equation can easily be solved for K (note that identical integral terms appear on both sides), and the classical result for K for the homogeneous orthotropic plate is obtained:

$$K = \frac{5}{6}. \tag{11.38}$$

Of course, this result cannot simply be used for arbitrary anisotropic surface structures or laminates. Rather, the shear correction factor depends on the number of individual layers, their properties and their positions in the laminate, so that the calculation of a shear correction factor must be carried out again for each new laminate.

There is a wealth of further literature on the determination of shear correction factors for composite laminates. We will not go into this topic further here, so interested readers are referred to the selected publications by Whitney and Pagano (1970), Chow (1971), Whitney (1973), Rohwer (1988), Laitinen et al. (1995), Rolfes and Rohwer (1997) or Altenbach (2000a, b).

11.3.5 Selected Solutions for Boundary Value Problems of Static Laminate Problems

In the following some solutions for boundary value problems of static laminate problems according to FSDT are presented. Even if the solutions presented are limited to quite simple geometries, they can be very valuable in practical applications, e.g. for the analysis of composite laminated components in aircraft construction, and are always preferable to extensive numerical analyses for reasons of computational efficiency.

For the sake of clarity, only the expressions used for the state variables u_0, v_0, w_0, ψ_x, ψ_y are shown below. The kinematic equations can then be used to calculate the strains of the laminate and, with the help of the constitutive relationships, the layerwise stresses.

11.3.5.1 Navier Solution for Cylindrical Bending of an Unsymmetric Laminate Strip

Consider a laminate with a purely orthotropic layup in which the laminate stiffness matrix is as follows:

$$\begin{bmatrix} \underline{\underline{A}} & \underline{\underline{B}} & \underline{\underline{0}} \\ \underline{\underline{B}} & \underline{\underline{D}} & \underline{\underline{0}} \\ \underline{\underline{0}} & \underline{\underline{0}} & \underline{\underline{A}}_S \end{bmatrix} = \begin{bmatrix} A_{11} & A_{12} & 0 & B_{11} & B_{12} & 0 & 0 & 0 \\ A_{12} & A_{22} & 0 & B_{12} & B_{22} & 0 & 0 & 0 \\ 0 & 0 & A_{66} & 0 & 0 & B_{66} & 0 & 0 \\ B_{11} & B_{12} & 0 & D_{11} & D_{12} & 0 & 0 & 0 \\ B_{12} & B_{22} & 0 & D_{12} & D_{22} & 0 & 0 & 0 \\ 0 & 0 & B_{66} & 0 & 0 & D_{66} & 0 & 0 \\ 0 & 0 & 0 & 0 & 0 & 0 & KA_{44} & 0 \\ 0 & 0 & 0 & 0 & 0 & 0 & 0 & KA_{55} \end{bmatrix}. \tag{11.39}$$

Let the laminate be infinitely extended in the y-direction, so that a plate strip is considered (Fig. 11.3) in which all state variables are only functions of the longitudinal coordinate x and which will deform like a cylinder segment under a transverse load $p = p(x)$. With regard to the xz-plane, a plane strain state therefore prevails. The laminate is simply supported at the points $x = 0$ and $x = a$. The load consists of a sinusoidally distributed load $p(x) = p_0 \sin\left(\frac{m\pi x}{a}\right)$ with amplitude p_0. We can conclude from the above conditions:

$$v_0 = \psi_y = 0, \quad u_0 = u_0(x), \quad \psi_x = \psi_x(x), \quad w_0 = w_0(x). \tag{11.40}$$

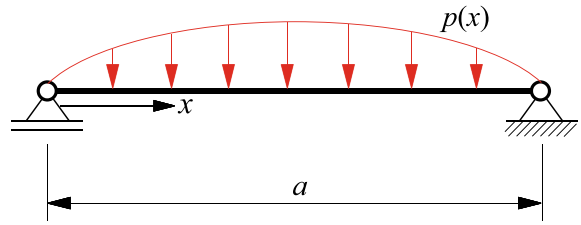


Fig. 11.3 Laminate under sinusoidal load $p(x)$, shown here for $m = 1$

The displacement differential equations (11.22) are then considerably simplified (whereby the second and fourth equations can be omitted), and it remains:

$$\begin{aligned} A_{11}\frac{\partial^2 u_0}{\partial x^2} + B_{11}\frac{\partial^2 \psi_x}{\partial x^2} &= 0, \\ B_{11}\frac{\partial^2 u_0}{\partial x^2} + D_{11}\frac{\partial^2 \psi_x}{\partial x^2} &= KA_{55}\left(\psi_x + \frac{\partial w_0}{\partial x}\right), \\ KA_{55}\left(\frac{\partial \psi_x}{\partial x} + \frac{\partial^2 w_0}{\partial x^2}\right) + p &= 0. \end{aligned} \tag{11.41}$$

The boundary conditions at the edges $x = 0$ and $x = a$ can be formulated as:

$$\begin{aligned} N^0_{xx} &= A_{11}\frac{\partial u_0}{\partial x} + B_{11}\frac{\partial \psi_x}{\partial x} = 0, \\ M^0_{xx} &= B_{11}\frac{\partial u_0}{\partial x} + D_{11}\frac{\partial \psi_x}{\partial x} = 0, \\ w_0 &= 0. \end{aligned} \tag{11.42}$$

It can be shown that the approaches

$$\begin{aligned} u_0 &= A_m\left[\cos\left(\frac{m\pi x}{a}\right) + 1\right], \\ \psi_x &= B_m \cos\left(\frac{m\pi x}{a}\right), \\ w_0 &= C_m \sin\left(\frac{m\pi x}{a}\right) \end{aligned} \tag{11.43}$$

for the state variables u_0, w_0, ψ_x fulfil both the differential equations (11.41) and the boundary conditions (11.42) identically and thus represent the exact solution for the problem currently under consideration if the constants A_m, B_m, C_m are chosen as follows:

$$A_m = \frac{B_{11}a^3 p_0}{m^3\pi^3\left(A_{11}D_{11} - B_{11}^2\right)},$$
$$B_m = -\frac{A_{11}a^3 p_0}{m^3\pi^3\left(A_{11}D_{11} - B_{11}^2\right)},$$
$$C_m = \frac{p_0 a^2}{m^2\pi^2}\left[\frac{A_{11}a^2}{m^2\pi^2\left(A_{11}D_{11} - B_{11}^2\right)} + \frac{1}{KA_{55}}\right]. \tag{11.44}$$

This allows, for example, the maximum deflection $w_{0,\max}$ of the laminate at the point $x = \frac{a}{2}$ to be analyzed in more detail, which can be calculated as follows for $m = 1$:

$$w_{0,\max} = \frac{p_0 a^4}{D_{11}\pi^4}\left(1 + \frac{B_{11}^2}{A_{11}D_{11} - B_{11}^2} + \frac{D_{11}\pi^2}{KA_{55}a^2}\right). \tag{11.45}$$

While the first two terms represent the solution according to CLPT, the third term represents the part due to transverse shear. For thick panels (e.g. $\frac{a}{h} < 10$) with corresponding transverse 'shear compliances', this can have serious effects on the deformation behaviour of laminates.

11.3.5.2 Bending of Symmetric Laminate Beams

We consider a laminated beam that has a symmetric layup. In this case, only the following terms need to be considered for pure bending in the constitutive law:

$$\begin{pmatrix} M_{xx}^0 \\ M_{yy}^0 \\ M_{xy}^0 \\ Q_y \\ Q_x \end{pmatrix} = \begin{bmatrix} D_{11} & D_{12} & D_{16} & 0 & 0 \\ D_{12} & D_{22} & D_{26} & 0 & 0 \\ D_{16} & D_{26} & D_{66} & 0 & 0 \\ 0 & 0 & 0 & KA_{44} & KA_{45} \\ 0 & 0 & 0 & KA_{45} & KA_{55} \end{bmatrix} \begin{pmatrix} \frac{\partial \psi_x}{\partial x} \\ \frac{\partial \psi_y}{\partial y} \\ \frac{\partial \psi_x}{\partial y} + \frac{\partial \psi_y}{\partial x} \\ \frac{\partial w_0}{\partial y} + \psi_y \\ \frac{\partial w_0}{\partial x} + \psi_x \end{pmatrix}. \tag{11.46}$$

In inverted form we obtain:

$$\begin{pmatrix} \frac{\partial \psi_x}{\partial x} \\ \frac{\partial \psi_y}{\partial y} \\ \frac{\partial \psi_x}{\partial y} + \frac{\partial \psi_y}{\partial x} \\ \frac{\partial w_0}{\partial y} + \psi_y \\ \frac{\partial w_0}{\partial x} + \psi_x \end{pmatrix} = \begin{bmatrix} \bar{D}_{11} & \bar{D}_{12} & \bar{D}_{16} & 0 & 0 \\ \bar{D}_{12} & \bar{D}_{22} & \bar{D}_{26} & 0 & 0 \\ \bar{D}_{16} & \bar{D}_{26} & \bar{D}_{66} & 0 & 0 \\ 0 & 0 & 0 & \frac{1}{K}\bar{A}_{44} & \frac{1}{K}\bar{A}_{45} \\ 0 & 0 & 0 & \frac{1}{K}\bar{A}_{45} & \frac{1}{K}\bar{A}_{55} \end{bmatrix} \begin{pmatrix} M_{xx}^0 \\ M_{yy}^0 \\ M_{xy}^0 \\ Q_y \\ Q_x \end{pmatrix}. \tag{11.47}$$

Quantities with a horizontal bar are inverted quantities, i.e. the inverse plate stiffnesses and transverse shear stiffnesses. Both the two moment flows M_{yy}^0 and M_{xy}^0 as well as the

shear force flow Q_y and the bending angle ψ_y are identical to zero for the present case, i.e.: $M^0_{yy} = M^0_{xy} = 0$, $Q_y = 0$, $\psi_y = 0$. We also assume that both the deflection w_0 of the beam and the bending angle ψ_x are exclusively functions of the longitudinal coordinate x of the beam, i.e. $w_0 = w_0(x)$, $\psi_x = \psi_x(x)$. Similarly, the load $p = p(x)$ is only a function of the coordinate x. If we are dealing with the case of pure bending with a symmetric layup, then the two displacements u_0 and v_0 of the laminate middle plane become zero, so that $u_0 = 0$, $v_0 = 0$. The displacement field of the laminate beam is therefore as follows:

$$u(x, z) = z\psi_x(x), \quad w(x, y) = w_0(x). \tag{11.48}$$

The strain field reads:

$$\varepsilon_{xx} = z\frac{\mathrm{d}\psi_x}{\mathrm{d}x}, \quad \gamma_{xz} = \frac{\mathrm{d}w_0}{\mathrm{d}x} + \psi_x. \tag{11.49}$$

By means of (11.47) it follows with $M^0_{yy} = M^0_{xy} = 0$:

$$\frac{\mathrm{d}\psi_x}{\mathrm{d}x} = \bar{D}_{11} M^0_{xx}, \quad \frac{\mathrm{d}w_0}{\mathrm{d}x} + \psi_x = \frac{1}{K}\bar{A}_{55} Q_x. \tag{11.50}$$

This can be written in terms of bending moment and transverse shear force $M(x) = M^0_{xx} b$ and $Q(x) = Q_x b$ in relation to the width b of the bar:

$$EI\frac{\mathrm{d}\psi_x}{\mathrm{d}x} = M, \quad KGA\left(\frac{\mathrm{d}w_0}{\mathrm{d}x} + \psi_x\right) = Q, \tag{11.51}$$

where $E = E^B_{xx} = \frac{12}{\bar{D}_{11} h^3}$ is the modulus of elasticity of the laminate with respect to bending about the y-axis. The quantity $I = I_{yy}$ is the corresponding moment of inertia of the beam cross-section. The expression G is the shear modulus G^B_{xz} of the laminate with $G^B_{xz} = \frac{1}{\bar{A}_{55} h}$. The cross-sectional area of the beam A is $A = bh$.

From equilibrium considerations, we conclude $\frac{dQ}{\mathrm{d}x} = -\bar{p}$, where $\bar{p}$ represents the line load on the beam. From the second equation in (11.51) then follows with $\bar{p} = pb$:

$$KGA\left(\frac{\mathrm{d}^2 w_0}{\mathrm{d}x^2} + \frac{\mathrm{d}\psi_x}{\mathrm{d}x}\right) = -\bar{p}. \tag{11.52}$$

Furthermore, $\frac{dM}{\mathrm{d}x} = Q$, so that:

$$EI\frac{\mathrm{d}^2\psi_x}{\mathrm{d}x^2} = Q, \tag{11.53}$$

or

$$EI\frac{\mathrm{d}^2\psi_x}{\mathrm{d}x^2} - KGA\left(\frac{\mathrm{d}w_0}{\mathrm{d}x} + \psi_x\right) = 0. \tag{11.54}$$

Integration of (11.52) leads to:

$$KGA\left(\frac{\mathrm{d}w_0}{\mathrm{d}x}+\psi_x\right)=-\int \bar{p}\mathrm{d}x+C_1, \tag{11.55}$$

where C_1 is an integration constant. Insertion into (11.54) results in:

$$EI\frac{\mathrm{d}^2\psi_x}{\mathrm{d}x^2}=-\int \bar{p}\mathrm{d}x+C_1. \tag{11.56}$$

We perform a double integration of this expression, which leads to ψ_x as follows:

$$\begin{aligned} EI\frac{\mathrm{d}\psi_x}{\mathrm{d}x} &= -\int\int \bar{p}\mathrm{d}x\mathrm{d}x+C_1x+C_2,\\ EI\psi_x &= -\int\int\int \bar{p}\mathrm{d}x\mathrm{d}x\mathrm{d}x+\frac{1}{2}C_1x^2+C_2x+C_3. \end{aligned} \tag{11.57}$$

Here, C_2 and C_3 are two further integration constants.
The expression (11.55) can be converted to $\frac{\mathrm{d}w_0}{\mathrm{d}x}$:

$$\frac{\mathrm{d}w_0}{\mathrm{d}x}=\frac{1}{KGA}\left(-\int q_z\mathrm{d}x+C_1\right)-\psi_x. \tag{11.58}$$

Inserting into the second equation of (11.57) results in:

$$\begin{aligned} \frac{\mathrm{d}w_0}{\mathrm{d}x} &= \frac{1}{KGA}\left(-\int \bar{p}\mathrm{d}x+C_1\right)\\ &\quad -\frac{1}{EI}\left(-\int\int\int \bar{p}\mathrm{d}x\mathrm{d}x\mathrm{d}x+\frac{1}{2}C_1x^2+C_2x+C_3\right). \end{aligned} \tag{11.59}$$

If a further integration is carried out here with regard to x, this results in the deflection of the laminate beam:

$$\begin{aligned} w_0 &= \frac{1}{KGA}\left(-\int\int \bar{p}\mathrm{d}x\mathrm{d}x+C_1x\right)\\ &\quad -\frac{1}{EI}\left(-\int\int\int\int \bar{p}\mathrm{d}x\mathrm{d}x\mathrm{d}x\mathrm{d}x+\frac{1}{6}C_1x^3+\frac{1}{2}C_2x^2+C_3x+C_4\right). \end{aligned} \tag{11.60}$$

The integration constants C_1, C_2, C_3, C_4 are adapted to the boundary conditions of the laminate beam. If the beam deflection $w(x)$ is available, the bending angle ψ_x can also be determined from (11.57).

A closer look at (11.60) shows that the deflection w_0 can be broken down into two parts, namely the expression that also results from CLPT and a second term that represents the shear deformation of the beam. If the beam is made of a material with sufficient shear stiffness, this second term tends to zero.

The intralaminar stresses $\sigma_{xx,k}$, $\sigma_{yy,k}$ and $\tau_{xy,k}$ in each layer k of the laminate beam under consideration can be determined from Hooke's law for the individual layer. The interlaminar shear stresses $\tau_{xz,k}$ and $\tau_{yz,k}$ can then be determined in a post-calculation using the local three-dimensional equilibrium. The stress determination is not discussed further here.

11.3.5.3 Navier Solution for the Bending of an Unsymmetric Cross-Ply Laminate

The consideration is now to be extended to an unsymmetric laminate with finite dimensions under biaxial bending. The laminate is rectangular with length a and width b. As before, the laminate stiffnesses are limited by $A_{16} = A_{26} = B_{16} = B_{26} = D_{16} = D_{26} = A_{45} = 0$. The load consists of an arbitrarily distributed surface load $p(x, y)$ and can be developed in the form of a Fourier series:

$$p = \sum_{m=1}^{m=\infty} \sum_{n=1}^{n=\infty} P_{mn} \sin\left(\frac{m\pi x}{a}\right) \sin\left(\frac{n\pi y}{b}\right), \tag{11.61}$$

where the coefficients P_{mn} can be calculated as:

$$P_{mn} = \frac{4}{ab} \int_0^b \int_0^a p\,(x, y) \sin\left(\frac{m\pi x}{a}\right) \sin\left(\frac{n\pi y}{b}\right) \mathrm{d}x\mathrm{d}y. \tag{11.62}$$

The following boundary conditions (so-called SS1 boundary conditions) apply:

$$\begin{array}{llll} u_0\,(y=0)=0, & u_0\,(y=b)=0, & v_0\,(x=0)=0, & v_0\,(x=a)=0, \\ w_0\,(x=0)=0, & w_0\,(x=a)=0, & w_0\,(y=0)=0, & w_0\,(y=b)=0, \\ \psi_x\,(y=0)=0, & \psi_x\,(y=b)=0, & \psi_y\,(x=0)=0, & \psi_y\,(x=a)=0, \\ N^0_{xx}\,(x=0)=0, & N^0_{xx}\,(x=a)=0, & N^0_{yy}\,(y=0)=0, & N^0_{yy}\,(y=b)=0, \\ M^0_{xx}\,(x=0)=0, & M^0_{xx}\,(x=a)=0, & M^0_{yy}\,(y=0)=0, & M^0_{yy}\,(y=b)=0. \end{array} \tag{11.63}$$

The boundary conditions (11.63) are then fulfilled by the following series developments for the state variables u_0, v_0, w_0, ψ_x, ψ_y:

$$
\begin{aligned}
u_0 &= \sum_{m=1}^{m=\infty}\sum_{n=1}^{n=\infty} U_{mn}\cos\left(\frac{m\pi x}{a}\right)\sin\left(\frac{n\pi y}{b}\right),\\
v_0 &= \sum_{m=1}^{m=\infty}\sum_{n=1}^{n=\infty} V_{mn}\sin\left(\frac{m\pi x}{a}\right)\cos\left(\frac{n\pi y}{b}\right),\\
w_0 &= \sum_{m=1}^{m=\infty}\sum_{n=1}^{n=\infty} W_{mn}\sin\left(\frac{m\pi x}{a}\right)\sin\left(\frac{n\pi y}{b}\right),\\
\psi_x &= \sum_{m=1}^{m=\infty}\sum_{n=1}^{n=\infty} X_{mn}\cos\left(\frac{m\pi x}{a}\right)\sin\left(\frac{n\pi y}{b}\right),\\
\psi_y &= \sum_{m=1}^{m=\infty}\sum_{n=1}^{n=\infty} Y_{mn}\sin\left(\frac{m\pi x}{a}\right)\cos\left(\frac{n\pi y}{b}\right).
\end{aligned}
\tag{11.64}
$$

The coefficients U_{mn}, V_{mn}, W_{mn}, X_{mn}, Y_{mn} can then be determined from the resulting system of linear equations after inserting (11.64) into the system of differential equations (11.22):

$$
\begin{bmatrix}
\lambda_{11} & \lambda_{12} & 0 & \lambda_{14} & \lambda_{15}\\
\lambda_{12} & \lambda_{22} & 0 & \lambda_{24} & \lambda_{25}\\
0 & 0 & \lambda_{33} & \lambda_{34} & \lambda_{35}\\
\lambda_{14} & \lambda_{24} & \lambda_{34} & \lambda_{44} & \lambda_{45}\\
\lambda_{15} & \lambda_{25} & \lambda_{35} & \lambda_{45} & \lambda_{55}
\end{bmatrix}
\begin{pmatrix} U_{mn}\\ V_{mn}\\ W_{mn}\\ X_{mn}\\ Y_{mn}\end{pmatrix}
=
\begin{pmatrix} 0\\ 0\\ P_{mn}\\ 0\\ 0\end{pmatrix},
\tag{11.65}
$$

where:

$$
\begin{aligned}
\lambda_{11} &= A_{11}\left(\frac{m\pi}{a}\right)^2 + A_{66}\left(\frac{n\pi}{b}\right)^2, \quad \lambda_{12} = (A_{12}+A_{66})\frac{m\pi}{a}\frac{n\pi}{b},\\
\lambda_{14} &= B_{11}\left(\frac{m\pi}{a}\right)^2 + B_{66}\left(\frac{n\pi}{b}\right)^2, \quad \lambda_{15} = (B_{12}+B_{66})\frac{m\pi}{a}\frac{n\pi}{b},\\
\lambda_{22} &= A_{66}\left(\frac{m\pi}{a}\right)^2 + A_{22}\left(\frac{n\pi}{b}\right)^2, \quad \lambda_{24} = (B_{12}+B_{66})\frac{m\pi}{a}\frac{n\pi}{b},\\
\lambda_{25} &= B_{66}\left(\frac{m\pi}{a}\right)^2 + B_{22}\left(\frac{n\pi}{b}\right)^2, \quad \lambda_{33} = K\left[A_{55}\left(\frac{m\pi}{a}\right)^2 + A_{44}\left(\frac{n\pi}{b}\right)^2\right],\\
\lambda_{34} &= KA_{55}\frac{m\pi}{a}, \quad \lambda_{35} = KA_{44}\frac{n\pi}{b},\\
\lambda_{44} &= D_{11}\left(\frac{m\pi}{a}\right)^2 + D_{66}\left(\frac{n\pi}{b}\right)^2 + KA_{55}, \quad \lambda_{45} = (D_{12}+D_{66})\frac{m\pi}{a}\frac{n\pi}{b},\\
\lambda_{55} &= D_{66}\left(\frac{m\pi}{a}\right)^2 + D_{22}\left(\frac{n\pi}{b}\right)^2 + KA_{44}.
\end{aligned}
\tag{11.66}
$$

Solving the system of linear equations (11.65) with (11.66) for each $m, n = 1, 2, 3, \ldots$ leads to the desired coefficients U_{mn}, V_{mn}, W_{mn}, X_{mn}, Y_{mn}, with which the state variables u_0, v_0, w_0, ψ_x, ψ_y are completely determined. The strains and stresses in the laminate can then be calculated from this.

11.3.5.4 Navier Solution for the Bending of a Symmetric Cross-Ply Composite

In the case of a symmetric cross-ply laminate, the bending problem is considerably simplified because the plate behaviour of the laminate is completely decoupled from the disk behaviour. It is therefore sufficient to make only an approach for the deflection w_0 and the two bending angles ψ_x and ψ_y, which may be of the form (11.64):

$$\begin{aligned} w_0 &= \sum_{m=1}^{m=\infty} \sum_{n=1}^{n=\infty} W_{mn} \sin\left(\frac{m\pi x}{a}\right) \sin\left(\frac{n\pi y}{b}\right), \\ \psi_x &= \sum_{m=1}^{m=\infty} \sum_{n=1}^{n=\infty} X_{mn} \cos\left(\frac{m\pi x}{a}\right) \sin\left(\frac{n\pi y}{b}\right), \\ \psi_y &= \sum_{m=1}^{m=\infty} \sum_{n=1}^{n=\infty} Y_{mn} \sin\left(\frac{m\pi x}{a}\right) \cos\left(\frac{n\pi y}{b}\right). \end{aligned} \tag{11.67}$$

The system of equations (11.65) is then reduced to the following form:

$$\begin{bmatrix} \lambda_{33} & \lambda_{34} & \lambda_{35} \\ \lambda_{34} & \lambda_{44} & \lambda_{45} \\ \lambda_{35} & \lambda_{45} & \lambda_{55} \end{bmatrix} \begin{pmatrix} W_{mn} \\ X_{mn} \\ Y_{mn} \end{pmatrix} = \begin{pmatrix} P_{mn} \\ 0 \\ 0 \end{pmatrix}, \tag{11.68}$$

whereby the abbreviations used herein are to be used in accordance with (11.66). This system of equations can then be easily solved for the required coefficients W_{mn}, X_{mn}, Y_{mn}.

11.3.5.5 Navier Solution for the Bending of an Unsymmetric Angle-Ply Laminate

The bending problem of an unsymmetric angle-ply laminate loaded by a surface load $p(x, y)$ is now to be considered. The boundary conditions considered here (so-called SS2 boundary conditions) are as follows:

$$\begin{array}{llll} u_0\,(x=0)=0, & u_0\,(x=a)=0, & v_0\,(y=0)=0, & v_0\,(y=b)=0, \\ w_0\,(x=0)=0, & w_0\,(x=a)=0, & w_0\,(y=0)=0, & w_0\,(y=b)=0, \\ \psi_x\,(y=0)=0, & \psi_x\,(y=b)=0, & \psi_y\,(x=0)=0, & \psi_y\,(x=a)=0, \\ N^0_{xy}\,(x=0)=0, & N^0_{xy}\,(x=a)=0, & N^0_{xy}\,(y=0)=0, & N^0_{xy}\,(y=b)=0, \\ M^0_{xx}\,(x=0)=0, & M^0_{xx}\,(x=a)=0, & M^0_{yy}\,(y=0)=0, & M^0_{yy}\,(y=b)=0. \end{array} \tag{11.69}$$

The stiffness properties of the laminate are such that the laminate stiffness matrix takes on the following form:

$$\begin{bmatrix} \underline{\underline{A}} & \underline{\underline{B}} & \underline{\underline{0}} \\ \underline{\underline{B}} & \underline{\underline{D}} & \underline{\underline{0}} \\ \underline{\underline{0}} & \underline{\underline{0}} & \underline{\underline{A}}_S \end{bmatrix} = \begin{bmatrix} A_{11} & A_{12} & 0 & 0 & 0 & B_{16} & 0 & 0 \\ A_{12} & A_{22} & 0 & 0 & 0 & B_{26} & 0 & 0 \\ 0 & 0 & A_{66} & B_{16} & B_{26} & 0 & 0 & 0 \\ 0 & 0 & B_{16} & D_{11} & D_{12} & 0 & 0 & 0 \\ 0 & 0 & B_{26} & D_{12} & D_{22} & 0 & 0 & 0 \\ B_{16} & B_{26} & 0 & 0 & 0 & D_{66} & 0 & 0 \\ 0 & 0 & 0 & 0 & 0 & 0 & KA_{44} & 0 \\ 0 & 0 & 0 & 0 & 0 & 0 & 0 & KA_{55} \end{bmatrix}. \tag{11.70}$$

The boundary conditions (11.69) are fulfilled by the following series expansions for the state variables u_0, v_0, w_0, ψ_x, ψ_y:

$$\begin{aligned} u_0 &= \sum_{m=1}^{m=\infty} \sum_{n=1}^{n=\infty} U_{mn} \sin\left(\frac{m\pi x}{a}\right) \cos\left(\frac{n\pi y}{b}\right), \\ v_0 &= \sum_{m=1}^{m=\infty} \sum_{n=1}^{n=\infty} V_{mn} \cos\left(\frac{m\pi x}{a}\right) \sin\left(\frac{n\pi y}{b}\right), \\ w_0 &= \sum_{m=1}^{m=\infty} \sum_{n=1}^{n=\infty} W_{mn} \sin\left(\frac{m\pi x}{a}\right) \sin\left(\frac{n\pi y}{b}\right), \\ \psi_x &= \sum_{m=1}^{m=\infty} \sum_{n=1}^{n=\infty} X_{mn} \cos\left(\frac{m\pi x}{a}\right) \sin\left(\frac{n\pi y}{b}\right), \\ \psi_y &= \sum_{m=1}^{m=\infty} \sum_{n=1}^{n=\infty} Y_{mn} \sin\left(\frac{m\pi x}{a}\right) \cos\left(\frac{n\pi y}{b}\right). \end{aligned} \tag{11.71}$$

The coefficients U_{mn}, V_{mn}, W_{mn}, X_{mn}, Y_{mn} can then be determined from the following system of equations:

$$\begin{bmatrix} \lambda_{11} & \lambda_{12} & 0 & \lambda_{14} & \lambda_{15} \\ \lambda_{12} & \lambda_{22} & 0 & \lambda_{24} & \lambda_{25} \\ 0 & 0 & \lambda_{33} & \lambda_{34} & \lambda_{35} \\ \lambda_{14} & \lambda_{24} & \lambda_{34} & \lambda_{44} & \lambda_{45} \\ \lambda_{15} & \lambda_{25} & \lambda_{35} & \lambda_{45} & \lambda_{55} \end{bmatrix} \begin{pmatrix} U_{mn} \\ V_{mn} \\ W_{mn} \\ X_{mn} \\ Y_{mn} \end{pmatrix} = \begin{pmatrix} 0 \\ 0 \\ P_{mn} \\ 0 \\ 0 \end{pmatrix}, \tag{11.72}$$

where:

$$\lambda_{11} = A_{11}\left(\frac{m\pi}{a}\right)^2 + A_{66}\left(\frac{n\pi}{b}\right)^2, \quad \lambda_{12} = (A_{12} + A_{66})\frac{m\pi}{a}\frac{n\pi}{b},$$
$$\lambda_{14} = 2B_{16}\frac{m\pi}{a}\frac{n\pi}{b}, \quad \lambda_{15} = B_{16}\left(\frac{m\pi}{a}\right)^2 + B_{26}\left(\frac{n\pi}{b}\right)^2,$$
$$\lambda_{22} = A_{66}\left(\frac{m\pi}{a}\right)^2 + A_{22}\left(\frac{n\pi}{b}\right)^2, \quad \lambda_{24} = B_{16}\left(\frac{m\pi}{a}\right)^2 + B_{26}\left(\frac{n\pi}{b}\right)^2,$$
$$\lambda_{25} = 2B_{26}\frac{m\pi}{a}\frac{n\pi}{b}, \quad \lambda_{33} = K\left[A_{55}\left(\frac{m\pi}{a}\right)^2 + A_{44}\left(\frac{n\pi}{b}\right)^2\right],$$
$$\lambda_{34} = KA_{55}\frac{m\pi}{a}, \quad \lambda_{35} = KA_{44}\frac{n\pi}{b},$$
$$\lambda_{44} = D_{11}\left(\frac{m\pi}{a}\right)^2 + D_{66}\left(\frac{n\pi}{b}\right)^2 + KA_{55},$$
$$\lambda_{45} = (D_{12} + D_{66})\frac{m\pi}{a}\frac{n\pi}{b},$$
$$\lambda_{55} = D_{66}\left(\frac{m\pi}{a}\right)^2 + D_{22}\left(\frac{n\pi}{b}\right)^2 + KA_{44}. \tag{11.73}$$

11.3.5.6 Lévy Solutions

Besides the Navier solutions shown for special bending problems of laminates according to FSDT, one can also derive so-called Lévy solutions for rectangular laminates. These are based on assuming boundary conditions for simply supported edges at two opposite edges of the laminate (such as the two edges at $y = 0$ and $y = b$, which run parallel to the x-axis) (whereby either the SS1 or SS2 conditions can be considered here depending on the layup of the laminate), while the two remaining edges can have any combination of boundary conditions (hinged, fixed, elastically restrained, free). Since an exact solution is known for the SS1 or SS2 conditions (see the previous sections), the system of partial differential equations (11.22) can be converted into a system of ordinary differential equations for which analytical solutions can be found. We will not go into this topic further at this point. Interested readers are referred to Reddy (2004), for example, where a wealth of further explanations and references to literature on this topic can be found.

11.3.6 The Ritz Method

In principle, all common approximation methods of mechanics can be used to solve general static laminate problems according to FSDT. In addition to classical methods limited to simple geometries, such as the Ritz method or the Galerkin method, the Finite Element Method should be mentioned here in particular, for which there is also a wealth of investigations for laminate problems according to FSDT. However, since the Ritz method is still very popular in the aerospace industry, its application to static problems will be briefly outlined. Again, a laminate with a rectangular form is given. At present, no restrictions are imposed with

regard to the constitutive law (11.17), so that all stiffness components may occur. The Ritz method is based on an approximation approach of the form

$$\begin{aligned}
u_0 &= \sum_{m=1}^{m=M_u} \sum_{n=1}^{n=N_u} U_{mn} U_{xm}(x)\, U_{yn}(y), \\
v_0 &= \sum_{m=1}^{m=M_v} \sum_{n=1}^{n=N_v} V_{mn} V_{xm}(x)\, V_{yn}(y), \\
w_0 &= \sum_{m=1}^{m=M_w} \sum_{n=1}^{n=N_w} W_{mn} W_{xm}(x)\, W_{yn}(y), \\
\psi_x &= \sum_{m=1}^{m=M_x} \sum_{n=1}^{n=N_x} X_{mn} X_{xm}(x)\, X_{yn}(y), \\
\psi_y &= \sum_{m=1}^{m=M_y} \sum_{n=1}^{n=N_y} Y_{mn} Y_{xm}(x)\, Y_{yn}(y)
\end{aligned} \tag{11.74}$$

where for the shape functions $U_{xm}(x)$, $U_{yn}(y)$, $V_{xm}(x)$, $V_{yn}(y)$, $W_{xm}(x)$, $W_{yn}(y)$, $X_{xm}(x)$, $X_{yn}(y)$, $Y_{xm}(x)$, $Y_{yn}(y)$ the requirement is made that they must fulfil all underlying geometric boundary conditions.

The Ritz method requires—assuming linear-elastic material behaviour—a minimum of the total elastic potential. While the inner potential Π_i has already been determined with (11.29), the external potential Π_a is in the case of a surface load $p(x, y)$:

$$\Pi_a = -\int_0^b \int_0^a p(x, y) w(x, y) \mathrm{d}x \mathrm{d}y. \tag{11.75}$$

The total potential Π then results from the sum of Π_i and Π_a:

$$\Pi = \Pi_i + \Pi_a = \text{Minimum}. \tag{11.76}$$

Using the approach (11.74), the potential Π takes the form

$$\Pi = \Pi\left(U_{mn}, V_{mn}, W_{mn}, X_{mn}, Y_{mn}\right), \tag{11.77}$$

so that the minimum requirement (11.76) can be expressed by the Ritz equations:

$$\frac{\partial \Pi}{\partial U_{mn}} = 0, \quad \frac{\partial \Pi}{\partial V_{mn}} = 0, \quad \frac{\partial \Pi}{\partial W_{mn}} = 0, \quad \frac{\partial \Pi}{\partial X_{mn}} = 0, \quad \frac{\partial \Pi}{\partial Y_{mn}} = 0. \tag{11.78}$$

If the partial derivatives of the total potential Π prescribed by (11.78) are analyzed, for a geometrically linear problem, we obtain a system of $M_u \cdot N_u + M_v \cdot N_v + M_w \cdot N_w + M_x \cdot N_x + M_y \cdot N_y$ linear equations for as many unknown initial coefficients U_{mn}, V_{mn},

W_{mn}, X_{mn}, Y_{mn}. The Ritz approach is then completely determined and approximate strains and approximate stresses can be calculated from this. The dynamic boundary conditions of the problem under consideration are then automatically fulfilled better and better with increasing quality of the approaches or with increasing degrees of series expansion due to the employed variation principle.

We now consider a symmetric, but otherwise completely arbitrary laminate, for which the constitutive law is as follows:

$$\begin{pmatrix} N^0_{xx} \\ N^0_{yy} \\ N^0_{xy} \\ M^0_{xx} \\ M^0_{yy} \\ M^0_{xy} \\ Q_y \\ Q_x \end{pmatrix} = \begin{bmatrix} A_{11} & A_{12} & A_{16} & 0 & 0 & 0 & 0 & 0 \\ A_{12} & A_{22} & A_{26} & 0 & 0 & 0 & 0 & 0 \\ A_{16} & A_{26} & A_{66} & 0 & 0 & 0 & 0 & 0 \\ 0 & 0 & 0 & D_{11} & D_{12} & D_{16} & 0 & 0 \\ 0 & 0 & 0 & D_{12} & D_{22} & D_{26} & 0 & 0 \\ 0 & 0 & 0 & D_{16} & D_{26} & D_{66} & 0 & 0 \\ 0 & 0 & 0 & 0 & 0 & 0 & KA_{44} & KA_{45} \\ 0 & 0 & 0 & 0 & 0 & 0 & KA_{45} & KA_{55} \end{bmatrix} \begin{pmatrix} \frac{\partial u_0}{\partial x} \\ \frac{\partial v_0}{\partial y} \\ \frac{\partial u_0}{\partial y} + \frac{\partial v_0}{\partial x} \\ \frac{\partial \psi_x}{\partial x} \\ \frac{\partial \psi_y}{\partial y} \\ \frac{\partial \psi_x}{\partial y} + \frac{\partial \psi_y}{\partial x} \\ \frac{\partial w_0}{\partial y} + \psi_y \\ \frac{\partial w_0}{\partial x} + \psi_x \end{pmatrix}. \tag{11.79}$$

The inner potential then results as:

$$\begin{aligned} \Pi_i = \frac{1}{2} \int_0^b \int_0^a \Bigg\{ & D_{11} \left(\frac{\partial \psi_x}{\partial x} \right)^2 + 2D_{12} \frac{\partial \psi_x}{\partial x} \frac{\partial \psi_y}{\partial y} + D_{22} \left(\frac{\partial \psi_y}{\partial y} \right)^2 + D_{66} \left(\frac{\partial \psi_x}{\partial y} + \frac{\partial \psi_y}{\partial x} \right)^2 \\ & + 2D_{16} \frac{\partial \psi_x}{\partial x} \left(\frac{\partial \psi_x}{\partial y} + \frac{\partial \psi_y}{\partial x} \right) + 2D_{26} \frac{\partial \psi_y}{\partial y} \left(\frac{\partial \psi_x}{\partial y} + \frac{\partial \psi_y}{\partial x} \right) + KA_{44} \left(\frac{\partial w_0}{\partial y} + \psi_y \right)^2 \\ & + 2KA_{45} \left(\frac{\partial w_0}{\partial x} + \psi_x \right) \left(\frac{\partial w_0}{\partial y} + \psi_y \right) + KA_{55} \left(\frac{\partial w_0}{\partial x} + \psi_x \right)^2 \Bigg\} \, \mathrm{d}x \mathrm{d}y. \end{aligned} \tag{11.80}$$

Due to the symmetry of the laminate, the disk and plate behaviour are decoupled from each other, so that the inplane displacements u_0 and v_0 under the given load case $p = p(x, y)$ are not included in the calculation.

The following approaches are used for the deflection w_0 and the bending angles ψ_x and ψ_y:

$$
\begin{aligned}
w_0 &= \sum_{m=1}^{m=M}\sum_{n=1}^{n=N} W_{mn} w_{1\,m}(x)\, w_{2n}(y)\,, \\
\psi_x &= \sum_{m=1}^{m=K}\sum_{n=1}^{n=L} X_{mn} \psi_{x1m}(x)\, \psi_{x2n}(y)\,, \\
\psi_y &= \sum_{m=1}^{m=I}\sum_{n=1}^{n=J} Y_{mn} \psi_{y1m}(x)\, \psi_{y2n}(y)\,.
\end{aligned} \tag{11.81}
$$

If we insert (11.81) into (11.80), then we obtain the inner potential Π_i:

$$
\begin{aligned}
\Pi_i = {} & \frac{1}{2} D_{11} \sum_{m=1}^{m=K}\sum_{n=1}^{n=L}\sum_{p=1}^{p=K}\sum_{q=1}^{q=L} X_{mn} X_{pq} \int_0^a \frac{\mathrm{d}\psi_{x1m}}{\mathrm{d}x}\frac{\mathrm{d}\psi_{x1p}}{\mathrm{d}x}\mathrm{d}x \int_0^b \psi_{x2n}\psi_{x2q}\mathrm{d}y \\
& + \frac{1}{2} D_{22} \sum_{m=1}^{m=I}\sum_{n=1}^{n=J}\sum_{p=1}^{p=I}\sum_{q=1}^{q=J} Y_{mn} Y_{pq} \int_0^a \psi_{y1m}\psi_{y1p}\mathrm{d}x \int_0^b \frac{\mathrm{d}\psi_{y2n}}{\mathrm{d}y}\frac{\mathrm{d}\psi_{y2q}}{\mathrm{d}y}\mathrm{d}y \\
& + D_{12} \sum_{m=1}^{m=K}\sum_{n=1}^{n=L}\sum_{p=1}^{p=I}\sum_{q=1}^{q=J} X_{mn} Y_{pq} \int_0^a \frac{\mathrm{d}\psi_{x1m}}{\mathrm{d}x}\psi_{y1p}\mathrm{d}x \int_0^b \frac{\mathrm{d}\psi_{y2q}}{\mathrm{d}y}\psi_{x2n}\mathrm{d}y \\
& + D_{16}\left[\sum_{m=1}^{m=K}\sum_{n=1}^{n=L}\sum_{p=1}^{p=K}\sum_{q=1}^{q=L} X_{mn} X_{pq} \int_0^a \frac{\mathrm{d}\psi_{x1m}}{\mathrm{d}x}\psi_{x1p}\mathrm{d}x \int_0^b \frac{\mathrm{d}\psi_{x2q}}{\mathrm{d}y}\psi_{x2n}\mathrm{d}y \right. \\
& \left. + \sum_{m=1}^{m=K}\sum_{n=1}^{n=L}\sum_{p=1}^{p=I}\sum_{q=1}^{q=J} X_{mn} Y_{pq} \int_0^a \frac{\mathrm{d}\psi_{x1m}}{\mathrm{d}x}\frac{\mathrm{d}\psi_{y1p}}{\mathrm{d}x}\mathrm{d}x \int_0^b \psi_{x2n}\psi_{y2q}\mathrm{d}y \right] \\
& + D_{26}\left[\sum_{m=1}^{m=K}\sum_{n=1}^{n=L}\sum_{p=1}^{p=I}\sum_{q=1}^{q=J} X_{mn} Y_{pq} \int_0^a \psi_{x1m}\psi_{y1p}\mathrm{d}x \int_0^b \frac{\mathrm{d}\psi_{x2n}}{\mathrm{d}y}\frac{\mathrm{d}\psi_{y2q}}{\mathrm{d}y}\mathrm{d}y \right. \\
& \left. + \sum_{m=1}^{m=I}\sum_{n=1}^{n=J}\sum_{p=1}^{p=I}\sum_{q=1}^{q=J} Y_{mn} Y_{pq} \int_0^a \frac{\mathrm{d}\psi_{y1m}}{\mathrm{d}x}\psi_{y1p}\mathrm{d}x \int_0^b \psi_{x2n}\frac{\mathrm{d}\psi_{y1q}}{\mathrm{d}y}\mathrm{d}y \right] \\
& + \frac{1}{2} D_{66}\left[\sum_{m=1}^{m=K}\sum_{n=1}^{n=L}\sum_{p=1}^{p=K}\sum_{q=1}^{q=L} X_{mn} X_{pq} \int_0^a \psi_{x1m}\psi_{x1p}\mathrm{d}x \int_0^b \frac{\mathrm{d}\psi_{x2n}}{\mathrm{d}y}\frac{\mathrm{d}\psi_{x2q}}{\mathrm{d}y}\mathrm{d}y \right. \\
& \left. + 2\sum_{m=1}^{m=K}\sum_{n=1}^{n=L}\sum_{p=1}^{p=I}\sum_{q=1}^{q=J} X_{mn} Y_{pq} \int_0^a \psi_{x1m}\frac{\mathrm{d}\psi_{y1p}}{\mathrm{d}x}\mathrm{d}x \int_0^b \frac{\mathrm{d}\psi_{x2n}}{\mathrm{d}y}\psi_{y2q}\mathrm{d}y \right.
\end{aligned}
$$

$$
\begin{aligned}
&+ \sum_{m=1}^{m=I}\sum_{n=1}^{n=J}\sum_{p=1}^{p=I}\sum_{q=1}^{q=J} Y_{mn}Y_{pq}\int_0^a \frac{\mathrm{d}\psi_{y1m}}{\mathrm{d}x}\frac{\mathrm{d}\psi_{y1p}}{\mathrm{d}x}\mathrm{d}x\int_0^b \psi_{y2n}\psi_{y2q}\mathrm{d}y\Bigg] \\
&+ \frac{1}{2}KA_{44}\Bigg[\sum_{m=1}^{m=M}\sum_{n=1}^{n=N}\sum_{p=1}^{p=M}\sum_{q=1}^{q=N} W_{mn}W_{pq}\int_0^a w_{1m}w_{1p}\mathrm{d}x\int_0^b \frac{\mathrm{d}w_{2n}}{\mathrm{d}y}\frac{\mathrm{d}w_{2q}}{\mathrm{d}y}\mathrm{d}y \\
&+ 2\sum_{m=1}^{m=M}\sum_{n=1}^{n=N}\sum_{p=1}^{p=I}\sum_{q=1}^{q=J} W_{mn}Y_{pq}\int_0^a w_{1m}\psi_{y1p}\mathrm{d}x\int_0^b \frac{\mathrm{d}w_{2n}}{\mathrm{d}y}\psi_{y2q}\mathrm{d}y \\
&+ \sum_{m=1}^{m=I}\sum_{n=1}^{n=J}\sum_{p=1}^{p=I}\sum_{q=1}^{q=J} Y_{mn}Y_{pq}\int_0^a \psi_{y1m}\psi_{y1p}\mathrm{d}x\int_0^b \psi_{y2n}\psi_{y2q}\mathrm{d}y\Bigg] \\
&+ KA_{45}\Bigg[\sum_{m=1}^{m=M}\sum_{n=1}^{n=N}\sum_{p=1}^{p=M}\sum_{q=1}^{q=N} W_{mn}W_{pq}\int_0^a \frac{\mathrm{d}w_{1m}}{\mathrm{d}x}w_{1p}\mathrm{d}x\int_0^b w_{2n}\frac{\mathrm{d}w_{2q}}{\mathrm{d}y}\mathrm{d}y \\
&+ \sum_{m=1}^{m=M}\sum_{n=1}^{n=N}\sum_{p=1}^{p=I}\sum_{q=1}^{q=J} W_{mn}Y_{pq}\int_0^a \frac{\mathrm{d}w_{1m}}{\mathrm{d}x}\psi_{y1p}\mathrm{d}x\int_0^b w_{2n}\psi_{y1q}\mathrm{d}y \\
&+ \sum_{m=1}^{m=M}\sum_{n=1}^{n=N}\sum_{p=1}^{p=K}\sum_{q=1}^{q=L} W_{mn}X_{pq}\int_0^a w_{1m}\psi_{x1p}\mathrm{d}x\int_0^b \frac{\mathrm{d}w_{2n}}{\mathrm{d}x}\psi_{x2q}\mathrm{d}y \\
&+ \sum_{m=1}^{m=K}\sum_{n=1}^{n=L}\sum_{p=1}^{p=I}\sum_{q=1}^{q=J} X_{mn}Y_{pq}\int_0^a \psi_{x1m}\psi_{y1p}\mathrm{d}x\int_0^b \psi_{x2m}\psi_{y2p}\mathrm{d}y\Bigg] \\
&+ \frac{1}{2}KA_{55}\Bigg[\sum_{m=1}^{m=M}\sum_{n=1}^{n=N}\sum_{p=1}^{p=M}\sum_{q=1}^{q=N} W_{mn}W_{pq}\int_0^a \frac{\mathrm{d}w_{1m}}{\mathrm{d}x}\frac{\mathrm{d}w_{1p}}{\mathrm{d}x}\mathrm{d}x\int_0^b w_{2n}w_{2q}\mathrm{d}y \\
&+ 2\sum_{m=1}^{m=M}\sum_{n=1}^{n=N}\sum_{p=1}^{p=K}\sum_{q=1}^{q=L} W_{mn}X_{pq}\int_0^a \frac{\mathrm{d}w_{1m}}{\mathrm{d}x}\psi_{x1p}\mathrm{d}x\int_0^b w_{2n}\psi_{x2q}\mathrm{d}y \\
&+ \sum_{m=1}^{m=K}\sum_{n=1}^{n=L}\sum_{p=1}^{p=K}\sum_{q=1}^{q=L} X_{mn}X_{pq}\int_0^a \psi_{x1m}\psi_{x1p}\mathrm{d}x\int_0^b \psi_{x2m}\psi_{x2p}\mathrm{d}y\Bigg]. \qquad (11.82)
\end{aligned}
$$

The following resultants of the shape functions are defined:

$$\Omega_{ij}^1 = \int_0^a \frac{\mathrm{d}^i \psi_{x1m}}{\mathrm{d}x^i} \frac{\mathrm{d}^j \psi_{x1p}}{\mathrm{d}x^j} \mathrm{d}x, \quad \Omega_{ij}^2 = \int_0^a \frac{\mathrm{d}^i \psi_{x1m}}{\mathrm{d}x^i} \frac{\mathrm{d}^j \psi_{y1p}}{\mathrm{d}x^j} \mathrm{d}x,$$

$$\Omega_{ij}^3 = \int_0^a \frac{\mathrm{d}^i \psi_{y1m}}{\mathrm{d}x^i} \frac{\mathrm{d}^j \psi_{y1p}}{\mathrm{d}x^j} \mathrm{d}x, \quad \Omega_{ij}^4 = \int_0^a \frac{\mathrm{d}^i w_{1m}}{\mathrm{d}x^i} \frac{\mathrm{d}^j w_{1p}}{\mathrm{d}x^j} \mathrm{d}x,$$

$$\Omega_{ij}^5 = \int_0^a \frac{\mathrm{d}^i w_{1m}}{\mathrm{d}x^i} \frac{\mathrm{d}^j \psi_{y1p}}{\mathrm{d}x^j} \mathrm{d}x, \quad \Omega_{ij}^6 = \int_0^a \frac{\mathrm{d}^i w_{1m}}{\mathrm{d}x^i} \frac{\mathrm{d}^j \psi_{x1p}}{\mathrm{d}x^j} \mathrm{d}x,$$

$$\Delta_{ij}^1 = \int_0^b \frac{\mathrm{d}^i \psi_{x2n}}{\mathrm{d}y^i} \frac{\mathrm{d}^j \psi_{x2q}}{\mathrm{d}y^j} \mathrm{d}y, \quad \Delta_{ij}^2 = \int_0^b \frac{\mathrm{d}^i \psi_{x2n}}{\mathrm{d}y^i} \frac{\mathrm{d}^j \psi_{y2q}}{\mathrm{d}y^j} \mathrm{d}y,$$

$$\Delta_{ij}^3 = \int_0^b \frac{\mathrm{d}^i \psi_{y2n}}{\mathrm{d}y^i} \frac{\mathrm{d}^j \psi_{y2q}}{\mathrm{d}y^j} \mathrm{d}y, \quad \Delta_{ij}^4 = \int_0^b \frac{\mathrm{d}^i w_{2n}}{\mathrm{d}y^i} \frac{\mathrm{d}^j w_{2q}}{\mathrm{d}y^j} \mathrm{d}y,$$

$$\Delta_{ij}^5 = \int_0^b \frac{\mathrm{d}^i w_{2n}}{\mathrm{d}y^i} \frac{\mathrm{d}^j \psi_{y2q}}{\mathrm{d}y^j} \mathrm{d}y, \quad \Delta_{ij}^6 = \int_0^b \frac{\mathrm{d}^i w_{2n}}{\mathrm{d}y^i} \frac{\mathrm{d}^j \psi_{x2q}}{\mathrm{d}y^j} \mathrm{d}y. \tag{11.83}$$

With the abbreviations

$$\begin{aligned}
\Gamma_i^{klkl} &= \frac{1}{2}\left(D_{11}\Omega_{11}^1\Delta_{00}^1 + D_{66}\Omega_{00}^1\Delta_{11}^1 + KA_{55}\Omega_{00}^1\Delta_{00}^1\right) + D_{16}\Omega_{10}^1\Delta_{01}^1,\\
\Gamma_i^{ijij} &= \frac{1}{2}\left(D_{22}\Omega_{00}^3\Delta_{11}^3 + D_{66}\Omega_{11}^3\Delta_{00}^3 + KA_{44}\Omega_{00}^3\Delta_{00}^3\right) + D_{26}\Omega_{10}^3\Delta_{01}^3,\\
\Gamma_i^{klij} &= D_{12}\Omega_{10}^2\Delta_{01}^2 + D_{16}\Omega_{11}^2\Delta_{00}^2 + D_{26}\Omega_{00}^2\Delta_{11}^2 + D_{66}\Omega_{01}^2\Delta_{10}^2 + KA_{45}\Omega_{00}^2\Delta_{00}^2,\\
\Gamma_i^{mnmn} &= \frac{K}{2}\left(A_{44}\Omega_{00}^4\Delta_{11}^4 + 2A_{45}\Omega_{10}^4\Delta_{01}^4 + A_{55}\Omega_{11}^4\Delta_{00}^4\right),\\
\Gamma_i^{mnij} &= K\left(A_{44}\Omega_{00}^5\Delta_{10}^5 + A_{45}\Omega_{10}^5\Delta_{00}^5\right),\\
\Gamma_i^{mnkl} &= K\left(A_{45}\Omega_{00}^6\Delta_{10}^6 + A_{55}\Omega_{10}^6\Delta_{00}^6\right)
\end{aligned} \tag{11.84}$$

the following representation for the inner potential Π_i results:

$$\Pi_i = \sum_{m=1}^{m=K}\sum_{n=1}^{n=L}\sum_{p=1}^{p=K}\sum_{q=1}^{q=L} X_{mn}X_{pq}\Gamma_i^{klkl} + \sum_{m=1}^{m=I}\sum_{n=1}^{n=J}\sum_{p=1}^{p=I}\sum_{q=1}^{q=J} Y_{mn}Y_{pq}\Gamma_i^{ijij}$$
$$+ \sum_{m=1}^{m=K}\sum_{n=1}^{n=L}\sum_{p=1}^{p=I}\sum_{q=1}^{q=J} X_{mn}Y_{pq}\Gamma_i^{klij} + \sum_{m=1}^{m=M}\sum_{n=1}^{n=N}\sum_{p=1}^{p=M}\sum_{q=1}^{q=N} W_{mn}W_{pq}\Gamma_i^{mnmn}$$
$$+ \sum_{m=1}^{m=M}\sum_{n=1}^{n=N}\sum_{p=1}^{p=I}\sum_{q=1}^{q=J} W_{mn}Y_{pq}\Gamma_i^{mnij} + \sum_{m=1}^{m=M}\sum_{n=1}^{n=N}\sum_{p=1}^{p=K}\sum_{q=1}^{q=L} W_{mn}X_{pq}\Gamma_i^{mnkl}. \quad (11.85)$$

The laminate under consideration is also assumed to be elastically restrained at the two edges at $y = 0$ and $y = b$ by elastic springs with stiffnesses k_l and k_r, respectively. The corresponding potential Π_s results as:

$$\Pi_s = \frac{1}{2}\int_0^a \left[k_l\left(\psi_y(y=0)\right)^2 + k_r\left(\psi_y(y=b)\right)^2\right]\mathrm{d}x. \quad (11.86)$$

With (11.81) we obtain:

$$\Pi_s = \frac{k_l}{2}\sum_{m=1}^{m=I}\sum_{n=1}^{n=J}\sum_{p=1}^{p=I}\sum_{q=1}^{q=J} Y_{mn}Y_{pq}\int_0^a \psi_{y1m}\psi_{y1p}\mathrm{d}x\left(\psi_{y2n}(y=0)\psi_{y2q}(y=0)\right)$$
$$+ \frac{k_r}{2}\sum_{m=1}^{m=I}\sum_{n=1}^{n=J}\sum_{p=1}^{p=I}\sum_{q=1}^{q=J} Y_{mn}Y_{pq}\int_0^a \psi_{y1m}\psi_{y1p}\mathrm{d}x\left(\psi_{y2n}(y=b)\psi_{y2q}(y=b)\right). \quad (11.87)$$

Using the abbreviations

$$\Phi_{11}^{nq} = \psi_{y2n}(y=0)\psi_{y2q}(y=0),$$
$$\Theta_{11}^{nq} = \psi_{y2n}(y=b)\psi_{y2q}(y=b) \quad (11.88)$$

and

$$\Gamma_s^{ijij} = \frac{1}{2}\Omega_{00}^3\left(k_l\Phi_{11}^{nq} + k_r\Theta_{11}^{nq}\right) \quad (11.89)$$

leads to:

$$\Pi_s = \sum_{m=1}^{m=I}\sum_{n=1}^{n=J}\sum_{p=1}^{p=I}\sum_{q=1}^{q=J} Y_{mn}Y_{pq}\Gamma_s^{ijij}. \quad (11.90)$$

The total elastic potential Π results from the summation of Π_i, Π_a and Π_s. The Ritz equations (11.78) then result in a linear system of equations for the Ritz constants. Once the approximated displacements are available, all other state variables of the laminate can be determined from them.

11.3.7 Nonlinear Equations of Motion

As already done in the context of CLPT, we also want to derive equations for FSDT that describe the nonlinear behaviour. Here, too, we follow the procedure described in Reddy (2004). The starting point of the considerations is the displacement field (11.5), which we present again here for better clarity:

$$\begin{aligned} u(x, y, z) &= u_0(x, y) + z\psi_x(x, y), \\ v(x, y, z) &= v_0(x, y) + z\psi_y(x, y), \\ w(x, y) &= w_0(x, y). \end{aligned} \tag{11.91}$$

The non-linear strains in the sense of v. Kármán's plate theory are then as follows:

$$\begin{aligned} \varepsilon_{xx} &= \frac{\partial u_0}{\partial x} + \frac{1}{2}\left(\frac{\partial w_0}{\partial x}\right)^2 + z\frac{\partial \psi_x}{\partial x}, \\ \varepsilon_{yy} &= \frac{\partial v_0}{\partial y} + \frac{1}{2}\left(\frac{\partial w_0}{\partial y}\right)^2 + z\frac{\partial \psi_y}{\partial y}, \\ \varepsilon_{zz} &= 0, \\ \gamma_{yz} &= \frac{\partial w_0}{\partial y} + \psi_y, \\ \gamma_{xz} &= \frac{\partial w_0}{\partial x} + \psi_x, \\ \gamma_{xy} &= \frac{\partial u_0}{\partial y} + \frac{\partial v_0}{\partial x} + \frac{\partial w_0}{\partial x}\frac{\partial w_0}{\partial y} + z\left(\frac{\partial \psi_x}{\partial y} + \frac{\partial \psi_y}{\partial x}\right). \end{aligned} \tag{11.92}$$

These kinematic equations can be represented in a vector matrix notation as:

$$\begin{pmatrix} \varepsilon_{xx} \\ \varepsilon_{yy} \\ \gamma_{yz} \\ \gamma_{xz} \\ \gamma_{xy} \end{pmatrix} = \begin{pmatrix} \varepsilon^0_{xx} \\ \varepsilon^0_{yy} \\ \gamma^0_{yz} \\ \gamma^0_{xz} \\ \gamma^0_{xy} \end{pmatrix} + z \begin{pmatrix} \varepsilon^1_{xx} \\ \varepsilon^1_{yy} \\ \gamma^1_{yz} \\ \gamma^1_{xz} \\ \gamma^1_{xy} \end{pmatrix} = \begin{pmatrix} \frac{\partial u_0}{\partial x} + \frac{1}{2}\left(\frac{\partial w_0}{\partial x}\right)^2 \\ \frac{\partial v_0}{\partial y} + \frac{1}{2}\left(\frac{\partial w_0}{\partial y}\right)^2 \\ \frac{\partial w_0}{\partial y} + \psi_y \\ \frac{\partial w_0}{\partial x} + \psi_x \\ \frac{\partial u_0}{\partial y} + \frac{\partial v_0}{\partial x} + \frac{\partial w_0}{\partial x}\frac{\partial w_0}{\partial y} \end{pmatrix} + z \begin{pmatrix} \frac{\partial \psi_x}{\partial x} \\ \frac{\partial \psi_y}{\partial y} \\ 0 \\ 0 \\ \frac{\partial \psi_x}{\partial y} + \frac{\partial \psi_y}{\partial x} \end{pmatrix}. \tag{11.93}$$

The equations of motion for a laminate in the context of FSDT are derived using Hamilton's principle:

$$\int_0^T (\delta\Pi_i + \delta\Pi_a - \delta K)\,\mathrm{d}t = 0, \tag{11.94}$$

with:

$$\begin{aligned}
\delta\Pi_i &= \int_{\Omega_0} \left\{ \int_{-\frac{h}{2}}^{\frac{h}{2}} \left[\sigma_{xx} \left(\delta\varepsilon^0_{xx} + z\delta\varepsilon^1_{xx} \right) + \sigma_{yy} \left(\delta\varepsilon^0_{yy} + z\delta\varepsilon^1_{yy} \right) \right.\right. \\
&\quad \left.\left. + \tau_{xy} \left(\delta\gamma^0_{xy} + z\delta\gamma^1_{xy} \right) + \tau_{xz}\delta\gamma^0_{xz} + \tau_{yz}\delta\gamma^0_{yz} \right] \mathrm{d}z \right\} \mathrm{d}x\mathrm{d}y, \\
\delta\Pi_a &= -\int_{\Omega_0} p\mathrm{d}y - \int_{\Gamma_\sigma} \int_{-\frac{h}{2}}^{\frac{h}{2}} \left[\hat{\sigma}_{nn} \left(\delta u_{0n} + z\delta\psi_n \right) + \hat{\tau}_{ns} \left(\delta u_{0s} + z\delta\psi_s \right) + \hat{\tau}_{nz}\delta w_0 \right] \mathrm{d}z\mathrm{d}s, \\
\delta K &= \int_{\Omega_0} \int_{-\frac{h}{2}}^{\frac{h}{2}} \rho_0 \left[\left(\dot{u}_0 + z\dot{\psi}_x \right) \left(\delta\dot{u}_0 + z\delta\dot{\psi}_x \right) + \left(\dot{v}_0 + z\dot{\psi}_y \right) \left(\delta\dot{v}_0 + z\delta\dot{\psi}_y \right) + \dot{w}_0\delta\dot{w}_0 \right] \mathrm{d}z\mathrm{d}x\mathrm{d}y.
\end{aligned} \tag{11.95}$$

Inserting (11.95) into (11.94) and carrying out the integration with regard to the thickness direction results in:

$$\begin{aligned}
\int_0^T \left\{ \int_{\Omega_0} \left[N^0_{xx}\delta\varepsilon^0_{xx} + M^0_{xx}\delta\varepsilon^1_{xx} + N^0_{yy}\delta\varepsilon^0_{yy} + M^0_{yy}\delta\varepsilon^1_{yy} + N^0_{xy}\delta\gamma^0_{xy} + M^0_{xy}\delta\gamma^1_{xy} \right.\right. \\
+ Q_x\delta\gamma^0_{xz} + Q_y\delta\gamma^0_{yz} - p\delta w_0 - I_0 \left(\dot{u}_0\delta\dot{u}_0 + \dot{v}_0\delta\dot{v}_0 + \dot{w}_0\delta\dot{w}_0 \right) \\
\left. - I_1 \left(\dot{\psi}_x\delta\dot{u}_0 + \dot{\psi}_y\delta\dot{v}_0 + \delta\dot{\psi}_x\dot{u}_0 + \delta\dot{\psi}_y\dot{v}_0 \right) - I_2 \left(\dot{\psi}_x\delta\dot{\psi}_x + \dot{\psi}_y\delta\dot{\psi}_y \right) \right] \mathrm{d}x\mathrm{d}y \\
\left. - \int_{\Gamma_\sigma} \left(\hat{N}^0_{nn}\delta u_{0n} + \hat{N}^0_{ns}\delta u_{0s} + \hat{M}_{nn}\delta\psi_n + \hat{M}_{ns}\delta\psi_s + \hat{Q}_n\delta w_0 \right) \mathrm{d}s \right\} \mathrm{d}t = 0.
\end{aligned} \tag{11.96}$$

Insertion of the virtual strains and partial integration results:

$$\begin{aligned}
\int_0^T \int_{\Omega_0} \Bigg[& -\left(\frac{\partial N^0_{xx}}{\partial x} + \frac{\partial N^0_{xy}}{\partial y} - I_0 \ddot{u}_0 - I_1 \ddot{\psi}_x \right) \delta u_0 \\
& -\left(\frac{\partial N^0_{xy}}{\partial x} + \frac{\partial N^0_{yy}}{\partial y} - I_0 \ddot{v}_0 - I_1 \ddot{\psi}_y \right) \delta v_0 \\
& -\left(\frac{\partial M^0_{xx}}{\partial x} + \frac{\partial M^0_{xy}}{\partial y} - Q_x - I_2 \ddot{\psi}_x - I_1 \ddot{u}_0 \right) \delta \psi_x \\
& -\left(\frac{\partial M^0_{xy}}{\partial x} + \frac{\partial M^0_{yy}}{\partial y} - Q_y - I_2 \ddot{\psi}_y - I_1 \ddot{v}_0 \right) \delta \psi_y \\
& -\left(\frac{\partial Q_x}{\partial x} + \frac{\partial Q_y}{\partial y} + p - I_0 \ddot{w}_0 \right. \\
& \left. + \frac{\partial}{\partial x} \left(N^0_{xx} \frac{\partial w_0}{\partial x} + N^0_{xy} \frac{\partial w_0}{\partial y} \right) + \frac{\partial}{\partial y} \left(N^0_{xy} \frac{\partial w_0}{\partial x} + N^0_{yy} \frac{\partial w_0}{\partial y} \right) \right) \delta w_0 \Bigg] \mathrm{d}x \mathrm{d}y \\
\int_0^T \int_\Gamma \Big[& \left(N^0_{nn} - \hat{N}^0_{nn} \right) \delta u_{0n} + \left(N^0_{ns} - \hat{N}^0_{ns} \right) \delta u_{0s} + \left(Q_n - \hat{Q}_n \right) \delta w_0 \\
& + \left(M^0_{nn} - \hat{M}^0_{nn} \right) \delta \psi_n + \left(M^0_{ns} - \hat{M}^0_{ns} \right) \delta \psi_s \Big] \mathrm{d}s \mathrm{d}t = 0.
\end{aligned} \tag{11.97}$$

The Euler-Lagrange equations of the given laminate problem in the context of FSDT result from the integral terms over Ω_0:

$$\begin{aligned}
\delta u_0 : & \frac{\partial N^0_{xx}}{\partial x} + \frac{\partial N^0_{xy}}{\partial y} = I_0 \ddot{u}_0 + I_1 \ddot{\psi}_x, \\
\delta v_0 : & \frac{\partial N^0_{xy}}{\partial x} + \frac{\partial N^0_{yy}}{\partial y} = I_0 \ddot{v}_0 + I_1 \ddot{\psi}_y, \\
\delta w_0 : & \frac{\partial Q_x}{\partial x} + \frac{\partial Q_y}{\partial y} + p \\
& + \frac{\partial}{\partial x} \left(N^0_{xx} \frac{\partial w_0}{\partial x} + N^0_{xy} \frac{\partial w_0}{\partial y} \right) + \frac{\partial}{\partial y} \left(N^0_{xy} \frac{\partial w_0}{\partial x} + N^0_{yy} \frac{\partial w_0}{\partial y} \right) = I_0 \ddot{w}_0, \\
\delta \psi_x : & \frac{\partial M^0_{xx}}{\partial x} + \frac{\partial M^0_{xy}}{\partial y} - Q_x = I_2 \ddot{\psi}_x + I_1 \ddot{u}_0, \\
\delta \psi_y : & \frac{\partial M^0_{xy}}{\partial x} + \frac{\partial M^0_{yy}}{\partial y} - Q_y = I_2 \ddot{\psi}_y + I_1 \ddot{v}_0.
\end{aligned} \tag{11.98}$$

The boundary conditions can be deduced from the remaining terms in (11.97).

If we insert the constitutive law

$$\begin{pmatrix} N^0_{xx} \\ N^0_{yy} \\ N^0_{xy} \\ M^0_{xx} \\ M^0_{yy} \\ M^0_{xy} \\ Q_y \\ Q_x \end{pmatrix} = \begin{bmatrix} A_{11} & A_{12} & A_{16} & B_{11} & B_{12} & B_{16} & 0 & 0 \\ A_{12} & A_{22} & A_{26} & B_{12} & B_{22} & B_{26} & 0 & 0 \\ A_{16} & A_{26} & A_{66} & B_{16} & B_{26} & B_{66} & 0 & 0 \\ B_{11} & B_{12} & B_{16} & D_{11} & D_{12} & D_{16} & 0 & 0 \\ B_{12} & B_{22} & B_{26} & D_{12} & D_{22} & D_{26} & 0 & 0 \\ B_{16} & B_{26} & B_{66} & D_{16} & D_{26} & D_{66} & 0 & 0 \\ 0 & 0 & 0 & 0 & 0 & 0 & KA_{44} & KA_{45} \\ 0 & 0 & 0 & 0 & 0 & 0 & KA_{45} & KA_{55} \end{bmatrix} \begin{pmatrix} \frac{\partial u_0}{\partial x} + \frac{1}{2}\left(\frac{\partial w_0}{\partial x}\right)^2 \\ \frac{\partial v_0}{\partial y} + \frac{1}{2}\left(\frac{\partial w_0}{\partial y}\right)^2 \\ \frac{\partial u_0}{\partial y} + \frac{\partial v_0}{\partial x} + \frac{\partial w_0}{\partial x}\frac{\partial w_0}{\partial y} \\ \frac{\partial \psi_x}{\partial x} \\ \frac{\partial \psi_y}{\partial y} \\ \frac{\partial \psi_x}{\partial y} + \frac{\partial \psi_y}{\partial x} \\ \frac{\partial w_0}{\partial y} + \psi_y \\ \frac{\partial w_0}{\partial x} + \psi_x \end{pmatrix} \tag{11.99}$$

into (11.98), then the nonlinear equations of motion of a laminate in the context of FSDT are obtained as follows:

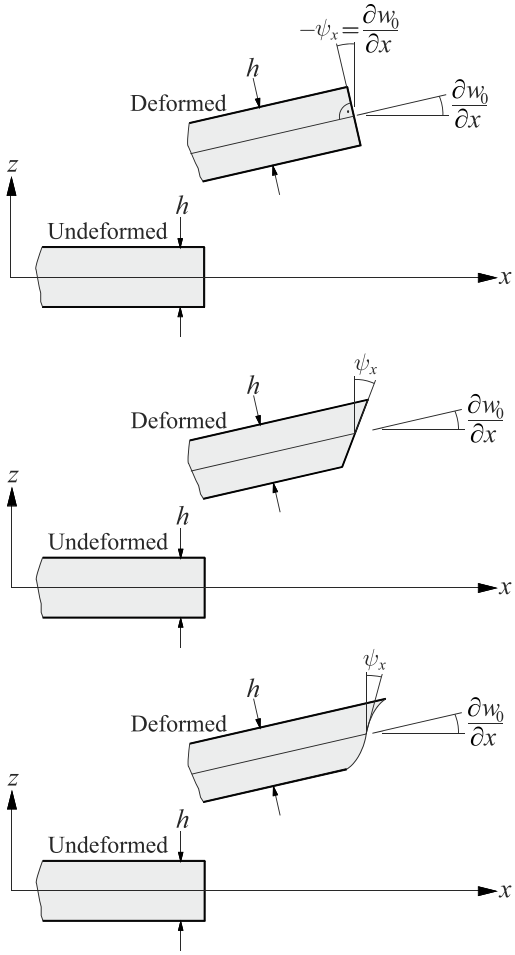
$$\begin{aligned}
&A_{11}\left(\frac{\partial^2 u_0}{\partial x^2} + \frac{\partial w_0}{\partial x}\frac{\partial^2 w_0}{\partial x^2}\right) + A_{12}\left(\frac{\partial^2 v_0}{\partial x \partial y} + \frac{\partial w_0}{\partial y}\frac{\partial^2 w_0}{\partial x \partial y}\right) \\
&+ A_{16}\left(\frac{\partial^2 u_0}{\partial x \partial y} + \frac{\partial^2 v_0}{\partial x^2} + \frac{\partial^2 w_0}{\partial x^2}\frac{\partial w_0}{\partial y} + \frac{\partial w_0}{\partial x}\frac{\partial^2 w_0}{\partial x \partial y}\right) \\
&+ B_{11}\frac{\partial^2 \psi_x}{\partial x^2} + B_{12}\frac{\partial^2 \psi_y}{\partial x \partial y} + B_{16}\left(\frac{\partial^2 \psi_x}{\partial x \partial y} + \frac{\partial^2 \psi_y}{\partial x^2}\right) \\
&+ A_{16}\left(\frac{\partial^2 u_0}{\partial x \partial y} + \frac{\partial w_0}{\partial x}\frac{\partial^2 w_0}{\partial x \partial y}\right) + A_{26}\left(\frac{\partial^2 v_0}{\partial y^2} + \frac{\partial w_0}{\partial y}\frac{\partial^2 w_0}{\partial y^2}\right) \\
&+ A_{66}\left(\frac{\partial^2 u_0}{\partial y^2} + \frac{\partial^2 v_0}{\partial x \partial y} + \frac{\partial^2 w_0}{\partial x \partial y}\frac{\partial w_0}{\partial y} + \frac{\partial w_0}{\partial x}\frac{\partial^2 w_0}{\partial y^2}\right) \\
&+ B_{16}\frac{\partial^2 \psi_x}{\partial x \partial y} + B_{26}\frac{\partial^2 \psi_y}{\partial y^2} + B_{66}\left(\frac{\partial^2 \psi_x}{\partial y^2} + \frac{\partial^2 \psi_y}{\partial x \partial y}\right) = I_0\frac{\partial^2 u_0}{\partial t^2} + I_1\frac{\partial^2 \psi_x}{\partial t^2}, \\
&A_{16}\left(\frac{\partial^2 u_0}{\partial x^2} + \frac{\partial w_0}{\partial x}\frac{\partial^2 w_0}{\partial x^2}\right) + A_{26}\left(\frac{\partial^2 v_0}{\partial x \partial y} + \frac{\partial w_0}{\partial y}\frac{\partial^2 w_0}{\partial x \partial y}\right) \\
&+ A_{66}\left(\frac{\partial^2 u_0}{\partial x \partial y} + \frac{\partial^2 v_0}{\partial x^2} + \frac{\partial^2 w_0}{\partial x^2}\frac{\partial w_0}{\partial y} + \frac{\partial w_0}{\partial x}\frac{\partial^2 w_0}{\partial x \partial y}\right) \\
&+ B_{16}\frac{\partial^2 \psi_x}{\partial x^2} + B_{26}\frac{\partial^2 \psi_y}{\partial x \partial y} + B_{66}\left(\frac{\partial^2 \psi_x}{\partial x \partial y} + \frac{\partial^2 \psi_y}{\partial x^2}\right) \\
&+ A_{12}\left(\frac{\partial^2 u_0}{\partial x \partial y} + \frac{\partial w_0}{\partial x}\frac{\partial^2 w_0}{\partial x \partial y}\right) + A_{22}\left(\frac{\partial^2 v_0}{\partial y^2} + \frac{\partial w_0}{\partial y}\frac{\partial^2 w_0}{\partial y^2}\right) \\
&+ A_{26}\left(\frac{\partial^2 u_0}{\partial y^2} + \frac{\partial^2 v_0}{\partial x \partial y} + \frac{\partial^2 w_0}{\partial x \partial y}\frac{\partial w_0}{\partial y} + \frac{\partial w_0}{\partial x}\frac{\partial^2 w_0}{\partial y^2}\right)
\end{aligned}$$

$$
\begin{aligned}
&+ B_{12}\frac{\partial^2\psi_x}{\partial x\partial y} + B_{22}\frac{\partial^2\psi_y}{\partial y^2} + B_{26}\left(\frac{\partial^2\psi_x}{\partial y^2} + \frac{\partial^2\psi_y}{\partial x\partial y}\right) = I_0\frac{\partial^2 v_0}{\partial t^2} + I_1\frac{\partial^2\psi_y}{\partial t^2},\\
&\quad KA_{55}\left(\frac{\partial^2 w_0}{\partial x^2} + \frac{\partial\psi_x}{\partial x}\right) + KA_{45}\left(\frac{\partial^2 w_0}{\partial x\partial y} + \frac{\partial\psi_y}{\partial x}\right)\\
&+ KA_{45}\left(\frac{\partial^2 w_0}{\partial x\partial y} + \frac{\partial\psi_x}{\partial y}\right) + KA_{44}\left(\frac{\partial^2 w_0}{\partial y^2} + \frac{\partial\psi_y}{\partial y}\right)\\
&+ \frac{\partial}{\partial x}\left(N^0_{xx}\frac{\partial w_0}{\partial x} + N^0_{xy}\frac{\partial w_0}{\partial y}\right) + \frac{\partial}{\partial y}\left(N^0_{xy}\frac{\partial w_0}{\partial x} + N^0_{yy}\frac{\partial w_0}{\partial y}\right) + p = I_0\frac{\partial^2 w_0}{\partial t^2},\\
&\quad B_{11}\left(\frac{\partial^2 u_0}{\partial x^2} + \frac{\partial w_0}{\partial x}\frac{\partial^2 w_0}{\partial x^2}\right) + B_{12}\left(\frac{\partial^2 v_0}{\partial x\partial y} + \frac{\partial w_0}{\partial y}\frac{\partial^2 w_0}{\partial x\partial y}\right)\\
&+ B_{16}\left(\frac{\partial^2 u_0}{\partial x\partial y} + \frac{\partial^2 v_0}{\partial x^2} + \frac{\partial^2 w_0}{\partial x^2}\frac{\partial w_0}{\partial y} + \frac{\partial w_0}{\partial x}\frac{\partial^2 w_0}{\partial x\partial y}\right)\\
&+ D_{11}\frac{\partial^2\psi_x}{\partial x^2} + D_{12}\frac{\partial^2\psi_y}{\partial x\partial y} + D_{16}\left(\frac{\partial^2\psi_x}{\partial x\partial y} + \frac{\partial^2\psi_y}{\partial x^2}\right)\\
&+ B_{16}\left(\frac{\partial^2 u_0}{\partial x\partial y} + \frac{\partial w_0}{\partial x}\frac{\partial^2 w_0}{\partial x\partial y}\right) + B_{26}\left(\frac{\partial^2 v_0}{\partial y^2} + \frac{\partial w_0}{\partial y}\frac{\partial^2 w_0}{\partial y^2}\right)\\
&+ B_{66}\left(\frac{\partial^2 u_0}{\partial y^2} + \frac{\partial^2 v_0}{\partial x\partial y} + \frac{\partial^2 w_0}{\partial x\partial y}\frac{\partial w_0}{\partial y} + \frac{\partial w_0}{\partial x}\frac{\partial^2 w_0}{\partial y^2}\right)\\
&+ D_{16}\frac{\partial^2\psi_x}{\partial x\partial y} + D_{26}\frac{\partial^2\psi_y}{\partial y^2} + D_{66}\left(\frac{\partial^2\psi_x}{\partial y^2} + \frac{\partial^2\psi_y}{\partial x\partial y}\right)\\
&- KA_{55}\left(\frac{\partial w_0}{\partial x} + \psi_x\right) - KA_{45}\left(\frac{\partial w_0}{\partial y} + \psi_y\right) = I_2\frac{\partial^2\psi_x}{\partial t^2} + I_1\frac{\partial^2 u_0}{\partial t^2},\\
&\quad B_{16}\left(\frac{\partial^2 u_0}{\partial x^2} + \frac{\partial w_0}{\partial x}\frac{\partial^2 w_0}{\partial x^2}\right) + B_{26}\left(\frac{\partial^2 v_0}{\partial x\partial y} + \frac{\partial w_0}{\partial y}\frac{\partial^2 w_0}{\partial x\partial y}\right)\\
&+ B_{66}\left(\frac{\partial^2 u_0}{\partial x\partial y} + \frac{\partial^2 v_0}{\partial x^2} + \frac{\partial^2 w_0}{\partial x^2}\frac{\partial w_0}{\partial y} + \frac{\partial w_0}{\partial x}\frac{\partial^2 w_0}{\partial x\partial y}\right)\\
&+ D_{16}\frac{\partial^2\psi_x}{\partial x^2} + D_{26}\frac{\partial^2\psi_y}{\partial x\partial y} + D_{66}\left(\frac{\partial^2\psi_x}{\partial x\partial y} + \frac{\partial^2\psi_y}{\partial x^2}\right)\\
&+ B_{12}\left(\frac{\partial^2 u_0}{\partial x\partial y} + \frac{\partial w_0}{\partial x}\frac{\partial^2 w_0}{\partial x\partial y}\right) + B_{22}\left(\frac{\partial^2 v_0}{\partial y^2} + \frac{\partial w_0}{\partial y}\frac{\partial^2 w_0}{\partial y^2}\right)\\
&+ B_{26}\left(\frac{\partial^2 u_0}{\partial y^2} + \frac{\partial^2 v_0}{\partial x\partial y} + \frac{\partial^2 w_0}{\partial x\partial y}\frac{\partial w_0}{\partial y} + \frac{\partial w_0}{\partial x}\frac{\partial^2 w_0}{\partial y^2}\right)\\
&+ D_{12}\frac{\partial^2\psi_x}{\partial x\partial y} + D_{22}\frac{\partial^2\psi_y}{\partial y^2} + D_{26}\left(\frac{\partial^2\psi_x}{\partial y^2} + \frac{\partial^2\psi_y}{\partial x\partial y}\right)\\
&- KA_{45}\left(\frac{\partial w_0}{\partial x} + \psi_x\right) - KA_{44}\left(\frac{\partial w_0}{\partial y} + \psi_y\right) = I_2\frac{\partial^2\psi_y}{\partial t^2} + I_1\frac{\partial^2 v_0}{\partial t^2}.
\end{aligned}
\tag{11.100}
$$

11.4 Third-Order Shear Deformation Theory According to Reddy

11.4.1 Introduction

Both CLPT and FSDT result in linear variations of the displacements u and v with respect to the thickness coordinate z (see Fig. 11.4). As a result, as already mentioned, constant transverse shear strains γ_{yz} and γ_{xz} as well as transverse shear stresses τ_{yz} and τ_{xz} result within the framework of FSDT. One can try to develop the displacement field with respect to z to an arbitrary degree, but of course this results in a sometimes considerably higher analysis



Classical Laminated Plate Theory (CLPT)

$$u = u_0 - z\frac{\partial w_0}{\partial x}$$
$$v = v_0 - z\frac{\partial w_0}{\partial y}$$
$$w = w_0$$

First-Order Shear Deformation Theory (FSDT)

$$u = u_0 + z\psi_x$$
$$v = v_0 + z\psi_y$$
$$w = w_0$$

Third-Order Shear Deformation Theory (TSDT)

$$u = u_0 + z\psi_x + z^2\theta_x + z^3\lambda_x$$
$$v = v_0 + z\psi_y + z^2\theta_y + z^3\lambda_y$$
$$w = w_0$$

Fig. 11.4 Undeformed and deformed laminate segment according to classical laminated plate theory (top), according to first-order shear deformation theory (middle) and according to third-order shear deformation theory (bottom)

effort. In addition, it is easy to show that a cubic development of the longitudinal displacements u and v with respect to the thickness coordinate z already provides a mechanically correct mapping of the quadratic distributions of τ_{yz} and τ_{xz} over the laminate cross-section, so that higher-order theories with a higher than cubic variation of u and v are rather rare. A quadratic variation of τ_{yz} and τ_{xz} also eliminates the need for a shear correction factor, which must be applied in FSDT and whose determination entails a certain 'arbitrariness'. An important representative of a third-order shear deformation theory goes back to Reddy[2] (1984a, 1984b, 1985, 1990c, 2004) and is described below. We will address this specific laminate theory as the so-called Third-Order Shear Deformation Theory (TSDT) in all that follows.

11.4.2 Kinematics

Reddy's Third-Order Shear Deformation Theory relaxes the assumptions of the laminate theories presented so far even further in that both the normal hypothesis and the hypothesis that the cross-sections remain plane are dropped. The following displacement field is assumed in order to describe the cross-sectional warping thus permitted:

$$\begin{aligned} u(x,y,z) &= u_0(x,y) + z\psi_x(x,y) + z^2\theta_x(x,y) + z^3\lambda_x(x,y), \\ v(x,y,z) &= v_0(x,y) + z\psi_y(x,y) + z^2\theta_y(x,y) + z^3\lambda_y(x,y), \\ w(x,y) &= w_0(x,y). \end{aligned} \tag{11.101}$$

Here, ψ_x, ψ_y, θ_x, θ_y, λ_x, λ_y are functions yet to be determined that describe the deformations of the laminate cross-section. This leads to a total of nine unknown variables with the displacements u_0, v_0, w_0 of the laminate middle plane.

The kinematic quantities occurring in (11.101) can be interpreted as follows. While u_0, v_0, w_0 are the displacements of the laminate middle plane as before, the bending angles ψ_x and ψ_y indicate the inclination of the cross-sectional warping at the point $z = 0$, i.e. on the laminate middle plane:

$$\psi_x = \left.\frac{\partial u}{\partial z}\right|_{z=0}, \quad \psi_y = \left.\frac{\partial v}{\partial z}\right|_{z=0}. \tag{11.102}$$

The remaining variables θ_x, θ_y, λ_x, λ_y can be interpreted as:

$$2\theta_x = \left.\frac{\partial^2 u}{\partial z^2}\right|_{z=0}, \quad 2\theta_y = \left.\frac{\partial^2 v}{\partial z^2}\right|_{z=0}, \quad 6\lambda_x = \left.\frac{\partial^3 u}{\partial z^3}\right|_{z=0}, \quad 6\lambda_y = \left.\frac{\partial^3 v}{\partial z^3}\right|_{z=0}. \tag{11.103}$$

The number of unknown kinematic variables can be reduced by placing certain requirements on the displacement field and the resulting strains and stresses. Currently, it is required

[2] Junuthula N. Reddy, born 1945, Indian-American engineering scientist.

that the transverse shear stresses τ_{yz} and τ_{xz} disappear at the free surfaces of the laminate (i.e. at the points $z = -\frac{h}{2}$ and $z = +\frac{h}{2}$):

$$\tau_{xz}\left(z = -\frac{h}{2}\right) = \tau_{xz}\left(z = +\frac{h}{2}\right) = \tau_{yz}\left(z = -\frac{h}{2}\right) = \tau_{yz}\left(z = +\frac{h}{2}\right) = 0. \quad (11.104)$$

Using Hooke's generalized law results in the following:

$$\begin{aligned}
\bar{C}_{45}\gamma_{yz}\left(z = -\frac{h}{2}\right) + \bar{C}_{55}\gamma_{xz}\left(z = -\frac{h}{2}\right) &= 0,\\
\bar{C}_{45}\gamma_{yz}\left(z = +\frac{h}{2}\right) + \bar{C}_{55}\gamma_{xz}\left(z = +\frac{h}{2}\right) &= 0,\\
\bar{C}_{44}\gamma_{yz}\left(z = -\frac{h}{2}\right) + \bar{C}_{45}\gamma_{xz}\left(z = -\frac{h}{2}\right) &= 0,\\
\bar{C}_{44}\gamma_{yz}\left(z = +\frac{h}{2}\right) + \bar{C}_{45}\gamma_{xz}\left(z = +\frac{h}{2}\right) &= 0. \qquad (11.105)
\end{aligned}$$

The shear strains γ_{yz} and γ_{xz} can be determined from the displacement field (11.101) as follows:

$$\begin{aligned}
\gamma_{yz} &= \frac{\partial v}{\partial z} + \frac{\partial w}{\partial y} = \frac{\partial w_0}{\partial y} + \psi_y + 2z\theta_y + 3z^2\lambda_y,\\
\gamma_{xz} &= \frac{\partial u}{\partial z} + \frac{\partial w}{\partial x} = \frac{\partial w_0}{\partial x} + \psi_x + 2z\theta_x + 3z^2\lambda_x. \qquad (11.106)
\end{aligned}$$

Insertion into (11.105) shows that the disappearance of the shear stresses τ_{yz} and τ_{xz} at the free surfaces of the laminate for any shear stiffness $\bar{C}_{44}$, $\bar{C}_{45}$, $\bar{C}_{55}$ can only be fulfilled if the shear strains γ_{yz} and γ_{xz} themselves become zero there. This then leads to the following four conditions:

$$\begin{aligned}
\frac{\partial w_0}{\partial y} + \psi_y - h\theta_y + \frac{3h^2}{4}\lambda_y &= 0,\\
\frac{\partial w_0}{\partial y} + \psi_y + h\theta_y + \frac{3h^2}{4}\lambda_y &= 0,\\
\frac{\partial w_0}{\partial x} + \psi_x - h\theta_x + \frac{3h^2}{4}\lambda_x &= 0,\\
\frac{\partial w_0}{\partial x} + \psi_x + h\theta_x + \frac{3h^2}{4}\lambda_x &= 0. \qquad (11.107)
\end{aligned}$$

From this, the kinematic variables $\theta_x, \theta_y, \lambda_x, \lambda_y$ can be determined as follows:

$$\theta_x = 0, \quad \theta_y = 0, \quad \lambda_x = -\frac{4}{3h^2}\left(\psi_x + \frac{\partial w_0}{\partial x}\right), \quad \lambda_y = -\frac{4}{3h^2}\left(\psi_y + \frac{\partial w_0}{\partial y}\right). \tag{11.108}$$

The displacement field (11.101) can then be represented as follows:

$$\begin{aligned} u(x, y, z) &= u_0(x, y) + z\psi_x(x, y) - \frac{4z^3}{3h^2}\left(\psi_x(x, y) + \frac{\partial w_0(x, y)}{\partial x}\right), \\ v(x, y, z) &= v_0(x, y) + z\psi_y(x, y) - \frac{4z^3}{3h^2}\left(\psi_y(x, y) + \frac{\partial w_0(x, y)}{\partial y}\right), \\ w(x, y) &= w_0(x, y). \end{aligned} \tag{11.109}$$

It can be seen that the number of unknown deformation functions is reduced to only five within the framework of the Third-Order Shear Deformation Theory according to Reddy. The number of degrees of freedom is thus identical to that according to FSDT.

11.4.3 Strains and Constitutive Equations

The following components of the infinitesimal strain tensor can be determined from the kinematic relationships:

$$\begin{aligned} \varepsilon_{xx} &= \frac{\partial u}{\partial x} = \frac{\partial u_0}{\partial x} + z\frac{\partial \psi_x}{\partial x} - \frac{4z^3}{3h^2}\left(\frac{\partial \psi_x}{\partial x} + \frac{\partial^2 w_0}{\partial x^2}\right), \\ \varepsilon_{yy} &= \frac{\partial v}{\partial y} = \frac{\partial v_0}{\partial y} + z\frac{\partial \psi_y}{\partial y} - \frac{4z^3}{3h^2}\left(\frac{\partial \psi_y}{\partial y} + \frac{\partial^2 w_0}{\partial y^2}\right), \\ \varepsilon_{zz} &= \frac{\partial w}{\partial z} = 0, \\ \gamma_{yz} &= \frac{\partial v}{\partial z} + \frac{\partial w}{\partial y} = \psi_y - \frac{4z^2}{h^2}\left(\psi_y + \frac{\partial w_0}{\partial y}\right) + \frac{\partial w_0}{\partial y}, \\ \gamma_{xz} &= \frac{\partial u}{\partial z} + \frac{\partial w}{\partial x} = \psi_x - \frac{4z^2}{h^2}\left(\psi_x + \frac{\partial w_0}{\partial x}\right) + \frac{\partial w_0}{\partial x}, \\ \gamma_{xy} &= \frac{\partial u}{\partial y} + \frac{\partial v}{\partial x} = \frac{\partial u_0}{\partial y} + \frac{\partial v_0}{\partial x} + z\left(\frac{\partial \psi_x}{\partial y} + \frac{\partial \psi_y}{\partial x}\right) - \frac{4z^3}{3h^2}\left(\frac{\partial \psi_x}{\partial y} + \frac{\partial \psi_y}{\partial x} + 2\frac{\partial^2 w_0}{\partial x \partial y}\right). \end{aligned} \tag{11.110}$$

We can summarize the strain components in a vector notation:

$$\underline{\varepsilon}^{(0)} = \begin{pmatrix} \varepsilon_{xx}^{(0)} \\ \varepsilon_{yy}^{(0)} \\ \gamma_{xy}^{(0)} \end{pmatrix} = \begin{pmatrix} \frac{\partial u_0}{\partial x} \\ \frac{\partial v_0}{\partial x} \\ \frac{\partial u_0}{\partial y} + \frac{\partial v_0}{\partial x} \end{pmatrix}, \quad \underline{\varepsilon}^{(1)} = \begin{pmatrix} \varepsilon_{xx}^{(1)} \\ \varepsilon_{yy}^{(1)} \\ \gamma_{xy}^{(1)} \end{pmatrix} = \begin{pmatrix} \frac{\partial \psi_x}{\partial x} \\ \frac{\partial \psi_y}{\partial y} \\ \frac{\partial \psi_x}{\partial y} + \frac{\partial \psi_y}{\partial x} \end{pmatrix},$$

$$\underline{\varepsilon}^{(3)} = \begin{pmatrix} \varepsilon_{xx}^{(3)} \\ \varepsilon_{yy}^{(3)} \\ \gamma_{xy}^{(3)} \end{pmatrix} = \begin{pmatrix} -\frac{4}{3h^2}\left(\frac{\partial \psi_x}{\partial x} + \frac{\partial^2 w_0}{\partial x^2}\right) \\ -\frac{4}{3h^2}\left(\frac{\partial \psi_y}{\partial y} + \frac{\partial^2 w_0}{\partial y^2}\right) \\ -\frac{4}{3h^2}\left(\frac{\partial \psi_x}{\partial y} + \frac{\partial \psi_y}{\partial x} + 2\frac{\partial^2 w_0}{\partial x \partial y}\right) \end{pmatrix},$$

$$\underline{\gamma}^{(0)} = \begin{pmatrix} \gamma_{yz}^{(0)} \\ \gamma_{xz}^{(0)} \end{pmatrix} = \begin{pmatrix} \psi_y + \frac{\partial w_0}{\partial y} \\ \psi_x + \frac{\partial w_0}{\partial x} \end{pmatrix}, \quad \underline{\gamma}^{(2)} = \begin{pmatrix} \gamma_{yz}^{(2)} \\ \gamma_{xz}^{(2)} \end{pmatrix} = \begin{pmatrix} -\frac{4}{h^2}\left(\psi_y + \frac{\partial w_0}{\partial y}\right) \\ -\frac{4}{h^2}\left(\psi_x + \frac{\partial w_0}{\partial x}\right) \end{pmatrix}. \tag{11.111}$$

Then the following applies to the strain field:

$$\begin{aligned} \underline{\varepsilon} &= \underline{\varepsilon}^{(0)} + z\underline{\varepsilon}^{(1)} + z^3\underline{\varepsilon}^{(3)}, \\ \underline{\gamma} &= \underline{\gamma}^{(0)} + z^2\underline{\gamma}^{(2)}. \end{aligned} \tag{11.112}$$

If the already known internal force and moment definitions are used again at this point

$$\begin{aligned} \underline{N}^0 &= \begin{pmatrix} N_{xx}^0 \\ N_{yy}^0 \\ N_{xy}^0 \end{pmatrix} = \int_{-\frac{h}{2}}^{+\frac{h}{2}} \begin{pmatrix} \sigma_{xx} \\ \sigma_{yy} \\ \tau_{xy} \end{pmatrix} \mathrm{d}z, \\ \underline{M}^0 &= \begin{pmatrix} M_{xx}^0 \\ M_{yy}^0 \\ M_{xy}^0 \end{pmatrix} = \int_{-\frac{h}{2}}^{+\frac{h}{2}} \begin{pmatrix} \sigma_{xx} \\ \sigma_{yy} \\ \tau_{xy} \end{pmatrix} z \mathrm{d}z, \\ \underline{Q} &= \begin{pmatrix} Q_y \\ Q_x \end{pmatrix} = \int_{-\frac{h}{2}}^{+\frac{h}{2}} \begin{pmatrix} \tau_{yz} \\ \tau_{xz} \end{pmatrix} \mathrm{d}z \end{aligned} \tag{11.113}$$

and the following new internal force quantities are also defined

$$\underline{P} = \begin{pmatrix} P_{xx} \\ P_{yy} \\ P_{xy} \end{pmatrix} = \int_{-\frac{h}{2}}^{+\frac{h}{2}} \begin{pmatrix} \sigma_{xx} \\ \sigma_{yy} \\ \tau_{xy} \end{pmatrix} z^3 \mathrm{d}z,$$

$$\underline{R} = \begin{pmatrix} R_y \\ R_x \end{pmatrix} = \int_{-\frac{h}{2}}^{+\frac{h}{2}} \begin{pmatrix} \tau_{yz} \\ \tau_{xz} \end{pmatrix} z^2 \mathrm{d}z, \tag{11.114}$$

the constitutive law for a laminate according to TSDT can be formulated as follows:

$$\begin{pmatrix} N_{xx}^0 \\ N_{yy}^0 \\ N_{xy}^0 \\ M_{xx}^0 \\ M_{yy}^0 \\ M_{xy}^0 \\ P_{xx} \\ P_{yy} \\ P_{xy} \\ Q_y \\ Q_x \\ R_y \\ R_y \end{pmatrix} = \begin{bmatrix} \underline{\underline{A}} & \underline{\underline{B}} & \underline{\underline{E}} & \underline{\underline{0}} & \underline{\underline{0}} \\ \underline{\underline{B}} & \underline{\underline{D}} & \underline{\underline{F}} & \underline{\underline{0}} & \underline{\underline{0}} \\ \underline{\underline{E}} & \underline{\underline{F}} & \underline{\underline{H}} & \underline{\underline{0}} & \underline{\underline{0}} \\ \underline{\underline{0}} & \underline{\underline{0}} & \underline{\underline{0}} & \underline{\underline{A}}_S & \underline{\underline{D}}_S \\ \underline{\underline{0}} & \underline{\underline{0}} & \underline{\underline{0}} & \underline{\underline{D}}_S & \underline{\underline{F}}_S \end{bmatrix} \begin{pmatrix} \frac{\partial u_0}{\partial x} \\ \frac{\partial v_0}{\partial x} \\ \frac{\partial u_0}{\partial y} + \frac{\partial v_0}{\partial x} \\ \frac{\partial \psi_x}{\partial x} \\ \frac{\partial \psi_y}{\partial y} \\ \frac{\partial \psi_x}{\partial y} + \frac{\partial \psi_y}{\partial x} \\ -\frac{4}{3h^2}\left(\frac{\partial \psi_x}{\partial x} + \frac{\partial^2 w_0}{\partial x^2}\right) \\ -\frac{4}{3h^2}\left(\frac{\partial \psi_y}{\partial y} + \frac{\partial^2 w_0}{\partial y^2}\right) \\ -\frac{4}{3h^2}\left(\frac{\partial \psi_x}{\partial y} + \frac{\partial \psi_y}{\partial x} + 2\frac{\partial^2 w_0}{\partial x \partial y}\right) \\ \psi_y + \frac{\partial w_0}{\partial y} \\ \psi_x + \frac{\partial w_0}{\partial x} \\ -\frac{4}{h^2}\left(\psi_y + \frac{\partial w_0}{\partial y}\right) \\ -\frac{4}{h^2}\left(\psi_x + \frac{\partial w_0}{\partial x}\right) \end{pmatrix}, \tag{11.115}$$

or in symbolic form:

$$\begin{pmatrix} \underline{N}^0 \\ \underline{M}^0 \\ \underline{P} \\ \underline{Q} \\ \underline{R} \end{pmatrix} = \begin{bmatrix} \underline{\underline{A}} & \underline{\underline{B}} & \underline{\underline{E}} & \underline{\underline{0}} & \underline{\underline{0}} \\ \underline{\underline{B}} & \underline{\underline{D}} & \underline{\underline{F}} & \underline{\underline{0}} & \underline{\underline{0}} \\ \underline{\underline{E}} & \underline{\underline{F}} & \underline{\underline{H}} & \underline{\underline{0}} & \underline{\underline{0}} \\ \underline{\underline{0}} & \underline{\underline{0}} & \underline{\underline{0}} & \underline{\underline{A}}_S & \underline{\underline{D}}_S \\ \underline{\underline{0}} & \underline{\underline{0}} & \underline{\underline{0}} & \underline{\underline{D}}_S & \underline{\underline{F}}_S \end{bmatrix} \begin{pmatrix} \underline{\varepsilon}^{(0)} \\ \underline{\varepsilon}^{(1)} \\ \underline{\varepsilon}^{(3)} \\ \underline{\gamma}^{(0)} \\ \underline{\gamma}^{(3)} \end{pmatrix}, \tag{11.116}$$

whereby the laminate stiffness matrix is composed as follows:

$$
\begin{bmatrix}
\underline{\underline{A}} & \underline{\underline{B}} & \underline{\underline{E}} & \underline{\underline{0}} & \underline{\underline{0}} \\
\underline{\underline{B}} & \underline{\underline{D}} & \underline{\underline{F}} & \underline{\underline{0}} & \underline{\underline{0}} \\
\underline{\underline{E}} & \underline{\underline{F}} & \underline{\underline{H}} & \underline{\underline{0}} & \underline{\underline{0}} \\
\underline{\underline{0}} & \underline{\underline{0}} & \underline{\underline{0}} & \underline{\underline{A}}_S & \underline{\underline{D}}_S \\
\underline{\underline{0}} & \underline{\underline{0}} & \underline{\underline{0}} & \underline{\underline{D}}_S & \underline{\underline{F}}_S
\end{bmatrix}
$$

$$
= \begin{bmatrix}
A_{11} & A_{12} & A_{16} & B_{11} & B_{12} & B_{16} & E_{11} & E_{12} & E_{16} & 0 & 0 & 0 & 0 \\
A_{12} & A_{22} & A_{26} & B_{12} & B_{22} & B_{26} & E_{12} & E_{22} & E_{26} & 0 & 0 & 0 & 0 \\
A_{16} & A_{26} & A_{66} & B_{16} & B_{26} & B_{66} & E_{16} & E_{26} & E_{66} & 0 & 0 & 0 & 0 \\
B_{11} & B_{12} & B_{16} & D_{11} & D_{12} & D_{16} & F_{11} & F_{12} & F_{16} & 0 & 0 & 0 & 0 \\
B_{12} & B_{22} & B_{26} & D_{12} & D_{22} & D_{26} & F_{12} & F_{22} & F_{26} & 0 & 0 & 0 & 0 \\
B_{16} & B_{26} & B_{66} & D_{16} & D_{26} & D_{66} & F_{16} & F_{26} & F_{66} & 0 & 0 & 0 & 0 \\
E_{11} & E_{12} & E_{16} & F_{11} & F_{12} & F_{16} & H_{11} & H_{12} & H_{16} & 0 & 0 & 0 & 0 \\
E_{12} & E_{22} & E_{26} & F_{12} & F_{22} & F_{26} & H_{12} & H_{22} & H_{26} & 0 & 0 & 0 & 0 \\
E_{16} & E_{26} & E_{66} & F_{16} & F_{26} & F_{66} & H_{16} & H_{26} & H_{66} & 0 & 0 & 0 & 0 \\
0 & 0 & 0 & 0 & 0 & 0 & 0 & 0 & 0 & A_{44} & A_{45} & D_{44} & D_{45} \\
0 & 0 & 0 & 0 & 0 & 0 & 0 & 0 & 0 & A_{45} & A_{55} & D_{45} & D_{55} \\
0 & 0 & 0 & 0 & 0 & 0 & 0 & 0 & 0 & D_{44} & D_{45} & F_{44} & F_{45} \\
0 & 0 & 0 & 0 & 0 & 0 & 0 & 0 & 0 & D_{45} & D_{55} & F_{45} & F_{55}
\end{bmatrix}. \tag{11.117}
$$

It is easy to see that already known quantities reappear in the relationships (11.115)–(11.117), namely the stiffness matrices $\underline{\underline{A}}$, $\underline{\underline{B}}$, $\underline{\underline{D}}$ according to CLPT and the matrix of transverse shear stiffnesses $\underline{\underline{A}}_S$ according to FSDT, as well as the sets of internal forces and moments $\underline{N}^0$, $\underline{M}^0$ and $\underline{Q}$, which are also already known from the previous theories. In addition, the submatrices $\underline{\underline{E}}$, $\underline{\underline{F}}$, $\underline{\underline{H}}$ and $\underline{\underline{D}}_S$ and $\underline{\underline{F}}_S$ (interpretable as transverse shear stiffnesses) as well as the new force variables $\underline{P}$ and $\underline{R}$ (interpretable as warping moments) occur. It can be seen that when using such a shear deformation theory, a significant additional effort in the calculation may be expected compared to the previously discussed laminate theories.

The new stiffnesses of the laminate introduced in (11.115)–(11.117) according to TSDT are defined as follows:

$$
\begin{aligned}
\underline{\underline{E}} &= \begin{bmatrix} E_{11} & E_{12} & E_{16} \\ E_{12} & E_{22} & E_{26} \\ E_{16} & E_{26} & E_{66} \end{bmatrix} = \sum_{k=1}^{k=N} \int_{z_{k-1}}^{z_k} \begin{bmatrix} \bar{Q}_{11} & \bar{Q}_{12} & \bar{Q}_{16} \\ \bar{Q}_{12} & \bar{Q}_{22} & \bar{Q}_{26} \\ \bar{Q}_{16} & \bar{Q}_{26} & \bar{Q}_{66} \end{bmatrix}_k z^3 \mathrm{d}z, \\
\underline{\underline{F}} &= \begin{bmatrix} F_{11} & F_{12} & F_{16} \\ F_{12} & F_{22} & F_{26} \\ F_{16} & F_{26} & F_{66} \end{bmatrix} = \sum_{k=1}^{k=N} \int_{z_{k-1}}^{z_k} \begin{bmatrix} \bar{Q}_{11} & \bar{Q}_{12} & \bar{Q}_{16} \\ \bar{Q}_{12} & \bar{Q}_{22} & \bar{Q}_{26} \\ \bar{Q}_{16} & \bar{Q}_{26} & \bar{Q}_{66} \end{bmatrix}_k z^4 \mathrm{d}z, \\
\underline{\underline{H}} &= \begin{bmatrix} H_{11} & H_{12} & H_{16} \\ H_{12} & H_{22} & H_{26} \\ H_{16} & H_{26} & H_{66} \end{bmatrix} = \sum_{k=1}^{k=N} \int_{z_{k-1}}^{z_k} \begin{bmatrix} \bar{Q}_{11} & \bar{Q}_{12} & \bar{Q}_{16} \\ \bar{Q}_{12} & \bar{Q}_{22} & \bar{Q}_{26} \\ \bar{Q}_{16} & \bar{Q}_{26} & \bar{Q}_{66} \end{bmatrix}_k z^6 \mathrm{d}z,
\end{aligned} \tag{11.118}
$$

and

$$\underline{\underline{D}}_S = \begin{bmatrix} D_{44} & D_{45} \\ D_{45} & D_{55} \end{bmatrix} = \sum_{k=1}^{k=N} \int_{z_{k-1}}^{z_k} \begin{bmatrix} \bar{C}_{44} & \bar{C}_{45} \\ \bar{C}_{45} & \bar{C}_{55} \end{bmatrix}_k z^2 \mathrm{d}z,$$

$$\underline{\underline{F}}_S = \begin{bmatrix} F_{44} & F_{45} \\ F_{45} & F_{55} \end{bmatrix} = \sum_{k=1}^{k=N} \int_{z_{k-1}}^{z_k} \begin{bmatrix} \bar{C}_{44} & \bar{C}_{45} \\ \bar{C}_{45} & \bar{C}_{55} \end{bmatrix}_k z^4 \mathrm{d}z. \tag{11.119}$$

If the integrations prescribed in (11.118) and (11.119) are carried out assuming constant elastic properties layer by layer, the newly added membrane and shear stiffnesses in (11.115)–(11.117) are obtained:

$$\begin{aligned} E_{ij} &= \frac{1}{4} \sum_{k=1}^{k=N} \bar{Q}_{ij,k} \left(z_k^4 - z_{k-1}^4 \right), \\ F_{ij} &= \frac{1}{5} \sum_{k=1}^{k=N} \bar{Q}_{ij,k} \left(z_k^5 - z_{k-1}^5 \right), \\ H_{ij} &= \frac{1}{7} \sum_{k=1}^{k=N} \bar{Q}_{ij,k} \left(z_k^7 - z_{k-1}^7 \right). \end{aligned} \tag{11.120}$$

It can be seen that the expressions obtained in this way contain fourth-order powers or higher, so that it can be expected that their influence may become very small, especially for 'thinner' laminates, but also for laminates with 'moderate' thickness. Therefore, when deciding for or against a specific laminate theory, one must always carefully consider which choice represents the best compromise between the additional computational effort required on the one hand and the resulting improvement in accuracy on the other. As far as the concrete application of the constitutive law (11.115)–(11.117) for various special laminates is concerned, Reddy (2004) provides a wealth of information.

11.4.4 Equilibrium Conditions

The equilibrium conditions in the context of TSDT can be derived from the principle of virtual displacements $\delta W_i = \delta W_a$. For the internal virtual work δW_i we obtain

$$\begin{aligned} \delta W_i = \int_0^b \int_0^a \int_{-\frac{h}{2}}^{\frac{h}{2}} \Bigg\{ & \sigma_{xx} \left[\delta \left(\frac{\partial u_0}{\partial x} \right) + z \delta \left(\frac{\partial \psi_x}{\partial x} \right) + \frac{16}{9h^4} z^3 \delta \left(\frac{\partial \psi_x}{\partial x} + \frac{\partial^2 w_0}{\partial x^2} \right) \right] \\ & + \sigma_{yy} \left[\delta \left(\frac{\partial v_0}{\partial y} \right) + z \delta \left(\frac{\partial \psi_y}{\partial y} \right) + \frac{16}{9h^4} z^3 \delta \left(\frac{\partial \psi_y}{\partial y} + \frac{\partial^2 w_0}{\partial y^2} \right) \right] \end{aligned}$$

$$
\begin{aligned}
&+ \tau_{xy}\left[\delta\left(\frac{\partial u_0}{\partial y}+\frac{\partial v_0}{\partial x}\right)+z\delta\left(\frac{\partial \psi_x}{\partial y}+\frac{\partial \psi_y}{\partial x}\right)+\frac{16}{9h^4}z^3\delta\left(\frac{\partial \psi_x}{\partial y}+\frac{\partial \psi_y}{\partial x}+2\frac{\partial^2 w_0}{\partial x\partial y}\right)\right]\\
&+ \tau_{xz}\left[\delta\left(\psi_x+\frac{\partial w_0}{\partial x}\right)-\frac{4}{h^2}z^2\delta\left(\psi_x+\frac{\partial w_0}{\partial x}\right)\right]\\
&+ \tau_{yz}\left[\delta\left(\psi_y+\frac{\partial w_0}{\partial y}\right)-\frac{4}{h^2}z^2\delta\left(\psi_y+\frac{\partial w_0}{\partial y}\right)\right]\Bigg\}\,\mathrm{d}z\mathrm{d}x\mathrm{d}y. \qquad (11.121)
\end{aligned}
$$

We carry out the integration over z and obtain

$$
\begin{aligned}
\delta W_i = \int_0^b\int_0^a\Bigg[&N_{xx}^0\delta\frac{\partial u_0}{\partial x}+M_{xx}^0\delta\frac{\partial \psi_x}{\partial x}+\frac{16}{9h^4}P_{xx}\delta\left(\frac{\partial \psi_x}{\partial x}+\frac{\partial^2 w_0}{\partial x^2}\right)\\
&+N_{yy}^0\delta\frac{\partial v_0}{\partial y}+M_{yy}^0\delta\left(\frac{\partial \psi_y}{\partial y}\right)+\frac{16}{9h^4}P_{yy}\delta\left(\frac{\partial \psi_y}{\partial y}+\frac{\partial^2 w_0}{\partial y^2}\right)\\
&+N_{xy}^0\delta\left(\frac{\partial u_0}{\partial y}+\frac{\partial v_0}{\partial x}\right)+M_{xy}^0\delta\left(\frac{\partial \psi_x}{\partial y}+\frac{\partial \psi_y}{\partial x}\right)+\frac{16}{9h^4}P_{xy}\delta\left(\frac{\partial \psi_x}{\partial y}+\frac{\partial \psi_y}{\partial x}+2\frac{\partial^2 w_0}{\partial x\partial y}\right)\\
&+Q_x\delta\left(\psi_x+\frac{\partial w_0}{\partial x}\right)-\frac{4}{h^2}R_x\delta\left(\psi_x+\frac{\partial w_0}{\partial x}\right)\\
&+Q_y\delta\left(\psi_y+\frac{\partial w_0}{\partial y}\right)-\frac{4}{h^2}R_y\delta\left(\psi_y+\frac{\partial w_0}{\partial y}\right)\Bigg]\mathrm{d}x\mathrm{d}y. \qquad (11.122)
\end{aligned}
$$

The virtual external work reads in the presence of a surface load $p = p(x, y)$:

$$
\delta W_a = \int_0^b\int_0^a p\delta w_0\mathrm{d}x\mathrm{d}y. \qquad (11.123)
$$

Using the principle of virtual displacements $\delta W_i = \delta W_a$, we obtain the equilibrium conditions after a few transformations and partial integration:

$$
\begin{aligned}
\frac{\partial N_{xx}^0}{\partial x}+\frac{\partial N_{xy}^0}{\partial y}&=0,\\
\frac{\partial N_{xy}^0}{\partial x}+\frac{\partial N_{yy}^0}{\partial y}&=0,\\
\frac{\partial Q_x}{\partial x}+\frac{\partial Q_y}{\partial y}-\frac{4}{h^2}\left(\frac{\partial R_x}{\partial x}+\frac{\partial R_y}{\partial y}\right)+\frac{4}{3h^2}\left(\frac{\partial^2 P_{xx}}{\partial x^2}+2\frac{\partial^2 P_{xy}}{\partial x\partial y}+\frac{\partial^2 P_{yy}}{\partial y^2}\right)+p&=0,\\
\frac{\partial M_{xx}^0}{\partial x}+\frac{\partial M_{xy}^0}{\partial y}-\frac{4}{3h^2}\left(\frac{\partial P_{xx}}{\partial x}+\frac{\partial P_{xy}}{\partial y}\right)-Q_x+\frac{4R_x}{h^2}&=0,\\
\frac{\partial M_{xy}^0}{\partial x}+\frac{\partial M_{yy}^0}{\partial y}-\frac{4}{3h^2}\left(\frac{\partial P_{xy}}{\partial x}+\frac{\partial P_{yy}}{\partial y}\right)-Q_y+\frac{4R_y}{h^2}&=0.
\end{aligned} \qquad (11.124)
$$

11.4.5 Special Laminates

11.4.5.1 Isotropic Single Layer

For the special case of an isotropic single layer, the terms B_{ij} and E_{ij} are omitted. For F_{ij} and H_{ij} $(i, j = 1, 2, 6)$ we obtain:

$$F_{ij} = \frac{h^5}{80} Q_{ij}, \quad H_{ij} = \frac{h^7}{448} Q_{ij}. \tag{11.125}$$

For D_{ij} and F_{ij} (with $i, j = 4, 5$) we have:

$$D_{ij} = \frac{h^3}{12} Q_{ij}, \quad F_{ij} = \frac{h^5}{80} Q_{ij}. \tag{11.126}$$

The following therefore applies:

$$\begin{aligned}
&F_{11} = F_{22} = \frac{Eh^5}{80(1-\nu^2)}, \quad F_{12} = \nu F_{11}, \quad F_{66} = \frac{1}{2}(1-\nu) F_{11}, \\
&H_{11} = H_{22} = \frac{Eh^7}{448(1-\nu^2)}, \quad H_{12} = \nu H_{11}, \quad H_{66} = \frac{1}{2}(1-\nu) H_{11}, \\
&D_{44} = D_{55} = \frac{Gh^3}{12}, \quad F_{44} = F_{55} = \frac{Gh^5}{80}.
\end{aligned} \tag{11.127}$$

11.4.5.2 Orthotropic Single Layer

If an orthotropic single layer is considered, then the components B_{ij} and E_{ij} are zero, and we obtain for F_{ij} and H_{ij} $(i, j = 1, 2, 6)$:

$$F_{ij} = \frac{Q_{ij} h^5}{80}, \quad H_{ij} = \frac{Q_{ij} h^7}{448}, \tag{11.128}$$

with $F_{16} = F_{26} = 0$ and $H_{16} = H_{26} = 0$. For D_{ij} and F_{ij} with $i, j = 4, 5$ we have:

$$D_{ij} = \frac{Q_{ij} h^3}{12}, \quad F_{ij} = \frac{Q_{ij} h^5}{80}, \tag{11.129}$$

with $D_{45} = 0$ and $F_{45} = 0$.

11.4.5.3 Anisotropic Single Layer

For an orthotropic single layer whose principal material axes do not coincide with the global reference system, for F_{ij} and H_{ij} $(i, j = 1, 2, 6)$:

$$F_{ij} = \frac{Q_{ij} h^5}{80}, \quad H_{ij} = \frac{Q_{ij} h^7}{448}. \tag{11.130}$$

For D_{ij} and F_{ij} with $i, j = 4, 5$ we have:

$$D_{ij} = \frac{Q_{ij}h^3}{12}, \quad F_{ij} = \frac{Q_{ij}h^5}{80}. \tag{11.131}$$

All other higher-order terms are zero.

11.4.5.4 Symmetric Laminates

For an arbitrary symmetric laminate, the terms B_{ij} and E_{ij} $(i, j = 1, 2, 6)$ disappear. All other terms in the constitutive law are generally not equal to zero and must be calculated according to the given stacking sequence. Whether any terms result in zero depends on the given layup.

11.4.6 Navier Solutions

Navier solutions can also be derived for TSDT for certain laminates under certain boundary conditions. The load is given in the form of a surface load $p = p(x, y)$.

11.4.6.1 Unsymmetric Cross-Ply Laminates

An unsymmetric cross-ply laminate is considered, for which the stiffnesses A_{16}, A_{26}, A_{45}, B_{16}, B_{26}, D_{16}, D_{26}, E_{16}, E_{26}, F_{16}, F_{26}, H_{16}, H_{26}, D_{45}, F_{45} result in zero. The surface load $p = p(x, y)$ is developed in the form of a Fourier series:

$$p(x, y) = \sum_{m=1}^{m=\infty} \sum_{n=1}^{n=\infty} P_{mn} \sin\left(\frac{m\pi x}{a}\right) \sin\left(\frac{n\pi y}{b}\right), \tag{11.132}$$

with:

$$P_{mn} = \frac{4}{ab} \int_0^b \int_0^a p(x, y) \sin\left(\frac{m\pi x}{a}\right) \sin\left(\frac{n\pi y}{b}\right) \mathrm{d}x\mathrm{d}y. \tag{11.133}$$

We assume the so-called SS1 boundary conditions, which are as follows:

$$\begin{gathered}
u_0\,(y = 0) = 0, \quad u_0\,(y = b) = 0, \quad v_0\,(x = 0) = 0, \quad v_0\,(x = a) = 0, \\
\psi_x\,(y = 0) = 0, \quad \psi_x\,(y = b) = 0, \quad \psi_y\,(x = 0) = 0, \quad \psi_y\,(x = a) = 0, \\
w_0\,(x = 0) = 0, \quad w_0\,(x = a) = 0, \quad w_0\,(y = 0) = 0, \quad w_0\,(y = b) = 0, \\
N^0_{xx}\,(x = 0) = 0, \; N^0_{xx}\,(x = a) = 0, \; N^0_{yy}\,(y = 0) = 0, \; N^0_{yy}\,(y = b) = 0, \\
\left(M^0_{xx} - \frac{4P_{xx}}{3h^2}\right)(x = 0) = 0, \; \left(M^0_{xx} - \frac{4P_{xx}}{3h^2}\right)(x = a) = 0, \\
\left(M^0_{yy} - \frac{4P_{yy}}{3h^2}\right)(y = 0) = 0, \; \left(M^0_{yy} - \frac{4P_{yy}}{3h^2}\right)(y = b) = 0.
\end{gathered} \tag{11.134}$$

The following series expansions fulfil the boundary conditions (11.134) identically:

$$
\begin{aligned}
u_0 &= \sum_{m=1}^{m=\infty}\sum_{n=1}^{n=\infty} U_{mn}\cos\left(\frac{m\pi x}{a}\right)\sin\left(\frac{n\pi y}{b}\right),\\
v_0 &= \sum_{m=1}^{m=\infty}\sum_{n=1}^{n=\infty} V_{mn}\sin\left(\frac{m\pi x}{a}\right)\cos\left(\frac{n\pi y}{b}\right),\\
w_0 &= \sum_{m=1}^{m=\infty}\sum_{n=1}^{n=\infty} W_{mn}\sin\left(\frac{m\pi x}{a}\right)\sin\left(\frac{n\pi y}{b}\right),\\
\psi_x &= \sum_{m=1}^{m=\infty}\sum_{n=1}^{n=\infty} X_{mn}\cos\left(\frac{m\pi x}{a}\right)\sin\left(\frac{n\pi y}{b}\right),\\
\psi_y &= \sum_{m=1}^{m=\infty}\sum_{n=1}^{n=\infty} X_{mn}\sin\left(\frac{m\pi x}{a}\right)\cos\left(\frac{n\pi y}{b}\right).
\end{aligned}
\tag{11.135}
$$

Inserting into the system of differential equations (11.124) leads to the following system of linear equations, from which the unknown coefficients $U_{mn}, V_{mn}, W_{mn}, X_{mn}, Y_{mn}$ can be determined:

$$
\begin{bmatrix}
\lambda_{11} & \lambda_{12} & \lambda_{13} & \lambda_{14} & \lambda_{15}\\
\lambda_{12} & \lambda_{22} & \lambda_{23} & \lambda_{24} & \lambda_{25}\\
\lambda_{13} & \lambda_{23} & \lambda_{33} & \lambda_{34} & \lambda_{35}\\
\lambda_{14} & \lambda_{24} & \lambda_{34} & \lambda_{44} & \lambda_{45}\\
\lambda_{15} & \lambda_{25} & \lambda_{35} & \lambda_{45} & \lambda_{55}
\end{bmatrix}
\begin{pmatrix} U_{mn}\\ V_{mn}\\ W_{mn}\\ X_{mn}\\ Y_{mn}\end{pmatrix}
=
\begin{pmatrix} 0\\ 0\\ P_{mn}\\ 0\\ 0\end{pmatrix},
\tag{11.136}
$$

wherein:

$$
\begin{aligned}
\lambda_{11} &= A_{11}\left(\frac{m\pi}{a}\right)^2 + A_{66}\left(\frac{n\pi}{b}\right)^2, \quad \lambda_{12} = (A_{12}+A_{66})\frac{m\pi}{a}\frac{n\pi}{b},\\
\lambda_{13} &= -\frac{4}{3h^2}\left[E_{11}\left(\frac{m\pi}{a}\right)^2 + (E_{12}+2E_{66})\left(\frac{n\pi}{b}\right)^2\right]\frac{m\pi}{a},\\
\lambda_{14} &= \left(B_{11}-\frac{4E_{11}}{3h^2}\right)\left(\frac{m\pi}{a}\right)^2 + \left(B_{66}-\frac{4E_{66}}{3h^2}\right)\left(\frac{n\pi}{b}\right)^2,\\
\lambda_{15} &= \left[\left(B_{12}-\frac{4E_{12}}{3h^2}\right)+\left(B_{66}-\frac{4E_{66}}{3h^2}\right)\right]\frac{m\pi}{a}\frac{n\pi}{b},\\
\lambda_{22} &= A_{66}\left(\frac{m\pi}{a}\right)^2 + A_{22}\left(\frac{n\pi}{b}\right)^2,\\
\lambda_{23} &= -\frac{4}{3h^2}\left[E_{22}\left(\frac{n\pi}{b}\right)^2 + (E_{12}+2E_{66})\left(\frac{m\pi}{a}\right)^2\right]\frac{n\pi}{b},\\
\lambda_{24} &= \left[\left(B_{12}-\frac{4E_{12}}{3h^2}\right)+\left(B_{66}-\frac{4E_{66}}{3h^2}\right)\right]\frac{m\pi}{a}\frac{n\pi}{b},\\
\lambda_{25} &= \left(B_{66}-\frac{4E_{66}}{3h^2}\right)\left(\frac{m\pi}{a}\right)^2 + \left(B_{22}-\frac{4E_{22}}{3h^2}\right)\left(\frac{n\pi}{b}\right)^2,
\end{aligned}
$$

$$
\begin{aligned}
\lambda_{33} &= \left(A_{55} - \frac{8D_{55}}{3h^2} + \frac{16F_{55}}{9h^4}\right)\left(\frac{m\pi}{a}\right)^2 + \left(A_{44} - \frac{8D_{44}}{3h^2} + \frac{16F_{44}}{9h^4}\right)\left(\frac{n\pi}{b}\right)^2 \\
&\quad + \frac{16}{9h^4}\left[H_{11}\left(\frac{m\pi}{a}\right)^4 + 2\left(H_{12} + 2H_{66}\right)\left(\frac{m\pi}{a}\right)^2\left(\frac{n\pi}{b}\right)^2 + H_{22}\left(\frac{n\pi}{b}\right)^4\right], \\
\lambda_{34} &= \left(A_{55} - \frac{8D_{55}}{3h^2} + \frac{16F_{55}}{9h^4}\right)\frac{m\pi}{a} - \frac{4}{3h^2}\left[\left(F_{11} - \frac{4H_{11}}{3h^2}\right)\left(\frac{m\pi}{a}\right)^3\right. \\
&\quad \left. + \left(F_{12} - \frac{4H_{12}}{3h^2} + 2\left\{F_{66} - \frac{4H_{66}}{3h^2}\right\}\right)\frac{m\pi}{a}\left(\frac{n\pi}{b}\right)^2\right], \\
\lambda_{35} &= \left(A_{44} - \frac{8D_{44}}{3h^2} + \frac{16F_{44}}{9h^4}\right)\frac{n\pi}{b} - \frac{4}{3h^2}\left[\left(F_{22} - \frac{4H_{22}}{3h^2}\right)\left(\frac{n\pi}{b}\right)^3\right. \\
&\quad \left. + \left(F_{12} - \frac{4H_{12}}{3h^2} + 2\left\{F_{66} - \frac{4H_{66}}{3h^2}\right\}\right)\left(\frac{m\pi}{a}\right)^2\frac{n\pi}{b}\right], \\
\lambda_{44} &= A_{55} - \frac{8D_{55}}{3h^2} + \frac{16F_{55}}{9h^4} + \left(D_{11} - \frac{8F_{11}}{3h^2} + \frac{16H_{11}}{9h^4}\right)\left(\frac{m\pi}{a}\right)^2 \\
&\quad + \left(D_{66} - \frac{8F_{66}}{3h^2} + \frac{16H_{66}}{9h^4}\right)\left(\frac{n\pi}{b}\right)^2, \\
\lambda_{45} &= \left[\left(D_{12} - \frac{8F_{12}}{3h^2} + \frac{16H_{12}}{9h^4}\right) + \left(D_{66} - \frac{8F_{66}}{3h^2} + \frac{16H_{66}}{9h^4}\right)\right]\frac{m\pi}{a}\frac{n\pi}{b}, \\
\lambda_{55} &= A_{44} - \frac{8D_{44}}{3h^2} + \frac{16F_{44}}{9h^4} + \left(D_{66} - \frac{8F_{66}}{3h^2} + \frac{16H_{66}}{9h^4}\right)\left(\frac{m\pi}{a}\right)^2 \\
&\quad + \left(D_{22} - \frac{8F_{22}}{3h^2} + \frac{16H_{22}}{9h^4}\right)\left(\frac{n\pi}{b}\right)^2.
\end{aligned} \tag{11.137}
$$

The coefficients $U_{mn}, V_{mn}, W_{mn}, X_{mn}, Y_{mn}$ can thus be determined. From this, the strains and stresses in the laminate can be calculated from the kinematic equations and the material law. The intralaminar stresses in the layer k follow as:

$$
\begin{aligned}
\begin{pmatrix}\sigma_{xx}\\ \sigma_{yy}\\ \tau_{xy}\end{pmatrix}_k &= \begin{bmatrix}\bar{Q}_{11} & \bar{Q}_{12} & 0\\ \bar{Q}_{12} & \bar{Q}_{22} & 0\\ 0 & 0 & \bar{Q}_{66}\end{bmatrix}_k \left[\begin{pmatrix}\frac{\partial u_0}{\partial x}\\ \frac{\partial v_0}{\partial y}\\ \frac{\partial u_0}{\partial y} + \frac{\partial v_0}{\partial x}\end{pmatrix}\right. \\
&\quad \left. + z\begin{pmatrix}\frac{\partial \psi_x}{\partial x}\\ \frac{\partial \psi_y}{\partial y}\\ \frac{\partial \psi_x}{\partial y} + \frac{\partial \psi_y}{\partial x}\end{pmatrix} - \frac{4}{3h^2}z^3\begin{pmatrix}\frac{\partial \psi_x}{\partial x} + \frac{\partial^2 w_0}{\partial x^2}\\ \frac{\partial \psi_y}{\partial y} + \frac{\partial^2 w_0}{\partial y^2}\\ \frac{\partial \psi_x}{\partial y} + \frac{\partial \psi_y}{\partial x} + 2\frac{\partial^2 w_0}{\partial x \partial y}\end{pmatrix}\right] \\
&= \sum_{m=1}^{\infty}\sum_{n=1}^{\infty}\begin{pmatrix}F_1(z)\sin\left(\frac{m\pi x}{a}\right)\sin\left(\frac{n\pi y}{b}\right)\\ F_2(z)\sin\left(\frac{m\pi x}{a}\right)\sin\left(\frac{n\pi y}{b}\right)\\ F_3(z)\cos\left(\frac{m\pi x}{a}\right)\cos\left(\frac{n\pi y}{b}\right)\end{pmatrix},
\end{aligned} \tag{11.138}
$$

with:

$$
\begin{aligned}
F_1(z) &= \frac{m\pi}{a}\left[-U_{mn} - zX_{mn} + \frac{4}{3h^2}z^3\left(X_{mn} + \frac{m\pi}{a}W_{mn}\right)\right],\\
F_2(z) &= \frac{n\pi}{b}\left[-V_{mn} - zY_{mn} + \frac{4}{3h^2}z^3\left(Y_{mn} + \frac{n\pi}{b}W_{mn}\right)\right],\\
F_3(z) &= \frac{n\pi}{b}U_{mn} + \frac{m\pi}{a}V_{mn} + z\left(\frac{n\pi}{b}X_{mn} + \frac{m\pi}{a}Y_{mn}\right)\\
&\quad - \frac{4}{3h^2}z^3\left(\frac{n\pi}{b}X_{mn} + \frac{m\pi}{a}Y_{mn} + 2\frac{m\pi}{a}\frac{n\pi}{b}W_{mn}\right).
\end{aligned}
\tag{11.139}
$$

For the interlaminar shear stresses τ_{xz} and τ_{yz} we obtain from the constitutive law:

$$
\begin{aligned}
\begin{pmatrix}\tau_{yz}\\ \tau_{xz}\end{pmatrix}_k &= \sum_{m=1}^{\infty}\sum_{n=1}^{\infty}\begin{bmatrix}\bar{C}_{44} & 0\\ 0 & \bar{C}_{55}\end{bmatrix}_k\begin{pmatrix}\psi_y + \frac{\partial w_0}{\partial y} - \frac{4}{h^2}z^2\left(\psi_y + \frac{\partial w_0}{\partial y}\right)\\ \psi_x + \frac{\partial w_0}{\partial x} - \frac{4}{h^2}z^2\left(\psi_x + \frac{\partial w_0}{\partial x}\right)\end{pmatrix}\\
&= \left(1 - \frac{4}{h^2}z^2\right)\sum_{m=1}^{\infty}\sum_{n=1}^{\infty}\begin{bmatrix}\bar{C}_{44} & 0\\ 0 & \bar{C}_{55}\end{bmatrix}_k\begin{pmatrix}\left(Y_{mn} + \frac{n\pi}{b}W_{mn}\right)\sin\left(\frac{m\pi x}{a}\right)\cos\left(\frac{n\pi y}{b}\right)\\ \left(X_{mn} + \frac{m\pi}{a}W_{mn}\right)\cos\left(\frac{m\pi x}{a}\right)\sin\left(\frac{n\pi y}{b}\right)\end{pmatrix}.
\end{aligned}
\tag{11.140}
$$

It can be seen that the interlaminar shear stresses occur as layerwise quadratic functions of the thickness coordinate z.

The interlaminar stresses τ_{xz}, τ_{yz} follow from the integration of the equilibrium conditions:

$$
\begin{aligned}
\tau_{xz,k} &= \sum_{m=1}^{\infty}\sum_{n=1}^{\infty}\left[(z - z_k)\,G_{mn1,k} + \frac{1}{2}\left(z^2 - z_k^2\right)G_{mn2,k}\right.\\
&\quad \left. + \frac{1}{3h^2}\left(z^4 - z_k^4\right)G_{mn3,k}\right]\cos\left(\frac{m\pi x}{a}\right)\sin\left(\frac{n\pi y}{b}\right) + \tau_{xz,k-1}(z = z_k),\\
\tau_{yz,k} &= \sum_{m=1}^{\infty}\sum_{n=1}^{\infty}\left[(z - z_k)\,G_{mn4,k} + \frac{1}{2}\left(z^2 - z_k^2\right)G_{mn5,k}\right.\\
&\quad \left. + \frac{1}{3h^2}\left(z^4 - z_k^4\right)G_{mn6,k}\right]\sin\left(\frac{m\pi x}{a}\right)\cos\left(\frac{n\pi y}{b}\right) + \tau_{yz,k-1}(z = z_k),
\end{aligned}
\tag{11.141}
$$

wherein:

$$
\begin{aligned}
G_{mn1,k} &= \left[\left(\frac{m\pi}{a}\right)^2\bar{Q}_{11,k} + \left(\frac{n\pi}{b}\right)^2\bar{Q}_{66,k}\right]U_{mn} + \frac{m\pi}{a}\frac{n\pi}{b}\left(\bar{Q}_{12,k} + \bar{Q}_{66,k}\right)V_{mn},\\
G_{mn2,k} &= \left[\left(\frac{m\pi}{a}\right)^2\bar{Q}_{11,k} + \left(\frac{n\pi}{b}\right)^2\bar{Q}_{66,k}\right]X_{mn} + \frac{m\pi}{a}\frac{n\pi}{b}\left(\bar{Q}_{12,k} + \bar{Q}_{66,k}\right)Y_{mn},\\
G_{mn3,k} &= -\left[\left(\frac{m\pi}{a}\right)^3\bar{Q}_{11,k} + \left(\frac{m\pi}{a}\right)\left(\frac{n\pi}{b}\right)^2\left(\bar{Q}_{12,k} + 2\bar{Q}_{66,k}\right)\right]W_{mn} - G_{mn2,k},
\end{aligned}
$$

$$
\begin{aligned}
G_{mn4,k} &= \frac{m\pi}{a}\frac{n\pi}{b}\left(\bar{Q}_{12,k}+\bar{Q}_{66,k}\right)U_{mn}+\left[\left(\frac{m\pi}{a}\right)^2\bar{Q}_{66,k}+\left(\frac{n\pi}{b}\right)^2\bar{Q}_{22,k}\right]V_{mn},\\
G_{mn5,k} &= \frac{m\pi}{a}\frac{n\pi}{b}\left(\bar{Q}_{12,k}+\bar{Q}_{66,k}\right)X_{mn}+\left[\left(\frac{m\pi}{a}\right)^2\bar{Q}_{66,k}+\left(\frac{n\pi}{b}\right)^2\bar{Q}_{22,k}\right]Y_{mn},\\
G_{mn6,k} &= -\left[\left(\frac{n\pi}{b}\right)^3\bar{Q}_{22,k}+\left(\frac{m\pi}{a}\right)^2\left(\frac{n\pi}{b}\right)\left(\bar{Q}_{12,k}+2\bar{Q}_{66,k}\right)\right]W_{mn}-G_{mn5,k}.
\end{aligned}
\tag{11.142}
$$

11.4.6.2 Symmetric Cross-Ply Laminates

The special case of the symmetric cross-ply laminate is included in the previously shown case of the unsymmetric cross-ply laminate and can be treated by a corresponding assignment of the constitutive law as well as neglecting the inplane displacements u_0 and v_0. This will not be explained in detail at this point.

11.4.6.3 Unsymmetric Angle-Ply Laminates

Now consider an unsymmetric angle-ply laminate in which the stiffnesses D_{45}, F_{45}, F_{16}, F_{26}, H_{16}, H_{26}, E_{11}, E_{22}, E_{12} and E_{66} become zero. The load on the laminate is in the form of a surface load $p = p(x, y)$, which is developed as a Fourier series as shown in (11.132) and (11.133). For the present case, we want to consider the so-called SS2 boundary conditions:

$$
\begin{gathered}
u_0\,(x=0)=0,\quad u_0\,(x=a)=0,\quad v_0\,(y=0)=0,\quad v_0\,(y=b)=0,\\
\psi_x\,(y=0)=0,\quad \psi_x\,(y=b)=0,\quad \psi_y\,(x=0)=0,\quad \psi_y\,(x=a)=0,\\
w_0\,(x=0)=0,\quad w_0\,(x=a)=0,\quad w_0\,(y=0)=0,\quad w_0\,(y=b)=0,\\
N^0_{xy}\,(x=0)=0,\quad N^0_{xy}\,(x=a)=0,\quad N^0_{xy}\,(y=0)=0,\quad N^0_{xy}\,(y=b)=0,\\
\left(M^0_{xx}-\frac{4P_{xx}}{3h^2}\right)(x=0)=0,\quad \left(M^0_{xx}-\frac{4P_{xx}}{3h^2}\right)(x=a)=0,\\
\left(M^0_{yy}-\frac{4P_{yy}}{3h^2}\right)(y=0)=0,\quad \left(M^0_{yy}-\frac{4P_{yy}}{3h^2}\right)(y=b)=0.
\end{gathered}
\tag{11.143}
$$

The following series expansions are used for the degrees of freedom that fulfil all the given conditions (11.143) identically:

$$
\begin{aligned}
u_0 &= \sum_{m=1}^{m=\infty}\sum_{n=1}^{n=\infty}U_{mn}\sin\left(\frac{m\pi x}{a}\right)\cos\left(\frac{n\pi y}{b}\right),\\
v_0 &= \sum_{m=1}^{m=\infty}\sum_{n=1}^{n=\infty}V_{mn}\cos\left(\frac{m\pi x}{a}\right)\sin\left(\frac{n\pi y}{b}\right),\\
w_0 &= \sum_{m=1}^{m=\infty}\sum_{n=1}^{n=\infty}W_{mn}\sin\left(\frac{m\pi x}{a}\right)\sin\left(\frac{n\pi y}{b}\right),
\end{aligned}
$$

$$\psi_x = \sum_{m=1}^{m=\infty} \sum_{n=1}^{n=\infty} X_{mn} \cos\left(\frac{m\pi x}{a}\right) \sin\left(\frac{n\pi y}{b}\right),$$
$$\psi_y = \sum_{m=1}^{m=\infty} \sum_{n=1}^{n=\infty} X_{mn} \sin\left(\frac{m\pi x}{a}\right) \cos\left(\frac{n\pi y}{b}\right). \tag{11.144}$$

Inserting these expressions into the system of differential equations (11.124) results in the following system of linear equations for determining the coefficients U_{mn}, V_{mn}, W_{mn}, X_{mn}, Y_{mn}:

$$\begin{bmatrix} \lambda_{11} & \lambda_{12} & \lambda_{13} & \lambda_{14} & \lambda_{15} \\ \lambda_{12} & \lambda_{22} & \lambda_{23} & \lambda_{24} & \lambda_{25} \\ \lambda_{13} & \lambda_{23} & \lambda_{33} & \lambda_{34} & \lambda_{35} \\ \lambda_{14} & \lambda_{24} & \lambda_{34} & \lambda_{44} & \lambda_{45} \\ \lambda_{15} & \lambda_{25} & \lambda_{35} & \lambda_{45} & \lambda_{55} \end{bmatrix} \begin{pmatrix} U_{mn} \\ V_{mn} \\ W_{mn} \\ X_{mn} \\ Y_{mn} \end{pmatrix} = \begin{pmatrix} 0 \\ 0 \\ P_{mn} \\ 0 \\ 0 \end{pmatrix}, \tag{11.145}$$

with:

$$\lambda_{11} = A_{11}\left(\frac{m\pi}{a}\right)^2 + A_{66}\left(\frac{n\pi}{b}\right)^2, \quad \lambda_{12} = (A_{12} + A_{66})\frac{m\pi}{a}\frac{n\pi}{b},$$
$$\lambda_{13} = -\frac{4}{3h^2}\left[3E_{16}\left(\frac{m\pi}{a}\right)^2 + E_{26}\left(\frac{n\pi}{b}\right)^2\right]\frac{n\pi}{b},$$
$$\lambda_{14} = 2\left(B_{16} - \frac{4}{3h^2}E_{16}\right)\frac{m\pi}{a}\frac{n\pi}{b},$$
$$\lambda_{15} = \lambda_{24} = \left(B_{16} - \frac{4}{3h^2}E_{16}\right)\left(\frac{m\pi}{a}\right)^2 + \left(B_{26} - \frac{4}{3h^2}E_{26}\right)\left(\frac{n\pi}{b}\right)^2,$$
$$\lambda_{22} = A_{66}\left(\frac{m\pi}{a}\right)^2 + A_{22}\left(\frac{n\pi}{b}\right)^2,$$
$$\lambda_{23} = -\frac{4}{3h^2}\left[E_{16}\left(\frac{m\pi}{a}\right)^2 + 3E_{26}\left(\frac{n\pi}{b}\right)^2\right]\frac{m\pi}{a},$$
$$\lambda_{25} = 2\left(B_{26} - \frac{4}{3h^2}E_{26}\right)\frac{m\pi}{a}\frac{n\pi}{b},$$
$$\lambda_{33} = \left(A_{55} - \frac{4}{3h^2}D_{55} - \frac{4}{h^2}\left(D_{55} - \frac{4}{3h^2}F_{55}\right)\right)\left(\frac{m\pi}{a}\right)^2$$
$$+ \left(A_{44} - \frac{4}{3h^2}D_{44} - \frac{4}{h^2}\left(D_{44} - \frac{4}{3h^2}F_{44}\right)\right)\left(\frac{n\pi}{b}\right)^2$$
$$+ \frac{16}{9h^4}\left[H_{11}\left(\frac{m\pi}{a}\right)^4 + 2\left(H_{12} + 2H_{66}\right)\left(\frac{m\pi}{a}\right)^2\left(\frac{n\pi}{b}\right)^2 + H_{22}\left(\frac{n\pi}{b}\right)^4\right],$$
$$\lambda_{34} = \left(A_{55} - \frac{4}{3h^2}D_{55} - \frac{4}{h^2}\left(D_{55} - \frac{4}{3h^2}F_{55}\right)\right)\frac{m\pi}{a}$$
$$- \frac{4}{3h^2}\left[\left(F_{11} - \frac{4}{3h^2}H_{11}\right)\left(\frac{m\pi}{a}\right)^3\right.$$

$$
\begin{aligned}
&+\left(F_{12}-\frac{4}{3h^2}H_{12}+2F_{66}-\frac{8}{3h^2}H_{66}\right)\frac{m\pi}{a}\left(\frac{n\pi}{b}\right)^2\Bigg],\\
\lambda_{34}&=\left(A_{44}-\frac{4}{3h^2}D_{44}-\frac{4}{h^2}\left(D_{44}-\frac{4}{3h^2}F_{44}\right)\right)\frac{n\pi}{b}\\
&-\frac{4}{3h^2}\Bigg[\left(F_{22}-\frac{4}{3h^2}H_{22}\right)\left(\frac{n\pi}{b}\right)^3\\
&+\left(F_{12}-\frac{4}{3h^2}H_{12}+2F_{66}-\frac{8}{3h^2}H_{66}\right)\left(\frac{m\pi}{a}\right)^2\frac{n\pi}{b}\Bigg],\\
\lambda_{44}&=A_{55}-\frac{4}{3h^2}D_{55}-\frac{4}{h^2}\left(D_{55}-\frac{4}{3h^2}F_{55}\right)\\
&+\left(D_{11}-\frac{4}{3h^2}F_{11}-\frac{4}{3h^2}\left(F_{11}-\frac{4}{3h^2}H_{11}\right)\right)\left(\frac{m\pi}{a}\right)^2\\
&+\left(D_{66}-\frac{4}{3h^2}F_{66}-\frac{4}{3h^2}\left(F_{66}-\frac{4}{3h^2}H_{66}\right)\right)\left(\frac{n\pi}{b}\right)^2,\\
\lambda_{45}&=\Bigg[D_{12}-\frac{4}{3h^2}F_{12}-\frac{4}{3h^2}\left(F_{12}-\frac{4}{3h^2}H_{12}\right)\\
&+D_{66}-\frac{4}{3h^2}F_{66}-\frac{4}{3h^2}\left(F_{66}-\frac{4}{3h^2}H_{66}\right)\Bigg]\frac{m\pi}{a}\frac{n\pi}{b},\\
\lambda_{55}&=A_{44}-\frac{4}{3h^2}D_{44}-\frac{4}{h^2}\left(D_{44}-\frac{4}{3h^2}F_{44}\right)\\
&+\left(D_{66}-\frac{4}{3h^2}F_{66}-\frac{4}{3h^2}\left(F_{66}-\frac{4}{3h^2}H_{66}\right)\right)\left(\frac{m\pi}{a}\right)^2\\
&+\left(D_{22}-\frac{4}{3h^2}F_{22}-\frac{4}{3h^2}\left(F_{22}-\frac{4}{3h^2}H_{22}\right)\right)\left(\frac{n\pi}{b}\right)^2.
\end{aligned}
\tag{11.146}
$$

From this, the coefficients U_{mn}, V_{mn}, W_{mn}, X_{mn}, Y_{mn} can be determined, and the strains and stresses in the laminate can be calculated from the kinematic equations and the material law.

We can calculate the intralaminar stresses σ_{xx}, σ_{yy} and τ_{xy} in the layer k as follows:

$$
\begin{aligned}
\begin{pmatrix}\sigma_{xx}\\ \sigma_{yy}\\ \tau_{xy}\end{pmatrix}_k&=\begin{bmatrix}\bar{Q}_{11}&\bar{Q}_{12}&\bar{Q}_{16}\\ \bar{Q}_{12}&\bar{Q}_{22}&\bar{Q}_{26}\\ \bar{Q}_{16}&\bar{Q}_{26}&\bar{Q}_{66}\end{bmatrix}_k\Bigg[\begin{pmatrix}\frac{\partial u_0}{\partial x}\\ \frac{\partial v_0}{\partial y}\\ \frac{\partial u_0}{\partial y}+\frac{\partial v_0}{\partial x}\end{pmatrix}\\
&+z\begin{pmatrix}\frac{\partial \psi_x}{\partial x}\\ \frac{\partial \psi_y}{\partial y}\\ \frac{\partial \psi_x}{\partial y}+\frac{\partial \psi_y}{\partial x}\end{pmatrix}-\frac{4}{3h^2}z^3\begin{pmatrix}\frac{\partial \psi_x}{\partial x}+\frac{\partial^2 w_0}{\partial x^2}\\ \frac{\partial \psi_y}{\partial y}+\frac{\partial^2 w_0}{\partial y^2}\\ \frac{\partial \psi_x}{\partial y}+\frac{\partial \psi_y}{\partial x}+2\frac{\partial^2 w_0}{\partial x\partial y}\end{pmatrix}\Bigg]\\
&=\begin{bmatrix}\bar{Q}_{11}&\bar{Q}_{12}&\bar{Q}_{16}\\ \bar{Q}_{12}&\bar{Q}_{22}&\bar{Q}_{26}\\ \bar{Q}_{16}&\bar{Q}_{26}&\bar{Q}_{66}\end{bmatrix}_k
\end{aligned}
$$

$$\times \left[\sum_{m=1}^{\infty} \sum_{n=1}^{\infty} \begin{pmatrix} \frac{m\pi}{a} U_{mn} \cos\left(\frac{m\pi x}{a}\right) \cos\left(\frac{n\pi y}{b}\right) \\ \frac{n\pi}{b} V_{mn} \cos\left(\frac{m\pi x}{a}\right) \cos\left(\frac{n\pi y}{b}\right) \\ -\left(\frac{n\pi}{b} U_{mn} + \frac{m\pi}{a} V_{mn}\right) \sin\left(\frac{m\pi x}{a}\right) \sin\left(\frac{n\pi y}{b}\right) \end{pmatrix} \right.$$
$$- z \sum_{m=1}^{\infty} \sum_{n=1}^{\infty} \begin{pmatrix} \frac{m\pi}{a} X_{mn} \sin\left(\frac{m\pi x}{a}\right) \sin\left(\frac{n\pi y}{b}\right) \\ \frac{n\pi}{b} Y_{mn} \sin\left(\frac{m\pi x}{a}\right) \sin\left(\frac{n\pi y}{b}\right) \\ -\left(\frac{n\pi}{b} X_{mn} + \frac{m\pi}{a} Y_{mn}\right) \cos\left(\frac{m\pi x}{a}\right) \cos\left(\frac{n\pi y}{b}\right) \end{pmatrix}$$
$$\left. + \frac{4}{3h^2} z^3 \sum_{m=1}^{\infty} \sum_{n=1}^{\infty} \begin{pmatrix} \frac{m\pi}{a} \left(X_{mn} + \frac{m\pi}{a} W_{mn}\right) \sin\left(\frac{m\pi x}{a}\right) \sin\left(\frac{n\pi y}{b}\right) \\ \frac{n\pi}{b} \left(Y_{mn} + \frac{n\pi}{b} W_{mn}\right) \sin\left(\frac{m\pi x}{a}\right) \sin\left(\frac{n\pi y}{b}\right) \\ -\left(\frac{n\pi}{b} X_{mn} + \frac{m\pi}{a} Y_{mn} + 2\frac{m\pi}{a}\frac{n\pi}{b} W_{mn}\right) \cos\left(\frac{m\pi x}{a}\right) \cos\left(\frac{n\pi y}{b}\right) \end{pmatrix} \right]. \tag{11.147}$$

For the interlaminar shear stresses τ_{xz} and τ_{yz} we use the three-dimensional local equilibrium and obtain by integration with respect to the thickness direction z:

$$\tau_{xz,k} = \sum_{m=1}^{\infty} \sum_{n=1}^{\infty} \left[(z - z_k) G_{mn1,k} + \frac{1}{2} \left(z^2 - z_k^2\right) G_{mn2,k} \right.$$
$$\left. + \frac{1}{3h^2} \left(z^4 - z_k^4\right) G_{mn3,k} \right] + \tau_{xz,k-1}(z = z_k),$$
$$\tau_{yz,k} = \sum_{m=1}^{\infty} \sum_{n=1}^{\infty} \left[(z - z_k) G_{mn4,k} + \frac{1}{2} \left(z^2 - z_k^2\right) G_{mn5,k} \right.$$
$$\left. + \frac{1}{3h^2} \left(z^4 - z_k^4\right) G_{mn6,k} \right] + \tau_{yz,k-1}(z = z_k), \tag{11.148}$$

wherein:

$$G_{mn1,k} = \left[\left[\left(\frac{m\pi}{a}\right)^2 \bar{Q}_{11,k} + \left(\frac{n\pi}{b}\right)^2 \bar{Q}_{66,k} \right] U_{mn} + \frac{m\pi}{a}\frac{n\pi}{b} \left(\bar{Q}_{12,k} + \bar{Q}_{66,k}\right) V_{mn} \right]$$
$$\times \sin\left(\frac{m\pi x}{a}\right) \cos\left(\frac{n\pi y}{b}\right)$$
$$+ \left[2\frac{m\pi}{a}\frac{n\pi}{b} \bar{Q}_{16,k} U_{mn} + \left(\left(\frac{m\pi}{a}\right)^2 \bar{Q}_{16,k} + \left(\frac{n\pi}{b}\right)^2 \bar{Q}_{26,k} \right) V_{mn} \right]$$
$$\times \cos\left(\frac{m\pi x}{a}\right) \sin\left(\frac{n\pi y}{b}\right),$$
$$G_{mn2,k} = \left[\left[\left(\frac{m\pi}{a}\right)^2 \bar{Q}_{11,k} + \left(\frac{n\pi}{b}\right)^2 \bar{Q}_{66,k} \right] X_{mn} + \frac{m\pi}{a}\frac{n\pi}{b} \left(\bar{Q}_{12,k} + \bar{Q}_{66,k}\right) Y_{mn} \right]$$
$$\times \cos\left(\frac{m\pi x}{a}\right) \sin\left(\frac{n\pi y}{b}\right)$$
$$+ \left[2\frac{m\pi}{a}\frac{n\pi}{b} \bar{Q}_{16,k} X_{mn} + \left(\left(\frac{m\pi}{a}\right)^2 \bar{Q}_{16,k} + \left(\frac{n\pi}{b}\right)^2 \bar{Q}_{26,k} \right) Y_{mn} \right]$$
$$\times \sin\left(\frac{m\pi x}{a}\right) \cos\left(\frac{n\pi y}{b}\right),$$

$$
\begin{aligned}
G_{mn3,k} = &-\left[\left(\frac{m\pi}{a}\right)^3 \bar{Q}_{11,k} + \frac{m\pi}{a}\left(\frac{n\pi}{b}\right)^2 \left(\bar{Q}_{12,k} + 2\bar{Q}_{66,k}\right)\right] W_{mn} \\
&\times \cos\left(\frac{m\pi x}{a}\right) \sin\left(\frac{n\pi y}{b}\right) \\
&-\left[3\left(\frac{m\pi}{a}\right)^2 \frac{n\pi}{b} \bar{Q}_{16,k} + \left(\frac{n\pi}{b}\right)^3 \bar{Q}_{26,k}\right] W_{mn} \\
&\times \sin\left(\frac{m\pi x}{a}\right) \cos\left(\frac{n\pi y}{b}\right) - G_{mn2,k}, \\
G_{mn4,k} = &\left[\left[\left(\frac{m\pi}{a}\right)^2 \bar{Q}_{16,k} + \left(\frac{n\pi}{b}\right)^2 \bar{Q}_{26,k}\right] U_{mn} + 2\frac{m\pi}{a}\frac{n\pi}{b} \bar{Q}_{16} V_{mn}\right] \\
&\times \sin\left(\frac{m\pi x}{a}\right) \cos\left(\frac{n\pi y}{b}\right) \\
&+\left[\frac{m\pi}{a}\frac{n\pi}{b}\left(\bar{Q}_{12,k} + \bar{Q}_{66,k}\right) U_{mn} + \left(\left(\frac{m\pi}{a}\right)^2 \bar{Q}_{66,k} + \left(\frac{n\pi}{b}\right)^2 \bar{Q}_{22,k}\right) V_{mn}\right] \\
&\times \cos\left(\frac{m\pi x}{a}\right) \sin\left(\frac{n\pi y}{b}\right), \\
G_{mn5,k} = &\left[\left[\left(\frac{m\pi}{a}\right)^2 \bar{Q}_{16,k} + \left(\frac{n\pi}{b}\right)^2 \bar{Q}_{66,k}\right] X_{mn} + 2\frac{m\pi}{a}\frac{n\pi}{b} \bar{Q}_{26} Y_{mn}\right] \\
&\times \cos\left(\frac{m\pi x}{a}\right) \sin\left(\frac{n\pi y}{b}\right) \\
&+\left[\frac{m\pi}{a}\frac{n\pi}{b}\left(\bar{Q}_{12,k} + \bar{Q}_{66,k}\right) X_{mn} + \left(\left(\frac{m\pi}{a}\right)^2 \bar{Q}_{66,k} + \left(\frac{n\pi}{b}\right)^2 \bar{Q}_{22,k}\right) Y_{mn}\right] \\
&\times \sin\left(\frac{m\pi x}{a}\right) \cos\left(\frac{n\pi y}{b}\right), \\
G_{mn6,k} = &-\left[\left(\frac{m\pi}{a}\right)^3 \bar{Q}_{16,k} + 3\frac{m\pi}{a}\left(\frac{n\pi}{b}\right)^2 \bar{Q}_{26,k}\right] W_{mn} \\
&\times \cos\left(\frac{m\pi x}{a}\right) \sin\left(\frac{n\pi y}{b}\right) \\
&-\left[\left(\frac{m\pi}{a}\right)^2 \frac{n\pi}{b}\left(\bar{Q}_{12,k} + 2\bar{Q}_{66,k}\right) + \left(\frac{n\pi}{b}\right)^3 \bar{Q}_{22,k}\right] W_{mn} \\
&\times \sin\left(\frac{m\pi x}{a}\right) \cos\left(\frac{n\pi y}{b}\right) - G_{mn5,k}.
\end{aligned}
\tag{11.149}
$$

11.4.7 The Ritz Method

The Ritz method uses the principle of the minimum of the total elastic potential Π. The inner potential is currently:

$$
\Pi_i = \frac{1}{2} \int_{-\frac{h}{2}}^{\frac{h}{2}} \int_0^b \int_0^a \left(\sigma_{xx}\varepsilon_{xx} + \sigma_{yy}\varepsilon_{yy} + \tau_{xy}\gamma_{xy} + \tau_{xz}\gamma_{xz} + \tau_{yz}\gamma_{yz}\right) \mathrm{d}x\mathrm{d}y\mathrm{d}z, \tag{11.150}
$$

or after performing the integration with respect to z and using the kinematic equations:

$$\begin{aligned}\Pi_i = \frac{1}{2}\int_0^b\int_0^a \Bigg[& N^0_{xx}\frac{\partial u_0}{\partial x} + N^0_{yy}\frac{\partial v_0}{\partial y} + N^0_{xy}\left(\frac{\partial u_0}{\partial y} + \frac{\partial v_0}{\partial x}\right) \\ & + M^0_{xx}\frac{\partial \psi_x}{\partial x} + M^0_{yy}\frac{\partial \psi_y}{\partial y} + M^0_{xy}\left(\frac{\partial \psi_x}{\partial y} + \frac{\partial \psi_y}{\partial x}\right) \\ & - \frac{4}{3h^2}P_{xx}\left(\frac{\partial \psi_x}{\partial x} + \frac{\partial^2 w_0}{\partial x^2}\right) - \frac{4}{3h^2}P_{yy}\left(\frac{\partial \psi_y}{\partial y} + \frac{\partial^2 w_0}{\partial y^2}\right) \\ & - \frac{4}{3h^2}P_{xy}\left(\frac{\partial \psi_x}{\partial y} + \frac{\partial \psi_y}{\partial x} + \frac{\partial^2 w_0}{\partial x \partial y}\right) \\ & + Q_x\left(\psi_x + \frac{\partial w_0}{\partial x}\right) + Q_y\left(\psi_y + \frac{\partial w_0}{\partial y}\right) \\ & - \frac{4}{h^2}R_y\left(\psi_y + \frac{\partial w_0}{\partial y}\right) - \frac{4}{h^2}R_x\left(\psi_x + \frac{\partial w_0}{\partial x}\right)\Bigg] \mathrm{d}x\mathrm{d}y. \end{aligned} \tag{11.151}$$

Only symmetric laminates are considered in the following. With the help of the constitutive equations follows:

$$\begin{aligned}\Pi_i = \frac{1}{2}\int_0^b\int_0^a \Bigg\{ & D_{11}\left(\frac{\partial \psi_x}{\partial x}\right)^2 + 2D_{12}\frac{\partial \psi_x}{\partial x}\frac{\partial \psi_y}{\partial y} + D_{22}\left(\frac{\partial \psi_y}{\partial y}\right)^2 \\ & + 2D_{16}\left(\frac{\partial \psi_x}{\partial y} + \frac{\partial \psi_y}{\partial x}\right)\frac{\partial \psi_x}{\partial x} + 2D_{26}\left(\frac{\partial \psi_x}{\partial y} + \frac{\partial \psi_y}{\partial x}\right)\frac{\partial \psi_y}{\partial y} \\ & + D_{66}\left(\frac{\partial \psi_x}{\partial y} + \frac{\partial \psi_y}{\partial x}\right)^2 \\ & - \frac{8}{3h^2}F_{11}\left(\frac{\partial \psi_x}{\partial x} + \frac{\partial^2 w_0}{\partial x^2}\right)\frac{\partial \psi_x}{\partial x} - \frac{8}{3h^2}F_{22}\left(\frac{\partial \psi_y}{\partial y} + \frac{\partial^2 w_0}{\partial y^2}\right)\frac{\partial \psi_y}{\partial y} \\ & - \frac{8}{3h^2}F_{12}\left(\frac{\partial^2 w_0}{\partial x^2}\frac{\partial \psi_y}{\partial y} + 2\frac{\partial \psi_x}{\partial y}\frac{\partial \psi_y}{\partial y} + \frac{\partial^2 w_0}{\partial y^2}\frac{\partial \psi_x}{\partial x}\right) \\ & - \frac{8}{3h^2}F_{16}\left[\left(\frac{\partial \psi_x}{\partial y} + \frac{\partial \psi_y}{\partial x}\right)\left(2\frac{\partial \psi_x}{\partial x} + \frac{\partial^2 w_0}{\partial x^2}\right) + 2\frac{\partial \psi_x}{\partial x}\frac{\partial^2 w_0}{\partial x \partial y}\right] \\ & - \frac{8}{3h^2}F_{26}\left[\left(\frac{\partial \psi_x}{\partial y} + \frac{\partial \psi_y}{\partial x}\right)\left(2\frac{\partial \psi_y}{\partial y} + \frac{\partial^2 w_0}{\partial y^2}\right) + 2\frac{\partial \psi_y}{\partial y}\frac{\partial^2 w_0}{\partial x \partial y}\right] \\ & - \frac{8}{3h^2}F_{66}\left[\left(\frac{\partial \psi_x}{\partial y} + \frac{\partial \psi_y}{\partial x}\right)^2 + 2\left(\frac{\partial \psi_x}{\partial y} + \frac{\partial \psi_y}{\partial x}\right)\frac{\partial^2 w_0}{\partial x \partial y}\right] \\ & + \frac{16}{9h^4}H_{11}\left(\frac{\partial \psi_x}{\partial x} + \frac{\partial^2 w_0}{\partial x^2}\right)^2 + \frac{16}{9h^4}H_{22}\left(\frac{\partial \psi_y}{\partial y} + \frac{\partial^2 w_0}{\partial y^2}\right)^2 \end{aligned}$$

$$
\begin{aligned}
&+ \frac{32}{9h^4} H_{12} \left(\frac{\partial \psi_x}{\partial x} \frac{\partial \psi_y}{\partial y} + \frac{\partial \psi_x}{\partial x} \frac{\partial^2 w_0}{\partial y^2} + \frac{\partial \psi_y}{\partial y} \frac{\partial^2 w_0}{\partial x^2} + \frac{\partial^2 w_0}{\partial x^2} \frac{\partial^2 w_0}{\partial y^2} \right) \\
&+ \frac{32}{9h^4} H_{16} \left(\frac{\partial \psi_x}{\partial x} + \frac{\partial^2 w_0}{\partial x^2} \right) \left(\frac{\partial \psi_x}{\partial y} + \frac{\partial \psi_y}{\partial x} + 2 \frac{\partial^2 w_0}{\partial x \partial y} \right) \\
&+ \frac{32}{9h^4} H_{26} \left(\frac{\partial \psi_y}{\partial y} + \frac{\partial^2 w_0}{\partial y^2} \right) \left(\frac{\partial \psi_x}{\partial y} + \frac{\partial \psi_y}{\partial x} + 2 \frac{\partial^2 w_0}{\partial x \partial y} \right) \\
&+ \frac{16}{9h^4} H_{66} \left[\left(\frac{\partial \psi_x}{\partial y} + \frac{\partial \psi_y}{\partial x} \right)^2 + 4 \left(\frac{\partial \psi_x}{\partial y} + \frac{\partial \psi_y}{\partial x} + \frac{\partial^2 w_0}{\partial x \partial y} \right) \frac{\partial^2 w_0}{\partial x \partial y} \right] \\
&+ A_{44} \left(\psi_y + \frac{\partial w_0}{\partial y} \right)^2 + A_{55} \left(\psi_x + \frac{\partial w_0}{\partial x} \right)^2 \\
&+ 2A_{45} \left(\psi_x \psi_y + \psi_x \frac{\partial w_0}{\partial y} + \psi_y \frac{\partial w_0}{\partial x} + \frac{\partial w_0}{\partial x} \frac{\partial w_0}{\partial y} \right) \\
&- \frac{8}{h^2} D_{44} \left(\psi_y + \frac{\partial w_0}{\partial y} \right)^2 - \frac{8}{h^2} D_{55} \left(\psi_x + \frac{\partial w_0}{\partial x} \right)^2 \\
&- \frac{16}{h^2} D_{45} \left(\psi_x \psi_y + \psi_x \frac{\partial w_0}{\partial y} + \psi_y \frac{\partial w_0}{\partial x} + \frac{\partial w_0}{\partial x} \frac{\partial w_0}{\partial y} \right) \\
&+ \frac{16}{h^2} F_{44} \left(\psi_y + \frac{\partial w_0}{\partial y} \right)^2 + \frac{16}{h^2} F_{55} \left(\psi_x + \frac{\partial w_0}{\partial x} \right)^2 \\
&+ \frac{32}{h^2} F_{45} \left(\psi_x \psi_y + \psi_x \frac{\partial w_0}{\partial y} + \psi_y \frac{\partial w_0}{\partial x} + \frac{\partial w_0}{\partial x} \frac{\partial w_0}{\partial y} \right) \Bigg\} \mathrm{d}x \mathrm{d}y. \qquad (11.152)
\end{aligned}
$$

It has already been taken into account here that no displacements u_0, v_0 occur in the laminate middle plane for symmetric laminate layups under a surface load $p = p(x, y)$.

We use the following approaches for the degrees of freedom w_0, ψ_x and ψ_y:

$$
\begin{aligned}
w_0 &= \sum_{m=1}^{m=M} \sum_{n=1}^{n=N} W_{mn} w_{1\,m}(x)\, w_{2n}(y), \\
\psi_x &= \sum_{m=1}^{m=K} \sum_{n=1}^{n=L} X_{mn} \psi_{x1m}(x)\, \psi_{x2n}(y), \\
\psi_y &= \sum_{m=1}^{m=I} \sum_{n=1}^{n=J} Y_{mn} \psi_{y1m}(x)\, \psi_{y2n}(y). \qquad (11.153)
\end{aligned}
$$

With the resultants of the functions w_{1m}, w_{2n}, ψ_{x1m}, ψ_{x2n}, ψ_{y1m} and ψ_{y2n}

$$\Omega_{ij}^{1} = \int_0^a \frac{\mathrm{d}^i \psi_{x1m}}{\mathrm{d}x^i} \frac{\mathrm{d}^j \psi_{x1p}}{\mathrm{d}x^j} \mathrm{d}x, \quad \Omega_{ij}^{2} = \int_0^a \frac{\mathrm{d}^i \psi_{x1m}}{\mathrm{d}x^i} \frac{\mathrm{d}^j \psi_{y1p}}{\mathrm{d}x^j} \mathrm{d}x,$$

$$\Omega_{ij}^{3} = \int_0^a \frac{\mathrm{d}^i \psi_{y1m}}{\mathrm{d}x^i} \frac{\mathrm{d}^j \psi_{y1p}}{\mathrm{d}x^j} \mathrm{d}x, \quad \Omega_{ij}^{4} = \int_0^a \frac{\mathrm{d}^i w_{1\,m}}{\mathrm{d}x^i} \frac{\mathrm{d}^j w_{1p}}{\mathrm{d}x^j} \mathrm{d}x,$$

$$\Omega_{ij}^{5} = \int_0^a \frac{\mathrm{d}^i w_{1\,m}}{\mathrm{d}x^i} \frac{\mathrm{d}^j \psi_{y1p}}{\mathrm{d}x^j} \mathrm{d}x, \quad \Omega_{ij}^{6} = \int_0^a \frac{\mathrm{d}^i w_{1\,m}}{\mathrm{d}x^i} \frac{\mathrm{d}^j \psi_{x1p}}{\mathrm{d}x^j} \mathrm{d}x,$$

$$\Delta_{ij}^{1} = \int_0^b \frac{\mathrm{d}^i \psi_{x2n}}{\mathrm{d}y^i} \frac{\mathrm{d}^j \psi_{x2q}}{\mathrm{d}y^j} \mathrm{d}y, \quad \Delta_{ij}^{2} = \int_0^b \frac{\mathrm{d}^i \psi_{x2n}}{\mathrm{d}y^i} \frac{\mathrm{d}^j \psi_{y2q}}{\mathrm{d}y^j} \mathrm{d}y,$$

$$\Delta_{ij}^{3} = \int_0^b \frac{\mathrm{d}^i \psi_{y2n}}{\mathrm{d}y^i} \frac{\mathrm{d}^j \psi_{y2q}}{\mathrm{d}y^j} \mathrm{d}y, \quad \Delta_{ij}^{4} = \int_0^b \frac{\mathrm{d}^i w_{2n}}{\mathrm{d}y^i} \frac{\mathrm{d}^j w_{2q}}{\mathrm{d}y^j} \mathrm{d}y,$$

$$\Delta_{ij}^{5} = \int_0^b \frac{\mathrm{d}^i w_{2n}}{\mathrm{d}y^i} \frac{\mathrm{d}^j \psi_{y2q}}{\mathrm{d}y^j} \mathrm{d}y, \quad \Delta_{ij}^{6} = \int_0^b \frac{\mathrm{d}^i w_{2n}}{\mathrm{d}y^i} \frac{\mathrm{d}^j \psi_{x2q}}{\mathrm{d}y^j} \mathrm{d}y, \tag{11.154}$$

and the abbreviations

$$\begin{aligned}
\Gamma_i^{klkl} &= \Omega_{11}^{1}\Delta_{00}^{1}\left(\frac{1}{2}D_{11} - \frac{4}{3h^2}F_{11} + \frac{8}{9h^4}H_{11}\right) \\
&\quad + \Omega_{00}^{1}\Delta_{11}^{1}\left(\frac{1}{2}D_{66} - \frac{4}{3h^2}F_{66} + \frac{8}{9h^4}H_{66}\right) \\
&\quad + \Omega_{10}^{1}\Delta_{01}^{1}\left(D_{16} - \frac{8}{3h^2}F_{16} + \frac{16}{9h^4}H_{16}\right) \\
&\quad + \Omega_{00}^{1}\Delta_{00}^{1}\left(\frac{1}{2}A_{55} + \frac{8}{h^4}F_{55} - \frac{4}{h^2}D_{55}\right), \\
\Gamma_i^{ijij} &= \Omega_{00}^{3}\Delta_{11}^{3}\left(\frac{1}{2}D_{22} - \frac{4}{3h^2}F_{22} + \frac{8}{9h^4}H_{22}\right) \\
&\quad + \Omega_{11}^{3}\Delta_{00}^{3}\left(\frac{1}{2}D_{66} - \frac{4}{3h^2}F_{66} + \frac{8}{9h^4}H_{66}\right) \\
&\quad + \Omega_{01}^{3}\Delta_{10}^{3}\left(D_{26} - \frac{8}{3h^2}F_{26} + \frac{16}{9h^4}H_{26}\right) \\
&\quad + \Omega_{00}^{3}\Delta_{00}^{3}\left(\frac{1}{2}A_{44} + \frac{8}{h^4}F_{44} - \frac{4}{h^2}D_{44}\right), \\
\Gamma_i^{klij} &= \Omega_{00}^{2}\Delta_{11}^{2}\left(D_{26} - \frac{8}{3h^2}F_{26} + \frac{16}{9h^4}H_{26}\right)
\end{aligned}$$

$$
\begin{aligned}
&+ \Omega_{11}^2 \Delta_{00}^2 \left(D_{16} - \frac{8}{3h^2} F_{16} + \frac{16}{9h^4} H_{16} \right) \\
&+ \Omega_{10}^2 \Delta_{01}^2 \left(D_{12} - \frac{8}{3h^2} F_{12} + \frac{16}{9h^4} H_{12} \right) \\
&+ \Omega_{01}^2 \Delta_{10}^2 \left(D_{66} - \frac{8}{3h^2} F_{66} + \frac{16}{9h^4} H_{66} \right) \\
&+ \Omega_{00}^2 \Delta_{00}^2 \left(A_{45} - \frac{8}{h^2} D_{45} + \frac{16}{h^4} F_{45} \right), \\
\Gamma_i^{mnmn} &= \Omega_{00}^4 \Delta_{11}^4 \left(\frac{1}{2} A_{44} - \frac{4}{h^2} D_{44} + \frac{8}{h^2} F_{44} \right) \\
&+ \Omega_{11}^4 \Delta_{00}^4 \left(\frac{1}{2} A_{55} - \frac{4}{h^2} D_{55} + \frac{8}{h^2} F_{55} \right) \\
&+ \frac{8}{9h^4} \left(\Omega_{22}^4 \Delta_{00}^4 H_{11} + 2\Omega_{20}^4 \Delta_{02}^4 H_{12} + \Omega_{00}^4 \Delta_{22}^4 H_{22} \right) \\
&+ \Omega_{10}^4 \Delta_{01}^4 \left(A_{45} - \frac{8}{h^2} D_{45} + \frac{16}{h^2} F_{45} \right) \\
&+ \frac{32}{9h^2} \left(\Omega_{11}^4 \Delta_{11}^4 H_{66} + \Omega_{12}^4 \Delta_{10}^4 H_{16} + \Omega_{01}^4 \Delta_{21}^4 H_{26} \right), \\
\Gamma_i^{mnij} &= \Omega_{00}^5 \Delta_{21}^5 \left(-\frac{4}{3h^2} F_{22} + \frac{16}{9h^4} H_{22} \right) \\
&+ \Omega_{11}^5 \Delta_{10}^5 \left(-\frac{8}{3h^2} F_{66} + \frac{32}{9h^4} H_{66} \right) \\
&+ \Omega_{21}^5 \Delta_{00}^5 \left(-\frac{4}{3h^2} F_{16} + \frac{16}{9h^4} H_{16} \right) \\
&+ \left(\Omega_{01}^5 \Delta_{20}^5 + 2\Omega_{10}^5 \Delta_{11}^5 \right) \left(-\frac{4}{3h^2} F_{26} + \frac{16}{9h^4} H_{26} \right) \\
&+ \Omega_{20}^5 \Delta_{01}^5 \left(-\frac{4}{3h^2} F_{12} + \frac{16}{9h^4} H_{12} \right) \\
&+ \Omega_{00}^5 \Delta_{10}^5 \left(A_{44} - \frac{8}{h^2} D_{44} + \frac{16}{h^4} F_{44} \right) \\
&+ \Omega_{10}^5 \Delta_{00}^5 \left(A_{45} - \frac{8}{h^2} D_{45} + \frac{16}{h^4} F_{45} \right), \\
\Gamma_i^{mnkl} &= \Omega_{21}^6 \Delta_{00}^6 \left(-\frac{4}{3h^2} F_{11} + \frac{16}{9h^4} H_{11} \right) \\
&+ \Omega_{10}^6 \Delta_{11}^6 \left(-\frac{8}{3h^2} F_{66} + \frac{32}{9h^4} H_{66} \right) \\
&+ \Omega_{00}^6 \Delta_{21}^6 \left(-\frac{4}{3h^2} F_{26} + \frac{16}{9h^4} H_{26} \right)
\end{aligned}
$$

$$
\begin{aligned}
&+ \left(\Omega_{20}^6 \Delta_{01}^6 + 2\Omega_{11}^6 \Delta_{10}^6\right)\left(-\frac{4}{3h^2}F_{16} + \frac{16}{9h^4}H_{16}\right) \\
&+ \Omega_{01}^6 \Delta_{20}^6 \left(-\frac{4}{3h^2}F_{12} + \frac{16}{9h^4}H_{12}\right) \\
&+ \Omega_{10}^6 \Delta_{00}^6 \left(A_{55} - \frac{8}{h^2}D_{55} + \frac{16}{h^4}F_{55}\right) \\
&+ \Omega_{00}^6 \Delta_{10}^6 \left(A_{45} - \frac{8}{h^2}D_{45} + \frac{16}{h^4}F_{45}\right)
\end{aligned} \tag{11.155}
$$

we obtain the following form for the inner potential Π_i:

$$
\begin{aligned}
\Pi_i = &\sum_{m=1}^{m=K}\sum_{n=1}^{n=L}\sum_{p=1}^{p=K}\sum_{q=1}^{q=L} X_{mn}X_{pq}\Gamma_i^{klkl} + \sum_{m=1}^{m=I}\sum_{n=1}^{n=J}\sum_{p=1}^{p=I}\sum_{q=1}^{q=J} Y_{mn}Y_{pq}\Gamma_i^{ijij} \\
&+ \sum_{m=1}^{m=K}\sum_{n=1}^{n=L}\sum_{p=1}^{p=I}\sum_{q=1}^{q=J} X_{mn}Y_{pq}\Gamma_i^{klij} + \sum_{m=1}^{m=M}\sum_{n=1}^{n=N}\sum_{p=1}^{p=M}\sum_{q=1}^{q=N} W_{mn}W_{pq}\Gamma_i^{mnmn} \\
&+ \sum_{m=1}^{m=M}\sum_{n=1}^{n=N}\sum_{p=1}^{p=I}\sum_{q=1}^{q=J} W_{mn}Y_{pq}\Gamma_i^{mnij} + \sum_{m=1}^{m=M}\sum_{n=1}^{n=N}\sum_{p=1}^{p=K}\sum_{q=1}^{q=L} W_{mn}X_{pq}\Gamma_i^{mnkl}.
\end{aligned} \tag{11.156}
$$

11.4.8 Equations of Motion

If a dynamic problem exists, then the following equations of motion apply within the framework of TSDT:

$$
\begin{aligned}
\frac{\partial N_{xx}^0}{\partial x} + \frac{\partial N_{xy}^0}{\partial y} &= I_0\ddot{u}_0 + J_1\ddot{\psi}_x - c_1 I_3 \frac{\partial \ddot{w}_0}{\partial x}, \\
\frac{\partial N_{xy}^0}{\partial x} + \frac{\partial N_{yy}^0}{\partial y} &= I_0\ddot{v}_0 + J_1\ddot{\psi}_y - c_1 I_3 \frac{\partial \ddot{w}_0}{\partial y}, \\
\frac{\partial \bar{Q}_x}{\partial x} + \frac{\partial \bar{Q}_y}{\partial y} + p + c_1\left(\frac{\partial^2 P_{xx}}{\partial x^2} + 2\frac{\partial^2 P_{xy}}{\partial x \partial y} + \frac{\partial^2 P_{yy}}{\partial y^2}\right) &= I_0\ddot{w}_0 - c_1^2 I_6\left(\frac{\partial^2 \ddot{w}_0}{\partial x^2} + \frac{\partial^2 \ddot{w}_0}{\partial y^2}\right) \\
&\quad + c_1\left[I_3\left(\frac{\partial \ddot{u}_0}{\partial x} + \frac{\partial \ddot{v}_0}{\partial y}\right) + J_4\left(\frac{\partial \ddot{\psi}_x}{\partial x} + \frac{\partial \ddot{\psi}_y}{\partial y}\right)\right], \\
\frac{\partial \bar{M}_{xx}^0}{\partial x} + \frac{\partial \bar{M}_{xy}^0}{\partial y} - \bar{Q}_x &= J_1\ddot{u}_0 + K_2\ddot{\psi}_x - c_1 J_4 \frac{\partial \ddot{w}_0}{\partial x}, \\
\frac{\partial \bar{M}_{xy}^0}{\partial x} + \frac{\partial \bar{M}_{yy}^0}{\partial y} - \bar{Q}_y &= J_1\ddot{v}_0 + K_2\ddot{\psi}_y - c_1 J_4 \frac{\partial \ddot{w}_0}{\partial y},
\end{aligned} \tag{11.157}
$$

with

$$\bar{M}^0_{xx} = M^0_{xx} - c_1 P_{xx}, \quad \bar{M}^0_{xy} = M^0_{xy} - c_1 P_{xy}, \quad \bar{M}^0_{yy} = M^0_{yy} - c_1 P_{yy},$$
$$\bar{Q}_x = Q_x - c_2 R_x, \quad \bar{Q}_y = Q_y - c_2 R_y,$$
$$I_i = \sum_{k=1}^{n} \int_{z_{k-1}}^{z_k} \rho_k z^i \mathrm{d}z \quad (i = 0, 1, 2, \ldots, 6),$$
$$J_i = I_i - c_1 I_{i+2}, \quad K_2 = I_2 - 2c_1 I_4 + c_1^2 I_6, \quad c_1 = \frac{4}{3h^2}, \quad c_2 = 3c_1. \quad (11.158)$$

11.5 Layerwise Approaches

11.5.1 Introduction

The laminate theories presented so far—i.e. the Classical Laminated Plate Theory, the First-Order Shear Deformation Theory and the Third-Order Shear Deformation Theory according to Reddy—attribute the behaviour of the laminate to effective stiffnesses, which relate the force variables of the laminate to the strain variables of the laminate middle plane. In the case of these stiffness variables, it should be noted that they represent 'effective' properties of the laminate with reference to the laminate middle plane, i.e. they are to a certain extent averaged variables that mathematically turn the actually layered surface structure into a single layer, namely the laminate middle plane. Their stiffness properties can then be regarded as 'averaged' or 'effective' laminate parameters. The laminate theories discussed so far are therefore also referred to as 'single-layer theories'.

Single-layer theories have proven themselves in many engineering applications, especially for the analysis of the rather 'global' behaviour of laminates, whereby global investigations refer to problem areas such as bending, buckling or vibrations. Laminate structures, on the other hand, are layered structures (which makes it necessary to analyse them on a mesoscopic level for a large number of problems) and have a pronounced microstructure (which in turn would make it necessary to analyse them on a microscopic level). In the context of a discussion of laminate theories, the first point is of interest. For example, it can be seen that three-dimensional stress states can occur, particularly in the context of damage in a laminate and the associated fracture processes, which cannot be treated with a global approach using a single-layer theory, or only to a very limited extent. Instead, an attempt must be made to find a modelling approach that is able to depict the individual layers of a laminate and the more 'local' events. The so-called layerwise theories are suitable for this purpose, in which each individual layer of a laminate is treated separately and the laminate as a whole is computationally composed by continuity conditions between adjacent layers. Depending on the requirements, both full three-dimensional kinematics and three-dimensional constitutive relationships should then be taken into account in each individual layer. The basics of modelling with the help of layerwise theories are presented in this section.

Another reason for the application of layerwise theories, especially when considering thicker laminates, lies in the continuity of the interlaminar stresses that is always required. If the stresses in the interface between the individual layers k and $k+1$ are considered, there will generally be discontinuities in the interface for the inplane/intralaminar stresses σ_{xx}, σ_{yy} and τ_{xy} due to the layer-by-layer differences in layer stiffness, i.e.:

$$\begin{aligned} \sigma_{xx,k}\,(z = z_k) &\neq \sigma_{xx,k+1}\,(z = z_k)\,, \\ \sigma_{yy,k}\,(z = z_k) &\neq \sigma_{yy,k+1}\,(z = z_k)\,, \\ \tau_{xy,k}\,(z = z_k) &\neq \tau_{xy,k+1}\,(z = z_k)\,. \end{aligned} \tag{11.159}$$

On the other hand, the stresses in the thickness direction/the interlaminar stresses τ_{yz}, τ_{xz} and σ_{zz} must run continuously from layer k via the interface into layer $k+1$, so that the following applies:

$$\begin{aligned} \tau_{xz,k}\,(z = z_k) &= \tau_{xz,k+1}\,(z = z_k)\,, \\ \tau_{yz,k}\,(z = z_k) &= \tau_{yz,k+1}\,(z = z_k)\,, \\ \sigma_{zz,k}\,(z = z_k) &= \sigma_{zz,k+1}\,(z = z_k)\,. \end{aligned} \tag{11.160}$$

However, since the stiffnesses of the individual layers k and $k+1$ are generally different, the transverse strains γ_{yz}, γ_{xz} and ε_{zz} must generally be discontinuous in the interface, i.e.:

$$\begin{aligned} \gamma_{xz,k}\,(z = z_k) &\neq \gamma_{xz,k+1}\,(z = z_k)\,, \\ \gamma_{yz,k}\,(z = z_k) &\neq \gamma_{yz,k+1}\,(z = z_k)\,, \\ \varepsilon_{zz,k}\,(z = z_k) &\neq \varepsilon_{zz,k+1}\,(z = z_k)\,. \end{aligned} \tag{11.161}$$

However, since all single-layer theories are based on an assumption for the displacement field, which is continuous over the entire thickness, the transverse strains γ_{yz}, γ_{xz} and ε_{zz} also result as continuous functions over the laminate thickness, which is contrary to the requirement (11.161). Thus, in the context of a single-layer theory, not only the intralaminar stresses σ_{xx}, σ_{yy} and τ_{xy} show discontinuities in the interfaces, but also the interlaminar stresses τ_{yz}, τ_{xz} and σ_{zz}, so that the condition (11.160) is violated. In such cases, it may be justified to give preference to a layerwise theory.

A literature study quickly shows that the application of layerwise theories for various analysis purposes has been documented in a large number of publications over about five decades. Examples of this are the publications by Mau (1973), Srinivas (1973) and Whitney (1973) from the early 1970s, which were followed by many other scientific papers up to the present day. It is noticeable that the layerwise theories can essentially be divided into two classes. On the one hand, these are layerwise theories in which only the inplane displacements u and v of the laminate are modelled by layerwise approaches, whereby an approach for the displacement w is still formulated globally over the entire laminate as in a single-layer theory. The disadvantage of this approach is that strains in the thickness direction are

neglected, which makes it correspondingly more difficult to make a statement about the interlaminar normal stress σ_{zz} (which is important for a failure assessment at free laminate edges, near holes or in the vicinity of cracks or delamination fronts). There are also layerwise theories in which all three displacement components are modelled using layer-by-layer approaches. There are also mixed forms of theories in which layer-by-layer formulations are superimposed on a single-layer theory. It is not possible to provide a precise overview of the layerwise approaches available here, so that interested readers are referred to the relevant specialist literature. The decision for or against a specific modelling approach always depends on the respective application purpose and cannot be answered universally.

11.5.2 Displacement Field

The layerwise laminate theory as formulated by Reddy (2004) is described below. The term 'zig-zag theory' is also frequently used in technical literature. The following approach is used for the displacements u_k, v_k, w_k in the single layer k:

$$\begin{aligned} u_k(x, y, z) &= \sum_{j=1}^{m} u_{j,k}(x, y)\, \phi_{j,k}(z), \\ v_k(x, y, z) &= \sum_{j=1}^{m} v_{j,k}(x, y)\, \phi_{j,k}(z), \\ w_k(x, y, z) &= \sum_{j=1}^{n} w_{j,k}(x, y)\, \psi_{j,k}(z), \end{aligned} \tag{11.162}$$

where $u_{j,k}$, $v_{j,k}$, $w_{j,k}$ are the displacements in the layer k at the grid point j, which depend only on the plane coordinates x and y. Furthermore, $\phi_{j,k}$ and $\psi_{j,k}$ are layerwise continuous shape functions (often in the form of Lagrangian interpolation functions) in the thickness direction z. For $u_{j,k}$ and $v_{j,k}$, identical shape functions $\phi_{j,k}$ and degrees/support points m are usually selected, while other approaches $\psi_{j,k}$ and a different approach degree n can also be used for $w_{j,k}$. In the simplest case, the shape functions $\phi_{j,k}$ and $\psi_{j,k}$ are linear, as shown in Fig. 11.5 qualitatively for the displacement u. In this case, the numbers of interpolation points m and n are defined as $m = n = 2$, and the functions $u_{j,k}$, $v_{j,k}$, $w_{j,k}$ represent the displacement functions in the interfaces of the individual layers. If we use higher-order shape functions through the thickness, then the functions $u_{j,k}$, $v_{j,k}$, $w_{j,k}$ represent the displacements of layer k at the grid point j. The approach (11.162) automatically ensures a continuous displacement field over z. Furthermore, when using layerwise approaches, it is also possible to proceed in such a way that a real physical layer is divided into a certain number of sublayers or so-called mathematical layers (Fig. 11.6, variant 2). This approach has proven to be particularly useful for the analysis of local effects such as stress concentration problems and can ensure that very good results are obtained locally, while in

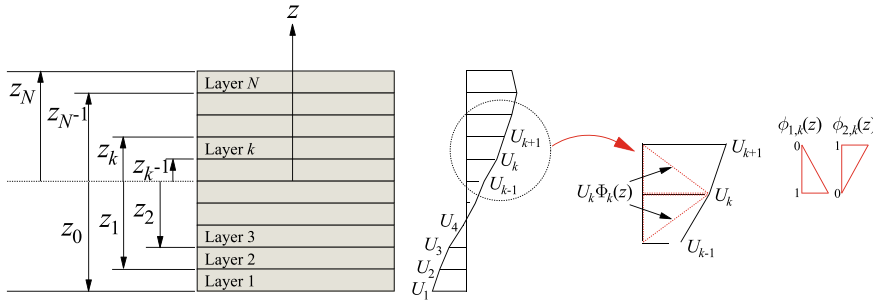


Fig. 11.5 Representation of the longitudinal displacements u using linear shape functions through the thickness

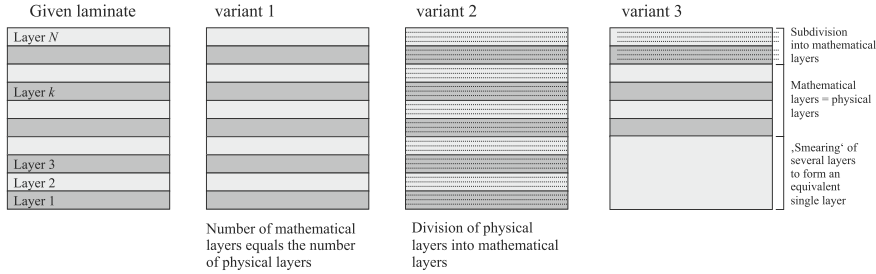


Fig. 11.6 Variants of layerwise approaches

areas of lesser interest it may be possible to dispense with a 'discretization' of the physical layers. Furthermore, when using such layerwise approaches, it is also possible to make a very fine local division into mathematical layers, while in less interesting areas several physical layers can be combined into a single effective layer (see Fig. 11.6, variant 3).

Although the displacement field described by (11.162) is continuous through the thickness of the laminate, discontinuous transverse strains γ_{yz}, γ_{xz} and ε_{zz} can occur across the individual layer interfaces. This in turn opens up the possibility of continuous distributions of the interlaminar stresses τ_{yz}, τ_{xz} and σ_{zz}, which fulfils the requirement (11.160).

The total displacements u, v, w at any point of the laminate can finally be calculated as follows:

$$
\begin{aligned}
u\,(x,\,y,\,z) &= \sum_{i=1}^{M_l} U_i\,(x,\,y)\,\Phi_i\,(z),\\
v\,(x,\,y,\,z) &= \sum_{i=1}^{M_l} V_i\,(x,\,y)\,\Phi_i\,(z),\\
w\,(x,\,y,\,z) &= \sum_{i=1}^{N_l} W_i\,(x,\,y)\,\Psi_i\,(z).
\end{aligned}
\tag{11.163}
$$

In this, M_l and N_l are the numbers of interfaces of the $M_e = M_l - 1$ mathematical layers for the inplane displacements u, v and the $N_e = N_l - 1$ mathematical layers for the thickness displacement w (whereby the surfaces of the laminate are also counted as interfaces), while the functions U_i, V_i, W_i are the displacement functions in the interfaces of the mathematical layers. The functions Φ_i and Ψ_i are the associated global interpolation functions. In the case of linear local interpolation functions, the following can be written:

$$\begin{aligned}
\Phi_1(z) &= \phi_{1,1}(z) \qquad z_0 \le z \le z_1, \\
\Phi_i(z) &= \begin{cases} \phi_{2,i-1}(z) & z_{i-2} \le z \le z_{i-1}, \\ \phi_{1,i}(z) & z_{i-1} \le z \le z_i, \end{cases} \\
\Phi_{M_l}(z) &= \phi_{2,M_e}(z) \qquad z_{M_e-1} \le z \le z_{M_e}.
\end{aligned} \tag{11.164}$$

Analogous expressions can be obtained for the global interpolation functions Ψ_i. The local shape functions $\phi_{1,i}$ and $\phi_{2,i}$ are defined as linear Lagrangian interpolation polynomials:

$$\phi_{1,i}(z) = \frac{z_i - z}{z_i - z_{i-1}}, \quad \phi_{2,i}(z) = \frac{z - z_{i-1}}{z_i - z_{i-1}}, \tag{11.165}$$

which have the properties

$$\begin{aligned}
\phi_{1,i}(z = z_{i-1}) &= 1, \quad \phi_{1,i}(z = z_i) = 0, \\
\phi_{2,i}(z = z_{i-1}) &= 0, \quad \phi_{2,i}(z = z_i) = 1.
\end{aligned} \tag{11.166}$$

11.5.3 Kinematics and Stresses

The strains of the laminate can be calculated from the displacement field (11.163):

$$\begin{aligned}
\varepsilon_{xx} &= \frac{\partial u}{\partial x} = \sum_{i=1}^{i=M_l} \frac{\partial U_i}{\partial x} \Phi_i, \\
\varepsilon_{yy} &= \frac{\partial v}{\partial y} = \sum_{i=1}^{i=M_l} \frac{\partial V_i}{\partial y} \Phi_i, \\
\varepsilon_{zz} &= \frac{\partial w}{\partial z} = \sum_{i=1}^{i=N_l} \frac{\partial W_i}{\partial z} \Psi_i, \\
\gamma_{xy} &= \frac{\partial u}{\partial y} + \frac{\partial v}{\partial x} = \sum_{i=1}^{i=M_l} \left(\frac{\partial U_i}{\partial y} + \frac{\partial V_i}{\partial x} \right) \Phi_i,
\end{aligned}$$

$$\gamma_{xz} = \frac{\partial u}{\partial z} + \frac{\partial w}{\partial x} = \sum_{i=1}^{i=M_l} U_i \frac{\partial \Phi_i}{\partial z} + \sum_{i=1}^{i=N_l} \frac{\partial W_i}{\partial x} \Psi_i ,$$
$$\gamma_{yz} = \frac{\partial v}{\partial z} + \frac{\partial w}{\partial y} = \sum_{i=1}^{i=M_l} V_i \frac{\partial \Phi_i}{\partial z} + \sum_{i=1}^{i=N_l} \frac{\partial W_i}{\partial y} \Psi_i . \tag{11.167}$$

From the strains obtained in this way, the layerwise stresses can be calculated using Hooke's generalised law (formulated here for monoclinic material behaviour in the xy-plane):

$$\begin{pmatrix} \sigma_{xx} \\ \sigma_{yy} \\ \sigma_{zz} \\ \tau_{yz} \\ \tau_{xz} \\ \tau_{xy} \end{pmatrix}_k = \begin{bmatrix} C_{11} & C_{12} & C_{13} & 0 & 0 & C_{16} \\ C_{12} & C_{22} & C_{23} & 0 & 0 & C_{26} \\ C_{13} & C_{23} & C_{33} & 0 & 0 & C_{36} \\ 0 & 0 & 0 & C_{44} & C_{45} & 0 \\ 0 & 0 & 0 & C_{45} & C_{55} & 0 \\ C_{16} & C_{26} & C_{36} & 0 & 0 & C_{66} \end{bmatrix}_k \begin{pmatrix} \varepsilon_{xx} \\ \varepsilon_{yy} \\ \varepsilon_{zz} \\ \gamma_{yz} \\ \gamma_{xz} \\ \gamma_{xy} \end{pmatrix}_k . \tag{11.168}$$

The approach described in the context of a layerwise theory can be used either to find closed-form analytical approximate solutions for special laminate problems, or purely numerical methods can be developed from this, usually in the sense of a finite element formulation. However, it should always be noted that although a layerwise formulation can in many cases achieve a high level of accuracy compared to single-layer theories, this gain comes at the cost of significantly higher computational effort. It is therefore always up to the user to decide what computational effort is required for which calculation purpose and whether a layerwise theory is preferable to 'simpler' laminate theories.

11.5.4 Cylindrical Bending of a Cross-Ply Laminate: Exact Solution According to Pagano (1969)

It is possible to find exact solutions for a few special cases within the framework of a layerwise laminate theory that exactly fulfil both the underlying differential equations and all boundary conditions. One such exact solution for the cylindrical bending of cross-ply laminates goes back to Pagano from 1969, which will be briefly outlined below. Even if such solutions are usually quite limited in their practical applicability, they are nevertheless extremely valuable, especially with regard to the verification of approximate numerical methods, so that the work of Pagano (1969), for example, now has many hundreds of citations from other scientists.

Consider a cross-ply laminate as shown in Fig. 11.7. The laminate is infinitely extended in the y-direction and is in a plane strain state with respect to the xz-plane. The individual layers have either the fibre orientations $\theta_k = 0°$ or $\theta_k = 90°$, otherwise no further requirements are placed on the layup or the layer properties and thicknesses. The laminate is stressed by a surface load $p(x)$ and there is a hinged support at the edges $x = 0$ and $x = l$.

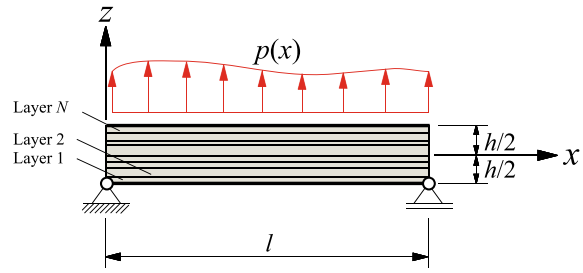


Fig. 11.7 Cross-ply laminate under cylindrical bending

The strains of each individual layer can be calculated as:

$$\begin{aligned} \varepsilon_{xx,k} &= R_{11,k}\sigma_{xx,k} + R_{12,k}\sigma_{zz,k}, \\ \varepsilon_{zz,k} &= R_{12,k}\sigma_{xx,k} + R_{22,k}\sigma_{zz,k}, \\ \gamma_{xz,k} &= R_{66,k}\tau_{xz,k}. \end{aligned} \tag{11.169}$$

Therein, $R_{11,k}$, $R_{22,k}$, $R_{12,k}$, $R_{66,k}$ are the reduced compliances of the single layer k for the plane strain state, which result when the transverse strain $\varepsilon_{yy,k}$ is eliminated from the material law. The remaining two equilibrium conditions are:

$$\frac{\partial \sigma_{xx,k}}{\partial x} + \frac{\partial \tau_{xz,k}}{\partial z} = 0, \quad \frac{\partial \tau_{xz,k}}{\partial x} + \frac{\partial \sigma_{zz,k}}{\partial z} = 0, \tag{11.170}$$

and assuming a geometrically linear problem, the strains in each individual layer can be calculated as:

$$\varepsilon_{xx,k} = \frac{\partial u_k}{\partial x}, \quad \varepsilon_{zz,k} = \frac{\partial w_k}{\partial z}, \quad \gamma_{xz,k} = \frac{\partial u_k}{\partial z} + \frac{\partial w_k}{\partial x}. \tag{11.171}$$

The boundary conditions on the surfaces of the laminate require that

$$\begin{aligned} \sigma_{zz}\left(z = \frac{h}{2}\right) &= p\,(x)\,, \quad \tau_{xz}\left(z = \frac{h}{2}\right) = 0, \\ \sigma_{zz}\left(z = -\frac{h}{2}\right) &= 0, \quad \tau_{xz}\left(z = -\frac{h}{2}\right) = 0 \end{aligned} \tag{11.172}$$

holds. At the edges $x = 0$ and $x = l$ it is required that the conditions

$$\sigma_{xx}\,(x = 0) = 0, \quad \sigma_{xx}\,(x = l) = 0, \quad w\,(x = 0) = 0, \quad w\,(x = l) = 0 \tag{11.173}$$

are fulfilled for all z. If we also introduce local reference axes x_k, z_k in the middle plane of each layer k with thickness h_k, where these have their origin at the edge $x = 0$, then the continuity conditions for the interlaminar stresses $\tau_{xz,k}$ and $\sigma_{zz,k}$ as well as for the displacements u_k and w_k can be formulated as follows:

$$\begin{aligned}
\tau_{xz,k}\left(z=\frac{h_k}{2}\right)&=\tau_{xz,k+1}\left(z=-\frac{h_{k+1}}{2}\right),\\
\sigma_{zz,k}\left(z=\frac{h_k}{2}\right)&=\sigma_{zz,k+1}\left(z=-\frac{h_{k+1}}{2}\right),\\
u_k\left(z=\frac{h_k}{2}\right)&=u_{k+1}\left(z=-\frac{h_{k+1}}{2}\right),\\
w_k\left(z=\frac{h_k}{2}\right)&=w_{k+1}\left(z=-\frac{h_{k+1}}{2}\right).
\end{aligned} \tag{11.174}$$

The load $p(x)$ is now assumed in the following form:

$$p\,(x)=p_0\sin\left(\frac{m\pi x}{l}\right). \tag{11.175}$$

At this point, Pagano proposed the following solution for the problem at hand

$$\begin{aligned}
\sigma_{xx,k}&=\frac{\partial^2 f_k}{\partial z^2}\sin\left(\frac{m\pi x}{l}\right),\\
\sigma_{zz,k}&=-\left(\frac{m\pi}{l}\right)^2 f_k\sin\left(\frac{m\pi x}{l}\right),\\
\tau_{xz,k}&=-\frac{m\pi}{l}\frac{\partial f_k}{\partial z}\cos\left(\frac{m\pi x}{l}\right)
\end{aligned} \tag{11.176}$$

for the stress components, where $f_k=f_k(z)$ is a layerwise function of the thickness coordinate z yet to be determined. It is easy to show that the approach (11.176) fulfils the equilibrium conditions (11.170) identically. The requirement for compatibility of the strains then ultimately leads to the following ordinary linear homogeneous differential equation of the fourth order for the still unknown stress function $f_k(z)$:

$$R_{11,k}\frac{\partial^4 f_k}{\partial z^4}-\left(\frac{m\pi}{l}\right)^2\left(2R_{12,k}+R_{66,k}\right)\frac{\partial^2 f_k}{\partial z^2}+R_{22,k}\left(\frac{m\pi}{l}\right)^4 f_k=0. \tag{11.177}$$

The solution can be given as:

$$f_k=\sum_{j=1}^{j=4}A_{j,k}e^{\lambda_{j,k}z_k}, \tag{11.178}$$

where the exponents $\lambda_{j,k}$ are defined as follows:

$$\lambda_{1,2,3,4,k}=\pm\frac{m\pi}{l}\sqrt{\frac{2R_{12,k}+R_{66,k}\pm\sqrt{\left(2R_{12,k}+R_{66,k}\right)^2-4R_{11,k}R_{22,k}}}{2R_{11,k}}}. \tag{11.179}$$

Assuming that all exponents $\lambda_{j,k}$ are real values, the constants $A_{j,k}$ will also be real values, and the stress functions in (11.176) can be specified as:

$$\sigma_{xx,k} = \sin\left(\frac{m\pi x}{l}\right) \sum_{j=1}^{j=4} \lambda_{j,k}^2 A_{j,k} e^{\lambda_{j,k} z_k},$$

$$\sigma_{zz,k} = -\left(\frac{m\pi}{l}\right)^2 \sin\left(\frac{m\pi x}{l}\right) \sum_{j=1}^{j=4} A_{j,k} e^{\lambda_{j,k} z_k},$$

$$\tau_{xz,k} = -\frac{m\pi}{l} \cos\left(\frac{m\pi x}{l}\right) \sum_{j=1}^{j=4} A_{j,k} \lambda_{j,k} e^{\lambda_{j,k} z_k}. \tag{11.180}$$

By integrating the strains, the displacements u_k and w_k can also be determined, but this is not discussed in detail. The stress functions (11.180) and the resulting displacements then fulfil the boundary conditions (11.173) identically. Evaluating the boundary and continuity conditions (11.172) and (11.174) then provides a linear system of equations for the still unknown coefficients $A_{j,k}$, whereby the exact solution of the bending problem is complete.

References

Altenbach H (1998): *Theories for laminated and sandwich plates, a review*, Mechanics of Composite Materials 34:243–252.

Altenbach H (2000a): *On the determination of transverse shear stiffnesses of orthotropic plates*, Zeitschrift für Angewandte Mathematik und Physik 51:629–649.

Altenbach H (2000b): *An alternative determination of transverse shear stiffnesses for sandwich and laminated plates*, International Journal of Solids and Structures 37:3503–3520.

Altenbach H, Becker W (2003): *Modern trends in composite laminates mechanics*, Springer Verlag, Wien et al., Austria.

Chow TS (1971): *On the propagation of flexural waves in an orthotropic laminated plate and its response to an impulsive load*, Journal of Composite Materials 5:306–319.

Hencky H (1947): *Über die Berücksichtigung der Schubverformung in ebenen Platten*, Ingenieur-Archiv 16:72–76.

Kant T, Swaminathan K (2000): *Estimation of transverse/interlaminar stresses in laminated composites - a selective review and survey of current developments*, Composite Structures 49:65–75.

Laitinen M, Lahtinen H, Sjölind SG (1995): *Transverse shear correction factors for laminates in cylindrical bending*, Communications in Numerical Methods in Engineering 11:41–47.

Mau ST (1973): *A refined laminated plate theory*, Journal of Applied Mechanics 40:606–607.

Mindlin RD (1951): *Influence of rotatory inertia and shear on flexural motions of isotropic, elastic plates*, Journal of Applied Mechanics 18:31–38.

Noor AK, Burton WS (1989): *Assessment of shear deformation theories for multilayered composite plates*, Applied Mechanics Reviews 42:1–13.

Noor AK, Burton WS (1990): *Assessment of computational models for multilayered anisotropic plates*, Composite Structures 14:233–265.

Pagano NJ (1969): *Exact solutions for composite laminates in cylindrical bending*, Journal of Composite Materials 3:398–411.
Reddy JN (1984a): *A simple higher-order theory for laminated composite plates*, Journal of Applied Mechanics 51:745–752.
Reddy JN (1984b): *A refined nonlinear theory of plates with transverse shear deformation*, International Journal of Solids and Structures 20:881–906.
Reddy JN, Phan ND (1985): *Stability and vibration of isotropic, orthotropic and laminated plates according to a higher-order shear deformation theory*, Journal of Sound and Vibration 98:157–170.
Reddy JN (1987): *A generalization of two-dimensional theories of laminated composite plates*, Communications in Applied Numerical Methods 3:173–180.
Reddy JN (1990a): *A review of refined theories of laminated composite plates*, Shock and Vibration Digest 22:3–17.
Reddy JN (1990b): *On refined theories of composite laminates*, Meccanica 25:230–238.
Reddy JN (1990c): *A general non-linear third-order theory of plates with moderate thickness*, International Journal of Non-Linear Mechanics 25:677–686.
Reddy JN, Robbins DH (1994): *Theories and computational models for composite laminates*, Applied Mechanics Reviews 47:147–169.
Reddy JN (2004): *Mechanics of laminated composite plates and shells (2nd edition)*, CRC Press Boca Raton et al., USA.
Reissner E (1945): *The effect of transverse shear deformation on the bending of elastic plates*, Journal of Applied Mechanics 12:69–77.
Rohwer K (1988): *Improved transverse shear stiffnesses for layered finite elements*. Research report DFVLR-FB 88-32, DFVLR, Institut für Strukturmechanik, Braunschweig, Germany.
Rohwer K (1996): *Modelle und Methoden zur Berechnung von Laminaten aus unidirektionalen Faserverbunden*. VDI Verlag, Düsseldorf, Germany.
Rolfes R, Rohwer K (1997): *Improved transverse shear stresses in composite finite elements based on first order shear deformation theory*, International Journal for Numerical Methods in Engineering 40:51–60.
Srinivas S (1973): *A refined analysis of composite laminates*, Journal of Sound and Vibration 30:495–507.
Sun CT, Whitney JM (1973): *Theories for the dynamic response of laminated plates*, AIAA Journal 11:178–183.
Whitney JM, Pagano NJ (1970): *Shear deformation in homogeneous anisotropic plates*, Journal of Applied Mechanics 37:1031–1036.
Whitney JM (1973): *Shear correction factors for orthotropic laminates under static load*, Journal of Applied Mechanics 40:302–304.

Part III
Buckling of Laminates

12 Navier-Type Solutions for Laminate Buckling Problems

In this chapter we consider plane, symmetric, orthotropic rectangular laminates under inplane compressive and biaxial loading, which are simply supported at all edges, and determine the critical buckling loads of these laminates wherein we assume Classical Laminated Plate Theory (CLPT) to be valid. This type of analysis is also referred to as a Navier solution. The considerations are later extended to unsymmetric cross-ply laminates and angle-ply laminates. Navier solutions are also considered in the context of First-Order Shear Deformation Theory (FSDT).

12.1 Basic Equations in the Context of Classical Laminated Plate Theory

Consider a laminate under the inplane edge loads N^0_{xx}, N^0_{yy}, N^0_{xy} according to Fig. 12.1, top left. The loads are plotted in such a way that N^0_{xx} and N^0_{yy} are counted as positive compressive forces. Correspondingly, N^0_{xy} is also counted as positive as given in Fig. 12.1, top left, contrary to the common sign convention.

As long as a given load combination is below a certain critical limit, there is essentially a plane stress state in the laminate, the so-called initial or pre-buckling stress state. For this, the inplane force equilibrium conditions must be fulfilled:

$$\begin{aligned} \frac{\partial N^0_{xx}}{\partial x} + \frac{\partial N^0_{xy}}{\partial y} &= 0, \\ \frac{\partial N^0_{xy}}{\partial x} + \frac{\partial N^0_{yy}}{\partial y} &= 0. \end{aligned} \tag{12.1}$$

The assumption that no deflections of the laminate due to the edge loads N^0_{xx}, N^0_{yy}, N^0_{xy} occur before the bifurcational buckling load is reached applies exactly to symmetric lami-

© The Author(s), under exclusive license to Springer-Verlag GmbH, DE, part of Springer Nature 2025

C. Mittelstedt, *Mechanics of Composite Structures*,
https://doi.org/10.1007/978-3-662-70788-3_12

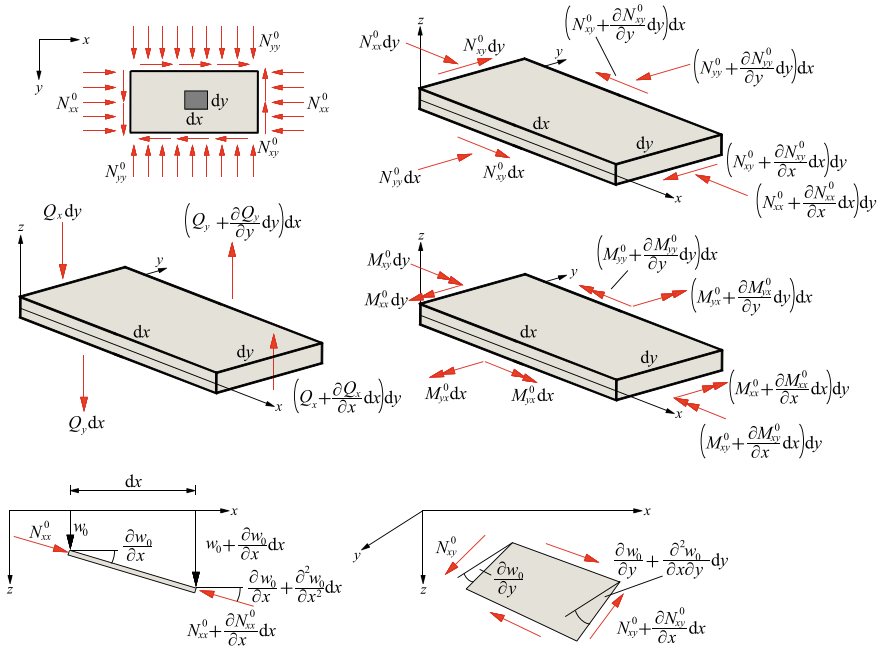


Fig. 12.1 Laminate under combined load and infinitesimal element (top and middle), section in the xz-plane (bottom left), contribution from the section force N^0_{xy} (bottom right)

nates without bending-extension coupling. In the case of unsymmetric laminates, however, it must always be kept in mind that the presence of bending-extension coupling means that even a plane stress state due to edge loads N^0_{xx}, N^0_{yy}, N^0_{xy} below the critical load combination will lead to curvatures and twist of the laminate. In this respect, the question is justified to what extent unsymmetric laminates may be treated at all within the framework of a bifurcation theory and whether such laminates do not rather represent a (potentially geometrically nonlinear) stress problem. However, a look at the relevant literature (e.g. Jones (1975), Reddy (2004)) shows that in many cases, unsymmetric laminates can also be treated in a good approximation within the framework of a bifurcational buckling analysis.

In all further explanations, it is assumed that the internal forces in the laminate correspond to the given respective edge loads at all points. In order to describe the bifurcational buckling problem of a laminate, the equilibrium at an infinitesimally deflected element or at the deformed system is considered, as is common in stability theory. Since it is assumed that the deflections of the infinitesimal element are very small, it can be assumed that the loads and thus also the initial stress state do not change due to the onset of buckling.

Firstly, the forces on the infinitesimal element are summed in the z-direction. If we first consider the section in the xz-plane (Fig. 12.1, bottom left), we obtain the following resulting force in the z-direction:

$$V_1 = N_{xx}^0 \mathrm{d}y \frac{\partial w_0}{\partial x} - \left(N_{xx}^0 + \frac{\partial N_{xx}^0}{\partial x} \mathrm{d}x \right) \left(\frac{\partial w_0}{\partial x} + \frac{\partial^2 w_0}{\partial x^2} \mathrm{d}x \right) \mathrm{d}y. \tag{12.2}$$

Neglecting higher-order terms provides the following resulting force V_1:

$$V_1 = - \left(N_{xx}^0 \frac{\partial^2 w_0}{\partial x^2} + \frac{\partial N_{xx}^0}{\partial x} \frac{\partial w_0}{\partial x} \right) \mathrm{d}x \mathrm{d}y. \tag{12.3}$$

Thus, V_1 is the force component in the z-direction that results from the force N_{xx}^0 due to the deflection of the infinitesimal element. Similarly, a resulting force V_2 can be determined at a section in the yz-plane as a result of N_{yy}^0:

$$V_2 = - \left(N_{yy}^0 \frac{\partial^2 w_0}{\partial y^2} + \frac{\partial N_{yy}^0}{\partial y} \frac{\partial w_0}{\partial y} \right) \mathrm{d}x \mathrm{d}y. \tag{12.4}$$

From the free-body image in Fig. 12.1, bottom right, the contribution of the shear force N_{xy}^0 to the total vertical force can be determined:

$$V_3 = N_{xy}^0 \mathrm{d}y \frac{\partial w_0}{\partial y} - \left(N_{xy}^0 + \frac{\partial N_{xy}^0}{\partial x} \mathrm{d}x \right) \mathrm{d}y \left(\frac{\partial w_0}{\partial y} + \frac{\partial^2 w_0}{\partial x \partial y} \mathrm{d}x \right). \tag{12.5}$$

Neglecting higher-order terms provides:

$$V_3 = - \left(N_{xy}^0 \frac{\partial^2 w_0}{\partial x \partial y} + \frac{\partial N_{xy}^0}{\partial x} \frac{\partial w_0}{\partial y} \right) \mathrm{d}x \mathrm{d}y. \tag{12.6}$$

Similarly, a contribution can be determined from $N_{yx}^0 = N_{xy}^0$. The result is

$$V_4 = - \left(N_{xy}^0 \frac{\partial^2 w_0}{\partial x \partial y} + \frac{\partial N_{xy}^0}{\partial y} \frac{\partial w_0}{\partial x} \right) \mathrm{d}x \mathrm{d}y. \tag{12.7}$$

The total resulting force component V in the z-direction due to the deflection of the infinitesimal element is then the result of the summation of the forces V_1, V_2, V_3, V_4. After a few short transformations, we obtain

$$\begin{aligned} V = & -N_{xx}^0 \frac{\partial^2 w_0}{\partial x^2} \mathrm{d}x \mathrm{d}y - 2N_{xy}^0 \frac{\partial^2 w_0}{\partial x \partial y} \mathrm{d}x \mathrm{d}y - N_{yy}^0 \frac{\partial^2 w_0}{\partial y^2} \mathrm{d}x \mathrm{d}y \\ & - \left(\frac{\partial N_{xx}^0}{\partial x} + \frac{\partial N_{xy}^0}{\partial y} \right) \frac{\partial w_0}{\partial x} \mathrm{d}x \mathrm{d}y - \left(\frac{\partial N_{xy}^0}{\partial x} + \frac{\partial N_{yy}^0}{\partial y} \right) \frac{\partial w_0}{\partial y} \mathrm{d}x \mathrm{d}y. \end{aligned} \tag{12.8}$$

The bracket terms in the second line of (12.8) occur in the equilibrium conditions (12.1) of the pre-buckling state and must therefore disappear. The following force component V therefore remains in the z-direction:

$$V = -\left(N_{xx}^0 \frac{\partial^2 w_0}{\partial x^2} + 2N_{xy}^0 \frac{\partial^2 w_0}{\partial x \partial y} + N_{yy}^0 \frac{\partial^2 w_0}{\partial y^2} \right) \mathrm{d}x\mathrm{d}y. \tag{12.9}$$

The force V can also be interpreted as the resultant of a load acting on the sectional element in the z-direction. If we form the shear force sum at the infinitesimal element in Fig. 12.1, then the following expression is obtained after elementary transformations:

$$\frac{\partial Q_x}{\partial x} + \frac{\partial Q_y}{\partial y} - N_{xx}^0 \frac{\partial^2 w_0}{\partial x^2} - 2N_{xy}^0 \frac{\partial^2 w_0}{\partial x \partial y} - N_{yy}^0 \frac{\partial^2 w_0}{\partial y^2} = 0. \tag{12.10}$$

The moment equilibrium is as follows:

$$\begin{aligned} \frac{\partial M_{xx}^0}{\partial x} + \frac{\partial M_{xy}^0}{\partial y} &= Q_x, \\ \frac{\partial M_{xy}^0}{\partial x} + \frac{\partial M_{yy}^0}{\partial y} &= Q_y. \end{aligned} \tag{12.11}$$

If the transverse shear forces in (12.10) are replaced by the moments in the laminate using (12.11), the following equation is obtained:

$$\frac{\partial^2 M_{xx}^0}{\partial x^2} + 2\frac{\partial^2 M_{xy}^0}{\partial x \partial y} + \frac{\partial^2 M_{yy}^0}{\partial y^2} - N_{xx}^0 \frac{\partial^2 w_0}{\partial x^2} - 2N_{xy}^0 \frac{\partial^2 w_0}{\partial x \partial y} - N_{yy}^0 \frac{\partial^2 w_0}{\partial y^2} = 0. \tag{12.12}$$

The plane equilibrium conditions (12.1) and the condensed plate equilibrium (12.12) then form the equations by which the equilibrium at the infinitesimally deflected laminate element is described. If the laminate forces and moments are replaced according to the constitutive law of CLPT

$$\begin{pmatrix} N_{xx}^0 \\ N_{yy}^0 \\ N_{xy}^0 \\ M_{xx}^0 \\ M_{yy}^0 \\ M_{xy}^0 \end{pmatrix} = \begin{bmatrix} A_{11} & A_{12} & A_{16} & B_{11} & B_{12} & B_{16} \\ A_{12} & A_{22} & A_{26} & B_{12} & B_{22} & B_{26} \\ A_{16} & A_{26} & A_{66} & B_{16} & B_{26} & B_{66} \\ B_{11} & B_{12} & B_{16} & D_{11} & D_{12} & D_{16} \\ B_{12} & B_{22} & B_{26} & D_{12} & D_{22} & D_{26} \\ B_{16} & B_{26} & B_{66} & D_{16} & D_{26} & D_{66} \end{bmatrix} \begin{pmatrix} \frac{\partial u_0}{\partial x} \\ \frac{\partial v_0}{\partial y} \\ \frac{\partial u_0}{\partial y} + \frac{\partial v_0}{\partial x} \\ -\frac{\partial^2 w_0}{\partial x^2} \\ -\frac{\partial^2 w_0}{\partial y^2} \\ -2\frac{\partial^2 w_0}{\partial x \partial y} \end{pmatrix}, \tag{12.13}$$

then the governing buckling differential equations for an arbitrary laminate are obtained as follows:

$$
\begin{aligned}
&A_{11}\frac{\partial^2 u_0}{\partial x^2}+2A_{16}\frac{\partial^2 u_0}{\partial x\partial y}+A_{66}\frac{\partial^2 u_0}{\partial y^2}+A_{16}\frac{\partial^2 v_0}{\partial x^2}+(A_{12}+A_{66})\frac{\partial^2 v_0}{\partial x\partial y}+A_{26}\frac{\partial^2 v_0}{\partial y^2}\\
&\qquad -B_{11}\frac{\partial^3 w_0}{\partial x^3}-3B_{16}\frac{\partial^3 w_0}{\partial x^2\partial y}-(B_{12}+2B_{66})\frac{\partial^3 w_0}{\partial x\partial y^2}-B_{26}\frac{\partial^3 w_0}{\partial y^3}=0,\\
&A_{16}\frac{\partial^2 u_0}{\partial x^2}+(A_{12}+A_{66})\frac{\partial^2 u_0}{\partial x\partial y}+A_{26}\frac{\partial^2 u_0}{\partial y^2}+A_{66}\frac{\partial^2 v_0}{\partial x^2}+2A_{26}\frac{\partial^2 v_0}{\partial x\partial y}+A_{22}\frac{\partial^2 v_0}{\partial y^2}\\
&\qquad -B_{16}\frac{\partial^3 w_0}{\partial x^3}-(B_{12}+2B_{66})\frac{\partial^3 w_0}{\partial x^2\partial y}-3B_{26}\frac{\partial^3 w_0}{\partial x\partial y^2}-B_{22}\frac{\partial^3 w_0}{\partial y^3}=0,\\
&\qquad -B_{11}\frac{\partial^3 u_0}{\partial x^3}-3B_{16}\frac{\partial^3 u_0}{\partial x^2\partial y}-(B_{12}+2B_{66})\frac{\partial^3 u_0}{\partial x\partial y^2}-B_{26}\frac{\partial^3 u_0}{\partial y^3}\\
&\qquad -B_{16}\frac{\partial^3 v_0}{\partial x^3}-(B_{12}+2B_{66})\frac{\partial^3 v_0}{\partial x^2\partial y}-3B_{26}\frac{\partial^3 v_0}{\partial x\partial y^2}-B_{22}\frac{\partial^3 v_0}{\partial y^3}\\
&+D_{11}\frac{\partial^4 w_0}{\partial x^4}+4D_{16}\frac{\partial^4 w_0}{\partial x^3\partial y}+2(D_{12}+2D_{66})\frac{\partial^4 w_0}{\partial x^2\partial y^2}+4D_{26}\frac{\partial^4 w_0}{\partial x\partial y^3}+D_{22}\frac{\partial^4 w_0}{\partial y^4}\\
&\qquad +N_{xx}^0\frac{\partial^2 w_0}{\partial x^2}+2N_{xy}^0\frac{\partial^2 w_0}{\partial x\partial y}+N_{yy}^0\frac{\partial^2 w_0}{\partial y^2}=0.
\end{aligned}
\tag{12.14}
$$

The displacements u_0, v_0, w_0 correspond to the displacements of the laminate middle plane that will occur when buckling occurs. In this context, one also speaks of the so-called buckling mode or the so-called buckling shape. Obviously, the differential equations (12.14) are coupled with each other and must therefore be solved simultaneously. If—as is very often the case in practice—a symmetric laminate is given, all coupling stiffnesses B_{op} $(o,\, p = 1, 2, 6)$ are omitted and the differential equations (12.14) are considerably simplified:

$$
\begin{aligned}
&A_{11}\frac{\partial^2 u_0}{\partial x^2}+2A_{16}\frac{\partial^2 u_0}{\partial x\partial y}+A_{66}\frac{\partial^2 u_0}{\partial y^2}+A_{16}\frac{\partial^2 v_0}{\partial x^2}+(A_{12}+A_{66})\frac{\partial^2 v_0}{\partial x\partial y}+A_{26}\frac{\partial^2 v_0}{\partial y^2}=0,\\
&A_{16}\frac{\partial^2 u_0}{\partial x^2}+(A_{12}+A_{66})\frac{\partial^2 u_0}{\partial x\partial y}+A_{26}\frac{\partial^2 u_0}{\partial y^2}+A_{66}\frac{\partial^2 v_0}{\partial x^2}+2A_{26}\frac{\partial^2 v_0}{\partial x\partial y}+A_{22}\frac{\partial^2 v_0}{\partial y^2}=0,\\
&D_{11}\frac{\partial^4 w_0}{\partial x^4}+4D_{16}\frac{\partial^4 w_0}{\partial x^3\partial y}+2(D_{12}+2D_{66})\frac{\partial^4 w_0}{\partial x^2\partial y^2}+4D_{26}\frac{\partial^4 w_0}{\partial x\partial y^3}+D_{22}\frac{\partial^4 w_0}{\partial y^4}\\
&\qquad +N_{xx}^0\frac{\partial^2 w_0}{\partial x^2}+2N_{xy}^0\frac{\partial^2 w_0}{\partial x\partial y}+N_{yy}^0\frac{\partial^2 w_0}{\partial y^2}=0.
\end{aligned}
\tag{12.15}
$$

While in the first two equations in (12.15) only partial derivatives of the inplane displacements u_0 and v_0 appear, the third equation in (12.15) is a partial differential equation in which only partial derivatives of the deflection w_0 appear. Thus, the first two equations

in (12.15) describe the disk behaviour of the laminate under the given edge loads, while the third equation in (12.15) describes the buckling behaviour.

12.2 Navier Solutions in the Context of Classical Laminated Plate Theory

For a few load cases in conjunction with special boundary conditions, it is possible to solve the governing equations (12.14) or the third equation in (12.15) exactly. One class of solutions are the so-called Navier solutions, which are discussed in more detail in this section.

12.2.1 Navier Solution for a Simply-Supported Symmetric Cross-Ply Laminate Under Uniaxial Compressive Load

Consider a rectangular symmetric cross-ply laminate (length a, width b) simply supported at all edges as shown in Fig. 12.2, which is subjected to a uniaxial edge load N^0_{xx}. The laminate is symmetric, balanced and orthotropic in its plate behaviour, so that the constitutive law (12.13) changes into the following form:

$$\begin{pmatrix} N^0_{xx} \\ N^0_{yy} \\ N^0_{xy} \\ M^0_{xx} \\ M^0_{yy} \\ M^0_{xy} \end{pmatrix} = \begin{bmatrix} A_{11} & A_{12} & 0 & 0 & 0 & 0 \\ A_{12} & A_{22} & 0 & 0 & 0 & 0 \\ 0 & 0 & A_{66} & 0 & 0 & 0 \\ 0 & 0 & 0 & D_{11} & D_{12} & 0 \\ 0 & 0 & 0 & D_{12} & D_{22} & 0 \\ 0 & 0 & 0 & 0 & 0 & D_{66} \end{bmatrix} \begin{pmatrix} \frac{\partial u_0}{\partial x} \\ \frac{\partial v_0}{\partial y} \\ \frac{\partial u_0}{\partial y} + \frac{\partial v_0}{\partial x} \\ -\frac{\partial^2 w_0}{\partial x^2} \\ -\frac{\partial^2 w_0}{\partial y^2} \\ -2\frac{\partial^2 w_0}{\partial x \partial y} \end{pmatrix}. \tag{12.16}$$

The buckling differential equation then takes the following form:

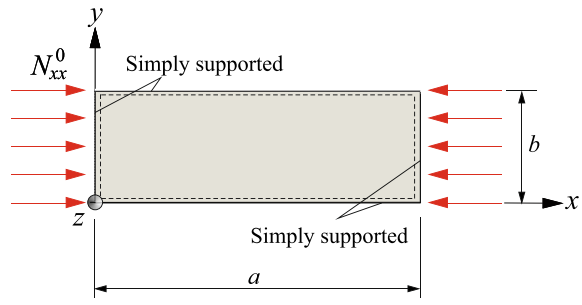


Fig. 12.2 Simply supported laminate under uniaxial compressive load

$$D_{11}\frac{\partial^4 w_0}{\partial x^4} + 2\left(D_{12} + 2D_{66}\right)\frac{\partial^4 w_0}{\partial x^2 \partial y^2} + D_{22}\frac{\partial^4 w_0}{\partial y^4} + N_{xx}^0\frac{\partial^2 w_0}{\partial x^2} = 0. \tag{12.17}$$

The laminate is simply supported so that the following boundary conditions must be fulfilled:

$$\begin{gathered} w_0\left(x=0\right)=0, \quad w_0\left(x=a\right)=0, \quad w_0\left(y=0\right)=0, \quad w_0\left(y=b\right)=0, \\ M_{xx}^0\left(x=0\right) = -D_{11}\left.\frac{\partial^2 w_0}{\partial x^2}\right|_{x=0} = 0, \quad M_{xx}^0\left(x=a\right) = -D_{11}\left.\frac{\partial^2 w_0}{\partial x^2}\right|_{x=a} = 0, \\ M_{yy}^0\left(y=0\right) = -D_{22}\left.\frac{\partial^2 w_0}{\partial y^2}\right|_{y=0} = 0, \quad M_{yy}^0\left(y=b\right) = -D_{22}\left.\frac{\partial^2 w_0}{\partial y^2}\right|_{y=b} = 0. \end{gathered} \tag{12.18}$$

This formulation already makes explicit use of the fact that the curvatures $\left.\frac{\partial^2 w_0}{\partial y^2}\right|_{x=0,a}$ or $\left.\frac{\partial^2 w_0}{\partial x^2}\right|_{y=0,b}$ disappear. An approach of the form

$$w_0 = W_{mn}\sin\left(\frac{m\pi x}{a}\right)\sin\left(\frac{n\pi x}{b}\right) \tag{12.19}$$

identically fulfills all boundary conditions (12.18). In (12.19), m and n are still unknown half-wave numbers of the applied sine functions, which must be positive and integer. If the approach (12.19) is inserted into the differential equation (12.17), the result is

$$\begin{aligned} &\left[D_{11}\frac{m^4\pi^4}{a^4} + 2\left(D_{12} + 2D_{66}\right)\frac{m^2\pi^2}{a^2}\frac{n^2\pi^2}{b^2} + D_{22}\frac{n^4\pi^4}{b^4} - N_{xx}^0\frac{m^2\pi^2}{a^2}\right] \\ &\qquad \times W_{mn}\sin\left(\frac{m\pi x}{a}\right)\sin\left(\frac{n\pi x}{b}\right) = 0. \end{aligned} \tag{12.20}$$

For a non-trivial solution W_{mn} it is necessary that the expression in the square bracket in (12.20) disappears:

$$D_{11}\frac{m^4\pi^4}{a^4} + 2\left(D_{12} + 2D_{66}\right)\frac{m^2\pi^2}{a^2}\frac{n^2\pi^2}{b^2} + D_{22}\frac{n^4\pi^4}{b^4} - N_{xx}^0\frac{m^2\pi^2}{a^2} = 0. \tag{12.21}$$

This can be solved immediately for the load N_{xx}^0:

$$N_{xx}^0 = \pi^2\left[D_{11}\frac{m^2}{a^2} + 2\left(D_{12} + 2D_{66}\right)\frac{n^2}{b^2} + D_{22}\frac{a^2}{m^2}\frac{n^4}{b^4}\right]. \tag{12.22}$$

The result (12.22) can be interpreted as follows. The edge load N_{xx}^0, which can be calculated by (12.22), is exactly the load at which there is an infinitesimally adjacent deformed equilibrium position for the previously plane laminate. The equilibrium becomes indifferent at exactly this load level. Accordingly, the edge load according to (12.22) is the desired load at which the laminate will buckle.

The solution (12.22) depends on the half-wave numbers m and n. For each pair of values m, n there is then a unique solution for the buckling load in conjunction with an associated buckling mode, which is described by (12.19). The laminate therefore buckles in the form of two sine functions, with m half-waves in the x-direction and n half-waves in the y-direction. There are therefore an infinite number of solutions to the given buckling problem. The solution that is relevant in the technical application is described by the pair of values m, n for which the minimum buckling load N_{xx}^0 results from (12.22). This is also referred to as the critical buckling load. A closer discussion of (12.22) shows that of all the values for n, only the value $n = 1$ can be used to obtain the minimum buckling load. The following therefore applies with $n = 1$:

$$N_{xx}^0 = \pi^2 \left[D_{11} \frac{m^2}{a^2} + \frac{2}{b^2} (D_{12} + 2D_{66}) + D_{22} \frac{a^2}{b^4 m^2} \right]. \tag{12.23}$$

Which value for the half-wave number m leads to the minimum buckling load cannot be answered this easily. To determine m, it can be required that the buckling load N_{xx}^0 assumes an extreme value with regard to m, i.e. $\frac{\partial N_{xx}^0}{\partial m} = 0$. The resulting equation can be solved directly for m and the following equation for the unknown half-wave number m is obtained:

$$m = \frac{a}{b} \sqrt[4]{\frac{D_{22}}{D_{11}}}. \tag{12.24}$$

Since Eq. (12.24) will only lead to an integer result in the rarest of cases, the numerical value resulting from (12.24) should be rounded down to the next lower integer as well as rounded up to the next higher integer. With these two numerical values, Eq. (12.23) is to be evaluated, and the smaller of the two numerical values for N_{xx}^0 then corresponds to the critical buckling load.

It should also be noted that the coefficient W_{mn} of the approach (12.19) remains undetermined, as is usual in the context of a bifurcational buckling theory. With the small deformations assumed here, there is also no possibility of determining this coefficient. This means that although the buckling shape/buckling mode of the laminate simply supported at all edges in the form of the two sine functions is known, the amplitude is not. In order to determine the amplitude, a geometrically nonlinear theory would have to be used, which is not dealt with in this chapter.

The limiting case of an infinitely long laminate ($a \to \infty$) is of particular interest. It can be seen that the buckling load N_{xx}^0 tends towards an asymptotic limit value with increasing length of the laminate and no longer changes with increasing a. The limit value sought is obtained by substituting the wave number m according to (12.24) into the solution (12.23), which leads to the following result:

$$N_{xx}^0 = \frac{2\pi^2}{b^2} \left(\sqrt{D_{11} D_{22}} + D_{12} + 2D_{66} \right). \tag{12.25}$$

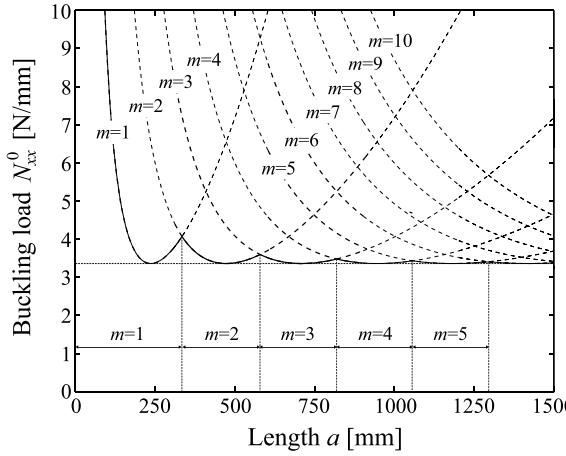


Fig. 12.3 Buckling curve for a cross-ply laminate $[0°/90°/0°/90°]_S$ under uniaxial load

Figure 12.3 contains a study of the buckling load N_{xx}^0 for a cross-ply composite laminate with the layup $[0°/90°/0°/90°]_S$, whereby the width of the laminate was fixed at $b = 200\,\text{mm}$ and the length a was varied. The elastic properties of the individual layers were defined as $E_{11} = 135{,}000\,\text{MPa}$, $E_{22} = 10{,}000\,\text{MPa}$, $G_{12} = 5000\,\text{MPa}$, $\nu_{12} = 0.27$, the individual layer thickness is 0.125 mm. Firstly, in Fig. 12.3 the results for the buckling load N_{xx}^0 according to (12.23) for different half-wave numbers m over the plate length a are plotted in dashed lines. It can be seen that all resulting curves have local minima and otherwise tend towards infinity with increasing distance from these minima. In addition, the individual curves have various points of intersection. For practical design, however, only the minimum possible buckling load is of interest for a fixed length a, so that the selection of practically relevant results for N_{xx}^0 is significantly reduced and is represented exclusively by the solid line. This form of result representation for the buckling load N_{xx}^0 of a plate is also addressed as buckling curve. The results of Fig. 12.3 can be interpreted as follows. For very short plates, the buckling load N_{xx}^0 increases beyond all limits and tends towards infinity. As the plate length a increases, the plate buckles in $m = 1$ half-waves and reaches a local minimum at about $a \approx 240\,\text{mm}$. At approximately $a \approx 330\,\text{mm}$ the buckling curves for $m = 1$ and $m = 2$ intersect and a local maximum occurs for the buckling curve. From this value for the plate length, the plate buckles in $m = 2$ half-waves (in this context, it is also said that a mode change from $m = 1$ half-waves to $m = 2$ half-waves has taken place at $a \approx 330\,\text{mm}$). The next mode change to $m = 3$ half-waves then takes place at about $a \approx 580\,\text{mm}$, and for higher plate lengths a further mode changes and local extrema can be observed. It can be seen that clear intervals for the plate length a can be specified for the current plate buckling problem, within which exactly one defined half-wave number m is relevant. Furthermore, it can be seen that the values of the local maxima at which the mode changes occur decrease overall as the plate length a increases. The curve therefore becomes increasingly flatter and approaches an asymptotic limit value for N_{xx}^0 from above, which corresponds exactly to Eq. (12.25). In the case of the buckling load according to (12.25),

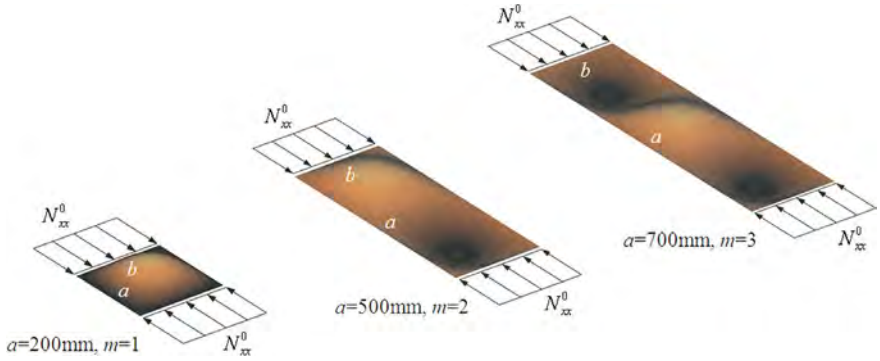


Fig. 12.4 Buckling modes for a cross-ply laminate $\left[0°/90°/0°/90°\right]_S$

one often speaks of the buckling load for the infinitely long or sufficiently long plate. In lightweight engineering practice, only the corresponding asymptotic solutions are used in a large number of applications due to the simplicity of the corresponding formulas.

Figure 12.4 contains graphical representations of the resulting buckling modes/buckling shapes for different lengths a for the discussed cross-ply laminate. The increase in the half-wave number m with increasing plate length a can be clearly seen.

Finally, the possibility of converting the results into a compact dimensionless form is considered. To do this, the coordinates x, y are transformed to the unit square using the natural coordinates ξ_1, ξ_2:

$$\xi_1 = \frac{x}{a}, \quad \xi_2 = \frac{y}{b}. \tag{12.26}$$

The differential equation (12.17) can then be transformed using $\frac{\partial^{i+j} w_0}{\partial x^i \partial y^j} = \frac{\partial^{i+j} w_0}{a^i b^j \partial \xi_1^i \partial \xi_2^j}$ and multiplication by the factor $\frac{a^2 b^2}{\sqrt{D_{11} D_{22}}}$ into the following form:

$$\frac{1}{\alpha^2} \frac{\partial^4 \bar{w}_0}{\partial \xi_1^4} + 2\beta \frac{\partial^4 \bar{w}_0}{\partial \xi_1^2 \partial \xi_2^2} + \alpha^2 \frac{\partial^4 \bar{w}_0}{\partial \xi_2^4} + \bar{N}_{xx}^0 \pi^2 \frac{\partial^2 \bar{w}_0}{\partial \xi_1^2} = 0. \tag{12.27}$$

The new dimensionless quantities introduced here are the aspect ratio α, the orthotropy factor/Seydel's orthotropy parameter β and the buckling load $\bar{N}_{xx}^0$, which are defined as follows:

$$\alpha = \frac{a}{b} \sqrt[4]{\frac{D_{22}}{D_{11}}}, \quad \beta = \frac{D_{12} + 2D_{66}}{\sqrt{D_{11} D_{22}}}, \quad \bar{N}_{xx}^0 = \frac{N_{xx}^0 b^2}{\pi^2 \sqrt{D_{11} D_{22}}}. \tag{12.28}$$

The buckling mode $\bar{w}_0$ introduced in (12.27) is basically freely available in the form of the dimensionless representation and has no influence on the solution of (12.27), but when using energy-based methods, it turns out that the following form is particularly useful:

$$\bar{w}_0 = \frac{w_0}{\sqrt{ab}}. \tag{12.29}$$

The boundary conditions (12.18) can be reformulated in a dimensionless form as follows:

$$\begin{gathered}\bar{w}_0\left(\xi_1 = 0\right) = 0, \quad \bar{w}_0\left(\xi_1 = 1\right) = 0, \quad \bar{w}_0\left(\xi_2 = 0\right) = 0, \quad \bar{w}_0\left(\xi_2 = 1\right) = 0, \\ \left.\frac{\partial^2 \bar{w}_0}{\partial \xi_1^2}\right|_{\xi_1=0} = 0, \quad \left.\frac{\partial^2 \bar{w}_0}{\partial \xi_1^2}\right|_{\xi_1=1} = 0, \quad \left.\frac{\partial^2 \bar{w}_0}{\partial \xi_2^2}\right|_{\xi_2=0} = 0, \quad \left.\frac{\partial^2 \bar{w}_0}{\partial \xi_2^2}\right|_{\xi_2=1} = 0.\end{gathered} \tag{12.30}$$

The approach suitable for the buckling shape is as follows:

$$\bar{w}_0 = W_{mn} \sin\left(m\pi\xi_1\right) \sin\left(n\pi\xi_2\right). \tag{12.31}$$

Inserting this into the differential equation (12.27) then results in

$$\pi^4 \left(\frac{m^4}{\alpha^2} + 2\beta m^2 n^2 + \alpha^2 n^4 - \bar{N}_{xx}^0 m^2\right) W_{mn} \sin\left(m\pi\xi_1\right) \sin\left(n\pi\xi_2\right) = 0. \tag{12.32}$$

The only relevant solution is the disappearance of the term in the round bracket:

$$\frac{m^4}{\alpha^2} + 2\beta m^2 n^2 + \alpha^2 n^4 - \bar{N}_{xx}^0 m^2 = 0. \tag{12.33}$$

This can be immediately solved for the required dimensionless buckling load $\bar{N}_{xx}^0$:

$$\bar{N}_{xx}^0 = \frac{m^2}{\alpha^2} + 2\beta n^2 + \frac{\alpha^2 n^4}{m^2}. \tag{12.34}$$

The minimum buckling load always results for $n = 1$:

$$\bar{N}_{xx}^0 = \frac{m^2}{\alpha^2} + 2\beta + \frac{\alpha^2}{m^2}. \tag{12.35}$$

The relevant half-wave number m can again be determined from the corresponding extreme value task $\frac{\partial \bar{N}_{xx}^0}{\partial m} = 0$ and follows as:

$$m = \alpha. \tag{12.36}$$

The asymptotic limit value of the buckling load $\bar{N}_{xx}^0$ is obtained by inserting the half-wave number m according to (12.36) into the solution (12.35). The following result is obtained:

$$\bar{N}_{xx}^0 = 2\left(1 + \beta\right). \tag{12.37}$$

It is interesting to note that there is a linear relationship between the dimensionless buckling load $\bar{N}_{xx}^0$ and the orthotropy parameter β.

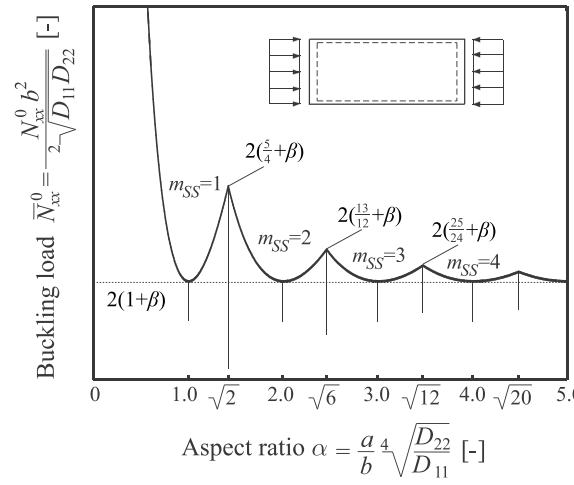


Fig. 12.5 Buckling curve for an orthotropic laminate in dimensionless form

The solution (12.35) for the dimensionless buckling load $\bar{N}^0_{xx}$ is shown in Fig. 12.5 plotted as a function of the aspect ratio. The characteristic shape of the buckling curve in Fig. 12.5 corresponds to that already discussed in Fig. 12.3. It can be shown that a mode change from m to $m+1$ half-waves always occurs at the point

$$\alpha = \sqrt{m^2 + m}. \tag{12.38}$$

At this point, the dimensionless buckling load $\bar{N}^0_{xx}$ is

$$\bar{N}^0_{xx} = 2\left[\frac{1}{m+1}\left(m + \frac{1}{2\,m} + 1\right) + \beta\right]. \tag{12.39}$$

Furthermore, there are various local minima, which for the curve section with m half-waves always occur at the point

$$\alpha = m. \tag{12.40}$$

The associated buckling load $\bar{N}^0_{xx}$ is also the minimum occurring value according to (12.37).

12.2.2 Navier Solution for a Simply-Supported Symmetric Cross-Ply Laminate Under Biaxial Load

We now consider a laminate as in the previous section which is now stressed by a biaxial compressive load in the form of the edge loads N^0_{xx} and N^0_{yy} (Fig. 12.6). Here, the edge load N^0_{yy} is a multiple of the edge load N^0_{xx}, i.e. $N^0_{yy} = \psi N^0_{xx}$. The buckling differential equation in (12.15) then takes the following form:

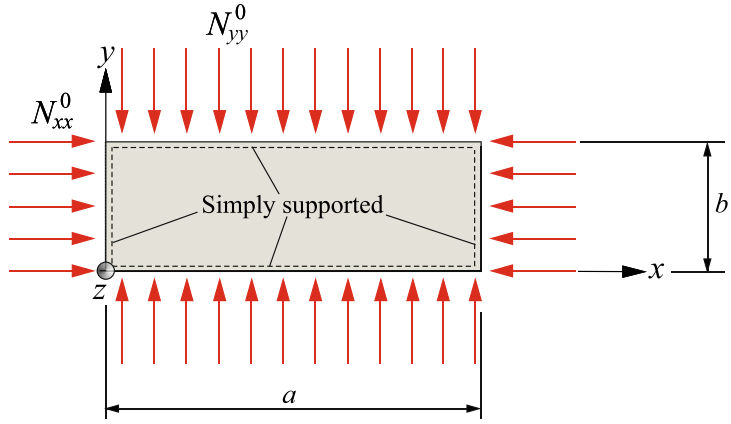


Fig. 12.6 Laminate under biaxial load

$$D_{11}\frac{\partial^4 w_0}{\partial x^4} + 2\left(D_{12} + 2D_{66}\right)\frac{\partial^4 w_0}{\partial x^2 \partial y^2} + D_{22}\frac{\partial^4 w_0}{\partial y^4} + N_{xx}^0\frac{\partial^2 w_0}{\partial x^2} + \psi N_{xx}^0\frac{\partial^2 w_0}{\partial y^2} = 0. \tag{12.41}$$

We use an approach of the form (12.19) and obtain the following closed-form solution:

$$N_{xx}^0 = \pi^2 \frac{D_{11}\frac{m^2}{a^2} + 2\left(D_{12} + 2D_{66}\right)\frac{n^2}{b^2} + D_{22}\frac{a^2}{m^2}\frac{n^4}{b^4}}{1 + \psi\frac{a^2}{m^2}\frac{n^2}{b^2}}. \tag{12.42}$$

The solution (12.42) depends on the half-wave numbers m and n. In contrast to the uniaxially compressed laminate, it is not easy to say which pair of values m and n leads to the minimum buckling load. Here, the relevant pair of values must be determined by trial and error.

An interesting case occurs when one of the two edge loads N_{xx}^0 or N_{yy}^0 is a tensile load. For example, if N_{yy}^0 is a tensile load, then the factor ψ is negative. If the solution (12.42) is discussed in more detail, it can be seen that this has a positive effect on the buckling load, i.e. the presence of a tensile load increases the buckling resistance. Figure 12.7 shows some selected buckling curves for the previously discussed cross-ply laminate $[0°/90°/0°/90°]_S$ under biaxial loading.

As expected, a positive tensile load N_{yy}^0 causes a significant increase in the buckling resistance. At the same time, it can be seen that more pronounced and more frequent mode changes occur in the buckling curves when the factor ψ decreases. In addition, for the case of equal edge loads N_{xx}^0 and N_{yy}^0, the two relevant half-wave numbers m and n are always fixed at $m = n = 1$, regardless of the length of the plate, which explains the continuous corresponding buckling curve in Fig. 12.7. Some selected buckling modes are shown in

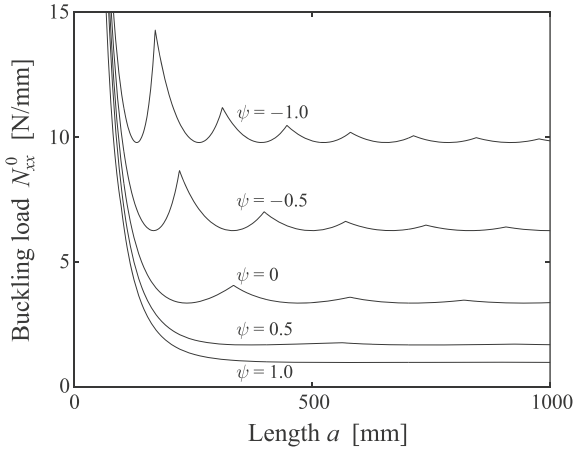


Fig. 12.7 Buckling curves for a cross-ply laminate $\left[0°/90°/0°/90°\right]_S$ under biaxial load

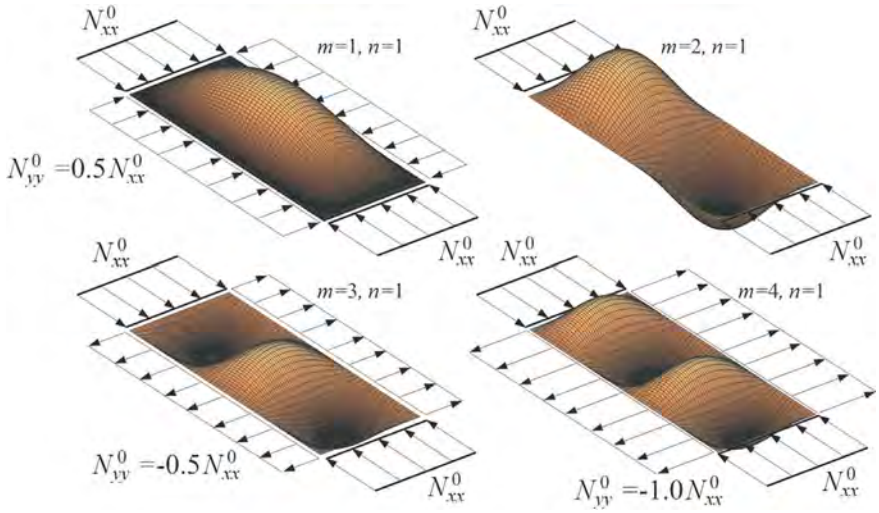


Fig. 12.8 Buckling modes for a cross-ply laminate $\left[0°/90°/0°/90°\right]_S$ under biaxial load

Fig. 12.8 for a laminate with $a = 500$ mm. An increase in the longitudinal half-wave number m can be clearly seen as the edge load N_{yy}^0 increases.

12.2.3 Navier Solution for a Simply-Supported Unsymmetric Cross-Ply Laminate Under Uniaxial Compressive Load

An unsymmetric cross-ply laminate is considered which is stressed by a uniaxial compressive edge load N^0_{xx}. The constitutive law (12.13) then takes the following form:

$$\begin{pmatrix} N^0_{xx} \\ N^0_{yy} \\ N^0_{xy} \\ M^0_{xx} \\ M^0_{yy} \\ M^0_{xy} \end{pmatrix} = \begin{bmatrix} A_{11} & A_{12} & 0 & B_{11} & 0 & 0 \\ A_{12} & A_{11} & 0 & 0 & -B_{11} & 0 \\ 0 & 0 & A_{66} & 0 & 0 & 0 \\ B_{11} & 0 & 0 & D_{11} & D_{12} & 0 \\ 0 & -B_{11} & 0 & D_{12} & D_{11} & 0 \\ 0 & 0 & 0 & 0 & 0 & D_{66} \end{bmatrix} \begin{pmatrix} \frac{\partial u_0}{\partial x} \\ \frac{\partial v_0}{\partial y} \\ \frac{\partial u_0}{\partial y} + \frac{\partial v_0}{\partial x} \\ -\frac{\partial^2 w_0}{\partial x^2} \\ -\frac{\partial^2 w_0}{\partial y^2} \\ -2\frac{\partial^2 w_0}{\partial x \partial y} \end{pmatrix}, \tag{12.43}$$

and the differential equation system (12.14) changes into:

$$\begin{aligned} A_{11}\frac{\partial^2 u_0}{\partial x^2} + A_{66}\frac{\partial^2 u_0}{\partial y^2} + (A_{12}+A_{66})\frac{\partial^2 v_0}{\partial x \partial y} - B_{11}\frac{\partial^3 w_0}{\partial x^3} &= 0, \\ (A_{12}+A_{66})\frac{\partial^2 u_0}{\partial x \partial y} + A_{66}\frac{\partial^2 v_0}{\partial x^2} + A_{11}\frac{\partial^2 v_0}{\partial y^2} + B_{11}\frac{\partial^3 w_0}{\partial y^3} &= 0, \\ B_{11}\left(\frac{\partial^3 v_0}{\partial y^3} - \frac{\partial^3 u_0}{\partial x^3}\right) + D_{11}\left(\frac{\partial^4 w_0}{\partial x^4} + \frac{\partial^4 w_0}{\partial y^4}\right) & \\ +2\,(D_{12}+2D_{66})\frac{\partial^4 w_0}{\partial x^2 \partial y^2} + N^0_{xx}\frac{\partial^2 w_0}{\partial x^2} &= 0. \end{aligned} \tag{12.44}$$

The solution presented here goes back to Jones (1973). The so-called SS1 boundary conditions are applied. The following is required at the edges at $x = 0$ and $x = a$ for $0 \leq y \leq b$:

$$\begin{aligned} v_0 = 0, \quad w_0 = 0, \\ M^0_{xx} = B_{11}\frac{\partial u_0}{\partial x} - D_{11}\frac{\partial^2 w_0}{\partial x^2} - D_{12}\frac{\partial^2 w_0}{\partial y^2} = 0, \\ N^0_{xx} = A_{11}\frac{\partial u_0}{\partial x} + A_{12}\frac{\partial v_0}{\partial y} - B_{11}\frac{\partial^2 w_0}{\partial x^2} = 0. \end{aligned} \tag{12.45}$$

The two edges at $y = 0$ and $y = b$ for $0 \leq x \leq a$ are subjected to the following boundary conditions:

$$u_0 = 0, \quad w_0 = 0,$$
$$M^0_{yy} = -B_{11}\frac{\partial v_0}{\partial y} - D_{12}\frac{\partial^2 w_0}{\partial x^2} - D_{22}\frac{\partial^2 w_0}{\partial y^2} = 0,$$
$$N^0_{yy} = A_{12}\frac{\partial u_0}{\partial x} + A_{11}\frac{\partial v_0}{\partial y} + B_{11}\frac{\partial^2 w_0}{\partial y^2} = 0. \tag{12.46}$$

It can be shown that with the following approach for the displacements u_0, v_0, w_0

$$u_0 = U_{mn}\cos\left(\frac{m\pi x}{a}\right)\sin\left(\frac{n\pi y}{b}\right),$$
$$v_0 = V_{mn}\sin\left(\frac{m\pi x}{a}\right)\cos\left(\frac{n\pi y}{b}\right),$$
$$w_0 = W_{mn}\sin\left(\frac{m\pi x}{a}\right)\sin\left(\frac{n\pi y}{b}\right) \tag{12.47}$$

all boundary conditions (12.45) and (12.46) are fulfilled identically. If the approach (12.47) is inserted into the differential equations (12.44), the result is

$$\left[-\left(A_{11}\frac{m^2\pi^2}{a^2} + A_{66}\frac{n^2\pi^2}{b^2}\right)U_{mn} - (A_{12}+A_{66})\frac{m\pi}{a}\frac{n\pi}{b}V_{mn} + B_{11}\frac{m^3\pi^3}{a^3}W_{mn}\right]$$
$$\times\cos\left(\frac{m\pi x}{a}\right)\sin\left(\frac{n\pi y}{b}\right) = 0,$$

$$\left[-(A_{12}+A_{66})\frac{m\pi}{a}\frac{n\pi}{b}U_{mn} - \left(A_{66}\frac{m^2\pi^2}{a^2} + A_{11}\frac{n^2\pi^2}{b^2}\right)V_{mn} - B_{11}\frac{n^3\pi^3}{b^3}W_{mn}\right]$$
$$\times\sin\left(\frac{m\pi x}{a}\right)\cos\left(\frac{n\pi y}{b}\right) = 0,$$

$$\left[-B_{11}\frac{m^3\pi^3}{a^3}U_{mn} + B_{11}\frac{n^3\pi^3}{b^3}V_{mn}\right.$$
$$\left. + \left\{D_{11}\left(\frac{m^4\pi^4}{a^4} + \frac{n^4\pi^4}{b^4}\right) + 2(D_{12}+2D_{66})\frac{m^2\pi^2}{a^2}\frac{n^2\pi^2}{b^2} - N^0_{xx}\frac{m^2\pi^2}{a^2}\right\}W_{mn}\right]$$
$$\times\sin\left(\frac{m\pi x}{a}\right)\sin\left(\frac{n\pi y}{b}\right) = 0. \tag{12.48}$$

The solution of these equations requires the disappearance of the terms in square brackets, i.e.:

$$\left(A_{11}\frac{m^2\pi^2}{a^2}+A_{66}\frac{n^2\pi^2}{b^2}\right)U_{mn}+(A_{12}+A_{66})\frac{m\pi}{a}\frac{n\pi}{b}V_{mn}-B_{11}\frac{m^3\pi^3}{a^3}W_{mn}=0,$$

$$(A_{12}+A_{66})\frac{m\pi}{a}\frac{n\pi}{b}U_{mn}+\left(A_{66}\frac{m^2\pi^2}{a^2}+A_{11}\frac{n^2\pi^2}{b^2}\right)V_{mn}+B_{11}\frac{n^3\pi^3}{b^3}W_{mn}=0,$$

$$-B_{11}\frac{m^3\pi^3}{a^3}U_{mn}+B_{11}\frac{n^3\pi^3}{b^3}V_{mn}$$
$$+\left[D_{11}\left(\frac{m^4\pi^4}{a^4}+\frac{n^4\pi^4}{b^4}\right)+2\,(D_{12}+2D_{66})\frac{m^2\pi^2}{a^2}\frac{n^2\pi^2}{b^2}-N^0_{xx}\frac{m^2\pi^2}{a^2}\right]W_{mn}=0. \tag{12.49}$$

This is a homogeneous system of three linear equations for the unknown coefficients U_{mn}, V_{mn}, W_{mn}. This can also be represented in a vector matrix notation as:

$$\begin{bmatrix}\lambda_{11} & \lambda_{12} & \lambda_{13}\\ \lambda_{12} & \lambda_{22} & \lambda_{23}\\ \lambda_{13} & \lambda_{23} & \lambda_{33}-N^0_{xx}\bar{\lambda}_{33}\end{bmatrix}\begin{pmatrix}U_{mn}\\ V_{mn}\\ W_{mn}\end{pmatrix}=\begin{pmatrix}0\\0\\0\end{pmatrix}, \tag{12.50}$$

wherein:

$$\lambda_{11}=A_{11}\frac{m^2\pi^2}{a^2}+A_{66}\frac{n^2\pi^2}{b^2},\quad \lambda_{12}=(A_{12}+A_{66})\frac{m\pi}{a}\frac{n\pi}{b},\quad \lambda_{13}=-B_{11}\frac{m^3\pi^3}{a^3},$$

$$\lambda_{22}=A_{66}\frac{m^2\pi^2}{a^2}+A_{11}\frac{n^2\pi^2}{b^2},\quad \lambda_{23}=B_{11}\frac{n^3\pi^3}{b^3},$$

$$\lambda_{33}=D_{11}\left(\frac{m^4\pi^4}{a^4}+\frac{n^4\pi^4}{b^4}\right)+2\,(D_{12}+2D_{66})\frac{m^2\pi^2}{a^2}\frac{n^2\pi^2}{b^2},\quad \bar{\lambda}_{33}=\frac{m^2\pi^2}{a^2}. \tag{12.51}$$

For a non-trivial solution, the determinant of the coefficient matrix must be zero. After a few transformations, the required buckling load N^0_{xx} can then be determined in an exact-analytical manner as:

$$N^0_{xx}=\frac{1}{\bar{\lambda}_{33}}\left[\lambda_{33}+\frac{2\lambda_{12}\lambda_{13}\lambda_{23}-\lambda_{11}\lambda^2_{23}-\lambda_{22}\lambda^2_{13}}{\lambda_{11}\lambda_{22}-\lambda^2_{12}}\right]. \tag{12.52}$$

As the matrix entries in (12.50) are dependent on the half-wave numbers m and n, it is not possible to make a generally valid statement about the relevant values for m and n for the minimum buckling load. Here again, trial and error is required to determine which half-wave numbers result in the technically relevant minimum buckling load N^0_{xx}. It is easy to show that (12.52) contains the solution (12.22) for the symmetric cross-ply laminate as a special case.

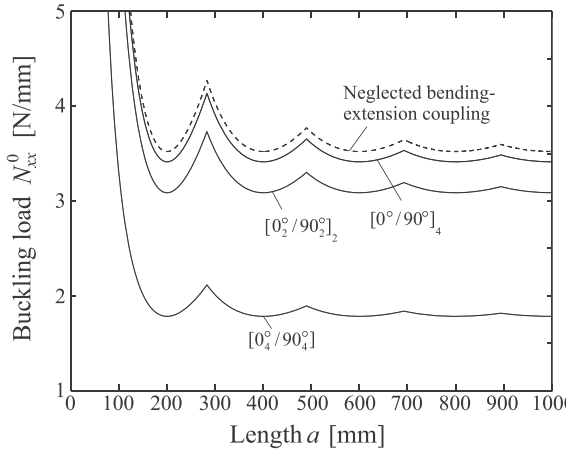


Fig. 12.9 Buckling curves for the eight-layered unsymmetric cross-ply laminates $[0^\circ/90^\circ]_4$, $\left[0_2^\circ/90_2^\circ\right]_2$ and $\left[0_4^\circ/90_4^\circ\right]$ under uniaxial loading

Figure 12.9 contains buckling curves for three different eight-layered unsymmetric cross-ply laminates, whereby the applied data correspond to those of the previous examples. The cross-ply laminates $[0^\circ/90^\circ]_4$, $\left[0_2^\circ/90_2^\circ\right]_2$ and $\left[0_4^\circ/90_4^\circ\right]$ are considered. For comparison, the buckling load according to (12.23) (i.e. if the bending-extensional coupling terms B_{11} and $B_{22} = -B_{11}$ are neglected) is also shown as a dashed line in Fig. 12.9. It should be noted that all three unsymmetric cross-ply laminates considered have identical plate stiffnesses D_{11}, D_{12}, D_{22}, D_{66}, so that the same comparative buckling load results for all three laminates. It can be seen that the cross-ply laminate $\left[0_4^\circ/90_4^\circ\right]$ has the weakest buckling resistance compared to the reference solution (dashed line). In contrast, the cross-ply laminate $\left[0_2^\circ/90_2^\circ\right]_2$ shows a significantly higher critical buckling load. The $[0^\circ/90^\circ]_4$-laminate shows the greatest buckling resistance, which is only slightly lower than the comparative buckling load. The results of Fig. 12.9 thus show that in the presence of unsymmetry and the associated bending-extension couplings, it is important to either concentrate the cause of the unsymmetry of the laminate as close as possible to the middle plane of the laminate or to mix the layers well so that the coupling effects are reduced if they cannot be completely avoided. In general, coupling effects should always be suitably taken into account in a stability analysis for a laminate structure in order to avoid errors in the calculation.

12.2.4 Navier Solution for a Simply-Supported Unsymmetric Angle-Ply Laminate Under Uniaxial Compressive Load

Another exact solution of the Navier type is the buckling problem of an unsymmetric angle-ply laminate. The constitutive law (12.13) is then:

$$\begin{pmatrix} N_{xx}^0 \\ N_{yy}^0 \\ N_{xy}^0 \\ M_{xx}^0 \\ M_{yy}^0 \\ M_{xy}^0 \end{pmatrix} = \begin{bmatrix} A_{11} & A_{12} & 0 & 0 & 0 & B_{16} \\ A_{12} & A_{22} & 0 & 0 & 0 & B_{26} \\ 0 & 0 & A_{66} & B_{16} & B_{26} & 0 \\ 0 & 0 & B_{16} & D_{11} & D_{12} & 0 \\ 0 & 0 & B_{26} & D_{12} & D_{22} & 0 \\ B_{16} & B_{26} & 0 & 0 & 0 & D_{66} \end{bmatrix} \begin{pmatrix} \frac{\partial u_0}{\partial x} \\ \frac{\partial v_0}{\partial y} \\ \frac{\partial u_0}{\partial y} + \frac{\partial v_0}{\partial x} \\ -\frac{\partial^2 w_0}{\partial x^2} \\ -\frac{\partial^2 w_0}{\partial y^2} \\ -2\frac{\partial^2 w_0}{\partial x \partial y} \end{pmatrix}. \tag{12.53}$$

The differential equation system (12.14) then takes the following form:

$$\begin{aligned} A_{11}\frac{\partial^2 u_0}{\partial x^2} + A_{66}\frac{\partial^2 u_0}{\partial y^2} + (A_{12} + A_{66})\frac{\partial^2 v_0}{\partial x \partial y} - 3B_{16}\frac{\partial^3 w_0}{\partial x^2 \partial y} - B_{26}\frac{\partial^3 w_0}{\partial y^3} = 0, \\ (A_{12} + A_{66})\frac{\partial^2 u_0}{\partial x \partial y} + A_{66}\frac{\partial^2 v_0}{\partial x^2} + A_{22}\frac{\partial^2 v_0}{\partial y^2} - B_{16}\frac{\partial^3 w_0}{\partial x^3} - 3B_{26}\frac{\partial^3 w_0}{\partial x \partial y^2} = 0, \\ -3B_{16}\frac{\partial^3 u_0}{\partial x^2 \partial y} - B_{26}\frac{\partial^3 u_0}{\partial y^3} - B_{16}\frac{\partial^3 v_0}{\partial x^3} - 3B_{26}\frac{\partial^3 v_0}{\partial x \partial y^2} \\ +D_{11}\frac{\partial^4 w_0}{\partial x^4} + 2(D_{12} + 2D_{66})\frac{\partial^4 w_0}{\partial x^2 \partial y^2} + D_{22}\frac{\partial^4 w_0}{\partial y^4} + N_{xx}^0\frac{\partial^2 w_0}{\partial x^2} = 0. \end{aligned} \tag{12.54}$$

The solution approach explained below goes back to the work of Whitney (1969) and is based on the so-called SS2 boundary conditions. The following is required at the boundaries at $x = 0$ and $x = a$ for $0 \leq y \leq b$:

$$\begin{aligned} u_0 = 0, \quad w_0 = 0, \\ M_{xx}^0 = B_{16}\left(\frac{\partial u_0}{\partial y} + \frac{\partial v_0}{\partial x}\right) - D_{11}\frac{\partial^2 w_0}{\partial x^2} - D_{12}\frac{\partial^2 w_0}{\partial y^2} = 0, \\ N_{xy}^0 = A_{66}\left(\frac{\partial u_0}{\partial y} + \frac{\partial v_0}{\partial x}\right) - B_{16}\frac{\partial^2 w_0}{\partial x^2} - B_{26}\frac{\partial^2 w_0}{\partial y^2} = 0. \end{aligned} \tag{12.55}$$

The two edges at $y = 0$ and $y = b$ for $0 \leq x \leq a$ are subjected to the following boundary conditions:

$$\begin{aligned} v_0 = 0, \quad w_0 = 0, \\ M_{yy}^0 = B_{26}\left(\frac{\partial u_0}{\partial y} + \frac{\partial v_0}{\partial x}\right) - D_{12}\frac{\partial^2 w_0}{\partial x^2} - D_{22}\frac{\partial^2 w_0}{\partial y^2} = 0, \\ N_{xy}^0 = A_{66}\left(\frac{\partial u_0}{\partial y} + \frac{\partial v_0}{\partial x}\right) - B_{16}\frac{\partial^2 w_0}{\partial x^2} - B_{26}\frac{\partial^2 w_0}{\partial y^2} = 0. \end{aligned} \tag{12.56}$$

An approach of the form

$$u_0 = U_{mn} \sin\left(\frac{m\pi x}{a}\right) \cos\left(\frac{n\pi y}{b}\right),$$
$$v_0 = V_{mn} \cos\left(\frac{m\pi x}{a}\right) \sin\left(\frac{n\pi y}{b}\right),$$
$$w_0 = W_{mn} \sin\left(\frac{m\pi x}{a}\right) \sin\left(\frac{n\pi y}{b}\right) \tag{12.57}$$

fulfils all boundary conditions (12.55) and (12.56) identically. Inserting the approach (12.57) into the differential equations (12.54) then results in

$$\begin{aligned}
&\left[\left(A_{11}\frac{m^2\pi^2}{a^2} + A_{66}\frac{n^2\pi^2}{b^2}\right) U_{mn} + (A_{12} + A_{66})\frac{m\pi}{a}\frac{n\pi}{b} V_{mn}\right.\\
&\left. - \left(3B_{16}\frac{m^2\pi^2}{a^2} + B_{26}\frac{n^2\pi^2}{b^2}\right)\frac{n\pi}{b} W_{mn}\right] \sin\left(\frac{m\pi x}{a}\right)\cos\left(\frac{n\pi y}{b}\right) = 0,\\
&\left[(A_{12} + A_{66})\frac{m\pi}{a}\frac{n\pi}{b} U_{mn} + \left(A_{66}\frac{m^2\pi^2}{a^2} + A_{22}\frac{n^2\pi^2}{b^2}\right) V_{mn}\right.\\
&\left. - \left(B_{16}\frac{m^2\pi^2}{a^2} + 3B_{26}\frac{n^2\pi^2}{b^2}\right)\frac{m\pi}{a} W_{mn}\right] \cos\left(\frac{m\pi x}{a}\right)\sin\left(\frac{n\pi y}{b}\right) = 0,
\end{aligned}$$

$$\begin{aligned}
&\left[-\left(3B_{16}\frac{m^2\pi^2}{a^2} + B_{26}\frac{n^2\pi^2}{b^2}\right)\frac{n\pi}{b} U_{mn} - \left(B_{16}\frac{m^2\pi^2}{a^2} + 3B_{26}\frac{n^2\pi^2}{b^2}\right)\frac{m\pi}{a} V_{mn}\right.\\
&\left. + \left\{D_{11}\frac{m^4\pi^4}{a^4} + 2(D_{12} + 2D_{66})\frac{m^2\pi^2}{a^2}\frac{n^2\pi^2}{b^2} + D_{22}\frac{n^4\pi^4}{b^4} - N^0_{xx}\frac{m^2\pi^2}{a^2}\right\} W_{mn}\right]\\
&\times \sin\left(\frac{m\pi x}{a}\right)\sin\left(\frac{n\pi y}{b}\right) = 0.
\end{aligned} \tag{12.58}$$

Again, this represents a homogeneous system of three linear equations for the unknown coefficients U_{mn}, V_{mn}, W_{mn}. In a vector-matrix notation it reads:

$$\begin{bmatrix} \lambda_{11} & \lambda_{12} & \lambda_{13} \\ \lambda_{12} & \lambda_{22} & \lambda_{23} \\ \lambda_{13} & \lambda_{23} & \lambda_{33} - N^0_{xx}\bar{\lambda}_{33} \end{bmatrix} \begin{pmatrix} U_{mn} \\ V_{mn} \\ W_{mn} \end{pmatrix} = \begin{pmatrix} 0 \\ 0 \\ 0 \end{pmatrix}, \tag{12.59}$$

wherein:

$$\lambda_{11} = A_{11}\frac{m^2\pi^2}{a^2} + A_{66}\frac{n^2\pi^2}{b^2}, \qquad \lambda_{12} = (A_{12} + A_{66})\,\frac{m\pi}{a}\frac{n\pi}{b},$$

$$\lambda_{13} = -\left(3B_{16}\frac{m^2\pi^2}{a^2} + B_{26}\frac{n^2\pi^2}{b^2}\right)\frac{n\pi}{b}, \quad \lambda_{22} = A_{66}\frac{m^2\pi^2}{a^2} + A_{22}\frac{n^2\pi^2}{b^2},$$

$$\lambda_{23} = -\left(B_{16}\frac{m^2\pi^2}{a^2} + 3B_{26}\frac{n^2\pi^2}{b^2}\right)\frac{m\pi}{a},$$

$$\lambda_{33} = D_{11}\frac{m^4\pi^4}{a^4} + 2\,(D_{12} + 2D_{66})\,\frac{m^2\pi^2}{a^2}\frac{n^2\pi^2}{b^2} + D_{22}\frac{n^4\pi^4}{b^4}, \quad \bar{\lambda}_{33} = \frac{m^2\pi^2}{a^2}. \tag{12.60}$$

Setting the coefficient determinant to zero then results in the following exact solution for the buckling load:

$$N^0_{xx} = \frac{1}{\bar{\lambda}_{33}}\left[\lambda_{33} + \frac{2\lambda_{12}\lambda_{13}\lambda_{23} - \lambda_{11}\lambda_{23}^2 - \lambda_{22}\lambda_{13}^2}{\lambda_{11}\lambda_{22} - \lambda_{12}^2}\right]. \tag{12.61}$$

As in the case of the unsymmetric cross-ply laminate, direct statements about the relevant half-wave numbers m and n are not possible. The minimum buckling load must again be determined by trial and error.

Figure 12.10 contains a study of the buckling load for three different unsymmetric eight-layered angle-ply laminates, namely with the layups $[+45°/-45°]_4$, $\left[+45°_2/-45°_2\right]_2$ and $\left[+45°_4/-45°_4\right]$. For comparison, the solution for a symmetric orthotropic laminate according to (12.23) is again shown as a dashed line. In this case, too, the plate stiffnesses D_{11}, D_{12}, D_{22}, D_{66} of all considered angle-ply laminates agree with each other, so that all reference calculations for an orthotropic symmetric laminate lead to the same result. The conclusions that can be drawn from Fig. 12.10 are similar to those of Fig. 12.9. Here, too, it can be

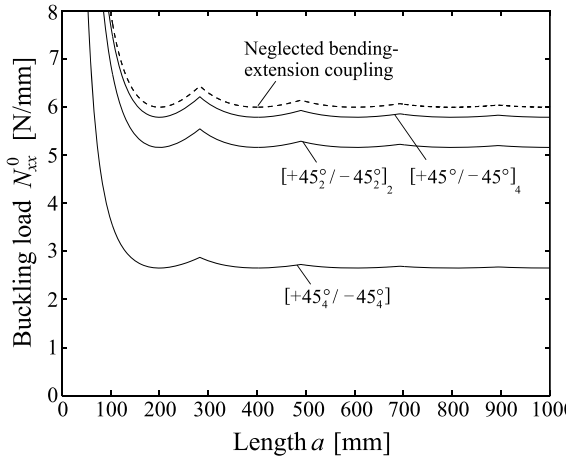


Fig. 12.10 Buckling curves for the eight-layered unsymmetric angle-ply laminates $[+45°/-45°]_4$, $\left[+45°_2/-45°_2\right]_2$ and $\left[+45°_4/-45°_4\right]$ under uniaxial loading

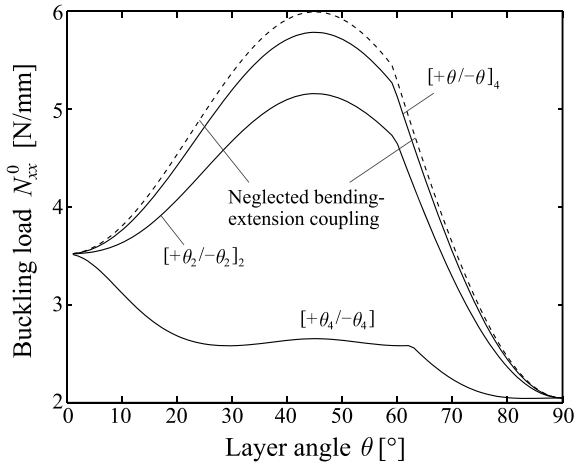


Fig. 12.11 Influence of the layer angle θ for the eight-layered unsymmetric angle-ply laminates $[+\theta/-\theta]_4$, $\left[+\theta_2/-\theta_2\right]_2$ and $\left[+\theta_4/-\theta_4\right]$ under uniaxial loading

seen that the angle-ply laminate with the greatest influence of unsymmetry (in this case the $\left[+45^\circ_4/-45^\circ_4\right]$ laminate) has the weakest buckling resistance. The driving factors here are the bending-extension coupling terms B_{16} and B_{26}.

A study of the influence of the layer angle θ for square angle-ply laminates $[+\theta/-\theta]_4$, $[+\theta_2/-\theta_2]_2$ and $[+\theta_4/-\theta_4]$ ($a = b = 200$ mm) can be found in Fig. 12.11. Again, it can be seen that the $\left[+\theta_4/-\theta_4\right]$ laminate offers by far the lowest buckling resistance - a clear indication of the weakening influence of bending-extension coupling, which is quite pronounced here. While no clear extreme values can be determined for this laminate as a function of the ply angle θ, the two laminates $[+\theta/-\theta]_4$ and $\left[+\theta_2/-\theta_2\right]_2$ exhibit maximum buckling resistances at around $\theta = 45^\circ$. All three laminates reach the minimum buckling resistance at $\theta = 90^\circ$.

12.3 Governing Equations for First-Order Shear Deformation Theory

Navier-type solutions for laminate buckling problems can also be derived within the framework of First-Order Shear Deformation Theory (FSDT). Before these solutions are discussed in detail, the governing equations are briefly examined.

To derive the governing equations according to FSDT, the equilibrium conditions already derived can be used:

$$\frac{\partial N_{xx}^0}{\partial x} + \frac{\partial N_{xy}^0}{\partial y} = 0, \quad \frac{\partial N_{xy}^0}{\partial x} + \frac{\partial N_{yy}^0}{\partial y} = 0,$$
$$\frac{\partial Q_x}{\partial x} + \frac{\partial Q_y}{\partial y} - N_{xx}^0 \frac{\partial^2 w_0}{\partial x^2} - 2N_{xy}^0 \frac{\partial^2 w_0}{\partial x \partial y} - N_{yy}^0 \frac{\partial^2 w_0}{\partial y^2} = 0,$$
$$\frac{\partial M_{xx}^0}{\partial x} + \frac{\partial M_{xy}^0}{\partial y} = Q_x, \quad \frac{\partial M_{xy}^0}{\partial x} + \frac{\partial M_{yy}^0}{\partial y} = Q_y. \tag{12.62}$$

Insertion of the constitutive relationship according to FSDT

$$\begin{pmatrix} N_{xx}^0 \\ N_{yy}^0 \\ N_{xy}^0 \\ M_{xx}^0 \\ M_{yy}^0 \\ M_{xy}^0 \\ Q_y \\ Q_x \end{pmatrix} = \begin{bmatrix} A_{11} & A_{12} & A_{16} & B_{11} & B_{12} & B_{16} & 0 & 0 \\ A_{12} & A_{22} & A_{26} & B_{12} & B_{22} & B_{26} & 0 & 0 \\ A_{16} & A_{26} & A_{66} & B_{16} & B_{26} & B_{66} & 0 & 0 \\ B_{11} & B_{12} & B_{16} & D_{11} & D_{12} & D_{16} & 0 & 0 \\ B_{12} & B_{22} & B_{26} & D_{12} & D_{22} & D_{26} & 0 & 0 \\ B_{16} & B_{26} & B_{66} & D_{16} & D_{26} & D_{66} & 0 & 0 \\ 0 & 0 & 0 & 0 & 0 & 0 & KA_{44} & KA_{45} \\ 0 & 0 & 0 & 0 & 0 & 0 & KA_{45} & KA_{55} \end{bmatrix} \begin{pmatrix} \frac{\partial u_0}{\partial x} \\ \frac{\partial v_0}{\partial y} \\ \frac{\partial u_0}{\partial y} + \frac{\partial v_0}{\partial x} \\ \frac{\partial \psi_x}{\partial x} \\ \frac{\partial \psi_y}{\partial y} \\ \frac{\partial \psi_x}{\partial y} + \frac{\partial \psi_y}{\partial x} \\ \frac{\partial w_0}{\partial y} + \psi_y \\ \frac{\partial w_0}{\partial x} + \psi_x \end{pmatrix} \tag{12.63}$$

then provides the following differential equations:

$$A_{11}\frac{\partial^2 u_0}{\partial x^2} + 2A_{16}\frac{\partial^2 u_0}{\partial x \partial y} + A_{66}\frac{\partial^2 u_0}{\partial y^2} + A_{16}\frac{\partial^2 v_0}{\partial x^2} + (A_{12} + A_{66})\frac{\partial^2 v_0}{\partial x \partial y} + A_{26}\frac{\partial^2 v_0}{\partial y^2}$$
$$+ B_{11}\frac{\partial^2 \psi_x}{\partial x^2} + 2B_{16}\frac{\partial^2 \psi_x}{\partial x \partial y} + B_{66}\frac{\partial^2 \psi_x}{\partial y^2} + B_{16}\frac{\partial^2 \psi_y}{\partial x^2} + (B_{12} + B_{66})\frac{\partial^2 \psi_y}{\partial x \partial y} + B_{26}\frac{\partial^2 \psi_y}{\partial y^2} = 0,$$
$$A_{16}\frac{\partial^2 u_0}{\partial x^2} + (A_{12} + A_{66})\frac{\partial^2 u_0}{\partial x \partial y} + A_{26}\frac{\partial^2 u_0}{\partial y^2} + A_{66}\frac{\partial^2 v_0}{\partial x^2} + 2A_{26}\frac{\partial^2 v_0}{\partial x \partial y} + A_{22}\frac{\partial^2 v_0}{\partial y^2}$$
$$+ B_{16}\frac{\partial^2 \psi_x}{\partial x^2} + (B_{12} + B_{66})\frac{\partial^2 \psi_x}{\partial x \partial y} + B_{26}\frac{\partial^2 \psi_x}{\partial y^2} + B_{66}\frac{\partial^2 \psi_y}{\partial x^2} + 2B_{26}\frac{\partial^2 \psi_y}{\partial x \partial y} + B_{22}\frac{\partial^2 \psi_y}{\partial y^2} = 0,$$
$$K\left[A_{55}\left(\frac{\partial \psi_x}{\partial x} + \frac{\partial^2 w_0}{\partial x^2}\right) + A_{45}\left(\frac{\partial \psi_x}{\partial y} + \frac{\partial \psi_y}{\partial x} + 2\frac{\partial^2 w_0}{\partial x \partial y}\right) + A_{44}\left(\frac{\partial \psi_y}{\partial y} + \frac{\partial^2 w_0}{\partial y^2}\right)\right]$$
$$- N_{xx}^0\frac{\partial^2 w_0}{\partial x^2} - 2N_{xy}^0\frac{\partial^2 w_0}{\partial x \partial y} - N_{yy}^0\frac{\partial^2 w_0}{\partial y^2} = 0,$$
$$B_{11}\frac{\partial^2 u_0}{\partial x^2} + 2B_{16}\frac{\partial^2 u_0}{\partial x \partial y} + B_{66}\frac{\partial^2 u_0}{\partial y^2} + B_{16}\frac{\partial^2 v_0}{\partial x^2} + (B_{12} + B_{66})\frac{\partial^2 v_0}{\partial x \partial y} + B_{26}\frac{\partial^2 v_0}{\partial y^2}$$
$$+ D_{11}\frac{\partial^2 \psi_x}{\partial x^2} + 2D_{16}\frac{\partial^2 \psi_x}{\partial x \partial y} + D_{66}\frac{\partial^2 \psi_x}{\partial y^2} + D_{16}\frac{\partial^2 \psi_y}{\partial x^2} + (D_{12} + D_{66})\frac{\partial^2 \psi_y}{\partial x \partial y} + D_{26}\frac{\partial^2 \psi_y}{\partial y^2}$$
$$= K\left[A_{55}\left(\psi_x + \frac{\partial w_0}{\partial x}\right) + A_{45}\left(\psi_y + \frac{\partial w_0}{\partial y}\right)\right],$$

$$
\begin{aligned}
&B_{16}\frac{\partial^2 u_0}{\partial x^2} + (B_{12}+B_{66})\frac{\partial^2 u_0}{\partial x\partial y} + B_{26}\frac{\partial^2 u_0}{\partial y^2} + B_{66}\frac{\partial^2 v_0}{\partial x^2} + 2B_{26}\frac{\partial^2 v_0}{\partial x\partial y} + B_{22}\frac{\partial^2 v_0}{\partial y^2} \\
&+ D_{16}\frac{\partial^2 \psi_x}{\partial x^2} + (D_{12}+D_{66})\frac{\partial^2 \psi_x}{\partial x\partial y} + D_{26}\frac{\partial^2 \psi_x}{\partial y^2} + D_{66}\frac{\partial^2 \psi_y}{\partial x^2} + 2D_{26}\frac{\partial^2 \psi_y}{\partial x\partial y} + D_{22}\frac{\partial^2 \psi_y}{\partial y^2} \\
&= K\left[A_{45}\left(\psi_x + \frac{\partial w_0}{\partial x}\right) + A_{44}\left(\psi_y + \frac{\partial w_0}{\partial y}\right)\right].
\end{aligned} \tag{12.64}
$$

In the case of symmetric laminate structures, this set of differential equations is reduced as follows:

$$
\begin{aligned}
&A_{11}\frac{\partial^2 u_0}{\partial x^2} + 2A_{16}\frac{\partial^2 u_0}{\partial x\partial y} + A_{66}\frac{\partial^2 u_0}{\partial y^2} + A_{16}\frac{\partial^2 v_0}{\partial x^2} + (A_{12}+A_{66})\frac{\partial^2 v_0}{\partial x\partial y} + A_{26}\frac{\partial^2 v_0}{\partial y^2} = 0, \\
&A_{16}\frac{\partial^2 u_0}{\partial x^2} + (A_{12}+A_{66})\frac{\partial^2 u_0}{\partial x\partial y} + A_{26}\frac{\partial^2 u_0}{\partial y^2} + A_{66}\frac{\partial^2 v_0}{\partial x^2} + 2A_{26}\frac{\partial^2 v_0}{\partial x\partial y} + A_{22}\frac{\partial^2 v_0}{\partial y^2} = 0, \\
&K\left[A_{55}\left(\frac{\partial \psi_x}{\partial x} + \frac{\partial^2 w_0}{\partial x^2}\right) + A_{45}\left(\frac{\partial \psi_x}{\partial y} + \frac{\partial \psi_y}{\partial x} + 2\frac{\partial^2 w_0}{\partial x\partial y}\right) + A_{44}\left(\frac{\partial \psi_y}{\partial y} + \frac{\partial^2 w_0}{\partial y^2}\right)\right] \\
&- N^0_{xx}\frac{\partial^2 w_0}{\partial x^2} - 2N^0_{xy}\frac{\partial^2 w_0}{\partial x\partial y} - N^0_{yy}\frac{\partial^2 w_0}{\partial y^2} = 0.
\end{aligned}
$$

$$
\begin{aligned}
&D_{11}\frac{\partial^2 \psi_x}{\partial x^2} + 2D_{16}\frac{\partial^2 \psi_x}{\partial x\partial y} + D_{66}\frac{\partial^2 \psi_x}{\partial y^2} + D_{16}\frac{\partial^2 \psi_y}{\partial x^2} + (D_{12}+D_{66})\frac{\partial^2 \psi_y}{\partial x\partial y} \\
&+ D_{26}\frac{\partial^2 \psi_y}{\partial y^2} = K\left[A_{55}\left(\psi_x + \frac{\partial w_0}{\partial x}\right) + A_{45}\left(\psi_y + \frac{\partial w_0}{\partial y}\right)\right], \\
&D_{16}\frac{\partial^2 \psi_x}{\partial x^2} + (D_{12}+D_{66})\frac{\partial^2 \psi_x}{\partial x\partial y} + D_{26}\frac{\partial^2 \psi_x}{\partial y^2} + D_{66}\frac{\partial^2 \psi_y}{\partial x^2} + 2D_{26}\frac{\partial^2 \psi_y}{\partial x\partial y} \\
&+ D_{22}\frac{\partial^2 \psi_y}{\partial y^2} = K\left[A_{45}\left(\psi_x + \frac{\partial w_0}{\partial x}\right) + A_{44}\left(\psi_y + \frac{\partial w_0}{\partial y}\right)\right].
\end{aligned} \tag{12.65}
$$

Accordingly, the disk behaviour is also decoupled from the plate behaviour in the buckling behaviour of laminates within the framework of FSDT. As in Classical Laminated Plate Theory (CLPT), the first two differential equations in (12.65) describe the disk behaviour (they only contain the plane displacements u_0 and v_0). The plate behaviour is described by the remaining three differential equations in (12.65), which are coupled with each other and contain the degrees of freedom w_0 (deflection / buckling shape) and ψ_x, ψ_y (cross-sectional bending angle).

12.4 Navier Solutions for First-Order Shear Deformation Theory

12.4.1 Navier Solution for a Simply Supported Symmetric Cross-Ply Laminate Under Uniaxial Compressive Load

Consider a symmetric cross-ply laminate under uniaxial compressive load N_{xx}^0 (see also Fig. 12.2). The constitutive law (12.63) is then as follows:

$$\begin{pmatrix} N_{xx}^0 \\ N_{yy}^0 \\ N_{xy}^0 \\ M_{xx}^0 \\ M_{yy}^0 \\ M_{xy}^0 \\ Q_y \\ Q_x \end{pmatrix} = \begin{bmatrix} A_{11} & A_{12} & 0 & 0 & 0 & 0 & 0 & 0 \\ A_{12} & A_{22} & 0 & 0 & 0 & 0 & 0 & 0 \\ 0 & 0 & A_{66} & 0 & 0 & 0 & 0 & 0 \\ 0 & 0 & 0 & D_{11} & D_{12} & 0 & 0 & 0 \\ 0 & 0 & 0 & D_{12} & D_{22} & 0 & 0 & 0 \\ 0 & 0 & 0 & 0 & 0 & D_{66} & 0 & 0 \\ 0 & 0 & 0 & 0 & 0 & 0 & KA_{44} & 0 \\ 0 & 0 & 0 & 0 & 0 & 0 & 0 & KA_{55} \end{bmatrix} \begin{pmatrix} \frac{\partial u_0}{\partial x} \\ \frac{\partial v_0}{\partial y} \\ \frac{\partial u_0}{\partial y} + \frac{\partial v_0}{\partial x} \\ \frac{\partial \psi_x}{\partial x} \\ \frac{\partial \psi_y}{\partial y} \\ \frac{\partial \psi_x}{\partial y} + \frac{\partial \psi_y}{\partial x} \\ \frac{\partial w_0}{\partial y} + \psi_y \\ \frac{\partial w_0}{\partial x} + \psi_x \end{pmatrix}. \tag{12.66}$$

The underlying boundary conditions (so-called SS1 boundary conditions) are currently as follows:

$$\begin{aligned} &w_0\,(x=0)=0, \quad w_0\,(x=a)=0, \quad w_0\,(y=0)=0, \quad w_0\,(y=b)=0, \\ &\psi_x\,(y=0)=0, \quad \psi_x\,(y=b)=0, \quad \psi_y\,(x=0)=0, \quad \psi_y\,(x=a)=0, \\ &M_{xx}^0\,(x=0)=0, \quad M_{xx}^0\,(x=a)=0, \quad M_{yy}^0\,(y=0)=0, \quad M_{yy}^0\,(y=b)=0. \end{aligned} \tag{12.67}$$

The differential equations (12.65) can then be expressed in the following form:

$$\begin{aligned} &K\left[A_{55}\left(\frac{\partial \psi_x}{\partial x}+\frac{\partial^2 w_0}{\partial x^2}\right)+A_{44}\left(\frac{\partial \psi_y}{\partial y}+\frac{\partial^2 w_0}{\partial y^2}\right)\right]-N_{xx}^0\frac{\partial^2 w_0}{\partial x^2}=0, \\ &D_{11}\frac{\partial^2 \psi_x}{\partial x^2}+D_{66}\frac{\partial^2 \psi_x}{\partial y^2}+(D_{12}+D_{66})\frac{\partial^2 \psi_y}{\partial x \partial y}=KA_{55}\left(\psi_x+\frac{\partial w_0}{\partial x}\right), \\ &(D_{12}+D_{66})\frac{\partial^2 \psi_x}{\partial x \partial y}+D_{66}\frac{\partial^2 \psi_y}{\partial x^2}+D_{22}\frac{\partial^2 \psi_y}{\partial y^2}=KA_{44}\left(\psi_y+\frac{\partial w_0}{\partial y}\right). \end{aligned} \tag{12.68}$$

It can be shown that an approach of the form

$$
\begin{aligned}
w_0 &= W_{mn} \sin\left(\frac{m\pi x}{a}\right) \sin\left(\frac{n\pi y}{b}\right), \\
\psi_x &= X_{mn} \cos\left(\frac{m\pi x}{a}\right) \sin\left(\frac{n\pi y}{b}\right), \\
\psi_y &= Y_{mn} \sin\left(\frac{m\pi x}{a}\right) \cos\left(\frac{n\pi y}{b}\right)
\end{aligned} \tag{12.69}
$$

fulfills all boundary conditions (12.67) identically. If the approach (12.69) is inserted into the differential equations (12.68), the result is

$$
\begin{aligned}
&\left[K\left(A_{55}\frac{m^2\pi^2}{a^2} + A_{44}\frac{n^2\pi^2}{b^2}\right) W_{mn} - N^0_{xx}\frac{m^2\pi^2}{a^2} W_{mn} + K A_{55}\frac{m\pi}{a} X_{mn} + K A_{44}\frac{n\pi}{b} Y_{mn}\right] \\
&\times \sin\left(\frac{m\pi x}{a}\right) \sin\left(\frac{n\pi y}{b}\right) = 0, \\
&\left[K A_{55}\frac{m\pi}{a} W_{mn} + \left(D_{11}\frac{m^2\pi^2}{a^2} + D_{66}\frac{n^2\pi^2}{b^2} + K A_{55}\right) X_{mn} + (D_{12} + D_{66})\frac{m\pi}{a}\frac{n\pi}{b} Y_{mn}\right] \\
&\times \cos\left(\frac{m\pi x}{a}\right) \sin\left(\frac{n\pi y}{b}\right) = 0, \\
&\left[K A_{44}\frac{n\pi}{b} W_{mn} + (D_{12} + D_{66})\frac{m\pi}{a}\frac{n\pi}{b} X_{mn} + \left(D_{66}\frac{m^2\pi^2}{a^2} + D_{22}\frac{n^2\pi^2}{b^2} + K A_{44}\right) Y_{mn}\right] \\
&\times \sin\left(\frac{m\pi x}{a}\right) \cos\left(\frac{n\pi y}{b}\right) = 0.
\end{aligned} \tag{12.70}
$$

As these equations must be fulfilled regardless of the choice of coordinates x, y, the terms in the square brackets must disappear:

$$
\begin{aligned}
K\left(A_{55}\frac{m^2\pi^2}{a^2} + A_{44}\frac{n^2\pi^2}{b^2}\right) W_{mn} - N^0_{xx}\frac{m^2\pi^2}{a^2} W_{mn} \\
+ K A_{55}\frac{m\pi}{a} X_{mn} + K A_{44}\frac{n\pi}{b} Y_{mn} = 0, \\
K A_{55}\frac{m\pi}{a} W_{mn} + \left(D_{11}\frac{m^2\pi^2}{a^2} + D_{66}\frac{n^2\pi^2}{b^2} + K A_{55}\right) X_{mn} \\
+ (D_{12} + D_{66})\frac{m\pi}{a}\frac{n\pi}{b} Y_{mn} = 0, \\
K A_{44}\frac{n\pi}{b} W_{mn} + (D_{12} + D_{66})\frac{m\pi}{a}\frac{n\pi}{b} X_{mn} \\
+ \left(D_{66}\frac{m^2\pi^2}{a^2} + D_{22}\frac{n^2\pi^2}{b^2} + K A_{44}\right) Y_{mn} = 0.
\end{aligned} \tag{12.71}
$$

This is a homogeneous system of three linear equations for the three unknown coefficients W_{mn}, X_{mn}, Y_{mn}. For a non-trivial solution, the vanishing of the coefficient determinant is required, which after some transformations leads to the following exact solution for the buckling load N^0_{xx}:

$$N_{xx}^{0} = \frac{a^2}{m^2\pi^2}\left[\frac{\lambda_1 + \left(\frac{m^2\pi^2}{a^2}\frac{1}{KA_{44}} + \frac{n^2\pi^2}{b^2}\frac{1}{KA_{55}}\right)\lambda_2}{1 + \frac{\lambda_2}{K^2A_{44}A_{55}} + \frac{\lambda_3}{KA_{55}} + \frac{\lambda_4}{KA_{44}}}\right], \tag{12.72}$$

in which the following abbreviations have been employed:

$$\lambda_1 = D_{11}\frac{m^4\pi^4}{a^4} + 2\,(D_{12} + 2D_{66})\,\frac{m^2\pi^2}{a^2}\frac{n^2\pi^2}{b^2} + D_{22}\frac{n^4\pi^4}{b^4}, \quad \lambda_2 = \lambda_3\lambda_4 - \lambda_5^2,$$
$$\lambda_3 = D_{11}\frac{m^2\pi^2}{a^2} + D_{66}\frac{n^2\pi^2}{b^2}, \quad \lambda_4 = D_{66}\frac{m^2\pi^2}{a^2} + D_{22}\frac{n^2\pi^2}{b^2}, \quad \lambda_5 = (D_{12} + D_{66})\,\frac{m\pi}{a}\frac{n\pi}{b}. \tag{12.73}$$

If all terms in (12.72) that contain the transverse shear stiffness are neglected (i.e. the shear stiffnesses A_{44}, A_{55} are allowed to approach infinity), then (12.72) becomes the solution (12.22) according to CLPT. As with some of the previous solutions, it is not possible to make a generally valid statement about the relevant half-wave numbers. Here, a parameter study must clarify for which pair of values m, n the buckling load N_{xx}^{0} becomes minimal.

Figure 12.12 contains studies on the effect of transverse shear strains on the buckling behaviour of cross-ply laminates of the type $\left[0_{2n}^{\circ}/90_{2n}^{\circ}\right]_S$ for different numbers of layers n, namely for $n = 1$ (Fig. 12.12, top left), $n = 5$ (Fig. 12.12, top right), $n = 10$ (Fig. 12.12, bottom left), and $n = 15$ (Fig. 12.12, bottom right). This corresponds to laminates with 8, 40, 80 and 120 individual layers, with total thicknesses $h = 1$ mm, $h = 5$ mm, $h = 10$ mm and $h = 15$ mm. The width was defined as $b = 100$ mm in all cases; all other properties correspond to those of the examples already discussed. The shear correction factor K was set to $K = \frac{5}{6}$, the values $G_{23} = 3972$ MPa and $G_{13} = 5000$ MPa were used as the transverse shear moduli of the individual layers. The influence of transverse shear strains only becomes apparent in the examples analysed above a certain total thickness h of the laminate. While the buckling curves according to CLPT and FSDT theory are indistinguishable for the case $n = 1$, slight deviations can already be observed for $n = 5$ (which corresponds to a ratio of width to thickness of 20). Obviously, the results according to CLPT are slightly higher than the results of FSDT. The deviations become more pronounced at $n = 10$ which corresponds to a ratio of width to thickness of 10. Particularly pronounced deviations in the results can be seen at $n = 15$. In general, the shorter and thicker the plate, the more the buckling curves according to CLPT and FSDT differ. In general, the ratio of the smallest length dimension a or b to the thickness h of the laminate is the decisive parameter that determines the influence of the transverse shear strains on the buckling resistance of a laminate. If $a < 100$ mm applies to the current example, then the ratio of length to thickness is decisive. From $a > 100$ mm, the ratio of width to thickness determines the influence of the transverse shear strains. In general, it can be stated that a considerable influence of the transverse shear strains on the buckling resistance is to be expected, especially for 'thick'

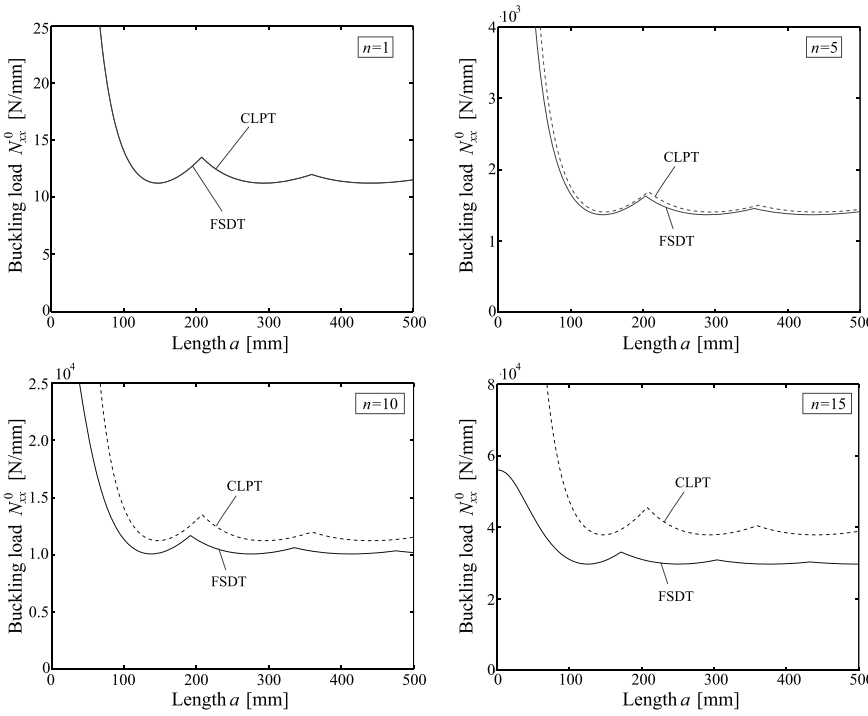


Fig. 12.12 Buckling curves for cross-ply laminates of the type $\left[0_{2n}^{\circ}/90_{2n}^{\circ}\right]_S$ under uniaxial load for different values of n

laminates. This influence will always have a weakening effect in any case. This means that a calculation of such laminates according to CLPT is always on the non-conservative side and the buckling resistance is always overestimated. However, it must be pointed out that a clearly defined ratio $\frac{a}{h}$ or $\frac{b}{h}$, at which the CLPT loses its validity, cannot be specified without further ado. In addition to the purely geometric conditions, the elastic properties, in particular the transverse shear stiffnesses, also play a very important role. Furthermore, the underlying load case also determines the influence of the transverse shear strains on the buckling resistance of a laminate quite considerably. The generally known rule of thumb 'Thick composite laminates may show a significant weakening influence of transverse shear strains on the buckling resistance' can certainly be confirmed as valid taking the results of Fig. 12.12 into account.

In the following, two further Navier solutions for buckling problems according to FSDT are presented, namely for unsymmetric cross-ply laminates and for unsymmetric angle-ply laminates.

12.4.2 Navier Solution for a Simply Supported Unsymmetric Cross-Ply Laminate Under Uniaxial Compressive Load

We consider an unsymmetric cross-ply laminate under uniaxial compressive load N_{xx}^0. Let the constitutive law (12.63) be given as follows:

$$\begin{pmatrix} N_{xx}^0 \\ N_{yy}^0 \\ N_{xy}^0 \\ M_{xx}^0 \\ M_{yy}^0 \\ M_{xy}^0 \\ Q_y \\ Q_x \end{pmatrix} = \begin{bmatrix} A_{11} & A_{12} & 0 & B_{11} & B_{12} & 0 & 0 & 0 \\ A_{12} & A_{22} & 0 & B_{12} & B_{22} & 0 & 0 & 0 \\ 0 & 0 & A_{66} & 0 & 0 & B_{66} & 0 & 0 \\ B_{11} & B_{12} & 0 & D_{11} & D_{12} & 0 & 0 & 0 \\ B_{12} & B_{22} & 0 & D_{12} & D_{22} & 0 & 0 & 0 \\ 0 & 0 & B_{66} & 0 & 0 & D_{66} & 0 & 0 \\ 0 & 0 & 0 & 0 & 0 & 0 & KA_{44} & 0 \\ 0 & 0 & 0 & 0 & 0 & 0 & 0 & KA_{55} \end{bmatrix} \begin{pmatrix} \frac{\partial u_0}{\partial x} \\ \frac{\partial v_0}{\partial y} \\ \frac{\partial u_0}{\partial y} + \frac{\partial v_0}{\partial x} \\ \frac{\partial \psi_x}{\partial x} \\ \frac{\partial \psi_y}{\partial y} \\ \frac{\partial \psi_x}{\partial y} + \frac{\partial \psi_y}{\partial x} \\ \frac{\partial w_0}{\partial y} + \psi_y \\ \frac{\partial w_0}{\partial x} + \psi_x \end{pmatrix}. \tag{12.74}$$

The differential equations (12.64) can be expressed in the following form:

$$\begin{aligned} A_{11}\frac{\partial^2 u_0}{\partial x^2} + A_{66}\frac{\partial^2 u_0}{\partial y^2} + (A_{12}+A_{66})\frac{\partial^2 v_0}{\partial x \partial y} + B_{11}\frac{\partial^2 \psi_x}{\partial x^2} + B_{66}\frac{\partial^2 \psi_x}{\partial y^2} + (B_{12}+B_{66})\frac{\partial^2 \psi_y}{\partial x \partial y} &= 0, \\ (A_{12}+A_{66})\frac{\partial^2 u_0}{\partial x \partial y} + A_{66}\frac{\partial^2 v_0}{\partial x^2} + A_{22}\frac{\partial^2 v_0}{\partial y^2} + (B_{12}+B_{66})\frac{\partial^2 \psi_x}{\partial x \partial y} + B_{66}\frac{\partial^2 \psi_y}{\partial x^2} + B_{22}\frac{\partial^2 \psi_y}{\partial y^2} &= 0, \\ K\left[A_{55}\left(\frac{\partial \psi_x}{\partial x} + \frac{\partial^2 w_0}{\partial x^2}\right) + A_{44}\left(\frac{\partial \psi_y}{\partial y} + \frac{\partial^2 w_0}{\partial y^2}\right)\right] - N_{xx}^0\frac{\partial^2 w_0}{\partial x^2} &= 0, \\ B_{11}\frac{\partial^2 u_0}{\partial x^2} + B_{66}\frac{\partial^2 u_0}{\partial y^2} + (B_{12}+B_{66})\frac{\partial^2 v_0}{\partial x \partial y} + D_{11}\frac{\partial^2 \psi_x}{\partial x^2} + D_{66}\frac{\partial^2 \psi_x}{\partial y^2} + (D_{12}+D_{66})\frac{\partial^2 \psi_y}{\partial x \partial y} & \\ = KA_{55}\left(\psi_x + \frac{\partial w_0}{\partial x}\right), & \\ (B_{12}+B_{66})\frac{\partial^2 u_0}{\partial x \partial y} + B_{66}\frac{\partial^2 v_0}{\partial x^2} + B_{22}\frac{\partial^2 v_0}{\partial y^2} + (D_{12}+D_{66})\frac{\partial^2 \psi_x}{\partial x \partial y} + D_{66}\frac{\partial^2 \psi_y}{\partial x^2} + D_{22}\frac{\partial^2 \psi_y}{\partial y^2} & \\ = KA_{44}\left(\psi_y + \frac{\partial w_0}{\partial y}\right). & \end{aligned} \tag{12.75}$$

The following SS1 boundary conditions are given:

$$
\begin{aligned}
&u_0\,(y=0)=0, \quad u_0\,(y=b)=0, \quad v_0\,(x=0)=0, \quad v_0\,(x=a)=0,\\
&w_0\,(x=0)=0, \quad w_0\,(x=a)=0, \quad w_0\,(y=0)=0, \quad w_0\,(y=b)=0,\\
&\psi_x\,(y=0)=0, \quad \psi_x\,(y=b)=0, \quad \psi_y\,(x=0)=0, \quad \psi_y\,(x=a)=0,\\
&N^0_{xx}\,(x=0)=0, \quad N^0_{xx}\,(x=a)=0, \quad N^0_{yy}\,(y=0)=0, \quad N^0_{yy}\,(y=b)=0,\\
&M^0_{xx}\,(x=0)=0, \quad M^0_{xx}\,(x=a)=0, \quad M^0_{yy}\,(y=0)=0, \quad M^0_{yy}\,(y=b)=0.
\end{aligned}
\tag{12.76}
$$

It can be shown that the following approach for u_0, v_0, w_0, ψ_x, ψ_y fulfils the boundary conditions (12.76) identically:

$$
\begin{aligned}
u_0 &= U_{mn}\cos\left(\frac{m\pi x}{a}\right)\sin\left(\frac{n\pi y}{b}\right),\\
v_0 &= V_{mn}\sin\left(\frac{m\pi x}{a}\right)\cos\left(\frac{n\pi y}{b}\right),\\
w_0 &= W_{mn}\sin\left(\frac{m\pi x}{a}\right)\sin\left(\frac{n\pi y}{b}\right),\\
\psi_x &= X_{mn}\cos\left(\frac{m\pi x}{a}\right)\sin\left(\frac{n\pi y}{b}\right),\\
\psi_y &= Y_{mn}\sin\left(\frac{m\pi x}{a}\right)\cos\left(\frac{n\pi y}{b}\right).
\end{aligned}
\tag{12.77}
$$

If the approach (12.77) is inserted into the differential equations (12.75), the following homogeneous linear system of equations is obtained after a few transformations to determine the coefficients U_{mn}, V_{mn}, W_{mn}, X_{mn}, Y_{mn}:

$$
\begin{bmatrix}
\lambda_{11} & \lambda_{12} & 0 & \lambda_{14} & \lambda_{15}\\
\lambda_{12} & \lambda_{22} & 0 & \lambda_{24} & \lambda_{25}\\
0 & 0 & \lambda_{33}-N^0_{xx}\bar{\lambda}_{33} & \lambda_{34} & \lambda_{35}\\
\lambda_{14} & \lambda_{24} & \lambda_{34} & \lambda_{44} & \lambda_{45}\\
\lambda_{15} & \lambda_{25} & \lambda_{35} & \lambda_{45} & \lambda_{55}
\end{bmatrix}
\begin{pmatrix} U_{mn}\\ V_{mn}\\ W_{mn}\\ X_{mn}\\ Y_{mn}\end{pmatrix}
=
\begin{pmatrix} 0\\ 0\\ 0\\ 0\\ 0\end{pmatrix},
\tag{12.78}
$$

wherein:

$$
\lambda_{11} = A_{11}\frac{m^2\pi^2}{a^2} + A_{66}\frac{n^2\pi^2}{b^2}, \quad \lambda_{12} = (A_{12}+A_{66})\frac{m\pi}{a}\frac{n\pi}{b}, \quad \lambda_{14} = B_{11}\frac{m^2\pi^2}{a^2} + B_{66}\frac{n^2\pi^2}{b^2},
$$

$$
\lambda_{15} = (B_{12}+B_{66})\frac{m\pi}{a}\frac{n\pi}{b}, \quad \lambda_{22} = A_{66}\frac{m^2\pi^2}{a^2} + A_{22}\frac{n^2\pi^2}{b^2}, \quad \lambda_{24} = (B_{12}+B_{66})\frac{m\pi}{a}\frac{n\pi}{b},
$$

$$
\lambda_{25} = B_{66}\frac{m^2\pi^2}{a^2} + B_{22}\frac{n^2\pi^2}{b^2}, \quad \lambda_{33} = K\left(A_{55}\frac{m^2\pi^2}{a^2} + A_{44}\frac{n^2\pi^2}{b^2}\right), \quad \bar{\lambda}_{33} = \frac{m^2\pi^2}{a^2},
$$

$$\lambda_{34} = KA_{55}\frac{m\pi}{a}, \quad \lambda_{35} = KA_{44}\frac{n\pi}{b}, \quad \lambda_{44} = D_{11}\frac{m^2\pi^2}{a^2} + D_{66}\frac{n^2\pi^2}{b^2} + KA_{55},$$

$$\lambda_{45} = (D_{12} + D_{66})\frac{m\pi}{a}\frac{n\pi}{b}, \quad \lambda_{55} = D_{66}\frac{m^2\pi^2}{a^2} + D_{22}\frac{n^2\pi^2}{b^2} + KA_{44}. \tag{12.79}$$

To avoid the trivial solution, the disappearance of the coefficient determinant is required again. A closed-form analytical solution for the buckling load is possible and can be given as follows after a few transformations:

$$N_{xx}^0 = \frac{a^2}{m^2\pi^2}\left[\lambda_{33} - \frac{\left(\lambda_{34}\bar{\lambda}_{55} - \lambda_{35}\bar{\lambda}_{45}\right)\lambda_{34} + \left(\lambda_{35}\bar{\lambda}_{44} - \lambda_{34}\bar{\lambda}_{45}\right)\lambda_{35}}{\bar{\lambda}_{44}\bar{\lambda}_{55} - \bar{\lambda}_{45}^2}\right], \tag{12.80}$$

with:

$$\begin{aligned}
\bar{\lambda}_{44} &= \lambda_{44} - \frac{\lambda_{14}\left(\lambda_{14}\lambda_{22} - \lambda_{12}\lambda_{24}\right) + \lambda_{24}\left(\lambda_{11}\lambda_{24} - \lambda_{12}\lambda_{14}\right)}{\lambda_{11}\lambda_{22} - \lambda_{12}^2}, \\
\bar{\lambda}_{45} &= \lambda_{45} - \frac{\lambda_{15}\left(\lambda_{14}\lambda_{22} - \lambda_{12}\lambda_{24}\right) + \lambda_{25}\left(\lambda_{11}\lambda_{24} - \lambda_{12}\lambda_{14}\right)}{\lambda_{11}\lambda_{22} - \lambda_{12}^2}, \\
\bar{\lambda}_{55} &= \lambda_{55} - \frac{\lambda_{15}\left(\lambda_{15}\lambda_{22} - \lambda_{12}\lambda_{25}\right) + \lambda_{25}\left(\lambda_{11}\lambda_{25} - \lambda_{12}\lambda_{15}\right)}{\lambda_{11}\lambda_{22} - \lambda_{12}^2}.
\end{aligned} \tag{12.81}$$

The relevant half-wave numbers m, n must again be determined by trial and error.

12.4.3 Navier Solution for a Simply Supported Unsymmetric Angle-Ply Laminate Under Uniaxial Compressive Load

As the last Navier-type solution according to FSDT, an unsymmetric angle-ply laminate is now considered, whose constitutive law is as follows:

$$\begin{pmatrix} N_{xx}^0 \\ N_{yy}^0 \\ N_{xy}^0 \\ M_{xx}^0 \\ M_{yy}^0 \\ M_{xy}^0 \\ Q_y \\ Q_x \end{pmatrix} = \begin{bmatrix} A_{11} & A_{12} & 0 & 0 & 0 & B_{16} & 0 & 0 \\ A_{12} & A_{22} & 0 & 0 & 0 & B_{26} & 0 & 0 \\ 0 & 0 & A_{66} & B_{16} & B_{26} & 0 & 0 & 0 \\ 0 & 0 & B_{16} & D_{11} & D_{12} & 0 & 0 & 0 \\ 0 & 0 & B_{26} & D_{12} & D_{22} & 0 & 0 & 0 \\ B_{16} & B_{26} & 0 & 0 & 0 & D_{66} & 0 & 0 \\ 0 & 0 & 0 & 0 & 0 & 0 & KA_{44} & 0 \\ 0 & 0 & 0 & 0 & 0 & 0 & 0 & KA_{55} \end{bmatrix} \begin{pmatrix} \frac{\partial u_0}{\partial x} \\ \frac{\partial v_0}{\partial y} \\ \frac{\partial u_0}{\partial y} + \frac{\partial v_0}{\partial x} \\ \frac{\partial \psi_x}{\partial x} \\ \frac{\partial \psi_y}{\partial y} \\ \frac{\partial \psi_x}{\partial y} + \frac{\partial \psi_y}{\partial x} \\ \frac{\partial w_0}{\partial y} + \psi_y \\ \frac{\partial w_0}{\partial x} + \psi_x \end{pmatrix}. \tag{12.82}$$

The governing differential equations then take the following form:

$$
\begin{aligned}
A_{11}\frac{\partial^2 u_0}{\partial x^2}+A_{66}\frac{\partial^2 u_0}{\partial y^2}+(A_{12}+A_{66})\frac{\partial^2 v_0}{\partial x\partial y}+2B_{16}\frac{\partial^2 \psi_x}{\partial x\partial y}+B_{16}\frac{\partial^2 \psi_y}{\partial x^2}+B_{26}\frac{\partial^2 \psi_y}{\partial y^2}&=0,\\
(A_{12}+A_{66})\frac{\partial^2 u_0}{\partial x\partial y}+A_{66}\frac{\partial^2 v_0}{\partial x^2}+A_{22}\frac{\partial^2 v_0}{\partial y^2}+B_{16}\frac{\partial^2 \psi_x}{\partial x^2}+B_{26}\frac{\partial^2 \psi_x}{\partial y^2}+2B_{26}\frac{\partial^2 \psi_y}{\partial x\partial y}&=0,\\
K\left[A_{55}\left(\frac{\partial \psi_x}{\partial x}+\frac{\partial^2 w_0}{\partial x^2}\right)+A_{44}\left(\frac{\partial \psi_y}{\partial y}+\frac{\partial^2 w_0}{\partial y^2}\right)\right]-N^0_{xx}\frac{\partial^2 w_0}{\partial x^2}&=0,\\
B_{16}\left(2\frac{\partial^2 u_0}{\partial x\partial y}+\frac{\partial^2 v_0}{\partial x^2}\right)+B_{26}\frac{\partial^2 v_0}{\partial y^2}+D_{11}\frac{\partial^2 \psi_x}{\partial x^2}&\\
+D_{66}\frac{\partial^2 \psi_x}{\partial y^2}+(D_{12}+D_{66})\frac{\partial^2 \psi_y}{\partial x\partial y}&=KA_{55}\left(\psi_x+\frac{\partial w_0}{\partial x}\right),\\
B_{16}\frac{\partial^2 u_0}{\partial x^2}+B_{26}\left(\frac{\partial^2 u_0}{\partial y^2}+2\frac{\partial^2 v_0}{\partial x\partial y}\right)+(D_{12}+D_{66})\frac{\partial^2 \psi_x}{\partial x\partial y}&\\
+D_{66}\frac{\partial^2 \psi_y}{\partial x^2}+D_{22}\frac{\partial^2 \psi_y}{\partial y^2}&=KA_{44}\left(\psi_y+\frac{\partial w_0}{\partial y}\right).
\end{aligned}
\tag{12.83}
$$

The following SS2 boundary conditions are assumed to apply:

$$
\begin{aligned}
&u_0\,(x=0)=0,\quad u_0\,(x=a)=0,\quad v_0\,(y=0)=0,\quad v_0\,(y=b)=0,\\
&w_0\,(x=0)=0,\quad w_0\,(x=a)=0,\quad w_0\,(y=0)=0,\quad w_0\,(y=b)=0,\\
&\psi_x\,(y=0)=0,\quad \psi_x\,(y=b)=0,\quad \psi_y\,(x=0)=0,\quad \psi_y\,(x=a)=0,\\
&N^0_{xy}\,(x=0)=0,\quad N^0_{xy}\,(x=a)=0,\quad N^0_{xy}\,(y=0)=0,\quad N^0_{xy}\,(y=b)=0,\\
&M^0_{xx}\,(x=0)=0,\quad M^0_{xx}\,(x=a)=0,\quad M^0_{yy}\,(y=0)=0,\quad M^0_{yy}\,(y=b)=0.
\end{aligned}
\tag{12.84}
$$

These boundary conditions are fulfilled identically by the following approaches:

$$
\begin{aligned}
u_0&=U_{mn}\sin\left(\frac{m\pi x}{a}\right)\cos\left(\frac{n\pi y}{b}\right),\\
v_0&=V_{mn}\cos\left(\frac{m\pi x}{a}\right)\sin\left(\frac{n\pi y}{b}\right),\\
w_0&=W_{mn}\sin\left(\frac{m\pi x}{a}\right)\sin\left(\frac{n\pi y}{b}\right),
\end{aligned}
$$

$$\psi_x = X_{mn} \cos\left(\frac{m\pi x}{a}\right) \sin\left(\frac{n\pi y}{b}\right),$$
$$\psi_y = Y_{mn} \sin\left(\frac{m\pi x}{a}\right) \cos\left(\frac{n\pi y}{b}\right). \tag{12.85}$$

Inserting this approach into the system of differential equations (12.83) yields the following homogeneous linear system of equations for the determination of the coefficients U_{mn}, V_{mn}, W_{mn}, X_{mn}, Y_{mn}:

$$\begin{bmatrix} \lambda_{11} & \lambda_{12} & 0 & \lambda_{14} & \lambda_{15} \\ \lambda_{12} & \lambda_{22} & 0 & \lambda_{24} & \lambda_{25} \\ 0 & 0 & \lambda_{33} - N^0_{xx}\bar{\lambda}_{33} & \lambda_{34} & \lambda_{35} \\ \lambda_{14} & \lambda_{24} & \lambda_{34} & \lambda_{44} & \lambda_{45} \\ \lambda_{15} & \lambda_{25} & \lambda_{35} & \lambda_{45} & \lambda_{55} \end{bmatrix} \begin{pmatrix} U_{mn} \\ V_{mn} \\ W_{mn} \\ X_{mn} \\ Y_{mn} \end{pmatrix} = \begin{pmatrix} 0 \\ 0 \\ 0 \\ 0 \\ 0 \end{pmatrix}, \tag{12.86}$$

wherein:

$$\lambda_{11} = A_{11}\frac{m^2\pi^2}{a^2} + A_{66}\frac{n^2\pi^2}{b^2}, \quad \lambda_{12} = (A_{12} + A_{66})\frac{m\pi}{a}\frac{n\pi}{b}, \quad \lambda_{14} = 2B_{16}\frac{m\pi}{a}\frac{n\pi}{b},$$
$$\lambda_{15} = B_{16}\frac{m^2\pi^2}{a^2} + B_{26}\frac{n^2\pi^2}{b^2}, \quad \lambda_{22} = A_{66}\frac{m^2\pi^2}{a^2} + A_{22}\frac{n^2\pi^2}{b^2},$$
$$\lambda_{24} = B_{16}\frac{m^2\pi^2}{a^2} + B_{26}\frac{n^2\pi^2}{b^2}, \quad \lambda_{25} = 2B_{26}\frac{m\pi}{a}\frac{n\pi}{b}, \quad \lambda_{33} = K\left(A_{55}\frac{m^2\pi^2}{a^2} + A_{44}\frac{n^2\pi^2}{b^2}\right),$$
$$\lambda_{34} = KA_{55}\frac{m\pi}{a}, \quad \lambda_{35} = KA_{44}\frac{n\pi}{b}, \quad \lambda_{44} = D_{11}\frac{m^2\pi^2}{a^2} + D_{66}\frac{n^2\pi^2}{b^2} + KA_{55},$$
$$\lambda_{45} = (D_{12} + D_{66})\frac{m\pi}{a}\frac{n\pi}{b}, \quad \lambda_{55} = D_{66}\frac{m^2\pi^2}{a^2} + D_{22}\frac{n^2\pi^2}{b^2} + KA_{44}. \tag{12.87}$$

If we require the coefficient determinant to vanish, we arrive at the following closed-form analytical solution for the buckling load after a few transformations:

$$N^0_{xx} = \frac{a^2}{m^2\pi^2}\left[\lambda_{33} - \frac{\left(\lambda_{34}\bar{\lambda}_{55} - \lambda_{35}\bar{\lambda}_{45}\right)\lambda_{34} + \left(\lambda_{35}\bar{\lambda}_{44} - \lambda_{34}\bar{\lambda}_{45}\right)\lambda_{35}}{\bar{\lambda}_{44}\bar{\lambda}_{55} - \bar{\lambda}^2_{45}}\right], \tag{12.88}$$

with:

$$\bar{\lambda}_{44} = \lambda_{44} - \frac{\lambda_{14}\left(\lambda_{14}\lambda_{22} - \lambda_{12}\lambda_{24}\right) + \lambda_{24}\left(\lambda_{11}\lambda_{24} - \lambda_{12}\lambda_{14}\right)}{\lambda_{11}\lambda_{22} - \lambda_{12}^2},$$
$$\bar{\lambda}_{45} = \lambda_{45} - \frac{\lambda_{15}\left(\lambda_{14}\lambda_{22} - \lambda_{12}\lambda_{24}\right) + \lambda_{25}\left(\lambda_{11}\lambda_{24} - \lambda_{12}\lambda_{14}\right)}{\lambda_{11}\lambda_{22} - \lambda_{12}^2},$$
$$\bar{\lambda}_{55} = \lambda_{55} - \frac{\lambda_{15}\left(\lambda_{15}\lambda_{22} - \lambda_{12}\lambda_{25}\right) + \lambda_{25}\left(\lambda_{11}\lambda_{25} - \lambda_{12}\lambda_{15}\right)}{\lambda_{11}\lambda_{22} - \lambda_{12}^2}. \tag{12.89}$$

The relevant half-wave numbers m, n are determined by trial and error.

References

Jones RM (1973): *Buckling and vibration of rectangular unsymmetrically laminated cross-ply plates*, AIAA Journal 11:1626–1632.

Jones RM (1975): *Mechanics of composite materials*, Scripta Book Co., Washington, USA.

Reddy JN (2004): *Mechanics of laminated composite plates and shells*, 2nd edition, CRC Press, Boca Raton et al., USA.

Whitney JM (1969): *Bending-extension coupling in laminated plates under transverse loading*, Journal of Composite Materials 3:20–28.

13 Lévy-Type Solutions for Laminate Buckling Problems

Besides the Navier solutions already described, Lévy-type solutions can also be used to analyze the buckling behaviour of composite laminates. The following explanations are initially limited to the case of symmetric balanced laminates with orthotropic plate behaviour within the framework of Classical Laminated Plate Theory (CLPT); an extension to the Third-Order Shear Deformation Theory (TSDT) will follow later. Interested readers will find some further Lévy solutions for other laminate types within the framework of various laminate theories, e.g. in Reddy (2004).

13.1 Introduction

A prerequisite for the existence of a Lévy solution is that the laminate under consideration is simply supported at two opposite edges (here these are the edges at $x = 0$ and $x = a$). This means that the following boundary conditions apply at these edges:

$$w_0 = 0, \quad M_{xx}^0 = -D_{11} \frac{\partial^2 w_0}{\partial x^2} = 0. \tag{13.1}$$

The two remaining edges at $y = 0$ and $y = b$ can each be subject to arbitrary and different boundary conditions, e.g. simply supported, free, clamped, elastically restrained, reinforced by edge stiffeners, etc. (see Fig. 13.1 for a possible selection of boundary conditions for $y = 0$ and $y = b$). The laminate is stressed by a uniaxial compressive edge load N_{xx}^0.

The differential equation describing the buckling behaviour of a symmetric laminate with orthotropic plate behaviour under a uniaxial compressive edge load N_{xx}^0 can be written as:

$$D_{11} \frac{\partial^4 w_0}{\partial x^4} + 2\,(D_{12} + 2D_{66}) \frac{\partial^4 w_0}{\partial x^2 \partial y^2} + D_{22} \frac{\partial^4 w_0}{\partial y^4} + N_{xx}^0 \frac{\partial^2 w_0}{\partial x^2} = 0. \tag{13.2}$$

© The Author(s), under exclusive license to Springer-Verlag GmbH, DE, part of Springer Nature 2025
C. Mittelstedt, *Mechanics of Composite Structures*,
https://doi.org/10.1007/978-3-662-70788-3_13

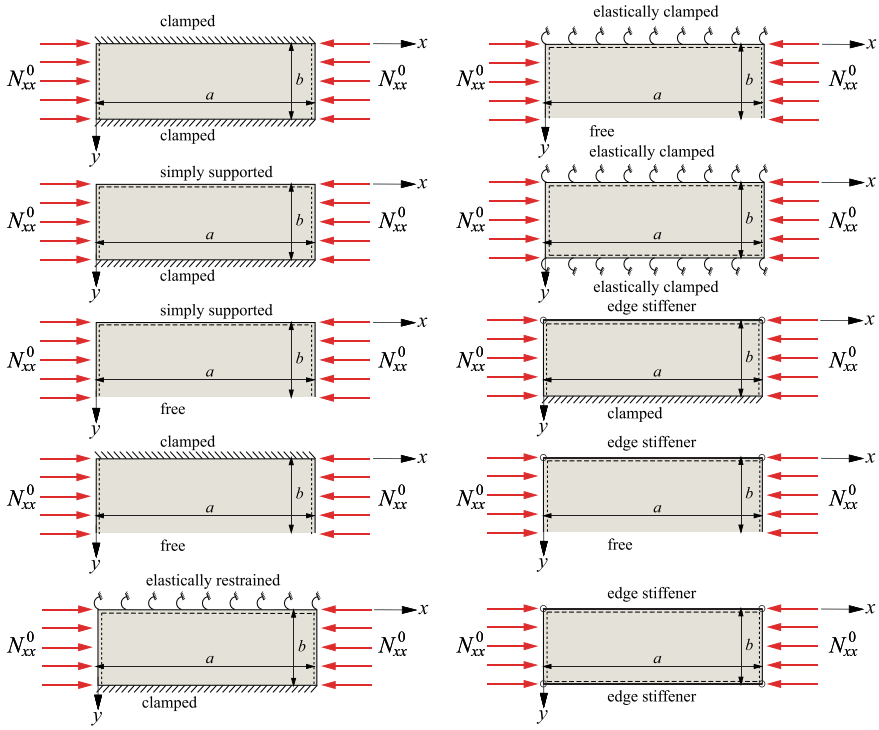


Fig. 13.1 Selected boundary conditions of the Lévy type

The following separation approach is used for the buckling mode w_0:

$$w_0 = \sin\left(\frac{m\pi x}{a}\right) W_m(y)\,. \tag{13.3}$$

Here, $W(y)$ is an as yet unknown function that describes the buckling mode in the y-direction. It is easy to see that the approach (13.3) fulfils the boundary conditions (13.1) identically. If the approach (13.3) is inserted into the partial differential equation (13.2), this leads to the following ordinary linear homogeneous differential equation of the fourth order:

$$\frac{\mathrm{d}^4 W_m}{\mathrm{d}y^4} - 2\frac{D_{12}+2D_{66}}{D_{22}}\frac{m^2\pi^2}{a^2}\frac{\mathrm{d}^2 W_m}{\mathrm{d}y^2} + \frac{1}{D_{22}}\frac{m^2\pi^2}{a^2}\left(D_{11}\frac{m^2\pi^2}{a^2} - N^0_{xx}\right) W_m = 0. \tag{13.4}$$

The general solution of (13.4) can be found in the form of an exponential approach:

$$W_m = Ce^{\lambda y}. \tag{13.5}$$

If this is inserted into the differential equation (13.4), the following characteristic polynomial is obtained to determine the exponents λ in (13.5):

$$\lambda^4 - 2\frac{D_{12}+2D_{66}}{D_{22}}\frac{m^2\pi^2}{a^2}\lambda^2 + \frac{1}{D_{22}}\frac{m^2\pi^2}{a^2}\left(D_{11}\frac{m^2\pi^2}{a^2} - N_{xx}^0\right) = 0. \tag{13.6}$$

The four roots of this polynomial then represent the unknown exponents in (13.5) and result as follows:

$$\lambda_{1,2,3,4} = \pm\frac{m\pi}{a}\frac{1}{\sqrt{D_{22}}}\sqrt{D_{12}+2D_{66} \pm \sqrt{(D_{12}+2D_{66})^2 + D_{22}\left(N_{xx}^0\frac{a^2}{m^2\pi^2} - D_{11}\right)}}. \tag{13.7}$$

The function $W(y)$ can thus be represented as:

$$W_m = C_1 e^{\lambda_1 y} + C_2 e^{\lambda_2 y} + C_3 e^{\lambda_3 y} + C_4 e^{\lambda_4 y}. \tag{13.8}$$

The entire solution for the buckling shape w_0 is then as follows:

$$w_0 = \sin\left(\frac{m\pi x}{a}\right)\left(C_1 e^{\lambda_1 y} + C_2 e^{\lambda_2 y} + C_3 e^{\lambda_3 y} + C_4 e^{\lambda_4 y}\right). \tag{13.9}$$

The constants $C_1, \ldots, C_4$ are finally adapted to the boundary conditions at the unloaded edges.

13.2 Case Distinctions and Alternative Solution Representations

Depending on the type (real-valued, complex) of the roots λ, a representation of the solution (13.9) using hyperbolic functions and trigonometric functions of the type $\sinh(\lambda y)$, $\cosh(\lambda y)$, $\sin(\lambda y)$, $\cos(\lambda y)$ is also very common. The advantage of such representations instead of the exponential functions in (13.9) is that when using such alternative notations with a skilful choice of coordinate system, it is often possible to write much more compact representations of the resulting buckling solutions than would be the case when using the representation (13.9). However, it must always be ensured that the correct alternative notation is selected by differentiating between the individual terms under the roots in (13.7). This is briefly described below. For further details, interested readers are referred to the works of Beerhorst (2013) and Dörfler (1993). At this point, a dimensionless notation is again used. The solution approach for the differential equation

$$\frac{1}{\alpha^2}\frac{\partial^4\bar{w}_0}{\partial\xi_1^4} + 2\beta\frac{\partial^4\bar{w}_0}{\partial\xi_1^2\partial\xi_2^2} + \alpha^2\frac{\partial^4\bar{w}_0}{\partial\xi_2^4} + \bar{N}_{xx}^0\pi^2\frac{\partial^2\bar{w}_0}{\partial\xi_1^2} = 0 \tag{13.10}$$

reads

$$\bar{w}_0 = \sin(m\pi\xi_1)\, W_m(\xi_2), \tag{13.11}$$

which, after insertion into (13.10), results in the following ordinary differential equation:

$$\frac{\mathrm{d}^4 W_m}{\mathrm{d}\xi_2^4} - 2\beta\frac{m^2\pi^2}{\alpha^2}\frac{\mathrm{d}^2 W_m}{\mathrm{d}\xi_2^2} + \frac{m^4\pi^4}{\alpha^4}\left(1 - \bar{N}_{xx}^0\frac{\alpha^2}{m^2}\right)W_m = 0. \tag{13.12}$$

An approach of the form

$$W_m = Ce^{\lambda\xi_2} \tag{13.13}$$

results in the following characteristic polynomial for determining the exponents λ after insertion into (13.12):

$$\lambda^4 - 2\beta\frac{m^2\pi^2}{\alpha^2}\lambda^2 + \frac{m^4\pi^4}{\alpha^4}\left(1 - \bar{N}_{xx}^0\frac{\alpha^2}{m^2}\right) = 0. \tag{13.14}$$

The roots are then as follows:

$$\lambda_{1,2,3,4} = \pm\frac{m\pi}{\alpha}\sqrt{\beta \pm \sqrt{\beta^2 - 1 + \bar{N}_{xx}^0\frac{\alpha^2}{m^2}}}. \tag{13.15}$$

By introducing the abbreviation

$$\Omega = \beta^2 - 1 + \bar{N}_{xx}^0\frac{\alpha^2}{m^2} \tag{13.16}$$

Equation (13.15) can be reformulated as follows:

$$\lambda_{1,2,3,4} = \pm\frac{m\pi}{\alpha}\sqrt{\beta \pm \sqrt{\Omega}}. \tag{13.17}$$

The type of roots depends heavily on the relationship between the variables β and $\sqrt{\Omega}$. Five different cases can be distinguished here, namely

$$\begin{aligned}
&1.\quad \sqrt{\Omega} > \beta,\\
&2.\quad \sqrt{\Omega} = \beta,\\
&3.\quad \beta > \sqrt{\Omega} > 0,\\
&4.\quad \sqrt{\Omega} = 0,\\
&5.\quad \Omega < 0.
\end{aligned} \tag{13.18}$$

If Ω is inserted into the case distinctions (13.18) according to (13.16) and solved for the buckling load $\bar{N}_{xx}^0$, the following relations are obtained:

$$
\begin{aligned}
&1.\quad \bar{N}^0_{xx} > \frac{m^2}{\alpha^2},\\
&2.\quad \bar{N}^0_{xx} = \frac{m^2}{\alpha^2},\\
&3.\quad \frac{m^2}{\alpha^2} > \bar{N}^0_{xx} > \frac{m^2}{\alpha^2}\left(1-\beta^2\right),\\
&4.\quad \bar{N}^0_{xx} = \frac{m^2}{\alpha^2}\left(1-\beta^2\right),\\
&5.\quad \bar{N}^0_{xx} < \frac{m^2}{\alpha^2}\left(1-\beta^2\right).
\end{aligned}
\tag{13.19}
$$

Since cases 2 and 4 only describe discrete points and not intervals, these cases will only be relevant in the rarest of cases. Therefore, only cases 1, 3 and 5 are considered in more detail below.

In case 1, there are two real-valued and two complex-conjugate exponents λ:

$$
\begin{aligned}
\lambda_{1,2} &= \pm\frac{m\pi}{\alpha}\sqrt{\beta+\sqrt{\Omega}} = \pm\lambda_1,\\
\lambda_{3,4} &= \pm i\frac{m\pi}{\alpha}\sqrt{\sqrt{\Omega}-\beta} = \pm i\lambda_3.
\end{aligned}
\tag{13.20}
$$

The solution (13.13) can then be represented as follows:

$$
W_m = C_1\cosh(\lambda_1\xi_2) + C_2\sinh(\lambda_1\xi_2) + C_3\cos(\lambda_3\xi_2) + C_4\sin(\lambda_3\xi_2)\,. \tag{13.21}
$$

In fact, the investigations in Beerhorst (2013) clearly show that the form (13.21) is the only significant one for large practically relevant parameter spaces and that the other cases only become relevant, for example, for very compact laminates with very small aspect ratios α. This also explains why the solution form (13.21) is assumed to be correct in a large number of literature references without further justification. In dimensional notation, (13.21) is written as:

$$
W_m = C_1\cosh(\lambda_1 y) + C_2\sinh(\lambda_1 y) + C_3\cos(\lambda_3 y) + C_4\sin(\lambda_3 y)\,, \tag{13.22}
$$

with:

$$
\begin{aligned}
\lambda_1 &= \frac{m\pi}{a}\frac{1}{\sqrt{D_{22}}}\sqrt{\sqrt{(D_{12}+2D_{66})^2 + D_{22}\left(N^0_{xx}\frac{a^2}{m^2\pi^2} - D_{11}\right)} + D_{12} + 2D_{66}},\\
\lambda_3 &= \frac{m\pi}{a}\frac{1}{\sqrt{D_{22}}}\sqrt{\sqrt{(D_{12}+2D_{66})^2 + D_{22}\left(N^0_{xx}\frac{a^2}{m^2\pi^2} - D_{11}\right)} - D_{12} - 2D_{66}}.
\end{aligned}
\tag{13.23}
$$

Case 3 leads to four real-valued and different exponents λ:

$$\lambda_{1,2} = \pm\frac{m\pi}{\alpha}\sqrt{\beta+\sqrt{\Omega}} = \pm\lambda_1,$$
$$\lambda_{3,4} = \pm\frac{m\pi}{\alpha}\sqrt{\beta-\sqrt{\Omega}} = \pm\lambda_3. \tag{13.24}$$

The solution (13.13) can then be written as follows:

$$W_m = C_1\cosh(\lambda_1\xi_2) + C_2\sinh(\lambda_1\xi_2) + C_3\cosh(\lambda_3\xi_2) + C_4\sinh(\lambda_3\xi_2)\,. \tag{13.25}$$

Finally, case 5 leads to four complex exponents λ, which occur as complex-conjugate pairs:

$$\lambda_{1,2} = \frac{m\pi}{\alpha}(\omega \pm i\psi)\,, \quad \lambda_{3,4} = \frac{m\pi}{\alpha}(-\omega \pm i\psi)\,, \tag{13.26}$$

with:

$$\omega = \sqrt{\frac{1}{2}\left(\sqrt{\beta^2-\Omega}+\beta\right)}, \quad \psi = \sqrt{\frac{1}{2}\left(\sqrt{\beta^2-\Omega}-\beta\right)}. \tag{13.27}$$

The solution (13.13) can then also be formulated as follows:

$$\begin{aligned} W_m = {} & C_1\cosh(\omega\xi_2)\cos(\psi\xi_2) + C_2\sinh(\omega\xi_2)\cos(\psi\xi_2) \\ & + C_3\cosh(\omega\xi_2)\sin(\psi\xi_2) + C_4\sinh(\omega\xi_2)\sin(\psi\xi_2)\,. \end{aligned} \tag{13.28}$$

13.3 Selected Lévy Solutions

13.3.1 Laminate with Three Simply Supported Edges and One Free Edge

To illustrate the procedure when using a Lévy-type solution, a laminate under uniaxial compressive load is considered, which is simply supported at the unloaded edge at $y = 0$. The unloaded edge at $y = b$ is free of any support (Fig. 13.2).

The boundary conditions at the unloaded edges are as follows:

$$\begin{aligned} & w_0(y=0) = 0, \quad M^0_{yy}(y=0) = -D_{22}\left.\frac{\partial^2 w_0}{\partial y^2}\right|_{y=0} = 0, \\ & M^0_{yy}(y=b) = -D_{12}\left.\frac{\partial^2 w_0}{\partial x^2}\right|_{y=b} - D_{22}\left.\frac{\partial^2 w_0}{\partial y^2}\right|_{y=b} = 0, \\ & \bar{Q}_y(y=b) = 2\left.\frac{\partial M^0_{xy}}{\partial x}\right|_{y=b} + \left.\frac{\partial M^0_{yy}}{\partial y}\right|_{y=b} \\ & = -D_{22}\left.\frac{\partial^3 w_0}{\partial y^3}\right|_{y=b} - (D_{12}+4D_{66})\left.\frac{\partial^3 w_0}{\partial x^2\partial y}\right|_{y=b} = 0. \end{aligned} \tag{13.29}$$

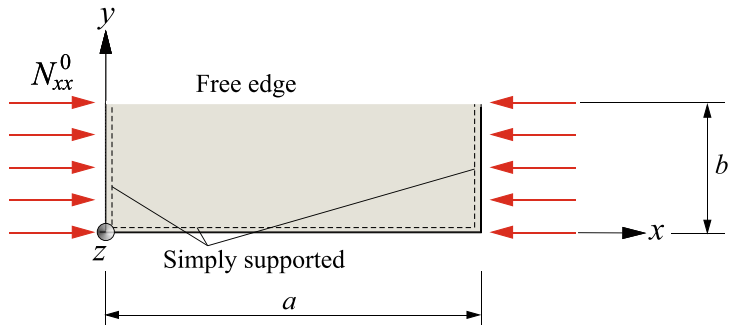


Fig. 13.2 Laminate with three simply supported edges and one free edge under uniaxial compressive load

Evaluating the boundary conditions (13.29) using the solution (13.9) leads to the following equations for determining the constants:

$$C_1 + C_2 + C_3 + C_4 = 0,$$

$$\lambda_1^2 C_1 + \lambda_2^2 C_2 + \lambda_3^2 C_3 + \lambda_4^2 C_4 = 0,$$

$$\left(D_{12}\frac{m^2\pi^2}{a^2} - D_{22}\lambda_1^2\right) e^{\lambda_1 b} C_1 + \left(D_{12}\frac{m^2\pi^2}{a^2} - D_{22}\lambda_2^2\right) e^{\lambda_2 b} C_2$$
$$+ \left(D_{12}\frac{m^2\pi^2}{a^2} - D_{22}\lambda_3^2\right) e^{\lambda_3 b} C_3 + \left(D_{12}\frac{m^2\pi^2}{a^2} - D_{22}\lambda_4^2\right) e^{\lambda_4 b} C_4 = 0,$$

$$\left[(D_{12} + 4D_{66})\frac{m^2\pi^2}{a^2} - D_{22}\lambda_1^2\right] \lambda_1 e^{\lambda_1 b} C_1$$
$$+ \left[(D_{12} + 4D_{66})\frac{m^2\pi^2}{a^2} - D_{22}\lambda_2^2\right] \lambda_2 e^{\lambda_2 b} C_2$$
$$+ \left[(D_{12} + 4D_{66})\frac{m^2\pi^2}{a^2} - D_{22}\lambda_3^2\right] \lambda_3 e^{\lambda_3 b} C_3$$
$$+ \left[(D_{12} + 4D_{66})\frac{m^2\pi^2}{a^2} - D_{22}\lambda_4^2\right] \lambda_4 e^{\lambda_4 b} C_4 = 0. \qquad (13.30)$$

This is a homogeneous system of equations for the four constants $C_1, \ldots, C_4$. For a non-trivial solution, the coefficient determinant is set to zero. The resulting expression is then the buckling condition from which the buckling load can be determined. However, the resulting equation is quite long and is not described in detail here.

For this example, it can be shown that a skilful reformulation of the solution (13.9) results in a solution representation that is easier to handle. It is assumed for the moment that the

exponents λ_1 and λ_2 are real-valued, while the exponents λ_3 and λ_4 are complex in nature and appear as a complex conjugate pair. The solution (13.22) is therefore valid:

$$w_0 = \sin\left(\frac{m\pi x}{a}\right)\left[C_1 \cosh(\lambda_1 y) + C_2 \sinh(\lambda_1 y) + C_3 \cos(\lambda_3 y) + C_4 \sin(\lambda_3 y)\right]. \tag{13.31}$$

If the boundary conditions (13.29) are analysed for this representation, the following equations are obtained from the first two boundary conditions:

$$C_1 + C_3 = 0, \quad \lambda_1^2 C_1 - \lambda_3^2 C_3 = 0. \tag{13.32}$$

From this we can immediately deduce $C_1 = C_3 = 0$. The solution (13.31) then reduces to:

$$w_0 = \sin\left(\frac{m\pi x}{a}\right)\left[C_2 \sinh(\lambda_1 y) + C_4 \sin(\lambda_3 y)\right]. \tag{13.33}$$

Evaluating the two remaining boundary conditions in (13.29) leads to the following two equations for determining the constants C_2 and C_4:

$$\begin{aligned}\left(D_{12}\frac{m^2\pi^2}{a^2} - D_{22}\lambda_1^2\right)\sinh(\lambda_1 b)\, C_2 + \left(D_{12}\frac{m^2\pi^2}{a^2} + D_{22}\lambda_3^2\right)\sin(\lambda_3 b)\, C_4 = 0,\\ \left[(D_{12}+4D_{66})\frac{m^2\pi^2}{a^2} - D_{22}\lambda_1^2\right]\lambda_1 \cosh(\lambda_1 b)\, C_2\\ + \left[(D_{12}+4D_{66})\frac{m^2\pi^2}{a^2} + D_{22}\lambda_3^2\right]\lambda_3 \cos(\lambda_3 b)\, C_4 = 0.\end{aligned} \tag{13.34}$$

In vector-matrix notation, the following results:

$$\begin{bmatrix} \left(D_{12}\frac{m^2\pi^2}{a^2} - D_{22}\lambda_1^2\right)\sinh(\lambda_1 b) & \left(D_{12}\frac{m^2\pi^2}{a^2} + D_{22}\lambda_3^2\right)\sin(\lambda_3 b) \\ \left[(D_{12}+4D_{66})\frac{m^2\pi^2}{a^2} - D_{22}\lambda_1^2\right]\lambda_1 \cosh(\lambda_1 b) & \left[(D_{12}+4D_{66})\frac{m^2\pi^2}{a^2} + D_{22}\lambda_3^2\right]\lambda_3 \cos(\lambda_2 b) \end{bmatrix} \times \begin{pmatrix} C_2 \\ C_4 \end{pmatrix} = \begin{pmatrix} 0 \\ 0 \end{pmatrix}. \tag{13.35}$$

To avoid the trivial solution, it is required that the coefficient determinant in (13.35) disappears. This leads to the following equation after a few elementary transformations:

$$\begin{aligned}&\left(D_{12}\frac{m^2\pi^2}{a^2} - D_{22}\lambda_1^2\right)\left[(D_{12}+4D_{66})\frac{m^2\pi^2}{a^2} + D_{22}\lambda_3^2\right]\lambda_3 \tanh(\lambda_1 b)\\ &- \left(D_{12}\frac{m^2\pi^2}{a^2} + D_{22}\lambda_3^2\right)\left[(D_{12}+4D_{66})\frac{m^2\pi^2}{a^2} - D_{22}\lambda_1^2\right]\lambda_1 \tan(\lambda_3 b) = 0.\end{aligned} \tag{13.36}$$

Equation (13.36) is the equation from which the buckling load N_{xx}^0 can be determined. This is also referred to as the so-called buckling condition. Since the solution (13.36) is based on the solution of the governing differential equation and even fulfils all underlying boundary conditions, it is exact in the sense of the assumptions of CLPT. However, the problem here is that it is not possible to explicitly solve the solution (13.36) for the buckling load N_{xx}^0. Rather, N_{xx}^0 appears in the two quantities λ_1 and λ_3 under a double root, which in turn are contained in trigonometric functions and hyperbolic functions, which is why the solution (13.36) is exact but implicit. This requires a numerical-iterative determination of the buckling load from the buckling condition (13.36). Experience shows that the automation of such a solution for everyday engineering use often encounters some difficulties, which is why Lévy-type solutions for buckling problems are of only minor value in practical engineering work. Nevertheless, such solutions—if they exist—are of great value if we either want to verify approximation methods or if we want to create generally valid results in the form of buckling diagrams from such exact buckling conditions. A few comments on this will follow later. In addition, Lévy-type solutions play a very significant role, for example, in the derivation of minimum stiffness requirements for stiffeners of thin-walled surface structures, which will be discussed at a later point.

13.3.2 Laminate with One Clamped and One Free Unloaded Edge

Next, a laminate under uniaxial compressive load is considered, which is clamped at the unloaded edge at $y = 0$. The unloaded edge at $y = b$ is again free of any support (Fig. 13.3). The exact buckling condition is sought using a Lévy-type solution. In this case, the boundary conditions at the unloaded edges are as follows

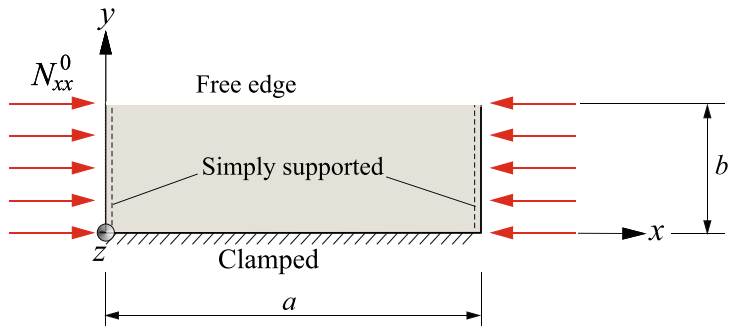


Fig. 13.3 Laminate with one clamped and one free unloaded edge

$$
\begin{aligned}
&w_0\,(y=0)=0, \quad \left.\frac{\partial w_0}{\partial y}\right|_{y=0}=0,\\
&M^0_{yy}\,(y=b)=-D_{12}\left.\frac{\partial^2 w_0}{\partial x^2}\right|_{y=b}-D_{22}\left.\frac{\partial^2 w_0}{\partial y^2}\right|_{y=b}=0,\\
&\bar{Q}_y\,(y=b)=2\left.\frac{\partial M^0_{xy}}{\partial x}\right|_{y=b}+\left.\frac{\partial M^0_{yy}}{\partial y}\right|_{y=b}\\
&=-D_{22}\left.\frac{\partial^3 w_0}{\partial y^3}\right|_{y=b}-(D_{12}+4D_{66})\left.\frac{\partial^3 w_0}{\partial x^2\partial y}\right|_{y=b}=0.
\end{aligned}
\tag{13.37}
$$

Once again, the validity of the following displacement solution is assumed:

$$
w_0=\sin\left(\frac{m\pi x}{a}\right)\Big[C_1\cosh(\lambda_1 y)+C_2\sinh(\lambda_1 y)+C_3\cos(\lambda_3 y)+C_4\sin(\lambda_3 y)\Big].
\tag{13.38}
$$

Analyzing the given boundary conditions leads to the following system of equations:

$$
\begin{aligned}
C_1+C_3&=0,\\
\lambda_1 C_2+\lambda_3 C_4&=0,\\
\left(D_{12}\frac{m^2\pi^2}{a^2}-D_{22}\lambda_1^2\right)\cosh(\lambda_1 b)\,C_1+\left(D_{12}\frac{m^2\pi^2}{a^2}-D_{22}\lambda_1^2\right)\sinh(\lambda_1 b)\,C_2&\\
+\left(D_{12}\frac{m^2\pi^2}{a^2}+D_{22}\lambda_3^2\right)\cos(\lambda_3 b)\,C_3+\left(D_{12}\frac{m^2\pi^2}{a^2}+D_{22}\lambda_3^2\right)\sin(\lambda_3 b)\,C_4&=0,\\
\left[-D_{22}\lambda_1^2+(D_{12}+4D_{66})\frac{m^2\pi^2}{a^2}\right]\lambda_1\sinh(\lambda_1 b)\,C_1&\\
+\left[-D_{22}\lambda_1^2+(D_{12}+4D_{66})\frac{m^2\pi^2}{a^2}\right]\lambda_1\cosh(\lambda_1 b)\,C_2&\\
+\left[-D_{22}\lambda_3^2-(D_{12}+4D_{66})\frac{m^2\pi^2}{a^2}\right]\lambda_3\sin(\lambda_3 b)\,C_3&\\
+\left[D_{22}\lambda_3^2+(D_{12}+4D_{66})\frac{m^2\pi^2}{a^2}\right]\lambda_3\cos(\lambda_3 b)\,C_4&=0.
\end{aligned}
\tag{13.39}
$$

In vector-matrix notation it reads:

$$
\begin{bmatrix}
1 & 0 & 1 & 0\\
0 & \lambda_1 & 0 & \lambda_3\\
\Lambda_1\cosh(\lambda_1 b) & \Lambda_1\sinh(\lambda_1 b) & \Lambda_2\cos(\lambda_3 b) & \Lambda_2\sin(\lambda_3 b)\\
\Lambda_3\sinh(\lambda_1 b) & \Lambda_3\cosh(\lambda_1 b) & \Lambda_4\sin(\lambda_3 b) & -\Lambda_4\cos(\lambda_3 b)
\end{bmatrix}
\begin{pmatrix}C_1\\C_2\\C_3\\C_4\end{pmatrix}=\begin{pmatrix}0\\0\\0\\0\end{pmatrix},
\tag{13.40}
$$

with:

$$\Lambda_1 = D_{12}\frac{m^2\pi^2}{a^2} - D_{22}\lambda_1^2, \quad \Lambda_2 = D_{12}\frac{m^2\pi^2}{a^2} + D_{22}\lambda_3^2,$$
$$\Lambda_3 = \left[-D_{22}\lambda_1^2 + (D_{12} + 4D_{66})\frac{m^2\pi^2}{a^2}\right]\lambda_1,$$
$$\Lambda_4 = \left[-D_{22}\lambda_3^2 - (D_{12} + 4D_{66})\frac{m^2\pi^2}{a^2}\right]\lambda_3. \tag{13.41}$$

For a non-trivial solution, the disappearance of the coefficient determinant is again required, which leads to the following equation after a few transformations:

$$(\lambda_1\Lambda_2\Lambda_3 + \lambda_3\Lambda_1\Lambda_4)\sinh(\lambda_1 b)\sin(\lambda_3 b) + (\lambda_1\Lambda_1\Lambda_4 - \lambda_3\Lambda_2\Lambda_3)\cosh(\lambda_1 b)\cos(\lambda_3 b) - \lambda_1\Lambda_2\Lambda_4 + \lambda_3\Lambda_1\Lambda_3 = 0. \tag{13.42}$$

13.3.3 Laminate with One Elastically Restrained and One Free Unloaded Edge

As a further solution of the Lévy type, the buckling problem of an elastically restrained laminate (spring stiffness k) according to Fig. 13.4 is considered.

The boundary conditions at the unloaded edges are as follows:

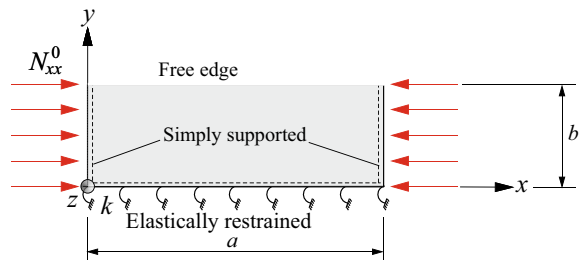


Fig. 13.4 Laminate with one elastically restrained and one free unloaded edge

$$w_0\,(y=0)=0,\quad M^0_{yy}\,(y=0)=-D_{22}\left.\frac{\partial^2 w_0}{\partial y^2}\right|_{y=0}=-k\left.\frac{\partial w_0}{\partial y}\right|_{y=0},$$
$$M^0_{yy}\,(y=b)=-D_{12}\left.\frac{\partial^2 w_0}{\partial x^2}\right|_{y=b}-D_{22}\left.\frac{\partial^2 w_0}{\partial y^2}\right|_{y=b}=0,$$

$$\bar{Q}_y\,(y=b)=2\left.\frac{\partial M^0_{xy}}{\partial x}\right|_{y=b}+\left.\frac{\partial M^0_{yy}}{\partial y}\right|_{y=b}$$
$$=-D_{22}\left.\frac{\partial^3 w_0}{\partial y^3}\right|_{y=b}-(D_{12}+4D_{66})\left.\frac{\partial^3 w_0}{\partial x^2\partial y}\right|_{y=b}=0. \tag{13.43}$$

A detailed description of the solution method is not provided here, only the resulting buckling condition is given as follows:

$$\begin{aligned}&k\,(\lambda_3\Lambda_2\Lambda_3-\lambda_1\Lambda_1\Lambda_4)\cosh(\lambda_1 b)\cos(\lambda_3 b)-k\,(\lambda_3\Lambda_1\Lambda_4+\lambda_1\Lambda_2\Lambda_3)\sinh(\lambda_1 b)\sin(\lambda_3 b)\\&-D_{22}\left(\lambda_1^2+\lambda_3^2\right)[\Lambda_1\Lambda_4\cos(\lambda_3 b)\sinh(\lambda_1 b)+\Lambda_2\Lambda_3\cosh(\lambda_1 b)\sin(\lambda_3 b)]\\&+k\,(\lambda_1\Lambda_2\Lambda_4-\lambda_3\Lambda_1\Lambda_3)=0.\end{aligned} \tag{13.44}$$

This buckling condition was used to provide generic buckling curves. These are shown in Fig. 13.5. This contains the two previously discussed special cases of the previous sections with $k=0$ and with $k\to\infty$.

In the diagrams in Fig. 13.5, a dimensionless notation was used. If the boundary conditions (13.43) are written in dimensionless form, the result is

$$\begin{aligned}\bar{w}_0\,(\xi_2=0)=0,\quad \left.\frac{\partial^2\bar{w}_0}{\partial\xi_2^2}\right|_{\xi_2=0}-\bar{k}\left.\frac{\partial\bar{w}_0}{\partial\xi_2}\right|_{\xi_2=0}&=0,\\ \zeta\beta\left.\frac{\partial^2\bar{w}_0}{\partial\xi_1^2}\right|_{\xi_2=1}+\alpha^2\left.\frac{\partial^2\bar{w}_0}{\partial\xi_2^2}\right|_{\xi_2=1}&=0,\\ \alpha^2\left.\frac{\partial^3\bar{w}_0}{\partial\xi_2^3}\right|_{\xi_2=1}-(\zeta-2)\,\beta\left.\frac{\partial^3\bar{w}_0}{\partial\xi_1^2\partial\xi_2}\right|_{\xi_2=1}&=0.\end{aligned} \tag{13.45}$$

Therein,

$$\bar{k}=\frac{kb}{D_{22}} \tag{13.46}$$

is the elastic restraint stiffness. Furthermore

$$\zeta=\frac{D_{12}}{D_{12}+2D_{66}} \tag{13.47}$$

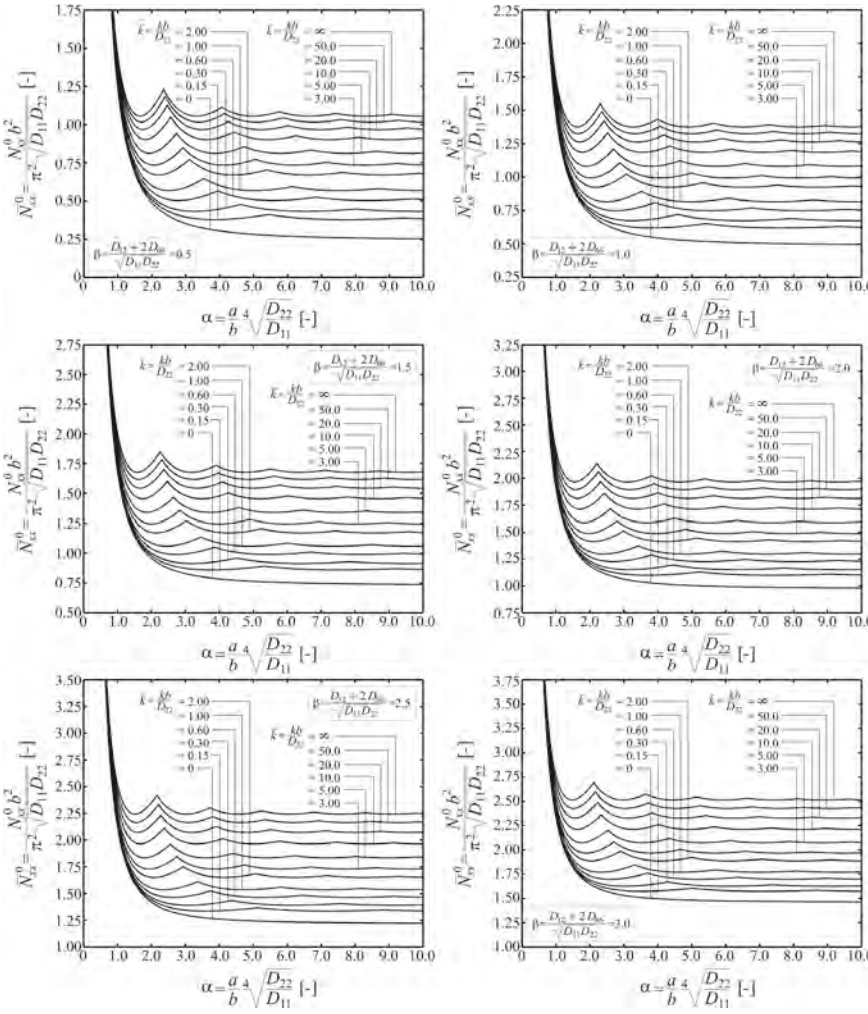


Fig. 13.5 Generic buckling curves for a laminate with an elastically restrained and a free unloaded edge ($\zeta = 0.2$)

is the so-called generalized Poisson's ratio of the laminate under consideration. Accordingly, a consistent dimensionless representation of the buckling curves for the elastically restrained laminate with regard to the elastic laminate properties must not only contain information about the orthotropy parameter β. Rather, the generalised Poisson's ratio ζ has an extremely important influence on the stability behaviour in the presence of free edges. In the diagrams in Fig. 13.5, $\zeta = 0.2$ was used. The buckling diagrams show the expected behaviour of the stability behaviour of the elastically restrained laminate, i.e. typical buckling curves result,

whereby not only a clear influence of the elastic properties of the laminate can be observed, but also the restraint stiffness k decisively influences the resulting buckling loads.

13.3.4 Laminate with Two Elastically Restrained Unloaded Edges

As a further solution of the Lévy type, the buckling problem of a laminate that is elastically restrained at both unloaded edges is treated (Fig. 13.6, restraint stiffnesses k_1 and k_2).

This includes various special cases, e.g. a laminate that is simply supported at all edges (where $k_1 = k_2 = 0$), or the laminate clamped at both unloaded edges (here the limit value considerations $k_1 \to \infty$ and $k_2 \to \infty$ would have to be carried out). The boundary conditions at the unloaded edges are currently as follows

$$\begin{aligned} w_0\,(y=0) &= 0, \quad M^0_{yy}\,(y=0) = -D_{22}\left.\frac{\partial^2 w_0}{\partial y^2}\right|_{y=0} = -k_1\left.\frac{\partial w_0}{\partial y}\right|_{y=0}, \\ w_0\,(y=b) &= 0, \quad M^0_{yy}\,(y=b) = -D_{22}\left.\frac{\partial^2 w_0}{\partial y^2}\right|_{y=b} = k_2\left.\frac{\partial w_0}{\partial y}\right|_{y=b}. \end{aligned} \tag{13.48}$$

The following equations for determining the constants $C_1, \ldots, C_4$ can be derived using the displacement solution (13.38) by evaluating the boundary conditions (13.48):

$$\begin{aligned} C_1 + C_3 &= 0, \\ D_{22}\lambda_1^2 C_1 - k_1\lambda_1 C_2 - D_{22}\lambda_3^2 C_3 - k_1\lambda_3 C_4 &= 0, \\ C_1\cosh(\lambda_1 b) + C_2\sinh(\lambda_1 b) + C_3\cos(\lambda_3 b) + C_4\sin(\lambda_3 b) &= 0, \\ [D_{22}\lambda_1\cosh(\lambda_1 b) + k_2\sinh(\lambda_1 b)]\,\lambda_1 C_1 + [D_{22}\lambda_1\sinh(\lambda_1 b) + k_2\cosh(\lambda_1 b)]\,\lambda_1 C_2 & \\ - [D_{22}\lambda_3\cos(\lambda_3 b) + k_2\sin(\lambda_3 b)]\,\lambda_3 C_3 - [D_{22}\lambda_3\sin(\lambda_3 b) - k_2\cos(\lambda_3 b)]\,\lambda_3 C_4 &= 0. \end{aligned} \tag{13.49}$$

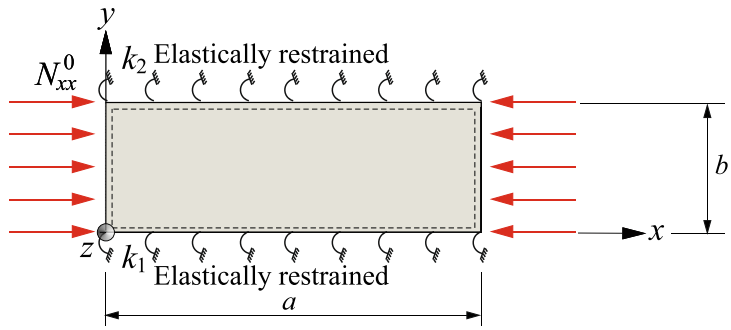


Fig. 13.6 Laminate with two elastically restrained unloaded edges

Setting the coefficient determinant to zero then provides the required buckling condition:

$$\begin{aligned}&\left[k_1\lambda_3\left(\Lambda_5-\Lambda_7\right)+D_{22}\Lambda_8\left(\lambda_1^2+\lambda_3^2\right)\right]\sinh\left(\lambda_1 b\right)\\&+\left[k_1\lambda_1\left(\Lambda_7-\Lambda_5\right)-D_{22}\Lambda_6\left(\lambda_1^2+\lambda_3^2\right)\right]\sin\left(\lambda_3 b\right)\\&+k_1\left(\lambda_1\Lambda_8-\lambda_3\Lambda_6\right)\left[\cosh\left(\lambda_1 b\right)-\cos\left(\lambda_3 b\right)\right]=0,\end{aligned}\tag{13.50}$$

wherein:

$$\begin{aligned}&\Lambda_5=\left[D_{22}\lambda_1\cosh\left(\lambda_1 b\right)+k_2\sinh\left(\lambda_1 b\right)\right]\lambda_1,\quad \Lambda_6=\left[D_{22}\lambda_1\sinh\left(\lambda_1 b\right)+k_2\cosh\left(\lambda_1 b\right)\right]\lambda_1,\\&\Lambda_7=\left[-D_{22}\lambda_3\cos\left(\lambda_3 b\right)-k_2\sin\left(\lambda_3 b\right)\right]\lambda_3,\quad \Lambda_8=\left[-D_{22}\lambda_3\sin\left(\lambda_3 b\right)+k_2\cos\left(\lambda_3 b\right)\right]\lambda_3.\end{aligned}\tag{13.51}$$

Figure 13.7 contains generic buckling curves that were determined numerically from the present Lévy solution. In order to keep the number of independent variables within reasonable limits in this section, the results of Fig. 13.7 were determined for the special case of identical degrees of elastic restraint at both unloaded edges, i.e. $k_1 = k_2 = k$. Here, too, the expected characteristic distributions of the resulting buckling curves can be seen. In addition, a massive influence of the elastic edge restraints on the buckling resistance can also be observed here.

13.3.5 Laminate with Two Clamped Unloaded Edges

For all subsequent laminate situations, Lévy-type solutions are given for a dimensionless notation, whereby the validity of the solution (13.21) is assumed.

For the laminate in Fig. 13.8, the boundary conditions at the unloaded edges are as follows:

$$\begin{aligned}&\bar{w}_0(\xi_2=0)=0,\quad \bar{w}_0(\xi_2=1)=0,\\&\left.\frac{\partial\bar{w}_0}{\partial\xi_2}\right|_{\xi_2=0}=0,\quad \left.\frac{\partial\bar{w}_0}{\partial\xi_2}\right|_{\xi_2=1}=0.\end{aligned}\tag{13.52}$$

Analyzing these equations results in the following system of linear equations:

$$\begin{aligned}C_1+C_3&=0,\\C_1\cosh\lambda_1+C_2\sinh\lambda_1+C_3\cos\lambda_3+C_4\sin\lambda_3&=0,\\\lambda_1 C_2+\lambda_3 C_4&=0,\\\lambda_1 C_1\sinh\lambda_1+\lambda_1 C_2\cosh\lambda_1-\lambda_3 C_3\sin\lambda_3+\lambda_3 C_4\cos\lambda_3&=0,\end{aligned}\tag{13.53}$$

or in vector-matrix notation:

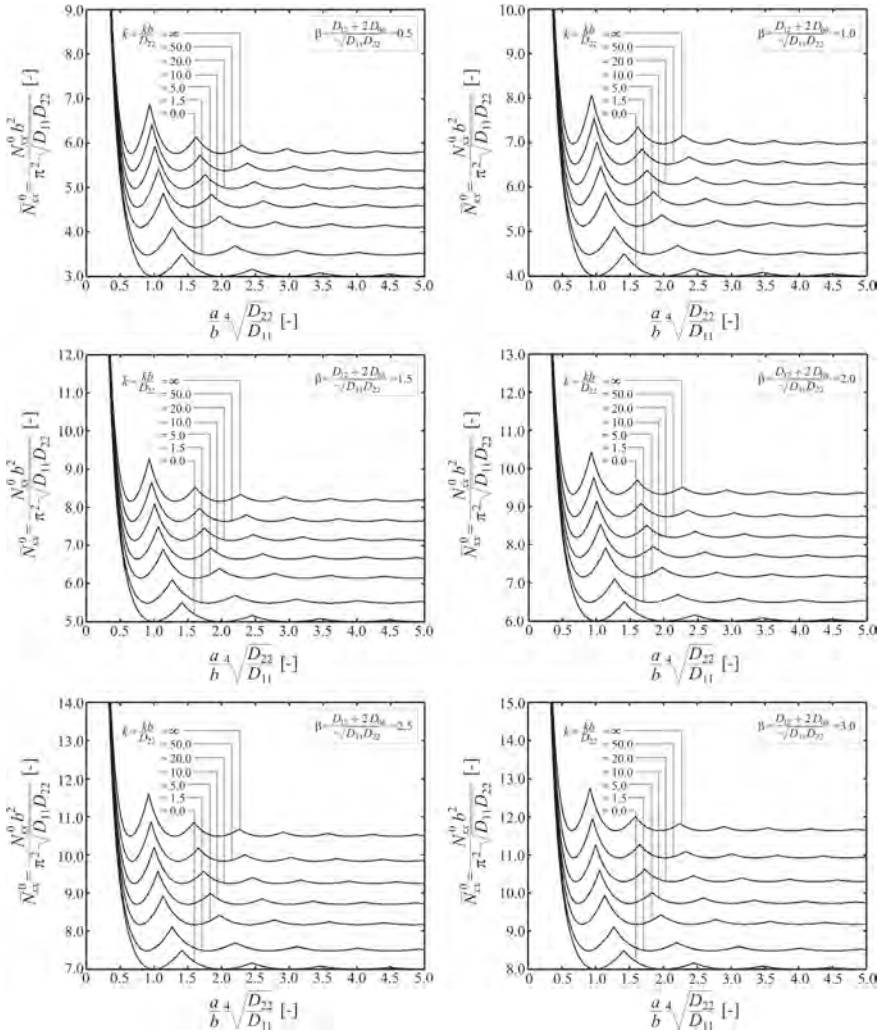


Fig. 13.7 Generic buckling curves for a laminate with two unloaded elastically restrained edges with identical restraint stiffnesses $k_1 = k_2 = k$

$$\begin{bmatrix} 1 & 0 & 1 & 0 \\ \cosh\lambda_1 & \sinh\lambda_1 & \cos\lambda_3 & \sin\lambda_3 \\ 0 & \lambda_1 & 0 & \lambda_3 \\ \lambda_1\sinh\lambda_1 & \lambda_1\cosh\lambda_1 & -\lambda_3\sin\lambda_3 & \lambda_3\cos\lambda_3 \end{bmatrix} \begin{pmatrix} C_1 \\ C_2 \\ C_3 \\ C_4 \end{pmatrix} = \begin{pmatrix} 0 \\ 0 \\ 0 \\ 0 \end{pmatrix}. \tag{13.54}$$

Developing and zeroing the coefficient determinant leads to the following buckling condition for the laminate considered here:

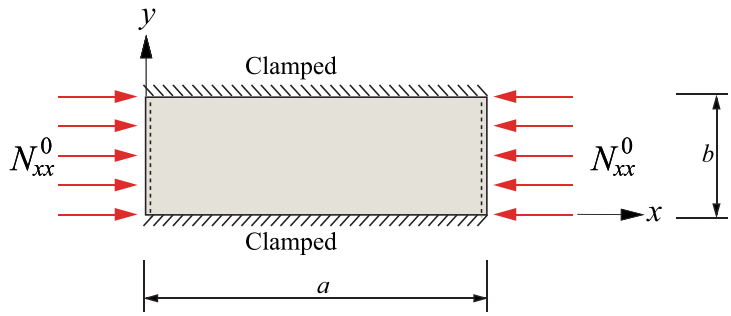


Fig. 13.8 Laminate with two clamped unloaded edges

$$2\lambda_1\lambda_3\,(1-\cos\lambda_3\cosh\lambda_1)+\left(\lambda_1^2-\lambda_3^2\right)\sin\lambda_3\sinh\lambda_1=0. \tag{13.55}$$

13.3.6 Laminate with One Clamped and One Simply Supported Unloaded Edge

The laminate shown in Fig. 13.9 is considered.

The boundary conditions at the unloaded edges are as follows for this case:

$$\begin{aligned}&\bar{w}_0(\xi_2=0)=0,\quad \bar{w}_0(\xi_2=1)=0,\\ &\left.\frac{\partial\bar{w}_0}{\partial\xi_2}\right|_{\xi_2=1}=0,\quad \left.\frac{\partial^2\bar{w}_0}{\partial\xi_2^2}\right|_{\xi_2=0}=0.\end{aligned} \tag{13.56}$$

Determining the coefficient determinant with the solution (13.21) leads to the following buckling condition for the laminate considered here after elementary transformations:

$$\lambda_3\sinh\lambda_1\cos\lambda_3-\lambda_1\cosh\lambda_1\sin\lambda_3=0. \tag{13.57}$$

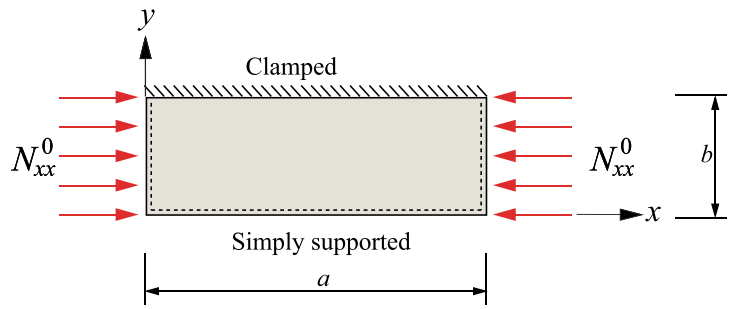


Fig. 13.9 Laminate with one clamped and one simply supported unloaded edge

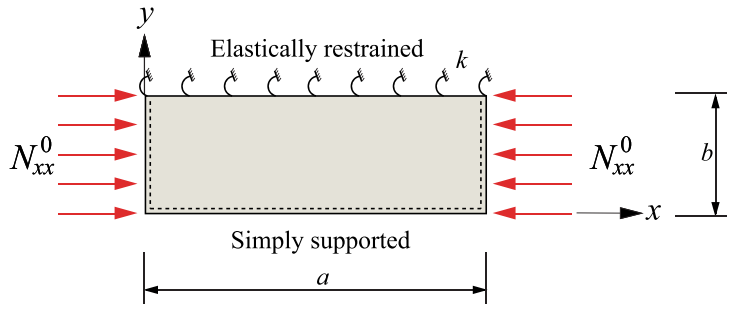


Fig. 13.10 Laminate with a simply supported and an elastically restrained unloaded edge

13.3.7 Laminate with One Elastically Restrained and One Simply Supported Unloaded Edge

Consider the situation of Fig. 13.10.

The boundary conditions for this laminate can be formulated as:

$$\begin{aligned} \bar{w}_0(\xi_2 = 0) = 0, \quad \bar{w}_0(\xi_2 = 1) = 0, \\ \left.\frac{\partial^2 \bar{w}_0}{\partial \xi_2^2}\right|_{\xi_2=0} = 0, \\ \left.\frac{\partial^2 \bar{w}_0}{\partial \xi_2^2}\right|_{\xi_2=1} + \bar{k} \left.\frac{\partial \bar{w}_0}{\partial \xi_2}\right|_{\xi_2=1} = 0. \end{aligned} \tag{13.58}$$

The buckling condition that can be derived from this is given by

$$\lambda_3 \sinh \lambda_1 \left(-\lambda_3 \sin \lambda_3 + \bar{k} \cos \lambda_3\right) - \lambda_1 \sin \lambda_3 \left(\lambda_1 \sinh \lambda_1 + \bar{k} \cosh \lambda_1\right) = 0. \tag{13.59}$$

13.3.8 Laminate with One Elastically Restrained and One Clamped Unloaded Edge

Finally, the situation of Fig. 13.11 is considered.

The boundary conditions for this case are as follows:

$$\begin{aligned} \bar{w}_0(\xi_2 = 0) = 0, \quad \bar{w}_0(\xi_2 = 1) = 0, \\ \left.\frac{\partial \bar{w}_0}{\partial \xi_2}\right|_{\xi_2=0} = 0, \\ \left.\frac{\partial^2 \bar{w}_0}{\partial \xi_2^2}\right|_{\xi_2=1} + \bar{k} \left.\frac{\partial \bar{w}_0}{\partial \xi_2}\right|_{\xi_2=1} = 0. \end{aligned} \tag{13.60}$$

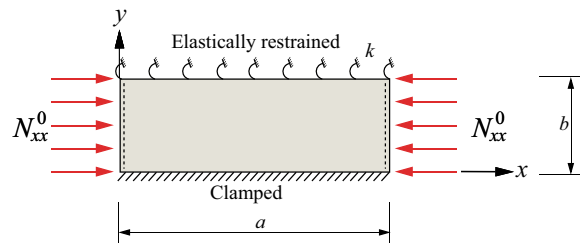


Fig. 13.11 Laminate with one clamped and one elastically restrained unloaded edge

This can be used to derive the following buckling condition:

$$\begin{aligned}&(\Lambda_{11} - \Lambda_9)\,\lambda_3 \sinh\lambda_1 + (\Lambda_{10}\lambda_3 - \Lambda_{12}\lambda_1)\cosh\lambda_1\\&+ (\Lambda_9 - \Lambda_{11})\,\lambda_1 \sin\lambda_3 + (\Lambda_{12}\lambda_1 - \Lambda_{10}\lambda_3)\cos\lambda_3 = 0.\end{aligned} \tag{13.61}$$

Therein, the following abbreviations have been defined:

$$\begin{aligned}\Lambda_9 &= \lambda_1^2 \cosh\lambda_1 + \bar{k}\lambda_1 \sinh\lambda_1,\\ \Lambda_{10} &= \lambda_1^2 \sinh\lambda_1 + \bar{k}\lambda_1 \cosh\lambda_1,\\ \Lambda_{11} &= -\lambda_3^2 \cos\lambda_3 - \bar{k}\lambda_3 \sin\lambda_3,\\ \Lambda_{12} &= -\lambda_3^2 \sin\lambda_3 + \bar{k}\lambda_3 \cos\lambda_3.\end{aligned} \tag{13.62}$$

13.4 Lévy Solutions for Shear-Deformable Laminates

Lévy-type solutions can also be derived within the framework of higher-order shear deformation theories. In this section, we discuss such a solution in the context of Reddy's Third-Order Shear Deformation Theory (TSDT, see Chap. 11, see also Khdeir (1988)). The governing equations that describe the buckling problem of a laminate within the framework of TSDT can be derived from the principle of the minimum of the total elastic potential of the buckled laminate. As an application, we consider the situation of Fig. 13.6, i.e. a laminate simply supported at all edges under unaxial compression with elastically restrained longitudinal edges (spring stiffnesses k_1 and k_2). The total elastic potential $\Pi = \Pi_i + \Pi_a + \Pi_s$ is made up of the following components:

$$\Pi_i = \frac{1}{2}\int_0^b \int_0^a \begin{pmatrix} \underline{\varepsilon}^{(0)} \\ \underline{\varepsilon}^{(1)} \\ \underline{\varepsilon}^{(3)} \\ \underline{\gamma}^{(0)} \\ \underline{\gamma}^{(3)} \end{pmatrix}^T \begin{pmatrix} \underline{N}^0 \\ \underline{M}^0 \\ \underline{P} \\ \underline{Q} \\ \underline{R} \end{pmatrix} \mathrm{d}x\,\mathrm{d}y,$$

$$\Pi_a = -\frac{N_{xx}^0}{2}\int_0^b \int_0^a \left(\frac{\partial w_0}{\partial x}\right)^2 \mathrm{d}x\,\mathrm{d}y,$$

$$\Pi_s = \frac{1}{2}\int_0^a \left(k_2\left[\psi_y(x,0)\right]^2 + k_1\left[\psi_y(x,b)\right]^2\right)\mathrm{d}x. \tag{13.63}$$

The variation of the potential $\delta\Pi = \delta\Pi_i + \delta\Pi_a + \delta\Pi_s = 0$ follows as:

$$\begin{aligned}
\delta\Pi = -\int_0^b \int_0^a \Bigg\{ & \left(\frac{\partial N_{xx}^0}{\partial x} + \frac{\partial N_{xy}^0}{\partial y}\right)\delta u_0 + \left(\frac{\partial N_{xy}^0}{\partial x} + \frac{\partial N_{yy}^0}{\partial y}\right)\delta v_0 \\
& + \left(-N_{xx}^0 \frac{\partial w_0^2}{\partial x^2} + \frac{4}{3h^2}\left[\frac{\partial^2 P_{xx}}{\partial x^2} + \frac{\partial^2 P_{yy}}{\partial y^2} + 2\frac{\partial^2 P_{xy}}{\partial x \partial y}\right]\right. \\
& \left. + \frac{\partial Q_x}{\partial x} + \frac{\partial Q_y}{\partial y} - \frac{4}{h^2}\left[\frac{\partial R_x}{\partial x} + \frac{\partial R_y}{\partial y}\right]\right)\delta w_0 \\
& + \left(\frac{\partial M_{xx}}{\partial x} + \frac{\partial M_{xy}}{\partial y} - \frac{4}{3h^2}\left[\frac{\partial P_{xx}}{\partial x} + \frac{\partial P_{xy}}{\partial y}\right] - Q_x + \frac{4}{h^2}R_x\right)\delta\psi_x \\
& + \left(\frac{\partial M_{xy}}{\partial x} + \frac{\partial M_{yy}}{\partial y} - \frac{4}{3t^2}\left[\frac{\partial P_{xy}}{\partial x} + \frac{\partial P_{yy}}{\partial y}\right] - Q_y + \frac{4}{h^2}R_y\right)\delta\psi_y \Bigg\}\,\mathrm{d}x\,\mathrm{d}y \\
& + \int_0^a \Bigg\{ \Bigg[N_{xy}^0\delta u + N_{yy}^0\delta v \\
& + \left(\frac{4}{3h^2}\left[\frac{\partial P_{yy}}{\partial y} + 2\frac{\partial P_{xy}}{\partial x}\right] + Q_y - \frac{4}{h^2}R_y\right)\delta w_0 \\
& + \left(M_{xy} - \frac{4}{3h^2}P_{xy}\right)\delta\psi_x + \left(M_{yy} - \frac{4}{3h^2}P_{yy}\right)\delta\psi_y - \frac{4}{3h^2}P_{yy}\delta\left(\frac{\partial w_0}{\partial y}\right)\Bigg]\Bigg|_0^b \\
& + k_2\psi_y(x,0)\,\delta\psi_y(x,0) + k_1\psi_y(x,b)\,\delta\psi_y(x,b)\Bigg\}\mathrm{d}x \\
& + \int_0^b \Bigg\{ N_{xx}^0\delta u + N_{xy}^0\delta v \\
& + \left(-N_{xx}^0\frac{\partial w_0}{\partial x} + \frac{4}{3h^2}\left[\frac{\partial P_{xx}}{\partial x} + 2\frac{\partial P_{xy}}{\partial y}\right] + Q_x - \frac{4}{h^2}R_x\right)\delta w_0 \\
& + \left(M_{xx} - \frac{4}{3h^2}P_{xx}\right)\delta\psi_x + \left(M_{xy} - \frac{4}{3h^2}P_{xy}\right)\delta\psi_y \\
& - \frac{4}{3h^2}P_{xx}\delta\left(\frac{\partial w_0}{\partial x}\right)\Bigg\}\Bigg|_0^a \mathrm{d}y - \left(\frac{8}{3h^2}P_{xy}\delta w_0\right)\Bigg|_0^a\Bigg|_0^b = 0.
\end{aligned} \tag{13.64}$$

In order for (13.64) to be fulfilled, the expressions from (13.64) must each disappear individually. Thus, the first five terms in brackets in (13.64) provide the equilibrium conditions and the remaining terms the boundary conditions of the system. Each boundary term can be

fulfilled in two ways. Either the variable to be varied $\delta(\ldots)$ disappears, or the corresponding term in brackets becomes zero. For the problem considered here, the following boundary conditions result. The following applies for the loaded laminate edges $x = 0$ and $x = a$:

$$\begin{aligned} w_0\,(0,y) &= 0, \quad w_0\,(a,y) = 0, \\ \psi_y\,(0,y) &= 0, \quad \psi_y\,(a,y) = 0, \\ P_{xx}\,(0,y) &= 0, \quad P_{xx}\,(a,y) = 0, \\ \left(M_{xx}^0 - \frac{4}{3h^2}P_{xx}\right)(0,y) &= 0, \\ \left(M_{xx}^0 - \frac{4}{3h^2}P_{xx}\right)(a,y) &= 0. \end{aligned} \tag{13.65}$$

The following boundary conditions apply at the unloaded and elastically clamped edges $y = 0$ and $y = b$:

$$\begin{aligned} w_0\,(x,0) &= 0, \quad w_0\,(x,b) = 0, \\ \psi_x\,(x,0) &= 0, \quad \psi_x\,(x,b) = 0, \\ P_{yy}\,(x,0) &= 0, \quad P_{yy}\,(x,b) = 0, \\ \left(-M_{yy}^0 + \frac{4}{3h^2}P_{yy} + k_2\psi_y\right)(x,0) &= 0, \\ \left(M_{yy}^0 - \frac{4}{3h^2}P_{yy} + k_1\psi_y\right)(x,b) &= 0. \end{aligned} \tag{13.66}$$

If we specialize the considerations to symmetric and orthotropic laminate structures, then the following stiffness components disappear:

$$\begin{aligned} A_{16} = A_{26} = B_{ij} = D_{16} = D_{26} = E_{ij} = F_{16} \\ = F_{26} = H_{16} = H_{26} = A_{45} = D_{45} = F_{45} = 0. \end{aligned} \tag{13.67}$$

The inner potential Π_i is then as follows:

$$\begin{aligned} \Pi_i = \frac{1}{2}\int_0^b \int_0^a \Bigg\{ & D_{11}\left(\frac{\partial\psi_x}{\partial x}\right)^2 + 2D_{12}\frac{\partial\psi_x}{\partial x}\frac{\partial\psi_y}{\partial y} + D_{22}\left(\frac{\partial\psi_y}{\partial y}\right)^2 + D_{66}\Bigg[\left(\frac{\partial\psi_x}{\partial y}\right)^2 \\ & + 2\frac{\partial\psi_x}{\partial y}\frac{\partial\psi_y}{\partial x} + \left(\frac{\partial\psi_y}{\partial x}\right)^2\Bigg] - \frac{8}{3h^2}\Bigg\{F_{11}\left[\left(\frac{\partial\psi_x}{\partial x}\right)^2 + \frac{\partial\psi_x}{\partial x}\frac{\partial^2 w_0}{\partial x^2}\right] \\ & + F_{12}\left[2\frac{\partial\psi_x}{\partial x}\frac{\partial\psi_y}{\partial y} + \frac{\partial\psi_x}{\partial x}\frac{\partial^2 w_0}{\partial y^2} + \frac{\partial\psi_y}{\partial y}\frac{\partial^2 w_0}{\partial x^2}\right] + F_{22}\left[\frac{\partial\psi_y}{\partial y}\frac{\partial^2 w_0}{\partial y^2} + \left(\frac{\partial\psi_y}{\partial y}\right)^2\right] \\ & + F_{66}\left[\left(\frac{\partial\psi_x}{\partial y}\right)^2 + \left(\frac{\partial\psi_y}{\partial x}\right)^2 + 2\frac{\partial\psi_x}{\partial y}\frac{\partial\psi_y}{\partial x} + 2\frac{\partial\psi_x}{\partial y}\frac{\partial^2 w_0}{\partial x\partial y} + 2\frac{\partial\psi_y}{\partial x}\frac{\partial^2 w_0}{\partial x\partial y}\right]\Bigg\} \end{aligned}$$

$$
\begin{aligned}
&+\frac{16}{9h^4}\left\{H_{11}\left[\left(\frac{\partial\psi_x}{\partial x}\right)^2+2\frac{\partial\psi_x}{\partial x}\frac{\partial^2 w_0}{\partial x^2}+\left(\frac{\partial^2 w_0}{\partial x^2}\right)^2\right]+2H_{12}\left[\frac{\partial\psi_x}{\partial x}\frac{\partial\psi_y}{\partial y}\right.\right.\\
&\left.+\frac{\partial\psi_x}{\partial x}\frac{\partial^2 w_0}{\partial y^2}+\frac{\partial\psi_y}{\partial y}\frac{\partial^2 w_0}{\partial x^2}+\frac{\partial^2 w_0}{\partial x^2}\frac{\partial^2 w_0}{\partial y^2}\right]+H_{22}\left[\left(\frac{\partial^2 w_0}{\partial y^2}\right)^2+2\frac{\partial\psi_y}{\partial y}\frac{\partial^2 w_0}{\partial y^2}\right.\\
&\left.+\left(\frac{\partial\psi_y}{\partial y}\right)^2\right]+H_{66}\left[4\left(\frac{\partial^2 w_0}{\partial y\partial x}\right)^2+\left(\frac{\partial\psi_x}{\partial y}\right)^2+4\frac{\partial\psi_y}{\partial x}\frac{\partial^2 w_0}{\partial x\partial y}+\left(\frac{\partial\psi_y}{\partial x}\right)^2\right.\\
&\left.\left.+2\frac{\partial\psi_x}{\partial y}\frac{\partial\psi_y}{\partial x}+4\frac{\partial\psi_x}{\partial y}\frac{\partial^2 w_0}{\partial x\partial y}\right]\right\}+A_{44}\left[\psi_y^2+2\psi_y\frac{\partial w_0}{\partial y}+\left(\frac{\partial w_0}{\partial y}\right)^2\right]\\
&+A_{55}\left[\psi_x^2+2\psi_x\frac{\partial w_0}{\partial x}+\left(\frac{\partial w_0}{\partial x}\right)^2\right]-\frac{8}{h^2}D_{44}\left[\psi_y^2+2\psi_y\frac{\partial w_0}{\partial y}+\left(\frac{\partial w_0}{\partial y}\right)^2\right]\\
&-\frac{8}{h^2}D_{55}\left[\psi_x^2+2\psi_x\frac{\partial w_0}{\partial x}+\left(\frac{\partial w_0}{\partial x}\right)^2\right]+\frac{16}{h^4}F_{44}\left[\psi_y^2+2\psi_y\frac{\partial w_0}{\partial y}+\left(\frac{\partial w_0}{\partial y}\right)^2\right]\\
&+\frac{16}{h^4}F_{55}\left[\psi_x^2+2\psi_x\frac{\partial w_0}{\partial x}+\left(\frac{\partial w_0}{\partial x}\right)^2\right]\Bigg\}\,\mathrm{d}x\,\mathrm{d}y. \qquad (13.68)
\end{aligned}
$$

The displacements u_0 and v_0 of the laminate middle plane were neglected, as only the out-of-plane displacement w_0 and the two bending angles ψ_x, ψ_y occur in the buckling modes of symmetric laminates.

The buckling problem is described by three partial differential equations that can be obtained by substituting the constitutive equations

$$
\begin{pmatrix} \underline{N}^0 \\ \underline{M}^0 \\ \underline{P} \\ \underline{Q} \\ \underline{R} \end{pmatrix} = \begin{bmatrix} \underline{\underline{A}} & \underline{\underline{B}} & \underline{\underline{E}} & \underline{\underline{0}} & \underline{\underline{0}} \\ \underline{\underline{B}} & \underline{\underline{D}} & \underline{\underline{F}} & \underline{\underline{0}} & \underline{\underline{0}} \\ \underline{\underline{E}} & \underline{\underline{F}} & \underline{\underline{H}} & \underline{\underline{0}} & \underline{\underline{0}} \\ \underline{\underline{0}} & \underline{\underline{0}} & \underline{\underline{0}} & \underline{\underline{A}}_{\mathrm{S}} & \underline{\underline{D}}_{\mathrm{S}} \\ \underline{\underline{0}} & \underline{\underline{0}} & \underline{\underline{0}} & \underline{\underline{D}}_{\mathrm{S}} & \underline{\underline{F}}_{\mathrm{S}} \end{bmatrix} \begin{pmatrix} \underline{\varepsilon}^{(0)} \\ \underline{\varepsilon}^{(1)} \\ \underline{\varepsilon}^{(3)} \\ \underline{\gamma}^{(0)} \\ \underline{\gamma}^{(2)} \end{pmatrix} \qquad (13.69)
$$

in the third, fourth and fifth expression of (13.64):

$$
\begin{aligned}
&\left(\frac{4}{3\,h^2}\right)^2\left[-H_{11}\left(\frac{\partial^4 w_0}{\partial x^4}+\frac{\partial^3\psi_x}{\partial x^3}\right)-H_{22}\left(\frac{\partial^4 w_0}{\partial y^4}+\frac{\partial^3\psi_y}{\partial y^3}\right)\right.\\
&-(H_{12}+2\,H_{66})\left(\frac{\partial^3\psi_y}{\partial y\partial x^2}+2\,\frac{\partial^4 w_0}{\partial y^2\partial x^2}+\frac{\partial^3\psi_x}{\partial y^2\partial x}\right)\\
&\left.+9\,F_{44}\left(\frac{\partial\psi_y}{\partial y}+\frac{\partial^2 w_0}{\partial y^2}\right)+9\,F_{55}\left(\frac{\partial\psi_x}{\partial x}+\frac{\partial^2 w_0}{\partial x^2}\right)\right]\\
&-\frac{4}{3\,h^2}\left[6\,D_{44}\left(\frac{\partial\psi_y}{\partial y}+\frac{\partial^2 w_0}{\partial y^2}\right)+6\,D_{55}\left(\frac{\partial\psi_x}{\partial x}+\frac{\partial^2 w_0}{\partial x^2}\right)\right.
\end{aligned}
$$

$$
\begin{aligned}
&- F_{11}\frac{\partial^3\psi_x}{\partial x^3} - F_{22}\frac{\partial^3\psi_y}{\partial y^3} - (F_{12}+2F_{66})\left(\frac{\partial^3\psi_y}{\partial y\partial x^2}+\frac{\partial^3\psi_x}{\partial y^2\partial x}\right)\Bigg] \\
&+A_{44}\left(\frac{\partial\psi_y}{\partial y}+\frac{\partial^2 w_0}{\partial y^2}\right)+A_{55}\left(\frac{\partial^2 w_0}{\partial x^2}+\frac{\partial\psi_x}{\partial x}\right)-N^0_{xx}\frac{\partial^2 w_0}{\partial x^2}=0, \\
&\left(\frac{4}{3h^2}\right)^2\Bigg[-H_{11}\left(\frac{\partial^3 w_0}{\partial x^3}+\frac{\partial^2\psi_x}{\partial x^2}\right)-(H_{12}+2H_{66})\left(\frac{\partial^3 w_0}{\partial y^2\partial x}+\frac{\partial^2\psi_y}{\partial y\partial x}\right) \\
&+H_{66}\left(\frac{\partial^2\psi_y}{\partial y\partial x}-\frac{\partial^2\psi_x}{\partial y^2}\right)+9F_{55}\left(\psi_x+\frac{\partial w_0}{\partial x}\right)\Bigg] \\
&+\frac{4}{3h^2}\Bigg[F_{11}\left(\frac{\partial^3 w_0}{\partial x^3}+2\frac{\partial^2\psi_x}{\partial x^2}\right)+(F_{12}+2F_{66})\left(\frac{\partial^3 w_0}{\partial y^2\partial x}+2\frac{\partial^2\psi_y}{\partial y\partial x}\right) \\
&+2F_{66}\left(\frac{\partial^2\psi_x}{\partial y^2}-\frac{\partial^2\psi_y}{\partial y\partial x}\right)-6D_{55}\left(\psi_x+\frac{\partial w_0}{\partial x}\right)\Bigg] \\
&+A_{55}\left(\psi_x+\frac{\partial w_0}{\partial x}\right)-D_{11}\frac{\partial^2\psi_x}{\partial x^2}-(D_{12}+2D_{66})\frac{\partial^2\psi_y}{\partial y\partial x} \\
&+D_{66}\left(\frac{\partial^2\psi_y}{\partial y\partial x}-\frac{\partial^2\psi_x}{\partial y^2}\right)=0, \\
&\left(\frac{4}{3h^2}\right)^2\Bigg[-H_{22}\left(\frac{\partial^3 w_0}{\partial y^3}+\frac{\partial^2\psi_y}{\partial y^2}\right)-(H_{12}+2H_{66})\left(\frac{\partial^3 w_0}{\partial y\partial x^2}+\frac{\partial^2\psi_x}{\partial y\partial x}\right) \\
&+H_{66}\left(\frac{\partial^2\psi_x}{\partial y\partial x}-\frac{\partial^2\psi_y}{\partial x^2}\right)+9F_{44}\left(\psi_y+\frac{\partial w_0}{\partial y}\right)\Bigg] \\
&+\frac{4}{3h^2}\Bigg[F_{22}\left(\frac{\partial^3 w_0}{\partial y^3}+2\frac{\partial^2\psi_y}{\partial y^2}\right)+(F_{12}+2F_{66})\left(\frac{\partial^3 w_0}{\partial y\partial x^2}+2\frac{\partial^2\psi_x}{\partial y\partial x}\right) \\
&2F_{66}\left(\frac{\partial^2\psi_y}{\partial x^2}-\frac{\partial^2\psi_x}{\partial y\partial x}\right)-6D_{44}\left(\psi_y+\frac{\partial w_0}{\partial y}\right)\Bigg] \\
&-D_{22}\frac{\partial^2\psi_y}{\partial y^2}-(D_{12}+2D_{66})\frac{\partial^2\psi_x}{\partial y\partial x}+D_{66}\left(\frac{\partial^2\psi_x}{\partial y\partial x}-\frac{\partial^2\psi_y}{\partial x^2}\right) \\
&+A_{44}\left(\psi_y+\frac{\partial w_0}{\partial y}\right)=0. \qquad (13.70)
\end{aligned}
$$

The boundary conditions considered below are the limit cases of the elastically restrained plate model, i.e. at the unloaded edges $y=0$ and $y=b$ we consider two different cases:

$$
\begin{aligned}
\text{simply supported: } & w_0=\psi_x=M_{yy}=P_{yy}=0, \\
\text{clamped: } & w_0=\frac{\partial w_0}{\partial y}=\psi_x=\psi_y=0. \qquad (13.71)
\end{aligned}
$$

The previously defined boundary conditions (13.65) apply at the loaded boundaries $x=0$ and $x=a$. The Lévy-type approaches fulfil the partial differential equations (13.70) and

the boundary conditions (13.71) as well as (13.65), i.e. it is an exact approach within the framework of the selected laminate theory. The method leads to a transcendental equation for the critical buckling load, which is not solved analytically but with numerical methods. The following approaches are used for the three displacements occurring here:

$$\begin{aligned} w_0 &= \sin\left(\frac{m\pi x}{a}\right) f_1(y), \\ \psi_x &= \cos\left(\frac{m\pi x}{a}\right) f_2(y), \\ \psi_y &= \sin\left(\frac{m\pi x}{a}\right) f_3(y). \end{aligned} \tag{13.72}$$

The partial differential equations (13.70) are simplified to three ordinary differential equations by substituting the approaches (13.72), which can be reduced to the following form:

$$\begin{aligned} f_1'''' &= c_1 f_1 + c_2 f_1'' + c_3 f_2 + c_4 f_3', \\ f_2'' &= c_5 f_1 + c_6 f_1'' + c_7 f_2 + c_8 f_3', \\ f_3'' &= c_9 f_1' + c_{10} f_1''' + c_{11} f_2' + c_{12} f_3, \end{aligned} \tag{13.73}$$

with $(\,)' = \frac{\partial}{\partial y}$. The constants $c_1..c_{12}$ contain both geometric and elastic properties and are as follows

$$\begin{aligned} c_1 &= \frac{e_1 e_{17} e_9 + e_{14} e_7 e_8 - e_{17} e_3 e_8}{e_{14}\,(e_1 e_{10} - e_2 e_8)}, \\ c_2 &= \frac{-e_1 e_{11} e_{14} + e_1 e_{15} e_9 + e_{14} e_4 e_8 - e_{15} e_3 e_8}{e_{14}\,(e_1 e_{10} - e_2 e_8)}, \\ c_3 &= \frac{e_1 e_{16} e_9 + e_{14} e_6 e_8 - e_{16} e_3 e_8}{e_{14}\,(e_1 e_{10} - e_2 e_8)}, \\ c_4 &= \frac{-e_1 e_{12} e_{14} + e_1 e_{13} e_9 - e_{13} e_3 e_8 + e_{14} e_5 e_8}{e_{14}\,(e_1 e_{10} - e_2 e_8)}, \\ c_5 &= -\frac{e_{17}}{e_{14}}, \quad c_6 = -\frac{e_{15}}{e_{14}}, \quad c_7 = -\frac{e_{16}}{e_{14}}, \quad c_8 = -\frac{e_{13}}{e_{14}}, \\ c_9 &= -\frac{e_{11}}{e_8}, \quad c_{10} = -\frac{e_{10}}{e_8}, \quad c_{11} = -\frac{e_9}{e_8}, \quad c_{12} = -\frac{e_{12}}{e_8}. \end{aligned} \tag{13.74}$$

The coefficients $e_1 \ldots e_{17}$ are:

$$
\begin{aligned}
e_1 &= \frac{4}{3\,h^2}\left(F_{22} - H_{22}\,\frac{4}{3\,h^2}\right),\\
e_2 &= -\left(\frac{4}{3\,h^2}\right)^2 H_{22},\\
e_3 &= \frac{4}{3\,h^2}\alpha\left[\frac{4}{3\,h^2}\,(H_{12}+2\,H_{66}) - F_{12} - 2\,F_{66}\right],\\
e_4 &= \left(\frac{4}{3\,h^2}\right)^2\left[(2\,H_{12}+4\,H_{66})\,\alpha^2 + 9\,F_{44}\right] - 2\,\frac{4}{h^2}\,D_{44} + A_{44},\\
e_5 &= \left(\frac{4}{h^2}\right)^2 F_{44} - 2\,\frac{4}{h^2}\,D_{44} + A_{44} + e_3\,\alpha,\\
e_6 &= -\alpha\left[\left(\frac{4}{3\,h^2}\right)^2\left(H_{11}\,\alpha^2 + 9\,F_{55}\right) - \frac{4}{3\,h^2}\left(F_{11}\,\alpha^2 + 6\,D_{55}\right) + A_{55}\right],\\
e_7 &= -\alpha^2\left[\left(\frac{4}{3\,h^2}\right)^2\left(H_{11}\,\alpha^2 + 9\,F_{55}\right) - 2\,D_{55}\,\frac{4}{h^2} + A_{55} - N^0_{xx}\right],\\
e_8 &= \left(\frac{4}{3\,h^2}\right)^2 H_{22} - 2\,\frac{4}{3\,h^2}\,F_{22} + D_{22},\\
e_9 &= -\alpha\left[\left(\frac{4}{3\,h^2}\right)^2 (H_{12}+H_{66}) - 2\,\frac{4}{3\,h^2}\,(F_{12}+F_{66}) + D_{12} + D_{66}\right],\\
e_{10} &= -e_1, \qquad e_{11} = -e_5,\\
e_{12} &= -\left(\frac{4}{3\,h^2}\right)^2\left(H_{66}\,\alpha^2 + 9\,F_{44}\right) + \frac{4}{3\,h^2}\left(2\,\alpha^2 F_{66} + 6\,D_{44}\right) - \alpha^2 D_{66} - A_{44},\\
e_{13} &= -e_9, \qquad e_{14} = \left(\frac{4}{3\,h^2}\right)^2 H_{66} - 2\,\frac{4}{3\,h^2}\,F_{66} + D_{66}, \qquad e_{15} = e_3,\\
e_{16} &= -\left(\frac{4}{3\,h^2}\right)^2\left(H_{11}\,\alpha^2 + 9\,F_{55}\right) + \frac{4}{3\,h^2}\left(2\,\alpha^2\,F_{11} + 6\,D_{55}\right) - \alpha^2 D_{11} - A_{55},\\
e_{17} &= e_6,
\end{aligned}
\tag{13.75}
$$

with

$$
\alpha = \frac{m\pi}{a}. \tag{13.76}
$$

The coupled ordinary differential equation system (13.73) is rewritten as a first-order system and can be represented in matrix notation as:

$$
\underline{Z}^{'}(y) = \underline{\underline{A}}\,\underline{Z}(y). \tag{13.77}
$$

The Eq. (13.77) can be written as follows:

$$\begin{bmatrix} Z_1' \\ Z_2' \\ Z_3' \\ Z_4' \\ Z_5' \\ Z_6' \\ Z_7' \\ Z_8' \end{bmatrix} = \begin{bmatrix} 0 & 1 & 0 & 0 & 0 & 0 & 0 & 0 \\ 0 & 0 & 1 & 0 & 0 & 0 & 0 & 0 \\ 0 & 0 & 0 & 1 & 0 & 0 & 0 & 0 \\ c_1 & 0 & c_2 & 0 & c_3 & 0 & 0 & c_4 \\ 0 & 0 & 0 & 0 & 0 & 1 & 0 & 0 \\ c_5 & 0 & c_6 & 0 & c_7 & 0 & 0 & c_8 \\ 0 & 0 & 0 & 0 & 0 & 0 & 0 & 1 \\ 0 & c_9 & 0 & c_{10} & 0 & c_{11} & c_{12} & 0 \end{bmatrix} \begin{bmatrix} Z_1 \\ Z_2 \\ Z_3 \\ Z_4 \\ Z_5 \\ Z_6 \\ Z_7 \\ Z_8 \end{bmatrix}, \quad \begin{bmatrix} Z_1 \\ Z_2 \\ Z_3 \\ Z_4 \\ Z_5 \\ Z_6 \\ Z_7 \\ Z_8 \end{bmatrix} = \begin{bmatrix} f_1 \\ f_1' \\ f_1'' \\ f_1''' \\ f_2 \\ f_2' \\ f_3 \\ f_3' \end{bmatrix}. \tag{13.78}$$

A solution of the Eq. (13.77) is given by:

$$\underline{Z}(y) = \underline{\underline{e}}^{Ay}\, \underline{K}. \tag{13.79}$$

Therein, the vector $\underline{K}$ contains constant coefficients and can be described by the boundary conditions, while $\underline{\underline{e}}^{Ay}$ is defined as follows:

$$\underline{\underline{e}}^{Ay} = \underline{\underline{L}} \begin{bmatrix} \mathrm{e}^{\lambda_1 y} & & 0 \\ & \ddots & \\ 0 & & \mathrm{e}^{\lambda_8 y} \end{bmatrix} \underline{\underline{L}}^{-1}. \tag{13.80}$$

The matrix $\underline{\underline{L}}$ contains the eigenvectors of $\underline{\underline{A}}$, and $\lambda_1, \ldots, \lambda_8$ represent the respective eigenvalues. Substituting the Eq. (13.79) into the corresponding boundary conditions results in a homogeneous system of equations of the type

$$\underline{\underline{M}}\, \underline{K} = 0. \tag{13.81}$$

Therein, $\underline{\underline{M}}$ is the coefficient matrix and has the dimension 8×8. For a non-trivial solution of (13.81), a vanishing determinant of the coefficient matrix is required:

$$\det(\underline{\underline{M}}) = 0. \tag{13.82}$$

This leads to a transcendental equation for the buckling load N_{xx}^0, which is exact with regard to the underlying theoretical framework. However, the described method can cause numerical problems. Firstly, the zero entries on the main diagonal of $\underline{\underline{A}}$ are problematic for the eigenvalue analysis. Secondly, the problem $\det(\underline{\underline{M}}) = 0$ is generally ill-conditioned. There are solution strategies for both problems, which were described by e.g. Nosier and Reddy (1992).

A constant value c is added to the main diagonal elements of $\underline{\underline{A}}$:

$$\overline{\underline{\underline{A}}} = \underline{\underline{A}} + \begin{bmatrix} c & & 0 \\ & \ddots & \\ 0 & & c \end{bmatrix}. \tag{13.83}$$

The relationship between the eigenvalues is as follows:

$$\lambda_i = \overline{\lambda}_i - c, \quad \text{for } i = 1, \ldots, 8. \tag{13.84}$$

The eigenvectors of $\overline{\underline{\underline{A}}}$ and $\underline{\underline{A}}$ are identical.

In addition, $\det(\underline{\underline{M}})$ is often poorly conditioned. Therefore, a method is presented that avoids the calculation of $\det(\underline{\underline{M}})$. Inserting (13.80) into (13.79) results in

$$\underline{Z}(y) = \underline{\underline{L}} \begin{bmatrix} \mathrm{e}^{\lambda_1 y} & & 0 \\ & \ddots & \\ 0 & & \mathrm{e}^{\lambda_8 y} \end{bmatrix} \underline{\underline{L}}^{-1}\, \underline{K}. \tag{13.85}$$

If we replace the last two terms in (13.85) with $\overline{\underline{K}} = \underline{\underline{L}}^{-1}\, \underline{K}$, we obtain the result:

$$\underline{Z}(y) = \underline{\underline{L}} \begin{bmatrix} \mathrm{e}^{\lambda_1 y} & & 0 \\ & \ddots & \\ 0 & & \mathrm{e}^{\lambda_8 y} \end{bmatrix} \overline{\underline{K}}. \tag{13.86}$$

The substitution of this solution in the boundary conditions leads to:

$$\overline{\underline{\underline{M}}}\, \overline{\underline{K}} = 0. \tag{13.87}$$

The resubstitution of $\overline{\underline{\underline{M}}}$ into the system of equations (13.87) results in:

$$\overline{\underline{\underline{M}}}\, \underline{\underline{L}}^{-1}\, \underline{K} = 0. \tag{13.88}$$

The non-trivial solution of (13.88) is given by:

$$\det(\overline{\underline{\underline{M}}}\, \underline{\underline{L}}^{-1}) = 0, \tag{13.89}$$

which can be divided into:

$$\det(\overline{\underline{\underline{M}}}\, \underline{\underline{L}}^{-1}) = \frac{\det(\overline{\underline{\underline{M}}})}{\det(\underline{\underline{L}})} = 0. \tag{13.90}$$

Equation (13.90) is the buckling condition for the critical load N_{xx}^0 and provides the same results as condition (13.82). The method shown avoids the calculation of $\underline{\underline{L}}^{-1}$ and calculates the determinant of $\overline{\underline{\underline{M}}}$ and $\underline{\underline{L}}$, which are better conditioned than $\underline{\underline{M}}$.

References

Beerhorst M (2013): *Entwicklung von hocheffizienten Berechnungsmethoden zur Beschreibung des Beul- und Nachbeulverhaltens von versteiften und unversteiften Flächentragwerken aus Faserverbundwerkstoffen*, Dissertation, Technische Universität Berlin, Fakultät V - Verkehrs- und Maschinensysteme, Berlin, Germany.

Dörfler T (1993): *Beulverhalten und Optimierung längsversteifter Gurtplatten unter Schub- und Druckbelastung*, Fortschrittsberichte VDI, Reihe 1, VDI-Verlag, Düsseldorf, Germany.

Khdeir AA (1988): *Free vibration and buckling of symmetric cross-ply laminated plates by an exact method*, Journal of Sound and Vibration 126:447–461.

Nosier A, Reddy JN (1992): *Vibration and stability analyses of cross-ply laminated circular cylindrical shells*, Journal of Sound and Vibration 157:139–159.

Reddy JN (2004): *Mechanics of laminated composite plates and shells*, 2nd edition, CRC Press, Boca Raton et al., USA.

Energy Methods for Laminate Buckling Problems 14

In the bifurcational buckling analysis of thin-walled composite lightweight structures, mathematically rigorous solutions can only be specified for a few idealized structures under certain boundary conditions and load cases. Therefore, the vast majority of engineering applications rely on approximate solutions. Common approximation methods are generally based on statements about the energy balance of the structure under consideration. This chapter is dedicated to an overview of such so-called energy methods. In addition to the presentation of the analysis methods, some typical problems that can be suitably treated with the help of energy-based methods are also discussed.

14.1 Energetic Derivation of the Governing Equations

The differential equations describing laminate buckling have so far been derived by considering the equilibrium of an infinitesimally deflected laminate element. In this section, the considerations will now be made in an energetic way. For this purpose, the total potential Π of a laminate in the buckled state is considered, which is composed of the inner potential Π_i and the potential Π_a of the applied load:

$$\Pi = \Pi_i + \Pi_a. \tag{14.1}$$

For the sake of simplicity, the laminate is assumed to be rectangular (length a, width b) and can have any arbitrary layup. The inner potential Π_i of the laminate can be written as follows within the framework of Classical Laminated Plate Theory (CLPT):

$$\begin{aligned}\Pi_i = \frac{1}{2}\int_0^a\int_0^b\left[N_{xx}^0\frac{\partial u_0}{\partial x} + N_{yy}^0\frac{\partial v_0}{\partial y} + N_{xy}^0\left(\frac{\partial u_0}{\partial y} + \frac{\partial v_0}{\partial x}\right)\right]\mathrm{d}y\mathrm{d}x \\ - \frac{1}{2}\int_0^a\int_0^b\left[M_{xx}^0\frac{\partial^2 w_0}{\partial x^2} + M_{yy}^0\frac{\partial^2 w_0}{\partial y^2} + 2M_{xy}^0\frac{\partial^2 w_0}{\partial x\partial y}\right]\mathrm{d}y\mathrm{d}x.\end{aligned} \tag{14.2}$$

© The Author(s), under exclusive license to Springer-Verlag GmbH, DE, part of Springer Nature 2025

C. Mittelstedt, *Mechanics of Composite Structures*,
https://doi.org/10.1007/978-3-662-70788-3_14

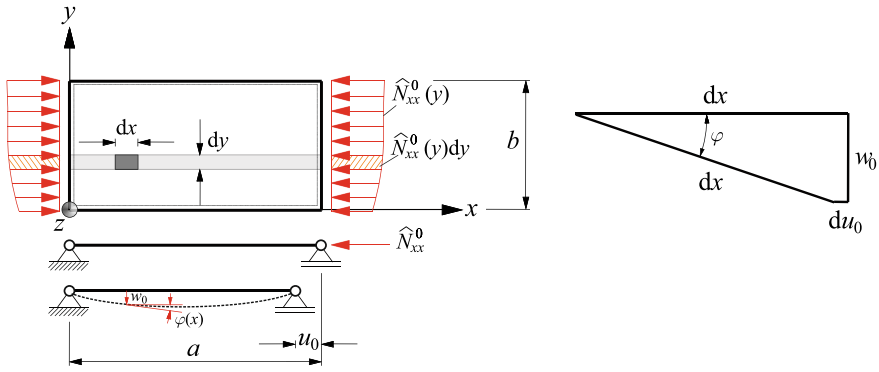


Fig. 14.1 On the potential of the edge load $\hat{N}^0_{xx}$

The potential of the edge loads—these are the two loads $\hat{N}^0_{xx}$ and $\hat{N}^0_{yy}$ normal to the edges as well as the shear edge load $\hat{N}^0_{xy}$—can be derived elementarily from the deformations at buckling onset. This is shown in detail here for the edge load $\hat{N}^0_{xx}$ (Fig. 14.1).

The potential Π_a of the variable edge load $\hat{N}^0_{xx}(y)$ over y is calculated as:

$$\Pi_a = -W_a = -\int_0^b \hat{N}^0_{xx}(y)\, u_0(y)\, \mathrm{d}y, \tag{14.3}$$

where $u_0(y)$ is the displacement of the laminate middle plane at the edge $x = a$. The integration prescribed in (14.3) indicates that all infinitesimal resulting edge forces $\hat{N}^0_{xx}(y)\,\mathrm{d}y$ from $y = 0$ to $y = b$ are to be summed up. In order to derive a suitable expression for the boundary displacement $u_0(y)$, the infinitesimal section element with the length $\mathrm{d}x$ (Fig. 14.1, left) is considered and the deformed state at the onset of buckling according to Fig. 14.1, right, is analyzed. It can be seen from this that the following applies to the displacement $\mathrm{d}u_0$:

$$\mathrm{d}u_0 = (1 - \cos(\varphi))\,\mathrm{d}x. \tag{14.4}$$

If we develop the cosine term in (14.4) into a Taylor series according to $\cos(\varphi) = 1 - \frac{1}{2}\varphi^2$, then we can also write

$$\mathrm{d}u_0 = \frac{1}{2}\varphi^2 \mathrm{d}x = \frac{1}{2}\left(\frac{\partial w_0}{\partial x}\right)^2 \mathrm{d}x. \tag{14.5}$$

Integration over the longitudinal coordinate x then leads to the boundary displacement $u_0(y)$:

$$u_0(y) = \frac{1}{2}\int_0^a \left(\frac{\partial w_0}{\partial x}\right)^2 \mathrm{d}x. \tag{14.6}$$

The potential Π_a of the edge load $\hat{N}^0_{xx}(y)$ can thus be written as follows:

$$\Pi_a = -\frac{1}{2}\int_0^b \hat{N}_{xx}^0(y)\left[\int_0^a \left(\frac{\partial w_0}{\partial x}\right)^2 \mathrm{d}x\right]\mathrm{d}y. \tag{14.7}$$

If we assume that the boundary load $\hat{N}_{xx}^0$ is constant, then we obtain

$$\Pi_a = -\frac{1}{2}\hat{N}_{xx}^0\int_0^a\int_0^b \left(\frac{\partial w_0}{\partial x}\right)^2 \mathrm{d}y\mathrm{d}x. \tag{14.8}$$

The same expression can also be derived by integrating over the displacement derivative $\frac{\partial u_0}{\partial x} = \varepsilon_{xx} - \frac{1}{2}\left(\frac{\partial w_0}{\partial x}\right)^2$ according to v. Kármán's theory and neglecting the ε_{xx} component due to the elongation of the laminate middle plane. We can proceed in the same way for the boundary loads $\hat{N}_{yy}^0$ and $\hat{N}_{xy}^0$, and we obtain the following expression if all three edge loads are present:

$$\Pi_a = -\frac{1}{2}\int_0^a\int_0^b \left[\hat{N}_{xx}^0\left(\frac{\partial w_0}{\partial x}\right)^2 + \hat{N}_{yy}^0\left(\frac{\partial w_0}{\partial y}\right)^2 + 2\hat{N}_{xy}^0\frac{\partial w_0}{\partial x}\frac{\partial w_0}{\partial y}\right]\mathrm{d}y\mathrm{d}x. \tag{14.9}$$

The infinitesimally deflected state is also a state of equilibrium, so that $\delta\Pi = \delta\Pi_i + \delta\Pi_a = 0$ also applies in the buckled state:

$$\begin{aligned}
\delta\Pi = &\int_0^a\int_0^b \left[N_{xx}^0\delta\frac{\partial u_0}{\partial x} + N_{yy}^0\delta\frac{\partial v_0}{\partial y} + N_{xy}^0\left(\delta\frac{\partial u_0}{\partial y} + \delta\frac{\partial v_0}{\partial x}\right)\right]\mathrm{d}y\mathrm{d}x\\
&-\int_0^a\int_0^b \left[M_{xx}^0\delta\frac{\partial^2 w_0}{\partial x^2} + M_{yy}^0\delta\frac{\partial^2 w_0}{\partial y^2} + 2M_{xy}^0\delta\frac{\partial^2 w_0}{\partial x\partial y}\right]\mathrm{d}y\mathrm{d}x\\
&-\frac{1}{2}\int_0^a\int_0^b \left[\hat{N}_{xx}^0\delta\left(\frac{\partial w_0}{\partial x}\right)^2 + \hat{N}_{yy}^0\delta\left(\frac{\partial w_0}{\partial y}\right)^2 + 2\hat{N}_{xy}^0\delta\left(\frac{\partial w_0}{\partial x}\frac{\partial w_0}{\partial y}\right)\right]\mathrm{d}y\mathrm{d}x = 0.
\end{aligned} \tag{14.10}$$

Consequent evaluation and partial integration then yields the following expression after a few elementary transformations:

$$\begin{aligned}
&-\int_0^a\int_0^b \left[\left(\frac{\partial N_{xx}^0}{\partial x} + \frac{\partial N_{xy}^0}{\partial y}\right)\delta u_0 + \left(\frac{\partial N_{xy}^0}{\partial x} + \frac{\partial N_{yy}^0}{\partial y}\right)\delta v_0\right.\\
&\left.+\left(\frac{\partial^2 M_{xx}^0}{\partial x^2} + 2\frac{\partial^2 M_{xy}^0}{\partial x\partial y} + \frac{\partial^2 M_{yy}^0}{\partial y^2} - \hat{N}_{xx}^0\frac{\partial^2 w_0}{\partial x^2} - 2\hat{N}_{xy}^0\frac{\partial^2 w_0}{\partial x\partial y} - \hat{N}_{yy}^0\frac{\partial^2 w_0}{\partial y^2}\right)\delta w_0\right]\mathrm{d}y\mathrm{d}x\\
&+\int_0^a\left\{\left[N_{xy}^0\delta u_0 + N_{yy}^0\delta v_0 - M_{yy}^0\delta\frac{\partial w_0}{\partial y} + \left(\frac{\partial M_{yy}^0}{\partial y} + 2\frac{\partial M_{xy}^0}{\partial x}\right)\delta w_0\right]\Big|_{y=0}^{y=b}\right\}\mathrm{d}x\\
&+\int_0^b\left\{\left[N_{xx}^0\delta u_0 + N_{xy}^0\delta v_0 - M_{xx}^0\delta\frac{\partial w_0}{\partial x} + \left(\frac{\partial M_{xx}^0}{\partial x} + 2\frac{\partial M_{xy}^0}{\partial y}\right)\delta w_0\right]\Big|_{x=0}^{x=a}\right\}\mathrm{d}y
\end{aligned}$$

$$
\begin{aligned}
&- \int_0^a \left\{ \left[\left(\hat{N}^0_{yy} \frac{\partial w_0}{\partial y} + \hat{N}^0_{xy} \frac{\partial w_0}{\partial x} \right) \delta w_0 \right] \Big|_{y=0}^{y=b} \right\} \mathrm{d}x \\
&- \int_0^b \left\{ \left[\left(\hat{N}^0_{xx} \frac{\partial w_0}{\partial x} + \hat{N}^0_{xy} \frac{\partial w_0}{\partial y} \right) \delta w_0 \right] \Big|_{x=0}^{x=a} \right\} \mathrm{d}y - 2 \left(M^0_{xy} \delta w_0 \right) \Big|_{x=0}^{x=a} \Big|_{y=0}^{y=b} = 0. \qquad (14.11)
\end{aligned}
$$

The first two lines in (14.11) show the differential equations of the presently considered buckling problem:

$$
\begin{aligned}
\frac{\partial N^0_{xx}}{\partial x} + \frac{\partial N^0_{xy}}{\partial y} &= 0, \\
\frac{\partial N^0_{xy}}{\partial x} + \frac{\partial N^0_{yy}}{\partial y} &= 0, \\
\frac{\partial^2 M^0_{xx}}{\partial x^2} + 2\frac{\partial^2 M^0_{xy}}{\partial x \partial y} + \frac{\partial^2 M^0_{yy}}{\partial y^2} - \hat{N}^0_{xx} \frac{\partial^2 w_0}{\partial x^2} - 2\hat{N}^0_{xy} \frac{\partial^2 w_0}{\partial x \partial y} - \hat{N}^0_{yy} \frac{\partial^2 w_0}{\partial y^2} &= 0.
\end{aligned} \qquad (14.12)
$$

We find that these equations agree with the corresponding equations that have already been derived from equilibrium considerations. After inserting the constitutive law for a laminate according to CLPT, one would obtain the governing differential equations, formulated in the displacements u_0, v_0, w_0 of the laminate middle plane, which will not be further elaborated here.

The remaining terms in (14.11) indicate the corresponding boundary conditions of the laminate. At the two edges at $x = 0$ and $x = a$, we have for all $0 \le y \le b$:

$$
\begin{aligned}
&\text{either} \quad N^0_{xx} = 0 \quad &&\text{or} \quad u_0 = \widehat{u}_0, \\
&\text{either} \quad N^0_{xy} = 0 \quad &&\text{or} \quad v_0 = \widehat{v}_0, \\
&\text{either} \quad M^0_{xx} = 0 \quad &&\text{or} \quad \frac{\partial w_0}{\partial x} = \widehat{\frac{\partial w_0}{\partial x}}, \\
&\text{either} \quad \frac{\partial M^0_{xx}}{\partial x} + 2\frac{\partial M^0_{xy}}{\partial y} - \hat{N}^0_{xx} \frac{\partial w_0}{\partial x} - \hat{N}^0_{xy} \frac{\partial w_0}{\partial y} = 0 \quad &&\text{or} \quad w_0 = \widehat{w}_0.
\end{aligned} \qquad (14.13)
$$

In the last condition (14.13), the first two terms are composed of Kirchhoff's equivalent shear force. The last two terms indicate that the edge loads $\hat{N}^0_{xx}$, $\hat{N}^0_{xy}$ in the buckled state have a component in the direction of the laminate shear force $\bar{Q}_x$. Similarly, the boundary conditions can be deduced for the two edges at $y = 0$ and $y = b$ for $0 \le x \le a$:

$$
\begin{aligned}
&\text{either} \quad N^0_{xy} = 0 \quad &&\text{or} \quad u_0 = \widehat{u}_0, \\
&\text{either} \quad N^0_{yy} = 0 \quad &&\text{or} \quad v_0 = \widehat{v}_0, \\
&\text{either} \quad M^0_{yy} = 0 \quad &&\text{or} \quad \frac{\partial w_0}{\partial y} = \widehat{\frac{\partial w_0}{\partial y}}, \\
&\text{either} \quad \frac{\partial M^0_{yy}}{\partial y} + 2\frac{\partial M^0_{xy}}{\partial x} - \hat{N}^0_{yy} \frac{\partial w_0}{\partial y} - \hat{N}^0_{xy} \frac{\partial w_0}{\partial x} = 0 \quad &&\text{or} \quad w_0 = \widehat{w}_0.
\end{aligned} \qquad (14.14)
$$

At all four laminate corners, either the twisting moment M_{xy}^0 must disappear or the deflection w_0 is specified there with the value $\widehat{w}_0$:

$$\text{either } M_{xy}^0 = 0 \text{ or } w_0 = \widehat{w}_0. \tag{14.15}$$

In the following of this chapter, the focus is mainly on symmetric laminates. This decouples the membrane and plate behaviour of the laminate, and the first two equilibrium conditions in (14.12) describe the inplane behaviour of the laminate under the given edge loads. The third differential equation in (14.12) then describes the buckling behaviour. After inserting the laminate material law

$$\begin{pmatrix} M_{xx}^0 \\ M_{yy}^0 \\ M_{xy}^0 \end{pmatrix} = \begin{bmatrix} D_{11} & D_{12} & D_{16} \\ D_{12} & D_{22} & D_{26} \\ D_{16} & D_{26} & D_{66} \end{bmatrix} \begin{pmatrix} -\dfrac{\partial^2 w_0}{\partial x^2} \\ -\dfrac{\partial^2 w_0}{\partial y^2} \\ -2\dfrac{\partial^2 w_0}{\partial x \partial y} \end{pmatrix} \tag{14.16}$$

it reads:

$$\begin{aligned} D_{11}\frac{\partial^4 w_0}{\partial x^4} + 4D_{16}\frac{\partial^4 w_0}{\partial x^3 \partial y} + 2\left(D_{12} + 2D_{66}\right)\frac{\partial^4 w_0}{\partial x^2 \partial y^2} + 4D_{26}\frac{\partial^4 w_0}{\partial x \partial y^3} + D_{22}\frac{\partial^4 w_0}{\partial y^4} \\ + N_{xx}^0\frac{\partial^2 w_0}{\partial x^2} + 2N_{xy}^0\frac{\partial^2 w_0}{\partial x \partial y} + N_{yy}^0\frac{\partial^2 w_0}{\partial y^2} = 0. \end{aligned} \tag{14.17}$$

In this case, the overlines for labelling the edge loads have been omitted, since after the constitutive law has been applied, there is no risk of confusion between edge loads and internal forces, at least for the buckling problems discussed in this chapter, since it is assumed that the stress state in the entire laminate is identical to the respective edge loads. In the following, $N_{xx}^0, N_{yy}^0, N_{xy}^0$ therefore always refer to the given edge loads or the associated buckling loads.

The corresponding potential formulation (14.1) for a symmetric laminate changes into the following form after inserting the material law (14.16):

$$\begin{aligned} \Pi = &\int_0^a \int_0^b \left[\frac{1}{2} D_{11} \left(\frac{\partial^2 w_0}{\partial x^2} \right)^2 + \frac{1}{2} D_{22} \left(\frac{\partial^2 w_0}{\partial y^2} \right)^2 + D_{12} \frac{\partial^2 w_0}{\partial x^2} \frac{\partial^2 w_0}{\partial y^2} + 2D_{66} \left(\frac{\partial^2 w_0}{\partial x \partial y} \right)^2 \right] \mathrm{d}y\mathrm{d}x \\ &+ 2\int_0^a \int_0^b \left[\left(D_{16} \frac{\partial^2 w_0}{\partial x^2} + D_{26} \frac{\partial^2 w_0}{\partial y^2} \right) \frac{\partial^2 w_0}{\partial x \partial y} \right] \mathrm{d}y\mathrm{d}x \\ &- \frac{1}{2}\int_0^a \int_0^b \left[N_{xx}^0 \left(\frac{\partial w_0}{\partial x} \right)^2 + N_{yy}^0 \left(\frac{\partial w_0}{\partial y} \right)^2 + 2N_{xy}^0 \frac{\partial w_0}{\partial x} \frac{\partial w_0}{\partial y} \right] \mathrm{d}y\mathrm{d}x, \end{aligned} \tag{14.18}$$

whereby only the plate terms are recognized as relevant here.

It is useful here as well to use a dimensionless representation. If the coordinates x and y are transformed by means of the substitution

$$\xi_1 = \frac{x}{a}, \quad \xi_2 = \frac{y}{b}, \tag{14.19}$$

then the potential (14.18) can also be written as follows:

$$\begin{aligned}\bar{\Pi} = \frac{1}{2}\int_0^1\int_0^1 \Bigg[&\frac{1}{\alpha^2}\left(\frac{\partial^2\bar{w}_0}{\partial\xi_1^2}\right)^2 + \alpha^2\left(\frac{\partial^2\bar{w}_0}{\partial\xi_2^2}\right)^2 + 2\beta\zeta\frac{\partial^2\bar{w}_0}{\partial\xi_1^2}\frac{\partial^2\bar{w}_0}{\partial\xi_2^2} \\ &+ 2(1-\zeta)\beta\left(\frac{\partial^2\bar{w}_0}{\partial\xi_1\partial\xi_2}\right)^2 + 4\left(\frac{\gamma}{\alpha}\frac{\partial^2\bar{w}_0}{\partial\xi_1^2} + \alpha\delta\frac{\partial^2\bar{w}_0}{\partial\xi_2^2}\right)\frac{\partial^2\bar{w}_0}{\partial\xi_1\partial\xi_2}\Bigg] \mathrm{d}\xi_2\mathrm{d}\xi_1 \\ &- \frac{1}{2}\pi^2\int_0^1\int_0^1\left[\bar{N}_{xx}^0\left(\frac{\partial\bar{w}_0}{\partial\xi_1}\right)^2 + \bar{N}_{yy}^0\left(\frac{\partial\bar{w}_0}{\partial\xi_2}\right)^2 + 2\bar{N}_{xy}^0\frac{\partial\bar{w}_0}{\partial\xi_1}\frac{\partial\bar{w}_0}{\partial\xi_2}\right]\mathrm{d}\xi_2\mathrm{d}\xi_1. \end{aligned} \tag{14.20}$$

Here, the characteristic dimensionless variables are the dimensionless potential

$$\bar{\Pi} = \frac{\Pi}{\sqrt{D_{11}D_{22}}}, \tag{14.21}$$

the dimensionless buckling mode

$$\bar{w}_0 = \frac{w_0}{\sqrt{ab}}, \tag{14.22}$$

the aspect ratio

$$\alpha = \frac{a}{b}\sqrt[4]{\frac{D_{22}}{D_{11}}}, \tag{14.23}$$

Seydel's orthotropy parameter

$$\beta = \frac{D_{12} + 2D_{66}}{\sqrt{D_{11}D_{22}}}, \tag{14.24}$$

the generalized Poisson's ratio

$$\zeta = \frac{D_{12}}{D_{12} + 2D_{66}}, \tag{14.25}$$

the bending-twisting ratios

$$\gamma = \frac{D_{16}}{\sqrt[4]{D_{11}^3 D_{22}}}, \quad \delta = \frac{D_{26}}{\sqrt[4]{D_{11}D_{22}^3}}, \tag{14.26}$$

and the edge loads or buckling loads

$$\bar{N}_{xx}^0 = \frac{N_{xx}^0 b^2}{\pi^2\sqrt{D_{11}D_{22}}}, \quad \bar{N}_{yy}^0 = \frac{N_{yy}^0 a^2}{\pi^2\sqrt{D_{11}D_{22}}}, \quad \bar{N}_{xy}^0 = \frac{N_{xy}^0 ab}{\pi^2\sqrt{D_{11}D_{22}}}. \tag{14.27}$$

The differential equation (14.17) can only be solved exactly in a few special cases with regard to the constitutive law, the load case and the boundary conditions. Therefore, in many

application cases, closed-form analytical, semi-analytical or purely numerical approximation solutions are used. Such approximation solutions are in the vast majority of cases energy-based and use the potential formulation (14.18) or (14.20). Energy-based methods and the problems that can be treated with them are discussed in detail in the following sections.

14.2 The Rayleigh Quotient for Laminates Without Bending-Twisting Coupling

14.2.1 Methodology

Starting point for the Rayleigh[1] quotient is the potential formulation (14.18) or (14.20). An approach for the buckling mode w_0 is used in the following form:

$$w_0 = \sum_{m=1}^{M} \sum_{n=1}^{N} W_{mn} w_{1m}(x) w_{2n}(y). \tag{14.28}$$

In this case, the shape functions w_{1m} and w_{2n} must fulfil all underlying static or geometric boundary conditions identically. The values W_{mn} are approach coefficients. An attempt should always be made to minimise the number M and N of approximation functions when using an approach of the form (14.28). If, as a special case of the representation (14.28), we even only use $M = N = 1$ shape functions, then the approach (14.28) is simplified:

$$w_0 = W w_1(x) w_2(y). \tag{14.29}$$

In the following, only laminates under a constant longitudinal compressive load N^0_{xx} are to be considered, the edge loads N^0_{yy} and N^0_{xy} are zero. In addition, only those laminates are considered for which the bending-twisting coupling terms D_{16} and D_{26} are either zero or at least negligible in good approximation. With the approach (14.29), the elastic potential of the buckled laminate (14.18) can be evaluated and obtained under the given conditions:

$$\begin{aligned}\Pi = \Bigg[& \frac{1}{2} D_{11} \int_0^a \left(\frac{\mathrm{d}^2 w_1}{\mathrm{d}x^2} \right)^2 \mathrm{d}x \int_0^b w_2^2 \mathrm{d}y + \frac{1}{2} D_{22} \int_0^a w_1^2 \mathrm{d}x \int_0^b \left(\frac{\mathrm{d}^2 w_2}{\mathrm{d}y^2} \right)^2 \mathrm{d}y \\ & + D_{12} \int_0^a w_1 \frac{\mathrm{d}^2 w_1}{\mathrm{d}x^2} \mathrm{d}x \int_0^b w_2 \frac{\mathrm{d}^2 w_2}{\mathrm{d}y^2} \mathrm{d}y + 2 D_{66} \int_0^a \left(\frac{\mathrm{d}w_1}{\mathrm{d}x} \right)^2 \mathrm{d}x \int_0^b \left(\frac{\mathrm{d}w_2}{\mathrm{d}y} \right)^2 \mathrm{d}y \\ & - \frac{1}{2} N^0_{xx} \int_0^a \left(\frac{\mathrm{d}w_1}{\mathrm{d}x} \right)^2 \mathrm{d}x \int_0^b w_2^2 \mathrm{d}y \Bigg] W^2. \end{aligned} \tag{14.30}$$

For the integrals of the shape functions, we introduce abbreviations as follows:

[1] John William Strutt, 3rd Baron Rayleigh, 1842–1919, English physicist.

$$\lambda_{x,ij} = \int_0^a \frac{\mathrm{d}^i w_1}{\mathrm{d}x^i} \frac{\mathrm{d}^j w_1}{\mathrm{d}x^j} \mathrm{d}x, \quad \lambda_{y,ij} = \int_0^b \frac{\mathrm{d}^i w_2}{\mathrm{d}y^i} \frac{\mathrm{d}^j w_2}{\mathrm{d}y^j} \mathrm{d}y. \tag{14.31}$$

Then (14.30) can also be represented as:

$$\Pi = \left[\frac{1}{2} D_{11} \lambda_{x,22} \lambda_{y,00} + \frac{1}{2} D_{22} \lambda_{x,00} \lambda_{y,22} + D_{12} \lambda_{x,02} \lambda_{y,02} + 2 D_{66} \lambda_{x,11} \lambda_{y,11} - \frac{1}{2} N_{xx}^0 \lambda_{x,11} \lambda_{y,00} \right] W^2. \tag{14.32}$$

Since in practical applications one will always endeavour to use mathematically easy to handle shape functions w_1 and w_2, the integrals (14.31) should be elementary solvable in the vast majority of cases.

The buckling condition $\delta \Pi = 0$ changes with the given approach (14.29) into the requirement for the disappearance of the first partial derivative of the potential Π with respect to the constant W:

$$\frac{\partial \Pi}{\partial W} = 0. \tag{14.33}$$

From (14.32) we obtain:

$$\left[D_{11} \lambda_{x,22} \lambda_{y,00} + D_{22} \lambda_{x,00} \lambda_{y,22} + 2 D_{12} \lambda_{x,02} \lambda_{y,02} + 4 D_{66} \lambda_{x,11} \lambda_{y,11} - N_{xx}^0 \lambda_{x,11} \lambda_{y,00} \right] W = 0. \tag{14.34}$$

In addition to the trivial solution $W = 0$, the case of interest here is that the bracket term in (14.34) is set to zero:

$$D_{11} \lambda_{x,22} \lambda_{y,00} + D_{22} \lambda_{x,00} \lambda_{y,22} + 2 D_{12} \lambda_{x,02} \lambda_{y,02} + 4 D_{66} \lambda_{x,11} \lambda_{y,11} - N_{xx}^0 \lambda_{x,11} \lambda_{y,00} = 0. \tag{14.35}$$

This can be solved immediately for the required buckling load N_{xx}^0:

$$N_{xx}^0 = \frac{D_{11} \lambda_{x,22} \lambda_{y,00} + D_{22} \lambda_{x,00} \lambda_{y,22} + 2 D_{12} \lambda_{x,02} \lambda_{y,02} + 4 D_{66} \lambda_{x,11} \lambda_{y,11}}{\lambda_{x,11} \lambda_{y,00}}. \tag{14.36}$$

This expression is the so-called 'Rayleigh quotient' for the approximate determination of the buckling load of a symmetric laminate without bending-twisting coupling under uniaxial compressive load. It is important to note that the solution (14.36) approximates the actual buckling load of a laminate 'from above'. This means that we always make an error that is on the non-conservative side.

The procedure will be briefly explained using a dimensionless notation. The approach for the buckling shape is as follows:

$$\bar{w}_0 = W \bar{w}_1 (\xi_1) \, \bar{w}_2 (\xi_2) \, . \tag{14.37}$$

The potential formulation is currently as follows:

$$\bar{\Pi} = \frac{1}{2}\int_0^1\int_0^1 \left[\frac{1}{\alpha^2}\left(\frac{\partial^2\bar{w}_0}{\partial\xi_1^2}\right)^2 + \alpha^2\left(\frac{\partial^2\bar{w}_0}{\partial\xi_2^2}\right)^2 + 2\beta\zeta\frac{\partial^2\bar{w}_0}{\partial\xi_1^2}\frac{\partial^2\bar{w}_0}{\partial\xi_2^2}\right]\mathrm{d}\xi_2\mathrm{d}\xi_1$$
$$+ \frac{1}{2}\int_0^1\int_0^1 \left[2(1-\zeta)\beta\left(\frac{\partial^2\bar{w}_0}{\partial\xi_1\partial\xi_2}\right)^2 - \pi^2\bar{N}_{xx}^0\left(\frac{\partial\bar{w}_0}{\partial\xi_1}\right)^2\right]\mathrm{d}\xi_2\mathrm{d}\xi_1. \tag{14.38}$$

Inserting (14.37) into (14.38) results in:

$$\bar{\Pi} = \left[\frac{1}{2}\frac{1}{\alpha^2}\int_0^1\left(\frac{\mathrm{d}^2\bar{w}_1}{\mathrm{d}\xi_1^2}\right)^2\mathrm{d}\xi_1\int_0^1\bar{w}_2^2\mathrm{d}\xi_2 + \frac{1}{2}\alpha^2\int_0^1\bar{w}_1^2\mathrm{d}\xi_1\int_0^1\left(\frac{\mathrm{d}^2\bar{w}_2}{\mathrm{d}\xi_2^2}\right)^2\mathrm{d}\xi_2\right.$$
$$+ \beta\zeta\int_0^1\bar{w}_1\frac{\mathrm{d}^2\bar{w}_1}{\mathrm{d}\xi_1^2}\mathrm{d}\xi_1\int_0^1\bar{w}_2\frac{\mathrm{d}^2\bar{w}_2}{\mathrm{d}\xi_2^2}\mathrm{d}\xi_2 + (1-\zeta)\beta\int_0^1\left(\frac{\mathrm{d}\bar{w}_1}{\mathrm{d}\xi_1}\right)^2\mathrm{d}\xi_1\int_0^1\left(\frac{\mathrm{d}\bar{w}_2}{\mathrm{d}\xi_2}\right)^2\mathrm{d}\xi_2$$
$$\left. - \frac{1}{2}\pi^2\bar{N}_{xx}^0\int_0^1\left(\frac{\mathrm{d}\bar{w}_1}{\mathrm{d}\xi_1}\right)^2\mathrm{d}\xi_1\int_0^1\bar{w}_2^2\mathrm{d}\xi_2\right]W^2. \tag{14.39}$$

With the abbreviations

$$\bar{\lambda}_{1,ij} = \int_0^1\frac{\mathrm{d}^i\bar{w}_1}{\mathrm{d}\xi_1^i}\frac{\mathrm{d}^j\bar{w}_1}{\mathrm{d}\xi_1^j}\mathrm{d}\xi_1, \quad \bar{\lambda}_{2,ij} = \int_0^1\frac{\mathrm{d}^i\bar{w}_2}{\mathrm{d}\xi_2^i}\frac{\mathrm{d}^j\bar{w}_2}{\mathrm{d}\xi_2^j}\mathrm{d}\xi_2 \tag{14.40}$$

we obtain:

$$\bar{\Pi} = \left(\frac{1}{2}\frac{1}{\alpha^2}\bar{\lambda}_{1,22}\bar{\lambda}_{2,00} + \frac{1}{2}\alpha^2\bar{\lambda}_{1,00}\bar{\lambda}_{2,22} + \beta\zeta\bar{\lambda}_{1,02}\bar{\lambda}_{2,02}\right.$$
$$\left. + (1-\zeta)\beta\bar{\lambda}_{1,11}\bar{\lambda}_{2,11} - \frac{1}{2}\pi^2\bar{N}_{xx}^0\bar{\lambda}_{1,11}\bar{\lambda}_{2,00}\right)W^2. \tag{14.41}$$

The buckling condition $\frac{\partial\bar{\Pi}}{\partial W} = 0$ then leads to the following expression for the buckling load:

$$\bar{N}_{xx}^0 = \frac{\frac{1}{\alpha^2}\bar{\lambda}_{1,22}\bar{\lambda}_{2,00} + \alpha^2\bar{\lambda}_{1,00}\bar{\lambda}_{2,22} + 2\beta\zeta\bar{\lambda}_{1,02}\bar{\lambda}_{2,02} + 2(1-\zeta)\beta\bar{\lambda}_{1,11}\bar{\lambda}_{2,11}}{\pi^2\bar{\lambda}_{1,11}\bar{\lambda}_{2,00}}. \tag{14.42}$$

Despite the simplicity of the procedure presented here for determining the bifurcational buckling load of a laminate using the Rayleigh quotient, this method continues to enjoy great popularity, especially in industrial applications. Therefore, the application of the presented method is demonstrated below using selected examples.

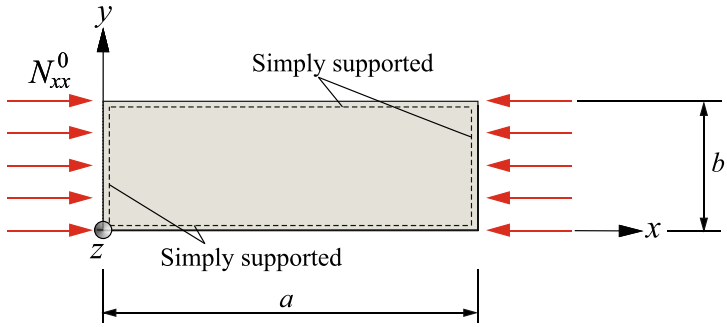


Fig. 14.2 Simply supported laminate under uniaxial compressive load

14.2.2 Simply Supported Laminate

The first example considered is a laminate that is simply supported at all four edges (Fig. 14.2).

The boundary conditions are for the current situation:

$$\begin{aligned} &w_0\,(x=0)=0, \quad w_0\,(x=a)=0, \quad w_0\,(y=0)=0, \quad w_0\,(y=b)=0,\\ &M_{xx}^0\,(x=0)=-D_{11}\left.\frac{\partial^2 w_0}{\partial x^2}\right|_{x=0}=0, \quad M_{xx}^0\,(x=a)=-D_{11}\left.\frac{\partial^2 w_0}{\partial x^2}\right|_{x=a}=0,\\ &M_{yy}^0\,(y=0)=-D_{22}\left.\frac{\partial^2 w_0}{\partial y^2}\right|_{y=0}=0, \quad M_{yy}^0\,(y=b)=-D_{22}\left.\frac{\partial^2 w_0}{\partial y^2}\right|_{y=b}=0. \end{aligned} \tag{14.43}$$

We choose an approach of the following form:

$$w_0 = W \sin\left(\frac{m\pi x}{a}\right)\sin\left(\frac{n\pi y}{b}\right). \tag{14.44}$$

It is easy to see that this approach not only fulfils the geometric boundary conditions in (14.43) identically, but also satisfies all given dynamic boundary conditions in (14.43). With the approach (14.44), the integrals in (14.31) can be written as follows:

$$\begin{aligned} \lambda_{x,00} &= \int_0^a w_1^2 \mathrm{d}x = \int_0^a \sin^2\left(\frac{m\pi x}{a}\right)\mathrm{d}x = \frac{a}{2},\\ \lambda_{x,11} &= \int_0^a \left(\frac{\mathrm{d}w_1}{\mathrm{d}x}\right)^2 \mathrm{d}x = \frac{m^2\pi^2}{a^2}\int_0^a \cos^2\left(\frac{m\pi x}{a}\right)\mathrm{d}x = \frac{m^2\pi^2}{2a},\\ \lambda_{x,02} &= \int_0^a w_1 \frac{\mathrm{d}^2 w_1}{\mathrm{d}x^2}\,\mathrm{d}x = -\frac{m^2\pi^2}{a^2}\int_0^a \sin^2\left(\frac{m\pi x}{a}\right)\mathrm{d}x = -\frac{m^2\pi^2}{2a},\\ \lambda_{x,22} &= \int_0^a \frac{\mathrm{d}^2 w_1}{\mathrm{d}x^2}\frac{\mathrm{d}^2 w_1}{\mathrm{d}x^2}\,\mathrm{d}x = \frac{m^4\pi^4}{a^4}\int_0^a \sin^2\left(\frac{m\pi x}{a}\right)\mathrm{d}x = \frac{m^4\pi^4}{2a^3}, \end{aligned}$$

$$\lambda_{y,00} = \int_0^b w_2^2 \mathrm{d}y = \int_0^b \sin^2\left(\frac{n\pi y}{b}\right) \mathrm{d}y = \frac{b}{2},$$
$$\lambda_{y,11} = \int_0^b \frac{\mathrm{d}w_2}{\mathrm{d}y}\frac{\mathrm{d}w_2}{\mathrm{d}y}\,\mathrm{d}y = \frac{n^2\pi^2}{b^2}\int_0^b \cos^2\left(\frac{n\pi y}{b}\right)\mathrm{d}y = \frac{n^2\pi^2}{2b},$$
$$\lambda_{y,02} = \int_0^b w_2\frac{\mathrm{d}^2 w_2}{\mathrm{d}y^2}\,\mathrm{d}y = -\frac{n^2\pi^2}{b^2}\int_0^b \sin^2\left(\frac{n\pi y}{b}\right)\mathrm{d}y = -\frac{n^2\pi^2}{2b},$$
$$\lambda_{y,22} = \int_0^b \frac{\mathrm{d}^2 w_2}{\mathrm{d}y^2}\frac{\mathrm{d}^2 w_2}{\mathrm{d}y^2}\,\mathrm{d}y = \frac{n^4\pi^4}{b^4}\int_0^b \sin^2\left(\frac{n\pi y}{b}\right)\mathrm{d}y = \frac{n^4\pi^4}{2b^3}. \tag{14.45}$$

The buckling load for the current laminate situation can be calculated as follows from (14.36):

$$N_{xx}^0 = \pi^2\left[D_{11}\frac{m^2}{a^2} + D_{22}\frac{a^2n^4}{b^4m^2} + \frac{2n^2}{b^2}\left(D_{12}+2D_{66}\right)\right]. \tag{14.46}$$

The minimum buckling load always occurs for $n = 1$, so that the following applies:

$$N_{xx}^0 = \pi^2\left[D_{11}\frac{m^2}{a^2} + D_{22}\frac{a^2}{b^4m^2} + \frac{2}{b^2}\left(D_{12}+2D_{66}\right)\right]. \tag{14.47}$$

This solution corresponds exactly to the exact solution of the current buckling problem, which can be derived from the solution of the differential equation and a corresponding approach for the buckling mode (the Navier solution). This result is not surprising, as the approach (14.44) happens to correspond exactly to the exact solution of the problem. Obviously, even with this type of solution, as is common with bifurcational buckling problems, the constant W remains undetermined.

In dimensionless notation, the approach is as follows:

$$\bar{w}_0 = W\sin\left(m\pi\xi_1\right)\sin\left(n\pi\xi_2\right). \tag{14.48}$$

The integrals (14.40) can then be written as follows:

$$\bar{\lambda}_{1,00} = \int_0^1 \bar{w}_1^2 \mathrm{d}\xi_1 = \int_0^1 \sin^2\left(m\pi\xi_1\right)\mathrm{d}\xi_1 = \frac{1}{2},$$
$$\bar{\lambda}_{1,11} = \int_0^1 \left(\frac{\mathrm{d}\bar{w}_1}{\mathrm{d}\xi_1}\right)^2 \mathrm{d}\xi_1 = m^2\pi^2\int_0^1 \cos^2\left(m\pi\xi_1\right)\mathrm{d}\xi_1 = \frac{m^2\pi^2}{2},$$
$$\bar{\lambda}_{1,02} = \int_0^1 \bar{w}_1\frac{\mathrm{d}^2\bar{w}_1}{\mathrm{d}\xi_1^2}\,\mathrm{d}\xi_1 = -m^2\pi^2\int_0^1 \sin^2\left(m\pi\xi_1\right)\mathrm{d}\xi_1 = -\frac{m^2\pi^2}{2},$$
$$\bar{\lambda}_{1,22} = \int_0^1 \left(\frac{\mathrm{d}^2\bar{w}_1}{\mathrm{d}\xi_1^2}\right)^2 \mathrm{d}\xi_1 = m^4\pi^4\int_0^1 \sin^2\left(m\pi\xi_1\right)\mathrm{d}\xi_1 = \frac{m^4\pi^4}{2},$$
$$\bar{\lambda}_{2,00} = \int_0^1 \bar{w}_2^2 \mathrm{d}\xi_2 = \int_0^1 \sin^2\left(n\pi\xi_2\right)\mathrm{d}\xi_2 = \frac{1}{2},$$

$$\bar{\lambda}_{2,11} = \int_0^1 \left(\frac{\mathrm{d}\bar{w}_2}{\mathrm{d}\xi_2}\right)^2 \mathrm{d}\xi_2 = n^2\pi^2 \int_0^1 \cos^2(n\pi\xi_2)\,\mathrm{d}\xi_2 = \frac{n^2\pi^2}{2},$$
$$\bar{\lambda}_{2,02} = \int_0^1 \bar{w}_2 \frac{\mathrm{d}^2\bar{w}_2}{\mathrm{d}\xi_2^2}\,\mathrm{d}\xi_2 = -n^2\pi^2 \int_0^1 \sin^2(n\pi\xi_2)\,\mathrm{d}\xi_2 = -\frac{n^2\pi^2}{2},$$
$$\bar{\lambda}_{2,22} = \int_0^1 \left(\frac{\mathrm{d}^2\bar{w}_2}{\mathrm{d}\xi_2^2}\right)^2 \mathrm{d}\xi_2 = n^4\pi^4 \int_0^1 \sin^2(n\pi\xi_2)\,\mathrm{d}\xi_2 = \frac{n^4\pi^4}{2}. \tag{14.49}$$

This allows the dimensionless buckling load (14.42) to be written after a few arithmetic operations as:

$$\bar{N}^0_{xx} = \frac{m^2}{\alpha^2} + 2\beta n^2 + \frac{\alpha^2 n^4}{m^2}. \tag{14.50}$$

The minimum buckling load occurs for $n = 1$:

$$\bar{N}^0_{xx} = \frac{m^2}{\alpha^2} + 2\beta + \frac{\alpha^2}{m^2}. \tag{14.51}$$

Apparently, this corresponds exactly to the solution already found in Chap. 12. In addition, the dimensionless notation reveals that the generalised Poisson's ratio ζ has no influence on the result of a stability analysis for a laminate that is simply supported at all edges.

14.2.3 Laminate with Clamped Unloaded Edges

Another elementary example is a laminate that is simply supported at the loaded edges, while the unloaded edges are clamped (Fig. 14.3).

The boundary conditions can currently be described as follows:

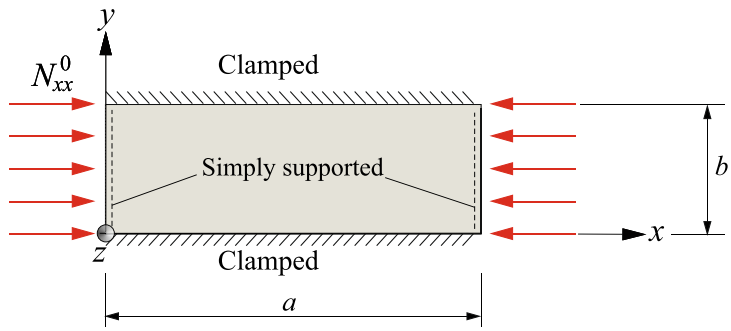


Fig. 14.3 Laminate under uniaxial compressive load with simply supported loaded edges and clamped unloaded edges

$$w_0\,(x=0)=0,\quad w_0\,(x=a)=0,\quad w_0\,(y=0)=0,\quad w_0\,(y=b)=0,$$
$$M^0_{xx}\,(x=0)=-D_{11}\left.\frac{\partial^2 w_0}{\partial x^2}\right|_{x=0}=0,\quad M^0_{xx}\,(x=a)=-D_{11}\left.\frac{\partial^2 w_0}{\partial x^2}\right|_{x=a}=0,$$
$$\left.\frac{\partial w_0}{\partial y}\right|_{y=0}=0,\quad \left.\frac{\partial w_0}{\partial y}\right|_{y=b}=0. \tag{14.52}$$

A suitable approach for the buckling shape w_0, which fulfils both the static and dynamic boundary conditions, is as follows:

$$w_0 = W\sin\left(\frac{m\pi x}{a}\right)\left\{\frac{1}{2}\left[1-\cos\left(\frac{2\pi y}{b}\right)\right]\right\}. \tag{14.53}$$

The integral formulations (14.31) can be taken directly from (14.45) with regard to the shape function w_1. The remaining expressions can be written as follows:

$$\lambda_{y,00}=\int_0^b w_2^2\mathrm{d}y=\frac{1}{4}\int_0^b\left[1-\cos\left(\frac{2\pi y}{b}\right)\right]^2\mathrm{d}y=\frac{3}{8}b,$$
$$\lambda_{y,11}=\int_0^b\left(\frac{\mathrm{d}w_2}{\mathrm{d}y}\right)^2\mathrm{d}y=\frac{\pi^2}{b^2}\int_0^b\sin^2\left(\frac{2\pi y}{b}\right)\mathrm{d}y=\frac{\pi^2}{2b},$$
$$\lambda_{y,02}=\int_0^b w_2\frac{\mathrm{d}^2w_2}{\mathrm{d}y^2}\mathrm{d}y=\frac{\pi^2}{b^2}\int_0^b\left[1-\cos\left(\frac{2\pi y}{b}\right)\right]\cos\left(\frac{2\pi y}{b}\right)\mathrm{d}y=-\frac{\pi^2}{2b},$$
$$\lambda_{y,22}=\int_0^b\frac{\mathrm{d}^2w_2}{\mathrm{d}y^2}\frac{\mathrm{d}^2w_2}{\mathrm{d}y^2}\mathrm{d}y=\frac{4\pi^4}{b^4}\int_0^b\cos^2\left(\frac{2\pi y}{b}\right)\mathrm{d}y=\frac{2\pi^4}{b^3}. \tag{14.54}$$

This means that the buckling load for this laminate situation can be written as:

$$N^0_{xx}=\pi^2\left[D_{11}\frac{m^2}{a^2}+\frac{16}{3}D_{22}\frac{a^2}{b^4m^2}+\frac{8}{3b^2}\left(D_{12}+2D_{66}\right)\right]. \tag{14.55}$$

The half-wave number m relevant for this laminate can again be determined from the extreme value task $\frac{\partial N^0_{xx}}{\partial m}=0$ and results as:

$$m=\frac{2}{\sqrt{3}}\frac{a}{b}\sqrt[4]{3\frac{D_{22}}{D_{11}}}. \tag{14.56}$$

In the present case, the resulting buckling load also converges towards an asymptotic limit value if a sufficiently long laminate with $a\to\infty$ is considered. This limit value can be determined by substituting the half-wave number m according to (14.56) into the buckling load (14.55). The result is obtained:

$$N^0_{xx}=\frac{8\pi^2}{3b^2}\left(\sqrt{3D_{11}D_{22}}+D_{12}+2D_{66}\right). \tag{14.57}$$

Table 14.1 Influence of edge restraints on the buckling loads of laminates for different values of Seydel's orthotropy factor β

	$\beta = 0.0$	$\beta = 0.5$	$\beta = 1.0$	$\beta = 1.5$	$\beta = 2.0$	$\beta = 2.5$	$\beta = 3.0$
ψ	0.43	0.57	0.54	0.47	0.39	0.33	0.28

The following approach is used in dimensionless notation:

$$\bar{w}_0 = W \sin(m\pi\xi_1) \left\{ \frac{1}{2} [1 - \cos(2\pi\xi_2)] \right\}. \tag{14.58}$$

Inserting this approach into the total potential (14.38) and evaluating the expression (14.42) then results in the following dimensionless buckling load:

$$\bar{N}^0_{xx} = \frac{m^2}{\alpha^2} + \frac{16}{3}\frac{\alpha^2}{m^2} + \frac{8}{3}\beta^2, \tag{14.59}$$

where the relevant half-wave number m can be written as follows:

$$m = \frac{2}{\sqrt[4]{3}}\alpha. \tag{14.60}$$

The asymptotic limit value of the buckling load for $\alpha \to \infty$ follows in this notation as:

$$\bar{N}^0_{xx} = \frac{8}{3}\left(\sqrt{3} + \beta^2\right). \tag{14.61}$$

The influence of the edge restraint can be discussed quite simply by comparing the two asymptotic limit values for the buckling loads of the laminate simply supported at all edges and the laminate with clamped unloaded edges. If the two buckling loads are compared with each other, the result is ('ss' stands for 'simply supported', i.e. simply supported unloaded edges, while 'cc' denotes the term 'clamped', i.e. clamped unloaded edges):

$$\psi = \frac{\bar{N}^0_{xx,\mathrm{ss}}}{\bar{N}^0_{xx,\mathrm{cc}}} = \frac{3}{4}\frac{\beta + 1}{\beta^2 + \sqrt{3}}. \tag{14.62}$$

If we evaluate this expression ψ for typical values of the Seydel orthotropy factor β, we obtain the numerical values in Table 14.1. It can be seen that, depending on the specific numerical value for β, a clamped edge ensures approximately a doubling of the buckling load compared to an identical laminate that is simply supported at all four edges. In this respect, this elementary example reveals that the correct consideration of the given boundary conditions in the idealization and analysis of a laminate structure is of great importance and has a massive influence on a stability analysis.

14.2.4 Laminate with Elastically Restrained Unloaded Edges

We now consider a laminate according to Fig. 14.4.

The laminate is elastically restrained at the unloaded edges (restraint stiffness k). The boundary conditions for the current situation are as follows:

$$w_0\,(x=0)=0,\quad w_0\,(x=a)=0,\quad w_0\,(y=0)=0,\quad w_0\,(y=b)=0,$$

$$M^0_{xx}\,(x=0)=-D_{11}\left.\frac{\partial^2 w_0}{\partial x^2}\right|_{x=0}=0,\quad M^0_{xx}\,(x=a)=-D_{11}\left.\frac{\partial^2 w_0}{\partial x^2}\right|_{x=a}=0,$$

$$M^0_{yy}\,(y=0)=-D_{22}\left.\frac{\partial^2 w_0}{\partial y^2}\right|_{y=0}+k\left.\frac{\partial w_0}{\partial y}\right|_{y=0}=0,$$

$$M^0_{yy}\,(y=b)=-D_{22}\left.\frac{\partial^2 w_0}{\partial y^2}\right|_{y=b}-k\left.\frac{\partial w_0}{\partial y}\right|_{y=b}=0. \tag{14.63}$$

In order to be able to solve this buckling problem in the manner of a Rayleigh quotient, the total elastic potential $\Pi=\Pi_i+\Pi_a+\Pi_s$ of the buckled laminate must be extended by the energy Π_s that is stored in the elastic restraints:

$$\Pi_i=\frac{1}{2}\int_0^a\int_0^b\left[D_{11}\left(\frac{\partial^2 w_0}{\partial x^2}\right)^2+D_{22}\left(\frac{\partial^2 w_0}{\partial y^2}\right)^2\right.$$

$$\left.+\;2D_{12}\frac{\partial^2 w_0}{\partial x^2}\frac{\partial^2 w_0}{\partial y^2}+4D_{66}\left(\frac{\partial^2 w_0}{\partial x\partial y}\right)^2\right]\mathrm{d}y\mathrm{d}x,$$

$$\Pi_a=-\frac{N^0_{xx}}{2}\int_0^a\int_0^b\left(\frac{\partial w_0}{\partial x}\right)^2\mathrm{d}y\mathrm{d}x,$$

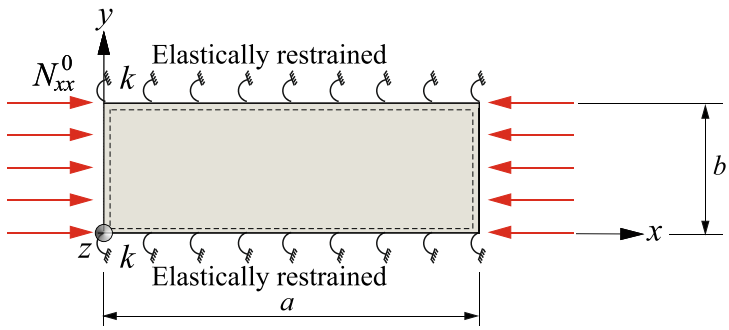


Fig. 14.4 Laminate under uniaxial compressive load with simply supported loaded edges and elastically restrained unloaded edges

$$\Pi_s = \frac{k}{2}\int_0^a \left[\left(\left.\frac{\partial w_0}{\partial y}\right|_{y=0} \right)^2 + \left(\left.\frac{\partial w_0}{\partial y}\right|_{y=b} \right)^2 \right] \mathrm{d}x. \tag{14.64}$$

Currently, a general approach for the buckling mode is chosen as follows:

$$w_0 = W w_1(x)\, w_2(y). \tag{14.65}$$

If this approach is used in the energy formulations (14.64), the result is

$$\begin{aligned}\Pi = {} & \frac{D_{11}}{2}W^2 \int_0^a \left(\frac{\mathrm{d}^2 w_1}{\mathrm{d}x^2}\right)^2 \mathrm{d}x \int_0^b w_2^2 \mathrm{d}y + \frac{D_{22}}{2}W^2 \int_0^a w_1^2 \mathrm{d}x \int_0^b \left(\frac{\mathrm{d}^2 w_2}{\mathrm{d}y^2}\right)^2 \mathrm{d}y \\ & + D_{12}W^2 \int_0^a \frac{\mathrm{d}^2 w_1}{\mathrm{d}x^2} w_1 \mathrm{d}x \int_0^b \frac{\mathrm{d}^2 w_2}{\mathrm{d}y^2} w_2 \mathrm{d}y + 2D_{66}W^2 \int_0^a \left(\frac{\mathrm{d}w_1}{\mathrm{d}x}\right)^2 \mathrm{d}x \int_0^b \left(\frac{\mathrm{d}w_2}{\mathrm{d}y}\right)^2 \mathrm{d}y \\ & - \frac{N_{xx}^0}{2}W^2 \int_0^a \left(\frac{\mathrm{d}w_1}{\mathrm{d}x}\right)^2 \mathrm{d}x \int_0^b w_2^2 \mathrm{d}y \\ & + \frac{k}{2}W^2 \int_0^a w_1^2 \mathrm{d}x \left[\left(\left.\frac{\mathrm{d}w_2}{\mathrm{d}y}\right|_{y=0} \right)^2 + \left(\left.\frac{\mathrm{d}w_2}{\mathrm{d}y}\right|_{y=b} \right)^2 \right]. \end{aligned} \tag{14.66}$$

With the abbreviations

$$\lambda_1 = \frac{k}{2}\left(\left.\frac{\mathrm{d}w_2}{\mathrm{d}y}\right|_{y=0} \right)^2, \quad \lambda_2 = \frac{k}{2}\left(\left.\frac{\mathrm{d}w_2}{\mathrm{d}y}\right|_{y=b} \right)^2, \tag{14.67}$$

after applying the buckling criterion $\frac{\partial \Pi}{\partial W} = 0$ the following expression for the buckling load is obtained:

$$N_{xx}^0 = \frac{D_{11}\lambda_{x,22}\lambda_{y,00} + D_{22}\lambda_{x,00}\lambda_{y,22} + 2D_{12}\lambda_{x,02}\lambda_{y,02} + 4D_{66}\lambda_{x,11}\lambda_{y,11} + 2\lambda_{x,00}(\lambda_1 + \lambda_2)}{\lambda_{x,11}\lambda_{y,00}}. \tag{14.68}$$

Since the current laminate situation assumes simply supported loaded edges at $x = 0$ and $x = a$, the following choice can be made for w_1, as with the solutions already discussed:

$$w_1 = \sin\left(\frac{m\pi x}{a}\right). \tag{14.69}$$

The shape function w_2 in the y-direction has to fulfil two requirements. Firstly, for the limiting case $k = 0$, it must contain the buckling function according to the Navier solution for the laminate simply supported at all edges. On the other hand, the shape function w_2 must be able to represent a rigid clamping of the unloaded edges for very high values of

the restraint stiffness $k \to \infty$. Against this background, the following choice for the shape function w_2 is appropriate:

$$w_2(x_2) = (1 - \Psi)\, w_2^{ss}(x_2) + \Psi w_2^{cc}(x_2)\,, \tag{14.70}$$

where the as yet unknown factor Ψ is used to interpolate between the functions w_2^{ss} (shape function for a laminate with simply supported unloaded edges) and w_2^{cc} (shape function for a laminate with clamped unloaded edges). It is obvious to use the functions already used in the previous subsections for the laminate that is simply supported at all edges and the laminate with clamped unloaded edges:

$$w_2^{ss}(y) = \sin\left(\frac{\pi y}{b}\right), \quad w_2^{cc}(y) = \frac{1}{2}\left[1 - \cos\left(\frac{2\pi y}{b}\right)\right]. \tag{14.71}$$

The approximated buckling mode can therefore be written as:

$$w_0 = W \sin\left(\frac{m\pi x}{a}\right)\left\{(1 - \Psi)\sin\left(\frac{\pi y}{b}\right) + \frac{\Psi}{2}\left[1 - \cos\left(\frac{2\pi y}{b}\right)\right]\right\}. \tag{14.72}$$

The unknown interpolation factor Ψ is determined from the moment boundary conditions for $y = 0$ and $y = b$ in (14.63). Evaluating the two conditions leads to the same result in both cases:

$$\Psi = \frac{kb}{kb + 2D_{22}\pi}. \tag{14.73}$$

It can be seen that the value $\Psi = 0$ results in the case of a vanishing restraint stiffness $k = 0$. For a rigid clamping with $k \to \infty$ we obtain $\Psi \to 1$. The approach thus ensures a physically meaningful interpolation between the two limit cases.

The integral formulations (14.31) with regard to the shape function w_1 can again be taken directly from (14.45). The remaining expressions are currently as follows:

$$\begin{aligned}
\lambda_{y,00} &= \int_0^b w_2^2 \mathrm{d}y = \frac{b\left(48D_{22}^2\pi^2 + 128kbD_{22} + 9k^2b^2\right)}{24\left(kb + 2D_{22}\pi\right)^2},\\
\lambda_{y,02} &= \int_0^b w_2 \frac{\mathrm{d}^2 w_2}{\mathrm{d}y^2}\mathrm{d}y = -\frac{\pi^2\left(12D_{22}^2\pi^2 + 32kbD_{22} + 3k^2b^2\right)}{6b\left(kb + 2D_{22}\pi\right)^2},\\
\lambda_{y,11} &= \int_0^b \left(\frac{\mathrm{d}w_2}{\mathrm{d}y}\right)^2 \mathrm{d}y = \frac{\pi^2\left(12D_{22}^2\pi^2 + 32kbD_{22} + 3k^2b^2\right)}{6b\left(kb + 2D_{22}\pi\right)^2},\\
\lambda_{y,22} &= \int_0^b \left(\frac{\mathrm{d}^2 w_2}{\mathrm{d}y^2}\right)^2 \mathrm{d}y = \frac{2\pi^4\left(3D_{22}^2\pi^2 + 8kbD_{22} + 3k^2b^2\right)}{3b^3\left(kb + 2D_{22}\pi\right)^2}.
\end{aligned} \tag{14.74}$$

For the constants λ_1 and λ_2 one obtains

$$\lambda_1 = \lambda_2 = \frac{2kD_{22}^2\pi^4}{b^2\left(2D_{22}\pi + kb\right)^2}. \tag{14.75}$$

The half-wave number m can be determined from the extreme value problem $\frac{\partial N_{xx}^0}{\partial m} = 0$ and results as:

$$m = \frac{2a}{b}\sqrt[4]{\frac{D_{22}}{D_{11}}\left(\frac{3D_{22}^2\pi^2 + 20kbD_{22} + 3k^2b^2}{48D_{22}^2\pi^2 + 128kbD_{22} + 9k^2b^2}\right)}. \tag{14.76}$$

It is of fundamental interest to consider the buckling behaviour of a sufficiently long or theoretically infinitely long laminate. Inserting the half-wave number m into the buckling load according to (14.68) results in:

$$N_{xx}^0 = \frac{8\pi^2}{b^2}\left(\sqrt{\frac{\tau_1}{\tau_2}D_{11}D_{22}} + \frac{\tau_3}{\tau_2}\left(D_{12} + 2D_{66}\right)\right), \tag{14.77}$$

wherein:

$$\begin{aligned}
\tau_1 &= 3D_{22}^2\pi^2 + 20kbD_{22} + 3k^2b^2,\\
\tau_2 &= 48D_{22}^2\pi^2 + 128kbD_{22} + 9k^2b^2,\\
\tau_3 &= 12D_{22}^2\pi^2 + 32kbD_{22} + 3k^2b^2.
\end{aligned} \tag{14.78}$$

The use of a dimensionless representation will also be briefly demonstrated for this example. The total elastic potential of the buckled laminate can be written as:

$$\begin{aligned}
\bar{\Pi} = \frac{1}{2}\int_0^1\int_0^1 \Bigg[&\frac{1}{\alpha^2}\left(\frac{\partial^2\bar{w}_0}{\partial\xi_1^2}\right)^2 + \alpha^2\left(\frac{\partial^2\bar{w}_0}{\partial\xi_2^2}\right)^2\\
&+ 2\beta\zeta\frac{\partial^2\bar{w}_0}{\partial\xi_1^2}\frac{\partial^2\bar{w}_0}{\partial\xi_2^2} + 2\left(1-\zeta\right)\beta\left(\frac{\partial^2\bar{w}_0}{\partial\xi_1\partial\xi_2}\right)^2\Bigg]\mathrm{d}\xi_2\mathrm{d}\xi_1\\
&- \frac{1}{2}\pi^2\int_0^1\int_0^1 \bar{N}_{xx}^0\left(\frac{\partial\bar{w}_0}{\partial\xi_1}\right)^2\mathrm{d}\xi_2\mathrm{d}\xi_1 + \frac{1}{2}\bar{k}\alpha^2\int_0^1\left[\left(\frac{\partial\bar{w}_0}{\partial\xi_2}\Big|_{\xi_2=0}\right)^2 + \left(\frac{\partial\bar{w}_0}{\partial\xi_2}\Big|_{\xi_2=1}\right)^2\right]\mathrm{d}\xi_1.
\end{aligned} \tag{14.79}$$

Therein,

$$\bar{k} = \frac{kb}{D_{22}} \tag{14.80}$$

is the dimensionless restraint stiffness. The buckling mode can be described as:

$$\bar{w}_0 = \bar{W}\sin\left(m\pi\xi_1\right)\left\{\left(1-\Psi\right)\sin\left(\pi\xi_2\right) + \frac{\Psi}{2}\left[1-\cos\left(2\pi\xi_2\right)\right]\right\}. \tag{14.81}$$

The boundary conditions are currently in dimensionless form:

$$\bar{w}_0(\xi_1 = 0) = 0, \quad \bar{w}_0(\xi_1 = 1) = 0, \quad \bar{w}_0(\xi_2 = 0) = 0, \quad \bar{w}_0(\xi_2 = 1) = 0,$$

$$\left.\frac{\partial^2 \bar{w}_0}{\partial \xi_1^2}\right|_{\xi_1=0} = 0, \quad \left.\frac{\partial^2 \bar{w}_0}{\partial \xi_1^2}\right|_{\xi_1=1} = 0,$$

$$\left.\frac{\partial^2 \bar{w}_0}{\partial \xi_2^2}\right|_{\xi_2=0} - \bar{k}\left.\frac{\partial \bar{w}_0}{\partial \xi_2}\right|_{\xi_2=0} = 0, \quad \left.\frac{\partial^2 \bar{w}_0}{\partial \xi_2^2}\right|_{\xi_2=1} + \bar{k}\left.\frac{\partial \bar{w}_0}{\partial \xi_2}\right|_{\xi_2=1} = 0. \tag{14.82}$$

Evaluating the moment boundary conditions at the unloaded edges results in the following expression for the interpolation factor Ψ in dimensionless notation:

$$\Psi = \frac{\bar{k}}{\bar{k} + 2\pi}. \tag{14.83}$$

Applying the buckling criterion $\frac{\partial \bar{\Pi}}{\partial W} = 0$ results in the following formulation for the buckling load of the infinitely long laminate after a few transformations:

$$\bar{N}_{xx}^0 = 8\pi^2 \left(\sqrt{\frac{3\pi^2 + 20\bar{k} + 3\bar{k}^2}{48\pi^2 + 128\bar{k} + 9\bar{k}^2}} + \frac{12\pi^2 + 32\bar{k} + 3\bar{k}^2}{48\pi^2 + 128\bar{k} + 9\bar{k}^2}\beta \right). \tag{14.84}$$

An alternative formulation for the buckling mode of an elastically restrained plate was proposed by Qiao and Shan (2005) in the form of a fourth-order polynomial in the y-direction:

$$w_0 = W \sin\left(\frac{m\pi x}{a}\right)\left[\frac{y}{b} + \psi_1\left(\frac{y}{b}\right)^2 + \psi_2\left(\frac{y}{b}\right)^3 + \psi_3\left(\frac{y}{b}\right)^4\right]. \tag{14.85}$$

The free constants ψ_1, ψ_2, and ψ_3 are determined from the boundary conditions (14.63) at the unloaded edges and ultimately result as:

$$\psi_1 = \frac{kb}{2D_{22}}, \quad \psi_2 = -\frac{kb + 2D_{22}}{D_{22}}, \quad \psi_3 = \frac{kb + 2D_{22}}{2D_{22}}. \tag{14.86}$$

The corresponding integral expressions in (14.31) can then be written as:

$$\lambda_{y,00} = \int_0^b w_2^2 \mathrm{d}y = \frac{b\left(124D_{22}^2 + 22D_{22}kb + k^2b^2\right)}{2520D_{22}^2},$$

$$\lambda_{y,02} = \int_0^b w_2 \frac{\mathrm{d}^2 w_2}{\mathrm{d}y^2}\mathrm{d}y = -\frac{102D_{22}^2 + 18D_{22}kb + k^2b^2}{210D_{22}^2 b},$$

$$\lambda_{y,11} = \int_0^b \left(\frac{\mathrm{d}w_2}{\mathrm{d}y}\right)^2 \mathrm{d}y = \frac{102D_{22}^2 + 18D_{22}kb + k^2b^2}{210D_{22}^2 b},$$

$$\lambda_{y,22} = \int_0^b \left(\frac{\mathrm{d}^2 w_2}{\mathrm{d}y^2}\right)^2 \mathrm{d}y = \frac{24D_{22}^2 + 4D_{22}kb + k^2b^2}{5D_{22}^2 b^3}. \tag{14.87}$$

The constants λ_1 and λ_2 are calculated as follows:

$$\lambda_1 = \lambda_2 = \frac{k}{2b^2}. \tag{14.88}$$

The buckling load N_{xx}^0 can then be calculated again from Eq. (14.68).

The reliability of both formulations presented here for the buckling modes and the resulting buckling loads was documented, for example, by Qiao and Shan (2005) or Mittelstedt and Beerhorst (2009) on the basis of various technical applications.

14.2.5 Laminate with Three Simply Supported Edges and One Free Unloaded Edge

The next laminate buckling problem is a laminate according to Fig. 14.5.

An approach for the buckling shape according to the following type (see Qiao and Shan 2005) is used:

$$w_0 = W \sin\left(\frac{m\pi x}{a}\right)\left[\frac{y}{b} + \psi_1\left(\frac{y}{b}\right)^2 + \psi_2\left(\frac{y}{b}\right)^3 + \psi_3\left(\frac{y}{b}\right)^4\right]. \tag{14.89}$$

This approach must be adapted to the given boundary conditions at the unloaded edges.

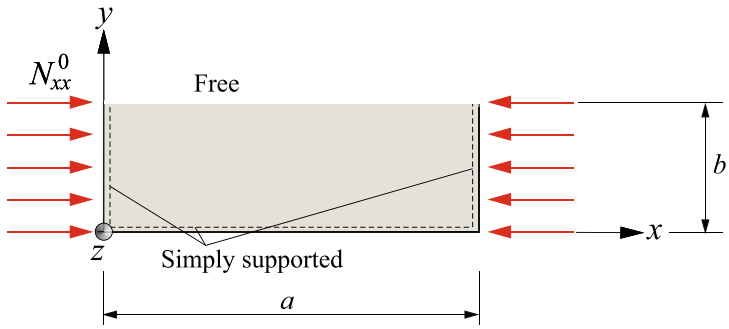


Fig. 14.5 Laminate under uniaxial compressive load with simply supported loaded edges, one simply supported unloaded edge and one free unloaded edge

$$w_0\,(y=0)=0,\quad M^0_{yy}\,(y=0)=-D_{22}\left.\frac{\partial^2 w_0}{\partial y^2}\right|_{y=0}=0,$$

$$M^0_{yy}\,(y=b)=-D_{12}\left.\frac{\partial^2 w_0}{\partial x^2}\right|_{y=b}-D_{22}\left.\frac{\partial^2 w_0}{\partial y^2}\right|_{y=b}=0,$$

$$\bar{Q}_y\,(y=b)=2\left.\frac{\partial M^0_{xy}}{\partial x}\right|_{y=b}+\left.\frac{\partial M^0_{yy}}{\partial y}\right|_{y=b}$$

$$=-D_{22}\left.\frac{\partial^3 w_0}{\partial y^3}\right|_{y=b}-(D_{12}+4D_{66})\left.\frac{\partial^3 w_0}{\partial x^2\partial y}\right|_{y=b}=0. \tag{14.90}$$

It is necessary for the fulfilment of (14.90) that the parameters ψ_1, ψ_2, ψ_3 all disappear, so that the following reduced approach remains:

$$w_0 = W\sin\left(\frac{m\pi x}{a}\right)\frac{y}{b}. \tag{14.91}$$

This shape function assumes that the buckling shape of the laminate in the y-direction can be described by a linear polynomial. Evaluating the Rayleigh quotient (14.36) then leads to the following expression for the buckling load after calculating the integrals

$$\lambda_{y,00}=\int_0^b w_2^2\mathrm{d}y=\int_0^b\frac{y^2}{b^2}\mathrm{d}y=\frac{b}{3},$$

$$\lambda_{y,11}=\int_0^b\left(\frac{\mathrm{d}w_2}{\mathrm{d}y}\right)^2\mathrm{d}y=\frac{1}{b^2}\int_0^b\mathrm{d}y=\frac{1}{b},$$

$$\lambda_{y,02}=\int_0^b w_2\frac{\mathrm{d}^2w_2}{\mathrm{d}y^2}\mathrm{d}y=0,$$

$$\lambda_{y,22}=\int_0^b\frac{\mathrm{d}^2w_2}{\mathrm{d}y^2}\frac{\mathrm{d}^2w_2}{\mathrm{d}y^2}\mathrm{d}y=0, \tag{14.92}$$

so that we obtain:

$$N^0_{xx}=\frac{D_{11}m^2\pi^2}{a^2}+\frac{12D_{66}}{b^2}. \tag{14.93}$$

It is easy to see that the minimum and therefore critical buckling load always occurs for $m=1$, so that the following applies in all cases:

$$N^0_{xx}=\frac{D_{11}\pi^2}{a^2}+\frac{12D_{66}}{b^2}. \tag{14.94}$$

In the case of the infinitely long laminate with $a\to\infty$, the first quotient in (14.94) can be neglected so that:

$$N^0_{xx}=\frac{12D_{66}}{b^2}. \tag{14.95}$$

For this case, the dimensionless representation of the problem will be discussed in a little more detail. The boundary conditions (14.90) with regard to the unloaded edges are obtained as follows:

$$\begin{aligned}
\bar{w}_0\,(\xi_2 = 0) = 0, \quad & \left.\frac{\partial^2 \bar{w}_0}{\partial \xi_2^2}\right|_{\xi_2=0} = 0, \\
\beta\zeta \left.\frac{\partial^2 \bar{w}_0}{\partial \xi_1^2}\right|_{\xi_2=1} + \alpha^2 & \left.\frac{\partial^2 \bar{w}_0}{\partial \xi_2^2}\right|_{\xi_2=1} = 0, \\
(\zeta - 2)\,\beta \left.\frac{\partial^3 \bar{w}_0}{\partial \xi_1^2 \partial \xi_2}\right|_{\xi_2=1} - \alpha^2 & \left.\frac{\partial^3 \bar{w}_0}{\partial \xi_2^3}\right|_{\xi_2=1} = 0.
\end{aligned} \tag{14.96}$$

This illustration shows that in the presence of a free edge, the generalised Poisson's ratio ζ will have an influence on the buckling behaviour in contrast to the plate situations considered so far and must be taken into account accordingly.

In dimensionless notation, the expression (14.94) results as:

$$\bar{N}_{xx}^0 = \frac{1}{\alpha^2} + \frac{6}{\pi^2}\,(1 - \zeta)\,\beta. \tag{14.97}$$

For sufficiently large aspect ratios α, the first quotient in (14.97) is also negligible in this representation, and it remains:

$$\bar{N}_{xx}^0 = \frac{6}{\pi^2}\,(1 - \zeta)\,\beta. \tag{14.98}$$

14.2.6 Laminate with One Clamped and One Free Unloaded Edge

A laminate that has a clamped unloaded edge at $y = 0$ and a free edge at $y = b$ is shown in Fig. 14.6.

The boundary conditions for the unloaded edges are as follows:

$$\begin{aligned}
w_0\,(y = 0) = 0, \quad & \left.\frac{\partial w_0}{\partial y}\right|_{y=0} = 0, \\
M_{yy}^0\,(y = b) = -D_{12} & \left.\frac{\partial^2 w_0}{\partial x^2}\right|_{y=b} - D_{22} \left.\frac{\partial^2 w_0}{\partial y^2}\right|_{y=b} = 0, \\
\bar{Q}_y\,(y = b) = 2 & \left.\frac{\partial M_{xy}^0}{\partial x}\right|_{y=b} + \left.\frac{\partial M_{yy}^0}{\partial y}\right|_{y=b} \\
= -D_{22} & \left.\frac{\partial^3 w_0}{\partial y^3}\right|_{y=b} - (D_{12} + 4D_{66}) \left.\frac{\partial^3 w_0}{\partial x^2 \partial y}\right|_{y=b} = 0.
\end{aligned} \tag{14.99}$$

An approach for the buckling shape is chosen in the following form:

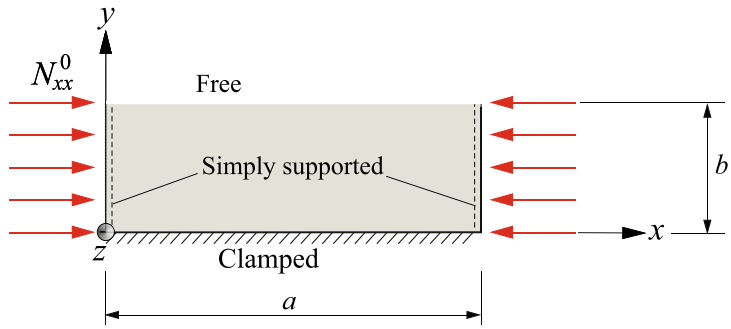


Fig. 14.6 Laminate under uniaxial compressive load with simply supported loaded edges, a clamped unloaded edge and a free unloaded edge

$$w_0 = W \sin\left(\frac{m\pi x}{a}\right)\left[\frac{3}{2}\left(\frac{y}{b}\right)^2 - \frac{1}{2}\left(\frac{y}{b}\right)^3\right]. \tag{14.100}$$

It should be noted that although this approach fulfils the first two conditions in (14.99) identically, it is only able to fulfil the boundary conditions at the free boundary at $y = b$ to the extent that the condition $\frac{\partial^2 w_0}{\partial y^2}\Big|_{y=b} = 0$ is satisfied. The integral expressions (14.31) with regard to the y-direction are obtained as follows:

$$\begin{aligned}
\lambda_{y,00} &= \int_0^b w_2^2 \mathrm{d}y = \int_0^b \left[\frac{3}{2}\left(\frac{y}{b}\right)^2 - \frac{1}{2}\left(\frac{y}{b}\right)^3\right]^2 \mathrm{d}y = \frac{33b}{140}, \\
\lambda_{y,11} &= \int_0^b \left(\frac{\mathrm{d}w_2}{\mathrm{d}y}\right)^2 \mathrm{d}y = \int_0^b \left[\frac{3y}{b^2} - \frac{3y^2}{2b^3}\right]^2 \mathrm{d}y = \frac{6}{5b}, \\
\lambda_{y,02} &= \int_0^b w_2 \frac{\mathrm{d}^2 w_2}{\mathrm{d}y^2} \mathrm{d}y = \int_0^b \left[\frac{3}{2}\left(\frac{y}{b}\right)^2 - \frac{1}{2}\left(\frac{y}{b}\right)^3\right]\left[\frac{3}{b^2} - \frac{3y}{b^3}\right] \mathrm{d}y = \frac{3}{10b}, \\
\lambda_{y,22} &= \int_0^b \frac{\mathrm{d}^2 w_2}{\mathrm{d}y^2} \frac{\mathrm{d}^2 w_2}{\mathrm{d}y^2} \mathrm{d}y = \int_0^b \left[\frac{3}{b^2} - \frac{3y}{b^3}\right]^2 \mathrm{d}y = \frac{3}{b^3},
\end{aligned} \tag{14.101}$$

and the Rayleigh quotient (14.36) then results in the following solution for the buckling load:

$$N_{xx}^0 = D_{11}\frac{m^2\pi^2}{a^2} + \frac{140}{11} D_{22} \frac{a^2}{m^2\pi^2 b^4} - \frac{28}{11b^2}\left(D_{12} - 8D_{66}\right). \tag{14.102}$$

The relevant half-wave number again results from the extreme value task $\frac{\partial N_{xx}^0}{\partial m} = 0$ and can be written as:

$$m = \frac{1}{\pi}\sqrt{\frac{2}{11}}\sqrt[4]{385\frac{D_{22}}{D_{11}}}\frac{a}{b}. \tag{14.103}$$

The asymptotic limit value of the buckling load can be specified as follows if the length a is sufficiently large:

$$N_{xx}^{0} = \frac{4}{11b^2}\left[\sqrt{385 D_{11} D_{22}} - 7\left(D_{12} - 8D_{66}\right)\right]. \tag{14.104}$$

In dimensionless representation, the approach (14.100) is:

$$\bar{w}_0 = W \sin\left(m\pi\xi_1\right)\left[\frac{3}{2}\xi_2^2 - \frac{1}{2}\xi_2^3\right]. \tag{14.105}$$

The buckling load can be written as:

$$\bar{N}_{xx}^{0} = \frac{m^2}{\alpha^2} + \frac{140}{11}\frac{\alpha^2}{m^2\pi^4} + \frac{28}{11\pi^2}\left(4 - 5\zeta\right)\beta. \tag{14.106}$$

The relevant half-wave number can be determined as:

$$m = \sqrt{\frac{2}{11}}\sqrt[4]{385}\frac{\alpha}{\pi}, \tag{14.107}$$

and thus the asymptotic limit value of the buckling load for $\alpha \to \infty$ can be determined as:

$$\bar{N}_{xx}^{0} = \frac{4}{11\pi^2}\left[\sqrt{385} + 7\left(4 - 5\zeta\right)\beta\right]. \tag{14.108}$$

14.2.7 Laminate with One Elastically Restrained and One Free Unloaded Edge

Another laminate buckling problem is the situation shown in Fig. 14.7. The laminate has an elastically restrained unloaded edge and a free unloaded edge.

The boundary conditions at the unloaded edges are as follows for the laminate situation considered here:

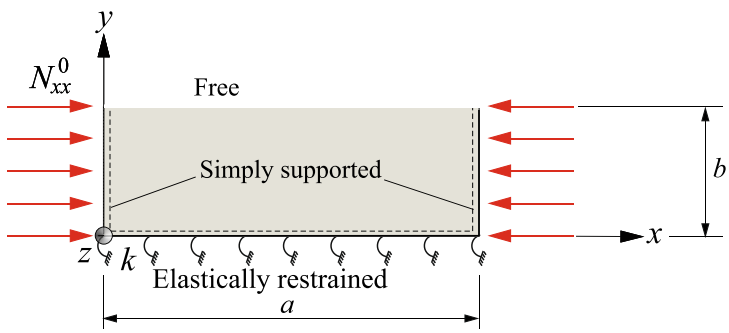


Fig. 14.7 Laminate under uniaxial compressive load with simply supported loaded edges, an elastically restrained unloaded edge and a free unloaded edge

$$w_0\,(y=0)=0,\quad M^0_{yy}\,(y=0)=-D_{22}\left.\frac{\partial^2 w_0}{\partial y^2}\right|_{y=0}=-k\left.\frac{\partial w_0}{\partial y}\right|_{y=0},$$

$$M^0_{yy}\,(y=b)=-D_{12}\left.\frac{\partial^2 w_0}{\partial x^2}\right|_{y=b}-D_{22}\left.\frac{\partial^2 w_0}{\partial y^2}\right|_{y=b}=0,$$

$$\bar{Q}_y\,(y=b)=2\left.\frac{\partial M^0_{xy}}{\partial x}\right|_{y=b}+\left.\frac{\partial M^0_{yy}}{\partial y}\right|_{y=b}$$

$$=-D_{22}\left.\frac{\partial^3 w_0}{\partial y^3}\right|_{y=b}-(D_{12}+4D_{66})\left.\frac{\partial^3 w_0}{\partial x^2\partial y}\right|_{y=b}=0. \tag{14.109}$$

An approach for the buckling mode is used as follows:

$$w_0=W\sin\left(\frac{m\pi x}{a}\right)\left[\frac{y}{b}+\psi_1\left(\frac{y}{b}\right)^2+\psi_2\left(\frac{y}{b}\right)^3+\psi_3\left(\frac{y}{b}\right)^4\right]. \tag{14.110}$$

An adequate representation of the solution is achieved by requiring that at least the vanishing of the partial derivative $\left.\frac{\partial^2 w_0}{\partial y^2}\right|_{y=b}$ is ensured. Then we obtain for ψ_1, ψ_2, ψ_3 (see Mittelstedt 2007a, b):

$$\psi_1=\frac{kb}{2D_{22}},\quad \psi_2=-\frac{kb}{3D_{22}},\quad \psi_3=\frac{kb}{12D_{22}}. \tag{14.111}$$

The energy formulation for the laminate must be extended accordingly to include the contribution by the elastic restraints:

$$\Pi_i=\frac{1}{2}\int_0^a\int_0^b\left[D_{11}\left(\frac{\partial^2 w_0}{\partial x^2}\right)^2+D_{22}\left(\frac{\partial^2 w_0}{\partial y^2}\right)^2\right.$$

$$\left.+\;2D_{12}\frac{\partial^2 w_0}{\partial x^2}\frac{\partial^2 w_0}{\partial y^2}+4D_{66}\left(\frac{\partial^2 w_0}{\partial x\partial y}\right)^2\right]\mathrm{d}y\mathrm{d}x,$$

$$\Pi_a=-\frac{N^0_{xx}}{2}\int_0^a\int_0^b\left(\frac{\partial w_0}{\partial x}\right)^2\mathrm{d}y\mathrm{d}x,\quad \Pi_s=\frac{k}{2}\int_0^a\left(\left.\frac{\partial w_0}{\partial y}\right|_{y=0}\right)^2\mathrm{d}x. \tag{14.112}$$

The corresponding Rayleigh quotient can then be specified for this buckling situation as:

$$N^0_{xx}=\frac{D_{11}\lambda_{x,22}\lambda_{y,00}+D_{22}\lambda_{x,00}\lambda_{y,22}+2D_{12}\lambda_{x,02}\lambda_{y,02}+4D_{66}\lambda_{x,11}\lambda_{y,11}+2\lambda_{x,00}\lambda_1}{\lambda_{x,11}\lambda_{y,00}}, \tag{14.113}$$

where the integral expressions (14.31) can be calculated with respect to the y-direction as:

$$\lambda_{y,00} = \int_0^b w_2^2 \mathrm{d}y = \int_0^b \left[\frac{y}{b} + \psi_1 \left(\frac{y}{b}\right)^2 + \psi_2 \left(\frac{y}{b}\right)^3 + \psi_3 \left(\frac{y}{b}\right)^4\right]^2 \mathrm{d}y$$
$$= \frac{b}{3}\left[1 + \frac{13kb}{30D_{22}}\left(1 + \frac{kb}{9D_{22}}\right)\right],$$
$$\lambda_{y,11} = \int_0^b \left(\frac{\mathrm{d}w_2}{\mathrm{d}y}\right)^2 \mathrm{d}y = \int_0^b \left[\frac{1}{b} + 2\psi_1 \frac{y}{b^2} + 3\psi_2 \frac{y^2}{b^3} + 4\psi_3 \frac{y^3}{b^4}\right]^2 \mathrm{d}y$$
$$= \frac{1}{b} + \frac{k}{2D_{22}}\left(1 + \frac{kb}{7D_{22}}\right),$$
$$\lambda_{y,02} = \int_0^b w_2 \frac{\mathrm{d}^2 w_2}{\mathrm{d}y^2}\mathrm{d}y$$
$$= \int_0^b \left[\frac{y}{b} + \psi_1 \left(\frac{y}{b}\right)^2 + \psi_2 \left(\frac{y}{b}\right)^3 + \psi_3 \left(\frac{y}{b}\right)^4\right]\left[\frac{2\psi_1}{b^2} + \frac{6\psi_2 y}{b^3} + \frac{12\psi_3 y^2}{b^4}\right]\mathrm{d}y$$
$$= \frac{k}{12D_{22}}\left(1 + \frac{kb}{7D_{22}}\right),$$
$$\lambda_{y,22} = \int_0^b \frac{\mathrm{d}^2 w_2}{\mathrm{d}y^2}\frac{\mathrm{d}^2 w_2}{\mathrm{d}y^2}\mathrm{d}y = \int_0^b \left[\frac{2\psi_1}{b^2} + \frac{6\psi_2 y}{b^3} + \frac{12\psi_3 y^2}{b^4}\right]^2 \mathrm{d}y = \frac{k^2}{5bD_{22}^2}. \quad (14.114)$$

The expression λ_1 follows as:

$$\lambda_1 = \frac{k}{2b^2}. \quad (14.115)$$

Evaluating the Rayleigh quotient (14.113) results in the following formulation for the buckling load:

$$N_{xx}^0 = D_{11}\frac{m^2\pi^2}{a^2} + \frac{1}{\lambda_{y,00}}\left[\frac{a^2}{m^2\pi^2}\left(D_{22}\lambda_{y,22} + 2\lambda_1\right) - 2\left(D_{12}\lambda_{y,02} - 2D_{66}\lambda_{y,11}\right)\right]. \quad (14.116)$$

The relevant wave number m follows as:

$$m = \frac{a}{\pi}\sqrt[4]{\frac{D_{22}\lambda_{y,22} + 2\lambda_1}{D_{11}\lambda_{y,00}}}, \quad (14.117)$$

which can then be used to write the asymptotic limit value of the buckling load for sufficiently long laminates:

$$N_{xx}^0 = \frac{2}{\lambda_{y,00}}\left[\sqrt{D_{11}\lambda_{y,00}\left(D_{22}\lambda_{y,22} + 2\lambda_1\right)} - D_{12}\lambda_{y,02} + 2D_{66}\lambda_{y,11}\right]. \quad (14.118)$$

In dimensionless notation, the following is obtained for the limit value (14.118):

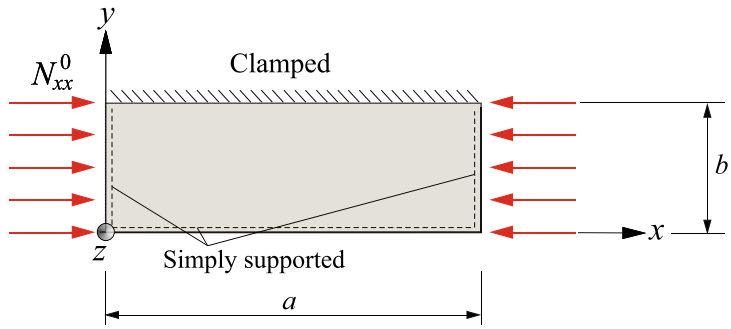


Fig. 14.8 Laminate under uniaxial compressive load with simply supported loaded edges, one simply supported unloaded edge and one clamped unloaded edge

$$\bar{N}_{xx}^0 = \frac{6}{\pi^2}\sqrt{\frac{18\left(\bar{k}+5\right)\bar{k}}{270+13\bar{k}\left(9+\bar{k}\right)}} - \frac{135}{7}\frac{\left[84\left(\zeta-1\right)+\left(7\zeta-6\right)\left(7+\bar{k}\right)\bar{k}\right]}{\pi^2\left(270+117\bar{k}+13\bar{k}^2\right)}\beta. \tag{14.119}$$

14.2.8 Laminate with One Simply Supported and One Clamped Unloaded Edge

We now consider the laminate shown in Fig. 14.8. The boundary conditions at the unloaded edges are currently as follows:

$$\begin{aligned} w_0\left(y=0\right)=0, \quad M_{yy}^0\left(y=0\right) = -D_{22}\left.\frac{\partial^2 w_0}{\partial y^2}\right|_{y=0} &= 0, \\ w_0\left(y=b\right)=0, \quad \left.\frac{\partial w_0}{\partial y}\right|_{y=b} &= 0. \end{aligned} \tag{14.120}$$

If a displacement approach of the type (14.110) is used again and the boundary conditions (14.120) are evaluated, then the free constants in (14.110) result as:

$$\psi_1 = 0, \quad \psi_2 = -3, \quad \psi_3 = 2. \tag{14.121}$$

This gives the approach (14.110) as follows:

$$w_0 = W\sin\left(\frac{m\pi x}{a}\right)\left[\frac{y}{b} - 3\left(\frac{y}{b}\right)^3 + 2\left(\frac{y}{b}\right)^4\right]. \tag{14.122}$$

The buckling load N_{xx}^0 can be written as follows after evaluating the Rayleigh quotient (14.36):

$$N_{xx}^0 = D_{11}\frac{m^2\pi^2}{a^2} + \frac{4536}{19}D_{22}\frac{a^2}{m^2\pi^2 b^4} + \frac{432}{19b^2}\left(D_{12}+2D_{66}\right), \tag{14.123}$$

and the corresponding relevant half-wave number m follows as:

$$m = \frac{3\sqrt{38}}{19\pi}\frac{a}{b}\sqrt[4]{266\frac{D_{22}}{D_{11}}}. \tag{14.124}$$

The asymptotic limit value for N_{xx}^0 for sufficiently long laminates is obtained as:

$$N_{xx}^0 = \frac{36}{19b^2}\left[\sqrt{266D_{11}D_{22}} + 12\left(D_{12}+2D_{66}\right)\right]. \tag{14.125}$$

In dimensionless notation, one obtains:

$$\bar{N}_{xx}^0 = \frac{36}{19\pi^2}\left(\sqrt{266}+12\beta\right). \tag{14.126}$$

14.2.9 Laminate with an Elastically Restrained and a Simply Supported Unloaded Edge

Furthermore, the buckling problem of Fig. 14.9 is considered.

For this situation, the boundary conditions at the unloaded edges can be written as follows:

$$\begin{aligned} &w_0\left(y=0\right)=0, \quad M_{yy}^0\left(y=0\right) = -D_{22}\left.\frac{\partial^2 w_0}{\partial y^2}\right|_{y=0} = -k\left.\frac{\partial w_0}{\partial y}\right|_{y=0}, \\ &w_0\left(y=b\right)=0, \quad M_{yy}^0\left(y=b\right) = -D_{22}\left.\frac{\partial^2 w_0}{\partial y^2}\right|_{y=b} = 0. \end{aligned} \tag{14.127}$$

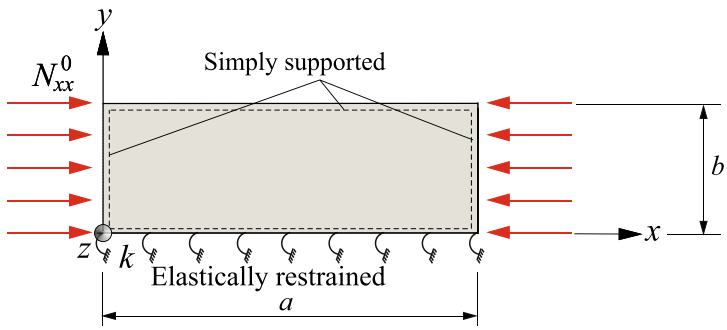


Fig. 14.9 Laminate under uniaxial compressive load with simply supported loaded edges, an elastically restrained unloaded edge and a simply supported unloaded edge

With the help of the displacement approach (14.110) and the free constants resulting from the boundary conditions (14.127)

$$\psi_1 = \frac{kb}{2D_{22}}, \quad \psi_2 = -\frac{5kb + 12D_{22}}{6D_{22}}, \quad \psi_3 = \frac{kb + 3D_{22}}{3D_{22}}, \tag{14.128}$$

after evaluating the potential expressions (14.112), the following formulation for the buckling load is obtained after some elementary transformations:

$$N_{xx}^0 = D_{11}\frac{m^2\pi^2}{a^2} + \frac{432}{b^2\left(19k^2b^2 + 1116D_{22}^2 + 285kbD_{22}\right)} \times \left[\frac{21D_{22}\,(kb + 3D_{22})\,(8D_{22} + kb)\,a^2}{2b^2m^2\pi^2} + \left(51D_{22}^2 + 13kbD_{22} + k^2b^2\right)(D_{12} + 2D_{66})\right]. \tag{14.129}$$

The relevant half-wave number m can be determined as:

$$m = \frac{3\sqrt{2}}{\pi}\frac{a}{b}\sqrt[4]{14\frac{D_{22}}{D_{11}}\frac{k^2b^2 + 24D_{22}^2 + 11kbD_{22}}{19k^2b^2 + 1116D_{22}^2 + 285kbD_{22}}}, \tag{14.130}$$

and thus the asymptotic limit value for the buckling load N_{xx}^0 follows in the case of sufficiently long laminates:

$$N_{xx}^0 = \frac{36}{b^2}\sqrt{14D_{11}D_{22}\frac{(kb + 3D_{22})\,(8D_{22} + kb)}{\left(19k^2b^2 + 1116D_{22}^2 + 285kbD_{22}\right)}} + \frac{432\left(51D_{22}^2 + 13kbD_{22} + k^2b^2\right)}{b^2\left(19k^2b^2 + 1116D_{22}^2 + 285kbD_{22}\right)}(D_{12} + 2D_{66})\,. \tag{14.131}$$

In dimensionless representation, we obtain for (14.131):

$$\bar{N}_{xx}^0 = \frac{36}{\pi^2}\left[\sqrt{\frac{14\left(3 + \bar{k}\right)\left(8 + \bar{k}\right)}{1116 + 285\bar{k} + 19\bar{k}^2}} + \frac{12\left(51 + 13\bar{k} + \bar{k}^2\right)}{1116 + 285\bar{k} + 19\bar{k}^2}\beta\right]. \tag{14.132}$$

14.2.10 Laminate with One Elastically Restrained and One Clamped Unloaded Edge

In the following, the buckling problem according to Fig. 14.10 will be considered.

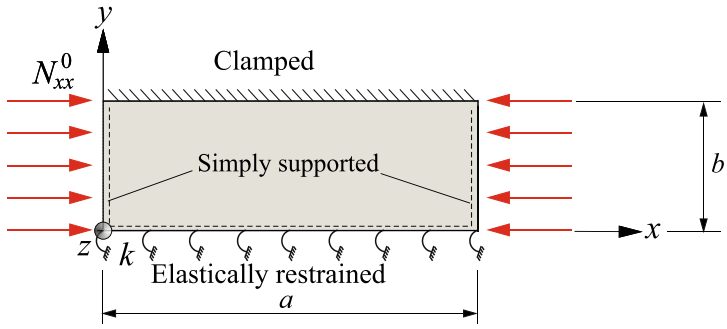


Fig. 14.10 Laminate under uniaxial compressive load with simply supported loaded edges, an elastically restrained unloaded edge and a clamped unloaded edge

In this case, the boundary conditions at the unloaded edges are as follows:

$$w_0\,(y=0)=0, \quad M_{yy}^0\,(y=0)=-D_{22}\left.\frac{\partial^2 w_0}{\partial y^2}\right|_{y=0}=-k\left.\frac{\partial w_0}{\partial y}\right|_{y=0},$$
$$w_0\,(y=b)=0, \quad \left.\frac{\partial w_0}{\partial y}\right|_{y=b}=0. \tag{14.133}$$

If a displacement approach of the form (14.110) is used here as well, then the free constants can be determined for the present case as:

$$\psi_1=\frac{kb}{2D_{22}}, \quad \psi_2=-\frac{kb+3D_{22}}{D_{22}}, \quad \psi_3=\frac{kb+4D_{22}}{2D_{22}}, \tag{14.134}$$

and evaluating the Rayleigh quotient (14.113) results in the following expression for the buckling load:

$$N_{xx}^0=D_{11}\frac{m^2\pi^2}{a^2}+\frac{24}{b^2\left(k^2b^2+76D_{22}^2+17kbD_{22}\right)}$$
$$\times\left[\frac{21D_{22}\,(kb+9D_{22})\,(4D_{22}+kb)\,a^2}{b^2m^2\pi^2}+\left(72D_{22}^2+15kbD_{22}+k^2b^2\right)(D_{12}+2D_{66})\right]. \tag{14.135}$$

The relevant half-wave number m can be determined as follows:

$$m=\frac{\sqrt{6}}{\pi}\frac{a}{b}\sqrt[4]{14\frac{D_{22}}{D_{11}}\frac{k^2b^2+36D_{22}^2+13kbD_{22}}{k^2b^2+76D_{22}^2+17kbD_{22}}}. \tag{14.136}$$

The asymptotic limit value for the buckling load N_{xx}^0 can be written as follows when considering a sufficiently long plate:

$$N_{xx}^0 = \frac{12}{b^2}\sqrt{14D_{11}D_{22}\frac{(kb+4D_{22})\,(9D_{22}+kb)}{\left(k^2b^2+76D_{22}^2+17kbD_{22}\right)}} + \frac{24\left(72D_{22}^2+15kbD_{22}+k^2b^2\right)}{b^2\left(k^2b^2+76D_{22}^2+17kbD_{22}\right)}\left(D_{12}+2D_{66}\right). \tag{14.137}$$

In dimensionless notation, we obtain for (14.137):

$$\bar{N}_{xx}^0 = \frac{12}{\pi^2}\left[\sqrt{\frac{14\left(4+\bar{k}\right)\left(9+\bar{k}\right)}{76+17\bar{k}+\bar{k}^2}} + \frac{2\left(72+15\bar{k}+\bar{k}^2\right)}{76+17\bar{k}+\bar{k}^2}\beta\right]. \tag{14.138}$$

14.3 The Rayleigh Quotient in the Framework of First-Order Shear Deformation Theory

In addition to the determination of approximate solutions for the buckling loads of laminates within the framework of Classical Laminated Plate Theory, it is also of great practical interest to provide approximate solutions within the framework of higher-order laminate theories that are easy to implement in engineering practice. One such approximation solution in the form of a Rayleigh quotient within the framework of First-Order Shear Deformation Theory (FSDT) is briefly described below. A laminate simply supported at all edges under uniaxial compression is considered, which is elastically clamped at the unloaded edges (restraint stiffness k). This corresponds to the situation shown in Fig. 14.4. This includes the special cases of a laminate simply supported at all edges and a laminate with clamped unloaded edges. The laminate is symmetric, balanced and orthotropic in its plate behaviour, so that the following form of the constitutive law applies:

$$\begin{pmatrix} N_{xx}^0 \\ N_{yy}^0 \\ N_{xy}^0 \\ M_{xx}^0 \\ M_{yy}^0 \\ M_{xy}^0 \\ Q_y \\ Q_x \end{pmatrix} = \begin{bmatrix} A_{11} & A_{12} & 0 & 0 & 0 & 0 & 0 & 0 \\ A_{12} & A_{22} & 0 & 0 & 0 & 0 & 0 & 0 \\ 0 & 0 & A_{66} & 0 & 0 & 0 & 0 & 0 \\ 0 & 0 & 0 & D_{11} & D_{12} & 0 & 0 & 0 \\ 0 & 0 & 0 & D_{12} & D_{22} & 0 & 0 & 0 \\ 0 & 0 & 0 & 0 & 0 & D_{66} & 0 & 0 \\ 0 & 0 & 0 & 0 & 0 & 0 & KA_{44} & 0 \\ 0 & 0 & 0 & 0 & 0 & 0 & 0 & KA_{55} \end{bmatrix} \begin{pmatrix} \frac{\partial u_0}{\partial x} \\ \frac{\partial v_0}{\partial y} \\ \frac{\partial u_0}{\partial y} + \frac{\partial v_0}{\partial x} \\ \frac{\partial \psi_x}{\partial x} \\ \frac{\partial \psi_y}{\partial y} \\ \frac{\partial \psi_x}{\partial y} + \frac{\partial \psi_y}{\partial x} \\ \frac{\partial w_0}{\partial y} + \psi_y \\ \frac{\partial w_0}{\partial x} + \psi_x \end{pmatrix}. \tag{14.139}$$

The boundary conditions are as follows:

$$
\begin{aligned}
&w_0\,(x=0)=0, \quad w_0\,(x=a)=0, \quad w_0\,(y=0)=0, \quad w_0\,(y=b)=0,\\
&\psi_x\,(y=0)=0, \quad \psi_x\,(y=b)=0, \quad \psi_y\,(x=0)=0, \quad \psi_y\,(x=a)=0,\\
&M^0_{xx}\,(x=0)=0, \quad M^0_{xx}\,(x=a)=0,\\
&M^0_{yy}\,(y=0)=k\psi_y\,(y=0)\,, \quad M^0_{yy}\,(y=b)=-k\psi_y\,(y=b)\,.
\end{aligned}
\tag{14.140}
$$

For this laminate situation, the following approach for the buckling shape w_0 and the bending angles ψ_x, ψ_y has proven to be suitable (Kühn et al. 2014):

$$
\begin{aligned}
w_0 &= W w_1\,(x)\,w_2\,(y) = W \sin\left(\frac{m\pi x}{a}\right)\left\{(1-\Psi)\sin\left(\frac{\pi y}{b}\right)+\frac{\Psi}{2}\left[1-\cos\left(\frac{2\pi y}{b}\right)\right]\right\},\\
\psi_x &= X\psi_{x1}\,(x)\,\psi_{x2}\,(y) = X\cos\left(\frac{m\pi x}{a}\right)\left\{(1-\Psi)\sin\left(\frac{\pi y}{b}\right)+\frac{\Psi}{2}\left[1-\cos\left(\frac{2\pi y}{b}\right)\right]\right\},\\
\psi_y &= Y\psi_{y1}\,(x)\,\psi_{y2}\,(y) = Y\sin\left(\frac{m\pi x}{a}\right)\left\{(1-\Psi)\cos\left(\frac{\pi y}{b}\right)+\Psi\sin\left(\frac{2\pi y}{b}\right)\right\}.
\end{aligned}
\tag{14.141}
$$

It is easy to see that this approach for the buckling mode w_0 corresponds exactly to the formulation (14.72) for the shear rigid laminate. Furthermore, it is easy to show that the approaches for the bending angles ψ_x, ψ_y include the special case of the laminate simply supported at all edges in the form of the corresponding Navier solution. The new terms added in Eq. (14.141) have the task of modelling the clamping effect due to the elastic edge restraints. Evaluating the boundary conditions (14.140) with regard to the edge restraints leads to the following result for the interpolation factor Ψ in both cases:

$$
\Psi = \frac{kb}{kb+2D_{22}\pi}. \tag{14.142}
$$

As before, the buckling load N^0_{xx} is determined from the principle of the minimum of the total elastic potential Π of the buckled laminate, whereby the potential Π can be written as follows in the present case:

$$
\begin{aligned}
\Pi = \frac{1}{2}\int_0^b\int_0^a &\left[D_{11}\left(\frac{\partial\psi_x}{\partial x}\right)^2+2D_{12}\frac{\partial\psi_x}{\partial x}\frac{\partial\psi_y}{\partial y}+D_{22}\left(\frac{\partial\psi_y}{\partial y}\right)^2+D_{66}\left(\frac{\partial\psi_x}{\partial y}+\frac{\partial\psi_y}{\partial x}\right)^2\right.\\
&\left.+\,KA_{44}\left(\frac{\partial w_0}{\partial y}+\psi_y\right)^2+KA_{55}\left(\frac{\partial w_0}{\partial x}+\psi_x\right)^2\right]\mathrm{d}x\mathrm{d}y-\frac{N^0_{xx}}{2}\int_0^a\int_0^b\left(\frac{\partial w_0}{\partial x}\right)^2\mathrm{d}y\mathrm{d}x\\
&+\frac{k}{2}\int_0^a\left\{\left[\psi_y\,(y=0)\right]^2+\left[\psi_y\,(y=b)\right]^2\right\}\mathrm{d}x.
\end{aligned}
\tag{14.143}
$$

The buckling condition $\delta\Pi = 0$ then results in the three following Ritz equations:

$$\frac{\partial \Pi}{\partial W} = 0, \quad \frac{\partial \Pi}{\partial X} = 0, \quad \frac{\partial \Pi}{\partial Y} = 0, \tag{14.144}$$

which, after inserting the approach (14.141), leads to the following homogeneous system of equations for the constants W, X, Y:

$$\begin{bmatrix} \lambda_{11} - N^0_{xx}\bar{\lambda}_{11} & \lambda_{12} & \lambda_{13} \\ \lambda_{12} & \lambda_{22} & \lambda_{23} \\ \lambda_{13} & \lambda_{23} & \lambda_{33} \end{bmatrix} \begin{pmatrix} W \\ X \\ Y \end{pmatrix} = \begin{pmatrix} 0 \\ 0 \\ 0 \end{pmatrix}. \tag{14.145}$$

The matrix entries are not specified in more detail here; interested readers can find information on this in Kühn et al. (2014).

For a non-trivial solution of the system of equations (14.145), the vanishing of the coefficient determinant is required, which after some transformations leads to the following closed-form analytical solution for the buckling load N^0_{xx}:

$$N^0_{xx} = \frac{\lambda_{11}}{\bar{\lambda}_{11}} + \frac{\lambda_{13}\left(\lambda_{12}\lambda_{23} - \lambda_{13}\lambda_{22}\right) - \lambda_{12}\left(\lambda_{12}\lambda_{33} - \lambda_{13}\lambda_{23}\right)}{\lambda_{22}\lambda_{33} - \lambda_{23}^2}. \tag{14.146}$$

The reliability of this solution for the local buckling analysis of beam structures consisting of shear-deformable composite laminates has been documented by Kühn et al. (2014). A more detailed discussion is omitted at this point, the general characteristics of the buckling behaviour of elastically restrained laminates (i.e. the influence of the thickness of the laminate and the degree of restraint) generally correspond to what has already been discussed in the previous chapters and therefore do not require a further discussion.

14.4 The Rayleigh Quotient in the Framework of Third-Order Shear Deformation Theory

In this section we discuss the derivation of a closed-form analytical method within the framework of a Rayleigh quotient for the Third-Order Shear Deformation Theory (see also Schreiber et al. (2020)). We consider the situation of Fig. 14.11. The total elastic potential $\Pi = \Pi_i + \Pi_a + \Pi_s$ consists of the following components:

$$\Pi_i = \frac{1}{2}\int_0^b \int_0^a \begin{pmatrix} \underline{\varepsilon}^{(0)} \\ \underline{\varepsilon}^{(1)} \\ \underline{\varepsilon}^{(3)} \\ \underline{\gamma}^{(0)} \\ \underline{\gamma}^{(2)} \end{pmatrix}^T \begin{pmatrix} \underline{N}^0 \\ \underline{M}^0 \\ \underline{P} \\ \underline{Q} \\ \underline{R} \end{pmatrix} \mathrm{d}x\,\mathrm{d}y,$$

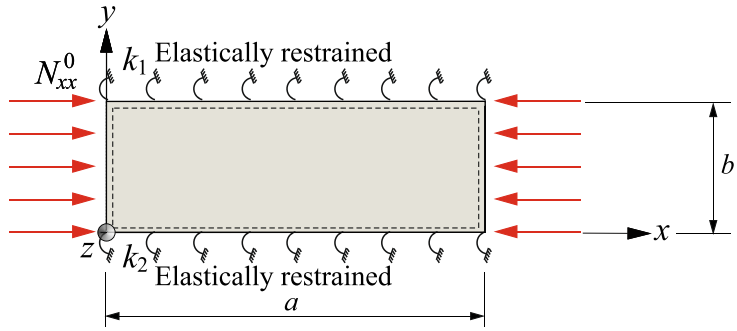


Fig. 14.11 Laminate under uniaxial compressive load with simply supported loaded edges and two elastically restrained unloaded edges

$$\Pi_a = -\frac{N_{xx}^0}{2}\int_0^b\int_0^a\left(\frac{\partial w_0}{\partial x}\right)^2 \mathrm{d}x\,\mathrm{d}y,$$
$$\Pi_\mathrm{s} = \frac{1}{2}\int_0^a\left(k_2\left[\psi_y\,(x,0)\right]^2 + k_1\left[\psi_y\,(x,b)\right]^2\right)\mathrm{d}x, \tag{14.147}$$

wherein

$$\underline{\varepsilon}^{(0)} = \begin{pmatrix}\varepsilon_{xx}^{(0)}\\ \varepsilon_{yy}^{(0)}\\ \gamma_{xy}^{(0)}\end{pmatrix} = \begin{pmatrix}\frac{\partial u_0}{\partial x}\\ \frac{\partial v_0}{\partial y}\\ \frac{\partial u_0}{\partial y}+\frac{\partial v_0}{\partial x}\end{pmatrix},\quad \underline{\varepsilon}^{(1)} = \begin{pmatrix}\varepsilon_{xx}^{(1)}\\ \varepsilon_{yy}^{(1)}\\ \gamma_{xy}^{(1)}\end{pmatrix} = \begin{pmatrix}\frac{\partial \psi_x}{\partial x}\\ \frac{\partial \psi_y}{\partial y}\\ \frac{\partial \psi_x}{\partial y}+\frac{\partial \psi_y}{\partial x}\end{pmatrix},$$

$$\underline{\varepsilon}^{(3)} = \begin{pmatrix}\varepsilon_{xx}^{(3)}\\ \varepsilon_{yy}^{(3)}\\ \gamma_{xy}^{(3)}\end{pmatrix} = \begin{pmatrix}-\frac{4}{3h^2}\left(\frac{\partial \psi_x}{\partial x}+\frac{\partial^2 w_0}{\partial x^2}\right)\\ -\frac{4}{3h^2}\left(\frac{\partial \psi_y}{\partial y}+\frac{\partial^2 w_0}{\partial y^2}\right)\\ -\frac{4}{3h^2}\left(\frac{\partial \psi_x}{\partial y}+\frac{\partial \psi_y}{\partial x}+2\frac{\partial^2 w_0}{\partial x\partial y}\right)\end{pmatrix},$$

$$\underline{\gamma}^{(0)} = \begin{pmatrix}\gamma_{yz}^{(0)}\\ \gamma_{xz}^{(0)}\end{pmatrix} = \begin{pmatrix}\psi_y+\frac{\partial w_0}{\partial y}\\ \psi_x+\frac{\partial w_0}{\partial x}\end{pmatrix},\quad \underline{\gamma}^{(2)} = \begin{pmatrix}\gamma_{yz}^{(2)}\\ \gamma_{xz}^{(2)}\end{pmatrix} = \begin{pmatrix}-\frac{4}{h^2}\left(\psi_y+\frac{\partial w_0}{\partial y}\right)\\ -\frac{4}{h^2}\left(\psi_x+\frac{\partial w_0}{\partial x}\right)\end{pmatrix}. \tag{14.148}$$

In the following, we consider symmetric and orthotropic laminate structures for which the following stiffness components become zero:

$$\begin{aligned}A_{16} = A_{26} = B_{ij} = D_{16} = D_{26} = E_{ij} = F_{16}\\ = F_{26} = H_{16} = H_{26} = A_{45} = D_{45} = F_{45} = 0.\end{aligned} \tag{14.149}$$

The inner potential Π_i is:

$$\begin{aligned}
\Pi_i = \frac{1}{2}\int_0^b \int_0^a \Bigg\{ & D_{11}\left(\frac{\partial \psi_x}{\partial x}\right)^2 + 2D_{12}\frac{\partial \psi_x}{\partial x}\frac{\partial \psi_y}{\partial y} + D_{22}\left(\frac{\partial \psi_y}{\partial y}\right)^2 + D_{66}\Bigg[\left(\frac{\partial \psi_x}{\partial y}\right)^2 \\
& + 2\frac{\partial \psi_x}{\partial y}\frac{\partial \psi_y}{\partial x} + \left(\frac{\partial \psi_y}{\partial x}\right)^2\Bigg] - \frac{8}{3h^2}\Bigg\{F_{11}\Bigg[\left(\frac{\partial \psi_x}{\partial x}\right)^2 + \frac{\partial \psi_x}{\partial x}\frac{\partial^2 w_0}{\partial x^2}\Bigg] \\
& + F_{12}\Bigg[2\frac{\partial \psi_x}{\partial x}\frac{\partial \psi_y}{\partial y} + \frac{\partial \psi_x}{\partial x}\frac{\partial^2 w_0}{\partial y^2} + \frac{\partial \psi_y}{\partial y}\frac{\partial^2 w_0}{\partial x^2}\Bigg] + F_{22}\Bigg[\frac{\partial \psi_y}{\partial y}\frac{\partial^2 w_0}{\partial y^2} + \left(\frac{\partial \psi_y}{\partial y}\right)^2\Bigg] \\
& + F_{66}\Bigg[\left(\frac{\partial \psi_x}{\partial y}\right)^2 + \left(\frac{\partial \psi_y}{\partial x}\right)^2 + 2\frac{\partial \psi_x}{\partial y}\frac{\partial \psi_y}{\partial x} + 2\frac{\partial \psi_x}{\partial y}\frac{\partial^2 w_0}{\partial x \partial y} + 2\frac{\partial \psi_y}{\partial x}\frac{\partial^2 w_0}{\partial x \partial y}\Bigg]\Bigg\} \\
& + \frac{16}{9h^4}\Bigg\{H_{11}\Bigg[\left(\frac{\partial \psi_x}{\partial x}\right)^2 + 2\frac{\partial \psi_x}{\partial x}\frac{\partial^2 w_0}{\partial x^2} + \left(\frac{\partial^2 w_0}{\partial x^2}\right)^2\Bigg] + 2H_{12}\Bigg[\frac{\partial \psi_x}{\partial x}\frac{\partial \psi_y}{\partial y} \\
& + \frac{\partial \psi_x}{\partial x}\frac{\partial^2 w_0}{\partial y^2} + \frac{\partial \psi_y}{\partial y}\frac{\partial^2 w_0}{\partial x^2} + \frac{\partial^2 w_0}{\partial x^2}\frac{\partial^2 w_0}{\partial y^2}\Bigg] + H_{22}\Bigg[\left(\frac{\partial^2 w_0}{\partial y^2}\right)^2 + 2\frac{\partial \psi_y}{\partial y}\frac{\partial^2 w_0}{\partial y^2} \\
& + \left(\frac{\partial \psi_y}{\partial y}\right)^2\Bigg] + H_{66}\Bigg[4\left(\frac{\partial^2 w_0}{\partial y \partial x}\right)^2 + \left(\frac{\partial \psi_x}{\partial y}\right)^2 + 4\frac{\partial \psi_y}{\partial x}\frac{\partial^2 w_0}{\partial x \partial y} + \left(\frac{\partial \psi_y}{\partial x}\right)^2 \\
& + 2\frac{\partial \psi_x}{\partial y}\frac{\partial \psi_y}{\partial x} + 4\frac{\partial \psi_x}{\partial y}\frac{\partial^2 w_0}{\partial x \partial y}\Bigg]\Bigg\} + A_{44}\Bigg[\psi_y^2 + 2\psi_y\frac{\partial w_0}{\partial y} + \left(\frac{\partial w_0}{\partial y}\right)^2\Bigg] \\
& + A_{55}\Bigg[\psi_x^2 + 2\psi_x\frac{\partial w_0}{\partial x} + \left(\frac{\partial w_0}{\partial x}\right)^2\Bigg] - \frac{8}{h^2}D_{44}\Bigg[\psi_y^2 + 2\psi_y\frac{\partial w_0}{\partial y} + \left(\frac{\partial w_0}{\partial y}\right)^2\Bigg] \\
& - \frac{8}{h^2}D_{55}\Bigg[\psi_x^2 + 2\psi_x\frac{\partial w_0}{\partial x} + \left(\frac{\partial w_0}{\partial x}\right)^2\Bigg] + \frac{16}{h^4}F_{44}\Bigg[\psi_y^2 + 2\psi_y\frac{\partial w_0}{\partial y} + \left(\frac{\partial w_0}{\partial y}\right)^2\Bigg] \\
& + \frac{16}{h^4}F_{55}\Bigg[\psi_x^2 + 2\psi_x\frac{\partial w_0}{\partial x} + \left(\frac{\partial w_0}{\partial x}\right)^2\Bigg]\Bigg\}\,\mathrm{d}x\,\mathrm{d}y. \qquad (14.150)
\end{aligned}$$

Here, the displacements u_0 and v_0 of the laminate middle plane were not considered further, as these do not play a role in a linear buckling analysis for symmetric laminates.

The current approach is based on a fairly simple formulation for the buckling modes w_0, ψ_x and ψ_y as follows:

$$\begin{aligned}
w_0 &= W\, w_1(x)\; w_2(y)\,, \\
\psi_x &= X\, \psi_{x_1}(x)\; \psi_{x_2}(y)\,, \\
\psi_y &= Y\, \psi_{y_1}(x)\; \psi_{y_2}(y)\,. \qquad (14.151)
\end{aligned}$$

In this case, each shape function was formulated as the product of two admissible one-dimensional shape functions w_1 and w_2, ψ_{x_1} and ψ_{x_2}, ψ_{y_1} and ψ_{y_2}, which must fulfil all the underlying geometric boundary conditions. The variables W, X and Y are free constants

and can be interpreted as the buckling mode amplitudes. Since the functions w_1, w_2, ψ_{x_1}, ψ_{x_2}, ψ_{y_1}, ψ_{y_2} are determined a priori for the best possible approximation of the buckling modes, it makes sense to define abbreviations for the above integral terms as follows:

$$
\begin{aligned}
I_1 &= \int_0^a \left(\frac{\mathrm{d}\psi_{x_1}}{\mathrm{d}x}\right)^2 \mathrm{d}x, \quad I_2 = \int_0^a \frac{\mathrm{d}\psi_{x_1}}{\mathrm{d}x}\psi_{y_1}\,\mathrm{d}x, \quad I_3 = \int_0^a \left(\psi_{y_1}\right)^2 \mathrm{d}x, \\
I_4 &= \int_0^a \left(\psi_{x_1}\right)^2 \mathrm{d}x, \quad I_5 = \int_0^a \psi_{x_1}\frac{\mathrm{d}\psi_{y_1}}{\mathrm{d}x}\,\mathrm{d}x, \quad I_6 = \int_0^a \left(\frac{\mathrm{d}\psi_{y_1}}{\mathrm{d}x}\right)^2 \mathrm{d}x, \\
I_7 &= \int_0^a \frac{\mathrm{d}\psi_{x_1}}{\mathrm{d}x}\frac{\mathrm{d}^2 w_1}{\mathrm{d}x^2}\,\mathrm{d}x, \quad I_8 = \int_0^a \frac{\mathrm{d}\psi_{x_1}}{\mathrm{d}x}w_1\,\mathrm{d}x, \quad I_9 = \int_0^a \frac{\mathrm{d}^2 w_1}{\mathrm{d}x^2}\psi_{y_1}\,\mathrm{d}x, \\
I_{10} &= \int_0^a \psi_{y_1} w_1\,\mathrm{d}x, \quad I_{11} = \int_0^a \psi_{x_1}\frac{\mathrm{d}w_1}{\mathrm{d}x}\,\mathrm{d}x, \quad I_{12} = \int_0^a \frac{\mathrm{d}\psi_{y_1}}{\mathrm{d}x}\frac{\mathrm{d}w_1}{\mathrm{d}x}\,\mathrm{d}x, \\
I_{13} &= \int_0^a \left(\frac{\mathrm{d}^2 w_1}{\mathrm{d}x^2}\right)^2 \mathrm{d}x, \quad I_{14} = \int_0^a \frac{\mathrm{d}^2 w_1}{\mathrm{d}x^2}w_1\,\mathrm{d}x, \quad I_{15} = \int_0^a (w_1)^2\,\mathrm{d}x, \\
I_{16} &= \int_0^a \left(\frac{\mathrm{d}w_1}{\mathrm{d}x}\right)^2 \mathrm{d}x
\end{aligned}
\tag{14.152}
$$

and

$$
\begin{aligned}
J_1 &= \int_0^b \left(\psi_{x_2}\right)^2 \mathrm{d}y, \quad J_2 = \int_0^b \frac{\mathrm{d}\psi_{y_2}}{\mathrm{d}y}\psi_{x_2}\,\mathrm{d}y, \quad J_3 = \int_0^b \left(\frac{\mathrm{d}\psi_{y_2}}{\mathrm{d}y}\right)^2 \mathrm{d}y, \\
J_4 &= \int_0^b \left(\frac{\mathrm{d}\psi_{x_2}}{\mathrm{d}y}\right)^2 \mathrm{d}y, \quad J_5 = \int_0^b \frac{\mathrm{d}\psi_{x_2}}{\mathrm{d}y}\psi_{y_2}\,\mathrm{d}y, \quad J_6 = \int_0^b \left(\psi_{y_2}\right)^2 \mathrm{d}y, \\
J_7 &= \int_0^b \psi_{x_2} w_2\,\mathrm{d}y, \quad J_8 = \int_0^b \psi_{x_2}\frac{\mathrm{d}{w_2}^2}{\mathrm{d}y^2}\,\mathrm{d}y, \quad J_9 = \int_0^b w_2\frac{\mathrm{d}\psi_{y_2}}{\mathrm{d}y}\,\mathrm{d}y, \\
J_{10} &= \int_0^b \frac{\mathrm{d}\psi_{y_2}}{\mathrm{d}y}\frac{\mathrm{d}^2 w_2}{\mathrm{d}y^2}\,\mathrm{d}y, \quad J_{11} = \int_0^b \frac{\mathrm{d}\psi_{x_2}}{\mathrm{d}y}\frac{\mathrm{d}w_2}{\mathrm{d}y}\,\mathrm{d}y, \quad J_{12} = \int_0^b \psi_{y_2}\frac{\mathrm{d}w_2}{\mathrm{d}y}\,\mathrm{d}y, \\
J_{13} &= \int_0^b (w_2)^2\,\mathrm{d}y, \quad J_{14} = \int_0^b w_2\frac{\mathrm{d}^2 w_2}{\mathrm{d}y^2}\,\mathrm{d}y, \quad J_{15} = \int_0^b \left(\frac{\mathrm{d}^2 w_2}{\mathrm{d}y^2}\right)^2 \mathrm{d}y, \\
J_{16} &= \int_0^b \left(\frac{\mathrm{d}w_2}{\mathrm{d}y}\right)^2 \mathrm{d}y.
\end{aligned}
\tag{14.153}
$$

Further we define:

$$
C_{2,\mathrm{rot}} = \left(\psi_{y_2}(0)\right)^2, \quad C_{1,\mathrm{rot}} = \left(\psi_{y_2}(b)\right)^2. \tag{14.154}
$$

The potential Π can then be given as follows:

$$
\begin{aligned}
\Pi = {} & \frac{1}{2}X^2 D_{11} I_1 J_1 + XY D_{12} I_2 J_2 + \frac{1}{2} D_{22} Y^2 I_3 J_3 + \frac{1}{2} D_{66} \left(X^2 I_4 J_4 \right. \\
& + \left. 2XY I_5 J_5 + Y^2 I_6 J_6 \right) - \frac{4}{3h^2} \left[F_{11} \left(X^2 I_1 J_1 - XW I_7 J_7 \right) \right. \\
& + F_{12} \left(2XY I_2 J_2 + XW I_8 J_8 + YW I_9 J_9 \right) + F_{22} \left(Y^2 I_3 J_3 + YW I_{10} J_{10} \right) \\
& + \left. F_{66} \left(2XW I_{11} J_{11} + 2YW I_{12} J_{12} + 2XY I_5 J_5 + X^2 I_4 J_4 + Y^2 I_6 J_6 \right) \right] \\
& + \frac{8}{9h^4} \left[H_{11} \left(X^2 I_1 J_1 + 2XW I_7 J_7 + W^2 I_{13} J_{13} \right) \right. \\
& + 2H_{12} \left(WY I_9 J_9 + XY I_2 J_2 + XW I_8 J_8 + W^2 I_{14} J_{14} \right) \\
& + H_{22} \left(Y^2 I_3 J_3 + W^2 I_{15} J_{15} + 2YW I_{10} J_{10} \right) + H_{66} \left(4XW I_{11} J_{11} \right. \\
& + \left. \left. 4YW I_{12} J_{12} + X^2 I_4 J_4 + 2XY I_5 J_5 + Y^2 I_6 J_6 + 4W^2 I_{16} J_{16} \right) \right] \\
& + \frac{1}{2} A_{44} \left(Y^2 I_3 J_6 + W^2 I_{15} J_{16} + 2YW I_{10} J_{12} \right) \\
& + \frac{1}{2} A_{55} \left(X^2 I_4 J_1 + W^2 I_{16} J_{13} + 2XW I_{11} J_7 \right) \\
& - \frac{4}{h^2} D_{44} \left(Y^2 I_3 J_6 + W^2 I_{15} J_{16} + 2WY I_{10} J_{12} \right) \\
& - \frac{4}{h^2} D_{55} \left(X^2 I_4 J_1 + W^2 I_{16} J_{13} + 2XW I_{11} J_7 \right) \\
& + \frac{8}{h^4} F_{44} \left(2WY I_{10} J_{12} + Y^2 I_3 J_6 + W^2 I_{15} J_{16} \right) \\
& + \frac{8}{h^4} F_{55} \left(W^2 I_{16} J_{13} + X^2 I_4 J_1 + 2XW I_{11} J_7 \right) \\
& - \frac{1}{2} N_{xx}^0 W^2 I_{16} J_{13} + \frac{1}{2} Y^2 \left(k_2 C_{2,rot} I_3 + k_1 C_{1,rot} I_3 \right) . \qquad (14.155)
\end{aligned}
$$

The onset of buckling and thus bifurcation of equilibrium, i.e. the infinitesimally deformed state of the considered laminate under uniaxial compressive load N_{xx}^0, is a state of indifferent equilibrium, which means that in this state the first variation of the total elastic potential Π disappears, i.e. $\delta\Pi = 0$. In the present case, this reduces to three Ritz equations as follows:

$$
\frac{\partial \Pi}{\partial W} = 0, \qquad \frac{\partial \Pi}{\partial X} = 0, \qquad \frac{\partial \Pi}{\partial Y} = 0. \qquad (14.156)
$$

The application of (14.156) to (14.155) leads to a linear system of equations as follows:

$$
\begin{bmatrix} \lambda_{11} - N_{xx}^0 \overline{\lambda}_{11} & \lambda_{12} & \lambda_{13} \\ \lambda_{12} & \lambda_{22} & \lambda_{23} \\ \lambda_{13} & \lambda_{23} & \lambda_{33} \end{bmatrix} \begin{bmatrix} W \\ X \\ Y \end{bmatrix} = \begin{bmatrix} 0 \\ 0 \\ 0 \end{bmatrix}, \qquad (14.157)
$$

where the following abbreviations were used for the components of the coefficient matrix:

$$
\begin{aligned}
\lambda_{11} &= \frac{16}{9\,h^4}\left[\,H_{11}\,I_{13}\,J_{13} + 2\,H_{12}\,I_{14}\,J_{14} + H_{22}\,I_{15}\,J_{15} + 4H_{66}I_{16}J_{16}\right] + A_{44}\,I_{15}\,J_{16} \\
&\quad + A_{55}\,I_{16}\,J_{13} - \frac{8}{h^2}\left[D_{44}I_{15}J_{16} + D_{55}I_{16}J_{13}\right] + \frac{16}{h^4}\left[F_{55}I_{16}J_{13} + F_{44}I_{15}J_{16}\right], \\
\overline{\lambda}_{11} &= I_{16}\,J_{13}, \\
\lambda_{12} &= \frac{16}{9\,h^4}\,[H_{11}\,I_7\,J_7 + H_{12}\,I_8\,J_8 + 2\,H_{66}\,I_{11}\,J_{11}] + A_{55}\,I_{11}\,J_7 - \frac{8}{h^2}D_{55}\,I_{11}\,J_7 \\
&\quad - \frac{4}{3\,h^2}\,[F_{11}\,I_7\,J_7 + F_{12}\,I_8\,J_8 + 2F_{66}\,I_{11}\,J_{11}] + \frac{16}{h^4}F_{55}\,I_{11}\,J_7, \\
\lambda_{13} &= -\frac{4}{3\,h^2}\,[F_{12}\,I_9\,J_9 + F_{22}\,I_{10}\,J_{10} + 2F_{66}\,I_{12}\,J_{12}] + A_{44}\,I_{10}\,J_{12} - \frac{8}{h^2}D_{44}\,I_{10}\,J_{12} \\
&\quad + \frac{16}{9\,h^4}\,[H_{12}\,I_9\,J_9 + H_{22}\,I_{10}\,J_{10} + 2\,H_{66}\,I_{12}\,J_{12}] + \frac{16}{h^4}F_{44}\,I_{10}\,J_{12}, \\
\lambda_{22} &= D_{11}\,I_1\,J_1 + D_{66}\,I_4\,J_4 - \frac{8}{3h^2}\,[F_{11}\,I_1\,J_1 + F_{66}\,I_4\,J_4] + A_{55}\,I_4\,J_1 \\
&\quad + \frac{16}{9\,h^4}\,[H_{11}\,I_1\,J_1 + H_{66}\,I_4\,J_4] - \frac{8}{h^2}D_{55}\,I_4\,J_1 + \frac{16}{h^4}F_{55}\,I_4\,J_1, \\
\lambda_{23} &= D_{12}\,I_2\,J_2 + D_{66}\,I_5\,J_5 - \frac{8}{3\,h^2}\left[F_{12}\,I_2\,J_2 + F_{66}\,I_5\,J_5\right] \\
&\quad + \frac{16}{9\,h^4}\left[H_{12}\,I_2\,J_2 + H_{66}\,I_5\,J_5\right], \\
\lambda_{33} &= D_{22}\,I_3\,J_3 + D_{66}\,I_6\,J_6 - \frac{8}{3\,h^2}\,[F_{22}\,I_3\,J_3 + F_{66}\,I_6\,J_6] \\
&\quad + \frac{16}{9\,h^4}\,[H_{22}\,I_3\,J_3 + H_{66}\,I_6\,J_6] + A_{44}\,I_3\,J_6 - \frac{8}{h^2}D_{44}\,I_3\,J_6 + \frac{16}{h^4}F_{44}\,I_3\,J_6 \\
&\quad + k_2\,C_{2,\mathrm{rot}}I_3 + k_1 C_{1,\mathrm{rot}}\,I_3.
\end{aligned}
\tag{14.158}
$$

In order to avoid a trivial solution for the system of equations (14.157), a vanishing coefficient determinant is required. From this, the following expression can be determined for the buckling load N^0_{xx}:

$$
N^0_{xx} = \frac{\lambda_{11}\,\left(\lambda_{22}\,\lambda_{33} - {\lambda_{23}}^2\right) + \lambda_{12}\,(\lambda_{13}\,\lambda_{23} - \lambda_{12}\lambda_{33}) + \lambda_{13}\,(\lambda_{12}\,\lambda_{23} - \lambda_{13}\lambda_{22})}{\overline{\lambda}_{11}\,\left(\lambda_{22}\,\lambda_{33} - {\lambda_{23}}^2\right)}. \tag{14.159}
$$

This expression represents the closed-form analytical solution for the buckling load N^0_{xx} of the considered laminate within the framework of the Third-Order Shear Deformation Theory. It is worth mentioning that no shape functions have yet been specified for the determination of this expression.

The shape functions w_1 and w_2, ψ_{x_1} and ψ_{x_2}, ψ_{y_1} and ψ_{y_2} are chosen equivalent to a study by Beerhorst and Thirusala Suresh Babu (2020):

$$
\begin{aligned}
w_0 &= W \sin\left(\frac{m\pi x}{a}\right)\left(\frac{y}{b} + W_2\,\frac{y^2}{b^2} + W_3\,\frac{y^3}{b^3} + W_4\,\frac{y^4}{b^4}\right),\\
\psi_x &= X\,\frac{m\pi}{a}\cos\left(\frac{m\pi x}{a}\right)\left(\frac{y}{b} + W_2\,\frac{y^2}{b^2} + W_3\,\frac{y^3}{b^3} + W_4\,\frac{y^4}{b^4}\right),\\
\psi_y &= Y \sin\left(\frac{m\pi x}{a}\right)\left(\frac{1}{b} + 2\,W_2\,\frac{y}{b^2} + 3\,W_3\,\frac{y^2}{b^3} + 4\,W_4\,\frac{y^3}{b^4}\right).
\end{aligned}
\tag{14.160}
$$

While the buckling modes in the longitudinal direction x are described by trigonometric functions that fulfil all underlying boundary conditions a priori, fourth- and third-order polynomials are used in the transverse direction. The free constants W_2, W_3 and W_4 are adapted to the boundary conditions at the unloaded edges. It is assumed that the shape functions (14.160) fulfil the geometric boundary conditions exactly and the dynamic boundary conditions approximately by neglecting the transverse shear stiffnesses ($H_{11} = H_{12} = H_{22} = H_{66} = F_{11} = F_{12} = F_{22} = F_{66} = 0$). The free constants W_2, W_3 and W_4 result as:

$$
\begin{aligned}
W_2 &= \frac{b k_2}{2\,D_{22}},\\
W_3 &= -\,\frac{12\,{D_{22}}^2 + b\,(5\,k_2 + 3\,k_1)\,D_{22} + b^2 k_2\,k_1}{(b k_1 + 6\,D_{22})\,D_{22}},\\
W_4 &= \frac{12\,{D_{22}}^2 + 4\,b\,(k_2 + k_1)\,D_{22} + b^2 k_2\,k_1}{2\,(b k_1 + 6\,D_{22})\,D_{22}}.
\end{aligned}
\tag{14.161}
$$

The expressions defined in (14.152), (14.153), (14.154) can then be written as follows:

$$
\begin{aligned}
&I_1 = \frac{1}{2}\,\frac{m^4\pi^4}{a^3}, \quad I_2 = -\frac{1}{2}\,\frac{m^2\pi^2}{a}, \quad I_3 = \frac{a}{2}, \quad I_1 = I_7 = I_{13},\\
&I_2 = -I_4 = -I_5 = -I_6 = I_8 = I_9 = -I_{11} = -I_{12} = I_{14} = -I_{16},\\
&I_3 = I_{10} = I_{15},\\
&J_1 = \frac{b}{5}\left[{W_2}^2 + \left(\frac{5}{3}\,W_3 + \frac{10\,W_4}{7} + \frac{5}{2}\right)W_2 + \frac{5}{7}\,{W_3}^2 + \left(\frac{5}{4}\,W_4 + 2\right)W_3\right.\\
&\qquad \left. +\ \frac{5}{9}\,{W_4}^2 + \frac{5}{3}\,W_4 + \frac{5}{3}\right],\\
&J_2 = \frac{1}{105\,b}\left[70\,{W_2}^2 + (210\,W_3 + 294\,W_4 + 105)\,W_2 + 126\,{W_3}^2\right.\\
&\qquad \left. +\ (315\,W_4 + 210)\,W_3 + 180\,{W_4}^2 + 315\,W_4\right],\\
&J_3 = \frac{20\,{W_2}^2 + (60\,W_3 + 80\,W_4)\,W_2 + 60\,{W_3}^2 + 180\,W_3\,W_4 + 144\,{W_4}^2}{5\,b^3},\\
&J_4 = \frac{1}{105\,b}\left[140\,{W_2}^2 + (315\,W_3 + 336\,W_4 + 210)\,W_2 + 189\,{W_3}^2\right.\\
&\qquad \left. +\ (420\,W_4 + 210)\,W_3 + 240\,{W_4}^2 + 210\,W_4 + 105\right],
\end{aligned}
$$

$$J_1 = J_7 = J_{13}, \qquad J_2 = J_8 = J_9 = J_{14}, \qquad J_3 = J_{10} = J_{15},$$
$$J_4 = J_5 = J_6 = J_{11} = J_{12} = J_{16},$$
$$C_{2,\mathrm{rot}} = \frac{1}{b^2}, \qquad C_{1,\mathrm{rot}} = \frac{(1 + 2\,W_2 + 3\,W_3 + 4\,W_4)^2}{b^2}. \tag{14.162}$$

Herrmann et al. (2018) used a similar Rayleigh quotient for the buckling analysis of shear-deformable laminates and used the following set of shape functions:

$$w_0 = W \sin\left(\frac{m\pi x}{a}\right)\left([1-\beta]\sin\left(\frac{\pi y}{b}\right) + \frac{1}{2}\beta\left[1 - \cos\left(2\,\frac{\pi y}{b}\right)\right]\right),$$
$$\psi_x = X \cos\left(\frac{m\pi x}{a}\right)\left([1-\beta]\sin\left(\frac{\pi y}{b}\right) + \frac{1}{2}\beta\left[1 - \cos\left(2\,\frac{\pi y}{b}\right)\right]\right),$$
$$\psi_y = Y \sin\left(\frac{m\pi x}{a}\right)\left([1-\beta]\cos\left(\frac{\pi y}{b}\right) + \beta\,\sin\left(2\,\frac{\pi y}{b}\right)\right), \tag{14.163}$$

with β as:

$$\beta = \frac{kb}{2\,D_{22}\,\pi + kb}. \tag{14.164}$$

The buckling results obtained with this set of shape functions are later used for comparison purposes. However, this approach only represents laminates with symmetric boundary conditions, i.e. the restraint stiffnesses at both edges must be identical: $k_1 = k_2 = k$.

It is easy to show that the current approach contains the Navier solution of the given laminate as a special case within the framework of the Third-Order Shear Deformation Theory. The Navier solution only applies to laminates that are simply supported at all edges. We consider the approach (14.163) again, which with $k_1 = k_2 = 0$ leads exactly to a Navier-type approach for the present case of the plate loaded under uniaxial compression:

$$w_0 = W \sin\left(\frac{m\pi x}{a}\right)\sin\left(\frac{\pi y}{b}\right),$$
$$\psi_x = X \cos\left(\frac{m\pi x}{a}\right)\sin\left(\frac{\pi y}{b}\right),$$
$$\psi_y = Y \sin\left(\frac{m\pi x}{a}\right)\cos\left(\frac{\pi y}{b}\right). \tag{14.165}$$

The Navier approach (14.165) fulfils the boundary conditions of the simply supported plate identically, where $k_1 = k_2 = 0$ applies. As already described, the determinant of the coefficient matrix must vanish for a non-trivial solution, and thus the buckling load can be calculated by Eq. (14.159) with (14.158), wherein:

Table 14.2 Aspect ratio b/h, laminate thickness h and number of sub-laminates n

b/h	200	100	50	20	10	5
t [mm]	0.5	1	2	5	10	20
n	1	2	4	10	20	40

$$
\begin{aligned}
&I_1 = \frac{1}{2}\frac{m^2\pi^2}{a}, \quad I_2 = -\frac{1}{2}m\pi, \quad I_3 = \frac{a}{2}, \quad I_7 = \frac{1}{2}\frac{m^3\pi^3}{a^2}, \quad I_{13} = \frac{1}{2}\frac{m^4\pi^4}{a^3},\\
&I_1 = I_6 = -I_9 = I_{12} = -I_{14} = I_{16}, \quad I_2 = -I_5 = I_8 = -I_{11},\\
&I_3 = I_4 = I_{10} = I_{15},\\
&J_1 = \frac{b}{2}, \quad J_2 = -\frac{\pi}{2}, \quad J_3 = \frac{1}{2}\frac{\pi^2}{b}, \quad J_{10} = \frac{1}{2}\frac{\pi^3}{b^2}, \quad J_{15} = \frac{1}{2}\frac{\pi^4}{b^3},\\
&J_1 = J_6 = J_7 = J_{13}, \quad J_2 = -J_5 = J_9 = -J_{12},\\
&J_3 = J_4 = -J_8 = J_{11} = -J_{14} = J_{16}, \qquad C_{0,\mathrm{rot}} = C_{b,\mathrm{rot}} = 0.
\end{aligned}
\tag{14.166}
$$

The results of the presented method are discussed below. The Lévy solution from Chap. 13 serves as a reference and is compared with the present solution and the solution by Herrmann et al. (2018). To represent the buckling loads, the dimensionless buckling load $\bar{N}^0_{xx}$ is introduced, which is related to the buckling load N^0_{xx} as follows:

$$
\bar{N}^0_{xx} = \frac{N^0_{xx} b^2}{\pi^2\sqrt{D_{11}D_{22}}}. \tag{14.167}
$$

In this parameter study, the characteristic geometric parameters are the aspect ratios a/b and b/h. The considered laminates consist of unidirectional layers with the elastic properties $E_{11} = 162{,}000\,\mathrm{MPa}$, $E_{22} = 10{,}000\,\mathrm{MPa}$, $\nu_{12} = 0.3$, $G_{12} = G_{13} = 5200\,\mathrm{MPa}$, $G_{23} = 4450\,\mathrm{MPa}$ with a constant layer thickness of 0.125mm. The laminate configurations considered are cross-ply laminates of the type $[(0°/90°)_n]_s$. The subscript n indicates the number of sub-laminates. In this study, the thickness h of the entire laminate is controlled by the multiplier n.

A total of 6 different laminate configurations are investigated, ranging from very thin laminates ($b/h = 200$) to medium-thick plates ($b/h = 20$) to very thick plates ($b/h = 5$). A detailed list of all 6 configurations can be found in Table 14.2. The aspect ratio of the aforementioned laminates is analysed in the range from $a/b = 0$ to $a/b = 5$.

As a starting point, the differences between Classical Laminated Plate Theory (CLPT), First-Order Shear Deformation Theory (FSDT) and Third-Order Shear Deformation Theory (TSDT) are considered. The comparison is carried out using the Navier solution for a cross-ply laminate that is simply supported at all edges and subjected to uniaxial compression. A shear correction factor of 5/6 is used in the FSDT analysis. The difference between the three theories becomes clear when different plate thicknesses are considered, as shown in

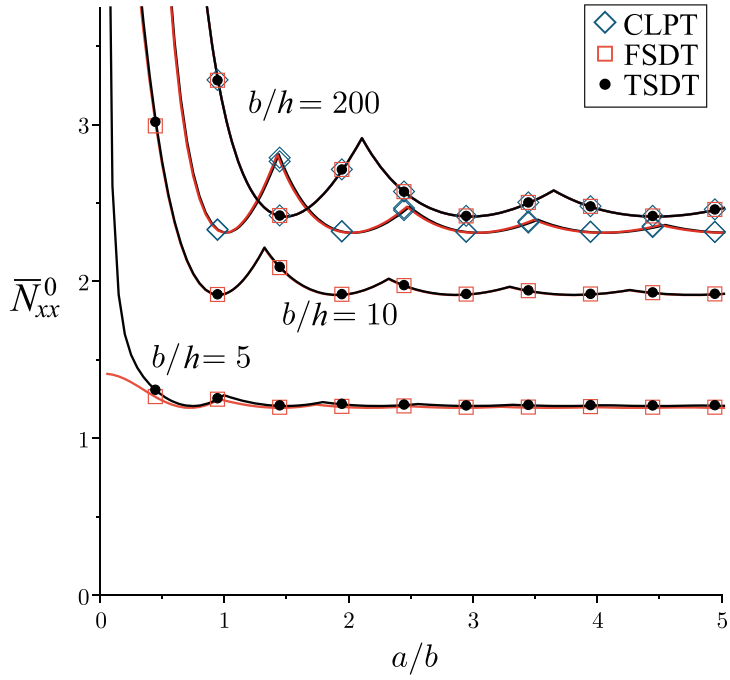


Fig. 14.12 Naviersche Lösung für die bezogene Beullast $\bar{N}^0_{xx}$ als Funktion des Seitenverhältnisses a/b

Fig. 14.12. For very thin plates ($b/h = 200$) there is no difference between the laminate theories. Due to the small thickness, the transverse shear deformations do not play a role, so that the critical load is almost identical according to all three theories. For moderately thick panels ($b/h = 10$) CLPT exceeds the critical load by up to 25.42%, as shown in Table 14.3. This is due to the assumption of a shear-rigid plate, which leads to an increase in bending stiffness for thick plates and thus also to an increase in the critical load. There is a difference of $-6.74\dot{\%}$ between FSDT and TSDT. For $b/h = 5$ the effects are even more pronounced, CLPT exceeds the buckling load by $98.79\dot{\%}$, while FSDT is $17.49\dot{\%}$ below TSDT and shows a levelling off for very short panels ($a/b < 0.5$). The results show that it is essential to use a higher-order laminate theory for thick laminates in order to achieve sufficiently accurate results.

In the following, the presented analysis methods for elastically restrained laminates are compared with each other. In this comparison, three sets of boundary conditions are considered at the unloaded edges of the laminate: both edges are simply supported, one edge is simply supported and the other edge is clamped, or both edges are clamped. These sets of boundary conditions are abbreviated as SSSS, SSSC and SCSC. These boundary conditions result in $k \to 0$ or $k \to \infty$ at the unloaded edges for simply supported or clamped edges.

Table 14.3 Minimum and maximum error of the dimensionless buckling load $\bar{N}_{xx}^0$ as well as location a/b and absolute values $\bar{N}_{xx}^0$ of the error (error $= \left(N_{xx}^0 - N_{xx}^{\mathrm{TSDT}}\right) 100/N_{xx}^{\mathrm{TSDT}}$). The errors were analysed in the range $a/b = 1, \ldots, 5$. The reference solution is the Navier solution within the framework of third-order shear deformation theory (TSDT)

		CLPT			FSDT		
b/h		Error in %	$\bar{N}_{xx}^0$	a/b	Error in %	$\bar{N}_{xx}^0$	a/b
200	min	0.02	2.90	2.10	0.00	3.08	1.00
	max	0.07	3.09	1.00	0.00	2.90	2.10
100	min	0.13	2.78	1.65	−0.01	2.79	1.70
	max	0.30	2.79	1.70	0.01	2.77	1.65
50	min	0.62	2.74	1.50	−0.03	2.75	1.55
	max	1.28	2.79	1.55	0.02	2.73	1.50
20	min	4.16	2.69	1.40	−0.10	2.61	1.45
	max	8.03	2.74	1.50	0.05	2.58	1.40
10	min	17.18	2.56	1.30	−0.30	2.18	1.35
	max	33.30	2.79	1.45	0.04	2.18	1.30
5	min	81.27	2.31	1.00	−2.60	1.24	1.00
	max	128.86	2.76	1.45	−0.66	1.21	1.70

The specified errors all relate to the Lévy-type solution. In the range $a/b = 0.5, \ldots, 5$, the minimum and maximum errors are evaluated and shown in the Tables 14.4, 14.5 and 14.6, where the values of error and $\bar{N}_{xx}^0$ are rounded to the second decimal digit. The corresponding $\bar{N}_{xx}^0$ and aspect ratios are given for the respective errors, so that a direct reference to the diagrams in Figs. 14.13, 14.14 and 14.15 can be established.

For the simply supported plate (SSSS plate), the present solution and the solution according to Herrmann et al. (2018) achieve a very high level of accuracy. Figure 14.13 shows the results for three different aspect ratios b/h.

It can be seen that the results of all analysis approaches are consistent. This high quality of results is also shown in Table 14.4. This solution shows minimum errors of 0.00 % to 0.01 % and maximum errors of only up to 0.10 %. The solution by Herrmann et al. (2018) shows practically no error. This is due to the form of the shape functions (14.163), which includes the exact solution of the SSSS plate ($k = 0$) as a special case. The results of the Navier solution and the Lévy-type solution show slight deviations, which can be attributed to the fact that the Navier solution is calculated analytically in closed form, while the Lévy-type solution is evaluated numerically.

Due to the asymmetric boundary conditions, the SSSC plate shows an asymmetric buckling shape, which the solution by Herrmann et al. (2018) cannot reproduce. Therefore, only the present solution and the Lévy-type solution are considered in the following comparison,

Table 14.4 Minimum and maximum error of the dimensionless buckling load $\bar{N}^0_{xx}$ as well as location a/b and absolute values $\bar{N}^0_{xx}$ of the error (error $= \left(N^0_{xx} - N^{\text{Lévy}}_{xx}\right) 100/N^{\text{Lévy}}_{xx}$) for the SSSS plate

		Present			Herrmann et al. (2018)		
b/t		Error in %	$\bar{N}^0_{xx}$	a/b	Error in %	$\bar{N}^0_{xx}$	a/b
200	min	0.00	5.85	0.65	0.00	2.41	4.45
	max	0.10	2.91	2.1	0.00	9.38	0.5
100	min	0.01	6.10	0.5	0.00	2.35	3.85
	max	0.10	2.78	1.65	0.00	6.10	0.5
50	min	0.01	5.10	0.5	0.00	2.30	1.1
	max	0.11	2.73	1.5	0.00	2.30	3.2
20	min	0.01	4.08	0.5	0.00	2.24	4.6
	max	0.10	2.59	1.4	0.00	2.53	1.5
10	min	0.01	2.76	0.5	0.00	1.93	3.5
	max	0.08	2.18	1.3	0.00	1.92	4.7
5	min	0.01	1.27	1	0.00	1.21	4.25
	max	0.04	1.25	0.95	0.00	1.21	2.2

Table 14.5 Minimum and maximum error of the dimensionless buckling load $\bar{N}^0_{xx}$ as well as location a/b and absolute values $\bar{N}^0_{xx}$ of the error (error $= \left(N^0_{xx} - N^{\text{Lévy}}_{xx}\right) 100/N^{\text{Lévy}}_{xx}$) for the SSSC plate

		Present		
b/h		Error in %	$\bar{N}^0_{xx}$	a/b
200	min	0.05	4.65	0.8
	max	0.20	4.30	1.65
100	min	0.05	6.40	0.5
	max	0.28	4.14	1.3
50	min	0.10	5.44	0.5
	max	0.53	4.12	1.2
20	min	0.48	4.41	0.5
	max	2.01	3.71	1.1
10	min	1.31	2.99	0.5
	max	4.90	2.83	1
5	min	1.45	1.39	0.85
	max	4.70	1.41	0.75

as shown in Fig. 14.14. For $b/h = 200$ there is a good match, the curves overlap. Up to moderately thick plates, the maximum error remains very small. The error increases with

Table 14.6 Minimum and maximum error of the dimensionless buckling load $\bar{N}^0_{xx}$ as well as location a/b and absolute values $\bar{N}^0_{xx}$ of the error (error $= \left(N^0_{xx} - N^{\text{Lévy}}_{xx}\right) 100/N^{\text{Lévy}}_{xx}$) for the SCSC plate

		Present			Herrmann et al. (2018)		
b/h		Error in %	$\bar{N}^0_{xx}$	a/b	Error in %	$\bar{N}^0_{xx}$	a/b
200	min	0.01	7.50	0.6	0.68	10.01	0.5
	max	0.31	5.96	1.35	3.33	6.14	1.35
100	min	0.04	6.90	0.5	1.00	6.97	0.5
	max	0.44	5.97	1.1	3.40	6.15	1.1
50	min	0.17	6.01	0.5	1.34	6.08	0.5
	max	0.75	5.81	1	3.78	5.98	1
20	min	0.88	4.90	0.5	2.31	4.97	0.5
	max	2.32	4.88	0.9	5.80	5.04	0.9
10	min	1.45	3.41	0.9	2.87	3.45	0.9
	max	4.47	3.41	0.85	8.67	3.55	0.85
5	min	0.94	1.46	0.7	1.98	1.48	0.7
	max	2.66	1.46	0.6	5.57	1.51	0.6

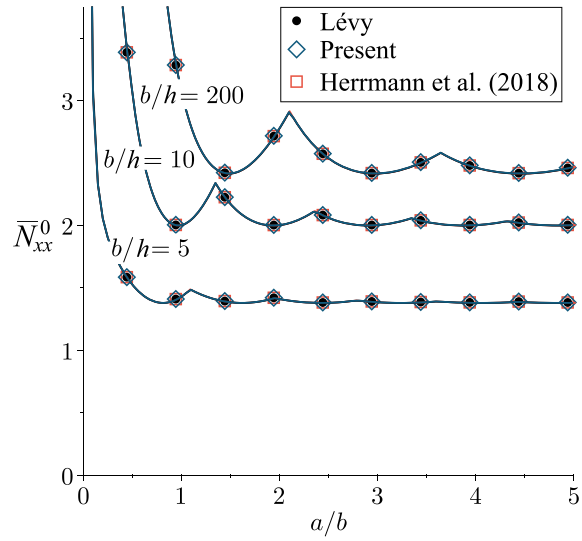


Fig. 14.13 Buckling curves for the SSSS plate, dimensionless buckling load $\bar{N}^0_{xx}$ as a function of the aspect ratio a/b

increasing thickness ratios, for $b/h = 20$ above 2% up to 4.70 % for very thick plates, see Table 14.5.

The SCSC plate is firmly clamped at both unloaded edges and therefore has the highest buckling load. The comparison between the present method and the analysis approach of

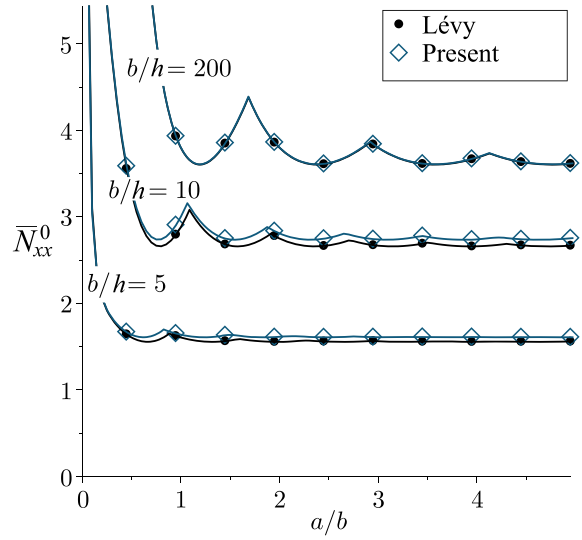


Fig. 14.14 Buckling curves for the SSSC plate, dimensionless buckling load $\bar{N}^0_{xx}$ as a function of the aspect ratio a/b

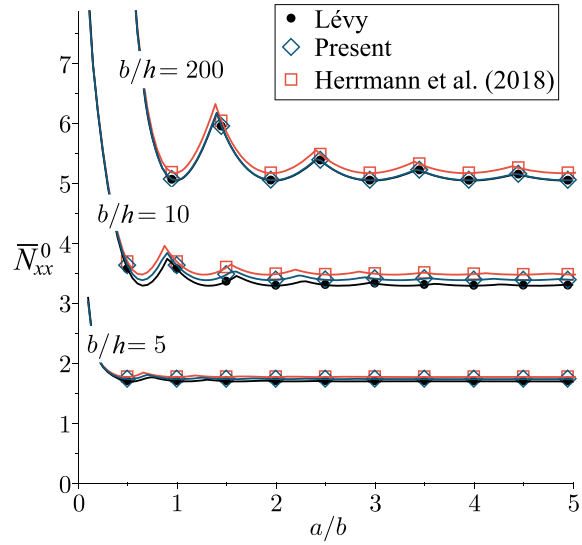


Fig. 14.15 Buckling curves for the SCSC plate, dimensionless buckling load $\bar{N}^0_{xx}$ as a function of the aspect ratio a/b

Herrmann et al. (2018) shows the clearest difference for very thin plates and becomes smaller for very thick plates, see Fig. 14.15. An error estimation is shown in Table 14.6.

So far, the limit cases $k = 0$ and $k \to \infty$ have been discussed for the restraint stiffnesses. In practice, the consideration of values between these two limiting factors is of interest. It is assumed that the elastic restraints at the unloaded edges of the plates have the same value ($k_1 = k_2$). In Fig. 14.16 the dimensionless buckling load for $a/b = 4$ is shown as a function of the elastic restraints (k_1, k_2) in a logarithmic scale. It can be observed that for

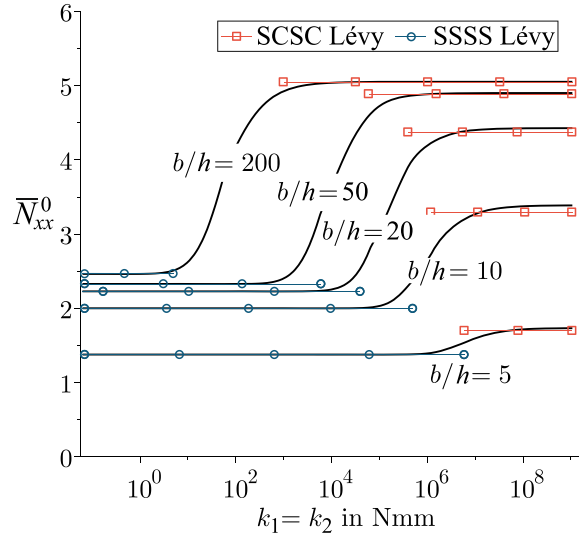


Fig. 14.16 Buckling curves for the SRSR plate, dimensionless buckling load $\bar{N}^0_{xx}$ as a function of the restraint stiffnesses ($k_1 = k_2$) for $a/b = 4$

small restraint values, all curves match the solution of the SSSS plate. The deviations are very small, as already mentioned above, see Table 14.4. The dimensionless buckling load $\bar{N}^0_{xx}$ shows a greater difference between the minimum and maximum values (k_1, k_2) for thin plates than for thick plates. A significant support effect of the restraints also occurs with thin plates at significantly lower restraint values than with thick plates. As expected, the buckling loads increase with increasing restraint stiffness. The slopes of the curves flatten out after a further increase in the degree of restraint and converge towards the results of the SCSC plate. After convergence is reached, the present solution systematically overestimates the Lévy-type solution as previously observed and shown in Table 14.6.

14.5 The Ritz Method for Arbitrary Symmetric Laminates

The previous sections dealt with the basics of the treatment of laminate buckling problems in the form of the so-called Rayleigh quotient. However, this approach is generally limited to rather simple types of load cases, laminate structures and boundary conditions, so it is of great practical interest to consider advanced energy-based methods. One such method is the Ritz method, which despite its relatively old origin is still very popular in engineering practice. Firstly, the basic formulaic relationships are explained in a compact manner. Afterwards, various load cases that can be treated with this method are considered and the basic characteristics of the respective buckling problems are explained. In addition, the influence of the bending-twisting coupling on the buckling behaviour of laminates under various load cases is investigated.

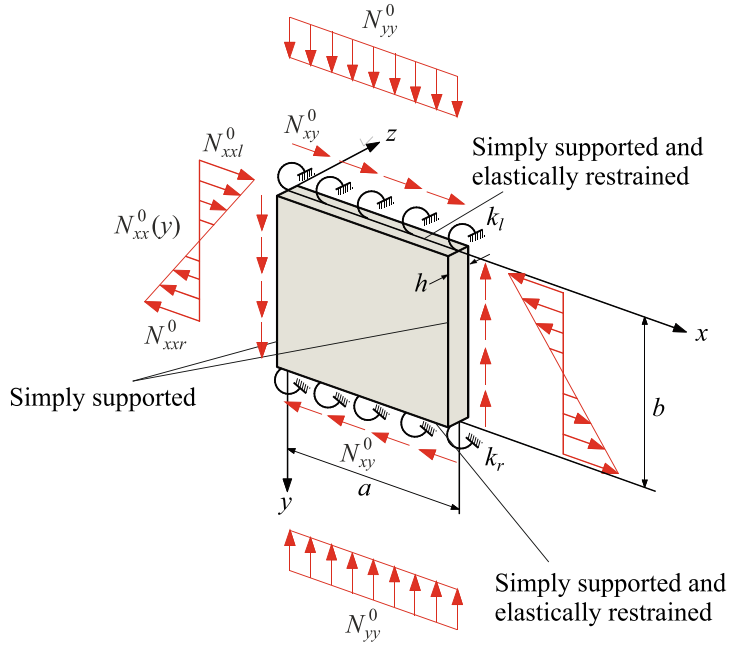


Fig. 14.17 Elastically restrained laminate under combined load

In the following, the Ritz method is used for the laminate situation shown in Fig. 14.17. The laminate has a symmetric layup, otherwise there are no further requirements for the employed stacking sequence. The laminate has the length a and the width b. The load consists of a linearly varying normal force flow $N^0_{xx}(y) = \frac{N^0_{xx}}{b}[(\psi - 1)\, y + b]$ with the edge values $N^0_{xxl} = N^0_{xx}(y = 0) = N^0_{xx}$ and $N^0_{xxr} = N^0_{xx}(y = b) = \psi N^0_{xx}$ (where ψ is a real number and is a multiple of the boundary value $N^0_{xxl} = N^0_{xx}(y = 0) = N^0_{xx}$), and the constant force flows N^0_{yy} and N^0_{xy}. The laminate is simply supported at all four edges. Furthermore, the two edges at $y = 0$ and $y = b$ are elastically restrained (spring stiffnesses k_l and k_r). However, the Ritz formulation to be developed can easily be extended to other boundary conditions without fundamental difficulties, as will be shown later.

Similar to the Rayleigh quotient already presented, the Ritz method is also based on analyzing the energy balance of the buckled laminate panel. At present, the total elastic potential Π of the buckled laminate is composed of the strain energy Π_i, the energy stored in the springs Π_s and the potential of the loads Π_a, i.e.

$$\Pi = \Pi_i + \Pi_a + \Pi_s, \tag{14.168}$$

wherein:

$$\Pi_i = \frac{1}{2}\int_0^a \int_0^b \left[D_{11}\left(\frac{\partial^2 w_0}{\partial x^2}\right)^2 + D_{22}\left(\frac{\partial^2 w_0}{\partial y^2}\right)^2 + 2D_{12}\frac{\partial^2 w_0}{\partial x^2}\frac{\partial^2 w_0}{\partial y^2}\right] \mathrm{d}y\mathrm{d}x$$
$$+ 2\int_0^a \int_0^b \left[\left(D_{16}\frac{\partial^2 w_0}{\partial x^2} + D_{26}\frac{\partial^2 w_0}{\partial y^2} + D_{66}\frac{\partial^2 w_0}{\partial x \partial y}\right)\frac{\partial^2 w_0}{\partial x \partial y}\right] \mathrm{d}y\mathrm{d}x,$$
$$\Pi_a = -\frac{1}{2}\int_0^a \int_0^b \left[\Lambda N_{xx}^0 \left(\frac{\partial w_0}{\partial x}\right)^2 + \Lambda N_{yy}^0 \left(\frac{\partial w_0}{\partial y}\right)^2 + 2\Lambda N_{xy}^0 \frac{\partial w_0}{\partial x}\frac{\partial w_0}{\partial y}\right] \mathrm{d}y\mathrm{d}x,$$
$$\Pi_s = \frac{1}{2}\int_0^a \left[k_l \left(\left.\frac{\partial w_0}{\partial y}\right|_{y=0}\right)^2 + k_r \left(\left.\frac{\partial w_0}{\partial y}\right|_{y=b}\right)^2\right] \mathrm{d}x. \tag{14.169}$$

Here, the given load case combination is multiplied by the unknown load multiplier Λ which is the load factor or load multiplier that indicates the multiple by which the given load can be increased before the laminate buckles. Some more details on this will follow later.

An approach for the buckling shape w_0 is now used as follows:

$$w_0 = \sum_{m=1}^{M}\sum_{n=1}^{N} W_{mn} w_{1m}(x)\, w_{2n}(y). \tag{14.170}$$

The shape functions w_{1m} and w_{2n} must at least fulfil all underlying static or geometric boundary conditions identically. The fulfilment of dynamic boundary conditions is not necessary, but is of course advantageous in terms of the accuracy of the results. The values W_{mn} are indeterminate coefficients. The number of shape functions is characterized by the integers M and N. As already shown above, the Ritz method reduces to the so-called Rayleigh quotient when using $M = 1$ and $N = 1$ shape functions. Inserting the approach (14.170) into the potential formulations (14.169) results in

$$\Pi_i = \frac{D_{11}}{2}\sum_{m=1}^{M}\sum_{n=1}^{N}\sum_{p=1}^{M}\sum_{q=1}^{N} W_{mn}W_{pq}\int_0^a \frac{\mathrm{d}^2 w_{1m}}{\mathrm{d}x^2}\frac{\mathrm{d}^2 w_{1p}}{\mathrm{d}x^2}\mathrm{d}x \int_0^b w_{2n}w_{2q}\mathrm{d}y$$
$$+ \frac{D_{22}}{2}\sum_{m=1}^{M}\sum_{n=1}^{N}\sum_{p=1}^{M}\sum_{q=1}^{N} W_{mn}W_{pq}\int_0^a w_{1m}w_{1p}\mathrm{d}x \int_0^b \frac{\mathrm{d}^2 w_{2n}}{\mathrm{d}y^2}\frac{\mathrm{d}^2 w_{2q}}{\mathrm{d}y^2}\mathrm{d}y$$
$$+ D_{12}\sum_{m=1}^{M}\sum_{n=1}^{N}\sum_{p=1}^{M}\sum_{q=1}^{N} W_{mn}W_{pq}\int_0^a \frac{\mathrm{d}^2 w_{1m}}{\mathrm{d}x^2}w_{1p}\mathrm{d}x \int_0^b w_{2n}\frac{\mathrm{d}^2 w_{2q}}{\mathrm{d}y^2}\mathrm{d}y,$$
$$+ 2D_{16}\sum_{m=1}^{M}\sum_{n=1}^{N}\sum_{p=1}^{M}\sum_{q=1}^{N} W_{mn}W_{pq}\int_0^a \frac{\mathrm{d}^2 w_{1m}}{\mathrm{d}x^2}\frac{\mathrm{d}w_{1p}}{\mathrm{d}x}\mathrm{d}x \int_0^b w_{2n}\frac{\mathrm{d}w_{2q}}{\mathrm{d}y}\mathrm{d}y$$
$$+ 2D_{26}\sum_{m=1}^{M}\sum_{n=1}^{N}\sum_{p=1}^{M}\sum_{q=1}^{N} W_{mn}W_{pq}\int_0^a w_{1m}\frac{\mathrm{d}w_{1p}}{\mathrm{d}x}\mathrm{d}x \int_0^b \frac{\mathrm{d}^2 w_{2n}}{\mathrm{d}y^2}\frac{\mathrm{d}w_{2q}}{\mathrm{d}y}\mathrm{d}y$$

$$+ 2D_{66} \sum_{m=1}^{M} \sum_{n=1}^{N} \sum_{p=1}^{M} \sum_{q=1}^{N} W_{mn} W_{pq} \int_0^a \frac{\mathrm{d}w_{1m}}{\mathrm{d}x} \frac{\mathrm{d}w_{1p}}{\mathrm{d}x} \mathrm{d}x \int_0^b \frac{\mathrm{d}w_{2n}}{\mathrm{d}y} \frac{\mathrm{d}w_{2q}}{\mathrm{d}y} \mathrm{d}y,$$

$$\begin{aligned}
\Pi_a = & -\Lambda \frac{N_{xx}^0}{2b} (\psi - 1) \sum_{m=1}^{M} \sum_{n=1}^{N} \sum_{p=1}^{M} \sum_{q=1}^{N} W_{mn} W_{pq} \int_0^a \frac{\mathrm{d}w_{1m}}{\mathrm{d}x} \frac{\mathrm{d}w_{1p}}{\mathrm{d}x} \mathrm{d}x \int_0^b w_{2n} w_{2q} y \mathrm{d}y \\
& - \Lambda \frac{N_{xx}^0}{2} \sum_{m=1}^{M} \sum_{n=1}^{N} \sum_{p=1}^{M} \sum_{q=1}^{N} W_{mn} W_{pq} \int_0^a \frac{\mathrm{d}w_{1m}}{\mathrm{d}x} \frac{\mathrm{d}w_{1p}}{\mathrm{d}x} \mathrm{d}x \int_0^b w_{2n} w_{2q} \mathrm{d}y \\
& - \frac{\Lambda N_{yy}^0}{2} \sum_{m=1}^{M} \sum_{n=1}^{N} \sum_{p=1}^{M} \sum_{q=1}^{N} W_{mn} W_{pq} \int_0^a w_{1m} w_{1p} \mathrm{d}x \int_0^b \frac{\mathrm{d}w_{2n}}{\mathrm{d}y} \frac{\mathrm{d}w_{2q}}{\mathrm{d}y} \mathrm{d}y \\
& - \Lambda N_{xy}^0 \sum_{m=1}^{M} \sum_{n=1}^{N} \sum_{p=1}^{M} \sum_{q=1}^{N} W_{mn} W_{pq} \int_0^a \frac{\mathrm{d}w_{1m}}{\mathrm{d}x} w_{1p} \mathrm{d}x \int_0^a w_{2n} \frac{\mathrm{d}w_{2q}}{\mathrm{d}y} \mathrm{d}y,
\end{aligned}$$

$$\begin{aligned}
\Pi_s = & \frac{k_l}{2} \sum_{m=1}^{M} \sum_{n=1}^{N} \sum_{p=1}^{M} \sum_{q=1}^{N} W_{mn} W_{pq} \int_0^a w_{1m} w_{1p} \mathrm{d}x \left(\frac{\mathrm{d}w_{2n}}{\mathrm{d}y} \frac{\mathrm{d}w_{2q}}{\mathrm{d}y} \right) \Big|_{y=0} \\
& + \frac{k_r}{2} \sum_{m=1}^{M} \sum_{n=1}^{N} \sum_{p=1}^{M} \sum_{q=1}^{N} W_{mn} W_{pq} \int_0^a w_{1m} w_{1p} \mathrm{d}x \left(\frac{\mathrm{d}w_{2n}}{\mathrm{d}y} \frac{\mathrm{d}w_{2q}}{\mathrm{d}y} \right) \Big|_{y=b}.
\end{aligned} \tag{14.171}$$

We can use a compact notation as follows:

$$\begin{aligned}
\Pi_i &= \sum_{m=1}^{M} \sum_{n=1}^{N} \sum_{p=1}^{M} \sum_{q=1}^{N} W_{mn} W_{pq} \Gamma_i^{mnpq}, \\
\Pi_a &= -\Lambda \sum_{m=1}^{M} \sum_{n=1}^{N} \sum_{p=1}^{M} \sum_{q=1}^{N} W_{mn} W_{pq} \Gamma_a^{mnpq}, \\
\Pi_s &= \sum_{m=1}^{M} \sum_{n=1}^{N} \sum_{p=1}^{M} \sum_{q=1}^{N} W_{mn} W_{pq} \Gamma_s^{mnpq},
\end{aligned} \tag{14.172}$$

with the following abbreviations:

$$\Gamma_i^{mnpq} = \frac{1}{2}\left(D_{11}R_{22}^{mp}S_{00}^{nq} + D_{22}R_{00}^{mp}S_{22}^{nq}\right) + D_{12}R_{20}^{mp}S_{02}^{nq} + 2\left(D_{16}R_{21}^{mp}S_{01}^{nq} + D_{26}R_{01}^{mp}S_{21}^{nq} + D_{66}R_{11}^{mp}S_{11}^{nq}\right),$$

$$\Gamma_a^{mnpq} = \frac{1}{2}N_{xx}^0 R_{11}^{mp}\left[S_{00}^{nq} + (\psi - 1)\,T_{00}^{nq}\right] + \frac{1}{2}N_{yy}^0 R_{00}^{mp}S_{11}^{nq} + N_{xy}^0 R_{10}^{mp}S_{01}^{nq},$$

$$\Gamma_s^{mnpq} = \frac{1}{2}R_{00}^{mp}\left(k_l U_{11}^{nq} + k_r V_{11}^{nq}\right). \tag{14.173}$$

For the resultants of the shape functions in (14.171) and (14.173), the following abbreviations were introduced:

$$R_{ij}^{mp} = \int_0^a \frac{\mathrm{d}^i w_{1m}}{\mathrm{d}x^i}\frac{\mathrm{d}^j w_{1p}}{\mathrm{d}x^j}\mathrm{d}x, \quad S_{ij}^{nq} = \int_0^b \frac{\mathrm{d}^i w_{2n}}{\mathrm{d}y^i}\frac{\mathrm{d}^j w_{2q}}{\mathrm{d}y^j}\mathrm{d}y,$$
$$T_{00}^{nq} = \frac{1}{b}\int_0^b w_{2n}w_{2q}\,y\mathrm{d}y,$$
$$U_{11}^{nq} = \left.\frac{\mathrm{d}w_{2n}}{\mathrm{d}y}\right|_{y=0}\left.\frac{\mathrm{d}w_{2q}}{\mathrm{d}y}\right|_{y=0}, \quad V_{11}^{nq} = \left.\frac{\mathrm{d}w_{2n}}{\mathrm{d}y}\right|_{y=b}\left.\frac{\mathrm{d}w_{2q}}{\mathrm{d}y}\right|_{y=b}. \tag{14.174}$$

The buckling condition $\delta\Pi = 0$ leads to the following Ritz equations

$$\frac{\partial\Pi}{\partial W_{mn}} = 0. \tag{14.175}$$

Performing the differentiations required here results in the following eigenvalue problem:

$$\left[\underline{\underline{K}}_i + \underline{\underline{K}}_s - \Lambda\underline{\underline{K}}_a\right]\underline{W} = \underline{0}. \tag{14.176}$$

Here, the load factor Λ plays the role of the eigenvalue, and the associated eigenvector $\underline{W}$ then contains the respective constants W_{mn}. The matrices $\underline{\underline{K}}_i$ and $\underline{\underline{K}}_s$, which in this context can be considered as stiffness matrices of the laminate and the edge restraints, as well as the matrix $\underline{\underline{K}}_a$, also known as the geometric stiffness matrix, can be represented as follows:

$$\underline{\underline{K}}_i = \begin{bmatrix} \underline{\underline{K}}_i^{11} & \underline{\underline{K}}_i^{12} & \underline{\underline{K}}_i^{13} & \cdots & \underline{\underline{K}}_i^{1M} \\ \underline{\underline{K}}_i^{21} & \underline{\underline{K}}_i^{22} & \underline{\underline{K}}_i^{23} & \cdots & \underline{\underline{K}}_i^{2M} \\ \underline{\underline{K}}_i^{31} & \underline{\underline{K}}_i^{32} & \underline{\underline{K}}_i^{33} & \cdots & \underline{\underline{K}}_i^{3M} \\ \vdots & \vdots & \vdots & \ddots & \vdots \\ \underline{\underline{K}}_i^{M1} & \underline{\underline{K}}_i^{M2} & \underline{\underline{K}}_i^{M3} & \cdots & \underline{\underline{K}}_i^{MM} \end{bmatrix} = \left[\underline{\underline{K}}_i^{\gamma\delta} \right],$$

$$\underline{\underline{K}}_s = \begin{bmatrix} \underline{\underline{K}}_s^{11} & \underline{\underline{K}}_s^{12} & \underline{\underline{K}}_s^{13} & \cdots & \underline{\underline{K}}_s^{1M} \\ \underline{\underline{K}}_s^{21} & \underline{\underline{K}}_s^{22} & \underline{\underline{K}}_s^{23} & \cdots & \underline{\underline{K}}_s^{2M} \\ \underline{\underline{K}}_s^{31} & \underline{\underline{K}}_s^{32} & \underline{\underline{K}}_s^{33} & \cdots & \underline{\underline{K}}_s^{3M} \\ \vdots & \vdots & \vdots & \ddots & \vdots \\ \underline{\underline{K}}_s^{M1} & \underline{\underline{K}}_s^{M2} & \underline{\underline{K}}_s^{M3} & \cdots & \underline{\underline{K}}_s^{MM} \end{bmatrix} = \left[\underline{\underline{K}}_s^{\gamma\delta} \right],$$

$$\underline{\underline{K}}_a = \begin{bmatrix} \underline{\underline{K}}_a^{11} & \underline{\underline{K}}_a^{12} & \underline{\underline{K}}_a^{13} & \cdots & \underline{\underline{K}}_a^{1M} \\ \underline{\underline{K}}_a^{21} & \underline{\underline{K}}_a^{22} & \underline{\underline{K}}_a^{23} & \cdots & \underline{\underline{K}}_a^{2M} \\ \underline{\underline{K}}_a^{31} & \underline{\underline{K}}_a^{32} & \underline{\underline{K}}_a^{33} & \cdots & \underline{\underline{K}}_a^{3M} \\ \vdots & \vdots & \vdots & \ddots & \vdots \\ \underline{\underline{K}}_a^{M1} & \underline{\underline{K}}_a^{M2} & \underline{\underline{K}}_a^{M3} & \cdots & \underline{\underline{K}}_a^{MM} \end{bmatrix} = \left[\underline{\underline{K}}_a^{\gamma\delta} \right]. \tag{14.177}$$

The components $K_{\varrho\omega,i}^{\gamma\delta}$, $K_{\varrho\omega,s}^{\gamma\delta}$, $K_{\varrho\omega,a}^{\gamma\delta}$ of the submatrices $\underline{\underline{K}}_i^{\gamma\delta} = \left[K_{\varrho\omega,i}^{\gamma\delta} \right]$, $\underline{\underline{K}}_s^{\gamma\delta} = \left[K_{\varrho\omega,s}^{\gamma\delta} \right]$, $\underline{\underline{K}}_a^{\gamma\delta} = \left[K_{\varrho\omega,a}^{\gamma\delta} \right]$, with N rows and N columns, can be written as:

$$K_{\varrho\omega,i}^{\gamma\delta} = \Gamma_i^{\varrho\gamma\omega\delta} + \Gamma_i^{\omega\delta\varrho\gamma}, \quad K_{\varrho\omega,s}^{\gamma\delta} = \Gamma_s^{\varrho\gamma\omega\delta} + \Gamma_s^{\omega\delta\varrho\gamma}, \quad K_{\varrho\omega,a}^{\gamma\delta} = \Gamma_a^{\varrho\gamma\omega\delta} + \Gamma_a^{\omega\delta\varrho\gamma}. \tag{14.178}$$

If, as assumed here, all edges of the laminate are simply supported, then an approach of the type

$$w_0 = \sum_{m=1}^{m=M} \sum_{n=1}^{n=N} W_{mn} w_{1m}(x)\, w_{2n}(y) = \sum_{m=1}^{m=M} \sum_{n=1}^{n=N} W_{mn} \sin\left(\frac{m\pi x}{a}\right) \sin\left(\frac{n\pi y}{b}\right) \tag{14.179}$$

can be employed which fulfils all geometric boundary conditions identically. The resultants of the shape functions (14.174) can then be written as follows:

$$R_{00}^{mp} = \int_0^a w_{1m} w_{1p} \mathrm{d}x = \int_0^a \sin\left(\frac{m\pi x}{a}\right) \sin\left(\frac{p\pi x}{a}\right) \mathrm{d}x$$
$$= \begin{cases} 0 & \text{if } m \neq p \\ \frac{a}{2} & \text{if } m = p \end{cases},$$

$$R_{01}^{mp} = \int_0^a w_{1m} \frac{\mathrm{d}w_{1p}}{\mathrm{d}x} \mathrm{d}x = \frac{p\pi}{a} \int_0^a \sin\left(\frac{m\pi x}{a}\right) \cos\left(\frac{p\pi x}{a}\right) \mathrm{d}x$$

$$= \begin{cases} 0 & \text{if } m+p = \text{even} \\ \dfrac{2mp}{m^2-p^2} & \text{if } m+p = \text{odd} \end{cases},$$

$$R_{02}^{mp} = \int_0^a w_{1m} \frac{\mathrm{d}^2 w_{1p}}{\mathrm{d}x^2} \mathrm{d}x = -\left(\frac{p\pi}{a}\right)^2 \int_0^a \sin\left(\frac{m\pi x}{a}\right) \sin\left(\frac{p\pi x}{a}\right) \mathrm{d}x$$
$$= \begin{cases} 0 & \text{if } m \neq p \\ -\dfrac{p^2\pi^2}{2a} & \text{if } m = p \end{cases},$$

$$R_{10}^{mp} = \int_0^a \frac{\mathrm{d}w_{1m}}{\mathrm{d}x} w_{1p} \mathrm{d}x = \frac{m\pi}{a} \int_0^a \cos\left(\frac{m\pi x}{a}\right) \sin\left(\frac{p\pi x}{a}\right) \mathrm{d}x$$
$$= \begin{cases} 0 & \text{if } m+p = \text{even} \\ \dfrac{2mp}{p^2-m^2} & \text{if } m+p = \text{odd} \end{cases},$$

$$R_{11}^{mp} = \int_0^a \frac{\mathrm{d}w_{1m}}{\mathrm{d}x} \frac{\mathrm{d}w_{1p}}{\mathrm{d}x} \mathrm{d}x = \frac{m\pi}{a} \frac{p\pi}{a} \int_0^a \cos\left(\frac{m\pi x}{a}\right) \cos\left(\frac{p\pi x}{a}\right) \mathrm{d}x$$
$$= \begin{cases} 0 & \text{if } m \neq p \\ \dfrac{mp\pi^2}{2a} & \text{if } m = p \end{cases},$$

$$R_{12}^{mp} = \int_0^a \frac{\mathrm{d}w_{1m}}{\mathrm{d}x} \frac{\mathrm{d}^2 w_{1p}}{\mathrm{d}x^2} \mathrm{d}x = -\frac{m\pi}{a} \left(\frac{p\pi}{a}\right)^2 \int_0^a \cos\left(\frac{m\pi x}{a}\right) \sin\left(\frac{p\pi x}{a}\right) \mathrm{d}x$$
$$= \begin{cases} 0 & \text{if } m+p = \text{even} \\ -\dfrac{2mp^3\pi^2}{a^2\left(p^2-m^2\right)} & \text{if } m+p = \text{odd} \end{cases},$$

$$R_{20}^{mp} = \int_0^a \frac{\mathrm{d}^2 w_{1m}}{\mathrm{d}x^2} w_{1p} \mathrm{d}x = -\left(\frac{m\pi}{a}\right)^2 \int_0^a \sin\left(\frac{m\pi x}{a}\right) \sin\left(\frac{p\pi x}{a}\right) \mathrm{d}x$$
$$= \begin{cases} 0 & \text{if } m \neq p \\ -\dfrac{m^2\pi^2}{2a} & \text{if } m = p \end{cases},$$

$$R_{21}^{mp} = \int_0^a \frac{\mathrm{d}^2 w_{1m}}{\mathrm{d}x^2} \frac{\mathrm{d}w_{1p}}{\mathrm{d}x} \mathrm{d}x = -\left(\frac{m\pi}{a}\right)^2 \frac{p\pi}{a} \int_0^a \sin\left(\frac{m\pi x}{a}\right) \cos\left(\frac{p\pi x}{a}\right) \mathrm{d}x$$
$$= \begin{cases} 0 & \text{if } m+p = \text{even} \\ -\dfrac{2m^3p\pi^2}{a^2\left(m^2-p^2\right)} & \text{if } m+p = \text{odd} \end{cases},$$

$$R_{22}^{mp} = \int_0^a \frac{\mathrm{d}^2 w_{1m}}{\mathrm{d}x^2} \frac{\mathrm{d}^2 w_{1p}}{\mathrm{d}x^2} \mathrm{d}x = \left(\frac{m\pi}{a}\right)^2 \left(\frac{p\pi}{a}\right)^2 \int_0^a \sin\left(\frac{m\pi x}{a}\right) \sin\left(\frac{p\pi x}{a}\right) \mathrm{d}x$$

$$= \begin{cases} 0 & \text{if } m \neq p \\ \dfrac{m^2 p^2 \pi^4}{2a^3} & \text{if } m = p \end{cases},$$

$$T_{00}^{nq} = \frac{1}{b}\int_0^b w_{2n} w_{2q}\, y \mathrm{d}y = \frac{1}{b}\int_0^b \sin\left(\frac{n\pi y}{b}\right)\sin\left(\frac{q\pi y}{b}\right) y \mathrm{d}y$$

$$= \begin{cases} \dfrac{b}{4} & \text{if } n = q \\ \dfrac{2bnq}{\pi^2\left(n^2 - q^2\right)^2}\left[(-1)^{n+q} - 1\right] & \text{if } n \neq q \end{cases},$$

$$U_{11}^{nq} = \left.\frac{\mathrm{d}w_{2n}}{\mathrm{d}y}\right|_{y=0} \left.\frac{\mathrm{d}w_{2q}}{\mathrm{d}y}\right|_{y=0} = nq\left(\frac{\pi}{b}\right)^2,$$

$$V_{11}^{nq} = \left.\frac{\mathrm{d}w_{2n}}{\mathrm{d}y}\right|_{y=b} \left.\frac{\mathrm{d}w_{2q}}{\mathrm{d}y}\right|_{y=b} = nq\left(\frac{\pi}{b}\right)^2 \cos(n\pi)\cos(q\pi)$$

$$= \begin{cases} nq\left(\dfrac{\pi}{b}\right)^2 & \text{if } n+q = \text{even} \\ -nq\left(\dfrac{\pi}{b}\right)^2 & \text{if } n+q = \text{odd} \end{cases}. \tag{14.180}$$

The resultants

$$S_{ij}^{nq} = \int_0^b \frac{\mathrm{d}^i w_{2n}}{\mathrm{d}y^i}\frac{\mathrm{d}^j w_{2q}}{\mathrm{d}y^j}\mathrm{d}y \tag{14.181}$$

can be determined from the already determined resultants R_{ij}^{mp} by replacing the length a with the width b in the corresponding expressions and also exchanging the indices m and p with the indices n and q. This remains here without further representation.

The Ritz method can be used to solve a number of practically relevant stability problems efficiently and yet with high precision, which will be discussed in detail later. Since the accuracy of the results, similar to a finite element calculation, strongly depends on the number of shape functions when using the Ritz method, convergence studies must always show whether the series expansion used (14.170) is sufficient or more shape functions are necessary.

In general, the procedure described is not limited to laminates with simply supported edges. In principle, all other possible combinations of boundary conditions can be treated with this method; for this purpose, only suitable shape functions must be found that fulfil at least all geometric boundary conditions. This will be discussed in more detail below. In order to make the explanations clearer, the elastic potential of the buckled laminate (whereby we will limit ourselves to laminates without elastic edge restraints and to constant edge loads for the sake of simplicity) is given in dimensionless notation, which results from the coordinate transformation

$$\xi_1 = \frac{x}{a}, \quad \xi_2 = \frac{y}{b}. \tag{14.182}$$

The approach for the buckling mode reads:

$$\bar{w}_0 = \sum_{m=1}^{M} \sum_{n=1}^{N} \bar{W}_{mn} \bar{w}_{1m}(\xi_1)\, \bar{w}_{2n}(\xi_2). \tag{14.183}$$

The following formulation can then be given for the dimensionless potential $\bar{\Pi}$:

$$\begin{aligned}\bar{\Pi} = \sum_{m=1}^{M} \sum_{n=1}^{N} \sum_{p=1}^{M} \sum_{q=1}^{N} \bar{W}_{mn} \bar{W}_{pq} \Bigg[& \frac{1}{2\alpha^2} \bar{R}_{22} \bar{S}_{00} + \frac{\alpha^2}{2} \bar{R}_{00} \bar{S}_{22} \\ & + \beta\zeta \bar{R}_{20} \bar{S}_{02} + (1-\zeta)\,\beta \bar{R}_{11} \bar{S}_{11} + 2\frac{\gamma}{\alpha} \bar{R}_{21} \bar{S}_{01} + 2\delta\alpha \bar{R}_{01} \bar{S}_{21} \\ & - \pi^2 \left(\frac{1}{2} \bar{N}^0_{xx} \bar{R}_{11} \bar{S}_{00} + \frac{1}{2} \bar{N}^0_{yy} \bar{R}_{00} \bar{S}_{11} + \bar{N}^0_{xy} \bar{R}_{10} \bar{S}_{01} \right) \Bigg]. \end{aligned} \tag{14.184}$$

The characteristic dimensionless variables already known from previous sections were used here. The resultants of the shape functions in the approach (14.183) are then:

$$\bar{R}^{mp}_{ij} = \int_0^1 \frac{\mathrm{d}^i \bar{w}_{1m}}{\mathrm{d}\xi_1^i} \frac{\mathrm{d}^j \bar{w}_{1p}}{\mathrm{d}\xi_1^j} \mathrm{d}\xi_1, \quad \bar{S}^{nq}_{ij} = \int_0^1 \frac{\mathrm{d}^i \bar{w}_{2n}}{\mathrm{d}\xi_2^i} \frac{\mathrm{d}^j \bar{w}_{2q}}{\mathrm{d}\xi_2^j} \mathrm{d}\xi_2. \tag{14.185}$$

The assignment of the individual matrices in the eigenvalue problem

$$\left[\underline{\underline{\bar{K}}}_i - \Lambda \underline{\underline{\bar{K}}}_a \right] \underline{\bar{W}} = \underline{0} \tag{14.186}$$

reads:

$$\begin{aligned} \underline{\underline{\bar{K}}}_i &= \begin{bmatrix} \underline{\underline{\bar{K}}}_i^{11} & \underline{\underline{\bar{K}}}_i^{12} & \underline{\underline{\bar{K}}}_i^{13} & \cdots & \underline{\underline{\bar{K}}}_i^{1M} \\ \underline{\underline{\bar{K}}}_i^{21} & \underline{\underline{\bar{K}}}_i^{22} & \underline{\underline{\bar{K}}}_i^{23} & \cdots & \underline{\underline{\bar{K}}}_i^{2M} \\ \underline{\underline{\bar{K}}}_i^{31} & \underline{\underline{\bar{K}}}_i^{32} & \underline{\underline{\bar{K}}}_i^{33} & \cdots & \underline{\underline{\bar{K}}}_i^{3M} \\ \vdots & \vdots & \vdots & \ddots & \vdots \\ \underline{\underline{\bar{K}}}_i^{M1} & \underline{\underline{\bar{K}}}_i^{M2} & \underline{\underline{\bar{K}}}_i^{M3} & \cdots & \underline{\underline{\bar{K}}}_i^{MM} \end{bmatrix} = \left[\underline{\underline{\bar{K}}}_i^{\gamma\delta} \right], \\ \underline{\underline{\bar{K}}}_a &= \begin{bmatrix} \underline{\underline{\bar{K}}}_a^{11} & \underline{\underline{\bar{K}}}_a^{12} & \underline{\underline{\bar{K}}}_a^{13} & \cdots & \underline{\underline{\bar{K}}}_a^{1M} \\ \underline{\underline{\bar{K}}}_a^{21} & \underline{\underline{\bar{K}}}_a^{22} & \underline{\underline{\bar{K}}}_a^{23} & \cdots & \underline{\underline{\bar{K}}}_a^{2M} \\ \underline{\underline{\bar{K}}}_a^{31} & \underline{\underline{\bar{K}}}_a^{32} & \underline{\underline{\bar{K}}}_a^{33} & \cdots & \underline{\underline{\bar{K}}}_a^{3M} \\ \vdots & \vdots & \vdots & \ddots & \vdots \\ \underline{\underline{\bar{K}}}_a^{M1} & \underline{\underline{\bar{K}}}_a^{M2} & \underline{\underline{\bar{K}}}_a^{M3} & \cdots & \underline{\underline{\bar{K}}}_a^{MM} \end{bmatrix} = \left[\underline{\underline{\bar{K}}}_a^{\gamma\delta} \right]. \end{aligned} \tag{14.187}$$

The components $\bar{K}^{\gamma\delta}_{\varrho\omega,i}$, $\bar{K}^{\gamma\delta}_{\varrho\omega,a}$ of the submatrices $\underline{\underline{\bar{K}}}_i^{\gamma\delta} = \left[\bar{K}^{\gamma\delta}_{\varrho\omega,i} \right]$, $\underline{\underline{\bar{K}}}_a^{\gamma\delta} = \left[\bar{K}^{\gamma\delta}_{\varrho\omega,a} \right]$, consisting of N rows and N columns, can be written as:

$$\begin{aligned}\bar{K}^{\gamma\delta}_{\varrho\omega,i} &= \frac{1}{\alpha^2}\bar{R}^{\gamma\delta}_{22}\bar{S}^{\varrho\omega}_{00} + \alpha^2\bar{R}^{\gamma\delta}_{00}\bar{S}^{\varrho\omega}_{22} + \beta\zeta\left(\bar{R}^{\gamma\delta}_{02}\bar{S}^{\varrho\omega}_{20} + \bar{R}^{\gamma\delta}_{20}\bar{S}^{\varrho\omega}_{02}\right)\\ &\quad + 2\beta(1-\zeta)\,\bar{R}^{\gamma\delta}_{11}\bar{S}^{\varrho\omega}_{11} + 2\frac{\gamma_{16}}{\alpha}\left(\bar{R}^{\gamma\delta}_{12}\bar{S}^{\varrho\omega}_{10} + \bar{R}^{\gamma\delta}_{21}\bar{S}^{\varrho\omega}_{01}\right)\\ &\quad + 2\gamma_{26}\alpha\left(\bar{R}^{\gamma\delta}_{10}\bar{S}^{\varrho\omega}_{12} + \bar{R}^{\gamma\delta}_{01}\bar{S}^{\varrho\omega}_{21}\right),\\ \bar{K}^{\gamma\delta}_{\varrho\omega,a} &= \pi^2\left[\bar{N}^0_{xx}\bar{R}^{\gamma\delta}_{11}\bar{S}^{\varrho\omega}_{00} + \bar{N}^0_{yy}\bar{R}^{\gamma\delta}_{00}\bar{S}^{\varrho\omega}_{11} + \bar{N}^0_{xy}\left(\bar{R}^{\gamma\delta}_{01}\bar{S}^{\varrho\omega}_{10} + \bar{R}^{\gamma\delta}_{10}\bar{S}^{\varrho\omega}_{01}\right)\right]. \end{aligned} \tag{14.188}$$

For better differentiation, we have used the notation $\gamma = \gamma_{16}$ and $\delta = \gamma_{26}$ for the two bending-twisting coupling degrees.

Let us now look again at the case of the simply supported plate. The shape functions are then as follows:

$$\bar{w}_0 = \sum_{m=1}^{M}\sum_{n=1}^{N}\bar{W}_{mn}\bar{w}_{1m}(\xi_1)\,\bar{w}_{2n}(\xi_2) = \sum_{m=1}^{M}\sum_{n=1}^{N}\bar{W}_{mn}\sin(m\pi\xi_1)\sin(n\pi\xi_2). \tag{14.189}$$

The resultants in (14.185) can then be explicitly specified as:

$$\begin{aligned}
\bar{R}^{mp}_{00} &= \int_0^1 \bar{w}_{1m}\bar{w}_{1p}\mathrm{d}\xi_1 &&= \begin{cases} 0 \text{ if } m \neq p \\ \frac{1}{2} \text{ if } m = p \end{cases},\\
\bar{R}^{mp}_{01} &= \int_0^1 \bar{w}_{1m}\frac{\mathrm{d}\bar{w}_{1p}}{\mathrm{d}\xi_1}\mathrm{d}\xi_1 &&= \begin{cases} 0 & \text{if } m+p = \text{even} \\ \frac{2mp}{m^2-p^2} & \text{if } m+p = \text{odd} \end{cases},\\
\bar{R}^{mp}_{02} &= \int_0^1 \bar{w}_{1m}\frac{\mathrm{d}^2\bar{w}_{1p}}{\mathrm{d}\xi_1^2}\mathrm{d}\xi_1 &&= \begin{cases} 0 \text{ if } m \neq p \\ -\frac{p^2\pi^2}{2} \text{ if } m = p \end{cases},\\
\bar{R}^{mp}_{10} &= \int_0^1 \frac{\mathrm{d}\bar{w}_{1m}}{\mathrm{d}\xi_1}\bar{w}_{1p}\mathrm{d}\xi_1 &&= \begin{cases} 0 & \text{if } m+p = \text{even} \\ \frac{2mp}{p^2-m^2} & \text{if } m+p = \text{odd} \end{cases},\\
\bar{R}^{mp}_{11} &= \int_0^1 \frac{\mathrm{d}\bar{w}_{1m}}{\mathrm{d}\xi_1}\frac{\mathrm{d}\bar{w}_{1p}}{\mathrm{d}\xi_1}\mathrm{d}\xi_1 &&= \begin{cases} 0 \text{ if } m \neq p \\ \frac{mp\pi^2}{2} \text{ if } m = p \end{cases},\\
\bar{R}^{mp}_{12} &= \int_0^1 \frac{\mathrm{d}\bar{w}_{1m}}{\mathrm{d}\xi_1}\frac{\mathrm{d}^2\bar{w}_{1p}}{\mathrm{d}\xi_1^2}\mathrm{d}\xi_1 &&= \begin{cases} 0 & \text{if } m+p = \text{even} \\ -\frac{2mp^3\pi^2}{p^2-m^2} & \text{if } m+p = \text{odd} \end{cases},\\
\bar{R}^{mp}_{20} &= \int_0^1 \frac{\mathrm{d}^2\bar{w}_{1m}}{\mathrm{d}\xi_1^2}\bar{w}_{1p}\mathrm{d}\xi_1 &&= \begin{cases} 0 \text{ if } m \neq p \\ -\frac{m^2\pi^2}{2} \text{ if } m = p \end{cases},\\
\bar{R}^{mp}_{21} &= \int_0^1 \frac{\mathrm{d}^2\bar{w}_{1m}}{\mathrm{d}\xi_1^2}\frac{\mathrm{d}\bar{w}_{1p}}{\mathrm{d}\xi_1}\mathrm{d}\xi_1 &&= \begin{cases} 0 & \text{if } m+p = \text{even} \\ -\frac{2m^3p\pi^2}{m^2-p^2} & \text{if } m+p = \text{odd} \end{cases},\\
\bar{R}^{mp}_{22} &= \int_0^1 \frac{\mathrm{d}^2\bar{w}_{1m}}{\mathrm{d}\xi_1^2}\frac{\mathrm{d}^2\bar{w}_{1p}}{\mathrm{d}\xi_1^2}\mathrm{d}\xi_1 &&= \begin{cases} 0 \text{ if } m \neq p \\ \frac{m^2p^2\pi^4}{2} \text{ if } m = p \end{cases}.
\end{aligned} \tag{14.190}$$

The resultants $\bar{S}_{ij}^{nq}$ can be obtained from this by exchanging the indices m and p for the indices n and q.

Now consider the case where the analyzed laminate is rigidly clamped at all four edges. The boundary conditions are then in dimensionless notation:

$$\begin{gathered}\bar{w}_0(\xi_1=0)=0,\quad \bar{w}_0(\xi_1=1)=0,\quad \bar{w}_0(\xi_2=0)=0,\quad \bar{w}_0(\xi_2=1)=0,\\ \frac{\partial\bar{w}_0}{\partial\xi_1}(\xi_1=0)=0,\quad \frac{\partial\bar{w}_0}{\partial\xi_1}(\xi_1=1)=0,\quad \frac{\partial\bar{w}_0}{\partial\xi_2}(\xi_2=0)=0,\quad \frac{\partial\bar{w}_0}{\partial\xi_2}(\xi_2=1)=0.\end{gathered} \tag{14.191}$$

In this case, it is advisable to use an approach of the following form for the buckling shape $\bar{w}_0$:

$$\begin{aligned}\bar{w}_0 &= \sum_{m=1}^{M}\sum_{n=1}^{N}\bar{W}_{mn}\bar{w}_{1m}(\xi_1)\,\bar{w}_{2n}(\xi_2)\\ &= \sum_{m=1}^{M}\sum_{n=1}^{N}\bar{W}_{mn}\{\cos[(m-2)\pi\xi_1]-\cos(m\pi\xi_1)\}\{\cos[(n-2)\pi\xi_2]-\cos(n\pi\xi_2)\}.\end{aligned} \tag{14.192}$$

The resultants $\bar{R}_{ij}^{mp}$ can be explicitly specified for this case as:

$$\bar{R}_{00}^{mp}=\begin{cases}\frac{3}{2} & \text{if } m=p=2\\ 1 & \text{if } m=p\\ -\frac{1}{2} & \text{if } p=m-2 \text{ or } m=p-2\\ 0 & \text{else}\end{cases},$$

$$\bar{R}_{01}^{mp}=\begin{cases}0 & \text{if } m+p=\text{even}\\ -\dfrac{32(p-1)(m-1)\left(m^2+p^2-2m-2p\right)}{(m-p)(m+p)(m+p-2)(m-p-2)(m-p+2)(m+p-4)} & \text{if } m+p=\text{odd}\end{cases},$$

$$\bar{R}_{02}^{mp}=\begin{cases}\pi^2\left(-m^2+2m-2\right) & \text{if } m=p\\ \frac{\pi^2m^2}{2} & \text{if } m=p-2\\ \frac{\pi^2p^2}{2} & \text{if } p=m-2\\ 0 & \text{else}\end{cases},$$

$$\bar{R}_{10}^{mp}=\begin{cases}0 & \text{if } m+p=\text{even}\\ \dfrac{32(m-1)(p-1)\left(m^2+p^2-2m-2p\right)}{(p-m)(m+p)(m+p-2)(p-m-2)(p-m+2)(m+p-4)} & \text{if } m+p=\text{odd}\end{cases},$$

$$\bar{R}_{11}^{mp}=\begin{cases}\pi^2\left(m^2-2m+2\right) & \text{if } m=p\\ -\frac{\pi^2m^2}{2} & \text{if } m=p-2\\ -\frac{\pi^2p^2}{2} & \text{if } p=m-2\\ 0 & \text{else}\end{cases},$$

$$\bar{R}_{12}^{mp} = \begin{cases} 0 & \text{if } m+p = \text{even} \\ -\dfrac{64\pi^2 (p-1)(m-1)\left[m^2p^2 - 2mp(m+p) + 2\left(m^2+p^2\right) + 4(mp-m-p)\right]}{(m+p-2)(m-p+2)(m-p-2)(m-p)(m+p)(m+p-4)} & \\ & \text{if } m+p = \text{odd} \end{cases},$$

$$\bar{R}_{20}^{mp} = \begin{cases} \pi^2\left(-m^2+2m-2\right) & \text{if } m = p \\ \dfrac{\pi^2 m^2}{2} & \text{if } m = p-2 \\ \dfrac{\pi^2 p^2}{2} & \text{if } p = m-2 \\ 0 & \text{else} \end{cases},$$

$$\bar{R}_{21}^{mp} = \begin{cases} 0 & \text{if } m+p = \text{even} \\ -\dfrac{64\pi^2 (m-1)(p-1)\left[m^2p^2 - 2mp(m+p) + 2\left(m^2+p^2\right) + 4(mp-m-p)\right]}{(m+p-2)(p-m+2)(p-m-2)(p-m)(m+p)(m+p-4)} & \\ & \text{if } m+p = \text{odd} \end{cases},$$

$$\bar{R}_{22}^{mp} = \begin{cases} \dfrac{\pi^4}{2}\left[(m-2)^4 - m^4\right] & \text{if } m = p \\ -\dfrac{\pi^4 m^4}{2} & \text{if } m = p-2 \\ -\dfrac{\pi^4 p^4}{2} & \text{if } p = m-2 \\ 0 & \text{else} \end{cases}. \tag{14.193}$$

The resultants $\bar{S}_{ij}^{nq}$ can be specified analogously if the indices m and p are exchanged for the indices n and q.

For further combinations of boundary conditions, the following approaches can be recommended for the buckling shape $\bar{w}_0$. If we consider a laminate that is simply supported at the edges at $x = 0$ and $x = a$ and clamped at the edges at $y = 0$ and $y = b$, we can use an approach of the following type:

$$\begin{aligned} \bar{w}_0 &= \sum_{m=1}^{M}\sum_{n=1}^{N} \bar{W}_{mn}\bar{w}_{1m}(\xi_1)\,\bar{w}_{2n}(\xi_2) \\ &= \sum_{m=1}^{M}\sum_{n=1}^{N} \bar{W}_{mn}\sin(m\pi\xi_1)\{\cos[(n-2)\pi\xi_2] - \cos(n\pi\xi_2)\}. \end{aligned} \tag{14.194}$$

The resultants $\bar{R}_{ij}^{mp}$ and $\bar{S}_{ij}^{nq}$ can then be taken directly from the two cases already discussed. A similar procedure can be used with a laminate that is clamped at the edges at $x = 0$ and $x = a$ and simply supported at the edges at $y = 0$ and $y = b$. In this case, the approach is:

$$\begin{aligned} \bar{w}_0 &= \sum_{m=1}^{M}\sum_{n=1}^{N} \bar{W}_{mn}\bar{w}_{1m}(\xi_1)\,\bar{w}_{2n}(\xi_2) \\ &= \sum_{m=1}^{M}\sum_{n=1}^{N} \bar{W}_{mn}\{\cos[(m-2)\pi\xi_1] - \cos(m\pi\xi_1)\}\sin(n\pi\xi_2). \end{aligned} \tag{14.195}$$

The shape functions discussed so far have proven themselves both in the case of ideally orthotropic laminates and in the case of laminates with bending-twisting coupling. With regard to the following combinations of boundary conditions, there is little experience to date with laminates that exhibit bending-twisting coupling, so that the use of the approaches briefly discussed below should either be limited to ideally orthotropic laminates or a certain degree of caution should be exercised when applying them to laminates with bending-twisting coupling. The following approaches in the form of so-called beam eigenfunctions and other relevant cases can be found, for example, in Berthelot (1998), Leissa (1969) or Reddy (2004).

If the laminate under consideration is clamped at $x = 0$, free at $x = a$ and simply supported at the edges at $y = 0$ and $y = b$, then the following approaches can be used:

$$\begin{aligned} \bar{w}_{1m}(\xi_1) &= \sin(\lambda_i \xi_1) - \sinh(\lambda_i \xi_1) + \alpha_i \left[\cosh(\lambda_i \xi_1) - \cos(\lambda_i \xi_1)\right], \\ \bar{w}_{2n}(\xi_2) &= \sin(n\pi \xi_2). \end{aligned} \tag{14.196}$$

The variables λ_i occurring here are the roots of the following transcendental equation:

$$\cos(\lambda_i)\cosh(\lambda_i) + 1 = 0. \tag{14.197}$$

The factor α_i can be determined as:

$$\alpha_i = \frac{\sinh(\lambda_i) + \sin(\lambda_i)}{\cosh(\lambda_i) + \cos(\lambda_i)}. \tag{14.198}$$

The resultants $\bar{R}_{ij}^{mp}$ and $\bar{S}_{ij}^{nq}$ can also be analysed in a closed form, but the resulting expressions (at least for $\bar{R}_{ij}^{mp}$) are relatively long, so we will not reproduce them here.

A laminate that is free of any support at the edges $x = 0$ and $x = a$, whereby the edges at $y = 0$ and $y = b$ are simply supported, can be analyzed using the following approaches:

$$\begin{aligned} \bar{w}_{1m}(\xi_1) &= \sin(\lambda_i \xi_1) + \sinh(\lambda_i \xi_1) - \alpha_i \left[\cosh(\lambda_i \xi_1) + \cos(\lambda_i \xi_1)\right], \\ \bar{w}_{2n}(\xi_2) &= \sin(n\pi \xi_2). \end{aligned} \tag{14.199}$$

In this case, the variables λ_i are the roots of the following transcendental equation:

$$\cos(\lambda_i)\cosh(\lambda_i) - 1 = 0. \tag{14.200}$$

The factor α_i reads:

$$\alpha_i = \frac{\sinh(\lambda_i) - \sin(\lambda_i)}{\cosh(\lambda_i) - \cos(\lambda_i)}. \tag{14.201}$$

A suitable approach for a laminate whose edges are simply supported at $x = 0$, $y = 0$ and $y = b$ and for which the remaining edge is free at $x = a$ is as follows:

$$\bar{w}_{1m}(\xi_1) = \sinh(\lambda_i)\sin(\lambda_i\xi_1) - \sin(\lambda_i)\sinh(\lambda_i\xi_1),$$
$$\bar{w}_{2n}(\xi_2) = \sin(n\pi\xi_2). \tag{14.202}$$

In the present case, the variables λ_i are the roots of the following transcendental equation:

$$\tan(\lambda_i) - \tanh(\lambda_i) = 0. \tag{14.203}$$

For shape functions with regard to further selected cases of combinations of boundary conditions of the type 'simply supported'—'fixed'—'free', the reader is referred to the available technical literature.

14.6 Laminates Under Inplane Shear Load

The Ritz method enables the consideration of load cases that go beyond the relatively easy-to-handle load case of uniaxial compression. For example, in composite lightweight construction, the load case of an inplane shear load is of outstanding importance if the laminate under consideration is interpreted, for example, as a skin field in the side shells of an aircraft fuselage. The resulting buckling shapes of an orthotropic laminate under inplane shear load are shown in Fig. 14.18. A laminate with the layup $[0°/90°/0°/90°]_S$ with the elastic single layer properties $E_{11} = 135{,}000\,\text{MPa}$, $E_{22} = 10{,}000\,\text{MPa}$, $G_{12} = 5000\,\text{MPa}$, $\nu_{12} = 0.27$ is considered. The laminate is simply supported at all four edges, the width of the laminate is $b = 200\,\text{mm}$, the total thickness is $h = 1.0\,\text{mm}$. In Fig. 14.18 the buckling modes for different laminate lengths a are shown. This shows that the buckling mode is skewed under the given shear load. The reason for this type of buckling mode can be found in the stress state in the laminate. The Ritz analysis assumes that there is a pure and uniform shear force flow $N^0_{xy} = \tau$ in the entire laminate. Such a stress state is equivalent to a pure normal stress state or normal force flow, in which a compressive force flow $N^0_{\xi\xi} = -\tau$ prevails at an angle of $\varphi = 45°$ and a tensile force flow $N^0_{\eta\eta} = \tau$ perpendicular to it (Fig. 14.19). The two normal force flows occurring at $\varphi = 45°$ have the same magnitude as the applied shear load. This force flow at an angle of $\varphi = 45°$ can be interpreted in such a way that a 'tension diagonal' builds up in the η-direction, while a 'compression diagonal' forms in the ξ-direction. The 'long axis' of the buckling waves, which are similar in shape to an ellipse, then runs in the direction of the tension diagonal. This means that the buckling behaviour of a laminate under shear is also comparable to the buckling behaviour of a bar in a truss structure as shown in Fig. 14.19. If the compression diagonal buckles when the critical buckling load is reached, the load must be carried further by the tension diagonal. The results of Fig. 14.18 show the expected result that the buckling loads N^0_{xy} depend on the length a of the laminate and tend towards an asymptotic limit value if the length is sufficient. With a length of $a = 400\,\text{mm}$, the critical buckling load is calculated as $N^0_{xy} = 5.64\,\frac{\text{N}}{\text{mm}}$, while for the lengths $a = 600\,\text{mm}$ and $a = 800\,\text{mm}$ the buckling loads amount to $N^0_{xy} = 4.91\,\frac{\text{N}}{\text{mm}}$

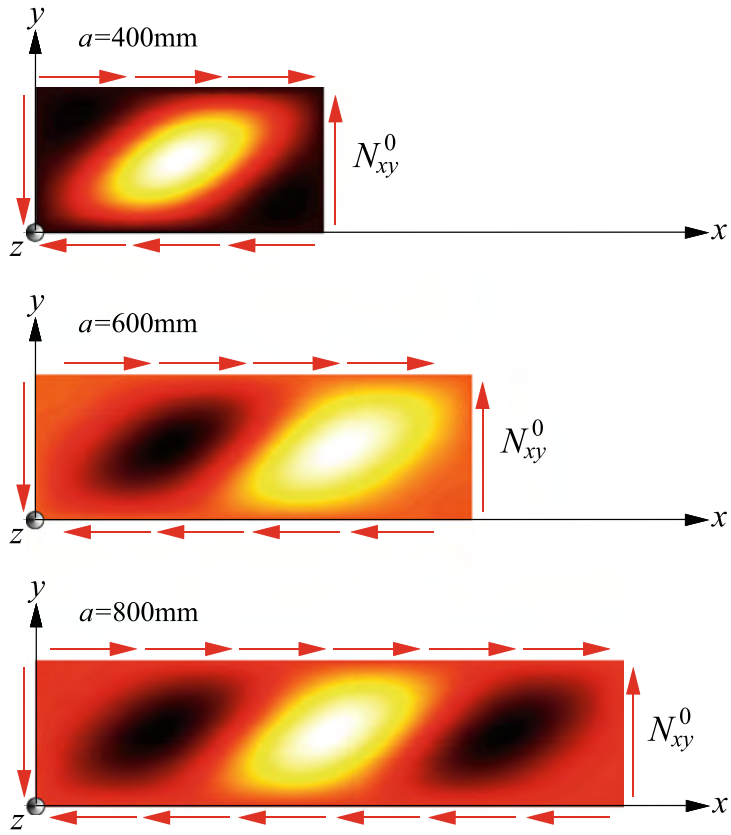


Fig. 14.18 Buckling modes for a cross-ply laminate $[0°/90°/0°/90°]_S$ under inplane shear load N_{xy}^0 for different lengths a

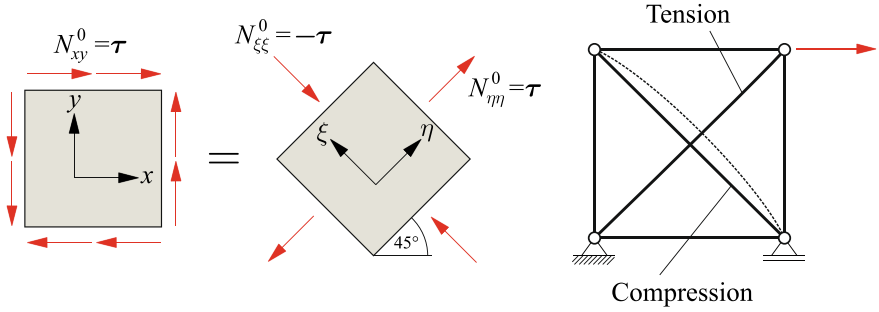


Fig. 14.19 Interpretation of the buckling behaviour of a laminate under inplane shear load

and $N_{xy}^0 = 4.71\,\frac{\mathrm{N}}{\mathrm{mm}}$, respectively. The relatively complex nature of the buckling modes that occur under inplane shear load compared to the buckling modes under compressive load (which are always associated with certain symmetry properties) are also a reason why closed-form analytical solutions for shear loads are often very difficult to develop.

Figure 14.20 contains generic buckling curves for an orthotropic laminated plate simply supported at all edges, where the dimensionless buckling load $\bar{N}_{xy}^0$ was plotted as a function of the inverted aspect ratio $\bar{\alpha}$ for different values β between $\beta = 0$ and $\beta = 3.0$.

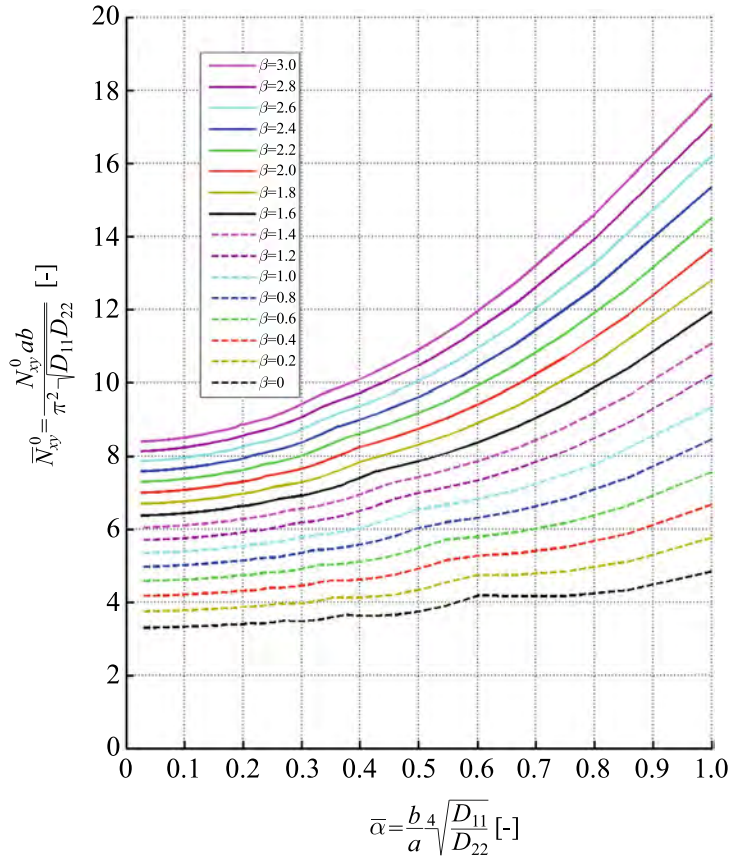


Fig. 14.20 Dimensionless buckling load $\bar{N}_{xy}^0$ as a function of the inverted aspect ratio $\bar{\alpha}$ for different values β

14.7 Laminates Under Inplane Bending

Another load case that can be handled with the presented Ritz formulation is the case of inplane bending, i.e. a linearly varying normal force $N^0_{xx}(y) = \frac{N^0_{xx}}{b}[(\psi - 1)\, y + b]$.

Figure 14.21 contains the buckling modes of a rectangular laminate simply supported at all edges ($a = 800\,\text{mm}$, $b = 200\,\text{mm}$, $h = 1.0\,\text{mm}$) with the layup $[0°/90°/0°/90°]_S$ and the elastic layer properties $E_{11} = 135{,}000\,\text{MPa}$, $E_{22} = 10{,}000\,\text{MPa}$, $G_{12} = 5000\,\text{MPa}$,

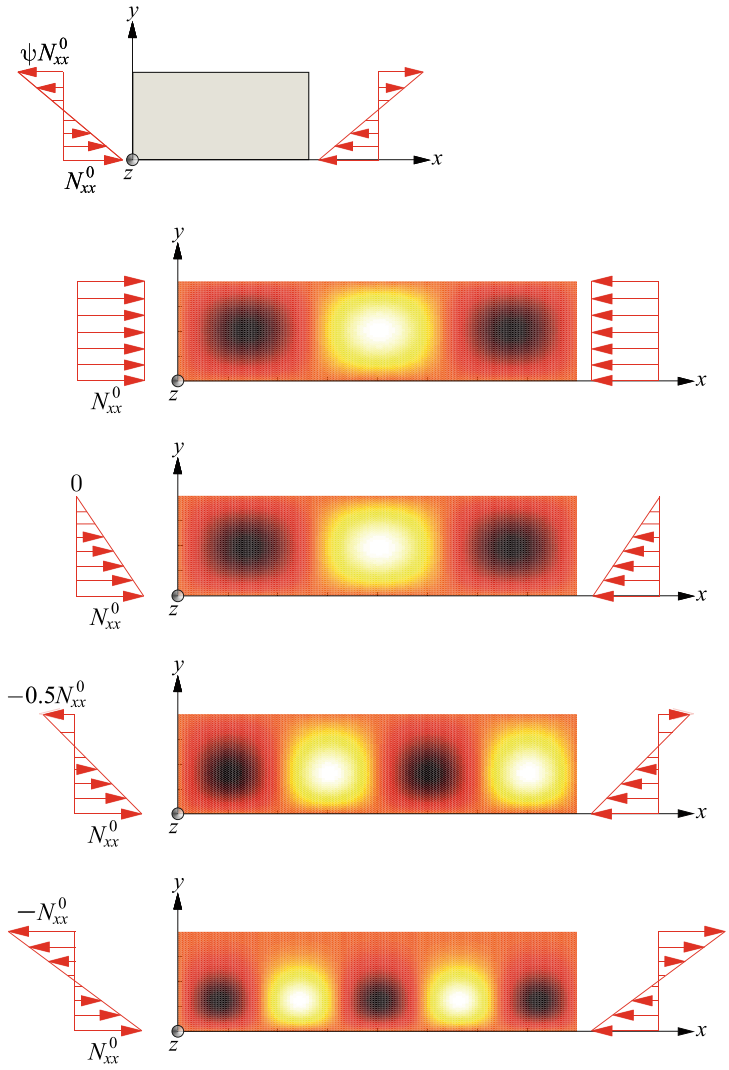


Fig. 14.21 Buckling modes for a cross-ply laminate $[0°/90°/0°/90°]_S$ under inplane bending load for different load parameters ψ

$\nu_{12} = 0.27$ for the case that the boundary value N^0_{xx} $(y = 0)$ is given and the boundary value N^0_{xx} $(y = b) = \psi N^0_{xx}$ $(y = 0)$ is varied with the values $\psi = 1$, $\psi = 0$, $\psi = -0.5$ and $\psi = -1$. In this example, the associated critical buckling loads are obtained as $N^0_{xx} = 3.44 \frac{\mathrm{N}}{\mathrm{mm}}$, $N^0_{xx} = 6.78 \frac{\mathrm{N}}{\mathrm{mm}}$, $N^0_{xx} = 11.74 \frac{\mathrm{N}}{\mathrm{mm}}$ and $N^0_{xx} = 21.74 \frac{\mathrm{N}}{\mathrm{mm}}$.

The increase in the buckling load N^0_{xx} with decreasing factor ψ can be explained as follows. The results show that the buckling resistance of the laminate is lowest at uniaxial compression with $\psi = 1$. This is contrasted by around a doubling of the buckling resistance at a factor of $\psi = 0$, and almost a tripling at $\psi = -0.5$ and around a six-fold increase at $\psi = -1$. At negative values ψ, the laminate is in a state of partial tensile stress, which is of course not critical in terms of buckling behaviour. If we look at the buckling mode for the case $\psi = -1$, we observe that the buckles that form are roughly limited to the area of the laminate that is actually under compressive stress. In this respect, the tensile area has a stabilizing effect and the actual width of the laminate, which is under compression and buckles accordingly, is much smaller in this case than in the case of $\psi = 1$, for example, in which the entire width of the laminate is involved in carrying compressive stresses.

14.8 Load Case Interactions

Up to now only separately acting load cases such as compression, inplane shear or inplane bending were considered. In lightweight construction practice, however, thin-walled laminate structures are usually subjected to a combination of such load cases. Although the Ritz method (or other energy-based methods such as the Finite Element Method) allows the consideration of almost any load cases and their combinations, it is very desirable for reasons of computational efficiency to find simple analysis rules that can be used to calculate the buckling resistances of combinations of the separately considered load cases (which are generally quite easy and quick to calculate) without great computational effort. For this purpose, some common interaction formulas are considered below. However, it should be noted at this point that these are only approximation formulas that do not originate from a strict physical background, so that they should only be used in the context of preliminary design. A detailed verification should then always be carried out with more detailed computations. Further details on the following explanations can be found, for example, in Petersen (1982).

A fairly simple approach for an interaction formula is the so-called Dunkerley interaction equation, which reads as follows:

$$\Lambda \sum_{i=1}^{i=n} \frac{N_i}{N_{i,\mathrm{crit}}} = 1. \tag{14.204}$$

Here, $N_{i,\mathrm{crit}}$ is the bifurcational buckling load that belongs to the i-th individual load N_i. The quantity Λ is the unknown load factor for the load combination under consideration. If

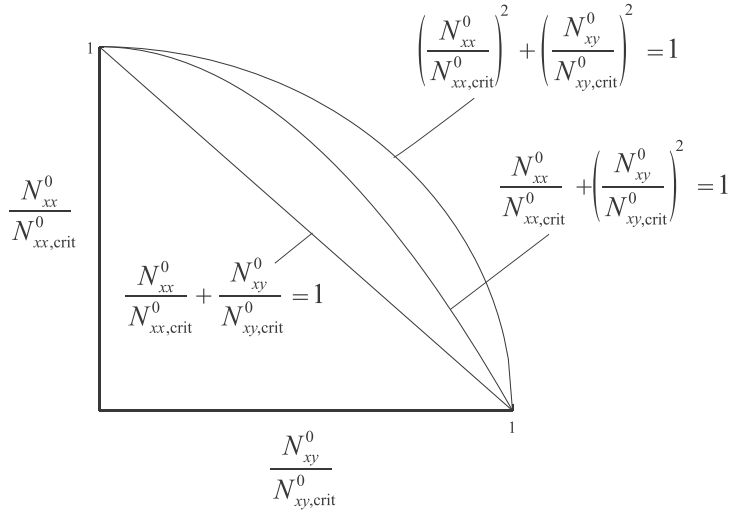


Fig. 14.22 Interaction formulas for combined load cases

this interaction formula is written out for two load cases, e.g. for the interaction between a compressive load and a shear load, then we obtain

$$\Lambda \frac{N^0_{xx}}{N^0_{xx,\text{crit}}} + \Lambda \frac{N^0_{xy}}{N^0_{xy,\text{crit}}} = 1. \tag{14.205}$$

If this relationship is depicted in an interaction diagram (see Fig. 14.22), it is also referred to as the so-called Dunkerley line. All load combinations occurring in the area delimited by Dunkerley's line are therefore permissible, i.e. no buckling occurs. Every load combination that lies on or beyond the interaction line is therefore critical: the structure buckles.

However, experience shows that an estimation of the interaction of compression and inplane shear load with the help of Dunkerley's line is generally overly conservative. A common extension of the interaction equation (14.205) is based on the consideration that the buckling behaviour (at least for ideally orthotropic laminates and isotropic plates) must not depend on the sign of the shear load. In this respect, the interaction curve must be mirror-symmetrical to the $\frac{N^0_{xx}}{N^0_{xx,\text{crit}}}$-axis and must therefore intersect the $\frac{N^0_{xx}}{N^0_{xx,\text{crit}}}$-axis with a horizontal tangent. This requirement can easily be met by a parabolic equation of the following form:

$$\Lambda \frac{N^0_{xx}}{N^0_{xx,\text{crit}}} + \Lambda^2 \left(\frac{N^0_{xy}}{N^0_{xy,\text{crit}}}\right)^2 = 1. \tag{14.206}$$

This type of interaction curve has proven itself many times over and is also popular in industrial applications; it is also shown in Fig. 14.22.

If there is an interaction of inplane bending with $\psi = 1$ and shear, it must also be required that the results from the interaction equation do not depend on the sign of the bending load. Accordingly, the interaction curve must not only be mirror-symmetrical to the $\frac{N^0_{xx}}{N^0_{xx,\mathrm{crit}}}$-axis and intersect it with a horizontal tangent, but also with respect to the $\dfrac{N^0_{xy}}{N^0_{xy,\mathrm{crit}}}$-axis. This can be easily ensured by a circle equation:

$$\Lambda^2 \left(\frac{N^0_{xx}}{N^0_{xx,\mathrm{crit}}} \right)^2 + \Lambda^2 \left(\frac{N^0_{xy}}{N^0_{xy,\mathrm{crit}}} \right)^2 = 1. \tag{14.207}$$

This interaction equation is also shown in Fig. 14.22.

Now consider the case where a combined load from inplane bending $N^0_{xx}(y) = \frac{N^0_{xx}}{b}[(\psi - 1)\, y + b]$ (with any factor ψ) and inplane shear N^0_{xy} occurs. Firstly, the bending load is divided into two components, namely the constant compressive component $N^0_{xx,C}$ and the pure bending component $N^0_{xx,B}$:

$$N^0_{xx,C} = \frac{1}{2}(1 + \psi)\, N^0_{xx}, \quad N^0_{xx,B} = \frac{1}{2}(1 - \psi)\, N^0_{xx}. \tag{14.208}$$

The corresponding interaction equation is then for this case:

$$\Lambda \frac{1 + \psi}{2} \frac{N^0_{xx}}{N^0_{xx,\mathrm{crit}}} + \Lambda^2 \frac{1 - \psi}{2} \left(\frac{N^0_{xx}}{N^0_{xx,\mathrm{crit}}} \right)^2 + \Lambda^2 \left(\frac{N^0_{xy}}{N^0_{xy,\mathrm{crit}}} \right)^2 = 1. \tag{14.209}$$

If we divide this equation by Λ^2, we obtain a quadratic equation for the load factor Λ, the solution of which is as follows:

$$\Lambda = \frac{1}{\dfrac{1 + \psi}{4} \dfrac{N^0_{xx}}{N^0_{xx,\mathrm{crit}}} + \sqrt{\left(\dfrac{3 - \psi}{4} \right)^2 \left(\dfrac{N^0_{xx}}{N^0_{xx,\mathrm{crit}}} \right)^2 + \left(\dfrac{N^0_{xy}}{N^0_{xy,\mathrm{crit}}} \right)^2}}. \tag{14.210}$$

Finally, it should be noted that the interaction formulas presented here are based on buckling analyses on isotropic plates and in most cases provide conservative results that can be used well in practice (see also Petersen (1982)). However, it should always be ensured that the applicability to orthotropic laminates or laminates with anisotropic plate behaviour is warranted. If necessary, this must be ensured by comparison with more precise analysis methods or with experimental findings.

14.9 Influence of Bending-Twisting Coupling on Buckling of Laminates

Up to now, only the buckling behaviour of laminates whose plate behaviour is ideally orthotropic has been considered. However, a look at common laminate structures in the aerospace industry shows that this requirement is almost never met and that the assumption of ideal orthotropy is often a strong simplification. For this reason, it is important to gain clarity about the general buckling behaviour of laminates in which bending-twisting coupling (caused by the terms D_{16}, D_{26}) occurs. Since no exact analytical solutions are generally known for such cases, this investigation can again be advantageously carried out using the Ritz method. The constitutive behaviour of a symmetric laminate with bending-twisting coupling is described as follows:

$$\begin{pmatrix} M_{xx}^0 \\ M_{yy}^0 \\ M_{xy}^0 \end{pmatrix} = \begin{bmatrix} D_{11} & D_{12} & D_{16} \\ D_{12} & D_{22} & D_{26} \\ D_{16} & D_{26} & D_{66} \end{bmatrix} \begin{pmatrix} \kappa_{xx}^0 \\ \kappa_{yy}^0 \\ \kappa_{xy}^0 \end{pmatrix}. \tag{14.211}$$

14.9.1 Influence of Bending-Twisting Coupling on Laminates Under Compression

As a first example, we consider a square angle-ply laminate ($a = b = 200\,\text{mm}$) simply supported at all edges with the layup $[\pm 45°]_S$, the thickness $h = 1.0\,\text{mm}$ and the elastic layer properties $E_{11} = 135{,}000\,\text{MPa}$, $E_{22} = 10{,}000\,\text{MPa}$, $G_{12} = 5000\,\text{MPa}$, $\nu_{12} = 0.27$. The laminate is under a uniaxial compressive load N_{xx}^0. In Fig. 14.23, the buckling modes for this laminate are shown on the one hand for the case where the bending-twisting coupling is taken into account (Fig. 14.23, left), and on the other hand for the case where the bending-twisting coupling was neglected in the Ritz method (Fig. 14.23, right).

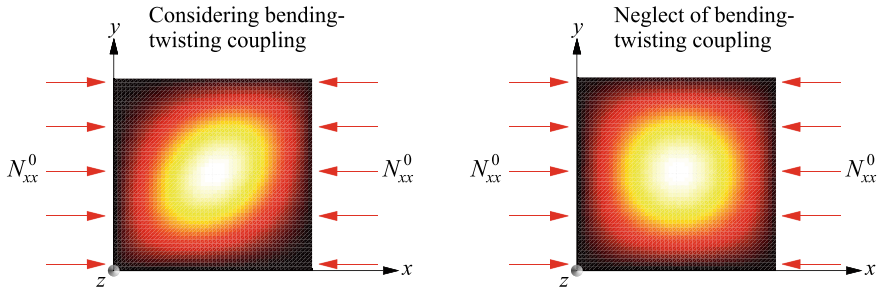


Fig. 14.23 Buckling modes for an angle-ply laminate $[\pm 45°]_S$ under compressive load N_{xx}^0; with consideration of bending-twisting coupling (left), without consideration of bending-twisting coupling (right)

Obviously, the buckling mode is very similar to that under an inplane shear load when bending-twisting coupling is taken into account (Fig. 14.23, left). The buckling pattern loses its symmetry properties which always occur in laminates with purely orthotropic plate behaviour under pure compressive loading. This effect can be explained quite simply from the constitutive law (14.211). If the applied load reaches the bifurcational buckling load, then the bending-twisting coupling not only causes the two curvatures $\kappa_{xx}^0, \kappa_{yy}^0$, but also the twist κ_{xy}^0 at the same time, which results in the skewed buckling pattern in Fig. 14.23, left. It can be seen here that bending-twisting coupling always leads to a reduction in the buckling load compared to a purely orthotropic laminate in the case of a purely compressive load. In the present example, this results in $N_{xx}^0 = 4.77 \, \frac{\mathrm{N}}{\mathrm{mm}}$ when taking bending-twisting coupling into account, whereas the buckling load is $N_{xx}^0 = 6.00 \, \frac{\mathrm{N}}{\mathrm{mm}}$ when neglecting bending-twisting coupling. The reason for this reduction lies in the resulting buckling modes. While only the two curvatures $\kappa_{xx}^0, \kappa_{yy}^0$ occur in a purely orthotropic laminate under compressive load, the twist κ_{xy}^0 also occurs in a laminate when taking bending-twisting coupling into account. In this respect, the laminate in the latter case behaves more compliant than the purely orthotropic laminate, and the buckling resistance is correspondingly lower. The complex buckling mode that arises here also explains why closed-form analytical approximation solutions, e.g. based on Rayleigh quotients, or exact analytical solutions for laminate buckling problems are difficult to derive or may not exist at all for such cases. Here, one is simply confronted with the mathematical difficulty of describing a relatively complicated buckling mode with simple functions.

The influence of bending-twisting coupling on the stability of laminates has been investigated by a number of scientists (see, for example, the works of Narita and Leissa (1990), Becker et al. (2000), Weaver (2004), Weaver and Nemeth (2007), Nemeth (1986, 1995, 2003a, b, 2010), Rohwer (1987, 1991) or Ovesy and Assaee (2007)). However, there is still a lack of systematic and practical investigations and, as a result, clear design rules that can be used in everyday engineering work to estimate the buckling resistance taking into account this rather complex coupling effect without great computational effort. A more recent work in this area was presented by Baucke and Mittelstedt (2015). In this work, characteristic buckling curves of laminates under uniaxial compressive load are found, which are subject to various boundary conditions. For this purpose, a dimensionless notation with the two bending-twisting coupling stiffnesses

$$\gamma = \frac{D_{16}}{\sqrt[4]{D_{11}^3 D_{22}}}, \quad \delta = \frac{D_{26}}{\sqrt[4]{D_{11} D_{22}^3}} \tag{14.212}$$

as well as the Seydel orthotropy parameter β and the aspect ratio α according to

$$\beta = \frac{D_{12} + 2D_{66}}{\sqrt{D_{11} D_{22}}}, \quad \alpha = \frac{a}{b} \sqrt[4]{\frac{D_{22}}{D_{11}}} \tag{14.213}$$

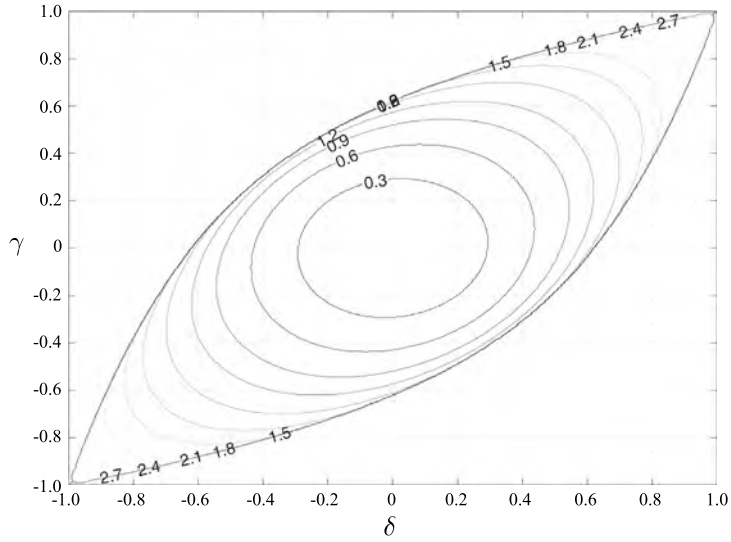


Fig. 14.24 Permissible values for γ and δ, according to Weaver and Nemeth (2007)

was employed. Note that the two anisotropy parameters γ and δ are generally not equal. However, it can be observed that even for angle-ply laminates, which tend to have a strongly anisotropic behaviour, the anisotropy parameters are the same for ply angles of $\theta = \pm 45°$. Values for different materials show that in many circumstances it is a reasonable approach to assume $\gamma \simeq \delta$. In general, γ and δ can vary in the ranges $-1 \leq \gamma \leq 1$ and $-1 \leq \delta \leq 1$. However, there are certain limits for γ and δ that result from thermodynamic requirements, as explained in detail by Weaver and Nemeth (2007). Without going into detail at this point, it is only mentioned here that the parameters γ and δ cannot assume arbitrary values depending on the value β, but are restricted as shown in Fig. 14.24. Consequently, the following buckling diagrams explicitly take these restrictions into account and only cover permissible value ranges for γ and β depending on the value β. The following buckling diagrams, in which the buckling load factor λ is shown as a function of the aspect ratio α for different permissible values $\delta = \gamma$, were developed for different types of boundary conditions using the Ritz method. The boundary conditions used are shown in Fig. 14.25. The results were verified using the Finite Element Method and the corresponding FEM results are also shown in Figs. 14.26, 14.27, 14.28, 14.29 and 14.30.

The results shown in Figs. 14.26, 14.27, 14.28, 14.29 and 14.30 allow the following general conclusions to be drawn:

– An increasing orthotropy parameter β leads to an increase in the buckling load.
– An increasing degree of anisotropy or bending-twisting coupling, which is characterised by the parameters γ and δ, leads to a decrease in the buckling load.

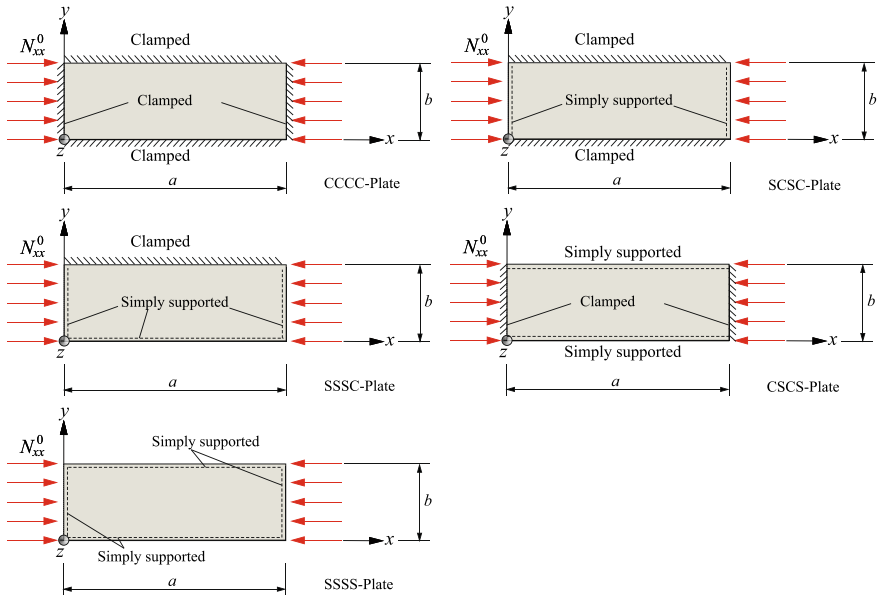


Fig. 14.25 Employed boundary conditions

– For relatively short plates (i.e. for low values of α), the buckling load increases and grows indefinitely, which is a well-known and typical observation in the context of plate buckling.
– For long plates (i.e. for high values of α), all buckling curves tend asymptotically to a constant limit value. Consequently, the buckling load decouples from α for $\alpha \to \infty$. This is also a typical observation in the treatment of plate buckling problems.
– All buckling curves show local maxima with a change in the curve gradient. These local maxima correspond to changes in the respective buckling modes.

14.9.2 Sign Dependence of the Buckling Load Under Inplane Shear Load

Under the load case of inplane shear there are some special features to consider with regard to the influence of the bending-twisting coupling. In order to illustrate this, the example of the previous section is now considered under an inplane shear load, once for a positive shear load (the buckling shape is shown in Fig. 14.31, left), and once for a negative shear load (the buckling shape can be found in Fig. 14.31, right). The influence of the bending-twisting coupling is particularly evident in the resulting buckling loads. In the case of positive shear (Fig. 14.31, left), this results in a buckling load of $N_{xy}^0 = 6.18\ \frac{\mathrm{N}}{\mathrm{mm}}$. This is contrasted by a significantly higher buckling load of $N_{xy}^0 = 19.64\ \frac{\mathrm{N}}{\mathrm{mm}}$ for negative shear. The explanation

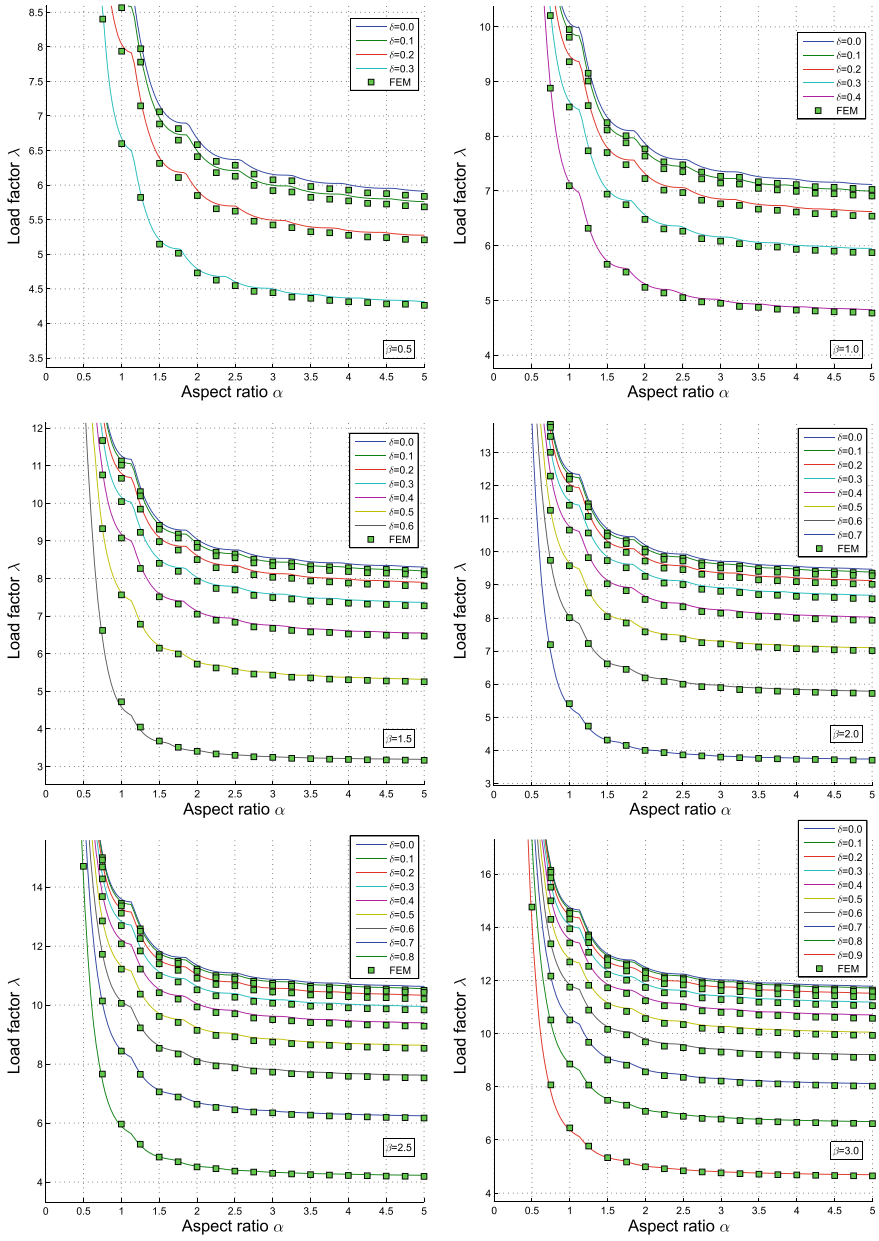


Fig. 14.26 Buckling curves for the CCCC plate

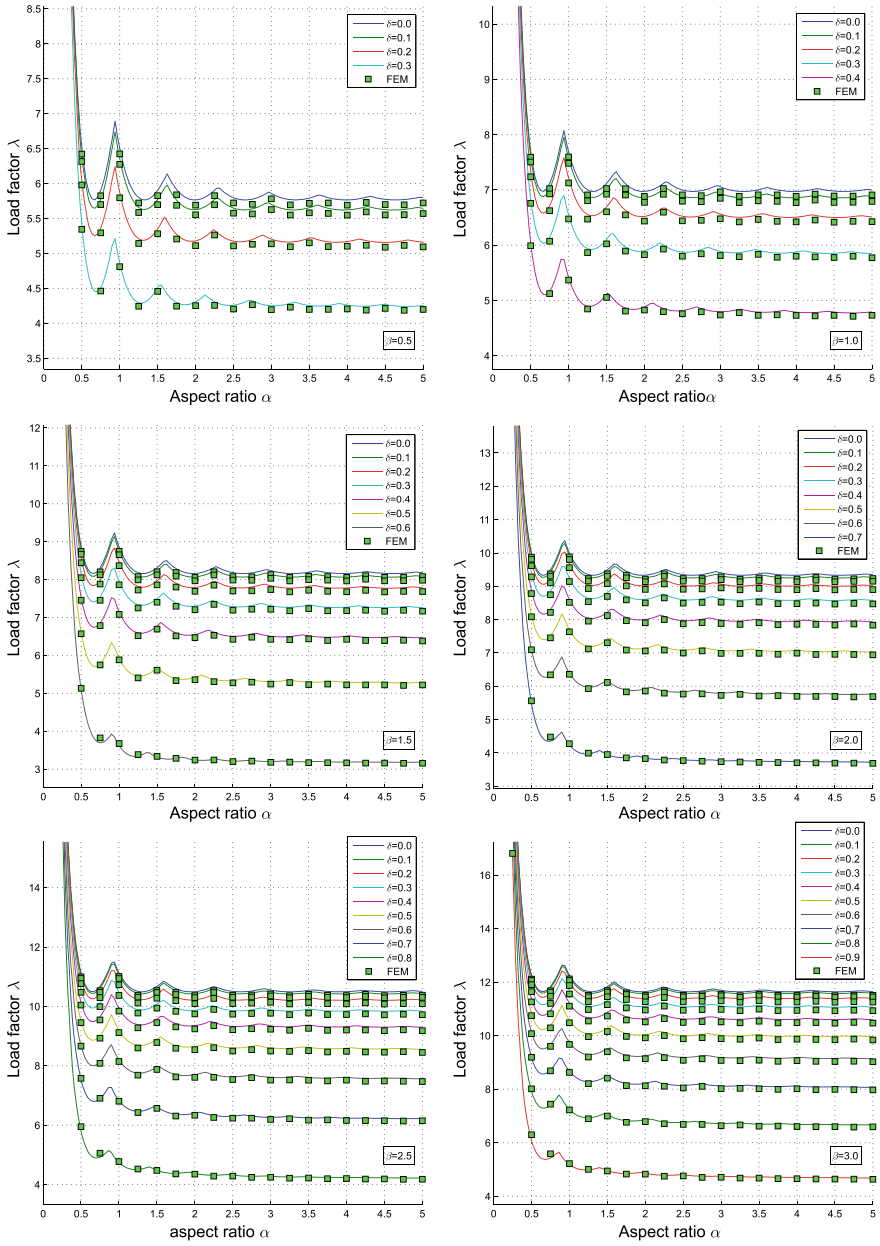


Fig. 14.27 Buckling curves for the SCSC plate

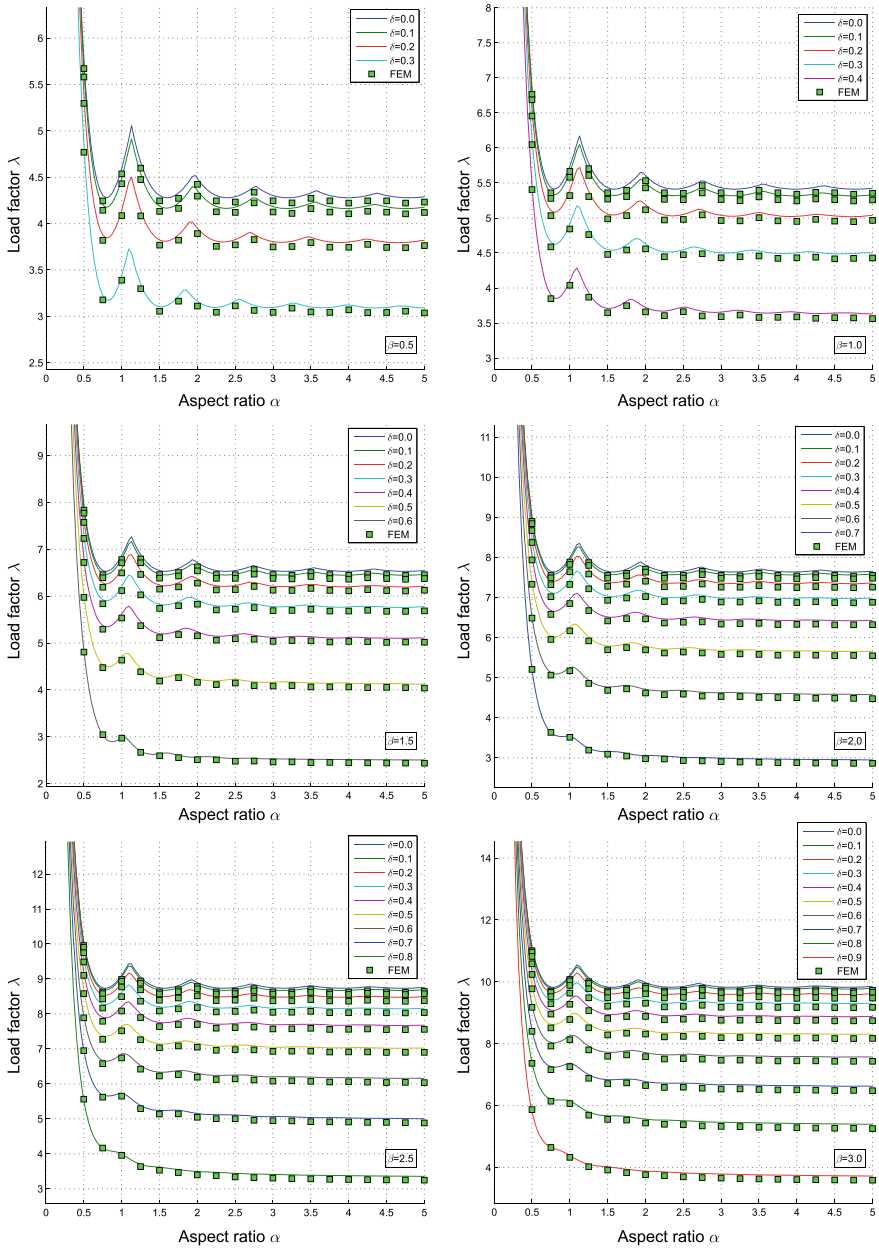


Fig. 14.28 Buckling curves for the SSSC plate

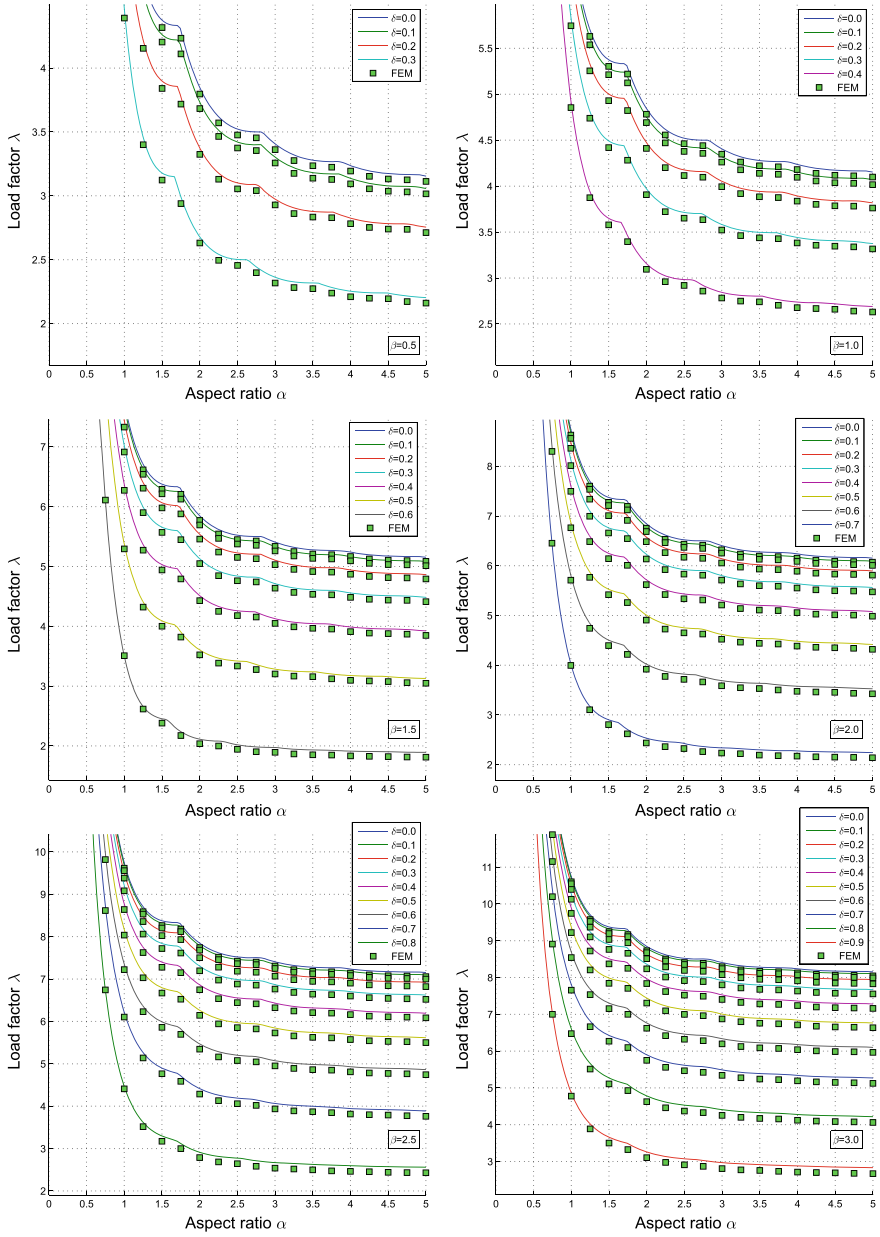


Fig. 14.29 Buckling curves for the CSCS plate

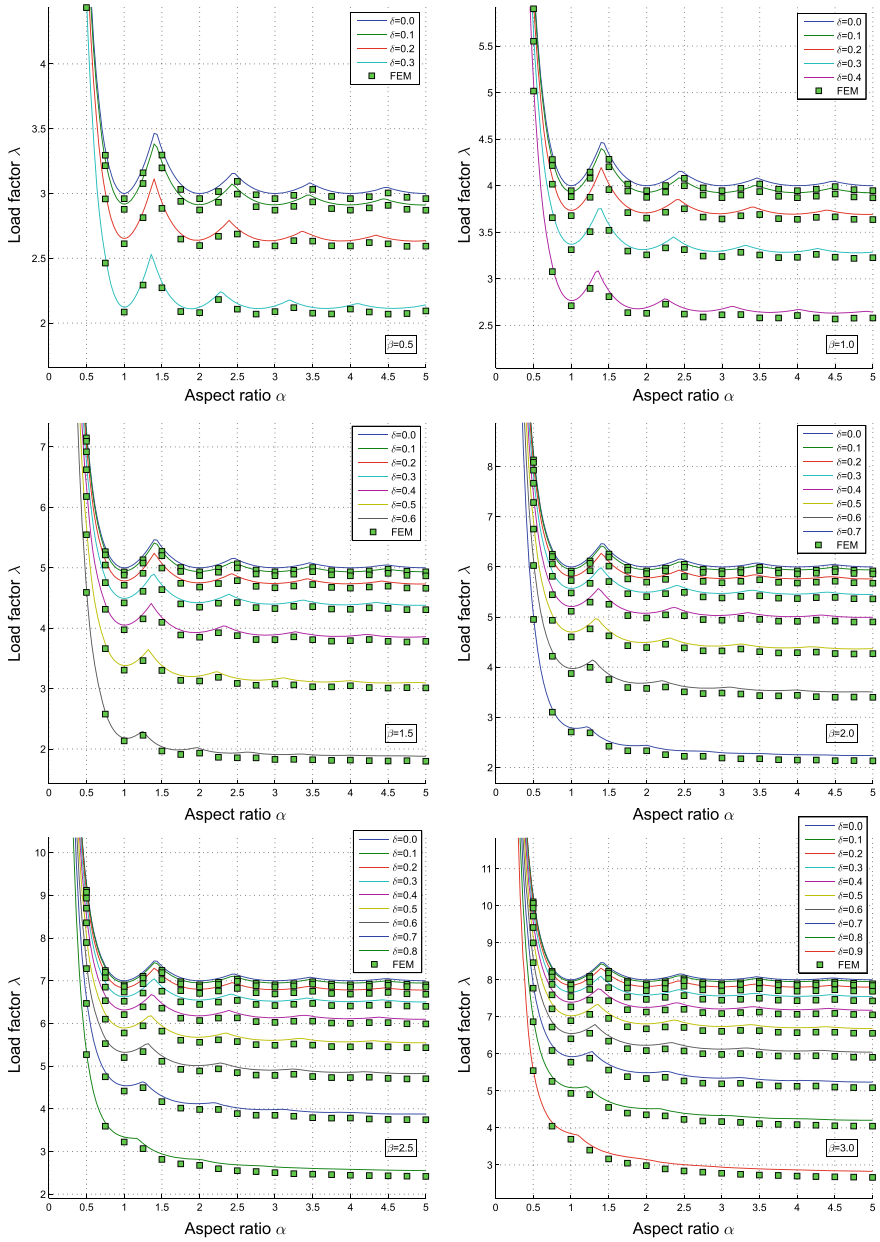


Fig. 14.30 Buckling curves for the SSSS plate

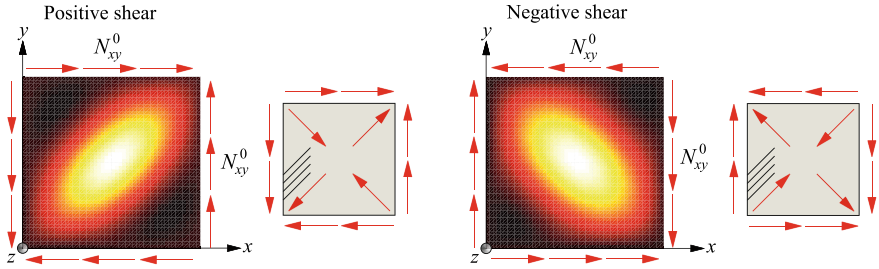


Fig. 14.31 Buckling modes for angle-ply laminates $\left[\pm 45°\right]_S$ under shear load N_{xy}^0; positive shear (left), negative shear (right)

is provided by a closer look at the layup (the decisive factors here are the $+45°$-plies) in conjunction with the stress state occurring in the laminate. While under the positive shear load, the equivalent compressive stresses (which are ultimately responsible for buckling) run at right angles to the fibers of the $+45°$-layers at the angle $\varphi = 45°$ and thus encounter a very low stiffness, in the case of negative shear, the compressive stresses run parallel to the fibers of the outer $+45°$-layers. In the latter case, the stiffness is particularly high and the buckling resistance of the laminate under negative shear is significantly higher than for positive shear. In this respect, it can be seen that bending-twisting coupling not only calls forth rather complex buckling modes, but also results in a sign dependence of the load in the case of shear loading, which does not occur in the case of ideally orthotropic laminates or isotropic structures.

Finally, it should be noted that bending-twisting coupling does not necessarily reduce the buckling resistance under shear loading, in contrast to pure compressive loading. For comparison, we consider the buckling load for a $[\pm 45°]_S$-laminate for which the bending-twisting coupling terms D_{16} and D_{26} were set to zero in the Ritz analysis. In this case, regardless of the sign of the shear load, this results in a buckling load of $N_{xy}^0 = 13.53 \frac{\mathrm{N}}{\mathrm{mm}}$. It can therefore be seen that bending-twisting coupling ensures a significant reduction in the buckling load compared to the orthotropic laminate in the case of positive shear, while negative shear results in a massive increase in the buckling resistance.

Figure 14.32 contains generic buckling curves for a laminate plate simply supported at all edges, in which the dimensionless buckling load $\bar{N}_{xy}^0$ as a function of the inverted aspect ratio $\bar{\alpha}$ for different values $\beta = 0$, $\beta = 1.0$, $\beta = 2.0$ and $\beta = 3.0$ for different permissible values $\delta = \gamma$ is shown. These buckling curves were generated using the Ritz method. The influence of the bending-twisting coupling in the form of the stiffness $\delta = \gamma$ on the buckling load can be clearly seen here. The symbols in the graphs are the results of accompanying finite element calculations used to verify the Ritz method. Apparently, the Ritz method produces a very good results accuracy compared to the Finite Element Method, which speaks in favour of the suitability and versatility of the method.

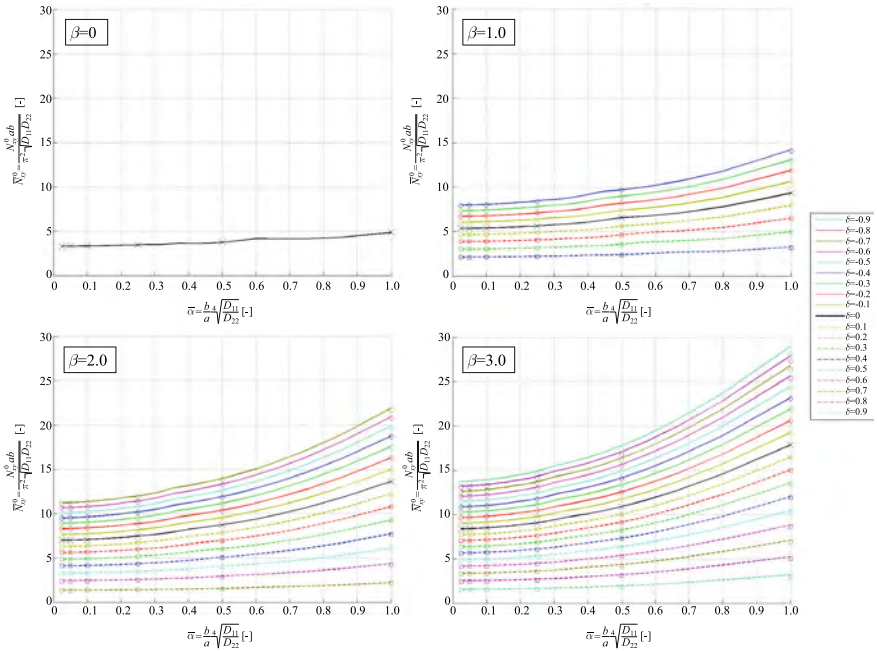


Fig. 14.32 Dimensionless buckling load $\bar{N}^0_{xy}$ as a function of the inverted aspect ratio $\bar{\alpha}$ for different values β and stiffnesses $\delta = \gamma$

14.10 The Finite Element Method for Linear Buckling Problems

Buckling problems with complex geometries, load cases and boundary conditions are generally analyzed using the Finite Element Method. In the following, we summarize the necessary equations for a finite element formulation within the framework of Classical Laminated Plate Theory, which can be found in detail in Reddy (2004). We consider the equations of motion (8.236) neglecting dynamic terms and transverse loads, multiply them by the virtual displacements δu_0, δv_0, δw_0 and integrate over the element e:

$$\int_{\Omega_e} \delta u_0 \left(\frac{\partial N^0_{xx}}{\partial x} + \frac{\partial N^0_{xy}}{\partial y} \right) \mathrm{d}x\mathrm{d}y = 0,$$

$$\int_{\Omega_e} \delta u_0 \left(\frac{\partial N^0_{xy}}{\partial x} + \frac{\partial N^0_{yy}}{\partial y} \right) \mathrm{d}x\mathrm{d}y = 0,$$

$$\int_{\Omega_e} \delta w_0 \left(-\frac{\partial^2 M^0_{xx}}{\partial x^2} - 2\frac{\partial^2 M^0_{xy}}{\partial x \partial y} - \frac{\partial M^0_{yy}}{\partial y^2} \right.$$

$$\left. - \frac{\partial}{\partial x}\left(\hat{N}^0_{xx} \frac{\partial w_0}{\partial x} + \hat{N}^0_{xy} \frac{\partial w_0}{\partial y} \right) - \frac{\partial}{\partial y}\left(\hat{N}^0_{xy} \frac{\partial w_0}{\partial x} + \hat{N}^0_{yy} \frac{\partial w_0}{\partial y} \right) \right) \mathrm{d}x\mathrm{d}y = 0. \quad (14.214)$$

This is the weak form of the equations of motion.

We use the following approach for the displacements of element e:

$$u_0(x, y, t) = \sum_{j=1}^{m} u_j^e(t)\psi_j^e(x, y),$$
$$v_0(x, y, t) = \sum_{j=1}^{m} v_j^e(t)\psi_j^e(x, y),$$
$$w_0(x, y, t) = \sum_{k=1}^{n} \Delta_k^e(t)\varphi_k^e(x, y). \tag{14.215}$$

Here, u_j^e, v_j^e are the nodal values of the inplane displacements of node j of the element. Similarly, Δ_k^e is the nodal value of w_0 in node k. The functions ψ_j^e, ψ_j^e are Lagrangian shape functions, whereas φ_k^e are Hermitian functions. Inserting this approach into the weak form (14.214) results in the following equations of motion for the element e:

$$\left(\begin{bmatrix} \underline{\underline{K}}_{11} & \underline{\underline{K}}_{12} & \underline{\underline{K}}_{13} \\ \underline{\underline{K}}_{12}^T & \underline{\underline{K}}_{22} & \underline{\underline{K}}_{23} \\ \underline{\underline{K}}_{13}^T & \underline{\underline{K}}_{23}^T & \underline{\underline{K}}_{33} \end{bmatrix} + \Lambda \begin{bmatrix} \underline{\underline{0}} & \underline{\underline{0}} & \underline{\underline{0}} \\ \underline{\underline{0}} & \underline{\underline{0}} & \underline{\underline{0}} \\ \underline{\underline{0}} & \underline{\underline{0}} & \underline{\underline{G}} \end{bmatrix} \right) \begin{pmatrix} \underline{u}_e \\ \underline{v}_e \\ \underline{\Delta}_e \end{pmatrix} = \begin{pmatrix} \underline{0} \\ \underline{0} \\ \underline{0} \end{pmatrix}. \tag{14.216}$$

This represents an eigenvalue problem for determining the load multiplier Λ. The specific assignment of the individual matrices occurring here is not presented at this point; interested readers are referred to Reddy (2004).

References

Bank LC, Yin J (1996): *Buckling of orthotropic plates with free and rotationally restrained edges*, Thin-Walled Structures 24:83–96.

Barbero EJ, Raftoyiannis IG (1993): *Local buckling of FRP beams and columns*, Journal of Materials in Civil Engineering 5:339–355.

Baucke A, Mittelstedt C (2015): *Closed-form analysis of the buckling loads of composite laminates under uniaxial compressive load explicitly accounting for bending-twisting-coupling*, Composite Structures 128:437–454.

Becker W, Hansel W, Oehm M (2000): *Buckling analysis of non-orthotropic laminates by means of B-spline functions*, Technische Mechanik 21:31–40.

Beerhorst M, Suresh Babu T (2020): *Closed-form approximate solution for linear buckling of Mindlin plates with SRSR-boundary conditions*, Composite Structures 240:112037.

Berthelot JM (1998): *Composite Materials: Mechanical Behavior and Structural Analysis*, Springer Verlag New York et al., USA.

Herrmann J, Kühn T, Müllenstedt T, Mittelstedt S, Mittelstedt C (2018): *A higher order shear deformation approach to the local buckling behavior of moderately thick composite laminated beams*, International Journal of Structural Stability and Dynamics 18:1850139-1–30.

Kollár LP (2002a): *Buckling of unidirectionally loaded composite plates with one free and one rotationally restrained unloaded edge*, Journal of Structural Engineering 128:1202–1211.

Kollár LP (2002b): *Local buckling of fiber reinforced plastic composite structural members with open and closed cross sections*, Journal of Structural Engineering 129:1503–1513.

Kühn T, Pasternak H, Mittelstedt C (2014): *Local buckling of shear-deformable laminated composite beams with arbitrary cross-sections using discrete plate analysis*, Composite Structures 113:236–248.

Leissa AW (1969): *Vibration of Plates*, Scientific and Technical Information Division, Washington D.C., USA, 20546: NASA - National Aeronautics and Space Administration, NASA SP-160.

Mittelstedt C (2007a): *Stability behaviour of arbitrarily laminated composite plates with free and elastically restrained unloaded edges*, International Journal of Mechanical Sciences 49:819–833.

Mittelstedt C (2007b): *Local buckling of wide-flange thin-walled anisotropic composite beams*, Archive of Applied Mechanics 77:439–452.

Mittelstedt C, Beerhorst M (2009): *Closed-form buckling analysis of compressively loaded composite plates braced by omega-stringers*, Composite Structures 88:424–435.

Narita Y, Leissa AW (1990): *Buckling studies for simply supported symmetrically laminated rectangular plates*, International Journal of Mechanical Sciences 11:909–924.

Nemeth MP (1986): *Importance of anisotropy on buckling of composite-loaded symmetric composites plates*, AIAA Journal 24:1831–1835.

Nemeth MP (1995): *Buckling behavior of long anisotropic plates subjected to combined loads*, NASA - National Aeronautics and Space Administration, Technical Paper 3568, Langley, USA.

Nemeth MP (2003a): *Buckling behavior of long anisotropic plates subjected to full restrained thermal expansion*, NASA - National Aeronautics and Space Administration, Technical Paper 212131, Langley, USA.

Nemeth MP (2003b): *Buckling of long compression loaded anisotropic plates restrained against inplane lateral and shear deformations*, Thin-Walled Structures 42:639–685.

Nemeth MP (2010): *Nondimensional parameters and equations for nonlinear and bifurcation analyses of thin anisotropic quasi-shallow shells*, NASA - National Aeronautics and Space Administration, Technical Paper 216726, Langley, USA.

Ovesy HR, Assaee H (2007): *The effects of bend-twist coupling on the post-buckling characteristics of composite laminated plates using semi-energy finite strip approach*, Thin-Walled Structures 45:209–220.

Petersen C (1982): *Statik und Stabilität der Baukonstruktionen*, 2. Auflage, Vieweg Verlag, Braunschweig / Wiesbaden, Germany.

Qiao P, Davalos JF, Wang J (2003): *Local buckling of composite FRP shapes by discrete plate analysis*, Journal of Structural Engineering 127:245–255.

Qiao P, Shan L (2005): *Explicit local buckling analysis and design of fiber-reinforced plastic composite structural shapes*, Composite Structures 70:468–483.

Reddy JN (2004): *Mechanics of laminated composite plates and shells (2nd edition)*, CRC Press Boca Raton et al., USA.

Rohwer K (1987): *Einfluss der Biege-Torsionskopplung auf die Beullasten symmetrisch geschichteter Platten*, Proceedings: Entwicklung und Anwendung von Faserverbund-Strukturen, Deutsche Gesellschaft für Luft- und Raumfahrt, Mai 1987, (DGLR-Symposium Report 87-02), S. 325–347.

Rohwer K (1991): *Reduction of the buckling loading of plates under compressive loading due to coupling of bending and torsion*, HSB - Handbuch für Strukturberechnung, Beitrag Nr. 45114-01, Issue B.

Schreiber P, Beerhorst M, Mittelstedt C (2020): *Buckling of shear-deformable orthotropic laminated plates with elastic restraints*, Thin Walled Structures 157:107071.

Weaver P (2004): *On optimisation of long anisotropic flat plates subject to shear buckling loads*, Proceedings of the 45th AIAA/ASME/ASCE/AHS/ASC Structures, Structural Dynamics and Materials Conference, 2004, Palm Springs, CA, USA.

Weaver P, Nemeth MP (2007): *Bounds on flexural properties and buckling response for symmetrically laminated composite plates*, Journal of Engineering Mechanics 133:1178–1191.

Webber JPH, Holt PJ, Lee DA (1985): *Instability of carbon fibre reinforced flanges of I section beams and columns*, Composite Structures 4:245–265.

Zureick A, Shih B (1998): *Local buckling of fiber-reinforced polymeric structural members under linearly-varying edge loading-part 1. Theoretical formulation*, Composite Structures 41:79–86.

The Ritz Method for Buckling Analysis of Shear-Deformable Laminates

15

The previous explanations on buckling of composite laminates only allow the consideration of laminates in which no transverse shear deformations occur. However, in many practical applications, layups with anisotropic properties and bending-twisting coupling are employed in which such shear deformations play a decisive role in the buckling response. This chapter is therefore dedicated to the development of the Ritz method for various laminate situations under consideration of transverse shear strains, based on the First-Order Shear Deformation Theory (FSDT) and the Third-Order Shear Deformation Theory (TSDT) (see also Mittelstedt and Mittelstedt (2019)).

15.1 The Ritz Method in the Framework of FSDT

15.1.1 Structural Situation and Basic Equations

Consider a rectangular laminate (length a, width b, Fig. 15.1) which is subject to the indicated force flows N_{xx}^0, N_{yy}^0 and N_{xy}^0, whereby the force flow N_{xx}^0 may vary linearly over y. The laminate is symmetric, but otherwise no further requirements are placed on the layup. The two longitudinal edges at $y = 0$ and $y = b$ are also elastically restrained (restraint stiffnesses k_r and k_l). In Fig. 15.1, hinged supports are provided as an example at all edges, but we will consider a number of other combinations of boundary conditions in the remainder of this chapter. We are now looking for the critical load combination at which the laminate enters the buckled state.

The constitutive law within the framework of FSDT is as follows, assuming symmetric laminates:

© The Author(s), under exclusive license to Springer-Verlag GmbH, DE, part of Springer Nature 2025

C. Mittelstedt, *Mechanics of Composite Structures*,
https://doi.org/10.1007/978-3-662-70788-3_15

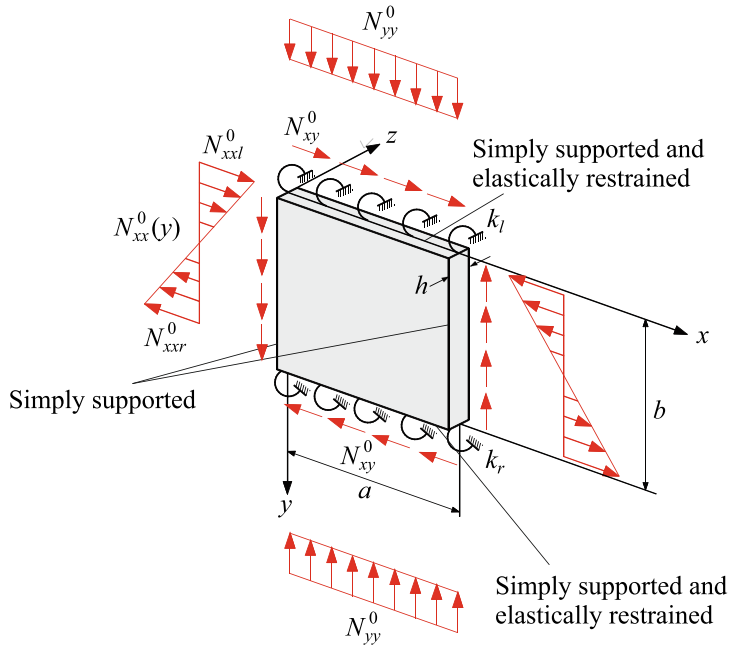


Fig. 15.1 Structural situation

$$\begin{pmatrix} N^0_{xx} \\ N^0_{yy} \\ N^0_{xy} \\ M^0_{xx} \\ M^0_{yy} \\ M^0_{xy} \\ Q_y \\ Q_x \end{pmatrix} = \begin{bmatrix} A_{11} & A_{12} & A_{16} & 0 & 0 & 0 & 0 & 0 \\ A_{12} & A_{22} & A_{26} & 0 & 0 & 0 & 0 & 0 \\ A_{16} & A_{26} & A_{66} & 0 & 0 & 0 & 0 & 0 \\ 0 & 0 & 0 & D_{11} & D_{12} & D_{16} & 0 & 0 \\ 0 & 0 & 0 & D_{12} & D_{22} & D_{26} & 0 & 0 \\ 0 & 0 & 0 & D_{16} & D_{26} & D_{66} & 0 & 0 \\ 0 & 0 & 0 & 0 & 0 & 0 & KA_{44} & KA_{45} \\ 0 & 0 & 0 & 0 & 0 & 0 & KA_{45} & KA_{55} \end{bmatrix} \begin{pmatrix} \frac{\partial u_0}{\partial x} \\ \frac{\partial v_0}{\partial y} \\ \frac{\partial u_0}{\partial y} + \frac{\partial v_0}{\partial x} \\ \frac{\partial \psi_x}{\partial x} \\ \frac{\partial \psi_y}{\partial y} \\ \frac{\partial \psi_x}{\partial y} + \frac{\partial \psi_y}{\partial x} \\ \frac{\partial w_0}{\partial y} + \psi_y \\ \frac{\partial w_0}{\partial x} + \psi_x \end{pmatrix}. \tag{15.1}$$

The total elastic potential Π of the buckled laminate is made up of the inner potential Π_i, the external potential Π_a and the energy Π_s stored in the edge restraints:

$$\Pi = \Pi_i + \Pi_a + \Pi_s. \tag{15.2}$$

The inner energy or inner potential Π_i required for the Ritz method is currently

$$\Pi_i = \frac{1}{2} \int_V \left(\sigma_{xx}\varepsilon_{xx} + \sigma_{yy}\varepsilon_{yy} + \tau_{xy}\varepsilon_{xy} + \tau_{xz}\varepsilon_{xz} + \tau_{yz}\varepsilon_{yz} \right) \mathrm{d}V, \tag{15.3}$$

or after performing the integration with respect to the thickness direction z and neglecting the inplane displacements u_0 and v_0:

$$\Pi_i = \frac{1}{2}\int_0^b \int_0^a \left[M_{xx}^0 \frac{\partial \psi_x}{\partial x} + M_{yy}^0 \frac{\partial \psi_y}{\partial y} + M_{xy}^0 \left(\frac{\partial \psi_x}{\partial y} + \frac{\partial \psi_y}{\partial x} \right) + Q_y \left(\frac{\partial w_0}{\partial y} + \psi_y \right) + Q_x \left(\frac{\partial w_0}{\partial x} + \psi_x \right) \right] \mathrm{d}x\mathrm{d}y. \tag{15.4}$$

Inserting the constitutive law according to FSDT then results in:

$$\begin{aligned} \Pi_i = \frac{1}{2}\int_0^b \int_0^a \Bigg[& D_{11} \frac{\partial \psi_x}{\partial x}\frac{\partial \psi_x}{\partial x} + 2D_{12} \frac{\partial \psi_y}{\partial y}\frac{\partial \psi_x}{\partial x} + D_{22} \frac{\partial \psi_y}{\partial y}\frac{\partial \psi_y}{\partial y} \\ & + 2D_{16} \left(\frac{\partial \psi_x}{\partial y}\frac{\partial \psi_x}{\partial x} + \frac{\partial \psi_y}{\partial x}\frac{\partial \psi_x}{\partial x} \right) + 2D_{26} \left(\frac{\partial \psi_x}{\partial y}\frac{\partial \psi_y}{\partial y} + \frac{\partial \psi_y}{\partial x}\frac{\partial \psi_y}{\partial y} \right) \\ & + D_{66} \left(\frac{\partial \psi_x}{\partial y}\frac{\partial \psi_x}{\partial y} + 2\frac{\partial \psi_x}{\partial y}\frac{\partial \psi_y}{\partial x} + \frac{\partial \psi_y}{\partial x}\frac{\partial \psi_y}{\partial x} \right) \\ & + KA_{44} \left(\frac{\partial w_0}{\partial y}\frac{\partial w_0}{\partial y} + 2\frac{\partial w_0}{\partial y}\psi_y + \psi_y^2 \right) \\ & + 2KA_{45} \left(\frac{\partial w_0}{\partial x}\frac{\partial w_0}{\partial y} + \frac{\partial w_0}{\partial x}\psi_y + \frac{\partial w_0}{\partial y}\psi_x + \psi_x\psi_y \right) \\ & + KA_{55} \left(\frac{\partial w_0}{\partial x}\frac{\partial w_0}{\partial x} + 2\frac{\partial w_0}{\partial x}\psi_x + \psi_x^2 \right) \Bigg] \mathrm{d}x\mathrm{d}y. \end{aligned} \tag{15.5}$$

The external potential Π_a results under the given boundary loads as:

$$\Pi_a = -\frac{1}{2}\int_0^b \int_0^a \left[\Lambda N_{xx}^0 \left(\frac{\partial w_0}{\partial x} \right)^2 + \Lambda N_{yy}^0 \left(\frac{\partial w_0}{\partial y} \right)^2 + 2\Lambda N_{xy}^0 \left(\frac{\partial w_0}{\partial x} \right) \left(\frac{\partial w_0}{\partial y} \right) \right] \mathrm{d}x\mathrm{d}y. \tag{15.6}$$

Herein, Λ is the load multiplier that indicates by how much the applied load may be increased before buckling occurs. The linearly varying force flow $N_{xx}^0(y)$ can be formulated as:

$$N_{xx}^0(y) = \frac{N_{xxl}^0}{b}\left[(\psi - 1)\, y + b \right], \tag{15.7}$$

if the boundary value N_{xxr}^0 is ψ times the multiple of the boundary value N_{xxl}^0.

Finally, the restraint energy Π_s must be considered, which can currently be specified as follows:

$$\Pi_s = \frac{1}{2}\int_0^a \left[k_l \left(\psi_y|_{y=0} \right)^2 + k_r \left(\psi_y|_{y=b} \right)^2 \right] \mathrm{d}x. \tag{15.8}$$

15.1.2 Shape Functions and Energy Formulations

For each of the types of boundary conditions considered later, a general approach for the buckling degrees of freedom is made as follows:

$$
\begin{aligned}
w_0 &= \sum_{m=1}^{M}\sum_{n=1}^{N} W_{mn} w_{1m}(x) w_{2n}(y)\,, \\
\psi_x &= \sum_{m=1}^{K}\sum_{n=1}^{L} X_{mn} \psi_{x1m}(x) \psi_{x2n}(y)\,, \\
\psi_y &= \sum_{m=1}^{I}\sum_{n=1}^{J} Y_{mn} \psi_{y1m}(x) \psi_{y2n}(y)\,,
\end{aligned}
\tag{15.9}
$$

whereby the requirement is made here that the shape functions must fulfil all geometric boundary conditions. The inner potential Π_i can thus be written as:

$$
\begin{aligned}
\Pi_i = {} & \frac{D_{11}}{2}\sum_{m=1}^{K}\sum_{n=1}^{L}\sum_{p=1}^{K}\sum_{q=1}^{L} X_{mn}X_{pq}\int_0^a \frac{d\psi_{x1m}}{\mathrm{d}x}\frac{d\psi_{x1p}}{\mathrm{d}x}\mathrm{d}x \int_0^b \psi_{x2n}\psi_{x2q}\mathrm{d}y \\
& + \frac{D_{22}}{2}\sum_{m=1}^{I}\sum_{n=1}^{J}\sum_{p=1}^{I}\sum_{q=1}^{J} Y_{mn}Y_{pq}\int_0^a \psi_{y1m}\psi_{y1p}\mathrm{d}x \int_0^b \frac{d\psi_{y2n}}{\mathrm{d}y}\frac{d\psi_{y2q}}{\mathrm{d}y}\mathrm{d}y \\
& + D_{12}\sum_{m=1}^{K}\sum_{n=1}^{L}\sum_{p=1}^{I}\sum_{q=1}^{J} X_{mn}Y_{pq}\int_0^a \frac{d\psi_{x1m}}{\mathrm{d}x}\psi_{y1p}\mathrm{d}x \int_0^b \frac{d\psi_{y2q}}{\mathrm{d}y}\psi_{x2n}\mathrm{d}y \\
& + D_{16}\sum_{m=1}^{K}\sum_{n=1}^{L}\sum_{p=1}^{K}\sum_{q=1}^{L} X_{mn}X_{pq}\int_0^a \frac{d\psi_{x1m}}{\mathrm{d}x}\psi_{x1p}\mathrm{d}x \int_0^b \frac{d\psi_{x2q}}{\mathrm{d}y}\psi_{x2n}\mathrm{d}y \\
& + D_{16}\sum_{m=1}^{K}\sum_{n=1}^{L}\sum_{p=1}^{I}\sum_{q=1}^{J} X_{mn}Y_{pq}\int_0^a \frac{d\psi_{x1m}}{\mathrm{d}x}\frac{d\psi_{y1p}}{\mathrm{d}x}\mathrm{d}x \int_0^b \psi_{x2n}\psi_{y2q}\mathrm{d}y \\
& + D_{26}\sum_{m=1}^{K}\sum_{n=1}^{L}\sum_{p=1}^{I}\sum_{q=1}^{J} X_{mn}Y_{pq}\int_0^a \psi_{x1m}\psi_{y1p}\mathrm{d}x \int_0^b \frac{d\psi_{x2n}}{\mathrm{d}y}\frac{d\psi_{y2q}}{\mathrm{d}y}\mathrm{d}y \\
& + D_{26}\sum_{m=1}^{K}\sum_{n=1}^{L}\sum_{p=1}^{I}\sum_{q=1}^{J} Y_{mn}Y_{pq}\int_0^a \frac{d\psi_{y1m}}{\mathrm{d}x}\psi_{y1p}\mathrm{d}x \int_0^b \psi_{x2n}\frac{d\psi_{y1q}}{\mathrm{d}y}\mathrm{d}y \\
& + \frac{D_{66}}{2}\sum_{m=1}^{K}\sum_{n=1}^{L}\sum_{p=1}^{K}\sum_{q=1}^{L} X_{mn}X_{pq}\int_0^a \psi_{x1m}\psi_{x1p}\mathrm{d}x \int_0^b \frac{d\psi_{x2n}}{\mathrm{d}y}\frac{d\psi_{x2q}}{\mathrm{d}y}\mathrm{d}y
\end{aligned}
$$

$$
\begin{aligned}
&+ D_{66} \sum_{m=1}^{K} \sum_{n=1}^{L} \sum_{p=1}^{I} \sum_{q=1}^{J} X_{mn} Y_{pq} \int_0^a \psi_{x1m} \frac{d\psi_{y1p}}{\mathrm{d}x} \mathrm{d}x \int_0^b \frac{d\psi_{x2n}}{\mathrm{d}y} \psi_{y2q} \mathrm{d}y \\
&+ \frac{D_{66}}{2} \sum_{m=1}^{I} \sum_{n=1}^{J} \sum_{p=1}^{I} \sum_{q=1}^{J} Y_{mn} Y_{pq} \int_0^a \frac{d\psi_{y1m}}{\mathrm{d}x} \frac{d\psi_{y1p}}{\mathrm{d}x} \mathrm{d}x \int_0^b \psi_{y2n} \psi_{y2q} \mathrm{d}y \\
&+ \frac{KA_{44}}{2} \sum_{m=1}^{M} \sum_{n=1}^{N} \sum_{p=1}^{M} \sum_{q=1}^{N} W_{mn} W_{pq} \int_0^a w_{1m} w_{1p} \mathrm{d}x \int_0^b \frac{dw_{2n}}{\mathrm{d}y} \frac{dw_{2q}}{\mathrm{d}y} \mathrm{d}y \\
&+ KA_{44} \sum_{m=1}^{M} \sum_{n=1}^{N} \sum_{p=1}^{I} \sum_{q=1}^{J} W_{mn} Y_{pq} \int_0^a w_{1m} \psi_{y1p} \mathrm{d}x \int_0^b \frac{dw_{2n}}{\mathrm{d}y} \psi_{y2q} \mathrm{d}y \\
&+ \frac{KA_{44}}{2} \sum_{m=1}^{I} \sum_{n=1}^{J} \sum_{p=1}^{I} \sum_{q=1}^{J} Y_{mn} Y_{pq} \int_0^a \psi_{y1m} \psi_{y1p} \mathrm{d}x \int_0^b \psi_{y2n} \psi_{y2q} \mathrm{d}y \\
&+ KA_{45} \sum_{m=1}^{M} \sum_{n=1}^{N} \sum_{p=1}^{M} \sum_{q=1}^{N} W_{mn} W_{pq} \int_0^a \frac{dw_{1m}}{\mathrm{d}x} w_{1p} \mathrm{d}x \int_0^b w_{2n} \frac{dw_{2q}}{\mathrm{d}y} \mathrm{d}y \\
&+ KA_{45} \sum_{m=1}^{M} \sum_{n=1}^{N} \sum_{p=1}^{I} \sum_{q=1}^{J} W_{mn} Y_{pq} \int_0^a \frac{dw_{1m}}{\mathrm{d}x} \psi_{y1p} \mathrm{d}x \int_0^b w_{2n} \psi_{y1q} \mathrm{d}y \\
&+ KA_{45} \sum_{m=1}^{M} \sum_{n=1}^{N} \sum_{p=1}^{K} \sum_{q=1}^{L} W_{mn} X_{pq} \int_0^a w_{1m} \psi_{x1p} \mathrm{d}x \int_0^b \frac{dw_{2n}}{\mathrm{d}y} \psi_{x2q} \mathrm{d}y \\
&+ KA_{45} \sum_{m=1}^{K} \sum_{n=1}^{L} \sum_{p=1}^{I} \sum_{q=1}^{J} X_{mn} Y_{pq} \int_0^a \psi_{x1m} \psi_{y1p} \mathrm{d}x \int_0^b \psi_{x2m} \psi_{y2p} \mathrm{d}y \\
&+ \frac{KA_{55}}{2} \sum_{m=1}^{M} \sum_{n=1}^{N} \sum_{p=1}^{M} \sum_{q=1}^{N} W_{mn} W_{pq} \int_0^a \frac{dw_{1m}}{\mathrm{d}x} \frac{dw_{1p}}{\mathrm{d}x} \mathrm{d}x \int_0^b w_{2n} w_{2q} \mathrm{d}y \\
&+ KA_{55} \sum_{m=1}^{M} \sum_{n=1}^{N} \sum_{p=1}^{K} \sum_{q=1}^{L} W_{mn} X_{pq} \int_0^a \frac{dw_{1m}}{\mathrm{d}y} \psi_{x1p} \mathrm{d}x \int_0^b w_{2n} \psi_{x2q} \mathrm{d}y \\
&+ \frac{KA_{55}}{2} \sum_{m=1}^{K} \sum_{n=1}^{L} \sum_{p=1}^{K} \sum_{q=1}^{L} X_{mn} X_{pq} \int_0^a \psi_{x1m} \psi_{x1p} \mathrm{d}x \int_0^b \psi_{x2m} \psi_{x2p} \mathrm{d}y.
\end{aligned}
\tag{15.10}
$$

It is appropriate to introduce at this point the following integral resultants of the shape functions in (15.9) and their derivatives as follows:

$$\begin{aligned}
\Omega_{ij}^{1} &= \int_0^a \frac{\partial^i \psi_{x1m}}{\partial x^i}\frac{\partial^j \psi_{x1p}}{\partial x^j}\mathrm{d}x,\\
\Omega_{ij}^{2} &= \int_0^a \frac{\partial^i \psi_{x1m}}{\partial x^i}\frac{\partial^j \psi_{y1p}}{\partial x^j}\mathrm{d}x,\\
\Omega_{ij}^{3} &= \int_0^a \frac{\partial^i \psi_{y1m}}{\partial x^i}\frac{\partial^j \psi_{y1p}}{\partial x^j}\mathrm{d}x,\\
\Omega_{ij}^{4} &= \int_0^a \frac{\partial^i w_{1m}}{\partial x^i}\frac{\partial^j w_{1p}}{\partial x^j}\mathrm{d}x,\\
\Omega_{ij}^{5} &= \int_0^a \frac{\partial^i w_{1m}}{\partial x^i}\frac{\partial^j \psi_{y1p}}{\partial x^j}\mathrm{d}x,\\
\Omega_{ij}^{6} &= \int_0^a \frac{\partial^i w_{1m}}{\partial x^i}\frac{\partial^j \psi_{x1p}}{\partial x^j}\mathrm{d}x,\\
\Delta_{ij}^{1} &= \int_0^b \frac{\partial^i \psi_{x2n}}{\partial y^i}\frac{\partial^j \psi_{x2q}}{\partial y^j}\mathrm{d}y,\\
\Delta_{ij}^{2} &= \int_0^b \frac{\partial^i \psi_{x2n}}{\partial y^i}\frac{\partial^j \psi_{y2q}}{\partial y^j}\mathrm{d}y,\\
\Delta_{ij}^{3} &= \int_0^b \frac{\partial^i \psi_{y2n}}{\partial y^i}\frac{\partial^j \psi_{y2q}}{\partial y^j}\mathrm{d}y,\\
\Delta_{ij}^{4} &= \int_0^b \frac{\partial^i w_{2n}}{\partial y^i}\frac{\partial^j w_{2q}}{\partial y^j}\mathrm{d}y,\\
\Delta_{ij}^{5} &= \int_0^b \frac{\partial^i w_{2n}}{\partial y^i}\frac{\partial^j \psi_{y2q}}{\partial y^j}\mathrm{d}y,\\
\Delta_{ij}^{6} &= \int_0^b \frac{\partial^i w_{2n}}{\partial y^i}\frac{\partial^j \psi_{x2q}}{\partial y^j}\mathrm{d}y.
\end{aligned} \tag{15.11}$$

With the abbreviations

$$\begin{aligned}
\Gamma_i^{klkl} &= \frac{1}{2}(D_{11}\Omega_{11}^{1}\Delta_{00}^{1} + D_{66}\Omega_{00}^{1}\Delta_{11}^{1} + kA_{55}\Omega_{00}^{1}\Delta_{00}^{1}) + D_{16}\Omega_{10}^{1}\Delta_{01}^{1},\\
\Gamma_i^{ijij} &= \frac{1}{2}\left(D_{22}\Omega_{00}^{3}\Delta_{11}^{3} + D_{66}\Omega_{11}^{3}\Delta_{00}^{3} + kA_{44}\Omega_{00}^{mp}\Delta_{00}^{nq}\right) + D_{26}\Omega_{10}^{3p}\Delta_{01}^{3},\\
\Gamma_i^{klij} &= D_{12}\Omega_{10}^{2}\Delta_{01}^{2} + D_{16}\Omega_{11}^{2}\Delta_{00}^{2} + D_{26}\Omega_{00}^{2}\Delta_{11}^{2} + D_{66}\Omega_{01}^{2}\Delta_{10}^{2} + kA_{45}\Omega_{00}^{2}\Delta_{00}^{2},\\
\Gamma_i^{mnmn} &= \frac{k}{2}\left(A_{44}\Omega_{00}^{4}\Delta_{11}^{4} + 2A_{45}\Omega_{10}^{4}\Delta_{01}^{4} + A_{55}\Omega_{11}^{4}\Delta_{00}^{4}\right),
\end{aligned}$$

$$\Gamma_i^{mnij} = \frac{k}{2}\left(2A_{44}\Omega_{00}^5\Delta_{10}^5 + 2A_{45}\Omega_{10}^5\Delta_{00}^5\right),$$
$$\Gamma_i^{mnkl} = \frac{k}{2}\left(2A_{45}\Omega_{00}^6\Delta_{10}^6 + 2A_{55}\Omega_{10}^6\Delta_{00}^6\right) \tag{15.12}$$

the inner potential Π_i can be represented in a compact manner as:

$$\begin{aligned}\Pi_i = &\sum_{m=1}^{K}\sum_{n=1}^{L}\sum_{p=1}^{K}\sum_{q=1}^{L} X_{mn}X_{pq}\Gamma_i^{klkl} \\ &+ \sum_{m=1}^{I}\sum_{n=1}^{J}\sum_{p=1}^{I}\sum_{q=1}^{J} Y_{mn}Y_{pq}\Gamma_i^{ijij} \\ &+ \sum_{m=1}^{K}\sum_{n=1}^{L}\sum_{p=1}^{I}\sum_{q=1}^{J} X_{mn}Y_{pq}\Gamma_i^{klij} \\ &+ \sum_{m=1}^{M}\sum_{n=1}^{N}\sum_{p=1}^{M}\sum_{q=1}^{N} W_{mn}W_{pq}\Gamma_i^{mnmn} \\ &+ \sum_{m=1}^{M}\sum_{n=1}^{N}\sum_{p=1}^{I}\sum_{q=1}^{J} W_{mn}Y_{pq}\Gamma_i^{mnij} \\ &+ \sum_{m=1}^{M}\sum_{n=1}^{N}\sum_{p=1}^{K}\sum_{q=1}^{L} W_{mn}X_{pq}\Gamma_i^{mnkl}.\end{aligned} \tag{15.13}$$

The external potential Π_a can also be specified in the same way:

$$\begin{aligned}\Pi_a = &-\Lambda\frac{N_{xx}^0}{2b}(\psi-1)\sum_{m=1}^{M}\sum_{n=1}^{N}\sum_{p=1}^{M}\sum_{q=1}^{N} W_{mn}W_{pq}\int_0^a \frac{\partial w_{1m}}{\partial x}\frac{\partial w_{1p}}{\partial x}\mathrm{d}x\int_0^b w_{2n}w_{2q}y\mathrm{d}y \\ &- \Lambda\frac{N_{xx}^0}{2}\sum_{m=1}^{M}\sum_{n=1}^{N}\sum_{p=1}^{M}\sum_{q=1}^{N} W_{mn}W_{pq}\int_0^a \frac{\partial w_{1m}}{\partial x}\frac{\partial w_{1p}}{\partial x}\mathrm{d}x\int_0^b w_{2n}w_{2q}\mathrm{d}y \\ &- \Lambda\frac{N_{yy}^0}{2}\sum_{m=1}^{M}\sum_{n=1}^{N}\sum_{p=1}^{M}\sum_{q=1}^{N} W_{mn}W_{pq}\int_0^a w_{1m}w_{1p}\mathrm{d}x\int_0^b \frac{\partial w_{2n}}{\partial y}\frac{\partial w_{2q}}{\partial y}\mathrm{d}y \\ &- \Lambda N_{xy}^0\sum_{m=1}^{M}\sum_{n=1}^{N}\sum_{p=1}^{M}\sum_{q=1}^{N} W_{mn}W_{pq}\int_0^a \frac{\partial w_{1m}}{\partial x}w_{1p}\mathrm{d}x\int_0^b w_{2n}\frac{\partial w_{2q}}{\partial y}\mathrm{d}y,\end{aligned} \tag{15.14}$$

or with (15.11) and the abbreviation

$$Q_{00} = \int_0^b w_{2n} w_{2q} y \mathrm{d}y \tag{15.15}$$

in the following form:

$$\begin{aligned}\Pi_a = &-\Lambda \frac{N_{xx}^0}{2} \sum_{m=1}^{M}\sum_{n=1}^{N}\sum_{p=1}^{M}\sum_{q=1}^{N} W_{mn} W_{pq} \left[\frac{(\psi-1)}{b}\Omega_{11}^4 Q_{00} + \Omega_{11}^4 \Delta_{00}^4\right] \\ &- \Lambda \frac{N_{yy}^0}{2} \sum_{m=1}^{M}\sum_{n=1}^{N}\sum_{p=1}^{M}\sum_{q=1}^{N} W_{mn} W_{pq} \Omega_{00}^4 \Delta_{11}^4 \\ &- \Lambda N_{xy}^0 \sum_{m=1}^{M}\sum_{n=1}^{N}\sum_{p=1}^{M}\sum_{q=1}^{N} W_{mn} W_{pq} \Omega_{10}^4 \Delta_{01}^4.\end{aligned} \tag{15.16}$$

With the abbreviation

$$\Gamma_a^{mnmn} = \frac{N_{xx}^0}{2}\left[\frac{(\psi-1)}{b}\Omega_{11}^4 Q_{00} + \Omega_{11}^4 \Delta_{00}^4\right] + \frac{N_{yy}^0}{2}\Omega_{00}^4 \Delta_{11}^4 + N_{xy}^0 \Omega_{10}^4 \Delta_{01}^4 \tag{15.17}$$

we obtain:

$$\Pi_a = -\Lambda \sum_{m=1}^{M}\sum_{n=1}^{N}\sum_{p=1}^{M}\sum_{q=1}^{N} W_{mn} W_{pq} \Gamma_a^{mnmn}. \tag{15.18}$$

Finally, the restraint energy Π_s can be specified in compact form:

$$\begin{aligned}\Pi_s = &\frac{k_l}{2} \sum_{m=1}^{I}\sum_{n=1}^{J}\sum_{p=1}^{I}\sum_{q=1}^{J} Y_{mn} Y_{pq} \int_0^a \psi_{y1m}\psi_{y1p}\mathrm{d}x \left(\psi_{y2n}\psi_{y2q}\right)\big|_{y=0} \\ &+ \frac{k_r}{2} \sum_{m=1}^{I}\sum_{n=1}^{J}\sum_{p=1}^{I}\sum_{q=1}^{J} Y_{mn} Y_{pq} \int_0^a \psi_{y1m}\psi_{y1p}\mathrm{d}x \left(\psi_{y2n}\psi_{y2q}\right)\big|_{y=b}.\end{aligned} \tag{15.19}$$

With the abbreviations

$$\begin{aligned}\Phi_{11} &= \psi_{y2n}\psi_{y2q}\big|_{y=0}, \\ \Theta_{11} &= \psi_{y2n}\psi_{y2q}\big|_{y=b}\end{aligned} \tag{15.20}$$

and

$$\Gamma_s^{ijij} = \frac{1}{2} T_{00}^{mp} \left(k_l \Phi_{11} + k_r \Theta_{11} \right) \tag{15.21}$$

we obtain:

$$\Pi_s = \sum_{m=1}^{I} \sum_{n=1}^{J} \sum_{p=1}^{I} \sum_{q=1}^{J} Y_{mn} Y_{pq} \Gamma_s^{ijij}. \tag{15.22}$$

15.1.3 Eigenvalue Problem

Reaching the bifurcational load or the critical load combination is described by an indifferent equilibrium state, which is equivalent to the vanishing of the first variation of the total elastic potential Π of the buckled laminate:

$$\delta \Pi = 0. \tag{15.23}$$

Since the mathematical form of the degrees of freedom has already been fully defined with the (not yet specified) shape functions, the variational statement (15.23) leads to the so-called Ritz equations:

$$\frac{\partial \Pi}{\partial W_{mn}} = 0, \quad \frac{\partial \Pi}{\partial X_{mn}} = 0, \quad \frac{\partial \Pi}{\partial Y_{mn}} = 0. \tag{15.24}$$

Performing the derivations required here and summarizing them in a vector-matrix notation produces the following system of equations:

$$\left[\underline{\underline{K}}_i + \underline{\underline{K}}_s - \Lambda \underline{\underline{K}}_a \right] \underline{W} = \underline{0}. \tag{15.25}$$

This is a linear eigenvalue problem, where the load multiplier Λ represents the eigenvalue and the vector $\underline{W}$ represents the eigenvector. The matrix $\underline{\underline{K}}_i$ is the stiffness matrix of the laminate under consideration, and $\underline{\underline{K}}_a$ is referred to as the geometric stiffness matrix. The matrix $\underline{\underline{K}}_s$ contains the stiffness contributions of the edge restraints.

The composition of the stiffness matrix $\underline{\underline{K}}_i$ is explained in more detail here. It is composed of several submatrices:

$$\underline{\underline{K}}_i = \begin{bmatrix} \underline{\underline{K}}_{1,w}^{mnmn} & \underline{\underline{K}}_{1,w}^{mnkl} & \underline{\underline{K}}_{1,w}^{mnij} \\ \underline{\underline{K}}_{1,x}^{mnkl} & \underline{\underline{K}}_{1,w}^{klkl} & \underline{\underline{K}}_{1,w}^{klij} \\ \underline{\underline{K}}_{1,y}^{mnij} & \underline{\underline{K}}_{1,y}^{ijkl} & \underline{\underline{K}}_{1,y}^{ijij} \end{bmatrix}, \tag{15.26}$$

whereby the following conditions apply:

$$\begin{aligned}\underline{\underline{K}}^{mnkl}_{1,x} &= \left(\underline{\underline{K}}^{mnkl}_{1,w}\right)^T,\\ \underline{\underline{K}}^{mnij}_{1,y} &= \left(\underline{\underline{K}}^{mnij}_{1,w}\right)^T,\\ \underline{\underline{K}}^{klij}_{1,y} &= \left(\underline{\underline{K}}^{klij}_{1,x}\right)^T.\end{aligned} \tag{15.27}$$

The individual submatrices in turn can be systematically broken down into further submatrices as follows:

$$\underline{\underline{K}}^{mnpq}_{i,w} = \begin{bmatrix} \underline{\underline{K}}^{11}_{i,w} & \underline{\underline{K}}^{12}_{i,w} & \underline{\underline{K}}^{13}_{i,w} & \cdots & \underline{\underline{K}}^{1P}_{i,w} \\ \underline{\underline{K}}^{21}_{i,w} & \underline{\underline{K}}^{22}_{i,w} & \underline{\underline{K}}^{23}_{i,w} & \cdots & \underline{\underline{K}}^{2P}_{i,w} \\ \underline{\underline{K}}^{31}_{i,w} & \underline{\underline{K}}^{32}_{i,w} & \underline{\underline{K}}^{33}_{i,w} & \cdots & \underline{\underline{K}}^{3P}_{i,w} \\ \vdots & \vdots & \vdots & \vdots & \vdots \\ \underline{\underline{K}}^{M1}_{i,w} & \underline{\underline{K}}^{M2}_{i,w} & \underline{\underline{K}}^{M3}_{i,w} & \cdots & \underline{\underline{K}}^{MP}_{i,w} \end{bmatrix},$$

$$\underline{\underline{K}}^{mnpq}_{i,x} = \begin{bmatrix} \underline{\underline{K}}^{11}_{i,x} & \underline{\underline{K}}^{12}_{i,x} & \underline{\underline{K}}^{13}_{i,x} & \cdots & \underline{\underline{K}}^{1P}_{i,x} \\ \underline{\underline{K}}^{21}_{i,x} & \underline{\underline{K}}^{22}_{i,x} & \underline{\underline{K}}^{23}_{i,x} & \cdots & \underline{\underline{K}}^{2P}_{i,x} \\ \underline{\underline{K}}^{31}_{i,x} & \underline{\underline{K}}^{32}_{i,x} & \underline{\underline{K}}^{33}_{i,x} & \cdots & \underline{\underline{K}}^{3P}_{i,x} \\ \vdots & \vdots & \vdots & \vdots & \vdots \\ \underline{\underline{K}}^{M1}_{i,x} & \underline{\underline{K}}^{M2}_{i,x} & \underline{\underline{K}}^{M3}_{i,x} & \cdots & \underline{\underline{K}}^{MP}_{i,x} \end{bmatrix},$$

$$\underline{\underline{K}}^{mnpq}_{i,y} = \begin{bmatrix} \underline{\underline{K}}^{11}_{i,y} & \underline{\underline{K}}^{12}_{i,y} & \underline{\underline{K}}^{13}_{i,y} & \cdots & \underline{\underline{K}}^{1P}_{i,y} \\ \underline{\underline{K}}^{21}_{i,y} & \underline{\underline{K}}^{22}_{i,y} & \underline{\underline{K}}^{23}_{i,y} & \cdots & \underline{\underline{K}}^{2P}_{i,y} \\ \underline{\underline{K}}^{31}_{i,y} & \underline{\underline{K}}^{32}_{i,y} & \underline{\underline{K}}^{33}_{i,y} & \cdots & \underline{\underline{K}}^{3P}_{i,y} \\ \vdots & \vdots & \vdots & \vdots & \vdots \\ \underline{\underline{K}}^{M1}_{i,y} & \underline{\underline{K}}^{M2}_{i,y} & \underline{\underline{K}}^{M3}_{i,y} & \cdots & \underline{\underline{K}}^{MP}_{i,y} \end{bmatrix}. \tag{15.28}$$

The components of the submatrices occurring here can be specified as:

$$\begin{aligned}\underline{\underline{K}}^{mp}_{i,w} &= \left[K^{mp}_{nq,i,w}\right],\\ \underline{\underline{K}}^{mp}_{i,x} &= \left[K^{mp}_{nq,i,x}\right],\\ \underline{\underline{K}}^{mp}_{i,y} &= \left[K^{mp}_{nq,i,y}\right],\end{aligned} \tag{15.29}$$

with:

$$\begin{aligned}K^{mp}_{nq,i,w} &= \Gamma^{mnpq}_i + \Gamma^{pqmn}_i,\\ K^{mp}_{nq,i,x} &= \Gamma^{mnpq}_i + \Gamma^{pqmn}_i,\\ K^{mp}_{nq,i,y} &= \Gamma^{mnpq}_i + \Gamma^{pqmn}_i.\end{aligned} \tag{15.30}$$

The other matrices of the eigenvalue problem can be constructed in a similar way, but this will not be explained further here.

15.2 Considered Boundary Conditions

The methodology described above in general terms using the Ritz method is described below for the four cases shown in Fig. 15.2 under the load case combination of Fig. 15.1.

The four cases are:

- case 1: Laminate simply supported at all edges with elastic edge restraints at the points $y = 0$ (restraint stiffness k_l) and $y = b$ (restraint stiffness k_r),
- case 2: Two simply supported edges at $x = 0$ and $x = a$, two rigidly clamped edges at $y = 0$ and $y = b$,
- case 3: Two simply supported edges at $x = 0$ and $x = a$, one elastically restrained edge at $y = 0$ (restraint stiffness k), one free edge at $y = b$,
- case 4: Two simply supported edges at $x = 0$ and $x = a$, one rigidly clamped edge at $y = 0$, one free edge at $y = b$.

15.2.1 Shape Functions for Case 1

The following shape functions are used for case 1:

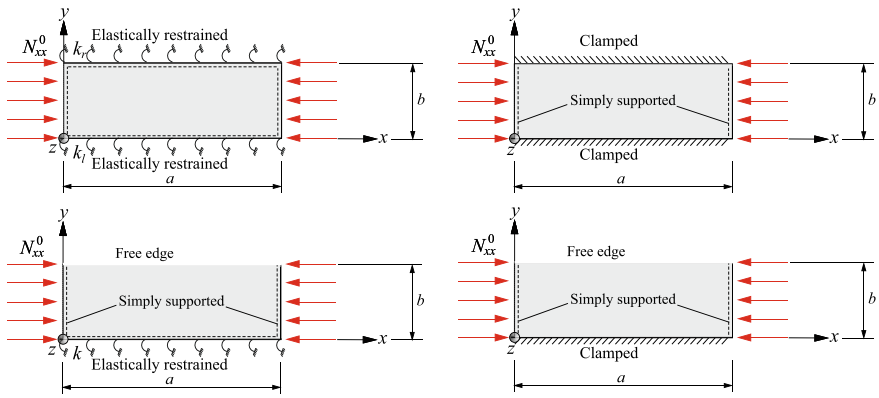


Fig. 15.2 Considered boundary conditions

$$
\begin{aligned}
w_0 &= \sum_{m=1}^{M}\sum_{n=1}^{N} W_{mn} w_{1m}(x) w_{2n}(y) \\
&= \sum_{m=1}^{M}\sum_{n=1}^{N} W_{mn} \sin\left(\frac{m\pi x}{a}\right) \sin\left(\frac{n\pi y}{b}\right), \\
\psi_x &= \sum_{m=1}^{K}\sum_{n=1}^{L} X_{mn} \psi_{x1m}(x) \psi_{x2n}(y) \\
&= \sum_{m=1}^{M}\sum_{n=1}^{N} X_{mn} \cos\left(\frac{m\pi x}{a}\right) \sin\left(\frac{n\pi y}{b}\right), \\
\psi_y &= \sum_{m=1}^{I}\sum_{n=1}^{J} Y_{mn} \psi_{y1m}(x) \psi_{y2n}(y) \\
&= \sum_{m=1}^{M}\sum_{n=1}^{N} Y_{mn} \sin\left(\frac{m\pi x}{a}\right) \cos\left(\frac{n\pi y}{b}\right).
\end{aligned} \tag{15.31}
$$

15.2.2 Shape Functions for Case 2

For case 2, the following shape functions have proven to be adequate:

$$
\begin{aligned}
w_0 &= \sum_{m=1}^{M}\sum_{n=1}^{N} W_{mn} w_{1m}(x) w_{2n}(y) \\
&= \sum_{m=1}^{M}\sum_{n=1}^{N} W_{mn} \sin\left(\frac{m\pi x}{a}\right) \left[\cos\left(\frac{(n-1)\pi y}{b}\right) - \cos\left(\frac{(n+1)\pi y}{b}\right)\right], \\
\psi_x &= \sum_{m=1}^{K}\sum_{n=1}^{L} X_{mn} \psi_{x1m}(x) \psi_{x2n}(y) \\
&= \sum_{m=1}^{M}\sum_{n=1}^{N} X_{mn} \cos\left(\frac{m\pi x}{a}\right) \left[\cos\left(\frac{(n-1)\pi y}{b}\right) - \cos\left(\frac{(n+1)\pi y}{b}\right)\right], \\
\psi_y &= \sum_{m=1}^{I}\sum_{n=1}^{J} Y_{mn} \psi_{y1m}(x) \psi_{y2n}(y) \\
&= \sum_{m=1}^{M}\sum_{n=1}^{N} Y_{mn} \sin\left(\frac{m\pi x}{a}\right) \left[\cos\left(\frac{(n-1)\pi y}{b}\right) - \cos\left(\frac{(n+1)\pi y}{b}\right)\right].
\end{aligned} \tag{15.32}
$$

15.2.3 Shape Functions for Case 3

Case 3 uses the following shape functions:

$$\begin{aligned}
w_0 &= \sum_{m=1}^{M}\sum_{n=1}^{N} W_{mn} w_{1m}(x) w_{2n}(y) \\
&= \sum_{m=1}^{M}\sum_{n=1}^{N} W_{mn} \sin\left(\frac{m\pi x}{a}\right)\left(\frac{y}{b}\right)^{n}, \\
\psi_x &= \sum_{m=1}^{K}\sum_{n=1}^{L} X_{mn} \psi_{x1m}(x) \psi_{x2n}(y) \\
&= \sum_{m=1}^{M}\sum_{n=1}^{N} X_{mn} \cos\left(\frac{m\pi x}{a}\right)\left(\frac{y}{b}\right)^{n}, \\
\psi_y &= \sum_{m=1}^{I}\sum_{n=1}^{J} Y_{mn} \psi_{y1m}(x) \psi_{y2n}(y) \\
&= \sum_{m=1}^{M}\sum_{n=1}^{N} Y_{mn} \sin\left(\frac{m\pi x}{a}\right)\left(\frac{y}{b}\right)^{n-1}.
\end{aligned} \tag{15.33}$$

15.2.4 Shape Functions for Case 4

Finally, for case 4, the following shape functions prove to be useful:

$$\begin{aligned}
w_0 &= \sum_{m=1}^{M}\sum_{n=1}^{N} W_{mn} w_{1m}(x) w_{2n}(y) \\
&= \sum_{m=1}^{M}\sum_{n=1}^{N} W_{mn} \sin\left(\frac{m\pi x}{a}\right)\left(\frac{y}{b}\right)^{n+1}, \\
\psi_x &= \sum_{m=1}^{K}\sum_{n=1}^{L} X_{mn} \psi_{x1m}(x) \psi_{x2n}(y) \\
&= \sum_{m=1}^{M}\sum_{n=1}^{N} X_{mn} \cos\left(\frac{m\pi x}{a}\right)\left(\frac{y}{b}\right)^{n+1}, \\
\psi_y &= \sum_{m=1}^{I}\sum_{n=1}^{J} Y_{mn} \psi_{y1m}(x) \psi_{y2n}(y)
\end{aligned}$$

$$= \sum_{m=1}^{M} \sum_{n=1}^{N} Y_{mn} \sin\left(\frac{m\pi x}{a}\right)\left(\frac{y}{b}\right)^{n+1}. \tag{15.34}$$

The resultants (15.11) as well as (15.15) and (15.20) for cases 1–4 are specifically defined in the following.

15.2.5 Resultants of the Shape Functions

15.2.5.1 Resultants with Respect to the x-Direction

The integral resultants Ω^1_{00}, Ω^1_{10}, …of the shape functions with respect to the x-direction according to (15.11) are identical for all four cases of boundary conditions considered here and are as follows:

$$\Omega^1_{00} = \int_0^a \psi_{x1m}\psi_{x1p}\mathrm{d}x = \int_0^a \cos\left(\frac{m\pi x}{a}\right)\cos\left(\frac{p\pi x}{a}\right)\mathrm{d}x$$
$$= \begin{cases} \frac{1}{2}a & \text{if} \quad m = p \\ 0 & \text{if} \quad m \neq p \end{cases},$$
$$\Omega^1_{10} = \int_0^a \frac{\partial\psi_{x1m}}{\partial x}\psi_{x1p}\mathrm{d}x = \frac{-m\pi}{a}\int_0^a \sin\left(\frac{m\pi x}{a}\right)\cos\left(\frac{p\pi x}{a}\right)\mathrm{d}x$$
$$= \begin{cases} 0 & \text{if} \quad m+p = \text{even} \\ \frac{-2m^2}{m^2-p^2} & \text{if} \quad m+p = \text{odd} \end{cases},$$
$$\Omega^1_{11} = \int_0^a \frac{\partial\psi_{x1p}}{\partial x}\frac{\partial\psi_{x1m}}{\partial x}\mathrm{d}x = \frac{m\pi}{a}\frac{p\pi}{a}\int_0^a \sin\left(\frac{m\pi x}{a}\right)\sin\left(\frac{p\pi x}{a}\right)\mathrm{d}x$$
$$= \begin{cases} \frac{m^2\pi^2}{2a} & \text{if} \quad m = p \\ 0 & \text{if} \quad m \neq p \end{cases},$$
$$\Omega^2_{00} = \int_0^a \psi_{x1m}\psi_{y1p}\mathrm{d}x = \int_0^a \cos\left(\frac{m\pi x}{a}\right)\sin\left(\frac{p\pi x}{a}\right)\mathrm{d}x$$
$$= \begin{cases} 0 & \text{if} \quad m+p = \text{even} \\ \frac{2pa}{(p^2-m^2)\pi} & \text{if} \quad m+p = \text{odd} \end{cases},$$
$$\Omega^2_{01} = \int_0^a \psi_{x1m}\frac{\partial\psi_{y1p}}{\partial x}\mathrm{d}x = \frac{p\pi}{a}\int_0^a \cos\left(\frac{m\pi x}{a}\right)\cos\left(\frac{p\pi x}{a}\right)\mathrm{d}x$$
$$= \begin{cases} \frac{p\pi}{2} & \text{if} \quad m = p \\ 0 & \text{if} \quad m \neq p \end{cases},$$
$$\Omega^2_{10} = \int_0^a \frac{\partial\psi_{x1m}}{\partial x}\psi_{y1p}\mathrm{d}x = \frac{-m\pi}{a}\int_0^a \sin\left(\frac{m\pi x}{a}\right)\sin\left(\frac{p\pi x}{a}\right)\mathrm{d}x$$
$$= \begin{cases} \frac{-m\pi}{2} & \text{if} \quad m = p \\ 0 & \text{if} \quad m \neq p \end{cases},$$

$$\Omega_{11}^{2} = \int_0^a \frac{\partial \psi_{x1m}}{\partial x}\frac{\partial \psi_{y1p}}{\partial x}\mathrm{d}x = -mp\left(\frac{\pi}{a}\right)^2 \int_0^a \cos\left(\frac{m\pi x}{a}\right)\cos\left(\frac{p\pi x}{a}\right)\mathrm{d}x$$
$$= \begin{cases} 0 & \text{if } m+p \ = \text{even} \\ \frac{-2m^2 p\pi}{a\,(m^2-p^2)} & \text{if } m+p \ = \text{odd} \end{cases},$$

$$\Omega_{00}^{3} = \int_0^a \psi_{y1m}\psi_{y1p}\mathrm{d}x = \int_0^a \sin\left(\frac{m\pi x}{a}\right)\sin\left(\frac{p\pi x}{a}\right)\,\mathrm{d}x$$
$$= \begin{cases} \frac{1}{2}a & \text{if} \quad m = p \\ 0 & \text{if} \quad m \neq p \end{cases},$$

$$\Omega_{10}^{3} = \int_0^a \frac{\partial \psi_{y1m}}{\partial x}\psi_{y1p}\mathrm{d}x = \frac{m\pi}{a}\int_0^a \cos\left(\frac{m\pi x}{a}\right)\sin\left(\frac{p\pi x}{a}\right)\,\mathrm{d}x$$
$$= \begin{cases} 0 & \text{if} \quad m+p \ = \text{even} \\ \frac{2mp}{p^2-m^2} & \text{if} \quad m+p \ = \text{odd} \end{cases},$$

$$\Omega_{11}^{3} = \int_0^a \frac{\partial \psi_{y1m}}{\partial x}\frac{\partial \psi_{y1p}}{\partial x}\mathrm{d}x = mp\left(\frac{\pi}{a}\right)^2 \int_0^a \cos\left(\frac{m\pi x}{a}\right)\cos\left(\frac{p\pi x}{a}\right)\mathrm{d}x$$
$$= \begin{cases} \frac{mp\pi^2}{2a} & \text{if} \quad m = p \\ 0 & \text{if} \quad m \neq p \end{cases},$$

$$\Omega_{00}^{4} = \int_0^a w_{1m}w_{1p}\mathrm{d}x = \int_0^a \sin\left(\frac{m\pi x}{a}\right)\sin\left(\frac{p\pi x}{a}\right)\mathrm{d}x$$
$$= \begin{cases} \frac{1}{2}a & \text{if} \quad m = p \\ 0 & \text{if} \quad m \neq p \end{cases},$$

$$\Omega_{10}^{4} = \int_0^a \frac{\partial w_{1m}}{\partial x}w_{1p}\mathrm{d}x = \frac{m\pi}{a}\int_0^a \cos\left(\frac{m\pi x}{a}\right)\sin\left(\frac{p\pi x}{a}\right)\mathrm{d}x$$
$$= \begin{cases} 0 & \text{if} \quad m+p \ = \text{even} \\ \frac{2pm}{p^2-m^2} & \text{if} \quad m+p \ = \text{odd} \end{cases},$$

$$\Omega_{11}^{4} = \int_0^a \frac{\partial w_{1m}}{\partial x}\frac{\partial w_{1p}}{\partial x}\mathrm{d}x = mp\left(\frac{\pi}{a}\right)^2 \int_0^b \cos\left(\frac{m\pi x}{a}\right)\cos\left(\frac{p\pi x}{a}\right)\mathrm{d}x$$
$$= \begin{cases} \frac{mp\pi^2}{2a} & \text{if} \quad m = p \\ 0 & \text{if} \quad m \neq p \end{cases},$$

$$\Omega_{00}^{5} = \int_0^a w_{1m}\psi_{y1p}\mathrm{d}x = \int_0^a \sin\left(\frac{m\pi x}{a}\right)\sin\left(\frac{p\pi x}{a}\right)\mathrm{d}x$$
$$= \begin{cases} \frac{a}{2} & \text{if} \quad m = p \\ 0 & \text{if} \quad m \neq p \end{cases},$$

$$\Omega_{10}^{5} = \int_0^a \frac{\partial w_{1m}}{\partial x}\psi_{y1p}\mathrm{d}x = \frac{m\pi}{a}\int_0^a \cos\left(\frac{m\pi x}{a}\right)\sin\left(\frac{p\pi x}{a}\right)\mathrm{d}x$$
$$= \begin{cases} 0 & \text{if} \quad m+p \ = \text{even} \\ \frac{2pm}{p^2-m^2} & \text{if} \quad m+p \ = \text{odd} \end{cases},$$

$$\Omega_{00}^{6} = \int_0^a w_{1m}\psi_{x1p}\mathrm{d}x = \int_0^a \sin\left(\frac{m\pi x}{a}\right)\cos\left(\frac{p\pi x}{a}\right)\mathrm{d}x$$
$$= \begin{cases} \frac{2ma}{\pi(m^2-p^2)} & \text{if} \quad m+p \quad = \text{odd} \\ 0 & \text{if} \quad m+p \quad = \text{even} \end{cases},$$
$$\Omega_{10}^{6} = \int_0^a \frac{\partial w_{1m}}{\partial x}\psi_{x1p}\mathrm{d}x = \frac{m\pi}{a}\int_0^a \cos\left(\frac{m\pi x}{a}\right)\cos\left(\frac{p\pi x}{a}\right)\mathrm{d}x$$
$$= \begin{cases} 0 & \text{if} \quad m \neq p \\ \frac{m\pi}{2} & \text{if} \quad m = p \end{cases}. \tag{15.35}$$

15.2.5.2 Resultants with Respect to the y-Direction, Case 1

The integral resultants (15.11) for case 1 according to FSDT are as follows:

$$\Delta_{00}^{1} = \int_0^b \psi_{x2n}\psi_{x2q}\mathrm{d}y = \int_0^b \sin\left(\frac{n\pi y}{b}\right)\sin\left(\frac{q\pi y}{b}\right)\mathrm{d}y$$
$$= \begin{cases} \frac{1}{2}b & \text{if} \quad n = q \\ 0 & \text{if} \quad n \neq q \end{cases},$$
$$\Delta_{01}^{1} = \int_0^b \psi_{x2n}\frac{\partial\psi_{x2q}}{\partial y}\mathrm{d}y = \frac{q\pi}{b}\int_0^b \sin\left(\frac{n\pi y}{b}\right)\cos\left(\frac{q\pi y}{b}\right)\mathrm{d}y$$
$$= \begin{cases} 0 & \text{if} \quad n+q \quad = \text{even} \\ \frac{2nq}{n^2-q^2} & \text{if} \quad n+q \quad = \text{odd} \end{cases},$$
$$\Delta_{11}^{1} = \int_0^b \frac{\partial\psi_{x2n}}{\partial y}\frac{\partial\psi_{x2q}}{\partial y}\mathrm{d}y = nq\left(\frac{\pi}{b}\right)^2\int_0^b \cos\left(\frac{n\pi y}{b}\right)\cos\left(\frac{q\pi y}{b}\right)\mathrm{d}y$$
$$= \begin{cases} \frac{nq\pi^2}{2b} & \text{if} \quad n = q \\ 0 & \text{if} \quad n \neq q \end{cases},$$
$$\Delta_{00}^{2} = \int_0^b \psi_{x2n}\psi_{y2q}\mathrm{d}y = \int_0^b \sin\left(\frac{n\pi y}{b}\right)\cos\left(\frac{q\pi y}{b}\right)\mathrm{d}y$$
$$= \begin{cases} 0 & \text{if} \quad n+q \quad = \text{even} \\ \frac{2bn}{\pi(n^2-q^2)} & \text{if} \quad n+q \quad = \text{odd} \end{cases},$$
$$\Delta_{01}^{2} = \int_0^b \psi_{x2n}\frac{\partial\psi_{y2q}}{\partial y}\mathrm{d}y = \frac{-q\pi}{b}\int_0^b \sin\left(\frac{n\pi y}{b}\right)\sin\left(\frac{q\pi y}{b}\right)\mathrm{d}y$$
$$= \begin{cases} \frac{-q\pi}{2} & \text{if} \quad n = q \\ 0 & \text{if} \quad n \neq q \end{cases},$$
$$\Delta_{10}^{2} = \int_0^b \frac{\partial\psi_{x2n}}{\partial y}\psi_{y2q}\mathrm{d}y = \frac{n\pi}{b}\int_0^b \cos\left(\frac{n\pi y}{b}\right)\cos\left(\frac{q\pi y}{b}\right)\mathrm{d}y$$

$$= \begin{cases} \frac{n\pi}{2} & \text{if} \quad n = q \\ 0 & \text{if} \quad n \neq q \end{cases},$$

$$\Delta_{11}^{2} = \int_0^b \frac{\partial \psi_{x2n}}{\partial y} \frac{\partial \psi_{y2q}}{\partial y} \mathrm{d}y = \frac{-n\pi}{b} \frac{q\pi}{b} \int_0^b \cos\left(\frac{n\pi y}{b}\right) \sin\left(\frac{q\pi y}{b}\right) \mathrm{d}y$$

$$= \begin{cases} 0 & \text{if} \quad n+q \ = \text{even} \\ \frac{-2nq^2\pi}{b(q^2-n^2)} & \text{if} \quad n+q \ = \text{odd} \end{cases},$$

$$\Delta_{00}^{3} = \int_0^b \psi_{y2n} \psi_{y2q} \mathrm{d}y = \int_0^b \cos\left(\frac{n\pi y}{b}\right) \cos\left(\frac{q\pi y}{b}\right) \mathrm{d}y$$

$$= \begin{cases} \frac{1}{2}b & \text{if} \quad n = q \\ 0 & \text{if} \quad n \neq q \end{cases},$$

$$\Delta_{01}^{3} = \int_0^b \psi_{y2n} \frac{\partial \psi_{y2q}}{\partial y} \mathrm{d}y = \frac{-q\pi}{b} \int_0^b \cos\left(\frac{n\pi y}{b}\right) \sin\left(\frac{q\pi y}{b}\right) \mathrm{d}y$$

$$= \begin{cases} 0 & \text{if} \quad n+q \ = \text{even} \\ \frac{2q^2}{(n^2-q^2)} & \text{if} \quad n+q \ = \text{odd} \end{cases},$$

$$\Delta_{11}^{3} = \int_0^b \frac{\partial \psi_{y2n}}{\partial y} \frac{\partial \psi_{y2q}}{\partial y} \mathrm{d}y = nq\left(\frac{\pi}{b}\right)^2 \int_0^b \sin\left(\frac{n\pi y}{b}\right) \sin\left(\frac{q\pi y}{b}\right) \mathrm{d}y$$

$$= \begin{cases} \frac{nq\pi^2}{2b} & \text{if} \quad n = q \\ 0 & \text{if} \quad n \neq q \end{cases},$$

$$\Delta_{00}^{4} = \int_0^b w_{2n} w_{2q} \mathrm{d}y = \int_0^b \sin\left(\frac{n\pi y}{b}\right) \sin\left(\frac{q\pi y}{b}\right) \mathrm{d}y$$

$$= \begin{cases} \frac{1}{2}b & \text{if} \quad n = q \\ 0 & \text{if} \quad n \neq q \end{cases},$$

$$\Delta_{01}^{4} = \int_0^b w_{2n} \frac{\partial w_{2q}}{\partial y} \mathrm{d}y = \frac{q\pi}{b} \int_0^b \sin\left(\frac{n\pi y}{b}\right) \cos\left(\frac{q\pi y}{b}\right) \mathrm{d}y$$

$$= \begin{cases} 0 & \text{if} \quad n+q \ = \text{even} \\ \frac{2nq}{n^2-q^2} & \text{if} \quad n+q \ = \text{odd} \end{cases},$$

$$\Delta_{11}^{4} = \int_0^b \frac{\partial w_{2n}}{\partial y} \frac{\partial w_{2q}}{\partial y} \mathrm{d}y = nq\left(\frac{\pi}{b}\right)^2 \int_0^b \cos\left(\frac{n\pi y}{b}\right) \cos\left(\frac{q\pi y}{b}\right) \mathrm{d}y$$

$$= \begin{cases} \frac{nq\pi^2}{2b} & \text{if} \quad n = q \\ 0 & \text{if} \quad n \neq q \end{cases},$$

$$\Delta_{00}^{5} = \int_0^b w_{2n} \psi_{y2q} \mathrm{d}y = \int_0^b \sin\left(\frac{n\pi y}{b}\right) \cos\left(\frac{q\pi y}{b}\right) \mathrm{d}y$$

$$= \begin{cases} 0 & \text{if} \quad n+q \ \text{ even} \\ \frac{2nb}{(n^2-q^2)\pi} & \text{if} \quad n+q \ \text{ odd} \end{cases},$$

$$\begin{aligned}
\Delta_{10}^{5} &= \int_0^b \frac{\partial w_{2n}}{\partial y}\psi_{y2q}\mathrm{d}y = \frac{n\pi}{b}\int_0^b \cos\left(\frac{n\pi y}{b}\right)\cos\left(\frac{q\pi y}{b}\right)\mathrm{d}y \\
&= \begin{cases} \frac{n\pi}{2} & \text{if} \quad n = q \\ 0 & \text{if} \quad n \neq q \end{cases}, \\
\Delta_{00}^{6} &= \int_0^b w_{2n}\psi_{x2q}\mathrm{d}y = \int_0^b \sin\left(\frac{n\pi y}{b}\right)\sin\left(\frac{q\pi y}{b}\right)\mathrm{d}y \\
&= \begin{cases} \frac{1}{2}b & \text{if} \quad n = q \\ 0 & \text{if} \quad n \neq q \end{cases}, \\
\Delta_{10}^{6} &= \int_0^b \frac{\partial w_{2n}}{\partial x}\psi_{y2q}\mathrm{d}y = \frac{n\pi}{b}\int_0^b \cos\left(\frac{n\pi y}{b}\right)\sin\left(\frac{q\pi y}{b}\right)\mathrm{d}y \\
&= \begin{cases} 0 & \text{if} \quad n+q \quad \text{even} \\ \frac{2nq}{(q^2-n^2)} & \text{if} \quad n+q \quad \text{odd} \end{cases}.
\end{aligned} \tag{15.36}$$

For (15.15) we have:

$$\begin{aligned}
Q_{00} &= \int_0^b w_{2n}w_{2q}y\mathrm{d}y = \int_0^b \sin\left(\frac{n\pi y}{b}\right)\sin\left(\frac{q\pi y}{b}\right)\mathrm{d}y \\
&= \begin{cases} \frac{1}{4}b^2 & \text{if} \quad n = q \\ \frac{2b^2nq}{\pi^2(n^2-q^2)^2}\left[(-1)^{n+q}-1\right] & \text{if} \quad n \neq q \end{cases}.
\end{aligned} \tag{15.37}$$

From (15.20) we obtain:

$$\begin{aligned}
\Phi_{11} &= \left.\psi_{y2n}\right|_{y=0}\left.\psi_{y2q}\right|_{y=0} = \cos(0)\cos(0) = 1, \\
\theta_{11} &= \left.\psi_{y2n}\right|_{y=b}\left.\psi_{y2q}\right|_{y=b} = \begin{cases} 1 & \text{if} \quad n+q = \text{even} \\ -1 & \text{if} \quad n+q = \text{odd} \end{cases}.
\end{aligned} \tag{15.38}$$

15.2.5.3 Resultants with Respect to the y-Direction, Case 2

The integral resultants (15.11) for case 2 according to FSDT are obtained as:

$$\begin{aligned}
\Delta_{00}^{1} &= \int_0^b \psi_{x2n}\psi_{x2q}\mathrm{d}y \\
&= \int_0^b \left\{\left[\cos\left((n-1)\,\pi\,\frac{y}{b}\right) - \cos\left((n+1)\,\pi\,\frac{y}{b}\right)\right]\right. \\
&\times \left.\left[\cos\left((q-1)\,\pi\,\frac{y}{b}\right) - \cos\left((q+1)\,\pi\,\frac{y}{b}\right)\right]\right\}\mathrm{d}y
\end{aligned}$$

$$= \begin{cases} \frac{-b}{2} & \text{if} \quad n = 2+q \\ b & \text{if} \quad n = q,\ q \neq 1 \\ \frac{-b}{2} & \text{if} \quad n = q-2 \text{ and } q \neq 1,\ q \neq 2 \\ \frac{3b}{2} & \text{if} \quad n = q = 1 \\ 0 & \text{else} \end{cases},$$

$$\Delta_{01}^{1} = \int_0^b \psi_{x2n} \frac{\partial \psi_{x2q}}{\partial y} \mathrm{d}y$$

$$= \int_0^b \left\{ \left[\cos\left((n-1)\pi\frac{y}{b}\right) - \cos\left((n+1)\pi\frac{y}{b}\right) \right] \right.$$

$$\left. \times \left[-\left((q-1)\frac{\pi}{b}\right) \sin\left((q-1)\pi\frac{y}{b}\right) + \left((q+1)\frac{\pi}{b}\right) \sin\left((q+1)\pi\frac{y}{b}\right) \right] \right\} \mathrm{d}y$$

$$= \frac{-32nq\left(-2+n^2+q^2\right)}{(-2+n-q)(n-q)(2+n-q)(-2+n+q)(2+n+q)(n+q)}$$

if $n+q =$ odd,

$$\Delta_{10}^{1} = \int_0^b \frac{\partial \psi_{x2n}}{\partial x} \psi_{y2q} \mathrm{d}y$$

$$= \int_0^b \left\{ \left[(1-n)\left(\frac{\pi}{b}\right) \sin\left((n-1)\pi\frac{y}{b}\right) + \left((n+1)\frac{\pi}{b}\right) \sin\left((n+1)\cdot\pi\cdot\frac{y}{b}\right) \right] \right.$$

$$\left. \times \left[\cos\left((q-1)\pi\frac{y}{b}\right) - \cos\left((q+1)\pi\frac{y}{b}\right) \right] \right\} \mathrm{d}y$$

$$= \frac{32\cdot n\cdot q\cdot(-2+n^2+q^2)}{(-2+n-q)\cdot(n-q)\cdot(2+n-q)\cdot(-2+n+q)\cdot(n+q)\cdot(2+n+q)}$$

if $n+q =$ odd,

$$\Delta_{11}^{1} = \int_0^b \frac{\partial \psi_{x2n}}{\partial y} \frac{\partial \psi_{x2q}}{\partial y} \mathrm{d}y$$

$$= \int_0^b \left[\left((1-n)\frac{\pi}{b}\right) \sin\left((n-1)\pi\frac{y}{b}\right) + \left((n+1)\frac{\pi}{y}\right) \sin\left((n+1)\pi\frac{y}{b}\right) \right]$$

$$\times \left[\left((1-q)\frac{\pi}{b}\right) \sin\left((q-1)\pi\frac{y}{b}\right) + \left((q+1)\frac{\pi}{y}\right) \sin\left((q+1)\pi\frac{y}{b}\right) \right] \mathrm{d}y$$

$$= \begin{cases} \frac{-\pi^2\left(1+q^2\right)}{2b} & \text{if } n = q+2 \\ \frac{\pi^2\left(1+q^2\right)}{b} & \text{if } n = q \\ \frac{-\pi^2(-1+q)^2}{2b} & \text{if } n = q-2 \quad \text{and} \quad q \geq 3 \\ 0 & \text{else} \end{cases},$$

$$\Delta_{00}^{2} = \int_0^b \psi_{x2n} \psi_{y2q} \mathrm{d}y$$

$$= \int_0^b \left\{ \left[\cos\left((n-1)\pi\frac{y}{b}\right) - \cos\left((n+1)\pi\frac{y}{b}\right) \right] \right.$$

$$\times \left[\cos\left((q-1)\,\pi\,\frac{y}{b}\right) - \cos\left((q+1)\,\pi\,\frac{y}{b}\right)\right]\Bigg\}\,\mathrm{d}y$$

$$= \begin{cases} \frac{-b}{2} & \text{if} \quad n = 2+q \\ b & \text{if} \quad n = q,\ q \neq 1 \\ \frac{-b}{2} & \text{if} \quad n = q-2 \text{ and } q \neq 1,\ q \neq 2 \\ \frac{3b}{2} & \text{if} \quad n = q = 1 \\ 0 & \text{else} \end{cases},$$

$$\Delta_{01}^{2} = \int_0^b \psi_{x2n}\frac{\partial \psi_{y2q}}{\partial y}\mathrm{d}y$$

$$= \int_0^b \left\{\left[\cos\left((n-1)\,\pi\,\frac{y}{b}\right) - \cos\left((n+1)\,\pi\,\frac{y}{b}\right)\right]\right.$$

$$\left.\times \left[-\left((q-1)\,\frac{\pi}{b}\right)\sin\left((q-1)\,\pi\,\frac{y}{b}\right) + \left((n+1)\,\frac{\pi}{b}\right)\sin\left((n+1)\,\pi\,\frac{y}{b}\right)\right]\right\}\mathrm{d}y$$

$$= \frac{-32\cdot n\cdot q\cdot\left(-2+n^2+q^2\right)}{(-2+n-q)\cdot(n-q)\cdot(2+n-q)\cdot(2+n+q)\cdot(-2+n+q)\cdot(n+q)}$$

$$\text{if} \quad n+q = \text{ odd},$$

$$\Delta_{00}^{3} = \int_0^b \psi_{y2n}\psi_{y2q}\mathrm{d}y$$

$$= \int_0^b \left\{\left[\cos\left((n-1)\,\pi\,\frac{y}{b}\right) - \cos\left((n+1)\,\pi\,\frac{y}{b}\right)\right]\right.$$

$$\left.\times \left[\cos\left((q-1)\,\pi\,\frac{y}{b}\right) - \cos\left((q+1)\,\pi\,\frac{y}{b}\right)\right]\right\}\mathrm{d}y$$

$$= \begin{cases} \frac{-b}{2} & \text{if} \quad n = 2+q \\ b & \text{if} \quad n = q,\ q \neq 1 \\ \frac{-b}{2} & \text{if} \quad n = q-2 \text{ and } q \neq 1,\ q \neq 2 \\ \frac{3b}{2} & \text{if} \quad n = q = 1 \\ 0 & \text{else} \end{cases},$$

$$\Delta_{01}^{3} = \int_0^b \psi_{x2n}\frac{\partial \psi_{y2q}}{\partial y}\mathrm{d}y$$

$$= \int_0^b \left\{\left[\cos\left((n-1)\,\pi\,\frac{y}{b}\right) - \cos\left((n+1)\,\pi\,\frac{y}{b}\right)\right]\right.$$

$$\left.\times \left[-\left((q-1)\,\frac{\pi}{b}\right)\sin\left((q-1)\,\pi\,\frac{y}{b}\right) + \left((q+1)\,\frac{\pi}{b}\right)\sin\left((q+1)\,\pi\,\frac{y}{b}\right)\right]\right\}\mathrm{d}y$$

$$= \frac{-32nq\left(-2+n^2+q^2\right)}{(-2+n-q)\,(n-q)\,(2+n-q)\,(-2+n+q)\,(2+n+q)\,(n+q)}$$

$$\text{if} \quad n+q = \text{ odd},$$

$$\Delta_{11}^{3} = \int_0^b \frac{\partial \psi_{y2n}}{\partial y}\frac{\partial \psi_{y2q}}{\partial y}\mathrm{d}y$$

$$
\begin{aligned}
&= \int_0^b \left\{ \left[\left((1-n)\,\frac{\pi}{b} \right) \sin\left((n-1)\,\pi\,\frac{y}{b} \right) + \left((n+1)\,\frac{\pi}{y} \right) \sin\left((n+1)\,\pi\,\frac{y}{b} \right) \right] \right. \\
&\left. \times \left[\left((1-q)\,\frac{\pi}{b} \right) \sin\left((q-1)\,\pi\,\frac{y}{b} \right) + \left((q+1)\,\frac{\pi}{y} \right) \sin\left((q+1)\,\pi\,\frac{y}{b} \right) \right] \right\} \mathrm{d}y \\
&= \begin{cases} \frac{-\pi^2\left(1+q^2\right)}{2b} & \text{if } n = q+2 \\ \frac{\pi^2\left(1+q^2\right)}{b} & \text{if } n = q \\ \frac{-\pi^2(-1+q)^2}{2b} & \text{if } n = q-2 \quad \text{and} \quad q \geq 3 \\ 0 & \text{else} \end{cases},
\end{aligned}
$$

$$
\begin{aligned}
\Delta_{00}^4 &= \int_0^b w_{2n} w_{2q} \mathrm{d}y \\
&= \int_0^b \left[\cos\left((n-1)\,\pi\,\frac{y}{b} \right) - \cos\left((n+1)\,\pi\,\frac{y}{b} \right) \right] \\
&\times \left[\cos\left((q-1)\,\pi\,\frac{y}{b} \right) - \cos\left((q+1)\,\pi\,\frac{y}{b} \right) \right] \mathrm{d}y \\
&= \begin{cases} \frac{-b}{2} & \text{if} \quad n = 2+q \\ b & \text{if} \quad n = q,\ q \neq 1 \\ \frac{-b}{2} & \text{if} \quad n = q-2 \text{ and } q \neq 1,\ q \neq 2 \\ \frac{3b}{2} & \text{if} \quad n = q = 1 \\ 0 & \text{else} \end{cases},
\end{aligned}
$$

$$
\begin{aligned}
\Delta_{01}^4 &= \int_0^b w_{2n} \frac{\partial w_{2q}}{\partial y} \mathrm{d}y \\
&= \int_0^b \left\{ \left[\cos\left((n-1)\,\pi\,\frac{y}{b} \right) - \cos\left((n+1)\,\pi\,\frac{y}{b} \right) \right] \right. \\
&\left. \times \left[-\left((q-1)\,\frac{\pi}{b} \right) \sin\left((q-1)\,\pi\,\frac{y}{b} \right) + \left((q+1)\,\frac{\pi}{b} \right) \sin\left((q+1)\,\pi\,\frac{y}{b} \right) \right] \right\} \mathrm{d}y \\
&= \frac{-32nq\left(-2+n^2+q^2\right)}{(-2+n-q)\,(n-q)\,(2+n-q)\,(-2+n+q)\,(2+n+q)\cdot(n+q)} \\
&\text{if} \quad n+q = \text{ odd},
\end{aligned}
$$

$$
\begin{aligned}
\Delta_{11}^4 &= \int_0^b \frac{\partial w_{2n}}{\partial y} \frac{\partial w_{2q}}{\partial y} \mathrm{d}y \\
&= \int_0^b \left\{ \left[\left((1-n)\,\frac{\pi}{b} \right) \sin\left((n-1)\,\pi\,\frac{y}{b} \right) + \left((n+1)\,\frac{\pi}{y} \right) \sin\left((n+1)\,\pi\,\frac{y}{b} \right) \right] \right. \\
&\left. \times \left[\left((1-q)\,\frac{\pi}{b} \right) \sin\left((q-1)\,\pi\,\frac{y}{b} \right) + \left((q+1)\,\frac{\pi}{y} \right) \sin\left((q+1)\,\pi\,\frac{y}{b} \right) \right] \right\} \mathrm{d}y
\end{aligned}
$$

$$= \begin{cases} \frac{-\pi^2\left(1+q^2\right)}{2b} & \text{if } n = q+2 \\ \frac{\pi^2\left(1+q^2\right)}{b} & \text{if } n = q \\ \frac{-\pi^2(-1+q)^2}{2b} & \text{if } n = q-2 \\ 0 & \text{else} \end{cases},$$

$$\Delta_{00}^{5} = \int_0^b w_{2n}\psi_{y2q}\mathrm{d}y$$

$$= \int_0^b \left\{\left[\cos\left((n-1)\,\pi\,\frac{y}{b}\right) - \cos\left((n+1)\,\pi\,\frac{y}{b}\right)\right]\right.$$

$$\left.\times\left[\cos\left((q-1)\,\pi\,\frac{y}{b}\right) - \cos\left((q+1)\,\pi\,\frac{y}{b}\right)\right]\right\}\mathrm{d}y$$

$$= \begin{cases} \frac{-b}{2} & \text{if } \; n = 2+q \\ b & \text{if } \; n = q,\; q \neq 1 \\ \frac{-b}{2} & \text{if } \; n = q-2 \text{ and } q \geq 3 \\ \frac{3b}{2} & \text{if } \; n = q = 1 \\ 0 & \text{else} \end{cases},$$

$$\Delta_{10}^{5} = \int_0^b \frac{\partial w_{2n}}{\partial x}\psi_{y2q}\mathrm{d}y$$

$$= \int_0^b \left\{\left[(1-n)\left(\frac{\pi}{b}\right)\sin\left((n-1)\,\pi\,\frac{y}{b}\right) + \left((n+1)\,\frac{\pi}{b}\right)\sin\left((n+1)\cdot\pi\cdot\frac{y}{b}\right)\right]\right.$$

$$\left.\times\left[\cos\left((q-1)\,\pi\,\frac{y}{b}\right) - \cos\left((q+1)\,\pi\,\frac{y}{b}\right)\right]\right\}\mathrm{d}y$$

$$= \frac{32\cdot n\cdot q\cdot\left(-2+n^2+q^2\right)}{(-2+n-q)\cdot(n-q)\cdot(2+n-q)\cdot(-2+n+q)\cdot(n+q)\cdot(2+n+q)}$$

$$\text{if} \quad n+q = \text{odd},$$

$$\Delta_{00}^{6} = \int_0^b w_{2n}\psi_{x2q}\mathrm{d}y$$

$$= \int_0^b \left\{\left[\cos((n-1)\,\pi\,\frac{y}{b}) - \cos\left((n+1)\,\pi\,\frac{y}{b}\right)\right]\right.$$

$$\left.\times\left[\cos\left((q-1)\,\pi\,\frac{y}{b}\right) - \cos\left((q+1)\,\pi\,\frac{y}{b}\right)\right]\right\}\mathrm{d}y$$

$$= \begin{cases} \frac{-b}{2} & \text{if } \; n = 2+q \\ b & \text{if } \; n = q,\; q \neq 1 \\ \frac{-b}{2} & \text{if } \; n = q-2 \text{ and } q \geq 3 \\ \frac{3b}{2} & \text{if } \; n = q = 1 \\ 0 & \text{else} \end{cases},$$

$$\Delta_{10}^{6} = \int_0^b \frac{\partial w_{2n}}{\partial x}\psi_{x2q}\mathrm{d}y$$

$$= \int_0^b \left\{\left[(1-n)\left(\frac{\pi}{b}\right)\sin\left((n-1)\,\pi\,\frac{y}{b}\right) + \left((n+1)\,\frac{\pi}{b}\right)\sin\left((n+1)\,\pi\,\frac{y}{b}\right)\right]\right.$$

$$\times \left[\cos\left((q-1)\,\pi\,\frac{y}{b}\right) - \cos\left((q+1)\,\pi\,\frac{y}{b}\right)\right]\Bigg\}\,\mathrm{d}y$$
$$= \frac{32\cdot n\cdot q\cdot(-2+n^2+q^2)}{(-2+n-q)\cdot(n-q)\cdot(2+n-q)\cdot(-2+n+q)\cdot(n+q)\cdot(2+n+q)}$$
$$\text{if}\quad n+q=\text{odd}. \tag{15.39}$$

For (15.15) results:

$$\begin{aligned}
Q_{00} &= \int_0^b w_{2n}\,w_{2q}\,y\,\mathrm{d}y \\
&= \int_0^b \Bigg\{\left[\cos\left((n-1)\,\pi\,\frac{y}{b}\right) - \cos\left((n+1)\,\pi\,\frac{y}{b}\right)\right] \\
&\times \left[\cos\left((q-1)\,\pi\,\frac{y}{b}\right) - \cos\left((q+1)\,\pi\,\frac{y}{b}\right)\right] y\Bigg\}\,\mathrm{d}y \\
&= \begin{cases}
\dfrac{b^2\left(-\frac{2}{(n-q)^2}+\frac{1}{(2+n-q)^2}+\frac{1}{(2-n+q)^2}-\frac{1}{(-2+n+q)^2}+\frac{2}{(n+q)^2}-\frac{1}{(2+n+q)^2}\right)}{\pi^2} & \text{if}\quad n+q=\text{odd} \\
\frac{-b^2}{4} & \text{if}\quad n=q+2 \\
\frac{-b^2}{4} & \text{if}\quad n=q-2 \\
\frac{b^2}{2} & \text{if}\quad n=q\neq 1 \\
\frac{3b^2}{4} & \text{if}\quad q=1
\end{cases}
\end{aligned} \tag{15.40}$$

Naturally, Eq. (15.20) leads to vanishing contributions of the edge restraints due to the clamped edges at $y=0$ and $y=b$:

$$\begin{aligned}
\Phi_{11} &= \psi_{y2n}\big|_{y=0}\psi_{y2q}\Big|_{y=0} = 0, \\
\theta_{11} &= \psi_{y2n}\big|_{y=b}\psi_{y2q}\Big|_{y=b} = 0.
\end{aligned} \tag{15.41}$$

15.2.5.4 Resultants with Respect to the y-Direction, Case 3

Here, the case is taken into account that there are no elastic edge restraints ($k_l = 0$) and that the laminate is simply supported at three edges. The integral resultants (15.11) for case 3 in the framework of FSDT are as follows:

$$\Delta_{00}^1 = \int_0^b \psi_{x2n}\psi_{x2q}\mathrm{d}y = \int_0^b \left(\frac{y}{b}\right)^n\left(\frac{y}{b}\right)^q\mathrm{d}y = \frac{b}{n+q+1},$$
$$\Delta_{01}^1 = \int_0^b \psi_{x2n}\frac{\partial\psi_{x2q}}{\partial y}\mathrm{d}y = \frac{q}{b}\int\left(\frac{y}{b}\right)^n\left(\frac{y}{b}\right)^{q-1}\mathrm{d}y = \frac{q}{n+q},$$

$$
\begin{aligned}
\Delta_{11}^{1} &= \int_0^b \frac{\partial \psi_{x2n}}{\partial y}\frac{\partial \psi_{x2q}}{\partial y}\mathrm{d}y = \frac{nq}{b^2}\int_0^b \left(\frac{y}{b}\right)^{(n+q-2)}\mathrm{d}y = \frac{nq}{b\,(n+q-1)},\\
\Delta_{00}^{2} &= \int_0^b \psi_{x2n}\psi_{y2q}\mathrm{d}y = \int_0^b \left(\frac{y}{b}\right)^{n}\left(\frac{y}{b}\right)^{q-1}\mathrm{d}y = \frac{b}{n+q},\\
\Delta_{01}^{2} &= \int_0^b \psi_{x2n}\frac{\partial \psi_{y2q}}{\partial y}\mathrm{d}y = \frac{q-1}{b}\int_0^b \left(\frac{y}{b}\right)^{n}\left(\frac{y}{b}\right)^{q-2}\mathrm{d}y = \frac{q-1}{n+q-1},\\
\Delta_{10}^{2} &= \int_0^b \frac{\partial \psi_{x2n}}{\partial y}\psi_{y2q}\mathrm{d}y = \frac{n}{b}\int_0^b \left(\frac{y}{b}\right)^{n-1}\left(\frac{y}{b}\right)^{q-1}\mathrm{d}y = \frac{n}{n+q-1},\\
\Delta_{11}^{2} &= \int_0^b \frac{\partial \psi_{x2n}}{\partial y}\frac{\partial \psi_{y2q}}{\partial y}\mathrm{d}y = \frac{(q-1)\,n}{b^2}\int_0^b \left(\frac{y}{b}\right)^{n-1}\left(\frac{y}{b}\right)^{q-2}\mathrm{d}y\\
&= \begin{cases} \frac{n(q-1)}{b(n+q-2)} & \text{if} \quad n+q \neq 2 \\ 0 & \text{if} \quad n=q=1 \end{cases},\\
\Delta_{00}^{3} &= \int_0^b \psi_{y2n}\psi_{y2q}\mathrm{d}y = \int_0^b \left(\frac{y}{b}\right)^{n-1}\left(\frac{y}{b}\right)^{q-1}\mathrm{d}y = \frac{b}{n+q-1},\\
\Delta_{01}^{3} &= \int_0^b \psi_{y2n}\frac{\partial \psi_{y2q}}{\partial y}\mathrm{d}y = \frac{q-1}{b}\int_0^b \left(\frac{y}{b}\right)^{n-1}\left(\frac{y}{b}\right)^{q-2}\mathrm{d}y\\
&= \begin{cases} \frac{(q-1)}{(n+q-2)} & \text{if} \quad n+q \neq 2 \\ 0 & \text{if} \quad n=q=1 \end{cases},\\
\Delta_{11}^{3} &= \int_0^b \frac{\partial \psi_{y2n}}{\partial y}\frac{\partial \psi_{y2q}}{\partial y}\mathrm{d}y = \frac{(n-1)\,(q-1)}{b^2}\int_0^b \left(\frac{y}{b}\right)^{n-2}\left(\frac{y}{b}\right)^{q-2}\mathrm{d}y\\
&= \frac{(n-1)\,(q-1)}{b\,(n+q-3)} \text{ if } n+q \quad \neq \quad 3,\\
\Delta_{00}^{4} &= \int_0^b w_{2n}w_{2q}\mathrm{d}y = \int_0^b \left(\frac{y}{b}\right)^{n}\left(\frac{y}{b}\right)^{q}\mathrm{d}y = \frac{b}{n+q+1},\\
\Delta_{01}^{4} &= \int_0^b w_{2n}\frac{\partial w_{2q}}{\partial y}\mathrm{d}y = \frac{q}{b}\int_0^b \left(\frac{y}{b}\right)^{n}\left(\frac{y}{b}\right)^{q-1}\mathrm{d}y = \frac{q}{n+q},\\
\Delta_{11}^{4} &= \int_0^b \frac{\partial w_{2n}}{\partial y}\frac{\partial w_{2q}}{\partial y}\mathrm{d}y = \frac{nq}{b^2}\int_0^b \left(\frac{y}{b}\right)^{n-1}\left(\frac{y}{b}\right)^{q-1}\mathrm{d}y = \frac{nq}{b\,(n+q-1)},\\
\Delta_{00}^{5} &= \int_0^b w_{2n}\psi_{y2q}\mathrm{d}y = \int_0^b \left(\frac{y}{b}\right)^{n}\left(\frac{y}{b}\right)^{q-1}\mathrm{d}y = \frac{b}{n+q},\\
\Delta_{10}^{5} &= \int_0^b \frac{\partial w_{2n}}{\partial y}\psi_{y2q}\mathrm{d}y = \frac{n}{b}\int_0^b \left(\frac{y}{b}\right)^{n-1}\left(\frac{y}{b}\right)^{q-1}\mathrm{d}y = \frac{n}{n+q-1},\\
\Delta_{00}^{6} &= \int_0^b w_{2n}\psi_{x2q}\mathrm{d}y = \int_0^b \left(\frac{y}{b}\right)^{n}\left(\frac{y}{b}\right)^{q}\mathrm{d}y = \frac{b}{n+q+1},\\
\Delta_{10}^{6} &= \int_0^b \frac{\partial w_{2n}}{\partial x}\psi_{y2q}\mathrm{d}y = \frac{n}{b}\int_0^b \left(\frac{y}{b}\right)^{n-1}\left(\frac{y}{b}\right)^{q}\mathrm{d}y = \frac{n}{n+q}.
\end{aligned}
\tag{15.42}
$$

From (15.15) we obtain:

$$Q_{00}^{nq} = \int_0^b w_{2n} w_{2q}\, y \mathrm{d}y = \int_0^b \left(\frac{y}{b}\right)^n \left(\frac{y}{b}\right)^q y \, \mathrm{d}y = \frac{b^2}{n+q+2}. \tag{15.43}$$

Equation (15.20) yields:

$$\Phi_{11} = \left.\psi_{y2n}\right|_{y=0} \left.\psi_{y2q}\right|_{y=0} = 0. \tag{15.44}$$

15.2.5.5 Resultants with Respect to the y-Direction, Case 4

The integral resultants (15.11) for case 4 in the case of FSDT result:

$$\Delta_{00}^1 = \int_0^b \psi_{x2n}\psi_{x2q}\mathrm{d}y = \int_0^b \left(\frac{y}{b}\right)^{n+1}\left(\frac{y}{b}\right)^{q+1}\mathrm{d}y = \frac{b}{n+q+3},$$

$$\Delta_{01}^1 = \int_0^b \psi_{x2n}\frac{\partial \psi_{x2q}}{\partial y}\mathrm{d}y = \frac{q+1}{b}\int \left(\frac{y}{b}\right)^{n+1}\left(\frac{y}{b}\right)^{q}\mathrm{d}y = \frac{1+q}{n+q+2},$$

$$\Delta_{11}^1 = \int_0^b \frac{\partial \psi_{x2n}}{\partial y}\frac{\partial \psi_{x2q}}{\partial y}\mathrm{d}y = \frac{(n+1)(q+1)}{b^2}\int_0^b \left(\frac{y}{b}\right)^{n+q}\mathrm{d}y = \frac{(1+n)\,(1+q)}{b\,(n+q+1)},$$

$$\Delta_{00}^2 = \int_0^b \psi_{x2n}\psi_{y2q}\mathrm{d}y = \int_0^b \left(\frac{y}{b}\right)^{n+1}\left(\frac{y}{b}\right)^{q+1}\mathrm{d}y = \frac{b}{n+q+3},$$

$$\Delta_{01}^2 = \int_0^b \psi_{x2n}\frac{\partial \psi_{y2q}}{\partial y}\mathrm{d}y = \frac{q+1}{b}\int_0^b \left(\frac{y}{b}\right)^{n+1}\left(\frac{y}{b}\right)^{q}\mathrm{d}y = \frac{1+q}{n+q+2},$$

$$\Delta_{10}^2 = \int_0^b \frac{\partial \psi_{x2n}}{\partial y}\psi_{y2q}\mathrm{d}y = \frac{n+1}{b}\int_0^b \left(\frac{y}{b}\right)^{n}\left(\frac{y}{b}\right)^{q+1}\mathrm{d}y = \frac{n+1}{n+q+2},$$

$$\Delta_{11}^2 = \int_0^b \frac{\partial \psi_{x2n}}{\partial y}\frac{\partial \psi_{y2q}}{\partial y}\mathrm{d}y = \frac{(q+1)\,(n+1)}{b^2}\int_0^b \left(\frac{y}{b}\right)^{n}\left(\frac{y}{b}\right)^{q}\mathrm{d}y = \frac{(q+1)\,(n+1)}{b\,(n+q+1)},$$

$$\Delta_{00}^3 = \int_0^b \psi_{y2n}\psi_{y2q}\mathrm{d}y = \int_0^b \left(\frac{y}{b}\right)^{n+1}\left(\frac{y}{b}\right)^{q+1}\mathrm{d}y = \frac{b}{n+q+3},$$

$$\Delta_{01}^3 = \int_0^b \psi_{y2n}\frac{\partial \psi_{y2q}}{\partial y}\mathrm{d}y = \frac{q+1}{b}\int_0^b \left(\frac{y}{b}\right)^{n+1}\left(\frac{y}{b}\right)^{q}\mathrm{d}y = \frac{1+q}{2+n+q},$$

$$\Delta_{11}^3 = \int_0^b \frac{\partial \psi_{y2n}}{\partial y}\frac{\partial \psi_{y2q}}{\partial y}\mathrm{d}y = \frac{(n+1)\,(q+1)}{b^2}\int_0^b \left(\frac{y}{b}\right)^{n}\left(\frac{y}{b}\right)^{q}\mathrm{d}y = \frac{(1+q)\,(1+n)}{b\,(1+n+q)},$$

$$\Delta_{00}^4 = \int_0^b w_{2n} w_{2q}\mathrm{d}y = \int_0^b \left(\frac{y}{b}\right)^{n+1}\left(\frac{y}{b}\right)^{q+1}\mathrm{d}y = \frac{b}{n+q+3},$$

$$\Delta_{01}^4 = \int_0^b w_{2n}\frac{\partial w_{2q}}{\partial y}\mathrm{d}y = \frac{q+1}{b}\int_0^b \left(\frac{y}{b}\right)^{n+1}\left(\frac{y}{b}\right)^{q}\mathrm{d}y = \frac{1+q}{n+q+2},$$

$$\Delta_{11}^4 = \int_0^b \frac{\partial w_{2n}}{\partial y}\frac{\partial w_{2q}}{\partial y}\mathrm{d}y = \frac{(1+n)\,(1+q)}{b^2}\int_0^b \left(\frac{y}{b}\right)^{n}\left(\frac{y}{b}\right)^{q}\mathrm{d}y = \frac{(1+n)\,(1+q)}{b\,(n+q+1)},$$

$$
\begin{aligned}
\Delta^5_{00} &= \int_0^b w_{2n}\psi_{y2q}\mathrm{d}y = \int_0^b \left(\frac{y}{b}\right)^{n+1}\left(\frac{y}{b}\right)^{q+1}\mathrm{d}y = \frac{b}{n+q+3},\\
\Delta^5_{10} &= \int_0^b \frac{\partial w_{2n}}{\partial y}\psi_{y2q}\mathrm{d}y = \frac{n+1}{b}\int_0^b \left(\frac{y}{b}\right)^{n}\left(\frac{y}{b}\right)^{q+1}\mathrm{d}y = \frac{1+n}{n+q+2},\\
\Delta^6_{00} &= \int_0^b w_{2n}\psi_{x2q}\mathrm{d}y = \int_0^b \left(\frac{y}{b}\right)^{n+1}\left(\frac{y}{b}\right)^{q+1}\mathrm{d}y = \frac{b}{n+q+3},\\
\Delta^6_{10} &= \int_0^b \frac{\partial w_{2n}}{\partial x}\psi_{y2q}\mathrm{d}y = \frac{n+1}{b}\int_0^b \left(\frac{y}{b}\right)^{n}\left(\frac{y}{b}\right)^{q+1}\mathrm{d}y = \frac{1+n}{n+q+2}.
\end{aligned}
\tag{15.45}
$$

Equation (15.15) results in:

$$
Q_{00} = \int_0^b w_{2n}w_{2q}\,y\mathrm{d}y = \int_0^b \left(\frac{y}{b}\right)^{n+1}\left(\frac{y}{b}\right)^{q+1} y\mathrm{d}y = \frac{b^2}{n+q+4}. \tag{15.46}
$$

Equation (15.20) naturally vanishes due to the clamped edge at $y = 0$ and the free edge at $y = b$.

15.3 The Ritz Method in the Framework of TSDT

The situation of Fig. 15.1 and the cases 1–4 of Fig. 15.2 are now considered in the framework of TSDT. Since the degrees of freedom within the framework of the TSDT are identical to those according to FSDT, many aspects of the procedure can be taken directly from the Ritz method according to the FSDT.

The constitutive law for a laminate in the framework of TSDT is as follows:

$$
\begin{pmatrix} N^0_{xx}\\ N^0_{yy}\\ N^0_{xy}\\ M^0_{xx}\\ M^0_{yy}\\ M^0_{xy}\\ P_{xx}\\ P_{yy}\\ P_{xy}\\ Q_y\\ Q_x\\ R_y\\ R_x \end{pmatrix}
=
\begin{pmatrix}
\underline{\underline{A}} & \underline{\underline{B}} & \underline{\underline{E}} & \underline{0} & \underline{0}\\
\underline{\underline{B}} & \underline{\underline{D}} & \underline{\underline{F}} & \underline{0} & \underline{0}\\
\underline{\underline{E}} & \underline{\underline{F}} & \underline{\underline{H}} & \underline{0} & \underline{0}\\
\underline{0} & \underline{0} & \underline{0} & \underline{\underline{A_S}} & \underline{\underline{D_S}}\\
\underline{0} & \underline{0} & \underline{0} & \underline{\underline{D_S}} & \underline{\underline{F_S}}
\end{pmatrix}
\begin{pmatrix}
\frac{\partial u_0}{\partial x}\\
\frac{\partial v_0}{\partial x}\\
\frac{\partial u_0}{\partial y}+\frac{\partial v_0}{\partial x}\\
\frac{\partial \psi_x}{\partial x}\\
\frac{\partial \psi_y}{\partial y}\\
\frac{\partial \psi_x}{\partial y}+\frac{\partial \psi_y}{\partial x}\\
-\frac{4}{3h^2}\left(\frac{\partial \psi_x}{\partial x}+\frac{\partial^2 w_0}{\partial x^2}\right)\\
-\frac{4}{3h^2}\left(\frac{\partial \psi_y}{\partial y}+\frac{\partial^2 w_0}{\partial y^2}\right)\\
-\frac{4}{3h^2}\left(\frac{\partial \psi_x}{\partial y}+\frac{\partial^2 \psi_y}{\partial x^2}+2\frac{\partial^2 w_0}{\partial x\partial y}\right)\\
\psi_y+\frac{\partial w_0}{\partial y}\\
\psi_x+\frac{\partial w_0}{\partial x}\\
-\frac{4}{h^2}\left(\psi_y+\frac{\partial w_0}{\partial y}\right)\\
-\frac{4}{h^2}\left(\psi_x+\frac{\partial w_0}{\partial x}\right)
\end{pmatrix},
\tag{15.47}
$$

where we want to assume symmetric but arbitrarily structured laminates so that $B_{ij} = 0$ and $E_{ij} = 0$.

The inner potential Π_i of a laminate in the context of TSDT is:

$$\Pi_i = \frac{1}{2}\int_V \sigma_{ij}\varepsilon_{ij}\mathrm{d}V = \frac{1}{2}\int_V \left(\sigma_{xx}\varepsilon_{xx} + \sigma_{yy}\varepsilon_{yy} + \tau_{xy}\gamma_{xy} + \tau_{xz}\gamma_{xz} + \tau_{yz}\gamma_{yz}\right)\mathrm{d}V. \tag{15.48}$$

By means of the kinematic relationships with respect to the infinitesimal strain tensor and after integration with respect to the thickness direction z, the following results:

$$\begin{aligned}
\Pi_i = \frac{1}{2}\int_0^b\int_0^a \Bigg[& N^0_{xx}\frac{\partial u_0}{\partial x} + N^0_{yy}\frac{\partial v_0}{\partial y} + N^0_{xy}\left(\frac{\partial u_0}{\partial y} + \frac{\partial v_0}{\partial x}\right) \\
& + M^0_{xx}\frac{\partial \psi_x}{\partial x} + M^0_{yy}\frac{\partial \psi_y}{\partial y} + M^0_{xy}\left(\frac{\partial \psi_x}{\partial y} + \frac{\partial \psi_y}{\partial x}\right) \\
& - \frac{4P_{xx}}{3t^2}\left(\frac{\partial \psi_x}{\partial x} + \frac{\partial^2 w_0}{\partial x^2}\right) - \frac{4P_{yy}}{3t^2}\left(\frac{\partial \psi_y}{\partial y} + \frac{\partial^2 w_0}{\partial y^2}\right) - \frac{4P_{xy}}{3t^2}\left(\frac{\partial \psi_x}{\partial y} + \frac{\partial \psi_y}{\partial x} + 2\frac{\partial^2 w_0}{\partial x \partial y}\right) \\
& + Q_y\left(\psi_y + \frac{\partial w_0}{\partial y}\right) + Q_x\left(\psi_x + \frac{\partial w_0}{\partial x}\right) \\
& + -\frac{4R_y}{t^2}\left(\psi_y + \frac{\partial w_0}{\partial y}\right) - \frac{4R_x}{t^2}\left(\psi_x + \frac{\partial w_0}{\partial x}\right)\Bigg]\mathrm{d}x\mathrm{d}y.
\end{aligned} \tag{15.49}$$

With $B_{ij} = 0$ and $E_{ij} = 0$ we get after inserting the constitutive law:

$$\begin{aligned}
\Pi_i = \frac{1}{2}\int_0^b\int_0^a \Bigg\{ & D_{11}\left(\frac{\partial \psi_x}{\partial x}\right)^2 + 2D_{12}\frac{\partial \psi_x}{\partial x}\frac{\partial \psi_y}{\partial y} + D_{22}\left(\frac{\partial \psi_y}{\partial y}\right)^2 + 2D_{16}\frac{\partial \psi_x}{\partial x}\left(\frac{\partial \psi_x}{\partial y} + \frac{\partial \psi_y}{\partial x}\right) \\
& + 2D_{26}\frac{\partial \psi_y}{\partial y}\left(\frac{\partial \psi_x}{\partial y} + \frac{\partial \psi_y}{\partial x}\right) + D_{66}\left(\frac{\partial \psi_x}{\partial y}\frac{\partial \psi_x}{\partial y} + 2\frac{\partial \psi_x}{\partial y}\frac{\partial \psi_y}{\partial x} + \frac{\partial \psi_y}{\partial x}\frac{\partial \psi_y}{\partial x}\right) \\
& - \frac{8}{3t^2}F_{11}\left[\left(\frac{\partial \psi_x}{\partial x}\right)^2 + \frac{\partial^2 w_0}{\partial x^2}\frac{\partial \psi_x}{\partial x}\right] - \frac{8}{3t^2}F_{22}\left[\left(\frac{\partial \psi_y}{\partial y}\right)^2 + \frac{\partial^2 w_0}{\partial y^2}\frac{\partial \psi_y}{\partial y}\right] \\
& - \frac{8}{3t^2}F_{12}\left(\frac{\partial^2 w_0}{\partial x^2}\frac{\partial \psi_y}{\partial y} + \frac{\partial^2 w_0}{\partial y^2}\frac{\partial \psi_x}{\partial x} + 2\frac{\partial \psi_x}{\partial x}\frac{\partial \psi_y}{\partial y}\right) \\
& - \frac{8}{3t^2}F_{16}\left[\frac{\partial^2 w_0}{\partial x^2}\left(\frac{\partial \psi_x}{\partial y} + \frac{\partial \psi_y}{\partial x}\right) + 2\frac{\partial \psi_x}{\partial x}\left(\frac{\partial^2 w_0}{\partial x \partial y} + \frac{\partial \psi_x}{\partial y} + \frac{\partial \psi_y}{\partial x}\right)\right] \\
& - \frac{8}{3t^2}F_{26}\left[\frac{\partial^2 w_0}{\partial y^2}\left(\frac{\partial \psi_x}{\partial y} + \frac{\partial \psi_y}{\partial x}\right) + 2\frac{\partial \psi_y}{\partial y}\left(\frac{\partial^2 w_0}{\partial x \partial y} + \frac{\partial \psi_x}{\partial y} + \frac{\partial \psi_y}{\partial x}\right)\right] \\
& - \frac{8}{3t^2}F_{66}\left[\left(\frac{\partial \psi_x}{\partial y}\right)^2 + \left(\frac{\partial \psi_y}{\partial x}\right)^2 + 2\left(\frac{\partial \psi_x}{\partial y} + \frac{\partial \psi_y}{\partial x}\right)\frac{\partial^2 w_0}{\partial x \partial y} + 2\frac{\partial \psi_x}{\partial y}\frac{\partial \psi_y}{\partial x}\right] \\
& + \frac{16}{9t^4}H_{11}\left(\frac{\partial \psi_x}{\partial x} + \frac{\partial^2 w_0}{\partial x^2}\right)^2 + \frac{16}{9t^4}H_{22}\left(\frac{\partial \psi_y}{\partial y} + \frac{\partial^2 w_0}{\partial y^2}\right)^2 \\
& + \frac{32}{9t^4}H_{12}\left[\frac{\partial \psi_x}{\partial x}\frac{\partial \psi_y}{\partial y} + \frac{\partial^2 w_0}{\partial x^2}\frac{\partial \psi_y}{\partial y} + \frac{\partial^2 w_0}{\partial y^2}\frac{\partial \psi_x}{\partial x} + \frac{\partial^2 w_0}{\partial x^2}\frac{\partial^2 w_0}{\partial y^2}\right]
\end{aligned}$$

$$
\begin{aligned}
&+\frac{32}{9t^4}\left[H_{16}\left(\frac{\partial\psi_x}{\partial x}+\frac{\partial^2 w_0}{\partial x^2}\right)+H_{26}\left(\frac{\partial\psi_y}{\partial y}+\frac{\partial^2 w_0}{\partial y^2}\right)\right]\left(\frac{\partial\psi_x}{\partial y}+2\frac{\partial^2 w_0}{\partial x\partial y}+\frac{\partial\psi_y}{\partial x}\right)\\
&+\frac{16}{9t^4}H_{66}\left[\left(\frac{\partial\psi_x}{\partial y}+\frac{\partial\psi_y}{\partial x}\right)^2+4\frac{\partial^2 w_0}{\partial y\partial x}\left(\frac{\partial^2 w_0}{\partial y\partial x}+\frac{\partial\psi_x}{\partial y}+\frac{\partial\psi_y}{\partial x}\right)\right]\\
&+A_{44}\left(\psi_y+\frac{\partial w_0}{\partial y}\right)^2+A_{55}\left(\psi_x+\frac{\partial w_0}{\partial x}\right)^2\\
&+2A_{45}\left[\psi_x\psi_y+\frac{\partial w_0}{\partial x}\psi_y+\frac{\partial w_0}{\partial y}\psi_x+\frac{\partial w_0}{\partial x}\frac{\partial w_0}{\partial y}\right]\\
&-\frac{8}{t^2}D_{44}\left(\psi_y+\frac{\partial w_0}{\partial y}\right)^2-\frac{8}{t^2}D_{55}\left(\psi_x+\frac{\partial w_0}{\partial x}\right)^2\\
&-\frac{16}{t^2}D_{45}\left(\psi_y\psi_x+\frac{\partial w_0}{\partial x}\psi_y+\frac{\partial w_0}{\partial y}\psi_x+\frac{\partial w_0}{\partial y}\frac{\partial w_0}{\partial x}\right)\\
&+\frac{16}{t^2}F_{44}\left(\psi_y+\frac{\partial w_0}{\partial y}\right)^2+\frac{16}{t^4}F_{55}\left(\psi_x+\frac{\partial w_0}{\partial x}\right)^2\\
&+\frac{32}{t^4}F_{45}\left(\psi_x\psi_y+\frac{\partial w_0}{\partial x}\psi_y+\frac{\partial w_0}{\partial y}\psi_x+\frac{\partial w_0}{\partial x}\frac{\partial w_0}{\partial y}\right)\Bigg\}\,\mathrm{d}x\mathrm{d}y. \qquad (15.50)
\end{aligned}
$$

The external potential Π_a remains unchanged compared to (15.6) and is as follows:

$$
\Pi_a=-\frac{1}{2}\int_0^b\int_0^a\left[\Lambda N_{xx}^0\left(\frac{\partial w_0}{\partial x}\right)^2+\Lambda N_{yy}^0\left(\frac{\partial w_0}{\partial y}\right)^2+2\Lambda N_{xy}^0\left(\frac{\partial w_0}{\partial x}\right)\left(\frac{\partial w_0}{\partial y}\right)\right]\mathrm{d}x\mathrm{d}y. \qquad (15.51)
$$

The restraint energy can also be directly taken from (15.8):

$$
\Pi_s=\frac{1}{2}\int_0^a\left[k_l\left(\psi_y|_{y=0}\right)^2+k_r\left(\psi_y|_{y=b}\right)^2\right]\mathrm{d}x. \qquad (15.52)
$$

The Ritz method according to TSDT works with identical approaches for the buckling degrees of freedom as already used in the FSDT, i.e. the following approximation is used:

$$
\begin{aligned}
w_0&=\sum_{m=1}^{M}\sum_{n=1}^{N}W_{mn}w_{1m}(x)w_{2n}(y),\\
\psi_x&=\sum_{m=1}^{K}\sum_{n=1}^{L}X_{mn}\psi_{x1m}(x)\psi_{x2n}(y),\\
\psi_y&=\sum_{m=1}^{I}\sum_{n=1}^{J}Y_{mn}\psi_{y1m}(x)\psi_{y2n}(y). \qquad (15.53)
\end{aligned}
$$

Here, too, integral results of the shape functions are introduced as follows:

$$\begin{aligned}
\Omega_{ij}^{1} &= \int_0^a \frac{\partial^i \psi_{x1m}}{\partial x^i}\frac{\partial^j \psi_{x1p}}{\partial x^j}\mathrm{d}x,\\
\Omega_{ij}^{2} &= \int_0^a \frac{\partial^i \psi_{x1m}}{\partial x^i}\frac{\partial^j \psi_{y1p}}{\partial x^j}\mathrm{d}x,\\
\Omega_{ij}^{3} &= \int_0^a \frac{\partial^i \psi_{y1m}}{\partial x^i}\frac{\partial^j \psi_{y1p}}{\partial x^j}\mathrm{d}x,\\
\Omega_{ij}^{4} &= \int_0^a \frac{\partial^i w_{1m}}{\partial x^i}\frac{\partial^j w_{1p}}{\partial x^j}\mathrm{d}x,\\
\Omega_{ij}^{5} &= \int_0^a \frac{\partial^i w_{1m}}{\partial x^i}\frac{\partial^j \psi_{y1p}}{\partial x^j}\mathrm{d}x,\\
\Omega_{ij}^{6} &= \int_0^a \frac{\partial^i w_{1m}}{\partial x^i}\frac{\partial^j \psi_{x1p}}{\partial x^j}\mathrm{d}x,\\
\Delta_{ij}^{1} &= \int_0^b \frac{\partial^i \psi_{x2n}}{\partial y^i}\frac{\partial^j \psi_{x2q}}{\partial y^j}\mathrm{d}y,\\
\Delta_{ij}^{2} &= \int_0^b \frac{\partial^i \psi_{x2n}}{\partial y^i}\frac{\partial^j \psi_{y2q}}{\partial y^j}\mathrm{d}y,\\
\Delta_{ij}^{3} &= \int_0^b \frac{\partial^i \psi_{y2n}}{\partial y^i}\frac{\partial^j \psi_{y2q}}{\partial y^j}\mathrm{d}y,\\
\Delta_{ij}^{4} &= \int_0^b \frac{\partial^i w_{2n}}{\partial y^i}\frac{\partial^j w_{2q}}{\partial y^j}\mathrm{d}y,\\
\Delta_{ij}^{5} &= \int_0^b \frac{\partial^i w_{2n}}{\partial y^i}\frac{\partial^j \psi_{y2q}}{\partial y^j}\mathrm{d}y,\\
\Delta_{ij}^{6} &= \int_0^b \frac{\partial^i w_{2n}}{\partial y^i}\frac{\partial^j \psi_{x2q}}{\partial y^j}\mathrm{d}y.
\end{aligned} \tag{15.54}$$

In addition, the following abbreviations are used:

$$\begin{aligned}
\Gamma_i^{klkl} &= \frac{1}{2}(D_{11}\Omega_{11}^{1}\Delta_{00}^{1} + D_{66}\Omega_{00}^{1}\Delta_{11}^{1}) + D_{16}\Omega_{10}^{1}\Delta_{01}^{1}\\
&\quad - \frac{4}{3h^2}F_{11}\Omega_{11}^{1}\Delta_{00}^{1} - \frac{8}{3h^2}F_{16}\Omega_{10}^{1}\Delta_{01}^{1} - \frac{4}{3h^2}F_{66}\Omega_{00}^{1}\Delta_{11}^{1}\\
&\quad + \frac{8}{9h^4}H_{11}\Omega_{11}^{1}\Delta_{00}^{1} + \frac{16}{9h^4}H_{16}\Omega_{10}^{1}\Delta_{01}^{1} + \frac{8}{9h^4}H_{66}\Omega_{00}^{1}\Delta_{11}^{1}\\
&\quad + \frac{1}{2}A_{55}\Omega_{00}^{1}\Delta_{00}^{1} + \frac{8}{h^4}F_{55}\Omega_{00}^{1}\Delta_{00}^{1} - \frac{4}{h^2}D_{55}\Omega_{00}^{1}\Delta_{00}^{1},\\
\Gamma_i^{ijij} &= \frac{1}{2}\left(D_{22}\Omega_{00}^{3}\Delta_{11}^{3} + D_{66}\Omega_{11}^{3}\Delta_{00}^{3}\right) + D_{26}\Omega_{10}^{3}\Delta_{01}^{3}\\
&\quad - \frac{4}{3h^2}F_{22}\Omega_{00}^{3}\Delta_{11}^{3} - \frac{8}{3h^2}F_{26}\Omega_{01}^{3}\Delta_{10}^{3} - \frac{4}{3h^2}F_{66}\Omega_{11}^{3}\Delta_{00}^{3}
\end{aligned}$$

$$
\begin{aligned}
&+\frac{8}{9h^4}H_{22}\Omega_{00}^3\Delta_{11}^3+\frac{16}{9h^4}H_{26}\Omega_{01}^3\Delta_{10}^3+\frac{8}{9h^4}H_{66}\Omega_{11}^3\Delta_{00}^3\\
&+\frac{1}{2}A_{44}\Omega_{00}^3\Delta_{00}^3-\frac{4}{h^2}D_{44}\Omega_{00}^3\Delta_{00}^3+\frac{8}{h^4}F_{44}\Omega_{00}^3\Delta_{00}^3,\\
\Gamma_i^{klij} &= D_{12}\Omega_{10}^2\Delta_{01}^2+D_{16}\Omega_{11}^2\Delta_{00}^2+D_{26}\Omega_{00}^2\Delta_{11}^2\\
&+D_{66}\Omega_{01}^2\Delta_{10}^2-\frac{8}{3h^2}F_{12}\Omega_{10}^2\Delta_{01}^2-\frac{8}{3h^2}F_{16}\Omega_{11}^2\Delta_{00}^2\\
&-\frac{8}{3h^2}F_{26}\Omega_{00}^2\Delta_{11}^2-\frac{8}{3h^2}F_{66}\Omega_{01}^2\Delta_{10}^2+\frac{16}{9h^4}H_{12}\Omega_{10}^2\Delta_{01}^2\\
&+\frac{16}{9h^4}H_{16}\Omega_{11}^2\Delta_{00}^2+\frac{16}{9h^4}H_{26}\Omega_{00}^2\Delta_{11}^2+\frac{16}{9h^4}H_{66}\Omega_{01}^2\Delta_{10}^2\\
&+A_{45}\Omega_{00}^2\Delta_{00}^2-\frac{8}{h^2}D_{45}\Omega_{00}^2\Delta_{00}^2+\frac{16}{h^4}F_{45}\Omega_{00}^2\Delta_{00}^2,\\
\Gamma_i^{mnmn} &= \frac{8}{9h^4}H_{11}\Omega_{22}^4\Delta_{00}^4+\frac{16}{9h^4}H_{12}\Omega_{20}^4\Delta_{02}^4\\
&+\frac{8}{9h^4}H_{22}\Omega_{00}^4\Delta_{22}^4+\frac{32}{9h^2}H_{16}\Omega_{12}^4\Delta_{10}^4+\frac{32}{9h^2}H_{26}\Omega_{01}^4\Delta_{21}^4\\
&+\frac{32}{9h^4}H_{66}\Omega_{11}^4\Delta_{11}^4+\frac{1}{2}A_{44}\Omega_{00}^4\Delta_{11}^4+A_{45}\Omega_{10}^4\Delta_{01}^4\\
&+\frac{1}{2}A_{55}\Omega_{11}^4\Delta_{00}^4-\frac{4}{h^2}D_{44}\Omega_{00}^4\Delta_{11}^4-\frac{8}{h^2}D_{45}\Omega_{10}^4\Delta_{01}^4\\
&+\frac{8}{h^4}F_{44}\Omega_{00}^4\Delta_{11}^4+\frac{16}{h^4}F_{45}\Omega_{10}^4\Delta_{01}^4+\frac{8}{h^4}F_{55}\Omega_{11}^4\Delta_{00}^4-\frac{4}{h^2}D_{55}\Omega_{11}^4\Delta_{00}^4,\\
\Gamma_i^{mnij} &= -\frac{4}{3h^2}F_{12}\Omega_{20}^5\Delta_{01}^5-\frac{4}{3h^2}F_{22}\Omega_{00}^5\Delta_{21}^5\\
&-\frac{4}{3h^2}F_{16}\Omega_{21}^5\Delta_{00}^5-\frac{4}{3h^2}F_{26}\Omega_{01}^5\Delta_{20}^5-\frac{8}{3h^2}F_{26}\Omega_{10}^5\Delta_{11}^5\\
&-\frac{8}{3h^2}F_{66}\Omega_{11}^5\Delta_{10}^5+\frac{16}{9h^4}H_{12}\Omega_{20}^5\Delta_{01}^5+\frac{16}{9h^4}H_{22}\Omega_{00}^5\Delta_{21}^5\\
&+\frac{16}{9h^4}H_{16}\Omega_{21}^5\Delta_{00}^5+\frac{32}{9h^4}H_{26}\Omega_{10}^5\Delta_{11}^5+\frac{16}{9h^4}H_{26}\Omega_{01}^5\Delta_{20}^5\\
&+\frac{32}{9h^4}H_{66}\Omega_{11}^5\Delta_{10}^5+A_{44}\Omega_{00}^5\Delta_{10}^5-\frac{8}{h^2}D_{44}\Omega_{00}^5\Delta_{10}^5\\
&-\frac{8}{h^2}D_{45}\Omega_{10}^5\Delta_{00}^5+\frac{16}{h^4}F_{44}\Omega_{00}^5\Delta_{10}^5+\frac{16}{h^4}F_{45}\Omega_{10}^5\Delta_{00}^5+A_{45}\Omega_{10}^5\Delta_{00}^5,\\
\Gamma_i^{mnkl} &= -\frac{4}{3h^2}F_{12}\Omega_{01}^6\Delta_{20}^6-\frac{8}{3h^2}F_{16}\Omega_{11}^6\Delta_{10}^6\\
&-\frac{4}{3h^2}F_{26}\Omega_{00}^6\Delta_{21}^6-\frac{8}{3h^2}F_{66}\Omega_{10}^6\Delta_{11}^6+\frac{16}{9h^4}H_{11}\Omega_{21}^6\Delta_{00}^6\\
&+\frac{16}{9h^4}H_{12}\Omega_{01}^6\Delta_{20}^6+\frac{16}{9h^4}H_{16}\Omega_{20}^6\Delta_{01}^6+\frac{32}{9h^4}H_{16}\Omega_{11}^6\Delta_{10}^6\\
&+\frac{16}{9h^4}H_{26}\Omega_{00}^6\Delta_{21}^6+\frac{32}{9h^4}H_{66}\Omega_{10}^6\Delta_{11}^6+A_{45}\Omega_{00}^6\Delta_{10}^6
\end{aligned}
$$

$$+ A_{55}\Omega_{10}^{6}\Delta_{00}^{6} - \frac{8}{h^2}D_{45}\Omega_{00}^{6}\Delta_{10}^{6} + \frac{16}{h^4}F_{45}\Omega_{00}^{6}\Delta_{10}^{6}$$
$$+ \frac{16}{h^4}F_{55}\Omega_{10}^{6}\Delta_{00}^{6} - \frac{4}{3h^2}F_{11}\Omega_{21}^{6}\Delta_{00}^{6} - \frac{4}{3h^2}F_{16}\Omega_{20}^{6}\Delta_{01}^{6} - \frac{8}{h^2}D_{55}\Omega_{10}^{6}\Delta_{00}^{6}. \tag{15.55}$$

Then the inner potential Π_i can be written as:

$$\begin{aligned}\Pi_i = &\sum_{m=1}^{K}\sum_{n=1}^{L}\sum_{p=1}^{K}\sum_{q=1}^{L} X_{mn}X_{pq}\Gamma_i^{klkl} \\ &+ \sum_{m=1}^{I}\sum_{n=1}^{J}\sum_{p=1}^{I}\sum_{q=1}^{J} Y_{mn}Y_{pq}\Gamma_i^{ijij} \\ &+ \sum_{m=1}^{K}\sum_{n=1}^{L}\sum_{p=1}^{I}\sum_{q=1}^{J} X_{mn}Y_{pq}\Gamma_i^{klij} \\ &+ \sum_{m=1}^{M}\sum_{n=1}^{N}\sum_{p=1}^{M}\sum_{q=1}^{N} W_{mn}W_{pq}\Gamma_i^{mnmn} \\ &+ \sum_{m=1}^{M}\sum_{n=1}^{N}\sum_{p=1}^{I}\sum_{q=1}^{J} W_{mn}Y_{pq}\Gamma_i^{mnij} \\ &+ \sum_{m=1}^{M}\sum_{n=1}^{N}\sum_{p=1}^{K}\sum_{q=1}^{L} W_{mn}X_{pq}\Gamma_i^{mnkl}.\end{aligned} \tag{15.56}$$

With the additional abbreviation

$$Q_{00}^{nq} = \int_0^b w_{2n}w_{2q}\,y\mathrm{d}y \tag{15.57}$$

the external potential Π_a changes into the following form:

$$\begin{aligned}\Pi_a = &-\Lambda\frac{N_{xx}^0}{2}\sum_{m=1}^{M}\sum_{n=1}^{N}\sum_{p=1}^{M}\sum_{q=1}^{N} W_{mn}W_{pq}\left[\frac{(\psi-1)}{b}\Omega_{11}^4 Q_{00}^{nq} + \Omega_{11}^4\Delta_{00}^4\right] \\ &- \Lambda\frac{N_{yy}^0}{2}\sum_{m=1}^{M}\sum_{n=1}^{N}\sum_{p=1}^{M}\sum_{q=1}^{N} W_{mn}W_{pq}\Omega_{00}^4\Delta_{11}^4 \\ &- \Lambda N_{xy}^0\sum_{m=1}^{M}\sum_{n=1}^{N}\sum_{p=1}^{M}\sum_{q=1}^{N} W_{mn}W_{pq}\Omega_{10}^4\Delta_{01}^4.\end{aligned} \tag{15.58}$$

We also introduce the abbreviations

$$\Phi_{11}^{nq} = \psi_{y2n}\psi_{y2q}\big|_{y=0},$$
$$\Theta_{11}^{nq} = \psi_{y2n}\psi_{y2q}\big|_{y=b} \tag{15.59}$$

and

$$\Gamma_s^{ijij} = \frac{1}{2}T_{00}^{mp}\left(k_l\Phi_{11}^{nq} + k_r\Theta_{11}^{nq}\right) \tag{15.60}$$

so that we obtain for the energy stored in the edge restraints Π_s:

$$\Pi_s = \sum_{m=1}^{I}\sum_{n=1}^{J}\sum_{p=1}^{I}\sum_{q=1}^{J} Y_{mn}Y_{pq}\Gamma_s^{ijij}. \tag{15.61}$$

For cases 1–4 of Fig. 15.2 taking into account the load case combination of Fig. 15.1, the same shape functions are employed as in the FSDT, i.e. Eqs. (15.31)–(15.34) are used again here. The derivation of the eigenvalue problem is analogous to the explanations of the FSDT, and the formulas given there are also valid for a calculation in the framework of TSDT.

The introduced resultants of the shape functions are specified in detail below for all four cases considered here.

15.3.1 Resultants of the Shape Functions

15.3.1.1 Resultants with Respect to the x-Direction

The integral resultants according to Eq. (15.54) with respect to the x-direction are obtained within the framework of TSDT as follows:

$$\Omega_{00}^{1} = \int_0^a \psi_{x1m}\psi_{x1p}\mathrm{d}x = \int_0^a \cos\left(\frac{m\pi x}{a}\right)\cos\left(\frac{p\pi x}{a}\right)\mathrm{d}x$$
$$= \begin{cases} \frac{1}{2}a & \text{if} \quad m = p \\ 0 & \text{if} \quad m \neq p \end{cases},$$
$$\Omega_{10}^{1} = \int_0^a \frac{\partial\psi_{x1m}}{\partial x}\psi_{x1p}\mathrm{d}x = \frac{-m\pi}{a}\int_0^a \sin\left(\frac{m\pi x}{a}\right)\cos\left(\frac{p\pi x}{a}\right)\mathrm{d}x$$
$$= \begin{cases} 0 & \text{if} \quad m+p = \text{even} \\ \frac{-2m^2}{m^2-p^2} & \text{if} \quad m+p = \text{odd} \end{cases},$$
$$\Omega_{11}^{1} = \int_0^a \frac{\partial\psi_{x1p}}{\partial x}\frac{\partial\psi_{x1m}}{\partial x}\mathrm{d}x = \frac{m\pi}{a}\frac{p\pi}{a}\int_0^a \sin\left(\frac{m\pi x}{a}\right)\sin\left(\frac{p\pi x}{a}\right)\mathrm{d}x$$
$$= \begin{cases} \frac{m^2\pi^2}{2a} & \text{if} \quad m = p \\ 0 & \text{if} \quad m \neq p \end{cases},$$
$$\Omega_{00}^{2} = \int_0^a \psi_{x1m}\psi_{y1p}\mathrm{d}x = \int_0^a \cos\left(\frac{m\pi x}{a}\right)\sin\left(\frac{p\pi x}{a}\right)\mathrm{d}x$$

$$= \begin{cases} 0 & \text{if} \quad m+p = \text{even} \\ \frac{2pa}{(p^2-m^2)\pi} & \text{if} \quad m+p = \text{odd} \end{cases},$$

$$\Omega_{10}^2 = \int_0^a \frac{\partial \psi_{x1m}}{\partial x} \psi_{y1p} \mathrm{d}x = \frac{-m\pi}{a} \int_0^a \sin\left(\frac{m\pi x}{a}\right) \sin\left(\frac{p\pi x}{a}\right) \mathrm{d}x$$

$$= \begin{cases} \frac{-m\pi}{2} & \text{if} \quad m = p \\ 0 & \text{if} \quad m \neq p \end{cases},$$

$$\Omega_{01}^2 = \int_0^a \psi_{x1m} \frac{\partial \psi_{y1p}}{\partial x} \mathrm{d}x = \frac{p\pi}{a} \int_0^a \cos\left(\frac{m\pi x}{a}\right) \cos\left(\frac{p\pi x}{a}\right) \mathrm{d}x$$

$$= \begin{cases} \frac{m\pi}{2} & \text{if} \quad m = p \\ 0 & \text{if} \quad m \neq p \end{cases},$$

$$\Omega_{11}^2 = \int_0^a \frac{\partial \psi_{x1m}}{\partial x} \frac{\partial \psi_{y1p}}{\partial x} \mathrm{d}x = -mp\left(\frac{\pi}{a}\right)^2 \int_0^a \sin\left(\frac{m\pi x}{a}\right) \cos\left(\frac{p\pi x}{a}\right) \mathrm{d}x$$

$$= \begin{cases} 0 & \text{if } m+p = \text{even} \\ \frac{-2m^2 p\pi}{a\,(m^2-p^2)} & \text{if } m+p = \text{odd} \end{cases},$$

$$\Omega_{00}^3 = \int_0^a \psi_{y1m} \psi_{y1p} \mathrm{d}x = \int_0^a \sin\left(\frac{m\pi x}{a}\right) \sin\left(\frac{p\pi x}{a}\right) \mathrm{d}x$$

$$= \begin{cases} \frac{1}{2}a & \text{if} \quad m = p \\ 0 & \text{if} \quad m \neq p \end{cases},$$

$$\Omega_{01}^3 = \int_0^a \psi_{y1m} \frac{\partial \psi_{y1p}}{\partial x} \mathrm{d}x = \frac{p\pi}{a} \int_0^a \sin\left(\frac{m\pi x}{a}\right) \cos\left(\frac{p\pi x}{a}\right) \mathrm{d}x$$

$$= \begin{cases} 0 & \text{if} \quad m+p = \text{even} \\ \frac{2mp}{m^2-p^2} & \text{if} \quad m+p = \text{odd} \end{cases},$$

$$\Omega_{10}^3 = \int_0^a \frac{\partial \psi_{y1m}}{\partial x} \psi_{y1p} \mathrm{d}x = \frac{m\pi}{a} \int_0^a \cos\left(\frac{m\pi x}{a}\right) \sin\left(\frac{p\pi x}{a}\right) \mathrm{d}x$$

$$= \begin{cases} 0 & \text{if} \quad m+p = \text{even} \\ \frac{2mp}{p^2-m^2} & \text{if} \quad m+p = \text{odd} \end{cases},$$

$$\Omega_{11}^3 = \int_0^a \frac{\partial \psi_{y1m}}{\partial x} \frac{\partial \psi_{y1p}}{\partial x} \mathrm{d}x = mp\left(\frac{\pi}{a}\right)^2 \int_0^a \cos\left(\frac{m\pi x}{a}\right) \cos\left(\frac{p\pi x}{a}\right) \mathrm{d}x$$

$$= \begin{cases} \frac{mp\pi^2}{2a} & \text{if} \quad m = p \\ 0 & \text{if} \quad m \neq p \end{cases},$$

$$\Omega_{00}^4 = \int_0^a w_{1m} w_{1p} \mathrm{d}x = \int_0^a \sin\left(\frac{m\pi x}{a}\right) \sin\left(\frac{p\pi x}{a}\right) \mathrm{d}x$$

$$= \begin{cases} \frac{1}{2}a & \text{if} \quad m = p \\ 0 & \text{if} \quad m \neq p \end{cases},$$

$$\Omega_{01}^4 = \int_0^a w_{1m} \frac{\partial w_{1p}}{\partial x} \mathrm{d}x = \frac{p\pi}{a} \int_0^a \sin\left(\frac{m\pi x}{a}\right) \cos\left(\frac{p\pi x}{a}\right) \mathrm{d}x$$

$$= \begin{cases} 0 & \text{if} \quad m+p = \text{even} \\ \frac{2pm}{m^2-p^2} & \text{if} \quad m+p = \text{odd} \end{cases},$$

$$\Omega_{10}^4 = \int_0^a \frac{\partial w_{1m}}{\partial x} w_{1p} \mathrm{d}x = \frac{m\pi}{a} \int_0^a \cos\left(\frac{m\pi x}{a}\right) \sin\left(\frac{p\pi x}{a}\right) \mathrm{d}x$$

$$= \begin{cases} 0 & \text{if} \quad m+p = \text{even} \\ \frac{2pm}{p^2-m^2} & \text{if} \quad m+p = \text{odd} \end{cases},$$

$$\Omega_{11}^4 = \int_0^a \frac{\partial w_{1m}}{\partial x} \frac{\partial w_{1p}}{\partial x} \mathrm{d}x = mp\left(\frac{\pi}{a}\right)^2 \int_0^a \cos\left(\frac{m\pi x}{a}\right) \cos\left(\frac{p\pi x}{a}\right) \mathrm{d}x$$

$$= \begin{cases} \frac{mp\pi^2}{2a} & \text{if} \quad m = p \\ 0 & \text{if} \quad m \neq p \end{cases},$$

$$\Omega_{12}^4 = \int_0^a \frac{\partial w_{1m}}{\partial x} \frac{\partial^2 w_{1p}}{\partial x^2} \mathrm{d}x = -mp^2\left(\frac{\pi}{a}\right)^3 \int_0^a \cos\left(\frac{m\pi x}{a}\right) \sin\left(\frac{p\pi x}{a}\right) \mathrm{d}x$$

$$= \begin{cases} \frac{2mp^3\pi^2}{a^2(m^2-p^2)} & \text{if} \quad m+p = \text{odd} \\ 0 & \text{if} \quad m+p = \text{even} \end{cases},$$

$$\Omega_{20}^4 = \int_0^a \frac{\partial^2 w_{1m}}{\partial x^2} w_{1p} \mathrm{d}x = -\frac{m^2\pi^2}{a^2} \int_0^a \sin\left(\frac{m\pi x}{a}\right) \sin\left(\frac{p\pi x}{a}\right) \mathrm{d}x$$

$$= \begin{cases} \frac{-m^2\pi^2}{2a} & \text{if} \quad m = p \\ 0 & \text{if} \quad m \neq p \end{cases},$$

$$\Omega_{22}^4 = \int_0^a \frac{\partial^2 w_{1m}}{\partial x^2} \frac{\partial^2 w_{1p}}{\partial x^2} \mathrm{d}x = \left(\frac{m\pi}{a}\right)^2 \left(\frac{p\pi}{a}\right)^2 \int_0^a \sin\left(\frac{m\pi x}{a}\right) \sin\left(\frac{p\pi x}{a}\right) \mathrm{d}x$$

$$= \begin{cases} \frac{m^4\pi^4}{2a^3} & \text{if} \quad m = p \\ 0 & \text{if} \quad m \neq p \end{cases},$$

$$\Omega_{00}^5 = \int_0^a w_{1m} w_{1p} \mathrm{d}x = \int_0^a \sin\left(\frac{m\pi x}{a}\right) \sin\left(\frac{p\pi x}{a}\right) \mathrm{d}x$$

$$= \begin{cases} \frac{a}{2} & \text{if} \quad m = p \\ 0 & \text{if} \quad m \neq p \end{cases},$$

$$\Omega_{01}^5 = \int_0^a w_{1m} \frac{\partial w_{1p}}{\partial x} \mathrm{d}x = \frac{p\pi}{a} \int_0^a \sin\left(\frac{m\pi x}{a}\right) \cos\left(\frac{p\pi x}{a}\right) \mathrm{d}x$$

$$= \begin{cases} 0 & \text{if} \quad m+p = \text{even} \\ \frac{2pm}{m^2-p^2} & \text{if} \quad m+p = \text{odd} \end{cases},$$

$$\Omega_{10}^5 = \int_0^a \frac{\partial w_{1m}}{\partial x} w_{1p} \mathrm{d}x = \frac{m\pi}{a} \int_0^a \cos\left(\frac{m\pi x}{a}\right) \sin\left(\frac{p\pi x}{a}\right) \mathrm{d}x$$

$$= \begin{cases} 0 & \text{if} \quad m+p = \text{even} \\ \frac{2pm}{p^2-m^2} & \text{if} \quad m+p = \text{odd} \end{cases},$$

$$\Omega_{11}^5 = \int_0^a \frac{\partial w_{1m}}{\partial x} \frac{\partial w_{1p}}{\partial x} \mathrm{d}x = \frac{p\pi}{a} \frac{m\pi}{a} \int_0^a \cos\left(\frac{m\pi x}{a}\right) \cos\left(\frac{p\pi x}{a}\right) \mathrm{d}x$$

$$
\begin{aligned}
&= \begin{cases} 0 & \text{if} \quad m \neq p \\ \frac{m^2\pi^2}{2a} & \text{if} \quad m = p \end{cases}, \\
\Omega_{20}^5 &= \int_0^a \frac{\partial^2 w_{1m}}{\partial x^2} w_{1p} \mathrm{d}x = -\left(\frac{m\pi}{a}\right)^2 \int_0^a \sin\left(\frac{m\pi x}{a}\right) \cos\left(\frac{p\pi x}{a}\right) \mathrm{d}x \\
&= \begin{cases} 0 & \text{if} \quad m \neq p \\ \frac{-m^2\pi^2}{2a} & \text{if} \quad m = p \end{cases}, \\
\Omega_{21}^5 &= \int_0^a \frac{\partial^2 w_{1m}}{\partial x^2} \frac{\partial w_{1p}}{\partial x} \mathrm{d}x = -\frac{p\pi}{a}\left(\frac{m\pi}{a}\right)^2 \int_0^a \sin\left(\frac{m\pi x}{a}\right) \cos\left(\frac{p\pi x}{a}\right) \mathrm{d}x \\
&= \begin{cases} \frac{2m^3\pi^2 p}{a^2(p^2-m^2)} & \text{if} \quad m+p = \text{odd} \\ 0 & \text{if} \quad m+p = \text{even} \end{cases}, \\
\Omega_{00}^6 &= \int_0^a w_{1m} \psi_{x1p} \mathrm{d}x = \int_0^a \sin\left(\frac{m\pi x}{a}\right) \cos\left(\frac{p\pi x}{a}\right) \mathrm{d}x \\
&= \begin{cases} \frac{2ma}{\pi(m^2-p^2)} & \text{if} \quad m+p = \text{odd} \\ 0 & \text{if} \quad m+p = \text{even} \end{cases}, \\
\Omega_{10}^6 &= \int_0^a \frac{\partial w_{1m}}{\partial x} \psi_{x1p} \mathrm{d}x = \frac{m\pi}{a} \int_0^a \cos\left(\frac{m\pi x}{a}\right) \cos\left(\frac{p\pi x}{a}\right) \mathrm{d}x \\
&= \begin{cases} 0 & \text{if} \quad m \neq p \\ \frac{m\pi}{2} & \text{if} \quad m = p \end{cases}, \\
\Omega_{01}^6 &= \int_0^a \psi_{x1m} \frac{\partial \psi_{x1p}}{\partial x} \mathrm{d}x = \frac{-p\pi}{a} \int_0^a \sin\left(\frac{m\pi x}{a}\right) \sin\left(\frac{p\pi x}{a}\right) \mathrm{d}x \\
&= \begin{cases} 0 & \text{if} \quad m \neq p \\ \frac{-m\pi}{2} & \text{if} \quad m = p \end{cases}, \\
\Omega_{11}^6 &= \int_0^a \frac{\partial w_{1m}}{\partial x} \frac{\partial \psi_{x1p}}{\partial x} \mathrm{d}x = \frac{-m\pi}{a} \frac{p\pi}{a} \int_0^a \cos\left(\frac{m\pi x}{a}\right) \sin\left(\frac{p\pi x}{a}\right) \mathrm{d}x \\
&= \begin{cases} \frac{2p^2 m\pi}{a(m^2-p^2)} & \text{if} \quad m+p = \text{odd} \\ 0 & \text{if} \quad m+p = \text{even} \end{cases}, \\
\Omega_{20}^6 &= \int_0^a \frac{\partial w_{1m}}{\partial x} \psi_{x1p} \mathrm{d}x = -\left(\frac{m\pi}{a}\right)^2 \int_0^a \sin\left(\frac{m\pi x}{a}\right) \cos\left(\frac{p\pi x}{a}\right) \mathrm{d}x \\
&= \begin{cases} 0 & \text{if} \quad m+p = \text{even} \\ \frac{2m^3\pi}{a(p^2-m^2)} & \text{if} \quad m+p = \text{odd} \end{cases}, \\
\Omega_{21}^6 &= \int_0^a \psi_{x1m} \frac{\partial \psi_{x1p}}{\partial x} \mathrm{d}x = \left(\frac{m\pi}{a}\right)^2 \frac{p\pi}{a} \int_0^a \sin\left(\frac{m\pi x}{a}\right) \sin\left(\frac{p\pi x}{a}\right) \mathrm{d}x \\
&= \begin{cases} 0 & \text{if} \quad m \neq p \\ \frac{m^3\pi^3}{2a^2} & \text{if} \quad m = p \end{cases}.
\end{aligned}
\tag{15.62}
$$

15.3.1.2 Resultants with Respect to the y-Direction, Case 1

Equation (15.54) gives the following result:

$$\Delta_{00}^{1} = \int_0^b \psi_{x2n}\psi_{x2q}\mathrm{d}y = \int_0^b \sin\left(\frac{n\pi y}{b}\right)\sin\left(\frac{q\pi y}{b}\right)\mathrm{d}y$$
$$= \begin{cases} \frac{1}{2}b & \text{if} \quad n = q \\ 0 & \text{if} \quad n \neq q \end{cases},$$

$$\Delta_{01}^{1} = \int_0^b \psi_{x2n}\frac{\partial\psi_{x2q}}{\partial y}\mathrm{d}y = \frac{q\pi}{b}\int_0^b \sin\left(\frac{n\pi y}{b}\right)\cos\left(\frac{q\pi y}{b}\right)\mathrm{d}y$$
$$= \begin{cases} 0 & \text{if} \quad n+q \ = \text{even} \\ \frac{2nq}{n^2-q^2} & \text{if} \quad n+q \ = \text{odd} \end{cases},$$

$$\Delta_{11}^{1} = \int_0^b \frac{\partial\psi_{x2n}}{\partial y}\frac{\partial\psi_{x2q}}{\partial y}\mathrm{d}y = nq\left(\frac{\pi}{b}\right)^2\int_0^b \cos\left(\frac{n\pi y}{b}\right)\cos\left(\frac{q\pi y}{b}\right)\mathrm{d}y$$
$$= \begin{cases} \frac{nq\pi^2}{2b} & \text{if} \quad n = q \\ 0 & \text{if} \quad n \neq q \end{cases},$$

$$\Delta_{00}^{2} = \int_0^b \psi_{x2n}\psi_{y2q}\mathrm{d}y = \int_0^b \sin\left(\frac{n\pi y}{b}\right)\cos\left(\frac{q\pi y}{b}\right)\mathrm{d}y$$
$$= \begin{cases} 0 & \text{if} \quad n+q \ = \text{even} \\ \frac{2bn}{\pi(n^2-q^2)} & \text{if} \quad n+q \ = \text{odd} \end{cases},$$

$$\Delta_{01}^{2} = \int_0^b \psi_{x2n}\frac{\partial\psi_{y2q}}{\partial y}\mathrm{d}y = \frac{-q\pi}{b}\int_0^b \sin\left(\frac{n\pi y}{b}\right)\sin\left(\frac{q\pi y}{b}\right)\mathrm{d}y$$
$$= \begin{cases} \frac{-q\pi}{2} & \text{if} \quad n = q \\ 0 & \text{if} \quad n \neq q \end{cases},$$

$$\Delta_{10}^{2} = \int_0^b \frac{\partial\psi_{x2n}}{\partial y}\psi_{y2q}\mathrm{d}y = \frac{n\pi}{b}\int_0^b \cos\left(\frac{n\pi y}{b}\right)\cos\left(\frac{q\pi y}{b}\right)\mathrm{d}y$$
$$= \begin{cases} \frac{n\pi}{2} & \text{if} \quad n = q \\ 0 & \text{if} \quad n \neq q \end{cases},$$

$$\Delta_{11}^{2} = \int_0^b \frac{\partial\psi_{x2n}}{\partial y}\frac{\partial\psi_{y2q}}{\partial y}\mathrm{d}y = \frac{-n\pi}{b}\frac{q\pi}{b}\int_0^b \cos\left(\frac{n\pi y}{b}\right)\sin\left(\frac{q\pi y}{b}\right)\mathrm{d}y$$
$$= \begin{cases} 0 & \text{if} \quad n+q \ = \text{even} \\ \frac{2nq^2\pi}{b(n^2-q^2)} & \text{if} \quad n+q \ = \text{odd} \end{cases},$$

$$\Delta_{00}^{3} = \int_0^b \psi_{y2n}\psi_{y2q}\mathrm{d}y = \int_0^b \cos\left(\frac{n\pi y}{b}\right)\cos\left(\frac{q\pi y}{b}\right)\mathrm{d}y$$
$$= \begin{cases} \frac{1}{2}b & \text{if} \quad n = q \\ 0 & \text{if} \quad n \neq q \end{cases},$$

$$\Delta_{01}^{3}=\int_0^b \psi_{y2n}\frac{\partial \psi_{y2q}}{\partial y}\mathrm{d}y=\frac{-q\pi}{b}\int_0^b \cos\left(\frac{n\pi y}{b}\right)\sin\left(\frac{q\pi y}{b}\right)\mathrm{d}y$$
$$=\begin{cases}0 & \text{if} \quad n+q=\text{even}\\ \frac{2q^2}{(n^2-q^2)} & \text{if} \quad n+q=\text{odd}\end{cases},$$

$$\Delta_{10}^{3}=\int_0^b \frac{\partial \psi_{y2n}}{\partial y}\cdot\psi_{y2q}\mathrm{d}y=\frac{-n\pi}{b}\int_0^b \sin\left(\frac{n\pi y}{b}\right)\cos\left(\frac{q\pi y}{b}\right)\mathrm{d}y$$
$$=\begin{cases}0 & \text{if} \quad n+q=\text{even}\\ \frac{2n^2}{(q^2-n^2)} & \text{if} \quad n+q=\text{odd}\end{cases},$$

$$\Delta_{11}^{3}=\int_0^b \frac{\partial \psi_{y2n}}{\partial y}\frac{\partial \psi_{y2q}}{\partial y}\mathrm{d}y=nq\left(\frac{\pi}{b}\right)^2\int_0^b \sin\left(\frac{n\pi y}{b}\right)\sin\left(\frac{q\pi y}{b}\right)\mathrm{d}y$$
$$=\begin{cases}\frac{nq\pi^2}{2b} & \text{if} \quad n=q\\ 0 & \text{if} \quad n\neq q\end{cases},$$

$$\Delta_{00}^{4}=\int_0^b w_{2n}w_{2q}\mathrm{d}y=\int_0^b \sin\left(\frac{n\pi y}{b}\right)\sin\left(\frac{q\pi y}{b}\right)\mathrm{d}y$$
$$=\begin{cases}\frac{1}{2}b & \text{if} \quad n=q\\ 0 & \text{if} \quad n\neq q\end{cases},$$

$$\Delta_{01}^{4}=\int_0^b w_{2n}\frac{\partial w_{2q}}{\partial y}\mathrm{d}y=\frac{q\pi}{b}\int_0^b \sin\left(\frac{n\pi y}{b}\right)\cos\left(\frac{q\pi y}{b}\right)\mathrm{d}y$$
$$=\begin{cases}0 & \text{if} \quad n+q=\text{even}\\ \frac{2nq}{n^2-q^2} & \text{if} \quad n+q=\text{odd}\end{cases},$$

$$\Delta_{10}^{4}=\int_0^b \frac{\partial w_{2n}}{\partial y}w_{2q}\mathrm{d}y=\frac{n\pi}{b}\int_0^b \cos\left(\frac{n\pi y}{b}\right)\sin\left(\frac{q\pi y}{b}\right)\mathrm{d}y$$
$$=\begin{cases}0 & \text{if} \quad n+q=\text{even}\\ \frac{2nq}{q^2-n^2} & \text{if} \quad n+q=\text{odd}\end{cases},$$

$$\Delta_{11}^{4}=\int_0^b \frac{\partial w_{2n}}{\partial y}\frac{\partial w_{2q}}{\partial y}\mathrm{d}y=nq\left(\frac{\pi}{b}\right)^2\int_0^b \cos\left(\frac{n\pi y}{b}\right)\cos\left(\frac{q\pi y}{b}\right)\mathrm{d}y$$
$$=\begin{cases}\frac{nq\pi^2}{2b} & \text{if} \quad n=q\\ 0 & \text{if} \quad n\neq q\end{cases},$$

$$\Delta_{02}^{4}=\int_0^b w_{2n}\frac{\partial^2 w_{2q}}{\partial x^2}\mathrm{d}y=-\left(\frac{q\pi}{b}\right)^2\int_0^b \sin\left(\frac{n\pi y}{b}\right)\sin\left(\frac{q\pi y}{b}\right)\mathrm{d}y$$
$$=\begin{cases}\frac{-n^2\pi^2}{2b} & \text{if} \quad n=q\\ 0 & \text{if} \quad n\neq q\end{cases},$$

$$\Delta_{21}^{4}=\int_0^b \frac{\partial^2 w_{2q}}{\partial y^2}\frac{\partial w_{2q}}{\partial y}\mathrm{d}y=-\left(\frac{n\pi}{b}\right)^2\frac{q\pi}{b}\int_0^b \sin\left(\frac{n\pi y}{b}\right)\cos\left(\frac{q\pi y}{b}\right)\mathrm{d}y$$

$$= \begin{cases} 0 & \text{if} \quad n+q \ = \text{even} \\ \frac{2n^3 q\pi^2}{b^2(q^2-n^2)} & \text{if} \quad n+q \ = \text{odd} \end{cases},$$

$$\Delta_{22}^4 = \int_0^b \frac{\partial^2 w_{2n}}{\partial y^2} \frac{\partial^2 w_{2q}}{\partial y^2} \mathrm{d}y = \left(\frac{n\pi}{b}\right)^2 \left(\frac{q\pi}{b}\right)^2 \int_0^b \sin\left(\frac{n\pi y}{b}\right) \sin\left(\frac{q\pi y}{b}\right) \mathrm{d}y$$

$$= \begin{cases} 0 & \text{if} \quad n \neq q \\ \frac{n^4\pi^4}{2b^3} & \text{if} \quad n = q \end{cases},$$

$$\Delta_{00}^5 = \int_0^b w_{2n} \psi_{y2q} \mathrm{d}y = \int_0^b \sin\left(\frac{n\pi y}{b}\right) \cos\left(\frac{q\pi y}{b}\right) \mathrm{d}y$$

$$= \begin{cases} 0 & \text{if} \quad n+q \ \text{ even} \\ \frac{2nb}{(n^2-q^2)\pi} & \text{if} \quad n+q \ \text{ odd} \end{cases},$$

$$\Delta_{01}^5 = \int_0^b w_{2n} \frac{\partial w_{2q}}{\partial y} \mathrm{d}y = \frac{-q\pi}{b} \int_0^b \sin\left(\frac{n\pi y}{b}\right) \sin\left(\frac{q\pi y}{b}\right) \mathrm{d}y$$

$$= \begin{cases} \frac{-q\pi}{2} & \text{if} \quad n = q \\ 0 & \text{if} \quad n \neq q \end{cases},$$

$$\Delta_{10}^5 = \int_0^b \frac{\partial w_{2n}}{\partial y} \psi_{y2q} \mathrm{d}y = \frac{n\pi}{b} \int_0^b \left(\frac{n\pi y}{b}\right) \cos\left(\frac{q\pi y}{b}\right) \ \mathrm{d}y$$

$$= \begin{cases} \frac{n\pi}{2} & \text{if} \quad n = q \\ 0 & \text{if} \quad n \neq q \end{cases},$$

$$\Delta_{11}^5 = \int_0^b \frac{\partial w_{2n}}{\partial y} \frac{\partial \psi_{y2q}}{\partial y} \mathrm{d}y = -\frac{n\pi}{b} \frac{q\pi}{b} \int_0^b \cos\left(\frac{n\pi y}{b}\right) \sin\left(\frac{q\pi y}{b}\right) \mathrm{d}y$$

$$= \begin{cases} 0 & \text{if} \quad n+q \ \text{ even} \\ \frac{2n\pi q^2}{b(n^2-q^2)} & \text{if} \quad n+q \ \text{ odd} \end{cases},$$

$$\Delta_{20}^5 = \int_0^b \frac{\partial^2 w_{2n}}{\partial y^2} \psi_{y2q} \mathrm{d}y = -\left(\frac{n\pi}{b}\right)^2 \int_0^b \sin\left(\frac{n\pi y}{b}\right) \cos\left(\frac{q\pi y}{b}\right) \mathrm{d}y$$

$$= \begin{cases} \frac{2n^3\pi}{b(q^2-n^2)} & \text{if} \quad n+q = \text{odd} \\ 0 & \text{if} \quad n+q = \text{even} \end{cases},$$

$$\Delta_{21}^5 = \int_0^b \frac{\partial^2 w_{2n}}{\partial y^2} \frac{\partial \psi_{y2q}}{\partial y} \mathrm{d}y = \left(\frac{n\pi}{b}\right)^2 \left(\frac{q\pi}{b}\right) \int_0^b \sin\left(\frac{n\pi y}{b}\right) \sin\left(\frac{q\pi y}{b}\right) \mathrm{d}y$$

$$= \begin{cases} \frac{n^3\pi^3}{2b^2} & \text{if} \quad n = q \\ 0 & \text{if} \quad n \neq q \end{cases},$$

$$\Delta_{00}^6 = \int_0^b w_{2n} \psi_{x2q} \mathrm{d}y = \int_0^b \sin\left(\frac{n\pi y}{b}\right) \sin\left(\frac{q\pi y}{b}\right) \mathrm{d}y$$

$$= \begin{cases} \frac{1}{2}b & \text{if} \quad n = q \\ 0 & \text{if} \quad n \neq q \end{cases},$$

$$\Delta_{10}^{6} = \int_0^b \frac{\partial w_{2n}}{\partial y}\psi_{x2q}\mathrm{d}y = \frac{n\pi}{b}\int_0^b \cos\left(\frac{n\pi y}{b}\right)\sin\left(\frac{q\pi y}{b}\right)\mathrm{d}y$$
$$= \begin{cases} 0 & \text{if} \quad n+q \ \text{ even} \\ \frac{2nq}{(q^2-n^2)} & \text{if} \quad n+q \quad \text{odd} \end{cases},$$
$$\Delta_{01}^{6} = \int_0^b w_{2n}\frac{\partial \psi_{x2q}}{\partial y}\mathrm{d}y = \frac{q\pi}{b}\int_0^b \sin\left(\frac{n\pi y}{b}\right)\cos\left(\frac{q\pi y}{b}\right)\mathrm{d}y$$
$$= \begin{cases} 0 & \text{if} \quad n+q \ \text{ even} \\ \frac{2nq}{(n^2-q^2)} & \text{if} \quad n+q \quad \text{odd} \end{cases},$$
$$\Delta_{11}^{6} = \int_0^b \frac{\partial w_{2n}}{\partial y}\frac{\partial \psi_{x2q}}{\partial y}\mathrm{d}y = nq\left(\frac{\pi}{b}\right)^2\int_0^b \cos\left(\frac{n\pi y}{b}\right)\cos\left(\frac{q\pi y}{b}\right)\mathrm{d}y$$
$$= \begin{cases} \frac{q^2\pi^2}{2b} & \text{if} \quad n=q \\ 0 & \text{if} \quad n\neq q \end{cases},$$
$$\Delta_{20}^{6} = \int_0^b \frac{\partial^2 w_{2n}}{\partial y^2}\psi_{x2q}\mathrm{d}y = -\left(\frac{n\pi}{b}\right)^2\int_0^b \sin\left(\frac{n\pi y}{b}\right)\sin\left(\frac{q\pi y}{b}\right)\mathrm{d}y$$
$$= \begin{cases} 0 & \text{if} \quad n\neq q \\ \frac{-n^2\pi^2}{2b} & \text{if} \quad n=q \end{cases},$$
$$\Delta_{21}^{6} = \int_0^b \frac{\partial^2 w_{2n}}{\partial y^2}\frac{\partial \psi_{x2q}}{\partial y}\mathrm{d}y = -\left(\frac{n\pi}{b}\right)^2\frac{q\pi}{b}\int_0^b \sin\left(\frac{n\pi y}{b}\right)\cos\left(\frac{q\pi y}{b}\right)\mathrm{d}y$$
$$= \begin{cases} 0 & \text{if} \quad n+q \ \text{ even} \\ \frac{2n^3q\pi^2}{b^2(q^2-n^2)} & \text{if} \quad n+q \quad \text{odd} \end{cases}. \tag{15.63}$$

With (15.57) we obtain:

$$Q_{00}^{nq} = \int_0^b w_{2n}w_{2q}y\mathrm{d}y = \int_0^b \sin\left(\frac{n\pi y}{b}\right)\sin\left(\frac{q\pi y}{b}\right)y\ \mathrm{d}y$$
$$= \begin{cases} \frac{1}{4}b^2 & \text{if} \quad n=q \\ \frac{2b^2nq}{\pi^2(n^2-q^2)^2}\left[(-1)^{n+q}-1\right] & \text{if} \quad n\neq q \end{cases}. \tag{15.64}$$

Equation (15.59) leads to:

$$\Phi_{11}^{nq} = \psi_{y2n}\big|_{y=0}\psi_{y2q}\Big|_{y=0} = \cos(0)\cos(0) = 1,$$
$$\theta_{11}^{nq} = \psi_{y2n}\big|_{y=b}\psi_{y2q}\Big|_{y=b} = \begin{cases} 1 & \text{if} \quad n+q = \text{even} \\ -1 & \text{if} \quad n+q = \text{odd} \end{cases}. \tag{15.65}$$

15.3.1.3 Resultants with Respect to the y-Direction, Case 2

With Eq. (15.54) we obtain:

$$
\begin{aligned}
\Delta_{00}^{1} &= \int_0^b \psi_{x2n}\psi_{x2q}\,\mathrm{d}y \\
&= \int_0^b \left\{\left[\cos\left((n-1)\,\pi\,\frac{y}{b}\right) - \cos\left((n+1)\pi\,\frac{y}{b}\right)\right]\right. \\
&\left.\times\left[\cos\left((q-1)\,\pi\,\frac{y}{b}\right) - \cos\left((q+1)\pi\,\frac{y}{b}\right)\right]\right\}\mathrm{d}y \\
&= \begin{cases} \frac{-b}{2} & \text{if} \quad n = 2+q \\ b & \text{if} \quad n = q,\ q \neq 1 \\ \frac{-b}{2} & \text{if} \quad n = q-2 \text{ and } q \geq 3 \\ \frac{3b}{2} & \text{if} \quad n = q = 1 \\ 0 & \text{else} \end{cases}, \\
\Delta_{01}^{1} &= \int_0^b \psi_{x2n}\frac{\partial\psi_{x2q}}{\partial y}\mathrm{d}y \\
&= \int_0^b \left\{\left[\cos\left((n-1)\,\pi\,\frac{y}{b}\right) - \cos\left((n+1)\pi\,\frac{y}{b}\right)\right]\right. \\
&\left.\times\left[-\left((q-1)\,\frac{\pi}{b}\right)\sin\left((q-1)\,\pi\,\frac{y}{b}\right) + \left((q+1)\frac{\pi}{b}\right)\sin\left((q+1)\pi\,\frac{y}{b}\right)\right]\right\}\mathrm{d}y \\
&= \frac{-32nq\left(-2+n^2+q^2\right)}{(-2+n-q)\,(n-q)\,(2+n-q)\,(-2+n+q)\,(2+n+q)\,(n+q)} \\
&\text{if} \quad n+q = \text{ odd}, \\
\Delta_{11}^{1} &= \int_0^b \frac{\partial\psi_{x2n}}{\partial y}\frac{\partial\psi_{x2q}}{\partial y}\mathrm{d}y \\
&= \int_0^b \left\{\left[\left((1-n)\,\frac{\pi}{b}\right)\sin\left((n-1)\,\pi\,\frac{y}{b}\right) + \left((n+1)\,\frac{\pi}{y}\right)\sin\left((n+1)\,\pi\,\frac{y}{b}\right)\right]\right. \\
&\left.\times\left[\left((1-q)\,\frac{\pi}{b}\right)\sin\left((q-1)\,\pi\,\frac{y}{b}\right) + \left((q+1)\,\frac{\pi}{y}\right)\sin\left((q+1)\,\pi\,\frac{y}{b}\right)\right]\right\}\mathrm{d}y \\
&= \begin{cases} \frac{-\pi^2(1+q)^2}{2b} & \text{if } n = q+2 \\ \frac{\pi^2\left(1+q^2\right)}{b} & \text{if } n = q \\ \frac{-\pi^2(-1+q)^2}{2b} & \text{if } n = q-2 \quad \text{and} \quad q \geq 3 \\ 0 & \text{else} \end{cases}, \\
\Delta_{00}^{2} &= \int_0^b \psi_{x2n}\psi_{y2q}\,\mathrm{d}y \\
&= \int_0^b \left\{\left[\cos\left((n-1)\,\pi\,\frac{y}{b}\right) - \cos\left((n+1)\pi\,\frac{y}{b}\right)\right]\right. \\
&\left.\times\left[\cos\left((q-1)\,\pi\,\frac{y}{b}\right) - \cos\left((q+1)\pi\,\frac{y}{b}\right)\right]\right\}\mathrm{d}y
\end{aligned}
$$

$$= \begin{cases} \frac{-b}{2} & \text{if} \quad n = 2+q \\ b & \text{if} \quad n = q,\ q \neq 1 \\ \frac{-b}{2} & \text{if} \quad n = q-2 \text{ and } q \neq 1,\ q \neq 2 \\ \frac{3b}{2} & \text{if} \quad n = q = 1 \\ 0 & \text{else} \end{cases},$$

$$\Delta_{01}^{2} = \int_0^b \psi_{x2n} \frac{\partial \psi_{y2q}}{\partial y} \mathrm{d}y$$

$$= \int_0^b \left\{ \left[\cos\left((n-1)\pi \frac{y}{b}\right) - \cos\left((n+1)\pi \frac{y}{b}\right) \right] \right.$$

$$\left. \times \left[-\left((q-1)\frac{\pi}{b}\right) \sin\left((q-1)\pi \frac{y}{b}\right) + \left((q+1)\frac{\pi}{b}\right) \sin\left((q+1)\pi \frac{y}{b}\right) \right] \right\} \mathrm{d}y$$

$$= \frac{-32nq\left(-2+n^2+q^2\right)}{(-2+n-q)(n-q)(2+n-q)(2+n+q)(-2+n+q)(n+q)}$$

if $n+q =$ odd,

$$\Delta_{10}^{2} = \int_0^b \frac{\partial \psi_{x2n}}{\partial x} \psi_{y2q} \mathrm{d}y$$

$$= \int_0^b \left\{ \left[(1-n)\left(\frac{\pi}{b}\right) \sin\left((n-1)\pi \frac{y}{b}\right) + \left((n+1)\frac{\pi}{b}\right) \sin\left((n+1)\pi \frac{y}{b}\right) \right] \right.$$

$$\left. \times \left[\cos\left((q-1)\pi \frac{y}{b}\right) - \cos\left((q+1)\pi \frac{y}{b}\right) \right] \right\} \mathrm{d}y$$

$$= \frac{32nq(-2+n^2+q^2)}{(-2+n-q)(n-q)(2+n-q)(-2+n+q)(n+q)(2+n+q)}$$

if $n+q =$ odd,

$$\Delta_{11}^{2} = \int_0^b \frac{\partial \psi_{x2n}}{\partial y} \frac{\partial \psi_{y2q}}{\partial y} \mathrm{d}y$$

$$= \int_0^b \left\{ \left[\left((1-n)\frac{\pi}{b}\right) \sin\left((n-1)\pi \frac{y}{b}\right) + \left((n+1)\frac{\pi}{y}\right) \sin\left((n+1)\pi \frac{y}{b}\right) \right] \right.$$

$$\left. \times \left[\left((1-q)\frac{\pi}{b}\right) \sin\left((q-1)\pi \frac{y}{b}\right) + \left((q+1)\frac{\pi}{y}\right) \sin\left((q+1)\pi \frac{y}{b}\right) \right] \right\} \mathrm{d}y$$

$$= \begin{cases} \frac{-\pi^2\left(1+q^2\right)}{2b} & \text{if } n = q+2 \\ \frac{\pi^2\left(1+q^2\right)}{b} & \text{if } n = q \\ \frac{-\pi^2(-1+q)^2}{2b} & \text{if } n = q-2 \quad \text{if} \quad q \neq 2 \\ 0 & \text{else} \end{cases},$$

$$\Delta_{00}^{3} = \int_0^b \psi_{y2n} \psi_{y2q} \mathrm{d}y$$

$$= \int_0^b \left\{ \left[\cos\left((n-1)\pi \frac{y}{b}\right) - \cos\left((n+1)\pi \frac{y}{b}\right) \right] \right.$$

$$\times \left[\cos\left((q-1)\,\pi\frac{y}{b}\right) - \cos\left((q+1)\pi\frac{y}{b}\right)\right]\Bigg\}\,\mathrm{d}y$$

$$= \begin{cases} \frac{-b}{2} & \text{if} \quad n = 2+q \\ b & \text{if} \quad n = q,\ q \neq 1 \\ \frac{-b}{2} & \text{if} \quad n = q-2 \text{ and } q \neq 1,\ q \neq 2 \\ \frac{3b}{2} & \text{if} \quad n = q = 1 \\ 0 & \text{else} \end{cases},$$

$$\Delta_{01}^{3} = \int_0^b \psi_{x2n}\frac{\partial \psi_{y2q}}{\partial y}\mathrm{d}y$$

$$= \int_0^b \left\{\left[\cos\left((n-1)\,\pi\frac{y}{b}\right) - \cos\left((n+1)\pi\frac{y}{b}\right)\right]\right.$$

$$\left.\times \left[-\left((q-1)\,\frac{\pi}{b}\right)\sin\left((q-1)\,\pi\frac{y}{b}\right) + \left((q+1)\frac{\pi}{b}\right)\sin\left((q+1)\pi\frac{y}{b}\right)\right]\right\}\mathrm{d}y$$

$$= \frac{-32nq\left(-2+n^2+q^2\right)}{(-2+n-q)\,(n-q)\,(2+n-q)\,(-2+n+q)\,(2+n+q)\,(n+q)}$$

if $n+q =$ odd,

$$\Delta_{10}^{3} = \int_0^b \psi_{x2n}\frac{\partial \psi_{y2q}}{\partial y}\mathrm{d}y$$

$$= \int_0^b \left\{\left[\cos\left((n-1)\,\pi\frac{y}{b}\right) - \cos\left((n+1)\pi\frac{y}{b}\right)\right]\right.$$

$$\left.\times \left[-\left((q-1)\,\frac{\pi}{b}\right)\sin\left((q-1)\,\pi\frac{y}{b}\right) + \left((q+1)\frac{\pi}{b}\right)\sin\left((q+1)\pi\frac{y}{b}\right)\right]\right\}\mathrm{d}y$$

$$= \frac{32nq\left(-2+n^2+q^2\right)}{(-2+n-q)\,(n-q)\,(2+n-q)\,(-2+n+q)\,(2+n+q)\cdot(n+q)}$$

if $n+q =$ odd,

$$\Delta_{11}^{3} = \int_0^b \frac{\partial \psi_{x2n}}{\partial y}\frac{\partial \psi_{y2q}}{\partial y}\mathrm{d}y$$

$$= \int_0^b \left\{\left[\left((1-n)\,\frac{\pi}{b}\right)\sin\left((n-1)\,\pi\frac{y}{b}\right) + \left((n+1)\,\frac{\pi}{y}\right)\sin\left((n+1)\,\pi\frac{y}{b}\right)\right]\right.$$

$$\left.\times \left[\left((1-q)\,\frac{\pi}{b}\right)\sin\left((q-1)\,\pi\frac{y}{b}\right) + \left((q+1)\,\frac{\pi}{y}\right)\sin\left((q+1)\,\pi\frac{y}{b}\right)\right]\right\}\mathrm{d}y$$

$$= \begin{cases} \frac{-\pi^2\left(1+q^2\right)}{2b} & \text{if } n = q+2 \\ \frac{\pi^2\left(1+q^2\right)}{b} & \text{if } n = q \\ \frac{-\pi^2(-1+q)^2}{2b} & \text{if } n = q-2 \quad \text{and } q \geq 3 \\ 0 & \text{else} \end{cases},$$

$$\Delta_{00}^{4} = \int_0^b w_{2n}\,w_{2q}\,\mathrm{d}y$$

$$
\begin{aligned}
&= \int_0^b \left\{ \left[\cos\left((n-1)\,\pi \frac{y}{b} \right) - \cos\left((n+1)\pi \frac{y}{b} \right) \right] \right. \\
&\left. \times \left[\cos\left((q-1)\,\pi \frac{y}{b} \right) - \cos\left((q+1)\pi \frac{y}{b} \right) \right] \right\} \mathrm{d}y \\
&= \begin{cases} \frac{-b}{2} & \text{if} \quad n = 2+q \\ b & \text{if} \quad n = q,\ q \neq 1 \\ \frac{-b}{2} & \text{if} \quad n = q-2 \text{ and } q \geq 3 \\ \frac{3b}{2} & \text{if} \quad n = q = 1 \\ 0 & \text{else} \end{cases},
\end{aligned}
$$

$$
\begin{aligned}
\Delta_{01}^4 &= \int_0^b w_{2n} \frac{\partial w_{2q}}{\partial y} \mathrm{d}y \\
&= \int_0^b \left\{ \left[\cos\left((n-1)\,\pi \frac{y}{b} \right) - \cos\left((n+1)\pi \frac{y}{b} \right) \right] \right. \\
&\left. \times \left[-\left((q-1)\,\frac{\pi}{b} \right) \sin\left((q-1)\,\pi \frac{y}{b} \right) + \left((q+1)\frac{\pi}{b} \right) \sin\left((q+1)\pi \frac{y}{b} \right) \right] \right\} \mathrm{d}y \\
&= \frac{-32nq\left(-2+n^2+q^2\right)}{(-2+n-q)\,(n-q)\,(2+n-q)\,(-2+n+q)\,(2+n+q)\,(n+q)} \\
&\quad \text{if} \quad n+q = \text{ odd},
\end{aligned}
$$

$$
\begin{aligned}
\Delta_{10}^4 &= \int_0^b \frac{\partial w_{2n}}{\partial y} w_{2q} \mathrm{d}y \\
&= \int_0^b \left\{ \left[-\left((n-1)\,\frac{\pi}{b} \right) \sin\left((n-1)\,\pi \frac{y}{b} \right) + \left((n+1)\frac{\pi}{b} \right) \sin\left((n+1)\pi \frac{y}{b} \right) \right] \right. \\
&\left. \times \left[\cos\left((q-1)\cdot\pi\cdot\frac{y}{b} \right) - \cos\left((q+1)\cdot\pi\cdot\frac{y}{b} \right) \right] \right\} \mathrm{d}y \\
&= \frac{32nq\left(-2+n^2+q^2\right)}{(-2+n-q)\,(n-q)\,(2+n-q)\,(-2+n+q)\,(2+n+q)\,(n+q)} \\
&\quad \text{if} \quad n+q = \text{ odd},
\end{aligned}
$$

$$
\begin{aligned}
\Delta_{11}^4 &= \int_0^b \frac{\partial w_{2n}}{\partial y} \frac{\partial w_{2q}}{\partial y} \mathrm{d}y \\
&= \int_0^b \left\{ \left[\left((1-n)\,\frac{\pi}{b} \right) \sin\left((n-1)\,\pi \frac{y}{b} \right) + \left((n+1)\,\frac{\pi}{y} \right) \sin\left((n+1)\,\pi \frac{y}{b} \right) \right] \right. \\
&\left. \times \left[\left((1-q)\,\frac{\pi}{b} \right) \sin\left((q-1)\,\pi \frac{y}{b} \right) + \left((q+1)\,\frac{\pi}{y} \right) \sin\left((q+1)\,\pi \frac{y}{b} \right) \right] \right\} \mathrm{d}y \\
&= \begin{cases} \frac{-\pi^2(1+q)^2}{2b} & \text{if } n = q+2 \\ \frac{\pi^2\left(1+q^2\right)}{b} & \text{if } n = q \\ \frac{-\pi^2(-1+q)^2}{2b} & \text{if } n = q-2 \text{ and } q \geq 3 \\ 0 & \text{else} \end{cases},
\end{aligned}
$$

$$\Delta_{02}^{4} = \int_0^b w_{2n} \frac{\partial^2 w_{2q}}{\partial y^2} \mathrm{d}y$$
$$= \int_0^b \left\{ \left[\cos\left((n-1)\,\pi \frac{y}{b}\right) - \cos\left((n+1)\pi \frac{y}{b}\right) \right] \right.$$
$$\left. \times \left[-\left((q-1)\,\frac{\pi}{b}\right)^2 \cos\left((q-1)\,\pi \frac{y}{b}\right) + \left((q+1)\frac{\pi}{b}\right)^2 \cos\left((q+1)\pi \frac{y}{b}\right) \right] \right\} \mathrm{d}y$$
$$= \begin{cases} \frac{\pi^2(1+q)^2}{2b} & \text{if} \quad n = q+2 \\ \frac{-\pi^2\left(1+q^2\right)}{b} & \text{if} \quad n = q \\ \frac{\pi^2(q-1)^2}{2b} & \text{if} \quad n = q-2 \text{ and } q \geq 3 \end{cases},$$

$$\Delta_{21}^{4} = \int_0^b \frac{\partial^2 w_{2n}}{\partial y^2} \frac{\partial w_{2q}}{\partial y} \mathrm{d}y$$
$$= \int_0^b \left\{ \left[-\left((n-1)\,\frac{\pi}{b}\right)^2 \cos\left((n-1)\,\pi \frac{y}{b}\right) + \left((n+1)\frac{\pi}{b}\right)^2 \cos\left((n+1)\pi \frac{y}{b}\right) \right] \right.$$
$$\left. \times \left[\left(-\left((q-1)\,\pi \frac{y}{b}\right) \sin\left((q-1)\,\pi \frac{y}{b}\right)\right) + \left(\left((q+1)\pi \frac{y}{b}\right) \sin\left((q+1)\pi \frac{y}{b}\right)\right) \right] \right\} \mathrm{d}y$$
$$= \frac{64\pi^2 nq\left(q^2+n^2+n^2q^2-3\right)}{b^2\,(-2+n-q)\;(n-q)\;(2+n-q)\;(-2+n+q)\;(n+q)\;(2+n+q)}$$
$$\text{if} \quad n+q = \text{odd},$$

$$\Delta_{22}^{4} = \int_0^b \frac{\partial^2 w_{2n}}{\partial y^2} \frac{\partial^2 w_{2q}}{\partial y^2} \mathrm{d}y$$
$$= \int_0^b \left\{ \left[-\left((n-1)\,\frac{\pi}{b}\right)^2 \cos\left((n-1)\,\pi \frac{y}{b}\right) + \left((n+1)\frac{\pi}{b}\right)^2 \cos\left((n+1)\pi \frac{y}{b}\right) \right] \right.$$
$$\left. \times \left[-\left((q-1)\,\frac{\pi}{b}\right)^2 \cos\left((q-1)\,\pi \frac{y}{b}\right) + \left((q+1)\frac{\pi}{b}\right)^2 \cos\left((q+1)\pi \frac{y}{b}\right) \right] \right\} \mathrm{d}y$$
$$= \begin{cases} \frac{-\pi^4(1+q)^4}{2b^3} & \text{if } n = q+2 \\ \frac{\pi^4\left(1+6q^2+q^4\right)}{b^3} & \text{if } n = q \\ \frac{-\pi^4(q-1)^4}{2b^3} & \text{if } n = q-2 \text{ and } q \geq 3 \end{cases},$$

$$\Delta_{00}^{5} = \int_0^b w_{2n} \psi_{y2q} \mathrm{d}y$$
$$= \int_0^b \left\{ \left[\cos\left((n-1)\,\pi \frac{y}{b}\right) - \cos\left((n+1)\pi \frac{y}{b}\right) \right] \right.$$
$$\left. \times \left[\cos\left((q-1)\,\pi \frac{y}{b}\right) - \cos\left((q+1)\pi \frac{y}{b}\right) \right] \right\} \mathrm{d}y$$

$$= \begin{cases} \frac{-b}{2} & \text{if} \quad n = 2+q \\ b & \text{if} \quad n = q,\ q \neq 1 \\ \frac{-b}{2} & \text{if} \quad n = q-2 \text{ and } q \neq 1,\ q \neq 2 \\ \frac{3b}{2} & \text{if} \quad n = q = 1 \\ 0 & \text{else} \end{cases},$$

$$\Delta_{10}^{5} = \int_0^b \frac{\partial w_{2n}}{\partial x} \psi_{y2q} \mathrm{d}y$$

$$= \int_0^b \left\{ \left[(1-n) \left(\frac{\pi}{b}\right) \sin\left((n-1)\pi\frac{y}{b}\right) + \left((n+1)\frac{\pi}{b}\right) \sin\left((n+1)\pi\frac{y}{b}\right) \right] \right.$$

$$\left. \times \left[\cos\left((q-1)\pi\frac{y}{b}\right) - \cos\left((q+1)\pi\frac{y}{b}\right) \right] \right\} \mathrm{d}y$$

$$= \frac{32nq(-2+n^2+q^2)}{(-2+n-q)(n-q)(2+n-q)(-2+n+q)(n+q)(2+n+q)}$$

if $n+q =$ odd,

$$\Delta_{01}^{5} = \int_0^b w_{2n} \frac{\partial \psi_{y2q}}{\partial y} \mathrm{d}y$$

$$= \int_0^b \left\{ \left[-\left((n-1)\frac{\pi}{b}\right) \sin\left((n-1)\pi\frac{y}{b}\right) + \left((n+1)\frac{\pi}{b}\right) \sin\left((n+1)\pi\frac{y}{b}\right) \right] \right.$$

$$\left. \times \left[\cos\left((q-1)\pi\frac{y}{b}\right) - \cos\left((q+1)\pi\frac{y}{b}\right) \right] \right\} \mathrm{d}y$$

$$= \frac{-32nq\left(-2+n^2+q^2\right)}{(-2+n-q)(n-q)(2+n-q)(-2+n+q)(2+n+q)(n+q)}$$

if $n+q =$ odd,

$$\Delta_{11}^{5} = \int_0^b \frac{\partial w_{2n}}{\partial y} \frac{\partial \psi_{y2q}}{\partial y} \mathrm{d}y$$

$$= \int_0^b \left\{ \left[\left((1-n)\frac{\pi}{b}\right) \sin\left((n-1)\pi\frac{y}{b}\right) + \left((n+1)\frac{\pi}{y}\right) \sin\left((n+1)\pi\frac{y}{b}\right) \right] \right.$$

$$\left. \times \left[\left((1-q)\frac{\pi}{b}\right) \sin\left((q-1)\pi\frac{y}{b}\right) + \left((q+1)\frac{\pi}{y}\right) \sin\left((q+1)\pi\frac{y}{b}\right) \right] \right\} \mathrm{d}y$$

$$= \begin{cases} \frac{-\pi^2\left(1+q^2\right)}{2b} & \text{if } n = q+2 \\ \frac{\pi^2\left(1+q^2\right)}{b} & \text{if } n = q \\ \frac{-\pi^2(-1+q)^2}{2b} & \text{if } n = q-2 \\ 0 & \text{else} \end{cases},$$

$$\Delta_{20}^{5} = \int_0^b \frac{\partial^2 w_{2n}}{\partial y^2} \psi_{y2q} \mathrm{d}y$$

$$= \int_0^b \left\{ \left[-\left((n-1)\frac{\pi}{b}\right)^2 \cos\left((n-1)\pi\frac{y}{b}\right) + \left((n+1)\frac{\pi}{b}\right)^2 \cos\left((n+1)\pi\frac{y}{b}\right) \right] \right.$$

$$\times \left[\cos\left((q-1)\pi\frac{y}{b}\right)-\cos\left((q+1)\pi\frac{y}{b}\right)\right]\Big\}\,\mathrm{d}y$$

$$= \begin{cases} \frac{\pi^2(1+q)^2}{2b} & \text{if} \quad n=q+2 \\ \frac{-\pi^2(1+q^2)}{b} & \text{if} \quad n=q \\ \frac{\pi^2(q-1)^2}{2b} & \text{if} \quad n=q-2 \text{ and } q\geq 3 \end{cases},$$

$$\Delta_{21}^5 = \int_0^b \frac{\partial^2 w_{2n}}{\partial y^2}\frac{\partial \psi_{y2q}}{\partial y}\mathrm{d}y$$

$$= \int_0^b \Big\{\Big[-\Big((n-1)\frac{\pi}{b}\Big)^2\cos\Big((n-1)\pi\frac{y}{b}\Big)+\Big((n+1)\frac{\pi}{b}\Big)^2\cos\Big((n+1)\pi\frac{y}{b}\Big)\Big]$$

$$\times \Big[\Big(-\Big((q-1)\pi\frac{y}{b}\Big)\sin\Big((q-1)\pi\frac{y}{b}\Big)\Big)+\Big(\Big((q+1)\pi\frac{y}{b}\Big)\sin\Big((q+1)\pi\frac{y}{b}\Big)\Big)\Big]\Big\}\,\mathrm{d}y$$

$$= \frac{64\pi^2 nq\left(q^2+n^2+n^2q^2-3\right)}{b^2\,(-2+n-q)\;(n-q)\;(2+n-q)\;(-2+n+q)\;(n+q)\;(2+n+q)}$$

if $n+q=$ odd,

$$\Delta_{00}^6 = \int_0^b w_{2n}\psi_{x2q}\mathrm{d}y$$

$$= \int_0^b \Big\{\Big[\cos\Big((n-1)\pi\frac{y}{b}\Big)-\cos\Big((n+1)\pi\frac{y}{b}\Big)\Big]$$

$$\times \Big[\cos\Big((q-1)\pi\frac{y}{b}\Big)-\cos\Big((q+1)\pi\frac{y}{b}\Big)\Big]\Big\}\,\mathrm{d}y$$

$$= \begin{cases} \frac{-b}{2} & \text{if} \quad n=2+q \\ b & \text{if} \quad n=q,\ q\neq 1 \\ \frac{-b}{2} & \text{if} \quad n=q-2 \text{ and } q\geq 3 \\ \frac{3b}{2} & \text{if} \quad n=q=1 \\ 0 & \text{else} \end{cases},$$

$$\Delta_{01}^6 = \int_0^b \frac{\partial w_{2n}}{\partial x}\psi_{x2q}\mathrm{d}y$$

$$= \int_0^b \Big\{\Big[\cos\Big((n-1)\pi\frac{y}{b}\Big)-\cos\Big((n+1)\pi\frac{y}{b}\Big)\Big]$$

$$\times \Big[(1-q)\Big(\frac{\pi}{b}\Big)\sin\Big((q-1)\pi\frac{y}{b}\Big)+\Big((q+1)\frac{\pi}{b}\Big)\sin\Big((q+1)\pi\frac{y}{b}\Big)\Big]\Big\}\,\mathrm{d}y$$

$$= \frac{-32nq(-2+n^2+q^2)}{(-2+n-q)\,(n-q)\,(2+n-q)\,(-2+n+q)\,(n+q)\,(2+n+q)}$$

if $n+q=$ odd,

$$\Delta_{10}^6 = \int_0^b \frac{\partial w_{2n}}{\partial x}\psi_{x2q}\mathrm{d}y$$

$$= \int_0^b \Big\{\Big[(1-n)\Big(\frac{\pi}{b}\Big)\sin\Big((n-1)\pi\frac{y}{b}\Big)+\Big((n+1)\frac{\pi}{b}\Big)\sin\Big((n+1)\pi\frac{y}{b}\Big)\Big]$$

$$\times \left[\cos\left((q-1)\,\pi\frac{y}{b}\right)-\cos\left((q+1)\,\pi\frac{y}{b}\right)\right]\Bigg\}\,\mathrm{d}y$$
$$=\frac{32nq\left(-2+n^2+q^2\right)}{(-2+n-q)\,(n-q)\,(2+n-q)\,(-2+n+q)\,(n+q)\,(2+n+q)}$$
if $n+q=$ odd,

$$\Delta_{11}^{6}=\int_0^b \frac{\partial w_{2n}}{\partial y}\frac{\partial \psi_{x2q}}{\partial y}\mathrm{d}y$$
$$=\int_0^b\left\{\left[-\left((n-1)\,\frac{\pi}{b}\right)\sin\left((n-1)\,\pi\frac{y}{b}\right)+\left((n+1)\,\frac{\pi}{y}\right)\sin\left((n+1)\,\pi\frac{y}{b}\right)\right]\right.$$
$$\left.\times\left[-\left((q-1)\,\frac{\pi}{b}\right)\sin\left((q-1)\,\pi\frac{y}{b}\right)+\left((q+1)\,\frac{\pi}{y}\right)\sin\left((q+1)\,\pi\frac{y}{b}\right)\right]\right\}\mathrm{d}y$$
$$=\begin{cases}\frac{-\pi^2(1+q)^2}{2b} & \text{if } n=q+2\\ \frac{\pi^2(1+q)^2}{b} & \text{if } n=q\\ \frac{-\pi^2(-1+q)^2}{2b} & \text{if } n=q-2 \text{ and } q\geq 3\\ 0 & \text{else}\end{cases},$$

$$\Delta_{20}^{6}=\int_0^b \frac{\partial^2 w_{2n}}{\partial y^2}\psi_{x2q}\mathrm{d}y$$
$$=\int_0^b\left\{\left[-\left((n-1)\,\frac{\pi}{b}\right)^2\cos\left((n-1)\,\pi\frac{y}{b}\right)+\left((n+1)\,\frac{\pi}{y}\right)^2\cos\left((n+1)\,\pi\frac{y}{b}\right)\right]\right.$$
$$\left.\times\left[\cos\left((q-1)\,\pi\frac{y}{b}\right)-\cos\left((q+1)\,\pi\frac{y}{b}\right)\right]\right\}\mathrm{d}y$$
$$=\begin{cases}\frac{\pi^2(1+q)^2}{2b} & \text{if } n=q+2\\ \frac{-\pi^2\left(1+q^2\right)}{b} & \text{if } n=q\\ \frac{\pi^2(-1+q)^2}{2b} & \text{if } n=q-2 \text{ and } q\geq 3\\ 0 & \text{else}\end{cases},$$

$$\Delta_{21}^{6}=\int_0^b \frac{\partial^2 w_{2n}}{\partial y^2}\frac{\partial \psi_{x2q}}{\partial y}\mathrm{d}y$$
$$=\int_0^b\left\{\left[-\left((n-1)\,\frac{\pi}{b}\right)^2\cos\left((n-1)\,\pi\frac{y}{b}\right)+\left((n+1)\frac{\pi}{b}\right)^2\cos\left((n+1)\pi\frac{y}{b}\right)\right]\right.$$
$$\left.\times\left[\left(-\left((q-1)\,\pi\frac{y}{b}\right)\sin\left((q-1)\,\pi\frac{y}{b}\right)\right)+\left(\left((q+1)\pi\frac{y}{b}\right)\sin\left((q+1)\pi\frac{y}{b}\right)\right)\right]\right\}\mathrm{d}y$$
$$=\frac{64\pi^2nq\left(q^2+n^2+n^2q^2-3\right)}{b^2\,(-2+n-q)\;(n-q)\;(2+n-q)\;(-2+n+q)\;(n+q)\;(2+n+q)}$$
if $n+q=$ odd.

(15.66)

From (15.57) we obtain:

$$
\begin{aligned}
Q_{00} &= \int_0^b w_{2n} w_{2q}\, y \, \mathrm{d}y \\
&= \int_0^b \left\{ \left[\cos\left((n-1)\,\pi \frac{y}{b} \right) - \cos\left((n+1)\pi \frac{y}{b} \right) \right] \right. \\
&\left. \times \left[\cos\left((q-1)\,\pi \frac{y}{b} \right) - \cos\left((q+1)\pi \frac{y}{b} \right) \right] \right\} y \mathrm{d}y \\
&= \begin{cases} \widehat{Q} & \text{if} \quad n+q = \text{odd} \\ \frac{-b^2}{4} & \text{if} \quad n = q+2 \\ \frac{-b^2}{4} \text{ if} & n = q-2 \quad \text{and} \quad q \geq 3 \\ \frac{b^2}{2} & \text{if} \quad n = q \quad \text{and} \quad q \neq 1 \\ \frac{3b^2}{4} & \text{if} \quad n = q = 1 \end{cases}, \\
&\textit{with} \\
\widehat{Q} &= \frac{b^2 \left(-\frac{2}{(n-q)^2} + \frac{1}{(2+n-q)^2} + \frac{1}{(2-n+q)^2} - \frac{1}{(-2+n+q)^2} + \frac{2}{(n+q)^2} - \frac{1}{(2+n+q)^2} \right)}{\pi^2}.
\end{aligned}
\tag{15.67}
$$

Equation (15.59) leads to vanishing values due to the fixed restraint at the edges $y = 0$ and $y = b$.

15.3.1.4 Resultants with Respect to the y-Direction, Case 3

Equation (15.54) leads to:

$$
\begin{aligned}
\Delta_{00}^1 &= \int_0^b \psi_{x2n} \psi_{x2q} \mathrm{d}y = \int_0^b \left(\frac{y}{b}\right)^n \left(\frac{y}{b}\right)^q \mathrm{d}y = \frac{b}{n+q+1}, \\
\Delta_{01}^1 &= \int_0^b \psi_{x2n} \frac{\partial \psi_{x2q}}{\partial y} \mathrm{d}y = \frac{q}{b} \int \left(\frac{y}{b}\right)^n \left(\frac{y}{b}\right)^{q-1} \mathrm{d}y = \frac{q}{n+q}, \\
\Delta_{11}^1 &= \int_0^b \frac{\partial \psi_{x2n}}{\partial y} \frac{\partial \psi_{x2q}}{\partial y} \mathrm{d}y = \frac{nq}{b^2} \int_0^b \left(\frac{y}{b}\right)^{n+q-2} \mathrm{d}y = \frac{nq}{b(n+q-1)}, \\
\Delta_{00}^2 &= \int_0^b \psi_{x2n} \psi_{y2q} \mathrm{d}y = \int_0^b \left(\frac{y}{b}\right)^n \left(\frac{y}{b}\right)^{q-1} \mathrm{d}y = \frac{b}{n+q}, \\
\Delta_{01}^2 &= \int_0^b \psi_{x2n} \frac{\partial \psi_{y2q}}{\partial y} \mathrm{d}y = \frac{q-1}{b} \int_0^b \left(\frac{y}{b}\right)^n \left(\frac{y}{b}\right)^{q-2} \mathrm{d}y = \frac{q-1}{n+q-1}, \\
\Delta_{10}^2 &= \int_0^b \frac{\partial \psi_{x2n}}{\partial y} \psi_{y2q} \mathrm{d}y = \frac{n}{b} \int_0^b \left(\frac{y}{b}\right)^{n-1} \left(\frac{y}{b}\right)^{q-1} \mathrm{d}y = \frac{n}{n+q-1}, \\
\Delta_{11}^2 &= \int_0^b \frac{\partial \psi_{x2n}}{\partial y} \frac{\partial \psi_{y2q}}{\partial y} \mathrm{d}y = \frac{(q-1)\,n}{b^2} \int_0^b \left(\frac{y}{b}\right)^{n-1} \left(\frac{y}{b}\right)^{q-2} \mathrm{d}y
\end{aligned}
$$

$$= \frac{(q-1)\,n}{b\,(n+q-2)} \text{ if } \quad n+q \neq 2,$$

$$\Delta_{00}^{3} = \int_0^b \psi_{y2n}\psi_{y2q}\mathrm{d}y = \int_0^b \left(\frac{y}{b}\right)^{n-1}\left(\frac{y}{b}\right)^{q-1}\mathrm{d}y = \frac{b}{n+q-1},$$

$$\Delta_{01}^{3} = \int_0^b \psi_{y2n}\frac{\partial \psi_{y2q}}{\partial y}\mathrm{d}y = \frac{q-1}{b}\int_0^b \left(\frac{y}{b}\right)^{n-1}\left(\frac{y}{b}\right)^{q-2}\mathrm{d}y$$

$$= \frac{q-1}{n+q-2} \text{ if } \quad n+q \neq 2,$$

$$\Delta_{10}^{3} = \int_0^b \frac{\partial \psi_{y2n}}{\partial y}\psi_{y2q}\mathrm{d}y = \frac{n-1}{b}\int_0^b \left(\frac{y}{b}\right)^{n-2}\left(\frac{y}{b}\right)^{q-1}\mathrm{d}y$$

$$= \frac{n-1}{n+q-2} \text{ if } \quad n+q \neq 2,$$

$$\Delta_{11}^{3} = \int_0^b \frac{\partial \psi_{y2n}}{\partial y}\frac{\partial \psi_{y2q}}{\partial y}\mathrm{d}y = \frac{(n-1)\,(q-1)}{b^2}\int_0^b \left(\frac{y}{b}\right)^{n-2}\left(\frac{y}{b}\right)^{q-2}\mathrm{d}y$$

$$= \frac{(n-1)\,(q-1)}{b\,(n+q-3)} \text{ if } n+q \neq 3,$$

$$\Delta_{00}^{4} = \int_0^b w_{2n}w_{2q}\mathrm{d}y = \int_0^b \left(\frac{y}{b}\right)^{n}\left(\frac{y}{b}\right)^{q}\mathrm{d}y = \frac{b}{n+q+1},$$

$$\Delta_{01}^{4} = \int_0^b w_{2n}\frac{\partial w_{2q}}{\partial y}\mathrm{d}y = \frac{q}{b}\int_0^b \left(\frac{y}{b}\right)^{n}\left(\frac{y}{b}\right)^{q-1}\mathrm{d}y = \frac{q}{n+q},$$

$$\Delta_{10}^{4} = \int_0^b \frac{\partial w_{2n}}{\partial y}w_{2q}\mathrm{d}y = \frac{n}{b}\int_0^b \left(\frac{y}{b}\right)^{n-1}\left(\frac{y}{b}\right)^{q}\mathrm{d}y = \frac{n}{n+q},$$

$$\Delta_{11}^{4} = \int_0^b \frac{\partial w_{2n}}{\partial y}\frac{\partial w_{2q}}{\partial y}\mathrm{d}y = \frac{nq}{b^2}\int_0^b \left(\frac{y}{b}\right)^{n-1}\left(\frac{y}{b}\right)^{q-1}\mathrm{d}y = \frac{nq}{b\,(n+q-1)},$$

$$\Delta_{02}^{4} = \int_0^b w_{2n}\frac{\partial^2 w_{2q}}{\partial y^2}\mathrm{d}y = \frac{q\,(q-1)}{b^2}\int_0^b \left(\frac{y}{b}\right)^{n}\left(\frac{y}{b}\right)^{q-2}\mathrm{d}y = \frac{q\,(q-1)}{b\,(n+q-1)},$$

$$\Delta_{21}^{4} = \int_0^b \frac{\partial^2 w_{2n}}{\partial y^2}\frac{\partial w_{2q}}{\partial y}\mathrm{d}y = \frac{nq\,(n-1)}{b^3}\int_0^b \left(\frac{y}{b}\right)^{n-2}\left(\frac{y}{b}\right)^{q-1}\mathrm{d}y$$

$$= \frac{nq\,(n-1)}{b^2\,(n+q-2)} \text{ if } n+q \neq 2,$$

$$\Delta_{22}^{4} = \int_0^b \frac{\partial^2 w_{2n}}{\partial y^2}\frac{\partial^2 w_{2q}}{\partial y^2}\mathrm{d}y = \frac{nq\,(q-1)\,(n-1)}{b^4}\int_0^b \left(\frac{y}{b}\right)^{n-2}\left(\frac{y}{b}\right)^{q-2}\mathrm{d}y$$

$$= \frac{nq\,(n-1)\,(q-1)}{b^3\,(n+q-3)} \text{ if } \quad n+q \neq 3,$$

$$\Delta_{00}^{5} = \int_0^b w_{2n}\psi_{y2q}\mathrm{d}y = \int_0^b \left(\frac{y}{b}\right)^{n}\left(\frac{y}{b}\right)^{q-1}\mathrm{d}y = \frac{b}{n+q},$$

$$\Delta_{01}^{5} = \int_0^b w_{2n}\frac{\partial \psi_{y2q}}{\partial y}\mathrm{d}y = \frac{q-1}{b}\int_0^b \left(\frac{y}{b}\right)^{n}\left(\frac{y}{b}\right)^{q-2}\mathrm{d}y = \frac{q-1}{n+q-1},$$

$$
\begin{aligned}
\Delta_{10}^{5} &= \int_0^b \frac{\partial w_{2n}}{\partial y}\psi_{y2q}\mathrm{d}y = \frac{n}{b}\int_0^b \left(\frac{y}{b}\right)^{n-1}\left(\frac{y}{b}\right)^{q-1}\mathrm{d}y = \frac{n}{n+q-1},\\
\Delta_{11}^{5} &= \int_0^b \frac{\partial w_{2n}}{\partial y}\frac{\partial \psi_{y2q}}{\partial y}\mathrm{d}y = \frac{n\,(q-1)}{b^2}\int_0^b \left(\frac{y}{b}\right)^{n-1}\left(\frac{y}{b}\right)^{q-2}\mathrm{d}y\\
&= \frac{n\,(q-1)}{b(n+q-2)} \text{ if } n+q \geq 3,\\
\Delta_{20}^{5} &= \int_0^b \frac{\partial^2 w_{2n}}{\partial y^2}\psi_{y2q}\mathrm{d}y = \frac{n\,(n-1)}{b^2}\int_0^b \left(\frac{y}{b}\right)^{n-2}\left(\frac{y}{b}\right)^{q-1}\mathrm{d}y\\
&= \frac{n\,(n-1)}{b(n+q-2)} \text{ if } \quad n+q \neq 2,\\
\Delta_{21}^{5} &= \int_0^b \frac{\partial^2 w_{2n}}{\partial y^2}\frac{\partial \psi_{y2q}}{\partial y}\psi_{y2q}\mathrm{d}y = \frac{n\,(n-1)\,(q-1)}{b^3}\int_0^b \left(\frac{y}{b}\right)^{n-2}\left(\frac{y}{b}\right)^{q-2}\mathrm{d}y\\
&= \frac{n\,(n-1)\,(q-1)}{b(n+q-3)} \text{ if } \quad n+q \neq 3,\\
\Delta_{00}^{6} &= \int_0^b w_{2n}\psi_{x2q}\mathrm{d}y = \int_0^b \left(\frac{y}{b}\right)^{n}\left(\frac{y}{b}\right)^{q}\mathrm{d}y = \frac{b}{n+q+1},\\
\Delta_{01}^{6} &= \int_0^b w_{2n}\frac{\partial \psi_{x2q}}{\partial y}\mathrm{d}y = \frac{q}{b}\int_0^b \left(\frac{y}{b}\right)^{n}\left(\frac{y}{b}\right)^{q-1}\mathrm{d}y = \frac{q}{n+q},\\
\Delta_{10}^{6} &= \int_0^b \frac{\partial w_{2n}}{\partial y}\psi_{x2q}\mathrm{d}y = \frac{n}{b}\int_0^b \left(\frac{y}{b}\right)^{n-1}\left(\frac{y}{b}\right)^{q}\mathrm{d}y = \frac{n}{n+q},\\
\Delta_{11}^{6} &= \int_0^b \frac{\partial w_{2n}}{\partial y}\frac{\partial \psi_{x2q}}{\partial y}\mathrm{d}y = \frac{nq}{b^2}\int_0^b \left(\frac{y}{b}\right)^{n-1}\left(\frac{y}{b}\right)^{q-1}\mathrm{d}y = \frac{nq}{b\,(n+q-1)},\\
\Delta_{20}^{6} &= \int_0^b \frac{\partial^2 w_{2n}}{\partial y^2}\psi_{x2q}\mathrm{d}y = \frac{n\,(n-1)}{b^2}\int_0^b \left(\frac{y}{b}\right)^{n-2}\left(\frac{y}{b}\right)^{q}\mathrm{d}y = \frac{n\,(n-1)}{b\,(n+q-1)},\\
\Delta_{21}^{6} &= \int_0^b \frac{\partial^2 w_{2n}}{\partial y^2}\frac{\partial \psi_{x2q}}{\partial y}\mathrm{d}y = \frac{nq\,(n-1)}{b^3}\int_0^b \left(\frac{y}{b}\right)^{n-2}\left(\frac{y}{b}\right)^{q-1}\mathrm{d}y\\
&= \frac{nq\,(n-1)}{b^2\,(n+q-2)} \text{ if } \quad n+q \neq 2.
\end{aligned}
\tag{15.68}
$$

From (15.57) we obtain:

$$
Q_{00}^{nq} = \int_0^b w_{2n}w_{2q}y\mathrm{d}y = \int_0^b \left(\frac{y}{b}\right)^{n}\left(\frac{y}{b}\right)^{q}y\mathrm{d}y = \frac{b^2}{n+q+2}. \tag{15.69}
$$

The case considered here is that there is no elastic restraint at the edge $y = 0$, but an ideal hinged support, so that Eq. (15.59) does not apply.

15.3.1.5 Resultants with Respect to the y-Direction, Case 4

With Eq. (15.54) we obtain:

$$\Delta_{00}^{1}=\int_0^b \psi_{x2n}\psi_{x2q}\mathrm{d}y=\int_0^b \left(\frac{y}{b}\right)^{n+1}\left(\frac{y}{b}\right)^{q+1}\mathrm{d}y=\frac{b}{n+q+3},$$

$$\Delta_{01}^{1}=\int_0^b \psi_{x2n}\frac{\partial\psi_{x2q}}{\partial y}\mathrm{d}y=\frac{q+1}{b}\int\left(\frac{y}{b}\right)^{n+1}\left(\frac{y}{b}\right)^{q}\mathrm{d}y=\frac{1+q}{n+q+2},$$

$$\Delta_{11}^{1}=\int_0^b \frac{\partial\psi_{x2n}}{\partial y}\frac{\partial\psi_{x2q}}{\partial y}\mathrm{d}y=\frac{(n+1)(q+1)}{b^2}\int_0^b \left(\frac{y}{b}\right)^{n+q}\mathrm{d}y=\frac{(n+1)(q+1)}{b(n+q+1)},$$

$$\Delta_{00}^{2}=\int_0^b \psi_{x2n}\psi_{y2q}\mathrm{d}y=\int_0^b \left(\frac{y}{b}\right)^{n+1}\left(\frac{y}{b}\right)^{q+1}\mathrm{d}y=\frac{b}{n+q+3},$$

$$\Delta_{01}^{2}=\int_0^b \psi_{x2n}\frac{\partial\psi_{y2q}}{\partial y}\mathrm{d}y=\frac{q+1}{b}\int_0^b \left(\frac{y}{b}\right)^{n+1}\left(\frac{y}{b}\right)^{q}\mathrm{d}y=\frac{q+1}{n+q+2},$$

$$\Delta_{10}^{2}=\int_0^b \frac{\partial\psi_{x2n}}{\partial y}\psi_{y2q}\mathrm{d}y=\frac{n+1}{b}\int_0^b \left(\frac{y}{b}\right)^{n}\left(\frac{y}{b}\right)^{q+1}\mathrm{d}y=\frac{n+1}{n+q+2},$$

$$\Delta_{11}^{2}=\int_0^b \frac{\partial\psi_{x2n}}{\partial y}\frac{\partial\psi_{y2q}}{\partial y}\mathrm{d}y=\frac{(q+1)(n+1)}{b^2}\int_0^b \left(\frac{y}{b}\right)^{n}\left(\frac{y}{b}\right)^{q}\mathrm{d}y=\frac{(q+1)(n+1)}{b(n+q+1)},$$

$$\Delta_{00}^{3}=\int_0^b \psi_{y2n}^{fc}\psi_{y2q}^{fc}\mathrm{d}y=\int_0^b \left(\frac{y}{b}\right)^{n+1}\left(\frac{y}{b}\right)^{q+1}\mathrm{d}y=\frac{b}{n+q+3},$$

$$\Delta_{01}^{3}=\int_0^b \psi_{y2n}^{fc}\frac{\partial\psi_{y2q}^{fc}}{\partial y}\mathrm{d}y=\frac{q+1}{b}\int_0^b \left(\frac{y}{b}\right)^{n+1}\left(\frac{y}{b}\right)^{q}\mathrm{d}y=\frac{q+1}{n+q+2},$$

$$\Delta_{10}^{3}=\int_0^b \frac{\partial\psi_{y2n}^{fc}}{\partial y}\psi_{y2q}^{fc}\mathrm{d}y=\frac{n+1}{b}\int_0^b \left(\frac{y}{b}\right)^{n}\left(\frac{y}{b}\right)^{q+1}\mathrm{d}y=\frac{n+1}{n+q+2},$$

$$\Delta_{11}^{3}=\int_0^b \frac{\partial\psi_{y2n}^{fc}}{\partial y}\frac{\partial\psi_{y2q}^{fc}}{\partial y}\mathrm{d}y=\frac{(n+1)(q+1)}{b^2}\int_0^b \left(\frac{y}{b}\right)^{n}\left(\frac{y}{b}\right)^{q}\mathrm{d}y=\frac{(n+1)(q+1)}{b(n+q+1)},$$

$$\Delta_{00}^{4}=\int_0^b w_{2n}w_{2q}\mathrm{d}y=\int_0^b \left(\frac{y}{b}\right)^{n+1}\left(\frac{y}{b}\right)^{q+1}\mathrm{d}y=\frac{b}{n+q+3},$$

$$\Delta_{01}^{4}=\int_0^b w_{2n}\frac{\partial w_{2q}}{\partial y}\mathrm{d}y=\frac{q+1}{b}\int_0^b \left(\frac{y}{b}\right)^{n+1}\left(\frac{y}{b}\right)^{q}\mathrm{d}y=\frac{1+q}{n+q+2},$$

$$\Delta_{10}^{4}=\int_0^b \frac{\partial w_{2n}}{\partial y}w_{2q}\mathrm{d}y=\frac{n+1}{b}\int_0^b \left(\frac{y}{b}\right)^{n}\left(\frac{y}{b}\right)^{q+1}\mathrm{d}y=\frac{n+1}{n+q+2},$$

$$\Delta_{11}^{4}=\int_0^b \frac{\partial w_{2n}}{\partial y}\frac{\partial w_{2q}}{\partial y}\mathrm{d}y=\frac{(n+1)(q+1)}{b^2}\int_0^b \left(\frac{y}{b}\right)^{n}\left(\frac{y}{b}\right)^{q}\mathrm{d}y=\frac{(n+1)(q+1)}{b(n+q+1)},$$

$$\Delta_{02}^{4}=\int_0^b w_{2n}\frac{\partial^2 w_{2q}}{\partial y^2}\mathrm{d}y=\frac{q(q+1)}{b^2}\int_0^b \left(\frac{y}{b}\right)^{n+1}\left(\frac{y}{b}\right)^{q-1}\mathrm{d}y=\frac{q(q+1)}{b(n+q+1)},$$

$$\Delta_{21}^{4}=\int_0^b \frac{\partial^2 w_{2n}}{\partial y^2}\frac{\partial w_{2q}}{\partial y}\mathrm{d}y=\frac{n(q+1)(n+1)}{b^3}\int_0^b \left(\frac{y}{b}\right)^{n-1}\left(\frac{y}{b}\right)^{q}\mathrm{d}y=\frac{n(n+1)(q+1)}{b^2(n+q)},$$

$$\Delta_{22}^{4} = \int_0^b \frac{\partial^2 w_{2n}}{\partial y^2}\frac{\partial^2 w_{2q}}{\partial y^2}\mathrm{d}y = \frac{nq\,(q+1)\,(n+1)}{b^4}\int_0^b \left(\frac{y}{b}\right)^{n-1}\left(\frac{y}{b}\right)^{q-1}\mathrm{d}y$$
$$= \frac{nq\,(n+1)\,(q+1)}{b^3\,(n+q-1)} \text{ if } \; n+q \neq 3,$$
$$\Delta_{00}^{5} = \int_0^b w_{2n}w_{2q}\mathrm{d}y = \int_0^b \left(\frac{y}{b}\right)^{n+1}\left(\frac{y}{b}\right)^{q+1}\mathrm{d}y = \frac{b}{n+q+3},$$
$$\Delta_{01}^{5} = \int_0^b w_{2n}\frac{\partial w_{2q}}{\partial y}\mathrm{d}y = \frac{q+1}{b}\int_0^b \left(\frac{y}{b}\right)^{n+1}\left(\frac{y}{b}\right)^{q}\mathrm{d}y = \frac{1+q}{n+q+2},$$
$$\Delta_{10}^{5} = \int_0^b \frac{\partial w_{2n}}{\partial y}w_{2q}\mathrm{d}y = \frac{n+1}{b}\int_0^b \left(\frac{y}{b}\right)^{n}\left(\frac{y}{b}\right)^{q+1}\mathrm{d}y = \frac{n+1}{n+q+2},$$
$$\Delta_{11}^{5} = \int_0^b \frac{\partial w_{2n}}{\partial y}\frac{\partial w_{2q}}{\partial y}\mathrm{d}y = \frac{(n+1)\,(q+1)}{b^2}\int_0^b \left(\frac{y}{b}\right)^{n}\left(\frac{y}{b}\right)^{q}\mathrm{d}y = \frac{(n+1)\,(q+1)}{b\,(n+q+1)},$$
$$\Delta_{20}^{5} = \int_0^b \frac{\partial^2 w_{2n}}{\partial y^2}w_{2q}\mathrm{d}y = \frac{n\,(n+1)}{b^2}\int_0^b \left(\frac{y}{b}\right)^{n-1}\left(\frac{y}{b}\right)^{q+1}\mathrm{d}y = \frac{n\,(n+1)}{b\,(n+q+1)},$$
$$\Delta_{21}^{5} = \int_0^b \frac{\partial^2 w_{2n}}{\partial y^2}\frac{\partial w_{2q}}{\partial y}\mathrm{d}y = \frac{n\,(q+1)\,(n+1)}{b^3}\int_0^b \left(\frac{y}{b}\right)^{n-1}\left(\frac{y}{b}\right)^{q}\mathrm{d}y = \frac{n\,(n+1)\,(q+1)}{b^2\,(n+q)},$$
$$\Delta_{00}^{6} = \int_0^b w_{2n}\psi_{x2q}\mathrm{d}y = \int_0^b \left(\frac{y}{b}\right)^{n+1}\left(\frac{y}{b}\right)^{q+1}\mathrm{d}y = \frac{b}{n+q+3},$$
$$\Delta_{01}^{6} = \int_0^b w_{2n}\frac{\partial \psi_{x2q}}{\partial y}\mathrm{d}y = \frac{q+1}{b}\int_0^b \left(\frac{y}{b}\right)^{n+1}\left(\frac{y}{b}\right)^{q}\mathrm{d}y = \frac{1+q}{n+q+2},$$
$$\Delta_{10}^{6} = \int_0^b \frac{\partial w_{2n}}{\partial y}\psi_{x2q}\mathrm{d}y = \frac{n+1}{b}\int_0^b \left(\frac{y}{b}\right)^{n}\left(\frac{y}{b}\right)^{q+1}\mathrm{d}y = \frac{n+1}{n+q+2},$$
$$\Delta_{11}^{6} = \int_0^b \frac{\partial w_{2n}}{\partial y}\frac{\partial \psi_{x2q}}{\partial y}\mathrm{d}y = \frac{(n+1)\,(q+1)}{b^2}\int_0^b \left(\frac{y}{b}\right)^{n}\left(\frac{y}{b}\right)^{q}\mathrm{d}y = \frac{(n+1)\,(q+1)}{b\,(n+q+1)},$$
$$\Delta_{20}^{6} = \int_0^b \frac{\partial^2 w_{2n}}{\partial y^2}\psi_{x2q}\mathrm{d}y = \frac{n\,(n+1)}{b^2}\int_0^b \left(\frac{y}{b}\right)^{n-1}\left(\frac{y}{b}\right)^{q+1}\mathrm{d}y = \frac{n\,(n+1)}{b\,(n+q+1)},$$
$$\Delta_{21}^{6} = \int_0^b \frac{\partial^2 w_{2n}}{\partial y^2}\frac{\partial \psi_{x2q}}{\partial y}\mathrm{d}y = \frac{n\,(q+1)\,(n+1)}{b^3}\int_0^b \left(\frac{y}{b}\right)^{n-1}\left(\frac{y}{b}\right)^{q}\mathrm{d}y = \frac{n\,(n+1)\,(q+1)}{b^2\,(n+q)}. \tag{15.70}$$

Equation (15.57) yields:

$$Q_{00}^{nq} = \int_0^b w_{2n}w_{2q}y\mathrm{d}y = \int_0^b \left(\frac{y}{b}\right)^{n+1}\left(\frac{y}{b}\right)^{q+1}y\mathrm{d}y = \frac{b^2}{n+q+4}. \tag{15.71}$$

Equation (15.59) leads to vanishing values due to the fixed restraint at the edge $y = 0$ and the free edge at $y = b$.

Reference

Mittelstedt S, Mittelstedt C (2019): *Globale Stabilität schubweicher anisotroper hochbelasteter Laminat-und Sandwich-Träger unter kombinierter Belastung im Brücken-und allgemeinen Ingenieurhochbau*, Abschlussbericht zum Projekt im Rahmen der Forschungsinitiative Zukunft Bau, SWD-10.08.18.7-15.62, Hamburg, Germany, November 2019.



Buckling of Unsymmetric Laminates

16

In this chapter we consider both a closed-form analysis approach and Lévy-type solutions for the buckling analysis of unsymmetric cross-ply and angle-ply laminates under two different types of boundary conditions (see Fig. 16.1). The configuration of Fig. 16.1, top (hereinafter referred to as SRSR plate), is a laminate that is simply supported at all edges and is also subject to elastic restraints at the two unloaded longitudinal edges, whereby the restraint stiffnesses are denoted as k_0 and k_b respectively. The second case shown in Fig. 16.1, bottom, is referred to as an SFSR plate. This is a laminate that is simply supported at three edges and free at the edge $y = b$. The simply supported unloaded longitudinal edge is subject to the clamping stiffness k_0. Both laminate configurations are subjected to a uniaxial compressive load. The solutions presented in this chapter are developed both for the Classical Laminated Plate Theory (abbreviated as CLPT) and for the First and Third-Order Shear Deformation Theories (referred to as FSDT and TSDT, respectively). This chapter is based on the two papers by Schreiber and Mittelstedt [11, 12].

16.1 Closed-Form Analysis Approach

16.1.1 Analysis Approach

The total potential of the considered laminates in the buckled state is composed of the inner potential Π_i and the external potential Π_a, which can be expressed as follows:

$$\Pi_i = \frac{1}{2}\int_0^b \int_0^a \underline{\varepsilon}^T \underline{\overline{N}}\, \mathrm{d}x\, \mathrm{d}y,$$
$$\Pi_a = -\frac{N_{xx}^0}{2}\int_0^b \int_0^a \left(\frac{\partial w_0}{\partial x}\right)^2 \mathrm{d}x\, \mathrm{d}y. \tag{16.1}$$

© The Author(s), under exclusive license to Springer-Verlag GmbH, DE, part of Springer Nature 2025

C. Mittelstedt, *Mechanics of Composite Structures*,
https://doi.org/10.1007/978-3-662-70788-3_16

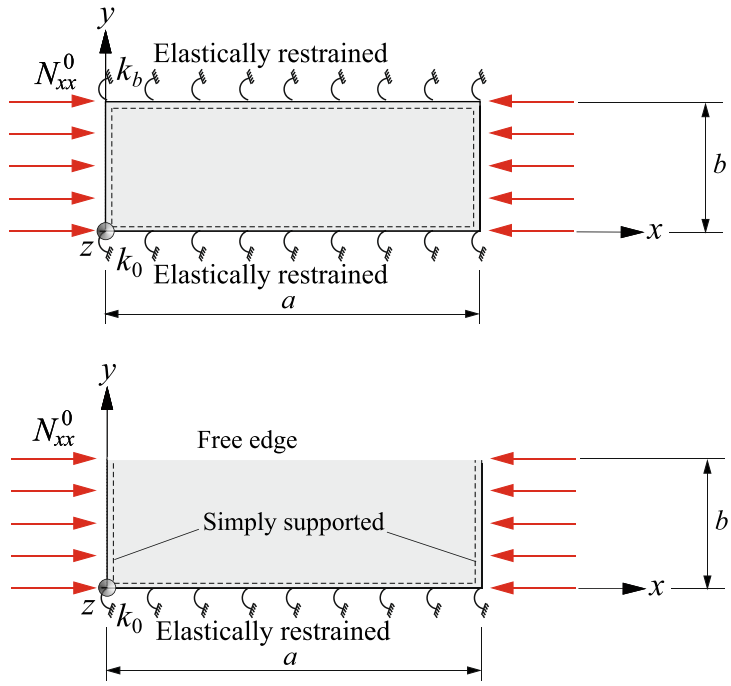


Fig. 16.1 Considered boundary conditions: SRSR plate (top), SFSR plate (bottom)

The constitutive law for the laminate theories considered here can be stated as:

$$\underline{\overline{N}} = \underline{\underline{C}}\,\underline{\varepsilon}. \tag{16.2}$$

Herein, $\underline{\overline{N}}$ is the vector of laminate forces and moments, whereas $\underline{\underline{C}}$ is the stiffness matrix and $\underline{\varepsilon}$ is the strain vector. For the laminate theories considered in this chapter, we obtain the following constitutive relations:

$$\text{CLPT:} \begin{pmatrix} \underline{N}^0 \\ \underline{M}^0 \end{pmatrix} = \begin{bmatrix} \underline{\underline{A}} & \underline{\underline{B}} \\ \underline{\underline{B}} & \underline{\underline{D}} \end{bmatrix} \begin{pmatrix} \underline{\varepsilon}^{(1)} \\ \underline{\kappa}^0 \end{pmatrix},$$

$$\text{FSDT:} \begin{pmatrix} \underline{N}^0 \\ \underline{M}^0 \\ \underline{Q} \end{pmatrix} = \begin{bmatrix} \underline{\underline{A}} & \underline{\underline{B}} & \underline{\underline{0}} \\ \underline{\underline{B}} & \underline{\underline{D}} & \underline{\underline{0}} \\ \underline{\underline{0}} & \underline{\underline{0}} & K\underline{\underline{A}}_S \end{bmatrix} \begin{pmatrix} \underline{\varepsilon}^{(1)} \\ \underline{\varepsilon}^{(2)} \\ \underline{\gamma}^{(1)} \end{pmatrix},$$

$$\text{TSDT:} \begin{pmatrix} \underline{N}^0 \\ \underline{M}^0 \\ \underline{P} \\ \underline{Q} \\ \underline{R} \end{pmatrix} = \begin{bmatrix} \underline{\underline{A}} & \underline{\underline{B}} & \underline{\underline{E}} & \underline{\underline{0}} & \underline{\underline{0}} \\ \underline{\underline{B}} & \underline{\underline{D}} & \underline{\underline{F}} & \underline{\underline{0}} & \underline{\underline{0}} \\ \underline{\underline{E}} & \underline{\underline{F}} & \underline{\underline{H}} & \underline{\underline{0}} & \underline{\underline{0}} \\ \underline{\underline{0}} & \underline{\underline{0}} & \underline{\underline{0}} & \underline{\underline{A}}_S & \underline{\underline{D}}_S \\ \underline{\underline{0}} & \underline{\underline{0}} & \underline{\underline{0}} & \underline{\underline{D}}_S & \underline{\underline{F}}_S \end{bmatrix} \begin{pmatrix} \underline{\varepsilon}^{(1)} \\ \underline{\varepsilon}^{(2)} \\ \underline{\varepsilon}^{(3)} \\ \underline{\gamma}^{(1)} \\ \underline{\gamma}^{(2)} \end{pmatrix}, \tag{16.3}$$

where K is the shear correction factor. The individual strain vectors are

$$\underline{\varepsilon}^{(1)} = \begin{pmatrix} \frac{\partial u_0}{\partial x} \\ \frac{\partial v_0}{\partial y} \\ \frac{\partial u_0}{\partial y} + \frac{\partial v_0}{\partial x} \end{pmatrix}, \quad \underline{\varepsilon}^{(2)} = \begin{pmatrix} \frac{\partial \psi_x}{\partial x} \\ \frac{\partial \psi_y}{\partial y} \\ \frac{\partial \psi_x}{\partial y} + \frac{\partial \psi_y}{\partial x} \end{pmatrix},$$

$$\underline{\varepsilon}^{(3)} = \begin{pmatrix} -\frac{4}{3h^2}\left(\frac{\partial \psi_x}{\partial x} + \frac{\partial^2 w_0}{\partial x^2}\right) \\ -\frac{4}{3h^2}\left(\frac{\partial \psi_y}{\partial y} + \frac{\partial^2 w_0}{\partial y^2}\right) \\ -\frac{4}{3h^2}\left(\frac{\partial \psi_x}{\partial y} + \frac{\partial \psi_y}{\partial x} + 2\frac{\partial^2 w_0}{\partial x \partial y}\right) \end{pmatrix}, \quad \underline{\kappa}^0 = \begin{pmatrix} -\frac{\partial^2 w_0}{\partial x^2} \\ -\frac{\partial^2 w_0}{\partial y^2} \\ -2\frac{\partial^2 w_0}{\partial x \partial y} \end{pmatrix},$$

$$\underline{\gamma}^{(1)} = \begin{pmatrix} \frac{\partial w_0}{\partial y} + \psi_y \\ \frac{\partial w_0}{\partial x} + \psi_x \end{pmatrix}, \quad \underline{\gamma}^{(2)} = \begin{pmatrix} -\frac{4}{h^2}\left(\psi_y + \frac{\partial w_0}{\partial y}\right) \\ -\frac{4}{h^2}\left(\psi_x + \frac{\partial w_0}{\partial x}\right) \end{pmatrix}. \tag{16.4}$$

In addition, the energy stored in the elastic restraints at the laminate edges must be added. Due to the different definition of the rotation angles in the context of CLPT and FSDT/TSDT, there are also different definitions of Π_s. The following applies within the framework of CLPT:

$$\Pi_s = \frac{1}{2}\int_0^a \left[k_0 \left(\left.\frac{\partial w_0}{\partial y}\right|_{y=0} \right)^2 + k_b \left(\left.\frac{\partial w_0}{\partial y}\right|_{y=b} \right)^2 \right] \mathrm{d}x. \tag{16.5}$$

For FSDT and TSDT we obtain:

$$\Pi_s = \frac{1}{2}\int_0^a \left(k_0 \left[\psi_y(x,0)\right]^2 + k_b \left[\psi_y(x,b)\right]^2 \right) \mathrm{d}x. \tag{16.6}$$

The total elastic potential Π then follows as:

$$\Pi = \Pi_i + \Pi_a + \Pi_s. \tag{16.7}$$

Two different types of boundary conditions are considered. The so-called SRSR plate is simply supported at the two opposing loaded edges and provided with additional elastic restraints at the two unloaded edges (restraint stiffnesses k_0 and k_b). The SFSR plate type is similar to the SRSR plate, with the difference that one of the unloaded edges is free of any support with no rotational restraints. For this case, $k_b = 0$ is applied. Due to the bending-extension coupling of unsymmetric laminates, inplane displacements occur in the deformed state. Therefore, in addition to the out-of-plane boundary conditions, boundary conditions must also be defined in the plane. At $x = 0, a$, the following applies to the simply supported edges (labelled with the letter S):

$$\left.\begin{array}{l}\text{Cross-ply:}\\ N^0_{xx}=v_0=0,\\ \text{Angle-ply:}\\ N^0_{xy}=u_0=0.\end{array}\right\}\left\{\begin{array}{l}\text{CLPT:}\\ w_0=M^0_{xx}=0,\\ \text{FSDT:}\\ w_0=M^0_{xx}=\psi_y=0,\\ \text{TSDT:}\\ w_0=M^0_{xx}=\psi_y=P_{xx}=0.\end{array}\right. \tag{16.8}$$

The following applies to the elastically restrained edges (labelled as R, based on the term 'rotational restraint') at the edges $y=0, b$:

$$\left.\begin{array}{l}\text{Cross-ply}\\ N^0_{yy}=u_0=0,\\ \text{Angle-ply:}\\ N^0_{xy}=v_0=0.\end{array}\right\}\left\{\begin{array}{l}\text{CLPT:}\\ w_0=\left\{\begin{array}{l}\left(-M^0_{yy}-k_0\frac{\partial w_0}{\partial y}\right)_{y=0}=0,\\ \left(M^0_{yy}-k_b\frac{\partial w_0}{\partial y}\right)_{y=b}=0.\end{array}\right.\\ \text{FSDT:}\\ w_0=\psi_x=\left\{\begin{array}{l}\left(-M^0_{yy}+k_0\psi_y\right)_{y=0}=0,\\ \left(M^0_{yy}+k_b\psi_y\right)_{y=b}=0.\end{array}\right.\\ \text{TSDT:}\\ w_0=\psi_x\\ =P_{yy}=\left\{\begin{array}{l}\left(-M^0_{yy}+\frac{4}{3h^2}P_{yy}+k_0\psi_y\right)_{y=0}=0,\\ \left(M^0_{yy}-\frac{4}{3h^2}P_{yy}+k_b\psi_y\right)_{y=b}=0.\end{array}\right.\end{array}\right. \tag{16.9}$$

At the edge $y=b$, the following applies for the free laminate edge (labelled as F):

$$\left.\begin{array}{c}\text{Cross-ply,}\\ \text{Angle-ply:}\\ N^0_{yy}=N^0_{xy}=0.\end{array}\right\}\left\{\begin{array}{l}\text{CLPT:}\\ M^0_{yy}=\frac{\partial M^0_{yy}}{\partial y}+2\frac{\partial M^0_{xy}}{\partial x}=0,\\ \text{FSDT:}\\ M^0_{yy}=M^0_{xy}=Q_y=0,\\ \text{TSDT:}\\ \left\{\begin{array}{l}M^0_{yy}-\frac{4}{3h^2}P_{yy}=P_{yy}=M^0_{xy}-\frac{4}{3h^2}P_{xy}\\ =\frac{4}{3h^2}\left(\frac{\partial P_{yy}}{\partial y}+2\frac{\partial P_{xy}}{\partial x}\right)+Q_y-\frac{4}{h^2}R_y=0.\end{array}\right.\end{array}\right. \tag{16.10}$$

The shape functions to be used for the closed-form analysis approach are applied in a separation form with regard to the x- and the y-direction. The approach can be written in general form as shown in Eq. (16.11):

$$\Phi_{1,\ldots,n} = c_{1,\ldots,n}\, \Phi^{(1)}_{1,\ldots,n} \Phi^{(2)}_{1,\ldots,n}, \begin{cases} n = 3 \text{ for CLPT} \\ n = 5 \text{ for FSDT and TSDT} \end{cases}, \tag{16.11}$$

wherein

$$\Phi_i = \begin{pmatrix} u_0\,(x,\,y) \\ v_0\,(x,\,y) \\ w_0\,(x,\,y) \\ \psi_x\,(x,\,y) \\ \psi_y\,(x,\,y) \end{pmatrix}, \quad c_i = \begin{pmatrix} U \\ V \\ W \\ X \\ Y \end{pmatrix},$$

$$\Phi^{(1)}_i = \begin{pmatrix} u_1\,(x) \\ v_1\,(x) \\ w_1\,(x) \\ \psi_{x_1}\,(x) \\ \psi_{y_1}\,(x) \end{pmatrix}, \quad \Phi^{(2)}_i = \begin{pmatrix} u_2\,(y) \\ v_2\,(y) \\ w_2\,(y) \\ \psi_{x_2}\,(y) \\ \psi_{y_2}\,(y) \end{pmatrix}. \tag{16.12}$$

Here, $\underline{c}$ is the vector of Ritz constants, which describe the amplitude of the shape functions.

If the shape functions (16.11) are inserted into the total elastic potential (16.7) for the different laminate theories CLPT, FSDT and TSDT, the following form results for all considered laminate theories:

$$\Pi = \frac{1}{2}\, \underline{c}^T\, \underline{\underline{\Lambda}}\, \underline{c} = \frac{1}{2}\, \Lambda_{ij} c_j c_i, \begin{cases} i,\, j = 1, 2, 3 \quad \text{for CLPT} \\ i,\, j = 1, \ldots, 5 \text{ for FSDT and TSDT} \end{cases}, \tag{16.13}$$

with

$$\Lambda_{ij} = \begin{bmatrix} \lambda_{11} & \lambda_{12} & \lambda_{13} & \lambda_{14} & \lambda_{15} \\ \lambda_{12} & \lambda_{22} & \lambda_{23} & \lambda_{24} & \lambda_{25} \\ \lambda_{13} & \lambda_{23} & N^0_{xx}\overline{\lambda}_{33} + \lambda_{33} & \lambda_{34} & \lambda_{35} \\ \lambda_{14} & \lambda_{24} & \lambda_{34} & \lambda_{44} & \lambda_{45} \\ \lambda_{15} & \lambda_{25} & \lambda_{35} & \lambda_{45} & \lambda_{55} \end{bmatrix}, \begin{cases} i,\, j = 1, 2, 3 \\ \text{for CLPT,} \\ i,\, j = 1, \ldots, 5 \\ \text{for FSDT} \\ \text{and TSDT.} \end{cases} \tag{16.14}$$

The entries Λ_{ij} of the above matrix representation contain stiffness parameters and integral quantities and are defined as follows. Due to the separation approach used, the integral expressions can be divided into integrals with respect to the x- and the y-direction. They are defined as follows:

$$I^{kl}_{ij} = \int_0^a \frac{\mathrm{d}^k \Phi^{(1)}_i}{\mathrm{d}x^k} \frac{\mathrm{d}^l \Phi^{(1)}_j}{\mathrm{d}x^l}\, \mathrm{d}x, \quad J^{kl}_{ij} = \int_0^b \frac{\mathrm{d}^k \Phi^{(2)}_i}{\mathrm{d}y^k} \frac{\mathrm{d}^l \Phi^{(2)}_j}{\mathrm{d}y^l}\, \mathrm{d}y, \tag{16.15}$$

with the shape functions $\Phi_i^{(1)}$ and $\Phi_i^{(2)}$. Here, i and j indicate the respective shape function, and k and l represent the respective derivative. For $k = 0$ or $l = 0$ no derivative exists.

There are differences between the employed laminate theories at the elastically restrained edges. In addition, the integration over y is not necessary here, since in Π_s only x has to be integrated. For CLPT we obtain:

$$C_{\mathrm{rot},0} = \left(\left. \frac{\mathrm{d}w_2}{\mathrm{d}y} \right|_{y=0} \right)^2, \quad C_{\mathrm{rot},b} = \left(\left. \frac{\mathrm{d}w_2}{\mathrm{d}y} \right|_{y=b} \right)^2. \tag{16.16}$$

For FSDT and TSDT we have:

$$C_{rot,0} = \left(\psi_{y_2}(0)\right)^2, \quad C_{rot,b} = \left(\psi_{y_2}(b)\right)^2. \tag{16.17}$$

The entries of Λ_{ij} that apply to CLPT, FSDT and TSDT together are given below:

$$\begin{aligned}
\lambda_{11} &= A_{11}\, I_{11}^{11} J_{11}^{00} + I_{11}^{00} J_{11}^{11} A_{66}, \\
\lambda_{12} &= A_{12}\, I_{12}^{10} J_{12}^{01} + I_{12}^{01} J_{12}^{10} A_{66}, \\
\lambda_{22} &= A_{22}\, I_{22}^{00} J_{22}^{11} + I_{22}^{11} J_{22}^{00} A_{66}, \\
\overline{\lambda}_{33} &= -I_{33}^{11} J_{33}^{00}.
\end{aligned} \tag{16.18}$$

Below we find the entries of Λ_{ij}, which differ for CLPT, FSDT and TSDT:

CLPT:

$$\begin{aligned}
\lambda_{13} &= -B_{11}\, I_{13}^{12} J_{13}^{00} - I_{13}^{10} J_{13}^{02} B_{12} - 2\, B_{16}\, I_{13}^{11} J_{13}^{01} - B_{16}\, I_{13}^{02} J_{13}^{10} \\
&\quad - B_{26} I_{13}^{00} J_{13}^{12} - 2\, B_{66} I_{13}^{01} J_{13}^{11}, \\
\lambda_{23} &= -B_{12} I_{23}^{02} J_{23}^{10} - B_{16} I_{23}^{12} J_{23}^{00} - B_{22}\, I_{23}^{00} J_{23}^{12} - 2\, B_{26}\, I_{23}^{01} J_{23}^{11} \\
&\quad - B_{26}\, I_{23}^{10} J_{23}^{02} - 2\, B_{66} I_{23}^{11} J_{23}^{01}, \\
\lambda_{33} &= \left(D_{22}\, J_{33}^{22} + k_0\, C_{\mathrm{rot},0} + k_b\, C_{\mathrm{rot},b}\right) I_{33}^{00} + 4\, D_{66}\, I_{33}^{11} J_{33}^{11} \\
&\quad + D_{11}\, J_{33}^{00} I_{33}^{22} + 2\, D_{12}\, I_{33}^{02} J_{33}^{02}.
\end{aligned} \tag{16.19}$$

FSDT:

$$\begin{aligned}
\lambda_{13} &= 0, \\
\lambda_{14} &= B_{11}\, I_{14}^{11} J_{14}^{00} + B_{16}\, I_{14}^{10} J_{14}^{01} + B_{16}\, I_{14}^{01} J_{14}^{10} + I_{14}^{00} J_{14}^{11} B_{66}, \\
\lambda_{15} &= I_{15}^{10} J_{15}^{01} B_{12} + B_{16}\, I_{15}^{11} J_{15}^{00} + B_{26}\, I_{15}^{00} J_{15}^{11} + B_{66}\, I_{15}^{01} J_{15}^{10}, \\
\lambda_{23} &= 0, \\
\lambda_{24} &= I_{24}^{01} J_{24}^{10} B_{12} + I_{24}^{11} J_{24}^{00} B_{16} + I_{24}^{00} J_{24}^{11} B_{26} + I_{24}^{10} J_{24}^{01} B_{66}, \\
\lambda_{25} &= B_{22}\, I_{25}^{00} J_{25}^{11} + B_{26}\, I_{25}^{10} J_{25}^{01} + B_{26}\, I_{25}^{01} J_{25}^{10} + I_{25}^{11} J_{25}^{00} B_{66}, \\
\lambda_{33} &= K \left(A_{44}\, I_{33}^{00} J_{33}^{11} + A_{55}\, I_{33}^{11} J_{33}^{00}\right),
\end{aligned}$$

$$
\begin{aligned}
\lambda_{34} &= A_{55}\, K\, I_{34}^{10}\, J_{34}^{00},\\
\lambda_{35} &= A_{44}\, K\, I_{35}^{00}\, J_{35}^{10},\\
\lambda_{44} &= \left(A_{55}\, K\, I_{44}^{00} + D_{11}\, I_{44}^{11}\right) J_{44}^{00} + I_{44}^{00}\, J_{44}^{11}\, D_{66},\\
\lambda_{45} &= D_{12}\, I_{45}^{10}\, J_{45}^{01} + D_{66}\, I_{45}^{01}\, J_{45}^{10},\\
\lambda_{55} &= \left(A_{44}\, K\, J_{55}^{00} + D_{22}\, J_{55}^{11} + k_0\, C_{\mathrm{rot},0} + k_b\, C_{\mathrm{rot},b}\right) I_{55}^{00}\\
&\quad + D_{66}\, J_{55}^{00} I_{55}^{11}.
\end{aligned}
\tag{16.20}
$$

TSDT:

$$
\begin{aligned}
\lambda_{13} &= -\tau\, \left(2\, E_{16}\, I_{13}^{11} J_{13}^{01} + E_{16}\, I_{13}^{02} J_{13}^{10} + E_{26}\, I_{13}^{00} J_{13}^{12}\right.\\
&\quad \left. +2\, E_{66}\, I_{13}^{01} J_{13}^{11} + E_{11}\, I_{13}^{12} J_{13}^{00} + E_{12}\, I_{13}^{10} J_{13}^{02}\right),\\
\lambda_{14} &= -\left(E_{11}\,\tau - B_{11}\right) J_{14}^{00} I_{14}^{11} - \left(E_{66}\,\tau - B_{66}\right) J_{14}^{11} I_{14}^{00}\\
&\quad - \left(E_{16}\,\tau - B_{16}\right)\left(J_{14}^{10} I_{14}^{01} + J_{14}^{01} I_{14}^{10}\right),\\
\lambda_{15} &= -\left(E_{26}\,\tau - B_{26}\right) J_{15}^{11} I_{15}^{00} - \left(E_{66}\,\tau - B_{66}\right) J_{15}^{10} I_{15}^{01}\\
&\quad - \left(E_{12}\,\tau - B_{12}\right) J_{15}^{01} I_{15}^{10} - \left(E_{16}\,\tau - B_{16}\right) J_{15}^{00} I_{15}^{11},\\
\lambda_{23} &= -\tau\, \left(E_{12}\, I_{23}^{02} J_{23}^{10} + E_{16}\, I_{23}^{12} J_{23}^{00} + E_{22}\, I_{23}^{00} J_{23}^{12}\right.\\
&\quad \left. +2\, E_{26}\, I_{23}^{01} J_{23}^{11} + E_{26}\, I_{23}^{10} J_{23}^{02} + 2\, E_{66}\, I_{23}^{11} J_{23}^{01}\right),\\
\lambda_{24} &= -\left(E_{26}\,\tau - B_{26}\right) J_{24}^{11} I_{24}^{00} - \left(E_{12}\,\tau - B_{12}\right) J_{24}^{10} I_{24}^{01}\\
&\quad - \left(E_{66}\,\tau - B_{66}\right) J_{24}^{01} I_{24}^{10} - \left(E_{16}\,\tau - B_{16}\right) J_{24}^{00} I_{24}^{11},\\
\lambda_{25} &= -\left(E_{22}\,\tau - B_{22}\right) J_{25}^{11} I_{25}^{00} - \left(E_{66}\,\tau - B_{66}\right) J_{25}^{00} I_{25}^{11}\\
&\quad - \left(E_{26}\,\tau - B_{26}\right)\left(J_{25}^{10} I_{25}^{01} + J_{25}^{01} I_{25}^{10}\right),\\
\lambda_{33} &= \left[\left(9\, F_{44}\,\tau^2 - 6\, D_{44}\,\tau + A_{44}\right) J_{33}^{11} + H_{22}\, J_{33}^{22}\tau^2\right] I_{33}^{00}\\
&\quad + \left[\left(9\, F_{55}\,\tau^2 - 6\, D_{55}\,\tau + A_{55}\right) J_{33}^{00} + 4\, H_{66}\, J_{33}^{11}\tau^2\right] I_{33}^{11}\\
&\quad + \tau^2\left(H_{11}\, J_{33}^{00} I_{33}^{22} + 2\, H_{12}\, J_{33}^{02} I_{33}^{02}\right),\\
\lambda_{34} &= \left[\left(9\, F_{55}\,\tau^2 - 6\, D_{55}\,\tau + A_{55}\right) J_{34}^{00} + 2\,\tau\left(H_{66}\,\tau - F_{66}\right) J_{34}^{11}\right] I_{34}^{10}\\
&\quad + \left[\left(H_{11}\,\tau - F_{11}\right) J_{34}^{00} I_{34}^{21} + \left(H_{12}\,\tau - F_{12}\right) J_{34}^{20} I_{34}^{01}\right]\tau,\\
\lambda_{35} &= \left[\left(9\, F_{44}\,\tau^2 - 6\, D_{44}\,\tau + A_{44}\right) J_{35}^{10} + \tau\, \left(H_{22}\,\tau - F_{22}\right) J_{35}^{21}\right] I_{35}^{00}\\
&\quad + \left[2\, \left(H_{66}\,\tau - F_{66}\right) J_{35}^{10} I_{35}^{11} + \left(H_{12}\,\tau - F_{12}\right) J_{35}^{01} I_{35}^{20}\right]\tau,\\
\lambda_{44} &= \left(9\, F_{55}\,\tau^2 - 6\, D_{55}\,\tau + A_{55}\right) J_{44}^{00} I_{44}^{00}\\
&\quad + \left(H_{66}\,\tau^2 - 2\, F_{66}\,\tau + D_{66}\right) J_{44}^{11} I_{44}^{00}\\
&\quad + \left(H_{11}\,\tau^2 - 2\, F_{11}\,\tau + D_{11}\right) J_{44}^{00} I_{44}^{11},\\
\lambda_{45} &= \left(H_{66}\,\tau^2 - 2\, F_{66}\,\tau + D_{66}\right) J_{45}^{10} I_{45}^{01}\\
&\quad + \left(H_{12}\,\tau^2 - 2\, F_{12}\,\tau + D_{12}\right) J_{45}^{01} I_{45}^{10},\\
\lambda_{55} &= \left(9\, F_{44}\,\tau^2 - 6\, D_{44}\,\tau + A_{44}\right) J_{55}^{00} I_{55}^{00}
\end{aligned}
$$

$$
\begin{aligned}
&+ \left(H_{22}\,\tau^2 - 2\,F_{22}\,\tau + D_{22}\right) J_{55}^{11}\, I_{55}^{00} \\
&+ \left(H_{66}\,\tau^2 - 2\,F_{66}\,\tau + D_{66}\right) I_{55}^{11}\, J_{55}^{00} \\
&+ \left(k_0 C_{\mathrm{rot},0} + k_b\, C_{\mathrm{rot},b}\right) I_{55}^{00}, \qquad (16.21)
\end{aligned}
$$

with $\tau = \frac{4}{3h^2}$.

The beginning of the bifurcation of the equilibrium, i.e. the infinitesimally deformed state of the considered laminate under uniaxial compressive load N_{xx}^0, is a state of indifferent equilibrium, which means that in this state the first variation of the total elastic potential Π disappears, i.e. $\delta\Pi = 0$. In the present case, this reduces to the Ritz equations as follows

$$
\frac{\partial \Pi}{\partial c_i} = \Lambda_{ij} c_j = 0, \begin{cases} i,j = 1,2,3 & \text{for CLPT,} \\ i,j = 1,\ldots,5 & \text{for FSDT and TSDT.} \end{cases} \qquad (16.22)
$$

In order to avoid a trivial solution for the system of equations (16.22), the coefficient determinant is required to vanish, i.e. $(\det(\Lambda_{ij}) = 0)$. Finally, for CLPT, the following expression for the buckling load N_{xx}^0 results:

$$
N_{xx}^0 = -\frac{\lambda_{11}\lambda_{22}\lambda_{33} - \lambda_{11}\lambda_{23}{}^2 - \lambda_{12}{}^2\lambda_{33} + 2\,\lambda_{12}\lambda_{13}\lambda_{23} - \lambda_{13}{}^2\lambda_{22}}{\bar{\lambda}_{33}\left(\lambda_{11}\lambda_{22} - \lambda_{12}{}^2\right)}. \qquad (16.23)
$$

The non-trivial solution in the context of FSDT and TSDT also results from $\det(\Lambda_{ij}) = 0$. In order to be able to represent this for a 5×5 matrix, we introduce a tensor notation. This requires the Levi-Civita symbol, which is defined as follows:

$$
\varepsilon_{ijklm} = \begin{cases} 1, & (i,j,k,\ldots) \text{ even permutation of } (1,2,3,\ldots), \\ -1, & (i,j,k,\ldots) \text{ odd Permutation of } (1,2,3,\ldots), \\ 0, & \text{else.} \end{cases} \qquad (16.24)
$$

Alternatively, (16.24) can also be represented as a product, as shown in (16.25):

$$
\varepsilon_{i_1\ldots i_n} = \prod_{p=1}^{n-1} \left(\prod_{q=p+1}^{n-1} \frac{i_p - i_q}{p - q} \right), \qquad (16.25)
$$

whereby the evaluation for the 5 indices leads to Eq. (16.26).

$$
\begin{aligned}
\varepsilon_{ijklm} = \frac{1}{288}\,&(i-j)\,(i-k)\,(i-l)\,(i-m)\,(j-k) \\
&(j-l)\,(j-m)\,(k-l)\,(k-m)\,(l-m)\,. \qquad (16.26)
\end{aligned}
$$

The solution for N_{xx}^0 in the context of FSDT and the TSDT can then be given as follows:

$$N_{xx}^0 = -\frac{\sum_{i=1}^{5}\sum_{j=1}^{5}\sum_{k=1}^{5}\sum_{l=1}^{5}\sum_{m=1}^{5}\varepsilon_{ijklm}\lambda_{1i}\lambda_{2j}\lambda_{3k}\lambda_{4l}\lambda_{5m}}{\sum_{i=1}^{5}\sum_{j=1}^{5}\sum_{l=1}^{5}\sum_{m=1}^{5}\varepsilon_{ij3lm}\lambda_{1i}\lambda_{2j}\bar{\lambda}_{33}\lambda_{4l}\lambda_{5m}}. \tag{16.27}$$

In Eq. (16.27) the symmetry property $\Lambda_{ij} = \Lambda_{ji}$ must be taken into account.

In the case of a symmetric laminate or when using the reduced bending stiffness method (RBS method for short, see Sect. 16.1.3), the solution for N_{xx}^0 can be simplified. The inplane displacements (u_0, v_0) are no longer required in connection with a buckling analysis. This results in the following solution for CLPT:

$$N_{xx}^0 = -\frac{\lambda_{33}}{\bar{\lambda}_{33}}. \tag{16.28}$$

For FSDT and TSDT follows:

$$N_{xx}^0 = -\frac{\lambda_{33}\lambda_{44}\lambda_{55} - \lambda_{33}\lambda_{45}{}^2 - \lambda_{34}{}^2\lambda_{55} + 2\,\lambda_{34}\lambda_{45}\lambda_{35} - \lambda_{35}{}^2\lambda_{44}}{\bar{\lambda}_{33}\left(\lambda_{44}\lambda_{55} - \lambda_{45}{}^2\right)}. \tag{16.29}$$

All solutions presented so far do not contain any further specifications of the shape functions and can therefore be used in general for any separation approach according to (16.11).

16.1.2 Shape Functions

The choice of shape functions is decisive for the quality of the results of the present analysis method. They must represent the buckling shape of the laminates and fulfil the boundary conditions as accurately as possible. The geometric boundary conditions must be fulfilled exactly, while the dynamic boundary conditions are fulfilled approximately. The approaches used are shown in (16.30) and (16.31). A distinction must be made between cross-ply and angle-ply laminates, as they have different boundary inplane conditions. In the x-direction, simple trigonometric functions are used that fulfil the boundary conditions at the simply supported edges $x = 0, a$ identically. In the y-direction, polynomials with the constants W_2, W_3 and W_4 are used. The approaches used below have already proven themselves in previous work. For example, Chai et al. (1991) and Qiao and Shan (2005) used approaches for w_1 and w_2 in the context of Classical Laminated Plate Theory. Studies on higher-order laminate theories using approaches for w_1, w_2, ψ_{x_1}, ψ_{x_2}, ψ_{y_1} and ψ_{y_2} can be found in Beerhorst and Suresh Babu (2020) and Schreiber et al. (2020). For the unsymmetric laminates investigated here, the inplane displacements must also be taken into account.

The following approaches are used for cross-ply laminates:

$$\begin{aligned}
u_1 &= \cos\left(\tfrac{m\pi x}{a}\right), \quad u_2 = \left(\tfrac{y}{b}\right) + W_2\left(\tfrac{y}{b}\right)^2 + W_3\left(\tfrac{y}{b}\right)^3 + W_4\left(\tfrac{y}{b}\right)^4,\\
v_1 &= \sin\left(\tfrac{m\pi x}{a}\right), \quad v_2 = 1 + 2\,W_2\left(\tfrac{y}{b}\right) + 3\,W_3\left(\tfrac{y}{b}\right)^2 + 4\,W_4\left(\tfrac{y}{b}\right)^3,\\
w_1 &= \sin\left(\tfrac{m\pi x}{a}\right), \quad w_2 = \left(\tfrac{y}{b}\right) + W_2\left(\tfrac{y}{b}\right)^2 + W_3\left(\tfrac{y}{b}\right)^3 + W_4\left(\tfrac{y}{b}\right)^4,\\
\psi_{x_1} &= \cos\left(\tfrac{m\pi x}{a}\right), \psi_{x_2} = \left(\tfrac{y}{b}\right) + W_2\left(\tfrac{y}{b}\right)^2 + W_3\left(\tfrac{y}{b}\right)^3 + W_4\left(\tfrac{y}{b}\right)^4,\\
\psi_{y_1} &= \sin\left(\tfrac{m\pi x}{a}\right), \psi_{y_2} = 1 + 2\,W_2\left(\tfrac{y}{b}\right) + 3\,W_3\left(\tfrac{y}{b}\right)^2 + 4\,W_4\left(\tfrac{y}{b}\right)^3.
\end{aligned} \tag{16.30}$$

For angle-ply laminates we employ the following shape functions:

$$\begin{aligned}
u_1 &= \sin\left(\tfrac{m\pi x}{a}\right), \quad u_2 = 1 + 2\,W_2\left(\tfrac{y}{b}\right) + 3\,W_3\left(\tfrac{y}{b}\right)^2 + 4\,W_4\left(\tfrac{y}{b}\right)^3,\\
v_1 &= \cos\left(\tfrac{m\pi x}{a}\right), \quad v_2 = \left(\tfrac{y}{b}\right) + W_2\left(\tfrac{y}{b}\right)^2 + W_3\left(\tfrac{y}{b}\right)^3 + W_4\left(\tfrac{y}{b}\right)^4,\\
w_1 &= \sin\left(\tfrac{m\pi x}{a}\right), \quad w_2 = \left(\tfrac{y}{b}\right) + W_2\left(\tfrac{y}{b}\right)^2 + W_3\left(\tfrac{y}{b}\right)^3 + W_4\left(\tfrac{y}{b}\right)^4,\\
\psi_{x_1} &= \cos\left(\tfrac{m\pi x}{a}\right), \psi_{x_2} = \left(\tfrac{y}{b}\right) + W_2\left(\tfrac{y}{b}\right)^2 + W_3\left(\tfrac{y}{b}\right)^3 + W_4\left(\tfrac{y}{b}\right)^4,\\
\psi_{y_1} &= \sin\left(\tfrac{m\pi x}{a}\right), \psi_{y_2} = 1 + 2\,W_2\left(\tfrac{y}{b}\right) + 3\,W_3\left(\tfrac{y}{b}\right)^2 + 4\,W_4\left(\tfrac{y}{b}\right)^3.
\end{aligned} \tag{16.31}$$

The constants W_2, W_3 and W_4 are determined by fulfilling the boundary conditions at the unloaded edges. The approaches fulfil the geometric boundary conditions exactly and the dynamic boundary conditions approximately:

$$\begin{aligned}
W_2 &= \frac{1}{2}\,\frac{bk_0}{D_{22}},\\
W_3 &= -\frac{b^2k_0\,k_b + 5\,D_{22}\,bk_0 + 3\,D_{22}\,bk_b + 12\,{D_{22}}^2}{(bk_b + 6\,D_{22})\,D_{22}},\\
W_4 &= \frac{1}{2}\,\frac{b^2k_0\,k_b + 4\,D_{22}\,bk_0 + 4\,D_{22}\,bk_b + 12\,{D_{22}}^2}{(bk_b + 6\,D_{22})\,D_{22}}.
\end{aligned} \tag{16.32}$$

For the SFSR plate, the right-hand side of (16.9) for $y = 0$ is considered. On the other hand, the boundary conditions (16.10) for $y = b$ apply, which are approximately fulfilled by $\frac{\partial^2 w_2}{\partial y^2} = \frac{\partial^3 w_2}{\partial y^3} = \frac{\partial \psi_{y_2}}{\partial y} = \frac{\partial^2 \psi_{y_2}}{\partial y^2} = 0$. This results in the following constants:

$$W_2 = \frac{1}{2}\,\frac{k_0\,b}{D_{22}}, \quad W_3 = -\frac{1}{3}\,\frac{k_0\,b}{D_{22}}, \quad W_4 = \frac{1}{12}\,\frac{k_0\,b}{D_{22}}. \tag{16.33}$$

The integral quantities of the respective approaches can be found below. The rotational parameters relating to the unloaded edges differ depending on the laminate theory used. For CLPT we obtain:

$$C_{rot1} = \frac{1}{b^2}, \quad C_{rot2} = \beta_0, \tag{16.34}$$

with

$$\beta_0 = \left(\frac{1}{b} + 2\,\frac{W_2}{b} + 3\,\frac{W_3}{b} + 4\,\frac{W_4}{b} \right)^2 . \tag{16.35}$$

For FSDT and TSDT the following applies:

$$C_{rot1} = 1, \quad C_{rot2} = \beta_0 b^2. \tag{16.36}$$

Evaluating (16.15) with the approach (16.30) for cross-ply laminates results in:

$$\begin{aligned}
I_{11}^{00} &= I_{14}^{00} = I_{22}^{00} = I_{23}^{00} = I_{25}^{00} \\
&= I_{33}^{00} = I_{35}^{00} = I_{44}^{00} = I_{55}^{00} = \alpha_4, \\
I_{13}^{00} &= I_{15}^{00} = I_{24}^{00} = I_{14}^{01} = I_{23}^{01} = I_{25}^{01} = I_{14}^{10} = I_{23}^{10} \\
&= I_{25}^{10} = I_{13}^{11} = I_{15}^{11} = I_{24}^{11} = I_{13}^{02} = I_{23}^{12} = 0, \\
I_{12}^{01} &= I_{13}^{01} = I_{15}^{01} = -I_{24}^{01} = -I_{34}^{01} = I_{45}^{01} = -I_{12}^{10} \\
&= -I_{13}^{10} = -I_{15}^{10} = I_{24}^{10} = I_{34}^{10} = -I_{45}^{10} = \alpha_2, \\
I_{11}^{11} &= I_{14}^{11} = I_{22}^{11} = I_{23}^{11} = I_{25}^{11} = I_{33}^{11} = I_{35}^{11} = I_{44}^{11} \\
&= I_{55}^{11} = -I_{23}^{02} = -I_{33}^{02} = -I_{35}^{20} = \alpha_1, \\
I_{13}^{12} &= I_{34}^{21} = \alpha_3, \quad I_{33}^{22} = \alpha_5,
\end{aligned} \tag{16.37}$$

$$\begin{aligned}
&J_{11}^{00} = J_{13}^{00} = J_{14}^{00} = J_{33}^{00} = J_{34}^{00} = J_{44}^{00} = \beta_2, \\
&J_{15}^{00} = J_{23}^{00} = J_{24}^{00} = J_{22}^{00} = J_{25}^{00} = J_{55}^{00} = \beta_3\, b, \\
&J_{22}^{00} = \beta_6\, b, \quad J_{12}^{01} = J_{15}^{01} = J_{35}^{01} = J_{45}^{01} = J_{23}^{10} = J_{24}^{10} = \beta_1\, b, \\
&J_{13}^{01} = J_{14}^{01} = J_{13}^{10} = J_{14}^{10} = \beta_3, \quad J_{23}^{01} = J_{24}^{01} = J_{12}^{10} = J_{15}^{10} = \beta_6, \\
&J_{25}^{01} = J_{25}^{10} = J_{35}^{10} = J_{45}^{10} = \beta_5\, b, \\
&J_{11}^{11} = J_{13}^{11} = J_{14}^{11} = J_{33}^{11} = J_{34}^{11} = J_{44}^{11} = \beta_7, \\
&J_{15}^{11} = J_{23}^{11} = J_{24}^{11} = J_{23}^{02} = \beta_5, \quad J_{22}^{11} = J_{25}^{11} = J_{55}^{11} = \beta_4\, b, \\
&J_{13}^{02} = J_{33}^{02} = J_{34}^{20} = \beta_1, \quad J_{13}^{12} = \frac{\beta_5}{b}, \quad J_{23}^{12} = J_{35}^{21} = \beta_4, \\
&J_{33}^{22} = \frac{\beta_4}{b}.
\end{aligned} \tag{16.38}$$

With the approach (16.31) for angle-ply laminates we obtain for (16.15):

$$\begin{aligned}
I_{11}^{00} &= I_{13}^{00} = I_{15}^{00} = I_{22}^{00} = I_{24}^{00} = I_{33}^{00} = I_{35}^{00} = I_{44}^{00} = I_{55}^{00} = \alpha_4, \\
I_{14}^{00} &= I_{23}^{00} = I_{25}^{00} = I_{13}^{01} = I_{15}^{01} = I_{24}^{01} = I_{13}^{10} = I_{15}^{10} \\
&= I_{24}^{10} = I_{14}^{11} = I_{23}^{11} = I_{25}^{11} = I_{23}^{02} = I_{13}^{12} = 0, \\
I_{12}^{01} &= I_{14}^{01} = -I_{23}^{01} = -I_{25}^{01} = I_{34}^{01} = -I_{45}^{01} = -I_{12}^{10} \\
&= -I_{14}^{10} = I_{23}^{10} = I_{25}^{10} = -I_{34}^{10} = I_{45}^{10} = -\alpha_2,
\end{aligned}$$

$$
\begin{aligned}
I_{11}^{11} &= I_{13}^{11} = I_{15}^{11} = I_{22}^{11} = I_{24}^{11} = I_{33}^{11} = I_{35}^{11} = I_{44}^{11} \\
&= I_{55}^{11} = -I_{13}^{02} = -I_{33}^{02} = -I_{35}^{20} = \alpha_1, \\
I_{23}^{12} &= I_{34}^{21} = \alpha_3, \quad I_{33}^{22} = \alpha_5,
\end{aligned} \tag{16.39}
$$

$$
\begin{aligned}
&J_{11}^{00} = J_{15}^{00} = J_{55}^{00} = \beta_6\, b, \quad J_{13}^{00} = J_{14}^{00} = J_{25}^{00} = \beta_3\, b, \\
&J_{22}^{00} = J_{23}^{00} = J_{24}^{00} = J_{33}^{00} = J_{34}^{00} = J_{44}^{00} = \beta_2, \\
&J_{12}^{01} = J_{13}^{01} = J_{14}^{01} = J_{25}^{10} = J_{35}^{10} = J_{45}^{10} = \beta_6, \\
&J_{15}^{01} = J_{15}^{10} = \beta_5\, b, \quad J_{23}^{01} = J_{24}^{01} = J_{23}^{10} = J_{24}^{10} = \beta_3, \\
&J_{25}^{01} = J_{35}^{01} = J_{45}^{01} = J_{12}^{10} = J_{13}^{10} = J_{14}^{10} = \beta_1\, b, \\
&J_{11}^{11} = J_{15}^{11} = J_{55}^{11} = \beta_4\, b, \quad J_{13}^{11} = J_{14}^{11} = J_{25}^{11} = J_{13}^{02} = \beta_5, \\
&J_{22}^{11} = J_{23}^{11} = J_{24}^{11} = J_{33}^{11} = J_{34}^{11} = J_{44}^{11} = \beta_7, \\
&J_{23}^{02} = J_{33}^{02} = J_{34}^{20} = \beta_1, \quad J_{13}^{12} = J_{35}^{21} = \beta_4, \\
&J_{23}^{12} = \frac{\beta_5}{b}, \quad J_{33}^{22} = \frac{\beta_4}{b}.
\end{aligned} \tag{16.40}
$$

The Eqs. (16.37)–(16.40) contain the following terms:

$$
\begin{aligned}
&\alpha_1 = \frac{1}{2}\,\frac{m^2\pi^2}{a}, \quad \alpha_2 = \frac{1}{2}\,m\,\pi, \quad \alpha_3 = \frac{1}{2}\,\frac{m^3\pi^3}{a^2}, \\
&\alpha_4 = \frac{a}{2}, \quad \alpha_5 = \frac{1}{2}\,\frac{m^4\pi^4}{a^3},
\end{aligned} \tag{16.41}
$$

and

$$
\begin{aligned}
\beta_1 &= \frac{1}{b}\left(\frac{2}{3}\,{W_2}^2 + \left(2\,W_3 + \frac{14}{5}\,W_4 + 1\right) W_2 + \frac{6}{5}\,{W_3}^2 \right. \\
&\quad \left. + (3\,W_4 + 2)\,W_3 + \frac{12}{7}\,{W_4}^2 + 3\,W_4\right), \\
\beta_2 &= \left(\frac{1}{5}\,{W_2}^2 + \left(\frac{1}{3}\,W_3 + \frac{2}{7}\,W_4 + \frac{1}{2}\right) W_2 + \frac{1}{7}\,{W_3}^2 \right. \\
&\quad \left. + \left(\frac{1}{4}\,W_4 + \frac{2}{5}\right) W_3 + \frac{1}{9}\,{W_4}^2 + \frac{1}{3}\,W_4 + \frac{1}{3}\right) b, \\
\beta_3 &= \frac{1}{2}\,(1 + W_2 + W_3 + W_4)^2, \\
\beta_4 &= \frac{1}{b^2}\left(4\,{W_2}^2 + (12\,W_3 + 16\,W_4)\,W_2 \right. \\
&\quad \left. + 12\,{W_3}^2 + 36\,W_3 W_4 + \frac{144}{5}\,{W_4}^2\right), \\
\beta_5 &= \frac{(4\,W_4 + 2 + 3\,W_3 + 2\,W_2)\,(4\,W_4 + 3\,W_3 + 2\,W_2)}{2\,b},
\end{aligned}
$$

$$\beta_6 = \frac{4}{3} W_2{}^2 + \left(3 W_3 + \frac{16}{5} W_4 + 2\right) W_2 + \frac{9}{5} W_3{}^2 + (4 W_4 + 2) W_3 + \frac{16}{7} W_4{}^2 + 2 W_4 + 1,$$

$$\beta_7 = \frac{1}{b}\left(\frac{4}{3} W_2{}^2 + \left(3 W_3 + \frac{16}{5} W_4 + 2\right) W_2 + \frac{9}{5} W_3{}^2 + (4 W_4 + 2) W_3 + \frac{16}{7} W_4{}^2 + 2 W_4 + 1\right). \tag{16.42}$$

At this point, the closed-form analytical approximate solutions for the buckling load N_{xx}^0 are now available for all three theories (CLPT, FSDT, TSDT) and the two structural situations (SRSR, SFSR). The solutions were developed for unsymmetric cross-ply laminates and unsymmetric angle-ply laminates. In the context of the CLPT, these correspond to the solutions by Qiao and Shan (2005) for the SRSR plate and Mittelstedt (2007) for the SFSR plate for symmetric laminates. The solutions in the context of FSDT and TSDT can be found in Beerhorst and Suresh Babu (2020) and Schreiber et al. (2020) for the SRSR plate. For the SFSR plate, there are no known investigations within the framework of the FSDT and TSDT as of yet that employ the approaches used in this chapter.

16.1.3 Reduced Bending Stiffness Method

The method of reduced bending stiffnesses (RBS) was developed as part of the CLPT in Reissner and Stavsky (1961). The RBS method reduces the bending stiffness of unsymmetric laminates by eliminating the bending-extension coupling stiffnesses, see e.g. Ashton (1969), Schilling and Mittelstedt (2020). This approximation method allows the calculation of unsymmetric laminates with the analysis methods for symmetric laminates, which can be found e.g. in the Eqs. (16.28) and (16.29). This method can also be applied directly to FSDT, as no further coupling occurs with respect to $\underline{N}$, as described in Whitney and Pagano (1970). There are additional coupling terms associated with the TSDT, however, and there is no known RBS method that takes these additional coupling terms into account. In the following, the development of the RBS method in the context of the TSDT is presented. Analogous to the procedure for the RBS method in the context of CLPT, the half-inverse of the constitutive law (16.3) is calculated with respect to $\underline{\varepsilon_1}$ and $\underline{N}$. This results in the following relationship:

$$\begin{pmatrix} \underline{\varepsilon_1} \\ \underline{M^0} \\ \underline{P} \\ \underline{Q} \\ \underline{R} \end{pmatrix} = \begin{bmatrix} \underline{\underline{A}}^* & -\underline{\underline{B}}^* & -\underline{\underline{E}}^* & \underline{\underline{0}} & \underline{\underline{0}} \\ \underline{\underline{B}}^{*T} & \underline{\underline{D}}^* & \underline{\underline{F}}^* & \underline{\underline{0}} & \underline{\underline{0}} \\ \underline{\underline{E}}^{*T} & \underline{\underline{F}}^{*T} & \underline{\underline{H}}^* & \underline{\underline{0}} & \underline{\underline{0}} \\ \underline{\underline{0}} & \underline{\underline{0}} & \underline{\underline{0}} & \underline{\underline{A}}_S & \underline{\underline{D}}_S \\ \underline{\underline{0}} & \underline{\underline{0}} & \underline{\underline{0}} & \underline{\underline{D}}_S & \underline{\underline{F}}_S \end{bmatrix} \begin{pmatrix} \underline{N^0} \\ \underline{\varepsilon_2} \\ \underline{\varepsilon_3} \\ \underline{\gamma_1} \\ \underline{\gamma_2} \end{pmatrix}, \tag{16.43}$$

with

$$\begin{aligned} \underline{\underline{A}}^* &= \underline{\underline{A}}^{-1}, \quad \underline{\underline{D}}^* = \underline{\underline{D}} - \underline{\underline{B}}\,\underline{\underline{A}}^{-1}\,\underline{\underline{B}}, \\ \underline{\underline{B}}^* &= \underline{\underline{A}}^{-1}\,\underline{\underline{B}}, \quad \underline{\underline{F}}^* = \underline{\underline{F}} - \underline{\underline{B}}\,\underline{\underline{A}}^{-1}\,\underline{\underline{E}}, \\ \underline{\underline{E}}^* &= \underline{\underline{A}}^{-1}\,\underline{\underline{E}}, \quad \underline{\underline{H}}^* = \underline{\underline{H}} - \underline{\underline{E}}\,\underline{\underline{A}}^{-1}\,\underline{\underline{E}}. \end{aligned} \tag{16.44}$$

The inner potential can be specified as:

$$\begin{aligned} \Pi_i = \frac{1}{2}\int_0^b \int_0^a \Big(& \underline{\varepsilon_1}^T \underline{\underline{A}}\,\underline{\varepsilon_1} + 2\,\underline{\varepsilon_1}^T \underline{\underline{B}}\,\underline{\varepsilon_2} + 2\,\underline{\varepsilon_1}^T \underline{\underline{E}}\,\underline{\varepsilon_3} \\ & + \underline{\varepsilon_2}^T \underline{\underline{D}}\,\underline{\varepsilon_2} + 2\,\underline{\varepsilon_2}^T \underline{\underline{F}}\,\underline{\varepsilon_3} + \underline{\varepsilon_3}^T \underline{\underline{H}}\,\underline{\varepsilon_3} \\ & + \underline{\gamma_1}^T \underline{\underline{A}}_S \underline{\gamma_1} + 2\,\underline{\gamma_1}^T \underline{\underline{D}}_S \underline{\gamma_2} + \underline{\gamma_2}^T \underline{\underline{F}}_S \underline{\gamma_2} \Big)\, \mathrm{d}x\, \mathrm{d}y. \end{aligned} \tag{16.45}$$

Inserting $\underline{\varepsilon}_1$ from Eq. (16.43) into (16.45) leads to the following expression:

$$\begin{aligned} \Pi_i = \frac{1}{2}\int_0^b \int_0^a \Big(& \underline{N}^{0,T} \underline{\underline{A}}^* \underline{N}^0 + \underline{\varepsilon_2}^T \underline{\underline{D}}^* \underline{\varepsilon_2} + 2\,\underline{\varepsilon_2}^T \underline{\underline{F}}^* \underline{\varepsilon_3} \\ & + \underline{\varepsilon_3}^T \underline{\underline{H}}^* \underline{\varepsilon_3} + \underline{\gamma_1}^T \underline{\underline{A}}_S \underline{\gamma_1} + 2\,\underline{\gamma_1}^T \underline{\underline{D}}_S \underline{\gamma_2} \\ & + \underline{\gamma_2}^T \underline{\underline{F}}_S \underline{\gamma_2} \Big)\, \mathrm{d}x\, \mathrm{d}y. \end{aligned} \tag{16.46}$$

In (16.46), $\underline{N}^0$ is now decoupled from $\underline{\varepsilon_2}, \underline{\varepsilon_3}, \underline{\gamma_1}, \underline{\gamma_2}$. The bending-extension coupling is decoupled in the potential (16.46). With this method, unsymmetric laminates can now be treated as effectively symmetric in the context of TSDT by reducing the stiffnesses as shown.

16.1.4 Results and Discussion

The following results using the closed-form analysis method (16.23) or (16.27) were generated with the elastic layer properties $E_{11} = 162{,}000$ MPa, $E_{22} = 10{,}000$ MPa, $\nu_{12} = 0.3$, $G_{12} = G_{13} = 5200$ MPa, $G_{23} = 4450$ MPa. The width of the plate is constant at $b = 100$ mm. The length a and the thickness h are varied and considered in a dimensionless manner in the form of the aspect ratio a/b or the relative width b/h. The RBS solutions contain the reduced stiffnesses as described in Sect. 16.1.3 and solved with Eqs. (16.28) and (16.29) for CLPT and FSDT or TSDT. The shear correction factor required for the FSDT is assumed to be constant with $K = 5/6$ in this study. The critical load is represented in dimensionless form as the buckling factor $k_x = \frac{N^0_{xx}\, b^2}{\pi^2 E_{22}\, h^3}$. The Tables 16.1, 16.2 and 16.3 show the deviations between the present solution and comparative FEM calculations. The deviations between the RBS method and the present solution are also shown. These are calculated with $\frac{N^{\text{present}}_{xx} - N^{\text{FEA}}_{xx}}{N^{\text{FEA}}_{xx}} 100$ or $\frac{N^{\text{RBS}}_{xx} - N^{\text{present}}_{xx}}{N^{\text{present}}_{xx}} 100$ and given in %.

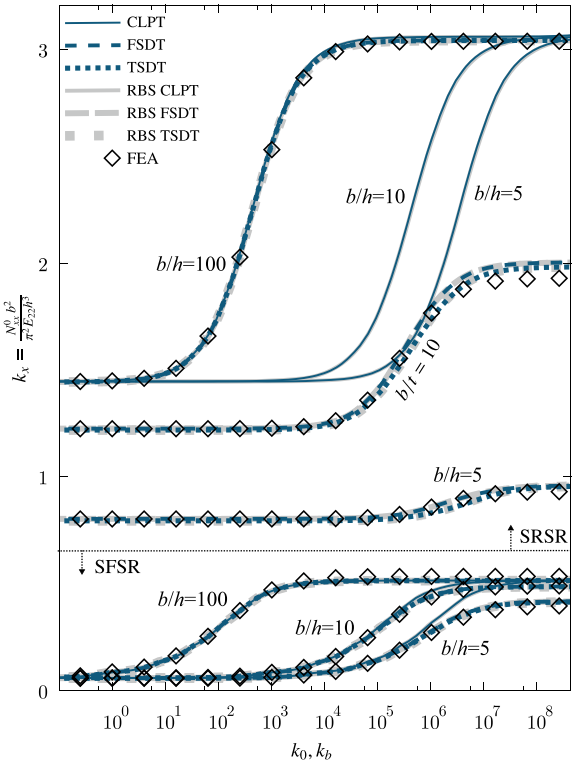


Fig. 16.2 Dimensionless buckling load k_x for a cross-ply laminate $\left[(0°/90°)_2\right]$ as a function of the restraint stiffnesses k_0, k_b for different ratios b/h (5, 10, 100) for SRSR and SFSR plates with the aspect ratio $a/b = 10$

In Figs. 16.2 and 16.3 the influence of the thickness and the degree of restraint on the buckling load is shown. The present solution, the RBS method and the results of accompanying FEM calculations for the boundary conditions SRSR and SFSR are taken into account here. The results for the cross-ply laminate $[(0°/90°)_2]$ can be seen in Fig. 16.2. For thin laminates ($b/h = 100$), the available solutions show very good agreement with the FEA (SRSR: $0.82\dot{\%}$, SFSR: $-3.26\dot{\%}$), as shown in Table 16.1. In addition to the comparison of the current solution and the FEA, Table 16.1 also shows the deviation of the RBS method from the current solution. The latter shows very good agreement between the two methods, with deviations between -0.14 and 0.12%. For $b/h = 10$ there is a clear overestimation of the buckling load when CLPT is used. Reducing the relative thickness to $b/h = 5$ increases this effect. This is due to the influence of transverse shear deformations, which are not taken into account by CLPT. However, it can also be seen that this effect is further increased by the restraint stiffness and, conversely, can be reduced by the free edge of the SFSR plate. This leads to relatively small deviations ($7.46\dot{\%}$) for the SFSR plate in connection with CLPT for low restraint stiffnesses, see Table 16.1. The higher order laminate theories take this effect into account and provide a very good agreement with the FEM. It can be observed that the deviations increase with decreasing b/h and that they are higher for the SFSR plate than for

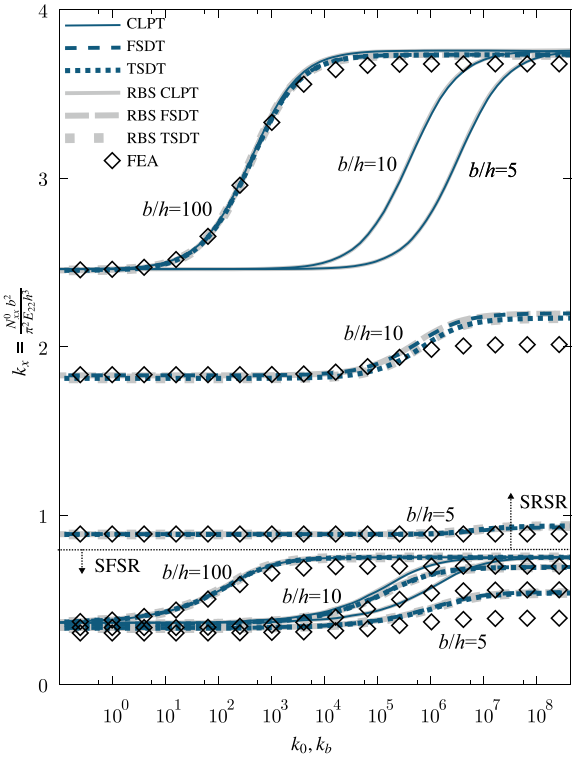


Fig. 16.3 Dimensionless buckling load k_x for an angle-ply laminate $\left[(45°/-45°)_2\right]$ as a function of the restraint stiffnesses k_0, k_b for different ratios b/h (5, 10, 100) for SRSR and SFSR plates with the aspect ratio $a/b = 10$

the SRSR plate. It can also be observed that the results of the TSDT agree slightly better with the FEA than those of the FSDT.

The angle-ply laminate shows the same behaviour as the cross-ply laminate, but the deviations are higher, see Table 16.1. However, the influence of the restraint stiffness is overestimated by the analytical solutions. This effect is more pronounced for the SFSR plate than for the SRSR plate and increases with increasing thickness. The agreement between the present solutions and the RBS method is very good and the deviations in relation to the TSDT for the newly developed RBS method are also between -0.05 and 0.04%.

Furthermore, the influence of the ply repetition n of a $[(0°/90°)_n]$ cross-ply laminate is considered. The laminate thickness and width remain constant, taking $b/h = 10$ into account. Therefore, n has no influence on the stiffnesses $\underline{\underline{A}}$, $\underline{\underline{D}}$, $\underline{\underline{F}}$ and $\underline{\underline{H}}$. Only the entries of the coupling matrices $\underline{\underline{B}}$ and $\underline{\underline{E}}$ become smaller with increasing n. For the case $n = \infty$, these are set to zero. Figure 16.4 shows the present solution and the RBS method in the context of the TSDT, which is compared with the FEA. Here, the restraint stiffnesses are selected as $k_0 = k_b = 10^5$ N for the SRSR plate and $k_0 = 10^4$ N for the SFSR plate. Figure 16.4 shows that the dimensionless buckling load increases with increasing n. This effect is large for the SRSR plate and small for the SFSR plate. The degree of symmetry therefore has

Table 16.1 Deviations of the present solution compared to the FEA $\frac{N_{xx}^{\text{present}} - N_{xx}^{\text{FEA}}}{N_{xx}^{\text{FEA}}} 100$ and deviations of the RBS-method compared to the present solution $\frac{N_{xx}^{\text{RBS}} - N_{xx}^{\text{present}}}{N_{xx}^{\text{present}}} 100$ for $a/b = 10$

b/h	k_0, k_b in N	CLPT		FSDT		TSDT	
		Present (FEA) in %	RBS (present) in %	Present (FEA) in %	RBS (present) in %	Present (FEA) in %	RBS (present) in %
SRSR cross-ply							
100	10^{-1}	0.24	0.00	0.06	0.00	0.06	0.00
	10^{8}	0.82	−0.14	0.28	−0.07	0.20	−0.01
10	10^{-1}	18.27	0.00	0.22	0.00	−0.32	0.00
	10^{8}	58.53	−0.03	3.91	−0.01	2.78	0.00
5	10^{-1}	80.65	0.00	0.36	−0.01	−0.81	−0.01
	10^{8}	224.10	−0.11	3.01	0.03	2.36	0.12
SFSR cross-ply							
100	10^{-1}	0.32	0.00	0.32	0.00	0.32	0.00
	10^{8}	−3.20	−0.02	−3.26	−0.02	−3.26	−0.02
10	10^{-1}	3.33	0.00	2.87	0.00	2.87	0.00
	10^{8}	5.66	−0.02	−0.03	−0.02	−0.21	−0.02
5	10^{-1}	7.46	0.00	5.56	0.00	5.54	0.00
	10^{8}	30.38	−0.06	6.02	−0.03	5.23	0.00
SRSR angle-ply							
100	10^{-1}	0.33	−0.02	0.03	−0.02	0.02	−0.02
	10^{8}	2.15	0.08	1.56	−0.01	1.54	−0.02
10	10^{-1}	34.33	−0.02	−0.05	−0.02	−1.03	−0.02
	10^{8}	86.58	−0.01	9.26	−0.02	7.87	−0.02
5	10^{-1}	177.31	−0.02	0.26	−0.05	0.06	−0.05
	10^{8}	318.33	0.04	4.55	−0.02	5.44	−0.02
SFSR angle-ply							
100	10^{-1}	1.04	0.00	1.01	0.00	1.01	0.00
	10^{8}	8.05	−0.01	7.96	−0.01	7.95	−0.01
10	10^{-1}	9.60	0.00	7.08	0.00	6.98	0.00
	10^{8}	35.20	−0.01	24.84	−0.01	24.48	−0.01
5	10^{-1}	21.28	0.00	10.85	0.00	10.48	0.00
	10^{8}	92.70	0.03	40.16	0.03	38.72	0.04

a greater influence on the SRSR plate than on the SFSR plate. There is a good agreement between the present solution and the FEA. As shown in Table 16.2, the maximum deviation for $n = 1$ is 3.75% and decreases with increasing n. For $n \to \infty$, the SRSR plate even shows negative deviations (−1.19%), and the SFSR plate always shows positive deviations (1.53%) compared to the FEA. The comparison between the RBS method and the present solution shows very good agreement. The deviations also become smaller with increasing n and decrease from −1.69% to values below 0.005%, see Table 16.2. For the material parameters and $n = 1$ used here, it can be observed that the RBS method is slightly closer to the FEA results than the present solution.

Finally, the influence of the ply angle θ and the ply repetition n on the unsymmetric angle-ply laminate $[(\theta°/-\theta°)_n]$ will be discussed. The laminate thickness and width are

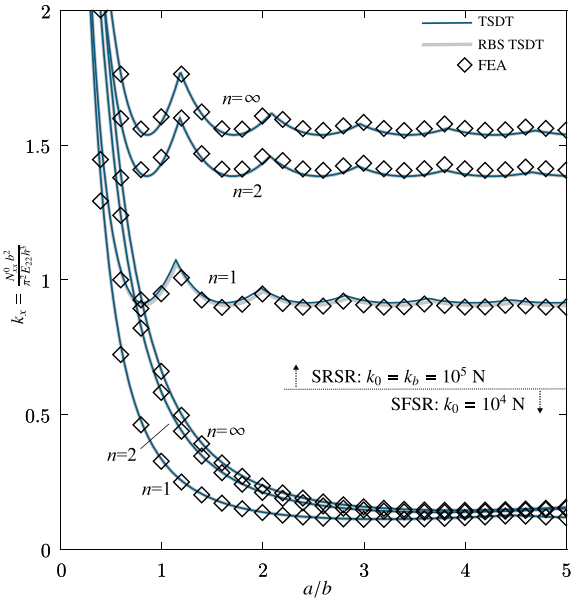


Fig. 16.4 Dimensionless buckling load k_x for a cross-ply laminate $\left[(0°/90°)_n\right]$ as a function of the aspect ratio a/b for the relative width $b/h = 10$ for different layer repetitions $n = 1, 2, \infty$ for SRSR and SFSR plates with the restraint stiffnesses $k_0 = k_b = 10^5$ N and $k_0 = 10^4$ N

Table 16.2 Cross-ply laminate $\left[(0°/90°)_n\right]$ within the scope of the TSDT: Maximum deviations of the present solution from the FEA $\frac{N_{xx}^{\text{present}} - N_{xx}^{\text{FEA}}}{N_{xx}^{\text{FEA}}} 100$ and deviations of the RBS-method from the present solution $\frac{N_{xx}^{\text{RBS}} - N_{xx}^{\text{present}}}{N_{xx}^{\text{present}}} 100$ for $b/h = 10$, $k_0 = k_b = 10^5$ N (SRSR plate) and $k_0 = 10^4$ N (SFSR plate)

n	present (FEA) in %	a/b	RBS (present) in %	a/b
SRSR Cross-ply				
1	3.35	0.6	−1.69	1
2	−1.51	2	−0.04	2
∞	−1.19	2	0.00	3
SFSR Cross-ply				
1	3.75	0.6	−0.79	4.4
2	1.70	4.4	−0.03	5
∞	1.53	4.4	0.00	5

constant, and a relative width $b/h = 10$ and the aspect ratio $a/b = 1$ are considered. The influence of the ply angle can be clearly seen in Fig. 16.5 for the SRSR plate. With increasing

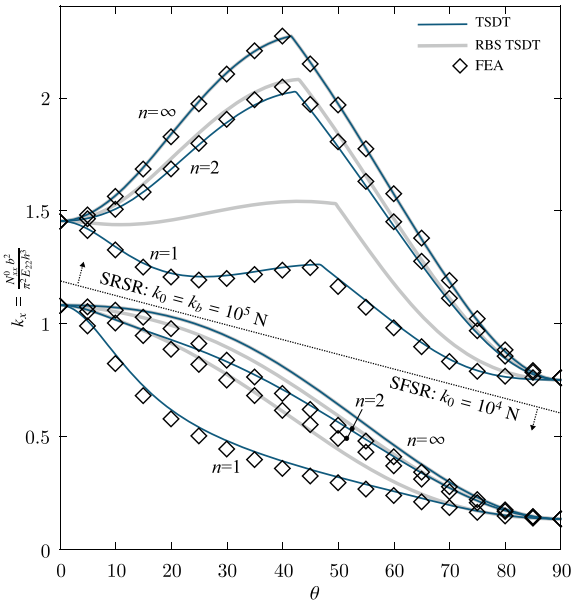


Fig. 16.5 Dimensionless buckling load k_x for angle-ply laminates $\left[(\theta°/-\theta°)_n\right]$ as a function of the ply angle θ for $b/t = 10$ and $a/b = 1$ with the ply repetitions $n = 1, 2, \infty$ for SRSR and SFSR plates with $k_0 = k_b = 10^5$ N and $k_0 = 10^4$ N

θ, the buckling load increases up to a certain angle and then continuously decreases again. This behaviour is very weak for $n = 1$, but clearly present from $n = 2$. The individual peaks in the curves can be explained by a change in the buckling modes or the half-wave number caused by the different fiber angles. For the parameter configurations shown here, the SFSR plate always shows a half-wave over the entire range for θ and the optimum fiber angle is 0°. The SRSR panel shows a similar behaviour to the cross-ply laminates in terms of deviations, see Table 16.3. The comparison between the present solution and the FEA shows the largest deviation of 3.02% for $n = 1$ and the smallest of -0.91% for $n \to \infty$. The RBS method shows very large deviations of 26.34% for $n = 1$ in relation to the present solution. These decrease rapidly with increasing n and drop to a value of less than 0.005% for $n \to \infty$. In the case of the SFSR plate, the comparison between the present solution and the FEA shows a significantly higher deviation. For $n = 1$ deviations of up to 9.56% are achieved, these increase with increasing n to 17.87%. Compared to the present solution, the RBS method for $n = 1$ shows a deviation of 60.98%, which decreases rapidly with increasing n and finally reaches a level of less than 0.005%.

The angle-ply laminate has different optimum fiber angles for different parameters, which is shown in Fig. 16.6 for TSDT. The curves SRSR (k_0, k_b) show the influence of the elastic restraints. A hinged support is shown for $k_0 = k_b = 0$ and the optimum fiber angle is 45°. With an increase in k_0, k_b, the optimum shifts to smaller angles. A similar effect can be observed for the curves SRSR (b/h). With a fixed clamping stiffness of $k_0 = k_b = 10^6$ N, the optimum shifts to smaller fiber angles when b/h is reduced. This thickness effect cannot be observed in the CLPT, it is only visible in the higher-order laminate theories. However,

Table 16.3 Angle-ply laminate $\left[(\theta°/-\theta°)_n\right]$ within the scope of the TSDT: Maximum deviations of the present solution from the FEA $\frac{N_{xx}^{\text{present}}-N_{xx}^{\text{FEA}}}{N_{xx}^{\text{FEA}}}100$ and deviation of the RBS-method from the present solution $\frac{N_{xx}^{\text{RBS}}-N_{xx}^{\text{present}}}{N_{xx}^{\text{present}}}100$ for $b/h = 10$, $a/b = 1$, $k_0 = k_b = 10^5$ N (SRSR plate) and $k_0 = 10^4$ N (SFSR plate)

n	Present (FEA) in %	θ in °	RBS (present) in %	θ in °
SRSR angle-ply				
1	3.02	50	26.34	50
2	−1.43	40	3.51	45
4	−0.92	80	0.76	45
∞	−0.91	90	0.00	60
SFSR angle-ply				
1	9.56	40	60.98	30
2	15.61	45	7.73	30
4	17.29	45	1.71	30
∞	17.87	45	0.00	25

the mentioned effects have a much smaller influence on the SFSR plate. The SFSR plate, on the other hand, shows a stronger influence of the aspect ratio a/b, as can be seen from the curve SFSR (a/b). For $a/b = 50$ and 100, the optimum is 0°. This shifts with increasing a/b to 45°.

16.2 Lévy Solutions

16.2.1 Fundamental Equations

In the following, we will derive Lévy-type solutions for the unsymmetric laminates discussed in the last section. This section contains the basic equations necessary to describe the stability problem considered here. With the formulation of the total elastic potential and its variation, the boundary conditions, the equilibrium conditions and the resulting partial differential equations can be formulated, which form the basis for the Lévy-type solutions presented in the following.

The total elastic potential is made up of the inner potential Π_i and the external potential Π_a, which can be expressed as follows:

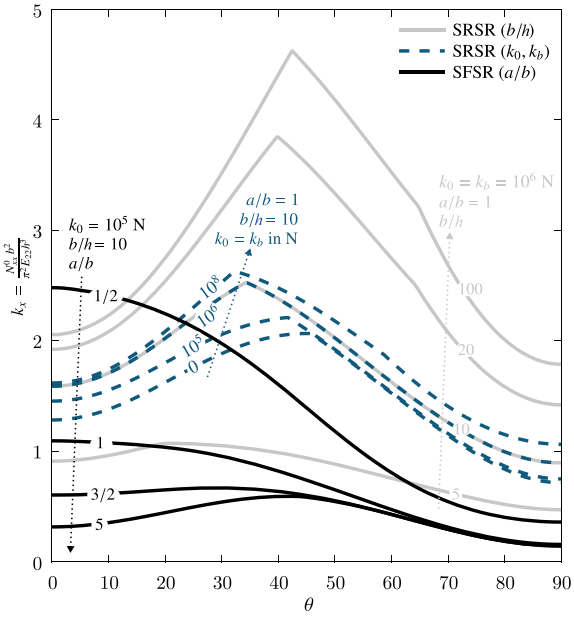


Fig. 16.6 Present TSDT solution for the angle-ply laminate $[(\theta^\circ/-\theta^\circ)_4]$: Dimensionless buckling load k_x as a function of the ply angle θ for different ratios b/h, a/b and (k_0, k_b)

$$\Pi_i = \frac{1}{2}\int_0^b \int_0^a \underline{\varepsilon}^{\mathrm{T}} \underline{\overline{N}}\, \mathrm{d}x\, \mathrm{d}y,$$

$$\Pi_a = -\frac{N_{\mathrm{crit}}}{2}\int_0^b \int_0^a \left\{ \xi_x \left(\frac{\partial w_0}{\partial x}\right)^2 + \xi_y \left(\frac{\partial w_0}{\partial y}\right)^2 \right\} \mathrm{d}x\, \mathrm{d}y. \tag{16.47}$$

In (16.47), the load factors ξ_x and ξ_y each represent the proportional values of the critical load N_{crit} to the two compressive loads; the following applies: $N_{xx}^0 = \xi_x N_{\mathrm{crit}}$ and $N_{yy}^0 = \xi_y N_{\mathrm{crit}}$. Further, the energy Π_{s} stored in the elastic edge restraints must be taken into account. The angle of rotation of the cross-section can be expressed as:

$$\overline{\varphi} = \frac{\partial v(x, y, z)}{\partial z}. \tag{16.48}$$

The evaluation of the Eq. (16.48) for the three laminate theories shows no dependence on the thickness direction for CLPT and FSDT. TSDT, on the other hand, shows a dependence in relation to z, as shown in the third equation of (16.49).

$$\begin{aligned}
&\text{CLPT:} \quad \overline{\varphi} = \frac{\partial w_0}{\partial y}, \\
&\text{FSDT:} \quad \overline{\varphi} = \psi_y, \\
&\text{TSDT:} \quad \overline{\varphi} = \psi_y(x, y) - \frac{4z^2}{h^2}\left(\psi_y(x, y) + \frac{\partial w_0(x, y)}{\partial y}\right).
\end{aligned} \tag{16.49}$$

The edge restraints are distributed over the entire cross-section, which has a constant stiffness per thickness h. The following relationship applies to the potential:

$$\Pi_{\mathrm{s}} = \frac{1}{2} \int_0^a \int_{-t/2}^{t/2} \left\{ \frac{k_0}{h} \left[\overline{\varphi}^2\right]_{y=0} + \frac{k_b}{h} \left[\overline{\varphi}^2\right]_{y=b} \right\} \mathrm{d}z \, \mathrm{d}x. \tag{16.50}$$

Evaluation of (16.50) yields:

$$\begin{aligned}
\text{CLPT:} \quad \Pi_s &= \frac{1}{2} \int_0^a \left\{ k_0 \left[\left. \frac{\partial w_0}{\partial y} \right|_{y=0} \right]^2 + k_b \left[\left. \frac{\partial w_0}{\partial y} \right|_{y=b} \right]^2 \right\} \mathrm{d}x, \\
\text{FSDT:} \quad \Pi_s &= \frac{1}{2} \int_0^a \left\{ k_0 \left[\psi_y(x,0)\right]^2 + k_b \left[\psi_y(x,b)\right]^2 \right\} \mathrm{d}x, \\
\text{TSDT:} \quad \Pi_s &= \frac{1}{2} \int_0^a \left\{ k_0 \left[\frac{8}{15} \psi_y^2 - \frac{4}{15} \psi_y \frac{\partial w_0}{\partial y} + \frac{1}{5} \left(\frac{\partial w_0}{\partial y} \right)^2 \right]_{y=0} \right. \\
&\quad \left. + k_b \left[\frac{8}{15} \psi_y^2 - \frac{4}{15} \psi_y \frac{\partial w_0}{\partial y} + \frac{1}{5} \left(\frac{\partial w_0}{\partial y} \right)^2 \right]_{y=b} \right\} \mathrm{d}x.
\end{aligned} \tag{16.51}$$

The total elastic potential Π results in:

$$\Pi = \Pi_i + \Pi_a + \Pi_s. \tag{16.52}$$

The variation of the potential

$$\delta\Pi = \delta\Pi_i + \delta\Pi_a + \delta\Pi_s = 0 \tag{16.53}$$

makes it possible to determine both the equilibrium conditions and the boundary conditions of the underlying buckling problem. For this purpose, the corresponding constitutive law of the respective laminate theory is inserted into the potential (16.52). This equation is then varied and the constitutive law is used. This is only shown here for TSDT. Particular attention is paid here to the new potential formulation (16.51) and the resulting boundary conditions.

$$\begin{aligned}
\delta\Pi_i + \delta\Pi_a = -\int_0^b \int_0^a \Bigg\{ & \left(\frac{\partial N_{xx}^0}{\partial x} + \frac{\partial N_{xy}^0}{\partial y} \right) \delta u_0 + \left(\frac{\partial N_{xy}^0}{\partial x} + \frac{\partial N_{yy}^0}{\partial y} \right) \delta v_0 \\
& + \left(-\xi_x N_{\mathrm{cr}} \frac{\partial w_0^2}{\partial x^2} - \xi_y N_{\mathrm{cr}} \frac{\partial w_0^2}{\partial y^2} - \frac{4}{h^2} \left[\frac{\partial R_x}{\partial x} + \frac{\partial R_y}{\partial y} \right] \right. \\
& \left. + \frac{4}{3h^2} \left[\frac{\partial^2 P_{xx}}{\partial x^2} + \frac{\partial^2 P_{yy}}{\partial y^2} + 2 \frac{\partial^2 P_{xy}}{\partial x \partial y} \right] + \frac{\partial Q_x}{\partial x} + \frac{\partial Q_y}{\partial y} \right) \delta w_0
\end{aligned}$$

$$
\begin{aligned}
&+\left(\frac{\partial M_{xx}}{\partial x}+\frac{\partial M_{xy}}{\partial y}-\frac{4}{3h^2}\left[\frac{\partial P_{xx}}{\partial x}+\frac{\partial P_{xy}}{\partial y}\right]-Q_x\right.\\
&\left.+\frac{4}{h^2}R_x\right)\delta\psi_x+\left(\frac{\partial M_{xy}}{\partial x}+\frac{\partial M_{yy}}{\partial y}-\frac{4}{3h^2}\left[\frac{\partial P_{xy}}{\partial x}+\frac{\partial P_{yy}}{\partial y}\right]\right.\\
&\left.-Q_y+\frac{4}{h^2}R_y\right)\delta\psi_y\Bigg\}\,\mathrm{d}x\,\mathrm{d}y+\int_0^a\Bigg\{\Bigg[N_{xy}^0\delta u+N_{yy}^0\delta v\\
&+\left(-\xi_y N_{\mathrm{cr}}\frac{\partial w_0}{\partial y}+\frac{4}{3h^2}\left[\frac{\partial P_{yy}}{\partial y}+2\frac{\partial P_{xy}}{\partial x}\right]+Q_y\right.\\
&\left.-\frac{4}{h^2}R_y\right)\delta\, w_0+\left(M_{xy}-\frac{4}{3h^2}P_{xy}\right)\delta\psi_x\\
&+\left(M_{yy}-\frac{4}{3h^2}P_{yy}\right)\delta\psi_y-\frac{4}{3h^2}P_{yy}\delta\left(\frac{\partial w_0}{\partial y}\right)\Bigg]\Bigg|_0^b\Bigg\}\mathrm{d}x\\
&+\int_0^b\Bigg\{N_{xx}^0\delta u+N_{xy}^0\delta v+\left(-\xi_x N_{\mathrm{cr}}\frac{\partial w_0}{\partial x}\right.\\
&\left.+\frac{4}{3h^2}\left[\frac{\partial P_{xx}}{\partial x}+2\frac{\partial P_{xy}}{\partial y}\right]+Q_x-\frac{4}{h^2}R_x\right)\delta\, w_0\\
&+\left(M_{xx}-\frac{4}{3h^2}P_{xx}\right)\delta\psi_x+\left(M_{xy}-\frac{4}{3h^2}P_{xy}\right)\delta\psi_y\\
&-\frac{4}{3h^2}P_{xx}\delta\left(\frac{\partial w_0}{\partial x}\right)\Bigg\}\Bigg|_0^a\mathrm{d}y-\left(\frac{8}{3h^2}P_{xy}\delta\, w_0\right)\Bigg|_0^a\Bigg|_0^b,
\end{aligned}
$$

$$
\begin{aligned}
\delta\Pi_s=\int_0^a\Bigg\{&k_0\left[\left(\frac{8}{15}\psi_y-\frac{2}{15}\frac{\partial w_0}{\partial y}\right)\delta\psi_y\right]_{y=0}\\
&+k_b\left[\left(\frac{8}{15}\psi_y-\frac{2}{15}\frac{\partial w_0}{\partial y}\right)\delta\psi_y\right]_{y=b}\\
&+k_0\left[\left(-\frac{2}{15}\psi_y+\frac{1}{5}\frac{\partial w_0}{\partial y}\right)\delta\left(\frac{\partial w_0}{\partial y}\right)\right]_{y=0}\\
&+k_b\left[\left(-\frac{2}{15}\psi_y+\frac{1}{5}\frac{\partial w_0}{\partial y}\right)\delta\left(\frac{\partial w_0}{\partial y}\right)\right]_{y=b}\Bigg\}\mathrm{d}x.
\end{aligned}
\tag{16.54}
$$

In order for (16.53) to be fulfilled, the terms from Eq. (16.54) must disappear individually. Consequently, the first five terms in brackets in (16.54) provide the equilibrium conditions and the remaining terms from (16.54) the boundary conditions of the given problem. Each boundary term can be fulfilled in two ways. Either the variable to be varied $\delta()$ disappears or the corresponding bracket term becomes zero. This results in the boundary conditions of the SRSR and SFSR plate described below. At the boundary $x = 0, a$ the following applies for the simply supported edges:

$$\left.\begin{array}{l}\text{Cross-ply:}\\ N^0_{xx} = v_0 = 0,\\ \text{Angle-ply:}\\ N^0_{xy} = u_0 = 0.\end{array}\right\} \left\{\begin{array}{l}\text{CLPT:}\\ w_0 = M^0_{xx} = 0,\\ \text{FSDT:}\\ w_0 = M^0_{xx} = \psi_y = 0,\\ \text{TSDT:}\\ w_0 = M^0_{xx} = \psi_y = P_{xx} = 0.\end{array}\right. \tag{16.55}$$

The following applies to the elastically restrained edges at $y = 0, b$:

$$\left.\begin{array}{l}\text{Cross-ply:}\\ N^0_{yy} = u_0 = 0,\\ \text{Angle-ply:}\\ N^0_{xy} = v_0 = 0.\end{array}\right\} \left\{\begin{array}{l}\text{CLPT:}\\ w_0 = \left\{\begin{array}{l}\left[-M^0_{yy} - k_0 \frac{\partial w_0}{\partial y}\right]_{y=0} = 0,\\ \left[M^0_{yy} - k_b \frac{\partial w_0}{\partial y}\right]_{y=b} = 0.\end{array}\right.\\ \text{FSDT:}\\ w_0 = \psi_x = \left\{\begin{array}{l}\left[-M^0_{yy} + k_0 \psi_y\right]_{y=0} = 0,\\ \left[M^0_{yy} + k_b \psi_y\right]_{y=b} = 0.\end{array}\right.\\ \text{TSDT:}\\ w_0 = \psi_x\\ = \left[\frac{4}{3h^2} P_{yy} + k_0 \left(-\frac{2}{15}\psi_y + \frac{1}{5}\frac{\partial w_0}{\partial y}\right)\right]_{y=0}\\ = \left[-\frac{4}{3h^2} P_{yy} + k_b \left(-\frac{2}{15}\psi_y + \frac{1}{5}\frac{\partial w_0}{\partial y}\right)\right]_{y=b}\\ = \left[-M^0_{yy} + \frac{4}{3h^2} P_{yy} + k_0 \left(\frac{8}{15}\psi_y - \frac{2}{15}\frac{\partial w_0}{\partial y}\right)\right]_{y=0}\\ = \left[M^0_{yy} - \frac{4}{3h^2} P_{yy} + k_b \left(\frac{8}{15}\psi_y - \frac{2}{15}\frac{\partial w_0}{\partial y}\right)\right]_{y=b}\\ = 0.\end{array}\right. \tag{16.56}$$

The new energetic consideration of the potential energy of the elastic restraint within the framework of the TSDT, see Eq. (16.51), results in new boundary conditions by varying the total potential, as described in Eq. (16.56). This boundary condition contains the simply supported boundary conditions ($w_0 = \psi_x = P_{yy} = M^0_{yy} = 0$) for the limiting case $k_0 = k_b = 0$. In the case $k_0 = k_b = \infty$, the values $\partial w_0/\partial y$ and ψ_y converge to zero, so that the sum of these values corresponds to the finite values P_{yy} and M^0_{yy}. This corresponds to the rigidly clamped boundary, for which $\partial w_0/\partial y = \psi_y = 0$ applies. These new boundary conditions can therefore represent both cases.

At the free edge $y = b$ the following applies:

$$\begin{array}{l} \text{Cross-ply,} \\ \text{Angle-ply:} \\ N^0_{yy} = N^0_{xy} = 0. \end{array} \left\{ \begin{array}{l} \text{CLPT:} \\ M^0_{yy} = \frac{\partial M^0_{yy}}{\partial y} + 2\frac{\partial M^0_{xy}}{\partial x} = 0, \\ \text{FSDT:} \\ M^0_{yy} = M^0_{xy} = Q_y = 0, \\ \text{TSDT:} \\ \left\{ \begin{array}{l} M^0_{yy} - \frac{4}{3h^2} P_{yy} = P_{yy} = M^0_{xy} - \frac{4}{3h^2} P_{xy} \\ = \frac{4}{3h^2} \left(\frac{\partial P_{yy}}{\partial y} + 2\frac{\partial P_{xy}}{\partial x} \right) + Q_y - \frac{4}{h^2} R_y = 0. \end{array} \right. \end{array} \right. \tag{16.57}$$

Due to the different coupling terms of unsymmetric cross-ply and angle-ply laminates, it is advisable to adapt the boundary conditions to the selected approaches. This leads to different boundary conditions in the plane, as shown in Eqs. (16.55)–(16.57).

The differential equations are obtained by inserting the constitutive law into the equilibrium conditions. For TSDT, the equilibrium conditions are shown in the first five terms of Eq. (16.54), and the constitutive law can be found in Eq. (16.3). The differential equations can be formulated for CLPT, FSDT and TSDT in compact matrix notation as follows:

$$L_{ij}\,\Phi_i = 0, \quad \left\{ \begin{array}{ll} i,\, j = 1, 2, 3 & \text{for CLPT} \\ i,\, j = 1, \ldots, 5 & \text{for FSDT and TSDT} \end{array} \right. \quad \text{with } \Phi_i = \begin{pmatrix} u_0\,(x,\, y) \\ v_0\,(x,\, y) \\ w_0\,(x,\, y) \\ \psi_x\,(x,\, y) \\ \psi_y\,(x,\, y) \end{pmatrix}. \tag{16.58}$$

It is important to note that L_{ij} is symmetric and therefore $L_{ij} = L_{ji}$ applies. The derivatives are specified below using the derivative operator $d_{i,\ldots}$. The operator $d_{i,\ldots}$ specifies a derivative to x $(\partial/\partial x)$ for $i = x$ and a derivative to y $(\partial/\partial y)$ for $i = y$. A repeated index indicates a multiple derivative. The different theories have the following entries, in which the TSDT contains the abbreviation $\tau = 4/\left(3\,h^2\right)$:

CLPT:

$$\begin{aligned} L_{11} &= A_{11}\,d_{x,x} + A_{66}\,d_{y,y}, \quad L_{12} = (A_{12} + A_{66})\,d_{x,y}, \\ L_{13} &= (-B_{12} - 2\,B_{66})\,d_{x,y,y} - B_{11}\,d_{x,x,x} - 3\,B_{16}\,d_{x,x,y} - B_{26}\,d_{y,y,y}, \\ L_{22} &= A_{22}\,d_{y,y} + A_{66}\,d_{x,x}, \\ L_{23} &= (-B_{12} - 2\,B_{66})\,d_{x,x,y} - B_{16}\,d_{x,x,x} - 3\,B_{26}\,d_{x,y,y} - B_{22}\,d_{y,y,y}, \\ L_{33} &= (2\,D_{12} + 4\,D_{66})\,d_{x,x,y,y} + \xi_x N_{\text{crit}}\,d_{x,x} \\ &\quad + \xi_y N_{\text{crit}}\,d_{y,y} + D_{11}\,d_{x,x,x,x} + D_{22}\,d_{y,y,y,y}, \end{aligned} \tag{16.59}$$

FSDT:

$$
\begin{aligned}
&L_{11} = A_{11}\, d_{x,x} + A_{66}\, d_{y,y}, \quad L_{12} = d_{x,y}\,(A_{12} + A_{66}), \quad L_{13} = 0,\\
&L_{14} = B_{11}\, d_{x,x} + 2\, B_{16}\, d_{x,y} + B_{66}\, d_{y,y},\\
&L_{15} = (B_{12} + B_{66})\, d_{x,y} + B_{16}\, d_{x,x} + B_{26}\, d_{y,y},\\
&L_{22} = A_{22}\, d_{y,y} + A_{66}\, d_{x,x}, \quad L_{23} = 0,\\
&L_{24} = (B_{12} + B_{66})\, d_{x,y} + B_{16}\, d_{x,x} + B_{26}\, d_{y,y},\\
&L_{25} = B_{22}\, d_{y,y} + 2\, B_{26}\, d_{x,y} + B_{66}\, d_{x,x},\\
&L_{33} = (-K A_{55} + \xi_x N_{\text{crit}})\, d_{x,x} - \left(K A_{44} - \xi_y N_{\text{crit}}\right)\, d_{y,y},\\
&L_{34} = -K A_{55}\, d_x, \quad L_{35} = -K A_{44}\, d_y,\\
&L_{44} = -K A_{55} + D_{11}\, d_{x,x} + D_{66}\, d_{y,y},\\
&L_{45} = (D_{12} + D_{66})\, d_{x,y},\\
&L_{55} = -K A_{44} + D_{22}\, d_{y,y} + D_{66}\, d_{x,x},
\end{aligned}
\tag{16.60}
$$

TSDT:

$$
\begin{aligned}
&L_{11} = A_{11}\, d_{x,x} + A_{66}\, d_{y,y}, \quad L_{12} = (A_{12} + A_{66})\, d_{x,y},\\
&L_{13} = -\tau \left[(E_{12} + 2\, E_{66})\, d_{x,y,y} + E_{11}\, d_{x,x,x}\right.\\
&\qquad \left. +3\, E_{16}\, d_{x,x,y} + E_{26}\, d_{y,y,y}\right],\\
&L_{14} = (-\tau\, E_{11} + B_{11})\, d_{x,x} - (2\,\tau\, E_{16} - 2\, B_{16})\, d_{x,y}\\
&\qquad - (\tau\, E_{66} - B_{66})\, d_{y,y},\\
&L_{15} = [\tau\,(-E_{66} - E_{12}) + B_{12} + B_{66}]\, d_{x,y} - (\tau\, E_{16} - B_{16})\, d_{x,x}\\
&\qquad - (E_{26}\,\tau - B_{26})\, d_{y,y}, \quad L_{22} = A_{22}\, d_{y,y} + A_{66}\, d_{x,x},\\
&L_{23} = -\tau \left[(E_{12} + 2\, E_{66})\, d_{x,x,y} + E_{16}\, d_{x,x,x}\right.\\
&\qquad \left. +3\, E_{26}\, d_{x,y,y} + E_{22}\, d_{y,y,y}\right],\\
&L_{24} = [\tau\,(-E_{66} - E_{12}) + B_{12} + B_{66}]\, d_{x,y} + (-\tau\, E_{16} + B_{16})\, d_{x,x}\\
&\qquad - (\tau\, E_{26} - B_{26})\, d_{y,y},\\
&L_{25} = (-\tau\, E_{66} + B_{66})\, d_{x,x} + (-2\tau\, E_{26} + 2\, B_{26})\, d_{x,y}\\
&\qquad - (\tau\, E_{22} - B_{22})\, d_{y,y},\\
&L_{33} = 2\,\tau^2\,(H_{12} + 2\, H_{66})\, d_{x,x,y,y} + \tau^2 H_{11}\, d_{x,x,x,x} + \tau^2 H_{22}\, d_{y,y,y,y}\\
&\qquad + \left(-9\,\tau^2 F_{55} + 6\,\tau\, D_{55} - A_{55} + \xi_x N_{\text{crit}}\right) d_{x,x}\\
&\qquad + \left(-9\,\tau^2 F_{44} + 6\,\tau\, D_{44} - A_{44} + \xi_y N_{\text{crit}}\right)\, d_{y,y},\\
&L_{34} = \tau\,[\tau\,(H_{12} + 2\, H_{66}) - F_{12} - 2\, F_{66}]\, d_{x,y,y}\\
&\qquad + \tau\,(\tau\, H_{11} - F_{11})\, d_{x,x,x} - \left(9\,\tau^2 F_{55} - 6\,\tau\, D_{55} + A_{55}\right)\, d_x,\\
&L_{35} = \tau\,[\tau\,(H_{12} + 2\, H_{66}) - F_{12} - 2\, F_{66}]\, d_{x,x,y}
\end{aligned}
$$

$$
\begin{aligned}
&+ \tau\ (\tau\, H_{22} - F_{22})\, d_{y,y,y} - \left(9\,\tau^2 F_{44} - 6\,\tau\, D_{44} + A_{44}\right) d_y, \\
L_{44} &= \left(\tau^2 H_{11} - 2\,\tau\, F_{11} + D_{11}\right) d_{x,x} \\
&+ \left(\tau^2 H_{66} - 2\,\tau\, F_{66} + D_{66}\right) d_{y,y} \\
&- \left(9\,\tau^2 F_{55} - 6\,\tau\, D_{55} + A_{55}\right), \\
L_{45} &= \left[\tau^2\,(H_{12} + H_{66}) - 2\,\tau\,(F_{12} + F_{66}) + D_{12} + D_{66}\right] d_{x,y}, \\
L_{55} &= \left(\tau^2 H_{66} - 2\,\tau\, F_{66} + D_{66}\right) d_{x,x} \\
&+ \left(\tau^2 H_{22} - 2\,\tau\, F_{22} + D_{22}\right) d_{y,y} \\
&- \left(9\,\tau^2 F_{44} - 6\,\tau\, D_{44} + A_{44}\right).
\end{aligned}
\tag{16.61}
$$

16.2.2 Lévy Solution

Based on the orthotropic laminate behaviour under consideration, the general form of the shape functions provides a separation of the variables in relation to the x- and y-direction. Due to the different coupling effects and boundary conditions, a distinction must be made between cross-ply and angle-ply laminates. The shape function Φ_i^{CP} from Eq. (16.62), which contains the abbreviation $\beta = m\,\pi\,/a$, applies to the unsymmetric cross-ply laminate.

$$
\Phi_i^{\mathrm{CP}} = \begin{pmatrix} \cos(\beta\, x)\, U(y) \\ \sin(\beta\, x)\, V(y) \\ \sin(\beta\, x)\, W(y) \\ \cos(\beta\, x)\, X(y) \\ \sin(\beta\, x)\, Y(y) \end{pmatrix}, \quad
\Phi_i^{\mathrm{AP}} = \begin{pmatrix} \sin(\beta\, x)\, U(y) \\ \cos(\beta\, x)\, V(y) \\ \sin(\beta\, x)\, W(y) \\ \cos(\beta\, x)\, X(y) \\ \sin(\beta\, x)\, Y(y) \end{pmatrix}.
\tag{16.62}
$$

The abbreviations CP and AP stand for cross-ply and angle-ply. For the unsymmetric angle-ply laminate, the shape functions Φ_i^{AP} result from Eq. (16.62). Both sets of shape functions fulfil the boundary conditions (16.55) at the edges $x = 0, a$ identically. The approaches also fulfil the differential equations in relation to the x-coordinate. If the approaches are inserted into the partial differential equations, these become ordinary differential equations in which only derivatives with respect to y occur ($(') = (\partial/\partial y)$). Since the approaches and coupling terms of cross-ply and angle-ply laminates differ, this results in different ordinary differential equations, which are shown below for CLPT, FSDT and TSDT.

16.2.2.1 CLPT Cross-Ply Laminate

The Eq. (16.58) with the components from (16.59) is considered in the framework of CLPT. The approach Φ_i^{CP} of the cross-ply laminate (16.62) is used here and the partial differential equation system is reduced to an ordinary differential equation system. The order of the resulting system can be reduced to the following system by some transformations:

$$\begin{aligned} U'' &= c_1\, U + c_2\, V' + c_3\, W + c_4\, W'', \\ V'' &= c_5\, U' + c_6\, V + c_7\, W' + c_8\, W''', \\ W'''' &= c_9\, U + c_{10}\, V' + c_{11}\, W + c_{12}\, W''. \end{aligned} \tag{16.63}$$

The following abbreviations are used at this point:

$$\begin{aligned} c_1 &= -\frac{k_1}{k_2}, \quad c_2 = -\frac{k_3}{k_2}, \quad c_3 = -\frac{k_4}{k_2}, \quad c_4 = -\frac{k_5}{k_2}, \\ c_5 &= \frac{k_3}{k_7}, \quad c_6 = -\frac{k_6}{k_7}, \quad c_7 = -\frac{k_8}{k_7}, \quad c_8 = -\frac{k_9}{k_7}, \\ c_9 &= \frac{k_1\, k_3\, k_9 - k_1\, k_5\, k_7 + k_4\, k_7\, k_2}{\left(k_7\, k_{12} - {k_9}^2\right) k_2}, \\ c_{10} &= \frac{k_2\, k_6\, k_9 - k_2\, k_7\, k_8 + {k_3}^2 k_9 - k_3\, k_5\, k_7}{\left(k_7\, k_{12} - {k_9}^2\right) k_2}, \\ c_{11} &= \frac{-k_{10}\, k_7\, k_2 + k_3\, k_4\, k_9 - k_4\, k_5\, k_7}{\left(k_7\, k_{12} - {k_9}^2\right) k_2}, \\ c_{12} &= \frac{-k_{11}\, k_2\, k_7 + k_2\, k_8\, k_9 + k_3\, k_5\, k_9 - {k_5}^2 k_7}{\left(k_7\, k_{12} - {k_9}^2\right) k_2}. \end{aligned} \tag{16.64}$$

As part of the state-space concept, the Eq. (16.63) is converted into a first-order system using the following transformation:

$$\begin{aligned} U &= Z_1, \quad U' = Z_2, \quad V = Z_3, \quad V' = Z_4, \\ W &= Z_5, \quad W' = Z_6, \quad W'' = Z_7, \quad W''' = Z_8. \end{aligned} \tag{16.65}$$

This results in the following first-order differential equation system:

$$\underline{Z}'\,(y) = \underline{\underline{A}}\,\underline{Z}, \tag{16.66}$$

which can be written as:

$$\begin{bmatrix} Z_1' \\ Z_2' \\ Z_3' \\ Z_4' \\ Z_5' \\ Z_6' \\ Z_7' \\ Z_8' \end{bmatrix} = \underbrace{\begin{bmatrix} 0 & 1 & 0 & 0 & 0 & 0 & 0 & 0 \\ c_1 & 0 & 0 & c_2 & c_3 & 0 & c_4 & 0 \\ 0 & 0 & 0 & 1 & 0 & 0 & 0 & 0 \\ 0 & c_5 & c_6 & 0 & 0 & c_7 & 0 & c_8 \\ 0 & 0 & 0 & 0 & 0 & 1 & 0 & 0 \\ 0 & 0 & 0 & 0 & 0 & 0 & 1 & 0 \\ 0 & 0 & 0 & 0 & 0 & 0 & 0 & 1 \\ c_9 & 0 & 0 & c_{10} & c_{11} & 0 & c_{12} & 0 \end{bmatrix}}_{\underline{\underline{A}}} \begin{bmatrix} Z_1 \\ Z_2 \\ Z_3 \\ Z_4 \\ Z_5 \\ Z_6 \\ Z_7 \\ Z_8 \end{bmatrix}. \tag{16.67}$$

16.2.2.2 CLPT Angle-Ply Laminate

If the approach Φ_i^{AP} of the unsymmetric angle-ply laminate (16.62) is inserted into the differential equation of CLPT (16.58) with (16.59), the following result is obtained after a few transformations:

$$\begin{aligned} U'' &= c_1\, U + c_2\, V' + c_3\, W' + c_4\, W''', \\ V'' &= c_5\, U' + c_6\, V + c_7\, W + c_8\, W'', \\ W'''' &= c_9\, U' + c_{10}\, V + c_{11}\, W + c_{12}\, W''. \end{aligned} \tag{16.68}$$

The following abbreviations were used here:

$$\begin{aligned} c_1 &= -\frac{k_1}{k_2}, \quad c_2 = \frac{k_3}{k_2}, \quad c_3 = -\frac{k_{13}}{k_2}, \quad c_4 = -\frac{k_{14}}{k_2}, \\ c_5 &= -\frac{k_3}{k_7}, \quad c_6 = -\frac{k_6}{k_7}, \quad c_7 = -\frac{k_{15}}{k_7}, \quad c_8 = -\frac{k_{16}}{k_7}, \\ c_9 &= \frac{k_1\, k_{14}\, k_7 - k_{13}\, k_2\, k_7 + k_{14}\, {k_3}^2 - k_{16}\, k_2\, k_3}{\left(k_2\, k_{12} - {k_{14}}^2\right) k_7}, \\ c_{10} &= \frac{k_{14}\, k_3\, k_6 + k_{15}\, k_2\, k_7 - k_{16}\, k_2\, k_6}{\left(k_2\, k_{12} - {k_{14}}^2\right) k_7}, \\ c_{11} &= \frac{-k_{10}\, k_2\, k_7 + k_{14}\, k_{15}\, k_3 - k_{15}\, k_{16}\, k_2}{\left(k_2\, k_{12} - {k_{14}}^2\right) k_7}, \\ c_{12} &= \frac{-k_{11}\, k_2\, k_7 + k_{13}\, k_{14}\, k_7 + k_{14}\, k_{16}\, k_3 - {k_{16}}^2 k_2}{\left(k_2\, k_{12} - {k_{14}}^2\right) k_7}. \end{aligned} \tag{16.69}$$

Equation (16.68) can be converted into the following first-order differential equation system using (16.65):

$$\begin{bmatrix} Z_1' \\ Z_2' \\ Z_3' \\ Z_4' \\ Z_5' \\ Z_6' \\ Z_7' \\ Z_8' \end{bmatrix} = \underbrace{\begin{bmatrix} 0 & 1 & 0 & 0 & 0 & 0 & 0 & 0 \\ c_1 & 0 & 0 & c_2 & 0 & c_3 & 0 & c_4 \\ 0 & 0 & 0 & 1 & 0 & 0 & 0 & 0 \\ 0 & c_5 & c_6 & 0 & c_7 & 0 & c_8 & 0 \\ 0 & 0 & 0 & 0 & 0 & 1 & 0 & 0 \\ 0 & 0 & 0 & 0 & 0 & 0 & 1 & 0 \\ 0 & 0 & 0 & 0 & 0 & 0 & 0 & 1 \\ 0 & c_9 & c_{10} & 0 & c_{11} & 0 & c_{12} & 0 \end{bmatrix}}_{\underline{\underline{A}}} \begin{bmatrix} Z_1 \\ Z_2 \\ Z_3 \\ Z_4 \\ Z_5 \\ Z_6 \\ Z_7 \\ Z_8 \end{bmatrix}. \tag{16.70}$$

16.2.2.3 FSDT Cross-Ply Laminate

In connection with FSDT, Eq. (16.58) is used with (16.60). If the approach Φ_i^{CP} of the cross-ply laminate (16.62) is inserted into this equation, then after a few transformations, the following system of differential equations is obtained:

$$\begin{aligned} U'' &= c_1\, U + c_2\, V' + c_3\, W + c_4\, X + c_5\, Y', \\ V'' &= c_6\, U' + c_7\, V + c_8\, W' + c_9\, X' + c_{10}\, Y, \\ W'' &= c_{11}\, W + c_{12}\, X + c_{13}\, Y', \\ X'' &= c_{14}\, U + c_{15}\, V' + c_{16}\, W + c_{17}\, X + c_{18}\, Y', \\ Y'' &= c_{19}\, U' + c_{20}\, V + c_{21}\, W' + c_{22}\, X' + c_{23}\, Y, \end{aligned} \tag{16.71}$$

with:

$$\begin{aligned} c_1 &= \frac{k_1\, k_{26} - k_{17}\, k_{18}}{{k_{18}}^2 - k_2\, k_{26}}, \quad c_2 = \frac{-k_{18}\, k_{19} + k_{26}\, k_3}{{k_{18}}^2 - k_2\, k_{26}}, \\ c_3 &= \frac{k_{23}\, k_{18}}{{k_{18}}^2 - k_2\, k_{26}}, \quad c_4 = \frac{k_{17}\, k_{26} - k_{18}\, k_{25}}{{k_{18}}^2 - k_2\, k_{26}}, \\ c_5 &= \frac{-k_{18}\, k_{27} + k_{19}\, k_{26}}{{k_{18}}^2 - k_2\, k_{26}}, \quad c_6 = \frac{k_{12}\, k_3 + k_{19}\, k_9}{k_7\, k_{12} - {k_9}^2}, \\ c_7 &= \frac{-k_{12}\, k_6 - k_{20}\, k_9}{k_7\, k_{12} - {k_9}^2}, \quad c_8 = -\frac{k_{24}\, k_9}{k_7\, k_{12} - {k_9}^2}, \\ c_9 &= \frac{k_{12}\, k_{19} + k_{27}\, k_9}{k_7\, k_{12} - {k_9}^2}, \quad c_{10} = \frac{-k_{12}\, k_{20} - k_{28}\, k_9}{k_7\, k_{12} - {k_9}^2}, \\ c_{11} &= -\frac{k_{21}}{k_{22}}, \quad c_{12} = -\frac{k_{23}}{k_{22}}, \quad c_{13} = -\frac{k_{24}}{k_{22}}, \\ c_{14} &= \frac{-k_1\, k_{18} + k_{17}\, k_2}{{k_{18}}^2 - k_2\, k_{26}}, \quad c_{15} = \frac{-k_{18}\, k_3 + k_{19}\, k_2}{{k_{18}}^2 - k_2\, k_{26}}, \\ c_{16} &= \frac{k_2\, k_{23}}{-{k_{18}}^2 + k_2\, k_{26}}, \quad c_{17} = \frac{-k_{17}\, k_{18} + k_2\, k_{25}}{{k_{18}}^2 - k_2\, k_{26}}, \end{aligned}$$

$$
\begin{aligned}
c_{18} &= \frac{-k_{18}\,k_{19} + k_2\,k_{27}}{{k_{18}}^2 - k_2\,k_{26}}, \quad c_{19} = \frac{k_{19}\,k_7 + k_3\,k_9}{k_7\,k_{12} - {k_9}^2}, \\
c_{20} &= \frac{-k_{20}\,k_7 - k_6\,k_9}{k_7\,k_{12} - {k_9}^2}, \quad c_{21} = -\frac{k_{24}\,k_7}{k_7\,k_{12} - {k_9}^2}, \\
c_{22} &= \frac{k_{19}\,k_9 + k_{27}\,k_7}{k_7\,k_{12} - {k_9}^2}, \quad c_{23} = \frac{-k_{20}\,k_9 - k_{28}\,k_7}{k_7\,k_{12} - {k_9}^2}.
\end{aligned} \tag{16.72}
$$

The following transformation converts the differential equation system of the FSDT from Eq. (16.71) into a first-order system:

$$
\begin{aligned}
U &= Z_1, \quad U' = Z_2, \quad V = Z_3, \quad V' = Z_4, \\
W &= Z_5, \quad W' = Z_6, \quad X = Z_7, \quad X' = Z_8, \\
Y &= Z_9, \quad Y' = Z_{10}.
\end{aligned} \tag{16.73}
$$

The first-order differential equation system resulting from the transformation has the form

$$
\begin{bmatrix} Z_1' \\ Z_2' \\ Z_3' \\ Z_4' \\ Z_5' \\ Z_6' \\ Z_7' \\ Z_8' \\ Z_9' \\ Z_{10}' \end{bmatrix} = \underbrace{\begin{bmatrix} 0 & 1 & 0 & 0 & 0 & 0 & 0 & 0 & 0 & 0 \\ c_1 & 0 & 0 & c_2 & c_3 & 0 & c_4 & 0 & 0 & c_5 \\ 0 & 0 & 0 & 1 & 0 & 0 & 0 & 0 & 0 & 0 \\ 0 & c_6 & c_7 & 0 & 0 & c_8 & 0 & c_9 & c_{10} & 0 \\ 0 & 0 & 0 & 0 & 0 & 1 & 0 & 0 & 0 & 0 \\ 0 & 0 & 0 & 0 & c_{11} & 0 & c_{12} & 0 & 0 & c_{13} \\ 0 & 0 & 0 & 0 & 0 & 0 & 0 & 1 & 0 & 0 \\ c_{14} & 0 & 0 & c_{15} & c_{16} & 0 & c_{17} & 0 & 0 & c_{18} \\ 0 & 0 & 0 & 0 & 0 & 0 & 0 & 0 & 0 & 1 \\ 0 & c_{19} & c_{20} & 0 & 0 & c_{21} & 0 & c_{22} & c_{23} & 0 \end{bmatrix}}_{\underline{\underline{A}}} \begin{bmatrix} Z_1 \\ Z_2 \\ Z_3 \\ Z_4 \\ Z_5 \\ Z_6 \\ Z_7 \\ Z_8 \\ Z_9 \\ Z_{10} \end{bmatrix}. \tag{16.74}
$$

16.2.2.4 FSDT Angle-Ply Laminate

For unsymmetric angle-ply laminates, the approach Φ_i^{AP} from Eq. (16.62) is used in the differential equation of FSDT (16.58) with (16.60). After a few transformations, this leads to the following ordinary differential equation system:

$$
\begin{aligned}
U'' &= c_1\,U + c_2\,V' + c_3\,W' + c_4\,X' + c_5\,Y, \\
V'' &= c_6\,U' + c_7\,V + c_8\,W + c_9\,X + c_{10}\,Y', \\
W'' &= c_{11}\,W + c_{12}\,X + c_{13}\,Y', \\
X'' &= c_{14}\,U' + c_{15}\,V + c_{16}\,W + c_{17}\,X + c_{18}\,Y',
\end{aligned}
$$

$$Y'' = c_{19}\,U + c_{20}\,V' + c_{21}\,W' + c_{22}\,X' + c_{23}\,Y, \tag{16.75}$$

wherein:

$$\begin{aligned}
c_1 &= \frac{-k_1\,k_{12} - k_{14}\,k_{30}}{k_2\,k_{12} - {k_{14}}^2}, \quad c_2 = \frac{k_{12}\,k_3 + k_{14}\,k_{31}}{k_2\,k_{12} - {k_{14}}^2},\\
c_3 &= -\frac{k_{24}\,k_{14}}{k_2\,k_{12} - {k_{14}}^2}, \quad c_4 = \frac{-k_{12}\,k_{29} + k_{14}\,k_{27}}{k_2\,k_{12} - {k_{14}}^2},\\
c_5 &= \frac{-k_{12}\,k_{30} - k_{14}\,k_{28}}{k_2\,k_{12} - {k_{14}}^2}, \quad c_6 = \frac{-k_{14}\,k_{29} + k_{26}\,k_3}{{k_{14}}^2 - k_7\,k_{26}},\\
c_7 &= \frac{k_{14}\,k_{30} + k_{26}\,k_6}{{k_{14}}^2 - k_7\,k_{26}}, \quad c_8 = \frac{k_{23}\,k_{14}}{-{k_{14}}^2 + k_7\,k_{26}},\\
c_9 &= \frac{k_{14}\,k_{25} + k_{26}\,k_{30}}{{k_{14}}^2 - k_7\,k_{26}}, \quad c_{10} = \frac{k_{14}\,k_{27} + k_{26}\,k_{31}}{{k_{14}}^2 - k_7\,k_{26}},\\
c_{11} &= -\frac{k_{21}}{k_{22}}, \quad c_{12} = -\frac{k_{23}}{k_{22}}, \quad c_{13} = -\frac{k_{24}}{k_{22}},\\
c_{14} &= \frac{k_{14}\,k_3 - k_{29}\,k_7}{{k_{14}}^2 - k_7\,k_{26}}, \quad c_{15} = \frac{k_{14}\,k_6 + k_{30}\,k_7}{{k_{14}}^2 - k_7\,k_{26}},\\
c_{16} &= \frac{k_{23}\,k_7}{-{k_{14}}^2 + k_7\,k_{26}}, \quad c_{17} = \frac{k_{14}\,k_{30} + k_{25}\,k_7}{{k_{14}}^2 - k_7\,k_{26}},\\
c_{18} &= \frac{k_{14}\,k_{31} + k_{27}\,k_7}{{k_{14}}^2 - k_7\,k_{26}}, \quad c_{19} = \frac{-k_1\,k_{14} - k_2\,k_{30}}{k_2\,k_{12} - {k_{14}}^2},\\
c_{20} &= \frac{k_{14}\,k_3 + k_2\,k_{31}}{k_2\,k_{12} - {k_{14}}^2}, \quad c_{21} = -\frac{k_2\,k_{24}}{k_2\,k_{12} - {k_{14}}^2},\\
c_{22} &= \frac{-k_{14}\,k_{29} + k_2\,k_{27}}{k_2\,k_{12} - {k_{14}}^2}, \quad c_{23} = \frac{-k_{14}\,k_{30} - k_2\,k_{28}}{k_2\,k_{12} - {k_{14}}^2}.
\end{aligned} \tag{16.76}$$

With the help of the transformation from Eq. (16.73), the system of differential equations can be transformed into the following first-order system:

$$\begin{bmatrix} {Z_1}' \\ {Z_2}' \\ {Z_3}' \\ {Z_4}' \\ {Z_5}' \\ {Z_6}' \\ {Z_7}' \\ {Z_8}' \\ {Z_9}' \\ {Z_{10}}' \end{bmatrix} = \underbrace{\begin{bmatrix} 0 & 1 & 0 & 0 & 0 & 0 & 0 & 0 & 0 & 0 \\ c_1 & 0 & 0 & c_2 & 0 & c_3 & 0 & c_4 & c_5 & 0 \\ 0 & 0 & 0 & 1 & 0 & 0 & 0 & 0 & 0 & 0 \\ 0 & c_6 & c_7 & 0 & c_8 & 0 & c_9 & 0 & 0 & c_{10} \\ 0 & 0 & 0 & 0 & 0 & 1 & 0 & 0 & 0 & 0 \\ 0 & 0 & 0 & 0 & c_{11} & 0 & c_{12} & 0 & 0 & c_{13} \\ 0 & 0 & 0 & 0 & 0 & 0 & 0 & 1 & 0 & 0 \\ 0 & c_{14} & c_{15} & 0 & c_{16} & 0 & c_{17} & 0 & 0 & c_{18} \\ 0 & 0 & 0 & 0 & 0 & 0 & 0 & 0 & 0 & 1 \\ c_{19} & 0 & 0 & c_{20} & 0 & c_{21} & 0 & c_{22} & c_{23} & 0 \end{bmatrix}}_{\underline{\underline{A}}} \begin{bmatrix} Z_1 \\ Z_2 \\ Z_3 \\ Z_4 \\ Z_5 \\ Z_6 \\ Z_7 \\ Z_8 \\ Z_9 \\ Z_{10} \end{bmatrix}. \tag{16.77}$$

16.2.2.5 TSDT Cross-Ply Laminate

For the cross-ply laminate in the context of TSDT, the substitution of the approach Φ_i^{CP} from Eq. (16.62) into the differential equation system (16.58) with (16.61) leads to:

$$
\begin{aligned}
U'' &= c_1\,U + c_2\,V' + c_3\,W + c_4\,W'' + c_5\,X + c_6\,Y',\\
V'' &= c_7\,U' + c_8\,V + c_9\,W' + c_{10}\,W''' + c_{11}\,X' + c_{12}\,Y,\\
W'''' &= c_{13}\,U + c_{14}\,V' + c_{15}\,W + c_{16}\,W'' + c_{17}\,X + c_{18}\,Y',\\
X'' &= c_{19}\,U + c_{20}\,V' + c_{21}\,W + c_{22}\,W'' + c_{23}\,X + c_{24}\,Y',\\
Y'' &= c_{25}\,U' + c_{26}\,V + c_{27}\,W' + c_{28}\,W''' + c_{29}\,X' + c_{30}\,Y.
\end{aligned}
\tag{16.78}
$$

The following abbreviations were used:

$$
\begin{aligned}
c_1 &= \frac{-k_1\,k_{49} + k_{34}\,k_{35}}{k_2\,k_{49} - {k_{35}}^2}, \quad c_2 = \frac{-k_3\,k_{49} + k_{35}\,k_{36}}{k_2\,k_{49} - {k_{35}}^2},\\
c_3 &= \frac{-k_{32}\,k_{49} - k_{35}\,k_{44}}{k_2\,k_{49} - {k_{35}}^2}, \quad c_4 = \frac{-k_{33}\,k_{49} - k_{35}\,k_{45}}{k_2\,k_{49} - {k_{35}}^2},\\
c_5 &= \frac{-k_{34}\,k_{49} + k_{35}\,k_{48}}{k_2\,k_{49} - {k_{35}}^2}, \quad c_6 = \frac{k_{35}\,k_{50} - k_{36}\,k_{49}}{k_2\,k_{49} - {k_{35}}^2},\\
c_7 &= \frac{-k_3\,k_{52} + k_{36}\,k_{40}}{{k_{40}}^2 - k_7\,k_{52}}, \quad c_8 = \frac{-k_{39}\,k_{40} + k_{52}\,k_6}{{k_{40}}^2 - k_7\,k_{52}},\\
c_9 &= \frac{k_{37}\,k_{52} - k_{40}\,k_{46}}{{k_{40}}^2 - k_7\,k_{52}}, \quad c_{10} = \frac{k_{38}\,k_{52} - k_{40}\,k_{47}}{{k_{40}}^2 - k_7\,k_{52}},\\
c_{11} &= \frac{-k_{36}\,k_{52} + k_{40}\,k_{50}}{{k_{40}}^2 - k_7\,k_{52}}, \quad c_{12} = \frac{k_{39}\,k_{52} - k_{40}\,k_{51}}{{k_{40}}^2 - k_7\,k_{52}},\\
c_{13} &= \frac{(-c_{11}\,k_{38} - c_{29}\,k_{47} - k_{45})\,c_{19} - c_1\,c_7\,k_{38}}{c_{10}\,k_{38} + c_{28}\,k_{47} + k_{43}}\\
&\quad + \frac{-c_1\,c_{25}\,k_{47} + c_1\,k_{33} + k_{32}}{c_{10}\,k_{38} + c_{28}\,k_{47} + k_{43}},\\
c_{14} &= \frac{(-c_{11}\,c_{20} - c_2\,c_7 - c_8)\,k_{38} + (-c_2\,c_{25} - c_{20}\,c_{29} - c_{26})\,k_{47}}{c_{10}\,k_{38} + c_{28}\,k_{47} + k_{43}}\\
&\quad \frac{+c_2\,k_{33} - c_{20}\,k_{45} - k_{37}}{c_{10}\,k_{38} + c_{28}\,k_{47} + k_{43}},\\
c_{15} &= \frac{(-c_{11}\,k_{38} - c_{29}\,k_{47} - k_{45})\,c_{21} - c_3\,c_7\,k_{38}}{c_{10}\,k_{38} + c_{28}\,k_{47} + k_{43}}\\
&\quad + \frac{-c_{25}\,c_3\,k_{47} + c_3\,k_{33} - k_{41}}{c_{10}\,k_{38} + c_{28}\,k_{47} + k_{43}},
\end{aligned}
$$

$$
\begin{aligned}
c_{16} &= \frac{(-c_{11}\,c_{22} - c_4\,c_7 - c_9)\,k_{38} + (-c_{22}\,c_{29} - c_{25}\,c_4 - c_{27})\,k_{47}}{c_{10}\,k_{38} + c_{28}\,k_{47} + k_{43}} \\
&\quad + \frac{+k_{33}\,c_4 - k_{45}\,c_{22} - k_{42}}{c_{10}\,k_{38} + c_{28}\,k_{47} + k_{43}}, \\
c_{17} &= \frac{(-c_{11}\,k_{38} - c_{29}\,k_{47} - k_{45})\,c_{23} - c_5\,c_7\,k_{38}}{c_{10}\,k_{38} + c_{28}\,k_{47} + k_{43}} \\
&\quad + \frac{-c_{25}\,c_5\,k_{47} + c_5\,k_{33} - k_{44}}{c_{10}\,k_{38} + c_{28}\,k_{47} + k_{43}}, \\
c_{18} &= \frac{(-c_{11}\,c_{24} - c_6\,c_7 - c_{12})\,k_{38} + (-c_{24}\,c_{29} - c_{25}\,c_6 - c_{30})\,k_{47}}{c_{10}\,k_{38} + c_{28}\,k_{47} + k_{43}} \\
&\quad + \frac{+c_6\,k_{33} - c_{24}\,k_{45} - k_{46}}{c_{10}\,k_{38} + c_{28}\,k_{47} + k_{43}}, \\
c_{19} &= \frac{k_1\,k_{35} - k_2\,k_{34}}{k_2\,k_{49} - {k_{35}}^2}, \quad c_{20} = \frac{-k_2\,k_{36} + k_3\,k_{35}}{k_2\,k_{49} - {k_{35}}^2}, \\
c_{21} &= \frac{k_2\,k_{44} + k_{32}\,k_{35}}{k_2\,k_{49} - {k_{35}}^2}, \quad c_{22} = \frac{k_2\,k_{45} + k_{33}\,k_{35}}{k_2\,k_{49} - {k_{35}}^2}, \\
c_{23} &= \frac{-k_2\,k_{48} + k_{34}\,k_{35}}{k_2\,k_{49} - {k_{35}}^2}, \quad c_{24} = \frac{-k_2\,k_{50} + k_{35}\,k_{36}}{k_2\,k_{49} - {k_{35}}^2}, \\
c_{25} &= \frac{k_3\,k_{40} - k_{36}\,k_7}{{k_{40}}^2 - k_7\,k_{52}}, \quad c_{26} = \frac{k_{39}\,k_7 - k_{40}\,k_6}{{k_{40}}^2 - k_7\,k_{52}}, \\
c_{27} &= \frac{-k_{37}\,k_{40} + k_{46}\,k_7}{{k_{40}}^2 - k_7\,k_{52}}, \quad c_{28} = \frac{-k_{38}\,k_{40} + k_{47}\,k_7}{{k_{40}}^2 - k_7\,k_{52}}, \\
c_{29} &= \frac{k_{36}\,k_{40} - k_{50}\,k_7}{{k_{40}}^2 - k_7\,k_{52}}, \quad c_{30} = \frac{-k_{39}\,k_{40} + k_{51}\,k_7}{{k_{40}}^2 - k_7\,k_{52}}.
\end{aligned}
\tag{16.79}
$$

With the transformation (16.80), the system of equations (16.78) can be transformed into the following first-order system (16.81).

$$
\begin{aligned}
&U = Z_1, \quad U' = Z_2, \quad V = Z_3, \quad V' = Z_4, \\
&W = Z_5, \quad W' = Z_6, \quad W'' = Z_7, \quad W''' = Z_8, \\
&X = Z_9, \quad X' = Z_{10}, \quad Y = Z_{11}, \quad Y' = Z_{12}.
\end{aligned}
\tag{16.80}
$$

$$\begin{bmatrix} Z_1' \\ Z_2' \\ Z_3' \\ Z_4' \\ Z_5' \\ Z_6' \\ Z_7' \\ Z_8' \\ Z_9' \\ Z_{10}' \\ Z_{11}' \\ Z_{12}' \end{bmatrix} = \underbrace{\begin{bmatrix} 0 & 1 & 0 & 0 & 0 & 0 & 0 & 0 & 0 & 0 & 0 & 0 \\ c_1 & 0 & 0 & c_2 & c_3 & 0 & c_4 & 0 & c_5 & 0 & 0 & c_6 \\ 0 & 0 & 0 & 1 & 0 & 0 & 0 & 0 & 0 & 0 & 0 & 0 \\ 0 & c_7 & c_8 & 0 & 0 & c_9 & 0 & c_{10} & 0 & c_{11} & c_{12} & 0 \\ 0 & 0 & 0 & 0 & 0 & 1 & 0 & 0 & 0 & 0 & 0 & 0 \\ 0 & 0 & 0 & 0 & 0 & 0 & 1 & 0 & 0 & 0 & 0 & 0 \\ 0 & 0 & 0 & 0 & 0 & 0 & 0 & 1 & 0 & 0 & 0 & 0 \\ c_{13} & 0 & 0 & c_{14} & c_{15} & 0 & c_{16} & 0 & c_{17} & 0 & 0 & c_{18} \\ 0 & 0 & 0 & 0 & 0 & 0 & 0 & 0 & 0 & 1 & 0 & 0 \\ c_{19} & 0 & 0 & c_{20} & c_{21} & 0 & c_{22} & 0 & c_{23} & 0 & 0 & c_{24} \\ 0 & 0 & 0 & 0 & 0 & 0 & 0 & 0 & 0 & 0 & 0 & 1 \\ 0 & c_{25} & c_{26} & 0 & 0 & c_{27} & 0 & c_{28} & 0 & c_{29} & c_{30} & 0 \end{bmatrix}}_{\underline{\underline{A}}} \begin{bmatrix} Z_1 \\ Z_2 \\ Z_3 \\ Z_4 \\ Z_5 \\ Z_6 \\ Z_7 \\ Z_8 \\ Z_9 \\ Z_{10} \\ Z_{11} \\ Z_{12} \end{bmatrix}. \tag{16.81}$$

16.2.2.6 TSDT Angle-Ply Laminate

The unsymmetric angle-ply laminate uses the approach Φ_i^{AP} from Eq. (16.62). This is used in Eq. (16.58) with (16.61) in the context of the TSDT. This results in an ordinary differential equation system whose order can be reduced by suitable transformation and can be represented as follows

$$\begin{aligned} U'' &= c_1\,U + c_2\,V' + c_3\,W' + c_4\,W''' + c_5\,X' + c_6\,Y, \\ V'' &= c_7\,U' + c_8\,V + c_9\,W + c_{10}\,W'' + c_{11}\,X + Y'\,c_{12}, \\ W'''' &= c_{13}\,U' + c_{14}\,V + c_{15}\,W + c_{16}\,W'' + c_{17}\,X + c_{18}\,Y', \\ X'' &= c_{19}\,U' + c_{20}\,V + c_{21}\,W + c_{22}\,W'' + c_{23}\,X + c_{24}\,Y', \\ Y'' &= c_{25}\,U + V'c_{26} + c_{27}\,W' + c_{28}\,W''' + c_{29}\,X' + c_{30}\,Y, \end{aligned} \tag{16.82}$$

with:

$$\begin{aligned} c_1 &= \frac{-k_1\,k_{52} + k_{56}\,k_{57}}{k_2\,k_{52} - {k_{57}}^2}, \quad c_2 = \frac{k_3\,k_{52} - k_{57}\,k_{60}}{k_2\,k_{52} - {k_{57}}^2}, \\ c_3 &= \frac{k_{46}\,k_{57} - k_{52}\,k_{53}}{k_2\,k_{52} - {k_{57}}^2}, \quad c_4 = \frac{k_{47}\,k_{57} - k_{52}\,k_{54}}{k_2\,k_{52} - {k_{57}}^2}, \\ c_5 &= \frac{-k_{50}\,k_{57} - k_{52}\,k_{55}}{k_2\,k_{52} - {k_{57}}^2}, \quad c_6 = \frac{k_{51}\,k_{57} - k_{52}\,k_{56}}{k_2\,k_{52} - {k_{57}}^2}, \\ c_7 &= \frac{-k_3\,k_{49} - k_{55}\,k_{57}}{k_7\,k_{49} - {k_{57}}^2}, \quad c_8 = \frac{-k_{49}\,k_6 + k_{56}\,k_{57}}{k_7\,k_{49} - {k_{57}}^2}, \\ c_9 &= \frac{-k_{44}\,k_{57} - k_{49}\,k_{58}}{k_7\,k_{49} - {k_{57}}^2}, \quad c_{10} = \frac{-k_{45}\,k_{57} - k_{49}\,k_{59}}{k_7\,k_{49} - {k_{57}}^2}, \end{aligned}$$

$$
\begin{aligned}
c_{11} &= \frac{k_{48}\,k_{57} - k_{49}\,k_{56}}{k_7\,k_{49} - {k_{57}}^2}, \quad c_{12} = \frac{-k_{49}\,k_{60} + k_{50}\,k_{57}}{k_7\,k_{49} - {k_{57}}^2},\\
c_{13} &= \frac{(-c_{19}\,c_{29} - c_{26}\,c_7 - c_{25})\,k_{47} + (-c_{19}\,c_5 - c_2\,c_7 - c_1)\,k_{54}}{c_{28}\,k_{47} + c_4\,k_{54} + k_{43}}\\
&\quad + \frac{-c_{19}\,k_{45} + c_7\,k_{59} - k_{53}}{c_{28}\,k_{47} + c_4\,k_{54} + k_{43}},\\
c_{14} &= \frac{(-c_{29}\,k_{47} - c_5\,k_{54} - k_{45})\,c_{20} - c_2\,c_8\,k_{54}}{c_{28}\,k_{47} + c_4\,k_{54} + k_{43}}\\
&\quad + \frac{-c_{26}\,c_8\,k_{47} + c_8\,k_{59} + k_{58}}{c_{28}\,k_{47} + c_4\,k_{54} + k_{43}},\\
c_{15} &= \frac{(-c_{29}\,k_{47} - c_5\,k_{54} - k_{45})\,c_{21} - c_2\,c_9\,k_{54}}{c_{28}\,k_{47} + c_4\,k_{54} + k_{43}}\\
&\quad + \frac{-c_{26}\,c_9\,k_{47} + c_9\,k_{59} - k_{41}}{c_{28}\,k_{47} + c_4\,k_{54} + k_{43}},\\
c_{16} &= \frac{(-c_{10}\,c_{26} - c_{22}\,c_{29} - c_{27})\,k_{47} + (-c_{10}\,c_2 - c_{22}\,c_5 - c_3)\,k_{54}}{c_{28}\,k_{47} + c_4\,k_{54} + k_{43}}\\
&\quad + \frac{-c_{22}\,k_{45} + c_{10}\,k_{59} - k_{42}}{c_{28}\,k_{47} + c_4\,k_{54} + k_{43}},\\
c_{17} &= \frac{(-c_2\,k_{54} - c_{26}\,k_{47} + k_{59})\,c_{11}}{c_{28}\,k_{47} + c_4\,k_{54} + k_{43}}\\
&\quad + \frac{+(-c_{29}\,k_{47} - c_5\,k_{54} - k_{45})\,c_{23} - k_{44}}{c_{28}\,k_{47} + c_4\,k_{54} + k_{43}},\\
c_{18} &= \frac{(-c_{12}\,c_{26} - c_{24}\,c_{29} - c_{30})\,k_{47} + (-c_{12}\,c_2 - c_{24}\,c_5 - c_6)\,k_{54}}{c_{28}\,k_{47} + c_4\,k_{54} + k_{43}}\\
&\quad + \frac{-c_{24}\,k_{45} + c_{12}\,k_{59} - k_{46}}{c_{28}\,k_{47} + c_4\,k_{54} + k_{43}},\\
c_{19} &= \frac{k_3\,k_{57} + k_{55}\,k_7}{k_7\,k_{49} - {k_{57}}^2}, \quad c_{20} = \frac{-k_{56}\,k_7 + k_{57}\,k_6}{k_7\,k_{49} - {k_{57}}^2},\\
c_{21} &= \frac{k_{44}\,k_7 + k_{57}\,k_{58}}{k_7\,k_{49} - {k_{57}}^2}, \quad c_{22} = \frac{k_{45}\,k_7 + k_{57}\,k_{59}}{k_7\,k_{49} - {k_{57}}^2},\\
c_{23} &= \frac{-k_{48}\,k_7 + k_{56}\,k_{57}}{k_7\,k_{49} - {k_{57}}^2}, \quad c_{24} = \frac{-k_{50}\,k_7 + k_{57}\,k_{60}}{k_7\,k_{49} - {k_{57}}^2},\\
c_{25} &= \frac{k_1\,k_{57} - k_2\,k_{56}}{k_2\,k_{52} - {k_{57}}^2}, \quad c_{26} = \frac{k_2\,k_{60} - k_3\,k_{57}}{k_2\,k_{52} - {k_{57}}^2},\\
c_{27} &= \frac{-k_2\,k_{46} + k_{53}\,k_{57}}{k_2\,k_{52} - {k_{57}}^2}, \quad c_{28} = \frac{-k_2\,k_{47} + k_{54}\,k_{57}}{k_2\,k_{52} - {k_{57}}^2},\\
c_{29} &= \frac{k_2\,k_{50} + k_{55}\,k_{57}}{k_2\,k_{52} - {k_{57}}^2}, \quad c_{30} = \frac{-k_2\,k_{51} + k_{56}\,k_{57}}{k_2\,k_{52} - {k_{57}}^2}.
\end{aligned}
\tag{16.83}
$$

With the transformation (16.80), the differential equation system (16.82) can be transformed into the following first-order system:

$$\begin{bmatrix} Z_1' \\ Z_2' \\ Z_3' \\ Z_4' \\ Z_5' \\ Z_6' \\ Z_7' \\ Z_8' \\ Z_9' \\ Z_{10}' \\ Z_{11}' \\ Z_{12}' \end{bmatrix} = \underbrace{\begin{bmatrix} 0 & 1 & 0 & 0 & 0 & 0 & 0 & 0 & 0 & 0 & 0 & 0 \\ c_1 & 0 & 0 & c_2 & 0 & c_3 & 0 & c_4 & 0 & c_5 & c_6 & 0 \\ 0 & 0 & 0 & 1 & 0 & 0 & 0 & 0 & 0 & 0 & 0 & 0 \\ 0 & c_7 & c_8 & 0 & c_9 & 0 & c_{10} & 0 & c_{11} & 0 & 0 & c_{12} \\ 0 & 0 & 0 & 0 & 0 & 1 & 0 & 0 & 0 & 0 & 0 & 0 \\ 0 & 0 & 0 & 0 & 0 & 0 & 1 & 0 & 0 & 0 & 0 & 0 \\ 0 & 0 & 0 & 0 & 0 & 0 & 0 & 1 & 0 & 0 & 0 & 0 \\ 0 & c_{13} & c_{14} & 0 & c_{15} & 0 & c_{16} & 0 & c_{17} & 0 & 0 & c_{18} \\ 0 & 0 & 0 & 0 & 0 & 0 & 0 & 0 & 0 & 1 & 0 & 0 \\ 0 & c_{19} & c_{20} & 0 & c_{21} & 0 & c_{22} & 0 & c_{23} & 0 & 0 & c_{24} \\ 0 & 0 & 0 & 0 & 0 & 0 & 0 & 0 & 0 & 0 & 0 & 1 \\ c_{25} & 0 & 0 & c_{26} & 0 & c_{27} & 0 & c_{28} & 0 & c_{29} & c_{30} & 0 \end{bmatrix}}_{\underline{\underline{A}}} \begin{bmatrix} Z_1 \\ Z_2 \\ Z_3 \\ Z_4 \\ Z_5 \\ Z_6 \\ Z_7 \\ Z_8 \\ Z_9 \\ Z_{10} \\ Z_{11} \\ Z_{12} \end{bmatrix}. \tag{16.84}$$

The Eq. (16.83) contain the following further abbreviations, where $\beta = m\pi/a$ and $\tau = 4/(3\,h^2)$:

$$\begin{aligned}
k_1 &= -A_{11}\,\beta^2, \quad k_2 = A_{66}, \quad k_3 = (A_{12} + A_{66})\,\beta, \\
k_4 &= B_{11}\,\beta^3, \quad k_5 = -(B_{12} + 2\,B_{66})\,\beta, \quad k_6 = -A_{66}\,\beta^2, \\
k_7 &= A_{22}, \quad k_8 = (B_{12} + 2\,B_{66})\,\beta^2, \quad k_9 = -B_{22}, \\
k_{10} &= D_{11}\,\beta^4 - \xi_x N_{\text{crit}}\,\beta^2, \quad k_{11} = -(2\,D_{12} + 4\,D_{66})\,\beta^2 + \xi_y N_{\text{crit}}, \\
k_{12} &= D_{22}, \quad k_{13} = 3\,B_{16}\,\beta^2, \quad k_{14} = -B_{26}, \quad k_{15} = B_{16}\,\beta^3, \\
k_{16} &= -3\,B_{26}\,\beta, \quad k_{17} = -B_{11}\,\beta^2, \quad k_{18} = B_{66}, \\
k_{19} &= (B_{12} + B_{66})\,\beta, \quad k_{20} = -B_{66}\,\beta^2, \\
k_{21} &= (K\,A_{55} - \xi_x N_{\text{crit}})\,\beta^2, \quad k_{22} = -K\,A_{44} + \xi_y N_{\text{crit}}, \\
k_{23} &= A_{55}\,K\,\beta, \quad k_{24} = -K\,A_{44}, \quad k_{25} = -D_{11}\,\beta^2 - K\,A_{55}, \\
k_{26} &= D_{66}, \quad k_{27} = (D_{12} + D_{66})\,\beta, \quad k_{28} = -D_{66}\,\beta^2 - K\,A_{44}, \\
k_{29} &= -2\,B_{16}\,\beta, \quad k_{30} = -B_{16}\,\beta^2, \quad k_{31} = 2\,B_{26}\,\beta, \\
k_{32} &= E_{11}\,\beta^3\tau, \quad k_{33} = -(E_{12} + 2\,E_{66})\,\beta\,\tau, \\
k_{34} &= (E_{11}\,\tau - B_{11})\,\beta^2, \quad k_{35} = -E_{66}\,\tau + B_{66}, \\
k_{36} &= (-(E_{66} + E_{12})\,\tau + B_{12} + B_{66})\,\beta, \\
k_{37} &= (E_{12} + 2\,E_{66})\,\beta^2\tau, \quad k_{38} = -\tau\,E_{22}, \\
k_{39} &= (E_{66}\,\tau - B_{66})\,\beta^2, \quad k_{40} = -\tau\,E_{22} + B_{22}, \\
k_{41} &= H_{11}\,\tau^2\beta^4 + \left(9\,F_{55}\,\tau^2 - 6\,D_{55}\,\tau + A_{55} - \xi_x N_{\text{crit}}\right)\beta^2, \\
k_{42} &= -2\,\tau^2\,(H_{12} + 2\,H_{66})\,\beta^2 - 9\,F_{44}\,\tau^2 + 6\,D_{44}\,\tau - A_{44} + \xi_y N_{\text{crit}}, \\
k_{43} &= H_{22}\,\tau^2, \\
k_{44} &= \tau\,(H_{11}\,\tau - F_{11})\,\beta^3 + \left(9\,F_{55}\,\tau^2 - 6\,D_{55}\,\tau + A_{55}\right)\beta,
\end{aligned}$$

$$
\begin{aligned}
k_{45} &= -\left((H_{12} + 2\,H_{66})\,\tau - F_{12} - 2\,F_{66}\right)\tau\,\beta,\\
k_{46} &= -\left((H_{12} + 2\,H_{66})\,\tau - F_{12} - 2\,F_{66}\right)\tau\,\beta^2 - 9\,F_{44}\,\tau^2\\
&\quad + 6\,D_{44}\,\tau - A_{44}, \quad k_{47} = \tau\,\left(H_{22}\,\tau - F_{22}\right),\\
k_{48} &= -\left(H_{11}\,\tau^2 - 2\,F_{11}\,\tau + D_{11}\right)\beta^2 - 9\,F_{55}\,\tau^2 + 6\,D_{55}\,\tau - A_{55},\\
k_{49} &= H_{66}\,\tau^2 - 2\,F_{66}\,\tau + D_{66},\\
k_{50} &= \left((H_{12} + H_{66})\,\tau^2 - (2\,F_{12} + 2\,F_{66})\,\tau + D_{12} + D_{66}\right)\beta,\\
k_{51} &= -\left(H_{66}\,\tau^2 - 2\,F_{66}\,\tau + D_{66}\right)\beta^2 - 9\,F_{44}\,\tau^2 + 6\,D_{44}\,\tau - A_{44},\\
k_{52} &= H_{22}\,\tau^2 - 2\,F_{22}\,\tau + D_{22}, \quad k_{53} = 3\,E_{16}\,\beta^2\tau,\\
k_{54} &= -E_{26}\,\tau, \quad k_{55} = (2\,E_{16}\,\tau - 2\,B_{16})\,\beta,\\
k_{56} &= (E_{16}\,\tau - B_{16})\,\beta^2, \quad k_{57} = -E_{26}\,\tau + B_{26},\\
k_{58} &= E_{16}\,\beta^3\tau, \quad k_{59} = -3\,E_{26}\,\beta\,\tau,\\
k_{60} &= (-2\,E_{26}\,\tau + 2\,B_{26})\,\beta.
\end{aligned}
\tag{16.85}
$$

For the presented differential equation systems, a solution method is presented in the next section.

16.2.2.7 The Transcendental Buckling Equation

The first-order differential equation systems described above can be solved with the so-called state-space concept, which can be found, for example, in Khdeir (1988) or Nosier and Reddy (1992). A general solution of the ordinary differential equation system is given by

$$\underline{Z}(y) = \mathrm{e}^{\underline{\underline{A}}\,y}\,\underline{K}. \tag{16.86}$$

The vector $\underline{K}$ contains constant coefficients and can be described by the boundary conditions. In the case that $\underline{\underline{A}}$ is diagonalizable, the matrix $\mathrm{e}^{\underline{\underline{A}}\,y}$ can be defined as follows:

$$\mathrm{e}^{\underline{\underline{A}}\,y} = \underline{\underline{L}}\begin{bmatrix} \mathrm{e}^{\lambda_1 y} & & 0 \\ & \ddots & \\ 0 & & \mathrm{e}^{\lambda_k y} \end{bmatrix}\underline{\underline{L}}^{-1}. \tag{16.87}$$

The matrix $\underline{\underline{L}}$ contains the eigenvectors of $\underline{\underline{A}}$, and $\lambda_{1\ldots k}$ represents the respective eigenvalues. The dimension of the matrix $\underline{\underline{A}}$ depends on the different laminate theories, therefore the number of eigenvalues is different, which leads to the following results: $k = 8$ for CLPT, $k = 10$ for FSDT and $k = 12$ for TSDT. Equation (16.87) is only valid as a solution if no multiple eigenvalues occur, i.e. the matrix $\underline{\underline{A}}$ is diagonalizable. The substitution of Eq. (16.86) into the corresponding boundary conditions leads to a homogeneous system of equations of the type

$$\underline{\underline{M}}\,\underline{K} = 0. \tag{16.88}$$

The coefficient matrix $\underline{\underline{M}}$ with the dimension $k \times k$ depends on the underlying theory, as described above. A non-trivial solution of (16.88) requires a vanishing determinant of the coefficient matrix:

$$\det\left(\underline{\underline{M}}\right) = 0. \tag{16.89}$$

This leads to a transcendental equation for the buckling load N_{xx}^0, which is exact with respect to the underlying theoretical framework. However, the described method can cause numerical problems. Firstly, zero entries on the main diagonal of $\underline{\underline{A}}$ are problematic for the eigenvalue analysis. Secondly, the problem $\det(\underline{\underline{M}}) = 0$ is generally ill-conditioned. There are solution strategies for both problems, which are described in the Chap. 13.

To solve the transcendental equation, it is useful to use a suitable initial value. For this purpose, the closed-form analytical solution from the first section of this chapter is used. This provides an initial value for the critical load and the half-wave number m. In the Lévy solution, only three values are calculated for the buckling load with $m-1, m, m+1$, where the smallest value represents the solution of interest. This method makes Lévy-type solutions much more efficient.

In addition, the very large gradients of $\det(\underline{\underline{M}})$ can cause difficulties for the solution algorithm. Therefore, the objective function is scaled with $\det(\underline{\underline{M}})^{-1}$ from the start value.

The solutions presented here can also be applied directly to symmetric orthotropic laminates without any modifications.

References

Ashton JE (1969): *An analogy for certain anisotropic plates*, Journal of Composite Materials 3:355–358.

Beerhorst M, Suresh Babu T (2020): *Closed-form approximate solution for linear buckling of Mindlin plates with SRSR-boundary conditions*, Composite Structures 240:112037.

Chai GB, Banks WM, Rhodes J (1991): *The instability behaviour of laminated panels with elastically rotationally restrined edges*, Composite Structures 19:41–65.

Khdeir AA (1988): *Free vibration and buckling of symmetric cross-ply laminated plates by an exact method*, Journal of Sound and Vibrarion 126:447–461.

Mittelstedt C (2007): *Local buckling of wide-flange thin-walled anisotropic composite beams*, Archive of Applied Mechanics 77:439–452.

Nosier A, Reddy JN (1992): *Vibration and stability analyses of cross-ply laminated circular cylindrical shells*, Journal of Sound and Vibration 157:139–159.

Qiao P, Shan L (2005): *Explicit local buckling analysis and design of fiber–reinforced plastic composite structural shapes*, Composite Structures 70:468–483.

Reissner E, Stavsky Y (1961): *Bending and stretching of certain types of heterogeneous aeolotropic elastic plates*, Journal of Applied Mechanics 28:402–408.

Schilling J, Mittelstedt C (2020): *Local buckling analysis of omega-stringer-stiffened composite panels using a new closed-form analytical approximate solution*, Thin-Walled Structures 147:106534.

Schreiber P, Mittelstedt C, Beerhorst M (2020): *Buckling of shear-deformable orthotropic laminated plates with elastic restraints*, Thin-Walled Structures 157:107071-1–14.

Schreiber P, Mittelstedt C (2022a): *Buckling of shear-deformable, unsymmetrically laminated plates*, International Journal of Mechanical Sciences 218:106995.

Schreiber P, Mittelstedt C (2022b): *Lévy-type solutions for the buckling analysis of unsymmetrically laminated plates with rotational restraints for various plate theories*, Archive of Applied Mechanics 93:2907–2935.

Whitney JM, Pagano NJ (1970): *Shear deformation in heterogeneous anisotropic plates*, Journal of Applied Mechanics 37:1031–1036.



Buckling of Stiffened Laminates

17

This chapter deals with the buckling behaviour of thin stiffened laminated structures. First, the Ritz method is presented as a suitable analysis method with which such stiffened laminates can be treated, and a detailed discussion of the buckling behaviour of such structures is carried out. Lévy-type solutions for longitudinally and transversely stiffened laminates under compressive loading are presented as a further method. For longitudinally stiffened laminates, closed-form analysis solutions are also given and generic buckling curves are presented. Another situation of practical relevance is the laminate with a stiffened free edge under compressive loading, and both the Lévy solution and the minimum stiffness of the edge stiffeners are discussed. Finally, a closed-form analytical approach is introduced for the buckling behaviour of a longitudinally stiffened laminate under compressive loading, taking into account the plate-stiffener interaction, and the buckling behaviour of stiffened laminates under shear loading is investigated using the Ritz method. The chapter concludes with a consideration of the global buckling behaviour of stiffened laminates.

17.1 Introduction

Large-scale structural parts in aircraft construction in composite design such as fuselage segments or tail planes and wing shells typically consist of a shell of moderate curvature, which is reinforced in the longitudinal and/or transverse direction by a number of stiffeners, the so-called stringers and frames or ribs (see Fig. 17.1, which shows a cross-section of an exemplary shell with various open-profile stiffeners). Since such components are generally classified as thin-walled, their stability behaviour is an important point in the analysis and design. This chapter is therefore dedicated to the stability of stiffened thin-walled load-bearing laminated structures.

© The Author(s), under exclusive license to Springer-Verlag GmbH, DE, part of Springer Nature 2025

C. Mittelstedt, *Mechanics of Composite Structures*,
https://doi.org/10.1007/978-3-662-70788-3_17

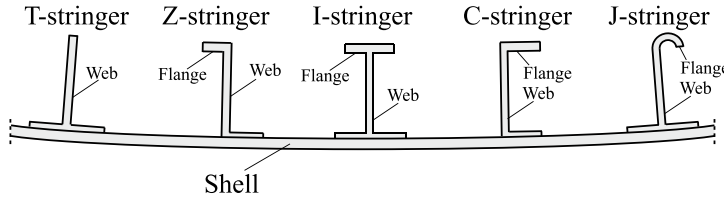


Fig. 17.1 Stiffened shell, reinforced by stiffeners with open profiles

The problem of the stability of stiffened plate structures under various load cases has been the subject of intensive research for about a century. One of the earliest works in this field goes back to Timoshenko in 1921, in which the stability analysis of stiffened and unstiffened isotropic plates using the Ritz method is reported. This fundamental work was followed by many other important papers in the subsequent decades, whereby the work of Schnadel (1930), Barbré (1936, 1937), Windenburg (1938), Chwalla (1944), Kromm (1944) and Seide and Stein (1949) can only represent a selection. More recent work in this field has been presented, for example, by Mittelstedt (2008a, b, 2009), Mittelstedt and Schagerl (2010), Weißgraeber et al. (2012), Mittelstedt (2021), Schilling and Mittelstedt (2020a, b), or Schilling et al. (2022).

If one specializes the considerations on isotropic stiffened plates, the question of the bending stiffness EI of the stiffeners, which is necessary to prevent simultaneous global buckling of the plate and the stiffeners, has always been asked in many investigations in addition to the actual calculation of buckling loads. If this specific value for the bending stiffness EI—also called minimum stiffness $EI_{\min}$—is reached, local buckling of the plate between the stiffeners is enforced, whereby the stiffeners themselves remain more or less undeformed and in their original position. Knowledge of this minimum stiffness $EI_{\min}$ is naturally of great relevance for many applications in lightweight construction, because it can be concluded that a buckling mode in which the stiffeners exhibit no or only very small deformations depends only on the properties of the individual plate sections and is ultimately decoupled from the properties of the stiffeners. It can be shown that when the minimum stiffness $EI_{\min}$ is reached, an upper limit value of the bending stiffness is reached, beyond which an increase in EI—at least from the point of view of the stability behaviour of the stiffened laminate—no longer brings any benefit, but would only mean an unnecessary increase in weight. This is a very important design criterion for the design of stiffened structures, especially in composite lightweight construction with its extreme demands on the weight of the structure.

17.2 The Ritz Method for Longitudinally and Transversely Stiffened Laminates

The stability behaviour of longitudinally and transversely stiffened plates or laminates can be advantageously investigated with the help of the Ritz method, whereby the formulation of the method already presented in Chap. 14 is to be extended accordingly by the influence of the stiffeners or more precisely by their internal and external potentials. Consider the situation shown in Fig. 17.2, in which an exemplary plate is shown, which is stiffened by stringers and frames. The stiffeners shown here are idealised as Euler-Bernoulli beams in the following Ritz formulation, whereby it is assumed that the centers of gravity of the beams are located exactly in the laminate middle plane. By taking into account the geometry and material properties in the cross-sectional values EA, EI and GI_T of the stringers and frames, a very good result accuracy can be achieved in many cases with such a relatively simple Ritz formulation. Let the stiffened plate be loaded by the force flows N^0_{xx}, N^0_{yy} and N^0_{xy}.

Let n_{ST} stringers and n_{FR} frames be given. Stringer i has the effective properties EA_i^{ST}, EI_i^{ST}, $GI_{T,i}^{\mathrm{ST}}$ and is positioned at the point y_i^{ST}. Stringer i is loaded by a normal force P_i^{ST}, which can be calculated from the compatibility of the longitudinal elongation of the stringer with the longitudinal elongation of the plate from the normal force flow N^0_{xx} acting on the plate. Similarly, frame i has the effective properties EA_i^{FR}, EI_i^{FR}, $GI_{T,i}^{\mathrm{FR}}$, is attached to the plate at the location x_i^{FR} and is loaded by the normal force P_i^{FR}. In order to consider the influence of the stiffeners on the buckling behaviour within the framework of the Ritz method, the internal and external total potential must be extended by the contributions of the stiffeners. Specifically, in addition to the inner potential of the plate, the inner potential of the stringers must be taken into account, which can be represented as follows:

$$\Pi_i^{\mathrm{ST}} = \frac{1}{2}\sum_{i=1}^{i=n_{\mathrm{ST}}} \int_0^a EI_i^{\mathrm{ST}} \left(\frac{\partial^2 w_0}{\partial x^2}\right)^2 \Bigg|_{y=y_i^{\mathrm{ST}}} \mathrm{d}x + \frac{1}{2}\sum_{i=1}^{i=n_{\mathrm{ST}}} \int_0^a GI_{T,i}^{\mathrm{ST}} \left(\frac{\partial^2 w_0}{\partial x \partial y}\right)^2 \Bigg|_{y=y_i^{\mathrm{ST}}} \mathrm{d}x. \tag{17.1}$$

In addition, the internal potential of the frames is as follows:

$$\Pi_i^{\mathrm{FR}} = \frac{1}{2}\sum_{i=1}^{i=n_{\mathrm{FR}}} \int_0^b EI_i^{\mathrm{FR}} \left(\frac{\partial^2 w_0}{\partial y^2}\right)^2 \Bigg|_{x=x_i^{\mathrm{FR}}} \mathrm{d}y + \frac{1}{2}\sum_{i=1}^{i=n_{\mathrm{FR}}} \int_0^b GI_{T,i}^{\mathrm{FR}} \left(\frac{\partial^2 w_0}{\partial x \partial y}\right)^2 \Bigg|_{x=x_i^{\mathrm{FR}}} \mathrm{d}y. \tag{17.2}$$

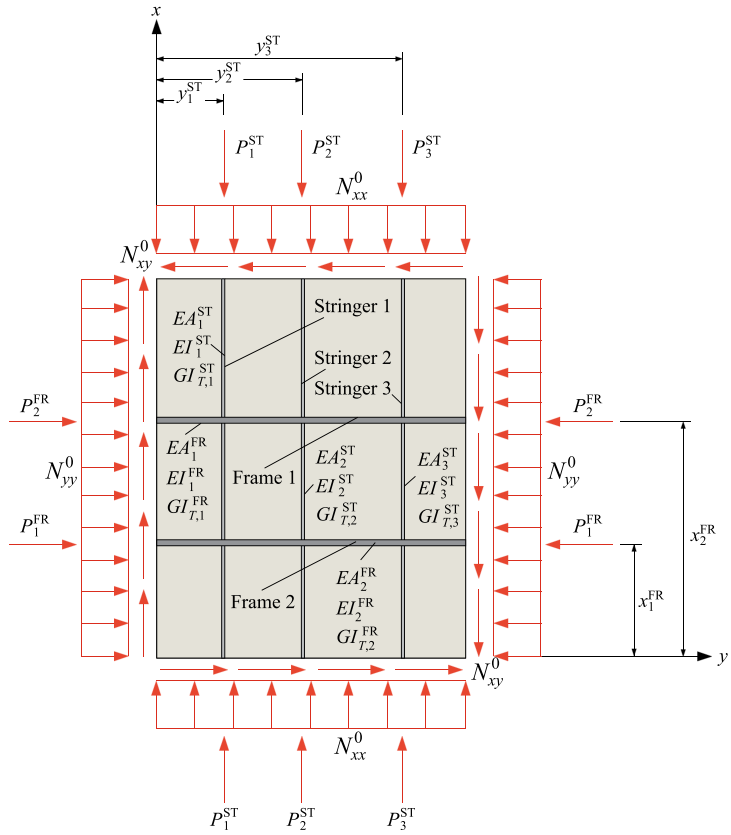


Fig. 17.2 Idealization of the stiffened plate

The potential of the stringer and frame forces then results as follows:

$$\Pi_a^{ST} = -\frac{1}{2}\Lambda \sum_{i=1}^{i=n_{ST}} P_i^{ST} \int_0^a \left(\frac{\partial w_0}{\partial x}\right)^2 |_{y=y_i^{ST}} \mathrm{d}x,$$

$$\Pi_a^{FR} = -\frac{1}{2}\Lambda \sum_{i=1}^{i=n_{FR}} P_i^{FR} \int_0^b \left(\frac{\partial w_0}{\partial y}\right)^2 |_{x=x_i^{FR}} \mathrm{d}y. \tag{17.3}$$

Adding up the potential contributions of the unstiffened plate already determined in Chap. 14 with the potential components due to the stiffeners then results in the total elastic potential of the buckled stiffened plate. The procedure for determining critical buckling loads then works in exactly the same way as already shown for the unstiffened plate, and no further details are given here.

In order to discuss the characteristic stability behaviour of stiffened plate structures in composite laminate construction in more detail, some selected configurations of plates simply supported at all edges are considered below. The following results were calculated with the presented Ritz formulation for degrees of series expansion of $M = 24$ and $N = 24$, whereby $GI_T = 0$ was assumed for all stiffeners for the sake of simplicity.

Figure 17.3 shows the buckling load for a centrically stiffened laminate plate with different stiffener heights h_S. A laminate with the dimensions $a = 300\,\text{mm}$, $b = 100\,\text{mm}$ and the layup $\left[(0°/90°)_{2S}\right]_S$ was considered, whereby for the sake of simplicity it was assumed that both the plate and the stiffener are made of composite laminates, which also have the same layups. The thickness of the plate and thus also the width of the stiffener cross-section was $h = 1.0\,\text{mm}$, and the elastic layer properties were assumed to be $E_{11} = 138{,}000\,\text{MPa}$, $E_{22} = 8960\,\text{MPa}$, $G_{12} = 7100\,\text{MPa}$, $\nu_{12} = 0.30$. It was also assumed that the center of gravity of the stiffener is located in the middle plane of the laminate. The graph $N^0_{xx}\,(h_S)$ shows that stiffeners with low cross-sectional heights contribute only slightly to an increase in the critical buckling load. Up to a value $h_S = 2.09\,\text{mm}$ the stiffened plate buckles in $m = 3$ longitudinal half-waves, with $n = 1$ half-waves occurring in the transverse direction (mode 1). In the interval $2.09\,\text{mm} \leq h_S \leq 8.63\,\text{mm}$, only $m = 2$ longitudinal half-waves occur with one half-wave in the transverse direction (mode 2), and a significant increase in the buckling load $N^0_{xx}\,(h_S)$ is noticeable. The change from $m = 3$ to $m = 2$ half-waves in the longitudinal direction can be clearly explained by the fact that the stiffener participates in the buckling resistance of the stiffened plate to an increasing extent with increasing cross-sectional height h_S and is also able to absorb potential energy accordingly. The plate is therefore prevented from buckling by the increasingly stiffer longitudinal stiffener and therefore the number of buckling half-waves that form continues to decrease. Accordingly, in the interval $8.63\,\text{mm} \leq h_S \leq 13.34\,\text{mm}$, only one longitudinal half-wave is encountered with one half-wave in the transverse direction (mode 3), and a further increase in the critical buckling load can be observed. An interesting observation is made for stiffener heights of $h_S \geq 13.34\,\text{mm}$. For such stiffener heights, regardless of the actual value for h_S, a purely localised buckling pattern results, in which the plate buckles on both sides of the stiffener in $m = 5$ half-waves in the longitudinal direction and $n = 2$ half-waves in the transverse direction. The longitudinal axis of the stiffener thus forms a perfect nodal line of the buckling mode that occurs (labelled here as mode 4). The buckling load of the stiffened plate thus decouples for $h_S \geq 13.34\,\text{mm}$ from the properties of the stiffener (the buckling load N^0_{xx} thus remains constant for such stiffener heights), and a purely local buckling of the plate takes place on both sides of the stiffener. The stiffener remains completely at rest and is not involved in any energy absorption at the onset of buckling. In buckling problems where a certain bending stiffness EI of the stiffener can be determined, above which the critical buckling load becomes completely independent of the stiffener properties, this specific bending stiffness is also referred to as the so-called minimum stiffness $EI_{\min}$. However, buckling problems in which the level of the critical buckling load is completely decoupled from the stiffness properties (which is why we want to speak of a 'real' minimum stiffness in

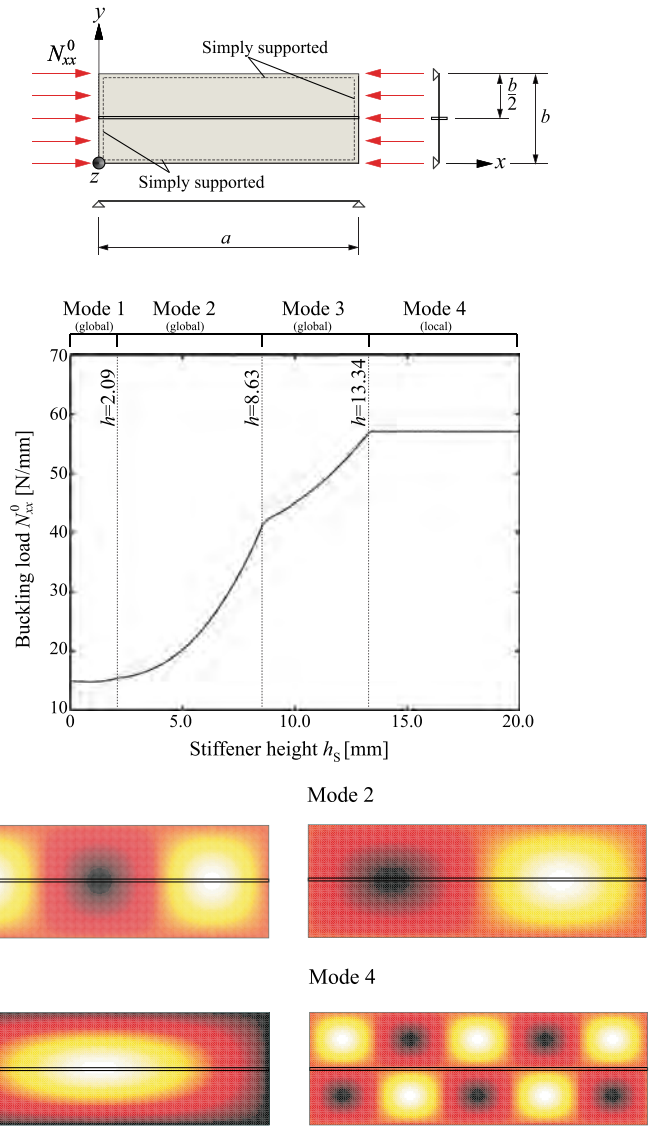


Fig. 17.3 Buckling load N_{xx}^0 and buckling modes of a centrically stiffened laminate under uniaxial compression as a function of the stiffener height h_S

such a case) are very rare. In fact, in many technically relevant problems, it will be possible to determine a certain limit value for the bending stiffness EI, above which an increase in EI only results in an insignificant increase in the buckling load, but without being able to prove a complete decoupling from the stiffener properties. This limit value would then

also be interpreted as a minimum stiffness $EI_{\min}$, but would then rather be described as an 'incomplete' minimum stiffness. Such examples will also be briefly discussed below.

Figure 17.4 shows the buckling load for a variable stiffener height h_S for a plate that is identical to the previous example, but here the stiffener is now arranged off-center at the

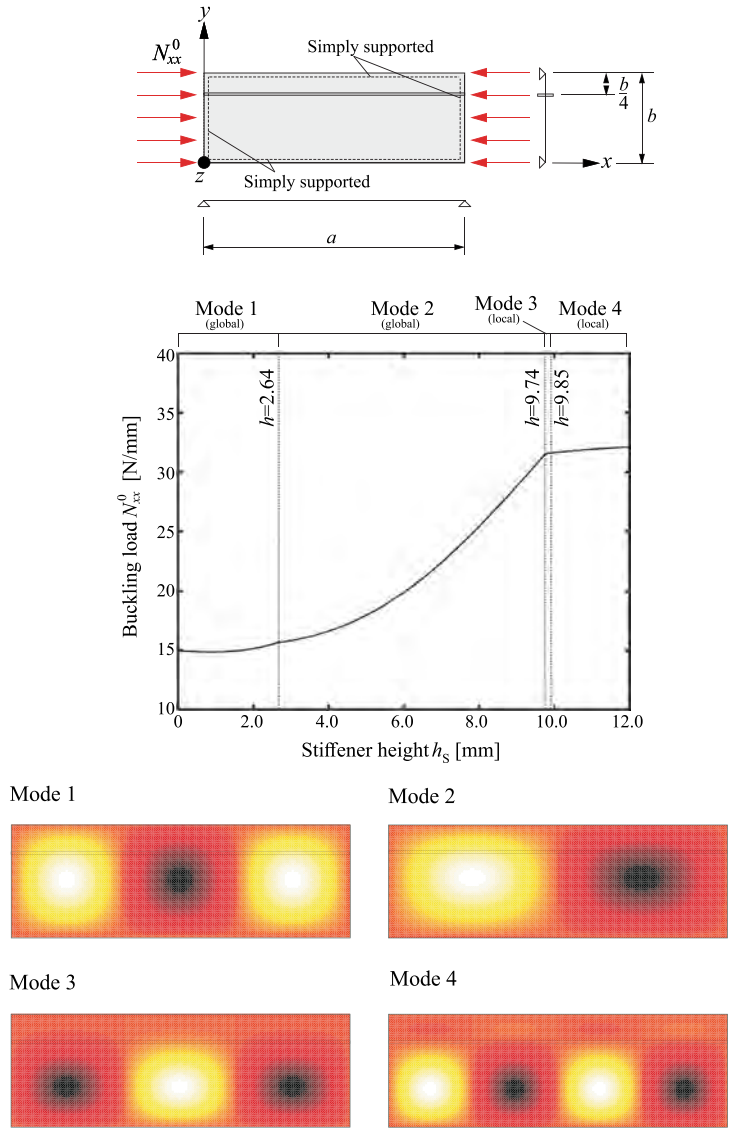


Fig. 17.4 Buckling load N_{xx}^0 and buckling modes of an eccentrically stiffened laminate under uniaxial compression as a function of the stiffener height h_S

point $y = \frac{3b}{4}$. Overall, the resulting graph $N_{xx}^0\,(h_S)$ is similar to that in Fig. 17.3, but with the two differences that, on the one hand, the resulting buckling load is significantly lower than for the centrically stiffened laminate and, on the other hand, no 'real' minimum stiffness $EI_{\min}$ can be determined. Rather, even after exceeding the limit value $h_S = 9.74\,\text{mm}$ or $h_S = 9.85\,\text{mm}$ (both stiffener heights lead to very localized buckling patterns in the wider partial field of the laminate), a slight increase in the critical buckling load N_{xx}^0 can be seen, so that in the case of the eccentrically stiffened laminate under uniaxial compressive load, an 'incomplete' minimum stiffness $EI_{\min}$ is present. Nevertheless, Fig. 17.4 clearly shows that increasing the stiffener height beyond the specified limit values would be uneconomical, because a significant increase in the structural weight would not be associated with a significant increase in the buckling load.

Similar conclusions can be drawn from Fig. 17.5, where a representation of the function $N_{xx}^0\,(h_S)$ and some resulting buckling modes for a centrically stiffened laminate under inplane bending can be found. Apparently, there is also an 'incomplete' minimum stiffness $EI_{\min}$ for this problem, which represents an important limit value for the design, beyond which no significant increase in the critical buckling load is possible.

The same applies to the results of Fig. 17.6, in which $N_{xx}^0\,(h_S)$ and some associated buckling modes for a centrically stiffened laminate under inplane shear load are shown. In the case of the shear-loaded laminate, the layer properties $E_{11} = 138{,}000\,\text{MPa}$, $E_{22} = 8960\,\text{MPa}$, $G_{12} = 7372\,\text{MPa}$, $\nu_{12} = 0.30$ were used.

Overall, it should be noted that the determination of optimal stiffener configurations in composite lightweight construction is an important design criterion, although there are still a number of open questions, especially if there is interest in simple, closed-form analytical and thus practical design methods. Some recent findings on this can be found, for example, in Mittelstedt (2008a, b).

17.3 Lévy Solution for Uniaxially Compressed Longitudinally Stiffened Laminates

17.3.1 Basic Equations

Consider a symmetric and orthotropic laminate (length a, width b, thickness h), which is under a uniaxial compressive load N_{xx}^0 and is reinforced by an arbitrary number of longitudinal stiffeners (Fig. 17.7). We assume $GI_T = 0$ for all stiffeners, i.e. the torsional stiffness is negligible.

The laminate is divided into $n + 1$ plate fields by the n stiffeners. Stiffener i has the bending stiffness EI_i and is loaded by the load P_i, which can be calculated from the requirement for compatibility of the longitudinal elongation of the laminate and the longitudinal elongation of the stiffener. Furthermore, local axes y_i are introduced as indicated.

If we start again from the buckling differential equation

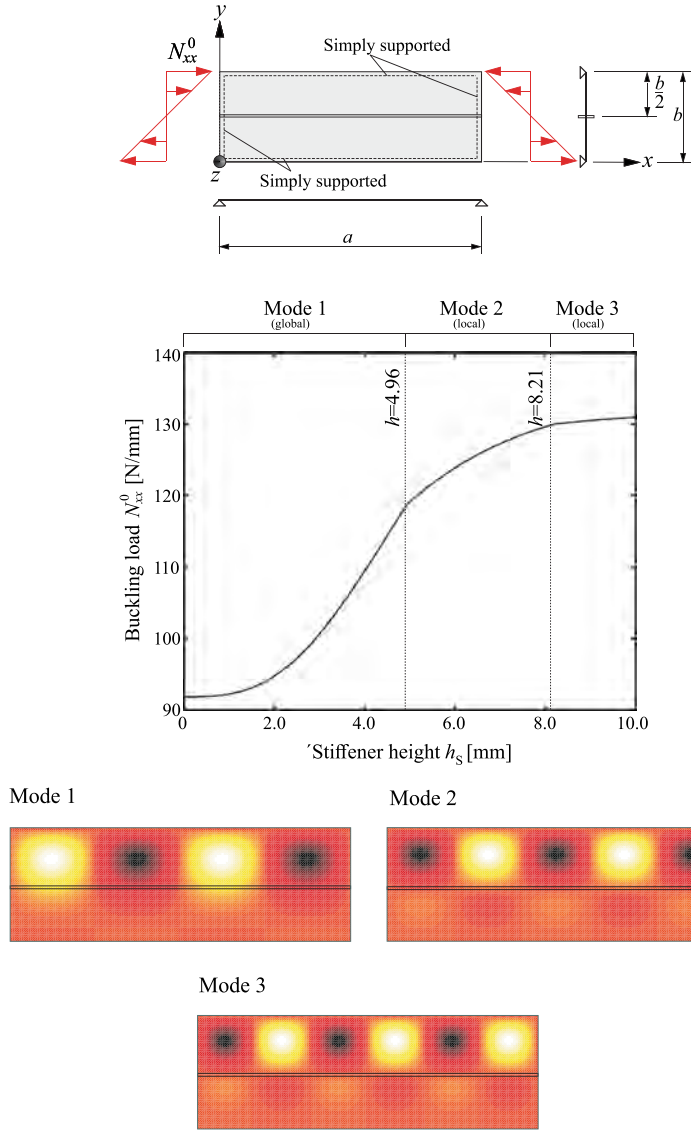


Fig. 17.5 Buckling load N_{xx}^0 and buckling modes of a centrically stiffened laminate under inplane bending as a function of the stiffener height h_S

$$D_{11}\frac{\partial^4 w_0}{\partial x^4} + D_{22}\frac{\partial^4 w_0}{\partial y^4} + 2\left(D_{12} + 2D_{66}\right)\frac{\partial^4 w_0}{\partial x^2 \partial y^2} + N_{xx}^0\frac{\partial^2 w_0}{\partial x^2} = 0 \tag{17.4}$$

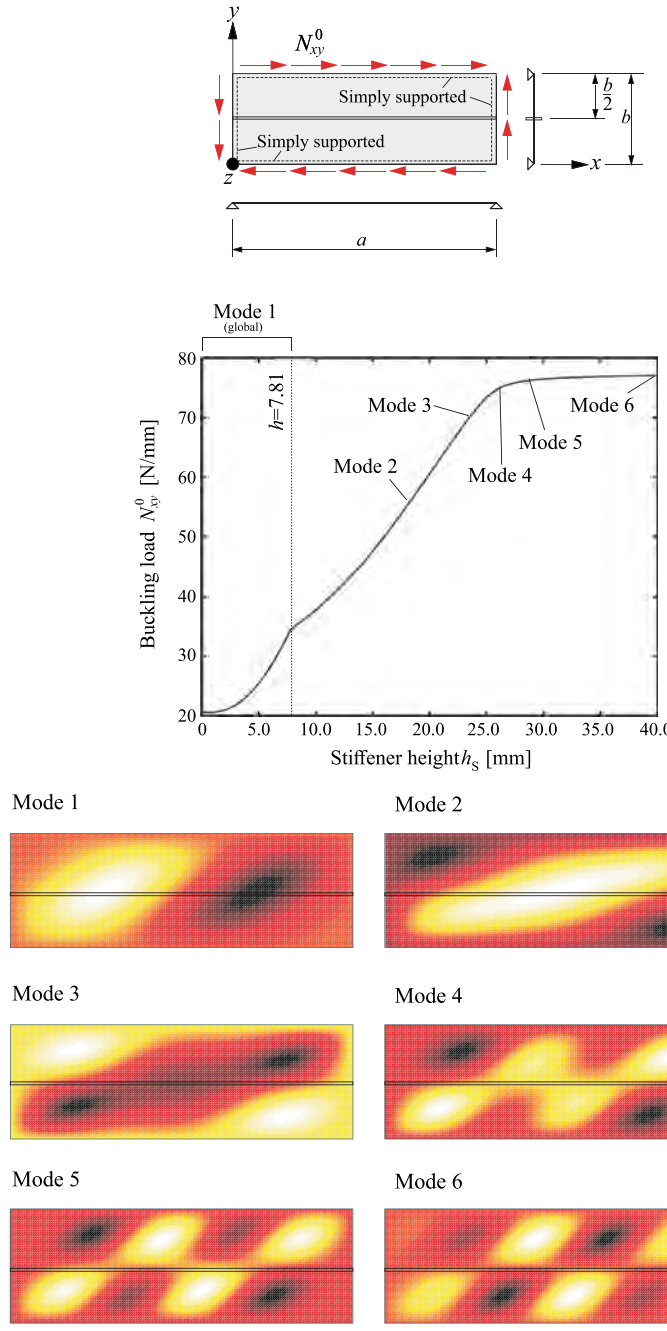


Fig. 17.6 Buckling load N^0_{xx} and buckling modes of a centrically stiffened laminate under shear load as a function of the stiffener height h_S

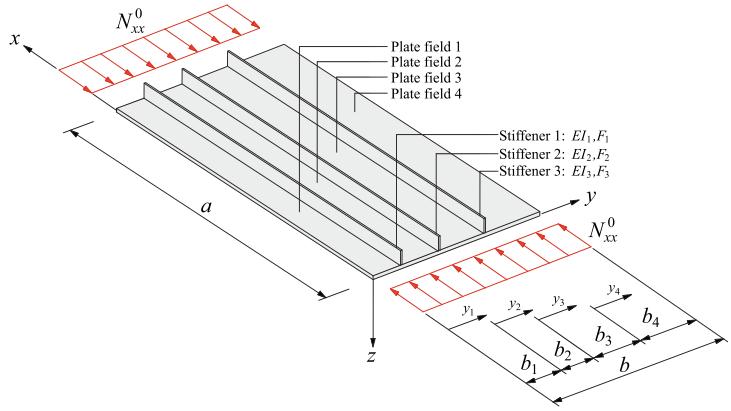


Fig. 17.7 Laminate reinforced by longitudinal stiffeners under uniaxial compressive load N_{xx}^0

and assuming that $N_{xx}^0 > \dfrac{D_{11}m^2\pi^2}{a^2}$ (see also the case distinctions in Chap. 13), then the following form of the solution w_0 can be given for (17.4):

$$w_0(x, y) = \sin\left(\frac{m\pi x}{a}\right) w(y), \tag{17.5}$$

where the function $w(y)$ can be specified as:

$$w(y) = C_1 \cosh\left(\frac{k_1 m\pi y}{a}\right) + C_2 \sinh\left(\frac{k_1 m\pi y}{a}\right) + C_3 \cos\left(\frac{k_2 m\pi y}{a}\right) + C_4 \sin\left(\frac{k_2 m\pi y}{a}\right). \tag{17.6}$$

The following abbreviations were introduced here:

$$k_{1,2} = \sqrt{\frac{1}{D_{22}}\left\{\sqrt{(D_{12}+2D_{66})^2 + D_{22}\left[N_{xx}^0\left(\frac{a}{m\pi}\right)^2 - D_{11}\right]} \pm (D_{12}+2D_{66})\right\}}. \tag{17.7}$$

17.3.2 Continuity Conditions at Stiffener *i*

Consider stiffener i at the point $y_i = b_i$, which is identical to the ordinate $y_{i+1} = 0$. With regard to this stiffener, the following continuity conditions between the plate fields i and $i+1$ can be formulated (see Fig. 17.8). Firstly, the displacements $w_{0,i}$ and $w_{0,i+1}$ of the two neighbouring subfields i and $i+1$ must be identical at the stiffener i:

$$w_{0,i}(y_i = b_i) - w_{0,i+1}(y_{i+1} = 0) = 0. \tag{17.8}$$

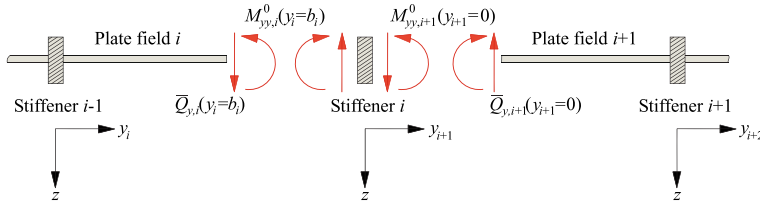


Fig. 17.8 Free body image of stiffener i

The same applies for the angular rotations of the plate fields i and $i+1$ at this stiffener location:

$$\left.\frac{\partial w_{0,i}}{\partial y_i}\right|_{y_i=b_i} - \left.\frac{\partial w_{0,i+1}}{\partial y_{i+1}}\right|_{y_{i+1}=0} = 0. \tag{17.9}$$

Furthermore, the balance of the moments around the x-axis must be ensured:

$$M^0_{yy,i}\,(y_i = b_i) - M^0_{yy,i+1}\,(y_{i+1} = 0) = 0. \tag{17.10}$$

If the constitutive law is used for a symmetric, balanced orthotropic laminate according to

$$\begin{pmatrix} N^0_{xx} \\ N^0_{yy} \\ N^0_{xy} \\ M^0_{xx} \\ M^0_{yy} \\ M^0_{xy} \end{pmatrix} = \begin{bmatrix} A_{11} & A_{12} & 0 & 0 & 0 & 0 \\ A_{12} & A_{22} & 0 & 0 & 0 & 0 \\ 0 & 0 & A_{66} & 0 & 0 & 0 \\ 0 & 0 & 0 & D_{11} & D_{12} & 0 \\ 0 & 0 & 0 & D_{12} & D_{22} & 0 \\ 0 & 0 & 0 & 0 & 0 & D_{66} \end{bmatrix} \begin{pmatrix} \varepsilon^0_{xx} \\ \varepsilon^0_{yy} \\ \gamma^0_{xy} \\ \kappa^0_{xx} \\ \kappa^0_{yy} \\ \kappa^0_{xy} \end{pmatrix}, \tag{17.11}$$

then the third condition at stiffener i can also be written as:

$$\begin{aligned} &D_{12}\left(\left.\frac{\partial^2 w_{0,i}}{\partial x^2}\right|_{y_i=b_i} - \left.\frac{\partial^2 w_{0,i+1}}{\partial x^2}\right|_{y_{i+1}=0}\right) \\ &+ D_{22}\left(\left.\frac{\partial^2 w_{0,i}}{\partial y_i^2}\right|_{y_i=b_i} - \left.\frac{\partial^2 w_{0,i+1}}{\partial y_{i+1}^2}\right|_{y_{i+1}=0}\right) = 0. \end{aligned} \tag{17.12}$$

Fourthly, it can be stated that the difference between the shear forces $\bar{Q}_{y,i}$ and $\bar{Q}_{y,i+1}$ acts as a distributed load q_i on the stiffener i. From Fig. 17.8 we obtain:

$$q_i = -\bar{Q}_{y,i}\,(y_i = b_i) + \bar{Q}_{y,i+1}\,(y_{i+1} = 0)\,. \tag{17.13}$$

The differential equation that describes the stability behaviour of the stiffener i when longitudinal and transverse loads occur simultaneously is as follows:

$$EI_i \left.\frac{\partial^4 w_{0,i+1}}{\partial x^4}\right|_{y_{i+1}=0} + F_i \left.\frac{\partial^2 w_{0,i+1}}{\partial x^2}\right|_{y_{i+1}=0} - q_i = 0. \tag{17.14}$$

The transverse shear forces $\bar{Q}_y$ (considered here as Kirchhoff's equivalent transverse forces) can also be expressed by the moments M^0_{yy} and M^0_{xy} as follows:

$$\bar{Q}_y = 2\frac{\partial M^0_{xy}}{\partial x} + \frac{\partial M^0_{yy}}{\partial y}. \tag{17.15}$$

Using the constitutive law (17.11) then finally results in the following fourth continuity condition at stiffener i: (i):

$$\begin{aligned} EI_i \left.\frac{\partial^4 w_{0,i+1}}{\partial x^4}\right|_{y_{i+1}=0} + F_i \left.\frac{\partial^2 w_{0,i+1}}{\partial x^2}\right|_{y_{i+1}=0} \\ + D_{22}\left(\left.\frac{\partial^3 w_{0,i+1}}{\partial y_{i+1}^3}\right|_{y_{i+1}=0} - \left.\frac{\partial^3 w_{0,i}}{\partial y_i^3}\right|_{y_i=b_i} \right) \\ + (D_{12}+4D_{66})\left(\left.\frac{\partial^3 w_{0,i+1}}{\partial x^2 \partial y_{i+1}}\right|_{y_{i+1}=0} - \left.\frac{\partial^3 w_{0,i}}{\partial x^2 \partial y_i}\right|_{y_i=b_i} \right) = 0. \end{aligned} \tag{17.16}$$

Due to the compressive load applied to the stiffened laminate, it is assumed that both the stiffeners and the laminate itself suffer the same longitudinal strain ε. Therefore, the force F_i acting on stiffener i can be assumed to be proportional to the compressive load N^0_{xx} on the laminate:

$$F_i = N^0_{xx}\frac{EA_i}{E_P h}, \tag{17.17}$$

where EA_i is the extensional stiffness of stiffener i. The quantity E_P is the plane modulus of elasticity of the laminate. If the auxiliary variable δ_i is introduced as follows

$$\delta_i = \frac{EA_i}{E_P bh}, \tag{17.18}$$

then the stiffener force F_i can be calculated as:

$$F_i = \delta_i N^0_{xx} b. \tag{17.19}$$

The quantity δ_i must not be confused with the variational operator (see Chap. 4). It should be noted that the stiffnesses EA_i and $E_P bh$ describe the material behaviour of the stiffener and the laminate before buckling. Accordingly, these values must also be calculated as a function of the membrane stiffnesses A_{op} $(o, p = 1, 2, 6)$ of the laminates involved.

17.3.3 Boundary Conditions

A hinged support is assumed at the loaded edges at $x = 0$ and $x = a$, so that the buckling shape $w_{0,i}$ of each plate field must have a nodal line and the bending moments $M^0_{xx,i}$ must disappear in each subplate i at the unloaded edges:

$$w_{0,i}\,(x = 0) = w_{0,i}\,(x = a) = M^0_{xx,i}\,(x = 0) = M^0_{xx,i}\,(x = a) = 0. \tag{17.20}$$

These boundary conditions are fulfilled identically in each plate field i by the approach (17.5) for the buckling shape $w_{0,i}$. At the unloaded longitudinal edge at $y_1 = 0$, the buckling deformations $w_{0,1}$ must also disappear:

$$w_{0,1}\,(y_1 = 0) = 0. \tag{17.21}$$

The bending moment $M^0_{yy,1}$ must also become zero at this point:

$$M^0_{yy,1}\,(y_1 = 0) = 0. \tag{17.22}$$

Inserting the constitutive law (17.11) results in $\left.\dfrac{\partial^2 w_{0,1}}{\partial x^2}\right|_{y_1=0} = 0$:

$$-\,D_{22}\left.\frac{\partial^2 w_{0,1}}{\partial y_1^2}\right|_{y_1=0} = 0. \tag{17.23}$$

Analogous boundary conditions apply in plate field $n + 1$ at $y_{n+1} = b_{n+1}$:

$$\begin{aligned} w_{0,n+1}\,(y_{n+1} = b_{n+1}) &= 0, \\ M^0_{yy,n+1}\,(y_{n+1} = b_{n+1}) &= 0. \end{aligned} \tag{17.24}$$

Using the constitutive law (17.11) results in the following expression for the second condition in (17.24):

$$-\,D_{22}\left.\frac{\partial^2 w_{0,n+1}}{\partial y_{n+1}^2}\right|_{y_{n+1}=b_{n+1}} = 0. \tag{17.25}$$

In total, at this point $4 + 4n = 4\,(n + 1)$ conditions are available for $4\,(n + 1)$ unknown constants C_1, C_2, C_3, and C_4.

17.3.4 Evaluation of the Boundary and Continuity Conditions

Evaluating the continuity conditions (17.8), (17.9), (17.12), and (17.16) results in the following expressions:

$$
\begin{aligned}
&\cosh\left(\frac{k_1 m\pi b_i}{a}\right) C_{1,i} + \sinh\left(\frac{k_1 m\pi b_i}{a}\right) C_{2,i} \\
&+\cos\left(\frac{k_2 m\pi b_i}{a}\right) C_{3,i} + \sin\left(\frac{k_2 m\pi b_i}{a}\right) C_{4,i} - C_{1,i+1} - C_{3,i+1} = 0, \\
&k_1\left[\sinh\left(\frac{k_1 m\pi b_i}{a}\right) C_{1,i} + \cosh\left(\frac{k_1 m\pi b_i}{a}\right) C_{2,i} - C_{2,i+1}\right] \\
&+k_2\left[-\sin\left(\frac{k_2 m\pi b_i}{a}\right) C_{3,i} + \cos\left(\frac{k_2 m\pi b_i}{a}\right) C_{4,i} - C_{4,i+1}\right] = 0, \\
&\left[\cosh\left(\frac{k_1 m\pi b_i}{a}\right) C_{1,i} + \sinh\left(\frac{k_1 m\pi b_i}{a}\right) C_{2,i} - C_{1,i+1}\right]\left(k_1^2 D_{22} - D_{12}\right) \\
&-\left[\cos\left(\frac{k_2 m\pi b_i}{a}\right) C_{3,i} + \sin\left(\frac{k_2 m\pi b_i}{a}\right) C_{4,i} - C_{3,i+1}\right]\left(k_2^2 D_{22} + D_{12}\right) = 0, \\
&-\frac{k_1 m\pi}{a}\left[\sinh\left(\frac{k_1 m\pi b_i}{a}\right) C_{1,i} + \cosh\left(\frac{k_1 m\pi b_i}{a}\right) C_{2,i}\right]\left[k_1^2 D_{22} - (D_{12} + 4D_{66})\right] \\
&+\frac{k_2 m\pi}{a}\left[-\sin\left(\frac{k_2 m\pi b_i}{a}\right) C_{3,i} + \cos\left(\frac{k_2 m\pi b_i}{a}\right) C_{4,i}\right]\left[k_2^2 D_{22} + (D_{12} + 4D_{66})\right] \\
&+\left(EI_i \frac{m^2\pi^2}{a^2} - F_i\right)\left(C_{1,i+1} + C_{3,i+1}\right) \\
&+\frac{k_1 m\pi}{a}\left[D_{22} k_1^2 - (D_{12} + 4D_{66})\right] C_{2,i+1} - \frac{k_2 m\pi}{a}\left[D_{22} k_2^2 + (D_{12} + 4D_{66})\right] C_{4,i+1} = 0.
\end{aligned}
\tag{17.26}
$$

The boundary conditions for plate field 1 result in the following two equations:

$$
C_{1,1} + C_{3,1} = 0, \quad k_1^2 C_{1,1} - k_2^2 C_{3,1} = 0, \tag{17.27}
$$

which leads to the following result:

$$
C_{1,1} = 0, \quad C_{3,1} = 0. \tag{17.28}
$$

The boundary conditions in plate field $n + 1$ finally result in

$$
\begin{aligned}
&\cosh\left(\frac{k_1 m\pi b_{i+1}}{a}\right) C_{1,n+1} + \sinh\left(\frac{k_1 m\pi b_{i+1}}{a}\right) C_{2,n+1} \\
&+\cos\left(\frac{k_2 m\pi b_{i+1}}{a}\right) C_{3,n+1} + \sin\left(\frac{k_2 m\pi b_{i+1}}{a}\right) C_{4,n+1} = 0, \\
&k_1^2\left[\cosh\left(\frac{k_1 m\pi b_{i+1}}{a}\right) C_{1,n+1} + \sinh\left(\frac{k_1 m\pi b_{i+1}}{a}\right) C_{2,n+1}\right] \\
&-k_2^2\left[\cos\left(\frac{k_2 m\pi b_{i+1}}{a}\right) C_{3,n+1} + \sin\left(\frac{k_2 m\pi b_{i+1}}{a}\right) C_{4,n+1}\right] = 0.
\end{aligned}
\tag{17.29}
$$

17.3.5 Buckling Conditions

The continuity conditions (17.26) and the boundary conditions (17.29) result in a homogeneous linear system of equations for the $4\,(n+1)-2$ constants C_1, C_2, C_3, and C_4 (note that $C_{1,1} = C_{3,1} = 0$). To obtain a non-trivial solution, it is required that the determinant of the coefficient matrix $\underline{\underline{M}}$ disappears. This finally yields the buckling condition for the currently considered buckling problem of a uniaxially compressed laminate with longitudinal stiffeners:

$$\det\left(\underline{\underline{M}}\right) = 0. \tag{17.30}$$

Evaluation results in a transcendental buckling condition to determine the buckling load N_{xx}^0. The buckling conditions for various special cases of the currently considered situation are given below.

17.3.5.1 Laminate with an Eccentric Single Stiffener

A laminate with a single longitudinal stiffener is considered ($n = 1$), i.e.

$$EI_i = EI, \quad F_i = F, \tag{17.31}$$

which is attached at an arbitrary location. Evaluating (17.30) results in the following buckling condition after a few elementary transformations:

$$\begin{aligned}
&\frac{k_2 \sinh\left(\frac{k_1 m\pi b_1}{a}\right) \sinh\left(\frac{k_1 m\pi b_2}{a}\right)}{\cosh\left(\frac{k_1 m\pi b_1}{a}\right) \sinh\left(\frac{k_1 m\pi b_2}{a}\right) + \sinh\left(\frac{k_1 m\pi b_1}{a}\right) \cosh\left(\frac{k_1 m\pi b_2}{a}\right)} \\
&- \frac{k_1 \sin\left(\frac{k_2 m\pi b_1}{a}\right) \sin\left(\frac{k_2 m\pi b_2}{a}\right)}{\cos\left(\frac{k_2 m\pi b_1}{a}\right) \sin\left(\frac{k_2 m\pi b_2}{a}\right) + \sin\left(\frac{k_2 m\pi b_1}{a}\right) \cos\left(\frac{k_2 m\pi b_2}{a}\right)} \\
&- \frac{D_{22} \frac{m\pi}{a} k_1 k_2 \left(k_1^2 + k_2^2\right)}{EI \frac{m^2\pi^2}{a^2} - F} = 0.
\end{aligned} \tag{17.32}$$

With the help of

$$\begin{aligned}
\sin(\alpha+\beta) &= \cos(\alpha)\sin(\beta) + \sin(\alpha)\cos(\beta), \\
\sinh(\alpha+\beta) &= \cosh(\alpha)\sinh(\beta) + \sinh(\alpha)\cosh(\beta),
\end{aligned} \tag{17.33}$$

the following form of the buckling condition is finally obtained:

$$\begin{aligned}
&\left(EI \frac{m^2\pi^2}{a^2} - F\right) \left[\frac{k_1 \sin\left(\frac{k_2 m\pi b_1}{a}\right) \sin\left(\frac{k_2 m\pi b_2}{a}\right)}{\sin\left(\frac{k_2 m\pi b}{a}\right)} - \frac{k_2 \sinh\left(\frac{k_1 m\pi b_1}{a}\right) \sinh\left(\frac{k_1 m\pi b_2}{a}\right)}{\sinh\left(\frac{k_1 m\pi b}{a}\right)} \right] \\
&\quad + D_{22} \frac{m\pi}{a} k_1 k_2 \left(k_1^2 + k_2^2\right) = 0.
\end{aligned} \tag{17.34}$$

17.3.5.2 Laminate with a Centric Single Stiffener

In the case of a single longitudinal stiffener that is positioned centrically on the laminate, the widths of the two plate fields are calculated as:

$$b_1 = b_2 = \frac{b}{n+1} = \frac{b}{2}. \tag{17.35}$$

The buckling condition (17.34) can then be expressed in the following form:

$$\left(EI\frac{m^2\pi^2}{a^2} - F\right)\left[\frac{k_1 \sin^2\left(\frac{k_2 m\pi b}{2a}\right)}{\sin\left(\frac{k_2 m\pi b}{a}\right)} - \frac{k_2 \sinh^2\left(\frac{k_1 m\pi b}{2a}\right)}{\sinh\left(\frac{k_1 m\pi b}{a}\right)}\right] + D_{22}\frac{m\pi}{a}k_1 k_2\left(k_1^2 + k_2^2\right) = 0. \tag{17.36}$$

By means of the relationships

$$\sin(2\alpha) = 2\sin(\alpha)\cos(\alpha), \quad \sinh(2\alpha) = 2\sinh(\alpha)\cosh(\alpha) \tag{17.37}$$

and

$$\tan(\alpha) = \frac{\sin(\alpha)}{\cos(\alpha)}, \quad \tanh(\alpha) = \frac{\sinh(\alpha)}{\cosh(\alpha)}, \tag{17.38}$$

the following buckling condition is finally obtained:

$$\left(EI\frac{m^2\pi^2}{a^2} - F\right)\left[k_1 \tan\left(\frac{k_2 m\pi b}{2a}\right) - k_2 \tanh\left(\frac{k_1 m\pi b}{2a}\right)\right] + 2D_{22}\frac{m\pi}{a}k_1 k_2\left(k_1^2 + k_2^2\right) = 0. \tag{17.39}$$

This buckling condition corresponds to an expression that can also be found in Wiedemann (1996).

17.3.5.3 Laminate with Two Longitudinal Stiffeners at Arbitrary Positions

The formulation of the boundary and continuity conditions for this case is analogous to the cases already considered with a single stiffener. After a few transformations, the buckling condition (17.30) is obtained as follows:

$$\det\begin{bmatrix} M_{11} & M_{12} & M_{13} & M_{14} \\ M_{21} & M_{22} & M_{23} & M_{24} \\ M_{31} & M_{32} & M_{33} & M_{34} \\ M_{41} & M_{42} & M_{43} & M_{44} \end{bmatrix} = 0, \tag{17.40}$$

where the components of the coefficient matrix $\underline{\underline{M}}$ can be written as:

$$
\begin{aligned}
M_{11} &= k_1 \frac{\tau_{1,1}}{\tau_{2,1}}, \quad M_{12} = -k_1, \quad M_{13} = k_2 \frac{\tau_{3,1}}{\tau_{4,1}}, \quad M_{14} = -k_2, \\
M_{21} &= EI_1 \frac{m^2\pi^2}{a^2} - F_1 - \frac{\tau_{1,1}}{\tau_{2,1}} \frac{k_1 m\pi}{a} \left(k_1^2 D_{22} - D_{12} - 4D_{66}\right), \\
M_{22} &= \frac{k_1 m\pi}{a} \left(k_1^2 D_{22} - D_{12} - 4D_{66}\right), \\
M_{23} &= EI_1 \frac{m^2\pi^2}{a^2} - F_1 + \frac{\tau_{3,1}}{\tau_{4,1}} \frac{k_2 m\pi}{a} \left(k_2^2 D_{22} + D_{12} + 4D_{66}\right), \\
M_{24} &= -\frac{k_2 m\pi}{a} \left(k_2^2 D_{22} + D_{12} + 4D_{66}\right), \\
M_{31} &= k_1 \left(\frac{\tau_{1,2}\tau_{1,3}}{\tau_{2,3}} + \tau_{2,2}\right), \quad M_{32} = k_1 \left(\frac{\tau_{2,2}\tau_{1,3}}{\tau_{2,3}} + \tau_{1,2}\right), \\
M_{33} &= k_2 \left(\frac{\tau_{3,2}\tau_{3,3}}{\tau_{4,3}} - \tau_{4,2}\right), \quad M_{34} = k_2 \left(\frac{\tau_{4,2}\tau_{3,3}}{\tau_{4,3}} + \tau_{3,2}\right), \\
M_{41} &= \tau_{1,2} \left(EI_2 \frac{m^2\pi^2}{a^2} - F_2\right) - \frac{k_1 m\pi}{a} \left(\frac{\tau_{1,2}\tau_{1,3}}{\tau_{2,3}} + \tau_{2,2}\right) \left[k_1^2 D_{22} - (D_{12} + 4D_{66})\right], \\
M_{42} &= \tau_{2,2} \left(EI_2 \frac{m^2\pi^2}{a^2} - F_2\right) - \frac{k_1 m\pi}{a} \left(\frac{\tau_{2,2}\tau_{1,3}}{\tau_{2,3}} + \tau_{1,2}\right) \left[k_1^2 D_{22} - (D_{12} + 4D_{66})\right], \\
M_{43} &= \tau_{3,2} \left(EI_2 \frac{m^2\pi^2}{a^2} - F_2\right) + \frac{k_2 m\pi}{a} \left(\frac{\tau_{3,2}\tau_{3,3}}{\tau_{4,3}} - \tau_{4,2}\right) \left[k_2^2 D_{22} + (D_{12} + 4D_{66})\right], \\
M_{44} &= \tau_{4,2} \left(EI_2 \frac{m^2\pi^2}{a^2} - F_2\right) + \frac{k_2 m\pi}{a} \left(\frac{\tau_{4,2}\tau_{3,3}}{\tau_{4,3}} + \tau_{3,2}\right) \left[k_2^2 D_{22} + (D_{12} + 4D_{66})\right],
\end{aligned}
\tag{17.41}
$$

with:

$$
\begin{aligned}
\tau_{1,i} &= \cosh\left(\frac{k_1 m\pi b_i}{a}\right), \quad \tau_{2,i} = \sinh\left(\frac{k_1 m\pi b_i}{a}\right), \\
\tau_{3,i} &= \cos\left(\frac{k_2 m\pi b_i}{a}\right), \quad \tau_{4,i} = \sin\left(\frac{k_2 m\pi b_i}{a}\right).
\end{aligned}
\tag{17.42}
$$

Further expansion of the determinant of the coefficient matrix $\underline{\underline{M}}$ is of course possible, but leads to very long and unwieldy expressions, so this is not presented here.

17.3.5.4 Laminate with Two Symmetrically Placed Identical Longitudinal Stiffeners

In the case that a laminate is considered that is stiffened by two identical longitudinal stiffeners symmetrically attached, the buckling condition (17.40) is considerably simplified:

$$M_0 + M_1 \left(EI \frac{m^2\pi^2}{a^2} - F \right) + M_2 \left(EI \frac{m^2\pi^2}{a^2} - F \right)^2 = 0, \tag{17.43}$$

in which the following abbreviations M_0, M_1 and M_2 were introduced:

$$\begin{aligned}
M_0 &= -\frac{\left(3\tau_1^2 + \tau_2^2\right)\left(3\tau_3^2 - \tau_4^2\right)}{\tau_2\tau_4} \left[k_1 k_2 D_{22} \frac{m\pi}{a} \left(k_1^2 + k_2^2\right) \right]^2, \\
M_1 &= 4k_1 k_2 D_{22} \frac{m\pi}{a} \left(k_1^2 + k_2^2\right) \left[\frac{\tau_1}{\tau_4} k_2 \left(3\tau_3^2 - \tau_4^2\right) - \frac{\tau_3}{\tau_2} k_1 \left(3\tau_1^2 + \tau_2^2\right) \right], \\
M_2 &= -k_1^2 \frac{\tau_4}{\tau_2} \left(3\tau_1^2 + \tau_2^2\right) - k_2^2 \frac{\tau_2}{\tau_4} \left(3\tau_3^2 - \tau_4^2\right) - 2k_1 k_2 \left(1 - 4\tau_1\tau_3\right),
\end{aligned} \tag{17.44}$$

with:

$$\tau_1 = \cosh\left(\frac{k_1 m\pi b}{3a}\right), \quad \tau_2 = \sinh\left(\frac{k_1 m\pi b}{3a}\right), \quad \tau_3 = \cos\left(\frac{k_2 m\pi b}{3a}\right), \quad \tau_4 = \sin\left(\frac{k_2 m\pi b}{3a}\right). \tag{17.45}$$

17.3.5.5 Laminate with n Arbitrary Longitudinal Stiffeners at Arbitrary Positions

The buckling condition (17.30) can be specified as follows for the most general case of a laminate with n longitudinal stiffeners with arbitrary properties at arbitrary positions:

$$\det \begin{bmatrix}
\underline{\underline{M}}_1 & \underline{\underline{M}}_{2,1} & \underline{\underline{0}}_{(4\times4)} & \underline{\underline{0}}_{(4\times4)} & \cdots & \underline{\underline{0}}_{(4\times4)} & \underline{\underline{0}}_{(4\times4)} \\
\underline{\underline{0}}_{(4\times2)} & \underline{\underline{M}}_{3,2} & \underline{\underline{M}}_{2,2} & \underline{\underline{0}}_{(4\times4)} & \cdots & \underline{\underline{0}}_{(4\times4)} & \underline{\underline{0}}_{(4\times4)} \\
\underline{\underline{0}}_{(4\times2)} & \underline{\underline{0}}_{(4\times4)} & \underline{\underline{M}}_{3,3} & \underline{\underline{M}}_{2,3} & \cdots & \underline{\underline{0}}_{(4\times4)} & \underline{\underline{0}}_{(4\times4)} \\
\underline{\underline{0}}_{(4\times2)} & \underline{\underline{0}}_{(4\times4)} & \underline{\underline{0}} & \underline{\underline{M}}_{3,4} & \cdots & \underline{\underline{0}}_{(4\times4)} & \underline{\underline{0}}_{(4\times4)} \\
\vdots & \vdots & \vdots & \vdots & \ddots & \vdots & \vdots \\
\underline{\underline{0}}_{(4\times2)} & \underline{\underline{0}}_{(4\times4)} & \underline{\underline{0}}_{(4\times4)} & \underline{\underline{0}}_{(4\times4)} & \underline{\underline{0}}_{(4\times4)} & \underline{\underline{M}}_{3,n} & \underline{\underline{M}}_{2,n} \\
\underline{\underline{0}}_{(2\times2)} & \underline{\underline{0}}_{(2\times4)} & \underline{\underline{0}}_{(2\times4)} & \underline{\underline{0}}_{(2\times4)} & \underline{\underline{0}}_{(2\times4)} & \underline{\underline{0}}_{(2\times4)} & \underline{\underline{M}}_4
\end{bmatrix} = 0. \tag{17.46}$$

The following submatrices have been introduced:

$$\underline{\underline{M}}_1 = \begin{bmatrix}
\tau_{2,1} & \tau_{4,1} \\
\tau_{1,1} k_1 & \tau_{3,1} k_2 \\
\tau_{2,1}\left(k_1^2 D_{22} - D_{12}\right) & -\tau_{4,1}\left(k_2^2 D_{22} + D_{12}\right) \\
-\tau_{1,1} \frac{k_1 m\pi}{a}\left[k_1^2 D_{22} - (D_{12} + 4D_{66})\right] & \tau_{3,1} \frac{k_2 m\pi}{a}\left[k_2^2 D_{22} + (D_{12} + 4D_{66})\right]
\end{bmatrix},$$

$$\underline{\underline{M}}_{2,i}^{T} = \begin{bmatrix} -1 & 0 & -k_1^2 D_{22} + D_{12} & EI_i \frac{m^2\pi^2}{a^2} - F_i \\ 0 & -k_1 & 0 & \frac{k_1 m\pi}{a}\left[k_1^2 D_{22} - (D_{12} + 4D_{66})\right] \\ -1 & 0 & k_2^2 D_{22} + D_{12} & EI_i \frac{m^2\pi^2}{a^2} - F_i \\ 0 & -k_2 & 0 & -\frac{k_2 m\pi}{a}\left[k_2^2 D_{22} + (D_{12} + 4D_{66})\right] \end{bmatrix},$$

$$\underline{\underline{M}}_{3,i}^{T} = \begin{bmatrix} \tau_{1,i} & \tau_{2,i}k_1 & \tau_{1,i}\left(k_1^2 D_{22} - D_{12}\right) & -\tau_{2,i}\frac{k_1 m\pi}{a}\left[k_1^2 D_{22} - (D_{12} + 4D_{66})\right] \\ \tau_{2,i} & \tau_{1,i}k_1 & \tau_{2,i}\left(k_1^2 D_{22} - D_{12}\right) & -\tau_{1,i}\frac{k_1 m\pi}{a}\left[k_1^2 D_{22} - (D_{12} + 4D_{66})\right] \\ \tau_{3,i} & -\tau_{4,i}k_2 & -\tau_{3,i}\left(k_2^2 D_{22} + D_{12}\right) & -\tau_{4,i}\frac{k_2 m\pi}{a}\left[k_2^2 D_{22} + (D_{12} + 4D_{66})\right] \\ \tau_{4,i} & \tau_{3,i}k_2 & -\tau_{4,i}\left(k_2^2 D_{22} + D_{12}\right) & \tau_{3,i}\frac{k_2 m\pi}{a}\left[k_2^2 D_{22} + (D_{12} + 4D_{66})\right] \end{bmatrix},$$

$$\underline{M}_4 = \begin{bmatrix} \tau_{1,n+1} & \tau_{2,n+1} & \tau_{3,n+1} & \tau_{4,n+1} \\ \tau_{1,n+1}k_1^2 & \tau_{2,n+1}k_1^2 & -\tau_{3,n+1}k_2^2 & -\tau_{4,n+1}k_2^2 \end{bmatrix}. \tag{17.47}$$

17.4 Closed-Form Analytical Solutions for Longitudinally Stiffened Laminates Under Uniaxial Compressive Load

The Lévy-type solutions presented in the previous section are indispensable when verifying approximate methods for buckling analysis of stiffened laminates. However, such implicit solutions are very cumbersome to use in engineering practice, which is why there is great practical interest in developing closed-form analytical approximate methods that can be used without great effort. In this section, the problem of buckling of a symmetric laminate reinforced by a longitudinal single stiffener under compressive loading is treated in a closed-form analytical way. In addition to providing simple equations for the buckling loads of such a stiffened laminate, the question of the minimum bending stiffness of the stiffening element is addressed. The laminate is assumed to be orthotropic so that bending-twisting coupling can be ruled out. Further stiffening patterns and load cases have been dealt with by Mittelstedt (2008a, b). The now decommissioned German standard DIN 4114 contains many other closed-form formulae for stiffened isotropic plates for a wide variety of stiffening patterns and load cases.

17.4.1 Determination of the Buckling Load

A single stiffener at the point $y = \frac{b}{2}$ divides the laminate into two equal subplates with the partial widths $b_1 = b_2 = \frac{b}{2}$. A simple approach for the buckling mode w_0 can be found in a separation form as follows:

$$w_0(x, y) = W \sin\left(\frac{m_1 \pi x}{a}\right) \sin\left(\frac{\pi y}{b}\right). \tag{17.48}$$

It is assumed here that the stiffened laminate buckles in a certain number m_1 of half-waves in the longitudinal direction x, whereas only a single half-wave is assumed in the transverse direction y. The quantity W is a constant and can be interpreted as the amplitude of the buckling mode. Bifurcation of equilibrium occurs when the first variation of the elastic potential Π_1 (where the index 1 symbolises the already buckled state) disappears in the buckled state:

$$\delta \Pi_1 = 0. \tag{17.49}$$

For the current situation of a stiffened laminate under compressive load, Π_1 can be written as:

$$\Pi_1 = \Pi_i^L + \Pi_i^S + \Pi_a^P + \Pi_a^S, \tag{17.50}$$

where Π_i^L and Π_i^S are the strain energies stored in the laminate and in the stiffener ('inner potential'). The portions Π_a^L and Π_a^S are the energy contributions of the applied load on the laminate and the stiffener ('external potential'). The following results for the individual components

$$\begin{aligned}
\Pi_i^L &= \int_0^a \int_0^b \left\{ \frac{1}{2} \left[D_{11} \left(\frac{\partial^2 w_0}{\partial x^2} \right)^2 + D_{22} \left(\frac{\partial^2 w_0}{\partial y^2} \right)^2 \right] \right. \\
&\quad \left. + D_{12} \frac{\partial^2 w_0}{\partial x^2} \frac{\partial^2 w_0}{\partial y^2} + 2 D_{66} \left(\frac{\partial^2 w_0}{\partial x \partial y} \right)^2 \right\} \mathrm{d}y \mathrm{d}x, \\
\Pi_i^S &= \frac{EI}{2} \int_0^a \left(\left. \frac{\partial^2 w_0}{\partial x^2} \right|_{y=\frac{b}{2}} \right)^2 \mathrm{d}x, \\
\Pi_a^L &= -\frac{N_{xx}^0}{2} \int_0^a \int_0^b \left(\frac{\partial w_0}{\partial x} \right)^2 \mathrm{d}y \mathrm{d}x, \\
\Pi_a^S &= -\frac{F}{2} \int_0^a \left(\left. \frac{\partial w_0}{\partial x} \right|_{y=\frac{b}{2}} \right)^2 \mathrm{d}x.
\end{aligned} \tag{17.51}$$

The laminate and the stiffener will suffer an identical longitudinal strain ε_{xx}^0 under the given compressive load, which means that the axial force F acting on the stiffener can be related to the plate load N_{xx}^0 as follows:

$$F = N_{xx}^0 \frac{EA}{E_P h}. \tag{17.52}$$

With the dimensionless variable

$$\delta = \frac{EA}{E_P bh} \tag{17.53}$$

we can also write for the stiffener force F:

$$F = \delta N^0_{xx} b. \tag{17.54}$$

Again, it should be noted that the variables E and E_P represent the inplane effective moduli of elasticity of the stiffener and the laminate before the onset of buckling, so that these must be calculated from the membrane stiffnesses A_{op} $(o, p = 1, 2, 6)$ of the underlying laminates.

Since the functional form of the buckling mode is already completely defined with the approach (17.48), the only unknown in (17.48) is the constant W, so that the variational problem (17.49) changes into the requirement for the disappearance of the first partial derivative of Π_1 with respect to W:

$$\frac{\partial \Pi_1}{\partial W} = 0. \tag{17.55}$$

If (17.48) is substituted into (17.51) and (17.55) is evaluated, the following approximate expression for the buckling load N^0_{xx} of the laminate with a centric stiffener is obtained:

$$N^0_{xx} = \frac{\pi^2 \left[D_{11} b^4 m_1^4 + D_{22} a^4 + 2a^2 b^2 m_1^2 (D_{12} + 2D_{66}) + 2EIb^3 m_1^4\right]}{a^2 b^4 m_1^2 (1 + 2\delta)}. \tag{17.56}$$

The quality of this approximate solution is later verified by comparison with calculations using the Ritz method. The special case of an unstiffened laminate can be derived from this by forming the limit values $EI \to 0$ and $\delta \to 0$. One obtains:

$$N^0_{xx} = \pi^2 \left[\frac{m_1^2}{a^2} D_{11} + \frac{a^2}{m_1^2 b^4} D_{22} + \frac{2}{b^2} (D_{12} + 2D_{66})\right]. \tag{17.57}$$

This corresponds to the Navier solution for the symmetric orthotropic laminate.

The number m_1 of buckling half-waves in the longitudinal direction x is obtained by deriving (17.56) with respect to m_1

$$\frac{\partial N^0_{xx}}{\partial m_1} = 0, \tag{17.58}$$

and the roots of the resulting function are determined. The only relevant result is obtained as:

$$m_1 = \frac{a}{b} \sqrt[4]{\frac{D_{22}}{D_{11}\left(1 + \frac{2EI}{D_{11} b}\right)}}. \tag{17.59}$$

It should be noted that m_1 does not usually result in an integer number, so the following procedure is suggested. First, m_1 is calculated according to (17.59). Then round down to the next lower integer m_u. In addition, round up to the next higher integer m_o. The buckling

load is calculated with both numbers m_u and m_o, and the resulting lower value for N_{xx}^0 is the required buckling load.

If sufficiently long plates are treated (theoretically, the aspect ratio $\frac{a}{b}$ tends to infinity), the limit value consideration $\frac{a}{b} \to \infty$ leads to the following expression for the buckling load:

$$N_{xx}^0 = \frac{2\pi^2}{b^2\,(1+2\delta)} \left[\sqrt{D_{11} D_{22} \left(1 + \frac{2EI}{D_{11} b}\right)} + D_{12} + 2D_{66} \right]. \tag{17.60}$$

If the bending stiffness EI of the stiffener exceeds the (as yet unknown) minimum stiffness $EI_{\min}$, the buckling load may be calculated as the buckling load of an identical but unstiffened plate with only half the width:

$$N_{xx}^0 = \pi^2 \left[\frac{m_2^2}{a^2} D_{11} + \frac{16a^2}{m_2^2 b^4} D_{22} + \frac{8}{b^2} \left(D_{12} + 2D_{66}\right) \right]. \tag{17.61}$$

Here m_2 is the number of buckling half-waves that occur, where $m_1 \neq m_2$ generally applies. The following relationship can be specified for m_2 analogous to (17.59):

$$m_2 = \frac{2a}{b} \sqrt[4]{\frac{D_{22}}{D_{11}}}. \tag{17.62}$$

17.4.2 Determination of the Minimum Stiffness

When the minimum stiffness $EI_{\min}$ is reached, there are two possible equilibrium positions. On the one hand, it is possible that the plate and the stiffener simultaneously assume a global buckling pattern, which is described by Eq. (17.56). On the other hand, it is possible that the stiffener remains in its original straight state, so that the buckling load N_{xx}^0 can be calculated according to Eq. (17.61) for the half laminate. This equation represents the upper limit for N_{xx}^0 since the buckling behaviour at $EI \geq EI_{\min}$ is completely decoupled from the properties of the stiffener. One way to determine the minimum stiffness is therefore to equate the expressions (17.56) and (17.61) for the buckling loads and solve for the bending stiffness EI. If the half-wave numbers and (17.59) and (17.62) are also used (which theoretically assumes infinitely long laminates in both cases), the following expression for $EI_{\min}$ is obtained after a few transformations:

$$EI_{\min} = H_0 + H_1\delta + H_2\delta^2, \tag{17.63}$$

wherein:

$$H_0 = \frac{3b}{D_{22}}\left[4\sqrt{D_{11}D_{22}}\,(D_{12}+2D_{66}) + \frac{5}{2}D_{11}D_{22} + \frac{3}{2}D_{12}^2 + 6D_{12}D_{66} + 6D_{66}^2\right],$$
$$H_1 = \frac{8b}{D_{22}}\left[7\sqrt{D_{11}D_{22}}\,(D_{12}+2D_{66}) + 4D_{11}D_{22} + 3D_{12}^2 + 12D_{12}D_{66} + 12D_{66}^2\right],$$
$$H_2 = \frac{32b}{D_{22}}\left[2\sqrt{D_{11}D_{22}}\,(D_{12}+2D_{66}) + D_{11}D_{22} + D_{12}^2 + 4D_{12}D_{66} + 4D_{66}^2\right]. \tag{17.64}$$

Obviously, (17.63) with (17.64) is decoupled from the plate length a. This form of equation for the minimum stiffness $EI_{\min}$ thus represents a limit value for infinitely long laminates.

A refined expression for the calculation of the minimum stiffness can be derived by equating the buckling load N_{xx}^0 according to (17.56) with the buckling load for half the plate field as before, but leaving the wave number m_1 in (17.56) as an unknown in the calculation, but as a simplification for the upper limit the expression

$$N_{xx}^0 = \frac{8\pi^2}{b^2}\left(\sqrt{D_{11}D_{22}} + D_{12} + 2D_{66}\right) \tag{17.65}$$

for a sufficiently long laminate with half the width is used. This ultimately leads to:

$$EI_{\min} = \frac{2a^2b^2m_1^2\left[4\,(1+2\delta)\sqrt{D_{11}D_{22}} + (3+8\delta)\,(D_{12}+2D_{66})\right] - D_{11}b^4m_1^4 - D_{22}a^4}{2b^3m_1^4}. \tag{17.66}$$

Obviously, this representation makes it possible to discuss the influence of the aspect ratio $\frac{a}{b}$ on the minimum stiffness $EI_{\min}$.

17.4.3 Verification and Discussion

An orthotropic laminate with a width of $b = 100\,\text{mm}$ and a total thickness of $h = 1\,\text{mm}$ consisting of eight layers of a typical carbon fiber-reinforced plastic with the layup $\left[(0°/90°)_2\right]_S$ is considered. The orthotropic properties of a single layer were assumed to be $E_{11} = 138{,}000\,\text{MPa}$, $E_{22} = 8960\,\text{MPa}$, $G_{12} = 7100\,\text{MPa}$ and $\nu_{12} = 0.30$. The plate is reinforced by a centric stiffener, also made of a fiber-reinforced plastic, with a rectangular cross-section of width $b_S = 1\,\text{mm}$ and variable height h_S, whereby the stiffener is arranged in such a way that its center of gravity coincides with the laminate middle plane. For the sake of simplicity, the stiffener and laminate are assumed to have identical layups.

It should be noted that the determination of the minimum stiffness according to both the simplified method and the refined method requires information about the cross-sectional

area A as an input variable, in the form of the dimensionless stiffness δ. The result of the calculation is then the minimum stiffness $EI_{\min}$, which also depends on the cross-section geometry in the form of the moment of inertia I. In general, the variables δ and $EI_{\min}$ will not be consistent with each other, so that in the most general case an iterative process must be carried out to determine $EI_{\min}$. If we turn to the example of a rectangular stiffener with variable height h_S but constant width $b_S = 1\text{mm}$ and invariable modulus of elasticity E, the requirement $EI \geq EI_{\min}$ can be reformulated as $h \geq h_{\min}$, where $h_{\min}$ is the minimum stiffener height from which local plate buckling without simultaneous stiffener buckling is guaranteed and which can be calculated from the minimum stiffness $EI_{\min}$ as:

$$h_{\min} = \sqrt[3]{\frac{12EI_{\min}}{Eb_S}}. \tag{17.67}$$

In order to calculate $EI_{\min}$, an input value h_0 is first estimated, from which an initial value A_0 of the cross-sectional area of the stiffener or the stiffness δ_0 can be calculated. An initial estimate of the minimum stiffness $EI_{\min,1}$ can then be made. This can then be used to calculate an improved estimate of the minimum stiffener height $h_{\min,1}$, which can be used as a new input variable for an improved cross-sectional area A_1 or stiffness δ_1. This can then be used to obtain a second and improved estimate of the minimum stiffness $EI_{\min,2}$ or the minimum stiffener height $h_{\min,2}$. This process is repeated until convergence of the results can be observed in iteration step n, so that $EI_{\min,n-1} \simeq EI_{\min,n}$ or currently $h_{\min,n-1} \simeq h_{\min,n}$ applies. In general, the results converge quickly after a few iteration steps.

Similarly, the procedure described applies to any shape of stiffener cross-section, although of course no iterative procedure would be necessary for the example of the stiffener with rectangular cross-section currently under consideration. Here, the stiffener height h_S is included in the moment of inertia I to the third power, while h_S appears as a linear term in the stiffness δ. In this specific case, this results in a third-order polynomial for the minimum stiffener height h_S, which is easy to solve. This remains without further illustration at this point.

In order to verify the methods developed for the minimum stiffness $EI_{\min}$ and the buckling loads N^0_{xx}, comparative calculations were carried out using the Ritz method. Figure 17.9, left, shows a comparison of the results for the minimum stiffness $EI_{\min}$ and the minimum stiffener height $h_{\min}$ for the currently considered centrically stiffened orthotropic laminate as a function of the length a. It can be seen that the simplified approach significantly overestimates the minimum stiffness $EI_{\min}$ in the range of small laminate lengths a, whereas the refined approach is able to reproduce the results of the Ritz method very well for all a. Obviously, the curve $EI_{\min}(a)$ or $h_{\min}(a)$ currently tends asymptotically towards the value predicted by the simplified method, so that the simplified method can be interpreted as a kind of upper limit for $EI_{\min}$ for sufficiently long plates. It should also be noted that the refined method must be limited 'downwards', as it can be seen that complex values for the minimum stiffness result for very small values, which can be explained by the underlying assumption

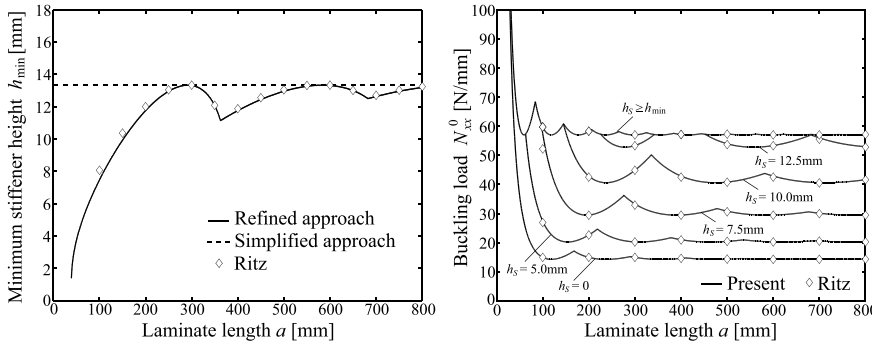


Fig. 17.9 Comparison of the results for the minimum stiffness $EI_{\min}$ or the minimum stiffener height $h_{\min}$ (left) and for the buckling load N_{xx}^0 (right) according to the current methods and according to the Ritz method for the centrically stiffened orthotropic laminate

of a constant local buckling load. The minimum length a, above which the refined method may be used, can be calculated by setting the expression for $EI_{\min}$ to zero according to the refined method and solving for the length. The following result is finally obtained:

$$a_{\min} = \frac{b}{\sqrt{D_{22}}} \left\{ 4\,(1+2\delta)\,\sqrt{D_{11}D_{22}} + (3+8\delta)\,(D_{12}+2D_{66}) \right. \\ \left. - \sqrt{\left[4\,(1+2\delta)\,\sqrt{D_{11}D_{22}} + (3+8\delta)\,(D_{12}+2D_{66}) \right]^2 - D_{11}D_{22}} \right\}^{\frac{1}{2}} . \quad (17.68)$$

In reality, however, a zero point for $EI_{\min}$ should only actually occur at the point $a = 0$. In order to gain a certain distance from the zero point $a_{\min}$, which does not occur in reality, it is recommended for practical application that the minimum plate length $a_{\min}$ be given the (arbitrarily chosen) factor 2, so that the following result is obtained:

$$a_{\min} = \frac{2b}{\sqrt{D_{22}}} \left\{ 4\,(1+2\delta)\,\sqrt{D_{11}D_{22}} + (3+8\delta)\,(D_{12}+2D_{66}) \right. \\ \left. - \sqrt{\left[4\,(1+2\delta)\,\sqrt{D_{11}D_{22}} + (3+8\delta)\,(D_{12}+2D_{66}) \right]^2 - D_{11}D_{22}} \right\}^{\frac{1}{2}} . \quad (17.69)$$

For values $a < a_{\min}$, the following can be conservatively assumed:

$$EI_{\min}\,(a < a_{\min}) = EI_{\min}\,(a = a_{\min})\,. \quad (17.70)$$

Figure 17.9, left, also shows that the minimum stiffness $EI_{\min}$ has local maxima at various points at which exactly the value according to the simplified method and thus also the asymptotic limiting case for sufficiently long laminates is reached. Obviously, after reaching the first maximum, there are only slight downward deflections of the minimum stiffness, so

that it seems justified, in the sense of a method that is easy to apply in practice, to use the refined approach for the interval $a_{\min} \leq a \leq a_0$, where $a = a_0$ indicates the point at which the curve $EI_{\min}(a)$ or currently $h_{\min}(a)$ reaches the first maximum. This point is obtained by setting the wave number $m_1 = 1$ in the refined approach, deriving the expression for $EI_{\min}$ with respect to the length a and searching for the roots of the resulting function. Finally, the following point $a = a_0$ is obtained:

$$a_0 = b\sqrt{\frac{1}{D_{22}}\left[4\left(1+2\delta\right)\sqrt{D_{11}D_{22}} + \left(3+8\delta\right)\left(D_{12}+2D_{66}\right)\right]}. \tag{17.71}$$

The minimum stiffness $EI_{\min}$ in the interval $a_{\min} \leq a \leq a_0$ can be calculated as:

$$EI_{\min} = \frac{1}{2b^3}\left\{2a^2b^2\left[4\left(1+2\delta\right)\sqrt{D_{11}D_{22}} + \left(3+8\delta\right)\left(D_{12}+2D_{66}\right)\right] - D_{11}b^4 - D_{22}a^4\right\}. \tag{17.72}$$

It should be emphasized that the calculation method presented for the minimum stiffness $EI_{\min}$ is of a completely closed-form analytical nature. If, on the other hand, the minimum stiffness were to be determined purely numerically, this would require an iterative process by determining the buckling load and the corresponding buckling mode for different stiffener configurations and differentiating between global or local buckling in a purely visual way. Depending on the quality of the input data and the complexity of the calculation method (Ritz, FEM), this process can require a considerable amount of calculation time for a single plate-stiffener configuration, whereas the results of Fig. 17.9, left, were generated within fractions of a second, although they contain several hundred data points. This emphasizes the value of such closed-form analytical methods.

Figure 17.9, right, shows a comparison of the results for the buckling load N_{xx}^0 for different stiffener heights h_S using both the closed-form analysis method and the Ritz method, where the length a was again kept variable. Tables 17.1, 17.2 and 17.3 show a comparison according to the current closed-form analytical method and iteratively determined values according to the Lévy solution.

Obviously, the agreement for all a and h_S is excellent, which emphasizes the value of the presented closed-form analytical method, especially with regard to the negligible computational effort. While the curves of Fig. 17.9, right, were available within a few seconds, both the Ritz method and the evaluation of the Lévy solution required a much greater computational effort, whereby the treatment of the transcendental buckling equations of the previous section in particular can be quite complicated and difficult to automate. Otherwise, the buckling curves show a characteristic behaviour that is generally to be expected for stiffened plates. While the buckling load N_{xx}^0 tends towards infinity for small laminate lengths a, increasing a results in several local maxima that characterize a mode change until the buckling load finally tends towards an asymptotic limit value for $a \to \infty$. However, it is interesting to note that, depending on the plate length a and stiffener height h_S, the solution can 'switch' between a global buckling of both the laminate and the stiffener and a purely

Table 17.1 Comparison of the results for the buckling load N_{xx}^0 [N/mm] according to the current analysis method and according to the Lévy solution for the centrically stiffened orthotropic laminate with $h_S = 5.0\,\text{mm}$

a [mm]	Present	Lévy
100	27.38	26.90
200	22.64	22.64
300	20.27	20.23
400	21.01	20.94
500	20.44	20.42
600	20.27	20.23
700	20.58	20.53
800	20.28	20.26

Table 17.2 Comparison of the results for the buckling load N_{xx}^0 [N/mm] according to the current analysis method and according to the Lévy solution for the centrically stiffened orthotropic laminate with $h_S = 7.5\,\text{mm}$

a [mm]	Present	Lévy
100	57.53	52.21
200	29.49	29.44
300	33.31	32.88
400	29.49	29.44
500	30.83	30.62
600	29.49	29.44
700	30.11	29.96
800	29.49	29.44

local buckling of the laminate. Such a point where a mode change between global and local buckling can be observed is shown in Fig. 17.9, right, e.g. at the point $a \simeq 100\,\text{mm}$ for the case $h_S = 7.5\,\text{mm}$, where the local two-wave buckling (curve for $h \geq h_{\min}$) changes into a global single-wave buckling. As the curve for $h_S = 12.5\,\text{mm}$ shows, for example, several such mode changes can occur over the laminate length, so that the stiffened laminate can exhibit both a local and a global buckling pattern depending on the length and stiffener geometry.

The results of Fig. 17.9, right, justify, as in the case of the minimum stiffness $EI_{\min}$, the formulation of the simplest possible and practically manageable method for calculating the buckling load N_{xx}^0 of an orthotropic laminate with centric stiffeners as long as $EI < EI_{\min}$. On the one hand, it can be seen that the buckling load in the range of smaller plate lengths a before reaching the first local maximum at the (still unknown) point $a = a_1$ has a pronounced

Table 17.3 Comparison of the results for the buckling load N_{xx}^0 [N/mm] according to the current analysis method and according to the Lévy solution for the centrically stiffened orthotropic laminate with $h_S = 10.0\,\text{mm}$

a [mm]	Present	Lévy
100	59.75	59.75
200	42.89	42.53
300	44.89	44.88
400	42.89	42.53
500	40.82	40.76
600	42.89	42.53
700	40.64	40.53
800	41.65	41.62

gradient, so that for all $a \leq a_1$ Eq. (17.56) can be used with a wave number m_1. On the other hand, it can also be seen that for all $a > a_1$, despite the occurrence of various local maxima, there are only small deflections in the curve $N_{xx}^0(a)$, so that it seems plausible to use the asymptotic limit value of the buckling load (17.60) after the occurrence of the first maximum for all $a > a_1$. One can therefore assume:

$$N_{xx}^0 = \frac{\pi^2 \left[D_{11} b^4 + D_{22} a^4 + 2a^2 b^2 \left(D_{12} + 2D_{66}\right) + 2EIb^3\right]}{a^2 b^4 \left(1 + 2\delta\right)}, \tag{17.73}$$

provided that $a \leq a_1$ applies. In the case $a \geq a_1$ results:

$$N_{xx}^0 = \frac{2\pi^2}{b^2 \left(1 + 2\delta\right)} \left[\sqrt{D_{11} D_{22} \left(1 + \frac{2EI}{D_{11} b}\right)} + D_{12} + 2D_{66}\right]. \tag{17.74}$$

The length a_1 follows from the associated extreme value task and can be written as:

$$a_1 = b \sqrt[4]{\frac{D_{11}}{D_{22}} \left(1 + \frac{2EI}{D_{11} b}\right)}. \tag{17.75}$$

An analogue procedure can be proposed if we consider the case that $EI \geq EI_{\min}$. Ultimately, $a \leq a_2$ is obtained in this case:

$$N_{xx}^0 = \frac{\pi^2 \left[D_{11} b^4 + 16 D_{22} a^4 + 8a^2 b^2 \left(D_{12} + 2D_{66}\right)\right]}{a^2 b^4}, \tag{17.76}$$

or if $a \geq a_2$:

$$N_{xx}^0 = \frac{8\pi^2}{b^2} \left(\sqrt{D_{11} D_{22}} + D_{12} + 2D_{66}\right). \tag{17.77}$$

The length a_2 is calculated as:

$$a_2 = \frac{b}{2}\sqrt[4]{\frac{D_{11}}{D_{22}}}. \tag{17.78}$$

17.4.4 Dimensionless Representation

It is useful to convert the presented closed-form analysis method into a dimensionless notation. At this point, only the final result is communicated; the conversion of the notation presented above into a dimensionless formulation is left to the reader at this point.

The following dimensionless parameters are required for the analysis. The aspect ratio α and Seydel's orthotropy factor β are already known from the previous considerations on stability:

$$\alpha = \frac{a}{b}\sqrt[4]{\frac{D_{22}}{D_{11}}}, \quad \beta = \frac{D_{12} + 2D_{66}}{\sqrt{D_{11}D_{22}}}. \tag{17.79}$$

Furthermore, the dimensionless extensional stiffness δ and the dimensionless bending stiffness γ of the stiffener are required:

$$\delta = \frac{EA}{E_P bh}, \quad \gamma = \frac{EI}{D_{11}b}. \tag{17.80}$$

Step 1: Select a suitable starting value for the extensional stiffness δ, where $\delta = 0.1$ is suggested. Calculate the limit values $\alpha_{\min}$ and $\alpha_{\max}$ as follows:

$$\begin{aligned}
\alpha_{\min} &= 2\sqrt{4\left(1+2\delta\right) + \left(3+8\delta\right)\beta - \sqrt{\left[4\left(1+2\delta\right) + \left(3+8\delta\right)\beta\right]^2 - 1}}, \\
\alpha_{\max} &= \sqrt{4\left(1+2\delta\right) + \left(3+8\delta\right)\beta}.
\end{aligned} \tag{17.81}$$

Step 2: Equations for determining the minimum stiffness. This analysis step can be divided into three cases. Case 1 occurs when $\alpha < \alpha_{\min}$. The following relationship is then obtained between δ and γ:

$$\gamma - 8\alpha_{\min}^2\left(1+\beta\right)\delta = \frac{1}{2}\alpha_{\min}^2\left(8 + 6\beta - \alpha_{\min}^2\right) - \frac{1}{2}. \tag{17.82}$$

Case 2 is when $\alpha_{\min} \leq \alpha \leq \alpha_{\max}$ applies:

$$\gamma - 8\alpha^2\left(1+\beta\right)\delta = \frac{1}{2}\alpha^2\left(8 + 6\beta - \alpha^2\right) - \frac{1}{2}. \tag{17.83}$$

Case 3 occurs when $\alpha > \alpha_{\max}$:

$$\gamma - 8\left(3\beta^2 + 7\beta + 4\right)\delta - 32\left(\beta^2 + 2\beta + 1\right)\delta^2 = \frac{3}{2}\left(3\beta^2 + 8\beta + 5\right). \tag{17.84}$$

In the most general case, the equations require an iterative solution process. For simple stiffener geometries, however, closed-form solutions will generally be possible.

After the minimum stiffness $\gamma_{\min}$ and the maximum extensional stiffness $\delta_{\max}$ have been found, it must finally be checked whether the limit values $\alpha_{\min}$ and $\alpha_{\max}$ calculated in step 1 are consistent with the determined value for $\delta_{\max}$ and whether the correct case distinctions were made in step 2.

Step 3: Calculate the buckling load. The dimensionless representation $\bar{N}^0_{xx}$ of the buckling load is as follows:

$$\bar{N}^0_{xx} = \frac{N^0_{xx} b^2}{\pi^2 \sqrt{D_{11} D_{22}}}. \tag{17.85}$$

The calculation of the buckling load differs according to the properties of the stiffener. If there is a stiffener with the optimum properties $\gamma = \gamma_{\min}$ and $\delta = \delta_{\max}$, or if the stiffener has properties $\gamma > \gamma_{\min}$ with simultaneous $\delta < \delta_{\max}$, then the buckling load $\bar{N}^0_{xx}$ can be determined as:

$$\bar{N}^0_{xx} = \frac{1}{\alpha^2} + 16\alpha^2 + 8\beta \quad \text{when} \quad \alpha < \frac{1}{2}, \tag{17.86}$$

or

$$\bar{N}^0_{xx} = 8\,(1 + \beta) \quad \text{when} \quad \alpha \geq \frac{1}{2}. \tag{17.87}$$

If, on the other hand, there is a stiffener for which the optimum properties are not achieved, then the buckling load is calculated as follows:

$$\bar{N}^0_{xx} = \frac{1}{1 + 2\delta}\left(\frac{1}{\alpha^2} + \alpha^2 + 2\beta + \frac{2\gamma}{\alpha^2}\right) \quad \text{when} \quad \alpha < \sqrt[4]{1 + 2\gamma}, \tag{17.88}$$

or

$$\bar{N}^0_{xx} = \frac{2}{1 + 2\delta}\left(\sqrt{1 + 2\gamma} + \beta\right) \quad \text{when} \quad \alpha \geq \sqrt[4]{1 + 2\gamma}. \tag{17.89}$$

17.5 Buckling Curves for Longitudinally Stiffened Laminates Under Compression

In this section we consider the linear buckling problem of longitudinally stiffened rectangular orthotropic plates that are loaded uniaxially by compression and are simply supported at all four edges (see also Werner and Mittelstedt (2010)). Buckling curves are provided for various elastic properties of the laminates, which were created using the Ritz method and can be used in practice in the manner of a buckling handbook. A dimensionless representation of all equations was used, whereby the parameters to be varied are reduced to a minimum. The laminates analysed here (length a, width b, thickness h, see Fig. 17.10, coordinate system

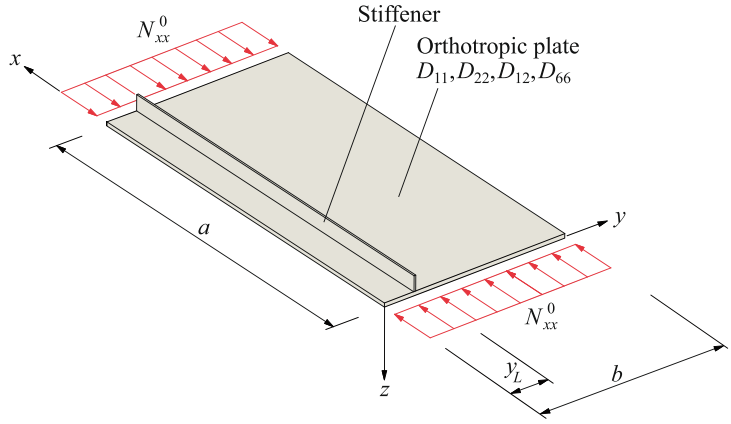


Fig. 17.10 Stiffened plate under uniaxial compression

x, y, z) are rectangular and simply supported at all four edges. In the longitudinal direction, the laminates are stiffened by a centric stiffener with an arbitrary cross-section (stiffener position at $y = y_L = \frac{b}{2}$). At this point, we only consider stiffeners with negligible torsional stiffness. The dimensionless parameters used here are Seydel's orthotropy parameter β, the aspect ratio α, the dimensionless bending stiffness of the stiffener γ and the dimensionless extensional stiffness δ. The following buckling Diagrams 17.11, 17.12 and 17.13 were created for $0 \leq \beta \leq 3.0$ with a step size of $\Delta\beta = 0.5$. The aspect ratio α is varied in the range $0 \leq \alpha \leq 5.0$, and in each diagram there are buckling curves for a large number of different values for the bending stiffness γ. The buckling load is given in a dimensionless form $\bar{N}^0_{xx}$ as

$$\bar{N}^0_{xx} = \frac{N^0_{xx} b^2}{\pi^2 \sqrt{D_{11} D_{22}}}. \tag{17.90}$$

17.6 Laminates with Transverse Stiffeners

17.6.1 Introduction

We now consider an orthotropic ($D_{16} = D_{26} = 0$) symmetric laminate (length a, width b) under uniaxial compressive load N^0_{xx}, which is stiffened by a number n of transverse stiffeners (position of stiffener k at $x = x_k$) in y-direction (Fig. 17.14). The buckling load is sought for this stiffened, simply supported laminate. The stiffeners are idealized as beams with the bending stiffness EI and the torsional stiffness GI_T.

For the given situation, a dimensionless notation in the natural coordinates $\xi = \frac{x}{a}, \xi_2 = \frac{y}{b}$ is used. The positions of the stiffeners are then converted to the following form:

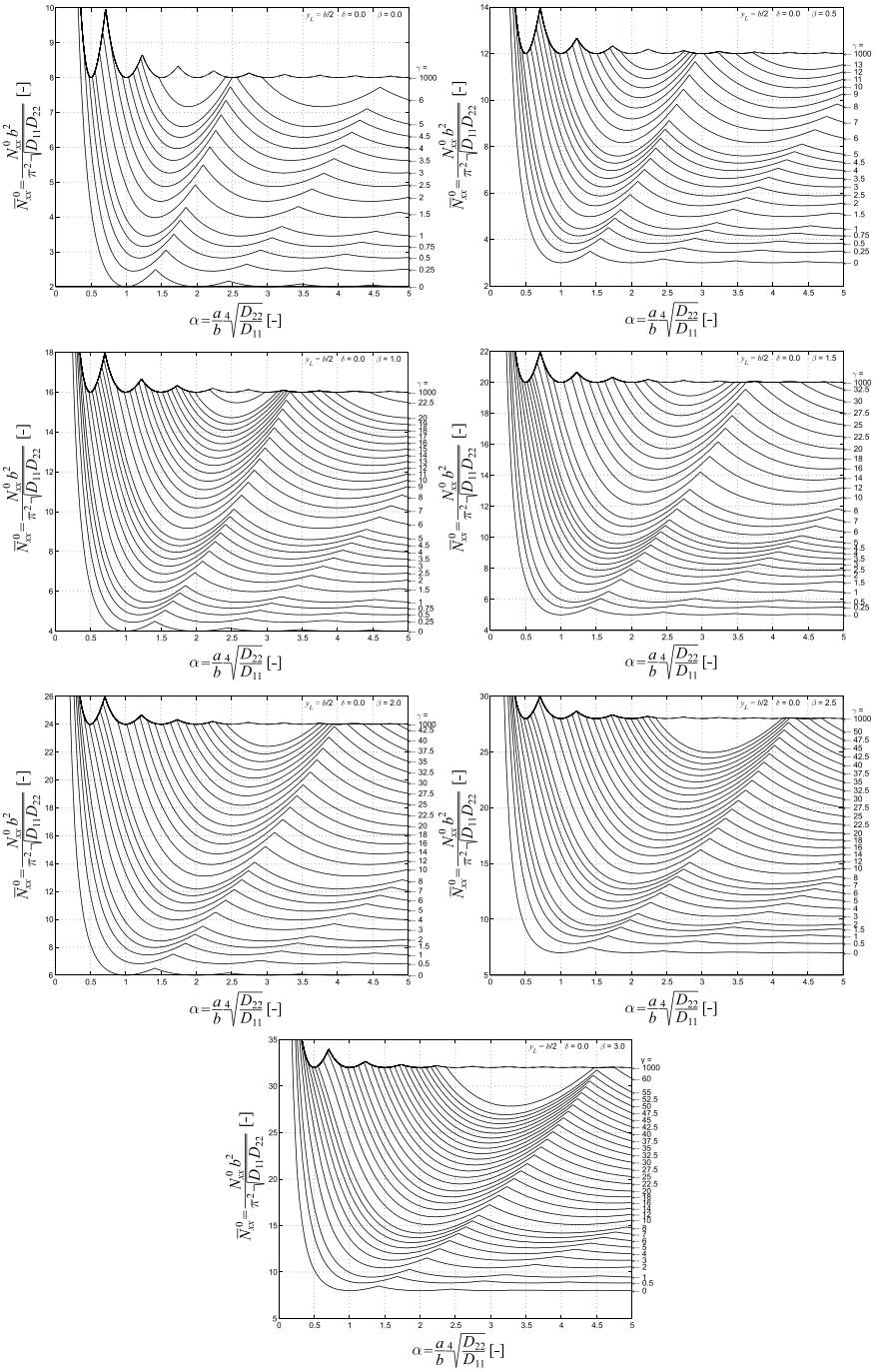


Fig. 17.11 Buckling diagrams for $y_L = \frac{b}{2}$ and $\delta = 0$

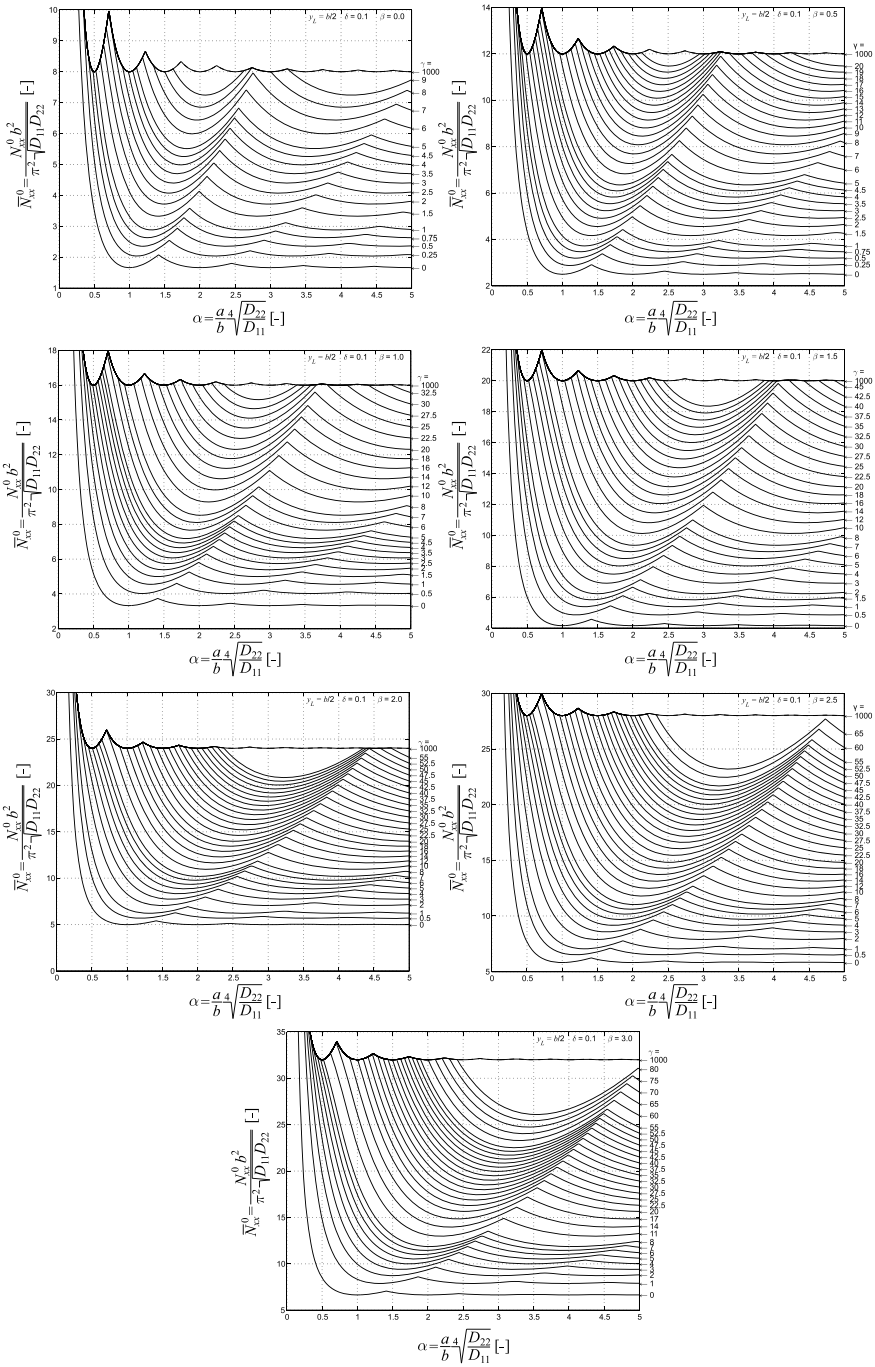


Fig. 17.12 Buckling diagrams for $y_L = \frac{b}{2}$ and $\delta = 0.1$

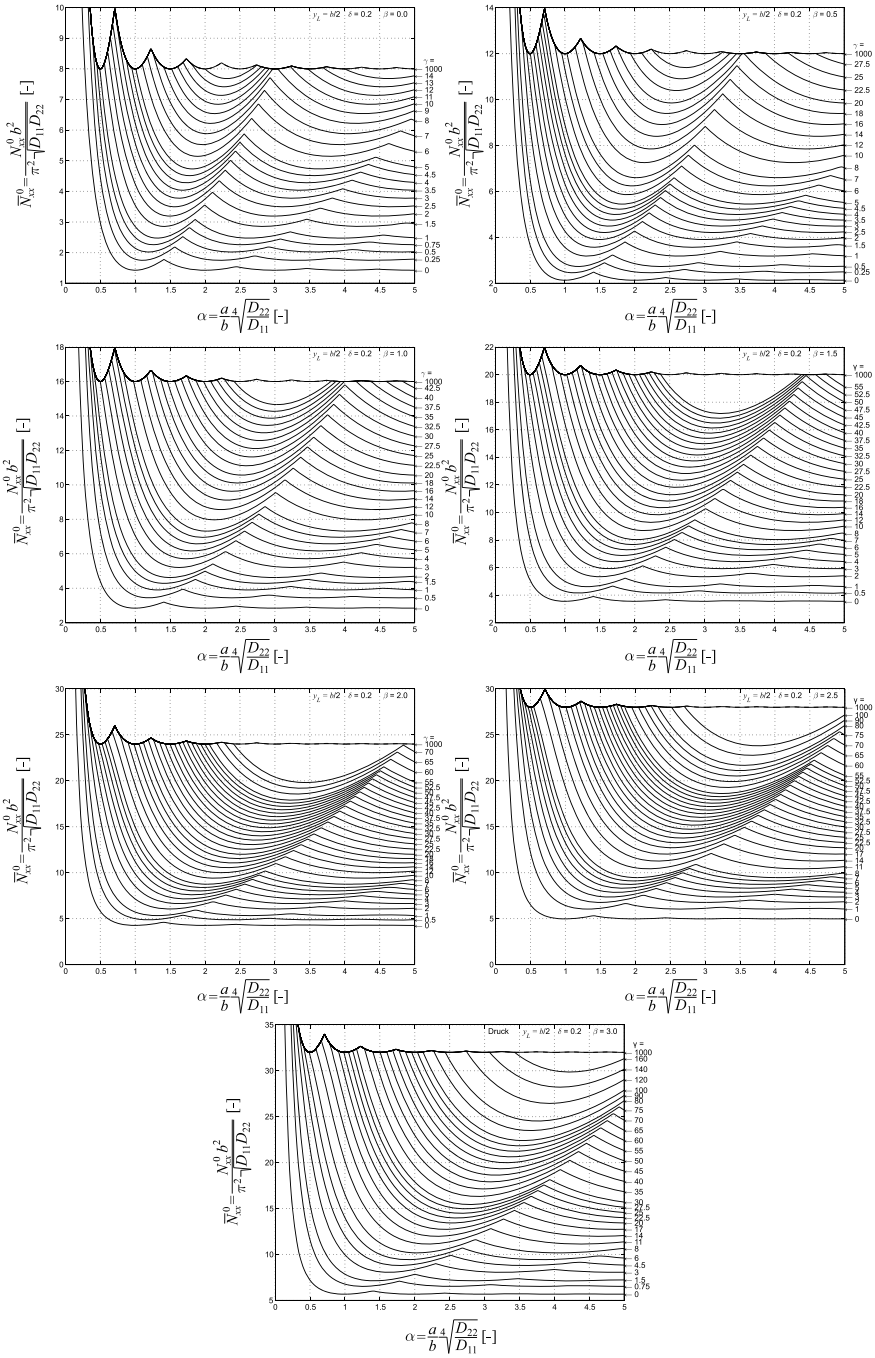


Fig. 17.13 Buckling diagrams for $y_L = \frac{b}{2}$ and $\delta = 0.2$

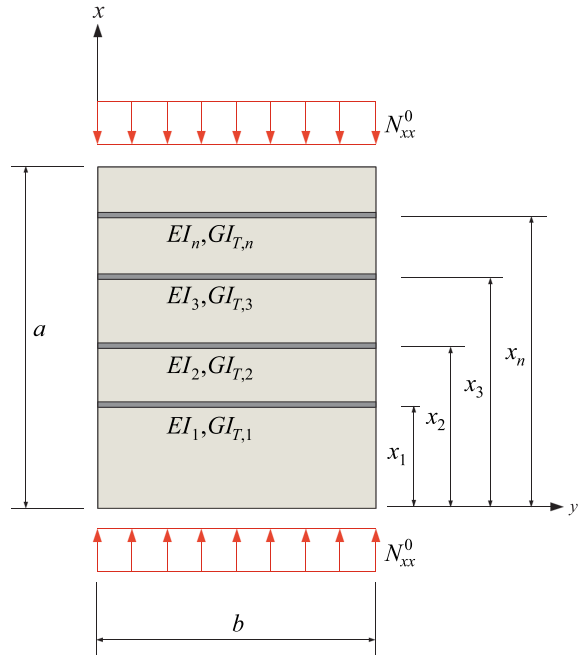


Fig. 17.14 Laminate with transverse stiffeners

$$a_1 = \frac{x_1}{a}, \quad a_2 = \frac{x_2}{a}, \quad \ldots \quad a_n = \frac{x_n}{a}. \tag{17.91}$$

The buckling differential equation that describes the given problem is in dimensionless form:

$$\frac{1}{\alpha^2}\frac{\partial^4 \bar{w}_0}{\partial \xi_1^4} + \alpha^2 \frac{\partial^4 \bar{w}_0}{\partial \xi_2^4} + 2\beta \frac{\partial^4 \bar{w}_0}{\partial \xi_1^2 \partial \xi_2^2} + \pi^2 \bar{N}_{xx}^0 \frac{\partial^2 \bar{w}_0}{\partial \xi_1^2} = 0, \tag{17.92}$$

with the following characteristic dimensionless variables:

$$\alpha = \frac{a}{b}\sqrt[4]{\frac{D_{22}}{D_{11}}}, \quad \beta = \frac{D_{12} + 2D_{66}}{\sqrt{D_{11}D_{22}}}, \quad \bar{N}_{xx}^0 = \frac{N_{xx}^0 b^2}{\sqrt{D_{11}D_{22}}}. \tag{17.93}$$

To solve the differential equation, we use an approach of the form

$$\bar{w}_0(\xi_1, \xi_2) = f(\xi_1) \sin n\pi\xi_2, \tag{17.94}$$

whereby the differential equation (17.92) changes into the following ordinary differential equation:

$$\frac{1}{\alpha^2}\frac{\mathrm{d}^4 f}{\mathrm{d}\xi_1^4} + \pi^2(\bar{N}_{xx}^0 - 2\beta)\frac{\mathrm{d}^2 f}{\mathrm{d}\xi_1^2} + \pi^4 \alpha^2 f = 0. \tag{17.95}$$

This equation is solved using an exponential approach:

$$f(\xi_1) = Ce^{\lambda\xi_1}, \tag{17.96}$$

which leads to the following form for (17.94) with $n = 1$:

$$\bar{w}_0(\xi_1, \xi_2) = \left(Ae^{\lambda_1\xi_1} + Be^{-\lambda_1\xi_1} + Ce^{\lambda_2\xi_1} + De^{-\lambda_2\xi_1}\right) \sin \pi\xi_2, \tag{17.97}$$

with

$$\lambda_{1,2} = \frac{\alpha\pi}{2}\sqrt{4\beta - 2\bar{N}^0_{xx} \pm 2\sqrt{\left(\bar{N}^0_{xx} - 2\beta\right)^2 - 4}}. \tag{17.98}$$

17.6.2 Boundary and Continuity Conditions

The underlying boundary and continuity conditions are specified below for the given situation.

The following boundary conditions apply at the unloaded longitudinal edges in each plate field i due to the hinged support:

$$\begin{aligned} \bar{w}_{0,i}(\xi_2 = 0) = \bar{w}_{0,i}(\xi_2 = 1) = 0, \\ M^0_{yy,i}(\xi_2 = 0) = M^0_{yy,i}(\xi_2 = 1) = 0. \end{aligned} \tag{17.99}$$

These conditions are already fulfilled with the separation approach (17.94).

The following applies at the two loaded edges of the plate fields 1 and $n + 1$:

$$\begin{aligned} \bar{w}_{0,1}(\xi_1 = 0) = \bar{w}_{0,n+1}(\xi_1 = 1) = 0, \\ M^0_{xx,1}(\xi_1 = 0) = M^0_{xx,n+1}(\xi_1 = 1) = 0, \end{aligned} \tag{17.100}$$

where the second equation can also be written as:

$$\left.\frac{\partial^2 \bar{w}_{0,1}}{\partial\xi_1^2}\right|_{\xi_1=0} = \left.\frac{\partial^2 \bar{w}_{0,n+1}}{\partial\xi_1^2}\right|_{\xi_1=1} = 0. \tag{17.101}$$

Furthermore, continuity conditions must be formulated at the stiffeners. They are as follows for stiffener i:

$$\begin{aligned} \bar{w}_{0,i}(\xi_1 = a_i) - \bar{w}_{0,i+1}(\xi_1 = a_i) = 0, \\ \left.\frac{\partial \bar{w}_{0,i}}{\partial\xi_1}\right|_{\xi_2=a_i} - \left.\frac{\partial \bar{w}_{0,i+1}}{\partial\xi_1}\right|_{\xi_2=a_i} = 0, \\ -\theta_i \left.\frac{\partial^3 \bar{w}_{0,i}}{\partial\xi_1\partial\xi_2^2}\right|_{\xi_1=a_i} - \left.\frac{\partial^2 \bar{w}_{0,i}}{\partial\xi_1^2}\right|_{\xi_1=a_i} + \left.\frac{\partial^2 \bar{w}_{0,i+1}}{\partial\xi_1^2}\right|_{\xi_1=a_i} = 0, \end{aligned}$$

$$\gamma_i \left.\frac{\partial^4 \bar{w}_{0,i}}{\partial \xi_2^4}\right|_{\xi_1=a_i} + \left.\frac{\partial^3 \bar{w}_{0,i+1}}{\partial \xi_1^3}\right|_{\xi_1=a_i} - \left.\frac{\partial^3 \bar{w}_{0,i}}{\partial \xi_1^3}\right|_{\xi_1=a_i} = 0, \tag{17.102}$$

where $\theta_i = \frac{GI_{T,i}a}{D_{11}b^2}$ is the dimensionless torsional stiffness of stiffener i. The expression $\gamma_i = \frac{EI_i a^3}{D_{11}b^4} = \frac{EI_i}{D_{22}a}\alpha^4$ is the dimensionless bending stiffness of stiffener i.

17.6.3 Buckling Condition

A total of $4(n+1)$ equations for determining the constants A_i, B_i, C_i, D_i can be determined with the boundary conditions at the plate edges and the continuity conditions at the stiffeners, which can be written in a vector matrix form as:

$$\underline{\underline{M}}\,\underline{C} = \underline{0}. \tag{17.103}$$

Here, the vector $\underline{C}$ is defined as:

$$\underline{C} = (A_1, B_1, C_1, D_1, A_2, B_2, C_2 - D_2, ..., A_{n+1}, B_{n+1}, C_{n+1}, D_{n+1})^T. \tag{17.104}$$

The coefficient matrix $\underline{\underline{M}}$ is as follows:

$$\underline{\underline{M}} = \begin{bmatrix} \underline{\underline{M}}_1 & \underline{\underline{0}}_{2\times4} & \underline{\underline{0}}_{2\times4} & \cdots & \underline{\underline{0}}_{2\times4} & \underline{\underline{0}}_{2\times4} \\ \underline{\underline{M}}_3^{i=1} & \underline{\underline{M}}_4^{i=1} & \underline{\underline{0}}_{4\times4} & \cdots & \underline{\underline{0}}_{4\times4} & \underline{\underline{0}}_{4\times4} \\ \underline{\underline{0}}_{4\times4} & \underline{\underline{M}}_3^{i=2} & \underline{\underline{M}}_4^{i=2} & \cdots & \underline{\underline{0}}_{4\times4} & \underline{\underline{0}}_{4\times4} \\ \vdots & \vdots & \vdots & \ddots & \vdots & \vdots \\ \underline{\underline{0}}_{4\times4} & \underline{\underline{0}}_{4\times4} & \underline{\underline{0}}_{4\times4} & \cdots & \underline{\underline{M}}_3^{i=n} & \underline{\underline{M}}_4^{i=n} \\ \underline{\underline{0}}_{2\times4} & \underline{\underline{0}}_{2\times4} & \underline{\underline{0}}_{2\times4} & \cdots & \underline{\underline{0}}_{4\times4} & \underline{\underline{M}}_2 \end{bmatrix}, \tag{17.105}$$

where the submatrices are defined as:

$$\underline{\underline{M}}_1 = \begin{bmatrix} 1 & 1 & 1 & 1 \\ \lambda_1^2 & \lambda_1^2 & \lambda_2^2 & \lambda_2^2 \end{bmatrix},$$

$$\underline{\underline{M}}_2 = \begin{bmatrix} e^{\lambda_1} & e^{-\lambda_1} & e^{\lambda_2} & e^{-\lambda_2} \\ \lambda_1^2 e^{\lambda_1} & \lambda_1^2 e^{-\lambda_1} & \lambda_2^2 e^{\lambda_2} & \lambda_2^2 e^{-\lambda_2} \end{bmatrix},$$

$$\underline{\underline{M}}_3^i = \begin{bmatrix} e^{\lambda_1 a_i} & e^{-\lambda_1 a_i} & e^{\lambda_2 a_i} & e^{-\lambda_2 a_i} \\ \lambda_1 e^{\lambda_1 a_i} & -\lambda_1 e^{-\lambda_1 a_i} & \lambda_2 e^{\lambda_2 a_i} & -\lambda_2 e^{-\lambda_2 a_i} \\ \left(\pi^2\theta_i\lambda_1 - \lambda_1^2\right) e^{\lambda_1 a_i} & \left(-\pi^2\theta_i\lambda_1 - \lambda_1^2\right) e^{-\lambda_1 a_i} & \left(\pi^2\theta_i\lambda_2 - \lambda_2^2\right) e^{\lambda_2 a_i} & \left(-\pi^2\theta_i\lambda_2 - \lambda_2^2\right) e^{-\lambda_2 a_i} \\ \left(\pi^4\gamma_i - \lambda_1^3\right) e^{\lambda_1 a_i} & \left(\pi^4\gamma_i + \lambda_1^3\right) e^{-\lambda_1 a_i} & \left(\pi^4\gamma_i - \lambda_2^3\right) e^{\lambda_2 a_i} & \left(\pi^4\gamma_i + \lambda_2^3\right) e^{-\lambda_2 a_i} \end{bmatrix},$$

$$\underline{\underline{M}}_4^i = \begin{bmatrix} -e^{\lambda_1 a_i} & -e^{-\lambda_1 a_i} & -e^{\lambda_2 a_i} & -e^{-\lambda_2 a_i} \\ -\lambda_1 e^{\lambda_1 a_i} & \lambda_1 e^{-\lambda_1 a_i} & -\lambda_2 e^{\lambda_2 a_i} & \lambda_2 e^{-\lambda_2 a_i} \\ \lambda_1^2 e^{\lambda_1 a_i} & \lambda_1^2 e^{-\lambda_1 a_i} & \lambda_2^2 e^{\lambda_2 a_i} & \lambda_2^2 e^{-\lambda_2 a_i} \\ \lambda_1^3 e^{\lambda_1 a_i} & -\lambda_1^3 e^{-\lambda_1 a_i} & \lambda_2^3 e^{\lambda_2 a_i} & -\lambda_2^3 e^{-\lambda_2 a_i} \end{bmatrix}.$$

To avoid the trivial solution, the coefficient determinant is set to zero:

$$\left|\underline{\underline{M}}\right| = 0. \tag{17.106}$$

This finally results in a transcendental equation from which the required buckling load of the transversely stiffened laminate can be determined numerically and iteratively.

17.6.4 Selected Configurations

17.6.4.1 Laminate with a Stiffener at Arbitrary Position

We first analyse a laminate under uniaxial compressive load, which exhibits a stiffener with $GI_T = 0$ at an arbitrary position x_1. The resulting system of equations (17.103) is as follows for this case:

$$\begin{bmatrix} \underline{\underline{M}}_1 & \underline{\underline{0}}_{2\times 4} \\ \underline{\underline{M}}_3^1 & \underline{\underline{M}}_4^1 \\ \underline{\underline{0}}_{2\times 4} & \underline{\underline{M}}_2 \end{bmatrix} \underline{C} = \underline{0}, \tag{17.107}$$

with

$$\underline{\underline{M}}_1 = \begin{bmatrix} 1 & 1 & 1 & 1 \\ \lambda_1^2 & \lambda_1^2 & \lambda_2^2 & \lambda_2^2 \end{bmatrix},$$

$$\underline{\underline{M}}_2 = \begin{bmatrix} e^{\lambda_1} & e^{-\lambda_1} & e^{\lambda_2} & e^{-\lambda_2} \\ \lambda_1^2 e^{\lambda_1} & \lambda_1^2 e^{-\lambda_1} & \lambda_2^2 e^{\lambda_2} & \lambda_2^2 e^{-\lambda_2} \end{bmatrix},$$

$$\underline{\underline{M}}_3^1 = \begin{bmatrix} e^{\lambda_1 a_1} & e^{-\lambda_1 a_1} & e^{\lambda_2 a_1} & e^{-\lambda_2 a_1} \\ \lambda_1 e^{\lambda_1 a_1} & -\lambda_1 e^{-\lambda_1 a_1} & \lambda_2 e^{\lambda_2 a_1} & -\lambda_2 e^{-\lambda_2 a_1} \\ -\lambda_1^2 e^{\lambda_1 a_1} & -\lambda_1^2 e^{-\lambda_1 a_1} & -\lambda_2^2 e^{\lambda_2 a_1} & -\lambda_2^2 e^{-\lambda_2 a_1} \\ \left(\pi^4\gamma_1 - \lambda_1^3\right) e^{\lambda_1 a_1} & \left(\pi^4\gamma_1 + \lambda_1^3\right) e^{-\lambda_1 a_1} & \left(\pi^4\gamma_1 - \lambda_2^3\right) e^{\lambda_2 a_1} & \left(\pi^4\gamma_1 + \lambda_2^3\right) e^{-\lambda_2 a_1} \end{bmatrix},$$

$$\underline{\underline{M}}_4^1 = \begin{bmatrix} -e^{\lambda_1 a_1} & -e^{-\lambda_1 a_1} & -e^{\lambda_2 a_1} & -e^{-\lambda_2 a_1} \\ -\lambda_1 e^{\lambda_1 a_1} & \lambda_1 e^{-\lambda_1 a_1} & -\lambda_2 e^{\lambda_2 a_1} & \lambda_2 e^{-\lambda_2 a_1} \\ \lambda_1^2 e^{\lambda_1 a_1} & \lambda_1^2 e^{-\lambda_1 a_1} & \lambda_2^2 e^{\lambda_2 a_1} & \lambda_2^2 e^{-\lambda_2 a_1} \\ \lambda_1^3 e^{\lambda_1 a_1} & -\lambda_1^3 e^{-\lambda_1 a_1} & \lambda_2^3 e^{\lambda_2 a_1} & -\lambda_2^3 e^{-\lambda_2 a_1} \end{bmatrix}.$$

Setting the coefficient determinant to zero results in the following buckling condition:

$$\begin{aligned} &\lambda_1\lambda_2\left(\lambda_1^2 - \lambda_2^2\right)\sinh\lambda_1 \sinh\lambda_2 \\ &+\gamma_1\pi^4\left[\lambda_1 \sinh\lambda_1 \sinh\lambda_2 a_1 \sinh(1-a_1)\lambda_2\right. \\ &\quad \left. + \lambda_2 \sinh\lambda_2 \sinh\lambda_1 a_1 \sinh(a_1 - 1)\lambda_1\right] = 0. \end{aligned} \tag{17.108}$$

If the special case $a_1 = 0.5$ exists, this results in the following:

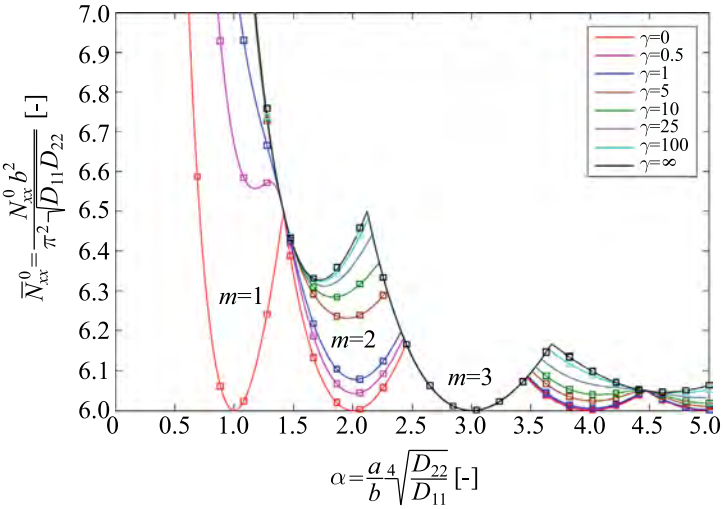


Fig. 17.15 Buckling curves for an orthotropic laminate ($\beta = 2.0$) with a transverse stiffener at $x_1 = \frac{a}{3}$

$$\lambda_1 \lambda_2 \left(\lambda_1^2 - \lambda_2^2\right) \sinh \lambda_1 \sinh \lambda_2$$
$$+\gamma_1 \pi^4 \left[\lambda_1 \sinh \lambda_1 \sinh^2 \frac{\lambda_2}{2} - \lambda_2 \sinh \lambda_2 \sinh^2 \frac{\lambda_1}{2}\right] = 0. \tag{17.109}$$

If we consider a stiffener with infinite bending stiffness γ_1, then it follows:

$$\lambda_1 \sinh \lambda_1 \sinh \lambda_2 a_1 \sinh(1 - a_1)\lambda_2$$
$$+\lambda_2 \sinh \lambda_2 \sinh \lambda_1 a_1 \sinh(a_1 - 1)\lambda_1 = 0. \tag{17.110}$$

Figure 17.15 shows the resulting buckling curves of an orthotropic laminate with $\beta = 2.0$ with a transverse stiffener at the point $x_1 = \frac{a}{3}$. All buckling curves shown here have infinite values for very short laminates with $\alpha \to 0$. For $\gamma = 0$, the corresponding curve approaches the smallest value $\bar{N}_{xx}^0$ of the unstiffened plate with increasing aspect ratio α. It can be seen that an increase in the bending stiffness leads to an increase in the buckling load. Mode changes between the individual buckling modes m can also be clearly recognized. It can be seen that the influence of the transverse stiffener on the buckling load continues to decrease as the aspect ratio α increases. In addition, it can be seen that the transverse stiffener has no influence at all on the buckling load at around $\alpha = 3.0$, which can be explained by the fact that at $m = 3$ a nodal line of the buckling mode occurs at the location of the transverse stiffener. This applies here for the following aspect ratios α:

$$\alpha = \frac{n}{a_1}, \quad \text{with} \quad n = 1, 2, 3, \ldots \tag{17.111}$$

If there is a nodal line at the stiffener location, this case is also referred to as local buckling. In this case, the plate buckles like an unstiffened plate, while the stiffener remains in its position. In the case of global buckling, on the other hand, the plate buckles together with the stiffener, which is a buckling mode that must generally be avoided in practical applications. The results show that local buckling always occurs for $\gamma \to \infty$, and the stiffened laminate exhibits at least $m = 2$ buckling half-waves. For stiffeners with a finite stiffness γ, global buckling modes with $m = 2$ or $m = 4$ occur with a sufficiently large distance of $\alpha = 3.0$. Local buckling with $m = 3$ only occurs for $\gamma = 1$ in the interval $2.41 < \alpha < 3.48$. Local buckling is only possible again for an aspect ratio of $\alpha = 6$ with $m = 6$ half-waves. It can be seen that the range of local buckling increases for finite γ to $\gamma \to \infty$, whereby the latter case changes from one local mode to the next. For the case $a_1 = \frac{1}{3}$, for example, this is the case for $\alpha = 2.12$, where there is a mode change from $m = 2$ to $m = 3$ half-waves.

For $\alpha = 2.41$ and $\alpha = 3.48$, the value $\gamma = 1$ represents the minimum stiffness of the stiffener. This is the stiffness above which a further increase in the bending stiffness of the stiffener does not lead to a further increase in the buckling load. For the transversely stiffened laminate considered here, a minimum stiffness can only be determined if a nodal line of the buckling shape results under the stiffener and the buckling shape corresponds to that of an unstiffened laminate.

Figure 17.15 contains not only the exact values according to the buckling condition (17.108) but also numerical results that were determined using the Ritz method. This shows a very good agreement, which speaks in favour of the accuracy of the Ritz method, whereby $M = N = 12$ shape functions were applied in both coordinate directions.

Figures 17.16 and 17.17 show buckling curves for orthotropic laminates ($\beta = 2.0$) with transverse stiffeners at $x_1 = \frac{a}{2}$ and $x_1 = \frac{a}{4}$, respectively. Here, too, a comparison of the exact solution (17.108) with the Ritz method was carried out, which is again very satisfactory.

17.6.4.2 Laminate with Two Stiffeners at Arbitrary Positions

As a further case, we consider an orthotropic laminate under uniaxial compressive load, which is reinforced by two stiffeners ($GI_{T,i} = 0$) at arbitrary positions x_1 and x_2. The system of equations to be solved here is as follows:

$$\begin{bmatrix} \underline{\underline{M}}_1 & \underline{\underline{0}}_{2\times4} & \underline{\underline{0}}_{2\times4} \\ \underline{\underline{M}}_3^1 & \underline{\underline{M}}_4^1 & \underline{\underline{0}}_{4\times4} \\ \underline{\underline{0}}_{4\times4} & \underline{\underline{M}}_3^2 & \underline{\underline{M}}_4^2 \\ \underline{\underline{0}}_{2\times4} & \underline{\underline{0}}_{2\times4} & \underline{\underline{M}}_2 \end{bmatrix} \underline{C} = \underline{0}, \tag{17.112}$$

with

$$\underline{\underline{M}}_1 = \begin{bmatrix} 1 & 1 & 1 & 1 \\ \lambda_1^2 & \lambda_1^2 & \lambda_2^2 & \lambda_2^2 \end{bmatrix},$$

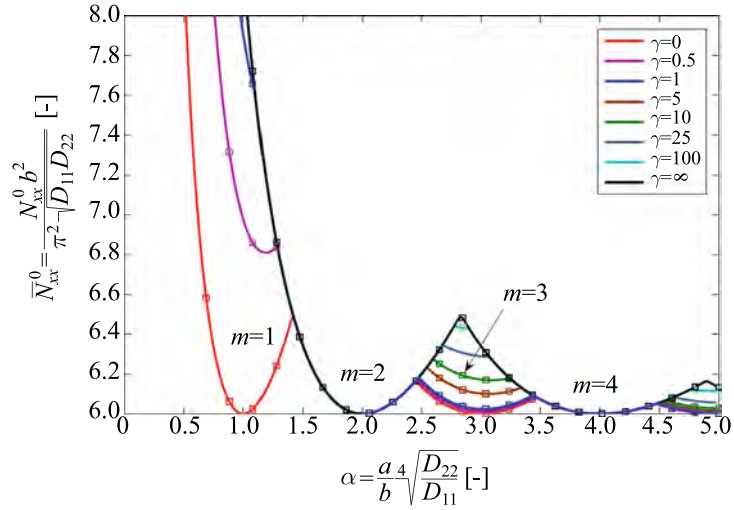


Fig. 17.16 Buckling curves for an orthotropic laminate ($\beta = 2.0$) with a transverse stiffener at $x_1 = \frac{a}{2}$

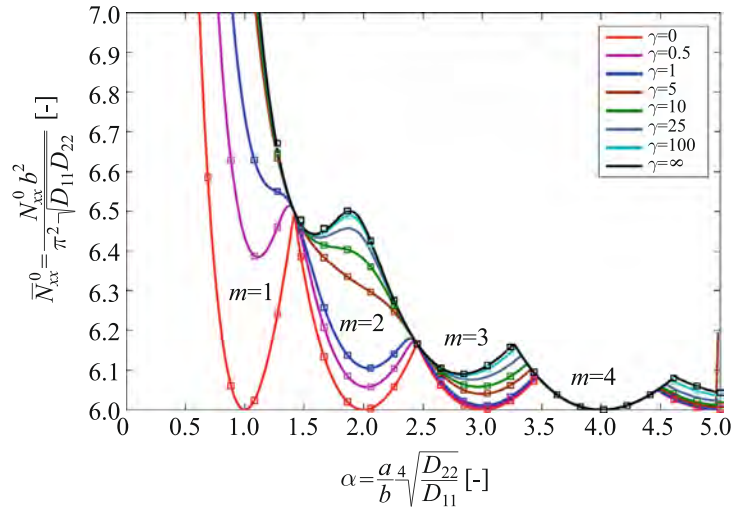


Fig. 17.17 Buckling curves for an orthotropic laminate ($\beta = 2.0$) with a transverse stiffener at $x_1 = \frac{a}{4}$

$$\underline{\underline{M}}_2 = \begin{bmatrix} e^{\lambda_1} & e^{-\lambda_1} & e^{\lambda_2} & e^{-\lambda_2} \\ \lambda_1^2 e^{\lambda_1} & \lambda_1^2 e^{-\lambda_1} & \lambda_2^2 e^{\lambda_2} & \lambda_2^2 e^{-\lambda_2} \end{bmatrix},$$

$$\underline{\underline{M}}_3^{1,2} = \begin{bmatrix} e^{\lambda_1 a_{1,2}} & e^{-\lambda_1 a_{1,2}} & e^{\lambda_2 a_{1,2}} & e^{-\lambda_2 a_{1,2}} \\ \lambda_1 e^{\lambda_1 a_{1,2}} & -\lambda_1 e^{-\lambda_1 a_{1,2}} & \lambda_2 e^{\lambda_2 a_{1,2}} & -\lambda_2 e^{-\lambda_2 a_{1,2}} \\ -\lambda_1^2 e^{\lambda_1 a_{1,2}} & -\lambda_1^2 e^{-\lambda_1 a_{1,2}} & -\lambda_2^2 e^{\lambda_2 a_{1,2}} & -\lambda_2^2 e^{-\lambda_2 a_{1,2}} \\ \left(\pi^4 \gamma_{1,2} - \lambda_1^3\right) e^{\lambda_1 a_{1,2}} & \left(\pi^4 \gamma_{1,2} + \lambda_1^3\right) e^{-\lambda_1 a_{1,2}} & \left(\pi^4 \gamma_{1,2} - \lambda_2^3\right) e^{\lambda_2 a_{1,2}} & \left(\pi^4 \gamma_{1,2} + \lambda_2^3\right) e^{-\lambda_2 a_1} \end{bmatrix},$$

$$\underline{\underline{M}}_4^{1,2} = \begin{bmatrix} -e^{\lambda_1 a_{1,2}} & -e^{-\lambda_1 a_{1,2}} & -e^{\lambda_2 a_{1,2}} & -e^{-\lambda_2 a_{1,2}} \\ -\lambda_1 e^{\lambda_1 a_{1,2}} & \lambda_1 e^{-\lambda_1 a_{1,2}} & -\lambda_2 e^{\lambda_2 a_{1,2}} & \lambda_2 e^{-\lambda_2 a_{1,2}} \\ \lambda_1^2 e^{\lambda_1 a_{1,2}} & \lambda_1^2 e^{-\lambda_1 a_{1,2}} & \lambda_2^2 e^{\lambda_2 a_{1,2}} & \lambda_2^2 e^{-\lambda_2 a_{1,2}} \\ \lambda_1^3 e^{\lambda_1 a_{1,2}} & -\lambda_1^3 e^{-\lambda_1 a_{1,2}} & \lambda_2^3 e^{\lambda_2 a_{1,2}} & -\lambda_2^3 e^{-\lambda_2 a_{1,2}} \end{bmatrix}.$$

Setting the coefficient determinant to zero leads to the following transcendental buckling condition:

$$\begin{aligned} &\lambda_1^2 \lambda_2^2 \left(\lambda_1^2 - \lambda_2^2\right)^2 \sinh \lambda_1 \sinh \lambda_2 \\ &+\pi^4 \lambda_1 \lambda_2 \left(\lambda_1^2 - \lambda_2^2\right) [\gamma_1 [\lambda_1 \sinh \lambda_1 \sinh a_1 \lambda_2 \sinh(1 - a_1)\lambda_1 \\ &\quad - \lambda_2 \sinh \lambda_2 \sinh a_1 \lambda_1 \sinh(1 - a_1)\lambda_1] \\ &\quad +\gamma_2 [\lambda_1 \sinh \lambda_1 \sinh a_2 \lambda_2 \sinh(1 - a_2)\lambda_2 \\ &\quad - \lambda_2 \sinh \lambda_2 \sinh a_2 \lambda_1 \sinh(1 - a_2)\lambda_1]] \\ &+\pi^8 \gamma_1 \gamma_2 \left[\lambda_1^2 \sinh \lambda_1 \sinh a_1 \lambda_2 \sinh(a_2 - a_1)\lambda_2 \sinh(1 - a_2)\lambda_2 \right. \\ &\quad +\lambda_2^2 \sinh \lambda_2 \sinh a_1 \lambda_1 \sinh(a_2 - a_1)\lambda_1 \sinh(1 - a_2)\lambda_1 \\ &\quad +\lambda_1 \lambda_2 [\sinh a_1 \lambda_1 \sinh(1 - a_2)\lambda_2 [\sinh a_1 \lambda_2 \sinh(1 - a_2)\lambda_1 \\ &\quad - \sinh a_2 \lambda_2 \sinh(1 - a_1)\lambda_1] \\ &\quad + \sinh a_1 \lambda_2 \sinh(1 - a_2)\lambda_1 [\sinh a_1 \lambda_1 \sinh(1 - a_2)\lambda_2 \\ &\quad \left. - \sinh a_2 \lambda_1 \sinh(1 - a_1)\lambda_2]]] = 0. \end{aligned} \tag{17.113}$$

For the special case of two identical stiffeners ($\gamma_1 = \gamma_2 = \gamma$) at arbitrary positions, this buckling condition is simplified as follows:

$$\begin{aligned} &\lambda_1^2 \lambda_2^2 \left(\lambda_1^2 - \lambda_2^2\right)^2 \sinh \lambda_1 \sinh \lambda_2 \\ &+\pi^4 \lambda_1 \lambda_2 \left(\lambda_1^2 - \lambda_2^2\right) \gamma [\lambda_1 \sinh \lambda_1 \sinh a_1 \lambda_2 \sinh(1 - a_1)\lambda_1 \\ &\quad -\lambda_2 \sinh \lambda_2 \sinh a_1 \lambda_1 \sinh(1 - a_1)\lambda_1 \\ &\quad +\lambda_1 \sinh \lambda_1 \sinh a_2 \lambda_2 \sinh(1 - a_2)\lambda_2 \\ &\quad - \lambda_2 \sinh \lambda_2 \sinh a_2 \lambda_1 \sinh(1 - a_2)\lambda_1] \\ &+\pi^8 \gamma^2 \left[\lambda_1^2 \sinh \lambda_1 \sinh a_1 \lambda_2 \sinh(a_2 - a_1)\lambda_2 \sinh(1 - a_2)\lambda_2 \right. \\ &\quad +\lambda_2^2 \sinh \lambda_2 \sinh a_1 \lambda_1 \sinh(a_2 - a_1)\lambda_1 \sinh(1 - a_2)\lambda_1 \\ &\quad +\lambda_1 \lambda_2 [\sinh a_1 \lambda_1 \sinh(1 - a_2)\lambda_2 [\sinh a_1 \lambda_2 \sinh(1 - a_2)\lambda_1 \\ &\quad - \sinh a_2 \lambda_2 \sinh(1 - a_1)\lambda_1] \\ &\quad + \sinh a_1 \lambda_2 \sinh(1 - a_2)\lambda_1 [\sinh a_1 \lambda_1 \sinh(1 - a_2)\lambda_2 \\ &\quad \left. - \sinh a_2 \lambda_1 \sinh(1 - a_1)\lambda_2]]] = 0. \end{aligned} \tag{17.114}$$

If two stiffeners are arranged symmetrically to the center line of the laminate at $a_1 = 1 - a_2$, then it follows:

$$\begin{aligned}
&\lambda_1^2\lambda_2^2\left(\lambda_1^2-\lambda_2^2\right)^2\sinh\lambda_1\sinh\lambda_2\\
+\pi^4\lambda_1\lambda_2&\left(\lambda_1^2-\lambda_2^2\right)(\gamma_1+\gamma_2)\left[\lambda_1\sinh\lambda_1\sinh a_1\lambda_2\sinh a_2\lambda_2\right.\\
&\left.-\lambda_2\sinh\lambda_2\sinh a_1\lambda_1\sinh a_2\lambda_1\right]\\
+\pi^8\gamma_1\gamma_2&\left[\lambda_1^2\sinh\lambda_1\sinh a_1\lambda_2\sinh(1-2a_1)\lambda_2\right.\\
&+\lambda_2^2\sinh\lambda_2\sinh^2 a_1\lambda_1\sinh(1-2a_1)\lambda_1\\
&+2\lambda_1\lambda_2\sinh a_1\lambda_1\sinh a_1\lambda_2\left[\sinh a_1\lambda_2\sinh a_1\lambda_1\right.\\
&\left.\left.-\sinh a_2\lambda_2\sinh a_2\lambda_1\right]\right]=0. \qquad (17.115)
\end{aligned}$$

If there are two stiffeners at $a_1 = \frac{1}{3}$ and $a_2 = \frac{2}{3}$, the following buckling condition results:

$$\begin{aligned}
&\lambda_1^2\lambda_2^2\left(\lambda_1^2-\lambda_2^2\right)^2\sinh\lambda_1\sinh\lambda_2\\
+\pi^4\lambda_1\lambda_2&\left(\lambda_1^2-\lambda_2^2\right)(\gamma_1+\gamma_2)\left[\lambda_1\sinh\lambda_1\sinh\frac{\lambda_2}{3}\sinh\frac{2\lambda_2}{3}\right.\\
&\left.-\lambda_2\sinh\lambda_2\sinh\frac{\lambda_1}{3}\sinh\frac{2\lambda_1}{3}\right]\\
+\pi^8\gamma_1\gamma_2&\left[\lambda_1^2\sinh\lambda_1\sinh^3\frac{\lambda_2}{3}+\lambda_2^2\sinh\lambda_2\sinh^3\frac{\lambda_1}{3}\right.\\
&+2\lambda_1\lambda_2\sinh\frac{\lambda_1}{3}\sinh\frac{\lambda_2}{3}\left[\sinh\frac{\lambda_2}{3}\sinh\frac{\lambda_1}{3}\right.\\
&\left.\left.-\sinh\frac{2\lambda_2}{3}\sinh\frac{2\lambda_1}{3}\right]\right]=0. \qquad (17.116)
\end{aligned}$$

17.6.4.3 Laminate with a Torsionally Stiff Stiffener at Arbitrary Position

Finally, we consider the case of an orthotropic laminate under uniaxial compression load, which is stiffened by a torsionally stiff stiffener at arbitrary position a_1. The following buckling condition can be derived for this case:

$$\begin{aligned}
&\lambda_1\lambda_2\left(\lambda_1^2-\lambda_2^2\right)\sinh\lambda_1\sinh\lambda_2\\
+\gamma\pi^4&\left[\lambda_1\sinh\lambda_1\sinh\lambda_2 a_1\sinh(1-a_1)\lambda_2\right.\\
&\left.+\lambda_2\sinh\lambda_2\sinh\lambda_1 a_1\sinh(a_1-1)\lambda_1\right]\\
+\theta\pi^2\lambda_1\lambda_2&\left[\lambda_1\sinh\lambda_2\cosh\lambda_1 a_1\cosh(1-a_1)\lambda_1\right.\\
&\left.-\lambda_2\sinh\lambda_1\cosh\lambda_2 a_1\cosh(a_1-1)\lambda_2\right]\\
+\gamma\theta\frac{\pi^6}{4}&\left[\frac{\lambda_1+\lambda_2}{\lambda_1-\lambda_2}\sinh a_1(\lambda_1-\lambda_2)\sinh(1-a_1)(\lambda_1-\lambda_2)\right.
\end{aligned}$$

$$+\frac{\lambda_1-\lambda_2}{\lambda_1+\lambda_2}\sinh a_1(\lambda_1+\lambda_2)\sinh(1-a_1)(\lambda_1+\lambda_2)$$
$$-\cosh\lambda_1\cosh(2a_1-1)\lambda_2+\cosh\lambda_2\cosh(2a_1-1)\lambda_1]=0. \tag{17.117}$$

17.7 Laminate Simply Supported at Three Edges with a Reinforced Free Edge

In this section we consider buckling of a laminate that is simply supported at three edges. The remaining edge is free, but reinforced by an edge stiffener (Fig. 17.18). Application examples for such a situation are stringers of a stiffened shell or plate with I-, Z-, C-profiles or stringers that are reinforced at the edge by flanges (see Fig. 17.1). A hinged support is provided at the resulting intersection edge between the stringer and shell/plate, whereby the clamping effect of the shell is neglected for the sake of a simple calculation method. This is a simplifying, but in all cases also a conservative assumption. The stiffener is subjected to a uniaxial compressive load in the form of a uniform line load N^0_{xx}. The upper edge of the stiffener is reinforced by a flange (extensional stiffness EA, bending stiffness EI, torsional stiffness GI_T) of arbitrary cross-section, but is otherwise free of any support. The flange is subjected to a compressive force. Figure 17.18 shows an example of an I-stiffener, but the analysis method presented in the following is not limited to this cross-sectional shape. The loaded edges of the stiffener are also assumed to be simply supported.

For the stiffener configuration shown in Fig. 17.18, two buckling modes are possible, provided that the flange is idealised as an Euler-Bernoulli beam with effective elastic prop-

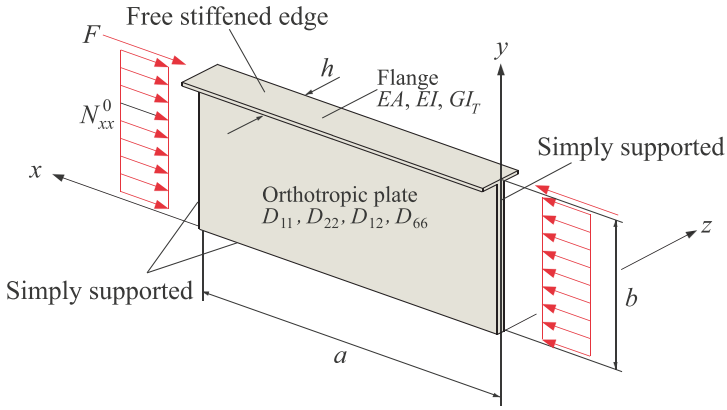


Fig. 17.18 Laminate with simply supported loaded edges, one simply supported unloaded edge and one free unloaded edge reinforced by a stiffener

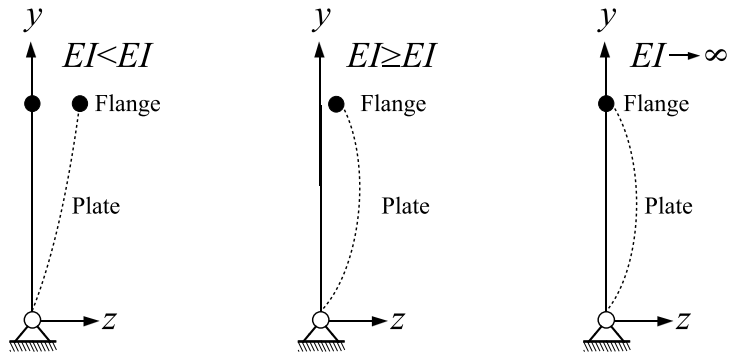


Fig. 17.19 Global and local buckling

erties. On the one hand, a global buckling mode can occur (Fig. 17.19, left), in which both the stiffening web (referred to as 'plate' in the rest of this section) and the flange buckle simultaneously. On the other hand, it is conceivable that the flange has sufficient bending stiffness EI (with regard to bending about the y-axis), so that the relevant buckling mode is a purely local buckling of the plate between the simply supported edge and the flange (Fig. 17.19, right). In addition to determining the buckling loads of such stiffened plates, the determination of this so-called minimum stiffness $EI_{\min}$ is another central topic that is analyzed in this section.

The first investigations into the buckling behaviour of three-sided simply supported isotropic plates with stiffened free edges under compression were carried out in 1938 by Windenburg, who also developed the well-known minimum stiffness criterion

$$\frac{2.73I}{bh^3} - \frac{A}{bh} \geq 5, \tag{17.118}$$

which establishes a relationship between the moment of inertia I and the cross-sectional area A of the flange on the one hand and the width b and thickness h of the plate on the other and, if it is fulfilled, it can be assumed that the flange represents an approximately rigid support and therefore the plate only buckles locally between the two unloaded edges. However, this criterion has two major disadvantages. Firstly, (17.118) is only valid for square plates, which generally limits its applicability. Secondly, the criterion (17.118) is only valid for isotropic plates whose Poisson's ratio is $\nu = 0.3$. For this reason, given the current state of the art in fiber composite lightweight construction, but also with regard to the current challenges in passenger aircraft construction, it seems justified to turn to this problem again and, in addition to a general discussion of the buckling behaviour of such plates, to create an extended form of the criterion (17.118) for orthotropic plates of arbitrary dimensions. For the sake of completeness, readers are referred to the publications by Goodman and Boyd (1947), Goodman (1949), Klöppel and Unger (1969) or Paik et al. (1998), which report on

similar investigations of edge-stiffened isotropic plate structures. This section is a summary of the publication by Mittelstedt and Schagerl (2010).

The underlying boundary conditions of the present problem require that at the loaded edges at $x = 0$ and $x = a$ the buckling shape w_0 has a nodal line and the plate bending moment M^0_{xx} disappears:

$$w_0\,(x = 0) = 0, \quad w_0\,(x = a) = 0, \quad M^0_{xx}\,(x = 0) = 0, \quad M^0_{xx}\,(x = a) = 0. \tag{17.119}$$

At the unloaded edge at $y = 0$, the buckling shape also assumes a zero value:

$$w_0\,(y = 0) = 0. \tag{17.120}$$

Furthermore, the bending moment M^0_{yy} must disappear there, which by observing $\left.\frac{\partial^2 w_0}{\partial x^2}\right|_{y=0} = 0$ leads to the following expression:

$$M^0_{yy}\,(y = 0) = -D_{22}\left.\frac{\partial^2 w_0}{\partial y^2}\right|_{y=0} = 0. \tag{17.121}$$

Two conditions must be observed at the free edge at the point $y = b$. Firstly, the plate bending moment M^0_{yy} acts like a torsional moment on the flange, which can be formulated as follows according to St. Venant's torsion theory:

$$M^0_{yy}\,(y = b) = -GI_T\left.\frac{\partial^3 w_0}{\partial x^2 \partial y}\right|_{y=b}. \tag{17.122}$$

Inserting the constitutive law for a symmetric laminate with an orthotropic plate quadrant then results in

$$-D_{12}\left.\frac{\partial^2 w_0}{\partial x^2}\right|_{y=b} - D_{22}\left.\frac{\partial^2 w_0}{\partial y^2}\right|_{y=b} + GI_T\left.\frac{\partial^3 w_0}{\partial x^2 \partial y}\right|_{y=b} = 0. \tag{17.123}$$

On the other hand, it can be stated that the plate shear force $\bar{Q}_y$ acts as a line load on the flange, which is described by the following equation:

$$EI\left.\frac{\partial^4 w_0}{\partial x^4}\right|_{y=b} + F\left.\frac{\partial^2 w_0}{\partial x^2}\right|_{y=b} + \bar{Q}_y\,(y = b) = 0. \tag{17.124}$$

This equation corresponds to the differential equation for the flexural buckling problem, i.e. the differential equation for a beam under normal and shear loading according to second-order theory. The shear force $\bar{Q}_y$ can be written as a Kirchhoff equivalent shear force:

$$\bar{Q}_y\,(y = b) = 2\left.\frac{\partial M^0_{xy}}{\partial x}\right|_{y=b} + \left.\frac{\partial M^0_{yy}}{\partial y}\right|_{y=b}. \tag{17.125}$$

Inserting the constitutive relations for the laminate finally leads to:

$$EI \left.\frac{\partial^4 w_0}{\partial x^4}\right|_{y=b} + F \left.\frac{\partial^2 w_0}{\partial x^2}\right|_{y=b} - D_{22} \left.\frac{\partial^3 w_0}{\partial y^3}\right|_{y=b} - (D_{12} + 4D_{66}) \left.\frac{\partial^3 w_0}{\partial x^2 \partial y}\right|_{y=b} = 0. \tag{17.126}$$

Both the plate and the flange suffer the same longitudinal strain ε_{xx} under the given load case. We can then derive a relationship between the plate load N^0_{xx} and the flange force F by requiring compatibility of the longitudinal strain of the plate and the longitudinal strain of the flange. This then leads to

$$F = N^0_{xx} \frac{EA}{E_P h}. \tag{17.127}$$

Here, E_P is the plane modulus of elasticity of the plate with respect to the x-direction, which, like the modulus of elasticity E of the flange, can be derived from the corresponding membrane stiffnesses A_{op} (o, $p = 1, 2, 6$) (only given here for E_P):

$$E_P = \frac{1}{d}\left(A_{11,P} - \frac{A^2_{12,P}}{A_{22,P}}\right). \tag{17.128}$$

If we use the abbreviation

$$\delta = \frac{EA}{E_P bh}, \tag{17.129}$$

for the ratio of the extensional stiffnesses of flange and plate, (17.127) can also be written as:

$$F = \delta N^0_{xx} b. \tag{17.130}$$

We consider the problem using a Lévy solution approach. Assuming $N^0_{xx} > D_{11}\left(\frac{m\pi}{a}\right)^2$, the Lévy solution is:

$$\begin{aligned} w_0 = \sin\left(\frac{m\pi x}{a}\right)\Bigg[C_1 \cosh\left(\frac{k_1 m\pi y}{a}\right) + C_2 \sinh\left(\frac{k_1 m\pi y}{a}\right) \\ + C_3 \cos\left(\frac{k_2 m\pi y}{a}\right) + C_4 \sin\left(\frac{k_2 m\pi y}{a}\right)\Bigg], \end{aligned} \tag{17.131}$$

wherein the following abbreviations were used:

$$k_{1,2} = \sqrt{\frac{1}{D_{22}}\left(\sqrt{(D_{12} + 2D_{66})^2 + D_{22}\left(N^0_{xx}\left(\frac{a}{m\pi}\right)^2 - D_{11}\right)} \pm (D_{12} + 2D_{66})\right)}. \tag{17.132}$$

The free constants $C_1, \ldots, C_4$ are determined from the boundary conditions at the unloaded edges of the plate. If the boundary conditions (17.120) and (17.121) at the simply supported unloaded edge are evaluated at $y = 0$, $C_1 = C_3 = 0$ is obtained immediately, so that the solution (17.131) is reduced to the following expression:

$$w_0 = \sin\left(\frac{m\pi x}{a}\right)\left[C_2 \sinh\left(\frac{k_1 m\pi y}{a}\right) + C_4 \sin\left(\frac{k_2 m\pi y}{a}\right)\right]. \tag{17.133}$$

With the solution (17.133), the following two equations for the remaining constants C_2 and C_4 are obtained from the two remaining boundary conditions at the free boundary (17.123) and (17.126) at $y = b$, taking into account (17.130):

$$\begin{aligned}
&\left[\sinh\left(\frac{k_1 m\pi b}{a}\right)\left(D_{12} - D_{22}k_1^2\right) - GI_T\frac{k_1 m\pi}{a}\cosh\left(\frac{k_1 m\pi b}{a}\right)\right]C_2 \\
&+\left[\sin\left(\frac{k_2 m\pi b}{a}\right)\left(D_{12} + D_{22}k_2^2\right) - GI_T\frac{k_2 m\pi}{a}\cos\left(\frac{k_2 m\pi b}{a}\right)\right]C_4 = 0, \\
&\left[\left(EI\frac{m^2\pi^2}{a^2} - \delta N_{xx}^0 b\right)\sinh\left(\frac{k_1 m\pi b}{a}\right)\right. \\
&\left.+\frac{k_1 m\pi}{a}\left(-D_{22}k_1^2 + D_{12} + 4D_{66}\right)\cosh\left(\frac{k_1 m\pi b}{a}\right)\right]C_2 \\
&+\left[\left(EI\frac{m^2\pi^2}{a^2} - \delta N_{xx}^0 b\right)\sin\left(\frac{k_2 m\pi b}{a}\right)\right. \\
&\left.+\frac{k_2 m\pi}{a}\left(D_{22}k_2^2 + D_{12} + 4D_{66}\right)\cos\left(\frac{k_2 m\pi b}{a}\right)\right]C_4 = 0.
\end{aligned} \tag{17.134}$$

To avoid a trivial solution of this homogeneous system of equations, its coefficient determinant is set to zero, which leads to the following equation after a few transformations:

$$\begin{aligned}
&A_1 \cosh\left(\frac{k_1 m\pi b}{a}\right)\cos\left(\frac{k_2 m\pi b}{a}\right) + A_2 \sinh\left(\frac{k_1 m\pi b}{a}\right)\sin\left(\frac{k_2 m\pi b}{a}\right) \\
&+A_3 \cosh\left(\frac{k_1 m\pi b}{a}\right)\sin\left(\frac{k_2 m\pi b}{a}\right) + A_4 \sinh\left(\frac{k_1 m\pi b}{a}\right)\cos\left(\frac{k_2 m\pi b}{a}\right) = 0,
\end{aligned} \tag{17.135}$$

where the coefficients $A_1, \ldots, A_4$ are abbreviations for:

$$\begin{aligned}
A_1 &= -D_{22}\frac{m^2\pi^2}{a^2}GI_T k_1 k_2\left(k_1^2 + k_2^2\right), \\
A_2 &= -D_{22}\left(EI\frac{m^2\pi^2}{a^2} - \delta N_{xx}^0 b\right)\left(k_1^2 + k_2^2\right), \\
A_3 &= \frac{k_1 m\pi}{a}\left[\left(k_1^2 D_{22} - D_{12} - 4D_{66}\right)\left(k_2^2 D_{22} + D_{12}\right) - GI_T\left(EI\frac{m^2\pi^2}{a^2} - \delta N_{xx}^0 b\right)\right], \\
A_4 &= -\frac{k_2 m\pi}{a}\left[\left(k_2^2 D_{22} + D_{12} + 4D_{66}\right)\left(k_1^2 D_{22} - D_{12}\right) - GI_T\left(EI\frac{m^2\pi^2}{a^2} - \delta N_{xx}^0 b\right)\right].
\end{aligned} \tag{17.136}$$

This represents the exact buckling condition from which the buckling load N_{xx}^0 of the currently considered stiffened plate can be determined. However, since the buckling condition with respect to N_{xx}^0 is highly nonlinear (as is typically the case when using a Lévy solution), no exact closed-form analytical solution for N_{xx}^0 can be determined. Instead, numerical methods must be used to provide solutions for (17.135) with (17.136).

In the further course of this section, we want to make the assumption that the torsional stiffness GI_T of the flange is small, so that we can set $GI_T = 0$ as an approximation. Then the transcendental equation (17.135) with (17.136) is simplified considerably, and the following result remains:

$$\begin{aligned} & D_{22}\left(EI\frac{m^2\pi^2}{a^2} - \delta N_{xx}^0 b\right)\left(k_1^2 + k_2^2\right) \\ & -\frac{k_1 m\pi}{a}\left(k_1^2 D_{22} - D_{12} - 4D_{66}\right)\left(k_2^2 D_{22} + D_{12}\right)\coth\left(\frac{k_1 m\pi b}{a}\right) \\ & +\frac{k_2 m\pi}{a}\left(k_2^2 D_{22} + D_{12} + 4D_{66}\right)\left(k_1^2 D_{22} - D_{12}\right)\cot\left(\frac{k_2 m\pi b}{a}\right) = 0. \end{aligned} \tag{17.137}$$

In Fig. 17.20 there are two exemplary buckling diagrams in which the dimensionless buckling load $\bar{N}_{xx}^0$ was plotted against the aspect ratio α. On the one hand, Fig. 17.20 contains the case $\beta = 0.5$ (Fig. 17.20, left), and on the other hand also the case $\beta = 3.0$ (Fig. 17.20, right). In both cases, the generalised Poisson's ratio was set to $\zeta = 0.3$. In the diagrams in Fig. 17.20 there are several graphs for different values of the bending stiffness γ, whereby the extensional stiffness was set to $\delta = 0.0$, $\delta = 0.1$, $\delta = 0.2$ and $\delta = 0.3$, so that for a certain value for γ there is a set of curves with four different graphs each. The characteristic behaviour of the solution (17.135) with (17.136) or the Eq. (17.137) can be concluded from the diagrams in Fig. 17.20 quite clearly. Obviously, the buckling load $\bar{N}_{xx}^0$ is limited in all cases to an interval whose lower limit is the case of the unstiffened plate with $\gamma = 0$, while the upper limit is given by the case of the infinitely stiff flange with $\gamma \to \infty$. This upper limit with $\gamma \to \infty$ also corresponds to the case of an identical plate simply supported at all edges. For finite values of the bending stiffness γ, the following characteristic behaviour of $\bar{N}_{xx}^0\,(\alpha, \gamma, \delta)$ always results. In a certain range of values for the aspect ratio α, $\bar{N}_{xx}^0\,(\alpha, \gamma, \delta)$ runs close to the upper limit $\bar{N}_{xx}^0\,(\alpha, \gamma \to \infty, \delta)$, until finally at a certain aspect ratio α a sharp drop in the buckling load $\bar{N}_{xx}^0\,(\alpha, \gamma, \delta)$ can be observed and $\bar{N}_{xx}^0\,(\alpha, \gamma, \delta)$ approaches the lower limit $\bar{N}_{xx}^0\,(\alpha, \gamma = 0, \delta)$ asymptotically for increasing α. Looking at the diagram in Fig. 17.20, left, for example, the function $\bar{N}_{xx}^0\,(\alpha, \gamma = 10.0, \delta = 0)$ in the interval $0 < \alpha \leq 1.5$ is very close to the upper limit $\bar{N}_{xx}^0\,(\alpha, \gamma \to \infty, \delta)$ and describes a single-wave buckling ($m = 1$). Obviously, the edge-stiffened plate behaves almost like a plate that is simply supported at all edges since the bending stiffness γ of the flange is sufficient to achieve an approximate effect like a rigid support at the free edge. At the point $\alpha \simeq 1.5$ an abrupt change in the gradient occurs and the plate buckles in the interval $1.5 \leq \alpha \leq 2.5$ in $m = 2$ half-waves. Such mode changes are, as already stated in previous sections, a typical observation when simply supported plates buckle. In the interval $2.5 \leq \alpha \leq 3.0$ $m = 3$ half-waves occur. From

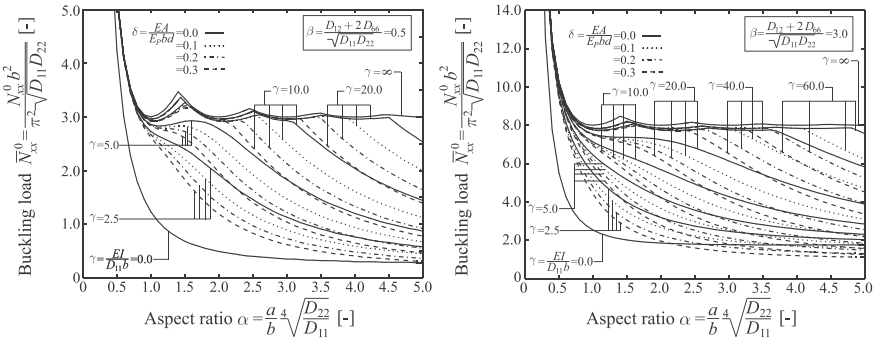


Fig. 17.20 Exemplary buckling diagrams

the aspect ratio $\alpha \simeq 3.0$, the plate reverts to a single-wave buckling pattern and the function graph $\bar{N}_{xx}^0\,(\alpha, \gamma = 10.0, \delta = 0)$ drops sharply with increasing α and approaches the lower limit $\bar{N}_{xx}^0\,(\alpha, \gamma = 0, \delta = 0)$. This phenomenon can be explained by the fact that when a certain aspect ratio is exceeded, the purely local plate buckling between the unloaded edge and the stiffened edge is no longer the relevant stability case, but rather a kind of single-wave Euler buckling of the flange occurs, which the plate is forced to follow. This means a considerable reduction in the resulting buckling load, because the flange loses its supporting effect in this case and the structure becomes more compliant overall. Obviously, in the case of $\gamma = 10.0$, $\delta = 0$ at the point $\alpha \simeq 3.0$, the bending stiffness of the flange is no longer sufficient to provide support at the free edge. The minimum stiffness was therefore not reached at this point. The direct comparison of the two diagrams in Fig. 17.20 also clearly shows the significant influence of β on the buckling load.

As Fig. 17.20 shows, the buckling behaviour of a simply supported plate with an edge stiffener is quite complex. In addition, the numerical evaluation of the transcendental buckling equation (17.135) with (17.136) or the Eq. (17.137) is not straightforward and difficult to automate, which proves to be problematic, especially in practical applications. In addition, it has been shown that a design in which the bending stiffness of the flange falls below the minimum stiffness is not optimal and may be considerably weaker than a design with sufficient flange bending stiffness would be. There is therefore an interest in adjusting the bending stiffness of the flange in an uncomplicated way so that precisely the minimum stiffness is achieved with which the given situation of the edge-reinforced plate can be treated approximately like a four-sided simply supported plate. This ensures that the resulting buckling load is maximized. In addition, this simplifies the calculation enormously, because for the four-sided simply supported orthotropic plate under uniaxial compression, we can dispense with the evaluation of a transcendental equation and use the known exact closed-form analytical solution for the buckling load ('ss' = simply supported, where m_{ss} is the number of buckling half-waves of the four-sided simply supported plate):

$$N^0_{xx,ss} = \pi^2 \left[D_{11} \frac{m_{ss}^2}{a^2} + D_{22} \frac{a^2}{m_{ss}^2 b^4} + \frac{2}{b^2} \left(D_{12} + 2D_{66} \right) \right]. \tag{17.138}$$

A simple criterion for the minimum stiffness can now be postulated by requiring that the buckling load N^0_{xx} of the edge-stiffened plate (which buckles with $m = 1$ half-waves in the insufficiently stiffened state) is equal to the buckling load $N^0_{xx,ss}$ of the four-sided simply supported plate, whereby an arbitrary factor ρ is applied to $N^0_{xx,ss}$, which must formally be in the interval $0 \leq \rho < 1$:

$$N^0_{xx} = \rho N^0_{xx,ss}. \tag{17.139}$$

If we substitute (17.139) into (17.137) and use the already known dimensionless quantities $\alpha, \gamma, \delta, \beta, \zeta, \bar{N}^0_{xx}$, we obtain the following representation for the buckling condition (17.137):

$$\begin{aligned} \gamma = \delta \rho \bar{N}^0_{xx,ss} \alpha^2 \quad & + \frac{\kappa_1 \alpha \left[\kappa_1^2 - (2 - \zeta)\, \beta \right] \left(\kappa_2^2 + \zeta \beta \right)}{\pi \left(\kappa_1^2 + \kappa_2^2 \right)} \coth \left(\frac{\kappa_1 \pi}{\alpha} \right) \\ & - \frac{\kappa_2 \alpha \left[\kappa_2^2 + (2 - \zeta)\, \beta \right] \left(\kappa_1^2 - \zeta \beta \right)}{\pi \left(\kappa_1^2 + \kappa_2^2 \right)} \cot \left(\frac{\kappa_2 \pi}{\alpha} \right), \end{aligned} \tag{17.140}$$

where the variables κ_1 and κ_2 are abbreviations for

$$\kappa_{1,2} = \sqrt{\sqrt{\beta^2 + \rho \bar{N}^0_{xx,ss} \alpha^2 - 1} \pm \beta}. \tag{17.141}$$

The dimensionless buckling load $\bar{N}^0_{xx,ss}$ can be specified as:

$$\bar{N}^0_{xx,ss} = \frac{m_{ss}^2}{\alpha^2} + \frac{\alpha^2}{m_{ss}^2} + 2\beta. \tag{17.142}$$

If we use the exact buckling condition (17.140) with (17.141) and then use the knowledge about the behaviour of the buckling load of a four-sided simply supported orthotropic plate, this leads to a continuous criterion using (17.139) and (17.142), from which the bending stiffness of the flange can be easily determined in such a way that a local buckling mode occurs and the buckling load N^0_{xx} assumes the value $N^0_{xx} = \rho N^0_{xx,ss}$, whereby the value ρ is to be determined by the user. It can be seen that with the choice $\rho = 0.98$ the current method includes the classic minimum stiffness criterion according to Windenburg as a special case (see also Mittelstedt and Schagerl (2010)).

Figure 17.21 contains diagrams for the bending stiffness γ of the flange, shown as a function of the aspect ratio α, the orthotropy parameter β and the generalised Poisson's ratio ζ. These diagrams can be used in practical applications as design diagrams and cover a parameter space in which almost all practically relevant cases can be found.

The determination of the minimum stiffness γ according to the explanations in the previous paragraphs, but also with the help of the generic design diagrams in Fig. 17.21 requires information about the cross-sectional area A of the flange as an input variable, in the form

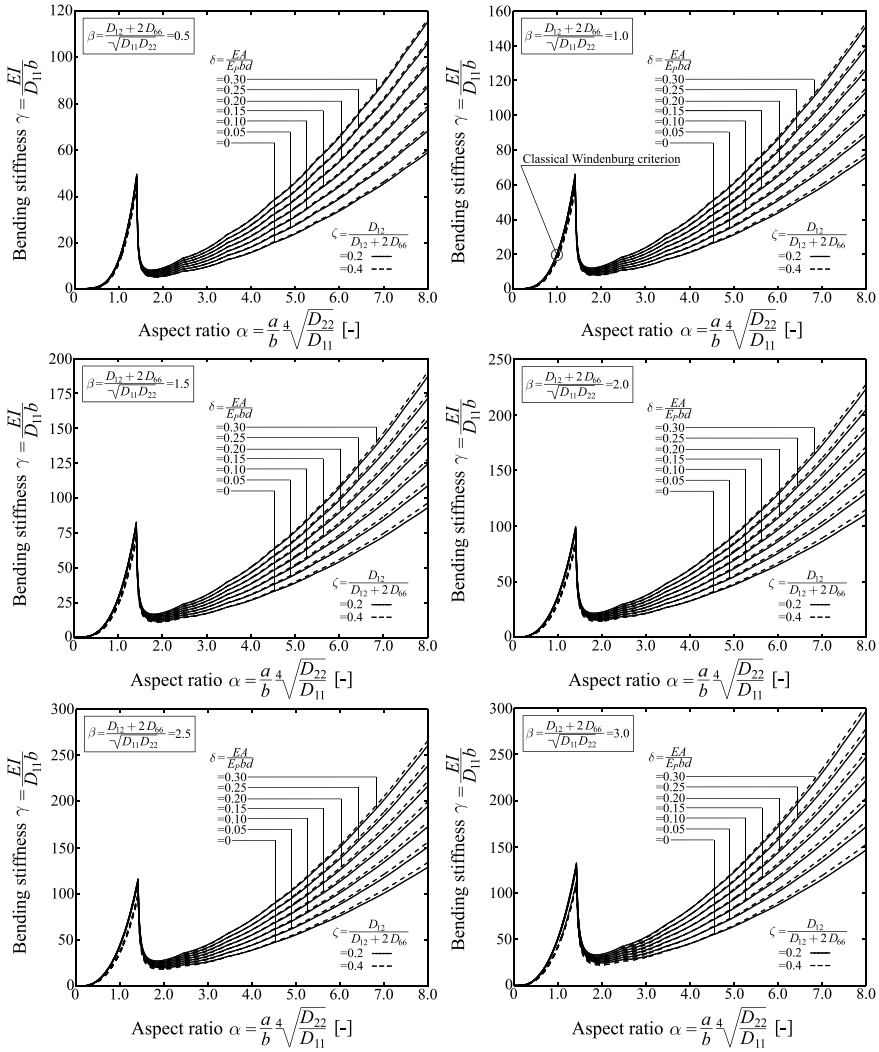


Fig. 17.21 Bending stiffness γ of the flange, represented as a function of the aspect ratio α, the orthotropy parameter β and the generalised Poisson's ratio ζ

of the dimensionless extensional stiffness δ. The result of the calculation is then the dimensionless bending stiffness γ, which in turn contains the bending stiffness EI of the flange and therefore also depends on the cross-sectional geometry due to the moment of inertia I. In general, the variables δ and γ will not be consistent with each other, so that an iterative process must be carried out to determine γ. In order to calculate the minimum stiffness, an input value A_0 of the cross-sectional area of the stiffener is first estimated, from which an initial value for the extensional stiffness δ_0 can be calculated. This can then be used to

determine an initial estimate γ_1 of the bending stiffness. This in turn can then be used to calculate an improved estimate A_1 of the cross-sectional area, which can be used as a new input variable for an improved related strain stiffness δ_1. From this, a second and improved estimate γ_2 of the bending stiffness can be obtained. This process is repeated until sufficient convergence of the results can be observed in iteration step n so that $\gamma_n \simeq \gamma_{n-1}$ applies. The value γ_n determined in this way then represents the dimensionless minimum stiffness, from which the actual minimum stiffness $EI_{\min}$ can be calculated in a practical application. For many technically relevant stiffener shapes, it may even be possible to dispense with an iterative process, and the minimum stiffness criterion derived above can be explicitly solved for the flange width for a flange with a rectangular cross-section, for example, if the flange thickness is specified and assumed to be invariable.

17.8 Laminate with Simply Supported Loaded Edges, One Elastically Restrained Unloaded Edge and One Reinforced Unloaded Free Edge

An extension of the case of the previous section exists if the simply supported, unloaded longitudinal edge is also subject to elastic restraint (restraint stiffness k, Fig. 17.22, see also Weißgraeber et al. (2012)). The boundary conditions at the unloaded longitudinal edges are as follows for this situation:

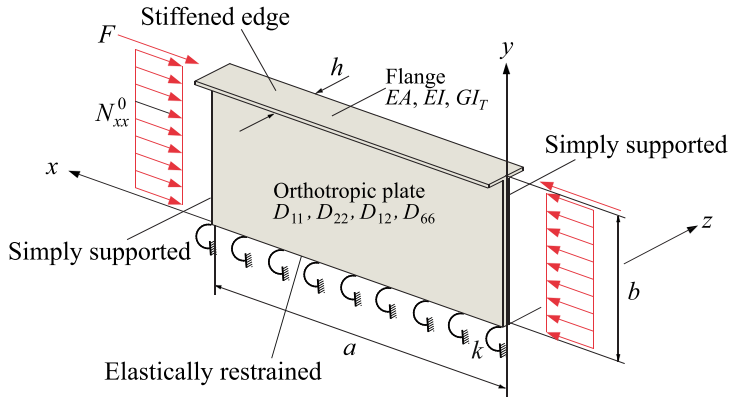


Fig. 17.22 Laminate with simply supported loaded edges, one elastically restrained unloaded edge and one reinforced unloaded free edge

$$
\begin{aligned}
w_0(y=0) &= 0,\\
D_{22}\left.\frac{\partial^2 w_0}{\partial y^2}\right|_{y=0} - k\left.\frac{\partial w_0}{\partial y}\right|_{y=0} &= 0,\\
EI\left.\frac{\partial^4 w_0}{\partial x^4}\right|_{y=b} + N^0_{xx}\frac{EA}{E_P bh}\left.\frac{\partial^2 w_0}{\partial x^2}\right|_{y=b} - D_{22}\left.\frac{\partial^3 w_0}{\partial y^3}\right|_{y=b} - (D_{12}+4D_{66})\left.\frac{\partial^3 w_0}{\partial x^2\partial y}\right|_{y=b} &= 0,\\
D_{12}\left.\frac{\partial^2 w_0}{\partial x^2}\right|_{y=b} + D_{22}\left.\frac{\partial^2 w_0}{\partial y^2}\right|_{y=b} - GI_T\left.\frac{\partial^3 w_0}{\partial x^2\partial y}\right|_{y=b} &= 0.
\end{aligned}
\tag{17.143}
$$

We introduce the following dimensionless variables at this point:

$$
\begin{aligned}
&\xi_1 = \frac{x}{a}, \quad \xi_2 = \frac{y}{b}, \quad \bar{w}_0 = \frac{w_0}{\sqrt{ab}},\\
&\beta = \frac{D_{12}+2D_{66}}{\sqrt{D_{11}D_{22}}}, \quad \zeta = \frac{D_{12}}{D_{12}+2D_{66}},\\
&\alpha = \frac{a}{b}\sqrt[4]{\frac{D_{22}}{D_{11}}}, \quad \bar{N}^0_{xx} = \frac{N^0_{xx}b^2}{\pi^2\sqrt{D_{11}D_{22}}},\\
&\delta = \frac{EA}{E_P bh}, \quad \gamma = \frac{EI}{D_{11}b}, \quad \theta = \frac{GI_T}{b\sqrt{D_{11}D_{22}}}, \quad \bar{k} = \frac{kb}{D_{22}}.
\end{aligned}
\tag{17.144}
$$

Here E_P is the modulus of elasticity of the plate:

$$
E_P = \frac{1}{h}\left(A_{11} - \frac{A_{12}^2}{A_{22}}\right). \tag{17.145}
$$

The boundary conditions (17.143) thus change to the following dimensionless form:

$$
\begin{aligned}
\bar{w}_0(\xi_2=0) &= 0,\\
\left.\frac{\partial^2 \bar{w}_0}{\partial \xi_2^2}\right|_{\xi_2=0} - \bar{k}\left.\frac{\partial \bar{w}_0}{\partial \xi_2}\right|_{\xi_2=0} &= 0,\\
\frac{\gamma}{\alpha^2}\left.\frac{\partial^4 \bar{w}_0}{\partial \xi_1^4}\right|_{\xi_2=1} + \bar{N}^0_{xx}\pi^2\delta\left.\frac{\partial^2 \bar{w}_0}{\partial \xi_1^2}\right|_{\xi_2=1} - \alpha^2\left.\frac{\partial^3 \bar{w}_0}{\partial \xi_2^3}\right|_{\xi_2=1} + (\zeta-2)\beta\left.\frac{\partial^3 \bar{w}_0}{\partial \xi_1^2\partial \xi_2}\right|_{\xi_2=1} &= 0,\\
\beta\zeta\left.\frac{\partial^2 \bar{w}_0}{\partial \xi_1^2}\right|_{\xi_2=1} + \alpha^2\left.\frac{\partial^2 \bar{w}_0}{\partial \xi_2^2}\right|_{\xi_2=1} - \theta\left.\frac{\partial^3 \bar{w}_0}{\partial \xi_1^2\partial \xi_2}\right|_{\xi_2=1} &= 0.
\end{aligned}
\tag{17.146}
$$

The buckling differential equation that describes the current plate buckling problem is in dimensionless form:

$$\frac{1}{\alpha^2}\frac{\partial^4\bar{w}_0}{\partial\xi_1^4}+2\beta\frac{\partial^4\bar{w}_0}{\partial\xi_1^2\partial\xi_2^2}+\alpha^2\frac{\partial^4\bar{w}_0}{\partial\xi_2^4}+\bar{N}_{xx}^0\pi^2\frac{\partial^2\bar{w}_0}{\partial\xi_1^2}=0. \tag{17.147}$$

With the solution approach

$$\bar{w}_0(\xi_1,\xi_2)=\sin(m\pi\xi_1)\,f(\xi_2) \tag{17.148}$$

the differential equation (17.147) changes into an ordinary differential equation as follows:

$$\alpha^2\frac{\mathrm{d}^4 f}{\mathrm{d}\xi_2^4}-2\beta(m\pi)^2\frac{\mathrm{d}^2 f}{\mathrm{d}\xi_2^2}+\left(\frac{1}{\alpha^2}-\frac{\bar{N}_{xx}^0}{m^2}\right)(m\pi)^4 f=0. \tag{17.149}$$

We assume the validity of the solution form (17.131) in dimensionless notation:

$$f(\xi_2)=C_1\cosh(m\pi k_1\xi_2)+C_2\sinh(m\pi k_1\xi_2)+C_3\cos(m\pi k_2\xi_2)+C_4\sin(m\pi k_2\xi_2), \tag{17.150}$$

with

$$k_{1,2}=\pm\frac{1}{\alpha}\sqrt{\pm\beta+\sqrt{\beta^2+\frac{\bar{N}_{xx}^0\alpha^2}{m^2}}-1}. \tag{17.151}$$

Evaluating the boundary conditions (17.146) leads to the following linear homogeneous system of equations:

$$\begin{aligned}
C_1+C_3&=0,\\
C_1 m\pi k_1^2-C_2\bar{k}k_1-C_3 m\pi k_2^2-C_4\bar{k}k_2&=0,\\
C_1\left[\cosh(m\pi k_1)\pi\left(\frac{\gamma m^2}{\alpha^2}-\bar{N}_{xx}^0\delta\right)+\sinh(m\pi k_1)m\left((2-\zeta)\beta k_1-k_1^3\alpha^2\right)\right]&\\
+C_2\left[\sinh(m\pi k_1)\pi\left(\frac{\gamma m^2}{\alpha^2}-\bar{N}_{xx}^0\delta\right)+\cosh(m\pi k_1)m\left((2-\zeta)\beta k_1-k_1^3\alpha^2\right)\right]&\\
+C_3\left[\cos(m\pi k_2)\pi\left(\frac{\gamma m^2}{\alpha^2}-\bar{N}_{xx}^0\delta\right)-\sin(m\pi k_2)m\left((2-\zeta)\beta k_2+k_2^3\alpha^2\right)\right]&\\
+C_4\left[\sin(m\pi k_2)\pi\left(\frac{\gamma m^2}{\alpha^2}-\bar{N}_{xx}^0\delta\right)+\cos(m\pi k_2)m\left((2-\zeta)\beta k_2+k_2^3\alpha^2\right)\right]&=0,\\
C_1\left[\cosh(m\pi k_1)\left(\alpha^2k_1^2-\zeta\beta\right)+\sinh(m\pi k_1)\theta m\pi\right]&\\
+C_2\left[\sinh(m\pi k_1)\left(\alpha^2k_1^2-\zeta\beta\right)+\cosh(m\pi k_1)\theta m\pi\right]&\\
+C_3\left[-\cos(m\pi k_2)\left(\alpha^2k_2^2+\zeta\beta\right)-\sin(m\pi k_2)\theta m\pi\right]&\\
+C_4\left[-\sin(m\pi k_2)\left(\alpha^2k_2^2+\zeta\beta\right)+\cos(m\pi k_2)\theta m\pi\right]&=0.
\end{aligned} \tag{17.152}$$

Expanding and zeroing the coefficient determinant leads to the following transcendental buckling condition for the problem at hand:

$$\begin{aligned}&\Lambda_1 + \cosh(k_1 m\pi)\left[\Lambda_2 \cos(k_2 m\pi) + \Lambda_3 \sin(k_2 m\pi)\right]\\&\quad + \sinh(k_1 m\pi)\left[\Lambda_4 \cos(k_2 m\pi) + \Lambda_5 \sin(k_2 m\pi)\right] = 0,\end{aligned} \tag{17.153}$$

with the abbreviations:

$$\begin{aligned}
\Lambda_1 &= \bar{k} k_1 k_2 m \Big[\left(k_1^4 + k_2^4\right)\alpha^6 + 2\left(-k_1^2 + k_2^2\right)\alpha^4\beta\\
&\quad - 2\alpha^2(-2+\zeta)\zeta\beta^2 + 2\pi^2\left(m^2\gamma - \bar{N}_{xx}^0\alpha^2\delta\right)\theta\Big],\\
\Lambda_2 &= k_1 k_2 m\Big[\left(k_1^2 + k_2^2\right)^2 m^2\pi^2\alpha^4\theta\\
&\quad + 2\bar{k}\left[-m^2\pi^2\gamma\theta + \alpha^2\left(k_1^2 k_2^2\alpha^4 + \left(k_1^2 - k_2^2\right)\alpha^2\beta + (-2+\zeta)\zeta\beta^2 + \bar{N}_{xx}^0\pi^2\delta\theta\right)\right]\Big],\\
\Lambda_3 &= -k_1\left(k_1^2 + k_2^2\right)\pi\Big[k_1^2 m^2\alpha^4\left(k_2^2\alpha^2 + \zeta\beta\right)\\
&\quad + m^2\left[\alpha^2(-2+\zeta)\beta\left(k_2^2\alpha^2 + \zeta\beta\right) + \pi^2\left(-m^2\gamma + \bar{N}_{xx}^0\alpha^2\delta\right)\theta\right]\\
&\quad - \bar{k}\alpha^2\left(-\bar{N}_{xx}^0\alpha^2\delta + m^2\left(\gamma + k_2^2\alpha^2\theta\right)\right)\Big],\\
\Lambda_4 &= k_2\left(k_1^2 + k_2^2\right)\pi\Big[\bar{k}\left(-m^2\alpha^2\gamma + \bar{N}_{xx}^0\alpha^4\delta\right)\\
&\quad + k_1^2 m^2\alpha^4\left[k_2^2\alpha^2 - (-2+\zeta)\beta + \bar{k}\theta\right] + m^2\Big[\alpha^2\zeta\beta\left(-k_2^2\alpha^2 + (-2+\zeta)\right)\\
&\quad + \pi^2\left(-m^2\gamma + \bar{N}_{xx}^0\alpha^2\delta\right)\theta\Big]\Big],\\
\Lambda_5 &= m\Big[\left(k_1^2 + k_2^2\right)^2\pi^2\alpha^2\left(m^2\gamma - \bar{N}_{xx}^0\alpha^2\delta\right)\\
&\quad - \bar{k}\Big[k_1^4\alpha^4\left(k_2^2\alpha^2 + \zeta\beta\right) + k_2^2\left(\alpha^2\zeta\beta\left(k_2^2\alpha^2 - (-2+\zeta)\beta\right) + \pi^2\left(m^2\gamma - \bar{N}_{xx}^0\alpha^2\delta\right)\theta\right)\\
&\quad + k_1^2\left[-k_2^4\alpha^6 + 2k_2^2\alpha^4(-2+\zeta)\beta + \alpha^2(-2+\zeta)\zeta\beta^2 + \pi^2\left(-m^2\gamma + \bar{N}_{xx}^0\alpha^2\delta\right)\theta\right]\Big]\Big].
\end{aligned} \tag{17.154}$$

The references Weißgraeber et al. (2012) and Weißgraeber (2009) contain a detailed discussion of the characteristic buckling behaviour of the currently discussed plate situation.

The above buckling condition can be used to derive an explicit expression for the bending stiffness of the flange. After solving for γ we obtain:

$$\gamma = \frac{B}{A}, \tag{17.155}$$

with

$$\begin{aligned}
B &= B_1 + \cosh k_1 m\pi\left[B_2 \cos k_2 m\pi + B_3 \sin k_2 m\pi\right]\\
&\quad + \sinh k_1 m\pi\left[B_4 \cos k_2 m\pi + B_5 \sin k_2 m\pi\right],\\
A &= A_1 \cosh k_1 m\pi \sin k_2 m\pi + A_2 \cos k_2 m\pi \sinh k_1 m\pi\\
&\quad + A_3 \sin k_2 m\pi \sinh k_1 m\pi,
\end{aligned} \tag{17.156}$$

and

$$
\begin{aligned}
A_1 &= \left(k_1^2 + k_2^2\right) m^2 \pi \bar{k} k_1, \\
A_2 &= -\left(k_1^2 + k_2^2\right) m^2 \pi \bar{k} k_2, \\
A_3 &= \left(k_1^2 + k_2^2\right)^2 m^3 \pi^2, \\
B_1 &= -\bar{k} k_1 k_2 m \left[\left(k_1^4 + k_2^4\right) \alpha^4 + 2\left(-k_1^2 + k_2^2\right) \alpha^2 \beta - 2\left(-2 + \zeta\right) \zeta \beta^2\right], \\
B_2 &= -2\bar{k} k_1 k_2 \left[k_1^2 k_2^2 \alpha^4 + \left(k_1^2 - k_2^2\right) \alpha^2 \beta + \left(-2 + \zeta\right) \zeta \beta^2\right], \\
B_3 &= k_1 \left(k_1^2 + k_2^2\right) \pi \left[\bar{k} \bar{N}_{xx}^0 \alpha^2 \delta + k_1^2 m^2 \alpha^2 \left(k_2^2 \alpha^2 + \zeta \beta\right) + m^2 \left(-2 + \zeta\right) \beta \left(k_2^2 \alpha^2 + \zeta \beta\right)\right], \\
B_4 &= -k_2 \left(k_1^2 + k_2^2\right) \pi \\
&\quad \times \left[\bar{k} \bar{N}_{xx}^0 \alpha^2 \delta + k_1^2 m^2 \alpha^2 \left(k_2^2 \alpha^2 - \left(-2 + \zeta\right) \beta\right) + m^2 \zeta \beta \left(-k_2^2 \alpha^2 + \left(-2 + \zeta\right) \beta\right)\right], \\
B_5 &= m \left(k_1^2 + k_2^2\right)^2 \bar{N}_{xx}^0 \pi^2 \alpha^2 \delta \\
&\quad + m \bar{k} \left[k_1^2 \left(k_1 - k_2\right) k_2^2 \left(k_1 + k_2\right) \alpha^4\right. \\
&\quad \left. + \alpha^2 \left[-4 k_1^2 k_2^2 + \left(k_1^2 + k_2^2\right)^2 \zeta\right] \beta + \left(k_1 - k_2\right) \left(k_1 + k_2\right) \left(-2 + \zeta\right) \zeta \beta^2\right]. \qquad (17.157)
\end{aligned}
$$

In Weißgraeber (2009) generic minimum stiffness diagrams can be found, determined with the solution (17.155). A discussion is omitted at this point.

17.9 Local Buckling Analysis Taking Into Account Plate-Stiffener Interaction

17.9.1 Structural Situation

This section describes a closed-form analytical method for the analysis of local buckling loads of stiffened laminated plates under longitudinal compression N_{xx}^0 (Mittelstedt 2009). Global buckling of the plate and the stiffeners is accordingly not considered here. We assume that the bending stiffnesses EI of the stiffeners fulfil the minimum stiffness requirements $EI \geq EI_{\min}$, so that purely local buckling modes can be assumed. It is assumed that the plates under consideration have an infinite width and are stiffened by longitudinal stiffeners with arbitrary open cross-sections that transfer their share of the compressive load N_{xx}^0. In the following, an explicit closed-form analysis approach is derived, which extends the analysis model of Fujikubo and Yao (1999) to the analysis of composite materials. Here, both the plate and the webs of the stiffener are treated as Kirchhoff plates, while the stiffener flanges are considered as Euler-Bernoulli beams (Mittelstedt 2021). The local buckling modes of the plate and the stiffeners are formulated separately and represented by simple shape functions in the form of trigonometric functions and linear polynomials, whereby the shape functions are selected in such a way that the periodicity of the structural situation is taken into account and a reduction of the considerations to a representative unit cell of the stiffened plate is made possible. The underlying continuity conditions are used to ensure the compatibility

and interaction between the plate segments and the stiffeners on the one hand and between the webs and flanges of the stiffener on the other. By using a solution approach according to Ritz in conjunction with the principle of the minimum of the total elastic potential of the stiffened plate in the buckled state, an explicit representation for the buckling load N^0_{xx} is achieved, which can be used in engineering practice in a simple manner. In addition, the Lévy solution of the considered buckling problem is derived and used to verify the analysis method. A comparison is also made with the results of other authors.

We consider an infinitely wide composite plate with a symmetric and orthotropic, but otherwise arbitrary layup. The plate is stiffened in the longitudinal direction by a series of identical stiffeners (Fig. 17.23). The cross-sections of the stiffeners are arbitrary, but must have a thin-walled cross-section with an open profile. Figure 17.23 shows an exemplary plate with I-stiffeners, but any other thin-walled cross-section with an open profile can also be modelled with the present approach. Extensions of this methodology to plates with closed-profile stiffeners have been presented e.g. by Schilling et al. (2020a, 2021, 2022). The load case considered here is uniaxial compression in the longitudinal direction x. The structural situation can be considered periodic since the equidistant stiffeners (distance b in transverse direction y) are assumed to be identical. In addition, the properties of the plate itself are assumed to be invariable. It is thus possible to extract a representative unit cell from the stiffened plate and to treat this unit cell with periodic boundary conditions. Let us consider a representative unit cell of the stiffened plate (Fig. 17.23, middle), consisting of two plate segments with the local coordinate systems x, y^I, z^I (left plate segment, segment 1) and x, y^{II}, z^{II} (right plate segment, segment 2), and of two stiffeners with the height h and the local coordinate systems x, y^{III}, z^{III} (left stiffener, stiffener 1) and x, y^{IV}, z^{IV} (right stiffener, stiffener 2). The thicknesses of the structural parts are denoted by d_P (plate), d_S (stiffener web) and d_F (flange), h_F is the width of the flange. The idealization used is shown in Fig. 17.23, bottom, where the flanges are represented by Euler-Bernoulli beams with the bending stiffness EI and the torsional stiffness GI_T.

Both the plate and the webs and flanges of the stiffeners are assumed to be symmetric, so that the disk and plate effects are decoupled. The resulting strain field in a symmetric laminated plate $\varepsilon^0_{xx}, \varepsilon^0_{yy}, \gamma^0_{xy}$ can be described by the curvatures $\kappa^0_{xx}, \kappa^0_{yy}$ and the twist κ^0_{xy} of the laminate middle plane:

$$\varepsilon^0_{xx} = z\kappa^0_{xx} = -z\frac{\partial^2 w_0}{\partial x^2}, \quad \varepsilon^0_{yy} = z\kappa^0_{yy} = -z\frac{\partial^2 w_0}{\partial y^2}, \quad \gamma^0_{xy} = z\kappa^0_{xy} = -2z\frac{\partial^2 w_0}{\partial x \partial y}, \tag{17.158}$$

where w_0 is the buckling mode. For all the following considerations, Classical Laminated Plate Theory (CLPT) is assumed to be valid, and the constitutive law for the orthotropic laminates considered here is as follows:

$$\begin{pmatrix} M^0_{xx} \\ M^0_{yy} \\ M^0_{xy} \end{pmatrix} = \begin{bmatrix} D_{11} & D_{12} & 0 \\ D_{12} & D_{22} & 0 \\ 0 & 0 & D_{66} \end{bmatrix} \begin{pmatrix} \kappa^0_{xx} \\ \kappa^0_{yy} \\ \kappa^0_{xy} \end{pmatrix}. \tag{17.159}$$

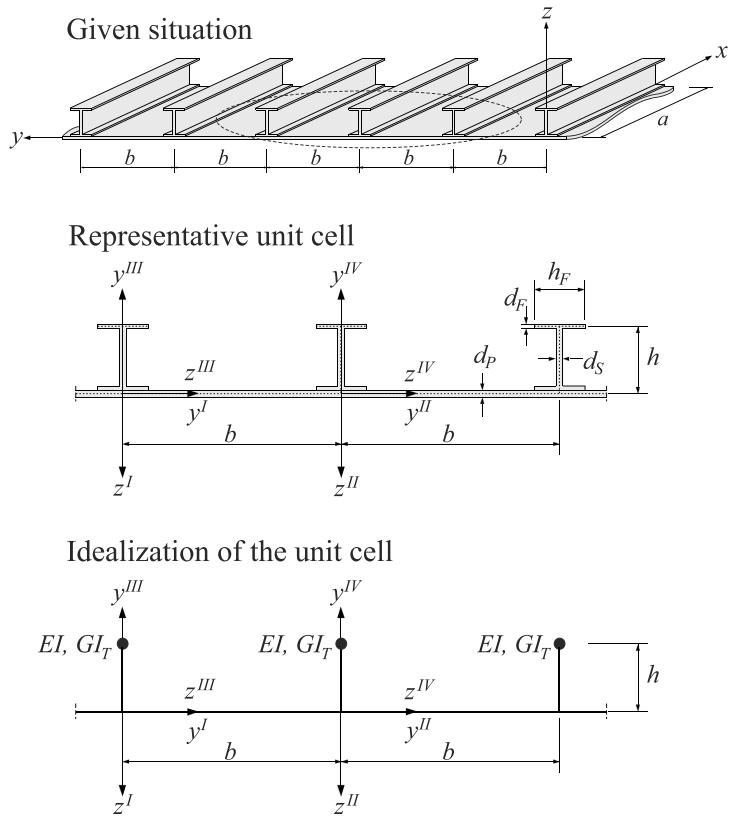


Fig. 17.23 Structural situation; nomenclature and coordinate systems; representative unit cell and its idealisation

In the present approach, the discontinuous nature of the plate due to the presence of the stiffener base is neglected, and a continuous plate structure with constant stiffness parameters for all y^I and y^{II} is assumed.

17.9.2 Boundary and Continuity Conditions

The following boundary conditions can be postulated for the two plate segments of the unit cell under consideration. Firstly, the displacements $w_1\left(x, y^I\right)$ of the left plate segment at the base of the left stiffener must disappear at $y^I = 0$, i.e.:

$$w_1\left(y^I = 0\right) = 0. \tag{17.160}$$

An analogous condition applies to the left plate segment at the base of the right stiffener at $y^I = b$:

$$w_1\left(y^I = b\right) = 0. \tag{17.161}$$

Similarly, the buckling mode $w_2\left(x, y^{II}\right)$ of the right-hand plate segment at the base of the right-hand stiffener must disappear at $y^{II} = 0$:

$$w_2\left(y^{II} = 0\right) = 0. \tag{17.162}$$

In addition, the buckling mode w_2 of the right-hand plate segment must disappear at $y^{II} = b$:

$$w_2\left(y^{II} = b\right) = 0. \tag{17.163}$$

The following continuity conditions can be formulated for the plate segments and the stiffener webs. Firstly, both plate segments must have identical rotations at the base of the left stiffener at $y^I = 0$:

$$\frac{\partial w_1}{\partial y^I}\left(y^I = 0\right) = \frac{\partial w_2}{\partial y^{II}}\left(y^{II} = b\right). \tag{17.164}$$

Note that this condition implies a structural periodicity by assuming that plate segment 2 also appears on the left side of plate segment 1, i.e. the coordinates $y^I = 0$ and $y^{II} = b$ describe the same location. Secondly, the rotations of the left plate segment and the left stiffener web at the stiffener base must be identical in order to ensure continuous rotations in both the plate and the stiffener, i.e.:

$$\frac{\partial w_1}{\partial y^I}\left(y^I = 0\right) = \frac{\partial u}{\partial y^{III}}\left(y^{III} = 0\right). \tag{17.165}$$

Here, $u\left(x, y^{III}\right)$ is the buckling mode of the left stiffener. In addition, the rotations of the two plate segments at the base of the right stiffener must be identical:

$$\frac{\partial w_1}{\partial y^I}\left(y^I = b\right) = \frac{\partial w_2}{\partial y^{II}}\left(y^{II} = 0\right). \tag{17.166}$$

In addition, continuous rotations between the right-hand plate segment and the web of the right-hand stiffener at the stiffener base must be assumed:

$$\frac{\partial w_2}{\partial y^{II}}\left(y^{II} = 0\right) = \frac{\partial v}{\partial y^{IV}}\left(y^{IV} = 0\right). \tag{17.167}$$

Therein, $v\left(x, y^{IV}\right)$ is the buckling mode of the right stiffener. In addition, the balance of the moments around the x-axis at the base of the left stiffener must be ensured:

$$M_{yy}^{II}\left(y^{II} = b\right) - M_{yy}^{I}\left(y^I = 0\right) - M_{yy}^{III}\left(y^{III} = 0\right) = 0. \tag{17.168}$$

Note that this formulation implies a periodicity of the bending moment distribution. An analogous expression applies to the equilibrium of the moments at the base of the right stiffener:

$$M_{yy}^{I}\left(y^{I}=b\right)-M_{yy}^{II}\left(y^{II}=0\right)-M_{yy}^{IV}\left(y^{IV}=0\right)=0. \tag{17.169}$$

The following boundary conditions can be postulated for the web plates of the stiffeners. The buckling mode u must disappear at the base of the left stiffener:

$$u\left(y^{III}=0\right)=0. \tag{17.170}$$

An analogous condition applies to the right-hand stiffener:

$$v\left(y^{IV}=0\right)=0. \tag{17.171}$$

In addition, the bending moment M_{yy}^{III} in the web at the flange of the left stiffener (i.e. at $y^{III}=h$) acts as a torsional moment on the flange. According to St. Venant's torsion theory (Mittelstedt 2021), the following relationship can be specified:

$$GI_T\frac{\partial^3 u}{\partial x^2\partial y^{III}}\left(y^{III}=h\right)+M_{yy}^{III}\left(y^{III}=h\right)=0. \tag{17.172}$$

The following also applies to the flange of the right-hand stiffener:

$$GI_T\frac{\partial^3 v}{\partial x^2\partial y^{IV}}\left(y^{IV}=h\right)+M_{yy}^{IV}\left(y^{IV}=h\right)=0. \tag{17.173}$$

Finally, the transverse shear force Q_2^{III} of the web of the left stiffener is assumed to be the shear load on the flange, i.e.:

$$EI\frac{\partial^4 u}{\partial x^4}\left(y^{III}=h\right)+P_{FL}\frac{\partial^2 u}{\partial x^2}\left(y^{III}=h\right)+Q_y^{III}\left(y^{III}=h\right)=0. \tag{17.174}$$

Therein, P_{FL} is the normal force acting on the flange. The same applies to the flange of the right-hand stiffener:

$$EI\frac{\partial^4 v}{\partial x^4}\left(y^{IV}=h\right)+P_{FL}\frac{\partial^2 v}{\partial x^2}\left(y^{IV}=h\right)+Q_y^{IV}\left(y^{IV}=h\right)=0. \tag{17.175}$$

17.9.3 Shape Functions

Both for the two plate segments and for the two stiffener webs, the assumption of simply supported loaded edges at $x=0$ and $x=a$ is made. Therefore, the buckling modes

$w_1\left(x, y^I\right)$, $w_2\left(x, y^{II}\right)$ and the web buckling modes $u\left(x, y^{III}\right)$, $v\left(x, y^{IV}\right)$ must disappear at the loaded edges:

$$\begin{aligned} w_1\,(x=0) = w_1\,(x=a) &= 0, \\ w_2\,(x=0) = w_2\,(x=a) &= 0, \\ u\,(x=0) = u\,(x=a) &= 0, \\ v\,(x=0) = v\,(x=a) &= 0. \end{aligned} \tag{17.176}$$

Similarly, the bending moments M_{xx} must disappear both in the plate segments and in the stiffener webs at the loaded edges:

$$\begin{aligned} M_{xx}^{I}\,(x=0) = M_{xx}^{I}\,(x=a) &= 0, \\ M_{xx}^{II}\,(x=0) = M_{xx}^{II}\,(x=a) &= 0, \\ M_{xx}^{III}\,(x=0) = M_{xx}^{III}\,(x=a) &= 0, \\ M_{xx}^{IV}\,(x=0) = M_{xx}^{IV}\,(x=a) &= 0. \end{aligned} \tag{17.177}$$

In order to derive a simple approach to solve the problem of local buckling of a stiffened laminate panel under compression, a set of shape functions must be found for both plate segments as well as for the web laminates of the two stiffeners considered in the representative unit cell. Given the fact that we want to derive a closed-form solution that can be efficiently used in daily engineering practice, the shape functions used must be as simple as possible to minimize the computational effort.

Let us first consider the local buckling behaviour of the plate segments. If we exclude the possibility of local buckling of the stiffeners for the moment, the buckling load of a segment is limited to a certain interval, whereby the case of a simply supported plate represents the lower limit and the case of a plate that is clamped at the stiffener feet represents the upper limit. The first case would occur if the stiffeners were very compliant and would not support the plate against rotation at the stiffener feet. On the other hand, the second case would theoretically occur if the stiffeners were rigidly clamping the plate segments. Of course, in all technically relevant cases, the actual buckling load of the plate segments must be found in this interval between these two theoretical limit values.

It can be shown for the given orthotropic plates under uniaxial compression that for both types of boundary conditions at the unloaded edges (i.e. simply supported and clamped plates), a single sin-function in the longitudinal direction x with an a priori unknown number of buckling half-waves m is sufficient to fully describe the buckling modes. For the transverse direction, we formulate the following buckling mode $w_1\left(x, y^I\right)$:

$$\begin{aligned} w_1\left(x, y^I\right) &= w_{11}\left(x, y^I\right) + w_{12}\left(x, y^I\right) \\ &= \sin\left(\frac{m\pi x}{a}\right)\left(W_1\overline{w}_{11}\left(y^I\right) + W_2\overline{w}_{12}\left(y^I\right)\right) \\ &= \sin\left(\frac{m\pi x}{a}\right)\left(W_1 \sin\left(\frac{\pi y^I}{b}\right) + \frac{1}{2}W_2\left(1 - \cos\left(\frac{2\pi y^I}{b}\right)\right)\right), \end{aligned} \tag{17.178}$$

where W_1 and W_2 are free constants. This rather simple approach for w_1 can be interpreted as an interpolation between the two limiting cases 'simply supported plate' and 'clamped plate'. Accordingly, we can formulate the following buckling mode $w_2\left(x, y^{II}\right)$ for the right-hand plate segment:

$$\begin{aligned} w_2\left(x, y^{II}\right) &= w_{21}\left(x, y^{II}\right) + w_{22}\left(x, y^{II}\right) \\ &= \sin\left(\frac{m\pi x}{a}\right)\left(W_3\overline{w}_{21}\left(y^I\right) + W_4\overline{w}_{22}\left(y^I\right)\right) \\ &= -\sin\left(\frac{m\pi x}{a}\right)\left(W_3 \sin\left(\frac{\pi y^{II}}{b}\right) + \frac{1}{2}W_4\left(1 - \cos\left(\frac{2\pi y^{II}}{b}\right)\right)\right), \end{aligned} \tag{17.179}$$

where the negative sign indicates that a periodic buckling mode of the two neighbouring plate segments occurs. Herein, W_3 and W_4 are free constants. Figure 17.24 shows the selected shape functions for the plate segments and the web plates. With regard to the buckling shape functions $u\left(x, y^{III}\right)$ and $v\left(x, y^{IV}\right)$ for the stiffener webs, analogous conclusions can be drawn as for the plate segments. If we initially focus our attention on T-stiffeners (i.e. stiffeners without flanges) and exclude the possibility of local buckling of the plate segments, then the buckling load of the web laminate of the left stiffener, for example, is limited to an interval in which the lower limit is formed by the case of a web laminate that is simply supported at three edges while the fourth edge is free. Utilising the fact that, by analogy with the plate segments, a single sin-function in the longitudinal direction x is sufficient, a suitable shape function for this case would consist of a linear buckling shape function in the transverse direction:

$$u_1\left(x, y^{III}\right) = U_1 \sin\left(\frac{m\pi x}{a}\right)\frac{y^{III}}{h}. \tag{17.180}$$

On the other hand, the upper limit of the interval for the buckling load of the web laminate is characterised by the case of a laminate that is fully clamped at the stiffener base. In this case, a shape function of the following form is an adequate approximation:

$$u_2\left(x, y^{III}\right) = U_2 \sin\left(\frac{m\pi x}{a}\right)\left(1 - \cos\left(\frac{\pi y^{III}}{2h}\right)\right). \tag{17.181}$$

Such an approach for the buckling modes of a web plate was used, for example, by Byklum (2002) or Buermann et al. (2006). Practically important examples, however, are often stiffeners with flanges (see also Figs. 17.23 and 17.24), which must be explicitly taken into account. A suitable approach would be to include another stiffener shape function as follows:

$$u_3\left(x, y^{III}\right) = U_3 \sin\left(\frac{m\pi x}{a}\right) \sin\left(\frac{\pi y^{III}}{2h}\right). \tag{17.182}$$

By adding this term to the displacement approach for the left stiffener, it is ensured that the influence of the inertia of the flange in the buckling shape $u\left(x_1, x_2^{III}\right)$ is taken into account. We can then write:

$$\begin{aligned} u\left(x, y^{III}\right) &= -u_1\left(x, y^{III}\right) - u_2\left(x, y^{III}\right) - u_3\left(x, y^{III}\right) \\ &= \sin\left(\frac{m\pi x}{a}\right)\left(U_1\overline{u}_1\left(y^{III}\right) + U_2\overline{u}_2\left(y^{III}\right) + U_3\overline{u}_3\left(y^{III}\right)\right), \\ &= -\sin\left(\frac{m\pi x}{a}\right)\left(U_1\frac{y^{III}}{h} + U_2\left(1 - \cos\left(\frac{\pi y^{III}}{2h}\right)\right) + U_3\sin\left(\frac{\pi y^{III}}{2h}\right)\right), \end{aligned} \tag{17.183}$$

where the negative sign was chosen to ensure compatibility with the shape functions $w_1\left(x, y^I\right)$ and $w_2\left(x, y^{II}\right)$ of the plate segments (see also Fig. 17.24). The variables U_1, U_2, and U_3 are free constants. Similarly, we can write the displacement formulation for the web laminate of the right stiffener:

$$\begin{aligned} v\left(x, y^{IV}\right) &= v_1\left(x, y^{IV}\right) + v_2\left(x, y^{IV}\right) + v_3\left(x, y^{IV}\right) \\ &= \sin\left(\frac{m\pi x}{a}\right)\left(V_1\overline{v}_1\left(y^{IV}\right) + V_2\overline{v}_2\left(y^{IV}\right) + V_3\overline{v}_3\left(y^{IV}\right)\right), \\ &= \sin\left(\frac{m\pi x}{a}\right)\left(V_1\frac{y^{IV}}{h} + V_2\left(1 - \cos\left(\frac{\pi y^{IV}}{2h}\right)\right) + V_3\sin\left(\frac{\pi y^{IV}}{2h}\right)\right), \end{aligned} \tag{17.184}$$

with the free constants V_1, V_2, and V_3. This special set of stiffener shape functions was used, for example, by Fujikubo and Yao (1999) for the buckling analysis of isotropic stiffened plates under biaxial compression.

The displacement approaches (17.178), (17.179), (17.183), and (17.184) have been postulated independently of each other. To ensure the continuity and the interaction between plate and stiffener, the conditions (17.164), (17.165), (17.166), (17.167), (17.168), (17.169), (17.172), and (17.173) are evaluated. Using the displacement approaches (17.178), (17.179), (17.183) and (17.184) as well as the constitutive relationship (17.159) for the bending moment flows M_{yy}^{I} and M_{yy}^{II} in the plate segments

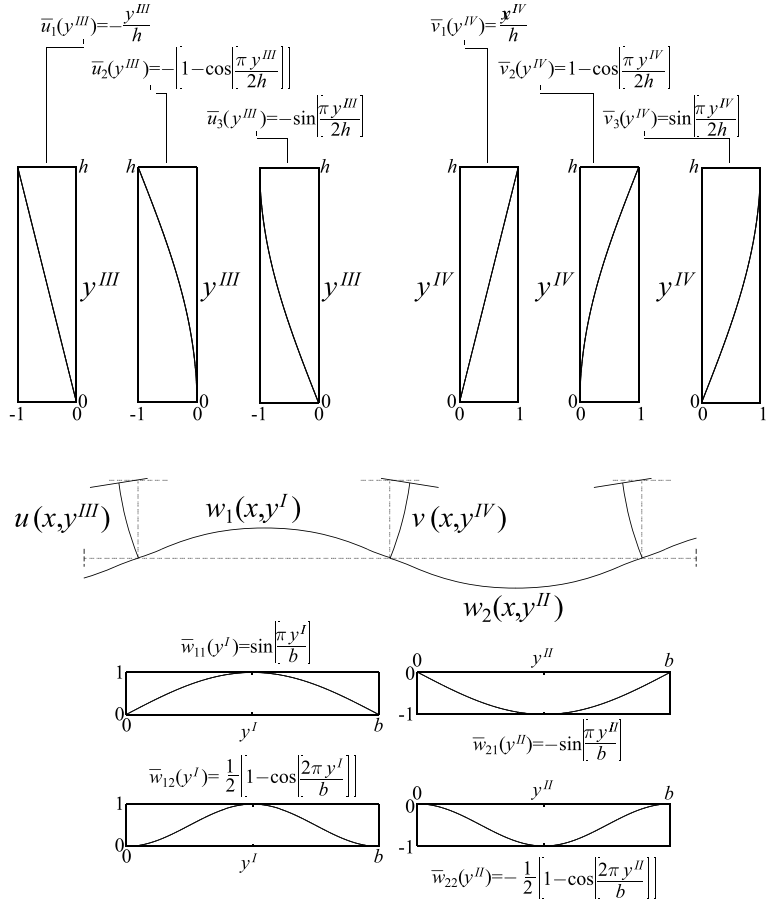


Fig. 17.24 Shape functions for plate segments and stiffener webs

$$M_{yy}^I = -D_{12}^P \frac{\partial^2 w_1}{\partial x^2} - D_{22}^P \frac{\partial^2 w_1}{\partial y^{I2}}, \quad M_{yy}^{II} = -D_{12}^P \frac{\partial^2 w_2}{\partial x^2} - D_{22}^P \frac{\partial^2 w_2}{\partial y^{II2}}, \tag{17.185}$$

and for the bending moment flows M_{yy}^{III} and M_{yy}^{IV} in the stiffening webs

$$M_{yy}^{III} = -D_{12}^S \frac{\partial^2 u}{\partial x^2} - D_{22}^S \frac{\partial^2 u}{\partial y^{III2}}, \quad M_{yy}^{IV} = -D_{12}^S \frac{\partial^2 v}{\partial x^2} - D_{22}^S \frac{\partial^2 v}{\partial y^{IV2}}, \tag{17.186}$$

we eventually obtain the following linear equations:

$$W_1 - W_3 = 0,$$
$$\frac{1}{h}U_1 + \frac{\pi}{2h}U_3 + \frac{\pi}{b}W_1 = 0,$$

$$
\begin{aligned}
\frac{1}{h}V_1 + \frac{\pi}{2h}V_3 + \frac{\pi}{b}W_1 &= 0,\\
-\frac{2D_{22}^P}{b^2}W_2 - \frac{2D_{22}^P}{b^2}W_4 + \frac{D_{22}^S}{4h^2}U_2 &= 0,\\
-\frac{2D_{22}^P}{b^2}W_2 - \frac{2D_{22}^P}{b^2}W_4 + \frac{D_{22}^S}{4h^2}V_2 &= 0,\\
\left(GI_Tm^2 - D_{12}^Sm^2h\right)U_1 + \left(\frac{1}{2}GI_Tm^2\pi - D_{12}^Sm^2h\right)U_2 - \left(D_{12}^Sm^2h + \frac{D_{22}^Sa^2}{4h}\right)U_3 &= 0,\\
\left(GI_Tm^2 - D_{12}^Sm^2h\right)V_1 + \left(\frac{1}{2}GI_Tm^2\pi - D_{12}^Sm^2h\right)V_2 - \left(D_{12}^Sm^2h + \frac{D_{22}^Sa^2}{4h}\right)V_3 &= 0,
\end{aligned}
\tag{17.187}
$$

where $D_{\alpha\beta}^P$ and $D_{\alpha\beta}^S$ $(\alpha, \beta = 1, 2)$ are the stiffness properties of the plate segments and the stiffener webs, respectively, according to the constitutive law of CLPT. From the first equation in (17.187) we obtain

$$W_3 = W_1. \tag{17.188}$$

Since the buckling modes of the plates have periodic properties, so that $w_1\left(x, y^I\right) = -w_2\left(x, y^{II}\right)$, we can also conclude that

$$W_4 = W_2. \tag{17.189}$$

Solving the remaining equations in (17.187) leads to the following expressions for the constants U_1, U_2, U_3, and V_1, V_2, V_3 of the shape functions of the web plates, expressed by the constants W_1 and W_2 of the buckling shapes of the plate segments:

$$U_1 = \varphi_1 W_1 + \varphi_2 W_2, \quad U_2 = \varphi_3 W_2, \quad U_3 = \varphi_4 W_1 + \varphi_5 W_2, \quad V_i = U_i, \tag{17.190}$$

(with $i = 1, 2, 3$), wherein:

$$
\begin{aligned}
\varphi_1 &= \frac{\frac{1}{b}\left(2D_{12}^Sm^2h^2 + \frac{D_{22}^Sa^2}{2}\right)}{m^2h\left(1 - \frac{2}{\pi}\right)D_{12}^S - \frac{D_{22}^Sa^2}{2\pi h} - GI_Tm^2},\\
\varphi_2 &= -\frac{\frac{8D_{22}^Pm^2h^2}{D_{22}^Sb^2}\left(-GI_T\pi + 2hD_{12}^S\right)}{m^2h\left(1 - \frac{2}{\pi}\right)D_{12}^S - \frac{D_{22}^Sa^2}{2\pi h} - GI_Tm^2},\\
\varphi_3 &= \frac{16D_{22}^Ph^2}{D_{22}^Sb^2}, \quad \varphi_4 = -2\left(\frac{\varphi_1}{\pi} + \frac{h}{b}\right), \quad \varphi_5 = -\frac{2\varphi_2}{\pi}.
\end{aligned}
\tag{17.191}
$$

We can therefore write the buckling shape functions in the following form:

$$
\begin{aligned}
w_1 &= \sin\left(\frac{m\pi x}{a}\right)\left(W_1 \sin\left(\frac{\pi y^I}{b}\right) + \frac{1}{2}W_2\left(1-\cos\left(\frac{2\pi y^I}{b}\right)\right)\right),\\
w_2 &= -\sin\left(\frac{m\pi x}{a}\right)\left(W_1 \sin\left(\frac{\pi y^{II}}{b}\right) + \frac{1}{2}W_2\left(1-\cos\left(\frac{2\pi y^{II}}{b}\right)\right)\right),\\
u &= -\sin\left(\frac{m\pi x}{a}\right)\left(\varphi_1\frac{y^{III}}{h} + \varphi_4 \sin\left(\frac{\pi y^{III}}{2h}\right)\right)W_1\\
&\quad -\sin\left(\frac{m\pi x}{a}\right)\left(\varphi_2\frac{y^{III}}{h} + \varphi_3\left(1-\cos\left(\frac{\pi y^{III}}{2h}\right)\right) + \varphi_5 \sin\left(\frac{\pi y^{III}}{2h}\right)\right)W_2,\\
v &= \sin\left(\frac{m\pi x}{a}\right)\left(\varphi_1\frac{y^{IV}}{h} + \varphi_4 \sin\left(\frac{\pi y^{IV}}{2h}\right)\right)W_1\\
&\quad +\sin\left(\frac{m\pi x}{a}\right)\left(\varphi_2\frac{y^{IV}}{h} + \varphi_3\left(1-\cos\left(\frac{\pi y^{IV}}{2h}\right)\right) + \varphi_5 \sin\left(\frac{\pi y^{IV}}{2h}\right)\right)W_2,
\end{aligned}
\tag{17.192}
$$

whereby the number of unknown coefficients was reduced to two constants, namely W_1 and W_2, which considerably simplifies the analysis approach.

17.9.4 Inner and External Potential

The elastic potential of the left plate segment in the buckled state is as follows:

$$
\begin{aligned}
\Pi_i^I &= \frac{1}{2}\int_0^a\int_0^b \left(D_{11}^P\left(\frac{\partial^2 w_1}{\partial x^2}\right)^2 + D_{22}^P\left(\frac{\partial^2 w_1}{\partial y^{I2}}\right)^2\right)\mathrm{d}y^I\mathrm{d}x\\
&\quad + \int_0^a\int_0^b \left(D_{12}^P\frac{\partial^2 w_1}{\partial x^2}\frac{\partial^2 w_1}{\partial y^{I2}} + 2D_{66}^P\left(\frac{\partial^2 w_1}{\partial x\partial y^I}\right)^2\right)\mathrm{d}y^I\mathrm{d}x.
\end{aligned}
\tag{17.193}
$$

An analogous formulation can be written for the right-hand plate segment:

$$
\begin{aligned}
\Pi_i^{II} &= \frac{1}{2}\int_0^a\int_0^b \left(D_{11}^P\left(\frac{\partial^2 w_2}{\partial x^2}\right)^2 + D_{22}^P\left(\frac{\partial^2 w_2}{\partial y^{I2}}\right)^2\right)\mathrm{d}x_2^{II}\mathrm{d}x_1\\
&\quad + \int_0^a\int_0^b \left(D_{12}^P\frac{\partial^2 w_2}{\partial x^2}\frac{\partial^2 w_2}{\partial y^{I2}} + 2D_{66}^P\left(\frac{\partial^2 w_2}{\partial x\partial y^{II}}\right)^2\right)\mathrm{d}y^{II}\mathrm{d}x.
\end{aligned}
\tag{17.194}
$$

The elastic potential of the left stiffener web is as follows:

$$\Pi_i^{III} = \frac{1}{2}\int_0^a\int_0^h \left(D_{11}^S \left(\frac{\partial^2 u}{\partial x^2}\right)^2 + D_{22}^S \left(\frac{\partial^2 u}{\partial y^{III2}}\right)^2 \right) \mathrm{d}y^{III}\mathrm{d}x + \int_0^a\int_0^h \left(D_{12}^S \frac{\partial^2 u}{\partial x^2}\frac{\partial^2 u}{\partial y^{III2}} + 2D_{66}^S \left(\frac{\partial^2 u}{\partial x \partial y^{III}}\right)^2 \right) \mathrm{d}y^{III}\mathrm{d}x. \tag{17.195}$$

We can write the same for the right-hand stiffener web:

$$\Pi_i^{IV} = \frac{1}{2}\int_0^a\int_0^h \left(D_{11}^S \left(\frac{\partial^2 v}{\partial x^2}\right)^2 + D_{22}^S \left(\frac{\partial^2 v}{\partial y^{IV2}}\right)^2 \right) \mathrm{d}y^{IV}\mathrm{d}x + \int_0^a\int_0^h \left(D_{12}^S \frac{\partial^2 v}{\partial x^2}\frac{\partial^2 v}{\partial y^{IV2}} + 2D_{66}^S \left(\frac{\partial^2 v}{\partial x \partial y^{IV}}\right)^2 \right) \mathrm{d}y^{IV}\mathrm{d}x. \tag{17.196}$$

The elastic potential of the left stiffener flange can be specified as follows:

$$\Pi_i^V = \frac{1}{2}\int_0^a \left(EI \left(\frac{\partial^2 u}{\partial x^2}\left(y^{III}=h\right)\right)^2 + GI_T \left(\frac{\partial^2 u}{\partial x \partial y^{III}}\left(y^{III}=h\right)\right)^2 \right) \mathrm{d}x. \tag{17.197}$$

An analogous formulation applies to the right-hand stiffener flange:

$$\Pi_i^{VI} = \frac{1}{2}\int_0^a \left(EI \left(\frac{\partial^2 v}{\partial x^2}\left(y^{IV}=h\right)\right)^2 + GI_T \left(\frac{\partial^2 v}{\partial x \partial y^{IV}}\left(y^{IV}=h\right)\right)^2 \right) \mathrm{d}x. \tag{17.198}$$

Inserting the buckling shapes (17.192) and performing the integrations as prescribed in (17.193)–(17.198) finally leads to the following expression for the total elastic potential Π_i of the representative unit cell of the stiffened plate:

$$\Pi_i = 2\left(\Gamma_1 + \Gamma_4 + \Gamma_7\right) W_1^2 + 2\left(\Gamma_2 + \Gamma_5 + \Gamma_8\right) W_2^2 + 2\left(\Gamma_3 + \Gamma_6 + \Gamma_9\right) W_1 W_2, \tag{17.199}$$

wherein the following abbreviations have been defined:

$$\Gamma_1 = \frac{\pi^4}{8a^3b^3}\left(D_{11}^P b^4 m^4 + D_{22}^P a^4 + 2\left(D_{12}^P + 2D_{66}^P\right)a^2 b^2 m^2\right),$$

$$\Gamma_2 = \frac{\pi^4}{32a^3b^3}\left(3D_{11}^P b^4 m^4 + 16D_{22}^P a^4 + 8\left(D_{12}^P + 2D_{66}^P\right)a^2 b^2 m^2\right),$$

$$\Gamma_3 = \frac{2\pi^3}{3a^3b^3}\left(D_{11}^P b^4 m^4 + D_{22}^P a^4 + 2\left(D_{12}^P + 2D_{66}^P\right)a^2b^2m^2\right),$$

$$\Gamma_4 = D_{11}^S \frac{hm^4\pi^2}{24a^3}\left(2\pi^2\varphi_1^2 + 48\varphi_1\varphi_4 + 3\pi^2\varphi_4^2\right) + D_{22}^S \frac{a\pi^4\varphi_4^2}{128h^3}$$
$$+ D_{12}^S \frac{m^2\pi^2\varphi_4}{16ah}\left(8\varphi_1 + \pi^2\varphi_4\right) + D_{66}^S \frac{m^2\pi^2}{8ah}\left(8\varphi_1^2 + 16\varphi_4\varphi_1 + \pi^2\varphi_4^2\right),$$

$$\Gamma_5 = D_{11}^S \frac{hm^4\pi^2}{24a^3}\left(2\pi^2\varphi_2^2 + 3\pi\left(3\pi - 8\right)\varphi_3^2 + 3\pi^2\varphi_5^2\right)$$
$$+ D_{11}^S \frac{hm^4\pi^2}{24a^3}\left(6\left(\pi^2 - 4\pi + 8\right)\varphi_2\varphi_3 + 48\varphi_2\varphi_5 + 12\pi\varphi_3\varphi_5\right)$$
$$+ D_{22}^S \frac{a\pi^3}{128h^3}\left(\pi\varphi_3^2 - 4\varphi_3\varphi_5 + \pi\varphi_5^2\right)$$
$$+ D_{12}^S \frac{m^2\pi^2}{16ah}\left(\pi\left(\pi - 4\right)\varphi_3^2 + \pi^2\varphi_5^2 + 4\left(2 - \pi\right)\varphi_2\varphi_3 + 8\varphi_2\varphi_5\right)$$
$$+ D_{66}^S \frac{m^2\pi^2}{8ah}\left(8\varphi_2^2 + \pi^2\left(\varphi_3^2 + \varphi_5^2\right) + 16\varphi_2\left(\varphi_3 + \varphi_5\right) + 4\pi\varphi_3\varphi_5\right),$$

$$\Gamma_6 = D_{11}^S \frac{hm^4\pi^2}{12a^3}\left(2\pi^2\varphi_1\varphi_2 + 3\left(\pi^2 - 4\pi + 8\right)\varphi_1\varphi_3\right)$$
$$+ D_{11}^S \frac{hm^4\pi^2}{12a^3}\left(24\varphi_1\varphi_5 + 3\left(8\varphi_2 + 2\pi\varphi_3 + \pi^2\varphi_5\right)\varphi_4\right)$$
$$+ D_{22}^S \frac{a\pi^3}{64h^3}\left(\pi\varphi_5 - 2\varphi_3\right)\varphi_4$$
$$+ D_{12}^S \frac{m^2\pi^2}{8ah}\left(2\left(2 - \pi\right)\varphi_1\varphi_3 + 4\varphi_1\varphi_5 + \left(4\varphi_2 + \pi^2\varphi_5\right)\varphi_4\right)$$
$$+ D_{66}^S \frac{m^2\pi^2}{4ah}\left(8\left(\varphi_2 + \varphi_3 + \varphi_5\right)\varphi_1 + \left(8\varphi_2 + 2\pi\varphi_3 + \pi^2\varphi_5\right)\varphi_4\right),$$

$$\Gamma_7 = \frac{m^2\pi^2}{4a^3h^2}\left(EIm^2\pi^2h^2\left(\varphi_1 + \varphi_4\right)^2 + GI_T\varphi_1^2a^2\right),$$

$$\Gamma_8 = EI\frac{m^4\pi^4}{4a^3}\left(2\left(\varphi_2\varphi_3 + \varphi_2\varphi_5 + \varphi_3\varphi_5\right) + \varphi_2^2 + \varphi_3^2 + \varphi_5^2\right)$$
$$+ GI_T\frac{m^2\pi^2}{16ah^2}\left(4\varphi_2^2 + 4\pi\varphi_2\varphi_3 + \pi^2\varphi_3^2\right),$$

$$\Gamma_9 = EI\frac{m^4\pi^4}{2a^3}\left(\varphi_1 + \varphi_4\right)\left(\varphi_2 + \varphi_3 + \varphi_5\right) + GI_T\frac{m^2\pi^2}{4ah^2}\varphi_1\left(2\varphi_2 + \pi\varphi_3\right). \tag{17.200}$$

At the onset of buckling, the longitudinal stress in the plate σ_{xxP} can be described as a function of the applied load $N_{xx}^0 = N_{xxP}^0$ ('P' = plate) as follows:

$$\sigma_{xxP} = \frac{N_{xxP}^0}{d_P}, \tag{17.201}$$

where d_P is the thickness of the plate. The corresponding longitudinal strain ε_{xx}^P in the plate is

$$\varepsilon_{xx}^P = \frac{N_{xxP}^0}{E_{xxP} d_P}, \tag{17.202}$$

where E_{xxP} is the modulus of elasticity of the plate, which can be calculated from the membrane stiffness A_{opP} of the plate in the laminate plane:

$$E_{xxP} = \frac{1}{d_P}\left(A_{11P} - \frac{A_{12P}^2}{A_{22P}}\right). \tag{17.203}$$

Enforcing the compatibility between the strains in the plate segments and in the stiffener webs (i.e. $\varepsilon_{xx}^P = \varepsilon_{xx}^S$) leads to the longitudinal force N_{xxS}^0 in the web plates as follows:

$$N_{xxS}^0 = \frac{E_{xxS} d_S}{E_{xxP} d_P} N_{xxP}^0, \tag{17.204}$$

where d_S and E_{xxS} are the thickness and the longitudinal modulus of elasticity of the stiffener webs. Note that E_{xxS} can be calculated in the same way as E_{xxP} (see (17.203)). With

$$\zeta_S = \frac{E_{xxS} d_S}{E_{xxP} d_P}, \tag{17.205}$$

results:

$$N_{xxS}^0 = \zeta_S N_{xxP}^0. \tag{17.206}$$

Assuming compatible strains of the plate and the flange, the force P_{FL} acting on the stiffener flange can be determined as:

$$P_{FL} = \zeta_{FL} N_{xxP}^0, \tag{17.207}$$

with

$$\zeta_{FL} = \frac{E_{xxFL} A_{FL}}{E_{xxP} d_P}, \tag{17.208}$$

where A_{FL} and E_{xxFL} are the cross-sectional area and the longitudinal modulus of elasticity of the flange.

The work performed by the forces in the plate segments, in the webs and in the stiffener flanges is then as follows:

$$\Pi_a^I = -\frac{N_{xxP}^0}{2} \int_0^a \int_0^b \left(\frac{\partial w_1}{\partial x}\right)^2 \mathrm{d}y^I \mathrm{d}x,$$

$$\Pi_a^{II} = -\frac{N_{xxP}^0}{2} \int_0^a \int_0^b \left(\frac{\partial w_2}{\partial x}\right)^2 \mathrm{d}y^{II} \mathrm{d}x,$$

$$\Pi_a^{III} = -\frac{\zeta_S N_{xxP}^0}{2} \int_0^a \int_0^h \left(\frac{\partial u}{\partial x}\right)^2 \mathrm{d}y^{III}\mathrm{d}x,$$

$$\Pi_a^{IV} = -\frac{\zeta_S N_{xxP}^0}{2} \int_0^a \int_0^h \left(\frac{\partial v}{\partial x}\right)^2 \mathrm{d}y^{IV}\mathrm{d}x,$$

$$\Pi_a^{V} = -\frac{\zeta_{FL} N_{xxP}^0}{2} \int_0^a \left(\frac{\partial u}{\partial x}\left(y^{III} = h\right)\right)^2 \mathrm{d}x,$$

$$\Pi_a^{VI} = -\frac{\zeta_{FL} N_{xxP}^0}{2} \int_0^a \left(\frac{\partial v}{\partial x}\left(y^{IV} = h\right)\right)^2 \mathrm{d}x. \tag{17.209}$$

The evaluation with (17.192) results in:

$$\begin{aligned}
\Pi_a^I = \Pi_a^{II} &= N_{xxP}^0 \left(\Phi_1 W_1^2 + \Phi_2 W_2^2 + \Phi_3 W_1 W_2\right), \\
\Pi_a^{III} = \Pi_a^{IV} &= N_{xxP}^0 \left(\Phi_4 W_1^2 + \Phi_5 W_2^2 + \Phi_6 W_1 W_2\right), \\
\Pi_a^V = \Pi_a^{VI} &= N_{xxP}^0 \left(\Phi_7 W_1^2 + \Phi_8 W_2^2 + \Phi_9 W_1 W_2\right),
\end{aligned} \tag{17.210}$$

with:

$$\begin{aligned}
\Phi_1 &= -\frac{bm^2\pi^2}{8a}, \quad \Phi_2 = -\frac{3bm^2\pi^2}{32a}, \quad \Phi_3 = -\frac{2bm^2\pi}{3a}, \\
\Phi_4 &= -\frac{\zeta_S h m^2}{24a}\left(2\pi^2\varphi_1^2 + 48\varphi_1\varphi_4 + 3\pi^2\varphi_4^2\right), \\
\Phi_5 &= -\frac{\zeta_S h m^2}{24a}\left(2\pi^2\varphi_2^2 + 3\pi\left(3\pi - 8\right)\varphi_3^2 + 3\pi^2\varphi_5^2\right) \\
&\quad - \frac{\zeta_S h m^2}{4a}\left(\left(\pi^2 - 4\pi + 8\right)\varphi_2\varphi_3 + 8\varphi_2\varphi_5 + 2\pi\varphi_3\varphi_5\right), \\
\Phi_6 &= -\frac{\zeta_S h m^2}{12a}\left(2\pi^2\varphi_2 + 3\left(\pi^2 - 4\pi + 8\right)\varphi_3 + 24\varphi_5\right)\varphi_1 \\
&\quad - \frac{\zeta_S h m^2}{4a}\left(8\varphi_2 + 2\varphi_3\pi + \varphi_5\pi^2\right)\varphi_4, \\
\Phi_7 &= -\frac{\zeta_{FL} m^2\pi^2}{4a}\left(\varphi_1^2 + 2\varphi_1\varphi_4 + \varphi_4^2\right), \\
\Phi_8 &= -\frac{\zeta_{FL} m^2\pi^2}{4a}\left(\varphi_2^2 + \varphi_3^2 + \varphi_5^2 + 2\varphi_2\varphi_3 + 2\varphi_2\varphi_5 + 2\varphi_3\varphi_5\right), \\
\Phi_9 &= -\frac{\zeta_{FL} m^2\pi^2}{2a}\left(\varphi_1 + \varphi_4\right)\left(\varphi_2 + \varphi_3 + \varphi_5\right).
\end{aligned} \tag{17.211}$$

The total potential of the internal forces can then be written as follows:

$$\Pi_a = \Pi_a^I + \Pi_a^{II} + \Pi_a^{III} + \Pi_a^{IV} + \Pi_a^V + \Pi_a^{VI}. \tag{17.212}$$

The total energy in the stiffened plate is finally:

$$\Pi = \Pi_i + \Pi_a. \tag{17.213}$$

Summing up (17.199) and (17.212) leads to:

$$\Pi = \left(\Omega_1 + N^0_{xxP}\Omega_4\right) W_1^2 + \left(\Omega_2 + N^0_{xxP}\Omega_5\right) W_2^2 + \left(\Omega_3 + N^0_{xxP}\Omega_6\right) W_1 W_2, \tag{17.214}$$

with:

$$\begin{aligned}
&\Omega_1 = 2\left(\Gamma_1 + \Gamma_4 + \Gamma_7\right), \quad \Omega_2 = 2\left(\Gamma_2 + \Gamma_5 + \Gamma_8\right), \quad \Omega_3 = 2\left(\Gamma_3 + \Gamma_6 + \Gamma_9\right), \\
&\Omega_4 = 2\left(\Phi_1 + \Phi_4 + \Phi_7\right), \quad \Omega_5 = 2\left(\Phi_2 + \Phi_5 + \Phi_8\right), \quad \Omega_6 = 2\left(\Phi_3 + \Phi_6 + \Phi_9\right).
\end{aligned} \tag{17.215}$$

17.9.5 Closed-Form Analytical Solution

With the approach (17.192), the equilibrium requirement $\delta\Pi = 0$ transforms into the following two Ritz equations:

$$\frac{\partial \Pi}{\partial W_1} = \frac{\partial \Pi}{\partial W_2} = 0. \tag{17.216}$$

If (17.216) is evaluated with (17.214), the following linear and homogeneous equations are obtained in a vector-matrix notation for the two remaining constants W_1 and W_2:

$$\begin{bmatrix} 2\left(\Omega_1 + N^0_{xxP}\Omega_4\right) & \Omega_3 + N^0_{xxP}\Omega_6 \\ \Omega_3 + N^0_{xxP}\Omega_6 & 2\left(\Omega_2 + N^0_{xxP}\Omega_5\right) \end{bmatrix} \begin{pmatrix} W_1 \\ W_2 \end{pmatrix} = \begin{pmatrix} 0 \\ 0 \end{pmatrix}. \tag{17.217}$$

To avoid a trivial solution, we demand the vanishing of the coefficient determinant and finally arrive at the following characteristic polynomial:

$$\Psi_1 N^0_{xxP} + \Psi_2 {N^0_{xxP}}^2 + \Psi_3 = 0, \tag{17.218}$$

with:

$$\Psi_1 = 2\left(2\Omega_1\Omega_5 + 2\Omega_2\Omega_4 - \Omega_3\Omega_6\right), \quad \Psi_2 = 4\Omega_4\Omega_5 - \Omega_6^2, \quad \Psi_3 = 4\Omega_1\Omega_2 - \Omega_3^2. \tag{17.219}$$

The minimum resulting value for N^0_{xxP} then represents the desired buckling load of the stiffened laminated plate:

$$N^0_{xxP} = \min \left\{ \frac{-\Psi_1 \pm \sqrt{\Psi_1^2 - 4\Psi_2\Psi_3}}{2\Psi_2} \right\}. \tag{17.220}$$

17.9.6 Lévy Solution

In addition to the derived approximate closed-form solution (17.220), the present buckling problem also allows the development of a Lévy-type solution. The starting point for the considerations is the following buckling differential equation:

$$D_{11}\frac{\partial^4 w}{\partial x^4} + 2\left(D_{12} + 2D_{66}\right)\frac{\partial^4 w}{\partial x^2 \partial y^2} + D_{22}\frac{\partial^4 w}{\partial y^4} + N^0_{xx}\frac{\partial^2 w}{\partial x^2} = 0. \tag{17.221}$$

A solution approach for $w\left(x_1, x_2\right)$ can be found in a separation form as follows:

$$w\left(x, y\right) = \sin\left(\frac{m\pi x}{a}\right)\widetilde{w}\left(y\right). \tag{17.222}$$

This approach fulfils the boundary conditions (17.176) and (17.177) identically at the loaded edges. Inserting (17.222) into the differential equation (17.221) results in the following ordinary and homogeneous differential equation of fourth order:

$$D_{22}\frac{\partial^4 \widetilde{w}}{\partial y^4} - 2\left(D_{12} + 2D_{66}\right)\left(\frac{m\pi}{a}\right)^2\frac{\partial^2 \widetilde{w}}{\partial y^2} + \left(\frac{m\pi}{a}\right)^2\left(D_{11}\left(\frac{m\pi}{a}\right)^2 - N^0_{xx}\right)\widetilde{w} = 0. \tag{17.223}$$

The general solution of this differential equation can be represented as follows:

$$\widetilde{w}\left(x_2\right) = A_1\cosh\left(\frac{k_1 m\pi y}{a}\right) + A_2\sinh\left(\frac{k_1 m\pi y}{a}\right) + A_3\cos\left(\frac{k_2 m\pi y}{a}\right) + A_4\sin\left(\frac{k_2 m\pi y}{a}\right), \tag{17.224}$$

with:

$$k_{1,2} = \sqrt{\frac{1}{D_{22}}\left(\sqrt{\left(D_{12} + 2D_{66}\right)^2 + D_{22}\left(N^0_{xx}\left(\frac{a}{m\pi}\right)^2 - D_{11}\right)} \pm D_{12} \pm 2D_{66}\right)}. \tag{17.225}$$

The variables A_1, A_2, A_3, and A_4 are free constants that can be adapted to the given boundary conditions.

We can use the solution (17.222) with (17.224) to formulate the solutions for the individual plate segments and the stiffener webs. For the plate segments we get

$$w_1\left(x, y^I\right) = \sin\left(\frac{m\pi x}{a}\right)\widetilde{w}_1\left(y^I\right), \quad w_2\left(x, y^{II}\right) = \sin\left(\frac{m\pi x}{a}\right)\widetilde{w}_2\left(y^{II}\right), \tag{17.226}$$

with:

$$\begin{aligned}\widetilde{w}_1\left(y^I\right) &= A_1\cosh\left(\frac{k_1 m\pi y^I}{a}\right) + A_2\sinh\left(\frac{k_1 m\pi y^I}{a}\right)\\ &\quad + A_3\cos\left(\frac{k_2 m\pi y^I}{a}\right) + A_4\sin\left(\frac{k_2 m\pi y^I}{a}\right),\\ \widetilde{w}_2\left(y^{II}\right) &= B_1\cosh\left(\frac{k_1 m\pi y^{II}}{a}\right) + B_2\sinh\left(\frac{k_1 m\pi y^{II}}{a}\right)\\ &\quad + B_3\cos\left(\frac{k_2 m\pi y^{II}}{a}\right) + B_4\sin\left(\frac{k_2 m\pi y^{II}}{a}\right),\end{aligned} \tag{17.227}$$

and

$$k_{1,2} = \sqrt{\frac{1}{D_{22}^P}\left(\sqrt{\left(D_{12}^P + 2D_{66}^P\right)^2 + D_{22}^P\left(N_{xxP}^0\left(\frac{a}{m\pi}\right)^2 - D_{11}^P\right)} \pm D_{12}^P \pm 2D_{66}^P\right)}.$$

Similarly, we can write down the following solutions for the stiffeners:

$$u\left(x, y^{III}\right) = \sin\left(\frac{m\pi x}{a}\right)\widetilde{u}\left(y^{III}\right), \quad v\left(x, y^{IV}\right) = \sin\left(\frac{m\pi x}{a}\right)\widetilde{v}\left(y^{IV}\right), \tag{17.228}$$

with

$$\begin{aligned}\widetilde{u}\left(y^{III}\right) &= C_1\cosh\left(\frac{k_3 m\pi y^{III}}{a}\right) + C_2\sinh\left(\frac{k_3 m\pi y^{III}}{a}\right)\\ &\quad + C_3\cos\left(\frac{k_4 m\pi y^{III}}{a}\right) + C_4\sin\left(\frac{k_4 m\pi y^{III}}{a}\right),\\ \widetilde{v}\left(y^{IV}\right) &= D_1\cosh\left(\frac{k_3 m\pi y^{IV}}{a}\right) + D_2\sinh\left(\frac{k_3 m\pi y^{IV}}{a}\right)\\ &\quad + D_3\cos\left(\frac{k_4 m\pi y^{IV}}{a}\right) + D_4\sin\left(\frac{k_4 m\pi y^{IV}}{a}\right),\end{aligned} \tag{17.229}$$

and

$$k_{3,4} = \sqrt{\frac{1}{D_{22}^S}\left(\sqrt{\left(D_{12}^S + 2D_{66}^S\right)^2 + D_{22}^S\left(\zeta_S N_{xxP}^0\left(\frac{a}{m\pi}\right)^2 - D_{11}^S\right)} \pm D_{12}^S \pm 2D_{66}^S\right)}.$$

There are a total of 16 unknown constants $A_1, \ldots, A_4$, $B_1, \ldots, B_4$, $C_1, \ldots, C_4$ and $D_1, \ldots, D_4$, which are adapted to the 16 underlying boundary and continuity conditions (17.160)–(17.175).

The evaluation of (17.160)–(17.163) leads to the following four equations:

$$\begin{aligned}
A_1 + A_3 &= 0,\\
A_1 \cosh\left(\frac{k_1 m\pi b}{a}\right) + A_2 \sinh\left(\frac{k_1 m\pi b}{a}\right) + A_3 \cos\left(\frac{k_2 m\pi b}{a}\right) + A_4 \sin\left(\frac{k_2 m\pi b}{a}\right) &= 0,\\
B_1 + B_3 &= 0,\\
B_1 \cosh\left(\frac{k_1 m\pi b}{a}\right) + B_2 \sinh\left(\frac{k_1 m\pi b}{a}\right) + B_3 \cos\left(\frac{k_2 m\pi b}{a}\right) + B_4 \sin\left(\frac{k_2 m\pi b}{a}\right) &= 0.
\end{aligned} \tag{17.230}$$

In addition, the evaluation of (17.164)–(17.167) leads to the following set of equations:

$$\begin{aligned}
A_2 k_1 + A_4 k_2 - B_1 k_1 \sinh\left(\frac{k_1 m\pi b}{a}\right) - B_2 k_1 \cosh\left(\frac{k_1 m\pi b}{a}\right)&\\
+ B_3 k_2 \sin\left(\frac{k_2 m\pi b}{a}\right) - B_4 k_2 \cos\left(\frac{k_2 m\pi b}{a}\right) &= 0,\\
A_2 k_1 + A_4 k_2 - C_2 k_3 - C_4 k_4 &= 0,\\
A_1 k_1 \sinh\left(\frac{k_1 m\pi b}{a}\right) + A_2 k_1 \cosh\left(\frac{k_1 m\pi b}{a}\right)&\\
- A_3 k_2 \sin\left(\frac{k_2 m\pi b}{a}\right) + A_4 k_2 \cos\left(\frac{k_2 m\pi b}{a}\right) - B_2 k_1 - B_4 k_2 &= 0,\\
B_2 k_1 + B_4 k_2 - D_2 k_3 - D_4 k_4 &= 0.
\end{aligned} \tag{17.231}$$

For the evaluation of (17.168) and (17.169) it is helpful to realize that no rotations $\frac{\partial w_1}{\partial x}$ and $\frac{\partial w_2}{\partial x}$ and no curvatures $\frac{\partial^2 w_1}{\partial x^2}$ and $\frac{\partial^2 w_2}{\partial x^2}$ are possible at the stiffener foot points. The bending moment flows at these points can then be written as

$$M_{yy}^{I} = -D_{22}^{P} \frac{\partial^2 w_1}{\partial y^{I2}}, \quad M_{yy}^{II} = -D_{22}^{P} \frac{\partial^2 w_2}{\partial y^{II2}}, \quad M_{yy}^{III} = -D_{22}^{S} \frac{\partial^2 u}{\partial y^{III2}}, \quad M_{yy}^{IV} = -D_{22}^{S} \frac{\partial^2 v}{\partial y^{IV2}}. \tag{17.232}$$

The two continuity conditions (17.168) and (17.169) finally lead to the following two equations:

$$\begin{aligned}
A_1 D_{22}^{P} k_1^2 - A_3 D_{22}^{P} k_2^2 - B_1 D_{22}^{P} k_1^2 \cosh\left(\frac{k_1 m\pi b}{a}\right) - B_2 D_{22}^{P} k_1^2 \sinh\left(\frac{k_1 m\pi b}{a}\right)&\\
+ B_3 D_{22}^{P} k_2^2 \cos\left(\frac{k_2 m\pi b}{a}\right) + B_4 D_{22}^{P} k_2^2 \sin\left(\frac{k_2 m\pi b}{a}\right) + C_1 D_{22}^{S} k_3^2 - C_3 D_{22}^{S} k_4^2 &= 0,\\
- A_1 D_{22}^{P} k_1^2 \cosh\left(\frac{k_1 m\pi b}{a}\right) - A_2 D_{22}^{P} k_1^2 \sinh\left(\frac{k_1 m\pi b}{a}\right)&
\end{aligned}$$

$$+A_3 D_{22}^P k_2^2 \cos\left(\frac{k_2 m\pi b}{a}\right) + A_4 D_{22}^P k_2^2 \sin\left(\frac{k_2 m\pi b}{a}\right)$$
$$+B_1 D_{22}^P k_1^2 - B_3 D_{22}^P k_2^2 + D_1 D_{22}^S k_3^2 - D_3 D_{22}^S k_4^2 = 0. \tag{17.233}$$

The conditions (17.170) and (17.171) lead to the following two equations:

$$\begin{aligned} C_1 + C_3 &= 0, \\ D_1 + D_3 &= 0. \end{aligned} \tag{17.234}$$

For the evaluation of (17.172) and (17.173) it must be taken into account that, in contrast to the bending moments at the stiffener feet, the following relationships must be considered:

$$M_{yy}^{III} = -D_{12}^S \frac{\partial^2 u}{\partial x^2} - D_{22}^S \frac{\partial^2 u}{\partial y^{III2}}, \quad M_{yy}^{IV} = -D_{12}^S \frac{\partial^2 v}{\partial x^2} - D_{22}^S \frac{\partial^2 v}{\partial y^{IV2}}. \tag{17.235}$$

The conditions (17.172) and (17.173) then lead to the following expressions:

$$\begin{aligned}
&\left(\left(D_{22}^S k_3^2 - D_{12}^S\right)\cosh\left(\frac{k_3 m\pi h}{a}\right) + GI_T \frac{k_3 m\pi}{a}\sinh\left(\frac{k_3 m\pi h}{a}\right)\right) C_1 \\
&+\left(\left(D_{22}^S k_3^2 - D_{12}^S\right)\sinh\left(\frac{k_3 m\pi h}{a}\right) + GI_T \frac{k_3 m\pi}{a}\cosh\left(\frac{k_3 m\pi h}{a}\right)\right) C_2 \\
&-\left(\left(D_{22}^S k_4^2 + D_{12}^S\right)\cos\left(\frac{k_4 m\pi h}{a}\right) + GI_T \frac{k_4 m\pi}{a}\sin\left(\frac{k_4 m\pi h}{a}\right)\right) C_3 \\
&-\left(\left(D_{22}^S k_4^2 + D_{12}^S\right)\sin\left(\frac{k_4 m\pi h}{a}\right) - GI_T \frac{k_4 m\pi}{a}\cos\left(\frac{k_4 m\pi h}{a}\right)\right) C_4 = 0, \\
&\left(\left(D_{22}^S k_3^2 - D_{12}^S\right)\cosh\left(\frac{k_3 m\pi h}{a}\right) + GI_T \frac{k_3 m\pi}{a}\sinh\left(\frac{k_3 m\pi h}{a}\right)\right) D_1 \\
&+\left(\left(D_{22}^S k_3^2 - D_{12}^S\right)\sinh\left(\frac{k_3 m\pi h}{a}\right) + GI_T \frac{k_3 m\pi}{a}\cosh\left(\frac{k_3 m\pi h}{a}\right)\right) D_2 \\
&-\left(\left(D_{22}^S k_4^2 + D_{12}^S\right)\cos\left(\frac{k_4 m\pi h}{a}\right) + GI_T \frac{k_4 m\pi}{a}\sin\left(\frac{k_4 m\pi h}{a}\right)\right) D_3 \\
&-\left(\left(D_{22}^S k_4^2 + D_{12}^S\right)\sin\left(\frac{k_4 m\pi h}{a}\right) - GI_T \frac{k_4 m\pi}{a}\cos\left(\frac{k_4 m\pi h}{a}\right)\right) D_4 = 0.
\end{aligned} \tag{17.236}$$

With reference to equations (17.174) and (17.175), the transverse shear forces in the stiffener webs can be described as follows:

$$Q_y^{III} = 2\frac{\partial M_{xy}^{III}}{\partial x} + \frac{\partial M_{yy}^{III}}{\partial y^{III}}, \quad Q_y^{IV} = 2\frac{\partial M_{xy}^{IV}}{\partial x} + \frac{\partial M_{yy}^{IV}}{\partial y^{IV}}. \tag{17.237}$$

We obtain the following for the web moments:

$$M_{xy}^{III} = -2D_{66}^{S}\frac{\partial^2 u}{\partial x \partial y^{III}}, \quad M_{yy}^{III} = -D_{12}^{S}\frac{\partial^2 u}{\partial x^2} - D_{22}^{S}\frac{\partial^2 u}{\partial y^{III2}},$$
$$M_{xy}^{IV} = -2D_{66}^{S}\frac{\partial^2 v}{\partial x \partial y^{IV}}, \quad M_{yy}^{IV} = -D_{12}^{S}\frac{\partial^2 v}{\partial x^2} - D_{22}^{S}\frac{\partial^2 v}{\partial y^{IV2}}. \tag{17.238}$$

Finally, we can write the relationships (17.174) and (17.175) as:

$$\begin{aligned}
&\left(\frac{k_3 m\pi}{a}\left(-D_{22}^{S}k_3^2 + D_{12}^{S} + 4D_{66}^{S}\right)\sinh\left(\frac{k_3 m\pi h}{a}\right) + \left(EI\frac{m^2\pi^2}{a^2} - P_{FL}\right)\cosh\left(\frac{k_3 m\pi h}{a}\right)\right)C_1 \\
&+\left(\frac{k_3 m\pi}{a}\left(-D_{22}^{S}k_3^2 + D_{12}^{S} + 4D_{66}^{S}\right)\cosh\left(\frac{k_3 m\pi h}{a}\right) + \left(EI\frac{m^2\pi^2}{a^2} - P_{FL}\right)\sinh\left(\frac{k_3 m\pi h}{a}\right)\right)C_2 \\
&+\left(\frac{k_4 m\pi}{a}\left(-D_{22}^{S}k_4^2 - D_{12}^{S} - 4D_{66}^{S}\right)\sin\left(\frac{k_4 m\pi h}{a}\right) + \left(EI\frac{m^2\pi^2}{a^2} - P_{FL}\right)\cos\left(\frac{k_4 m\pi h}{a}\right)\right)C_3 \\
&+\left(\frac{k_4 m\pi}{a}\left(D_{22}^{S}k_4^2 + D_{12}^{S} + 4D_{66}^{S}\right)\cos\left(\frac{k_4 m\pi h}{a}\right) + \left(EI\frac{m^2\pi^2}{a^2} - P_{FL}\right)\sin\left(\frac{k_4 m\pi h}{a}\right)\right)C_4 \\
&= 0, \\
&\left(\frac{k_3 m\pi}{a}\left(-D_{22}^{S}k_3^2 + D_{12}^{S} + 4D_{66}^{S}\right)\sinh\left(\frac{k_3 m\pi h}{a}\right) + \left(EI\frac{m^2\pi^2}{a^2} - P_{FL}\right)\cosh\left(\frac{k_3 m\pi h}{a}\right)\right)D_1 \\
&+\left(\frac{k_3 m\pi}{a}\left(-D_{22}^{S}k_3^2 + D_{12}^{S} + 4D_{66}^{S}\right)\cosh\left(\frac{k_3 m\pi h}{a}\right) + \left(EI\frac{m^2\pi^2}{a^2} - P_{FL}\right)\sinh\left(\frac{k_3 m\pi h}{a}\right)\right)D_2 \\
&+\left(\frac{k_4 m\pi}{a}\left(-D_{22}^{S}k_4^2 - D_{12}^{S} - 4D_{66}^{S}\right)\sin\left(\frac{k_4 m\pi h}{a}\right) + \left(EI\frac{m^2\pi^2}{a^2} - P_{FL}\right)\cos\left(\frac{k_4 m\pi h}{a}\right)\right)D_3 \\
&+\left(\frac{k_4 m\pi}{a}\left(D_{22}^{S}k_4^2 + D_{12}^{S} + 4D_{66}^{S}\right)\cos\left(\frac{k_4 m\pi h}{a}\right) + \left(EI\frac{m^2\pi^2}{a^2} - P_{FL}\right)\sin\left(\frac{k_4 m\pi h}{a}\right)\right)D_4 \\
&= 0,
\end{aligned} \tag{17.239}$$

with P_{FL} according to (17.207).

The Eqs. (17.230), (17.231), (17.233), (17.234), (17.236), and (17.239) form the 16 equations required to determine the coefficients $A_1, \ldots, A_4$, $B_1, \ldots, B_4$, $C_1, \ldots, C_4$ and $D_1, \ldots, D_4$. Since the resulting system of equations is homogeneous, we require a vanishing coefficient determinant to avoid the trivial solution for $A_1, \ldots, A_4$, $B_1, \ldots, B_4$, $C_1, \ldots, C_4$ and $D_1, \ldots, D_4$. After a few transformations, this finally leads to the following exact buckling condition of the stiffened plate:

$$\begin{aligned}
&2\left(\lambda_1\lambda_4 - \lambda_3\lambda_2\right)\left(\lambda_6\lambda_7 - \lambda_5\lambda_8\right) + 2\left(\lambda_1\lambda_2 - \lambda_3\lambda_4\right)\left(\lambda_5\lambda_6 - \lambda_7\lambda_8\right) \\
&\qquad - \left(\lambda_1^2 - \lambda_3^2\right)\left(\lambda_6^2 - \lambda_8^2\right) - \left(\lambda_2^2 - \lambda_4^2\right)\left(\lambda_5^2 - \lambda_7^2\right) = 0,
\end{aligned} \tag{17.240}$$

with the abbreviations

$$
\begin{aligned}
\lambda_1 &= \frac{k_2 m\pi}{a}\left(\frac{\cosh\left(\frac{k_1 m\pi b}{a}\right)}{\sin\left(\frac{k_2 m\pi b}{a}\right)} - \cot\left(\frac{k_2 m\pi b}{a}\right)\right),\\
\lambda_2 &= \frac{m\pi}{a}\left(k_2\frac{\sinh\left(\frac{k_1 m\pi b}{a}\right)}{\sin\left(\frac{k_2 m\pi b}{a}\right)} - k_1\right),\\
\lambda_3 &= \frac{k_1 m\pi}{a}\sinh\left(\frac{k_1 m\pi b}{a}\right)\\
&\quad + \frac{k_2 m\pi}{a}\left(\sin\left(\frac{k_2 m\pi b}{a}\right) - \left(\cosh\left(\frac{k_1 m\pi b}{a}\right) - \cos\left(\frac{k_2 m\pi b}{a}\right)\right)\cot\left(\frac{k_2 m\pi b}{a}\right)\right),\\
\lambda_4 &= \frac{m\pi}{a}\left(k_1\cosh\left(\frac{k_1 m\pi b}{a}\right) - k_2\sinh\left(\frac{k_1 m\pi b}{a}\right)\cot\left(\frac{k_2 m\pi b}{a}\right)\right),\\
\lambda_5 &= \frac{m^2\pi^2}{a^2}\left(D_{22}^P\left(k_1^2+k_2^2\right) - k_2\frac{\cosh\left(\frac{k_1 m\pi b}{a}\right) - \cos\left(\frac{k_2 m\pi b}{a}\right)}{\sin\left(\frac{k_2 m\pi b}{a}\right)}\frac{D_{22}^S\left(k_3^2+k_4^2\right)}{\lambda_9 k_3 + \lambda_{10} k_4}\right),\\
\lambda_6 &= \frac{m^2\pi^2}{a^2}\frac{D_{22}^S\left(k_3^2+k_4^2\right)}{\lambda_9 k_3 + \lambda_{10} k_4}\left(k_1 - \frac{\sinh\left(\frac{k_1 m\pi b}{a}\right)}{\sin\left(\frac{k_2 m\pi b}{a}\right)}k_2\right),\\
\lambda_7 &= -D_{22}^P\frac{m^2\pi^2}{a^2}\cosh\left(\frac{k_1 m\pi b}{a}\right)\left(k_1^2+k_2^2\right),\\
\lambda_8 &= -D_{22}^P\frac{m^2\pi^2}{a^2}\sinh\left(\frac{k_1 m\pi b}{a}\right)\left(k_1^2+k_2^2\right),
\end{aligned}
\tag{17.241}
$$

with:

$$
\lambda_9 = \frac{\left(\lambda_{15}-\lambda_{17}\right)\lambda_{14} + \left(-\lambda_{11}+\lambda_{13}\right)\lambda_{18}}{\lambda_{12}\lambda_{18} - \lambda_{14}\lambda_{16}}, \quad \lambda_{10} = \frac{\left(-\lambda_{15}+\lambda_{17}\right)\lambda_{12} + \left(\lambda_{11}-\lambda_{13}\right)\lambda_{16}}{\lambda_{12}\lambda_{18} - \lambda_{14}\lambda_{16}},
\tag{17.242}
$$

and

$$
\begin{aligned}
\lambda_{11} &= \left(D_{22}^S k_3^2 - D_{12}^S\right)\cosh\left(\frac{k_3 m\pi h}{a}\right) + GI_T\frac{k_3 m\pi}{a}\sinh\left(\frac{k_3 m\pi h}{a}\right),\\
\lambda_{12} &= \left(D_{22}^S k_3^2 - D_{12}^S\right)\sinh\left(\frac{k_3 m\pi h}{a}\right) + GI_T\frac{k_3 m\pi}{a}\cosh\left(\frac{k_3 m\pi h}{a}\right),\\
\lambda_{13} &= -\left(\left(D_{22}^S k_4^2 + D_{12}^S\right)\cos\left(\frac{k_4 m\pi h}{a}\right) + GI_T\frac{k_4 m\pi}{a}\sin\left(\frac{k_4 m\pi h}{a}\right)\right),\\
\lambda_{14} &= -\left(\left(D_{22}^S k_4^2 + D_{12}^S\right)\sin\left(\frac{k_4 m\pi h}{a}\right) - GI_T\frac{k_4 m\pi}{a}\cos\left(\frac{k_4 m\pi h}{a}\right)\right),
\end{aligned}
$$

$$\lambda_{15} = \frac{k_3 m\pi}{a}\left(-D_{22}^S k_3^2 + D_{12}^S + 4D_{66}^S\right)\sinh\left(\frac{k_3 m\pi h}{a}\right) + \left(EI\frac{m^2\pi^2}{a^2} - P_{FL}\right)\cosh\left(\frac{k_3 m\pi h}{a}\right),$$
$$\lambda_{16} = \frac{k_3 m\pi}{a}\left(-D_{22}^S k_3^2 + D_{12}^S + 4D_{66}^S\right)\cosh\left(\frac{k_3 m\pi h}{a}\right) + \left(EI\frac{m^2\pi^2}{a^2} - P_{FL}\right)\sinh\left(\frac{k_3 m\pi h}{a}\right),$$
$$\lambda_{17} = \frac{k_4 m\pi}{a}\left(-D_{22}^S k_4^2 - D_{12}^S - 4D_{66}^S\right)\sin\left(\frac{k_4 m\pi h}{a}\right) + \left(EI\frac{m^2\pi^2}{a^2} - P_{FL}\right)\cos\left(\frac{k_4 m\pi h}{a}\right),$$
$$\lambda_{18} = \frac{k_4 m\pi}{a}\left(D_{22}^S k_4^2 + D_{12}^S + 4D_{66}^S\right)\cos\left(\frac{k_4 m\pi h}{a}\right) + \left(EI\frac{m^2\pi^2}{a^2} - P_{FL}\right)\sin\left(\frac{k_4 m\pi h}{a}\right). \tag{17.243}$$

17.9.7 Verification

The developed closed-analysis approach is verified using reference results available in the literature. Fujikubo and Yao (1999) developed a similar approach for isotropic plates under biaxial compression and performed calculations for several typical ship hull plates (isotropic, $E = 210{,}000$ MPa, $\nu = 0.3$) with T- and I-stiffeners. A comparison between the present solution (17.220) and some of the results of Fujikubo and Yao (1999) can be found in Table 17.4. Obviously, a very satisfactory agreement is achieved in all cases where the highest deviation

$$\Delta = 100\left[\frac{N^0_{xx,\text{present}} - N^0_{xx\text{ref.}}}{N^0_{xx,\text{ref.}}}\right] \tag{17.244}$$

is $\Delta = 3,92\%$.

Yao et al. (1997) performed finite element calculations for the linear and nonlinear stability analysis of stiffened plates with T- and Z-stiffeners under longitudinal compression, considering a unit cell with periodic boundary conditions. The isotropic material data used are $E = 205{,}800$ MPa and $\nu = 0.3$. The geometric plate data and the resulting buckling

Table 17.4 Comparison of the current approach with the results of Fujikubo and Yao (1999)

a [mm]	b [mm]	d_P [mm]	h [mm]	d_S [mm]	h_F [mm]	d_F [mm]	N^0_{xx}, present [N/mm]	N^0_{xx}, Ref [N/mm]	Δ [%]
3200	850	18.5	250	25	–	–	8191	8022	2.11
5630	955	20.5	400	11	150	19	7597	7444	2.06
5630	955	22.0	700	14	200	25	7791	7726	0.84
5095	850	18.0	650	13.5	150	25	5502	5514	0.22
4000	795	22.0	330	25	–	–	13,327	12,824	3.92

Table 17.5 Comparison of the present analytical approach with the results of Yao et al. (1997) ($a = 2400$ mm, $b = 800$ mm, $d_P = 10.0$ mm)

h [mm]	d_S [mm]	h_F [mm]	d_F [mm]	N^0_{xx}, present [N/mm]	N^0_{xx}, Ref. [N/mm]	Δ [%]
195	10.0	–	–	1252	1280	2.19
150	12.0	90	12	1746	1845	5.37
156	19.5	–	–	1738	1769	1.75
322	10.0	–	–	1139	1142	0.26
250	12.0	90	16	1672	1794	6.80
395	20.0	–	–	1846	1890	2.33
400	11.5	100	16	1575	1650	4.55

loads according to Yao et al. (1997) and the present closed solution are shown in Table 17.5. Here, too, there is a very satisfactory agreement between the reference results and the results of the present analytical approach.

A comparison of the closed-form solution with results obtained with the Lévy solution can be found in Table 17.6, where the plate and the webs of the stiffener as well as the stiffener flanges were applied as laminates with the identical layups $[45°/-45°/0°/90°]_S$. The material parameters of the individual laminate layers were assumed to be $E_{11} = 135{,}000$ MPa, $E_{22} = 10{,}000$ MPa, $G_{12} = 5000$ MPa, $\nu_{12} = 0.27$ at a layer thickness of 0.125 mm. The geometry under consideration is a plate stiffened with I-stiffeners, whereby the plate length a and the width h_F of the flange were varied. The torsional stiffness GI_T of the flange was assumed to be negligible ($GI_T \to 0$). Obviously, the agreement between the two approaches is very good with a maximum deviation of $\Delta = 2.13\%$. The numbers in brackets stand for the respective number m of buckling half-waves in the longitudinal direction. It is obvious that both the closed-form analysis approach and the exact solution have the same number of half-waves m for all plate geometries considered.

Another study can be found in Table 17.7, in which the plate width b was varied while all other parameters were kept constant. Laminate structures and material data correspond to those used previously. Again, the agreement between the exact solution and the analytical approach is very convincing with a maximum deviation of $\Delta = 2.23\%$.

To gain an insight into the behaviour of the closed-form solution when the plate and stiffeners do not have the same layup and thickness, a study was carried out in which the plate was assumed to be an eight-layered plate $[\Theta/-\Theta/0°/90°]_S$, while the web plate of the stiffener was assumed to be a laminate with the layup $[\Theta/-\Theta/0°/90°/-\Theta/\Theta]_S$, consisting of 12 layers. All material data corresponds to that used previously. The geometric data of the stiffened plate as well as the results of the closed approach and the Lévy solution can be found in Table 17.8. Here, too, the results are in excellent agreement. At present, the highest deviation between the results is $\Delta = 4.52\%$.

Table 17.6 Comparison of the present analytical approach with the Lévy solution for varying plate length a and flange width h_F ($b = 150$ mm, $d_P = 1.0$ mm, $h = 40$ mm, $d_S = 1.0$ mm

a [mm]	h_F [mm]	d_F [mm]	N^0_{xx}, present [N/mm]	N^0_{xx}, Lévy [N/mm]	Δ [%]
100	–	–	$12.73^{(1)}$	$12.64^{(1)}$	0.71
200	–	–	$11.60^{(1)}$	$11.57^{(1)}$	0.26
300	–	–	$11.26^{(2)}$	$11.21^{(2)}$	0.45
400	–	–	$11.43^{(3)}$	$11.37^{(3)}$	0.53
500	–	–	$11.26^{(3)}$	$11.22^{(3)}$	0.36
600	–	–	$11.26^{(4)}$	$11.21^{(4)}$	0.45
100	10	1.0	$13.53^{(1)}$	$13.27^{(1)}$	1.96
200	10	1.0	$13.53^{(2)}$	$13.27^{(2)}$	1.96
300	10	1.0	$12.86^{(2)}$	$12.65^{(2)}$	1.66
400	10	1.0	$12.75^{(3)}$	$12.53^{(3)}$	1.76
500	10	1.0	$12.79^{(4)}$	$12.56^{(4)}$	1.83
600	10	1.0	$12.85^{(5)}$	$12.61^{(5)}$	1.90
100	20	1.0	$13.58^{(1)}$	$13.31^{(1)}$	2.03
200	20	1.0	$13.58^{(2)}$	$13.31^{(2)}$	2.03
300	20	1.0	$13.21^{(2)}$	$12.94^{(2)}$	2.09
400	20	1.0	$12.95^{(3)}$	$12.69^{(3)}$	2.05
500	20	1.0	$12.94^{(4)}$	$12.67^{(4)}$	2.13
600	20	1.0	$12.97^{(5)}$	$12.71^{(5)}$	2.05

Table 17.7 Comparison of the present analytical approach with the Lévy solution for a varying plate width b ($a = 600$ mm, $d_P = 1.0$mm, $h = 40$ mm, $d_S = 1.0$ mm, $h_F = 20$ mm, $d_F = 1.0$ mm)

b [mm]	N^0_{xx}, present [N/mm]	N^0_{xx}, Lévy [N/mm]	Δ [%]
100.0	$28.33^{(7)}$	$27.78^{(7)}$	1.98
112.5	$22.54^{(6)}$	$22.11^{(6)}$	1.94
125.0	$18.47^{(6)}$	$18.11^{(6)}$	1.99
137.5	$15.30^{(5)}$	$14.99^{(5)}$	2.07
150.0	$12.97^{(5)}$	$12.71^{(5)}$	2.05
175.0	$9.62^{(4)}$	$9.41^{(4)}$	2.23

Table 17.8 Comparison of the present analytical approach with the Lévy solution for a varying layer orientation angle Θ ($a = 600$ mm, $b = 150$ mm, $d_P = 1.0$ mm, $h = 40$ mm, $d_S = 1.5$ mm, $h_F = 20$ mm, $d_F = 1.5$ mm)

Θ [deg]	N^0_{xx}, present [N/mm]	N^0_{xx}, Lévy [N/mm]	Δ [%]
0	$7.32^{(3)}$	$7.15^{(3)}$	2.38
15	$9.03^{(3)}$	$8.73^{(3)}$	3.44
30	$12.73^{(4)}$	$12.18^{(4)}$	4.52
45	$15.02^{(5)}$	$14.39^{(5)}$	4.38
60	$13.45^{(7)}$	$12.97^{(7)}$	3.70
75	$10.31^{(8)}$	$10.05^{(8)}$	2.59
90	$8.91^{(8)}$	$8.73^{(8)}$	2.06

17.10 Buckling of Stiffened Laminates Under Shear Load

Besides the load case of uniaxial compression considered so far, an inplane shear load is also of considerable practical relevance. This section deals with the linear buckling problem of longitudinally stiffened rectangular orthotropic plates that are subjected to a homogeneous plane shear load and are simply supported at all four edges (see also Werner and Mittelstedt (2010)). Such a situation can be considered representative for a skin panel of an aircraft component, for example in the fuselage or in the wings. The buckling problem under consideration is approached numerically using the Ritz method, and buckling curves are provided for various geometric situations, stiffener positions and elastic properties of the laminate panels, which users can apply in practice in the form of a buckling handbook. A dimensionless representation allows the necessary parameter spaces to be reduced to a minimum and the results to be presented in a generic way so that all practically relevant laminate layups are covered with just a few buckling diagrams.

The laminated plates under consideration (length a, width b, thickness h, see Fig. 17.25, coordinate system x, y, z) are rectangular, are assumed to be simply supported at all four edges and are stiffened in the longitudinal direction by a stiffener with an arbitrary cross-section (stiffener position at $y = y_L$). For simplification, only stiffeners with negligible torsional stiffness are treated, which is an obvious and conservative assumption for stiffeners with an open profile. In order to obtain practical results, it is advisable to use dimensionless parameters that fully describe the buckling behaviour of stiffened laminated plates. Specifically, these are the orthotropy parameter β, the aspect ratio α of the laminate and the bending stiffness of the stiffener γ:

$$\beta = \frac{D_{12} + 2D_{66}}{\sqrt{D_{11}D_{22}}}, \quad \alpha = \frac{a}{b}\sqrt[4]{\frac{D_{22}}{D_{11}}}, \quad \gamma = \frac{EI}{D_{11}b}. \tag{17.245}$$

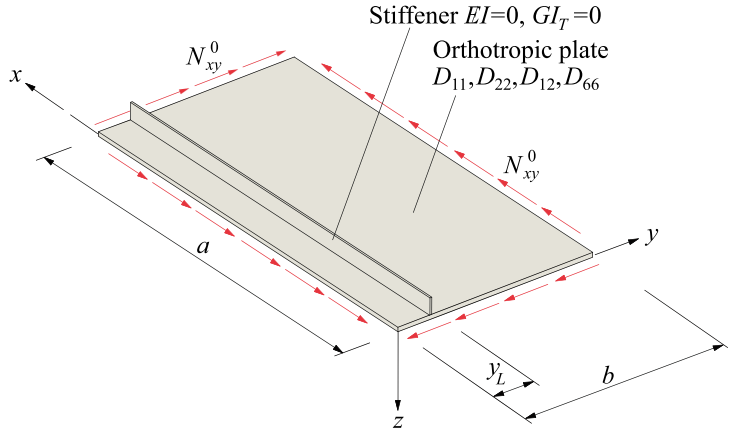


Fig. 17.25 Stiffened plate under inplane shear

The buckling diagrams contained in this section were created for $0 \leq \beta \leq 3.0$ with a step size of $\Delta\beta = 0.5$. The aspect ratio α was varied in the range of $0 \leq \alpha \leq 5.0$. In order to present a wide range of results, a relatively large number of buckling curves were plotted in each diagram for different values of the bending stiffness γ. In each diagram, the resulting buckling load is given in a dimensionless form $\bar{N}_{xy}^0$ as

$$\bar{N}_{xy}^0 = \frac{N_{xy}^0 b^2}{\pi^2 \sqrt[4]{D_{11} D_{22}^3}}. \tag{17.246}$$

Three different stiffener positions were analysed, namely $y_L = \frac{b}{2}$, $y_L = \frac{b}{3}$ and $y_L = \frac{b}{4}$. From the diagrams in Figs. 17.26, 17.27 and 17.28, intermediate values for the buckling loads can be determined by linear interpolation.

The following conclusions can be drawn from the results of the buckling diagrams:

(1) The buckling curves tend to infinite values when the aspect ratio α tends towards zero. In addition, the buckling curves tend asymptotically to a certain limit value with increasing aspect ratio α, i.e. in intermediate areas, the individual buckling curves show local maxima at certain aspect ratios, which are associated with a discontinuous slope, which corresponds to a change in the buckling mode.
(2) For a fixed stiffener position and fixed bending stiffness, an increase in the orthotropy parameter β leads to an increase in the dimensionless buckling load $\bar{N}_{xy}^0$. In addition, an increase in the bending stiffness γ leads to an increase in the resulting buckling load in all cases.

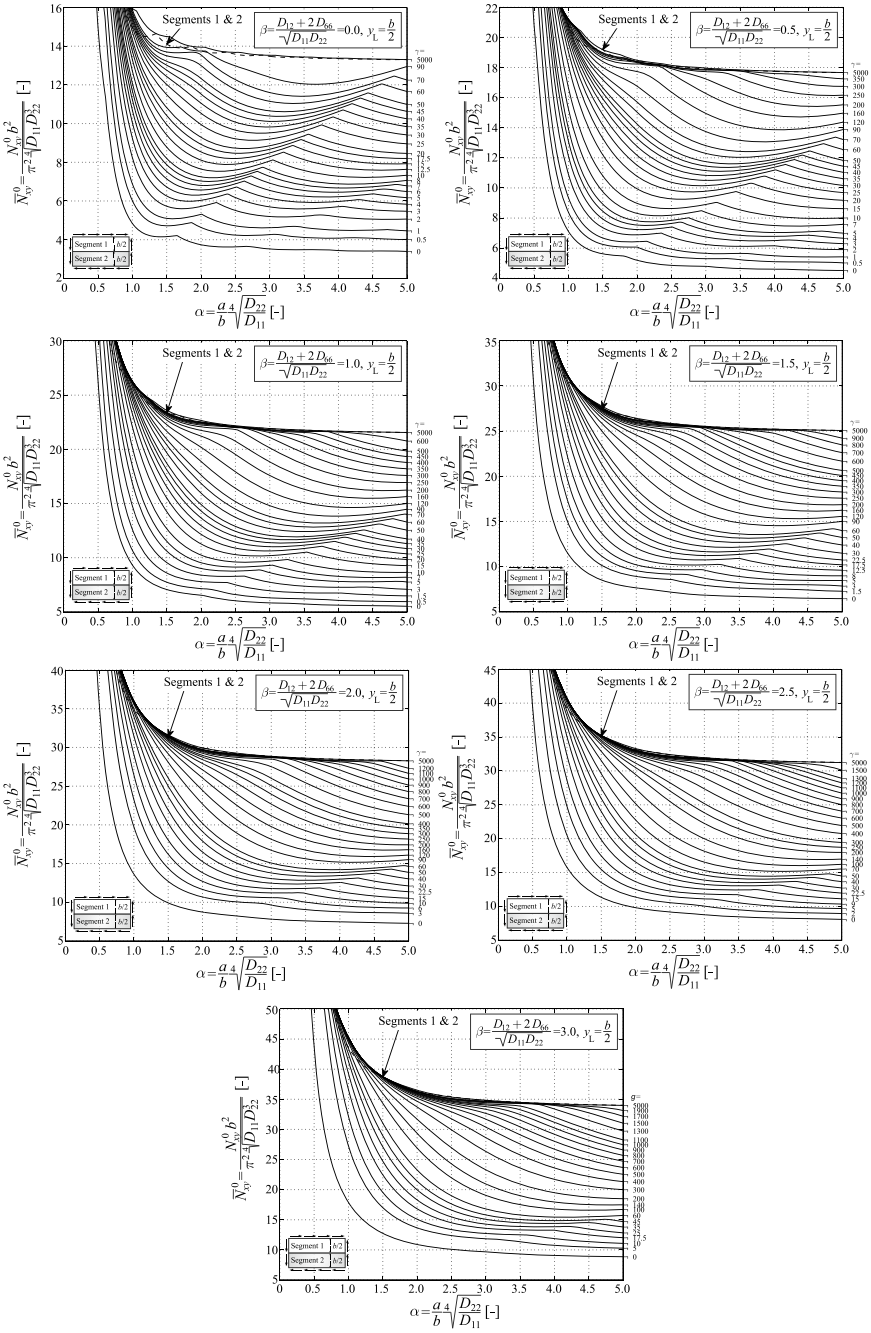


Fig. 17.26 Buckling diagrams of stiffened laminates under inplane shear load for $y_L = \frac{b}{2}$

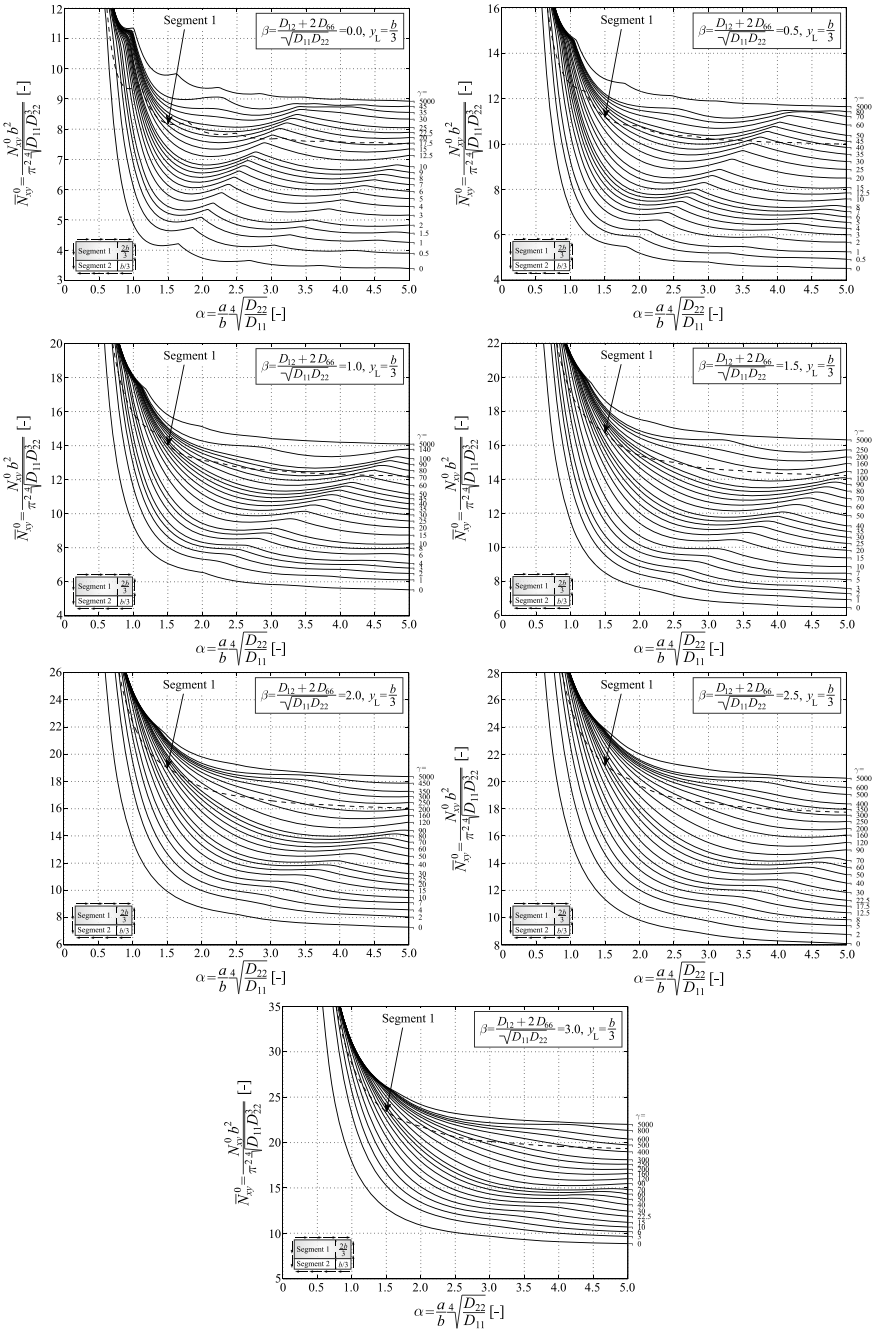


Fig. 17.27 Buckling diagrams of stiffened laminates under inplane shear load for $y_L = \frac{b}{3}$

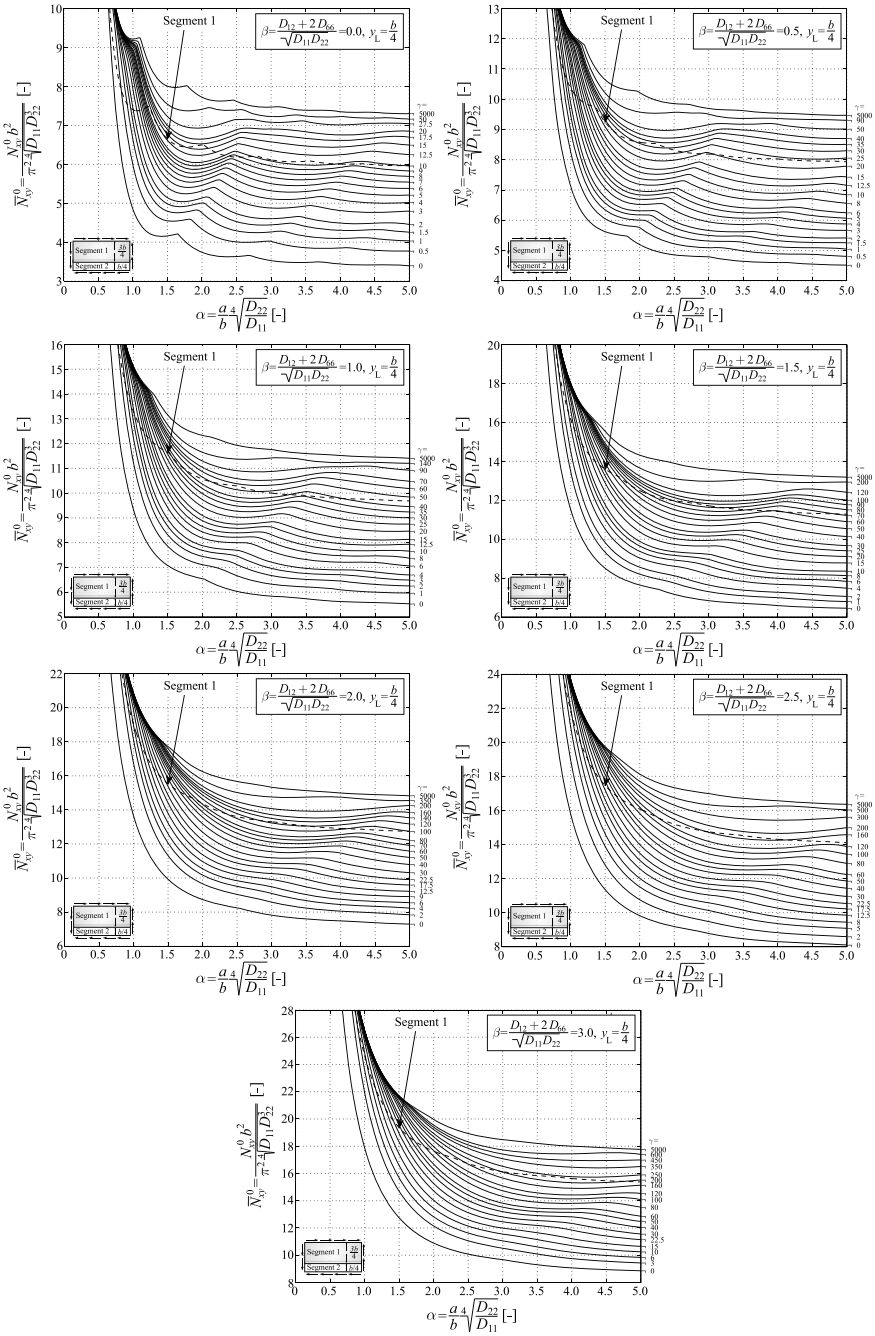


Fig. 17.28 Buckling diagrams of stiffened laminates under inplane shear load for $y_L = \frac{b}{4}$

(3) Reducing the value for the stiffener position leads to a reduction in the resulting buckling loads, which means that a centrically stiffened plate offers the maximum buckling resistance.
(4) In engineering practice, it is desirable to find a certain minimum bending stiffness of the stiffener. A bending stiffness in excess of this specific value generally does not lead to a significant increase in the buckling behaviour of the stiffened panel, but leads to unnecessary additional weight. In the absence of a more specific criterion for determining the minimum bending stiffness, it is usually postulated that the stiffener has sufficient bending stiffness if the buckling load of the entire stiffened plate is equal to the buckling load of the plate segment in question, calculated assuming hinged supports at all four edges of the plate. For this purpose, all buckling diagrams also contain the buckling curves of the relevant plate segment (i.e. the plate segment with the greatest width), which are shown with dashed lines. At the points where the buckling curves of the stiffened plates (solid lines) for a fixed bending stiffness intersect with the buckling curves of the plate segment in question (dashed lines), the minimum bending stiffness for maximizing the buckling load for a given aspect ratio is found. It is then assumed that the stiffener has sufficient bending stiffness to remain approximately straight and undeformed even in the buckled state, so that only the plate itself buckles locally.

17.11 Global Buckling of Stiffened Plates

In the design of stiffened laminates, the stability behaviour is crucial and both types of stability, namely global buckling and local buckling, must be considered to avoid panel configurations where the minimum stiffness of the stringers is not achieved. In this section, a simple analysis model is presented that can be used to calculate the critical stiffener buckling load of a plate stiffened with omega stringers with periodic boundary conditions. This is achieved by determining the effective stiffness properties of an equivalent composite stiffener. The model is able to conservatively predict the buckling of the stiffeners (Fig. 17.29) and to attribute this rather complex situation to the buckling of an equivalent beam (Schilling and Mittelstedt 2020b).

The basic idea of the following approach is to idealize the buckling of plates stiffened with omega stiffeners as a beam that is simply supported at both ends, as shown in Fig. 17.29. The corresponding Euler formula for the buckling of beams is

$$F_{\text{crit}} = \frac{\pi^2 E I}{a^2}. \tag{17.247}$$

Consequently, two steps are required to obtain an expression for the critical buckling load N_{crit}. First, the critical buckling force F_{crit} is converted into a line load related to the plate by requiring that the elongation due to the force is equal to the line load, as shown in Eq. (17.248):

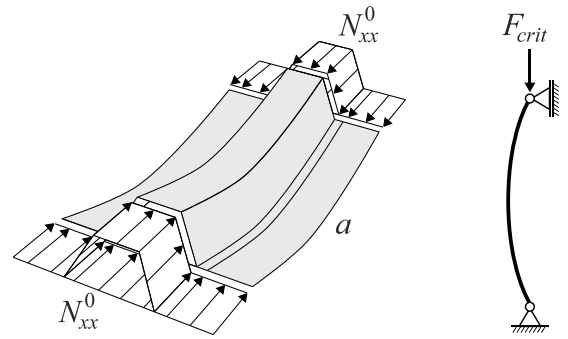


Fig. 17.29 Situation under consideration

$$\varepsilon = \frac{F}{EA} = \frac{Nb_1}{E_{\mathrm{sk}} b_1 t_{\mathrm{sk}}} \quad \text{with} \quad E_{\mathrm{sk}} = \frac{1}{t_{\mathrm{sk}} a_{11,\,\mathrm{sk}}}. \tag{17.248}$$

If we combine Eq. (17.248) with Eq. (17.247) and solve for N_{crit}, we obtain the following expression:

$$N_{\mathrm{crit}} = \frac{\pi^2 \, E_{\mathrm{sk}} \, b_1 \, t_{\mathrm{sk}} \, EI}{EA \, b_1 \, a^2}. \tag{17.249}$$

In the second step, expressions for the effective stiffnesses EI and EA are determined for the laminated plate according to the method described by Kollár and Springer (2003) (see also Chap. 24). The cross-section is divided into partial plates whose respective contribution to the effective bending stiffness is summed up. For the present case, this leads to the following equations:

$$\begin{aligned} EI &= \sum_{k=1}^{K} \left[\left(\frac{b_k \, z_k^2}{a_{11,\,k}} + \frac{b_k^3 \sin^2 \alpha_k}{12 \, a_{11,\,k}} \right) + \frac{b_k \, \cos^2 \alpha_k}{d_{11,\,k}} \right], \\ EA &= \sum_{k=1}^{K} \frac{b_k}{a_{11,\,k}} \qquad z_k = \bar{z}_k - z_{\mathrm{c}} = \bar{z}_k - \frac{\sum_{k=1}^{K} \bar{z}_k \, \frac{b_k}{a_{11,\,k}}}{\sum_{k=1}^{K} \frac{b_k}{a_{11,\,k}}}. \end{aligned} \tag{17.250}$$

In Fig. 17.30 the $\bar{z}$-coordinates are given in relation to the arbitrary coordinate system for each partial laminate. The index k indicates the number of the partial plate and K the total number of partial plates. This ultimately leads to the following expression for the critical global buckling load:

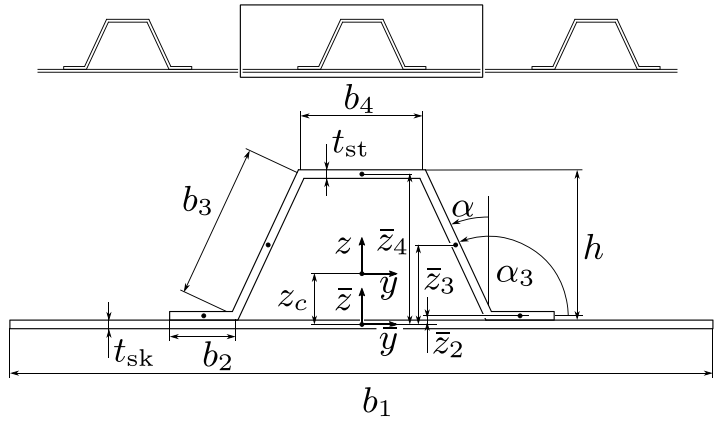


Fig. 17.30 Geometry of omega stringer and plate in a unit cell with $\bar{z}_1 = 0,\ \bar{z}_2 = \frac{1}{2}\left(t_{\mathrm{st}} + t_{\mathrm{P}}\right),\ \bar{z}_3 = \frac{h}{2}$ and $\bar{z}_4 = h$

$$N_{\mathrm{crit}} = \frac{\pi^2}{a^2\, a_{11,\mathrm{sk}} \left(\frac{2\,b_2 + 2\,b_3 + b_4}{a_{11,\mathrm{st}}} + \frac{b_1}{a_{11,\mathrm{sk}}} \right)} \left(\frac{b_1}{d_{11,\mathrm{sk}}} + \frac{\frac{1}{6}\,{b_3}^3 \cos(\alpha)^2 + 2\,b_3\,{z_3}^2 + 2\,b_2\,{z_2}^2 + b_4\,{z_4}^2}{a_{11,\mathrm{st}}} + \frac{2\,b_2 + b_4 - 2\,b_3\,\left(\cos(\alpha)^2 - 1\right)}{d_{11,\mathrm{st}}} + \frac{b_1\,{z_1}^2}{a_{11,\mathrm{sk}}} \right). \tag{17.251}$$

In this formula, the geometric parameters can be taken from Fig. 17.30, and a_{11} and d_{11} are elements of the compliance matrices resulting from the constitutive relationships for cross-ply laminates based on Classical Laminated Plate Theory.

The analytical solution is evaluated in combination with a paper on local buckling behaviour (Schilling and Mittelstedt 2020a). Exemplary results are shown in Fig. 17.31 for different widths b_1 for a cross-ply laminate with a different number of layers for skin and stringer. It is clear that the local buckling mode is modelled with good agreement and the global buckling load prediction is able to capture the stability behaviour for high aspect ratios $\frac{a}{b_1}$. It is noteworthy that the present method provides a conservative result compared to finite element analyses as the edges are modelled freely and consequently are not stiffened by the adjacent plates as implied by periodic boundary conditions.

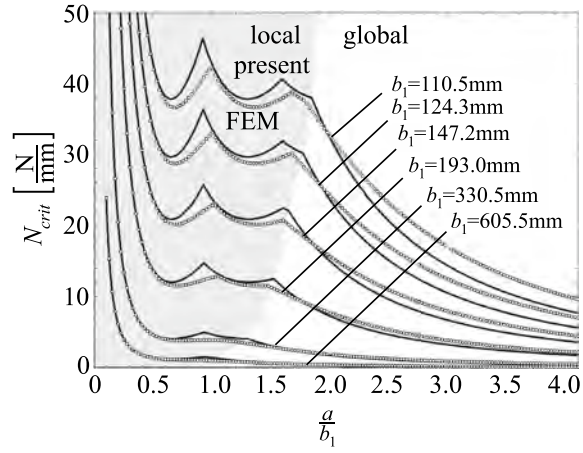


Fig. 17.31 Buckling curves for different stringer distances b_1 of a stringer with $b_2 = 0.1(b_1 - 10.5\,\text{mm})$, $b_3 = 6.263$ mm, $b_4 = 5.206$ mm, $h = 5.676$ mm, $\alpha = 25°$; Stringer laminate [0°/90°/0°/90°/0°]; Skin laminate [0°/90°/0°/90°]

References

Barbre R (1936): *Beulspannungen von Rechteckplatten mit Längssteifen bei gleichmässiger Druckbeanspruchung*, Der Bauingenieur 17:268–273.

Barbre R (1937): *Stabilität gleichmäßig gedrückter Rechteckplatten mit Längs- oder Quersteifen*, Ingenieur-Archiv 8:117–150.

Buermann P, Rolfes R, Tessmer J, Schagerl M (2006): *A semi-analytical model for local post-buckling analysis of stringer- and frame-stiffened cylindrical panels*, Thin-Walled Structures 44:102–14.

Byklum E (2002): *Ultimate strength analysis of stiffened steel and aluminium panels using semi-analytical methods*, Dissertation thesis, Norwegian University of Science and Technology, Trondheim, Norway.

Chwalla E (1944): *Über die Biegebeulung der längsversteiften Platte und das Problem der Mindeststeifigkeit*, Der Stahlbau 17:84–88.

DIN - Deutsches Institut für Normung e.V. (1953): *DIN 4114-2 (02/53) Stahlbau; Stabilitätsfälle (Knickung, Kippung, Beulung*, DIN - Deutsches Institut für Normung e.V., Berlin, Germany.

Fujikubo M, Yao T (1999): *Elastic local buckling strength of stiffened plate considering plate/stiffener interaction and welding residual stress*, Marine Structures 12:543–64.

Goodman S, Boyd E (1947): *Instability of outstanding angles simply supported at one edge and reinforced by bulbs at other edge*, NACA - National Advisory Committee for Aeronautics - Technical Note No. 1433, Washington, USA.

Goodman S (1949): *Elastic buckling of outstanding angles clamped at one edge and reinforced by bulbs at other edge*, NACA - National Advisory Committee for Aeronautics - Technical Note No. 1985, Washington, USA.

Klöppel K, Unger B (1969): *Das Ausbeulen einer am freien Rand versteiften, dreiseitig momentenfrei gelagerten Platte unter Verwendung der nichtlinearen Beultheorie*, Der Stahlbau 38:289–299.

Kollár LP, Springer GS (2003): *Mechanics of Composite Structures*, Cambridge University Press, Cambridge, UK.

Kromm A (1944): *Zur Frage der Mindeststeifigkeiten von Plattenaussteifungen*, Der Stahlbau 17:81–84.

Mittelstedt C (2008a): *Closed-form buckling analysis of stiffened composite plates and identification of minimum stiffener requirements*, International Journal of Engineering Science 46:1011–1034.

Mittelstedt C (2008b): *Explicit analysis and design equations for buckling loads and minimum stiffener requirements of orthotropic and isotropic plates under compressive load braced by longitudinal stiffeners*, Thin-Walled Structures 46:1409–1429.

Mittelstedt C (2009): *Explicit local buckling analysis of stiffened composite plates accounting for periodic boundary conditions and stiffener–plate interaction*, Composite Structures 91:249–265.

Mittelstedt C, Schagerl M (2010): *A composite view on Windenburg's problem: buckling and minimum stiffness requirements of compressively loaded orthotropic plates with edge reinforcements*, International Journal of Mechanical Sciences 52:471–484.

Mittelstedt C (2021): *Structural Mechanics in Lightweight Engineering*, Springer Nature, Cham, Switzerland.

Paik JK, Thayamballo AK, Park YE (1998): *Local buckling of stiffeners in ship plating*, Journal of Ship Research 42:56–67.

Schilling JC, Mittelstedt C (2020a): *Local buckling analysis of omega-stringer-stiffened composite panels using a new closed-form analytical approximate solution*, Thin-Walled Structures 147:106534.

Schilling JC, Mittelstedt C (2020b): *A simple closed-form analytical model for the column buckling of omega-stinger-stiffened panels with periodic boundary conditions*, Results in Engineering 6:100120.

Schilling JC, Mittelstedt C (2021): *Shear buckling of omega-stringer stiffened panels*, International Journal of Mechanical Sciences 207:106646.

Schilling JC, Atamann D, Voges J, Mittelstedt C (2022): *Local buckling of omega-stringer-stiffened composite panels under compression–shear interaction*, Thin-Walled Structures 180:109838.

Schnadel G (1930): *Knickung von Schiffsplatten*, Werft, Reederei, Hafen 6:461–465 und 6:493–497.

Seide P, Stein M (1949): *Compressive buckling of simply supported plates with longitudinal stiffeners*, NACA - National Advisory Committee for Aeronautics - Technical Note No. 1825, Washington, USA.

Timoshenko SP (1921): *Über die Stabilität versteifter Platten*, Eisenbau 12:147–163.

Weißgraeber P (2009): *Analytische Behandlung des linearen Beulproblems elastisch eingespannter, dreiseitig gelenkig gelagerter, gedrückter, orthotroper Platten mit Randversteifung*, Diplomarbeit, Technische Universität Darmstadt, Germany.

Weißgraeber P, Mittelstedt C, Becker W (2012): *Buckling of composite panels: A criterion for optimum stiffener design*, Aerospace Science and Technology 16:10–18.

Werner S, Mittelstedt C (2010): *Generic buckling curves for stiffened composite plates under inplane shear load*, Luftfahrttechnisches Handbuch (LTH), Abt. Faserverbund-Leichtbau, Blatt Nr. FL 33100-28.

Wiedemann J (1996): *Leichtbau - Band 1: Elemente*, Zweite Auflage, Springer-Verlag, Berlin et al., Germany.

Windenburg DW (1938): *The elastic stability of tee stiffeners*, Proceedings of the Fifth Congress on Applied Mechanics, 12.-16. September 1938, Cambridge, Massachusetts, USA, 54–61.

Yao T, Fujikubo M, Yanagihara D (1997): *Buckling/plastic collapse behaviour and strength of stiffened plates under thrust*, Seventh international offshore and polar engineering conference. The International Society of Offshore and Polar Engineers, Honolulu, Hawaii, USA, 25.–30. Mai 1997, 353–360.



Postbuckling of Laminates

18

This chapter is dedicated to the postbuckling analysis of laminated plates, focussing on the presentation of the fundamentals and the provision of closed-form analytical and semi-analytical computational methods. For orthotropic laminates under compression and shear under different types of boundary conditions, closed-form analytical approaches are presented, which can be used to treat the postbuckling behaviour of such laminates in a computationally efficient way. Subsequently, a semi-analytical method based on series expansions for the state variables in the postbuckling state is presented, which can be used to treat more complex problems. The chapter concludes with a computational method for analysing the postbuckling behaviour of shear-deformable laminates under compressive load in the context of First-Order Shear Deformation Theory (FSDT) and Third-Order Shear Deformation Theory (TSDT).

18.1 Introduction

The layout and design of modern passenger aircraft structures are increasingly dominated by composite laminated structures, which are characterized by stability problems due to their thin-walled nature. In order to be able to compete with the classic metal designs, it will be necessary to go beyond the determination of classic-ideal bifurcational buckling loads (see also the previous chapters). It will thus be necessary to provide calculation methods for the postcritical (i.e. the geometrically nonlinear) range, such as those that have existed for metallic fuselage structures for a long time. Practically relevant analysis methods, especially in the field of optimization and pre-design, must meet the requirements that, on the one hand, a good accuracy of the results should be achieved and, on the other hand, only little

© The Author(s), under exclusive license to Springer-Verlag GmbH, DE, part of Springer Nature 2025

C. Mittelstedt, *Mechanics of Composite Structures*,
https://doi.org/10.1007/978-3-662-70788-3_18

computational effort should be required. In the best case, calculation methods for this purpose are of a purely closed-form analytical nature and do not require any numerical effort. The current chapter is therefore dedicated to the problem area of the closed-form analysis of the so-called postbuckling, taking imperfections (i.e. pre-deformations that may result from the manufacturing process of the component or from assembly inaccuracies) into account, and the postbuckling behaviour of imperfect rectangular orthotropic plates under longitudinal compressive loading and under shear is dealt with. Such a plate is representative e.g. for a skin panel in an aircraft fuselage structure and thus represents an important geometric situation. This chapter concludes with the description of a semi-analytical method for laminates under combined loads and a closed-form analysis method for the postbuckling analysis of shear-deformable laminates.

The postcritical behaviour of orthotropic plates and anisotropic laminates has been the subject of intensive research in recent decades, in particular using complex analysis methods with an iterative character such as the Ritz method, the Finite Strip Method or the Finite Element Method. A detailed overview cannot be given in this chapter; interested readers are referred to the books by Chia (1980) and Turvey and Marshall (1995), which contain a wealth of further explanations and relevant literature references.

18.2 Postbuckling Behaviour of Laminates Under Uniaxial Compression

18.2.1 Material Law and Boundary Conditions

The laminate under consideration (length a, width b, thickness h, reference coordinate system x, y, z, see Fig. 18.1) is assumed to be simply supported at the loaded edges at $x = 0$ and $x = a$ with regard to the displacements w_0 in the thickness direction. It then applies that both the displacements w_0 and the laminate bending moments M^0_{xx} must disappear at these edges:

$$w_0\,(x = 0) = 0, \quad w_0\,(x = a) = 0, \quad M^0_{xx}\,(x = 0) = 0, \quad M^0_{xx}\,(x = a) = 0. \tag{18.1}$$

With regard to the unloaded edges at $y = 0$ and $y = b$, two possibilities are considered. On the one hand, the case is analyzed in which there is also a simple support at the unloaded edges with respect to w_0 (Fig. 18.1, top). This leads to:

$$w_0\,(y = 0) = 0, \quad w_0\,(y = b) = 0, \quad M^0_{yy}\,(y = 0) = 0, \quad M^0_{yy}\,(y = b) = 0. \tag{18.2}$$

On the other hand, the case is considered where the unloaded edges are clamped (Fig. 18.1, bottom):

$$w_0\,(y = 0) = 0, \quad w_0\,(y = b) = 0, \quad \left.\frac{\partial w_0}{\partial y}\right|_{y=0} = 0, \quad \left.\frac{\partial w_0}{\partial y}\right|_{y=b} = 0. \tag{18.3}$$

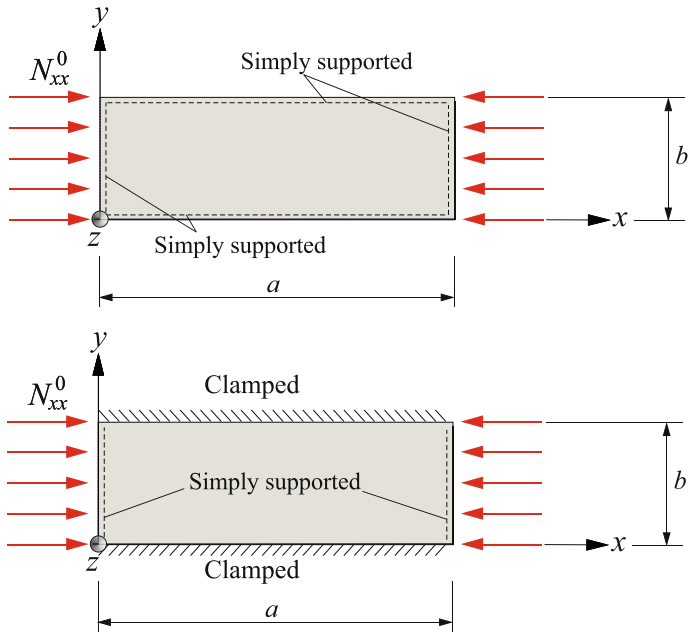


Fig. 18.1 Considered boundary conditions with regard to the displacement w_0 in the thickness direction: laminate simply supported at all edges (top) and laminate clamped at the unloaded edges (right)

The laminates discussed in this section are part of a thin plate structure stiffened by a stiffener grid (Fig. 18.2, left). If we turn to the specific situation of an aircraft fuselage, for example, the stiffening elements would be given by the stringers and the frames, and the analyzed laminates according to Fig. 18.1 could be considered representative of a skin field if the curvature of the skin field, which is always present in reality, is neglected in the interest of an easy-to-use analysis method. Since even small curvatures of a skin field significantly increase the buckling loads compared to a flat plate, this is a valid and permissible simplification.

The laminates discussed in this section are symmetric, balanced and free of bending-twisting coupling, as is the case with symmetric cross-ply laminates, for example. It is also assumed that the laminates are sufficiently thin so that the validity of the Classical Laminated Plate Theory (CLPT) can be assumed. The constitutive law can then be written as:

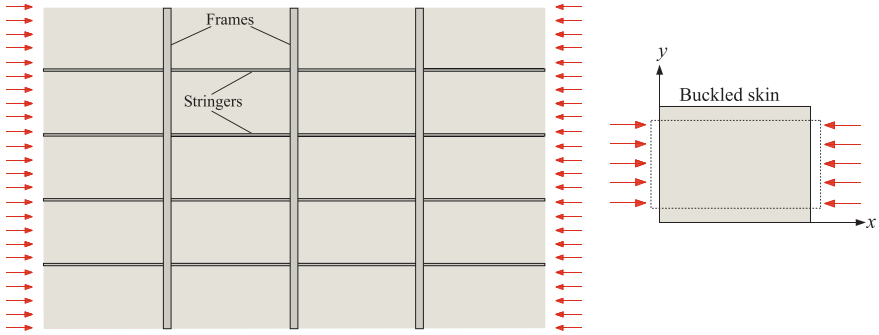


Fig. 18.2 Laminate stiffened by stringers and frames (left), representative skin field in the deformed state (right)

$$\begin{pmatrix} N^0_{xx} \\ N^0_{yy} \\ N^0_{xy} \\ M^0_{xx} \\ M^0_{yy} \\ M^0_{xy} \end{pmatrix} = \begin{bmatrix} A_{11} & A_{12} & 0 & 0 & 0 & 0 \\ A_{12} & A_{22} & 0 & 0 & 0 & 0 \\ 0 & 0 & A_{66} & 0 & 0 & 0 \\ 0 & 0 & 0 & D_{11} & D_{12} & 0 \\ 0 & 0 & 0 & D_{12} & D_{22} & 0 \\ 0 & 0 & 0 & 0 & 0 & D_{66} \end{bmatrix} \begin{pmatrix} \varepsilon^0_{xx} \\ \varepsilon^0_{yy} \\ \gamma^0_{xy} \\ \kappa^0_{xx} \\ \kappa^0_{yy} \\ \kappa^0_{xy} \end{pmatrix}. \tag{18.4}$$

If one assumes that all other skin fields in a certain area around the skin field under consideration have identical or very similar properties, it follows that with a pure compressive load at the onset of buckling, all skin fields transition to the buckled state at the same time. At the same time, a certain reciprocal supporting effect develops along the edges of the skin panel/laminate in such a way that the skin panel laminate undergoes compression in the compressive direction and expansion in the transverse direction, but retains a rectangular shape overall (Fig. 18.2, right). Of course, this also assumes that the laminates are balanced and do not exhibit shear coupling. The following then applies to the boundary conditions with regard to the inplane displacements u_0 and v_0:

$$\left.\frac{\partial u_0}{\partial y}\right|_{x=0} = 0, \quad \left.\frac{\partial u_0}{\partial y}\right|_{x=a} = 0, \quad \left.\frac{\partial v_0}{\partial x}\right|_{y=0} = 0, \quad \left.\frac{\partial v_0}{\partial x}\right|_{y=b} = 0. \tag{18.5}$$

18.2.2 Fundamental Equations: Strains, Equilibrium and Compatibility

The strains of the laminate, consisting of the strains ε_{xx}, ε_{yy} and the shear strain γ_{xy}, can be derived from the strains ε^0_{xx}, ε^0_{yy}, γ^0_{xy} and the curvatures and twist κ^0_{xx}, κ^0_{yyy}, κ^0_{xy} of the laminate middle plane as follows:

$$\varepsilon_{xx} = \varepsilon^0_{xx} + z\kappa^0_{xx}, \quad \varepsilon_{yy} = \varepsilon^0_{yy} + z\kappa^0_{yy}, \quad \gamma_{xy} = \gamma^0_{xy} + z\kappa^0_{xy}. \tag{18.6}$$

The membrane strains in the sense of v. Kármán's plate theory (see also Chap. 2 of this book) are as follows:

$$\varepsilon^0_{xx} = \frac{\partial u_0}{\partial x} + \underbrace{\frac{1}{2}\left(\frac{\partial w_0}{\partial x}\right)^2}_{(a)}, \quad \varepsilon^0_{yy} = \frac{\partial v_0}{\partial y} + \underbrace{\frac{1}{2}\left(\frac{\partial w_0}{\partial y}\right)^2}_{(b)}, \quad \gamma^0_{xy} = \frac{\partial u_0}{\partial y} + \frac{\partial v_0}{\partial x} + \underbrace{\frac{\partial w_0}{\partial x}\frac{\partial w_0}{\partial y}}_{(c)}. \tag{18.7}$$

In addition to the geometrically linear theory and the associated infinitesimal strains, the components labelled (a), (b) and (c) must also be taken into account. The curvatures and the twist of the laminate middle plane remain unchanged compared to the linear theory and can be written as a function of the laminate deflection w_0:

$$\kappa^0_{xx} = -\frac{\partial^2 w_0}{\partial x^2}, \quad \kappa^0_{yy} = -\frac{\partial^2 w_0}{\partial y^2}, \quad \kappa^0_{xy} = -2\frac{\partial^2 w_0}{\partial x \partial y}. \tag{18.8}$$

For the reasons mentioned in the introduction, imperfect plates are to be considered, so that the plate deflection is composed of the variable part w_0 and the a priori known and invariable part w_i (the index i stands for the term 'imperfection'). The substitution $w_0 \to w_0 + w_i$ is introduced into the Eqs. (18.7) and (18.8) and neglecting terms of the order

$$\left(\frac{\partial w_i}{\partial x}\right)^2, \quad \left(\frac{\partial w_i}{\partial y}\right)^2, \quad \frac{\partial w_i}{\partial x}\frac{\partial w_i}{\partial y}, \quad \frac{\partial^2 w_i}{\partial x^2}, \quad \frac{\partial^2 w_i}{\partial y^2}, \quad \frac{\partial^2 w_i}{\partial x \partial y}, \tag{18.9}$$

after differentiation, the following nonlinear strain field for the imperfect laminated plate is finally obtained:

$$\begin{aligned}
\varepsilon_{xx} &= \frac{\partial u_0}{\partial x} + \frac{1}{2}\left(\frac{\partial w_0}{\partial x}\right)^2 + \frac{\partial w_0}{\partial x}\frac{\partial w_i}{\partial x} - z\frac{\partial^2 w_0}{\partial x^2}, \\
\varepsilon_{yy} &= \frac{\partial v_0}{\partial y} + \frac{1}{2}\left(\frac{\partial w_0}{\partial y}\right)^2 + \frac{\partial w_0}{\partial y}\frac{\partial w_i}{\partial y} - z\frac{\partial^2 w_0}{\partial y^2}, \\
\gamma_{xy} &= \frac{\partial u_0}{\partial y} + \frac{\partial v_0}{\partial x} + \frac{\partial w_0}{\partial x}\frac{\partial w_0}{\partial y} + \frac{\partial w_0}{\partial x}\frac{\partial w_i}{\partial y} + \frac{\partial w_i}{\partial x}\frac{\partial w_0}{\partial y} - 2z\frac{\partial^2 w_0}{\partial x \partial y}.
\end{aligned} \tag{18.10}$$

The equilibrium conditions for a deflected plate are as follows:

$$\begin{aligned}
\frac{\partial N^0_{xx}}{\partial x} + \frac{\partial N^0_{xy}}{\partial y} &= 0, \\
\frac{\partial N^0_{xy}}{\partial x} + \frac{\partial N^0_{yy}}{\partial y} &= 0,
\end{aligned}$$

$$\frac{\partial^2 M_{xx}^0}{\partial x^2} + \frac{\partial^2 M_{xy}^0}{\partial x \partial y} + \frac{\partial^2 M_{yy}^0}{\partial y^2} + N_{xx}^0 \frac{\partial^2 w_0}{\partial x^2} + 2N_{xy}^0 \frac{\partial^2 w_0}{\partial x \partial y} + N_{yy}^0 \frac{\partial^2 w_0}{\partial y^2} = 0. \tag{18.11}$$

In contrast to linear plate buckling analyses, tensile forces were assumed to be positive forces. The Airy stress function F according to

$$N_{xx}^0 = \frac{\partial^2 F}{\partial y^2}, \quad N_{yy}^0 = \frac{\partial^2 F}{\partial x^2}, \quad N_{xy}^0 = -\frac{\partial^2 F}{\partial x \partial y} \tag{18.12}$$

is introduced. The first two equilibrium conditions in (18.11) are fulfilled identically for any choice of F. If we again assume an imperfect structure and neglect terms of order

$$\frac{\partial^4 w_i}{\partial x^4}, \quad \frac{\partial^4 w_i}{\partial y^4}, \quad \frac{\partial^4 w_i}{\partial x^2 \partial y^2}, \tag{18.13}$$

the third equilibrium condition with the material law (18.4) leads to the following form:

$$\begin{aligned} D_{11} \frac{\partial^4 w_0}{\partial x^4} + 2\left(D_{12} + 2D_{66}\right) \frac{\partial^4 w_0}{\partial x^2 \partial y^2} + D_{22} \frac{\partial^4 w_0}{\partial y^4} - \frac{\partial^2 F}{\partial y^2} \left(\frac{\partial^2 w_0}{\partial x^2} + \frac{\partial^2 w_i}{\partial x^2} \right) \\ + 2 \frac{\partial^2 F}{\partial x \partial y} \left(\frac{\partial^2 w_0}{\partial x \partial y} + \frac{\partial^2 w_i}{\partial x \partial y} \right) - \frac{\partial^2 F}{\partial x^2} \left(\frac{\partial^2 w_0}{\partial y^2} + \frac{\partial^2 w_i}{\partial y^2} \right) = 0. \end{aligned} \tag{18.14}$$

This is the first differential equation that describes the postbuckling problem currently under consideration.

The second necessary equation is obtained from the requirement for compatibility of the plane strains $\varepsilon_{xx}^0, \varepsilon_{yyy}^0, \gamma_{xy}^0$:

$$\frac{\partial^2 \varepsilon_{xx}^0}{\partial y^2} + \frac{\partial^2 \varepsilon_{yy}^0}{\partial x^2} - \frac{\partial^2 \gamma_{xy}^0}{\partial x \partial y} = 0. \tag{18.15}$$

The following results are obtained by solving the material law (18.4) for the strains ε_{xx}^0, $\varepsilon_{yy}^0, \gamma_{xy}^0$ and inserting the definition (18.12) of Airy's stress function:

$$\varepsilon_{xx}^0 = a_{12} \frac{\partial^2 F}{\partial x^2} + a_{11} \frac{\partial^2 F}{\partial y^2}, \quad \varepsilon_{yy}^0 = a_{22} \frac{\partial^2 F}{\partial x^2} + a_{12} \frac{\partial^2 F}{\partial y^2}, \quad \gamma_{xy}^0 = -a_{66} \frac{\partial^2 F}{\partial x \partial y}. \tag{18.16}$$

The inverted membrane stiffnesses can be specified as:

$$a_{11} = \frac{A_{22}}{A_{11}A_{22} - A_{12}^2}, \quad a_{22} = \frac{A_{11}}{A_{11}A_{22} - A_{12}^2}, \quad a_{12} = \frac{A_{12}}{A_{12}^2 - A_{11}A_{22}}, \quad a_{66} = \frac{1}{A_{66}}. \tag{18.17}$$

The compatibility condition (18.15) with (18.16) can then also be written as:

$$\frac{\partial^2 \varepsilon_{xx}^0}{\partial y^2} + \frac{\partial^2 \varepsilon_{yy}^0}{\partial x^2} - \frac{\partial^2 \gamma_{xy}^0}{\partial x \partial y} = a_{22} \frac{\partial^4 \psi}{\partial x^4} + a_{11} \frac{\partial^4 \psi}{\partial y^4} + (2a_{12} + a_{66}) \frac{\partial^4 \psi}{\partial x^2 \partial y^2}. \tag{18.18}$$

On the other hand, the definitions (18.7) of the plane strains can also be used to evaluate the compatibility condition (18.15). Assuming an imperfect structure and neglecting terms of order

$$\left(\frac{\partial^2 w_i}{\partial x \partial y} \right)^2, \quad \frac{\partial^2 w_i}{\partial x^2} \frac{\partial^2 w_i}{\partial y^2}, \tag{18.19}$$

eventually yields:

$$\begin{aligned} \frac{\partial^2 \varepsilon_{xx}^0}{\partial y^2} + \frac{\partial^2 \varepsilon_{yy}^0}{\partial x^2} - \frac{\partial^2 \gamma_{xy}^0}{\partial x \partial y} &= \left(\frac{\partial^2 w_0}{\partial x \partial y} \right)^2 \\ - \frac{\partial^2 w_0}{\partial x^2} \frac{\partial^2 w_0}{\partial y^2} - \frac{\partial^2 w_0}{\partial x^2} \frac{\partial^2 w_i}{\partial y^2} + 2 \frac{\partial^2 w_0}{\partial x \partial y} \frac{\partial^2 w_i}{\partial x \partial y} - \frac{\partial^2 w_i}{\partial x^2} \frac{\partial^2 w_0}{\partial y^2}. \end{aligned} \tag{18.20}$$

Equating (18.18) and (18.20) provides:

$$\begin{aligned} a_{22} \frac{\partial^4 \psi}{\partial x^4} + a_{11} \frac{\partial^4 \psi}{\partial y^4} + (2a_{12} + a_{66}) \frac{\partial^4 \psi}{\partial x^2 \partial y^2} &= \left(\frac{\partial^2 w_0}{\partial x \partial y} \right)^2 \\ - \frac{\partial^2 w_0}{\partial x^2} \frac{\partial^2 w_0}{\partial y^2} - \frac{\partial^2 w_0}{\partial x^2} \frac{\partial^2 w_i}{\partial y^2} + 2 \frac{\partial^2 w_0}{\partial x \partial y} \frac{\partial^2 w_i}{\partial x \partial y} - \frac{\partial^2 w_i}{\partial x^2} \frac{\partial^2 w_0}{\partial y^2}. \end{aligned} \tag{18.21}$$

The coupled differential equations (18.14) and (18.21) thus describe the behaviour of an orthotropic plate/a symmetric cross-ply composite laminate in the postbuckling range and are the subject of the following investigations.

For the further treatment of the considered postbuckling problem, it is advantageous to reduce all equations to dimensionless quantities. For this purpose, natural coordinates ξ_1 and ξ_2 are introduced as follows:

$$\xi_1 = \frac{x}{a}, \quad \xi_2 = \frac{y}{b}. \tag{18.22}$$

Use of the following characteristic dimensionless quantities (see also Brunelle and Oyibo 1983, Mittelstedt and Schröder 2010a, b, Stein 1983, Wiedemann 1996)

$$\begin{aligned} \bar{F} &= \frac{F}{\sqrt{D_{11} D_{22}}}, \quad \alpha_D = \frac{a}{b} \sqrt[4]{\frac{D_{22}}{D_{11}}}, \quad \alpha_A = \frac{a}{b} \sqrt[4]{\frac{a_{11}}{a_{22}}}, \\ \beta_D &= \frac{D_{12} + 2D_{66}}{\sqrt{D_{11} D_{22}}}, \quad \beta_A = \frac{2a_{12} + a_{66}}{\sqrt{a_{11} a_{22}}}, \\ \bar{u}_0 &= \frac{a u_0}{\sqrt{a_{11} a_{22} D_{11} D_{22}}}, \quad \bar{w}_0 = \frac{w_0}{\sqrt[4]{a_{11} a_{22} D_{11} D_{22}}}, \quad \bar{w}_i = \frac{w_i}{\sqrt[4]{a_{11} a_{22} D_{11} D_{22}}} \end{aligned} \tag{18.23}$$

leads to the following transformed form of the differential equations (18.14) and (18.21):

$$\frac{1}{\alpha_D^2}\frac{\partial^4\bar{w}_0}{\partial\xi_1^4}+2\beta_D\frac{\partial^4\bar{w}_0}{\partial\xi_1^2\partial\xi_2^2}+\alpha_D^2\frac{\partial^4\bar{w}_0}{\partial\xi_2^4}=\frac{\partial^2\bar{\psi}}{\partial\xi_2^2}\left(\frac{\partial^2\bar{w}_0}{\partial\xi_1^2}+\frac{\partial^2\bar{w}_i}{\partial\xi_1^2}\right)$$
$$-2\frac{\partial^2\bar{\psi}}{\partial\xi_1\partial\xi_2}\left(\frac{\partial^2\bar{w}_0}{\partial\xi_1\partial\xi_2}+\frac{\partial^2\bar{w}_i}{\partial\xi_1\partial\xi_2}\right)+\frac{\partial^2\bar{\psi}}{\partial\xi_1^2}\left(\frac{\partial^2\bar{w}_0}{\partial\xi_2^2}+\frac{\partial^2\bar{w}_i}{\partial\xi_2^2}\right),$$
$$\frac{1}{\alpha_A^2}\frac{\partial^4\bar{\psi}}{\partial\xi_1^4}+\beta_A\frac{\partial^4\bar{\psi}}{\partial\xi_1^2\partial\xi_2^2}+\alpha_A^2\frac{\partial^4\bar{\psi}}{\partial\xi_2^4}=\left(\frac{\partial^2\bar{w}_0}{\partial\xi_1\partial\xi_2}\right)^2-\frac{\partial^2\bar{w}_0}{\partial\xi_1^2}\frac{\partial^2\bar{w}_0}{\partial\xi_2^2}$$
$$+2\frac{\partial^2\bar{w}_0}{\partial\xi_1\partial\xi_2}\frac{\partial^2\bar{w}_i}{\partial\xi_1\partial\xi_2}-\frac{\partial^2\bar{w}_0}{\partial\xi_1^2}\frac{\partial^2\bar{w}_i}{\partial\xi_2^2}-\frac{\partial^2\bar{w}_i}{\partial\xi_1^2}\frac{\partial^2\bar{w}_0}{\partial\xi_2^2}. \tag{18.24}$$

A dimensionless representation of the laminate forces

$$\bar{N}_{xx}^0=\frac{N_{xx}^0b^2}{\pi^2\sqrt{D_{11}D_{22}}},\quad \bar{N}_{yy}^0=\frac{N_{yy}^0a^2}{\pi^2\sqrt{D_{11}D_{22}}},\quad \bar{N}_{xy}^0=\frac{N_{xy}^0ab}{\pi^2\sqrt{D_{11}D_{22}}}, \tag{18.25}$$

then provides the following transformed relationship between the laminate forces and Airy's stress function:

$$\bar{N}_{xx}^0=\frac{1}{\pi^2}\frac{\partial^2\bar{\psi}}{\partial\xi_2^2},\quad \bar{N}_{yy}^0=\frac{1}{\pi^2}\frac{\partial^2\bar{\psi}}{\partial\xi_1^2},\quad \bar{N}_{xy}^0=-\frac{1}{\pi^2}\frac{\partial^2\bar{\psi}}{\partial\xi_1\partial\xi_2}. \tag{18.26}$$

18.2.3 Postbuckling Behaviour of the Simply Supported Plate

The plate situation as shown in Fig. 18.1, top, is considered. The boundary conditions (18.2) at the unloaded edge are as follows in the natural coordinate system ξ_1 and ξ_2:

$$\bar{w}_0\,(\xi_2=0)=0,\quad \bar{w}_0\,(\xi_2=1)=0,\quad \bar{M}_{yy}^0\,(\xi_2=0)=0,\quad \bar{M}_{yy}^0\,(\xi_2=1)=0. \tag{18.27}$$

The following approach is chosen for the buckling mode $\bar{w}_{0,\mathrm{init}}$ of the perfect laminate when the bifurcational buckling load $\bar{N}_{xx,\mathrm{init}}^0$ is reached:

$$\bar{w}_{0,\mathrm{init}}=\sin\left(m\pi\xi_1\right)\sin\left(\pi\xi_2\right). \tag{18.28}$$

The suffix 'init' is intended to make it clear that the quantities labelled this way refer to the ideal bifurcational problem. It can easily be shown that the form (18.28) actually represents the exact solution of the problem of the currently considered plate situation and leads to the following exact solution for the linear buckling load $\bar{N}_{xx,\mathrm{init}}^0$:

$$\bar{N}_{xx,\mathrm{init}}^0=\frac{m^2}{\alpha_D^2}+\frac{\alpha_D^2}{m^2}+2\beta_D. \tag{18.29}$$

In accordance with the literature, the bifurcational buckling load $\bar{N}^0_{xx,\text{init}}$ is always considered to be positive, although a buckling load must of course always act as a compressive force for the plate geometries under consideration. The number m of buckling half-waves follows from the condition $\frac{\partial \bar{N}^0_{xx,\text{init}}}{\partial m} = 0$ and provides the following only relevant root:

$$m = \alpha_D . \tag{18.30}$$

The following fundamental assumptions always apply to the postbuckling analyses discussed in this section: Firstly, it is assumed that the deflection $\bar{w}_0$ of the laminate in the postbuckling state is proportional to the linear buckling mode $\bar{w}_{0,\text{init}}$ and that this functional description of the postbuckling shape $\bar{w}_0$ does not change, regardless of the magnitude of the applied compressive force $\bar{N}^0_{xx}$. On the other hand, it is assumed that the number m of buckling half-waves no longer changes after buckling occurs, also independent of the applied compressive force $\bar{N}^0_{xx}$. Although these assumptions will allow the implementation of a practically feasible method and lead to closed-form analytical expressions, it must also be accepted as a certain limitation that the current calculation methods will provide certain deviations from the real structural response, especially for large degrees of postbuckling. On the one hand, it is always to be expected that with increasing loads $\bar{N}^0_{xx}$ buckling modes $\bar{w}_0$ will form that deviate significantly from the buckling mode $\bar{w}_{0,\text{init}}$ according to the bifurcational buckling theory, on the other hand, it is known that the number m of buckling half-waves can also increase with increasing compressive forces $\bar{N}^0_{xx}$, which is generally associated with mode changes. However, the analysis results to be discussed later will show that the assumptions made for slight degrees of postbuckling are entirely justifiable. The following formulation is therefore proposed for the postbuckling shape $\bar{w}_0$:

$$\bar{w}_0 = \bar{f}\,\bar{w}_{0,\text{init}} = \bar{f}\,\sin(m\pi\xi_1)\sin(\pi\xi_2)\,. \tag{18.31}$$

Here, $\bar{f}$ is the postbuckling amplitude, the determination of which is the actual aim of the calculations. The imperfections $\bar{w}_i$ are, as is common practice, also assumed to be proportional to the linear buckling shape, whereby the amplitude $\bar{f}_i$ is assumed to be known and determined by the user:

$$\bar{w}_i = \bar{f}_i\,\bar{w}_{0,\text{init}} = \bar{f}_i\,\sin(m\pi\xi_1)\sin(\pi\xi_2)\,. \tag{18.32}$$

Of the two equations (18.24), the compatibility condition is now considered first. As is well known, the solution of this differential equation splits into a homogeneous solution $\bar{F}_\text{h}$ and a particular solution $\bar{F}_\text{p}$ for the Airy stress function $\bar{F}$. The homogeneous form of the compatibility condition is

$$\frac{1}{\alpha_A^2}\frac{\partial^4 \bar{F}_\text{h}}{\partial \xi_1^4} + \beta_A \frac{\partial^4 \bar{F}_\text{h}}{\partial \xi_1^2 \partial \xi_2^2} + \alpha_A^2 \frac{\partial^4 \bar{F}_\text{h}}{\partial \xi_2^4} = 0. \tag{18.33}$$

This equation describes the membrane problem prior to buckling and is therefore particularly easy to solve. If the relationship (18.26) is observed and it is assumed that the laminate is under a uniaxial compressive load $\bar{N}_{xx}^0$ before buckling (where $\bar{N}_{yy}^0 = \bar{N}_{xy}^0 = 0$), the solution for (18.33) can be determined by integrating the applied compressive force $\bar{N}_{xx}^0$ twice:

$$\bar{F}_\mathrm{h} = \int \left(\int \bar{N}_{xx}^0 \pi^2 \mathrm{d}\xi_2 \right) \mathrm{d}\xi_2 + C_1 + C_2 \xi_2. \tag{18.34}$$

The integration constants C_1 and C_2 can be neglected without loss of generality. Performing the integrations then provides:

$$\bar{F}_\mathrm{h} = \frac{\bar{N}_{xx}^0 \pi^2 \xi_2^2}{2}. \tag{18.35}$$

The particular solution $\bar{F}_\mathrm{p}$ is obtained from the inhomogeneous form of the compatibility condition (18.24), where the approaches (18.31) and (18.32) were used for $\bar{w}_0$ and $\bar{w}_i$:

$$\frac{1}{\alpha_A^2} \frac{\partial^4 \bar{F}_\mathrm{p}}{\partial \xi_1^4} + \beta_A \frac{\partial^4 \bar{F}_\mathrm{p}}{\partial \xi_1^2 \partial \xi_2^2} + \alpha_A^2 \frac{\partial^4 \bar{F}_\mathrm{p}}{\partial \xi_2^4} = \bar{f} \left(\bar{f} + 2 \bar{f}_i \right) m^2 \pi^4 \left[\cos^2 (m\pi\xi_1) + \cos^2 (\pi\xi_2) - 1 \right]. \tag{18.36}$$

An approach of the right-hand side type

$$\bar{F}_\mathrm{p} = B_1 \cos^2 (m\pi\xi_1) + B_2 \cos^2 (\pi\xi_2) \tag{18.37}$$

provides the following constants after insertion and coefficient comparison:

$$B_1 = \frac{\bar{f} \left(\bar{f} + 2 \bar{f}_i \right) \alpha_A^2}{16 m^2}, \quad B_2 = \frac{\bar{f} \left(\bar{f} + 2 \bar{f}_i \right) m^2}{16 \alpha_A^2}. \tag{18.38}$$

The total solution $\bar{F}$ for the Airy stress function then results from the sum of the homogeneous and the particular solution:

$$\bar{F} = \bar{F}_\mathrm{h} + \bar{F}_\mathrm{p} = \frac{\bar{N}_{xx}^0 \pi^2 \xi_2^2}{2} + \frac{\bar{f} \left(\bar{f} + 2 \bar{f}_i \right)}{16} \left[\frac{\alpha_A^2}{m^2} \cos^2 (m\pi\xi_1) + \frac{m^2}{\alpha_A^2} \cos^2 (\pi\xi_2) \right]. \tag{18.39}$$

Thus, Airy's stress function has been determined by using a simple closed-form analytical approach, and the only remaining unknown is the postbuckling amplitude $\bar{f}$. This is obtained from the remaining equation (18.24), whereby an exact fulfilment of this equation is not possible, but rather an approximate solution must be used, currently in the form of a Galerkin formulation. It is required that

$$\int_0^1 \left\{ \int_0^1 \left[\frac{1}{\alpha_D^2} \frac{\partial^4 \bar{w}_0}{\partial \xi_1^4} + 2\beta_D \frac{\partial^4 \bar{w}_0}{\partial \xi_1^2 \partial \xi_2^2} + \alpha_D^2 \frac{\partial^4 \bar{w}_0}{\partial \xi_2^4} - \frac{\partial^2 \bar{F}}{\partial \xi_2^2} \left(\frac{\partial^2 \bar{w}_0}{\partial \xi_1^2} + \frac{\partial^2 \bar{w}_i}{\partial \xi_1^2} \right) \right.\right.$$
$$\left.\left. + 2\frac{\partial^2 \bar{F}}{\partial \xi_1 \partial \xi_2} \left(\frac{\partial^2 \bar{w}_0}{\partial \xi_1 \partial \xi_2} + \frac{\partial^2 \bar{w}_i}{\partial \xi_1 \partial \xi_2} \right) - \frac{\partial^2 \bar{F}}{\partial \xi_1^2} \left(\frac{\partial^2 \bar{w}_0}{\partial \xi_2^2} + \frac{\partial^2 \bar{w}_i}{\partial \xi_2^2} \right) \right] \bar{w}_{0,\text{init}} \mathrm{d}\xi_2 \right\} \mathrm{d}\xi_1 = 0. \tag{18.40}$$

Inserting (18.31), (18.32) and (18.39) finally yields the following cubic equation for the postbuckling amplitude $\bar{f}$:

$$\frac{16m^2\alpha_A^2 \bar{f}_i \bar{N}_{xx}^0}{m^4 + \alpha_A^4} + 2\left[\frac{8\left(\bar{N}_{xx,\text{init}}^0 + \bar{N}_{xx}^0\right) m^2 \alpha_A^2}{m^4 + \alpha_A^4} + \bar{f}_i^2 \right] \bar{f} + 3\bar{f}_i \bar{f}^2 + \bar{f}^3 = 0. \tag{18.41}$$

Equation (18.41) can be solved in a closed-form analytical manner. The only relevant real solution is:

$$\bar{f} = \frac{1}{3\gamma} \left[\bar{f}_i^2 - \frac{16m^2\alpha_A^2 \left(\bar{N}_{xx,\text{init}}^0 + \bar{N}_{xx}^0\right)}{m^4 + \alpha_A^4} \right] + \gamma - \bar{f}_i, \tag{18.42}$$

wherein the following abbreviation was introduced:

$$\gamma = \frac{1}{3} \sqrt[3]{\frac{3}{m^4 + \alpha_A^4}} \left(72\bar{f}_i m^2 \alpha_A^2 \bar{N}_{xx,\text{init}}^0 + \left[\frac{1}{m^4 + \alpha_A^4} \left\{ 96m^2\alpha_A^2 \left(\bar{N}_{xx,\text{init}}^0 + \bar{N}_{xx}^0\right) \right.\right.\right.$$
$$\times \left[m^4 \alpha_A^4 \left\{ 128 \left(\bar{N}_{xx,\text{init}}^0 + \bar{N}_{xx}^0\right)^2 + 3\bar{f}_i^4 \right\} + \frac{3\bar{f}_i^4}{2} \left(m^8 + \alpha_A^8\right) \right] \Bigg\}$$
$$\left.\left.\left. - 3\bar{f}_i^2 \left\{ 192m^4 \alpha_A^4 \left(5\bar{N}_{xx,\text{init}}^0 + 2\bar{N}_{xx}^0\right) \left(-\bar{N}_{xx,\text{init}}^0 + 2\bar{N}_{xx}^0\right) + \bar{f}_i^4 \left(m^4 + \alpha_A^4\right)^2 \right\} \right]^{\frac{1}{2}} \right)^{\frac{1}{3}}. \tag{18.43}$$

This provides a closed-form analytical expression for the postbuckling amplitude $\bar{f}$ as a function of the elastic and geometric properties of the laminate, of the linear buckling behaviour, of the applied compressive force $\bar{N}_{xx}^0$ and of the type and magnitude of the imperfections. In the case of a perfect plate with $\bar{f}_i = 0$, Eq. (18.41) reduces to:

$$\frac{16\left(\bar{N}_{xx,\text{init}}^0 + \bar{N}_{xx}^0\right) m^2 \alpha_A^2}{m^4 + \alpha_A^4} \bar{f} + \bar{f}^3 = 0. \tag{18.44}$$

In addition to the trivial solution $\bar{f} = 0$, the following two solutions result:

$$\bar{f} = \pm \frac{4m\alpha_A}{m^4 + \alpha_A^4} \sqrt{-\left(m^4 + \alpha_A^4\right)\left(\bar{N}^0_{xx,\text{init}} + \bar{N}^0_{xx}\right)}. \tag{18.45}$$

The alternating sign indicates that when considering a postbuckling problem of a perfect plate, it is irrelevant in which direction the buckling of the plate takes place, both solutions are equally valid and correct. Furthermore, Eq. (18.45) only results in real-valued solutions if the compressive force $\bar{N}^0_{xx}$ reaches or exceeds a certain value, namely exactly the ideal bifurcational buckling load $\bar{N}^0_{xx,\text{init}}$.

If we write Eq. (18.45) in the original coordinates x, y, we obtain the following result:

$$f = \pm \frac{4ab^2 m}{\pi} \sqrt{-\frac{a_{11}a_{22}}{a^4 a_{11} + m^4 b^4 a_{22}}\left(N^0_{xx,\text{init}} + N^0_{xx}\right)}. \tag{18.46}$$

This equation coincides with an expression given by Meyer-Piening et al. (1991) for perfect plates.

It is of interest for practical structural design to calculate the change in length u_0. This can be easily done by integrating the plane strain component ε^0_{xx} over the plate length a with respect to the length coordinate x. From (18.7), (18.10) and (18.16):

$$u_0 = \int_0^a \left[a_{11}\frac{\partial^2 F}{\partial y^2} + a_{12}\frac{\partial^2 F}{\partial x^2} - \frac{1}{2}\left(\frac{\partial w_0}{\partial x}\right)^2 - \frac{\partial w_0}{\partial x}\frac{\partial w_i}{\partial x} \right] \mathrm{d}x. \tag{18.47}$$

Performing the integration then provides the following edge displacement of the plate:

$$u_0 = a_{11} N^0_{xx} a - \frac{f\,(f + 2f_i)\,m^2\pi^2}{8a}. \tag{18.48}$$

In the normalized coordinate system the following expression is obtained:

$$\bar{u}_0 = \pi^2 \left[\bar{N}^0_{xx}\alpha_A^2 - \frac{\bar{f}\left(\bar{f} + 2\bar{f}_i\right)m^2}{8} \right]. \tag{18.49}$$

An important point in the design of compressed composite laminates in the postbuckling range is the calculation of the effective width b_{eff}. The basic idea behind this important geometric parameter is shown in Fig. 18.3 (see also e.g. Wiedemann (1996)). A force flow $\bar{N}^0_{xx,\text{post}}$ will occur in the postbuckling range, which, in contrast to the prebuckling state, will not develop uniformly, but will rather show a nonlinear distribution over the plate width. Figure 18.3 clearly shows that if the bifurcational buckling load is exceeded in the center of the plate, the membrane stresses will no longer increase in the longitudinal direction. The additional load applied above the bifurcational buckling load will then be redistributed to the unloaded plate edges, where it will become noticeable in stress concentrations, so that the stress concentration shown in Fig. 18.3 results. If the plate under consideration is

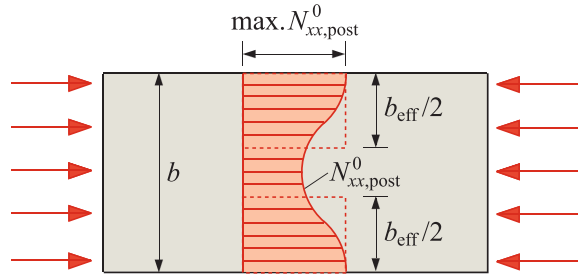


Fig. 18.3 Determination of the effective width of the plate under compressive load in the postbuckling range

representative of a skin field in a stiffener grid (Fig. 18.2), the stress concentrations at the edges of the plate must primarily be carried by the stiffeners in the longitudinal direction (the so-called stringers). The dimensioning of the longitudinal stiffeners must then also ensure the load-bearing capacity in the postbuckling range of the stiffened plate.

The force flow $\bar{N}^0_{xx,\text{post}}$ can be written in the normalized coordinate system as follows:

$$\bar{N}^0_{xx,\text{post}} = \frac{1}{\pi^2}\frac{\partial^2 \bar{F}}{\partial \xi_2^2} = \bar{N}^0_{xx} - \frac{\bar{f}\left(\bar{f}+2\bar{f}_i\right)m^2\left[2\cos^2(\pi\xi_2)-1\right]}{8\alpha_A^2}. \tag{18.50}$$

The maximum values max . $\bar{N}^0_{xx,\text{post}}$ of the membrane force $\bar{N}^0_{xx,\text{post}}$ will naturally occur at the longitudinal edges and are calculated as:

$$\max.\bar{N}^0_{xx,\text{post}} = \bar{N}^0_{xx} - \frac{\bar{f}\left(\bar{f}+2\bar{f}_i\right)m^2}{8\alpha_A^2}. \tag{18.51}$$

The effective width b_{eff} is now defined in such a way that instead of the nonlinear curve $\bar{N}^0_{xx,\text{post}}$ two stress blocks of the still unknown width $\frac{1}{2}\,b_{\text{eff}}$ and the magnitude max . $\bar{N}^0_{xx,\text{post}}$ can be assumed. For reasons of equilibrium, the area of the two stress blocks must match the area of the membrane force $\bar{N}^0_{xx,\text{post}}$. The following therefore applies:

$$\max.\bar{N}^0_{xx,\text{post}}\bar{b}_{\text{eff}} = \frac{1}{\pi^2}\int_0^1 \frac{\partial^2 \bar{F}}{\partial \xi_2^2}\mathrm{d}\xi_2. \tag{18.52}$$

The effective width is therefore a measure of the part of the laminate that is still available for the transfer of additional loads beyond the bifurcational buckling load after the buckling load has been exceeded. The effective width is $b_{\text{eff}} = b$ for an unbuckled plate. Inserting (18.39) and (18.51) and performing the integration finally yields the following closed-form analytical expression for the effective width $\bar{b}_{\text{eff}} = b_{\text{eff}}/b$ as a function of the applied load $\bar{N}^0_{xx}$:

$$\bar{b}_{\text{eff}} = \frac{8\bar{N}^0_{xx}\alpha_A^2}{8\bar{N}^0_{xx}\alpha_A^2 - \bar{f}\left(\bar{f}+2\bar{f}_i\right)m^2}. \tag{18.53}$$

18.2.4 Postbuckling Behaviour of the Clamped Plate

The case of the simply supported plate represents an extreme case insofar as such a plate represents a lower limit and thus a conservative case with regard to the buckling load and the postbuckling stiffness. An upper limit, on the other hand, is reached when the unloaded longitudinal edges are rigidly clamped (see Fig. 18.1, bottom). The boundary conditions at the unloaded edge are then as follows

$$\bar{w}_0\,(\xi_2 = 0) = 0, \quad \bar{w}_0\,(\xi_2 = 1) = 0, \quad \frac{\partial \bar{w}_0}{\partial \xi_2}\,(\xi_2 = 0) = 0, \quad \frac{\partial \bar{w}_0}{\partial \xi_2}\,(\xi_2 = 1) = 0. \tag{18.54}$$

A plausible assumption for the buckling mode $\bar{w}_{0,\mathrm{init}}$ is in this case:

$$\bar{w}_{0,\mathrm{init}} = \frac{1}{2}\sin\left(m\pi\xi_1\right)\left[1 - \cos\left(2\pi\xi_2\right)\right]. \tag{18.55}$$

While a single sine function was again assumed in the longitudinal direction, a cosine function is used in the transverse direction in this case, which exactly fulfils the boundary conditions (18.54). The buckling load $\bar{N}^0_{xx,\mathrm{init}}$ associated with this buckling shape can be calculated from the principle of the minimum of the elastic potential in the buckled state with $\bar{\Pi} = \Pi/\sqrt{D_{11}D_{22}}$ and $\bar{w}_0 = w_0/\sqrt{ab}$:

$$\begin{aligned}\delta\bar{\Pi} = \delta\Bigg\{ &\int_0^1\int_0^1 \Bigg[\frac{1}{2\alpha_D^2}\left(\frac{\partial^2\bar{w}_0}{\partial\xi_1^2}\right)^2 + \frac{\alpha_D^2}{2}\left(\frac{\partial^2\bar{w}_0}{\partial\xi_2^2}\right)^2 \\ &+ \beta_D\zeta\left(\frac{\partial^2\bar{w}_0}{\partial\xi_1^2}\right)\left(\frac{\partial^2\bar{w}_0}{\partial\xi_2^2}\right) + \beta_D\left(1-\zeta\right)\left(\frac{\partial^2\bar{w}_0}{\partial\xi_1\partial\xi_2}\right)^2\Bigg]\mathrm{d}\xi_2\mathrm{d}\xi_1 \\ &- \frac{\pi^2\bar{N}^0_{xx,\mathrm{init}}}{2}\int_0^1\int_0^1\left(\frac{\partial\bar{w}_0}{\partial\xi_1}\right)^2\mathrm{d}\xi_2\mathrm{d}\xi_1\Bigg\} = 0.\end{aligned} \tag{18.56}$$

After a short calculation, this leads to the following representation of $\bar{N}^0_{xx,\mathrm{init}}$:

$$\bar{N}^0_{xx,\mathrm{init}} = \frac{m^2}{\alpha_D^2} + \frac{16\alpha_D^2}{3m^2} + \frac{8\beta_D}{3}. \tag{18.57}$$

As before, the number m of buckling half-waves is determined from the condition $\partial\bar{N}^0_{xx,\mathrm{init}}/\partial m = 0$. The only relevant solution is obtained as:

$$m = \frac{2\alpha_D}{\sqrt[4]{3}}. \tag{18.58}$$

As in the case of the simply supported plate, the postbuckling shape and the plate imperfections are assumed to be proportional to the buckling mode:

$$\bar{w}_0 = \bar{f}\bar{w}_{0,\text{init}} = \frac{\bar{f}}{2}\sin(m\pi\xi_1)\left[1-\cos(2\pi\xi_2)\right],$$
$$\bar{w}_i = \bar{f}_i\bar{w}_{0,\text{init}} = \frac{\bar{f}_i}{2}\sin(m\pi\xi_1)\left[1-\cos(2\pi\xi_2)\right]. \tag{18.59}$$

The compatibility condition in (18.24) thus changes to the following form:

$$\frac{1}{\alpha_A^2}\frac{\partial^4\bar{F}}{\partial\xi_1^4} + \beta_A\frac{\partial^4\bar{F}}{\partial\xi_1^2\partial\xi_2^2} + \alpha_A^2\frac{\partial^4\bar{F}}{\partial\xi_2^4}$$
$$= \frac{1}{2}\bar{f}\left(\bar{f}+2\bar{f}_i\right)m^2\pi^4\left\{\cos^2(2m\pi\xi_1)\left[1-\cos(2\pi\xi_2)\right]+\cos(2\pi\xi_2)-\cos(4\pi\xi_2)\right\}. \tag{18.60}$$

The homogeneous solution corresponds to Eq. (18.35). The particular solution can currently be determined as follows:

$$\bar{F}_\text{p} = \frac{\bar{f}\left(\bar{f}+2\bar{f}_i\right)\alpha_A^2}{32m^2}\left\{\cos(2m\pi\xi_1)\left[1-\frac{m^4\cos(2\pi\xi_2)}{m^4+\beta_A m^2\alpha_A^2+\alpha_A^4}\right]+\frac{m^4}{\alpha_A^4}\left[\cos(2\pi\xi_2)-\frac{\cos(4\pi\xi_2)}{16}\right]\right\}. \tag{18.61}$$

With (18.59) and (18.61), the Galerkin method provides the following cubic determination equation for the postbuckling amplitude $\bar{f}$:

$$\gamma_1\bar{f}^2\left(\bar{f}+3\bar{f}_i\right)+\left[2\gamma_1\bar{f}_i^2+\frac{3m^2\pi^4}{16}\left(\bar{N}^0_{xx,\text{init}}+\bar{N}^0_{xx}\right)\right]\bar{f}+\frac{3\bar{f}_i m^2\pi^4}{16}\bar{N}^0_{xx}=0, \tag{18.62}$$

wherein:

$$\gamma_1 = \frac{\pi^4\left[17m^6\left(m^2+\beta_A\alpha_A^2\right)+41m^4\alpha_A^4+16\alpha_A^6\left(\alpha_A^2+\beta_A m^2\right)\right]}{1024\left(m^4+\beta_A m^2\alpha_A^2+\alpha_A^4\right)\alpha_A^2}. \tag{18.63}$$

Again, there is only one relevant solution:

$$\bar{f} = \bar{f}_i\left(\frac{\bar{f}_i}{3\gamma}-1\right)+\gamma-\frac{64\left(\bar{N}^0_{xx,\text{init}}+\bar{N}^0_{xx}\right)m^2\alpha_A^2\left(m^4+\beta_A m^2\alpha_A^2+\alpha_A^4\right)}{\gamma\left[17m^6\left(m^2+\beta_A\alpha_A^2\right)+41m^4\alpha_A^4+16\alpha_A^6\left(\alpha_A^2+\beta_A m^2\right)\right]}, \tag{18.64}$$

wherein the following abbreviation was introduced:

$$\gamma = \sqrt[3]{\frac{3\bar{N}^0_{xx,\text{init}}m^2\pi^4\bar{f}_i}{32\gamma_1}+\frac{\sqrt{3}}{18\gamma_1}\sqrt{\frac{\gamma_2}{\gamma_1}\left[4\gamma_2^2-9\gamma_1\bar{f}_i\left(\gamma_2\bar{f}_i+6\gamma_3\right)\right]+27\gamma_3\left(4\gamma_1\bar{f}_i^3+\gamma_3\right)}}, \tag{18.65}$$

with:

$$\gamma_2 = 2\gamma_1\bar{f}_i^2+\frac{3m^2\pi^4}{16}\left(\bar{N}^0_{xx,\text{init}}+\bar{N}^0_{xx}\right),\quad \gamma_3 = \frac{3\bar{f}_i m^2\pi^4}{16}\bar{N}^0_{xx}. \tag{18.66}$$

In the case of a perfect plate with $\bar{f}_i = 0$, the following equation is obtained:

$$\frac{192\left(m^4+\beta_A\alpha_A^2m^2+\alpha_A^4\right)m^2\alpha_A^2\left(\bar{N}^0_{xx,\text{init}}+\bar{N}^0_{xx}\right)}{17m^6\left(m^2+\beta_A\alpha_A^2\right)+41m^4\alpha_A^4+16\alpha_A^6\left(\alpha_A^2+\beta_Am^2\right)}\bar{f}+\bar{f}^3=0. \tag{18.67}$$

In addition to the trivial solution $\bar{f} = 0$, the following results:

$$\bar{f}=\pm8\sqrt{3}\alpha_Am\sqrt{-\frac{\left(m^4+\beta_A\alpha_A^2m^2+\alpha_A^4\right)\left(\bar{N}^0_{xx,\text{init}}+\bar{N}^0_{xx}\right)}{17m^6\left(m^2+\beta_A\alpha_A^2\right)+41m^4\alpha_A^4+16\alpha_A^6\left(\alpha_A^2+\beta_Am^2\right)}}. \tag{18.68}$$

The edge displacement $\bar{u}_0$ is obtained analogously to the simply supported laminate as:

$$\bar{u}_0=\pi^2\left[\bar{N}^0_{xx}\alpha_A^2-\frac{3\bar{f}\left(\bar{f}+2\bar{f}_i\right)m^2}{32}\right]. \tag{18.69}$$

The membrane force distribution in the postbuckling state is the same as before:

$$\bar{N}^0_{xx,\text{post}}=\frac{1}{\pi^2}\frac{\partial^2\bar{F}}{\partial\xi_2^2}=\bar{N}^0_{xx}+\frac{\bar{f}\left(\bar{f}+2\bar{f}_i\right)m^2}{8}$$
$$\times\left\{\frac{1}{\alpha_A^2}\left[-\cos\left(2\pi\xi_2\right)+\frac{1}{4}\cos\left(4\pi\xi_2\right)\right]+\frac{\alpha_A^2}{m^4+\alpha_A^2\beta_Am^2+\alpha_A^4}\cos\left(2m\pi\xi_1\right)\cos\left(2\pi\xi_2\right)\right\}. \tag{18.70}$$

The maximum values are again to be expected at the plate edges:

$$\max.\bar{N}^0_{xx,\text{post}}=\bar{N}^0_{xx}+\frac{\bar{f}\left(\bar{f}+2\bar{f}_i\right)m^2}{8}\left[-\frac{3}{4\alpha_A^2}+\frac{\alpha_A^2}{m^4+\alpha_A^2\beta_Am^2+\alpha_A^4}\cos\left(2m\pi\xi_1\right)\right]. \tag{18.71}$$

The effective width $\bar{b}_{\text{eff}} = \frac{b_{\text{eff}}}{b}$ then results analogously to the laminate simply supported at all edges as:

$$\bar{b}_{\text{eff}}=\frac{8\bar{N}^0_{xx}}{8\bar{N}^0_{xx}+\bar{f}\left(\bar{f}+2\bar{f}_i\right)m^2\left[-\frac{3}{4\alpha_A^2}+\frac{\alpha_A^2}{m^4+\alpha_A^2\beta_Am^2+\alpha_A^4}\cos\left(2m\pi\xi_1\right)\right]}. \tag{18.72}$$

It is interesting to note that, in contrast to the plate with simply supported edges, the maximum value of the membrane force flow and thus also the effective width remains dependent on the longitudinal coordinate ξ_1. It is therefore at the discretion of the user to decide at which point the Eq. (18.72) should be evaluated.

18.2.5 Verification of the Closed-Form Analysis Methods

After all the necessary equations for the calculation of the postbuckling behaviour of symmetric orthotropic laminates have been given in the two previous sections, the accuracy and applicability of the derived methods will be examined and assessed by comparing them with reference results from the literature.

18.2.5.1 Imperfect Isotropic Plate with Simply Supported Unloaded Edges (Zou and Qiao 2002)

Zou and Qiao (2002) used the finite strip method to analyse imperfect isotropic and anisotropic plates under uniaxial compressive load. A comparison of the results for the postbuckling amplitude $\bar{f} + \bar{f}_i$ and the edge displacement $\bar{u}_0$ as a function of the applied load $\bar{N}^0_{xx}$ for a square isotropic plate with $\frac{a}{h} = 120$ and $\nu = \frac{1}{3}$ with various imperfections $\frac{f_i}{h}$ can be found in Fig. 18.4. It should be noted here that although Zou and Qiao also assumed that constant boundary displacements $\bar{u}_0$ occur at the loaded edges, no restrictions were provided for the membrane displacements $\bar{v}_0$ at the unloaded edges. This means that the current method for the simply supported plate assumes a greater stiffness for the system than the finite strip method according to Zou and Qiao. In particular, it will be the case that the conditions assumed in the current formulation

$$\left.\frac{\partial v_0}{\partial x}\right|_{y=0} = 0, \quad \left.\frac{\partial v_0}{\partial x}\right|_{y=b} = 0 \tag{18.73}$$

cannot be maintained—the edge displacements v_0 will then not be constant. The postbuckling situation considered in this way then proves to be potentially more compliant than a plate for which it is required in the postbuckling range that all edges remain straight. This assumption is also supported by the results of Fig. 18.4, left, which shows a comparison between the current method and the finite strip calculations according to Zou and Qiao for the postbuckling amplitudes $\bar{f} + \bar{f}_i$. Overall, the agreement of the results for low postbuckling amplitudes is quite satisfactory. On the other hand, however, it can also be seen that certain deviations in the results occur as the buckling load $\bar{N}^0_{xx,\text{init}}$ is exceeded. This is the result of the different inplane boundary conditions, which, according to the approach of Zou and Qiao, probably only inadequately represent the conditions in a skin field of a stiffened plate. Nevertheless, it can be seen that the current method for slight degrees of postbuckling is able to reproduce the postbuckling behaviour of an imperfect plate not only qualitatively but also quantitatively quite well. This also applies to the results of Fig. 18.4, right, in which the results for the edge displacement $\bar{u}_0$ are given. Here, the slopes of the postbuckling curves clearly show that the current method overestimates the stiffness of the system - again a result of the deviating inplane boundary conditions. Overall, this example underlines the importance of the boundary conditions with regard to the inplane displacements $\bar{u}_0$ and $\bar{v}_0$ if one wants to investigate the postbuckling behaviour of composite laminates.

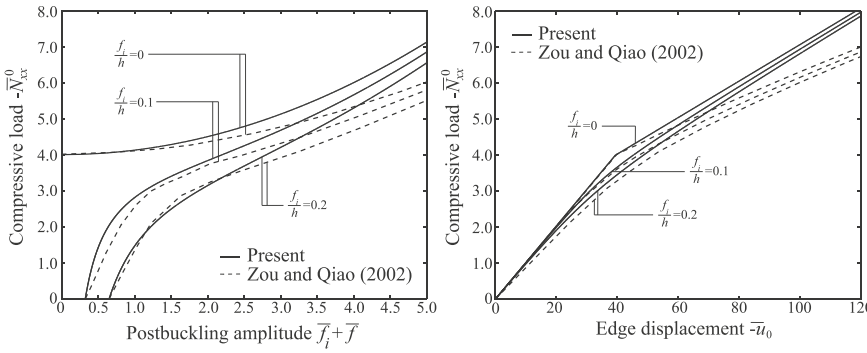


Fig. 18.4 Comparison of the results according to the present method with the results according to Zou and Qiao for an isotropic imperfect square plate; postbuckling amplitude $\bar{f}+\bar{f}_i$ (left) and edge displacement $\bar{u}_0$ (right) as functions of the applied compressive load $\bar{N}^0_{xx}$

18.2.5.2 Perfect Isotropic Plates with Simply Supported Unloaded Edges (Ovesy et al. 2004)

Ovesy et al. (2004) used the finite strip method for the postbuckling analysis of perfect isotropic plates under uniaxial compressive load and studied the influence of the inplane boundary conditions with regard to the displacements $\bar{v}_0$ at the unloaded edges of a square isotropic plate with $\frac{a}{h}=120$ and $\nu=\frac{1}{3}$. Figure 18.5 shows the edge displacement $\bar{u}_0$ as a function of the applied load $\bar{N}^0_{xx}$ for a plate in which the unloaded longitudinal edges are free with respect to the edge displacements $\bar{v}_0$. Furthermore, Fig. 18.5 includes results for a plate in which the unloaded longitudinal edges are required to remain straight even in the postbuckling state, which corresponds precisely to the assumptions of the current method (Fig. 18.2, right). Obviously, the agreement between the results according to the latter

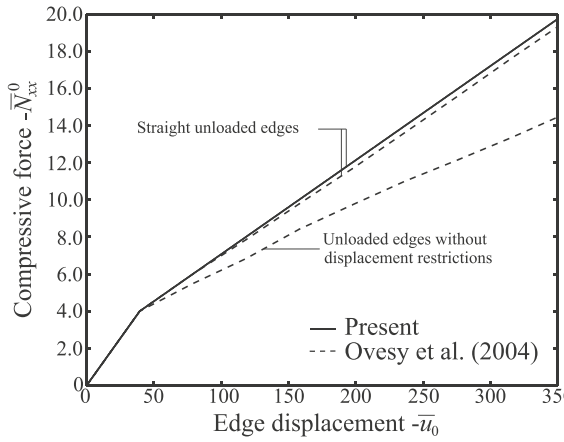


Fig. 18.5 Comparison of the results according to the current method for the boundary displacement $\bar{u}_0$ for different inplane boundary conditions at the unloaded longitudinal edges with the results according to Ovesy et al. for an isotropic perfect square plate as a function of the applied compressive load $\bar{N}^0_{xx}$

assumption and the current method is excellent, even for large degrees of postbuckling. The results emphasize the importance of the boundary conditions for the inplane displacements $\bar{u}_0$ and $\bar{v}_0$. Against this background, the results of Fig. 18.4 must be considered anew.

18.2.5.3 Imperfect Isotropic Plates with Simply Supported and Clamped Unloaded Longitudinal Edges (Yamaki 1959)

As early as 1959, Yamaki investigated the postbuckling behaviour of imperfect isotropic plates under uniaxial compressive load and used series expansions for the plate deflection $\bar{w}_0$ with an otherwise identical procedure as described in the derivation of the current closed-form analytical methods. Yamaki's methodology allowed for various boundary conditions at the loaded and unloaded edges. For square plates with the Poisson's ratio $\nu = \frac{1}{3}$, Yamaki determined a large number of numerical results for the postbuckling amplitude $\bar{f}$, the edge displacement $\bar{u}_0$ and the effective width $\bar{b}_{\text{eff}}$. Figure 18.6 shows a comparison of the current methods for the postbuckling amplitude $\bar{f} + \bar{f}_i$ as a function of the applied compressive load $\bar{N}^0_{xx}$, whereby both perfect plates and imperfect plates with $\frac{f_0}{h} = 0.1$ were considered. In both cases, the agreement is also very good for higher degrees of postbuckling. Certain deviations are noticeable in the case of the plate with clamped unloaded longitudinal edges (Fig. 18.6, right), which are due to the approximation of the buckling mode and the associated inaccuracy in the bifurcational buckling load. Nevertheless, the present results impressively underline the applicability of the derived methods for postbuckling problems of imperfect plates. A comparison of the results according to the current method with the results according to Yamaki for the edge displacement $\bar{u}_0$ and the effective width $\bar{b}_{\text{eff}}$ of a square isotropic plate with simply supported unloaded longitudinal edges can be found in Fig. 18.7. In the left part of this figure, the results according to Yamaki were only provided for the perfect

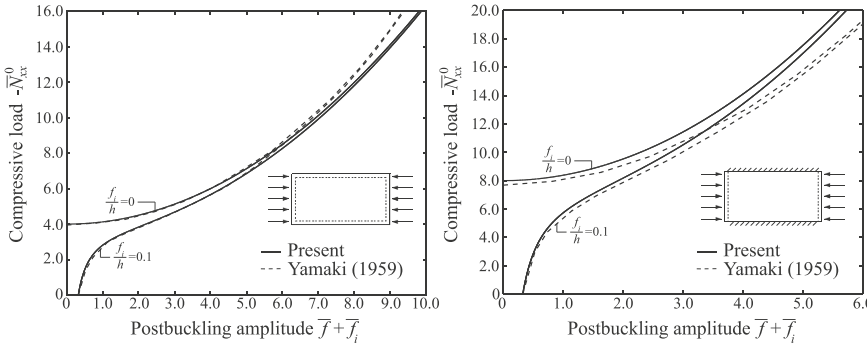


Fig. 18.6 Comparison of the results according to the current method for the postbuckling amplitude $\bar{f} + \bar{f}_i$ with the results according to Yamaki for isotropic imperfect square plates as a function of the applied compressive load $\bar{N}^0_{xx}$; Plate with simply supported unloaded plate edges (left), plate with clamped unloaded plate edges (right)

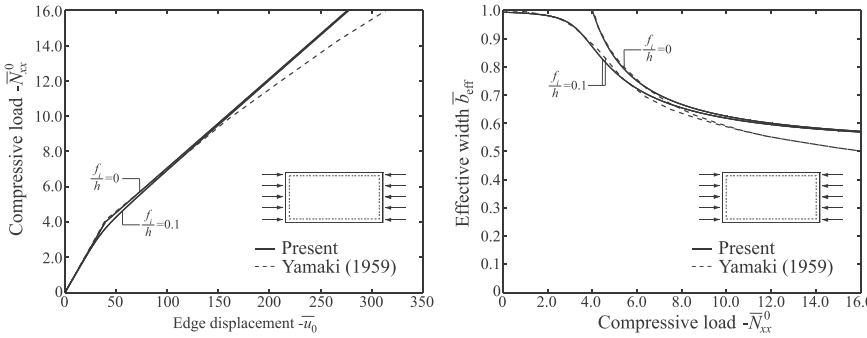


Fig. 18.7 Comparison of the results according to the present method with the results according to Yamaki for the edge displacement $\bar{u}_0$ (left) and the effective width $\bar{b}_{\text{eff}}$ (right) of a square isotropic imperfect plate as a function of the applied compressive load $\bar{N}_{xx}^0$

plate, as they are almost identical to the results for the imperfect plate for this example. Also, for the results shown in Fig. 18.7 for the state variables of the plate in the postbuckling range, there is a very good match between the present method and the results according to Yamaki.

18.2.5.4 Perfect Angle-Ply Laminates with Simply Supported Unloaded Edges (Shin et al. 1993)

Shin et al. (1993) carried out postbuckling analyses on symmetric angle-ply laminates simply supported at all edges under uniaxial compressive load and used a Fourier series expansion for the postbuckling amplitude $\bar{f}$. Airy's stress function was determined from the requirement for compatibility of the membrane strains. Finally, free constants were determined from the principle of the minimum of the elastic potential. Nonlinear finite element analyses were also carried out for comparison purposes. It is noteworthy that the methodology according to Shin et al. automatically leads to straight unloaded plate edges in the postbuckling state (see also Fig. 18.2, right), so that a direct comparability with the current closed-form analysis method is possible. Figure 18.8 shows the resulting edge displacement $\bar{u}_0$ as a function of the postbuckling amplitude $\bar{f}$ for a square four-ply laminate with the layup $[+45°/-45°]_S$. Overall, the results are in satisfactory agreement. Greater deviations are found at higher degrees of postbuckling, which is probably due to the bending-twisting coupling (expressed by the terms D_{16} and D_{26} in the material law), which is quite significant for the laminate considered here and has been neglected so far. In order to estimate the influence of bending-twisting coupling, Shin et al. also considered laminates with higher numbers of layers. It is known that the influence of the terms D_{16} and D_{26} decreases as the number of layers increases. A comparison for laminates with the layups $\left[(+45°/-45°)_6\right]_S$ and $\left[(+45°/-45°)_{24}\right]_S$ can be found in Fig. 18.9. It can be seen that the influence of the bending-twisting coupling on the postbuckling behaviour is indeed strongly reduced and that

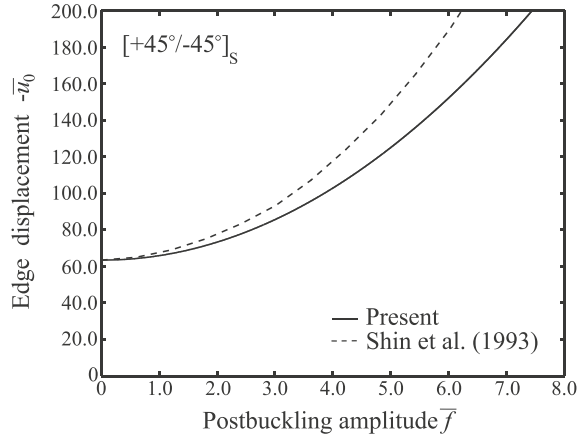


Fig. 18.8 Comparison of the results according to the present method with the results according to Shin et al. for a perfect square laminate with the layup $[+45°/-45°]_S$; edge displacement $\bar{u}_0$ as a function of the postbuckling amplitude $\bar{f}$

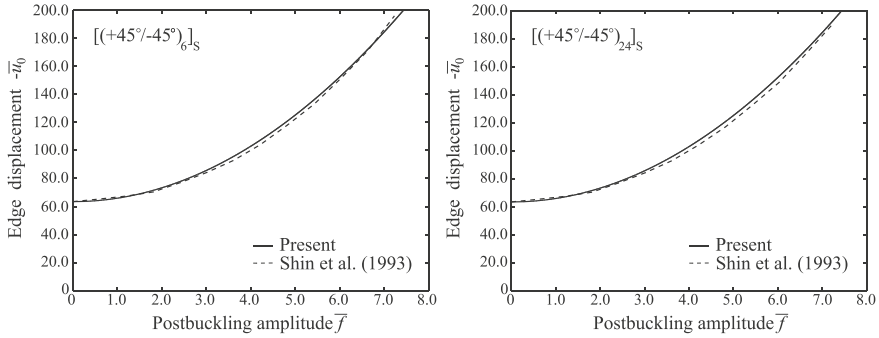


Fig. 18.9 Comparison of the results according to the present method with the results according to Shin et al. for perfect square laminates with the layups $[(+45°/-45°)_6]_S$ (left) and $[(+45°/-45°)_{24}]_S$ (right); edge displacement $\bar{u}_0$ as a function of the postbuckling amplitude $\bar{f}$

both the present method and the approach by Shin et al. produce almost identical results, which speaks in favour of the credibility of the analysis method presented here.

18.3 Postbuckling Behaviour of Laminates Under Shear

In the following, an analysis approach is outlined that can be used to investigate the postbuckling behaviour of laminates under inplane shear loading (Mittelstedt et al. 2011).

18.3.1 Given Situation and Boundary Conditions

We consider a laminate (Fig. 18.10) with length a and width b under a constant inplane shear load N^0_{xy}. To enable a closed-form analytical solution under this complex load case, we assume an infinitely long laminate strip with $a \to \infty$. The present laminates are symmetric cross-ply laminates for which we can state the constitutive law as:

$$\begin{pmatrix} N^0_{xx} \\ N^0_{yy} \\ N^0_{xy} \\ M^0_{xx} \\ M^0_{yy} \\ M^0_{xy} \end{pmatrix} = \begin{bmatrix} A_{11} & A_{12} & 0 & 0 & 0 & 0 \\ A_{12} & A_{22} & 0 & 0 & 0 & 0 \\ 0 & 0 & A_{66} & 0 & 0 & 0 \\ 0 & 0 & 0 & D_{11} & D_{12} & 0 \\ 0 & 0 & 0 & D_{12} & D_{22} & 0 \\ 0 & 0 & 0 & 0 & 0 & D_{66} \end{bmatrix} \begin{pmatrix} \varepsilon^0_{xx} \\ \varepsilon^0_{yy} \\ \gamma^0_{xy} \\ \kappa^0_{xx} \\ \kappa^0_{yy} \\ \kappa^0_{xy} \end{pmatrix}. \tag{18.74}$$

Two types of boundary conditions are considered. For the first plate, simply supported longitudinal edges are considered (so-called SSSS plate, Fig. 18.10, top right), while for the second plate situation, clamped longitudinal edges are assumed (CCCC plate, Fig. 18.10, bottom right). The boundary conditions for both the SSSS plate and the CCCC plate at the longitudinal edges are as follows:

$$w_0(y = 0) = 0, \quad w_0\,(y = b) = 0. \tag{18.75}$$

The boundary conditions at the unloaded edges of the SSSS plate with regard to the bending moments M^0_{yy} are as follows:

$$M^0_{yy}(y = 0) = -D_{22}\left.\frac{\partial^2 w_0}{\partial y^2}\right|_{y=0} = 0, \quad M^0_{yy}(x_2 = b) = -D_{22}\left.\frac{\partial^2 w_0}{\partial y^2}\right|_{y=b} = 0. \tag{18.76}$$

Here we have utilized the fact that $\frac{\partial^2 w_0}{\partial x^2}$ disappears at the edges $y = 0$ and $y = b$.

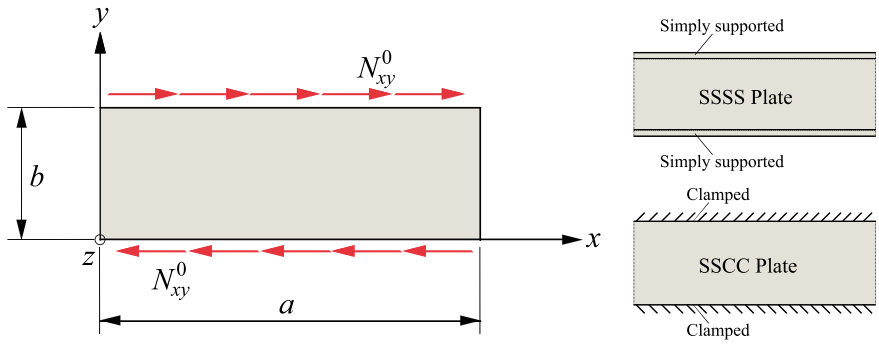


Fig. 18.10 Given situation and boundary conditions

In the case of CCCC plates, the edge rotations must become zero:

$$\left.\frac{\partial w_0}{\partial y}\right|_{y=0} = 0, \quad \left.\frac{\partial w_0}{\partial y}\right|_{y=b} = 0. \tag{18.77}$$

Since the considered laminates are assumed to be infinitely long, no boundary conditions are specified at the transverse edges.

18.3.2 Basic Equations

Buckling of a symmetric orthotropic laminate under inplane shear load N_{xy}^0 is governed by the following homogeneous partial differential equation of fourth order:

$$D_{11}\frac{\partial^4 w_0}{\partial x^4} + D_{22}\frac{\partial^4 w_0}{\partial y^4} + 2\left(D_{12} + 2D_{66}\right)\frac{\partial^4 w_0}{\partial x^2 \partial y^2} + 2N_{xy}^0\frac{\partial^2 w_0}{\partial x \partial y} = 0. \tag{18.78}$$

Since this equation does not allow an exact solution for the given load case, we will use an energy formulation instead. The elastic potential Π of the buckled laminate, consisting of the internal potential Π_i and the external potential Π_a of the applied load, can be written as follows:

$$\begin{aligned}\Pi_i = \int_0^b \int_0^{\lambda_1} \Bigg[&\frac{D_{11}}{2}\left(\frac{\partial^2 w_0}{\partial x^2}\right)^2 + \frac{D_{22}}{2}\left(\frac{\partial^2 w_0}{\partial y^2}\right)^2 \\ &+ D_{12}\frac{\partial^2 w_0}{\partial x^2}\frac{\partial^2 w_0}{\partial y^2} + 2D_{66}\left(\frac{\partial^2 w_0}{\partial x \partial y}\right)^2\Bigg] \mathrm{d}x\mathrm{d}y, \\ \Pi_a = -N_{xy}^0 \int_0^b \int_0^{\lambda_1} &\frac{\partial w_0}{\partial x}\frac{\partial w_0}{\partial y}\mathrm{d}x\mathrm{d}y. \end{aligned} \tag{18.79}$$

This formulation, together with suitable shape functions for the buckling mode $w_{0,\mathrm{init}}$, is later used for the derivation of closed-form analytical expressions for the buckling load $N_{xy,\mathrm{init}}^0$.

The postbuckling problem is treated as a geometrically nonlinear problem in the v. Kármán sense, which leads to the two coupled partial differential equations (18.14) and (18.21) with respect to the unknown postbuckling mode w_0 and Airy's stress function F. The imperfections w_i can be regarded as known a priori and must be defined in advance.

18.3.3 Laminates with Simply Supported Longitudinal Edges (SSSS Plates)

18.3.3.1 Buckling Analysis

Before an approximation approach for the postbuckling analysis is discussed, it is important to determine a closed-form solution for the bifurcational buckling load $N^0_{xy,\text{init}}$, which appears later in all postbuckling equations. For this purpose, the buckling mode $w_{0,\text{init}}$ is assumed in the following form:

$$w_{0,\text{init}} = W \sin\left[\frac{\pi}{\lambda_1}(x - \lambda_2 y)\right] \sin\left(\frac{\pi y}{b}\right), \tag{18.80}$$

where W represents the buckling amplitude, whereas λ_1 and λ_2 describe the length of a buckling half-wave and the inclination of the buckling pattern respectively. A graphical representation of (18.80) is shown in Fig. 18.11. The buckling mode according to (18.80) is a generalization of a shape function as it was used by Timoshenko for the buckling analysis of isotropic plates under inplane shear (Timoshenko and Gere 1961). Insertion of (18.80) into the potential formulation (18.79) and evaluation of the buckling condition

$$\frac{\partial}{\partial W}(\Pi_i + \Pi_a) = 0 \tag{18.81}$$

finally leads to the following closed-form analytical solution for the buckling load $N^0_{xy,\text{init}}$:

$$N^0_{xy,\text{init}} = -\pi^2 \frac{D_{11}b^4 + D_{22}\left(\lambda_1^4 + 6\lambda_1^2\lambda_2^2 b^2 + \lambda_2^4 b^4\right) + 2\left(D_{12} + 2D_{66}\right)\left(\lambda_1^2 + \lambda_2^2 b^2\right) b^2}{2\lambda_1^2\lambda_2 b^4}. \tag{18.82}$$

The unknown quantities λ_1 and λ_2 are determined from the requirement that the minimum is sought among all possible solutions $N^0_{xy,\text{init}}(\lambda_1, \lambda_2)$, which leads to the following two requirements for the buckling load $N^0_{xy,\text{init}}$:

$$\frac{\partial N^0_{xy,\text{init}}}{\partial \lambda_1} = 0, \quad \frac{\partial N^0_{xy,\text{init}}}{\partial \lambda_2} = 0. \tag{18.83}$$

Evaluating (18.83) leads to the following two equations:

$$\begin{aligned} \lambda_1 &= b\sqrt[4]{\frac{D_{11} + D_{22}\lambda_2^4 + 2\left(D_{12} + 2D_{66}\right)\lambda_2^2}{D_{22}}}, \\ \lambda_2 &= -\frac{\sqrt{\lambda_3 - 3D_{22}\lambda_1^2 - \left(D_{12} + 2D_{66}\right)b^2}}{\sqrt{3D_{22}}b}, \end{aligned} \tag{18.84}$$

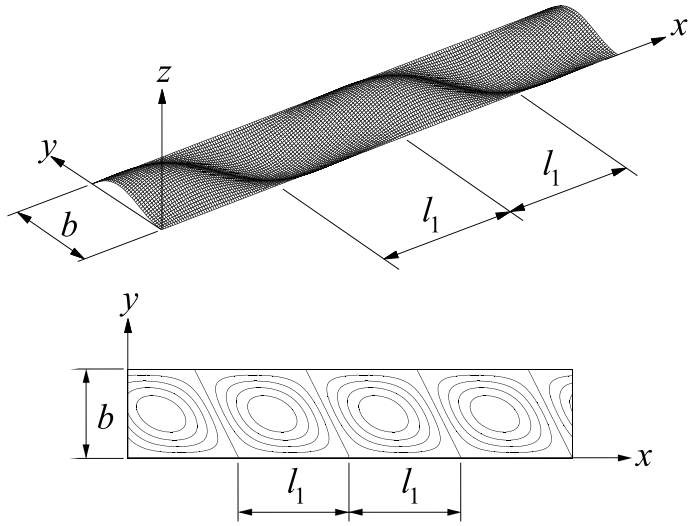


Fig. 18.11 Buckling mode of the SSSS plate

with

$$\lambda_3 = \sqrt{12 D_{22} \lambda_1^2 \left[D_{22} \lambda_1^2 + (D_{12} + 2D_{66})\, b^2 \right] + \left[3 D_{11} D_{22} + (D_{12} + 2D_{66})^2 \right] b^4}. \tag{18.85}$$

Obviously, explicit expressions for λ_1 and λ_2 are difficult to determine from (18.84) with (18.85), so that the following iterative approach is suitable. An initial value $\lambda_1 = \lambda_{1,0}$ is estimated, whereby for the sake of simplicity it is suggested that $\lambda_{1,0}$ is equal to the plate width b. Using $\lambda_{1,0} = b$, the first iteration leads to a first estimate of $\lambda_2 = \lambda_{2,1}$. This results in a new value $\lambda_1 = \lambda_{1,1}$, which leads to an updated value $\lambda_2 = \lambda_{2,2}$, and so on. This process is repeated until, in iteration step i, $\lambda_{1,i} \simeq \lambda_{1,i-1}$ and $\lambda_{2,i} \simeq \lambda_{2,i-1}$, with a desired degree of accuracy. For all subsequent examples, no more than 4–5 iterations were required to obtain convergent results for λ_1 and λ_2.

18.3.3.2 Postbuckling Analysis

The postbuckling mode w_0 and the imperfection w_i are assumed to be identical to the buckling mode $w_{0,\text{init}}$:

$$\begin{aligned} w_0 &= f \sin\left[\frac{\pi}{\lambda_1}(x - \lambda_2 y)\right] \sin\left(\frac{\pi y}{b}\right), \\ w_i &= f_0 \sin\left[\frac{\pi}{\lambda_1}(x - \lambda_2 y)\right] \sin\left(\frac{\pi y}{b}\right). \end{aligned} \tag{18.86}$$

Here, f is the unknown postbuckling amplitude that must be determined, while f_0 is the amplitude of the imperfections and can be considered a known quantity.

The homogeneous equation (18.21) describes the stress state in the laminate before buckling begins and results in the homogeneous solution by double integration of the applied load N_{xy}^0:

$$F_h = -\int \left(\int N_{xy}^0 \mathrm{d}x \right) \mathrm{d}y + B_1 y + B_2. \tag{18.87}$$

Without loss of generality of the solution, the constants B_1 and B_2 can be neglected. Performing the integration according to (18.87) leads to:

$$F_h = -N_{xy}^0 xy. \tag{18.88}$$

The particular solution F_p is determined by inserting (18.86) into (18.21) and using the relationships $\cos^2(a) = \frac{1}{2}(1 + \cos(2a))$, $\sin^2(a) = \frac{1}{2}(1 - \cos(2a))$, which finally leads to the following representation of (18.21):

$$\begin{aligned} a_{22}\frac{\partial^4 F_p}{\partial x^4} + a_{11}\frac{\partial^4 F_p}{\partial y^4} + (2a_{12} + a_{66})\frac{\partial^4 F_p}{\partial x^2 \partial y^2} \\ = \frac{f\,(f + 2f_0)\,\pi^4}{2\lambda_1^2 b^2}\left\{ \cos\left[\frac{2\pi}{\lambda_1}(x - \lambda_2 y)\right] + \cos\left(\frac{2\pi y}{b}\right)\right\}. \end{aligned} \tag{18.89}$$

With the help of a solution approach for F_p in the form of the right-hand side term of (18.89)

$$F_p = C_1 \cos\left[\frac{2\pi}{\lambda_1}(x - \lambda_2 y)\right] + C_2 \cos\left(\frac{2\pi y}{b}\right) \tag{18.90}$$

the following representation for the constants C_1 and C_2 results from (18.89) by comparing the coefficients:

$$C_1 = \frac{f\,(f + 2f_0)\,\lambda_1^2}{32b^2\left[a_{11}\lambda_2^4 + a_{22} + (2a_{12} + a_{66})\,\lambda_2^2\right]}, \quad C_2 = \frac{f\,(f + 2f_0)\,b^2}{32a_{11}\lambda_1^2}. \tag{18.91}$$

The total solution for the Airy stress function F then results from the addition of (18.88) and (18.90) with (18.91):

$$\begin{aligned} F = F_h + F_p = -N_{xy}^0 xy \\ + \frac{f\,(f + 2f_0)\,\lambda_1^2}{32b^2\left[a_{11}\lambda_2^4 + a_{22} + (2a_{12} + a_{66})\,\lambda_2^2\right]} \cos\left[\frac{2\pi}{\lambda_1}(x - \lambda_2 y)\right] \\ + \frac{f\,(f + 2f_0)\,b^2}{32a_{11}\lambda_1^2} \cos\left(\frac{2\pi y}{b}\right). \end{aligned} \tag{18.92}$$

The remaining equation (18.14) cannot be solved in closed form, but is fulfilled in an integral sense by a Galerkin formulation as follows:

$$\int_0^{\lambda_1} \left(\int_0^b L\left(w_0,\, F\right) w_{0,\mathrm{init}} \mathrm{d}y \right) \mathrm{d}x = 0. \tag{18.93}$$

The operator $L\left(w_0,\, F\right)$ is defined as:

$$\begin{aligned} L\left(w_0,\, F\right) = {} & D_{11}\frac{\partial^4 w_0}{\partial x^4} + 2\left(D_{12}+2D_{66}\right)\frac{\partial^4 w_0}{\partial x^2 \partial y^2} + D_{22}\frac{\partial^4 w_0}{\partial y^4} - \frac{\partial^2 F}{\partial y^2}\left(\frac{\partial^2 w_0}{\partial x^2}+\frac{\partial^2 w_i}{\partial x^2}\right) \\ & + 2\frac{\partial^2 F}{\partial x \partial y}\left(\frac{\partial^2 w_0}{\partial x \partial y}+\frac{\partial^2 w_i}{\partial x \partial y}\right) - \frac{\partial^2 F}{\partial x^2}\left(\frac{\partial^2 w_0}{\partial y^2}+\frac{\partial^2 w_i}{\partial y^2}\right). \end{aligned} \tag{18.94}$$

Inserting the postbuckling shape w_0, the imperfection w_i and the Airy stress function F according to (18.86) or (18.92) and performing the integrations as prescribed in (18.93) with (18.94) with the abbreviation

$$\gamma = \frac{b}{a_{11}\lambda_1^3} + \frac{\lambda_1}{\left[a_{11}\lambda_2^4 + a_{22} + \left(2a_{12}+a_{66}\right)\lambda_2^2\right] b^3} \tag{18.95}$$

finally leads to the following cubic polynomial for the unknown postbuckling amplitude f:

$$\frac{\pi^2\gamma}{64} f^3 + \frac{3\pi^2\gamma}{64} f^2 f_0 + \frac{1}{2}\left[\frac{\pi^2\gamma f_0^2}{16} - \frac{\left(N_{xy}^0 + N_{xy,\mathrm{init}}^0\right)\lambda_2 b}{\lambda_1}\right] f - \frac{\lambda_2 b f_0}{2\lambda_1} N_{xy}^0 = 0. \tag{18.96}$$

This equation has only one relevant real root:

$$f = f_0\left(\frac{f_0}{3\gamma_1} - 1\right) + \gamma_1 + \frac{32 a_{11}\lambda_1^2\lambda_2\left[a_{11}\lambda_2^4 + a_{22} + \left(2a_{12}+a_{66}\right)\lambda_2^2\right]\left(N_{xy,\mathrm{init}}^0 + N_{xy}^0\right)}{3\pi^2\gamma_1\left[\frac{a_{11}}{b^4}\left(\lambda_1^4 + \lambda_2^4 b^4\right) + a_{22} + \left(2a_{12}+a_{66}\right)\lambda_2^2\right]}, \tag{18.97}$$

in which the following abbreviations were used:

$$\begin{aligned} \gamma_1 &= \sqrt[3]{\frac{\sqrt{\gamma_2}}{9\pi^3\lambda_1\gamma} - \frac{16 N_{xy,\mathrm{init}}^0 \lambda_2 b f_0}{\pi^2\lambda_1\gamma}}, \\ \gamma_2 &= -3\pi^6\lambda_1^2\gamma^2 f_0^6 - 288\pi^4\lambda_1\lambda_2 b f_0^4\gamma\left(N_{xy}^0 + N_{xy,\mathrm{init}}^0\right) - 98304\frac{\lambda_2^3 b^3}{\lambda_1\gamma}\left(N_{xy}^0 + N_{xy,\mathrm{init}}^0\right)^3 \\ &\quad - 2304\pi^2\lambda_2^2 b^2 f_0^2\left(2N_{xy}^0 + 5N_{xy,\mathrm{init}}^0\right)\left(2N_{xy}^0 - N_{xy,\mathrm{init}}^0\right). \end{aligned} \tag{18.98}$$

In the case of a perfect plate with $f_0 = 0$, the characteristic polynomial (18.96) for determining the postbuckling amplitude f can be simplified as follows:

$$\frac{\pi^4\left[a_{11}\left(\lambda_1^4+\lambda_2^4b^4\right)+a_{22}b^4+\left(2a_{12}+a_{66}\right)\lambda_2^2b^4\right]}{64a_{11}\left[a_{11}\lambda_2^4+a_{22}+\left(2a_{12}+a_{66}\right)\lambda_2^2\right]\lambda_1^3b^3}f^3-\frac{\lambda_2b\pi^2\left(N^0_{xy,\text{init}}+N^0_{xy}\right)}{2\lambda_1}f=0. \tag{18.99}$$

In addition to the trivial solution $f = 0$, the following two roots can be specified:

$$f=\pm\frac{4b^2\lambda_1}{\pi}\sqrt{\frac{2a_{11}\left[a_{11}\lambda_2^4+a_{22}+\left(2a_{12}+a_{66}\right)\lambda_2^2\right]\left(N^0_{xy}+N^0_{xy,\text{init}}\right)\lambda_2}{a_{11}\left(\lambda_1^4+\lambda_2^4b^4\right)+a_{22}b^4+\left(2a_{12}+a_{66}\right)\lambda_2^2b^4}}. \tag{18.100}$$

Ultimately, the membrane force flows in the buckled plate can be determined as follows:

$$\begin{aligned}
N^0_{xx,post}&=\frac{\partial^2F}{\partial y^2}=-\frac{f\left(f+2f_0\right)\pi^2}{8}\\
&\quad\times\left\{\frac{\lambda_2^2\cos\left[\frac{2\pi}{\lambda_1}\left(x-\lambda_2y\right)\right]}{b^2\left[a_{11}\lambda_2^4+a_{22}+\left(2a_{12}+a_{66}\right)\lambda_2^2\right]}+\frac{\cos\left(\frac{2\pi y}{b}\right)}{a_{11}\lambda_1^2}\right\},\\
N^0_{yy,post}&=\frac{\partial^2F}{\partial x^2}=-\frac{f\left(f+2f_0\right)\pi^2\cos\left[\frac{2\pi}{\lambda_1}\left(x-\lambda_2y\right)\right]}{8b^2\left[a_{11}\lambda_2^4+a_{22}+\left(2a_{12}+a_{66}\right)\lambda_2^2\right]},\\
N^0_{xy,post}&=-\frac{\partial^2F}{\partial x\partial y}=N^0_{xy}-\frac{f\left(f+2f_0\right)\lambda_2\pi^2\cos\left[\frac{2\pi}{\lambda_1}\left(x-\lambda_2y\right)\right]}{8b^2\left[a_{11}\lambda_2^4+a_{22}+\left(2a_{12}+a_{66}\right)\lambda_2^2\right]}.
\end{aligned} \tag{18.101}$$

18.3.4 Laminates with Clamped Longitudinal Edges (CCCC Plates)

18.3.4.1 Buckling Analysis

The following buckling mode is assumed for the buckling analysis of the CCCC plate:

$$w_{0,\text{init}}=\frac{W}{2}\sin\left[\frac{\pi}{\lambda_1}\left(x-\lambda_2y\right)\right]\left[1-\cos\left(\frac{2\pi y}{b}\right)\right]. \tag{18.102}$$

Inserting (18.102) into the potential formulation (18.79) and evaluating the buckling condition (18.81) yields:

$$N^0_{xy,\text{init}}=-\pi^2\frac{3D_{11}b^4+D_{22}\left(16\lambda_1^4+24\lambda_1^2\lambda_2^2b^2+3\lambda_2^4b^4\right)+2\left(D_{12}+2D_{66}\right)\left(4\lambda_1^2+3\lambda_2^2b^2\right)b^2}{6\lambda_1^2\lambda_2b^4}.$$

The requirements (18.83) lead to the following two expressions for the unknown variables λ_1 and λ_2:

$$\lambda_1 = \frac{b}{2}\sqrt[4]{3\frac{D_{11} + D_{22}\lambda_2^4 + 2\left(D_{12} + 2D_{66}\right)\lambda_2^2}{D_{22}}},$$
$$\lambda_2 = -\frac{\sqrt{\lambda_3 - 4D_{22}\lambda_1^2 - \left(D_{12} + 2D_{66}\right)b^2}}{\sqrt{3D_{22}}b}, \tag{18.103}$$

with

$$\lambda_3 = \sqrt{16D_{22}\left[2D_{22}\lambda_1^2 + \left(D_{12} + 2D_{66}\right)b^2\right]\lambda_1^2 + \left[3D_{11}D_{22} + \left(D_{12} + 2D_{66}\right)^2\right]b^4}. \tag{18.104}$$

The iterative determination of λ_1 and λ_2 can be carried out as described in the previous section.

18.3.4.2 Postbuckling Analysis

For the postbuckling analysis of the CCCC plate, the postbuckling mode w_0 and the imperfection w_i are again assumed in the same functional form as the buckling mode $w_{0,\text{init}}$:

$$w_0 = \frac{f}{2}\sin\left[\frac{\pi}{\lambda_1}\left(x - \lambda_2 y\right)\right]\left[1 - \cos\left(\frac{2\pi y}{b}\right)\right],$$
$$w_i = \frac{f_0}{2}\sin\left[\frac{\pi}{\lambda_1}\left(x - \lambda_2 y\right)\right]\left[1 - \cos\left(\frac{2\pi y}{b}\right)\right]. \tag{18.105}$$

Analogous to the SSSS plate, the solution for the Airy stress function can again be composed of a homogeneous and a particular solution. At present, one obtains

$$\begin{aligned} F = &-N_{xy}^0 xy \\ &+ f\left(f + 2f_0\right)\left\{D_1\cos\left(\frac{2\pi y}{b}\right) + D_2\cos\left(\frac{4\pi y}{b}\right) + D_3\cos\left[\frac{2\pi}{\lambda_1}\left(x - \lambda_2 y\right)\right]\right. \\ &\left. + D_4\cos\left[\frac{2\pi}{\lambda_1}\left(x - \lambda_2 y\right)\right]\cos\left(\frac{2\pi y}{b}\right) + D_5\sin\left[\frac{2\pi}{\lambda_1}\left(x - \lambda_2 y\right)\right]\sin\left(\frac{2\pi y}{b}\right)\right\}, \end{aligned} \tag{18.106}$$

with:

$$D_1 = \frac{b^2}{32a_{11}\lambda_1^2}, \quad D_2 = -\frac{b^2}{512a_{11}\lambda_1^2}, \quad D_3 = \frac{\lambda_1^2}{32\left[a_{11}\lambda_2^4 + a_{22} + \lambda_2^2\left(2a_{12} + a_{66}\right)\right]b^2},$$
$$D_4 = -\frac{\overline{D}_1}{32\overline{D}_2}, \quad D_5 = \frac{\overline{D}_3}{16\overline{D}_2}, \tag{18.107}$$

and:

$$\begin{aligned}
\overline{D}_1 &= \lambda_1^2 b^2 \left[a_{11}\left(\lambda_1^4 + 6b^2\lambda_1^2\lambda_2^2 + b^4\lambda_2^4\right) + a_{22}b^4 + (2a_{12} + a_{66})\left(\lambda_1^2 + b^2\lambda_2^2\right)b^2\right], \\
\overline{D}_2 &= a_{11}^2 (b\lambda_2 - \lambda_1)^4 (b\lambda_2 + \lambda_1)^4 + a_{22}^2 b^8 + \left(a_{66}^2 + 4a_{12}^2\right)(b\lambda_2 - \lambda_1)^2 (b\lambda_2 + \lambda_1)^2 b^4 \\
&\quad + 2a_{11}a_{22}\left(6b^2\lambda_1^2\lambda_2^2 + b^4\lambda_2^4 + \lambda_1^4\right)b^4 \\
&\quad + 2a_{11}(2a_{12} + a_{66})\left(b^2\lambda_2^2 + \lambda_1^2\right)(b\lambda_2 - \lambda_1)^2 (b\lambda_2 + \lambda_1)^2 b^2 \\
&\quad + 2a_{22}(2a_{12} + a_{66})\left(b^2\lambda_2^2 + \lambda_1^2\right)b^6 + 4a_{12}a_{66}(b\lambda_2 - \lambda_1)^2 (b\lambda_2 + \lambda_1)^2 b^4, \\
\overline{D}_3 &= \lambda_1^3\lambda_2\left[2a_{11}\left(b^2\lambda_2^2 + \lambda_1^2\right) + b^2(2a_{12} + a_{66})\right]b^3.
\end{aligned} \tag{18.108}$$

Evaluating the Galerkin formulation (18.93) with (18.94) and introducing the abbreviation

$$\gamma = \frac{3b^2\lambda_2}{2\pi^2(2D_1 - 2D_2 + 2D_3 - D_4)} \tag{18.109}$$

finally leads to the following cubic polynomial for the unknown postbuckling amplitude f in the case of the CCCC plate:

$$f(f + 2f_0)(f + f_0) - \gamma\left[f\left(N_{xy,\text{init}}^0 + N_{xy}^0\right) + N_{xy}^0 f_0\right] = 0. \tag{18.110}$$

Equation (18.110) has only one relevant and real root:

$$f = \gamma_1 + \frac{f_0^2 + \gamma\left(N_{xy,\text{init}}^0 + N_{xy}^0\right)}{3\gamma_1} - f_0, \tag{18.111}$$

whereby the following abbreviations were used for the sake of simplicity:

$$\begin{aligned}
\gamma_1 &= \sqrt[3]{-\frac{f_0 N_{xy,\text{init}}^0 \gamma}{2} + \frac{\sqrt{\gamma_2}}{18}}, \\
\gamma_2 &= -12\gamma^3\left(N_{xy,\text{init}}^0 + N_{xy}^0\right)^3 - 12f_0^6 - 36f_0^4\gamma\left(N_{xy,\text{init}}^0 + N_{xy}^0\right) \\
&\quad - 9f_0^2\gamma^2\left(2N_{xy}^0 + 5N_{xy,\text{init}}^0\right)\left(2N_{xy}^0 - N_{xy,\text{init}}^0\right).
\end{aligned} \tag{18.112}$$

In the case of a perfect plate with $f_0 = 0$, the following characteristic polynomial (18.110) is used to determine the postbuckling amplitude:

$$f^3 - \gamma f\left(N_{xy,\text{init}}^0 + N_{xy}^0\right) = 0. \tag{18.113}$$

In addition to the trivial solution $f = 0$, the following two roots can be specified:

$$f = \pm\sqrt{\gamma\left(N_{xy,\text{init}}^0 + N_{xy}^0\right)}. \tag{18.114}$$

The membrane forces in the buckled plate can be determined as:

$$
\begin{aligned}
N^0_{xx,post} &= 4f\,(f+2f_0)\,\pi^2\Psi_1\,(x,y)\,,\\
N^0_{yy,post} &= -\frac{4f\,(f+2f_0)\,\pi^2}{\lambda_1^2}\Psi_2\,(x,y)\,,\\
N^0_{xy,post} &= N^0_{xy} - \frac{4f\,(f+2f_0)\,\pi^2}{\lambda_1}\Psi_3\,(x,y)\,,
\end{aligned}
\tag{18.115}
$$

in which the following abbreviations have been introduced for the sake of simplicity:

$$
\begin{aligned}
\Psi_1\,(x,y) = &-\frac{D_1}{b^2}\cos\left(\frac{2\pi y}{b}\right) - \frac{4D_2}{b^2}\cos\left(\frac{4\pi y}{b}\right)\\
&- \frac{1}{\lambda_1^2}\left[\frac{D_4\left(\lambda_1^2+\lambda_2^2b^2\right)+2D_5\lambda_1\lambda_2 b}{b^2}\cos\left(\frac{2\pi y}{b}\right) + D_3\lambda_2^2\right]\cos\left[\frac{2\pi\,(\lambda_2 y - x)}{\lambda_1}\right]\\
&+ \frac{2D_4\lambda_1\lambda_2 b + D_5\left(\lambda_1^2+\lambda_2^2b^2\right)}{\lambda_1^2 b^2}\sin\left[\frac{2\pi\,(\lambda_2 y - x)}{\lambda_1}\right]\sin\left(\frac{2\pi y}{b}\right),\\
\Psi_2\,(x,y) = &\left[D_3 + D_4\cos\left(\frac{2\pi x_2}{b}\right)\right]\cos\left[\frac{2\pi\,(x-\lambda_2 y)}{\lambda_1}\right]\\
&+ D_5\sin\left[\frac{2\pi\,(x-\lambda_2 y)}{\lambda_1}\right]\sin\left(\frac{2\pi y}{b}\right),\\
\Psi_3\,(x,y) = &\left(\frac{D_4}{b} + \frac{D_5\lambda_2}{\lambda_1}\right)\sin\left[\frac{2\pi\,(x-\lambda_2 y)}{\lambda_1}\right]\sin\left(\frac{2\pi y}{b}\right)\\
&+ \left[\frac{D_3\lambda_2}{\lambda_1} + \left(\frac{D_4\lambda_2}{\lambda_1} + \frac{D_5}{b}\right)\cos\left(\frac{2\pi y}{b}\right)\right]\cos\left[\frac{2\pi\,(x-\lambda_2 y)}{\lambda_1}\right].
\end{aligned}
\tag{18.116}
$$

18.3.5 Results and Discussion

The results for the buckling analysis are compared with FEM calculations. For comparison purposes, the width b of the plates was chosen based on typical aircraft skin parts with $b = 200\,\text{mm}$. It should be remembered that, strictly speaking, the methods of buckling analysis shown only apply to infinitely long plates. For this reason, the length a of the finite element model was kept variable in order to investigate the influence of the length a on the accuracy of the analytical approaches. Isotropic aluminium plates (modulus of elasticity $E = 73{,}800\,\text{MPa}$, Poisson's ratio $\nu = 0.33$) and symmetric cross-ply laminates $[0°/90°/90°/0°/90°]_S$ with unidirectional fiber-reinforced layers (elastic properties $E_{11} = 157{,}000\,\text{MPa}$, $E_{22} = 8500\,\text{MPa}$, $G_{12} = 4200\,\text{MPa}$, $\nu_{12} = 0.35$) were investigated.

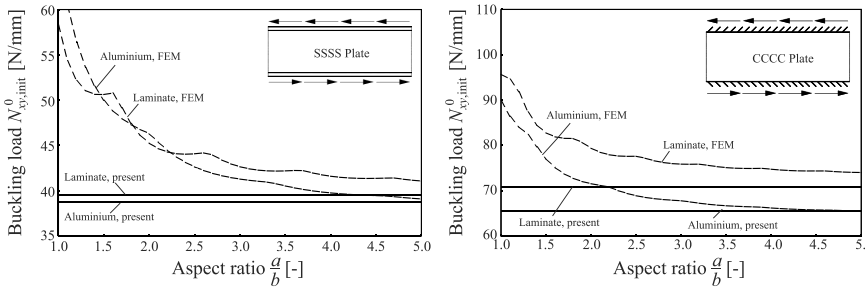


Fig. 18.12 Bifurcational buckling load $N^0_{xy,\text{init}}$ for aluminium plates and laminates

Figure 18.12 shows a comparison of the theoretical results for the buckling loads $N^0_{xy,\text{init}}$ with the results from the finite element calculations. Since the plate length a is not included in the analytical equations, the results from the closed-form analytical solution are constant, regardless of the length a.

For all plates and boundary conditions considered, the following conclusions can be drawn from the results shown in Fig. 18.12. Obviously, the analytical approach underestimates the buckling load $N^0_{xy,\text{init}}$ when plates with low aspect ratios $\frac{a}{b}$ are considered. This is an expected result as it is known that for $\frac{a}{b} \to 0$ the plate buckling loads $N^0_{xy,\text{init}}$ tend to infinite values. At high aspect ratios, the numerical results tend to an asymptotic value, i.e. $N^0_{xy,\text{init}}\,(a \to \infty) = \text{const}$. If aspect ratios of about $\frac{a}{b} \simeq 3.5$ are approximated, as they are realistic for skin sections in aircraft fuselage structures, the differences between the results and the finite element calculations become very small, and apparently the closed-form analytical method provides a quite reasonable estimate of the asymptotic value for $N^0_{xy,\text{init}}\,(a \to \infty)$. Note that in all cases the closed-form analysis approach provides lower values $N^0_{xy,\text{init}}\,(a \to \infty)$ than the FEM analysis, i.e. it is a conservative approach compared to the numerical analysis.

In order to estimate the accuracy of the postbuckling analysis presented in this chapter, the post-buckling deformations and their amplitudes f are analysed. All the following results were determined for plates with length $a = 640\,\text{mm}$. Figure 18.13 contains results for the maximum postbuckling amplitude f of perfect and imperfect ($f_0 = 0.1h$) aluminium plates and orthotropic cross-ply laminates determined with the present method and with finite element analyses for simply supported longitudinal edges (SSSS plates). Analogous results for CCCC plates can be found in Fig. 18.14.

In the finite element calculations, the imperfections w_i were selected in the form of the first buckling mode. In order to obtain numerical postbuckling results for perfect plates, the finite element models were fitted with initial imperfections using a very small amplitude of $f_0 = 0.01h$. The results show that the present analytical approach satisfactorily reproduces the postbuckling deflections in load ranges not too far beyond the bifurcational buckling load $N^0_{xy,\text{init}}$, where the closed-form analytical approach obviously overestimates the post-

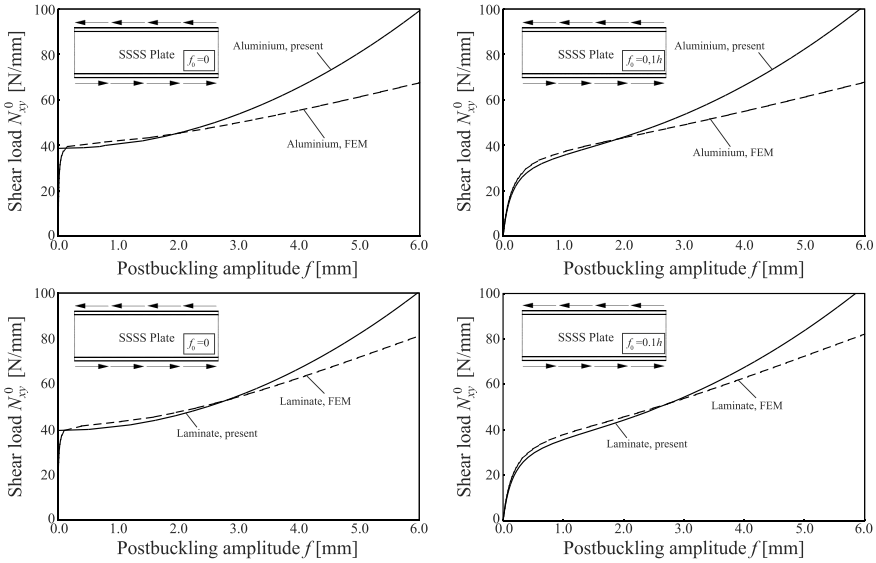


Fig. 18.13 Results for the deflections of perfect and imperfect SSSS plates made of aluminium and orthotropic composites

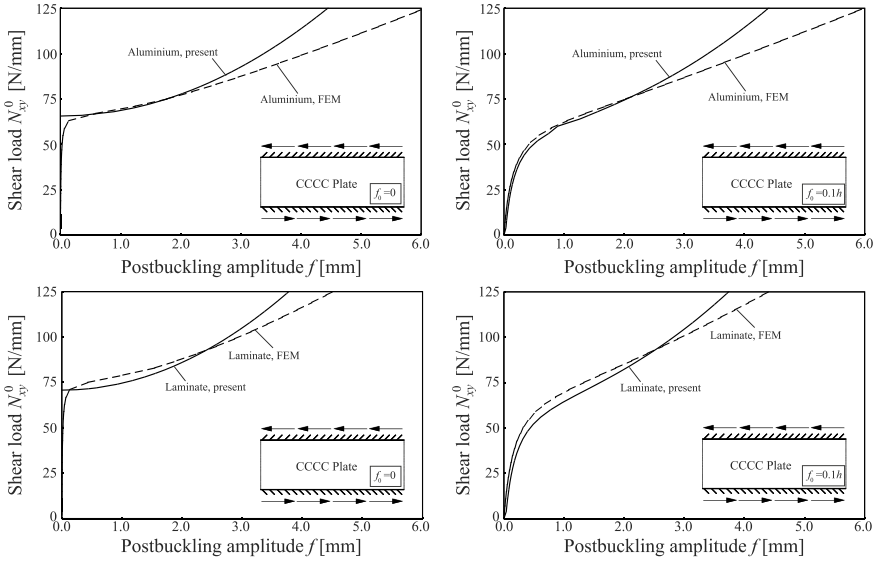


Fig. 18.14 Results for the deflections of perfect and imperfect CCCC plates made of aluminium and orthotropic composites

buckling stiffness of the considered plates. The results show that the outlined analytical approach is valid for load levels that lie within a certain range, where the upper bound is characterised by approximately $N^0_{xy} \simeq \frac{3}{2} N^0_{xy,\text{init}}$ to $N^0_{xy} \simeq 2N^0_{xy,\text{init}}$, depending on the plate material. While this seems to be a strong limitation of the outlined analysis approach, it is important to note that the state of the art in the design of modern aircraft structures allows only a small amount of postbuckling of the skin of a fuselage panel, so that the load levels that can be analyzed with the presented method are sufficient from a lightweight design point of view. The presented closed-form analytical solutions therefore prove to be valuable and fast analysis methods that can be used for such applications that are limited by computational time and effort. This applies in particular to analysis purposes such as pre-design, optimisation procedures or extensive parameter studies.

18.4 Semi-analytical Method

The presented closed-form analysis approaches to the postbuckling behaviour of laminates are naturally limited in their applicability. In order to make more complex load situations and layups accessible to an efficient calculation, semi-analytical methods have been developed in the past, with the help of which postbuckling analyses can be carried out and which not only lead to improved results accuracy, but can generally also treat any laminate structure. Such methods, usually based on a Ritz or Galerkin formulation, require numerical-iterative methods for their solution due to the nonlinear character of the governing equations. In the following, the general procedure is described using symmetric orthotropic laminates under combined loads N^0_{xx}, N^0_{yyy}, N^0_{xy}. The treatment of other layups generally leads to significantly more extensive equations, but does not pose a problem in principle. Let the laminate under consideration be rectangular with length a and width b. In addition, all four edges are simply supported, whereby the consideration of other boundary conditions is generally unproblematic, but requires the provision of suitable shape functions. Again, an imperfect laminate with the imperfections w_i is considered.

The starting point for the considerations are again the differential equations (18.24). For the presently considered case of the symmetric, orthotropic and simply supported laminate, the following series expansions are suitable for the postbuckling deformations as well as for the imperfections:

$$\begin{aligned} \bar{w}_0 &= \sum_{m=1}^{M} \sum_{n=1}^{N} A_{mn} \sin(m\pi\xi_1) \sin(n\pi\xi_2) , \\ \bar{w}_i &= \sum_{m=1}^{M} \sum_{n=1}^{N} B_{mn} \sin(m\pi\xi_1) \sin(n\pi\xi_2) . \end{aligned} \tag{18.117}$$

Here, the coefficients A_{mn} are unknown and the actual goal of the calculation, while the coefficients B_{mn}, which concern the imperfections, can be assumed to be known. If these series expansions are inserted into the compatibility equation in (18.24), the result is

$$\begin{aligned}
&\frac{1}{\alpha_A^2}\frac{\partial^4 \bar{F}}{\partial \xi_1^4} + \alpha_A^2 \frac{\partial^4 \bar{F}}{\partial \xi_2^4} + 2\beta_A \frac{\partial^4 \bar{F}}{\partial \xi_1^2 \partial \xi_2^2} \\
&= \pi^4 \sum_{m=1}^{M}\sum_{n=1}^{N}\sum_{p=1}^{M}\sum_{q=1}^{N} mnpq A_{mn}\left(A_{pq} + 2B_{pq}\right) \\
&\times \cos\left(m\pi\xi_1\right)\cos\left(p\pi\xi_1\right)\cos\left(n\pi\xi_2\right)\cos\left(q\pi\xi_2\right) \\
&\quad - \pi^4 \sum_{m=1}^{M}\sum_{n=1}^{N}\sum_{p=1}^{M}\sum_{q=1}^{N} A_{mn}\left[A_{pq}m^2q^2 + \left(q^2m^2 + p^2n^2\right)B_{pq}\right] \\
&\times \sin\left(m\pi\xi_1\right)\sin\left(p\pi\xi_1\right)\sin\left(n\pi\xi_2\right)\sin\left(q\pi\xi_2\right). \qquad (18.118)
\end{aligned}$$

Firstly, the homogeneous form of (18.118) is considered:

$$\frac{1}{\alpha_A^2}\frac{\partial^4 \bar{F}_\mathrm{h}}{\partial \xi_1^4} + \alpha_A^2 \frac{\partial^4 \bar{F}_\mathrm{h}}{\partial \xi_2^4} + 2\beta_A \frac{\partial^4 \bar{F}_\mathrm{h}}{\partial \xi_1^2 \partial \xi_2^2} = 0. \qquad (18.119)$$

This differential equation describes the membrane state of stress in the laminate before the onset of buckling. Therefore, the individual components of the homogeneous solution $\bar{F}_\mathrm{h}$ can be calculated by integrating the membrane force flows as:

$$\begin{aligned}
\bar{F}_{\mathrm{h}11} &= \int\left(\int \bar{N}_{xx}^0 \pi^2 \mathrm{d}\xi_2\right)\mathrm{d}\xi_2, \\
\bar{F}_{\mathrm{h}22} &= \int\left(\int \bar{N}_{yy}^0 \pi^2 \mathrm{d}\xi_1\right)\mathrm{d}\xi_1, \\
\bar{F}_{\mathrm{h}12} &= -\int\left(\int \bar{N}_{xy}^0 \pi^2 \mathrm{d}\xi_1\right)\mathrm{d}\xi_2. \qquad (18.120)
\end{aligned}$$

Carrying out the integrations prescribed in (18.120) and adding up the individual solution components results in:

$$\bar{F}_\mathrm{h} = \frac{\bar{N}_{xx}^0 \pi^2 \xi_2^2}{2} + \frac{\bar{N}_{yy}^0 \pi^2 \xi_1^2}{2} - \bar{N}_{xy}^0 \pi^2 \xi_1 \xi_2, \qquad (18.121)$$

in which the integration constants that actually appear were neglected without loss of generality.

To find a particular solution, it is useful to rewrite the right-hand side of (18.118) using the following relations:

$$\begin{aligned}
\cos(m\pi\xi_1)\cos(p\pi\xi_1) &= \frac{1}{2}\cos(m\pi\xi_1 - p\pi\xi_1) + \frac{1}{2}\cos(m\pi\xi_1 + p\pi\xi_1)\,,\\
\cos(n\pi\xi_2)\cos(q\pi\xi_2) &= \frac{1}{2}\cos(n\pi\xi_2 - q\pi\xi_2) + \frac{1}{2}\cos(n\pi\xi_2 + q\pi\xi_2)\,,\\
\sin(m\pi\xi_1)\sin(p\pi\xi_1) &= \frac{1}{2}\cos(m\pi\xi_1 - p\pi\xi_1) - \frac{1}{2}\cos(m\pi\xi_1 + p\pi\xi_1)\,,\\
\sin(n\pi\xi_2)\sin(q\pi\xi_2) &= \frac{1}{2}\cos(n\pi\xi_2 - q\pi\xi_2) - \frac{1}{2}\cos(n\pi\xi_2 + q\pi\xi_2)\,.
\end{aligned} \tag{18.122}$$

The following expression then results from the compatibility condition (18.118):

$$\begin{aligned}
&\frac{1}{\alpha_A^2}\frac{\partial^4\bar{F}}{\partial\xi_1^4} + \alpha_A^2\frac{\partial^4\bar{F}}{\partial\xi_2^4} + 2\beta_A\frac{\partial^4\bar{F}}{\partial\xi_1^2\partial\xi_2^2}\\
&= \frac{\pi^4}{4}\sum_{m=1}^{M}\sum_{n=1}^{N}\sum_{p=1}^{M}\sum_{q=1}^{N} mnpq\,A_{mn}\left(A_{pq} + 2B_{pq}\right)\\
&\times\left[\cos(m\pi\xi_1 - p\pi\xi_1)\cos(n\pi\xi_2 - q\pi\xi_2) + \cos(m\pi\xi_1 - p\pi\xi_1)\cos(n\pi\xi_2 + q\pi\xi_2)\right.\\
&\quad\left. + \cos(m\pi\xi_1 + p\pi\xi_1)\cos(n\pi\xi_2 - q\pi\xi_2) + \cos(m\pi\xi_1 + p\pi\xi_1)\cos(n\pi\xi_2 + q\pi\xi_2)\right]\\
&\quad - \frac{\pi^4}{4}\sum_{m=1}^{M}\sum_{n=1}^{N}\sum_{p=1}^{M}\sum_{q=1}^{N} A_{mn}\left[A_{pq}m^2q^2 + \left(q^2m^2 + p^2n^2\right)B_{pq}\right]\\
&\times\left[\cos(m\pi\xi_1 - p\pi\xi_1)\cos(n\pi\xi_2 - q\pi\xi_2) - \cos(m\pi\xi_1 - p\pi\xi_1)\cos(n\pi\xi_2 + q\pi\xi_2)\right.\\
&\quad\left. - \cos(m\pi\xi_1 + p\pi\xi_1)\cos(n\pi\xi_2 - q\pi\xi_2) + \cos(m\pi\xi_1 + p\pi\xi_1)\cos(n\pi\xi_2 + q\pi\xi_2)\right].
\end{aligned} \tag{18.123}$$

The particular solution for the Airy stress function can be suitably written in the form of a series expansion as:

$$\bar{F}_{\mathrm{p}} = \sum_{m=0}^{2M}\sum_{n=0}^{2N} f_{mn}\cos(m\pi\xi_1)\cos(n\pi\xi_2)\,. \tag{18.124}$$

If we insert (18.124) into (18.123), sort by terms of the same order and perform a coefficient comparison, we obtain the following expression for the coefficients f_{mn}:

$$f_{mn} = \frac{\alpha_A^2}{4\left(m^4 + \alpha_A^4 n^4 + 2\beta_A m^2 n^2 \alpha_A^2\right)}\sum_{p=1}^{M}\sum_{q=1}^{N}\sum_{r=1}^{M}\sum_{s=1}^{N} b_{mnpqrs}\left(A_{pq}A_{rs} + A_{pq}B_{rs} + B_{pq}A_{rs}\right). \tag{18.125}$$

Here the coefficients b_{mnpqrs} result as:

$$b_{mnpqrs} = \begin{cases} pqrs - r^2q^2 & \text{if} \quad |p-r| = m \text{ and } |q-s| = n \\ pqrs - r^2q^2 & \text{if} \quad p+r = m \quad \text{and } q+s = n \\ pqrs + r^2q^2 & \text{if} \quad |p-r| = m \text{ and } q+s = n \\ pqrs + r^2q^2 & \text{if} \quad p+r = m \quad \text{and } |q-s| = n \\ 0 & \text{else} \end{cases} . \tag{18.126}$$

This gives the following solution for the Airy stress function:

$$\bar{F} = \bar{F}_\mathrm{h} + \bar{F}_\mathrm{p} = \frac{\bar{N}^0_{xx}\pi^2\xi_2^2}{2} + \frac{\bar{N}^0_{yy}\pi^2\xi_1^2}{2} - \bar{N}^0_{xy}\pi^2\xi_1\xi_2 + \sum_{m=0}^{2M}\sum_{n=0}^{2N} f_{mn}\cos(m\pi\xi_1)\cos(n\pi\xi_2)\,. \tag{18.127}$$

At this point, the only unknowns are the coefficients A_{mn} in the series expansion for the postbuckling deformations $\bar{w}_0$. These can be determined, for example, from an energy analysis using the principle of the minimum of the total elastic potential, or with the help of the Galerkin method. Both methods lead to a cubic nonlinear system of equations for the coefficients A_{mn}, which can be solved using a suitable solution method such as the Newton-Raphson method or the arc length method.

Semi-analytical methods of the type described in this section have been used in the past by a number of authors to investigate the postbuckling behaviour of isotropic and anisotropic, stiffened and unstiffened plates or shells in a semi-analytical and thus computationally efficient way. In addition to the publications already mentioned, examples of this include the works of Chandra and Raju (1973), Chia and Prabhakara (1973), Zhang and Matthews (1984, 1985), Kunz (1989), Byklum (2002), Mijuskovic et al. (1999), Romeo and Frulla (1997), Byklum (2002), Diaconu and Weaver (2005, 2006), Brubak and Hellesland (2007a, b), Brubak et al. (2007), Brubak (2008), to which interested readers are referred for more in-depth details.

18.5 Postbuckling Analysis of Shear-Deformable Laminates

In this section, a closed-form analytical approach for the postbuckling analysis of simply supported shear-deformable laminates under uniaxial compression is presented (Schilling and Mittekstedt 2024). The analysis is based on Classical Laminated Plate Theory (CLPT) as the basic case and the First-Order Shear Deformation Theory (FSDT) and the Third-Order Shear Deformation Theory (TSDT) for modelling shear deformations. The strain fields are shown below. For CLPT, $\psi_x = -\frac{\partial w}{\partial x}$ and $\psi_y = -\frac{\partial w}{\partial y}$ result in the expressions $\underline{\varepsilon}^{(0)}$ and $\underline{\varepsilon}^{(1)}$. For FSDT, $\underline{\varepsilon}^{(0)}$ and $\underline{\varepsilon}^{(1)}$ are to be used. In addition, the shear strains $\underline{\gamma}^{(0)}$ must be taken into account. As the last case, TSDT uses all the strain components shown here.

$$
\begin{aligned}
\underline{\varepsilon}^{(0)} &= \begin{pmatrix} \frac{\partial u_0}{\partial x} + \frac{1}{2}\left(\frac{\partial w_0}{\partial x}\right)^2 + \frac{\partial w_i}{\partial x}\,\frac{\partial w_0}{\partial x} \\ \frac{\partial v_0}{\partial y} + \frac{1}{2}\left(\frac{\partial w_0}{\partial y}\right)^2 + \frac{\partial w_i}{\partial y}\,\frac{\partial w_0}{\partial y} \\ \frac{\partial u_0}{\partial y} + \frac{\partial v_0}{\partial x} + \frac{\partial^2 w_0}{\partial y \partial x} + \frac{\partial w_i}{\partial y}\,\frac{\partial w_0}{\partial x} + \frac{\partial w_0}{\partial y}\,\frac{\partial w_i}{\partial x} \end{pmatrix}, \\
\underline{\varepsilon}^{(1)} &= \begin{pmatrix} \frac{\partial \psi_x}{\partial x} \\ \frac{\partial \psi_y}{\partial y} \\ \frac{\partial \psi_y}{\partial x} + \frac{\partial \psi_x}{\partial y} \end{pmatrix}, \\
\underline{\varepsilon}^{(3)} &= -\frac{4}{3\,h^2} \begin{pmatrix} \frac{\partial \psi_x}{\partial x} + \frac{\partial^2 w_0}{\partial x^2} \\ \frac{\partial \psi_y}{\partial y} + \frac{\partial^2 w_0}{\partial y^2} \\ \frac{\partial \psi_y}{\partial x} + \frac{\partial \psi_x}{\partial y} + 2\,\frac{\partial^2 w_0}{\partial x \partial y} \end{pmatrix}, \\
\underline{\gamma}^{(0)} &= \begin{pmatrix} \frac{\partial w_0}{\partial y} + \psi_y \\ \frac{\partial w_0}{\partial x} + \psi_x \end{pmatrix}, \\
\underline{\gamma}^{(2)} &= -\frac{4}{h^2} \begin{pmatrix} \frac{\partial w_0}{\partial y} + \psi_y \\ \frac{\partial w_0}{\partial x} + \psi_x \end{pmatrix}.
\end{aligned} \tag{18.128}
$$

The presence of simply supported edges for symmetric orthotropic cross-ply laminates requires the fulfilment of the following boundary conditions:

$$
\begin{aligned}
x = 0, a: &\quad w_0 = M^0_{xx} = \psi_y = P_{xx} = 0, \\
y = 0, b: &\quad w_0 = M^0_{yy} = \psi_x = P_{yy} = 0.
\end{aligned} \tag{18.129}
$$

While the analysis within the framework of CLPT only requires the consideration of the postbuckling deflection w_0, the approach for both FSDT and TSDT must include both w_0 and the bending angles ψ_x and ψ_y, which represent independent degrees of freedom within the framework of these higher-order shear deformation theories. With the given boundary conditions, the following set of trigonometric shape functions is suitable:

$$
\begin{aligned}
w_0 &= W\, w_1(x)\; w_2(y) = W\, \sin\left(\frac{\pi\, m\, x}{a}\right) \sin\left(\frac{\pi\, n\, y}{b}\right), \\
\psi_x &= X\, \psi_{x,1}(x)\; \psi_{x,2}(y) = X\, \frac{\pi\, m}{a}\, \cos\left(\frac{\pi\, m\, x}{a}\right) \sin\left(\frac{\pi\, n\, y}{b}\right), \\
\psi_y &= Y\, \psi_{y,1}(x)\; \psi_{y,2}(y) = Y\, \frac{\pi\, n}{b}\, \cos\left(\frac{\pi\, n\, y}{b}\right) \sin\left(\frac{\pi\, m\, x}{a}\right).
\end{aligned} \tag{18.130}
$$

Here W, X, Y are Ritz constants that are unknown and must be determined. We use an analogous formulation for the imperfections:

$$
w_{\mathrm{i}} = W_{\mathrm{i}}\, w_1(x)\; w_2(y) = W_{\mathrm{i}}\, \sin\left(\frac{\pi\, m\, x}{a}\right) \sin\left(\frac{\pi\, n\, y}{b}\right). \tag{18.131}
$$

The present approach is based on the use of Airy's stress function F to map the inplane resulting force flows N^0_{xx}, N^0_{yy}, N^0_{xy} and to fulfil the equilibrium conditions a priori. The relationship between F and the force flows N^0_{xx}, N^0_{yy}, N^0_{xy} is given by:

$$N^0_{xx} = \frac{\partial^2 F}{\partial y^2}, \quad N^0_{yy} = \frac{\partial^2 F}{\partial x^2}, \quad N^0_{xy} = -\frac{\partial^2 F}{\partial x \partial y}. \tag{18.132}$$

The plane strains depend on the inverse membrane stiffnesses a_{ij}, which result from the constitutive relationships:

$$\begin{aligned} \varepsilon^0_{xx} &= a_{12} \frac{\partial^2 F}{\partial x^2} + a_{11} \frac{\partial^2 F}{\partial y^2}, \\ \varepsilon^0_{yy} &= a_{22} \frac{\partial^2 F}{\partial x^2} + a_{12} \frac{\partial^2 F}{\partial y^2}, \\ \gamma^0_{xy} &= -a_{66} \frac{\partial^2 F}{\partial x \partial y}. \end{aligned} \tag{18.133}$$

For the given problem, the compatibility according to the equation (18.134) must be ensured:

$$\frac{\partial^2 \varepsilon^0_{xx}}{\partial y^2} + \frac{\partial^2 \varepsilon^0_{yy}}{\partial x^2} - \frac{\partial^2 \gamma^0_{xy}}{\partial x \partial y} = 0. \tag{18.134}$$

We can now express the compatibility requirement by the strains given in Eq. (18.133), which are based on the von Kármán strains for CLPT, FSDT and TSDT (Eq. (18.128), neglecting higher-order terms. We obtain:

$$\begin{aligned} a_{22} \frac{\partial^4 F}{\partial x^4} + (2\, a_{12} + a_{66}) \frac{\partial^2 F}{\partial y^2 \partial x^2} + a_{11} \frac{\partial^4 F}{\partial y^4} = \\ \left(\frac{\partial^2 w_0}{\partial x \partial y} \right)^2 - \frac{\partial^2 w_0}{\partial x^2} \frac{\partial^2 w_0}{\partial y^2} - \frac{\partial^2 w_0}{\partial x^2} \frac{\partial^2 w_i}{\partial y^2} \\ + 2 \frac{\partial^2 w_0}{\partial x \partial y} \frac{\partial^2 w_i}{\partial x \partial y} - \frac{\partial^2 w_i}{\partial x^2} \frac{\partial^2 w_0}{\partial y^2}. \end{aligned} \tag{18.135}$$

wherein

$$a_{11} = \frac{A_{22}}{A_{11} A_{22} - A_{12}^2}, \quad a_{22} = \frac{A_{11}}{A_{11} A_{22} - A_{12}^2}, \quad a_{12} = \frac{A_{12}}{A_{12}^2 - A_{11} A_{22}}, \quad a_{66} = \frac{1}{A_{66}}. \tag{18.136}$$

The solution of the Airy stress function for the given postbuckling problem is identical and known for each laminate theory considered here (see e.g. Mittelstedt and Schröder 2010a). The following applies:

$$F_h = N_{xx}\,\frac{y^2}{2},$$
$$F_p = \left(W^2 + 2\,W\,W_\mathrm{i}\right)\left[\cos\left(\frac{\pi\,m\,x}{a}\right)^2 \frac{a^2\,n^2}{16\,a_{22}\,b^2\,m^2} + \cos\left(\frac{\pi\,n\,y}{b}\right)^2 \frac{b^2\,m^2}{16\,a_{11}\,a^2\,n^2}\right]. \tag{18.137}$$

It can be stated at this point that the present approach fulfils both the boundary conditions of shear-free longitudinal edges and the requirement that the longitudinal edges of the buckled plate remain straight:

$$N^0_{xy}\,(x,\,y=0,b) = 0, \quad v\,(x,\,y=0,b) = \text{const.} \tag{18.138}$$

For the closed-form analytical approach, we need the total elastic potential of the considered laminate in the buckled state. It consists of three individual contributions, namely a part Π_m, which takes into account the membrane deformations, a part Π_b, which takes into account the bending deformations, and the part Π_a of the applied load. It can be seen that only the contribution Π_b differs for the laminate theories considered here. The different theories CLPT, FSDT and TSDT are labelled with the indices C, F and T respectively. The individual contributions are then as follows:

$$\Pi_\mathrm{m} = \frac{1}{2}\int_\Omega \underline{N}^{0T}\,\underline{\underline{a}},\,\underline{N}^0 \mathrm{d}\Omega \quad \text{mit } \underline{N}^{(0)} = \begin{pmatrix} \frac{\partial^2\psi}{\partial y^2} \\ \frac{\partial^2\psi}{\partial x^2} \\ \frac{\partial^2\psi}{\partial x\,\partial y} \end{pmatrix},$$
$$\Pi_\mathrm{a} = \int_\Omega \left[-N_{xx}\left(a_{12}\frac{\partial^2\psi}{\partial x^2} + a_{11}\frac{\partial^2\psi}{\partial y^2}\right)\right]\mathrm{d}\Omega,$$
$$\Pi_{\mathrm{b,\,C}} = \frac{1}{2}\int_\Omega \underline{\varepsilon}^{(1)\mathrm{T}}\,\underline{\underline{D}}\,\underline{\varepsilon}^{(1)}\mathrm{d}\Omega,$$
$$\Pi_{\mathrm{b,\,F}} = \frac{1}{2}\int_\Omega \begin{pmatrix} \underline{\varepsilon}^{(1)} \\ \underline{\gamma}^{(0)} \end{pmatrix}^\mathrm{T} \begin{bmatrix} \underline{\underline{D}} & \underline{\underline{0}} \\ \underline{\underline{0}} & K\,\underline{\underline{A}}_\mathrm{S} \end{bmatrix} \begin{pmatrix} \underline{\varepsilon}^{(1)} \\ \underline{\gamma}^{(0)} \end{pmatrix} \mathrm{d}\Omega,$$
$$\Pi_{\mathrm{b,\,T}} = \frac{1}{2}\int_\Omega \begin{pmatrix} \underline{\varepsilon}^{(1)} \\ \underline{\varepsilon}^{(3)} \\ \underline{\gamma}^{(0)} \\ \underline{\gamma}^{(2)} \end{pmatrix}^\mathrm{T} \begin{bmatrix} \underline{\underline{D}} & \underline{\underline{F}} & \underline{\underline{0}} & \underline{\underline{0}} \\ \underline{\underline{F}} & \underline{\underline{H}} & \underline{\underline{0}} & \underline{\underline{0}} \\ \underline{\underline{0}} & \underline{\underline{0}} & \underline{\underline{A}}_\mathrm{S} & \underline{\underline{D}}_\mathrm{S} \\ \underline{\underline{0}} & \underline{\underline{0}} & \underline{\underline{D}}_\mathrm{S} & \underline{\underline{F}}_\mathrm{S} \end{bmatrix} \begin{pmatrix} \underline{\varepsilon}^{(1)} \\ \underline{\varepsilon}^{(3)} \\ \underline{\gamma}^{(0)} \\ \underline{\gamma}^{(2)} \end{pmatrix} \mathrm{d}\Omega. \tag{18.139}$$

The total elastic potential of the buckled laminate is then the sum of these contributions:

$$\Pi\,(W,\,X,\,Y) = \Pi_\mathrm{m} + \Pi_\mathrm{b,C,F,T} + \Pi_\mathrm{a}. \tag{18.140}$$

The basis for the closed-form analysis approach for postbuckling analysis is the principle of the minimum of the total elastic potential, from which the following three Ritz equations result:

$$\frac{\partial \Pi}{\partial W} = 0, \quad \frac{\partial \Pi}{\partial X} = 0, \quad \frac{\partial \Pi}{\partial Y} = 0. \tag{18.141}$$

This leads to a system of nonlinear equations as follows:

$$\begin{aligned} &\left\{ \underline{\underline{K}}_{\mathrm{m}} \left(4\, W^2 + 12\, W\, W_i + 8\, {W_i}^2\right) + \underline{\underline{K}}_{\mathrm{b,C,F,T}} \right. \\ &\left. + \underline{\underline{K}}_{\mathrm{a}}\, N_{xx} \right\} \underline{Q} + \underline{\underline{K}}_{a}\, N_{xx}\, W_i = \underline{0}, \end{aligned} \tag{18.142}$$

with $\underline{Q} = [W, X, Y]^{\mathrm{T}}$. The matrices $\underline{\underline{K}}_{\mathrm{m}}$, $\underline{\underline{K}}_{\mathrm{b,C,F,T}}$ and $\underline{\underline{K}}_{\mathrm{e}}$ result from the integration in Eq. (18.139) and contain the integrated shape functions as well as the material and geometric properties of the analyzed laminates. The matrices $\underline{\underline{K}}_{\mathrm{m}}$ and $\underline{\underline{K}}_{\mathrm{a}}$ are identical for all three laminate theories considered and are as follows:

$$\begin{aligned} \underline{\underline{K}}_{\mathrm{m}} &= \begin{bmatrix} K_{\mathrm{m},1} & 0 & 0 \\ 0 & 0 & 0 \\ 0 & 0 & 0 \end{bmatrix}, \\ \underline{\underline{K}}_{\mathrm{a}} &= \begin{bmatrix} 2\, K_{\mathrm{a},1} & 0 & 0 \\ 0 & 0 & 0 \\ 0 & 0 & 0 \end{bmatrix}, \end{aligned} \tag{18.143}$$

with

$$K_{\mathrm{m},1} = \frac{\pi^4 \left(a_{11}\, a^4\, n^4 + a_{22}\, b^4\, m^4\right)}{256\, a_{11}\, a_{22}\, a^3\, b^3}, \quad K_{\mathrm{a},1} = \frac{b\, m^2\, \pi^2}{8\, a}.$$

The elements of the matrix $\underline{\underline{K}}_{\mathrm{b}}$ are defined differently for each laminate theory considered. The following applies:

$$\underline{\underline{K}}_{\mathrm{b,C,F,T}} = \begin{bmatrix} 2\, K_{\mathrm{b},6} & K_{\mathrm{b},3} & K_{\mathrm{b},5} \\ K_{\mathrm{b},3} & 2\, K_{\mathrm{b},1} & K_{\mathrm{b},2} \\ K_{\mathrm{b},5} & K_{\mathrm{b},2} & 2\, K_{\mathrm{b},4} \end{bmatrix}_{\mathrm{C,F,T}}. \tag{18.144}$$

For CLPT we obtain:

$$\begin{aligned} K_{\mathrm{b},1} &= R^{22}_{w_1,w_1}\, S^{00}_{w_2,w_2}\, \eta_1 + R^{20}_{w_1,w_1}\, S^{20}_{w_2,w_2}\, \eta_2 + R^{11}_{w_1,w_1}\, S^{11}_{w_2,w_2}\, 4\, \eta_3 + R^{00}_{w_1,w_1}\, S^{22}_{w_2,w_2}\, \eta_4, \\ K_{\mathrm{b},2} &= K_{\mathrm{b},3} = K_{\mathrm{b},4} = K_{\mathrm{b},5} = K_{\mathrm{b},6} = 0, \end{aligned} \tag{18.145}$$

with

$$\eta_1 = \frac{D_{1,1}}{2}, \quad \eta_2 = D_{1,2}, \quad \eta_3 = 2\, D_{3,3}, \quad \eta_4 = \frac{D_{2,2}}{2}. \tag{18.146}$$

For FSDT, the following results:

$$
\begin{aligned}
K_{\mathrm{b},1} &= R^{11}_{\psi_{x,1},\psi_{x,1}}\, S^{00}_{\psi_{x,2},\psi_{x,2}}\, \eta_1 + R^{00}_{\psi_{x,1},\psi_{x,1}}\, S^{11}_{\psi_{x,2},\psi_{x,2}}\, \eta_3 + R^{00}_{\psi_{x,1},\psi_{x,1}}\, S^{00}_{\psi_{x,2},\psi_{x,2}}\, \eta_5,\\
K_{\mathrm{b},2} &= R^{10}_{\psi_{x,1},\psi_{y,1}}\, S^{01}_{\psi_{x,2},\psi_{y,2}}\, \eta_2 + 2\, R^{01}_{\psi_{x,1},\psi_{y,1}}\, S^{10}_{\psi_{x,2},\psi_{y,2}}\, \eta_3,\\
K_{\mathrm{b},3} &= 2\, R^{10}_{w_1,\psi_{x,1}}\, S^{00}_{w_2,\psi_{x,2}}\, \eta_5,\\
K_{\mathrm{b},4} &= R^{11}_{\psi_{y,1},\psi_{y,1}}\, S^{00}_{\psi_{y,2},\psi_{y,2}}\, \eta_3 + R^{00}_{\psi_{y,1},\psi_{y,1}}\, S^{11}_{\psi_{y,2},\psi_{y,2}}\, \eta_4 + R^{00}_{\psi_{y,1},\psi_{y,1}}\, S^{00}_{\psi_{y,2},\psi_{y,2}}\, \eta_6,\\
K_{\mathrm{b},5} &= 2\, R^{00}_{w_1,\psi_{y,1}}\, S^{10}_{w_2,\psi_{y,2}}\, \eta_6,\\
K_{\mathrm{b},6} &= R^{11}_{w_1,w_1}\, S^{00}_{w_2,w_2}\, \eta_5 + R^{00}_{w_1,w_1}\, S^{11}_{w_2,w_2}\, \eta_6,
\end{aligned}
\tag{18.147}
$$

wherein:

$$
\eta_5 = \frac{A_{\mathrm{S}2,2}}{2}\, K, \quad \eta_6 = \frac{A_{\mathrm{S}1,1}}{2}\, K. \tag{18.148}
$$

Finally, the following applies to TSDT:

$$
\begin{aligned}
K_{\mathrm{b},1} &= R^{11}_{\psi_{x,1},\psi_{x,1}}\, S^{00}_{\psi_{x,2},\psi_{x,2}}\, \beta_1 + R^{00}_{\psi_{x,1},\psi_{x,1}}\, S^{11}_{\psi_{x,2},\psi_{x,2}}\, \beta_5,\\
&\quad + R^{00}_{\psi_{x,1},\psi_{x,1}}\, S^{00}_{\psi_{x,2},\psi_{x,2}}\, \beta_9,\\
K_{\mathrm{b},2} &= R^{10}_{\psi_{x,1},\psi_{y,1}}\, S^{01}_{\psi_{x,2},\psi_{y,2}}\, \beta_2 + 2\, R^{01}_{\psi_{x,1},\psi_{y,1}}\, S^{10}_{\psi_{x,2},\psi_{y,2}}\, \beta_5,\\
K_{\mathrm{b},3} &= R^{21}_{w_1,\psi_{x,1}}\, S^{00}_{w_2,\psi_{x,2}}\, \beta_3 + R^{01}_{w_1,\psi_{x,1}}\, S^{20}_{w_2,\psi_{x,2}}\, \beta_4\\
&\quad + R^{10}_{w_1,\psi_{x,1}}\, S^{11}_{w_2,\psi_{x,2}}\, \beta_6 + 2\, R^{10}_{w_1,\psi_{x,1}}\, S^{00}_{w_2,\psi_{x,2}}\, \beta_9,\\
K_{\mathrm{b},4} &= R^{11}_{\psi_{y,1},\psi_{y,1}}\, S^{00}_{\psi_{y,2},\psi_{y,2}}\, \beta_5 + R^{00}_{\psi_{y,1},\psi_{y,1}}\, S^{11}_{\psi_{y,2},\psi_{y,2}}\, \beta_7\\
&\quad + R^{00}_{\psi_{y,1},\psi_{y,1}}\, S^{00}_{\psi_{y,2},\psi_{y,2}}\, \beta_{10},\\
K_{\mathrm{b},5} &= R^{20}_{w_1,\psi_{y,1}}\, S^{01}_{w_2,\psi_{y,2}}\, \beta_4 + R^{11}_{w_1,\psi_{y,1}}\, S^{10}_{w_2,\psi_{y,2}}\, \beta_6\\
&\quad + R^{00}_{w_1,\psi_{y,1}}\, S^{21}_{w_2,\psi_{y,2}}\, \beta_8 + 2\, R^{00}_{w_1,\psi_{y,1}}\, S^{10}_{w_2,\psi_{y,2}}\, \beta_{10},\\
K_{\mathrm{b},6} &= R^{11}_{w_1,w_1}\, S^{00}_{w_2,w_2}\, \beta_9 + R^{00}_{w_1,w_1}\, S^{11}_{w_2,w_2}\, \beta_{10}\\
&\quad + R^{22}_{w_1,w_1}\, S^{00}_{w_2,w_2}\, \beta_{11} + R^{20}_{w_1,w_1}\, S^{20}_{w_2,w_2}\, \beta_{12}\\
&\quad + R^{11}_{w_1,w_1}\, S^{11}_{w_2,w_2}\, \beta_{13} + R^{00}_{w_1,w_1}\, S^{22}_{w_2,w_2}\, \beta_{14},
\end{aligned}
\tag{18.149}
$$

with:

$$
\begin{aligned}
\beta_1 &= \eta_1 - \frac{4\, F_{1,1}}{3\, h^2} + \frac{8\, H_{1,1}}{9\, h^4}, & \beta_2 &= \eta_2 - \frac{8\, F_{1,2}}{3\, h^2} + \frac{16\, H_{1,2}}{9\, h^4},\\
\beta_3 &= \frac{16\, H_{1,1}}{9\, h^4} - \frac{4\, F_{1,1}}{3\, h^2}, & \beta_4 &= \frac{16\, H_{1,2}}{9\, h^4} - \frac{4\, F_{1,2}}{3\, h^2},\\
\beta_5 &= \eta_3 - \frac{4\, F_{3,3}}{3\, h^2} + \frac{8\, H_{3,3}}{9\, h^4}, & \beta_6 &= \frac{32\, H_{3,3}}{9\, h^4} - \frac{8\, F_{3,3}}{3\, h^2},
\end{aligned}
$$

$$\beta_7 = \eta_4 - \frac{4\,F_{2,2}}{3\,h^2} + \frac{8\,H_{2,2}}{9\,h^4}, \qquad \beta_8 = \frac{16\,H_{2,2}}{9\,h^4} - \frac{4\,F_{2,2}}{3\,h^2},$$
$$\beta_9 = \frac{A_{\mathrm{S}2,2}}{2} - \frac{4\,D_{\mathrm{S}2,2}}{h^2} + \frac{8\,F_{\mathrm{S}2,2}}{h^4}, \qquad \beta_{11} = \frac{8\,H_{1,1}}{9\,h^4},$$
$$\beta_{10} = \frac{A_{\mathrm{S}1,1}}{2} - \frac{4\,D_{\mathrm{S}1,1}}{h^2} + \frac{8\,F_{\mathrm{S}1,1}}{h^4}, \qquad \beta_{12} = \frac{16\,H_{1,2}}{9\,h^4},$$
$$\beta_{13} = \frac{32\,H_{3,3}}{9\,h^4}, \qquad \beta_{14} = \frac{8\,H_{2,2}}{9\,h^4}.$$

The expressions $R^{ij}_{f(y),g(y)}$ and $S^{ij}_{f(x),g(x)}$ result from the integration of the shape functions according to x and y, respectively, where $f(y)$ and $g(y)$ are placeholders for the different shape functions:

$$S^{ij}_{f(y),g(y)} = \int_0^b \frac{\partial^i f(y)}{\partial y^i} \frac{\partial^j g(y)}{\partial y^j}\,\mathrm{d}y, \tag{18.150}$$

$$R^{ij}_{f(x),g(x)} = \int_0^a \frac{\partial^i f(x)}{\partial x^i} \frac{\partial^j g(x)}{\partial x^j}\,\mathrm{d}x. \tag{18.151}$$

For the buckling analysis of the considered shear-deformable laminates, we neglect the nonlinear contributions and imperfections in the above formulations and obtain a simplified linear eigenvalue problem as follows:

$$\left\{ \underline{\underline{K}}_{b,\mathrm{C,F,T}} + \underline{\underline{K}}_{a}\, N_{xx} \right\} \underline{W} = \underline{0}. \tag{18.152}$$

This eigenvalue problem can be simplified by eliminating X and Y from the first line and solving the remaining expression for N^0_{xx}:

$$N^0_{xx} = -\frac{K_{\mathrm{b},6}}{K_{\mathrm{e},1}} - \frac{K_{\mathrm{b},1}\,{K_{\mathrm{b},5}}^2 - K_{\mathrm{b},2}\,K_{\mathrm{b},3}\,K_{\mathrm{b},5} + {K_{\mathrm{b},3}}^2\,K_{\mathrm{b},4}}{K_{\mathrm{e},1}\left(-4\,K_{\mathrm{b},1}\,K_{\mathrm{b},4} + {K_{\mathrm{b},2}}^2\right)}. \tag{18.153}$$

Since the buckling functions used correspond to the exact Navier solution of the given buckling problem, the resulting expression is identical to the Navier solution in the context of the laminate theories considered here. The buckling analysis is the starting point for the postbuckling analysis, since the mode shape and the critical half-wave number m are also assumed to be valid in the postbuckling range, as will be shown below.

The starting point of the postbuckling analysis is the nonlinear system of equations in (18.142). We simplify the problem again by eliminating X and Y from the first line, resulting in a single nonlinear equation in which the postbuckling amplitude W is the only remaining unknown quantity.

$$\begin{aligned}&\left(-8\,K_{\mathrm{b},1}\,K_{\mathrm{b},4}\,K_{\mathrm{m},1}+2\,{K_{\mathrm{b},2}}^2\,K_{\mathrm{m},1}\right)\left(W^3+3\,W^2\,W_i\right.\\&\left.+2\,W\,{W_i}^2\right)+W\,\left(-4\,K_{\mathrm{b},1}\,K_{\mathrm{b},4}\,K_{\mathrm{b},6}+K_{\mathrm{b},1}\,{K_{\mathrm{b},5}}^2\right.\\&\left.+{K_{\mathrm{b},2}}^2\,K_{\mathrm{b},6}-K_{\mathrm{b},2}\,K_{\mathrm{b},3}\,K_{\mathrm{b},5}+{K_{\mathrm{b},3}}^2\,K_{\mathrm{b},4}\right)+\left(N_{xx}\,W\right.\\&\left.+N_{xx}\,W_i\right)\,\left(-4\,K_{\mathrm{b},1}\,K_{\mathrm{b},4}\,K_{\mathrm{e},1}+{K_{\mathrm{b},2}}^2\,K_{\mathrm{e},1}\right)=0.\end{aligned}\tag{18.154}$$

This can be translated into the following appropriate form:

$$\begin{aligned}&L_3\,W+L_2\,\left(N_{xx}\,W+N_{xx}\,W_i\right)\\&+L_1\,\left(W^3+3\,W^2\,W_i+2\,W\,{W_i}^2\right)=0,\end{aligned}\tag{18.155}$$

with:

$$\begin{aligned}L_1=&-8\,K_{\mathrm{b},1}\,K_{\mathrm{b},4}\,K_{\mathrm{m},1}+2\,{K_{\mathrm{b},2}}^2\,K_{\mathrm{m},1},\\L_2=&-4\,K_{\mathrm{b},1}\,K_{\mathrm{b},4}\,K_{\mathrm{e},1}+{K_{\mathrm{b},2}}^2\,K_{\mathrm{e},1},\\L_3=&-4\,K_{\mathrm{b},1}\,K_{\mathrm{b},4}\,K_{\mathrm{b},6}+K_{\mathrm{b},1}\,{K_{\mathrm{b},5}}^2+{K_{\mathrm{b},2}}^2\,K_{\mathrm{b},6}\\&-K_{\mathrm{b},2}\,K_{\mathrm{b},3}\,K_{\mathrm{b},5}+{K_{\mathrm{b},3}}^2\,K_{\mathrm{b},4}.\end{aligned}\tag{18.156}$$

This expression can be further simplified by introducing the expressions

$$O_1=3\,W_{\mathrm{i}},\quad O_2=2\,{W_i}^2+\frac{L_2\,N_{xx}+L_3}{L_1},\quad O_3=\frac{L_2\,N_{xx}\,W_i}{L_1}.$$

The expression (18.155) thus takes the following form:

$$W^3+W^2\,O_1+W\,O_2+O_3=0.\tag{18.157}$$

This is a cubic equation for the determination of W. This equation can be solved by closed-form analysis, and the only relevant zero is

$$W=-\left(\beta_2-\beta_1\right)-\frac{O_1}{3},\tag{18.158}$$

with

$$\begin{aligned}\beta_1=&\left(\sqrt{\left(\frac{{O_1}^3}{27}-\frac{O_1\,O_2}{6}+\frac{O_3}{2}\right)^2+\left(-\frac{{O_1}^2}{9}+\frac{O_2}{3}\right)^3}\right.\\&\left.-\frac{{O_1}^3}{27}-\frac{O_3}{2}+\frac{O_1\,O_2}{6}\right)^{1/3},\\\beta_2=&-\frac{1}{\beta_1}\left(\frac{{O_1}^2}{9}+\frac{O_2}{3}\right).\end{aligned}$$

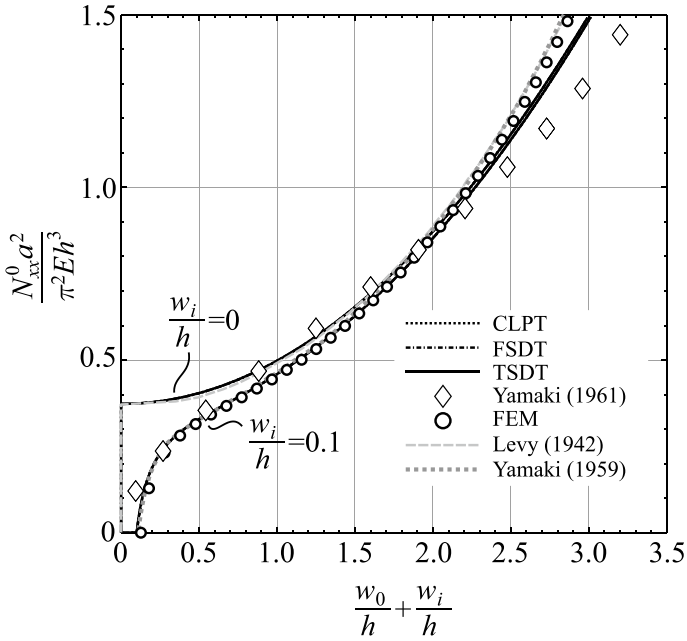


Fig. 18.15 Load-deflection behaviour of a simply supported isotropic plate, comparison of the present method with literature results

At this point, the closed-form analytical solution for the postbuckling behaviour of the shear-deformable laminates considered here is complete. With the determination of the postbuckling amplitude W, all other state variables of the buckled plate can also be determined analytically in closed form.

The closed-form analysis approach is illustrated in Fig. 18.15 by a comparison with the finite element method and with literature results for the load-deflection behaviour of an isotropic plate simply supported at all edges. This figure contains results from Yamaki (1961), who conducted an experimental study of isotropic square plates. In addition, Yamaki (1959) carried out numerical investigations of the postbuckling behaviour of isotropic plates for various boundary conditions. Finally, the results of Levy (1942) are also shown, who presented theoretically exact solutions for the postbuckling behaviour of isotropic simply supported plates. The results are presented for perfect and imperfect plates, where the imperfection is defined as 0.1 of the total thickness h. The material parameters used are $E = 68200\text{MPa}$, $\nu = 0.326$, with a thickness $h = 1.27$ mm and an edge length of $a = 299.72$ mm. The results show a very satisfactory agreement between the present method and the FEM as well as the reference results. Obviously, the result plots for CLPT, FSDT and TSDT are difficult to distinguish from each other as this example is a very thin plate.

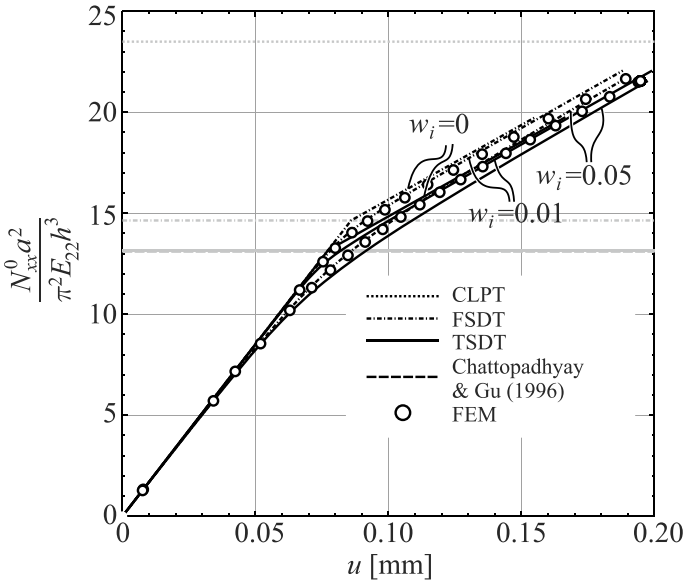


Fig. 18.16 Edge displacement of the buckled laminate

As a further example, a cross-ply laminate with the layup [0° /90° /0°] is considered. The layerwise elastic properties are $E_{22} = 10000\,\text{MPa}$, $E_{11} = 25\,E_{22}$, $\nu = 0.25$, $G_{12} = 0,5\,E_{22}, G_{13} = 0.5\,E_{22}$, $\frac{G_{23}}{G_{13}} = 0.2$, the laminate thickness is $h = 1$ mm. Figure 18.16 shows the edge displacement of the buckled plate, where three different graphs, namely $w_\text{i} = 0,\ 0.01,\ 0.05$, for $\frac{a}{h} = 10$ are considered. The critical buckling loads are shown in grey. The results are compared with the FEM only for imperfect laminates, and it can be seen that the FEM agrees very well with the FSDT results and deviates slightly at higher loads. Overall, these results show that the nonlinear postbuckling behaviour of the considered laminate is well predicted by the closed-form analytical approach.

Figure 18.17 shows load-displacement curves for the investigated laminate for the three laminate theories considered here in comparison with FEM calculations and results from the literature for $\frac{a}{h} = 10$.

In this case as well, the FEM corresponds to the analytical results for FSDT and deviates slightly for higher loads. Apparently, this predicts the geometrically nonlinear behaviour of laminate panels very well. The results show that the maximum deflection values vary considerably between the solutions based on FSDT and TSDT.

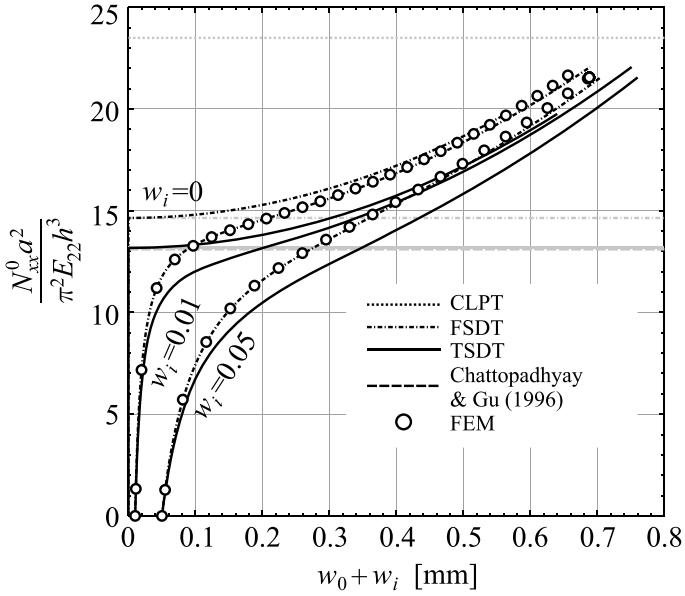


Fig. 18.17 Deflection of the buckled laminate

References

Brubak L, Hellesland J (2007a): *Semi-analytical postbuckling and strength analysis of arbitrarily stiffened plates in local and global bending*, Thin-Walled Structures 45:620–633.

Brubak L, Hellesland J (2007b): *Approximate buckling strength analysis of arbitrarily stiffened, stepped plates*,Engineering Structures 29:2321–2333.

Brubak L, Hellesland J, Steen E (2007): *Semi-analytical buckling strength analysis of plates with arbitrary stiffener arrangements*, Journal of Constructional Steel Research 63:532–543.

Brubak L (2008): *Semi-analytical postbuckling analysis of stiffened plates with a free edge*, Research report No. 03, University of Oslo, Department of mathematics, Mechanics division, Oslo, Norway.

Brunelle EJ, Oyibo GA (1983): *Generic buckling curves for specially orthotropic rectangular plates*, AIAA Journal 21:1150–1156.

Buermann P, Rolfes R, Tessmer J, Schagerl M (2006): *A semi-analytical model for local post-buckling analysis of stringer-and frame-stiffened cylindrical panels*, Thin-Walled Structures 44:102–114.

Buermann P (2006): *A semi-analytical model for the post-buckling analysis of stringer- and frame-stiffened cylindrical panels under combined loading*, Dissertation, Technische Universität Braunschweig, Braunschweig, Germany.

Byklum E (2002): *Ultimate strength analysis of stiffened steel and aluminium panels using semi-analytical methods*, Dissertation, Norwegian University of Science and Technology, Trondheim, Norway.

Byklum E, Amdahl J (2002): *A simplified method for elastic large deflection analysis of plates and stiffened panels due to local buckling*, Thin-Walled Structures 40:925–953.

Chandra R, Raju B (1973): *Postbuckling analysis of rectangular orthotropic plates*, International Journal of Mechanical Sciences 15:81–97.

Chattopadhyay A, Gu H (1996): *Exact elasticity solution for buckling of composite laminates*, Composite Structures 34:291–299.

Chia CY, Prabhakara MK (1973): *Postbuckling behaviour of unsymmetrically layered anisotropic rectangular plates*, Journal of Applied Mechanics 41:155–162.

Chia CY (1980): *Nonlinear analysis of plates*, McGraw-Hill, New York et al., USA.

Diaconu CG, Weaver PM (2005): *Approximate solution and optimum design of compression-loaded, postbuckled laminated composite plates*, AIAA Journal 43:906–914.

Diaconu CG, Weaver PM (2006): *Postbuckling of long unsymmetrically laminated composite plates under axial compression*, International Journal of Solids and Structures 43:6978–6997.

Kunz RK (1989): *Postbuckling of stiffened composite plates under combined loading*, Proceedings of the *8th DoD / NASA / FFA Conference on fibrous composites in structural design*, NASA CP-3087, pp. 591–608.

Levy S (1942): *Bending of Rectangular Plates with Large Deflections*, National Advisory Committee for Aeronautics, NACA-TN-846, Washington, USA.

Meyer-Piening HR, Geier B, Rohwer K (1991): *Remarks on the effective-width concept for orthotropic thin shells*, Proceedings: International Colloquium on Buckling of Shell Structures, on Land, in the Sea and in the Air, Lyon, France, 17–19 September 1991.

Mijuskovic O, Coric B, Pavlovic MN (1999): *Transverse-stiffener requirements for the post-buckling behaviour of a plate in shear*, Thin-Walled Structures 34:43–63.

Mittelstedt C, Schröder KU (2010a): *Postbuckling of compressively loaded imperfect composite plates: closed-form approximate solutions*, International Journal of Structural Stability and Dynamics 10:761–778.

Mittelstedt C, Schröder KU (2010b): *Local postbuckling of hat-stringer stiffened composite laminated plates under transverse compression*, Composite Structures 92:2830–2844.

Mittelstedt C, Erdmann H, Schröder KU (2011): *Postbuckling of composite plates under inplane shear: closed-form approximate solutions*, Archive of Applied Mechanics 81: 1409–1426.

Nemeth MP (1995): *Buckling behavior of long anisotropic plates subjected to combined loads*, National Aeronautics and Space Administration, NASA TP 3568, Hampton, Virginia, USA.

Ovesy HR, Loughlan J, Assaee H (2004): *The compressive post-local buckling behaviour of thin plates using a semi-energy finite-strip approach*, Thin-Walled Structures 42:449–474.

Romeo G, Frulla G (1997): *Post-buckling behaviour of graphite/epoxy stiffened panels with initial imperfections subjected to eccentric biaxial compression loading*, International Journal of Non-Linear Mechanics 32:1017–1033.

Schilling JC, Mittekstedt C (2024): *Closed-form postbuckling analysis of shear deformable composite laminated panels*, Archive of Applied Mechanics, accepted for publication, in press.

Shin DK, Griffin, OH jr, Gürdal, Z (1993): *Postbuckling response of laminated plates under uniaxial compression*, International Journal of Non-Linear Mechanics 28:95–115.

Stein M (1983): *Postbuckling of orthotropic composite plates loaded in compression*, AIAA Journal 21:1729–1735.

Timoshenko SP, Gere JM (1961): *Theory of elastic stability*, 2nd edition, McGraw-Hill, New York, USA.

Turvey GJ, Marshall IH (1995): *Buckling and postbuckling of composite plates*, Chapman and Hall, London, UK.

Wiedemann J (1996): *Leichtbau - Band 1: Elemente*, Zweite Auflage, Springer-Verlag, Berlin et al., Germany.

Yamaki N (1959): *Postbuckling behaviour of rectangular plates with small initial curvature loaded in edge compression*, Journal of Applied Mechanics 81:407–414.

Yamaki N (1961): *Experiments on the postbuckling behavior of square plates loaded in edge compression*, Journal of Applied Mechanics 28:238–244.

Zhang Y, Matthews FL (1984): *Postbuckling behaviour of anisotropic laminated plates under pure shear and shear combined with compressive loading*, AIAA Journal 22:281–286.

Zhang Y, Matthews FL (1985): *Large deflection behaviour of simply supported laminated panels under in-plane loading*, Journal of Applied Mechanics 52:553–558.

Zou G, Qiao P (2002): *Higher-order finite strip method for postbuckling analysis of imperfect composite plates*, Journal of Engineering Mechanics 128:1008–1015.

Part IV
Advanced Topics

Sandwich Structures

19

A sandwich is a structure that is made up of two so-called facesheets and a so-called core (Fig. 19.1). Sandwiches are generally designed in such a way that the facesheets exhibit high stiffness and strength, whereas the core has significantly weaker properties. If the sandwich is subjected to a bending load, the facesheets are significantly involved in the transfer of the bending moments, namely in the form of tensile and compressive forces in the facesheet plane. However, the core is responsible for the transfer of shear stresses and is generally not or only very little involved in the transfer of bending moments. A sandwich therefore obviously has a very clear division of tasks between the individual components, which will be discussed in detail later on. We begin this chapter with a fundamental discussion of the load-bearing behaviour of sandwich structures. Afterwards, the considerations are detailed using the example of an orthotropic sandwich panel. We end the chapter by analysing a completely arbitrary sandwich structure.

Fundamental literature on the mechanical behaviour of sandwich structures is available with Allen (1969), Altenbach et al. (1996, 2004), Klein (1994), Plantema (1966), Stamm and Witte (1974), Wiedemann (2006) and Zenkert (1995).

19.1 Load-Bearing Behaviour of Sandwich Structures

We begin the discussion of the load-bearing behaviour of sandwich structures (cf. Zenkert 1995) using the example of a sandwich beam (Fig. 19.2). In this introductory example, for the sake of simplicity, identical materials are provided in the two facesheets of the same thickness (modulus of elasticity E_f, thicknesses $h_1 = h_2 = h_f$). The core has the thickness h_c and behaves isotropically for the sake of simplicity (modulus of elasticity E_c). The distance between the two facesheets in relation to their middle planes is d. The total thickness of the sandwich structure under consideration is h. In the explanations of this section, we relate all

© The Author(s), under exclusive license to Springer-Verlag GmbH, DE, part of Springer Nature 2025

C. Mittelstedt, *Mechanics of Composite Structures*,
https://doi.org/10.1007/978-3-662-70788-3_19

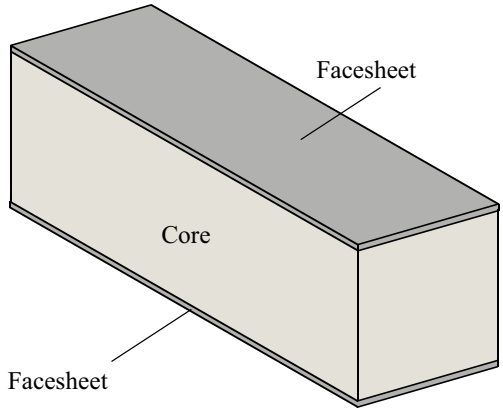


Fig. 19.1 Sandwich

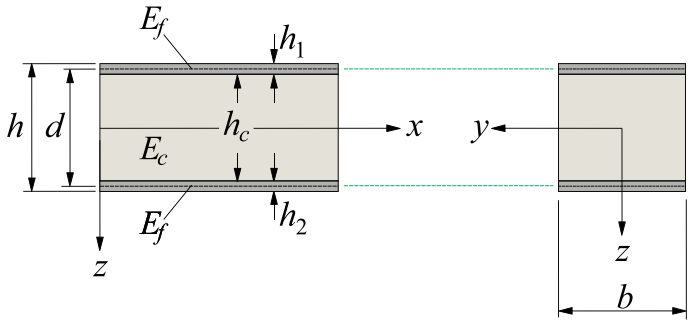


Fig. 19.2 Sandwich beam

loads and stiffness variables to the unit width b of the beam cross-section. The coordinate origin is in the center of the core.

Let us first consider the strain ε_{xx} in pure bending. It is calculated from the distance z on the z-axis multiplied by the beam curvature κ:

$$\varepsilon_{xx} = z\kappa. \tag{19.1}$$

The bending moment M_y is obtained by integrating the normal stress σ_{xx} multiplied by the lever arm z:

$$M_y = \int \sigma_{xx} z \mathrm{d}z. \tag{19.2}$$

Inserting (19.1) when using Hooke's law $\sigma_{xx} = E\varepsilon_{xx}$ results in:

$$M_y = \kappa \int E z^2 \mathrm{d}z. \tag{19.3}$$

Let $(EI)_{eff}$ be the effective bending stiffness of the beam cross-section:

$$(EI)_{eff} = \int E z^2 \mathrm{d}z = D, \tag{19.4}$$

where we use the abbreviation D for better readability:

$$M_y = (EI)_{eff}\, \kappa = D\kappa. \tag{19.5}$$

With $\kappa = \frac{M_y}{D}$ we obtain from (19.1):

$$\varepsilon_{xx} = \frac{M_y}{D} z. \tag{19.6}$$

We now analyze the effective bending stiffness D. It follows after a short calculation as:

$$D = \int_{-\frac{h}{2}}^{+\frac{h}{2}} E z^2 \mathrm{d}z = \frac{E_f h_f^3}{6} + \frac{E_f h_f d^2}{2} + \frac{E_c h_c^3}{12} = 2D_f + D_0 + D_c. \tag{19.7}$$

Therein, $2D_f$ is the bending stiffness of the two facesheets, D_0 is the out-of-plane component of the two facesheets. The quantity D_c is the bending stiffness of the core.

We now discuss various simplifications with regard to the bending stiffness D. As a rule, the facesheets are thinner than the core, so that $h_f \ll h_c$. The term $2D_f$ is less than or equal to 1% of D_0 if:

$$3\left(\frac{d}{h_f}\right)^2 > 100, \quad \text{or} \quad \frac{d}{h_f} > 5,77. \tag{19.8}$$

Furthermore, in many cases the core material is significantly less stiff than the facesheet material ($E_c \ll E_f$). The third term in (19.7) is less than or equal to 1% of the second term if:

$$\frac{6E_f h_f d^2}{E_c h_c^3} > 100. \tag{19.9}$$

As a consequence of these simplifications, the following applies to the effective bending stiffness:

$$D = D_0 = \frac{E_f h_f d^2}{2} = (EI)_{eff}\,. \tag{19.10}$$

The bending stresses in the two facesheets and in the core are as follows:

$$\sigma_f = \frac{M_y E_f}{D} z, \quad \left(\frac{h_c}{2} \leq |z| \leq \frac{h_c}{2} + h_f \right)$$
$$\sigma_c = \frac{M_y E_c}{D} z. \quad \left(|z| \leq \frac{h_c}{2} \right) \tag{19.11}$$

The normal stress σ is linear over z and will exhibit a discontinuity at the interfaces between the facesheets and the core due to the different elastic properties E_f and E_c.

If a pure normal force load is present, the strain ε_{xx} results as:

$$\varepsilon_{xx} = \frac{N}{2E_f h_f + E_c h_c}. \tag{19.12}$$

With the effective extensional stiffness $(EA)_{eff}$

$$(EA)_{eff} = 2E_f h_f + E_c h_c \tag{19.13}$$

we have:

$$\varepsilon_{xx} = \frac{N}{(EA)_{eff}}. \tag{19.14}$$

The normal stresses in the facesheets and in the core are calculated as follows:

$$\sigma_{xx,f} = \frac{N E_f}{(EA)_{eff}}, \quad \sigma_{xx,c} = \frac{N E_c}{(EA)_{eff}}. \tag{19.15}$$

We consider the shear stress τ_{xz}, which we can determine from the free-body diagram in Fig. 19.3. A sectional element of length dx is shown, which we have cut out of the sandwich at an arbitrary point z. In addition to the required shear stress τ_{xz}, this also releases the normal stress σ_{xx} on the negative cutting edge and the normal stress σ_{xx} with an infinitesimal increase $\mathrm{d}\sigma_{xx} = \frac{\partial \sigma_{xx}}{\partial x} \mathrm{d}x$ on the positive cutting edge. The sum of the horizontal forces is as follows:

$$\tau_{xz} = \int_z^{\frac{d+h_f}{2}} \frac{\mathrm{d}\sigma_{xx}}{dx} \mathrm{d}z. \tag{19.16}$$

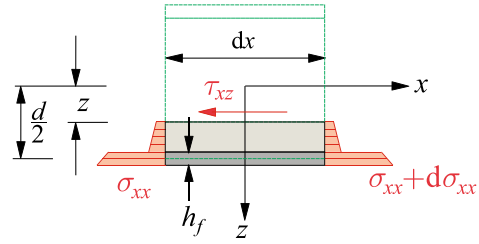


Fig. 19.3 Determination of the shear stress τ_{xz}

With $\frac{\mathrm{d}M_y}{\mathrm{d}x} = Q_z$ and $\sigma_{xx} = \frac{M_y E}{D} z$ the derivation of σ_{xx} follows:

$$\frac{\mathrm{d}\sigma_{xx}}{dx} = \frac{Q_z E}{D} z. \tag{19.17}$$

For the shear stress τ_{xz} we then obtain

$$\tau_{xz} = \frac{Q_z}{D} \int_z^{\frac{d+h_f}{2}} E z \mathrm{d}z = \frac{Q_z}{D} \left(E S_y\right)_{eff}, \tag{19.18}$$

where $\left(E S_y\right)_{eff}$ is the effective static moment. In essence, it reads:

$$\left(E S_y\right)_{eff,c} = \frac{E_f h_f d}{2} + \frac{E_c}{2} \left(\frac{h_c}{2} - z\right) \left(\frac{h_c}{2} + z\right). \tag{19.19}$$

The core shear stress is then:

$$\tau_c = \frac{Q_z}{D} \left[\frac{E_f h_f d}{2} + \frac{E_c}{2} \left(\frac{h_c^2}{4} - z^2\right)\right]. \tag{19.20}$$

In the facesheets with $\frac{h_c}{2} \leq |z| \leq \frac{h_c}{2} + h_f$, the static moment results as:

$$\left(E S_y\right)_{eff,f} = \frac{E_f}{2} \left(\frac{h_c}{2} + h_f - z\right) \left(\frac{h_c}{2} + h_f + z\right). \tag{19.21}$$

This results in the shear stress in the facesheets as:

$$\tau_f = \frac{Q_z}{D} \frac{E_f}{2} \left(\frac{h_c^2}{4} + h_c h_f + h_f^2 - z^2\right). \tag{19.22}$$

The maximum shear stress in the core occurs at the point $z = 0$:

$$\tau_{c,\max} = \frac{Q_z}{D} \left(\frac{E_f h_f d}{2} + \frac{E_c h_c^2}{8}\right). \tag{19.23}$$

A common approximation for the core shear stress is to assume that the deviation between the maximum and minimum shear stress is very small. This deviation is less than or equal to 1% if the following applies

$$\frac{4 E_f h_f d}{E_c h_c^2} > 100. \tag{19.24}$$

The simplifications described so far can be summarised as follows. If the core of the sandwich structure under consideration is quite compliant, i.e. $E_c \ll E_f$, then the stresses in the sandwich are as follows:

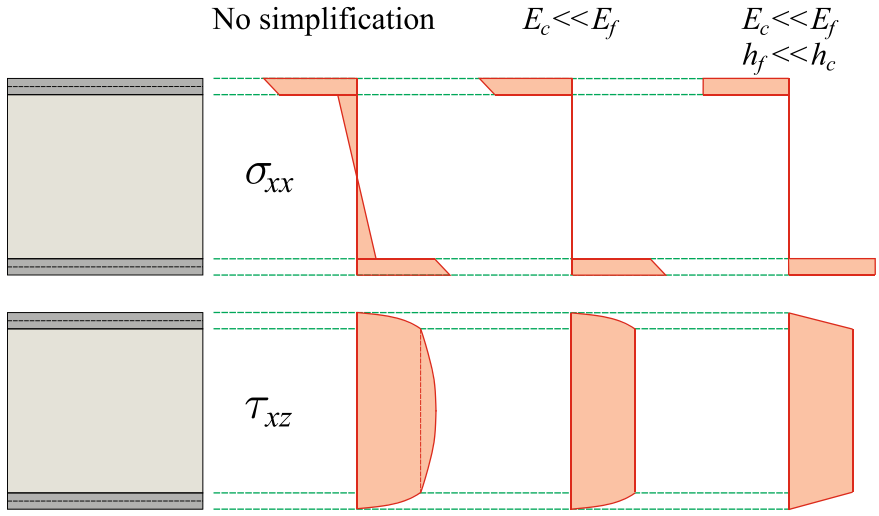


Fig. 19.4 Overview of the simplifications introduced and their effects on the stress distributions in the sandwich

$$\sigma_c = 0, \quad \sigma_f = \frac{M_y E_f}{2D_f + D_0} z,$$
$$\tau_c = \frac{Q_z E_f h_f d}{2(2D_f + D_0)}, \quad \tau_f = \frac{Q_z E_f}{2(2D_f + D_0)} \left(\frac{h_f^2}{4} + h_c h_f + h_f^2 - z^2 \right). \tag{19.25}$$

If, in addition, thin facesheets with $h_f \ll h_c$ are involved, further simplifications can be made:

$$\sigma_c = 0, \quad \sigma_f = \pm \frac{M_y}{h_f d}, \quad \tau_c = \frac{Q_z}{d}, \quad \tau_f = 0. \tag{19.26}$$

These simplifications are shown in Fig. 19.4. This shows the aforementioned division of tasks between the individual sandwich components: Facesheets are fully responsible for carrying the bending moments, and the core is responsible for carrying transverse shear forces. The core also acts as a spacer for the two facesheets, whose out-of-plane components of the bending stiffness make up the effective bending stiffness of the sandwich structure.

19.2 Idealization for an Orthotropic Sandwich Panel

We extend our considerations in this section to an orthotropic sandwich plate (Fig. 19.5), which consists of a core and two facesheets. The two facesheets have the thicknesses h_1 (upper facesheet) and h_2 (lower facesheet), the distance between the middle planes of the

facesheets is d. It can be shown that for an ideal-orthotropic sandwich, analogous to the neutral fiber of a beam, a neutral plane can be found in which plane forces or force flows must act so that no bending effect occurs. We assume that (as in many technical applications) the two facesheets are made of identical material but can have different thicknesses. The distance of the facesheets from the neutral plane is e_1 (upper facesheet) or e_2 (lower facesheet), where e_1 and e_2 are to be determined.

We assume that the core is not involved in the transmission of planar force flows and moment flows. In addition, the contribution of the facesheets to the bending stiffness is only taken into account by their out-of-plane components, their inherent bending stiffness is neglected. The normal stresses in the facesheets resulting from bending are therefore assumed to be constant (Figs. 19.4 and 19.6). Similarly, shear force flows are transmitted exclusively by shear through the core and the transverse shear stress occurring in the core is assumed to be constant over the core thickness. Furthermore, the core is incompressible and therefore does not experience any change in thickness due to the applied load. The force and moment quantities M^0_{xx}, M^0_{yy}, M^0_{xy}, Q_x, Q_y and N^0_{xx}, N^0_{yy}, N^0_{xy} are assumed to occur. For the following idealization, the First-Order Shear Deformation Theory (FSDT) (Chap. 11) is used.

We determine the position of the neutral plane and set the reference axis $\bar{z}$ as shown in Fig. 19.5. The position $\bar{z}_s$ of the elastic center of gravity is obtained as:

$$\bar{z}_s = \frac{\sum_{i=1}^{3} E_i \int_{A_i} \bar{z}_i \mathrm{d}A_i}{\sum_{i=1}^{3} E_i \int_{A_i} \mathrm{d}A_i} = \frac{\left(ES_{\bar{y}}\right)_{eff}}{(EA)_{eff}}. \tag{19.27}$$

The effective static moment $\left(ES_{\bar{y}}\right)_{eff}$ is:

$$\left(ES_{\bar{y}}\right)_{eff} = E_f dbh_2 + E_c \frac{d}{2} bd. \tag{19.28}$$

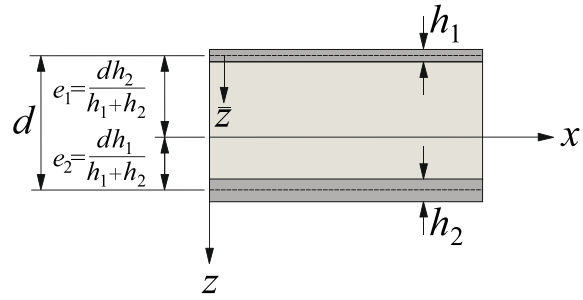


Fig. 19.5 Determination of the neutral plane for an orthotropic sandwich

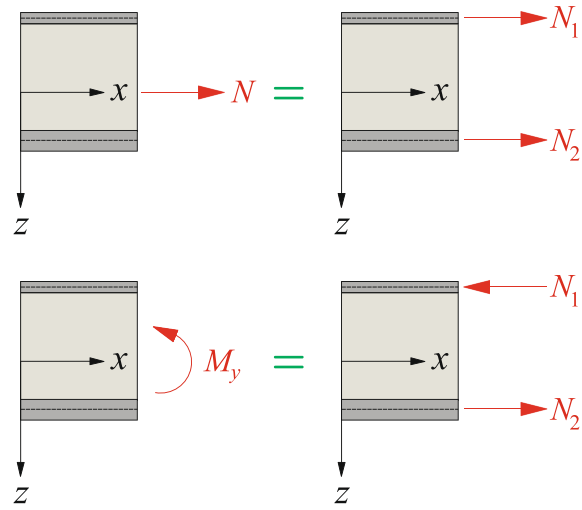


Fig. 19.6 Force flows in the sandwich due to normal force and bending

With $E_f \gg E_c$ we have:

$$\left(ES_{\bar{y}}\right)_{eff} = E_f dbh_2. \tag{19.29}$$

The effective extensional stiffness $(EA)_{eff}$ is calculated as:

$$(EA)_{eff} = E_f bh_1 + E_f bh_2 + E_c bd, \tag{19.30}$$

or if the contribution of the core is neglected:

$$(EA)_{eff} = E_f b(h_1 + h_2). \tag{19.31}$$

The position of the ideal center of gravity $\bar{z}_s$ is then:

$$\bar{z}_s = \frac{dh_2}{h_1 + h_2} = e_1. \tag{19.32}$$

From this follows e_2 as:

$$e_2 = \frac{dh_1}{h_1 + h_2}. \tag{19.33}$$

We consider the given orthotropic sandwich in the context of FSDT. In order to keep this section self-contained, the most important basics are repeated here. The main difference between Classical Laminated Plate Theory (CLPT) and FSDT is the omission of the normal hypothesis while retaining the hypothesis that the cross-sections remain plane, which leads to the following displacement field:

$$\begin{aligned} u(x, y, z) &= u_0(x, y) + z\psi_x(x, y), \\ v(x, y, z) &= v_0(x, y) + z\psi_y(x, y), \\ w(x, y) &= w_0(x, y). \end{aligned} \tag{19.34}$$

Here, u_0, v_0, w_0 are the displacements of the neutral plane of the sandwich under consideration, and the two bending angles ψ_x and ψ_y describe the rotation of the cross-section about the y- and x-axes respectively. There are therefore five degrees of freedom, namely u_0, v_0, w_0 and ψ_x, ψ_y.

The strain field follows from the displacement field shown above as:

$$\begin{aligned} \varepsilon_{xx} &= \frac{\partial u}{\partial x} = \frac{\partial u_0}{\partial x} + z\frac{\partial \psi_x}{\partial x}, \\ \varepsilon_{yy} &= \frac{\partial v}{\partial y} = \frac{\partial v_0}{\partial y} + z\frac{\partial \psi_y}{\partial y}, \\ \varepsilon_{zz} &= \frac{\partial w}{\partial z} = 0, \\ \gamma_{xy} &= \frac{\partial u}{\partial y} + \frac{\partial v}{\partial x} = \frac{\partial u_0}{\partial y} + \frac{\partial v_0}{\partial x} + z\left(\frac{\partial \psi_x}{\partial y} + \frac{\partial \psi_y}{\partial x}\right), \\ \gamma_{xz} &= \frac{\partial u}{\partial z} + \frac{\partial w}{\partial x} = \frac{\partial w_0}{\partial x} + \psi_x, \\ \gamma_{yz} &= \frac{\partial v}{\partial z} + \frac{\partial w}{\partial y} = \frac{\partial w_0}{\partial y} + \psi_y. \end{aligned} \tag{19.35}$$

In addition to the plane strain components ε_{xx}, ε_{yy} and γ_{xy}, the two transverse shear strains γ_{xz} and γ_{yz}, which are constant over the sandwich thickness, also occur. The strain ε_{zz} assumes a value zero due to the assumed incompressibility of the core and the facesheets.

From the displacement and strain field, the layerwise stresses σ_{xx}, σ_{yy} and τ_{xy} in segment k of the sandwich can be calculated from Hooke's law in the plane stress state:

$$\begin{pmatrix} \sigma_{xx} \\ \sigma_{yy} \\ \tau_{xy} \end{pmatrix}_k = \begin{bmatrix} Q_{11} & Q_{12} & 0 \\ Q_{12} & Q_{22} & 0 \\ 0 & 0 & Q_{66} \end{bmatrix}_k \begin{pmatrix} \varepsilon_{xx} \\ \varepsilon_{yy} \\ \gamma_{xy} \end{pmatrix}. \tag{19.36}$$

Only the contributions from the facesheets of the sandwich are taken into account here. The reduced stiffnesses Q_{11}, Q_{22}, Q_{12}, Q_{66} are as follows:

$$Q_{11} = \frac{E_{xx}}{1 - \nu_{xy}\nu_{yx}}, \quad Q_{22} = \frac{E_{yy}}{1 - \nu_{xy}\nu_{yx}}, \quad Q_{12} = \frac{\nu_{xy}E_{yy}}{1 - \nu_{xy}\nu_{yx}}. \quad Q_{66} = G_{xy}. \tag{19.37}$$

Here, E_{xx}, E_{yy}, ν_{xy}, ν_{yx}, G_{xy} are the elastic properties of the segment under consideration.

The interlaminar shear stresses τ_{xz} and τ_{yz} can be calculated from the generalised Hooke's law:

$$\begin{pmatrix} \tau_{yz} \\ \tau_{xz} \end{pmatrix}_k = \begin{bmatrix} C_{44} & 0 \\ 0 & C_{55} \end{bmatrix}_k \begin{pmatrix} \gamma_{yz} \\ \gamma_{xz} \end{pmatrix}, \tag{19.38}$$

where C_{44} and C_{55} are the transverse shear stiffnesses. At this point, only the core properties are considered later.

The force flows N^0_{xx}, N^0_{yy}, N^0_{xy}, the moment flows M^0_{xx}, M^0_{yy}, M^0_{xy} and the shear force flows Q_x, Q_y occur as internal forces. For the force flows N^0_{xx}, N^0_{yy}, N^0_{xy} we obtain:

$$\begin{pmatrix} N^0_{xx} \\ N^0_{yy} \\ N^0_{xy} \end{pmatrix} = \int_h \begin{pmatrix} \sigma_{xx} \\ \sigma_{yy} \\ \tau_{xy} \end{pmatrix} \mathrm{d}z = \int_h \begin{bmatrix} Q_{11} & Q_{12} & 0 \\ Q_{12} & Q_{22} & 0 \\ 0 & 0 & Q_{66} \end{bmatrix} \left[\begin{pmatrix} \varepsilon^0_{xx} \\ \varepsilon^0_{yy} \\ \gamma^0_{xy} \end{pmatrix} + z \begin{pmatrix} \kappa^0_{xx} \\ \kappa^0_{yy} \\ \kappa^0_{xy} \end{pmatrix} \right] \mathrm{d}z. \tag{19.39}$$

The moment flows M^0_{xx}, M^0_{yy}, M^0_{xy} are as follows:

$$\begin{pmatrix} M^0_{xx} \\ M^0_{yy} \\ M^0_{xy} \end{pmatrix} = \int_h \begin{pmatrix} \sigma_{xx} \\ \sigma_{yy} \\ \tau_{xy} \end{pmatrix} z\mathrm{d}z = \int_h \begin{bmatrix} Q_{11} & Q_{12} & 0 \\ Q_{12} & Q_{22} & 0 \\ 0 & 0 & Q_{66} \end{bmatrix} \left[\begin{pmatrix} \varepsilon^0_{xx} \\ \varepsilon^0_{yy} \\ \gamma^0_{xy} \end{pmatrix} + z \begin{pmatrix} \kappa^0_{xx} \\ \kappa^0_{yy} \\ \kappa^0_{xy} \end{pmatrix} \right] z\mathrm{d}z. \tag{19.40}$$

Since neither the reduced stiffnesses nor the strains quantities are functions of the coordinate z when the core layer is neglected, these expressions can also be written as:

$$\begin{pmatrix} N^0_{xx} \\ N^0_{yy} \\ N^0_{xy} \end{pmatrix} = \begin{bmatrix} Q_{11} & Q_{12} & 0 \\ Q_{12} & Q_{22} & 0 \\ 0 & 0 & Q_{66} \end{bmatrix} \left[\begin{pmatrix} \varepsilon^0_{xx} \\ \varepsilon^0_{yy} \\ \gamma^0_{xy} \end{pmatrix} \int_h \mathrm{d}z + \begin{pmatrix} \kappa^0_{xx} \\ \kappa^0_{yy} \\ \kappa^0_{xy} \end{pmatrix} \int_h z\mathrm{d}z \right]. \tag{19.41}$$

We split the integral over the cross-sectional height h into the proportions of the upper and lower facesheet as follows:

$$\begin{aligned} \begin{pmatrix} N^0_{xx} \\ N^0_{yy} \\ N^0_{xy} \end{pmatrix} = \begin{bmatrix} Q_{11} & Q_{12} & 0 \\ Q_{12} & Q_{22} & 0 \\ 0 & 0 & Q_{66} \end{bmatrix} \Bigg[& \begin{pmatrix} \varepsilon^0_{xx} \\ \varepsilon^0_{yy} \\ \gamma^0_{xy} \end{pmatrix} \left(\int_{-e_1-\frac{h_1}{2}}^{-e_1+\frac{h_1}{2}} \mathrm{d}z + \int_{e_2-\frac{h_2}{2}}^{e_2+\frac{h_2}{2}} \mathrm{d}z \right) \\ & + \begin{pmatrix} \kappa^0_{xx} \\ \kappa^0_{yy} \\ \kappa^0_{xy} \end{pmatrix} \left(\int_{-e_1-\frac{h_1}{2}}^{-e_1+\frac{h_1}{2}} z\mathrm{d}z + \int_{e_2-\frac{h_2}{2}}^{e_2+\frac{h_2}{2}} z\mathrm{d}z \right) \Bigg]. \end{aligned} \tag{19.42}$$

For the moment flows M^0_{xx}, M^0_{yy}, M^0_{xy} follows analogously:

$$\begin{pmatrix} M^0_{xx} \\ M^0_{yy} \\ M^0_{xy} \end{pmatrix} = \begin{bmatrix} Q_{11} & Q_{12} & 0 \\ Q_{12} & Q_{22} & 0 \\ 0 & 0 & Q_{66} \end{bmatrix} \left[\begin{pmatrix} \varepsilon^0_{xx} \\ \varepsilon^0_{yy} \\ \gamma^0_{xy} \end{pmatrix} \begin{pmatrix} \int\limits_{-e_1-\frac{h_1}{2}}^{-e_1+\frac{h_1}{2}} z\mathrm{d}z + \int\limits_{e_2-\frac{h_2}{2}}^{e_2+\frac{h_2}{2}} z\mathrm{d}z \end{pmatrix} + \begin{pmatrix} \kappa^0_{xx} \\ \kappa^0_{yy} \\ \kappa^0_{xy} \end{pmatrix} \begin{pmatrix} \int\limits_{-e_1-\frac{h_1}{2}}^{-e_1+\frac{h_1}{2}} z^2\mathrm{d}z + \int\limits_{e_2-\frac{h_2}{2}}^{e_2+\frac{h_2}{2}} z^2\mathrm{d}z \end{pmatrix} \right], \tag{19.43}$$

with

$$\begin{aligned} \int\limits_{-e_1-\frac{h_1}{2}}^{-e_1+\frac{h_1}{2}} \mathrm{d}z + \int\limits_{e_2-\frac{h_2}{2}}^{e_2+\frac{h_2}{2}} \mathrm{d}z &= h_1 + h_2, \\ \int\limits_{-e_1-\frac{h_1}{2}}^{-e_1+\frac{h_1}{2}} z\mathrm{d}z + \int\limits_{e_2-\frac{h_2}{2}}^{e_2+\frac{h_2}{2}} z\mathrm{d}z &= -e_1 h_1 + e_2 h_2 = 0, \\ \int\limits_{-e_1-\frac{h_1}{2}}^{-e_1+\frac{h_1}{2}} z^2\mathrm{d}z + \int\limits_{e_2-\frac{h_2}{2}}^{e_2+\frac{h_2}{2}} z^2\mathrm{d}z &= e_1^2 h_1 + e_2^2 h_2 + \frac{h_1^3}{12} + \frac{h_2^3}{12}. \end{aligned} \tag{19.44}$$

In the last expression, the two terms $\frac{h_1^3}{12}$ and $\frac{h_2^3}{12}$ can be neglected as moments of inertia of the facesheets:

$$\int\limits_{-e_1-\frac{h_1}{2}}^{-e_1+\frac{h_1}{2}} z^2\mathrm{d}z + \int\limits_{e_2-\frac{h_2}{2}}^{e_2+\frac{h_2}{2}} z^2\mathrm{d}z = e_1^2 h_1 + e_2^2 h_2 = d^2 \frac{h_1 h_2}{h_1 + h_2}. \tag{19.45}$$

The shear force flows Q_x and Q_y result from the integration of the transverse shear stresses τ_{xz} and τ_{yz} over the sandwich thickness, whereby we only take into account the core:

$$\begin{aligned} \begin{pmatrix} Q_y \\ Q_x \end{pmatrix} &= \int\limits_{-e_1}^{e_2} \begin{pmatrix} \tau_{yz} \\ \tau_{xz} \end{pmatrix} \mathrm{d}z = \int\limits_{-e_1}^{e_2} \begin{bmatrix} C_{44} & 0 \\ 0 & C_{55} \end{bmatrix} \begin{pmatrix} \gamma_{yz} \\ \gamma_{xz} \end{pmatrix} \mathrm{d}z \\ &= d \begin{bmatrix} C_{44} & 0 \\ 0 & C_{55} \end{bmatrix} \begin{pmatrix} \gamma_{yz} \\ \gamma_{xz} \end{pmatrix} = d \begin{bmatrix} G_{yz} & 0 \\ 0 & G_{xz} \end{bmatrix} \begin{pmatrix} \gamma_{yz} \\ \gamma_{xz} \end{pmatrix}. \end{aligned} \tag{19.46}$$

The quantities G_{yz} and G_{xz} are the two transverse shear moduli of the sandwich core. The constitutive law in the context of FSDT

$$\begin{pmatrix} N_{xx}^0 \\ N_{yy}^0 \\ N_{xy}^0 \\ M_{xx}^0 \\ M_{yy}^0 \\ M_{xy}^0 \\ Q_y \\ Q_x \end{pmatrix} = \begin{bmatrix} A_{11} & A_{12} & A_{16} & B_{11} & B_{12} & B_{16} & 0 & 0 \\ A_{12} & A_{22} & A_{26} & B_{12} & B_{22} & B_{26} & 0 & 0 \\ A_{16} & A_{26} & A_{66} & B_{16} & B_{26} & B_{66} & 0 & 0 \\ B_{11} & B_{12} & B_{16} & D_{11} & D_{12} & D_{16} & 0 & 0 \\ B_{12} & B_{22} & B_{26} & D_{12} & D_{22} & D_{26} & 0 & 0 \\ B_{16} & B_{26} & B_{66} & D_{16} & D_{26} & D_{66} & 0 & 0 \\ 0 & 0 & 0 & 0 & 0 & 0 & A_{44} & A_{45} \\ 0 & 0 & 0 & 0 & 0 & 0 & A_{45} & A_{55} \end{bmatrix} \begin{pmatrix} \frac{\partial u_0}{\partial x} \\ \frac{\partial v_0}{\partial y} \\ \frac{\partial u_0}{\partial y} + \frac{\partial v_0}{\partial x} \\ \frac{\partial \psi_x}{\partial x} \\ \frac{\partial \psi_y}{\partial y} \\ \frac{\partial \psi_x}{\partial y} + \frac{\partial \psi_y}{\partial x} \\ \frac{\partial w_0}{\partial y} + \psi_y \\ \frac{\partial w_0}{\partial x} + \psi_x \end{pmatrix} \tag{19.47}$$

can be specified for the sandwich considered here as:

$$\begin{aligned} \begin{bmatrix} A_{11} & A_{12} & A_{16} \\ A_{12} & A_{22} & A_{26} \\ A_{16} & A_{26} & A_{66} \end{bmatrix} &= (h_1 + h_2) \begin{bmatrix} Q_{11} & Q_{12} & 0 \\ Q_{12} & Q_{22} & 0 \\ 0 & 0 & Q_{66} \end{bmatrix} \\ &= (h_1 + h_2) \begin{bmatrix} \frac{E_{xx}}{1-\nu_{xy}\nu_{yx}} & \frac{\nu_{xy}E_{yy}}{1-\nu_{xy}\nu_{yx}} & 0 \\ \frac{\nu_{xy}E_{yy}}{1-\nu_{xy}\nu_{yx}} & \frac{E_{yy}}{1-\nu_{xy}\nu_{yx}} & 0 \\ 0 & 0 & G_{xy} \end{bmatrix}, \\ \begin{bmatrix} B_{11} & B_{12} & B_{16} \\ B_{12} & B_{22} & B_{26} \\ B_{16} & B_{26} & B_{66} \end{bmatrix} &= \begin{bmatrix} 0\,0\,0 \\ 0\,0\,0 \\ 0\,0\,0 \end{bmatrix}, \\ \begin{bmatrix} D_{11} & D_{12} & D_{16} \\ D_{12} & D_{22} & D_{26} \\ D_{16} & D_{26} & D_{66} \end{bmatrix} &= d^2 \frac{h_1 h_2}{h_1 + h_2} \begin{bmatrix} \frac{E_{xx}}{1-\nu_{xy}\nu_{yx}} & \frac{\nu_{xy}E_{yy}}{1-\nu_{xy}\nu_{yx}} & 0 \\ \frac{\nu_{xy}E_{yy}}{1-\nu_{xy}\nu_{yx}} & \frac{E_{yy}}{1-\nu_{xy}\nu_{yx}} & 0 \\ 0 & 0 & G_{xy} \end{bmatrix}, \\ \begin{bmatrix} A_{44} & A_{45} \\ A_{45} & A_{55} \end{bmatrix} &= d \begin{bmatrix} G_{yz} & 0 \\ 0 & G_{xz} \end{bmatrix}. \end{aligned} \tag{19.48}$$

Obviously, all stiffnesses B_{ij} are eliminated if all considerations are related to the neutral plane. An orthotropic sandwich is therefore free of bending-extension coupling in relation to the neutral plane. In addition, the stiffnesses A_{16}, A_{26}, D_{16}, D_{26} and A_{45} are also eliminated for such a sandwich. Summarized, this results in the following form of the constitutive law (19.47):

$$\begin{pmatrix} N_{xx}^0 \\ N_{yy}^0 \\ N_{xy}^0 \\ M_{xx}^0 \\ M_{yy}^0 \\ M_{xy}^0 \\ Q_y \\ Q_x \end{pmatrix} = \begin{bmatrix} A_{11} & A_{12} & 0 & 0 & 0 & 0 & 0 & 0 \\ A_{12} & A_{22} & 0 & 0 & 0 & 0 & 0 & 0 \\ 0 & 0 & A_{66} & 0 & 0 & 0 & 0 & 0 \\ 0 & 0 & 0 & D_{11} & D_{12} & 0 & 0 & 0 \\ 0 & 0 & 0 & D_{12} & D_{22} & 0 & 0 & 0 \\ 0 & 0 & 0 & 0 & 0 & D_{66} & 0 & 0 \\ 0 & 0 & 0 & 0 & 0 & 0 & A_{44} & 0 \\ 0 & 0 & 0 & 0 & 0 & 0 & 0 & A_{55} \end{bmatrix} \begin{pmatrix} \frac{\partial u_0}{\partial x} \\ \frac{\partial v_0}{\partial y} \\ \frac{\partial u_0}{\partial y} + \frac{\partial v_0}{\partial x} \\ \frac{\partial \psi_x}{\partial x} \\ \frac{\partial \psi_y}{\partial y} \\ \frac{\partial \psi_x}{\partial y} + \frac{\partial \psi_y}{\partial x} \\ \frac{\partial w_0}{\partial y} + \psi_y \\ \frac{\partial w_0}{\partial x} + \psi_x \end{pmatrix}. \tag{19.49}$$

The equilibrium conditions for the sandwich considered here are as follows:

$$\begin{aligned} A_{11}\frac{\partial^2 u_0}{\partial x^2} + A_{66}\frac{\partial^2 u_0}{\partial y^2} + (A_{12} + A_{66})\frac{\partial^2 v_0}{\partial x \partial y} &= 0, \\ (A_{12} + A_{66})\frac{\partial^2 u_0}{\partial x \partial y} + A_{66}\frac{\partial^2 v_0}{\partial x^2} + A_{22}\frac{\partial^2 v_0}{\partial y^2} &= 0, \\ D_{11}\frac{\partial^2 \psi_x}{\partial x^2} + D_{66}\frac{\partial^2 \psi_x}{\partial y^2} + (D_{12} + D_{66})\frac{\partial^2 \psi_y}{\partial x \partial y} - A_{55}\left(\psi_x + \frac{\partial w_0}{\partial x}\right) &= 0, \\ (D_{12} + D_{66})\frac{\partial^2 \psi_x}{\partial x \partial y} + D_{66}\frac{\partial^2 \psi_y}{\partial x^2} + D_{22}\frac{\partial^2 \psi_y}{\partial y^2} - A_{44}\left(\psi_y + \frac{\partial w_0}{\partial y}\right) &= 0, \\ A_{55}\left(\frac{\partial \psi_x}{\partial x} + \frac{\partial^2 w_0}{\partial x^2}\right) + A_{44}\left(\frac{\partial \psi_y}{\partial y} + \frac{\partial^2 w_0}{\partial y^2}\right) + p &= 0. \end{aligned} \tag{19.50}$$

Since the coupling terms B_{ij} result in zero, the disk and plate behaviour are decoupled from each other here.

The strain energy for a rectangular sandwich is

$$\begin{aligned} \Pi_i = \frac{1}{2}\int_0^b \int_0^a \Bigg\{ & A_{11}\left(\frac{\partial u_0}{\partial x}\right)^2 + 2A_{12}\frac{\partial u_0}{\partial x}\frac{\partial v_0}{\partial y} + A_{22}\left(\frac{\partial v_0}{\partial y}\right)^2 + A_{66}\left(\frac{\partial u_0}{\partial y} + \frac{\partial v_0}{\partial x}\right)^2 \\ & + D_{11}\left(\frac{\partial \psi_x}{\partial x}\right)^2 + 2D_{12}\frac{\partial \psi_x}{\partial x}\frac{\partial \psi_y}{\partial y} + D_{22}\left(\frac{\partial \psi_y}{\partial y}\right)^2 + D_{66}\left(\frac{\partial \psi_x}{\partial y} + \frac{\partial \psi_y}{\partial x}\right)^2 \\ & + A_{44}\left(\frac{\partial w_0}{\partial y} + \psi_y\right)^2 + A_{55}\left(\frac{\partial w_0}{\partial x} + \psi_x\right)^2 \Bigg\} \mathrm{d}x\mathrm{d}y. \end{aligned} \tag{19.51}$$

It turns out that all analysis methods for orthotropic disks and orthotropic plates can be used for such an orthotropic sandwich. More detailed explanations can be omitted at this point.

19.3 General Formulation

For a sandwich with arbitrary structure with linear-elastic material properties in facesheets and core, in general no neutral plane can be determined. For this case, a general formulation of the constitutive law (19.47) in the context of FSDT can be given as follows. First, the stiffness matrices $\underline{\underline{A}}_1$, $\underline{\underline{B}}_1$, $\underline{\underline{D}}_1$ of facesheet 1 and $\underline{\underline{A}}_2$, $\underline{\underline{B}}_2$, $\underline{\underline{D}}_2$ of facesheet 2 are determined with respect to their middle planes:

$$A_{ij,1} = \int_{-\frac{h_1}{2}}^{+\frac{h_1}{2}} \bar{Q}_{ij,1} \mathrm{d}z_1, \quad B_{ij,1} = \int_{-\frac{h_1}{2}}^{+\frac{h_1}{2}} \bar{Q}_{ij,1} z \mathrm{d}z_1, \quad D_{ij,1} = \int_{-\frac{h_1}{2}}^{+\frac{h_1}{2}} \bar{Q}_{ij,1} z^2 \mathrm{d}z_1 \tag{19.52}$$

and

$$A_{ij,2} = \int_{-\frac{h_2}{2}}^{+\frac{h_2}{2}} \bar{Q}_{ij,2} \mathrm{d}z_2, \quad B_{ij,2} = \int_{-\frac{h_2}{2}}^{+\frac{h_2}{2}} \bar{Q}_{ij,2} z \mathrm{d}z_2, \quad D_{ij,2} = \int_{-\frac{h_2}{2}}^{+\frac{h_2}{2}} \bar{Q}_{ij,2} z^2 \mathrm{d}z_2. \tag{19.53}$$

It should be noted here that the facesheets can also have a laminate-like structure and therefore in such a case the above integrals must be broken down into partial integrals over the individual layers of the facesheet laminates. The reference axes z_1 and z_2 are local facesheet axes with origin in the middle plane of the facesheet laminates.

To determine the stiffness matrices $\underline{\underline{A}}$, $\underline{\underline{B}}$, $\underline{\underline{D}}$ of the sandwich, the parallel axis theorem (see e.g. Kollár and Springer 2003) is used (Fig. 19.7). Let the two reference planes 1 and 2 be given with the distance e, whereby the stiffness matrices $\underline{\underline{A}}$, $\underline{\underline{B}}$, $\underline{\underline{D}}$ are given in relation to plane 1. The relationship $\bar{z} = z - e$ exists between the two axes z and $\bar{z}$. The stiffness matrices $\underline{\underline{A}}^e$, $\underline{\underline{B}}^e$, $\underline{\underline{D}}^e$ in relation to plane 2 result from the constitutive law

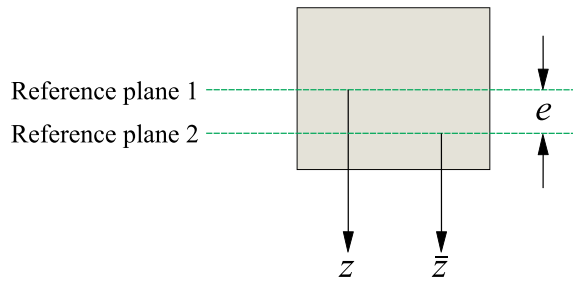


Fig. 19.7 Parallel axis theorem

$$A_{ij} = \sum_{k=1}^{N} \bar{Q}_{ij,k} \left(z_k - z_{k-1}\right),$$
$$B_{ij} = \frac{1}{2} \sum_{k=1}^{N} \bar{Q}_{ij,k} \left(z_k^2 - z_{k-1}^2\right),$$
$$D_{ij} = \frac{1}{3} \sum_{k=1}^{N} \bar{Q}_{ij,k} \left(z_k^3 - z_{k-1}^3\right), \tag{19.54}$$

by replacing z_k with $z_k - e$:

$$\begin{aligned}
A_{ij}^e &= \sum_{k=1}^{N} \bar{Q}_{ij,k} \left[(z_k - e) - (z_{k-1} - e)\right] \\
&= \sum_{k=1}^{N} \bar{Q}_{ij,k} \left(z_k - z_{k-1}\right) \\
&= A_{ij}, \\
B_{ij}^e &= \frac{1}{2} \sum_{k=1}^{N} \bar{Q}_{ij,k} \left[(z_k - e)^2 - (z_{k-1} - e)^2\right] \\
&= \sum_{k=1}^{N} \bar{Q}_{ij,k} \left[\frac{z_k^2 - z_{k-1}^2}{2} - e(z_k - z_{k-1})\right] \\
&= B_{ij} - eA_{ij}, \\
D_{ij}^e &= \frac{1}{3} \sum_{k=1}^{N} \bar{Q}_{ij,k} \left[(z_k - e)^3 - (z_{k-1} - e)^3\right] \\
&= \sum_{k=1}^{N} \bar{Q}_{ij,k} \left[\frac{z_k^3 - z_{k-1}^3}{3} - 2e\frac{z_k^2 - z_{k-1}^2}{2} + e^2(z_k - z_{k-1})\right] \\
&= D_{ij} - 2eB_{ij} + e^2 A_{ij}.
\end{aligned} \tag{19.55}$$

In the case of a sandwich with arbitrary reference plane (distances e_1 and e_2 from the upper and lower facesheet, Fig. 19.8), the stiffness matrices follow as:

$$\begin{bmatrix} A_{11} & A_{12} & A_{16} \\ A_{12} & A_{22} & A_{26} \\ A_{16} & A_{26} & A_{66} \end{bmatrix} = \begin{bmatrix} A_{11,1} & A_{12,1} & A_{16,1} \\ A_{12,1} & A_{22,1} & A_{26,1} \\ A_{16,1} & A_{26,1} & A_{66,1} \end{bmatrix} + \begin{bmatrix} A_{11,2} & A_{12,2} & A_{16,2} \\ A_{12,2} & A_{22,2} & A_{26,2} \\ A_{16,2} & A_{26,2} & A_{66,2} \end{bmatrix},$$
$$\begin{bmatrix} B_{11} & B_{12} & B_{16} \\ B_{12} & B_{22} & B_{26} \\ B_{16} & B_{26} & B_{66} \end{bmatrix} = \begin{bmatrix} B_{11,1} & B_{12,1} & B_{16,1} \\ B_{12,1} & B_{22,1} & B_{26,1} \\ B_{16,1} & B_{26,1} & B_{66,1} \end{bmatrix} + \begin{bmatrix} B_{11,2} & B_{12,2} & B_{16,2} \\ B_{12,2} & B_{22,2} & B_{26,2} \\ B_{16,2} & B_{26,2} & B_{66,2} \end{bmatrix}$$

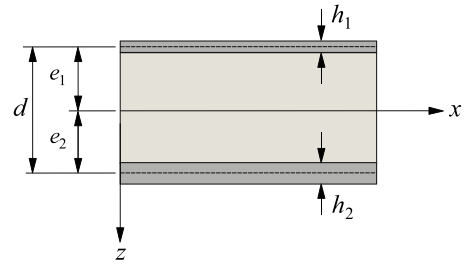


Fig. 19.8 Sandwich with arbitrary reference plane

$$
\begin{aligned}
&+ e_1 \begin{bmatrix} A_{11,1} & A_{12,1} & A_{16,1} \\ A_{12,1} & A_{22,1} & A_{26,1} \\ A_{16,1} & A_{26,1} & A_{66,1} \end{bmatrix} - e_2 \begin{bmatrix} A_{11,2} & A_{12,2} & A_{16,2} \\ A_{12,2} & A_{22,2} & A_{26,2} \\ A_{16,2} & A_{26,2} & A_{66,2} \end{bmatrix}, \\
\begin{bmatrix} D_{11} & D_{12} & D_{16} \\ D_{12} & D_{22} & D_{26} \\ D_{16} & D_{26} & D_{66} \end{bmatrix} &= \begin{bmatrix} D_{11,1} & D_{12,1} & D_{16,1} \\ D_{12,1} & D_{22,1} & D_{26,1} \\ D_{16,1} & D_{26,1} & D_{66,1} \end{bmatrix} + \begin{bmatrix} D_{11,2} & D_{12,2} & D_{16,2} \\ D_{12,2} & D_{22,2} & D_{26,2} \\ D_{16,2} & D_{26,2} & D_{66,2} \end{bmatrix} \\
&+ 2e_1 \begin{bmatrix} B_{11,1} & B_{12,1} & B_{16,1} \\ B_{12,1} & B_{22,1} & B_{26,1} \\ B_{16,1} & B_{26,1} & B_{66,1} \end{bmatrix} - 2e_2 \begin{bmatrix} B_{11,2} & B_{12,2} & B_{16,2} \\ B_{12,2} & B_{22,2} & B_{26,2} \\ B_{16,2} & B_{26,2} & B_{66,2} \end{bmatrix} \\
&+ e_1^2 \begin{bmatrix} A_{11,1} & A_{12,1} & A_{16,1} \\ A_{12,1} & A_{22,1} & A_{26,1} \\ A_{16,1} & A_{26,1} & A_{66,1} \end{bmatrix} + e_2^2 \begin{bmatrix} A_{11,2} & A_{12,2} & A_{16,2} \\ A_{12,2} & A_{22,2} & A_{26,2} \\ A_{16,2} & A_{26,2} & A_{66,2} \end{bmatrix}.
\end{aligned}
\tag{19.56}
$$

For the shear stiffnesses in (19.47) we have with $i, j = 4.5$:

$$A_{ij} = d\bar{C}_{ij}. \tag{19.57}$$

References

Allen HG (1969): *Analysis and design of structural sandwich panels*, Pergamon Press, Oxford, UK.

Altenbach H, Altenbach J, Rikards R (1996): *Einführung in die Mechanik der Laminat- und Sandwichtragwerke*, Deutscher Verlag für Grundstoffindustrie, Stuttgart, Germany.

Altenbach H, Altenbach J, Kissing W (2004): *Mechanics of composite structural elements*, Springer, Berlin et al., Germany.

Klein B (1994): *Leichtbau-Konstruktion*, 2nd edition, Vieweg, Braunschweig Wiesbaden, Germany.

Kollár L, Springer GS (2003): *Mechanics of composite structures*, Cambridge University Press, Cambridge et al., UK.

Mittelstedt C (2021): *Rechenmethoden des Leichtbaus*, Springer Vieweg, Berlin, Germany.

Plantema FJ (1966): *Sandwich construction. The bending and buckling of sandwich beams, plates and shells*, Wiley, New York, USA.

Stamm K, Witte H (1974): *Sandwichkonstruktionen*, Springer, Wien et al., Austria.
Wiedemann J (2006): *Leichtbau, Elemente und Konstruktion*, 3rd edition, Springer, Berlin et al., Germany.
Zenkert D (1995): *An introduction to sandwich construction*, EMAS Publishing, Warrington, UK.



The Free-Edge Effect

20

This chapter deals with the occurrence of localized and potentially singular interlaminar stresses at free edges of laminates. This phenomenon is usually referred to as the so-called free-edge effect and requires special consideration when analyzing and designing laminate structures. After a basic introduction to the problem, some closed-form analytical and numerical approaches are considered and related problems are discussed.

20.1 Introduction

The deformation and stress analysis of laminates is usually carried out (unless a higher theory is required) within the framework of Classical Laminated Plate Theory (CLPT), in which a plane stress state is assumed for the individual layers of the laminate. The strength assessment of a laminate is also usually based on the individual layer stresses of CLPT. As proven as this procedure may be for the 'interior' of a laminate, it can be inadmissible in the area of the edges of laminates, especially if they are free edges, i.e. unloaded from the outside. Although a free laminate edge may intuitively seem quite harmless, it is precisely here that strongly localized interlaminar stresses can occur, which make up the so-called 'free-edge effect'. These interlaminar stresses can easily lead to premature laminate failure, especially in the form of edge delaminations, and therefore require special consideration.

This chapter aims to introduce the reader to the free-edge effect in composite laminates and its evaluation, particularly with regard to the fact that constructive freedom in the choice of laminate layups is used to make the free-edge effect as harmless as possible. Firstly, the nature of the free-edge effect and the mechanisms of its generally undesirable development are introduced. Several different practical methods for analyzing the free-edge effect are

© The Author(s), under exclusive license to Springer-Verlag GmbH, DE, part of Springer Nature 2025

C. Mittelstedt, *Mechanics of Composite Structures*,
https://doi.org/10.1007/978-3-662-70788-3_20

then presented. On the one hand, this is the evaluation with the help of delamination forces and moments, which can be calculated quite easily from the plane stress fields according to CLPT. Furthermore, there is always the possibility of detailed numerical analysis using the Finite Element Method, but due to the singular character of the edge stress field, very complex meshing is often required and one therefore quickly reaches the limits of practical feasibility. A closed-form analytical method is the so-called Force-Balance-Method, which is based on layerwise stress approaches and an energy analysis. Alternatively, the implementation of a specially developed semi-analytical method is presented, which has proven to be extremely efficient and yet comparable to finite element calculations in terms of accuracy. In this method, the individual laminate layers are divided into virtual sub-layers or so-called mathematical layers. In each mathematical layer, a displacement approach is formulated whose unknowns are determined from the principle of the minimum of the total elastic potential and from the given boundary conditions. The methods described make it possible to find out how the free-edge effect problem given in a specific case can be minimised as far as possible. Some general recommendations for practice and an outlook on further approaches and problems round off this chapter.

20.2 The Nature of the Free-Edge Effect

To clarify the occurrence of interlaminar stresses in the vicinity of free laminate edges, we consider two simple examples. Consider the situation of a laminate consisting of four layers under uniaxial strain ε_{xx} (Fig. 20.1). We assume the coordinate axes x, y, z so that the middle plane of the laminate is formed by the x- and y-axes, where y is measured from the free edge inwards. The laminate structure is assumed to be symmetric with respect to the middle plane. CLPT predicts inplane or intralaminar stresses, namely the two inplane normal stresses σ_{xx} and σ_{yy} and the inplane shear stress τ_{xy}. The interlaminar stresses, i.e. the two interlaminar shear stresses τ_{xz} and τ_{yz} and the interlaminar normal stress σ_{zz}, are neglected in a calculation within the framework of CLPT, although their concentrated occurrence in the vicinity of free laminate edges can be easily deduced from very basic equilibrium considerations in connection with the discontinuous change of the elastic material properties in the interfaces between unequal laminate layers. We assume that the laminate under consideration is sufficiently long in the longitudinal direction x. It follows that, according to St. Venant's principle, both the strains and stresses as well as the transverse displacement components v and w are decoupled from the x-direction and thus depend exclusively on the transverse coordinates y and z. Let h be the total thickness of the laminate. In the following, it is assumed that all layers have the same thickness $\frac{h}{4}$.

20.2.1 The Free-Edge Effect in a Cross-Ply Laminate

As a first example, we consider the case of a cross-ply laminate with the layup $[0°/90°]_S$ under uniaxial strain ε_{xx} as shown in Fig. 20.1. Let us first consider the case where the laminate layers are not bonded to form a laminate (see Fig. 20.1, top) so that they can deform independently of each other under the uniaxial strain. Due to the different transverse contraction properties of the 0°- and the 90°-layers, the 0°-layers have higher transverse strains ε_{yy} than the inner 90°-layers, as the contraction in the y-direction runs against the principal material directions of the 0°-layers. It follows that the resulting layerwise

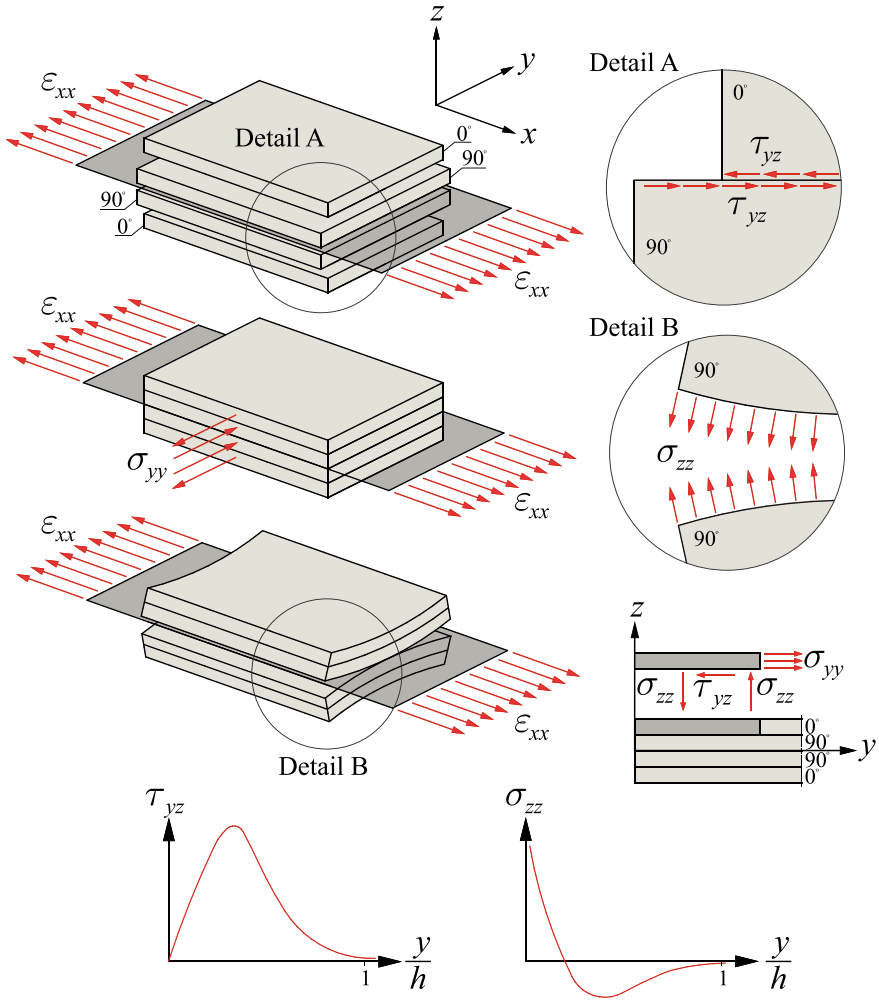


Fig. 20.1 The free-edge effect in a cross-ply laminate $[0°/90°]_S$ under uniaxial strain

displacements v will be discontinuous in the interfaces of the layers. Note, however, that in the actual laminate structure, the displacements at the interfaces must be continuous, since we assume a perfect bond between all individual laminate layers. Consequently, we would have to apply tensile stresses σ_{yy} to the 0°-layers (see also Fig. 20.1, middle, where σ_{yy} is shown as an edge stress), while compressive stresses must be applied to the inner 90°-layers in order to ensure the continuity of the layerwise displacements v. These stresses σ_{yy}, which maintain the compatibility of the transverse displacements v, are exactly the values predicted by a calculation using CLPT. Their absolute values are identical in the 0°- and 90°-layers, so that the resulting total stress over the thickness disappears under the present load:

$$\int_{-\frac{h}{2}}^{\frac{h}{2}} \sigma_{yy} \mathrm{d}z = 0. \tag{20.1}$$

Note also that at the free edges the stresses σ_{yy} must actually disappear due to the given boundary conditions at the free laminate edge in order to maintain the equilibrium of the forces in the y-direction according to the free body diagram of the upper 0°-layer shown in Fig. 20.1. As a result, the interlaminar shear stresses τ_{yz} must also occur in the interface at $z = \frac{h}{4}$ in the given cross-ply laminate (see Fig. 20.1, detail A). A typical distribution of τ_{yz} in y-direction in the interface between the 0°- and 90°-layers at $z = \frac{h}{4}$ is shown in Fig. 20.1, bottom. The following relationship applies between σ_{yy} and τ_{yz} for sufficiently high values for y:

$$\int_0^y \tau_{yz} \mathrm{d}\hat{y} = \int_{\frac{h}{4}}^{\frac{h}{2}} \sigma_{yy} \mathrm{d}z. \tag{20.2}$$

However, the above-mentioned stress results do not have a common line of action, so that in order to maintain the equilibrium of the moments with respect to the x-axis, the interlaminar normal stresses σ_{zz} in the interface between the 0°- and the 90°-layer at $z = \frac{d}{4}$ (see Fig. 20.1, detail B) must occur according to the condition

$$\int_0^y \sigma_{zz} \hat{y} \mathrm{d}\hat{y} = -\int_{\frac{h}{4}}^{\frac{h}{2}} \sigma_{yy} \left(z - \frac{h}{4} \right) \mathrm{d}z. \tag{20.3}$$

Since the interlaminar stress component σ_{zz} is the only stress acting in the z-direction in the interface at $z = \frac{h}{4}$, the resulting integral must disappear with respect to the y-direction, i.e.

$$\int_0^y \sigma_{zz} \mathrm{d}\hat{y} = 0. \tag{20.4}$$

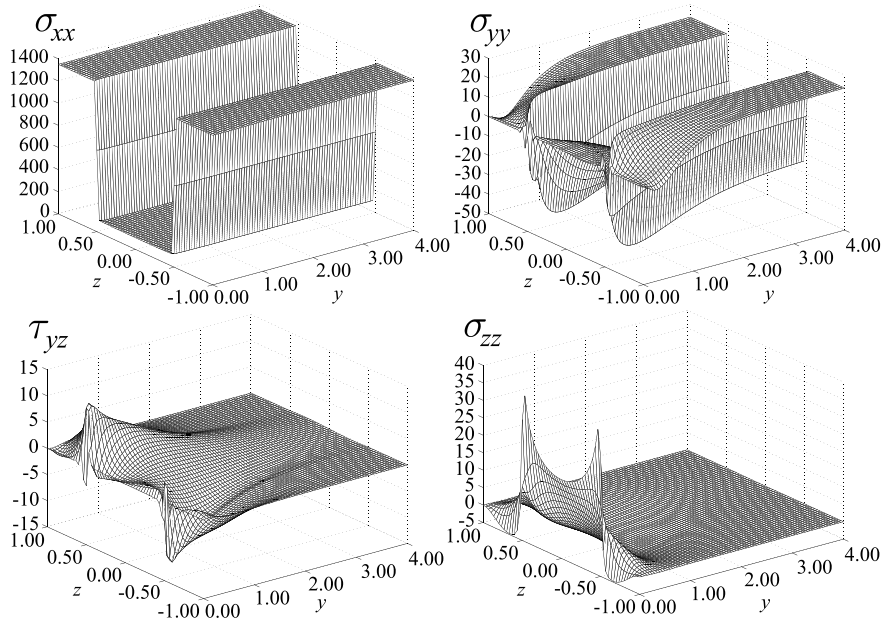


Fig. 20.2 Stress distributions for the free-edge effect in a cross-ply laminate $\left[0°/90°\right]_S$ under uniaxial strain ε_{xx} according to Mittelstedt and Becker (2007b)

This means that σ_{zz} must change its sign at least once along the y-axis to ensure the force equilibrium in the thickness direction (see Fig. 20.1, bottom, where a typical distribution of σ_{zz} in the interface between the 0°-layer and the 90°-layer is shown). It is important to note that the interlaminar normal stress σ_{zz} has its maximum tensile value directly at the free laminate edge in the interface between the 0°- and the 90°-layer. In fact, a mathematical singularity occurs at this point at the free laminate edge for the stress σ_{zz}, which makes this location particularly susceptible to the occurrence of interlaminar failure, e.g. due to delamination.

Figure 20.2 shows typical stress distributions for the free-edge effect in a cross-ply laminate $[0°/90°]_S$ under uniaxial strain ε_{xx} according to Mittelstedt and Becker (2007b). This clearly shows the localized character of the free-edge effect, i.e. the occurrence of the two interlaminar stresses τ_{yz} and σ_{zz}.

In summary, it can be said that a three-dimensional and singular stress state occurs in the interfaces between two neighbouring unequal laminate layers near the free laminate edge of cross-ply laminates, which is primarily explained by the inequality of the elastic properties of the layers, in particular the different Poisson's ratios of the 0°- and 90°-layers.

20.2.2 The Free-Edge Effect in an Angle-Ply Laminate

As in the case of the cross-ply laminate, interlaminar free-edge stress fields also occur in symmetric angle-ply laminates. We consider the situation of an angle-ply laminate $[\pm 45°]_S$ under uniaxial strain ε_{xx} (Fig. 20.3). Firstly, the case is again considered in which the individual layers are not connected to each other and can deform freely and independently of each other. Under uniaxial strain, the individual layers exhibit different shear strains in the plane, as shown in Fig. 20.3, top. In order to maintain the compatibility of the resulting displacement fields in the interfaces of the actual laminate, the inplane shear stresses τ_{xy}, as predicted by CLPT, will have to be applied (see Fig. 20.3, middle, here τ_{xy} is shown as boundary stress). Here, too, the total resultant through the thickness must vanish, so that

$$\int_{-\frac{h}{2}}^{\frac{h}{2}} \tau_{xy} \mathrm{d}z = 0. \tag{20.5}$$

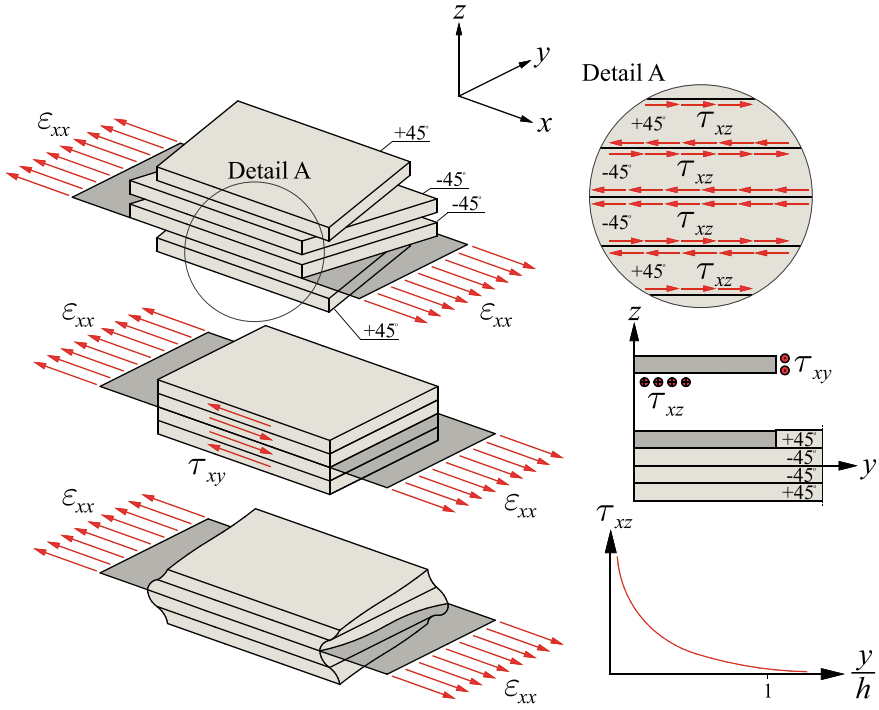


Fig. 20.3 The free-edge effect in an angle-ply laminate $[\pm 45°]_S$ under uniaxial strain

This is achieved by this stress occurring in the individual layers with identical absolute values of τ_{xy} according to CLPT, but with the opposite sign: in the outer $+45°$-layers, τ_{xy} must be positive, whereas in the inner $-45°$-layers τ_{xy} must have a negative sign in order to compensate for the inequality of the shear properties of the individual layers in the plane. However, since the intralaminar shear stress τ_{xy} in a laminate must disappear at the free laminate edge, the interlaminar shear stress τ_{xz} must also occur in the interface between the $+45°$- and the $-45°$-layer at $z = \frac{h}{4}$ for reasons of equilibrium of forces in the x-direction, as shown in Fig. 20.3 in the free-body diagram of the upper $+45°$-layer (see also detail A).

Here, too, the upper laminate layer shown in the free-body diagram is assumed to be sufficiently long in the y-direction so that CLPT applies at its inner end. The force equilibrium relates the two shear stresses τ_{xy} and τ_{xz} by their resultants according to the free body diagram in Fig. 20.3 as follows:

$$\int_0^y \tau_{xz} \mathrm{d}\hat{y} = \int_{\frac{h}{4}}^{\frac{h}{2}} \tau_{xy} \mathrm{d}z. \tag{20.6}$$

A typical distribution of τ_{xz} in the interface with respect to the y-axis is shown in Fig. 20.3, bottom. In the vicinity of the free laminate edge, τ_{xz} generally has steep gradients and is characterized by a mathematical singularity at the interface point at the free laminate edge. Due to the different shear properties in each layer, characteristic deformations occur at the laminate edge and in the cross-section of the laminate, as shown in Fig. 20.3. The free-edge effect present here in angle-ply laminates is of a pronounced three-dimensional and singular nature and also finds its main cause in the mismatch of the elastic material properties of neighbouring unequal layers, here in particular the discontinuous change in the shear properties in the interface between the $+45°$- and the $-45°$-layers.

Figure 20.4 shows stress distributions according to Mittelstedt and Becker (2007b) for the free-edge effect in an angle-ply laminate $[\pm 45°]_S$ under uniaxial strain ε_{xx}. Here, too, the very localized occurrence of singular interlaminar stresses can be observed.

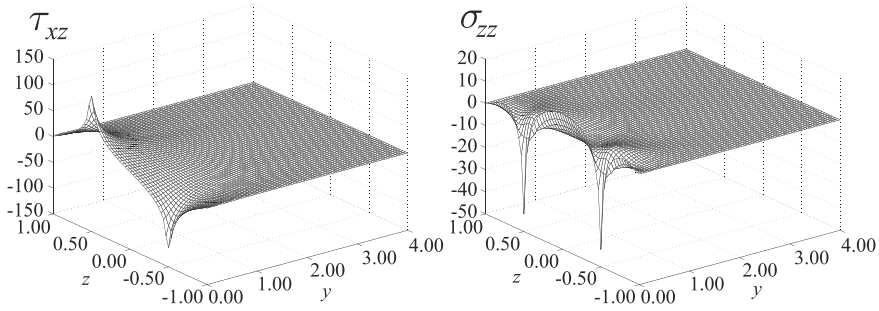


Fig. 20.4 Stress distributions for the free-edge effect in an angle-ply laminate $[\pm 45°]_S$ under uniaxial strain ε_{xx} according to Mittelstedt and Becker (2007b)

As a rule, it can be assumed that after a distance from the free laminate edge of approximately one laminate thickness h, the predictions of CLPT are essentially correct and a plane state of stress is restored. Therefore, the effects of free edges are generally limited to a very small edge area. Nevertheless, the occurrence of interlaminar stress concentrations at free edges is of great practical importance for the design and application of layered structural elements, as such stress concentrations can lead to interlaminar delamination failure.

20.2.3 The Free-Edge Effect in an Arbitrary Symmetric Laminate

20.2.3.1 State Variables and Governing Equations

We consider a symmetric laminate, consisting of N orthotropic layers, under uniaxial strain ε_{xx} (Fig. 20.5). It is assumed that the laminate is sufficiently long in the longitudinal direction x so that at a sufficient distance from the load application the displacement components v and w are independent of the longitudinal coordinate x due to St. Venant's principle. The longitudinal displacement component u, on the other hand, has a linear dependence on x due to the applied uniaxial strain ε_{xx}. We can therefore assume a displacement field of the following form in the laminate (see also Pipes and Pagano (1970)):

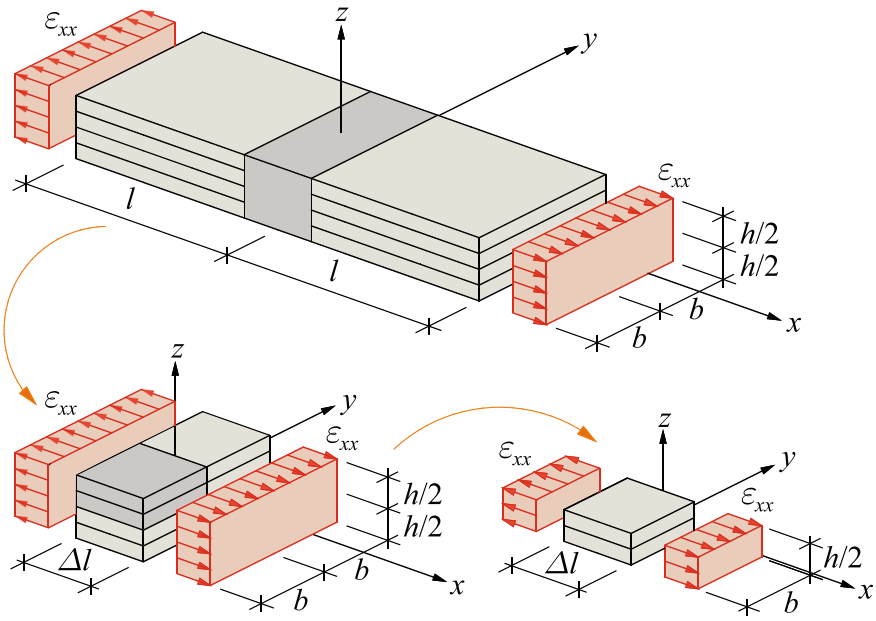


Fig. 20.5 Symmetric four-layered laminate under uniaxial strain (top), investigation of a laminate strip (bottom left) and consideration of a quarter model (bottom right)

$$
\begin{aligned}
u &= \varepsilon_{xx} x + U_1(y,z)\,, \\
v &= U_2(y,z)\,, \\
w &= U_3(y,z)\,.
\end{aligned} \tag{20.7}
$$

Here, the three unknown displacement functions $U_i(y,z)$ appear, which must be determined in order to fully describe the given free-effect problem. In the context of a geometrically linear theory, all strain components will be completely independent of the length coordinate x, so that:

$$
\begin{aligned}
\varepsilon_{xx} &= \frac{\partial u}{\partial x} = \text{const.}, \\
\varepsilon_{yy} &= \frac{\partial v}{\partial y} = \varepsilon_{yy}(y,z)\,, \\
\varepsilon_{zz} &= \frac{\partial w}{\partial z} = \varepsilon_{zz}(y,z)\,, \\
\gamma_{yz} &= \frac{\partial v}{\partial z} + \frac{\partial w}{\partial y} = \gamma_{yz}(y,z)\,, \\
\gamma_{xz} &= \frac{\partial u}{\partial z} + \frac{\partial w}{\partial x} = \gamma_{xz}(y,z)\,, \\
\gamma_{xy} &= \frac{\partial u}{\partial y} + \frac{\partial v}{\partial x} = \gamma_{xy}(y,z)\,.
\end{aligned} \tag{20.8}
$$

Assuming physical linearity, we apply Hooke's generalized law in the three-dimensional case, assuming a monoclinic material due to the arbitrary orientation of the individual laminate layers:

$$
\begin{pmatrix} \sigma_{xx} \\ \sigma_{yy} \\ \sigma_{zz} \\ \sigma_{yz} \\ \sigma_{xz} \\ \sigma_{xy} \end{pmatrix}
=
\begin{bmatrix}
C_{11} & C_{12} & C_{13} & 0 & 0 & C_{16} \\
C_{12} & C_{22} & C_{23} & 0 & 0 & C_{26} \\
C_{13} & C_{23} & C_{33} & 0 & 0 & C_{36} \\
0 & 0 & 0 & C_{44} & C_{45} & 0 \\
0 & 0 & 0 & C_{45} & C_{55} & 0 \\
C_{16} & C_{26} & C_{36} & 0 & 0 & C_{66}
\end{bmatrix}
\begin{pmatrix} \varepsilon_{xx} \\ \varepsilon_{yy} \\ \varepsilon_{zz} \\ \gamma_{yz} \\ \gamma_{xz} \\ \gamma_{xy} \end{pmatrix}. \tag{20.9}
$$

Accordingly, analogous to the strain components, all occurring stresses are also independent of the longitudinal coordinate x:

$$
\sigma_{ij} = \sigma_{ij}(y,z)\,. \tag{20.10}
$$

From now on, we want to use a layerwise notation. The k-th layer has the thickness h_k and the orientation angle θ_k in the xy-plane. The stress field of the k-th layer must fulfil the three-dimensional equilibrium conditions, which in the absence of volume forces and with $\frac{\partial \sigma_{i1,k}}{\partial x} = 0$ read:

$$\frac{\partial \tau_{xy,k}}{\partial y} + \frac{\partial \tau_{xz,k}}{\partial z} = 0,$$
$$\frac{\partial \sigma_{yy,k}}{\partial y} + \frac{\partial \tau_{yz,k}}{\partial z} = 0,$$
$$\frac{\partial \tau_{yz,k}}{\partial y} + \frac{\partial \sigma_{zz,k}}{\partial z} = 0. \tag{20.11}$$

Using the relations (20.8) and (20.9), the following coupled homogeneous partial differential equations of second order in the layer k follow from the equilibrium conditions (20.11), which determine the displacement field for the given free-edge effect situation:

$$C_{66,k}\frac{\partial^2 U_{1,k}}{\partial y^2} + C_{55,k}\frac{\partial^2 U_{1,k}}{\partial z^2} + C_{26,k}\frac{\partial^2 U_{2,k}}{\partial y^2} + C_{45,k}\frac{\partial^2 U_{2,k}}{\partial z^2} + \left(C_{36,k} + C_{45,k}\right)\frac{\partial^2 U_{3,k}}{\partial y \partial z} = 0,$$
$$C_{26,k}\frac{\partial^2 U_{1,k}}{\partial y^2} + C_{45,k}\frac{\partial^2 U_{1,k}}{\partial z^2} + C_{22,k}\frac{\partial^2 U_{2,k}}{\partial y^2} + C_{44,k}\frac{\partial^2 U_{2,k}}{\partial z^2} + \left(C_{23,k} + C_{44,k}\right)\frac{\partial^2 U_{3,k}}{\partial y \partial z} = 0,$$
$$\left(C_{36,k} + C_{45,k}\right)\frac{\partial^2 U_{1,k}}{\partial y \partial z} + \left(C_{23,k} + C_{44,k}\right)\frac{\partial^2 U_{2,k}}{\partial y \partial z} + C_{44,k}\frac{\partial^2 U_{3,k}}{\partial y^2} + C_{33,k}\frac{\partial^2 U_{3,k}}{\partial z^2} = 0. \tag{20.12}$$

20.2.3.2 Boundary and Continuity Conditions, Symmetry Properties

The continuity conditions with regard to displacements and interlaminar stresses must be fulfilled in the interfaces of the laminate. In addition, the conditions for traction-free laminate edges and surfaces of the outer layers must be fulfilled under the given uniaxial strain. The conditions for traction-free laminate edges with the inplane coordinate y measured from the center of the laminate (see Fig. 20.5) for each layer k result as:

$$\tau_{xy,k}\,(x,\, y = \pm b,\, z) = 0,$$
$$\sigma_{yy,k}\,(y,\, z = \pm b,\, z) = 0,$$
$$\tau_{yz,k}\,(x,\, y = \pm b,\, z) = 0. \tag{20.13}$$

Similarly, the interlaminar stresses τ_{xz}, τ_{yz} and σ_{zz} must disappear at the surfaces of the laminate:

$$\tau_{xz,1}\left(x, y, z = -\tfrac{h}{2}\right) = \tau_{xz,n}\left(x, y, z = +\tfrac{h}{2}\right) = 0,$$
$$\tau_{yz,1}\left(x, y, z = -\tfrac{h}{2}\right) = \tau_{yz,n}\left(x, y, z = +\tfrac{h}{2}\right) = 0,$$
$$\sigma_{zz,1}\left(x, y, z = -\tfrac{h}{2}\right) = \sigma_{zz,n}\left(x, y, z = +\tfrac{h}{2}\right) = 0. \tag{20.14}$$

The continuity conditions regarding the interlaminar stresses in the interface between the layer k and the layer $k + 1$ are as follows:

$$\begin{aligned}
\tau_{xz,k}\,(x,\,y,\,z=z_k) &= \tau_{xz,k+1}\,(x,\,y,\,z=z_k)\,,\\
\tau_{yz,k}\,(x,\,y,\,z=z_k) &= \tau_{yz,k+1}\,(x,\,y,\,z=z_k)\,,\\
\sigma_{zz,k}\,(x,\,y,\,z=z_k) &= \sigma_{zz,k+1}\,(x,\,y,\,z=z_k)\,.
\end{aligned} \tag{20.15}$$

We must also formulate analogous continuity conditions for the displacements in the interface between the layers k and $k+1$:

$$\begin{aligned}
U_{1,k}\,(x,\,y,\,z=z_k) &= U_{1,k+1}\,(x,\,y,\,z=z_k)\,,\\
U_{2,k}\,(x,\,y,\,z=z_k) &= U_{2,k+1}\,(x,\,y,\,z=z_k)\,,\\
U_{3,k}\,(x,\,y,\,z=z_k) &= U_{3,k+1}\,(x,\,y,\,z=z_k)\,.
\end{aligned} \tag{20.16}$$

Unfortunately, there is no exact solution for the differential equations (20.12) in conjunction with the given boundary and continuity conditions (20.13)–(20.16). Therefore, a considerable international research effort has been invested in the analytical and numerical investigation of free-edge effects over a period of more than 50 years.

Certain symmetry and invariance properties of the given situation of a symmetric laminate under uniaxial strain can be used to simplify the calculations, especially when using methods that are very computationally intensive. Consider a center section with width and thickness $2b$ and h and infinitesimal length Δl as shown in Fig. 20.5. Then all state variables—displacements, strains and stresses—on the two resulting cross-sections (Fig. 20.5, bottom left) parallel to the yz-plane at $x = \pm\frac{\Delta l}{2}$ must be identical. In order to create a numerical model, e.g. in the context of finite element calculations, it is therefore sufficient to restrict all considerations to this central laminate section, provided that the laminate has a sufficient length in the longitudinal direction x. In addition, the displacements also have certain symmetry properties due to the symmetry of the laminate under consideration. If we dispense with the layerwise notation of the displacement components at this point, the following symmetry properties can be determined with regard to the xy-plane:

$$\begin{aligned}
U_1\,(x,\,y,\,z) &= U_1\,(x,\,y,\,-z)\,,\\
U_2\,(x,\,y,\,z) &= U_2\,(x,\,y,\,-z)\,,\\
U_3\,(x,\,y,\,z) &= -U_3\,(x,\,y,\,-z)\,,
\end{aligned} \tag{20.17}$$

which means that the displacement functions U_1 and U_2 are even functions of the thickness coordinate z, whereas U_3 is an odd function of z. With respect to the xz-plane, we can state that

$$\begin{aligned}
U_1\,(x,\,y,\,z) &= -U_1\,(x,\,-y,\,z)\,,\\
U_2\,(x,\,y,\,z) &= -U_2\,(x,\,-y,\,z)\,,\\
U_3\,(x,\,y,\,z) &= U_3\,(x,\,-y,\,z)\,.
\end{aligned} \tag{20.18}$$

Obviously, U_1 and U_2 are both odd functions and U_3 is an even function of y. Therefore, it is sufficient to restrict the analysis to a quarter section of the center section of the laminate with the dimensions Δl, b, $\frac{h}{2}$ as shown in Fig. 20.5, bottom right, since the properties of the displacement field lead to the conclusion that in the plane $(x, y = 0, z)$ the displacement functions U_1 and U_2 must vanish. In addition, the transverse displacement function U_3 must become zero in the laminate middle plane $(x, y, z = 0)$. We can therefore write:

$$\begin{aligned} U_1\,(x, y = 0, z) &= 0, \\ U_2\,(x, y = 0, z) &= 0, \\ U_3\,(x, y, z = 0) &= 0. \end{aligned} \tag{20.19}$$

20.3 Methods for Analyzing the Free-Edge Effect

While the free-edge effect has been the subject of intensive research since the fundamental work of Pipes and Pagano (1970), no general elasticity solution is known to date that exactly fulfils all governing differential equations as well as the underlying boundary and continuity conditions. It can be assumed that such an exact solution does not exist. Nevertheless, there is a whole series of closed-form analytical approximation solutions and countless purely numerical investigations. For an overview, see for example Mittelstedt (2006a) and Mittelstedt and Becker (2007a) as well as Mittelstedt et al. (2022). Several different approximation methods for analyzing the free-edge edge effect are discussed below.

20.3.1 Delamination Forces and Moments

For a given laminate, the plane stresses σ_{xx}, σ_{yy} and τ_{xy} are first calculated in the edge region according to CLPT. Of course, these do not correspond to the actual boundary conditions directly at the edge, which is why interlaminar stresses must arise. It is assumed that the free edge is given by $y = 0$ and for a laminate with N individual layers, the layer boundaries (interfaces) are located at the z-coordinates $z_1, z_2, \ldots, z_{N-1}$, while the lower surface of the laminate is given by $z_0 = -\frac{h}{2}$ and the upper surface of the laminate is given by $z_N = \frac{h}{2}$, as shown in Fig. 20.6. The following delamination forces $N_{yy,k}$ are then introduced as measures for the interlaminar shear stresses τ_{yz} occurring in the interface k at the free edge:

$$N_{yy,k} = \int_{z_k}^{z_N} \sigma_{yy} \mathrm{d}z. \tag{20.20}$$

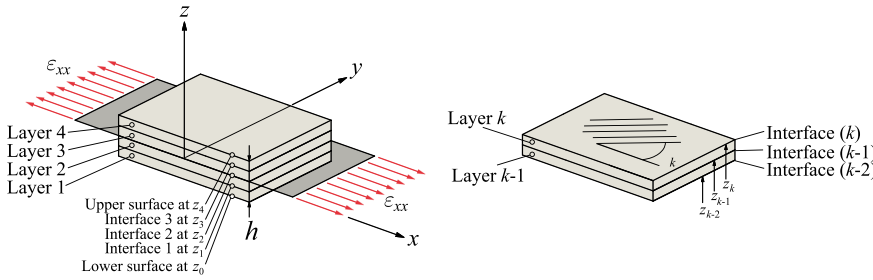


Fig. 20.6 Individual layers and interfaces in the laminate

Similarly, the following delamination forces $N_{xy,k}$ are introduced as measures for the interlaminar shear stresses τ_{xz} occurring in the interface k at the edge:

$$N_{xy,k} = \int_{z_k}^{z_N} \tau_{xy} \mathrm{d}z. \tag{20.21}$$

Furthermore, the following delamination moments $M_{yy,k}$ are introduced as measures for the interlaminar normal stresses σ_{zz} occurring along the interface k at the edge of the same interface:

$$M_{yy,k} = \int_{z_k}^{z_N} \sigma_{yy} \, (z - z_k) \, \mathrm{d}z. \tag{20.22}$$

With a positive delamination moment $M_{yy,k} > 0$, a positive normal stress $\sigma_{zz} > 0$ directly at the edge in the interface k can be expected, and thus also a corresponding delamination tendency. With a negative delamination moment $M_{yy,k} < 0$, a negative normal stress $\sigma_{zz} < 0$ directly at the edge can be concluded, i.e. a compressive stress that does not give rise to any delamination tendency.

The evaluation of the delamination tendency with the help of the delamination forces and delamination moments boils down to the question of whether the most critical interfaces can endure the delamination forces and moments acting there. The free-edge effect problem can be optimized by switching to laminate layups which entail lower delamination forces and moments.

20.3.2 Finite Element Analyses

As a quite universal purely numerical method, the Finite Element Method is of course also available for analyzing the free-edge effect. However, this requires a very problem-conscious and targeted modelling and discretization, on the one hand to adequately capture the free-edge effect, and on the other hand to keep the numerical effort within reasonable limits. Along a straight free laminate edge, it is appropriate to perform the free-edge effect analysis within a representative laminate strip of arbitrarily chosen length Δx and width $\frac{b}{2}$ (if b is the

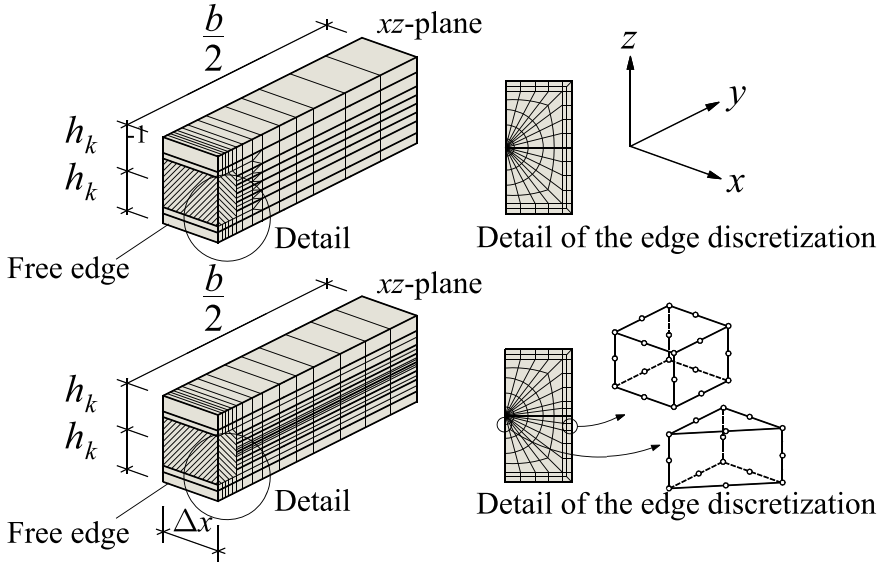


Fig. 20.7 Two different finite element discretizations for the analysis of the free-edge effect in an exemplary two-ply laminate

total width of the laminate), whereby this strip is limited by two flat surfaces perpendicular to the free laminate edge, as shown in Fig. 20.7 for a two-layer composite as an example. Within this strip, the finite element discretization can be carried out using volume elements, whereby the discretization can be limited to a single element in the direction of the strip length Δx. In the individual laminate layers sufficiently far away from the edge, the discretization can also be relatively coarse, as the conditions of CLPT will apply here. In the vicinity of the free edge, however, a considerable mesh refinement is required, and this applies in particular in the area of the layer interfaces at the edge. A more precise description of all occurring local state variables easily requires an extreme mesh refinement and a correspondingly large numerical effort. Figure 20.8 shows a finite element modelling as carried out by Raju and Crews (1981).

After all, with computers becoming more and more powerful, the possibilities here are already quite extensive. In order to capture the real conditions in the laminate, it is still necessary to use multi-point constraints to ensure that the two surfaces of the laminate strip deform in the same way, whereby deformations of the surfaces that are flat in the undeformed state must be permitted. The actual load application to the laminate is usually carried out via these multi-point constraints, e.g. by converting the effective longitudinal strain parallel to the free laminate edge into a corresponding displacement difference of the corresponding nodes on the cut surfaces.

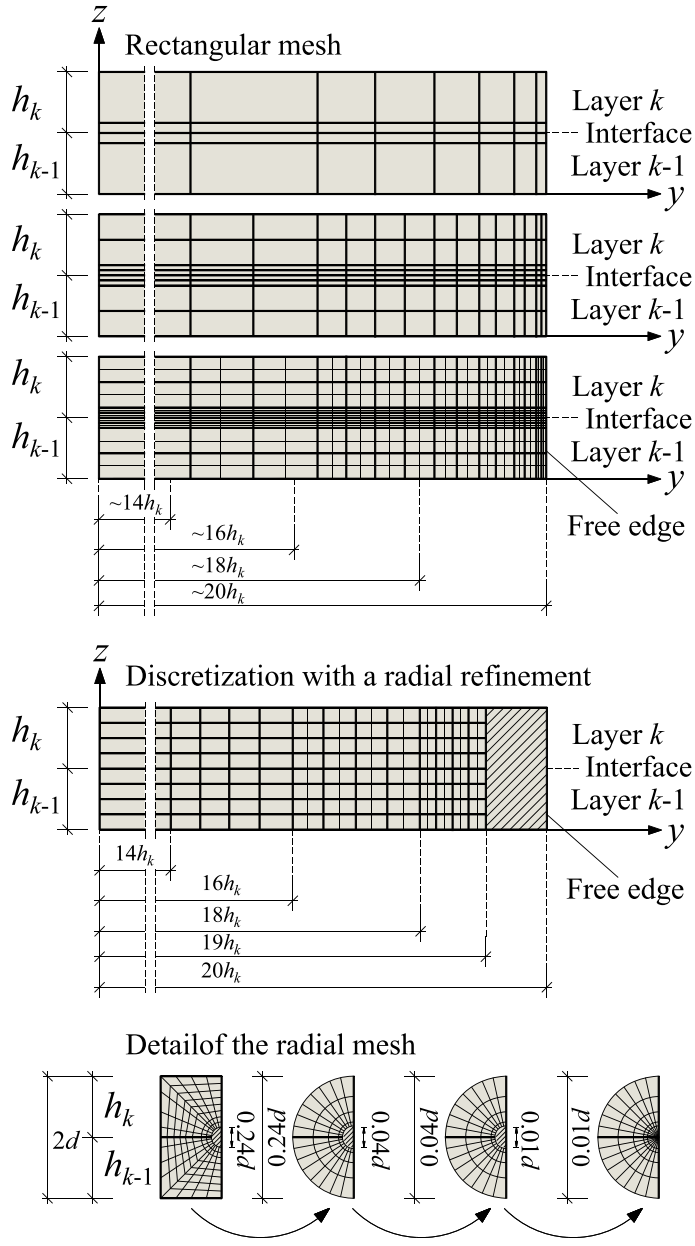


Fig. 20.8 Exemplary finite element modelling for the free-edge effect according to Raju and Crews (1981), rectangular element scheme (top), mesh refinement running radially towards the interface at the free edge (bottom)

20.3.3 Closed-Form Analysis According to Kassapoglou and Lagace (1986)

A well-known and widely used method for the closed-form analysis of free-edge effects in laminates that goes back to Kassapoglou and Lagace (1986) is the so-called Force-Balance-Method. The method is based on layerwise stress analyses, which are used to estimate the free-edge stress fields of mechanically loaded symmetric laminates. It is briefly described below.

The starting point of the Force-Balance-Method is an approach for the stress components in each layer, in the following form:

$$\begin{aligned} \sigma_{xx,k} &= f_{xx,k}(y)\, g_{xx,k}(z), \quad \sigma_{yy,k} = f_{yy,k}(y)\, g_{yy,k}(z), \\ \sigma_{zz,k} &= f_{zz,k}(y)\, g_{zz,k}(z), \quad \tau_{xy,k} = f_{xy,k}(y)\, g_{xy,k}(z), \\ \tau_{xz,k} &= f_{xz,k}(y)\, g_{xz,k}(z), \quad \tau_{yz,k} = f_{yz,k}(y)\, g_{yz,k}(z). \end{aligned} \tag{20.23}$$

Explicit use was made here of the fact that the stress state in a simple laminate tensile specimen is not a function of the x-axis, provided that edge effects are considered at points of the tensile specimen that are sufficiently far away from the force application points. The stress functions f and g must be determined for each layer k.

Since all stress components are independent of the longitudinal coordinate x as a result of the considered free-edge effect situation, the layerwise equilibrium conditions are significantly reduced, whereby the longitudinal normal stress $\sigma_{xx,k}$ is even completely eliminated:

$$\frac{\partial \tau_{xy,k}}{\partial y} + \frac{\partial \tau_{xz,k}}{\partial z} = 0, \quad \frac{\partial \sigma_{yy,k}}{\partial y} + \frac{\partial \tau_{yz,k}}{\partial z} = 0, \quad \frac{\partial \tau_{yz,k}}{\partial y} + \frac{\partial \sigma_{zz,k}}{\partial z} = 0. \tag{20.24}$$

If the stress approach (20.23) is inserted into (20.24), the following relationships between the stress functions f and g are obtained:

$$\begin{aligned} \frac{\partial f_{xy,k}}{\partial y} &= f_{xz,k}, \quad \frac{\partial f_{yy,k}}{\partial y} = f_{yz,k}, \quad \frac{\partial f_{yz,k}}{\partial y} = f_{zz,k}, \\ \frac{\partial g_{xz,k}}{\partial z} &= g_{xy,k}, \quad \frac{\partial g_{yz,k}}{\partial z} = g_{yy,k}, \quad \frac{\partial g_{zz,k}}{\partial z} = g_{yz,k}. \end{aligned} \tag{20.25}$$

Here, the plane stress functions f must now be determined in order to map the typical distributions of the free-edge effect stresses in the y-direction. In particular, the functions for f must be chosen in such a way that the characteristic decay behaviour of the free-edge stress fields into the laminate interior can be mapped. Decaying exponential functions, for example, are suitable for this purpose:

$$f_{yy,k} = A_{1,k} e^{-\varphi_1 x_2} + A_{2,k} e^{-\varphi_1 \varphi_2 x_2} + A_{3,k}, \quad f_{xy,k} = A_{4,k} + A_{5,k} e^{-\varphi_1 x_2}. \tag{20.26}$$

This definition results in the following remaining stress functions:

$$\begin{aligned} f_{xz,k} &= -\varphi_1 A_{5,k} e^{-\varphi_1 x_2}, \\ f_{yz,k} &= -A_{1,k}\varphi_1 e^{-\varphi_1 x_2} - \varphi_1\varphi_2 A_{2,k} e^{-\varphi_1\varphi_2 x_2}, \\ f_{zz,k} &= A_{1,k}\varphi_1^2 e^{-\varphi_1 x_2} + \varphi_1^2\varphi_2^2 A_{2,k} e^{-\varphi_1\varphi_2 x_2}. \end{aligned} \tag{20.27}$$

The quantities φ_1 and φ_2 appearing here are still unknown decay coefficients, which are finally determined from an energy principle. The constants $A_{1,k}$, $A_{2,k}$, $A_{3,k}$, $A_{4,k}$, $A_{5,k}$ are determined from the condition that the free-edge effect stresses must decay completely with increasing distance from the free laminate edge, so that the conditions according to CLPT prevail in the laminate interior. Furthermore, the stress functions must fulfil the boundary conditions at the free laminate edge. Finally, the following is obtained:

$$\begin{aligned} A_{1,k} &= -\frac{\varphi_2 \sigma^0_{yy,k}}{\varphi_2 - 1}, \quad A_{2,k} = \frac{\sigma^0_{yy,k}}{\varphi_2 - 1}, \\ A_{3,k} &= \sigma^0_{yy,k}, \quad A_{4,k} = \tau^0_{xy,k}, \quad A_{5,k} = -\tau^0_{xy,k}. \end{aligned} \tag{20.28}$$

Here, $\sigma^0_{yy,k}$ and $\tau^0_{xy,k}$ are the layerwise stresses that result in the considered laminate tensile specimen according to CLPT.

The stress functions g are determined in the same way. If we assume that the plane stresses $\sigma_{yy,k}$ and $\tau_{xy,k}$ are constant over the layer thickness, the following approach for $g_{xy,k}$ and $g_{yy,k}$ is plausible:

$$g_{xy,k} = B_{1,k}, \quad g_{yy,k} = B_{3,k}. \tag{20.29}$$

Integration with respect to the thickness direction z then results in:

$$\begin{aligned} g_{xz,k} &= B_{1,k} z + B_{2,k}, \\ g_{yz,k} &= B_{3,k} z + B_{4,k}, \\ g_{zz,k} &= \frac{1}{2} B_{3,k} z^2 + B_{4,k} z + B_{5,k}. \end{aligned} \tag{20.30}$$

The constants $B_{1,k}$, $B_{2,k}$, $B_{3,k}$, $B_{4,k}$, $B_{5,k}$ are determined by the requirement for continuous distribution of the interlaminar stresses τ_{xz}, τ_{yz}, σ_{zz} across the layer interfaces and the requirement for stress-free laminate surfaces. The final result is as follows:

$$\begin{aligned} &B_{1,k} = 1, \quad B_{2,k} = \sum_{r=k+1}^{N} \tau^0_{xy,r} h_r, \quad B_{3,k} = 1, \\ &B_{4,k} = \sum_{r=k+1}^{N} \sigma^0_{yy,r} h_r, \quad B_{5,k} = \sum_{p=k+1}^{N} \sigma^0_{yy,p} h_p \left(\frac{1}{2} h_p + \sum_{q=k+1}^{q=p-1} h_q \right). \end{aligned} \tag{20.31}$$

The stress field in the layer k can then be fully specified as:

$$\begin{aligned}
\sigma_{yy,k} &= \sigma^0_{yy,k}\left[1 - \frac{\varphi_2}{\varphi_2 - 1}\left(e^{-\varphi_1 y} - \frac{1}{\varphi_2}e^{-\varphi_1\varphi_2 y}\right)\right], \\
\sigma_{zz,k} &= \frac{\varphi_1^2\varphi_2}{\varphi_2 - 1}\left(\varphi_2 e^{-\varphi_1\varphi_2 y} - e^{-\varphi_1 y}\right) \\
&\quad \times \left[\frac{1}{2}\sigma^0_{yy,k}z^2 + z\sum_{r=k+1}^{N}\sigma^0_{yy,r}h_r + \sum_{p=k+1}^{N}\sigma^0_{yy,p}h_p\left(\frac{1}{2}h_p + \sum_{q=k+1}^{q=p-1}h_q\right)\right], \\
\tau_{yz,k} &= \frac{\varphi_1\varphi_2}{\varphi_2 - 1}\left(e^{-\varphi_1 y} - e^{-\varphi_1\varphi_2 y}\right)\left(\sigma^0_{yy,k}z + \sum_{r=k+1}^{N}\sigma^0_{yy,r}h_r\right), \\
\tau_{xz,k} &= \varphi_1 e^{-\varphi_1 y}\left(\tau^0_{xy,k}z + \sum_{r=k+1}^{N}\tau^0_{xy,r}h_r\right), \\
\tau_{xy,k} &= \tau^0_{xy}\left(1 - e^{-\varphi_1 y}\right).
\end{aligned} \tag{20.32}$$

Finally, the plane normal stress $\sigma_{xx,k}$ is determined from the requirement that the longitudinal strains ε_{xx} are identical according to both CLPT and the current free-edge effect analysis. The only remaining unknowns in the stress approach are then the decay parameters φ_1 and φ_2. Kassapoglou and Lagace determined them from the principle of the minimum of the complementary potential. However, more detailed information is not provided here and reference is made to the original work by Kassapoglou and Lagace.

20.3.4 Semi-Analytical Free-Edge Effect Analysis According to Mittelstedt and Becker (2006a, 2007a)

In the recent past, a semi-analytical method for the analysis of the free-edge effect has been developed, which manages with a relatively simple boundary discretisation, while it is of a closed-form analytical nature in the laminate interior and therefore proves to be numerically extremely effective. This method will be outlined here, for further details the reader is referred to Mittelstedt and Becker (2006a, 2007b).

As shown in Fig. 20.9 for a simple cross-ply laminate, this method involves discretizing each physical laminate single layer into a not too large number of (e.g. 10) 'mathematical layers', which are then numbered consecutively with the index k ($k = 1, 2, 3, \ldots, n_L$), whereby, with regard to the coordinate system used in Fig. 20.9 their individual layer interfaces are located at the points z_{k-1} and z_k and, for simpler mathematical formulation, the surfaces of the cover layers are counted as 'fictitious interfaces'. Within each mathematical layer, the following displacement representation is used for the three spatial displacement components u, v, w:

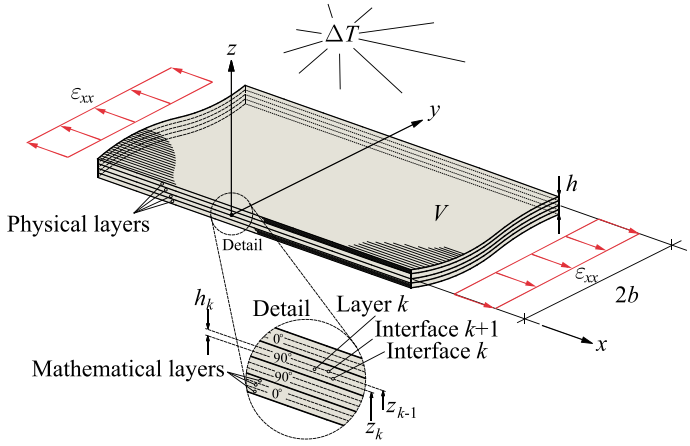


Fig. 20.9 Laminate under thermomechanical load, notation and introduction of mathematical layers

$$\begin{aligned} u_k &= U_k^0(x,y) + U_k^1(y,z), \\ v_k &= V_k^0(y) + V_k^1(y,z), \\ w_k &= W_k^0(z) + W_k^1(y,z). \end{aligned} \tag{20.33}$$

Here, the quantities U_k^0 and V_k^0 denote the inplane displacements according to CLPT, and the quantity W_k^0 is a layerwise linear displacement function resulting from the requirement of the plane stress state by integrating the transverse thickness strain $\varepsilon_{zz,k}$. The other variables U_k^1, V_k^1 and W_k^1 are displacement functions yet to be determined, which are intended to represent the stresses emanating from the free edge. In the following way, these displacement functions are reduced to functions $\hat{U}_k$, $\hat{V}_k$, $\hat{W}_k$ of only one variable, which are defined exclusively in the interfaces:

$$\begin{aligned} U_k^1(y,z) &= \hat{U}_k(y)\,\psi_{1,k}(z) + \hat{U}_{k+1}(y)\,\psi_{2,k}(z), \\ V_k^1(y,z) &= \hat{V}_k(y)\,\psi_{1,k}(z) + \hat{V}_{k+1}(y)\,\psi_{2,k}(z), \\ W_k^1(y,z) &= \hat{W}_k(y)\,\psi_{1,k}(z) + \hat{W}_{k+1}(y)\,\psi_{2,k}(z). \end{aligned} \tag{20.34}$$

The interpolation polynomials $\psi_{1,k}(z)$ and $\psi_{2,k}(z)$ are required to fulfil the conditions

$$\begin{aligned} \psi_{1,k}(z = z_{k-1}) = 1, \quad \psi_{1,k}(z = z_k) = 0, \\ \psi_{2,k}(z = z_{k-1}) = 0, \quad \psi_{2,k}(z = z_k) = 1 \end{aligned} \tag{20.35}$$

where the interpolation is linear in the simplest case:

$$\psi_{1,k}(z) = \frac{1}{h_k}(z_k - z), \quad \psi_{2,k}(z) = \frac{1}{h_k}(z - z_{k-1}). \tag{20.36}$$

With the help of the approach chosen in this way, the layerwise stresses can be determined within the framework of geometric linearity and under the assumption of linear-elastic material behaviour:

$$\begin{pmatrix} \sigma_{xx,k} \\ \sigma_{yy,k} \\ \sigma_{zz,k} \\ \tau_{yz,k} \\ \tau_{xz,k} \\ \tau_{xy,k} \end{pmatrix} = \begin{bmatrix} C_{11,k} & C_{12,k} & C_{13,k} & 0 & 0 & C_{16,k} \\ C_{12,k} & C_{22,k} & C_{23,k} & 0 & 0 & C_{26,k} \\ C_{13,k} & C_{23,k} & C_{33,k} & 0 & 0 & C_{36,k} \\ 0 & 0 & 0 & C_{44,k} & C_{45,k} & 0 \\ 0 & 0 & 0 & C_{45,k} & C_{55,k} & 0 \\ C_{16,k} & C_{26,k} & C_{36,k} & 0 & 0 & C_{66,k} \end{bmatrix} \times \left(\begin{pmatrix} \frac{\partial u_k}{\partial x} \\ \frac{\partial v_k}{\partial y} \\ \frac{\partial w_k}{\partial z} \\ \frac{\partial v_k}{\partial z} + \frac{\partial w_k}{\partial y} \\ \frac{\partial u_k}{\partial z} + \frac{\partial w_k}{\partial x} \\ \frac{\partial u_k}{\partial y} + \frac{\partial v_k}{\partial x} \end{pmatrix} - \Delta T \begin{pmatrix} \alpha_{11t,k} \\ \alpha_{22t,k} \\ \alpha_{33t,k} \\ 0 \\ 0 \\ \alpha_{12t,k} \end{pmatrix} \right). \tag{20.37}$$

The principle of the minimum of the total elastic potential Π is used to determine the previously unknown displacement functions $\hat{U}_k, \hat{V}_k, \hat{W}_k$. For the case of a thermomechanical load with specified deformation, the following applies to the total potential

$$\Pi = \frac{1}{2} \sum_{k=1}^{n_L} \left(\int \int \int_{V_k} \underline{\varepsilon}_k{}^T \underline{\underline{C}}_k \underline{\varepsilon}_k \mathrm{d}V_k \right) - \sum_{k=1}^{n_L} \left(\int \int \int_{V_k} \underline{\varepsilon}_k{}^T \underline{\underline{C}}_k \underline{\alpha}_{t,k} \Delta T_k \mathrm{d}V_k \right) + \frac{1}{2} \sum_{k=1}^{n_L} \left(\int \int \int_{V_k} \underline{\alpha}_{t,k}{}^T \Delta T_k \underline{\underline{C}}_k \underline{\alpha}_{t,k} \Delta T_k \mathrm{d}V_k \right) = \text{Min.} \tag{20.38}$$

Execution of the integration in x- and in z-direction and evaluation of the total potential Π then leads to the Euler-Lagrange differential equations of the problem for the unknown displacement functions, which can be summarized in the following form:

$$\begin{aligned} \underline{\underline{K}}_1 \underline{U} + \underline{\underline{K}}_2 \frac{\partial^2 \underline{U}}{\partial y^2} + \underline{\underline{K}}_3 \underline{V} + \underline{\underline{K}}_4 \frac{\partial^2 \underline{V}}{\partial y^2} + \underline{\underline{K}}_5 \frac{\partial \underline{W}}{\partial y} &= \underline{0}, \\ \underline{\underline{K}}_6 \underline{U} + \underline{\underline{K}}_7 \frac{\partial^2 \underline{U}}{\partial y^2} + \underline{\underline{K}}_8 \underline{V} + \underline{\underline{K}}_9 \frac{\partial^2 \underline{V}}{\partial y^2} + \underline{\underline{K}}_{10} \frac{\partial \underline{W}}{\partial y} &= \underline{0}, \\ \underline{\underline{K}}_{11} \frac{\partial \underline{U}}{\partial y} + \underline{\underline{K}}_{12} \frac{\partial \underline{V}}{\partial y} + \underline{\underline{K}}_{13} \underline{W} + \underline{\underline{K}}_{14} \frac{\partial^2 \underline{W}}{\partial y^2} &= \underline{R}. \end{aligned} \tag{20.39}$$

The unknown displacement functions are summarised in the column vectors $\underline{U}$, $\underline{V}$, $\underline{W}$. The vector of the right-hand side $\underline{R}$ and the coefficient matrices $\underline{\underline{K}}_1, \ldots, \underline{\underline{K}}_{14}$, can be found in more detail in Mittelstedt and Becker (2007b). This is a linear system of differential equations with constant coefficients whose general solution is made up of homogeneous solution components of the type $Ae^{\lambda y}$, i.e. it results in

$$\underline{U}_{\text{hom}} = \begin{pmatrix} \underline{U} \\ \underline{V} \\ \underline{W} \end{pmatrix} = \sum_{r=1}^{r=3(n_L+1)} b_r \underline{A}_r e^{\lambda_r y}, \tag{20.40}$$

with free constants b_r $(r = 1, 2, \ldots, 3(n_L + 1))$. Inserting (20.40) into the system of differential equations (20.39) results in all exponential functions being cancelled out and the following quadratic eigenvalue problem for determining the exponents λ is obtained:

$$\left(\lambda^2 \begin{bmatrix} \underline{\underline{K}}_2 & \underline{\underline{K}}_4 & \underline{\underline{0}} \\ \underline{\underline{K}}_7 & \underline{\underline{K}}_9 & \underline{\underline{0}} \\ \underline{\underline{0}} & \underline{\underline{0}} & \underline{\underline{K}}_{14} \end{bmatrix} + \lambda \begin{bmatrix} \underline{\underline{0}} & \underline{\underline{0}} & \underline{\underline{K}}_5 \\ \underline{\underline{0}} & \underline{\underline{0}} & \underline{\underline{K}}_{10} \\ \underline{\underline{K}}_{11} & \underline{\underline{K}}_{12} & \underline{\underline{0}} \end{bmatrix} + \begin{bmatrix} \underline{\underline{K}}_1 & \underline{\underline{K}}_3 & \underline{\underline{0}} \\ \underline{\underline{K}}_6 & \underline{\underline{K}}_8 & \underline{\underline{0}} \\ \underline{\underline{0}} & \underline{\underline{0}} & \underline{\underline{K}}_{13} \end{bmatrix} \right) \underline{A} = \underline{0}. \tag{20.41}$$

Finally, the constants b_r result from the given boundary conditions of a traction-free laminate edge, which can be fulfilled in a suitably integrated form. For further details, the reader is referred to Mittelstedt and Becker (2007b).

The semi-analytical procedure now described requires the independent programming of the corresponding equations and relationships, which involves a certain amount of effort. On the other hand, the numerical efficiency of the method is far superior to a corresponding finite element analysis with the same accuracy of the results, which quickly pays off in parameter studies and optimizations.

20.4 Benefits of the Free-Edge Effect Analyses

In the case of the free-edge effect, the occurrence of singular stresses means that discretizing methods (such as the Finite Element Method or the semi-analytical methods described) show higher stresses the finer the discretization is chosen. In this respect, a laminate with a correspondingly fine discretization is predicted to fail with a purely stress-based failure criterion in connection with the free-edge effect, even if it does not fail in reality. The situation here is similar to that of the stress singularities at crack tips within linear-elastic fracture mechanics, whereby the stress singularities of the free-edge effect are usually of considerably lower order than the $\frac{1}{\sqrt{r}}$ stress singularities at the tip of a crack. Ultimately, the stress singularities are a result of the underlying linear-elastic idealizations.

If a reliable failure or non-failure statement also requires a fracture mechanics evaluation, the value of the presented free-edge effect analyses lies above all in the possibility of a comparative evaluation of laminate design alternatives. Trend statements can also be obtained via corresponding sensitivity analyses and it is possible to find out in which way the free-edge effect problem can be optimized such that low edge stresses occur.

20.5 Results and Discussion

Figures 20.10 and 20.11 show some selected results for the free-edge effect, which were generated by Rohwer (1996) with the help of detailed finite element analyses. The stress images impressively show the rather complex three-dimensional, but also highly localized character of the free-edge stress state. The singular influences for the interlaminar edge stresses at the interfaces can be clearly recognized.

Figure 20.12 shows a comparison of some results according to the semi-analytical method of Mittelstedt and Becker with finite element calculations according to Reddy (2004) for a longitudinal strain $\varepsilon_{xx} = 0.01$ for an $[\pm 45°]_S$ angle-ply laminate made of typical carbonfiber-reinforced plastic, namely for the interlaminar stresses τ_{xz} and σ_{zz} classically occurring there in the direct edge area over the thickness coordinate z. For more details on these calculations, the reader is referred to Mittelstedt and Becker (2007b). Overall, it can be seen that the semi-analytical method produces almost identical results to the purely

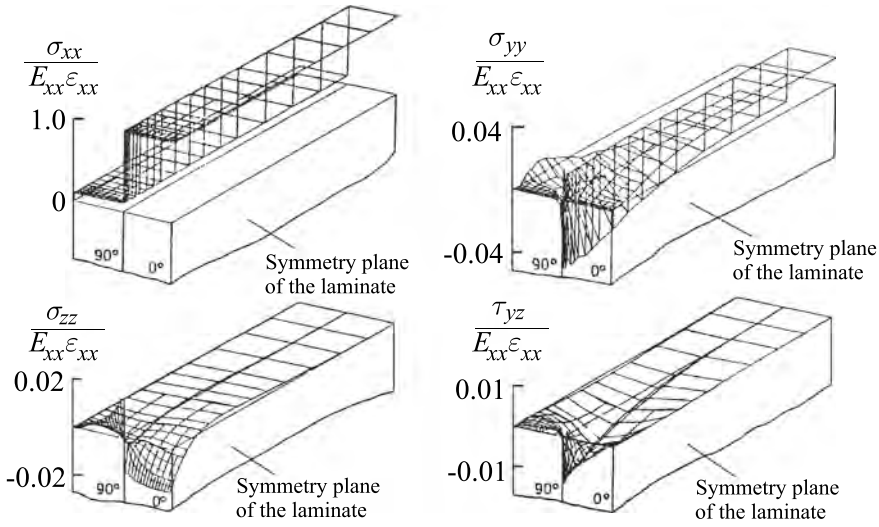


Fig. 20.10 Free-edge effect stresses in a $[90°/0°]_S$ cross-ply laminate (Rohwer 1996)

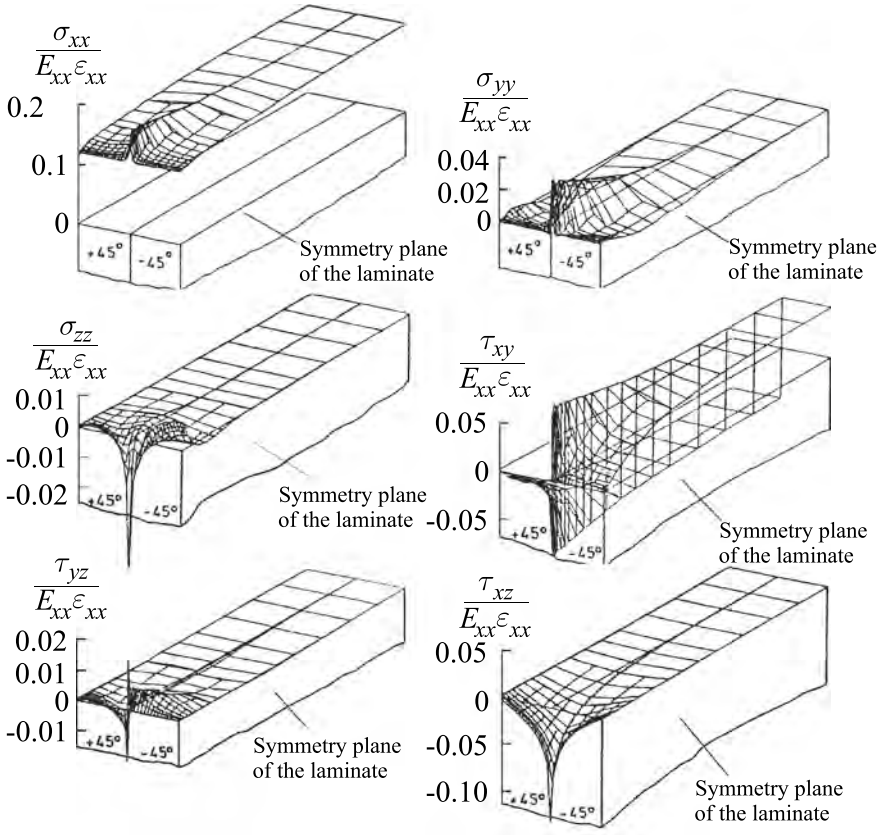


Fig. 20.11 Free-edge effect stresses in a $[\pm 45°]_S$ angle-ply laminate (Rohwer 1996)

numerical finite element analysis. In particular, it should be emphasized that the semi-analytical method provides results within a few seconds, whereas the computing time of well-converged finite element results in the case of free-edge effect analyses is at least in the range of minutes, which underlines the benefits of alternative semi-analytical approaches. Otherwise, Fig. 20.12 shows the typical distributions of the interlaminar stresses τ_{xz} and σ_{zz} for this class of laminates, i.e. maximum values at the interfaces of the [±45°]-layers, which are caused by the stress singularities, as well as disappearing interlaminar stresses at the free laminate surfaces. Obviously, in this example, under the given load case, only negative normal stresses σ_{zz} occur in the interfaces at the free edge, so that it can be concluded that we are probably not dealing with a delamination failure in the form of a classic Mode I crack opening. On the other hand, positive and thus potentially critical shear stresses σ_{zz} can be seen in the area of the laminate middle plane. In addition, there are considerable interlaminar

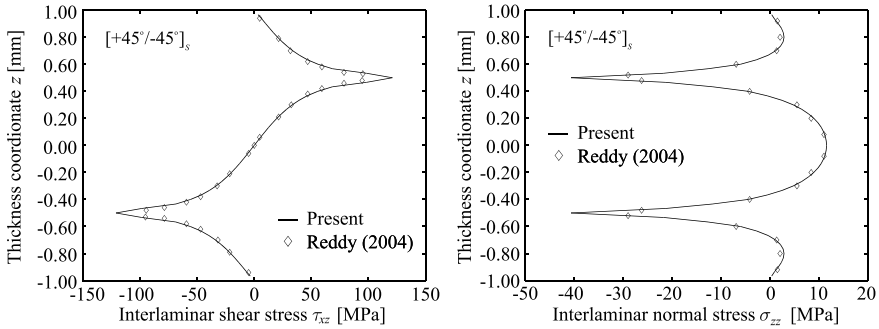


Fig. 20.12 Comparison of the results according to the semi-analytical method with finite element calculations by Reddy (2004) for a $\left[\pm 45°\right]_S$ angle-ply laminate under uniaxial tensile load $\varepsilon_{xx} = 0.01$

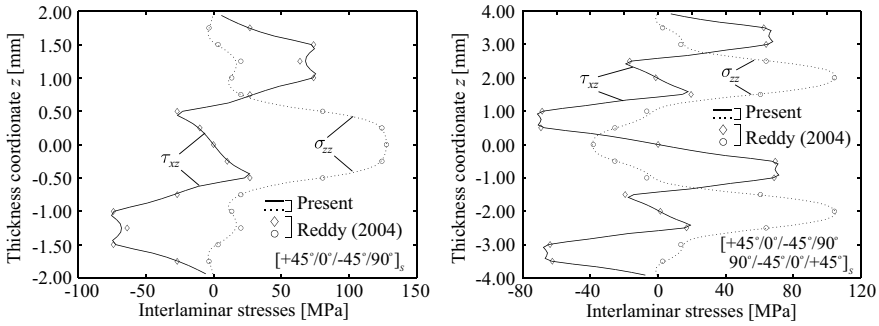


Fig. 20.13 Comparison of the results according to the semi-analytical method with finite element calculations by Reddy (2004) for an 8-ply $\left[+45°/0°/-45°/90°\right]_S$-laminate (left) and for a 16-ply laminate $\left[\left[+45°/0°/-45°/90°\right]_S\right]_S$ (right) under uniaxial tensile load $\varepsilon_{xx} = 0.01$

shear stresses τ_{xz} in the area of the interfaces of the $[\pm 45°]$-layers, the presence of which can also favour premature laminate failure and must therefore also be included in an assessment of the interlaminar stress state.

Figure 20.13 shows a comparison for an 8-ply $[+45°/0°/-45°/90°]_S$-laminate (Fig. 20.13, left) and a 16-ply laminate with the layup $\left[[+45°/0°/-45°/90°]_S\right]_S$ (Fig. 20.13, right). Here, too, the load case is a uniaxial tensile strain $\varepsilon_{xx} = 0.01$. Again, the comparison of the results according to the semi-analytical method and the finite element calculations according to Reddy is extremely positive, which emphasizes the value of such alternative analysis methods. Of course, this is especially true with regard to the necessary computing time, which is particularly important for finite element analyses in the presence of singular stresses and can easily lead to unacceptable effort.

Finally, the method of delamination forces and moments will be briefly examined, whereby we will currently only consider the delamination moments for the 8-ply $[+45°/0°/-45°/90°]_S$-laminate. Here, a calculation according to CLPT yields the fol-

lowing values for the delamination moments in the interfaces (only given here for interfaces 4–7 for reasons of symmetry):

$$M_{yy,4} = \int_{z_4}^{z_8} \sigma_{yy}\,(z - z_4)\,\mathrm{d}z = 191.32\,\mathrm{N},$$

$$M_{yy,5} = \int_{z_5}^{z_8} \sigma_{yy}\,(z - z_5)\,\mathrm{d}z = 143.49\,\mathrm{N},$$

$$M_{yy,6} = \int_{z_6}^{z_8} \sigma_{yy}\,(z - z_6)\,\mathrm{d}z = 71.78\,\mathrm{N},$$

$$M_{yy,7} = \int_{z_7}^{z_8} \sigma_{yy}\,(z - z_7)\,\mathrm{d}z = 23.95\,\mathrm{N}. \tag{20.42}$$

A comparison with the corresponding distribution of the normal stress σ_{zz} in Fig. 20.13, left, shows that with the help of delamination moments it is possible to estimate, at least qualitatively, to what extent one is dealing with positive or negative interlaminar normal stresses in the interface under consideration, and in which order of magnitude the interlaminar normal stress will turn out in comparison with other interfaces. Obviously, the largest delamination moment occurs in interface 4 (which coincides here with the laminate middle plane), while the smallest delamination moment occurs in interface 7. This is in good agreement with the results in Fig. 20.13, left, where the maximum and minimum interlaminar normal stresses σ_{zz} also occur in interfaces 4 and 7 respectively.

20.6 Recommendations for Practical Applications

Whether and in what way the free-edge effect can lead to premature failure depends heavily on the individual layer material used, the individual layup, the existing geometric conditions and the load cases to be considered (mechanical, thermal, moisture). Nevertheless, the following general recommendations can be given for practical use:

(a) When determining the laminate layup, an attempt should be made to avoid excessive differences in stiffness between directly neighbouring individual layers, in particular differences in stiffness caused by different individual layer orientations.
(b) In the case of unidirectionally fiber-reinforced individual layers, there should be as few angular differences as possible in the fiber directions of immediately adjacent individual layers.
(c) The laminate layers should be as thin as possible.

(d) One should avoid joining (or clustering) several immediately neighbouring thin individual layers of the same reinforcement direction. The existing thin individual layers should be 'well mixed' (with not too large fiber angle differences).
(e) If necessary, an attempt should be made to achieve that interlaminar normal stresses occur directly at the laminate edge as far as possible as compressive stresses by permutation of the existing individual laminate layers.
(f) If necessary, an existing edge delamination tendency must be countered by suitable additional constructive measures (e.g. mutual seaming of the individual layers or the use of an edge clamping).

All of the above recommendations are measures that aim to minimize the free-edge stress fields due to the free-edge effect or to bring them into ranges that are less critical. However, when designing a composite laminate, it is always necessary to check whether such measures do not conflict with other design requirements. Sometimes it may be that a laminate design can be assessed as positive with regard to the free-edge effect, while it has weaknesses in terms of stability or general static strength, for example. The reverse can also be true. It is then the task of the designing engineer to find a solution that represents a good compromise between all requirements.

20.7 Related Problems

For various reasons (e.g. for cable ducts), it may be necessary to provide a laminate with a hole, the simplest case being that of a circular hole (Fig. 20.14). If such a hole is not used for load introduction or load transmission (e.g. by a bolt connection), but is free of external loads, there is again the case of a free laminate edge along the edge of the hole, along which a corresponding free-edge effect can form. Since a laminate hole also represents the case of a stress concentrator (along the edge of the hole, stress components tangential to the edge occur with a layup- and load-dependent hole stress concentration factor), the free-edge effect is correspondingly more pronounced and easily leads to edge delaminations that progress from the edge of the hole into the laminate. The corresponding stress fields have not yet been exhaustively investigated (see e.g. Hu et al. 1997; Kharghani and Mittelstedt 2022, 2023). If necessary, the Finite Element Method can of course be used for this purpose, whereby the required mesh refinement in the area of the hole edge quickly leads to comparatively large finite element models.

Another situation that frequently occurs in practice is that of free laminate corners, e.g. right-angled laminate corners, as also shown in Fig. 20.14. Here, a so-called 'free-corner effect' occurs as a quasi-superposition of the free-edge effects forming along the adjacent straight laminate edges, which can only be analysed with a fully three-dimensional elasticity-theoretical structural analysis. Depending on the laminate layup and load case, the free-corner effect can occur in the form of both harmless or more critical, more pro-

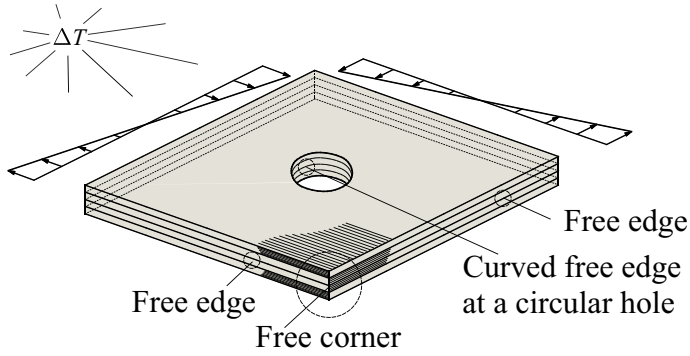


Fig. 20.14 Laminate with a circular hole problem; right-angled free laminate corner

nounced interlaminar stresses when compared to the involved free-edge effects. For further investigations and corresponding different approaches to analysis, the reader is referred to Mittelstedt (2006a) and Mittelstedt and Becker (2004, 2005a).

20.8 Free-Edge Effects in Piezoelectric Laminates

Adaptive laminate structures often contain piezoelectric layers for the active control of such structures as well as for sensory purposes. It must be assumed that the free-edge effect also occurs in such piezoelectric laminates. The analysis of such stress concentration problems can be treated with closed-form analytical methods, semi-analytical approaches or purely numerical methods such as the Finite Element Method, all of which are based on the following energetic considerations (see e.g. Artel and Becker 2005). The mechanical and electrical quantities are linked by the following equations in a Cartesian system x_1, x_2, x_3:

$$\begin{aligned} \underline{\sigma} &= \underline{\underline{C}}\,\underline{\varepsilon} - \underline{e}^T \underline{E}, \\ \underline{D} &= \underline{\underline{e}}\,\underline{\varepsilon} + \underline{\phi}\,\underline{E}, \end{aligned} \tag{20.43}$$

where the stress and strain components in the vectors $\underline{\sigma}$ and $\underline{\varepsilon}$ are summarised as

$$\begin{aligned} \underline{\sigma} &= (\sigma_{11}, \sigma_{22}, \sigma_{33}, \sigma_{23}, \sigma_{13}, \sigma_{12})^T, \\ \underline{\varepsilon} &= (\varepsilon_{11}, \varepsilon_{22}, \varepsilon_{33}, \gamma_{23}, \gamma_{13}, \gamma_{12})^T. \end{aligned} \tag{20.44}$$

The electrical quantities, i.e. the electrical flux vector $\underline{D}$ and the field vector $\underline{E}$, are defined as:

$$\underline{D} = (D_1, D_2, D_3)^T ,$$
$$\underline{E} = (E_1, E_2, E_3)^T . \tag{20.45}$$

The matrices $\underline{\underline{C}}$, $\underline{\underline{e}}$ and $\underline{\underline{\phi}}$ in (20.43) are the stiffness matrix, the piezoelectric coupling matrix and the dielectric matrix, respectively, defined as:

$$\underline{\underline{C}} = \begin{bmatrix} C_{11} & C_{12} & C_{13} & C_{14} & C_{15} & C_{16} \\ C_{12} & C_{22} & C_{23} & C_{24} & C_{25} & C_{26} \\ C_{13} & C_{23} & C_{33} & C_{34} & C_{35} & C_{36} \\ C_{14} & C_{24} & C_{34} & C_{44} & C_{45} & C_{46} \\ C_{15} & C_{25} & C_{35} & C_{45} & C_{55} & C_{56} \\ C_{16} & C_{26} & C_{36} & C_{46} & C_{56} & C_{66} \end{bmatrix},$$
$$\underline{\underline{e}} = \begin{bmatrix} e_{11} & e_{12} & e_{13} & e_{14} & e_{15} & e_{16} \\ e_{21} & e_{22} & e_{23} & e_{24} & e_{25} & e_{26} \\ e_{31} & e_{32} & e_{33} & e_{34} & e_{35} & e_{36} \end{bmatrix},$$
$$\underline{\underline{\phi}} = \begin{bmatrix} \phi_{11} & \phi_{12} & \phi_{13} \\ \phi_{12} & \phi_{22} & \phi_{23} \\ \phi_{13} & \phi_{23} & \phi_{33} \end{bmatrix}. \tag{20.46}$$

The equilibrium equations for the mechanical and electrical variables are as follows:

$$\frac{\partial \sigma_{i1}}{\partial x_1} + \frac{\partial \sigma_{i2}}{\partial x_2} + \frac{\partial \sigma_{i3}}{\partial x_3} + f_i = 0,$$
$$\frac{\partial D_1}{\partial x_1} + \frac{\partial D_2}{\partial x_2} + \frac{\partial D_3}{\partial x_3} - q = 0, \tag{20.47}$$

with $i = 1, 2, 3$. The quantities f_i and q are volume forces and the electric charge respectively.

The weak form of (20.47) can be given in the form of volume integrals over the domain Ω with admissible virtual displacements δu_i ($i = 1, 2, 3$) and electric potential changes $\delta\varphi$:

$$\int_\Omega \sum_{i=1}^{3} \left[\left(\frac{\partial \sigma_{i1}}{\partial x_1} + \frac{\partial \sigma_{i2}}{\partial x_2} + \frac{\partial \sigma_{i3}}{\partial x_3} + f_i \right) \delta u_i \right] \mathrm{d}\Omega$$
$$+ \int_\Omega \left(\frac{\partial D_1}{\partial x_1} + \frac{\partial D_2}{\partial x_2} + \frac{\partial D_3}{\partial x_3} - q \right) \delta\varphi \mathrm{d}\Omega = 0. \tag{20.48}$$

Taking into account the material and electrical linearity, the following kinematic equations and relationships between the vector components of the electric field E_i and the electric potential φ ($i, j = 1, 2, 3$) apply:

$$\varepsilon_{ii} = \frac{\partial u_i}{\partial x_i},$$
$$\gamma_{ij} = \frac{\partial u_i}{\partial x_j} + \frac{\partial u_j}{\partial x_i},$$
$$E_i = -\frac{\partial \varphi}{\partial x_i}. \tag{20.49}$$

With the help of (20.49) and (20.43) and by applying the divergence theorem, (20.48) can be converted into the following form:

$$\underbrace{\int_\Omega \underline{\varepsilon}^T \underline{\underline{C}} \delta \underline{\varepsilon} \mathrm{d}\Omega}_{(a)} - \underbrace{\int_\Omega \left(\underline{\varepsilon}^T \underline{\underline{e}} \delta \underline{E} + \underline{E}^T \underline{\underline{e}} \delta \underline{\varepsilon} \right) \mathrm{d}\Omega}_{(b)}$$
$$+ \underbrace{\int_\Omega \underline{E}^T \underline{\underline{\phi}} \delta \underline{E} \mathrm{d}\Omega}_{(c)} = \underbrace{\int_\Omega \underline{f} \delta \underline{u} \mathrm{d}\Omega + \int_\Gamma \underline{t} \delta \underline{u} \mathrm{d}\Gamma}_{(d)}$$
$$+ \underbrace{\int_\Omega q \delta \varphi \mathrm{d}\Omega + \int_\Gamma Q \delta \varphi \mathrm{d}\Gamma}_{(e)}. \tag{20.50}$$

Therein, $\underline{t}$ are the surface loads, while Q denotes the surface electric charges on the surface Γ. Equation (20.50) thus represents the variational expression required for piezoelectric calculations. The part labelled (a) is the internal virtual energy of the considered piezoelectric solid, while (b) and (c) represent the piezoelectric part and the electrical part of the virtual internal energy. Parts (d) and (e) are the mechanical and electrical virtual works. In a fundamental work, Artel and Becker (2005) addressed the effect of electromechanical coupling on the stress fields at free laminate edges and the electric field strengths near the free edges of composite laminates under uniaxial strain with piezoelectric material properties. The analyses were performed using the Finite Element Method and a comparison was made between coupled and uncoupled piezoelectric analyses. This work provides the reader with a good overview of the free-edge effect behaviour in piezoelectric laminates.

20.9 The Scaled Boundary Finite Element Method

For the numerical analysis of the free-edge effect, the Finite Element Method is currently probably the most frequently used tool. This is due to the general availability, the universal character of this method and the fact that almost all engineers are familiar with this method. However, due to the strong localization of the free-edge stresses, in most cases a sophisticated and well-adapted mesh refinement is required in the finite element discretization near the

free edges. In particular, if the interlaminar normal stress σ_{zz} and/or the interlaminar shear stress τ_{xz} occur as singularities, it is a major challenge to obtain sufficiently accurate stress predictions using finite elements. Also, there is no good access to the orders of the occurring stress singularities using finite elements.

For the numerical analysis of free-edge stresses, the so-called Scaled Boundary Finite Element Method (SBFEM) is a much more efficient method in many cases. Although this method is not as well known as the Finite Element Method, it has proven its favourable properties in a large number of applications for linear systems. Strictly speaking, the SBFEM is a semi-analytical method that combines the advantages of the standard Finite Element Method (FEM) and the boundary element method (BEM). Similar to the BEM, only the boundary (or part of the boundary) needs to be discretised in the SBFEM, so that the problem dimension is reduced by one and the discretization is much simpler than in a full FEM discretization. Like the FEM, the SBFEM is also based on a variational principle, but unlike the BEM, without the need for a fundamental solution. Song and Wolf (1995, 1997) can be regarded as pioneers of the SBFEM. Since the method is able to efficiently compute stress singularities, it has been used favourably for linear elastic fracture mechanics problems (Mittelstedt and Becker 2005b, c, 2006b; Song 2005; Song et al. 2010; Saputra et al. 2015). A good overview of the application of SBFEM for linear-elastic fracture mechanics problems can be found in Song et al. (2018). It is worth mentioning that the SBFEM can also be applied to complex three-dimensional crack problems where cracks, interfaces and edges coincide, and it allows a deep insight into the combined occurrence of stress singularities of different orders (Hell and Becker 2015). Of course, the application of the SBFEM is also very beneficial for stress analysis and the evaluation of the free-edge effect. In a recent publication, for example, this was shown by Dölling et al. (2020) for the example of angle-ply laminates.

To get an idea of the SBFEM and the associated analysis approach, a $[\pm\vartheta]_S$ laminate under tensile load is considered. To analyse the free-edge effect, it is sufficient to focus on the indicated quarter model (see Fig. 20.5). A cross-section in the yz-plane can be analysed using the scaled coordinates ξ and η as shown in Fig. 20.15, where the coordinate ξ starts at the point of stress singularity (the so-called similarity center) and the coordinate η runs along the edge part shown in red. For the unknown displacements $\underline{u}(\xi, \eta)$ a representation of the following type is used:

$$\underline{u}(\xi, \eta) = \underline{\underline{N}}(\xi)\underline{\hat{u}}(\eta), \tag{20.51}$$

where $\underline{\underline{N}}$ denotes a matrix of shape functions within the line elements along the boundary as used in the standard Finite Element Method. The quantities $\underline{\hat{u}}(\xi)$ are unknown functions for each of the line elements shown in Fig. 20.15 specified in the boundary nodes. The substitution of the representation (20.51) into the principle of virtual work and the consideration of the kinematics and Hooke's law leads after some calculations to a system of Euler-Cauchy differential equations of the type

$$\xi^2 \underline{\underline{E}}_0 \underline{\hat{u}}_{,\xi\xi}(\xi) + \xi(\underline{\underline{E}}_0 + \underline{\underline{E}}_1^T - \underline{\underline{E}}_1)\underline{\hat{u}}_{,\xi}(\xi) - \underline{\underline{E}}_2 \underline{\hat{u}}(\xi) = -\xi(\underline{S}_\xi - \underline{S}_\eta), \tag{20.52}$$

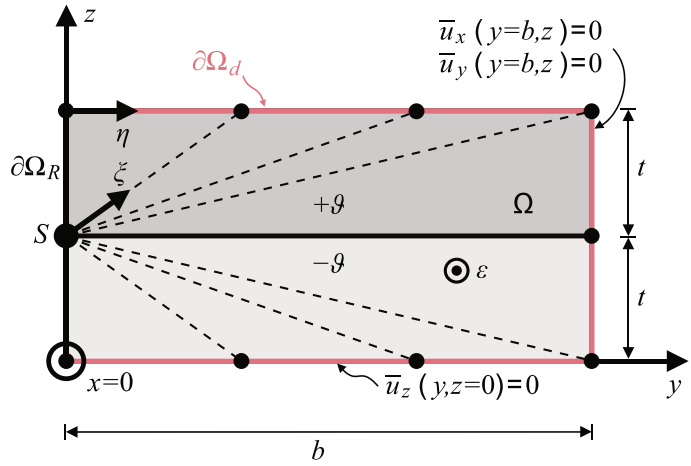


Fig. 20.15 SBFEM discretization with global axes x, y, z and local axes ξ, η; In SBFEM, it is sufficient to discretise only the boundary Ω_d of the considered area Ω

together with corresponding boundary conditions. In (20.52), the variables $\underline{\underline{E}}_0$, $\underline{\underline{E}}_1$ and $\underline{\underline{E}}_2$ are matrices, which result from the given material stiffnesses, and the variables $\underline{S}_\xi$ and $\underline{S}_\eta$ are vectors that represent the given load. For further details, the reader is referred to Dölling et al. (2020), for example. The general homogeneous solution of the system (20.52) is a linear combination of power functions ξ^λ, where the lowest exponents λ correspond to the existing stress singularities. The particular solution is of the type of the right-hand side of (20.52). The coefficients of the general solution can be determined from the given boundary conditions.

The advantage of SBFEM is that even a relatively small number of boundary elements leads to surprisingly accurate stress results, especially in the vicinity of stress concentrations. This makes this method highly interesting and advantageous for analyzing the free-edge effect. Further works dealing with the application of SBFEM to problems in the context of linear-elastic fracture mechanics and the investigation of stress concentration phenomena can be found in Hell and Becker (2015), Artel and Becker (2006), Goswami and Becker (2012), or Dieringer and Becker (2015).

References

Artel J, Becker W (2005): *Coupled and uncoupled analyses of piezoelectric free-edge effect in laminated plates*. Composite Structures 69:329–335.

Artel J, Becker W (2006): *On kinematic coupling equations within the scaled boundary finite-element method*. Archive of Applied Mechanics 76:617–633.

Dieringer R, Becker W (2015): *A new scaled boundary finite element formulation for the computation of singularity orders at cracks and notches in arbitrarily laminated composites*. Composite Structures 123:263–270.

Dölling S, Hahn J, Felger J, Bremm S, Becker W (2020): *A scaled boundary finite element method model for interlaminar failure in composite laminates*. Composite Structures 241:111865.

Goswami S, Becker W (2012): *Computation of 3-D stress singularities for multiple cracks and crack intersections by the Scaled Boundary Finite Element Method*. International Journal of Fracture 175:13–25.

Hell S, Becker W (2015): *The scaled boundary finite element method for the analysis of 3D crack interaction*. Journal of Computational Science 9:76–81.

Hu FZ, Soutis C, Edge EC (1997): *Interlaminar stresses in composite laminates with a circular hole*. Composite Structures 37:223–232.

Kassapoglou C, Lagace (1986): *An efficient method for the calculation of interlaminar stresses in composite materials*. Journal of Applied Mechanics 53:744–750.

Kharghani N, Mittelstedt C (2022): *Reduction of free-edge effects around a hole of a composite plate using a numerical layup optimization*. Composite Structures 284:115139.

Kharghani N, Mittelstedt C (2023): *Free-edge effects at circular holes in composite laminates under hygrothermomechanical load*. Journal of Composite Materials 57:3991–4007.

Mittelstedt C, Becker W (2004): *Interlaminar stress concentrations in layered structures - part II: closed-form analysis of stresses at laminated rectangular wedges with arbitrary non-orthotropic layup*. Journal of Composite Materials 38:1063–1090.

Mittelstedt C, Becker W (2005a): *Thermoelastic fields in boundary layers of isotropic laminates*. Journal of Applied Mechanics 72:86–101.

Mittelstedt C, Becker W (2005b): *Semi-analytical computation of 3D stress singularities in linear elasticity*. Communications in Numerical Methods in Engineering 21:247–257.

Mittelstedt C, Becker W (2005c): *Asymptotic analysis of stress singularities in composite laminates by the boundary finite element method*. Composite Structures 71:210–219.

Mittelstedt C (2006a): *Free-edge and free-corner effects in composite laminates - Closed-form analytical and semi-analytical approaches*. Fortschritt-Berichte VDI, Reihe 18, Nr. 307. VDI-Verlag, Düsseldorf, Germany.

Mittelstedt C, Becker W (2006b): *Fast and reliable analysis of free-edge stress fields in a thermally loaded composite strip by a layerwise laminate theory*. International Journal for Numerical Methods in Engineering 67:747–770.

Mittelstedt C, Becker W (2006c): *Efficient computation of order and mode of three-dimensional stress singularities in linear elasticity by the boundary finite element method*. International Journal of Solids and Structures 43:2868–2903.

Mittelstedt C, Becker W (2007a): *Free-edge effects in composite laminates*. Applied Mechanics Reviews 60:217–245.

Mittelstedt C, Becker W (2007b): *The Pipes-Pagano problem revisited: Elastic fields in boundary layers of plane laminated specimens under combined thermomechanical load*. Composite Structures 80:373–395.

Mittelstedt C, Becker W, Kappel A, Kharghani N (2022): *Free-edge effects in composite laminates a review of recent developments 2005–2020*. Applied Mechanics Reviews 74:010801.

Pipes RB, Pagano NJ (1970): *Interlaminar stresses in composite laminates under uniform axial extension*. Journal of Composite Materials 4:538–548.

Raju IS, Crews JH (1981): *Interlaminar stress singularities at a straight free edge in composite laminates*. Computers and Structures 14:21–28.

Reddy JN (2004): *Mechanics of laminated composite plates and shells (Zweite Auflage)*. CRC Press Boca Raton et al., USA.

Rohwer K (1996): *Modelle und Methoden zur Berechnung von Laminaten aus unidirektionalen Faserverbunden*. VDI Verlag, Düsseldorf, Germany.

Saputra AA, Birk C, Song C (2015): *Computation of three-dimensional fracture parameters at interface cracks and notches by the scaled boundary finite element method*. Engineering Fracture Mechanics 148:213–242.

Song C, Wolf JP (1995): *Consistent infinitesimal finite-element-cell method: out-of-plane motion*. Journal of Engineering Mechanics 121:613–619.

Song C, Wolf JP (1997): *The scaled boundary finite-element method - alias consistent infinitesimal finite-element cell method - for elastodynamics*. Computer Methods in Applied Mechanics and Engineering 147:329–355.

Song C (2005): *Evaluation of power-logarithmic singularities, T-stresses and higher order terms of in-plane singular stress fields at cracks and multi-material corners*. Engineering Fracture Mechanics 72:1498–1530.

Song C, Tin-Loi F, Gao W (2010): *A definition and evaluation procedure of generalized stress intensity factors at cracks and multi-material wedges*. Engineering Fracture Mechanics 77:2316–2336.

Song C, Ooi ET, Natarajan S (2018): *A review of the scaled boundary finite element method for two-dimensional linear elastic fracture mechanics*. Engineering Fracture Mechanics 187:45–73.



Laminated Shells

21

This chapter is devoted to the static and dynamic behaviour of laminated shells, i.e. thin curved layered surface structures. After an introduction to shells in general, the so-called membrane theory of layered shells is discussed, i.e. the state in which a shell essentially transfers its loads through membrane force flows. This is followed by the general consideration of the so-called bending theory, i.e. the state that arises in shells when moment and shear force flows are taken into account. These considerations are later extended to layered cross-ply cylindrical shells within the framework of Classical Laminated Plate Theory (CLPT) and First-Order Shear Deformation Theory (FSDT). After a brief consideration of sandwich shells, vibrations and buckling of layered circular cylindrical shells are discussed before this chapter concludes with the analysis of the postbuckling behaviour of circular cylindrical shells. The analysis of shell structures is the subject of a number of textbooks, a selection of which is included in the reference list at the end of this chapter and which the reader can consult for deeper information.

21.1 Introduction

Shells are curved surface structures and have considerable technical significance. By a shell we mean a thin load-bearing structure curved arbitrarily in space, which is mathematically characterised by its mid-plane, whereby we assume that the thickness of the shell is small compared to its other dimensions. In the case of disks and plates, the corresponding load-bearing effects can be considered separately from each other under the condition of geometric linearity. However, this cannot generally be assumed for a shell. This can make it considerably more difficult to analyze shell structures.

© The Author(s), under exclusive license to Springer-Verlag GmbH, DE, part of Springer Nature 2025

C. Mittelstedt, *Mechanics of Composite Structures*,
https://doi.org/10.1007/978-3-662-70788-3_21

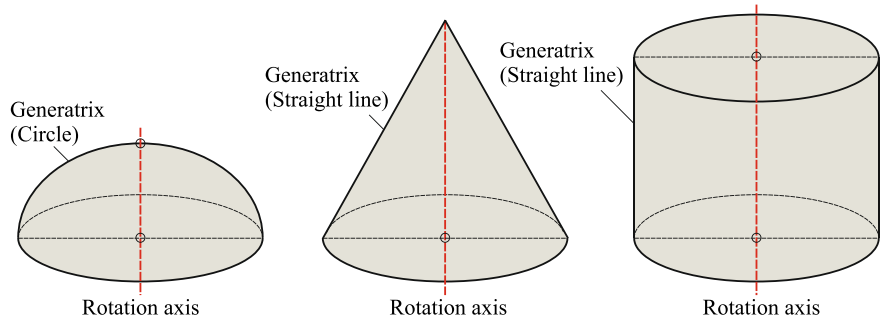


Fig. 21.1 Selected shells of revolution: spherical shell, conical shell, cylindrical shell

In this chapter, we only consider the so-called shells of revolution. Shells of revolution are shells that are created by rotating a plane curve around a rotation axis, whereby this axis lies in the plane of the generatrix. Selected shells of revolution are shown in Fig. 21.1.

In all further explanations, we assume layered and sufficiently thin shell structures. In addition to geometric linearity, material linearity is also assumed. We restrict ourselves to analyzing shells of revolution where both the shell shape and the boundary conditions are rotationally symmetric. The shell has the thickness h, which does not necessarily have to be constant. The shell is described via the mathematical reduction to the shell middle surface. The thickness direction of the shell is z and points in the direction of the normal to the shell middle surface at every point of the shell.

To describe surfaces of revolution, which represent the shell middle surface for the shells of revolution considered here, a number of geometric parameters must be defined (see Fig. 21.2). We consider a point P on the surface of revolution (see Fig. 21.2, top). The corresponding normal vector to the surface is called $\underline{n}$. On the one hand, the surface is described by its longitudinal circle or its meridian, which is also the generatrix. In addition, the so-called latitude circle is considered, which can be interpreted as the trajectory of the generatrix. Meridians and latitude circle are always perpendicular to each other and are used as coordinates. The position of the point P on the latitude circle is described by the angle ϑ, i.e. the angle of the meridian plane relative to a reference meridian plane. The inclination of the normal vector to the axis of rotation and thus also the position of the point P is characterized by the angle φ, i.e. the angle of the normal of the plane of rotation relative to the axis of rotation. The corresponding radii of curvature are labelled r_ϑ and r_φ. As these are the principal radii of curvature of the surface under consideration, the designations $r_1 = r_\varphi$ and $r_2 = r_\vartheta$ can also be used. The following applies:

$$r = r_2 \sin \varphi. \tag{21.1}$$

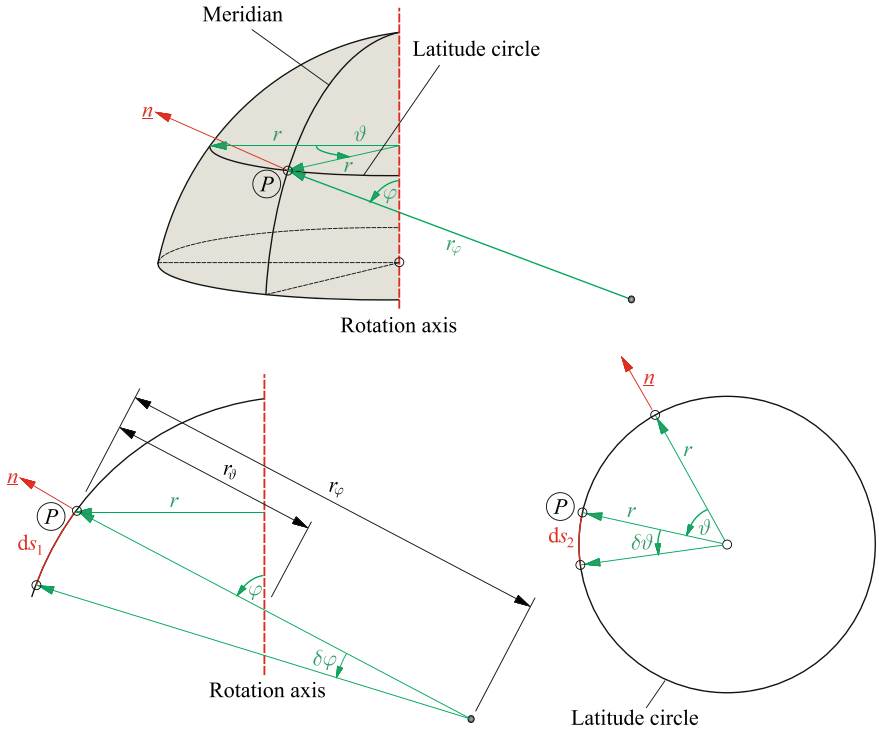


Fig. 21.2 Surface of revolution

At the meridian section shown in Fig. 21.2, bottom left, an infinitesimal point neighbouring P is shown on the surface of revolution. The angle is $\mathrm{d}\varphi$. The length $\mathrm{d}s_1$ of the meridian section is then:

$$\mathrm{d}s_1 = r_1 \mathrm{d}\varphi. \tag{21.2}$$

In the same way, at Fig. 21.2, bottom right, with $\varphi = \text{const.}$ the length $\mathrm{d}s_2$ can be determined:

$$\mathrm{d}s_2 = r \mathrm{d}\vartheta, \tag{21.3}$$

or with (21.1):

$$\mathrm{d}s_2 = r_2 \sin\varphi \mathrm{d}\vartheta. \tag{21.4}$$

The infinitesimal surface element $\mathrm{d}A$ of the surface of revolution is then (Fig. 21.3, left):

$$\mathrm{d}A = \mathrm{d}s_1 \mathrm{d}s_2 = r_1 r_2 \sin\varphi \mathrm{d}\varphi \mathrm{d}\vartheta. \tag{21.5}$$

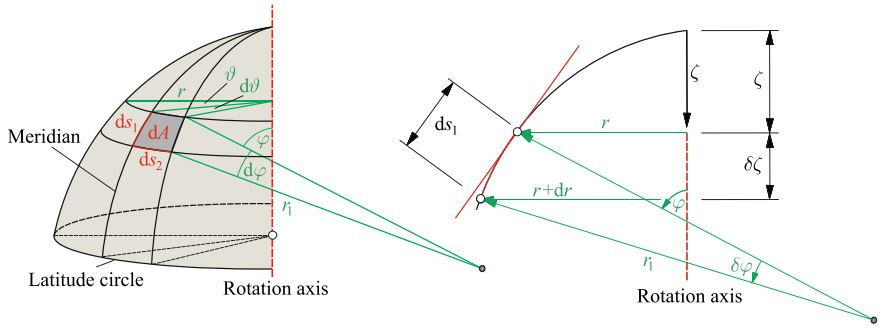


Fig. 21.3 Infinitesimal surface element of a surface of revolution (left), relationship between ζ and $r(\zeta)$ (right)

To describe the surface of revolution, the radius r is described using the vertical coordinate ζ along the axis of rotation as $r = r(\zeta)$. From Fig. 21.3, right, we can conclude:

$$\mathrm{d}r = \cos\varphi \mathrm{d}s_1 = r_1 \cos\varphi \mathrm{d}\varphi. \tag{21.6}$$

For $\mathrm{d}\zeta$ follows:

$$\mathrm{d}\zeta = r_1 \sin\varphi \mathrm{d}\varphi. \tag{21.7}$$

The change in r via ζ therefore follows as:

$$\frac{\mathrm{d}r}{\mathrm{d}\zeta} = r' = \cot\varphi. \tag{21.8}$$

The surface A of a body of revolution is:

$$A = 2\pi \int_{\zeta_0}^{\zeta_1} r\sqrt{1 + r'^2}\mathrm{d}\zeta, \tag{21.9}$$

where ζ can assume values between $\zeta = \zeta_0$ and $\zeta = \zeta_1$.

The radii of curvature of the meridian are considered next. The following applies:

$$r_1 = -\frac{\left(1 + r'^2\right)^{\frac{3}{2}}}{r''}. \tag{21.10}$$

With $r_2 = \frac{r}{\sin\varphi}$ and $\sin\varphi = \frac{1}{\sqrt{1+\cot^2\varphi}} = \frac{1}{\sqrt{1+r'^2}}$ we obtain:

$$r_2 = r\sqrt{1 + r'^2}. \tag{21.11}$$

This results in the corresponding curvatures as:

$$\kappa_1 = \frac{1}{r_1} = -\frac{r''}{\left(1+r'^2\right)^{\frac{3}{2}}}, \quad \kappa_2 = \frac{1}{r_2} = \frac{1}{r\sqrt{1+r'^2}}. \tag{21.12}$$

The so-called Gaussian curvature κ can thus be specified as:

$$\kappa = \frac{1}{r_1}\frac{1}{r_2} = -\frac{r''}{r\left(1+r'^2\right)^2}. \tag{21.13}$$

This curvature is not only decisive for the description of a surface, but also for the assessment of the static behaviour of a shell of revolution. If it is assumed that $r > 0$ applies, the sign of κ is determined by the sign of r''. The case that $r'' < 0$ applies leads to a curvature $\kappa > 0$. Such a surface of revolution is called elliptical, and the center of curvature M is then on the side of the axis of rotation as seen from the point of the curve. Examples of this are spherical surfaces (see Fig. 21.4, left). If the case $r'' = 0$ is present, the Gaussian curvature κ is also zero. The center of the curvature is then at infinity. We refer to such surfaces as parabolic, examples are conical shells (Fig. 21.4, middle) or cylindrical surfaces (Fig. 21.4, right). The case $r'' > 0$ with $\kappa < 0$ is referred to as hyperbolic. The center of curvature is on the side facing away from the axis of rotation as seen from the curve point, and such a surface is called a rotational hyperboloid.

Loads on shells of revolution can be in the form of surface loads, whereby these can act both tangentially on the shell surface (p_ϑ, p_φ) and normal to the shell surface (surface load p_z, where z is the direction of the surface normal). This is shown in Fig. 21.5. Examples of rotationally symmetric surface loads with $p = f(\varphi)$ and $\frac{\partial p}{\partial \vartheta} = 0$ are shown in Fig. 21.6. Rotationally symmetric loads can also occur in the form of force and moment flows and as individual forces and moments (Fig. 21.7).

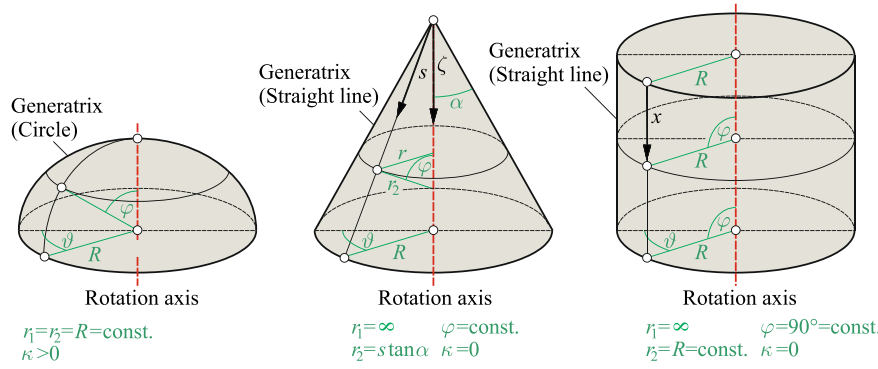


Fig. 21.4 Examples of surfaces of revolution: Spherical shell (left), conical shell (middle), cylindrical shell (right)

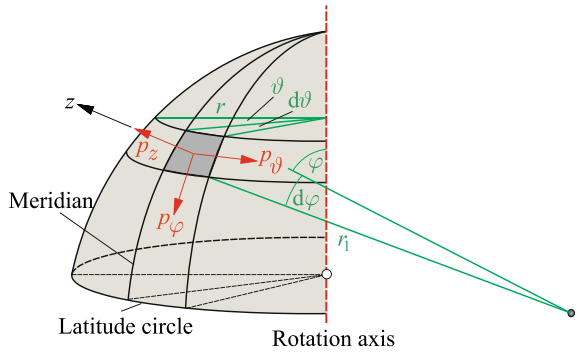


Fig. 21.5 Surface loads p_ϑ, p_φ, p_z

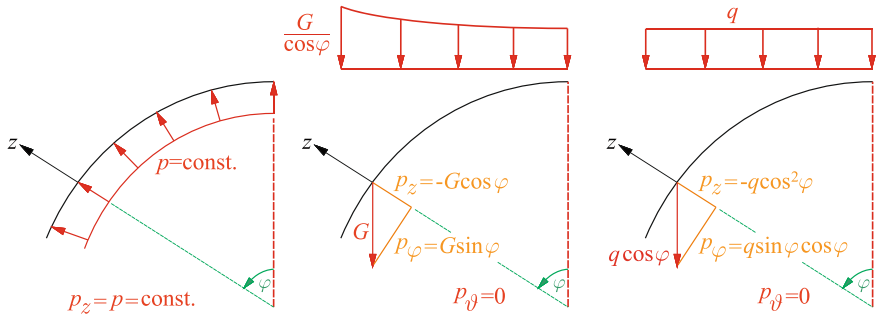


Fig. 21.6 Selected surface loads: constant internal pressure (left), dead weight (centre), load evenly distributed over the floor plan (right)

We make the following assumptions for the analysis of shells of revolution:

(i) We start from a geometrically and materially linear theory. Therefore, we can linearize all kinematic relationships. In addition, Hooke's law applies without restriction, the considerations are initially limited to shells within the framework of Classical Laminated Plate Theory (CLPT) where it should be pointed out that the term 'plate' included in CLPT contains a certain redundancy since we are dealing with shells in this chapter and not plates. However, since the assumptions made in the following correspond to CLPT and also apply to shells we will keep the denomination as CLPT.

(ii) The shell thickness h is very small compared to the dimensions of the shell. This makes it possible to reduce the considerations to the middle surface of the shell.

(iii) As with the Kirchhoff plate, we assume that the hypothesis that the cross-sections remain plane and the normal hypothesis are valid. A straight line that is perpendicular to the shell middle surface before deformation also remains a straight line in the deformed state and is also perpendicular to the deformed shell middle surface. It is also

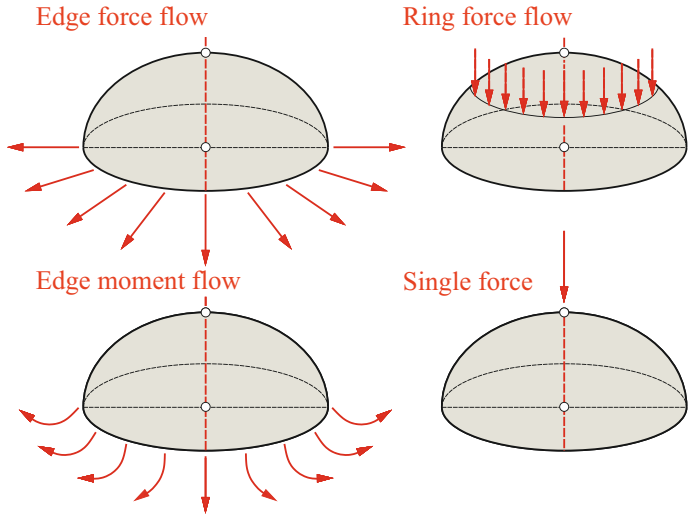


Fig. 21.7 Selected rotationally symmetric loads

assumed that the thickness of the shell does not change compared to the undeformed configuration.

(iv) We assume a plane stress state with respect to the thickness direction of the shell.

The stress tensor for the shell is (Fig. 21.8):

$$\underline{\underline{\sigma}} = \begin{bmatrix} \sigma_{\varphi\varphi} & \tau_{\varphi\vartheta} & \tau_{\varphi z} \\ \tau_{\varphi\vartheta} & \sigma_{\vartheta\vartheta} & \tau_{\vartheta z} \\ \tau_{\varphi z} & \tau_{\vartheta z} & \sigma_{zz} \end{bmatrix} . \tag{21.14}$$

By integrating the stress components over the shell thickness h, shell forces and moments can be calculated in the form of force and moment fluxes, which are shown in Fig. 21.8. These are the normal force flows $N_{\varphi\varphi}$, $N_{\vartheta\vartheta}$, the shear force flows $N_{\varphi\vartheta}$, $N_{\vartheta\varphi}$, the shear force flows Q_{φ}, Q_{ϑ}, the bending moment flows $M_{\varphi\varphi}$, $M_{\vartheta\vartheta}$ and the twisting moment flows $M_{\varphi\vartheta}$, $M_{\vartheta\varphi}$. It should be noted that the shear force flows $N_{\varphi\vartheta}$, $N_{\vartheta\varphi}$ and the twisting moment flows $M_{\varphi\vartheta}$, $M_{\vartheta\varphi}$ are generally not identical for the shell, unlike in the case of laminated plates.

We consider the shell section element of Fig. 21.9. The perspective is tangential to the shell plane in the direction of the angle φ. The length of the segment of the shell middle plane shown here is the unit length 1. The surface element $\mathrm{d}A$ results as:

$$\mathrm{d}A = \mathrm{d}z \left(1 + \frac{z}{r_2}\right) . \tag{21.15}$$

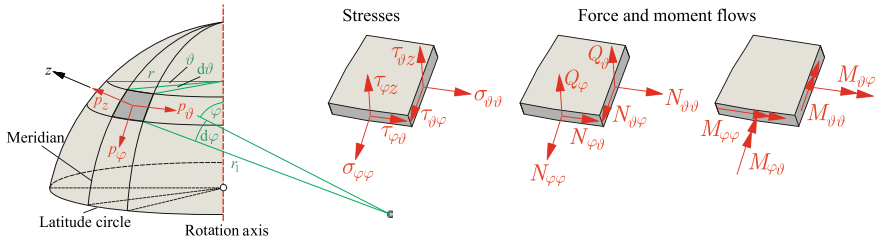


Fig. 21.8 Stress state and force and moment quantities of a shell

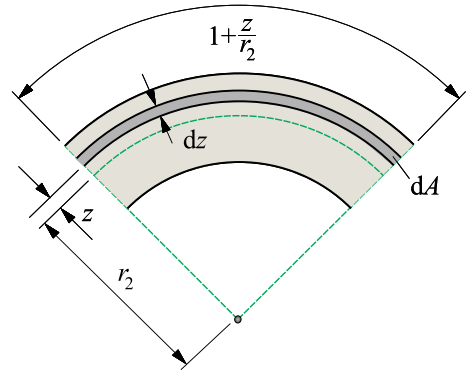


Fig. 21.9 On the determination of shell forces and moments

As an example, the normal force flow $N_{\varphi\varphi}$ is considered:

$$N_{\varphi\varphi} = \int_{-\frac{h}{2}}^{\frac{h}{2}} \sigma_{\varphi\varphi} \mathrm{d}A = \int_{-\frac{h}{2}}^{\frac{h}{2}} \sigma_{\varphi\varphi} \left(1 + \frac{z}{r_2}\right) \mathrm{d}z. \tag{21.16}$$

The bending moment flow $M_{\varphi\varphi}$, for example, can be determined in exactly the same way:

$$M_{\varphi\varphi} = \int_{-\frac{h}{2}}^{\frac{h}{2}} \sigma_{\varphi\varphi} z \mathrm{d}A = \int_{-\frac{h}{2}}^{\frac{h}{2}} \sigma_{\varphi\varphi} z \left(1 + \frac{z}{r_2}\right) \mathrm{d}z. \tag{21.17}$$

This is also referred to as the trapezoid effect. The force and moment quantities of the shell can be determined as follows:

$$N_{\varphi\varphi} = \int_{-\frac{h}{2}}^{\frac{h}{2}} \sigma_{\varphi\varphi} \left(1 + \frac{z}{r_2}\right) \mathrm{d}z, \quad N_{\vartheta\vartheta} = \int_{-\frac{h}{2}}^{\frac{h}{2}} \sigma_{\vartheta\vartheta} \left(1 + \frac{z}{r_1}\right) \mathrm{d}z,$$

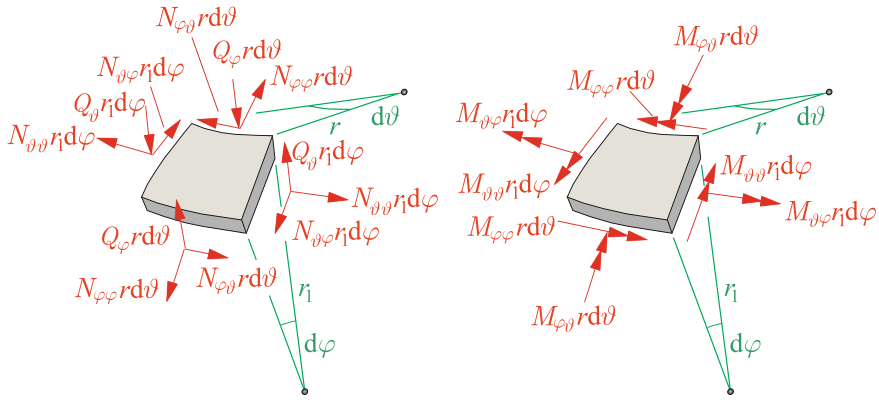


Fig. 21.10 Force and moment flows of the shell

$$
\begin{aligned}
N_{\varphi\vartheta} &= \int_{-\frac{h}{2}}^{\frac{h}{2}} \tau_{\varphi\vartheta} \left(1 + \frac{z}{r_2}\right) \mathrm{d}z, \quad N_{\vartheta\varphi} = \int_{-\frac{h}{2}}^{\frac{h}{2}} \tau_{\vartheta\varphi} \left(1 + \frac{z}{r_1}\right) \mathrm{d}z, \\
M_{\varphi\varphi} &= \int_{-\frac{h}{2}}^{\frac{h}{2}} \sigma_{\varphi\varphi} z \left(1 + \frac{z}{r_2}\right) \mathrm{d}z, \quad M_{\vartheta\vartheta} = \int_{-\frac{h}{2}}^{\frac{h}{2}} \sigma_{\vartheta\vartheta} z \left(1 + \frac{z}{r_1}\right) \mathrm{d}z, \\
M_{\varphi\vartheta} &= \int_{-\frac{h}{2}}^{\frac{h}{2}} \tau_{\varphi\vartheta} z \left(1 + \frac{z}{r_2}\right) \mathrm{d}z, \quad M_{\vartheta\varphi} = \int_{-\frac{h}{2}}^{\frac{h}{2}} \tau_{\vartheta\varphi} z \left(1 + \frac{z}{r_1}\right) \mathrm{d}z, \\
Q_\varphi &= \int_{-\frac{h}{2}}^{\frac{h}{2}} \tau_{\varphi z} \left(1 + \frac{z}{r_2}\right) \mathrm{d}z, \quad Q_\vartheta = \int_{-\frac{h}{2}}^{\frac{h}{2}} \tau_{\vartheta z} \left(1 + \frac{z}{r_1}\right) \mathrm{d}z.
\end{aligned} \tag{21.18}
$$

For the shell, the shear force flows $N_{\varphi\vartheta}$ and $N_{\vartheta\varphi}$ as well as the two twisting moment flows $M_{\varphi\vartheta}$ and $M_{\vartheta\varphi}$ will not be identical due to the generally different radii r_1 and r_2, despite the equality of the shear stresses $\tau_{\varphi\vartheta}$ and $\tau_{\vartheta\varphi}$ that determine them. An exception is the spherical shell, for example, where $r_1 = r_2$. The bending moment flows $M_{\varphi\varphi}$ and $M_{\vartheta\vartheta}$ are defined in such a way that a positive moment causes tensile stresses in the range $z > 0$. The twisting moment flow $M_{\varphi\vartheta}$ is positive for shear stresses $\tau_{\varphi\vartheta} = \tau_{\vartheta\varphi}$ that act for $z > 0$ on sections with positive outer normal in the positive coordinate direction. The force flows are positive if they act on a section with a positive normal in the positive coordinate direction.

Figure 21.10 shows the force and moment flows of the shell on an infinitesimal section element in an overview.

It should be noted that bending and twisting moments can occur in a shell, even if the stresses in the cross-section are constant. This is explained by the curvature of the shell and the governing equations (21.18).

In many technically relevant cases, it can be assumed that the expressions $\frac{z}{r_1}$ and $\frac{z}{r_2}$ occurring in (21.18) are negligibly small compared to the value 1. This is known as the Kirchhoff-Love[1]-approximation. For the shell force and moment flows then follows:

$$
\begin{aligned}
N_{\varphi\varphi} &= \int_{-\frac{h}{2}}^{\frac{h}{2}} \sigma_{\varphi\varphi} \mathrm{d}z, \quad N_{\vartheta\vartheta} = \int_{-\frac{h}{2}}^{\frac{h}{2}} \sigma_{\vartheta\vartheta} \mathrm{d}z, \\
N_{\varphi\vartheta} &= \int_{-\frac{h}{2}}^{\frac{h}{2}} \tau_{\varphi\vartheta} \mathrm{d}z = N_{\vartheta\varphi}, \quad M_{\varphi\varphi} = \int_{-\frac{h}{2}}^{\frac{h}{2}} \sigma_{\varphi\varphi} z \mathrm{d}z, \\
M_{\vartheta\vartheta} &= \int_{-\frac{h}{2}}^{\frac{h}{2}} \sigma_{\vartheta\vartheta} z \mathrm{d}z, \quad M_{\varphi\vartheta} = \int_{-\frac{h}{2}}^{\frac{h}{2}} \tau_{\varphi\vartheta} z \mathrm{d}z = M_{\vartheta\varphi}, \\
Q_{\varphi} &= \int_{-\frac{h}{2}}^{\frac{h}{2}} \tau_{\varphi z} \mathrm{d}z, \quad Q_{\vartheta} = \int_{-\frac{h}{2}}^{\frac{h}{2}} \tau_{\vartheta z} \mathrm{d}z.
\end{aligned}
\tag{21.19}
$$

If the trapezoidal effect is neglected, the shear force flows $N_{\varphi\vartheta}$ and $N_{\vartheta\varphi}$ as well as the two twisting moment flows $M_{\varphi\vartheta}$ and $M_{\vartheta\varphi}$ are identical.

If the shell force and moment flows are known, then the corresponding layerwise stresses of the laminated shell can be determined from Hooke's law. In the context of CLPT, the following constitutive relationship applies:

$$
\begin{pmatrix} N_{\varphi\varphi} \\ N_{\vartheta\vartheta} \\ N_{\varphi\vartheta} \\ M_{\varphi\varphi} \\ M_{\vartheta\vartheta} \\ M_{\varphi\vartheta} \end{pmatrix} = \begin{bmatrix} A_{11} & A_{12} & A_{16} & B_{11} & B_{12} & B_{16} \\ A_{12} & A_{22} & A_{26} & B_{12} & B_{22} & B_{26} \\ A_{16} & A_{26} & A_{66} & B_{16} & B_{26} & B_{66} \\ B_{11} & B_{12} & B_{16} & D_{11} & D_{12} & D_{16} \\ B_{12} & B_{22} & B_{26} & D_{12} & D_{22} & D_{26} \\ B_{16} & B_{26} & B_{66} & D_{16} & D_{26} & D_{66} \end{bmatrix} \begin{pmatrix} \varepsilon^0_{\varphi\varphi} \\ \varepsilon^0_{\vartheta\vartheta} \\ \gamma^0_{\varphi\vartheta} \\ \kappa^0_{\varphi\varphi} \\ \kappa^0_{\vartheta\vartheta} \\ \kappa^0_{\varphi\vartheta} \end{pmatrix}. \tag{21.20}
$$

The shell strains can be determined by inversion, which can be used to determine the layerwise stresses from Hooke's law.

The infinitesimal strain tensor $\underline{\underline{\varepsilon}}$ can be specified in the reference coordinates given here as:

[1] Augustus Edward Hough Love, 1863–1940, English mathematician and physicist.

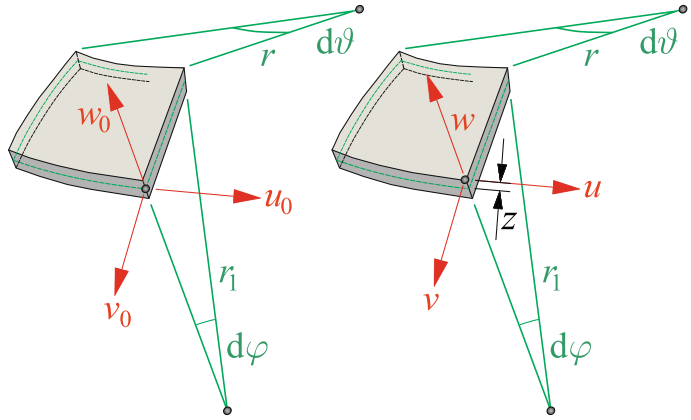


Fig. 21.11 Displacements of the shell

$$\underline{\underline{\varepsilon}} = \begin{bmatrix} \varepsilon_{\varphi\varphi} & \gamma_{\varphi\vartheta} & \gamma_{\varphi z} \\ \gamma_{\vartheta\varphi} & \varepsilon_{\vartheta\vartheta} & \gamma_{\vartheta z} \\ \gamma_{\varphi z} & \gamma_{\vartheta z} & \varepsilon_{zz} \end{bmatrix}. \tag{21.21}$$

Due to the hypothesis that the cross-sections remain plane and the normal hypothesis, the transverse shear strains $\gamma_{\varphi z}$ and $\gamma_{\vartheta z}$ are omitted here as a prerequisite. The assumption that the shell thickness h does not change during the deformation process also leads to $\varepsilon_{zz} = 0$. The deformation state of a shell in the context of CLPT is therefore determined by the strains $\varepsilon_{\varphi\varphi}$ (strain in meridian direction) and $\varepsilon_{\vartheta\vartheta}$ (strain in ring direction) and the shear strain $\gamma_{\varphi\vartheta} = \gamma_{\vartheta\varphi}$ (angle change between the coordinate lines φ and ϑ). We also define the corresponding strain quantities in relation to the middle surface $\varepsilon^0_{\varphi\varphi}$, $\varepsilon^0_{\vartheta\vartheta}$, $\gamma^0_{\varphi\vartheta} = \gamma^0_{\vartheta\varphi}$, which are not dependent on the thickness coordinate z.

The displacements u, v and w (Fig. 21.11) of a shell point outside the shell middle plane are the displacement u in the ring direction, the displacement v in the meridian direction and the displacement w in the thickness direction z. These quantities are functions of the two angles φ and ϑ as well as the thickness coordinate z. In addition, we consider the displacements u_0, v_0 and w_0 of the shell middle surface, which are not functions of z.

21.2 Membrane Theory of Shells of Revolution

A very useful simplification of shell problems is the assumption that a considered shell structure carries a given load by a pure membrane effect and that no bending effect occurs. This is comparable to a disk in which only membrane force flows occur. This state is known as the membrane stress state and the associated theory is known as membrane theory. It is based on the following assumptions:

(i) It is assumed that the plane stress components $\sigma_{\varphi\varphi}$, $\sigma_{\vartheta\vartheta}$, $\tau_{\varphi\vartheta} = \tau_{\vartheta\varphi}$ are the only acting stresses. Further, it is assumed that the moment flows $M_{\vartheta\vartheta}$, $M_{\vartheta\vartheta}$, $M_{\varphi\vartheta} = M_{\vartheta\varphi}$, which generally also occur, are negligibly small. This is accompanied by the disappearance of the shear force flows Q_φ and Q_ϑ.

(ii) The bending and twisting stiffnesses of the shell are considered negligible compared to the membrane stiffnesses. However, this assumes that the shell is thin. The shell can therefore be mathematically reduced to its middle surface.

The assumptions described correspond to the requirement that the terms $\frac{z}{r_1}$ and $\frac{z}{r_2}$ disappear. This is referred to as the Kirchhoff-Love-approximation. For the remaining force flows we obtain

$$N_{\varphi\varphi} = \int_{-\frac{h}{2}}^{\frac{h}{2}} \sigma_{\varphi\varphi} \mathrm{d}z, \quad N_{\vartheta\vartheta} = \int_{-\frac{h}{2}}^{\frac{h}{2}} \sigma_{\vartheta\vartheta} \mathrm{d}z, \quad N_{\varphi\vartheta} = N_{\vartheta\varphi} = \int_{-\frac{h}{2}}^{\frac{h}{2}} \tau_{\varphi\vartheta} \mathrm{d}z. \tag{21.22}$$

If we neglect all curvature and twisting influences on the stresses, the strains of the laminate result as:

$$\begin{pmatrix} \varepsilon_{\varphi\varphi} \\ \varepsilon_{\vartheta\vartheta} \\ \gamma_{\varphi\vartheta} \end{pmatrix} = \begin{pmatrix} \varepsilon^0_{\varphi\varphi} \\ \varepsilon^0_{\vartheta\vartheta} \\ \gamma^0_{\varphi\vartheta} \end{pmatrix} = \begin{bmatrix} A_{11} & A_{12} & A_{16} \\ A_{12} & A_{22} & A_{26} \\ A_{16} & A_{26} & A_{66} \end{bmatrix}^{-1} \begin{pmatrix} N_{\varphi\varphi} \\ N_{\vartheta\vartheta} \\ N_{\varphi\vartheta} \end{pmatrix}. \tag{21.23}$$

This applies to both symmetric and unymmetric layups. The layerwise stresses then read:

$$\begin{pmatrix} \sigma_{\varphi\varphi} \\ \sigma_{\vartheta\vartheta} \\ \tau_{\varphi\vartheta} \end{pmatrix} = \begin{bmatrix} \bar{Q}_{11} & \bar{Q}_{12} & \bar{Q}_{16} \\ \bar{Q}_{12} & \bar{Q}_{22} & \bar{Q}_{26} \\ \bar{Q}_{16} & \bar{Q}_{26} & \bar{Q}_{66} \end{bmatrix} \begin{pmatrix} \varepsilon_{\varphi\varphi} \\ \varepsilon_{\vartheta\vartheta} \\ \gamma_{\varphi\vartheta} \end{pmatrix}. \tag{21.24}$$

The equilibrium conditions are accordingly the force equilibria with regard to the meridian direction φ, the ring direction ϑ and the thickness direction z. The moment equilibria give no result due to the omission of all moment quantities (moment balances with respect to φ and ϑ) or have already been employed in establishing the equality of the plane shear force flows $N_{\varphi\vartheta}$ and $N_{\vartheta\varphi}$ (moment equilibrium with respect to the z-axis).

With the three force flows and the three force balances, the considered membrane problem of the shell proves to be statically determinate. It is therefore not necessary to consider the deformation state if only the determination of the stress state of the shell is of interest and there is no shell structure that is internally statically indeterminate or statically indeterminately supported.

In addition to the formal requirements mentioned above, however, a number of other aspects must be taken into account under which a shell can be regarded as free of bending and twisting and which must be assumed to be mandatory for the validity of the membrane theory.

(i) The middle surface of the shell must meet the requirement that it is continuous in terms of its shape, gradient and curvature. The surface shown in Fig. 21.12, left, would therefore be suitable for an analysis using membrane theory, the one shown in Fig. 21.12, right, would not. The reason for this is that due to the discontinuous inclination of the shell middle surface shown here, the local equilibrium can no longer be ensured with the membrane force flows alone and a local bending effect occurs there.

(ii) For the shell thickness h, which can vary over φ and ϑ, the requirement applies that it does not change abruptly (Fig. 21.13). According to this, the shell shown in Fig. 21.13 on the left would be permissible in the context of membrane theory, while the shell shown in Fig. 21.13 on the right is not permissible. It must also be ensured that the layups of the shell laminates do not change abruptly.

(iii) The applied surface loads must be evenly distributed and must not exhibit any large variability or excessive waviness. The calculation of shells under single loads is therefore not possible according to membrane theory. Both single forces and strongly varying surface loads cause forces inside the shell that in turn cause a bending effect.

(iv) Edge force flows of a shell must be applied in such a way that they act tangentially to the middle surface of the shell. Accordingly, only longitudinal and transverse forces are permissible (Fig. 21.14, left), but not transverse forces that would lead to a bending effect (Fig. 21.14, right). This must be ensured by suitable supports.

(v) Deformations that occur at bearings or at transitions to other components may only be limited to the extent that the tangential direction of action of the forces occurring there is not cancelled out (Fig. 21.15, left). Otherwise, a local bending effect occurs at such points (Fig. 21.15, right), which can no longer be assessed within the framework of membrane theory.

For derivation of the equilibrium conditions, we consider an infinitesimal element of the shell middle surface with the edge lengths $\mathrm{d}s_1 = r_1 \mathrm{d}\varphi$ and $\mathrm{d}s_2 = r\mathrm{d}\vartheta$. We introduce the membrane force flows $N_{\varphi\varphi}$, $N_{\vartheta\vartheta}$ and $N_{\varphi\vartheta}$ with their infinitesimal increments at the respective cutting edges of the element and form the force equilibria in the direction of the meridian tangent and the ring tangent and also with regard to the thickness direction. Figure 21.16

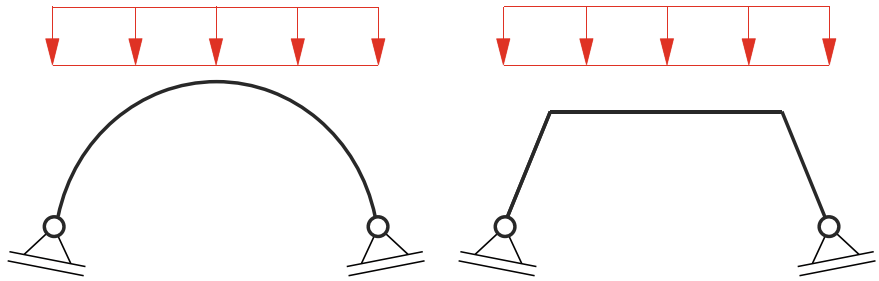


Fig. 21.12 On the shape of the shell middle surface

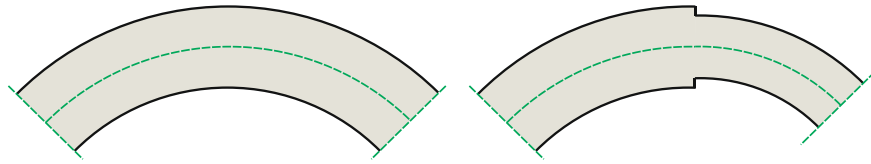


Fig. 21.13 On the distribution of the shell thickness h

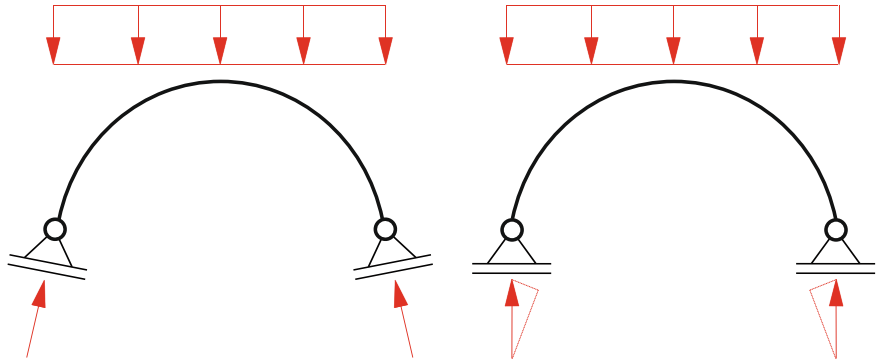


Fig. 21.14 Introduction of edge forces

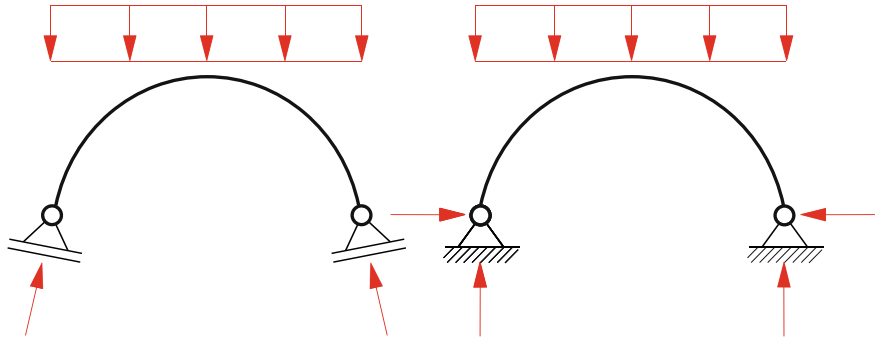


Fig. 21.15 Edge displacements

shows a meridian section at a point $\vartheta = \text{const.}$ where the corresponding parts of the force flow $N_{\varphi\varphi}$ can be identified. To improve readability, the resulting force $\bar{N}_{\varphi\varphi} = N_{\varphi\varphi} r \mathrm{d}\vartheta$ and the abbreviation $(\ldots.)^{\cdot}$ for a partial derivative $\frac{\partial}{\partial\varphi}(\ldots)$ of a given quantity with respect to φ have been introduced. Due to the smallness of the angle $\mathrm{d}\varphi$, $\sin\frac{\mathrm{d}\varphi}{2} \simeq \frac{\mathrm{d}\varphi}{2}$ and $\cos\frac{\mathrm{d}\varphi}{2} \simeq 1$. The force component in the direction of the meridian tangent is then $\bar{N}_{\varphi\varphi}\mathrm{d}\varphi$. In the normal direction, the component $-\bar{N}_{\varphi\varphi}\mathrm{d}\varphi$ remains.

In Fig. 21.17 the force components due to the shear forces $\bar{N}_{\vartheta\varphi} = N_{\vartheta\varphi} r_1 \mathrm{d}\varphi$ and $\bar{N}_{\varphi\vartheta} = N_{\varphi\vartheta} r \mathrm{d}\vartheta$ are shown. We again consider small angles and the abbreviation $(\ldots)'$ for a partial

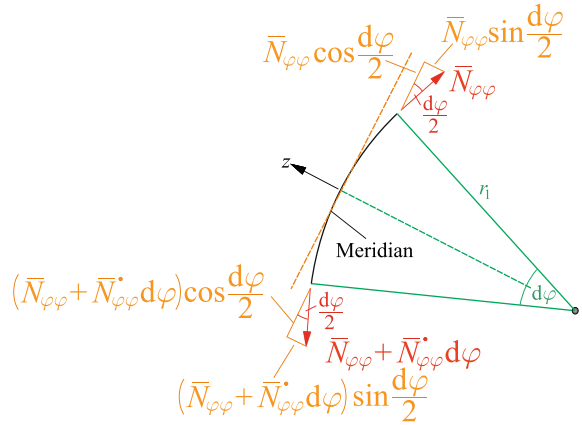


Fig. 21.16 Meridian section

derivative $\frac{\partial}{\partial\vartheta}(\ldots)$ with respect to ϑ. Terms of a higher order in the angles $d\varphi$ and $d\vartheta$ can be neglected. The force component in the direction of the meridian tangent is calculated as $\bar{N}'_{\vartheta\varphi}d\vartheta$. In the ring direction, we obtain $\bar{N}_{\vartheta\varphi}d\vartheta\cos\varphi + N^{\cdot}_{\varphi\vartheta}d\varphi$.

The decomposition of the force $\bar{N}_{\vartheta\vartheta}$ is shown in Fig. 21.18, using a circular section with $\varphi = \text{const.}$ and a meridian section. The force component remaining in the meridional direction is $-\bar{N}_{\vartheta\vartheta}\cos\varphi d\vartheta$, whereas in the ring direction we obtain the component $\bar{N}'_{\vartheta\vartheta}d\vartheta$. In the normal direction, the component $-\bar{N}_{\vartheta\vartheta}\sin\varphi d\vartheta$ remains.

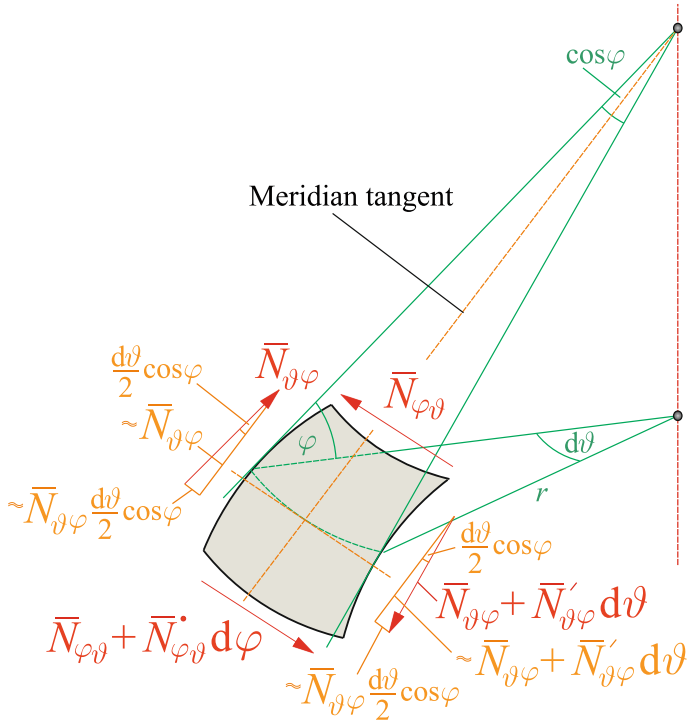


Fig. 21.17 Decomposition of the forces $\bar{N}_{\varphi\vartheta}$ and $\bar{N}_{\vartheta\varphi}$

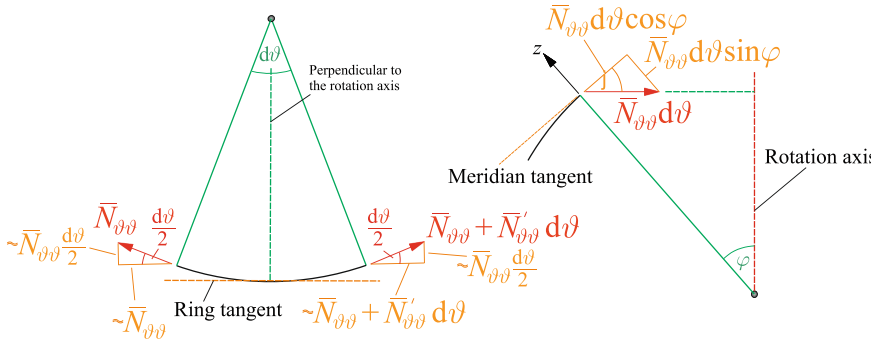


Fig. 21.18 Decomposition of the force $\bar{N}_{\vartheta\vartheta}$

When forming the force balances in the meridian, ring and normal directions, the contributions by the surface loads p_φ, p_ϑ and p_z, each multiplied by $dA = r_1 r \mathrm{d}\varphi \mathrm{d}\vartheta$, must be taken into account. We obtain:

$$\begin{aligned}
\frac{\partial}{\partial \varphi}\left(N_{\varphi\varphi} r\right) + \frac{\partial N_{\varphi\vartheta}}{\partial \vartheta} r_1 - N_{\vartheta\vartheta} \cos\varphi r_1 + p_\varphi r_1 r = 0, \\
\frac{\partial}{\partial \varphi}\left(N_{\varphi\vartheta} r\right) + \frac{\partial N_{\vartheta\vartheta}}{\partial \vartheta} r_1 + N_{\vartheta\varphi} \cos\varphi r_1 + p_\vartheta r_1 r = 0, \\
N_{\varphi\varphi} r_2 + N_{\vartheta\vartheta} r_1 - p_z r_1 r_2 = 0.
\end{aligned} \tag{21.25}$$

These are three coupled differential equations for the three force flows $N_{\varphi\varphi}$, $N_{\vartheta\vartheta}$, $N_{\varphi\vartheta} = N_{\vartheta\varphi}$ in the framework of membrane theory.

We specialize the equilibrium conditions below for technically relevant special cases. For the spherical shell with $r_1 = r_2 = R$ and $r = R \sin\varphi$ we obtain

$$\begin{aligned}
\frac{\partial}{\partial \varphi}\left(N_{\varphi\varphi} \sin\varphi\right) + \frac{\partial N_{\vartheta\varphi}}{\partial \vartheta} - N_{\vartheta\vartheta} \cos\varphi + p_\varphi R \sin\varphi = 0, \\
\frac{\partial}{\partial \varphi}\left(N_{\varphi\vartheta} \sin\varphi\right) + \frac{\partial N_{\vartheta\vartheta}}{\partial \vartheta} + N_{\vartheta\varphi} \cos\varphi + p_\vartheta R \sin\varphi = 0, \\
N_{\varphi\varphi} + N_{\vartheta\vartheta} - p_z R = 0.
\end{aligned} \tag{21.26}$$

In the case of the conical shell with the opening angle α with the reference axis s tangential to the meridian, we obtain with $\mathrm{d}s = r_1 \mathrm{d}\varphi$, $r_1 \to \infty$ and $r_2 = s \tan\alpha$ and with $r = r_2 \sin\varphi = s \sin\alpha$ and $\cos\varphi = \sin\alpha$:

$$\begin{aligned}
\frac{\partial}{\partial s}\left(N_{ss} s\right) + \frac{1}{\sin\alpha} \frac{\partial N_{\vartheta s}}{\partial \vartheta} - N_{\vartheta\vartheta} + p_s s = 0, \\
\frac{\partial}{\partial s}\left(N_{\vartheta s} s\right) + \frac{1}{\sin\alpha} \frac{\partial N_{\vartheta\vartheta}}{\partial \vartheta} + N_{\vartheta s} + p_\vartheta s = 0, \\
N_{\vartheta\vartheta} - p_z s \tan\alpha = 0.
\end{aligned} \tag{21.27}$$

For the circular cylindrical shell, $r_1 \to \infty$, $r_2 = R$ and $\varphi = 90°$. With the vertical reference axis x with $r_1 \mathrm{d}\varphi = \mathrm{d}x$ and $r = r_2 \sin\varphi = s \sin\alpha$ and $\cos\varphi = \sin\alpha$ follows:

$$\begin{aligned}
\frac{\partial N_{xx}}{\partial x} + \frac{1}{R} \frac{\partial N_{\vartheta x}}{\partial \vartheta} + p_x = 0, \\
\frac{\partial N_{x\vartheta}}{\partial x} + \frac{1}{R} \frac{\partial N_{\vartheta\vartheta}}{\partial \vartheta} + p_\vartheta = 0, \\
N_{\vartheta\vartheta} - p_z R = 0.
\end{aligned} \tag{21.28}$$

We now want to analyze the special case of a shell of revolution under a rotationally symmetrical load. Then all derivatives with respect to ϑ result in zero. The membrane force flows of the shell are then only functions of the angle φ, and the equilibrium conditions (21.25) are as follows:

$$\begin{aligned}
\frac{\mathrm{d}}{\mathrm{d}\varphi}\left(N_{\varphi\varphi} r\right) - N_{\vartheta\vartheta}\cos\varphi r_1 + p_\varphi r_1 r = 0,\\
\frac{\mathrm{d}}{\mathrm{d}\varphi}\left(N_{\varphi\vartheta} r\right) + N_{\vartheta\varphi}\cos\varphi r_1 + p_\vartheta r_1 r = 0,\\
N_{\varphi\varphi} r_2 + N_{\vartheta\vartheta} r_1 - p_z r_1 r_2 = 0.
\end{aligned} \tag{21.29}$$

It can be seen that the first and third differential equations in (21.29) are coupled with each other and describe the membrane force flows $N_{\varphi\varphi}$ and $N_{\vartheta\vartheta}$ that will occur due to the surface loads p_φ and p_z. The second differential equation, on the other hand, is decoupled from the other two equations and describes the membrane force flow $N_{\varphi\vartheta} = N_{\vartheta\varphi}$, which results from the surface load p_ϑ. This can be interpreted as a torsional load case, which we will not discuss further. We will focus on solving the first and third differential equation in (21.29).

The equilibrium conditions can again be specified for various technically relevant shell types. For the spherical shell with $r_1 = r_2 = R$ it follows from (21.29):

$$\begin{aligned}
\frac{\mathrm{d}}{\mathrm{d}\varphi}\left(N_{\varphi\varphi}\sin\varphi\right) - N_{\vartheta\vartheta}\cos\varphi + p_\varphi R\sin\varphi = 0,\\
\frac{\mathrm{d}}{\mathrm{d}\varphi}\left(N_{\varphi\vartheta}\sin\varphi\right) + N_{\vartheta\varphi}\cos\varphi + p_\vartheta R\sin\varphi = 0,\\
N_{\varphi\varphi} + N_{\vartheta\vartheta} - p_z R = 0.
\end{aligned} \tag{21.30}$$

For the conical shell with the opening angle α and the reference axis s tangential to the meridian, the following applies with $\mathrm{d}s = r_1\mathrm{d}\varphi$ and $r_1 \to \infty$ and $r_2 = s\tan\alpha$ and $r = r_2\sin\varphi = s\sin\alpha$ and $\cos\varphi = \sin\alpha$:

$$\begin{aligned}
\frac{\mathrm{d}}{\mathrm{d}s}\left(N_{ss} s\right) - N_{\vartheta\vartheta} + p_s s = 0,\\
\frac{\mathrm{d}}{\mathrm{d}s}\left(N_{\vartheta s} s\right) + N_{\vartheta s} + p_\vartheta s = 0,\\
N_{\vartheta\vartheta} - p_z s\tan\alpha = 0.
\end{aligned} \tag{21.31}$$

If we consider a circular cylindrical shell with $r_1 \to \infty$, $r_2 = R$ and $\varphi = 90°$ and considering the vertical reference axis x with $r_1\mathrm{d}\varphi = \mathrm{d}x$ and $r = r_2\sin\varphi = s\sin\alpha$ and $\cos\varphi = \sin\alpha$, then it follows from (21.29):

$$\begin{aligned}
\frac{\mathrm{d}N_{xx}}{\mathrm{d}x s} + p_x = 0,\\
\frac{\mathrm{d}N_{x\vartheta}}{\mathrm{d}x} + p_\vartheta = 0,\\
N_{\vartheta\vartheta} - p_z R = 0.
\end{aligned} \tag{21.32}$$

In the following, we solve the differential equation system (21.29) and consider the first and third equations occurring there. The surface load p_ϑ is excluded. It follows:

$$\frac{\mathrm{d}}{\mathrm{d}\varphi}\left(N_{\varphi\varphi} r\right) - N_{\vartheta\vartheta}\cos\varphi r_1 + p_\varphi r_1 r = 0,$$
$$N_{\varphi\varphi} r_2 + N_{\vartheta\vartheta} r_1 - p_z r_1 r_2 = 0. \tag{21.33}$$

The second equation in (21.33) results in

$$N_{\vartheta\vartheta} = r_2\left(p_z - \frac{N_{\varphi\varphi}}{r_1}\right). \tag{21.34}$$

The first equation in (21.33) can then be transformed as follows:

$$\frac{\mathrm{d}}{\mathrm{d}\varphi}\left(N_{\varphi\varphi} r_2\right) + 2N_{\varphi\varphi} r_2\cot\varphi + \left(p_\varphi - p_z\cot\varphi\right) r_1 r_2 = 0. \tag{21.35}$$

This is a first-order linear inhomogeneous differential equation with non-constant coefficients for the membrane force flow $N_{\varphi\varphi}$ which is multiplied by the radius r_2. With

$$\frac{1}{\sin^2\varphi}\frac{\mathrm{d}}{\mathrm{d}\varphi}\left(N_{\varphi\varphi} r_2 \sin^2\varphi\right) = \frac{\mathrm{d}}{\mathrm{d}\varphi}\left(N_{\varphi\varphi} r_2\right) + 2N_{\varphi\varphi} r_2\cot\varphi \tag{21.36}$$

we obtain:

$$\frac{\mathrm{d}}{\mathrm{d}\varphi}\left(N_{\varphi\varphi} r_2 \sin^2\varphi\right) = \sin^2\varphi\left(p_z\cot\varphi - p_\varphi\right) r_1 r_2. \tag{21.37}$$

This differential equation is solved by integration:

$$N_{\varphi\varphi} = \frac{1}{r_2\sin^2\varphi}\left[\int_\varphi \left(p_z\cot\varphi - p_\varphi\right) r_1 r_2 \sin^2\varphi \mathrm{d}\varphi + C_1\right]. \tag{21.38}$$

This provides the solution for the membrane force flow $N_{\varphi\varphi}$. The quantity C_1 is an integration constant that must be determined from specified boundary conditions. If we use the solution for $N_{\varphi\varphi}$ in (21.34), then the membrane force flow $N_{\vartheta\vartheta}$ results as:

$$N_{\vartheta\vartheta} = r_2\left\{p_z - \frac{1}{r_1 r_2\sin^2\varphi}\left[\int_\varphi \left(p_z\cot\varphi - p_\varphi\right) r_1 r_2 \sin^2\varphi \mathrm{d}\varphi + C_1\right]\right\}. \tag{21.39}$$

For the previously discussed cases of spherical, conical and cylindrical shells, these equations can be specialized. The following applies to the spherical shell:

$$N_{\varphi\varphi} = \frac{1}{R\sin^2\varphi}\left[R^2\int_\varphi \left(p_z\cot\varphi - p_\varphi\right)\sin^2\varphi \mathrm{d}\varphi + C_1\right],$$
$$N_{\vartheta\vartheta} = p_z R - N_{\varphi\varphi}. \tag{21.40}$$

In the case of the conical shell, we obtain:

$$N_{ss} = \frac{1}{s}\left[\int_s (p_z \tan\alpha - p_s)\, s\,\mathrm{d}s + C_1\right],$$
$$N_{\vartheta\vartheta} = p_z s \tan\alpha. \tag{21.41}$$

Finally, the following results for the cylindrical shell:

$$N_{xx} = -\int_x p_x \mathrm{d}x + C_1,$$
$$N_{\vartheta\vartheta} = R p_z. \tag{21.42}$$

Solutions for the membrane force flows of rotational shells can be found in large numbers in the available literature, and these solutions also apply to the laminated shells considered here. An explicit specification of such solutions is omitted here and reference is made to the specialist literature a selection of which is given in the reference list at the end of this chapter.

To determine the strain and deformation state of a shell, it is necessary to consider the shell kinematics. The following displacement quantities are defined for this purpose:

- Let the displacements u, v and w be displacements of a shell point outside the shell middle plane $z = 0$. Here, u is the displacement in the direction of the ring tangent, v the displacement in the direction of the meridian tangent and w the displacement in the normal direction z, which are functions of the two angles φ and ϑ as well as the thickness coordinate z.
- The displacements u_0, v_0 and w_0 are the displacements of a point on the middle surface of the shell, which depend only on φ and ϑ and not on z.

We further have the strain in the meridian direction $\varepsilon^0_{\varphi\varphi}$, the strain in the ring direction $\varepsilon^0_{\vartheta\vartheta}$ and the shear strain $\gamma^0_{\varphi\vartheta}$ of the shell middle surface, which are functions of φ and ϑ, but not of z. We consider this in Fig. 21.19 of the infinitesimal element $\mathrm{d}A$ of the shell middle surface with the edge lengths $\mathrm{d}s_1$ and $\mathrm{d}s_2$. The corner points of the element are referred to as points 1–4. The displacements of the corner points are labelled $u_{0,i}$, $v_{0,i}$ and $w_{0,i}$ ($i = 1, 2, 3, 4$). The displacements of points 2, 3 and 4 are expressed by the displacements of point 1 and developed as Taylor series, which are terminated after the first term in each case. The following then applies to the displacements at point 2:

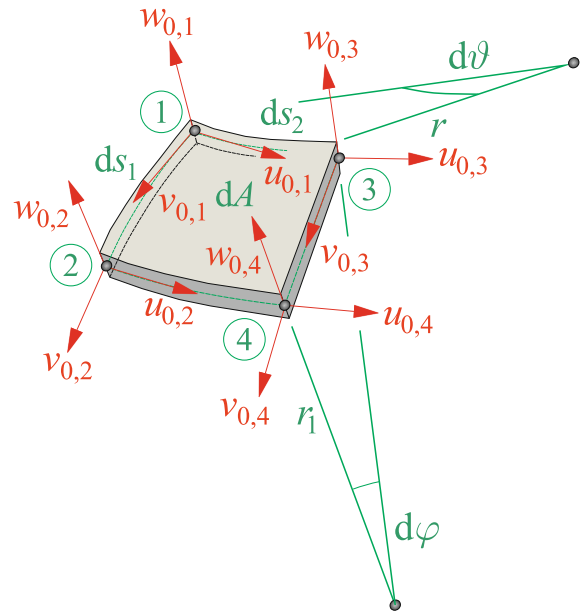


Fig. 21.19 Infinitesimal surface element of the shell middle surface and the displacements of vertices 1–4

$$
\begin{aligned}
u_{0,2} &= u_0 + \frac{\partial u_0}{\partial \varphi}\mathrm{d}\varphi, \\
v_{0,2} &= v_0 + \frac{\partial v_0}{\partial \varphi}\mathrm{d}\varphi, \\
w_{0,2} &= w_0 + \frac{\partial w_0}{\partial \varphi}\mathrm{d}\varphi.
\end{aligned}
\tag{21.43}
$$

For point 3 we obtain:

$$
\begin{aligned}
u_{0,3} &= u_0 + \frac{\partial u_0}{\partial \vartheta}\mathrm{d}\vartheta, \\
v_{0,3} &= v_0 + \frac{\partial v_0}{\partial \vartheta}\mathrm{d}\vartheta, \\
w_{0,3} &= w_0 + \frac{\partial w_0}{\partial \vartheta}\mathrm{d}\vartheta.
\end{aligned}
\tag{21.44}
$$

For point 4 it follows:

$$
\begin{aligned}
u_{0,4} &= u_0 + \frac{\partial u_0}{\partial \varphi}\mathrm{d}\varphi + \frac{\partial u_0}{\partial \vartheta}\mathrm{d}\vartheta, \\
v_{0,4} &= v_0 + \frac{\partial v_0}{\partial \varphi}\mathrm{d}\varphi + \frac{\partial v_0}{\partial \vartheta}\mathrm{d}\vartheta, \\
w_{0,4} &= w_0 + \frac{\partial w_0}{\partial \varphi}\mathrm{d}\varphi + \frac{\partial w_0}{\partial \vartheta}\mathrm{d}\vartheta.
\end{aligned}
\tag{21.45}
$$

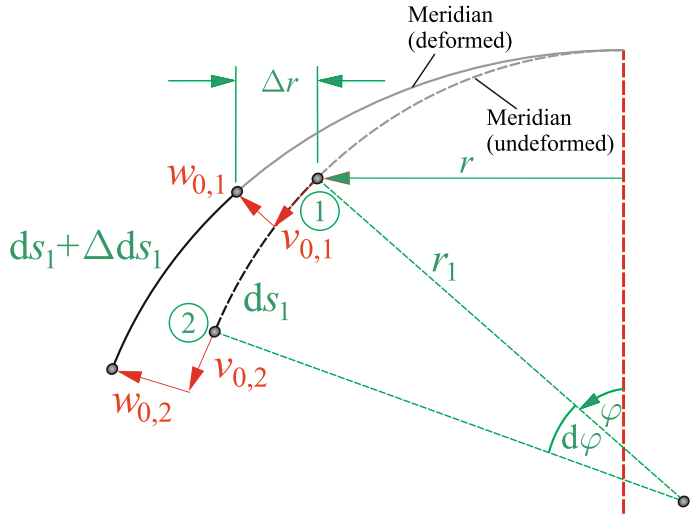


Fig. 21.20 Meridian section of the infinitesimal surface element of the shell middle surface through the two points 1 and 2

The strains of the shell middle surface are then as follows:

$$\varepsilon^0_{\varphi\varphi} = \frac{(\mathrm{d}s_1 + \Delta\mathrm{d}s_1) - \mathrm{d}s_1}{\mathrm{d}s_1}, \quad \varepsilon^0_{\vartheta\vartheta} = \frac{(\mathrm{d}s_2 + \Delta\mathrm{d}s_2) - \mathrm{d}s_2}{\mathrm{d}s_2}. \tag{21.46}$$

Here, $\Delta\mathrm{d}s_1$ and $\Delta\mathrm{d}s_2$ are the changes of the edge lengths of the element $\mathrm{d}A$. The shear strain $\gamma^0_{\varphi\vartheta}$ corresponds to the change in the right angle between the section element edges.

To determine the kinematic quantities, we again consider different sections through the shell and determine the respective contributions of the individual displacements, using the relationships $\mathrm{d}s_1 = r_1\mathrm{d}\varphi$ and $\mathrm{d}s_2 = r\mathrm{d}\vartheta$ and neglecting terms of a higher order. In Fig. 21.20 a meridian section for $\vartheta = \text{const.}$ is shown through the two points 1 and 2, both in the undeformed and deformed state. This results in the length of the edge piece in the deformed state:

$$\mathrm{d}s_1 + \Delta\mathrm{d}s_1 = \left(\mathrm{d}s_1 + \frac{\partial v_0}{\partial\varphi}\mathrm{d}\varphi\right)\left(1 + \frac{\Delta r_1}{r_1}\right). \tag{21.47}$$

With $\Delta r_1 = w_0$ and neglecting the term $\frac{w}{r_1}\frac{\partial v_0}{\partial\varphi}\mathrm{d}\varphi$ this expression can be written as follows:

$$\mathrm{d}s_1 + \Delta\mathrm{d}s_1 = \mathrm{d}s_1\left(1 + \frac{w_0}{r_1}\right) + \frac{\partial v_0}{\partial\varphi}\mathrm{d}\varphi. \tag{21.48}$$

With (21.46), the strain $\varepsilon^0_{\varphi\varphi}$ results as:

$$\begin{aligned}\varepsilon^0_{\varphi\varphi} &= \frac{(\mathrm{d}s_1 + \Delta\mathrm{d}s_1) - \mathrm{d}s_1}{\mathrm{d}s_1} \\ &= \frac{\mathrm{d}s_1\left(1 + \frac{w_0}{r_1}\right) + \frac{\partial v_0}{\partial\varphi}\mathrm{d}\varphi - \mathrm{d}s_1}{\mathrm{d}s_1} \\ &= \frac{1}{r_1}\left(\frac{\partial v_0}{\partial\varphi} + w_0\right).\end{aligned} \tag{21.49}$$

Here $\mathrm{d}s_1 = r_1\mathrm{d}\varphi$ was used. The expansion Δr of the radius r can be determined as:

$$\Delta r = v_0\cos\varphi + w_0\sin\varphi. \tag{21.50}$$

Figure 21.21 contains an annular circle section for $\varphi = \text{const.}$ through points 1 and 3, where the undeformed and the deformed annular circle segment of length $\mathrm{d}s_2$ is shown here, which in the deformed state has the length $\mathrm{d}s_2 + \Delta\mathrm{d}s_2$. For the length $\mathrm{d}s_2 + \Delta\mathrm{d}s_2$ of the deformed section element applies:

$$\mathrm{d}s_2 + \Delta\mathrm{d}s_2 = \left(\mathrm{d}s_2 + \frac{\partial u_0}{\partial\vartheta}\mathrm{d}\vartheta\right)\left(1 + \frac{\Delta r}{r}\right). \tag{21.51}$$

This can be written as follows with (21.50) by neglecting the term $\frac{\partial u_0}{\partial\vartheta}\mathrm{d}\vartheta\frac{\Delta r}{r}$:

$$\mathrm{d}s_2 + \Delta\mathrm{d}s_2 = \mathrm{d}s_2\left(1 + \frac{v_0}{r}\cos\varphi + \frac{w_0}{r}\sin\varphi\right) + \frac{\partial u_0}{\partial\vartheta}\mathrm{d}\vartheta. \tag{21.52}$$

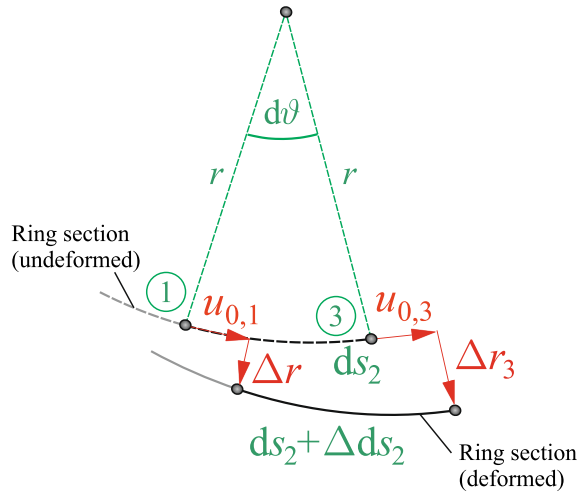


Fig. 21.21 Circular section of the infinitesimal surface element of the shell middle surface through the two points 1 and 3

The strain $\varepsilon^0_{\vartheta\vartheta}$ in (21.46) then results in:

$$\begin{aligned}\varepsilon^0_{\vartheta\vartheta} &= \frac{(\mathrm{d}s_2 + \Delta\mathrm{d}s_2) - \mathrm{d}s_2}{\mathrm{d}s_2} \\ &= \frac{1}{r}\left(\frac{\partial u_0}{\partial\vartheta} + v_0\cos\varphi + w_0\sin\varphi\right),\end{aligned} \tag{21.53}$$

wherein $r = \frac{\mathrm{d}s_2}{\mathrm{d}\vartheta}$.

Figure 21.22 shows the deformation state of an infinitesimal element of the shell middle surface. For the two angles γ_1 and γ_2 it follows with $\Delta u_0 = u_0\left(1 + \frac{\mathrm{d}r}{r}\right)$:

$$\begin{aligned}\gamma_1 &= \frac{\frac{\partial v_0}{\partial\vartheta}\mathrm{d}\vartheta}{\mathrm{d}s_2 + \Delta\mathrm{d}s_2} \simeq \frac{\frac{\partial v_0}{\partial\vartheta}\mathrm{d}\vartheta}{\mathrm{d}s_2}, \\ \gamma_2 &= \frac{u_0 + \frac{\partial u_0}{\partial\varphi}\mathrm{d}\varphi - u_0\left(1 + \frac{\mathrm{d}r}{r}\right)}{\mathrm{d}s_1 + \Delta\mathrm{d}s_1} \simeq \frac{\frac{\partial u_0}{\partial\varphi}\mathrm{d}\varphi - u_0\frac{\mathrm{d}r}{r}}{\mathrm{d}s_1}.\end{aligned} \tag{21.54}$$

The shear strain $\gamma_{\varphi\vartheta}$ represents the sum of the two angles γ_1 and γ_2 and with $\mathrm{d}r = \mathrm{d}s_1\cos\varphi$ results in:

$$\gamma_{\varphi\vartheta} = \gamma_1 + \gamma_2 = \frac{\frac{\partial v_0}{\partial\vartheta}\mathrm{d}\vartheta}{\mathrm{d}s_2} + \frac{\frac{\partial u_0}{\partial\varphi}\mathrm{d}\varphi}{\mathrm{d}s_1} - \frac{u_0\cos\varphi}{r}. \tag{21.55}$$

With $\mathrm{d}s_1 = r_1\mathrm{d}\varphi$ and $\mathrm{d}s_2 = r\mathrm{d}\vartheta$ it follows:

$$\gamma_{\varphi\vartheta} = \frac{1}{r}\frac{\partial v_0}{\partial\vartheta} + \frac{1}{r_1}\frac{\partial u_0}{\partial\varphi} - \frac{u_0\cos\varphi}{r}. \tag{21.56}$$

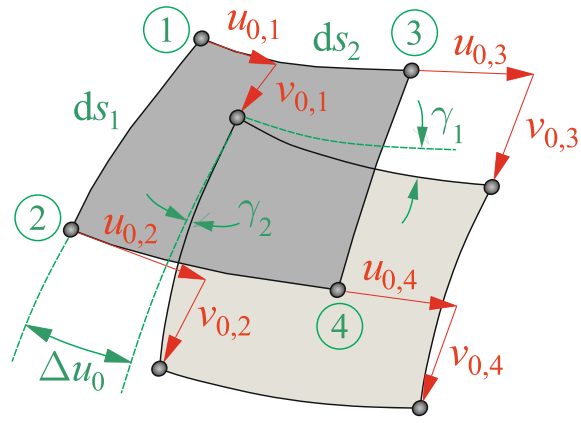


Fig. 21.22 Deformation of an infinitesimal element of the shell middle surface

The kinematic equations for the shell of revolution are summarized as follows

$$\begin{aligned}
\varepsilon^0_{\varphi\varphi} &= \frac{1}{r_1}\left(\frac{\partial v_0}{\partial \varphi} + w_0\right), \\
\varepsilon^0_{\vartheta\vartheta} &= \frac{1}{r}\left(\frac{\partial u_0}{\partial \vartheta} + v_0 \cos\varphi + w_0 \sin\varphi\right), \\
\gamma^0_{\varphi\vartheta} &= \frac{1}{r}\frac{\partial v_0}{\partial \vartheta} + \frac{1}{r_1}\frac{\partial u_0}{\partial \varphi} - \frac{u_0 \cos\varphi}{r}.
\end{aligned} \tag{21.57}$$

The constitutive equations of the membrane shell are given by (21.23).

In the case of a rotationally symmetric load, the kinematic relationships (21.57) are simplified. Since all state variables in this case depend exclusively on φ, all partial derivatives relating to ϑ are omitted and the following applies:

$$\begin{aligned}
\varepsilon^0_{\varphi\varphi} &= \frac{1}{r_1}\left(\frac{\mathrm{d}v_0}{\mathrm{d}\varphi} + w_0\right), \\
\varepsilon^0_{\vartheta\vartheta} &= \frac{1}{r}\left(v_0 \cos\varphi + w_0 \sin\varphi\right), \\
\gamma^0_{\varphi\vartheta} &= \frac{1}{r_1}\frac{\mathrm{d}u_0}{\mathrm{d}\varphi} - \frac{u_0 \cos\varphi}{r}.
\end{aligned} \tag{21.58}$$

For this case, closed-form analytical solutions for the deformations can be given for elementary shell shapes. The case described by the third equation in (21.58) can be interpreted as a torsion of the shell and will not be further analyzed here.

The displacement w_0 from the first equation can be eliminated from the second equation in (21.58):

$$\frac{\mathrm{d}v_0}{\mathrm{d}\varphi} - v_0 \cot\varphi = r_1 \varepsilon^0_{\varphi\varphi} - r_2 \varepsilon^0_{\vartheta\vartheta}, \tag{21.59}$$

or

$$\frac{\mathrm{d}}{\mathrm{d}\varphi}\left(\frac{v_0}{\sin\varphi}\right) = \frac{1}{\sin\varphi}\left(r_1 \varepsilon^0_{\varphi\varphi} - r_2 \varepsilon^0_{\vartheta\vartheta}\right). \tag{21.60}$$

This is an inhomogeneous differential equation for the displacement v_0. The particular solution results from direct integration:

$$v_{0,p} = \sin\varphi \int_{\varphi} \left(r_1 \varepsilon^0_{\varphi\varphi} - r_2 \varepsilon^0_{\vartheta\vartheta}\right) \frac{\mathrm{d}\varphi}{\sin\varphi}. \tag{21.61}$$

We obtain the homogeneous solution by setting the right-hand side of (21.60) to zero:

$$v_{0,h} = C_2 \sin\varphi. \tag{21.62}$$

This expression describes a pure rigid body translation of the shell.
The total solution for v_0 is obtained as follows:

$$v_0 = v_{0,h} + v_{0,p} = \sin\varphi \left[\int_{\varphi} \left(r_1 \varepsilon^0_{\varphi\varphi} - r_2 \varepsilon^0_{\vartheta\vartheta} \right) \frac{\mathrm{d}\varphi}{\sin\varphi} + C_2 \right]. \tag{21.63}$$

From (21.58) we obtain the displacement w_0 as:

$$w_0 = r_2 \varepsilon^0_{\vartheta\vartheta} - v_0 \cot\varphi. \tag{21.64}$$

The constitutive law (21.23) can now be employed here, whereby we refrain from explicitly specifying the result.

21.3 Bending Theory of Shells of Revolution

In addition to the membrane stress state that is always desirable for thin-walled shell structures, in many technically relevant situations there is a state in which the loads on the shell can no longer be transferred exclusively by membrane stresses. Instead, a bending effect also occurs and the corresponding analysis model is referred to as bending theory. Here, too, we want to restrict ourselves to shells of revolution and consider shells whose thickness h, which is assumed to be constant, is small compared to the other characteristic dimensions r_1, r_2 of the shell. We therefore assume the Kirchhoff-Love approximation and define the force and moment quantities of the shell as already given by (21.19):

$$\begin{aligned}
N_{\varphi\varphi} &= \int_{-\frac{h}{2}}^{\frac{h}{2}} \sigma_{\varphi\varphi} \mathrm{d}z, \quad N_{\vartheta\vartheta} = \int_{-\frac{h}{2}}^{\frac{h}{2}} \sigma_{\vartheta\vartheta} \mathrm{d}z, \\
N_{\varphi\vartheta} &= \int_{-\frac{h}{2}}^{\frac{h}{2}} \tau_{\varphi\vartheta} \mathrm{d}z = N_{\vartheta\varphi}, \quad M_{\varphi\varphi} = \int_{-\frac{h}{2}}^{\frac{h}{2}} \sigma_{\varphi\varphi} z \mathrm{d}z, \\
M_{\vartheta\vartheta} &= \int_{-\frac{h}{2}}^{\frac{h}{2}} \sigma_{\vartheta\vartheta} z \mathrm{d}z, \quad M_{\varphi\vartheta} = \int_{-\frac{h}{2}}^{\frac{h}{2}} \tau_{\varphi\vartheta} z \mathrm{d}z = M_{\vartheta\varphi}, \\
Q_{\varphi} &= \int_{-\frac{h}{2}}^{\frac{h}{2}} \tau_{\varphi z} \mathrm{d}z, \quad Q_{\vartheta} = \int_{-\frac{h}{2}}^{\frac{h}{2}} \tau_{\vartheta z} \mathrm{d}z.
\end{aligned} \tag{21.65}$$

Accordingly, there are a total of eight force and moment quantities.

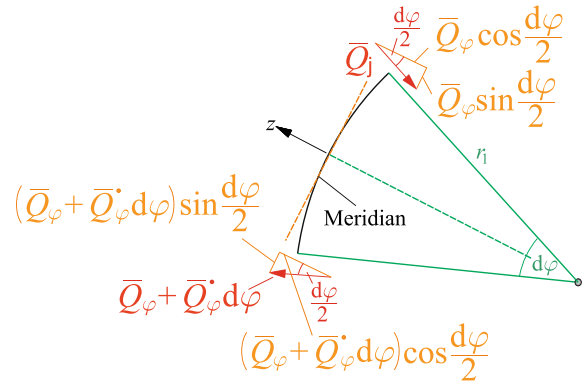


Fig. 21.23 Contribution of the shear force flow to the force equilibrium in the meridian direction

Firstly, the force equilibrium in the direction of the meridian tangent is considered. This equilibrium condition is made up of contributions from the increase in the membrane force flow $N_{\varphi\vartheta}$ in the ϑ-direction and the increase in $N_{\varphi\varphi}$ in the φ-direction. In addition, the load p_φ must be taken into account as well as the contribution of the membrane force flow $N_{\vartheta\vartheta}$ in the φ-direction. In addition, a contribution of the shear force flow Q_φ must be taken into account within the framework of the bending theory (Fig. 21.23, here the resultant $\bar{Q}_\varphi = Q_\varphi r \mathrm{d}\vartheta$ is shown). We decompose the two shear force flows, use the small-angle approximation and neglect higher-order terms. The remaining component of Q_φ acting in the meridional direction then is $Q_\varphi r \mathrm{d}\varphi \mathrm{d}\vartheta$. The equilibrium of forces (21.25) then changes into:

$$\frac{\partial}{\partial\varphi}\left(N_{\varphi\varphi} r\right) + \frac{\partial N_{\varphi\vartheta}}{\partial\vartheta} r_1 - N_{\vartheta\vartheta}\cos\varphi r_1 + Q_\varphi r + p_\varphi r_1 r = 0. \tag{21.66}$$

In the same way, the two other force equilibrium equations in (21.25) can be extended by the shear force flow components:

$$\begin{aligned} \frac{\partial}{\partial\varphi}\left(N_{\varphi\vartheta} r\right) + \frac{\partial N_{\vartheta\vartheta}}{\partial\vartheta} r_1 + N_{\vartheta\varphi}\cos\varphi r_1 + Q_\vartheta r_1 \sin\varphi + p_\vartheta r_1 r = 0, \\ \frac{\partial}{\partial\varphi}\left(Q_\varphi r\right) + \frac{\partial Q_\vartheta}{\partial\vartheta} r_1 - N_{\varphi\varphi} r - N_{\vartheta\vartheta} r_1 \sin\varphi + p_z r_1 r = 0. \end{aligned} \tag{21.67}$$

With regard to the moment equilibrium conditions, it should be noted that the equilibrium condition with regard to the normal axis does not lead to any new result due to the equality of $N_{\varphi\vartheta}$ and $N_{\vartheta\varphi}$. This leaves only the two moment equilibria relating to the meridian axis and the annular circle axis. The moment equilibrium with respect to the latitude direction follows as:

$$\frac{\partial}{\partial\varphi}\left(M_{\varphi\varphi} r\right) + \frac{\partial M_{\varphi\vartheta}}{\partial\vartheta} r_1 - M_{\vartheta\vartheta} r_1 \cos\varphi - Q_\varphi r_1 r = 0. \tag{21.68}$$

For the moment equilibrium around the meridian tangent we obtain:

$$\frac{\partial}{\partial\varphi}\left(M_{\varphi\vartheta}r\right)+\frac{\partial M_{\vartheta\vartheta}}{\partial\vartheta}r_1+M_{\varphi\vartheta}r_1\cos\varphi-Q_\vartheta r_1 r=0. \tag{21.69}$$

The five resultant equilibrium conditions are summarized as follows:

$$\begin{aligned}
\frac{\partial}{\partial\varphi}\left(N_{\varphi\varphi}r\right)+\frac{\partial N_{\varphi\vartheta}}{\partial\vartheta}r_1-N_{\vartheta\vartheta}\cos\varphi r_1+Q_\varphi r+p_\varphi r_1 r=0,\\
\frac{\partial}{\partial\varphi}\left(N_{\varphi\vartheta}r\right)+\frac{\partial N_{\vartheta\vartheta}}{\partial\vartheta}r_1+N_{\vartheta\varphi}\cos\varphi r_1+Q_\vartheta r_1\sin\varphi+p_\vartheta r_1 r=0,\\
\frac{\partial}{\partial\varphi}\left(Q_\varphi r\right)+\frac{\partial Q_\vartheta}{\partial\vartheta}r_1-N_{\varphi\varphi}r-N_{\vartheta\vartheta}r_1\sin\varphi+p_z r_1 r=0,\\
\frac{\partial}{\partial\varphi}\left(M_{\varphi\varphi}r\right)+\frac{\partial M_{\varphi\vartheta}}{\partial\vartheta}r_1-M_{\vartheta\vartheta}r_1\cos\varphi-Q_\varphi r_1 r=0,\\
\frac{\partial}{\partial\varphi}\left(M_{\varphi\vartheta}r\right)+\frac{\partial M_{\vartheta\vartheta}}{\partial\vartheta}r_1+M_{\varphi\vartheta}r_1\cos\varphi-Q_\vartheta r_1 r=0.
\end{aligned} \tag{21.70}$$

These equations are not sufficient to determine the eight force and moment flows to be determined. A shell problem in the context of bending theory is therefore statically indeterminate, and we must use both kinematic and constitutive relationships to solve a bending theory problem.

The equilibrium conditions (21.70) can be specialized for technically relevant special cases. For the spherical shell with the radius R, for which $r_1=r_2=R$ and $r=R\sin\varphi$ apply, the following equilibrium conditions result:

$$\begin{aligned}
\frac{\partial}{\partial\varphi}(N_{\varphi\varphi}\sin\varphi)+\frac{\partial N_{\varphi\vartheta}}{\partial\vartheta}-N_{\vartheta\vartheta}\cos\varphi+Q_\varphi\sin\varphi+p_\varphi R\sin\varphi=0,\\
\frac{\partial}{\partial\varphi}(N_{\varphi\vartheta}\sin\varphi)+\frac{\partial N_{\vartheta\vartheta}}{\partial\vartheta}+N_{\varphi\vartheta}\cos\varphi+Q_\vartheta\sin\varphi+p_\vartheta R\sin\varphi=0,\\
\frac{\partial}{\partial\varphi}(Q_\varphi\sin\varphi)+\frac{\partial Q_\vartheta}{\partial\vartheta}-N_{\varphi\varphi}\sin\varphi-N_{\vartheta\vartheta}\sin\varphi+p_z R\sin\varphi=0,\\
\frac{\partial}{\partial\varphi}(M_{\varphi\varphi}\sin\varphi)+\frac{\partial M_{\varphi\vartheta}}{\partial\vartheta}-M_{\vartheta\vartheta}\cos\varphi-Q_\varphi R\sin\varphi=0,\\
\frac{\partial}{\partial\varphi}(M_{\varphi\vartheta}\sin\varphi)+\frac{\partial M_{\vartheta\vartheta}}{\partial\vartheta}+M_{\varphi\vartheta}\cos\varphi-Q_\vartheta R\sin\varphi=0.
\end{aligned} \tag{21.71}$$

If we consider a rotationally symmetrically loaded spherical shell with $p_\vartheta=0$ and $N_{\varphi\vartheta}=0$, $M_{\varphi\vartheta}=0$, $Q_\vartheta=0$, then the following applies:

$$\frac{\mathrm{d}}{\mathrm{d}\varphi}(N_{\varphi\varphi}\sin\varphi) - N_{\vartheta\vartheta}\cos\varphi + Q_\varphi\sin\varphi + p_\varphi R\sin\varphi = 0,$$
$$\frac{\mathrm{d}}{\mathrm{d}\varphi}(Q_\varphi\sin\varphi) - N_{\varphi\varphi}\sin\varphi - N_{\vartheta\vartheta}\sin\varphi + p_z R\sin\varphi = 0,$$
$$\frac{\mathrm{d}}{\mathrm{d}\varphi}(M_{\varphi\varphi}\sin\varphi) - M_{\vartheta\vartheta}\cos\varphi - Q_\varphi R\sin\varphi = 0. \tag{21.72}$$

For the circular cylindrical shell with $r_1 \to \infty$, $r_2 = r = R$, $\varphi = \frac{\pi}{2}$ and the relationship $r_1\mathrm{d}\varphi = \mathrm{d}x$ follows:

$$\frac{\partial N_{xx}}{\partial x} + \frac{1}{R}\frac{\partial N_{x\vartheta}}{\partial\vartheta} + p_x = 0,$$
$$\frac{\partial N_{x\vartheta}}{\partial x} + \frac{1}{R}\frac{\partial N_{\vartheta\vartheta}}{\partial\vartheta} + \frac{Q_\vartheta}{R} + p_\vartheta = 0,$$
$$\frac{\partial Q_x}{\partial x} + \frac{1}{R}\frac{\partial Q_\vartheta}{\partial\vartheta} - \frac{N_{\vartheta\vartheta}}{R} + p_z = 0,$$
$$\frac{\partial M_{xx}}{\partial x} + \frac{1}{R}\frac{\partial M_{x\vartheta}}{\partial\vartheta} - Q_x = 0,$$
$$\frac{\partial M_{x\vartheta}}{\partial x} + \frac{1}{R}\frac{\partial M_{\vartheta\vartheta}}{\partial\vartheta} - Q_\vartheta = 0. \tag{21.73}$$

For the special case of the rotationally symmetrically loaded circular cylindrical shell with $p_\vartheta = 0$ and $N_{x\vartheta} = 0$, $M_{x\vartheta} = 0$, $Q_\vartheta = 0$ we obtain:

$$\frac{\mathrm{d}N_{xx}}{\mathrm{d}x} + p_x = 0,$$
$$\frac{\mathrm{d}Q_x}{\mathrm{d}x} - \frac{N_{\vartheta\vartheta}}{R} + p_z = 0,$$
$$\frac{\mathrm{d}M_{xx}}{\mathrm{d}x} - Q_x = 0. \tag{21.74}$$

In addition to the displacement quantities u_0, v_0, w_0 and the strains $\varepsilon^0_{\varphi\varphi}$, $\varepsilon^0_{\vartheta\vartheta}$ already known from membrane theory, the bending theory also includes $\gamma^0_{\varphi\vartheta}$, $\gamma^0_{\varphi\vartheta}$ and also the curvatures $\kappa^0_{\varphi\varphi}$ (meridian curvature), $\kappa^0_{\vartheta\vartheta}$ (circumferential curvature) and the twist $\kappa^0_{\varphi\vartheta}$. The corresponding kinematic equations are given below without further derivation; the reader is referred to the specialist literature in this field. The following kinematic equations result:

$$
\begin{aligned}
\varepsilon^0_{\varphi\varphi} &= \frac{1}{r_1}\left(\frac{\partial v_0}{\partial \varphi} + w_0\right),\\
\varepsilon^0_{\vartheta\vartheta} &= \frac{1}{r}\left(\frac{\partial u_0}{\partial \vartheta} + v_0\cos\varphi + w_0\sin\varphi\right),\\
\gamma^0_{\varphi\vartheta} &= \frac{1}{r}\frac{\partial v_0}{\partial \vartheta} + \frac{1}{r_1}\frac{\partial u_0}{\partial \varphi} - \frac{u_0\cos\varphi}{r},\\
\kappa^0_{\varphi\varphi} &= \frac{1}{r_1}\frac{\partial \chi}{\partial \varphi} = \frac{1}{r_1}\frac{\partial}{\partial \varphi}\left(\frac{v_0 - \frac{\partial w_0}{\partial \varphi}}{r_1}\right),\\
\kappa^0_{\vartheta\vartheta} &= \frac{1}{r^2}\frac{\partial}{\partial \vartheta}\left(u_0\sin\varphi - \frac{\partial w_0}{\partial \vartheta}\right) + \frac{\cos\varphi}{rr_1}\left(v_0 - \frac{\partial w_0}{\partial \varphi}\right),\\
\kappa^0_{\varphi\vartheta} &= \frac{1}{rr_1}\frac{\partial v_0}{\partial \vartheta} - \frac{2}{rr_1}\frac{\partial^2 w_0}{\partial \varphi \partial \vartheta} + 2\frac{\cos\varphi}{r^2}\frac{\partial w_0}{\partial \vartheta} - 2\frac{\cos\varphi}{rr_2}u_0 + \frac{1}{r_1 r_2}\frac{\partial u_0}{\partial \varphi} + \frac{\cos\varphi}{rr_1}u_0.
\end{aligned}
\tag{21.75}
$$

If the special case of rotationally symmetrical loading with $\gamma^0_{\varphi\vartheta} = 0$ and $\kappa^0_{\varphi\vartheta} = 0$ applies, then we have:

$$
\begin{aligned}
\varepsilon^0_{\varphi\varphi} &= \frac{1}{r_1}\left(\frac{\mathrm{d}v_0}{\mathrm{d}\varphi} + w_0\right),\\
\varepsilon^0_{\vartheta\vartheta} &= \frac{1}{r}\left(v_0\cos\varphi + w_0\sin\varphi\right),\\
\kappa^0_{\varphi\varphi} &= \frac{1}{r_1}\frac{\mathrm{d}}{\mathrm{d}\varphi}\left(\frac{v_0 - \frac{\mathrm{d}w_0}{\mathrm{d}\varphi}}{r_1}\right),\\
\kappa^0_{\vartheta\vartheta} &= \frac{\cos\varphi}{rr_1}\left(v_0 - \frac{\mathrm{d}w_0}{\mathrm{d}\varphi}\right).
\end{aligned}
\tag{21.76}
$$

For the spherical shell with the radius $r_1 = r_2 = R$ and $r = R\sin\varphi$ it follows from (21.75):

$$
\begin{aligned}
\varepsilon^0_{\varphi\varphi} &= \frac{1}{R}\left(\frac{\partial v_0}{\partial \varphi} + w_0\right),\\
\varepsilon^0_{\vartheta\vartheta} &= \frac{1}{R}\left(\frac{1}{\sin\varphi}\frac{\partial u_0}{\partial \vartheta} + v_0\cot\varphi + w_0\right),\\
\gamma^0_{\varphi\vartheta} &= \frac{1}{R\sin\varphi}\frac{\partial v_0}{\partial \vartheta} + \frac{1}{R}\frac{\partial u_0}{\partial \varphi} - \frac{u_0}{R}\cot\varphi,\\
\kappa^0_{\varphi\varphi} &= \frac{1}{R^2}\frac{\partial}{\partial \varphi}\left(v_0 - \frac{\partial w_0}{\partial \varphi}\right),\\
\kappa^0_{\vartheta\vartheta} &= \frac{1}{R^2\sin^2\varphi}\frac{\partial}{\partial \vartheta}\left(u_0\sin\varphi - \frac{\partial w_0}{\partial \vartheta}\right) + \frac{\cot\varphi}{R^2}\left(v_0 - \frac{\partial w_0}{\partial \varphi}\right),\\
\kappa^0_{\varphi\vartheta} &= \frac{1}{R^2\sin\varphi}\left(\frac{\partial v_0}{\partial \vartheta} - 2\frac{\partial^2 w_0}{\partial \varphi \partial \vartheta} + 2\cot\varphi\frac{\partial w_0}{\partial \vartheta} - \cos\varphi u_0 + \sin\varphi\frac{\partial u_0}{\partial \varphi}\right).
\end{aligned}
\tag{21.77}
$$

If the load is rotationally symmetrical, the following remains:

$$\begin{aligned}
\varepsilon^0_{\varphi\varphi} &= \frac{1}{R}\left(\frac{\mathrm{d}v_0}{\mathrm{d}\varphi} + w_0\right),\\
\varepsilon^0_{\vartheta\vartheta} &= \frac{1}{R}\left(v_0 \cot\varphi + w_0\right),\\
\kappa^0_{\varphi\varphi} &= \frac{1}{R^2}\frac{\mathrm{d}}{\mathrm{d}\varphi}\left(v_0 - \frac{\mathrm{d}w_0}{\mathrm{d}\varphi}\right),\\
\kappa^0_{\vartheta\vartheta} &= \frac{\cot\varphi}{R^2}\left(v_0 - \frac{\mathrm{d}w_0}{\mathrm{d}\varphi}\right).
\end{aligned} \tag{21.78}$$

For the circular cylindrical shell with the radius $r = r_2 = R$ and with $r_1 \to \infty$ and $\varphi = \frac{\pi}{2}$ it follows with $r_1 \mathrm{d}\varphi = \mathrm{d}x$:

$$\begin{aligned}
\varepsilon^0_{xx} &= \frac{\partial v_0}{\partial x},\\
\varepsilon^0_{\vartheta\vartheta} &= \frac{1}{R}\left(\frac{\partial u_0}{\partial \vartheta} + w_0\right),\\
\gamma^0_{x\vartheta} &= \frac{1}{R}\frac{\partial v_0}{\partial \vartheta} + \frac{\partial u_0}{\partial x},\\
\kappa^0_{xx} &= -\frac{\partial^2 w_0}{\partial x^2},\\
\kappa^0_{\vartheta\vartheta} &= \frac{1}{R^2}\frac{\partial}{\partial \vartheta}\left(u_0 - \frac{\partial w_0}{\partial \vartheta}\right),\\
\kappa^0_{x\vartheta} &= \frac{1}{R}\left(\frac{\partial u_0}{\partial x} - 2\frac{\partial^2 w_0}{\partial x \partial \vartheta}\right).
\end{aligned} \tag{21.79}$$

In the case of rotationally symmetrical loading, these equations are reduced as follows:

$$\begin{aligned}
\varepsilon^0_{xx} &= \frac{\mathrm{d}v_0}{\mathrm{d}x},\\
\varepsilon^0_{\vartheta\vartheta} &= \frac{w_0}{R},\\
\kappa^0_{xx} &= -\frac{\mathrm{d}^2 w_0}{\mathrm{d}x^2}.
\end{aligned} \tag{21.80}$$

The constitutive equations in the context of bending theory are given by (21.20).

It turns out that a problem for a shell of revolution in the context of bending theory is described by 17 unknown quantities. These are the membrane force flows $N_{\varphi\varphi}$, $N_{\vartheta\vartheta}$, $N_{\varphi\vartheta}$, the shear force flows Q_φ, Q_ϑ, the moment flows $M_{\varphi\varphi}$, $M_{\vartheta\vartheta}$, $M_{\varphi\vartheta}$, the displacements u_0, v_0, w_0 of the shell middle surface, as well as the six strain quantities $\varepsilon^0_{\varphi\varphi}$, $\varepsilon^0_{\vartheta\vartheta}$, $\gamma_{\varphi\vartheta}$, $\kappa^0_{\varphi\varphi}$, $\kappa^0_{\vartheta\vartheta}$, $\kappa^0_{\varphi\vartheta}$. With the equilibrium conditions (21.70), the kinematic equations (21.75) and the material law (21.20), a total of 17 equations are available. Accordingly, a solution to a given shell problem is possible, taking into account the given boundary conditions. However,

experience shows that the closed-form analytical solution of a shell problem within the framework of bending theory is only possible in a few and often highly idealised cases. Shell problems therefore often require numerical methods for their solution.

21.4 Bending Theory of a Cross-Ply Circular Cylindrical Shell Within the Framework of Classical Laminated Plate Theory

In the following we consider layered circular cylindrical shells, whose layups for the time being can be arbitrary (Fig. 21.24).

We assume the applicability of classical shell theory and the validity of the Kirchhoff-Love-hypothesis. The total strains, which are composed of the strains as well as the curvatures and the twist of the shell middle surface, are as follows:

$$\begin{aligned} \varepsilon_{xx} &= \varepsilon^0_{xx} + z\kappa^0_{xx}, \\ \varepsilon_{\vartheta\vartheta} &= \varepsilon^0_{\vartheta\vartheta} + z\kappa^0_{\vartheta\vartheta}, \\ \gamma_{x\vartheta} &= \gamma^0_{x\vartheta} + z\kappa^0_{x\vartheta}. \end{aligned} \tag{21.81}$$

The following form for Hooke's law applies in each individual layer k of the laminated shell:

$$\begin{aligned} \begin{pmatrix} \sigma_{xx} \\ \sigma_{\vartheta\vartheta} \\ \tau_{x\vartheta} \end{pmatrix}_k &= \begin{bmatrix} \bar{Q}_{11} & \bar{Q}_{12} & \bar{Q}_{16} \\ \bar{Q}_{12} & \bar{Q}_{22} & \bar{Q}_{26} \\ \bar{Q}_{16} & \bar{Q}_{26} & \bar{Q}_{66} \end{bmatrix}_k \begin{pmatrix} \varepsilon_{xx} \\ \varepsilon_{\vartheta\vartheta} \\ \gamma_{x\vartheta} \end{pmatrix} \\ &= \begin{bmatrix} \bar{Q}_{11} & \bar{Q}_{12} & \bar{Q}_{16} \\ \bar{Q}_{12} & \bar{Q}_{22} & \bar{Q}_{26} \\ \bar{Q}_{16} & \bar{Q}_{26} & \bar{Q}_{66} \end{bmatrix}_k \left[\begin{pmatrix} \varepsilon^0_{xx} \\ \varepsilon^0_{\vartheta\vartheta} \\ \gamma^0_{x\vartheta} \end{pmatrix} + z \begin{pmatrix} \kappa^0_{xx} \\ \kappa^0_{\vartheta\vartheta} \\ \kappa^0_{x\vartheta} \end{pmatrix} \right], \end{aligned} \tag{21.82}$$

with $z_{k-1} \le z \le z_k$.

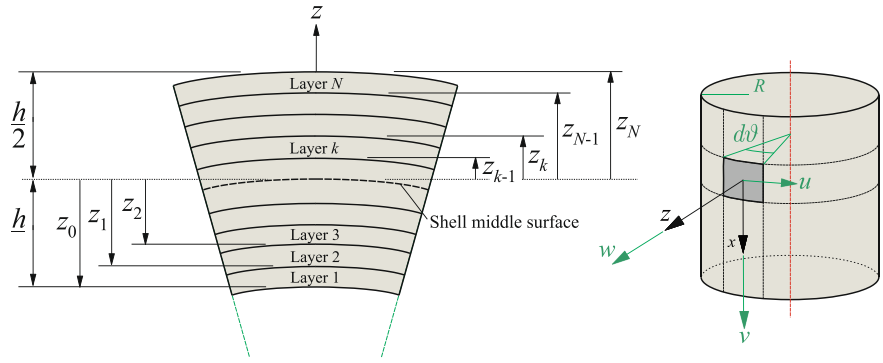


Fig. 21.24 Nomenclature (left); laminated shell (right)

We assume the validity of the constitutive law according to CLPT:

$$\begin{pmatrix} N_{xx} \\ N_{\vartheta\vartheta} \\ N_{x\vartheta} \\ M_{xx} \\ M_{\vartheta\vartheta} \\ M_{x\vartheta} \end{pmatrix} = \begin{bmatrix} A_{11} & A_{12} & A_{16} & B_{11} & B_{12} & B_{16} \\ A_{12} & A_{22} & A_{26} & B_{12} & B_{22} & B_{26} \\ A_{16} & A_{26} & A_{66} & B_{16} & B_{26} & B_{66} \\ B_{11} & B_{12} & B_{16} & D_{11} & D_{12} & D_{16} \\ B_{12} & B_{22} & B_{26} & D_{12} & D_{22} & D_{26} \\ B_{16} & B_{26} & B_{66} & D_{16} & D_{26} & D_{66} \end{bmatrix} \begin{pmatrix} \varepsilon_{xx}^0 \\ \varepsilon_{\vartheta\vartheta}^0 \\ \gamma_{x\vartheta}^0 \\ \kappa_{xx}^0 \\ \kappa_{\vartheta\vartheta}^0 \\ \kappa_{x\vartheta}^0 \end{pmatrix}. \tag{21.83}$$

The force and moment flows here are as follows:

$$\begin{aligned} N_{xx} &= \int_{-\frac{h}{2}}^{+\frac{h}{2}} \sigma_{xx} \mathrm{d}z, \quad N_{\vartheta\vartheta} = \int_{-\frac{h}{2}}^{+\frac{h}{2}} \sigma_{\vartheta\vartheta} \mathrm{d}z, \quad N_{x\vartheta} = \int_{-\frac{h}{2}}^{+\frac{h}{2}} \tau_{x\vartheta} \mathrm{d}z, \\ M_{xx} &= \int_{-\frac{h}{2}}^{+\frac{h}{2}} \sigma_{xx} z \mathrm{d}z, \quad M_{\vartheta\vartheta} = \int_{-\frac{h}{2}}^{+\frac{h}{2}} \sigma_{\vartheta\vartheta} z \mathrm{d}z, \quad M_{x\vartheta} = \int_{-\frac{h}{2}}^{+\frac{h}{2}} \tau_{x\vartheta} z \mathrm{d}z. \end{aligned} \tag{21.84}$$

We therefore assume the Love assumption $1 + \frac{z}{R} \simeq 1$ to be valid, i.e. differences between the shell areas above and below the middle shell area $z = 0$ are negligible. The condensed equilibrium conditions result as follows after elimination of the shear force flows:

$$\begin{aligned} \frac{\partial N_{xx}}{\partial x} + \frac{1}{R} \frac{\partial N_{x\vartheta}}{\partial \vartheta} + p_x &= 0, \\ \frac{\partial N_{x\vartheta}}{\partial x} + \frac{1}{R} \frac{\partial N_{\vartheta\vartheta}}{\partial \vartheta} + \frac{1}{R} \left(\frac{1}{R} \frac{\partial M_{\vartheta\vartheta}}{\partial \vartheta} + \frac{\partial M_{x\vartheta}}{\partial x} \right) + p_\vartheta &= 0, \\ \frac{\partial^2 M_{xx}}{\partial x^2} + \frac{2}{R} \frac{\partial^2 M_{x\vartheta}}{\partial x \partial \vartheta} + \frac{1}{R^2} \frac{\partial^2 M_{\vartheta\vartheta}}{\partial \vartheta^2} - \frac{N_{\vartheta\vartheta}}{R} + p_z &= 0. \end{aligned} \tag{21.85}$$

Inserting the constitutive law (21.83) with the kinematic equations (21.79) results in the following coupled differential equation system, which describes the static behaviour of an arbitrarily layered circular cylindrical shell:

$$\begin{aligned} \left[\left(A_{16} + \frac{B_{16}}{R} \right) \frac{\partial^2}{\partial x^2} + \frac{1}{R} \left(A_{12} + A_{66} + \frac{B_{12} + B_{66}}{R} \right) \frac{\partial^2}{\partial x \partial \vartheta} \right. \\ \left. + \frac{1}{R^2} \left(A_{26} + \frac{B_{26}}{R} \right) \frac{\partial^2}{\partial \vartheta^2} \right] u_0 \\ + \left[A_{11} \frac{\partial^2}{\partial x^2} + \frac{2A_{16}}{R} \frac{\partial^2}{\partial x \partial \vartheta} + \frac{A_{66}}{R^2} \frac{\partial^2}{\partial \vartheta^2} \right] v_0 \\ + \left[-B_{11} \frac{\partial^3}{\partial x^3} - \frac{3B_{16}}{R} \frac{\partial^3}{\partial x^2 \partial \vartheta} - \frac{B_{12} + 2B_{66}}{R^2} \frac{\partial^3}{\partial x \partial \vartheta^2} \right. \end{aligned}$$

$$
\begin{aligned}
&- \frac{B_{26}}{R^3}\frac{\partial^3}{\partial\vartheta^3} + \frac{A_{12}}{R}\frac{\partial}{\partial x} + \frac{A_{26}}{R^2}\frac{\partial}{\partial\vartheta}\Bigg] w_0 = -p_x,\\
&\Bigg[\left(A_{66} + \frac{2B_{66}}{R} + \frac{D_{66}}{R^2}\right)\frac{\partial^2}{\partial x^2} + \frac{2}{R}\left(A_{26} + \frac{2B_{26}}{R} + \frac{D_{26}}{R^2}\right)\frac{\partial^2}{\partial x\partial\vartheta}\\
&\quad + \frac{1}{R^2}\left(A_{22} + \frac{2B_{22}}{R} + \frac{D_{22}}{R^2}\right)\frac{\partial^2}{\partial\vartheta^2}\Bigg] u_0 + \Bigg[\left(A_{16} + \frac{B_{16}}{R}\right)\frac{\partial^2}{\partial x^2}\\
&+ \frac{1}{R}\left(A_{12} + A_{66} + \frac{B_{12} + B_{66}}{R^2}\right)\frac{\partial^2}{\partial x\partial\vartheta} + \frac{1}{R^2}\left(A_{26} + \frac{B_{26}}{R}\right)\frac{\partial^2}{\partial\vartheta^2}\Bigg] v_0\\
&+ \Bigg[-\left(B_{16} + \frac{D_{16}}{R}\right)\frac{\partial^3}{\partial x^3} - \frac{1}{R}\left(B_{12} + 2B_{66} + \frac{D_{12} + 2D_{66}}{R}\right)\frac{\partial^3}{\partial x^2\partial\vartheta}\\
&\quad - \frac{3}{R^2}\left(B_{26} + \frac{D_{26}}{R}\right)\frac{\partial^3}{\partial x\partial\vartheta^2} - \frac{1}{R^3}\left(B_{22} + \frac{D_{22}}{R}\right)\frac{\partial^3}{\partial\vartheta^3}\\
&\quad + \frac{1}{R}\left(A_{26} + \frac{B_{26}}{R}\right)\frac{\partial}{\partial x} + \frac{1}{R^2}\left(A_{22} + \frac{B_{22}}{R}\right)\frac{\partial}{\partial\vartheta}\Bigg] w_0 = -p_\vartheta,\\
&\Bigg[\left(B_{16} + \frac{D_{16}}{R}\right)\frac{\partial^3}{\partial x^3} + \frac{1}{R}\left(B_{12} + 2B_{66} + \frac{D_{12} + 2D_{66}}{R}\right)\frac{\partial^3}{\partial x^2\partial\vartheta}\\
&\quad + \frac{3}{R^2}\left(B_{26} + \frac{D_{26}}{R}\right)\frac{\partial^3}{\partial x\partial\vartheta^2} + \frac{1}{R^3}\left(B_{22} + \frac{D_{22}}{R}\right)\frac{\partial^3}{\partial\vartheta^3}\\
&\quad - \frac{1}{R}\left(A_{26} + \frac{B_{26}}{R}\right)\frac{\partial}{\partial x} - \frac{1}{R^2}\left(A_{22} + \frac{B_{22}}{R}\right)\frac{\partial}{\partial\vartheta}\Bigg] u_0\\
&\quad \Bigg[B_{11}\frac{\partial^3}{\partial x^3} + \frac{3B_{16}}{R}\frac{\partial^3}{\partial x^2\partial\vartheta} + \frac{1}{R^2}\left(B_{12} + 2B_{66}\right)\frac{\partial^3}{\partial x\partial\vartheta^2}\\
&\quad\quad + \frac{B_{26}}{R^3}\frac{\partial^3}{\partial\vartheta^3} - \frac{A_{12}}{R}\frac{\partial}{\partial x} - \frac{A_{26}}{R^2}\frac{\partial}{\partial\vartheta}\Bigg] v_0\\
&+ \Bigg[-D_{11}\frac{\partial^4}{\partial x^4} - \frac{4D_{16}}{R}\frac{\partial^4}{\partial x^3\partial\vartheta} - \frac{2}{R^2}\left(D_{12} + 2D_{66}\right)\frac{\partial^4}{\partial x^2\partial\vartheta^2}\\
&\quad - \frac{4D_{26}}{R^3}\frac{\partial^4}{\partial x\partial\vartheta^3} - \frac{D_{22}}{R^4}\frac{\partial^4}{\partial\vartheta^4} + \frac{2B_{12}}{R}\frac{\partial^2}{\partial x^2}\\
&\quad + \frac{4B_{26}}{R^2}\frac{\partial^2}{\partial x\partial\vartheta} + \frac{2B_{22}}{R^3}\frac{\partial^2}{\partial\vartheta^2} - \frac{A_{22}}{R^2}\Bigg] w_0 = -p_z.
\end{aligned}
\tag{21.86}
$$

In the following, we consider the case of a cross-ply shell with $A_{16} = A_{26} = 0$ and $D_{16} = D_{26} = 0$ under rotationally symmetrical load. We restrict the load case to $p_x = 0$, $p_s = 0$ and $p_z = p_z(x)$, i.e. there is a rotationally symmetrical load p_z. In this case, all partial derivatives $\frac{\partial}{\partial\vartheta}$ as well as the state variables u_0, $N_{x\vartheta}$, $M_{x\vartheta}$ disappear. The equilibrium conditions (21.85) are then reduced as follows after elimination of the shear force flow Q_x:

$$\frac{\mathrm{d}N_{xx}}{\mathrm{d}x} = 0, \quad \frac{\mathrm{d}^2 M_{xx}}{\mathrm{d}x^2} - \frac{N_{\vartheta\vartheta}}{R} = -p_z. \tag{21.87}$$

The corresponding kinematic equations are given by:

$$\varepsilon^0_{xx} = \frac{\mathrm{d}v_0}{\mathrm{d}x}, \quad \varepsilon^0_{\vartheta\vartheta} = \frac{w_0}{R}, \quad \kappa^0_{xx} = -\frac{\mathrm{d}^2 w_0}{\mathrm{d}x^2}. \tag{21.88}$$

All other strain quantities are zero.

The constitutive law reads:

$$\begin{aligned} N_{xx} &= A_{11}\varepsilon^0_{xx} + A_{12}\varepsilon^0_{\vartheta\vartheta} + B_{11}\kappa^0_{xx}, \\ N_{\vartheta\vartheta} &= A_{12}\varepsilon^0_{xx} + A_{22}\varepsilon^0_{\vartheta\vartheta} + B_{12}\kappa^0_{xx}, \\ M_{xx} &= B_{11}\varepsilon^0_{xx} + B_{12}\varepsilon^0_{\vartheta\vartheta} + D_{11}\kappa^0_{xx}, \\ M_{\vartheta\vartheta} &= B_{12}\varepsilon^0_{xx} + B_{22}\varepsilon^0_{\vartheta\vartheta} + D_{12}\kappa^0_{xx}. \end{aligned} \tag{21.89}$$

With the equilibrium conditions (21.87) it follows with (21.89) and (21.88):

$$\begin{aligned} &A_{11}\frac{\mathrm{d}^2 v_0}{\mathrm{d}x^2} + \frac{A_{12}}{R}\frac{\mathrm{d}w_0}{\mathrm{d}x} - B_{11}\frac{\mathrm{d}^3 w_0}{\mathrm{d}x^3} = 0, \\ &\left(\frac{A_{11}D_{11} - B_{11}^2}{A_{11}}\right)\frac{\mathrm{d}^4 w_0}{\mathrm{d}x^4} + \frac{2}{R}\left(\frac{A_{12}B_{11} - A_{11}B_{12}}{A_{11}}\right)\frac{\mathrm{d}^2 w_0}{\mathrm{d}x^2} \\ &\quad + \frac{1}{R^2}\left(\frac{A_{11}A_{22} - A_{12}^2}{A_{11}}\right)w_0 = p_z - \frac{A_{12}}{A_{11}}\frac{N_{xx}}{R}. \end{aligned} \tag{21.90}$$

With the abbreviations

$$D^R = \frac{A_{11}D_{11} - B_{11}^2}{A_{11}}, \quad 4\lambda^4 = \frac{1}{D^R R^2}\frac{A_{11}A_{22} - A_{12}^2}{A_{11}} \tag{21.91}$$

the second equation in (21.90) takes the following form:

$$\frac{\mathrm{d}^4 w_0}{\mathrm{d}x^4} + \frac{2}{D^R R}\left(\frac{A_{12}B_{11} - A_{11}B_{12}}{A_{11}}\right)\frac{\mathrm{d}^2 w_0}{\mathrm{d}x^2} + 4\lambda^4 w_0 = \frac{1}{D^R}\left(p_z - \frac{A_{12}}{A_{11}}\frac{N_{xx}}{R}\right). \tag{21.92}$$

For the special case of a symmetric cross-ply laminate with $B_{ij} = 0$ and $D^R = D_{11}$ it follows

$$\frac{\mathrm{d}^4 w_0}{\mathrm{d}x^4} + 4\lambda^4 w_0 = \frac{1}{D_{11}}\left(p_z - \frac{A_{12}}{A_{11}}\frac{N_{xx}}{R}\right), \tag{21.93}$$

with the abbreviation:

$$4\lambda^4 = \frac{1}{D_{11}R^2}\frac{A_{11}A_{22} - A_{12}^2}{A_{11}}. \tag{21.94}$$

The solution of the Eq. (21.93) consists of a homogeneous solution and a load-dependent particular solution, i.e. $w_0 = w_{0,h} + w_{0,p}$. The homogeneous solution is:

$$w_{0,h} = e^{-\lambda x} \left(C_1 \cos \lambda x + C_2 \sin \lambda x\right) + e^{\lambda x} \left(C_3 \cos \lambda x + C_4 \sin \lambda x\right). \tag{21.95}$$

21.5 Bending Theory of a Cross-Ply Circular Cylindrical Shell in the Context of First-Order Shear Deformation Theory

We now also consider the case of the cross-ply circular cylindrical shell, whereby we now want to start from the First-Order Shear Deformation Theory (FSDT). This case was considered by Altenbach et al. (2004), and the most important relations from this reference are summarized below.

The case of a rotationally symmetrical situation is considered, i.e. all derivatives relating to the coordinate $s = R\vartheta$ are identical to zero. In addition, the shear strain γ_{xs}, the warping κ^0_{ss} and the twist κ^0_{xs} disappear. The force and moment quantities N_{xs} and M_{xs} also disappear in this situation. Only a surface load p_z is considered which is only dependent on x: $p_z = p_z(x)$. The displacement field then reads:

$$\begin{aligned} u(x,z) &= 0, \\ v(x,z) &= v_0(x,z) + z\psi_x, \\ w(x,z) &= w_0(x). \end{aligned} \tag{21.96}$$

For the non-vanishing strains, we obtain:

$$\begin{aligned} \varepsilon_{xx} &= \frac{\mathrm{d}v_0}{\mathrm{d}x} + z\frac{\mathrm{d}\psi_x}{\mathrm{d}x}, \\ \varepsilon_{ss} &= \frac{w_0}{R+z}, \\ \gamma_{xz} &= \psi_x + \frac{\mathrm{d}w_0}{\mathrm{d}x}. \end{aligned} \tag{21.97}$$

Once the strains are given, the layerwise stresses of the laminated shell can be calculated:

$$\begin{pmatrix} \sigma_{xx} \\ \sigma_{ss} \\ \tau_{xz} \end{pmatrix} \begin{bmatrix} Q_{11} & Q_{12} & 0 \\ Q_{12} & Q_{22} & 0 \\ 0 & 0 & Q_{66} \end{bmatrix} \begin{pmatrix} \frac{\mathrm{d}v_0}{\mathrm{d}x} + z\frac{\mathrm{d}\psi_x}{\mathrm{d}x} \\ \frac{w_0}{R+z} \\ \psi_x + \frac{\mathrm{d}w_0}{\mathrm{d}x} \end{pmatrix}. \tag{21.98}$$

With the resulting force and moment quantities

$$
\begin{aligned}
N_{xx} &= \sum_{k=1}^{n} \int_{h_k} \sigma_{xx,k} \left(1 + \frac{z}{R}\right) \mathrm{d}z, \\
N_{ss} &= \sum_{k=1}^{n} \int_{h_k} \sigma_{ss,k} \mathrm{d}z, \\
M_{xx} &= \sum_{k=1}^{n} \int_{h_k} \sigma_{xx,k} z \left(1 + \frac{z}{R}\right) \mathrm{d}z, \\
M_{ss} &= \sum_{k=1}^{n} \int_{h_k} \sigma_{ss,k} z \mathrm{d}z, \\
Q_x &= \sum_{k=1}^{n} \int_{h_k} \tau_{xz,k} z \left(1 + \frac{z}{R}\right) \mathrm{d}z
\end{aligned}
\tag{21.99}
$$

taking into account the trapezoidal effect, the following constitutive relationship results for the shell considered here:

$$
\begin{aligned}
N_{xx} &= A_{11} \frac{\mathrm{d}v_0}{\mathrm{d}x} + A_{12} \frac{w_0}{R} + \frac{1}{R} D_{11} \frac{\mathrm{d}\psi_x}{\mathrm{d}x}, \\
N_{ss} &= A_{12} \frac{\mathrm{d}v_0}{\mathrm{d}x} + T_{22} w_0, \\
M_{xx} &= D_{11} \left(\frac{1}{R} \frac{\mathrm{d}v_0}{\mathrm{d}x} + \frac{\mathrm{d}\psi_x}{\mathrm{d}x} \right), \\
M_{ss} &= D_{12} \frac{\mathrm{d}\psi_x}{\mathrm{d}x} + \bar{T}_{22} w_0, \\
Q_x &= K A_{55} \left(\psi_x + \frac{\mathrm{d}w_0}{\mathrm{d}x} \right),
\end{aligned}
\tag{21.100}
$$

wherein $T_{22} = \frac{A_{22}}{R} + \frac{D_{22}}{R^3}$ and $\bar{T}_{22} = \frac{D_{22}}{R^2}$.

The equations of motion of the laminated shell under consideration can be derived from Hamilton's principle, whereby a detailed specification of their determination is omitted. The final result is given below:

$$
\begin{aligned}
\frac{\partial N_{xx}}{\partial x}+\frac{\partial N_{xs}}{\partial s}+p_x &= \rho_0\frac{\partial^2 v_0}{\partial t^2}+\rho_1\frac{\partial^2 \psi_x}{\partial t^2},\\
\frac{\partial N_{xs}}{\partial x}+\frac{\partial N_{ss}}{\partial s}+\frac{Q_s}{R}+p_s &= \rho_0\frac{\partial^2 u_0}{\partial t^2}+\rho_1\frac{\partial^2 \psi_s}{\partial t^2},\\
\frac{\partial Q_x}{\partial x}+\frac{\partial Q_s}{\partial s}-\frac{N_{ss}}{R}+p_z &= \rho_0\frac{\partial^2 w_0}{\partial t^2},\\
\frac{M_{xx}}{\partial x}+\frac{\partial M_{xs}}{\partial s}-Q_x &= \rho_2\frac{\partial^2 \psi_x}{\partial t^2}+\rho_1\frac{\partial^2 v_0}{\partial t^2},\\
\frac{M_{xs}}{\partial x}+\frac{\partial M_{ss}}{\partial s}-Q_s &= \rho_2\frac{\partial^2 \psi_s}{\partial t^2}+\rho_1\frac{\partial^2 u_0}{\partial t^2},
\end{aligned}
\tag{21.101}
$$

with

$$
\begin{aligned}
\rho_0 &= \sum_{k=1}^{n}\rho_k\left(z_k-z_{k-1}\right),\\
\rho_1 &= \sum_{k=1}^{n}\rho_k\left(z_k^2-z_{k-1}^2\right),\\
\rho_2 &= \sum_{k=1}^{n}\rho_k\left(z_k^3-z_{k-1}^3\right).
\end{aligned}
\tag{21.102}
$$

Insertion of the constitutive equations

$$
\begin{pmatrix} N_{xx}\\ N_{ss}\\ N_{xs}\\ M_{xx}\\ M_{ss}\\ M_{xs}\\ Q_s\\ Q_x \end{pmatrix}
=
\begin{bmatrix}
A_{11} & A_{12} & A_{16} & B_{11} & B_{12} & B_{16} & 0 & 0\\
A_{12} & A_{22} & A_{26} & B_{12} & B_{22} & B_{26} & 0 & 0\\
A_{16} & A_{26} & A_{66} & B_{16} & B_{26} & B_{66} & 0 & 0\\
B_{11} & B_{12} & B_{16} & D_{11} & D_{12} & D_{16} & 0 & 0\\
B_{12} & B_{22} & B_{26} & D_{12} & D_{22} & D_{26} & 0 & 0\\
B_{16} & B_{26} & B_{66} & D_{16} & D_{26} & D_{66} & 0 & 0\\
0 & 0 & 0 & 0 & 0 & 0 & KA_{44} & KA_{45}\\
0 & 0 & 0 & 0 & 0 & 0 & KA_{45} & KA_{55}
\end{bmatrix}
\begin{pmatrix} \varepsilon_{xx}^0\\ \varepsilon_{ss}^0\\ \gamma_{xs}^0\\ \kappa_{xx}^0\\ \kappa_{ss}^0\\ \kappa_{xs}^0\\ \gamma_{sz}\\ \gamma_{xz} \end{pmatrix}
\tag{21.103}
$$

gives the equations of motion in the following form:

$$
\begin{bmatrix}
L_{11} & L_{12} & L_{13} & L_{14} & L_{15}\\
L_{21} & L_{22} & L_{23} & L_{24} & L_{25}\\
L_{31} & L_{32} & L_{33} & L_{34} & L_{35}\\
L_{41} & L_{42} & L_{43} & L_{44} & L_{45}\\
L_{51} & L_{52} & L_{53} & L_{54} & L_{55}
\end{bmatrix}
\begin{pmatrix} v_0\\ u_0\\ \psi_x\\ \psi_s\\ w_0 \end{pmatrix}
= -\begin{pmatrix} p_x\\ p_s\\ 0\\ 0\\ p_z \end{pmatrix}
+\begin{bmatrix}
\rho_0 & 0 & \rho_1 & 0 & 0\\
0 & \rho_0 & 0 & \rho_1 & 0\\
\rho_1 & 0 & \rho_2 & 0 & 0\\
0 & \rho_1 & 0 & \rho_2 & 0\\
0 & 0 & 0 & 0 & \rho_0
\end{bmatrix}
\frac{\partial^2}{\partial t^2}
\begin{pmatrix} v_0\\ u_0\\ \psi_x\\ \psi_s\\ w_0 \end{pmatrix}.
\tag{21.104}
$$

The operators appearing here are:

$$
\begin{aligned}
L_{11} &= A_{11}\frac{\partial^2}{\partial x^2} + 2A_{16}\frac{\partial^2}{\partial x\partial s} + A_{66}\frac{\partial^2}{\partial s^2},\\
L_{12} &= A_{16}\frac{\partial^2}{\partial x^2} + (A_{12}+A_{66})\frac{\partial^2}{\partial x\partial s} + A_{26}\frac{\partial^2}{\partial s^2},\\
L_{13} &= B_{11}\frac{\partial^2}{\partial x^2} + 2B_{16}\frac{\partial^2}{\partial x\partial s} + B_{66}\frac{\partial^2}{\partial s^2},\\
L_{14} &= B_{16}\frac{\partial^2}{\partial x^2} + (B_{12}+B_{66})\frac{\partial^2}{\partial x\partial s} + B_{26}\frac{\partial^2}{\partial s^2},\\
L_{15} &= \frac{A_{12}}{R}\frac{\partial}{\partial x} + \frac{A_{26}}{R}\frac{\partial}{\partial s},\\
L_{22} &= A_{66}\frac{\partial^2}{\partial x^2} + 2A_{26}\frac{\partial^2}{\partial x\partial s} + A_{22}\frac{\partial^2}{\partial s^2} - \frac{KA_{44}}{R^2},\\
L_{23} &= B_{16}\frac{\partial^2}{\partial x^2} + (B_{16}+B_{66})\frac{\partial^2}{\partial x\partial s} + B_{26}\frac{\partial^2}{\partial s^2} + \frac{KA_{45}}{R},\\
L_{24} &= B_{66}\frac{\partial^2}{\partial x^2} + 2B_{26}\frac{\partial^2}{\partial x\partial s} + B_{22}\frac{\partial^2}{\partial s^2} + \frac{KA_{44}}{R},\\
L_{25} &= (A_{12}+KA_{55})\frac{1}{R}\frac{\partial}{\partial x} + (A_{26}+KA_{45})\frac{1}{R}\frac{\partial}{\partial s},\\
L_{33} &= D_{11}\frac{\partial^2}{\partial x^2} + 2D_{16}\frac{\partial^2}{\partial x\partial s} + D_{66}\frac{\partial^2}{\partial s^2} - KA_{55},\\
L_{34} &= D_{16}\frac{\partial^2}{\partial x^2} + (D_{12}+D_{66})\frac{\partial^2}{\partial x\partial s} + D_{26}\frac{\partial^2}{\partial s^2} - KA_{45},\\
L_{35} &= \left(\frac{B_{12}}{R} - KA_{55}\right)\frac{\partial}{\partial x} + \left(\frac{B_{26}}{R} - KA_{45}\right)\frac{\partial}{\partial s},\\
L_{44} &= D_{66}\frac{\partial^2}{\partial x^2} + 2D_{26}\frac{\partial^2}{\partial x\partial s} + D_{22}\frac{\partial^2}{\partial s^2} - KA_{44},\\
L_{45} &= \left(\frac{B_{26}}{R} - KA_{45}\right)\frac{\partial}{\partial x} + \left(\frac{B_{22}}{R} - KA_{44}\right)\frac{\partial}{\partial s},\\
L_{55} &= KA_{55}\frac{\partial^2}{\partial x^2} + 2KA_{45}\frac{\partial^2}{\partial x\partial s} - \frac{A_{22}}{R^2},\\
L_{51} &= -L_{15}, \quad L_{52} = -L_{25}, \quad L_{53} = -L_{35}, \quad L_{54} = -L_{45}.
\end{aligned}
\tag{21.105}
$$

In the following, we consider the case of a static problem with $p_z = p_z(x)$. For the equilibrium conditions then remains:

$$\begin{aligned} \frac{\mathrm{d}N_{xx}}{\mathrm{d}x} &= 0, \\ \frac{\mathrm{d}M_{xx}}{\mathrm{d}x} - Q_x &= 0, \\ \frac{\mathrm{d}Q_x}{\mathrm{d}x} - \frac{N_{ss}}{R} + p_z &= 0. \end{aligned} \tag{21.106}$$

The kinematic equations are as follows:

$$\varepsilon_{xx}^0 = \frac{\mathrm{d}v_0}{\mathrm{d}x}, \quad \varepsilon_{ss}^0 = \frac{w_0}{R}, \quad \kappa_{xx}^0 \frac{\mathrm{d}\psi_x}{\mathrm{d}x}, \quad \gamma_{xz} = \psi_x + \frac{\mathrm{d}w_0}{\mathrm{d}x}. \tag{21.107}$$

For the constitutive equations we have:

$$\begin{aligned} N_{xx} &= A_{11} \frac{\mathrm{d}v_0}{\mathrm{d}x} + A_{12} \frac{w_0}{R}, \\ N_{ss} &= A_{12} \frac{\mathrm{d}v_0}{\mathrm{d}x} + A_{22} \frac{w_0}{R}, \\ M_{xx} &= D_{11} \frac{\mathrm{d}\psi_x}{\mathrm{d}x}, \\ Q_x &= K A_{55} \left(\psi_x + \frac{\mathrm{d}w_0}{\mathrm{d}x} \right). \end{aligned} \tag{21.108}$$

If we assume $\frac{\mathrm{d}N_{xx}}{\mathrm{d}x} = 0$, i.e. the normal force flow N_{xx} is constant with the value N_0, then the following applies:

$$\frac{\mathrm{d}v_0}{\mathrm{d}x} = \frac{1}{A_{11}} \left(N_0 - A_{12} \frac{w_0}{R} \right). \tag{21.109}$$

From the third equilibrium condition in (21.106) we obtain

$$\begin{aligned} \frac{\mathrm{d}}{\mathrm{d}x} \left(\psi_x + \frac{\mathrm{d}w_0}{\mathrm{d}x} \right) &= \frac{1}{K A_{55}} \left(\frac{N_{ss}}{R} - p_z \right) \\ &= \frac{1}{K A_{55}} \left[\frac{1}{R} \left(A_{12} \frac{\mathrm{d}v_0}{\mathrm{d}x} + A_{22} \frac{w_0}{R} \right) - p_z \right]. \end{aligned} \tag{21.110}$$

For the second equilibrium condition in (21.106) follows:

$$D_{11} \frac{\mathrm{d}^2 \psi_x}{\mathrm{d}x^2} - K A_{55} \left(\psi_x + \frac{\mathrm{d}w_0}{\mathrm{d}x} \right) = 0. \tag{21.111}$$

This results in the following two differential equations to describe w_0 and ψ_x:

$$\frac{\mathrm{d}\psi_x}{\mathrm{d}x} = -\frac{\mathrm{d}^2 w_0}{\mathrm{d}x^2} + \frac{1}{KA_{55}}\left[\frac{1}{R}\left(\frac{A_{12}}{A_{11}}N_0 - \frac{A_{12}^2 - A_{11}A_{22}}{A_{11}}\frac{w_0}{R}\right) - p_z\right],$$
$$\frac{\mathrm{d}w_0}{\mathrm{d}x} = \frac{D_{11}}{KA_{55}}\frac{\mathrm{d}^2\psi_x}{\mathrm{d}x^2} - \psi_x. \tag{21.112}$$

From this, the following differential equation for the shell deflection w_0 can be obtained:

$$\frac{\mathrm{d}^4 w_0}{\mathrm{d}x^4} - \frac{1}{KA_{55}}\frac{1}{R^2}\frac{A_{11}A_{22} - A_{12}^2}{A_{11}}\frac{\mathrm{d}^2 w_0}{\mathrm{d}x^2} + \frac{1}{R^2}\frac{A_{11}A_{22} - A_{12}^2}{D_{11}A_{11}}w_0$$
$$= \frac{1}{D_{11}}\left(-\frac{A_{12}}{A_{11}}\frac{N_0}{R} + p_z\right) - \frac{1}{KA_{55}}\frac{\mathrm{d}^2 p_z}{\mathrm{d}x^2}. \tag{21.113}$$

The solution of this differential equation, consisting of a homogeneous solution and a particular solution, is largely determined by the type of roots of the characteristic polynomial. No further details are given here; interested readers are referred to Altenbach et al. (2004).

21.6 Sandwich Shells

In this section, we consider the equations of motion of a cylindrically curved sandwich shell (Fig. 21.25). The sandwich shell with the radius R has two facesheets with the thicknesses h_f and a core with the thickness h_c. The total thickness of the shell is $h = 2h_f + h_c$. In the following, laminated facesheets and an ideally orthotropic core are assumed (see also Hwu (2024), on which the following equations in this section are based). The displacement field (assumed here to be time-dependent) is for the circular cylindrical shell in the context of FSDT:

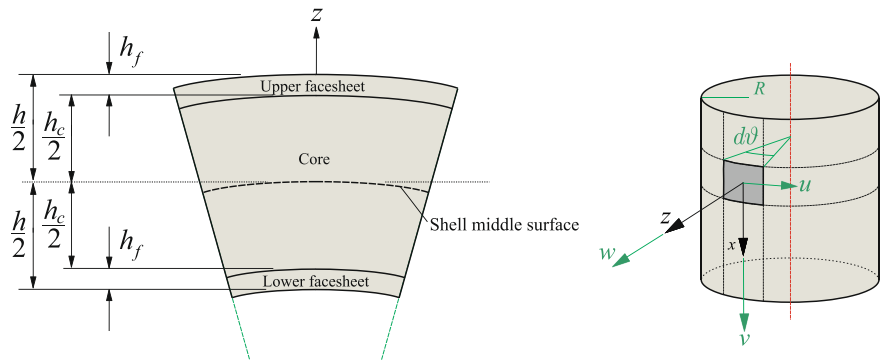


Fig. 21.25 Circular cylindrical sandwich shell

$$
\begin{aligned}
u(x,\vartheta,z,t) &= u_0(x,\vartheta,z,t) + z\psi_\vartheta(x,\vartheta,t),\\
v(x,\vartheta,z,t) &= v_0(x,\vartheta,z,t) + z\psi_x(x,\vartheta,t),\\
w(x,\vartheta,z,t) &= w_0(x,\vartheta,t).
\end{aligned}
\tag{21.114}
$$

The two rotation angles ψ_x and ψ_ϑ are related to the two transverse shear strains γ_{xz} and $\gamma_{\vartheta z}$ as follows:

$$
\psi_x = \gamma_{xz} - \frac{\partial w}{\partial x}, \quad \psi_\vartheta = \gamma_{\vartheta z} - \frac{1}{R}\frac{\partial w}{\partial \vartheta} + \frac{u_0}{R}.
\tag{21.115}
$$

The strain field reads:

$$
\begin{aligned}
\varepsilon_{xx} &= \varepsilon^0_{xx} + z\kappa^0_{xx},\\
\varepsilon_{\vartheta\vartheta} &= \varepsilon^0_{\vartheta\vartheta} + z\kappa^0_{\vartheta\vartheta},\\
\gamma_{x\vartheta} &= \gamma^0_{x\vartheta} + z\kappa^0_{x\vartheta},
\end{aligned}
\tag{21.116}
$$

with

$$
\begin{aligned}
\varepsilon^0_{xx} &= \frac{\partial v_0}{\partial x},\\
\varepsilon^0_{\vartheta\vartheta} &= \frac{1}{R}\frac{\partial u_0}{\partial \vartheta} + \frac{w}{R},\\
\gamma^0_{x\vartheta} &= \frac{1}{R}\frac{\partial v_0}{\partial \vartheta} + \frac{\partial u_0}{\partial x},\\
\kappa^0_{xx} &= \frac{\partial \psi_x}{\partial x},\\
\kappa^0_{\vartheta\vartheta} &= \frac{1}{R}\frac{\partial \psi_\vartheta}{\partial \vartheta},\\
\kappa^0_{x\vartheta} &= \frac{1}{R}\frac{\partial \psi_x}{\partial \vartheta} + \frac{\partial \psi_\vartheta}{\partial x}.
\end{aligned}
\tag{21.117}
$$

The formulation (11.17) according to FSDT is used as the constitutive law:

$$
\begin{pmatrix} N_{xx}\\ N_{\vartheta\vartheta}\\ N_{x\vartheta}\\ M_{xx}\\ M_{\vartheta\vartheta}\\ M_{x\vartheta}\\ Q_\vartheta\\ Q_x \end{pmatrix}
=
\begin{bmatrix}
A_{11} & A_{12} & A_{16} & B_{11} & B_{12} & B_{16} & 0 & 0\\
A_{12} & A_{22} & A_{26} & B_{12} & B_{22} & B_{26} & 0 & 0\\
A_{16} & A_{26} & A_{66} & B_{16} & B_{26} & B_{66} & 0 & 0\\
B_{11} & B_{12} & B_{16} & D_{11} & D_{12} & D_{16} & 0 & 0\\
B_{12} & B_{22} & B_{26} & D_{12} & D_{22} & D_{26} & 0 & 0\\
B_{16} & B_{26} & B_{66} & D_{16} & D_{26} & D_{66} & 0 & 0\\
0 & 0 & 0 & 0 & 0 & 0 & A_{44} & 0\\
0 & 0 & 0 & 0 & 0 & 0 & 0 & A_{55}
\end{bmatrix}
\begin{pmatrix} \varepsilon^0_{xx}\\ \varepsilon^0_{\vartheta\vartheta}\\ \gamma^0_{x\vartheta}\\ \kappa^0_{xx}\\ \kappa^0_{\vartheta\vartheta}\\ \kappa^0_{x\vartheta}\\ \gamma_{\vartheta z}\\ \gamma_{xz} \end{pmatrix}.
\tag{21.118}
$$

The equations of motion of the circular cylindrical sandwich shell are as follows:

$$\begin{aligned}
\frac{\partial N_{xx}}{\partial x}+\frac{1}{R}\frac{\partial N_{\vartheta x}}{\partial \vartheta}&=\rho h\frac{\partial^2 v_0}{\partial t^2},\\
\frac{\partial N_{x\vartheta}}{\partial x}+\frac{1}{R}\frac{N_{\vartheta\vartheta}}{\partial \vartheta}+\frac{Q_\vartheta}{R}&=\rho h\frac{\partial^2 u_0}{\partial t^2},\\
\frac{\partial Q_x}{\partial x}+\frac{1}{R}\frac{\partial Q_\vartheta}{\partial \vartheta}-\frac{N^0_{\vartheta\vartheta}}{R}+p&=\rho h\frac{\partial^2 w}{\partial t^2},\\
\frac{\partial M_{xx}}{\partial x}+\frac{1}{R}\frac{\partial M_{x\vartheta}}{\partial \vartheta}-Q_x&=I\frac{\partial^2 \psi_x}{\partial t^2},\\
\frac{\partial M_{x\vartheta}}{\partial x}+\frac{1}{R}\frac{\partial M_{\vartheta\vartheta}}{\partial \vartheta}-Q_\vartheta&=I\frac{\partial^2 \psi_\vartheta}{\partial t^2}.
\end{aligned}\tag{21.119}$$

If we assume the special case $A_{16}=A_{26}=B_{ij}=D_{16}=D_{26}=0$, then the following equations of motion result for the sandwich shell:

$$\begin{aligned}
A_{11}\frac{\partial^2 v_0}{\partial x^2}+(A_{12}+A_{66})\frac{1}{R}\frac{\partial^2 u_0}{\partial\vartheta\partial x}+A_{66}\frac{1}{R^2}\frac{\partial^2 v_0}{\partial\vartheta^2}+\frac{A_{12}}{R}\frac{\partial w}{\partial x}&=\rho h\frac{\partial^2 v_0}{\partial t^2},\\
A_{66}\frac{\partial^2 u_0}{\partial x^2}+(A_{12}+A_{66})\frac{1}{R}\frac{\partial^2 v_0}{\partial\vartheta\partial x}+A_{22}\frac{1}{R^2}\frac{\partial^2 u_0}{\partial\vartheta^2}&\\
+(A_{22}+A_{44})\frac{1}{R^2}\frac{\partial w}{\partial\vartheta}+\frac{A_{44}}{R}\left(\psi_\vartheta-\frac{u_0}{R}\right)&=\rho h\frac{\partial^2 u_0}{\partial t^2},\\
A_{55}\frac{\partial^2 w}{\partial x^2}+A_{44}\frac{1}{R^2}\frac{\partial w^2}{\partial\vartheta^2}+A_{55}\frac{\partial\psi_x}{\partial x}+A_{44}\frac{1}{R}\frac{\partial\psi_\vartheta}{\partial\vartheta}&\\
-(A_{22}+A_{44})\frac{1}{R^2}\frac{\partial u_0}{\partial\vartheta}-\frac{A_{12}}{R}\frac{\partial v_0}{\partial x}-\frac{A_{22}}{R^2}w+p&=\rho h\frac{\partial^2 w}{\partial t^2},\\
D_{11}\frac{\partial^2\psi_x}{\partial x^2}+(D_{12}+D_{66})\frac{1}{R}\frac{\partial^2\psi_\vartheta}{\partial\vartheta\partial x}+D_{66}\frac{1}{R^2}\frac{\partial^2\psi_x}{\partial\vartheta^2}&\\
-A_{55}\left(\psi_x+\frac{\partial w}{\partial x}\right)&=I\frac{\partial^2\psi_x}{\partial t^2},\\
D_{66}\frac{\partial^2\psi_\vartheta}{\partial x^2}+(D_{12}+D_{66})\frac{1}{R}\frac{\partial^2\psi_x}{\partial\vartheta\partial x}+D_{22}\frac{1}{R^2}\frac{\partial^2\psi_\vartheta}{\partial\vartheta^2}&\\
-A_{44}\left(\psi_\vartheta+\frac{1}{R}\frac{\partial w}{\partial\vartheta}-\frac{u_0}{R}\right)&=I\frac{\partial^2\psi_\vartheta}{\partial t^2}.
\end{aligned}\tag{21.120}$$

If the circular cylindrical shell under consideration is simply suported at both shell ends, then the following boundary conditions apply at these two ends at $x=0$ and $x=l$ (l is the length of the shell):

$$N^0_{xx}=0,\quad u_0=0,\quad w=0,\quad M^0_{xx}=0,\quad \psi_\vartheta=0.\tag{21.121}$$

The following approach fulfils these boundary conditions:

$$
\begin{aligned}
u_0(x\vartheta,t) &= \sum_{m=1}^{\infty}\sum_{n=1}^{\infty} U_{mn}\sin\left(\frac{m\pi x}{l}\right)\sin(\vartheta)\,e^{i\omega_{mn}t},\\
v_0(x\vartheta,t) &= \sum_{m=1}^{\infty}\sum_{n=1}^{\infty} V_{mn}\cos\left(\frac{m\pi x}{l}\right)\cos(\vartheta)\,e^{i\omega_{mn}t},\\
w(x\vartheta,t) &= \sum_{m=1}^{\infty}\sum_{n=1}^{\infty} W_{mn}\sin\left(\frac{m\pi x}{l}\right)\cos(\vartheta)\,e^{i\omega_{mn}t},\\
\psi_x(x\vartheta,t) &= \sum_{m=1}^{\infty}\sum_{n=1}^{\infty} X_{mn}\cos\left(\frac{m\pi x}{l}\right)\cos(\vartheta)\,e^{i\omega_{mn}t},\\
\psi_\vartheta(x\vartheta,t) &= \sum_{m=1}^{\infty}\sum_{n=1}^{\infty} X_{mn}\sin\left(\frac{m\pi x}{l}\right)\sin(\vartheta)\,e^{i\omega_{mn}t}.
\end{aligned}
\tag{21.122}
$$

If this approach is used in the equations of motion (21.120), a system of equations of the form $\left(\underline{\underline{K}}-\omega^2\underline{\underline{I}}_0\right)\underline{u}=\underline{0}$ is obtained. This represents an eigenvalue problem from which the natural frequencies ω and eigenmodes can be determined. The specific entries of this system of equations are not specified here.

21.7 Vibrations of Circular Cylindrical Shells

Dong (1968) investigated the vibration behaviour of unsymmetric cross-ply circular cylindrical shells with radius R and gave the equations of motion of the shell with the z-axis pointing inwards as follows:

$$
\begin{aligned}
L_{11}v_0 + L_{12}u_0 + L_{13}w_0 + p_x &= \rho_0\ddot{v}_0,\\
L_{12}v_0 + L_{22}u_0 + L_{23}w_0 + p_\vartheta &= \rho_0\ddot{u}_0,\\
L_{13}v_0 + L_{23}u_0 + L_{33}w_0 + \rho_0\ddot{w} &= p_z,
\end{aligned}
\tag{21.123}
$$

with $\rho_0 = \int_h \rho(z)\mathrm{d}z$. The operators occurring here are defined as:

$$
\begin{aligned}
L_{11} &= A_{11}\frac{\partial^2}{\partial x^2} + \frac{A_{66}}{R^2}\frac{\partial^2}{\partial s^2},\\
L_{12} &= \frac{A_{12}+A_{66}}{R}\frac{\partial^2}{\partial x\partial s},\\
L_{13} &= -B_{11}\frac{\partial^3}{\partial x^3} - \frac{B_{12}+2B_{66}}{R^2}\frac{\partial^3}{\partial x\partial s^2} - \frac{A_{12}}{R}\frac{\partial}{\partial x},\\
L_{22} &= A_{66}\frac{\partial^2}{\partial x^2} + \frac{A_{22}}{R^2}\frac{\partial^2}{\partial s^2},
\end{aligned}
$$

$$
\begin{aligned}
L_{23} &= -\frac{B_{12}+2B_{66}}{R}\frac{\partial^3}{\partial x^2 \partial s} - \frac{B_{22}}{R^3}\frac{\partial^3}{\partial s^3} - \frac{A_{22}}{R^2}\frac{\partial}{\partial s}, \\
L_{33} &= D_{11}\frac{\partial^4}{\partial x^4} + \frac{2}{R^2}\left(D_{12}+2D_{66}\right)\frac{\partial^4}{\partial x^2 \partial s^2} + \frac{D_{22}}{R^4}\frac{\partial^4}{\partial s^4} \\
&\quad + \frac{2}{R}\left(B_{12}\frac{\partial^2}{\partial x^2} + \frac{B_{22}}{R^2}\frac{\partial^2}{\partial s^2}\right) + \frac{A_{22}}{R^2},
\end{aligned} \tag{21.124}
$$

with $s = R\vartheta$.

For the case of the simply supported shell of length l with boundary conditions $N_{xx} = 0$, $u_0 = 0$, $w_0 = 0$, $M_{xx} = 0$, the following approach is used for the displacements:

$$
\begin{aligned}
u_0 &= U e^{i\omega t} \sin\left(\frac{m\pi x}{l}\right) \sin\left(ns\right), \\
v_0 &= V e^{i\omega t} \cos\left(\frac{m\pi x}{l}\right) \cos\left(ns\right), \\
w_0 &= W e^{i\omega t} \sin\left(\frac{m\pi x}{l}\right) \cos\left(ns\right).
\end{aligned} \tag{21.125}
$$

Inserting this approach into the equations of motion (21.123) results in the following system of equations:

$$
\begin{bmatrix}
\lambda_{11} - \rho_0\omega^2 & \lambda_{12} & \lambda_{13} \\
\lambda_{12} & \lambda_{22} - \rho_0\omega^2 & \lambda_{23} \\
\lambda_{13} & \lambda_{23} & \lambda_{33} - \rho_0\omega^2
\end{bmatrix}
\begin{pmatrix} V \\ U \\ W \end{pmatrix} =
\begin{pmatrix} 0 \\ 0 \\ 0 \end{pmatrix}, \tag{21.126}
$$

with the abbreviations

$$
\begin{aligned}
\lambda_{11} &= A_{11}k_m^2 + A_{66}\bar{n}^2, \\
\lambda_{12} &= -\left(A_{12}+A_{66}\right)k_m\bar{n}, \\
\lambda_{13} &= k_m\left[\frac{A_{12}}{R} - B_{11}k_m^2 + \left(B_{12}+2B_{66}\right)\bar{n}^2\right], \\
\lambda_{22} &= A_{22}\bar{n}^2 + A_{66}k_m^2, \\
\lambda_{23} &= \bar{n}\left[\left(B_{12}+2B_{66}\right)k_m + B_{22}\bar{n}^2 - \frac{A_{22}}{a}\right], \\
\lambda_{33} &= D_{11}k_m^4 + 2\left(D_{12}+2D_{66}\right)k_m^2\bar{n}^2 + D_{22}\bar{n}^4 \\
&\quad - \frac{2}{R}\left(B_{12}k_m^2 + B_{22}\bar{n}^2\right) + \frac{A_{22}}{R^2},
\end{aligned} \tag{21.127}
$$

with $k_m = \frac{m\pi}{l}$ and $\bar{n} = \frac{n}{R}$. Developing and zeroing the coefficient determinant allows the natural frequencies of the given circular cylindrical shell to be determined.

21.8 Buckling of Circular Cylindrical Shells

Starting from Donnel's equations (Mittelstedt 2024) with the z-axis pointing outwards

$$\begin{aligned}
\frac{\partial N_{xx}}{\partial x} + \frac{\partial N_{xy}}{\partial y} &= 0, \\
\frac{\partial N_{xy}}{\partial x} + \frac{\partial N_{yy}}{\partial y} &= 0, \\
\frac{\partial^2 M_{xx}}{\partial x^2} + 2\frac{\partial^2 M_{xy}}{\partial x \partial y} + \frac{\partial^2 M_{yy}}{\partial y^2} - N_{xx}\frac{\partial^2 w_0}{\partial x^2} &= 0
\end{aligned} \tag{21.128}$$

the following buckling differential equations for the shell under longitudinal compression N_{xx} can be derived for circular cylindrical shells with unsymmetric cross-ply layups ($A_{16} = A_{26} = B_{16} = B_{26} = D_{16} = D_{26} = 0$, radius R) within the framework of CLPT (Jones 2006):

$$\begin{aligned}
A_{11}\frac{\partial^2 v_0}{\partial x^2} + A_{12}\left(\frac{\partial^2 u_0}{\partial x \partial y} + \frac{1}{R}\frac{\partial w_0}{\partial x}\right) + A_{66}\left(\frac{\partial^2 v_0}{\partial y^2} + \frac{\partial^2 u_0}{\partial x \partial y}\right) \\
- B_{11}\frac{\partial^3 w_0}{\partial x^3} - (B_{12} + 2B_{66})\frac{\partial^3 w_0}{\partial x \partial y^2} = 0, \\
A_{12}\frac{\partial^2 v_0}{\partial x \partial y} + A_{22}\left(\frac{\partial^2 u_0}{\partial y^2} + \frac{1}{R}\frac{\partial w_0}{\partial y}\right) + A_{66}\left(\frac{\partial^2 v_0}{\partial x \partial y} + \frac{\partial^2 u_0}{\partial x^2}\right) \\
- B_{22}\frac{\partial^3 w_0}{\partial y^3} - (B_{12} + 2B_{66})\frac{\partial^3 w_0}{\partial x^2 \partial y} = 0, \\
\frac{A_{12}}{R}\frac{\partial v_0}{\partial x} - B_{11}\frac{\partial^3 v_0}{\partial x^3} - (B_{12} + 2B_{66})\left(\frac{\partial^3 v_0}{\partial x \partial y^2} + \frac{\partial^3 u_0}{\partial x^2 \partial y}\right) \\
+ \frac{A_{22}}{R}\left(\frac{\partial u_0}{\partial y} + \frac{w_0}{R}\right) + B_{22}\frac{\partial^3 u_0}{\partial y^3} - \frac{2B_{12}}{R}\frac{\partial^2 w_0}{\partial x^2} \\
+ \frac{2B_{22}}{R}\frac{\partial^2 w_0}{\partial y^2} + D_{11}\frac{\partial^4 w_0}{\partial x^4} + 2(D_{12} + 2D_{66})\frac{\partial^4 w_0}{\partial x^2 \partial y^2} + D_{22}\frac{\partial^4 w_0}{\partial y^4} + N_{xx}\frac{\partial^2 w_0}{\partial x^2} = 0.
\end{aligned} \tag{21.129}$$

The following boundary conditions are considered at the shell ends:

$$N_{xx} = 0, \quad u_0 = 0, \quad w_0 = 0, \quad M_{xx} = 0. \tag{21.130}$$

The following approach fulfils these boundary conditions:

$$\begin{aligned}
u_0 &= U_{mn}\sin\left(\frac{m\pi x}{l}\right)\sin(ny), \\
v_0 &= V_{mn}\cos\left(\frac{m\pi x}{l}\right)\cos(ny), \\
w_0 &= W_{mn}\sin\left(\frac{m\pi x}{l}\right)\cos(ny).
\end{aligned} \tag{21.131}$$

Inserting into (21.129), developing and setting the coefficient determinant to zero finally results in the following expression for the buckling load N_{xx}:

$$N_{xx}\left(\frac{m\pi}{l}\right)^2 = \lambda_{33} + \frac{2\lambda_{12}\lambda_{13}\lambda_{23} + \lambda_{11}\lambda_{23}^2 + \lambda_{22}\lambda_{13}^2}{\lambda_{11}\lambda_{22} - \lambda_{12}^2}, \tag{21.132}$$

with:

$$\begin{aligned}
\lambda_{11} &= A_{11}\left(\frac{m\pi}{l}\right)^2 + A_{66}\left(\frac{n}{R}\right)^2,\\
\lambda_{12} &= (A_{12} + A_{66})\,\frac{m\pi}{l}\frac{n}{R},\\
\lambda_{13} &= \frac{A_{12}}{R}\frac{m\pi}{l} + B_{11}\left(\frac{m\pi}{l}\right)^3 + (B_{12} + 2B_{66})\,\frac{m\pi}{l}\left(\frac{n}{R}\right)^2,\\
\lambda_{22} &= A_{66}\left(\frac{m\pi}{l}\right)^2 + A_{22}\left(\frac{n}{R}\right)^2,\\
\lambda_{23} &= (B_{12} + 2B_{66})\left(\frac{m\pi}{l}\right)^2\frac{n}{R} + \frac{A_{22}}{R}\frac{n}{R} + B_{22}\left(\frac{n}{R}\right)^3,\\
\lambda_{33} &= D_{11}\left(\frac{m\pi}{l}\right)^4 + 2\,(D_{12} + 2D_{66})\left(\frac{m\pi}{l}\right)^2\left(\frac{n}{R}\right)^2 + D_{22}\left(\frac{n}{R}\right)^4\\
&\quad + \frac{2B_{12}}{R}\left(\frac{m\pi}{l}\right)^2 + \frac{2B_{22}}{R}\left(\frac{n}{R}\right)^2 + \frac{A_{22}}{R^2}.
\end{aligned} \tag{21.133}$$

21.9 Postbuckling Behaviour of Imperfect Circular Cylindrical Shells

21.9.1 Introduction

The buckling and postbuckling behaviour of layered shells is usually treated with iterative-numerical methods such as the Ritz method or the Galerkin method (see e.g. Shin et al. 1993), but also with methods such as the finite strip method (Zou and Qiao 2002) or the Finite Element Method (Reddy 2004). In engineering practice, however, closed-form analytical methods prove to be the better and more time-efficient methodology, especially in the case of optimization routines or in the preliminary design stage. This section introduces the closed-form analytical treatment of the buckling and postbuckling problem of a laminated shell in the form of a section of a circular cylindrical shell. The methodology presented here is based on the publication by Beerhorst et al. (2011) and is an extension of a methodology presented in Mittelstedt and Schröder (2010).

Consider a shell as shown in Fig. 21.26. The shell has the length a and width b as well as the constant radius R. The coordinate system is introduced as indicated. Initially we want to consider an arbitrarily layered laminate shell. The load consists of a constant axial longitudinal compressive load N_{xx}. Of the numerous available shell theories (see e.g. Donnell 1933; Sanders 1959; Koiter 1959; Love 1927; Flügge 1973), Donnell's shell theory is selected here. Comparative investigations on individual available shell theories can be found, for example, in Simitses et al. (1985) and Jauncky and Knight (1999).

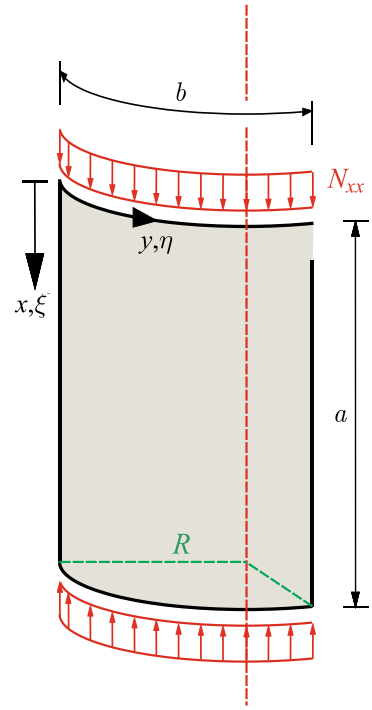


Fig. 21.26 Cylindrically curved cylindrical shell segment under uniaxial compressive load

21.9.2 Basic Equations

Our considerations are based on the validity of CLPT. The constitutive law is stated again here for the sake of clarity:

$$\begin{pmatrix} N_{xx} \\ N_{yy} \\ N_{xy} \\ M_{xx} \\ M_{yy} \\ M_{xy} \end{pmatrix} = \begin{bmatrix} A_{11} & A_{12} & A_{16} & B_{11} & B_{12} & B_{16} \\ A_{12} & A_{22} & A_{26} & B_{12} & B_{22} & B_{26} \\ A_{16} & A_{26} & A_{66} & B_{16} & B_{26} & B_{66} \\ B_{11} & B_{12} & B_{16} & D_{11} & D_{12} & D_{16} \\ B_{12} & B_{22} & B_{26} & D_{12} & D_{22} & D_{26} \\ B_{16} & B_{26} & B_{66} & D_{16} & D_{26} & D_{66} \end{bmatrix} \begin{pmatrix} \varepsilon_{xx}^0 \\ \varepsilon_{yy}^0 \\ \varepsilon_{xy}^0 \\ \kappa_{xx}^0 \\ \kappa_{yy}^0 \\ \kappa_{xy}^0 \end{pmatrix}. \tag{21.134}$$

In a symbolic notation we have:

$$\begin{pmatrix} \underline{N} \\ \underline{M} \end{pmatrix} = \begin{bmatrix} \underline{\underline{A}} & \underline{\underline{B}} \\ \underline{\underline{B}} & \underline{\underline{D}} \end{bmatrix} \begin{pmatrix} \underline{\varepsilon}^0 \\ \underline{\kappa}^0 \end{pmatrix}. \tag{21.135}$$

The corresponding partially inverted form is as follows:

$$\begin{pmatrix} \underline{\varepsilon}^0 \\ \underline{M} \end{pmatrix} \begin{bmatrix} \underline{\underline{\widehat{A}}} & \underline{\underline{\widehat{B}}} \\ \underline{\underline{\widehat{B}}} & \underline{\underline{\widehat{D}}} \end{bmatrix} \begin{pmatrix} \underline{N} \\ \underline{\kappa}^0 \end{pmatrix}, \tag{21.136}$$

wherein:

$$\underline{\underline{\widehat{A}}} = \underline{\underline{A}}^{-1}, \quad \underline{\underline{\widehat{B}}} = -\underline{\underline{A}}^{-1}\underline{\underline{B}}, \quad \underline{\underline{\widehat{D}}} = \underline{\underline{D}} - \underline{\underline{B}}\,\underline{\underline{A}}^{-1}\underline{\underline{B}}. \tag{21.137}$$

At this point, the strains and the formulations for the shell curvatures and the twist apply as follows:

$$\kappa_{xx}^0 = -\frac{\partial^2 w_0}{\partial x^2}, \quad \kappa_{yy}^0 = -\frac{\partial^2 w_0}{\partial y^2}, \quad \kappa_{xy}^0 = -2\frac{\partial^2 w_0}{\partial x \partial y}. \tag{21.138}$$

The equilibrium conditions of the circular cylindrical shell can also be used here. The definition of the Airy stress function F is as follows:

$$N_{xx} = \frac{\partial^2 F}{\partial y^2}, \quad N_{yy} = \frac{\partial^2 F}{\partial x^2}, \quad N_{xy} = -\frac{\partial^2 F}{\partial x \partial y}. \tag{21.139}$$

With the partially inverted material law (21.136) and the above definition (21.139) for the Airy stress function F we obtain the moment flows of the shell as:

$$\begin{aligned}
M_{xx} &= -\widehat{B}_{11}\frac{\partial^2 F}{\partial y^2} - \widehat{B}_{21}\frac{\partial^2 F}{\partial x^2} + \widehat{B}_{61}\frac{\partial^2 F}{\partial x \partial y} - \widehat{D}_{11}\frac{\partial^2 w_0}{\partial x^2} - \widehat{D}_{12}\frac{\partial^2 w_0}{\partial y^2} - 2\widehat{D}_{16}\frac{\partial^2 w_0}{\partial x \partial y}, \\
M_{yy} &= -\widehat{B}_{12}\frac{\partial^2 F}{\partial y^2} - \widehat{B}_{22}\frac{\partial^2 F}{\partial x^2} + \widehat{B}_{62}\frac{\partial^2 F}{\partial x \partial y} - \widehat{D}_{12}\frac{\partial^2 w_0}{\partial x^2} - \widehat{D}_{22}\frac{\partial^2 w_0}{\partial y^2} - 2\widehat{D}_{26}\frac{\partial^2 w_0}{\partial x \partial y}, \\
M_{xy} &= -\widehat{B}_{16}\frac{\partial^2 F}{\partial y^2} - \widehat{B}_{26}\frac{\partial^2 F}{\partial x^2} + \widehat{B}_{66}\frac{\partial^2 F}{\partial x \partial y} - \widehat{D}_{16}\frac{\partial^2 w_0}{\partial x^2} - \widehat{D}_{26}\frac{\partial^2 w_0}{\partial y^2} - 2\widehat{D}_{66}\frac{\partial^2 w_0}{\partial x \partial y}.
\end{aligned} \tag{21.140}$$

Insertion into the shell equilibrium results in:

$$\begin{aligned}
&\widehat{B}_{21}\frac{\partial^4 F}{\partial x^4} + \left(\widehat{B}_{11} + \widehat{B}_{22} - 2\widehat{B}_{66}\right)\frac{\partial^4 F}{\partial x^2 \partial y^2} + \widehat{B}_{12}\frac{\partial^4 F}{\partial y^4} + \left(2\widehat{B}_{26} - \widehat{B}_{61}\right)\frac{\partial^4 F}{\partial x^3 \partial y} \\
&+ \left(2\widehat{B}_{16} - \widehat{B}_{62}\right)\frac{\partial^4 F}{\partial x \partial y^3} + \widehat{D}_{11}\frac{\partial^4 w_0}{\partial x^4} + 2\left(\widehat{D}_{12} + 2\widehat{D}_{66}\right)\frac{\partial^4 w_0}{\partial x^2 \partial y^2} + \widehat{D}_{22}\frac{\partial^4 w_0}{\partial y^4} \\
&+ 4\widehat{D}_{16}\frac{\partial^4 w_0}{\partial x^3 \partial y} + 4\widehat{D}_{26}\frac{\partial^4 w_0}{\partial x^2 \partial y^2} - \frac{\partial^2 F}{\partial y^2}\left(\frac{\partial^2 w_0}{\partial x^2} + \frac{\partial^2 w_i}{\partial x^2}\right) \\
&+ 2\frac{\partial^2 F}{\partial x \partial y}\left(\frac{\partial^2 w_0}{\partial x \partial y} + \frac{\partial^2 w_i}{\partial x \partial y}\right) - \frac{\partial^2 F}{\partial x^2}\left(\frac{\partial^2 w_0}{\partial y^2} + \frac{\partial^2 w_i}{\partial y^2} - \frac{1}{R}\right) + p = 0.
\end{aligned} \tag{21.141}$$

Here, p is a radial compressive load.

The membrane strains are given by the partially inverted material law (21.136):

$$\begin{aligned}
\varepsilon_{xx} &= \widehat{A}_{11}\frac{\partial^2 F}{\partial y^2} + \widehat{A}_{12}\frac{\partial^2 F}{\partial x^2} - \widehat{A}_{16}\frac{\partial^2 F}{\partial x\partial y} - \widehat{B}_{11}\frac{\partial^2 w_0}{\partial x^2} - \widehat{B}_{12}\frac{\partial^2 w_0}{\partial y^2} - 2\widehat{B}_{16}\frac{\partial^2 w_0}{\partial x\partial y},\\
\varepsilon_{yy} &= \widehat{A}_{12}\frac{\partial^2 F}{\partial y^2} + \widehat{A}_{22}\frac{\partial^2 F}{\partial x^2} - \widehat{A}_{26}\frac{\partial^2 F}{\partial x\partial y} - \widehat{B}_{21}\frac{\partial^2 w_0}{\partial x^2} - \widehat{B}_{22}\frac{\partial^2 w_0}{\partial y^2} - \widehat{B}_{26}\frac{\partial^2 w_0}{\partial x\partial y},\\
\varepsilon_{xy} &= \widehat{A}_{16}\frac{\partial^2 F}{\partial y^2} + \widehat{A}_{26}\frac{\partial^2 F}{\partial x^2} - \widehat{A}_{66}\frac{\partial^2 F}{\partial x\partial y} - \widehat{B}_{61}\frac{\partial^2 w_0}{\partial x^2} - \widehat{B}_{62}\frac{\partial^2 w_0}{\partial y^2} - 2\widehat{B}_{66}\frac{\partial^2 w_0}{\partial x\partial y}.
\end{aligned} \tag{21.142}$$

Insertion into the compatibility condition results in:

$$\begin{aligned}
&\widehat{A}_{22}\frac{\partial^4 F}{\partial x^4} + \widehat{A}_{11}\frac{\partial^4 F}{\partial y^4} + \left(2\widehat{A}_{12} + \widehat{A}_{66}\right)\frac{\partial^4 F}{\partial x^2\partial y^2} - 2\widehat{A}_{16}\frac{\partial^4 F}{\partial x\partial y^3}\\
&\quad - \widehat{A}_{26}\frac{\partial^4 F}{\partial x^3\partial y} - \widehat{B}_{21}\frac{\partial^4 w_0}{\partial x^4} - \widehat{B}_{12}\frac{\partial^4 w_0}{\partial y^4} + \left(2\widehat{B}_{66} - \widehat{B}_{11} - \widehat{B}_{22}\right)\frac{\partial^4 w_0}{\partial x^2\partial y^2}\\
&\quad + \left(\widehat{B}_{62} - 2\widehat{B}_{16}\right)\frac{\partial^4 w_0}{\partial x\partial y^3} + \left(\widehat{B}_{61} - 2\widehat{B}_{26}\right)\frac{\partial^4 w_0}{\partial x^3\partial y} = 0.
\end{aligned} \tag{21.143}$$

An alternative formulation of the compatibility equation is obtained by inserting the membrane strains. It follows:

$$\begin{aligned}
&\left(\frac{\partial^2 w_0}{\partial x\partial y}\right)^2 - \frac{\partial^2 w_0}{\partial x^2}\frac{\partial^2 w_0}{\partial y^2} - \frac{\partial^2 w_0}{\partial x^2}\frac{\partial^2 w_i}{\partial y^2} - \frac{\partial^2 w_0}{\partial y^2}\frac{\partial^2 w_i}{\partial x^2}\\
&\quad + 2\frac{\partial^2 w_0}{\partial x\partial y}\frac{\partial^2 w_i}{\partial x\partial y} + \frac{1}{R}\frac{\partial^2 w_0}{\partial x^2} = 0.
\end{aligned} \tag{21.144}$$

The two expressions (21.143) and (21.144) are equated to obtain a relationship between the Airy stress function and the shell deflections as follows:

$$\begin{aligned}
&\widehat{A}_{22}\frac{\partial^4 F}{\partial x^4} + \widehat{A}_{11}\frac{\partial^4 F}{\partial y^4} + \left(2\widehat{A}_{12} + \widehat{A}_{66}\right)\frac{\partial^4 F}{\partial x^2\partial y^2} - 2\widehat{A}_{16}\frac{\partial^4 F}{\partial x\partial y^3} - \widehat{A}_{26}\frac{\partial^4 F}{\partial x^3\partial y}\\
&\quad - \widehat{B}_{21}\frac{\partial^4 w_0}{\partial x^4} - \widehat{B}_{12}\frac{\partial^4 w_0}{\partial y^4} + \left(2\widehat{B}_{66} - \widehat{B}_{11} - \widehat{B}_{22}\right)\frac{\partial^4 w_0}{\partial x^2\partial y^2} + \left(\widehat{B}_{62} - 2\widehat{B}_{16}\right)\frac{\partial^4 w_0}{\partial x\partial y^3}\\
&\quad + \left(\widehat{B}_{61} - 2\widehat{B}_{26}\right)\frac{\partial^4 w_0}{\partial x^3\partial y} = \left(\frac{\partial^2 w_0}{\partial x\partial y}\right)^2 - \frac{\partial^2 w_0}{\partial x^2}\frac{\partial^2 w_0}{\partial y^2} - \frac{\partial^2 w_0}{\partial x^2}\frac{\partial^2 w_i}{\partial y^2}\\
&\quad - \frac{\partial^2 w_0}{\partial y^2}\frac{\partial^2 w_i}{\partial x^2} + 2\frac{\partial^2 w_0}{\partial x\partial y}\frac{\partial^2 w_i}{\partial x\partial y} + \frac{1}{R}\frac{\partial^2 w_0}{\partial x^2}.
\end{aligned} \tag{21.145}$$

21.9.3 Dimensionless Notation

A more compact notation can be achieved if a dimensionless notation is introduced instead of the previous notation (see e.g. Diaconu and Weaver 2006). For this purpose, the natural coordinate system

$$\xi = \frac{x}{a}, \quad \eta = \frac{y}{b} \tag{21.146}$$

is introduced. In addition, the dimensionless radius and radial pressure are introduced as follows:

$$\overline{R} = R\frac{\widehat{AD}}{b^2}, \overline{p} = p\frac{a^2 b^2}{\widehat{AD}\sqrt{\widehat{D}_{11}\widehat{D}_{22}}}. \tag{21.147}$$

The following abbreviation was used here:

$$\widehat{AD} = \sqrt[4]{\widehat{A}_{11}\widehat{A}_{22}\widehat{D}_{11}\widehat{D}_{22}}. \tag{21.148}$$

The Airy stress function and the elastic total potential to be applied later can also be specified in dimensionless notation:

$$\overline{F} = \frac{F}{\sqrt{\widehat{D}_{11}\widehat{D}_{22}}}, \quad \overline{\Pi} = \Pi\frac{ab}{\widehat{AD}^2\sqrt{\widehat{D}_{11}\widehat{D}_{22}}}. \tag{21.149}$$

The displacement quantities can be specified as:

$$\overline{u} = \frac{ua}{\widehat{AD}^2}, \quad \overline{v} = \frac{vb}{\widehat{AD}^2}, \quad \overline{w} = \frac{w_0}{\widehat{AD}}, \quad \overline{w}_i = \frac{w_i}{\widehat{AD}}. \tag{21.150}$$

In addition, there are further dimensionless quantities as follows (Diaconu and Weaver 2006):

$$\alpha_A = \frac{a}{b}\sqrt[4]{\frac{\widehat{A}_{11}}{\widehat{A}_{22}}}, \quad \alpha_B = \frac{b^2}{a^2}\frac{\widehat{B}_{21}}{\widehat{AD}}, \quad \alpha_D = \frac{a}{b}\sqrt[4]{\frac{\widehat{D}_{22}}{\widehat{D}_{11}}},$$

$$\beta_A = \frac{2\widehat{A}_{12} + \widehat{A}_{66}}{2\sqrt{\widehat{A}_{11}\widehat{A}_{22}}}, \quad \beta_B = \frac{\widehat{B}_{11} + \widehat{B}_{22} - 2\widehat{B}_{66}}{\widehat{AD}}, \quad \beta_D = \frac{\widehat{D}_{12} + 2\widehat{D}_{66}}{\sqrt{\widehat{D}_{11}\widehat{D}_{22}}},$$

$$\gamma_A = \frac{\widehat{A}_{16}}{\sqrt[4]{\widehat{A}_{11}^3\widehat{A}_{22}}}, \quad \gamma_B = \frac{b}{a}\frac{2\widehat{B}_{26} - \widehat{B}_{61}}{\widehat{AD}}, \quad \gamma_D = \frac{\widehat{D}_{16}}{\sqrt[4]{\widehat{D}_{11}^3\widehat{D}_{22}}},$$

$$\delta_A = \frac{\widehat{A}_{26}}{\sqrt[4]{\widehat{A}_{11}\widehat{A}_{22}^3}}, \quad \delta_B = \frac{a}{b}\frac{2\widehat{B}_{16} - \widehat{B}_{62}}{\widehat{AD}}, \quad \delta_D = \frac{\widehat{D}_{26}}{\sqrt[4]{\widehat{D}_{11}\widehat{D}_{22}^3}},$$

$$\eta_A = \frac{\widehat{A}_{12}}{\sqrt{\widehat{A}_{11}\widehat{A}_{22}}}, \quad \eta_B = \frac{a^2}{b^2}\frac{\widehat{B}_{12}}{\widehat{AD}}, \quad \eta_D = \frac{\widehat{D}_{12}}{\sqrt{\widehat{D}_{11}\widehat{D}_{22}}},$$

$$\mu_B = \frac{\widehat{B}_{11}}{\widehat{AD}}, \quad \rho_B = \frac{\widehat{B}_{22}}{\widehat{AD}}, \quad \omega_B = \frac{\widehat{B}_{66}}{\widehat{AD}}, \quad \nu_B = \frac{a}{b}\frac{\widehat{B}_{16}}{\widehat{AD}}, \quad \tau_B = \frac{a}{b}\frac{\widehat{B}_{62}}{\widehat{AD}},$$
$$\theta_B = \frac{b}{a}\frac{\widehat{B}_{61}}{\widehat{AD}}, \quad \zeta_B = \frac{b}{a}\frac{2\widehat{B}_{26}}{\widehat{AD}}, \quad k_1 = \frac{a^2b^2}{\widehat{AD}\sqrt{\widehat{D}_{11}\widehat{D}_{22}}}, \quad k_2 = \frac{a^2b^2}{\widehat{AD}^2}. \tag{21.151}$$

A dimensionless representation of the equilibrium condition (21.141) results if the above dimensionless quantities are used consistently and the resulting equation is multiplied by k_1:

$$\begin{aligned}\alpha_B \frac{\partial^4 \overline{F}}{\partial\xi^4} + \beta_B \frac{\partial^4 \overline{F}}{\partial\xi^2\partial\eta^2} + \eta_B \frac{\partial^4 \overline{F}}{\partial\eta^4} + \gamma_B \frac{\partial^4 \overline{F}}{\partial\xi^3\partial\eta} + \delta_B \frac{\partial^4 \overline{F}}{\partial\xi\partial\eta^3} + \frac{1}{\alpha_D^2}\frac{\partial^4 \overline{w}}{\partial\xi^4} + 2\beta_D \frac{\partial^4 \overline{w}}{\partial\xi^2\partial\eta^2} \\ + \alpha_D^2 \frac{\partial^4 \overline{w}}{\partial\eta^4} + 4\frac{\gamma_D}{\alpha_D}\frac{\partial^4 \overline{w}}{\partial\xi^3\partial\eta} + 4\alpha_D\delta_D \frac{\partial^4 \overline{w}}{\partial\xi\partial\eta^3} - \frac{\partial^2 \overline{F}}{\partial\eta^2}\left(\frac{\partial^2 \overline{w}}{\partial\xi^2} + \frac{\partial^2 \overline{w}_i}{\partial\xi^2}\right) \\ + 2\frac{\partial^2 \overline{F}}{\partial\xi\partial\eta}\left(\frac{\partial^2 \overline{w}}{\partial\xi\partial\eta} + \frac{\partial^2 \overline{w}_i}{\partial\xi\partial\eta}\right) - \frac{\partial^2 \overline{F}}{\partial\xi^2}\left(\frac{\partial^2 \overline{w}}{\partial\eta^2} + \frac{\partial^2 \overline{w}_i}{\partial\eta^2} - \frac{1}{\overline{R}}\right) + \overline{p} = 0.\end{aligned} \tag{21.152}$$

The compatibility equation results in the same way, whereby k_2 is now multiplied here:

$$\begin{aligned}&\frac{1}{\alpha_A^2}\frac{\partial^4 \overline{F}}{\partial\xi^4} + \alpha_A^2 \frac{\partial^4 \overline{F}}{\partial\eta^4} + 2\beta_A \frac{\partial^4 \overline{F}}{\partial\xi^2\partial\eta^2} - 2\alpha_A\gamma_A \frac{\partial^4 \overline{F}}{\partial\xi\partial\eta^3} - 2\frac{\delta_A}{\alpha_A}\frac{\partial^4 \overline{F}}{\partial\xi^3\partial\eta} \\ &- \alpha_B \frac{\partial^4 \overline{w}}{\partial\xi^4} - \eta_B \frac{\partial^4 \overline{w}}{\partial\eta^4} - \beta_B \frac{\partial^4 \overline{w}}{\partial\xi^2\partial\eta^2} - \delta_B \frac{\partial^4 \overline{w}}{\partial\xi\partial\eta^3} - \gamma_B \frac{\partial^4 \overline{w}}{\partial\xi^3\partial\eta} \\ &= \left(\frac{\partial^2 \overline{w}}{\partial\xi\partial\eta}\right)^2 - \frac{\partial^2 \overline{w}}{\partial\xi^2}\frac{\partial^2 \overline{w}}{\partial\eta^2} - \frac{\partial^2 \overline{w}}{\partial\xi^2}\frac{\partial^2 \overline{w}_i}{\partial\eta^2} - \frac{\partial^2 \overline{w}}{\partial\eta^2}\frac{\partial^2 \overline{w}_i}{\partial\xi^2} + 2\frac{\partial^2 \overline{w}}{\partial\xi\partial\eta}\frac{\partial^2 \overline{w}_i}{\partial\xi\partial\eta} + \frac{1}{\overline{R}}\left(\frac{\partial^2 \overline{w}}{\partial\xi^2}\right).\end{aligned} \tag{21.153}$$

A transformed representation of the definition of Airy's stress function can be given as:

$$\overline{N}_{xx}\pi^2 = \frac{\partial^2 \overline{F}}{\partial\eta^2}, \quad \overline{N}_{yy}\pi^2 = \frac{\partial^2 \overline{F}}{\partial\xi^2}, \quad \overline{N}_{xy}\pi^2 = -\frac{\partial^2 \overline{F}}{\partial\xi\partial\eta}, \tag{21.154}$$

wherein:

$$\overline{N}_{xx} = \frac{N_{xx}b^2}{\pi^2\sqrt{\widehat{D}_{11}\widehat{D}_{22}}}, \quad \overline{N}_{yy} = \frac{N_{yy}a^2}{\pi^2\sqrt{\widehat{D}_{11}\widehat{D}_{22}}}, \quad \overline{N}_{xy} = \frac{N_{xy}ab}{\pi^2\sqrt{\widehat{D}_{11}\widehat{D}_{22}}}. \tag{21.155}$$

If the special case of a symmetric orthotropic laminate is given, then the two Eqs. (21.152) and (21.153) simplify considerably. Specifically, the dimensionless variables γ_A, δ_A, γ_D, δ_D and all variables in (21.151) that have the index B disappear. The equilibrium condition (21.152) then changes to the following form

$$\frac{1}{\alpha_D^2}\frac{\partial^4\overline{w}}{\partial\xi^4}+2\beta_D\frac{\partial^4\overline{w}}{\partial\xi^2\partial\eta^2}+\alpha_D^2\frac{\partial^4\overline{w}}{\partial\eta^4}-\frac{\partial^2\overline{F}}{\partial\eta^2}\left(\frac{\partial^2\overline{w}}{\partial\xi^2}+\frac{\partial^2\overline{w}_i}{\partial\xi^2}\right)$$
$$+2\frac{\partial^2\overline{F}}{\partial\xi\partial\eta}\left(\frac{\partial^2\overline{w}}{\partial\xi\partial\eta}+\frac{\partial^2\overline{w}_i}{\partial\xi\partial\eta}\right)-\frac{\partial^2\overline{F}}{\partial\xi^2}\left(\frac{\partial^2\overline{w}}{\partial\eta^2}+\frac{\partial^2\overline{w}_i}{\partial\eta^2}-\frac{1}{\overline{R}}\right)+\overline{p}=0. \tag{21.156}$$

The compatibility condition (21.153) takes the following form:

$$\frac{1}{\alpha_A^2}\frac{\partial^4\overline{F}}{\partial\xi^4}+\alpha_A^2\frac{\partial^4\overline{F}}{\partial\eta^4}+2\beta_A\frac{\partial^4\overline{F}}{\partial\xi^2\partial\eta^2}=\left(\frac{\partial^2\overline{w}}{\partial\xi\partial\eta}\right)^2-\frac{\partial^2\overline{w}}{\partial\xi^2}\frac{\partial^2\overline{w}}{\partial\eta^2}$$
$$-\frac{\partial^2\overline{w}}{\partial\xi^2}\frac{\partial^2\overline{w}_i}{\partial\eta^2}-\frac{\partial^2\overline{w}}{\partial\eta^2}\frac{\partial^2\overline{w}_i}{\partial\xi^2}+2\frac{\partial^2\overline{w}}{\partial\xi\partial\eta}\frac{\partial^2\overline{w}_i}{\partial\xi\partial\eta}+\frac{1}{\overline{R}}\left(\frac{\partial^2\overline{w}}{\partial\xi^2}\right). \tag{21.157}$$

21.9.4 Inplane Displacements

In the context of the practical design of a shell structure, one is not only interested in the consideration of the shell deflection in the postbuckling state, but also endeavours to obtain a statement about the displacements u and v. From the kinematic equations

$$\begin{aligned}\frac{\partial u}{\partial x}&=\varepsilon_x^0-\frac{1}{2}\left(\frac{\partial w}{\partial x}\right)^2-\frac{\partial w}{\partial x}\frac{\partial w_i}{\partial x},\\ \frac{\partial v}{\partial y}&=\varepsilon_y^0-\frac{1}{2}\left(\frac{\partial w}{\partial y}\right)^2-\frac{\partial w}{\partial y}\frac{\partial w_i}{\partial y}-\frac{w}{\overline{R}},\\ \frac{\partial u}{\partial y}+\frac{\partial v}{\partial x}&=\varepsilon_{xy}^0-\frac{\partial w}{\partial x}\frac{\partial w}{\partial y}-\frac{\partial w}{\partial x}\frac{\partial w_i}{\partial y}-\frac{\partial w}{\partial y}\frac{\partial w_i}{\partial x}\end{aligned} \tag{21.158}$$

we obtain by inserting (21.142) and transforming into a dimensionless notation:

$$\begin{aligned}\frac{\partial\overline{u}}{\partial\xi}&=\alpha_A^2\frac{\partial^2\overline{F}}{\partial\eta^2}+\eta_A\frac{\partial^2\overline{F}}{\partial\xi^2}-\frac{1}{2}\left(\frac{\partial\overline{w}}{\partial\xi}\right)^2-\frac{\partial\overline{w}}{\partial\xi}\frac{\partial\overline{w}_i}{\partial\xi},\\ \frac{\partial\overline{v}}{\partial\eta}&=\eta_A\frac{\partial^2\overline{F}}{\partial\eta^2}+\frac{1}{\alpha_A^2}\frac{\partial^2\overline{F}}{\partial\xi^2}-\frac{1}{2}\left(\frac{\partial\overline{w}}{\partial\eta}\right)^2-\frac{\partial\overline{w}}{\partial\eta}\frac{\partial\overline{w}_i}{\partial\eta}-\frac{\overline{w}}{\overline{R}},\\ \frac{\partial\overline{u}}{\partial\eta}+\frac{\partial\overline{v}}{\partial\xi}&=2(\eta_A-\beta_A)\frac{\partial^2\overline{F}}{\partial\xi\partial\eta}-\frac{\partial\overline{w}}{\partial\xi}\frac{\partial\overline{w}}{\partial\eta}-\frac{\partial\overline{w}}{\partial\xi}\frac{\partial\overline{w}_i}{\partial\eta}-\frac{\partial\overline{w}}{\partial\eta}\frac{\partial\overline{w}_i}{\partial\xi},\end{aligned} \tag{21.159}$$

provided we have a symmetric and orthotropic laminate.

The changes in the length of the shell can then be calculated as:

$$\Delta\overline{a}=\int_0^1\left(\alpha_A^2\frac{\partial^2\overline{F}}{\partial\eta^2}+\eta_A\frac{\partial^2\overline{F}}{\partial\xi^2}-\frac{1}{2}\left(\frac{\partial\overline{w}}{\partial\xi}\right)^2-\frac{\partial\overline{w}}{\partial\xi}\frac{\partial\overline{w}_i}{\partial\xi}\right)\mathrm{d}\xi, \tag{21.160}$$

and:

$$\Delta\overline{b} = \int_0^1 \left(\eta_A \frac{\partial^2 \overline{F}}{\partial \eta^2} + \frac{1}{\alpha_A^2} \frac{\partial^2 \overline{F}}{\partial \xi^2} - \frac{1}{2} \left(\frac{\partial \overline{w}}{\partial \eta} \right)^2 - \frac{\partial \overline{w}}{\partial \eta} \frac{\partial \overline{w}_i}{\partial \eta} - \frac{\overline{w}}{\overline{R}} \right) \mathrm{d}\eta. \tag{21.161}$$

If these values are related to the dimensionless length $\overline{a}$ and width $\overline{b}$ of the shell, then the mean strains result as:

$$\varepsilon_a = \frac{\Delta\overline{a}}{\overline{a}} = \frac{\Delta a}{a}, \quad \varepsilon_b = \frac{\Delta\overline{b}}{\overline{b}} = \frac{\Delta b}{b}. \tag{21.162}$$

The dimensionless lengths $\overline{a}$ and $\overline{b}$ result from (21.150) by exchanging u with a and v with b.

21.9.5 Closed-Form Analytical Solution

21.9.5.1 Boundary Conditions

We consider a shell that is simply supported at all edges. Therefore the following boundary conditions apply:

$$\begin{aligned}
&\overline{w}\,(\xi = 0, \eta) = 0, \quad \overline{M}_\xi\,(\xi = 0, \eta) = 0,\\
&\overline{w}\,(\xi = 1, \eta) = 0, \quad \overline{M}_\xi\,(\xi = 1, \eta) = 0,\\
&\overline{w}\,(\xi, \eta = 0) = 0, \quad \overline{M}_\eta\,(\xi, \eta = 0) = 0,\\
&\overline{w}\,(\xi, \eta = 1) = 0, \quad \overline{M}_\eta\,(\xi, \eta = 1) = 0.
\end{aligned} \tag{21.163}$$

No boundary conditions are specified here with regard to the inplane displacements. The edges can therefore move freely in the shell plane.

21.9.5.2 Bifurcational Buckling Load

In order to be able to discuss the later results appropriately, the bifurcational buckling load of the shells under consideration is also required. It can be specified for an orthotropic circular cylindrical shell segment as:

$$\overline{N}_{xx} = n^2 \left[\left(\frac{m}{n} \frac{1}{\alpha_D} \right)^2 + 2\beta_D + \left(\frac{n}{m} \alpha_D \right)^2 + \frac{1}{(\pi n)^4 \overline{R}^2 \left(\left(\frac{m}{n} \frac{1}{\alpha_A} \right)^2 + 2\beta_A + \left(\frac{n}{m} \alpha_A \right)^2 \right)} \right]. \tag{21.164}$$

The wave numbers m and n are generally determined by trial and error.

21.9.5.3 Closed-Form Analytical Solution

We first consider the compatibility equation (21.157) to determine a closed-form analytical solution for the postbuckling behaviour of a laminate shell with orthotropic and symmetric layup. We use the following approaches for the shell deflection $\overline{w}$ and the shell imperfection $\overline{w}_i$:

$$\begin{aligned} \overline{w} &= A \sin(m\pi\xi) \sin(n\pi\eta), \\ \overline{w}_i &= B \sin(m\pi\xi) \sin(n\pi\eta). \end{aligned} \tag{21.165}$$

Here, A and B are the unknown amplitude of the postbuckling deformation and the predetermined amplitude of the geometric imperfection respectively. The number of half-waves m in the longitudinal direction and the number of half-waves n in the circumferential direction are set as they result from the linear bifurcation load. Inserting (21.165) into (21.157) results in

$$\begin{aligned} \frac{1}{\alpha_A^2}\frac{\partial^4 \overline{F}}{\partial \xi^4} + \alpha_A^2 \frac{\partial^4 \overline{F}}{\partial \eta^4} + 2\beta_A \frac{\partial^4 \overline{F}}{\partial \xi^2 \partial \eta^2} &= -\pi^2 \frac{m^2}{\overline{R}} A \sin(m\pi\xi) \sin(n\pi\eta) \\ &+ \pi^4 m^2 n^2 A(A+2B)\left(\cos^2(m\pi\xi) + \cos^2(n\pi\eta) - 1\right). \end{aligned} \tag{21.166}$$

This differential equation can be solved in an exact manner, and the solution is composed of a homogeneous and a particular solution:

$$\overline{F} = \overline{F}_h + \overline{F}_{p1} + \overline{F}_{p2}. \tag{21.167}$$

The homogeneous solution corresponds to a shell without deflection. It can be determined by direct integration:

$$\overline{F}_h = \int \left(\int \overline{N}_{xx} \pi^2 d\eta \right) \mathrm{d}\xi, \tag{21.168}$$

which leads to the following expression:

$$\overline{F}_h = \frac{\overline{N}_x^0 \pi^2 \eta^2}{2}. \tag{21.169}$$

The particular solution is made up of two parts:

$$\overline{F}_{p1} = C \sin(m\pi\xi) \sin(n\pi\eta), \quad \overline{F}_{p2} = D \cos^2(m\pi\xi) + E \cos^2(n\pi\eta). \tag{21.170}$$

A coefficient comparison results in:

$$\begin{aligned} C &= \frac{-A}{\overline{R}\pi^2 \left(\frac{m^2}{\alpha_A^2} + \alpha_A^2 \frac{n^4}{m^2} + 2\beta_A n^2 \right)}, \\ D &= \frac{\alpha_A^2 n^2 A(A+2B)}{16m^2}, \quad E = \frac{m^2 A(A+2B)}{16\alpha_A^2 n^2}. \end{aligned} \tag{21.171}$$

However, the equilibrium condition (21.156) cannot be solved in an exact analytical manner, so that instead of an exact solution, an energy analysis is used. In principle, there are two conceivable ways of doing this, one using the Ritz method and one using the Galerkin method. Both methods are briefly described below.

The Ritz method uses the principle of the minimum of the total elastic potential Π, which assumes a minimum when the partial derivatives of Π disappear according to the constants A_i:

$$\frac{\partial \overline{\Pi}}{\partial A_i} = 0. \tag{21.172}$$

In this case, the total elastic potential is made up of the inner potential and the external potential:

$$\overline{\Pi} = \overline{\Pi}_i + \overline{\Pi}_a. \tag{21.173}$$

At present, the inner potential $\overline{\Pi}_i$ can be specified as:

$$\Pi_i = \frac{1}{2} \int \int \int_V \left(\sigma_{xx} \varepsilon_{xx} + \sigma_{yy} \varepsilon_{yy} + \tau_{xy} \gamma_{xy} \right) \mathrm{d}V. \tag{21.174}$$

Insertion of the strains and integration over the thickness of the laminate results in:

$$\Pi_i = \frac{1}{2} \int_0^a \int_0^b \left(N_{xx} \varepsilon_{xx}^0 + N_{yy} \varepsilon_{yy}^0 + N_{xy} \gamma_{xy}^0 + M_{xx} \kappa_{xx}^0 + M_{yy} \kappa_{yy}^0 + M_{xy} \kappa_{xy}^0 \right) \mathrm{d}y \mathrm{d}x. \tag{21.175}$$

The force and moment flows as well as strains, curvatures and twist are now replaced by their respective expressions:

$$\begin{aligned} \Pi_i = \frac{1}{2} \int_0^a \int_0^b \Bigg[& \widehat{A}_{11} \left(\frac{\partial^2 F}{\partial y^2} \right)^2 + 2 \widehat{A}_{12} \frac{\partial^2 F}{\partial x^2} \frac{\partial^2 F}{\partial y^2} \\ & + \widehat{A}_{22} \left(\frac{\partial^2 F}{\partial x^2} \right)^2 + \widehat{A}_{66} \left(\frac{\partial^2 F}{\partial x \partial y} \right)^2 \\ & + \widehat{D}_{11} \left(\frac{\partial^2 w}{\partial x^2} \right)^2 + 2 \widehat{D}_{12} \frac{\partial^2 w}{\partial x^2} \frac{\partial^2 w}{\partial y^2} \\ & + \widehat{D}_{22} \left(\frac{\partial^2 w}{\partial y^2} \right)^2 + 4 \widehat{D}_{66} \left(\frac{\partial^2 w}{\partial x \partial y} \right)^2 \Bigg] \mathrm{d}y \mathrm{d}x. \end{aligned} \tag{21.176}$$

In dimensionless notation we obtain:

$$\begin{aligned}\overline{\Pi}_i = \frac{1}{2}\int_0^1\int_0^1 \Bigg[& \alpha_A^2\left(\frac{\partial^2\overline{F}}{\partial\eta^2}\right)^2 + 2\eta_A\frac{\partial^2\overline{F}}{\partial\xi^2}\frac{\partial^2\overline{F}}{\partial\eta^2} \\ & + \frac{1}{\alpha_A^2}\left(\frac{\partial^2\overline{F}}{\partial\xi^2}\right)^2 + 2\left(\beta_A - \eta_A\right)\left(\frac{\partial^2\overline{F}}{\partial\xi\partial\eta}\right)^2 \\ & + \frac{1}{\alpha_D^2}\left(\frac{\partial^2\overline{w}}{\partial\xi^2}\right)^2 + 2\eta_D\frac{\partial^2\overline{w}}{\partial\xi^2}\frac{\partial^2\overline{w}}{\partial\eta^2} \\ & + \alpha_D^2\left(\frac{\partial^2\overline{w}}{\partial\eta^2}\right)^2 + 2\left(\beta_D - \eta_D\right)\left(\frac{\partial^2\overline{w}}{\partial\xi\partial\eta}\right)^2 \Bigg] \mathrm{d}\eta\mathrm{d}\xi. \end{aligned} \tag{21.177}$$

The external potential is as follows:

$$\overline{\Pi}_a = -\int_0^1\int_0^1 \overline{N}_{xx}\frac{\mathrm{d}\overline{u}}{\mathrm{d}\xi}\mathrm{d}\eta\mathrm{d}\xi. \tag{21.178}$$

or:

$$\overline{\Pi}_a = -\int_0^1\int_0^1 \overline{N}_{xx}\left(\alpha_A^2\frac{\partial^2\overline{F}}{\partial\eta^2} + \eta_A\frac{\partial^2\overline{F}}{\partial\xi^2} - \frac{1}{2}\left(\frac{\partial\overline{w}}{\partial\xi}\right)^2 - \frac{\partial\overline{w}}{\partial\xi}\frac{\partial\overline{w}_i}{\partial\xi}\right)\mathrm{d}\eta\mathrm{d}\xi. \tag{21.179}$$

At present, the only unknown is the postbuckling amplitude A, resulting in the following Ritz equation:

$$\frac{\partial\overline{\Pi}}{\partial A} = 0. \tag{21.180}$$

This leads to a cubic equation in A and linear terms in the external load $\overline{N}_{xx}^0$.

There are now basically two ways to find a relationship between the load and the postbuckling amplitude:

- Load-controlled determination: The load is specified and the postbuckling amplitude is determined from this, which results as the maximum real root of the cubic polynomial in A.
- Displacement-controlled determination: The Eq. (21.172) is solved for $\overline{N}_{xx}^0$, and the resulting expression is used to calculate the load for a given amplitude.

The advantage of the load-controlled approach lies in the intuitive methodology: Engineers in practice are often interested in the behaviour of a structure in a certain interval of the applied load. On the other hand, the second approach is particularly suitable for investigating

the postbuckling behaviour of circular cylindrical shells, where in many cases a decrease in amplitude can be observed with increasing load.

An further possibility to fulfil the given equilibrium condition at least approximately lies in the application of the Galerkin method, in which the weighted residual of the differential equation is set to zero in an integral sense. At present, this leads to the following:

$$\int_0^1 \int_0^1 R\left[\overline{w}\left(\xi,\eta\right)\right] W(\xi,\eta)\mathrm{d}\eta\mathrm{d}\xi = 0, \tag{21.181}$$

where the first factor of the integrand represents the residual:

$$\begin{aligned} R\left[\overline{w}\left(\xi,\eta\right)\right] = {} & \frac{1}{\alpha_D^2}\frac{\partial^4\overline{w}}{\partial\xi^4} + 2\beta_D\frac{\partial^4\overline{w}}{\partial\xi^2\partial\eta^2} + \alpha_D^2\frac{\partial^4\overline{w}}{\partial\eta^4} - \frac{\partial^2\overline{F}}{\partial\eta^2}\left(\frac{\partial^2\overline{w}}{\partial\xi^2} + \frac{\partial^2\overline{w}_i}{\partial\xi^2}\right) \\ & + 2\frac{\partial^2\overline{F}}{\partial\xi\partial\eta}\left(\frac{\partial^2\overline{w}}{\partial\xi\partial\eta} + \frac{\partial^2\overline{w}_i}{\partial\xi\partial\eta}\right) - \frac{\partial^2\overline{F}}{\partial\xi^2}\left(\frac{\partial^2\overline{w}}{\partial\eta^2} + \frac{\partial^2\overline{w}_i}{\partial\eta^2} - \frac{1}{\overline{R}}\right). \end{aligned} \tag{21.182}$$

The weighting function corresponds to the approach function for the shell deflection, whereby the amplitude was set to unity:

$$W(\xi,\eta) = \sin(m\pi\xi)\sin(n\pi\eta). \tag{21.183}$$

Evaluating (21.181) after some transformations again leads to a third-order polynomial for the postbuckling amplitude A, which in turn contains linear terms of the applied load $\overline{N}_{xx}^0$. The evaluation can be load-controlled or displacement-controlled.

21.9.6 Results and Discussion

In order to enable a comparison of the results of the described closed-form solution, a comparison is carried out with a solution method in which both the shell deflections and the shell imperfections are approximated as Fourier series.

$$\begin{aligned} \overline{w} &= \sum_{m=1}^{M}\sum_{n=1}^{N} A_{mn}\sin\left(m\pi\xi\right)\sin\left(n\pi\eta\right), \\ \overline{w}_i &= \sum_{m=1}^{M}\sum_{n=1}^{N} B_{mn}\sin\left(m\pi\xi\right)\sin\left(n\pi\eta\right). \end{aligned} \tag{21.184}$$

A similar approach is used for the particular components of the Airy stress function F:

$$\overline{F}_{p1} = \sum_{m=0}^{2M} \sum_{n=0}^{2N} C_{mn} \sin(m\pi\xi) \sin(n\pi\eta), \tag{21.185}$$

$$\overline{F}_{p2} = \sum_{m=0}^{2M} \sum_{n=0}^{2N} D_{mn} \cos(m\pi\xi) \cos(n\pi\eta). \tag{21.186}$$

A similar approach was also proposed by Byklum (2002) and Buermann (2006) for isotropic stiffened plates and shells. Details of this methodology will not be presented here. Since this series-based approach is also able to treat unsymmetric laminates, the term PBUS (**P**ost**b**uckling of **u**nsymmetric **s**hells) is used. Similarly, the presented closed-form analysis method is referred to as PBOS (**P**ost**b**uckling of **o**rthotropic **s**hells). The results are evaluated at the shell point at which the largest amplitude of the buckling eigenmode occurs.

The investigations are carried out using a laminated shell consisting of T300/913C UD-Prepreg with the layerwise engineering constants $E_{11} = 93000$ MPa, $E_{22} = 7300$ MPa, $G_{12} = 4700$ MPa, $\nu_{12} = 0.3$, whereby the layer thickness was set to 0.25mm in all cases. The selected layup is $[90/90/0/0]_s$. The numbers of buckling half-waves m and n result from the linear bifurcation analysis. The amplitude B of the imperfections is set at 10.4% of the laminate thickness. Shells with $a = 500$mm, $b = 200$ mm and $R = 2000$mm are considered. The linear buckling analysis results in a buckling load of $\overline{N}_{xx} = -3.8$, the corresponding buckling mode leads to $m = 4$ and $n = 1$. A convergence analysis using PBUS showed that the use of 6×6 series terms is sufficient for the problem at hand.

Figure 21.27 shows the deformation history of the point $\xi = 5/8$ and $\eta = 0.5$. It is shown that the shell deflections increase sharply with increasing load and that the results according to the current closed-form analysis method (PBOS) and by means of series development (PBUS) are in very good agreement in the subcritical range. The calculations show that the results using the Ritz method and the Galerkin method are identical. Overall, the shell shows a stiffer behaviour than the results of a comparative calculation for a plate with identical dimensions and properties. For the postcritical region, on the other hand, the Fourier series expansion shows a significantly stiffer behaviour than the closed-form analytical method, and the results show greater deviations the greater the applied compressive load is. The reason for this is that the absolute values of the deflection for the two analysis methods do not match, as can easily be seen in Fig. 21.28, where the shell deflection along the ξ-axis in the center of the shell is shown at $\eta = 0.5$ for $\overline{N}_{xx} = -12$. In contrast to the plate, the shell shows the effect that, due to the curved character of the shell, the deflections against the radial direction are larger than those in the radial direction, which cannot be mapped by the closed-form analysis method. The results of the closed-form analysis method can therefore be regarded as a kind of mean value of the values of the PBUS method. Figure 21.27 shows the averaging of the deflection, which leads to a very good agreement with the results of the closed-form analysis method.

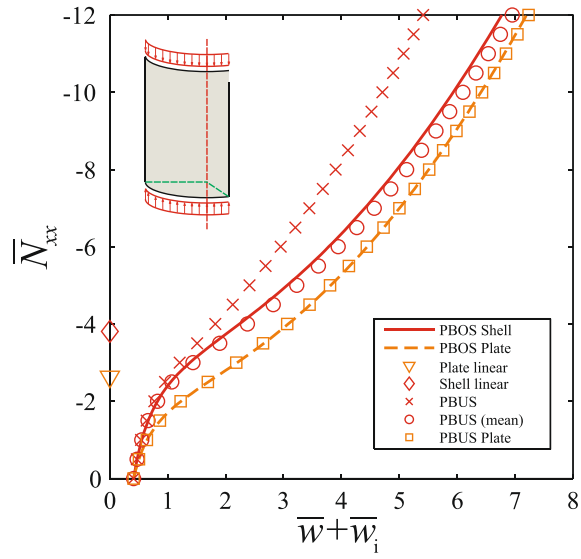


Fig. 21.27 Deformation history at the point $\xi = 5/8$, $\eta = 0.5$

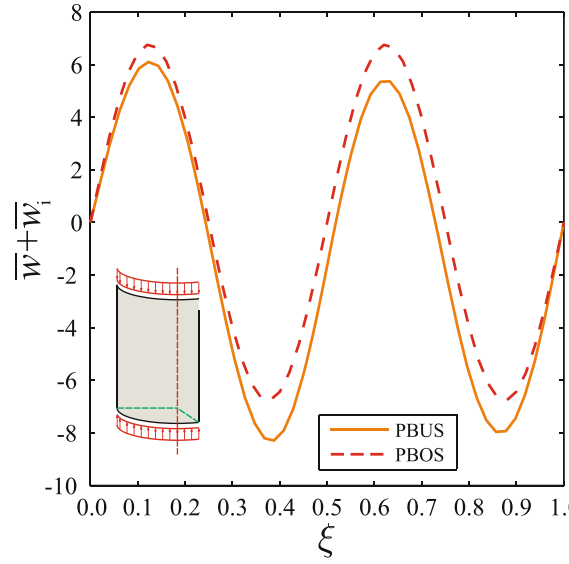


Fig. 21.28 Shell deflection along the ξ-axis along the shell center line $\eta = 0.5$ for $\overline{N}_{xx} = -12$

Another interesting aspect of the calculations is the shape of the buckling modes that occur. While in the range of the bifurcational buckling load for shell buckling (Fig. 21.29) a shape results that can be well described by the product of two sine functions, for high degrees of buckling (Fig. 21.30) a postbuckling shape results that has a clearly unsymmetric shape.

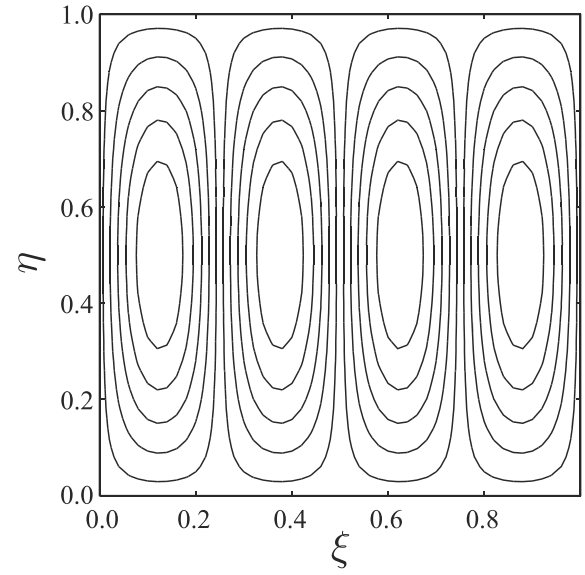


Fig. 21.29 Contour plot of the buckling mode

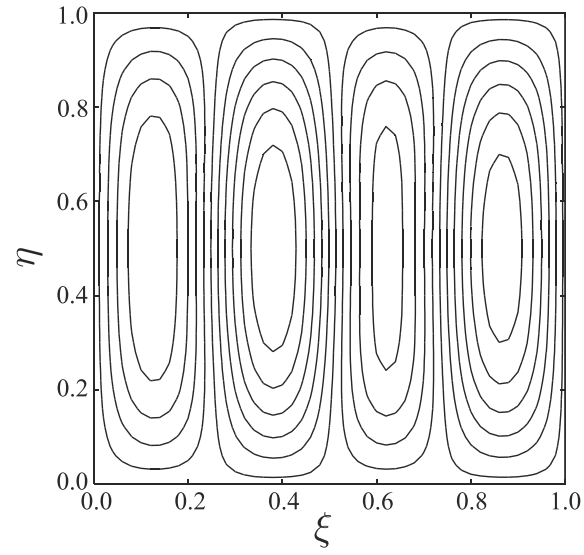


Fig. 21.30 Contour plot of the postbuckling mode for $(\overline{N}_{xx} = -12)$

A comparison of the average strains in the longitudinal and transverse directions is shown in Figs. 21.31 and 21.32 for $\overline{N}_{xx} = -6$, which means a postbuckling ratio of about 1.5 times the buckling load and represents an important design case in aircraft construction. The predictions according to PBOS and PBUS for the average strain ε_a are of a similar order of magnitude, whereby PBOS, in contrast to PBUS, results in a constant strain. The

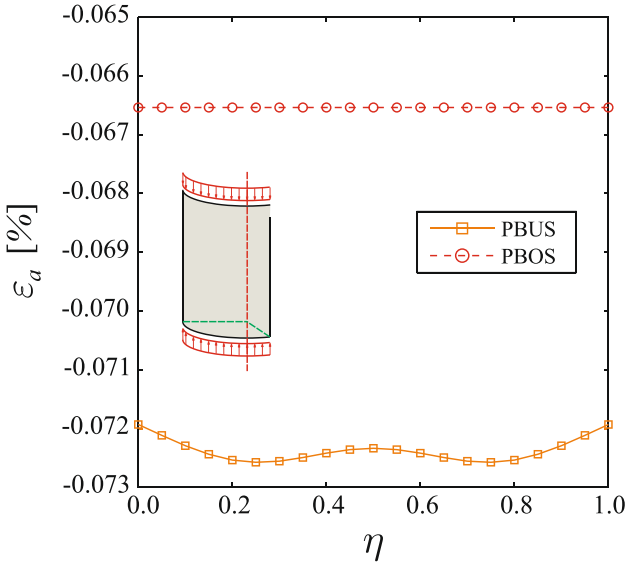
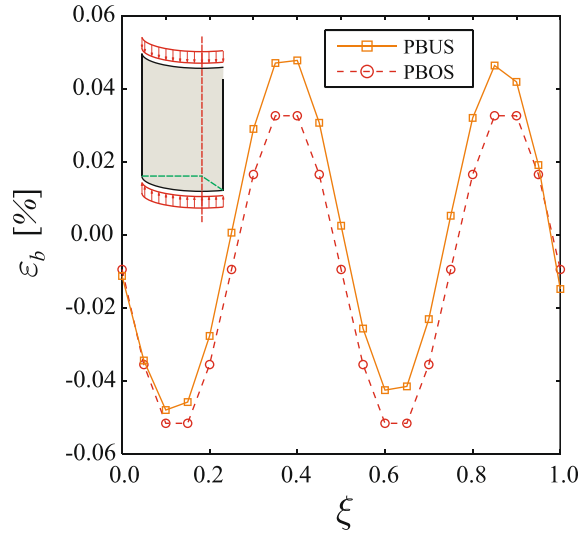


Fig. 21.31 Averaged strain ε_a for $\overline{N}_{xx} = -6$

Fig. 21.32 Averaged strain ε_b for $\overline{N}_{xx} = -6$



relative deviation is around 10%. For ε_b, the qualitative agreement is again quite satisfactory, although there are more significant deviations of up to -30%.

Figure 21.33 shows the average longitudinal strain ε_a in the center of the shell at $\eta = 0.5$ as a function of the applied load. Overall, this results in a satisfactory agreement, whereby the closed-form solution predicts a stiffer shell behaviour.

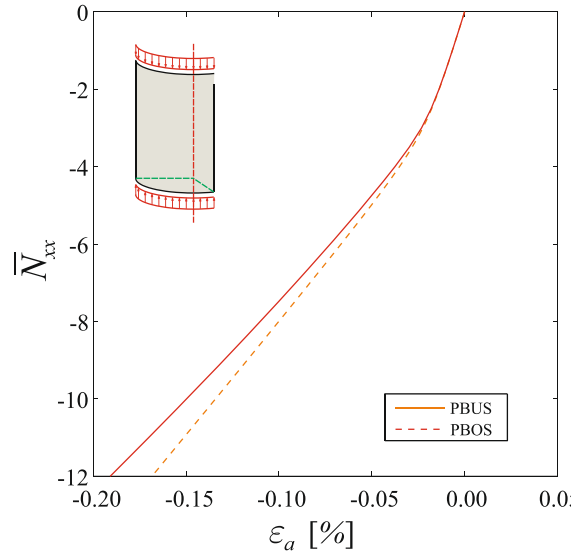


Fig. 21.33 Strain ε_a in the center of the shell

References

Altenbach H, Altenbach J, Kissing W (2004): *Mechanics of Composite Structural Elements*, Springer, Berlin et al., Germany.

Ambartsumyan SA (1964): *Theory of anisotropic shells*, NASA Technical Translation TT F-118. Washington DC, USA.

Axelrad EL (1983): *Schalentheorie*, Teubner, Stuttgart, Germany.

Axelrad EL (1987): *Theory of flexible shells*, North-Holland Amsterdam et al., The Netherlands.

Baker EH, Kovalevsky L, Rish FL (1972): *Structural analysis of shells*, McGraw Hill New York et al., USA.

Becker W, Gross D (2002): *Mechanik elastischer Körper und Strukturen*, Springer, Berlin et al., Germany.

Beerhorst M, Seibel M, Mittelstedt C (2011): *Closed-form Approximate Solution for the Postbuckling Behavior of Orthotropic Shallow Shells Under Axial Compression*, In: Shell-Like Structures, Springer Berlin, Heidelberg, Germany, 103–124.

Beles AA, Soare MV (1972): *Berechnung von Schalentragwerken*, Bauverlag, Wiesbaden et al., Germany.

Born J (1968): *Praktische Schalenstatik, Band I: Die Rotationsschalen*, 2nd edition, Ernst und Sohn, Berlin et al., Germany.

Buermann P (2006): *A semi-analytical model for the post-buckling analysis of stringer- and frame-stiffened cylindrical panels under combined loading*, Dissertation, TU Braunschweig, Braunschweig, Germany.

Byklum E (2002): *Ultimate strength analysis of stiffened steel and aluminium panels using semi-analytical methods*, Dissertation, NTNU Trondheim, Norway.

Calladine CR (1983): *Theory of shell structures*, Cambridge University Press, Cambridge et al., UK.

Czerwenka G, Schnell W (1970a): *Einführung in die Rechenmethoden des Leichtbaus, Band 1*, Bibliographisches Institut, Mannheim et al., Germany.
Czerwenka G, Schnell W (1970b): *Einführung in die Rechenmethoden des Leichtbaus, Band 2*, Bibliographisches Institut, Mannheim et al., Germany.
Diaconu CG, Weaver PM (2006): *Postbuckling of long unsymmetrically laminated composite plates under axial compression*, International Journal of Solids and Structures 43:6978–6997.
Dong, SB (1968): *Free vibration of laminated orthotropic cylindrical shells*, The Journal of the Acoustical Society of America 44:1628–1635.
Donnell LH (1933): *Stability if Thin-Walled Tubes under Torsion*, NACA - National Advisory Committe for Aeronautics, Technical Report No. 479, Washington DC, USA.
Dym CL (1990): *Introduction to the theory of shells*, Hemisphere Publishing Co., New York et al., USA.
Eschenauer H, Schnell W (1993): *Elastizitätstheorie*, Bibliographisches Institut, Mannheim et al., Germany.
Eschenauer H, Olhoff N, Schnell W (1997): *Applied structural mechanics*, Springer, Berlin et al., Germany.
Flügge W (1973): *Stresses in shells*, Springer, Berlin, Germany.
Gibson JE (1965): *Linear elastic theory of thin shells*, Pergamon Press, Oxford et al., UK.
Gibson JE (1980): *Thin shells: computing and theory*, Pergamon Press, Oxford et al., UK.
Girkmann K (1974): *Flächentragwerke*, 6th edition, Springer, Wien et al., Austria.
Göldner H, Altenbach J, Eschke K, Garz KF, Sähn S (1979): *Lehrbuch Höhere Festigkeitslehre Band 1*, Physik Verlag, Weinheim, Germany.
Göldner H, Altenbach J, Eschke K, Garz KF, Sähn S (1985): *Lehrbuch Höhere Festigkeitslehre Band 2*, Physik Verlag, Weinheim, Germany.
Gould PL (1977): *Static analysis of shells*, DC Heath and Company, Lexington, USA.
Hake E (2007): *Statik der Flächentragwerke*, 2nd edition, Springer, Berlin et al., Germany.
Hampe E (1963): *Statik Rotationssymmetrischer Flächentragwerke Band 1: Allgemeine Rotationsschale, Kreis- und Kreisringscheibe, Kreis- und Kreisringplatte*, 3. Auflage, Verlag für Bauwesen, Berlin, Germany.
Hampe, E (1964): *Statik Rotationssymmetrischer Flächentragwerke Band 2: Kreiszylinderschale*, 3. Auflage, Verlag für Bauwesen, Berlin, Germany.
Hampe E (1968): *Statik Rotationssymmetrischer Flächentragwerke Band 3: Kegelschale. Kugelschale*, 3. Auflage, Verlag für Bauwesen, Berlin, Germany.
Hampe E (1971): *Statik Rotationssymmetrischer Flächentragwerke Band 4: Zusammengesetzte Flächentragwerke. Zahlentafeln*, 3. Auflage, Verlag für Bauwesen, Berlin, Germany.
Hampe E (1973): *Statik Rotationssymmetrischer Flächentragwerke Band 5: Hyperbelschalen*, 3. Auflage, Verlag für Bauwesen, Berlin, Germany.
Hwu C (2024): *Mechanics of laminated composite structures*, CRC Press, Boca Raton et al., USA.
Jauncky N, Knight NF (1999): *An assessment of shell theories for buckling of circular cylindrical laminated composite panels loaded in axial compression*, International Journal of Solids and Structures 36:3799–3820.
Jones RM (2006): *Buckling of bars, plates, and shells*, Bull Ridge Publishing, Blacksburg, USA.
Koiter WT (1959): *A consistent first approximation in general theory of thin elastic shells. The theory of thin elastic shells*, Proceedings of the IUTAM Symposium on the theory of thin elastic shells, 24–28 August 1959, Delft, The Netherlands.
Love AEH (1927): *A treatise on the mathematical theory of elasticity*, Dover, New York, NY, USA.
Mazurkiewicz EM, Nagorski RT (1991): *Shells of revolution*, Elsevier, Amsterdam, The Netherlands.
Møllmann H (1981): *Introduction to the theory of thin shells*, Wiley, Chichester et al., UK.

Mittelstedt C, Schröder KU (2010): *Postbuckling of compressively loaded imperfect composite plates: closed-form approximate solutions*, International Journal of Structural Stability and Dynamics 10:761–778.
Mittelstedt C (2023): *Theory of plates and shells*, Springer Vieweg, Berlin et al., Germany.
Mittelstedt C (2024): *Buckling of beams, plates and shells*, Springer, Berlin et al., Germany.
Novozhilov VV (1959): *The theory of thin shells*, Springer Vieweg, Berlin et al., Germany.
Pflüger A (1967): *Elementare Schalenstatik*, 4th edition, Springer, Berlin et al., Germany.
Reddy JN (2004): *Mechanics of laminated composite plates and shells*, CRC Press, Boca Raton et al., FL, USA.
Reddy JN (2006): *Theory and analysis of elastic plates and shells*, CRC Press, Boca Raton et al., FL, USA.
Sanders JL (1959): *An improved first-approximation theory for thin shells*, NASA - National Aeronautics and Space Administration, Technical Report TR-R-24, Washington DC, USA.
Simitses G, Shaw D, Sheinman I (1985): *Stability of cylindrical shells, by various nonlinear shell theories*, Zeitschrift für Angewandte Mathematik und Mechanik 65:159–166.
Timoshenko S, Woinowsky-Krieger S (1964): *Theory of plates and shells*, 2nd edition, McGraw Hill, New York et al., USA.
Turner CE (1965): *Introduction to plate and shell theory*, Longmans Green and Co. Ltd., London, UK.
Ugural AC (1981): *Stresses in plates and shells*, McGraw Hill, New York et al., USA.
Vinson JR (1974): *The behaviour of plates and shells*, Wiley, New York et al., USA.
Vinson JR (1989): *The behaviour of thin walled structures: beams, plates, and shells*, Kluwer, Dordrecht et al., The Netherlands.
Vinson JR (1993): *The behaviour of shells composed of isotropic and composite materials*, Kluwer, Dordrecht et al., The Netherlands.
Wiedemann J (2007): *Leichtbau 1: Elemente*, Springer, Berlin et al., Germany.
Wlassow WS (1958): *Allgemeine Schalentheorie und ihre Anwendung in der Technik*, Akademie-Verlag, Berlin, Germany.
Zou G, Qiao P (2002): *Higher-Order Finite Strip Method for Postbuckling Analysis of Imperfect Composite Plates*, Journal of Engineering Mechanics 128:1008–1015.

Check for updates

Interlaminar Stresses in Curved Laminates 22

In this chapter, we investigate the occurrence of interlaminar stresses in curved laminates. This is a phenomenon that is of great practical relevance, as stresses in the thickness direction of a laminate generally face very weak strength properties. The associated failure mode due to delamination is often referred to as 'unfolding'. After a brief motivation of this problem, we will investigate the closed-form analytical two-dimensional treatment of this problem area by means of a disk analysis. Finally, a three-dimensional analysis method is presented, which is based on a layerwise approach and is also able to suitably treat the free-edge effect.

22.1 Interlaminar Stresses in Curved Laminates

The occurrence of interlaminar stresses in curved composite laminates is a phenomenon that is not only caused by the free-edge effect, but rather results from the curved character of a shell in itself. For motivation, we consider a cylindrically curved shell under end moments M_0, as shown in Fig. 22.1. The shell is assumed to be isotropic for this introductory example. In this situation, it can be seen that the tangential normal stress $\sigma_{\varphi\varphi}$ will show a nonlinear distribution over the shell thickness (Fig. 22.1, right). In addition, the normal stress σ_{rr} occurs, which naturally must become zero at the two shell surfaces $r = R_i$ and $r = R_a$ and will assume its maximum at a certain point r. The qualitative behaviour of the stresses is shown in Fig. 22.1, right. In contrast to the free-edge effect situation, these are not singular stresses.

As we will show later on, the stress field in such a curved laminate depends both on the degree of orthotropy of the individual layers and on the specific layup. In particular, the occurrence of the interlaminar normal stress σ_{rr} must be taken into account in the design and verification of curved laminates, as this stress component is associated with rather weak

© The Author(s), under exclusive license to Springer-Verlag GmbH, DE, part of Springer Nature 2025

C. Mittelstedt, *Mechanics of Composite Structures*,
https://doi.org/10.1007/978-3-662-70788-3_22

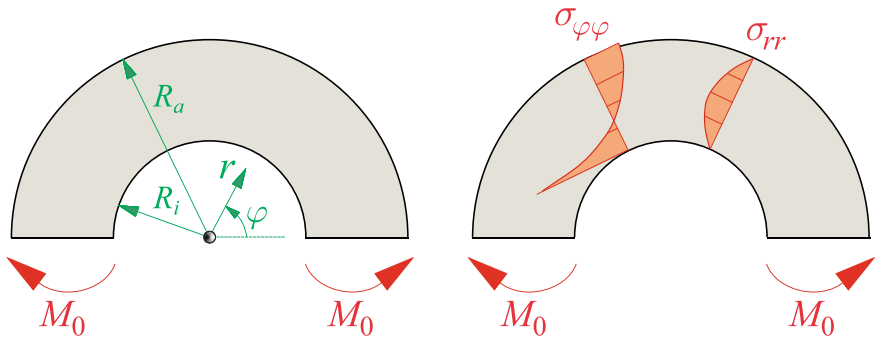


Fig. 22.1 Isotropic circular cylindrical shell under bending (left), qualitative stress distributions (right)

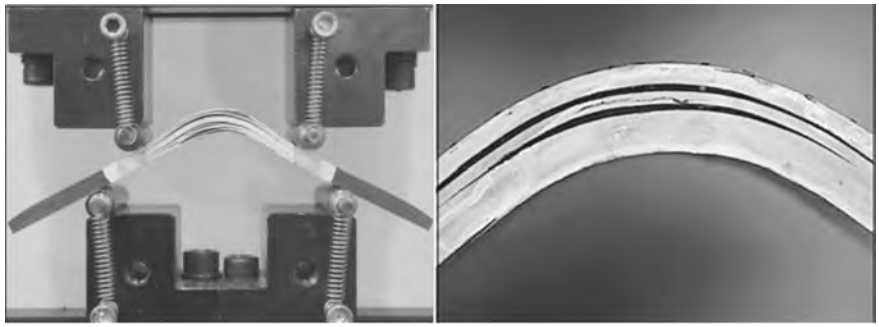


Fig. 22.2 Typical test setup for investigating the interlaminar tensile strength of a composite laminate using a four-point bending test (left), characteristic failure mode in the form of delaminations in the curved area (right), from Ju et al. (2017)

strength properties in the case of composite laminates. The problem here is that this stress component is not included in the shell theories commonly used in practice and therefore requires special analysis methods. A typical failure pattern due to interlaminar stresses in a four-point bending test is shown in Fig. 22.2.

The static strength of curved composite structures has attracted increased interest in research and industry, particularly in the last two decades. This can certainly also be attributed to the development of newer generation aircraft by Boeing (Boeing 787, 'Dreamliner') and Airbus (Airbus A350XWB), which consist of composite materials in large parts of their primary structures. By nature, such large-scale composite structures contain a large number of curved components, so that there is also a particular interest from an industrial point of view in providing analysis methods that can be used to investigate the stress fields in curved laminates or in layered shells, taking interlaminar stresses into account. The occurrence of delamination in curved laminates is often referred to as 'unfolding' and has been recognised as a relevant problem area, as the publications of authors with an industrial

background clearly show Zimmermann et al. (2010), Gözlüklü and Coker (2012), Charrier et al. (2016), Most et al. (2015). However, it is evident that there are hardly any analysis methods available to date that are capable of capturing the stress field of a curved structure while simultaneously taking free-edge effects into account, as well as enabling a corresponding strength assessment. Typically, a pure disk analysis is used in practical applications, or high-resolution FEM calculations are carried out. While the first method only provides a very incomplete picture of the conditions, the second option is usually extremely time-consuming and not very effective in application.

22.2 Isotropic Cylindrically Curved Shells

We consider a cylindrically curved shell structure (thickness h), as already shown in Fig. 22.1. Let the coordinate system be labelled r, φ, z, where z is the reference axis perpendicular to r. The following analysis equations can also be found, for example, in Lekhnitskii (1968), Girkmann (1974), Blumer (1979), Altenbach et al. (1998), Mittelstedt (2023) and assume a plane stress state with respect to z.

The local equilibrium conditions are as follows for the given situation:

$$\begin{aligned} \frac{\partial \sigma_{rr}}{\partial r} + \frac{1}{r}\frac{\partial \tau_{r\varphi}}{\partial \varphi} + \frac{1}{r}\left(\sigma_{rr} - \sigma_{\varphi\varphi}\right) + f_r = 0, \\ \frac{\partial \tau_{r\varphi}}{\partial r} + \frac{1}{r}\frac{\partial \sigma_{\varphi\varphi}}{\partial \varphi} + \frac{2}{r}\tau_{r\varphi} + f_\varphi = 0. \end{aligned} \tag{22.1}$$

Here, σ_{rr}, $\sigma_{\varphi\varphi}$ and $\tau_{r\varphi}$ are the stress components, f_r and f_φ are volume forces. The corresponding kinematic equations are as follows:

$$\begin{aligned} \varepsilon_{rr} &= \frac{\partial u_r}{\partial r}, \\ \varepsilon_{\varphi\varphi} &= \frac{1}{r}\left(\frac{\partial u_\varphi}{\partial \varphi} + u_r\right), \\ \gamma_{r\varphi} &= \frac{1}{r}\left(\frac{\partial u_r}{\partial \varphi} - u_\varphi\right) + \frac{\partial u_\varphi}{\partial r}, \end{aligned} \tag{22.2}$$

where ε_{rr} and $\varepsilon_{\varphi\varphi}$ are the two normal strains and $\gamma_{r\varphi}$ is the shear strain. The two displacement components relevant here are referred to as u_r and u_φ. The corresponding compatibility condition in the $r\varphi$ plane is:

$$\frac{\partial^2 \varepsilon_{rr}}{\partial \varphi^2} + r\frac{\partial^2\left(r\varepsilon_{\varphi\varphi}\right)}{\partial r^2} - \frac{\partial^2\left(r\gamma_{r\varphi}\right)}{\partial r \partial \varphi} - r\frac{\partial \varepsilon_{rr}}{\partial r} = 0. \tag{22.3}$$

In the case of linear-elastic and isotropic material behaviour, Hooke's law can be written as:

$$\begin{pmatrix} \varepsilon_{rr} \\ \varepsilon_{\varphi\varphi} \\ \gamma_{r\varphi} \end{pmatrix} = \begin{bmatrix} \frac{1}{E} & -\frac{\nu}{E} & 0 \\ -\frac{\nu}{E} & \frac{1}{E} & 0 \\ 0 & 0 & \frac{1}{G} \end{bmatrix} \begin{pmatrix} \sigma_{rr} \\ \sigma_{\varphi\varphi} \\ \tau_{r\varphi} \end{pmatrix}. \tag{22.4}$$

Here, E and ν are the isotropic engineering constants of the material under consideration. Note that the formulation for a plane stress state was used here. If there is interest in working out results for a plane strain state, then all equations are valid with the exception of Hooke's law (22.4) in which E and ν are then to be replaced by the corresponding replacement quantities for the plane strain state Altenbach et al. (1998), Mittelstedt (2021).

If the situation is rotationally symmetric (as shown in Fig. 22.1), then all state variables are decoupled from the circumferential coordinate φ, and the equations are considerably simplified:

$$\begin{aligned} \frac{\partial \sigma_{rr}}{\partial r} + \frac{1}{r}\left(\sigma_{rr} - \sigma_{\varphi\varphi}\right) + f_r &= 0, \\ \varepsilon_{rr} &= \frac{\partial u_r}{\partial r}, \\ \varepsilon_{\varphi\varphi} &= \frac{u_r}{r}, \\ \frac{\partial^2 \varepsilon_{\varphi\varphi}}{\partial r^2} + \frac{2}{r}\frac{\partial \varepsilon_{\varphi\varphi}}{\partial r} - \frac{1}{r}\frac{\partial \varepsilon_{rr}}{\partial r} &= 0, \\ \begin{pmatrix} \varepsilon_{rr} \\ \varepsilon_{\varphi\varphi} \end{pmatrix} &= \begin{bmatrix} \frac{1}{E} & -\frac{\nu}{E} \\ -\frac{\nu}{E} & \frac{1}{E} \end{bmatrix} \begin{pmatrix} \sigma_{rr} \\ \sigma_{\varphi\varphi} \end{pmatrix}. \end{aligned} \tag{22.5}$$

Note that due to $u_\varphi = 0$ in this case $\gamma_{r\varphi} = 0$ and therefore $\tau_{r\varphi} = 0$ also applies.

The majority of analysis methods in this particular field of knowledge use the so-called force method, i.e. the formulation of suitable expressions for the stress field and the determination of strains and displacements based on them. This method has its origins in the treatment of disk structures, which can obviously be directly transferred to the problem of cylindrically curved shells presented here. The force method uses Airy's stress function F, which is related to the stress components σ_{rr}, $\sigma_{\varphi\varphi}$ and $\tau_{r\varphi}$ as follows:

$$\begin{aligned} \sigma_{rr} &= \frac{1}{r}\frac{\partial F}{\partial r} + \frac{1}{r^2}\frac{\partial^2 F}{\partial \varphi^2}, \\ \sigma_{\varphi\varphi} &= \frac{\partial^2 F}{\partial r^2}, \\ \tau_{r\varphi} &= -\frac{\partial^2}{\partial r \partial \varphi}\left(\frac{F}{r}\right) = \frac{1}{r^2}\frac{\partial F}{\partial \varphi} - \frac{1}{r}\frac{\partial^2 F}{\partial r \partial \varphi}. \end{aligned} \tag{22.6}$$

Using the compatibility condition (22.3) in conjunction with Hooke's law (22.4), the following differential equation, the so-called disk equation, can then be derived to determine F:

$$\frac{\partial^4 F}{\partial r^4} + \frac{2}{r}\frac{\partial^3 F}{\partial r^3} - \frac{1}{r^2}\left(\frac{\partial^2 F}{\partial r^2} - 2\frac{\partial^4 F}{\partial r^2 \partial \varphi^2}\right) + \frac{1}{r^3}\left(\frac{\partial F}{\partial r} - 2\frac{\partial^3 F}{\partial r \partial \varphi^2}\right) + \frac{1}{r^4}\left(4\frac{\partial^2 F}{\partial \varphi^2} + \frac{\partial^4 F}{\partial \varphi^4}\right) = 0, \tag{22.7}$$

or in compact form:

$$\Delta\Delta F = 0, \tag{22.8}$$

with the Laplace operator

$$\Delta = \frac{\partial^2}{\partial r^2} + \frac{1}{r^2}\frac{\partial^2}{\partial \varphi^2} + \frac{1}{r}\frac{\partial}{\partial r}. \tag{22.9}$$

In the case of a rotationally symmetric situation, the disk equation is reduced to an Euler equation as follows:

$$\frac{\mathrm{d}^4 F}{\mathrm{d}r^4} + \frac{2}{r}\frac{\mathrm{d}^3 F}{\mathrm{d}r^3} - \frac{1}{r^2}\frac{\mathrm{d}^2 F}{\mathrm{d}r^2} + \frac{1}{r^3}\frac{\mathrm{d}F}{\mathrm{d}r} = 0. \tag{22.10}$$

It has the following general solution:

$$F(r) = C_1 + C_2 \ln r + C_3 r^2 + C_4 r^2 \ln r. \tag{22.11}$$

The constants $C_1, \ldots, C_4$ are then adapted to the given boundary conditions.
For the present case of Fig. 22.1, the stress field can be specified as

$$\begin{aligned}
\sigma_{rr} &= \frac{1}{r}\frac{\mathrm{d}F}{\mathrm{d}r} = 2C_3 + \frac{C_2}{r_2} + C_4\left[2\ln\left(\frac{r}{R_a}\right) + 1\right], \\
\sigma_{\varphi\varphi} &= \frac{\mathrm{d}^2 F}{\mathrm{d}r^2} = 2C_3 - \frac{C_2}{r^2} + C_4\left[2\ln\left(\frac{r}{R_a}\right) + 3\right], \\
\tau_{r\varphi} &= 0,
\end{aligned} \tag{22.12}$$

where we have exchanged r for $\frac{r}{R_a}$ in the logarithmic terms. The relevant constants C_2, C_3 and C_4 are adapted to the conditions that the radial normal stress σ_{rr} on both surfaces $r = R_i$ and $r = R_a$ must become zero and that the bending moment caused by the circumferential normal stress $\sigma_{\varphi\varphi}$ is in equilibrium with the applied moment M_0. Thus:

$$\begin{aligned}
\sigma_{rr}\,(r = R_i) &= 0,\\
\sigma_{rr}\,(r = R_a) &= 0,\\
\int_{R_i}^{R_a} \sigma_{\varphi\varphi} r \mathrm{d}r &= -M_0.
\end{aligned} \tag{22.13}$$

After a short calculation, this leads to the following expressions for the stresses in Fig. 22.1 for the current situation:

$$\begin{aligned}
\sigma_{rr} &= 4M_0 \frac{\frac{R_i^2 R_a^2}{r^2} \ln\left(\frac{R_a}{R_i}\right) - R_i^2 \ln\left(\frac{r}{R_i}\right) - R_a^2 \ln\left(\frac{R_a}{r}\right)}{\left(R_i^2 - R_a^2\right)^2 - 4R_i^2 R_a^2 \ln^2\left(\frac{R_a}{R_i}\right)},\\
\sigma_{\varphi\varphi} &= 4M_0 \frac{-\frac{R_i^2 R_a^2}{r^2} \ln\left(\frac{R_a}{R_i}\right) - R_i^2 \ln\left(\frac{r}{R_i}\right) - R_a^2 \ln\left(\frac{R_a}{r}\right) - R_i^2 + R_a^2}{\left(R_i^2 - R_a^2\right)^2 - 4R_i^2 R_a^2 \ln^2\left(\frac{R_a}{R_i}\right)},\\
\tau_{r\varphi} &= 0.
\end{aligned} \tag{22.14}$$

The qualitative stress distributions are shown in Fig. 22.1.

22.3 Orthotropic Cylindrically Curved Shells

We now consider the situation of a cylindrically curved anisotropic shell. In this case, the generalised Hooke's law can be expressed as:

$$\begin{aligned}
\begin{pmatrix} \sigma_{rr} \\ \sigma_{\varphi\varphi} \\ \tau_{r\varphi} \end{pmatrix} &= \begin{bmatrix} Q_{11} & Q_{12} & Q_{16} \\ Q_{12} & Q_{22} & Q_{26} \\ Q_{16} & Q_{26} & Q_{66} \end{bmatrix} \begin{pmatrix} \varepsilon_{rr} \\ \varepsilon_{\varphi\varphi} \\ \gamma_{r\varphi} \end{pmatrix},\\
\begin{pmatrix} \varepsilon_{rr} \\ \varepsilon_{\varphi\varphi} \\ \gamma_{r\varphi} \end{pmatrix} &= \begin{bmatrix} S_{11} & S_{12} & S_{16} \\ S_{12} & S_{22} & S_{26} \\ S_{16} & S_{26} & S_{66} \end{bmatrix} \begin{pmatrix} \sigma_{rr} \\ \sigma_{\varphi\varphi} \\ \tau_{r\varphi} \end{pmatrix}.
\end{aligned} \tag{22.15}$$

Here, Q_{ij} $(i, j = 1, 2, 6)$ are the so-called reduced stiffnesses that result when considering a plane stress state. The quantities S_{ij}, on the other hand, are the compliances that describe the given problem. For the special case of polar orthotropy, i.e. the existence of two symmetry axes of the material under consideration with respect to the rz-plane and the φz-plane, the terms Q_{16}, Q_{26} and S_{16}, S_{26} disappear, and the disk equation can be given as:

$$\frac{1}{E_{\varphi\varphi}}\frac{\partial^4 F}{\partial r^4}+\left(\frac{1}{G_{r\varphi}}-\frac{2\nu_{r\varphi}}{E_{rr}}\right)\frac{1}{r^2}\frac{\partial^4 F}{\partial r^2\partial\varphi^2}+\frac{1}{E_{rr}}\frac{1}{r^4}\frac{\partial^4 F}{\partial\varphi^4}+\frac{2}{E_{\varphi\varphi}}\frac{1}{r}\frac{\partial^3 F}{\partial r^3}$$
$$-\left(\frac{1}{G_{r\varphi}}-\frac{2\nu_{r\varphi}}{E_{rr}}\right)\frac{1}{r^3}\frac{\partial^3 F}{\partial r\partial\varphi^2}-\frac{1}{E_{rr}}\frac{1}{r^2}\frac{\partial^2 F}{\partial r^2}$$
$$+\left(\frac{2}{E_{rr}}-\frac{2\nu_{r\varphi}}{E_{rr}}+\frac{1}{G_{r\varphi}}\right)\frac{1}{r^4}\frac{\partial^2 F}{\partial\varphi^2}+\frac{1}{E_{rr}}\frac{1}{r^3}\frac{\partial F}{\partial r}=0, \tag{22.16}$$

where the engineering constants E_{rr}, $E_{\varphi\varphi}$, $G_{r\varphi}$ and $\nu_{r\varphi}$ were used, which are related to the compliances as follows:

$$S_{11}=\frac{1}{E_{rr}},\quad S_{22}=\frac{1}{E_{\varphi\varphi}},\quad S_{66}=\frac{1}{G_{r\varphi}},\quad S_{12}=-\frac{\nu_{\varphi r}}{E_{\varphi\varphi}}=-\frac{\nu_{r\varphi}}{E_{rr}}. \tag{22.17}$$

We now look at the example of Fig. 22.1 again and assume polar orthotropy. A solution approach of the type

$$F(r)=r^{\lambda} \tag{22.18}$$

results in the following characteristic equation for determining the exponent λ after insertion into the disk equation (22.16):

$$\lambda(\lambda-2)(\lambda+k-1)(-\lambda+k+1)=0, \tag{22.19}$$

with the abbreviation:

$$k^2=\frac{S_{11}}{S_{22}}=\frac{E_{\varphi\varphi}}{E_{rr}}. \tag{22.20}$$

The roots of (22.19) are $\lambda=0$, $\lambda=2$, $\lambda=1\pm k$, so that the final result is

$$F=A_0+B_0r^2+C_0r^{1+k}+D_0r^{1-k}. \tag{22.21}$$

With the help of the boundary conditions (22.13), the following stress field results with (22.6) in the considered cylindrically curved shell:

$$\sigma_{rr}=-\frac{M_0}{R_a^2h\eta}\left[1-\frac{1-\left(\frac{R_i}{R_a}\right)^{k+1}}{1-\left(\frac{R_i}{R_a}\right)^{2k}}\left(\frac{r}{R_a}\right)^{k-1}-\frac{1-\left(\frac{R_i}{R_a}\right)^{k-1}}{1-\left(\frac{R_i}{R_a}\right)^{2k}}\left(\frac{R_i}{R_a}\right)^{k+1}\left(\frac{R_a}{r}\right)^{k+1}\right],$$
$$\sigma_{\varphi\varphi}=-\frac{M_0}{R_a^2h\eta}\left[1-\frac{1-\left(\frac{R_i}{R_a}\right)^{k+1}}{1-\left(\frac{R_i}{R_a}\right)^{2k}}k\left(\frac{r}{R_a}\right)^{k-1}+\frac{1-\left(\frac{R_i}{R_a}\right)^{k-1}}{1-\left(\frac{R_i}{R_a}\right)^{2k}}k\left(\frac{R_i}{r}\right)^{k+1}\right],$$
$$\tau_{r\varphi}=0, \tag{22.22}$$

with:

$$\eta = \frac{1}{2}\left[1-\left(\frac{R_i}{R_a}\right)^2\right] - \frac{k}{k+1}\frac{\left[1-\left(\frac{R_i}{R_a}\right)^{k+1}\right]^2}{1-\left(\frac{R_i}{R_a}\right)^{2k}} + \frac{k}{k-1}\left(\frac{R_i}{R_a}\right)^2\frac{\left[1-\left(\frac{R_i}{R_a}\right)^{k-1}\right]^2}{1-\left(\frac{R_i}{R_a}\right)^{2k}}. \tag{22.23}$$

22.4 Layered Cylindrically Curved Shells

We now extend our considerations to a layered circular cylindrical shell under boundary moments M_0 (Fig. 22.3), whereby we assume that the shell consists of N perfectly bonded polar orthotropic layers. Layer j ($j = 1, 2, \ldots, N$) is bounded by the two interfaces at the points $r = R_{j-1}$ and $r = R_j$. The following solution methodology goes back to Tolf (1983) and Ko and Jackson (1989).

The solution (22.21) for Airy's stress function is now formulated separately for each individual layer:

$$F_j = A_{0j} + B_{0j}r^2 + C_{0j}r^{1+k_j} + D_{0j}r^{1-k_j}. \tag{22.24}$$

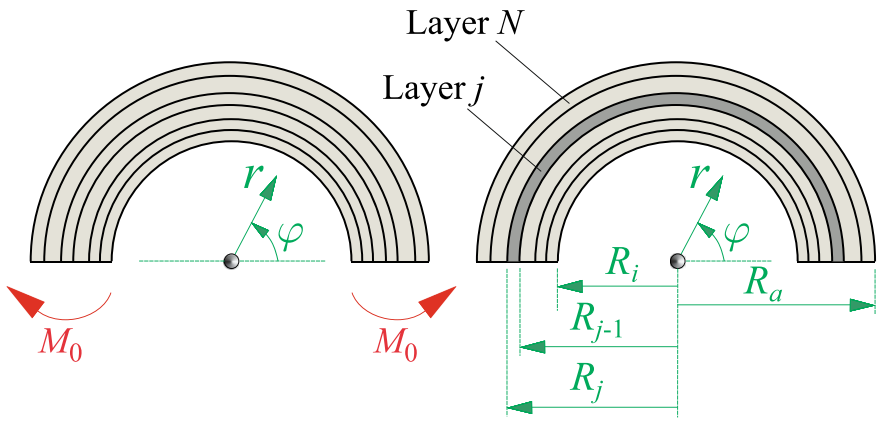


Fig. 22.3 Layered circular cylindrical shell under edge moments

The layerwise stress components can then be specified as:

$$\begin{aligned}\sigma_{rrj} &= 2B_{0j} + C_{0j}\left(k_j + 1\right) r^{k_j - 1} + D_{0j}\left(1 - k_j\right) r^{-k_j - 1},\\ \sigma_{\varphi\varphi j} &= 2B_{0j} + C_{0j} k_j \left(k_j + 1\right) r^{k_j - 1} - D_{0j} k_j \left(1 - k_j\right) r^{-k_j - 1},\\ \tau_{r\varphi j} &= 0.\end{aligned} \tag{22.25}$$

The layerwise displacement components can be obtained by inserting the stresses into Hooke's law and then integrating the kinematic equations as follows:

$$\begin{aligned}u_{rj} &= 2B_{0j}\left(S_{11j} + S_{12j}\right) r + C_{0j}\left(\frac{1}{k_j} S_{11j} + S_{12j}\right)\left(k_j + 1\right) r^{k_j}\\ &\quad - D_{0j}\left(\frac{1}{k_j} S_{11j} - S_{12j}\right)\left(1 - k_j\right) r^{-k_j},\\ u_{\varphi j} &= 2B_{0j}\left(S_{22j} - S_{11j}\right) r\varphi.\end{aligned} \tag{22.26}$$

The boundary and continuity conditions to be applied here can be formulated as follows. Firstly, it must be required that the radial stress σ_{rr} at the two free shell surfaces $r = R_i = R_0$ and $r = R_a = R_n$ becomes zero:

$$\begin{aligned}\sigma_{rr1}\left(r = R_0\right) &= 0,\\ \sigma_{rrn}\left(r = R_n\right) &= 0.\end{aligned} \tag{22.27}$$

Evaluation leads to the following conditions:

$$\begin{aligned}2B_{01} + C_{01}\left(k_1 + 1\right) R_0^{k_1 - 1} + D_{01}\left(1 - k_1\right) R_0^{-k_1 - 1} &= 0,\\ 2B_{0n} + C_{0n}\left(k_n + 1\right) R_a^{k_n - 1} + D_{0n}\left(1 - k_n\right) R_a^{-k_n - 1} &= 0.\end{aligned} \tag{22.28}$$

Furthermore, it is required that the radial normal stress σ_{rr} and the two displacements u_r and u_φ are continuous in the interface between the layers j and $j + 1$:

$$\begin{aligned}\sigma_{rrj}\left(r = R_j\right) &= \sigma_{rrj+1}\left(r = R_j\right),\\ u_{rj}\left(r = R_j\right) &= u_{rj+1}\left(r = R_j\right),\\ u_{\varphi j}\left(r = R_j\right) &= u_{\varphi j+1}\left(r = R_j\right).\end{aligned} \tag{22.29}$$

This leads to the following conditions:

$$
\begin{aligned}
2B_{0j} + C_{0j}\left(k_j + 1\right) R_j^{k_j - 1} + D_{0j}\left(1 - k_j\right) R_j^{-k_j - 1} \\
-2B_{0j+1} - C_{0j+1}\left(k_{j+1} + 1\right) R_j^{k_{j+1} - 1} - D_{0j+1}\left(1 - k_{j+1}\right) R_j^{-k_{j+1} - 1} = 0, \\
2B_{0j}\left(S_{11j} + S_{12j}\right) R_j + C_{0j}\left(\frac{1}{k_j} S_{11j} + S_{12j}\right)\left(k_j + 1\right) R_j^{k_j} \\
-D_{0j}\left(\frac{1}{k_j} S_{11j} - S_{12j}\right)\left(1 - k_j\right) R_j^{-k_j} - 2B_{0j+1}\left(S_{11j+1} + S_{12j+1}\right) R_j \\
-C_{0j+1}\left(\frac{1}{k_{j+1}} S_{11j+1} + S_{12j+1}\right)\left(k_{j+1} + 1\right) R_j^{k_{j+1}} \\
+D_{0j+1}\left(\frac{1}{k_{j+1}} S_{11j+1} - S_{12j+1}\right)\left(1 - k_{j+1}\right) R_j^{-k_{j+1}} = 0, \\
B_{0j}\left(S_{22j} - S_{11j}\right) - B_{0j+1}\left(S_{22j+1} - S_{11j+1}\right) = 0.
\end{aligned}
\tag{22.30}
$$

The last condition is that in each radial section through the laminate the circumferential stresses from all layers are in equilibrium with the applied moment M_0, i.e.:

$$
\sum_{j=1}^{n} \int_{R_{j-1}}^{R_j} \sigma_{\varphi\varphi j} r \, \mathrm{d}r = -M_0. \tag{22.31}
$$

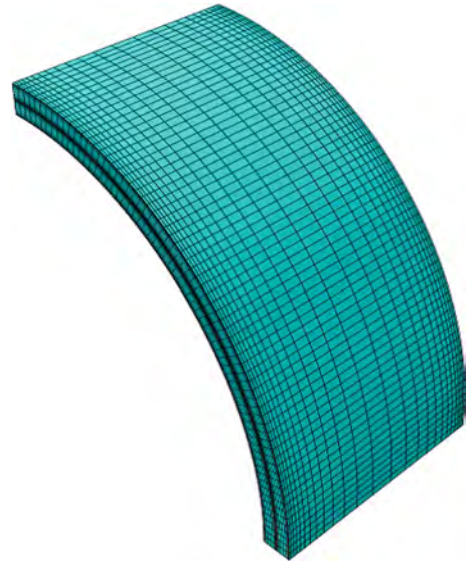
This results in:

$$
\sum_{j=1}^{n} \left[B_{0j}\left(R_j^2 - R_{j-1}^2\right) + C_{0j} k_j \left(R_j^{k_j+1} - R_{j-1}^{k_j+1}\right) - D_{0j} k_j \left(R_j^{-k_j+1} - R_{j-1}^{-k_j+1}\right) \right] = -M_0. \tag{22.32}
$$

Thus, a total of $3(n+1)$ conditions are available for the $3(n+1)$ constants.

Schnabel et al. (2017) investigated free-edge effects in layered shells under bending and also considered the reliability of the shell solution presented above by comparison with high-resolution finite element simulations. A typical FEM mesh is shown in Fig. 22.4. Some selected results for the stress components σ_{rr} and $\sigma_{\varphi\varphi}$ are shown in Figs. 22.5 and 22.6. The material properties used are shown in Table 22.1. The layer thickness was assumed as 0.125 mm. The layups [0/90] and $[0/90]_S$ are considered here, which then leads to the shell thicknesses $h = 0.5$ mm and $h = 1.0$ mm. The auxiliary coordinate $\bar{r}$ used here has its origin at the lower shell surface at $r = R_i = R_0$, so that $0 \le \bar{r} \le R_a = R_N$. Overall, the results show an excellent agreement between the shell solution and the numerical results, although it should be noted that the analytical method is clearly superior to purely numerical calculations in terms of computational efficiency, which also explains its popularity in practical applications. It is noticeable here that the 0°-layers, which are significantly stiffer in

Fig. 22.4 Finite element mesh



the circumferential direction, are significantly more involved in carrying the circumferential stress $\sigma_{\varphi\varphi}$ than the more compliant 90°-layers. As expected, $\sigma_{\varphi\varphi}$ shows discontinuities in the interfaces between the 0° layers and the 90° layers, which can be explained by the abrupt changes in stiffness.

22.5 Three-Dimensional Stress Analysis

It is a fundamental concern to develop efficient yet highly accurate computational methods for estimating free-edge effects in layered shells that can be used in industrial practice. One such method, based on Schnabel et al. (2017), is briefly presented below. A cylindrically curved cross-ply laminate is considered, which is under pure bending load due to the boundary moment flow M_0 (Fig. 22.7, top) and consists of N layers. The analysis method is based on the division of the given physical layers into a number m of mathematical layers (Fig. 22.7, bottom), which corresponds to a discretization of the individual layers into a number of sublayers. The total number of mathematical layers within the analysis model then amounts to $m \cdot n$. The mathematical layer k is limited by the two interfaces k and $k + 1$, which are located at the points $r = R_{k-1}$ and R_k.

Only laminates that consist of unidirectional fiber-reinforced layers and have an orthotropic layer structure are considered below. The fibers are therefore located in the φz-plane and have either a ply angle of 0° or 90°. A fiber direction of 0° means that the fibers run parallel to the φ-direction, whereas in the case of the fiber angle 90° the fibers are oriented parallel to the z-axis. For the examples considered later, the inner radius of

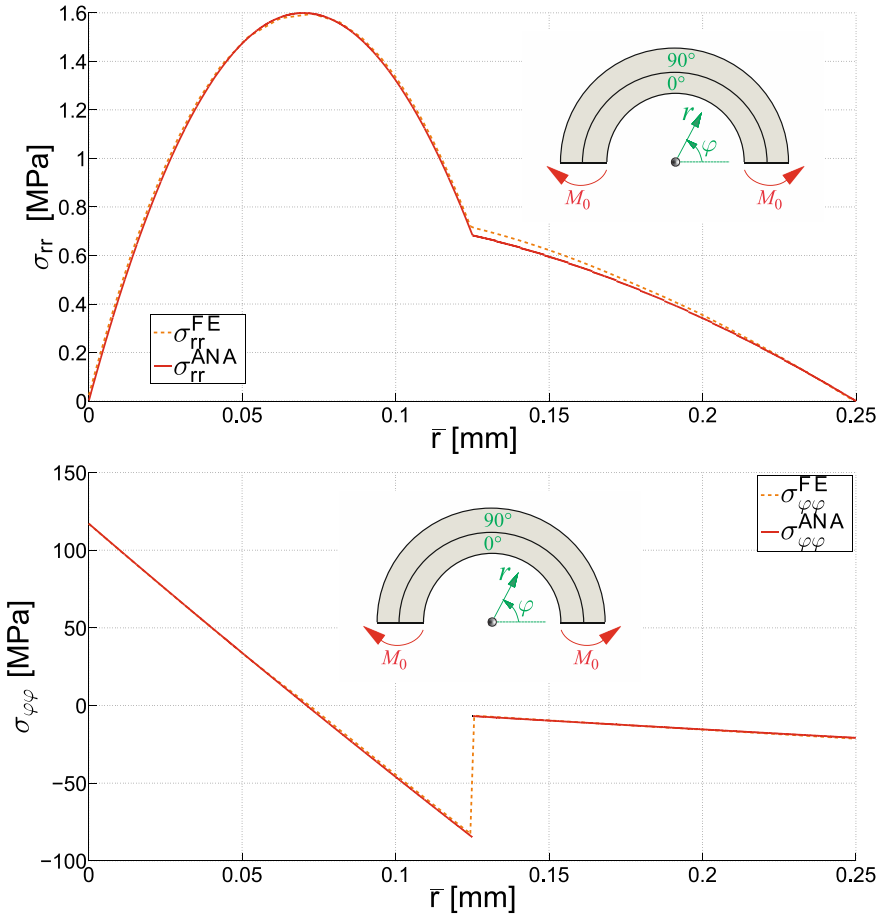


Fig. 22.5 Comparison of the shell solution for the unsymmetric [0/90]-laminate with FEM calculations

the shell is assumed to be $r_0 = 2.5$ mm. All layers have a uniform thickness of 0.125 mm. The applied moment flow M_0 is defined as $M = 0.5$ N and the width of the laminate is 2 mm. The employed material properties are shown in Table 22.1. The analysis method is later verified using finite element calculations, an exemplary mesh for a two-layer laminate is shown in Fig. 22.4.

We consider a cylindrically orthotropic material whose principal directions are characterised by r, φ, z. We assume material linearity in all further explanations, so that we can assume the generalized Hooke's law to be valid. It currently reads:

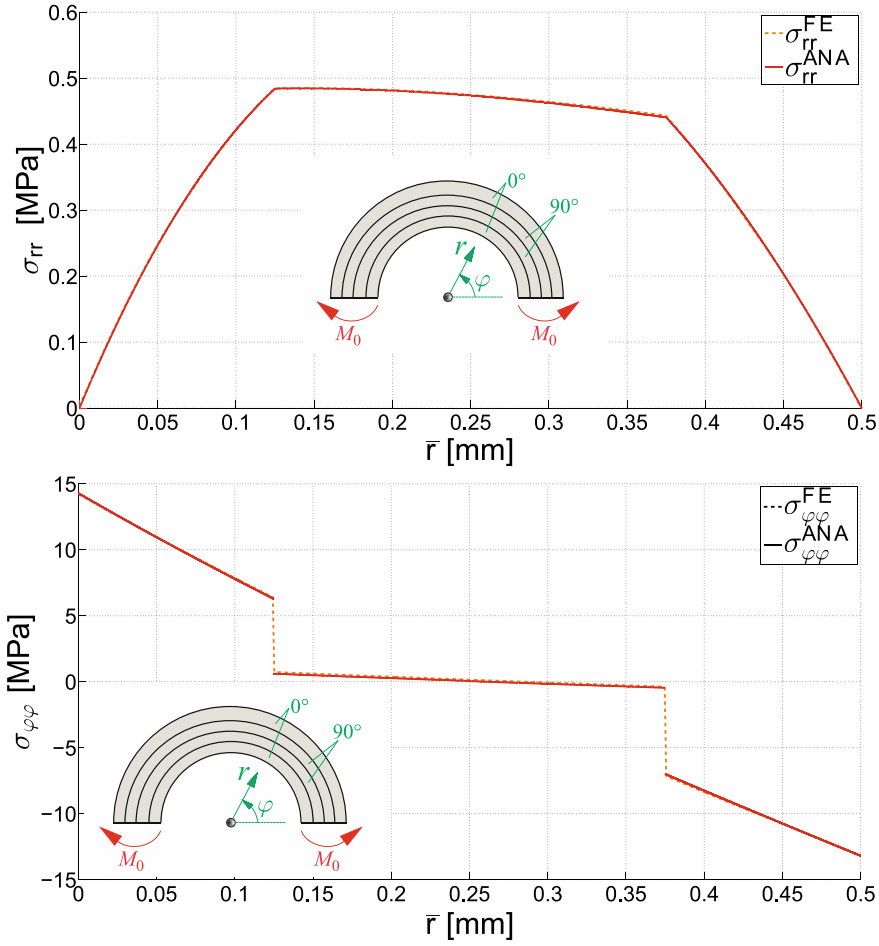


Fig. 22.6 Comparison of the shell solution for the symmetric $[0/90]_S$-laminate with FEM calculations

$$\begin{pmatrix} \varepsilon_{rr} \\ \varepsilon_{\varphi\varphi} \\ \varepsilon_{zz} \\ \gamma_{\varphi z} \\ \gamma_{rz} \\ \gamma_{r\varphi} \end{pmatrix} = \begin{bmatrix} S_{11} & S_{12} & S_{13} & 0 & 0 & 0 \\ S_{12} & S_{22} & S_{23} & 0 & 0 & 0 \\ S_{13} & S_{23} & S_{33} & 0 & 0 & 0 \\ 0 & 0 & 0 & S_{44} & 0 & 0 \\ 0 & 0 & 0 & 0 & S_{55} & 0 \\ 0 & 0 & 0 & 0 & 0 & S_{66} \end{bmatrix} \begin{pmatrix} \sigma_{rr} \\ \sigma_{\varphi\varphi} \\ \sigma_{zz} \\ \tau_{\varphi z} \\ \tau_{rz} \\ \tau_{r\varphi} \end{pmatrix}, \tag{22.33}$$

wherein ε_{rr}, $\varepsilon_{\varphi\varphi}$, ε_{zz}, $\gamma_{\varphi z}$, γ_{rz}, $\gamma_{r\varphi}$ are the strain components. The stress components are denoted as and σ_{rr}, $\sigma_{\varphi\varphi}$, σ_{zz}, $\tau_{\varphi z}$, τ_{rz}, $\tau_{r\varphi}$. The quantities S_{ij} (with $i, j = 1, 2, \ldots, 6$) are

Table 22.1 Material properties

0°-layer			90°-layer		
E_φ	132,000	[MPa]	E_φ	10,800	[MPa]
E_r	10,800	[MPa]	E_r	10,800	[MPa]
E_z	10,800	[MPa]	E_z	132,000	[MPa]
$\nu_{r\varphi}$	0.0195	[–]	$\nu_{r\varphi}$	0.238	[–]
ν_{rz}	0.238	[–]	ν_{rz}	0.0195	[–]
$\nu_{\varphi z}$	0.238	[–]	$\nu_{\varphi z}$	0.0195	[–]
$G_{r\varphi}$	5650	[MPa]	$G_{r\varphi}$	3360	[MPa]
G_{rz}	3360	[MPa]	G_{rz}	5650	[MPa]
$G_{\varphi z}$	5650	[MPa]	$G_{\varphi z}$	5650	[MPa]

the compliances of the orthotropic material under consideration and can be defined by the engineering constants $E_{rr}, E_{\varphi\varphi}, E_{zz}, G_{\varphi z}, G_{rz}, G_{r\varphi}, \nu_{r\varphi}, \nu_{rz}, \nu_{\varphi z}$ as follows:

$$\begin{aligned} S_{11} &= \frac{1}{E_{rr}}, \quad S_{22} = \frac{1}{E_{\varphi\varphi}}, \quad S_{33} = \frac{1}{E_{zz}}, \\ S_{44} &= \frac{1}{G_{\varphi z}}, \quad S_{55} = \frac{1}{G_{rz}}, \quad S_{66} = \frac{1}{G_{r\varphi}}, \\ S_{12} &= -\frac{\nu_{r\varphi}}{E_{rr}}, \quad S_{13} = -\frac{\nu_{rz}}{E_{rr}}, \quad S_{23} = -\frac{\nu_{\varphi z}}{E_{\varphi\varphi}}. \end{aligned} \tag{22.34}$$

The stiffness matrix $\underline{\underline{S}}$ can be determined from the compliance matrix $\underline{\underline{C}}$ by inversion:

$$\underline{\underline{C}} = \underline{\underline{S}}^{-1}. \tag{22.35}$$

The analysis method to be developed here consists of two parts, namely an 'inner' solution and a 'outer' solution. The inner solution aims to describe the state variables inside the shell at a sufficient distance from the shell edge, where we can assume that free-edge effects have completely decayed and no longer influence the stress and strain state. This inner solution corresponds to the solution we have already considered for the layered shell under boundary moments. Since we have to assume a plane strain state in the case of the inner solution, the following representation for the plane strain state follows from the requirement $\varepsilon_{zz} = 0$ in Hooke's law:

$$\begin{pmatrix} \varepsilon_{rr} \\ \varepsilon_{\varphi\varphi} \\ \gamma_{r\varphi} \end{pmatrix} = \begin{bmatrix} R_{11} & R_{12} & 0 \\ R_{12} & R_{22} & 0 \\ 0 & 0 & R_{66} \end{bmatrix} \begin{pmatrix} \sigma_{rr} \\ \sigma_{\varphi\varphi} \\ \tau_{r\varphi} \end{pmatrix}, \tag{22.36}$$

where the quantities R_{op} $(o, p = 1, 2, 6)$ are the so-called reduced compliances, which can be calculated from the compliances S_{ij} $(i, j = 1, 2, \ldots, 6)$ as:

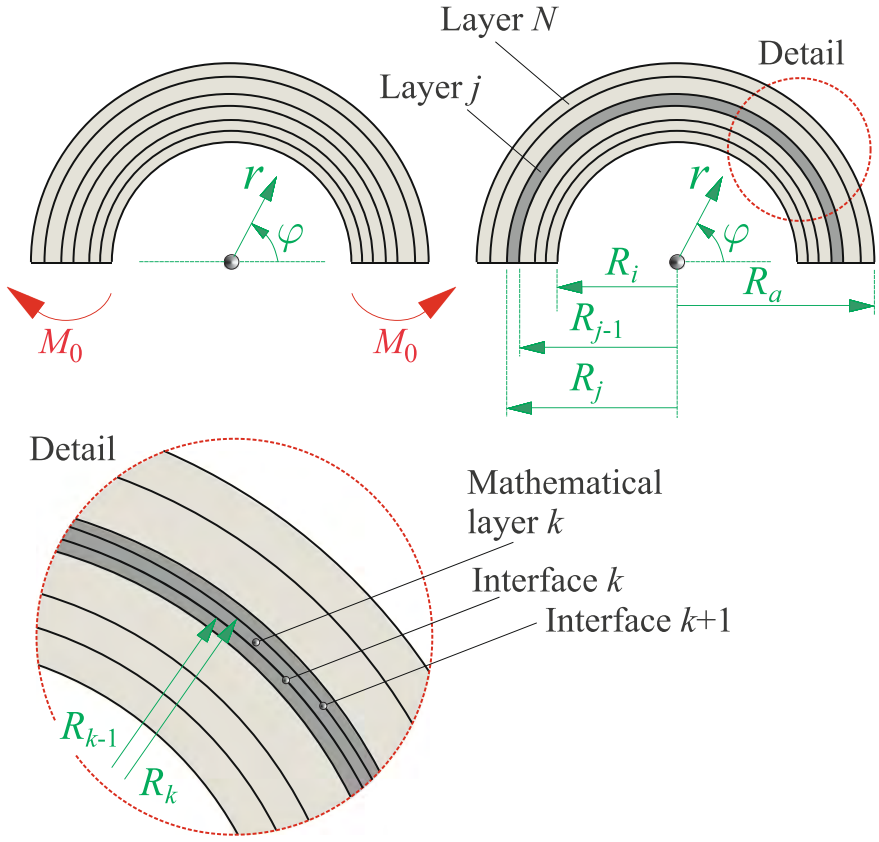


Fig. 22.7 The semi-analytical model

$$R_{ij} = S_{ij} - \frac{S_{i3}S_{j3}}{S_{33}}. \tag{22.37}$$

The following strain field can be calculated from the displacements u, v and w with respect to the reference directions r, φ and z:

$$\varepsilon_{rr} = \frac{\partial u}{\partial r}, \quad \varepsilon_{\varphi\varphi} = \frac{1}{r}\left(\frac{\partial v}{\partial \varphi} + u\right), \quad \varepsilon_{zz} = \frac{\partial w}{\partial z},$$
$$\gamma_{r\varphi} = \frac{1}{r}\left(\frac{\partial u}{\partial \varphi} - v\right) + \frac{\partial v}{\partial r}, \quad \gamma_{rz} = \frac{\partial w}{\partial r} + \frac{\partial u}{\partial z}, \quad \gamma_{\varphi z} = \frac{\partial v}{\partial z} + \frac{1}{r}\frac{\partial w}{\partial \varphi}. \tag{22.38}$$

The aim of the 'outer' solution to be considered now is to extend the state variables of the 'inner' solution in such a way that the typical three-dimensional stress field, which is characteristic of free-edge effects, can be suitably modelled. The solution must therefore be able to describe the strong stress gradients of the edge stress fields and their decay behaviour.

It is important to note that the dependence of the state variables on the z-coordinate is neglected in the inner solution, but this is an important characteristic of the free-edge effects occurring here and will have to be taken into account by the outer solution. The solution now assumes that the N physical layers are each divided into m mathematical layers, within each of which a suitable displacement approach is formulated that has to map the free-edge effects. The mathematical layer k has the thickness h_k and is limited by the radial coordinates R_{k-1} and R_k.

A displacement field is now defined in each mathematical layer as follows:

$$u_{L,k} = U_{0,k}(r, \varphi) + U_{1,k}(r, z), \tag{22.39}$$

$$v_{L,k} = V_{0,k}(r, \varphi) + V_{1,k}(r, z), \tag{22.40}$$

$$w_{L,k} = W_{1,k}(r, z). \tag{22.41}$$

Here, $U_{0,k}$ and $V_{0,k}$ are the displacement functions that result from the inner solution and that can be assumed to be known at this point. They are exclusively functions of r and φ. In order to take into account the actual dependence of the displacement field on z in the boundary region, further as yet unknown displacement functions $U_{1,k}$, $V_{1,k}$ and $W_{1,k}$ are added, which are functions of r and z. These functions are to be determined.

The mathematical form of these additional displacement functions is currently chosen as follows:

$$U_{1,k}(r, z) = U_k(z)\psi_{1,k}(r) + U_{k+1}(z)\psi_{2,k}(r), \tag{22.42}$$

$$V_{1,k}(r, z) = V_k(z)\psi_{1,k}(r) + V_{k+1}(z)\psi_{2,k}(r), \tag{22.43}$$

$$W_{1,k}(r, z) = W_k(z)\psi_{1,k}(r) + W_{k+1}(z)\psi_{2,k}(r), \tag{22.44}$$

with $k = 1, \ldots, n_L = N \cdot m$. The structure of this approach is briefly explained using $U_{1,k}$. This function consists of the two functions $U_k(z)$ and $U_{k+1}(z)$, which depend exclusively on z. They are multiplied by interpolation functions $\psi_{1,k}(r)$ and $\psi_{2,k}(r)$, which only depend on the radial coordinate r. This means that the additional displacement function $U_{1,k}$ consists of two unknown functions $U_k(z)$ and $U_{k+1}(z)$, which are defined in the interfaces of the mathematical layer k and between which linear interpolation is performed using $\psi_{1,k}(r)$ and $\psi_{2,k}(r)$. The other displacement functions $V_{1,k}(r, z)$ and $W_{1,k}(r, z)$ of the inner solution are constructed in the same way.

The following requirements are placed on the shape functions $\psi_{1,k}(r)$ and $\psi_{2,k}(r)$:

$$\psi_{1,k}(r = R_{k-1}) = 1, \quad \psi_{1,k}(r = R_k) = 0, \tag{22.45}$$

$$\psi_{2,k}(r = R_{k-1}) = 0, \quad \psi_{2,k}(r = R_k) = 1. \tag{22.46}$$

The result is then:

$$\psi_{1,k}(r) = \frac{1}{h_k}(R_k - r), \quad \psi_{2,k}(r) = \frac{1}{h_k}(r - R_{k-1}) \tag{22.47}$$

for $k = 1, 2, \ldots, n_L$.

Using the kinematic relationships (22.38), the strain field in each mathematical layer can be determined as follows:

$$\begin{aligned}
\varepsilon_{rr,k} &= \varepsilon^0_{rr,k} + U_k \frac{\partial \psi_{1,k}}{\partial r} + U_{k+1} \frac{\partial \psi_{2,k}}{\partial r}, \\
\varepsilon_{\varphi\varphi,k} &= \varepsilon^0_{\varphi\varphi,k} + \frac{1}{r}\left(U_k \psi_{1,k} + U_{k+1}\psi_{2,k}\right), \\
\varepsilon_{zz,k} &= \frac{\partial W_k}{\partial z}\psi_{1,k} + \frac{\partial W_{k+1}}{\partial z}\psi_{2,k}, \\
\gamma_{r\varphi,k} &= -\frac{1}{r}\left(V_k \psi_{1,k} + V_{k+1}\psi_{2,k}\right) + V_k \frac{\partial \psi_{1,k}}{\partial r} + V_{k+1}\frac{\partial \psi_{2,k}}{\partial r}, \\
\gamma_{rz,k} &= W_k \frac{\partial \psi_{1,k}}{\partial r} + W_{k+1}\frac{\partial \psi_{2,k}}{\partial r} + \frac{\partial U_k}{\partial z}\psi_{1,k} + \frac{\partial U_{k+1}}{\partial z}\psi_{2,k}, \\
\gamma_{\varphi z,k} &= \frac{\partial V_k}{\partial z}\psi_{1,k} + \frac{\partial V_{k+1}}{\partial z}\psi_{2,k}.
\end{aligned} \tag{22.48}$$

Once the layerwise strains are known, the layerwise stress field can also be determined as follows:

$$\begin{pmatrix} \sigma_{rr,k} \\ \sigma_{\varphi\varphi,k} \\ \sigma_{zz,k} \\ \tau_{\varphi z,k} \\ \tau_{rz,k} \\ \tau_{r\varphi,k} \end{pmatrix} = \begin{bmatrix} C_{11,k} & C_{12,k} & C_{13,k} & 0 & 0 & 0 \\ C_{12,k} & C_{22,k} & C_{23,k} & 0 & 0 & 0 \\ C_{13,k} & C_{23,k} & C_{33,k} & 0 & 0 & 0 \\ 0 & 0 & 0 & C_{44,k} & 0 & 0 \\ 0 & 0 & 0 & 0 & C_{55,k} & 0 \\ 0 & 0 & 0 & 0 & 0 & C_{66,k} \end{bmatrix} \begin{pmatrix} \varepsilon_{rr,k} \\ \varepsilon_{\varphi\varphi,k} \\ \varepsilon_{zz,k} \\ \gamma_{\varphi z,k} \\ \gamma_{rz,k} \\ \gamma_{r\varphi,k} \end{pmatrix}. \tag{22.49}$$

The outer solution is now treated using the principle of the minimum of the total elastic potential Π of the cross-ply shell under consideration. The total elastic potential Π consists of the inner potential Π_i and the external potential Π_a, where Π_i results from adding up the contributions of all mathematical layers. The following applies here:

$$\Pi = \overbrace{\frac{1}{2}\sum_{j=1}^{n_L} \int_{V_j} \underline{\varepsilon}_j^T \underbrace{\underline{\underline{C}}_j \underline{\varepsilon}_j}_{\underline{\sigma}_j} \mathrm{d}V^{(j)}}^{\Pi_i} - \underbrace{\frac{1}{2} M \frac{\partial v_j}{\partial r}}_{\Pi_a} = \text{Min.} \tag{22.50}$$

The volume integral in Π_i with respect to V_j of the layer (j) is split into three integrals with respect to z, φ and r:

$$\Pi_i = \frac{1}{2}\sum_{j=1}^{n_L} \int_{R_{j-1}}^{R_j} \int_0^{\psi} \int_0^{\hat{z}} \underline{\varepsilon}_j^T \underline{\underline{C}}_j \underline{\varepsilon}_j \mathrm{d}z \mathrm{d}\varphi \mathrm{d}r. \tag{22.51}$$

Since both the stresses and the strains do not depend on φ in the context of the solution, the corresponding integration can be carried out easily and provides the value φ. In addition, the integrations with respect to r can be performed in an exact-analytical manner due to the simplicity of the shape functions $\psi_{1,k}(r)$ and $\psi_{2,k}(r)$. What ultimately remains is a variation task with regard to those terms that have a dependence on z:

$$\frac{1}{2}\sum_{j=1}^{n_L}\int_0^{\hat{z}} F_j \mathrm{d}z = \text{Min.} \tag{22.52}$$

Here, the integrand F_k with respect to the mathematical layer k is of the following general form:

$$F_k = f\Bigg(z, U_k, U_{k+1}, V_k, V_{k+1}, W_k, W_{k+1}, \frac{\partial U_k}{\partial z}, \frac{\partial U_{k+1}}{\partial z}, \frac{\partial V_k}{\partial z}, \frac{\partial V_{k+1}}{\partial z}, \frac{\partial W_k}{\partial z}, \frac{\partial W_{k+1}}{\partial z}\Bigg). \tag{22.53}$$

The corresponding Euler-Lagrange equations can be given as:

$$\frac{\partial F}{\partial U_k} - \frac{\mathrm{d}}{\mathrm{d}z}\left(\frac{\partial F}{\frac{\partial U_k}{\partial z}}\right) = 0, \tag{22.54}$$

$$\frac{\partial F}{\partial V_k} - \frac{\mathrm{d}}{\mathrm{d}z}\left(\frac{\partial F}{\frac{\partial V_k}{\partial z}}\right) = 0, \tag{22.55}$$

$$\frac{\partial F}{\partial W_k} - \frac{\mathrm{d}}{\mathrm{d}z}\left(\frac{\partial F}{\frac{\partial W_k}{\partial z}}\right) = 0, \tag{22.56}$$

where $F = \sum_{r=1}^{n_L} F_r$. Evaluating the Euler-Lagrange equations results in the following coupled system of differential equations for the unknown displacement functions:

$$\underline{\underline{K}}_1 \frac{\partial^2}{\partial z^2}\underline{U} + \underline{\underline{K}}_2 \frac{\partial}{\partial z}\underline{W} + \underline{\underline{K}}_3 \underline{U} = \underline{R}_1, \tag{22.57}$$

$$\underline{\underline{K}}_4 \frac{\partial^2}{\partial z^2}\underline{V} + \underline{\underline{K}}_5 \underline{V} = \underline{R}_2, \tag{22.58}$$

$$\underline{\underline{K}}_6 \frac{\partial^2}{\partial z^2}\underline{W} + \underline{\underline{K}}_7 \frac{\partial}{\partial z}\underline{U} + \underline{\underline{K}}_8 \underline{W} = \underline{R}_3. \tag{22.59}$$

The coefficient matrices $\underline{\underline{K}}_i$ occurring here have the dimensions $(n_L + 1) \times (n_L + 1)$ and are shown next to the vectors $\underline{R}_i$ on the right-hand side at the end of this chapter. The as yet unknown displacement functions are summarized in the vectors $\underline{U}$, $\underline{V}$ and $\underline{W}$:

$$\underline{U} = \begin{pmatrix} U_1 \\ \vdots \\ U_{n_L+1} \end{pmatrix}, \quad \underline{V} = \begin{pmatrix} V_1 \\ \vdots \\ V_{n_L+1} \end{pmatrix}, \quad \underline{W} = \begin{pmatrix} W_1 \\ \vdots \\ W_{n_L+1} \end{pmatrix}. \tag{22.60}$$

If the vectors $\underline{U}$, $\underline{V}$ and $\underline{W}$ are summarized in the vector $\underline{\hat{U}}$ as follows

$$\underline{\hat{U}} = \begin{pmatrix} \underline{U} \\ \underline{V} \\ \underline{W} \end{pmatrix}, \tag{22.61}$$

then the given system of differential equations can be written in condensed form as:

$$\underbrace{\begin{bmatrix} \underline{\underline{K}}_1 & \underline{\underline{0}} & \underline{\underline{0}} \\ \underline{\underline{0}} & \underline{\underline{K}}_4 & \underline{\underline{0}} \\ \underline{\underline{0}} & \underline{\underline{0}} & \underline{\underline{K}}_6 \end{bmatrix}}_{\underline{\overline{K}}_1} \frac{\partial^2}{\partial z^2}\underline{\hat{U}} + \underbrace{\begin{bmatrix} \underline{\underline{0}} & \underline{\underline{0}} & \underline{\underline{K}}_2 \\ \underline{\underline{0}} & \underline{\underline{0}} & \underline{\underline{0}} \\ \underline{\underline{K}}_7 & \underline{\underline{0}} & \underline{\underline{0}} \end{bmatrix}}_{\underline{\overline{K}}_2} \frac{\partial}{\partial z}\underline{\hat{U}}$$
$$+ \underbrace{\begin{bmatrix} \underline{\underline{K}}_3 & \underline{\underline{0}} & \underline{\underline{0}} \\ \underline{\underline{0}} & \underline{\underline{K}}_5 & \underline{\underline{0}} \\ \underline{\underline{0}} & \underline{\underline{0}} & \underline{\underline{K}}_8 \end{bmatrix}}_{\underline{\overline{K}}_3} \underline{\hat{U}} = \underbrace{\begin{pmatrix} \underline{R}_1 \\ \underline{R}_2 \\ \underline{R}_3 \end{pmatrix}}_{\underline{\overline{R}}}. \tag{22.62}$$

The matrices $\underline{\overline{K}}_i$ have the dimensions $3(n_L + 1) \times 3(n_L + 1)$.

We first solve the homogeneous differential equation system by using the following approach for $\underline{\hat{U}}_{hom}$:

$$\underline{\hat{U}}_{hom} = \underline{A} e^{\lambda z}. \tag{22.63}$$

Inserting into (22.62) results in the exponential functions being cancelled out, and ultimately a quadratic eigenvalue problem for the exponents λ is obtained as follows:

$$\left(\lambda^2 \underline{\overline{K}}_1 + \lambda \underline{\overline{K}}_2 + \underline{\overline{K}}_3\right) \underline{A} = \underline{0}. \tag{22.64}$$

Here, the exponents λ play the role of eigenvalues, whereas $\underline{A}$ represents the corresponding eigenvector. This eigenvalue problem can be solved numerically and leads to $6(n_L + 1)$ eigenvalues, which always appear in pairs with opposite signs. Since we are basically interested in considering only the decaying behaviour of the lower solution, only the $3(n_L + 1)$ eigenvalues with negative signs are considered. However, it can be observed that multiple zero eigenvalues always result, which correspond to rigid body motions. As this result is physically nonsensical, the system of equations (22.62) is slightly modified as follows. Very small numbers Δ_i are subtracted from each coefficient matrix $\underline{\underline{K}}_i$, which are determined as follows:

$$\Delta_{1,k} = \int_{R_{k-2}}^{R_{k-1}} \psi_{1,k-1}\psi_{2,k-1}\mathrm{d}r, \tag{22.65}$$

$$\Delta_{2,k} = \int_{R_{k-2}}^{R_{k-1}} \psi_{1,k-1}\psi_{2,k-1}\mathrm{d}r + \int_{R_{k-1}}^{R_{k}} \psi_{1,k}\psi_{2,k}\mathrm{d}r, \tag{22.66}$$

$$\Delta_{3,k} = \int_{R_{k-1}}^{R_{k}} \psi_{1,k}\psi_{2,k}\mathrm{d}r, \tag{22.67}$$

or in matrix form:

$$\underline{\underline{K}}_{\Delta} = \begin{bmatrix} \Delta_{2,1} & \Delta_{3,1} & 0 & 0 & 0 \\ \Delta_{1,2} & \Delta_{2,2} & \Delta_{3,2} & 0 & 0 \\ \vdots & \vdots & \ddots & \vdots & \vdots \\ 0 & 0 & \Delta_{1,n_L-1} & \Delta_{2,n_L-1} & \Delta_{3,n_L-1} \\ 0 & 0 & 0 & \Delta_{1,n_L} & \Delta_{2,n_L} \end{bmatrix}. \tag{22.68}$$

This matrix $\underline{\underline{K}}_{\Delta}$ is then multiplied by the small factor k_k and subtracted from the coefficient matrix $\overline{\underline{\underline{K}}}_i$:

$$\underline{\underline{K}}_i^{mod} = \underline{\underline{K}}_i - k_k \underline{\underline{K}}_{\Delta}. \tag{22.69}$$

This minor numerical manipulation converts all zero eigenvalues into very small non-zero numbers, which also makes the solution physically meaningful. Parameter studies have shown that a value of $k_k = 10^{-3}$ is already completely sufficient.

The displacement field can ultimately be determined as:

$$\underline{U}_{hom} = \sum_{j=1}^{3(n_L+1)} b_j \underline{A}_j e^{\lambda_j z}, \tag{22.70}$$

where b_j are free constants that are later adapted to the given boundary conditions at the free shell edges.

Furthermore, it is necessary to consider the particular solution of the system of equations (22.62). Since all members in (22.62) are constant terms, a particular solution would also have to consist of constant terms. However, since constant displacement terms mean rigid body translations and rotations, which are nonsensical in the given context, the particular solution is neglected in the following:

$$\underline{\hat{U}}_{part} = \underline{0}. \tag{22.71}$$

The free constants b_j are determined from the boundary conditions at the free shell edges. These are for each layer k:

$$\sigma_{zz,k}(z=0)=0, \quad \tau_{rz,k}(z=0)=0, \quad \tau_{\varphi z,k}(z=0)=0. \tag{22.72}$$

The current free-edge effect solution cannot be adapted exactly to these conditions in a pointwise fashion, so that an integral formulation is used instead:

$$\int_{R_{k-2}}^{R_{k-1}} \sigma_{zz,k-1}(z=0)\psi_{2,k-1}\mathrm{d}r + \int_{R_{k-1}}^{R_k} \sigma_{zz,k}(z=0)\psi_{1,k}\mathrm{d}r = 0, \tag{22.73}$$

$$\int_{R_{k-2}}^{R_{k-1}} \tau_{\varphi z,k-1}(z=0)\psi_{2,k-1}\mathrm{d}r + \int_{R_{k-1}}^{R_k} \tau_{\varphi z,k}(z=0)\psi_{1,k}\mathrm{d}r = 0, \tag{22.74}$$

$$\int_{R_{k-2}}^{R_{k-1}} \tau_{rz,k-1}(z=0)\psi_{2,k-1}\mathrm{d}r + \int_{R_{k-1}}^{R_k} \tau_{rz,k}(z=0)\psi_{1,k}\mathrm{d}r = 0. \tag{22.75}$$

This leads to a total of $3\,(n_L+1)$ conditions for the $3\,(n_L+1)$ constants b_j.

A comparison between the current method and FEM calculations is shown in Fig. 22.8 for the two unsymmetric two-layer cross-ply shells with the layups [0/90] and [90/0] based on the interlaminar normal stress σ_{rr}. There is very satisfactory agreement between the results, although it should be noted that the present method is significantly more computationally efficient than the Finite Element Method. While the developed semi-analytical method delivers results within seconds, the Finite Element Method requires a significantly higher effort, which is in the range of minutes. Overall, the results show the behaviour characteristic of free-edge effects, i.e. the occurrence of steep stress gradients in the edge region and a complete decay with increasing distance from the shell edge until the conditions according to the inner solution are restored at a certain distance from the edge. The results also show that the free-edge effect, depending on the layup, can be both more critical and less harmful than the stress fields in the interior, which must be taken into account when designing such shell structures.

For further results, readers are referred to the original work by Schnabel et al. (2017). In follow-up publications, Kappel and Mittelstedt (2020, 2021, 2022) investigated the influence of higher-order shape functions and mathematical layers of different arrangements and were able to determine a further increase in the efficiency and accuracy of the methodology. In addition, extended load cases were considered.

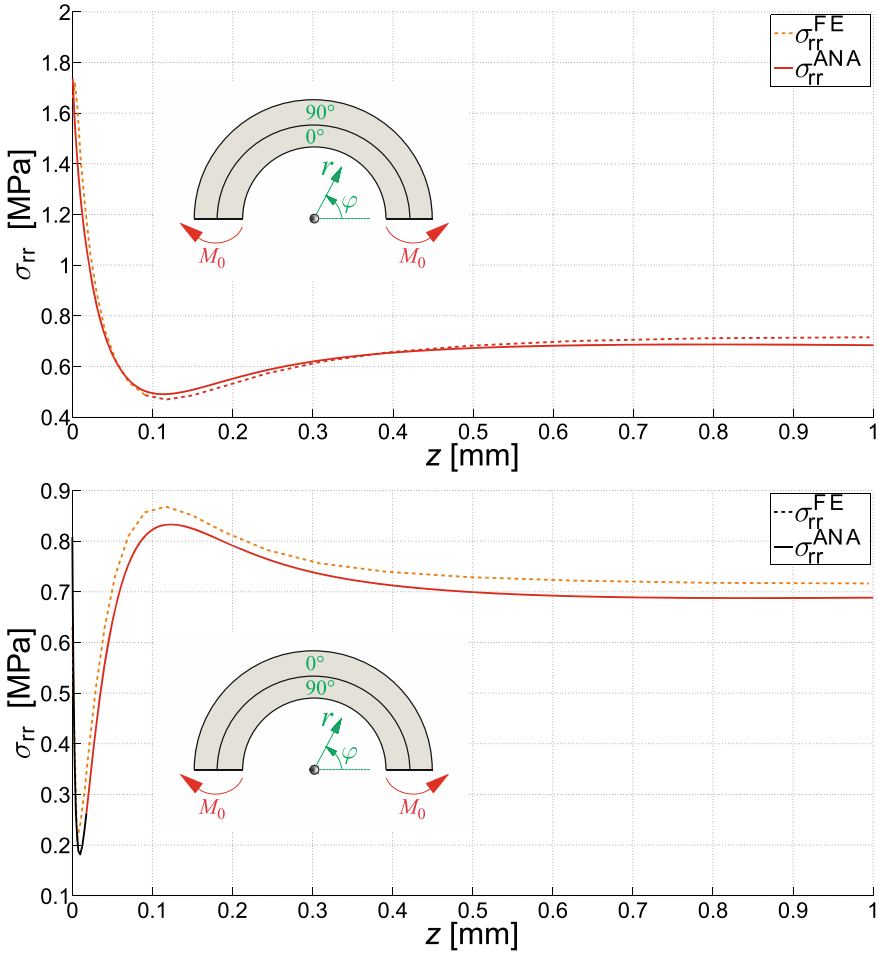


Fig. 22.8 Comparison of the results for the radial normal stress σ_{rr} according to the semi-analytical method and the Finite Element Method for the unsymmetric [0/90]-laminate and the unsymmetric [90/0]-laminate in the interface between the two laminate single layers

22.6 Coefficient Matrices and Perturbation Terms

The matrices $\underline{\underline{K}}_i$ are given as:

$$\underline{\underline{K}}_1 = -\begin{bmatrix} E^{(1)}_{5511} & E^{(1)}_{5512} & 0 & 0 & 0 \\ E^{(1)}_{5512} & E^{(2)}_{5511} + E^{(1)}_{5522} & E^{(2)}_{5512} & 0 & 0 \\ \vdots & \vdots & \ddots & \vdots & \vdots \\ 0 & 0 & E^{(n_L-1)}_{5512} & E^{(n_L)}_{5511} + E^{(n_L-1)}_{5522} & E^{(n_L)}_{5512} \\ 0 & 0 & 0 & E^{(n_L)}_{5512} & E^{(n_L)}_{5522} \end{bmatrix}, \tag{22.76}$$

$$\underline{\underline{K}}_2 = \begin{bmatrix} F^{(1)}_{1311}+H^{(1)}_{2311} & F^{(1)}_{1321}+H^{(1)}_{2312} & 0 & 0 & 0 \\ -F^{(1)}_{5511} & -F^{(1)}_{5512} & & & \\ F^{(1)}_{1312}+H^{(1)}_{2312} & F^{(2)}_{1311}+F^{(1)}_{1322} & F^{(2)}_{1321}+H^{(2)}_{2312} & 0 & 0 \\ -F^{(1)}_{5521} & +H^{(1)}_{2322}+H^{(2)}_{2311} & -F^{(2)}_{5512} & & \\ & -F^{(2)}_{5511}-F^{(1)}_{5522} & & & \\ \vdots & \vdots & \ddots & \vdots & \vdots \\ 0 & 0 & F^{(nL-1)}_{1312}+H^{(n_L-1)}_{2312} & F^{(n_L)}_{1311}+F^{(n_L-1)}_{1322} & F^{(n_L)}_{1321}+H^{(n_L)}_{2312} \\ & & -F^{(n_L-1)}_{5521} & +H^{(n_L-1)}_{2322}+H^{(n_L)}_{2311} & -F^{(n_L)}_{5512} \\ & & & -F^{(n_L-1)}_{5522}-F^{(n_L)}_{5511} & \\ 0 & 0 & 0 & F^{(n_L)}_{1312}+H^{(n_L)}_{2312} & F^{(n_L)}_{1322}+H^{(n_L)}_{2322} \\ & & & -F^{(n_L)}_{5521} & -F^{(n_L)}_{5522} \end{bmatrix}, \tag{22.77}$$

$$\underline{\underline{K}}_3 = \begin{bmatrix} 2I^{(1)}_{1211}+G^{(1)}_{1111} & G^{(1)}_{1112}+I^{(1)}_{1221} & 0 & 0 & 0 \\ +J^{(1)}_{2211} & +I^{(1)}_{1212}+J^{(1)}_{2212} & & & \\ G^{(1)}_{1112}+I^{(1)}_{1221} & 2I^{(2)}_{1211}+2I^{(1)}_{1222} & G^{(2)}_{1112}+I^{(2)}_{1221} & 0 & 0 \\ +I^{(1)}_{1212}+J^{(1)}_{2212} & +G^{(1)}_{1122}+G^{(2)}_{1111} & +I^{(2)}_{1212}+J^{(2)}_{2212} & & \\ & +J^{(1)}_{2222}+J^{(2)}_{2211} & & & \\ \vdots & \vdots & \ddots & \vdots & \vdots \\ 0 & 0 & G^{(n_L-1)}_{1112}+I^{(n_L-1)}_{1221} & 2I^{(n_L-1)}_{1222}+2I^{(n_L)}_{1211} & G^{(n_L)}_{1112}+I^{(n_L)}_{1221} \\ & & +I^{(n_L-1)}_{1212}+J^{(n_L-1)}_{2212} & +G^{(n_L)}_{1111}+G^{(n_L-1)}_{1122} & +I^{(n_L)}_{1212}+J^{(n_L)}_{2212} \\ & & & +J^{(n_L)}_{2211}+J^{(n_L-1)}_{2222} & \\ 0 & 0 & 0 & G^{(n_L)+}_{1112}I^{(n_L)}_{1221} & 2I^{(n_L)}_{1222}+G^{(n_L)}_{1122} \\ & & & +I^{(n_L)}_{1212}+J^{(n_L)}_{2212} & +J^{(n_L)}_{2222} \end{bmatrix}, \tag{22.78}$$

$$\underline{\underline{K}}_4 = -\begin{bmatrix} E^{(1)}_{4411} & E^{(1)}_{4412} & 0 & 0 & 0 \\ E^{(1)}_{4412} & E^{(2)}_{4411}+E^{(1)}_{4422} & E^{(2)}_{4412} & 0 & 0 \\ \vdots & \vdots & \ddots & \vdots & \vdots \\ 0 & 0 & E^{(n_L-1)}_{4412} & E^{(n_L)}_{4411}+E^{(n_L-1)}_{4422} & E^{(n_L)}_{4412} \\ 0 & 0 & 0 & E^{(n_L)}_{4412} & E^{(n_L)}_{4422} \end{bmatrix}, \tag{22.79}$$

$$\underline{\underline{K}}_5 = \begin{bmatrix} G_{6611}^{(1)} - 2I_{6611}^{(1)} & J_{6612}^{(1)} - I_{6612}^{(1)} & 0 & 0 & 0 \\ J_{6611}^{(1)} & G_{6612}^{(1)} - I_{6621}^{(1)} & & & \\ J_{6612}^{(1)} - I_{6612}^{(1)} & G_{6611}^{(2)} + G_{6622}^{(1)} & J_{6612}^{(2)} - I_{6612}^{(2)} & 0 & 0 \\ +G_{6612}^{(1)} - I_{6621}^{(1)} & -2I_{6622}^{(1)} - 2I_{6611}^{(2)} & +G_{6612}^{(2)} - I_{6621}^{(2)} & & \\ & +J_{6611}^{(2)} + J_{6622}^{(1)} & & & \\ \vdots & \vdots & \ddots & \vdots & \vdots \\ 0 & 0 & J_{6612}^{(n_L-1)} - I_{6612}^{(n_L-1)} & G_{6611}^{(n_L)} + G_{6622}^{(n_L-1)} & J_{6612}^{(n_L)} - I_{6612}^{(n_L)} \\ & & +G_{6612}^{(n_L-1)} - I_{6621}^{(n_L-1)} & -2I_{6622}^{(nL-1)} - 2I_{6611}^{(n_L)} & +G_{6612}^{(n_L)} - I_{6621}^{(n_L)} \\ & & & J_{6611}^{(n_L)} + J_{6622}^{(n_L-1)} & \\ 0 & 0 & 0 & J_{6612}^{(n_L)} - I_{6612}^{(n_L)} & G_{6622}^{(n_L)} - 2I_{6622}^{(n_L)} \\ & & & +G_{6612}^{(n_L)} - I_{6621}^{(n_L)} & +J_{6622}^{(n_L)} \end{bmatrix}, \tag{22.80}$$

$$\underline{\underline{K}}_6 = -\begin{bmatrix} E_{3311}^{(1)} & E_{3312}^{(1)} & 0 & 0 & 0 \\ E_{3312}^{(1)} & E_{3311}^{(2)} + E_{3322}^{(1)} & E_{3312}^{(2)} & 0 & 0 \\ \vdots & \vdots & \ddots & \vdots & \vdots \\ 0 & 0 & E_{3312}^{(n_L-1)} & E_{3311}^{(n_L)} + E_{3322}^{(n_L-1)} & E_{3312}^{(n_L)} \\ 0 & 0 & 0 & E_{3312}^{(n_L)} & E_{3322}^{(n_L)} \end{bmatrix}, \tag{22.81}$$

$$\underline{\underline{K}}_7 = \begin{bmatrix} -H_{2311}^{(1)} - F_{1311}^{(1)} & -H_{2312}^{(1)} - F_{1312}^{(1)} & 0 & 0 & 0 \\ +F_{5511}^{(1)} & +F_{5521}^{(1)} & & & \\ -H_{2312}^{(1)} - F_{1321}^{(1)} & -H_{2311}^{(2)} - H_{2322}^{(1)} & -H_{2312}^{(2)} - F_{1312}^{(2)} & 0 & 0 \\ +F_{5512}^{(1)} & -F_{1311}^{(2)} - F_{1322}^{(1)} & +F_{5521}^{(2)} & & \\ & +F_{5511}^{(2)} + F_{5522}^{(1)} & & & \\ \vdots & \vdots & \ddots & \vdots & \vdots \\ 0 & 0 & -H_{2312}^{(n_L-1)} - F_{1321}^{(n_L-1)} & -H_{2311}^{(n_L)} - H_{2322}^{(n_L-1)} & -H_{2312}^{(n_L)} - F_{1312}^{(n_L)} \\ & & +F_{5512}^{(n_L-1)} & -F_{1311}^{(nL)} - F_{1322}^{(n_L-1)} & +F_{5521}^{(n_L)} \\ & & & +F_{5511}^{(n_L)} - F_{5522}^{(n_L-1)} & \\ 0 & 0 & 0 & -H_{2312}^{(n_L)} - F_{1321}^{(n_L)} & -H_{2322}^{(n_L)} - F_{1322}^{(n_L)} \\ & & & +F_{5512}^{(n_L)} & +F_{5522}^{(n_L)} \end{bmatrix}, \tag{22.82}$$

$$\underline{\underline{K}}_8 = \begin{bmatrix} G_{5511}^{(1)} & G_{5512}^{(1)} & 0 & 0 & 0 \\ G_{5512}^{(1)} & G_{5511}^{(2)} + G_{5522}^{(1)} & G_{5512}^{(2)} & 0 & 0 \\ \vdots & \vdots & \ddots & \vdots & \vdots \\ 0 & 0 & G_{5512}^{(n_L-1)} & G_{5511}^{(n_L)} + G_{5522}^{(n_L-1)} & G_{5512}^{(n_L)} \\ 0 & 0 & 0 & G_{5512}^{(n_L)} & G_{5522}^{(n_L)} \end{bmatrix}. \tag{22.83}$$

The following abbreviations were used:

$$C_{opij\gamma}^{(k)} = \int_{R_{k-1}}^{R_k} C_{op,k} \varepsilon_{ij,k}^0 \frac{\partial \psi_{\gamma,k}}{\partial r} \mathrm{d}r, \qquad D_{opij\gamma}^{(k)} = \int_{R_{k-1}}^{R_k} C_{op,k} \varepsilon_{ij,k}^0 \frac{\psi_{\gamma,k}}{r} \mathrm{d}r,$$

$$E_{op\gamma\delta}^{(k)} = \int_{R_{k-1}}^{R_k} C_{op,k} \psi_{\gamma,k} \psi_{\delta,k} \mathrm{d}r, \qquad F_{op\gamma\delta}^{(k)} = \int_{R_{k-1}}^{R_k} C_{op,k} \psi_{\gamma,k} \frac{\partial \psi_{\delta,k}}{\partial r} \mathrm{d}r,$$

$$G_{op\gamma\delta}^{(k)} = \int_{R_{k-1}}^{R_k} C_{op,k} \frac{\partial \psi_{\gamma,k}}{\mathrm{d}r} \frac{\partial \psi_{\delta,k}}{\mathrm{d}r} \mathrm{d}r, \qquad H_{op\gamma\delta}^{(k)} = \int_{R_{k-1}}^{R_k} C_{op,k} \frac{\psi_{\gamma,k} \psi_{\delta,k}}{r} \mathrm{d}r,$$

$$I_{op\gamma\delta}^{(k)} = \int_{R_{k-1}}^{R_k} C_{op,k} \frac{\psi_{\gamma,k} \frac{\partial \psi_{\delta,k}}{\partial r}}{r} \mathrm{d}r, \qquad J_{op\gamma\delta}^{(k)} = \int_{R_{k-1}}^{R_k} C_{op,k} \frac{\psi_{\gamma,k} \psi_{\delta,k}}{r^2} \mathrm{d}r. \tag{22.84}$$

The perturbation terms R_1, R_2, R_3 can be specified as:

$$\underline{R}_1 = \begin{bmatrix} C_{12221}^{(1)} + C_{11111}^{(1)} + D_{12111}^{(1)} + D_{22221}^{(1)} \\ C_{12221}^{(2)} + C_{11111}^{(2)} + D_{12111}^{(2)} + D_{22221}^{(2)} \\ + C_{11112}^{(1)} + C_{12222}^{(1)} + D_{12112}^{(1)} + D_{22222}^{(1)} \\ \vdots \\ C_{12221}^{(n_L)} + C_{11111}^{(n_L)} + D_{12111}^{(n_L)} + D_{22221}^{(n_L)} \\ + C_{11112}^{(n_L-1)} + C_{12222}^{(n_L-1)} + D_{12112}^{(n_L-1)} + D_{22222}^{(n_L-1)} \\ C_{11112}^{(n_L)} + C_{12222}^{(n_L)} + D_{12112}^{(n_L)} + D_{22222}^{(n_L)} \end{bmatrix}, \quad \underline{R}_2 = \underline{0}, \quad \underline{R}_3 = \underline{0}. \tag{22.85}$$

References

Altenbach H, Altenbach J, Naumenko K (1998): *Ebene Flächentragwerke*, Springer, Berlin et al., Germany.

Blumer H (1979): *Spannungsberechnungen an anisotropen Kreisbogenscheiben und Sattelträgern konstanter Dicke*, Technischer Bericht, Technische Universität Karlsruhe, Karlsruhe, Germany.

Charrier JS, Laurin F, Carrere N, Mahdi S (2016): *Determination of the out-of-plane tensile strength using four-point bending tests on laminated L-angle specimens with different stacking sequences and total thicknesses*, Composites Part A 81A:243–253.

Girkmann K (1974): *Flächentragwerke*, 6th edition, Springer Verlag, Wien et al., Austria.

Gözlüklü B, Coker D (2012): *Modeling of the dynamic delamination of L-shaped unidirectional laminated composites*, Composite Structures 94:1430–1442.

Ju H, Nguyen KH, Chae SS, Kweon JH (2017): *Delamination strength of composite curved beams reinforced by grooved stainless-steel Z-pins*, Composite Structures 180:497–506.

Kappel A, Dillen S, Mittelstedt C (2022): *Hygrothermomechanical analysis of the free-edge stress fields in circular cylindrical cross-ply laminated shells*, Mechanics of Advanced Materials and Structures, https://doi.org/10.1080/15376494.2021.2022256.

Kappel A, Mittelstedt C (2020): *Free-edge stress fields in cylindrically curved cross-ply laminated shells*, Composites Part B 183:107693.

Kappel A, Mittelstedt C (2021): *Interlaminar stress fields in circular cylindrical cross-ply laminated shells subjected to transverse loads*, International Journal of Solids and Structures 228:111096.

Ko WL, Jackson RH (1989): *Multilayer theory for delamination analysis of a compsite curved bar subjected to end forces and end moments*, Technical Memorandum No. 4139, NASA Research Center, Edwards, CA, USA.

Lekhnitskii SG (1968): *Anisotropic plates*, Gordon and Breach, New York et al., USA.

Mittelstedt C (2021): *Structural mechanics in lightweight engineering*, Springer Nature, Cham, Switzerland.

Mittelstedt C (2023): *Theory of plates and shells*, Springer Vieweg, Berlin, Germany.

Most J, Stegmair D, Petry D (2015): *Error estimation between simple, closed-form analytical formulae and full-scale FEM for interlaminar stress prediction in curved laminates*, Composite Structures 131:72–81.

Schnabel JE, Yousfi M, Mittelstedt C (2017): *Free-edge stress fields in cylindrically curved symmetric and unsymmetric cross-ply laminates under bending*, Composite Structures 180:862–875.

Tolf G (1983): *Stresses in a curved laminated beam*, Fibre Science and Technology 19:243–267.

Zimmermann K, Zenkert D, Siemetzki M (2010): *Testing and analysis of ultra thick composites*, Composites Part B 41:326–336.

Part V
Laminated Beams



Laminate and Sandwich Beams

23

This chapter deals with the fundamentals for the analytical and numerical treatment of laminated and sandwich beams. Both Classical Laminated Plate Theory (CLPT) and First-Order Shear Deformation Theory (FSDT) are treated and all necessary equations are provided for the analytical treatment of such laminated beams. In addition, beams in sandwich construction are considered and the basis for analytical treatment is also presented for this case. The chapter concludes with the consideration of finite elements for laminated rods as well as for beams within the framework of CLPT and FSDT.

23.1 Classical Laminated Plate Theory

A laminated beam (Fig. 23.1) is a linear structural element that consists of an arbitrary number N of individual layers. Each individual layer can have an arbitrary thickness and arbitrary linear elastic properties. In this section, we specialize the previous explanations of CLPT to layered beams. We consider a laminate consisting of N layers (Fig. 23.2). Layer k has the elastic modulus E_k, the interface coordinates are z_{k-1} and z_k. The laminated beam has a constant width b and thickness h and is subsequently treated in the context of CLPT (see Altenbach et al. (2018), Ambartsumyan (1970), Ashton and Whitney (1970), Becker and Gross (2002), Jones (1975), Lekhnitskii (1968), Reddy (2004) and the explanations in Chap. 7). Uniaxial bending in the xz-plane with normal force is considered. The coordinate origin is located in the laminate middle plane. The displacement u_P of an arbitrary point P at z_P in the x-direction follows as (cf. (7.14)):

$$u_P = u - z_P w'. \tag{23.1}$$

© The Author(s), under exclusive license to Springer-Verlag GmbH, DE, part of Springer Nature 2025

C. Mittelstedt, *Mechanics of Composite Structures*,
https://doi.org/10.1007/978-3-662-70788-3_23

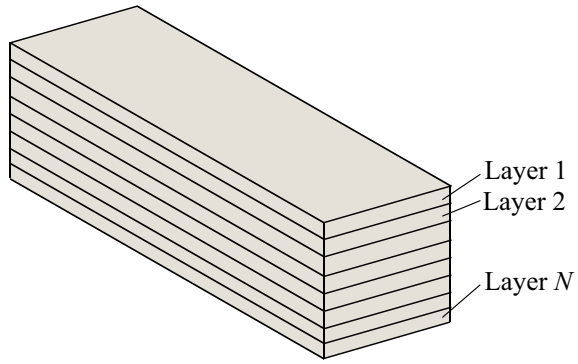


Fig. 23.1 Laminated beam

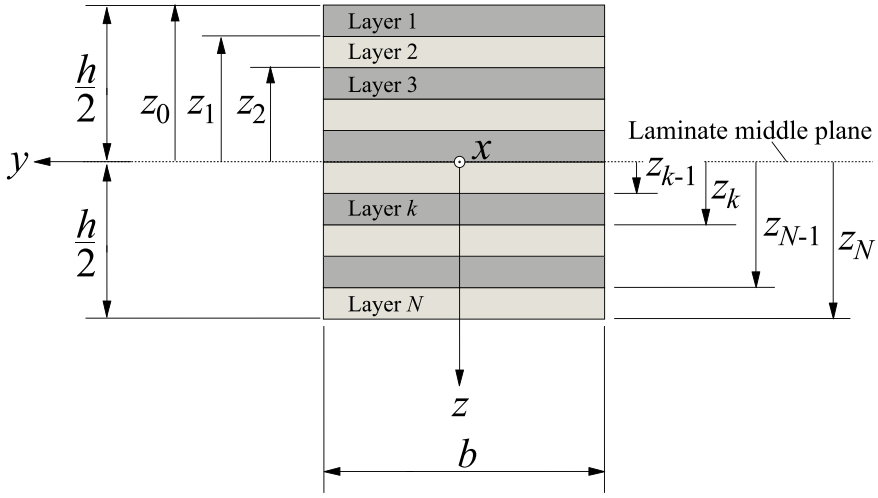


Fig. 23.2 Nomenclature for the laminated beam

The deflection w_P follows analogously to (7.11):

$$w_P = w. \tag{23.2}$$

For better readability, we drop the index P from here on. The longitudinal strain ε_{xx} results as:

$$\varepsilon_{xx} = u' - zw''. \tag{23.3}$$

In the layer k, the normal stress $\sigma_{xx,k}$ follows as:

$$\sigma_{xx,k} = E_k \varepsilon_{xx} = E_k \left(u' - z w'' \right). \tag{23.4}$$

The following normal force and bending moment are present in the laminated beam under consideration:

$$N = \int_A \sigma_{xx} \mathrm{d}A, \quad M_y = \int_A \sigma_{xx} z \mathrm{d}A. \tag{23.5}$$

Firstly, we consider the normal force N. The integration prescribed in (23.5) is divided into N partial integrals:

$$N = \sum_{k=1}^{N} \int_{A_k} \sigma_{xx,k} \mathrm{d}A_k. \tag{23.6}$$

With $\mathrm{d}A_k = b \mathrm{d}z$ it follows:

$$N = b \sum_{k=1}^{N} \int_{z_{k-1}}^{z_k} \sigma_{xx,k} \mathrm{d}z. \tag{23.7}$$

With (23.4) this results in:

$$N = b \sum_{k=1}^{N} E_k \int_{z_{k-1}}^{z_k} \left(u' - z w'' \right) \mathrm{d}z, \tag{23.8}$$

or

$$N = b \sum_{k=1}^{N} E_k \left(z_k - z_{k-1} \right) u' - \frac{b}{2} \sum_{k=1}^{N} E_k \left(z_k^2 - z_{k-1}^2 \right) w''. \tag{23.9}$$

Introduction of the following stiffnesses

$$\begin{aligned} \bar{A}_{11} &= b \sum_{k=1}^{N} E_k \left(z_k - z_{k-1} \right), \\ \bar{B}_{11} &= \frac{b}{2} \sum_{k=1}^{N} E_k \left(z_k^2 - z_{k-1}^2 \right) \end{aligned} \tag{23.10}$$

then provides the following expression for the normal force N:

$$N = \bar{A}_{11} u' - \bar{B}_{11} w''. \tag{23.11}$$

Similarly, the following expression can be derived for the bending moment M_y:

$$M_y = \bar{B}_{11} u' - \bar{D}_{11} w'', \tag{23.12}$$

wherein:

$$\bar{D}_{11} = \frac{b}{3} \sum_{k=1}^{N} E_k \left(z_k^3 - z_{k-1}^3 \right). \tag{23.13}$$

The constitutive law for the laminated beam is then summarised in vector-matrix-notation:

$$\begin{pmatrix} N \\ M_y \end{pmatrix} = \begin{bmatrix} \bar{A}_{11} & \bar{B}_{11} \\ \bar{B}_{11} & \bar{D}_{11} \end{bmatrix} \begin{pmatrix} u' \\ -w'' \end{pmatrix}. \tag{23.14}$$

The stiffnesses $\bar{A}_{11}$, $\bar{B}_{11}$, $\bar{D}_{11}$ are referred to as extensional stiffness, Coupling stiffness and flexural stiffness of the laminated beam. As already discussed for laminates in the context of CLPT, the constitutive law (23.14) shows that an arbitrary laminate structure leads to a coupling of the extensional and the bending load-bearing effect due to the coupling stiffness $\bar{B}_{11}$. Thus, the longitudinal strain u' and the curvature w'' generally lead to the occurrence of a normal force N and a bending moment M_y. At this point, one speaks of the so-called coupling effects, here specifically in the form of the so-called bending-extension coupling. The corresponding stiffness parameter $\bar{B}_{11}$ disappears in the case of symmetric layups, as can easily be concluded from (23.10).

The equilibrium conditions of the laminated beam result from (Mittelstedt 2021):

$$N' = -n, \quad Q_z' = -q_z, \quad M_y' = Q_z, \tag{23.15}$$

whereby in the following we consider the case that no longitudinal line load n occurs. With the help of the constitutive law (23.14) follows:

$$\begin{aligned} \left(\bar{A}_{11} u'\right)' - \left(\bar{B}_{11} w''\right)' &= 0, \\ \left(\bar{B}_{11} u'\right)' - \left(\bar{D}_{11} w''\right)' &= Q_z, \\ \left(\bar{B}_{11} u'\right)'' - \left(\bar{D}_{11} w''\right)'' &= -q_z. \end{aligned} \tag{23.16}$$

If we consider a prismatic beam whose properties are invariable along the longitudinal axis, then the following results:

$$\begin{aligned} \bar{A}_{11} u'' - \bar{B}_{11} w''' &= 0, \\ \bar{B}_{11} u'' - \bar{D}_{11} w''' &= Q_z, \\ \bar{B}_{11} u''' - \bar{D}_{11} w'''' &= -q_z. \end{aligned} \tag{23.17}$$

In the following, we want to determine an expression for the normal stress $\sigma_{xx,k}$ in layer k. If we invert the constitutive law (23.14), the result is

$$u' = \frac{\bar{D}_{11}}{\bar{A}_{11}\bar{D}_{11} - \bar{B}_{11}^2} N - \frac{\bar{B}_{11}}{\bar{A}_{11}\bar{D}_{11} - \bar{B}_{11}^2} M_y,$$
$$w'' = \frac{\bar{B}_{11}}{\bar{A}_{11}\bar{D}_{11} - \bar{B}_{11}^2} N - \frac{\bar{A}_{11}}{\bar{A}_{11}\bar{D}_{11} - \bar{B}_{11}^2} M_y, \tag{23.18}$$

or in vector-matrix-notation:

$$\begin{pmatrix} u' \\ -w'' \end{pmatrix} = \frac{1}{\bar{A}_{11}\bar{D}_{11} - \bar{B}_{11}^2} \begin{bmatrix} \bar{D}_{11} & -\bar{B}_{11} \\ -\bar{B}_{11} & \bar{A}_{11} \end{bmatrix} \begin{pmatrix} N \\ M_y \end{pmatrix}. \tag{23.19}$$

We then obtain the normal stress $\sigma_{xx,k}$ in layer k from (23.4) by inserting the corresponding expressions (23.18) for u' and w'':

$$\sigma_{xx,k} = \frac{E_k}{\bar{A}_{11}\bar{D}_{11} - \bar{B}_{11}^2} \left[\bar{D}_{11} N - \bar{B}_{11} M_y + z \left(\bar{A}_{11} M_y - \bar{B}_{11} N\right)\right]. \tag{23.20}$$

For the symmetric laminate follows:

$$\sigma_{xx,k} = E_k \left(\frac{N}{\bar{A}_{11}} + \frac{M_y}{\bar{D}_{11}} z\right). \tag{23.21}$$

If the special case of the homogeneous beam with rectangular cross-section (width b, height h) is given, then $\bar{A}_{11} = EA$ and $\bar{D}_{11} = EI_{yy}$:

$$\sigma_{xx} = \frac{N}{A} + \frac{M_y}{I_{yy}} z. \tag{23.22}$$

This corresponds to the classic beam formulation of uniaxial bending with normal force (Mittelstedt 2021).

The transverse shear stresses τ_{xz} can be obtained by analyzing the equilibrium of the forces on an infinitesimal section element. For this purpose, we consider the infinitesimal section element of Fig. 23.3, in which an element of length $\mathrm{d}x$ is shown, which is cut free in the interface between layer $k-1$ and k. The shear stress $\tau_{xz,k}$ of layer k occurs at this element. The balance of forces in the x-direction yields:

$$\tau_{xz,k}\mathrm{d}x + \sum_{i=1}^{k-1} \int_{z_{i-1}}^{z_i} \left[\left(\sigma_{xx,i} + \frac{\mathrm{d}\sigma_{xx,i}}{\mathrm{d}x}\mathrm{d}x\right) - \sigma_{xx,i}\right] \mathrm{d}z = 0. \tag{23.23}$$

This expression can be solved for the shear stress $\tau_{xz,k}$:

$$\tau_{xz,k} = -\sum_{i=1}^{k-1} \int_{z_{i-1}}^{z_i} \frac{\mathrm{d}\sigma_{xx,i}}{\mathrm{d}x}\mathrm{d}z. \tag{23.24}$$

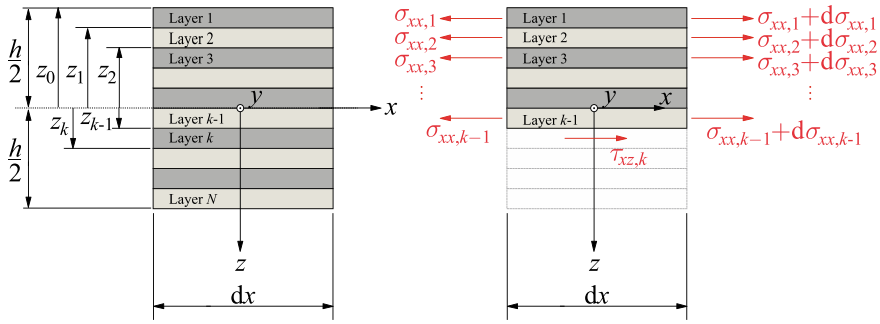


Fig. 23.3 Determination of the shear stress $\tau_{xz,k}$

If the special case of a symmetric laminated beam with $\bar{B}_{11} = 0$ is given, for $n = 0$ we then obtain taking $M_y' = Q_z$ into account:

$$\frac{\mathrm{d}\sigma_{xx,i}}{\mathrm{d}x} = \frac{E_i}{\bar{D}_{11}} z Q_z. \tag{23.25}$$

Hence:

$$\tau_{xz,k} = -\sum_{i=1}^{k-1} \int_{z_{i-1}}^{z_i} \frac{E_i}{\bar{D}_{11}} z Q_z \mathrm{d}z = -\frac{Q_z}{\bar{D}_{11}} \sum_{i=1}^{k-1} E_i \int_{z_{i-1}}^{z_i} z \mathrm{d}z = -\frac{Q_z}{2\bar{D}_{11}} \sum_{i=1}^{k-1} E_i \left(z_i^2 - z_{i-1}^2\right). \tag{23.26}$$

If we again consider the homogeneous beam cross-section with $\bar{D}_{11} = EI_{yy}$, then for the rectangular cross-section with width b and height h follows:

$$\tau_{xz} = \frac{3Q_z}{2bh}\left[1 - 4\left(\frac{z}{h}\right)^2\right]. \tag{23.27}$$

We also want to deal with the deformation behaviour of a laminated beam and consider the differential equations (23.17). Deriving the first equation in (23.17) with respect to x results in

$$\bar{A}_{11} u''' - \bar{B}_{11} w'''' = 0, \tag{23.28}$$

or

$$u''' = \frac{\bar{B}_{11}}{\bar{A}_{11}} w''''. \tag{23.29}$$

If we insert this expression into the second equation in (23.17), the result is as follows:

$$\left(\bar{D}_{11} - \frac{\bar{B}_{11}^2}{\bar{A}_{11}}\right) w'''' = q_z, \tag{23.30}$$

or with the abbreviation $\hat{D}_{11} = \bar{D}_{11} - \frac{\bar{B}_{11}^2}{\bar{A}_{11}}$:

$$\hat{D}_{11} w'''' = q_z. \tag{23.31}$$

The deflection w can be determined from this expression by quadruple integration:

$$\begin{aligned}
\hat{D}_{11} w'''' &= q_z, \\
\hat{D}_{11} w''' &= -Q_z = \int q_z \mathrm{d}x + C_1, \\
\hat{D}_{11} w'' &= -M_y = \int\int q_z \mathrm{d}x\mathrm{d}x + C_1 x + C_2, \\
\hat{D}_{11} w' &= \int\int\int q_z \mathrm{d}x\mathrm{d}x\mathrm{d}x + \frac{1}{2} C_1 x^2 + C_2 x + C_3, \\
\hat{D}_{11} w &= \int\int\int\int q_z \mathrm{d}x\mathrm{d}x\mathrm{d}x\mathrm{d}x + \frac{1}{6} C_1 x^3 + \frac{1}{2} C_2 x^2 + C_3 x + C_4.
\end{aligned} \tag{23.32}$$

The integration constants C_1, C_2, C_3, C_4 are adapted to the given boundary conditions. The longitudinal displacement u can be determined in a post calculation from (23.29).

In the following, we determine the strain energy Π_i of a laminated beam. The following applies in general:

$$\Pi_i = \frac{1}{2} \int_V \sigma_{xx} \varepsilon_{xx} \mathrm{d}V. \tag{23.33}$$

We decompose the volume integral into an area integral and an integral with respect to the longitudinal axis:

$$\Pi_i = \frac{1}{2} \int_A \int_0^l \sigma_{xx} \varepsilon_{xx} \mathrm{d}x\mathrm{d}A. \tag{23.34}$$

With $\mathrm{d}A = b\mathrm{d}z$ this results in:

$$\Pi_i = \frac{b}{2} \int_{-\frac{h}{2}}^{+\frac{h}{2}} \int_0^l \sigma_{xx} \varepsilon_{xx} \mathrm{d}x\mathrm{d}z. \tag{23.35}$$

The normal stress is not a continuous function of z, so that the integration with regard to the thickness coordinate z must be carried out layer by layer:

$$\Pi_i = \frac{b}{2} \int_0^l \sum_{k=1}^N \int_{z_{k-1}}^{z_k} \sigma_{xx,k} \varepsilon_{xx,k} \mathrm{d}z \mathrm{d}x. \tag{23.36}$$

We express the normal stress $\sigma_{xx,k}$ by the strain $\varepsilon_{xx,k}$:

$$\Pi_i = \frac{b}{2} \int_0^l \sum_{k=1}^N E_k \int_{z_{k-1}}^{z_k} \varepsilon_{xx,k}^2 \mathrm{d}z \mathrm{d}x = \frac{b}{2} \int_0^l \sum_{k=1}^N E_k \int_{z_{k-1}}^{z_k} \left(u' - z w''\right)^2 \mathrm{d}z \mathrm{d}x. \tag{23.37}$$

After a brief transformation, this leads to the following expression for the inner potential Π_i:

$$\Pi_i = \frac{1}{2} \bar{A}_{11} \int_0^l \left(u'\right)^2 \mathrm{d}x - \bar{B}_{11} \int_0^l u' w'' \mathrm{d}x + \frac{1}{2} \bar{D}_{11} \int_0^l \left(w''\right)^2 \mathrm{d}x. \tag{23.38}$$

The principle of the minimum of the total elastic potential $\delta \Pi = 0$ can be used to derive both the governing differential equations and all potential combinations of boundary conditions. With the requirement $\delta \Pi = \delta \left(\Pi_i + \Pi_a\right) = 0$, the following results with

$$\Pi_a = - \int_0^l q w \mathrm{d}x \tag{23.39}$$

for the case of an arbitrary but continuously distributed line load $q_z = q_z(x)$:

$$\begin{aligned} &\int_0^l \left(-\bar{A}_{11} u'' + \bar{B}_{11} w'''\right) \delta u \mathrm{d}x + \int_0^l \left(-\bar{B}_{11} u''' + \bar{D}_{11} w'''' - q_z\right) \delta w \mathrm{d}x \\ &+ \left(\bar{A}_{11} u' - \bar{B}_{11} w''\right) \delta u \Big|_0^l + \left(\bar{B}_{11} u'' - \bar{D}_{11} w'''\right) \delta w \Big|_0^l + \left(-\bar{B}_{11} u' + \bar{D}_{11} w''\right) \delta w' \Big|_0^l = 0. \end{aligned} \tag{23.40}$$

The equilibrium conditions, which have already been provided with (23.17), follow from the integral terms:

$$\begin{aligned} \bar{A}_{11} u'' - \bar{B}_{11} w''' &= 0, \\ \bar{B}_{11} u''' - \bar{D}_{11} w'''' &= -q_z. \end{aligned} \tag{23.41}$$

From the boundary terms in (23.40) follow the boundary conditions for the laminated beam. At the points $x = 0$ and $x = l$ the following applies:

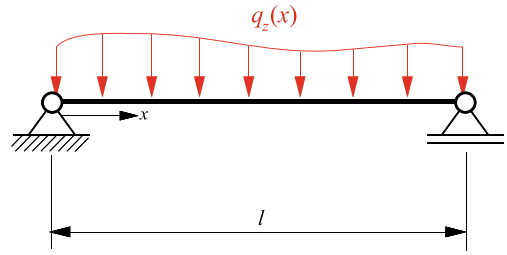


Fig. 23.4 Beam under line load q_z

$$\begin{aligned} &\text{Either} \quad \bar{A}_{11}u' - \bar{B}_{11}w'' = 0 \quad \text{or} \quad \delta u = 0, \\ &\text{Either} \quad \bar{B}_{11}u'' - \bar{D}_{11}w''' = 0 \quad \text{or} \quad \delta w = 0, \\ &\text{Either} \quad \bar{B}_{11}u' - \bar{D}_{11}w'' = 0 \quad \text{or} \quad \delta w' = 0. \end{aligned} \tag{23.42}$$

A formulation for the Ritz method for the laminated beam can be derived from the previous energy considerations. Consider the prismatic laminated beam of Fig. 23.4 with length l, which is subject to a line load q_z that is arbitrarily but continuously distributed over l. The stiffnesses $\bar{A}_{11}$, $\bar{B}_{11}$, $\bar{D}_{11}$ are known. The starting point of the considerations are the expressions (23.38) and (23.39) for the inner and the external potential. We use approaches for the displacements u and w of the following form:

$$w(x) \simeq W(x) = \sum_{i=1}^{N} C_i W_i(x), \quad u(x) \simeq U(x) = \sum_{i=1}^{M} D_i U_i(x). \tag{23.43}$$

The shape functions $W_i(x)$ and $U_i(x)$ must at least fulfil the given static boundary conditions. Inserting the approaches (23.43) into (23.38) and (23.39) results in:

$$\begin{aligned} \Pi_i = &\frac{1}{2}\bar{A}_{11}\int_0^l \sum_{i=1}^{M}\sum_{j=1}^{M} D_i D_j U_i' U_j' \mathrm{d}x \\ &- \bar{B}_{11}\int_0^l \sum_{i=1}^{M}\sum_{j=1}^{N} D_i C_j U_i' W_j'' \mathrm{d}x \\ &+ \frac{1}{2}\bar{D}_{11}\int_0^l \sum_{i=1}^{N}\sum_{j=1}^{N} C_i C_j W_i'' W_j'' \mathrm{d}x, \\ \Pi_a = &-\int_0^l q_z \sum_{i=1}^{N} C_i W_i \mathrm{d}x. \end{aligned} \tag{23.44}$$

From the Ritz equations

$$\frac{\partial \Pi}{\partial C_i} = 0, \quad \frac{\partial \Pi}{\partial D_i} = 0 \tag{23.45}$$

follows a linear system of equations of the type

$$\underline{\underline{K}}\,\underline{C} = \underline{F}, \tag{23.46}$$

or

$$\begin{bmatrix} \underline{\underline{K}}_1 & \underline{\underline{K}}_3^T \\ \underline{\underline{K}}_3 & \underline{\underline{K}}_2 \end{bmatrix} \begin{pmatrix} C_1 \\ C_2 \\ \vdots \\ C_N \\ D_1 \\ D_2 \\ \vdots \\ D_M \end{pmatrix} = \begin{pmatrix} F_1 \\ F_2 \\ \vdots \\ F_N \\ 0 \\ 0 \\ \vdots \\ 0 \end{pmatrix}, \tag{23.47}$$

with:

$$F_i = \int_0^l q_i W_i \mathrm{d}x. \tag{23.48}$$

The submatrices $\underline{\underline{K}}_1, \underline{\underline{K}}_2, \underline{\underline{K}}_3$ of the stiffness matrix $\underline{\underline{K}}$ are as follows:

$$\begin{aligned}
\underline{\underline{K}}_1 &= \begin{bmatrix} K_{11}^1 & K_{12}^1 & K_{13}^1 & \cdots & K_{1N}^1 \\ K_{12}^1 & K_{22}^1 & K_{23}^1 & \cdots & K_{2N}^1 \\ K_{13}^1 & K_{23}^1 & K_{33}^1 & \cdots & K_{3N}^1 \\ \vdots & \vdots & \vdots & \ddots & \vdots \\ K_{1N}^1 & K_{2N}^1 & K_{3N}^1 & \cdots & K_{NN}^1 \end{bmatrix}, \\
\underline{\underline{K}}_2 &= \begin{bmatrix} K_{11}^2 & K_{12}^2 & K_{13}^2 & \cdots & K_{1M}^2 \\ K_{12}^2 & K_{22}^2 & K_{23}^2 & \cdots & K_{2M}^2 \\ K_{13}^2 & K_{23}^2 & K_{33}^2 & \cdots & K_{3M}^2 \\ \vdots & \vdots & \vdots & \ddots & \vdots \\ K_{1M}^2 & K_{2M}^2 & K_{3M}^2 & \cdots & K_{MM}^2 \end{bmatrix}, \\
\underline{\underline{K}}_3 &= \begin{bmatrix} K_{11}^3 & K_{12}^3 & K_{13}^3 & \cdots & K_{1N}^3 \\ K_{21}^3 & K_{22}^3 & K_{23}^3 & \cdots & K_{2N}^3 \\ K_{31}^3 & K_{32}^3 & K_{33}^3 & \cdots & K_{3N}^3 \\ \vdots & \vdots & \vdots & \ddots & \vdots \\ K_{M1}^3 & K_{M2}^3 & K_{M3}^3 & \cdots & K_{MN}^3 \end{bmatrix},
\end{aligned} \tag{23.49}$$

with

$$K_{ij}^{1} = \bar{D}_{11} \int_0^l W_i'' W_j'' \mathrm{d}x,$$

$$K_{ij}^{2} = \bar{A}_{11} \int_0^l U_i' U_j' \mathrm{d}x,$$

$$K_{ij}^{3} = -\bar{B}_{11} \int_0^l U_i' W_j'' \mathrm{d}x. \tag{23.50}$$

The two submatrices $\underline{\underline{K}}_1$ and $\underline{\underline{K}}_2$ are symmetric, whereas $\underline{\underline{K}}_3$ has no symmetry properties.

23.2 First-Order Shear Deformation Theory

In the following, we consider laminated beams within the framework of First-Order Shear Deformation Theory (FSDT), which is a generalization of Timoshenko's beam theory (see Mittelstedt 2021). We assume a displacement field analogous to Chap. 11 and obtain the displacements of a point P at an arbitrary point of the cross-section:

$$u_P = u + z_P \varphi_y, \quad w_P = w. \tag{23.51}$$

The resulting strain components are as follows:

$$\varepsilon_{xx} = u' + z\varphi_y', \quad \gamma_{xz} = \varphi_y + w'. \tag{23.52}$$

The following stress components result in layer k:

$$\begin{aligned} \sigma_{xx,k} &= E_k \varepsilon_{xx} = E_k \left(u' + z\varphi_y' \right), \\ \tau_{xz,k} &= G_k \gamma_{xz} = G_k \left(\varphi_y + w' \right). \end{aligned} \tag{23.53}$$

While the normal stress $\sigma_{xx,k}$ within the layer k is linear over z and discontinuities occur at the interfaces between different laminate layers, the shear stress $\tau_{xz,k}$ in each individual layer k is constant over the layer thickness. The force quantities N, M_y, Q_z can be determined from (23.53):

$$N = \int_A \sigma_{xx} \mathrm{d}A, \quad M_y = \int_A \sigma_{xx} z \mathrm{d}A, \quad Q_z = \int_A \tau_{xz} \mathrm{d}A. \tag{23.54}$$

For the normal force N we obtain with the area element $\mathrm{d}A = b\mathrm{d}z$:

$$N = b \int_{-\frac{h}{2}}^{+\frac{h}{2}} \sigma_{xx} \mathrm{d}z. \tag{23.55}$$

We decompose the integral into integrals over the individual layer thicknesses and apply the expression (23.53) for the normal stress $\sigma_{xx,k}$:

$$N = b \sum_{k=1}^{N} E_k \int_{z_{k-1}}^{z_k} \left(u' + z\varphi_y' \right) \mathrm{d}z. \tag{23.56}$$

After the integrations have been carried out we obtain:

$$N = \bar{A}_{11} u' + \bar{B}_{11} \varphi_y'. \tag{23.57}$$

Herein, $\bar{A}_{11}$ and $\bar{B}_{11}$ are the stiffnesses already known from CLPT.

The bending moment M_y is calculated in the same way:

$$M_y = \bar{B}_{11} u' + \bar{D}_{11} \varphi_y'. \tag{23.58}$$

Here, the bending stiffness $\bar{D}_{11}$ is identical to the stiffness already derived in the framework of CLPT.

We determine the shear force Q_z by integrating the shear stress over the cross-sectional area. With $\mathrm{d}A = b\mathrm{d}z$ follows:

$$Q_z = b \int_{-\frac{h}{2}}^{+\frac{h}{2}} \tau_{xz} \mathrm{d}z. \tag{23.59}$$

We can use (23.53) to express the shear stress using the displacement variables φ_y and w:

$$Q_z = b \sum_{k=1}^{N} G_k \int_{z_{k-1}}^{z_k} \left(\varphi_y + w' \right) \mathrm{d}z, \tag{23.60}$$

or

$$Q_z = b \left(\varphi_y + w' \right) \sum_{k=1}^{N} G_k \left(z_{k-1} - z_k \right). \tag{23.61}$$

At this point, the shear stiffness of the laminate in the thickness direction is introduced, which we refer to as $\bar{A}_{55}$:

$$\bar{A}_{55} = b \sum_{k=1}^{N} G_k \left(z_{k-1} - z_k \right). \tag{23.62}$$

For the shear force Q_z then follows:

$$Q_z = K \bar{A}_{55} \left(\varphi_y + w' \right). \tag{23.63}$$

Here, the so-called shear correction factor K was introduced within the framework of Timoshenko's beam theory (Mittelstedt 2021). The determination of K in the case of laminated beams is not discussed in more detail here; the interested reader is referred to the available specialist literature.

For a laminated beam in the context of FSDT, the constitutive law can be expressed in a vector-matrix notation as follows:

$$\begin{pmatrix} N \\ M_y \\ Q_z \end{pmatrix} = \begin{bmatrix} \bar{A}_{11} & \bar{B}_{11} & 0 \\ \bar{B}_{11} & \bar{D}_{11} & 0 \\ 0 & 0 & K \bar{A}_{55} \end{bmatrix} \begin{pmatrix} u' \\ \varphi_y' \\ \varphi_y + w' \end{pmatrix}. \tag{23.64}$$

The equilibrium conditions (23.15) can also be applied here, and they are given again here for the sake of clarity:

$$N' = -n, \quad Q_z' = -q_z, \quad M_y' = Q_z. \tag{23.65}$$

If we assume a symmetric laminate with $\bar{B}_{11} = 0$, then with (23.64) it follows:

$$\begin{aligned} \left(\bar{A}_{11} u' \right)' &= -n, \\ \left[K \bar{A}_{55} \left(\varphi_y + w' \right) \right]' &= -q_z, \\ \left(\bar{D}_{11} \varphi_y' \right)' &= K \bar{A}_{55} \left(\varphi_y + w' \right). \end{aligned} \tag{23.66}$$

For the prismatic beam with properties that do not change over x we have:

$$\begin{aligned} \bar{A}_{11} u'' &= -n, \\ K \bar{A}_{55} \left(\varphi_y' + w'' \right) &= -q_z, \\ \bar{D}_{11} \varphi_y'' &= K \bar{A}_{55} \left(\varphi_y + w' \right). \end{aligned} \tag{23.67}$$

If we consider a homogeneous beam with $\bar{A}_{11} = EA$, $\bar{D}_{11} = EI_{yy}$ and $K \bar{A}_{55} = KGA$, then the equations known from the Timoshenko beam theory result:

$$
\begin{aligned}
EAu'' &= -n, \\
KGA\left(\varphi_y' + w''\right) &= -q_z, \\
EI_{yy}\varphi_y'' &= KGA\left(\varphi_y + w'\right).
\end{aligned} \tag{23.68}
$$

Expressions for the normal stress $\sigma_{xx,k}$ and the shear stress $\tau_{xz,k}$ can be determined by inverting the constitutive law (23.64), whereby the layup under consideration is arbitrarily unsymmetric:

$$
\begin{pmatrix} u' \\ \varphi_y' \\ \varphi_y + w' \end{pmatrix} = \begin{bmatrix} \dfrac{\bar{D}_{11}}{\bar{A}_{11}\bar{D}_{11} - \bar{B}_{11}^2} & -\dfrac{\bar{B}_{11}}{\bar{A}_{11}\bar{D}_{11} - \bar{B}_{11}^2} & 0 \\ -\dfrac{\bar{B}_{11}}{\bar{A}_{11}\bar{D}_{11} - \bar{B}_{11}^2} & \dfrac{\bar{A}_{11}}{\bar{A}_{11}\bar{D}_{11} - \bar{B}_{11}^2} & 0 \\ & & \dfrac{1}{K\bar{A}_{55}} \end{bmatrix} \begin{pmatrix} N \\ M_y \\ Q_z \end{pmatrix}. \tag{23.69}
$$

If this is inserted into (23.53), the following expressions result for the normal stress $\sigma_{xx,k}$ and the shear stress $\tau_{xz,k}$:

$$
\begin{aligned}
\sigma_{xx,k} &= \frac{E_k}{\bar{A}_{11}\bar{D}_{11} - \bar{B}_{11}^2}\left[\bar{D}_{11}N - \bar{B}_{11}M_y + z\left(\bar{A}_{11}M_y - \bar{B}_{11}N\right)\right], \\
\tau_{xz,k} &= \frac{G_k Q_z}{\bar{A}_{55}}.
\end{aligned} \tag{23.70}
$$

It can be seen that the expression for the normal stress $\sigma_{xx,k}$ is identical to (23.20).

In the following, we consider the deformations for symmetric layups. The displacement u can be calculated by integrating the first equation in (23.66) or (23.67):

$$
\begin{aligned}
\bar{A}_{11}u'' &= -n, \\
\bar{A}_{11}u' &= -\int n\mathrm{d}x + D_1, \\
\bar{A}_{11}u &= -\int\int n\mathrm{d}x\mathrm{d}x + D_1 x + D_2.
\end{aligned} \tag{23.71}
$$

The integration constants D_1 and D_2 are adapted to given boundary conditions.

To determine the beam deflection w, we use the equilibrium conditions $Q_z' = -q_z$ and $M_y' = Q_z$, from which the following results:

$$
\bar{D}_{11}\varphi_y''' = -q_z. \tag{23.72}
$$

With $Q_z = K\bar{A}_{55}\left(\varphi_y + w'\right)$ we have:

$$
\bar{D}_{11}\varphi_y'' - K\bar{A}_{55}\left(\varphi_y + w'\right) = 0. \tag{23.73}
$$

We integrate the expression

$$K\bar{A}_{55}\left(\varphi_y' + w''\right) = -q_z \tag{23.74}$$

once with respect to x:

$$K\bar{A}_{55}\left(\varphi_y + w'\right) = -\int q_z \mathrm{d}x + C_1. \tag{23.75}$$

This expression is used in (23.73):

$$\bar{D}_{11}\varphi_y'' = -\int q_z \mathrm{d}x + C_1. \tag{23.76}$$

From this, φ_y can be determined by twofold integration:

$$\begin{aligned}\bar{D}_{11}\varphi_y' &= -\int\int q_z \mathrm{d}x\mathrm{d}x + C_1 x + C_2,\\ \bar{D}_{11}\varphi_y &= -\int\int\int q_z \mathrm{d}x\mathrm{d}x\mathrm{d}x + \frac{1}{2}C_1 x^2 + C_2 x + C_3.\end{aligned} \tag{23.77}$$

With (23.75) the following expression for w' results:

$$w' = \frac{1}{K\bar{A}_{55}}\left(-\int q_z \mathrm{d}x + C_1\right) - \varphi_y. \tag{23.78}$$

We insert (23.77) and obtain:

$$\begin{aligned}w' = &\frac{1}{K\bar{A}_{55}}\left(-\int q_z \mathrm{d}x + C_1\right)\\ &- \frac{1}{\bar{D}_{11}}\left(-\int\int\int q_z \mathrm{d}x\mathrm{d}x\mathrm{d}x + \frac{1}{2}C_1 x^2 + C_2 x + C_3\right).\end{aligned} \tag{23.79}$$

Integration with respect to x then leads to the deflection w of the beam:

$$\begin{aligned}w = &\frac{1}{K\bar{A}_{55}}\left(-\int\int q_z \mathrm{d}x\mathrm{d}x + C_1 x\right)\\ &- \frac{1}{\bar{D}_{11}}\left(-\int\int\int\int q_z \mathrm{d}x\mathrm{d}x\mathrm{d}x\mathrm{d}x + \frac{1}{6}C_1 x^3 + \frac{1}{2}C_2 x^2 + C_3 x + C_4\right).\end{aligned} \tag{23.80}$$

The integration constants C_1, C_2, C_3, C_4 are again adapted to the given boundary conditions.

In the following, the strain energy Π_i is derived within the framework of FSDT. The following applies in general:

$$\Pi_i = \frac{1}{2}\int_V \left(\sigma_{xx}\varepsilon_{xx} + \tau_{xz}\gamma_{xz}\right)\mathrm{d}V. \tag{23.81}$$

We split the volume integral into a line integral with respect to x and an area integral with respect to A. With the area element $\mathrm{d}A = b\mathrm{d}z$ follows:

$$\Pi_i = \frac{b}{2} \int_0^l \int_{-\frac{h}{2}}^{+\frac{h}{2}} (\sigma_{xx}\varepsilon_{xx} + \tau_{xz}\gamma_{xz}) \, \mathrm{d}z\mathrm{d}x. \tag{23.82}$$

Inserting the stresses according to $\sigma_{xx,k} = E_k\varepsilon_{xx}$ and $\tau_{xz,k} = G_k\gamma_{xz}$ results in:

$$\Pi_i = \frac{b}{2} \int_0^l \sum_{k=1}^{N} \int_{z_{k-1}}^{z_k} \left(E_k\varepsilon_{xx}^2 + G_k\gamma_{xz}^2\right) \mathrm{d}z\mathrm{d}x. \tag{23.83}$$

We can apply the strains $\varepsilon_{xx} = u' + z\varphi_y'$ and $\gamma_{xz} = \varphi_y + w'$, and the following result is obtained:

$$\begin{aligned} \Pi_i = {} & \frac{1}{2}\bar{A}_{11} \int_0^l \left(u'\right)^2 \mathrm{d}x + \bar{B}_{11} \int_0^l u'\varphi_y' \mathrm{d}x \\ & + \frac{1}{2}\bar{D}_{11} \int_0^l \left(\varphi_y'\right)^2 \mathrm{d}x + \frac{1}{2}K\bar{A}_{55} \int_0^l \left(\varphi_y + w'\right)^2 \mathrm{d}x. \end{aligned} \tag{23.84}$$

The governing differential equations as well as all potential combinations of boundary conditions can also be derived with the help of the principle of the minimum of the total elastic potential $\delta\Pi = 0$ for the case of a beam under the line load q_z (Fig. 23.4). The external potential Π_a does not change compared to (23.39), and the requirement for the vanishing of the first variation $\delta\Pi = \delta\left(\Pi_i + \Pi_a\right) = 0$ eventually yields:

$$\begin{aligned} & -\int_0^l \left(\bar{A}_{11}u'' + \bar{B}_{11}\varphi_y''\right)\delta u \mathrm{d}x - \int_0^l \left(K\bar{A}_{55}\left(\varphi_y' + w''\right) + q_z\right)\delta w \mathrm{d}x \\ & \quad - \int_0^l \left(\bar{B}_{11}u'' + \bar{D}_{11}\varphi_y'' - K\bar{A}_{55}\left(\varphi_y + w'\right)\right)\delta\varphi_y \mathrm{d}x \\ & \quad + \left(\bar{A}_{11}u' + \bar{B}_{11}\varphi_y'\right)\delta u\Big|_0^l + K\bar{A}_{55}\left(\varphi_y + w'\right)\delta w\Big|_0^l \\ & \quad + \left(\bar{D}_{11}\varphi_y' + \bar{B}_{11}u'\right)\delta\varphi_y\Big|_0^l = 0. \end{aligned} \tag{23.85}$$

The integral terms contain the governing differential equations:

$$\begin{aligned} \bar{A}_{11}u'' + \bar{B}_{11}\varphi_y'' &= 0, \\ K\bar{A}_{55}\left(\varphi_y' + w''\right) &= -q_z, \\ \bar{B}_{11}u'' + \bar{D}_{11}\varphi_y'' &= K\bar{A}_{55}\left(\varphi_y + w'\right). \end{aligned} \tag{23.86}$$

The boundary terms remaining in (23.85) describe the boundary conditions of the beam in the context of FSDT.

23.3 Sandwich Beams

We now consider beams in sandwich construction (Fig. 23.5). In the following, we analyze sandwich structures consisting of two facesheets made of identical material (modulus of elasticity E_f), but which can have different thicknesses (thicknesses t_1 and t_2). The core has the thickness d measured between the skeleton lines of the two facesheets, and its elastic properties are given by E_c and G_c. We assume that $E_f >> E_c$ applies. The center of gravity of the sandwich cross-section under consideration has the distance e_1 from the top facesheet and the distance e_2 from the bottom facesheet. We introduce the $\bar{z}$-axis as shown in Fig. 23.5. The origin of the reference system x, z is located in the center of gravity of the cross-section.

In accordance with the explanations in Chap. 19, we assume that the sandwich core is rather compliant in comparison to the facesheets. It is therefore exclusively involved in carrying transverse shear stresses. We also want to assume that the facesheets are significantly thinner than the sandwich core, so that $t_1, t_2 << d$ applies. Consequently, the inherent bending stiffness of the facesheets can be neglected and only the out-of-plane stiffnesses of the facesheets are taken into account when determining the bending stiffness of the sandwich beam. The bending moment $M_y = N_2 e_2 - N_1 e_1$ acts in the form of a pair of forces ($N_1 = N_2 = \frac{M_y}{d}$) in the facesheets, and the resulting forces are carried by the facesheets by tension and compression (Fig. 23.6). This also applies to the normal force $N = N_1 + N_2$ acting in the sandwich beam. Accordingly, it is assumed that the normal stresses acting in the facesheets as a result of the normal force N and the bending moment M_y are constant over the thickness of the facesheets. Furthermore, the facesheets do not participate in carrying of transverse forces, which are only carried by the core. Here we assume that the shear stresses

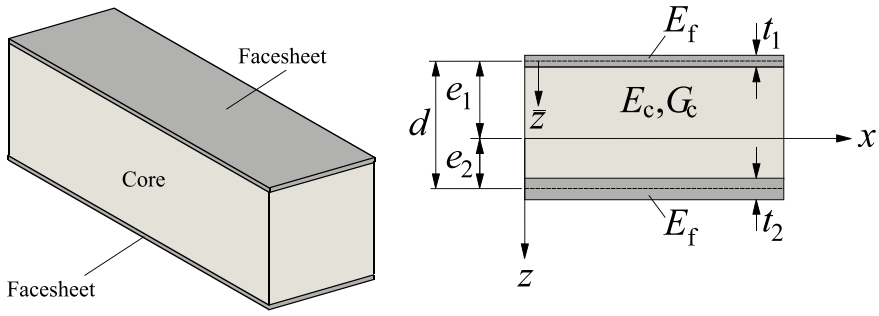


Fig. 23.5 Sandwich beam

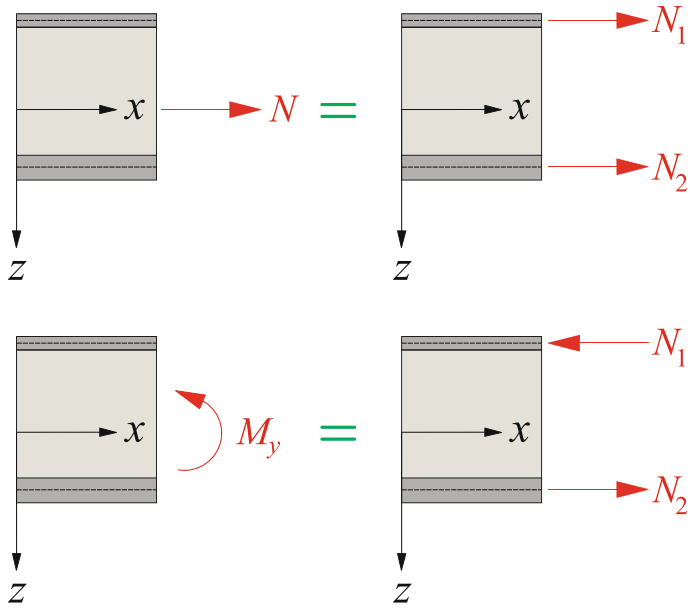


Fig. 23.6 Transfer of normal force N and bending moment M_y in the sandwich beam

are constantly distributed over the entire core. The core is incompressible in the thickness direction and there are no strains in the thickness direction in the sandwich beam under consideration.

The described analysis model corresponds to the application of the shear field beam model (Mittelstedt 2021) to the calculation of sandwich beams. Further literature on sandwich structures is available e.g. with Stamm and Witte (1974), Wiedemann (2007), or Zenkert (1995).

We first determine the position of the ideal center of gravity $\bar{z}_S$ of the sandwich beam and apply the calculation rules for hybrid cross-sections (Mittelstedt 2021):

$$\bar{z}_s = \frac{\sum_{i=1}^{3} E_i \int_{A_i} \bar{z} \mathrm{d}A_i}{\sum_{i=1}^{3} E_i \int_{A_i} \mathrm{d}A_i} = \frac{\left(E S_{\bar{y}}\right)_{eff}}{(EA)_{eff}}. \tag{23.87}$$

The effective static moment $\left(E S_{\bar{y}}\right)_{eff}$ follows as:

$$\left(E S_{\bar{y}}\right)_{eff} = E_f \cdot d \cdot b \cdot t_2 + E_c \cdot \frac{d}{2} \cdot b \cdot d. \tag{23.88}$$

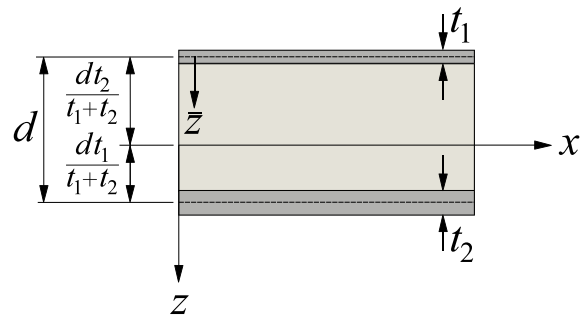


Fig. 23.7 Location of the center of gravity of the sandwich beam

With $E_f >> E_c$ the second term can be neglected:

$$\left(ES_{\bar{y}}\right)_{eff} = E_f dbt_2. \tag{23.89}$$

The effective extensional stiffness $(EA)_{eff}$ is calculated as:

$$(EA)_{eff} = E_f bt_1 + E_f bt_2 + E_c bd, \tag{23.90}$$

or if the last term is neglected:

$$(EA)_{eff} = E_f b\left(t_1 + t_2\right). \tag{23.91}$$

For the center of gravity $\bar{z}_S$ follows (Fig. 23.7):

$$\bar{z}_s = \frac{dt_2}{t_1 + t_2} = e_1. \tag{23.92}$$

The distance of the center of gravity $e_2 = d - e_1$ then results as:

$$e_2 = \frac{dt_1}{t_1 + t_2}. \tag{23.93}$$

We want to assume that a sandwich beam behaves like a shear-compliant beam within the framework of Timoshenko's beam theory (Mittelstedt 2021) or First-Order Shear Deformation Theory. The displacement field is as follows:

$$\begin{aligned} u_P &= u + z_P \varphi_y, \\ w_P &= w. \end{aligned} \tag{23.94}$$

For the strains ε_{xx} and γ_{xz} we obtain:

$$\begin{aligned} \varepsilon_{xx} &= u' + z\varphi_y', \\ \gamma_{xz} &= \varphi_y + w'. \end{aligned} \tag{23.95}$$

The stresses in segment k of the sandwich beam are then as follows:

$$\begin{aligned} \sigma_{xx,k} &= E_k \varepsilon_{xx} = E_k \left(u' + z\varphi_y' \right), \\ \tau_{xz,k} &= G_k \gamma_{xz} = G_k \left(\varphi_y + w' \right). \end{aligned} \tag{23.96}$$

We consider the normal force N:

$$N = \int_A \sigma_{xx} \mathrm{d}A. \tag{23.97}$$

The area integral can be broken down into two integrals concerning the two facesheets, whereby we note here that the core is not involved in carrying the normal force:

$$N = \int_{A_1} \sigma_{xx,1} \mathrm{d}A_1 + \int_{A_2} \sigma_{xx,2} \mathrm{d}A_2. \tag{23.98}$$

With (23.96) follows:

$$\begin{aligned} N &= E_f \int_{A_1} \left(u' + z\varphi_y' \right) \mathrm{d}A_1 + E_f \int_{A_2} \left(u' + z\varphi_y' \right) \mathrm{d}A_2 \\ &= E_f \left(A_1 + A_2 \right) u' + E_f b \left(e_2 t_2 - e_1 t_1 \right) \varphi_y'. \end{aligned} \tag{23.99}$$

With (23.92) and (23.93) the second term disappears, and with $A_1 = bt_1$ and $A_2 = bt_2$ the following remains:

$$N = E_f b \left(t_1 + t_2 \right) u'. \tag{23.100}$$

The expression $E_f b \left(t_1 + t_2 \right)$ is the effective tensile stiffness of the sandwich beam:

$$N = (EA)_{eff} \, u'. \tag{23.101}$$

The bending moment M_y can be determined in the same way:

$$M_y = \int_A \sigma_{xx} z \mathrm{d}A. \tag{23.102}$$

The area integral is broken down into two integrals:

$$M_y = \int_{A_1} \sigma_{xx,1} z \mathrm{d}A_1 + \int_{A_2} \sigma_{xx,2} z \mathrm{d}A_2. \tag{23.103}$$

With (23.96) we obtain:

$$\begin{aligned} M_y &= E_f \int_{A_1} \left(u'z + z^2\varphi_y'\right) \mathrm{d}A_1 + E_f \int_{A_2} \left(u'z + z^2\varphi_y'\right) \mathrm{d}A_2 \\ &= E_f u' \int_{A_1} z \mathrm{d}A_1 + E_f u' \int_{A_2} z \mathrm{d}A_2 + E_f \varphi_y' \int_{A_1} z^2 \mathrm{d}A_1 + E_f \varphi_y' \int_{A_2} z^2 \mathrm{d}A_2 \\ &= E_f u' \left(e_2 A_2 - e_1 A_1\right) + E_f \varphi_y' \left(e_1^2 A_1 + e_2^2 A_2\right). \end{aligned} \tag{23.104}$$

With (23.92) and (23.93) the first term disappears, and we have:

$$M_y = E_f d^2 b \frac{t_1 t_2}{t_1 + t_2} \varphi_y'. \tag{23.105}$$

This is the constitutive relationship for the bending moment M_y, where the effective bending stiffness is as follows:

$$(EI)_{eff} = E_f d^2 b \frac{t_1 t_2}{t_1 + t_2}. \tag{23.106}$$

We now determine an expression for the transverse shear force Q_z:

$$Q_z = \int_A \tau_{xz} \mathrm{d}A. \tag{23.107}$$

We assume that shear is only transferred via the core, and therefore:

$$Q_z = \int_{A_c} \tau_{xz} \mathrm{d}A_c. \tag{23.108}$$

With (23.96) we obtain:

$$Q_z = G_c \int_{A_c} \left(\varphi_y + w'\right) \mathrm{d}A_c = G_c A_c \left(\varphi_y + w'\right) = G_c b d \left(\varphi_y + w'\right). \tag{23.109}$$

The expression $G_c bd$ is the effective shear stiffness $(GA)_{eff}$ of the sandwich beam. The constitutive relationships for the sandwich beam are thus as follows:

$$N = E_f b\,(t_1 + t_2)\,u',$$
$$M_y = E_f d^2 b \frac{t_1 t_2}{t_1 + t_2}\varphi_y',$$
$$Q_z = G_c A_c\left(\varphi_y + w'\right). \tag{23.110}$$

Next we determine the stress components in the components of the sandwich beam. Firstly, we take into account that the normal force N is only transferred via the facesheets. From Eq. (23.101), the normal stress in the facesheets is given by

$$\sigma_{xx,k} = \frac{E_k N}{(EA)_{eff}}, \tag{23.111}$$

with $k = 1$ (upper facesheet) or $k = 2$ (lower facesheet). Since we assume identical material in both facesheets, the normal stresses in both facesheets are identical:

$$\sigma_{xx,1} = \sigma_{xx,2} = \frac{E_f N}{E_f b\,(t_1 + t_2)} = \frac{N}{b\,(t_1 + t_2)}. \tag{23.112}$$

We also consider the normal stresses in the facesheets due to the bending moment M_y. The following applies:

$$\sigma_{xx,k} = \frac{E_k M_y z}{\left(EI_{yy}\right)_{eff}}. \tag{23.113}$$

With $\left(EI_{yy}\right)_{eff}$ according to (23.106) we have:

$$\sigma_{xx,1} = -\frac{M_y}{bt_1 d}, \quad \sigma_{xx,2} = \frac{M_y}{bt_2 d}. \tag{23.114}$$

The shear stresses of the core result from the assumption of constant distribution over the cross-sectional area of the core as:

$$\tau_c = \frac{Q_z}{A_c} = \frac{Q_z}{bd}. \tag{23.115}$$

23.4 Finite Rod and Beam Elements

We derive finite element formulations for beam and rod elements for layered beam structures below, whereby we restrict ourselves to symmetric beams and rods in all cases, so that $\bar{B}_{11} = 0$ applies.

23.4.1 The Two-Noded Rod Element

We consider a rod of length l with an arbitrarily variable but continuously distributed extensional stiffness $\bar{A}_{11}(x)$, which is loaded by the arbitrarily but continuously distributed axial line load $n(x)$ (Fig. 23.8). The rod is divided into a number of finite elements over its length. An approach for the element displacements is formulated in each of these finite elements. We first consider finite rod elements that have two nodes, so that linear interpolation is performed between the two nodal displacements $u_{K,e}$ and $u_{L,e}$, which represent the element degrees of freedom, by means of the shape functions $N_{1,e}(s_e)$ and $N_{2,e}(s_e)$ (Fig. 23.9). This approximates the displacement field u in the straight rod in a polygonal manner. In the following, we assume that the line load n and extensional stiffness $\bar{A}_{11}$ can vary over x but are constant within each finite element.

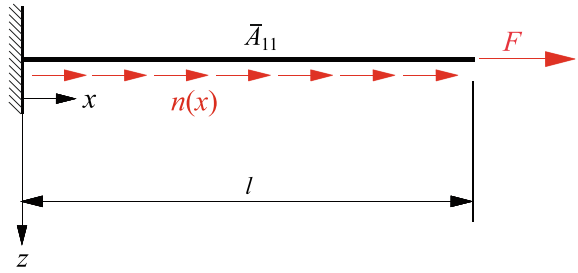


Fig. 23.8 Rod under axial line load and single force

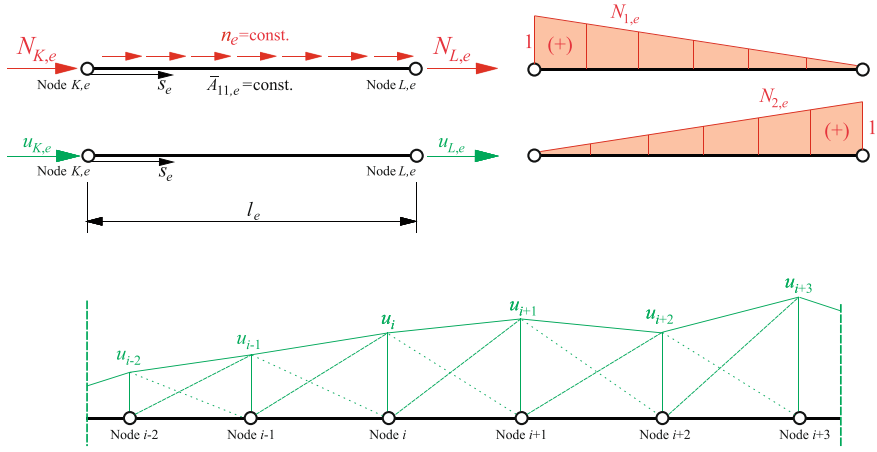


Fig. 23.9 Two-noded finite rod element taking into account the axial line load n (top), approximation of the axial rod displacement u (bottom)

The following approach is used for the displacement $u_e(s_e)$:

$$u_e(s_e) = u_{K,e} N_{1,e}(s_e) + u_{L,e} N_{2,e}(s_e). \tag{23.116}$$

The element shape functions $N_{1,e}$ and $N_{2,e}$ are shown in Fig. 23.9. The following requirements are placed on the shape functions:

$$N_{1,e}(s_e = 0) = 1, \quad N_{1,e}(s_e = l_e) = 0, \quad N_{2,e}(s_e = 0) = 0, \quad N_{2,e}(s_e = l_e) = 1. \tag{23.117}$$

They thus read as follows:

$$N_{1,e}(s_e) = 1 - \frac{s_e}{l_e}, \quad N_{2,e}(s_e) = \frac{s_e}{l_e}. \tag{23.118}$$

Accordingly, linear interpolation between the nodal displacements $u_{K,e}$ and $u_{L,e}$ is performed with the aid of these shape functions.

The total elastic potential Π of the rod element is formulated next. The inner potential Π_i is:

$$\begin{aligned} \Pi_i &= \frac{1}{2} \bar{A}_{11,e} \int_0^{l_e} \left(u_e'\right)^2 \mathrm{d}s_e = \frac{1}{2} \bar{A}_{11,e} \int_0^{l_e} \left(-\frac{u_{K,e}}{l_e} + \frac{u_{L,e}}{l_e} \right)^2 \mathrm{d}s_e \\ &= \frac{\bar{A}_{11,e}}{2 l_e} \left(u_{K,e}^2 - 2 u_{K,e} u_{L,e} + u_{L,e}^2 \right). \end{aligned} \tag{23.119}$$

The external potential Π_a contains both the negative work of the nodal forces $N_{K,e}$ and $N_{L,e}$ along the nodal displacements $u_{K,e}$ and $u_{L,e}$ as well as a contribution of the line load n_e, which is assumed to be constant along the element length:

$$\Pi_a = -N_{K,e} u_{K,e} - N_{L,e} u_{L,e} - \int_0^{l_e} n_e u_e(s_e) \mathrm{d}s_e. \tag{23.120}$$

Execution of the integration results:

$$\Pi_a = -N_{K,e} u_{K,e} - N_{L,e} u_{L,e} - \frac{1}{2} n_e l_e (u_{K,e} + u_{L,e}). \tag{23.121}$$

From the principle of the minimum of the total elastic potential $\delta\Pi = \delta(\Pi_i + \Pi_a) = 0$ we obtain:

$$\begin{aligned} \delta\Pi = \frac{\bar{A}_{11,e}}{2 l_e} &\left(2 u_{K,e} \delta u_{K,e} - 2 \delta u_{K,e} u_{L,e} - 2 u_{K,e} \delta u_{L,e} + 2 u_{L,e} \delta u_{L,e} \right) \\ &- N_{K,e} \delta u_{K,e} - N_{L,e} \delta u_{L,e} - \frac{1}{2} n_e l_e \delta u_{K,e} - \frac{1}{2} n_e l_e \delta u_{L,e} = 0, \end{aligned} \tag{23.122}$$

or sorted according to the variations $\delta u_{K,e}$ and $\delta u_{L,e}$:

$$\left[\frac{\bar{A}_{11,e}}{l_e}\left(u_{K,e}-u_{L,e}\right)-N_{K,e}-\frac{1}{2}n_e l_e\right]\delta u_{K,e} + \left[\frac{\bar{A}_{11,e}}{l_e}\left(-u_{K,e}+u_{L,e}\right)-N_{L,e}-\frac{1}{2}n_e l_e\right]\delta u_{L,e}=0. \tag{23.123}$$

Zeroing the terms in brackets gives the element equations as:

$$\begin{aligned}\frac{\bar{A}_{11,e}}{l_e}\left(u_{K,e}-u_{L,e}\right)&=N_{K,e}+\frac{1}{2}n_e l_e,\\ \frac{\bar{A}_{11,e}}{l_e}\left(-u_{K,e}+u_{L,e}\right)&=N_{L,e}+\frac{1}{2}n_e l_e,\end{aligned} \tag{23.124}$$

or in vector matrix form:

$$\frac{\bar{A}_{11,e}}{l_e}\begin{bmatrix}1 & -1\\ -1 & 1\end{bmatrix}\begin{pmatrix}u_{K,e}\\ u_{L,e}\end{pmatrix}=\begin{pmatrix}N_{K,e}+\frac{1}{2}n_e l_e\\ N_{L,e}+\frac{1}{2}n_e l_e\end{pmatrix}. \tag{23.125}$$

Accordingly, the constant line load n_e is converted into statically equivalent nodal forces $\frac{1}{2}n_e l_e$, which are applied in the element nodes.

23.4.2 The Three-Noded Rod Element

We now determine the element equations for a three-noded rod element. The element load is again a constant line load n_e. This element is shown in Fig. 23.10. The nodes are assumed to be equidistant, so that they divide the element of length l_e into two halves with lengths $\frac{l_e}{2}$. Let the extensional stiffness $\bar{A}_{11,e}$ be constant. The three-noded rod element has three nodes K, L and M with the nodal degrees of freedom $u_{K,e}$, $u_{L,e}$ and $u_{M,e}$. The corresponding nodal forces are $N_{K,e}$, $N_{L,e}$ and $N_{M,e}$. The displacement approach is:

$$u_e(s_e)=u_{K,e}N_{1,e}(s_e)+u_{L,e}N_{2,e}(s_e)+u_{M,e}N_{3,e}(s_e). \tag{23.126}$$

The following requirements are placed on the shape functions $N_{1,e}(s_e)$, $N_{2,e}(s_e)$ and $N_{3,e}(s_e)$:

$$
\begin{aligned}
&N_{1,e}\,(s_e=0)=1, \quad N_{1,e}\left(s_e=\frac{l_e}{2}\right)=0, \quad N_{1,e}\,(s_e=l_e)=0,\\
&N_{2,e}\,(s_e=0)=0, \quad N_{2,e}\left(s_e=\frac{l_e}{2}\right)=1, \quad N_{2,e}\,(s_e=l_e)=0,\\
&N_{3,e}\,(s_e=0)=0, \quad N_{3,e}\left(s_e=\frac{l_e}{2}\right)=0, \quad N_{3,e}\,(s_e=l_e)=1.
\end{aligned}
\tag{23.127}
$$

With a parabolic approach of the type $f(s_e)=as_e^2+bs_e+c$, the shape functions $N_{1,e}(s_e)$, $N_{2,e}(s_e)$, $N_{3,e}(s_e)$ result after adjustment to the above conditions (23.127) as:

$$
N_{1,e}\,(s_e)=1-3\frac{s_e}{l_e}+2\frac{s_e^2}{l_e^2}, \quad N_{2,e}\,(s_e)=4\left(\frac{s_e}{l_e}-\frac{s_e^2}{l_e^2}\right), \quad N_{3,e}\,(s_e)=-\frac{s_e}{l_e}+2\frac{s_e^2}{l_e^2}.
\tag{23.128}
$$

They are shown in Fig. 23.10.

The element equations again follow from the principle of the minimum of the total elastic potential $\delta\Pi=\delta\Pi_i+\delta\Pi_a=0$:

$$
\begin{aligned}
\delta\Pi_i &= \frac{1}{2}\bar{A}_{11,e}\delta\int_0^{l_e}\left((u_e(s_e))'\right)^2\,\mathrm{d}s_e=\frac{\bar{A}_{11,e}}{l_e}\left[\left(\frac{7}{3}u_{K,e}-\frac{8}{3}u_{L,e}+\frac{1}{3}u_{M,e}\right)\delta u_{K,e}\right.\\
&\left.+\left(-\frac{8}{3}u_{K,e}+\frac{16}{3}u_{L,e}-\frac{8}{3}u_{M,e}\right)\delta u_{L,e}+\left(\frac{1}{3}u_{K,e}-\frac{8}{3}u_{L,e}+\frac{7}{3}u_{M,e}\right)\delta u_{M,e}\right],\\
\delta\Pi_a &= -N_{K,e}\delta u_{K,e}-N_{L,e}\delta u_{L,e}-N_{M,e}\delta u_{M,e}-\frac{n_e l_e}{6}\left(\delta u_{K,e}+4\delta u_{L,e}+\delta u_{M,e}\right).
\end{aligned}
\tag{23.129}
$$

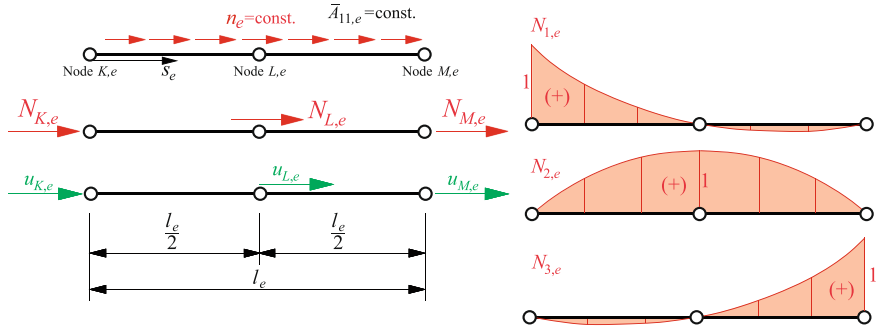


Fig. 23.10 Three-noded rod element

From $\delta\Pi = 0$ we obtain:

$$\begin{aligned}
&\left[\frac{\bar{A}_{11,e}}{3l_e}\left(7u_{K,e} - 8u_{L,e} + u_{M,e}\right) - N_{K,e} - \frac{n_e l_e}{6}\right]\delta u_{K,e} \\
&+\left[\frac{\bar{A}_{11,e}}{3l_e}\left(-8u_{K,e} + 16u_{L,e} - 8u_{M,e}\right) - N_{L,e} - \frac{2n_e l_e}{3}\right]\delta u_{L,e} \\
&+\left[\frac{\bar{A}_{11,e}}{3l_e}\left(u_{K,e} - 8u_{L,e} + 7u_{M,e}\right) - N_{M,e} - \frac{n_e l_e}{6}\right]\delta u_{M,e} = 0. \qquad (23.130)
\end{aligned}$$

Zeroing of the bracket terms yields:

$$\begin{aligned}
\frac{\bar{A}_{11,e}}{3l_e}\left(7u_{K,e} - 8u_{L,e} + u_{M,e}\right) &= N_{K,e} + \frac{n_e l_e}{6}, \\
\frac{\bar{A}_{11,e}}{3l_e}\left(-8u_{K,e} + 16u_{L,e} - 8u_{M,e}\right) &= N_{L,e} + \frac{2n_e l_e}{3}, \\
\frac{\bar{A}_{11,e}}{3l_e}\left(u_{K,e} - 8u_{L,e} + 7u_{M,e}\right) &= N_{M,e} + \frac{n_e l_e}{6}. \qquad (23.131)
\end{aligned}$$

In vector-matrix-notation, we obtain

$$\frac{\bar{A}_{11,e}}{3l_e}\begin{bmatrix} 7 & -8 & 1 \\ -8 & 16 & -8 \\ 1 & -8 & 7 \end{bmatrix}\begin{pmatrix} u_{K,e} \\ u_{L,e} \\ u_{M,e} \end{pmatrix} = \begin{pmatrix} N_{K,e} + \dfrac{n_e l_e}{6} \\ N_{L,e} + \dfrac{2n_e l_e}{3} \\ N_{M,e} + \dfrac{n_e l_e}{6} \end{pmatrix}. \qquad (23.132)$$

These are the element equations for the three-noded rod element.

23.4.3 The Two-Noded Beam Element in the Framework of Classical Laminated Plate Theory

We now consider beam elements where the loads are applied exclusively in the plane of the structure. We assume that one of the two principal cross-sectional axes is also located in the plane of the structure so that we can assume uniaxial bending. We are looking for the element equations for the beam element shown in Fig. 23.11.

The beam element under consideration has the nodes K and L with the nodal force and moment values $N_{K,e}$, $Q_{K,e}$, $M_{K,e}$ or $N_{L,e}$, $Q_{L,e}$, $M_{L,e}$ and the assigned nodal degrees of freedom $u_{K,e}$, $w_{K,e}$, $\varphi_{K,e}$ or $u_{L,e}$, $w_{L,e}$, $\varphi_{L,e}$. The element has the length l_e. The constant extensional stiffness is $\bar{A}_{11,e}$, and the constant flexural stiffness has the value $\bar{D}_{11,e}$. The loads are assumed to be constant line loads n_e and q_e.

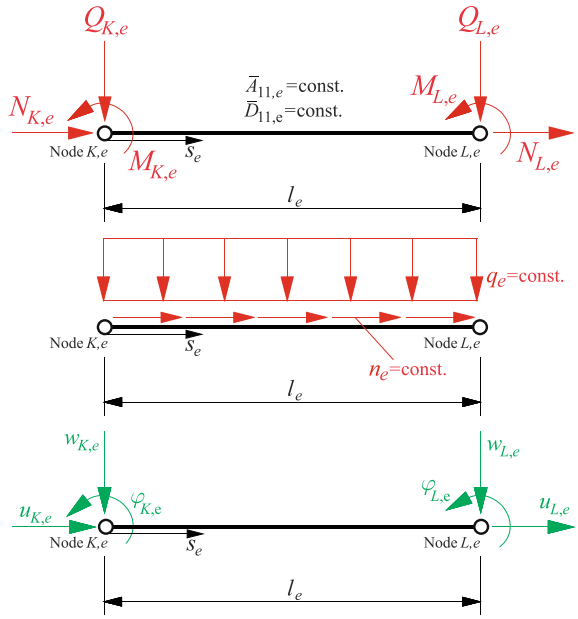


Fig. 23.11 Two-noded beam element

As far as the element equations concerning the two longitudinal displacements $u_{K,e}$ and $u_{L,e}$ are concerned, we can directly adopt (23.125):

$$\frac{\bar{A}_{11,e}}{l_e}\begin{bmatrix} 1 & -1 \\ -1 & 1 \end{bmatrix}\begin{pmatrix} u_{K,e} \\ u_{L,e} \end{pmatrix} = \begin{pmatrix} N_{K,e} + \dfrac{1}{2} n_e l_e \\ N_{L,e} + \dfrac{1}{2} n_e l_e \end{pmatrix}. \tag{23.133}$$

The following formulation is used for the element deflection $w_e(s_e)$:

$$w_e(s_e) = N_{1,e}(s_e)\, w_{K,e} + N_{2,e}(s_e)\, \varphi_{K,e} + N_{3,e}(s_e)\, w_{L,e} + N_{4,e}(s_e)\, \varphi_{L,e}. \tag{23.134}$$

The shape functions $N_{1,e}(s_e)$, $N_{2,e}(s_e)$, $N_{3,e}(s_e)$, $N_{4,e}(s_e)$ are the so-called Hermitian polynomials:

$$\begin{aligned} N_{1,e}(s_e) &= 1 - 3\frac{s_e^2}{l_e^2} + 2\frac{s_e^3}{l_e^3}, \quad N_{2,e}(s_e) = s_e - 2\frac{s_e^2}{l_e} + \frac{s_e^3}{l_e^2}, \\ N_{3,e}(s_e) &= 3\frac{s_e^2}{l_e^2} - 2\frac{s_e^3}{l_e^3}, \quad N_{4,e}(s_e) = -\frac{s_e^2}{l_e} + \frac{s_e^3}{l_e^2}. \end{aligned} \tag{23.135}$$

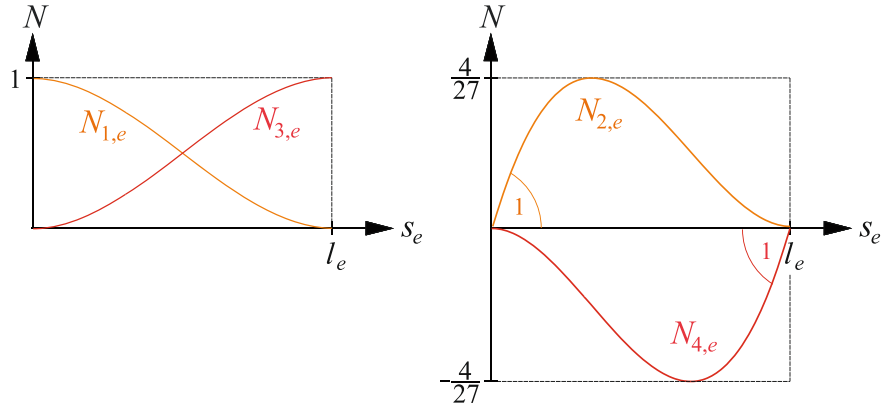


Fig. 23.12 The Hermitian polynomials for a two-noded beam element

They are shown in Fig. 23.12 and have the following properties:

$$\begin{aligned}
&N_{1,e}\,(s_e=0)=1, \quad N'_{1,e}\,(s_e=0)=0, \quad N_{1,e}\,(s_e=l_e)=0, \quad N'_{1,e}\,(s_e=l_e)=0,\\
&N_{2,e}\,(s_e=0)=0, \quad N'_{2,e}\,(s_e=0)=1, \quad N_{2,e}\,(s_e=l_e)=0, \quad N'_{2,e}\,(s_e=l_e)=0,\\
&N_{3,e}\,(s_e=0)=0, \quad N'_{3,e}\,(s_e=0)=0, \quad N_{3,e}\,(s_e=l_e)=1, \quad N'_{3,e}\,(s_e=l_e)=0,\\
&N_{4,e}\,(s_e=0)=0, \quad N'_{4,e}\,(s_e=0)=0, \quad N_{4,e}\,(s_e=l_e)=0, \quad N'_{4,e}\,(s_e=l_e)=1.
\end{aligned} \tag{23.136}$$

The inner potential Π_i of the beam element is as follows:

$$\begin{aligned}
\Pi_i &= \frac{1}{2}\bar{D}_{11,e}\int_0^{l_e}\left(w''_e(s_e)\right)^2\,\mathrm{d}s_e\\
&= \frac{1}{2}\bar{D}_{11,e}\int_0^{l_e}\left(N''_{1,e}w_{K,e}+N''_{2,e}\varphi_{K,ei}+N''_{3,e}w_{L,e}+N''_{4,e}\varphi_{L,e}\right)^2\,\mathrm{d}s_e.
\end{aligned} \tag{23.137}$$

Inserting (23.135) and performing the integrations as well as forming the first variation $\delta\Pi_i$ results in:

$$\begin{aligned}\delta\Pi_i = &\frac{2\bar{D}_{11,e}}{l_e^3}\left(6w_{K,e}+3\varphi_{K,e}l_e-6w_{L,e}+3\varphi_{L,e}l_e\right)\delta w_{K,e}\\ &+\frac{2\bar{D}_{11,e}}{l_e^3}\left(3w_{K,e}l_e+2\varphi_{K,e}l_e^2-3w_{L,e}l_e+\varphi_{L,e}l_e^2\right)\delta\varphi_{K,e}\\ &+\frac{2\bar{D}_{11,e}}{l_e^3}\left(-6w_{K,e}-3\varphi_{K,e}l_e+6w_{L,e}-3\varphi_{L,e}l_e\right)\delta w_{L,e}\\ &+\frac{2\bar{D}_{11,e}}{l_i e^3}\left(3w_{K,e}l_e+\varphi_{K,e}l_e^2-3w_{L,e}l_e+2\varphi_{L,e}l_e^2\right)\delta\varphi_{L,e}. \end{aligned} \tag{23.138}$$

The external potential Π_a results as:

$$\Pi_a = -Q_{K,e}w_{K,e}-Q_{L,e}w_{L,e}-M_{K,e}\varphi_{K,e}-M_{L,e}\varphi_{L,e}-\int_0^{l_e} q_e w_e(s_e)\mathrm{d}s_e. \tag{23.139}$$

The first variation $\delta\Pi_a$ is:

$$\begin{aligned}\delta\Pi_a = &\left(-Q_{K,e}-\frac{1}{2}q_e l_e\right)\delta w_{K,e}+\left(-M_{K,e}-\frac{1}{12}q_e l_e^2\right)\delta\varphi_{K,e}\\ &+\left(-Q_{L,e}-\frac{1}{2}q_e l_e\right)\delta w_{L,e}+\left(-M_{L,e}+\frac{1}{12}q_e l_e^2\right)\delta\varphi_{L,e}. \end{aligned} \tag{23.140}$$

We demand the disappearance of the first variation $\delta\Pi$, which leads to the following expressions with (23.138) and (23.140):

$$\begin{aligned}\frac{2\bar{D}_{11,e}}{l_e^3}\left(6w_{K,e}+3\varphi_{K,e}l_e-6w_{L,e}+3\varphi_{L,e}l_e\right) &= Q_{K,e}+\frac{1}{2}q_e l_e,\\ \frac{2\bar{D}_{11,e}}{l_e^3}\left(3w_{K,e}l_e+2\varphi_{K,e}l_e^2-3w_{L,e}l_e+\varphi_{L,e}l_e^2\right) &= M_{K,e}+\frac{1}{12}q_e l_e^2,\\ \frac{2\bar{D}_{11,e}}{l_e^3}\left(-6w_{K,e}-3\varphi_{K,e}l_e+6w_{L,e}-3\varphi_{L,e}l_e\right) &= Q_{L,e}+\frac{1}{2}q_e l_e,\\ \frac{2\bar{D}_{11,e}}{l_i e^3}\left(3w_{K,e}l_e+\varphi_{K,e}l_e^2-3w_{L,e}l_e+2\varphi_{L,e}l_e^2\right) &= M_{L,e}-\frac{1}{12}q_e l_e^2, \end{aligned} \tag{23.141}$$

or in vector-matrix-notation:

$$\frac{\bar{D}_{11,e}}{l_e^3}\begin{bmatrix} 12 & 6l_e & -12 & 6l_e \\ 6l_e & 4l_e^2 & -6l_e & 2l_e^2 \\ -12 & -6l_e & 12 & -6l_e \\ 6l_e & 2l_e^2 & -6l_e & 4l_e^2 \end{bmatrix}\begin{pmatrix} w_{K,e} \\ \varphi_{K,e} \\ w_{L,e} \\ \varphi_{L,e} \end{pmatrix} = \begin{pmatrix} Q_{K,e} + \frac{1}{2}q_e l_e \\ M_{K,e} + \frac{1}{12}q_e l_e^2 \\ Q_{L,e} + \frac{1}{2}q_e l_e \\ M_{L,e} - \frac{1}{12}q_e l_e^2 \end{pmatrix}. \tag{23.142}$$

The line load q_e was converted into equivalent static nodal forces and nodal moments (Fig. 23.13).

The Eq. (23.142) apply to uniaxial bending and do not take any longitudinal displacements u into account up to this point. In the case of a beam which, in addition to the load q, also has the axial line load n, the element equations (23.142) can be superimposed with the rod element equations (23.133):

$$\begin{bmatrix} \frac{\bar{A}_{11,e}}{l_e} & 0 & 0 & -\frac{\bar{A}_{11,e}}{l_e} & 0 & 0 \\ 0 & 12\frac{\bar{D}_{11,e}}{l_e^3} & 6\frac{\bar{D}_{11,e}}{l_e^2} & 0 & -12\frac{\bar{D}_{11,e}}{l_e^3} & 6\frac{\bar{D}_{11,e}}{l_e^2} \\ 0 & 6\frac{\bar{D}_{11,e}}{l_e^2} & 4\frac{\bar{D}_{11,e}}{l_e} & 0 & -6\frac{\bar{D}_{11,e}}{l_e^2} & 2\frac{\bar{D}_{11,e}}{l_e} \\ -\frac{\bar{A}_{11,e}}{l_e} & 0 & 0 & \frac{\bar{A}_{11,e}}{l_e} & 0 & 0 \\ 0 & -12\frac{\bar{D}_{11,e}}{l_e^3} & -6\frac{\bar{D}_{11,e}}{l_e^2} & 0 & 12\frac{\bar{D}_{11,e}}{l_e^3} & -6\frac{\bar{D}_{11,e}}{l_e^2} \\ 0 & 6\frac{\bar{D}_{11,e}}{l_e^2} & 2\frac{\bar{D}_{11,e}}{l_e} & 0 & -6\frac{\bar{D}_{11,e}}{l_e^2} & 4\frac{\bar{D}_{11,e}}{l_e} \end{bmatrix}\begin{pmatrix} u_{K,e} \\ w_{K,e} \\ \varphi_{K,e} \\ u_{L,e} \\ w_{L,e} \\ \varphi_{L,e} \end{pmatrix}$$

$$= \begin{pmatrix} N_{K,e} + \frac{1}{2}n_e l_e \\ Q_{K,e} + \frac{1}{2}q_e l_e \\ M_{K,e} + \frac{1}{12}q_e l_e^2 \\ N_{L,e} + \frac{1}{2}n_e l_e \\ Q_{L,e} + \frac{1}{2}q_e l_e \\ M_{K,e} - \frac{1}{12}q_e l_e^2 \end{pmatrix}. \tag{23.143}$$

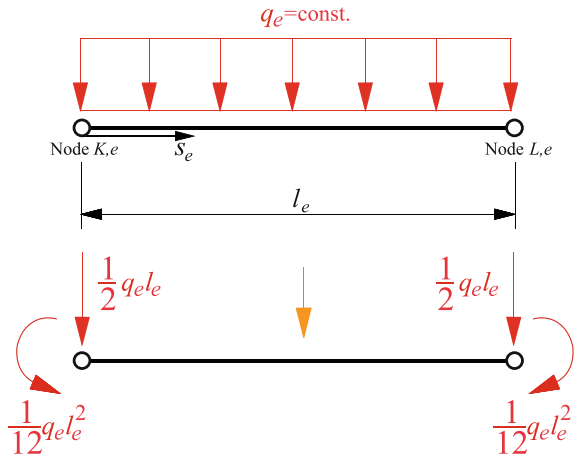


Fig. 23.13 Conversion of the line load q_e into equivalent static nodal forces and moments

23.4.4 The Three-Noded Beam Element in the Framework of Classical Laminated Plate Theory

We derive the stiffness matrix $\underline{\underline{K}}$ for a three-noded beam element below. The considered element with equidistant nodes is shown in Fig. 23.14. We consider bending at this point exclusively, normal forces are not present.

The given finite element has the deflections $w_{K,e}$, $w_{L,e}$, $w_{M,e}$ and the rotations $\varphi_{K,e}$, $\varphi_{L,e}$, $\varphi_{M,e}$ as nodal degrees of freedom. The corresponding nodal forces and moments are

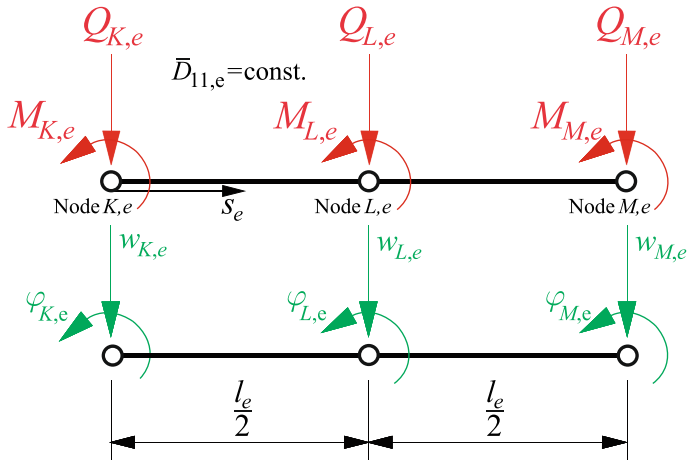


Fig. 23.14 Three-noded beam element

the transverse forces $Q_{K,e}$, $Q_{L,e}$, $Q_{M,e}$ and the bending moments $M_{K,e}$, $M_{L,e}$, $M_{M,e}$. The following approach is used for the element deflection $w_e(s_e)$:

$$w_e(s_e) = w_{K,e}N_{1,e} + \varphi_{K,e}N_{2,e} + w_{L,e}N_{3,e} + \varphi_{L,e}N_{4,e} + w_{M,e}N_{5,e} + \varphi_{M,e}N_{6,e}. \tag{23.144}$$

The shape functions $N_{1,e}$, $N_{2,e}$, $N_{3,e}$, $N_{4,e}$, $N_{5,e}$, $N_{6,e}$ are chosen as fifth-order polynomials:

$$w_e(s_e) = as_e^5 + bs_e^4 + cs_e^3 + ds_e^2 + es_e + f, \tag{23.145}$$

whereby the following conditions must be met:

$$\begin{aligned}
&N_{1,e}\,(s_e = 0) = 1, \quad N_{1,e}\left(s_e = \frac{l_e}{2}\right) = 0, \quad N_{1,e}\,(s_e = l_e) = 0,\\
&N'_{1,e}\,(s_e = 0) = 0, \quad N'_{1,e}\left(s_e = \frac{l_e}{2}\right) = 0, \quad N'_{1,e}\,(s_e = l_e) = 0,\\
&N_{2,e}\,(s_e = 0) = 0, \quad N_{2,e}\left(s_e = \frac{l_e}{2}\right) = 0, \quad N_{2,e}\,(s_e = l_e) = 0,\\
&N'_{2,e}\,(s_e = 0) = 1, \quad N'_{2,e}\left(s_e = \frac{l_e}{2}\right) = 0, \quad N'_{2,e}\,(s_e = l_e) = 0,\\
&N_{3,e}\,(s_e = 0) = 0, \quad N_{3,e}\left(s_e = \frac{l_e}{2}\right) = 1, \quad N_{3,e}\,(s_e = l_e) = 0,\\
&N'_{3,e}\,(s_e = 0) = 0, \quad N'_{3,e}\left(s_e = \frac{l_e}{2}\right) = 0, \quad N'_{3,e}\,(s_e = l_e) = 0,\\
&N_{4,e}\,(s_e = 0) = 0, \quad N_{4,e}\left(s_e = \frac{l_e}{2}\right) = 0, \quad N_{4,e}\,(s_e = l_e) = 0,\\
&N'_{4,e}\,(s_e = 0) = 0, \quad N'_{4,e}\left(s_e = \frac{l_e}{2}\right) = 1, \quad N'_{4,e}\,(s_e = l_e) = 0,\\
&N_{5,e}\,(s_e = 0) = 0, \quad N_{5,e}\left(s_e = \frac{l_e}{2}\right) = 0, \quad N_{5,e}\,(s_e = l_e) = 1,\\
&N'_{5,e}\,(s_e = 0) = 0, \quad N'_{5,e}\left(s_e = \frac{l_e}{2}\right) = 0, \quad N'_{5,e}\,(s_e = l_e) = 0,\\
&N_{6,e}\,(s_e = 0) = 0, \quad N_{6,e}\left(s_e = \frac{l_e}{2}\right) = 0, \quad N_{6,e}\,(s_e = l_e) = 0,\\
&N'_{6,e}\,(s_e = 0) = 0, \quad N'_{6,e}\left(s_e = \frac{l_e}{2}\right) = 0, \quad N'_{6,e}\,(s_e = l_e) = 1.
\end{aligned} \tag{23.146}$$

The shape functions are then as follows:

$$
\begin{aligned}
N_{1,e}(s_e) &= 1 - 23\left(\frac{s_e}{l_e}\right)^2 + 66\left(\frac{s_e}{l_e}\right)^3 - 68\left(\frac{s_e}{l_e}\right)^4 + 24\left(\frac{s_e}{l_e}\right)^5, \\
N_{2,e}(s_e) &= s_e\left[1 - \frac{s_e}{l_e} + 13\left(\frac{s_e}{l_e}\right)^2 - 12\left(\frac{s_e}{l_e}\right)^3 + 4\left(\frac{s_e}{l_e}\right)^4\right], \\
N_{3,e}(s_e) &= \left(\frac{s_e}{l_e}\right)^2\left[16 - 32\frac{s_e}{l_e} + 16\left(\frac{s_e}{l_e}\right)^2\right], \\
N_{4,e}(s_e) &= \frac{s_e^2}{l_e}\left[-8 + 32\frac{s_e}{l_e} - 40\left(\frac{s_e}{l_e}\right)^2 + 16\left(\frac{s_e}{l_e}\right)^3\right], \\
N_{5,e}(s_e) &= \left(\frac{s_e}{l_e}\right)^2\left[7 - 34\frac{s_e}{l_e} + 52\left(\frac{s_e}{l_e}\right)^2 - 24\left(\frac{s_e}{l_e}\right)^3\right], \\
N_{6,e}(s_e) &= \frac{s_e^2}{l_e}\left[-1 + 5\frac{s_e}{l_e} - 8\left(\frac{s_e}{l_e}\right)^2 + 4\left(\frac{s_e}{l_e}\right)^3\right].
\end{aligned}
\tag{23.147}
$$

They are shown in Fig. 23.15. The inner potential Π_i can be specified as:

$$
\Pi_i = \frac{1}{2}\bar{D}_{11,e}\int_0^{l_e}\left(w_e''(s_e)\right)^2 \mathrm{d}s_e. \tag{23.148}
$$

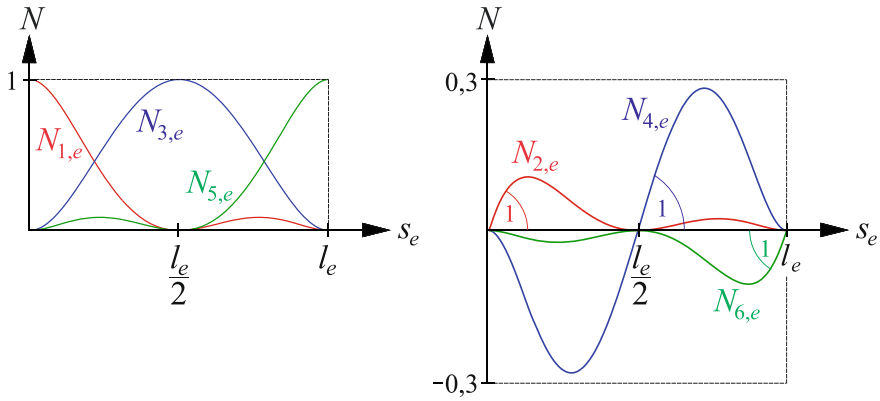


Fig. 23.15 Shape functions for the three-noded beam element

The Ritz equations

$$\begin{aligned} \frac{\partial \Pi_i}{\partial w_{K,e}} &= 0, \quad \frac{\partial \Pi_i}{\partial \varphi_{K,e}} = 0, \quad \frac{\partial \Pi_i}{\partial w_{L,e}} = 0, \\ \frac{\partial \Pi_i}{\partial \varphi_{L,e}} &= 0, \quad \frac{\partial \Pi_i}{\partial w_{M,e}} = 0, \quad \frac{\partial \Pi_i}{\partial \varphi_{M,e}} = 0 \end{aligned} \tag{23.149}$$

result in the following stiffness matrix $\underline{\underline{K}}_e$ of the beam element under consideration after a few transformations:

$$\underline{\underline{K}}_e = \frac{2\bar{D}_{11,e}}{35 l_e} \begin{bmatrix} 2546 & 569 l_e & -1792 & 960 l_e & -754 & 121 l_e \\ 569 l_e & 166 l_e^2 & -448 l_e & 160 l_e^2 & -121 l_e & 19 l_e^2 \\ -1792 & -448 l_e & 3584 & 0 & -1792 & 448 l_e \\ 960 l_e & 160 l_e^2 & 0 & 640 l_e^2 & -960 l_e & 160 l_e^2 \\ -754 & -121 l_e & -1792 & -960 l_e & 2546 & -569 l_e \\ 121 l_e & 19 l_e^2 & 448 l_e & 160 l_e^2 & -569 l_e & 166 l_e^2 \end{bmatrix}. \tag{23.150}$$

Similarly, the force vector $\underline{F}$ can be derived for this element, which is not explained further here.

23.4.5 Finite Beam Element in the Framework of First-Order Shear Deformation Theory

We now consider a beam element according to FSDT (see Fig. 23.16). The element has the length l_e and m equidistant nodes that divide the element into sections of lengths $\frac{l_e}{m-1}$. The nodes $(1, e)$, $(2, e)$, $(3, e)$, $\ldots$, $(m-1, e)$, (m, e) have the degrees of freedom $w_{1,e}, w_{2,e}, w_{3,e}, \ldots, w_{m-1,e}, w_{m,e}$ and $\varphi_{1,e}, \varphi_{2,e}, \varphi_{3,e}, \ldots, \varphi_{m-1,e}, \varphi_{m,e}$. The stiffnesses $\bar{D}_{11,e}$ and $K\bar{A}_{55,e}$ are assumed to be constant over the element length. The line load q_e is also assumed to be constant within the element.

We determine the total elastic potential $\Pi_e = \Pi_{i,e} + \Pi_{a,e}$ of the finite element e:

$$\begin{aligned} \Pi_{i,e} &= \frac{1}{2} \int_0^{l_e} \left[\bar{D}_{11,e} \left(\varphi_e'\right)^2 + K\bar{A}_{55,e} \left(\varphi_e^2 + 2 w_e' \varphi_e + \left(w_e'\right)^2 \right) \right] \mathrm{d}s_e, \\ \Pi_{a,e} &= - \int_0^{l_e} q_e w_e \mathrm{d}s_e. \end{aligned} \tag{23.151}$$

Here, $w_e(s_e)$ and $\varphi_e(s_e)$ are the element deflections and the element bending angles.

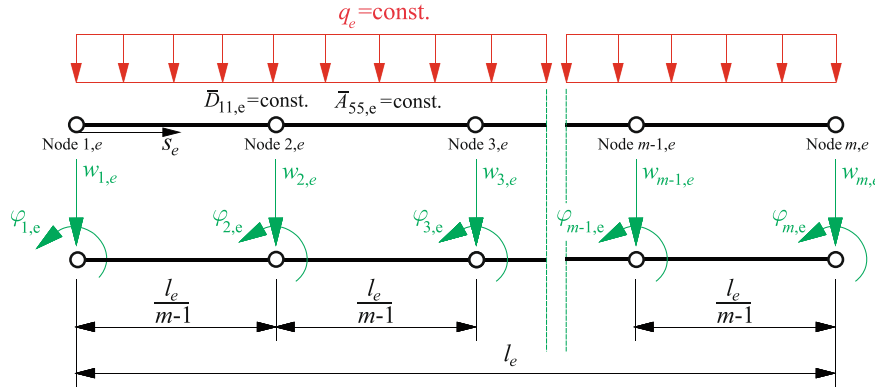


Fig. 23.16 Finite element with m nodes in the framework of First-Order Shear Deformation Theory

We now use approaches of the following form for $w_e(s_e)$ and $\varphi_e(s_e)$:

$$w_e(s_e) = w_{1,e}N_{1,e}(s_e) + w_{2,e}N_{2,e}(s_e) + \cdots + w_{m,e}N_{m,e}(s_e) = \sum_{i=1}^{m} w_{i,e}N_{i,e}(s_e),$$
$$\varphi_e(s_e) = \varphi_{1,e}N_{1,e}(s_e) + \varphi_{2,e}N_{2,e}(s_e) + \cdots + \varphi_{m,e}N_{m,e}(s_e) = \sum_{i=1}^{m} \varphi_{i,e}N_{i,e}(s_e), \tag{23.152}$$

where $N_{1,e}(s_e)$, $N_{2,e}(s_e)$, $N_{3,e}(s_e)$, ..., $N_{m,e}(s_e)$ are the m shape functions belonging to the respective element nodes, which are applied in the form of polynomials. The shape function of node k, e assumes the value 1 in node k, e and the value zero in all other nodes.

For an element with $m = 2$ nodes, the shape functions $N_{1,e}$ and $N_{2,e}$ can be formulated as follows:

$$N_{1,e}(s_e) = 1 - \frac{s_e}{l_e}, \quad N_{2,e}(s_e) = \frac{s_e}{l_e}. \tag{23.153}$$

For $m = 3$ nodes, the shape functions are $N_{1,e}$, $N_{2,e}$ and $N_{3,e}$:

$$N_{1,e}\,(s_e) = 1 - 3\frac{s_e}{l_e} + 2\frac{s_e^2}{l_e^2}, \quad N_{2,e}\,(s_e) = 4\left(\frac{s_e}{l_e} - \frac{s_e^2}{l_e^2}\right), \quad N_{3,e}\,(s_e) = -\frac{s_e}{l_e} + 2\frac{s_e^2}{l_e^2}. \tag{23.154}$$

For $m = 4$ nodes, the shape functions $N_{1,e}$, $N_{2,e}$, $N_{3,e}$ and $N_{4,e}$ are cubic polynomials:

$$
\begin{aligned}
N_{1,e}(s_e) &= 1 - \frac{11}{2}\frac{s_e}{l_e} + 9\left(\frac{s_e}{l_e}\right)^2 - \frac{9}{2}\left(\frac{s_e}{l_e}\right)^3, \\
N_{2,e}(s_e) &= 9\frac{s_e}{l_e} - \frac{45}{2}\left(\frac{s_e}{l_e}\right)^2 + \frac{27}{2}\left(\frac{s_e}{l_e}\right)^3, \\
N_{3,e}(s_e) &= -\frac{9}{2}\frac{s_e}{l_e} + 18\left(\frac{s_e}{l_e}\right)^2 - \frac{27}{2}\left(\frac{s_e}{l_e}\right)^3, \\
N_{4,e}(s_e) &= \frac{s_e}{l_e} - \frac{9}{2}\left(\frac{s_e}{l_e}\right)^2 + \frac{9}{2}\left(\frac{s_e}{l_e}\right)^3.
\end{aligned} \tag{23.155}
$$

Inserting (23.152) into the potential formulations (23.151) results in:

$$
\begin{aligned}
\Pi_e = {} & \frac{1}{2}\int_0^{l_e} \bar{D}_{11,e} \sum_{i=1}^{m}\sum_{j=1}^{m} \varphi_{i,e}\varphi_{j,e}N'_{i,e}N'_{j,e}\mathrm{d}s_e + \frac{1}{2}\int_0^{l_e} K\bar{A}_{55,e} \sum_{i=1}^{m}\sum_{j=1}^{m} \varphi_{i,e}\varphi_{j,e}N_{i,e}N_{j,e}\mathrm{d}s_e \\
& + \int_0^{l_e} K\bar{A}_{55,e} \sum_{i=1}^{m}\sum_{j=1}^{m} w_{i,e}\varphi_{j,e}N'_{i,e}N_{j,e}\mathrm{d}s_e + \frac{1}{2}\int_0^{l_e} K\bar{A}_{55,e} \sum_{i=1}^{m}\sum_{j=1}^{m} w_{i,e}w_{j,e}N'_{i,e}N'_{j,e}\mathrm{d}s_e \\
& - \int_0^{l_e} q_e \sum_{i=1}^{m} w_{i,e}N_{i,e}(s_e)\mathrm{d}s_e.
\end{aligned} \tag{23.156}
$$

From the Ritz equations

$$
\frac{\partial \Pi_e}{\partial w_{i,e}} = 0, \quad \frac{\partial \Pi_e}{\partial \varphi_{i,e}} = 0 \tag{23.157}
$$

(with $i = 1, 2, \ldots, m$) the following system of linear equations results:

$$
\underline{\underline{K}}_e \underline{v}_e = \underline{F}_e, \tag{23.158}
$$

or

$$
\begin{bmatrix} \underline{\underline{K}}_{1,e} & \underline{\underline{K}}_{3,e} \\ \underline{\underline{K}}^T_{3,e} & \underline{\underline{K}}_{2,e} \end{bmatrix}
\begin{pmatrix} w_{1,e} \\ w_{2,e} \\ \vdots \\ w_{m,e} \\ \varphi_{1,e} \\ \varphi_{2,e} \\ \vdots \\ \varphi_{m,e} \end{pmatrix}
=
\begin{pmatrix} F_{1,e} \\ F_{2,e} \\ \vdots \\ F_{m,e} \\ 0 \\ 0 \\ \vdots \\ 0 \end{pmatrix}. \tag{23.159}
$$

Here, the quantities $F_{i,e}$ are the resultants of the line load q_e:

$$F_{i,e} = \int_0^l q_e N_i \mathrm{d}s_e. \tag{23.160}$$

The element stiffness matrix $\underline{\underline{K}}_e$ is composed of the submatrices $\underline{\underline{K}}_{1,e}$, $\underline{\underline{K}}_{2,e}$, $\underline{\underline{K}}_{3,e}$ (m rows and m columns each):

$$\underline{\underline{K}}_{1,e} = \begin{bmatrix} K^1_{11,e} & K^1_{12,e} & K^1_{13,e} & \cdots & K^1_{1m,e} \\ K^1_{12,e} & K^1_{22,e} & K^1_{23,e} & \cdots & K^1_{2m,e} \\ K^1_{13,e} & K^1_{23,e} & K^1_{33,e} & \cdots & K^1_{3m,e} \\ \vdots & \vdots & \vdots & \ddots & \vdots \\ K^1_{1m,e} & K^1_{2m,e} & K^1_{3m,e} & \cdots & K^1_{mm,e} \end{bmatrix},$$

$$\underline{\underline{K}}_{2,e} = \begin{bmatrix} K^2_{11,e} & K^2_{12,e} & K^2_{13,e} & \cdots & K^2_{1m,e} \\ K^2_{12,e} & K^2_{22,e} & K^2_{23,e} & \cdots & K^2_{2m,e} \\ K^2_{13,e} & K^2_{23,e} & K^2_{33,e} & \cdots & K^2_{3m,e} \\ \vdots & \vdots & \vdots & \ddots & \vdots \\ K^2_{1m,e} & K^2_{2m,e} & K^2_{3m,e} & \cdots & K^2_{mm,e} \end{bmatrix},$$

$$\underline{\underline{K}}_{3,e} = \begin{bmatrix} K^3_{11,e} & K^3_{12,e} & K^3_{13,e} & \cdots & K^3_{1m,e} \\ K^3_{21,e} & K^3_{22,e} & K^3_{23,e} & \cdots & K^3_{2m,e} \\ K^3_{31,e} & K^3_{32,e} & K^3_{33,e} & \cdots & K^3_{3m,e} \\ \vdots & \vdots & \vdots & \ddots & \vdots \\ K^3_{m1,e} & K^3_{m2,e} & K^3_{m3,e} & \cdots & K^3_{mm,e} \end{bmatrix}. \tag{23.161}$$

The two submatrices $\underline{\underline{K}}_{1,e}$ and $\underline{\underline{K}}_{2,e}$ are symmetric, but the submatrix $\underline{\underline{K}}_{3,e}$ is not. The entries of the submatrices are as follows:

$$\begin{aligned} K^1_{ij,e} &= \int_0^{l_e} K \bar{A}_{55,e} N_i' N_j' \mathrm{d}s_e, \\ K^2_{ij,e} &= \int_0^{l_e} \bar{D}_{11,e} N_i' N_j' \mathrm{d}s_e + \int_0^{l} K \bar{A}_{55,e} N_i N_j \mathrm{d}s_e, \\ K^3_{ij,e} &= \int_0^{l_e} K \bar{A}_{55,e} N_i' N_j \mathrm{d}s_e. \end{aligned} \tag{23.162}$$

References

Altenbach H, Altenbach J, Kissing W (2018): *Mechanics of composite structural elements*, 2nd edition, Springer Nature, Singapore.

Ambartsumyan SA (1970): *Theory of anisotropic plates*, Technomic Publishing Co., Inc., Stamford, USA.

Ashton JE, Whitney JM (1970): *Theory of laminated plates*, Technomic Publishing Co., Inc., Stamford, USA.

Becker W, Gross D (2002): *Mechanik elastischer Körper und Strukturen*, Springer Verlag, Berlin et al., Germany.

Jones RM (1975): *Mechanics of composite materials*, Scripta Book Co., Washington, USA.

Lekhnitskii SG (1968): *Anisotropic plates*, Gordon and Breach, New York et al., USA.

Mittelstedt C (2021): *Structural Mechanics in Lightweight Engineering*, Springer Nature, Cham, Switzerland.

Reddy JN (2004): *Mechanics of laminated composite plates and shells*, 2nd edition, CRC Press, Boca Raton et al., USA.

Stamm K, Witte H (1974): *Sandwichkonstruktionen*, Springer Verlag, Wien et al., Austria.

Wiedemann J (2007): *Leichtbau 1: Elemente*, Springer Verlag, Berlin et al., Germany.

Zenkert D (1995): *An introduction to sandwich construction*, EMAS - Engineering Materials Advisory Services Ltd., UK.



Thin-Walled Laminated Beams

24

In this chapter, we focus on the consideration of thin-walled beams whose walls are made of composite laminates and, in addition to bending with normal force, we also consider the topics of transverse shear force and torsion. The treatment of the elementary load-bearing behaviour of thin-walled composite beams is a very lively field of work and research, for which a large number of research papers are available. Interested readers can gain an overview of this field of knowledge with the review paper by Mittelstedt (2020).

24.1 Introduction

In this chapter, we consider beam structures for which we want to assume linear elasticity in all cases. At this point, we limit ourselves to beam structures in which only normal forces, bending moments and shear forces occur (Fig. 24.1, left). Torsion and the associated stresses and deformations are considered later. The beam under consideration is loaded by the two line loads q_y and q_z, whereby the indexing indicates the direction of the acting line loads. Both line loads can be an arbitrary function of the longitudinal coordinate x. In addition, any number of individual forces F_y and F_z can occur, which can act at any point x. Individual bending moments can also act, but for the sake of clarity these are not shown in Fig. 24.1. Torsional loading is excluded here for the time being. We relate the considerations in this chapter exclusively to very thin-walled beam cross-sections, which we can then represent in very good approximation by their respective skeleton lines (Fig. 24.2). The skeleton line halves the cross-section thickness at each point.

© The Author(s), under exclusive license to Springer-Verlag GmbH, DE, part of Springer Nature 2025

C. Mittelstedt, *Mechanics of Composite Structures*,
https://doi.org/10.1007/978-3-662-70788-3_24

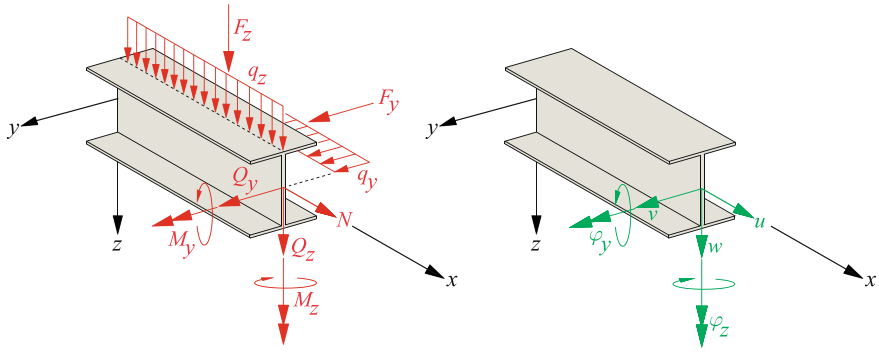


Fig. 24.1 Load and internal forces and moments of the beam (left), associated displacement and rotations (right)

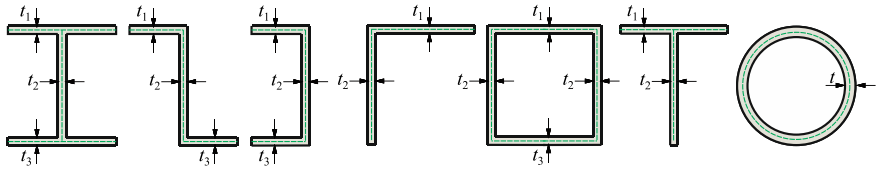


Fig. 24.2 Thin-walled cross-sections and their skeleton lines (dashed lines)

The applied load leads to internal stresses, which in turn can be summarized as internal forces and moments. The internal forces and moments (Fig. 24.1, left) are the normal force N, the two bending moments M_y and M_z and the two transverse shear forces Q_y and Q_z. The associated displacements are the three displacements u, v and w in the directions x, y and z on the one hand and the two rotations φ_y and φ_z on the other (the so-called bending angles), as shown in Fig. 24.1, right. Torsion ϑ of the cross-section around the x-axis is excluded for the time being.

The forces and moments N, M_y, M_z, Q_y and Q_z are linked to the stress components occurring in the isotropic beam (normal stress σ_{xx} and shear stress τ) as shown in Fig. 24.3. The loads q_z and F_z cause the internal bending moment M_y and the transverse shear force Q_z. The loads q_y and F_y, on the other hand, are responsible for the bending moment M_z and the transverse shear force Q_y. A normal force N can also occur. Figure 24.3, top right, shows that the normal force N exclusively causes the normal stress σ_{xx}, which is distributed constantly over the cross-section under certain conditions that are still to be discussed. In addition, the bending moment M_y also causes the normal stress σ_{xx}, which is distributed linearly across the cross-section (Fig. 24.3, center left). The transverse shear force Q_z that also occurs is the cause of the shear stress τ (Fig. 24.3, center right), which is linear in the flanges of the I-beam shown here and quadratic in the web. Their direction of action is indicated by arrows. Finally, the bending moment M_z also occurs, which causes the normal stress σ_{xx}, which also runs linearly across the cross-section, as shown in Fig. 24.3, bottom left. Added to this is the

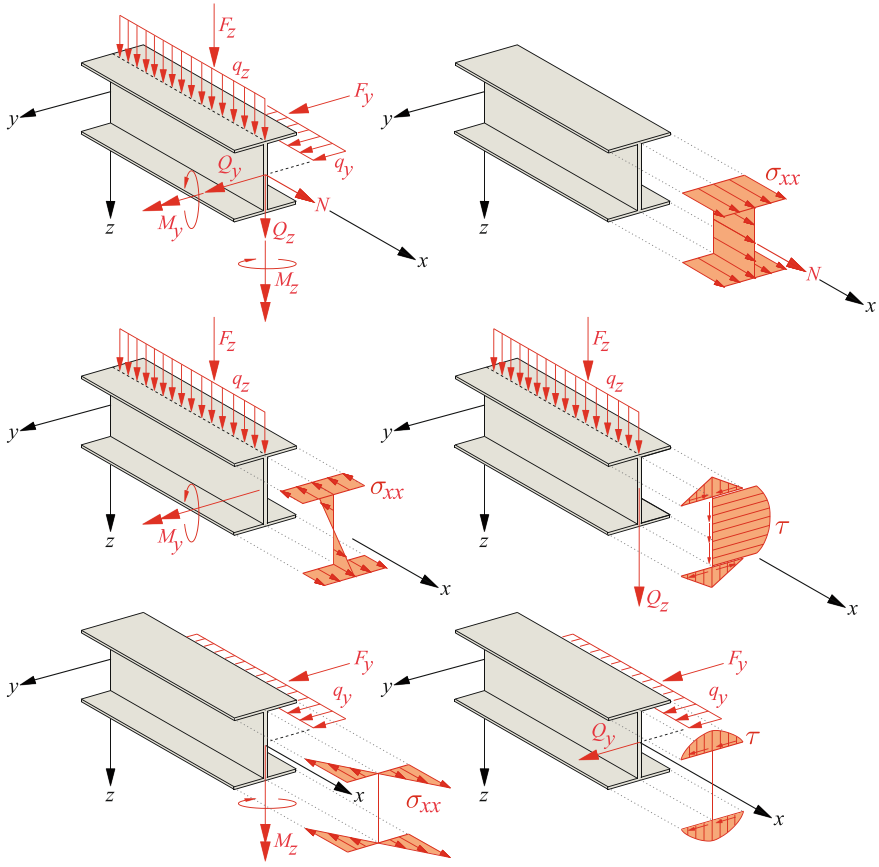


Fig. 24.3 Forces and moments on the isotropic thin-walled beam and the stress components assigned to them

transverse shear force Q_y, which in turn is the cause of the shear stress τ (Fig. 24.3, bottom right). It is then the main task of engineers to determine these stresses and to verify their maximum values against a failure of the material (this can be both yielding or fracture). In addition, the deformations of the beam structure under consideration must be verified against permissible maximum values. It must also be verified that there is no global or local stability failure of the beam. The following section first deals with the determination of the normal stresses σ_{xx} as well as the development of the necessary analytical methods and the calculation of the deformations of beams whose walls consist of composite laminates. The determination of the shear stresses due to the transverse forces that also occur and the investigation of the torsion of beams are dealt with later.

24.2 Beams Under Normal Force and Bending

24.2.1 Basic Equations for an Arbitrary Reference System

In the following, we consider laminated prismatic beam structures that have an arbitrary open-profiled cross-section (Fig. 24.4). The walls can be both flat and curved, the layup of the wall can be variable over the circumference of the cross-section. For the following considerations, we first introduce a right-handed coordinate system $\bar{x}$, $\bar{y}$, $\bar{z}$ at an arbitrary point of the cross-section. Furthermore, a coordinate system x, y, z is arranged at the center of gravity (to be determined). Furthermore, let a local coordinate system ξ, η, ζ be defined in an infinitesimal element (angle of inclination α to the y-axis) as indicated.

In the following, we assume the beam theory according to Euler and Bernoulli and make the following assumptions:

- We assume the hypothesis that the cross-sections remain flat, and also assume that the so-called normal hypothesis is valid. This means that the cross-sections do not deform when the beam deflects and that the cross-sections are orthogonal to the longitudinal axis of the beam even when deformed (Fig. 24.5). Shear strains in the beam are therefore excluded.

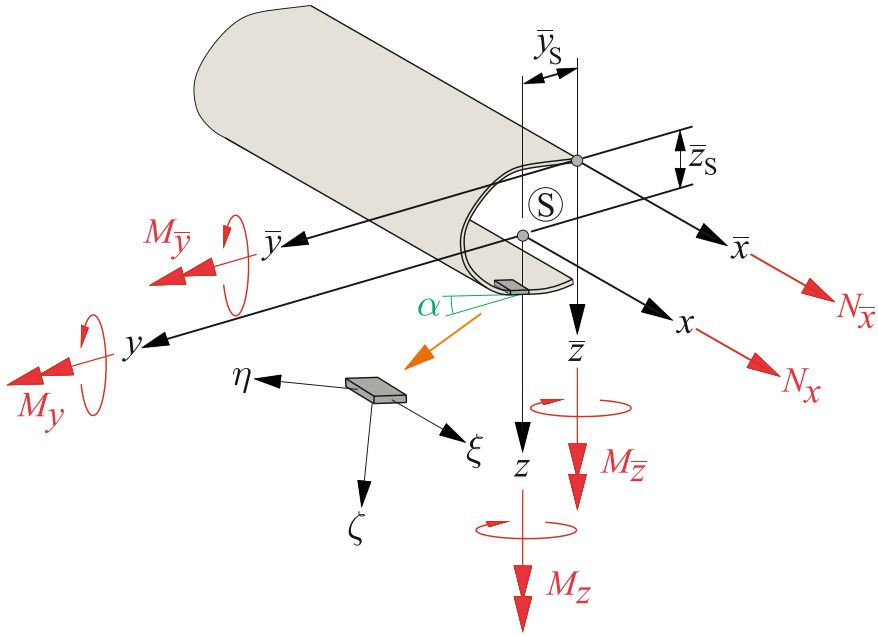


Fig. 24.4 Thin-walled laminated beam with open cross-section

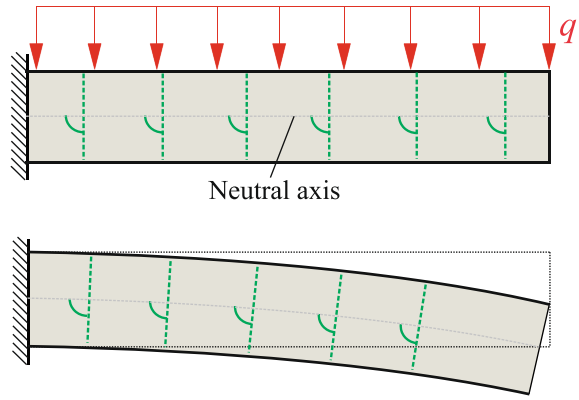


Fig. 24.5 Illustration of the hypothesis of plane cross-sections and the normal hypothesis

However, we will see later that this assumption can lead to contradictory results, but for now we will accept it as a suitable working hypothesis.

- In addition, we assume linear elastic material behaviour, so that Hooke's law applies without restrictions.
- The dimensions of the cross-section are significantly smaller than the length of the beam, so that an idealization within the framework of a beam theory is justified.
- In all further explanations, it is assumed that the cross-sectional shape is completely maintained during deformation due to a given load. We also assume that the cross-sectional shape does not change at the load application points.
- We are working within the framework of a geometrically linear theory, i.e. the deformations are small compared to the length of the beam, but also compared to the dimensions of its cross-section.
- In this chapter, we only analyze straight beam structures.

In the works of Bauchau and Craig (2009), Czerwenka and Schnell (1970), Kindmann and Frickel (2017), Kollár and Springer (2003), Linke and Nast (2015), Megson (1999), Mittelstedt (2021), Petersen (1997) or Roik (1978), the interested reader will find further information on beams under normal force and bending.

The starting point for the following considerations is Fig. 24.6. We introduce a reference system $\bar{x}$, $\bar{y}$, $\bar{z}$ at an arbitrary point of the cross-section and want to determine both the deflection $\bar{w}_P$ and the longitudinal displacement $\bar{u}_P$ of the point P. The displacement $\bar{v}_P$ is taken into account later. It should be noted that the coordinate origin is not at the center of gravity of the cross-section. The displacements to be considered are the displacements $\bar{u}$, $\bar{v}$ and $\bar{z}$ as well as the two cross-sectional rotations or bending angles $\varphi_{\bar{y}}$ and $\varphi_{\bar{z}}$. We first consider the kinematics of the beam in the context of the Euler-Bernoulli theory according to Fig. 24.7, in which a sectional element of the beam is shown in its undeformed and deformed state. There is both a normal force and a bending load, so that the sectional element experiences both a deflection $\bar{w}$ and a longitudinal displacement $\bar{u}$. In the deformed

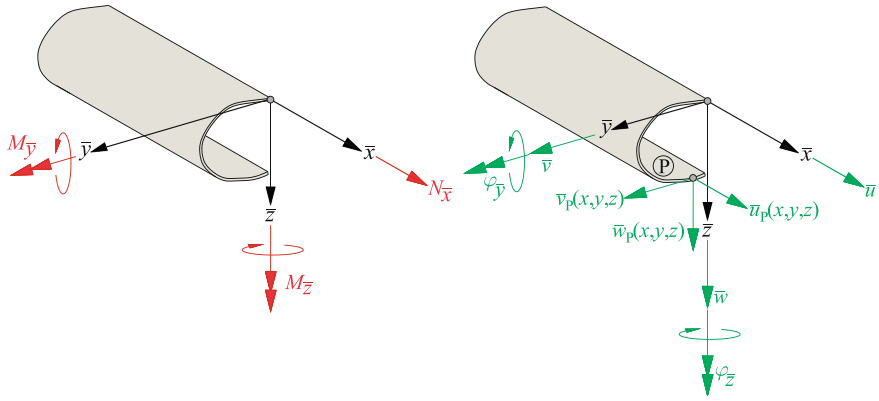


Fig. 24.6 Moment and displacement quantities in an arbitrary reference system $\bar{x}, \bar{y}, \bar{z}$ as well as displacements $\bar{u}_P$, $\bar{v}_P$ and $\bar{w}_P$ of the point P

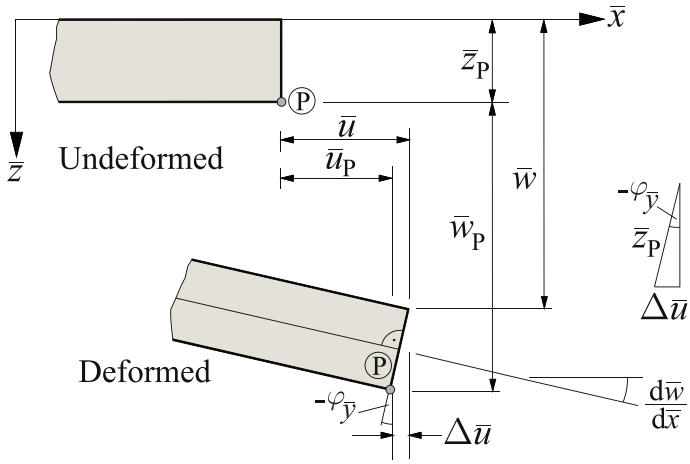


Fig. 24.7 Kinematics of the Euler-Bernoulli beam theory

state, there is also an inclination $\frac{\mathrm{d}\bar{w}}{\mathrm{d}\bar{x}} = \bar{w}'$. We denote the corresponding displacements of the point P as $\bar{w}_P$ and $\bar{u}_P$. Due to the rotation angle $-\varphi_{\bar{y}}$, the coordinate origin undergoes a displacement $\bar{u}$ that is different from the displacement $\bar{u}_P$ of point P. We want to denote the difference between these two displacement values as $\Delta\bar{u}$. To calculate the difference $\Delta\bar{u}$, we look at the right-angled triangle in Fig. 24.7, on the right. We note:

$$\sin(-\varphi_{\bar{y}}) = \frac{\Delta\bar{u}}{\bar{z}_P}. \tag{24.1}$$

Since we assume small deformations and thus also small rotations $\varphi_{\bar{y}}$ and $\varphi_{\bar{z}}$, we can assume $\sin(-\varphi_{\bar{y}}) \simeq -\varphi_{\bar{y}}$ so that:

$$\Delta\bar{u} = -\bar{z}_P \varphi_{\bar{y}}. \tag{24.2}$$

Since we also assume that no warping of the cross-section occurs due to the bending deformation and the normal hypothesis also applies, we can equate the inclination $\frac{\mathrm{d}\bar{w}}{\mathrm{d}\bar{x}} = \bar{w}'$ of the beam deflection $\bar{w}$ and the bending angle $-\varphi_{\bar{y}}$ so that:

$$\Delta\bar{u} = \bar{z}_P \bar{w}'. \tag{24.3}$$

We can therefore write the longitudinal displacement $\bar{u}_P$ of the point P as:

$$\bar{u}_P = \bar{u} - \Delta\bar{u} = \bar{u} - \bar{z}_P \bar{w}'. \tag{24.4}$$

This relationship applies to the case of so-called uniaxial bending, i.e. to the case where only deformations $\bar{u}$ and $\bar{w}$ occur in the $\bar{x}\bar{z}$-plane.

If, on the other hand, the given load leads to the deformations $\bar{u}$ and $\bar{w}$ as well as to the displacement $\bar{v}$ (so-called biaxial bending), Eq. (24.4) expands as follows:

$$\bar{u}_P = \bar{u} - \bar{z}_P \bar{w}' - \bar{y}_p \bar{v}', \tag{24.5}$$

where $\bar{y}_p$ is the distance of the point P from the origin of the reference system $\bar{x}$, $\bar{y}$, $\bar{z}$, analogous to the previous explanations.

Finally, a statement must be made about the relationship between the deflection $\bar{w}$ of the coordinate origin and the deflection $\bar{w}_P$ of point P. Since we assume that the cross-sectional dimensions do not change due to the deformations of the beam, we can equate $\bar{w}$ and $\bar{w}_P$:

$$\bar{w}_P = \bar{w}. \tag{24.6}$$

This applies analogously for the deflections in the $\bar{y}$-direction:

$$\bar{v}_P = \bar{v}. \tag{24.7}$$

Once we have determined the displacement field of the beam, we can turn our attention to the strain field. Since we assume that we are dealing with a slender component with a significantly large length compared to the cross-sectional dimensions and we have also excluded any shear strains, the only strain component that occurs will be the strain $\varepsilon_{\bar{x}\bar{x}P} = \varepsilon^0_{\bar{\xi}\bar{\xi}}$. It is calculated as follows:

$$\varepsilon^0_{\bar{\xi}\bar{\xi}} = \frac{\mathrm{d}\bar{u}_P}{\mathrm{d}\bar{x}} = \bar{u}'_P = \bar{u}' - \bar{z}_P \bar{w}'' - \bar{y}_p \bar{v}''. \tag{24.8}$$

In the following, we use the notations $\kappa^0_{\bar{y}\bar{y}} = -w''$ and $\kappa^0_{\bar{z}\bar{z}} = -v''$ as well as $\varepsilon^0_{\bar{x}\bar{x}} = \bar{u}'$, so that

$$\varepsilon^0_{\bar{\xi}\bar{\xi}} = \varepsilon^0_{\bar{x}\bar{x}} + \bar{z}_P \kappa^0_{\bar{y}\bar{y}} + \bar{y}_p \kappa^0_{\bar{z}\bar{z}}. \tag{24.9}$$

In addition, the following applies to the curvature $\kappa^0_{\xi\xi}$:

$$\kappa^0_{\xi\xi} = \kappa^0_{\bar{y}\bar{y}} \cos\alpha - \kappa^0_{\bar{z}\bar{z}} \sin\alpha. \tag{24.10}$$

In the following, we assume that the forces $N^0_{\eta\eta}$, $N^0_{\xi\eta}$ and the moment $M^0_{\eta\eta}$ disappear in the walls of the cross-section:

$$N^0_{\eta\eta} = N^0_{\xi\eta} = M^0_{\eta\eta} = 0. \tag{24.11}$$

We also want to assume that there is no twisting of the laminate walls:

$$\kappa^0_{\xi\eta} = 0. \tag{24.12}$$

In the following, we will start from three different cases and draw on the explanations in Kollár and Springer (2003):

- Orthotropic, unsymmetric layups with arbitrary cross-section
- Orthotropic, symmetric layups with arbitrary cross-section
- Arbitrary layups with simply symmetric beam cross-section with respect to the $\bar{z}$-axis, load leads to uniaxial bending in the $\bar{x}\bar{z}$-plane.

The constitutive law for the laminates under consideration reads in its inverted form:

$$\begin{pmatrix} \varepsilon^0_{\xi\xi} \\ \varepsilon^0_{\eta\eta} \\ \gamma^0_{\xi\eta} \\ \kappa^0_{\xi\xi} \\ \kappa^0_{\eta\eta} \\ \kappa^0_{\xi\eta} \end{pmatrix} = \begin{bmatrix} \alpha_{11} & \alpha_{22} & 0 & \beta_{11} & \beta_{22} & 0 \\ \alpha_{12} & \alpha_{22} & 0 & \beta_{12} & \beta_{22} & 0 \\ 0 & 0 & \alpha_{66} & 0 & 0 & \beta_{66} \\ \beta_{11} & \beta_{12} & 0 & \delta_{11} & \delta_{12} & 0 \\ \beta_{12} & \beta_{22} & 0 & \delta_{12} & \delta_{22} & 0 \\ 0 & 0 & \beta_{66} & 0 & 0 & \delta_{66} \end{bmatrix} \begin{pmatrix} N^0_{\xi\xi} \\ N^0_{\eta\eta} \\ N^0_{\xi\eta} \\ M^0_{\xi\xi} \\ M^0_{\eta\eta} \\ M^0_{\xi\eta} \end{pmatrix}. \tag{24.13}$$

With the simplifications discussed above, the following results for the three cases mentioned above:

$$\begin{pmatrix} \varepsilon^0_{\xi\xi} \\ \kappa^0_{\xi\xi} \end{pmatrix} = \begin{bmatrix} \alpha_{11} & \beta_{11} \\ \beta_{11} & \delta_{11} \end{bmatrix} \begin{pmatrix} N^0_{\xi\xi} \\ M^0_{\xi\xi} \end{pmatrix}. \tag{24.14}$$

If (24.14) is solved for $N^0_{\xi\xi}$ and $M^0_{\xi\xi}$, then we obtain for orthotropic and unsymmetric layups:

$$\begin{aligned} N^0_{\xi\xi} &= \frac{\delta_{11}}{D}\varepsilon^0_{\xi\xi} - \frac{\beta_{11}}{D}\kappa^0_{\xi\xi}, \\ M^0_{\xi\xi} &= -\frac{\beta_{11}}{D}\varepsilon^0_{\xi\xi} + \frac{\alpha_{11}}{D}\kappa^0_{\xi\xi}, \\ M^0_{\xi\eta} &= 0, \end{aligned} \tag{24.15}$$

with $D = \alpha_{11}\delta_{11} - \beta^2_{11}$.

If we consider a symmetric orthotropic layup, then we obtain:

$$\begin{aligned} N^0_{\xi\xi} &= \frac{1}{a_{11}}\varepsilon^0_{\xi\xi}, \\ M^0_{\xi\xi} &= \frac{1}{d_{11}}\kappa^0_{\xi\xi}, \\ M^0_{\xi\eta} &= 0. \end{aligned} \tag{24.16}$$

Herein, the expressions a_{ij} are the inverted membrane stiffnesses:

$$\begin{pmatrix} \varepsilon^0_{\xi\xi} \\ \varepsilon^0_{\eta\eta} \\ \gamma^0_{\xi\eta} \end{pmatrix} = \begin{bmatrix} a_{11} & a_{22} & 0 \\ a_{12} & a_{22} & 0 \\ 0 & 0 & a_{66} \end{bmatrix} \begin{pmatrix} N^0_{\xi\xi} \\ N^0_{\eta\eta} \\ N^0_{\xi\eta} \end{pmatrix}. \tag{24.17}$$

The expressions d_{ij} are the inverted plate stiffnesses:

$$\begin{pmatrix} \kappa^0_{\xi\xi} \\ \kappa^0_{\eta\eta} \\ \kappa^0_{\xi\eta} \end{pmatrix} = \begin{bmatrix} d_{11} & d_{12} & 0 \\ d_{12} & d_{22} & 0 \\ 0 & 0 & d_{66} \end{bmatrix} \begin{pmatrix} M^0_{\xi\xi} \\ M^0_{\eta\eta} \\ M^0_{\xi\eta} \end{pmatrix}. \tag{24.18}$$

For the arbitrary layup we have:

$$\begin{aligned} N^0_{\xi\xi} &= \frac{\bar{\delta}_{11}}{\bar{D}}\varepsilon^0_{\xi\xi} - \frac{\bar{\beta}_{11}}{\bar{D}}\kappa^0_{\xi\xi}, \\ M^0_{\xi\xi} &= -\frac{\bar{\beta}_{11}}{\bar{D}}\varepsilon^0_{\xi\xi} + \frac{\bar{\alpha}_{11}}{\bar{D}}\kappa^0_{\xi\xi}, \\ M^0_{\xi\eta} &= -\frac{\beta_{16}}{\delta_{66}}N^0_{\xi\xi} - \frac{\delta_{16}}{\delta_{66}}M^0_{\xi\xi}, \end{aligned} \tag{24.19}$$

with

$$\begin{aligned} \bar{\alpha}_{11} &= \alpha_{11} - \frac{\beta^2_{16}}{\delta_{66}}, \\ \bar{\beta}_{11} &= \beta_{11} - \frac{\beta_{16}\delta_{16}}{\delta_{66}}, \\ \bar{\delta}_{11} &= \delta_{11} - \frac{\delta^2_{16}}{\delta_{66}}, \\ \bar{D} &= \bar{\alpha}_{11}\bar{\delta}_{11} - \bar{\beta}^2_{11}. \end{aligned} \tag{24.20}$$

We next consider the force and moment definitions as they are relevant for the present beam situation and first examine the beam with orthotropic and usymmetric layup. For the normal force $N_{\bar{x}}$ we obtain

$$
\begin{aligned}
N_{\bar{x}} &= \oint N^0_{\xi\xi}\mathrm{d}\eta \\
&= \oint \left(\frac{\delta_{11}}{D}\varepsilon^0_{\xi\xi} - \frac{\beta_{11}}{D}\kappa^0_{\xi\xi}\right)\mathrm{d}\eta \\
&= \oint \left[\frac{\delta_{11}}{D}\left(\varepsilon^0_{\bar{x}\bar{x}} + \bar{z}\kappa^0_{\bar{y}\bar{y}} + \bar{y}\kappa^0_{\bar{z}\bar{z}}\right) - \frac{\beta_{11}}{D}\left(\kappa^0_{\bar{y}\bar{y}}\cos\alpha - \kappa^0_{\bar{z}\bar{z}}\sin\alpha\right)\right]\mathrm{d}\eta \\
&= \oint \frac{\delta_{11}}{D}\varepsilon^0_{\bar{x}\bar{x}}\mathrm{d}\eta + \oint \left(\frac{\delta_{11}}{D}\bar{z} - \frac{\beta_{11}}{D}\cos\alpha\right)\kappa^0_{\bar{y}\bar{y}}\mathrm{d}\eta + \oint \left(\frac{\delta_{11}}{D}\bar{y} + \frac{\beta_{11}}{D}\sin\alpha\right)\kappa^0_{\bar{z}\bar{z}}\mathrm{d}\eta.
\end{aligned}
\tag{24.21}
$$

We proceed in the same way for the bending moment $M_{\bar{y}}$ and obtain:

$$
\begin{aligned}
M_{\bar{y}} &= \oint M^0_{\xi\xi}\cos\alpha\mathrm{d}\eta + \oint \bar{z}N^0_{\xi\xi}\mathrm{d}\eta \\
&= \oint \left(-\frac{\beta_{11}}{D}\varepsilon^0_{\xi\xi} + \frac{\alpha_{11}}{D}\kappa^0_{\xi\xi}\right)\cos\alpha\mathrm{d}\eta + \oint \bar{z}\left(\frac{\delta_{11}}{D}\varepsilon^0_{\xi\xi} - \frac{\beta_{11}}{D}\kappa^0_{\xi\xi}\right)\mathrm{d}\eta \\
&= \oint \left(\frac{\delta_{11}}{D}\bar{z} - \frac{\beta_{11}}{D}\cos\alpha\right)\varepsilon^0_{\bar{x}\bar{x}}\mathrm{d}\eta \\
&\quad + \oint \left(\frac{\delta_{11}}{D}\bar{z}^2 - 2\frac{\beta_{11}}{D}\cos\alpha\bar{z} + \frac{\alpha_{11}}{D}\cos^2\alpha\right)\kappa^0_{\bar{y}\bar{y}}\mathrm{d}\eta \\
&\quad + \oint \left(\frac{\delta_{11}}{D}\bar{y}\bar{z} + \frac{\beta_{11}}{D}\left(\bar{z}\sin\alpha - \bar{y}\cos\alpha\right) - \frac{\alpha_{11}}{D}\sin\alpha\cos\alpha\right)\kappa^0_{\bar{z}\bar{z}}\mathrm{d}\eta.
\end{aligned}
\tag{24.22}
$$

Finally, the following results for the bending moment $M_{\bar{z}}$:

$$
\begin{aligned}
M_{\bar{z}} &= \oint M^0_{\xi\xi}\sin\alpha\mathrm{d}\eta - \oint \bar{y}N^0_{\xi\xi}\mathrm{d}\eta \\
&= -\oint \left(\frac{\delta_{11}}{D}\bar{y} + \frac{\beta_{11}}{D}\sin\alpha\right)\varepsilon^0_{\bar{x}\bar{x}}\mathrm{d}\eta \\
&\quad + \oint \left(-\frac{\delta_{11}}{D}\bar{y}\bar{z} + \frac{\beta_{11}}{D}\left(-\bar{z}\sin\alpha + \bar{y}\cos\alpha\right) + \frac{\alpha_{11}}{D}\cos\alpha\sin\alpha\right)\kappa^0_{\bar{y}\bar{y}}\mathrm{d}\eta \\
&\quad - \oint \left(\frac{\delta_{11}}{D}\bar{y}^2 + 2\frac{\beta_{11}}{D}\bar{y}\sin\alpha + \frac{\alpha_{11}}{D}\sin^2\alpha\right)\kappa^0_{\bar{z}\bar{z}}\mathrm{d}\eta.
\end{aligned}
\tag{24.23}
$$

In a vector-matrix-notation, the relationships (24.21)–(24.23) can be summarized as:

$$
\begin{pmatrix} N_{\bar{x}} \\ M_{\bar{y}} \\ -M_{\bar{z}} \end{pmatrix} = \begin{bmatrix} EA & ES_{\bar{y}} & ES_{\bar{z}} \\ ES_{\bar{y}} & EI_{\bar{y}\bar{y}} & EI_{\bar{y}\bar{z}} \\ ES_{\bar{z}} & EI_{\bar{y}\bar{z}} & EI_{\bar{z}\bar{z}} \end{bmatrix} \begin{pmatrix} \varepsilon^0_{\bar{x}\bar{x}} \\ \kappa^0_{\bar{y}\bar{y}} \\ \kappa^0_{\bar{z}\bar{z}} \end{pmatrix}. \tag{24.24}
$$

Here EA is the effective extensional stiffness of the beam under consideration:

$$EA = \oint \frac{\delta_{11}}{D} \mathrm{d}\eta. \tag{24.25}$$

The quantities $EI_{\bar{y}\bar{y}}$, $EI_{\bar{z}\bar{z}}$ and $EI_{\bar{y}\bar{z}}$ are the two effective bending stiffnesses and the effective deviation stiffness of the beam:

$$\begin{aligned}
EI_{\bar{y}\bar{y}} &= \oint \left(\frac{\delta_{11}}{D} \bar{z}^2 - 2\frac{\beta_{11}}{D} \bar{z} \cos\alpha + \frac{\alpha_{11}}{D} \cos^2\alpha \right) \mathrm{d}\eta, \\
EI_{\bar{z}\bar{z}} &= \oint \left(\frac{\delta_{11}}{D} \bar{y}^2 + 2\frac{\beta_{11}}{D} \bar{y} \sin\alpha + \frac{\alpha_{11}}{D} \sin^2\alpha \right) \mathrm{d}\eta, \\
EI_{\bar{y}\bar{z}} &= \oint \left(\frac{\delta_{11}}{D} \bar{y}\bar{z} + \frac{\beta_{11}}{D} (\bar{z} \sin\alpha - \bar{y} \cos\alpha) - \frac{\alpha_{11}}{D} \sin\alpha \cos\alpha \right) \mathrm{d}\eta.
\end{aligned} \tag{24.26}$$

The quantities $ES_{\bar{y}}$ and $ES_{\bar{z}}$ can be interpreted as effective static moments of the cross-section, which must become zero in a center of gravity reference system:

$$\begin{aligned}
ES_{\bar{y}} &= \oint \left(\frac{\delta_{11}}{D} \bar{z} - \frac{\beta_{11}}{D} \cos\alpha \right) \mathrm{d}\eta, \\
ES_{\bar{z}} &= \oint \left(\frac{\delta_{11}}{D} \bar{y} + \frac{\beta_{11}}{D} \sin\alpha \right) \mathrm{d}\eta.
\end{aligned} \tag{24.27}$$

24.2.2 First Cross-Sectional Normalization

We now shift the coordinate system by the amounts $\bar{y}_S$, $\bar{z}_S$ to the center of gravity S of the cross-section (Fig. 24.4). The following relationship exists between the center of gravity axes x, y, z and the previously used axes $\bar{x}$, $\bar{y}$, $\bar{z}$:

$$x = \bar{x}, \quad y = \bar{y} - \bar{y}_S, \quad z = \bar{z} - \bar{z}_S. \tag{24.28}$$

We require that the two effective static moments ES_y and ES_z become zero when the considerations are related to a center of gravity coordinate system:

$$\begin{aligned}
\oint \left(\frac{\delta_{11}}{D} z - \frac{\beta_{11}}{D} \cos\alpha \right) \mathrm{d}\eta &= \oint \left(\frac{\delta_{11}}{D} (\bar{z} - \bar{z}_S) - \frac{\beta_{11}}{D} \cos\alpha \right) \mathrm{d}\eta = 0, \\
\oint \left(\frac{\delta_{11}}{D} y + \frac{\beta_{11}}{D} \sin\alpha \right) \mathrm{d}\eta &= \oint \left(\frac{\delta_{11}}{D} (\bar{y} - \bar{y}_S) + \frac{\beta_{11}}{D} \sin\alpha \right) \mathrm{d}\eta = 0.
\end{aligned} \tag{24.29}$$

which can be solved for the center of gravity coordinates $\bar{y}_S$ and $\bar{z}_S$:

$$\bar{y}_S = \frac{\oint \left(\frac{\delta_{11}}{D} \bar{y} + \frac{\beta_{11}}{D} \sin\alpha \right) \mathrm{d}\eta}{\oint \frac{\delta_{11}}{D} \mathrm{d}\eta},$$
$$\bar{z}_S = \frac{\oint \left(\frac{\delta_{11}}{D} \bar{z} - \frac{\beta_{11}}{D} \cos\alpha \right) \mathrm{d}\eta}{\oint \frac{\delta_{11}}{D} \mathrm{d}\eta}. \tag{24.30}$$

The effective extensional stiffness EA of the considered beam remains unchanged during the first cross-section normalization:

$$EA = \oint \frac{\delta_{11}}{D} \mathrm{d}\eta. \tag{24.31}$$

On the other hand, the effective bending stiffnesses EI_{yy}, EI_{zz} and the effective deviation stiffness EI_{yz} require separate consideration. For the bending stiffness EI_{yy} we obtain

$$\begin{aligned} EI_{yy} &= \oint \left(\frac{\delta_{11}}{D} z^2 - 2\frac{\beta_{11}}{D} z\cos\alpha + \frac{\alpha_{11}}{D}\cos^2\alpha \right) \mathrm{d}\eta \\ &= \oint \left(\frac{\delta_{11}}{D} (\bar{z} - \bar{z}_S)^2 - 2\frac{\beta_{11}}{D} (\bar{z} - \bar{z}_S)\cos\alpha + \frac{\alpha_{11}}{D}\cos^2\alpha \right) \mathrm{d}\eta \\ &= \oint \left(\frac{\delta_{11}}{D} \bar{z}^2 - 2\bar{z}\frac{\beta_{11}}{D}\cos\alpha + \frac{\alpha_{11}}{D}\cos^2\alpha \right) \mathrm{d}\eta \\ &\quad + \bar{z}_S^2 \oint \frac{\delta_{11}}{D} \mathrm{d}\eta \\ &\quad + 2\bar{z}_S \oint \left(\frac{\beta_{11}}{D}\cos\alpha - \frac{\delta_{11}}{D}\bar{z} \right) \mathrm{d}\eta \\ &= EI_{\bar{y}\bar{y}} + \bar{z}_S^2 EA - 2\bar{z}_S ES_{\bar{y}}. \end{aligned} \tag{24.32}$$

With $ES_{\bar{y}} = \bar{z}_S EA$ it follows:

$$EI_{yy} = EI_{\bar{y}\bar{y}} - \bar{z}_S^2 EA. \tag{24.33}$$

Analogously we obtain:

$$\begin{aligned} EI_{zz} &= EI_{\bar{z}\bar{z}} - \bar{y}_S^2 EA, \\ EI_{yz} &= EI_{\bar{y}\bar{z}} - \bar{y}_S \bar{z}_S EA. \end{aligned} \tag{24.34}$$

This is Steiner's theorem[1] or the parallel axis theorem for the thin-walled laminated cross-section considered here with unsymmetric orthotropic layup.

In many technical applications, the center of gravity coordinates $\bar{y}_S$ and $\bar{z}_S$ are first determined using (24.30) and then the necessary cross-sectional properties are determined from the center of gravity system. For the cross-section of arbitrary shape with an orthotropic unsymmetric layup, we obtain

$$\begin{aligned}
EA &= \oint \frac{\delta_{11}}{D} \mathrm{d}\eta, \\
EI_{yy} &= \oint \left(\frac{\delta_{11}}{D} z^2 - 2\frac{\beta_{11}}{D} z \cos\alpha + \frac{\alpha_{11}}{D} \cos^2\alpha \right) \mathrm{d}\eta, \\
EI_{zz} &= \oint \left(\frac{\delta_{11}}{D} y^2 + 2\frac{\beta_{11}}{D} y \sin\alpha + \frac{\alpha_{11}}{D} \sin^2\alpha \right) \mathrm{d}\eta, \\
EI_{yz} &= \oint \left(\frac{\delta_{11}}{D} yz + \frac{\beta_{11}}{D} (z\sin\alpha - y\cos\alpha) - \frac{\alpha_{11}}{D} \sin\alpha\cos\alpha \right) \mathrm{d}\eta.
\end{aligned} \tag{24.35}$$

The constitutive law of the beam can then be written as:

$$\begin{pmatrix} N_x \\ M_y \\ -M_z \end{pmatrix} = \begin{bmatrix} EA & 0 & 0 \\ 0 & EI_{yy} & EI_{yz} \\ 0 & EI_{yz} & EI_{zz} \end{bmatrix} \begin{pmatrix} \varepsilon^0_{xx} \\ \kappa^0_{yy} \\ \kappa^0_{zz} \end{pmatrix}. \tag{24.36}$$

Apparently, after the first cross-sectional normalization, the normal force effect is completely decoupled from the bending effect. However, the two bending effects, characterized by the two bending moments M_y and M_z as well as the two curvatures κ^0_{yy} and κ^0_{zz}, are still coupled with each other.

For the cross-section of arbitrary shape with a symmetric orthotropic layup, we obtain the effective stiffnesses as:

$$\begin{aligned}
EA &= \oint \frac{\mathrm{d}\eta}{a_{11}}, \\
EI_{yy} &= \oint \left(\frac{1}{a_{11}} z^2 + \frac{1}{d_{11}} \cos^2\alpha \right) \mathrm{d}\eta, \\
EI_{zz} &= \oint \left(\frac{1}{a_{11}} y^2 + \frac{1}{d_{11}} \sin^2\alpha \right) \mathrm{d}\eta, \\
EI_{yz} &= \oint \left(\frac{1}{a_{11}} yz + \frac{1}{d_{11}} \sin\alpha\cos\alpha \right) \mathrm{d}\eta.
\end{aligned} \tag{24.37}$$

[1] Jakob Steiner (1796–1863), Swiss mathematician.

The center of gravity coordinates in this case follow as:

$$\bar{y}_S = \frac{\oint \frac{\bar{y}}{a_{11}} \mathrm{d}\eta}{\oint \frac{1}{a_{11}} \mathrm{d}\eta}, \quad \bar{z}_S = \frac{\oint \frac{\bar{z}}{a_{11}} \mathrm{d}\eta}{\oint \frac{1}{a_{11}} \mathrm{d}\eta}. \tag{24.38}$$

If we are dealing with a simply symmetric cross-section under uniaxial bending with arbitrary layup of the beam walls, then the required effective stiffnesses result as follows:

$$\begin{aligned} EA &= \oint \frac{\bar{\delta}_{11}}{\bar{D}} \mathrm{d}\eta, \\ EI_{yy} &= \oint \left(\frac{\bar{\delta}_{11}}{\bar{D}} z^2 - 2\frac{\bar{\beta}_{11}}{\bar{D}} z \cos\alpha + \frac{\bar{\alpha}_{11}}{\bar{D}} \cos^2\alpha \right) \mathrm{d}\eta. \end{aligned} \tag{24.39}$$

The location of the center of gravity follows as:

$$\bar{y}_S = 0, \quad \bar{z}_S = \frac{\oint \left(\frac{\bar{\delta}_{11}}{\bar{D}} \bar{z} - \frac{\bar{\beta}_{11}}{\bar{D}} \cos\alpha \right) \mathrm{d}\eta}{\oint \frac{\bar{\delta}_{11}}{\bar{D}} \mathrm{d}\eta}. \tag{24.40}$$

If the cross-section is composed of a number n of straight segments (see Fig. 24.2), then the previous calculation equations with

$$\oint (\ldots)\, \mathrm{d}\eta = \sum_{k=1}^{n} \int_{-\frac{l_k}{2}}^{\frac{l_k}{2}} (\ldots)\, \mathrm{d}\eta_k \tag{24.41}$$

lead to the following calculation rule for the beam with arbitrary cross-sectional shape and orthotropic layup (see Fig. 24.8). For the location of the center of gravity we obtain:

$$\begin{aligned} \bar{y}_S &= \frac{\sum_{k=1}^{n} \left(\frac{\delta_{11,k}}{D_k} \bar{y}_{S,k} l_k + \frac{\beta_{11,k}}{D_k} l_k \sin\alpha_k \right)}{\sum_{k=1}^{n} \frac{\delta_{11,k}}{D_k} l_k}, \\ \bar{z}_S &= \frac{\sum_{k=1}^{n} \left(\frac{\delta_{11,k}}{D_k} \bar{z}_{S,k} l_k - \frac{\beta_{11,k}}{D_k} l_k \cos\alpha_k \right)}{\sum_{k=1}^{n} \frac{\delta_{11,k}}{D_k} l_k}. \end{aligned} \tag{24.42}$$

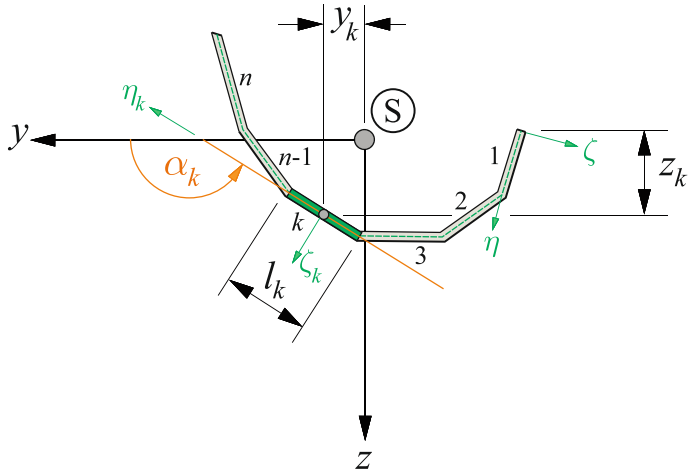


Fig. 24.8 Cross-section consisting of n straight segments

The effective stiffnesses follow as:

$$
\begin{aligned}
EA &= \sum_{k=1}^{n} \frac{\delta_{11,k} l_k}{D_k}, \\
EI_{yy} &= \sum_{k=1}^{n} \left[\frac{\delta_{11,k}}{D_k} \left(l_k z_k^2 + \frac{l_k^3 \sin^2 \alpha_k}{12} \right) - 2 \frac{\beta_{11,k}}{D_k} z_k l_k \cos \alpha_k + \frac{\alpha_{11,k}}{D_k} l_k \cos^2 \alpha_k \right], \\
EI_{zz} &= \sum_{k=1}^{n} \left[\frac{\delta_{11,k}}{D_k} \left(l_k y_k^2 + \frac{l_k^3 \cos^2 \alpha_k}{12} \right) + 2 \frac{\beta_{11,k}}{D_k} y_k l_k \sin \alpha_k + \frac{\alpha_{11,k}}{D_k} l_k \sin^2 \alpha_k \right], \\
EI_{yz} &= \sum_{k=1}^{n} \left[\frac{\delta_{11,k}}{D_k} \left(l_k y_k z_k + \frac{l_k^3 \cos \alpha_k \sin \alpha_k}{12} \right) \right. \\
&\quad \left. + \frac{\beta_{11,k}}{D_k} l_k \left(z_k \sin \alpha_k - y_k \cos \alpha_k \right) - \frac{\alpha_{11,k}}{D_k} l_k \sin \alpha_k \cos \alpha_k \right].
\end{aligned}
\tag{24.43}
$$

24.2.3 Selected Cross-Sections

An overview (Fig. 24.9) of selected practically relevant cross-sections can be found below (according to Kollár and Springer (2003), w = web, f = flange). The formulas were analyzed for very thin-walled cross-sections whose profiles can be described using their skeleton lines.

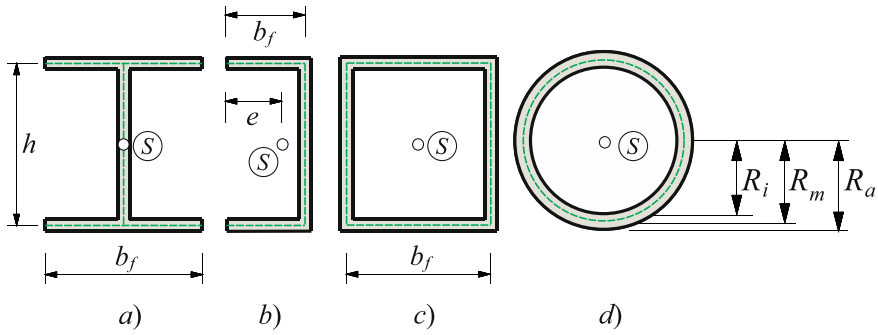


Fig. 24.9 Selected cross-sections with orthotropic symmetric layups

24.2.3.1 Orthotropic Symmetric Layups

For the doubly symmetric I-cross-section of Fig. 24.9a we obtain:

$$\begin{aligned} EA &= \frac{2b_f}{a_{11,f}} + \frac{h}{a_{11,w}}, \\ EI_{yy} &= \frac{b_f}{a_{11,f}}\frac{h^2}{2} + \frac{2b_f}{d_{11,f}} + \frac{h^3}{12a_{11,w}}, \\ EI_{zz} &= \frac{h}{d_{11,w}} + \frac{2b_f^3}{12a_{11,f}}, \\ EI_{yz} &= 0. \end{aligned} \tag{24.44}$$

The effective stiffnesses for the C-section of Fig. 24.9b are as follows:

$$\begin{aligned} EA &= \frac{2b_f}{a_{11,f}} + \frac{h}{a_{11,w}}, \\ EI_{yy} &= \frac{b_f}{a_{11,f}}\frac{h^2}{2} + \frac{2b_f}{d_{11,f}} + \frac{h^3}{12a_{11,w}}, \\ EI_{zz} &= \frac{h}{a_{11,w}}\left(b_f - e\right)^2 + \frac{h}{d_{11,w}} + \frac{2}{a_{11,f}}\left(\frac{e^3}{3} + \frac{\left(b_f - e\right)^3}{3}\right), \\ EI_{yz} &= 0, \\ e &= \frac{1}{EA}\left(\frac{2b_f}{a_{11,f}}\frac{b_f}{2} + \frac{h}{a_{11,w}}b_f\right). \end{aligned} \tag{24.45}$$

For the box cross-section of Fig. 24.9c results:

$$
\begin{aligned}
EA &= \frac{2b_f}{a_{11,f}} + \frac{2h}{a_{11,w}}, \\
EI_{yy} &= \frac{b_f}{a_{11,f}}\frac{h^2}{2} + \frac{2b_f}{d_{11,f}} + \frac{2h^3}{12a_{11,w}}, \\
EI_{zz} &= \frac{h}{a_{11,w}}\frac{b_f^2}{2} + \frac{2h}{d_{11,w}} + \frac{2b_f^3}{12a_{11,f}}, \\
EI_{yz} &= 0.
\end{aligned} \tag{24.46}
$$

At the circular cross-section of Fig. 24.9d follows:

$$
\begin{aligned}
EA &= \frac{2R_m\pi}{a_{11}}, \\
EI_{yy} &= \pi\left(\frac{R_m^3}{a_{11}} + \frac{R_m}{d_{11}}\right), \\
EI_{zz} &= \pi\left(\frac{R_m^3}{a_{11}} + \frac{R_m}{d_{11}}\right), \\
EI_{yz} &= 0.
\end{aligned} \tag{24.47}
$$

24.2.3.2 Orthotropic Unsymmetric Layups

We also consider open-profile cross-sections with orthotropic and unsymmetric layups (Fig. 24.10). Here, the expressions α_{11} and δ_{11} are to be evaluated in the neutral plane of the walls, which is located at the point $e = -\frac{\beta_{11}}{\delta_{11}}$, where in the expression for e the stiffnesses in the middle plane of the wall are to be evaluated.

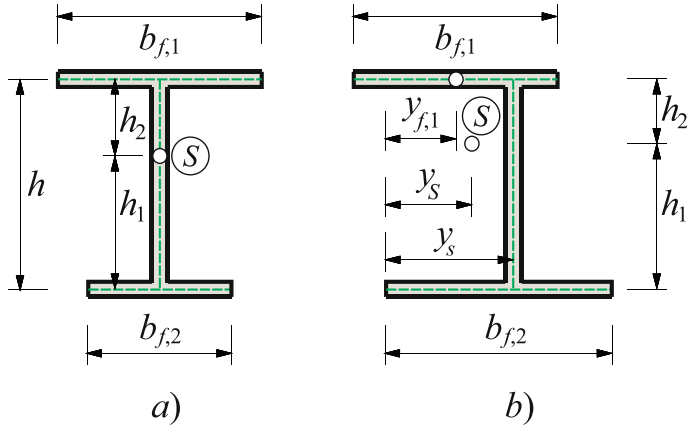


Fig. 24.10 Selected open-profile cross-sections with orthotropic unsymmetric layups

For the cross-section of Fig. 24.10a the effective stiffnesses are:

$$
\begin{aligned}
EA &= \frac{b_{f,1}}{\alpha_{11,f,1}} + \frac{b_{f,2}}{\alpha_{11,f,2}} + \frac{h}{\alpha_{11,w}}, \\
EI_{yy} &= \frac{b_{f,1}}{\alpha_{11,f,1}} (h-h_1)^2 + \frac{b_{f,2}}{\alpha_{11,f,2}} h_1^2 + \frac{b_{f,1}}{\delta_{11,f,1}} + \frac{b_{f,2}}{\delta_{11,f,2}} + \frac{1}{\alpha_{11,w}} \frac{h_1^3 + h_2^3}{3}, \\
EI_{zz} &= \frac{h}{\delta_{11,w}} + \frac{1}{\alpha_{11,f,1}} \frac{b_{f,1}^3}{12} + \frac{1}{\alpha_{11,f,2}} \frac{b_{f,2}^3}{12}, \\
EI_{yz} &= 0, \\
h_1 &= \frac{1}{EA} \left(\frac{b_{f,1}}{\alpha_{11,f,1}} h + \frac{h}{\alpha_{11,w}} \frac{h}{2} \right).
\end{aligned}
\tag{24.48}
$$

The effective stiffnesses for the cross-section of Fig. 24.10b are as follows:

$$
\begin{aligned}
EA &= \frac{b_{f,1}}{\alpha_{11,f,1}} + \frac{b_{f,2}}{\alpha_{11,f,2}} + \frac{h}{\alpha_{11,w}}, \\
EI_{yy} &= \frac{b_{f,1}}{\alpha_{11,f,1}} (h-h_1)^2 + \frac{b_{f,2}}{\alpha_{11,f,2}} h_1^2 + \frac{b_{f,1}}{\delta_{11,f,1}} + \frac{b_{f,2}}{\delta_{11,f,2}} + \frac{1}{\alpha_{11,w}} \frac{b_{f,1} + b_{f,2}}{3}, \\
EI_{zz} &= \frac{h}{\alpha_{11,w}} (y_s - y_S)^2 + \frac{h}{\delta_{11,w}} + \frac{1}{\alpha_{11,f,1}} \frac{b_{f,1}^3}{12} + \frac{1}{\alpha_{11,f,2}} \frac{b_{f,2}^3}{12} \\
&\quad + \frac{b_{f,1}}{\alpha_{11,f,1}} \left(y_S - y_{f,1} \right)^2 + \frac{b_{f,2}}{\alpha_{11,f,2}} \left(y_S - \frac{b_{f,2}}{2} \right)^2, \\
EI_{yz} &= \frac{b_{f,1}}{\alpha_{11,f,1}} \left(y_{f,1} - y_S \right) (h-h_1) - \frac{b_{f,2}}{\alpha_{11,f,2}} \left(\frac{b_{f,2}}{2} - y_S \right) h_1 \\
&\quad + \frac{h}{\alpha_{11,w}} (y_s - y_S) \left(\frac{h}{2} - h_1 \right), \\
h_1 &= \frac{1}{EA} \left(\frac{b_{f,1}}{\alpha_{11,f,1}} h + \frac{h}{\alpha_{11,w}} \frac{h}{2} \right), \\
y_S &= \frac{1}{EA} \left(\frac{b_{f,1}}{\alpha_{11,f,1}} y_{f,1} + \frac{b_{f,2}}{\alpha_{11,f,2}} \frac{b_{f,2}}{2} + \frac{h}{\alpha_{11,w}} y_s \right).
\end{aligned}
\tag{24.49}
$$

For the thin-walled closed cross-sections of Fig. 24.11 we obtain the following effective stiffnesses. Here, the quantity $\hat{\alpha}_{11} = \alpha_{11} - \frac{\beta_{12}^2}{\delta_{22}}$ is evaluated at the point $e = -\frac{\hat{\beta}_{11}}{\hat{\delta}_{11}}$ (with $\hat{\beta}_{11} = \beta_{11} - \frac{\beta_{12}\delta_{12}}{\delta_{22}}$ and $\hat{\delta}_{11} = \delta_{11} - \frac{\delta_{12}^2}{\delta_{22}}$, evaluated in the middle plane of the wall). The stiffnesses α_{11} and δ_{11} are to be determined at the point $e = -\frac{\beta_{11}}{\delta_{11}}$, whereby the stiffnesses in the middle plane of the wall are to be evaluated in the expression for e. The box cross-section of Fig. 24.11a has the following effective stiffnesses:

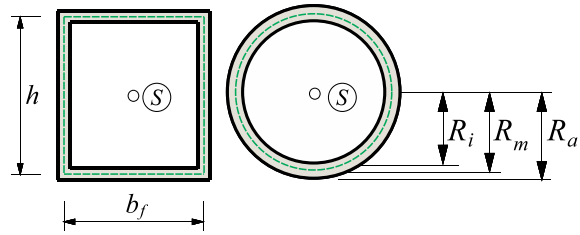


Fig. 24.11 Selected closed cross-sections with orthotropic unsymmetric layups

$$
\begin{aligned}
EA &= \frac{2b_f}{\hat{\alpha}_{11,f}} + \frac{2h}{\hat{\alpha}_{11,w}}, \\
EI_{yy} &= \frac{b_f}{\alpha_{11,f}}\frac{h^2}{2} + \frac{2b_f}{\delta_{11,f}} + \frac{2h^3}{12\alpha_{11,w}}, \\
EI_{zz} &= \frac{h}{\alpha_{11,w}}\frac{b_f^2}{2} + \frac{2h}{\delta_{11,w}} + \frac{2b_f^3}{12\alpha_{11,f}}, \\
EI_{yz} &= 0.
\end{aligned}
\tag{24.50}
$$

For the circular cross-section of Fig. 24.11b results:

$$
\begin{aligned}
EA &= \frac{2R_m\pi}{\hat{\alpha}_{11}}, \\
EI_{yy} &= \pi\left(\frac{R_m^3}{\alpha_{11}} + \frac{R_m}{\delta_{11}}\right), \\
EI_{zz} &= \pi\left(\frac{R_m^3}{\alpha_{11}} + \frac{R_m}{\delta_{11}}\right), \\
EI_{yz} &= 0.
\end{aligned}
\tag{24.51}
$$

24.2.3.3 Arbitrary Layups

Finally, the simply symmetric cross-sections of Fig. 24.12 with arbitrary layups are considered. Here, the variables $\bar{\alpha}_{11}$ and $\bar{\delta}_{11}$ are evaluated at the point $e = -\frac{\bar{\beta}_{11}}{\bar{\delta}_{11}}$, with $\bar{\beta}_{11} = \beta_{11} - \frac{\beta_{16}\delta_{16}}{\delta_{66}}$ and $\bar{\delta}_{11} = \delta_{11} - \frac{\delta_{16}^2}{\delta_{66}}$ (evaluated in the middle plane of the wall).

For the cross-section of Fig. 24.12a we obtain:

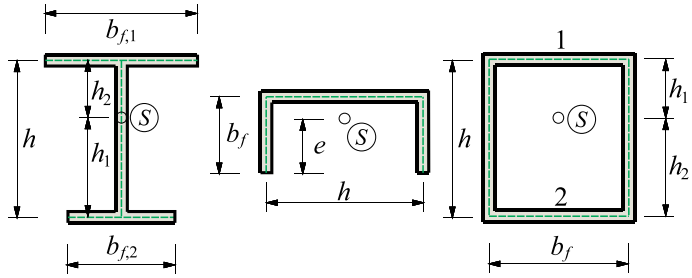


Fig. 24.12 Selected single symmetric cross-sections with arbitrary layups

$$
\begin{aligned}
EA &= \frac{b_{f,1}}{\bar{\alpha}_{11,f,1}} + \frac{b_{f,2}}{\bar{\alpha}_{11,f,2}} + \frac{h}{\alpha_{11,w}}, \\
EI_{yy} &= \frac{b_{f,1}}{\bar{\alpha}_{11,f,1}} (h - h_1)^2 + \frac{b_{f,2}}{\bar{\alpha}_{11,f,2}} h_1^2 + \frac{b_{f,1}}{\bar{\delta}_{11,f,1}} + \frac{b_{f,2}}{\bar{\delta}_{11,f,2}} + \frac{1}{\alpha_{11,w}} \frac{h_1^3 + h_2^2}{3}, \\
h_1 &= \frac{1}{EA} \left(\frac{b_{f,1}}{\bar{\alpha}_{11,f,1}} + \frac{h}{\alpha_{11,w}} \frac{h}{2} \right).
\end{aligned} \tag{24.52}
$$

The stiffnesses for the cross-section of Fig. 24.12b are as follows:

$$
\begin{aligned}
EA &= \frac{2b_f}{\bar{\alpha}_{11,f}} + \frac{h}{\bar{\alpha}_{11,w}}, \\
EI_{yy} &= \frac{2}{\bar{\alpha}_{11,f}} \frac{b_f^3}{12} + \frac{2}{\bar{\alpha}_{11,f}} b_f \left(\frac{b_f}{2} - e \right)^2 + \frac{h}{\bar{\alpha}_{11,w}} (b_f - e)^2 + \frac{h}{\bar{\delta}_{11,w}}, \\
e &= \frac{1}{EA} \left(\frac{2b_f}{\bar{\alpha}_{11,f}} \frac{b_f}{2} + \frac{h}{\bar{\alpha}_{11,w}} b_f \right).
\end{aligned} \tag{24.53}
$$

For the box cross-section of Fig. 24.12c follows:

$$
\begin{aligned}
EA &= \frac{b_f}{\bar{\alpha}_{11,f,1}} + \frac{b_f}{\bar{\alpha}_{11,f,2}} + \frac{2h}{\bar{\alpha}_{11,w}}, \\
EI_{yy} &= \frac{b_f}{\bar{\delta}_{11,f,1}} + \frac{b_f}{\bar{\delta}_{11,f,2}} + \frac{2h^3}{12\bar{\alpha}_{11,w}} \\
&\quad + \frac{b_f}{\bar{\alpha}_{11,f,1}} (h - h_2)^2 + \frac{b_f}{\bar{\alpha}_{11,f,2}} h_2^2 + \frac{2h}{\bar{\alpha}_{11,w}} \left(\frac{h}{2} - h_2 \right)^2, \\
h_1 &= \frac{1}{EA} \left(\frac{b_f}{\bar{\alpha}_{11,f,1}} h + \frac{2h}{\bar{\alpha}_{11,w}} \frac{h}{2} \right).
\end{aligned} \tag{24.54}
$$

24.2.4 Second Cross-Sectional Normalization

We now want to determine the principal axis system x_p, y_p, z_p for the types of cross-sections considered so far. We obtain this principal axis system by rotating the reference system x, y, z by the principal axis angle φ_0 around the center of gravity axis x. The principal axis system is characterized by a vanishing deviation stiffness EI_{yz}. In the principal axis system, the two effective bending stiffnesses assume extremal values.

The coordinate system x, y, z is rotated by an arbitrary angle φ into a new reference system $\hat{x}$, $\hat{y}$, $\hat{z}$ (Fig. 24.13). The corresponding transformation rules can be specified as:

$$y = \hat{y}\cos\varphi + \hat{z}\sin\varphi, \quad z = -\hat{y}\sin\varphi + \hat{z}\cos\varphi. \tag{24.55}$$

The transformation equations for the effective bending stiffnesses and the effective deviation stiffness during the transition from the reference system x, y, z to the new system $\hat{x}$, $\hat{y}$, $\hat{z}$ by means of rotation around the fixed axis $x = \hat{x}$ by the angle φ are as follows:

$$\begin{aligned}
EI_{\hat{y}\hat{y}} &= \frac{1}{2}\left(EI_{yy} + EI_{zz}\right) + \frac{1}{2}\left(EI_{yy} - EI_{zz}\right)\cos 2\varphi - EI_{yz}\sin 2\varphi, \\
EI_{\hat{z}\hat{z}} &= \frac{1}{2}\left(EI_{yy} + EI_{zz}\right) - \frac{1}{2}\left(EI_{yy} - EI_{zz}\right)\cos 2\varphi + EI_{yz}\sin 2\varphi, \\
EI_{\hat{y}\hat{z}} &= \frac{1}{2}\left(EI_{yy} - EI_{zz}\right)\sin 2\varphi + EI_{yz}\cos 2\varphi.
\end{aligned} \tag{24.56}$$

The angle $\varphi = \varphi_0$, under which the effective deviation stiffness EI_{yz} becomes zero, follows from the requirement $EI_{yz} = 0$, which after a short transformation leads to the following expression:

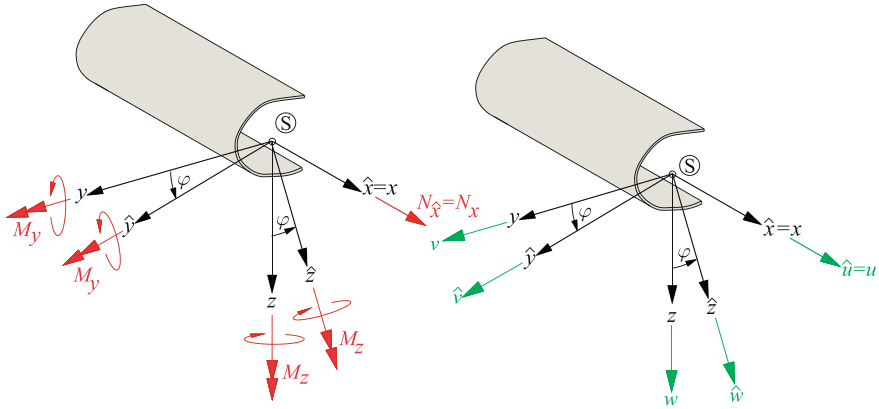


Fig. 24.13 Rotation of the reference system

$$\tan 2\varphi_0 = \frac{2EI_{yz}}{EI_{zz} - EI_{yy}}. \tag{24.57}$$

The following extremal values can then be specified for the effective bending stiffnesses:

$$EI_{1,2} = \frac{EI_{yy} + EI_{zz}}{2} \pm \sqrt{\left(\frac{EI_{zz} - EI_{yy}}{2}\right)^2 + EI_{yz}^2}. \tag{24.58}$$

Due to the vanishing deviation moment, not only the rod and beam load-bearing effects are decoupled from each other in the principal axis system, but the two bending effects are also no longer coupled with each other.

24.2.5 Stresses and Strains

In an isotropic beam under normal force and bending, only the normal stress $\sigma_{\xi\xi}$ occurs. In a laminated beam, on the other hand, the normal stress $\sigma_{\eta\eta}$ and the shear stress $\tau_{\xi\eta}$ must be determined in addition to the normal stress $\sigma_{\xi\xi}$ due to the layered nature of the structure. We first consider beam structures with unsymmetric orthotropic layups. The strain and the two curvatures of the beam axis, related to the center of gravity of the cross-section, are as follows

$$\begin{aligned}
\varepsilon_{xx}^0 &= \frac{N}{EA}, \\
\kappa_{yy}^0 &= \frac{EI_{zz}M_y + EI_{yz}M_z}{EI_{yy}EI_{zz} - EI_{yz}^2}, \\
\kappa_{zz}^0 &= -\frac{EI_{yz}M_y + EI_{yy}M_z}{EI_{yy}EI_{zz} - EI_{yz}^2}.
\end{aligned} \tag{24.59}$$

For an arbitrary point on the cross-section follows:

$$\begin{aligned}
\varepsilon_{\xi\xi}^0 &= \varepsilon_{xx}^0 + z\kappa_{yy}^0 + y\kappa_{zz}^0, \\
\kappa_{\xi\xi}^0 &= \kappa_{yy}^0 \cos\alpha - \kappa_{zz}^0 \sin\alpha.
\end{aligned} \tag{24.60}$$

As we assume an orthotropic layup, the following applies:

$$N_{\eta\eta}^0 = N_{\xi\eta}^0 = M_{\eta\eta}^0 = M_{\xi\eta}^0 = 0. \tag{24.61}$$

For the remaining normal force and bending moment we obtain

$$\begin{aligned}
N_{\xi\xi}^0 &= \frac{\delta_{11}}{D}\varepsilon_{\xi\xi}^0 - \frac{\beta_{11}}{D}\kappa_{\xi\xi}^0, \\
M_{\xi\xi}^0 &= -\frac{\beta_{11}}{D}\varepsilon_{\xi\xi}^0 + \frac{\alpha_{11}}{D}\kappa_{\xi\xi}^0.
\end{aligned} \tag{24.62}$$

Thus:

$$N^0_{\xi\xi} = \kappa^0_{yy}\left(z\frac{\delta_{11}}{D} - \cos\alpha\frac{\beta_{11}}{D}\right) + \kappa^0_{zz}\left(y\frac{\delta_{11}}{D} + \sin\alpha\frac{\beta_{11}}{D}\right) + \frac{N}{EA}\frac{\delta_{11}}{D},$$
$$M^0_{\xi\xi} = \kappa^0_{yy}\left(-z\frac{\beta_{11}}{D} + \cos\alpha\frac{\alpha_{11}}{D}\right) - \kappa^0_{zz}\left(y\frac{\beta_{11}}{D} + \sin\alpha\frac{\alpha_{11}}{D}\right) - \frac{N}{EA}\frac{\beta_{11}}{D}, \tag{24.63}$$

with κ^0_{yy} and κ^0_{zz} according to (24.59). The constitutive law is for the present case:

$$\begin{pmatrix} \varepsilon^0_{\xi\xi} \\ \varepsilon^0_{\eta\eta} \\ \gamma^0_{\xi\eta} \\ \kappa^0_{\xi\xi} \\ \kappa^0_{\eta\eta} \\ \kappa^0_{\xi\eta} \end{pmatrix} = \begin{bmatrix} \alpha_{11} & \beta_{11} \\ \alpha_{12} & \beta_{21} \\ 0 & 0 \\ \beta_{11} & \delta_{11} \\ \beta_{12} & \delta_{12} \\ 0 & 0 \end{bmatrix} \begin{pmatrix} N^0_{\xi\xi} \\ M^0_{\xi\xi} \end{pmatrix}. \tag{24.64}$$

This results in the strains in each layer as:

$$\begin{pmatrix} \varepsilon_{\xi\xi} \\ \varepsilon_{\eta\eta} \\ \gamma_{\xi\eta} \end{pmatrix} = \begin{pmatrix} \varepsilon^0_{\xi\xi} \\ \varepsilon^0_{\eta\eta} \\ \gamma^0_{\xi\eta} \end{pmatrix} + \zeta \begin{pmatrix} \kappa^0_{\xi\xi} \\ \kappa^0_{\eta\eta} \\ \kappa^0_{\xi\eta} \end{pmatrix}. \tag{24.65}$$

From this, the stresses in each layer of the wall can be determined:

$$\begin{pmatrix} \sigma_{\xi\xi} \\ \sigma_{\eta\eta} \\ \tau_{\xi\eta} \end{pmatrix} = \begin{bmatrix} \bar{Q}_{11} & \bar{Q}_{12} & 0 \\ \bar{Q}_{12} & \bar{Q}_{22} & 0 \\ 0 & 0 & \bar{Q}_{66} \end{bmatrix} \begin{pmatrix} \varepsilon_{\xi\xi} \\ \varepsilon_{\eta\eta} \\ \gamma_{\xi\eta} \end{pmatrix}. \tag{24.66}$$

Since $\gamma_{\xi\eta} = 0$ applies to the present case, the shear stress $\tau_{\xi\eta}$ disappears in each layer. If, on the other hand, symmetric orthotropic layups are involved, the following applies:

$$N^0_{\xi\xi} = \frac{1}{a_{11}}\varepsilon^0_{\xi\xi}, \quad M^0_{\xi\xi} = \frac{1}{d_{11}}\kappa^0_{\xi\xi}, \tag{24.67}$$

or

$$N^0_{\xi\xi} = \frac{1}{a_{11}}\left(z\kappa^0_{yy} + y\kappa^0_{zz} + \frac{N}{EA}\right),$$
$$M^0_{\xi\xi} = \frac{1}{d_{11}}\left(\kappa^0_{yy}\cos\alpha - \kappa^0_{zz}\sin\alpha\right). \tag{24.68}$$

With $\beta_{ij} = 0$ and $\alpha_{ij} = a_{ij}$ as well as $\delta_{ij} = d_{ij}$ the constitutive law follows as:

$$\begin{pmatrix} \varepsilon^0_{\xi\xi} \\ \varepsilon^0_{\eta\eta} \\ \gamma^0_{\xi\eta} \\ \kappa^0_{\xi\xi} \\ \kappa^0_{\eta\eta} \\ \kappa^0_{\xi\eta} \end{pmatrix} = \begin{bmatrix} a_{11} & 0 \\ a_{12} & 0 \\ 0 & 0 \\ 0 & d_{11} \\ 0 & d_{12} \\ 0 & 0 \end{bmatrix} \begin{pmatrix} N^0_{\xi\xi} \\ M^0_{\xi\xi} \end{pmatrix}. \tag{24.69}$$

The layerwise stresses then result from (24.65) and (24.66).

The last case we consider is the simply symmetric cross-section with arbitrary layup. The constitutive law then takes the following form:

$$\begin{pmatrix} \varepsilon^0_{\xi\xi} \\ \varepsilon^0_{\eta\eta} \\ \gamma^0_{\xi\eta} \\ \kappa^0_{\xi\xi} \\ \kappa^0_{\eta\eta} \\ \kappa^0_{\xi\eta} \end{pmatrix} = \begin{bmatrix} \alpha_{11} & \beta_{11} & \beta_{16} \\ \alpha_{12} & \beta_{21} & \beta_{26} \\ \alpha_{16} & \beta_{61} & \beta_{66} \\ \beta_{11} & \delta_{11} & \delta_{16} \\ \beta_{12} & \delta_{12} & \delta_{26} \\ \beta_{16} & \delta_{16} & \delta_{66} \end{bmatrix} \begin{pmatrix} N^0_{\xi\xi} \\ M^0_{\xi\xi} \\ M^0_{\xi\eta} \end{pmatrix}, \tag{24.70}$$

wherein:

$$\begin{aligned} N^0_{\xi\xi} &= \frac{M_y}{EI_{yy}} \left(z \frac{\bar{\delta}_{11}}{\bar{D}} - \cos\alpha \frac{\bar{\beta}_{11}}{\bar{D}} \right) + \frac{N}{EA} \frac{\bar{\delta}_{11}}{\bar{D}}, \\ M^0_{\xi\xi} &= \frac{M_y}{EI_{yy}} \left(-z \frac{\bar{\beta}_{11}}{\bar{D}} + \cos\alpha \frac{\bar{\alpha}_{11}}{\bar{D}} \right) - \frac{N}{EA} \frac{\bar{\beta}_{11}}{\bar{D}}, \\ M^0_{\xi\eta} &= -\frac{\beta_{16}}{\delta_{66}} N^0_{\xi\xi} - \frac{\delta_{16}}{\delta_{66}} M^0_{\xi\xi}. \end{aligned} \tag{24.71}$$

The layer stresses then result as:

$$\begin{pmatrix} \sigma_{\xi\xi} \\ \sigma_{\eta\eta} \\ \tau_{\xi\eta} \end{pmatrix} = \begin{bmatrix} \bar{Q}_{11} & \bar{Q}_{12} & \bar{Q}_{16} \\ \bar{Q}_{12} & \bar{Q}_{22} & \bar{Q}_{26} \\ \bar{Q}_{16} & \bar{Q}_{26} & \bar{Q}_{66} \end{bmatrix} \begin{pmatrix} \varepsilon_{\xi\xi} \\ \varepsilon_{\eta\eta} \\ \gamma_{\xi\eta} \end{pmatrix}. \tag{24.72}$$

24.2.6 Arbitrary Cross-Sections

The previous explanations are also valid for closed cross-sections of arbitrary shape with orthotropic symmetric layups. For arbitrary closed cross-sections with arbitrary layups, the reader is referred to Kollár and Springer (2003) for further information.

24.3 Transverse Shear

In the previous section, we dealt with straight beams under normal force and bending and, in particular, with the determination of the stresses due to the normal force N and the two bending moments M_y and M_z. On the other hand, consideration of the equilibrium conditions of such a beam shows that the transverse forces Q_y and Q_z must also occur in order to maintain equilibrium. Figure 24.3 has shown that the transverse shear forces are related to the shear stresses τ, the determination of which on thin-walled laminated cross-sections is the subject of this section. However, a problem that arises in connection with the Euler-Bernoulli beam theory is the requirement for the validity of the hypothesis that the cross-sections remain plane and the normal hypothesis, which is synonymous with vanishing shear strains γ, so that with vanishing shear strains γ also vanishing shear stresses τ follow. This is a contradiction of the Euler-Bernoulli beam theory which cannot be resolved. This means that we have to obtain statements about the shear stress τ from equilibrium considerations.

In the following, we consider the determination of the transverse shear stresses in thin-walled layered cross-sections and want to assume that the acting loads all act on the shear center axis M. This means that the loads are applied in such a way that they do not cause any additional torsional effect in addition to the bending effect. Specifically, cross-sections with orthotropic layups or beams with simply symmetric cross-sections that can have arbitrary layups are considered here. For other arbitrary types of cross-sections, the reader is referred to Kollár and Springer (2003) for further information.

24.3.1 Shear Flow in Open Cross-Sections

In order to derive the necessary basic equations, we consider the situation in Fig. 24.14 in which a straight beam is shown which can have any arbitrary cross-section and has been represented here as a doubly symmetric I-section for the sake of simplicity. For the moment, this beam is only loaded by the line load $q_z(x)$, resulting in the transverse shear force $Q_z(x)$ and the bending moment $M_y(x)$, which can be represented as functions of the beam longitudinal axis x. We now cut out an infinitesimal section element of length $\mathrm{d}x$ and consider the section element shown in Fig. 24.14, middle. Due to the given load, the bending moment M_y causes the normal stress σ_{xx} distributed linearly over z, which is depicted as constant in the flanges for the sake of simplicity. Since the stress σ_{xx} is a function of the coordinate x in addition to its variable distribution over the cross-section, the normal stress is plotted with the infinitesimal part $\frac{\mathrm{d}\sigma_{xx}}{\mathrm{d}x}\mathrm{d}x$ on the positive cutting edge. This also applies analogously to the transverse shear force Q_z and bending moment M_y. We now want to obtain the distribution of the shear stress τ over the cross-section if the normal stress σ_{xx} is known. For this purpose, we introduce the circumferential coordinate η. It is advisable not to work with the shear stress τ for the time being, but to introduce a new force quantity at

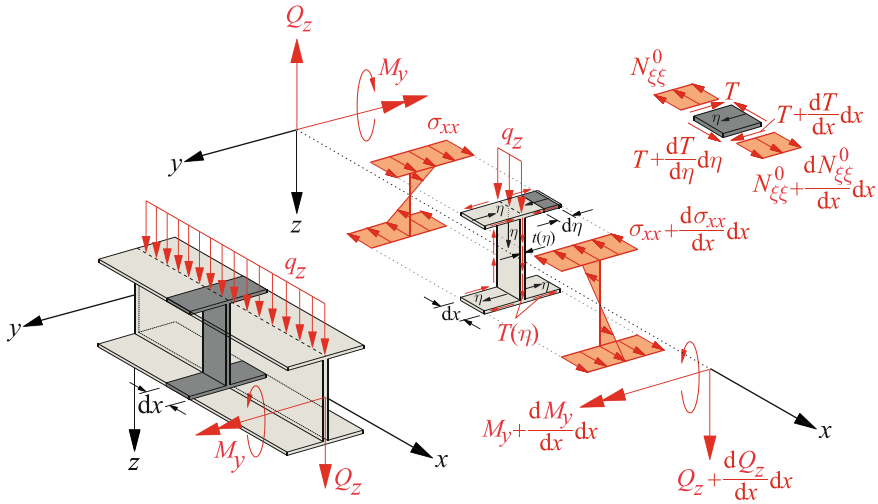


Fig. 24.14 On the determination of the shear stress τ

this point, namely the so-called shear flow T. The shear flow represents the resultant of the shear stress τ over the cross-section thickness t, which can be determined as:

$$T = \int_h \tau_{\xi\eta} \mathrm{d}\zeta = N^0_{\xi\eta}. \tag{24.73}$$

Accordingly, T is present in the unit of a force per unit length. Let us now consider the free body diagram of Fig. 24.14, right, in which an infinitesimal section element of width $\mathrm{d}\eta$ is shown, which we have cut out from the element of Fig. 24.14, middle. In addition to the shear flow T and its respective directions, we have also plotted the resulting force flow $N^0_{\xi\xi}$, which can be interpreted as the resultant of the normal stress σ_{xx} over the cross-section thickness t. The equilibrium of forces in the x-direction results in

$$\left(N^0_{\xi\xi} + \frac{\mathrm{d}N^0_{\xi\xi}}{\mathrm{d}x}\mathrm{d}x\right)\mathrm{d}\eta - N^0_{\xi\xi}\mathrm{d}\eta + \left(T + \frac{\mathrm{d}T}{\mathrm{d}\eta}\mathrm{d}\eta\right)\mathrm{d}x - T\mathrm{d}x = 0, \tag{24.74}$$

which can be solved as follows:

$$\frac{\mathrm{d}N^0_{\xi\xi}}{\mathrm{d}x}\mathrm{d}x\mathrm{d}\eta + \frac{\mathrm{d}T}{\mathrm{d}\eta}\mathrm{d}\eta\mathrm{d}x = 0. \tag{24.75}$$

Division by $\mathrm{d}x$ and integration over η from a starting point $\eta = \eta_A$ to an arbitrary point η results in:

$$\int_{\eta_A}^{\eta} \frac{\mathrm{d}T}{\mathrm{d}\eta}\mathrm{d}\eta = T(\eta) - T(\eta = \eta_A) = -\int_{\eta_A}^{\eta} \frac{\mathrm{d}N^0_{\xi\xi}}{\mathrm{d}x}\mathrm{d}\eta, \tag{24.76}$$

where we can set the initial value $T(\eta = \eta_A)$ to zero in the case of open cross-sections, provided that we start the integration at a free end of the cross-section and no tangential loads are applied. From here on, we consider biaxial bending, i.e. both bending moments M_y and M_z may occur. For $N^0_{\xi\xi}$ then applies:

$$\begin{aligned} N^0_{\xi\xi} = &\frac{EI_{zz}M_y + EI_{yz}M_z}{EI_{yy}EI_{zz} - EI^2_{yz}}\left(z\frac{\delta_{11}}{D} - \cos\alpha\frac{\beta_{11}}{D}\right) \\ &- \frac{EI_{yz}M_y + EI_{yy}M_z}{EI_{yy}EI_{zz} - EI^2_{yz}}\left(y\frac{\delta_{11}}{D} + \sin\alpha\frac{\beta_{11}}{D}\right) + \frac{N}{EA}\frac{\delta_{11}}{D}. \end{aligned} \tag{24.77}$$

The equilibrium conditions for the beam are:

$$M'_y = Q_z, \quad M'_z = -Q_y. \tag{24.78}$$

Assuming a constant or only slightly varying normal force N, the shear flow T then follows as:

$$\begin{aligned} T = &-\frac{EI_{zz}Q_z - EI_{yz}Q_y}{EI_{yy}EI_{zz} - EI^2_{yz}}\int_{\eta_A}^{\eta}\left(z\frac{\delta_{11}}{D} - \cos\alpha\frac{\beta_{11}}{D}\right)\mathrm{d}\eta \\ &- \frac{-EI_{yz}Q_z + EI_{yy}Q_y}{EI_{yy}EI_{zz} - EI^2_{yz}}\int_{\eta_A}^{\eta}\left(y\frac{\delta_{11}}{D} + \sin\alpha\frac{\beta_{11}}{D}\right)\mathrm{d}\eta. \end{aligned} \tag{24.79}$$

This provides an expression for determining the shear flow $T(s)$, depending on the transverse shear forces Q_y and Q_z acting on the cross-section, the two bending stiffnesses and the deviation stiffness, as well as the two effective static moments of the cross-section between the point η and the start of the integration $\eta = \eta_A$. If the cross-section is simply symmetric with arbitrary layup, the following applies:

$$T = -\frac{Q_z}{EI_{yy}}\int_{\eta_A}^{\eta}\left(z\frac{\bar{\delta}_{11}}{\bar{D}} - \cos\alpha\frac{\bar{\beta}_{11}}{\bar{D}}\right)\mathrm{d}\eta. \tag{24.80}$$

24.3.2 Shear Force Flow in Single-Cell Closed Cross-Sections

In this section we want to investigate the extent to which we can also use the previous findings for the calculation of the shear flow $T(\eta)$ on open cross-sections for the calculation of closed cross-sections. To motivate the method, we consider the closed box cross-section

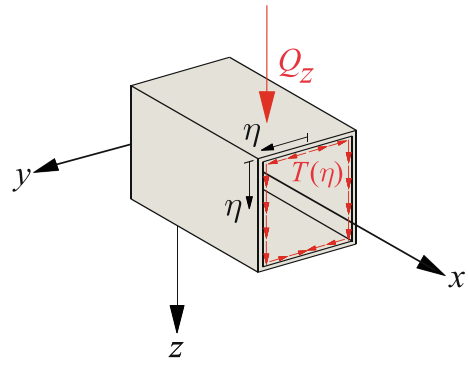


Fig. 24.15 Determination of the shear flow on a symmetric box cross-section under the shear force Q_z

shown in Fig. 24.15, on which a transverse shear force Q_z acts. The resulting shear flow $T(\eta)$ is also indicated here by arrows.

The problem that arises with a closed cross-section is that, in contrast to an open cross-section, we cannot a priori set the term $T(\eta = \eta_A)$ to zero. We therefore have to work with compatibility conditions, which we will explain below. We initially assume an exclusive loading by the shear force Q_z, but the analysis can be extended quite easily to the additional shear force Q_y. Further, a principal axis system is assumed.

We treat the problem in the form of a statically indeterminate calculation and initially consider symmetric orthotropic cross-section walls. We consider the closed thin-walled box cross-section and perform an imaginary section along the longitudinal direction at an arbitrary point (Fig. 24.16, top). The shear flow $T_0(\eta)$ due to the shear force Q_z can then be easily determined at this now open cross-section using the methods already derived. However, due to the cross-sectional warping $u(\eta)$, a displacement discontinuity Δu_{10} occurs at the location of the longitudinal cutting line, which must not occur at the actually closed cross-section. We can calculate the displacement discontinuity Δu_{10} by integrating over the entire cross-section perimeter as follows:

$$\Delta u_{10} = \oint \frac{T_0(\eta)}{A_{66}} \mathrm{d}\eta. \tag{24.81}$$

In order to compensate for this incompatibility, we apply the constant shear flow T_1 to the cross-section, which we initially apply as a unit shear flow $T_1 = 1$ and which also causes a discontinuity Δu_{11} in the longitudinal displacement. This displacement discontinuity can be calculated as:

$$\Delta u_{11} = \oint \frac{1}{A_{66}} \mathrm{d}\eta. \tag{24.82}$$

The shear flow T_1 is plotted here as a unit shear flow, but its final value is still unknown at this point. It is now quite easy to find a determining equation for T_1 by requiring that the

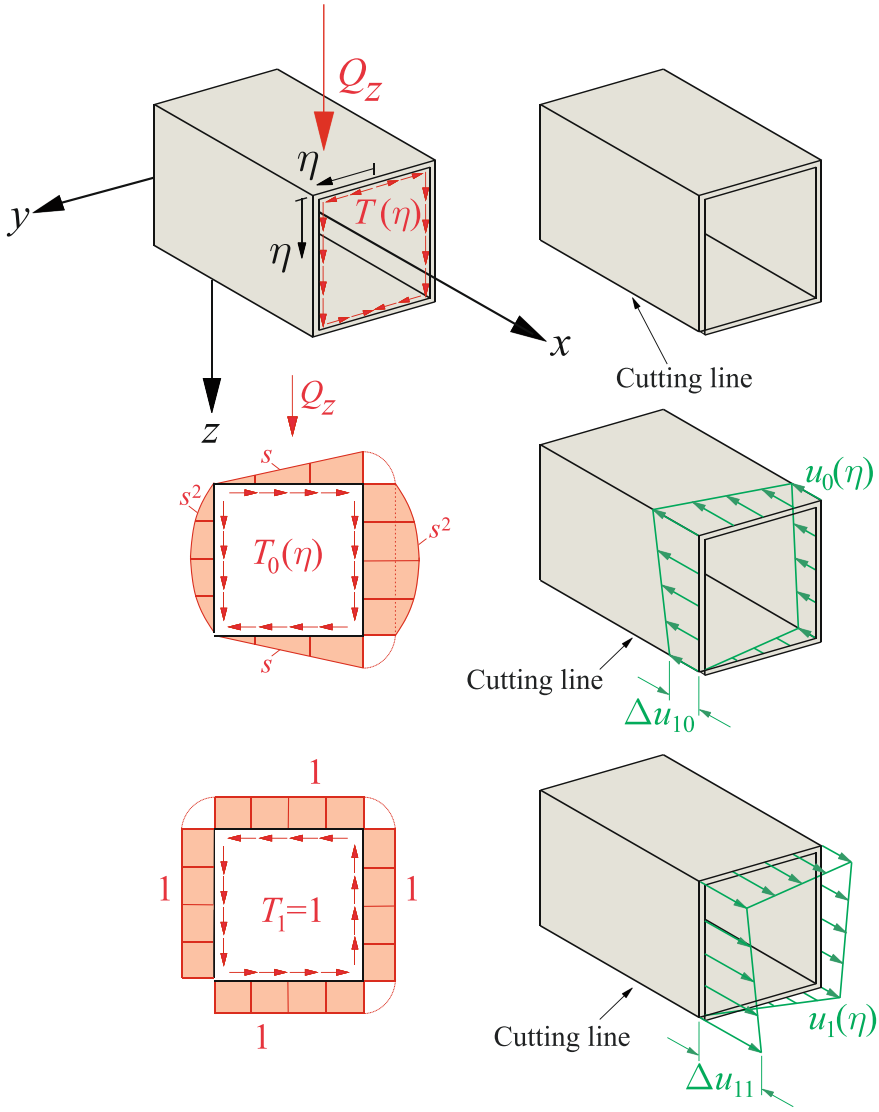


Fig. 24.16 Determination of the shear flow in a symmetric closed box cross-section under the shear force Q_z

sum of Δu_{10} and Δu_{11} is zero, whereby we multiply the displacement discontinuity Δu_{11} by the (still unknown) shear flow T_1:

$$\Delta u_{10} + T_1 \Delta u_{11} = 0. \tag{24.83}$$

Since the two displacement discontinuities Δu_{10} and Δu_{11} are known from (24.81) and (24.82), we can immediately solve for T_1 and obtain the result:

$$T_1 = -\frac{\Delta u_{10}}{\Delta u_{11}} = -\frac{\oint \frac{T_0}{A_{66}} \mathrm{d}\eta}{\oint \frac{1}{A_{66}} \mathrm{d}\eta}. \tag{24.84}$$

The shear flow $T(\eta)$ acting in the closed cross-section is then the sum of $T_0(\eta)$ and the shear flow T_1 determined with (24.84):

$$T(\eta) = T_0(\eta) + T_1. \tag{24.85}$$

If, on the other hand, there is an unsymmetric orthotropic layup, or if we consider a simply symmetric cross-section with arbitrary layup, then the following expression results for T_1:

$$T_1 = -\frac{\oint \alpha^e_{66} T_0 \mathrm{d}\eta}{\oint \alpha^e_{66} \mathrm{d}\eta}. \tag{24.86}$$

Herein, α^e_{66} is to be evaluated at the point $e = -\frac{\beta_{66}}{\delta_{66}}$, so that $\alpha^e_{66} = \alpha_{66} - \frac{\beta^2_{66}}{\delta_{66}}$.

24.3.3 Shear Flow in Multicellular Closed Cross-Sections

For the case of a multicellular closed cross-section under the shear force Q_z, the method just described can be generalized in this respect. We discuss the case of a two-cell closed cross-section shown in Fig. 24.17, top left, whereby we want to limit ourselves here to symmetric orthotropic layups of the walls and a principal coordinate system. We now apply a longitudinal cut to each cell, as shown in Fig. 24.17, top right. This results in a completely open cross-section on which the shear flow $T_0(\eta)$ can be calculated. However, the cuts have made displacement discontinuities possible, which can be calculated as follows. Firstly, the displacement discontinuity Δu_{10} results in cell 1:

$$\Delta u_{10} = \oint \frac{T_0(\eta)}{A_{66}} \mathrm{d}\eta. \tag{24.87}$$

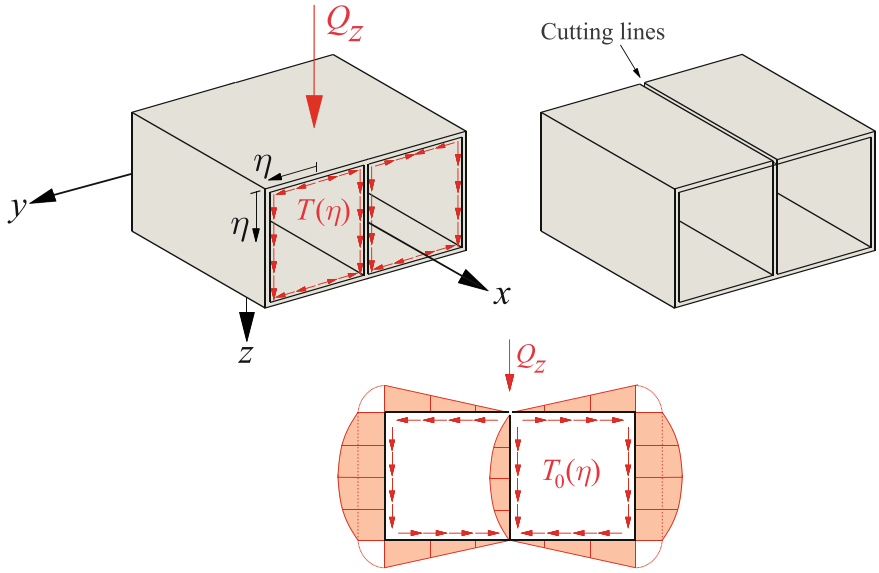


Fig. 24.17 Determination of shear flow $T_0(\eta)$ on the two-cell box cross-section under the shear force Q_z. A symmetric cross-section is shown, but the analysis method outlined here applies to any two-cell cross-section

The integration over the perimeter prescribed here refers exclusively to the perimeter of cell 1. Analogously we have for Δu_{20}:

$$\Delta u_{20} = \oint \frac{T_0(\eta)}{A_{66}} \mathrm{d}\eta. \tag{24.88}$$

Here we have to integrate over the circumference of the second cell.

We now apply a unit shear flow $T_1 = 1$ in cell 1, as shown in Fig. 24.18, top. This results in a displacement discontinuity Δu_{11}. We proceed in exactly the same way for cell 2 (Fig. 24.18, middle). These displacement discontinuities are calculated as:

$$\Delta u_{11} = \oint \frac{1}{A_{66}} \mathrm{d}\eta, \quad \Delta u_{22} = \oint \frac{1}{A_{66}} \mathrm{d}\eta, \tag{24.89}$$

whereby the integrations must be carried out exclusively for cell 1 or cell 2. The indexes of the displacement discontinuities indicate both the location (first index) and the cause (second index) of the displacement discontinuity. Accordingly, for example, Δu_{11} is the displacement discontinuity in cell 1 as a result of the unit shear flow T_{s1}. The values Δu_{ii} ($i = 1, 2, \ldots, n$ for n cells) are always positive.

At the same time, however, it must also be noted that due to the two unit shear flows T_{s1} and T_{s2}, there are not only differences in the longitudinal displacements within the two cells,

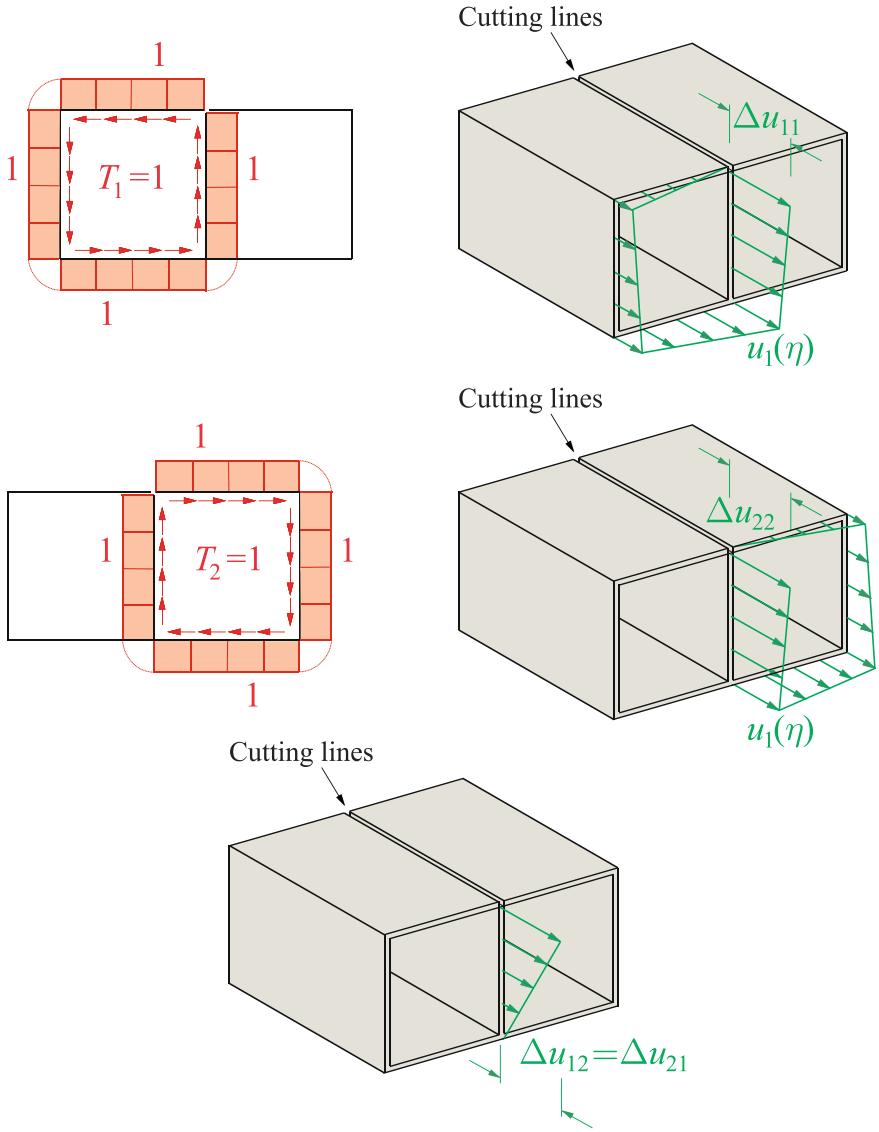


Fig. 24.18 Determination of the displacement discontinuities of a symmetric two-cell box cross-section

but also an incompatibility or a displacement discontinuity between the two cells, which we want to denote as $\Delta u_{12} = \Delta u_{21}$. This results in the following:

$$\Delta u_{12} = \Delta u_{21} = -\oint \frac{\mathrm{d}s}{A_{66}}, \tag{24.90}$$

whereby the integration is to be carried out exclusively via cell walls which are common to both cells.

We can now formulate two compatibility conditions from which we can determine the two shear flows T_{s1} and T_{s2}:

$$\begin{aligned} \Delta u_{10} + T_1 \Delta u_{11} + T_2 \Delta u_{12} &= 0, \\ \Delta u_{20} + T_1 \Delta u_{12} + T_2 \Delta u_{22} &= 0, \end{aligned} \tag{24.91}$$

where $\Delta u_{12} = \Delta u_{21}$ applies. The final shear flow on the two-cell closed cross-section then follows from the sum of the individual shear flows:

$$T(\eta) = T_0(\eta) + T_1 + T_2. \tag{24.92}$$

The qualitative distribution for the two-cell cross-section under consideration is shown in Fig. 24.19.

The method described in the context of a statically indeterminate calculation can be extended to cross-sections with n cells. The resulting compatibility equations can be expressed in a vector matrix notation as follows:

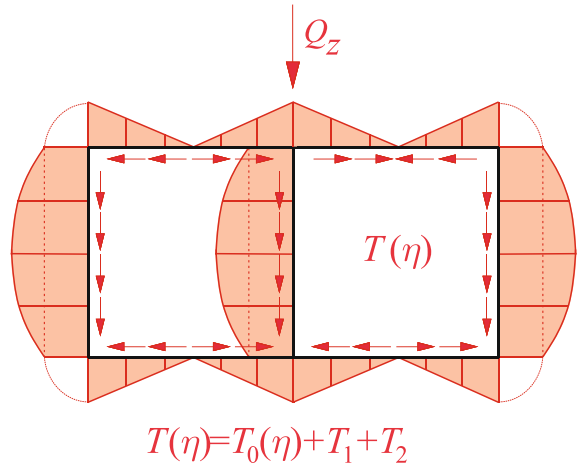


Fig. 24.19 Shear flow $T(\eta)$ in the two-cell symmetric closed cross-section under the shear force Q_z

$$\begin{bmatrix} \Delta u_{11} & \Delta u_{12} & \Delta u_{13} & \cdots & \Delta u_{1n} \\ \Delta u_{12} & \Delta u_{22} & \Delta u_{23} & \cdots & \Delta u_{2n} \\ \Delta u_{13} & \Delta u_{23} & \Delta u_{33} & \cdots & \Delta u_{3n} \\ \vdots & \vdots & \vdots & \ddots & \vdots \\ \Delta u_{1n} & \Delta u_{2n} & \Delta u_{3n} & \cdots & \Delta u_{nn} \end{bmatrix} \begin{pmatrix} T_1 \\ T_2 \\ T_3 \\ \vdots \\ T_n \end{pmatrix} = - \begin{pmatrix} \Delta u_{10} \\ \Delta u_{20} \\ \Delta u_{30} \\ \vdots \\ \Delta u_{n0} \end{pmatrix}, \tag{24.93}$$

or in symbolic form:

$$\underline{\underline{\Delta}} \, \underline{T} = -\underline{\Delta}_0. \tag{24.94}$$

The matrix $\underline{\underline{\Delta}}$ is always symmetric. The shear flow $T(\eta)$ follows analogously to (24.92):

$$T_s(s) = T_0(s) + T_1 + T_2 + \cdots + T_n. \tag{24.95}$$

24.3.4 Shear Center

As in the case of isotropic beams, a shear center can also be determined for cross-sections with layered walls, in which shear loads must act in order to avoid unwanted torsion. This is not explained in detail here; the determination of the shear center is explained in detail in Mittelstedt (2021), for example. Reference is also made here to Kollár and Springer (2003).

24.4 Torsion

24.4.1 Introduction

We first consider the so-called St. Venant torsion, which is based on the following assumptions in addition to geometric and material linearity:

- Only bars with a straight bar axis are treated.
- If the bar is twisted, the cross-section twists. We assume that the so-called axis of rotation is free and is not forced by design measures.
- We assume that only rotations $\vartheta(x)$ around the member axis x occur as a result of the torsional load. We assume that torsion and bending can be treated independently of each other and that there is no coupling of these phenomena. Furthermore, we assume that the cross-section of the beam twists due to torsion and that this is expressed by the torsion angle $\vartheta(x)$ around the longitudinal axis x, but that the cross-section retains its shape and dimensions completely even in the twisted state. This assumption is often referred to as the straight radii hypothesis. We assume warping-free cross-sections that do not exhibit any longitudinal displacements u when torsion ϑ about the member axis x occurs. The fact that this does not apply in many cases is discussed in Sect. 24.4.6.

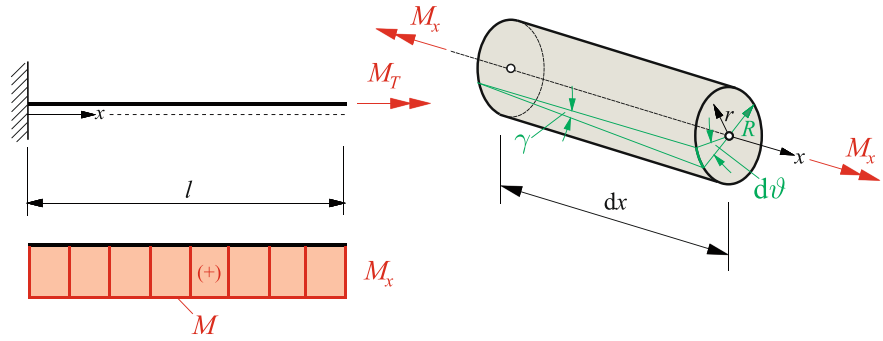


Fig. 24.20 Bar with circular cross-section under torsional moment M_T and corresponding moment distribution M_x (left), sectional element (right)

We first consider the elementary case of a bar with a circular cross-section (first described by Coulomb[2]), on which a torsional moment M_T acts, causing a constant torsional moment M_x in the bar (see Fig. 24.20, left). We consider an infinitesimal section element of length $\mathrm{d}x$ cut out of the beam (Fig. 24.20, right). The shear strain γ of the shell surface and the torsional increment $d\vartheta$ of the cross-section are also shown there. The radius of the cross-section is R and the radial coordinate, measured from the center of gravity of the cross-section, is r. The shear strain γ and ϑ are related as follows:

$$\gamma \mathrm{d}x = r \mathrm{d}\vartheta. \tag{24.96}$$

Solving for the shear strain γ yields:

$$\gamma = r \frac{\mathrm{d}\vartheta}{\mathrm{d}x} = r\vartheta'. \tag{24.97}$$

The first derivative of the rotation ϑ to x is referred to as the so-called twist ϑ' of the bar.

Once the shear strain γ is given, the shear stress in the cross-section can be determined from the constitutive law $\tau = G\gamma$, where G is the shear modulus of the material:

$$\tau = G\gamma = Gr\vartheta'. \tag{24.98}$$

The shear stress is therefore distributed linearly over the radial coordinate r. It becomes zero at the center of gravity of the cross-section and assumes its maximum value at the edge, which is yet to be determined.

The resulting torsional moment M_x follows as:

$$M_x = \int_A \tau r \mathrm{d}A = \int_A Gr^2\vartheta' \mathrm{d}A = G\vartheta' \int_A r^2 \mathrm{d}A. \tag{24.99}$$

[2] Charles Augustin de Coulomb, 1736–1806, French physicist.

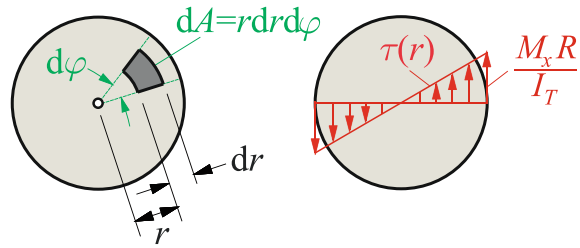


Fig. 24.21 Infinitesimal area element dA of the circular cross-section (left), shear stress $\tau(r)$ over the circular cross-section (right)

The surface integral occurring here can be broken down into two integrals with $\mathrm{d}A = r\mathrm{d}r\mathrm{d}\varphi$ (Fig. 24.21, left):

$$M_x = G\vartheta' \int_0^{2\pi} \int_0^R r^3 \mathrm{d}r\mathrm{d}\varphi = G\vartheta' \frac{R^4}{4} \int_0^{2\pi} \mathrm{d}\varphi = G\vartheta' \frac{\pi R^4}{2}. \tag{24.100}$$

With the torsional moment of inertia I_T

$$I_T = \frac{\pi R^4}{2} \tag{24.101}$$

we obtain:

$$M_x = G I_T \vartheta'. \tag{24.102}$$

The quantity GI_T that occurs here is the so-called torsional stiffness of the beam. Equation (24.102) is the constitutive law for St. Venant torsion. The following can then be written for (24.98):

$$\tau = Gr\vartheta' = \frac{M_x}{I_T} r. \tag{24.103}$$

The maximum value of the torsional stress τ at the cross-section edge (Fig. 24.21, right) then follows as:

$$\tau = \frac{M_x R}{I_T}. \tag{24.104}$$

In the following sections, we will primarily address the question of which stress states we encounter in thin-walled laminate beams under torsion and how the effective torsional stiffness GI_T can be determined for such beam structures. The torsion of isotropic bars is discussed in various works on structural mechanics, e.g. Bauchau and Craig (2009), Czerwenka and Schnell (1970), Franke and Friemann (2005), Hanswille (1995), Kindmann and Frickel (2017), Kollbrunner and Hajdin (1963), Kollbrunner and Basler (1963),(1966), Linke and Nast (2015), Megson (1999), Mittelstedt (2021), Petersen (1997), Roik et al. (1972), Roik (1978), Shama (2010), Wiedemann (2007), or Wlassow (1964, 1965).

24.4.2 Closed Single-Cell Profiles

We consider a thin-walled closed cross-section of arbitrary shape (Fig. 24.22). The axis around which the cross-section is twisted is called the axis of rotation D. We introduce the shear flow T at this point:

$$T = \int_{-\frac{h}{2}}^{\frac{h}{2}} \tau_{\xi\eta} \mathrm{d}\zeta = N^0_{\xi\eta}. \tag{24.105}$$

The shear flow thus represents the resultant of the shear stress over the cross-section thickness. With the help of the free body diagram in Fig. 24.22 the force equilibrium in x-direction:

$$\frac{\partial T}{\partial \eta} = 0. \tag{24.106}$$

It can be seen that the shear flow T is constant at every point η.

In order to establish a relationship between the shear flow T and the torsional moment M_x, we consider the free body diagram in Fig. 24.23, in which a sectional element of the cross-section with the length $\mathrm{d}\eta$ and the constant shear flow T is shown. The lever arm of the shear flow with respect to the axis of rotation is r_t, where r_t is the distance of the cutting element from the axis of rotation, measured from the tangent to the skeleton line. The section element has the distance $r(s)$ from the axis of rotation. The shear flow shown here now causes the infinitesimal part $\mathrm{d}M_x$ of the torsional moment M_x:

$$\mathrm{d}M_x = T \mathrm{d}\eta r_t. \tag{24.107}$$

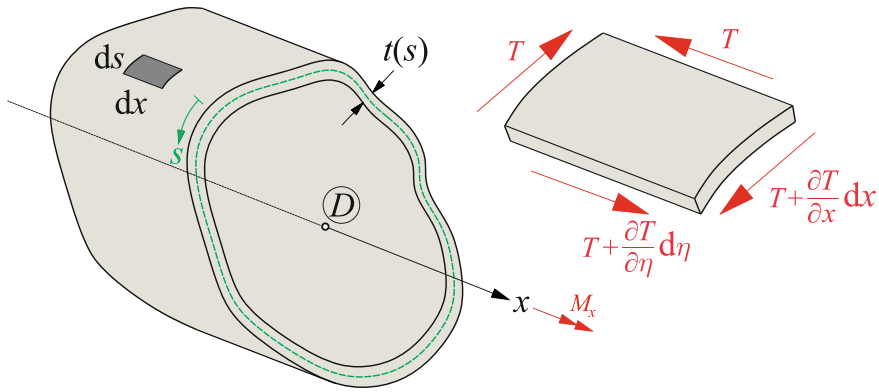


Fig. 24.22 Arbitrary thin-walled closed cross-section

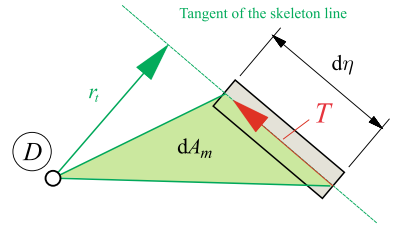


Fig. 24.23 Free-body image of a cross-sectional section ds

If this is summed up over the entire cross-section, the torsional moment M_x is obtained:

$$M_x = \oint T r_t \mathrm{d}\eta. \tag{24.108}$$

With the relation

$$\mathrm{d}A_m = \frac{1}{2} r_t \mathrm{d}\eta \tag{24.109}$$

we obtain for dη:

$$\mathrm{d}\eta = 2\frac{\mathrm{d}A_m}{r_t}. \tag{24.110}$$

Insert into (24.108) yields:

$$M_x = 2\,T \oint_{A_m} \mathrm{d}A_m \tag{24.111}$$

or

$$M_x = 2TA_m. \tag{24.112}$$

Here, A_m is the area of the cross-section enclosed by the skeleton line. The shear flow T due to the torsional moment M_x can then be specified as:

$$T = \frac{M_x}{2A_m}. \tag{24.113}$$

This is the so-called 1st Bredt formula.[3]

In the next step, we determine the torsional stiffness GI_T of the cross-section and consider the shear strain of the wall:

$$\gamma^0_{\xi\eta} = \alpha_{66} N^0_{\xi\eta} + \beta_{66} M^0_{\xi\eta}. \tag{24.114}$$

We now determine the plane at the point e at which β_{66} becomes zero (Fig. 24.24):

$$\beta^e_{66} = \beta_{66} + e\delta_{66} = 0. \tag{24.115}$$

It follows:

$$e = -\frac{\beta_{66}}{\delta_{66}}. \tag{24.116}$$

[3] Rudolf Bredt, 1842–1900, German engineer.

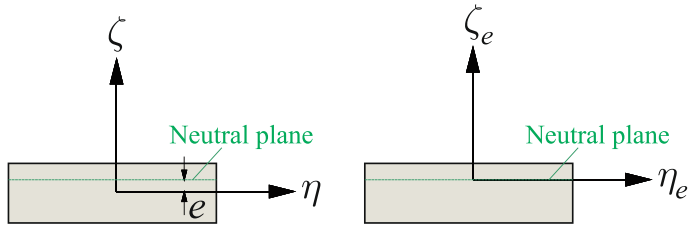


Fig. 24.24 Position of the neutral plane

Thus:

$$\gamma^0_{\xi\eta} = \alpha^e_{66} N^0_{\xi\eta} = \alpha^e_{66} T, \tag{24.117}$$

with

$$\alpha^e_{66} = \alpha_{66} + 2e\beta_{66} + e^2\delta_{66} = \alpha_{66} - \frac{\beta^2_{66}}{\delta_{66}}. \tag{24.118}$$

We now want to determine an expression for the torsional stiffness GI_T for the thin-walled closed cross-section considered here and examine the cross-section twisted around the axis of rotation D. The displacements of the point P are considered according to Fig. 24.25, which is displaced by the dimension dr perpendicular to the radius r. Projected onto the tangent of the skeleton line, this is the displacement dv. Assuming small angles we have:

$$\mathrm{d}r = r\,\mathrm{d}\vartheta. \tag{24.119}$$

The following also applies:

$$\cos\alpha = \frac{\mathrm{d}v}{\mathrm{d}r} = \frac{\mathrm{d}v}{r\,\mathrm{d}\vartheta}. \tag{24.120}$$

Thus:

$$\cos\alpha = \frac{r_t}{r}. \tag{24.121}$$

Equating (24.120) and (24.121) results in the following:

$$\mathrm{d}v = r_t\,\mathrm{d}\vartheta. \tag{24.122}$$

We derive (24.122) once with respect to x under the assumption that r_t is independent of x for a prismatic bar, and obtain

$$\frac{\mathrm{d}v}{\mathrm{d}x} = r_t \frac{\mathrm{d}\vartheta}{\mathrm{d}x} = r_t\,\mathrm{d}\vartheta'. \tag{24.123}$$

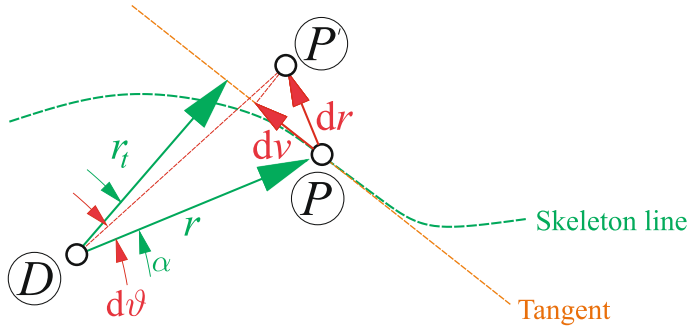


Fig. 24.25 Displacement of a point P on the skeleton line

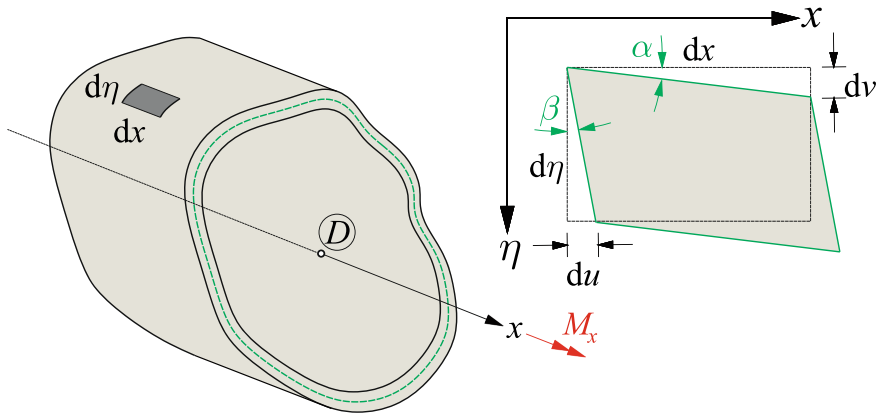


Fig. 24.26 Shear strain of an infinitesimal sectional element

We now analyze the shear strain of an infinitesimal section element of the bar (Fig. 24.26). The angles α and β read:

$$\alpha = \frac{\mathrm{d}v}{\mathrm{d}x}, \quad \beta = \frac{\mathrm{d}u}{\mathrm{d}\eta}, \tag{24.124}$$

so that

$$\gamma^0_{\xi\eta} = \alpha + \beta = \frac{\mathrm{d}v}{\mathrm{d}x} + \frac{\mathrm{d}u}{\mathrm{d}\eta} = r_t\vartheta' + \frac{\mathrm{d}u}{\mathrm{d}\eta}. \tag{24.125}$$

The following also applies:

$$\gamma^0_{\xi\eta} = \alpha^e_{66} N^0_{\xi\eta}. \tag{24.126}$$

Equating (24.125) and (24.126) and integrating over η results in:

$$\oint \alpha^e_{66} N^0_{\xi\eta}\mathrm{d}\eta = \oint r_t\vartheta'\mathrm{d}\eta + \oint \frac{\mathrm{d}u}{\mathrm{d}\eta}\mathrm{d}\eta. \tag{24.127}$$

The second integral term on the right-hand side disappears, as this is a closed cross-section, and it remains:

$$N^0_{\xi\eta} \oint \alpha^e_{66} \mathrm{d}\eta = \vartheta' \oint r_t \mathrm{d}\eta. \tag{24.128}$$

For the expression of the right-hand side follows:

$$\vartheta' \oint r_t \mathrm{d}\eta = 2A_m \vartheta' = 2A_m \frac{M_x}{GI_T} = 2A_m \frac{2N^0_{\xi\eta} A_m}{GI_T}. \tag{24.129}$$

We solve for the torsional stiffness and obtain:

$$GI_T = \frac{4A_m^2}{\oint \alpha^e_{66} \mathrm{d}\eta}. \tag{24.130}$$

This is the 2nd Bredt's formula for the single-cell cross-section.
The strains, curvatures and twist of the neutral plane follow as:

$$\begin{pmatrix} \varepsilon^0_{\xi\xi} \\ \varepsilon^0_{\eta\eta} \\ \gamma^0_{\xi\eta} \\ \kappa^0_{\xi\xi} \\ \kappa^0_{\eta\eta} \\ \kappa^0_{\xi\eta} \end{pmatrix} = \begin{pmatrix} 0 \\ 0 \\ \alpha^e_{66} \\ 0 \\ 0 \\ 0 \end{pmatrix} N^0_{\xi\eta} = \begin{pmatrix} 0 \\ 0 \\ \alpha^e_{66} \\ 0 \\ 0 \\ 0 \end{pmatrix} T, \tag{24.131}$$

and the layerwise stresses result as:

$$\begin{pmatrix} \sigma_{\xi\xi} \\ \sigma_{\eta\eta} \\ \tau_{\xi\eta} \end{pmatrix} = \begin{pmatrix} 0 \\ 0 \\ \bar{Q}_{66} \end{pmatrix} \gamma^0_{\xi\eta}. \tag{24.132}$$

24.4.3 Closed Multi-cell Profiles

We now consider multicellular cross-sections under torsion with n cells. Figure 24.27 shows an exemplary two-cell ($n = 2$) box cross-section. Clearly, this is a parallel connection of cells 1 and 2, whose torsional stiffnesses will ultimately add up. Equation (24.113) is also valid here for cells 1 and 2, so that $M_{x,1}$ and $M_{x,2}$ can be calculated from the shear flows $T_{s,1}$ and $T_{s,2}$ of the two cells:

$$M_{x,1} = 2A_{m,1} T_1, \quad M_{x,2} = 2A_{m,2} T_2, \tag{24.133}$$

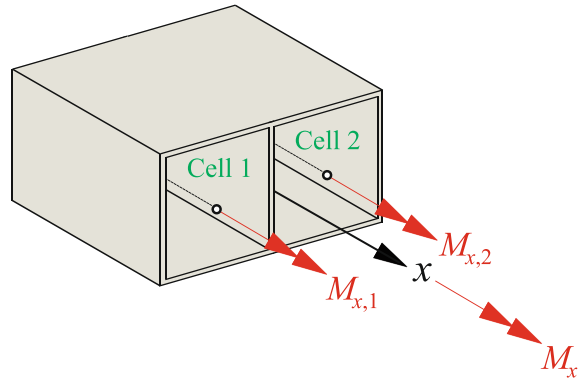


Fig. 24.27 Two-cell closed box cross-section

with the areas $A_{m,1}$ and $A_{m,2}$ enclosed by the two cells. The partial torsional moments are added together to form the total torsional moment M_x, i.e. generally for n cells:

$$M_x = \sum_{i=1}^{n} M_{x,i} = 2 \sum_{i=1}^{n} A_{m,i} T_{s,i}. \tag{24.134}$$

The following correlation applies to both cells:

$$\begin{aligned} 2A_{m,1}\vartheta_1' &= \oint \alpha_{66}^e T_1 \mathrm{d}\eta, \\ 2A_{m,2}\vartheta_2' &= \oint \alpha_{66}^e T_2 \mathrm{d}\eta. \end{aligned} \tag{24.135}$$

The twists ϑ_1' and ϑ_2' are identical to the twist ϑ' of the total cross-section:

$$\vartheta_1' = \vartheta_2' = \vartheta'. \tag{24.136}$$

Thus:

$$\begin{aligned} 2A_{m,1} &= \frac{T_1}{\vartheta'} \oint \alpha_{66}^e \mathrm{d}\eta, \\ 2A_{m,2} &= \frac{T_2}{\vartheta'} \oint \alpha_{66}^e \mathrm{d}\eta. \end{aligned} \tag{24.137}$$

At this point, we introduce the so-called torsion function ψ_i as follows:

$$\psi_1 = \frac{T_1}{\vartheta'}, \quad \psi_2 = \frac{T_2}{\vartheta'}. \tag{24.138}$$

Then for (24.137) applies:

$$2A_{m,1} = \psi_1 \oint \alpha_{66}^e \mathrm{d}\eta,$$
$$2A_{m,2} = \psi_2 \oint \alpha_{66}^e \mathrm{d}\eta. \tag{24.139}$$

Compatibility between cells 1 and 2 is ensured by requiring that the difference between the shear flow T_1 and T_2 acts in those parts of the cross-section that are common to both cells. This is ensured by the following compatibility conditions:

$$\psi_1 \oint_1 \alpha_{66}^e \mathrm{d}\eta - \psi_2 \oint_{1,2} \alpha_{66}^e \mathrm{d}\eta = 2A_{m,1},$$
$$-\psi_1 \oint_{1,2} \alpha_{66}^e \mathrm{d}\eta + \psi_2 \oint_2 \alpha_{66}^e \mathrm{d}\eta = 2A_{m,2}. \tag{24.140}$$

The integral $\oint_{1,2} \frac{\mathrm{d}s}{t(s)}$ extends over those parts of the cross-section that are common to the two cells 1 and 2. Equation (24.140) is a linear system of equations from which the two torsion functions ψ_1 and ψ_2 can be determined. Generalised for the n-cell cross-section, the compatibility conditions are as follows

$$\begin{bmatrix} \oint_1 \alpha_{66}^e \mathrm{d}\eta & -\oint_{1,2} \alpha_{66}^e \mathrm{d}\eta & -\oint_{1,3} \alpha_{66}^e \mathrm{d}\eta & \cdots & -\oint_{1,n} \alpha_{66}^e \mathrm{d}\eta \\ -\oint_{2,1} \alpha_{66}^e \mathrm{d}\eta & \oint_2 \alpha_{66}^e \mathrm{d}\eta & -\oint_{2,3} \alpha_{66}^e \mathrm{d}\eta & \cdots & -\oint_{2,n} \alpha_{66}^e \mathrm{d}\eta \\ -\oint_{3,1} \alpha_{66}^e \mathrm{d}\eta & -\oint_{3,2} \alpha_{66}^e \mathrm{d}\eta & \oint_3 \alpha_{66}^e \mathrm{d}\eta & \cdots & -\oint_{3,n} \alpha_{66}^e \mathrm{d}\eta \\ \vdots & \vdots & \vdots & \ddots & \vdots \\ -\oint_{n,1} \alpha_{66}^e \mathrm{d}\eta & -\oint_{n,2} \alpha_{66}^e \mathrm{d}\eta & -\oint_{n,3} \alpha_{66}^e \mathrm{d}\eta & \cdots & \oint_n \alpha_{66}^e \mathrm{d}\eta \end{bmatrix} \begin{pmatrix} \psi_1 \\ \psi_2 \\ \psi_3 \\ \vdots \\ \psi_n \end{pmatrix} = \begin{pmatrix} 2A_{m,1} \\ 2A_{m,2} \\ 2A_{m,3} \\ \vdots \\ 2A_{m,n} \end{pmatrix}, \tag{24.141}$$

or in symbolic form:

$$\underline{\underline{A}}\underline{\psi} = -\underline{a}. \tag{24.142}$$

The torsional stiffness for the two-cell cross-section follows from the constitutive law:

$$GI_T = \frac{M_x}{\vartheta'} = \frac{1}{\vartheta'} \left(2A_{m,1}T_1 + 2A_{m,2}T_2\right) = 2A_{m,1}\psi_1 + 2A_{m,2}\psi_2. \tag{24.143}$$

For the cross-section with n cells we obtain:

$$GI_T = 2\sum_{i=1}^{n} A_{m,i}\psi_i. \tag{24.144}$$

The shear flows of cells 1 and 2 follow as:

$$T_1 = \psi_1 \vartheta' = \frac{M_x}{GI_T}\psi_1,$$
$$T_2 = \psi_2 \vartheta' = \frac{M_x}{GI_T}\psi_2, \tag{24.145}$$

or generally for the cell i of an n-cell cross-section:

$$T_i = \frac{M_x}{GI_T}\psi_i. \tag{24.146}$$

24.4.4 Open Thin-Walled Cross-Sections

We now consider the torsion of an open thin-walled laminated cross-section with arbitrary layup with the dimensions h and t as shown in Fig. 24.28, where $t << h$ is assumed.

Due to the applied torsional moment M_x, the shear stresses $\tau_{\xi\eta}$ are formed as shown in Fig. 24.28, which can be translated into the torsional moment flow $M^0_{\xi\eta}$. This leads to the shear flow T as indicated, which is formed on the length $\bar{h}$ and the thickness $\bar{t}$. The torsional moment M_x can then be specified as:

$$M_x = T\bar{h}\bar{t} + T\bar{t}\bar{h}, \tag{24.147}$$

or under the assumption $\bar{h} \simeq h$:

$$M_x = 2T\bar{t}h. \tag{24.148}$$

The twisting moment flow $M^0_{\xi\eta}$ follows:

$$M^0_{\xi\eta} = -T\bar{t}. \tag{24.149}$$

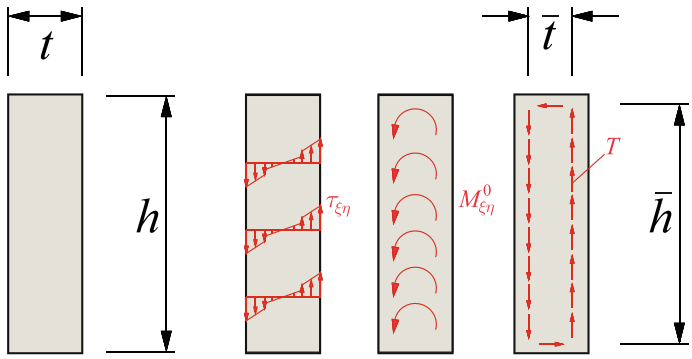


Fig. 24.28 Open thin-walled cross-section

Thus:

$$M_x = -2hM^0_{\xi\eta}. \tag{24.150}$$

For the twist $\kappa^0_{\xi\eta}$ applies:

$$\kappa^0_{\xi\eta} = \delta_{66} M^0_{\xi\eta}. \tag{24.151}$$

In addition, we have the following relation:

$$\vartheta' = -\frac{1}{2}\kappa^0_{\xi\eta}. \tag{24.152}$$

Thus:

$$\vartheta' = \frac{\delta_{66}}{4h} M_x. \tag{24.153}$$

The comparison with the constitutive law $M_x = GI_T\vartheta'$ then gives the required torsional stiffness GI_T as follows:

$$GI_T = \frac{4h}{\delta_{66}}. \tag{24.154}$$

If we consider a curved cross-section, then the following applies:

$$GI_T = 4\int_0^s \frac{1}{\delta_{66}} \mathrm{d}\eta, \tag{24.155}$$

where s is the length of the skeleton line of the cross-section.

24.4.5 Thin-Walled Cross-Sections

As a further case, we consider thin-walled cross-sections that are composed of different parts, whereby both open and closed parts are possible. Since it is assumed that all cross-section parts undergo the same torsion ϑ and twist ϑ', we can write for the partial cross-sections:

$$\vartheta'_i = \frac{M_{x,i}}{GI_{T,i}} = \vartheta'. \tag{24.156}$$

The same applies to the total cross-section:

$$\vartheta' = \frac{M_x}{GI_T}, \tag{24.157}$$

or

$$M_x = GI_T\vartheta'. \tag{24.158}$$

The torsional moment M_x is made up of the partial moments of the partial cross-sections:

$$M_x = \sum_{i=1}^{n} M_{x,i} = \sum_{i=1}^{n} \vartheta' G I_{T,i} = \vartheta' \sum_{i=1}^{n} G I_{T,i}. \tag{24.159}$$

Equating (24.158) and (24.159) results in the following:

$$G I_T \vartheta' = \vartheta' \sum_{i=1}^{n} G I_{T,i}, \tag{24.160}$$

or

$$G I_T = \sum_{i=1}^{n} G I_{T,i}. \tag{24.161}$$

The torsional stiffness of a cross-section composed of several different parts is therefore calculated by adding up the contributions of the individual segments.

24.4.6 Warping Torsion

We have so far dealt with the St. Venant torsion of thin-walled layered cross-sections. In particular, we have assumed cross-sections free of warping and assumed that the cross-sections remain flat or assumed cross-sections in which warping is not restrained. We now want to explore in which cases we need to treat the torsion problem of thin-walled laminated beams with a more advanced theory. The corresponding term for this is the so-called warping torsion.

In order to motivate the concept of warping torsion, we consider the cantilever of Fig. 24.29, which is loaded at its free end by the torsional moment M_T. Let the beam initially consist of isotropic and homogeneous material. The I-cross-section under consideration has the flange width b and the web height h. For the sake of simplicity, let the wall thickness t be constant. The applied torsional moment M_T leads to the internal torsional moment M_x, which is constant over the entire length with $M_x = M_T$. In Fig. 24.30 we decompose the torsional moment M_x into a pair of forces with $M_x = Fh$. Due to the acting torsional moment, there is a twist ϑ of the cross-section around the rotation axis which we denote as D. The pair of forces F in the upper and lower flange of the beam induces transverse forces and moments and also a deflection v of the flanges in the y-direction. As a consequence, this also results in a longitudinal displacement u as shown in Fig. 24.31. The considered beam is firmly clamped at its left end, so that the moments in the flanges also cause bending stresses, which we refer to as warping stresses $\sigma_{\omega\omega}$. The resulting cross-sectional warping is shown in Fig. 24.31.

This elementary example shows that, in addition to the newly added axial normal stress, further shear stresses occur due to axial force torsion, as shown in Fig. 24.32. In order to

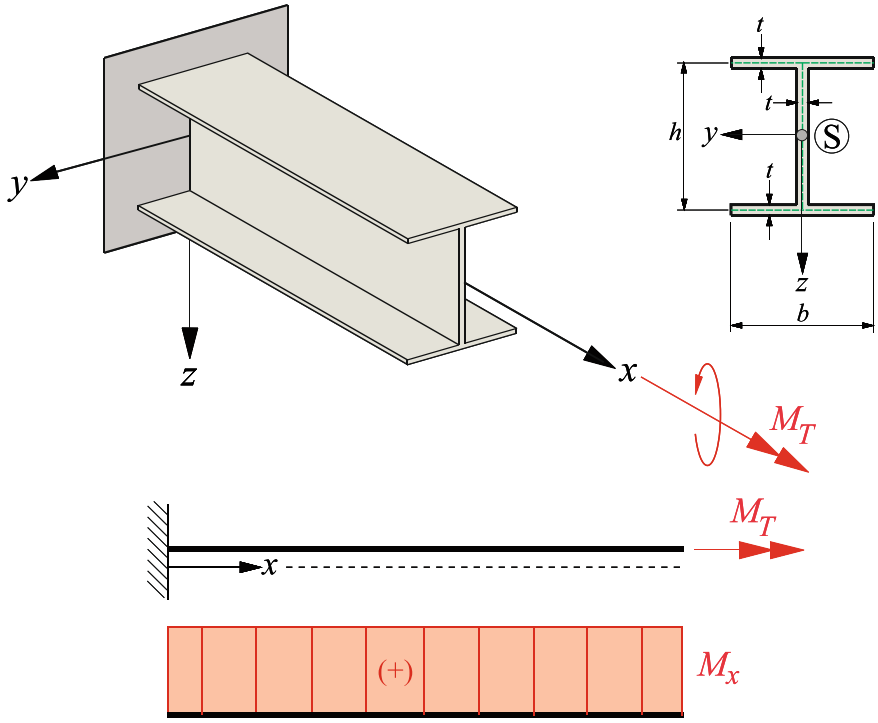


Fig. 24.29 I-beam clamped on one side under torsional moment M_T

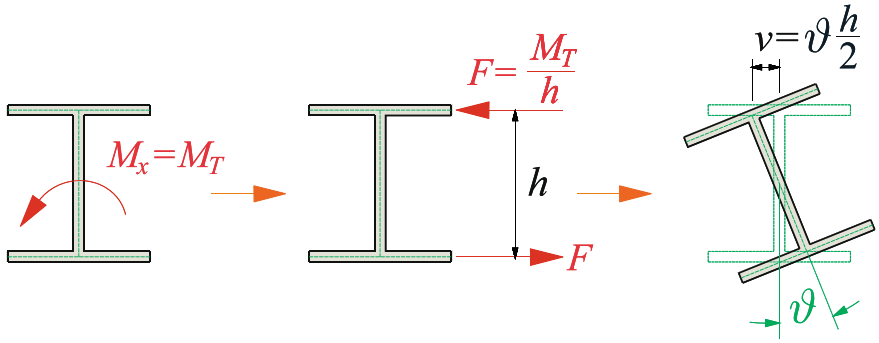


Fig. 24.30 Decomposing the torsional moment M_x into a pair of forces, resulting torsion and displacement

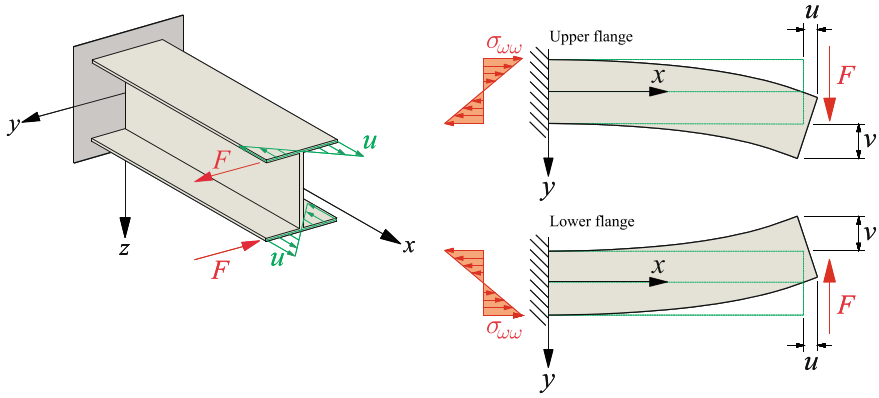


Fig. 24.31 Resulting warping of the flanges of the I-beam and warping stresses $\sigma_{\omega\omega}$

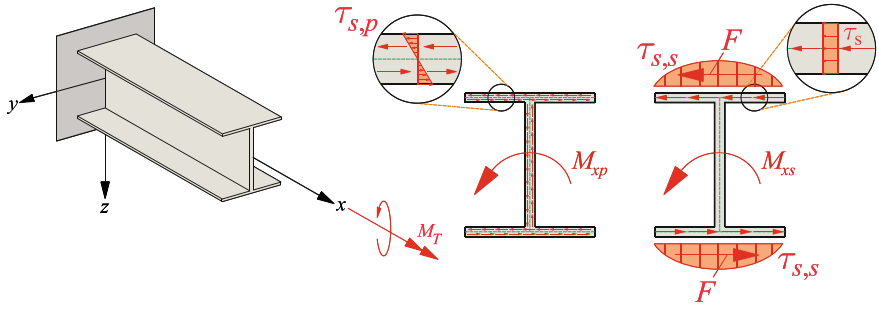


Fig. 24.32 Development of shear stresses due to primary torsion (M_{xp}) and secondary torsion (M_{xs})

clearly distinguish between St. Venant torsion and warping torsion, we denote the corresponding section moments M_x as M_{xp} (for primary torsion, i.e. St. Venant torsion) and as M_{xs} (for secondary torsion, i.e. warping torsion). The applied torsional moment M_T is therefore dissipated by St. Venant torsion and by warping torsion. The total torsional moment M_x is the sum of the two components M_{xp} and $M_{xs} = Fh$:

$$M_x = M_{xp} + M_{xs}. \tag{24.162}$$

The secondary torsional moment M_{xs} is correspondingly the resultant of the shear stresses $\tau_{s,s}$ caused by warping torsion with lever arm on the rotation axis D. The warping stresses $\sigma_{\omega\omega}$ resulting from the flange bending moment M_{Fl} are shown in Fig. 24.33.

If we look again at the assumptions of St. Venant's torsion theory, we find that it is only applicable if the treated cross-section is free of warping, i.e. we can assume that the cross-sections remain flat, or if the warping of the cross-section can occur freely and is not hindered by support conditions or the like. However, the simple example discussed above already shows that in practical applications, we only rarely have to deal with cross-sections

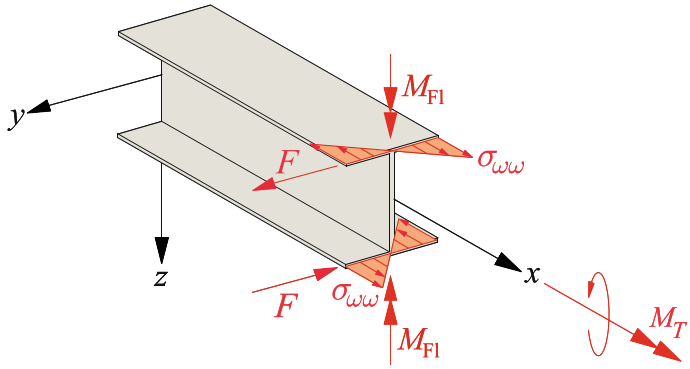


Fig. 24.33 Development of warping stresses due to secondary torsion M_{xs}

that are free of warping, which makes it necessary to take warping torsion into account. As a result, we have to drop the assumption of the validity of the hypothesis that the cross-sections remain plane when considering warping torsion. However, this hypothesis is retained at least for individual segments of the beam cross-section under consideration, i.e. for flanges and webs.

The section moment M_x was broken down into the force pair $F = \frac{M_{xs}}{h}$, whereby both the flange bending moment M_{Fl} and the flange shear force Q_{Fl} are generated in the two flanges if we consider the two flanges as beams under bending about the z-axis. For the flange bending moment M_{Fl} we obtain

$$M_{Fl}(x) = -EI_{zz}v''(x), \tag{24.163}$$

where I_{zz} is the moment of inertia of the flange cross-section with respect to bending about the z-axis. With $v = \vartheta\frac{h}{2}$ we have:

$$M_{Fl}(x) = -EI_{zz}\vartheta''(x)\frac{h}{2}. \tag{24.164}$$

The flange shear force Q_{Fl} follows as the first derivative of the flange moment M_{Fl}:

$$Q_{Fl}(x) = -EI_{zz}v'''(x) = -EI_{zz}\vartheta'''(x)\frac{h}{2}. \tag{24.165}$$

From this, the secondary torsional moment M_{xs} can be determined as:

$$M_{xs} = Q_{Fl}h = -EI_{zz}\vartheta'''(x)\frac{h^2}{2}. \tag{24.166}$$

The product $I_{zz}\frac{h^2}{2}$ corresponds to the warping moment of inertia $I_{\omega\omega}$, so that with $I_{zz} = \frac{tb^3}{12}$:

$$M_{xs} = -EI_{\omega\omega}\vartheta'''(x). \tag{24.167}$$

The two flange moments M_{Fl}, multiplied by the distance h, represent the so-called warping moment M_ω:

$$M_\omega = M_{Fl}h = -EI_{\omega\omega}\vartheta''(x). \tag{24.168}$$

The total torsional moment M_x results from the addition of M_{xp} and M_{xs}:

$$M_x = M_{xp} + M_{xs} = GI_T\vartheta'(x) - EI_{\omega\omega}\vartheta'''(x). \tag{24.169}$$

With the equilibrium condition

$$M_x' = -m_T \tag{24.170}$$

the differential equation of warping torsion follows in the case of a prismatic beam:

$$EI_{\omega\omega}\vartheta''''(x) - GI_T\vartheta''(x) = m_T. \tag{24.171}$$

This equation was derived here using the example of the isotropic I-beam. However, it also applies in the form given here for any other prismatic isotropic beam and also for thin-walled laminate beams with orthotropic layups. The corresponding warping stiffness $EI_{\omega\omega}$ must therefore be determined at this point. Section 24.4.7 contains an overview of common practically relevant cross-sections.

The general solution of the differential equation (24.171) is as follows:

$$\vartheta(x) = \frac{C_1}{\lambda^2}\sinh(\lambda x) + \frac{C_2}{\lambda^2}\cosh(\lambda x) + C_3x + C_4 + F(x). \tag{24.172}$$

Here, $F(x)$ represents the term that results from the particular solution of (24.171). For the special case $m_T = \text{const.}$ results:

$$\vartheta(x) = \frac{C_1}{\lambda^2}\sinh(\lambda x) + \frac{C_2}{\lambda^2}\cosh(\lambda x) + C_3x + C_4 - \frac{m_Tx^2}{2GI_T}. \tag{24.173}$$

The quantity λ is the so-called decay factor:

$$\lambda = \sqrt{\frac{GI_T}{EI_{\omega\omega}}}. \tag{24.174}$$

The solution (24.172) of the differential equation of warping torsion (24.171) requires the formulation of boundary conditions to determine the constants C_1, C_2, C_3 and C_4. Typical cases of boundary conditions are shown in Fig. 24.34. If we consider a fork restraint

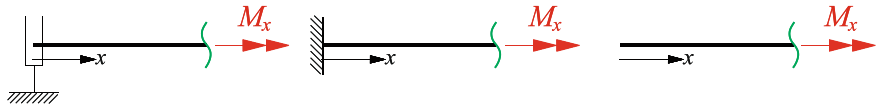


Fig. 24.34 Typical boundary conditions at the point $x = 0$: Fork restraint (left), clamped end (middle), free end (right)

(Fig. 24.34, left), the torsion ϑ is zero at this point. In addition, the second derivative of ϑ disappears there, as the warping M_ω becomes zero:

$$\vartheta = 0, \quad \vartheta'' = 0. \tag{24.175}$$

A fork restraint is thus a type of bearing in which torsional moments can be absorbed, but no torsion ϑ is possible. The warping of the cross-section can occur unhindered with a fork restraint.

If we have a firmly clamped beam (Fig. 24.34, middle), then both the torsion ϑ and its first derivative ϑ' disappear at this point:

$$\vartheta = 0, \quad \vartheta' = 0. \tag{24.176}$$

If there is a free unloaded end (Fig. 24.34, right), then the warping moment M_ω and correspondingly the second derivative ϑ'' of ϑ disappear there. In addition, M_x becomes zero:

$$\vartheta'' = 0, \quad GI_T\vartheta'(x) - EI_{\omega\omega}\vartheta'''(x) = 0. \tag{24.177}$$

24.4.7 Selected Cross-Sections

The following is an overview of selected practically relevant cross-sections. The position of the shear center, the torsional stiffness GI_T and the warping stiffness $EI_{\omega\omega}$ are given (according to Kollár and Springer (2003), w = web, f = flange).

24.4.7.1 Open Cross Sections

Figure 24.35 shows some selected thin-walled open cross-sections. The layups of the walls are orthotropic and unsymmetric. The properties δ_{66} and δ_{11} are evaluated in the neutral plane, which is located at the point $e = -\frac{\beta_{11}}{\delta_{11}}$. Here, β_{11} and δ_{11} are evaluated in the middle plane of the wall.

For the doubly symmetric I-section of Fig. 24.35a, the shear center M lies exactly in the center of gravity of the cross-section. The torsional stiffness and the warping stiffness follow as:

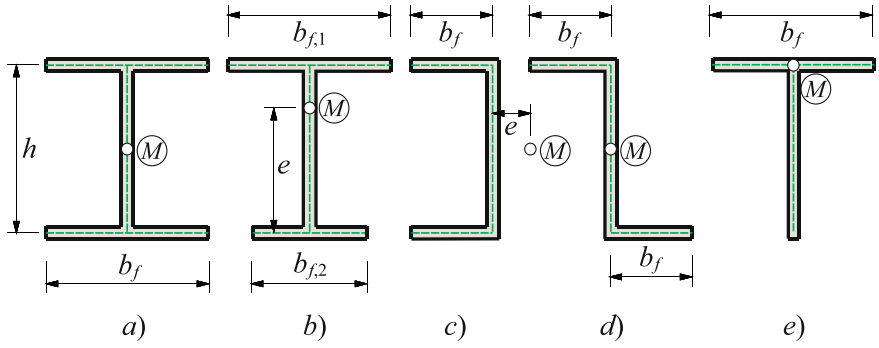


Fig. 24.35 Selected open thin-walled cross-sections

$$GI_T = 4\left(\frac{2b_f}{\delta_{66,f}} + \frac{h}{\delta_{66,w}}\right),$$
$$EI_{\omega\omega} = \frac{1}{\alpha_{11,f}}\frac{h^2 b_f^3}{24}. \tag{24.178}$$

In the case of the simply symmetric I-section of Fig. 24.35b follows:

$$GI_T = 4\left(\frac{b_{f,1}}{\delta_{66,f,1}} + \frac{b_{f,2}}{\delta_{66,f,2}} + \frac{b_s}{\delta_{66,w}}\right),$$
$$EI_{\omega\omega} = \frac{1}{12}\frac{b_{f,2}^3}{\alpha_{11,f,2}}eh,$$
$$e = h\frac{\frac{b_{f,1}^3}{\alpha_{11,f,1}}}{\frac{b_{f,1}^3}{\alpha_{11,f,1}} + \frac{b_{f,2}^3}{\alpha_{11,f,2}}}. \tag{24.179}$$

For the simply symmetric C-section (Fig. 24.35c) we obtain:

$$GI_T = 4\left(\frac{2b_f}{\delta_{66,f}} + \frac{h}{\delta_{66,w}}\right),$$
$$EI_{\omega\omega} = \frac{b_f^3 h^2}{12}\frac{1}{\alpha_{11,f}}\frac{\frac{3b_f}{\alpha_{11,f}} + \frac{2h}{\alpha_{11,w}}}{\frac{6b_f}{\alpha_{11,f}} + \frac{h}{\alpha_{11,w}}},$$
$$e = \frac{\frac{3b_f^2}{\alpha_{11,f}}}{\frac{6b_f}{\alpha_{11,f}} + \frac{h}{\alpha_{11,w}}}. \tag{24.180}$$

For the Z cross-section as shown in Fig. 24.35d we have:

$$GI_T = 4\left(\frac{2b_f}{\delta_{66,f}} + \frac{h}{\delta_{66,w}}\right),$$
$$EI_{\omega\omega} = \frac{b_f^3 h^2}{12\left(2b_f + h\right)^2}\left(2\frac{b_f^2 + b_f h + h^2}{\alpha_{11,f}} + 3\frac{b_f h}{\alpha_{11,w}}\right). \tag{24.181}$$

Finally, the T-cross-section of Fig. 24.35e is considered:

$$GI_T = 4\left(\frac{2b_f}{\delta_{66,f}} + \frac{h}{\delta_{66,w}}\right),$$
$$EI_{\omega\omega} = 0. \tag{24.182}$$

24.4.7.2 Closed Cross-Sections

For the box cross-section of Fig. 24.36a follows:

$$GI_T = \frac{2b_f^2 h^2}{\alpha^e_{66,f} b_f + \alpha^e_{66,w} h},$$
$$EI_{\omega\omega} \simeq 0. \tag{24.183}$$

In the case of the circular cross-section (Fig. 24.36b), the result is:

$$GI_T = \frac{2R_m^3 \pi}{\alpha^e_{66}},$$
$$EI_{\omega\omega} = 0. \tag{24.184}$$

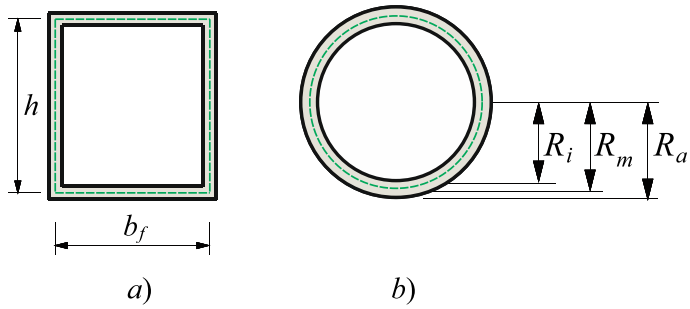


Fig. 24.36 Selected closed thin-walled cross-sections

References

Bauchau OA, Craig JI (2009): *Structural analysis: with applications to aerospace structures*, Springer, Dordrecht et al., The Netherlands.

Czerwenka G, Schnell W (1970): *Einführung in die Rechenmethoden des Leichtbaus, Band 1*, Bibliographisches Institut, Mannheim et al., Germany.

Franke W, Friemann H (2005): *Schub und Torsion in geraden Stäben*, 3rd edition, Vieweg + Teubner Verlag, Wiesbaden, Germany.

Hanswille G (1995): *Vorlesungen über Stahl- und Verbundbau*, Fachbereich Bauingenieurwesen, Bergische Universität Wuppertal, Wuppertal, Germany.

Kindmann R, Frickel J (2017): *Elastische und plastische Querschnittstragfähigkeit*, Online edition 2017, https://kindmann.de, last retrieved march 2020.

Kollár LP, Springer GS (2003): *Mechanics of composite structures*, Cambridge University Press, Cambridge et al., USA.

Kollbrunner CF, Hajdin N (1963): *Die St.-Venantsche Torsion*, Mitteilungen der Technischen Kommission der Schweizer Stahlbau-Vereinigung, Heft 26, Verlag der Schweizer Stahlbau-Vereinigung, Zürich, Switzerland.

Kollbrunner CF, Basler K (1963): *Torsionsmomente und Stabverdrehung bei St.-Venantscher Torsion*, Mitteilungen der Technischen Kommission der Schweizer Stahlbau-Vereinigung, Heft 27, Verlag der Schweizer Stahlbau-Vereinigung, Zürich, Switzerland.

Kollbrunner CF, Basler K (1966): *Torsion*, Springer Verlag, Berlin et al., Germany.

Linke M, Nast E (2015): *Festigkeitslehre für den Leichtbau*, Springer-Verlag, Berlin, Heidelberg, Germany.

Megson THG (1999): *Aircraft structures for engineering students*, 3rd edition, Arnold, London, UK.

Mittelstedt C (2020): *Buckling and Post-Buckling of Thin-Walled Composite Laminated Beams - A Review of Engineering Analysis Methods*, Applied Mechanics Reviews 72:020802.

Mittelstedt C (2021): *Structural mechanics in lightweight engineering*, Springer Nature, Cham, Switzerland.

Petersen C (1997): *Stahlbau*, 3rd edition, Vieweg Verlag, Braunschweig, Wiesbaden, Germany.

Roik KH, Carl J, Lindner J (1972): *Biegetorsionsprobleme gerader dünnwandiger Stäbe*, Ernst & Sohn, Berlin et al., Germany.

Roik KH (1978): *Vorlesungen über Stahlbau*, Ernst & Sohn, Berlin et al., Germany.

Shama M (2010): *Torsion and shear stresses in ships*, Springer Verlag, Heidelberg et al., Germany.

Wiedemann J (2007): *Leichtbau 1: Elemente*, Springer Verlag, Berlin et al., Germany.

Wlassow WS (1964): *Dünnwandige elastische Stäbe, Band I*, VEB Verlag für Bauwesen, Berlin, Germany.

Wlassow WS (1965): *Dünnwandige elastische Stäbe, Band II*, VEB Verlag für Bauwesen, Berlin, Germany.



Buckling of Laminated Beams

25

This chapter provides an overview of the stability behaviour of thin-walled layered beams, distinguishing between global and local stability. For the case of a beam under combined loads, all necessary equations for the global stability behaviour are provided and a distinction is made between global cases such as column buckling, torsional buckling, flexural-torsional buckling and lateral stability. For some selected cases, exact analytical solutions can be given, whereas for non-elementary solvable cases, approximation methods such as the Ritz method or the Finite Element Method will be used, both of which are discussed. Regarding the local stability of thin-walled layered beams, an analytical approach based on plate analysis and using appropriate equivalent restraint stiffnesses is discussed.

25.1 Introduction

Thin-walled beams are the most elementary structural elements in many technical applications and can be designed in any desired shape and cross-section to fulfil specific purposes. Some exemplary cross-sections with an open profile, which are relevant in the following, are shown in Fig. 25.1. The structural analysis of such thin-walled beam structures is very often determined by their stability behaviour, i.e. by the determination of the critical buckling loads at which an originally straight beam suddenly experiences lateral deformations under a certain load combination. As soon as such deformations occur, the beam is said to have reached its buckling load. Figure 25.2 shows exemplary finite element results for the different modes of a double-symmetric I-beam under axial compressive load in the x-direction. While local buckling is to be expected for rather short beams (Fig. 25.2, left), i.e. a buckling mode in which the beam longitudinal axis remains straight and the individual segments (web and flanges) buckle locally, global buckling becomes relevant for beams of sufficient length

© The Author(s), under exclusive license to Springer-Verlag GmbH, DE, part of Springer Nature 2025

C. Mittelstedt, *Mechanics of Composite Structures*,
https://doi.org/10.1007/978-3-662-70788-3_25

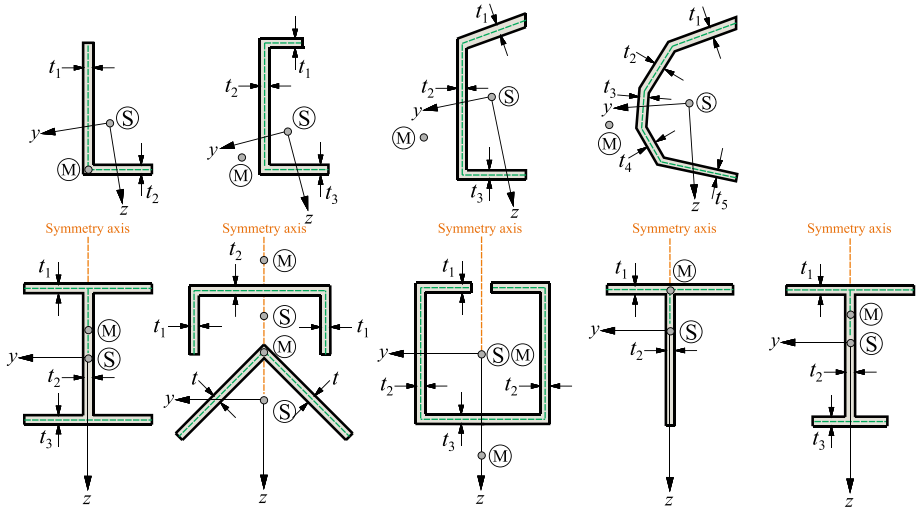


Fig. 25.1 Exemplary open profile cross-sections of thin-walled beams with the principal axes y and z as well as the positions of the center of gravity S and the shear center M

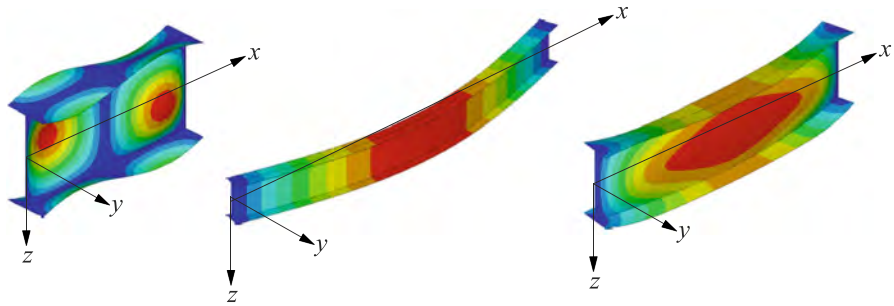


Fig. 25.2 Buckling modes for a thin-walled I-beam under longitudinal compressive load in the x-direction: local buckling (left), global buckling (middle), interactive buckling (right)

(Fig. 25.2, middle), which is particularly relevant here in the form of flexural buckling, i.e. a buckling mode in which the longitudinal axis of the beam deforms sinusoidally and the web and flanges do not exhibit any local buckling deformations. However, for medium-length beams, an interaction between local and global buckling modes can occur, which is commonly referred to as interactive buckling (Fig. 25.2, right).

Depending on the cross-sectional properties of the beam under consideration, other forms of stability problems can occur during global buckling in addition to flexural buckling. A (rather rare) buckling problem under compressive loading appears in the form of a cross-sectional twist ϑ while the beam axis remains straight. This type of buckling can be prevalent in beams under compression with a double-symmetric cross-section and weak flanges and

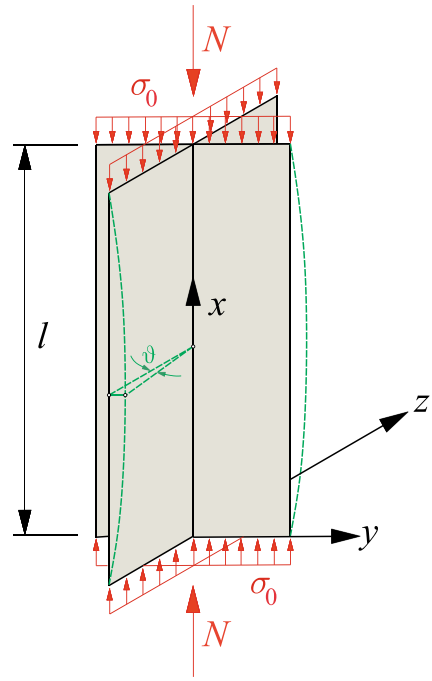


Fig. 25.3 Torsional buckling of a double-symmetric beam under axial compressive load

is referred to as torsional buckling (Fig. 25.3). For beams that are under centric compressive load and whose cross-section has only one axis of symmetry or no symmetry properties at all, a combination of torsional and flexural buckling occurs, which is generally referred to as flexural-torsional buckling. Figure 25.4 shows the possible buckling modes for a beam with a simply symmetric C-section. Depending on the actual geometric properties of the cross-section, either flexural buckling around the z-axis or flexural-torsional buckling occurs as a superposition of flexural buckling in the z-direction and torsional buckling.

Another global stability failure of thin-walled beams occurs when the beam is subjected to loads that cause bending. Figure 25.5 shows a beam loaded by end moments M_0. A buckling problem occurs when there are bending moments around the major cross-sectional axis that lead to a combined buckling mode consisting of lateral displacements in the y-direction combined with a rotation of the cross-section around the longitudinal axis of the beam. This buckling phenomenon is commonly referred to as lateral buckling. Figure 25.6 shows the lateral buckling of a cantilever beam under a single force F.

It should be noted that the terms lateral buckling and flexural-torsional buckling contain a certain redundancy. Both stability cases are not only very similar, they are actually described by the same differential equations and boundary conditions. In order to make a clear distinction, however, the term lateral buckling is used below when both axial and transverse loads can be present, whereas the term flexural-torsional buckling is only used when a centric axial compressive load occurs.

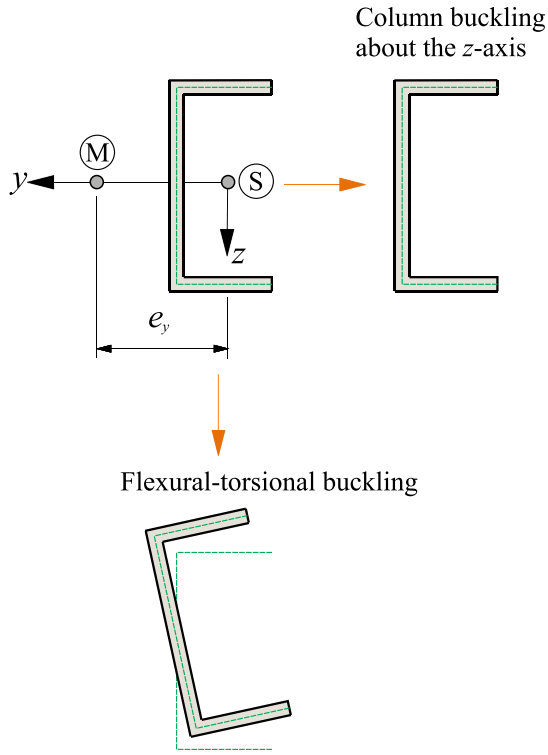


Fig. 25.4 Flexural buckling and flexural-torsional buckling of a beam under centric compressive load with a single symmetric C-section

All the global buckling problems mentioned—flexural buckling, torsional buckling, flexural-torsional buckling, lateral buckling—have in common that they can be described within the framework of a suitable beam theory. While for many cases, in particular for isotropic thin-walled structures, the classical Euler-Bernoulli beam theory is sufficient in many practically relevant cases, taking into account warping torsion (commonly referred to as Vlasov's beam theory, see Vlasov (1961)), where the beam behaviour is described by effective stiffness properties, the analysis of thin-walled composite beams requires more refined means of analysis to describe phenomena such as shear deformations or inherent coupling effects, which do not occur in isotropic beams.

The occurrence of local buckling modes, on the other hand, is usually described with the help of plate analysis. While Kirchhoff's classical plate theory is sufficient for many isotropic beam structures and provides local buckling results of sufficient accuracy, the treatment of beams consisting of segments of laminated composite materials requires the use of adequate laminate theories to capture, for example, coupling effects and the influence of transverse shear deformations. The analysis of interactive buckling processes requires, of course, the

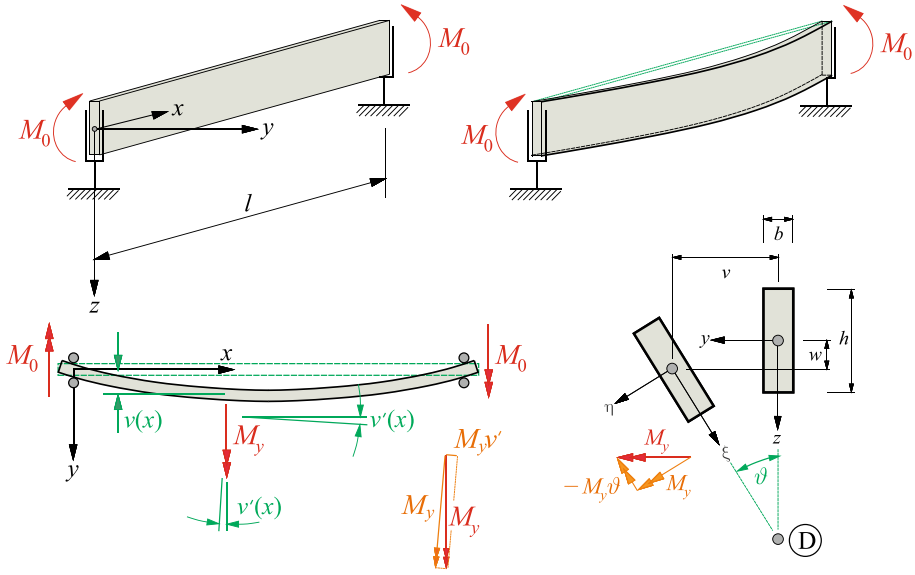


Fig. 25.5 Lateral buckling of a slender beam under end moments M_0

simultaneous consideration of local and global buckling with appropriate analytical tools which is not dealt with in this chapter.

This chapter deals with the global and local stability of thin-walled composite beams and gives an overview of common analysis methods. Comprehensive research reports on the topic dealt with in this chapter can be found in Becker (1957), Gerard and Becker (1957) for isotropic structures and Barbero (1992) for composite beams, the latter reference containing an overview of common analytical methods and numerous experimental results. Further works with comprehensive literature reviews can be found in Almroth (1981), Beerhorst (2013), Bonnani et al. (1988, 1991), Kolakowski and Teter (2016), Mittelstedt (2011), Shan (2007), Simoes Da Silva Dias Simao (2007), Xu et al. (2013) and Russo (2017). In 2019, Mittelstedt presented a review paper on the buckling problems discussed here, citing more than 400 references in this field. Textbooks on the theory of stability that are relevant in the context of this chapter are available with the works of Alfutov (1999), Bleich (1952), Chen and Lui (1987), Pflüger (1975), Reddy (2004), Singer et al. (1998, 2002), Jones (2006), Timoshenko and Gere (1961), Trahair (1993), Turvey and Marshall (1995), and Mittelstedt (2024).

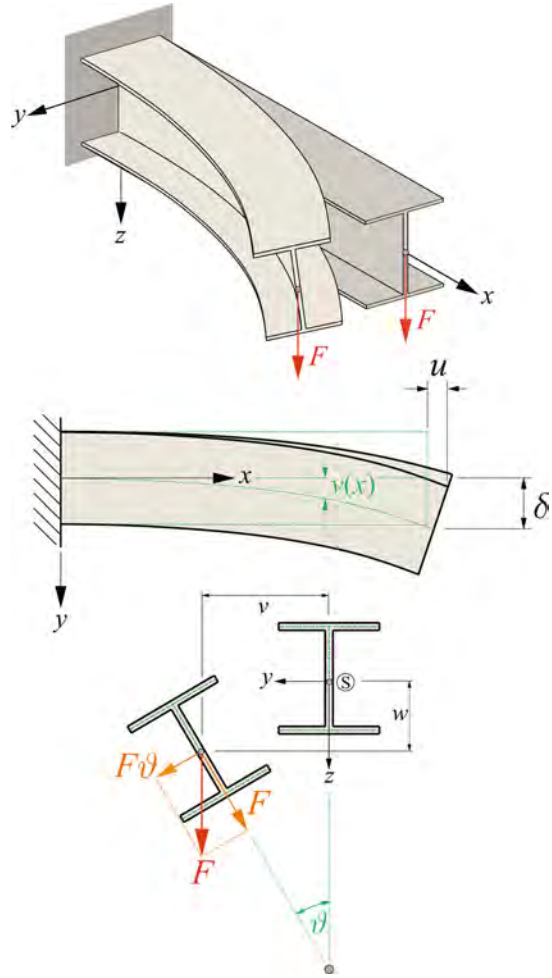


Fig. 25.6 Lateral buckling of a cantilever beam under a force F

25.2 Global Buckling of Thin-Walled Beams

25.2.1 Basic Equations

We consider the buckling equations within the framework of the Euler-Bernoulli beam theory (Mittelstedt 2021), including warping torsion, and consider prismatic beams made of linear-elastic material, where the material and geometry properties are assumed to be homogeneous with respect to the longitudinal direction of the beam. Local buckling, i.e. changes in the cross-sectional shape during buckling, are excluded at this point and will be discussed later. The coordinate axes x, y, z are assumed to be the principal axes of the cross-section. We consider the beam in an infinitesimally deformed configuration, i.e. we

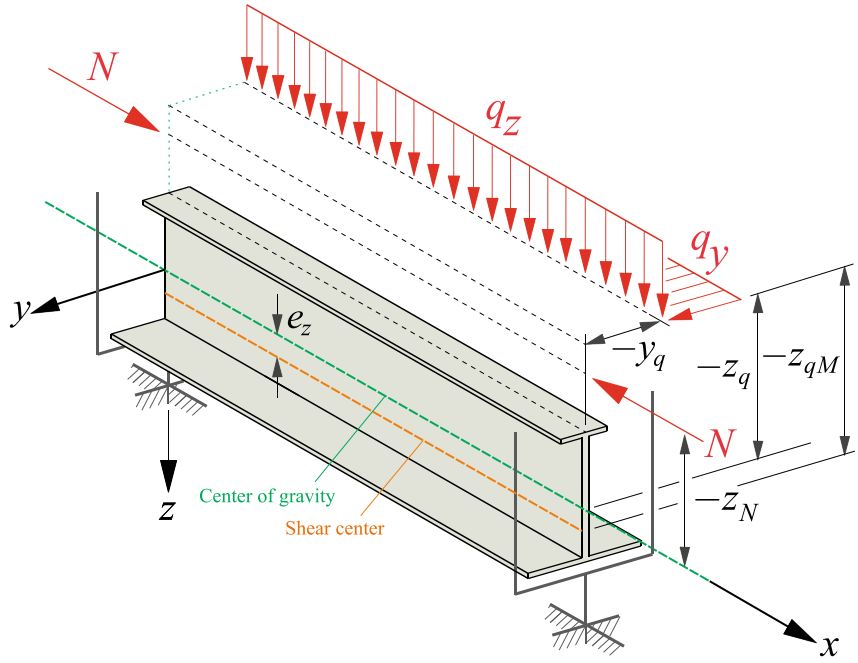


Fig. 25.7 Structural situation

carry out our considerations within the framework of the so-called second-order theory. Consequently, we assume that all deformations and rotations are small, which allows us to linearize all considerations.

The structural situation under consideration is shown in Fig. 25.7. It is assumed that the beam is loaded by line loads $q_y(x)$ and $q_z(x)$ in the y- and z-directions. Individual loads and individual moments are also permissible, but are not depicted here for the sake of simplicity. The line loads q_y and q_z are assumed to be eccentric along a line with the coordinates y_q and z_q relative to the center of gravity S of the cross-section. The distances with respect to the shear center M of the cross-section are referred to as y_{qM} and z_{qM}. In addition, an eccentric normal force $N(x)$ is assumed at the location y_N, z_N. Figure 25.7 shows an example of a beam that exhibits fork restraints at both ends, although no boundary conditions are specified at this point in the derivation. It should be noted that Fig. 25.7 shows a beam with a simple symmetric cross-section for the sake of simplicity. However, all the following equations are valid for arbitrary cross-sections. The offset between the center of gravity S and the shear center M is described by e_y and e_z.

The governing differential equations and all potential combinations of boundary conditions can be derived from the principle of the minimum of the total elastic potential $\Pi = \Pi_i + \Pi_a$ (see also e.g. Roik et al. (1972) and Roik (1978)), where Π_i is the strain

energy/inner potential of the buckled beam in the second order analysis, and Π_a is the potential of the applied loads. For the given situation, the inner potential Π_i is:

$$\begin{aligned}\Pi_i = &\frac{1}{2}\int_0^l EI_{yy}\left(w_M''\right)^2 \mathrm{d}x + \frac{1}{2}\int_0^l EI_{zz}\left(v_M''\right)^2 \mathrm{d}x \\ &+ \frac{1}{2}\int_0^l GI_T\left(\vartheta'\right)^2 \mathrm{d}x + \frac{1}{2}\int_0^l EI_{\omega\omega}\left(\vartheta''\right)^2 \mathrm{d}x \\ &- \frac{1}{2}\int_0^l N\left[2e_z v_M'\vartheta' - 2e_y w_M'\vartheta' + \left(v_M'\right)^2 + \left(w_M'\right)^2 + i_M^2\left(\vartheta'\right)^2\right]\mathrm{d}x \\ &+ \frac{1}{2}\int_0^l M_z\left[-2w_M''\vartheta + r_{My}\left(\vartheta'\right)^2\right]\mathrm{d}x + \frac{1}{2}\int_0^l M_y\left[2v_M''\vartheta + r_{Mz}\left(\vartheta'\right)^2\right]\mathrm{d}x, \qquad (25.1)\end{aligned}$$

where i_M is the radius of gyration with respect to the shear center M, and r_{My} and r_{Mz} are third-order moments of gyration.

The external potential Π_a contains the potential loss of the applied line loads q_y and q_z:

$$\Pi_a = -\int_0^l \left(q_y v_M + q_z w_M\right)\mathrm{d}x + \frac{1}{2}\int_0^l \left(q_y y_{qM} + q_z z_{qM}\right)\vartheta^2 \mathrm{d}x. \qquad (25.2)$$

Since we assume unrestrained rotation of the cross-section, the displacements v_M and w_M are measured in relation to the shear center M. The equilibrium of an elastic system requires that the first variation $\delta\Pi$ of the total elastic potential disappears, i.e. $\delta\Pi = \delta\Pi_i + \delta\Pi_a = 0$, so that:

$$\begin{aligned}&\int_0^l \left[EI_{zz}v_M'''' + \left(Ne_z\vartheta'\right)' + \left(Nv_M'\right)' + \left(M_y\vartheta\right)'' - q_y\right]\delta v_M \mathrm{d}x \\ &+ \int_0^l \left[EI_{yy}w_M'''' - \left(Ne_y\vartheta'\right)' + \left(Nw_M'\right)' + \left(M_z\vartheta\right)'' - q_z\right]\delta w_M \mathrm{d}x \\ &+ \int_0^l \Big[EI_{\omega\omega}\vartheta'''' - GI_T\vartheta'' + \left(Ne_z v_M'\right)' - \left(Ne_y w_M'\right)' \\ &+ \left(Ni_M^2\vartheta'\right)' + M_z w_M'' + M_y v_M'' + \left(M_z r_{My}\vartheta'\right)' \\ &- \left(M_y r_{Mz}\vartheta'\right)' + q_y y_{qM}\vartheta + q_z z_{qM}\vartheta\Big]\delta\vartheta \mathrm{d}x\end{aligned}$$

$$
\begin{aligned}
&- \left[EI_{zz} v_M''' + N \left(v_M' + e_z \vartheta' \right) + \left(M_y \vartheta \right)' \right] \delta v_M \Big|_0^l \\
&+ \left[EI_{zz} v_M'' + M_y \vartheta \right] \delta v_M' \Big|_0^l \\
&- \left[EI_{yy} w_M''' + N \left(w_M' - e_y \vartheta' \right) + (M_z \vartheta)' \right] \delta w_M \Big|_0^l \\
&+ \left[EI_{yy} w_M'' + M_z \vartheta \right] \delta w_M' \Big|_0^l \\
&- \left[EI_{\omega\omega} \vartheta''' - N \left(e_y w_M' - e_z v_M' \right) \right. \\
&- \left. \left(GI_T - Ni_M^2 + M_y r_{Mz} - M_z r_{My} \right) \vartheta' \right] \delta \vartheta \Big|_0^l \\
&+ EI_{\omega\omega} \vartheta'' \delta \vartheta' \Big|_0^l = 0.
\end{aligned} \tag{25.3}
$$

From the integral terms in (25.3), the governing differential equations can be derived, which describe the global buckling behaviour of the considered beam:

$$
\begin{aligned}
EI_{zz} v_M'''' + \left[N \left(v_M' + e_z \vartheta' \right) \right]' + \left(M_y \vartheta \right)'' &= q_y, \\
EI_{yy} w_M'''' + \left[N \left(w_M' - e_y \vartheta' \right) \right]' + (M_z \vartheta)'' &= q_z, \\
EI_{\omega\omega} \vartheta'''' - GI_T \vartheta'' + \left(N e_z v_M' \right)' - \left(N e_y w_M' \right)' & \\
+ M_y v_M'' + M_z w_M'' + \left[\vartheta' \left(Ni_M^2 - M_y r_{Mz} + M_z r_{My} \right) \right]' & \\
+ q_y y_{qM} \vartheta + q_z z_{qM} \vartheta &= 0.
\end{aligned} \tag{25.4}
$$

Obviously, buckling under transverse and normal loading is described by three coupled differential equations that must be solved simultaneously. The boundary terms contained in (25.3) form the boundary conditions for the given global buckling problem:

$$
\begin{aligned}
\left[EI_{zz} v_M''' + N \left(v_M' + e_z \vartheta' \right) + \left(M_y \vartheta \right)' \right] \delta v_M \Big|_0^l &= 0, \\
\left[EI_{yy} w_M''' + N \left(w_M' - e_y \vartheta' \right) + (M_z \vartheta)' \right] \delta w_M \Big|_0^l &= 0, \\
\left[EI_{zz} v_M'' + M_y \vartheta \right] \delta v_M' \Big|_0^l &= 0, \\
\left[EI_{yy} w_M'' + M_z \vartheta \right] \delta w_M' \Big|_0^l &= 0, \\
\left[EI_{\omega\omega} \vartheta''' - N \left(e_y w_M' - e_z v_M' \right) \right. & \\
\left. - \left(GI_T - Ni_M^2 + M_y r_{Mz} - M_z r_{My} \right) \vartheta' \right] \delta \vartheta \Big|_0^l &= 0, \\
EI_{\omega\omega} \vartheta'' \delta \vartheta' \Big|_0^l &= 0.
\end{aligned} \tag{25.5}
$$

25.2.2 Flexural-Torsional Buckling

We now consider the special case of a beam under a centric compressive load N so that $M_y = M_z = 0$ and $q_y = q_z = 0$. In the following derivations, it is assumed that the normal compressive force N is constant over the length of the beam, so that $N' = 0$. The differential equations (25.4) then take the following form:

$$\begin{aligned} EI_{zz} v_M'''' + N\left(v_M'' + e_z \vartheta''\right) &= 0, \\ EI_{yy} w_M'''' + N\left(w_M'' - e_y \vartheta''\right) &= 0, \\ EI_{\omega\omega} \vartheta'''' - GI_T \vartheta'' + N e_z v_M'' - N e_y w_M'' + N i_M^2 \vartheta'' &= 0. \end{aligned} \tag{25.6}$$

Obviously, this set of differential equations describes the buckling modes with simultaneous occurrence of the transverse displacements v_M and w_M and the torsion ϑ of the cross-section, which is referred to as flexural-torsional buckling. The boundary conditions (25.5) are simplified as follows:

$$\begin{aligned} \left[EI_{zz} v_M''' + N\left(v_M' + e_z \vartheta'\right)\right] \delta v_M \Big|_0^l &= 0, \\ \left[EI_{yy} w_M''' + N\left(w_M' - e_y \vartheta'\right)\right] \delta w_M \Big|_0^l &= 0, \\ \left[EI_{zz} v_M''\right] \delta v_M' \Big|_0^l &= 0, \\ \left[EI_{yy} w_M''\right] \delta w_M' \Big|_0^l &= 0, \\ \left[EI_{\omega\omega} \vartheta''' - N\left(e_y w_M' - e_z v_M'\right) - \left(GI_T - N i_M^2\right) \vartheta'\right] \delta \vartheta \Big|_0^l &= 0, \\ EI_{\omega\omega} \vartheta'' \delta \vartheta' \Big|_0^l &= 0. \end{aligned} \tag{25.7}$$

25.2.3 Flexural Buckling and Torsional Buckling

If we assume that the cross-section under consideration is doubly symmetric or has polar symmetry, so that $S = M$ and consequently $e_y = e_z = 0$, the differential equations are simplified further:

$$\begin{aligned} EI_{zz} v_M'''' + N v_M'' &= 0, \\ EI_{yy} w_M'''' + N w_M'' &= 0, \\ EI_{\omega\omega} \vartheta'''' - GI_T \vartheta'' + N i_M^2 \vartheta'' &= 0. \end{aligned} \tag{25.8}$$

It is worth noting that in this particular case the equations are fully decoupled, so that the global buckling behaviour of such beams is described by two flexural buckling modes associated with v_M and w_M and a torsional buckling mode describing a twist ϑ of the cross-section, referred to as torsional buckling. The boundary conditions are simplified as follows

$$
\begin{aligned}
\left[EI_{zz}v_M''' + Nv_M'\right]\delta v_M\big|_0^l &= 0,\\
\left[EI_{yy}w_M''' + Nw_M'\right]\delta w_M\big|_0^l &= 0,\\
\left[EI_{zz}v_M''\right]\delta v_M'\big|_0^l &= 0,\\
\left[EI_{yy}w_M''\right]\delta w_M'\big|_0^l &= 0,\\
\left[EI_{\omega\omega}\vartheta''' - \left(GI_T - Ni_M^2\right)\vartheta'\right]\delta\vartheta\big|_0^l &= 0,\\
EI_{\omega\omega}\vartheta''\delta\vartheta'\big|_0^l &= 0.
\end{aligned}
\tag{25.9}
$$

25.2.4 Exact Solutions

The system of differential equations (25.4) allows exact closed-form solutions only for very few special cases. Let us further consider the set of differential equations (25.6) for flexural-torsional buckling and assume fork restraints at both ends of the beam at $x = 0$ and $x = l$, where $v_M = 0$, $v_M'' = 0$, $w_M = 0$, $w_M'' = 0$, $\vartheta = 0$, $\vartheta'' = 0$. Then the following approaches for the transverse displacements v_M, w_M and the angle ϑ are permissible:

$$
\begin{aligned}
v_M &= C_1 \sin\left(\frac{\pi x}{l}\right),\\
w_M &= C_2 \sin\left(\frac{\pi x}{l}\right),\\
\vartheta &= C_3 \sin\left(\frac{\pi x}{l}\right),
\end{aligned}
\tag{25.10}
$$

where C_1, C_2, C_3 are the buckling amplitudes. If (25.10) is inserted into the Eq. (25.6) and the coefficient determinant of the resulting homogeneous linear system of equations is formed and set to zero, the following third-order polynomial for N is finally obtained:

$$
\begin{aligned}
&\left(\frac{\pi^2 EI_{yy}}{l^2} - N\right)\left(\frac{\pi^2 EI_{zz}}{l^2} - N\right)\left(\frac{\pi^2 EI_{\omega\omega}}{l^2} + GI_T - I_p\frac{N}{A}\right)\\
&\quad -(Ne_z)^2\left(\frac{\pi^2 EI_{yy}}{l^2} - N\right) - (Ne_y)^2\left(\frac{\pi^2 EI_{zz}}{l^2} - N\right) = 0.
\end{aligned}
\tag{25.11}
$$

Therein, I_p is the polar moment of inertia. The smallest resulting value for N then constitutes the critical buckling load N_{crit}.

In the special case of a cross-section with $e_y = e_z = 0$, Eq. (25.11) reduces to:

$$
\left(\frac{\pi^2 EI_{yy}}{l^2} - N\right)\left(\frac{\pi^2 EI_{zz}}{l^2} - N\right)\left(\frac{\pi^2 EI_{\omega\omega}}{l^2} + GI_T - I_p\frac{N}{A}\right) = 0.
\tag{25.12}
$$

In this case, an explicit solution for N is possible as follows:

$$N = \begin{cases} \dfrac{\pi^2 E I_{yy}}{l^2} \\ \dfrac{\pi^2 E I_{zz}}{l^2} \\ \dfrac{A}{I_p}\left(\dfrac{\pi^2 E I_{\omega\omega}}{l^2} + G I_T\right) \end{cases} . \tag{25.13}$$

While the first two resulting expressions are the classical Euler column buckling loads, the third expression represents the torsional buckling load. The smallest resulting value in (25.13) is then the critical global buckling load N_{crit} for the structural situation under consideration.

25.2.5 Approximate Methods

Exact closed-form solutions for the considered global stability problems are only possible for a few selected cases. This can be attributed to the fact that even if the presented equations are also valid for laminate structures, exact solutions can only be determined for a few specific cases of boundary and load conditions, and that coupling effects due to the considered laminate structures might make the exact solution of a given global buckling problem difficult or even impossible. As a result, approximation methods have been frequently used by many authors. In this subsection, two approximate analysis approaches, namely the Ritz method and the Finite Element Method, are discussed using the example of the flexural-torsional buckling problem under the assumption that the governing equations (25.6) are applicable. Both methods can then be derived from the energy formulations given by (25.1) and (25.2).

The Ritz method is based on the assumption of a set of shape functions that can be represented in the following form:

$$\begin{aligned} v_M(x) &\simeq \sum_{i=1}^{N_v} V_i v_i(x), \\ w_M(x) &\simeq \sum_{i=1}^{N_w} W_i w_i(x), \\ \vartheta(x) &\simeq \sum_{i=1}^{N_\vartheta} X_i \vartheta_i(x), \end{aligned} \tag{25.14}$$

where V_i, W_i, X_i are a priori unknown coefficients and $v_i(x)$, $w_i(x)$, $\vartheta_i(x)$ are admissible shape functions that must fulfil all underlying geometric constraints of the given global stability problem. The quantities N_v, N_w, N_ϑ are the degrees of the series expansions used for v_M, w_M, ϑ. Inserting the shape functions for v_M, w_M, ϑ into (25.1) and (25.2) and evaluating the Ritz equations

$$\frac{\partial \Pi}{\partial V_i} = 0, \quad \frac{\partial \Pi}{\partial W_i} = 0, \quad \frac{\partial \Pi}{\partial X_i} = 0 \tag{25.15}$$

eventually leads to an eigenvalue problem of the following form:

$$\left[\underline{\underline{K}} - N\underline{\underline{K}}_{\mathrm{G}}\right]\underline{U} = \underline{0}, \tag{25.16}$$

where the stiffness matrix $\underline{\underline{K}}$ and the geometric stiffness matrix $\underline{\underline{K}}_{\mathrm{G}}$ can be represented as follows:

$$\underline{\underline{K}} = \begin{bmatrix} EI_{zz}\underline{\underline{K}}_1 & \underline{\underline{0}} & \underline{\underline{0}} \\ \underline{\underline{0}} & EI_{yy}\underline{\underline{K}}_2 & \underline{\underline{0}} \\ \underline{\underline{0}} & \underline{\underline{0}} & EI_{\omega\omega}\underline{\underline{K}}_3 \end{bmatrix} + \begin{bmatrix} \underline{\underline{0}} & \underline{\underline{0}} & \underline{\underline{0}} \\ \underline{\underline{0}} & \underline{\underline{0}} & \underline{\underline{0}} \\ \underline{\underline{0}} & \underline{\underline{0}} & GI_T\underline{\underline{K}}_4 \end{bmatrix},$$

$$\underline{\underline{K}}_{\mathrm{G}} = \begin{bmatrix} \underline{\underline{K}}_5 & \underline{\underline{0}} & e_z\underline{\underline{K}}_8 \\ \underline{\underline{0}} & \underline{\underline{K}}_6 & -e_y\underline{\underline{K}}_9 \\ e_z\underline{\underline{K}}_8^T & -e_y\underline{\underline{K}}_9^T & \frac{I_p}{A}\underline{\underline{K}}_7 \end{bmatrix}. \tag{25.17}$$

The submatrices $\underline{\underline{K}}_1 - \underline{\underline{K}}_9$ contain the resultants of the shape functions $v_i(x)$, $w_i(x)$, $\vartheta_i(x)$ and their derivatives. For reasons of brevity, these submatrices will not be discussed in more detail here. The resulting eigenvalue problem generally requires a numerical evaluation. The smallest positive real eigenvalue then represents the critical buckling load N_{crit} of the given structural situation.

The Finite Element Method (FEM) is the most commonly used approximate analysis method for the treatment of global buckling problems today. The Finite Element Method divides the beam length l into an arbitrary number n_e of elements with length l_e. In each element, shape functions are used to interpolate between the nodal degrees of freedom of the finite element, and by using the potential formulas (25.1) and (25.2) and evaluating the equilibrium condition $\delta\Pi = 0$, the governing equations for the element e can be derived. By combining the equations of the individual elements into a global set of equations, an eigenvalue problem can be set up, which can be solved numerically to determine the critical global buckling load N_{crit} of such a discretized beam. We will briefly discuss the FEM using the example of a beam with arbitrary and possibly unsymmetric cross-section with $e_y \neq 0$ and $e_z \neq 0$. An exemplary beam is shown in Fig. 25.8, top, and the discretization used is shown in Fig. 25.8, middle.

We consider two-noded straight finite elements (Fig. 25.8, bottom), where the element e has the two nodes K, e and L, e. The element load consists of a normal force N_e, which is assumed to be constant over the element length l_e. A local coordinate system s_e, y_e, z_e is introduced as indicated. At the two element nodes K, e and L, e, the nodal degrees of freedom are introduced in the form of the translations $v_{K,e}$, $w_{K,e}$ and $v_{L,e}$, $w_{L,e}$ as well as in the form of the rotations $\vartheta_{K,e}$, $\vartheta_{L,e}$. In addition, the first derivatives of these quantities with respect to the element axis are also defined as degrees of freedom, i.e. $v'_{K,e}$. i.e. $v'_{K,e}$, $w'_{K,e}$, $\vartheta'_{K,e}$, $v'_{L,e}$, $w'_{L,e}$, $\vartheta'_{L,e}$ are assumed to be unknown degrees of freedom. The element

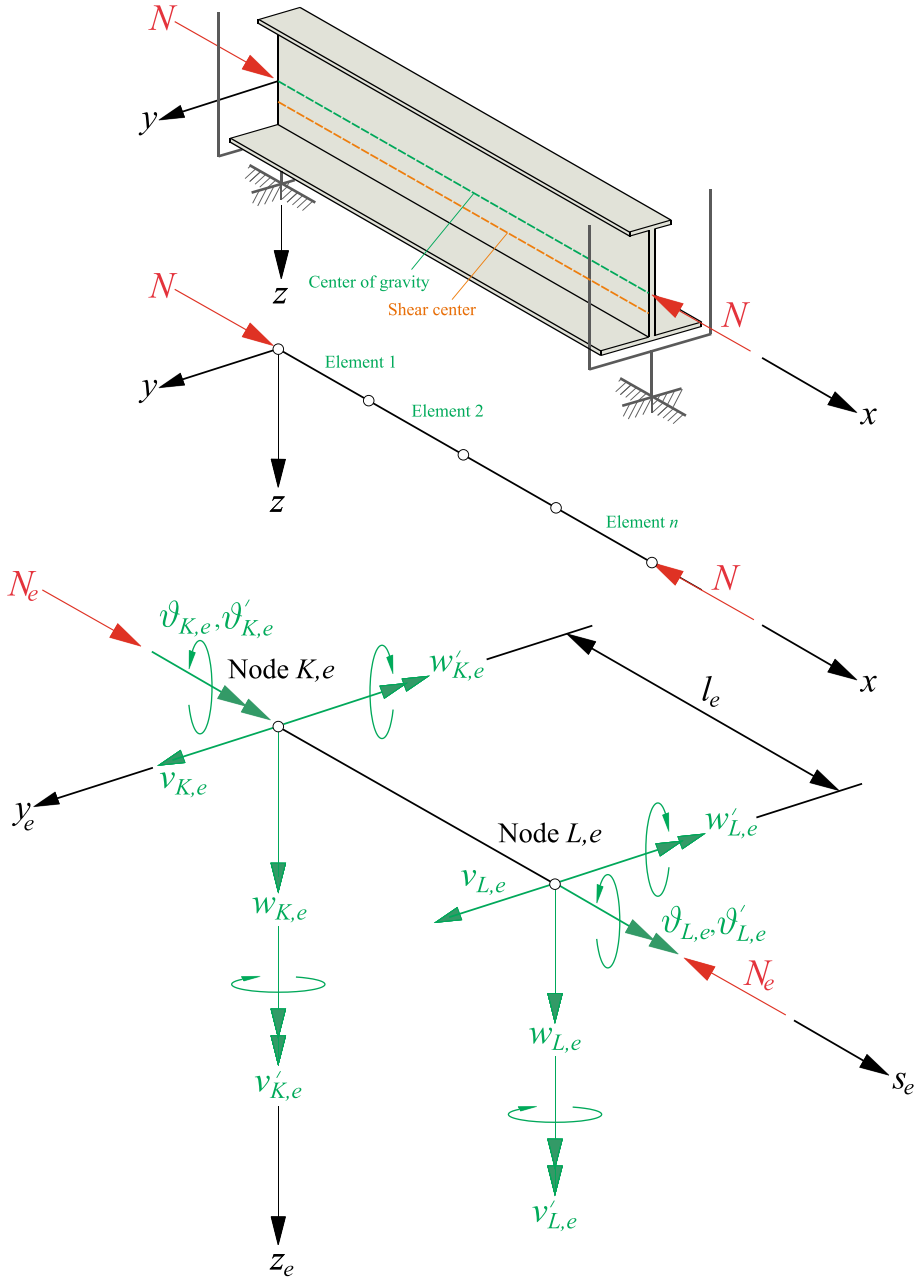


Fig. 25.8 Finite beam element for the flexural-torsional buckling of a straight beam under centric normal force

e has the properties $EI_{yy,e}$, $EI_{zz,e}$, $GI_{T,e}$, $EI_{\omega\omega,e}$, $I_{p,e}$, A_e as well as the eccentricities $e_{y,e}$ and $e_{z,e}$. The total elastic potential of the element e in the buckled state is then

$$\begin{aligned}\Pi_e = &\frac{1}{2}EI_{yy,e}\int_0^{l_e}\left(w_e''\right)^2\,\mathrm{d}s_e + \frac{1}{2}EI_{zz,e}\int_0^{l_e}\left(v_e''\right)^2\,\mathrm{d}s_e\\ &+\frac{1}{2}GI_{T,e}\int_0^{l_e}\left(\vartheta_e'\right)^2\,\mathrm{d}s_e + \frac{1}{2}EI_{\omega\omega,e}\int_0^{l_e}\left(\vartheta_e''\right)^2\,\mathrm{d}s_e\\ &-\frac{F_e}{2}\int_0^{l_e}\left[\left(v_e'\right)^2+\left(w_e'\right)^2+2e_{z,e}v_e'\vartheta_e'-2e_{y,e}w_e'\vartheta_e'+\frac{I_{p,e}}{A_e}\left(\vartheta_e'\right)^2\right]\mathrm{d}s_e. \end{aligned} \tag{25.18}$$

The buckling modes of the element e are approximated as follows:

$$\begin{aligned} v_e(s_e) &= N_{1,e}v_{K,e} + N_{2,e}v_{K,e}' + N_{3,e}v_{L,e} + N_{4,e}v_{L,e}',\\ w_e(s_e) &= N_{1,e}w_{K,e} + N_{2,e}w_{K,e}' + N_{3,e}w_{L,e} + N_{4,e}w_{L,e}',\\ \vartheta_e(s_e) &= N_{1,e}\vartheta_{K,e} + N_{2,e}\vartheta_{K,e}' + N_{3,e}\vartheta_{L,e} + N_{4,e}\vartheta_{L,e}'. \end{aligned} \tag{25.19}$$

Therein, the shape functions $N_{1,e}$, $N_{2,e}$, $N_{3,e}$ and $N_{4,e}$ are third-order Hermitian polynomials. If (25.19) is inserted into (25.18) and the condition $\delta\Pi_e = 0$ is imposed, an eigenvalue problem of the following form is obtained:

$$\left[\underline{\underline{K}}_e - N_e\underline{\underline{K}}_{\mathrm{G,e}}\right]\begin{pmatrix}\underline{v_e}\\ \underline{w_e}\\ \underline{\vartheta_e}\end{pmatrix} = \underline{0}, \tag{25.20}$$

where $\underline{\underline{K}}_e$ and $\underline{\underline{K}}_{\mathrm{G,e}}$ are the stiffness matrix and the geometric stiffness matrix of the finite element e. The vectors $\underline{v_e}$, $\underline{w_e}$ and $\underline{\vartheta_e}$ contain the nodal degrees of freedom. The matrices $\underline{\underline{K}}_e$ and $\underline{\underline{K}}_{\mathrm{G,e}}$ can be specified as follows:

$$\begin{aligned}\underline{\underline{K}}_e = &\begin{bmatrix}\frac{2EI_{zz,e}}{l_e^3}\underline{\underline{K}}_{1,e} & \underline{\underline{0}} & \underline{\underline{0}}\\ \underline{\underline{0}} & \frac{2EI_{yy,e}}{l_e^3}\underline{\underline{K}}_{1,e} & \underline{\underline{0}}\\ \underline{\underline{0}} & \underline{\underline{0}} & \frac{2EI_{\omega\omega,e}}{l_e^3}\underline{\underline{K}}_{1,e}\end{bmatrix}\\ &+\begin{bmatrix}\underline{\underline{0}} & \underline{\underline{0}} & \underline{\underline{0}}\\ \underline{\underline{0}} & \underline{\underline{0}} & \underline{\underline{0}}\\ \underline{\underline{0}} & \underline{\underline{0}} & GI_{T,e}\underline{\underline{K}}_{2,e}\end{bmatrix},\\ \underline{\underline{K}}_{\mathrm{G,e}} = &\begin{bmatrix}\underline{\underline{K}}_{2,e} & \underline{\underline{0}} & e_{z,e}\underline{\underline{K}}_{2,e}\\ \underline{\underline{0}} & \underline{\underline{K}}_{2,e} & -e_{y,e}\underline{\underline{K}}_{2,e}\\ e_{z,e}\underline{\underline{K}}_{2,e} & -e_{y,e}\underline{\underline{K}}_{2,e} & \frac{I_{p,e}}{A_e}\underline{\underline{K}}_{2,e}\end{bmatrix}, \end{aligned} \tag{25.21}$$

with the submatrices $\underline{\underline{K}}_{1,e}$ und $\underline{\underline{K}}_{2,e}$ as:

$$\underline{\underline{K}}_{1,e} = \begin{bmatrix} 6 & 3l_e & -6 & 3l_e \\ 3l_e & 2l_e^2 & -3l_e & l_e^2 \\ -6 & -3l_e & 6 & -3l_e \\ 3l_e & l_e^2 & -3l_e & 2l_e^2 \end{bmatrix},$$

$$\underline{\underline{K}}_{2,e} = \begin{bmatrix} \frac{6}{5l_e} & \frac{1}{10} & -\frac{6}{5l_e} & \frac{1}{10} \\ \frac{1}{10} & \frac{2l_e}{15} & -\frac{1}{10} & -\frac{l_e}{30} \\ -\frac{6}{5l_e} & -\frac{1}{10} & \frac{6}{5l_e} & -\frac{1}{10} \\ \frac{1}{10} & -\frac{l_e}{30} & -\frac{1}{10} & \frac{2l_e}{15} \end{bmatrix}. \tag{25.22}$$

The combination of all element matrices that form the beam structure under consideration leads to a global system of equations of the form $\left[\underline{\underline{K}} - N\underline{\underline{K}}_{\mathrm{G}}\right]\underline{u} = \underline{0}$, from which the buckling load N_{crit} can be determined.

25.3 Local Buckling of Thin-Walled Beam Structures

The approximate solutions for laminate buckling problems derived in Chap. 14 can be used for many technical applications. In this section, the local buckling behaviour of thin-walled beam structures, for example with I, Z, C cross-sections or with box cross-sections, will be considered under uniaxial longitudinal compressive load (Fig. 25.9). For the sake of simplicity, the beams are assumed to have non-varying properties and cross-sectional shapes along the longitudinal axis.

In addition to the verification of safety against typical global stability cases such as column buckling and flexural-torsional buckling, it must be ensured in the design of such components that no local buckling modes in the form of web and flange buckling occur. For this purpose, the structural element to be considered—i.e. either the web or the flange—is

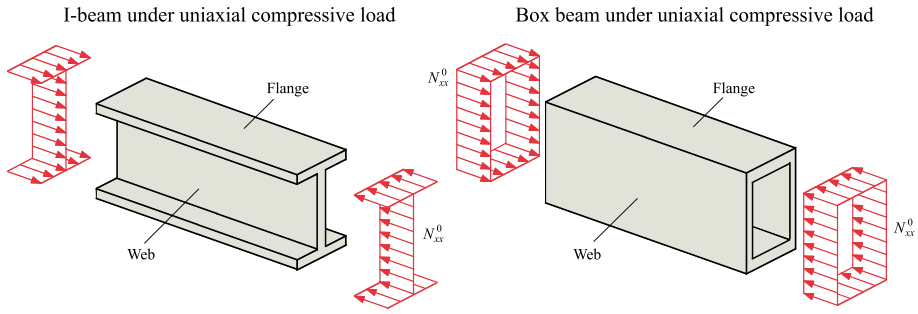


Fig. 25.9 Thin-walled beams under uniaxial compressive load: I-beam (left), box beam (right)

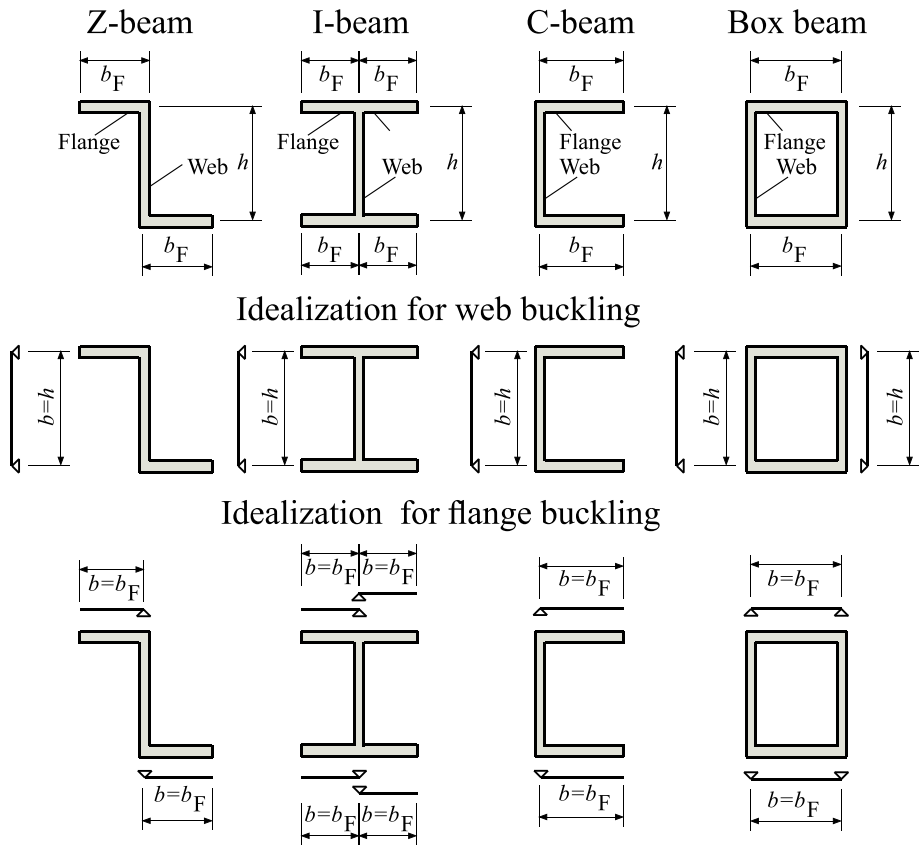


Fig. 25.10 Idealization for local buckling analyses of thin-walled beam structures

cut out of the beam and simply supported boundary conditions are assumed at the cutting edges. In the case of the web of an I-beam, this then leads to a replacement model in the form of a Navier plate, i.e. a plate with simple supports at all edges. In the case of the flange, the buckling behaviour of a plate simply supported at three edges with a free edge is then investigated (Fig. 25.10). In the case of web buckling, the width of the plate is then set to $b = h$ if h is the height of the web under consideration. If flange buckling is to be analysed, $b = b_{\mathrm{F}}$ should be used if the flange width is denoted by b_{F}. In both cases, the plate length a is then identical to the beam length.

However, it is important to note that the separately considered structural elements are always stiffened to a certain extent by the adjacent beam segments, which can be taken into account quite easily, for example, by arranging elastic restraints at the cutting edges (Fig. 25.11). The elastic restraint stiffnesses can then be calculated from the properties of the neighbouring structural elements, which will be discussed in more detail below. The

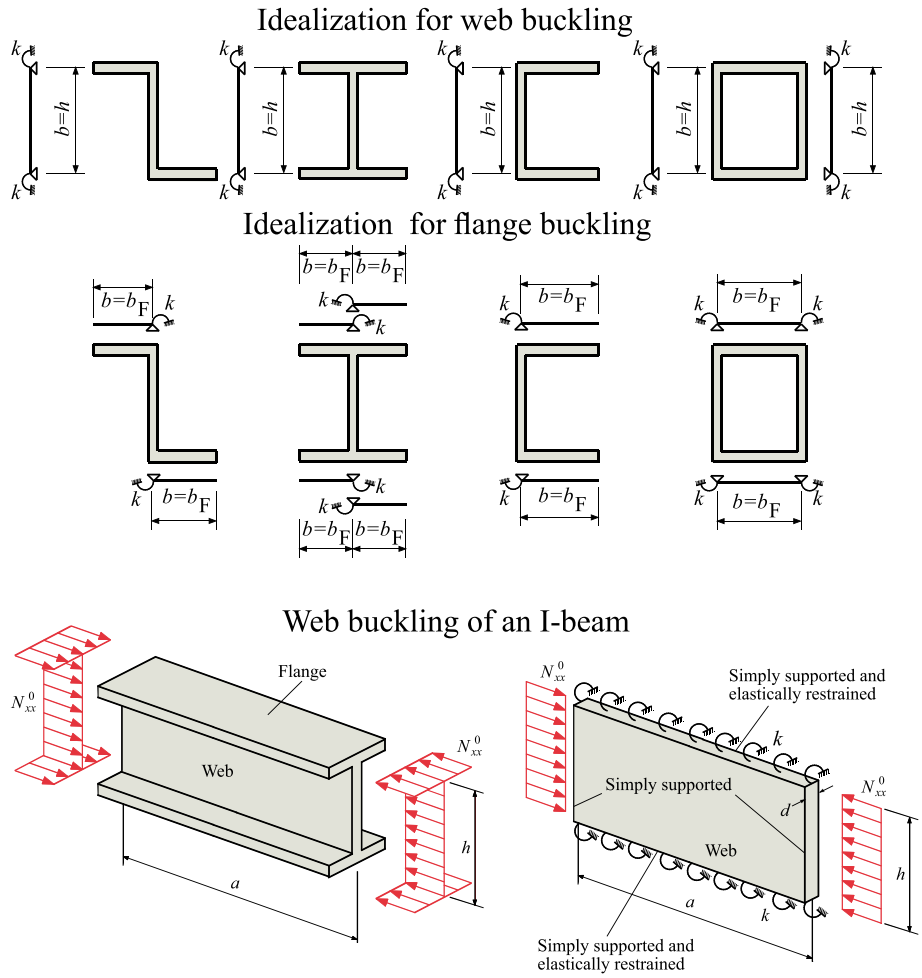


Fig. 25.11 Improved idealization for local buckling analyses of thin-walled beam structures

corresponding buckling loads can then be calculated, for example, using the simple closed-form analytical solutions already derived e.g. in Chap. 14. More recent investigations (see e.g. Mittelstedt (2007a), Qiao and Shan (2005)) also show that taking this stiffening effect into account can lead to sometimes considerable increases in the calculated load-bearing capacity compared to idealizations with simply supported cutting edges and should not be neglected, especially in applications where the structural weight plays a significant role.

In the following, the procedure for the local buckling analysis of thin-walled beam structures is treated at the examples of the cross-sectional shapes shown in Fig. 25.11. Here, we essentially follow the approach of Qiao and co-workers. Related work on this topic can be

found, for example, in Qiao et al. (2003), Kollár (2002a, b), Bank and Yin (1996), Barbero and Raftoyiannis (1993), Webber et al. (1985) or Zureick and Shih (1998).

If local buckling occurs in a web or flange of a box beam, then the flanges or webs of the beam act as stiffeners. It then becomes apparent that the stiffening elements exhibit deformations that are affine to the buckling shapes of the buckled beam segments. If, for example, the web of a box beam of length a buckles in m half-waves in the longitudinal direction x, then the flanges will exhibit bending deformations with m half-waves in the longitudinal direction x. In this case, the bending deformations of the flanges will alternately form upwards or downwards, analogous to the buckling mode of the web, so that nodal lines of the bending deformations form at intervals of $\lambda = \frac{a}{m}$. Here, $\lambda = \frac{a}{m}$ is the length of a buckling half-wave. The stiffening flanges can then be idealised by considering the flanges as Navier plates that are loaded by a bending moment M_{yy}^0 at the edges adjacent to the webs. This bending moment is proportional to $\sin\left(\frac{m\pi x}{a}\right)$ according to the functional structure of the buckling mode of the web in the longitudinal direction and, like the bending surfaces of the flange, has nodal lines at distances of $\lambda = \frac{a}{m}$. The bending surface w_0 of such a hinged Navier plate under edge bending moments M_{yy}^0 is given by Qiao and Shan (2005) as follows:

$$w_0 = \frac{b\lambda}{2\pi D_{22} \sinh\left(\frac{\pi y}{\lambda}\right)} \left[\frac{y}{b} \cosh\left(\frac{\pi\,(y-b)}{\lambda}\right) + \left(1 - \frac{y}{b}\right) \cosh\left(\frac{\pi y}{\lambda}\right) - \frac{\sinh\left(\frac{\pi y}{\lambda}\right) + \sinh\left(\frac{\pi\,(y-b)}{\lambda}\right)}{\sinh\left(\frac{\pi y}{\lambda}\right)} \right] M_{yy}^0. \tag{25.23}$$

The transverse bending stiffness D_{22} of the stiffening segment that braces the buckling segment must be applied here. The width b must then be assigned either $b = b_F$ (web buckling) or $b = h$ (flange buckling). The rotation angle can be calculated as a function of the bending moment using (25.23):

$$\varphi = -\frac{\lambda}{2\pi D_{22}} \left(1 + \frac{\frac{\pi b}{\lambda}}{\sinh\left(\frac{\pi b}{\lambda}\right)}\right) \tanh\left(\frac{\pi b}{2\lambda}\right) M_{yy}^0 = -\frac{\lambda}{D_{22}} \rho\left(\frac{b}{\lambda}\right) M_{yy}^0. \tag{25.24}$$

The half-wave length λ is still unknown in this case. For the sake of simplicity, it can be determined that the half-wave length λ corresponds exactly to the width $b = b_R$ of the stiffened buckled beam segment. The error thus made is relatively small and is always 'on the safe side'. The auxiliary function $\rho\left(\frac{b}{\lambda}\right)$ can then be approximated by $\rho\left(\frac{b}{b_R}\right)$ and one obtains:

$$\varphi = -\frac{b_R}{D_{22}} \rho\left(\frac{b}{b_R}\right) M_{yy}^0. \tag{25.25}$$

If we consider local buckling of the web of a box beam, the flange will stiffen the web. The edge rotation of the flange then amounts to with the assumptions made above:

$$\varphi = -\frac{h}{D_{22}^{\mathrm{F}}} \rho \left(\frac{b_{\mathrm{F}}}{h} \right) M_{yy}^{0}. \tag{25.26}$$

Here, D_{22}^{F} is the transverse bending stiffness of the flange. The moment boundary condition $M_{yy}^{0} = -k\varphi$ is then used to obtain the following expression for the stiffness k of the edge restraint in the case of local web buckling:

$$k = \frac{D_{22}^{\mathrm{F}}}{h\rho \left(\frac{b_{\mathrm{F}}}{h} \right)}. \tag{25.27}$$

In order to take into account the influence of the longitudinal compressive forces acting on the individual beam segments, Qiao and Shan (2005) introduced a reduction factor of the form

$$r = 1 - \frac{N_{xx,\mathrm{buckling}}^{0}}{N_{xx,\mathrm{stiffening}}^{0}}, \tag{25.28}$$

with which the restraint stiffness k of the edge restraint is to be multiplied. The buckling loads $N_{xx,\mathrm{buckling}}^{0}$ and $N_{xx,\mathrm{stiffening}}^{0}$ are the local buckling loads of the web or the flange of the box beam, which can be determined in a simplified manner assuming Navier-type boundary conditions. If the beam length a is sufficiently large, we can then write

$$r = 1 - \frac{b_{\mathrm{F}}^{2}}{h^{2}} \frac{\sqrt{D_{11}^{\mathrm{W}} D_{22}^{\mathrm{W}}} + D_{12}^{\mathrm{W}} + 2D_{66}^{\mathrm{W}}}{\sqrt{D_{11}^{\mathrm{F}} D_{22}^{\mathrm{F}}} + D_{12}^{\mathrm{F}} + 2D_{66}^{\mathrm{F}}}, \tag{25.29}$$

where the variables $D_{\mathrm{op}}^{\mathrm{W}}$ are the plate stiffnesses of the web and $D_{\mathrm{op}}^{\mathrm{F}}$ are the plate stiffnesses of the flange. The stiffness k of the edge restraint in the case of local web buckling then finally follows as:

$$k = \frac{D_{22}^{\mathrm{F}}}{h\rho \left(\frac{b_{\mathrm{F}}}{h} \right)} \left(1 - \frac{b_{\mathrm{F}}^{2}}{h^{2}} \frac{\sqrt{D_{11}^{\mathrm{W}} D_{22}^{\mathrm{W}}} + D_{12}^{\mathrm{W}} + 2D_{66}^{\mathrm{W}}}{\sqrt{D_{11}^{\mathrm{F}} D_{22}^{\mathrm{F}}} + D_{12}^{\mathrm{F}} + 2D_{66}^{\mathrm{F}}} \right). \tag{25.30}$$

In connection with Eq. (14.77) or (14.84), the local buckling load N_{xx}^{0} of the web of a box beam under longitudinal compressive load can then be determined analytically.

It should also be noted here that Eq. (25.30) is only applicable if $N_{xx,\mathrm{buckling}}^{0} < N_{xx,\mathrm{stiffening}}^{0}$ applies, which explicitly assumes that the buckling load of the stiffening support element is not decisive for the local buckling. Otherwise, the factor r would not result in a reduction but, on the contrary, an increase in restraint stiffness. A factor $r < 0$ is therefore an indicator that the segment under consideration is not at risk of buckling, but rather that the neighbouring segment must be considered.

If local buckling of the flange of the box beam is to be considered, the following expression for the restraint stiffness k is obtained:

$$k = \frac{D_{22}^{\mathrm{W}}}{b_{\mathrm{F}}\rho\left(\frac{h}{b_{\mathrm{F}}}\right)}\left(1 - \frac{h^2}{b_{\mathrm{F}}^2}\frac{\sqrt{D_{11}^{\mathrm{F}}D_{22}^{\mathrm{F}}} + D_{12}^{\mathrm{F}} + 2D_{66}^{\mathrm{F}}}{\sqrt{D_{11}^{\mathrm{W}}D_{22}^{\mathrm{W}}} + D_{12}^{\mathrm{W}} + 2D_{66}^{\mathrm{W}}}\right). \tag{25.31}$$

Qiao and Shan (2005) also presented the restraint stiffness k for I-beams, the derivation of which is based on very similar considerations as shown above. Detailed documentation of the derivation is omitted at this point, only the restraint stiffnesses are given here. In the case of local flange buckling of an I-beam, the restraint stiffness k is calculated as follows:

$$k = \frac{D_{22}^{\mathrm{W}}}{h}\left(1 - \frac{6h^2}{\pi^2 b_{\mathrm{F}}^2}\frac{D_{66}^{\mathrm{F}}}{\sqrt{D_{11}^{\mathrm{W}}D_{22}^{\mathrm{W}}} + D_{12}^{\mathrm{W}} + 2D_{66}^{\mathrm{W}}}\right). \tag{25.32}$$

If, on the other hand, local buckling of the web is relevant, then k can be determined as:

$$k = \frac{D_{22}^{\mathrm{F}}}{h\rho\left(\frac{b_{\mathrm{F}}}{h}\right)}\left(1 - \frac{\pi^2 b_{\mathrm{F}}^2}{6h^2}\frac{\sqrt{D_{11}^{\mathrm{W}}D_{22}^{\mathrm{W}}} + D_{12}^{\mathrm{W}} + 2D_{66}^{\mathrm{W}}}{D_{66}^{\mathrm{F}}}\right). \tag{25.33}$$

Here the auxiliary function $\rho\left(\frac{b_{\mathrm{F}}}{h}\right)$ is:

$$\rho\left(\frac{b_{\mathrm{F}}}{h}\right) = \frac{1}{4\pi}\frac{3\cosh^2\left(\frac{\pi b_{\mathrm{F}}}{h}\right) + \left(\frac{\pi b_{\mathrm{F}}}{h}\right)^2 + 1}{\frac{\pi b_{\mathrm{F}}}{h} + 3\sinh\left(\frac{\pi b_{\mathrm{F}}}{h}\right)\cosh\left(\frac{\pi b_{\mathrm{F}}}{h}\right)}. \tag{25.34}$$

The corresponding local buckling loads can then be determined with the solutions (14.118) for local flange buckling or (14.77) for local web buckling or their dimensionless counterparts.

Furthermore, analysis rules are also available for the restraint stiffness of beams with C- or Z-profiles. If local flange buckling in a C- or Z-beam is considered, then the restraint stiffness k is calculated as:

$$k = \frac{2D_{22}^{\mathrm{W}}}{h}\left(1 - \frac{6h^2}{\pi^2 b_{\mathrm{F}}^2}\frac{D_{66}^{\mathrm{F}}}{\sqrt{D_{11}^{\mathrm{W}}D_{22}^{\mathrm{W}}} + D_{12}^{\mathrm{W}} + 2D_{66}^{\mathrm{W}}}\right). \tag{25.35}$$

If, on the other hand, the web buckles, then Eq. (25.33) is applicable.

References

Alfutov NA (1999): *Stability of elastic structures*, Springer, Berlin et al., Germany.

Almroth BO (1981): *Design of composite material structures for buckling - an evaluation of the state-of-the-art*, Forschungsbericht, Lockheed Space and Missiles Company, Palo Alto, CA, USA.

Bank LC, Yin J (1996): *Buckling of orthotropic plates with free and rotationally restrained edges*, Thin-Walled Structures 24:83–96.

Barbero EJ (1992): *Buckling of FRP columns*, Forschungsbericht, West Virginia University, Morgantown, WV, USA.

Barbero EJ, Raftoyiannis IG (1993): *Local buckling of FRP beams and columns*, Journal of Materials in Civil Engineering 5:339–355.

Becker H (1957): *Handbook of structural stability part II - buckling of composite elements*, NACA - National Advisory Committee for Aeronautics, Technical Note 3782, Washington DC, USA.

Beerhorst M (2013): *Entwicklung von hocheffizienten Berechnungsmethoden zur Beschreibung des Beul- und Nachbeulverhaltens von versteiften und unversteiften Flächentragwerken aus Faserverbundwerkstoffen*, Dissertation, Technische Universität Berlin, Fakultät V - Verkehrs- und Maschinensysteme, Berlin, Germany.

Bleich F (1952): *Buckling Strength of metal structures*, McGraw-Hill Inc., USA.

Bonnani DL, Johnson ER, Starnes JH (1988): *Local buckling and crippling of composite stiffener sections*, Research report, Virginia Polytechnic Institute and State University, College of Engineering, Department of Aerospace and Ocean Engineering, Blacksburg, VA, USA.

Bonnani DL, Johnson ER, Starnes JH (1991): *Local Crippling of Thin-Walled Graphite-Epoxy Stiffeners*, AIAA Journal 29:1951–1959.

Chen WF, Lui EM (1987): *Structural stability*, Elsevier, New York et al., USA.

Gerard G, Becker H (1957): *Handbook of structural stability, part I - Buckling of flat plates*, NACA - National Advisory Committee for Aeronautics - Technical Note No. 3781, Washington, USA.

Jones RM (2006): *Buckling of bars, plates and shells*, Bull Ridge Publishing, Blacksburg, VA, USA.

Kolakowski Z, Teter A (2016): *Coupled static and dynamic buckling modelling of thin-walled structures in elastic range, review of selected problems*, Acta Mechanica et Automatica 10:141–149.

Kollár LP (2002a): *Buckling of unidirectionally loaded composite plates with one free and one rotationally restrained unloaded edge*, Journal of Structural Engineering 128:1202–1211.

Kollár LP (2002b): *Local buckling of fiber reinforced plastic composite structural members with open and closed cross sections*, Journal of Structural Engineering 129:1503–1513.

Mittelstedt C (2007a): *Stability behaviour of arbitrarily laminated composite plates with free and elastically restrained unloaded edges*, International Journal of Mechanical Sciences 49:819–833.

Mittelstedt C (2011): *Local Buckling and postbuckling of thin-walled stiffened composite panels - Efficient analysis methods for lightweight engineering*, Habilitation thesis, Technische Universität Darmstadt, Darmstadt, Germany.

Mittelstedt C (2019): *Buckling and post-buckling of thin-walled composite laminated beams - A review of engineering analysis methods*, Applied Mechanics Reviews 72:020802-1.

Mittelstedt C (2021): *Structural mechanics in lightweight engineering*, Springer Vieweg, Berlin, Germany.

Mittelstedt C (2024): *Buckling of beams, plates and shells*, Springer, Berlin, Germany.

Pflüger A (1975): *Stabilitätsprobleme der Elastostatik*, Springer, Berlin et al., Germany.

Qiao P, Shan L (2005): *Explicit local buckling analysis and design of fiber-reinforced plastic composite structural shapes*, Composite Structures 70:468–483.

Qiao P, Davalos JF, Wang J (2003): *Local buckling of composite FRP shapes by discrete plate analysis*, Journal of Structural Engineering 127:245–255.

Reddy JN (2004): *Mechanics of laminated composite plates and shells*, 2nd edition, CRC Press, Boca Raton et al., USA.

Roik KH, Carl J, Lindner J (1972): *Biegetorsionsprobleme gerader dünnwandiger Stäbe*, Wilhelm Ernst und Sohn, Berlin et al., Germany.

Roik KH (1978): *Vorlesungen über Stahlbau*, Wilhelm Ernst und Sohn, Berlin et al., Germany.

Russo S (2017): *A review on buckling collapses of simple and complex columns made from pultruded frp material*, Composites: Mechanics 8:1–34.

Shan L (2007): *Explicit buckling analysis of fiber-reinforced plactic (FRP) composite structures*, Dissertation, Washington State University, Department of Civil and Environmental Engineering, WA, USA.

Simoes Da Silva Dias Simao FP (2007): *Post-buckling bifurcational analysis of thin-walled prismatic members in the context of the Generalized Beam Theory*, Dissertation, University of Coimbra, Department of Civil Engineering, Coimbra, Portugal.

Singer J, Arbocz J, Weller T (1998): *Buckling experiments: experimental methods in buckling of thin-walled structures, volume 1: basic concepts, columns, beams and plates*, John Wiley and sons, New York, USA.

Singer J, Arbocz J, Weller T (2002): *Buckling experiments: experimental methods in buckling of thin-walled structures, volume 2: shells, built-up structures, composites and additional topics*, John Wiley and sons, New York, USA.

Timoshenko SP, Gere JM (1961): *Theory of elastic stability*, McGraw-Hill, New York, NY, USA.

Trahair NS (1993): *Flexural-torsional buckling of structures*, CRC Press, Boca Raton et al., USA.

Turvey GJ, Marshall I (1995): *Buckling and postbuckling of composite plates*, Chapman and Hall, London, UK.

Vlasov VZ (1961): *Thin-walled elastic beams*, Office of Technical Services, US Department of Commerce, Washington DC, USA.

Webber JPH, Holt PJ, Lee DA (1985): *Instability of carbon fibre reinforced flanges of I section beams and columns*, Composite Structures 4:245–265.

Xu J, Zhao Q, Qiao P (2013): *A critical review on buckling and post-buckling analysis of composite structures*, Frontiers in Aerospace Engineering 2:157–168.

Zureick A, Shih B (1998): *Local buckling of fiber-reinforced polymeric structural members under linearly-varying edge loading-part 1. Theoretical formulation*, Composite Structures 41:79–86.



Generalized Beam Theory

26

This chapter presents the basic features of the so-called Generalized Beam Theory (GBT), introduced and formalized by R. Schardt at the Technische Universität Darmstadt, Germany. The governing equations within the framework of conventional GBT are derived and the prerequisites for basic static and dynamic problems as well as for problems within the framework of second-order theory are created. The chapter concludes with an outlook on the treatment of anisotropic layered beam structures.

26.1 Introduction

Thin-walled structures, as they are common in many engineering applications such as civil engineering or aerospace engineering, require analysis methods that are able to take into account all specific aspects of their load-bearing behaviour. For thin-walled structures such as composite laminated beams, e.g. in modern aircraft construction, the behaviour within the framework of the first-order theory as well as the buckling resistance must be taken into account. The trend towards optimized material usage and lighter and thinner structures reveals effects in the structural response, such as cross-sectional distortions, which complicate the analysis and must be adequately taken into account. This requires the development of advanced analysis approaches that can be reliably used by engineers in practice. The most well-known analysis method is certainly the Finite Element Method (FEM) due to its versatility, and FEM is part of every engineering industry where structural elements and load-bearing parts are designed, analyzed and optimized. Nevertheless, even with the computer resources available today, analysis methods that work efficiently are still very much in demand, and this is where the so-called Generalized Beam Theory (GBT), which

© The Author(s), under exclusive license to Springer-Verlag GmbH, DE, part of Springer Nature 2025

C. Mittelstedt, *Mechanics of Composite Structures*,
https://doi.org/10.1007/978-3-662-70788-3_26

is the topic of this chapter, comes into play for those structural elements where one dimension is significantly larger than the other two dimensions, i.e. beam-like structures, and where the thickness of the cross-sectional segments is significantly smaller than all other dimensions. In such thin-walled structures, strong cross-sectional distortions often occur and the assumptions of classical beam theory become invalid. Deformations of the cross-section can strongly influence the mechanical behaviour of thin-walled structures, so that this aspect must be adequately taken into account in the analysis and design of such parts. GBT is a method of analysis that is capable of capturing such effects. The importance of considering cross-sectional distortions was already recognised in the seminal work of Vlasov (1961).

The Generalized Beam Theory has been developed since 1966 (Schardt 1966) and was introduced and formalized by Prof. Richard Schardt from the Technical University of Darmstadt, Germany, and summarized in a groundbreaking book publication (Schardt 1989) (hereinafter referred to as conventional GBT). The conventional GBT decomposes the deformation behaviour of the thin-walled component under consideration into a linear combination of cross-sectional deformation modes, which can be subdivided into local, global and distortion modes and which are directly related to the deformation behaviour of the component under consideration. These modes are determined in a so-called cross-sectional analysis. In order to achieve a complete representation of the displacements, the displacement modes are multiplied by axial shape functions as part of the so-called beam analysis and these axial functions are determined from the resulting differential equations of the GBT either analytically in closed form or by any numerical means suitable for the application under consideration. The GBT thus reduces the order of the given problem to one and is therefore a suitable alternative to the FEM in cases where prismatic thin-walled structures are to be considered, especially when cross-sectional distortions are important. Literature reviews on the GBT can be found, for example, in Carrera et al. (2015), Andreassen (2012), Ferrarotti (2018), Camotim et al. (2006), Gonçalves et al. (2023), or Mittelstedt (2024). The latter reference summarizes the state of research in the field of GBT and cites over 400 references.

26.2 Conventional GBT According to Schardt

26.2.1 The Elementary Cases for the Straight Prismatic Beam

Schardt defines the elementary static behaviour of linear elastic straight prismatic beams by four elementary states, namely rod behaviour (state 1), bending about the two principal axes (states 2 and 3) and torsion (state 4), see Fig. 26.1. These four elementary states are determined by the following differential equations in Cartesian coordinates x, y, z, assuming a principal axis system (Mittelstedt 2021):

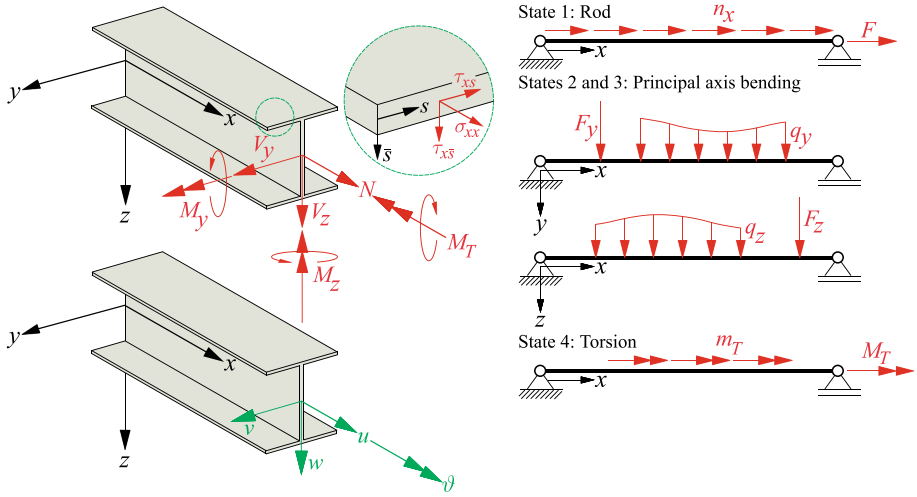


Fig. 26.1 The four elementary states of a beam: rod (state 1), principal axis bending (states 2 and 3) and torsion (state 4)

$$\begin{aligned} EAu'' &= -n_x, \\ EI_{zz}v'''' &= q_y, \\ EI_{yy}w'''' &= q_z, \\ EC_M\vartheta'''' - GI_T\vartheta'' &= m_T, \end{aligned} \tag{26.1}$$

where EA is the extensional stiffness of the beam, EI_{yy} and EI_{zz} are the principal bending stiffnesses, $EC_M = EI_{\omega\omega}$ is the warping stiffness and GI_T is the torsional stiffness. The notation $(\ldots)'$ denotes a derivative with respect to x. The constitutive relationships for states 1–4 can be written as follows:

$$\begin{aligned} N = EAu', \quad M_z = -EI_{zz}v'', \\ M_y = -EI_{yy}w'', \quad W = -EC_M\vartheta'', \end{aligned} \tag{26.2}$$

where N is the normal force, M_z and M_y are the bending moments about the principal cross-sectional axes and W is the warping moment. The degrees of freedom of these four elementary states are the three displacements u, v, w in the x-, y- and z-directions as well as the rotation ϑ of the cross-section about the x-axis. At this point, the state variables of the thin-walled beam under consideration are decomposed in relation to the x-axis on the one hand and the yz-plane on the other, whereby the function describing the yz-plane depends on the cross-section of the beam. The longitudinal displacement u of the beam is for the four elementary cases:

$$
\begin{aligned}
u(x, y, z) &= u, \\
u(x, y, z) &= -yv'(x), \\
u(x, y, z) &= -zw'(x), \\
u(x, y, z) &= \omega(y, z)\vartheta'(x),
\end{aligned} \tag{26.3}
$$

where $\omega(y, z)$ is the unit warping of the cross-section. Schardt treats all these displacements as warping of the cross-section associated with the four elementary states, regardless of whether the cross-section remains plane or not, and introduces the following so-called unit warpings ${}^k\tilde{u}(y, z)$ $(k = 1, 2, 3, 4)$

$$
\begin{aligned}
{}^1\tilde{u}(y, z) &= -1, \quad {}^2\tilde{u}(y, z) = -y, \\
{}^3\tilde{u}(y, z) &= -z, \quad {}^4\tilde{u}(y, z) = \omega,
\end{aligned} \tag{26.4}
$$

where the superscript numbers denote states 1–4 and the tilde means that they are unit functions. The displacements v and w can also be interpreted as multiples of a unit function at any position x on the bar axis. For state 2, this leads to

$$
\begin{aligned}
v(x, y, z) &= {}^2\tilde{v}(y, z)v(x), \\
w(x, y, z) &= {}^2\tilde{w}(y, z)v(x),
\end{aligned} \tag{26.5}
$$

with ${}^2\tilde{v}(y, z) = 1$ and ${}^2\tilde{w}(y, z) = 0$. For state 3 follows:

$$
\begin{aligned}
v(x, y, z) &= {}^3\tilde{v}(y, z)w(x) = 0, \\
w(x, y, z) &= {}^3\tilde{w}(y, z)w(x) = w(x).
\end{aligned} \tag{26.6}
$$

For state 4, the following is obtained:

$$
\begin{aligned}
v(x, y, z) &= {}^4\tilde{v}(y, z)\vartheta(x) = (z_M - z)\vartheta(x), \\
w(x, y, z) &= {}^4\tilde{w}(y, z)\vartheta(x) = (y - y_M)\vartheta(x).
\end{aligned} \tag{26.7}
$$

In the case of state 1, ${}^1\tilde{v} = {}^1\tilde{w} = 0$, i.e. no transverse displacements occur. The unit warping functions and unit displacements are shown for three elementary cross-sections in Fig. 26.2.

For the normal stress σ_{xx}, the one-dimensional relationship $\sigma_{xx} = Eu'$ applies, which leads to the following stress formulations for the four elementary states in separation form:

$$
\begin{aligned}
\sigma_{xx}(x, y, z) &= E\,{}^1\tilde{u}(y, z)u'(x), \\
\sigma_{xx}(x, y, z) &= E\,{}^2\tilde{u}(y, z)v''(x), \\
\sigma_{xx}(x, y, z) &= E\,{}^3\tilde{u}(y, z)w''(x), \\
\sigma_{xx}(x, y, z) &= E\,{}^4\tilde{u}(y, z)\vartheta''(x).
\end{aligned} \tag{26.8}
$$

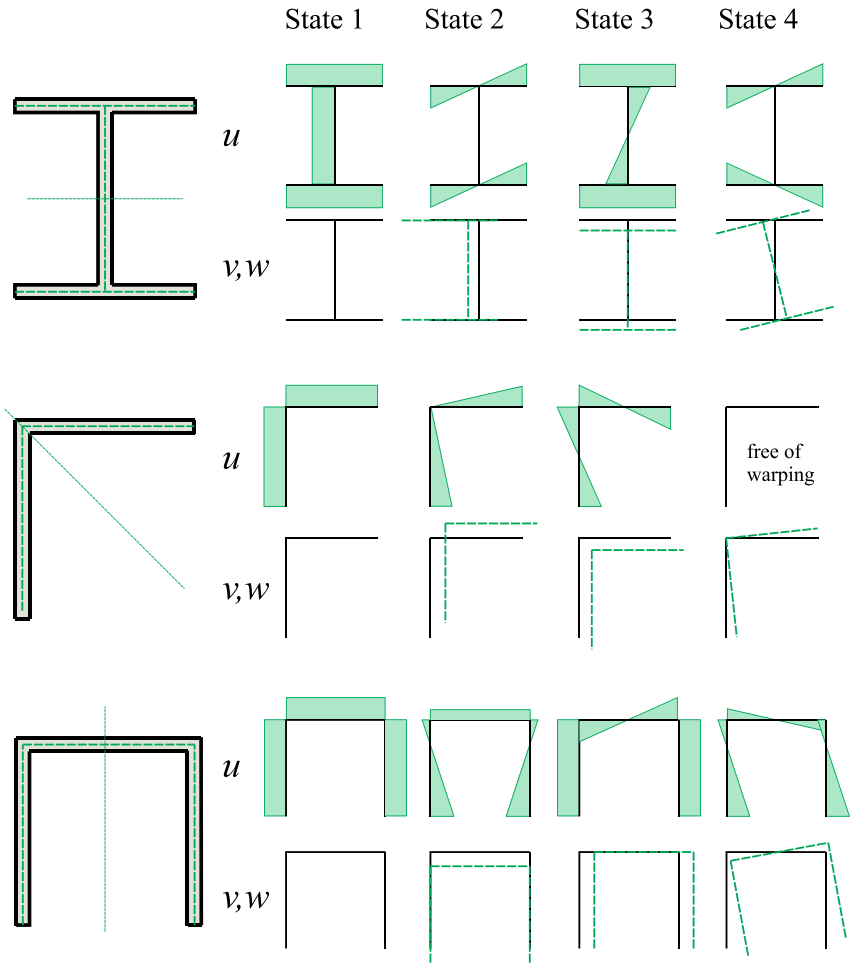


Fig. 26.2 Unit warping functions and unit displacements for three elementary cross-sections

This means that the distribution of σ_{xx} over the cross-section is described by the unit warpings ${}^{k}\tilde{u}(y, z)$. The shear force flow $T = \tau_{xs} h$ (where τ_{xs} is the shear stress acting parallel to the skeleton line of the cross-section and h is the wall thickness, Fig. 26.1) of the thin-walled cross-section can be expressed on the basis of elementary equilibrium considerations as

$$T = -\int_0^s h\sigma'_{xx}\mathrm{d}s, \tag{26.9}$$

where s is a local circumferential coordinate that encompasses the entire cross-section. With (26.8) we obtain e.g. for state 2:

$$T = -\int_s h\left(E^2\tilde{u}v''\right)' \mathrm{d}s = -E\int_s {}^2\tilde{u}h\mathrm{d}sv'''. \tag{26.10}$$

The functions $v(x)$, $w(x)$ and $\vartheta(x)$ are the shape functions of the state variables v, w and ϑ in relation to the beam longitudinal axis x. The introduction of the designations

$$\begin{aligned} u(x) &= {}^1V(x), \quad v(x) = {}^2V(x), \\ w(x) &= {}^3V(x), \quad \vartheta(x) = {}^4V(x) \end{aligned} \tag{26.11}$$

leads to the following expressions for u, v, w, σ_{xx} and τ_{xs}:

$$\begin{aligned} u(x,y,z) &= {}^k\tilde{u}(y,z)^kV'(x), \\ v(x,y,z) &= {}^k\tilde{v}(y,z)^kV(x), \\ w(x,y,z) &= {}^k\tilde{w}(y,z)^kV(x), \\ \sigma_{xx} &= E^k\tilde{u}(y,z)^kV''(x), \\ \tau_{xs} &= -E\int_s {}^k\tilde{u}(y,z)t\mathrm{d}s^kV'''(x), \end{aligned} \tag{26.12}$$

with $k = 1, 2, 3, 4$. With the definitions

$$\begin{aligned} N &= \int_A \sigma_{xx}\mathrm{d}A = {}^1W(x), \\ M_z &= \int_A \sigma_{xx}y\mathrm{d}A = {}^2W(x), \\ M_y &= \int_A \sigma_{xx}z\mathrm{d}A = {}^3W(x), \\ W &= -\int_A \sigma_{xx}\omega\mathrm{d}A = {}^4W(x) \end{aligned} \tag{26.13}$$

the following formulation can be developed for the normal force, the bending moments and the warping moment:

$${}^kW = -\int_A \sigma_{xx}{}^k\tilde{u}\mathrm{d}A. \tag{26.14}$$

This can be interpreted as the work of the normal stress σ_{xx} along the unit displacement ${}^k\tilde{u}$. The transverse forces V_y, V_z and the torsional moment M_T are then $V_y = {}^2W'$, $V_z = {}^3W'$, $M_T = {}^4W'$.

Assignment of the cross-sectional properties A, I_{zz}, I_{yy}, C_M with the designations

$$A = {}^1C, \quad I_{zz} = {}^2C, \quad I_{yy} = {}^3C, \quad C_M = {}^4C \tag{26.15}$$

allows the following standardized definition:

$${}^kC = \int_A {}^k\tilde{u}^2 \mathrm{d}A. \tag{26.16}$$

With this notation, the extensional stiffness EA can be interpreted as a stiffness with respect to a constant deformation, while the bending stiffnesses EI_{yy} and EI_{zz} can be interpreted as stiffnesses with respect to linear deformations over the cross-section. This gives us the following notation for the constitutive law for each elementary state:

$${}^kW(x) = -E^kC^kV''(x). \tag{26.17}$$

For the stresses we obtain:

$${}^k\sigma_{xx}(x, y, z) = -\frac{{}^kW(x){}^k\tilde{u}(y, z)}{{}^kC}, \tag{26.18}$$

$${}^k\tau_{xs}t = \frac{{}^kW'(x)}{{}^kC} \int_s {}^k\tilde{u}(y, z)t\mathrm{d}s. \tag{26.19}$$

The differential equations for the four elementary states can be written in uniform notation as follows:

$$E^kC^kV'''' = {}^kq, \tag{26.20}$$

where the term on the right-hand side ${}^kq$ can be interpreted as the sum of the work of the external load q with respect to the unit displacements ${}^k\tilde{v}$ and ${}^k\tilde{w}$.

At this point, Schardt introduces the concept of orthogonality , which is the prerequisite for treating the four individual states separately and describing them by separate decoupled differential equations. The decoupling of the bending effects and the rod effect is achieved by relating all considerations to the center of gravity, so that

$$\int_A y\mathrm{d}A = 0, \quad \int_A z\mathrm{d}A = 0. \tag{26.21}$$

By using the principal axes of the cross-section, the two bending states are also decoupled so that the deviation moment must disappear:

$$\int_A yz\mathrm{d}A = 0. \tag{26.22}$$

Finally, the shear center M of the cross-section is determined so that state 4 (torsion) can be treated independently of states 1–3. This requires.

$$\int_A \omega\mathrm{d}A = 0, \quad \int_A \omega y\mathrm{d}A = 0, \quad \int_A \omega z\mathrm{d}A = 0. \tag{26.23}$$

These orthogonality requirements can be written in a standardized form as:

$$\int_A {}^i\tilde{u}^k\tilde{u}\omega\mathrm{d}A = 0, \tag{26.24}$$

for $i \neq k$.

26.2.2 Introduction of Higher-Order Deformation Terms

The idea of the conventional GBT is to extend the consideration of straight prismatic thin-walled beams with open unbranched cross-section beyond the described elementary four cases to deformations by including additional cases that can also be described uniformly. If we want to consider a case where we have an additional fifth state with a deformation function ${}^5\tilde{u}$ that satisfies (26.24), we can also determine the unit deformations ${}^5\tilde{v}$ and ${}^5\tilde{w}$. Since all rigid body motions have already been taken into account in the four elementary cases, ${}^5\tilde{v}$ and ${}^5\tilde{w}$ must describe a distortion of the cross-section. The differential equation for ${}^5V(x)$ is then as follows:

$$E{}^5C{}^5V'''' = {}^5q, \tag{26.25}$$

with the warping stiffness ${}^5C$ determined from (26.16). The complete solution for the considered thin-walled beam is then obtained by superimposing the elementary cases 1–4 and the new distortion case 5. In the same way, further cases 6, 7, … can be constructed in the same way. Since the deformations of the individual segments of the cross-sections are assumed to be linear functions of the circumferential coordinate s, the number of additional cases is determined by the number of nodes of the cross-section, where nodes are the intersection points between segments of the cross-section. End points are also counted as nodes. A cross-section that consists of n segments therefore has $n + 1$ independent warping functions and has $n - 3$ additional states in addition to the four elementary states. The warping functions are therefore the basis for the introduction of additional deformations. Figure 26.3 contains the unit warping functions and unit displacements for a cross-section consisting of $n = 4$ segments with $n + 1 = 5$ nodes, so that $n - 1 = 1$ distortion cases must exist.

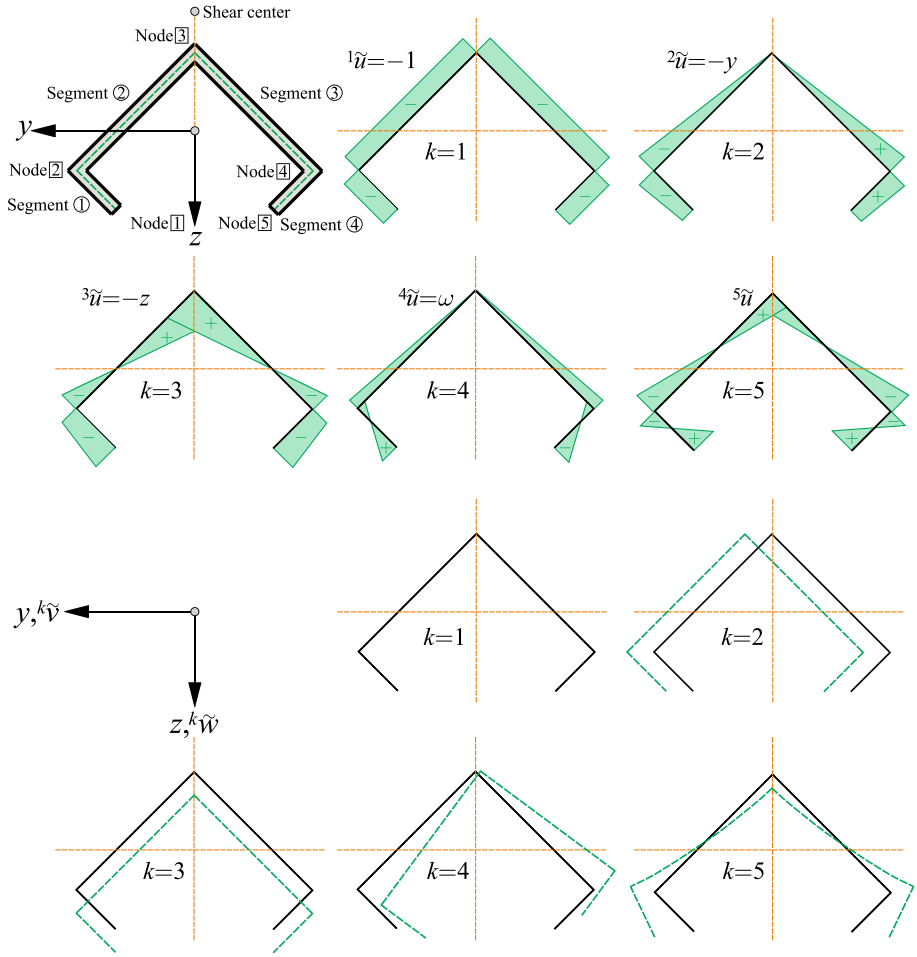


Fig. 26.3 Unit warping functions and unit displacements for a cross-section consisting of four segments with five nodes (after Schardt (1989))

26.2.3 Cross-Sectional Analysis

The conventional GBT formulation considers the following structural situation. Consider an open, unbranched, thin-walled cross-section consisting of n segments (width b_r, constant thickness h_r, orientation angle α_r) with $n + 1$ nodes. The segments are rigidly connected and the segments $r - 1$ and r include the angle $\Delta\alpha_r$ (Fig. 26.4). Schardt lists the following assumptions for the conventional GBT:

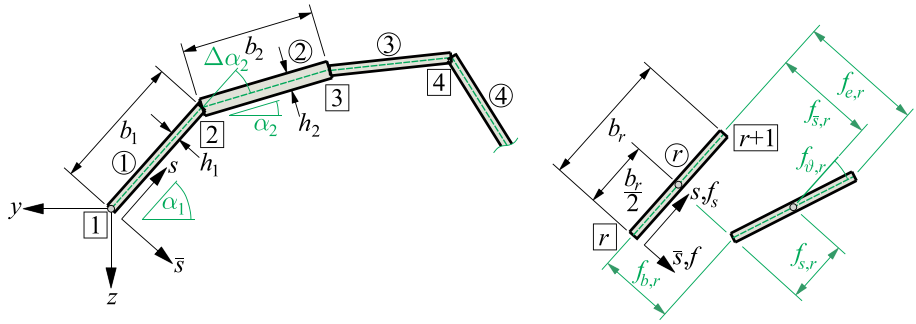


Fig. 26.4 Nomenclature for the conventional GBT formulation (left), deformed segment r (right) (after Schardt (1989))

- Geometric and material linearity is assumed. The deformations are assumed to be small and Hooke's law is assumed to apply.
- For the bending of the cross-section segments, the assumptions of Kirchhoff's plate theory apply. As a result, the transverse shear strains $\gamma_{x\bar{s}}$ and $\gamma_{s\bar{s}}$ disappear.
- The circumferential membrane strain ε_{ss}^M is taken into account, but neglected when considering the deformations. It is assumed that ε_{ss}^M is only associated with the stress component σ_{xx}^M.
- The membrane shear strains γ^M are assumed to vanish, so that the associated stresses σ_{ss}^M and τ^M can only be determined from equilibrium conditions.
- The longitudinal normal stress σ_{xx}^M is linked to the strain components by $\sigma_{xx}^M = E\varepsilon_{xx}^M$.
- The loads are applied to the inner nodes of the cross-section.
- The longitudinal bending stiffness of the individual segments is assumed to be negligible.

The following derivations are restricted to first-order theory, i.e. all equations are formulated in the undeformed state. Let u_r, v_r, w_r be the displacements of the node r with respect to x, y, z and f the displacements associated with the coordinate s, where $f(s_r)$ is the displacement of the segment r perpendicular to the segment plane, i.e. in the $\bar{s}_r$-direction, which results as a cubic function of s. The displacement $f_s(s_r)$ is the displacement in the s_r-direction, which is constant in each segment, so that it is sufficient to use the value $f_{s,r}$ in each segment. Thus, the deformed state of the segment r can be fully described by the displacements $f_{s,r}$, $f_{\bar{s},r}$ and the rotation $f_{\vartheta,r}$ (Fig. 26.4, right). The strains are divided into a membrane part and a bending part, i.e. $\varepsilon_{xx} = \varepsilon_{xx}^M + \varepsilon_{xx}^B$, $\varepsilon_{ss} = \varepsilon_{ss}^M + \varepsilon_{ss}^B$, $\gamma_{xs} = \gamma = \gamma^M + \gamma^B$. The same is assumed for the stresses, so that e.g. $\sigma_{xx} = \sigma_{xx}^M + \sigma_{xx}^B$. The stresses can be converted into their resultants, i.e. into the membrane force flows N_{xx}, N_{ss}, N_{xs} and the moment flows M_{xx}, M_{ss}, M_{xs}. The membrane strains are defined as:

$$\varepsilon_{xx}^M = u', \quad \varepsilon_{ss}^M = \dot{f}_s, \quad \gamma_{xs}^M = f_s' + \dot{u}, \tag{26.26}$$

while the bending strains follow as:

$$\varepsilon_{xx}^{B} = -f''\bar{s}, \quad \varepsilon_{ss}^{B} = -\ddot{f}\bar{s}, \quad \gamma_{xs}^{B} = -2\dot{f}'\bar{s}. \tag{26.27}$$

A superscript denotes a derivative with respect to s. The membrane force flow N_{xx} is determined from Hooke's law as $N_{xx} = \sigma_{xx}^{M} t = Eh\varepsilon_{xx} = Ehu'$. There is no constitutive relationship for the two force flows N_{ss} and N_{xs}, so that these quantities must be determined from equilibrium conditions. For the moment flows, the bending moment flow M_{xx} is neglected so that only M_{ss} and M_{xs} remain. The strain ε_{ss}^{M} is not taken into account in the deformation analysis, so that $\dot{f}_s = 0$, i.e. f_s is constant over each segment. It is also assumed that the shear strain γ_{xs}^{M} disappears, resulting in a dependency between the deformation and f_s, which ultimately leads to linearly varying deformations across the width of each segment. As a result, the variables f_s, $f_{\bar{s}}$, f_ϑ are not independent of each other, but can be determined from the shear deformations u_r, as will be explained below. Since all these quantities assume discrete values, they can be conveniently represented in vector-matrix notation. From the definition of the shear strain $\gamma_{xs}^{M} = \frac{\partial u}{\partial s} + \frac{\partial f_s}{\partial x} = 0$, the derivative of u with respect to s can be expressed by the deformation coordinates of the nodes of the cross-section. It is constant in each segment. Summing the node circumferential displacements $f_{s,r}$ and the warping ordinates u_r in vectors $\underline{f}_s = \left(f_{s,1}, \ldots, f_{s,n}\right)^T$ and $\underline{u} = (u_1, \ldots, u_{n+1})^T$, this allows a representation of the relationship between circumferential displacements and warping in the following form:

$$\underline{f}_s' = \underline{\underline{F}}_s \underline{u}. \tag{26.28}$$

The assignment of the matrix $\underline{\underline{F}}_s$ is not given here, the reader is referred to Schardt (1989). We can write in a similar way:

$$\underline{f}_{\bar{s}}' = \underline{\underline{F}}_{\bar{s}} \underline{u}, \quad \underline{f}_{\vartheta}' = \underline{\underline{F}}_{\vartheta} \underline{u}, \quad \Delta\underline{f}_{\vartheta}' = \Delta\underline{\underline{F}}_{\vartheta} \underline{u}. \tag{26.29}$$

In order to harmonize the GBT formulation with classical beam theory (see Sect. 26.2.1), all state variables are expressed in a separation form. For this purpose, a basic deformation function ${}^{r}\bar{u}(s)$ is introduced (Fig. 26.5), which reaches the unit value 1 at node r and is zero in all other nodes, with the overline introduced to distinguish this function from the unit deformations introduced at a later point. Any warping function $u(s, x)$ can then be formulated in a separation form as:

$$u(s, x) = \sum_{r=1}^{n+1} {}^{r}\bar{u}(s)\, {}^{r}\bar{V}'(x). \tag{26.30}$$

At this point, the warping vectors ${}^{r}\underline{\bar{u}} = (0, \ldots, 0, 1, 0, \ldots, 0)^T$ are introduced. They are summarized in the warping matrix $\underline{\underline{\bar{U}}}$, and further the vectors $\underline{\bar{V}}(x) = ({}^{1}\bar{V}(x), \ldots, {}^{n+1}\bar{V}(x))^T$, $\underline{u} = (u_1(x), \ldots, u_{n+1}(x))^T$ are defined, which allows the following product form for $\underline{u}(x)$:

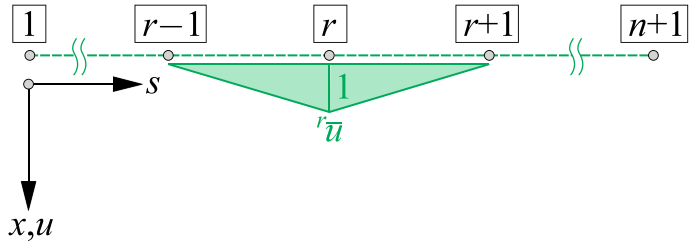


Fig. 26.5 Deformation function in relation to the node r (after Schardt (1989))

$$\underline{u}(x) = \underline{\underline{\bar{U}}}\,\underline{\bar{V}}'(x). \tag{26.31}$$

Due to (26.31), the previously defined displacement quantities can also be written in a similar product form, and after integration with respect to x, the following representations finally result:

$$\begin{aligned}
\underline{f}_s(x) &= \underline{\underline{F}}_s\,\underline{\underline{\bar{U}}}\,\underline{\bar{V}}(x) = \underline{\underline{\bar{F}}}_s\,\underline{\bar{V}}(x),\\
\underline{f}_{\bar{s}}(x) &= \underline{\underline{F}}_{\bar{s}}\,\underline{\underline{\bar{U}}}\,\underline{\bar{V}}(x) = \underline{\underline{\bar{F}}}_{\bar{s}}\,\underline{\bar{V}}(x),\\
\underline{f}_{\vartheta}(x) &= \underline{\underline{F}}_{\vartheta}\,\underline{\underline{\bar{U}}}\,\underline{\bar{V}}(x) = \underline{\underline{\bar{F}}}_{\vartheta}\,\underline{\bar{V}}(x),\\
\Delta\underline{f}_{\vartheta}(x) &= \Delta\underline{\underline{F}}_{\vartheta}\,\underline{\underline{\bar{U}}}\,\underline{\bar{V}}(x) = \Delta\underline{\underline{\bar{F}}}_{\vartheta}\,\underline{\bar{V}}(x).
\end{aligned} \tag{26.32}$$

Similar product representations are possible for those forces and moments for which a constitutive relationship exists.

26.2.4 Differential Equations and Boundary Conditions

The principle of virtual displacements $\delta W_i = \delta W_a$ is used in the following. In this way, the governing differential equations and all boundary conditions can be derived. The virtual internal work δW_i results from

$$\delta W_i = \int_0^l \int_A \left(\sigma_{xx}\delta\varepsilon_{xx} + \sigma_{ss}\delta\varepsilon_{ss} + \tau_{xs}\delta\gamma_{xs}\right) \mathrm{d}A\mathrm{d}x, \tag{26.33}$$

or when split into membrane and bending part with $\delta\varepsilon_{ss}^M = 0$ and $\delta\gamma_{xs}^M = 0$:

$$\delta W_i = \int_0^l \int_A \left(\sigma_{xx}^M\delta\varepsilon_{xx}^M + \sigma_{xx}^B\delta\varepsilon_{xx}^B + \sigma_{ss}^B\delta\varepsilon_{ss}^B + \tau_{xs}^B\delta\gamma_{xs}^B\right) \mathrm{d}A\mathrm{d}x. \tag{26.34}$$

The stress components can be expressed as follows using the kinematic equations (26.26) and (26.27) and Hooke's law:

$$\begin{aligned}
\sigma_{xx}^{M} &= Eu', \\
\sigma_{xx}^{B} &= -\frac{E}{1-\nu^2}\left(f'' + \nu\ddot{f}\right)\bar{s}, \\
\sigma_{ss}^{B} &= -\frac{E}{1-\nu^2}\left(\ddot{f} + \nu f''\right)\bar{s}, \\
\tau_{xs}^{B} &= -2G\dot{f}'\bar{s}.
\end{aligned} \tag{26.35}$$

In accordance with the previous derivations, the following series expansion is used in separation form for the displacements:

$$\begin{aligned}
u(s,x) &= \sum_{k=1}^{n+1} {}^{k}u(s)\,{}^{k}V'(x), \\
f_s(s,x) &= \sum_{k=1}^{n+1} {}^{k}f_s(s)\,{}^{k}V(x), \\
f(s,x) &= \sum_{k=1}^{n+1} {}^{k}f(s)\,{}^{k}V(x).
\end{aligned} \tag{26.36}$$

Here, ${}^{k}f_s$ and ${}^{k}f$ depend on ${}^{k}u$, whereby the latter is given as a continuous linear function over s (Fig. 26.5), so that continuous constant functions ${}^{k}f_s$ and cubic functions ${}^{k}f$ result. The number $n+1$ of linearly independent warping functions ${}^{k}u$ corresponds to the number $n+1$ of nodes of the cross-section under consideration. At this point, the only unknown variables are the functions ${}^{k}V(x)$, so that the following variations only affect ${}^{k}V(x)$. For the portion $\int_0^l \int_A \sigma_{xx}^{M}\delta\varepsilon_{xx}^{M}\mathrm{d}A\mathrm{d}x$ we obtain:

$$\begin{aligned}
\int_0^l \int_A \sigma_{xx}^{M}\delta\varepsilon_{xx}^{M}\mathrm{d}A\mathrm{d}x &= E\int_0^l \int_A u'\delta u'\mathrm{d}A\mathrm{d}x \\
&= E\sum_{i=1}^{n+1}\sum_{k=1}^{n+1}\int_0^l \int_A {}^{i}u^{k}u^{i}V''\delta^{k}V''\mathrm{d}A\mathrm{d}x \\
&= E\sum_{i=1}^{n+1}\sum_{k=1}^{n+1}\int_0^l \int_A {}^{ik}C^{Mi}V''\delta^{k}V''\mathrm{d}A\mathrm{d}x,
\end{aligned} \tag{26.37}$$

with ${}^{ik}C^M = \int_A {}^i u^k u \mathrm{d}A$. In a similar way, we obtain for the other expressions in (26.34):

$$\begin{aligned}
\int_0^l \int_A \sigma_{xx}^B \delta\varepsilon_{xx}^B \mathrm{d}A\mathrm{d}x &= E \sum_{i=1}^{n+1}\sum_{k=1}^{n+1} \int_0^l \int_A \left({}^{ik}C^{Bi} V'' + \nu {}^{ik}D_2{}^i V\right)\delta^k V'' \mathrm{d}A\mathrm{d}x, \\
\int_0^l \int_A \sigma_{ss}^B \delta\varepsilon_{ss}^B \mathrm{d}A\mathrm{d}x &= \sum_{i=1}^{n+1}\sum_{k=1}^{n+1} \int_0^l \left({}^{ik}B^i V + \nu E^{ik} D_2{}^i V''\right)\delta^k V \mathrm{d}x, \\
\int_0^l \int_A \tau_{xs}^B \delta\gamma_{xs}^B \mathrm{d}A\mathrm{d}x &= G \sum_{i=1}^{n+1}\sum_{k=1}^{n+1} \int_0^l {}^{ik}D_1{}^i V' \delta^k V' \mathrm{d}x,
\end{aligned} \tag{26.38}$$

with ${}^{ik}B = \int_s K^i \ddot{f}^k \ddot{f} \mathrm{d}s$, ${}^{ik}C^B = E^{-1} \int_s K^i f^k f \mathrm{d}s$ (K is the plate stiffness), ${}^{ik}D_1 = \frac{1}{3}\int_h^{3i} \dot{f}^k \dot{f} \mathrm{d}s$, ${}^{ik}D_2 = E^{-1} \int_s K^i \ddot{f}^k f \mathrm{d}s$. The virtual work performed by the external loads is taken into account later on. Partial integration leads to the following equations and boundary conditions:

$$\begin{aligned}
\sum_{i=1}^{n+1} \left(E^{ik} C^i V'''' - G^{ik} D^i V'' + {}^{ik}B^i V\right) &= 0, \\
\sum_{i=1}^{n+1} \left(E^{ik} C^i V'' + \nu E^{ik} D_2{}^i V\right) \delta^k V' \Big|_0^l &= 0, \\
\sum_{i=1}^{n+1} \left(-E^{ik} C^i V''' - \nu E^{ik} D_2{}^i V' + G^{ik} D_1{}^i V'\right) \delta^k V \Big|_0^l &= 0,
\end{aligned} \tag{26.39}$$

for $k = 1, \ldots, n+1$ with ${}^{ik}C = {}^{ik}C^M + {}^{ik}C^B$ and ${}^{ik}D = {}^{ik}D_1 - \frac{\nu E}{G}\left({}^{ik}D_2 + {}^{ki}D_2\right)$. The first set of equations in (26.39) can also be written in a vector-matrix-notation as follows:

$$E\underline{\underline{C}}\,\underline{V}'''' - G\underline{\underline{D}}\,\underline{V}'' + \underline{\underline{B}}\,\underline{V} = \underline{0}. \tag{26.40}$$

By diagonalizing the matrices $\underline{\underline{B}}$, $\underline{\underline{C}}$, $\underline{\underline{D}}$ (see Schardt 1989) with the help of the Jacobi transformation, the system of Eq. (26.40) can be brought into the following form:

$$E\underline{\underline{\tilde{C}}}\,\underline{\tilde{V}}'''' - G\underline{\underline{\tilde{D}}}\,\underline{\tilde{V}}'' + \underline{\underline{\tilde{B}}}\,\underline{\tilde{V}} = \underline{0}. \tag{26.41}$$

Due to the diagonal form of the matrices $\underline{\underline{\tilde{B}}}$, $\underline{\underline{\tilde{C}}}$, $\underline{\underline{\tilde{D}}}$, this system of equations is now decoupled, and the equation for the form function ${}^k\tilde{V}$ is as follows:

$$E^k \tilde{C}^k \tilde{V}'''' - G^k \tilde{D}^k \tilde{V}'' + {}^k\tilde{B}^k \tilde{V} = {}^k\tilde{q} + {}^k\tilde{q}'_x, \tag{26.42}$$

where now the virtual work δW_a of the generalized line loads ${}^k\tilde{q}$ and ${}^k\tilde{q}_x$ acting in the plane and in the longitudinal direction with respect to the nodal lines of the beam has been taken into account. Finally, the boundary terms in (26.39) also take a simplified form, which is not given here for reasons of brevity. The stress resultant ${}^kW$ is defined as:

$$\begin{aligned} {}^kW(x) &= -\int_A {}^k\sigma_{xx}(x,s)\,{}^k\tilde{u}(s)\mathrm{d}A \\ &= -E\int_A {}^kV''(x)\,{}^k\tilde{u}\,{}^k\tilde{u}\mathrm{d}A = -E\,{}^k\tilde{C}\,{}^k\tilde{V}''(x), \end{aligned} \tag{26.43}$$

and the stress $\sigma_{xx}(x,s)$ results as:

$$\sigma_{xx}(x,s) = -\sum_{k=1}^{n+1} \frac{{}^kW(x)\,{}^k\tilde{u}(s)}{{}^k\tilde{C}}. \tag{26.44}$$

For the solution of the Eq. (26.42), Schardt presents an analytical approach in closed-form based on solution methods for beams under bending and tensile loading on elastic foundation. The finite difference method is introduced as a solution method for complex applications.

This concludes the overview of conventional GBT as outlined by Schardt.

26.2.5 Further Work from Schardt's Working Group

Schardt supervised a considerable number of dissertations on topics of Generalised Beam Theory, a selection of which is cited below.

A first work on the extension of GBT to problems according to second-order theory was presented by Okur (1971). Steingass (1972) considered the buckling behaviour of isotropic thin-walled cylindrical shells. Saal (1974) investigated the vibration behaviour of prismatic shells using GBT, interpreting the shells as composed of plate segments. This approach required an extension of the GBT to closed thin-walled structures, and Saal also introduced membrane shear strains as degrees of freedom. Miosga (1976) considered imperfect thin-walled beams and plates under predominantly longitudinal load with finite deformations. Usuki (1976) investigated the torsional behaviour of closed-profile box beams considering cross-sectional deformations using VTB, taking into account in-plane shear strains and the influence of torsional stiffness. The nonlinear analysis of shells was considered by Kahmer (1981). In his doctoral thesis, Möller (1982) extended the scope of conventional GBT to the static and dynamic analysis of thin-walled prismatic structures with arbitrary open and closed branched or unbranched cross-sections under mechanical and thermal loading, taking into account shear deformations. Schrade (1984) dealt with the buckling behaviour of beams under longitudinal load with open U-sections with flanges and stiffeners between

the flanges at intermediate positions along the beam length. In 1984, Girmscheid submitted his doctoral thesis and extended the scope of the GBT to include transverse normal strains, shear strains and large deformations. Hanf submitted his dissertation in 1989. He derived the equilibrium and boundary conditions of the GBT within the framework of second-order theory using the principle of virtual work, whereby beams primary under longitudinal loads were assumed to be in a constant initial stress state with negligible deformations. Since the boundary conditions can be clearly derived in this way, this aspect is briefly described below. The normal stresses at the beam ends perform work along the displacements and the corresponding work is

$$W_a = -\int_A \sigma_{xx}^M \int_0^l \frac{1}{2}\left((v')^2 + (w')^2\right) \mathrm{d}x\mathrm{d}A, \tag{26.45}$$

wherein $(v')^2 + (w')^2 = (f_s')^2 + (f')^2$. With an approach of the type

$$\begin{aligned} f_s(s,x) &= \sum_{k=1}^{n+1} {}^k\tilde{f}_s(s)^k V(x), \\ f(s,x) &= \sum_{k=1}^{n+1} {}^k\tilde{f}(s)^k V(x) \end{aligned} \tag{26.46}$$

one obtains:

$$(v')^2 + (w')^2 = \sum_{j=1}^{n+1}\sum_{k=1}^{n+1} \left({}^j\tilde{f}_s{}^k\tilde{f}_s + {}^j\tilde{f}^k\tilde{f}\right) {}^jV'^kV'. \tag{26.47}$$

With the membrane stress $\sigma_{xx}^M = -\sum_{i=1}^{n+1} {}^iW \frac{{}^i\tilde{u}}{{}^iC}$ one obtains:

$$W_a = \sum_{i=1}^{n+1} {}^iW \sum_{j=1}^{n+1}\sum_{k=1}^{n+1} \left({}^{ijk}\kappa_\sigma \int_0^l \frac{1}{2} {}^jV'^kV'\mathrm{d}x\right), \tag{26.48}$$

with ${}^{ijk}\kappa_\sigma = \int_A \frac{{}^i\tilde{u}}{{}^iC}\left({}^j\tilde{f}_s{}^k\tilde{f}_s + {}^j\tilde{f}^k\tilde{f}\right)\mathrm{d}A$. If imperfections are also taken into account, then the external work takes the following form:

$$W_a = -\int_A \sigma_{xx}^M \int_0^l \frac{1}{2}\left((v_g')^2 + (w_g')^2 - (v_0')^2 - (w_0')^2\right)\mathrm{d}x\mathrm{d}A. \tag{26.49}$$

If this expression is used in the total work and the principle of virtual displacements $\delta W_i = \delta W_a$ is applied, this results in the following system of differential equations:

$$E^k C^k V'''' - \sum_{j=1}^{n+1} G^{jk} D^j V'' + \sum_{i=1}^{n+1} {}^i W \sum_{j=1}^{n+1} {}^{ijk}\kappa_\sigma{}^j V'' + {}^k B^k V = -\sum_{i=1}^{n+1} {}^i W \sum_{j=1}^{n+1} {}^{ijk}\kappa_\sigma{}^j V_0'', \tag{26.50}$$

for $k = 1, \ldots, n+1$. This is a fourth-order linear differential equation system. The boundary conditions are as follows:

$$\begin{aligned} &- E^k C^k V'' - \sum_{j=1}^{n+1} \nu E^{jk} D_2{}^j V = 0 \quad \text{or} \quad {}^k V' = 0, \\ &-E^k C^k V''' + \sum_{j=1}^{n+1} \left(G^{jk} D_1 - \nu E^{jk} D_2 \right) {}^j V' \\ &\qquad + \sum_{i=1}^{n+1} {}^i W \sum_{j=1}^{n+1} {}^{ijk}\kappa_\sigma \left({}^j V' + {}^j V_0' \right) = 0 \\ &\qquad\qquad \text{or} \quad {}^k V = 0, \end{aligned} \tag{26.51}$$

for $k = 1, \ldots, n+1$. Hanf went on to solve the system of differential equations in a closed-form analytical manner by using an exponential function approach for the homogeneous solution:

$$\underline{V} = \underline{t} e^{\lambda x}, \tag{26.52}$$

where $\underline{t}$ is the amplitude vector. Special solutions were derived for two practically relevant load cases. Finally, Hanf extended the scope of GBT to the analysis of thin-walled beams in which plasticity occurs.

Zhang presented his dissertation in 1989 and discussed the local and global buckling behaviour of thin-walled beams with U-sections under longitudinal loading in the plane of symmetry using the GBT. In addition to the static behaviour of structures, Mörschardt (1989) also investigated the buckling and dynamic behaviour of thin-walled prismatic beams using the GBT. C. Schardt (1995) investigated the natural frequencies of prismatic beams and folded structures, including cracks, with the aid of classical beam theory and the GBT, whereby in the latter the beam under consideration was divided into two areas, in each of which a GBT formulation was used. In his dissertation submitted in 1997, Gamal-Eldin (1997) investigated cold-formed thin-walled profiles with open unbranched cross-sections with special consideration of the influence of local buckling on the global stability behaviour. Gamal-Eldin investigated thin-walled beams in the postcritical range under two different load applications. Heppner (1997) investigated the dynamic behaviour of prismatic thin-walled shells with the aid of GBT, taking geometric nonlinearities into account. The analysis of plate structures using the GBT was carried out by Conchon (2001). Haakh (2004) aimed in his work to find a common basis for the selection of different deformation approaches in

addition to the rotations of the nodal lines and allowed the treatment of arbitrary open or closed cross-sections with membrane shear strains, circumferential strains and rotations of the nodal lines. Haakh solved the resulting differential equations by power series expansion. In this way, variable coefficients can also be treated and Haakh presents formulations for first and second order theory.

In a conference paper, Schardt and Heinz (1991) extended the scope of GBT to the dynamic analysis of thin-walled prismatic structures and presented an example for the determination of natural frequencies and mode shapes of a stiffened plate. The additional components δW_{dyn} in the principle of virtual work can be given as follows:

$$\begin{aligned}\delta W_{dyn} &= \int_l \int_s \rho h\left(\ddot{u}\delta u + \ddot{f}\delta f + \ddot{f}_s \delta f_s\right) \mathrm{d}s\,\mathrm{d}x \\ &= \int_l \int_s \rho h\Big(\sum_{i,k} {}^{i}u^{i}\,\ddot{V}'^{k}u\delta^{k}V' + {}^{i}f^{i}\,\ddot{V}^{k}f\delta^{k}V + {}^{i}f_s{}^{i}\,\ddot{V}^{k}f_s\delta^{k}V\Big)\mathrm{d}s\,\mathrm{d}x, \end{aligned} \tag{26.53}$$

where a superscript denotes a partial derivative with respect to time t. The integration over the cross-section leads to

$$\delta W_{dyn} = \sum_j \left(-{}^{ij}\kappa_{dyn,u}{}^{j}V'' + {}^{jk}\kappa_{dyn,f}{}^{j}V\right)\delta^{k}V, \tag{26.54}$$

with

$$\begin{aligned} {}^{ij}\kappa_{dyn,u} &= \int_s \rho h\,{}^{i}u^{k}u\,\mathrm{d}s + \sum_n m_n\,{}^{i}u(s_n)^{k}u(s_n), \\ {}^{jk}\kappa_{dyn,f} &= \int_S \rho h\left({}^{i}f^{k}f + {}^{i}f_s{}^{k}f_s\right)\mathrm{d}s \\ &\quad + \sum_n m_n\left({}^{i}f(s_n)^{k}f(s_n) + {}^{i}f_s(s_n)^{k}f_s(s_n)\right), \end{aligned} \tag{26.55}$$

where m_n are concentrated masses along lines in the longitudinal direction. Partial integration and summarizing terms of the same order finally leads to the following system of differential equations in vector-matrix-notation:

$$\begin{aligned} &E\underline{\underline{C}}\,\underline{V}'''' - G\underline{\underline{D}}\,\underline{V}'' + \underline{\underline{B}}\,\underline{V} \\ &\quad + \sum_i \sum_j {}^{ijk}\kappa_\sigma \left({}^{i}W^{j}V'\right)' + \sum_j \left(-{}^{jk}\kappa_{dyn,u}{}^{j}\ddot{V}'' + {}^{jk}\kappa_{dyn,f}{}^{j}\ddot{V}\right) = \underline{q}. \end{aligned} \tag{26.56}$$

26.3 Application of the Generalized Beam Theory to Layered Thin-Walled Beams

Schardt and colleagues published their research results largely in German and limited their considerations to isotropic structures. Accordingly, there have been considerable efforts by international working groups, especially in about the last 20 years, to make the GBT usable for laminated structures as well. The first work in this area was presented by Silvestre and Camotim (2002a, b), in which an extension of the GBT to orthotropic and laminated materials is described within the framework of first- and second-order theory. In the first paper, the general concepts of GBT are revisited and the assumptions of classical GBT are retained, while the material law in a plane stress state for each laminate layer is given as follows:

$$\begin{pmatrix} \sigma_{xx} \\ \sigma_{yy} \\ \tau_{xy} \end{pmatrix} = \begin{bmatrix} \bar{Q}_{11} & \bar{Q}_{12} & \bar{Q}_{16} \\ \bar{Q}_{12} & \bar{Q}_{22} & \bar{Q}_{26} \\ \bar{Q}_{16} & \bar{Q}_{26} & \bar{Q}_{66} \end{bmatrix} \begin{pmatrix} \varepsilon_{xx} \\ \varepsilon_{yy} \\ \gamma_{xy} \end{pmatrix}. \tag{26.57}$$

For a beam cross-section consisting of n discrete plate-like segments, the displacement field can be specified as follows (summation over k):

$$u(x,s) = u_k(s)\phi_{k,x}(x), \quad v(x,s) = v_k(s)\phi_k(x), \quad w(x,s) = w_k(x)\phi_k(x), \tag{26.58}$$

with $1 \le k \le n+1$, where $u_k(s)$ is a segmentwise linear function of s, and $\phi_k(x) = u(s_k)\psi(x)$. The functions $v_k(s)$ and $w_k(s)$ can be expressed a priori by $u_k(s)$ due to the assumptions of classical GBT. The strain field then reads:

$$\varepsilon_{xx} = (u_k - z w_k)\,\phi_{k,xx}, \quad \varepsilon_{ss} = -z w_{k,ss}\phi_k, \quad \gamma_{xs} = -2z w_{k,s}\phi_{k,x}. \tag{26.59}$$

Hooke's law (26.57) then changes into the following form:

$$\begin{aligned} \sigma_{xx} &= \bar{Q}_{11}\,(u_k - z w_k)\,\phi_{k,xx} - z\left(\bar{Q}_{12} w_{k,ss}\phi_k + 2\bar{Q}_{16} w_{k,s}\phi_{k,x}\right), \\ \sigma_{yy} &= \bar{Q}_{12}\,(u_k - z w_k)\,\phi_{k,xx} - z\left(\bar{Q}_{22} w_{k,ss}\phi_k + 2\bar{Q}_{26} w_{k,s}\phi_{k,x}\right), \\ \sigma_{xx} &= \bar{Q}_{16}\,(u_k - z w_k)\,\phi_{k,xx} - z\left(\bar{Q}_{26} w_{k,ss}\phi_k + 2\bar{Q}_{66} w_{k,s}\phi_{k,x}\right). \end{aligned} \tag{26.60}$$

The governing equations were derived from the principle of virtual displacements $\delta W_i = \delta W_a$, whereby the virtual internal work δW_i is composed of the contributions of the individual stress components:

$$\delta W_i = \int_V (\sigma_{xx}\delta\varepsilon_{xx} + \sigma_{ss}\delta\varepsilon_{ss} + \tau_{xs}\delta\gamma_{xs})\,\mathrm{d}V = \delta W_{i,xx} + \delta W_{i,ss} + \delta W_{i,xs}, \tag{26.61}$$

where the virtual strains are:

$$\begin{aligned}
\delta\varepsilon_{xx} &= (u_i - zw_i)\,\delta\phi_{i,xx},\\
\delta\varepsilon_{ss} &= -zw_{i,ss}\delta\phi_i,\\
\delta\gamma_{xs} &= -2zw_{i,s}\delta\phi_{i,x}.
\end{aligned} \tag{26.62}$$

Inserting (26.60) and (26.62) into (26.61) then leads to the following representations for the three components of the internal work (26.61):

$$\begin{aligned}
\delta W_{i,xx} = \int_0^l & \left[\left(C_{ik}^1 + C_{ik}^2 - C_{ik}^3 - C_{ki}^3\right)\phi_{k,xxxx}\right.\\
&+ \left(D_{ik}^2 - D_{ik}^3\right)\phi_{k,xx} + \left(H_{ik}^1 - H_{ik}^2\right)\phi_{k,xxx}\Big]\,\mathrm{d}x\,\delta\phi_i\\
&+ \Big[\left(C_{ik}^1 + C_{ik}^2 - C_{ik}^3 - C_{ki}^3\right)\phi_{k,xx}\\
&+ \left(D_{ik}^2 - D_{ik}^3\right)\phi_k + \left(H_{ik}^1 - H_{ik}^2\right)\phi_{k,x}\Big]\,\delta\phi_{i,x}\Big|_0^l\\
&- \Big[\left(C_{ik}^1 + C_{ik}^2 - C_{ik}^3 - C_{ki}^3\right)\phi_{k,xxx}\\
&+ \left(D_{ik}^2 - D_{ik}^3\right)\phi_{k,x} + \left(H_{ik}^1 - H_{ik}^2\right)\phi_{k,xx}\Big]\,\delta\phi_i\Big|_0^l,\\
\delta W_{i,ss} = \int_0^l & \left[\left(H_{ki}^2 - H_{ki}^1\right)\phi_{k,xxx} - F_{ki}^1\phi_{k,x} - D_{ik}^1\phi_{k,xx}\right]\mathrm{d}x\,\delta\phi_i\\
&+ \left[\left(H_{ki}^1 - H_{ki}^2\right)\phi_{k,xx} + F_{ki}^1\phi_k + D_{ik}^1\phi_{k,x}\right]\delta\phi_i\Big|_0^l,\\
\delta W_{i,xs} = \int_0^l & \left[\left(D_{ki}^2 - D_{ki}^3\right)\phi_{k,xx} + B_{ik}\phi_k + F_{ik}^1\phi_{k,x}\right]\mathrm{d}x\,\delta\phi_i.
\end{aligned} \tag{26.63}$$

The quantities B_{ik}, C_{ik}^1, C_{ik}^2, C_{ik}^3, D_{ik}^1, D_{ik}^2, D_{ik}^3, F_{ik}^1, H_{ik}^1, H_{ik}^2 are stiffness resultants, which represent the products of the membrane stiffnesses A_{ik}, coupling stiffnesses B_{ik}, and plate stiffnesses D_{ik} as well as the displacements u_i and w_i. Their details are not given here.

The virtual work δW_a can be specified with the surface loads q_x, q_y, q_z as:

$$\delta W_a = \int_A \left(q_x\delta u + q_s\delta v + q_z\delta w\right)\mathrm{d}s\mathrm{d}x. \tag{26.64}$$

The following system of differential equations arises from the principle of virtual displacements:

$$C_{ik}\phi_{k,xxxx} + H_{ik}\phi_{k,xxx} - D_{ik}\phi_{k,xx} + F_{ik}\phi_{k,x} + B_{ik}\phi_k = q_i. \tag{26.65}$$

The underlying boundary conditions follow as:

$$\left[C_{ik}\phi_{k,xxx} + H_{ik}\phi_{k,xx} - \left(D^1_{ik} - D^2_{ik} + D^3_{ik}\right)\phi_{k,x} - F^1_{ki} + q_i u_i\right]\delta\phi_i\Big|_0^l = 0,$$
$$\left[C_{ik}\phi_{k,xx} + \left(H^1_{ik} - H^2_{ik}\right)\phi_{k,x} + \left(D^2_{ik} - D^3_{ik}\right)\phi_k\right]\delta\phi_{i,x}\Big|_0^l = 0, \qquad (26.66)$$

where C_{ik}, H_{ik}, D_{ik} and F_{ik} are additional stiffness resultants.

The above equations show that the structures of the laminates under consideration have a very significant influence on the structural analysis using the GBT. The remaining calculation steps, in particular the diagonalization of the system matrices and the resulting decoupling of the system of equations, essentially correspond to those of the conventional GBT, so that further explanations can be omitted at this point.

The second contribution by Silvestre and Camotim (2002b) extends the considerations to the GBT within the framework of second-order theory in order to analyse the stability behaviour of thin-walled orthotropic and layered structures. The principle of virtual displacements is used to derive the governing equations and boundary conditions, and the resulting equations are compared with the results of other authors. The implications of the GBT second-order analysis are discussed in detail before the analysis approach is illustrated using examples for fiber-reinforced plastics. In Silvestre and Camotim (2003), the derived second-order GBT analysis approach for orthotropic materials is revisited and a finite element formulation is established to solve the eigenvalue problem that arises when solving the resulting system of equilibrium equations. In another paper (Silvestre and Camotim 2004a), the vibration behaviour of thin-walled composite beams is treated using the GBT.

In addition to the contributions already mentioned, a large number of other international publications are available on the analysis of thin-walled composite structures using the GBT. At this point, the works by Silvestre and Camotim (2004b, 2009, 2013a, b), Silvestre and Freitas Silva (2006), De Miranda et al. (2013, 2014), Gutierrez (2014), Nunes et al. (2013), Silva and Silvestre (2007), Silva et al. (2006, 2008, 2010a, b, 2011), Silva (2013), and Melchionda (2016) should be mentioned.

References

Andreassen MJ (2012): *Distortional Mechanics of Thin-Walled Structural Elements*. Dissertation, Technical University of Denmark, Denmark.

Camotim D, Silvestre N, Gonçalves R, Dinis PB (2006): *GBT-based structural analysis of thin-walled members: overview, recent progress and future developments*. In: Pandey M, Xie WC (Eds.): Advances in Engineering Structures, Mechanics and Construction. Proceedings of an International Conference on Advances in Engineering Structures, Mechanics and Construction, Waterloo, Kanada, 14.-17. Mai 2006, pp. 187-204.

Carrera E, Pagani A, Petrolo M, Zappino E (2015): *Recent developments on refined theories for beams with applications*. Mechanical Engineering Reviews 2:14-00298.

Conchon R (2001): *Berechnung von Platten mit der Verallgemeinerten Technischen Biegetheorie*. Dissertation, Technische Universität Darmstadt, Darmstadt, Germany.

De Miranda S, Gutierrez A, Miletta R, Ubertini F (2013): *A generalized beam theory with shear deformation*. Thin-Walled Structures 67:88–100.

De Miranda S, Gutierrez A, Miletta R (2014): *Equilibrium-based reconstruction of three-dimensional stresses in GBT*. Thin-Walled Structures 74:146–154.

Ferrarotti A (2018): *New approaches for linear and nonlinear analyses of thin-walled members in the framework of the generalized beam theory*. Dissertation, University of Genoa, Italy / University of Sydney, Australia.

Gamal-Eldin A (1997): *Der Einfluss der lokalen Instabilität auf die globale Instabilität dünnwandiger offener Querschnitte unter zwei verschiedenen Lasteinleitungen*. Dissertation, Technische Universität Darmstadt, Darmstadt, Germany.

Girmscheid G (1984): *Ein Beitrag zur Verallgemeinerten Technischen Biegetheorie unter Berücksichtigung der Umfangsdehnungen, Schubverzerrungen und großer Verformungen*. Dissertation, Technische Universität Darmstadt, Darmstadt, Germany.

Gonçalves R, Camotim D, Basaglia C, Martins AD, Peres N (2023): *Latest developments on the analysis of thin-walled structures using Generalised Beam Theory (GBT)*. Journal of Constructional Steel Research 204:107858.

Gutierrez A (2014): *Modelling and analysis of thin-walled beams in the context of the Generalized Beam Theory*. Dissertation, University of Bologna, Italy.

Haakh A (2004): *Die Erweiterung der VTB für allgemeine dünnwandige Querschnitte sowie die Lösung des Differentialgleichungssystems mit Potenzreihen*. Dissertation, Technische Universität Darmstadt, Darmstadt, Germany.

Hanf M (1989): *Die geschlossene Lösung der linearen Differentialgleichungssysteme der Verallgemeinerten Technischen Biegetheorie mit einer Anwendung auf die Ermittlung plastischer Grenzlasten*. Dissertation, Technische Universität Darmstadt, Darmstadt, Germany.

Heppner KU (1997): *Die Berechnung von geometrisch und statisch nichtlinearen Schwingungen von vorwiegend längs beanspruchten, prismatischen Schalen mit Hilfe der Verallgemeinerten Technischen Biegetheorie*. Dissertation, Technische Universität Darmstadt, Darmstadt, Germany.

Kahmer H (1981): *Zum Tragverhalten der Kreiszylinderschale mit endlichen, elastischen Formänderungen*. Dissertation, Technische Universität Darmstadt, Darmstadt, Germany.

Melchionda D (2016): *First-order and buckling analysis of thin-walled members with deformable cross-section within the Generalized Beam Theory*. Dissertation, University of Bologna, Italy.

Miosga G (1976): *Vorwiegend längsbeanspruchte dünnwandige prismatische Stäbe und Platten mit endlichen elastischen Verformungen*. Dissertation, Technische Universität Darmstadt, Darmstadt, Germany.

Mittelstedt C (2021): *Structural mechanics in lightweight engineering*. Springer Nature, Cham, Switzerland.

Mittelstedt C (2024): *Generalized Beam Theory for the analysis of thin-walled structures - a state-of-the-art survey*. Thin-Walled Structures 200:111849.

Möller R (1982): *Zur Berechnung prismatischer Strukturen mit beliebigem nicht formtreuem Querschnitt*. Dissertation, Technische Universität Darmstadt, Darmstadt, Germany.

Mörschardt S (1989): *Zur Abschätzung der Lösung von zusammengesetzten Verzweigungsproblemen aus der Kenntnis von Teillösungen*. Dissertation, Technische Universität Darmstadt, Darmstadt, Germany.

Nunes F, Correia M, Correia JR, Silvestre N, Moreira A (2013): *Experimental and numerical study on the structural behavior of eccentrically loaded GFRP columns*. Thin-Walled Structures 72:175–187.

Okur H (1971): *Eine statische Methode zur Lösung von nichtlinearen Differentialgleichungssystemen 4. Ordnung mit ihrer hauptsächlichen Anwendung auf die Untersuchung der Stabilität von Faltwerken und Schalen*. Dissertation, Technische Universität Darmstadt, Darmstadt, Germany.

Saal G (1974): *Ein Beitrag zur Schwingungsberechnung von dünnwandigen, prismatischen Schalentragwerken mit unverzweigtem Querschnitt*. Dissertation, Technische Universität Darmstadt, Darmstadt, Germany.

Schardt C (1995): *Ein Beitrag zur Berechnung gekoppelter Eigenschwingungen angerissener prismatischer Stäbe unter Berücksichtigung von Querschnittsverformungen*. Dissertation, Technische Universität Darmstadt, Darmstadt, Germany.

Schardt R (1966): *Eine Erweiterung der technischen Biegelehre für die Berechnung biegesteifer prismatischer Faltwerke*. Der Stahlbau 35:161–171.

Schardt R (1989): *Verallgemeinerte Technische Biegetheorie*. Springer, Berlin et al., Germany.

Schardt R, Heinz D (1991): *Vibrations of thin-walled prismatic structures under simultaneous static load using Generalized Beam Theory*. In: Krätzig WB et al. (Eds.): Structural Dynamics, Volume 2. Proceedings of the European conference on structural dynamics Eurodyn '90, 5.–7. Juni 1990. Balkema, Rotterdam, Brookfield, pp. 921-927.

Schrade W (1984): *Ein Beitrag zum Stabilitätsnachweis dünnwandiger, durch Bindebleche versteifter Stäbe mit offenem Querschnitt*. Dissertation, Technische Universität Darmstadt, Darmstadt, Germany.

Silva NF, Silvestre N, Camotim D (2006): *GBT formulation to analyse the buckling behaviour of FRP composite branched thin-walled members*. III European Conference on Computational Mechanics, Solids, Structures and Coupled Problems in Engineering, Lissabon, Portugal, 5.–8. Juni 2006.

Silva NF, Silvestre N (2007): *On the influence of material couplings on the linear and buckling behavior of I-section composite columns*. International Journal of Structural Stability and Dynamics 7:243–272.

Silva NM, Degenhardt R, Camotim D, Silvestre N (2008): *Application of generalised beam theory to the study of the stability behaviour of laminated CFRP cylindrical stiffened panels*. Proceedings of the 2nd International Conference on Buckling and Postbuckling Behaviour of Composite Laminated Shell Structures, 3.–5. September 2008, Braunschweig, Germany.

Silva NMF, Camotim D, Silvestre N, Degenhardt R (2010a): *On the use of Generalised Beam Theory to assess the buckling and postbuckling behaviour of laminated CFRP cylindrical stiffened panels*. International Journal of Structural Stability and Dynamics 10:737–760.

Silva NMF, Silvestre N, Camotim D (2010b): *GBT formulation to analyse the buckling behaviour of FRP composite open-section thin-walled columns*. Composite Structures 93:79–92.

Silva NMF, Camotim D, Silvestre N, Correia JR, Branco FA (2011): *First-order, buckling and post-buckling behaviour of GFRP pultruded beams. Part 2: Numerical simulation*. Computers and Structures 89:2065–2078.

Silva NF (2013): *Behaviour and Strength of Thin-Walled Laminated FRP Composite Structural Elements*. Dissertation, University of Lisbon, Portugal.

Silvestre N, Camotim D (2002a): *First-order generalised beam theory for arbitrary orthotropic materials*. Thin-Walled Structures 40:755–789.

Silvestre N, Camotim D (2002b): *Second-order generalised beam theory for arbitrary orthotropic materials*. Thin-Walled Structures 40:791–820.

Silvestre N, Camotim D (2003): *GBT buckling analysis of pultruded FRP lipped channel members*. Computers and structures 81:1889–1904.

Silvestre N, Camotim D (2004a): *Generalised Beam Theory to analyse the vibration behaviour of orthotropic thin-walled members*. Thin-Walled Structures, 1. Auflage, CRC Press, Boca Raton et al., USA.

Silvestre N, Camotim D (2004b): *Generalized Beam Theory formulation to analyze the post-buckling behaviour of orthotropic laminated plate thin-walled members*. Proceedings of the XXI International Congress of Theoretical and Applied Mechanics, 15.–21. August 2004, Warsaw, Poland.

Silvestre N, Camotim D (2009): *Vibration analysis of composite folded-plate members*. International Journal of Vehicle Structures and Systems 1:39–44.

Silvestre N, Camotim D (2013a): *Generalized Beam Theory to analyze the vibration of open-section thin-walled composite members*. Journal of Engineering Mechanics 139:992–1009.

Silvestre N, Camotim D (2013b): *Shear deformable Generalized Beam Theory for the analysis of thin-walled composite members*. Journal of Engineering Mechanics 139:1010–1024.

Silvestre N, Freitas Silva N (2006): *On the influence of material couplings on the buckling behaviour of FRP thin-walled columns - a GBT-based approach*. III European Conference on Computational Mechanics - Solids, Structures and Coupled Problems in Engineering. 5.–8. Juni 2006, Lisbon, Portugal.

Steingass J (1972): *Ein Beitrag zur Klärung des Tragverhaltens von geschlossenen isotropen Kreiszylinderschalen*. Dissertation, Technische Universität Darmstadt, Darmstadt, Germany.

Usuki T (1976): *Torsion und Profilverformung des einzelligen Kastenträgers mit vier Wänden unter Berücksichtigung der Schubverformungen und der Drillsteifigkeit der Wände*. Dissertation, Technische Universität Darmstadt, Darmstadt, Germany.

Vlasov VZ (1961): *Thin-walled elastic beams*. Office of Technical Services, US Department of Commerce, Washington DC, USA.

Zhang X (1989): *Ein Beitrag zur Bestimmung der Traglast dünnwandiger, durch Knicken und Beulen gefährdeter U-Profile unter Längsdruckbelastung in der Symmetrieebene*. Dissertation, Technische Universität Darmstadt, Darmstadt, Germany.

Index

A
ABD matrix, 176
Airy stress function, 61, 702, 849, 870
Angle-ply laminate, 182
Approximation methods, 85, 104
Aspect ratio, 210

B
Beam element
  three-noded beam element, 926
  two-noded beam element, 921
Beltrami strain energy hypothesis, 128
Bending-extension coupling, 176, 193, 898
Bending stiffness, 945
Bending-twisting coupling, 176, 497
Bending-twisting coupling ratio, 210
Boundary conditions, 201
Boundary value problems, 312
1st Bredt formula, 972
2nd Bredt formula, 975
Brittle material behaviour, 126
Buckling, 846, 989
  basic equations, 369
  bending-twisting coupling, 497
  boundary conditions, 434
  buckling curve, 377
  buckling differential equations, 372
  elastic potential, 431
  energy methods, 431
  finite element method, 507
  first-order shear deformation theory, 390, 461
  Lévy solution, 403
  load case interactions, 494
  Navier solution, 369
  Rayleigh quotient, 437
  Ritz method, 477, 511
  shear, 490, 500
  third-order shear deformation theory, 421, 463
  unsymmetric laminates, 565

C
Cauchy's theorem, 22
Cauchy stress tensor, 21
Circular cylindrical shell, 832, 836
Classical laminated plate theory, 165, 810, 832, 895
  ABD matrix, 176
  angle-ply laminate, 182
  assumptions, 167
  balanced laminate, 177
  bending-extension coupling, 178, 193
  bending-twisting coupling, 178
  boundary conditions, 201
  change of reference plane, 184
  condensed plate equilibrium, 200
  constitutive law, 173
  coupling effects, 176
  coupling stiffnesses, 175
  cross-ply laminate, 182

© The Editor(s) (if applicable) and The Author(s), under exclusive license to Springer-Verlag GmbH, DE, part of Springer Nature 2025

C. Mittelstedt, *Mechanics of Composite Structures*,
https://doi.org/10.1007/978-3-662-70788-3

curvatures, 171
dimensionless notation, 209
disk equilibrium, 199
displacement differential equations, 200
displacements, 168
effective laminate properties, 185
finite element method, 269
kinematics, 167
laminate code, 166
laminate internal forces, 173
laminate middle plane, 167
laminate stiffness matrix, 176
Lévy solution, 224
local equilibrium, 198
membrane stiffnesses, 175
Navier solution, 213, 263
nomenclature, 167
nonlinear equations of motion, 252
plate equilibrium, 199
plate stiffnesses, 175
principle of the minimum of the total elastic potential, 203
quasi-isotropic laminates, 183
reduced plate stiffnesses, 194
Ritz method, 229
shear coupling, 177
special laminates, 180
strain energy, 190, 203, 210
strains, 170
stresses, 171
symmetric laminates, 181
symmetry plane, 167
twist, 171
vibrations, 263
Coefficient of thermal expansion, 47, 290
Compatibility conditions, 37
Condensed plate equilibrium, 200, 372
Constitutive law, 38
Coulomb-Mohr hypothesis, 131
Coupling effects, 41, 143, 176, 898
Coupling quadrant, 176
Coupling stiffnesses, 175, 898
Cross-ply laminate, 182
Cuntze's failure mode concept, 135, 283
Curved laminates, 867
Cylindrical bending, 312

D

Deviation stiffness, 945
Dimensionless notation, 209
Disk, 52
Airy stress function, 61
bipotential equation, 61
disk equation, 60, 61
internal forces, 53
potential equation, 60
stresses, 53
Disk equation, 61, 871, 872
Drucker-Prager hypothesis, 134
Ductile material behaviour, 125

E

Effective laminate properties, 185
Effective width, 708
Einstein's summation convention, 10
Engineering constants, 148
Equivalent stiffnesses, 57
Extensional stiffness, 898, 945
External complementary potential, 92
External potential, 91
Extremal principles, 91

F

Failure criteria, 123
Beltrami strain energy hypothesis, 128
Coulomb-Mohr hypothesis, 131
Cuntze's failure mode concept, 135, 283
Drucker-Prager hypothesis, 134
Hashin criterion, 278
maximum strain criterion, 274
maximum stress criterion, 274
Mohr failure hypothesis, 133
principal strain hypothesis, 127
principal stress hypothesis, 126
Puck criterion, 277
Puck's action plane fracture criterion, 279
strength, 273
Tresca yield criterion, 131
Tsai-Hill criterion, 275
Tsai-Wu criterion, 275
von Mises strain energy hypothesis, 129
Failure criterion, 126
Failure function, 126

Fiber fracture, 277
Finite Element Method, 115, 269, 507, 916, 1001
  beam elements, 921, 926
  rod elements, 917, 919
First cross-sectional normalisation, 945
First-order shear deformation theory, 302, 390, 461, 511, 755, 836, 905
  bending of symmetric beams, 314
  boundary conditions, 308
  boundary value problems, 312
  constitutive law, 306
  differential equations, 307
  displacement field, 303
  equilibrium conditions, 307
  Lévy solutions, 321
  Navier solution, 312, 317, 319
  nonlinear equations of motion, 328
  Ritz method, 321
  shear correction factor, 305, 310
  strain energy, 309
  stresses, 304
  transverse shear forces, 304
Flexural stiffness, 898
Flexural-torsional buckling, 991, 998
Force-balance-method, 782
Frame, 607
Free-corner effect, 792
Free-edge effect, 767
  analysis methods, 778
  angle-ply laminates, 772
  arbitrary laminate, 774
  cross-ply laminates, 769
  delamination forces and moments, 778
  finite element method, 779
  force-balance-method, 782
  free-corner effect, 792
  hole edge effect, 792
  piezoelectric laminates, 793
  scaled boundary finite element method, 795
  singularity, 771, 787
Full anisotropy, 142

G

Galerkin equations, 115
Galerkin method, 114, 858
Gaussian curvature, 805
Generalized beam theory, 1013
  assumptions, 1021
  boundary conditions, 1024
  cross-sectional analysis, 1021
  diagonalization, 1026
  differential equations, 1019, 1024
  distortions, 1020
  elementary states, 1014
  laminated structures, 1031
  orthogonality, 1019
  second-order theory, 1028
  stresses, 1019
  unit warping, 1016
  vibrations, 1030
Generalized Poisson's ratio, 211
General theorem of work, 86
Global buckling, 994
  approximate methods, 1000
  finite element method, 1001
  Ritz method, 1000
Green-Dirichlet minimum principle, 92
Green-Lagrange strain tensor, 32

H

Hamilton's principle, 252
Hashin criterion, 278
Higher-order laminate theories, 299
  first-order shear deformation theory, 302
  layerwise approaches, 357
  third-order shear deformation theory, 333
  three-dimensional local equilibrium, 301
Hygromechanical problems, 293
Hygrothermal problems, 289
Hypothesis of plane cross-sections, 67, 168, 806, 938

I

Index notation, 11
Infinitesimal strain tensor, 34
Inner complementary potential, 92
Inner potential, 91
Interactive buckling, 990
Interface, 167
Inter fiber fracture, 277
Interlaminar stresses, 767, 867
Isotropy, 41, 147

K
Kinematic equations, 36
Kirchhoff plate theory, 67

L
Laminate, 165
Laminate code, 166
Laminated beams, 895
  approximate methods, 1000
  bending angles, 936
  bending stiffness, 945
  boundary conditions, 902
  1st Bredt formula, 972
  2nd Bredt formula, 975
  buckling, 989
  center of gravity, 945
  constitutive law, 898, 907
  decay factor, 984
  deviation stiffness, 945
  Euler-Bernoulli beam theory, 938
  extensional stiffness, 945
  finite element method, 1001
  finite elements, 916
  first cross-sectional normalisation, 945
  first-order shear deformation theory, 905
  flexural buckling, 998
  flexural-torsional buckling, 991, 998
  forces and moments, 943
  global buckling, 994
  kinematics, 939
  lateral buckling, 991
  local buckling, 992, 1004
  parallel axis theorem, 947
  principal axis transformation, 955
  Ritz method, 903, 1000
  second cross-sectional normalization, 955
  shear correction factor, 907
  shear force flow, closed cross-section, 961
  shear stiffness, 907
  stability, 989
  static moments, 945
  Steiner's theorem, 947
  strain energy, 901, 909
  stresses, 908, 936
  St. Venant torsion, 968
  torsion, 968
  torsional buckling, 991, 998
  torsional moment of inertia, 970
  torsional stiffness, 970, 975, 977, 979
  torsion, multicellular cross-section, 975
  torsion, open profiles, 978
  torsion, single-cell cross-section, 971
  transverse shear, open cross-section, 959
  twist, 969
  warping moment, 984
  warping moment of inertia, 984
  warping stiffness, 984
  warping torsion, 980
Laminate internal forces, 173
Laminate middle plane, 167
Laminate stiffness matrix, 176
Lateral buckling, 991
Layerwise approaches, 357
Lévy solution, 224, 321, 403, 584, 612, 678
Load case interactions, 494
Local buckling, 992, 1004

M
Mass moment of inertia, 256
Material law, 38
Material symmetries, 143
Maximum strain criterion, 274
Maximum stress criterion, 274
Membrane quadrant, 176
Membrane stiffnesses, 175
Membrane theory, 811
Minimum stiffness, 609, 627
Mohr failure hypothesis, 133
Moisture expansion coefficient, 294
Moisture forces, 294
Monoclinic material, 143

N
Natural coordinates, 209
Natural frequency, 263
Navier solution, 76, 213, 263, 312, 343, 369
Nonlinear equations of motion, 252
Normal hypothesis, 67, 168, 806, 938

O
Off-axis system, 151
On-axis system, 141
Orthotropy, 145

P
Parallel axis theorem, 947
Piezoelectric laminates, 793
Plane state of strain, 56
Plane state of stress, 58
Plate, 52
  assumptions, 67
  boundary conditions, 73
  condensed plate equilibrium, 72
  constitutive equations, 70
  corner force, 75
  displacements, 69
  equilibrium conditions, 71
  hypothesis of plane cross-sections, 67
  internal forces, 53, 70
  Kirchhoff equivalent transverse shear forces, 73
  Kirchhoff plate theory, 67
  Lévy solution, 79
  Navier solution, 76
  normal hypothesis, 67
  plate equation, 73
  plate stiffness, 71
  strains, 69
  stresses, 53, 70
Plate quadrant, 176
Plate stiffnesses, 175
Postbuckling, 697
  clamped plate, 710
  compression, 698
  effective width, 708
  governing equations, 700
  semi-analytical method, 730
  shear, 717
  shear-deformable laminates, 733
  simply supported plate, 704
Principal axes, 141
Principal strain hypothesis, 127
Principal stress hypothesis, 126
Principle of Castigliano and Menabrea, 93
Principle of the minimum of the total complementary potential, 93
Principle of the minimum of the total potential, 92
Principle of the stationary value of the total complementary potential, 92
Principle of the stationary value of the total potential, 91
Principle of the virtual total complementary potential, 92
Principle of the virtual total potential, 91
Principle of virtual displacements, 88
Principle of virtual forces, 89
Puck criterion, 277
Puck's action plane fracture criterion, 279

Q
Quasi-isotropic laminates, 183

R
Rayleigh quotient, 437
Reduced bending stiffness method, 577
Reduced compliances, 880
Reduced plate stiffnesses, 194
Reduced stiffnesses, 155
Representative unit cell, 158
Ritz equations, 106, 232
Ritz method, 105, 229, 321, 351, 477, 511, 607, 856, 903, 1000
  shape functions, 233
Rod element
  three-noded rod element, 919
  two-noded rod element, 917
Rules of mixture, 157

S
Sandwich, 749, 841, 895
  bending stiffness, 915
  constitutive law, 759, 915
  effective bending stiffness, 751
  effective extensional stiffness, 752
  effective static moment, 753
  extensional stiffness, 914
  general formulation, 762
  load-bearing behaviour, 749
  neutral plane, 755
  orthotropic plate, 754
  shear stiffness, 915
  simplifications, 751
  strain energy, 761
  stresses, 916
Sandwich beam, 749
Scaled boundary finite element method, 795
Second cross-sectional normalization, 955

Seydel's orthotropy parameter, 210
Shear correction factor, 907
Shear coupling, 176
Shear deformation theories, 299
Shells, 55, 801, 867
  bending theory, 826
  buckling, 846
  circular cylindrical shell, 832, 836
  classical laminated plate theory, 810, 832
  equations of motion, 837
  equilibrium, 828
  equilibrium conditions, 813
  first-order shear deformation theory, 836
  Galerkin method, 858
  inverted constitutive law, 849
  isotropic, 869
  kinematic equations, 825, 829
  kinematics, 820
  Kirchhoff-Love-approximation, 810
  latitude circle, 802
  layered shell, 874
  loads, 805
  membrane theory, 811
  meridian, 802
  orthotropic shell, 872
  Ritz method, 856
  sandwich, 841
  shells of revolution, 802
  strain tensor, 810
  stresses, 807
  trapezoidal effect, 808, 837
  vibrations, 844
Single layer, 141
  coupling effects, 143
  effective properties, 157
  engineering constants, 148
  full anisotropy, 142
  isotropy, 147
  material law, 142
  material symmetries, 143
  monoclinic material, 143
  off-axis system, 151
  on-axis system, 141
  orthotropy, 145
  plane case, 154
  reduced stiffnesses, 155
  transformation rules, 150
  transformed reduced stiffnesses, 156
  transversal isotropy, 146
Single-layer theory, 176, 357
Singularity, 771
State of stress, 18
Static moments, 945
Steiner's theorem, 947
Stiffened laminates, 605
  buckling curves, 635
  compressive load, 612
  edge stiffener, 649, 658
  global buckling, 692
  Lévy solution, 612, 678
  minimum stiffness, 609, 627
  plate-stiffener interaction, 662
  Ritz method, 607
  shear load, 687
  transverse stiffeners, 636
  uniaxial compression, 624
Stiffness matrix, 111, 119
Strain energy, 42, 190, 901, 909
Strength, 273
Strength hypotheses, 123
Stress singularity, 787
Stringer, 607
St. Venant torsion, 968
Surface structures, 52
Swelling coefficient, 294

T

Theoretical strength, 123
Theory of elasticity, 15
  boundary conditions, 46
  boundary value problems, 45
  Cauchy's formula, 22
  Cauchy stress tensor, 21
  coefficient of thermal expansion, 47
  compatibility conditions, 37
  compliance matrix, 41
  compliance tensor, 41
  constitutive equation, 17
  constitutive law, 38
  coupling effects, 41
  deformation state, 29
  direction cosine, 23
  displacement gradient, 32
  displacements, 30
  elasticity tensor, 39
  equilibrium conditions, 28
  Eulerian approach, 31

governing equations, 46
Green-Lagrange strain tensor, 32
hydrostatic stress state, 26
infinitesimal strain tensor, 34
invariants, 25, 27
isotropy, 41
kinematic equations, 17, 18, 36
Lagrangian approach, 30
modulus of elasticity, 17
Mohr's circles, 26
normal strain, 16
normal stress, 16, 20
principal axes, 24
principal shear stresses, 25
shear modulus, 18
shear strain, 17
shear stress, 17, 20
spherical tensor, 27
state of stress, 18
stiffness matrix, 40
strain energy, 42
strain energy density, 44
strain transformation, 36
stress deviator, 26
stress vector, 19
surface forces, 19
technical shear strains, 35
thermal strains, 47
transformation matrix, 23, 36
transverse normal strain, 17
volume forces, 18
von-Kármán strains, 34
Thermal forces, 292
Thermal strains, 47
Thermomechanical problems, 290
Third-order shear deformation theory, 333, 421, 463
constitutive law, 338
equations of motion, 356
equilibrium conditions, 340
internal forces, 337
kinematics, 334
Navier solution, 343
Ritz method, 351
strain energy, 351
transverse shear stiffnesses, 339
warping moments, 339
Three-dimensional local equilibrium, 301
Torsion, 968
Torsional buckling, 991, 998
Torsional moment of inertia, 970
Torsional stiffness, 970, 975, 977, 979
Total complementary potential, 92
Total elastic potential, 91
Transformation rules, 150
compliances, 152
stiffnesses, 153
Transformed reduced stiffnesses, 156
Transversal isotropy, 146
Trapezoidal effect, 837
Tresca yield criterion, 131
Tsai-Hill criterion, 275
Tsai-Wu criterion, 275
Twist, 969

U

Unfolding, 867
Unsymmetric laminates
buckling, 565
closed-form analysis method, 565
Lévy solution, 584
reduced bending stiffness method, 577

V

Variation, 93
Variational principles, 85
Variation operator, 93
Vibrations, 263, 844
Virtual complementary work, 90
Virtual displacements, 88
Virtual forces, 90
Virtual work, 89
von-Kármán strains, 34
von Mises strain energy hypothesis, 129

W

Warping moment, 984
Warping moment of inertia, 984
Warping stiffness, 984
Warping torsion, 980